MATTHEW A. WALLIG WANDA M. HASCHEK
COLIN G. ROUSSEAUX BRAD BOLON BETH W. MAHLER

FUNDAMENTALS OF

TOXICOLOGIC PATHOLOGY

THIRD EDITION

FUNDAMENTALS OF TOXICOLOGIC PATHOLOGY

This page intentionally left blank

FUNDAMENTALS OF TOXICOLOGIC PATHOLOGY

THIRD EDITION

Edited by

MATTHEW A. WALLIG
University of Illinois at Urbana-Champaign, Urbana, IL, United States

WANDA M. HASCHEK
University of Illinois at Urbana-Champaign, Urbana, IL, United States

COLIN G. ROUSSEAUX
University of Ottawa, Ottawa, ON, Canada

BRAD BOLON
GEMpath Inc., Longmont, CO, United States

Illustrations Editor

BETH W. MAHLER
Experimental Pathology Laboratories Inc., Research Triangle Park, NC, United States

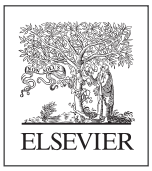

ACADEMIC PRESS
An imprint of Elsevier

Academic Press is an imprint of Elsevier
125 London Wall, London EC2Y 5AS, United Kingdom
525 B Street, Suite 1800, San Diego, CA 92101-4495, United States
50 Hampshire Street, 5th Floor, Cambridge, MA 02139, United States
The Boulevard, Langford Lane, Kidlington, Oxford OX5 1GB, United Kingdom

Notices
Knowledge and best practice in this field are constantly changing. As new research and experience broaden our understanding, changes in research methods, professional practices, or medical treatment may become necessary.

Practitioners and researchers must always rely on their own experience and knowledge in evaluating and using any information, methods, compounds, or experiments described herein. In using such information or methods they should be mindful of their own safety and the safety of others, including parties for whom they have a professional responsibility.

To the fullest extent of the law, neither the Publisher nor the authors, contributors, or editors, assume any liability for any injury and/or damage to persons or property as a matter of products liability, negligence or otherwise, or from any use or operation of any methods, products, instructions, or ideas contained in the material herein.

Library of Congress Cataloging-in-Publication Data
A catalog record for this book is available from the Library of Congress

British Library Cataloguing-in-Publication Data
A catalogue record for this book is available from the British Library

ISBN: 978-0-12-809841-7

Publisher: Mica Haley
Acquisition Editor: Rob Sykes
Editorial Project Manager: Fenton Coulthurst
Production Project Manager: Anusha Sambamoorthy
Cover Designer: Mark Rogers

Typeset by MPS Limited, Chennai, India

“To teach is to learn. . .” Japanese Proverb

This page intentionally left blank

We are profoundly grateful to those individuals responsible for our love of pathology and who mentored us during our careers as well as to our colleagues and students who inspired and supported us along this journey.

We also thank our partners, who encouraged and sustained us during our efforts to complete this revision.

This page intentionally left blank

Contents

†In Memoriam

List of Contributors

Carl L. Alden Mayflower Consulting, Wrenceburg, IN, United States

Brian R. Berridge GlaxoSmithKline Research & Development, King of Prussia, PA, United States

Brad Bolon GEMpath, Inc., Longmont, CO, United States

Denise I. Bounous Bristol-Myers Squibb Co., Princeton, NJ, United States

Mark T. Butt Tox Path Specialists, LLC, Frederick, MD, United States

Russell C. Cattley Auburn University, Auburn, AL, United States

Robert E. Chapin Retired, Pfizer Global R&D, Groton, CT, United States

Sandrine F. Chebekoue University of Montreal, Montreal, QC, Canada

Dianne M. Creasy Dianne Creasy Consulting, Norfolk, United Kingdom

John M. Cullen North Carolina State University, Raleigh, NC, United States

Dimitry M. Danilenko Genentech, South San Francisco, CA, United States

Barbara Davis Innogenics, Inc., Harvard, MA, United States

Kelly L. Diegel GlaxoSmithKline Research & Development, King of Prussia, PA, United States

David C. Dorman North Carolina State University, Raleigh, NC, United States

Richard R. Dubielzig University of Wisconsin-Madison, Madison, WI, United States

Susan A. Elmore National Toxicology Program/NIEHS, Research Triangle Park, NC, United States

Suzanne E. Fenton National Institute of Environmental Health Sciences, Research Triangle Park, NC, United States

Duncan C. Ferguson University of Illinois at Urbana-Champaign, Urbana, IL, United States

George L. Foley Abbvie, Chicago, IL, United States

Robert H. Garman Consultants in Veterinary Pathology, Inc., Murrysville, PA, United States

Kathryn E. Gropp Pfizer Inc., Groton, CT, United States

Diane Gunson Novartis Pharmaceuticals Corporation, East Hanover, NJ, United States

Gordon C. Hard Toxicologic Pathology Consulting, Tairua, New Zealand

Jack R. Harkema Michigan State University, East Lansing, MI, United States

Wanda M. Haschek University of Illinois at Urbana-Champaign, Urbana, IL, United States

Eugene Herman National Cancer Institute, Bethesda, MD, United States

Mark J. Hoenerhoff University of Michigan, Ann Arbor, MI, United States

Evan B. Janovitz Bristol-Meyer Squibb Company, Princeton, NJ, United States

Kanwar N.M. Khan Worldwide R&D, Pfizer, Groton, CT, United States

Kannan Krishnan Risk Sciences International, Ottawa, ON, Canada; University of Montreal, Montreal, QC, Canada

C. Frieke Kuper TNO, Zeist, The Netherlands

Lois D. Lehman-McKeeman Bristol-Myers Squibb Company, Princeton, NJ, United States

Xiantang Li Worldwide R&D, Pfizer, Groton, CT, United States

David E. Malarkey National Institute of Environmental Health Sciences, Research Triangle Park, NC, United States

Robert R. Maronpot Maronpot Consulting LLC, Raleigh, NC, United States

Kristen J. Nikula Seventh Wave Laboratories, LLC, Maryland Heights, MO, United States

Ricardo Ochoa Pre-Clinical Safety, Inc., Niantic, CT, United States

George A. Parker Charles River Laboratories, Inc., Hillsborough, NC, United States

Lila Ramaiah Bristol-Myers Squibb Co., New Brunswick, NJ, United States

Colin G. Rousseaux University of Ottawa, Ottawa, ON, Canada

Daniel G. Rudmann Flagship Biosciences, Westminster, CO, United States

Christine Ruehl-Fehlert Bayer AG, Wuppertal, Germany

Stefan U. Ruepp Bristol-Myers Squibb Company, Princeton, NJ, United States

Kenneth A. Schafer Vet Path Services, Inc., Mason, OH, United States

John M. Sullivan Eli Lilly & Company, Indianapolis, IN, United States

Leandro Teixeira University of Wisconsin-Madison, Madison, WI, United States

John F. Van Vleet[†] Purdue University, West Lafayette, IN, United States

Aurore Varela Charles River Laboratories, Inc., Senneville, QC, Canada

Matthew A. Wallig University of Illinois at Urbana-Champaign, Urbana, IL, United States

Zbigniew W. Wojcinski Drug Development Preclinical Services, LLC, Ann Arbor, MI, United States

[†]In Memoriam

Preface

Fundamentals of Toxicologic Pathology, as stated in the preface of its first edition, "examines the interface between toxicology and pathology, providing an overview of structural alterations caused by toxicants and the mechanisms which result in those changes." It is designed as a "textbook" with easy and ready access to core information about toxicologic pathology. It is divided into two sections, Part I containing basic information pertaining to toxicology and pathology, and Part II in an organ systems format. The basis for this textbook is the *Handbook of Toxicologic Pathology*, a much larger reference work that comprehensively addresses virtually all aspects of toxicologic pathology and its multiple interfaces with numerous-related scientific disciplines. This edition updates and expands information presented in the second edition of *Fundamentals of Toxicologic Pathology*, not only to provide additional necessary core information regarding essential toxicologic principles, core mechanisms of injury, and basic tissue responses to toxic injury (Part I) but also to provide organ system-specific mechanisms of toxicity, responses to toxic injury, and basic methods of evaluating injury (Part II). The mammary gland and special senses have been added to the organ systems section.

As with the first and second editions, this third edition is focused toward entry-level professionals in the field of toxicologic pathology, mainly pathology/toxicology residents and graduate students, who require a brief but comprehensive overview that addresses the integration of structural and functional changes, which occur with toxic injury. In addition, this textbook is also a useful reference for more experienced pathologists, toxicologists, and other health professionals. Whether you are new to the field or already an accomplished practitioner, the editors and chapter authors hope that this volume serves you well.

The editors wish to acknowledge the efforts of the original authors of the chapters in the *Handbook of Toxicologic Pathology*, third edition, many of whom actively participated in updating and revising the chapters for this book.

Matthew A. Wallig
Wanda M. Haschek
Colin G. Rousseaux
Brad Bolon
Beth W. Mahler

This page intentionally left blank

CHAPTER

1

An Overview of Toxicologic Pathology

Colin G. Rousseaux[1], *Matthew A. Wallig*[2], *Wanda M. Haschek*[2], *and Brad Bolon*[3]

[1]University of Ottawa, Ottawa, ON, Canada [2]University of Illinois at Urbana-Champaign, Urbana, IL, United States
[3]GEMpath, Inc., Longmont, CO, United States

OUTLINE

INTRODUCTION

Humans, animals, and/or the environment are exposed to dozens of xenobiotics (exogenous compounds or materials) each day, and thousands of xenobiotics over the course of time. These agents may be encountered as a single substance or in complex mixtures, in doses large or small, and for a limited period, intermittently or continuously over time. The impact of xenobiotics ranges from no detectable effect to toxicity of various severity to death. Toxicologic pathologists are instrumental in protecting the well-being of humans, animals, and the environment.

Even though toxicologic pathology was practiced for decades prior to the 1970s, widespread use of toxicologic pathology did not begin until the declaration of the "War on Cancer" in the United States by President Richard Nixon under the National Cancer Act in 1971. Over the past 50 years, this effort led to a major effort to identify carcinogens and toxicants that occur in the environment and workplace. At this time the National Cancer Institute (NCI), a subdivision of the US National Institutes of Health (NIH), initiated the first large-scale testing program, known as the bioassay program. In 1978 this program was transferred to the National Toxicology Program (NTP), located within the National Institute of Environmental Health Sciences (NIEHS), another subdivision of the NIH. To date, over 500 two-year rodent toxicity and carcinogenicity studies have been conducted by the NCI/NTP, resulting in identification of numerous environmental and workplace hazards.

Other federal agencies in the United States participating in this effort through the use of animal models, *in vitro* toxicology and molecular biology include the National Institute for Occupational Safety and Health (NIOSH) and the Environmental Protection

Fundamentals of Toxicologic Pathology.
DOI: http://dx.doi.org/10.1016/B978-0-12-809841-7.00001-0

Agency (EPA). In addition the US Food and Drug Administration (FDA) is responsible for ensuring the safety and efficacy of human and veterinary drugs, biological products, and medical devices as well as the safety of the food supply, cosmetics, products that emit radiation, and tobacco products. Similar programs to address concerns about the impact of environmental toxicants on human health also have been created in other countries, with well-known laboratories including the Fraunhofer Institute for Toxicology and Experimental Medicine in Hannover, Germany; the Institute for Applied Scientific Research (TNO) in the Netherlands; the Maltoni Institute in Bologna, Italy; and the British Industrial Biological Research Association (BIBRA). Together, these programs have substantially decreased human exposure to potentially harmful agents and thus have improved public health throughout the world.

Societies in developed countries have responded to concerns raised by focus groups and the general public by introducing legislation to address a number of issues regarding not only the effects of chemical dispersal on the environment but also the safety of products developed for industrial use. The increasing demands placed on industry to demonstrate that their products are "safe" have catalyzed an expanded interest in toxicologic pathology as a key means to develop better assessments of safety.

Industry, whether chemical or pharmaceutical, must provide safety assessment of their products to appropriate government agencies for approval prior to marketing. To address this requirement, an increasing number of pathologists have been recruited to evaluate anatomic pathology (morphologic) and clinical pathology (biochemical and hematologic) changes following exposure to xenobiotics of concern under controlled experimental conditions (i.e., safety testing). Since long-term exposure is anticipated with many environmental contaminants, a major focus of testing has been carcinogenesis using the 2-year rodent bioassay. Good Laboratory Practices (GLP) regulations, central to the industrial toxicologic pathologist's work, have been developed and implemented following exposure of fraud in laboratory testing of chemicals in the late 1970s. These regulations ensure the uniformity, reliability, and integrity of the data produced during safety assessment. Periodically, GLP regulations are revised to ensure that animal-derived data used to predict potential human responses are of the highest possible quality.

Because of the ability of toxicologic pathologists to integrate and interpret information from a broad range of disciplines, their efforts are considered critical to the identification, interpretation, and integration of functional and morphological changes from laboratory animals into safety assessment and risk management for agents to which humans might be exposed. The ability of the pathologist to work and communicate effectively in a team setting with scientists in other disciplines (toxicologists, pharmacologists, and physicians, to name a few) is essential for a successful product development and risk assessment program—as well as for a fruitful career for the pathologist. In the process of acquiring a knowledge base concerning the safety and efficacy of agents for potential use by humans, or to which they may be exposed, communal experience over time has shown it to be necessary to describe the structural and functional effects caused by these compounds in a consistent manner, and to be able to predict the likelihood of these effects and whether or not they are harmful (or "adverse") under various conditions. Thus, dose−response characterizations and adversity decisions have become an integral and important part of the field of toxicologic pathology (Chapter 2: Biochemical and Molecular Basis of Toxicity). Because an understanding of the biology of diseases that are caused by xenobiotics is necessary at the molecular level to be able to predict low-dose effects of exposure, a considerable amount of research has gone into developing appropriate models that will envisage these adverse effects.

Toxicologic pathologists are involved in many functions that protect society. A principal role is safety assessment of many materials, including drugs, chemicals, biotechnology-derived products (e.g., biomolecules, cells, gene therapy vectors, and vaccines), medical devices (e.g., implantable devices, companion diagnostic kits), and nanoparticles. Toxicologic pathologists also participate in laboratory animal disease surveillance programs; drug discovery including identification and validation of therapeutic targets; phenotypic analysis of transgenic animals; characterization and validation of animal models; evaluation of product efficacy (Chapter 7: Design of Studies and Risk Management in Toxicologic Pathology), often using animal models; and the investigation of mechanisms of toxicity (Chapter 5: Morphologic Manifestations of Toxic Cell Injury). An underappreciated task for toxicologic pathologists is to accurately and clearly communicate the meaning of their work, to many audiences: other scientists, corporate managers, regulators, and even members of the general public.

Toxicologic pathologists have many career opportunities. The largest number of toxicologic pathologists is employed by industry, be it pharmaceutical, agrochemical, chemical, or contract research organizations (CROs). Toxicologic pathologists also work for regulatory agencies, academia, research organizations (private foundations and governments), and as consultants. Societies of toxicologic pathology (STPs) in many countries provide a "home" for those working in the

discipline in regions such as North America, the United Kingdom, Europe, Japan, Latin America, China, and India. The key activities undertaken by these STPs are to provide their members with professional development opportunities (continuing education and networking) and to influence public policy by providing opinions ("best practice" and "points to consider" papers) designed to positively influence governmental policies that protect human, animal, and environmental health. Worldwide cooperation among STPs and an increasing emphasis on global harmonization promises job security to toxicologic pathologists for the foreseeable future.

WHAT IS TOXICOLOGIC PATHOLOGY?

Toxicologic pathology integrates the disciplines of pathology and toxicology most often in an experimental setting. Pathologists study the nature of disease (pathophysiology), evaluating changes produced in cells, tissues, organs, or body fluids in response to a "challenge," whether it is metabolic, infectious, neoplastic, immune-mediated, physical, or toxic in origin. Most diseases leave significant "footprints" in cells, fluids, and tissues (Chapter 5: Morphologic Manifestations of Toxic Cell Injury). Toxicologists, on the other hand, focus on the biochemical basis of the science of poisons (Chapter 2: Biochemical and Molecular Basis of Toxicity). The discipline of toxicologic pathology requires knowledge of both pathology and toxicology, as well as other related disciplines, such as statistics and experimental design, so that integration of anatomic pathology data, clinical pathology findings, and functional changes can be accomplished in a logical manner with respect to their biological significance. Contemporary toxicologic pathology also relies on an understanding of molecular biology, metabolomics, toxicogenomics, epigenetics, imaging, biomarkers, specialized techniques (such as immunohistochemistry), and quantitative approaches (e.g., morphometry, stereology, and digital image analysis) to pathology. The ability of modern biologists, including toxicologic pathologists, to relate these new platforms for gaining biological knowledge is driving the 21st century transformation from generalized to personalized medicine.

Pathologists are well versed in evaluating the manifestations of diseases, whether they occur in humans (medical) or in animals (veterinary). The toxicologic pathologist must have a mastery of both "experimental pathology" (i.e., disease investigations by which an appropriately designed study is undertaken to test a hypothesis) and "comparative pathology" (i.e., the relationship of anatomic, physiological, and pathological characteristics among various species) in the context of data interpretation and extrapolation from animals to the human population (Chapter 7: Design of Studies and Risk Management in Toxicologic Pathology). Another related but more expansive term is "environmental pathology," a branch of toxicologic pathology concerned with abiotic (unrelated to living organisms) environmental agents that influence human or animal health.

The perspective of a toxicologic pathologist differs from that of other pathologists. For example, a diagnostic pathologist interprets changes in tissues and body fluids from an individual or group to determine the cause of disease or death in that individual or wider population. However, the diagnostic pathologist must consider toxic agents as a possible cause of disease and may find evidence of contamination in the environment (polybrominated biphenyls in cattle, dichlorodiphenyltrichloroethane in raptors) or food (melamine in dogs and cats); in instances where both humans and animals may be exposed to the same toxic agent, findings by diagnostic pathologists may permit animals to serve as sentinels of disease for humans.

A forensic pathologist specializes in the investigation of death or disease that is "suspicious" in nature, with toxic agents as a possible cause of the condition. In contrast, the main role of the toxicologic pathologist, by contrast, is to determine the biological significance of alterations in form, function, or both, as manifested by altered structure of cells and tissues (lesions) or composition of body fluids (biomarkers), induced by a known chemical entity (often called the "test article" in the industrial setting). Toxicologic pathology is an essential part of hazard identification, dose–response data generation, and risk characterization, all of which are essential for risk analysis and assessment as well as risk management of human and animal exposure to potentially toxic agents (Chapter 7: Design of Studies and Risk Management in Toxicologic Pathology). Since these activities are largely confined to the industrial setting, toxicologic pathology is sometimes referred to as "industrial" pathology.

THE BASIS OF TOXICOLOGIC PATHOLOGY

The foundation of pathology is the art and science of observation, with descriptions of altered morphology still an important basis for understanding diseased tissue. Pathology has its roots in common with other medical specialties dating back to antiquity. However, modern pathology began to develop during the 19th century, with Rudolf Virchow being considered the "father of pathology" due to his use of the microscope to view cellular changes in diseased tissues. The quest to understand the causes of disease resulted in efforts

to associate lesions with their cause(s). As the discipline of pathology grew, associations were made between gross and microscopic lesions, alterations in body fluids (especially blood and urine), clinical alterations, and potential etiologies, resulting in the use of pathology as a routine diagnostic tool in medicine, initially for forensic purposes.

Observations of altered morphology were initially based on findings at autopsy or necropsy. With the development of the light microscope and later the electron microscope, novel morphologic observations could be made at the cellular and subcellular levels (Chapter 4: Principles of Pharmacodynamics and Toxicodynamics). More recent techniques have been developed to detect changes at the tissue, cellular, molecular, and gene levels such as *in vivo* small animal imaging and toxicogenomics. Importantly, enhanced techniques for examination of altered components in blood and other body fluids from living animals have led to the development of biomarkers that can be used to predict the presence, severity, and progression of toxic injury.

Toxicologic pathology requires additional working knowledge of disciplines other than anatomic and clinical pathology, and toxicology. Disciplines that form a foundation for the toxicologic pathologist include cellular and molecular biology, biochemistry, physiology, microbiology, immunology, pharmacokinetics, pharmacodynamics, risk assessment, experimental design, and statistical evaluation. These disciplines are important in integration of clinical, biochemical, morphological, and functional changes to understand the biological significance and investigate mechanisms of action (MOAs).

A working knowledge of what the body does to a xenobiotic agent (Chapter 2: Biochemical and Molecular Basis of Toxicity; Chapter 3: Pharmacokinetics and Toxicokinetics) and what the agent can do to the body (Chapter 4: Principles of Pharmacodynamics and Toxicodynamics; Chapter 5: Morphologic Manifestations of Toxic Cell Injury) is essential. In both cases, there are many factors that affect these interactions. Examples include the route of exposure and the chemical form or composition of the toxic agent or test article, as well as the species, breed/strain (race), and individual variations in absorption, distribution, metabolism, and excretion.

Exposure to toxic substances may occur by a variety of routes. Dermal and inhalation exposures are the most common routes of unintentional exposure, while intentional exposure is frequently via the oral route. Fat-soluble substances such as phenolic compounds, vitamins D and K, and steroid hormones are readily absorbed through the skin; thus, it is important to recognize the chemical characteristics of the compounds in question (Chapter 23: Bone and Joints). Widespread inhalation exposure to potentially toxic gases and particles occurs in the workplace as well as in everyday life. In addition, exposures to gases are complicated by particles that may facilitate pulmonary exposure and add to the insult of the respiratory system as well as cardiovascular system (Chapter 14: Respiratory System). The oral (per os [PO]) route is a common route by which a toxic substance or drug may enter the body. Absorption of a substance across the gastrointestinal wall depends on its lipid solubility, pH, and ionization constant, and the nature of the mucosal lining at the site of absorption (Chapter 2: Biochemical and Molecular Basis of Toxicity; Chapter 15: Digestive System). Parenteral injections of toxins (noxious agents or biological origin, such as venoms) and therapeutic agents into dermal tissues (subcutaneous, SC); muscle bellies (intramuscular, IM); or blood vessels (intravascular, IV) represent other possible routes of exposure. The rates at which toxic agents rise and fall in blood and tissue as well as the persistence of agents within the body are affected by the route of exposure.

The route of exposure to be used in toxicity testing is determined by many parameters. Key factors include the chemical and physical properties of the compound, the route for its intended use or common exposure, and natural protective barriers, such as hair or skin. The route of administration may also be governed by special biological attributes of the test species and its environment, which is particularly important for fish and insects. Toxicity testing programs often incorporate bioassays using several routes of exposure with different pharmacokinetic profiles based on the peak test article accumulation (termed the "maximum concentration," or C_{max}) and the total accumulation over time (integrated as the "area under the curve," or AUC) (see Chapter 3: Pharmacokinetics and Toxicokinetics).

THE CHALLENGES FACING TOXICOLOGIC PATHOLOGY

As one contemplates the dimensions of the problem of safety assessment and evaluation of risk, one is reminded of Albert Einstein's remark, "No amount of experimentation could ever prove me right; a single experiment can prove me wrong." This comment epitomizes the dilemma of toxicologic pathology: the data may indicate that a substance is likely to be toxic or carcinogenic, but there is never the certainty to say that it is not.

Development of lesions that can be evaluated by the toxicologic pathologist is influenced by numerous genetic, epigenetic, microbial, environmental, and

experimental factors. The importance of the microbiome in health and disease is only now starting to be appreciated and may be at least partly responsible for individual differences in response to toxic agents. As such, the toxicologic pathologist needs to understand how factors associated with the laboratory animal, the animal care and use program, the research facility environment, and the study conditions contribute to study findings so that the results of toxicity experiments can be properly interpreted. The issue of species variation in the handling of test substances makes extrapolation of results from rodents to humans difficult at best and at worst a tenuous process (Chapter 3: Pharmacokinetics and Toxicokinetics). It is doubtful whether a toxic response to a test substance administered at a high dose in a rat necessarily reflects the action of the same compound at a low dose in humans. At best, animal toxicity studies (high doses over short periods) represent a worst-case scenario for compound exposure in humans, and frequently is not an accurate representation of reality (low doses over long periods, and often multiple agents at a time). Such discrepancies may be exacerbated by the inherent genetic properties of inbred animal species versus typically outbred human populations; this situation often is handled in toxicity testing by using outbred rodent stocks (which are genetically heterogenous, like people) rather than highly inbred strains. Yet, given the state of our present knowledge and economic constraints, this method is the best we have on which to base social, political, legislative, and financial decisions.

Risk assessment characterizes potentially adverse findings (clinical, clinical pathology, and anatomic pathology) for a given species, usually humans. The risk assessment process has four main components: (1) hazard identification (does an agent cause toxicity?), (2) dose–response determination (at what doses is it toxic?), (3) exposure assessment (will individuals encounter the agent, and if so when and where), and (4) risk characterization (how likely is it that individuals will encounter the agent at a dose that may cause toxicity?). For most industrial toxicity studies, hazard identification and dose–response assessment for a test substance are central to the toxicologic pathologist's work. In contrast, exposure assessment and risk characterization are key tasks for environmental toxicologic pathologists.

Toxicologic pathologists and toxicologists participate in the risk assessment process on a daily basis. The toxicologic pathologist, together with the input from colleagues in toxicology, initially identifies the potential adverse health effects of test articles in laboratory animal species, defines the dose–response of the adverse effects, and then determines whether or not these effects are likely to express themselves in humans. An adverse health effect can only develop when exposure to a hazard occurs. However, it is important to keep in mind that not all test article–related effects are adverse, some effects are adaptive or actually desirable (i.e., pharmacological). Thus, the risk from test article exposure is the probability that a harmful response will manifest. The estimate regarding how likely it is that an adverse reaction will develop is termed risk characterization.

For many practicing toxicologic pathologists, the bioassay for determining the 2-year rodent carcinogenicity of compounds is central to their day-to-day work. The general approach to carcinogenicity testing involves treating large numbers of male and female rats and mice (50 animals per group to start, due to animal attrition over time) at several dose levels over a lifetime, followed by pathology evaluation. Unfortunately, the results are often equivocal or difficult to interpret, not least because some rodent carcinogens act by mechanisms that are not found in human cells. Given the high cost and questions regarding the relevance of the rodent cancer bioassay, a search for more predictive alternative assays continues. For example, genetically engineered mouse (GEM) models are starting to be used; these models have been designed with built-in molecular defects that predispose the animals to develop cancer at an early age, thereby allowing for smaller numbers of animals and a shorter exposure period (6 months). Nonetheless, the GEM models still are not widely used for a variety of reasons. Accordingly, the search continues for alternatives that would limit or replace animal use. Toxicologic pathologists will be integral to the identification and validation of alternative animal models.

The validity of toxicity study data is only as good as the quality of that data. Therefore, it is important for the toxicologic pathologist to be familiar with and participate in development of the study design and methods to be utilized, including sample collection, and to understand the methodologies and interpretation of statistical evaluation. Furthermore, toxicologic pathologists who assess anatomic or clinical pathology endpoints for GLP studies must work closely with quality assurance (QA) specialists to ensure that the study data set is compiled correctly and documented according to established regulatory guidelines for multiple regions of the world.

Toxicologic pathology is an interpretive discipline, and anatomic pathology diagnoses in particular are subjective evaluations that may differ even among well-trained individuals. Furthermore, morphologic lesions seen in carcinogenicity studies can be confounded by a number of factors and often require negotiation among pathologists to obtain scientific consensus regarding their relevance. For this reason, it is

now standard practice to use pathology peer-review and pathology working groups (PWGs) to validate the quality of the anatomic pathology data.

Due to the fact that anatomic pathology evaluation is an interpretive science that generates qualitative data and typically is not based on mechanical production of exact (quantitative) data, it is of paramount importance to utilize consistent nomenclature for lesions, such as that devised by the International Harmonization of Nomenclature and Diagnostic Criteria (INHAND). The communication of the interpretation for the study findings requires careful consideration as well as succinct and accurate communication skills. Interpretation of clinical pathology data may be qualitative (e.g., morphologic findings for cytological preparations) or quantitative (e.g., clinical chemistry or hematology values measured on automated high-throughput analytical instruments), but often still requires cooperation among multiple toxicologic pathologists when deciding on its final significance in assessing risk.

Additional challenges in toxicologic pathology lie with laboratory animal issues, including the advancement of the 3Rs (Replacement, Reduction, and Refinement) to minimize the numbers of animals used in research and testing in toxicology, and changes in animal husbandry related to animal welfare. In conjunction with the 3Rs, emphasis now is being placed on the development of high-throughput screening assays such as in silico algorithms (computer modeling) and *in vitro* methods (e.g., cell cultures and tissue slices), and decreased use of nonrodent species (especially nonhuman primate models) in non-GLP studies. However, rodent use is increasing in toxicity testing due to the increased utilization of GEM models to assess basic biological mechanisms as well as test article efficacy and toxicity, and also the increasing sophistication in animal monitoring systems such as telemetric assessment of physiological parameters and noninvasive imaging methods, both of which can now be applied to rodents.

When the toxicity study is complete, the toxicologic pathologist must be able to synthesize the data into a comprehensive pathology report that communicates not only the main test article–related findings but also the pathologist's interpretation regarding their meaning (adverse vs nonadverse) to the test species under the conditions of the bioassay. This pathology report is combined with documents compiled by other scientists (biochemists, pharmacokineticists, etc.) to produce a final study report that describes the outcome of the entire study. Multiple study reports from toxicity tests undertaken in multiple species ultimately are considered together to produce an overview document that communicates the risk posed by exposure to a test article; such compilations are submitted to regulatory agencies as part of a product registration package.

The data in the pathology report also may be part of the grant documentation submitted to funding agencies, or may be adapted for publication in a scientific journal. The language used in the report needs to keep in mind the audience at which it is aimed. Will it need to be understood by other scientists who are not trained in pathology? Will it need to be understood by nonscientists? Excellent communication skills, both written and verbal, are important to the success of the toxicologic pathologist.

The toxic impact of a test article requires an accurate assessment of its risk, which entails a broad scientific knowledge concerning the nature of the harm and under what conditions its potential for harm may manifest. The main challenge today often is to compile biologically based mechanistic information for several species (ideally including human cells or tissues), the possession of which permits better estimations of how cells and organisms may respond to test articles. Mechanistic information helps to determine whether or not the hazard will be likely to develop in humans and may give quantitative information to suggest under what conditions a risk may actually occur. This information may also help identify subpopulations (based on genetic, geographic, or other differences) that are at greater or lesser risk. Thus, there is a critical need for a scientific understanding of the MOAs to reduce the extent of uncertainty associated with the assessment of risk.

Finally, the globalization of markets and corporations needs to be taken into consideration when considering modern challenges faced by toxicologic pathologists. As companies extend across multiple sites, often across multiple states and countries, and as outsourcing of discovery research and safety evaluation continues to increase, there is a need for harmonization of regulations and pathology nomenclature, as well as more uniform standards for professional training and practices. In the past, each country tended to have different regulations as well as training opportunities and requirements. The International Conference on Harmonisation of Technical Requirements for Registration of Pharmaceuticals for Human Use (ICH), a consortium of European, Japanese, and US regulatory agencies and pharmaceutical industries, has brought some uniformity to international regulations to ensure the quality, efficacy, and safety of pharmaceuticals. On a smaller scale, the STP, the European STP (ESTP), the British STP (BSTP), and the Japanese STP (JSTP) collaborate regularly to standardize toxicologic pathology nomenclature through the INHAND initiative. However, a unified global standard for training of toxicologic pathologists still needs to be defined.

Globalization also has created a need for instant communication, with data- and image-sharing capabilities that often require toxicologic pathologists to become familiar with new technologies such as digital pathology. As the 21st century rolls on, toxicologic pathologists increasingly will need to adapt to new roles and technical innovations.

Resources required to address the various challenges faced by toxicologic pathologists are being developed by STP, based in North America, and other STPs around the world. The STP regularly circulates new information in *Toxicologic Pathology* and in the Society's website (www.toxpath.org). Key categories that are addressed in the STP outreach effort include continuing education for its members, affiliated societies, and regulators; up-to-date scientific reviews; position ("best practice" and "points to consider") papers for important issues facing the toxicologic pathology community, and opinion pieces on current regulatory issues. Similar publications are available from the BSTP, ESTP, and JSTP as well as in other related journals (*Experimental and Toxicologic Pathology* and the *Journal of Toxicologic Pathology*).

TRAINING AND CERTIFICATION IN TOXICOLOGIC PATHOLOGY

A toxicologic pathologist is a biomedical scientist with extensive clinical training, specialized training in comparative pathology, and subspecialization in toxicologic pathology. The majority of toxicologic pathologists worldwide are veterinarians with a veterinary medical degree (DVM or equivalent) and pathology training through a residency program, which generally culminates with board certification in general pathology [e.g., diplomate status in the American or European College of Veterinary Pathology (ACVP or ECVP, respectively)]. In the United States, pathology training focuses on anatomic pathology and/or clinical pathology (depending on the training program), although there is some overlap both in training and the content of the ACVP board examination.

Very few training institutions provide training in toxicologic pathology per se, although trainees may be exposed to some toxicology courses and occasional diagnostic cases involving toxicant exposure. To a lesser extent, medically trained pathologists (MD or equivalent) or comparative/experimental pathologists (PhD or equivalent) are also involved in the practice of toxicologic pathology, especially in countries such as China and Japan; scientists with doctoral degrees alone (PhD) make up a very small group of current toxicologic pathologists. Research training may be obtained through an MS, PhD, or other postdoctoral training. Because of the differing scopes of training in diagnostic pathology (i.e., a medical-oriented degree and/or residency) versus experimental pathology (i.e., a research-oriented degree), individuals with both experiences generally enter the toxicologic pathology work force with more self-confidence and often require less time to gain proficiency.

Formal certification in toxicologic pathology is only available in Japan (diplomate, JSTP) and in some European countries. Many pathologists engaged in toxicologic pathology have chosen to demonstrate their expertise in toxicology by obtaining certification in toxicology [e.g., diplomate status provided through the American Board of Toxicology (ABT) in the United States or as a European Registered Toxicologist (ERT)]. For more experienced toxicologic pathologists, recognition as a Fellow by the International Academy of Toxicologic Pathology (IATP) is an option for showcasing their long-term expert practice in this profession.

Traditionally trained veterinary and medical pathologists encounter many unanticipated challenges in the transition from diagnostic pathologist to the experimental, regulatory-driven environment of the industrial toxicologic pathologist. During their years of training and diagnostic effort, pathologists typically provide both clinical and public health services in a diagnostic, hospital, or private laboratory setting. In such settings, they also serve the clinical community to support therapeutic approaches and prognoses. These laboratories generally function by internal work practices and procedures based on professionally recognized best practices with a degree of governmental oversight. However, the work practices of the diagnostic pathologist in these environments are not as severely constrained by the extensive GLP regulations mandating proper management and storage of data, QA review, peer review, animal welfare standards, organizational structure and personnel, and study design, except in the case of forensics. Adaptation to this enhanced degree of regulatory oversight represents one of the significant challenges faced by diagnostic pathologists who choose to make the transition to an industrial toxicologic pathology role.

THE "PRACTITIONER" OF TOXICOLOGIC PATHOLOGY

A "practitioner" of toxicological pathology utilizes toxicologic pathology, on a daily basis regardless of the employment sector. As discussed earlier, the majority of toxicologic pathologists are employed by industry (including CROs), with smaller numbers in government, academia, and private consulting practices.

Regulatory (Industrial) Toxicologic Pathology

The majority of toxicologic pathologists in industry participate in regulatory-type, nonclinical studies performed in an experimental setting (applied research) in support of development of bio/pharmaceuticals and, to a lesser extent, agricultural and other chemicals, and medical devices. Anatomic pathology is usually a key part of these studies, whereby a standard tissue set (Table 1.1) is examined histologically for potential lesions. Toxicologic pathologists also participate in other aspects of drug development, particularly drug discovery (especially target discovery and validation), or can move up the corporate ladder into management (of pathology and/or toxicology departments, or sometimes of whole product development divisions). Optimal qualifications for entry-level industrial toxicologic pathologists in developed countries include a DVM (or equivalent) medical degree, board certification in veterinary pathology, and a degree (PhD) demonstrating research training. The PhD degree is valued because it fits its holders to face many of the challenges in toxicologic pathology stemming from new technologies (e.g., advanced molecular methods, innovative analytical instrumentation) and also provides some understanding of experimental design and statistical considerations.

Industrial toxicologic pathologists play a vital role in risk assessment. As new methods become validated and implemented, resulting in sophisticated visualization of altered morphology, new biomarkers, and gene-based technologies, toxicologic pathologists are expected to provide more than unambiguous diagnoses and a dose–response assessment via interpretation of routine hematoxylin and eosin–stained tissue sections and standard clinical pathology parameters. As toxicologic pathologists more frequently assume a greater role in product development, such as serving as Study Director for compounds under development as pharmaceutical agents, the impact of their observations, interpretations, and expert comments will become even greater. Therefore, issues such as consistency of terminology, study design (Chapter 7: Design of Studies and Risk Management in Toxicologic Pathology), statistical interpretation, integration of data into meaningful assessments of health risks, communication of risk, and risk management (Chapter 7: Design of Studies and Risk Management in Toxicologic Pathology) will need to be familiar to the toxicologic pathologist. The value of research skills is becoming of greater importance as more toxicologic pathologists in industry are becoming involved in the discovery arena, developing models for toxicity and efficacy testing and also investigating mechanisms of toxicity. The whole-animal focus of veterinary or medical training provides a critical viewpoint for product development teams that help in integrating data provided by other team members with more reductionist (molecule- or cell-oriented) perspectives.

TABLE 1.1 Society of Toxicologic Pathology Recommended Core List of Tissues to be Examined Histopathologically in Repeat-Dose Toxicity and Carcinogenicity Studies (for All Species Where Applicable)[a]

Adrenal gland	Pancreas
Aorta	Parathyroid gland
Bone with bone marrow[b]	Peripheral nerve
Brain	Pituitary
Cecum	Prostate
Colon	Salivary gland
Duodenum	Seminal vesicle
Epididymis	Skeletal muscle
Esophagus	Skin
Eye	Spinal cord
Gallbladder	Spleen
Harderian gland	Stomach
Heart	Testis
Ileum	Thymus
Jejunum	Thyroid gland
Kidney	Trachea
Liver	Urinary bladder
Lung	Uterus
Lymph node(s)	Vagina
Mammary gland[c]	Other organs or tissues with gross lesions
Ovary	Tissue masses

[a]*This tissue list is intended to be a minimum core list that can be used for all types of repeat-dose toxicity and carcinogenicity studies, regardless of route of administration, species or strain of mammalian laboratory animal, duration of study, or class of drug to be tested. It is recommended that the route of administration be considered at the time of study design and that tissues relevant to the route of administration be added to this core list. For example, the addition of nasal cavity and turbinates, larynx, and tracheobronchial lymph nodes may be considered for inclusion in the tissue list for nasal inhalation studies. Likewise, depending upon the species or strain of laboratory animal, the addition of organs or tissues unique to or characteristic of that species or strain may be selected, as appropriate. It is also recommended that additional tissues that are known to be targets of the test article or those of its class be added to this core tissue list.*
[b]*For nonrodents, either rib or sternum. For rodents, femur including articular cartilage.*
[c]*Females only.*
From Bregman, C.L., Alder, R.R., Morton, D.G., Regan, K.S., Yano, B.L., 2003. Recommended tissue list for histopathologic examination in repeat-dose toxicity and carcinogenicity studies: a proposal of the Society of Toxicologic Pathology (STP). Toxicol. Pathol. 31 (2), 252–253.

Toxicologic Pathology Related to the Environment and Food Safety

Toxicologic pathologists involved in environmental pathology and food safety are generally employed by government agencies, such as the US EPA; US National Institute of Environmental Health Sciences (NIEHS, a division of the NIH); FDA; and US Department of Agriculture (USDA). However, some pathologists filling these roles are professionals in academia. There has been increasing recognition that the practice of toxicologic pathology can add valuable information for diagnosing environmental problems, detailing background disease prevalence, investigating mechanisms of toxicity, and developing alternate animal models for evaluating toxicity.

Human activities are the major source of environmental contaminants. Some contaminants, such as chlorinated or brominated organics and heavy metals as well as radioactive wastes, persist in the environment for indefinite periods and threaten human, wildlife, and domestic animal health. Environmental pathology deals with workplace exposures as well as air, water, and ground contaminants. Examples of workplace toxicants include asbestos, which causes asbestosis, lung cancer and mesothelioma, and diacetyl from popcorn butter flavoring, which can cause bronchiolitis obliterans (popcorn worker's lung). Air pollutants include sulfur dioxide, nitrogen oxides, ozone, and fine particulates, largely produced by industry and motor vehicles; these agents affect the respiratory and cardiovascular systems as well as possibly playing a role in metabolic syndrome and diabetes. Recently, lead from corroding water distribution pipes has been under the spotlight in Detroit and other cities, although lead exposure from chips of old paint is probably as important source in many communities. New environmental concerns include pharmaceuticals and antibiotics found in drinking water and industrial effluents, endocrine-disrupting chemicals, and the effect of "lifestyle" drugs (e.g., alcohol, marijuana, tobacco) on human populations (including those exposed by second-hand smoke).

The adverse effects of nutritional components and contaminants in food products are also important areas to which the toxicologic pathologist can add value. Nutritive and nonnutritive (typically preservative) chemicals are integral components of foods; indeed, foods may contain, intentionally or unintentionally, a wide range of chemicals from many sources that could be a potential health hazard. Toxicants (including toxins such as phycotoxins and mycotoxins) can enter the food chain at various levels of the food web, after which they can interact with other chemicals and compounds present in food, bio-accumulate, be metabolized into bio-products, or be modified during food processing and cooking. Knowledge of the chemical properties of substances and understanding their biological effects, MOAs, and pharmacokinetics (absorption, distribution, metabolism, bioaccumulation, and elimination) are important in assessing food safety.

Diagnostic Toxicologic Pathology

Diagnostic pathology identifies the cause of disease based on morphologic and/or clinical pathology findings, as well as history, clinical signs, and ancillary test results. It is important in all areas of pathology, both in spontaneous and in experimentally induced disease, including conditions associated with toxicant exposure. In experimental studies, it is important to separate out the effects of spontaneous disease and those induced by the experimental agent/test article. Diagnostic pathology is essential to investigate unexpected disease or death in laboratory animal colonies or prior to the termination of a study.

Diagnostic pathologists in academia and government also need to be familiar with the basics of toxicologic pathology since exposure to toxic agents is not uncommon in both companion and agricultural animals. Diagnostic pathologists working in human and veterinary medicine need to be familiar with tissue responses to drugs, harmful industrial and agricultural chemicals, environmental contaminants, and toxins produced by a wide variety of microbes, algae, fungi, and plants. Exposure to such agents may be accidental or intentional, and may occur in a single individual or in a group setting. Accidental exposure in humans may occur in an occupational setting or from environmental contamination, whereas intentional exposure or overdose can occur in malicious poisoning or suicide. Genetic susceptibility or underlying disease in exposed individuals or populations can increase risk posed by exposure to toxic agents.

In the veterinary diagnostic laboratory, toxicologic pathology will continue to be central to diagnosis and prevention of spontaneous, toxicant or toxin-induced disease. Since animals can serve as sentinels for human disease, the diagnostic laboratory is uniquely situated to identify sources of environmental contamination whether they are related to food, water, or other forms of exposure. Such contamination may affect the local animal population or may also affect human health. In addition, the utility of naturally occurring chemically induced diseases as models should not be underestimated, as it is often that diagnostic cases add crucial information to inform our understanding of the mechanisms of toxicity of these and similar chemical groups. One

example of this paradigm was the identification of melamine and cyanuric acid (present in pet food) as the cause of acute nephrotoxicity in dogs and cats. Research based on such an outbreak in the United States led to the identification of melamine as the cause of nephrotoxicity in children in China due to contamination of milk formula (Chapter 11: Urinary System).

Investigative Toxicologic Pathology

Research in toxicologic pathology is essential for understanding the mechanisms of toxic injury (e.g., Chapter 6: Carcinogenesis: Manifestation and Mechanisms) and to fill data gaps that impede risk assessment. In addition, by obtaining an understanding of the pathogenesis of altered structure and function associated with toxicant exposure, normal physiological processes are often elucidated. For example, the use of teratogenic substances has aided our understanding of embryonic and fetal development (Chapter 25: Embryo, Fetus, and Placenta), and even helped to devise mechanism-based treatments to reduce or prevent certain classes of birth defects.

Toxicologic pathologists participate in research in many settings, including industry, academia, and government. Their unique skill set, which includes descriptive and comparative pathology, problem-solving, and broad-based education with a "whole-animal" orientation, brings an added dimension to many research areas.

Research in toxicologic pathology ranges from simple associative types of work including retrospective studies using archived tissues, cross-sectional surveys, and longitudinal studies of disease progression and remission to evaluation of the importance of toxicant-induced gene changes in initiating and sustaining various human diseases. In prospective investigations, the etiology is known, but the pathologist still uses morphological diagnoses to describe the disease process. Familiarity with experimental design and an understanding of statistical analysis are essential skills in investigative pathology. This output is considered in light of the key experimental variable(s), usually exposure to a xenobiotic at a particular dose. The output is a tested hypothesis as to the effect of the treatment by the experimental variable—xenobiotic "X"—generally by determining a difference between treated and untreated (negative control) animals as well as the relationship of xenobiotic exposure to the dose level. This relationship is essential in risk assessment.

The ongoing advent of new techniques and animal models will allow the field of investigative toxicologic pathology to progress and expand in scope and importance. Molecular biology and genomic techniques being used to probe the mechanisms of toxic injury. For example, activated oncogenes have been found in both human and animal tumors (Chapter 6: Carcinogenesis: Manifestation and Mechanisms), and so tumorigenesis associated with expression of constitutively activated oncogenes can be studied in transgenic mice, where the engineered proteins have been modified to always be functioning. Identification of an oncogene specifically activated by a given xenobiotic may aid in the extrapolation of data from bioassays conducted in rodents to predict human responses to that xenobiotic. In the case of genetically altered mice, the information obtained from studies using these animals has led to alternative models to study and test for carcinogenic potential. In fact, the p53 knockout mouse is presently being used to aid in identification of carcinogens.

Today's rapid pace of scientific advancement and the development of new technologies that can be exploited to address toxicological issues means that large strides will continue to be made in understanding mechanisms of xenobiotic-induced alterations and diseases. The combination of morphological techniques, which provide topographic specificity, with novel technologies that permit large-scale assessments of metabolic intermediates, proteins, and mRNA but generally lack topographic specificity, can be used to facilitate the study of mechanisms underlying xenobiotic-induced, microscopically detectable lesions. The combination of traditional lesion identification with laser capture microdissection, for example, will permit the direct molecular assessment of lesions by a variety of such new technologies.

Management Roles for Toxicologic Pathologists

As their careers progress, many scientists involved in product discovery and development find themselves moving toward more managerial roles, where they need to make decisions on compound development that necessitates the incorporation of techniques for risk management (Chapter 7: Design of Studies and Risk Management in Toxicologic Pathology). In fact, they may attain positions in upper management themselves. The toxicologic pathologist is well poised by both training and prior experience to fill such positions, as the management of scientific issues concerning product discovery and development is often best served by the integration of information arising from many interrelated disciplines (Figure 1.1).

However, a manager requires more than just a solid toxicologic pathology background to succeed in such a role. Toxicologic pathologists in managerial positions

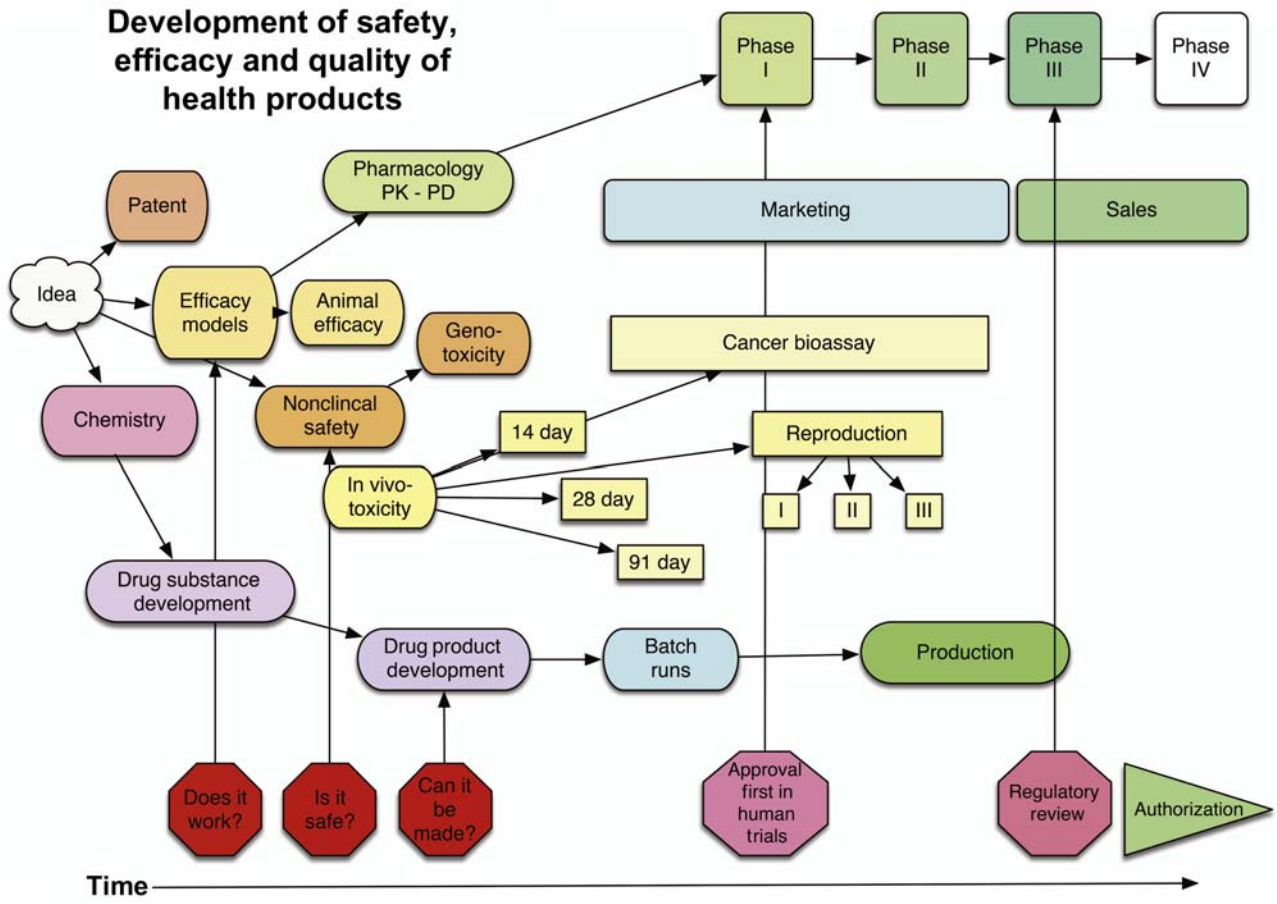

FIGURE 1.1 An example of the multidisciplinary understanding required for risk management in the development of health products. Source: *From Haschek, W.M., Rousseaux, C.G., Wallig, M.A. (Eds.), 2013. Handbook of Toxicologic Pathology, third ed. Academic Press, Figure 21.3, p. 653, with permission.*

also require strong oral and written communication skills to deal with upper-level managers (i.e., senior executives), regulators, corporate (including patent) lawyers, and external stakeholders, including prospective investors. In particular, genuine prowess in communication is a prerequisite for success in a managerial role, particularly when it comes to risk management (Chapter 7: Design of Studies and Risk Management in Toxicologic Pathology).

SUMMARY

In summary, toxicologic pathologists are well suited to play many pivotal roles in decision-making within the framework of hazard identification and risk assessment/management. Their broad and thorough understanding of most biological processes, their perspective of biology as an integrative (i.e., whole animal) rather than reductionist (molecule- or cell-oriented) discipline, their ability to generate detailed data for decision-making, and their familiarity with the many limitations on the biological significance of such inherently subjective data make the toxicologic pathologist a critical member of the modern product discovery and development process. The growing number of new products being developed and produced worldwide as well as the many novel roles that will arise in this field during the next decades will offer toxicologic pathologists long and vibrant careers in serving to protect public health. For further information and details regarding specific aspects of toxicologic pathology (e.g., GLPs, quality assurance and quality control; a pathologist's role in drug discovery and development; peer review and PWGs), it is suggested that the reader refer to "*Haschek and Rousseaux's Handbook of Toxicologic Pathology*," Third Edition, Volumes I, II, and III, Elsevier, San Diego, CA (2013).

Further Reading

Aeffner, F., Wilson, K., Bolon, B., Kanaly, S., Mahrt, C.R., Rudmann, D., et al., 2016. Commentary: roles for pathologists in a high-throughput image analysis team. Toxicol. Pathol. 44, 825–834.

Bolon, B., Barale-Thomas, E., Bradley, A., Ettlin, R.A., Franchi, C.A., George, C., et al., 2010. International recommendations for training future toxicologic pathologists participating in regulatory-type, nonclinical toxicity studies. Toxicol. Pathol. 38, 984–992.

Bucher, J.R., 2013. Regulatory Forum Opinion Piece: Tox21 and toxicologic pathology. Toxicol. Pathol. 41, 125–127.

Cohen, S.M., Arnold, L.L., 2016. Critical role of toxicologic pathology in a short-term screen for carcinogenicity. J. Toxicol. Pathol. 29, 215–227.

Ettlin, R.A., 2013. Toxicologic pathology in the 21st century. Toxicol. Pathol. 41, 689–708.

Mann, P.C., Vahle, J., Keenan, C.M., Baker, J.F., Bradley, A.E., Goodman, D.G., et al., 2012. International harmonization of toxicologic pathology nomenclature: an overview and review of basic principles. Toxicol. Pathol. 40 (4 Suppl.), 7S–13S.

Maronpot, R.R., 2012. Regulatory Forum Opinion Piece: the role of the toxicologic pathologist in the postgenomic era: challenges and opportunities. Toxicol. Pathol. 40, 1082–1086.

Turner, P.V., Haschek, W.M., Bolon, B., Diegel, K., Hayes, M.A., McEwen, B., et al., 2015. Commentary: the role of the toxicologic pathologist in academia. Vet. Pathol. 52, 7–17.

van Tongeren, S., Fagerland, J.A., Conner, M.W., Diegel, K., Donnelly, K., Grubor, B., et al., 2011. The role of the toxicologic pathologist in the biopharmaceutical industry. Int. J. Toxicol. 30, 568–582.

Weber, K., 2014. Role of the study pathologist. Toxicol. Pathol. 42, 276–277.

PART I

PRINCIPLES OF TOXICOLOGIC PATHOLOGY

This page intentionally left blank

CHAPTER

2

Biochemical and Molecular Basis of Toxicity

Lois D. Lehman-McKeeman and Stefan U. Ruepp

Bristol-Myers Squibb Company, Princeton, NJ, United States

OUTLINE

INTRODUCTION

The cellular basis of toxicity encompasses the identification of a target organ of toxicity coupled with the features of how that organ responds to toxic stress. Since most organs are a composite of different cell types with a variety of functions, cellular targets of toxicity are determined by the type of insult and the mechanism of toxicity. The molecular basis of toxicity encompasses the breadth of changes from transcriptional, translational, and signal transduction pathways that are causally related to toxic responses. Although defined separately, molecular and cellular events are intertwined and contribute to sensitivity to toxicity, the nature of the toxic response, and the type of repair mechanisms that may ensue. An overarching concept in considering any mechanism of toxicity is that xenobiotic disposition plays a central role in the development of toxicity and is often a major determinant of the dose–response relationship for toxicity and a potential source for species differences in toxic responses.

In light of the breadth of target cells, target organs, and molecular pathways underlying toxic mechanisms, it is difficult to adequately address the multitude of mechanisms and pathways by which toxicants elicit adverse effects in cells or organs. This chapter focuses on the fundamental principles that contribute broadly to toxic or pathologic effects, starting with the characteristics that determine how a toxicant is delivered to its target, the major factors that determine toxic outcome and concluding with those that determine whether repair or regeneration occurs after toxic insult.

Fundamentals of Toxicologic Pathology.
DOI: http://dx.doi.org/10.1016/B978-0-12-809841-7.00002-2

GENERAL PRINCIPLES OF XENOBIOTIC DISPOSITION

The disposition of a xenobiotic is defined as the integrated action of its absorption, distribution, biotransformation, and elimination. The quantitative determination of these properties comprises the field of pharmacokinetics (or toxicokinetics), and collectively, disposition and kinetics ultimately determine the concentration of a compound at a target site for toxicity and dictate whether adverse effects will occur.

General Properties of Absorption

Biological Membranes

Cell membranes are comprised of a phospholipid bilayer wherein the polar head groups of the lipids are oriented toward the outer and inner surfaces of the membrane and the lipid tails are oriented inward forming a hydrophobic inner space. Cell membranes are typically 7–9 nm thick, and phosphatidylcholine and phosphatidylethanolamine are the primary phospholipids in the outer and inner leaflets, respectively. Membranes also contain a variety of transmembrane proteins that function as receptors for many endogenous ligands, form pores, or ion channels in the membrane, or transport endogenous and exogenous compounds into and out of cells. The processes involved in the passage of compounds across membranes include those that require no energy, and include direct passage through pores, filtration or simple diffusion. In addition, there are numerous active transport processes, which require energy utilization to move solutes across membranes against a concentration gradient.

Simple Diffusion

Diffusion occurs down a concentration gradient, moving from regions of higher concentration to lower concentration (Fick's law). Large, hydrophobic molecules diffuse directly across the lipid domain of the membrane. In contrast, smaller water-soluble molecules can pass through aqueous pores in a process referred to as paracellular diffusion. The two principal factors that govern the rate of transport across membranes for organic molecules are lipid solubility and the degree to which a compound is in its nonionized form at physiological pH. Lipid solubility is frequently expressed as the octanol–water partition coefficient (or log P), where a very lipid-soluble molecule has a positive log P. For example, the highly lipophilic compound, 2,3,7,8-tetrachlorodibenzodioxin (TCDD), has a log P of 7.05, whereas the water-soluble metal salt, lead acetate, has negative log P (−0.63). Ionization is determined by the Henderson–Hasselbalch equation, which defines the relationship between the pH and the pK (the pH at which a weak organic acid or base is 50% ionized). Only the nonionized form of a compound is available for diffusion across membranes. In this manner, a weak base, such as aniline (pK = 5), is 50% ionized at pH 5, but it is essentially in its nonionized form at pH 7. Thus, physiological pH favors the absorbance of weak bases more so than weak acids.

Filtration

Filtration is the bulk movement of water across a porous membrane, and any solute that is small enough to pass through membrane pores will flow with it. Overall, filtration is governed by hydrostatic and osmotic pressures along with the pores that allow small molecules to pass through them. Pore sizes are typically 2–7 Å, and as pressure rises on one side of the membrane, small molecules are forced through the pores. The renal glomerulus is a major site of filtration, and its pores are typically in range of 70–80 Å, large enough for numerous solutes and some low-molecular-weight proteins to be filtered. In some endothelial beds, there are larger pores that form interendothelial gaps to allow larger molecules to move from the plasma to extracellular space. In contrast, such pores are absent in the brain, where the blood–brain barrier (BBB) is formed by tight junctions between cells.

Specialized Transport: Active Transport and Facilitated Diffusion

The sequencing of the human genome revealed that there are at least 500 genes likely to function in membrane transport. These systems contribute to uptake and efflux of compounds and contribute to the homeostasis of endogenous compounds and xenobiotics. There are active transporters that utilize energy (typically adenosine triphosphate, ATP) to move chemicals against a concentration gradient. They demonstrate some substrate selectivity, can be saturated at high concentrations and are inhibited by compounds that compete for transport.

The first ATP-dependent transporter identified to play a role in xenobiotic disposition was a phosphoglycoprotein identified in tumor cells that developed resistance to cancer chemotherapy. The protein was called P-glycoprotein or multidrug resistance protein (Mdr1), and the basis for cell resistance is that Mdr1 is an efflux pump that actively removes toxic compounds from cells. Meanwhile several transporter families have been identified that contribute to the disposition of xenobiotics and influence toxicant exposure and outcome. A summary of these gene families is provided in Table 2.1. The process of facilitated diffusion is also a carrier-mediated process but it does not require ATP consumption. In facilitated diffusion, a

TABLE 2.1 Summary of Major Transporters That Contribute to Xenobiotic Disposition

Name	Gene family	Function	Common name	Tissue expression
Multidrug resistance protein; P-glycoprotein	*Abcb1*	Efflux pump	Mdr1a, 1b	Liver, kidney, brain small intestine
Bile sale export pump	*Abcb11*	Efflux pump for bile salts	Bsep	Liver
Multidrug resistance protein (Mrp)	*Abcc*	Efflux pumps; apical; and/or basolateral	Mrp1	Choroid plexus
			Mrp2	Liver, kidney, brain small intestine
			Mrp3	Liver, small intestine
			Mrp4	Liver, kidney, brain, choroid plexus
			Mrp5	Brain
			Mrp6	Liver
Breast cancer resistance protein (Bcrp)	*Abcg2*	Efflux pump on bile canaliculus	Bcrp	Liver, kidney, brain, placenta
Organic anion transporting polypeptide (Oatp)	*Slco*	Influx pump; organic anions substrates	Oatp1a1	Liver, kidney, choroid plexus
			Oatp1a4	Liver, kidney choroid plexus, brain
			Oatp1b2	Liver
			Oatp2a1	Kidney
Organic anion transporter (Oat)	*Slc22*	Uptake of organic anions	Oat1	Kidney
			Oat2	Liver, kidney
			Oat3	Kidney, brain
Organic cation transporter (Oct)	*Slc22*	Uptake of organic cations	Oct1	Liver, kidney jejunum, testis
			Oct2	Kidney, lung, choroid plexus
			Oct3	Testis
Organic cation/carnitine transporter	*Slc22*	Carnitine transport	Octn1	Kidney
		Carnitine transport	Octn2	Kidney, small intestine
Multidrug and toxin extrusion transporter (Mate)	*Slc47*	Efflux pump for cations	Mate1	Kidney, liver
		H^+/cation antiporter	MATE2K	Human kidney

Genes listed represent major transporters in rats involved in xenobiotic disposition (except where noted for MATE2K). Several transporter families including those that contribute to nucleoside or peptide transport are not included but are discussed in the text.
From Haschek, W.M., Rousseaux, C.G., Wallig, M.A. (Eds.), 2013. Handbook of Toxicologic Pathology, third ed. Academic Press, Table 1.1, p. 18, with permission.

substrate moves with a concentration gradient, and carrier proteins, typically integral membrane proteins, are responsible for the passage of molecules or ions across the membrane. Classically, the transport of glucose occurs by facilitated diffusion.

In addition to transporters that contribute to the disposition of xenobiotics, there are numerous transporter families that are specifically involved in the distribution of important endogenous compounds. These include the glucose and nucleoside transporters, transporters that serve to move basic or neutral amino acids, including neurotransmitters, and transporters involved in the distribution of essential elements such as calcium, iron, and copper. Although such transporters are associated with important endogenous nutrients, they can influence exposure to toxicants. For example, lead is a substrate for the facilitated transporters involved in calcium and iron uptake.

Routes of Absorption

Absorption From the Gastrointestinal Tract

Absorption can occur all along the gastrointestinal (GI) tract, but as noted earlier, the nonionized fraction is most readily absorbed. As such, some weak acids may be absorbed in the acid pH of the stomach, whereas most weak bases are not absorbed until reaching the more neutral environment of the small intestine.

Numerous xenobiotic transporters are expressed in the GI tract, where they function to increase or decrease absorption of xenobiotics (Table 2.1). Influx transporters are predominantly localized on the apical brush border membranes of the enterocytes and increase uptake from the lumen into the enterocytes. These include the Oatps, Octs, and peptide transporters (Pept1). The primary active efflux transporters such as P-gp, Mrp2, and Bcrp are also expressed on enterocyte brush border membranes, where they function to excrete their substrates into the lumen, thereby decreasing the net absorption of xenobiotics.

Particles can also be absorbed by the GI epithelium. Particle size is the primary determinant of absorption, and smaller particles are more likely to be absorbed. Absorption into gut-associated lymphoid tissue (such as Peyer's patches) and the mesenteric lymph supply is key to systemic absorption of particles.

The amount of a chemical that enters the systemic circulation after oral administration depends on the amount absorbed into the cells of the GI tract, the action of transporters on uptake or efflux from the cells, and the potential for biotransformation. An important concept in this regard is presystemic elimination, referred to as a first-pass effect, which is the potential for removal of chemicals before entrance into the systemic circulation. Chemicals that have a high first-pass effect will appear to have a lower absorption because they are eliminated as quickly as they are absorbed.

Absorption From the Respiratory Tract

Agents that are absorbed by the lungs include gases, vapors of volatile liquids, aerosols, and particulates. The absorption of inhaled gases takes place mainly in the lungs, but they first must pass through the nose, where some molecules are retained if they react with cell surface components. Although such actions may reduce systemic exposure or protect the lungs, they also increase the potential for the nose to be adversely affected.

Absorption of gases in the lungs is determined primarily by the respiration rate. It differs from GI absorption because most ionized molecules have low volatility and do not achieve significant concentrations in normal ambient air. Overall, any chemical absorbed by the lungs is removed rapidly by the blood, which moves very quickly through the extensive capillary network in the lungs.

Absorption of aerosols and particles is determined by the aerosol size and water solubility of any chemical in the aerosol. In general, the smaller the particle, the further into the respiratory tree the particle will deposit. Particles $\geq 5\,\mu m$ usually are deposited in the nasopharyngeal region, whereas those with diameters of approximately $2.5\,\mu m$ distribute to the tracheobronchial and bronchiolar regions. Particles $\leq 1\,\mu m$ penetrate to the alveolar sacs of the lungs, and nanoparticles that are 10–20 nm in diameter tend to deposit in the alveolar region, where they may be absorbed into blood or cleared through the lymphatics after being scavenged by alveolar macrophages.

Absorption Through the Skin

As the largest organ in the body, skin comes into contact with many chemicals, but exposure is usually limited due to its relatively impermeable nature. The stratum corneum is the single most important barrier to preventing fluid loss from the body while also serving as the major barrier that prevents the absorption of xenobiotics into the body. Chemicals move across the stratum corneum by passive diffusion, and in general, diffusion is proportional to lipid solubility and inversely related to molecular weight. Once absorbed across the stratum corneum, the vascular network within the dermis allows absorbed compounds to enter the body.

Dermal absorption varies widely across species. In general, dermal absorption across rodent skin is much greater than human skin, whereas the cutaneous permeability characteristics of guinea pigs, pigs, and monkeys are often similar to those observed in humans. Species differences in dermal absorption of xenobiotics result from several anatomic, physiologic, and biochemical factors. Importantly, the stratum corneum is much thicker in humans than in most laboratory animals. However, the thinner stratum corneum in animals is often compensated for by a relatively thick hair cover, diminishing direct contact of the skin with a xenobiotic.

General Principles of Distribution

Once absorbed, a compound rapidly distributes throughout the body. The rate of distribution to organs or tissues is determined primarily by blood flow and the rate of diffusion out of capillary beds into cells of a particular organ. The final distribution depends on the affinity of a xenobiotic for various tissues, and this factor often determines the target organ of toxicity.

Volume of Distribution

A fundamental concept for understanding xenobiotic disposition is the volume of distribution (V_d), which quantifies the distribution of a xenobiotic throughout the body. It is defined as the volume in which the amount of compound would need to be uniformly dissolved in order to produce the observed blood concentration. For example, if a chemical is only in the plasma compartment and not distributed into organs, it would have a higher plasma concentration and a low V_d. In contrast, if a compound distributes throughout the body, it would have a much lower concentration in the blood and a high V_d. Similarly, if a compound is extensively concentrated in an organ, it will typically show a high volume of distribution.

The distribution and storage of many compounds are determined by the extent of binding to plasma proteins or accumulation in organelles or tissues. Serum albumin is present in plasma at a concentration of about 500−600 μM and is a major tissue-binding site. A second relevant serum protein is α_1-acid glycoprotein, which, although present at a much lower concentration than albumin, binds compounds like the numerous endogenous steroids and certain basic compounds. The binding of chemicals to plasma proteins can determine toxicity because only the unbound fraction can enter tissues to cause toxicity. Therefore, a compound that is highly bound to plasma protein may not show toxicity when compared to one that is not bound to plasma proteins. Ironically, a high degree of protein binding can increase the risk of adverse effects resulting from interactions with other highly bound compounds. In particular, severe toxic reactions can occur if a toxicant with a high degree of protein binding is displaced from plasma proteins by another agent, increasing the free fraction of the toxicant in plasma. For example, the anticoagulant warfarin is highly bound to plasma protein and if it is displaced by another highly protein bound drug, increased bleeding can result.

The liver and kidney have a high capacity for binding many chemicals. These two organs probably concentrate more toxicants than do all other organs combined, and in most cases, active transport or binding to tissue components are likely to be involved. The heavy metal-binding protein, metallothionein (MT), sequesters both essential and toxic metals, including zinc and cadmium (Cd), with high affinities in the kidney and liver.

Adipose tissue is a storage site for chemicals that have a high lipid/water partition coefficient. This is an issue for environmental bio-accumulation and is a critical factor in the toxicity of pesticides such as chlordane and dichlorodiphenyltrichloroethane (DDT), along with the large class of polychlorinated and polybrominated biphenyls, dioxins, and furans. The potential for these compounds to produce toxicity, including carcinogenic, developmental, and endocrine effects, is related to their accumulation and storage in body fat. Although storage in fat may reduce the amount that reaches target organs, there is a risk that mobilization from fat storage will increase the concentration of a chemical in blood and in the target organ of toxicity.

Bone is an important depot for compounds such as fluoride, lead, and strontium, all of which may be incorporated and stored in the bone matrix. For example, 90% of the lead in the body is eventually found in the skeleton, although it is not toxic to bone. In contrast, deposition in bone is an important determinant of the toxicity fluoride and radioactive strontium.

Barriers Affecting Distribution

Several organs, most notably the brain, have barriers that restrict entry to toxicants. The BBB is formed primarily by endothelial cells with tight junctions between adjacent cells that prevent diffusion of polar compounds through paracellular pathways. Four ATP-dependent transporters have also been identified as part of the BBB including P-gp, Mrp2, Mrp4, and Bcrp, and they can prevent distribution to the brain by pumping xenobiotics absorbed into the capillary endothelial cells back out into the blood.

Genetically modified mice illustrate the importance of transport processes to the maintenance of the BBB and the restriction of compounds from the brain. For example, compounds that are substrates for P-gp achieve much higher brain levels in P-gp null ($Mdr1a^{-/-}/Mdr1b^{-/-}$) mice relative to wild-type mice. Seminal studies demonstrated that compounds like ivermectin and vinblastine accumulated in the brains of P-gp null mice and produce marked neurotoxicity and increased lethality.

The Placental Barrier

The placenta is a specialized structure that serves to both nourish and protect the developing fetus. Although its organization differs markedly across species, the major cellular elements are the syncytiotrophoblast and cytotrophoblast layers. Xenobiotic transporters are differentially expressed in various cells of the placental unit and contribute to the barrier function that restricts distribution of toxicants to the fetus. Importantly, the expression of breast cancer resistance protein (Bcrp) is highest in the placenta relative to any other organ, and plays a pivotal role in protecting the fetus from exposure to toxicants.

Metabolism: Activation and Detoxification

Although some xenobiotics are directly toxic, many require metabolism to the penultimate or ultimate toxic moiety. In general, biotransformation serves to increase the water solubility of a compound and thereby enhance its excretion and limit its toxicity. However, in some cases, biotransformation leads to the formation of a variety of reactive intermediates that can be directly cytotoxic or mutagenic. Examples of such reactive intermediates include electrophiles, free radicals, and redox-reactive intermediates.

Electrophiles are molecules that contain an electron-deficient atom with a partial or full positive charge that can react by sharing electron pairs with an electron-rich atom. Electrophiles include reactive epoxides, arene oxides, aldehydes, quinones, and acyl halides. Examples of compounds that can be activated in this way include acetaminophen (to a reactive quinoneimine), aflatoxin (to a reactive epoxide intermediate), and ethanol (to acetaldehyde).

Free radicals are molecules that contain unpaired electrons in their outer orbit. They are reactive because they can accept electrons, transfer that electron to molecular oxygen, and ultimately form the superoxide anion radical ($O_2^{-\bullet}$). The hydroxyl radical ($HO^{\bullet}$) is an important toxicologic moiety that can be generated from hydrogen peroxide (HOOH) as illustrated in Figure 2.1. Importantly, this reactive intermediate can be formed by numerous toxic agents that are free radicals or by endogenous sources including NADPH oxidase, which is highly abundant in activated macrophages and other cells during toxic or inflammatory reactions. Figure 2.1 also illustrates the Fenton reaction, a process that generates hydroxyl free radical.

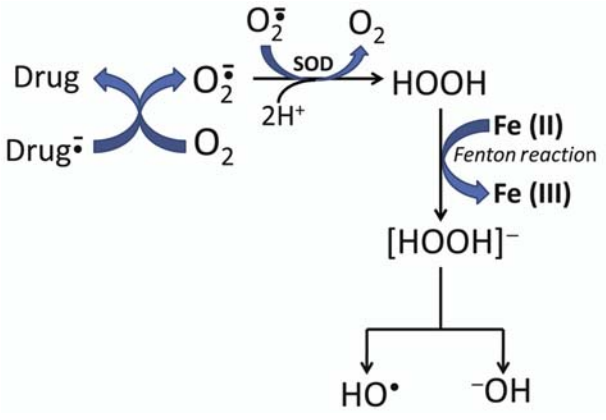

FIGURE 2.1 Schematic illustration of the formation of the hydroxy radical ($HO^{\bullet}$) through a reaction involving hydrogen peroxide (HOOH). The generation of free radicals can be a significant contributor to toxicity. Source: *From Haschek, W.M., Rousseaux, C.G., Wallig, M.A. (Eds.), 2013. Handbook of Toxicologic Pathology, third ed. Academic Press, Figure 1.1, p. 22, with permission.*

This is an important process catalyzed by transition metals including iron (illustrated) or by other metals such as copper, chromium, nickel, or manganese.

Biotransformation is described in two phases, with Phase I including oxidative, reductive, and hydrolytic reactions. In general, these reactions introduce small changes in the water solubility of the compound. In contrast, Phase II reactions are typically some type of conjugation reaction wherein a large change in water solubility is introduced through the addition of different types of hydrophilic moieties such as UDP-glucuronic acid (Uridine diphosphate glucuronic acid, UDPGA) (glucuronidation), sulfate (sulfation), or the tripeptide glutathione (GSH).

Phase I Metabolism

The most important enzymes involved in the Phase I biotransformation of xenobiotics are the cytochromes P450 (CYPs), a family of more than 50 heme-containing enzymes. Binding of ligands such as oxygen or carbon monoxide (CO) occurs when the iron in the heme moiety is in the reduced ferrous form (Fe^{2+}), and the name CYP 450 was derived from the observation that the CO-saturated protein absorbs light maximally at 450 nm. The basic reaction catalyzed by CYPs is monooxygenation and is summarized by the following equation:

$$\text{Substrate (RH)} + O_2 + \text{NADPH} + H^+ \longrightarrow \text{Product (ROH)} + H_2O + \text{NADP}^+$$

Overall, the reactions that are catalyzed by CYPs include: (1) hydroxylation of an aliphatic or aromatic carbon; (2) epoxidation across a double bond; (3) oxidation of a heteroatom such as S or N or N-hydroxylation; (4) dealkylation of a heteroatom such as O−, S−, or N−; (5) oxidative group transfer; (6) cleavage of esters; and (7) dehydrogenation.

Given its major role in biotransformation, the liver expresses high levels of a variety of CYPs, and the enzymes involved in xenobiotic metabolism are localized to the endoplasmic reticulum (microsomal fraction). Expression of these enzymes is higher in the hepatic centrilobular zones (more so than the midzonal or periportal regions), and for this reason, many xenobiotics that are metabolized to reactive intermediates in the liver show toxicity in the centrilobular regions. In addition, CYPs are localized intracellularly to the smooth endoplasmic reticulum (SER) such that enzyme activity is often studied from the SER-rich microsomal fraction obtained by differential centrifugation of tissue homogenates.

Of the many CYP families and subfamilies, the CYP3A enzymes are typically the most constitutively abundant in all species. Other enzyme families are

more highly expressed in extra-hepatic tissues. For example, the CYP2F enzymes are more abundant in the lung than liver, particularly in the metabolically competent nonciliated exocrine bronchiolar (Clara or club) cells. In this manner, toxicants that are metabolically activated in the lung, such as naphthalene or ipomeanol, show marked toxicity in these bronchiolar cells. The major families of CYP enzymes involved in xenobiotic metabolism are summarized in Table 2.2. It should be noted that a variety of CYPs are also critical to or rate-limiting in the metabolism of endogenous compounds such as cholesterol, steroid, vitamin D, bile acids, and fatty acids.

Another family of Phase I biotransformation enzymes are the flavin monooxygenases (FMOs). These enzymes, which are also located in the microsomal fraction, catalyze the oxidation of nitrogen, sulfur, or phosphorous in a variety of xenobiotics, and are distinguished from CYPs in that they are heat labile (inactivated by heating to 50°C for 1 minute) and detergent-resistant, whereas as CYPs are inactivated by nonionic detergents. FMOs catalyze the formation of N-oxides from tertiary amines or hydroxylamines from primary or secondary amines, as well as the formation of S-oxides or P-oxides from sulfur- and phosphorous-containing compounds. They play an important role in the metabolism of drugs such as cimetidine as well as endogenous substrates such as trimethylamine.

Other Phase I reactions include hydrolysis, which is important in the biotransformation of esters. A major hydrolytic reaction is that involved in the fate of epoxide intermediates. A wide range of alkene or aromatic compounds can be oxidized by CYPs to epoxides, many of which are potentially reactive. Epoxide hydrolases catalyze the *trans*-addition of water to an epoxide forming a dihydrodiol metabolite that is generally less reactive than its epoxide precursor, thereby functioning as an important detoxification mechanism. However, epoxide hydrolase works in concert with CYPs to form bay region diol-epoxides from polyaromatic hydrocarbons (such as benzo[*a*]pyrene), the penultimate toxicant for this class of compounds.

TABLE 2.2 Cytochrome P450 Enzymes Families and General Function

Gene family	Tissue distribution (major organs)	Substrate examples
CYP1A	Liver, kidney, lung, intestine	Aromatic hydrocarbons
CYP1A2	Liver, kidney, lung, intestine	Xanthines (caffeine, theophylline), phenacetin, APAP
CYP1B	Adrenal gland, ovary, testis, liver	Estradiol
CYP2A	Liver, testis, skin, nasal mucosa	Testosterone (rat), coumarin, nitrosamines, nicotine
CYP2B	Liver, lung, kidney, intestine	Bupropion, 7-benzyloxyresorufin
CYP2C	Liver, lung, kidney, intestine	Warfarin, diclofenac
CYP2D	Liver, lung, intestine	Debrisoquine, codeine, imipramine
CYP2E	Liver, lung, kidney, intestine	Chlorzoxazone, APAP, ethanol
CYP2F	Lung, nasal mucosa, liver	Naphthalene, styrene, 3-methylindole
CYP2J	Liver, nasal mucosa, lung, kidney, intestine	Arachidonic acid metabolites
CYP3A	Liver, lung, intestine	APAP, aflatoxin, erythromycin, lovastatin
CYP4A	Liver, kidney, lung	Fatty acids (omega hydroxylation)
CYP4B	Lung, kidney, liver	Fatty acids (omega hydroxylation), valproic acid, aromatic amines
CYP7A	Liver	Bile acid metabolism
CYP11A	Adrenal cortex, ovary, testis, placenta	Cholesterol side-chain cleavage
CYP11B	Adrenal cortex	Steroid 11β-hydroxylation
CYP17	Testis, ovary, kidney	Androgen synthesis
CYP21	Adrenal cortex	Glucocorticoid synthesis
CYP24	Kidney	Vitamin D metabolism
CYP26	Liver, brain	Vitamin A metabolism

Tissue distribution summarizes the major organs of constitutive expression of P450s in rats. In most cases, these enzymes are highly abundant in liver, and for those families, the liver is listed first. When the liver is noted but preceded by other tissues, it is present but not highly abundant. Some organs that are not listed may also express low levels of these enzymes (e.g., heart, spleen, pancreas, brain).

From Haschek, W.M., Rousseaux, C.G., Wallig, M.A. (Eds.), 2013. Handbook of Toxicologic Pathology, third ed. Academic Press, Table 1.2, p. 24, with permission.

Alcohol and aldehyde dehydrogenases are a large family of enzymes that catalyze the oxidation of alcohols to aldehydes and aldehydes to carboxylic acids, respectively. These reactions are classically illustrated by the metabolism of ethanol wherein alcohol dehydrogenase converts ethanol to acetaldehyde, which is subsequently oxidized to acetic acid by aldehyde dehydrogenase as follows:

$$CH_3CH_2OH \rightarrow CH_3CHO \rightarrow CH_3COOH$$

Reductive mechanisms are important for some metals, such as arsenic or xenobiotics containing aldehyde, ketone, nitro or azo groups. Furthermore, the reduction of nitro- and azo-containing compounds is generally catalyzed by intestinal microflora particularly in the anaerobic environment of the lower GI tract. This is the case for compounds such as 2,6-nitrotoluene, in which reduction by intestinal bacterial produces mutagenic metabolites.

Phase II Metabolism

Phase II metabolic reactions are primarily conjugation reactions, generally occurring in the cytosol, with glucuronidation, sulfation, and GSH conjugation being the most important in xenobiotic toxicity. The cofactors used in these conjugation reactions are illustrated in Figure 2.2. Glucuronidation and sulfation require UDPGA and 3′-phosphoadenosine-5′-phosphosulfate (PAPS), respectively. UDPGA is synthesized from glucose 1-phosphate with concentrations of at least 200 μM detected in liver. In contrast, cysteine is the major source of PAPS. Since free cysteine concentrations are limited, PAPS levels are considerably lower than levels of UDPGA. The lower availability of the cofactors renders sulfation a low capacity system relative to glucuronidation.

Glucuronidation and sulfation reactions are catalyzed by UDP-glucuronosyltransferases (UGTs) and sulfotransferases (SULTs), respectively. SULTs are localized in the cytosol, whereas UGTs are localized to the microsomal fraction. In rats, there are two major families of UGTs (UGT1 and 2) and three predominant families of SULTs (SULT1, 2, and 4). Substrates for both conjugation reactions typically contain functional groups such as alcohols (aliphatic and aromatic), carboxylic acids, and amines, although phenolic and aliphatic alcohols are the major substrates for SULTs. Glucuronide and sulfate conjugates markedly increase the water solubility of compounds and thereby facilitate excretion. Although urinary excretion is favored, glucuronide conjugates are also excreted to a large extent in bile. In most cases, conjugation reactions detoxify xenobiotics and facilitate excretion. However, there are notable cases of increased toxicity or adverse

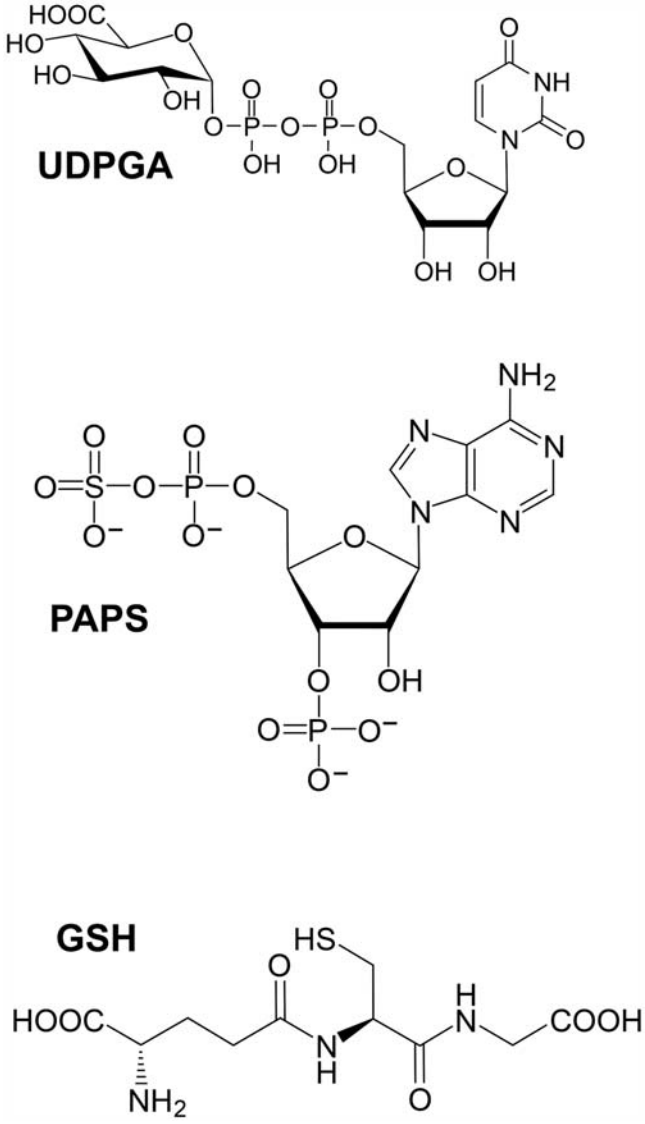

FIGURE 2.2 Structures of cofactors for glucuronidation (UDPGA), sulfation (PAPS), and GSH conjugation reactions.

reactions related to Phase II metabolism. For example, bilirubin is glucuronidated by reactions catalyzed primarily by UGT1A1. Compounds that compete with bilirubin for conjugation by this enzyme can cause hyperbilirubinemia as a direct consequence of enzyme inhibition. In addition, glucuronidation or sulfation of aromatic amines (or the hydroxylamine metabolites of aromatic amines) can increase the potential tumorigenic activity of these compounds. Finally, some acylglucuronides are reactive intermediates that increase the likelihood of toxicity. This is the case for a variety of nonsteroidal antiinflammatory drugs.

Finally, there are significant species differences in glucuronidation and sulfation reactions. Most notably, glucuronidation is the major Phase II metabolic

pathway in all mammalian species except for cats, whereas in cats, SULT activity is quite high, a biochemical difference that likely serves to offset their low capacity to form glucuronide conjugates. GSH conjugation is a major pathway involved in the detoxification of electrophilic compounds, thereby reducing toxicity from these potentially reactive species. GSH is a tripeptide composed of glycine, cysteine, and glutamic acid, with glutamic acid linked to cysteine via a γ-carboxyl group (γ-glutamine-cysteinylglycine). It is a major nonprotein sulfhydryl moiety in most tissues, and in liver its concentration is extremely high ($\approx 5-10$ mM). In light of its high concentration, some compounds can be directly conjugated with GSH, representing a nonenzymatic addition, whereas most reactions are catalyzed by glutathione S-transferases (GSTs).

There is a large family of GSTs classified as alpha, mu, pi, sigma, theta, zeta, and omega forms. The functional activity of GSTs is a major determinant of certain species differences in toxicity, the most notable example of which is the fungal toxicant, aflatoxin B1 (AFB1). Specifically, very low doses of AFB1 are hepatotoxic and tumorigenic in rats but not in mice, even though both species metabolize this fungal contaminant to a highly reactive epoxide (AFB1 8,9-epoxide) at similar rates. The species difference in toxic outcome is determined by the fact that mice conjugate the 8,9-epoxide with GSH up to 50 times faster than rats.

Other conjugation pathways that contribute to xenobiotic fate include methylation, acetylation, and amino acid conjugation reactions. Methylation is generally a minor pathway that differs from most other Phase II reactions in that metabolites formed are typically less water soluble than the parent compound. Methylation requires S-adenosylmethionine as a cofactor, with a variety of methyltransferases responsible for catalyzing the reaction.

Acetylation is particularly important for compounds such as aromatic amines and is catalyzed by *N*-acetyltransferases with acetyl coenzyme A as the required cofactor. These cytosolic enzymes are found in most mammals with the notable exception of dogs (and foxes), which are unable to acetylate xenobiotics. This enzyme family is also characterized by the prevalence of genetic polymorphisms, as "fast" and "slow" acetylators have been described in humans, hamsters, rabbits, and mice. Compounds such as p-aminobenzene, isoniazid, and sulfamethazine are recognized substrates for acetylation.

Amino acid conjugation is classically illustrated by the glycine conjugation of benzoic acid to form hippuric acid (hippurate). This reaction, which requires activation of the substrate by conjugation with acetyl CoA, typically occurs in the mitochondria where numerous acyl-CoA synthetases are present. Bile acids are endogenous substrates for conjugation with glycine or taurine, but this reaction is catalyzed by a family of bile acid-CoA:amino acid *N*-acetyltransferases that are localized to the microsomal fraction. Marked species differences in the conjugation of bile acids are recognized, as rabbits and pigs form predominantly glycine-conjugated metabolites, whereas rats form predominantly taurine conjugates and humans and primates form both types of conjugates in variable proportions.

The metabolic fate of the widely used analgesic, acetaminophen (N-acetyl-p-aminophenol, APAP), encompasses both Phase I and II biotransformations and is illustrated in Figure 2.3. The biotransformation of this compound provides a general summary of the biotransformation and conjugation reactions and, as described in this chapter, reflects how the biotransformation pathways change with increasing dose of APAP, and illustrates how metabolic fate limits or ultimately results in toxicity.

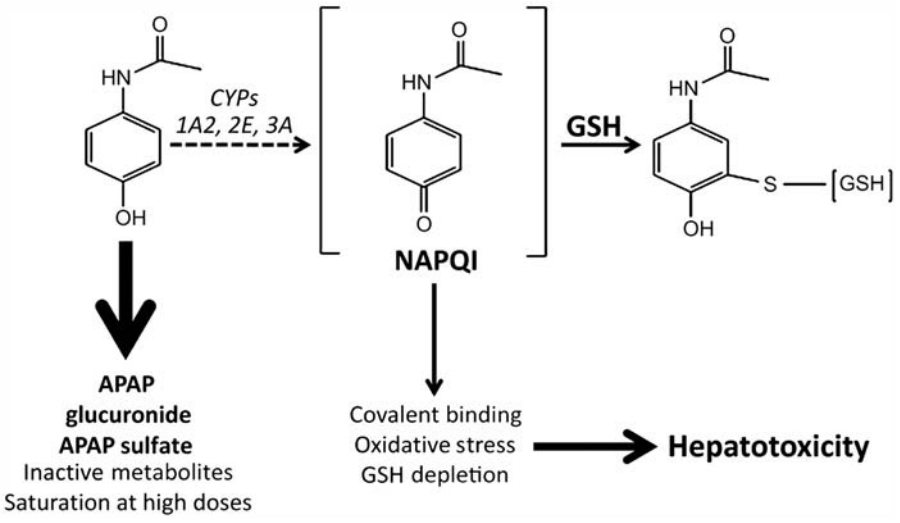

FIGURE 2.3 Outline of the contribution of Phase I and Phase II biotransformation reactions in contributing to the metabolic activation and detoxification of acetaminophen. Source: *From Haschek, W.M., Rousseaux, C.G., Wallig, M.A. (Eds.), 2013. Handbook of Toxicologic Pathology, third ed. Academic Press, Figure 1.2, p. 27, with permission.*

Elimination of Toxicants

The major routes of elimination are urinary and fecal excretion, with biliary elimination contributing to the net excretion in feces. Gases are eliminated primarily by exhalation. Compounds are also excreted in body secretions and can be found in sweat, saliva, tears, and breast milk.

Urinary Excretion

The kidneys comprise about 4% of total body weight, but receive nearly 25% of the cardiac output. The net result is that urinary excretion is a major route of elimination for a diverse group of compounds and electrolytes. Filtration at the glomerulus is driven by pressure differences between the afferent and efferent arteriole, the presence of large pores in the glomerular capillaries and the degree of plasma protein binding. The molecular weight cut-off for filtration is approximately 60 kDa but varies across species. Glomerular filtration rates are determined by the relative number of nephrons (normalized to body weight) and range from a high of approximately 10 mL/min/kg in mice to about 1.8 mL/min/kg in humans.

Once filtered, a compound may remain in the tubular lumen and be excreted with urine or be reabsorbed back into the bloodstream. Reabsorption of toxicants occurs primarily in the proximal tubules and is governed by the principles described earlier for passive diffusion including lipid solubility and ionization. Thus, toxicants with a high log *P* are reabsorbed more efficiently than polar compounds and ions. The pH of urine is normally slightly acidic (approximately 6–6.5), such that excretion of organic bases is favored whereas organic acids may be reabsorbed.

Xenobiotics can also be excreted into urine by active secretion, a process that involves uptake from the blood into the cells of the renal proximal tubule and subsequent efflux from the cell into the tubular fluid. Transporters play an important role in the net secretion, reabsorption, and ultimately urinary excretion of xenobiotics, and are expressed on the luminal side of the cell, where they contribute to tubular secretion and reabsorption, or are localized to the basolateral membranes, serving to transport xenobiotics to and from the circulation, and the renal tubular cells (Figure 2.4).

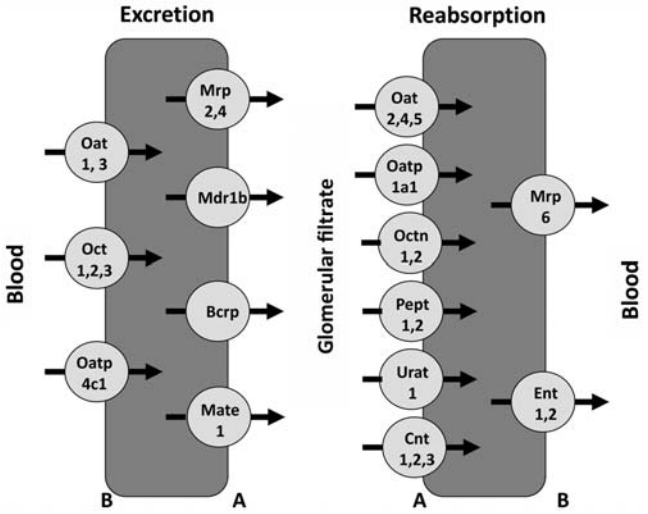

FIGURE 2.4 Expression and membrane localization of xenobiotic transporters in the rat kidney. Source: *From Haschek, W.M., Rousseaux, C.G., Wallig, M.A. (Eds.), 2013. Handbook of Toxicologic Pathology, third ed. Academic Press, Figure 1.3, p. 28, with permission.*

Fecal Excretion

Fecal excretion is a major pathway for the elimination of xenobiotics from the body. The two processes that contribute to fecal excretion are direct excretion (from lack of absorption in the GI tract after oral exposure) and biliary elimination, which is a significant source of fecal excretion of xenobiotics and their metabolites.

The factors that determine whether a chemical is excreted into bile are not fully understood. A general rule is that low-molecular-weight compounds (<325) are poorly excreted into bile, whereas compounds with molecular weights exceeding about 325 can be excreted in appreciable quantities. GSH and glucuronide conjugates have a high predilection for excretion into bile. In addition, rats and mice tend to excrete compounds in bile more than other species.

Xenobiotic transporters play a critical role in biliary excretion (Figure 2.5). (The excretion of metabolic conjugates via transporters is sometimes called "phase III" metabolism.) P-gp, Mrp2, and Bcrp are important in the biliary excretion of a wide range of xenobiotics, whereas Bsep is critical for the secretion of bile and the regulation of bile flow. Mate1 transports cationic compounds.

Mrp2 is extremely important in biliary excretion because it is largely responsible for the transport of organic anions including the glucuronide and GSH conjugates of many xenobiotics. Its role in biliary excretion of toxicants was established in part by the characterization of two naturally occurring mutant strains of rat, the Groningen/Yellow transport deficient (TR^-) and the Eisai hyperbilirubinemic rat (EHBR), both of which lack functional Mrp2 protein. These rats are phenotypically similar to humans suffering from Dubin–Johnson syndrome, a rare inherited disorder associated with mutations in MRP2 and characterized by chronic conjugated hyperbilirubinemia.

The biliary excretion of xenobiotics mediated by Mrp2, Bcrp, and P-gp usually results in increased

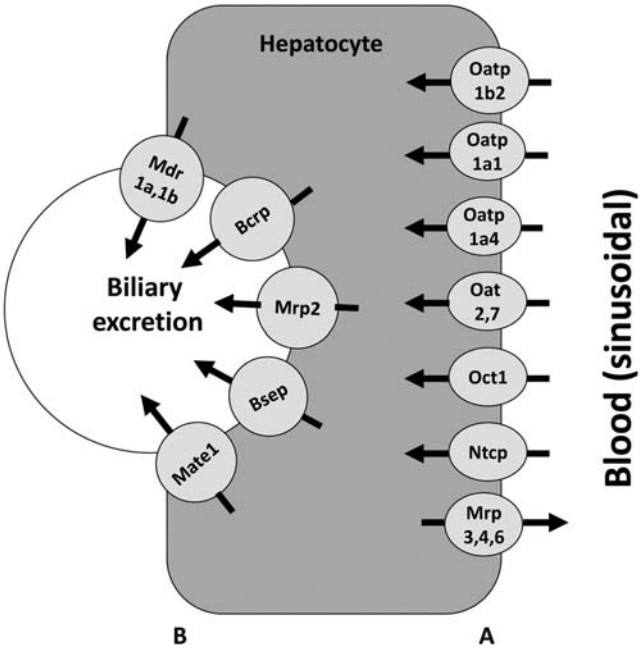

FIGURE 2.5 Expression and membrane localization of xenobiotic transporters in rat liver. Source: *From Haschek, W.M., Rousseaux, C.G., Wallig, M.A. (Eds.), 2013. Handbook of Toxicologic Pathology, third ed. Academic Press, Figure 1.4, p. 28, with permission.*

excretion of toxicants out of hepatocytes and into bile. In doing so, these transporters can reduce the likelihood of toxicity in the liver. However, adverse reactions can occur if the function of these transporters is inhibited. For example, compounds that inhibit the transport function of Bsep cause a net decrease in the biliary excretion of bile acids leading to cholestasis and liver injury.

Several influx transporters are located in the basolateral membrane of hepatocytes, where they contribute to the hepatic uptake of many organic anions. Numerous Oatps are expressed in liver and contribute to the uptake of organic anions including conjugated metabolites. Oatp1b2 is highly expressed in liver and is directly involved in the uptake of the mushroom toxin, phalloidin, and the blue-green algal toxin, microcystin. Oatp1b2$^{-/-}$ mice are resistant to phalloidin- and microcystin-induced toxicity as a direct result of reduced hepatic uptake.

An important concept relating to biliary excretion and hepatic disposition is the phenomenon of enterohepatic circulation. This is a cycle in which a compound excreted into bile reenters the intestine to be reabsorbed again and returned to liver. Many compounds excreted into bile are conjugated with UDPGA, sulfate, or GSH, and enzymes found in the intestinal microflora hydrolyze the glucuronide and sulfate conjugates, to facilitate reabsorption from the gut. Reabsorption and uptake into the liver completes a cycle where it can again be metabolized and excreted back into bile. Repeated enterohepatic cycling results in very long half-lives for some xenobiotics. Therefore, it is desirable to interrupt this cycle to hasten the elimination of a toxicant from the body.

Exhalation

Substances that exist predominantly in the gas phase at body temperature are eliminated mainly by the lungs. Because volatile liquids are in equilibrium with their gas phase in the alveoli, they may also be excreted via the lungs. The amount of a liquid eliminated via the lungs is proportional to its vapor pressure. A practical application of this principle is seen in the breath analyzer test for determining the amount of ethanol in the body. Highly volatile liquids such as diethyl ether and certain volatile anesthetics (nitrous oxide) are excreted almost exclusively by the lungs.

Other Routes of Elimination

Although urine and feces are the major routes of excretion for most xenobiotics, some elimination can occur in other body fluids such as sweat, saliva, breast milk, and cerebrospinal fluid. Of these minor routes, secretion of toxic compounds into milk is notable because it allows for the materials to be passed from the mother to her nursing offspring or for compounds to be passed from cows to people via dairy products. Many compounds that can accumulate in fat such as aldrin, chlordane, DDT, polychlorinated and polybrominated biphenyls, dibenzo-p-dioxins, and furans have been found in milk.

INTERACTIONS OF TOXICANTS WITH CELLULAR AND MOLECULAR TARGETS

Covalent Modification

A major contributor to toxicity is the covalent modification of cellular macromolecules. Covalent adducts are typically formed with cellular nucleophiles including proteins, DNA, RNA, and phospholipids. Covalent modifications impair protein function by altering conformation or structure and ultimately disrupt cellular energy homeostasis and/or signal transduction mechanisms. These effects may activate cell death pathways (discussed later), or in some cases, evoke an immune response. Such adverse effects are exemplified by APAP (Figure 2.3) wherein metabolic activation leads to reactive intermediates that covalently bind to numerous macromolecules and ultimately cause marked hepatocellular necrosis. In most cases the precise identity of intracellular targets of covalent binding has not been fully characterized. Moreover, although

analytical methods have been developed to assess covalent binding and to detect specific modifications in individual peptides or proteins, establishing a causal link between covalent modification and toxic response is far more difficult. In the case of APAP, covalent modification of mitochondrial proteins appears to be an important initiating event in the cascade that leads to cell death.

Covalent binding of xenobiotics to endogenous proteins has also been implicated as a key event in the development of skin sensitization and allergic contact dermatitis. Specifically, the formation of an adducted protein may be recognized as a hapten to ultimately invoke an allergic response.

Reactive toxicants can also interfere with the DNA template. Covalent binding to DNA causes nucleotide mispairing during replication, a pro-mutagenic event resulting from incorrect codon formation that alters amino acid sequence and protein function. This is the case with the epoxide intermediates of aflatoxin as they specifically modify the coding sequences of proteins that increase the likelihood of liver tumor development (including p53 and *h*-ras). Some agents also intercalate into DNA to cause frame shifts that terminate normal DNA synthesis.

A fundamental principle of covalent-binding mechanisms of toxicity is that the effects are dose-dependent. For example, oxidative metabolites of APAP are conjugated with UDPGA or PAPS until these essential cofactors are depleted. As dose increases and Phase I and II pathways are saturated, GSH conjugation serves as a secondary defense mechanism to bind up reactive metabolites. However, at very high doses, even GSH can be depleted so that cellular macromolecules are now vulnerable to covalent modification and toxicity ensues. Understanding this mechanistic underpinning can be used in two important ways. First, trapping reactive metabolites as GSH conjugates is widely used to determine the extent to which a compound is metabolized to potentially toxic intermediates. In addition, the treatment for APAP overdose in any species is *N*-acetyl cysteine, a sulfhydryl source that increases hepatic levels of cysteine and replenishes intracellular GSH.

Free radicals (described earlier) often initiate lipid peroxidation that disrupts membrane integrity. End products resulting from lipid peroxidation include malondialdehyde (MDA) and 4-hydroxynonenal (HNE), and both can contribute to toxicity. For illustration, HNE can bind to many proteins by addition to histidine, cysteine, or lysine residues, forming protein adducts or cross-linking proteins (Figure 2.6). HNE and MDA also react with DNA to generate mutagenic adducts (not illustrated), many of which are detected

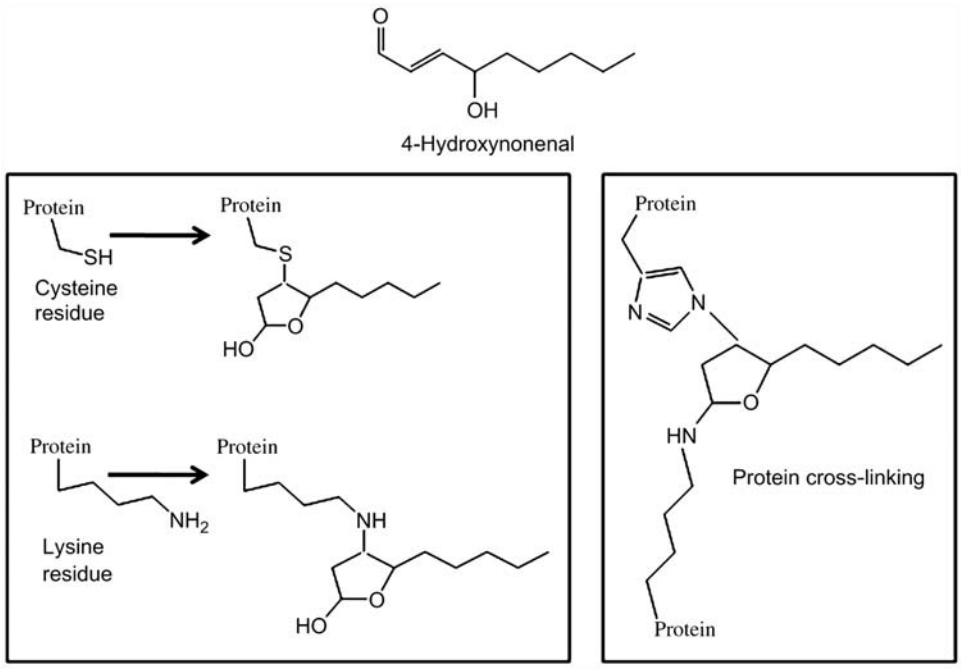

FIGURE 2.6 Illustration of the types of protein adducts that can be formed from HNE, an end product of lipid peroxidation. HNE can adduct proteins or form protein crosslinks leading to cellular damage. HNE can also adduct DNA to generate mutagenic adducts (not illustrated here). Source: *From Haschek, W.M., Rousseaux, C.G., Wallig, M.A. (Eds.), 2013. Handbook of Toxicologic Pathology, third ed. Academic Press, Figure 15 p. 31, with permission.*

constitutively as a result of endogenous formation. Such adducts can cause DNA damage, particularly strand breaks.

Toxic Stressors

A major pathway involved in toxicity is oxidative stress, operationally defined as a disturbance in the redox state of the cell resulting from an imbalance between the production of reactive oxygen species and the cell's ability to detoxify these intermediates or to repair the damage that may result. Examples of oxidative stress include covalent-binding, free radical formation, and lipid peroxidation as described earlier. Oxidative stress is also a critical pathway underlying mitochondrial dysfunction and cell death. Moreover, oxidative stress appears to be involved in many diseases, including neurodegenerative diseases, atherosclerosis, and the general process of aging. Oxidative stress is often detected by cellular levels of MDA (a general marker) or 8-hydroxydeoxyguanosine, a marker of oxidative DNA damage. In addition, there are redox-sensitive transcription factors that are activated by oxidative stress and drive expression of a family of cytoprotective genes (Table 2.3 and discussed later).

There are other important stress responses involved in toxicity (summarized in Table 2.3). These mechanisms are associated with specific changes in cells resulting from a variety of stressors that are distinguished by histopathologic presentation and alterations in gene expression or signal transduction pathways (discussed later). These stress responses are also important mechanisms of toxicity and include responses elicited by the following types of stress: (1) DNA damage, associated with chemicals that directly affect DNA sequence or alter the fidelity of DNA replication; (2) hypoxia, caused by any adverse effect that lowers oxygen tension or affects the cellular utilization of oxygen; (3) heat shock, a generalized stress response observed with many insults including heavy metals and temperature alterations; (4) endoplasmic reticulum (ER) stress, elicited by agents that perturb ER function to disrupt essential lipid and protein biosynthesis and normal protein folding; (5) metal stress, a specific response elicited by heavy metals secondary to alterations in the homeostasis of essential metals such as zinc and copper; (6) osmotic stress, evoked by compounds that alter cellular environments by disrupting cellular water or osmolyte movement (particularly important in the kidney); and (7) inflammatory stress, a physiologically important pathway that can also exert adverse effects on cells.

Altered Gene Expression

Toxicants alter gene expression by increasing or decreasing transcriptional activity of numerous targets or by modifying the activity of cellular proteins by posttranscriptional events including phosphorylation state. A major group of ligand-activated transcription factors are the family of nuclear receptors that regulate gene expression in response to endogenous hormones and vitamins such as the androgen, estrogen, and glucocorticoid receptors. In general, these receptors remain outside the nucleus when not engaged by ligands, but are translocated to the nucleus following ligand interaction where they bind to the consensus

TABLE 2.3 Common Stress Response Pathways

Cellular stress mechanism	Transcription factor(s) regulating response	Examples of induced response genes
Oxidative stress	Nrf2	Heme oxygenase, quinone oxidoreductase
DNA damage	p53	Growth arrest and DNA damage repair (GADD)45, mdm2, p21
Hypoxia	HIF-1	Vascular endothelial growth factors, erythropoietin
Heat shock	HSF-1	Heat shock proteins
Endoplasmic reticulum stress	XBP-1, ATF4, 6	Heat shock proteins 90B1, A5, DNAJb9
Metal stress	MTF-1	Metallothioneins
Osmotic stress	NFAT5 (TonEBP)	Betaine/GABA transporter (SLC6A12)
		Na-myoinositol transporter (SLC5A3)
Inflammation	NF-κB	Interleukin-1, TNFα

Abbreviations: Nrf2, nuclear factor (erythroid-derived 2)-like; HIF-1, hypoxia inducible factor 1; HSF-1, heat shock transcription factor; XBP-1, X-box binding protein 1; ATF, activating transcription factor; MTF-1, metal transcription factor 1; NFAT5, nuclear factor of activated T cells (also known as tonicity enhancer binding protein; TonEBP).

From Haschek, W.M., Rousseaux, C.G., Wallig, M.A. (Eds.), 2013. Handbook of Toxicologic Pathology, third ed. Academic Press, Table 1.3, p. 32, with permission.

sequences in gene promoters to initiate transcriptional activity. Chemicals that interact with these receptors cause adverse effects by mimicking the action of the endogenous ligands. For example, compounds that can bind to the estrogen receptor (ER) can mimic the effects of estrogen, including abnormal developmental programming, inappropriate feminization of male sex organs, or altered mammary proliferation that increases the likelihood of breast cancer. It is speculated that the adverse effects of a variety of environmental compounds, described as endocrine disruptors (such as DDT or bisphenol-A), are manifested through their ability to engage the ER.

Several NRs, including the aryl hydrocarbon receptor (AhR), constitutive androstane receptor (CAR), pregnane X receptor (PXR), and the peroxisome proliferator-activated receptor α (PPARα) are widely recognized to control expression of various cytochrome P450 enzymes, UDPGTs, and transporters. Ligands that activate these receptors induce the expression of many genes involved in xenobiotic metabolism and can markedly alter xenobiotic disposition. Examples of compounds that engage these receptors as a primary mechanism of their toxic effects include TCDD and other polyaromatic hydrocarbons that bind to AhR, phenobarbital and 1,4-bis[2-(3,5-dichloropyridyloxy)]benzene (TCPOBOP) are ligands for CAR, pregnenolone 16α-carbonitrile, and rifampicin bind to PXR and phthalate esters bind to PPARα. In addition, activation of CAR and PPARα increases cell proliferation, particularly in liver. Increased proliferation results in hepatocellular hyperplasia and hypertrophy and in rodents, is often associated with liver tumor development. Two other important mechanisms underlying altered gene expression patterns are DNA methylation and microRNA (miRNA) regulation. Briefly, DNA is frequently methylated at cytosine residues, and the pattern of methylation, particularly in regulatory regions (promoters or enhancers), affects gene expression. Methylation patterns in coding sequences can affect gene expression, and in general, the extent of DNA methylation is inversely correlated to the level of gene expression, although this is not an absolute relationship. Such changes are described as epigenetic alterations and represent nongenetic events that alter cell phenotype. Importantly, epigenetic changes are associated mechanistically with adverse outcomes not only in the developing fetus, but also with changes that persist through adulthood.

miRNAs are small noncoding RNA sequences (21−23 nucleotides) that bind to complementary regions of target mRNAs and repress translation of the mRNA. There is growing evidence that miRNAs markedly influence the posttranscriptional regulation of gene expression, and more than 1000 miRNAs have been described. Tissue expression patterns for miRNAs have been determined, revealing several organ-specific (or predominant) miRNAs. One such example is miR-122, a liver-predominant miRNA that appears to alter hepatic expression of numerous transcripts, including many that are important for normal mitochondrial function. This miRNA is implicated to have a role in the pathology of hepatitis C, liver carcinogenesis, and with respect to toxicity, is markedly increased in response to hepatic toxicants such as APAP.

Mechanisms of Cell Death

Although necrotic cell death was long considered the ultimate consequence of toxicity, it is now clear that chemical toxicity is associated with multiple modes of cell death. For some toxicants, the mode of cell death is dose-dependent, progressing from autophagy at low, toxic doses to apoptosis and necrosis with increasing dose and severity. It is also clear that these distinct pathways may coexist in a damaged organ. The pathways of cell death are complex, but the triggering events and general features of the major modes of death are described here.

Autophagy

Autophagy is a lysosomal process in which intracellular substrates are degraded within the lysosomal compartment. It is unique among cell death mechanisms in that there is no evidence of chromatin condensation, but is characterized by the presence of cytoplasmic vacuoles resulting from engulfment of cellular components. Autophagy is a constitutive and rapid process, and most autophagosomes are very short-lived, with a half-life of no more than 10 minutes. It is also distinct from apoptosis and necrosis in that the clearance of "debris" is an intracellular process, and there is no involvement of other phagocytic cells. Autophagy occurs by the engulfment of cellular constituents (macroautophagy), membrane uptake of smaller amounts of cytoplasm, and organelles (microautophagy) or by chaperone-mediated events that enable specific protein substrates to be taken into the lysosome for degradation. Autophagy is an important mechanism for survival in the fasting state. With respect to toxicity, autophagy is an important mechanism for removing misfolded proteins from cells resulting from oxidative stress or ER stress. ER stress (Table 2.3) is an adaptive mechanism that is designed to trigger transcriptional activation of a genetic program that will enhance autophagy and the capacity for normal protein folding in the ER. However, if excessive or prolonged, ER stress ultimately triggers cell death, typically in the form of apoptosis.

Apoptosis

Apoptosis is characterized by chromatin condensation, cytoplasmic shrinkage, nuclear fragmentation, and outpouching (blebbing) of cell membranes. Apoptotic cells ultimately disperse as membrane-enclosed fragments called apoptotic bodies. There are two major pathways that lead to apoptosis in mammalian cells referred to as the extrinsic and intrinsic pathways (Figure 2.7), with caspase activation the hallmark of both pathways. The extrinsic pathway is a receptor-mediated pathway in which activation of caspases, particularly procaspases 8 or 9, occurs following ligation of membrane receptors (CD95, TNFR1). Pro-caspase 8 is activated directly from receptor ligation through formation of the death-inducible signaling complex, and caspase 8 activates caspase 3, which cleaves target proteins leading to apoptosis. Pro-caspase 9 is also activated in the extrinsic pathway subsequent to pro-caspase 8 activation and mitochondrial membrane changes, leading again to activation of caspase 3. In the intrinsic pathway, signals for cell death act directly on mitochondria to stimulate the release of pro-apoptotic proteins including cytochrome *c*, with activation of pro-caspase 9 and activation of caspase 3. This pathway is controlled by Bcl-2 proteins, which regulate the release of cytochrome *c* by inhibiting mitochondrial permeability transition (MPT) pore formation (see later), along with several other intracellular apoptotic regulatory proteins.

Necrosis

Necrotic cell death is comprised of a continuum of effects, culminating in nuclear pyknosis, karyorhexis or karyolysis, rupture of cell membranes, and dispersal of cellular contents (see Chapter 5: Morphologic Manifestations of Toxic Cell Injury). Numerous toxicants have been shown to cause both apoptosis and necrosis, with necrosis associated with higher doses and more severe toxicity.

MPT is a critical change underlying necrosis. MPT occurs when permeability transition (PT) pores in the mitochondrial inner membrane are opened, leading to mitochondrial depolarization, uncoupling and organelle swelling. When the PT pores are opened in all mitochondria, ATP is depleted and necrotic cell death ensues from the lack of energy.

There are additional pathways of cell death now recognized that differ from autophagic, apoptotic, or necrotic mechanisms discussed earlier. These pathways include necroptosis, pyroptosis, and parthanatos (Table 2.4). Although they involve many of the events outlined already (such as oxidative stress or caspase

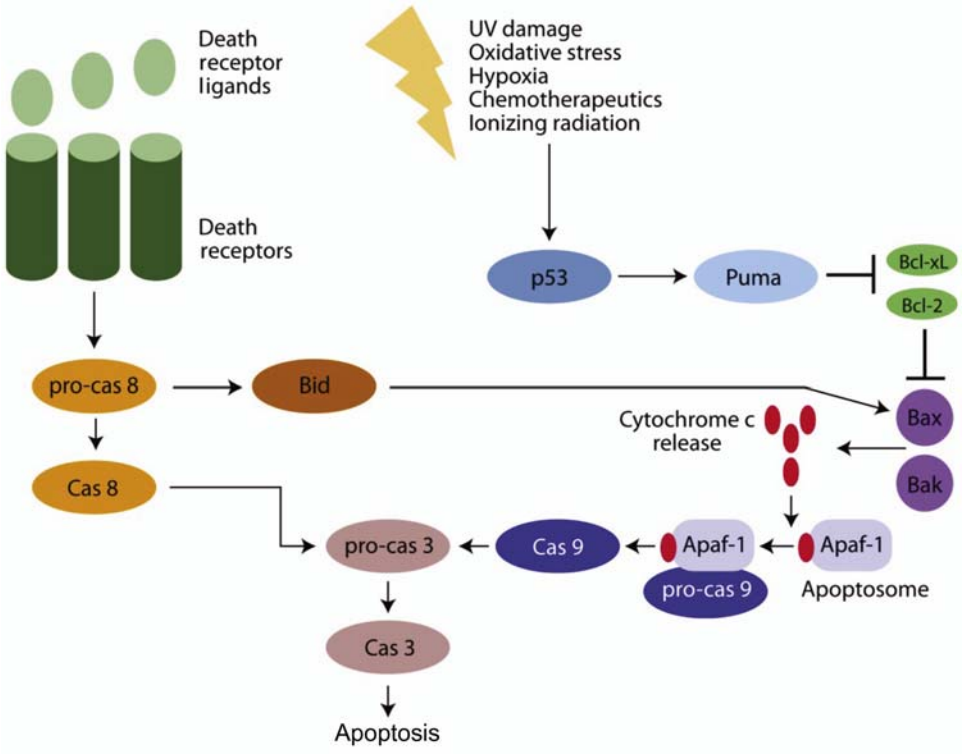

FIGURE 2.7 The extrinsic pathway of apoptosis is triggered by activation of death receptors, leading to pro-caspase 8 activation. The intrinsic pathway can be triggered by a variety of stimuli that ultimately result in release of cytochrome *c* from mitochondria, leading to formation of an apoptosome and activation of caspase 9. Extrinsic and intrinsic pathways converge at the level of caspase 3 activation.

TABLE 2.4 Mechanisms of Cell Death

Cell death mechanism	Major pathways and tissue response
Autophagy[a]	Lysosomal-mediated intracellular consumption with vacuolation
Apoptosis[a]	Intrinsic and extrinsic pathways of caspase activation illustrated in Figure 1.7 with characteristic nuclear fragmentation patterns
Necrosis[a]	Common pathway of mitochondrial changes leading to nuclear pyknosis, karyorrhexis, and karyolysis
Necroptosis	Kinase-mediated necrosis: involves receptor-interacting kinase-1 and mixed lineage kinase domain-like leading to cell rupture and inflammatory phenotype
Pyroptosis	Involves inflammasomes and caspase-1 activation: mediated by immune cells that release IL-18 and IL-1β in response to bacterial infection
Pyronecrosis	Mediated by cathepsin B activity: inflammation involved but distinguished from pyroptosis by lack of involvement of caspases or interleukin release
Parthanatos	Mediated by poly(ADP-ribose)polymerase-1 (PARP1): death pathway in response to genomic stress with transactivation of apoptosis inducing factor to induce DNA fragmentation
Ferroptosis	Iron- and reactive oxygen-dependent process: regulated by loss of glutathione peroxidase 4

[a]*Discussed in more detail in the text of this chapter. Other less well-defined mechanisms are summarized to illustrate the complexity of pathways that lead to cell death.*

activation), they are primarily differentiated by the agents that induce the effects and the mediators of cell death. Morphologically, at the microscopic level, these types of cell death resemble necrosis or apoptosis whereas ultrastructurally the variations between the various forms of death are sometimes subtle and challenging to discern (see Chapter 5: Morphologic Manifestations of Toxic Cell Injury).

Major Metabolic Events in Cell Death

Regardless of the mechanism of cell death, altered calcium homeostasis and mitochondrial changes are critical events in any toxic cell death. The energy state of the cell is regulated by ATP; it drives all biochemical processes, is a required cofactor for energy-dependent transport including many of the xenobiotic transporters, and is essential for the overall maintenance of cell morphology. Toxicants disrupt mitochondrial ATP synthesis by affecting numerous steps involved in oxidative phosphorylation or damaging mitochondrial DNA to alter expression of mitochondrial-specific genes.

It is also well established that intracellular calcium levels or alterations in Ca^{2+} compartmentalization are involved in cell death. There is about a 10,000-fold difference between extracellular and cytoplasmic Ca^{2+} levels, and toxicants that increase cytosolic Ca^{2+} levels by stimulating influx or preventing efflux can cause cell death by stimulating a variety of cytotoxic mechanisms.

Disruption of mitochondrial function, and particularly MPT, is a critical event in cell death. Biochemical changes that increase MPT include increase Ca^{2+} uptake, low transmembrane potential, generation of reactive oxygen species, and ATP depletion. Ca^{2+} depletion triggers the widespread opening of permeability transition pores, large protein complexes that traverse both the outer and inner mitochondrial membranes, which ultimately leads to mitochondrial swelling and eventually rupture.

PROTECTIVE MECHANISMS, REPAIR MECHANISMS, AND ADAPTATION

Protective Cellular Constituents

Cells have a variety of systems that provide protection from toxicity. GSH (discussed previously) is a major cellular nucleophile that protects against a wide array of reactive metabolites. GSH is constitutively abundant in essentially all cells, with the highest concentrations in the liver. *N*-acetylcysteine can be used to increase GSH to help protect against toxicity. In the same manner, some chemicals, including *N*-ethylmaleamide and buthionine sulfoximine, are often used to intentionally deplete GSH, an action that increases the likelihood of toxicity.

Another major source for cell protection, particularly for heavy metals, is MT, a small, cytosolic protein that contains 20 cysteine residues (1/3 of its amino acids) with high affinity for essential and toxic metals (Zn, Cu, Cd). MT is also a highly inducible protein, and exposure to these metals increases transcriptional activity through metal-responsive transcription factor 1

(MTF-1; Table 2.3). Each mole of MT binds up to 7 moles of metal, so that with induction, the capacity to bind a toxic metal is increased.

Induction of MT is causally related to the development of tolerance to heavy metal toxicity. For example, when pretreated with Zn, a dose of Cd that would be toxic to an untreated animal shows reduced or no toxicity. This is because increased tissue levels of MT provide a sink to bind the toxic metal and protect cellular organelles. Although MT is most frequently associated with protection from heavy metal toxicity, it also affords protection from other types of cellular stress.

Stress Response Pathways

Table 2.3 summarizes the types of pathways that are activated in response to cell stress and toxicity. In all cases, activation of transcription factors drives a program of gene expression changes that are designed to protect cells from further damage. There are two major pathways for protection against oxidative stress or DNA damage that are described here.

Keap1-Nrf2 Regulatory Pathway

The transcription factor Nrf2 (NF-E2-related factor 2) plays a central role in the induction of cytoprotective genes in response to oxidative stress (Figure 2.8). Under normal conditions, Nrf2 is bound to Keap1 (Kelch-like ECH-associated protein 1) in the cytoplasm, and binding to Keap1 targets Nrf2 for proteosomal degradation to maintain low intracellular levels. In the presence of electrophiles or oxidative stress, Keap1 is inactivated by direct modification of reactive cysteine residues, causing the release of active, stabilized Nrf2 that translocates to the nucleus to activate transcription of a variety of antioxidant and detoxification genes. Nrf2 activity is normally repressed by Keap1, and it accumulates in response to cell stress because the constitutive repression of Keap1 is removed. Genes that are activated via the Nrf2 pathway include numerous genes involved in xenobiotic disposition, protection from electrophiles and general stress responses.

Some xenobiotics can induce Nrf2, most notably the sulforaphane metabolites derived from broccoli sprouts, along with oltipraz and butylated hydroxytoluene. Induction of Nrf2 has been shown to protect

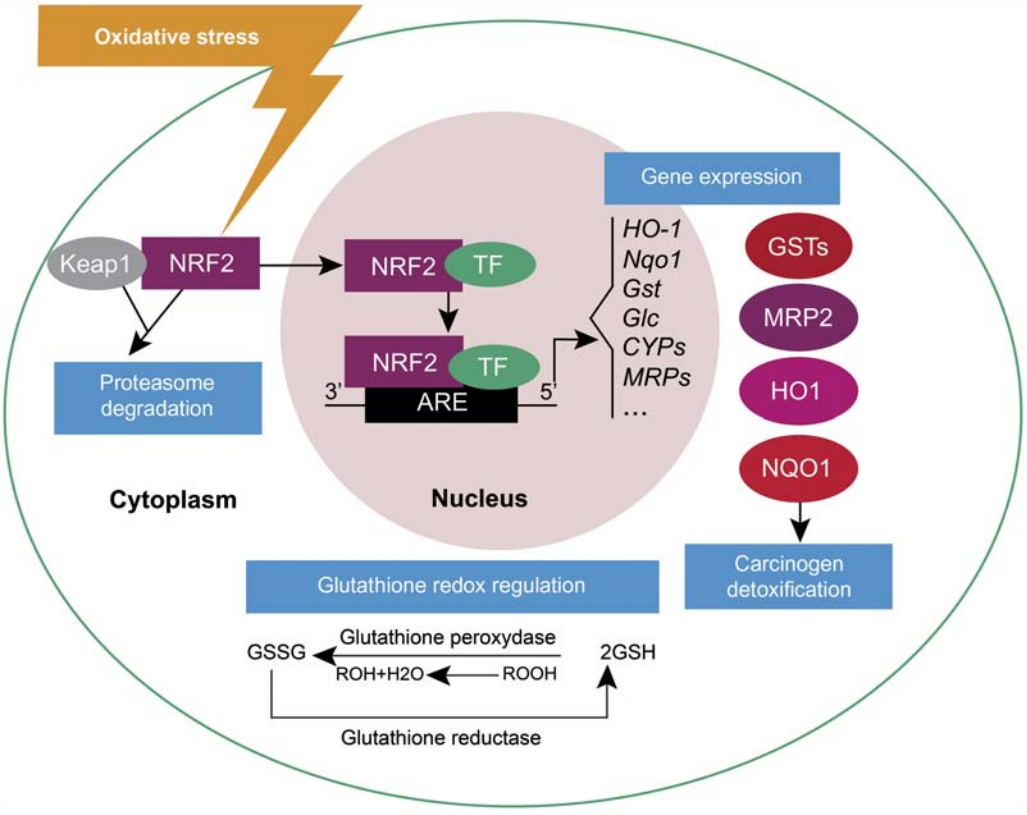

FIGURE 2.8 Under normal conditions, Keap1 acts as an adapter between Nrf2 and the ubiquitin ligase Cullin-3 and promotes the proteasomal degradation of Nrf2. Oxidative stress leads to the modification of specific thiols, resulting in dissociation of Nrf2 from Keap1 and translocation of Nrf2 into the nucleus, where Nrf2 binding to the antioxidant response element (ARE) in the regulatory region of a wide array genes involved in antioxidative responses and xenobiotic disposition leads their transcriptional activation.

against the risk of liver cancer associated with exposure to aflatoxin-contaminated food sources.

p53 Pathway

The major pathway involved in protecting against DNA damage is the p53 pathway. Under normal conditions, p53 activity is bound by mdm2 (double minute 2), a ubiquitin ligase that targets p53 for proteosomal degradation and prevents its intracellular accumulation. In the presence of DNA damage, p53 is phosphorylated and its binding to mdm2 is disrupted. Cellular levels of p53 increase dramatically with DNA damage, and with movement to the nucleus, a generalized cellular program to enable DNA repair is transcriptionally activated (Table 2.3). This response includes cell cycle arrest (in G1) to afford more time for DNA repair, along with induction of DNA repair enzymes and increased levels of ribonucleotide reductase to provide deoxyribonucleotides for DNA synthesis. A major p53-dependent gene is the cyclin-dependent kinase inhibitor, p21, which plays a critical role in cell cycle arrest. Importantly, p53 activation induces mdm2, serving to terminate p53-dependent programming when DNA repair is complete.

Although the stress response pathways have been described independently, it is clear that toxicity and any form of cell stress can affect multiple pathways concurrently. Thus, transcriptional activation of Nrf2 may be seen along with MT induction in response to heavy metals. Furthermore, it is now established that there is some interaction between the p53 and Nrf2 pathways.

Cell Proliferation

An almost immediate response to tissue injury is that undamaged cells enter the cell cycle to begin the process of tissue repair. It is likely that this process is initiated by mediators released from damaged cells, including a variety of cytokines and growth factors involved in cell replication. In the classical model of liver regeneration following partial hepatectomy, the early regeneration phase is regulated primarily by TNFα and IL-6. These factors are likely produced by the resident Kupffer cells rather than by hepatocytes. A variety of other growth factors (e.g., hepatocyte growth factor, transforming growth factor-α) increase and drive the cells into mitotic division. In addition, increased expression of genes that function in growth arrest is also observed, thereby terminating the cell cycle, to maintain a tight regulation on the regenerative process.

In response to various types of injury, tissue-specific stem cells are the primary source of early replication, and these cells can further differentiate into the mature cell type. This is the case for highly proliferative target organs such as bone marrow and the intestinal mucosa. In addition, in liver, oval cells localized within the portal triad appear to be the source for tissue renewal and repair. Similarly, in lung, Type II pneumocytes and bronchiolar club cells function to replace the differentiated Type I pneumocyte and bronchiolar epithelium, respectively.

One early feature of tissue repair is that the regenerating tissue is often refractory to additional tissue damage. This phenomenon of tolerance has been illustrated in many tissues. As one example, a number of xenobiotics are toxic to bronchiolar club cells, usually as a result of localized formation of reactive metabolites. Chemicals such as naphthalene, coumarin, ipomeanol, and 3-methylindole cause marked bronchioloar club cell toxicity accompanied by cell proliferation and repair. However, whereas as a single dose of these compounds causes nonciliated exocrine bronchiolar cell necrosis, after repeated dosing (1–2 weeks), there is no histological evidence of club cell toxicity. The mechanism(s) underlying this phenomenon is not well understood, but is thought to reflect changes in detoxification pathways or altered differentiation of the cells that renders them resistant to toxicity.

As described earlier, xenobiotics that activate CAR and PPARα stimulate cell proliferation without evidence of cytotoxicity or cell death. Proliferation is primarily observed in liver and is associated with induction of CYPs and peroxisome proliferation, respectively. The stimulus for induction of cell proliferation is not fully understood, but in both cases, $CAR^{-/-}$ and $PPAR\alpha^{-/-}$ mice are refractory to both enzyme induction and increased cell proliferation confirming that both the biochemical changes and hepatocellular proliferation are dependent on NR activation.

SUMMARY

There are many different mechanisms of toxicity. Unraveling complex mechanisms of toxicity requires an understanding of basic principles that govern whether and how a toxic chemical reaches its target site along with information on how the target organ or target cell responds to the toxicant. Furthermore, the integration of morphologic, biochemical, and molecular changes provides insight into mechanisms of toxicity. Ultimately, understanding toxic mechanisms is relevant for addressing species differences in toxicity, characterizing the potential risk for toxicity resulting from chemical exposure, and developing approaches to prevent or treat adverse effects.

Further Reading

Conrad, M., Angeli, J.P., Vandenabeele, P., Stockwell, B.R., 2016. Regulated necrosis: disease relevance and therapeutic opportunities. Nat. Rev. Drug Discov. 15, 348–366.

Jacobs, A.T., Marnett, L.J., 2010. Systems analysis of protein modification and cellular responses induced by electrophile stress. Accounts Chem. Res. 43, 673–683.

Jaeschke, H., Gores, G.J., Cederbaum, A.I., Hinson, J.A., Pessayre, D., Lemasters, J.J., 2002. Mechanisms of hepatotoxicity. Toxicol. Sci. 65, 166–176.

Klaassen, C., 2013. Casarett and Doull's Toxicology, eighth ed. McGraw-Hill, New York. [Particularly chapters 3, 5 and 6].

Klaassen, C.D., Aleksunes, L.M., 2010. Xenobiotic, bile acid and cholesterol transporters: function and regulation. Pharmacol. Rev. 62, 1–96.

Lehman-McKemman, L.D., 2013. Biochemical and molecular basis of toxicity. In: third ed Haschek, W., Rousseaux, C., Wallig, M., Ochoa, R., Bolon, B. (Eds.), Handbook of Toxicologic Pathology, vol. I. Elsevier, Amsterdam, pp. 15–38. Chapter 1.

Nelson, D.R., Zeldin, D.C., Hoffman, S.M., Mathias, L.J., Wain, N.M., Nebert, D.W., 2004. Comparison of cytochrome P450 (CYP) genes from the mouse and human genomes including nomenclature recommendations for genes, pseudogenes and alternative-splice variants. Pharmacogenetics. 14, 1–18.

Orrenius, S., Nicotera, P., Zhibotovsky, B., 2011. Cell death mechanisms and their implications in toxicology. Toxicol. Sci. 119, 3–19.

Simmons, S.O., Fan, C.-Y., Ramabhadran, R., 2009. Cellular stress response pathway system as a sentinel ensemble in toxicological screening. Toxicol. Sci. 111, 202–225.

Szyf, M., 2011. The implications of DNA methylation for toxicology: toward toxicomethylomics, the toxicology of DNA methylation. Toxicol. Sci. 120, 235–255.

Wakabayashi, N., Slocum, S.L., Skoko, J.J., Shin, S., Kensler, T.W., 2010. When Nrf2 talks, who's listening? Antioxid. Redox Signal. 13, 1649–1663.

Yokoi, T., Nakajima, M., 2013. microRNAs as mediators of drug toxicity. Annu. Rev. Pharmacol. Toxicol. 53, 377–400.

This page intentionally left blank

CHAPTER

3

Pharmacokinetics and Toxicokinetics

Kannan Krishnan[1,2] *and Sandrine F. Chebekoue*[2]

[1]Risk Sciences International, Ottawa, ON, Canada [2]University of Montreal, Montreal, QC, Canada

OUTLINE

INTRODUCTION

The interpretation of the outcome of *in vivo* toxicological studies can be challenging when the *tissue response* is analyzed as a function of *administered dose* (i.e., dose in mg/kg/d) or *exposure concentration* (e.g., chemical concentration in dosing solution or exposure medium). The biological responses are more closely related to the concentration of the active form of the chemical present in the target tissue, rather than the amount administered to the animal. The critical importance of the relationship between tissue (or blood) concentrations and tissue responses in exposed organisms has long been recognized in pharmacology and drug development.

In toxicology and risk assessment, the target tissue dose or the internal dose that most closely relates to an adverse response is referred to as a *dose metric*. Consistent with the current understanding of the mode of action, a *dose metric* reflects the intensity and level of the biologically active form of a chemical (i.e., parent chemical or metabolite(s)) in a target tissue (or a surrogate matrix such as blood) for a specific duration. Here, the *intensity* refers to peak, average, or integral measures, whereas the *level* refers to concentration or amount; the *duration* corresponds to an exposure time frame of relevance, for example, instantaneous, daily, lifetime, or a specific period during development (such as exposure window corresponding to a particular gestational event). Thus, a variety of dose metrics could be of potential relevance in interpreting tissue response data for a given chemical. Typically, these include the maximal concentration (C_{max}), the area under the concentration versus time curve ($AUC_{0\text{-}t}$), or the time-averaged concentration (C_{av}) of the parent chemical or metabolite(s) in the blood (plasma) or a specific tissue. The experimental measurement, or model-based calculation, of such dose metrics for interpreting toxicity studies is facilitated by pharmacokinetics (PK) and toxicokinetics (TK).

PK involves the study of absorption, distribution, metabolism, and excretion (ADME) in view of

Fundamentals of Toxicologic Pathology.
DOI: http://dx.doi.org/10.1016/B978-0-12-809841-7.00003-4

characterizing the time-course of the level of parent chemical or its metabolite(s) in biological matrices. TK is synonymous to PK but the latter term is used when PK principles are applied to toxicants or when kinetic data for therapeutic agents are collected and analyzed at doses that elicit toxicity. In essence then, both PK and TK are fields of study that relate to *kinetics*, which refers to the change in one or more variables as a function of time.

This chapter presents the basic principles and models used for characterizing the PK and TK of chemicals in experimental animals, with emphasis on their critical role in designing toxicity studies. For more elaborate mathematical treatment of the subject as well as for more complex modeling approaches, the reader is referred to specialized textbooks and monographs on this subject matter (see Further Reading).

PHARMACOKINETICS: PROCESSES AND DETERMINANTS

The dose metrics of relevance (e.g., AUC_{0-t}, C_{max}) in interpreting response data from toxicological studies depend upon the competing processes of ADME. The time-course of the blood and/or target tissue concentration of a substance or its metabolite(s) in the exposed organism depends upon the mechanism, magnitude, and rate of each of these processes (Figure 3.1). These processes as well as the underlying mechanisms are discussed in detail in Chapter 2: Biochemical and Molecular Basis of Toxicity. The following paragraphs then focus on the quantitative aspects of ADME, highlighting their key mechanistic determinants.

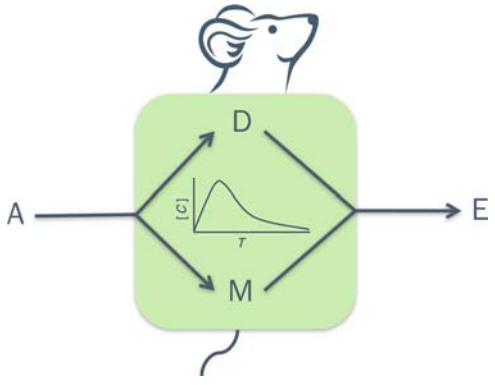

FIGURE 3.1 An illustration of the key processes determining the time-course of the concentration of a chemical in target site ([C] versus *T*). A, absorption from the dosing or exposure medium; D, distribution into blood components and rest of the body; M, metabolism by hepatic and extrahepatic tissues; E, excretion.

Absorption

Absorption is the process by which the chemical in the dosing solution or exposure medium moves across the biological membranes to get into systemic circulation. Depending upon the purpose of the study, the chemical may be administered by a variety of routes such as dermal/topical, oral, intraperitoneal (ip), intramuscular (im), intravenous (iv), pulmonary (inhalation), or subcutaneous (sc) (Figure 3.2). An iv administration does not comport an absorption phase since the chemical is introduced directly into systemic circulation. For all other routes of administration, the kinetics of absorption is dependent primarily upon the route-specific rate of absorption and bioavailable fraction.

For the dermal route, the flux of a chemical through a membrane following passive diffusion from the immediate environment (e.g., water) can be computed according to Fick's first law, as follows:

$$\text{Rate of the amount of chemical absorbed via skin (mg/}h) = K_p \times S_a \times C_{in} \quad (3.1)$$

where C_{in} is the applied concentration (mg/mL), K_p is the membrane permeability coefficient (cm/h), and S_a is the exposed surface area (cm^2).

The value of K_p reflects the relative importance of both transcellular (lipidic) and paracellular (movement through the water-filled gaps between adjacent cells) transport of chemicals.

For the inhalation route, the concentration of a chemical in alveolar space and arterial blood, at any time, depends upon the total input and output (or loss) from the lung compartment. Figure 3.3 illustrates a simple case of a volatile organic chemical (e.g., toluene) that equilibrates quickly between alveolar space and blood and for which there is no significant

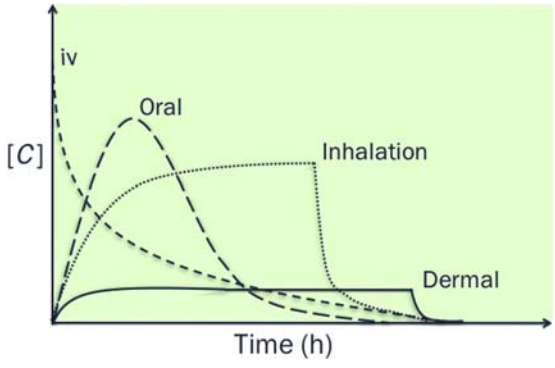

FIGURE 3.2 An illustration of the blood time-course curves of a hypothetical chemical following its absorption through various routes. [C], blood concentration.

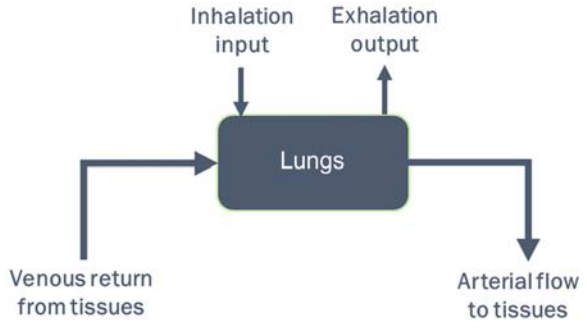

FIGURE 3.3 Mass conservation and flux of inhaled volatile organic chemicals in the lung compartment.

metabolism or storage by the lung tissue. The mass conservation in this case can be written as follows:

Amount inhaled from the air
+ amount received via venous blood
= amount exiting through arterial blood
+ amount removed from lung by metabolism/exhalation (3.2)

Notationally,

$$Q_p \times C_{inh} + Q_c \times C_v = Q_c \times C_a + Q_p \times C_{alv} \quad (3.3)$$

where C_a is the arterial concentration, C_{alv} is the alveolar air concentration, C_{inh} is the inhaled concentration, C_v is the venous blood concentration, Q_c is the cardiac output, and Q_p is the alveolar ventilation rate.

Since the lung equilibrates vapor between alveolar air and blood, the alveolar concentration and arterial blood concentration are related by the blood:air partition coefficient (P_b), that is, $C_{alv} = C_a/P_b$. A partition coefficient, in general terms, represents the ratio of chemical concentration in two matrices at equilibrium, and in this case, between blood and air. If P_b is 10, that would imply that the chemical concentration in blood would be 10 times greater than that of the inhaled air at equilibrium. Based on this principle then, Eq. (3.3) can be rewritten to calculate arterial blood concentration C_a, resulting from inhalation exposures as follows:

$$C_a = \frac{Q_p \times C_{inh} + Q_c \times C_v}{Q_c + (Q_p/P_b)} \quad (3.4)$$

A close examination of this equation would indicate that, for highly blood-soluble chemicals (i.e., with high P_b), the pulmonary absorption will be influenced by P_b and Q_p but not Q_c. Given the extensive blood solubility of these chemicals, the delivery rate is essentially the key factor determining C_a, such that an increase in Q_p would translate to a corresponding increase in the amount absorbed. Examples of chemicals exhibiting high blood solubility would be 1,4-dioxane (rat $P_b = 1861$) and 2-butoxyethanol (rat $P_b = 7965$).

In the case of chemicals that are poorly soluble in blood (i.e., chemicals with low P_b), the rate of pulmonary absorption is influenced by blood perfusion rate (Q_c) and P_b rather than Q_p. So, for a given exposure concentration of a chemical with low P_b such as carbon tetrachloride (rat $P_b = 4.52$), the pulmonary absorption is enhanced further only by increases in Q_c (facilitating greater systemic entry).

For the oral route, the amount entering the liver following absorption can be calculated as follows:

$$R_{abs} = K_a \times A_{stomach} \quad (3.5)$$

where $A_{stomach}$ is the amount in the stomach (mg), K_a is the first-order absorption rate constant (h^{-1}), and R_{abs} is the rate of amount absorbed (mg/h).

In Eq. (3.5), $A_{stomach}$ is initially determined by the dose administered and thereafter by the amount remaining to be absorbed (i.e., nonionized form). In the case of chemicals metabolized by the liver, the fraction of the dose escaping the liver unmetabolized (i.e., fraction that is not subject to metabolism upon entry, also referred to as *first pass effect*) is accounted for. The use of K_a (h^{-1}) is conceptually similar to the first-order uptake rate described in Eq. (3.1) for dermal pathway. In essence, K_a reflects the proportion of the dose that is absorbed per unit time. For example, if $K_a = 0.1\ h^{-1}$, it implies that 10% of the amount in the stomach is absorbed per hour. Thus, after 1 h of oral dosing, an amount equal to 90% will remain unabsorbed; similarly, after the second hour, 10% of the remaining 90% is absorbed (i.e., 9%), leaving 81% of the dose in the stomach/gut, and so on. If the amount absorbed per unit time is constant (e.g., 10 mg/h), regardless of the magnitude of the dose administered (1, 5, 10, or 100 g), then it is said to follow a *zero-order process*. Dietary exposure to chemicals is sometimes described by a zero-order (or constant) input process, since it results in a fairly constant input dose to the exposed animals. The concepts of proportionality (i.e., first order) and constant input (i.e., zero order) explained here are applicable to all other phases of PK, thereby being critical in interpreting toxicity data.

Distribution

Distribution is the process by which a chemical in systemic circulation moves into the various organs, including metabolizing organs (e.g., liver), excretory organs (e.g., kidney), storage depots (e.g., fat, bone), and target sites (e.g., placenta, brain). Lipid solubility, ionization, and protein binding are key factors determining the extent to which a chemical is distributed in the body.

The volume of distribution (V_d) or the apparent volume of blood (or volume of plasma water as reported

in the pharmaceutical literature) in which the chemical is distributed or diluted throughout the body determines the resulting chemical concentration. V_d would be equal to the volume of blood if the chemical resided solely and uniformly in the blood components (plasma, erythrocytes). However, V_d would increase as a chemical exhibits greater affinity for binding proteins and lipidic tissues, and thus moves from the plasma water (or blood) into these depots. In this regard, the affinity of a chemical for tissues relative to blood is represented by the tissue:blood partition coefficient (P_{tb}). The P_{tb}, with units of mL blood/mL tissue, represents the ratio of the concentration of a chemical in the tissue and blood, at equilibrium. The volume of a tissue (V_t) multiplied by the corresponding P_{tb} yields the blood-equivalent volume in which the chemical is distributed.

For example, in the case of a chemical with a P_{tb} of 1, the total V_d is 30 mL if it is distributed in the blood and tissue compartment with volumes of 15 and 15 mL, respectively (Figure 3.4). However, if the P_{tb} of the chemical is 10, then the physical volumes of tissues and blood remain at 15 and 15 mL, respectively, but the physiological apparent volume of the tissue compartment becomes 150 mL (i.e., $V_t \times P_{tb} = 15$ mL tissue $\times$ 10 mL blood/mL tissue = 150 mL blood; Figure 3.4) to yield a total distribution volume of 165 mL. Accordingly then, the sum of blood volume (V_b) and tissue volumes (expressed as blood-equivalent volume, i.e., $V_t \times P_{tb}$) is considered to be a reasonable approximation of the V_d of chemicals, as follows:

$$V_d = V_b + \text{sum}(V_t \times P_{tb}) \tag{3.6}$$

where P_{tp} is the tissue:blood partition coefficient, V_d is the volume of distribution (units of volume, e.g., L, mL), V_b is the volume of blood (or plasma), and V_t is the volume of tissue.

Thus, for 1,1,1,2-tetrachloroethane, a chemical with P_{tb} of 2.1, 51.5, and 0.95 for the liver, fat, and muscle compartments, the computed V_d in the rat would be 1.14 L even though its body weight (i.e., physical volume) is only 0.25 kg. The units of V_d are frequently mL or L, but it is also sometimes reported as volume per kg body weight (mL/kg, L/kg). Empirically, V_d is calculated with knowledge of dose administered (Dose, mg) and the initial blood concentration (C_0, mg/L), estimated using PK models (see "Pharmacokinetic (Time-Course) Data and Derivation of Dose Metrics" section), as follows:

$$C_0 = \frac{\text{Dose}}{V_d} \tag{3.7}$$

where C_0 is the initial blood concentration (mg/L); Dose is the dose administrated (mg), and V_d is the volume of distribution (unit of volume).

Accordingly, the extensively distributed chemicals (e.g., those that exhibit a marked affinity for fat depots and those that bind to tissue proteins) will have very large V_d, whereas hydrophilic substances exhibit smaller V_d, often close to 0.6 L/kg (approximately equaling the total water content of body, i.e., 60% of the body weight). This water content is the sum total of the content of plasma, intracellular fluid, and interstitial fluid, which correspond to 4%, 35%, and 21% of the body weight, respectively. Depending upon how well or how little the substances distribute within various components of the tissues and blood (i.e., water, lipids, proteins), the apparent V_d differs from chemical to chemical, and from one species to another.

Despite the comparable rate of absorption and V_d of any two chemicals, the resulting blood (or target tissue) concentration and half-life ($t_{1/2}$) could be different depending upon the extent of the elimination processes, namely metabolism and excretion, as discussed later.

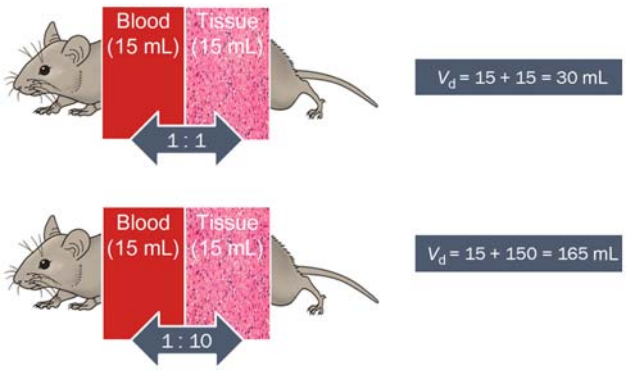

FIGURE 3.4 An illustration of the physical volume and physiological volume of distribution of chemicals. P_{tb} is the tissue:blood partition coefficient.

Metabolism

Metabolism or biotransformation in organs such as liver is limited by the delivery (blood flow to the organ) and/or capacity (i.e., of metabolizing enzymes). The enzyme content, the catalytic efficiency of the enzyme, and the binding affinity of the substrate determine the intrinsic metabolic capacity of an organ. The rate of the amount of chemical metabolized per unit time (RAM) is frequently computed on the basis of the maximal velocity (V_{max}), affinity for the metabolizing enzyme (K_m), and free concentration of the substrate ([S]), as per the Michaelis–Menten equation:

$$\text{RAM} = \frac{V_{max} \times [S]}{K_m + [S]} \tag{3.8}$$

where K_m is the affinity for the metabolizing enzyme, RAM is the rate of the amount of chemical metabolized per unit time (or rate of metabolism), [S] is the concentration of free substrate, and V_{max} is the maximal velocity (mass unit/time unit; e.g., mg/h).

In Eq. (3.8), the ability of the enzyme machinery (in an organ *in vivo* or in an experimental system *in vitro*) to remove a substance and thereby clear the exposure (or carrier) medium in which it is present (e.g., blood) is determined by V_{max} and K_m, or intrinsic clearance (CL_{int}). CL_{int} is expressed in units of volume/time (e.g., L/h) and estimated as follows:

$$CL_{int} = \frac{V_{max}}{K_m + [S]} \tag{3.9}$$

where CL_{int} is the intrinsic clearance (units of volume/time, e.g., L/h).

Considering Eqs. (3.8) and (3.9) together, it can be seen that RAM can be calculated as the product of [S] and CL_{int}. Then, as [S] increases (i.e., [S] $\gg$ K_m), the RAM approximates the V_{max}, that is, the maximal-metabolizing capacity of the enzyme. On the other hand, at very low substrate concentrations (i.e., [S] $\ll$ K_m), the RAM is proportional to [S] because CL_{int} is essentially a constant (being approximately equal to V_{max}/K_m). The values of CL_{int} (calculated as V_{max}/K_m) vary from chemical to chemical (e.g., CL_{int} of endosulfan = 39 L/h, whereas CL_{int} of 1,1,1-trichloroethane = 0.02 L/h in rats).

Figure 3.5 illustrates that the RAM for a hypothetical chemical as per Eqs. (3.8) and (3.9) approaches a constant value equal to the V_{max} (100 μg/h). So, for this hypothetical chemical, responses seen at high doses (that yield blood concentrations > 100 μg/L) should not be extrapolated linearly to predict metabolic rate or response incidence at lower doses. The amount metabolized as calculated per Eqs. (3.8) and (3.9) does not account for physiological limitations, particularly the delivery to the metabolizing tissue *in vivo*. The latter is determined by the rate of blood flow (Q) to the organ. For example, considering a rate of blood flow to the liver (Q_l) in the rat of 1.3 L/h, the implication would be that the rat liver cannot metabolize more than the amount of chemical delivered by 1.3 L blood per hour. This physiological limitation and its relevance to the RAM of a chemical will become evident upon integrating the intrinsic enzyme capacity, CL_{int}, with the Q_l, to calculate hepatic clearance ($CL_{hepatic}$). $CL_{hepatic}$ is defined as the volume of blood (or plasma) from which chemical is removed per unit time and calculated as follows:

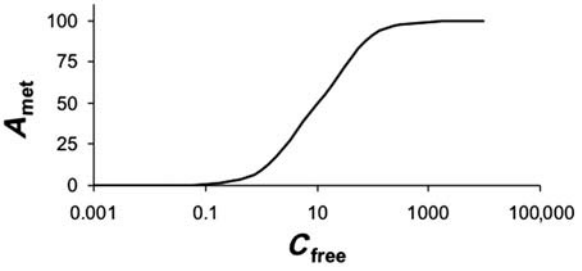

FIGURE 3.5 Rate of the amount metabolized (A_{met}, μg/h) as a function of the free concentration of a hypothetical chemical (C_{free}, μg/L). $A_{met} = CL_{int} \times C_{free}$ and CL_{int} (L/h) is based on V_{max} of 100 μg/h and K_m of 10 μg/L for this hypothetical chemical.

$$CL_{hepatic} = \frac{CL_{int} \times Q_l}{CL_{int} + Q_l} \tag{3.10}$$

where $CL_{hepatic}$ is the hepatic clearance (units of volume/time) and Q_l is the rate of blood flow to the liver (units of volume per time).

$CL_{hepatic}$ is expressed in units of volume per time (e.g., mL/min, L/h) or sometimes in units of volume per time normalized to the weight of the organ or body (e.g., L/h/kg). Furthermore, the RAM can be estimated from $CL_{hepatic}$ as follows:

$$RAM = CL_{hepatic} \times C_a \tag{3.11}$$

$CL_{hepatic}$ can also be computed with knowledge of the fraction of chemical in hepatic blood removed by metabolism during its passage (i.e., hepatic extraction ratio) and Q_l:

$$CL_{hepatic} = E_h \times Q_l \tag{3.12}$$

where E_h, hepatic extraction ratio [i.e., amount metabolized by liver/amount delivered to liver, fractional difference in arteriovenous concentration of a chemical ($C_{arterial} - C_{venous}$)/$C_{arterial}$], or ratio of hepatic clearance to hepatic blood flow [i.e., $CL_{hepatic}/Q_l$ or $CL_{int}/(Q_l + CL_{int})$].

The values of $CL_{hepatic}$ and E_h vary among chemicals. For example, in the rat, $E_h = 0.02$ for 1,1,1-trichloroethane and $E_h = 0.92-0.97$ for endosulfan and trichloroethylene. A high E_h value (≥ 0.7) would suggest that the chemical is highly cleared by the liver, implying that Q_l rather than the enzyme content is the limiting factor of metabolic clearance. The metabolic clearance of a chemical exhibiting a small E_h value (< 0.1) would be limited by the enzyme capacity and not delivery, that is, even if more chemical enters the liver, the metabolism will only occur at a low rate characterized by its CL_{int}. The concepts of nonlinearity and physiological limitation discussed earlier are also applicable to other elimination processes, including urinary excretion (*vide infra*).

Excretion

The elimination of a chemical from the systemic circulation of a treated animal depends not only upon

metabolic clearance but also upon other excretion processes. These include exhalation, urinary excretion, biliary and fecal excretion, and transfer via milk, hair, saliva, etc.

The total clearance (CL_{total}) of a chemical from systemic circulation then equals the sum of all individual clearance (elimination) processes occurring in parallel. Accordingly,

$$CL_{total} = CL_{pulmonary} + CL_{renal} + CL_{hepatic} + CL_{other} \quad (3.13)$$

where CL_{total} is the total clearance, $CL_{pulmonary}$ is the pulmonary clearance, CL_{renal} is the renal clearance, $CL_{hepatic}$ is the hepatic clearance, and CL_{other} is the elimination from other potential metabolism organs.

In the "Metabolism" section, Eq. (3.10) was presented and described for its use in calculating $CL_{hepatic}$. Similar calculations of the number of liters of blood cleared of a substance per unit time can also be performed for other elimination processes. Thus, the pulmonary clearance is calculated as Q_p/P_b. Accordingly, chemicals with low P_b show high $CL_{pulmonary}$ (e.g., cyclohexane with $P_b = 1.4$ and $CL_{pulmonary} = 3.2$ L/h, in the rat), whereas the reverse is true for VOCs with high P_b values (e.g., 2-butoxyethanol with $P_b = 7965$ and $CL_{pulmonary} = 0.0007$ L/h).

In the case of urinary excretion, glomerular filtration, tubular reabsorption, and tubular secretion together determine the overall rate and amount of chemical excreted. Accordingly then, CL_{renal} is equal to the glomerular filtration rate (GFR) if there is no tubular reabsorption or secretion. However, when these processes are not negligible, CL_{renal} is calculated as follows:

$$CL_{renal} = f_u \times (GFR + CL_{secretion}) \times (1 - F_{reabsorbed}) \quad (3.14)$$

where $CL_{secretion}$ is the clearance by tubular secretion, $F_{reabsorbed}$ is the fraction reabsorbed, f_u is the unbound fraction of the chemical in systemic circulation, and GFR is the glomerular filtration rate.

The competing and net influence of ADME processes results in a certain time-course profile (e.g., AUC_{0-t}) of the chemical concentration in the target organ of experimental animals. The exposure of the target organ to the chemical and its metabolites can be assessed, where feasible, by measuring them in selected biological matrices. Such derivations of dose metrics from PK data and their usefulness relative to the administered dose are discussed in the following section.

PHARMACOKINETIC (TIME-COURSE) DATA AND DERIVATION OF DOSE METRICS

The tissue responses observed in toxicity studies is a result of the toxic form of the chemical (parent or metabolite) being delivered in some quantity over a specific duration (t) to the target organ. For systemically acting chemicals (which induce toxicity in organs other than the portals of entry), the measure of dose to the target is critical not only for interpreting the toxicity data but also for extrapolating to other test or exposure systems (e.g., route, scenario, dose, exposure matrix, species). In this regard, the administered dose or daily intake (mg/kg/d) was used in the past because it was the most readily available measure of dose and for which measurement methods (development and implementation) were least tedious. Even though this dose measure accounts for body weight differences between animals, it does not take into account any qualitative or quantitative differences in PK processes across doses, routes, and species (on the basis of toxic moiety of chemicals). Therefore it is the least relevant measure of dose to the target tissue.

The next level of refinement in terms of the dose measure for analyzing responses in a toxicology study would involve the use of *absorbed dose*, which accounts for differences in body weight as well as species-specific differences in absorption efficiency and bioavailability. While this dose measure is more closely related to the tissue response than administered dose, it does not account for the potential dose-, route-, time-, and/or species-specific differences in unbound concentration in plasma or distribution to target tissues. Furthermore, such a dose measure does not explicitly account for the rate or extent of formation of active metabolite(s). Therefore, the maximal, average, or integrated concentration of the chemical or its metabolite(s) in blood (or plasma water) is increasingly used for monitoring internal exposure, and for extrapolating/interpreting toxicity data.

This approach reflects the basic tenet of PK that the unbound or active form of the chemical in blood is a key determinant of tissue responses. Blood (or plasma), besides being a convenient sampling site, represents a reasonable reference biological fluid for kinetic calculations as it reflects the net impact of bioavailability, uptake, distribution, and elimination processes in the organism. Since the tissues equilibrate with blood (i.e., as reflected by the P_{tb}), it further effectively reflects the extent of target exposure.

Two common measures of dose metric based on blood are: C_{max} and AUC_{0-t}. Whereas C_{max} represents the maximal concentration (or the peak concentration) in a time-course curve, AUC_{0-t} is the integral measure of internal exposure over a given period of time. When the parent chemical is the toxic moiety, C_{max} correlates well with acute responses (e.g., neurotoxicity of toluene), whereas AUC_{0-t} is the better internal dose metric for chronic effects (e.g., cancer). The selection of appropriate dose metrics is critical to a sound interpretation and extrapolation of toxicological data collected under one set of exposure conditions.

Let us consider the measurements of 0, 0.5, 1.2, 0.6, and 0.3 mg/L of a substance at 0, 2, 4, 8, and 12 h post-administration (Figure 3.6). In this case, based on the measurements made in the exposed animal, the C_{max} is 1.2 mg/L. The AUC_{0-t} is calculated by integrating the concentrations over the duration of interest. As shown in Figure 3.6, determining the area under each trapezoid and then adding them together can compute AUC_{0-t}. This is done by: (1) taking the average concentration during two consecutive sampling times and (2) multiplying it with the corresponding time interval. Thus, the *AUC* of the first trapezoid would be: $[(0 + 0.5)/2] \times (2 - 0)$, or 0.5 mg/L × h. The *AUC* for the subsequent trapezoids are: 1.7, 3.6, and 1.8 mg/L × h, respectively. The total *AUC* then corresponds to 7.6 mg/L × h $(= 0.5 + 1.7 + 3.6 + 1.8)$. This *AUC*, for example, can be used as a basis for comparing responses across dose groups, studies, or even species. With knowledge of elimination constant, the *AUC* for extended periods of time can be calculated.

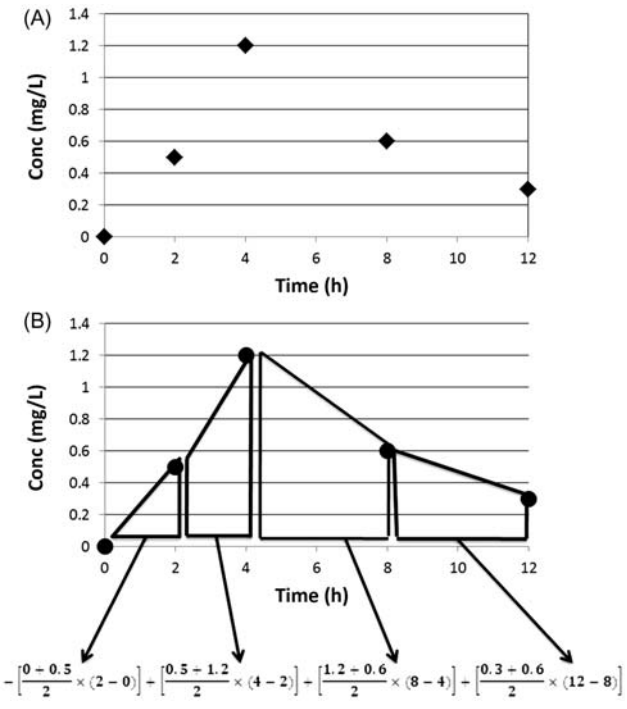

FIGURE 3.6 Illustration of (A) measured blood concentrations (Conc, mg/L) following a single oral dose, and (B) the construction of trapezoids for calculating area under the curve (AUC_{0-t}) for a hypothetical chemical.

In order to obtain reliable estimates of C_{max} and AUC_{0-t}, appropriate design of TK studies is essential. Collection of PK data in the main study groups or a satellite group can be done in these studies. However, the sampling times should permit the characterization of C_{max}; also, sufficient blood samples should be collected during critical phases to calculate AUC_{0-t}. But care should be taken not to take more than 10% of the total blood volume from the small laboratory animals, in a given week.

At least five, and preferably seven, time points are used to characterize the entire time-course of the kinetics of a chemical. Of these, at least two time points should be in the early (absorption/distribution) phase and at least three time points in the terminal elimination phase. In case of an oral-dosing study, at least one sample should be obtained before the t_{max} to facilitate reliable characterization of the TK profile of a substance, including the absorption phase. In terms of the sampling during elimination phase, the time interval between the first and last sampling time points should at least be twice the $t_{1/2}$ of the substance. For the estimation of AUC_{0-t}, sampling during at least three $t_{1/2}$ beyond t_{max} is considered reliable. Specialized designs and statistical analyses can be employed to strike a balance between sampling time intervals and minimization of the number of samples while focusing to get a reasonable estimate of the dose metrics.

Since the collection of all desired data on blood or tissue concentrations as a function of time, dose, duration, and species is not routinely possible, mathematical tools are used to construct the required time-course curves. These tools, referred to as PK models, are quantitative descriptions based on either empirical modeling of PK data or mechanistic understanding of the critical determinants of the ADME processes, as described below.

PHARMACOKINETIC MODELS AND COMPUTATION OF DOSE METRICS

When the dose metrics of interest (e.g., AUC_{0-t}, C_{max}) cannot be measured at all desired time points and matrices in the treated animals, they can be computed using PK models based on available data or parameters. These PK models range from a simple, one-compartmental model to complex multicompartmental models.

One-Compartment Model

The *one-compartment PK model* considers the body as a single homogeneous compartment (Figure 3.7). This model is based on the assumption that the absorbed chemical is distributed uniformly in all tissues and at all times. In the simplest case illustrated here, the amount of a chemical in the body results from the input rate corresponding to the administered dose (mg/h) minus the output (or elimination, mg/h). The chemical concentration in tissues and blood can then be determined by dividing the amount in body by the volume in which the chemical is distributed (V_d). The basic equations underlying the one compartment model are listed in Table 3.1.

Figure 3.8A presents a plot of the plasma concentration data collected for a hypothetical chemical at various time intervals following a single iv dose. The measured concentrations were 1.2, 0.6, 0.3, and 0.15 mg/L at 2, 4, 6, and 8 h postdosing. Therefore, the initial concentration, namely C_0, is not known and needs to be estimated by extrapolation. In order to do that, and to estimate the eliminate rate constant (K_{el}), logarithmic transformation of the data is applied (Figure 3.8B). The intercept ($\ln C_0 = 0.8755$; or upon linear transformation equals 2.4 mg/L) equals the initial plasma concentration, whereas the slope ($= 0.437\ h^{-1}$) corresponds to the K_{el}. The elimination or terminal half-life ($t_{1/2}$, in units of minutes, hours, weeks, months, years, etc.), defined as the time taken for the concentration (or body burden) to decline by 50% of the initial value, is obtained from K_{el} as shown in the following equation:

$$t_{1/2} = \frac{\ln 0.5}{-K_{el}} = \frac{0.693}{K_{el}} \tag{3.15}$$

where K_{el} is the elimination rate constant and $t_{1/2}$ is the elimination or terminal half-life (units of minutes, hours, weeks, months, years).

Accordingly, after one $t_{1/2}$, the initial concentration would have come down by 50%. After the second $t_{1/2}$, half of the remaining quantity (i.e., 50% ÷ 2 = 25%) is eliminated such that the total elimination amounts to 75%. After the third $t_{1/2}$, half of the remaining amount (i.e., 12.5%) is eliminated such that the total eliminated at the end of the third $t_{1/2}$ is 87.5% of the initial quantity. Continuing this calculation would indicate that after 4, 5, 6, and 7 $t_{1/2}$, a total of 93.7%, 96.9%, 98.5%, and 99.25% would be eliminated, respectively. Figure 3.9 is a pictorial representation of the percent dose eliminated as a function of $t_{1/2}$. From this figure, one can formulate that, at about five $t_{1/2}$, the substance in the body is nearly fully eliminated.

Even though the K_{el} value for a given chemical can be estimated by modeling the time-course data in a biological matrix taken from treated animals, attention should be given to planning the data collection. For example, estimating K_{el} from just two C_t values obtained from the elimination phase might be unreliable due to inadequate consideration of within-animal and between-animal variability, as well as uncertainty in estimates. Therefore, when estimating K_{el} or $t_{1/2}$, the time interval between the two measured concentrations should be equal to at least one $t_{1/2}$, and it is preferable to collect such data during time spanning at least three to four $t_{1/2}$.

The compartmental PK model described earlier and associated parameters (Table 3.1) are "data-driven," and require that the time-course data on chemical (or its metabolite(s)) concentration be collected in a biological matrix (blood, plasma, tissue, urine, or exhaled air) for each dosing regimen in each species. An alternative to such an intensively data-based approach is

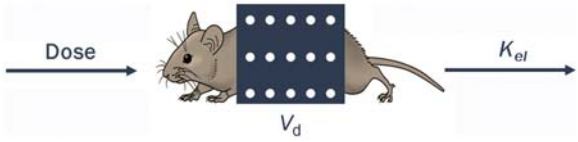

FIGURE 3.7 Conceptual representation of the one-compartment PK model. V_d is the volume of distribution and K_{el} is the elimination constant.

TABLE 3.1 Summary of Equations Associated With, and Derived From, the Simplest One-Compartmental PK Model. Dose indicates absorbed oral dose.

Output	Model equation
Rate of change in the amount of chemical (dA_t/dt, mg/h)	$\text{Dose} - (A_t \times K_{el})$
Amount or body burden at specific time t (A_t)	$A_0 \times e^{-K_{el} \times t}$
Concentration in blood or tissue at specific time t (C_t)	$C_t = C_0 \times e^{-K_{el} \times t}$
Half-life ($t_{1/2}$; h or min)	$t_{1/2} = \frac{0.693}{K_{el}}$
Clearance (Cl; L/h or L/min)	$K_{el} \times V_d$
Amount or body burden *(A)*	$\frac{\text{Dose (mg/h)}}{K_{el}\ (h^{-1})}$
Concentration in blood at steady-state (C_{ss})	$\frac{\text{Dose (mg/h)}}{\text{CL (L/h)}}$
Area under the blood concentration vs time curve (*AUC*; mg/Lxh)	$\frac{\text{Dose (mg)}}{\text{CL (L/h)}}$
Fraction eliminated (F_{elim})	$1 - e^{-k_{el} \times t}$
($C_{max_{ss}}$)	$\frac{\text{Dose}}{V_d} \times \left(\frac{1}{1 - F_{elim}}\right)$
($C_{min_{ss}}$)	$C_{max_{ss}} \times F_{elim}$

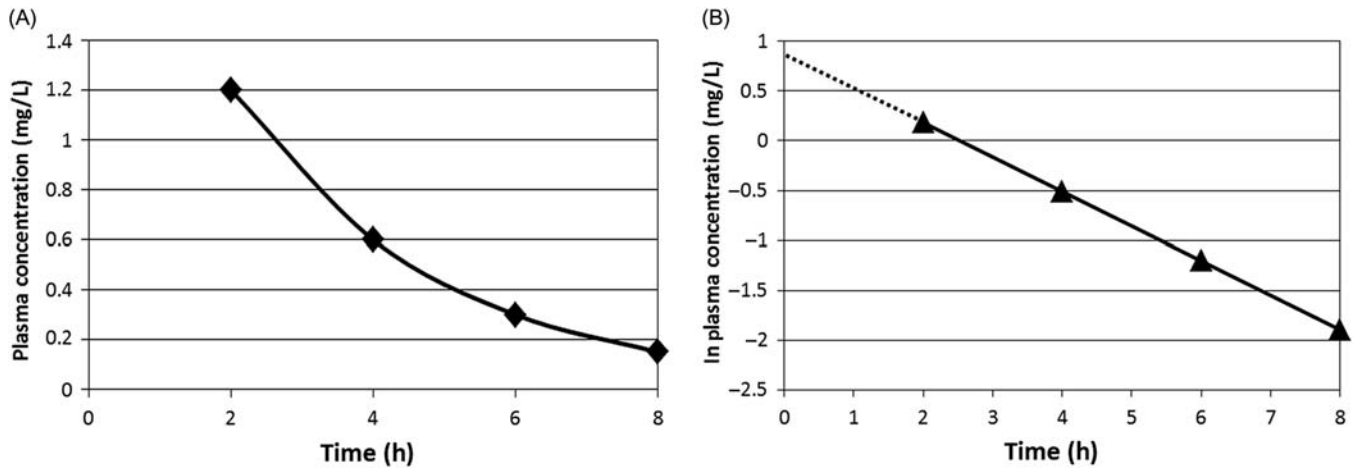

FIGURE 3.8 Plots of the measured plasma concentration versus time (A) and of the transformed data (natural log (ln)) for PK analysis with a one-compartment model (B).

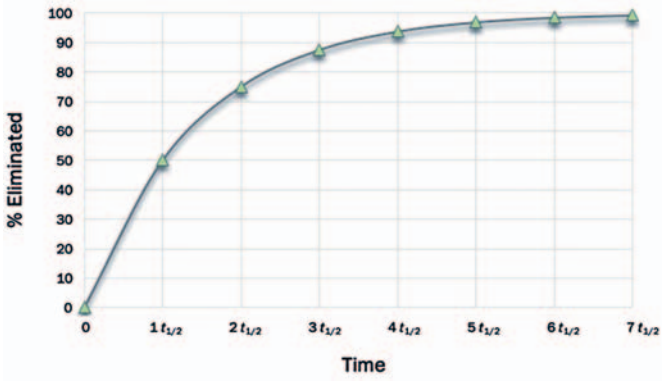

FIGURE 3.9 Percent eliminated as a function of the elimination half-life ($t_{1/2}$) of a chemical.

physiologically based pharmacokinetic (PBPK) modeling, described in the next section.

Physiologically Based Pharmacokinetic Models

The PBPK models are quantitative descriptions of the interrelationship among the determinants of ADME, based on the concepts of clearance and volume of distribution, discussed earlier. The initial step in the construction of PBPK models involves development of a conceptual representation—the complexity of which is consistent with the goals and intended end-use of the model. In this process the organism is represented as a network of compartments, each of which is physically, physiologically, and biochemically characterized. The exposure and elimination routes are indicated by adding arrows to the appropriate compartments (Figure 3.10). Each compartment may represent a single tissue or a group of tissues with similar kinetic characteristics. For example, tissues with poor or slow blood perfusion characteristics (such as the muscle and skin) are frequently grouped within a compartment referred to as "slowly perfused tissues." Since the skeletal and structural components of the body have negligible perfusion and are not key determinants of the kinetics of many organic chemicals, they have not been routinely included in the PBPK models for this subset of chemicals. However, while modeling the kinetics of certain metals and metalloids, a detailed characterization of the bone/skeletal compartments is included.

Each compartment in a PBPK model is described using a mass-balance differential equation of the following form:

$$\begin{aligned}&\text{Rate of change in the amount of the chemical in the compartment}\\&= \text{input rate (mg/h)} - \text{output rate (mg/h)}\\&- \text{elimination rate (mg/h)}\end{aligned} \tag{3.16}$$

Considering the "internal" tissues described in the model, the chemical input is via the arterial blood whereas the output occurs via the venous blood flow. The rate of change in the amount of chemical in a nonmetabolizing tissue then equals the arterial−venous difference (Figure 3.11).

The free concentration of chemical leaving the tissue is computed with the knowledge of the tissue concentration (i.e., amount/tissue volume) and tissue:blood partition coefficient. The greater the partitioning into a tissue or the rate of metabolism in a tissue, the less would be the amount of chemical leaving that tissue. The simplest form of PBPK models then are based on compartment-specific input parameters that correspond to the tissue volumes, tissue blood flow rates, partition coefficients, and metabolism rates. These

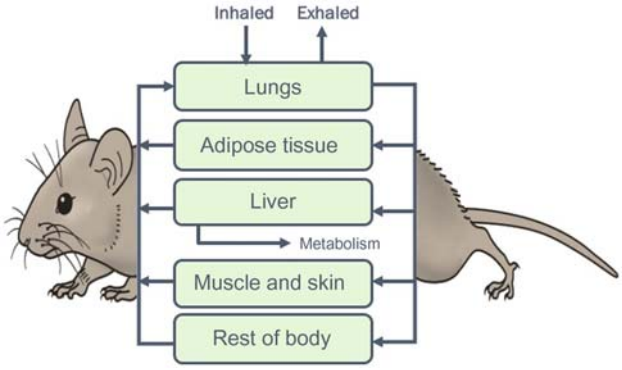

FIGURE 3.10 Conceptual representation of a PBPK model for exposure to a volatile organic chemical in the rat.

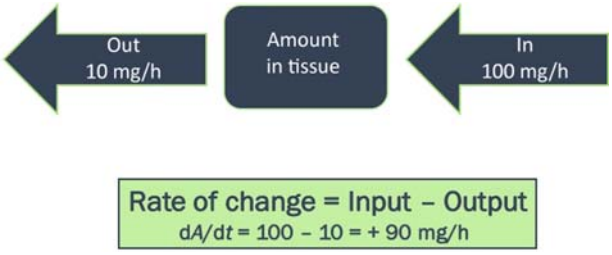

FIGURE 3.11 Representation of the mass-balance differential equation to calculate the rate of change in the amount of chemical in a tissue compartment (dA/dt) of a PBPK model.

parameters as well as corresponding mass-balance equations are integrated and solved using commercially available software or freeware to simulate the kinetic behavior of a chemical in the test animal species.

The generic input parameters of PBPK models are physiological, biochemical, or physicochemical in nature. The key physiological parameters include alveolar ventilation rate, cardiac output, tissue volumes and tissue perfusion rates, and GFR. Some or all of these parameters can be measured in the experimental animals or obtained from biomedical literature. The physicochemical parameters required for PBPK models refer primarily to the blood:air and tissue:blood partition coefficients, which together with the volumes of tissues and blood facilitate the calculation of the V_d. Unlike the classical compartmental PK models, the V_d specific to each tissue is calculated in PBPK models with the use of tissue:blood or tissue:plasma partition coefficients. Several *in vitro*, *in vivo*, and *in silico* (algorithm) methods are available for estimating the partition coefficients of chemicals required for PBPK modeling. The biochemical parameters required for PBPK modeling, such as the rates of absorption, biotransformation, macromolecular binding, and excretion, have been determined either by conducting time-course analysis *in vivo* or upon extrapolation of data collected *in vitro*.

A critical aspect in PBPK modeling relates to the evaluation and selection of models that are fit for the purpose. It is important to select a PBPK model that can adequately address a particular issue at hand (e.g., route-to-route extrapolation, high dose to low dose extrapolation, species to species extrapolation). This process, in the context of PBPK model use for animal toxicity testing, would require the consideration of the following aspects:

1. The species for which the PBPK model has been constructed versus the species used in the toxicity study requiring interpretation.
2. The developmental stage(s) for which the PBPK model has been parameterized and evaluated versus the life-stage for which the model is intended to be used for interpreting/designing a toxicity study.
3. The exposure route used in the toxicity tests versus exposure route(s) described in the model.
4. The exposure duration and maximal dose for which the model has been tested versus the exposure protocol of the proposed toxicity study.

The compartmental models including the PBPK models are useful in the estimation of blood and tissue concentrations associated with a single dose or repeated doses given by various routes, and this can frequently be accomplished using a single set of parameters. In other instances, reestimation or adjustment of parameter values might be necessary to accommodate the observed or anticipated change in input parameters with time (e.g., change in V_d due to body fat content, change in CL_{int} due to enzyme induction). Even though temporal changes in dose metrics can be effectively modeled with these kinetic models, often in reality the rate of change in the blood concentration approaches zero during repeated (or lifetime) exposures. This situation is termed as *steady-state*, that is, the numerical value of a variable remains constant during a given interval of time. The "steady-state" should not be confused with "equilibrium," which implies the cancellation of driving forces on either side. At steady-state, the input (dose rate) equals elimination rate such that the observed internal concentration is a constant value or range. The steady-state situation then requires fewer parameters than the full-fledged kinetic models (Table 3.1).

PHARMACOKINETICS AND ITS USE IN DESIGNING TOXICITY STUDIES

Animal toxicity studies use various dosing regimens and protocols ranging from a single-dose (acute) study

to lifetime (chronic) exposure studies. It is critical to take into account the PK characteristics of the chemical in selecting doses, dosing regimens, and sampling times. In this regard the available ADME data or PK models can be used to evaluate the following aspects/questions:

Absorption

1. What is the rate of absorption for the dose levels, route, and vehicle chosen for the study, i.e., what fraction is absorbed during a given time frame?
2. What are the blood:air and skin:air partition coefficients of the chemical?
3. What percentage of the chemical remains in the nonionized form at physiological pH?
4. Are there significant bioavailability issues for the route and vehicle of exposure used in the experiment? If so what is the most critical factor influencing it?

Distribution

1. What is the volume of distribution (or tissue:blood partition coefficient) of the test chemical?
2. How does the volume of distribution compare to the body weight of the animal?
3. Are there specific binding/transport phenomena demonstrated or suspected for this chemical?
4. Does the extent of binding/transport appear to vary as a function of dose or species?
5. Is the distribution limited by membrane diffusion or blood flow to tissues?

Metabolism

1. What are the key pathways and enzymes involved in the metabolism of the chemical?
2. Are there quantitative estimates of metabolism parameters for the chemical (V_{max}, K_m, or CL_{int}) as a function of species, life-stage, and duration of exposure?
3. What dose level corresponds to the deflection point of the linear kinetics in the test species of interest?
4. How does the CL_{int} of the chemical compare with the hepatic blood flow?
5. What is the significance of extrahepatic metabolism pathways and rates?

Excretion

1. What are the major excretion pathways in the test species of interest?
2. Are the rates known for each of the major excretion pathways?
3. If so, how do they compare with the physiological limits for organ clearance (i.e., blood flow rates)?

An understanding of these aspects is key to the interpretation of the kinetic behavior of a chemical in terms of the critical dose metrics across dose, routes, and species. In this regard, the above ADME factors can be integrated within a PK model to facilitate predictions of their impact on a given dose metric, under various hypothetical dosing scenarios. Thus, the quantitative use of PK data/model can help select the spacing and number of doses. Such PK information is also critical in planning future/supplementary studies by a different route or in a different species. In this regard, PBPK models or steady-state algorithms can be used to compute the pharmacokinetically equivalent dose for one route of exposure from another (e.g., inhalation to oral).

The PK data and models are also useful in choosing dose levels that will remain in the linear range, and in selection of appropriate sampling times during which the concentrations of parent chemical and/or metabolite(s) are likely to remain well above the limit of quantitation of the analytical method. In this regard, predictive models, such as PBPK models, are uniquely useful in providing *a priori* simulation of concentration versus time-course data, based on independent estimates of parameters using *in vitro* or *in silico* approaches. This particular application facilitates the selection of blood or tissue sampling times corresponding to critical phases of the PK curve so that reliable calculations of AUC_{0-t} can be made, avoiding the assignment of unequal weighting to selected portions of the PK curve.

CONCLUDING REMARKS

PK data and models are essential for effective design and interpretation of toxicity studies. Dose metrics of relevance to the mode of action of chemicals (e.g., C_{max}, AUC_{0-t}) are more effective than the administered dose, in relating to the response seen in systemic toxicity studies and cancer bioassays. The PK data collected in test animals or in satellite groups should be analyzed to develop parameters and/or models, given the intended end-use. In this regard, PBPK models are powerful tools for integrating the determinants of absorption, metabolism, protein binding, etc., obtained *in vitro* with animal physiology for providing simulations of outcome in intact animals. The integration of PBPK models with biologically based pharmacodynamic models would enhance the potential of simulating the time-course of the relevant dose metrics and toxicological responses in exposed animals and humans based on kinetic and dynamic mechanisms.

Further Reading

Boroujerdi, M., 2002. Pharmacokinetics. Principles and Applications. McGraw Hill, New York.

Curry, S.H., Whelpton, R., 2011. Drug Disposition and Pharmacokinetics. From Principles to Applications. Wiley-Blackwell, Chichester.

DiPiro, J.T., Spruill, W.J., Wade, W.E., Blouin, R.A., Pruemer, J.M., 2005. Concepts in Clinical Pharmacokinetics, fourth ed. American Society of Health-System Pharmacists, Bethesda, MD.

Kenakin, T.P., 2009. A Pharmacology Primer, third edition Elsevier, Amsterdam.

Krishnan, K., Andersen, M.E., 2010. Quantitative Modeling in Toxicology. Wiley, Chichester.

Kwon, Y., 2001. Handbook of Essential Pharmacokinetics, Pharmacodynamics and Drug Metabolism for Industrial Scientists. Springer, New York.

Lodola, A., Stedler, J. (Eds.), 2011. Pharmaceutical Toxicology in Practice: A Guide to Nonclinical Development. Wiley, Hoboken, NY.

Rosenbaum, A., 2011. Basic Pharmacokinetics and Pharmacodynamics. An Integrated Textbook and Computer Simulations. Wiley, Hoboken, NJ.

Rowland, M., Tozer, T.N., 2011. Clinical Pharmacokinetics and Pharmacodynamics: Concepts and Applications. Lippincott William & Wilkins, Philadelphia, PA.

Somogyi, A.A., 1988. Clinical pharmacokinetics and issues in therapeutics. In: Minneman, K.P., Wecker, L. (Eds.), Brody's Human Pharmacology. Elsevier, Philadelphia, PA, pp. 41–56.

CHAPTER

4

Principles of Pharmacodynamics and Toxicodynamics

Duncan C. Ferguson

University of Illinois at Urbana-Champaign, Urbana, IL, United States

OUTLINE

INTRODUCTION: PHARMACODYNAMICS AND TOXICODYNAMICS DEFINED

In simple terms, while *pharmacokinetics* (PK, Chapter 2: Biochemical and Molecular Basis of Toxicity) describes the *concentration* of a drug or toxin over a time course, *pharmacodynamics* (PD) and *toxicodynamics* describe a drug or toxin's *effect* on the body over a time course. The underlying premise is that, in the majority of cases, the drug concentration in plasma or tissue fluid drives a reversible mass–action interaction with a protein, most often a receptor, enzyme, or ion channel. In whole organism terms, PK predicts a *linear* relationship between a compound's dosage and the concentration achieved initially and at steady-state (see Figure 4.1). However, the mass–action process of binding predicts a *nonlinear* dose response curve, which is hyperbolic, and can be classically linearized within a certain range by the log–dose (concentration)-response curve, demonstrating a sigmoidal shape, with a *threshold* and *maximal effect* (E_{max}; Figure 4.2). This process only describes toxicodynamic responses, which are dose (concentration) dependent (*Type A toxicities* of therapeutic agents);

Fundamentals of Toxicologic Pathology.
DOI: http://dx.doi.org/10.1016/B978-0-12-809841-7.00004-6

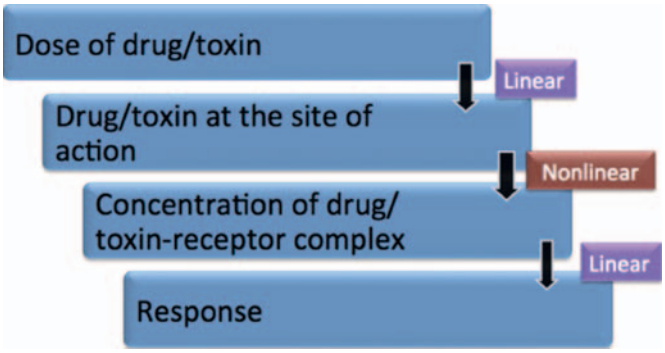

FIGURE 4.1 Demonstration of linear and nonlinear steps associated with dose of a drug or toxin leading to a tissue or clinical response or effect.

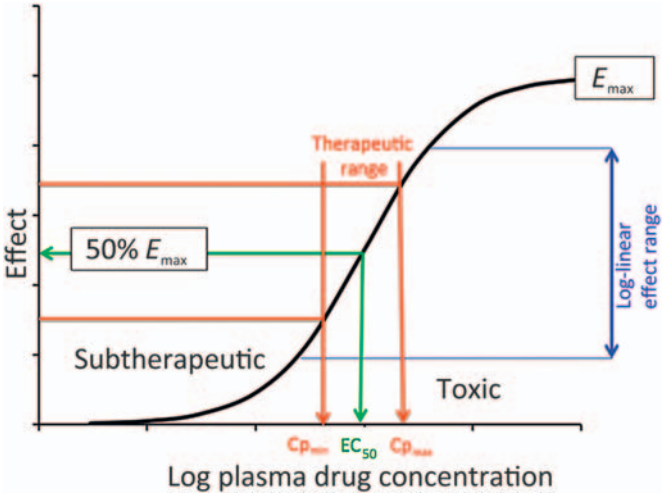

FIGURE 4.2 Classical relationship between dose and concentration determining the efficacy and safety of a therapeutic drug.

that is, are an extension of the therapeutic effect (see Figure 4.2). *Type B toxicities* are idiosyncratic or nondose dependent, and these are not described by a mass–action relationship. Type B toxicities will not be discussed. In more complex interactions, with multiple receptors or signal transduction mechanisms and feedback loops, the dose-response curve may have be even more complex (e.g., inverted U-shaped), such as may be seen with disruptors of the endocrine system.

RELEVANCE TO TOXICOLOGICAL PATHOLOGY

The adverse effect of a therapeutic (drug) or toxic agent is determined by its (1) mechanism of action and (2) duration of action. Together with PK considerations and tissue levels, the mechanism of action will determine the tissue sites at which most severe pathological consequences will occur. The continuous nature of the effect of a drug from subtherapeutic to therapeutic and then toxic range is shown in Figure 4.2. The mid-therapeutic or median effective dose (ED_{50}) is not just a PD parameter but is defined by drug clearance (CI), bioavailability (F) and the median effective concentration (EC_{50}) for that drug's action:

$$ED_{50} = \frac{Cl}{F} \times EC_{50}$$

When the logarithm of the dosage of an agent is plotted on the x-axis and effect on the y-axis, the relationship is most often sigmoidal, with a clear "threshold" at the upward curve and maximum effect (E_{max}) at the plateau at the highest doses. However, within this range, one finds a relatively linear log (dose) versus effect relationship and nestled within that range is the therapeutic range, bounded by the minimum plasma concentration required for an effect ($C_{p,min}$) and the upper therapeutic/lowest toxic dose ($C_{p,max}$). If an agent's action is via a single receptor, the concentration range necessary to move from threshold to E_{max} is observed over about 100-fold concentration range, with the EC_{50} at the inflection of the sigmoidal plot, achievable by a drug dosage, which also coincides with mid-therapeutic effects. For example, if the EC_{50} for a drug is 10 nM, the effect of a concentration of 1 nM would be 9.1% of maximum and at 100 nM, it would be 90.9%. Log–dose effect curves with greater slopes would be potentially associated with receptor and/or signal transduction mechanisms associated with cooperativity. Drugs with narrow therapeutic response ranges are often difficult to adapt to safe clinical use.

DRUG/TOXIN–RECEPTOR INTERACTIONS LEAD TO SIGNAL TRANSDUCTION AND EFFECT

In most cases, drugs or toxins act on target proteins on or in cells, in particular receptors, enzymes, carrier molecules (cell-associated transporters), and ion channels.

For the sake of the following discussion, drug interaction with these protein targets will be collectively characterized according to *receptor theory* to explain the dose nonlinear interactions leading to drug or toxin action. Key characteristics of receptors include structural *specificity* for a class of compound (and vice versa), finite in number (i.e., *saturable*), and linked to a distinct *biological effect*.

Specificity is a relative term and it is important to recognize that as the dose and concentration of a drug increases, it may increase its interaction with nontarget receptors, leading to adverse clinical effects.

Receptor Occupancy Theory: Driven by Mass–Action

The vast majority of drugs or toxins (either abbreviated by D) interact reversibly with their cellular protein targets (hereafter called receptors, and abbreviated R). Drugs or toxins combine with their receptors at a rate dependent on the concentration of the drug and receptor, and the resulting drug–receptor complex breaks down at a rate proportional to the number of complexes formed (see equations in Figure 4.3).

The mass–action relationship between a drug and a receptor is defined by the affinity of binding, defined by the equilibrium association constant (K_A) or, more commonly, its inverse, the equilibrium dissociation constant (K_D). K_D is used more frequently because its units are in concentration units, and it describes the mid-range of concentrations over which the receptor "operates" in detecting circulating or local concentrations of a physiological signal or xenobiotic.

$$[D] + [R] \underset{k_2}{\overset{k_1}{\rightleftharpoons}} [DR]$$

k_1 = association rate constant
k_2 = disassociation rate constant

$$K_A = \text{association equilibrium constant} = \frac{[DR]}{[D][R]}$$

$$K_D = \text{disassociation equilibrium constant} = \frac{[D][R]}{[DR]} = \frac{1}{K_A}$$

FIGURE 4.3 Mass–action equations describing reversible interaction between a ligand (drug, toxin) with a receptor.

Characterizing Drug–Receptor Binding

In order to determine the characteristics of drug–receptor affinity (K_A) and maximal binding (capacity; B_{max}), broken cell preparations of a tissue are often incubated with a drug and allowed to come to equilibrium *in vitro*. Although the technical details are beyond the scope of this discussion, only *saturable* binding is relevant for analysis of receptor–drug interaction. Figure 4.4 shows the log–concentration versus saturable binding plot to reveal a positive sigmoidal relationship with the inflection of the curve being equal to K_D or $1/K_A$, and an approximately log–linear relationship from 0.1- to 10-fold the concentration represented by the K_D.

It is more common to express binding data by starting with the equation for K_D in Figure 4.3 and expressing bound drug ([*DR*] as a function of free drug ([*D*], [*D*]free, or *F*)) resulting in the saturation equations shown in Figure 4.7. Illustrating the relevance and similarity of drug–receptor binding equations to those describing drug–effect relationships, the homologous equation for the latter is also shown (more later).

However, curvilinear plots are prone to bias in interpretation or even computer data fitting, particularly if binding studies reveal targets of multiple affinities. Therefore, the saturation curve equations are commonly transformed by dividing the left-hand side

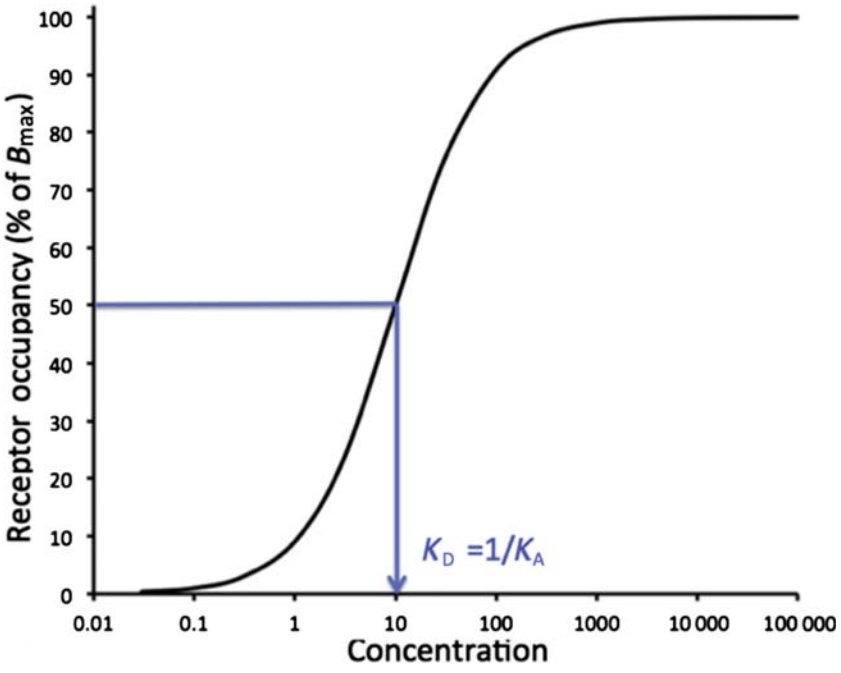

FIGURE 4.4 **Sigmoidal log–concentration—receptor occupancy curve.** This figure represents the log transformation of the Figure 4.5. In an ideal single-receptor experiment, the receptor occupancy will rise from a threshold to maximum in a concentration range of about 100-fold, and the inflection of the sigmoidal curve represents is observed at (approximately) the equilibrium dissociation constant (K_D) if the experimental conditions are ideal. K_D is the inverse of the equilibrium association constant (K_A).

Drug receptor binding

$$[DR] = B = \text{Bound} = \frac{B_{max} \times [D]\text{free}}{[D]\text{free} + K_D}$$

Drug dose–response relationship

$$\text{Response} = \text{Effect} = E = \frac{E_{max} \times [D]\text{free}}{[D]\text{free} + EC_{50}}$$

FIGURE 4.5 **Comparison of receptor occupancy and response–effect equations.** The equations describing the concentration of bound drug (also called [*DR*] or *B*) as a function of unbound (free) drug is shown. The sigmoidal curve describing the classical dose-response (effect) relationship produced when the nonlinear portion of the curve is represented by ligand binding to the receptor shows the homology between E_{max} and B_{max} and EC_{50} and K_D.

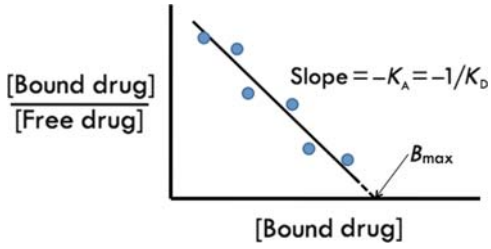

FIGURE 4.6 **Scatchard plot.** The Scatchard plot of a ligand interacting with a single receptor with a finite-binding capacity (B_{max}) and an equilibrium dissociation constant defined by K_D. The slope of the curve is the negative reciprocal of K_D and the *x*-intercept is equivalent to B_{max}, usually expressed as moles/mg protein, where the protein amount represents the total tissue protein added to the binding reaction.

of the equation by the free drug (shown as [*D*]free but equivalent to F). When *B* is plotted on the *x*-axis and *B*/*F* on the *y*-axis, the outcome is the traditional *Scatchard plot* (Figure 4.6). *B* is commonly in moles of drug bound per amount of protein in the binding reaction, and *B*/*F* is unitless as a ratio of mass or concentration. The Scatchard plot linearizes the data for a single binding site with the slope equal to $-K_A$, which equals $-1/K_D$. Extrapolation to the *x*-intercept reveals the maximal amount of drug bound (B_{max}), which represents the finite capacity of a true receptor system. When there is one or two breaks in the slope of the Scatchard plot, it suggests multiple drug-binding sites. The highest affinity sites are represented by a larger negative slope and generally are felt to be most relevant for biological activity.

Mechanisms of Drug Action: General Categories

Drugs and toxins may cause their effects through *physical* or *biological* interactions. Biological actions can be divided into *receptor-mediated* signal transduction and *nonreceptor-mediated* mechanisms.

Physical Interaction

Examples of drugs that interact through physical or chemical reactions with body fluids or tissues include the osmotic diuretic mannitol and orally administered antacids. These compounds are designed to alter, respectively, osmolarity and pH, but do not interact directly with cellular processes.

Nonreceptor Interaction

Drugs or toxins may directly target enzymes, carrier proteins like ion transporters, ion channels, DNA, and cellular structures like microtubules. Enzyme inhibitors include nonsteroidal antiinflammatory drugs, which inhibit cyclooxygenases, the anticancer drug methotrexate, which inhibits tetrahydrolate reductase, acetylcholinesterase inhibitors like the drug physostigmine or the toxin sarin, and digoxin, an inhibitor of Na^+/K^+ ATPase. Direct inhibitors of ion channels include Na^+ channel blockers such as local anesthetics and calcium channel blockers. Drugs directly inhibiting membrane ion transporters include the proton pump inhibitors omeprazole (Na^+/H^+ ATPase in gastric parietal cells) and most of the diuretics, such as the thiazides (Na^+/Cl^- cotransport in distal convoluted renal tubule) and loop diuretics ($Na^+/K^+/2Cl^-$ symport in the thick ascending limb of the renal loop of Henle). Examples of drugs, which interact with DNA, include the anticancer drugs, like lomustine CCNU = 1-(2-chloroethyl)-3-cyclohexyl-1-nitrosourea (CCNU), which alkylates DNA, and the fluoroquinolones, which interact with DNA gyrase resulting in alteration of the three-dimensional structure of DNA leading to reduced bacterial replication and death. Drugs interacting with microtubules include the anticancer drugs vincristine and vinblastine. Through this mechanism, the mitotic spindle of the cell is disrupted.

Receptor Interaction

Through interaction with a receptor, a drug often alters the receptor protein's three-dimensional structure triggering signal transduction processes within the cell resulting in a biological effect. Understanding the details of signal transduction leads to understanding of the timeframe and persistence of the biological effect of drug or toxin, sometimes long after removal of the agent. Signal transduction mechanisms also underlie the phenomena of the cell's adaptation to a drug or toxin following chronic exposure. These clinically observed phenomena will be described later in this chapter.

Cellular Processes Linking Drug Concentration and Receptor Binding to Cellular Effect

Although a complete review of cellular signal transduction is beyond the scope of this chapter, the reader is directed to a web database maintained by the International Union of Basic and Clinical Pharmacology (IUPHAR), which maintains updated information on signal transduction systems linked with receptors (http://www.iuphar-db.org/). This resource is particularly useful because it tracks information about *orphan receptors*, which are receptor proteins identified by genome sequencing and molecular biology with homology to known receptors, but which, to date, have not been unequivocally linked to a known effect.

Signal transduction is usually accomplished with one or more of the following key cellular processes, each of which results in allowing a signal (drug) to move its effect from outside the cell to the intracellular compartment. Transmembrane receptors are classified as either *ionotropic* (linked to ion channels) or *metabotropic* (linked to biochemical processes). *Intracellular receptors* include cytosolic and nuclear receptors.

Ionotropic receptors or ligand-gated transmembrane ion channels include γ-aminobutyric acid ($GABA_A$) and ionotropic glycine receptors linked to chloride channels, nicotinic acetylcholine, and glutamate receptors [AMPA = 2-amino-2-(3-hydroxy-5-methyl-isoxazol-4-yl)propanoic acid, kainate, and *N*-methyl-D-aspartate (NMDA)] linked to sodium channels, and serotonin 3 ($5HT_3$) receptors are linked to cation currents. There are also subtypes of GABA ($GABA_B$), glutamate, and serotonin receptors that are metabotropic.

Metabotropic receptors either act directly or indirectly as signal transduction enzymes, or are linked to enzymes that have an extracellular domain recognizing a drug and an intracellular domain that catalyzes a biochemical response. Transmembrane metabotropic receptors include the following:

1. *G-protein-coupled receptors (GPCRs)*
   - **a.** Gs—stimulatory—e.g., coupled to adenylate cyclase.
   - **b.** Gi/o—inhibitory—inhibit adenylate cyclase or close Ca^{++} and open K^+ channels.
   - **c.** Gq—coupled to phospholipase C-β.
2. *Receptors with associated enzymatic activity*
   - **a.** *Plasma membrane kinase-linked receptors*: Enzyme activity is part of the receptor's intracellular domain. Tyrosine or serine kinases phosphorylate a cellular substrate including other kinases that phosphorylate proteins associated with cellular action often through altered gene transcription. For example, insulin receptor.
   - **b.** *Cytosolic kinase-linked receptors*: Janus kinase (a tyrosine kinase) is phosphorylated by the activated plasma membrane receptor. Examples include: cytokines interferons (α, β, and γ), interleukin-2, growth hormone, and leptin.
   - **c.** *Guanylyl cyclase (GC)-linked*: Plasma membrane receptors have GC activity and the cyclic GMP formed activates protein kinase G (PKG) that phosphorylates proteins associated with cellular action. Nitric oxide (NO) can also directly activate cytosolic GC. Examples include atrial natriuretic factor, nitric oxide (directly or via muscarinic receptors).
3. *Intracellular receptors (nuclear or cytosolic)*: Compounds permeate plasma membrane bind to cytosolic and/or nuclear receptors that bind to a DNA response element, which then results in inhibition or activation of mRNA and then protein transcription.

   Examples: Lipid soluble drugs/toxins (polychlorinated biphenyls) or lipophilic hormones (e.g., thyroid hormone, steroid hormones).

Characterizing Biological Effects of a Drug or Toxin

As described earlier, for an effect mediated by a single receptor, the log–dose effect relationship parallels that of the log–dose receptor-binding relationship. The term encompassing all factors determining the actual effect is the drug's intrinsic *efficacy*, defined as the characteristic that results in a tissue response when that ligand interacts with a receptor. The greater the maximal effect (E_{max}) of a drug, the greater is the efficacy of that drug.

Efficacy should be distinguished from *potency*, a term used to compare the receptor affinity or the EC_{50} of two compounds. The more potent compound has a lower K_D or lower EC_{50}, defined as 50% of E_{max}. EC_{50} represents the middle of the linear part of the log–dose (concentration)-response curve, and therefore the middle of the "operating" concentration range for the biological effect of a compound.

Agonists

Compounds interacting with receptors are divided into distinct pharmacological types based upon their intrinsic efficacy on a receptor-signal transduction system. A *full agonist* is a compound that achieves the largest biological effect at its maximally effective concentration. Empirically, this compound has the *highest intrinsic efficacy* known at that time. A *partial agonist* is a compound for which the E_{max}, and therefore the intrinsic efficacy, is less than that of a full agonist. It is

important to note that a partial agonist may be more potent than a full agonist, and therefore induces a greater biological effect at a given concentration than a full agonist. A classical example of a partial agonist is buprenorphine, a mu opioid partial agonist. Its activity is compared with morphine, a pure mu agonist. In fact, buprenorphine is about 30-fold more potent than morphine.

Antagonists

Antagonists are any compounds that act to counteract a specific biological action. However, in terms of receptor interaction, they are defined as compounds that do not cause a biological effect alone, and, therefore, have zero intrinsic efficacy. For a pure antagonist, its biological effect is only seen in the presence of an agonist. Antagonists are generally divided into those that are *competitive antagonists*, that is, they interact reversibly with the receptor and, in a concentration-dependent and affinity-dependent manner, block the binding of an agonist. In the presence of a competitive antagonist, an increased dosage or concentration of an agonist can completely reverse the effect of the antagonist. An example of a competitive antagonist is atenolol for the β1 adrenergic receptor. Most clinically used antagonists are competitive. *Noncompetitive antagonists* are compounds that allosterically or irreversibly bind with a receptor protein to block the effect of an agonist. Increasing the concentration of an agonist does not reverse the effect of a noncompetitive antagonist through mass–action principles. For irreversible antagonists that might covalently alter a receptor, the effect is indistinguishable from receptor downregulation (*vide infra*). An example of an irreversible antagonist is phenoxybenzamine, which covalently links with α adrenergic receptor binding site, and an example of an allosteric inhibitor is the benzodiazepine diazepam, which binds noncompetitively to the chloride channel normally activated by GABA resulting in enhancing the effect of GABA on channel chloride conductance and therefore, enhancing membrane hyperpolarization.

Inverse agonists are compounds that interact with receptor-signal transduction systems that have a constitutive level of activity, and through interaction with the receptor, reduce the activity in the direction opposite of that of a pure agonist. Historically, some inverse agonists were previously clinically characterized as pure antagonists. Constitutive activation has been demonstrated for GABA, cannabinoid, histamine, and serotonin receptors. Some Histamine 1 (H_1) antagonists have been shown to also be inverse agonists, which can downregulate H_1 receptor synthesis.

Reversible Two-State Model of Receptor Activation

The receptor occupancy theory does not fully account for the existence of partial or inverse agonists, and it does not address the observation that the maximal response of some receptor systems was achieved well before theoretical saturation of the receptor binding. It was not sufficient to characterize receptors as static entities, and this led to a two-state model of receptor activation where receptors are in an equilibrium between resting (R) and activated (R^*) states. Figure 4.7A–E illustrates the nonliganded receptor (7a), the full agonist (7b), the full or "neutral" antagonist (7c), the partial agonist (7d), and the inverse agonist (7e). When a full agonist interacts with a receptor, it shifts the equilibrium toward R^* and it has a preferential affinity for R^* over R, which means that the $[D-R^*]/[D-R]$ ratio will be greater than the R^*/R ratio. The greater the conformational selectivity for R^*, the greater the efficacy. A compound, which binds with equal affinity to R and R^*, will not shift the conformational equilibrium, and so will lead to no effect on its own but will act as a competitive antagonist for a full or partial agonist. A partial agonist, while favoring R^*, does not shift the conformational equilibrium toward R^* as effectively as a pure agonist. An inverse agonist binds with greater affinity to R shifting the conformational equilibrium to R and when interacting with a system where the unliganded receptor has constitutive activity, serves to decrease the effect below constitutive levels, that is, it moves the effect in the opposite direction of a pure or partial agonist.

Figure 4.8 shows the log–dose (concentration) versus effect curves for the same five drug activation scenarios, and also shows the impact of a competitive antagonist in the presence of a full or inverse agonist. It is now apparent that receptors are not restricted to only two conformational states, and that there may be more than one resting or active form of some receptors. Modeling of this level of complexity (ternary models or higher) requires consideration of the details of signal transduction associated with the cellular effects, and is beyond the scope of this review.

Spare Receptors

Some drugs have their maximal biological effect at much lower concentrations than expected based upon the receptor-binding affinity. The classical example is with neuromuscular relaxants that are nicotinic acetylcholine receptor antagonists, like D-tubocurarine that competitively block nicotinic receptors in the postsynaptic plasma membrane of skeletal muscle. The nicotinic receptors are linked to Na^+ channels. Once depolarized, these receptors/channels undergo

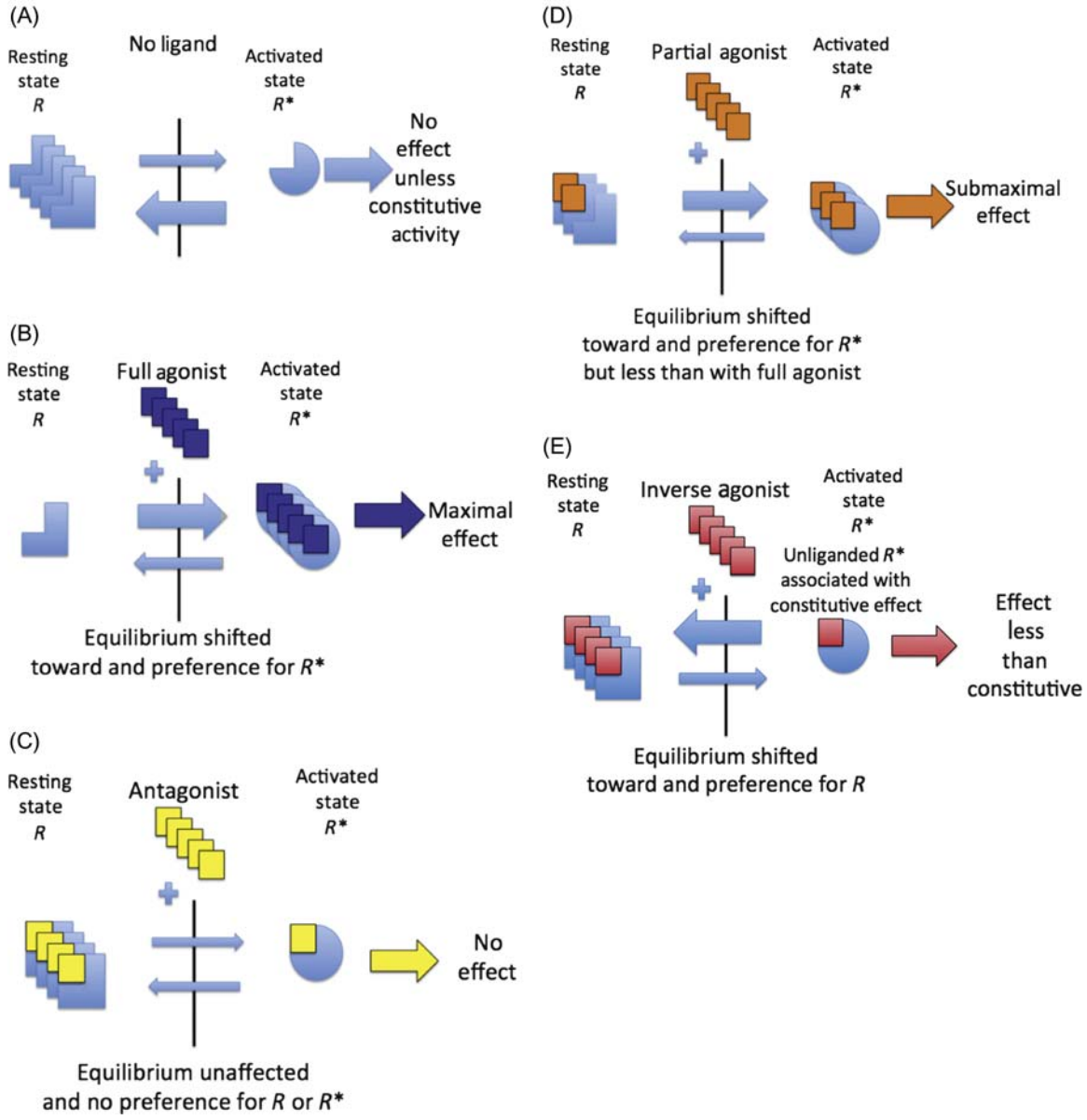

FIGURE 4.7 **The reversible two-state receptor activation model.** This figure represents the receptor system in the absence of a ligand (A), the impact of addition of a receptor full agonist (B), a competitive antagonist (C), a partial agonist (D), and an inverse agonist (E). Binding of the full agonist (B) moves the equilibrium most effectively toward the active form of the receptor (R^*) with no effect by an antagonist (C), which nonetheless can bind equally to both resting (R) and active (R^*) forms of the receptor to block the effect of an agonist. A partial agonist (D) is less effective than a full agonist at activating receptors and, therefore, the maximal effect (E_{max}) will be less than a full agonist. An inverse agonist (E) is an agent, which is capable of moving the effect in the opposite direction of a full or partial agonist, and has been described in systems with constitutive activity in the absence of a ligand. (A) Receptor system in the absence of a ligand (drug or toxin). (B) Receptor system in presence of a full agonist. (C) Receptor system in presence of a competitive antagonist. (D) Receptor system in the presence of a partial agonist. (E) Receptor system in the presence of an inverse agonist.

temporary desensitization. As a result, to maintain the potential for repetitive stimulation at normal physiological rates, additional receptors must be recruited to maintain contraction. These additional receptors are called *spare receptors*. Because occupancy of only a small fraction of the receptors is required for maximal muscle contraction, the EC_{50} for the agonist acetylcholine is much lower than the K_D. Because the maximal biological effect is achieved at low percentages of receptor occupancy, it allows a system with apparently high sensitivity because much lower levels of receptor occupancy are needed to achieve maximal effects. To initiate its action, D-tubocurarine must therefore block not only the active receptors, but also the spare receptors.

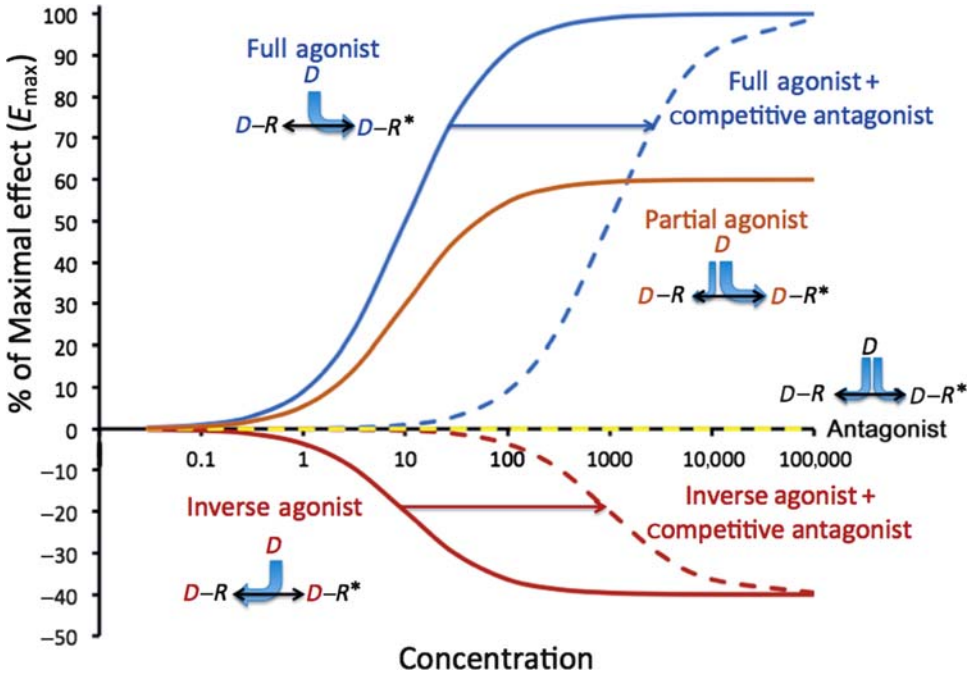

FIGURE 4.8 Summary of log−dose effect curves for full agonist, antagonist, partial agonist, and inverse agonists according to reversible two-state receptor theory. *R* and *R** represent the equilibrium between resting (*R*) and activated (*R**) receptor forms.

SELECTIVITY AND SAFETY: THERAPEUTIC VERSUS TOXIC EFFECT OF DRUGS

The structural specificity of drug−receptor(s) interaction predicts the clinical selectivity of drug action. More precisely, the ability of receptors or enzymes to recognize and respond to a given drug or toxin is based upon the three-dimensional structure of the protein's binding pocket. Absolute specificity is not common. For those involved in preclinical phases of drug development, it is important to screen for binding and activity to a variety of receptor types in a variety of tissues to help predict the therapeutic and potentially adverse effects. Most drugs interact with a variety of receptors with varying affinities. However, eventually, it is important to evaluate the drug's effect *in vivo*, because relative tissue effects, integrated tissue responses, and counter-responses to a drug are harder to predict. When a drug's dosage and concentration is increased, "spill-over" effects then occur on lower affinity receptors in the same or other tissues and may contribute to adverse effects. For example, when used clinically, dopamine stimulates renal dopaminergic D_1 receptors to induce renovascular dilation at low-dosage infusion rates, but stimulates cardiac β1 adrenergic receptors at intermediate rates causing tachycardia as a side effect, and at even higher dosage infusion rates, stimulates arterial α1 receptors causing vasoconstriction and counteracting the renovascular dilatory effect.

Drugs may interact with tissues not targeted therapeutically, but with the same receptor−effector machinery. A drug may target a different cellular mechanism at higher concentrations. For example, promethazine is a phenothiazine derivative with multiple mechanisms of action: it is an H_1 receptor antagonist, a muscarinic, serotoninergic, dopaminergic, and α1-adrenergic receptor antagonist, as well as being a local anesthetic blocking sodium channels. For drugs with a narrow therapeutic window, individual patient therapeutic drug monitoring may be indicated to optimize efficacy while minimizing toxicity (please review Figure 4.2).

QUANTAL DOSE−EFFECT CURVES

To this point, it has been assumed that dose−effect curves are graded. Across a population of patients, the pharmacological/toxicological effect may appear as an all-or-none (quantal) phenomenon. Examples might be when the endpoint is the occurrence of arrhythmias, seizures, or even mortality. In this case, it is more relevant to know the population statistics regarding such a quantal event. For example, the dose might be plotted against the cumulative percent occurrence of the therapeutic effect, and a second plot of the dosage against the cumulative incidence of adverse effects. For

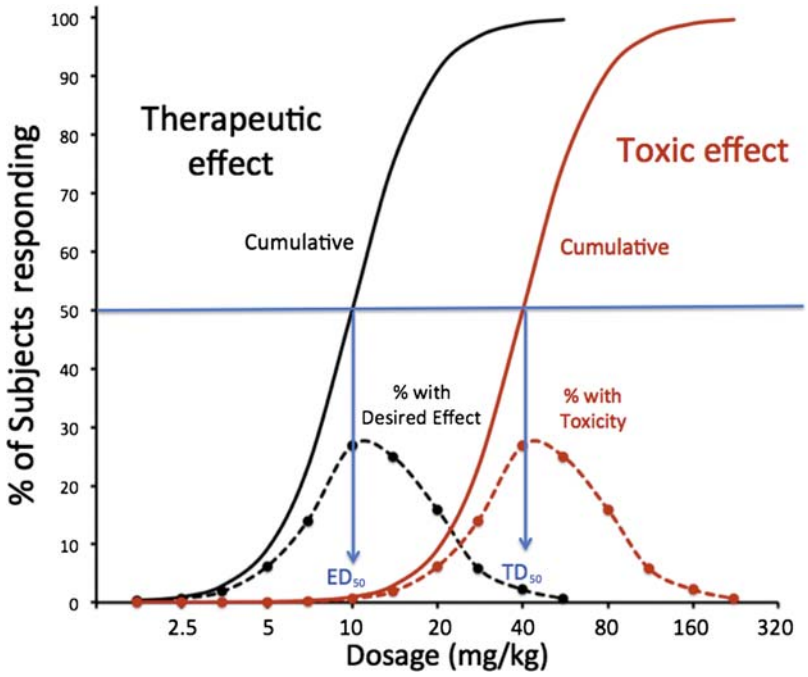

FIGURE 4.9 Appearance of dose-titration study evaluating the TI of a drug across a population of patients. The solid lines represent the cumulative percentage of patients showing either the Therapeutic Effect (black) or Toxic Effect (red). The dotted lines represent the proportion of subjects showing signs at a given dosage. The safety margin may be characterized by the ratio of TD_{50}:ED_{50}.

example, with a β receptor 1 agonist, the quantal therapeutic endpoint might be achievement of a 20% increase in heart rate, and for the toxic effects, the incidence of premature ventricular contractions. Such a plot is shown in Figure 4.9. In this plot, the *median effective dosage (ED_{50})* is the dosage at which 50% of the subjects have cumulatively demonstrated the therapeutic effect. Likewise, the *median toxic dosage (TD_{50})* is the dosage at which 50% of the subjects demonstrate the toxic effect. If the toxic effect is death, the *median lethal dose* is termed LD_{50}. In modern nonclinical safety studies, achieving LD_{50} is now rarely an endpoint because of animal welfare considerations. The ratio of TD_{50}: $ED5_0$ represents a useful way to characterize the *therapeutic index (TI)* for a therapeutic compound. Standard safety margin is also used to characterize a drug's safety in a more conservative manner:

$$(LD_1 - ED_{99}) \times ED_{99} \times 100$$

The standard safety margin is the percentage by which the ED_{99} must be increased before an LD_1 is observed.

FORMS OF ANTAGONISM AT THE TISSUE OR ORGANISM LEVEL

Receptor antagonism and *inverse agonism* are not the only mechanisms leading to reversal of a biological effect. *Physiological antagonism* is the result of receptor activation with opposing physiological effects. An example would be muscarinic receptor stimulation reducing heart rate and antagonizing β1 receptor agonism that would increase heart rate. *Chemical antagonism* involves a direct interaction of two molecules within the body. Agents used to treat intoxication often fall into this category. For example, penicillamine chelates Cu^{++}, $Pb+^{+}$, or $Hg+^{+}$.

DYNAMIC RECEPTOR PHENOMENA RESULTING IN ALTERED EFFICACY FOLLOWING CHRONIC DOSING

Hyporeactivity

The body has multiple mechanisms to adapt to the administration of multiple doses of a drug or toxin. The general term for developed hyporeactivity is *tolerance*. When it occurs in relatively short timeframe (hours to days), the term *tachypylaxis* is used, and usually this is associated with the phenomenon of receptor *desensitization* (see later). However, the mechanism leading to tolerance after chronic dosing may be difficult to distinguish in the individual patient unless a complete dose-response study is performed, which is generally impractical. However, the

cellular or tissue studies may uncover the following mechanisms:

1. *Desensitization*: When GPCRs are stimulated, the cellular response may diminish over seconds or minutes, even when the agonist remains present. Exemplified by the β adrenergic receptor, rapid desensitization is usually associated with receptor phosphorylation. In a desensitized state, the dose–effect curve would be shifted in parallel to higher concentrations (to the right), and the apparent EC_{50} would be higher.

   Homologous desensitization occurs only when from the stimulated receptor is affected and is mediated by receptor-specific kinases. *Heterologous desensitization* may occur when unrelated receptors share a similar signal transduction mechanism, such as adenylate cyclase, and is usually mediated by PKA = protein kinase A, which is not receptor specific.
2. *Downregulation*: With some GPCRs, including BARs = beta adrenergic receptor more chronic stimulation leads to trafficking of the phosphorylated receptor to lysosomes, which effectively reduces the available number of receptors (downregulation) available on the plasma membrane and reduces B_{max} and E_{max} in receptor binding and effect studies, respectively.
3. *Exhaustion of Mediators*: The action of a drug given chronically can be reduced by the exhaustion of mediators of action. For example, tyramine and amphetamine lead to the release of synaptic catecholamines. Chronic administration may lead to the eventual depletion of catecholamine stores.
4. *Hyperreactivity*: Hyperreactivity may also occur but mainly with a reduction of endogenous physiological ligands and either *super-sensitization* (reduced K_D and/or EC_{50}) or *upregulation* (increased B_{max} and/or E_{max}) of receptors. For example, β adrenergic blockers such as propranolol reduce signaling through the G-protein-coupled receptor. Reduction of signaling through adenylate cyclase eventually results in a recruitment and upregulation of β receptors on the cell membrane. Withdrawal of a drug or toxin ligand is recommended when possible to return the normal responsiveness of a receptor-transduction system.

VARIATION IN DRUG/TOXIN RESPONSIVENESS

The actual observed effect of a drug or toxin will be impacted by a number of factors, starting with the individual's genetic makeup with regard to receptor and signal transduction as well as drug distribution and metabolism. The following list summarizes the main factors impacting a drug or toxin's ultimate effect on an organism:

1. *Alteration in Drug Reaching Target*: For the most part, differences or disease-induced changes in PK parameters will reduce the plasma, and therefore, local tissue concentrations of the drug or toxin. An example might be seen with the induction of cytochrome P450 enzymes associated with metabolism of phenobarbital.
2. *Alteration in Number or Function of Receptors*: The cellular mechanisms leading to hypo- or hyperreactivity are described earlier.
3. *Variation in Endogenous Receptor Agonists*: The effect of drugs interacting with receptors that have significant physiological ligands will vary depending upon the concentration of endogenous ligands. An example of this phenomenon would be the effect of the α1 receptor competitive antagonist prazosin to reduce blood pressure would be determined by the amount of endogenous catecholamines.
4. *Physiological Adaptation*: A number of physiological mechanisms unrelated to a specific receptor-transduction system may also impact the observed effect in the whole organism. For example, when diuretics are used as antihypertensive drugs, they reduce whole body sodium concentrations and blood pressure. In response, the renin-angiotensin-aldosterone system may be activated resulting in increased renal sodium retention, angiotensin, and aldosterone, counteracting the beneficial diuretic effect.

NONMONOTONIC DOSE–EFFECT CURVES

Standard toxicology testing generally involves the evaluation of relatively high concentrations of a compound to establish a threshold below, which no adverse effects are observed. As more low-dose toxicology studies are performed with compounds suspected of disruption of the endocrine or neurotransmitter systems, it has become apparent that not all dose-response curves are characterized by graded responses from low concentrations to toxic at higher concentrations. Instead, the dose-response is best represented as an inverted U-shaped curve (Figure 4.10). For example, at the cellular level, growth of estrogen-dependent human breast cancer cells in culture has been shown to increase their replication rate in response to increasing estradiol concentrations reaching a maximal response with higher concentrations then

slowing growth and eventually leading to direct cytotoxicity. The lowest concentration range reflects the physiological response to estrogen and is dependent upon the presence of estrogen receptors. The high-dose effects are not estrogen-dependent.

Inverted U-shaped dose–effect curves have also been described in animal and human cognitive functions such as spatial working memory. In fact, dopamine 1 (D_1) receptor agonist stimulation or direct dopaminergic neuron stimulation in the prefrontal cortex has demonstrated that too little or too much D_1 receptor stimulation will impair spatial working memory (Vijayraghavan et al., 2007). Of increasing regulatory significance, for some toxicities described by an inverted U-shaped dose–effect curve, there is no threshold of adverse effect upon which to establish a no adverse effect level of a toxin.

PRINCIPLES OF PHARMACOKINETIC/PHARMACODYNAMIC MODELING

PK/PD modeling has been proposed as a more systematic alternative to dose-titration trials. Toutain (2009) provides an excellent review of the process. Three major parts constitute an integrated PK/PD model: a PK model that transforms a given dose to a concentration versus time profile, a link model representing the transfer of the drug from plasma into the a concentration in the compartment associated with the effect (e.g., tissue receptor) and a PD model describing the relationship between drug concentration in this compartment to the effect.

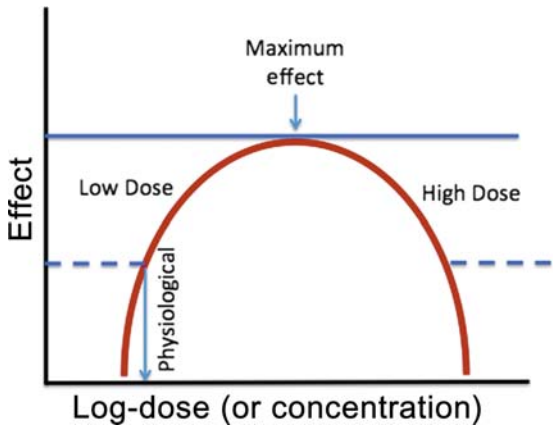

FIGURE 4.10 Classical appearance of an inverted U-shaped dose-response curve. The curve shows no threshold response and shows a maximum beneficial or toxic effect with low concentrations demonstrating an effect or toxicity, which is lost at higher concentrations. This particular example also shows physiological concentrations, which might be achieved under normal physiological conditions (e.g., plasma estradiol or synaptic dopamine concentrations).

In linking PK time course data to such PD data in a PK/PD model, the modeling process must recognize that PK and PD data are not in phase, so a feedback (hysteresis) loop must be included to account for the delay in drug effect. PK models have been described in Chapter 3: Pharmacokinetics and Toxicokinetics. The link model is designed when the source of the delay is known. If it is determined that the delay is associated with the rate of transfer from the plasma to the tissue site of drug action, then a first order rate constant (K_{e0}) may be sufficient to describe the link model. If the delay is associated with a time-dependent process in signal transduction and action, then the equations used may represent the kinetics of appearance and disappearance of the effect. Drug effects may be represented by stimulation or inhibition.

PD models may be graded or quantal, as previously described. If graded, studies are designed to establish *in vivo* the parameters E_{max}, EC_{50}, and the slope (sensitivity) of the linear portion of the sigmoidal log–dose effect curve. Graded PD models are commonly described by the sigmoidal E_{max} model: $E(t) = E_0 + E_{max} \times C^n(t)/(EC_{50}{}^n + C^n(t))$. $E(t)$ is the effect for a concentration at time t ($C(t)$), and E_0 is either the basal or placebo effect. E_{max} and EC_{50} have been previously described, and n is the Hill coefficient, which is the slope of the dose–effect relationship. When the drug is an inhibitor, median inhibitory concentration IC_{50} is utilized and the effect is subtracted from E_0. In summary, the goal of PK/PD modeling is aid the appropriate clinical trial design for a drug.

Further Reading

Boothe, D.M., 2012. Small animal, Clinical Pharmacology and Therapeutics, second ed. Elsevier, St Louis, MO, pp. 1–4.

de Ligt, R.A.F., Kourounakis, A.P., IJzerman, A.P., 2000. Inverse agonism at G protein-coupled receptors: (patho)physiological relevance and implications for drug discovery. Br. J. Pharmacol. 130, 1–12.

International Union of Basic and Clinical Pharmacology (IUPHAR) Committee on Receptor Nomenclature and Drug Classification website. <http://www.iuphar-db.org/>.

Leff, P., 1995. The two-state model of receptor activation. Trends Pharmacol. Sci. 16, 89–97.

Negus, S.S., 2006. Some implications of receptor theory for *in vivo* assessment of agonists, antagonists and inverse agonists. Biochem. Pharmacol. 71, 1663–1670.

Rang, H.P., 2006. The receptor concept: pharmacology's big idea. Br. J. Pharmacol. 247, S9–S16.

Rang, H.P., Dale, M.M., Ritter, J.M., Flower, R.J., 2007. Rang and Dale's Pharmacology, sixth ed. Churchill-Livingstone, New York, pp. 8–53.

Toutain, P.-L., 2009. Mechanisms of drug action and pharmacokinetics/pharmacodynamics integration in dosage regimen optimization for veterinary medicine. In: Riviere, J.E., Papich, M.G. (Eds.), Veterinary Pharmacology and Therapeutics, ninth ed. Wiley-Blackwell, Ames, IA, pp. 75–96.

Vijayraghavan, S., Wang, M., Birnbaum, S.G., Williams, G.V., Arnsten, A.F.T., 2007. Inverted-U dopamine D1 receptor actions

on prefrontal neurons engaged in working memory. Nat. Neurosci. 10 (3), 376–384.

Von Zastrow, M., Bourne, H.R., 2009. Drug receptors and pharmacodynamics. In: Katzung, B.G., Masters, S.B., Trevor, A.J. (Eds.), Basic and Clinical Pharmacology, 11th ed. McGraw-Hill, New York, pp. 15–35.

Welshons, W.V., Thayer, K.A., Judy, B.M., Taylor, J.A., Curran, E.M., vom Saal, F.S., 2003. Large effects from small exposures. I. Mechanisms for endocrine-disrupting chemicals with estrogenic activity. Env. Health Persp. 111, 994–1006.

CHAPTER

5

Morphologic Manifestations of Toxic Cell Injury

Matthew A. Wallig[1] *and Evan B. Janovitz*[2]

[1]University of Illinois at Urbana-Champaign, Urbana, IL, United States [2]Bristol-Meyer Squibb Company, Princeton, NJ, United States

OUTLINE

INTRODUCTION

Structural and Functional Components of Cell Injury

Living cells are complex structures comprising an interdependent array of many essential components including organelles, fluids, proteins, electrolytes, signaling molecules, and plasma membrane receptors. Although injury to any one of these components can ultimately result in death of the entire cell, some are particularly critical for cell survival: the plasma membrane is the site of osmotic, electrolyte and water regulation, and receptor-ligand signal transduction; the mitochondrion is the site of aerobic respiration and adenosine triphosphate (ATP) generation; the endoplasmic reticulum (ER) is the site of most protein synthesis and calcium storage; and the nucleus, where DNA transcription occurs. The biochemical consequences of damage to these structures have been discussed in Chapter 2, Biochemical and Molecular Basis of Toxicity. Other structures, such as lysosomes, peroxisomes, secretory granules, microtubules, microfilaments, and even the extracellular matrix (ECM), may be altered in cell injury, but these generally reflect penultimate changes rather than the proximate cause of cell death.

Cell Injury in Context

The onset and progression of cell injury depend on the nature of the noxious insult, including its severity and duration. If injury to the cell is mild and not persistent, recovery is usually rapid and complete; a morphologic manifestation may be absent or imperceptible although a temporary functional disruption and/or a brief biochemical alteration may be detectable. For example, transient release of alanine aminotransferase

Fundamentals of Toxicologic Pathology.
DOI: http://dx.doi.org/10.1016/B978-0-12-809841-7.00005-8

(ALT) from hepatocytes into plasma after administration of a mild hepatotoxic compound for a short period of time may not be evident microscopically. At the other extreme, a potent hepatotoxic compound may cause such widespread necrosis that hepatocyte ALT content is no longer sufficient to be detectable in serum even though the lesion is obvious at the macroscopic level. If the compound is still detectable in blood or tissue by analytical techniques, a presumptive diagnosis is possible. But with chronic tissue injury, such as glomerulosclerosis or retinal atrophy, the etiology may be indeterminable. Cell injury can be manifested exclusively by functional deficits without perceptible morphologic manifestations. Such injury could even result in death of the animal. The complete disruption of oxidative phosphorylation by acute cyanide toxicity is such an example.

The metabolic rate of a cell has a significant effect on lesion development. Cells with high metabolic activity are generally more sensitive to noxious injury than cells with low energy needs. For example, neurons are quite sensitive to hypoxia while fibroblasts are quite resistant. Metabolically active cells absolutely depend on a continuous supply of oxygen (O_2) and functional mitochondria to generate ATP for sustaining cell function. Toxic injuries that break the link between O_2 diffusion from inhaled air across pulmonary alveoli, to the O_2-carrying capacity of red blood cells, to blood vessels, to mitochondria where oxidative phosphorylation and ATP generation occur can subsequently injure cells with high energy needs. Adequate cellular ATP is necessary to maintain normal structure and function of many vital, specialized cell populations, such as neurons that require energy to sustain membrane integrity and polarity as well as neurotransmitter production, myocardial cells that require energy for myofilament contraction/relaxation and Ca^{+2} transport, and renal tubular epithelial cells that require energy for transport of fluids, electrolytes, and metabolites. Even small changes in cellular O_2 tension leading to mildly decreased ATP production can cause serious alterations in essential functions of these cell types, with severe consequences for survival. Shifting to anaerobic glycolysis is inefficient and leads to lactic acidosis. By contrast, cells with low metabolic activity, such as fibroblasts and adipocytes, are resistant to low O_2 supply and can tolerate hypoxic conditions. Hence, these connective tissue elements can play prominent roles in regeneration and scarring.

Highly specialized cells are generally more sensitive to toxic insult than connective tissue cells. The latter, such as fibroblasts, are "plastic" in their adaptability to a variety of conditions, assuming an assortment of different roles due to their relatively undifferentiated nature and broad functional capabilities. These cells can tolerate anaerobic conditions and many types of toxic insults. In contrast, highly specialized cells, such as retinal rods and cones, must expend abundant energy to maintain their membranes in conformations capable of trapping photons (see Chapter 22a: Special Senses—Eye). Hence, they are exquisitely sensitive to injury.

The specialized functions of a given cell may predispose it to a particular type of noxious insult. Specific receptors on a cell population may render it susceptible to insults that would not impact neighboring cell types. For instance, cells expressing the *fas* receptor may undergo apoptosis when *fas* ligand binds to their receptors, whereas cells without this receptor will be unaffected. Some cells may accumulate toxicants because they have specific transporters that facilitate uptake of the molecule. For example, the nephrotoxicity of gentamicin, and similar aminoglycoside antibiotics, depends on the organic cation transport system that leads to gentamycin accumulation in lysosomes. Lysosomes eventually rupture hastening cell death. Pancreatic acinar cells are especially sensitive to excessive dietary intake of lysine or arginine. Toxicity may be further enhanced if the target cell is incapable of metabolic detoxification or metabolizes the toxicant to a more reactive chemical species. Phase I metabolism, especially by certain members of the cytochromes P450 (CYP) family, is particularly important in bioactivation of xenobiotics to toxic intermediates. For example, the presence in the hepatocyte of CYP 2E1 makes it uniquely susceptible to damage by acetaminophen, which is bioactivated to a highly reactive quinone imine by this CYP isozyme.

The "innate" ability of a cell to counter an injurious stimulus can be critical for resisting a toxic insult. For example, cells with high levels of antioxidants are typically resistant to oxidative injury. The liver, which receives 60% of its blood supply directly from the gastrointestinal tract through the portal vein, can generally tolerate a remarkably high level of potential noxious agents originating from the gut. This tolerability is attributable to high concentrations of antioxidants such as reduced glutathione and vitamins C and E, and a broad array of phase I and phase II detoxification enzymes within hepatocytes. Of course, being rich in metabolizing enzymes is a "double-edged sword" since otherwise innocuous compounds may be metabolized to highly bioactive, toxic intermediates, which deplete glutathione and then bind to proteins or nucleic acids. Cells lacking high concentrations of endogenous antioxidants and/or antioxidant enzymes or that are missing the appropriate quantities or combinations of phase I and phase II enzymes can be especially prone to toxic injury. This vulnerability is

heightened if cells tasked with detoxification, like the hepatocyte or the bronchiolar exocrine (club or Clara) cell in the lung, fail to detoxify harmful substances before they reach the general circulation.

Host Reactions to Cell Injury

Host reactions to injured or dead cells often play a key role in the morphologic manifestation of toxic cell injury. The inflammatory reaction to injured cells can amplify the original toxic injury to a more substantial lesion or even a life-threatening condition. Thus what could have been a relatively mild and recoverable injury can progress to a severe, nonresolving lesion. For example, acute necrotizing pancreatitis induced by acinar cell toxicants is exacerbated by activated neutrophils attracted by released zymogen granules. Neutrophils release a variety of preformed and de novo-generated chemicals that indiscriminately destroy even previously unaffected cells in the vicinity of the original injury. With necrotic cell death, the inflammatory reaction is provoked by leakage of intracellular contents and signaling proteins from disintegrating (parenchymal and inflammatory) cells. This process especially attracts neutrophils, the "foot soldiers" of the acute inflammatory response. In contrast, with apoptotic cell death, an orderly sequence of cell senescence preserves membrane integrity. The sequestration of intracellular materials within the debris (apoptotic bodies) permits macrophages to scavenge potential pro-inflammatory products before they can be released. Therefore, it is important to remember that the inflammatory reaction to apoptotic (so-called "programmed") cell death is muted or even absent altogether.

All the aforementioned factors and more contribute to the varied susceptibility of different cells and tissues to injury. Regardless of the type of injury or the factors present that mitigate or exacerbate that injury, a given cell population has only a limited number of responses available for survival and repair.

Adaptation

A cell exists within a narrow range of physiochemical conditions necessary to maintain a viable state. Thus, a cell, even a highly specialized one, dedicates much of its resources toward maintaining this homeostatic internal environment. Ion gradients, intracellular pH, and cytosolic osmolarity are vigorously maintained by the cell, even at the cost of its own specialized functions. A cell threatened with a loss of homeostasis will often jettison its specialized structures and cut back on its specialized functions, regardless of whether these functions are critical to the survival of the host, in order to maintain homeostasis of the cell. Substantial deviations from homeostasis lead to death of the cell. Less substantial deviations may lead to a new, usually reduced, level of function or metabolic activity in an attempted compromise between overall cell survival and specialized cell function. The response of a cell to disrupted homeostasis while maintaining some degree of function and avoiding death is called adaptation.

Atrophy

Atrophy is an adaptive change characterized by a reduction in the size of a cell, tissue, or organ. Cell atrophy can simply result from lack of use, such as occurs in skeletal muscle fibers after denervation or with immobilization. The lack of muscle contraction leads to a reduction in sarcoplasmic contractile proteins, which is evident microscopically as a decrease in myofiber diameter (Figure 5.1). Atrophy can also result from a lack of hormone stimulation. Deficiencies in pituitary trophic hormones, such as thyroid stimulating hormone (TSH) or adrenocorticotropic hormone (ACTH), lead to atrophy of thyroid follicular and adrenal cortical epithelial cells, respectively, resulting in atrophy of that portion of each gland where unstimulated cells reside. The severity of atrophic changes is dependent on both the degree and duration of stimulus withdrawal. Complete loss of stimulation for an

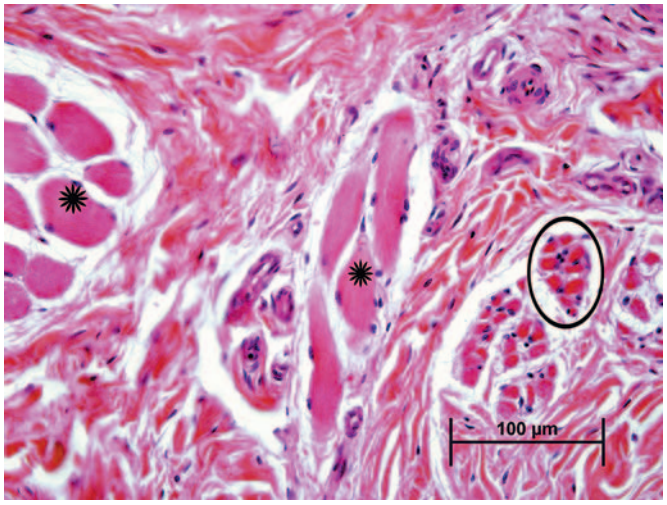

FIGURE 5.1 Atrophy due to loss of cellular mass. Photomicrograph of skeletal muscle from the tongue of a young horse. Portions of the tongue atrophied secondary to impairment of the regional blood supply. Affected muscle bundles (*circled*) are reduced in size, as are individual myofibers. Normal fibers are indicated by *asterisks*. Hematoxylin and eosin. Source: *From Haschek, W. M., Rousseaux, C.G., Wallig, M.A. (Eds.), 2013. Handbook of Toxicologic Pathology, third ed. Academic Press, San Diego, CA, Fig. 4.1, p. 80, with permission.*

extended period of time can lead to autophagy (see below) and senescence. Cell atrophy can also result from an insufficient supply of energy or substrates required to maintain structure and function. For example, pressure from an adjacent tumor can disrupt normal circulation leading to hypoxia or insufficient delivery of glucose for ATP generation or amino acids to maintain structural proteins. Cells that are capable of surviving in such an adverse environment will undergo atrophy. Cells in the immediate vicinity of the tumor may be compressed and distorted by physical displacement.

At the subcellular level, an atrophied cell may show morphologic evidence of an adaptive catabolic state reflecting the reduced demand for use or supply of substrates. Affected cells not only may be reduced in size but also may lack organellar features typical for a fully functional cell of that particular phenotype (Figure 5.2). Often atrophy is accomplished by a process termed autophagy. Autophagy is characterized by sequestration of degenerate organelles in a vesicle (defined by an "induction membrane"), termed an "autophagosome" (or autophagic vacuole). Autophagosomes ultimately fuse with a lysosome to form autophagolysosomes, where enzymatic digestion of the vesicle contents can provide a source of recycled macromolecules. The autophagocytic process is observable by transmission electron microscopy (TEM). Initially, enveloped organelles may be structurally disrupted but remain largely intact and recognizable within discrete double-layered membrane-bound vesicles, a process termed "macroautophagy." As degradation proceeds, organelles lose their distinctive structural features, and the vesicles tend to be defined by a single-layered membrane. Amorphous vesicles containing electron-dense granular material often represent residual bodies, an end-stage of autophagolysosomes, or a process termed "microautophagy," which is characterized by tubular proteasome formation associated with ubiquitin-mediated destruction of proteins. Autophagy can be so severe that the cell undergoes cell death in a modified form of apoptosis, termed "autophagic cell death." In this case, the ultrastructural and histologic morphology of the affected cell resembles closely the classical form of apoptosis (see later), but without the nuclear changes typical of apoptosis. Cells undergoing autophagic cell death are generally not removed by macrophage ingestion.

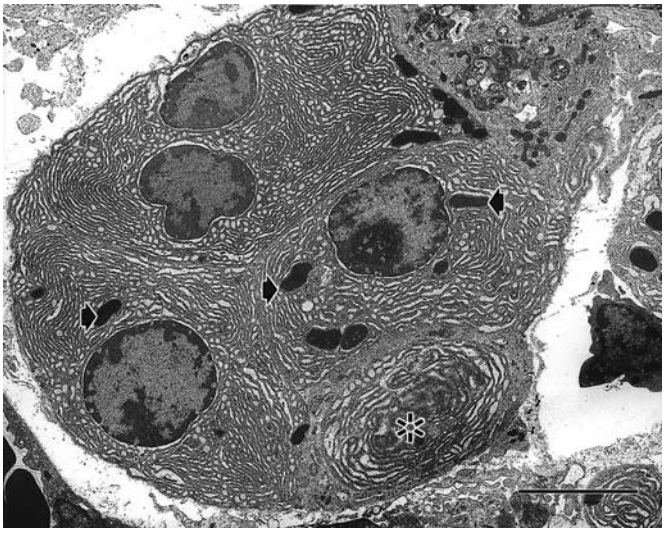

FIGURE 5.2 Atrophy due to loss of cellular mass. Electron photomicrograph of an atrophic pancreatic acinus from a male Fischer 344 (F344) rat after a bout of edematous pancreatitis induced by the phytochemical crambene. Acinar cells are reduced in size, lack polarity, are devoid of granules, and have few mitochondria (*arrows*). An autophagic vacuole containing acinar cell cytoplasm (*asterisk*) is present in one cell. Bar = 10 μm. Source: *From Haschek, W.M., Rousseaux, C.G., Wallig, M.A. (Eds.), 2002. Handbook of Toxicologic Pathology, second ed. Academic Press, San Diego, CA, Fig. 2, p. 43, with permission.*

The contents of residual bodies are typically nondegradable complex lipids and lipoproteins that collectively may be termed lipofuscin or ceroid "wear and tear" pigments (Figure 5.3). Residual bodies are particularly common in longer lived, metabolically active cells that have a high turnover of membrane components, such as striated muscle cells, neurons, and hepatocytes.

Atrophic cells may lose some, or all, of their specialized structures such as microvilli, cilia, contractile apparatuses, or secretory granules. In the extreme, an atrophic cell may not be recognizable as a specialized cell at all (Figure 5.4). Under light microscopy with standard hematoxylin and eosin (H&E) staining, an atrophic cell is typically small with reduced amounts of cytoplasm that may contain eosinophilic droplets, reflective of retained autophagosomes, or red-brown or golden-brown pigment granules, which represent residual bodies filled with lipofuscin and ceroid pigments. Grossly, an atrophic organ may simply appear small and pale but with normal conformation, such as thyroid glands following prolonged lack of TSH stimulation, or may be shrunken and deformed as a reflection of the underlying etiology, such as shrunken, irregularly contoured, gray, and firm kidneys resulting from chronic interstitial inflammation and fibrosis.

Tissue or organ atrophy can also result from a decrease in the number of normal-sized cells subsequent to cell death, for example, by apoptosis or necrosis (discussed in more detail later), or insufficient cell replacement. Atrophic tissue often displays the mechanism of cell death. When cell loss has occurred via widespread apoptosis, tissue macrophages may be prominent within the atrophic tissue (Figure 5.5).

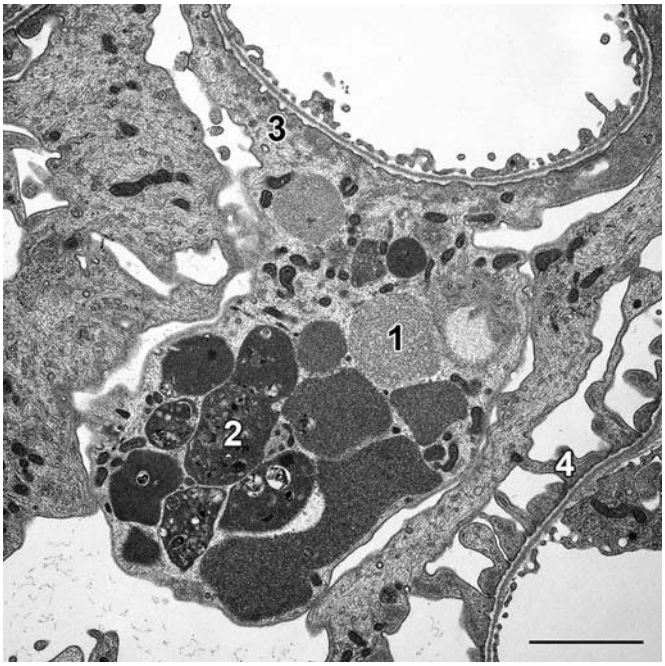

FIGURE 5.3 Residual bodies. Electron photomicrograph of the renal glomerulus from a rat with xenobiotic-induced podocytopathy. Note the degenerate podocyte with enlarged phagolysosomes (*1*) and residual bodies (*2*). Also note diffuse fusion of blunted podocyte foot processes (*3*), in contrast with the distinct and elongate processes (*4*) of an adjacent, normal podocyte. Bar = 2 μm. Source: *From Haschek, W.M., Rousseaux, C.G., Wallig, M.A. (Eds.), 2013. Handbook of Toxicologic Pathology, third ed. Academic Press, San Diego, CA, Fig. 4.3, p. 81, with permission.*

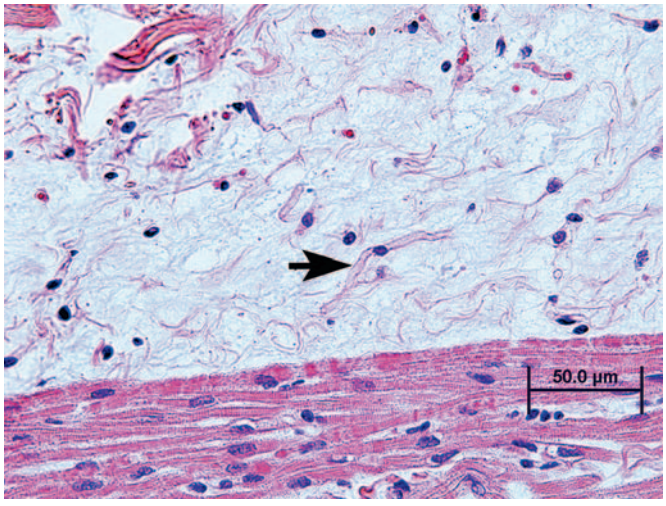

FIGURE 5.4 Atrophy due to loss of cellular mass. Photomicrograph of epicardial adipose tissue from a severely emaciated sheep. The arrow points to a severely atrophied adipocyte that no longer retains its normal morphologic features (i.e., round contour with large, central, clear cytoplasmic fat droplet). Note the abundant pale ground substance between the atrophied adipocytes. Hematoxylin and eosin. Source: *From Haschek, W.M., Rousseaux, C.G., Wallig, M.A. (Eds.), 2013. Handbook of Toxicologic Pathology, third ed. Academic Press, San Diego, CA, Fig. 4.4, p. 82, with permission.*

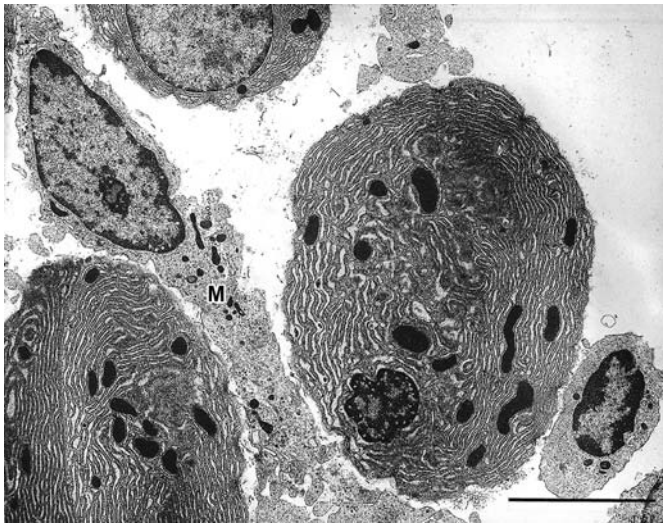

FIGURE 5.5 Atrophy due to loss of cells. Electron photomicrograph of a single remaining atrophied pancreatic acinar cell from a Fischer 344 (F344) rat treated with crambene, resulting in extensive apoptosis of most acinar cells in the pancreas. A tissue macrophage (M) is present near the atrophied cell. Bar = 10 μm. Source: *From Haschek, W.M., Rousseaux, C.G., Wallig, M.A. (Eds.), 2002. Handbook of Toxicologic Pathology, second ed. Academic Press, San Diego, CA, Fig. 3, p. 44, with permission.*

Vacuoles, representing phagolysosomes or residual bodies containing remnants of dead cells in various stages of degradation, may be evident within surviving cells or within nearby tissue macrophages. Apoptotic bodies may be observed (Figure 5.6), but if apoptosis has waned inflammation is usually absent. Grossly, atrophic organs resulting from loss of cell numbers may be indistinguishable from atrophic tissue resulting from reduction in cell mass, but when subtle the decrease in organ size may only be revealed by reductions in absolute or relative organ weight.

Tissue or organ atrophy resulting from overt cell necrosis is evident by light microscopy by the presence of swollen or lysed cells, with spillage of the cells content (Figure 5.7). Where patent capillary beds remain, inflammatory cell infiltration is typical. Chronically, after necrotic cells are removed, fibrosis, evident grossly as firmness and pallor, will ensue to replace the void left by the lost parenchymal tissue.

Hypertrophy

Hypertrophy is an adaptive increase in the mass of a cell, tissue, or organ that does not result from cell proliferation, that is, hyperplasia. The most common example of hypertrophy in toxicologic pathology is xenobiotic induction of hepatocyte metabolizing enzyme systems, which leads to expansion of hepatocyte cytoplasm. Elevations in serum transaminases (due to leakage across the plasma membranes of swollen cells) or

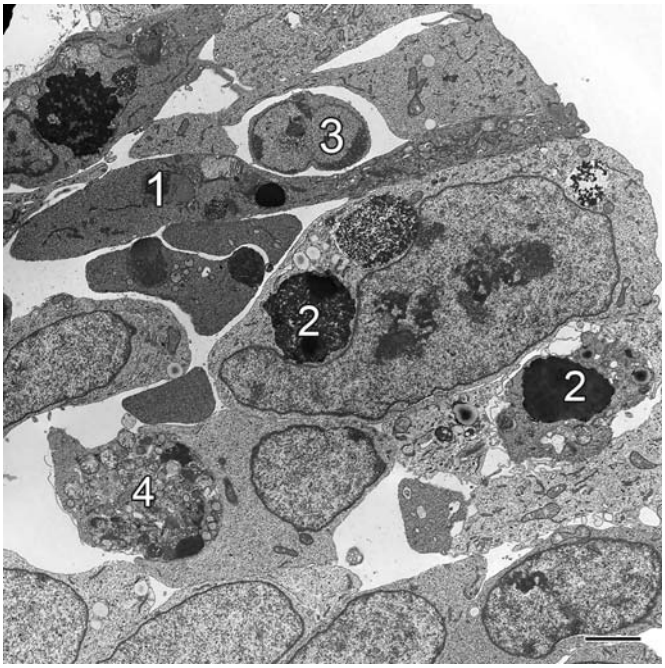

FIGURE 5.6 Atrophy due to loss of cells. Electron photomicrograph of neuroepithelium from the forebrain of a mouse embryo in which xenobiotic-induced organ atrophy has occurred. Note numerous shrunken cells with increased electron density of the cytoplasm, characteristic of apoptosis (*1*). Note also that many cells contain clumps of condensed chromatin (2). In one cell, peripherally clumped, crescent-shaped chromatin caps a portion of the remaining nucleus (*3*). An apoptotic cell with degenerate organelles has been phagocytized (*4*). Bar = 2 μm. Source*: From Haschek, W.M., Rousseaux, C.G., Wallig, M.A. (Eds.), 2013. Handbook of Toxicologic Pathology, third ed. Academic Press, San Diego, CA, Fig. 4.6, p. 83, with permission.*

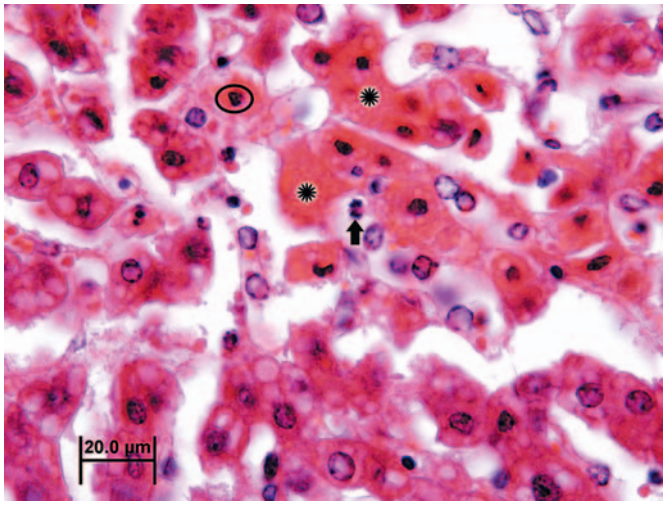

FIGURE 5.7 Necrosis. Photomicrograph of liver from a cow that died of endotoxemia. Foci of necrosis were present throughout the liver. The starbursts indicate hypereosinophilic, swollen hepatocytes with irregular profiles; these have most likely ruptured. Encircled is an irregularly shrunken nucleus typical of pyknosis (nuclear condensation and shrinkage), a change associated with necrosis. The *arrow* indicates a neutrophil attracted to the partially degraded cellular material released from the dying cell. Less severely affected, viable hepatocytes are present in the lower right hand corner of the image. Hematoxylin and eosin. Source*: From Haschek, W.M., Rousseaux, C.G., Wallig, M.A. (Eds.), 2013. Handbook of Toxicologic Pathology, third ed. Academic Press, San Diego, CA, Fig. 4.7, p. 83, with permission.*

even hepatocyte necrosis can result from handling of mice with severely enlarged livers after xenobiotic treatment.

Endogenously, hypertrophy is commonly a response to increased demand for the specialized function provided by the particular cell population. Endocrine cells responsive to trophic hormones often undergo hypertrophy when stimulated by the appropriate hormonal ligand. Hypertrophy of gonadotrophic adenohypophyseal cells in response to gonadotropin-releasing hormone (GnRH) from the hypothalamus at the onset of puberty is a classic example. By light microscopy, hypertrophy appears as an increase in the volume of cytoplasm, which may be more granular if accompanied by organelle hyperplasia. The nuclei of hypertrophied cells are often enlarged and contain a prominent nucleolus. By TEM, hypertrophied cells are usually replete with morphologically normal organelles, although certain organelles may also be enlarged or more numerous, for examples, peroxisomes, ER, or cytoskeletal microfilaments. Diffuse but subtle cell hypertrophy may be imperceptible by standard microscopy but can be discerned grossly by organ weight increases or by morphometry if necessary.

In toxicologic pathology, hepatocyte peroxisome proliferation is the classic, although now somewhat historical, example of organelle hyperplasia causing cell and organ hypertrophy. Xenobiotics that agonize peroxisome proliferator-activated receptors (PPARs, especially PPAR-α) on the nuclear membrane induce activation of particular transcription factors, which subsequently lead to such widespread proliferation of peroxisomes that hepatocytes are noticeably enlarged, with abundant granular eosinophilic cytoplasm (Figure 5.8).

Although not necessarily considered hypertrophy by every pathologist, phospholipidosis is another common cause of xenobiotic-induced cell enlargement due to organelle accumulation. Cationic amphiphilic compounds accumulating in lysosomes can alter degradation of phospholipid-rich membranes. With standard processing for light microscopy, most of the retained lipid-soluble breakdown products dissolve leaving abundant, finely vacuolated, or "moth-eaten" appearing, cytoplasm. With processing for TEM, the lipids

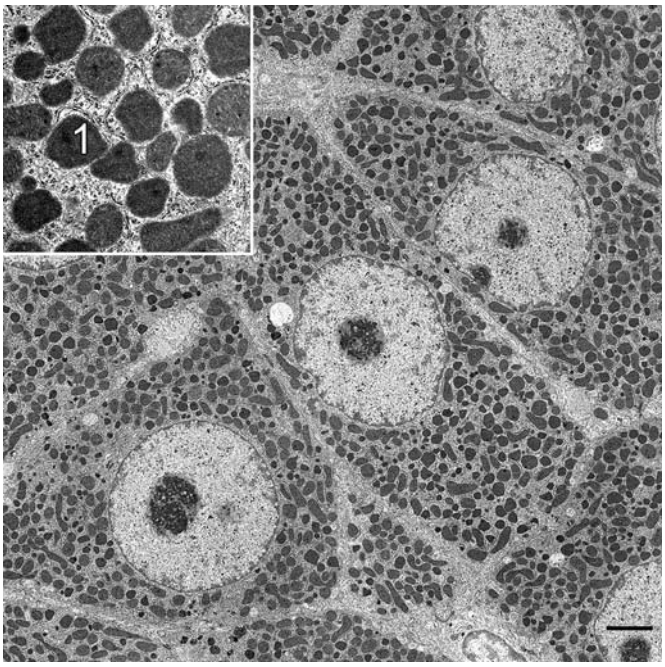

FIGURE 5.8 Organellar hypertrophy. Electron photomicrograph of hepatocytes from a rat treated with a peroxisome proliferator-activated receptors (PPAR)-α agonist, leading to a dramatic increase in the numbers of electron-dense granules (peroxisomes) in the cytoplasm. Bar = 2 μm. Inset: Peroxisomes are identifiable by the presence of a distinctive nucleoid (inset, *1*). Source: *From Haschek, W.M., Rousseaux, C.G., Wallig, M.A. (Eds.), 2013. Handbook of Toxicologic Pathology, third ed. Academic Press, San Diego, CA, Fig. 4.8, p. 84, with permission.*

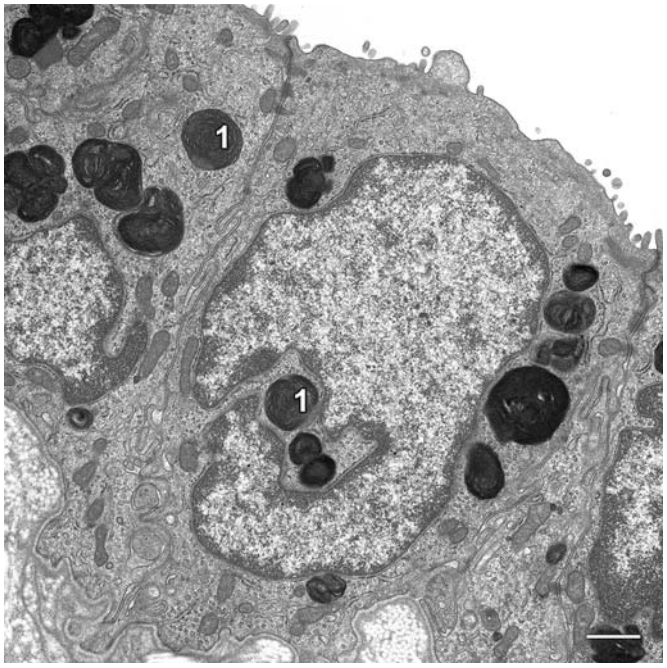

FIGURE 5.9 Phospholipid accumulation. Electron photomicrograph of biliary epithelium from a rat treated with a xenobiotic that induces phospholipidosis. Note the numerous enlarged, electron-dense lysosomes expanded by lamellar or myelinoid bodies (*1*). These bodies are the ultrastructural hallmark of phospholipidosis. Bar = 1 μm. Source: *From Haschek, W.M., Rousseaux, C.G., Wallig, M.A. (Eds.), 2013. Handbook of Toxicologic Pathology, third ed. Academic Press, San Diego, CA, Fig. 4.9, p. 84, with permission.*

are retained so that "vacuoles" appear as enlarged, discrete, membrane-bound bodies containing laminated whorls of partially degraded membranes, termed "myelin whorls" (Figure 5.9).

Often cell or even organ hypertrophy is not injurious, especially in the short term, and merely reflects a physiologic response to an increased demand on a tissue for its specialized function. However, organelle proliferation can interfere with other cell functions leading to so-called pathologic hypertrophy; this is fairly common in toxicologic pathology. For example, hypertrophy of smooth endoplasmic reticulum (sER) of hepatocytes chronically exposed to phenobarbital or other anticonvulsant drugs (Figure 5.10) can impair other hepatocyte functions such as urea production or bile excretion, leading to hyperammonemia or bilirubinemia, respectively. Hypertrophy of sER is not necessarily pathologic. In investigative toxicologic pathology, treatment of experimental animals with 1-aminobenzotriazole used to inhibit phase I metabolism can lead to nonpathologic hypertrophy of affected hepatocytes secondary to mild sER hypertrophy (Figure 5.11).

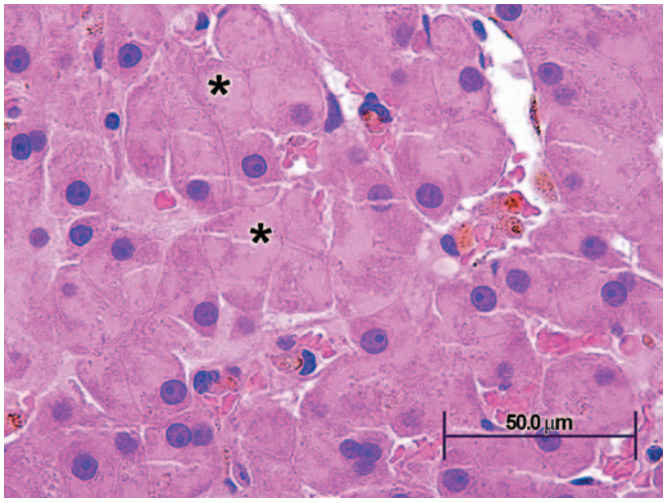

FIGURE 5.10 Pathologic hypertrophy. Photomicrograph of liver from a dog treated for a prolonged period of time with oral phenobarbital to control convulsions. The enlarged hepatocytes contain an increased quantity of pale, hyalin cytoplasm (*asterisk*) due to profound expansion of the smooth endoplasmic reticulum (sER). Hematoxylin and eosin. Source: *From Haschek, W.M., Rousseaux, C.G., Wallig, M.A. (Eds.), 2007. Handbook of Toxicologic Pathology, second ed. Academic Press, San Diego, CA, Fig. 2.3, p. 13, with permission.*

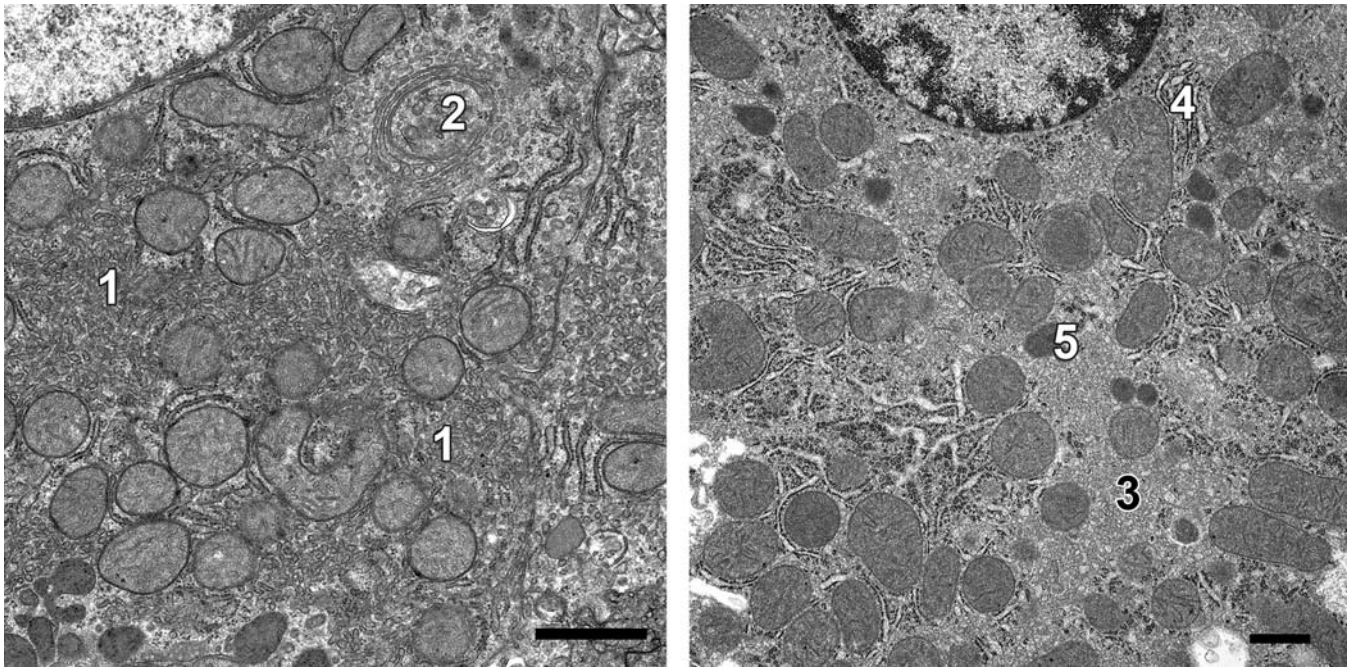

FIGURE 5.11 Adaptive hypertrophy with organellar hyperplasia. Electron photomicrograph of a hypertrophic centrilobular hepatocyte from a rat treated with a xenobiotic (1-aminobenzotriazole) that induces smooth endoplasmic reticulum (sER) proliferation (*left panel*), compared to a normal centrilobular hepatocyte from a control rat (*right panel*). Note numerous profiles of sER (*1*) and a prominent Golgi complex (*2*) in the hepatocyte from the treated rat. This contrasts with the normal complement of smooth (*3*) and rough (*4*) ER, and other organelles such as peroxisomes (*5*), in the hepatocyte from the control rat. Bar = 1 μm. Source*: From Haschek, W.M., Rousseaux, C.G., Wallig, M.A. (Eds.), 2013. Handbook of Toxicologic Pathology, third ed. Academic Press, San Diego, CA, Fig. 4.8, p. 84, with permission.*

IRREVERSIBLE VERSUS REVERSIBLE CELL INJURY

Cell injury is any physical or chemical insult that results in the loss of a cell's capacity to maintain homeostasis, in either a normal or adapted state. In toxicologic pathology, cell injury is often in the context of exposure to a noxious stimulus that prevents the cell from maintaining its physiologic parameters within survivable limits. Defining these limits for an injured cell, that is, detecting the "point of no return," at the biochemical level is a complex undertaking. However, it is clear that alteration of mitochondrial membrane permeability leading to leakage of the electron transport chain enzyme cytochrome *c* into the cytosol is a critical step for both necrosis and apoptosis. The leakage of cytochrome *c* is a nonrecoverable event.

Recognizing whether an injured cell is destined to die as compared to one that will survive can be challenging via light microscopy. There is a time lag between those biochemical events that inevitably lead to cell death and the obvious morphological manifestations of necrosis or apoptosis. With TEM, morphologic changes of irreversible cell injury are generally evident somewhat earlier than with light microscopy. Fortunately, it is rarely necessary for a toxicologic pathologist to be concerned with the potential fate of an individual cell because other cells within the affected tissue will typically manifest the morphologic features of irreversible cell injury.

Reversible cell injury simply indicates that the affected cell has the potential to survive following a noxious insult. A reversibly injured cell may be morphologically recognizable by a variety of changes depending on its phenotype. For example, specialized cells may lose their unique phenotypic structures, such as cilia from injured respiratory epithelium. More generally, reversibly injured cells may exhibit classic morphologic features of what has been termed cell "degeneration." For example, hydropic degeneration refers to a swollen cell with pale cytoplasm attributed to excessive accumulation of fluid resulting from a disruption in water balance. Even reversible cell injury can be fatal to the entire organism if a vital function is impaired or the consequences of cell injury are catastrophic. Examples of this concept include neuronal or neuroglial swelling in the central nervous system leading to respiratory arrest, and cardiac myofiber swelling leading to loss of contractility and altered

depolarization, repolarization, or electrical conductance. In contrast, hepatocyte swelling in the liver can be quite marked but, considering the reserve and regenerative capacity of the liver, still have little impact on the animal's viability.

Two classic morphologic features of reversible cell injury are cell swelling and fatty change. Both can progress to cell death.

Cell Swelling

Cell swelling is an early degenerative change that occurs in many types of acute cell injury. It may be a prelude to more drastic changes or may resolve as the cell adapts and repairs the damage.

By light microscopy, cell swelling is characterized by expanded, pale cytoplasm. The cell nucleus and/or adjacent cells may be displaced. Occasionally, cell swelling resulting from reversible cell injury may resemble organelle hyperplasia or hypertrophy. While special histochemical stains or electron microscopy may be necessary to distinguish between these processes, microscopic evaluation of the affected tissue overall is usually sufficient to allow for accurate interpretation. By TEM, cell swelling is usually characterized by dilution of cytoplasmic elements and dispersion of organelles; dilated cisternae of ER may also be evident. Rarely, extreme organelle hyperplasia/hypertrophy of organelles may lead to swelling so that both processes occur simultaneously. As cell swelling progresses, clear spaces or vacuoles may form in the cytoplasm; these usually represent dilated portions of the ER and/or Golgi apparatus. If severe enough, cisternae may rupture and "cytoplasmic lakes" may form. Solubilized or denatured proteins that accumulate in these "lakes" are eosinophilic and appear as so-called hyaline droplets. This type of change is termed "vacuolar degeneration" or "vacuolar change." Diffuse cytoplasmic swelling with minimal vacuolation is also termed "ballooning degeneration" or "cloudy swelling" (Figure 5.12).

The nucleus of reversibly injured cells is often morphologically normal. However, nuclei of affected cells may undergo chromatin clumping, rarefaction, and peripheral nucleolar migration as an indication of more severe cell injury.

Cell swelling occurs when the cell loses its ability to maintain the balance between cytosolic influx of sodium (Na^+) ions and water, and efflux of potassium (K^+) ions. Swelling reflects the influx of excessive water as a consequence of ineffective membrane ATPases required to actively exchange Na^+ for K^+. The optimum osmotic gradient is lost, and water follows Na^+ into the cell cytoplasm. The pathophysiology

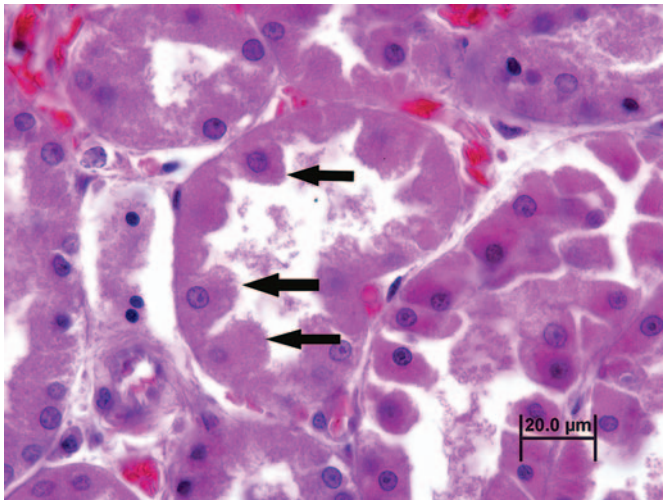

FIGURE 5.12 Cell swelling. Photomicrograph demonstrating swollen renal tubular epithelial cells from a dog in septic shock. Note the bulging of the apical portions of the cells (*arrows*), loss of brush border, and elevation of the nuclei away from their normal basal positions in the affected cells. Hematoxylin and eosin. Source: *From Haschek, W.M., Rousseaux, C.G., Wallig, M.A. (Eds.), 2007. Handbook of Toxicologic Pathology, second ed. Academic Press, San Diego, CA, Fig. 2.3, p. 13, with permission.*

of cell swelling can result from direct damage to these ATP-dependent "pumps," an inadequate supply of ATP substrate, or an overwhelming influx of Na^+ after direct damage to the plasma membrane. Cytoplasmic vacuoles may also form directly from the ER if the Na^+/K^+ ATPases in the ER membrane are sufficiently functional to import excess Na^+ (followed by water) out of the cytoplasm into ER cisternae (Figure 5.13).

The morphologic changes associated with cell swelling are also due to the influx of calcium (Ca^{++}) via the diminished capacity or function of the ATP-dependent Na^+/Ca^{++} exchange pumps. The dissociation of cytoskeletal elements and the loss of intercellular junctions that result from excessively high cytosolic levels of free Ca^{++} leads to additional loss of normal shape and a tendency for the cell to assume a spherical profile (Figure 5.14).

Cell swelling is not lethal per se but may indicate an early phase of a lethal process. In other words, a lethally injured cell may be fixed at the stage of cell swelling. Alternative interpretations for what appears as cell swelling or vacuolar change by light microscopy include hepatocytes with glycogen accumulation, commonly observed when liver samples are obtained from animals in the fed state. Glycogen is typically stored within the hepatocyte cytosol as aggregates, recognized by TEM as "rosettes." A large portion of these rosettes dissolve during processing for light microscopy, leaving behind swollen hepatocytes with clear or "feathery" cytoplasm that resembles vacuolar change

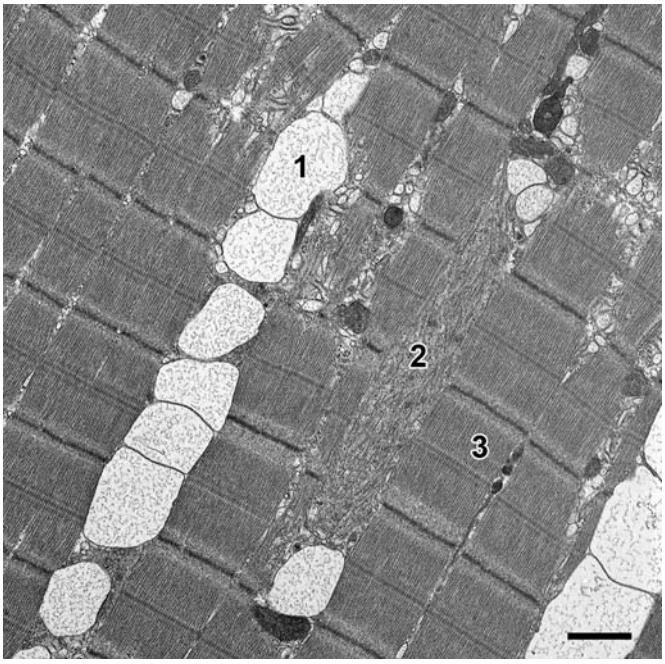

FIGURE 5.13 Vacuolar change. Electron photomicrograph of rat skeletal muscle damaged by a xenobiotic. Note the degenerate myofibers with markedly dilated sarcoplasmic reticulum containing amorphous granular material (*1*) and disaggregated myofibrils (*2*). Contrast with normal sarcomeres in adjacent myofibers (*3*). Bar = 1 μm. Source: *From Haschek, W.M., Rousseaux, C.G., Wallig, M.A. (Eds.), 2013. Handbook of Toxicologic Pathology, third ed. Academic Press, San Diego, CA, Fig. 4.13, p. 87, with permission.*

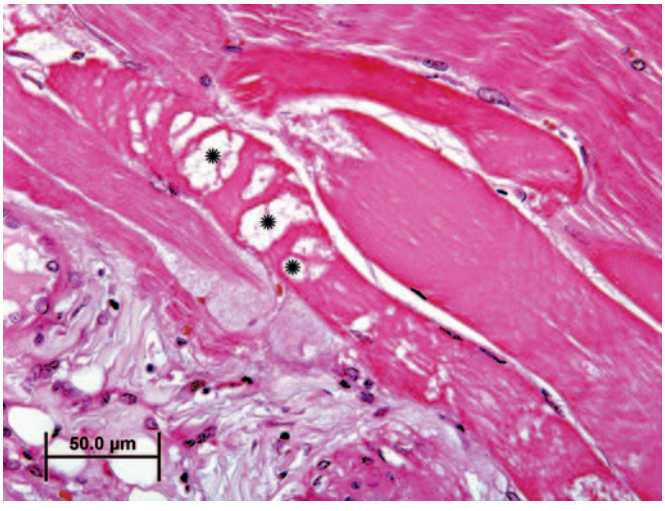

FIGURE 5.14 Vacuolar change. Photomicrograph of injured gluteal muscle of a horse. In addition to swelling, the sarcoplasm of affected myofibers is characterized by clear vacuoles (*starbursts*) as well as separation of myofibrils with loss of striations. Hematoxylin and eosin. Source: *From Haschek, W.M., Rousseaux, C.G., Wallig, M.A. (Eds.), 2013. Handbook of Toxicologic Pathology, third ed. Academic Press, San Diego, CA, Fig. 4.8, p. 87, with permission.*

but is not an indication of cell injury. Partially degraded complex carbohydrates that accumulate within neuronal lysosomes with inherited or acquired lysosomal enzyme deficiency, such as swainsonine toxicosis (locoism) in sheep, can also appear as vacuolar degeneration. In principle, such acquired lysosomal storage diseases are reversible following withdrawal of the toxic etiology. However, resolution may be incomplete in highly specialized cells such as neurons.

Fatty Change

Fatty change, also termed fatty degeneration, lipidosis or "steatosis," is a second manifestation of reversible cell injury. It occurs in cells that are capable of storing and metabolizing lipid, usually in the form of triglycerides, and is especially common in hepatocytes but also affects myocardial cells and renal tubular epithelium. Whether fatty change represents a degenerative or adaptive change depends on the pathogenesis, although severe fatty change can lead to irreversible cell injury regardless of etiology.

Excessive influx or inadequate efflux of triglycerides will lead to accumulation of lipid droplets throughout the cytoplasm. Mitochondrial dysfunction can lead to insufficient β-oxidation of triglycerides and accumulation of non-metabolized triglycerides, typically adjacent to affected mitochondria. Inadequate protein synthesis secondary to a noxious insult or hypoxia can result in a deficiency of apolipoproteins for lipid transport or oxidative enzymes necessary for β-oxidation of fatty acids; consequently, lipid droplets accumulate within the cytoplasm. Cells with fatty degeneration can be swollen enough to occlude vascular supply. Lipid droplets may be so abundant or large that organelles necessary for normal cell function are compromised.

By TEM, fatty change is characterized by accumulation of spherical, often homogenous, cytoplasmic inclusions of varying electron density. These arise from the sER, forming between the inner and outer membrane leaflets. Hence lipid droplets are usually surrounded by a single layer of phospholipids derived from the outer membrane leaflet of the sER (Figure 5.15). Lipid droplets occur in a wide range of sizes. They can be relatively small and dispersed, so-called "microvesicular" lipidosis, which often occurs in the context of an acute insult (Figure 5.16). Lipid droplets can also be quite large, so-called "macrovesicular" lipidosis, occupying almost the entire cell and displacing organelles, including the nucleus, peripherally (Figure 5.17); this type of fatty change typically requires a longer time to develop. Microscopically, cells that have undergone fatty degeneration are swollen with one large to

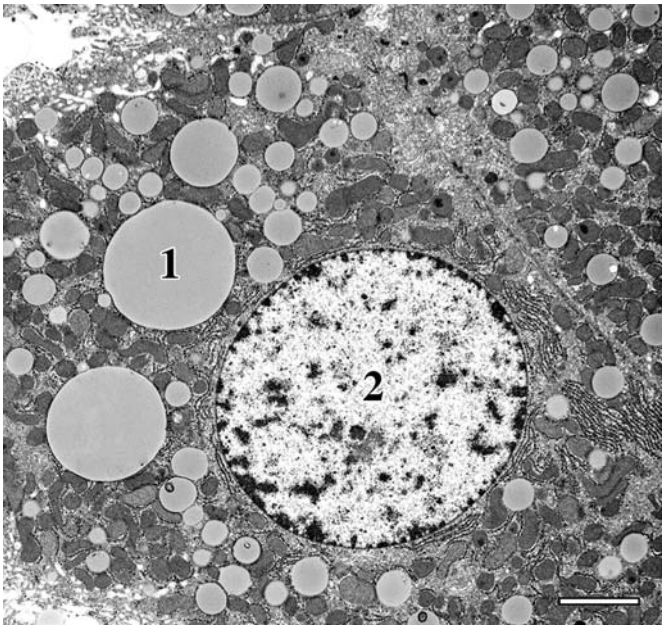

FIGURE 5.15 Lipidosis. Electron photomicrograph of xenobiotic-induced lipidosis in a mouse hepatocyte. Note that numerous, variably sized, membrane-bound lipid droplets (*1*) are widely dispersed throughout the cytoplasm. Also note that lipid droplets are smaller than the nucleus (*2*). Bar = 2 μm. Source*: From Haschek, W.M., Rousseaux, C.G., Wallig, M.A. (Eds.), 2013. Handbook of Toxicologic Pathology, third ed. Academic Press, San Diego, CA, Fig. 4.15, p. 88, with permission.*

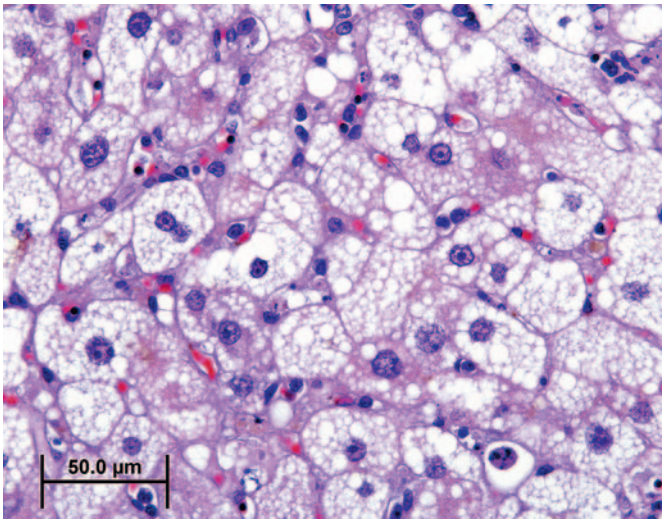

FIGURE 5.16 Microvesicular lipidosis. Photomicrograph of liver from a cat with acute hepatic lipidosis. Most hepatocytes contain many variably sized but usually small round, clear, colorless vacuoles dispersed throughout the cytoplasm. Hematoxylin and eosin. Source*: From Haschek, W.M., Rousseaux, C.G., Wallig, M.A. (Eds.), 2013. Handbook of Toxicologic Pathology, third ed. Academic Press, San Diego, CA, Fig. 4.16, p. 89, with permission.*

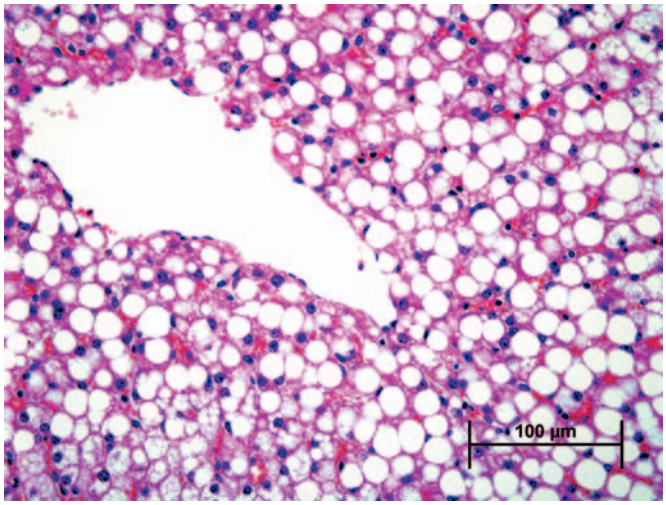

FIGURE 5.17 Macrovesicular lipidosis. Photomicrograph of liver from a goat with chronic hepatic lipidosis as a consequence of pregnancy toxemia. Most hepatocytes contain one large round, clear, colorless lipid vacuole. Other structures (e.g., nuclei) are displaced to the periphery of the cell, and often are indented by the encroaching vacuoles. Hematoxylin and eosin. Source*: From Haschek, W.M., Rousseaux, C.G., Wallig, M.A. (Eds.), 2007. Handbook of Toxicologic Pathology, second ed. Academic Press, San Diego, CA, Fig. 2.4, p. 14, with permission.*

numerous, variably sized, perfectly round, clear spaces compressing the residual cytosol and nucleus to the periphery of the cell. Lipid droplets dissolve when tissue is routinely processed for light microscopy, but are easily recognized. If confirmation of their lipid component is necessary, frozen sections can be stained with Oil Red O (orange droplets), Sudan black (black droplets), or osmium tetroxide (black droplets).

Macroscopically, a fresh liver with fatty change is easily recognized as one of the classic lesions in pathology. It is orange to yellow, evenly reticulated with a distinct lobular pattern, friable, and greasy. Lipidosis in the heart or kidney appears as pale whitish-yellow areas. In the heart, lipidosis may occur in the myocardium bordering an infarct where mitochondrial β-oxidation pathways are impaired. In the kidney, triglycerides may accumulate in renal tubular epithelium in the context of hyperlipidemia with diabetes mellitus. In areas of inflammation involving lipid-rich tissue, macrophages sequester lipids in discrete round vacuoles. A prototypic instance of this is necrosis of infarcted brain or spinal cord tissue, especially white matter, with the recruitment of numerous foamy "gitter cells" to remove the lipid-rich debris (see Chapter 21: Nervous System). While replete foamy macrophages may degenerate and elicit phagocytosis by adjacent macrophages, this type of lipid accumulation is considered a normal cell function and not primary cell injury.

IRREVERSIBLE CELL INJURY

Irreversible cell injury denotes the "point-of-no-return" from which a damaged cell is incapable of recovery and is committed to die. Functionally, this occurs when the physiology of an irreversibly injured cell is disrupted enough that homeostasis cannot be maintained. Once a cell has reached this state, cell death, whether via a passive process, that is, necrosis (or more formally, "oncotic necrosis"), or an active process, that is, apoptosis (more formally, "apoptotic necrosis"), is inevitable. The dead cell ultimately degrades, lyses, and dissolves, or is phagocytized.

Defining the precise physiologic criteria necessary for a cell to become irreversibly injured is virtually impossible, but an irreversibly injured cell exhibits stereotypical morphologic features that can clearly indicate the lethal aspect of its injury. In some instances, such features reveal the pathogenesis or even etiology of the noxious insult, and these may provide the only clues regarding why the cell was in the process of dying (Table 5.1). The morphologic progression of a dead cell's breakdown and removal can be termed generically as "necrosis," regardless of the mechanism of cell death.

Generally, the process of post-necrotic cell degradation is also termed degeneration and can be recognized by various gross or light microscopic features after lethal cell injury. Viable tissue surrounding necrotic cells will often exhibit a host reaction, such as hemorrhage or inflammation, which allows a pathologist to distinguish antemortem from postmortem cell death. The latter, also termed autolysis, encompasses many of the end-stage physiologic and some of the morphologic manifestations of antemortem cell death. Importantly, autolysis affects large contiguous portions of whole organs, while necrosis typically affects distinct areas. Autolysis proceeds at different rates depending on internal and external factors. For example, autolysis of intestinal mucosa is rapid because bacteria are already

TABLE 5.1 Necrosis Versus Apoptosis

Characteristic	Necrosis	Apoptosis
Gross changes	Grossly evident with disruption of normal tissue structure and detail, scarring if long-term	Minimal or atrophy without scarring
Histologic changes	Whole fields of cells affected	Individual cells scattered throughout the affected tissue
	Hypereosinophilia	Hyperbasophilia or hypereosinophilia
	Loss of cell borders with irregular fragmentation	Formation of round bodies, often within a clear halo
	Irregular chromatin clumping, pyknosis, karyorrhexis and/or karyolysis; rupture of nuclear envelope	Chromatin condensation into caps or crescents, within round nuclear bodies; preservation of nuclear envelope
Ultrastructural changes	Swelling and loss of surface structures with blebbing and loss of apical portions of cytoplasm	Condensation followed by rapid zeiosis (formation of membrane blebs or buds in degenerating cells)
	Rarefaction of cytoplasm followed by condensation after death	Condensation of cytoplasm followed by rarefaction after ingestion by phagocytes
	Swelling and loss of organellar morphology	Preservation of organellar morphology
	Low-amplitude swelling of mitochondria followed by high-amplitude swelling and rupture	Preservation of mitochondrial ultrastructure
	Rupture and degradation of internal and external membranes with bursting of the cell and leakage of cell contents	Preservation of internal and external membranes with preservation of membrane around apoptotic bodies
	Irregular clumping and degradation of chromatin; disintegration of nuclear envelope	Migration of uniformly degraded chromatin to margins of nuclear envelope; preservation of nuclear envelope
Sequelae	Release of intracellular enzymes into extracellular millieu	Retention of intracellular enzymes within the apoptotic bodies
	Release of pro-inflammatory cell breakdown products (*damage-associated molecular patterns* [DAMPs])	No release of pro-inflammatory products
	Ingress of neutrophils followed by macrophages	Ingestion by tissue macrophages or adjacent parenchymal cells
	Active inflammation with scarring	Atrophy with stromal collapse but *no* scarring

From Haschek, W.M., Rousseaux, C.G., Wallig, M.A. (Eds.), 2007. Handbook of Toxicologic Pathology, second ed. Academic Press, San Diego, CA, Table 2.1, p. 16.

present and abdominal viscera retain their warmth after death. In contrast, autolysis of the brain may be quite slow, especially if the ambient temperature is low, since heat rapidly dissipates from the skull.

Necrosis

Ultrastructural features of necrosis mimic some of those characteristic of reversible cell injury, including cytoplasmic swelling and rarefaction of the cytosol, dilation of the ER or formation of cytoplasmic lakes, loss or deformation of specialized structures such as microvilli, and/or dissociation from adjacent cells or the extracellular matrix (ECM). Subcellular changes of lethal cell injury may be evident hours before they are recognizable histologically.

Plasma membrane alterations are an early indication of lethal injury. These include loss of microvilli and cilia (Figure 5.18) and disruption of intercellular junctions (e.g., gap junctions separate, the maculae densae and zonulae adherentes degrade, and the terminal cytoskeletal web dissolves). As the cell swells and the intricate substructure of the plasma membrane is disturbed, cytoplasmic "blebs" or "out-pouchings" may form on the surfaces of lethally injured cells (Figure 5.19). Such cytoplasmic fragments may detach from the bulging surface of the swollen cell and slough into an adjacent lumen or interstitial space, where they eventually lyse and release their contents, which include lytic enzymes and pro-inflammatory chemicals.

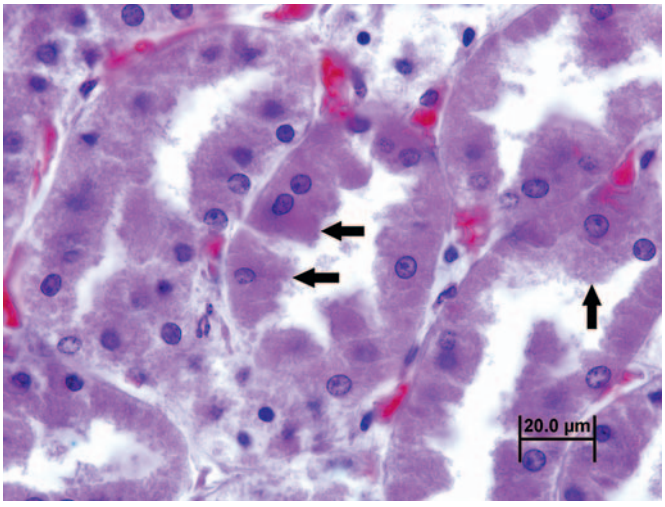

FIGURE 5.18 Loss of specialized structures after injury. Photomicrograph of injured renal tubular epithelial cells in a cat with lily (*Lilium longiflorum*) toxicosis, demonstrating loss of microvillous borders (*arrows*) and swelling of the cytoplasm. Hematoxylin and eosin. Source: *From Haschek, W.M., Rousseaux, C.G., Wallig, M.A. (Eds.), 2013. Handbook of Toxicologic Pathology, third ed. Academic Press, San Diego, CA, Fig. 4.16, p. 89, with permission.*

The aforementioned pro-inflammatory chemicals include damage-associated molecular pattern molecules (DAMPs), which trigger inflammatory and immunologic responses, but these are generally mild in comparison to the responses invoked by an infectious agent (discussed later). DAMPs include both proteins and non-protein substances that are normally sequestered within a viable cell or as part of the ECM. Intracellular DAMP proteins include heat shock proteins (HSPs), S-100, and the chromatin-associated protein high mobility group box 1 (HMGB1). Non-protein DAMPs include ATP, adenosine, uric acid, and DNA itself. ECM-derived DAMPs include hyaluronan fragments and heparan sulfate.

Lethal cell injury commonly leads to cell swelling with disruption of plasma membrane integrity. Cell

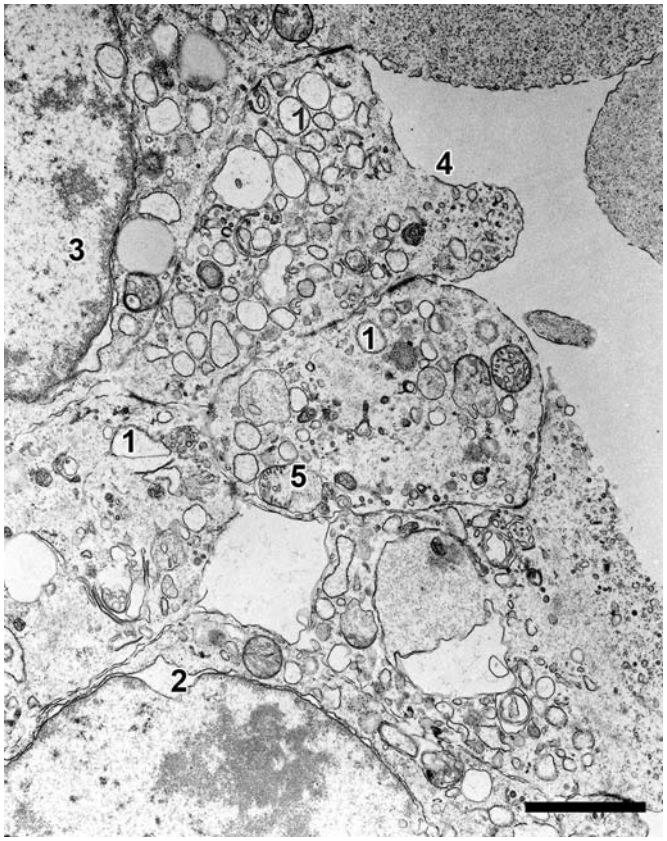

FIGURE 5.19 Necrosis. Electron photomicrograph of a necrotic neuroepithelial cell in a rat embryo with ischemia secondary to xenobiotic-induced toxicity to the dam. Note the widespread dilatation of the cytocavity network, including the endoplasmic reticulum (*1*) and nuclear envelope (2); dissolution of nuclear chromatin (i.e., karyolysis) (*3*), cytoplasmic bleb formation with loss of plasma membrane integrity (*4*), and swollen mitochondria with lysis of the cristae (*5*). These ultrastructural changes of end-stage cell death are not specific as they also occur with postmortem autolysis. Bar = 2 µm. Source: *From Haschek, W.M., Rousseaux, C.G., Wallig, M.A. (Eds.), 2013. Handbook of Toxicologic Pathology, third ed. Academic Press, San Diego, CA, Fig. 4.19, p. 92, with permission.*

swelling often reflects loss of energy-dependent, membrane-bound ion exchange proteins, but it also may reflect enzymatic digestion of the plasma membrane by phospholipases activated by uncontrolled Ca^{+2} influx. Other causes of plasma membrane injury include free radicals generated by dysfunctional mitochondria and noxious agents that are directly toxic to plasma membrane phospholipids (Figure 5.19). By TEM, portions of partially degraded, bilayered plasma membrane characteristically roll into laminated myelin whorls (Figure 5.9).

Mitochondria exhibit a variety of dramatic morphologic changes during the process of necrosis. These organelles first undergo a form of distension termed "low-amplitude" swelling, which develops as ATP production diminishes and ATP-dependent ion pumps in the mitochondrial outer membrane become incapable of maintaining water balance. Low-amplitude swelling refers to expansion of the outer mitochondrial compartment as water and electrolytes flow from the inner compartment and sequester in the intermembranous space. Concurrently, the inner mitochondrial compartment condenses, becoming electron-dense when observed by TEM. This state is recoverable if the noxious insult halts. With persistent injury, electron-dense calcium phosphate deposits form as Ca^{+2} homeostatic mechanisms fail, and over time these enlarge to form "flocculent densities" composed of partially degraded protein and membrane elements.

"High-amplitude" mitochondrial swelling is an indication that the necrotic processes have progressed to the "point-of-no-return." It is characterized by massive swelling of both inner and outer compartments, loss of cristae (cristolysis), and accumulation of precipitated mineral and protein (Figure 5.19). As the inner mitochondrial compartment expands to contact the outer compartment, an irreversible state termed mitochondrial permeability transition (MPT) ensues. Once MTP begins, ATP-generating particles on the inner mitochondrial membrane detach, ATP production ceases, and molecules of adenine nucleotide transporter (ANT) are released. ANT binds to the mitochondrial matrix protein cyclophilin D. This complex binds to an outer membrane ion transport protein, the voltage-dependent anion channel, forming the MPT pore, which allows the passage of small molecules between the cytosol and the mitochondrial matrix. At this stage, Ca^{+2} salt precipitates are especially prominent, especially when vascular perfusion replenishes interstitial fluid Ca^{+2} and phosphate into the extracellular interstitial fluid surrounding the injured cells. With MPT pore formation, the mitochondrial outer membrane ruptures, and the mitochondrion is no longer viable. For most cell types, necrosis quickly follows complete depletion of energy storage and production.

Coincident with the morphologic and functional deterioration of mitochondria that portends imminent necrosis, water continues to accumulate in the cytoplasm. Distension of the rough and smooth ER may reflect a temporary accommodation for the excess fluid; however, ER fragmentation typically ensues as ribosomes detach from the rough ER and adaptive protein synthesis ceases. Recovery is now impossible. Once organelle membranes rupture, releasing lysosomal enzymes, degradation of cellular components accelerates, leaving condensed cellular remnants. The sequence of cell swelling followed by condensation is characteristic of necrosis. In contrast, cell death by apoptosis is characterized initially by condensation followed by fragmentation and ingestion by adjacent phagocytes.

In the cell nucleus, morphologic changes of irreversible cell injury are manifested mainly by changes in chromatin and the nuclear membrane. Chromatin clumps along the nuclear membrane so that the distinction between light-staining euchromatin (i.e., the regions with more active gene transcription) and dark-staining heterochromatin are lost. This is considered a consequence of decreasing nuclear pH that occurs during the process of necrosis. The nuclear membrane pores break down, severing normal connections between the nucleus and the ER cytocavitary network. After the nuclear membrane ruptures, the nucleus typically shrinks and condenses, a morphologic hallmark of necrosis termed pyknosis, while the swollen cytosol and enlarged perinuclear space impinge on the nucleus (Figure 5.20). Eventually the nuclear membrane breaks down completely, leading to rarefaction of the remaining nucleoplasm and dispersion of the aggregated bits of degraded chromatin while attached to plasma membrane fragments; this change is another morphologic hallmark of necrosis, termed karyorrhexis (Figure 5.20). Eventually all the chromatin, nucleoplasm, and nuclear membrane are completely degraded, a change that is termed karyolysis (Figure 5.20).

Once an irreversibly injured cell is no longer physiologically active, lysosomes swell, their membranes leak, and their enzymes are released into the cytosol, triggering a process termed autolysis. Because lysosomal enzymes require sequestration to prevent their leakage into a viable cell's cytoplasm, lysosomal membranes are relatively resilient to noxious stimuli, so that their constituent enzymes are typically released into the cytosol quite late in the process of necrosis. However, there are a few examples of primary lysosomal damage leading to cell injury. For example, hepatotoxicity occurs when excessive amounts of copper accumulate in hepatocyte lysosomes, predisposing them to increased lysosomal membrane permeability.

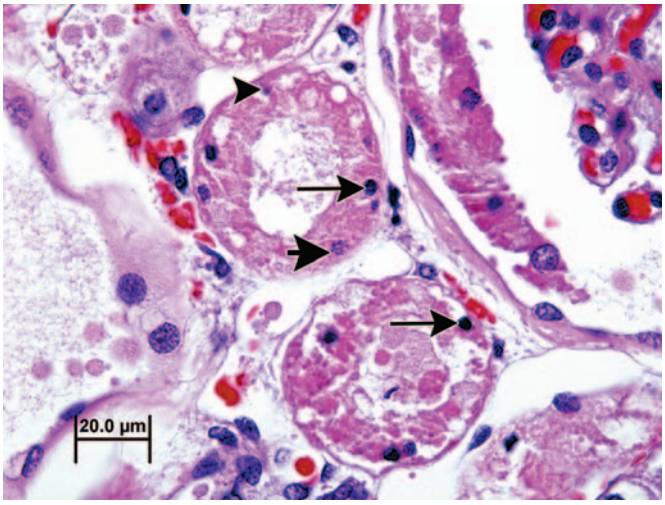

FIGURE 5.20 Nuclear changes associated with necrosis. Photomicrograph of renal tubules from a dog with raisin toxicosis. Pyknosis [nuclear consolidation (*long thin arrows*)], karyorhexis [nuclear fragmentation (*short thick arrow*)], and karyolysis (*arrowhead*) are present in necrotic tubular epithelial cells. Hematoxylin and eosin. Source: *From Haschek, W.M., Rousseaux, C.G., Wallig, M.A. (Eds.), 2013. Handbook of Toxicologic Pathology, third ed. Academic Press, San Diego, CA, Fig. 4.20, p. 94, with permission.*

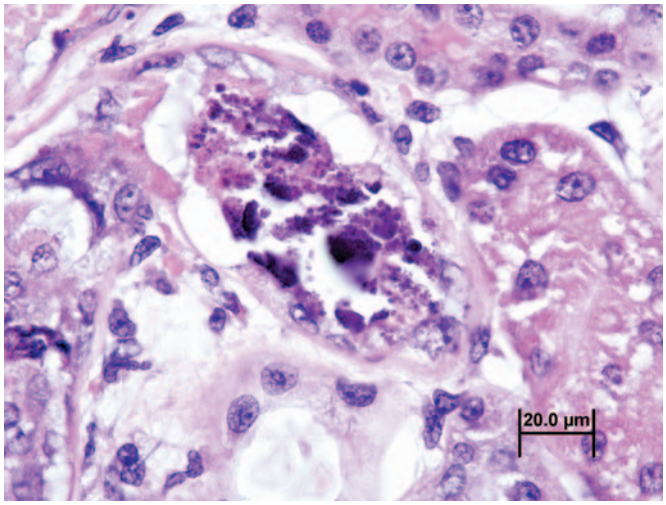

FIGURE 5.21 Post-necrotic mineralization. Photomicrograph a necrotic renal tubule from a cat with lily (*Lilium longiflorum*) toxicosis. Mineralized necrotic tubular epithelium presents as angular deposits of blue-violet granules (center of the image). Hematoxylin and eosin. Source: *From Haschek, W.M., Rousseaux, C.G., Wallig, M.A. (Eds.), 2013. Handbook of Toxicologic Pathology, third ed. Academic Press, San Diego, CA, Fig. 4.21, p. 94, with permission.*

Release of enzymes and highly oxidative cupric cations into the cytosol then leads to uncontrolled degradation of cell constituents.

When degradation of cell components by lysosomal enzymes nears completion, the cell is clearly recognizable by light microscopy as necrotic (Table 5.1). The morphology of necrosis is quite stereotypical, although features do vary depending on biochemical, functional, or structural traits specific to the particular cell, tissue, or organ. Most necrotic cells are characterized by diffusely hypereosinophilic cytoplasm as a consequence of coagulated proteins. The cytoplasm may become "glassy" in appearance, that is, hyalinized, as reactive peptides released from degrading proteins bind to eosin. Eosinophilia is also enhanced by the loss of normally hematoxylin-staining, that is, basophilic, nucleic acids, such as ribosomal RNA. Cytoplasmic granules, representing mitochondria laden with Ca^{+2} deposits, may also be observed by light microscopy. As the degradation of a necrotic cell progresses, its cytoplasm becomes "moth-eaten" and fragmented. In tissues with a large influx of Ca^{+2}, a necrotic cell's cytoplasm may calcify, or mineralize, yielding a strong basophilic, stippled, fragmented, or even crystalline appearance (Figure 5.21). The morphologic progression of necrosis as manifested in the injured cell cytoplasm and nucleus does not necessarily occur in a predictable sequence, so several permutations are possible. Viable tissue adjacent to necrotic cells typically reacts to the injury with an inflammatory response.

The macroscopic, that is, gross, characteristics of necrotic tissue are almost as diverse as the number of specialized tissues. The nature of the lethal injury and the reaction of surrounding viable tissues to the lethal injury can complicate the gross pathology further. Necrotic tissue is often pale, friable, and shrunken, especially if its blood supply was lost antemortem. If blood supply was maintained, necrotic tissue may become swollen, soft, and dark as a consequence of dilated vasculature and exuded blood-derived fluid. A clear indication of antemortem necrosis is a discrete area of pallor demarcated by a dark-red rim, which represents hemorrhage and congestion often with some degree of inflammation in response to the core of necrotic tissue.

Necrotic tissue can be classified based on gross and histologic characteristics. Coagulation, or coagulative, necrosis refers to necrotic tissue that has retained its basic structural features. The necrotic tissue remains discernable by light microscopy; necrotic cells are distinct and lightly eosinophilic but lack detail so that they appear ghost- or shadow-like. "Coagulation" necrosis is generally acute and, therefore, is seen with many toxicities. Cells with few lysosomes may be prone to coagulation necrosis because they lack a primary source for enzymes that accelerate the degradative process. The inflammatory response in viable tissue surrounding areas of coagulation necrosis may be somewhat diminished with toxicant-induced injury

since the DAMPs required to trigger a more substantial inflammatory response have yet to be released in abundant quantities. Pro-inflammatory proteins, such as active complement fragments, and antigen-antibody binding, are also typically not a prominent feature of toxicant-induced injury.

Liquefactive necrosis occurs when neutrophils and activated macrophages infiltrate necrotic tissue, adding their extensive lytic enzyme pools to the process of tissue degradation. This is common with several bacterial infections and related to pathogen-associated molecular patterns (PAMPs), molecular motifs—usually of microbial origin—that activate Toll-like receptors on neutrophils and macrophages as well as complement pathways. Activated neutrophils characteristically release their lysosomal enzymes into the extracellular milieu, accelerating tissue digestion and producing a lesion that is typically soft and semiliquefied. Some lipid-rich tissues, particularly the central nervous system, undergo liquefactive necrosis since denatured lipids become greasy or oily. The end result of liquefaction is removal of tissue, leaving a space.

Caseous necrosis is the term used when necrotic tissue has the consistency of dry cheese (i.e., consists of crumbling, amorphous debris). It is most common with infections that release PAMPs. Necrotic tissue is typically pale yellow or light green, sometimes with a white tint, quite soft or pasty, and friable but generally does not spontaneously fall apart.

Apoptosis

Cell death by apoptosis contrasts with cell death by necrosis in a variety of important morphologic and molecular ways, and is a common mechanism of toxicant-induced injury. At a basic morphologic level, apoptosis is characterized by cell condensation and fragmentation, while necrosis is characterized by cell swelling. Apoptosis is a morphologically ordered and mechanistically regulated process. Synonyms for apoptosis include apoptotic necrosis, single cell necrosis, programmed cell death, cell suicide, and necrobiosis. Apoptosis is quite common but tends to be morphologically less conspicuous than necrosis for two reasons: apoptosis is a rapid process, and apoptotic cells are quickly ingested by adjacent parenchymal cells or macrophages; and apoptosis typically affects only a small fraction of a cell population at any one time. Apoptosis has several causes and triggering mechanisms, which progress along generally common biochemical pathways. While generally stereotypical in its morphological evolution, apoptosis is manifested somewhat uniquely in some specialized cells or tissues.

The ultrastructural morphology of apoptosis is quite distinctive and clearly contrasts with necrosis (Table 5.1). Initially a cell undergoing apoptosis detaches from adjacent cells or stroma, and rapidly condenses into spherical body, losing any specialized surface structures. Secretory cells disgorge their storage granules as they condense. Initial dilation of the ER may be observed as Na^+ ions and water are pumped into the cisternae prior to condensation of the cytoplasm. As the cytosol condenses, organelles are drawn closer together. Portions of the cell pinch off into spherical, membrane-bound fragments or apoptotic bodies, a process of bleb formation termed zeiosis (Figure 5.22). The integrity of the plasma membrane is generally preserved, even after fragmentation, so organelles such as mitochondria may be visible within detached apoptotic bodies (Figure 5.22). Ribosomes may even remain attached to the rough ER.

Nuclear changes of apoptosis occur before, during or after cytoplasmic changes and zeiosis. While the nuclear envelope is usually preserved, the nucleolus segregates from the chromatin, which uniformly condenses into crescent-shaped or smooth-edged clusters

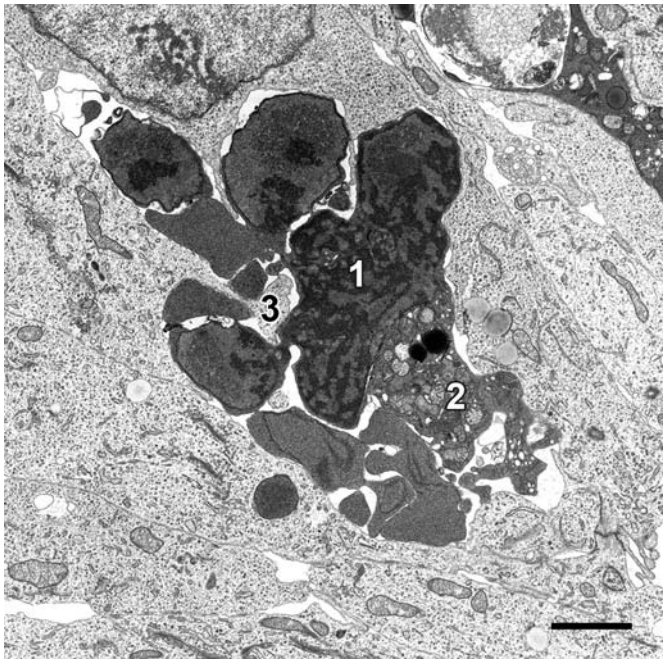

FIGURE 5.22 Apoptosis. Electron photomicrograph of xenobiotic-induced apoptosis in the forebrain of a rat embryo. Note the shrunken and fragmented cell with condensed chromatin (*1*), and several mitochondria concentrated in the reduced volume of condensed (more electron-dense) cytoplasm (*2*). Note also the partial phagocytosis of this apoptotic cell by cytoplasmic extensions of an adjacent normal cell (*3*). Bar = 2 μm. Source*: From Haschek, W.M., Rousseaux, C.G., Wallig, M.A. (Eds.), 2013. Handbook of Toxicologic Pathology, third ed. Academic Press, San Diego, CA, Fig. 4.16, p. 96, with permission.*

along the nuclear envelope. The nucleus may also undergo zeiosis, forming small, round to oval bodies of densely packed chromatin enveloped by an intact nuclear membrane. After phagocytosis by adjacent cells, apoptotic cells or bodies swell and degrade within phagolysosomes, where their remnants are indistinguishable from those of a necrotic cell.

By light microscopy, the morphology of an apoptotic cell is quite distinctive. A key feature is that an apoptotic cell almost always appears isolated, small, spherical, and densely stained. In H&E-stained sections, an apoptotic cell is often demarcated by a thick, clear pericellular halo. Its nuclear remnants are darkly stained by hematoxylin and its cytoplasm by eosin. Apoptotic bodies have clearly defined cell boundaries, reflective of their intact plasma membranes. The surrounding halo may actually be a phagocytic vacuole (Figure 5.23). A particularly characteristic nuclear feature of apoptosis occurs when chromatin condenses as a crescent- or cap-shaped mass along one edge of the nuclear envelope.

Because the apoptosis is morphologically a rapid process and apoptotic cells are efficiently removed, apoptotic cells are rarely numerous. Even in tissues with toxicologically significant apoptosis, usually only 1%–2% at most of the total cell population are recognizable as apoptotic in any tissue section.

Apoptosis can be triggered by a wide variety of physiologic or toxicologic mechanisms. Injured cells that retain enough function to forestall overt necrosis can be stimulated to undergo apoptosis. The mechanism underlying this form of apoptosis is mediated by caspase 9, reflecting a progressive loss of mitochondrial function, and is referred to as the intrinsic pathway of apoptosis. Examples of this process include oxidative stress with decreased sulfide–disulfide ratios, disrupted ion gradients, or structural damage to proteins on the inner mitochondrial membrane. MPT pores, that is, contact points between the inner and outer mitochondrial membranes, are not a prominent feature of mitochondrial-mediated apoptosis. MPT pores seem to form through dimerization of pro-apoptotic proteins, such as Bax and Bak, from the cytosol and/or outer mitochondrial membrane. These proteins are normally in an inactive, monomeric state docked to the anti-apoptotic protein, Bcl-2, in the outer mitochondrial membrane. As with necrosis, mitochondrial cytochrome *c* passes through the pores and binds to Apaf-1, a protein that also is "docked" to anti-apoptotic proteins such as Bcl-2. The Apaf-1/cytochrome *c* complex forms a hexamer that binds to pre-caspase 9, also located on the outer mitochondrial membrane, to form the apoptosome leading to activation of caspase 9. This enzyme in turn activates cytosolic caspase 3, the effector protein that serves as the final common "master molecule" for induction of apoptosis.

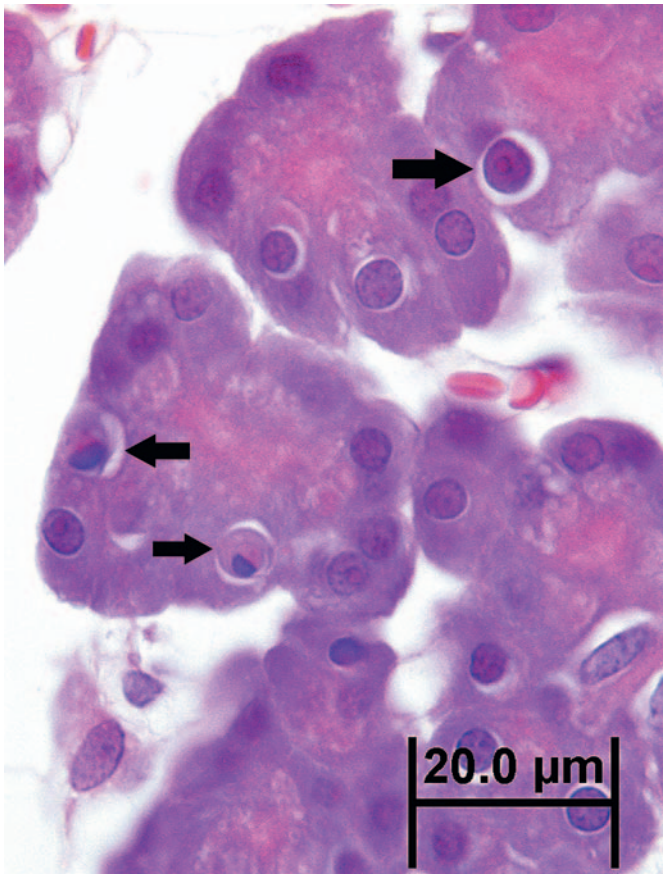

FIGURE 5.23 Apoptosis. Photomicrograph of pancreas from a Fischer 344 (F344) rat 12 hours after treatment with the pancreatic toxicant crambene. *Arrows* point to apoptotic exocrine acinar cells, each with its characteristic clear pericellular halo and round shape (indicative of cell contraction) as well as shrunken, condensed nucleus. Hematoxylin and eosin. Source: *From Haschek, W.M., Rousseaux, C.G., Wallig, M.A. (Eds.), 2013. Handbook of Toxicologic Pathology, third ed. Academic Press, San Diego, CA, Fig. 4.23, p. 97, with permission.*

Another mechanism of apoptosis depends on activation of Fas ligand (FasL), a homodimer which trimerizes with Fas receptor (FasR) to form a "death-inducing signaling complex" (DISC) that spans the cell membrane. This mechanism is termed the extrinsic pathway of apoptosis. Intracellular attachments to DISC include proteins such as Fas-associated protein with death domain (FADD) or tumor necrosis factor (TNF) receptor type 1-associated death domain protein (TRADD). These are bound to pre-caspase 8. When trimerization of the FasL/FasR complex occurs, pre-caspase 8 is cleaved, releasing active caspase 8 into the cytosol where it also activates caspase 3. Caspase 8 also activates the cytosolic protein Bid to tBid, which then binds to Bcl-2, causing it to release bound Bax

and/or Bak, which dimerize and form MPT pores. Therefore, although the FasL mechanism of apoptosis is initiated outside mitochondria, mitochondria are critical in completing the process.

Although not completely understood, another apoptotic mechanism of toxicologic relevance is initiated by activation of caspase 12, when the severity of ER stress exceeds the injured cell's adaptive capacity, for example, through NFκB activation. ER stress is manifested by accumulation of misfolded or unfolded proteins within cisternae with subsequent induction of "sensor" proteins, release of Ca^{+2}, and activation of pre-caspase 12 on the cytosolic side of the ER. Caspase 12 then activates caspase 3, leading to apoptosis.

Activated caspase 3 initiates a variety of downstream events that mediate the morphological changes of apoptosis. These include promoting degradation of the cytoskeleton via cleavage of β-catenin, fodrin, actin, lamin, and gel-solin, and inactivating several cell cycle pathways such as protein kinase b/Akt. Caspase 3 also activates pro-apoptotic proteins such as scramblase, which promotes eversion of phosphatidylserine (PS) from the inner plasma membrane leaflet to the outer leaflet.

Caspase 3 regulates the fate of the genome during apoptosis via caspase-activated DNase, an endonuclease that cleaves DNA into 180 base pair units. It also inactivates certain key enzymes involved in DNA repair, for example, Poly[ADP-ribose] polymerase 1 (PARP-1), DNA phosphokinase C, and topoisomerases I and II. Indirectly, histones are released from the nucleosome, further exposing DNA to degradation. In this way, caspase 3 is also linked to p53-initiated apoptosis when toxicant-induced injury to the genome overwhelms DNA repair mechanisms.

As additional molecular mechanisms involved in cell death are discovered, classification schemes and nomenclature are updated. For example, the Nomenclature Committee on Cell Death recommends using biochemical and/or signaling pathways rather than morphologic criteria to this end (see Chapter 2: Biochemical and Molecular Basis of Toxicity). Morphologic criteria may no longer be precise enough because only "autophagic" cell death, apoptosis, and necrosis can be recognized regardless of which of many mechanisms of cell death may be responsible. However, since several biochemical mechanisms of cell death only occur in certain cell types or only have been described *in vitro*, whether new classifications are fully accepted by the community of pathologists ultimately will depend on their translational relevance to toxicant-induced cell injury *in vivo*. For now, morphologic criteria, as well characterized by conventional light and electron microscopy, remain the mainstay for toxicologic pathologists (see Elmore et al., 2016).

Toxicant-induced injury to a tissue rarely leads exclusively to apoptosis or necrosis. Instead, these two manifestations of irreversible cell injury commonly occur simultaneously. Less severely injured cells, such as those that maintain the functional elements necessary to complete the apoptotic process because they are exposed to a lower dose of the toxicant or are closer to an intact blood supply near the edge of a lesion, tend to undergo apoptosis. Examples of required functional elements that might allow this to happen include sufficient ATP, glutathione, and Ca^{+2} regulation necessary for caspase activity. In contrast, more severely injured cells or those less capable of maintaining these functional elements tend to lose osmoregulation and proceed to non-caspase-mediated cell death, that is, necrosis. Therefore, toxicant-induced lesions manifested by irreversible cell injury can present with apoptotic cells near the outer limits of a larger focus of overt necrosis, particularly in the liver.

Consequences of Irreversible Cell Injury

Necrosis

In most instances, necrosis elicits an inflammatory response, the extent and nature of which depend on variety of factors, the most obvious being the time elapsed between the initial injury and the actual pathologic evaluation. For example, inflammation will not be observed in the heart when sudden death results from acute myocardial infarction. Alternatively, when death occurs several days after the infarct, an inflammatory response is often quite elaborate.

Neutrophils are generally the first inflammatory cell type to infiltrate an area of necrosis. Macrophages, from differentiated blood-derived monocytes and resident precursors, typically predominate within a few days (Figure 5.24). Neutrophils play a critical role in the progressive morphogenesis of a necrotic lesion since their release of lysosomal enzymes into the ECM during phagocytosis of necrotic cell remnants often results in indiscriminate degradation of stroma and lysis of viable "innocent bystander" cells, including neutrophils themselves. This process can exacerbate the severity of the initial parenchymal tissue injury. Neutrophils also produce soluble mediators of inflammation, for example, cytokines that attract more neutrophils, and eventually macrophages, to the site of injury.

In many organs, extensive tissue damage that cannot be repaired by parenchymal regeneration stimulates fibrosis, for example, scar formation, a process characterized by replacement of lost tissue with nonfunctional stroma. In contrast to normal supporting stroma, which comprises Type IV collagen, elastin, and

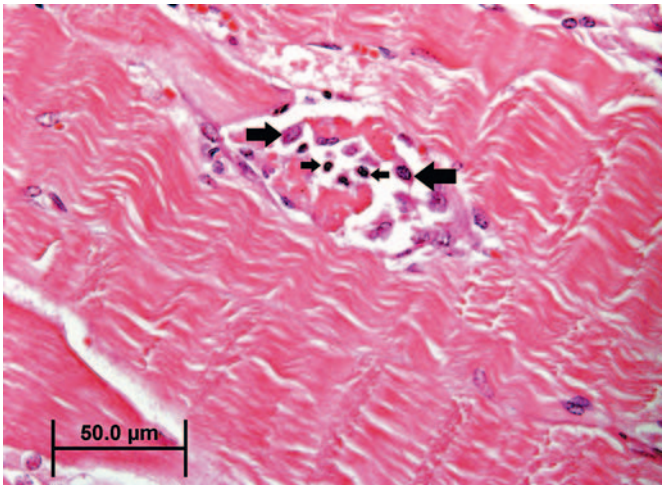

FIGURE 5.24 Postnecrotic inflammation. Photomicrograph of gluteal muscle of a horse with extensive myonecrosis. Neutrophils (*small arrows*) and macrophages (*large arrows*) are infiltrating and phagocytosing the remnants of a necrotic myocyte. Hematoxylin and eosin. Source*: From Haschek, W.M., Rousseaux, C.G., Wallig, M.A. (Eds.), 2013. Handbook of Toxicologic Pathology, third ed. Academic Press, San Diego, CA, Fig. 4.24, p. 99, with permission.*

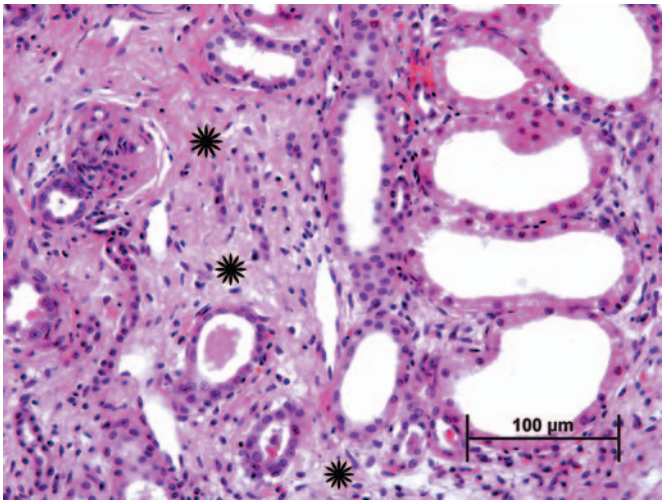

FIGURE 5.25 Postnecrotic fibrosis. Renal cortex from a dog following a bout of severe, widespread renal necrosis due to ethylene glycol intoxication. Tubules lined by flattened, incompletely differentiated epithelium are entrapped within extensive dense collagen matrix [interstitial scar tissue (*starburst*)]. Hematoxylin and eosin. Source*: From Haschek, W.M., Rousseaux, C.G., Wallig, M.A. (Eds.), 2013. Handbook of Toxicologic Pathology, third ed. Academic Press, San Diego, CA, Fig. 4.25, p. 100, with permission.*

laminin, fibrotic tissue is predominantly of Type I collagen, which is generally resistant to restoration of functional parenchyma (Figure 5.25). Extensive fibrosis leads to permanent loss of function in the affected tissue. In some organs, such as the liver or kidney, a substantial reserve capacity provides a buffer between multifocal fibrosis and organ failure, but progressive or recurring injury eventually erodes this capacity.

The specialized function and structure of some organs dictates the nature of an inflammatory response to a toxic injury. For example, necrotic pancreatic acinar cells release proteases, which stimulate a dramatic influx of neutrophils. A vicious cycle can ensue, with neutrophils inciting further acinar cell necrosis so that a localized lesion can rapidly progress to an extensive one. The inflammatory response also depends on the extent of the initial tissue damage and the degree of tissue vascularization. For example, a large renal infarct typically elicits a more intense inflammatory response than a lesion localized to only part of one nephron. Injury to well vascularized tissue, such as the pulmonary parenchyma, often elicits a stronger inflammatory cell infiltrate than does damage to a poorly vascularized tissue, such as articular cartilage. However, a better blood supply can also lead to faster and more complete tissue repair.

When supporting stroma is retained following tissue injury, the inflammatory response tends to be muted. For example, inflammation subsequent to gastric erosion (i.e., loss of part or all of the mucosa) is generally less intense than is the response to a gastric ulcer (i.e, a full thickness penetration of the wall), and the latter is more likely to result in a scar.

Secondary or opportunistic infections can complicate the inflammatory response to a toxicant-induced lesion. Bacteria are an additional source of toxins and PAMPs that cause further cell injury, inhibit regeneration, and attract more inflammatory cells, especially neutrophils. Those tissues with a so-called barrier function, such as the skin and gastrointestinal tract, are at particular risk for opportunistic bacterial infections following a toxic insult. Hematogenous dissemination of bacteria from the damaged intestinal mucosa can lead to secondary hepatitis or even septicemia.

Complete structural restoration of injured tissue is predicated on viable supporting architectural stroma. For example, following a toxic injury, the basement membrane of an epithelial tissue must remain intact or, if damaged, be adequately resynthesized before the epithelium can effectively regenerate. Typically this type of tissue restoration proceeds from the lateral or deep margins of a resolving necrotic lesion, where vascular ingrowth is initiated. Incomplete restoration of parenchymal tissue, also termed repair, may be evident microscopically as fibrosis for an extended period of time even if the overall organ function is maintained.

The process leading to repair mirrors that of regeneration. The initial neutrophil-predominant response is followed by a macrophage-predominant one. Macrophages, derived from circulating monocytes and

resident macrophage precursors, scavenge cell debris, including effete neutrophils, and secrete mediators of cell differentiation and migration. These cytokines and chemokines include a variety of growth factors that drive the repair process. Tissue repair in mice depleted of resident macrophages or lacking certain macrophage functions is defective.

The number of macrophage-derived chemokines is enormous. Of particular importance in tissue repair are platelet-derived growth factor (PDGF), epithelial growth factor (EGF), fibroblast growth factors (FGFs), and transforming growth factor-beta (TGF-β). Epithelial cells, fibroblasts, and endothelial cells are also sources of chemokines. Chemokine-mediated activation of fibroblasts at the site of tissue injury temporally coincides with the influx of macrophages, typically within a few days after the initial injury. These fibroblasts produce a matrix rich in fibronectin, hyaluronan, glycosaminoglycans, and Type III collagen, a matrix that serves as a scaffold for fibroblasts and capillary-forming endothelial cells. The matrix is also well hydrated, and therefore conducive to diffusion of oxygen and amino acids. Many fibroblasts express smooth muscle actin and acquire a contractile function. These myofibroblasts promote contraction of tissue undergoing repair, which accelerates lesion resolution but sometimes results in tissue distortion.

Vascular endothelial growth factor (VEGF) is another important chemokine involved in tissue repair. VEGF is secreted by a variety of cell types under hypoxic conditions and stimulates budding of endothelial cells from intact adjacent capillaries into the area of tissue injury. The purpose of this response is obvious: to reestablish the blood supply required for supplying essential nutrients to regenerating parenchymal cells and proliferating fibroblasts. Provided tissue injury has ceased, endothelial buds form tubular structures that merge with the intact capillary network and interweave with newly deposited collagen fibers. By light microscopy, interwoven neocapillaries and immature collagen fibers present a "basket-weave" pattern, termed granulation tissue (Figure 5.26). Neocapillaries are porous, allowing protein-rich plasma to leak into the well-hydrated ECM. Hence, in life, young granulation tissue is typically pink, somewhat gelatinous, quite friable, and bleeds easily. Granulation tissue is more suited for scar formation than parenchymal cell regeneration, but over time may be partially remodeled so that partial resolution is possible. With type I collagen maturation, cross-linking condensation and reduced vascularization allow tissue contraction to proceed beyond that mediated by myofibroblast function. At this time, the lesion can be recognized grossly as a firm, tough, white scar. This scar tissue serves as a near-permanent barrier to regeneration (i.e., complete parenchymal restoration). For a comprehensive insight regarding how tissue repair versus regeneration occurs in a damaged tissue, refer to Chapter 15: Digestive System.

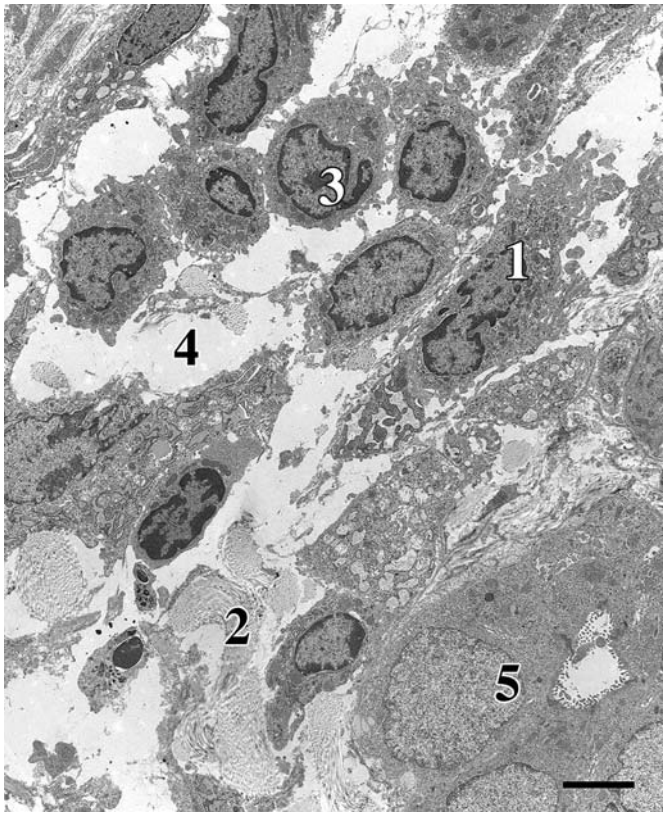

FIGURE 5.26 Postnecrotic fibrosis. Electron photomicrograph of a portal triad from a rat with xenobiotic-induced periportal hepatic damage leading to fibrosis. Note the increase in fibroblasts (*1*), increased deposition of collagen fibers (*2*), and influx of macrophages (*3*) within the interstitial space, which is expanded by edema fluid [clear spaces (*4*)]. Epithelial cells lining a bile duct (*5*) are enlarged, indicating a hypertrophic response due to increased cell mass. Bar = 5 μm. Source: *From Haschek, W.M., Rousseaux, C.G., Wallig, M.A. (Eds.), 2013. Handbook of Toxicologic Pathology, third ed. Academic Press, San Diego, CA, Fig. 4.26, p. 101, with permission.*

Apoptosis

In contrast to necrosis, which usually provokes a robust inflammatory response, the tissue response to apoptosis is quite benign. One explanation for this difference is that apoptotic cells do not release quantities of DAMPs sufficient enough to attract inflammatory cells, in particular neutrophils and blood-derived monocytes. Instead, the membranes of the apoptotic bodies are targeted for rapid phagocytosis by adjacent parenchymal cells and resident tissue macrophages (Figures 5.27 and 5.28). The molecular basis for this targeting is complex and appears to depend on a number of factors. Phosphatidylserine (PS) is normally confined to the inner leaflet of the plasma membrane by a

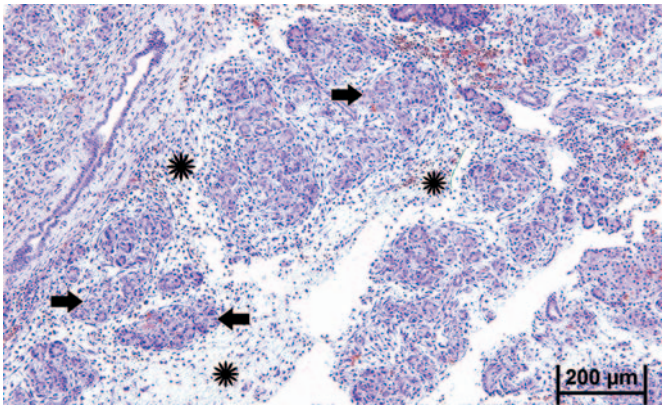

FIGURE 5.27 Postapoptotic atrophy. Photomicrograph of atrophied acinar pancreas in a Fischer 344 (F344) rat 4 days after extensive apoptosis due to administration of the pancreatic toxicant crambene. Small acini (*arrows*) containing shrunken, non-functional acinar cells are scattered throughout the section. Numerous histiocytic macrophages (*starbursts*) occupy the loose preexisting lobular stroma between acini. Hematoxylin and eosin. Source: *From Haschek, W.M., Rousseaux, C.G., Wallig, M.A. (Eds.), 2013. Handbook of Toxicologic Pathology, third ed. Academic Press, San Diego, CA, Fig. 4.27, p. 102, with permission.*

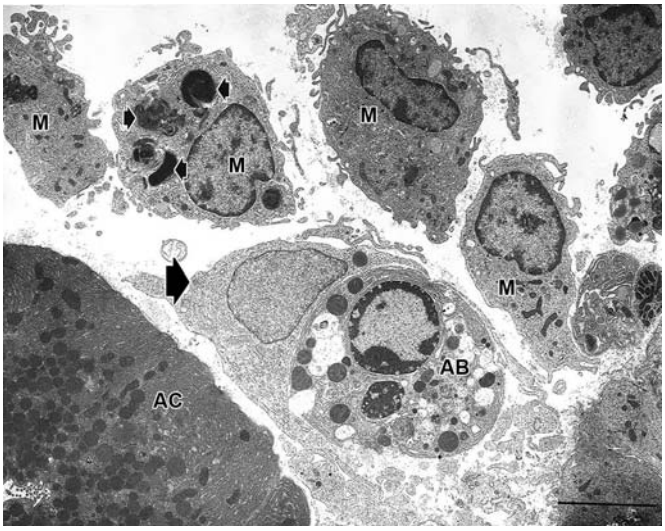

FIGURE 5.28 Sequela to apoptosis. Electron photomicrograph of a macrophage (*large arrow*) ingesting an apoptotic body (*AB*) within the pancreas of a Fischer 344 (F344) rat in which extensive apoptosis has occurred. Tissue macrophages (*M*) containing ingested apoptotic bodies (*small arrows*) appearing as inclusions are present as well. Intact pancreatic acinar cells (*AC*) are also present. Bar = 15 µm. Source: *From Haschek, W.M., Rousseaux, C.G., Wallig, M.A. (Eds.), 2002. Handbook of Toxicologic Pathology, second ed. Academic Press, San Diego, CA, Fig. 22, p. 63.*

β-catenin bridge to the actin cytoskeleton. During zeiosis, PS everts to the outer leaflet of the plasma membrane. Macrophages loosely bind to externalized PS, along with "immature" glycans, facilitating phagocytosis of apoptotic bodies. Other external macromolecules apparently recognized by macrophages include lysophosphatidyl choline, calreticulin, and annexin. Macrophage receptors, such as LOX-1 and CD61, appear to be necessary for binding to apoptotic cells. Phagocytosis of an apoptotic body after engulfment by a macrophage has been described as a "big gulp" to contrast with the "zipper" type of engulfment that typically precedes phagocytosis of bacteria; the latter is characterized by tight binding of the macrophage membrane to specific ligands on the bacterial membrane. The "big gulp" mode of phagocytosis is thought to involve three signaling pathways: Rac-1, CD91/LRP→hCED/GULP→ABCA, and ELMO.

The precise mechanisms involved in digestion of the apoptotic body are uncertain, but the overall process depends on gradual acidification and protease degradation of the phagosome. Interleukin (IL)-10 synthesis and release by macrophages with engulfed apoptotic bodies partially explain the dampened inflammatory response to apoptosis. IL-10 inhibits synthesis of pro-inflammatory cytokines such as interferon-gamma (IFN-γ), IL-2, IL-3, TNF-α, and granulocyte/macrophage colony stimulating factor (GM-CSF). The net effect of is to block antigen presentation by those macrophages with engulfed apoptotic bodies. Furthermore, while apoptotic bodies remain in their phagosomes, macrophages have markedly reduced phagocytic capability. In total, phagocyte-derived release of intracellular inflammatory chemokines, those that enhance endothelial permeability and activate or attract neutrophils, is minimal.

Widespread apoptosis within a tissue leads to atrophy (Figure 5.5). Once the cause of apoptosis is addressed, for example, by removing a noxious insult or adding a trophic hormone, full regeneration is usually achievable provided a residual precursor cell population survives. Regeneration potential is particularly high in tissues with constant cell turnover such as lymph nodes, intestinal epithelium, and liver. However, in those tissues with so-called permanent cell populations, such as the retina, significant apoptosis will result in a permanent lesion, retinal atrophy, with some loss of function.

Hyperplasia

As part of the regenerative process subsequent to widespread cell loss, cell proliferation is necessary and often recognizable temporarily as compensatory hyperplasia. However, compensatory hyperplasia can predispose to an ominous molecular event, namely the permanent establishment, that is, fixation, of genetic mutations that can lead to cancer. Hyperplasia in this context is discussed in Chapter 6, Carcinogenesis:

Manifestation and Mechanisms. Tissues vary widely in their capacity for compensatory hyperplasia with those composed of so-called labile cell populations most capable followed by those with stable cell populations. Tissues with labile cell populations include lymph nodes and bone marrow; tissues with stable cell populations include lung, liver, and kidney. Retaining precursor cells with the capacity to reenter the active cell cycle as well as adequate stromal and vascular support are prerequisites. Initiation and maintenance of a hyperplastic response among surviving parenchymal cells is mediated at the molecular level by a myriad of protein and small molecule ligands interacting with an array of receptors and downstream signal transduction pathways. Some of these are tissue-specific, such as hepatocyte growth factor (HGF), and others are nonselective, such as epidermal growth factor (EGF) and TGF-β. Compensatory hyperplasia can result in peculiar lesions such as hyperplastic nodules with cirrhosis or hyperplastic polyps with chronic colitis. While such proliferative lesions are benign, they can harbor genetic mutations, such as those that may arise from exposure to mutagenic toxicants, and predispose to carcinomas.

Metaplasia

A less common response to tissue injury than hyperplasia, but quite important from a disease perspective, is metaplasia. Metaplasia is generally defined as the replacement of mature fully specialized cells with mature but less specialized cells. It occurs in certain tissues when conditions for complete regeneration are suboptimal, particularly in the context of persistent but relatively limited injury. Classic examples are squamous metaplasia of ciliated bronchial epithelium in response to chronic injury by tobacco smoke and intestinal metaplasia of the esophageal mucosa in response to chronic injury by gastric acid reflux. In both examples, metaplastic cells are more resistant to the inciting injury than are the elements in the normal specialized cell population. Paradoxically, in the bronchus, columnar epithelium is commonly replaced by squamous epithelium, while in the esophagus, squamous epithelium is replaced by goblet cell-rich columnar epithelium. Metaplastic tissue is a stop-gap measure for regeneration, having less functional efficiency than normal tissue. Metaplastic tissue arises in the context of hyperplasia since the new cell type must arise from a precursor cell type and then proliferate. Therefore, metaplastic tissue is also predisposed to neoplastic transformation. In fact, metaplastic tissue is generally more likely to undergo neoplastic transformation than is hyperplastic tissue. This is not surprising since the process of metaplasia requires activation of genes normally suppressed and suppression of genes that are normally active; for example, proto-oncogenes could be newly activated, and tumor suppressor genes newly suppressed. Finally, metaplastic cells may metabolize xenobiotics through substantially different enzymatic pathways than do normal specialized cells. The nature of such metabolites, for example, whether they form protein or DNA adducts, can impact the eventual pathologic outcome of a metaplastic lesion. Metaplasia is further discussed in Chapter 6, Carcinogenesis: Manifestation and Mechanisms.

Clinical Pathology

When a sufficient number of cells in an organ or tissue, such as liver or muscle, are necrotic, specific biomarkers reflecting such damage may be measurable in the plasma or other biofluids. Cytoplasmic blebs released from injured or dying cells can break away and rupture, releasing a variety of cell constituents, such as enzymes, structural proteins, or ribosomal RNA, directly into the blood or interstitial fluid. The identity and quantity of these released constituents often allows a clinical pathologist to determine which organ or tissue is affected, and how severely, while the individual is still alive. In general, during the progression of necrosis, unbound cytosolic enzymes are released earliest, followed by mitochondrial membrane-bound enzymes and finally by lysosomal enzymes. Analysis of isoenzymes may provide exquisite specificity for determining the site of injury. While clinical pathology analyses can provide the sensitivity and even specificity to detect necrosis in certain tissues, the nature of the apoptotic process precludes any widespread usefulness of clinical biomarkers in detecting this process during life. This is understandable considering that apoptotic bodies are rapidly dispatched by adjacent cells, thus minimizing the opportunity for apoptotic cell constituents to reach the interstitial fluid let alone the systemic circulation.

Clinical pathology evaluations can also reflect functional consequences of irreversible cell injury. A classic example is bilateral adrenal cortical necrosis, which may be caused by a variety of toxic and nontoxic injuries. Without the damaged zona glomerulosa, mineralocorticoids are not synthesized, leading to life-threatening hyperkalemia and hyponatremia.

SUMMARY

The morphologic features of an injured cell are complex but generally stereotypical in form and often independent of the etiology. Occasionally, they are distinctive enough to provide an indication of the pathogenesis, particularly when the time course of

subcellular changes is known. The terminology used to classify, and subclassify, the stages and manifestations of cell injury is in constant flux as modern molecular techniques are used to correlate morphology, including ultrastructural pathology, with biochemical alterations. This chapter provides a synopsis of concepts in cell injury formulated from observations and experiences (communicated since the early 20th century) that are widely accepted by toxicologic pathologists. No synopsis can be complete because the number of variables, including those that can render injured cells more or less sensitive to noxious stimuli, is impossible to estimate. The succeeding chapters in this book will focus on many of these variables, including those that are dependent on the mechanism of toxicity and on the organ system affected.

Further Readings

Cheville, N.F., 2009. Structural basis of cell injury of acute cell injury. In: Cheville, N. (Ed.), Ultrastructural Pathology: The Comparative Cellular Basis of Disease, second Ed Wiley-Blackwell, Ames, IA, pp. 3–73. Part 1.

Cheville, N.F., 2009. Organellar pathology. Consequences of acute cell injury: necrosis, recovery and hypertrophy. In: Cheville, N. (Ed.), Ultrastructural Pathology: The Comparative Cellular Basis of Disease, second ed. Wiley-Blackwell, Ames, IA, pp. 75–198. Part 2.

Elmore, S.A., Dixon, D., Hailey, J.R., Harada, T., Herbert, R.A., Maronpot, R.R., et al., 2016. Recommendations from the INHAND apoptosis/necrosis working group. Toxicol. Pathol. 44 (2), 173–188.

Miller, M.A., Zachary, J.F., 2016. Cellular adaptation, injury and death: mechanisms and morphology of cellular injury, adaptation and death. In: Zachary, J., McGavin, M.D. (Eds.), Pathologic Basis of Veterinary Disease, sixth ed Elsevier (Mosby), St. Louis, MO, pp. 2–43. Section 1, Chapter 1.

Orrenius, S., Nicotera, P., Zhivotovsky, B., 2011. Cell death: Mechanisms and their implication in toxicology. Toxicol. Sci. 119 (1), 3–19.

Vanlangenakker, N., Vanden Berghe, T., Vandenabeele, P., 2012. Many stimuli pull the necrotic trigger, an overview. Cell Death Differ. 19 (1), 75–86.

Wallig, M.A., Janovitz, E., 2013. Morphologic manifestations of toxic cell injury. In: third ed. Haschek, W., Rousseaux, C., Wallig, M., Ochoa, R., Bolon, B. (Eds.), Handbook of Toxicologic Pathology, vol. I. Elsevier, Waltham, MA, pp. 77–105. Chapter 4.

This page intentionally left blank

CHAPTER

6

Carcinogenesis: Manifestation and Mechanisms

David E. Malarkey[1], *Mark J. Hoenerhoff*[2], *and Robert R. Maronpot*[3]

[1]National Institute of Environmental Health Sciences, Research Triangle Park, NC, United States
[2]University of Michigan, Ann Arbor, MI, United States [3]Maronpot Consulting LLC, Raleigh, NC, United States

OUTLINE

OVERVIEW OF CARCINOGENESIS

Cancer is a major cause of debilitation and death in humans and animals. The development of cancer is influenced by a number of factors, including age, environmental exposures, diet, gender, and genetic makeup. As humans reach their sixth decade, they face an exponentially increased risk for developing cancer. A similar window of increased susceptibility exists in aged rodents either spontaneously or when exposed to single, multiple, or continuous carcinogen(s). Therefore, identification of potential human carcinogens through the use of rodent bioassays has been a major focus of the field of toxicologic pathology.

Our understanding of cancer biology is evolving at a rapid rate. Conceptual views of carcinogenesis are formed by the piece-by-piece discovery of key elements of the complex biological puzzle that this disease entails, including the early evidence of clonal evolution of cancer, the Knudsen two-hit hypothesis, progression from benign to malignant growth, discovery of oncogenes and tumor suppressor genes, the somatic mutation theory, the Fearon-Vogelstein multistep colon cancer mutation model, mutator phenotype, and the cancer stem-cell

Fundamentals of Toxicologic Pathology.
DOI: http://dx.doi.org/10.1016/B978-0-12-809841-7.00006-X

(CSC) theory. With the adventof new technologies in molecular analysis, such as gene expression profiling, genomic sequencing, microRNAs (miRNAs), principal component analysis (PCA), hierarchical cluster analysis (HCA), next generation sequencing, exome sequencing, and pathway analysis, carcinogenesis is proving to be much more complex than being simply a clonal evolution of a cell that sustained two genetic "hits" by a carcinogen or inherited genetic susceptibility. The current multistep model of carcinogenesis involves numerous cancer gene mutations or functional alterations (at least 80 by some reports); about a dozen of which are "drivers" of cancer growth pathways, the results of which are manifested as the well-accepted "hallmarks of carcinogenesis" developed by Hanahan and Weinberg (2011). These hallmarks include: (1) sustained proliferative signaling, (2) evasion of growth suppressors, (3) resistance to cell death, (4) replicative immortality, (5) induction of angiogenesis, (6) acquisition of invasive and metastatic capability, (7) reprogramming of energy metabolism pathways, and (8) evasion of destruction by the immune system.

Environmental Causes of Cancer

Besides hereditary causes, an important factor influencing cancer development is that of chemical exposures, whether environmental, occupational, dietary, medicinal, or lifestyle-driven. Of those human cancers, which arise secondary to nonhereditary factors, it is estimated that 5% are caused by certain viral infections, 5% by radiation exposure, and the remaining 90% by exposures to certain chemicals. Of those induced by chemicals, an estimated 30% are secondary to tobacco use, and the remainder secondary to chemicals associated with diet, lifestyle, and the environment. The importance of chemical products in the etiology of cancer is reflected in the fact that up to 8% of all human cancers are related to occupational chemical exposure. Most chemical carcinogens are highly reactive electrophiles, which have electron-deficient atoms that can react with nucleophilic, electron-rich sites in the cell. Deoxyribonucleic acid (DNA), in particular, is made up of an array of nucleophilic centers at which these DNA-damaging agents can form adducts through one or more covalent bonds, resulting in DNA mutations and resultant cellular transformation and oncogenesis.

Millions of chemicals have been identified and registered with the chemical abstracts services. Of these, more than an estimated 50,000 are used regularly in commerce and industry. Less than 2000, however, have been examined for their carcinogenic potential. According to the International Agency of Research on Cancer (IARC), the United States Environmental Protection Agency (EPA), and the United States National Toxicology Program's Report on Carcinogens (RoC), there are slightly more than 100 known human carcinogens, and virtually all of these also cause cancer in animals. Animal and human cancers are fundamentally similar and frequently share morphological, biological, and molecular features. In fact, approximately 30% of human carcinogens were first identified in animal studies. Two Japanese pathologists, Yamagiwa and Ichikawa, are credited with the original demonstration that a chemical could produce cancer in animals. In 1915 they showed that chronic exposure of the skin (pinnae) of rabbits to coal tars induced squamous cell carcinomas, some of which metastasized. These findings confirmed Percival Pott's strong epidemiological observations in 1775 of increased rates of cutaneous scrotal squamous cell carcinoma in chimney sweeps, and demonstrated through the use of their animal model that chronic exposures were necessary for the induction of some cancers. The rabbit studies are the basis for the approach used today in the study of environmental carcinogenesis.

Chronic inflammation and infectious agents have also been implicated in the development of a number of human and animal cancers. Nobel laureates Drs. Robin Warren and Barry Marshall were credited with determining that infection with *Helicobacter pylori* was a common cause of gastric inflammation and ulcers in man. Some skeptical scientists were not convinced that *H. pylori* was infectious until Dr. Marshall developed gastritis soon after consuming the contents of a Petri dish containing the bacteria, and recovered only after treatment with antibiotics. In subsequent years, it was shown that chronic helicobacter gastritis is associated with the development of gastric lymphomas and carcinomas, and thereby *H. pylori* has been listed as a human carcinogen. Some of the lymphomas induced by *H. pylori* appear to be reversible, and they can regress following antibiotic treatment. Similarly, certain strains of mice (including A/JCr and B6C3F1/N) with chronic hepatitis due to *Helicobacter hepaticus* infection develop significantly higher rates of liver cancer compared to uninfected controls. Such animal models are useful in the study of infectious causes of human cancers, but also need to be considered as potential confounders of the results of cancer occurrence in animal bioassays or human epidemiological studies.

Initiation/Promotion and Progression Models

In early studies on carcinogenesis, it was observed that a long latent period could elapse from exposure to carcinogens to the development of cancer. In 1941

Rous and Kidd induced skin tumors by "painting" the skin of rabbits with carcinogens, and found that if this painting were interrupted, the tumors would disappear, only to reappear if the application of the carcinogen was reestablished. It seemed, therefore, that a reversible process was taking place in those cells that did not attain the complete neoplastic state.

These cells had undergone what Rous called *initiation* (Figure 6.1). Further development of tumors would then require what was termed *promotion*, the process by which the initiated cell expands clonally into a detectable preneoplastic or benign neoplastic cell mass. Finally, cells must undergo additional changes in their *progression* from preneoplasia or benign neoplasm to a malignant neoplasm. This capacity for autonomous growth remains latent for weeks, months, or years, during which time the initiated cell may be phenotypically indistinguishable from other parenchymal cells in that tissue. Today it is known that for a normal cell to evolve into a malignant one,

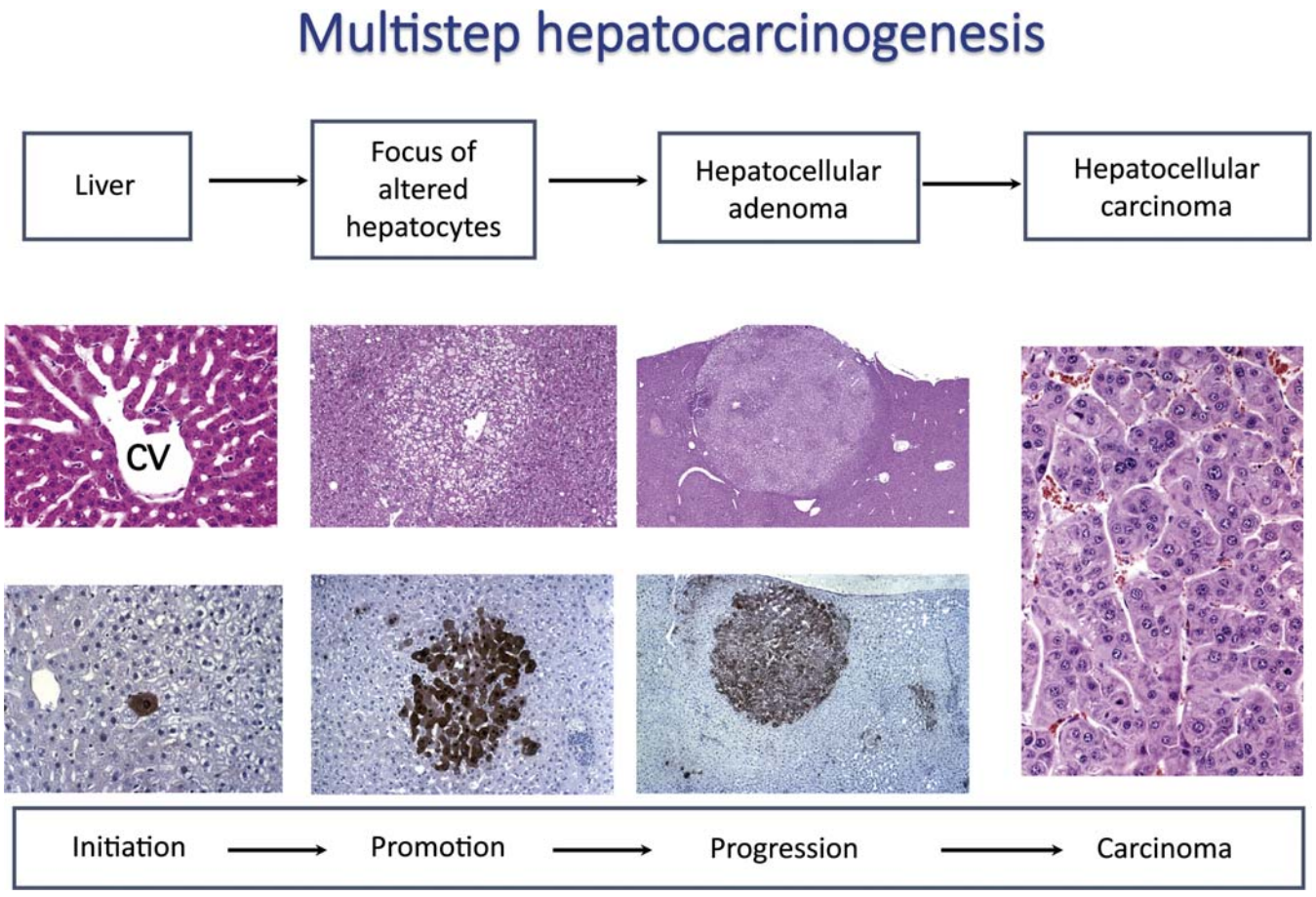

FIGURE 6.1 This figure depicts the overlapping concepts in the development, progression, and multistep evolution of hepatocarcinogenesis in the rat and mouse. The top row represents the diagnostic terminology for the progressive proliferative liver lesions arising from normal liver to the putative preneoplastic lesion called focus of altered hepatocytes (FAH), clear cell type, to hepatocellular adenoma, and then hepatocellular carcinoma (HCC) is depicted on the far right. In the second row are representative H&E histologic sections of each stage from benign to malignant liver cancer. Notice how the FAH is a group of vacuolated cells that merge imperceptibly with surrounding liver, while the adenoma is expansile, well-demarcated, noninvasive, and slightly compresses the surrounding liver. The photomicrograph of HCC demonstrates the pleomorphic (variably shaped) cancer cells forming trabeculae, typical of HCC in man and animals. HCC are generally expansile, invasive into surrounding tissues, and about 25% of rodent HCCs metastasize, usually to lung. The bottom row demonstrates the positive immunohistochemical findings of rat hepatocytes with abundant glutathione-S-transferase Pi (GST-Pi). In the normal-appearing liver scattered individual cells with abundant GST-Pi are found spontaneously or at increased frequency when treated with an initiator in the rat. It is proposed that these individual cells are initiated and prone to promotion and/or progression to neoplasia. Essentially all the cells are positive for GST-Pi in the hepatocellular adenoma, supporting a clonal expansion of initiated hepatocytes in the promotion and progression stages of tumor growth. The HCCs with GST-Pi (not shown) are generally variably positive to negative for GST-Pi supporting the concept of the stem-cell theory—subclones arise within neoplasms and contribute to heterogeneous populations within tumors and progression to malignancy. Note that benign or malignant growth is generally not the fate of every preneoplastic lesion, since they, by far, outnumber the neoplasms (by hundreds to thousands fold in the mouse and rat liver, respectively). Source: *Photomicrographs are from the collection and courtesy of Drs. Robert Maronpot and Dave Malarkey of the US National Toxicology Program, Research Triangle Park, NC.*

genetic changes involving multiple, independent genes are required. This "multihit" model is consistent with the evidence demonstrating that incidence rates of cancer increase exponentially with age. The concepts of initiation and promotion have since been applied to a variety of other tissues and species.

Based on the hypothesis that most initiators are mutagenic or genotoxic, a battery of short-term *in vitro* and *in vivo* mutagenicity tests has been developed to permit the detection of chemicals with potential initiating activity. Identification of initiating agents is especially important due to the irreversible and hereditary nature of alterations that occur during initiation. While useful when positive results are obtained, the predictive ability of short-term mutagenicity tests for the ultimate carcinogenic potential of compounds is not absolute.

Exposure of experimental animals to chemicals with initiating activity may ultimately result in the induction of multiple neoplasms in a given tissue. Each individual neoplasm is often found to be monoclonal in origin, having arisen independently from a single initiated cell. Application of techniques such as identification of cell surface immunoglobulin markers and glucose-6-phosphatase dehydrogenase variants, restriction fragment length polymorphisms, cytogenetic studies, single-cell transplantation studies, and identification of chromosome inactivation mosaics has permitted identification of both the monoclonal and heterogeneous nature of individual neoplasms.

Promotion of an initiated cell may result in hyperplasia and/or inflammation. This is particularly true in skin initiation–promotion studies using phorbol esters as promoters, and has also been observed in hyperplasia of hepatocytes in rodents following treatment with mitogenic agents such as phenobarbital. However, while some promoters may induce hyperplasia or inflammation, it should be remembered that other compounds may induce hyperplasia or inflammation but lack the promotion effects that result in clonal expansion of initiated cells.

In the classical mouse skin carcinogenesis model (Figure 6.2), the first stage of promotion occurs as a phorbol ester binds to its membrane receptor, and induces protein kinase C expression. This effect is induced by a single application, and is at least partially irreversible. Weak or nonpromoting agents such as mezerein are effective as second-stage promoters, but require multiple applications and do not always have receptor-binding properties. Similar multistage promotion has not yet been demonstrated in other experimental carcinogenesis model systems.

Progression is a multistep neoplastic process associated with the development of an initiated cell into a biologically malignant cell population and is a term used to signify the stages whereby a benign proliferation becomes malignant or as a result of which a neoplasm develops from a low-grade to a high-grade malignancy. During progression, neoplasms show

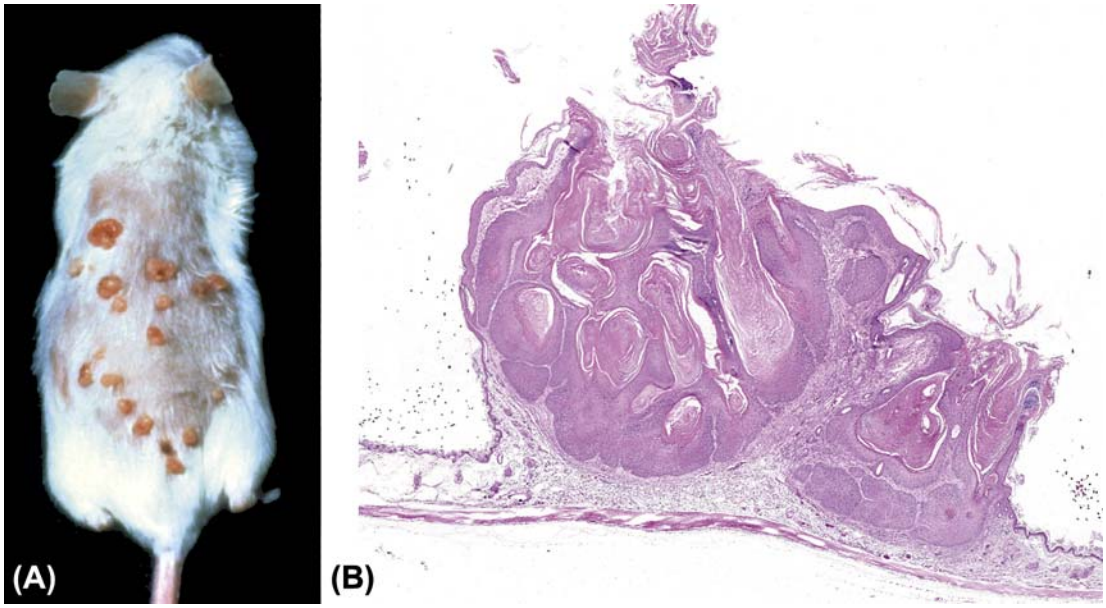

FIGURE 6.2 The initiation–promotion–progression skin tumor model is the most studied. Depicted in this figure is a transgenic TgAC mouse, which has a mutated human H-RAS gene transfected into its genome. These mice are considered to be born "initiated" and after application of only a promoter, 12-*O*-tetradecanoylphorbol 13-acetate, they develop clinically apparent benign squamous cell papillomas of the skin (A). The papillomas are exophytic cutaneous masses that histologically appear well-differentiated and noninvasive (B). Source: *Courtesy: The US National Toxicology Program, Research Triangle Park, NC.*

increased invasive behavior, develop the ability to metastasize, and develop alterations in biochemical, metabolic, and morphologic characteristics (Figure 6.1).

Tumor cell heterogeneity is an important characteristic of tumor progression. Heterogeneity allows for antigenic and protein product variants, the ability to elaborate angiogenic factors, emergence of chromosomal variants, development of metastatic capability, altered metabolism, and decreased sensitivity to radiation. The development of intraneoplastic diversity may come about as a consequence of genetic change such as loss of polymorphic restriction fragments in DNA of malignant tumors or similar random processes such as additional genomic "hits" by genotoxic agents. Alternatively, the heterogeneity observed in tumor progression may be generated by epigenetic regulatory mechanisms operative as a continuation of the process of promotion. More than likely, genetic and epigenetic events subsequent to initiation operate in a nonmutually exclusive manner during progression, possibly in an ordered cascade of latter epigenetic events superimposed on earlier genetic events. Tumor cell heterogeneity is one of the characteristics of tumors with regards to the CSC theory, discussed later in this chapter.

The most plausible mechanism of progression invokes the notion that during the process of tumor growth, there is selection that favors enhanced growth of a subpopulation of neoplastic cells. In support of this mechanism is the observation of increased phenotypic heterogeneity that is observed in malignant versus benign neoplastic proliferations. Presumably a variety of subpopulations arise, and over time a subpopulation with more malignant biological characteristics or a differential growth advantage emerges as the predominant population. This can occasionally be observed during early stages of experimental hepatocarcinogenesis when phenotypically distinguishable neoplasms arise within existing foci of altered hepatocytes (FAH).

Associated with progression is the development of an increased degree of karyotypic instability and aneuploidy. This latter phenomenon may be supported by the not infrequent observation of abnormal mitoses in malignant neoplasms. Finally, chromosomal rearrangement is associated with several clinically malignant neoplasms, especially leukemias, in humans. It is probable that such rearrangements are a consequence of karyotypic instability and that apposition of critical portions of genes upstream or downstream from genomic enhancers or derepressors impart a proliferative advantage and metastatic capability to affected cells within an evolving neoplastic lesion.

Neither structural genomic changes nor biochemical alterations associated with tumor progression or promotion can be defined by conventional histopathology. Ancillary technologies centered on histochemistry, immunocytochemistry, genomics to identify products of proto-oncogenes and activated oncogenes offer promise in distinguishing the various stages of progression in the evolution from benign to malignant neoplasms.

Preneoplasia

Most neoplasms are believed to be derived from the clonal proliferation of a single initiated cell. Usually at some point early in the clonal expansion, the differentially proliferating cells may become phenotypically distinguishable from the surrounding normal parenchyma. Although such lesions may not as yet have sufficient phenotypic characteristics to qualify as neoplasms, their recognition as potential precursors of a true neoplasm has led many to regard them as "preneoplastic." According to the multistage model of carcinogenesis (Figure 6.1), there is a morphological continuum from hyperplasia/preneoplasia to adenoma and carcinoma, which is reflected in the pattern observed in many tumor types.

Humans or animals with preneoplastic lesions are at increased risk of developing neoplasms at the preneoplastic tissue site. Some of the preneoplastic lesions themselves are believed to progress to neoplasia, although unequivocal proof for this is difficult to obtain. In humans, examples of preneoplasia include leukoplakia of the oral cavity/vulva or actinic keratosis, precursors to squamous cell carcinoma, and *xeroderma pigmentosum*, which is a precursor to melanoma.

Numerous putative preneoplastic lesions have been identified in laboratory animals. One well-studied example is that of preneoplasia in experimental studies of liver neoplasia using rats or mice exposed to potent hepatocarcinogens. The initial change detected in liver tissue consists of FAH (Figure 6.1). These foci consist of nests or islands of altered hepatocytes that differ phenotypically from adjacent normal hepatocytes due to the altered tinctorial quality of the cytoplasm. There are several phenotypes of FAH, including eosinophilic, basophilic, clear cell, and mixed, and neoplasms which arise from them may resemble them phenotypically. Because of their consistent production by known hepatocarcinogens and their temporal relationship with ultimate neoplasia, FAH are regarded operationally as preneoplastic lesions. However, because the number of neoplasms eventually generated represents a very small proportion of the number of foci produced (estimates range from 1 neoplasm for every hundreds to thousands of foci, depending on the rodent species), conservative pathologists regard the foci as "putatively preneoplastic."

Benign Versus Malignant Neoplasms

A benign neoplasm is a localized growth of well-differentiated, noninvasive tissue (Figures 6.1 and 6.2). Its growth is by expansion, and it may produce compression of adjacent normal tissues. Benign neoplasms ordinarily grow very slowly and are usually not life-threatening unless they interfere with vital functions, such as a cardiac Schwannoma or a so-called "benign" meningioma severely compressing vital areas in the brain or spinal cord.

Controversy regarding the significance of benign neoplasia with respect to the development of malignancy is similar to that associated with preneoplastic lesions. In chemical carcinogenicity studies using rodents, carcinogens frequently produce both benign and malignant neoplasms in a given tissue, and morphological evidence exists that benign lesions progress to malignancy in some studies (Figure 6.3).

Malignant neoplasms (Figure 6.1) grow rapidly and are characterized by disorganized cells, invasive growth, and metastasis. Malignant neoplasms may spread by extension into adjacent tissues or by metastasis to distant sites via blood and/or lymphatic circulation (Figure 6.4). Some malignant neoplasms, particularly carcinomas, at some time in their evolution are at an in situ stage. In situ carcinomas have microscopic cytological criteria of malignancy, but are localized and have not invaded beyond their associated basement membrane. Areas of necrosis seen in some malignant neoplasms presumably result when growth is so rapid that the neoplastic tissue outgrows the existing blood supply. Hemorrhage is also common as neoplasms may have a fragile vasculature and/or varying intratumoral blood pressure. Intratumoral lymphocytes are indicative of an immune reaction and attempts of the individual to rid the body of tumor cells.

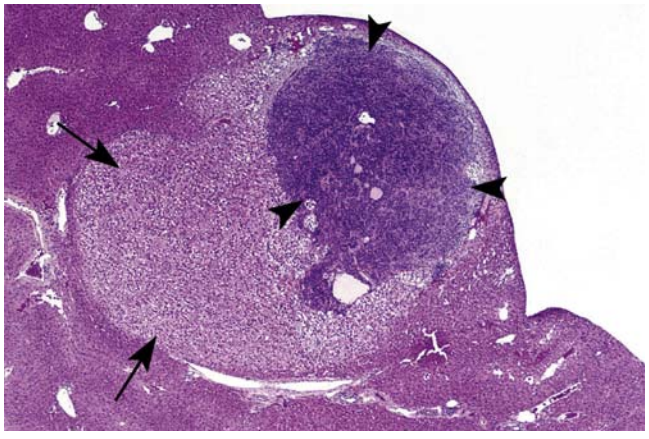

FIGURE 6.3 This is a mass in the liver of a B6C3F1 adult male mouse with an hepatoblastoma (a more malignant liver tumor variant of hepatocellular origin delineated by *arrowheads*), which is arising from an hepatocellular adenoma (*arrows*). These findings support the belief that subclone precursor cells can progress through the processes of promotion and progression toward malignant transformation. Source: *Courtesy: The U.S. National Toxicology Program, Research Triangle Park, NC.*

MECHANISMS OF CARCINOGENESIS

Oncogenes, Tumor Suppressors, Apoptosis, and Repair Genes

The carcinogenic process also follows the "Somatic Mutation Theory" and involves alterations in function in four broad categories of cancer genes, namely activation of oncogenes, inactivation of tumor suppressor genes, alterations in apoptosis genes, and DNA repair gene dysfunction (Table 6.1). Of the approximately 20,000 genes in the mammalian genome, hundreds are known or proposed as oncogenes; however, relatively fewer are tumor suppressor genes. Fewer still are involved in resistance to apoptosis or DNA repair. Other fundamental cellular alterations occur, including limitless replicative potential, ability to trigger sustained angiogenesis, and the ability to invade and metastasize; these, too, are involved in the multistep process of neoplastic transformation. Multistage models of carcinogenesis have proven useful for defining these events in the neoplastic process, and form the cornerstone of current hypotheses of biological mechanisms of carcinogenesis. These models have been used to demonstrate the multistep process of transformation in a variety of organ systems, such as the skin, liver, urinary bladder, lung, kidney, intestine, mammary gland, and pancreas. They have utilized various methods, in order to categorize various agents as initiators, promoters, and complete carcinogens capable of both initiating and promoting. The operationally defined phases of carcinogenesis—initiation, promotion, and progression—are useful for discussion and understanding of carcinogenesis, but in fact each of these phases in the process of neoplastic transformation may likely consist of multiple and overlapping stages.

Since the mid-1980s, oncogenes have been identified in the tumor DNA of many human neoplasms as well as in spontaneous and chemically induced neoplasms in animals. Proto-oncogene and tumor suppressor gene mutation assays have become a popular tool for investigating tumor etiology in humans using rodent models mainly because mutations tend to be chemical specific. Study of the patterns of oncogene activation in spontaneous versus chemically induced rodent neoplasms has provided data suggesting that the

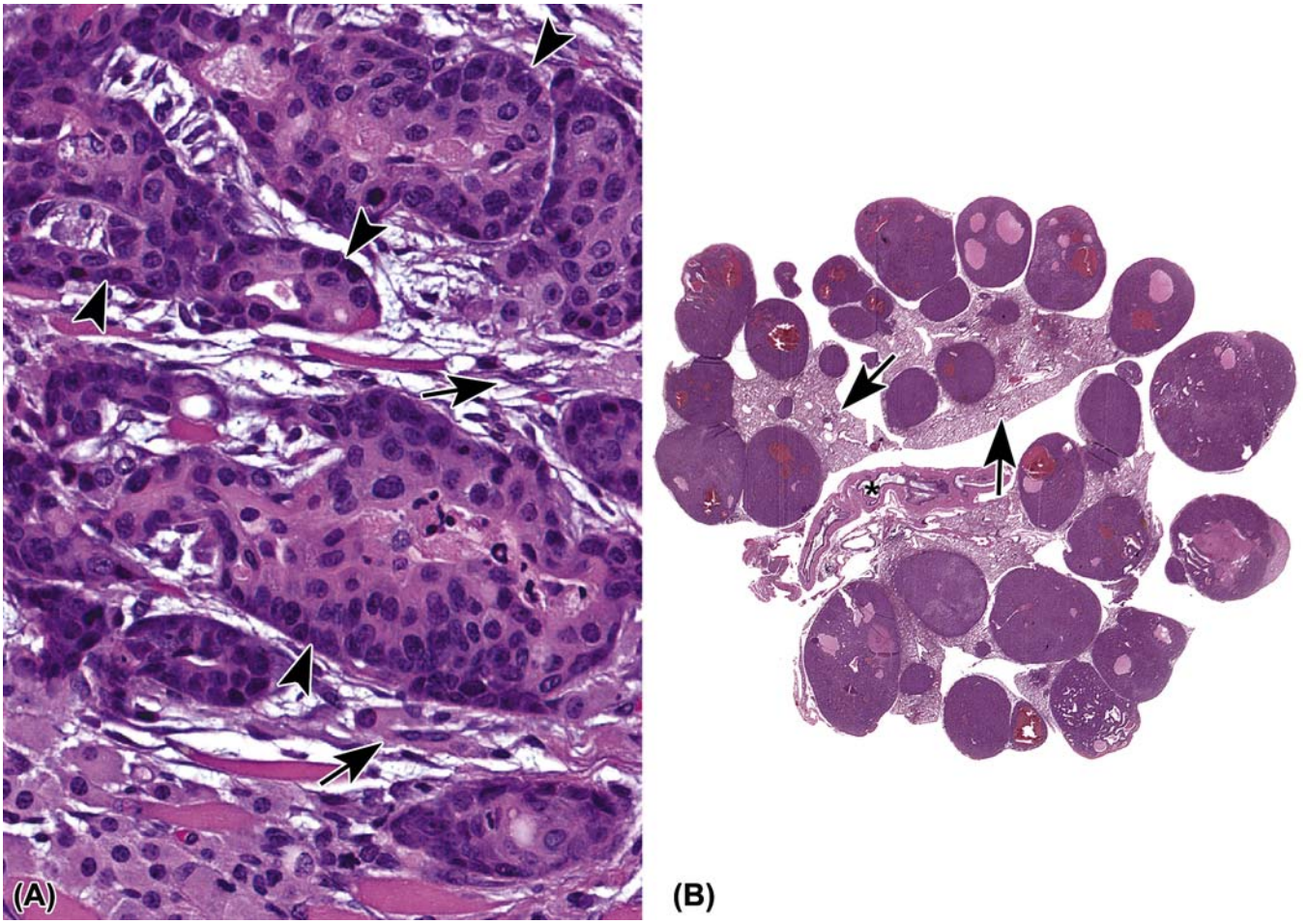

FIGURE 6.4 Panel A demonstrates the features of extensive invasion by malignant epithelial cells (*arrowheads*) and desmoplasia, the fibrous reaction to neoplastic cells in the stroma (*arrows*), by a urethral (transitional cell) carcinoma in a mouse. The primary site was in the proximal urethra of this male B6C3F1 mouse. Panel B is a low magnification photomicrograph of a male B6C3F1 mouse demonstrating multiple, nodular metastases in the lung (*arrows*) originating from a primary hepatoblastoma. (For orientation, the *asterisk* is located in the normal esophagus.) Source*: Courtesy: The US National Toxicology Program, Research Triangle Park, NC.*

TABLE 6.1 Selected Examples of Genes Involved With Cancer Classified by Mechanism(s) of Action

Oncogenes
Growth factors (Sis)
Growth factor receptors (EGFR, PDGFR, HER2/neu)
Signal transduction (*ras*, *abl*, Beta-catenin)
Cell-cycle regulators (cyclin D, cdk4)
Transcription factors (*myc*)
Tumor suppressors
Cell surface (TGF-R)
Cytoskeleton (NF2)
Cytosol (APC/Beta-catenin, PTEN, Smad 2)
Transcription factors (Rb1, p53, Brca1)
Cell-cycle regulators
Apoptosis evasion (p53, bcl-2, bcl-xl, bax)
Defective DNA repair (XP, HNPCC, MLH1, ATM, Brca1, Brca2)

From Haschek, W.M., Rousseaux, C.G., Wallig, M.A. (Eds.), 2013. Handbook of Toxicologic Pathology, third ed. Academic Press, San Diego, CA, Table 5.7, p. 120, with permission.

molecular lesions associated with chemically induced cancer are sometimes different from those documented in spontaneous cancer. Furthermore, the patterns of oncogene activation in several rodent model systems appear not only to be carcinogen-specific but are also consistent with known or expected DNA adduct formation. In some cases, there are even similar patterns of oncogene activation to those documented in human neoplasms.

Alterations in *RAS* gene expression are perhaps the best studied of altered oncogene function in carcinogenesis. Mutations in the *RAS* gene from human skin tumors related to sun-exposed areas appear to be consistent with pyrimidine dimer formation induced by UV irradiation; on the other hand, *KRAS* mutations in human lung and colon tumors may be the result of adduct formation due to carcinogens from cigarette smoke.

It has been proposed that the carcinogen-specific patterns of *RAS* gene mutation observed in tumors reflect the mechanisms of carcinogenesis, and some patterns of *Hras* mutations in mouse liver tumors suggest that they occur from direct chemical–*Ras* gene (genotoxic) interactions.

The B6C3Fl mouse liver is a model in which many genotoxic and nongenotoxic chemicals induce hepatocellular tumors. *RAS* activation is an early and common event in tumorigenesis, and activated *RAS* oncogenes frequently differ from their homologous proto-oncogene by virtue of a single point mutation (Figure 6.5). The frequency and pattern of activating mutations can be compared between tumors that are chemically induced and spontaneous to help in determining possible mechanisms by which chemicals induce tumors. Some genotoxic compounds cause mutations that can be explained by the type of DNA adducts formed and some nongenotoxic carcinogens induce tumors that have the same mutational spectra as spontaneous tumors, suggesting that these chemicals act by promoting the spontaneously initiated hepatocytes.

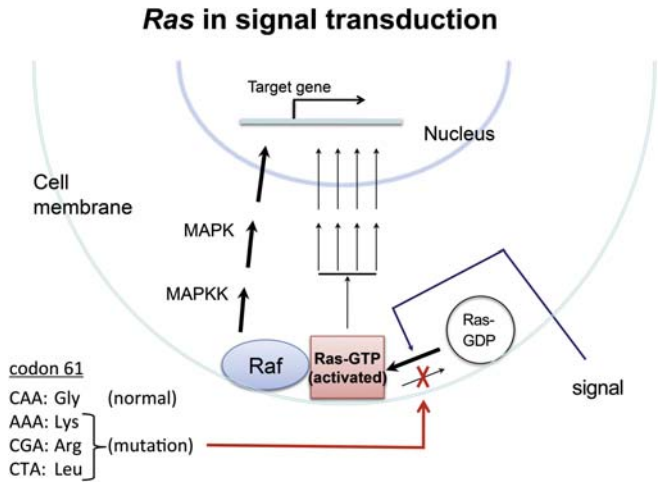

FIGURE 6.5 In this oversimplified diagram of mutational oncogene activation, we show how H-ras, a commonly activated proto-oncogene in human and animal cancer, acts through signal transduction pathways in order to promote oncogenic growth. It is a typical example of proto-oncogene activation. Normally, a signal triggers activation of ras-GDP which converts to ras-GTP, an activated form, that binds with Raf, which further stimulates growth promoting signals, including MAP Kinase (MAPK) and MAPK Kinase. In the normal state, ras-GTP is rapidly inactivated to ras-GDP. When H-ras harbors a mutation, such as a base substitution in codon 61, specific mutant forms of H-*ras* protein remain in the activated state with its partner Raf and stimulates cell proliferation. There are a number of ras codons and mutant codon sequences that can activate ras and contribute to tumor growth. Abbreviations: Ras, a G protein involved in signal transduction; Raf, an enzyme; GDP, guanosine diphosphate; GTP, guanosine triphosphate; MAPK, mitogen-activated protein kinase; MAPKK, MAPK kinase; A, adenine, T, thymine, C, cytosine, G, guanine; Leu, leucine, Gly, glycine, Lys, lysine, Arg, Arginine. Source: *Diagram by Dave Malarkey.*

However, while it can be argued that activation of proto-oncogenes may be a necessary event in the genesis of some cancers, it is not believed that a single point mutation associated with an activated oncogene is sufficient in and of itself for the development of cancer, and other genetic modifications (up to 80 or more!) in tumor suppressor genes, apoptosis genes (such as the antiapoptic gene *BCL2*), or DNA repair genes (such as *BRCA1/2* and *CHEK1/2*) are needed to achieve neoplastic transformation.

In common human cancers, multiple tumor suppressor genes may be affected, supporting the notion that cancer development involves perturbation of multiple levels of growth control. Inactivation of the tumor suppressor gene *TP53* is a frequent occurrence in a variety of human cancers. Because the inactivating mutations of the *TP53* gene are primarily missense mutations (90%) and there are many "hotspot" mutation sites, it is well-suited for investigation of genotoxic mechanisms involving alterations of this gene in human and animal tumors. Thus, inactivation or loss of tumor suppressor genes, working in concert with the activation of oncogenes and with a variety of endogenous and exogenous stimuli, plays an important part in the complex process of carcinogenesis. One of the major roles of TP53 is to ensure that, in response to genotoxic damage, cells arrest in the cell cycle and attempt to repair their DNA before it is replicated. Lack of functional TP53 permits synthesis of damaged DNA and increases the incidence of selected types of mutations. This increased incidence has been shown after a variety of DNA damage mechanisms, such as ionizing radiation (strand breaks), ultraviolet irradiation (photo-dimers), and a variety of environmental carcinogens.

The pivotal role of cell proliferation in all phases (e.g., initiation, promotion, progression) of the multistep process of carcinogenesis is inextricably linked to positive and negative cell cycle control mechanisms as influenced by oncogenes, tumor suppressor genes, growth factors and their cognate receptors, hormones and their receptors, and the action of exogenous agents (e.g., chemicals and viruses) on cell cycle control. Uncontrolled cellular proliferation is the hallmark of neoplasia, and many cancer cells demonstrate damage to genes that regulate their cell cycles directly.

Epigenetics

Epigenetics refers to reversible changes in gene expression that occur without alteration to the underlying genetic code. Such changes include posttranslational modification of histones, miRNAs, and DNA methylation, all of which affect gene expression. In

normal, differentiated cells, the majority of the genome is not expressed. Some portions of the genome are silenced by DNA methylation and histone modifications that lead to the condensation of DNA into heterochromatin. On the other hand, cancer cells are often characterized by a global DNA *hypo*methylation and selective promoter-localized hypermethylation. Indeed, it has become evident during the past few years that tumor suppressor genes are sometimes silenced by hypermethylation of promoter sequences rather than by mutation.

Hypomethylation is believed to influence the regulation of transcription and gene expression and may be associated with cellular differentiation. miRNAs are small noncoding RNA molecules (~22 nucleotides) found in the nucleus or cytoplasm of cells (or sometimes extracellular) that function in RNA silencing and posttranscriptional regulation of gene expression. Unfortunately, as with many abnormalities that are associated with cancer cells, we are faced with a dilemma in deciding whether miRNA regulation and/or hypomethylation of genes is a cause of the malignancy or whether these processes are consequences of the altered metabolism of the malignant cells.

Cancer Stem Cell Theory

There is extensive evidence that multiple types of cancers arise from transformation of stem and/or multipotent progenitor cells during carcinogenesis. The CSC theory states that CSCs are neoplastic cells that have stem-cell properties, including the ability to self-renew, in order to propagate additional malignant stem cells that drive tumorigenesis and differentiate to give rise to phenotypically diverse noncarcinogenic cells that comprise the bulk of a tumor.

The formal CSC hypothesis was first proposed over 150 years ago: that there are dormant embryonic components, which exist in adult tissues and which may be activated to later become tumorigenic. Over the decades, the idea that tissue-specific stem cells may be the cell of origin of various cancers and that cancers may represent a maturation arrest of stem cells advanced the study of carcinogenesis, and the study of CSCs continues today as an enormous focus of the field of cancer research.

Through the ability to self-renew, a small population of CSCs within a neoplasm has the ability to maintain malignant clones. Self-renewal is a process by which a stem-cell pool maintains its numbers through symmetric and asymmetric division. In symmetric cell division, the progeny is identical to the initial stem cell; in asymmetric stem-cell self-renewal, one of the two progenies is identical to the initial stem cell, whereas the other cell is a committed progenitor cell, which eventually undergoes cellular differentiation.

The traditional clonal origin of carcinogenesis states that transformation occurs through a series of sequential mutations resulting in preneoplastic lesions that progress to neoplasia and, finally, metastasis. However, in many tissue sites in which cancers arise, cell populations have a high rate of cell turnover and thus individual cells do not persist for a sufficient length of enough time to accumulate the necessary number of mutations for cellular transformation. On the other hand, through the tightly regulated process of self-renewal, normal stem cells are able to function over the lifespan of the host, and thus their longevity and continued mitotic activity makes them a significant target, and potential reservoir for, the accumulation of the numerous genetic mutations needed for transformation. Furthermore, many similarities between normal stem cells and tumor cells exist, including indefinite proliferative potential and the ability to give rise to new tissues (although disorganized and atypical in the case of tumorigenesis). In addition, both stem cells and various neoplastic cells express telomerase (which imparts longevity), have antiapoptotic mechanisms to prevent cell death, share common embryonic and developmental metabolic pathways, and have increased membrane transporter activity (allowing them to efflux chemicals from the intracellular compartment). Both stem cells and neoplastic cells also have the ability to migrate (metastasize in the case of neoplastic cells), and share embryonic and stem-cell markers such as β-HCG, AFP, c-KIT, and CD34, among others.

In many ways, neoplastic cells differ from stem cells in terms of their unrestricted and disordered growth and genetic alterations. Perhaps the major difference between these two cell types is that the process of tumorigenesis in many types of cancer involves dysregulation of embryonic and developmental pathways, cell differentiation, and stem-cell maintenance. Some of these key pathways include *Wnt*, *Notch*, and *Sonic Hedgehog*, all vital for normal embryogenesis and stem-cell maintenance.

Significant evidence exists for the presence of tissue-specific CSCs in various organs, consistent with the theory that cancers arising in various tissues originate from transformation of tissue-specific stem or progenitor cells. However, identification of these cells can be problematic, because stem cells represent a very small proportion of the overall cell population in an organ. In order to identify CSCs, investigators have used a stem-cell immunophenotype based on immunocytologic and immunohistochemical expression of various stem-cell markers and cell surface markers, followed by cell sorting to identify a CSC population. Stem-cell

populations have been identified using panels of a number of immunocytochemical markers, including CD133, CD34, CD38, CD24, CD44, SOX2, OCT4, BMI1, ESA, NANOG, NES, and CKIT.

While the earliest evidence of CSCs comes from studies in hematologic malignancies such as human acute and chronic leukemia and myeloma, multiple researchers have provided evidence for the existence of CSCs in solid tumors, including brain, lung, colon, ovarian, pancreas, and prostate tumors, as well as in breast cancer and melanoma, among others. Through molecular investigation, the use of stem-cell markers, developmental pathways, and xenograft transplantation experiments in mouse models, numerous studies have provided significant evidence for the relevance of CSCs as initiators of various types of cancer in humans.

The CSC origin hypothesis does not discount the somatic mutation theory, and it is possible that each paradigm could be contributing to transformation and ultimate formation of a neoplasm. The CSC hypothesis accepts the contribution of genetic instability, mutation, and epigenetic factors that influence the evolution of heterogeneity in a malignancy, but the target of the genetic alteration is the stem cell rather than the somatic cell. Furthermore, the concept of initiation and promotion that is a significant part of the somatic mutation theory applies to the CSC hypothesis; mutations that lead to clonal expansion of a neoplasm may initially occur in a stem or progenitor cell.

A major cause of cancer-related death, metastasis, is currently considered to occur through sequential acquisition of mutations leading to selection of clones with metastatic potential. However, it has been shown that in certain cancers a small number of individual cancer cells disseminate and lie dormant at distant sites in a state of quiescence for up to several years, until triggered to outbreak. Alternatively, some disseminated tumor cells never activate to cause formation of metastatic tumors and ultimately undergo anchorage-dependent cell death (anoikis). One explanation is that these cells are destroyed by immune surveillance. An alternative explanation, according to the CSC hypothesis, is that a majority of tumor cells are transformed but poorly proliferative and thus unable to withstand anoikis; only a small proportion of the transformed cells, the CSC subpopulation, is able to evade anoikis and establish metastases.

Finally, the idea that the growth of a solid tumor is driven by proliferation of CSCs has profound implications for cancer therapy. Treatment of cancer as a homogeneous population of proliferative clones with unlimited growth potential is problematic because many tumors may initially respond to therapy only to recur, often months to years later in life. Rather, if tumors are composed of a heterogeneous population of tumor cells driven by a small subpopulation of transformed stem cells, this would account for the recurrence of tumors following an initial regression period, since this subpopulation of CSCs is more resistant to current chemotherapeutics.

If, according to the CSC hypothesis, the growth and metastasis of tumors are driven by a small fraction of highly tumorigenic CSCs within a heterogeneous population of tumor cells, this may explain the failure to develop therapies that are able to consistently eradicate solid tumors. Therefore, a paradigm shift in cancer therapy is beginning to be realized, in which therapy is directed towards killing CSCs. This approach may result in much more effective therapies.

Cell Proliferation and Apoptosis

Current data strongly suggest that cell death may be as essential as cell proliferation in carcinogenesis. The ratio between cell "birth" and counterbalancing cell death determines tumor growth. Two forms of cell death are commonly observed in cancer development: necrosis and apoptosis. Necrosis typically occurs when a developing cancer outgrows its blood supply, resulting in hypoxia and deprivation of nutrients necessary for tumor cell survival. Apoptosis is an energy-dependent process that involves active gene transcription and translation and relatively intact cellular metabolic machinery. In preneoplastic lesions, apoptosis is the predominant form of cell death that is observed. Enhanced apoptosis may be triggered in experimental *in vivo* models by chemical exposure; food deprivation; certain cytokines, growth factors, and tumor suppressor gene actions; and withdrawal of mitogenic agents. Loss of the ability to undergo apoptosis during progression can result in tumor "growth" even when there is no increase in the rate of proliferation. For example, it has been reported that the growth of dioxin-promoted preneoplastic liver foci in rats is secondary to inhibition of apoptosis, rather than enhanced cell proliferation. In addition, an underlying principle of cancer chemotherapy is the selective induction of apoptosis in neoplastic cells.

Some compounds, such as those classified as nongenotoxic carcinogens (see later), often act through enhancement of cell proliferation or interference with apoptosis via mechanisms unrelated to changes in genomic sequence. Confirmation of whether altered cell turnover alone is a realistic explanation for observed carcinogenicity of nongenotoxic carcinogens will require carefully conducted studies that demonstrate enhanced cell turnover (i.e., proliferation) at doses that result in cancer, and a lack of an increase in cell turnover at noncarcinogenic doses. If enhanced

neoplasia in an animal test system is a consequence of increased cell proliferation, and if that cell proliferation is related to exposure to excessive amounts of certain chemicals, then it becomes important to place the study results into the context of expected environmental exposure in assessing potential risk to human health.

Hypertrophy

While not technically a proliferative change, hypertrophy deserves mention because it is sometimes diagnosed incorrectly as hyperplasia. Hypertrophy and hyperplasia may occur together, and several factors link hypertrophy to rodent hepatocarcinogenesis. Hypertrophy is under various regulatory controls, and thus is limited in amount and duration. Hypertrophy may be classified in a manner similar to how hyperplasia is classified. Compensatory, or adaptive, hypertrophy represents a physiological response to a stimulus, such as is seen with muscle hypertrophy subsequent to prolonged exercise or hepatocellular hypertrophy due to enzyme induction in the liver following exposure to chemical inducers such as phenobarbital. Along with degenerative changes, such as necrosis and vacuolization, hepatocyte hypertrophy is associated with the development of hepatocellular neoplasms in rats and mice. However, hypertrophy may not be consistently observed in the development of other types of neoplasms.

Exposure of animals to liver enzyme inducers results in a signature of toxicological changes characterized by an increase in liver weight, hepatocellular hypertrophy, cell proliferation, and frequently hepatocarcinogenesis in chronic 2-year studies. Hepatic enzyme induction is generally an adaptive response, and is associated with the induction of gene expression and resultant morphological changes in hepatocytes. The additive growth and functional demands that initiate the response to hepatic enzyme induction cover a wide range of stimuli, including pregnancy and lactation, hormonal fluctuations, dietary constituents, infections associated with acute phase proteins, and responses to xenobiotic exposure. Common xenobiotic enzyme inducers in rodents trigger pathways involving the constitutive androstane receptor, the peroxisome proliferator-activated receptor, the aryl hydrocarbon receptor, and the pregnane-X-receptor. Liver enlargement in response to hepatic enzyme induction in rodents is typically associated with hepatocellular hypertrophy, and often with transient hepatocyte hyperplasia as well. The hypertrophy may show a lobular distribution, with the pattern of lobular zonation and severity reflecting species, strain, and gender differences in addition to effects from specific xenobiotics. Toxicity and hepatocarcinogenicity may occur when liver responses exceed adaptive changes. These undesirable consequences are influenced by the type and dose of xenobiotics, and show considerable species differences in susceptibility and severity that need to be understood for assessing the potential effects on human health from similar exposures to specific xenobiotics.

Hormones

Hormones are chemical messengers that bind to specific cellular receptors and form a hormone–receptor complex that triggers a cellular response. The cellular response is specific for both the hormone and the target cell. The target-cell response to hormone stimulation is typically an increase or decrease in cell division, or an acceleration or deceleration in differentiation. There has been recently almost continual discovery of new endogenous messenger substances and growth factors that fit the broad definition of "hormone." Like hormones, hormone-related peptides, commonly referred to as growth factors, play an important role in the control of growth and differentiation of cells, tissues, and organs. A major difference between hormones and growth factors is that hormones are produced in an endocrine tissue and act on cells at a distant site, whereas growth factors are secreted by a variety of normal and abnormal tissues and act on nearby responsive cells.

Endogenous and exogenous hormones have long been known to be associated with the development of specific neoplasms (e.g., diethylstilbestrol, DES) but also in some cases with the inhibition of carcinogenesis. Hormones or hormone imbalances undoubtedly play a major causative role in cancers of certain hormone-sensitive tissues (ovary, uterus, prostate, testes, and endocrine organs). However, it is unlikely that they play a major causative role in the development of neoplasia in nonhormone-sensitive tissues. Through the use of two-stage animal models for mammary and thyroid cancer, hormones have been demonstrated to function as tumor promoters of certain neoplasms. There is little evidence that there is direct interaction of endogenous hormones with DNA, although minimal DNA binding has been shown with some synthetic estrogens, and some hormones do bind to proteins other than receptors.

Hormones can also induce hypertrophy. For example, injection of growth hormone from the anterior pituitary induces hypertrophy of liver cells, which have an increase in their RNA content. Whether the various types of hypertrophy are considered physiological, adaptive, or pathological depends on the philosophy of the person making the judgment. For example, because hypertension is a disease, then cardiac hypertrophy that occurs secondary to the hypertension can be

considered pathologic. However, one could argue that cardiac hypertrophy is an adaptive physiological response to an increased demand for work, regardless of the proximate cause.

Genotoxic and Nongenotoxic Carcinogens

Supportive of the arguments for the mutational hypotheses of cancer causation are the correlation between mutagenicity and carcinogenicity, the correlation between faulty DNA repair and some cancers, and the genetic nature of neoplastic transformation. While the correlation between mutagenicity and carcinogenicity is not perfect, many chemical carcinogens are mutagenic, either alone or after metabolic activation.

Because it is well known that some mutagens are not carcinogens and some carcinogens are not mutagens, the association between mutagenicity and carcinogenicity is not absolute and necessarily must be qualified. Practical considerations logically compel the admission that no single mutagenicity test or even battery of mutagenicity tests can be expected to reflect the complexity and diverse mechanisms of carcinogenesis. Nonetheless, the association between mutagenicity and carcinogenicity, where it occurs, is intuitively appealing as a potential mechanism for the genesis of some cancers.

Endogenous hereditary defects in mutational repair in the face of exposure to environmental mutagenic factors are known to lead to some cancers. Most notable is the occurrence of carcinomas and melanomas of the skin in *xeroderma pigmentosum* patients who sustain mutations caused by ultraviolet radiation. Because a constellation of biochemical abnormalities may be present in the same cells that have defective excision repair of pyrimidine dimers, it cannot be adamantly stated that the observed skin cancers result exclusively from the accumulation of mutations resulting from deficient DNA repair. However, the strong association between defective DNA repair and carcinogenesis in *xeroderma pigmentosum patients* lends support to the somatic mutation hypothesis of cancer formation.

Nonalkylating Genotoxic Agents

This class of carcinogen directly substitutes for exocyclic amino groups of nucleosides. The substitution occurs either through oxidative mechanisms or by direct electrophilic attack, and results in a change of base pairing because of deamination or a shift in tautomeric (structural isomer) equilibrium. Examples include nitrous oxide (NO), which causes oxidative deamination, and formaldehyde, which forms crosslinks within DNA. Formaldehyde also causes hydroxymethyl adducts, and thus may also act as an alkylating agent.

Alkylating Genotoxic Agents

Alkylating chemical carcinogens either interact directly with cellular genomic material (direct acting carcinogens) or must first be metabolized by the host to a reactive species (indirect acting carcinogens) that then interacts with the genome. Examples of direct alkylating agents include methylnitrosourea, ethylnitrosourea, methylmethane sulfonate, ethylmethane, and sulfonate. Indirectly acting alkylating agents requiring metabolic activation to an electrophilic intermediate include chemicals such as diethylnitrosamine, benzo*[a]*pyrene, nitrofurans, nitroquinoline oxide, ethylene dibromide, ethylene dichloride, *N*-acetyl-2-aminofluorene, and dimethylhydrazine. Pathways for activation involve cytochrome P450, reduction with NADPH dehydrogenase, reaction with glutathione, or oxidation mediated by peroxidases or via prostaglandin synthase.

For both direct and indirect acting genotoxic agents, the reactive form of the carcinogen is an electron-deficient species (electrophile) that interacts nonenzymatically with electron-rich or nucleophilic molecular sites in the cell. These nucleophilic sites are not limited to DNA but also include RNA and cellular proteins. Thus, the reaction is not specific for genomic material or for nucleic acids. The interaction of electrophilic forms of the carcinogen with host cellular material results in the formation of covalent adducts (addition products). These interactions take place primarily between the electrophilic form of the carcinogen and electron−rich nitrogen, oxygen, and sulfur atoms in cellular macromolecules. Adducts formed may be small, as is seen with simple alkylating agents, or large, so-called "bulky adducts," as occur with polycyclic aromatic hydrocarbons. In either case, configurational or conformational changes occur in the DNA, which can lead to steric hindrance and result in infidelity of DNA replication.

The electrophilic forms of carcinogens react at sites to produce DNA adducts and mutations throughout the genome. Some of these mutations may be lethal and the cell dies; hence, there is no initiation. Nonlethal reactions with cellular targets are the most relevant for carcinogenesis in that initiation occurs when one of these is in a critical genomic site. Nonlethal alteration in the somatic cell genotype is consistent with the genetic changes observed in cancer cells.

Evidence of alteration of the cellular genome is supported by the observation of chromosomal abnormalities and altered gene expression in cancer cells. Furthermore, adduct formation at DNA nucleophilic sites such as phosphate residues and hydrogen-bonding sites between base pairs can also result in

miscoding or in sufficient distortion of DNA structure to result in infidelity of DNA replication. Because DNA damage (adduct formation) can be repaired efficiently by cellular enzymes, it is necessary for cell proliferation to occur prior to repair of the DNA damage in order for a genetic change to occur. Once a round of cell proliferation takes place, the genomic alteration is said to be "fixed" and the affected cell(s) is initiated. The round or rounds of cell replication that serve to fix the molecular lesions may occur de novo, may be induced by the inherent toxicity of the chemical carcinogen, or may be induced by the promoting activity of the chemical carcinogen.

Molecular Epidemiology

One objective of this field is to identify cancer-causing agents to which individuals may be exposed, based on the occurrence of predictable molecular alterations, which are found in a particular neoplasm. This is based on the hypothesis that there are carcinogen-specific patterns of mutations that reflect direct interactions of the carcinogen with specific cancer genes. For example, lung and colon cancers from people who smoke tend to have a specific mutation in the *RAS* oncogene or *TP53* tumor suppressor gene (mostly a G to T nucleotide base substitution) and that this mutation is likely due to direct interaction of a carcinogen in tobacco smoke, benzo*[a]*pyrene, with DNA.

Such chemical-specific mutational profiles (or "molecular signatures") have been used to establish causality between particular genetic events in tumors and the carcinogen in question, as has been established with neoplasms associated with exposure to radon, aflatoxin B_1, vinyl chloride, and the nitrosamines. The strongest evidence for linkage between a cancer-causing agent and a specific type of neoplasm is that of the CC to TT double base changes observed in skin neoplasms of man and animals exposed to UV radiation. The mutational pattern in these neoplasms is consistent with predicted UV-induced formation of dipyrimidine dimers. In liver tumors from persons living in geographic areas where there is high exposure to aflatoxin B_1, there is a frequent mutation at the third nucleotide pair of codon 249 in the TP53 gene, suggesting the mutation is chemical-specific and imparts a specific growth or survival advantage to the mutated liver cells.

Animal studies have confirmed that there are certainly chemical-specific mutational profiles in neoplasms; however, there are many examples where the mutational profile varies by strain, species, dose, or dosing regimen. For example, diethylnitrosamine, a strong, cross-species hepatocarcinogen, induces liver neoplasms in mice, rats, and rainbow trout, but the frequency and type of *ras* mutation in the neoplasm vary widely, and the mutations are not simply a reflection of direct DNA interaction.

In some studies using *in vitro* mutation assays to predict cancer risk, there was poor correlation between positive *in vitro* data and subsequent liver tumor mutation profiles in the mouse. Therefore, in the complex process of carcinogenesis, other than direct mutational events, carcinogens may also be influencing events such as DNA repair, oxidative DNA damage, methylation, cell death, and proliferation, or maybe inducing a hypermutable state by interfering with DNA repair, all factors which might alter the original mutational profile.

Other factors can affect the mutational profile of certain oncogenes, specifically *Hras*, in mouse liver tumors. These include genetic background (strain) of mouse, dose of carcinogen, dosing regimen or route of exposure, and time of sampling, thus adding an additional level of complexity in the evaluation of chemical genotoxicity in tumor DNA. In addition, in some instances when humans and rodents are exposed to the same mutagenic carcinogen, such as vinyl chloride, the specific cells or tissue at risk and specific mutations differ.

Tumor Regression

A large body of experimental data supports the contention that malignant neoplasia is generally irreversible. Even in initiation–promotion studies, the initial mutational changes constituting initiation may remain latent for weeks or months before being expressed by administration of a promoting agent. This "memory effect" is compatible with a stable somatic mutation.

Regression of hepatocellular neoplasms, including hepatocellular carcinomas (HCCs), has occasionally been described in humans, rats, and mice. Mechanisms for tumor regression are unclear, but this phenomenon suggests that some histologically appearing benign and malignant "neoplasms" depend on the sustained presence of the inciting chemical. For example, in a study of chlordane exposure in B6C3F1 mice, there was evidence of regression of benign and malignant hepatocellular neoplasms after cessation of exposure. *Hras* mutations, which commonly occur in up to 60% of neoplasms in this strain of mouse, were not present, suggesting that this common alteration associated with the development of these particular tumors did not play a role in their genesis.

Other nongenotoxic murine hepatocarcinogens that do not appear to induce tumors through *Hras* mutation include hexachlorobenzene, aroclor, phenobarbital,

ciprofibrate, dieldrin, chloroform, oxazepam, and methyl clofenapate. The absence of *Ras* mutations and evidence for regression implies that the reversible "neoplasms" may lack the appropriate genomic alterations necessary for autonomous proliferation. Alternatively, chlordane may provide a selective growth advantage to the hepatocellular lesions without *Ras* mutations, may eliminate *Ras* mutated cells through hepatocyte necrosis or apoptosis, or may induce tumorigenic pathways that do not involve *Ras* activation. There was no histological evidence of immune-mediated rejection of any neoplasms in the study. Interestingly, *Bcl2* and *Bclx*, proteins that inhibit apoptotic pathways, were elevated in hypertrophied centrilobular hepatocytes (Figure 6.6) and in liver neoplasms from rodents treated with chlordane, phenobarbital, or clofibrate. In addition, a gene array profiling study supported the involvement of other growth-promoting factors and oncogenes in chlordane hepatocarcinogenesis.

Complete regression of HCCs occurs rarely in humans with cirrhosis or in children after cessation of androgen therapy. Benign liver tumors have regressed after withdrawal of oral contraceptives in women. The latter two examples suggest a role for sex hormones in this regression. Indeed, recent evidence suggests that chlordane can act by mimicking sex steroids, or by altering the synthesis and elimination of sex steroids or their receptors. Taken in toto, these findings suggest that chlordane appears to act through enzyme induction as well as nongenotoxic, hormone-like mechanisms that promote cell survival and inhibit cell death. If such mechanisms can be further elucidated, then risks that chemicals such as chlordane pose to humans can be more accurately assessed.

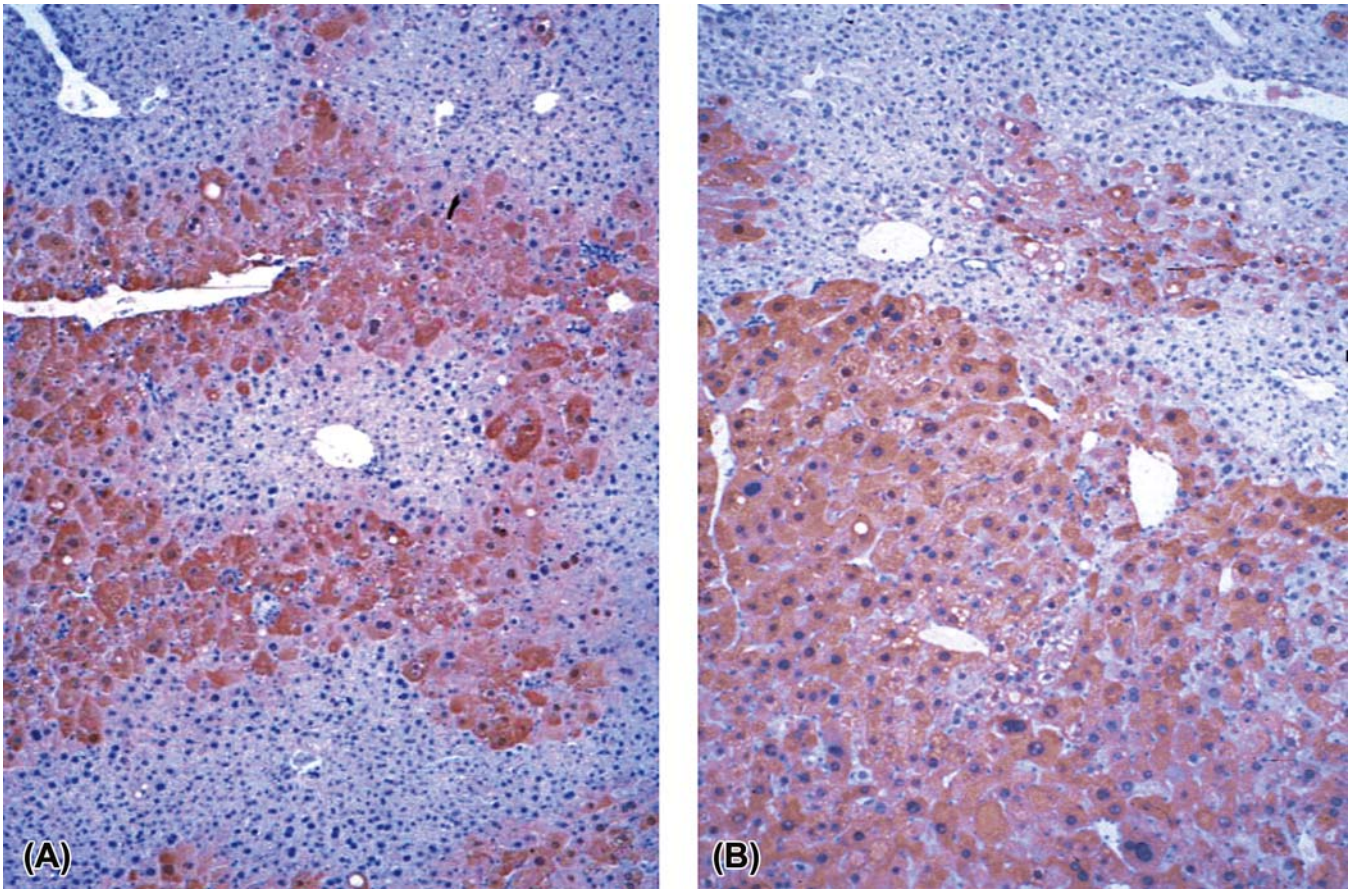

FIGURE 6.6 These photomiocrographs depict immunohistochemical positivity for antiapoptotic proteins Bcl-2 (A) and Bcl-XL (B) in the livers of B6C3F1 mice treated with phenobarbital for 30 days (A) and 2 years (B). In panel A, there is marked centrilobular to midzonal hypertrophy of hepatocytes, which concurrently accumulated cytoplasmic bcl-2 (red/brown color) and in panel B there is red-brown staining in the hepatocellular adenoma in the lower half of the photo. There are two smaller proliferative lesions above. These data strongly support an antiapoptotic role in the nongenotoxic mechanism of phenobarbital hepatocarcinogenesis. It is also indicating that hepatocyte hypertrophy and enzyme induction are also risk factors for mouse hepatocarcinogenesis and regression (Hematoxylin counterstain). Source*: From Christensen et al., 1999. Altered bcl-2 family expression during non-genotoxic hepatocarcinogenesis in mice. Carcinogenesis 20, 1583–1590, with permission.*

Omics Revolution

The advent of "-omics" technology (e.g., transcriptomics, genomics, proteomics, and metabolomics) has revolutionized the way we study toxicity and define the mechanisms of disease. This section covers how these technologies are being applied to enhance the understanding of carcinogenesis in toxicological pathology.

Gene Expression Microarray Data Analysis

During the last several years, much effort has been undertaken to understand alterations in global gene expression, which occur during the process of carcinogenesis. With the development of microarray technology, and more recently next-generation sequencing, a single sample of tumor mRNA can be used to assess alterations in the expression of tens of thousands of genes at a single time. The study of global gene expression has been an important tool in the characterization of neoplasia, not only as a means to better understand alterations leading to cancer, but also as a method to develop molecular signatures of tumors, with the goal of personalized treatment of individuals with cancer.

The basic functional concept of microarray technology is through mRNA binding to complementary DNA strands (probes) from its respective coding region of the gene of interest. By attaching these probes representing hundreds to thousands of genes to solid substrata, RNA transcripts can be hybridized and measured as an output of relative or absolute gene expression at a given point in time, allowing investigators to detect alterations in the genomic landscape in a particular disease state, including cancer.

Depending on the application, genomics studies in the cancer setting may be used to better elucidate cellular or animal models of neoplasia, or, in the clinical setting, to better understand underlying mechanisms of carcinogenesis driving tumorigenesis and to develop targeted therapies. Two primary methods of gene expression analysis, predictive and mechanistic, are often applied in the research setting. Mechanistic toxicogenomics is used to define the genomic alterations, which occur during the process of neoplastic transformation to better understand mode of action, and pathophysiology. They are also employed to identify potential therapeutic targets. For example, the National Toxicology Program (NTP) has used microarray analysis in numerous 2-year chronic bioassay studies in B6C3F1 mice as well as F344 and Sprague Dawley rats to provide insights into molecular mechanisms of tumorigenesis for chemicals eliciting a tumor response in these particular species. They also have also provided insights into the relevance of these animal models to the human disease. Through these types of studies, the NTP has gathered data on the relevance of rodent exposure studies on compounds of importance to humans in terms of occupational and environmental health. The demonstration that a chemically induced tumor in rodent species harbors the same genetic alterations and pathway dysregulation leading to neoplastic transformation as the disease in humans provides additional supportive mechanistic evidence that the chemical may pose a similar cancer risk to humans. Other investigators have demonstrated similar genomic endpoints relevant to human exposure; for example, Yoon et al. (2003) showed that exposure of mice to benzene resulted in bone marrow toxicity and leukemia development in mice through *TP53*-dependent mechanisms associated with cell cycle dysregulation and defective DNA repair. These types of studies provide supporting evidence for a shared mechanism of TP53 tumorigenesis between rodent models and the human disease.

In addition, genomics may be used as a tool to help predict a carcinogenic response in models of carcinogen exposure. Disruption of normal global gene expression due to exposure to such compounds may provide clues as to the subsequent induction of neoplastic transformation prior to the onset of clinical or histopathologic alterations. Prediction of a cancer outcome in these models requires the development of a database of gene expression alterations induced by various chemicals that are known to induce a cancer response by certain mechanisms (class prediction). Compounds with suspected but unknown carcinogenic properties can then be tested against these databases to determine if there are similarities in gene expression profiles with known carcinogens. Numerous studies have been performed using this technique to differentiate carcinogens from noncarcinogens, as well as differentiating carcinogens with genotoxic and nongenotoxic mechanisms of action. For example, much work has been invested in the predictive value of short-term bioassays as an adjunct to the costly and long "gold standard" 2-year rodent carcinogenicity bioassay. Based on chemically induced gene expression signatures from precancer time points, several investigators have developed predictive signatures of tumorigenesis for chronic time points, which have good predictive accuracy. Several 90-day studies in mice have shown that animals exposed to lung or liver carcinogens have identifiable biomarkers that permit discrimination between carcinogenic and noncarcinogenic compounds. In addition, these genomic biomarkers have been able to predict a lung tumor response occurring after 2 years of exposure. It is hoped that at shorter exposures (5, 14, 28 days) predictive genomics may

differentiate carcinogens from noncarcinogens and correctly predict genotoxic and nongenotoxic chemicals based on their genomic signatures.

Predictive profiles such as these are of great interest in hazard identification and risk assessment by providing an efficient and cost-effective way to identify potential carcinogens that may pose a risk to human populations, and to provide mode of action data critical in the determination of relevance of exposures to human health.

Principal Component Analysis (PCA)

A robust, statistically based, system biology approach to data analysis is critical for understanding the complex datasets that are generated in a large-scale genomics assay. Primary methods used to organize microarray data into a biologically meaningful form to ascertain similarities and differences between samples based on their gene expression patterns include Principal Component Analysis (PCA) and Hierarchical Cluster Analysis (HCA) (Figure 6.7).

PCA is a statistical method employed to visualize differences in global gene expression between samples in a spatial manner. Using this method, samples are represented by individual points in space, and their similarities and differences are reflected in their proximity to one another. For example, samples which cluster very closely together in space have very little biologic variability, indicating that gene expression between these samples is very similar. Conversely, those samples which are separated in space represent marked differences in overall gene expression. This method provides a "first look" at the big picture of the data, and the ability to understand similarities and differences between samples in terms of their overall gene expression.

Hierarchical Cluster Analysis

HCA is another way to visualize differences between samples based on their overall gene expression profiles, represented by a heat map depicting the expression of analyzed genes in each sample (Figure 6.7). This format provides a way to cluster genes based on their function, and show how these groups of genes differ between samples, in order to provide a higher-level understanding of pathway and functionality differences between samples, while maintaining a more "global" picture of the data. PCA and HCA analysis is an effective way to rapidly identify alterations in gene expression in an efficient manner. These methods can highlight group differences related to exposure, treatment, or differences in etiology, and are therefore very useful when applied to the field of cancer research, hazard identification, or risk assessment.

Pathway Analysis

Once the identification of differentially expressed genes in a microarray experiment is completed, data analysis must be performed in order to accurately identify functional pathways that correlate with alterations in gene expression that are biologically meaningful (Figure 6.8). A variety of different software programs

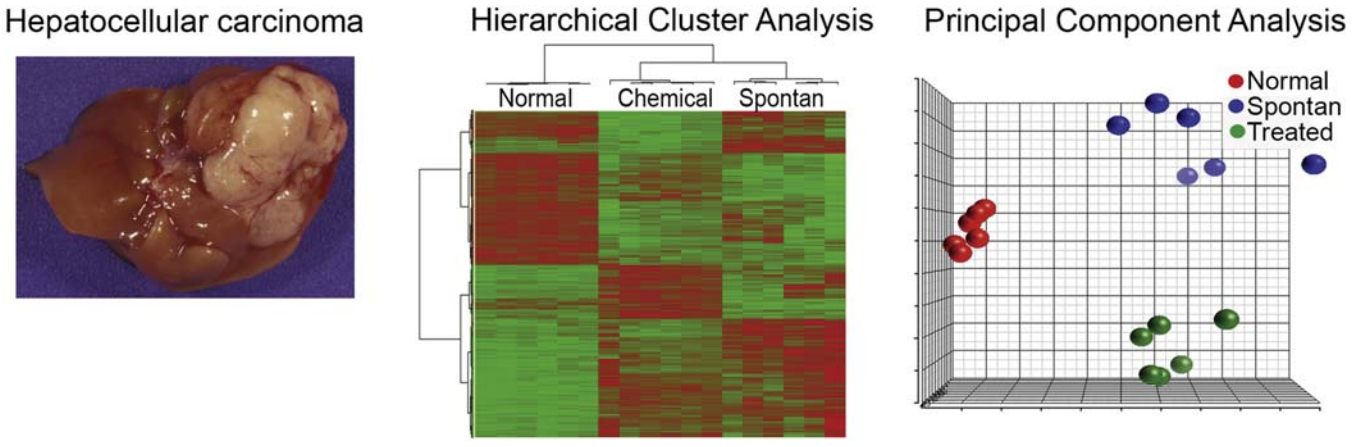

FIGURE 6.7 HCA and PCA of spontaneous and chemically induced HCC in a 2-year chronic B6C3F1 mouse bioassay. HCA illustrates distinct differences in global gene expression between experimental groups, with directionality of gene expression (green = downregulated, red = upregulated) depicted in a heat map. PCA of experimental groups demonstrates similarities and differences in global gene expression between control liver, spontaneous HCC, and HCC from chemically treated mice based on spatial organization; the closer proximity samples are to one another, the more similar their overall global gene expression profiles. Source: *From Hoenerhoff, et al., 2013. Hepatocellular carcinomas in B6C3F1 mice treated with Ginkgo biloba extract for two years differ from spontaneous liver tumors in cancer gene mutations and genomic pathways. Toxicol. Pathol. 41, 826–841, with permission.*

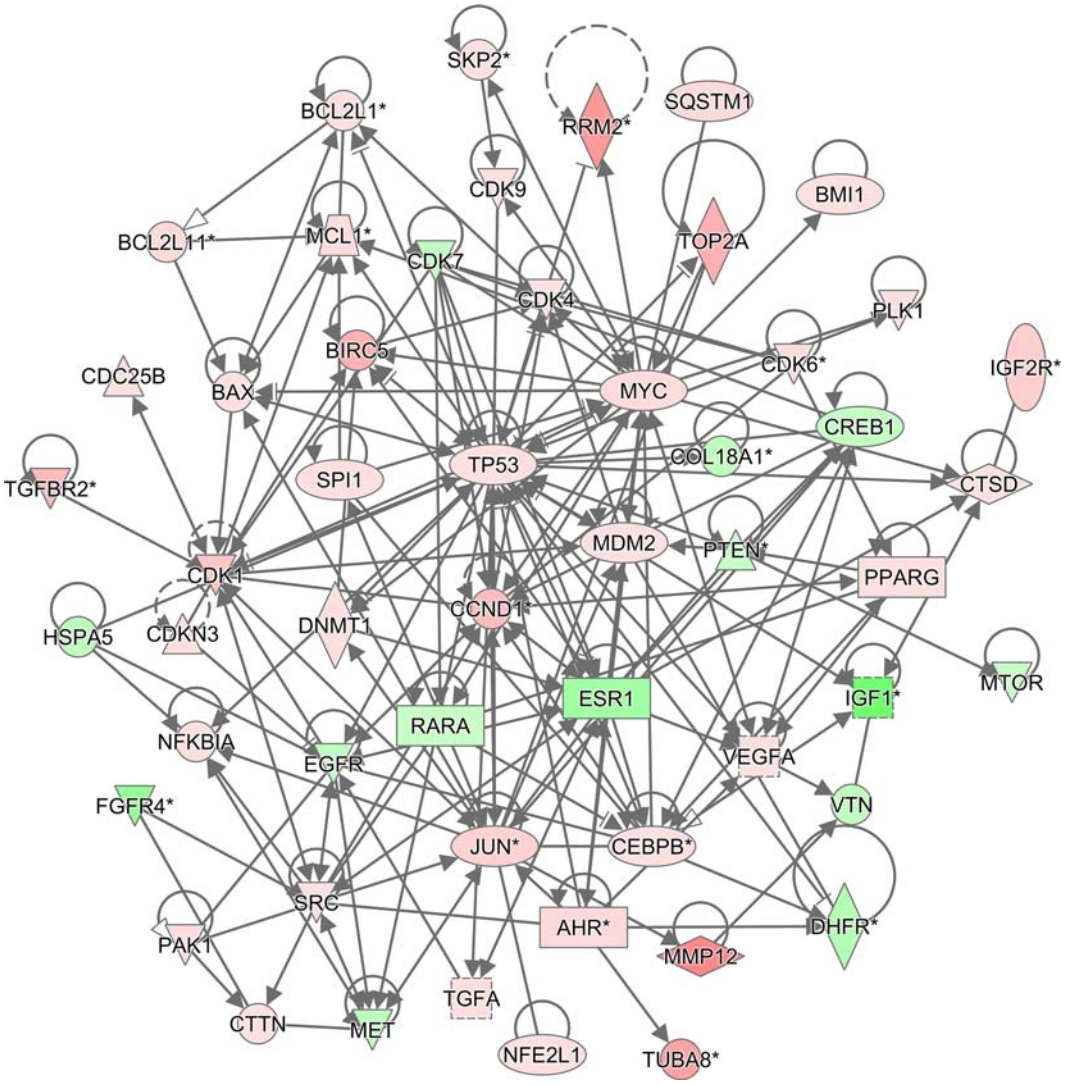

FIGURE 6.8 Ingenuity Pathway Analysis network of differentially expressed cancer genes in HCC from chemically treated B6C3F1 mice. Upregulated genes are in red and downregulated genes are in green. Linear connections indicate relationships between genes that inform on biologically relevant pathways in cancer. Networks containing differentially expressed genes in this mouse HCC dataset relevant for human cancer include upregulated oncogenes (*Myc*, *Fos*, *Jun*, *Src*), dysregulated tumor suppressor genes (*Pten*, *Tp53*, *Esr1*), cell cycle regulators (*Cdk1*, *Ccnd1*, *Cdk4*/*6*), and apoptosis genes (*Bcl2*, *Bax*, *Birc5*, *Mcl1*), growth factors (*Nfkb*, *Vegfa*, *Tgfa*, *Tgfbr*), and matrix remodeling genes (*Mmp12*, *Cola1*), among others. Pathway analysis provides network information on differentially expressed genes, which enables investigation of biologically relevant pathways, molecular characterization of neoplasia, and animal model validation.

[Ingenuity Pathways Analysis (IPA), NextBio meta-analysis software, GeneGO, Gene Ontology (GO) Analysis, GeneSpring] are used to perform these analyses to identify biologically relevant categories of gene expression. For example, when comparing gene expression of a neoplasm to normal control tissue, pathway analysis software can group significantly altered groups of genes into relevant biologic pathways characterized by increased cellular growth and proliferation, oncogenesis, or alterations in apoptosis. In like fashion, comparison of chemically induced tumors to spontaneously arising neoplasms in animal models can provide information on altered pathways which may correlate with chemical exposure. This type of pathway-based analysis of gene expression is a valuable tool to convert gene expression data into biologically meaningful information that can offer insight into mechanism of action, molecular characterization, and chemically induced carcinogenesis.

Next Generation Sequencing

Next generation sequencing technologies have expedited the characterization of neoplasia at the DNA, RNA, and epigenetic level. Also known as "massively parallel sequencing," this technology utilizes repeated

nucleotide amplification to generate hundreds of megabases or even gigabases of nucleotide sequences by utilizing solid substrata or bead-based methods to allow for millions of parallel reactions to occur simultaneously. Subsequent improvements to this method have substantially reduced the time and cost of sequencing, leading to next-generation sequencing that can be used to decipher targeted genomic DNA sequences or the entire genome. Furthermore, it can be used to sequence specific regions of the transcriptome or provide whole transcriptomic assessment, including investigation of changes in small RNAs, noncoding RNAs, genome-wide methylation, and chromatin immunoprecipitation. This technology allows the assessment of the structure and expression of any nucleic acid in a high-throughput manner at relatively low cost. Next generation sequencing of DNA enables the identification of alterations in unmapped regions of the genome, rapidly and exponentially increasing the ability to identify genomic mutations, alterations in DNA copy number, and somatic rearrangements in various types of neoplasms. It has enabled researchers to rapidly sequence entire genomes of various cancers, identifying known and novel mutations in cancer genes, detect novel single nucleotide polymorphisms as well as large insertions, deletions, and rearrangements.

Exome Sequencing

In addition to its applications for genomic sequencing and identification of novel variations and mutations in genomic sequence, next-generation sequencing technologies have been applied to whole transcriptomic or exome sequencing, permitting assessment of gene expression changes for known or novel genes. RNA-Seq, for example, is a powerful method to examine targeted transcriptomic sequences, or even to assess the entire transcriptome in a quantitative manner. This has led to the identification of new splice variants and gene rearrangements, as well as novel fusion genes, in cancer. RNA-Seq has provided significant insights into changes associated with gene expression related to various complex diseases, including cancer. This technology has several advantages over traditional microarray platforms for use in gene expression studies. Microarrays require hybridization and probe-based assays, which are limited to detecting transcripts that correspond to *predetermined* RNA sequences. Therefore, microarray technology is based on expression patterns of *known* segments of the genome. In contrast, RNA-Seq does not rely on previously known sequences to generate probes for hybridization; rather it directly determines cDNA sequence, allowing for de novo generation of sequences independent of a known reference or genomic origin of transcription. This allows for an unbiased approach to gene expression, greater sensitivity, and discovery of previously unannotated genes and rare transcripts. In addition to transcriptomic alterations, other changes such as alternative splicing, sequence variation, and variants of known genes arising from alterations in posttranscriptional RNA processing can be evaluated. RNA-Seq has a better ability to identify RNA isoforms and sequence variants, as well as differences in allelic expression. Moreover, RNA-Seq has single-base resolution capability, and has a greater dynamic range for detecting expression level differences than microarray.

SUMMARY

Genomics has expanded the capabilities of researchers to better understand disease mechanisms, discover novel transcripts and genetic mutations, and develop novel therapies based on patients' individual molecular profiles, even at the single cell level. This technology offers improvements over traditional microarray analysis in terms of depth of analysis, and in recent years has become increasingly cost-effective for use in research and diagnostics. As these technologies continue to be developed and refined, their utility with be of increasing value in cancer research, diagnostics, and therapy. Next-generation sequencing has expanded the understanding of cancer classifications, the prediction of cancer outcomes, and provided the background for effective cancer treatments and personalized medicine for cancer patients.

IDENTIFYING CARCINOGENS

Chronic 2-Year Bioassays

Widespread and routine evaluation of chemicals for their carcinogenic potential began in the mid-1960s with the use of a standardized protocol for the "bioassay" program by the National Cancer Institute (NCI). The original NCI "bioassay" has evolved to the present-day NTP 2-year and perinatal carcinogenicity studies.

Throughout this period a variety of alternative *in vivo* and *in vitro* assay schemes also were introduced in hopes of identifying potential carcinogens in less time and for decreased cost. Some of these alternative testing models have become highly beneficial tools to explore the processes of carcinogenesis in order to identify types of carcinogens, to elucidate the genotoxicity of carcinogenic chemicals, and to discovery the specific mechanisms whereby given agents produce a

carcinogenic response. As adjuncts to the standard 2-year bioassay, testing batteries, tier approaches, and decision-point analyses have been proposed to provide a basis for prioritizing chemicals in the testing queue and to provide a larger database for risk assessment.

These efforts serve to emphasize that there is no ideal model or test for identifying potential human carcinogens. In general, efforts to supplant the long-term cancer "bioassay" with less costly short-term tests have been frustrated by poor concordance of the latter with the traditional long-term test results. In the meantime, increasing costs for conducting long-term carcinogenicity studies have resulted in fewer chemicals being tested annually for potential carcinogenicity. During the 1990s, a high number of medium-term tests, such as 6- to 9-month studies in genetically modified mice, were performed by private industries as well as agencies of the US Federal Government. Both groups concluded that genetically altered mouse models were not adequate because the models generally had decreased concordance with rodent chronic studies and with identifying human carcinogens. These models also needed increasingly higher number of samples for achieving adequate statistical power, and there was decreased sensitivity for identifying some known human carcinogens. Furthermore, some models were criticized for exhibiting transgene- or knockout gene-specific pathways purportedly not relevant to human cancer.

Therefore, the current strategy for identifying the potential carcinogenicity of chemicals remains the systemic (including dermal) exposure of male and female rats and mice to high doses and fractions thereof of suspected carcinogenic chemicals over a 2-year period. At the end of 2 years, the carcinogenicity of the chemical being studied is assessed by measuring the relative incidence and multiplicity of neoplastic lesions above background levels, documenting the occurrence of rare neoplasms with negligible background levels, or demonstrating a reduced latency in neoplasm development.

If increased incidence of neoplasia occurs in experimental animals exposed to a given agent, that agent is regarded as a potential human carcinogen. In countries throughout the world, legal requirements mandate that all new chemical agents and drugs be tested in animal bioassays to determine if they cause cancer in test animals. In addition, since the mid-1960s in the United States, the NCI and currently the NTP have collectively conducted animal bioassays on more than 600 chemical agents to assess their potential to cause cancer. Of those 600 agents, about half (290) have been identified as rodent carcinogens. Twenty-one of them are considered known or suspect human carcinogens. Of the 21 of approximately 100 known human carcinogens studied by the NTP, 7 had at least a liver-tumor response. Of the 290 rodent carcinogens examined by the NTP, there was at least a positive (or elevated) liver tumor response in 57% of studies (primarily representing B6C3F1 mice), a lung tumor response in 22% of the studies, renal tumor response in 14% (primarily representing studies using the F344/N rat), mammary gland tumors in 13%, hematopoietic neoplasia in 13%, and forestomach, thyroid, and endothelial tumors in 12%, 10%, and 9% of studies, respectively (Table 6.2).

TABLE 6.2 Frequency of Tissue Response in 290 Positive NTP Chronic, 2-Year Rat and Mouse Cancer Studies[a]

Liver	57%
Lung	22%
Kidney	22%
Mammary gland	14%
Hematopoeitic	13%
Forestomach	12%
Thyroid	10%
Vascular system	9%

[a]*Data gathered from the National Toxicology Program, Research Triangle Park, NC and represents data from nearly 600 NTP Technical Reports including at least 400,000 rodents.*
From Haschek, W.M., Rousseaux, C.G., Wallig, M.A. (Eds.), 2013. Handbook of Toxicologic Pathology, third ed. Academic Press, San Diego, CA, Table 5.12, p. 135, with permission.

To fully characterize the toxicity of chemicals, modifications to the chronic rodent carcinogenicity study protocol have been selectively introduced by the NTP. Interim sacrifices and "stop studies" are incorporated into the design of many carcinogenicity studies to better define the pathogenesis and biological relevance of the anticipated response. The route of administration of chemicals is chosen to mimic natural routes of human exposure whenever possible. Consequently, corn-oil gavage of chemicals is rarely used in contemporary study design. Ancillary studies, such as chemical disposition and metabolism, toxicokinetics, toxicogenomics and gene expression studies, reproductive toxicity, teratology, behavioral testing, and immunotoxicity, frequently complement and run concurrently with contemporary 2-year carcinogenicity studies. In addition, *in vitro* and *in vivo* genotoxicity tests are conducted for each chemical.

Short-Term Models

Over the years, it has become apparent that there is no panacea for identifying potential human carcinogens, there is no absolute reference for carcinogenicity, and there is virtually no "ideal" human surrogate

immune to criticism. Equivocal results can occur in any animal model no matter how well the carcinogenicity study is designed. In the end, carcinogenicity data are most relevant to the test model employed. The greatest potential of the various "short-term" organ-specific animal carcinogenesis models is in understanding the underpinnings of the carcinogenic process.

When used with potent carcinogens, a preneoplastic or neoplastic response may be observed in only a few weeks, hence the designation "short term." However, for less potent carcinogens and for noncarcinogens, tests are typically conducted for several months. In the case of the mouse skin-painting model, lifetime studies may sometimes be conducted to assess carcinogenicity. Because of the sharp contrast in the study duration for these so-called "short-term" *in vivo* test models relative to truly "short-term" (days or weeks) *in vivo* test systems, they have more recently been referred to as "medium-term" bioassays for carcinogens, indicating a study shorter than the conventional 2-year rodent carcinogenicity study.

Various investigators have proposed batteries of specific "short-term" or "medium-term" *in vivo* rodent models to supplant the more costly chronic rodent carcinogenicity bioassay. However, in those instances where appropriate validation studies have been conducted, these models have shown unacceptable concordance with results obtained using the "gold standard" chronic rodent carcinogenicity bioassay. In many cases, consideration of simple questions such as, "Why would a short-duration lung tumor assay system be expected to identify chemicals that produce renal cancer in a chronic rodent study?" has not been broached. Despite these unfortunate shortcomings, alternative *in vivo* carcinogenicity models can play an important role in defining chemical carcinogenesis.

First, *in vivo* "short-term" tests are useful in defining the nature of the carcinogenic response observed in a chronic rodent carcinogenicity study. For specific target tissues, they can identify whether a chemical is an initiator or promoter, and they can help define the relative potency of the carcinogen. Second, they can help elucidate the mechanistic basis of carcinogenesis. Third, when used as part of a battery or tier approach to carcinogen testing, they help set priorities for more extensive carcinogenicity testing of chemicals.

Additional carcinogenicity models have been developed to study specific cancers, including urinary bladder, pancreatic, gastric, and thyroid cancer models in rats, a fish liver neoplasm model, and rat and mouse colon cancer models. A short-term multiorgan test system for carcinogens has been proposed in which rats are treated by multiple carcinogens to cause initiation in several target tissues followed by administration of the test chemical for 12 weeks. Endpoints that lend themselves to quantitation include preneoplastic lesions in the liver, thyroid, lung, forestomach, urinary bladder, and esophagus. Each has its own limitations.

Data Evaluation and Interpretation

Interpretation of results from human epidemiological studies and animal bioassays to identify carcinogenic agents has often proven difficult and controversial. Humans are rarely exposed to only one potential cancer-causing agent in their lifetime, and the amount and duration of that exposure may be difficult or impossible to quantify rigorously. Many years may intervene between exposure to a potential carcinogen and ultimate development of neoplasia, making accurate assessment of cause and effect almost impossible. Relative to humans, rodents infrequently develop prostate, colon, pancreatic, cervical, and uterine carcinomas, but do develop lung, mammary, hematopoietic, and skin tumors at similar rates. Neoplasms of the liver and kidney are much more frequent in rodents than in humans.

Despite limitations, human epidemiological studies that clearly show an association between a given chemical exposure or lifestyle habit and an enhanced rate of a specific cancer are regarded as the most relevant method for identification of human carcinogens. While animal bioassays have proven useful for identification of agents that can cause cancer in the laboratory rodent, they only identify an agent as potentially hazardous to human health. Additional information must be considered in classifying such an agent as a likely human carcinogen.

The current approach for assessing the scientific relevance of either epidemiological or animal bioassay results to human health risk involves a "weight-of-evidence" process in which national and international panels of expert scientists from multiple disciplines examine all available information on the suspect agent and reach a consensus opinion. Included in this analysis are the strength of the epidemiological evidence, the dose−response curve of the animal response, comparative species metabolism, ability to extrapolate between species, likely mechanism of cancer induction for the agent in question, the genotoxicity of the agent, the amount of the agent in the environment, and the number of people potentially exposed to the agent. Based on this type of analysis, more than 100 agents so far have been classified as known human carcinogens by the International Agency for Research on Cancer (IARC), the Environmental Protection Agency (EPA), and the National Institute of Environmental Health

Sciences (NIEHS) US Health and Human Services Annual Report on Carcinogens (ROC); virtually all of these 100 agents are carcinogenic in animals. In addition, due to the limitations of animal studies, there remains a lack of certainty in determining if a chemical negative in a standard bioassay system is truly *not* carcinogenic to either humans or animals. Thus, the interpretation of animal carcinogenicity results has proven difficult and controversial because there are concerns about adequacy of the rodent bioassay to represent the potential human risk.

The central issues for interpretation are those data dealing with interspecies and low-dose extrapolation. For example, the chemical induction of renal tumors in the male rat by some chemicals appears dependent on a pathway involving the deposition of α_{2u}-globulin in the renal tubular epithelium; α_{2u}-globulin is not found in humans. Hence, there is less concern about potential carcinogenic effects of such chemicals in humans when they induce only kidney tumors in male rats by that specific mode of action. Another example is the occurrence of thyroid neoplasms in rats treated with nongenotoxic enzyme-inducing agents that in turn increase the amount of UDP-glucuronosyl transferase, which inactivates thyroxine (T4) by catalyzing its glucuronidation. The glucuronidated form of T4 is excreted in the feces, and hence there are lower circulating levels of T4 and elevated thyroid stimulating hormone (TSH), which is released as part of the endocrine feedback process. The constant elevation of TSH results in secondary proliferation of thyroid follicle cells, leading to the formation of hyperplastic and ultimately neoplastic lesions of the thyroid.

Using discriminatory and balanced judgment and scaling in assessing the significance of the carcinogenicity findings should qualify even this endpoint. For example, a chemical that causes a clear increase in malignant neoplasia in multiple sites and in both sexes of rats and mice should be given different consideration than a chemical that causes a marginal increase of a benign neoplasm with a background incidence that is normally quite variable in one sex of one species. This approach is referred to as the "weight-of-evidence" method of interpretation, and it goes further than just simple evaluation of neoplasm incidence data.

The judgment of whether a chemical poses a carcinogenic hazard should be made in light of the total evidence provided by all sources of available relevant information. The "maximum tolerated dose" (MTD) concept continues to be one of the most debated and controversial issues in toxicology. Studies that are negative for carcinogenicity but were conducted with doses below the MTD leave doubt about the adequacy of the test. There can be doubt as to whether the animals were sufficiently exposed to the chemical to unmask its carcinogenicity.

On the other hand, studies conducted at or above the MTD may compromise host homeostasis to such a degree that secondary mechanisms intervene; therefore, a positive result may have little relevance to human exposure situations. Because it is not always possible to determine what the MTD will be prior to exposure of the animals over much of their lifespans, the real problem comes with how the study results are used in risk assessment. Thus, conclusions regarding carcinogenicity or lack thereof as determined in chronic rodent tests must be qualified as occurring under conditions of the specific study in question. The limitations of the particular study should be pointed out as they relate to MTD, the original design and purpose of the study, study conduct, confounding toxicity, and other study conditions.

OVERALL SUMMARY

Our understanding of cancer biology is evolving at a rapid rate. Animal and human cancers are fundamentally similar and animal models are revealing the complexities of cancer and leading to identification of human carcinogens. This, in turn, is leading to cancer prevention and cures. Conceptual views of carcinogenesis have been formed by the piece-by-piece discovery of key elements of the complex biological puzzle that cancer presents. These include the early evidence for clonal evolution of cancer, the Knudsen two-hit hypothesis of cancer induction, the observed progression of neoplastic lesions from benign to malignant growth and metastasis, discovery of oncogenes and tumor suppressor genes, advancement of the somatic mutation theory, and the evolution of the CSC theory. With the advent of new technologies in molecular analysis, such as gene expression profiling, genomic sequencing, PCA, HCA, next generation sequencing, exome sequencing, and pathway analysis, carcinogenesis is proving to be much more complex than being simply the clonal evolution of a cell that sustained two genetic "hits" into a full blown malignant neoplasm.

Acknowledgments

The authors wish to thank Drs. Gordon Flake, Arun Pandiri, and Ramesh Kovi and all of the National Institute of Environmental Health Sciences, Research Triangle Park, North Carolina for their helpful comments and suggestions in reviewing and improving this chapter. Also our gratitude to Beth Mahler of Experimental Pathology Laboratories, Inc., of Research Triangle Park, North Carolina for her help with the figures.

Further Reading

Overview of Carcinogenesis

Bannasch, P., 1986. Preneoplastic lesions as end points in carcinogenicity testing. II. Preneoplasia in various nonhepatic tissues. Carcinogenesis. 7, 849–852.

Cardiff, R.D., Anver, M.R., Boivin, G.P., Bosenberg, M.W., Maronpot, R.R., Molinolo, A.A., et al., 2006. Precancer in mice: animal models used to understand, prevent, and treat human precancers. Toxicol. Pathol. 34, 699–707.

Hanahan, D., Weinberg, R.A., 2011. Hallmarks of cancer: the next generation. Cell. 144, 652–674.

Vogelstein, B., Kinzler, K.W., 2004. Cancer genes and the pathways they control. Nat. Med. 10, 789–799.

Mechanisms of Carcinogenesis

Al-Hajj, M., Becker, M.W., Wicha, M., Weissman, I., Clarke, M.F., 2004. Therapeutic implications of cancer stem cells. Curr. Opin. Genet. Dev. 14, 43–47.

Allen, D.G., Pearse, G., Haseman, J.K., Maronpot, R.R., 2004. Prediction of rodent carcinogenesis: an evaluation of prechronic liver lesions as forecasters of liver tumors in NTP carcinogenicity studies. Toxicol. Pathol. 32, 393–401.

Malarkey, D.E., Devereux, T.R., Dinse, G.E., Mann, P.C., Maronpot, R.R., 1995. Hepatocarcinogenicity of chlordane in B6C3F1 and B6D2F1 male mice: evidence for regression in B6C3F1 mice and carcinogenesis independent of *ras* proto-oncogene activation. Carcinogenesis. 16, 2617–2625.

Maronpot, R.R., Fox, T., Malarkey, D.E., Goldsworthy, T., 1995. Mutations in the *ras* proto-oncogene: clues to etiology and molecular pathogenesis of mouse liver tumors. Toxicology. 101, 125–156.

Maronpot, R.R., Yoshizawa, K., Nyska, A., Harada, T., Flake, G., Mueller, G., et al., 2010. Hepatic enzyme induction: histopathology. Toxicol. Pathol. 38, 776.

Pathak, S., 2002. Organ- and tissue-specific stem cells and carcinogenesis. Anticancer Res. 22, 1353–1356.

Reya, T., Morrison, S.J., Clarke, M.F., Weissman, I.L., 2001. Stem cells, cancer, and cancer stem cells. Nature. 414, 105–111.

Sell, S., 2004. Stem cell origin of cancer and differentiation therapy. Crit. Rev. Oncol. Hematol. 51, 1–28.

Omics Revolution

Boorman, G.A., Anderson, S.P., Casey, W.M., et al., 2002. Toxicogenomics, drug discovery, and the pathologist. Toxicol. Pathol. 30 (1), 15–27.

Ellinger-Ziegelbauer, H., Aubrecht, J., Kleinjans, J.C., Ahr, H.J., 2009. Application of toxicogenomics to study mechanisms of genotoxicity and carcinogenicity. Toxicol. Lett. 186 (1), 36–44.

Hoenerhoff, M.J., Pandiri, A.R., Lahousse, S.A., Hong, H.H., Ton, T.V., Masinde, T., et al., 2011. Global gene profiling of spontaneous hepatocellular carcinoma in B6C3F1 mice: similarities in the molecular landscape with human liver cancer. Toxicol. Pathol. 39, 678–699.

Hoenerhoff, M.J., Pandiri, A.R., Snyder, S.A., et al., 2013. Hepatocellular carcinomas in B6C3F1 mice treated with ginkgo biloba extract for two years differ from spontaneous liver tumors in cancer gene mutations and genomic pathways. Toxicol. Pathol. 41, 826–841.

Reis-Filho, J.S., 2009. Next-generation sequencing. Breast Cancer Res. 11 (Suppl 3), S12.

Wang, Z., Gerstein, M., Snyder, M., 2009. RNA-Seq: a revolutionary tool for transcriptomics. Nat. Rev. Genet. 10 (1), 57–63.

Waters, M.D., Jackson, M., Lea, I., 2010. Characterizing and predicting carcinogenicity and mode of action using conventional and toxicogenomics methods. Mutat. Res. 705 (3), 184–200.

Yoon, B.I., Li, G.X., Kitada, K., et al., 2003. Mechanisms of benzene-induced hematotoxicity and leukemogenicity: cDNA microarray analyses using mouse bone marrow tissue. Environ. Health Perspect. 111 (11), 1411–1420.

Identifying Carcinogens

Beyer, L.A., Beck, B.D., Lewandowski, T.A., 2011. Historical perspective on the use of animal bioassays to predict carcinogenicity: evolution in design and recognition of utility. Crit. Rev. Toxicol. 41, 321–338.

Hoenerhoff, M.J., Hong, H.H., Ton, T.V., Lahousse, S.A., Sills, R.C., 2009. A review of the molecular mechanisms of chemically induced neoplasia in rat and mouse models in National Toxicology Program bioassays and their relevance to human cancer. Toxicol. Pathol. 37, 835–848.

Huff, J., Cirvello, J., Haseman, J., Bucher, J., 1991. Chemicals associated with site-specific neoplasia in 1394 long-term carcinogenesis experiments in laboratory rodents. Environ. Health Perspect. 93, 247–270.

Huff, J., Haseman, J., 1991. Long-term chemical carcinogenesis experiments for identifying potential human cancer hazards: collective database of the National Cancer Institute and National Toxicology Program (1976–1991). Environ. Health Perspect. 96, 23–31.

Huff, J., Jacobson, M.F., Davis, D.L., 2008. The limits of two-year bioassay exposure regimens for identifying chemical carcinogens. Environ. Health Perspect. 116, 1439–1442.

Pritchard, J.B., French, J.E., Davis, B.J., Haseman, J.K., 2003. The role of transgenic mouse models in carcinogen identification. Environ. Health Perspect. 111, 444–454.

Tennant, R.W., Margolin, B.H., Shelby, M.D., Zeiger, E., Haseman, J.K., Spalding, J., et al., 1987. Prediction of chemicall carcinogenicity in rodents from *in vitro* genetic toxicity assays. Science. 236, 933–941.

CHAPTER

7

Design of Studies and Risk Management in Toxicologic Pathology: Addressing Risks in Product Discovery and Development

Ricardo Ochoa

Pre-Clinical Safety, Inc., Niantic, CT, United States

OUTLINE

Fundamentals of Toxicologic Pathology.
DOI: http://dx.doi.org/10.1016/B978-0-12-809841-7.00007-1

INTRODUCTION

Risk is a generic term used to describe the probability, or chance, of a specific event occurring. For example, when gambling (e.g., games of "chance," like blackjack), the risk applies to the possibility of winning offset by the potential for losing. Both the positive and negative outcomes depend to some extent on random chance, so both may be considered risks, though in many settings the term "risk" is applied to the negative consequence while the positive result is accorded an honorific like "benefit" or "opportunity."

Toxicologic pathology is a key discipline in identifying, characterizing, and managing benefit versus risk (the "risk:benefit ratio") when discovering and developing new products (e.g., chemicals, drugs, medical devices, modified cells and genes, and many other entities), and in particular the adverse (i.e., harmful) health outcomes that may afflict humans, animals, and their environments. An important additional consideration is to balance the health effects (beneficial and potentially hazardous) of the new product with the financial opportunities and risks faced by the firms developing and commercializing the new products.

Evaluating the health and financial risks involves a logical, measured approach to product development. The five principal aspects of the product development pathway are to identify possible negative effects (hazard identification), to determine their complete spectrum and the mechanism(s) and pathogeneses that lead to their initiation and progression (hazard characterization), to develop an interpretation concerning the likelihood that a risk will develop in a given setting (risk assessment), to devise means for reducing or ideally preventing negative outcomes from occurring (risk management), and to communicate with the consumer of the product what the risk is and how it compares to its benefits (risk communication). Risk of an adverse health effect can only be determined in the context of a potential exposure to a particular test article. The practice of toxicologic pathology is instrumental to successfully undertaking all of these tasks. For most industrial toxicological studies, hazard identification and dose–response assessment for xenobiotics (i.e., a foreign chemical substance) are the central work of the toxicologic pathologist, whereas exposure assessment and risk characterization also are important elements of environmental toxicologic pathology.

The toxicologic pathologist applies his expertise in many fashions during the product discovery and development process. Perhaps the most common roles are to determine morphologic (anatomic pathology) and biochemical (clinical pathology) alterations that are produced by exposure to a potential new product (termed a "test article"). Identification and characterization of such changes (an objective dataset) coupled with experience gained during the course of professional toxicologic pathology practice (a subjective, individual-specific or communal "database"), subsequently permits an interpretation to be made regarding whether or not an effect caused by a test article should be considered harmful (adverse) or incidental (nonadverse). As such, the toxicologic pathologist is in a unique position to help in the interpretation of data originating from nonclinical studies in many animal species that will have an often-decisive impact on the product development process with respect to management of health and financial risks.

This chapter concerns the nonclinical issues of health risks; the significance of toxicologic pathology findings as they impact the development process from the impact on human clinical risk; and provides strategies for management of these risks. The information in this chapter lies at the very core of professional toxicologic pathology practice.

RISK ASSESSMENT: THE PROCESS

Pathologists and toxicologists participate in evaluating risk on a daily basis. The pathologist, together with the input from colleagues in toxicology, initially identifies the potential adverse health effects of products in laboratory animals (of many species, but most typically rodents, rabbits, dogs, pigs, and nonhuman primates), defines the dose–response of the adverse effects in test animals, and then determines whether or not these effects are likely to express themselves in a given population (generally human patients with some disease). Estimation of risk is a multipronged analytical problem, involving a series of steps.

Hazard Identification

Hazard identification is a qualitative process utilized to discover potential adverse health effects (e.g., carcinogenicity, neurotoxicity, and developmental toxicity) for humans following exposure to a particular test article under a given set of conditions. The output of hazard identification is the detection of an abnormal finding, sometimes with a preliminary estimate of how the finding (or response) varies with the exposure level (or dose). Hazard statements are usually short (e.g., "Agent X is a known human carcinogen"). Adequate identification of a hazard incorporates numerous datasets, including structure–activity relationships; *in vitro* analyses; ADME (absorption, distribution, metabolism, and excretion) evaluations; genotoxicity; animal toxicity bioassays; and epidemiological (usually human or environmental) information. Part of the hazard

identification is the detailed description of lesions that typify a reproducible treatment effect of the test article. Integration of these findings with knowledge about the pharmacology and clinical toxicology of the test article allows the pathologist to determine whether or not the treatment-associated effect is in fact a test article–related effect.

Hazard Characterization

Hazard characterization expands on the hazard identification step to more fully define "under what conditions the hazard is present." Hazard characterization explores the complete constellation of changes that result from exposure to a test article. A common approach is to assess variations in structural changes (anatomic pathology data) and various biochemical and cellular alterations (clinical pathology data), and where possible to make mechanistic correlations between these types of findings under various exposure conditions: acute versus chronic, low-dose versus high-dose, different routes of exposure, different species, progression, regression or persistence of changes, etc. In modern practice, product registration packages for novel test articles emphasize inclusion of more extensive datasets than would be required for simple hazard identification.

Dose–Response Assessment

Dose–response assessment is a critical element of hazard characterization. Nonclinical toxicity studies are designed to evaluate the conditions under which exposure to the test article might induce an effect, and particularly an adverse effect (i.e., "toxicity"). It characterizes the relationship between variable levels of exposure to a test substance and the shifts in incidence and severity in any responses. Dose–response assessments incorporate both qualitative data (e.g., does a lesion exist, and if so what is its severity grade) and quantitative data (e.g., organ weights, cell numbers, and other end points). Conventional nonclinical studies in animals incorporate four dose groups (negative control, and low, medium, and high doses of the test article); in some cases, additional groups are included (e.g., additional doses of the test article, or a positive control cohort, or even a second negative control group). Dose–response relationships characterize development and progression of effects over a broad range of exposure periods, including acute, subchronic, and chronic effects. The intended goal of a dose–response assessment is to define a threshold of exposure above which the test article will cause adverse effects. Many calculated values have been defined to provide a numerical estimate of this threshold, including the "benchmark dose" (BMD, commonly used for chemicals) and the "no observed adverse effect level" (NOAEL, typically employed for drug candidates). Dose–responses may be linear or nonlinear.

Exposure Assessment

Exposure assessment is another aspect of hazard characterization, which is specific to agents that might be present in the environment. Such analyses entail the determination of the source, amount, and duration of potential exposure (usually to humans, but sometimes to wildlife and their habitat) to the agent of concern. In general, toxicologic pathologists do not obtain such data.

Risk Assessment: The Outcome

Risk assessment is the systematic integration of data regarding potential hazards and their relationship to exposure. This step is essential to predict the potential for adverse effects on human health. Risk assessments are based on results of many studies conducted in multiple species, in which each individual study examines the hazard posed by a specific exposure to a test article at a given level for a set period of time. Such analyses use the frequency and severity of effects seen in the exposed population under specific exposure conditions to estimate whether or not similar effects might be expected to develop in another species (usually humans) under a different set of exposure conditions. Such predictions culminate in calculations of a margin of safety (for chemicals) or therapeutic indices (for drugs, the difference between a minimally toxic dose and a lethal dose). Such assessments may be linked to a formal probability statement. For example, the lifetime exposure (cumulative dose) to a compound might result in a probability statement for developing cancer [Probability of cancer development is 10^{-6} (1 chance in 1,000,000)]. Alternatively, the assessment may rely on qualitative interpretation (a "weight of evidence" approach) of what is considered adverse, culminating in a simple statement of harm rather than a statistical calculation. In this case, not all observations are considered to have equal value (i.e., some outcomes are more undesirable than others), so the weight given to assess the risk depends on the potential extent of the negative health impact. For example, the outcome hepatocellular carcinoma is of greater concern than hepatic inflammation alone.

RISK ASSESSMENT: THE ELEMENTS

Product Discovery and Development Programs: General Features

The series of studies performed during product discovery and development programs are designed to optimize the quality of the products that enter the testing process and eventually become available for use. As the number of products that are explored for possible development increases, it becomes more critical to make decisions based on accurate data, and ideally to make "go—no go" decisions as early as possible during the development process. Obtaining accurate data is often not straightforward, especially in the pathology discipline where the data are based on the professional opinion of the pathologist making the interpretation of morphologic and clinical pathology findings.

Studies undertaken to support the eventual registration of new products [especially new chemical entities (NCEs) being developed as pharmaceuticals for intended human administration] collectively must provide information regarding many parameters. For NCEs, the most critical considerations addressed in nonclinical studies characterize the:

1. distribution of the target in various tissues;
2. distribution of the compound within various tissues (that contain or do not contain the target) in both animals and humans;
3. compound's intrinsic toxicity for individual species (including any effects that occur in multiple test species); and
4. variations in toxicity based on changes in the:
   a. route of exposure;
   b. length of administration;
   c. dose;
   d. absorption, metabolism, and elimination; and
   e. initial dose for humans.

Ultimately, the data are integrated to permit estimation of the initial dose (for NCEs) or margin of safety for humans, together with a statement of the risk–benefit ratio.

Product Discovery Studies

Discovery studies optimize the nature of the products being prepared for commercial use. Many institutions use toxicologic pathologists in discovery studies merely as special-purpose consultants to solely provide diagnoses for possible toxic effects. Inclusion of toxicologic pathologists as integral members of discovery teams (not as outside consultants) is vital to ensure the proper collection and processing of tissue and fluid samples (which is essential to making well-informed development decisions) as well as the identification and (as necessary) exclusion of potential lead candidates, and to document efficacy of the early candidates.

Studies that are carried out in animals during the discovery process are of two major categories: screening studies and exploratory toxicology studies. Due to low availability and high cost of novel test articles, these studies generally use rodents, unless they are inadequate for lack of therapeutic targets for the specific compound.

Screening studies are intended to select among several possible lead compounds to choose the ones with better likelihood of surviving development hurdles to become new products. Such studies often include demonstrating the efficacy of a test article in an animal model of a human condition; diseases in such animal models may be produced by surgical, infectious, or genetic modifications, or may arise spontaneously. The understanding of comparative pathophysiology, which is the core of the pathologist's training, is instrumental in selecting the best animal model to use in the selection of candidates. The key result of screening studies is to show efficacy (i.e., that a test article can alleviate or even cure a disease). However, other important outcomes are to identify the optimal formulation and regimen (i.e., route of exposure) for delivering the compound, undesirable effects (toxicity) that can be eliminated, and biomarkers that can be used to follow the course of a disease and course of treatment.

The other main type of discovery study is the exploratory toxicology assay. These studies are intended to detect adverse effects of a test article, thereby allowing an analysis of its chances of successful development. These studies mimic, on a small scale, the safety assessment studies undertaken in development to satisfy regulatory requirements. While generally done in rodents, dogs or nonhuman primates may be utilized if prior *in vitro* or *in vivo* screens suggest that a species-specific response needs to be investigated.

Safety Assessment Studies

Regulatory animal studies most frequently used in pharmaceutical development may be divided into several categories (Table 7.1). Short-term tests explore such responses as acute toxicity (at high doses for NCEs) and mutagenic potential. A specialized short-term assay, the dose range-finding study, is undertaken in rodents (typically rats) and nonrodents (usually rabbits or dogs) as a means of establishing the spectrum of doses that will be employed in subsequent safety

TABLE 7.1 Accepted Duration of Animal Toxicology Studies to Support Human Clinical Trials of Various Durations[a]

Duration of clinical trial	Rodents	Nonrodents
SINGLE DOSE		
Unites States	1–14 days	1–14 days
European Community	2 weeks	2 weeks
Japan	4 weeks	2 weeks
Up to 2 weeks	2 weeks (Japan: 4 weeks)	2 weeks
Up to 1 month	1 month	1 month
Up to 3 months	3 months	3 months
Up to 6 months	6 months	6 months
>6 months	6 months	Chronic (EC: 6 months; US and Japan: 6, 9, or 12 months)

[a]*Guidance reflects the consensus recognized by the ICH (International Conference on Harmonization of Technical Requirements for Registration of Pharmaceuticals for Human Use).*

Abbreviations: EC, European Community; US, United States.

Adapted from Ochoa, R., 2013. Pathology issues in the design of toxicology studies. In: Haschek, W.M., Rousseaux, C.G., Wallig, M.A., Bolon, B., Ochoa, R., Mahler, B.W. (Eds.), Haschek and Rousseaux's Handbook of Toxicologic Pathology, third ed. Academic Press (Elsevier), San Diego, CA, pp. 595–618 (Table 19.1).

studies. Short-term studies may last for up to 4 weeks; dose range-finding studies generally are 2 weeks in length. Longer toxicity studies are conducted in rodents and nonrodents for weeks ("subchronic," usually 13 weeks); months ("chronic," typically 6 months in rodents, and 6–12 months in nonrodents); or life ("carcinogenicity bioassay" in rodents, 2 years). Special safety studies may be required for critical functions (e.g., developmental and reproductive toxicity, neurotoxicity). Most exploratory toxicology short-term studies are called "Dose-Range Finding Studies" and are undertaken outside of compliance with Good Laboratory Practices (GLP, a set of guidelines designed to ensure that study datasets used to make regulatory decisions are of highest quality). However, successful product approval generally requires that some short-term (2–4-week) studies and all longer-term studies used to assess safety must be conducted in compliance with GLP guidance.

With the exception of some biological products, safety assessment generally requires that product candidates be tested in both rodents and nonrodents. The rodents usually are outbred rats, where their genetic heterogeneity (mimicking that in human populations) and relatively larger size render them preferable to inbred mouse strains. The nonrodents typically are dogs (purpose-bred Beagles), nonhuman primates, rabbits, and, increasingly, minipigs. The choice of model depends on the nature of the test article. For example, nonhuman primates often are employed to evaluate biomolecules [fully human or humanized (i.e., chimeric test articles having a human-origin active domain attached to a backbone of animal derivation)] intended for administration to humans based on the phylogenetic proximity of simians to humans, while rodent studies are often not recommended for use with human biomolecules. The rationale is that conserved molecular properties among these primate groups will minimize rejection reactions and aberrant target interactions of heterologous proteins. However, claims that only primate studies will better predict human responses may be accepted by regulatory agencies only after presentation of relevant justification.

Many individual countries have their own regulatory guidelines for conducting safety studies, which will vary based on the type of product being developed. For example, the guidance provided by the U.S. Environmental Protection Agency (US EPA) for developing agricultural chemicals differs from that given by the U.S. Food and Drug Administration (US FDA) for developing pharmaceutical agents. Within the US FDA, guidance varies with the nature of the potential product (NCE vs medical device vs cell therapy, etc.). The trend toward product registration in multiple geographic regions has led to efforts toward standardizing regulatory requirements around the globe. Examples of such collaborative international rule-making include the ICH (International Conference on Harmonisation of Technical Requirements for Registration of Pharmaceuticals for Human Use) and the OECD (Organisation for Economic Co-operation and Development).

Wide consensus exists that nonclinical safety assessment studies support human clinical trials of equal length. Some exceptions exist to these rules, particularly when the risk–benefit analysis reveals that exposure to the potential harmful effects of a compound is less detrimental to the patient than the withdrawal of a drug providing obvious benefit. Such exceptions often are made for compounds being developed to treat life-threatening diseases for which there is no alternative treatment, such as terminal cancer or lethal genetic diseases. In contrast, decreased tolerance for risk is present when dealing with diseases considered "minor" or cosmetic, or for which there are safe alternatives (e.g., asthma, diabetes).

Experimental Design for Discovery and Safety Studies

Studies undertaken during product discovery and development generally should be designed in advance. Discovery studies may be planned informally, using

an outline, while GLP-type safety studies are conducted according to signed protocols that detail all aspects of the experiment. Specific sections of standard study protocols describe the test article and control materials, the animal demographics, methods, and how data quality will be assured. The toxicologic pathologist will be instrumental in ensuring the accuracy of tissue and fluid sampling as well as the analytical battery to be used (i.e., anatomic pathology and clinical pathology endpoints). In addition, the pathologist should review other portions of the study protocol (e.g., choices of species/strain, sex, and age) so that obvious errors are avoided. For example, acute studies in nonhuman primates may be designed in which the test subjects are immature (younger than 3.5 years), which may confound the assessment of toxic responses in the gonads.

Perhaps the key consideration for developing NCE products is defining the dose range that will be tested in the nonclinical setting. In general, doses for animal studies are chosen that are a multiple of the effective dose as predicted from *in vitro* and efficacy discovery studies, where doses were escalated until intolerance was observed. From this starting point, doses are decreased and given over several days (often varying between 5 and 14 days, depending on compound availability). The dose range for safety studies in animals typically will exceed the proposed human dose by a large amount (ideally with a high dose that is 20-fold or greater than the intended human dose).

In general, GLP-type safety studies have the following design features with respect to the toxicologic pathology examination. Typical pathology endpoints are organ weights; clinical chemistry and hematologic parameters (comparable to the test panels performed in the diagnostic pathology setting) in blood samples; and histopathologic changes in specimens from all major organs as well as demonstrably unique organ regions (e.g., in brain, specimens are taken specifically from multiple cerebral zones that serve distinct functions). Special pathology procedures (electron microscopy, urinalysis, blood smears, etc.) may be undertaken if necessary, either as part of the original study protocol (based on prior experience with the test article or a structurally related compound) or by *post hoc* protocol amendment (due to in-life clinical signs seen during the course of the study). Where possible, baseline data collection (prior to initial treatment) is obtained for noninvasive (clinical pathology values, total body weight) or minimally invasive (e.g., needle biopsies) parameters; thus, each animal also can serve as its own control as an additional means of evaluating biological responses. The full constellation of pathology endpoints generally is examined at the end of the treatment period (the "terminal necropsy") and also after a treatment-free period (the "recovery necropsy").

The number of animals per treatment group is impacted by several factors. The group sizes for scheduled necropsies depend on the timing with respect to the final treatment. For terminal necropsies, the numbers of animals for all groups (including the control cohort) usually are set at 5 males for rodents and 2 males for nonrodents for discovery studies, and 10 per sex for rodents and 4–5 per sex for nonrodents for regulatory studies. For recovery necropsies, these sizes are halved (i.e., five per sex for rodents, and two per sex for nonrodents). The group sizes in rodent studies typically are increased for longer studies so that early, unexpected (unscheduled) deaths do not deplete the animal numbers so much that statistical calculations are thwarted. For example; initial group sizes in 2-year carcinogenicity studies in rodents usually are set at 50–65 per sex per treatment dose for a final per group count of 25 at termination.

Toxicologic pathologists are essential members of the discovery and development program, particularly through their advocacy to avoid major experimental errors. For instance, pathologists can ensure that sampling practices will permit acquisition of both morphologic and clinical pathology parameters, and avoid interference from other sampling on these parameters. Failure to collect these data, including during discovery studies, in the belief that they are either irrelevant or too expensive to obtain can make interpretation of the results difficult or impossible. Pathologists also can argue against the common practice of returning animals from discovery studies to the colony for reuse, since residual changes from the prior experiment complicate the interpretation of changes observed in later studies.

TOXICOLOGIC PATHOLOGY ISSUES IN RISK ASSESSMENT

Diagnoses

Diagnoses of structural lesions (for anatomic pathology) or cellular and chemical changes (for clinical pathology) are the interpretations of a pathologist. Such interpretations represent a combination of objective criteria (e.g., appearance of a lesion) and subjective opinion (based on the training and unique experiences of the individual). Toxicologic pathologists are divided into those who believe that the diagnoses for different variations of the condition should be consolidated (the "lumpers") and those who advocate that every feature should be represented individually in the text description and data tables (the "splitters"). Generally, diagnoses should be the synthesis of different descriptive

components placed into perspective. When the pathologist provides multiple diagnoses to a common pathological response, the diagnosis may be obscured and the data tables greatly expanded, making interpretation difficult. However, occasionally splitting the diagnosis will clarify the interpretation of a response, and in those situations splitting is appropriate. A good example of this dilemma is the use of multiple diagnoses for different components of chronic progressive nephropathy (CPN) in rats, which can encompass varying degrees of regenerative (basophilic) tubules, proteinaceous content in tubules, interstitial fibrosis, interstitial lymphocytic infiltration, and glomerular sclerosis, among others. The separation of these components into individual diagnoses may make the detection of another renal effect difficult by masking a potential compound-related effect on the behavior of a background lesion.

Toxicologic pathology evaluation is undertaken to discriminate genuine treatment effects from incidental findings ("background pathology" or "normal abnormalities"). Accordingly, certain findings in pathology samples are not diagnosed. Examples include minimal elevations in serum activities of hepatocellular leakage enzymes [e.g., alanine (ALT) and aspartate (AST) aminotransferases] in many animal species and small foci of extramedullary hematopoiesis (EMH) in the liver and spleen of rodents. Such changes fall within the expected range of interindividual variability ["within normal limits" (WNL)] and do not impact organ function. Thus, ignoring such minor findings is a means of avoiding the expansion of pathology data tables with incidental changes that do not indicate the presence of an adverse effect. However, if the degree of such changes is increased in a dose-related fashion (e.g., EMH fills the parenchyma or leads to bulging of the splenic contours), such findings should be accorded a formal diagnosis so that their potential biological importance may be assessed. Of course, variability among pathologists in whether or not these changes are recorded may impact the historical control data tables, which are occasionally used to interpret the incidence and severity of these types of changes if the findings in the concurrent control group are confusing, inconclusive, or skewed.

Validation of Diagnoses

Masked (Blinded) Evaluation of Slides

Information regarding the treatment group, clinical signs, necropsy findings, clinical pathology, and any other relevant information should be taken into consideration when making diagnoses. Therefore, the initial evaluation of the changes in toxicology studies should not use masking (coded or "blind" reading), as the ancillary information is critical to arrive at a specific diagnosis. The most important role of the pathologist follows the clinical model, where all the available information is used to achieve an accurate diagnosis. Performing a masked (blinded) assessment becomes useful when a subtle change is identified and one wants to decide (1) whether or not the treated animals have a higher incidence or severity of the change relative to the controls and (2) to establish a NOAEL (i.e., at what dose the adverse finding is not present) or NOEL ("no observed effect level," the lowest dose at which no treatment-related change—adverse or not—is seen). In such situations, the findings seen during the unblinded initial evaluation are used to define the grading criteria that will be utilized during the subsequent blinded examination. Blinding the slide assessment for that organ allows the pathologist to remove the possible unintentional bias of knowing which animals were treated and which animals were controls. Of course, review of specific slides in special-purpose studies, such as efficacy or mechanistic endpoint, can and should be done blindly in order to eliminate observer bias. In regulatory toxicology studies, masking (blinding) is a second-tier mechanism to clarify subtle changes in the diagnosis.

Peer Review

Because of the subjective nature of the diagnostic interpretation, the toxicologic pathology community has developed the process of formal peer review of histology slides and study data. Pathology peer review verifies and improves the accuracy and quality of pathology diagnoses and interpretations. Peer review is conducted at the discretion of the sponsoring organization, and may be planned in advance (by inclusion in the original study protocol) or undertaken retrospectively (by amending the protocol). In general, pathology peer review is recommended when important risk assessment or business decisions are based on data from nonclinical studies.

The peer review pathologist reviews sufficient slides and pathology data to assist the study pathologist in refining pathology diagnoses and interpretations before study completion. Consultations with additional experts or a formal (documented) pathology working group may be used to resolve discrepancies. The importance of pathology peer review to assuring data quality has resulted in the establishment of recommended (best) practices, which provide standardization while retaining flexibility.

Quality Assurance

Delivering defective samples to the pathologist (e.g., hemolyzed blood samples; slides with artifacts and with

incomplete tissues or tissues that are unfit for evaluation due to staining, cutting, or overall processing defects) increases the time for analysis and reporting while obscuring evaluation. The pathologist, in such situations, has the further role of quality controller for the necropsy team and processing laboratory. For example, slides with defects identified by the toxicologic pathologist should be recut or reprocessed before microscopic evaluation of the tissue, while hemolysis may require remedial training of the necropsy team prior to the next study.

Adverse Events

Risk assessment requires data from toxicology studies that identify the nature of any adverse events and the doses at which they occur. Defining adverse events is core to a toxicologic pathologist's job, though decisions regarding whether or not an effect is adverse is far from clear-cut when real data are presented. Many morphological changes (lesions) are routinely recognized as adverse (e.g., cancer, blindness, reproductive failure). Unfortunately, most treatment-related morphological changes are not obviously adverse, but nonetheless need to be addressed with respect to why they are or are not considered adverse. For example, the presence of increased liver weights as an expression of enhanced metabolic activity in hepatocytes to detoxify a NCE (i.e., "hepatic enzyme induction") is a common event in rodent toxicology studies but seldom is observed in nonrodents (or human patients). Regardless, most toxicologic pathologists do not consider this treatment-associated effect to be adverse, even though liver cytosolic aminotransferases (e.g., ALT, AST) and other biomarkers of hepatic injury may leak into the circulation. This change becomes adverse in rodents when it interferes with critical functions or leads over time to neoplasia. As this adaptive response progresses and hepatocytes become swollen diffusely, adversity is indicated by an increased probability of liver rupture during handling of the animal and eventually increased susceptibility to liver neoplasia, both benign and malignant. A related finding is thyroid neoplasia, which is a secondary response to enhanced hepatocyte metabolism of thyroid hormone (T_4) that leads to increased secretion of thyroid stimulating hormone by the pituitary gland and ultimately follicular cell hyperplasia in the thyroid gland. So, when do such findings become "adverse"?

First, an event is considered to be adverse only when there is a negative health impact (harm) to the animal that suffers the event. The presence of a detectable biomarker that demonstrates that a response has occurred is not necessarily proof of adversity. Second, the event may be adverse in one species, but not in other species where the compound is used. An example of such a finding is $\alpha 2\mu$-globulin nephropathy, in which exposure to certain agents causes accumulation of hyaline droplets in renal proximal convoluted tubules only of male rats leading to renal dysfunction and neoplasia. Therefore, the designation of adversity is limited to the specific conditions of a given study in which the adverse event is found, and is not relevant to other species, lengths of treatment, doses, etc. Third, it is unacceptable to report that a finding is *not* adverse in a test species based on the known lack of applicability to human beings (as is the case with enzyme-induced liver hypertrophy and $\alpha 2\mu$-globulin nephropathy, which are limited to rodents and may be adverse in these animals). Finally, data regarding morphological changes should not be extrapolated based on an assumed (known) course of future lesion progression.

Reversibility (Recovery)

In general, a reversible lesion is considered to have a lower risk than a nonreversible one, which may also be progressive. In many cases, the pathologist can address whether or not the given change is generally accepted as reversible and can even suggest what amount of time would be required for its reversal. Recovery must be assessed in the context of the treatment and the incidences of incidental findings. For example, some treatments may modify the pattern of age-related background changes (e.g., CPN, thymic involution), but such effects may not be reversible as the animals continue to age throughout the study.

For certain changes, the potential for reversibility is not very well understood (e.g., some new compound-induced changes through novel mechanisms), so there is a need to document whether and when the change resolves. How to document the reversibility of findings in toxicology studies that have a limited preplanned time course becomes an issue. One common approach is to increase the number of animals in each treatment group [generally by 50% (five animals per sex in rodent studies and two animals per sex in nonrodent studies)], with the extra animals allocated to the recovery necropsy.

Determining the numbers of animals dedicated to assessment of reversibility is tricky. If the morphological change occurs in 100% of the animals in the high-dose group, a few additional animals will suffice. In contrast, if the incidence is low (e.g., 1 out of 10 animals shows the change) and there is no reliable biomarker of the compound-induced effect, reversibility cannot be determined using only a small number of additional animals as there may not be any evidence

that the animals expressed the lesion at the end of dosing. Hence, one cannot say that the change "reversed," as one cannot determine if it was there in the first place. The practice varies among institutions; some study directors explore reversibility only in the high-dose and control groups, while others use recovery animals in all dose groups to find out at what dose level the change becomes reversible. In general, the reversibility groups are kept without dosing for a specified time following compound exposure—usually the same duration as dosing for short-term (4-week) studies, and shorter than dosing (one-third to one-half) for longer studies.

Deciding on the appropriate length of time to conduct the recovery necropsy can impact the evaluation of reversibility. Even short-term studies might have changes that require an extended time for recovery; hence, a 2-week recovery period may be insufficient to determine whether or not reversibility occurs at all, let alone occurs completely. If there is a biomarker that can be used to predict the presence of a morphological alteration, the length of the recovery period may be adjusted during the course of the study, until the biomarker comes down to normal levels. If no biomarker exists, and if the time of recovery necropsy is too early, lack of reversibility (or at best incomplete reversibility) may be evident. Risk managers often interpret this scenario as lack of reversibility. General practice for assessing reversibility is to have the pathologist review only tissues identified as targets during tissue evaluation for the terminal necropsy (i.e., encompassing the treatment period, and ending in the scheduled terminal necropsy), as the main study has already identified that there are no test article–related effects in nontarget organs.

Severity Grading

Toxicologic pathologists use severity grades to score changes observed. Such grades are semiquantitative in nature and generally follow a 4-point to 6-point scale, in which a term for lesion severity (ideally based on a set of specific descriptive criteria) is matched to a number (to permit statistical calculations). Possible ways to define such scales are:

- *4-point scale*: WNLs (Within Normal Limits) (0), minimal (1), modest or moderate (2), and marked (3) changes;
- *5-point scale*: WNLs (0), or minimal (1), mild (2), moderate (3), or marked or severe (4) changes; or
- *6-point scale*: WNLs (0), or minimal (1), mild (2), moderate (3), marked (4), or severe (5) changes.

The only way that these diagnostic terms have any relevance is if the pathologist follows an *a priori* system that is preferably written and somewhat universally understandable before tissue evaluations start. The choice of scale (including the terms used for each grade) typically is decided by the pathologist, the 5-point scale is probably the one that is used most. For commonly seen lesions (especially if they occur reliably in a given animal model), pathologists are encouraged to either follow recognized scales gleaned from the literature or base their own scales on objectively defined criteria tempered by prior experience—and ideally publish them, or at least define the scale in the study report.

The severity grades should be independent of the study, and applicable to any lesions observed. For example, minimal severity may be defined as a change that is barely discernible from background morphology or that involves less than 10% of the organ surface and is not expected to affect the functionality of the organ. In contrast, a severe score may be defined as a visually apparent change that involves 75% or more of the organ surface and is expected to affect the functionality of the organ. The other severity grades are placed somewhere in between these two extremes, and should be divided into logical sections using recognizable structural attributes (the character of the finding, the number of affected cells, etc.).

As there is no universal system of severity scores to date, it is important to ask colleagues for the systems that they use when faced with devising a novel scoring scheme of your own. It is also essential to remember that these agreed-on severity grades constitute ranges of morphological features, which may include changes that are visibly distinguishable within the different grades, but that are not distinct enough to warrant a change in the severity grade. The adoption of severity grades based on the changes present in the individual study, by adopting the highest score for the most severe lesion observed in that study, leads to complications because the scale would be unique in different studies of the same compound, and therefore not universally understandable. The severity grade descriptors and the criteria used to define them should be part of an institutional standard operating procedure (SOP) or listed in the pathology report.

What Constitutes a Risk—Is the Risk Real?

When encountering an adverse effect, the development management team should make sure that the effect is "real" before making conclusions regarding safety and efficacy. Poorly designed studies can endanger the development plan and may lead to radical and perhaps rash decisions by the team. The following factors need to be considered when determining the implications of treatment-related effects.

Statistical Versus Biological Significance

Absolute reliance on statistical calculations does not address the biological relevance of the statistically significant effect recorded using multiple stars in pathology data tables. Given the large number of statistical analyses performed in nonclinical studies, and given the inherent physiological variation among members of the heterogeneous sample population, it is not unusual to see statistical significance in parameters that may have limited biological significance. These findings may be a statistical artifact (Type I error erroneous rejection of a "false positive" result). Statistical artifacts often are seen in clinical pathology and organ weight datasets.

Is the "No-Effect" Outcome Real?

The toxicologic pathologist needs to remember that the absence of evidence does not constitute evidence of absence. Failure to show a statistical difference for a biologically evident effect, referred to as a Type II error (erroneous acceptance of a "false negative" result), may occur if the power of the study (i.e., animal numbers in each treatment group) was inadequate. Therefore, the process of analyzing data from a study should first check that the computer-generated statistical probability for a given finding is consistent with its potential biological impact. This exercise requires an understanding of the design, execution, and objective results of the study, ultimately culminating in a part-objective/part-subjective segregation of the biologically important results from the spurious ones.

Inconsistent Nomenclature

Since pathology is an interpretive science, there is a high degree of variability in the application of diagnostic terms. Using incorrect nomenclature when describing treatment-related findings can either raise a false risk or ignore a true one. Misdiagnosis of findings can occur due to inexperience of the pathologist. Diagnostic drift (i.e., assigning two or more diagnoses or inconsistent severity to identical lesions during the course of a study) is an error sometimes made even by experienced pathologists. Pathologists should employ considerable care in avoiding these problems when evaluating nonclinical studies including masked review.

The discipline of toxicologic pathology provides two solutions to this problem. The first is the production of consensus terminology. The most consequential effort in this regard is the INHAND initiative (International Harmonization of Nomenclature and Diagnostic Criteria for Lesions), in which pathologists with organ-specific expertise from around the globe have defined descriptive terms and criteria for nonproliferative and proliferative lesions. The second solution is the introduction of pathology peer review as a routine component of the safety assessment process.

Splitting Diagnoses

The perils of dividing complex lesions (e.g., CPN or murine progressive cardiomyopathy) into separate diagnoses for each of the specific components (e.g., renal tubular degeneration, renal tubular regeneration, interstitial inflammation, interstitial fibrosis) have been mentioned earlier, but it warrants mentioning again. The practice may lead to identification of phantom issues that either will require correction during data interpretation or may obscure possible treatment-related effects characterized by specific induction of a related change (e.g., isolated interstitial inflammation or fibrosis in the absence of CPN).

Compound-Related Versus Compound Effects

Not all changes observed in toxicologic studies are a toxic reaction due to the compound. A compound can have an effect that is deleterious to the animal, but this effect is an expected exaggeration of the intended "on-target" biological effect (referred to as "exaggerated pharmacology"). In terms of toxic off-target responses, some effects are primary (caused by the compound directly), while others are secondary (caused by complications from a primary effect).

EXAGGERATED PHARMACOLOGY

Since toxicological studies are designed to expose individuals to doses of compounds at many multiples of intended therapeutic doses, the organism may show adverse effects due to excessive activation of the test article's molecular target. Such predictable but heightened effects are not expected in the clinical setting, or at least not with the same severity. Of course, product developers are accustomed to extrapolating safety margins for anticipated physiological reactions, using data from nonclinical studies to estimate the potential response of tissues having a comparable molecular target following treatment of patients with the test article in the clinical setting. A possible problem occurs when such pharmacologic changes in humans may be new and/or unexpected and/or persistent. For example, it is very difficult to find a NOEL in glucocorticoids because these compounds impact endocrine and immune organ function at therapeutic doses. When given to excess (in terms of either dose or treatment length), these pharmacologic effects are adverse even though they are an expected consequence of glucocorticoid exposure.

PRIMARY TOXICITY

These effects can be ascribed to direct action of the test article. Off-target actions are effects on tissues or molecular pathways where the compound acts at an unintended site. The concept of an off-target effect implies that the test article interacts with a new target that is not the originally intended one, that the distribution of the original target was not well understood, or that the target has a different distribution in the toxicology test species. These off-target effects can be identified early during development by assessing expression of the pharmacologic target. Such expression studies (usually done for the functional protein) are essential components of selecting among possible lead candidates.

SECONDARY EFFECTS

These outcomes are a very common reason for adverse compound effects, some of which can be devastating. These effects are indeed compound-related, but they are a downstream effect from an initial impact of the compound on systems that lead to a cascade of follow-on effects. It is not unusual that secondary effects will lead to major organ dysfunction and mortality, yet frequently they are confused with direct (primary) effects of the test article. Perhaps the most common secondary effect of compound exposure is "stress," which is often definitely related to test article concentration and occurs in a dose-dependent fashion. Consequences of compound-related stress are deficient immunologic function (via the lympholytic action of glucocorticoids in the circulation and lymphoid organs), listlessness, and a general feeling of discomfort, which may depress the appetite, lower food consumption, and promote weight loss. These outcomes may be mediated by release of cytokines and chemokines. Once listlessness and low appetite manifest, the situation can intensify as indicated by increasing severity and incidence in the affected groups related to the release of endogenous glucocorticoids and other hormones (e.g., catecholamines), which in turn result in catecholamine-induced focal myocardial necrosis (termed "murine progressive cardiomyopathy") or even sepsis and death.

More drastic immunosuppression has pronounced effects on the ability of the organism to fight opportunistic bacteria or viruses, so that generalized infection (sepsis) and later death may follow. In these situations, it is imperative to determine whether or not the immunosuppressive effects are solely the result of stress or alternatively a component of immunotoxicity caused by the compound. Similarly, septicemic conditions can affect multiple organs such as liver, lungs, and kidneys, although these infected sites are not considered "target" organs of the test article.

RISK PERCEPTION AND ACCEPTABILITY

Perception of risk varies considerably among different populations and the conditions under which the perceived risk has occurred. Cultural norms in the society where the risk is assessed influence its perception, and the decisions that people take to decrease this risk. The accurate assessment of risk is often difficult because it requires the weighing of multiple factors that may combine in variable fashions to produce an adverse effect. Two of the most important characteristics in evaluating risk are assessment of its probability and of its severity. Ultimately, communities must decide what level of risk is acceptable. Negation of all risk is very difficult to achieve (if possible at all), and is associated with rapidly rising costs for relatively small gains.

Acceptability of the Risk

Perception of risk is a subjective, individual-specific process that is essential for survival. Scientists are often surprised by the reaction of various audiences to a potential risk. In some cases, findings that are thought to be of limited biologic relevance end up causing great concern from colleagues within the laboratory, regulators, or the general public. This diversity of perspective is better understood when we look at a number of factors that affect the ways in which different people under differing conditions perceive risk, which impacts whether or not they are willing or not to accept that risk. Some common attributes of the risk that influence the perception of its acceptability are outlined in the following sections.

Likelihood (Probability) of the Adverse Effect

The likelihood of a risk being realized as an adverse effect is one factor that affects how that risk is perceived. In many cases, risks that have a very small likelihood of affecting a person will be perceived to be less important than risks that are more likely to impact their health and life. However, some extremely unlikely effects may be deemed unacceptable due to the other factors discussed later. To further complicate the matter, some relatively large risks (e.g., dying of a smoking-related illness, or dying in a car accident) are perceived by many as being relatively acceptable to society as a whole since the decision to smoke or drive is an individual choice that incurs individual responsibility for the outcome.

The toxicologic pathologist is often ideally suited to help inform our communal understanding of the relative likelihood or severity of an adverse effect. In some instances, a specific morphologic diagnosis taken at

face value may sound ominous, but when put in context with the relative severity of the effect, margin of safety, and other information, rational consideration permits the decision that the seemingly menacing risk is acceptable. An example of this scenario is use of Non-Steroidal Anti-inflammatory Drugs (NSAIDs). There has been mounting evidence that the use of these products for the long-term treatment of chronic pain may increase the probability of significant cardiovascular events. However, the risk is marginal and the prospects of living with crippling chronic pain make people disregard the small probability of increased cardiovascular events and continue taking the medication.

Permanent or Reversible Nature of the Adverse Effect

Different types of risk are usually perceived differently, and for obvious reasons (e.g., cancer vs transient nausea). Most people are more willing to accept the risk of effects that are relatively minor, and reversible or temporary (e.g., nausea). On the other hand, they are less likely to accept an increased risk of serious negative effects that are less reversible or lethal, and that a serious negative impact on the quality or length of life (e.g., cancer). This concern highlights the importance of understanding the reversibility of key test article−related toxicities.

Risk/Benefit

Knowledge of the severity of the adverse effect is required for accurate assessment and management of risk. There are multiple examples of acceptable risks in daily life (e.g., driving), and the development of new products is no exception. If the likelihood or impact of an adverse effect (risk) is of less concern than the test article's ability to reduce or cure a disease (benefit), the existence of an adverse event may not prevent the approval and use of the treatment. The balance between risk and benefit will depend on the severity of any adverse event. For example, if the probability of a severe reaction is low (1/1000) relative to the devastation produced by a disease (say, 20%), the occurrence of the severe adverse reaction may be catastrophic to that one individual in a thousand. This possibility therefore creates ethical complications with respect to what risks should be taken by the many, and how to avoid the adverse event in the one.

Who Benefits From Acceptance of a Risk?

People who may benefit from accepting a risk tend to be more willing to tolerate that risk than people who do not benefit. This becomes particularly important when the people who face the risk (e.g., residents who live in an industrial area affected by factory emissions) are different from those who stand to reap the greatest financial benefit (i.e., the owners and operators of the factory). In this case, even very small risks may be completely unacceptable to nearby residents, due to the lack of perceived benefits. This concept highlights a key difference in the approach required for a toxicologic pathologist engaged in environmental risk assessment compared to a toxicologic pathologist involved in safety assessment for biomedical products (drugs, devices, cell therapies, etc.). In drug safety assessment, prescribers and patients typically are willing to accept certain risks given the benefit that the patients expect to receive by accepting the intentional exposure.

A fundamental challenge to risk communication is the fact that actual risks that bring harm are often completely different from the perceived risks about which the public is concerned. This dilemma has been highlighted by Covello and Sandman (2001) (see Further Reading), who define "Risk" as the sum of "Hazard" and "Outrage." In their paradigm, "hazard" represents the data-driven assessment a scientist would use to identify and understand potential harm while "outrage" represents those factors, often emotional, that influence the public's perception of risk. Positions held by the lay public, which trained scientists would view as irrational fears, may primarily be due to a lack of context for the general citizenry. For example, consider a molecule that, when inhaled in sufficient quantity, is fatal, and where accidental inhalation resulted in over 3000 deaths in 2007. Without appropriate context, the public might consider this molecule—common everyday water!—a highly toxic substance. Thus, to effectively communicate and manage risk, toxicologic pathologists need to understand that an individual's perception of risk goes far beyond the data-driven, reasoned analysis that governs scientific dialogue. Understanding the emotional factors that influence how a risk is perceived will aid the toxicologic pathologist to more effectively communicate and manage risk.

RISK COMMUNICATION

When communicating potential risk to different audiences, it is important the discourse be conducted as thoughtfully and rigorously as the experiments which provide the scientific basis for the risk assessment. The effectiveness and impact of a rigorous safety assessment program can be markedly diminished if the risks are not portrayed in a clear and concise manner. Communicating sensitive, technical information to a nonscientific audience can be one of the most difficult challenges that a scientist faces today. This is

especially true for communicating with the general public given the public's growing distrust of corporations, academic institutions, and government agencies charged with protecting the health and safety of our communities.

Risk communication has developed into a distinct discipline, so the toxicologic pathologist should have a basic understanding of certain key principles in this field. The following definition of "risk management" developed by the National Research Council (NRC) and US EPA provides useful insight into this field, which is relevant to individuals in both environmental risk assessment and safety assessment of novel biomedical products. According to these two groups, "risk communication is an interactive process of exchange of information and opinions among individuals, groups, and institutions." The US EPA acknowledges specifically the key role of risk communication in the risk management process, stating that risk communication is "any purposeful exchange of information and interaction between interested parties regarding health, safety, or environmental risks." In addition, the US EPA has defined "Seven Cardinal Rules of Risk Communication" outlining the critical steps to effective dialogue with the public. These points are:

1. accept and involve the public as a legitimate partner;
2. listen to their concerns;
3. be honest, candid, and open;
4. coordinate and collaborate with credible sources;
5. speak clearly, concisely, with care and compassion;
6. plan carefully, and evaluate your efforts continually; and
7. meet the needs of the media (where appropriate).

While these steps are focused on information being delivered to the lay public, they are useful to consider when communicating risk to scientific audiences as well (including decision makers like managers and regulators).

Challenges and Obstacles to Effective Risk Communication

To effectively communicate risk, it is important to be aware of various issues that complicate such communications. Overcoming these obstacles will help create a "common language" that can be understood by both the communicator and the intended audience(s).

Data Versus Information

Scientists are trained to deal effectively with data. Experiments are designed and conducted; the data are collected, organized, and analyzed; and the investigator reaches a conclusion about the meaning of the data. In other words, a "data" set is a collection of single observations that, when synthesized, provides "information."

The public and other lay audiences are at a disadvantage compared to scientists when it comes to interpreting data. They often do not have the technical knowledge to synthesize data into information, let alone understand the meaning of a single data point. This lack of understanding can lead to misinterpretation of data, or to the inappropriate focusing of attention upon a single experimental result—both of which may lead to an incorrect interpretation regarding potential risk.

More data may be perceived by nonscientists to mean "more concern." Therefore, the public should be provided with information in understandable language, and not just data. For a lay or public audience, it is important to avoid presenting excessive amounts of data when summarizing risks, particularly at the expense of providing integrated information. Effective communicators understand the needs of their audience, examine their data carefully, and present the data in a manner that provides information in language that is accessible to their audience. Accessibility of the language is key: information that is presented in unintelligible language does not impart knowledge, does not empower involvement in decision-making, and instead may be perceived to be a tactic designed to hide or conceal important risks from the audience. This dilemma can be a particular concern for toxicologic pathologists in that, for both scientific and lay audiences, the "language" of pathology (with its diverse array of diagnostic and descriptive terms that are assigned by subjective criteria) can often be confusing at best, and misleading at worst.

Public Expectations of Science

A scientist must communicate with many of the "lay" audiences, which may have unrealistic expectations regarding what science can provide and also preconceived notions regarding scientists in general. The media frequently report scientific failures and impending threats, such as the withdrawal of a marketed drug due to previously undiscovered side effects or the discovery of chemical contaminants in drinking water that may cause cancer.

At the same time, people seem to have serious doubts about the positive role of science in their lives. Many members of the lay public consider scientists to inaccessible (at best) and/or aloof. This impression is often a result of the inability, or unwillingness, on the part of scientists to learn and use clear, simple language to explain what they do, how they do it, and

what they have found. It is not surprising that scientists have difficulty in meeting the public's expectations of science: the public desires simple and absolute answers, while given complex interacting factors in the real-world science can generally only identify likely and unlikely outcomes but not what is guaranteed to happen. Thus, scientists resist distilling information down to simple "yes" or "no" answers, preferring instead to present probabilities and theories while recounting all the evidence in support and against them. This is an important disconnect in communication between technical experts and the public. The public understanding of the word "safe" as in categorizing the probability of a compound to produce adverse effects is simpler than the meaning of "safe" as understood by scientists. The public expectation is that a "safe" product has no deleterious effects, but the scientist knows that the word safe is just the beginning of a sentence that describes when, how, and in what circumstances the compound can be given to avoid adverse events.

Contradictory Expert Opinions

The scientific method is rooted in hypothesis testing, in healthy debate that validates interpretations of data through experimentation, and through reasoned argument about alternative explanations. Interpretations that withstand this rigorous scrutiny become established as the most plausible explanation, and become a platform for further expansion of knowledge. Unfortunately, the public rarely has an opportunity to see this constructive and (usually) collegial process, and do not comprehend how expert scientists can interpret the same objective dataset differently. This dynamic is particularly relevant to anatomic toxicologic pathologists in that histopathology is an interpretive science based on assigning subjective diagnostic terminology and thresholds; differences among pathology practitioners create confusion and, at times, distrust of the dataset and final interpretation. To forestall such objections, pathologists should seek to deliver peer-reviewed, consensus datasets rather than disparate subjective opinions on the effects of a test article.

RISK MANAGEMENT

Risk management encompasses the systematic scientific identification, evaluation, and prioritization of risks with respect to adverse health effects resulting from human or environmental exposure to hazardous agents or situations. The goal of risk management is the economical application of finite investigative and corrective resources to minimize, monitor, and control the probability and/or impact of the adverse events. The positioning of the toxicologic pathology findings is an important aspect of risk management.

Risk management practices differ depending on the context. In the case of pharmaceutical products, the risks are managed by making sure that the benefits outweigh the risks and that the individuals who are to be exposed to the NCEs understand the risks inherent to receiving the intended exposure (a process designated "informed consent"). A similar situation applies to the chemical industry, except that the potential risk is determined primarily by the likelihood that exposure will cause harm rather than the benefit offered by use of the product. The reason for the difference in regulatory approach to risk in these two industries is the management of exposure. Health products represent a risk that the individual takes knowingly and voluntarily, whereas environmental exposure to chemical hazards typically is involuntary and often unexpected.

The US FDA has defined risk management activities in the following progressive fashion:

- Risk Assessment: Estimation and evaluation of risk.
- Risk Confrontation: Determining an acceptable level of risk in a larger context.
- Risk Intervention: Risk control action.
- Risk Communication: Interactive process of exchanging information.
- Risk Management Evaluation: Measuring and ensuring effectiveness of risk management efforts.

Risk impact is evaluated as the probability (likelihood) of an event occurring, and the severity of that event if it occurs. An adverse event can be considered to have a high probability but low impact (when it will occur often but with little effect), or such events may have a low probability but high impact (when the effects of an event are high but the likelihood of it occurring is low). Differentiation between these two scenarios is essential in communicating risk, as they should be managed in different fashions.

Problems in Risk Management Caused by Toxicologic Pathology Data

Ineffective Reporting

Reports (both for the entire study and for its various component parts, including the pathology subreport) fail when they just enumerate findings based on the statistics and incidence tables without providing a cohesive interpretation for the reader. Frequently, the study report's narrative may fail to address the relationship of different compound-related effects to each other and the potential mechanisms responsible for their evolution. Ineffectual reports may be worse than

useless, because they not only fail to provide a usable interpretation but also may obscure findings of potential importance to the risk assessment and management activities.

Lack of Data Cohesiveness

It is essential to find the underlying causes and biological significance of the effects observed, not just provide a list of these effects. Failure to provide an expert evaluation of all relevant information to support interpretation of findings may result in inaccurate assessment of risks. The lack of cohesive interpretation regarding the biological relevance by a toxicologic pathologist may create difficulty for the development of the test article and cause confusion for scientists who are not trained in comparative pathology, whether these scientists are at drug and chemical companies, serving as managers, or in regulatory agencies. It is also important to expressly address the kinds of background lesions observed and their lack of relevance to the evaluation of the specific compound as a way to clear confusion from reviewers, who are often not versed in the normal laboratory animal findings.

Species Relationships: Is the Animal Finding Relevant to Humans?

OVERPREDICTION

Although animal studies are an important part of understanding the nature of toxic effects, their use to assess potential risk to humans has met with qualified success. In addition, assessment of human risk continues to be a challenge due to the increased complexity of the pharmaceutical and chemical compounds under development. The perils of extrapolation are not only based in the inadequacy of many animal models, which incompletely recapitulate human biological responses, but also in the need for accurate, enlightened, and unbiased evaluation of the data arising from animal models.

For example, it is clear that animal models overpredict carcinogenic risk to humans, particularly from exposure to nongenotoxic compounds (i.e., agents that cause parenchymal cells to proliferate). The ability to induce tumors is often based on mechanistic responses that are either not present in human subjects (e.g., $\alpha 2\mu$-globulin nephropathy) or may occur at exposure levels, which exceed the human dose by such large multiples that it would be highly improbable that such compounds will be able to do harm to an individual. Compounds categorized as nongenotoxic carcinogens in rodents, which exhibit florid proliferative responses in liver, are considered to have a negligible risk of inducing neoplasia in humans, because human liver does not respond to exposure with excessive proliferation to the same extent as rodent liver. In contrast, both rodents and humans exhibit sensitivity for genotoxic carcinogens (i.e., agents that initiate mutations by damaging DNA).

UNDERPREDICTION

Some conditions are not easily addressed by animal models. For instance, the presence of hives and other cutaneous hypersensitivity reactions in humans are underpredicted by animal models. Similarly, developmental toxicology studies in rodents using thalidomide (marketed in Europe as an over-the-counter antinausea therapy for "morning sickness" of pregnancy) failed to predict the extreme sensitivity of the limb primordia in human embryos, leading to an epidemic of phocomelia (lack or underdevelopment of the proximal limbs). Instead, such species-specific differences in adverse reactions often are better addressed by specialized testing using human tissue samples or human volunteers. Notably, the regular battery of nonclinical toxicology studies utilized for development of compounds do not often alert the scientist to this and similar risks. The possibility that datasets derived from animal experimentation do not predict human biological responses emphasizes the critical importance of risk assessment and risk management.

Managing the Identified Risk—Remediation

Treating the Adverse Effect

If the effect is real and if there are health risks to the patient, understanding of the condition that is produced by the compound, regardless of how the product is to be used, is essential. One sometimes can avoid the initiation and progression of an adverse event by coadministration of the compound together with some treatment to mitigate or prevent the adverse effect. For example, coadministration of antiemetics with cancer treatments is used to remediate nausea and vomiting. Similarly, probiotics (i.e., living bacteria or yeast extracts) are commonly coadministered with oral antibiotics to prevent and treat the development of diarrhea that is associated with their use. Thorough understanding of the mechanisms present in the induction of the adverse event is necessary to formulate a treatment strategy for this kind of remediation.

Remediation of Biological Risk

Some severe adverse effects do not necessarily impede development and marketing of a product due to a perceived advantageous risk/benefit profile. The US FDA defines a "safe" product as "one with reasonable risks given the magnitude of the expected benefit and the available alternatives." This definition means

that there must be an acceptance of reasonable risks, based on the benefits that the patient and society will accrue from the use of the given substance; no pharmaceutical agent could be developed if one were to insist on avoiding all risks. The repurposing of thalidomide, a most feared teratogenic compound, for use in the treatment of erythema nodosum leprosum in nonpregnant human patients by careful monitoring and licensing of distribution, is a good example that a compound's toxicity depends on the context in which exposure is to occur. Indeed, many compounds can be safely administered when the mechanisms of toxicity and the conditions of exposure are well understood.

FINANCIAL RISK AND TOXICOLOGIC PATHOLOGY

The pharmaceutical, chemical, and food additive industries are businesses, and as such must produce a profit for survival. This financial motive must be integrated with the expectation that product development decisions must meet society's need for efficacious and safe solutions regarding the health and other needs of its members. In order to attract operating capital, these industries need to convince their investors that the money they pay for their stock will produce more revenue than a similar amount of money invested in other opportunities. This reward is linked to success in developing new products, and in particular unique and/or better products that offer greater benefits or a better risk/benefit ratio to individuals and society as a whole. Discovery and development programs leading to approval of one new product may cost hundreds of millions or even billions of dollars, the cost of which must be recouped if more products are to be produced in the future. As the patents for old products expire, the reduced sales typically associated with competing products from other firms will impact the revenue that the companies can return to their investors. Although there is altruism in the search for new and better medications for patients, the bottom line is that companies engaged in product development cannot survive unless profits are made.

Risk of financial damage by errors of commission (i.e., taking an ineffective or mistaken action) often reflects the identification of false signals or the overconservative interpretation of the data. Errors of commission are not unusual, and typically are more prevalent in small companies and with test articles that are very early in development. Due to the fear of losing the compound later in development and interest in cutting financial losses early, compounds often are removed from the development pathway before enough data have been collected to rationally make a reasoned decision about its viability. For example, the history of the pharmaceutical industry is replete with compounds abandoned due to perceived risks, as well as with the ones that were successful because health risks were effectively managed. Many innovative "first-in-class" (FIC) compounds are at the verge of being dropped due to difficulties in the development program. Since the mechanism of activity is novel, FIC compounds generally face new problems that require considerable expenditure of funds and technical resources to be understood. Only by having a good grasp of these issues, gained in large part by toxicologic experimentation, can enough understanding be obtained to permit product development to proceed.

Risk of financial damage by errors of omission (i.e., not gathering certain data and/or taking timely action) corresponds to making the decision to avoid obtaining critical toxicity data in order to maintain the compound in the development portfolio. Obtaining relevant information for reasoned decision-making is necessary so that the compound may be placed in the appropriate relation to other competing development opportunities. However, gathering such data is risky; frequently, companies choose not to seek nonclinical data because it could be harmful to the compound's success, or there is financial reward (i.e., bonus payments) in keeping several compounds in development at the same time. This approach consumes resources in the short term and, more critically, moves the critical decision regarding a compound's fate to a later, and costlier, stage of development, thereby magnifying the cost of failure. Later in development, companies have a stronger commitment to work on elucidating and explaining away (or mitigating) adverse findings to ensure a path forward for late development compounds. This strategy reflects the prior financial cost, which cannot be lightly cast aside, but risk mitigation as an alternative to "killing" (ceasing development for) a compound is ethically and morally acceptable if sufficient efficacy and safety data are available to ensure that the molecule—a costly asset to the company—has a chance to continue in development and thereby benefit both society and the corporate coffers.

Societal costs occur when compounds helpful in solving health needs do not get developed, or when the public may be put at risk of adverse effects by exposure to potentially hazardous products. It is difficult to articulate and measure societal costs associated with halting development of a pharmaceutical candidate or chemical agent (e.g., herbicide, insecticide). Indeed, this cost is generally ignored.

The contribution of pharmaceuticals and chemicals to society is best understood by comparing the mortality rate of populations before and after the introduction of specific products. Obvious examples in the

biomedical arena are the increase in longevity and the decrease in mortality due to cardiovascular disease and many infections that have been wrought since the introduction of compounds to treat hypercholesterolemia and routine childhood vaccination, respectively. Similarly, longevity and mortality have been positively impacted by the regular utilization of selective herbicides to increase crop production. It is clear from epidemiological studies that society at large has benefited substantially from the use of these products, certainly in comparison to the possible risks posed by unintended exposure of nontarget human and animal populations and their habitats. However, it is difficult to assess the societal cost of the lack of treatments for conditions for which there are no treatments or for which the treatments are inappropriate.

SUMMARY

The critical role of the Toxicologic Pathologists in product development in the pharmaceutical and chemical industries is based on the training and experience of the pathologist to interpret morphologic and biochemical findings observed in animal studies that are preliminary to human or environmental exposure to the same compounds. Pathology is an interpretive science melding a practitioner's objective observations with his subjective judgments, and as such does not have the rigor of the exact numerical determinations of other disciplines. This inherent flexibility in pathology interpretations creates an opportunity for errors and differences of opinion on the data resulting from these studies, and can produce damage to patients and product developers if the findings are not accurately evaluated. Understanding of the risks (health and financial) of the development process is of great benefit to the toxicologic pathologist and the compound development teams. The way that the pathologist perceives, interprets, and communicates the observed effect of the compound has a direct effect in regulatory acceptance or rejection of the compound for human experimentation or marketing authorization. This perception needs to be consistent with the highest standards of scientific

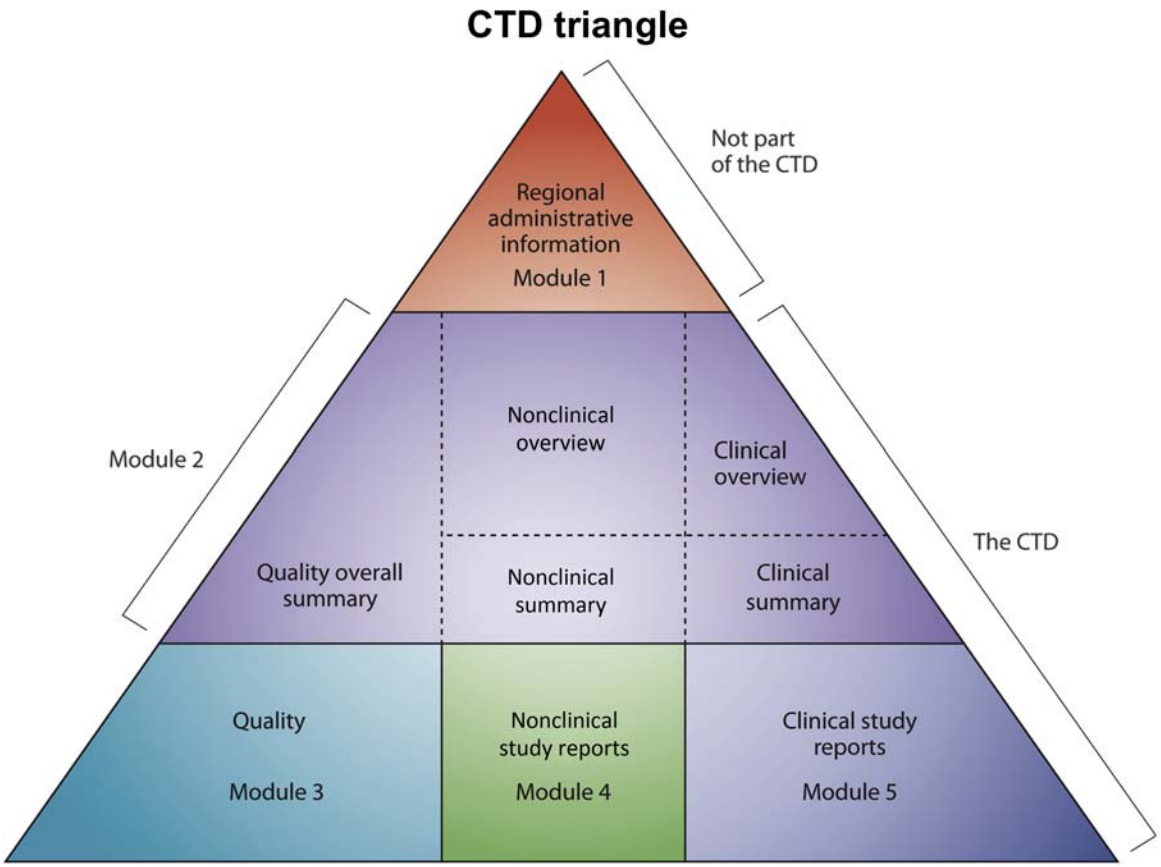

FIGURE 7.1 Diagrammatic representation of the modules required to prepare the Common Technical Document (CTD) for Marketing Authorization of pharmaceutical products. The CTD is organized into five modules. Module 1 is region specific and modules 2–5 are intended to be common for all regions. Source: *From the International Committee on Harmonisation (ICH) website. http://www.ich.org/products/ctd.html (accessed 02.04.17.).*

discipline, and often is bolstered by seeking a consensus interpretation among multiple pathologists through rigorous peer review. Following the generally accepted nomenclature, application of the principles of scientific communication in presenting and interpreting data to the sponsors and regulators, and clear and comprehensive evaluation of the findings is the first step in the process. Participation in the early development programs to address efficacy in animal models, interaction with clinical pharmacologists to make sure that the nonclinical data are appropriately interpreted, addressing adverse events and developing hypothesis to be tested in elucidating the causes and mechanisms involved in the adverse event, and finally developing a strategy to manage and remediate the adverse events are important aspects of the practice of Toxicologic Pathology discussed in this chapter (Figure 7.1).

Acknowledgments

The author acknowledges the contributions of Drs. Colin Rouseaux, Stephen Durham, James Swenberg, and John Vahle for the materials from their chapters that are included in this chapter.

Further Reading

Covello, V., Allen, F., 1988. Seven Cardinal Rules of Risk Communication. U.S. Environmental Protection Agency, Washington, DC, <https://www.atsdr.cdc.gov/risk/riskprimer/references.ht> (accessed 02.04.17.).

Covello, V., Sandman, P., 2001. Risk communication: evolution and revolution. In: Wolbarst, A. (Ed.), Solutions to an Environment in Peril. John Hopkins University Press, Baltimore, MD, pp. 164–178. , <http://www.psandman.com/articles/covello.htm> (accessed 02.04.17.).

Covello, V., Slovic, P., von Winterfeldt, D., 1988. Risk communication: a review of the literature. Risk Abstracts. 3 (4), 172–182.

Durham, S.K., Swenberg, J.A., 2013. Risk Assessment. In: Haschek, W.M., Rousseaux, C.G., Wallig, M.A., Bolon, B., Ochoa, R., Mahler, B.W. (Eds.), Haschek and Rousseaux's Handbook of Toxicologic Pathology, 3rd ed. Academic Press (Elsevier), San Diego, CA, pp. 989–998.

McCallum, D.B., Santos, S.L., 1995. Participation and persuasion: a communication perspective on risk management. Risk Assessment and Management Handbook for Environmental, Health and Safety Professionals. McGraw-Hill, New York.

Ochoa, R., 2013. Pathology issues in the design of toxicology studies. In: Haschek, W.M., Rousseaux, C.G., Wallig, M.A., Bolon, B., Ochoa, R., Mahler, B.W. (Eds.), Haschek and Rousseaux's Handbook of Toxicologic Pathology, third ed. Academic Press (Elsevier), San Diego, CA, pp. 595–618.

Ochoa, R., Sills, R.C., 2013. Risk management in non-clinical drug development. In: Haschek, W.M., Rousseaux, C.G., Wallig, M.A., Bolon, B., Ochoa, R., Mahler, B.W. (Eds.), Haschek and Rousseaux's Handbook of Toxicologic Pathology, third ed. Academic Press (Elsevier), San Diego, CA, pp. 1009–1025.

Rousseaux, C.G., Bracken, W.M., 2013. Overview of drug development. In: Haschek, W.M., Rousseaux, C.G., Wallig, M.A., Bolon, B., Ochoa, R., Mahler, B.W. (Eds.), Haschek and Rousseaux's Handbook of Toxicologic Pathology, 3rd ed. Academic Press (Elsevier), San Diego, CA, pp. 647–685.

Schmid, E.F., Smith, D.A., Ryder, S.W., 2007. Communicating the risks and benefits of medicines. Drug Discov. Today. 12 (9–10), 355–364.

Slovic, P., 1987. Perception of risk. Science. 236, 280–285.

Vahle, J.L., 2013. Risk communication for toxicologic pathologists. In: Haschek, W.M., Rousseaux, C.G., Wallig, M.A., Bolon, B., Ochoa, R., Mahler, B.W. (Eds.), Haschek and Rousseaux's Handbook of Toxicologic Pathology, 3rd ed. Academic Press (Elsevier), San Diego, CA, pp. 999–1008.

PART II

SYSTEMS TOXICOLOGIC PATHOLOGY

This page intentionally left blank

CHAPTER

8

Liver and Gall Bladder

Russell C. Cattley[1] *and John M. Cullen*[2]

[1]Auburn University, Auburn, AL, United States [2]North Carolina State University, Raleigh, NC, United States

OUTLINE

INTRODUCTION

The liver is generally regarded as the most important organ in the evaluation of toxicity. As such, the evaluation, interpretation, and contextualization of liver lesions is an important concern for pathologists, toxicologists, and other scientists engaged in hazard identification and dose–response characterization of unknown or potentially toxic entities. By virtue of the source and volume of its blood supply, the liver receives a much higher exposure of orally administered chemical substances than other organs. In addition, the liver's capacity for metabolizing and eliminating these substances is very extensive, exposing the liver to a wide variety of potentially injurious metabolites compared with similar activities in other tissues.

Chemicals affecting the liver have been identified from across the spectrum of structural characteristics and commercial applications. This includes drugs and biotherapeutics that are very early in the discovery process, or in advancing stages of clinical development and commercialization. In addition, a variety of commodity and specialty chemicals, as well as agricultural and veterinary products and product candidates, may have hepatotoxic activity. Liver function is critical to the survival of the organism, so exposure to any potentially hepatotoxic entity is a concern.

By convention, chemical substances that are hepatotoxic are often considered to be either intrinsically or extrinsically toxic. Intrinsically toxic substances generally cause a high incidence of dose-dependent toxicity in more than one species (e.g., humans and experimental animals). A gallery of commodity chemicals (chloroform, carbon tetrachloride, vinyl chloride), dietary-associated chemicals (aflatoxin, pyrrolizidine alkaloids (PAs)), and drugs (acetaminophen, fialuridine, ethanol)

Fundamentals of Toxicologic Pathology.
DOI: http://dx.doi.org/10.1016/B978-0-12-809841-7.00008-3

have received historical and/or current recognition as intrinsic hepatotoxicants. Extrinsically toxic substances generally cause a low incidence of toxicity that is not predicted by dose or by studies in experimental animals. These chemical entities are typically drugs, and the risk of liver injury sometimes is not recognized until a significantly high number of patients have been treated.

Another source of concern regarding hepatotoxic substances is that the susceptibility of humans to hepatotoxicity is quite variable, making the prediction of a safe dose or exposure challenging. This variable susceptibility may have genetic and environmental components, although the relative importance of these two components, and the numerous as yet unidentified factors comprising each makes the prediction of susceptibility difficult. Among the environmental components, typical in many populations are underlying liver injuries or susceptibilities that may be related to diet, dietary contaminants, dietary supplements, ethanol intake, and conventional and homeopathic medications, as well as hepatitis virus infections. These environmental components serve as confounders for attempting to assess toxicity of a particular drug or chemical substance that is newly introduced in a population.

Given its susceptibility to toxic effects and the serious health consequences associated with the loss of its function, the liver is one of the most important target organs of toxicity. As a result, the recognition of lesions and the understanding of their pathogenesis are often important for understanding the implications of toxicity.

STRUCTURE, FUNCTION, AND CELL BIOLOGY

Liver

The liver is located in the cranial abdomen; in rats and mice it accounts for approximately 4% of the body weight, while in dogs and humans the weight is usually 3%–4% and 2.5%–3.5% of body weight, respectively. The liver is formed by lobes, and the number of lobes and the shape of each lobe is consistent within species but differs among species. In mice, dogs, and primates the gall bladder is located adjacent to the median lobe of the liver and stores and concentrates bile. It collects bile from the hepatic duct via the cystic duct, which then continues to the duodenum as the common bile duct. Rats, lacking a gall bladder, continuously secrete unconcentrated bile.

The microscopic and functional anatomy of the liver is remarkably similar across animals typically encountered in toxicologic pathology (rodents, dogs, primates, and other mammalian species, as well as humans). In each of these species the parenchymal cell of the liver is the hepatocyte, which accounts for approximately 65% of the number of the cells in the liver, and about 90% of its mass. The hepatocyte is the principal cell responsible for many of the specialized functions of the liver, making it a key participant in glucose regulation, production of plasma proteins, lipid metabolism, urea production, xenobiotic metabolism, and bile formation (see later).

Hepatocytes are arranged in plates along blood-containing sinusoids. Adjacent hepatocytes are attached via tight junctions and gap junctions, except at two surfaces: (1) where they form small channels called bile canaliculi into which hepatocytes excrete bile and (2) where they face the gap formed underneath the sinusoidal endothelial cells (the so-called "space of Disse").

The hepatocytes are a key location of xenobiotic metabolizing enzymes. Between the numerous enzyme entities and the magnitude of their expression, the liver easily exceeds the metabolic capacity of all other organs. These enzyme entities and their associated activities are broadly associated with phase 1 and phase 2 reaction classes. Phase 1 reactions promote oxidation, reduction, hydrolysis, cyclization, and decyclization of the substrates. Phase 1 reactions may either enhance or eliminate the biological activity of the xenobiotic substrate, while phase 2 reactions typically inactivate the phase 1 metabolite and facilitate its export by transforming lipophilic substrates into water-soluble molecules that can be transported into the circulation or the bile.

Hepatocytes also possess a variety of membrane transporters, some that are preferentially located along the sinusoidal segments and others that are located along the canalicular segments of the cell membrane. These transporters have a range of occasionally overlapping substrates including bile acids and conjugates of glutathione (GSH) and glucuronate and sulfonate.

The hepatic blood supply is unique in that it is comprised of arterial blood supply via the hepatic artery (~20% of total hepatic blood flow) and portal venous blood supply (venous drainage of abdominal viscera including gastrointestinal tract, pancreas, and spleen, ~80% of total hepatic blood flow). This accounts for the so-called first-pass effect, wherein orally administered chemical substances that are absorbed in the venous blood of the gastrointestinal tract reach the liver at a relatively high concentration that is effectively reduced by uptake in the liver before they ever reach the systemic circulation.

The sinusoids that comprise the vascular component of the liver parenchyma form the architectural framework for the nonparenchymal cells of the liver,

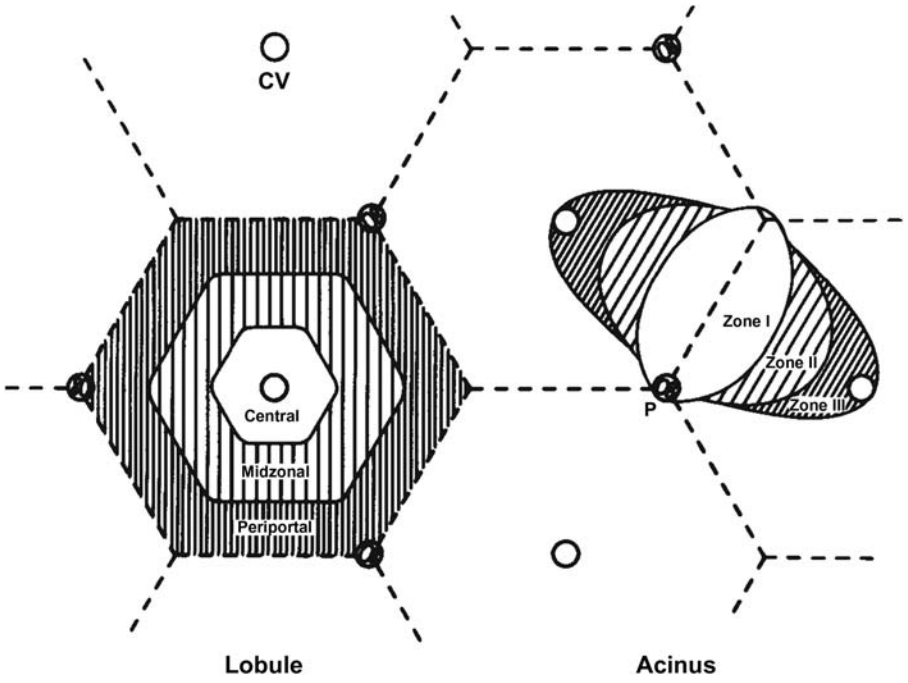

FIGURE 8.1 Hepatic architecture, organization of parenchyma according to concepts of lobular and acinar organization. CV, central vein; P, portal vein. Source: *From Haschek, W.M., Rousseaux, C.G., Wallig, M.A. (Eds.), 2002. Handbook of Toxicologic Pathology, second ed., vol. 2. Academic Press, San Diego, CA, Figure. 8.2, p. 189, with permission.*

including endothelial cells, Kupffer cells, stellate cells (also formerly known as Ito cells), and NK/NKT cells (also known as pit cells). Sinusoidal endothelial cells form a continuous lining of the sinusoids, but are fenestrated and have little or no basement membrane, allowing free exchange of blood solutes into the perisinusoidal space (space of Disse) and up to the microvillar surface of the hepatocytes. Stellate cells, also called Ito cells, are distributed within the space of Disse. These cells normally store vitamin A, but upon activation in liver injury they will adopt a phenotype resembling that of myofibroblasts.

Kupffer cells, resident macrophages, are distributed along the surface of the endothelium facing the sinusoidal lumen. Kupffer cells are effective in removing small particles as well as proteins from the circulation. Kupffer cells also collaborate with endothelial cells in the clearance of endotoxin, an active component of bacterial lipopolysaccharide. NK (natural killer) and NKT (natural killer T lymphocyte) cells also reside and migrate along the sinusoidal endothelial cells and collaborate with Kupffer cells in immune functions. The immune cells of the liver are thought to be more likely to favor tolerance as opposed to acquired immunity.

The lobular architecture of the liver is subdivided by the portal tracts, which each contain small structures (portal veins, bile ducts, and arteries), which are arrayed around a draining central (or terminal hepatic) venule forming microscopically recognizable structures called lobules that are approximately 1 mm in diameter (Figure 8.1). Lobules are bounded by five to six portal tracts. The constituents of the portal tracts are distributing branches of the larger portal veins and hepatic arteries that first enter the liver at the hilus. In contrast, bile flows toward the portal tracts, within the canaliculi to the canals of Hering and then into the interlobular bile ducts. These ducts are lined by simple cuboidal epithelium and drain into progressively larger ducts, drain the individual lobes, and terminate in the hepatic duct. In species with a gall bladder, the cystic duct and the hepatic duct merge to form the common bile duct that communicates with the duodenum. At the center of each lobule is a small hepatic vein that collects blood into larger hepatic veins that eventually join to form the hepatic vein and exit the liver, draining into the caudal vena cava.

The organization of the liver into lobules forms the basis of a well-established approach to delineating morphological changes in the parenchymal tissue (and will be used in this chapter). An alternative approach to describing the parenchymal tissue is reflected by the hepatic acinus, which is defined as the microscopic region of tissue defined by receiving the blood flow from the terminal arterial and portal venous blood vessels within a given portal region. The acinus is divided into three zones, with Zones 1, 2, and 3 reflecting

proximal, intermediate, and distal location relative to these blood vessels, respectively. The lobule and acinus are compared in Figure 8.1. One key consequence of the liver architecture is that hepatocytes are functionally heterogeneous due to their different locations within the lobule, presumably due to gradients of oxygen tension and hormone and nutrient concentrations that form as sinusoidal blood flows across the lobule.

Molecular Aspects of Bile Formation

Hepatobiliary transport of organic ions including bilirubin and bile acids has been increasingly better understood as new molecular transport molecules have been identified, cloned, and evaluated for function. Normal bile formation and elimination require normal function of the hepatobiliary transport system. Regulation of the uptake and excretion of the constituents of bile, including bilirubin, bile acids, cholesterol, phospholipids, hormones, drugs, and toxins, requires specific substrate–transporter interactions. Transporters situated on the basolateral surface of hepatocytes are involved in the uptake of bile constituents from the blood. In health and in disease the regulation of transcription of the various transporters is controlled by the interaction of bilirubin or bile acids with several nuclear receptors (NRs). In cholestasis, cytoplasmic bile acids bind to several NRs, but the most important is FXR (Farnesoid-X-Receptor). Movement of bile constituents across the canalicular membrane is driven by bile salt-dependent and bile salt-independent mechanisms.

Gall Bladder

The gall bladder is a hollow, blindly ending organ that is part of the extrahepatic biliary system. The gall bladder is histologically composed of three layers: a mucosa, a muscular layer, and a serosa. The mucosa is lined by simple cuboidal to columnar epithelium, and is folded except when the gall bladder is distended. This system includes the hepatic duct from the liver, which joins the cystic duct arising from the neck of the gall bladder to form the common bile duct. The common bile duct continues to the wall of the duodenum and ends at a mucosal papilla where it opens into the duodenal lumen. Spontaneous lesions of the gall bladder include heterotopic rests of parenchymal cells of liver (hepatocytes) and pancreas (acinar cells), within the wall of the gall bladder. These lesions are incidental, and in toxicology studies have not been associated with a test article.

The gall bladder functions to store and modify bile between meals, concentrating bile via bile salt-dependent mechanisms between meals and adding bicarbonate and other secretions during digestion. Bile is important in the digestive process, as the bile acids found in bile promote emulsification of lipid constituents of the diet.

EVALUATION OF LIVER TOXICITY

A variety of methodologies have been advanced and applied to the evaluation of liver toxicity. While these methodologies may vary in sensitivity and specificity, a more important consideration in the selection of methods for evaluating liver toxicity is defining the question being addressed. An overview of clinical pathology and morphology methods is provided in the following section. For additional information, see Cattley and Cullen (2013).

Biochemical-Clinical Pathology

Indicators of Hepatocellular Injury

In most species used in toxicological studies, that is, rats, dogs, and nonhuman primates, hepatic function or hepatic injury is monitored by evaluation of liver-related enzymes, bilirubin, bile acids, serum proteins, and dye excretion. The most common enzymes that are evaluated to assess hepatocellular injury are the transaminases, alanine aminotransferase (ALT) and aspartate aminotransferase (AST). Both are considered to be useful markers of hepatocellular injury.

Of the two markers, ALT is regarded as the more specific and sensitive. ALT is a "leakage" enzyme, and may be elevated as a result of hepatocellular necrosis, injury, or repair. ALT is the more useful marker of hepatocyte injury without necrosis. Increases of two- to fourfold in dogs, rats, and, likely, nonhuman primates have been proposed to indicate hepatocellular injury. Higher increases are indicative of more hepatocytes being injured or of lethal injury. Interpretation of ALT increases should be taken in context with other changes. It is possible to have quite modest but statistically significant increases in ALT that are not toxicologically relevant.

Hepatic drug metabolizing enzyme induction in rats does not generally lead to elevation of ALT when hepatocytic hypertrophy is the only histologic change evident. There is no consistent response in these parameters in dogs or monkeys during drug metabolizing enzyme induction either. Alternatively, serum levels of ALT may decrease in rats with induction of the smooth endoplasmic reticulum (SER) when, presumably, endogenous catabolism is increased. Skeletal muscle is also a source of ALT, so interpretation of serum chemistry results can be confounded by restraint, handling, or possible injury. However, AST

activity is typically increased to a greater extent than ALT when the muscle is a significant source of serum transaminase increase.

In addition to ALT and AST, other serum enzymes such as serum sorbitol dehydrogenase (SDH), ornithine carbamoyltransferase, paraoxonase-1, and glutamate dehydrogenase (GDH) can be evaluated. SDH and GDH can be particularly useful in nonstandard species such as swine, guinea pigs, woodchucks, and possibly others, where ALT activity is not suitable.

Indicators of Biliary Injury

The two more useful analytes for the evaluation of biliary injury in standard laboratory animals are serum bile acids (SBA) and total bilirubin (TBILI). Alkaline phosphatase (ALP) and gamma glutamyl transferase (GGT) are less sensitive markers in rodents (although ALP is a useful marker for peroxisome proliferation). ALT can also be secondarily elevated in cases of biliary injury.

TBILI is increased in the serum when there is either a reduced excretion of bilirubin or an increased production of bilirubin, typically due to increased red cell destruction or alterations in bilirubin metabolism. Concurrent elevations of TBILI in addition to elevations of ALT should warrant concern, as this combination of alterations in humans is linked to a risk of severe liver injury.

SBA, mainly cholic acid and chenodeoxycholic acid (although there are significant species-specific variations), are synthesized from cholesterol. In the liver bile acids are conjugated to amino acids, often taurine or glycine, and excreted in bile where they assist in lipid digestion. SBA levels are affected by the rate of hepatic synthesis, removal by the hepatocytes, extrahepatic obstruction, and various forms of liver disease. Consequently, altered bile acid levels can indicate hepatocellular or biliary tree injury.

Total ALP measured in serum is a relatively poor marker of biliary injury in the rat. GGT is distributed within the biliary canalicular membrane and serum levels increase when there is reduced bile flow or biliary necrosis. Progressive GGT elevation in chronic toxicity may be more useful than GGT assessment in acute injury.

Other Parameters and Contemporary Biomarkers

There are a number of additional indicators of liver or biliary injury (ALP isoenzymes, 5′ nucleotidase (5′-NT), alpha-glutathione-(*S*)-transferase (GST), and lactate dehydrogenase), but they are not typically employed because, in general, they do not offer an improvement over the standard analyses.

Interpretation

While the relevant data from the analysis of serum can be clearly displayed, an accurate and meaningful interpretation of these data is often a significant challenge. Statistical analysis can be useful, but some caution is warranted, Clinical pathology measurements should be interpreted as a part of the larger circumstance including in-life observations; information on absorption, distribution, metabolism, and elimination; histology; and possible drug class effects. When studies contain relatively small numbers of animals, interanimal variation should be considered. Recommended guidelines from a review of laboratory animal clinical pathology in preclinical studies include the following:

1. ALT elevations of two- to fourfold in rats or dogs and greater than 40 U/L absolute value in nonhuman primates are a threshold for concern, but must be evaluated in context, as mentioned earlier.
2. When TBILI is elevated, causes other than cholestasis, such as sepsis and hemolysis, and drug interactions with bilirubin conjugating enzymes (UDP-glucuronosyltransferase family 1, polypeptide A1), should be eliminated. Only when increased TBILI is accompanied with another hepatic parameter is the finding likely to be adverse.
3. ALP elevations are difficult to interpret with confidence due to a variety of nonhepatic factors.

Morphology

Liver Mass (Liver Weight)

The routine assessment of liver mass (liver weight) is a commonly applied endpoint in toxicology studies. Liver weights are often characterized as absolute liver weights and as ratios to body weight in individual animals. If body weights are significantly affected by treatment, normalization of liver weights can be a useful approach since, in the absence of other treatment effects, liver-weight:body-weight ratios are fairly constant within adults for the given species being studied. Changes in liver weights relative to brain weights can be used for comparison in instances where significant shifts in body weight occur, as brain weight is generally not affected in typical studies.

Changes in liver weights can be useful to detect and quantitate the effects of hepatotoxins, although these changes are rarely specific. Increases in liver weights are more commonly observed than decreases and in some cases may reflect generalized accumulations (fat, glycogen, water). Significant increases in liver weight are more commonly observed in conjunction with adaptive changes such as hypertrophy and/or hyperplasia. Liver weight can also be affected by primary or

secondary neoplasia, so its use as a parameter is not as informative in chronic studies conducted to detect carcinogenic potential of test articles.

Microscopy

Routine microscopic evaluation uses immersion fixation with 10% buffered formalin, paraffin embedment, and hematoxylin and eosin (H&E) staining of 4- to 6-μm sections. Hematoxylin and eosin–stained sections demonstrate many alterations of hepatocytes and bile duct epithelial cells. However, this staining technique provides limited information on nonparenchymal cells of the liver. In addition to focal gross lesions, representative samples that include capsule and underlying parenchyma should be prepared. These samples should be taken in a uniform fashion with respect to lobe, site, and orientation, and more than one lobe should be sampled. Although the possible mechanisms of interlobar variability are not well characterized, the portal streamlining of toxic agents absorbed via segments of the gastrointestinal tract, as well as transperitoneal migration of volatile toxicants out of the stomach, has been suggested.

The assignment of diagnoses in the practice of toxicologic pathology is typically based upon the microscopic examination of H&E-stained sections. For rats and mice, the terms and criteria for these diagnoses have been the subject of initiatives for international harmonization (http://www.toxpath.org/inhand.asp). For liver and gall bladder, a harmonized diagnostic lexicon with criteria has been published (Thoolen et al., 2010).

Exsanguination of the animal prior to removing the liver is adequate for routine examination. However, perfusion of the liver with buffered saline to remove blood constituents is preferred in some laboratories. Perfusion of the liver with fixative, generally via the portal vein, is often chosen for ultrastructural examination, but immersion fixation may be adequate for some studies.

There are a variety of antigens or enzymes that can be best appreciated in frozen sections of liver. Sections of frozen liver can be used to evaluate cellular lipid and bile more accurately than routinely processed tissue because lipid is removed in processing and bile can be removed in aqueous fixatives and processing solutions. In addition, various enzymes of interest in toxicological studies can be detected using histochemical techniques. For immunohistochemistry, there are a number of cell surface markers, as well as other antigens, that require the use of frozen sections because currently available antibodies will only bind to the native conformation of the antigens and will not bind if they are altered during routine fixation and processing.

Hepatocytes in young and adult animals retain the capacity for self-renewal, and cell proliferation in the liver may represent either replacement of lost hepatocytes or an absolute increase in hepatocyte numbers. Frequently, the toxicologic significance of chemically induced hepatocellular proliferation is of interest. Increased rates of hepatocellular turnover may indicate cytotoxicity or adaptive hyperplasia and may be mechanistically related to neoplastic development. Quantitation of cell replication has usually been approached by determining the fraction of cells in mitosis or replicative DNA synthesis (S-phase).

A variety of methods are utilized to measure the frequency of hepatocellular replication. To determine the S-phase of DNA replication, *in vivo* incorporation of a nucleoside into DNA over a specified time period can be determined. Bromodeoxyuridine (BrdU), a thymidine analog, can be detected by monoclonal antibody, making it applicable for quantitative immunohistochemistry or cell sorter analysis of suspensions of individual hepatocytes. The administration of BrdU may be by pulse or continuous dosing regimens.

As a surrogate for detection of S-phase nuclei by labeling techniques, some investigations have utilized the immunohistochemical detection of Ki-67 or proliferating cell nuclear antigen (PCNA). Ki-67 is a protein associated with ribosomal transcription, and is expressed throughout all phases of cell cycle except interphase. PCNA is a protein associated with DNA polymerase, and its expression begins in late G1 cells and continues through S-phase and beyond.

RESPONSE TO INJURY

Nonneoplastic Responses to Toxicant Injury

Nonneoplastic responses to toxicant injury include hepatocellular degeneration and necrosis, hepatocellular adaptation, infiltrations and pigments, hepatocellular inclusions, phospholipidosis, cholestasis, biliary epithelial degeneration and necrosis, biliary hyperplasia, and cholangiofibrosis.

Hepatocellular Degeneration and Necrosis

Hepatocellular degeneration and necrosis is a frequent and significant concern in preclinical and clinical toxicology. Given the fundamentally vital functions of the liver, and the difficulty in supplementing or replacing its capabilities, the appearance of unanticipated hepatocellular injury is a significant liability for drugs and other commercially valued chemical entities if exposure of people is anticipated.

Hepatocellular degeneration and necrosis results from a variety of mechanisms by which chemical

substances may injure the liver (see "Mechanisms of Toxicity in Liver" section). Depending upon the magnitude of injury, hepatocytes may undergo degeneration, which is reversible. If the injury is more substantial, hepatocytes may progress to an irreversible course leading to necrosis. Degeneration is not a uniform or consistent process leading to necrosis, and within the liver an injurious agent that causes necrosis in some hepatocytes may cause degeneration in others, presumably due to differential sensitivity of hepatocytes or distribution of the agent within the liver.

In hepatocytes, degeneration is limited to instances where the homeostatic mechanisms of the hepatocyte are compromised to the point where fluid and ion balance within the cell is disrupted, leading to increased accumulation of electrolytes and water within hepatocytes, sometimes referred to as *vacuolar or hydropic degeneration*. Histologically, this appears as hepatocellular enlargement with cytoplasmic pallor and/or vacuolation (Figure 8.2). By electron microscopy, the accumulation of fluid appears as dilated endoplasmic reticulum and/or mitochondria. During this phase of injury the cell membrane of the hepatocyte may undergo blebbing and release of cytoplasmic blebs into the circulation. Blebbing may account for the elevations in circulating aminotransferases and lactic dehydrogenase (albeit subtle in some cases) that may be observed in the absence of hepatocellular necrosis.

Besides degenerative changes in hepatocytes, sublethal injury may lead to accumulation of cytoplasmic lipids, a change that is termed *lipidosis* or *steatosis*. Histologically, this change is reflected by the presence of clear space within hepatocytes, reflecting the extraction of lipid during tissue processing prior to paraffin impregnation and embedment. Hepatocellular lipidosis is often characterized as either macrovesicular or microvesicular in nature. Macrovesicular lipidosis appears as a single large vacuole in the center of the cell and peripheral displacement of the nucleus (Figure 8.3). Microvesicular lipidosis appears as multiple small vacuoles or foamy cytoplasm, and nuclear displacement does not typically occur (Figure 8.4). Besides its association with hepatocellular injury, lipidosis is also observed when there is accelerated mobilization of lipids stored in adipose tissue. The mechanisms of lipidosis associated with hepatocellular injury are described later in this chapter.

When injury to the hepatocyte results in irreversible damage of cells, histological evidence of hepatocellular necrosis will be evident. In hepatocytes, two types of necrosis have been described: apoptosis and oncotic necrosis. In theory, these types of necrosis are separable. Apoptosis is considered to represent an active, energy-dependent process that depends upon molecular signaling through a variety of receptors, which eventually converge upon a final pathway that causes activation of a series of proteolytic enzymes known as caspases. Apoptotic hepatocytes are fragmented into so-called "apoptotic bodies" (Figure 8.5) that contain intact cellular organelles upon ultrastructural examination. This differs from oncotic necrosis, wherein the cell is depleted of ATP and consequently lacks sufficient energy to maintain membrane-associated ionic pumps, leading to swelling and gross calcium fluxes resulting in disruption of the mitochondrial and plasma membrane.

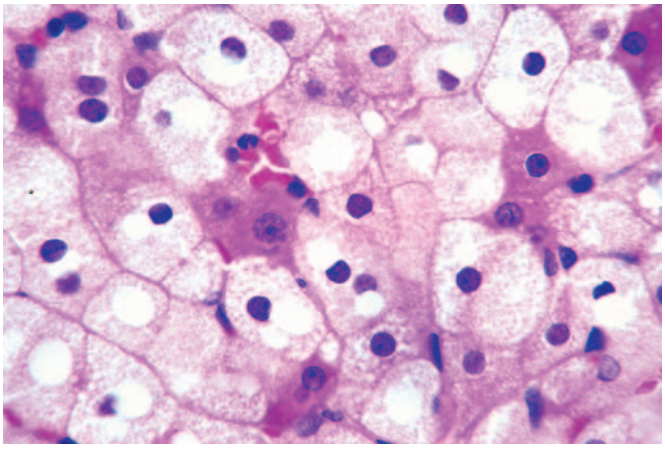

FIGURE 8.2 Hepatocyte degeneration, often described as vacuolar or hydropic degeneration, associated with organellar (usually endoplasmic reticulum and/or mitochondrial) accumulation of fluid (not lipid). Rat, administered carbon tetrachloride. Source: *From Haschek, W.M., Rousseaux, C.G., Wallig, M.A. (Eds.), 2013. Haschek and Rousseaux's Handbook of Toxicologic Pathology, third ed. Academic Press (Elsevier), San Diego, CA, Figure 45.2, p. 1523, with permission.*

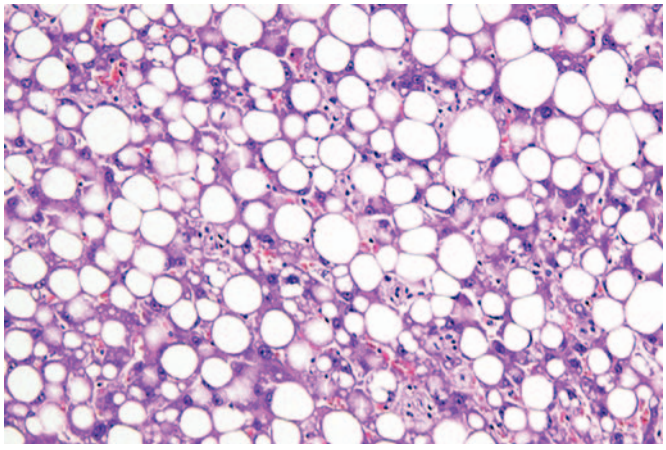

FIGURE 8.3 Macrovesicular lipidosis, typically appearing as a single large vacuole in the center of the hepatocyte and peripheral displacement of the nucleus. Rat, administered furan. Source: *Courtesy: The National Toxicology Program. From Haschek, W.M., Rousseaux, C.G., Wallig, M.A. (Eds.), 2013. Haschek and Rousseaux's Handbook of Toxicologic Pathology, third ed. Academic Press (Elsevier), San Diego, CA, Figure 45.4, p. 1523, with permission.*

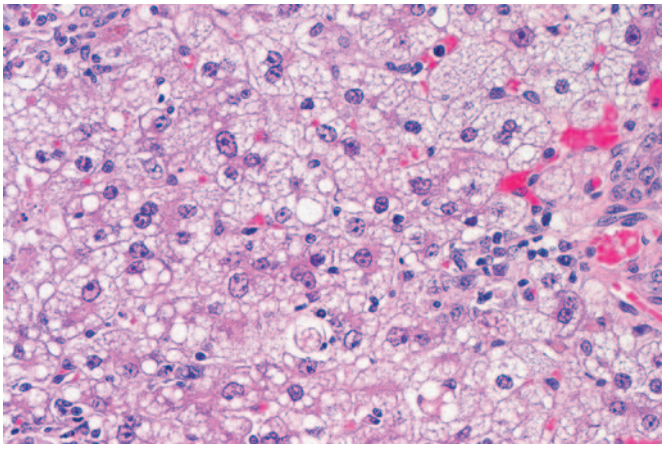

FIGURE 8.4 Microvesicular lipidosis, typically appearing as multiple small vacuoles or foamy cytoplasm (note absence of nuclear displacement). Rat, administered carbon tetrachloride. Source: *Courtesy: The National Toxicology Program. From Haschek, W.M., Rousseaux, C.G., Wallig, M.A. (Eds.), 2013. Haschek and Rousseaux's Handbook of Toxicologic Pathology, third ed. Academic Press (Elsevier), San Diego, CA, Figure 45.5, p. 1524, with permission.*

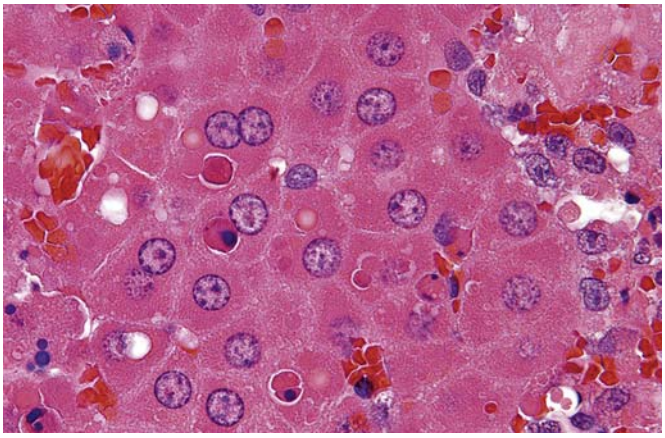

FIGURE 8.5 Apoptosis of hepatocytes characterized by the appearance of "apoptotic bodies," usually within the cytoplasm of adjacent cells. The apoptotic bodies appear as round eosinophilic fragments of hepatocytic cytoplasm, with variable presence of basophilic nuclear fragments. Rat, administered galactosamine HCl. Source: *From Haschek, W.M., Rousseaux, C.G., Wallig, M.A. (Eds.), Haschek and Rousseaux's Handbook of Toxicologic Pathology, third ed. Academic Press (Elsevier), San Diego, CA, Figure 45.6, p. 1524, with permission.*

In practice the histological differentiation of oncotic necrosis from apoptosis may be difficult, and for several reasons. First of all, light microscopy does not consistently differentiate cells undergoing apoptosis from oncotic necrosis, since both may be characterized by increased cytoplasmic eosinophilia and nuclear fragmentation. Secondly, both processes may occur among hepatocytes within the same liver. Thirdly, the same toxicant can produce both apoptosis and oncotic necrosis depending on the dose. Furthermore, the appearance of apoptotic bodies is a very transient event that may be missed if timing of tissue sampling is not optimal. Finally, although inflammatory cell response is less likely to be observed in association with cells in apoptotic versus oncotic necrosis, this is not a consistent discriminator. For these reasons, many toxicological pathologists avoid any definitive diagnosis of apoptotic necrosis or oncotic necrosis, preferring to use the inclusive term *hepatocellular necrosis* and addressing evidence for apoptotic versus oncotic necrosis in their associated comments. Elevations in ALT and AST activities are more typically observed in the presence of oncotic necrosis, since apoptotic cells are less likely to release these intracellular enzymes upon fragmentation into apoptotic bodies.

The response of the liver to hepatocellular necrosis involves several processes. Following oncotic necrosis, affected hepatocytes are typically removed from the liver by phagocytic inflammatory cells, primarily neutrophils and macrophages. The neutrophils are derived from the circulating pool, while the macrophages may be derived from activation and recruitment of circulating monocytes and from local activation of Kupffer cells. Unlike hepatocytes undergoing oncotic necrosis, remnant bodies from apoptotic hepatocytes are generally observed to undergo phagocytosis by adjacent hepatocytes.

The presence of neutrophils and macrophages in association with necrotic hepatocytes may resemble an inflammatory response in the liver, also known as "hepatitis." In practice, this assessment and terminology are avoided if (1) observation of neutrophils and macrophages is limited to necrotic areas, (2) accumulation of additional inflammatory cells such as lymphocytes (especially T cells but possibly including B cells) and/or eosinophils is not observed, and (3) hepatic NK cells are not activated. Small foci of inflammation also can be found as a background lesion, particularly in mice and not infrequently in rats. The presence of extramedullary hematopoiesis may be observed in adult liver, and must be differentiated from inflammatory cell infiltration or inflammation. Extramedullary hematopoiesis, more commonly observed in rodents than in other species, is characterized by the irregular presence of hematopoietic cells in hepatic sinusoids and around central veins and portal areas. Erythroid, myeloid, and megakaryocytic lineages may be variably present.

Another major response of the liver in resolution of toxic hepatocellular injury is the restoration of the functional liver mass by replacing lost hepatocytes. In most cases, this involves the process of hepatocellular regeneration. In regeneration, new hepatocytes are derived from replication of existing fully differentiated hepatocytes, even in adulthood when the liver is no

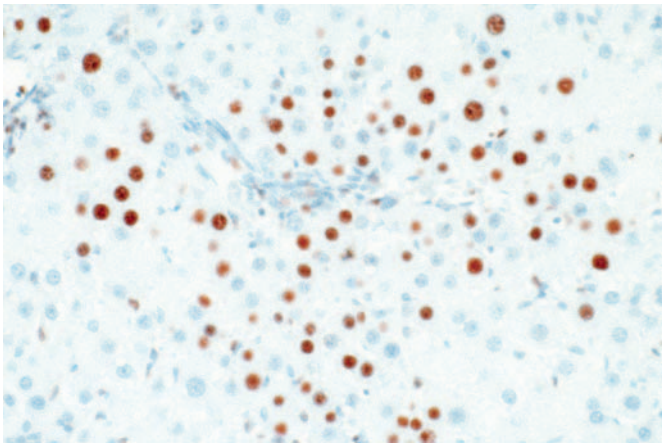

FIGURE 8.6 Immunohistochemical staining of nuclei containing 5-BrdU. This technique demonstrates the nuclei in S-phase during the period of *in vivo* labeling prior to tissue collection. Rat. Source: *From Haschek, W.M., Rousseaux, C.G., Wallig, M.A. (Eds.), 2013. Haschek and Rousseaux's Handbook of Toxicologic Pathology, third ed. Academic Press (Elsevier), San Diego, CA, Figure 45.9, p. 1526, with permission.*

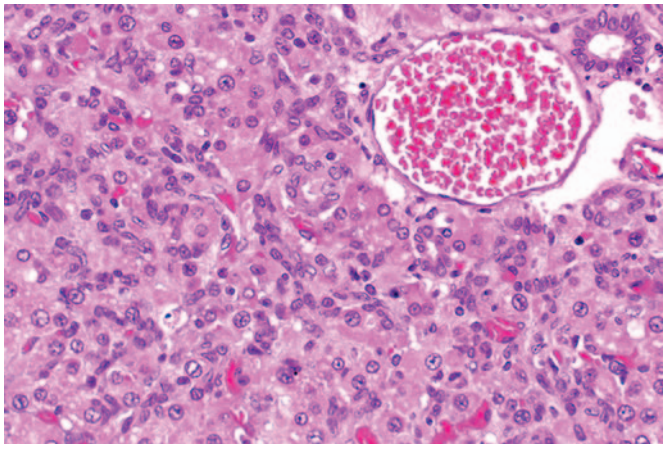

FIGURE 8.7 Oval cell proliferation, characterized by the presence of epithelial cells, with small oval nuclei and minimal basophilic cytoplasm, accumulating along the rows of hepatocytes. These cells are often most numerous in periportal areas. Mouse. Source: *From Haschek, W.M., Rousseaux, C.G., Wallig, M.A. (Eds.), 2013. Haschek and Rousseaux's Handbook of Toxicologic Pathology, third ed. Academic Press (Elsevier), San Diego, CA, Figure 45.10, p. 1527, with permission.*

longer increasing in size. The process of regeneration is often assessed by in-life labeling of hepatocytes in replicative DNA synthesis. Hepatocytes in S-phase can be readily demonstrated by immunohistochemical detection of BrdU labeling (Figure 8.6).

Exceptionally, some hepatotoxicants may inhibit DNA replication and block regeneration. One response observed in liver injury with toxicants that block regeneration is the formation of megalocytes, which are hepatocytes that are enlarged by dramatic increases in both cytoplasmic and nuclear volume, and readily detected by light microscopy. Megalocyte formation, sometimes called megalocytosis, has been linked to a group of plant-derived toxins known as PAs. Upon ingestion of high levels of PA-containing vegetation, the PA is converted to pyrols, which bind and crosslink DNA and proteins.

Another response observed in liver injury with toxicants that block regeneration is the proliferation of oval cells within the liver parenchyma. Oval cells are considered to be bipotential precursor cells. Histologically, these epithelial cells are characterized by small oval nuclei and minimal basophilic cytoplasm (Figure 8.7). These cells appear to derive from a small population of cells located at the site of transition from canaliculi to bile ducts at the periphery of the portal track localized in the area of the canals of Herring. Although not a common response to hepatotoxicants, oval cell proliferation is most readily induced in rodents, and is rarely reported in other species. The use of the diagnostic term "ductular reaction" has been considered to more accurately characterize oval cell proliferation.

Significant ongoing or repetitive hepatocellular necrosis will often result in fibrosis in the hepatic parenchyma. Often this change is recognized as the deposition of collagen fibers and other extracellular matrix proteins. The cells primarily responsible for hepatic fibrosis are the stellate cells, with potential participation of perivascular fibroblasts in periportal and centrilobular regions. Stellate cells respond to inflammatory cytokines, principally TGF-β, by undergoing differentiation into myofibroblasts. Because of their location within the space of Disse, these cells deposit collagen and matrix proteins in this location, which forms a barrier to diffusion between the sinusoidal circulation and the hepatocyte surface.

Hepatocellular degeneration and necrosis induced by toxicants may occur in either a defined lobular pattern or in a pattern independent of lobular location. In a lobular pattern, hepatocytes in the central or the midzonal or the periportal regions of the lobule are preferentially affected. The lobular patterns of injury derive from the lobular heterogeneity of hepatocytes and their tissue microenvironment. Among nonlobular patterns, affected hepatocytes may be either distributed as random foci or simultaneously affected throughout the liver lobule in a pattern that has been termed *massive*. The distribution pattern of hepatocellular necrosis indicates a susceptibility pattern (or lack thereof) that is linked to the mechanism of injury.

Among patterns of lobular hepatocellular degeneration and necrosis, the central lobular pattern is most commonly elicited following administration of toxic chemical substances. These include carbon tetrachloride, acetaminophen, thioacetamide, and bromobenzene. As the term implies, *central lobular necrosis* occurs in the central lobular area, with the necrotic hepatocytes

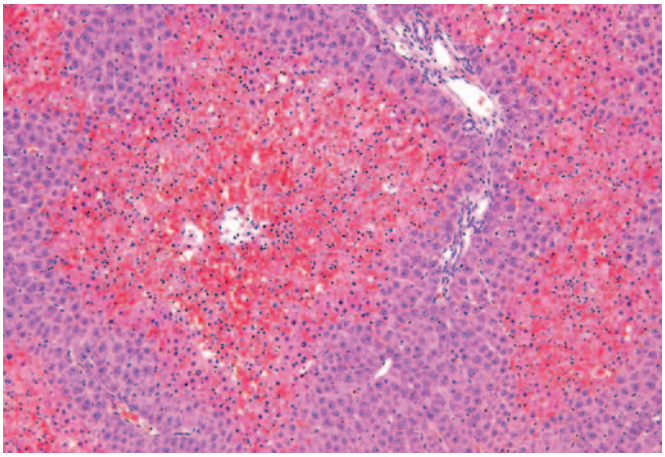

FIGURE 8.8 Central lobular necrosis, with areas of coagulative hepatocellular necrosis and sinusoidal congestion surrounding central veins. Rat, administered carbon tetrachloride. Source: *Courtesy: The National Toxicology Program. From Haschek, W.M., Rousseaux, C.G., Wallig, M.A. (Eds.), 2013. Haschek and Rousseaux's Handbook of Toxicologic Pathology, third ed. Academic Press (Elsevier), San Diego, CA, Figure 45.11, p. 1528, with permission.*

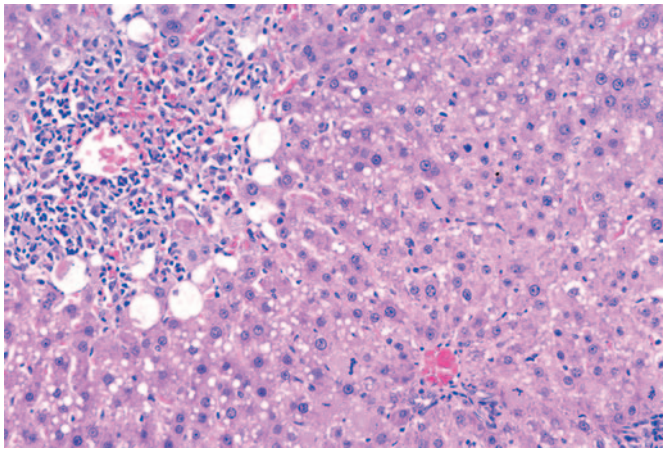

FIGURE 8.9 Hepatocellular degeneration characterized by a rim of cells with enlarged and completely vacuolated cytoplasm, which is present immediately surrounding a region of central lobular necrosis and accumulated macrophages. Peripheral to the degenerated cells, hepatocytes variably contain small lipid vacuoles, and several mitotic hepatocytes are present. Rat, administered carbon tetrachloride. Source: *From Haschek, W.M., Rousseaux, C.G., Wallig, M.A. (Eds.), 2013. Haschek and Rousseaux's Handbook of Toxicologic Pathology, third ed. Academic Press (Elsevier), San Diego, CA, Figure 45.12, p. 1529, with permission.*

completely encircling the central vein (terminal hepatic venule) (Figure 8.8). Based on this morphologic distribution, central lobular necrosis has also been referred to as *periacinar*, indicating based upon the relationship to metabolic zonation or *perivenous* based upon the distribution around the central vein. The lesion is generally found throughout the liver, with the central areas of many, if not all, lobules affected. Within each lobule, the percentage of cells involved depends on the inciting agent and the dose. The demarcation between necrotic hepatocytes and adjacent normal-appearing hepatocytes is frequently abrupt when examined by light microscopy. Any necrotic cells are readily identified by light microscopy, and nonnecrotic cells immediately adjacent to the necrotic cells but slightly further away from the lobule center may undergo enlargement and cytoplasmic vacuolation indicative of degeneration, suggesting less extensive and potentially reversible injury (Figure 8.9).

Although a variety of mechanisms may be responsible for the preferential susceptibility of central lobular hepatocytes, it is their higher activity of xenobiotic metabolism, particularly phase 1 enzymatic activity, which leads to higher concentrations of biologically active metabolites that result in injury. Cellular injury induced by central lobular hepatotoxicants is frequently restricted to the hepatocytes, as occurs after the administration of acetaminophen. With this toxicant, endothelial cells and Kupffer cells appear to be normal while the adjacent hepatocytes are undergoing necrosis. The swollen and necrotic hepatocytes appear to compress the vascular spaces so that little blood is

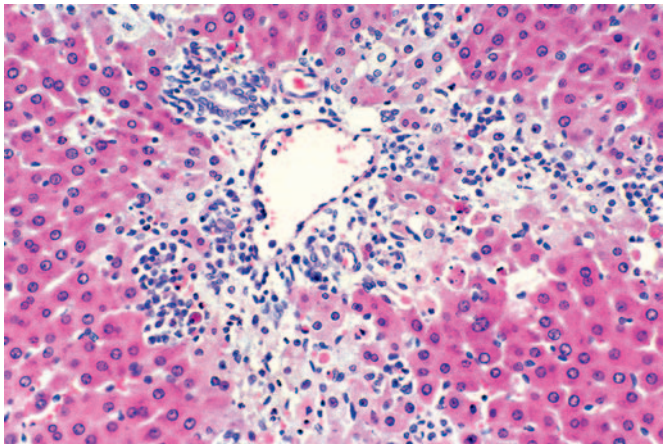

FIGURE 8.10 Periportal necrosis, with areas of coagulative hepatocellular necrosis and mixed phagocytic inflammatory cells, surrounding a portal region. Rat, administered *N*-hydroxy-2-acetylaminofluorene. Source: *From Haschek, W.M., Rousseaux, C.G., Wallig, M.A. (Eds.), 2013. Haschek and Rousseaux's Handbook of Toxicologic Pathology, third ed. Academic Press (Elsevier), San Diego, CA, Figure 45.13, p. 1529, with permission.*

observed in the sinusoids in the necrotic central lobular areas. With other toxicants, such as dimethylnitrosamine, the endothelial cells lining the sinusoids adjacent to the necrotic hepatocytes are also destroyed.

Degeneration and necrosis of periportal hepatocytes is a much less common pattern of lobular injury than that of central lobular hepatocytes as a consequence of toxicant exposure (Figure 8.10). Several potential

factors have been proposed to account for the susceptibility of periportal hepatocytes to toxicant-induced injury when it occurs, but it should be noted that these factors cannot be discerned from the light-microscopic appearance of the lesion. One factor is the lack of dependence of CYP-mediated activation for toxicity. Another factor is the concentration gradient of substances in the blood across the sinusoids, so that periportal hepatocytes usually experience and may extract higher concentrations of toxicants than hepatocytes in downstream regions of the lobule. The same gradient exists for oxygen tension, so if metabolic activation is uniquely dependent upon oxygen concentration, a higher level could form in periportal hepatocytes. Another factor responsible for the periportal selectivity of necrosis is the putative participation of Kupffer cells in hepatocellular injury, as these cells reportedly may be more numerous and more readily activated in periportal regions than in downstream regions of the lobule.

Midzonal hepatocellular degeneration and necrosis is the rarest pattern of lobular injury caused by hepatotoxicants. It is characterized by the appearance of affected hepatocytes in a pattern that spares the periportal and central lobular hepatocytes. Due to the rarity of this pattern, examples are infrequent. It has been described following furan treatment of mice and aflatoxin treatment of rabbits. As the name implies, this pattern of necrosis is found as a band of necrosis equidistant between the portal triad and the central vein (Figure 8.11). The factors underlying the susceptibility of hepatocytes in the midzonal region are unknown, and it should be noted that some toxicants that induce midzonal hepatocytes in one species may fail to replicate the same lobular distribution in other species. A recent report evaluated the possible induction of midzonal ischemia as a contributing factor to hepatocellular injury in this region, as the result of lipopolysaccharide-mediated production of iNOS (inducible Nitric Oxide Synthase) and resulting changes in sinusoidal circulation due to increased nitric oxide concentrations.

One pattern of hepatocellular injury, typically manifested as necrosis, affects all hepatocytes within several, often adjacent, lobules. This is referred to as *massive necrosis*. Although not every lobule may be equally affected, the extensive necrosis extends from the central vein to the portal area in at least some lobules (Figure 8.12). Due to the massive reserve in liver function, destruction of a large portion of the liver is still compatible with life. The complete (or nearly complete) destruction of hepatocytes in a lobule renders that lobule incapable of participating in the reparative process so the lobule is permanently lost from the liver. Where complete or substantial destruction of the lobule occurs, fibrosis will constitute the major reparative effort.

Massive necrosis is clearly evident on gross observation. In the early phase the affected liver areas are abnormal in color (frequently pale) and appear slightly swollen. After several days the affected area is depressed below the surface of the adjacent tissue. As the repair process progresses to fibrosis, the areas become firm.

Various factors are speculated to contribute to the distribution of susceptible hepatocytes in different lobes or sublobar locations. Massive necrosis may be noted when toxicants are delivered directly into the vascular system, particularly into the portal vein or a

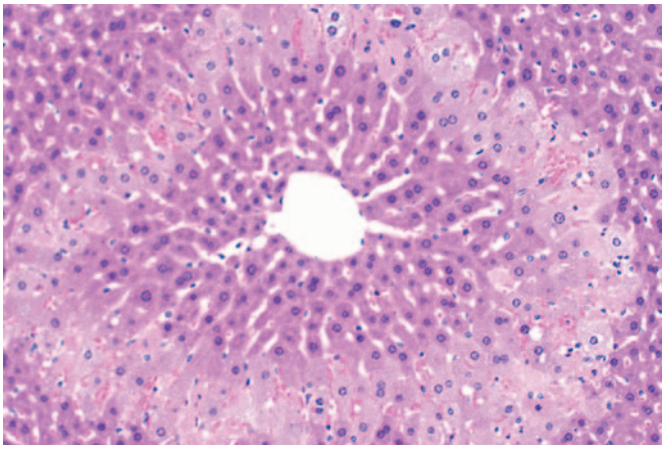

FIGURE 8.11 Midzonal necrosis, with continuous region of coagulative hepatocellular necrosis, located between central and periportal regions. Mouse, administered furan. Source: *From Haschek, W.M., Rousseaux, C.G., Wallig, M.A. (Eds.), 2013. Haschek and Rousseaux's Handbook of Toxicologic Pathology, third ed. Academic Press (Elsevier), San Diego, CA, Figure 45.14, p. 1530, with permission.*

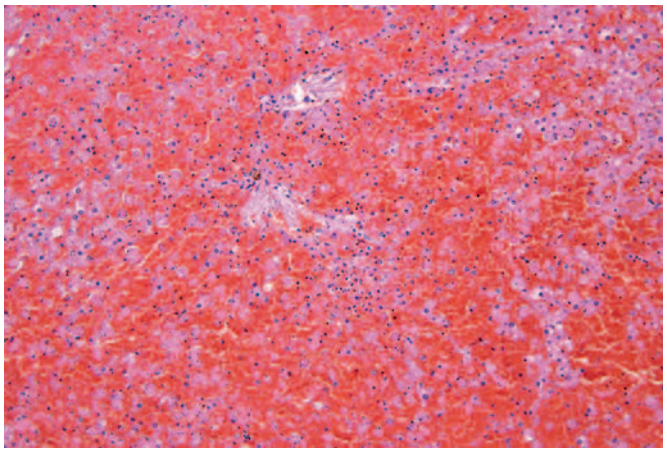

FIGURE 8.12 Massive necrosis, characterized by disassociated and necrotic hepatocytes and hemorrhage, completely involving adjacent lobules. Rat, administered monocrotaline. Source: *Courtesy: The National Toxicology Program. From Haschek, W.M., Rousseaux, C.G., Wallig, M.A. (Eds.), 2013. Haschek and Rousseaux's Handbook of Toxicologic Pathology, third ed. Academic Press (Elsevier), San Diego, CA, Figure 45.15, p. 1530, with permission.*

major tributary. In these instances, the important factor is the potential incomplete mixing of portal blood in the relatively short portal vein, which could lead to preferential streaming of the toxic agent to certain lobes or portions of lobes in the liver. Another putative factor that has been hypothesized to contribute to the appearance of massive subcapsular necrosis in rodents is the possible pressure-induced ischemia that might result from rapidly developing hepatomegaly. However, evidence for this mechanism is not substantial.

Focal hepatocellular degeneration and necrosis refers to an infrequently observed pattern of injury affecting individual cells and small groups of cells in which there is no selective lobular distribution. It is typically recognized as multiple foci of necrosis that randomly occur in all three regions of the liver lobules (central, midzonal, and periportal regions) (Figure 8.13). Factors leading to this pattern of necrosis have not been identified. Since this pattern resembles that observed in infectious processes in the liver, a role for the immune response and cytokine-mediated injury are considered possible.

Hepatocellular Adaptation

The liver undergoes a variety of adaptive changes in response to xenobiotic exposure. These adaptive changes may include increased liver size, microscopic changes, ultrastructural changes, and functional metabolic changes. In many instances, the magnitude and character of these adaptive changes are species-dependent. Adaptive changes are reversible, and the process of reversibility may be rapid unless the casual xenobiotic agent persists in the tissue.

An increased liver size, typically determined by increased liver weight, is referred to as *hepatomegaly*. While accumulation of fat or glycogen may cause modest increases in liver weight, the adaptive changes leading to xenobiotic-mediated hepatomegaly at the tissue level include hypertrophy and hyperplasia. Conceptually these processes represent distinct mechanisms of liver enlargement, although they often are concurrently present and are often species-specific.

Hypertrophy is the term used for the increase in liver size that may result from an increase in the size of the hepatocytes due to the expansion of one or more organellar components of the hepatocytes. Hypertrophy may occur in defined lobular regions or may affect the entire lobules, depending upon the activity and dose level of the xenobiotic. Even when it is restricted to a lobular region (central lobular is most common), it usually involves the entire liver. The increase in hepatocyte size is often, but not universally, associated with preferential increase in SER, peroxisomes, or mitochondria. The expansion in number and/or volume of these organelles is sometimes referred to as *proliferation* (SER proliferation, peroxisome proliferation, mitochondrial proliferation).

The light-microscopic appearance of hypertrophy upon routine H&E staining will sometimes suggest the selective involvement of one organelle. If total SER volume is increased, the cytoplasm is often noted to have an eosinophilic ground-glass appearance upon light microscopy (Figure 8.14). If total peroxisomal volume is increased, the cytoplasm is often noted to have an eosinophilic granular appearance (Figure 8.15). Changes in organellar composition may be definitively

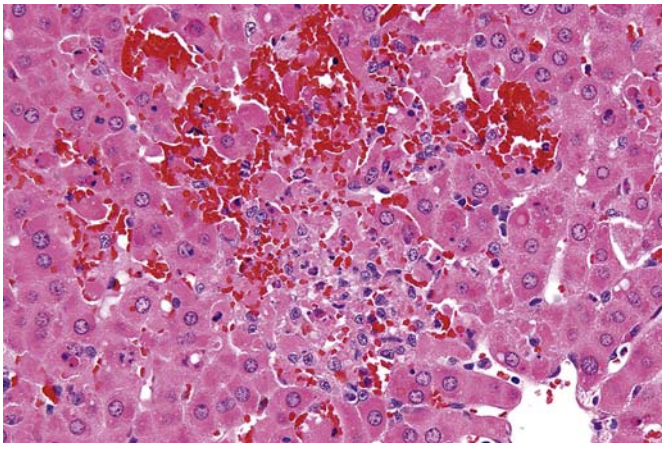

FIGURE 8.13 Focal necrosis, characterized by coagulative hepatocellular necrosis, congestion, and hemorrhage, with no discernible zonal distribution. Rat, administered galactosamine HCl. Source: *Courtesy: The National Toxicology Program. From Haschek, W.M., Rousseaux, C.G., Wallig, M.A. (Eds.), 2013. Haschek and Rousseaux's Handbook of Toxicologic Pathology, third ed. Academic Press (Elsevier), San Diego, CA, Figure 45.16, p. 1531, with permission.*

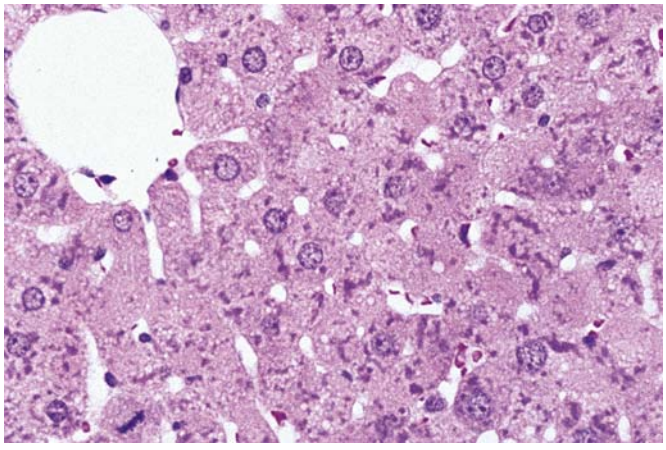

FIGURE 8.14 Central lobular hypertrophy characterized by enlarged hepatocytes with amorphous eosinophilic cytoplasm, typical for proliferation of SER. Rat, administered phenobarbital. Source: *From Haschek, W.M., Rousseaux, C.G., Wallig, M.A. (Eds.), 2013. Haschek and Rousseaux's Handbook of Toxicologic Pathology, third ed. Academic Press (Elsevier), San Diego, CA, Figure 45.19, p. 1533, with permission.*

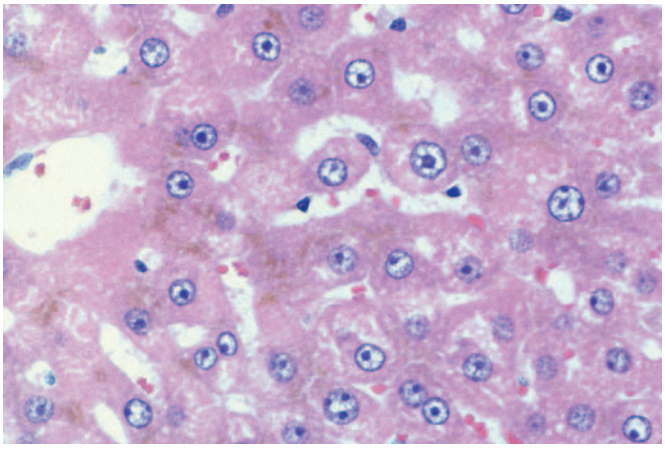

FIGURE 8.15 Central lobular hypertrophy, characterized by enlarged hepatocytes with granular eosinophilic cytoplasm, typical for proliferation of peroxisomes. Brown pigment accumulation in pericanalicular regions of adjacent hepatocytes is lipofuscin. Rat, administered WY-14,643. Source: *From Haschek, W.M., Rousseaux, C.G., Wallig, M.A. (Eds.), 2013. Haschek and Rousseaux's Handbook of Toxicologic Pathology, third ed. Academic Press (Elsevier), San Diego, CA, Figure 45.20, p. 1533, with permission.*

detected by subjective or morphometric assessment of hepatocytes using either electron micrography, or light microscopy assisted by immunohistochemical detection of organelle-specific markers.

Hyperplasia is the term used for the increase in liver size that results from an increase in the number of the hepatocytes, due primarily to an increased rate of cell replication but in some instances supplemented by a decreased rate of attrition of the hepatocytes. Hyperplasia may be detected by light microscopy as increased mitosis, but often more sensitive methods are employed, such as immunohistochemical assessment of BrdU incorporation (similarly to regeneration, as described earlier). Like hypertrophy, hyperplasia may occur in defined lobular regions or across entire lobules. The cell replication accounting for hyperplasia is often transient, so that detection of an increased cell replication among hepatocytes is not possible even though their increase in absolute number (and associated increase in liver weight) may be sustained throughout repeated administration of the xenobiotic. Following cessation of dosing, the xenobiotic agent diminishes below threshold levels, and loss of hepatocytes through apoptosis has been reported to reverse the increase in hepatocyte numbers and associated increased liver weight. Beyond hypertrophy and hyperplasia, an additional manifestation of hepatocellular adaptive change is the increased expression and activity of specific enzymes related to intermediary or xenobiotic metabolism.

The mechanism by which drugs may cause as hypertrophy and hyperplasia has been attributed to the activation of NRs that function as transcription factors including AHR (Aryl Hydrocarbon Receptor), constitutive androstane receptor (CAR), pregnane X receptor, FXR, and peroxisome proliferator-activated receptor (PPAR)-α. NRs constitute the largest family of transcription factors in humans and other mammals studied. NRs respond to a broad variety of intracellular small molecules, including steroids, fatty acids, bile acids, cholesterol, and vitamins formed endogenously, as well as exogenous substances such as drugs and toxins.

The significance of hepatic adaptive changes should be considered from several points of reference. The changes are typically reversible as tissue levels of the causative agent decrease below the threshold for response. Furthermore, the changes in isolation do not typically result in tissue damage or compromised function, and therefore are not considered adverse (although the adaptive response may occur coincidentally with other effects that might or might not be considered adverse). However, the adaptive responses often indicate shifts in xenobiotic metabolism, which raise the likelihood of altered drug metabolism.

Infiltrations and Pigments

Hydropic change is an accumulation of water within the cytosolic matrix or rough endoplasmic reticulum of hepatocytes. Hydropic change of the latter type occurs in the liver of rats given either carbon tetrachloride or carbon disulfide (CS_2). It is characterized by enlarged, pale-staining cytoplasm with narrowing of the sinusoids and the perisinusoidal space of Disse. This form of injury is reversible, and can be attributed to a failure to maintain an intracellular sodium ion balance. Glycogen is usually depleted. In its mildest form, hydropic change may be difficult to observe by light microscopy. When routine histologic stains are used, hydropic change may not be distinguished easily from mild lipidosis or glycogen accumulation. Although glycogen content of the liver is variable depending on the physiologic state of the animal, glycogen accumulation may be observed in hepatocytes as a manifestation of toxicity. Glycogen accumulation results in a clear cytoplasm with indistinct vacuoles; this is apparently due to the impairment of enzymatic activity for glycogen catabolism, or an increase in glycogen synthesis.

Small amounts of lipofuscin pigment accumulate in hepatocytes with aging. However, several chemicals, most notably the peroxisome proliferators, result in dramatic lipofuscin accumulation. The pigment is granular and brown in unstained or routinely stained sections, and is located adjacent to bile canaliculi (see Figure 8.15).

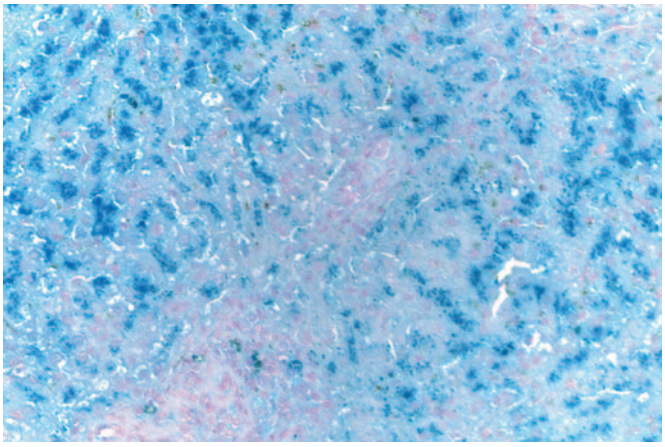

FIGURE 8.16 Lipofuscin accumulation in hepatocytes located in pericanalicular cytoplasm. Schmorl's histochemical stain. Dog. Source: *From Haschek, W.M., Rousseaux, C.G., Wallig, M.A. (Eds.), 2013. Haschek and Rousseaux's Handbook of Toxicologic Pathology, third ed. Academic Press (Elsevier), San Diego, CA, Figure 45.22, p. 1537, with permission.*

Lipofuscin can be distinguished from other liver pigments by staining positively with Schmorl's technique (Figure 8.16) or by autofluorescence under ultraviolet light. Lipofuscin is believed to represent lysosomal accumulation of poorly digested or oxidized lipid, and can be detected as the accumulation of secondary lysosomes by electron microscopy.

Excess storage of iron in hepatocytes may occur as a consequence of excessive dietary intake, or treatment with hepatotoxins. Iron is stored in hepatocytes in the form of ferritin, ferric iron bound to the protein apoferritin. Excess ferritin aggregates are observed as gold-brown hemosiderin granules. Ultrastructural studies demonstrate that these membrane-bound granules, siderosomes, may derive from secondary lysosomes and are often pericanalicular. Biliary excretion of iron from lysosomes may represent an important route for the excretion of excess iron.

Excess storage of hepatic copper may occur as a consequence of increased copper intake, or rarely from previous damage. Copper storage may be demonstrated in histologic sections by either rubeanic acid or rhodamine staining. In rats fed a high-copper diet, copper is localized in the periportal and sometimes midzonal hepatocytes. Sufficient copper accumulation is associated with enlarged hyperchromatic hepatocytes and necrosis, with accumulation of neutrophils and mononuclear inflammatory cells. In mice, copper intoxication has been associated with Mallory body formation. In some species (e.g., sheep), excessive storage may be followed by the eventual release of copper into the circulation, from the liver, often following ingestion of toxic plants, leading to an acute and often fatal hemolytic crisis.

Hepatocellular Inclusions

Cytoplasmic inclusions have been described in hepatocytes of mice following treatment with a variety of drugs and chemicals. They are generally described as round eosinophilic structures within otherwise normal cytoplasm. Depending upon the context, they have been characterized as Mallory bodies, lamellated inclusions, or crystalloid inclusions. The presence of Mallory bodies has been described following griseofulvin or dieldrin administration, and these inclusions have been demonstrated to be composed of cytokeratin intermediate filaments.

Intranuclear inclusions have been described in hepatocytes of various species. They may represent accumulated components of viruses in certain infectious diseases, and have also been described in lead poisoning (but less commonly than in other tissues, e.g., renal tubular epithelium). However, they are most often observed as a background finding in many contexts. Microscopically, these spontaneous nonviral intranuclear inclusions appear as round eosinophilic structures within otherwise normal nuclei. Upon investigation, these inclusions are composed of membrane-bound cytoplasm, and the inclusion therefore represents the invagination of cytoplasm within the nucleus. The attribution of these intranuclear invagination-inclusions to any toxic or adaptive response has been considered highly unlikely.

Phospholipidosis

Hepatic phospholipidosis is an excessive accumulation of phospholipids within the cytoplasm of hepatocytes. This condition is an acquired storage disorder caused by numerous drugs and chemicals, including amiodarone and chlorfentermine. Despite the diversity of agents capable of causing phospholipidosis, these agents share a common chemical feature; they are all cationic amphipathic molecules. These agents disrupt the normal trafficking of cell membrane phospholipids through autophagosomes to lysosomes for degradation. This leads to an accumulation of lysosomal phospholipids. Differences in phospholipid composition (in different organs and in different species) should be taken into account when assessing the mechanism and significance in toxicologic studies.

The histologic appearance of phospholipidosis can be quite variable, but often hepatocellular cytoplasm contains numerous round clear vacuoles that can be smaller than the diameter of the nucleus or larger, imparting a foamy appearance to the cytoplasm. Fine vacuoles are most often apparent adjacent to canaliculi. Zonal distribution can vary depending on the type of drug or chemical. Biliary epithelium can also be affected, with or without hepatocellular involvement.

The clear vacuoles can be confused with microvesicular lipidosis (steatosis), although at the ultrastructural level, there is a characteristic multilaminated whorl of material with a "fingerprint" pattern, termed a *myeloid body*, within affected lysosomes. Phospholipidosis can develop in Kupffer cells within the liver. The potential for phospholipidosis to cause cytotoxicity is unclear. In most cases, phospholipidosis is reversible upon discontinuation of the drug or chemical.

Cholestasis

Cholestasis is defined as disrupted or arrested bile flow. Defined biochemically, cholestasis consists of altered serum constituents, that is, hyperbilirubinemia, bile acidemia, and elevated enzymes such as alkaline phosphatase and gamma-glutamyl transpeptidase.

Morphologically, acute cholestasis is characterized by the presence of greenish yellow-orange waxy plugs in hepatocellular canaliculi, most evident in the centrilobular areas (Figure 8.17). The differentiation of bile from other pigments may be confirmed using histochemical stains such as Hall's. Bile may also be evident in Kupffer cells and in cases of marked cholestasis, within the cytoplasm of hepatocytes. In cases of marked obstruction, bile may also be evident in the lumen of cholangioles and small-caliber bile ducts. Cholestasis can cause vacuolization of hepatocytes, often with bile pigmentation, in some rodent species, but rarely in the dog. Canalicular cholestasis is rarely, if ever, seen in rats, and is only occasionally seen in mice.

Cholestasis can develop from intrahepatic and extrahepatic causes. Extrahepatic cholestasis can arise from obstruction of the common bile duct via intraductal and extraductal causes. In contrast, intrahepatic cholestasis has a number of possible causes and appearances. Bland cholestasis is a category in which cholestasis is evident, but there is no coexisting histologic injury of the biliary tree or hepatocytes. Bland cholestasis can arise from the presence of sepsis caused by endotoxin or some drugs. Drugs and chemicals that can produce both acute cholangitis and cholestasis include alpha-napthylisothiocyanate (ANIT), chlorpromazine, allopurinol, and amoxicillin-clavulanate. Histologically, neutrophils and edema are present within the portal tract connective tissue and there is evidence of injury or necrosis of the biliary epithelium.

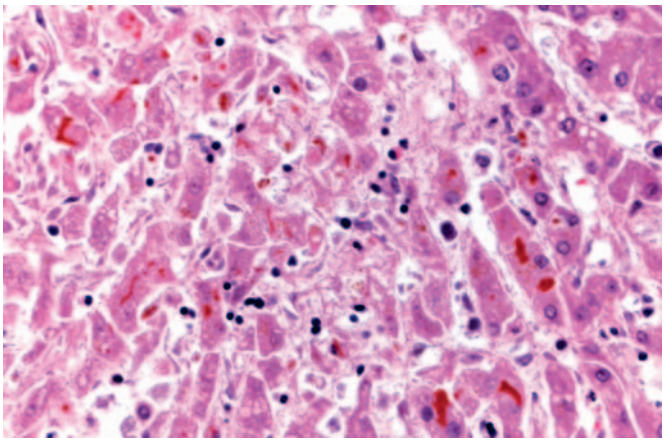

FIGURE 8.17 Canalicular cholestasis characterized by the presence of bile plugs in canaliculi between adjacent hepatocytes. Dog. Source: *From Haschek, W.M., Rousseaux, C.G., Wallig, M.A. (Eds.), 2013. Haschek and Rousseaux's Handbook of Toxicologic Pathology, third ed. Academic Press (Elsevier), San Diego, CA, Figure 45.27, p. 1540, with permission.*

Biliary Epithelial Degeneration and Necrosis

Specific targeting of the biliary epithelium by toxic drugs is uncommon. Biliary epithelium may be more often injured in circumstances of significant hepatocellular injury. However, there are a few notable chemicals that can cause biliary epithelial degeneration or necrosis. Because the biliary tree is lined with functionally heterogeneous epithelial cells, the site of injury produced by a particular toxin can vary from species to species. One of the better known toxicants is ANIT. Only large bile ducts are injured in rats and mice, while the small-caliber ducts are spared. Extrahepatic ducts of mice are injured, but not those of rats. Single doses of phenylene diisothiocyanate given to rats result in extensive destruction of the epithelium of the common bile duct and major intrahepatic ducts, but not of the epithelium of the bile ductules found in the portal triads. Phenylisothiocyanate causes acute necrosis of epithelium in the interlobar ducts but not in the epithelium of the bile ductules found in the portal triad.

Biliary Hyperplasia

Bile duct hyperplasia is a common finding in the liver of rodents. Hyperplastic ducts may be restricted to the immediate periportal area, or may extend from the immediate periportal area and form foci of proliferated ducts. To assess bile duct hyperplasia, the toxicologic pathologist must have a clear appreciation of normal bile duct numbers. In the young rodent, one or two bile ductules are found in each portal triad. However, with increasing age, a typical portal triad will have several bile ductules that will continue to be restricted to the triad.

Histologically, there are three subdivisions of biliary proliferation based on morphological criteria. These include typical hyperplasia, atypical hyperplasia, and oval cell proliferation (ductular reaction).

"Typical" biliary hyperplasia is characterized histologically by proliferation of well-differentiated biliary epithelium forming an increase in number of small-caliber ducts with a well-defined lumen within the

portal tracts or occasionally extending into the adjacent parenchyma (Figure 8.18). This change can be caused by obstruction of bile flow, but is often a nonspecific response to hepatic injury. In laboratory animals, "typical" cholangiocyte proliferation can occur as an aging change in rats and hamsters. In general, this lesion poses little risk as it has no evidence of functional alteration or progression.

"Atypical" biliary hyperplasia is characterized by an irregular proliferation of bile ducts, which extends beyond the portal region, occasionally appearing to merge with adjacent hepatocytes. Some biliary epithelial hyperplasia may exhibit slight atypia and/or may occur outside the portal tract. There appears to be an increased risk of neoplasia following prolonged "atypical" biliary hyperplasia, as observed in studies of the carcinogen thioacetamide where histologic atypia or biliary dysplasia was observed by the ninth week of treatment in a study in rats.

The third category of biliary proliferation, "oval cell" proliferation, is characterized by disorganized tubular structures with poorly defined lumens formed by oval-shaped, basophilic cells that are smaller than typical bile duct epithelium (see oval cell proliferation and Figure 8.7). This response is also termed *ductular reaction*. Ductular reaction is believed to be a proliferation of bipotential precursor cells with the ability to form mature biliary epithelium or hepatocytes. The different categories may represent a continuum that is dose- and/or time-dependent. Ductular reaction (oval cell proliferation) may occur as the result of massive or chronic liver injury, or may be associated with inhibition of hepatocyte proliferation.

Cholangiofibrosis

Cholangiofibrosis occurs in rats and is generally considered to be part of a continuum of biliary epithelial injury that starts with oval cell proliferation (ductular reaction). The lesions of cholangiofibrosis include ducts that are frequently incompletely lined by hyperchromatic cuboidal to columnar cells (Figure 8.19). Mucus, necrotic debris, and desquamated epithelial cells may accumulate within the bile ducts. As the lesion progresses, there are peribiliary fibrosis and a mixed inflammatory cell infiltrate. Large areas of hepatic lobe may be affected. Over time, dense connective tissue develops with spotty retention of biliary epithelium surrounding residual pools of mucus. Persisting biliary epithelium may become reduced in height and number, eventually forming cysts lined by a few flattened cells or devoid of epithelium altogether. The original bile duct epithelial component may no longer be visible, while the collagenous component remains and is never completely resolved. The ultimate lesion may be a focus of scar tissue. In distinct contrast to regression, some studies have demonstrated progressive lesions resulting in cholangiocarcinoma. For example, treatment of rats with furan for 90 days resulted in cholangiofibrosis. Progression to cholangiocarcinoma, in the absence of further treatment, was observed when these rats were maintained for several months after stopping furan administration. Because the spectrum of lesions generally classified as cholangiofibrosis, cholangiofibroma, and cholangiocarcinoma in the rat is a morphological continuum,

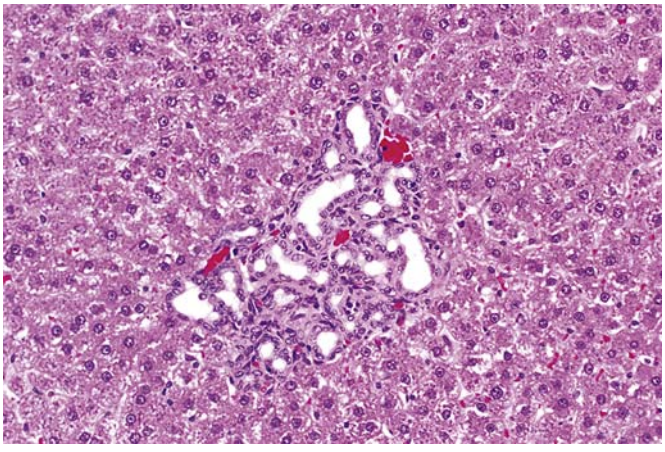

FIGURE 8.18 Bile duct hyperplasia characterized by numerous bile duct profiles within the portal region. Rat, untreated. Source: *From Haschek, W.M., Rousseaux, C.G., Wallig, M.A. (Eds.), 2013. Haschek and Rousseaux's Handbook of Toxicologic Pathology, third ed. Academic Press (Elsevier), San Diego, CA, Figure 45.29, p. 1541, with permission.*

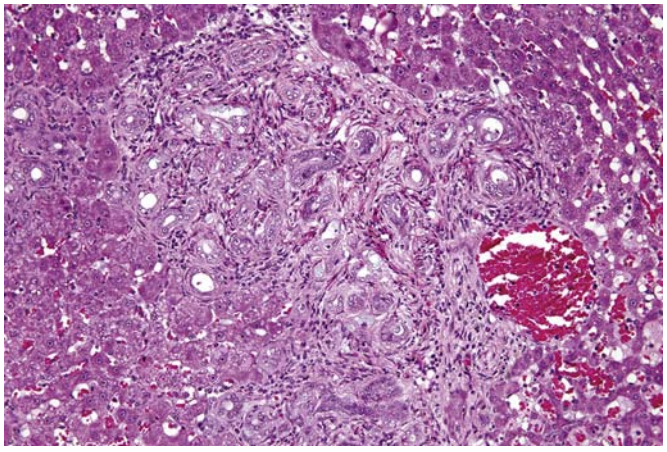

FIGURE 8.19 Cholangiofibrosis characterized by numerous bile ducts that are lined by hyperchromatic cuboidal to columnar cells, peribiliary fibrosis, and a mixed inflammatory cell infiltrate. Rat, administered furan. Source: *Courtesy: The National Toxicology Program. From Haschek, W.M., Rousseaux, C.G., Wallig, M.A. (Eds.), 2013. Haschek and Rousseaux's Handbook of Toxicologic Pathology, third ed. Academic Press (Elsevier), San Diego, CA, Figure 45.30, p. 1542, with permission.*

identifying specific criteria for separation of the various categories is difficult and controversial.

Nonparenchymal Cell Injury

While the liver mass is composed predominantly of hepatocytes, several other cell types are found in the liver. Although nonparenchymal cells are less conspicuous and probably affected less frequently by hepatotoxins, they are nevertheless occasionally involved in toxic responses. When nonparenchymal injury is noted, it is associated most frequently with hepatocytic injury.

Sinusoidal Endothelial Cells

Hepatic sinusoidal endothelial cells constitute approximately one-half of the hepatic sinusoidal cell population and are characterized by a specialized phenotype that includes fenestrations and lack of a basement membrane. Injury to this cell population can have significant effects on hepatic perfusion, and the cells also participate in a variety of immunologic and inflammatory reactions. Only a few chemicals have been identified that target this cell population. Arsenic compounds can damage the hepatic sinusoidal epithelium via oxidative injury to the extent that the sinusoids resemble capillaries with loss of fenestration, and deposition of basement membrane material.

Necrosis of endothelial cells may be observed within regions of central lobular hepatocellular necrosis with agents such as dimethylnitrosamine, as discussed earlier under hepatocellular necrosis. The mechanism is thought to result from diffusion of toxic metabolites, formed in central lobular hepatocytes, into endothelial cells, and is often accompanied by localized hemorrhage.

Very rapid destruction of hepatic endothelial cells follows the administration of microcystin-LR, a toxin produced by the cyanobacterium *Microcystis aeruginosa*. Destruction of the endothelium can result in the embolization of hepatocytes to the lung. Evidence suggests that hepatocyte dissociation, probably related to the aggregation of actin filaments, precedes endothelial cell injury.

Other chemicals that have a selective toxicity for sinusoidal endothelial cells in rodents include azathioprine and the PA monocrotaline. Monocrotaline and other PAs cause a condition in humans referred to in the past as veno-occlusive disease, and in a recently described rat model as sinusoidal obstruction syndrome (SOS). In SOS caused by monocrotaline, lesions are initially characterized by loss of sinusoidal lining cells, sinusoidal hemorrhage, and mild damage to central vein endothelium. This phase is followed by centrilobular coagulative necrosis of hepatocytes, and severe injury to sinusoids and endothelium of central veins. Inflammation (monocytes and macrophages) may be marked at this stage. This is followed by subendothelial and adventitial fibrosis of central veins.

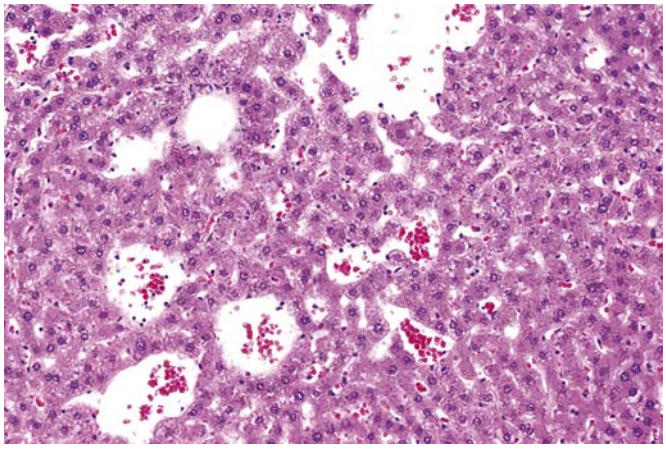

FIGURE 8.20 Peliosis hepatis, also referred to as angiectasis, consisting of clusters of dilated blood-filled sinusoids usually occurring randomly throughout the liver parenchyma. Rat, untreated. Source: *From Haschek, W.M., Rousseaux, C.G., Wallig, M.A. (Eds.), 2013. Haschek and Rousseaux's Handbook of Toxicologic Pathology, third ed. Academic Press (Elsevier), San Diego, CA, Figure 45.31, p. 1543, with permission.*

Peliosis hepatis, sometimes referred to as angiectasis, is characterized by clusters of greatly dilated sinusoids usually occurring randomly throughout the liver parenchyma. The resultant lacunae are filled by blood and may be either lined by or devoid of endothelium (Figure 8.20). Peliosis hepatis is generally a spontaneous lesion in laboratory animals, although it is rarely reported to be associated with hepatotoxicants, particularly toxicants that induce endothelial injury.

Peliosis hepatis (angiectasis) must be differentiated from a rare lesion known as intrahepatocellular erythrocytes (hepatocellular erythrophagocytosis). This lesion appears as individual hepatocytes or small groups of hepatocytes that are enlarged and contain intact erythrocytes with margination of hepatocellular nuclei. The presence of intrahepatocellular erythrocytes has been observed exclusively in mice, usually in studies greater than 1 year in duration. It has been considered as a spontaneous lesion that may in some instances be exacerbated or possibly caused by treatment, although information on pathogenesis is lacking.

Kupffer Cells and Other Nonparenchymal Cells

Little is known about toxicant-induced injury of Kupffer cells. Following endocytosis of the naturally occurring toxin ricin, found in castor beans, Kupffer cell necrosis results, possibly via ribosome inactivation and/or oxidative stress. Other experimental systems causing Kupffer cell injury include intravenous injection of gadolinium, beryllium phosphate, or liposomal clodronate.

Hepatic Stellate Cells

Hepatic stellate cells are minority cells in the liver, constituting only 5% of the total hepatic cell numbers. Despite the rather small number of stellate cells in the liver, compared with other cell types, this cell plays a central role in several toxicant-induced hepatic lesions.

Because the stellate cell is the vitamin A storage site in the liver of many species, including rodent species, its response is central in the development of hepatic lesions associated with hypervitaminosis A. On ingestion or administration of excessive doses of vitamin A, stellate cells enlarge due to the development of large cytoplasmic lipid deposits. With continued treatment, collagen is formed by the activated stellate cells, and severe hepatic fibrosis may ensue.

Stellate cells are responsive to hepatic injury induced by variety of hepatic necrogenic agents. When carbon tetrachloride induces central lobular necrosis, or when ethionine causes periportal necrosis, stellate cells accumulate in the local area of injury, apparently because of a proliferation of the local population of stellate cells. These cells participate in the reparative process by producing collagen. It appears now well established that hepatic fibrosis occurring within the lobule is due to collagen production by the stellate cells.

Cystic degeneration (spongiosis hepatis) is a spontaneous lesion of aging rats and is more frequent in male rats than female rats. Mice are infrequently affected. Cystic degeneration arises from altered hepatic stellate cells that form uni- or multilocular cyst-like structures filled with finely granular to flocculent acidophilic material (Figure 8.21). The lesion tends to replace, rather than compress, adjacent hepatic parenchyma or interdigitate between hepatocytes. The cystic spaces are lined by extracellular matrix components. These components include collagens III and IV, but not collagen I, which would be formed by activated stellate cells. Immediately adjacent to the extracellular matrix, there are fibroblast-like cells that contain small lipid vacuoles typical of hepatic stellate cells. These cells may be stained immunohistochemically with markers such as desmin and, less often, smooth muscle actin, which are typical for hepatic stellate cells. The pathogenesis of cystic degeneration is not clear. It is recognized as a spontaneous aging lesion, but can also occur in carcinogen-treated rats.

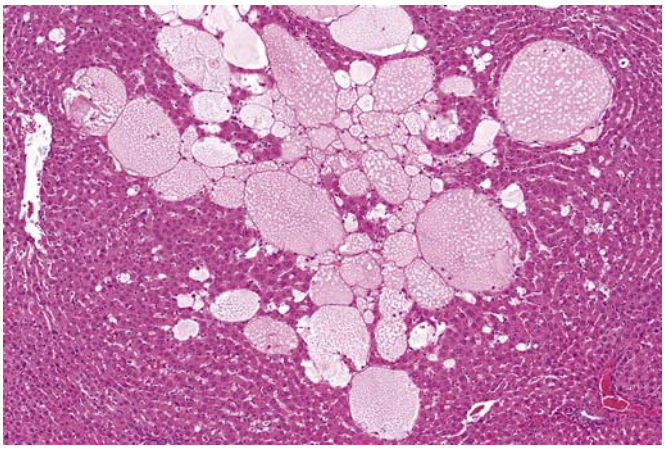

FIGURE 8.21 Cystic degeneration (spongiosis hepatis) appearing as uni- or multilocular cyst-like structures filled with finely granular to flocculent acidophilic material. Rat. Source: *From Haschek, W.M., Rousseaux, C.G., Wallig, M.A. (Eds.), 2013. Haschek and Rousseaux's Handbook of Toxicologic Pathology, third ed. Academic Press (Elsevier), San Diego, CA, Figure 45.32, p. 1544, with permission.*

Hepatic Neoplasia Due to Toxicant Injury

Hepatocellular Neoplasia

The induction of hepatocellular neoplasia by drugs and chemicals is a significant and common finding in toxicologic pathology. In rats and mice (without specific genetic modification), species commonly used in long-term carcinogenicity studies for hazard identification, the liver, and specifically the hepatocyte, represents the most common test article–related target of tumorigenesis.

The pathogenesis of hepatocellular neoplasia has been mostly characterized in rats and mice, and is considered in many instances to represent a progression of lesions from preneoplastic lesions to benign neoplasia to malignant neoplasia. The early preneoplastic lesion is referred to as a focus of cellular alteration. These lesions may occur spontaneously and increase in frequency in aging rats and mice, but may also reflect a response to a xenobiotic. Foci are recognized by routine light microscopy as a collection of hepatocytes with altered cytoplasmic staining. The altered cytoplasmic staining appears as either increased basophilia or eosinophilia in H&E–stained sections, or in some instances as the lack of cytoplasmic staining. Four general categories of hepatocellular foci have been defined including basophilic (Figure 8.22), eosinophilic (Figure 8.23), mixed basophilic/eosinophilic, and clear cell (Figure 8.24). The mixed cell type includes a mixture of cells of which some are basophilic and others eosinophilic. The clear-cell type is characterized by extremely vacuolated or clear nonstaining cytoplasm. In some classification schemes, the number of types of foci is expanded by further subdividing these four general categories of foci. Foci of cellular alteration may be detected by a variety of specialized histochemical and immunohistochemical markers. In the rat, positive markers include gamma-glutamyl transferase (GGT, membrane associated) and placental glutathione-S-transferase (GST cytoplasmic). Negative markers include adenosine triphosphatase (ATPase,

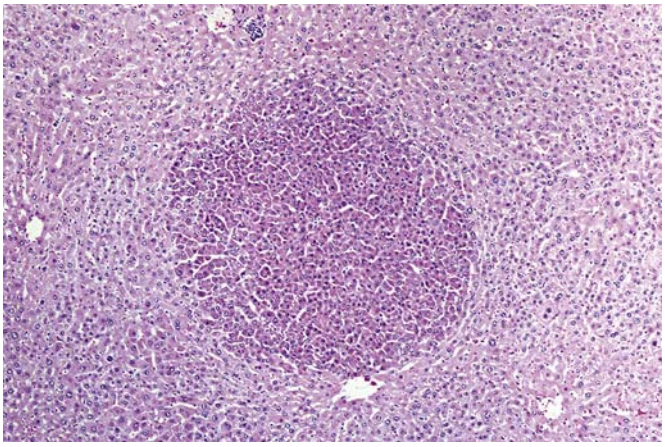

FIGURE 8.22 Focus of cellular alteration, basophilic type. Rat, administered WY-14,643. Source: *From Haschek, W.M., Rousseaux, C.G., Wallig, M.A. (Eds.), 2013. Haschek and Rousseaux's Handbook of Toxicologic Pathology, third ed. Academic Press (Elsevier), San Diego, CA, Figure 45.33, p. 1545, with permission.*

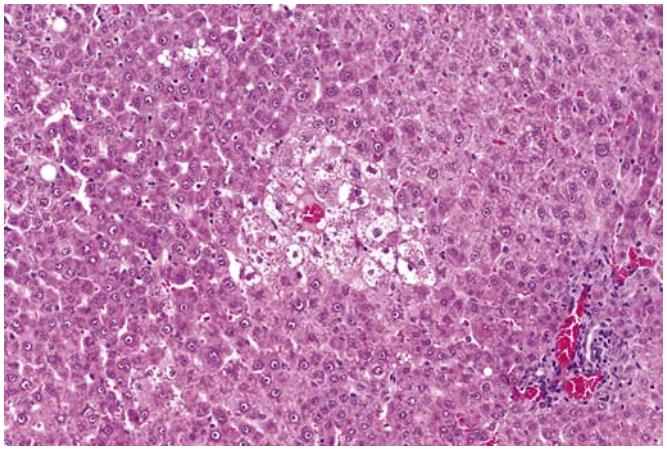

FIGURE 8.24 Focus of cellular alteration, clear-cell type. Rat. Source: *From Haschek, W.M., Rousseaux, C.G., Wallig, M.A. (Eds.), 2013. Haschek and Rousseaux's Handbook of Toxicologic Pathology, third ed. Academic Press (Elsevier), San Diego, CA, Figure 45.35, p. 1546, with permission.*

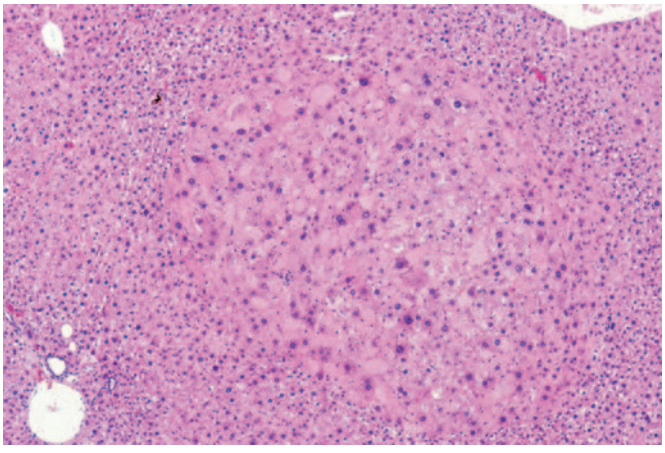

FIGURE 8.23 Focus of cellular alteration, eosinophilic type. Source: *From Haschek, W.M., Rousseaux, C.G., Wallig, M.A. (Eds.), 2013. Haschek and Rousseaux's Handbook of Toxicologic Pathology, third ed. Academic Press (Elsevier), San Diego, CA, Figure 45.34, p. 1546, with permission.*

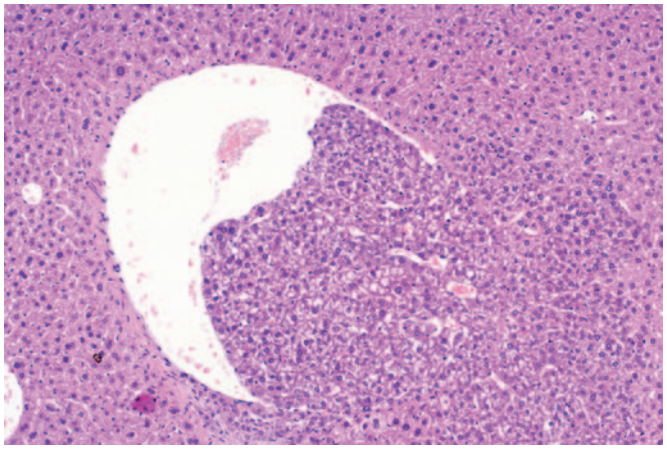

FIGURE 8.25 Basophilic focus of cellular alteration forming a projection from the adjacent parenchyma into a hepatic vein. Mouse. Source: *From Haschek, W.M., Rousseaux, C.G., Wallig, M.A. (Eds.), 2013. Haschek and Rousseaux's Handbook of Toxicologic Pathology, third ed. Academic Press (Elsevier), San Diego, CA, Figure 45.39, p. 1547, with permission.*

membrane associated) and glucose-6-phophatase (G6P, cytoplasmic). These and similar markers also have been used to characterize foci in mice, although results have tended to be more variable. In both species, the appearance of some markers may be correlated to the altered staining characteristics detected in H&E-stained sections.

The characterization of foci using H&E staining characteristics and marker analysis suggests that the mode of action of a carcinogen may exert a profound influence upon the prevalence of certain phenotypes. For example, in rats, foci increased by the CAR activator, phenobarbital, tend to be eosinophilic and GGT-positive, while foci increased by the PPAR-α activator, clofibrate, tend to be basophilic and GGT-negative. However, the mechanistic explanation for these types of observations remains incomplete.

In mice, intravascular protrusion of hepatocytes from basophilic foci has been observed following nitrosamine administration. In this lesion, hepatocytes appear to form projections from the adjacent parenchyma into the hepatic veins (Figure 8.25). These projections may be contained in subendothelial locations, but in some cases appear to extend beyond the endothelial lining of the veins. Some of the earlier literature debated whether this finding represented an invasive process linked to metastatic potential. However, it is generally accepted that these are nonneoplastic lesions

that have no metastatic potential. Foci of cellular alteration are considered to represent potential precursors to hepatocellular neoplasms.

Hepatocellular neoplasms are divided into benign lesions called adenomas and malignant lesions called carcinomas. Hepatocellular adenomas are very similar in appearance to foci of cellular alteration. The key difference is that adenomas tend to be larger and cause a greater degree of compression of adjacent hepatic parenchyma, while foci tend to be smaller and merge with adjacent parenchyma, causing only modest, if any, compression. Hepatocellular adenomas also must be distinguished from focal hyperplasia of hepatocytes that may be related to previous or ongoing liver injury or other liver lesions. Unlike adenomas and foci, the lobular structure in focal hyperplasia is usually maintained, even if in some cases it may be distorted. Although hepatocytes in focal hyperplasia may be enlarged, they often stain similarly to hepatocytes in the surrounding liver, and are typically recognized due to compression of adjacent tissues.

Hepatocellular carcinomas are malignant neoplasms of hepatocytes. They are readily diagnosed as primary lesions, and the metastatic potential varies. When metastasis occurs, it most typically involves the lung. Carcinomas are most readily differentiated due to their growth pattern, which most commonly appears as trabeculae of neoplastic hepatocytes ranging in some areas from three to eight hepatocytes in width (Figure 8.26). This common pattern is termed a *trabecular pattern*. Especially wide trabecular structures tend to undergo central (presumably ischemic) necrosis, and loss of necrotic centers may result in a pseudoglandular pattern of growth. Some hepatocellular carcinomas are characterized by rarer cellular arrangements including sheets, glands, and mixed cholangiocellular patterns.

Occasionally, some hepatocellular neoplasms may have the typical appearance of adenomas except for one or few select areas within the lesion, where a nodule of neoplastic hepatocytes compresses the adjacent adenoma tissue, and contains a trabecular pattern and/or possesses a distinct, usually more basophilic, cytoplasm staining. Current diagnostic conventions designate these lesions as hepatocellular carcinomas.

In rats and mice, hepatocellular neoplasms may occur spontaneously and are often observed as incidental findings in aging untreated animals in standard laboratory environments. The incidence in most rat strains is low. However, in mice, some strains such as the C3H are known to have a fairly high incidence (30%–50% in males) while other strains such as the C57Bl/6 have a fairly low incidence (<5% in males). In the F1 hybrid of these strains, an intermediate incidence is observed. The incidence is lower in females than in males.

Rats occasionally have spontaneous hepatodiaphragmatic nodules of the median lobe, with the incidence varying by strain. These are often grossly visible lesions, appearing as a single nodule up to 1 cm in diameter located on the diaphragmatic surface of the liver near the diaphragmatic attachment (Figure 8.27). They are composed of hepatic lobular parenchyma, often with hepatocytes possessing unusual linear chromatin patterns. The incidence appears strain dependent (example, 0.7% in F344 rats and 5.5% in Han:WIST rats). In long-term studies of carcinogenicity, hepatodiaphragmatic nodules are important only in that they

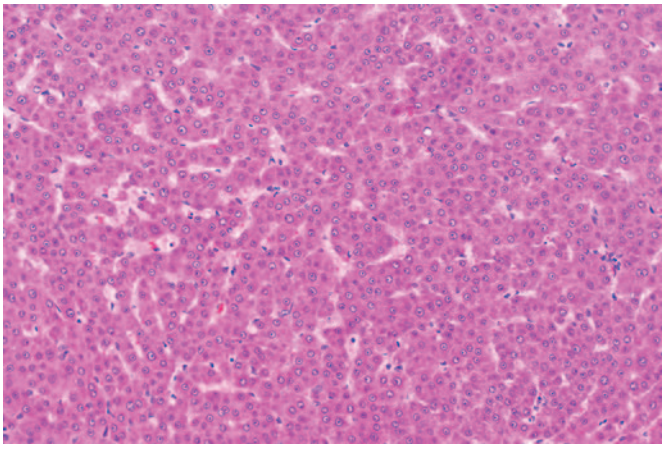

FIGURE 8.26 Hepatocellular carcinoma characterized by typical trabecular growth pattern, in some areas forming trabeculae of three or more hepatocytes in width. Rat. Source: *From Haschek, W.M., Rousseaux, C.G., Wallig, M.A. (Eds.), 2013. Haschek and Rousseaux's Handbook of Toxicologic Pathology, third ed. Academic Press (Elsevier), San Diego, CA, Figure 45.40, p. 1548, with permission.*

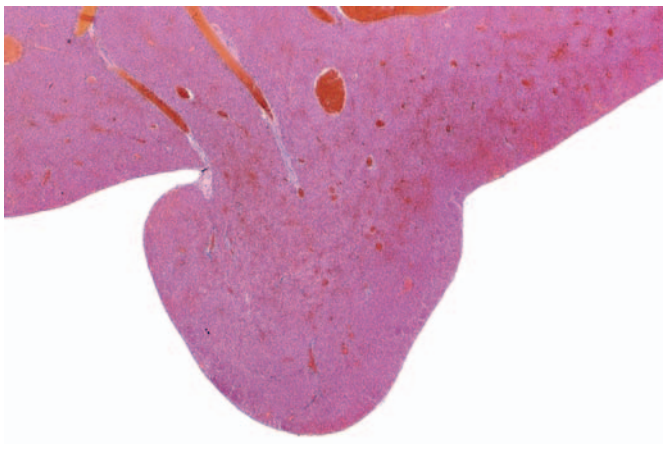

FIGURE 8.27 Hepato-diaphragmatic nodule of the median lobe appearing as a single nodule located on the diaphragmatic surface of the liver. Rat. Source: *Courtesy: The National Toxicology Program. From Haschek, W.M., Rousseaux, C.G., Wallig, M.A. (Eds.), 2013. Haschek and Rousseaux's Handbook of Toxicologic Pathology, third ed. Academic Press (Elsevier), San Diego, CA, Figure 45.41, p. 1549, with permission.*

must not be confused with grossly visible hepatocellular neoplasms.

A rare lesion that may be confused with hepatocellular neoplasia is glandular metaplasia of hepatocytes. This lesion may have a variable appearance, with formation of a few too many glands of diverse size that are lined by cells resembling hepatocytes or cuboidal epithelial cells which resemble bile duct epithelium. The glands may contain granular eosinophilic material or blood cells. The partial replacement of hepatic parenchyma by glandular structures with features resembling hepatocytes has been observed in chronic studies of some pentachlorobiphenyls. The pathogenesis and significance of this lesion is unknown.

Hepatoblastoma is a distinct form of hepatic neoplasm that has been described in aging mice as a spontaneous lesion, or in some instances attributed to a test article. Among aged untreated control B6C3F1 mice, the incidence of hepatoblastoma was approximately 2% in males and <1% in females. Hepatoblastomas are usually detected in mice with concurrent hepatocellular adenoma or carcinoma. When associated with a test article, affected treatment groups with an increased incidence of hepatoblastoma often also have an increased incidence of hepatocellular neoplasia. Hepatoblastomas often occur within hepatocellular adenomas and carcinomas.

Hepatoblastomas present histologically as masses composed of islands and sheets of poorly demarcated elongated cells with oval, deeply basophilic nuclei and scant cytoplasm (Figure 8.28). The lesions typically include endothelial-lined cystic spaces that contain blood and/or eosinophilic material. Central areas of necrosis with hemosiderin-laden macrophages, calcium deposits, and cholesterol crystals may also be present. On occasion, there are focal areas with cells arranged in an embryonal-like organoid pattern or form rosettes and ribbons. In some studies, focal areas of squamous differentiation or osteoid differentiation have been noted.

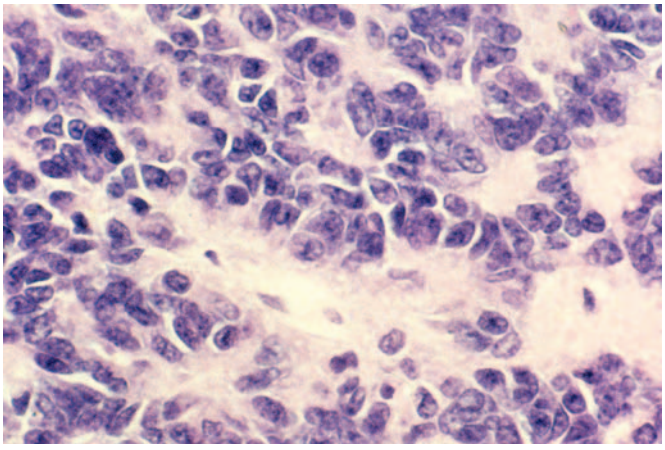

FIGURE 8.28 Hepatoblastoma, composed of islands and sheets of poorly demarcated elongated cells with oval, deeply basophilic nuclei and scant cytoplasm, with occasional arrangement of cells in an embryonal-like organoid pattern, rosettes or ribbons. Mouse. Source: *From Haschek, W.M., Rousseaux, C.G., Wallig, M.A. (Eds.), 2013. Haschek and Rousseaux's Handbook of Toxicologic Pathology, third ed. Academic Press (Elsevier), San Diego, CA, Figure 45.42, p. 1550, with permission.*

Biliary Neoplasia

Neoplasms of the biliary epithelium may be apparent by gross inspection. Typically, they form raised, pale, white to beige masses that may be cystic or contain areas of necrosis. Cholangioma (biliary adenoma) is a benign lesion of bile duct epithelium that is characterized by a distinct border and composed of numerous irregular bile ducts. Cholangiomas have scant connective tissue stroma and may have a thin connective tissue capsule. Although the individual bile ducts may be slightly irregular in shape, the epithelium lining these ducts is usually homogeneous in cell size and shape. The cells are cuboidal, similar to normal intrahepatic bile duct epithelium. The cytoplasm is lightly basophilic, and nuclei are uniform in size and shape. Mitotic figures are rare. Cystic cholangiomas are characterized by irregular cystic cavities usually lined by a uniformly low cuboidal to squamous epithelium. These lesions may have more connective tissue stroma than the simple cholangioma.

Cholangiofibroma

Cholangiofibroma is a benign liver tumor that has some characteristics in common with the cholangiocarcinoma. The cholangiofibroma has an extensive collagenous connective tissue stroma surrounding atypical bile ducts composed of several different cell types. Most cells have bile duct epithelial characteristics, including a basophilic cytoplasm and vesicular nucleus, and goblet cells are observed frequently. In addition, cells resembling Paneth cells and enterochromaffin cells are not infrequent. The duct-like structures are usually filled with necrotic cellular debris from sloughed epithelial cells and mucous substances. In the center of cholangiofibromas, the bile duct epithelium may be completely denuded from the surface of the gland-like structure, leaving a mucus-filled cyst surrounded by connective tissue. Cholangiofibromas are benign lesions and consequently they do not metastasize.

Cholangiocarcinoma

Cholangiocarcinomas are malignant neoplasms of biliary epithelium. The malignant biliary epithelium is pleomorphic, with an increased nuclear–cytoplasmic ratio and basophilic cytoplasm. Mitotic figures are

common. The malignant biliary epithelium may form ducts, glandular structures (often with papillary projections), or solid sheets of neoplastic cells. Cholangiocarcinomas often have a very invasive growth pattern. These tumors tend to be quite firm due to the presence of abundant scirrhous response. Chemically induced biliary neoplasms are uncommon in rodents, and when they do occur they are often associated with significant liver toxicity.

The differential diagnosis of bile duct neoplasms is frequently difficult, at least in comparison with other primary liver neoplasms. The cholangiocarcinoma should always be distinguished from the cholangiofibroma. The malignant lesion is identified primarily by evidence of invasion into vessels or by metastasis. Extreme atypia of the cells may be helpful but has limited diagnostic significance because the cells of cholangiofibromas also display considerable atypia. Two features, the smaller amount of collagen in the stroma and the less abundant accumulation of mucus in neoplastic glands, aid in differentiating the cholangiocarcinoma from the nonneoplastic lesion of cholangiofibrosis. The unitized structure of the lesion with distinct borders, particularly the presence of a thin capsule, helps distinguish the cholangioma. The biological potential, as well as the pathogenesis of the various bile duct proliferative lesions, has generated a moderate amount of research interest and an even greater degree of speculation. Cholangiofibrosis, cholangiofibromas, and cholangiocarcinomas are generally believed to represent a continuous spectrum of lesions.

Neoplasms of bile duct epithelium are extremely rare as spontaneous lesions in the rodent, even though bile duct proliferation is relatively common. Although early bile duct proliferation, including oval cell proliferation and cholangiofibrosis, is associated with the development of bile duct neoplasms, bile duct carcinogenesis should not be predicted based on bile duct proliferation.

Endothelial Cell Neoplasia

Hemangiomas are benign neoplasms formed by endothelial cells. They form fairly well circumscribed but rarely encapsulated masses of vascular channels lined by a single layer of well-differentiated endothelial cells. Mitotic figures are rare. Hemangiomas may assume a capillary form composed of multiple small-caliber vessels compressed into a mass. The cavernous variant is composed of distended larger-caliber vessels.

By gross inspection, hemangiosarcomas may appear as single or multiple raised, dark red, solid to fluid-filled masses. Histologically, there are multiple irregular vascular channels lined by moderately pleomorphic endothelial cells that may be arranged in single or multiple cell thickness (Figure 8.29). More solid areas may be scattered through the mass. Mitotic figures may be common. Local invasion into adjacent parenchyma or distant metastasis may occur.

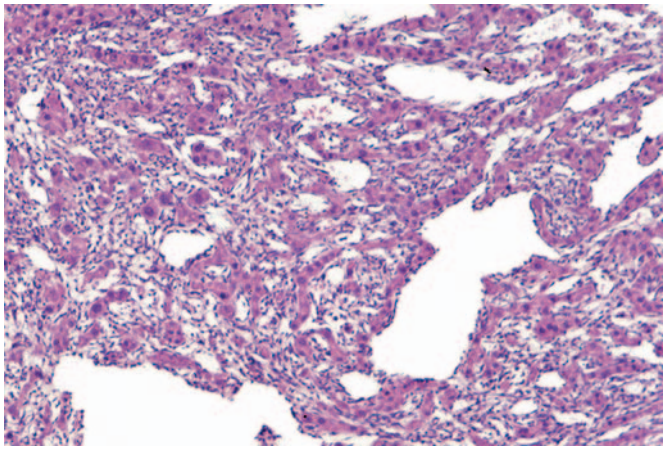

FIGURE 8.29 Hemangiosarcoma composed of multiple irregular vascular channels lined by moderately pleomorphic neoplastic endothelial cells that may be arranged in single or multiple cell layers. Mouse. Source: *From Haschek, W.M., Rousseaux, C.G., Wallig, M.A. (Eds.), 2013. Haschek and Rousseaux's Handbook of Toxicologic Pathology, third ed. Academic Press (Elsevier), San Diego, CA, Figure 45.46, p. 1552, with permission.*

There are several agents associated with an increased risk of hemangiosarcoma in rodents, particularly mice. Iron overload, vinyl chloride, and exposure to the pyrrolizidine, riddelliine, can cause hemangiosarcomas in mice.

The differential diagnosis of hepatic endothelial neoplasms presents few problems. The distinction between benign and malignant endothelial neoplasms of the liver is based primarily on the relatively normal cellular appearance and the uniform single-cell pavementing of hepatocyte surfaces by the benign hemangioma. Hemangiomas must be distinguished from dilated vascular spaces such as telangiectasia and peliosis hepatis. This distinction is relatively simple because the nonneoplastic lesions do not have proliferated endothelial cells lining the abnormal vascular spaces.

Stellate Cell Neoplasia

Stellate cell neoplasms are quite rare. They can from a single or multiple pale, soft, unencapsulated masses. Neoplastic cells may form a discrete mass, or dissect through the parenchyma. Typically, the mass compresses normal adjacent parenchyma, inducing atrophy. Tumor cells may grow in isolated clusters, as sheets, or along the sinusoids. Cells may differ in size, but contain prominent lipid droplets that may also vary in size (Figure 8.30). Some extracellular matrix components are usually distributed within the mass.

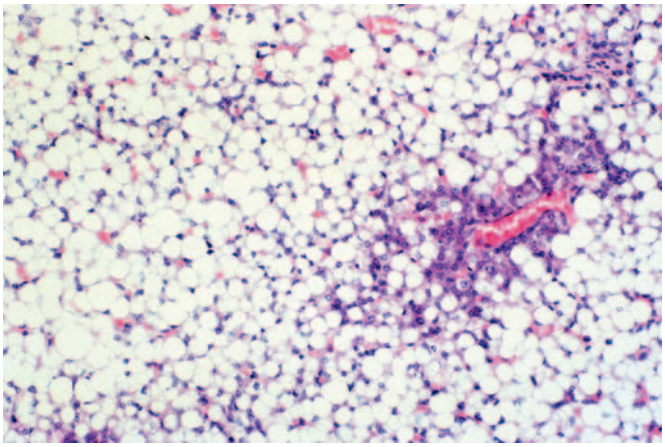

FIGURE 8.30 Stellate cell neoplasm with growth pattern in sheets or along the sinusoids. Neoplastic cells vary in size, but contain prominent lipid droplets. Mouse. Source: *From Haschek, W.M., Rousseaux, C.G., Wallig, M.A. (Eds.), 2013. Haschek and Rousseaux's Handbook of Toxicologic Pathology, third ed. Academic Press (Elsevier), San Diego, CA, Figure 45.47, p. 1553, with permission.*

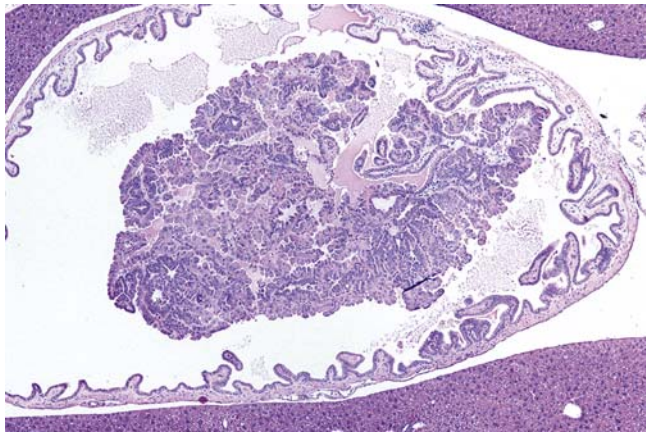

FIGURE 8.31 Gall bladder adenoma appearing as a well-differentiated solitary lesion with irregular papillary growth pattern. Mouse. Source: *From Haschek, W.M., Rousseaux, C.G., Wallig, M.A. (Eds.), 2013. Haschek and Rousseaux's Handbook of Toxicologic Pathology, third ed. Academic Press (Elsevier), San Diego, CA, Figure 45.48, p. 1555, with permission.*

The pathogenesis and behavior of these lesions is unknown due to their rarity.

Kupffer Cell Sarcoma

Kupffer cell sarcomas may form pale masses within the liver that are visible by gross observation and may have an area of central necrosis. Kupffer cell sarcomas may arise as primary neoplasms from the resident Kupffer cell population. Typically, Kupffer cell sarcomas form single or multiple pale nodules within the liver. Histologically, Kupffer cell sarcomas are composed of round to oval uniform cells with abundant foamy eosinophilic cytoplasm. Cell borders may be indistinct. Enlarged multinucleate cells may be scattered throughout the mass, and can be frequent. The growth pattern can also be invasive, and tumor cells may dissect along sinusoids or blood vessels. These tumors are uncommon in the liver, and their pathogenesis and behavior are not well characterized.

Gall Bladder

The gall bladder represents an uncommon consideration in the assessment of toxicity.

Among nonneoplastic lesions of the gall bladder, cholecystitis (inflammation of the gall bladder) and mucosal proliferation without cholelithiasis is a commonly identifiable lesion in dogs associated with so-called statin drugs that inhibit HMG-CoA reductase, such as atorvastatin and fluvastatin. The lesions include edema, ulceration, transmural inflammation, and granulation tissue formation. The pathogenesis of this lesion is unknown.

Inflammatory lesions of the gall bladder wall may also appear in association with conditions that cause vasculitis. In toxicology studies, treatment-related vasculitis should be readily differentiated from cholecystitis based upon the appearance of typical vascular lesions in gall bladder, and usually in other tissues. Dogs are also susceptible to an unusual lesion, cystic mucinous hyperplasia, of the gall bladder mucosa. This lesion occurs spontaneously, but is uncommon in recent experience. In toxicology studies, it has been reported to result from long-term administration of progestagens such as oral contraceptives and corticosteroids. The lesion is characterized by extensive hyperplasia of mucosal epithelium forming numerous long intraluminal projections with cysts that may contain varying, sometime abundant, accumulation of mucus.

Cytoplasmic changes in gall bladder mucosal epithelium have been reported as a manifestation of toxicity in some studies. In mice, accumulation of eosinophilic crystalline material, also known as hyalinosis, was observed in gall bladder and stomach mucosal epithelium following long-term administration of Penicillin V. The material was reminiscent of YM1 (also called Chi313), a chitinase-like protein. The hyalinosis resulting from accumulation of this protein has been described as a rare spontaneous finding in a variety of tissues.

Mice are often utilized in long-term studies for carcinogenicity assessment, and spontaneous occurrences of hyperplasias, adenomas (papillomas), and carcinomas in gall bladder have been reported, although uncommonly. The typical adenoma is a well-differentiated solitary lesion with irregular papillary growth pattern (Figure 8.31). The typical carcinoma is

a broad-based mucosal lesion with evidence of mural invasion and advanced cytological atypia.

Glandular metaplasia has been reported as a spontaneous finding in mouse gall bladder. This lesion is characterized by thickened mucosa with proliferation of tall columnar cells that form numerous glands in the lamina propria. The hypertrophic columnar cells may undergo hyalinosis and the gland lumens may contain eosinophilic crystals. Chronic inflammation of the gall bladder may be present in association with glandular metaplasia.

MECHANISMS OF TOXICITY IN LIVER

Metabolic Activation

While some chemical entities are directly hepatotoxic, many require physicochemical modification, within the susceptible organism, to biologically active substances. This process is called *metabolic activation*. The liver is a major site of CYP enzymes that catalyze the addition of oxygen or removal of hydrogen from the parent compound. While these reactions may ultimately promote further reactions that favor the elimination of the substance, they often produce metabolites that react with endogenous biomolecules in either specific or nonspecific ways.

In the liver, a variety of specific interactions may lead to toxicity, including receptor interactions (which may result in functional agonism or antagonism) and enzyme interactions (which may inhibit endogenous metabolic pathways). An example of an enzyme affected by noncovalent binding is phospho-inositol-3 kinase (PI3K). Drugs designed to inhibit certain isoforms of PI3K (for treatment of cancer) have the potential to cause hepatotoxicity because PI3K mediates survival (antiapoptotic) pathways in hepatocytes. These specific interactions usually involve low-energy, noncovalent binding that is typically reversible. In contrast, nonspecific interactions leading to hepatotoxicity generally involve covalent binding that is typically nonreversible.

Covalent Binding

Covalent binding is an important outcome of the metabolism of toxic substances to reactive metabolites. This typically occurs on susceptible functional moieties of proteins and nucleic acids. It is nonreversible, so affected endogenous molecules are permanently altered. In most instances, the drug or chemical hepatotoxicant is metabolically activated to electrophiles (phase 1 metabolism), which can subsequently react with nucleophilic groups such as sulfur in thiols and methionine in proteins, nitrogen in amino groups of amino acids in proteins and purine bases of nucleic acids, and oxygen in purines and pyrimidine bases or in phosphate groups in nucleic acids. An example of a hepatotoxicant leading to covalent binding to protein is the active metabolite of acetaminophen, *N*-acetyl-p-benzoquinone imine, which covalently binds to GSH and to protein sulfhydryls. An example of a hepatotoxicant leading to covalent binding to nucleic acid is diethylnitrosamine, which is activated to the very reactive ethyl carbonium ion, resulting in ethyl adduct formation in DNA bases. The result of covalent binding is the replacement of physiologically functional endogenous molecules with either nonfunctional or dysfunctional endogenous molecules.

Free Radical Injury

The formation of neutral free radicals can be an important step in the mechanism of hepatotoxicity. Free radicals contain one or more unpaired electrons, and are reactive in biological systems. Carbon tetrachloride (CCl4) is an example of a hepatotoxicant that is activated to produce the trichloromethyl free radical that can react with molecular oxygen to form trichloromethylperoxy radical. Xenobiotic chemicals may also produce superoxide anion radicals by accepting electrons from reductases such as P450 reductase, and transferring them to molecular oxygen and regenerating the parent molecule. This means that a molecule of the xenobiotic may generate several superoxide anion radicals through a process known as *redox cycling*. Superoxide anion may undergo conversion to hydrogen peroxide either spontaneously or through the activity of the enzyme superoxide dismutase. Hydrogen peroxide can be neutralized by enzymatic pathways including gluthione peroxidase and catalase, or it can undergo the metal-ion based Fenton reaction to form hydroxyl radicals, which may damage cellular macromolecules and cell membranes.

One of the more toxicologically significant results of free radical formation is the initiation of lipid peroxidation. Lipid peroxidation damages lipids and compromises membrane functions, and is a self-propagating pathway in the presence of lipid and molecular oxygen.

Glutathione

GSH is a key endogenous molecule in hepatocytes and other cell types. It is an essential factor in the elimination of xenobiotic-derived electrophiles and peroxides. GSH is a tripeptide formed in a two-step enzymatic process from cysteine, glutamate, and glycine. In normal

hepatocytes, it is a major reducing molecule. In the process of its enzymatically catalyzed reactions with electrophiles (via GST) or peroxides (via glutathione peroxidases or GPx), GSH is oxidized to glutathione disulfide (GSSG). In the presence of adequate reducing equivalents provided by NADPH, GSSG may be converted to GSH through the activity of glutathione reductase.

Cellular Targets of Hepatotoxicity

Mitochondria

Mitochondria provide the majority of energy for the hepatocyte, and, consequently, injury to the mitochondria leads to hepatocyte dysfunction. Hepatocyte injury induced by mitochondrial dysfunction includes oxidative stress, energy shortage, accumulation of lipids and fatty acids, and eventually death via apoptosis or necrosis. A broad variety of drugs or their metabolites can damage mitochondrial function.

Damage to mitochondria can lead to the opening of mitochondrial permeability pores (MTP). This loss of integrity of the mitochondrial membrane has several consequences. The consequences range from mild to fulminant hepatocellular necrosis, as well as a characteristic microvesicular steatosis. If a high proportion of mitochondria is damaged, there is a prominent loss of ATP production. Since the plasma membrane calcium ATPase is dependent on adequate ATP, deficiency can drive calcium influx leading to hepatocyte death. If the number of mitochondria damaged is lower, apoptosis may result due to the release of several pro-apoptotic proteins from mitochondria, such as apoptosis inducing factor, cytochrome *c*, and several caspases.

As stated, a variety of drugs can damage mitochondrial function. Several mechanisms of injury are recognized, including MTP opening, direct inhibition of mitochondrial fatty acid oxidation, uncoupling of oxidative phosphorylation, direct inhibition of the mitochondrial respiratory chain, and depletion of mitochondrial DNA.

Hypertrophy of mitochondria, termed *megamitochondria*, may be induced by a variety of chemicals, including cuprizone, ethionine, and orotic acid. In the case of cuprizone and isonicotinic acid derivatives, large mitochondria result from the fusion of preexisting ones. By light microscopy, mitochondrial hypertrophy usually is not discernible. However, by electron microscopy, hypertrophic mitochondria have normal cristae and normal matrix density. Mitochondrial hypertrophy should be distinguished from mitochondrial swelling, which is characterized by swollen cristae and irregular densities in the matrix by electron microscopy.

Cytoskeleton

There are a few naturally occurring chemicals that can cause hepatocellular injury by direct injury to the cytoskeleton. Microcystins are among the better characterized toxins that target the cytoskeleton. They have an unusual molecular composition, forming monocyclic heptapeptides, and there are more than 50 related toxins. The major source of microcystins comes from *M. aeruginosa*, one of several fresh water cyanobacteria that produce the toxin microcystin-LR. Microcystin-LR inhibits hepatocellular protein phosphatases 1 and 2A and disrupts the cytoskeleton, leading to massive hepatic necrosis.

The *Amanita* sp. mushroom toxin phalloidin binds to actin and disrupts the cell cytoskeleton, resulting in increased plasma membrane permeability. However, this toxin is likely more significant in the gastrointestinal system than it is in the liver, as the mushroom toxin amanitin is a much more significant cause of hepatocyte injury. Pectenotoxins, found in marine dinoflagellates, also directly damage the hepatocellular cytoskeleton.

Nucleus

The nucleus is a target for several hepatotoxins where the principle activity is the inhibition of DNA transcription. The inhibition of transcription may result from extensive covalent binding from electrophilic metabolites (for toxins such as aflatoxin and some nitrosamines) or the specific inhibition of RNA polymerase (for toxins such as α-amanitin and actinomycin D). Another hepatotoxicant, ethionine, traps ATPase also inhibits RNA synthesis. The nucleolus, the site of active ribosomal RNA synthesis, is usually affected early in response to inhibition of RNA synthesis and, by light microscopy, is reduced in size. At the ultrastructural level, the nucleolus may either be fragmented, or undergo a process of segregation of its granular and fibrillar components.

Nuclear size typically increases with increased DNA content. In the liver, this may occur by two mechanisms. The first is polyploidization, which is a normal aging change in many mammalian species, but especially prominent in aging mice. It also may be caused by drugs that produce hyperplasia, through the process of amitotic cytokinesis of binucleated cells into mononucleated cells after DNA replication.

Cytoplasm

Polysome breakdown is a frequent cytoplasmic manifestation of hepatocellular toxicity when transcription is inhibited. Polysomes are aggregates of numerous ribosomes that are in the process of actively translating mRNA into protein. By light microscopy

polysomes appear as basophilic cytoplasmic granules, but are extremely labile during postmortem change in the liver. As a result, polysomes are observed only in rapidly fixed liver tissue. Polysome breakdown appears as the loss of basophilic cytoplasmic granules, but its attribution to hepatotoxicity can only be confirmed with rapid fixation such as perfusion fixation.

Glycogen is a polymer of glucose that serves as a storage form in the cytoplasm of hepatocytes and other cells. Hepatocytes typically vary in the amount of glycogen that is present in the cytoplasm. In untreated animals, this variability is typically related to recent feeding history. Glycogen accumulation is recognized histologically as indistinct clear vacuoles in the cytoplasm of hepatocytes, due to its water solubility and removal during tissue processing. Because of the variability related to the timing of food intake, carefully controlled studies are needed to ascertain the effect of hepatotoxicants on hepatic glycogen levels.

Lipid Metabolism

The liver plays a key role in systemic lipid metabolism by regulating the synthesis, oxidization, transport, and excretion of lipids. Consequently, various perturbations of hepatocellular homeostasis can lead to accumulation of lipids within hepatocytes. A variety of drugs or chemicals can produce steatosis, or, as it is also known fatty change or hepatic lipidosis. Lipid vacuoles are typically distinct, round, and clear when viewed in H&E sections as lipid is extracted during tissue processing. The size of the vacuoles can have pathogenic significance as discussed later. Lipid can accumulate in hepatocytes by three main routes: excess deposition, which is usually a dietary rather than a toxicity issue; altered metabolism of lipids; and impaired excretion of cellular lipids as lipoproteins due to impaired protein synthesis. Intrahepatocytic lipid accumulation can be classified histologically as macrovesicular or microvesicular.

Mitochondrial injury is a frequent cause of microvesicular steatosis, although there are other causes and the change can be nonspecific. Mitochondria serve as the main site of lipid oxidation, and the process leads to ATP generation to power the cell. Mechanisms of mitochondrial injury have been discussed earlier. In mitochondrial dysfunction, partially metabolized triglycerides yield amphipathic free fatty acids that enter cytoplasmic vacuoles along with triglycerides, altering the surface tension qualities of the vacuoles and leading to smaller, microvesicular lipid vacuoles (Figure 8.4). Typically, the nucleus is not displaced by these vacuoles.

Macrovesicular lipid is the more common manifestation of altered lipid metabolism in injured cells. Histologically, there is a single or occasionally multiple large, round, clear vacuoles that displace the nucleus in routine H&E sections (Figure 8.3). Special stains establish the lipid nature of the inclusions. There are a number of toxic chemicals or drugs that can cause macrovesicular lipidosis by various mechanisms, including (1) disruption of protein synthesis, (2) trapping of adenosyl moieties normally utilized for S-adenosylmethionine, (3) disruption of lipoprotein secretion, (4) impaired fatty acid synthesis and oxidation, and (5) endoplasmic reticulum stress leading to "Unfolded Protein Response."

Immunological Mechanisms of Toxic Hepatic Injury

In humans, idiosyncratic drug reactions are attributed to two possible causes. One is idiosyncratic metabolism of the drug in question; the other is immunological idiosyncrasy. Both the innate and the acquired branches of the immune system can play a role in liver injury.

Innate Immunity

The resident cellular components of the hepatic innate immune system include Kupffer cells, resident macrophages, NK lymphocytes, and NKTs. Neutrophils and monocytes can be recruited in times of hepatic inflammation. The participation of the innate immune system can significantly influence the extent of injury that a toxic chemical or drug can produce. There are a number of studies demonstrating both pro- and anti-inflammatory effects of Kupffer cells following drug-induced injury. Resolution of this conundrum has been facilitated by the identification of subsets of intrahepatic macrophages following injury. In addition to the resident Kupffer cells, a population of infiltrating macrophages or monocytes may also modulate injury. Stimulation of NK cells also accentuate toxicity, as seen with acetaminophen.

There are few animal models of innate immune system-mediated idiosyncratic hepatic injury. One interesting model involves stimulation of the immune system with endotoxin prior to drug exposure. In rats, several drugs associated with idiosyncratic liver injury, that are nontoxic in the absence of endotoxin, produce hepatic injury when they are administered following exposure to endotoxin.

Acquired Immunity

Hypersensitivity-related liver injury is thought to be due to immunological idiosyncrasy of the individual animal or patient. Typically, the response develops after a relatively brief period of exposure. There is need for animal models of this type of liver injury. In

humans there is often an associated rash, along with hematologic abnormalities, and an eosinophilic or granulomatous infiltrate of the liver, although acute inflammation and necrosis may also develop. In humans there are a number of drugs, such as tienilic acid, which in some affected patients produced antibodies that will react to tienilic acid altered hepatocyte proteins. This response suggests that certain drug metabolites interact with cellular proteins, yielding adducts that can produce neoantigens, which in turn are recognized by the host immune system.

SUMMARY

The liver represents a key target organ for toxicity. The recognition of the diverse patterns of liver injury following experimental or natural exposures to drug and chemical agents is an important step toward understanding the implications of toxicity. As such, characterizing the pattern of injury represents an important contribution of the toxicologic pathologist, who must then actively participate in the characterization of safety or risk, in collaboration with other scientists (toxicologists, molecular biologists, toxicokinetics and metabolism scientists, and clinicians).

The hepatocyte is a critical target for acute toxicity as well as chronic toxicity, including carcinogenic responses. In many instances, acute responses may allow some prediction of chronic responses. This predictive process is optimal when a mechanism of action for the drug or chemical at the level of the hepatocyte can be inferred, and ultimately extrapolated to various scenarios of exposure. Furthermore, while much of our understanding of liver toxicity is related to hepatocellular toxicity, other cell types are also critical to understanding target organ toxicity, and may be targeted directly and/or mediate acute and chronic responses.

Further Reading

Amacher, D.E., Chalasani, N., 2014. Drug-induced hepatic steatosis. Semin. Liver Dis. 34, 205–214.

Cattley, R.C., Cullen, J.M., 2013. Liver and gall bladder. In: third ed. Haschek, W.M., Rousseaux, C.G., Wallig, M.A. (Eds.), Haschek and Rousseaux's Handbook of Toxicologic Pathology, vol. 3. Academic Press, San Diego, CA, pp. 1509–1566.

Ennulat, D., Magid-Slav, M., Rehm, S., Tatsuoka, K.S., 2010. Diagnostic performance of traditional hepatobiliary biomarkers of drug-induced liver injury in the rat. Toxicol. Sci. 116, 397–412.

Ingawale, D.K., Mandlik, S.K., Naik, S.R., 2014. Models of hepatotoxicity and the underlying cellular, biochemical and immunological mechanism(s): a critical discussion. Environ. Toxicol. Pharmacol. 37, 118–133.

Maes, M., Vinken, M., Jaeschke, H., 2016. Experimental models of hepatotoxicity related to acute liver failure. Toxicol. Appl. Pharmacol. 290, 86–97.

Maronpot, R.R., Yoshizawa, K., Nyska, A., Harada, T., Flake, G., Mueller, G., et al., 2010. Hepatic enzyme induction: histopathology. Toxicol. Pathol. 38, 776–795.

McGill, M.R., Jaeschke, H., 2014. Mechanistic biomarkers in acetaminophen-induced hepatotoxicity and acute liver failure: from preclinical models to patients. Expert Opin. Drug Metab. Toxicol. 10, 1005–1017.

Michalopoulos, G.K., 2014. Advances in liver regeneration. Expert Rev. Gastroenterol. Hepatol. 8, 897–907.

Thoolen, B., Maronpot, R.R., Harada, T., Nyska, A., Rousseaux, C., Nolte, T., et al., 2010. Proliferative and nonproliferative lesions of the rat and mouse hepatobiliary system. Toxicol. Pathol. 38 (Suppl. 7), 5S–81S.

This page intentionally left blank

CHAPTER

9

Cardiovascular System

Brian R. Berridge[1], *John F. Van Vleet (In Memoriam)*[2], *and Eugene Herman*[3]

[1]GlaxoSmithKline Research & Development, King of Prussia, PA, United States
[2]Purdue University, West Lafayette, IN, United States
[3]National Cancer Institute, Bethesda, MD, United States

OUTLINE

INTRODUCTION

The cardiovascular (CV) system is a common target for both naturally occurring disease and toxic injury. The environment, diet, and practices of Western cultures that are spreading throughout the world contribute to CV and cardiopulmonary disease, which are collectively the number one cause of mortality in the United States and globally. Naturally occurring diseases increase the susceptibility of patients to injuries from drugs that may intentionally or unintentionally target the CV system. Cardiovascular safety liabilities are among the more important causes of pre- and postmarketing drug development attrition. Companion and farm animals are also susceptible to CV toxicity induced by a broad array of natural and man-made xenobiotics.

The CV system is particularly susceptible to toxic xenobiotics because of its role in circulating a primary substrate (i.e., blood) for absorbed substances, its dynamic function and its significant interdependencies with both its own component parts (i.e., heart and blood vessels) and other organ systems. Manifestations of toxicity are influenced by the adaptability and functional reserve of the system. The consequences are complicated by a general lack of regenerative capacity. This chapter

Fundamentals of Toxicologic Pathology.
DOI: http://dx.doi.org/10.1016/B978-0-12-809841-7.00009-5

contextualizes the causes and consequences of toxic injury due to the unique anatomic and physiologic features of the CV system, explores the diversity of responses to injury, and known mechanisms for those injuries.

HEART

Introduction

The heart, the dynamic center of a vast network of circulatory conduits, is subject to structural and functional alterations from exposure to a long list of potentially toxic xenobiotics. Alterations in cardiac function may result from changes in ion movements, membrane function, autonomic controls, energy-producing systems, or structural injuries. Structural alterations include changes in cardiac mass (e.g., hypertrophy), injury to cellular elements of the heart, or even "repair" mechanisms (e.g., fibrosis) that may result from direct xenobiotic effects or as a consequence of changes in cardiac work or the heart's ability to do work. In human patients, the presence of preexisting CV disease may predispose some individuals to toxic cardiac injury and dysfunction.

Structure and Function

Gross and Microscopic Anatomy

The heart is a conical-shaped muscular organ that, in mammals, birds, and reptiles is divided into four chambers separated by cardiac valves that ensure unidirectional flow of blood. The heart is interposed as a pump into the vascular system; the right side receives systemic venous blood and shunts it through the pulmonary circulation while the left side receives blood from the lungs and circulates it through the systemic arterial system.

A detailed description of the gross anatomy of the heart is deferred to other texts but a few salient features are worth mentioning. The walls of the cardiac chambers are composed of three layers: the epicardium, the myocardium, and the endocardium. The myocardium is the prominent striated muscular layer of the heart. It is composed of cardiac muscle cells or myocytes arranged in interdigitating fascicles. The myocardial thickness is related to the pressures present in each chamber; the atria are thin and the ventricles are thick. The thickness of the left ventricular free wall is approximately threefold greater than that of the right ventricle when measured in a transverse section across the middle of the chambers. This is because the pressures are higher in the systemic circulation than in the pulmonary circuit.

The arterial supply to the heart consists of left and right coronary arteries, which arise from the aorta at the sinuses of Valsalva behind the left and right cusps of the aortic valves. The arteries tend to form a ring or crown as they encircle the base of the heart in the atrioventricular (coronary) groove. They then radiate over the heart in the subepicardium and give off perforating intramyocardial arteries that supply a rich capillary bed throughout the myocardium. Extensive anastomoses occur between capillaries that tend to run parallel to the cardiac muscle cells. On histologic cross-section, the ratio of capillaries to muscle cells is approximately 1:1. There are differences among species with respect to the level of vascular anastomoses that influences their individual susceptibility to the ischemic injury of arterial occlusion.

The cardiac conduction system is a primary conduit of electrical impulses that stimulate an orchestrated and rhythmic contraction of the myocardium. Components include the sinoatrial node at the junction of the anterior vena cava and the right atrium; the atrioventricular node and bundle located beneath the septal leaflet of the tricuspid valve and traversing the lower atrial septum onto the upper portion of the muscular ventricular septum; and the right and left bundle branches that descend on each side of the muscular ventricular septum and eventually ramify over the ventricles as the Purkinje fiber network.

Normal features in animal hearts may occasionally be misinterpreted as lesions. The overall shape of normal hearts may vary from the elongated somewhat flattened conical profile in the horse, cow, and chicken to the somewhat shortened and rounded shape of the pig and dog. Cardiac weight (as % body weight) varies greatly among species; pigs and rats have small hearts (approximately 0.3% of body weight), cows, mice, and guinea pigs have intermediate-sized hearts (approximately 0.5% of body weight), and dogs, cats, and horses have large hearts (from 0.75% of body weight in nonathletic dog breeds to 1.25% in athletic breeds).

Cellular and Extracellular Elements of the Heart

Atrial and ventricular myocardia are composed of a variety of cells, of which the myocytes are the primary force-generating cells. Cardiomyocytes comprise 80% of heart volume but only 25% of the cellular content by number. Myocytes are elongated and joined to one another by intercellular junctions. The latter mediate electrical coupling of the myocytes and render them able to act as a functional syncytium. The myocytes are surrounded by a rich network of blood vessels and capillaries embedded in a matrix of connective tissue. Also present in this matrix are nerves and lymphatics, as well as connective tissue cells such as mast cells,

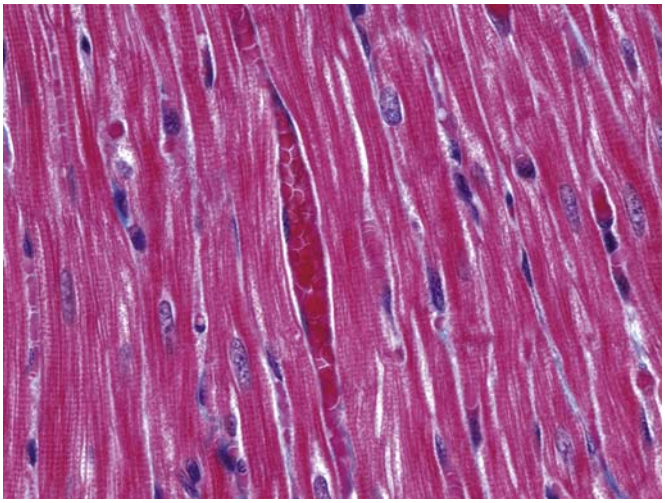

FIGURE 9.1 Longitudinal section of rat myocardium with a central capillary filled with erythrocytes. Paraffin-embedded, Masson's trichrome stain. Original magnification ×60. Source: *From Haschek, W.M., Rousseaux, C.G., Wallig, M.A. (Eds.), 2013. Handbook of Toxicologic Pathology, third ed. Academic Press, San Diego, CA, Figure 9.1, p. 1571, with permission.*

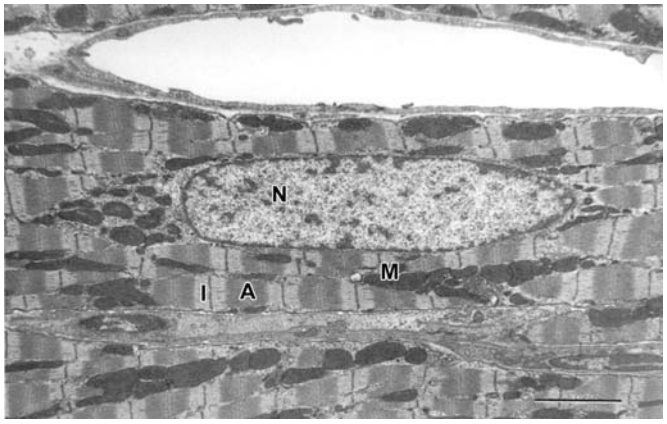

FIGURE 9.2 Electron micrograph of perfused rat myocardium. Several myocytes lie adjacent to an open capillary (*top*). Sarcomeres are relaxed and have prominent A (dark) and I (light) bands. N, nucleus; M, mitochondria. Bar = 5 μm. Source: *From Haschek, W.M., Rousseaux, C.G., Wallig, M.A. (Eds.), 2002. Handbook of Toxicologic Pathology, second ed. Academic Press, San Diego, CA, Figure 9.2, p. 367, with permission.*

histiocytes, fibroblasts, pericytes, and poorly differentiated mesenchymal cells.

VENTRICULAR MYOCYTES

Ventricular myocytes are approximately cylindrical, branch freely, 80–100 μm in length and 10–20 μm in width (Figures 9.1 and 9.2). The ends of myocytes have a step-like appearance, which corresponds to the intercalated discs and is best appreciated in scanning electron micrographs of isolated enzymatically dissociated myocytes.

Myocytes are limited by the sarcolemma, a structure formed by the plasma membrane (plasmalemma) and the external lamina (laminar coat, basement membrane, basal lamina, glycocalyx). The external lamina contains basement membrane collagens (types IV and V) and noncollagen glycoproteins that have not been well characterized in cardiac muscle.

The T-tubule system is a network of tubular invaginations of the sarcolemma. T-tubules extend from the free surface throughout the cells, in a generally transverse direction, coursing around the myofibrils at the levels of the Z bands. However, longitudinally oriented branches interconnect adjacent transversely oriented T-tubules. The T-tubule system allows close direct contact between the extracellular environment and the deeper regions of the cells functioning in facilitating the inward spread of electrical events at the cell surface, in ionic exchange with the interstitium and in the excitation–contraction coupling in the ventricular myocardium.

Neighboring myocytes are connected end-to-end and, to a lesser extent, side-to-side by intercellular junctions. These mediate intercellular adhesions and transmission of the electrical impulse. The end-to-end junctions are known as intercalated discs, the side-to-side junctions as lateral junctions.

Myocytes contain one or two nuclei that are centrally located and oblong. The nuclear contours are smooth when the cells are relaxed and wrinkled when the cells are contracted. Myofibrils course around the nucleus, leaving at the nuclear poles a conical area free of contractile elements but densely packed with other cellular organelles, including the Golgi complex, mitochondria, glycogen, lysosomes, and lipofuscin granules.

The contractile elements occupy about 50% of the cytoplasm of myocytes and form a continuous mass, which is separated into myofibrils of varying size by the interfibrillar matrix. This matrix contains mitochondria, sarcoplasmic reticulum (SR) and T-tubules, glycogen particles, and other organelles. Myofibrils are highly ordered arrays of contractile elements. They exhibit a periodicity that is clearly evident by light microscopy in the form of dark anisotropic A bands and light less anisotropic I bands. The I bands are bisected by a thick dark Z band. The array of contractile elements between two adjacent Z bands is known as a sarcomere and constitutes the contractile unit of cardiac muscle (Figure 9.2).

The A band is composed of thick filaments, which are aggregates of myosin molecules and measure 1.5 μm in length and 10–15 nm in diameter. The I band is composed of thin myofilaments, which are

formed by aggregates of the fibrous form of actin and various other proteins. The myofilaments measure 1 μm in length and 4–8 nm in diameter.

Z bands of adjacent myofibrils tend to be in register. They are connected to each other and to the internal surface of the plasmalemma by bundles of transversely oriented cytoskeletal filaments that average 10 nm in diameter. Because of these connections, the sarcolemma in contracted cells assumes a scalloped appearance, with indentations in register with the Z bands.

The ultrastructural orientation of the SR is closely related to that of the myofibrils and the T system. An important function of the SR is to cyclically take up, store, and release calcium ions by mechanisms that involve the calcium release channels (Ryanodine receptors; release), SR Ca^{2+} ATPase (SERCA; reuptake), and calsequestrin (storage) during the contraction–relaxation cycle of the myocyte. The SR also functions in the metabolism of glycogen and lipids.

Ventricular myocytes are rich in mitochondria roughly constituting 35% of the cell volume. Mitochondria are situated between the myofibrils, immediately subjacent to the sarcolemma and in perinuclear areas. Mitochondria are the sites of oxidative phosphorylation and of synthesis of high-energy phosphates and thus provide the energy needed for muscular contraction. Cardiac mitochondria are very sensitive to noxious influences; at the ultrastructural level, they can be drastically changed even by short periods of ischemia.

Lysosomes, phagosomes, and multivesicular bodies are commonly observed in myocytes, as are residual bodies of lysosomal origin (lipofuscin granules); all of these structures are usually located in the perinuclear region. The Golgi apparatus in ventricular myocytes is usually found in the form of multiple stacks of cisterns and associated vesicles in the perinuclear areas. It is less extensively developed than in atrial myocytes.

Ventricular myocytes contain moderate amounts of glycogen found in the beta or monoparticulate form in the interfibrillar spaces and perinuclear areas and between the myofilaments.

ATRIAL MYOCYTES

The architecture of atrial myocytes basically resembles that of ventricular myocytes; however, the two cell types differ in a number of fine structural features, including the intercellular junctions, the T system, the SR, the mitochondria, and the presence of specific "atrial" granules.

The arrangement of atrial myocytes is less regular than that of ventricular myocytes. The length is in the same range, but the diameter of the atrial myocytes (6–12 μm in humans) is smaller than that of ventricular myocytes.

Atrial myocytes contain a population of cytoplasmic granules. These atrial granules are round or oval, are limited by single membranes, and have a moderately dense core, which is slightly retracted from the surrounding membrane. Granules are formed in the rather extensive Golgi vesicles of atrial myocytes. The granules are the source of important regulatory hormones, the atrial natriuretic peptides. The prohormone pro-atrial natriuretic peptide is released in response to elevated vascular volume or atrial wall stretch. Natriuresis and diuresis are produced by the mature atrial natriuretic peptide acting to increase glomerular filtration rate, renal blood flow, urine volume, and urinary sodium excretion and to decrease plasma renin activity.

Conduction System The conduction system of the heart consists of the sinoatrial node, the atrioventricular node, and the bundle of His, which becomes subdivided into the main left and right branches and their peripheral ramifications. The morphology of the specialized conducting cells shows great variation, not only among different species but also in different components of the conduction system in a given species.

Cellular Components of the Myocardial Interstitium Fibroblasts are spindle-shaped connective tissue cells with a few cytoplasmic processes that extend in various directions and for varying distances into the surrounding connective tissue. Myofibroblasts resemble fibroblasts in most of their ultrastructural features but can be distinguished from the latter by their nuclear indentations and by the abundance of actin filaments in their cytoplasm. Myofibroblasts are thought to represent a type of cellular differentiation intermediate between fibroblasts and smooth muscle cells. In the heart, myofibroblasts are present in valvular and endocardial connective tissue.

Macrophages (histiocytes) are normally present in small numbers in the myocardial interstitium and in the connective tissue of endocardium and valves. Mast cells are found in small numbers in myocardial interstitium, usually in perivascular locations, and in the endocardium.

Extracellular Components of Myocardial Interstitium The collagen fibrils in the myocardial interstitium have been shown by scanning electron microscopy to have a highly organized three-dimensional arrangement; small bundles of collagen fibrils (collagen struts) constitute a fibrous skeleton that mechanically interconnects adjacent myocytes and also connects myocytes to neighboring capillaries. Thus, these connections provide sarcomere alignment from cell to cell and prevent slippage during contraction.

Cellular Components of the Myocardial Vasculature The detailed structure of the various types of vascular

cells is presented subsequently with the discussion of the vessels.

Myocardial Innervation Unmyelinated nerve fibers are commonly found in cardiac muscle, where they course adjacent to blood vessels.

Pericardium The parietal pericardium is composed of three layers: the serosa, the fibrosa, and the epipericardial connective tissue layer. The serosa consists of the surface lining layer of mesothelial cells and of a narrow subendothelial space that separates the serosa from the underlying fibrosa.

The visceral pericardium consists of a mesothelial cell layer and a submesothelial layer that varies considerably in composition from one area to another. In some regions, particularly in the atria, it has a layer of elastic tissue and a deeper layer that is rich in collagen fibrils.

Endocardium The endocardium is a delicate layer that invests the entire inner surface of the heart. Its structure and thickness are variable from one chamber to another and even within different regions of a given chamber. The ventricular endocardium is composed of five distinct layers: the endothelial layer, the inner connective tissue layer, the elastic tissue layer, the smooth muscle cell layer, and the outer connective tissue layer or subendocardial layer.

Cardiac Valves Cardiac valves ensure unidirectional flow of blood through the four chambers of the heart. Two morphologic subtypes are typical: atrioventricular valve leaflets and semilunar valve cusps. Atrioventricular valves separate atria from ventricles and semilunar valves ensure blood flow out of the aorta and pulmonary artery.

The atrioventricular valves consist of the mitral and tricuspid valves. The mitral valvular apparatus consists of the annulus, the leaflets, the chordae tendineae, and the papillary muscles.

The annulus itself is composed of a ring of circumferentially oriented collagen and elastic fibers, with connections that extend into the ventricle and the atrium. The bundles of collagen that constitute the fibrous core of the leaflet extend from the annulus, first forming a broad sheet (known as the fibrosa) that shows a basket-weave arrangement throughout the leaflet, then continuing into the chordae tendineae, and finally spreading out into a network that covers the tips of the papillary muscles.

The architecture of the tricuspid valve apparatus and the layered arrangement of the tricuspid valve leaflets are generally similar to those in the mitral valve; however, the individual layers of connective tissue are thinner in the tricuspid valve.

The semilunar valves also have a well-defined layered structure, which differs in some respects from that of the atrioventricular valves. Three layers are recognizable in semilunar valves: the fibrosa, the spongiosa, and the ventricularis. These layers are similar in distribution in the aortic and pulmonary valves but are thinner and more delicate in the latter.

Physiology and Functional Considerations

The heart propels blood through the lungs and peripheral circulatory system providing oxygen and nutrients to all tissues. The efficiency of the heart and its ability to perform its task depend on the coordinated and rhythmic conduction of electrical impulses coupled with rapid coordinated activation of the contractile apparatus. The functional units of the myocardium are the cylindrically shaped striated muscle fibers described earlier.

Resting and Action Potential

Electrical activity in the heart is generated at the level of individual muscle cells as self-propagating, depolarizing, and repolarizing action potentials across the cell membrane (Figure 9.3). The principal diffusible ions responsible for these action potentials are sodium, potassium, calcium, and chloride. The time course of de- and repolarization occurs in two basic patterns in discrete populations of cardiomyocytes: slow response and fast response.

A steady resting membrane potential of approximately −90 mV (inside to outside) is recorded from fast response cardiac muscle cells. This potential depends primarily on the differences in concentration of potassium and sodium ions across the cell membrane and the differential permeability of the cell membrane to the ions. When the membrane potential reaches a critical value of −60 to −70 mV (threshold potential) the fast sodium channels open and initiate the action potential (phase 0). Conduction velocity is directly related to the rate of rise of phase 0, and fast response cells conduct impulses rapidly. At the end of

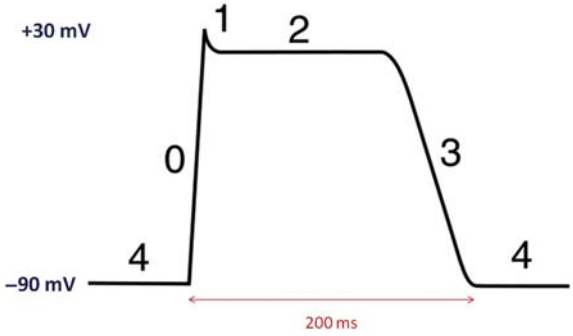

FIGURE 9.3 Cardiomyocyte action potential representing changes in membrane potential over time. Discrete phases of the action potential (phases 0–4) are under the influence of a number of cardiomyocyte sarcolemmal ion channels.

phase 0, the cell is completely polarized, with an inside voltage of approximately +30 mV. During phase 1 and early phase 2 of the action potential, the influx of sodium markedly declines and the membrane potential begins to fall. The commencement of repolarization during phase 1 of the fast-type action potential is thought to be due to a transient influx of negatively charged chloride ions and outflux of positively charged potassium ions. During the plateau phase (phase 2), calcium and sodium enter the cell through slow channels. The influx of calcium at this time is believed to initiate the excitation–contraction coupling process. During phase 3, the potassium permeability increases and the slow sodium and calcium channels are inactivated. The final result is the repolarization of the membrane and the return of the resting action potential (phase 4). Disease processes and certain drugs and other chemicals, which alter membrane properties, can convert a fast-response cell to a cell with properties similar to those of a slow-response cell.

Slow-response fibers normally are found in only a few specific locations in the heart [e.g., sinoatrial (SA) and atrioventricular (AV) nodes]. The resting potential in slow-response cells is near −60 mV. At this level, fast sodium channels are virtually inactive and thus only slow sodium and calcium channels are functional. The slow channels are activated when the transmembrane potential reaches −40 mV. As a result, depolarization proceeds slowly by diffusion of sodium and calcium into the cell. Slow-response cells can act as pacemakers because the membrane potential in phase 4 is constantly decreasing in these cells. Some conducting fibers of the right atrium, AV node, and Purkinje system may exhibit pacemaker potentials and can initiate cardiac activity if the SA node is not functioning normally. The SA node normally overrides other pacemaker cells because its rate of diastolic depolarization is more rapid than that of other cells.

Initiation and Conduction of Cardiac Impulse

Rhythmicity in the heart is normally controlled by pacemaker cells in the SA node and conducting tissue. Both slow- and fast-response fibers are involved in this impulse initiation and subsequent conduction to other parts of the heart. The impulse originating in the SA node travels rapidly to all parts of the atria and AV node. Conduction of the impulse through the AV node is slow and limits the frequency with which impulses can enter the ventricles. Once past the AV node, the impulse is again conducted rapidly through the specialized conducting fibers of the bundle of His. This bundle subdivides into the many branches forming the subendocardial Purkinje system, which ultimately delivers the impulse to the ventricular muscle cells. The propagation of excitation initiates the contractile process in both ventricles.

Excitation–Contraction Coupling

Myocellular contraction is initiated by an increase in intracellular calcium triggered by the opening of L-type membrane calcium channels during depolarization. Influx of extracellular calcium also triggers the release of large intracellular calcium stores from the SR. Rising intracellular concentrations of calcium stimulate release of the regulatory proteins tropomyosin and troponin on the thin filament. Myosin ATPase is activated. Adenosine triphosphate (ATP) is hydrolyzed and the energy is used to form cross-bridges between actin and myosin resulting in "filament sliding" and contraction. The force and velocity of contraction are influenced by the amount of calcium that reaches the contractile sites. Relaxation of the contracted cardiomyocye results from an ATP-driven process of intracellular reuptake and extracellular extrusion of calcium.

Myocardial Metabolism

The heart muscle uses chemical energy to initiate and sustain the work of contraction. The majority of the energy liberated from fuel substances occurs as a result of the production of ATP. Energy sources such as lactate, glucose, triglycerides, and fatty acids ultimately enter the tricarboxylic acid (TCA) cycle to generate ATP. Within the TCA cycle, the carbons from pyruvate are oxidized through intermediate steps to carbon dioxide and oxidative phosphorylation is initiated in the mitochondria. The energy produced by the reactions is stored in the heart as ATP or creatine phosphate. The process of energy utilization also involves calcium ions. The action potential allows both externally and internally sequestered calcium to move into the cytosol of the myofibrils. The released calcium then activates the myofilaments by binding ATP into reactive sites between the myosin and the actin filaments. An ATPase enzyme splits ATP in the presence of magnesium and the myofibril contracts.

Innervation of the Heart

Neural control of the heart is mediated by the parasympathetic and sympathetic divisions of the autonomic nervous system. Vagus nerve fibers (parasympathetic) supply the SA node, atrial muscle fibers, AV node, and, to a limited degree, the ventricles. The main effects of acetylcholine, released from the vagus nerve, are a decrease in the force of atrial and ventricular contraction (negative inotropy), a decrease in conduction velocity through the AV node and a decrease in heart rate (decreased chronotropy). The effect of acetylcholine results primarily from a decrease in the

slope (phase 4) of the pacemaker potential and from the production of a more negative diastolic potential. This hyperpolarization may be caused by an increase in potassium permeability.

The release of norepinephrine by sympathetic nerve stimulation increases the slope of diastolic depolarization so the threshold potential is reached more quickly and the rate of SA nodal discharge is increased (increased chronotropy). This effect is attributed to an augmentation of slow inward calcium currents. The effects on the AV node and other conducting fibers are similar to those of the SA node. Sympathetic stimulation of myocardial contractile fibers leads to an increase in force of contraction (positive inotropic response). This effect is mediated by cyclic adenosine monophosphate (cAMP). cAMP is thought to activate a kinase enzyme (protein kinase A) that ultimately makes more calcium available for the contractile proteins.

Xenobiotic Exposure

The heart and blood vessels are susceptible to injury or dysfunction caused by a variety of chemicals and drugs. Some agents exert myocardial effects directly while many may produce CV alterations through indirect actions involving other organ systems. As with other organs, the blood provides the primary vehicle by which exposure can occur. The CV system's unique role in circulating blood and xenobiotic metabolites may result in unique and prolonged exposure to toxic agents. Consequently, progressive and irreversible effects may occur with repeated exposure. Substances producing myocardial effects may enter the vascular compartment from any exposure route. For example, inhaled carbon monoxide (CO) competes with hemoglobin-binding of O_2 leading to decreased O_2 availability, hypoxia, tachycardia, and other electrocardiographic changes. Likewise, inhaled low molecular weight halogenated alkanes used for industrial purposes as well as volatile anesthetics can cause arrhythmias and sensitize the heart to sympatho-adrenal discharge or to exogenous catecholamines. A substance in the blood capable of producing myocardial toxicity need not have a direct effect on CV function. Chemically induced alterations in other organs such as the kidney could lead to acid-base imbalance and electrolyte concentration changes of sufficient magnitude to cause significant alterations in CV function.

Testing for Toxicity

A number of well-characterized methods are available for detecting and characterizing toxicity in the CV system. These methods include *in vitro*, *ex vivo*, and *in vivo* assessments of varying usefulness depending on their context of use. Contemporary drug safety assessment involves a fairly regimented battery of evaluations that can be modified or complemented as needed to address specific issues or needs.

Accurately predicting clinical outcomes from nonclinical animal modeling can be challenging. Though the mammalian system exhibits significant biological conservation across species, there are physiologic differences that can impact the ability to model toxicity in animals and also the potential for a toxicity to occur in animals that is not a risk for human patients. Contributing to this are significant differences in disease context between human patients and animal models commonly used for safety testing. The animal models most commonly used in toxicity testing studies are young and healthy while patients often have a wide spectrum of morbidities and comorbidities that can have a significant influence on the toxicity potential of a xenobiotic.

Given the spectrum of ways CV toxicity can manifest, a holistic approach to evaluation should be considered with assessments of cardiac and vascular function as well as structure. Functional measures should include contractility, electrophysiology, and blood pressure. Morphologic assessments should include all regions of the heart (e.g., myocardium, valves, atria, ventricles, major vessels) as well as blood vessels inside and outside of the heart.

Functional Evaluation of Toxicity

Monitoring Myocardial Contractile Function

Mechanical energy in cardiac muscle is reflected in two measurable contractile properties of the muscle; the ability to shorten and the ability to develop force. All indices of the contractile state are based on these two characteristics of muscle contraction or some derivative of them. A positive inotropic agent will increase both the magnitude and velocity of muscle shortening and the magnitude and rate of force development. In the intact animal, contractile force can be impacted by ventricular loading conditions as a result of effects on arterial blood pressure and ventricular chamber size. In order to accurately quantitate a change in myocardial contractility, the influence of changes in muscle loading conditions must either be eliminated or taken into account.

Isolated Muscle Preparations There are a variety of isolated muscle preparations that have been developed for evaluating myocardial contractility. Because there is a complex relationship between inotropism and chronotropism, force of contraction measurements are

best made in test systems where the cardiac tissue is electrically stimulated at a constant rate. The papillary muscle, the left atrium, and atrial or ventricular trabeculae from the cat, guinea pig, or rabbit are the most frequently used areas of the heart for this purpose.

Isolated Perfused Heart It is often difficult to separate the interaction of one major organ system from another in intact organisms or to single out the action of any substance on a specific functional unit such as the heart. In an attempt to resolve this problem, Langendorff in 1895 devised the isolated perfused heart technique in which the mammalian heart was isolated from the remainder of the body and maintained in a viable beating condition. Subsequently, many modifications have been described and the hearts of several species have been perfused with blood or a variety of physiological solutions. These isolated heart preparations are advantageous for toxicity studies for a number of reasons. The isolated heart allows a definitive evaluation of chemical effects directly on the heart without interference or interactions with other tissues and organs present in the body. In addition, it is possible to maintain control over variables, such as perfusion pressure and blood flow, that are likely to change during the course of an experiment in an intact animal. The structural composition of the heart is retained in such an isolated system. The principle limitation of isolated organ preparations is that adequate physiological and biochemical integrity can be retained for only limited periods of time (up to 4 hours).

In Vivo Invasive Preparations A major advantage of *in vitro* studies is that the determinants of cardiac performance such as heart rate, preload, and afterload may be fixed. For intact animal studies the analysis of drug effects on myocardial contractility is more difficult unless these three functions are carefully controlled. However, studies with intact animals will provide information concerning acute adaptive responses to xenobiotics. In a closed-chest anesthetized dog, cat, or pig, indirect assessment of contractility is possible if certain variables such as heart rate, arterial blood pressure, and cardiac output are recorded simultaneously. Methods for detecting changes in myocardial contraction are dependent on monitoring intravascular and intracardiac pressures and cardiac output. Estimates of the contractile state can be derived from the rate of intraventricular pressure development.

Noninvasive Methods A variety of clinical imaging modalities have been applied to laboratory animals for assessing cardiac structure and function. The most common method is echocardiography using an ultrasound instrument with image capture rate capabilities appropriate for the heart rate of the species being evaluated. Echocardiography is a staple of human clinical medicine and commonly used to assess both structural and functional changes in the human heart. Echocardiography has been successfully used to detect drug-induced myocardial alterations in dogs and is even now increasingly used in rodents as newer technologies have gained the resolution and image capture rates necessary to look at these small and rapidly beating hearts.

Though echocardiography does permit quantitative and qualitative evaluation of a number of structural and functional parameters, it allows most sensitive assessment of left ventricular function. Measured and/or derived values include ejection fraction, end-diastolic and end-systolic ventricular volumes, stroke volume, and cardiac output. Ventricular mass can also be quantitated using 3D capabilities or 2D slices and an appropriate algorithm that considers the 3D cardiac architecture of the species being evaluated. Valve function can also be evaluated using Doppler capabilities common on most instruments.

In addition to echocardiography, magnetic resonance imaging (MRI) and computed tomography (CT) have also been applied to laboratory animals to assess cardiac function noninvasively. MRI and CT have the advantage of being isotropic and less limited in their ability to image all regions of the heart but the disadvantage of requiring special equipment—particularly for rodent capabilities. Nonetheless, instrumentation with the appropriate resolution for rodent applications is available and has been used to assess heart function in xenobiotic-treated animals.

Monitoring Myocardial Electrical Activity

Cardiac arrhythmias are a common and important presentation for cardiotoxicity. Xenobiotics can interfere with the formation and conduction of cardiac impulses and thereby initiate supraventricular and ventricular premature contractions, disturbance of conduction, bradycardia, or tachycardia. Disturbances of impulse formation may be due to changes in normal automaticity of the specialized conduction tissues or to abnormal autonomic activity generated in any area of the heart. The most important arrhythmogenic actions of xenobiotics can be reproduced and monitored in heart muscle preparations, isolated heart preparations, and intact animals.

Heart Muscle Preparation The use of isolated Purkinje fibers to evaluate toxic effects of substances can provide important information. Purkinje fibers from dogs and sheep are the most frequently used, though fibers have also been obtained from calves, pigs, goats, and rabbits. Long-term continuous recording from cardiac Purkinje fibers is possible because they contract less vigorously than atrial or ventricular muscle.

In contrast to Purkinje fibers, contractile myocytes suitable for isolated tissue studies can be obtained. Papillary muscles small enough to insure adequate oxygenation can be found in cats, guinea pigs, and rabbits. Normally these muscle cells are not spontaneously active and must be electrically stimulated to evoke action potentials. The electrical activity of contractile muscle fibers is often studied concurrently with Purkinje fibers. Alterations in membrane potentials can be used to evaluate arrhythmic activity. While the various phases of the action potential from Purkinje and contractile muscle fibers are the same, the action potentials from these tissues do differ in amplitude, duration, and rate of depolarization. Membrane action potentials are a reflection of and result from changes in membrane ionic permeability.

Since atrial and ventricular muscle can react differently to xenobiotics, both atrial and papillary muscles have been examined simultaneously. A potential screening method, which includes simultaneous stimulation of atrial and papillary muscle fibers, allows monitoring of the myocardial functional refractory period. The functional refractory period is derived from the interval between consecutive electrical pulses that cause a distinct increase in the force of contraction. All xenobiotics that shorten the functional refractory period are potentially arrhythmogenic.

Cultured Heart Cells *In vitro* cell culture systems have been used for many years in cardiotoxicity screening and mechanistic assays. The cellular substrates have varied and include explanted adult rodent cardiomyocytes, explanted neonatal or fetal rat cardiomyocytes, and immortalized cell lines like H9c2 cells. Likewise, the physiologic focus of these studies has varied and includes electrophysiology, contractility, hypertrophy, viability, and mitochondrial function. Significant limitations exist for each of these systems with respect to how well they reflect the *in vivo* state. Neonatal or fetal cells continue to beat and retain some capacity for cell division but are metabolically very different from adult cardiomyocytes since they are more adapted to an anaerobic form of metabolism than the oxidative bias of adult cells. Adult cells may also continue to beat but are challenging to harvest, do undergo some dedifferentiation and have limited survival in culture systems. A significant challenge for any explanted culture system is the difficulty in excluding "nontarget" cells (e.g., fibroblasts) from the system that often overgrow the intended cell population. H9c2 cells are immortalized and more straightforward to establish in culture but are relatively undifferentiated and may weakly recapitulate the differentiated adult cardiomyocyte.

More recently, significant focus has shifted to embryonic (ESC) and induced-pluripotential stem (iPS) cell systems as a source of cellular substrates that would have good culture stability, relevant differentiation traits, and can even be of human origin thus addressing concerns about translatability of animal models to human patients. Significant progress has been made in driving *ex vivo* differentiation of stem cells along specific cellular lineages like cardiomyocytes. The iPS cell systems harvest differentiated cells (e.g., fibroblasts) from human donors, dedifferentiate them to a pluripotent state, and then redifferentiate them into specific cell types. In addition, these approaches allow one to model genotypic variability or even disease states *in vitro* by harvesting source cells from patients with varying genotypic or phenotypic backgrounds. Although this technology is still being refined, it is likely to significantly impact *in vitro* modeling in the future.

Intact AnimalsIsolated tissue studies should ultimately be correlated with whole animal studies. Electrophysiologic information from whole animal studies is most often obtained from electrocardiographic recordings.

ECGs in large or small animals can be collected in conscious-restrained, anesthetized, or instrumented animals. Use of implanted and telemeterized instrumentation for sensitive measures of ECG, blood pressure, and even left ventricular pressures have become common in drug development settings. This instrumentation allows remote monitoring (i.e., outside the room) of basic measures of cardiac function for prolonged periods of time (e.g., 24 hours to repeated measures over days or weeks) without the influence of handling or human interaction.

Significant changes in the electrocardiogram following exposure to xenobiotics may result from functional alterations to the myocyte cell membrane or structural damage to the myocyte. Drugs or other substances can alter the transmembrane potential by modifying the electrophysiological properties of the myocardial cell membrane. Alterations in resting membrane potential, membrane responsiveness, conduction velocity, action potential duration, duration of the refractory period, slope of diastolic depolarization and threshold level (automaticity), and sensitivity to external stimuli (excitability) could occur.

Monitoring Arterial Blood Pressure

The recording of arterial blood pressure in toxicity studies complements electrocardiography by adding a hemodynamic variable to routinely monitored CV functions. A majority of the toxicity studies in which blood pressure is recorded are carried out in the dog and rat. Single and multiple blood pressure measurements have been reported in these and other species using both direct and indirect methods.

Direct blood pressure measurements entail either direct percutaneous puncture or exposure and catheterization of a major artery. Direct measurement of arterial blood pressure from an arterial cannula is a widely used technique in both anesthetized and conscious rats, dogs, and other animals. However, anesthesia impairs reflex blood pressure regulation and, thus, less marked changes in pressure can generally be expected to occur in conscious animals than in those which are anesthetized.

As mentioned above with methods for evaluating electrical activity in intact animals, implanted telemetered instrumentation that includes a pressure cathether in a major artery to get sensitive measures of arterial blood pressure is common in drug development settings. This instrumentation allows longitudinal monitoring in conscious and unrestrained animals without the artifactual distraction of human intervention.

A widely used indirect method to measure systemic arterial blood pressure in the rat is tail cuff sphygmomanometry. This technique necessitates restraint of the animal and heating and immobilization of the tail. A good correlation appears to exist between direct and indirect methods of blood pressure assessment in the rat. A major disadvantage to all tail cuff techniques is that it is not possible to record blood pressures continuously.

Morphologic Evaluation of Toxicity

Toxic injuries to the heart that result in morphologic alterations can be detected by careful gross and microscopic evaluation. In specific instances, further study may be desirable, including ultrastructural evaluation, special staining or labeling procedures, and morphometric analysis. Special attention must be given to problems that accompany morphologic evaluations. These include (1) possible sampling errors, (2) presence of postmortem alterations, (3) misinterpretation of tissue artifacts, and (4) failure to recognize normal variations in structure, incidental lesions, and lesions of spontaneous diseases.

Gross Examination

Many thorough descriptions have been published on the methods of gross dissection and examination of the exterior and interior features of the heart at necropsy. Any one of these methods can be used successfully and will result in a systematic and thorough evaluation of the heart for gross lesions. Care must be taken to avoid misinterpretation of postmortem alterations including rigor mortis, prerigor and postrigor muscular relaxation, imbibition of blood, alterations from terminal intracardiac injection, postmortem blanching of the myocardium, and intracardiac blood clots. Hearts should be weighed following removal of blood clots from the chambers and the data recorded as absolute weight and relative weight as a ratio with body weight, brain weight, or tibial length. Optional procedures include determinations of weights of walls of individual chambers and the septum. The conduction system may be evaluated microscopically by collection of a series of blocks of tissue that include the SA node, AV node, His bundle, and specialized conduction fibers.

Microscopic Examination

Tissue specimens for microscopic study may be obtained at the time of necropsy or by endomyocardial biopsy from living patients. Endomyocardial biopsies, though used in human medicine, have had limited application in animal studies except for occasional use in dogs and nonhuman primates. Multiple samples should be collected from the heart at necropsy to detect lesions that are not diffusely distributed and lesions that are not grossly apparent. Tissue blocks should include samples of any gross lesion and routine collection of specimens from both atria including auricles, both ventricular free walls, ventricular septum, left ventricular papillary muscle, and the coronary arterial tree. Sampling should be increased in regions where lesions are predicted to be produced by a specific compound. In small laboratory animals, a longitudinal section through the heart taken perpendicular to the ventricular septum is often sufficient. Sampling of the conduction system is not routinely done but appropriate techniques have been described.

Tissue fixation is generally with immersion of samples or the entire heart for small animals in 10% neutral buffered formalin. Perfusion fixation may be used to optimize fixation quality if ultrastructural studies are to be done. Samples are routinely processed and embedded in paraffin and sections stained with hematoxylin and eosin. Special stains that are often useful to optimally visualize microscopic alterations include phosphotungstic acid hematoxylin, Masson's trichrome, periodic acid-Schiff, and various elastin stains. Application of lipid stains to frozen sections may be of value. A variety of enzyme (e.g., acid phosphatase) and immunohistochemical (e.g., Factor VIII, vascular endothelial growth factor, endothelin, actin, myosin, desmin) procedures are also available for application to cardiac tissue.

Ultrastructural Examination

Many cardiac lesions of toxic origin have been studied by transmission electron microscopy to detect subcellular alterations and to obtain information that may

suggest the pathogenesis of the damage. It is important to appreciate the limitations and possible artifacts associated with ultrastructural study. Thus, fixation should be optimal (preferably by perfusion) and tissue artifacts should be avoided. Hypercontracted myocytes are often seen at the margin of immersion-fixed-tissue blocks; these areas should be avoided in ultrastructural study. Extensive sampling may be necessary if the cardiac alterations are not diffusely distributed. Even under optimal conditions, some cardiotoxicities may not have remarkable alterations since death may have occurred rapidly from functional alterations and morphologic alterations did not have sufficient time to evolve.

Quantitation of Morphologic Alterations

Morphometry is being used increasingly to quantitatively evaluate the extent of cardiac damage induced by a wide variety of insults. This technique is especially useful for study of tissues prepared for electron microscopy with optimal fixation and embedding methods to avoid artifacts. Stereological analysis, using random sampling and adequate sample sizes, allows determination of various parameters such as volume density, surface density, and numerical density of an organelle or subcellular component and subsequent statistical analysis to detect significant differences among treatment groups.

Response to Injury

The heart's response to toxic injury is varied but finite much like other important target organs. These responses can involve changes in function (rhythmicity or contractility), structure (change in mass, cardiomyocellular injury), or both. As noted previously, changes in cardiac work can lead to structural injuries and structural injuries to the heart can lead to dysfunction (Figure 9.4). Accordingly, toxicity assessment strategies generally integrate approaches for assessing CV function as well as morphology.

Developmental Cardiotoxicities

Abnormal cardiac function in the newborn is usually a consequence of a structural malformation. Ventricular and atrial septal defects are the most common. These have been associated with prenatal treatments with diphenylhydantoin and thalidomide in human infants, with phenobarbital and caffeine in rats, and with acetylsalicylic acid and cortisone in dogs.

Chemicals can also influence the functional development of the heart. Central control of CV reflexes is established prenatally, but the peripheral sympathetic system develops over the first postnatal weeks. Administration of reserpine to pregnant rats caused a permanent elevation of sympathetic tone in their offspring. Neonatal treatment with reserpine or with glucocorticoids slowed development of the sympathetic nervous system. Perinatal exposure to ethanol, opiates, or thyroid hormone accelerated development of the sympathetic nervous system in rats but a deficit in the number of nerve terminals and neurotransmitter receptors occurred, resulting in reduced sensitivity to sympathetic stimulation that persisted in adulthood.

Treatment with CV drugs during pregnancy can cause adverse effects on the fetus or the newborn. For example, a β-agonist given as a tocolytic (antilabor) agent can cause arrhythmia and a β-blocker given as an antihypertensive may cause cardiac depression in the newborn child. Delayed or long-lasting effects have also been demonstrated in animal experiments. Exposure of neonatal rats to low concentrations of lead caused an enhanced response to the arrhythmia-inducing effect of norepinephrine later. These findings indicate the need for evaluation of effects of this nature in preclinical studies, particularly when the drug is destined for use during pregnancy or in neonates.

Cardiac Dysfunction as a Manifestation of Toxicity

The heart's intrinsic properties of automaticity, excitability, conductivity, and contractility endow it with a variety of drug-sensitive targets. Consequently, exposure of the heart to certain agents could produce functional changes in rhythm and the force of contraction that might be severe enough to result in death.

Arrhythmias Arrhythmias are among the most serious immediate cardiac functional abnormalities. Disturbances of impulse formation and of impulse conduction, either singly or in combination, are the main causes of cardiac arrhythmias.

A key factor in the occurrence of arrhythmias is the relationship between the resting potential of a cell and the action potential that can be evoked. Since the ability of an action potential to propagate to an adjacent cell is directly related to the rate of rise and the amplitude of the action potential, changes in the membrane potential level also affect conductivity. Normal cardiac function depends on conduction of the impulse over specialized pathways, through the AV node, and over the His-Purkinje system to reach ventricular muscle fibers. Exposure to certain agents or ischemic conditions can lower the resting membrane potential of the myocardial cell. These alterations decrease the speed of conduction and favor production of block. Paradoxically the effects of quinidine and other antiarrhythmic agents on the heart may be to initiate rhythm disturbances. This action can occur as a result of a diminution in fast sodium channel activity, thereby allowing the development of slow responses.

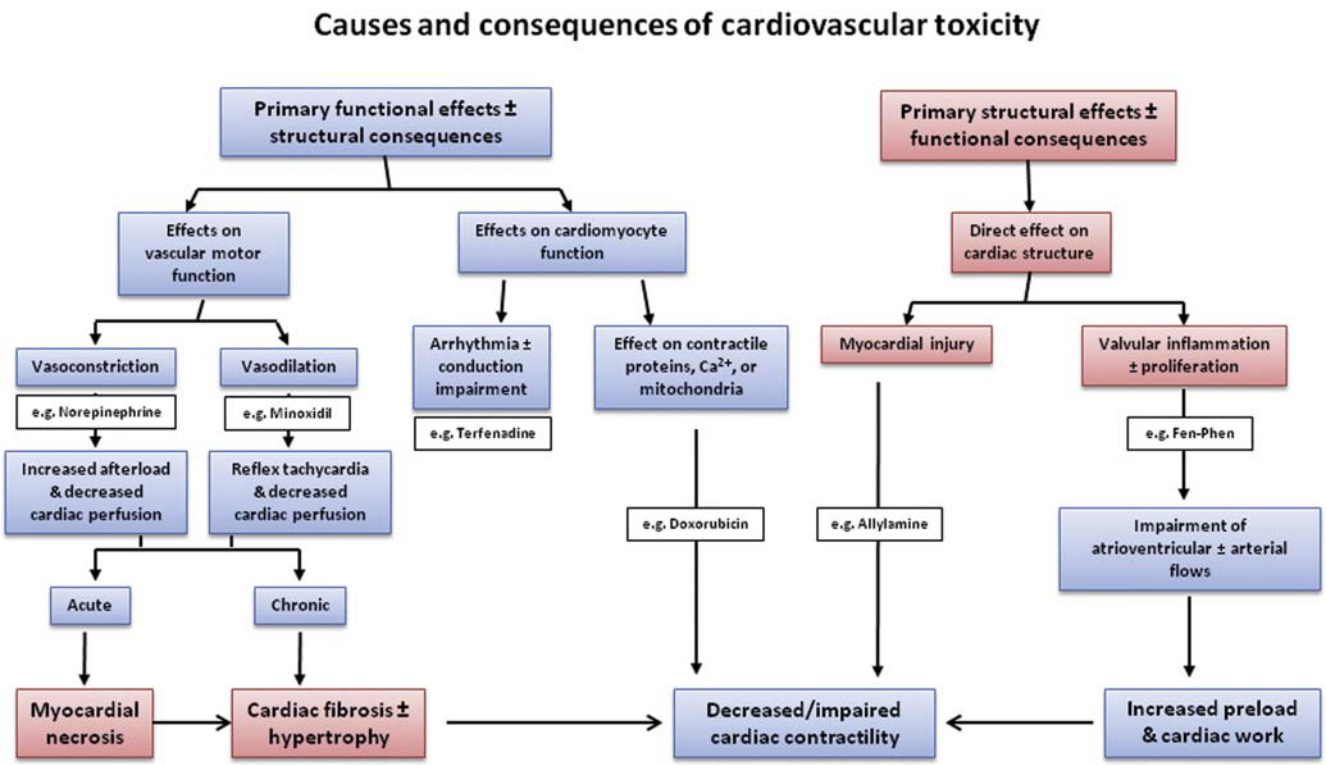

FIGURE 9.4 Interrelationship of functional and structural injuries in the CV system. The potential for structural injury to occur secondary to functional changes or functional changes as a consequence of structural injury emphasizes the importance of assessing both when characterizing xenobiotic toxicity. Xenobiotics inserted as examples may induce the spectrum of changes illustrated. Red shading, structural injuries; blue shading, functional changes.

The most common site of conduction disturbance is the AV node, but similar disturbances may occur between the SA node and the atria, in either of the main branches of the bundle of His or in the more peripheral Purkinje network. Conduction delay and block can lead to tachyarrhythmias because an impulse may reenter and excite the heart more than once. A marked reduction in conduction velocity due to depressed sodium current, slow calcium current, or both, is the alteration that permits reentry. Reentry can occur at many sites in the heart; common examples are the SA node (premature atrial beats), the atria (atrial flutter or fibrillation), the AV node (paroxysmal supraventricular tachycardia), and the ventricles (premature beats, ventricular tachycardia).

Electrocardiographic alterations are infrequent effects seen with antidepressants such as the tricyclic antidepressants, phenothiazine, lithium, and the selective serotonin reuptake inhibitors.

Changes in Contractility Cardiac contraction is closely linked to action potential propagation in a process known as "excitation–contraction coupling." Ionic movements in and out of the cell during the action potential trigger an increase in intracellular free calcium concentration. Myocardial contractility increases when more calcium is available inside the cell. Catecholamines activate the adenyl cyclase system by stimulating membrane β-adrenergic receptors. The resulting increase in cAMP affects the SR that provides calcium ions to the contractile proteins. This action leads to a positive inotropic effect (i.e., an increase in the force of contraction). By interfering with the actions of norepinephrine, β-adrenergic blocking agents, such as propranolol, exert negative inotropic, and chronotropic effects. Vagal impulses or cholinergic substances can also produce negative inotropic and chronotropic effects.

Impaired contractility may be the result of a decrease in cardiac energetics (availability of fuel substrate, oxygen extraction, energy production, or utilization of energy) or impairment of the process of excitation–contraction coupling.

A number of agents can interfere with the process of energy liberation, storage, or use. For example, ergot derivatives and vasopressin can all produce coronary vasoconstriction and decrease the myocardial oxygen supply. Some substances may affect oxyhemoglobin association or dissociation, thereby interfering with oxygen delivery. When coronary blood flow or oxygen extraction is reduced, the metabolism and function of

the heart can be disrupted at all levels. Agents can alter the energy liberation and supply process by interfering with the rate-limiting steps in the TCA cycle. For example, some anesthetics and several cytotoxins (rotenone, cyanide) interfere with electron transport systems or uncouple phosphorylation.

Cardioactive compounds can alter myocardial contractility by affecting any of the structures or steps involved in the excitation–contraction process. The sarcolemma constitutes the permeability barrier of the cell to nutrients, substrates, metabolites, and ions. Disturbances in sarcolemmal permeability to ions or alterations in the activity of membrane enzymes (adenyl cyclase, Na^+-K^+-ATPase, and calcium-activated ATPase) can change the action potential and influence myocardial contractile strength. The ATP-dependent sodium pump (Na^+-K^+-ATPase), which maintains the normal transmembrane gradients of sodium and potassium ions, is extremely sensitive to cardiac glycosides. Verapamil blocks the slow inward calcium current and thereby decreases intracellular calcium stores available to combine with contractile proteins.

The SR is intimately involved in modulating intracellular calcium flux as a primary intracellular store of calcium. Quinidine exerts a depressant effect on cardiac contractility, which has been attributed to an inhibitory effect on SR calcium regulation.

The heart contains an abundance of mitochondria. Since the energy used in the process of excitation–contraction coupling is derived from mitochondrial ATP, agents, which affect myocardial oxidative phosphorylation, would be expected to alter cardiac function.

Lateral movement due to cross-bridge formation between actin and myosin is responsible for contraction. In order for cross-bridges of the contractile proteins to form and lead to contraction, chemical energy must be supplied to the system in the form of ATP. The myosin protein possesses ATPase activity and this activity correlates with the ability of myosin to bind to actin. Anesthetic agents such as halothane depress cardiac contractility; this effect may result, in part, from the inhibition of myosin ATPase activity.

Changes in Cardiac Mass as a Response to Toxicity

Cardiac mass can increase or decrease in response to a variety of endogenous and exogenous stimuli. Xenobiotic-induced changes in cardiac mass are usually an increase in mass and will be the primary focus of this section. Decreases in mass are uncommon but may occur with mechanical unloading or increased catabolism as might occur with cachexia.

Cardiac hypertrophy is an increase in the mass of the heart muscle beyond the normal limits for age, sex, and body weight. An increase in heart mass may result from an increase in workload (e.g., increased chronotropy, inotropy), an increase in mechanical wall stress (e.g., increased preload or afterload), decreased energy production (i.e., energetic stress) or when primary growth pathways are stimulated in cardiomyocytes (e.g., anabolic steroids). All of these scenarios may be induced by toxic xenobiotics. Importantly, changes that are initially compensatory can progress to maladaptive hypertrophy (i.e., cardiomyopathies) with time, progression, or persistence of the stress. An increase in cardiac mass beyond normal limits does represent an independent risk factor for cardiac dysfunction and even sudden death.

Hyperthyroidism Hyperthyroidism has been experimentally induced or occurs as a spontaneous disease in various animal species including the rat, cat, dog, rabbit, and guinea pig. Cardiac hypertrophy, the result of enhanced protein anabolism, is consistently produced but regresses with restoration of normal thyroid functional status. Cats given thyroxine (0.75 mg/kg/day for 10 months) had biventricular hypertrophy with weight increases of 86% in the left ventricle and 60% in the right ventricle. Light microscopic and ultrastructural studies demonstrated hypertrophy of cardiac muscle cells and increased numbers of mitochondria that showed densely packed cristae.

In rats with thyroid hormone-induced myocardial hypertrophy, angiogenesis of myocardial capillaries preceded ventricular enlargement. Presumably, a coincident induction of angiogenesis would more closely mimic the remodeling of the athletic heart resulting in less opportunity for pathologic outcomes.

Growth Hormone Excess In rats implanted with a growth hormone-secreting tumor, cardiomegaly develops with prominent ventricular hypertrophy. Similar cardiac lesions occur in human patients with acromegaly.

Oxfenicine Dogs and rats developed myocardial hypertrophy following chronic treatment with oxfenicine, an inhibitor of long-chain fatty acid oxidation. Increased cardiac mass in this situation would result from "energetic stress" since an increased reliance on energy production from glucose substrates (i.e., secondary to decreased fatty acid oxidation) would be less efficient. Cardiomyocytes respond to energetic and mechanical stresses by increasing mass.

Drug-Induced Cardiomyopathies

A cardiomyopathic heart is one that is structurally altered (e.g., enlarged, remodeled heart muscle) and dysfunctional. Dilated cardiomyopathies are a heterogeneous group of heart muscle diseases that have congestive heart failure (systolic pump failure) and dilatation of both ventricular chambers as common features. Mural thrombi and focal endocardial thickening are common consequences of disordered blood

flow as are small foci of myocytolysis and myocardial fibrosis.

The etiology of the disorder remains unknown in many human patients (idiopathic dilated cardiomyopathy) but this cardiac injury can be associated with chronic alcoholism (alcoholic cardiomyopathy), viral infection or administration of toxic agents.

Alcoholic Cardiomyopathy Ethyl alcohol has several detrimental effects on myocardial metabolism; nevertheless, the pathogenic mechanisms of alcoholic cardiomyopathy remain uncertain. Cardiomyopathy develops only in a small percentage of alcoholics. It appears likely that the toxic effect of ethanol on the myocardium is modified by other factors and that the "alcoholic" cardiomyopathy observed clinically in human patients is a multifactorial disease. A metallothionein-knockout mouse model fed an alcohol-containing liquid diet for 2 months appears to replicate the cardiac hypertrophy and fibrosis seen in human alcoholic cardiomyopathy and may provide a model for understanding this pathogenesis better.

Histologic findings in myocardial biopsy specimens from patients with dilated cardiomyopathy are nonspecific and do not differ significantly among patients with or without a history of chronic alcoholism. Alcoholic cardiomyopathy can be complicated by concomitant deficiency of thiamine or other nutrients and by other toxic materials ingested along with ethanol. The most striking example of this was illustrated by the epidemics of severe acute cardiomyopathy with pericardial effusion that developed in chronically malnourished alcoholic patients who had ingested large amounts of beer to which cobalt salts had been added during the manufacturing process to improve the quality of the foam. Structural cardiomyocyte findings in these patients included prominent vacuolization, myofibrillar lysis, glycogen accumulation, and edema of the muscle cells. Experiments in animals showed that protein deficiency was an important factor increasing the absorption of cobalt from the gastrointestinal (GI) tract.

Cardiomyopathy Induced by Antineoplastic Drugs Although anthracycline chemotherapeutics can produce acute (ventricular arrhythmias and depression of contractility) and subacute (pericarditis and myocarditis) cardiac toxicity, these antineoplastic agents are well known for the distinctive type of chronic dilated cardiomyopathy that they produce in humans and experimental animals. Gross lesions of doxorubicin cardiotoxicity described in pigs, rabbits, and dogs are hydropericardium, hydrothorax, and ascites. In pigs, fibrinous pericarditis is occasionally present. The myocardium is often pale and the hearts dilated when compared with control hearts; however, many animals have no gross evidence of cardiotoxicity at necropsy. The microscopic and ultrastructural alterations in the myocardium of pigs, rabbits, and dogs with chronic doxorubicin cardiotoxicity are similar to those in humans and in other species of animals.

The pathogenesis of anthracycline cardiotoxicity, which generally is dose dependent (usually at least 400 mg/m^2 total cumulative dose), remains uncertain; however, a number of possible mechanisms have been proposed, including drug binding by intercalation into the DNA of cardiac muscle cells; inhibition of several enzyme systems; and promotion of peroxidative damage mediated by free radicals to cell membranes, mitochondrial membranes, DNA, enzymes, and membranes of SR. Recent work has supported a potential role for anthracycline inhibition of topoisomerase 2β as a primary mediator of cardiotoxicity. This drug toxicity leads to two major lesions; cardiomyocyte degeneration characterized by intracellular loss of myofibrils with cytoplasmic vacuolization and ventricular dilation (Figures 9.5 and 9.6). Ultrastructurally, cardiomyocyte vacuolation is caused by massive dilatation of the SR. These changes can also involve the conduction system of the heart.

Considerable effort has been made to develop or identify cardioprotective therapies that would diminish the cardiotoxicity of anthracyclines without compromising their therapeutic effectiveness. Most of these efforts related to the anthracyclines have focused on the presumed oxidative injury pathogenesis. The most successful of these is the iron chelating agent dexrazoxane, which is marketed in the United States for coadministration to adult cancer patients.

Doxorubicin is also known to cause very late, delayed ventricular dysfunction in young adults who underwent antineoplastic therapy successfully during childhood and survived for 10 years or longer. Cardiac morphologic findings in these patients have not been consistent, and the exact mechanisms mediating this greatly delayed cardiotoxicity remain to be determined. It has been suggested that previous therapy with doxorubicin prevents proper growth of the heart during adolescence. It is thought that the selective cardiotoxicity of anthracyclines is due to the fact that the heart, unlike other organs such as the liver, has very limited defenses (i.e., low levels of superoxide dismutase, catalase, and glutathione peroxidase) against peroxidative damage.

Antineoplastic agents other than the anthracyclines are also capable of producing cardiac damage, but only rarely. Among these are cyclophosphamide, busulfan, mitomycin C, cisplatin, 5-fluorouracil, and vincristine. Cyclophosphamide is cardiotoxic only when administered in massive doses. This is the case in patients being prepared for bone marrow transplantation in whom cyclophosphamide has been reported

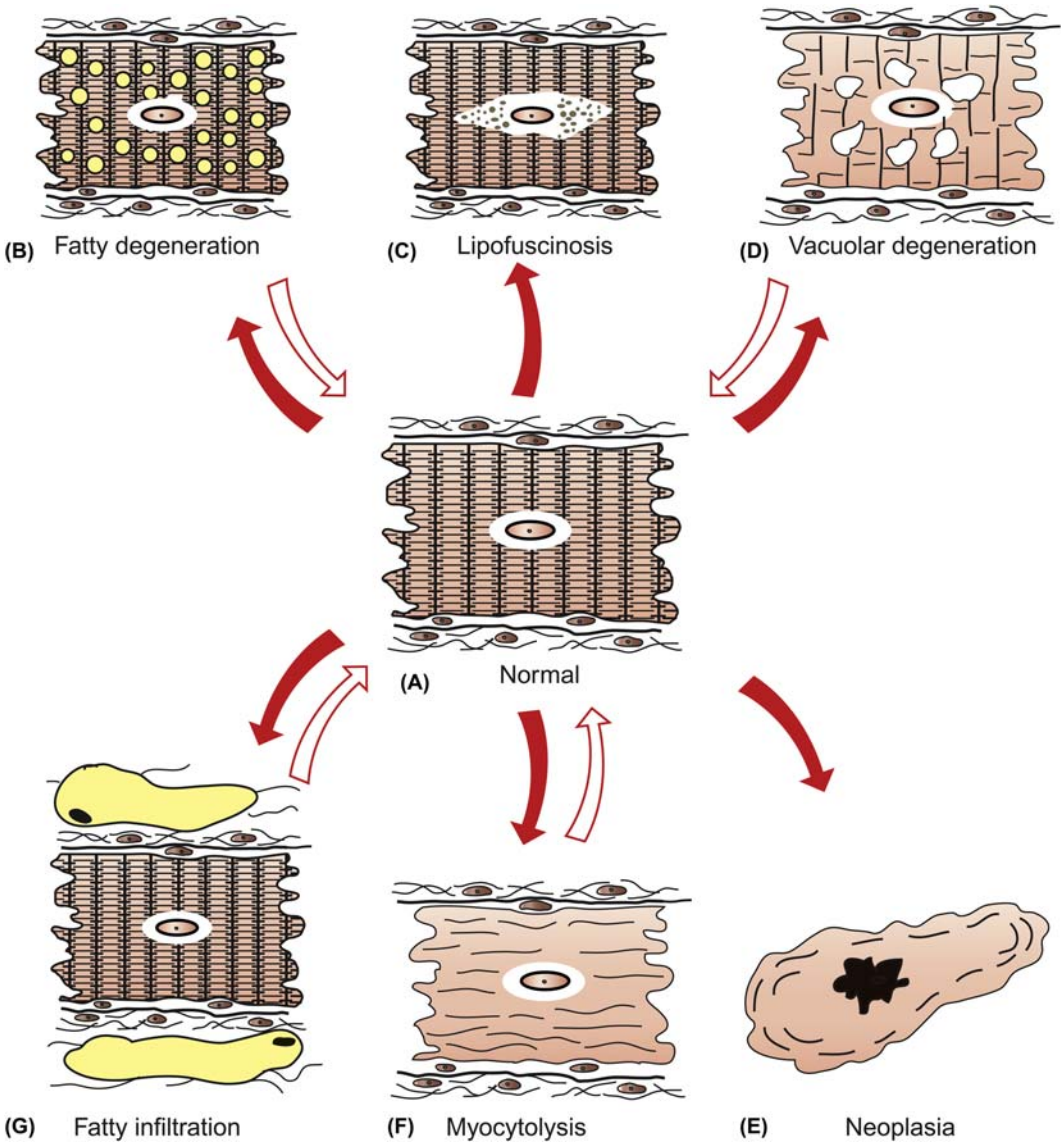

FIGURE 9.5 Schematic diagram of various sublethal cardiac muscle cell injuries. (A) Normal muscle cell, (B) fatty degeneration, (C) lipofuscinosis, (D) vacuolar degeneration, (F) myocytolysis. Also illustrated is fatty infiltration of interstitium (G) and neoplastic transformation of myocytes (E). Source*: Redrawn with permission from School of Veterinary Medicine, Purdue University. From Van Vleet, J.F., Ferrans, V.J., 2007. Cardiovascular system. In: McGavin, M., Zachary, J.F. (Eds.), Pathologic Basis of Veterinary Disease, fourth ed. Mosby Elsevier, St. Louis, MO, Figure 10–6, p. 563.*

to precipitate an acute cardiomyopathy characterized by hemorrhagic myocardial necrosis and pericardial effusion. Busulfan has caused endocardial fibrosis and mitomycin C provokes myocardial fibrosis. Myocardial infarctions have followed the administration of vincristine and 5-fluorouracil. Electrocardiographic changes have been reported after cisplatin therapy.

A popular and emerging class of cancer drugs that inhibit endogenous tyrosine kinases, upregulated in some forms of neoplasia, has also been associated with clinical incidences of cardiac contractile dysfunction (decreased ejection fractions) and congestive heart failure in treated patients. Tyrosine kinases (TKs) are important mediators of cellular signaling in neoplastic and nonneoplastic cells. Small molecule and biologic therapies (e.g., monoclonal antibodies like trastuzumab) frequently have varying levels of activity on kinases beyond those, which are specifically targeted. Accordingly, effects on normal cell signaling are possible with deleterious consequences. More detail on the developing experience with tyrosine kinase-inhibitor cardiotoxicity is included in "Mechanisms of Toxicity."

Cardiotoxicity has also been observed with various cytokines used for cancer immunotherapy including

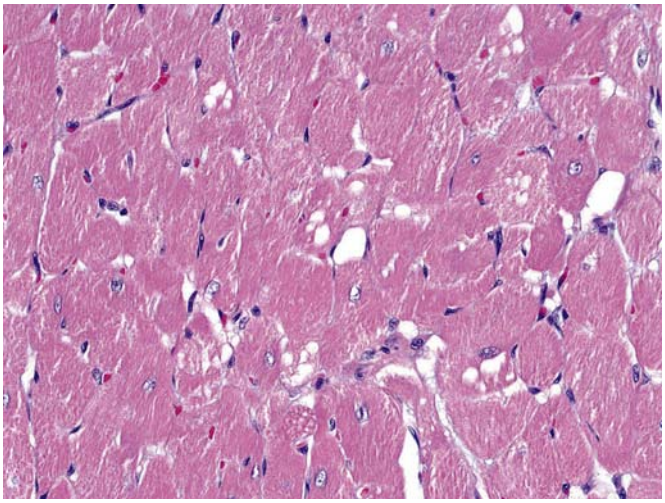

FIGURE 9.6 Prominent large vacuoles in myocytes of a rat 6 weeks after given a single bolus dose of doxorubicin. Paraffin-embedded; hematoxylin and eosin stain. Original magnification ×40. Source: *From Haschek, W.M., Rousseaux, C.G., Wallig, M.A. (Eds.), 2013. Handbook of Toxicologic Pathology, third ed. Academic Press, San Diego, CA, Figure 9.3, p. 1591, with permission.*

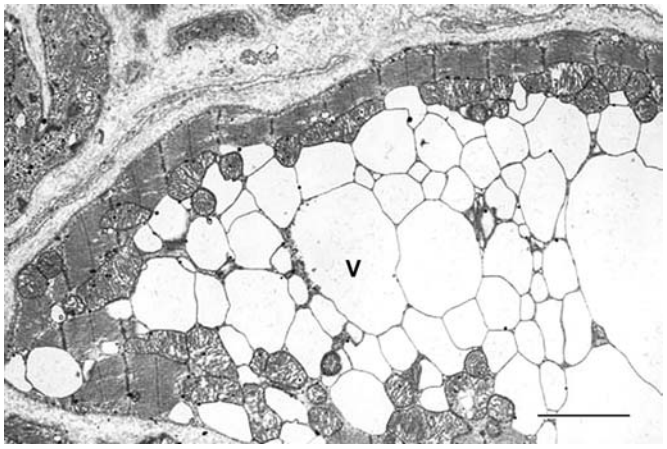

FIGURE 9.7 Electron micrograph of myocyte with vacuolar (V) degeneration as in Figure 9.6. Severe distention of SR is present. Bar = 2 μm. Source: *From Haschek, W.M., Rousseaux, C.G., Wallig, M.A. (Eds.), 2002. Handbook of Toxicologic Pathology, second ed. Academic Press, San Diego, CA, Figure 9.4, p. 388, with permission.*

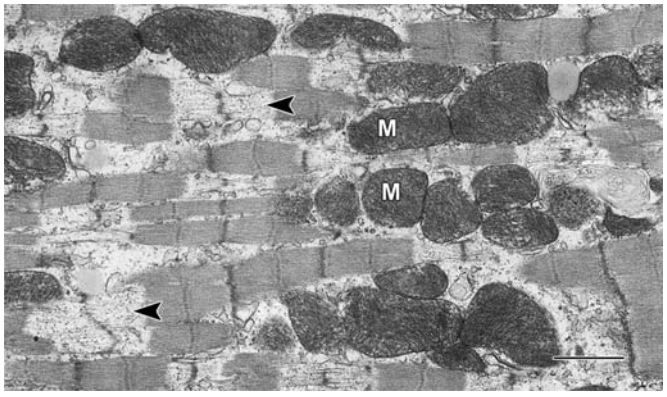

FIGURE 9.8 Selective disruption and lysis of I bands (*arrowheads*) in left ventricular myocardium of a rat with acute plasmocid toxicosis. M, mitochondria. Bar = 1 μm. Source: *From Haschek, W.M., Rousseaux, C.G., Wallig, M.A. (Eds.), 2002. Handbook of Toxicologic Pathology, second ed. Academic Press, San Diego, CA, Figure 9.8, p. 391, with permission.*

interleukin-2 (IL-2), IL-1, IL-4, and interferon. The most frequently recognized CV complication of cancer immunotherapy provoked by IL-2 is the vascular leak syndrome, which is thought to result, at least in part, from the interaction between IL-2-activated lymphocytes (lymphokine-activated killer cells or LAK cells) and endothelial cells. The vascular leak syndrome is characterized by an increase in vascular permeability with fluid retention, peripheral edema, ascites, pleural effusion, and pulmonary edema.

Cardiomyocellular Injury

Xenobiotic-induced cardiomyocellular injury can manifest in a variety of ways depending on the mechanism, pathogenesis, and organellar target of toxicity (Figure 9.5). These injuries can range from sublethal injuries (e.g., degeneration) to cell death by apoptosis or necrosis. Cardiomyocellular necrosis is often accompanied by an inflammatory cell reaction and possibly interstitial connective tissue deposition depending on the magnitude of the lesion. Widely disseminated or cumulative injury may result in measureable changes in cardiac function detectable with either an ECG or contractility assessment (e.g., echocardiography).

Vacuolar Degeneration Vacuolar degeneration is a distinctive microscopic alteration in cardiac muscle cells characterized by variably sized and well-delineated clear spaces within the cardiomyocyte cytoplasm. This change is best associated with the chronic progressive toxicity of anthracyclines (Figure 9.6). Vacuoles at the light microscopic level are revealed to be dilated elements of SR with ultrastructural examination (Figure 9.7). In mildly affected myocytes, the vacuoles vary from 0.1 to 1 μm in diameter, but in severely affected cells the vacuoles can be 1−5 μm in diameter. Lysis of contractile elements also often accompanies the progression of cellular injury.

Myofibrillar Degeneration Myofibrillar degeneration (myocytolysis) is a distinctive sublethal injury of cardiac muscle cells. Affected fibers have pale eosinophilic sarcoplasm and lack cross striations. Ultrastructurally, myofibrils have a varying extent of dissolution (myofibrillar lysis). This lesion has been described with anthracycline cardiomyopathy, furazolidone (FZ) cardiotoxicity in birds, potassium deficiency in rats, and plasmocid toxicosis in rats (Figures 9.8 and 9.9).

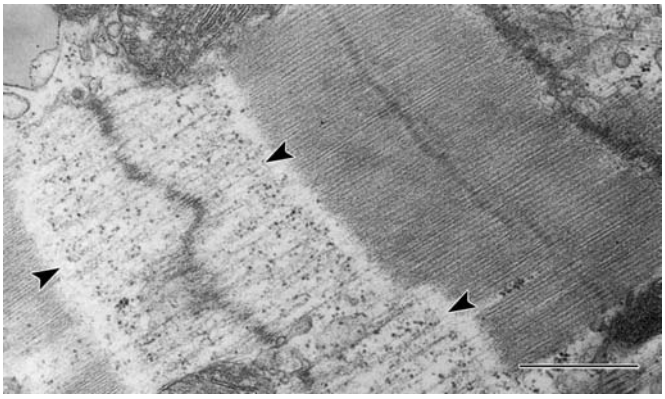

FIGURE 9.9 Higher magnification of portion of Figure 9.8 shows lysis of actin filaments and disruption of myofibril at the junction of A and I bands (*arrowheads*). Bar = 1 μm. Source*: From Haschek, W.M., Rousseaux, C.G., Wallig, M.A. (Eds.), 2002. Handbook of Toxicologic Pathology, second ed. Academic Press, San Diego, CA, Figure 9.9, p. 391, with permission.*

Often accompanying the vacuolar changes of anthracycline cardiotoxicosis is disruption of elements of the contractile apparatus. Myocytolysis is best seen ultrastructurally and can be present in damaged myocytes with or without sarcoplasmic vacuolization. Thick myofilaments are preferentially lysed and irregular clumps of Z-band material may be present. Accumulation of glycogen granules and elements of SR occur in some fibers undergoing myofibrillar lysis. Affected myocytes may also have mitochondrial alterations consisting of swelling and disruption of membranes and scattered accumulations of residual bodies.

Congestive cardiomyopathy is produced in turkeys, ducklings, and chickens by excessive intake of FZ (Figure 9.10). This disease was first reported in 1972 in turkey poults accidentally exposed to excessive amounts of this antibacterial drug. Since then, numerous studies have been reported on the clinical, pathologic, and biochemical alterations of FZ-induced cardiomyopathy. Gross changes of heart failure (ascites, hydropericardium, liver, and lung congestion) were accompanied by ultrastructural changes of cardiomyocyte myofibrillar lysis without overt evidence of necrosis, inflammation, or fibrosis.

Fatty Degeneration Fatty degeneration (fatty change) or myocardial steatosis is characterized by the accumulation of abundant lipid droplets in the cytoplasm of cardiomyocytes. In severe cases, the myocardium will be grossly pale and flabby. Microscopically, affected myocytes have numerous small spherical droplets that appear as empty vacuoles in paraffin sections but stain for lipids with lipid-soluble stains in frozen sections (e.g., Oil Red O). This lesion may occur with systemic disorders such as severe anemia,

FIGURE 9.10 Cardiac dilatation and congestive heart failure in a duckling with FZ toxicosis. Serous fluid accumulation is present in the body cavities and fibrin deposits are present over the liver. Source: *From Van Vleet, J.F., Ferrans, V.J., 2007. Cardiovascular system. In: McGavin, M., Zachary, J.F. (Eds.) Pathologic Basis of Veterinary Disease, fourth ed. Mosby Elsevier, St. Louis, MO, Figure 10.13, p. 566.*

toxemia, and copper deficiency but is less often seen in the heart than in the liver and kidney.

Myocardial lesions occur in a number of species (rats, rabbits, monkeys, gerbils, turkeys, chickens, ducklings, pigs) fed diets containing long-chain monoenoic fatty acids such as erucic acid, which is found in rapeseed oil. Male rats were more susceptible than females to the cardiac lesions. Light and electron microscopic studies revealed early lesions of myocellular lipid accumulation. Later lesions were focal myocardial necrosis, macrophage invasion, and fibrosis. Ducklings and chicks, but not turkey poults, were highly susceptible to the cardiotoxicity and developed prominent hydropericardium, ascites, and myocardial pallor. New varieties of rape plants produce rapeseed oil that contain only small amounts of erucic acid.

Lipofuscinosis Lipofuscin is a lipid-containing product of lysosomal digestion. Lipofuscinosis or brown atrophy of the myocardium occurs in healthy aged animals and in animals with severe cachexia, as well as a hereditary lesion in healthy Ayrshire cattle. Affected hearts appear brown grossly and have clusters of yellowish-brown granules at the nuclear poles of myocytes microscopically. Ultrastructurally, these granules appear as intralysosomal accumulation of membranous and amorphous debris (residual bodies).

Phospholipidosis Another lipid-containing degradation product that might accumulate as a drug or toxicant-related change is phospholipid, which ultrastructurally appears as concentric lamellar whorls in the cytoplasm of affected cells (which might include cardiomyocytes and endothelial cells). These accumulations have been described in myocytes of rats given Brown FK, a food-coloring agent, and in rats, mice, and human patients given chloroquine (Figure 9.11).

Cardiomyocyte Necrosis Necrosis of cardiac muscle cells is generally followed by inflammatory cell infiltration and phagocytosis of sarcoplasmic debris. In lesions with severe disruption of the myocardium, repair may involve fibroblast proliferation and collagen deposition to form scar tissue. Regeneration of cardiac muscle cells is generally not observed. Rarely, in very young animals and especially in avian hearts, a limited amount of myocyte regeneration will occur. Proliferation of myocytes is a normal component of cardiac growth in the first several months of life but then ceases; the remainder of growth is the result of hypertrophy of myocytes until normal cell sizes are reached.

Two basic forms of cardiac muscle cell necrosis are distinguishable: coagulation necrosis and necrosis with contraction bands (myofibrillar damage leading to myocytolysis). Short periods of ischemia (e.g., less than 20 minutes) produce damage characterized by glycogen depletion, mitochondrial swelling, mild intracellular edema, and relaxation of sarcomeres (reflecting loss of contractility). These changes are reversible upon reflow. However, longer periods of ischemia cause irreversible injury with the features of coagulation necrosis. Coagulation necrosis is characterized by flocculent intramitochondrial precipitates thought to be derived from mitochondrial lipids, margination of nuclear chromatin indicating irreversible nuclear damage, small holes or defects in the plasma membrane with loss of its permeability barrier function, relaxed myofibrils with indistinct myofilaments, and various degrees of dissociation of the intercellular junctions. Coagulation necrosis is limited to central areas of infarcts, in which reflow does not occur following ischemic damage.

In contrast to coagulation necrosis, areas peripheral to infarcts show a different type of necrosis known as contraction band necrosis, which is characterized by hypercontraction of myofibrils, intramitochondrial electron-dense calcific deposits, and progression to myocytolysis. The distinctive features of this type of necrosis are related to the entry of large amounts of calcium ions, which originate from partial perfusion of peripheral areas of ischemic lesions, into cells which

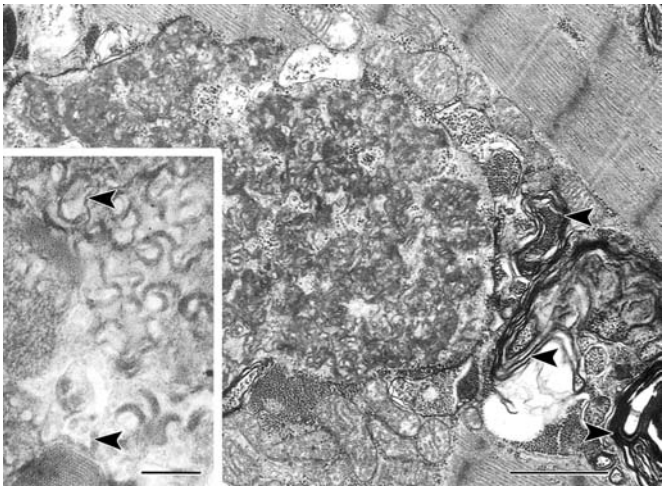

FIGURE 9.11 Electron micrograph of right ventricular myocardial biopsy from a human patient who had received chloroquine for several years for treatment of lupus erythematosis and developed cardiomyopathy. There are large accumulations of curvilinear bodies (*left center*) and membranous lamellae (*arrowheads*). Bar = 1 μm. (*Inset*) Higher magnification of curvilinear bodies (*arrowheads*). Bar = 0.2 μm. Source*: From Haschek, W.M., Rousseaux, C.G., Wallig, M.A. (Eds.), 2002. Handbook of Toxicologic Pathology, second ed. Academic Press, San Diego, CA, Figure 9.11, p. 393, with permission.*

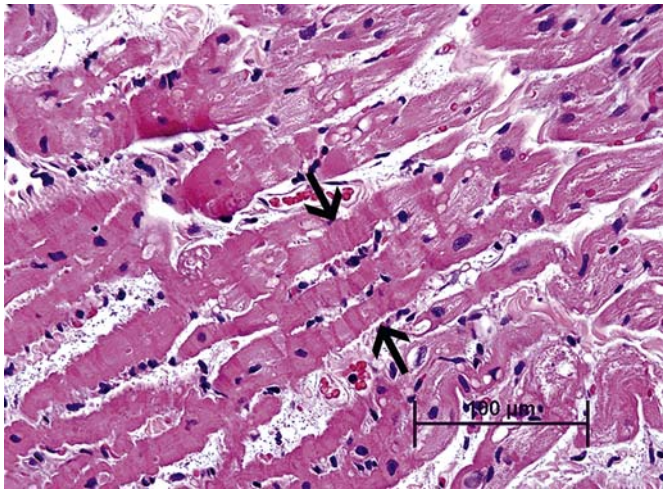

FIGURE 9.12 Myocardium with contraction bands in a rat. Transverse bands (*arrows*) of densely eosinophilic material are separated by pale, sometimes granular or vacuolated sarcoplasm. Paraffin-embedded, hematoxylin and eosin stain. Source*: From Haschek, W.M., Rousseaux, C.G., Wallig, M.A. (Eds.), 2010. Fundamentals of Toxicologic Pathology, second ed. Academic Press, San Diego, CA, Figure 12.12, p. 345, with permission.*

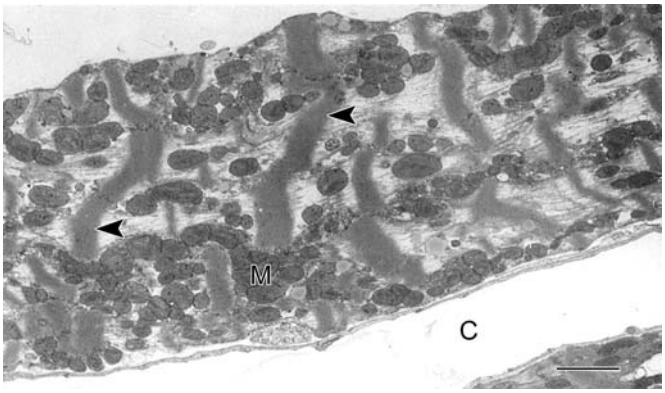

FIGURE 9.13 Contraction band necrosis in ventricular myocyte of a rat with acute plasmocid toxicosis. Dense transverse masses of contractile material are prominent (*arrowheads*). M, mitochondria; C, capillary. Bar = 2 μm. Source: *From Haschek, W.M., Rousseaux, C.G., Wallig, M.A. (Eds.), 2002. Handbook of Toxicologic Pathology, second ed. Academic Press, San Diego, CA, Figure 9.15, p. 398, with permission.*

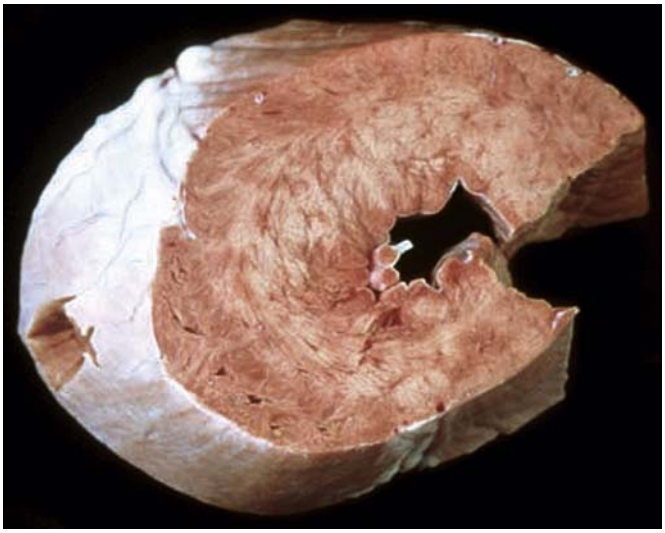

FIGURE 9.14 Myocardial necrosis due to acute monensin toxicosis in a calf. Cross-section of the left ventricular myocardium; mottled areas due to necrosis. Source: *From Haschek, W.M., Rousseaux, C.G., Wallig, M.A. (Eds.), 2010. Fundamentals of Toxicologic Pathology, second ed. Academic Press, San Diego, CA, Figure 12.10A, p. 342, with permission.*

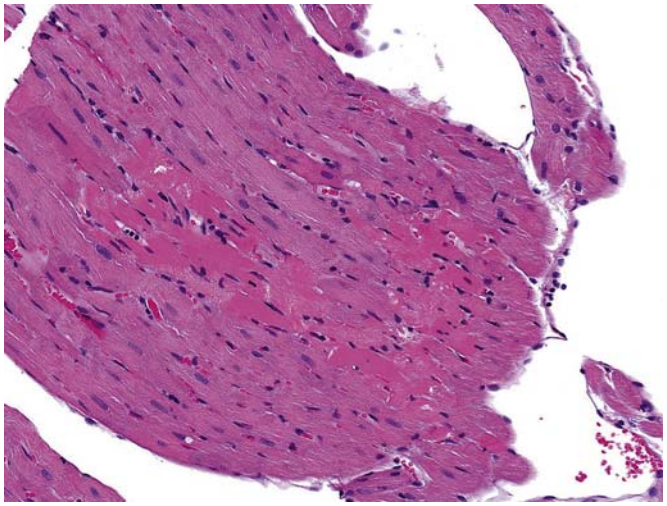

FIGURE 9.15 Section of myocardium from a rat given a high dose of isoproterenol 4 hours ago. Discrete hypereosinophilia of a subset of cardiomyocytes is an early stage of necrosis. Paraffin-embedded, hematoxylin and eosin stain. Original magnification ×20. Source: *From Haschek, W.M., Rousseaux, C.G., Wallig, M.A. (Eds.), 2013. Handbook of Toxicologic Pathology, third ed. Academic Press, San Diego, CA, Figure 9.14, p. 1598, with permission.*

are damaged by ischemia. The passage of calcium through damaged and abnormally permeable plasma membranes is responsible for the hypercontraction. This passage occurs either when severely but temporarily ischemic tissue is reperfused with arterial blood or when necrosis develops because of factors not related to a reduction in coronary blood flow. For these reasons, necrosis with contraction bands is seen in many forms of cardiac toxic injury, including the lesions caused by catecholamines, vasodilating antihypertensive agents, and other cardiotoxic compounds (Figures 9.12 and 9.13). Progression of necrosis with contraction bands to myocytolysis is mediated through lysis of the myofilaments, a change that results in an empty appearance of the cells. The time course of this progression is highly variable.

Progression of Morphologic Alterations Following Cardiomyocyte Necrosis Grossly, areas of necrosis generally appear pale initially and may progress to prominent yellow to white dry gritty areas with dystrophic mineralization (Figure 9.14). The lesions may be focal, multifocal, or diffuse. If the lesions are of ischemic or energy-work mismatch origin, the most frequent sites of focal lesions are the left ventricular papillary muscles and the subendocardial myocardium. These lesions may be overlooked at necropsy unless multiple incisions are made in the ventricular myocardium. Sampling of the left ventricular papillary muscles should be included in any thorough microscopic assessment of the heart. In diseases with diffuse necrosis, such as so-called "white muscle disease" of calves and lambs with selenium-vitamin E deficiency, the pale lesions may be readily observed on the epicardial and endocardial surfaces.

Microscopically, fibers in areas of recent necrosis often appear swollen and hypereosinophilic (hyaline necrosis) (Figure 9.15). Striations are indistinct and nuclei are pyknotic. Necrotic fibers often have scattered basophilic granules that represent mitochondrial accumulation of calcium salts as confirmed by electron microscopy.

Areas of necrosis will have infiltration of inflammatory cells 24–48 hours after injury. These cells are mainly macrophages, with occasional neutrophils, that

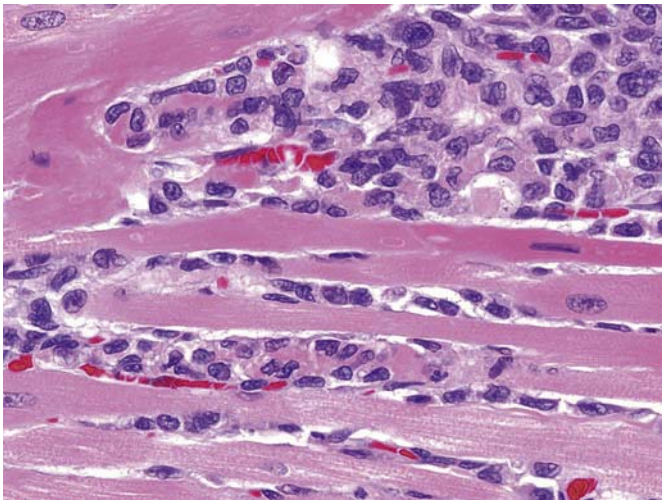

FIGURE 9.16 Cardiomyocyte necrosis in a rat given a single subcutaneous dose of isoproterenol 24 hours previously. Macrophages have infiltrated the myocardium and are phagocytizing the fragmented cardiomyocytes. This stage of myocardial necrosis follows that illustrated in Figure 9.15. Paraffin-embedded, hematoxylin and eosin stain. Original magnification ×40. Source: *From Haschek, W.M., Rousseaux, C.G., Wallig, M.A. (Eds.), 2013. Handbook of Toxicologic Pathology, third ed. Academic Press, San Diego, CA, Figure 9.14, p. 1599, with permission.*

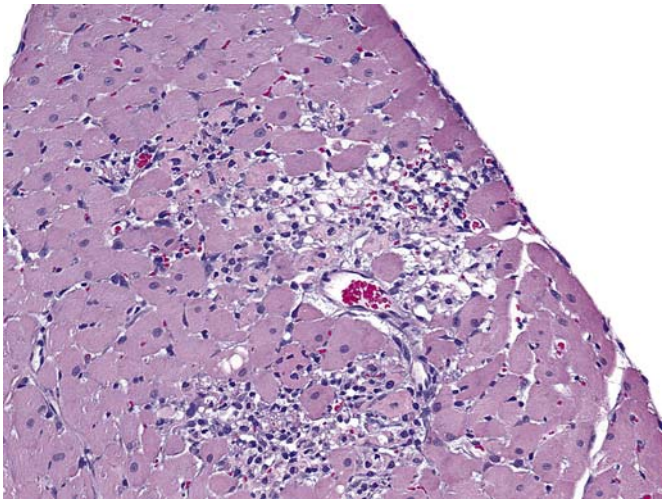

FIGURE 9.17 Cardiomyocyte necrosis in a rat given a single subcutaneous dose of isoproterenol 48 hours previously. Macrophages have removed fragmented cellular material leaving empty "sarcolemmal tubes." This stage of myocardial necrosis follows that illustrated in Figure 9.15. Paraffin-embedded, hematoxylin and eosin stain. Original magnification ×20. Source: *From Haschek, W.M., Rousseaux, C.G., Wallig, M.A. (Eds.), 2013. Handbook of Toxicologic Pathology, third ed. Academic Press, San Diego, CA, Figure 9.15, p. 1599, with permission.*

phagocytize and lyse the necrotic cellular debris (Figure 9.16). In early stages of resolution of necrosis, it may be difficult to distinguish the lesions from those produced by some types of myocarditis or primary myocardial inflammation. Later lesions of resolving necrosis will have persistent stromal tissues (interstitial fibroblasts and collagen, capillaries) and empty "tubes" of basal laminae from necrotic myocytes (Figure 9.17). The healing phase is further characterized by proliferation of connective tissue cells (fibroblasts, capillary endothelial cells) and by deposition of connective tissue (collagen, elastic tissue, acid mucopolysaccharides) (Figure 9.18). Grossly, these areas will appear as white scars.

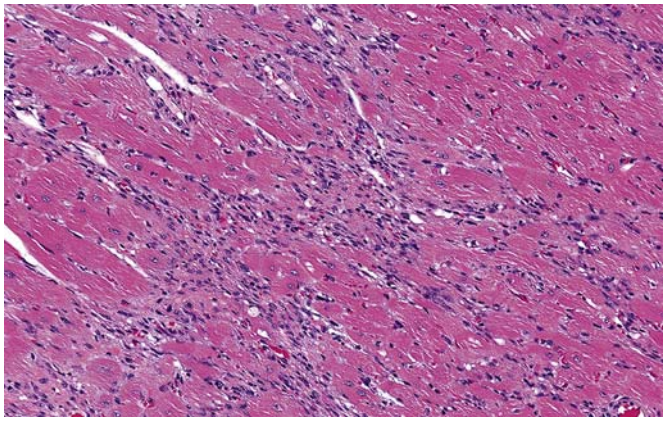

FIGURE 9.18 Myocardial fibrosis. Substantive areas of cardiomyocyte necrosis are replaced by fibrosis in a rat given a single subcutaneous dose of isoproterenol 2 weeks previously. These scars lack the contractile properties of normal myocardium creating regional areas of altered ventricular wall motion if large enough. Paraffin-embedded, hematoxylin and eosin stain. Original magnification ×20. Source: *From Haschek, W.M., Rousseaux, C.G., Wallig, M.A. (Eds.), 2013. Handbook of Toxicologic Pathology, third ed. Academic Press, San Diego, CA, Figure 9.16, p. 1599, with permission.*

The outcome of cases with myocardial necrosis will vary depending on the extent of the damage. Many animals will die acutely from cardiac failure if the extent of myocardial damage is extensive. Sudden death from necrosis-related arrhythmias may also occur. Some cases may eventually develop cardiac decompensation with cardiac dilatation and scarring as well as changes typical of chronic congestive failure in non-CV organs (e.g., chronic passive congestion in the liver). Finally, with minimal damage, only microscopically detectable residual myocardial lesions may be found when death eventually occurs from other causes.

Agents That Produce Myocardial Necrosis

Chemicals can cause more extensive myocardial injury by direct toxic effects that result in cardiomyocyte damage as well as changes in the myocardial interstitium. This type of drug toxicity is dose related and may present either as acute toxic injury or a more chronic drug-induced cardiomyopathy. Acute toxic myocardial injuries may exhibit interstitial edema, multifocal areas of cardiac muscle cell necrosis with contraction bands, and an inflammatory cell infiltrate

consisting of lymphocytes, plasma cells, and polymorphonuclear leukocytes. Eosinophils may be present, but seldom are prominent. The paucity of eosinophils and the presence of various stages of cell death and healing by fibrosis serve to differentiate direct toxic myocardial injury from hypersensitivity myocarditis. Although vascular injury is generally not present, microthrombi have been reported with adenosine diphosphate, cyclophosphamide, catecholamines, and thromboxane A. It should be remembered that a cellular inflammatory reaction may be poorly developed or totally absent in toxic myocardial injuries that involve immunosuppressive agents.

Myocardial Infarction Associated With Toxic Reactions Myocardial infarcts are most commonly associated with unstable atherosclerotic coronary artery disease in human patients. But, myocardial infarction may occur in drug-induced coronary arterial injury (as from amphetamines), fibromuscular intimal proliferation (estrogen- and/or progesterone-containing oral contraceptives), embolization from infective endocarditis (associated with intravenous drug abuse) or in patients with normal coronary arteries following exposure to toxic levels of carbon monoxide, nitrates, thyroid preparations, methylsergide or ergot derivatives and certain antineoplastic agents.

Large areas of necrosis, not related to obstruction of large extramural coronary arteries, have been produced in experimental animals by the administration of toxic doses of isoproterenol. It is likely that this necrosis results from isoproterenol-induced increases in heart rate, contractility, and oxidative metabolism beyond the limits of the oxygen supply system. However, isoproterenol also produces other highly complex effects including a marked increase in calcium uptake, stimulation of the adenyl cyclase system, aggregation of platelets, and formation of free radicals capable of causing peroxidative damage. Other sympathomimetic amines (norepinephrine, epinephrine) are capable of inducing lesions of myocardial necrosis, which are small, multifocal, and usually localized in the left ventricular subendocardium.

Catecholamine-induced cardiac lesions in experimental animals occur in conjunction with pheochromocytomas, tetanus, subarachnoid hemorrhage, and other central nervous system (CNS) lesions. In these conditions, release of large amounts of catecholamines can lead to focal cardiac damage. Ischemic cardiac damage can be aggravated by high circulating levels of catecholamines in patients with acute myocardial infarction.

Hypersensitivity Myocarditis Hypersensitivity myocarditis represents the most common form of drug-induced heart disease in human patients. The clinical criteria for the diagnosis of this disorder are (1) previous use of the drug without incident; (2) the hypersensitivity reaction bears no relationship to the dose of the drug; (3) the reaction is characterized by clinical signs consistent with classic allergy, serum sickness, or infectious disease; (4) immunologic confirmation; and (5) persistence of symptoms until the drug is discontinued.

Hypersensitivity myocarditis associated with drug therapy is characterized by infiltration of the heart muscle with numerous eosinophils admixed with mononuclear cells, predominantly lymphocytes and plasma cells. The cellular infiltrate may be focal or diffuse and is associated with foci of myocytolysis. Fibrotic changes are absent and all lesions are similar in age and appearance. Vascular involvement is frequent and consists of medial necrosis and inflammation affecting small arteries, arterioles, and venules. The inflammatory reaction may also involve the pericardium but characteristically spares the cardiac valves. The absence of extensive myocardial necrosis or fibrosis distinguishes drug-related hypersensitivity myocarditis from other forms of myocarditis in which eosinophils are prominent. Endocardial fibrosis is not a feature of hypersensitivity myocarditis. The pathogenesis of drug-induced hypersensitivity myocarditis remains unclear. The condition appears to be immunologically mediated, perhaps as a reaction in which the drug or one of its metabolites acts as a hapten and combines with an endogenous macromolecule; it is this combination that is antigenic. Hypersensitivity myocarditis also has developed after injection of horse serum, tetanus toxoid, and smallpox vaccine.

Endocardium

Morphologic endocardial alterations are infrequently associated with cardiotoxic agents but endocardial fibrosis and atrial thrombosis have been described with xenobiotic treatment. "Endocardium" in this discussion is distinguished from toxic effects on valves, which are discussed in the following.

Fibrosis Endocardial mural fibrosis can occur in association with toxic or ischemic myocardial necrosis. Large regions of subendocardial necrosis as might be seen with high doses of isoproterenol could be expected to be replaced by fibrosis. Morphologically similar lesions may occur with coronary artery occlusions as seen in human patients with myocardial infarctions. Mural endocardial thickening occurs in the late stages of allylamine cardiotoxicity and in radiation-induced myocardial fibrosis.

Endocardial fibrosis may also be a sequela to altered laminar flow of blood in the cardiac chambers. These "jet" lesions are most commonly seen in atria with valvular dysfunction that allows "jets" of regurgitant blood flow back into the atria when ventricles contract.

Thrombosis Atrial thrombosis that may result from endocardial/endothelial effects has been reported with a spectrum of chemicals tested by the National Toxicology Program of the National Institute of Environmental Sciences. Putative mechanisms for this change include endothelial damage, altered hemodynamics, altered platelet function, and changes in clotting factors.

Neoplasia

Chemically induced cardiac neoplasms are infrequent but have been described in rats, mice, and hamsters. The compounds involved included carbamates (1,1-diphenyl-2-butynyl-*N*-cyclohexyl carbamate), fluorenylacetamide, urethane, ethylnitrosourea, methylnitrosourea, dimethylnitrosamine, methylnitrosamine, ethyl methanesulfonate, ethylnitrosobiuret, hydrazine, triazene, diethylnitrosamine, and 1,3-butadiene. Most of the induced neoplasms were of endocardial origin (endocardial mesenchymal tumors; mostly Schwannomas) but a few arose from the vasculature of the myocardium or pericardium (hemangiosarcoma).

Valves

Drug-induced heart valve injury has and continues to hamper the development of a few classes of drugs. Valve injury can involve any or all of the cellular elements of the valve leaflets or cusps and be proliferative, degenerative, and/or inflammatory. Valve injuries that alter normal valve structure or compliance can lead to a disruption in unidirectional blood flow creating workload challenges for the heart (e.g., increased preload) and consequential changes in the myocardium like hypertrophy and decreased contractility.

Proliferative Valvulopathies The best known drug-induced valvulopathy is that which occurred in human patients taking the anorexigenic diet drug combination fenfluramine−phentermine. A subset of patients taking these drugs for varying periods of time presented with clinical signs of heart failure and/or murmurs. Echocardiography revealed morphologically distorted and dysfunctional atrioventricular valves while microscopic evaluation of a few explanted valves demonstrated valve thickening with stromal proliferation and increased myxomatous matrix. These drugs were subsequently removed from the market.

Similar valve lesions have been described in patients with naturally occurring carcinoid tumors or who have received ergot alkaloid-derived drugs for migraines or Parkinson's disease (e.g., methylsergide, pergolide). Carcinoid tumors (malignant tumors of the intestinal tract) can produce and secrete high concentrations of serotonin. Similarly, ergot alkaloids and the fenfluramine metabolite norfenfluramine have been demonstrated to be agonists of the 5HT2B serotonin receptor, which is expressed on and demonstrated to be mitogenic for valve stromal cells. Accordingly, 5HT2B agonism has been implicated as the cause of these natural or xenobiotic-induced valve injuries. But, animal modeling of this effect has been challenging and with mixed success making it very difficult to discharge this risk in the nonclinical safety assessment setting.

Degenerative/Inflammatory Valvulopathies More recently, a more destructive valvulopathy has been described in rats given ALK5 inhibitors. ALK5 receptors are type I TGFβ receptors targeted for a number of therapeutic indications like cancer, chronic inflammatory disease, and progressive renal disease. Treatment with an ALK5 inhibitor was found to quickly induce hemorrhage, inflammation, and stromal cell proliferation in multiple heart valves of rats. Interestingly, physeal dysplasia was also present in these animals. Similar lesions have been seen but not published by others developing drugs with a similar target.

The lesions described with ALK5 inhibitors are distinguished from those described with 5HT2B agonists by their consistent and rapid development in animal models and their more inflammatory and destructive character.

Mechanisms of Toxicity

Cardiotoxic reactions are potentially life-threatening; for this reason their detection in preclinical safety studies of drug candidates or in premarketing safety studies of other chemicals is of great importance. The detectability of cardiotoxic reactions in these studies significantly depends on the mechanism of action of the chemical on the heart. Although reactions due to exaggerated pharmacological effects are readily elicited in laboratory animals, those due to unrelated mechanisms may or may not develop under the conditions of safety studies. The latter, and particularly those reactions that require predisposing factors for their occurrence, are often detected only in clinical trials or with extensive postmarketing use of the product. Nevertheless, many of these reactions can be reproduced in laboratory animals and the identification of appropriate animal models is instrumental in the development of new drugs that are devoid of cardiotoxic effects. Table 9.1 summarizes known cardiotoxic agents by chemical class or use, their effects and presumptive mechanism of action.

Mechanisms of Functional Alterations

The intrinsic properties of myocardial tissue such as automaticity, excitability, and conductivity endow the heart with a variety of chemically and biologically

TABLE 9.1 Selected Cardiotoxic Agents

Agents	Structural/functional effects	Proposed mechanism(s)
SUBSTITUTED ALIPHATIC HYDROCARBONS		
Haloanesthetics (halothane, methoflurane, and enflurane)	Negative chronotropic, inotropic, and dromotropic effects: possible cardiac arrest	Myocardial depression
Ethanol	Decreases cardiac contraction; causes arrhythmias and ventricular fibrillation with sudden death (after chronic exposure); cardiomegaly	Depression of oxidative phosphorylation in heart mitochrondria
HEAVY METALS		
Cobalt	Cardiomyopathy; heart failure	Antagonism of endogenous Ca^{2+}; complexes of cobalt with macromolecules
Manganese	Arrhythmia	Blocks Ca^{2+} channels
Nickel	Arrhythmia	Blocks Ca^{2+} channels
Gases		
Carbon monoxide (acute)	Tachycardia; bradycardia; extra systoles; increased demand for oxygen by the heart; production of angina pectoris; myocardial infarction	Interference with myocardial energy metabolism; decreased oxygen availability
DRUGS		
(A) Cardioactive drugs		
1. Antiarrhythmics		
Quinidine and procainamide	Prolongation of QRS and QT intervals; ventricular fibrillation after iv injection; extra systoles; low doses accelerate while large doses prolong AV conduction; cardiac arrest	Decreased conductivity and automaticity of the myocardium
Lidocaine	Sinus bradycardia; depressed automaticity of Purkinje fibers and myocardial cells; depresses myocardial contractility	Shortened action potentials of Purkinje fibers and myocardial cells
2. Adrenergic agonists		
Epinephrine and isoproterenol	Positive inotropic and chronotropic effects; ST segment deviation, ectopic beats, and subendocardial necrosis	Relative myocardial hypoxia (work-energy mismatch); cellular Ca^{2+} overload
3. Glycosides of digitalis, strophanthin, and oleandrin	Increase in cardiac contractility, irritability, and arrhythmias; premature ventricular contractions; prolonged PR interval	Inhibit the sarcolemmal Na^+ pump (Na^+-K^+ ATPase) with elevation of intracellular Ca^{2+} via Na^+-Ca^{2+} pump; ventricular fibrillation; complete heart block
4. Vasodilators and antihypertensives (hydralazine, diazoxide, minoxidil, adenosine agonist)	Hypotension, reflex tachycardia; vascular injury, myocardial injury	Suppresses K^+ conductance
5. Endothelin receptor antagonist	Coronary artery medial necrosis and hemorrhage; hypotension, reflex tachycardia	Hyperpharmacology, vasodilation
6. Ca^{2+} antagonists		
Verapamil and nifedipine	Negative chronotropic and inotropic effects	Excitation–contraction uncoupling; block both slow Ca^{2+} and Na^+ channels; depress or block Ca^{2+} influx into myocardial cells
(B) CNS active drugs		
Amphetamine and cocaine	Increased heart rate; blood pressure increase causing great risk when there is preexisting angina, hypertension, and atherosclerosis	Increased workload on the heart; sympathomimetic effects

(*Continued*)

TABLE 9.1 (Continued)

Agents	Structural/functional effects	Proposed mechanism(s)
Imipramine and amitriptyline	Low doses enhance cardiac contractility, whereas high doses depress it as well as coronary flow and heart rate; prolongation of the PR, QRS, and QT interval; bundle branch block; supraventricular; and ventricular arrhythmias	Catecholamine reuptake inhibition; anticholinergic effects
Methylsergide	Endomyocardial fibrosis; valvular defects	Serotonin receptor (5HT2B) receptor agonism
Barbiturates	Depression of myocardial contractility	Inserts in lipid bilayer of membrane; stabilizes membranes
(C) Chemotherapeutic agents		
Anthracyclines (doxorubicin and daunorubicin)	Arrhythmias (acute); dilated cardiomyopathy and congestive heart failure (chronic)	Mitochondrial injury/dysfunction; generation of reactive oxygen; peroxidation of membrane lipids and consequent changes in membrane structure; topoisomerase 2β inhibition
5-Fluorouracil	Myocardial ischemia; cardiac arrest	Mitochondrial dysfunction
Cyclophosphamide (large doses)	Myocardial capillary microthrombosis; pericarditis	Endothelial injury
Monensin, lasalocid, narasin, salinomycin, maduramicin	Positive inotropic effect; increased cardiac output; occasional increase in heart rate and automaticity; increased coronary blood flow	Increased excitation–contraction coupling; enhanced metabolism of cardiac cells; increased sarcolemmal cationic trap for Na^+ (lasalocid: cationic trap for K^+)
Penicillin and sulfonamide	Focal or diffuse interstitial infiltration with eosinophils, lymphocytes, and plasma cells	Hypersensitivity myocarditis
(D) Growth promoting agents		
Clenbuterol	Cardiac hypertrophy	B_2 adrenergic agonism
(E) Cationic amphiphilic drugs		
Chloroquine	Interaction of xenobiotics on synthesis and metabolism of phospholipids	Phospholipidosis in multiple organs
(F) Appetite suppressants		
Fenfluramine–phentermine	Valvular heart disease	Serotonin receptor (5HT2B) agonism on valvular interstitial cells
(G) Cytokines		
IL-2	Myocardial edema, myocyte injury, hemorrhage	Lymphocyte-mediated endothelial damage; hypersensitivity; decreased cAMP
(H) Antiviral agents		
NRTIs	Cardiomyopathy	Inhibition of mitochondrial biogenesis
(I) Carcinogenic agents		
3-Butadiene and nitrosamines	Sarcoma formation within heart	Induction of chemical carcinogenesis
(J) Agents and drugs producing CV teratogenesis		
Dextroamphetamine	Ventricular and atrial septal defects	Unknown
Ethanol	Ventricular septal defects	Unknown
TOXINS		
Endotoxin	Reduced coronary perfusion; depression of contractility; negative inotropic and chronotropic responses to NE and histamine	Depression of Ca^{2+} ATPase activity; depression of Ca^{2+} uptake; reduced Ca^{2+} release by action potentials

(*Continued*)

TABLE 9.1 (Continued)

Agents	Structural/functional effects	Proposed mechanism(s)
Tetrodotoxin and saxitoxin	Conduction defects	Blocks fast Na^+ channels
Gossypol	Myocardial necrosis/fibrosis; congestive heart failure	Na + , K + -ATPase inhibition
Moniliformin	Bradycardia	Myocardial necrosis/fibrosis and sudden death syndrome in chicks and turkey poults
Fumonisin B_1	Left-sided heart failure and pulmonary edema in swine	Altered sphingolipid biosynthesis causes decreased CV function

Source: *Originally modified from Cohen (1986). Table modified from Haschek, W.M., Rousseaux, C.G., Wallig, M.A. (Eds.), 2013. Handbook of Toxicologic Pathology, third ed. Elsevier, San Diego, CA, Table 46.3, pp. 1602–1608, with permission.*

sensitive pathophysiologic targets. Disruptions in normal cardiac function can arise from alterations in membrane function, energy production, contractility, vascular tone, or autonomic influences.

Changes in Rate and Rhythm Changes in heart rate induced by xenobiotics are generally secondary to some change in autonomic signaling to pacemaker centers in the heart (particularly the SA node). That change in signaling can be direct or indirect. Direct effects may result from xenobiotic influences on brain centers of the autonomic nervous system or target organ receptor activity (e.g., β-adrenergic receptors). Indirect effects result from drug effects outside the heart. For example, drugs that cause vasodilation and lower blood pressure often have the indirect effect of increasing heart rate as normal CV compensatory mechanisms are activated.

Arrhythmias are among the most serious immediate functional cardiac abnormalities. Abnormalities in action potential formation or conduction, individually or in combination, are primary causes of arrhythmias. Substances can directly influence the initiation or propagation of the cardiac action potential by altering the ionic gradients and fluxes that are involved in these processes. Ions such as barium and strontium carry current through the slow channels in place of calcium ions. This action initially leads to cardiac stimulation but subsequently these two ions cause serious arrhythmias followed by cardiac arrest. These latter adverse effects are thought to be due to an impairment of the efflux of potassium ions from myocardial cells.

The two types of electrical activity (fast and slow responses) that have been detected in cardiac tissue and in chemically altered cells have a major role in the precipitation of arrhythmias. Fast-response cells are located in the working atria and ventricles and in most portions of the conducting system except the SA and AV nodes. Exposure to certain agents or ischemic conditions can reduce the resting membrane potential of the cardiac cell. The reduction in membrane potential causes a decrease in the speed of impulse conduction and enhances the chance for a block in conduction of electrical activity. The fast-response fibers possess a second slow inward current carried by Ca^{2+} ions that develops only when the fast Na^+ depolarizing current has decreased the membrane potential. Sustained partial depolarization of the membrane to about −60 mV by abnormal conditions such as increased extracellular potassium concentration or hypoxia, inactivate the fast sodium channel while leaving the slow calcium component functional. The initiation and conduction of the slow-response action potential in fibers that are partially depolarized by damage or hypoxia may provoke abnormalities of cardiac rhythm.

Probably the most studied drug-induced arrhythmia in the past 15 years is that related to drugs that block the cardiomyocyte repolarizing hERG (*human Ether Related-a- go-go gene*) K + channel. Congenital mutations in the hERG gene that result in dysfunction of this K + channel cause prolongation of the repolarization phase of the action potential and prolongation of the ECG QT interval (congenital long QT syndrome) (Figure 9.19). Patients with this electrophysiologic abnormality are recognized to be predisposed to a fatal form of ventricular arrhythmia called *Torsades de Pointes* (TdP) (i.e., QT prolongation is a surrogate measure of TdP risk). The recognition that a number of commonly used drugs belonging to a variety of therapeutic classes could induce an acquired form of long QT syndrome with putative risk for fatal arrhythmia instigated new regulatory guidances and a number of nonclinical and clinical assays to characterize this risk potential (Table 9.2). Currently, a battery of *in vitro* and *in vivo*, nonclinical and clinical assessments is required for drugs intended for human clinical use. Since not all QT prolongation induces an inherent risk of TdP and QT prolongation itself is not injurious to the heart, there is much controversy about the validity of this surrogate measure

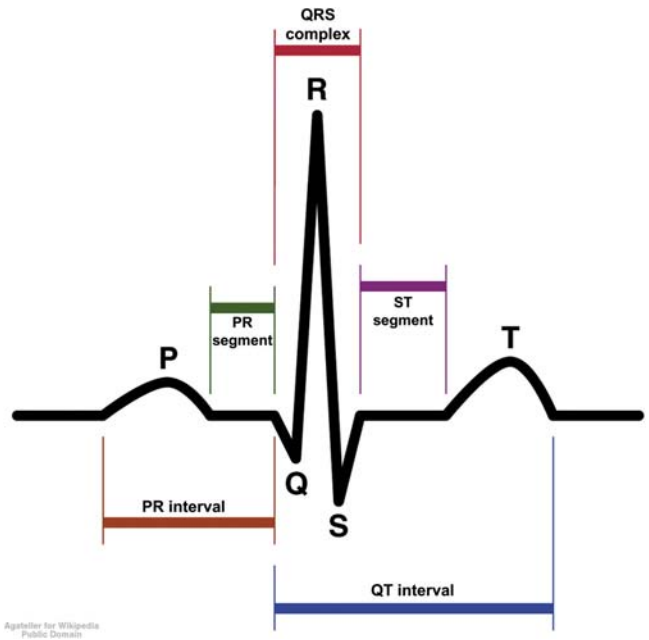

FIGURE 9.19 A typical Lead II electrocardiographic trace indicating segments of the electrical cardiac cycle. https://commons.wikimedia.org/wiki/File:SinusRhythmLabels.svg

TABLE 9.2 Drugs Associated with QT Prolongation and Possible Risk of *Torsades des Pointes* in Patients

Drug	Therapeutic class
Quinidine	Antiarrhythmic
Sotalol	Antiarrhythmic
Amiodarone	Antiarrhythmic
Erythromycin	Macrolide antibiotic
Azithromycin	Macrolide antibiotic
Moxifloxacin	Quinolone antibiotic
Ketoconazole	Antifungal
Terfenadine	Antihistamine
Chloroquine	Antimalarial
Ritonavir	Antiretroviral
Vandetanib	Oncology chemotherapy
Furosemide	Diuretic
Cisapride	Gastroprokinetic
Apopmorphine	Opioid
Haloperidol	Psychoactive
Risperidone	Psychoactive
Thioridazine	Psychoactive

and its contribution to drug attrition pre- and post-marketing. Table 9.2 lists drugs that are known to induce QT prolongation and have putative risks of inducing TdP.

Contractility Contractile work by the myocardium requires the concerted integration of both structural and biochemical components of the myocardium. Cardiac contractility is most quickly influenced by changes in autonomic adrenergic stimulation, which may be an intended pharmacologic activity of some cardiac-directed drugs but may also occur as an "off-target effect." Changes in autonomic adrenergic stimulation affect contractile force largely by influencing calcium flux into and out of the cardiomyocyte. Likewise, xenobiotic inhibition of energetic pathways that affect ATP production (e.g., mitochondrial injury, substrate utilization) can also alter calcium fluxes and change contractility. More chronically, loss of cardiomyocytes through apoptosis or necrosis with or without replacement by less contractile interstitial fibrosis will affect contractile function either regionally or within the organ as a whole.

Mechanisms of Direct Cellular Injury

Direct cardiotoxic effects are the result of a selective or random interaction of a xenobiotic with molecules of vital importance in cardiomyocytes. These interactions may be facilitated by metabolic pathways, drug transporters, or physiologic functions unique to the beating heart.

The high energy requirement of the heart predisposes the myocardium to the adverse effects of metabolic poisons. Toxic reactions may involve suppression of an enzyme system. For example, cobalt-induced cardiotoxicity is due to inhibition of certain mitochondrial energy-generating systems.

Adverse myocardial effects may be elicited when a compound or a reactive metabolite of a compound interacts with structural macromolecules in the myocyte. Since myocardial enzymes that metabolize endogenous substances may also use xenobiotics as substrates, biotransformation can occur in the heart. The role of metabolically derived, chemically reactive substances in the initiation of certain myocardial toxicities has been described. Following acute exposure to the industrial chemical allylamine, rats develop multifocal cardiomyocyte degeneration and necrosis, whereas prolonged dosing leads to myocardial and vascular fibrosis. An amine oxidase enzyme found in the heart and blood vessels metabolizes allylamine to acrolein, which is responsible for the cardiac injury. Acrolein is conjugated by glutathione and is excreted as a mercapturic acid conjugate. It is likely that the extent of injury is a function of the rate of acrolein

formation and the availability of glutathione at the site of biotransformation.

The role of reactive chemical species in myocardial toxicity is of considerable consequence in other ways. As with acrolein, two factors significantly influence the development of reactive metabolite-induced injury—the rate of formation of the reactive products and the availability of sufficient amounts of protective substances. Some agents can stimulate the formation of reactive oxygen radicals in the heart and induce myocyte injury. Anthracycline antineoplastic agents such as doxorubicin produce a distinctive type of chronic congestive cardiomyopathy in humans and experimental animals. Two major morphological lesions are seen in the myocyte: dilation of the sacroplasmic reticulum and loss of myofibrils. The pathogenesis of these lesions is believed to be linked at least in part to the generation of toxic oxygen free radicals. A key factor in this concept was the finding that doxorubicin can form a complex with iron that is capable of mediating production of reactive oxygen radicals. This complex can bind to cell membranes and, by reacting with endogenous thiols, is capable of oxidative destruction of structural macromolecules such as those found in the cell membrane. The unique sensitivity of the heart to the cardiotoxic effects of doxorubicin may be secondary to the low cellular concentrations of enzymes such as catalase that are capable of preventing accumulation of damaging reactive oxygen radicals. In addition, doxorubicin suppresses the activity of glutathione peroxidase, another enzyme capable of protecting against injury by oxygen free radicals. Thus the low levels of potential protective enzymatic activity make the myocardium quite vulnerable to the effects of certain reactive substances.

Another mechanism of direct cardiotoxicity is related to small molecule or biologic (e.g., monoclonal antibodies) therapeutics that may unintentionally target mediators of normal cardiomyocyte physiology. TK enzymes modulate a variety of signaling pathways concerned with important cellular functions such as metabolism, cell cycle progression, proliferation, differentiation, and survival. In nonproliferating cells, TK activity is tightly controlled and is present only at low levels in normal cells. However, increased TK expression can facilitate the transformation to neoplasia in certain tissues. Tyrosine kinase inhibitors (TKIs) are a relatively new category of small molecule drugs that act intracellularly to interfere with specific pathways influenced by upregulated kinase enzymes. TKI compounds target the kinase ATP-binding pocket and thus prevent ATP from binding to the upregulated kinase enzyme. It is this action that attenuates kinase signaling activity in tumor cells. Because the configuration of the ATP-binding pocket is conserved across most human kinases, TKIs that target the ATP-binding pocket tend to be promiscuous in their activity. Thus, although treatment with TKIs is intended to target specific over-expressing kinases in certain types of tumor cells, these agents have also been found to exert inhibitory actions against off-target kinases in normal tissues. The experimental and clinical reports of cardiotoxicity following treatment with TKIs indicate that some of these off-target kinases also serve important functions in the heart.

Direct cardiomyocyte toxicants may target specific subcellular organelles leading to whole cell dysfunction and even cell death. The heart easily compensates for individual cell dysfunction and death but large-scale cardiomyocyte loss will lead to clinically detectable whole-organ dysfunction and possibly death of the patient. Subcellular organelles of cardiac muscle cells subject to specific damage by toxic agents include:

1. Mitochondria—Xenobiotics may interfere with mitochondrial enzymes (cyanide, thyroid hormone), uncouple oxidative phosphorylation (dinitrophenol, cobalt, lead, mercury), bind to mitochondrial DNA (acriflavin), produce mitochondrial mineralization (dehydrotachysterol, sodium phosphate), or produce selective mitochondrial damage by undetermined mechanisms (monensin, *Cassia occidentalis*, bis(2-chloroethoxy)methane).
2. Sarcoplasmic reticulum—Toxic agents may cause selective dilatation of SR elements (anthracyclines) and other SR alterations (guanidine, volvatoxin A).
3. Contractile material—Myofibrilysis can occur (sympathomimetic amines, plasmocid, diuretics, or other conditions leading to potassium deficiency, FZ in birds, halothane, corticosteroids).
4. Sarcolemma—Compounds which selectively affect the sarcolemma (tetrodotoxin, verapamil, cardiac glycosides).
5. Nucleus/nucleolus—Compounds which selectively affect the nucleus/nucleolus through mechanisms like DNA intercalation (anthracyclines).
6. Lysosomes/residual bodies—Compounds that cause drug-induced phospholipidosis result in accumulations of electron-dense lamellae (chloroquine).

Organellar injuries may give some insight into the molecular mechanisms of toxicity. Many of the changes in the contractile apparatus, nucleus, or membrane system (plasma membrane, T-tubules, and SR) are associated with complex alterations in the concentrations of Ca^{2+}, Mg^{2+}, Na^{+}, and K^{+}, as well as with changes in the intracellular compartmentalization of these ions. In addition, these changes and changes in intracellular pH can be associated with activation and

release of lysosomal hydrolytic enzymes, including cathepsin D and other proteases, and phospholipases. This cascade of changes, coupled with alterations in the permeability of plasma membranes, acts as determinants of whether or not cellular injury progresses to the point of irreversibility—i.e., cellular necrosis.

Mechanisms of Indirect Injury

Some cardiac injuries associated with xenobiotic exposure may occur secondary to effects outside the heart itself and result from changes in the metabolic milieu of circulating plasma or changes in cardiac workload. For example, drug-induced kidney injury may result in altered cardiac function and myocellular injury. Related to the kidney's role in electrolyte conservation and elimination, electrolyte imbalances often accompany kidney dysfunction and can lead to arrhythmias. Uremia resulting from severe kidney dysfunction can cause direct cardiomyocyte injury (necrosis and mineralization) or vascular endothelial injury that leads to cardiac ischemia (e.g., secondary to thrombosis).

Also, drugs that alter vascular activity (i.e., constriction or dilation) change cardiac workloads and may alter blood perfusion of the cardiac muscle. For example, drugs like the potassium channel inhibitor, minoxidil, are potent vasodilators. Vasodilation causes a drop in blood pressure initiating a compensatory increase in heart rate and increase in plasma volume secondary to renal fluid retention. Ultimately, the heart sees an increase in work (increased heart rate), an increase in the volume of blood that is pumped (plasma volume expansion), and possibly a decrease in coronary perfusion (decreased systemic vascular resistance, decrease in diastolic interval). The results may be an increase in cardiac mass and ischemic cardiomyocellular injury.

Drugs like the mixed β-adrenergic agonist isoproterenol have direct effects on the heart as well as effects on the peripheral vascular system that can synergize to cause cardiac injury at toxic doses. Isoproterenol causes an increase in both the rate (chronotropy) and force of cardiac contraction (inotropy) resulting in increased cardiac work. It also causes peripheral vasodilation that decreases coronary perfusion pressures. High doses of isoproterenol classically produce acute, regionally extensive to multifocal myocardial necrosis in animal models (Figure 9.14).

Weight loss herbals containing natural forms of ephedra (Ma Huang) and caffeine have been associated with adverse clinical events that ultimately led to their market withdrawal in 2004. Ephedra is a potent sympathomimetic amine with activity on both α- and β-adrenergic receptors. Caffeine is a centrally acting stimulant that increases endogenous catecholamine release and causes vasoconstriction. Modeling of these effects with ephedrine/caffeine combinations in laboratory rodents reveals rapid increases in heart rate and blood pressure with secondary myocardial hemorrhage and necrosis. The observation that 14-week-old rats are more sensitive to the effects of this combination than 7-week-old rats is consistent with similar observations for the hyperpharmacologic effects of isoproterenol.

Cardiotoxicity of Cardiac Drugs

Adverse cardiac reactions are common with CV drugs like digitalis glycoside, antiarrhythmics, and antihypertensives. These reactions are the result of exaggerated pharmacological effects following an overdose or occurring because of an unusual sensitivity to the patient brought about by young or advanced age, comorbidities, or drug interactions. The heart can also be a target of unintended pharmacologic side effects when the drug acts on an organ other than the desired one. Examples of cardiac effects of drugs that act on the CNS are the neuroleptic and antidepressant-induced arrhythmias.

If the desired pharmacological effect occurs in a laboratory animal species, it is likely that the exaggerated or "superpharmacologic" effect can also be elicited. Effects of this nature are dose related and may appear only at doses that are nearly lethal in laboratory animals. However, they could occur at therapeutic doses in humans, since several conditions may predispose to their development. Of particular significance are those conditions that are frequently encountered in the greatest users of drugs, the elderly. Altered physiological functions that may be associated with adverse effects are decreased glomerular filtration rate or preexisting heart disease. For example, the toxicity of digoxin is increased with a decreased glomerular filtration rate, and β-adrenergic blocking agents cause potentially fatal effects in patients with congestive heart failure. Life-threatening CV effects may develop following a therapeutic dose of β-blockers in patients whose cardiac function depends upon the maintenance of sympathetic drive.

Arrhythmias and QT-interval prolongation have occurred in patients receiving overdoses or even therapeutic doses of tricyclic antidepressants or neuroleptics. However, several conditions sensitize to these effects. Sudden cardiac deaths associated with ventricular fibrillation have occurred in patients who had preexisting heart disease and were taking therapeutic doses of these drugs.

Thioridazine is one of the most cardiotoxic phenothiazine neuroleptic drugs. One of its metabolites, a ring sulfoxide, appears to be responsible for cardiotoxicity. Patients at risk are those who rapidly

metabolize thioridazine to this cardiotoxic metabolite. Neuroleptic-induced electrocardiographic changes may be enhanced by glucose loading that increases the intracellular to extracellular ratio of potassium in response to an increase in insulin.

Hypersensitivity Reactions

The heart is also a target of immune-mediated effects of xenobiotics. Allergic skin reactions are occasionally accompanied by subtle electrocardiographic changes and, in rare instances, by hypersensitivity myocarditis. Diagnostic testing for suspected allergens in humans carries some risk of cardiac reaction. In systemic anaphylaxis, mediators such as histamine and leukotrienes cause constriction of coronary arteries and decrease the force of contraction of the heart muscle; thus, a primary cardiac event occurs and can include arrhythmia or even heart failure. Penicillin has now replaced horse serum as the most frequent cause (1%–10%) of anaphylaxis in humans. Fatal reactions, however, are less than one per one million injections.

In addition to anaphylaxis, cytotoxic immune-complex-elicited injuries can affect the heart. Methyldopa-induced myocarditis fits into this category. Numerous drugs can cause immune-complex-mediated reactions in the coronary vessels (e.g., sulfonamides, penicillin, procainamide, quinidine), and autoimmune mechanisms have been implicated with some of these drugs. Development of the reactions in humans has been associated in some instances with a specific gene haplotype (a set of alleles) of the major histocompatibility complex. The great polymorphism of the gene product is responsible for variability in the sensitivity to antigens. Animal models are generally not predictive for hypersensitivity-related cardiotoxicities in human patients.

Xenobiotic Interactions

Drug–drug interactions play a significant role in the development of serious cardiotoxic reactions. The myocardial sensitivity to the arrhythmogenic actions of cardiac glycosides is increased by diuretic agents that deplete potassium and magnesium. Digitalis glycosides and extracellular potassium have competitive affinities for the membrane Na^+-K^+-ATPase enzyme. Exposure to potassium may simultaneously increase Na^+-K^+-ATPase activity and decrease the binding of glycosides to this enzyme. A decrease in extracellular K^+ would intensify the inhibitory effect of glycosides on the Na^+-K^+-ATPase system, resulting in an increase in intracellular sodium concentration. As a result, the magnitude of the membrane potential may approach the threshold for initiation of diastolic depolarization and thus initiate serious arrhythmias. Concurrent exposure to CV agents that have similar effects, but which act by different mechanisms, can cause potentiation of specific adverse effects. For example, the simultaneous administration of propranolol, a β-adrenergic receptor blocker, and verapamil, a calcium channel antagonist, has caused profound AV block and marked hypotension.

Normally, catecholamine administration causes a predictable series of dose-related myocardial effects. Initially, sinus tachycardia occurs but a variety of arrhythmias are induced as the dose is increased (ventricular bigemeny, multifocal premature ventricular contractions, ventricular tachycardia) and finally, at high concentrations, ventricular fibrillation ensues. Exposure to certain halogenated hydrocarbon chemicals reduces the amount of catecholamines necessary to cause these arrhythmias.

Two additional potential targets for adverse drug–-drug interactions in the heart are cytochrome P450 metabolizing enzymes and membrane drug transporters. A number of P450 enzymes are known to be expressed in the mammalian heart and have roles in metabolizing xenobiotics as well as endogenous substrates as they do in other tissues. Though a specific role in facilitating direct cellular toxicity in the heart through generation of a toxic metabolite is speculated, this mechanism is poorly explored. Also, a number of drug transporters including the well-characterized transporters P-glycoprotein (ABCB1; endothelial cells) and BCRP (Breast Cancer Resistance Protein; ABCG2) are expressed in the heart. Transmembrane ATP-binding cassette (ABC) proteins are efflux transporters of substrates against a concentration gradient and out of the cell. Normal function of these transporters protects the cellular components of the heart from harmful accumulation of toxic xenobiotics. Alternatively, inhibition of transporters may enhance toxicity. This effect is best exemplified in the observations of enhanced doxorubicin toxicity in mice and rats coadministered the transporter inhibitors verapamil or cyclosporine A.

Modifying Factors in Toxicity

Individual responses to cardiotoxic xenobiotics can be variable, particularly in heterogeneous human patient populations. Modifying influences include demographic factors like age, sex, gender, and race; biological factors like genetic polymorphisms in key metabolizing enzymes or transporters; pathobiological factors like preexisting disease in or out of the CV system; and coadministration of other xenobiotics (i.e., polypharmacy).

The role of some sensitizing factors has been demonstrated in laboratory animals. For example, age- or weight-dependent susceptibility to the cardiotoxicity of β-adrenergic agonist and vasodilating antihypertensive agents occurs in the rat and to some extent in other laboratory animal species. Young weaned

rats are fairly resistant to the cardiotoxicity of isoproterenol. The LD_{50} of subcutaneously (sc) injected isoproterenol hydrochloride is about 1 g/kg in these rats and focal subendocardial necrosis occurs at 100 mg/kg. The 6-month-old rat, particularly of the Sprague-Dawley strain that can reach 500–600 g body weight, develops an increased sensitivity to the cardiotoxicity of isoproterenol. The sc LD_{50} of isoproterenol is about 0.6 mg/kg, with death preceded by ventricular fibrillation and myocardial necrosis at a dose as low as 50 μg/kg. The mechanism of this difference in the sensitivity of young weanling rats and older heavier rats has not been established. Their sensitivity to the positive chronotropic effect of the drug is similar. Electrophysiological events in isolated papillary muscles are comparable in both groups before and after isoproterenol treatment. It is conceivable that the susceptibility to the consequence of isoproterenol treatment, that is, to hypoxia, differs. Hypoxia is most likely responsible for the development of cardiac lesions and perhaps also for the preceding fibrillation.

The cardiotoxicity of isoproterenol was overlooked in preclinical safety studies because the investigators used young weanling rats. The older heavier rats, described earlier, and adult beagle dogs develop focal subendocardial necrosis after suprapharmacological doses of drugs which, like isoproterenol, produce tachycardia and hypotension.

BLOOD VESSELS

Introduction

Blood vessels, subdivided into arteries, veins, capillaries, and lymphatic, have remarkable adaptations of their structure to achieve required functions. Xenobiotics may provoke vascular alterations that may be unique to the vessels of a particular organ or have tropism for a particular segment of specific types of vessels. A spectrum of morphologic reactions is induced by vascular toxicoses including accelerated atherosclerosis, medial and intimal proliferation, calcification, aneurysms, medial hemorrhagic necrosis, fibrinoid necrosis, microangiopathy, and vasculitis. The outcome of vascular injuries may be dominated by repair processes rather than regeneration and may be complicated by development of thrombosis, aneurysm formation, and vascular rupture.

Structure and Function

Microscopic Anatomy

The vascular system is subdivided into arterial, capillary, venous, and lymphatic segments. The arteries are classified into three types: elastic arteries, muscular arteries, and arterioles. Interposed between the arterial and venous segments are the capillary beds. Some authors prefer to further define a vascular segment termed the microcirculation that includes arterioles, capillaries, and venules and serves as the major area of exchange between the circulating blood and the peripheral tissues. The lymphatic vasculature includes lymph capillaries and lymphatic vessels.

The overall design of the blood and lymphatic vessels is similar except that lumenal diameter, wall thickness, and the presence of other anatomic features such as valves will vary between the different segments of the system. The lumenal surface of all vessels is lined by longitudinally aligned endothelial cells lying over a basal lamina. Vascular walls are divided into three layers: intima, media, and adventitia. However, some or all of the layers may be absent or thinned in some segments of the vascular system depending on the intravascular pressures. The large elastic arteries such as the aorta have an intimal layer composed of endothelium and subendothelial connective tissue; and a very thick medial layer composed of concentrically arranged layers of smooth muscle cells alternating with fenestrated elastic laminae and small amounts of ground substance. The media are demarcated by the internal and external elastic laminae. The outermost layer, the adventitia, is composed of collagen, elastic fibers, and connective tissue cells with penetrating blood vessels termed the vasa vasorum that supply nutrition to the adventitia and the outer half of the media. In muscular arteries and arterioles the media are largely composed of smooth muscle cells arranged in a circumferential pattern (Figure 9.20).

Arterioles are the smallest arterial channels and are generally recognized as vessels of less than 100 μm in diameter surrounded by one to three layers of smooth muscle cells.

Capillaries are 5–10 μm in diameter and have an endothelium of one of three types: continuous, fenestrated (as in the endocrine glands), and porous (as in renal glomeruli). The endothelium rests on an external lamina surrounded by pericytes. Lesions in the endothelium may require electron microscopy to be visualized.

Veins have thin walls in relation to their lumenal size when compared with arteries where blood pressures are higher (Figure 9.21). The adventitia is the thickest layer. Valves are present to prevent retrograde blood flow away from the heart.

Lymphatic capillaries lack basal laminae. Large lymphatic vessels appear similar to veins with large lumina, thin walls, and intimal valves but will contain lymph, evident as eosinophilic serum protein deposits devoid of erythrocytes, rather than blood as in veins.

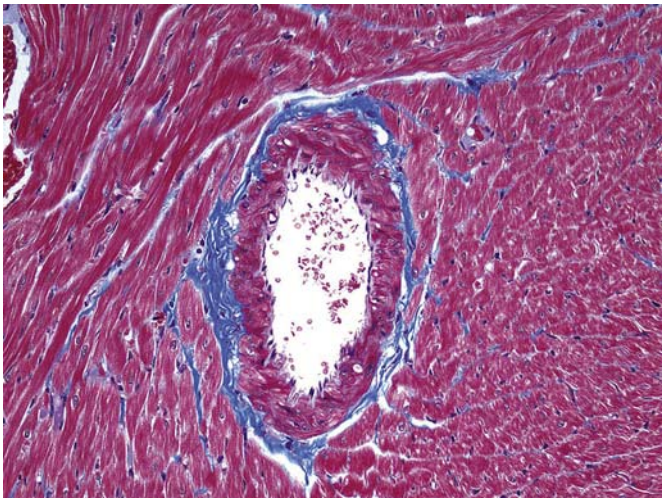

FIGURE 9.20 Cross-section of a coronary artery in a section of myocardium from a rat. The undulating tunica intima lining the luminal surface is surrounded by concentrically arranged smooth muscle cells. Paraffin-embedded, Masson's trichrome stain. Original magnification ×20. Source: *From Haschek, W.M., Rousseaux, C.G., Wallig, M.A. (Eds.), 2013. Handbook of Toxicologic Pathology, third ed. Academic Press, San Diego, CA, Figure 9.18, p. 1618, with permission.*

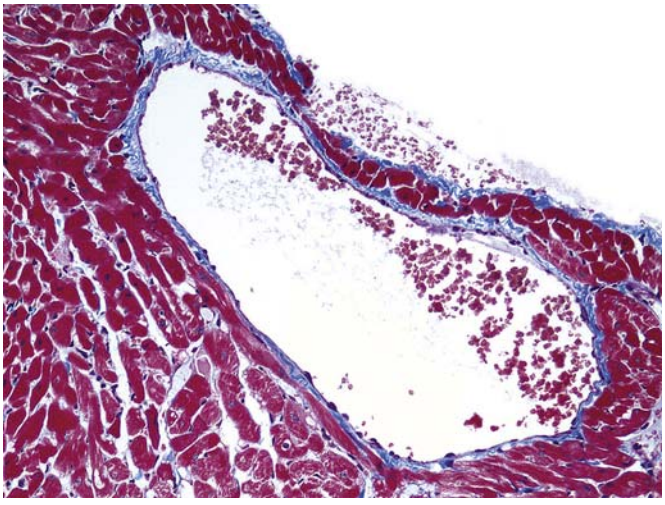

FIGURE 9.21 Section of normal coronary vein from the heart of a rat. Venular walls are thin and lined by endothelial cells along the luminal surface. Paraffin-embedded, Masson's trichrome stain. Original magnification ×20. Source: *From Haschek, W.M., Rousseaux, C.G., Wallig, M.A. (Eds.), 2013. Handbook of Toxicologic Pathology, third ed. Academic Press, San Diego, CA, Figure 9.19, p. 1618, with permission.*

Cellular and Extracellular Components of the Vasculature

Endothelial Cells

Endothelial cells are flattened and measure <3 μm in thickness in their central part, which contains the nucleus and most of the cellular organelles. Peripheral areas are much thinner and contain only a few organelles. The lumenal surfaces are covered with a thin glycocalyx that is demonstrable only by special staining procedures such as cationic ferritin and peroxidase-coupled lectins. Microvilli and filopodia extend from the endothelial surface into the vascular lumen. The numbers of these structures vary considerably from one region to another. The ablumenal surfaces are invested by a well-defined external lamina, rich in types III and IV collagen. In addition to the usual organelles, the cytoplasm of endothelial cells contains transport vesicles, mitochondria, free ribosomes, cisterns of rough endoplasmic reticulum, the Golgi complex, lysosomes, multivesicular bodies, glycogen particles, cytoskeletal filaments (which may be arranged in bundles), microtubules (which are arranged parallel to the longitudinal axis of the vessel), and Weibel–Palade bodies (not present in all species). Weibel–Palade bodies are membrane-bound granules with a dense matrix in which clear tubular spaces 20 nm in diameter are present. These structures constitute qualitatively specific cytological markers for endothelial cells containing the clotting factor Von Willebrand Factor (Factor VIII).

The endothelium comprises a single layer of cells that act as a barrier and a thrombosis-resistant surface. Alteration of this monolayer may provoke changes in transendothelial permeability and initiation of thrombosis. The junctions of endothelial cells also play an important role in maintaining the functional integrity of the vascular surface. They can be disrupted by various pharmacologic agents and other toxicants resulting in leakage of intravascular content. The junctions are also subject to dynamic changes representing another route of transendothelial transport. The patterns of organization of the junctions of endothelial cells differ in arterioles, capillaries, venules, and muscular venules. These differences account for regional variations in endothelial permeability along the microvascular network.

Smooth Muscle Cells

Smooth muscle cells are spindle-shaped and have single elongated nuclei. As in cardiac muscle cells, the configuration of the nuclear membranes in smooth muscle cells changes during contraction and relaxation. Smooth muscle cells contain thin (actin) and thick (myosin) contractile filaments as well as cytoskeletal filaments. The thin filaments are the most conspicuous feature of smooth muscle cells. They fill most of the cytoplasm, are easily demonstrable in electron microscopic preparations, are 4–8 nm thick, and insert into condensations of electron-dense material (dense bodies) located subjacent to the plasma membranes. The external laminae of smooth muscle cells are well developed with transport vesicles numerous along their surfaces.

Pericytes and Veil Cells

Pericytes are perivascular mesenchymal cells that surround capillaries and postcapillary venules. Veil cells are similar cells present in the adventitial layers of large vessels.

Connective Tissue Cells

The connective tissue cells are concentrated in the intima as the subendothelial connective tissue and in the adventitia where, in large vessels, they surround blood vessels, lymphatics, and nerves.

Connective Tissue Fibers and Ground Substance

Elastic fibers allow the resilient rebound of the stretched vessel wall while collagen fibers provide tensile strength to the vessel wall. The elastic fibers may be isolated but are more often arranged in sheets as distinct laminae or layers (internal and external elastic lamina) or as fenestrated lamellae in the walls of elastic arteries. Collagen fibers are scattered in the intima, media, and adventitia. Collagen, mainly type III, is especially abundant in the walls of veins.

The extracellular spaces of the vessel wall contain glycosaminoglycans such as chondroitin sulfate and dermatan sulfate. Arteries contain higher concentrations of ground substance than veins. The ground substance affects permeability across the wall and contributes to the physical properties of the vessel wall.

Physiology and Functional Considerations

Blood Circulation and Tissue Perfusion

The circulatory system of multicellular organisms has evolved to distribute blood through a closed circuit of branching vessels with propulsion provided by the muscular heart (a modified portion of the vascular system) delivering nutrients to and removing cell products and wastes from all the cells of the body. Blood is ejected from the heart during systole into large elastic arteries, the aorta, and pulmonary arteries, under considerable pressure that causes stretching of elastic tissue in the vessel walls. During diastole, elastic recoil occurs and hydrostatic pressure is maintained to allow blood to be conducted into the muscular (distributing) arteries. The potential volume of the circulatory system is considerably greater than the blood volume. To allow distribution to meet the needs of each of the different parts of the body, the muscular arteries and arterioles contract or distend appropriately under the influence of nervous stimulation and autoregulation via local metabolic stimuli. Thus, blood is delivered to the capillary beds in necessary amounts but at low pressure where rapid blood–tissue exchanges occur across the endothelial layer that serves as a thin semipermeable barrier. Blood then enters the venous portion of the circulatory system at low pressure and flows slowly. The veins distend greatly and serve as a blood reservoir; the blood volume in veins is approximately 4–5 times greater than in the corresponding arteries.

Endothelial Permeability

The transvascular exchange of water and solutes represents a large volume of material with net outward movement at the arteriolar end of the capillary and net inflow at the venous end. Most of the exchange occurs by diffusion and less by filtration–absorption processes. Intravascular forces that govern transcapillary exchanges include hydrostatic pressure, osmotic pressure of plasma proteins, and concentration gradients of molecules. Endothelium has a unique, bidirectional permeability to water and solutes provided by a modulating transport system involving vesicles, channels, fenestrae, and diaphragms via transcytosis and endocytosis. The extent of transcapillary exchange may vary greatly among various capillary beds. High permeability occurs across beds with fenestrated or discontinuous endothelia. Low permeability occurs in those with continuous endothelium and unique blood–tissue barriers, as in the brain and eye. Sophisticated studies of endothelial transport mechanisms using various macromolecular tracers have established a complicated regional localization of transport sites over the cell surfaces. For example, fenestrae are primarily associated with permeability to water and solutes while plasmalemmal vesicles and channels are selectively permeable to anionic proteins.

Metabolic Activities in Vascular Cells

The integrity of the endothelium is essential to maintain the normal structure and function of the vessel wall. Exposure of the subendothelial tissues will initiate platelet aggregation and subsequent thrombus formation. In addition to functioning as a semipermeable barrier, the endothelium has a number of metabolic activities that can have both local and systemic ramifications and which vary according to the location in the body. These include a role in hemostasis and thrombosis by production of procoagulant substances (Factor VIII, plasminogen inhibitor) and anticoagulant substances (prostacyclin, plasminogen inhibitor), a role in the modulation of vascular tone (prostacyclin, angiotensin II, nitric oxide, endothelin), a role in the metabolism of vasoactive substances (angiotensin-converting enzyme; enzymatic degradation of norepinephrine, serotonin, and bradykinin); a role in vascular growth and remodeling (transforming growth factor-B, heparin sulfate, glycosaminoglycans, thrombospondin, vascular endothelial growth factor, insulin-like growth

factors), a role in inflammatory and immune reactions (nitric oxide, prostacyclin, complement regulatory factors, cytokines, chemokines, adhesion molecules, selectins), secretion of type III and IV collagen to form basal lamina and production of fibronectin, laminin, elastin, glycosaminoglycans, and blood group antigens A and B. In addition, endothelial cells can secrete matrix-metalloproteinases and their specific tissue inhibitors that regulate the turnover of connective tissue proteins and the remodeling of tissues during normal growth and repair of tissue injury. Endothelial cells are able to contract and possess receptors for compounds such as angiotensin and insulin.

Vascular smooth muscle is similar to the smooth muscle of other organs like the GI tract (the actin and myosin components are not aligned into a striated configuration). Vascular smooth muscle cells are numerous in the media and less numerous in the intima and adventitia. Each cell is surrounded by basal lamina and often attached by gap junctions. These cells are metabolically active and produce various types of collagen (I and III), elastin, and glycosaminoglycans. When stimulated, vascular smooth muscle cells may elaborate growth factors and cytokines, proliferate, migrate, and assume phagocytic activity.

Vascular smooth muscle cells are usually situated circumferentially around blood vessels and vary in numbers depending on vessel type and circulatory location. The presence of these smooth muscle cells in the medial portion of the vascular walls of arteries, arterioles, and veins provides the means by which changes in vessel tone can occur. The normal functioning of vascular smooth muscle is dependent on a variety of physiological influences. As a result, many factors are responsible for the diverse pharmacologic and toxicologic responses observed in different types of vascular smooth muscle.

Vascular Function

Neural Influences Neural control of the vasculature is exerted mainly by the sympathetic division of the autonomic nervous system. Sympathetic fibers innervate most arteries, arterioles, and veins. These are mostly adrenergic fibers although some vessels receive cholinergic sympathetic fibers. Both α and β adrenegic receptors exist in the same vessels and share the same neurotransmitter (norepinephrine). Whether the smooth muscle constricts or dilates depends on the affinity and numbers of the two classes of adrenergic receptors. Muscarinic cholinergic receptors are present on both smooth muscle cells and endothelial cells. Receptors for histamine, serotonin, ATP, and other vasoactive substance are also found in many portions of the vasculature. It has been shown that nerves do not penetrate the entire thickness of blood vessels. In small arteries, innervation is limited to the adventitia while in larger arteries, there are nerve-free regions that include the innermost quarter to half of the smooth muscle layer. As a result, there is a significant difference in sensitivity to all common vasoconstrictor substances between those outer portions of the vessel, which are innervated and the nerve-free inner layer of muscle. Only the inner layer of muscle is sensitive enough to react to circulating levels of vasoconstrictor hormones (norepinephine, epinephrine), whereas the outer portion of the vessels requires high concentrations of norepinephrine released by sympathetic nerves to provoke a response. Muscle and skin vasculature is controlled by sympathetic innervation. In other tissues, the role of blood vessel control by the autonomic nervous system is less clear, but some studies suggest that autonomic nerves may exert control in renal, cerebral, and coronary blood vessels. In certain situations, adjustment of vascular tone by the autonomic nervous system is less important than other control systems or mediators. It appears that a number of vasoconstrictor and vasodilator substances that act directly on vascular smooth muscle cells also exert an indirect action by altering the release of norepinephrine from sympathetic nerves. Endogenous substances that appear to act at specific presynaptic receptors and decrease norepinephrine release include acetylcholine, adenosine, histamine, dopamine, prostaglandins of the E series, and norepinephrine itself. Other endogenous substances such as angiotensin and prostaglandins of the F series potentiate the release of norepinephrine.

Local Humoral and Environmental Influences Blood vessels are capable of both synthesizing and metabolizing vasoactive hormones and as a result are not entirely dependent on circulating substances or neurotransmitters for control of vascular tone. The endothelium is the source of many potent endogenous vasoactive substances including the vasodilator, nitric oxide, and the vasoconstrictor, endothelin-1. Endothelial cells also produce prostacyclin, a substance that causes vasodilation and prevents the adhesion of platelets to the vascular endothelium. In addition, the endothelium may contribute to the local control of vascular tone by secreting other relaxing and contracting factors such as angiotensin II and platelet-derived growth factor (PDGF). Angiotensin II is produced in the lungs and also, to a certain extent, in limb vessels themselves. Regardless of the source, angiotensin II reacts directly with resistance vessels (arterioles) to cause vasoconstriction. PDGF, in addition to its mitogenic properties, also acts as a smooth muscle contractile agonist. It is likely that local metabolites (e.g., potassium, ATP, adenosine, oxygen, carbon dioxide) are also available to act on the vascular smooth muscle.

Responses of Blood Vessels to Vasoactive Substances Blood vessels of different types and from

different areas do not react uniformly to the presence of certain drugs and other xenobiotics. Norepinephrine induces uniform contraction of all types of blood vessels but angiotensin exerts more constrictor activity in the resistance vessels than in the veins. Ergot alkaloids, at low doses, demonstrate preferential constrictor activity in veins with little increase in resistance vessel tone. A selectivity of action is also seen with xenobiotics that dilate vessels. Hydralazine mainly relaxes resistance vessels, while glyceryl trinitrate preferentially exerts this action on veins.

Electrical Activity and Intracellular Calcium Responses to Vasoactive Substances Heterogeneity in smooth muscle responses resulting from exposure to xenobiotics relates in part to the varying patterns of cellular electrical activity and to the variety of mechanisms that are involved in the control of the cytoplasmic concentration of calcium. Smooth muscle cells are characterized by a low resting membrane potential (−40 to −60 mV). The action potential of vascular smooth muscle is mainly driven by an inward flux of calcium ions. Excitation spikes can be detected as calcium enters the cell and the membrane potential becomes more positive. Some types of smooth muscle display phasic activity, an effect which is associated with the generation of spike action potentials. Calcium is also critical to the contractile process. The SR appears to be the major cellular compartment for calcium storage; both contraction and relaxation are influenced by the levels of calcium in the cytoplasm. Critical levels of cytoplasmic calcium are achieved by entrance through voltage-dependent membrane channels and through release of the cation from intracellular storage sites. Spontaneous contractile activity resulting from calcium entry in this manner is not present in all smooth muscle; some types develop sustained contractions only in response to agonists such as norepinephrine and angiotensin. Agents that stimulate contraction have the potential to produce greater depolarization and to increase the frequency of spike potentials. However, vascular contractile activity can be induced without membrane depolarization and in these instances alterations in membrane permeability are important. Vascular contraction as a result of changes in membrane permeability appears to involve the movement of calcium through a receptor-mediated channel and the subsequent release of additional calcium from intracellular stores. Varying combinations of phasic and sustained contraction are found in the smooth muscle cells from different types of vessels. It has been suggested that entrance of calcium through channels may have limited importance and that agonist-induced contraction may depend entirely on release of calcium from intracellular storage sites. Dependence of the contractile response on calcium influx appears to vary considerably at different points along the vascular tree. The dependence is least in the aorta where contractile responses appear to rely almost entirely on the release of calcium from intracellular storage sites. In contrast, calcium influx is essential for contraction of small resistance arteries. Differences in pharmacologic and toxicologic responses are thought to be related to the varying intrinsic smooth muscle properties found in vessels of different types. The primary action of calcium antagonists such as verapamil and nifedipine on resistance vessels may be related to the greater importance of phasic activity associated with entry of calcium through voltage-dependent calcium channels. In contrast, the preferential action of sodium nitroprusside in veins is an indication of the importance of the receptor-operated sustained contraction mechanism.

Effects of Endothelial Cell Function and Damage on Blood Vessel Activity Vascular endothelial cells serve as a protective barrier in blood vessel walls and serve as an active source for the synthesis, metabolism, uptake, storage, and degradation of a number of vasoactive substances. Endothelial cell damage can be a factor in diseases that affect the vasculature. Endothelial cells from certain arteries and veins seem to be directly involved in the decrease of vascular tone noted in these vessels as a result of exposure to naturally occurring vasodilator substances such as acetylcholine, bradykinin, arachidonic acid, substance P, and ATP. When endothelial cells are destroyed, the vessels lose the ability to relax on exposure to most of these dilator substances. In addition, the loss of functional endothelial cells seems to transform normal vasodilator responses into potent vasoconstrictor activity. A substance that damages or destroys endothelial cells to the extent that vasodilatory responses are altered could conceivably cause significant decreases in blood flow and subsequent tissue damage in certain organs.

Evaluation of Vasotoxic Effects

Xenobiotic-induced vascular dysfunction or injury may be systemic or localized to a particular organ or vascular bed. Effects may also be seen at varying levels of the vascular hierarchy (e.g., arteries, veins, capillaries). Studies of vascular function and structure have been done using a variety of *in vivo* and *in vitro* methods.

Physiologic Methods for Testing

Blood Flow Measurements Measurement of blood flow can be done with electromagnetic or ultrasonic Doppler flow meters. These devices are able to detect flow through the walls of intact blood vessels avoiding

the artifact of interrupted flow. In addition, the probes can be chronically implanted so measurements can be made continuously or over long periods of time without the interference of anesthetics. The electromagnetic flow meter and the Doppler ultrasonic techniques provide moment-to-moment phasic flow information. This type of information is important in situations where the vascular effects of a substance either are transient or where changes occur over a period of time. These techniques have been used successfully in monitoring blood flows from large arteries such as the aorta as well as from smaller vessels such as the renal, mesenteric, femoral, carotid, and coronary arteries.

Dilution Methods Measurements of organ perfusion can be made with the aid of dilution methods utilizing the Fick principle. All methods use an indicator substance that may be an inert gas, a natural metabolite, a nondiffusable dye, or a radioactive tracer. The indicator substance is injected into the blood and its concentration measured by an appropriate detector at a downstream sampling site. The indicator dilution method is useful for the measurement of mean organ blood flow if the indicators used are removed from the blood by these organs. For example, the liver removes bromsulfalein and the kidneys remove *p*-aminohippurate while the brain and heart absorb nitrous oxide.

Direct Measurement of Blood Flow Direct *in vivo* measurement of blood flow is possible by using a semiisolated dog biceps muscle preparation. The advantage of this preparation is that the principle components (muscle, blood vessels, and nerve) are all part of a single system. A nearly identical type of biceps muscle preparation uses the cat as the experimental model. Measurement of blood flow and vascular reactivity in these preparations are most reliable under normal flow conditions. A cat hindlimb preparation was developed for situations where blood flow is low. This preparation allows monitoring of the effects of vasoactive substances on the resistance and capacitance vessels at times when the circulation to the area is compromised. Perfusion of isolated hindlimb preparations at a constant rate allows a means of detecting substance-induced alterations in vascular resistance.

Angiography Alterations in vascular tone can be detected when a suitable contrast medium is injected into a vessel and the vessel or associated organ imaged with radiography, CT, or MRI. This technique has allowed identification of substances that possess vasoactive effects. However, it is not possible to determine whether this activity is due to a direct or indirect effect on the vascular smooth muscle.

Direct Observations of Blood Vessels Direct microscopic observations of microvascular beds can be achieved in easily transilluminated thin membranes. Studies of this type are usually limited to acute experiments in anesthetized animal preparations such as the hamster cheek pouch, the rat and mouse ear, or mesenteric beds. A transparent chamber for use in the rabbit ear considerably lengthens the period for direct observation of substance effects on blood vessels in unanesthetized animals. This technique allows measurement of changes in vessel wall thickness, lumen diameter, and total vessel diameter in both isolated tissues and the intact vascular beds.

In Vitro Methods for Detecting Vascular Toxicity

Mechanistic insights into a particular vascular effect may be aided by studies in an isolated system rather than on the entire vascular bed. *Ex vivo* and *in vivo* rat mesenteric preparations have been used in vascular studies. Though *in vitro* preparations allow a more controlled analysis of the potential toxic vascular effects, results obtained from isolated or even perfused tissues do not always completely represent the action of the xenobiotic on the vasculature in the intact organism, particularly if cellular components of the blood are involved in the activity of the substance.

Isolated Vascular Muscle Strip *In vitro* studies can be conducted on strips obtained from large arteries of laboratory animals such as rabbits and rats. The method involves suspending spiral cut strips of vessels, usually aorta, in a physiological solution. The arterial strip preparation makes it possible to study changes induced in the tone of vascular smooth muscle due to xenobiotics added to the bathing solution. Information concerning the action of substances on microscopic resistance and capacitance vessels has also been obtained from isolated strip preparations. Direct effects of substances on veins can also be detected in isolated venous strip preparations.

Isolated Preparations for Determining Endothelial-Dependent Vascular Responses The use of *in vitro* strip preparations has also provided a means for determining the extent to which endothelial-dependent responses are responsible for the activity of vasoactive xenobiotics. Rings of vascular smooth muscle, with and without endothelium, are usually examined in a parallel system so the activity of vasoactive substances can be compared. The endothelial cells are removed from the intimal surface of the blood vessel by gently rubbing with a small forceps. Substances have been identified, which interfere with the production, release, or action of endothelium-derived relaxing factors. The potential role of endothelial cells in vascular activity can also be assessed in a perfused preparation that uses a blood vessel ring without endothelial cells. The perfusion of the vessel ring occurs via a steel cannula or through blood vessels with or without endothelial

cells. Agents causing the release of vasoactive substances from endothelial cells can be identified by means of this type of bioassay technique.

Cellular Electrophysiological Methods Vascular effects of some xenobiotics may be mediated by changes in smooth muscle membrane potential, action potential, or contractile activity. Use of an intracellular microelectrode (micropuncture studies) can determine the transmembrane potential and whether a substance causes changes in membrane potential. Micropuncture studies can also be used to determine cell membrane resistance. This type of information can be obtained by applying a known current through the electrode and subsequently measuring the voltage change after the resistance of the electrode itself has balanced out. Any changes in the resistance following exposure to vasoactive substances are indicative of alterations in membrane permeability. Intracellular microelectrode techniques can be used for examining the effect of substances on the relationship between electrical and mechanical activities. Information obtained from this preparation is useful only if the membrane response of the impaled cell represents a uniform single-unit behavior.

Cultured Vascular Smooth Muscle Cells Methods similar to those described for cultured cardiac muscle cells have produced cultured reaggregates of endothelial and spontaneously contracting vascular smooth muscle cells. The cells for these cultures are obtained from arteries and veins isolated from 10 to 20-day-old chicken embryos. Other sources of cultured smooth muscle cells have been the rat or rabbit aorta, guinea pig vas deferens, and canine coronary artery. Reaggregated cells have been maintained in primary cultures for a number of weeks and these cells retain both electrical and mechanical properties resembling those of smooth muscle cells from intact adult blood vessels. These cultured cell preparations can be used to examine the electrophysiological and toxicological effects of substances acting directly on endothelial cells and noninnervated vascular smooth muscle cells. However, a major disadvantage to use of these cells is that they are much more difficult to propagate than are cultured heart cells.

Morphologic Evaluation

Gross Examination At necropsy, large vessels, including the large elastic arteries and great veins near the heart, can be examined grossly. Longitudinal incision will expose the intimal surface for inspection and may allow detection of degenerative lesions of the walls that may be accompanied by mineralization, fibrosis, or lipid deposition. Other grossly apparent lesions include aneurysms, thrombosis, and vascular rupture. Indirect evidence of vascular disease may be suggested by hemorrhage or infarction. However, many vascular lesions will not be detectable by gross examination. Intravenous injection of Monastral blue, Evan's blue, or horseradish peroxidase prior to necropsy can be utilized to detect sites of compromised vascular permeability. Subsequent screening of these sites by microscopic evaluation can determine the extent and type of injury.

Microscopic and Biochemical Evaluation The evaluation procedures described for the heart may also be used for study of blood vessels and include light microscopy, electron microscopy, and biochemical analysis. Light microscopic study should include use of special staining procedures for elastic fibers (Verhoeff's elastica), collagen (Masson's trichrome, Movat's pentachrome), and mucopolysaccharides (periodic acid-Schiff). Lipid stains on frozen sections are essential for lipid-containing lesions. Immunohistochemical methods can be used for both light and electron microscopic study. Scanning electron microscopy is especially suited for morphologic evaluation of lesions of the lumenal surface.

Response to Injury

Vascular injuries may be primary or secondary. Secondary lesions develop as an extension of a disease process in surrounding tissues. However, primary vascular diseases are the most frequent type and the lesions may be generalized or regional in distribution. Arteries, the high pressure segment of the circulatory system, tend to develop significant alterations more frequently than veins, capillaries, and lymphatics. The spectrum of pathologic alterations observed includes (1) degenerative conditions with accumulations of lipid, mineral deposits, or fibrous connective tissue; (2) degeneration or necrosis of vascular smooth muscle; (3) proliferative lesions of the intima, media, or endothelial basal lamina; and (4) immune-mediated inflammation (Figure 9.22). The etiology of any of these vascular injuries is multifactorial and often in part due to aging. Many of these disorders have a slow progressive course and do not become clinically apparent until a secondary event such as thrombosis and subsequent ischemic injury occurs. However, some of the vascular diseases that are initiated by toxic injury, infectious agents, or immunologically mediated mechanisms develop rapidly and may produce widespread lesions.

Atherosclerosis Accelerated by Toxic Agents

There is epidemiologic evidence in human patients and direct evidence from studies on animal models of atherosclerosis that exposure to certain chemical agents along with the presence of atherogenic risk factors

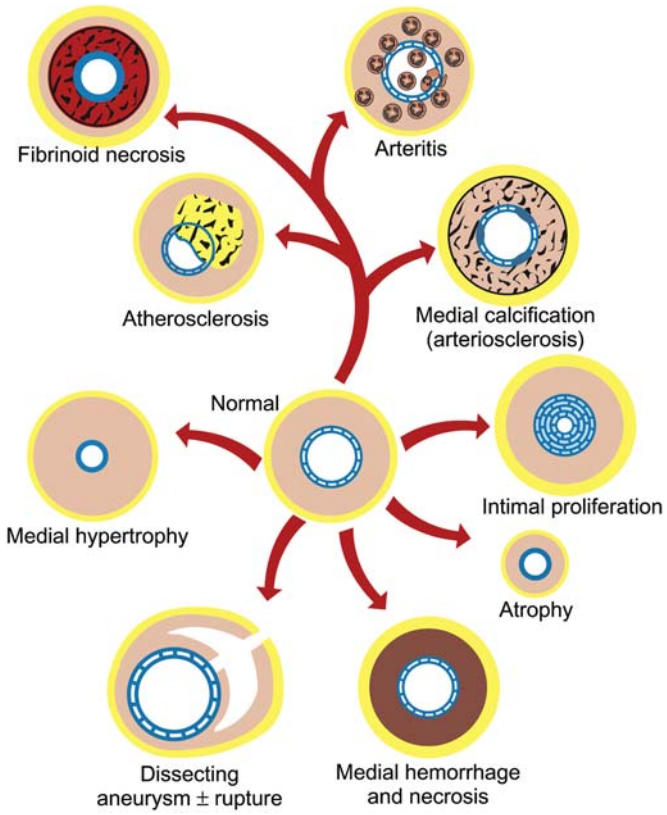

FIGURE 9.22 Schematic diagram of major arterial injuries. Source: *Redrawn with permission from School of Veterinary Medicine, Purdue University. From Van Vleet, J.F., Ferrans, F.J., 2007. Cardiovascular system. In: McGavin, M., Zachary, J.F. (Eds.), Pathologic Basis of Veterinary Disease, fourth ed. Mosby Elsevier, St. Louis, MO, Figure 10.106, p. 608.*

may enhance the development of atherosclerosis. Chemical substances that have been incriminated include goitrogenic agents, carbon disulfide, benz[*a*]pyrene, dimethylbenz[*a*]anthracene, homocysteine, carbon monoxide, fluorocarbons, oral contraceptives (especially those containing mainly progestins), combined hydrochlorothiazide and propranolol therapy, calcium, lead, and soft water.

The lesions and sequelae of atherosclerosis are well described. The vessels with the most severe alterations tend to be the muscular and elastic arteries. The pig, rabbit, and chicken are more susceptible to lesion development than the dog, cat, cow, or rat. The initial lesions are fatty streaks (intimal aggregations of foam cells with vacuolated cytoplasm derived from both macrophages and smooth muscle cells), which are most readily detected grossly by application of fat stains such as Sudan IV. The hallmark lesion is the raised intimal atheromatous plaque. The plaque is composed of lipid deposits together with cells (smooth muscle cells, monocytes/macrophages, and a few lymphocytes) and connective tissue fibers and matrix. Atherosclerotic lesions may evolve over time into complicated plaques.

Air pollutants are another class of toxicants with well-recognized potential for exacerbating preexisting CV disease. Air pollution has a strong epidemiologic correlation with increased rates of CV morbidity and mortality. Air pollutants are a heterogeneous mix of particulate and nonparticulate (predominately gases) and organic and inorganic materials of varying size. The smaller particulate components ($\leq$2.5 μm diameter) are thought to be primary mediators of systemic endothelial injury, oxidative stress, and inflammation. Though electrocardiographic abnormalities are possible, vascular effects are likely most important with increased risk of thrombosis, changes in physiologic vasoactivity, and increase in the severity of atherosclerotic plaques.

Medial Proliferation

Hyperplasia and hypertrophy of smooth muscle cells in small muscular arteries and arterioles may result from hypertension or exposure to ergot alkaloids and pyrrolizidine alkaloids. The chronic vasoconstrictor action of the ergot compounds is the basis for their induction of proliferative lesions. In cattle with ergotism and fescue toxicity, the distinctive clinical feature is ischemic necrosis or dry gangrene of the extremities including the tail, limbs, ears, and nose. These signs are usually present within 10–14 days of exposure to fescue pasture. The ergot alkaloids are produced by *Claviceps purpurea*, a fungus that infects rye and other grains and grasses. Tall fescue (*Festuca arundinacea*) parasitized by endophytic fungi such as *Neotyphodium coenophialum* (previously *Epichloe typhina*, *Acremonium coenophialum*) will also produce ergot alkaloids. Arterioles in the ischemic tissue of the extremities will have prominent medial thickening due to proliferated smooth muscle cells and may also have fibromuscular intimal proliferation.

Intimal Proliferation

Intimal proliferative lesions of arteries (influx and proliferation of smooth muscle cells, glycosaminoglycan production, and endothelial hypertrophy) have been observed with use of estrogen- or progesterone-containing oral contraceptives in women, chronic administration of ergotamine and methylsergide maleate in human patients, talc or magnesium silicate exposure in intravenous drug users, and administration of allylamine or phosphodiesterase inhibitors to rats. The intimal lesions produced by ergotamine and methylsergide maleate are primarily fibroblastic in elastic and large muscular arteries but involve fibromuscular hyperplasia in medium and small arteries; similar

fibrotic lesions may also occur in cardiac valves and endocardium of affected patients. The pathogenesis of the intimal proliferative lesions is not clear but it is suggested that these agents directly stimulate fibroblastic proliferation or act indirectly via serotonin mediation of the proliferative response.

Calcification

Arterial medial calcification is a frequent lesion in animals. The vascular lesions may involve both elastic and muscular arteries and often occur concurrently with endocardial mineralization. The toxic etiologies for arterial calcification include calcinogenic plant and vitamin D toxicoses. Vitamin D toxicosis may occur acutely as it does in dogs that consume cholecalciferol-containing rodenticides or from chronic ingestion of food containing excess vitamin D fortification. Affected arteries appear grossly as solid dense pipe-like structures or as raised white solid intimal plaques. Microscopically, prominent basophilic granular mineral deposits are present either on elastic fibers of the media of elastic arteries or as a complete ring of mineralization involving the internal elastic lamina and the medial musculature of muscular arteries (Figure 9.23).

The calcinogenic plants (*Cestrum diurnum*, *Trisetum flavescens*, *Solanum malacoxylon*, *Solanum torvum*) contain the active metabolite of vitamin D3 (1,25-dihydroxycholecalciferol) or its glycoside. Different names have been given to these plant-induced syndromes in various areas of the world including "Manchester wasting disease" in Jamaica, "enzootic calcinosis" in Europe, "naahelu disease" in Hawaii, "enteque seco" in Argentina, and "espichamento" in Brazil.

Aneurysms

Localized weakening of the wall of large elastic arteries results in formation of aneurysms. The lesion is produced by administration of *Lathyrus* sp. (termed lathyrism), β-aminoproprionitrile (the active principle of *Lathyrus* sp.), penicillamine or aminoacetonitrile (copper chelators), and copper deficiency. Dissecting aneurysms of the aorta are produced in turkeys fed β-aminoproprionitrile. The mechanisms of lesion production by these compounds is inhibition of lysyl oxidase, a copper-containing enzyme involved in cross-linking of collagen and elastin, which are essential ingredients for normal strength of the walls of elastic arteries.

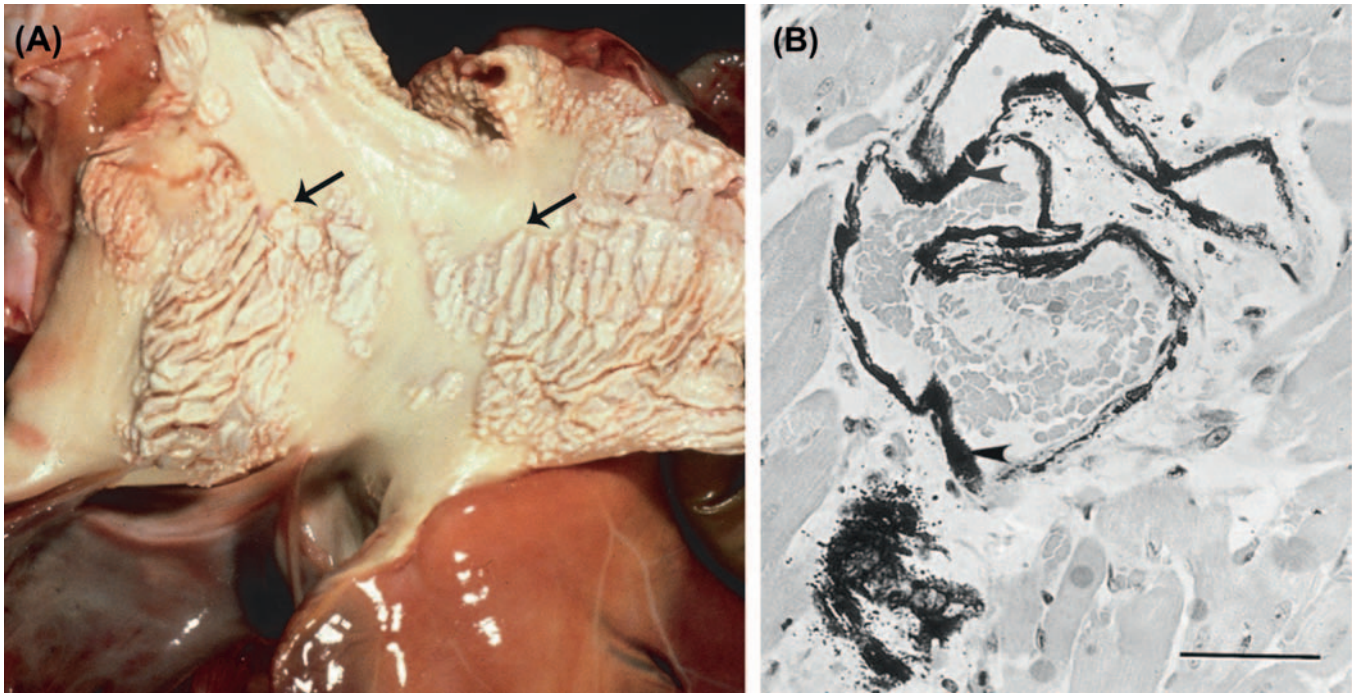

FIGURE 9.23 (A) Aortic mineralization in a calf. The surface of the aorta has raised plaque-like lesions due to mineralization; the heart is present below the aorta. (B) Medial calcification (*arrowheads*) and focal myocyte calcification (bottom left) in the ventricular myocardium of a rat with acute vitamin D toxicosis. Paraffin-embedded, von Kossa stain. Bar = 100 μm. Source: *(A) From Haschek, W.M., Rousseaux, C.G., Wallig, M.A. (Eds.), 2010. Fundamentals of Toxicologic Pathology, second ed. Academic Press, San Diego, CA, Figure 12.19A, p. 361. (B) From Haschek, W.M., Rousseaux, C.G., Wallig, M.A. (Eds.), 2002. Handbook of Toxicologic Pathology, second ed. Academic Press, San Diego, CA, Figure 9.21, p. 421, with permission.*

Medial Hemorrhagic Necrosis

Arterial lesions with necrosis of medial smooth muscle and medial hemorrhage have been observed following treatment with a variety of vasoactive substances. The vascular injury may be severe enough to be accompanied by hemorrhage in adjacent tissues as is the case with minoxidil where lesions in atrial arteries may be accompanied by grossly observable hemorrhage. Vasodilating drugs tend to be overrepresented as causes of medial arterial necrosis, can be demonstrated experimentally in a number of species and may have varying anatomic sites of predilection. Right atrial lesions are common in dogs and mesenteric arteries are a common site in rodents but lesions may also be seen in ventricular, hepatic, and renal arteries. Vascular injury may be accompanied by myocardial injury, which is likely due, in part, to the hemodynamic changes associated with vasoactivity (e.g., reflex tachycardia, decreased coronary perfusion).

Fibrinoid Necrosis

Accumulation of serum proteins and polymerized fibrin in the wall of small arteries following endothelial damage results in a distinctive eosinophilic homogenous appearance of the media of the affected vessels (Figure 9.24). This lesion has been described in cerebral vessels of pigs and guinea pigs with organic mercury toxicosis, and in those of nonhuman primates and dogs with lead toxicosis.

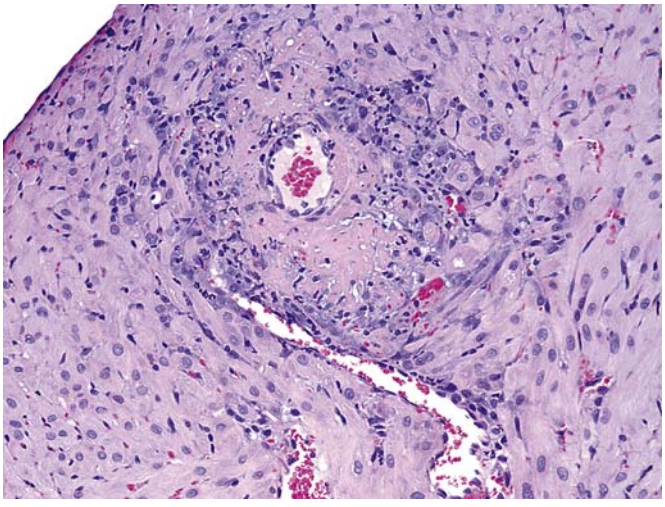

FIGURE 9.24 Fibrinoid necrosis of a coronary artery in a rat given a VEGF inhibitor. The wall of the artery is replaced by homogeneous pink material representing fibrin and plasma proteins that extend into the periarterial tissues. Paraffin embedded. Hematoxylin and eosin stain. Original magnification ×20. Source: *From Haschek, W.M., Rousseaux, C.G., Wallig, M.A. (Eds.), 2013. Handbook of Toxicologic Pathology, third ed. Academic Press, San Diego, CA, Figure 9.24, p. 1631, with permission.*

Fibrinoid necrosis of small veins was considered the primary lesion in horses with phenylbutazone toxicosis. This appeared to be the basis for renal medullary necrosis and oral and GI ulceration. The loss of endothelial cells and formation of thrombi may also occur.

Microangiopathy

Xenobiotic-induced injury may also occur in microcirculatory vessels, where the endothelium is the likely cellular target. Cadmium administration to rats results in hemorrhagic testicular necrosis due to selective damage to testicular capillary endothelium. Microthrombosis and hemorrhage have been produced in the heart by administration of cyclophosphamide.

Immune-Mediated Vascular Inflammation

Vascular injury is often accompanied by inflammatory cell infiltrations as a response to primary injury to smooth muscle or endothelial cells. But, vascular inflammation (vasculitis) may also be a primary process induced by some drugs. Vascular inflammatory lesions associated with drugs are associated with drug-induced hypersensitivity reactions and lupus-like syndromes. Drug-induced vascular inflammation usually affects all three layers of mainly small-sized vessels. Medium-sized muscular arteries are occasionally involved, but large arteries and veins are usually not targets of drug-induced vasculitis.

Hypersensitivity Vasculitis This condition commonly includes the vascular lesions associated with serum sickness, systemic bacterial infections, protozoal infections, reactions to influenza vaccines, and drug-related vasculitides. The lesions are characterized by a predominantly mononuclear leukocytic infiltrate with occasional eosinophils, in the absence of fibrinoid necrosis or necrotizing lesions of the vessel wall. The endothelial lining of involved arterial and venous channels is intact and free of thrombi.

A variety of drugs have been found to induce an immune-mediated vascular injury (ampicillin, procainamide, dextran, hydralazine, penicillin, sulfonamide, tetracycline, propylthiouracil, quinidine, allopurinol, phenylbutazone). This type of drug-induced vasculitis is neither dose- nor time-dependent. The lack of a dose-dependent response and the clinical presentation suggest that this form of drug-related vasculitis is a delayed hypersensitivity phenomenon.

Lupus-Like Syndromes Considerable evidence now exists that drug-induced lupus erythematosus occurs, not in a random population that develops drug hypersensitivity, but among individuals with an intrinsic tendency to the syndrome. The mechanism by which these drugs cause or unmask the lupus-like syndrome is unknown. It is suggested that the drug either modifies nucleoprotein antigenicity or reinforces the

antigenicity of circulating DNA, which is normally present in small amounts.

Regeneration and Repair

The consequences of vascular injury are multiple. Most injuries will heal by repair with fibrosis rather than by regeneration to restore normal structure to the affected vessel. Vascular endothelial cells are an exception to this generalization. When the affected area of the vessel is small, the endothelium is repaired by spreading and migration of neighboring endothelial cells. If lesions are extensive, cell proliferation is also required in addition to cell migration to replace irreversible damaged cells and reestablish the continuity of the endothelium. However, residual damage often follows vascular injuries. Damage to the endothelial layer and the other layers of arterial walls may initiate thrombosis with subsequent regional ischemic injury of the organ in the circulatory field. Other injuries may result in damage to the vessel wall with dilatation and potential rupture of the vessel. Some healed lesions will result in only minor structural and functional alterations of the affected vessels and will be detected only as incidental lesions by microscopic study.

Mechanisms of Toxicity

Vasoactive xenobiotics that reach systemic circulation are widely distributed throughout the vascular tree and are therefore capable of system-wide activity. However, rapid metabolism, such as that of acetycholine in the blood, or effective removal, such as that of the prostaglandins in the lung, can lead to limitations of the effects of these substances. Likewise, if a significant amount of a xenobiotic is bound to plasma albumin, as occurs with diazoxide, the concentration of the substance reaching the vessel will be less than expected.

Exposure to certain chemical substances can initiate degenerative or inflammatory alterations in vascular smooth muscle. These toxic effects could occur as a result of excessive pharmacologic activity or by direct reaction of xenobiotics with structural or functional macromolecules in the vascular wall. Ergotamine intoxication leads to sustained arterial vasoconstriction. With continued exposure, ergotamine induces occlusive vascular lesions such as intimal proliferation, medial hypertrophy, and hyalinization in some peripheral vessels. Vascular toxicity can also be demonstrated with allylamine. Fibromuscular intimal proliferation in small- and medium-sized arteries (such as coronary arteries) occurs in rats given this agent. Metabolism of allylamine yields acrolein, a substance that is capable of denaturing protein and disrupting nucleic acid synthesis. This metabolite is thought to be responsible for other more subtle changes such as medial hypertrophy and proliferation of vascular smooth muscle. Acetylsalicylic acid given to rats produces early alterations in the basement membrane of the endothelial cells of capillaries and postcapillary venules. These changes subsequently may cause small vessel damage in the gastric mucosa. Under certain conditions, sympathomimetic agents are capable of eliciting toxic effects on arterial vasculature. For example, subintimal alterations (medial smooth muscle cell necrosis and calcification) in large- and medium-sized arteries have been induced following administration of large doses of norepinephrine. These effects could be due to the excessive stimulation of adrenergic receptors.

Morphologic changes of considerable importance are induced by drugs or chemicals that modify atherosclerotic lesions, either by changes in plasma lipids and lipoproteins or by more direct effects on vascular walls. Carbon monoxide increases capillary permeability and hastens plaque formation in animals fed high cholesterol diets. The effect of carbon monoxide might also be due to decreased availability of oxygen, since plaque formation is also accelerated in animals exposed to hypoxic conditions. Excessive amounts of homocysteine have been implicated in the pathogenesis of thrombotic and arteriosclerotic vascular disease. Homocysteine can react directly with nitric oxide to form highly reactive S-nitroso-thiol compounds that may mediate potentially harmful secondary biochemical effects. Homocysteine appears to induce a sequence of alterations, which includes platelet adhesion, smooth muscle cell proliferation, formation of foam cells, and ultimately loss of the endothelial layer at the site of atherogenic lesions. Vascular changes are also associated with exposure to carbon disulfide. Long-term exposure of industrial workers has been associated with a two- to threefold increase in coronary heart disease. Carbon disulfide has been shown to accelerate the development of atherosclerosis in rabbits maintained on a high cholesterol diet. There are at least two mechanisms by which carbon disulfide might enhance the formation of atherogenic lesions in blood vessels: direct injury to the endothelium and induction of hypothyroidism with resulting alterations in lipid metabolism. Thiocarbamide, a potent antithyroid substance, is the principal urinary metabolite detected after exposure to carbon disulfide and may be responsible for the carbon-disulfide-mediated suppression of thyroid glandular activity.

Other toxic substances such as penicillamine and β-aminoproprionitrile can cause vascular alterations by inducing changes in connective tissue, an effect which ultimately results in the formation of nonatherosclerotic aneurysms in the aorta and other large arterial

TABLE 9.3 Drugs Associated with Vascular Injury

Drug	Pharmacology	Vascular effect
Vasopressin	Antidiuretic hormone	Vasoconstriction
5-Hydroxytryptamine	Serotonin receptor agonist	Vasoconstriction
Epinephrine	α and β adrenergic receptor agonist	Vasoconstriction
Yohimbine	α2 adrenergic receptor antagonist	Vasoconstriction
Amphetamine	α and β adrenergic receptor agonist	Vasoconstriction
Minoxidil	K + channel opener	Vasodilation
Nitroprusside	cGMP agonist	Vasodilation
SB-217242	Endothelin receptor antagonist	Vasodilation
Fenoldopam	DA1 selective agonist	Vasodilation
Prazosin	α1 adrenergic receptor antagonist	Vasodilation
SKF-95654	PDE3 inhibitor	Vasodilation
GSK-157007	PDE4 inhibitor	Vasodilation
Hyrdralazine	NO inducer	Vasodilation
Colchicine	Tubulin inhibitor	Endothelial cell cycle arrest
Vincristine	Tubular inhibitor	Endothelial cell cycle arrest
Cyclophosphamide	Alkylating agent	Endothelial DNA intercalation/cross-linking
Monocrotaline	Alkylating agent	Endothelial DNA intercalation/cross-linking, vasoconstriction
Penicillin	Antibiotic	Hypersensitivity reaction
Sulfonamide	Antibiotic	Hypersensitivity reaction

vessels. These agents apparently inhibit specific steps in the connective tissue protein biosynthetic pathway. Chromium seems to have a significant role in maintaining the integrity of the vasculature. Serum cholesterol levels are elevated and the incidence of atherosclerotic plaques increases when chromium is deficient.

Aside from direct toxicity, immune-mediated vasculitis can result from exposure to sensitizing compounds, which act as haptens, presumably combining with the host's own proteins and inducing formation of appropriate antibodies. Usually, only small vessels (arterioles, venules, and capillaries) are affected, but in some instances the coronary arteries can also develop lesions. Predominant components involved in the inflammatory reaction include eosinophils and mononuclear cells. The induction of vasculitis is not dose- or time-dependent and appears related to the deposition of soluble immune complexes in the vessel wall and to the activation of the complement system. Penicillin, sulfonamides, methyldopa, procainamide, quinidine, and a number of other drugs and chemicals have been implicated in causing this type of reaction in humans.

Table 9.3 summarizes a selection of drugs of varying pharmacologic activity recognized to cause vascular injury either experimentally or in human patients (e.g., hypersensitivity reactions).

SUMMARY

Cardiovascular toxicity is an important environmental and drug development public health concern. The significant physiologic adaptability of the CV system, variability in presentation, and high incidence of predisposing natural disease can make it very difficult to detect xenobiotic injuries. Accordingly, a thorough understanding of these features and a holistic approach to assessment is critical. Though the presentations and pathogeneses for an ever expanding portfolio of cardiac and vascular toxicants are described, their mechanisms of action are still often unknown. This chapter aimed to provide a general overview and introduction to the subject. Further study is encouraged for deeper and contemporary understanding of specific toxic injuries and rapidly developing approaches to their assessment.

Further Reading

Berridge, B.R., Mowat, V., Nagai, H., Nyska, A., Okazaki, Y., Clements, P.J., et al., 2016. Non proliferative and proliferative lesions of the cardiovascular system of the rat and mouse. J. Toxicol. Pathol. 29 (3 Suppl), 1S–47S.

Berridge, B.R., Van Vleet, J.F., Herman, E., 2013. Cardiac, vascular, and skeletal muscle systems. In: Haschek, W.M., Rousseaux, C.G., Wallig, M.A. (Eds.), Haschek and Rousseaux's Handbook of Toxicologic Pathology. Elsevier, Inc., Academic Press, San Diego, CA, pp. 1567–1665.

Bers, D.M., 2002. Cardiac excitation-contraction coupling. Nature 415 (6868), 198–205.

Bishop, S.P., 1999. Necropsy techniques for the heart and great vessels. In: Fox, P., Sisson, D., Moise, N. (Eds.), Textbook of Canine and Feline Cardiology, second ed. Saunders, Philadelphia, PA.

Ferri, N., Siegl, P., Corsini, A., Herrmann, J., Lerman, A., Benghozi, R., 2013. Drug attrition during preclinical and clinical development: understanding and managing drug-induced cardiotoxicity. Pharm. Ther. 138, 470–484.

Lenneman, C.G., Sawyer, D.B., 2016. Cardio-oncology: an update on cardiotoxicity of cancer-related treatments. Circ. Res. 118, 1008–1020.

Mills, N.L., Donaldson, K., Hadoke, P.W., Boon, N.A., MacNee, W., Cassee, F.R., et al., 2009. Adverse cardiovascular effects of air pollution. Nat. Clin. Pract. Cardiovasc. Med. 6, 36–44.

Morton, D., Houle, C.D., Tomlinson, L., 2014. Perspectives on drug-induced vascular injury. Toxicol. Pathol. 42, 633–634.

CHAPTER

10

Skeletal Muscle System

Brian R. Berridge[1], *Brad Bolon*[2], *and Eugene Herman*[3]

[1]GlaxoSmithKline Research & Development, King of Prussia, PA, United States [2]GEMpath, Inc., Longmont, CO, United States [3]National Cancer Institute, Bethesda, MD, United States

OUTLINE

Skeletal muscle is a unique tissue with the role of support and movement of the body. The mass of the skeletal musculature is large, and constitutes 40%–50% of the total body weight. Recognition of gross pathologic alterations in muscular diseases is complicated by the normal variation in color and consistency observed among the muscles of various animal species and animals of differing ages. Detailed study of the skeletal musculature during routine necropsies generally is not performed. In fact, prosectors often overlook examination of the skeletal muscles in their haste to expose and observe the visceral organs.

Skeletal muscle fibers have unique structural features. Each fiber represents a syncytium formed during myogenesis by fusion of hundreds to thousands of individual myoblasts. The fibers are highly specialized, with approximately 80% of their cell volume occupied by contractile elements. Normal function of these fibers is dependent on normal nervous system function to initiate contraction, and further involves intricate control mechanisms to direct movement of calcium ions in and out of the sarcoplasmic reticulum (SR) during the contraction–relaxation cycle. Muscle fibers have high energy requirements, often needed on short notice; this metabolic feature may predispose these cells to injury from certain chemicals and drugs. Use of histochemical staining procedures allows recognition of several fiber types, each with unique metabolic and functional features that may render a specific population of fibers susceptible to certain insults. Critical nutrients needed to maintain the structural integrity of muscle fibers include adequate dietary intake of selenium, vitamin E, and protein. Thus the skeletal muscle fiber possesses a number of unique metabolic and

Fundamentals of Toxicologic Pathology.
DOI: http://dx.doi.org/10.1016/B978-0-12-809841-7.00010-1

structural features that will influence the pathological reactions observed in skeletal muscle diseases.

STRUCTURE AND FUNCTION

Anatomy of Skeletal Muscle

Skeletal muscle arises from mesodermal somites in the embryo during the first trimester of gestation. The somites give rise to myotomes, sites where embryonic muscle cells or myoblasts aggregate, that roughly correspond to the segments of the vertebral column; each somite receives a spinal nerve. Skeletal muscles of the adult will often contain muscle fibers from several myotomes following migration and fusion of embryonic myoblasts, and thus will also receive nerve supply from several myotomes.

Myoblasts, the primitive mononuclear precursor cells of skeletal muscle fibers, elongate and fuse with each other to form myotubes. These cells rapidly evolve to form the early cytoplasmic components of mature muscle cells by production of thin (actin intertwined with troponin and tropomyosin) and thick (myosin) myofilaments and Z-band material that aggregate into sarcomeres; the sarcotubular membrane systems that propagate depolarizing ion gradients into the myofiber interior are also formed at this stage. Myotubes subsequently fuse with each other, and sarcomerogenesis continues as nuclei migrate to the subsarcolemmal positions. Finally, myofiber innervation occurs and individual fibers become organized into small groups for coordinated contractile function. Further growth of these fibers in width and length occurs during fetal life. Increased numbers of muscle fibers are produced by waves of growth in late gestation. This expansion is presumed to be the result of proliferation and activation of satellite cells to form new myofibers, which recapitulate the events of myoblast-associated muscle fiber development and maturation as just described.

Skeletal Muscle Fibers. Individual muscle fibers generally extend linearly from tendon to tendon in a muscle and do not branch or form syncytia. In cross-sections, skeletal myofibers have a polygonal or multifaceted shape in muscles of adults. Many factors, such as species, breed, age, sex, body weight, nutritional status, position and function of the muscle, and exercise, influence the diameter of muscle fibers. Measurements of fiber diameters in individual muscles will vary in size as a bell-shaped curve on a histogram. Differences in fiber size in various species are not directly related to body weight (typical fiber diameter: pig > human, cow, rabbit, dog, rat > mouse). Fiber size is greater in males than females, and tends to increase with age to maturity. Fiber size decreases with senescence.

The cellular features of skeletal muscle fibers are best appreciated in longitudinal sections. The fibers are bounded by the plasma membrane or sarcolemma, which is covered by an external lamina that is stained by the periodic acid-Schiff (PAS) reaction. Myofibers contain multiple thin, elongated nuclei, which are generally positioned immediately beneath the sarcolemma in a spiral pattern spaced 10–50 μm apart along the entire myofiber. At myotendinous junctions, however, muscle fibers have numerous centrally located nuclei. Nuclei of satellite cells are positioned between the sarcolemma and the external lamina.

Skeletal muscle fibers contain hundreds of longitudinally aligned myofibrils composed of repeating sarcomeres. The characteristic transverse striations of skeletal muscle fibers results from parallel alignment of the bands in adjacent myofibrils (Figure 10.1). Bands are named according to their appearance in polarized light. The largest are A bands (anisotropic or birefringent, appear bright) and I bands (iostropic, appear dark). The I bands, composed of thin myofilaments (made of actin, troponin, and tropomyosin), are bisected by Z lines (disks, bands) that form the end of each sarcomere; the A bands, composed of thick myosin myofilaments, are bisected by the less-birefringent H bands. The banding pattern, named for the appearance in polarized light, is reversed when studied by light microscopy with phase contrast optics, light microscopy with conventional optics on sections stained with the usual cationic dyes, or transmission electron microscopy.

Application of histochemical stains (described later) to frozen sections of unfixed skeletal muscle will allow demonstration of various fiber-type populations that cannot be distinguished in paraffin-embedded sections stained with conventional histologic stains such as hematoxylin and eosin (H&E). The histochemical uniqueness of these fiber types correlates with differences in their physiologic features, such as contraction speed and fatigability; their biochemical and metabolic activities; their gross color; and their structure as revealed ultrastructurally (Table 10.1).

Most skeletal muscles will have a mixture of all fiber types to produce the so-called "checkerboard" pattern that becomes evident with differential histochemical staining. Fibers innervated by the same nerve branches will have the same fiber type, although reinnervated fibers may show reversal of fiber types depending on which nerve endings reach the restored fiber. Some muscles will have a preponderance of one fiber type; e.g., the soleus is a "red" muscle high in type I (or "slow twitch") fibers that are capable of sustained action or weight bearing, while the gastrocnemius is a "white" muscle high in type II (or "fast twitch") fibers that are capable of sudden action and purposeful motion. The proportions of the various fiber types in a

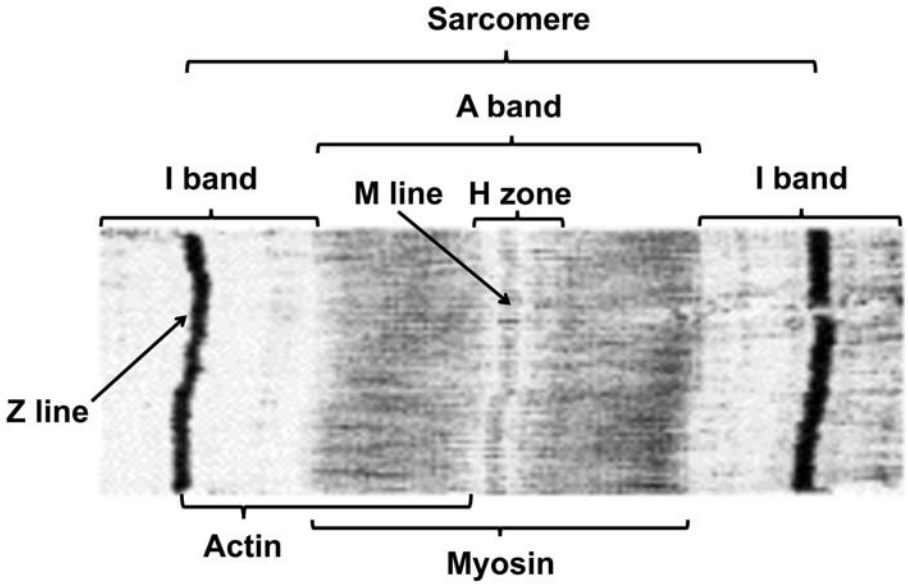

FIGURE 10.1 The sarcomere, the structural unit of skeletal muscle myofibrils, are bounded by dense Z lines and banded due to the different overlapping patterns of interdigitating thin myofilaments (formed of actin) and thick myofilaments (made of myosin). Thin myofilaments are anchored to the Z lines, from which they extend on both sides as the I bands. The sarcomere core harbors the thick myofilaments, which form the A band. The dark part of the A band consists of overlapping thick and thin myofilaments; the light central part of the A band, termed the H zone, contains only thick myofilaments and is bisected by the dense M line. Myofiber contraction leads to shortening of the sarcomeres and (as here) narrowing of the H zone and I band. Source: *Transmission electron micrograph acquired by Dr. H.E. Huxley, and reproduced from Kimball's Biology Pages (http://www.biology-pages.info/M/Muscles.html), with permission of Dr. John Kimball.*

TABLE 10.1 Characteristics of Major Skeletal Muscle Fiber Types in Mammals

	Type I	Type IIA	Type IIB
MORPHOLOGIC CHARACTERISTICS			
Natural color	Dark	Dark	Pale
Glycogen content	Low	High	High
Myoglobin content	High	High	Low
Lipid globules	Numerous	Numerous	Few
Mitochondrial content	High	Intermediate	Low
PHYSIOLOGICAL FEATURES			
Twitch speed	Slow	Fast	Fast
Fatigability	Resistant	Resistant	Susceptible

Table reproduced from Haschek, W.M., Rousseaux, C.G., Wallig, M.A. (Eds.) 2010. Fundamentals of Toxicologic Pathology, second ed. Academic Press, Table 12.9, p. 366 with permission.

given muscle may vary with species, breed, age, and exercise, and also in certain muscular diseases.

Ultrastructurally the myofiber surface is covered by the sarcolemma, which in turn is encompassed by an external lamina. The elongated subsarcolemmal nuclei are surrounded by accumulations of mitochondria, lipid droplets, glycogen granules, elements of sarcoplasmic (endoplasmic) reticulum, and collections of Golgi apparatuses. The myofiber contains abundant contractile elements that are organized as many parallel myofibrils of 0.5–1.0 μm in diameter. Myofibrils are composed of repeating units, termed sarcomeres, of 2–3 μm in length (Figure 10.1). Sarcomeres end at dense Z lines that contain α-actinin, actin, and tropomyosin. Thin 6-nm-diameter myofilaments containing actin, troponin, and tropomyosin extend on both sides of the Z line to form the I bands. The middle half of the sarcomere contains thick (16 nm diameter) myofilaments that are composed of myosin and interdigitate with the adjacent thin filaments. The center of the sarcomere, with only thick filaments, is the H band and is bisected by the relatively dense M line, which represents interconnecting elements of the cytoskeleton. Fiber contraction results in shortening of sarcomeres due to sliding of bulbous heads of thick filaments along the length of thin filaments to produce narrowed I and H bands. Cross-sections of myofibrils show variable appearance depending on the location in the sarcomere, but the edges of the A band will have thick filaments surrounded by a hexagonal array of thin filaments. The sarcoplasm surrounding myofibrils contains elements of the transverse (T) tubular system and SR, mitochondria, lipid droplets, glycogen granules, and cytosol. The T tubules are invaginations of the sarcolemma that are often seen at the edge of the I band with two adjacent elements of SR to form a "triad." The T-tubular system functions as a channel to allow rapid spread of an electrical impulse from the motor

end plate (i.e., the junction between a nerve terminus and the surface of a myofiber) on the sarcolemma to the interior of the fiber to elicit release of calcium (Ca^{2+}) stored in the SR. Increasing concentrations of cytoplasmic Ca^{2+} will bind to regulatory troponin proteins on the thin myofilament, thereby releasing binding sites on actin that will interact with myosin to initiate myofiber contraction.

Satellite Cells. Satellite cells are thin cells with a nucleus and a scant amount of sarcoplasm that are interposed between the sarcolemma of myofibers and the external lamina (Figure 10.2). They are abundant in newborn animals; in muscle of mature animals, 3%–5% of nuclei in muscle fibers belong to satellite cells. These cells play an important role in normal development of myofibers and also in regeneration of damaged fibers during adult life by serving as stem cells that can be activated to undergo mitosis and subsequently differentiate to myoblasts, myotubes, and, eventually, mature myofibers.

Motor End Plates. Motor end plates (i.e., neuromuscular junctions) represent a complex and intimate attachment site of the motor nerve fiber on the surface of the skeletal muscle fiber. The end of the nerve fiber is unmyelinated and branches into axon terminals that invaginate into a synaptic cleft, which is characterized by a thickened zone of subsarcolemmal sarcoplasm with numerous nuclei. The axon terminal has abundant synaptic vesicles containing the neurotransmitter acetylcholine (ACh). Release of ACh with binding to receptors on the postsynaptic sarcolemmal membrane results in increased sodium (Na^+) and potassium (K^+) conductance, depolarization of the sarcolemma, mobilization of intracellular Ca^{2+} stores, and myofiber contraction. Motor end plates generally are recognized in muscle tissue only by use of special techniques such as metallic impregnation, intravital dyes, histochemical procedures, or transmission electron microscopy.

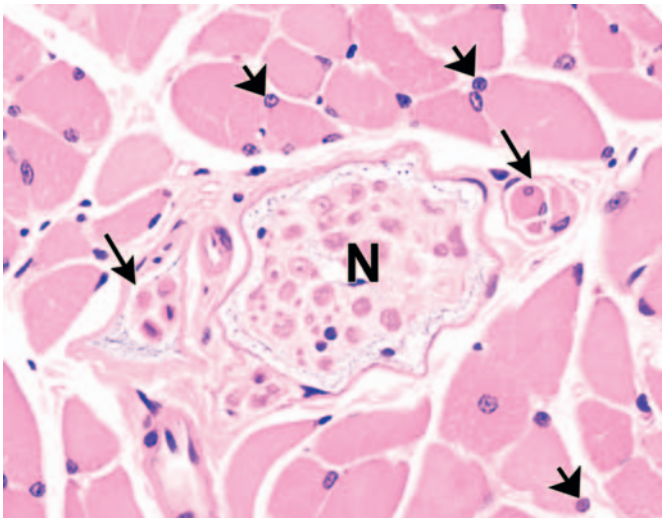

FIGURE 10.2 Normal microscopic anatomy of a skeletal muscle fasciculus (i.e., a bundle of myofibers), demonstrating skeletal myofibers, a somatic nerve (N), and two muscle spindles (arrows) in cross section. Satellite cells are denoted by arrowheads. Formalin fixation, paraffin embedding, H&E staining.

Muscle Spindles. Muscle spindles are fusiform sensory receptors approximately 0.5–3.0 mm in length oriented longitudinally near the edges of muscle fasciculi. Their function is to detect changes in the length of muscle bellies; they regulate muscle contraction via the stretch reflex by activating motor neurons in the central nervous system to counter muscle stretch. The muscle spindle has a thick fibrous capsule and contains multiple small, variably sized, intrafusal muscle fibers, nerve fibers, specialized nerve endings, and blood vessels (Figure 10.2).

Connective Tissue. The interstitial connective tissue of skeletal muscle is subdivided into the epimysium (surrounds the entire muscle), perimysium (surrounds large angular fascicles divided into primary fascicles of 10–100 fibers), and endomysium (surrounds individual muscle fibers). The endomysium contains capillaries, nerve fibers, fibroblasts, and collagen fibrils. Larger amounts of collagen fibrils and larger blood vessels and nerves are in the perimysium.

Tendons are thick bands of dense fibrous connective tissue that connect muscles to bones. The collagen type I fibers in tendons, which are secreted by fibroblast-like tenocytes, are oriented parallel to their length and the lines of tension that are applied to the tendon during contraction of the muscle. Tendons not only serve in locomotion, as the anchor through which skeletal muscles fulfill their role, but also provide additional stability to nearby joints (as an adjunct to ligaments, which connect bone to bone). Basic functional and structural attributes of tendons as well as their responses to toxic insult are covered elsewhere in this volume (see Chapter 23: Bone and Joints).

Physiology and Function of Skeletal Muscle

The unique structural differentiation of skeletal muscle fibers is closely integrated with their highly developed, specialized contractile function for locomotion and maintenance of posture by conversion of chemical energy into mechanical energy. Further specialization in form and function is provided by the differentiation of myofibers into various fiber types, each of which is specifically suited for certain physiologic applications.

The functional unit of the neuromuscular system is the motor unit, consisting of (1) nerve cell bodies in the spinal cord ventral horns or brainstem, (2) axons

of these neurons that course to the muscles and terminate as motor end plates, and (3) the group of histochemical type-specific skeletal muscle fibers that are innervated by the neuron. The number of muscle fibers supplied by a neuron of a motor unit varies widely depending on the degree of refined movement needed by the muscle. For example, 10 fibers are innervated by a single neuron in extrinsic eye muscles, which require exquisite control, while 2000 fibers are supplied per neuron in large limb muscles where actions are performed by large cooperating groups of fibers.

Contraction of muscle is the result of sarcomere shortening by interdigitation of thin and thick myofilaments. According to the *sliding filament hypothesis*, the force of contraction is generated by the movement of cross-bridges formed by heads that project from myosin molecules in thick myofilaments to actin molecules (the main portion of thin myofilaments), leading to migration of the myosin-based filaments along the actin-based filaments. The chemical energy for contraction is supplied by high-energy phosphate compounds (i.e., adenosine triphosphate (ATP) and creatine phosphate (CP)). In type I (slow twitch) fibers, these compounds are largely generated by mitochondrial oxidative phosphorylation via the electron transport system following the oxidation of fatty acids and glucose via the citric acid (or Krebs) cycle, while in type II (fast twitch) fibers they are produced mainly by sarcoplasmic anaerobic glycolysis and glycogenolysis. Thus the metabolic differences of the various fiber types are correlated with differences in their functional features, such as speed of contraction and resistance to fatigue.

EVALUATION OF SKELETAL MUSCLE TOXICITY

The techniques for assessing the toxic effects of xenobiotics on skeletal muscle vary from detection of biochemical constituents in the blood to sophisticated direct evaluation of isolated muscle tissue. Routine toxicity studies rely on assessment of muscle histopathology and analysis of serum creatine kinase (CK) activity.

Biochemical Evaluation. Certain enzymes present in high concentrations in the sarcoplasm can leak into the blood and serve as biomarkers of myotoxicity. The most sensitive enzyme is CK. This enzyme is released from muscle cells in a number of myopathies. Three isoenzymes (MM, MB, and BB) can be detected in blood; MM is the main isoenzyme found in skeletal muscle. A greater than 10-fold increase in CK concentration is usually indicative of muscle origin following myofiber injury. Smaller increases in CK occur at times during exercise or in response to localized damage resulting from intramuscular injections. CK levels usually are not elevated in those instances where the myopathy is due to denervation or myoneural junctional disorders. The serum values for other intramuscular constituents also may be increased following damage to skeletal muscle, including the enzymes alanine (ALT) and aspartate (AST) aminotransferase, lactic dehydrogenase (LDH), and aldolase as well as 3-methylhistidine (a component of actin in all types of muscle fibers, and of heavy and light myosin chains of the fast-twitch fibers). Hypo- or hyperkalemia can lead to episodes of flaccid muscle paralysis.

Other proteins may be indicative of skeletal muscle toxicity when found in circulation as well. The most abundant protein in skeletal muscle is myoglobin, a low molecular weight, oxygen-binding heme protein that constitutes up to 5%−10% of all the cytoplasmic proteins found in muscle cells. In blood, myoglobin is bound primarily to plasma globulins. If the plasma concentration exceeds the plasma-binding capacity (1.5 mg/dL in humans), myoglobin begins to appear in the urine. Myoglobin is rapidly released after muscle damage and thus can be a useful biomarker in the early phases of injury. Because myoglobin has a short half-life (2−3 hours) and undergoes rapid renal clearance, changes in serum concentrations usually occur over a shorter time course than do changes in serum levels of CK (i.e., myoglobin is elevated sooner and returns to normal at a more rapid rate). Dip stick urine tests are not specific as they cannot discern between myoglobin and hemoglobin. Troponins are important regulatory proteins present in both cardiac and skeletal muscles. Cardiac troponin isoforms (e.g., I, T) are widely used as biomarkers of cardiac muscle injury and can be measured in serum or plasma with a number of commercially available assays. Assays for skeletal muscle troponin isoforms are less specific and thus are not used as widely.

Electrophysiological Evaluation. Electromyography (EMG) involves placing two electrodes on the skin or inserting needle electrodes into the muscle to measure the summated electrical potentials of action potentials traveling along muscle fibers. Detection of muscle abnormalities depends on the analysis of spontaneous or evoked electrical potentials; properly calibrated, the readouts can distinguish muscle-centered from nerve-centered anomalies. A disadvantage of EMG is that recorded changes may be difficult to quantify. Electrophysiological analysis of isolated whole muscles or individual muscle cells may be used to evaluate the excitability of muscle cell membranes in response to chemical exposure *in vitro*.

Gross Examination. Complete examination of the skeletal muscles is rarely done at necropsy. The large mass of the skeletal musculature (40%−50% of body weight) precludes complete dissection of each individual muscle. In necropsies of animals without any historical

evidence of clinical disease of the skeletal musculature, the prosector should at least inspect the muscles exposed during the necropsy procedure. In animals with clinical suspicion of muscle disease, a more detailed examination of the musculature should be carried out, with particularly careful inspection of those muscles presumed to be responsible for the clinical signs. Gross alterations in color, shape, size, and consistency should be sought by viewing the uncut surface and cut sections of the muscles. Prosectors should avoid over-interpretation of gross findings such as color and size of muscles, which may be a function of the normal variation associated with species, age, particular muscle, and state of nutrition seen among animals.

Following somatic death, skeletal muscle will generally remain in relaxation for 2–4 hours until muscle glycogen stores are metabolized and sufficient energy reserves are no longer present to maintain the relaxed state. Rigor mortis then ensues as stiffness of the muscles and immobility of the joints, and will persist for at least 24–48 hours. Subsequently, muscle rigor will dissipate as autolysis occurs. The onset of rigor mortis will be rapid if the muscle is kept at low pH and high temperature, while rigor will be delayed if abundant muscular glycogen stores at the time of death and will be weak if the animal was debilitated at the time of death.

Microscopic Evaluation. Histologic analysis of skeletal muscle sections can reveal changes associated with xenobiotics causing (1) myopathic or neurogenic alterations, (2) specific muscular structural alterations, or (3) specific muscular metabolic alterations. A number of pathologic muscular alterations can be detected in routine paraffin sections of muscle. Muscle fiber necrosis and regeneration are common features of myotoxicity. If necrosis is substantial and chronic, regeneration may fail, resulting in progressive myofiber loss and replacement by fat and fibrous tissue. Degeneration of muscle fibers without overt necrosis causes structural alteration of myofibrils and sarcoplasm. Pathologic changes may be restricted to one type of fiber in the muscle.

Sample collection must be done carefully to avoid hypercontraction artifacts that are inevitable in fresh muscle collected in biopsy samples and in samples taken from animals soon after death. To prevent contraction artifacts, isolated longitudinal strips of muscle are dissected and clamped or ligated to a strip of wood (e.g., tongue depressor) at isometric length (i.e., in a slightly stretched position) and then excised. Placing the clamped sample in physiologic saline solution for 20 minutes will further decrease problems with contraction artifacts.

Morphologic analysis of skeletal muscle typically is undertaken using conventional tissue preparation techniques. For routine light microscopy, the clamped sample is fixed in neutral buffered 10% formalin, embedded in paraffin, sectioned at 4–5 μm, and stained with H&E. Other stains frequently used to evaluate skeletal muscle structures include Gomori or Masson's trichrome (for connective tissue) and phosphotungstic acid hematoxylin (PTAH, to demonstrate myofibrils and cross-striations of muscle fibers). Application of lipid stains (e.g., oil red O) to frozen sections may be useful. Each muscle sample should have longitudinal and cross-sections prepared for microscopic study. Tissue samples to be used for high-resolution light microscopy or transmission electron microscopy are immersed in buffered 3% glutaraldehyde or Trump's universal fixative, post-fixed in 1% osmium tetroxide, and then embedded in either methacrylate ("soft plastic") or epoxy ("hard plastic") resins.

Myofiber isotype characterization requires special histochemical techniques applied to fresh-frozen muscle sections. Key morphologic endpoints include myofiber dimensions, the distribution and quantity of mitochondria, lipid and glycogen content, myofibrillar enzymes, and the distribution of the fiber types. Muscle units differ both in size and in certain biochemical properties of their fibers. Two primary types of muscle fibers are characterized (Table 10.1): type I (slow twitch, fatigue resistant) and type II (fast twitch, fatigable); classically, the type II fibers have been further classified as types 2A (fast twitch oxidative) and 2B (fast twitch glycolytic), although modern fiber typing techniques have shown that this scheme is an oversimplification. Special histochemical stains used for categorizing fiber types include myosin ATPase activity at three different pH levels, to differentiate fast- and slow-contracting myofibers, and NADH-tetrazolium reductase (NADH-TR) activity and succinic dehydrogenase (SDH) activity, both of which are indicators of mitochondrial oxidative potential. Analysis of myosin heavy chain (myHC) composition also can be used to define fiber types, although some fibers are hybrids containing multiple myHC isoforms. Fiber-type differentiation may be useful in evaluating myotoxic effects since some agents injure only one fiber type.

Ultrastructural examination is useful for characterizing subcellular changes leading to myofiber degeneration or death. Vacuolation at the light microscopic level may represent accumulations of either neutral (nonpolar) lipids (i.e., accretion of potential energy substrates) or polar phospholipids (i.e., accrual of undigested membrane constituents), or even mitochondrial swelling and degeneration. Swollen muscle fibers with a "lacy" cytoplasm at the light microscopic level might have cytoplasmic glycogen accumulation. Pale staining or loss of discrete cross-striations at the light microscopic level may reflect myofibril lysis. Though some of these changes may be characterized at the

light microscopic level using special stains (e.g., lipid, glycogen), they are all best examined at the ultrastructural level to ensure that the components that can be stained are not present as well (e.g., lipid accumulation with mitochondrial swelling).

Numerous artifacts may be observed in muscle sections prepared for either light or electron microscopic evaluation. These artifacts include hypercontracted fibers from improper collection and fixation procedures, mitochondrial vacuolation, distention of elements of SR and glycogen loss from faulty fixation, and occurrence of knife marks, chatter, and wrinkles from sectioning problems.

RESPONSE TO INJURY

Skeletal muscle will respond to insults with a limited number of morphological reactions. In fact diseases of differing etiologies may exhibit similar types of lesions. Thus it may not be possible to render a specific etiologic diagnosis for a given skeletal muscle lesion even following careful microscopic study from a given case.

Many injuries of skeletal muscle heal by regeneration rather than by fibrosis—which is a distinguishing feature of repair in skeletal versus cardiac muscle. This is especially true for the common monophasic or polyphasic polyfocal myopathies (see subsequent text) such as those associated with nutritional deficiencies, metabolic disorders, and myotoxicities. In these diseases, although extensive muscle fiber necrosis may occur, the scaffolding of external lamina that surrounds the degenerated muscle fiber and the innervation and blood supply to the damaged muscle are preserved, permitting myofiber regeneration within the external lamina (which is often virtually complete). Regeneration is further promoted in these conditions by the short-term nature of the insult responsible for the muscle injury. In contrast, prolonged insults such as denervation or genetic derangements often induce muscular diseases in which regeneration is limited. In severe myopathic diseases (i.e., those in which muscle tissue is directly damaged), extensive disruption of endomysial connective tissues and "tubes" of external laminae from damaged myofibers may occur from trauma, hemorrhage, or infection. In such cases, the outcome of healing will be limited regeneration accompanied by extensive fibrosis and scarring.

The cellular events of skeletal muscle regeneration are well characterized and center on the proliferation of mononucleated myogenic stem cells, termed myoblasts (Figure 10.3). Myoblasts arise from satellite cells, a population of resting and undifferentiated cells that persist in mature skeletal muscle and appear

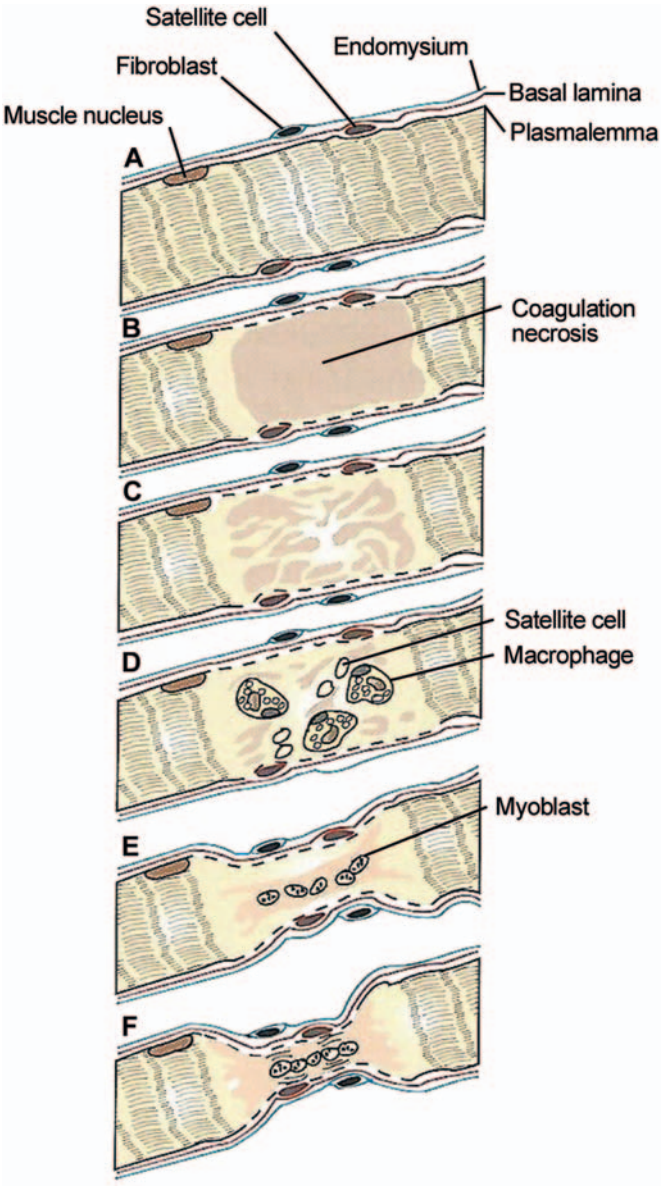

FIGURE 10.3 Schematic diagram of segmental myofiber necrosis and regeneration. (A) Myofiber, longitudinal section, demonstrating normal histologic features. (B) Segmental coagulation necrosis. (C) The necrotic segment of the myofiber has become floccular (i.e., dissolving) and detached from the adjacent viable portions of the myofiber. The satellite cells are enlarging. (D) The necrotic segment of the myofiber has been invaded by macrophages to remove the necrotic debris, and satellite cells are migrating to the center to develop into myoblasts. The sarcolemma (cell membrane) of the necrotic segment has disappeared. (E) Myoblasts have formed a myotube, which has produced sarcoplasm. This extends out to meet the viable ends of the myofiber. The integrity of the myofiber is maintained by the sarcolemmal tube formed by the basal lamina and endomysium. (F) Regenerating myofibers have a reduced diameter and central rowing of nuclei. There is early formation of sarcomeres (cross-striations), and the sarcolemma has reformed. Such fibers stain basophilic with routine hematoxylin and eosin (H&E) staining. Source: *A–F, Redrawn with permission from Dr. M.D. McGavin, College of Veterinary Medicine, University of Tennessee.*

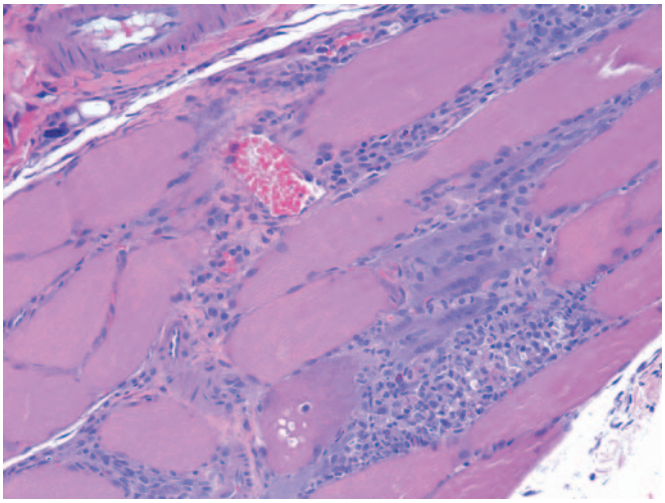

FIGURE 10.4 Section of soleus muscle from a rat given a myotoxic xenobiotic. The necrotic muscle fibers are replaced by a mixed mononuclear inflammatory cell infiltrate. Regenerating myoblasts are basophilic and multinucleated. Formalin fixation, paraffin embedding, hematoxylin and eosin (H&E) staining. Source: *Figure reproduced from Haschek, W.M., Rousseaux, C.G., Wallig, M.A. (Eds.), 2013. Handbook of Toxicologic Pathology, third ed. Academic Press, Fig. 46.25, p. 1647, with permission.*

morphologically as very thin subsarcolemmal cells that lie between the sarcolemma and the external lamina of myofibers. For unknown reasons, satellite cells tend to be resistant to many insults that destroy mature myofibers. Following selective destruction of skeletal muscle fibers, the sarcoplasmic debris is removed rapidly by invasion of macrophages and phagocytic lysis (Figure 10.4). The persisting sarcolemmal "tubes" of external laminae rapidly become populated by elongated myoblasts with large vesicular nuclei and prominent basophilic sarcoplasm that reflects the numerous polyribosomes supporting intense synthesis of cellular proteins in these cells. Myoblasts fuse to form multinucleated cells termed sarcoblasts, which further elongate to form myotubes that rapidly bridge the gap of disrupted sarcoplasm in damaged myofibers. Myotubes have rows of centrally located nuclei and peripheral masses of forming contractile myofilaments that soon become oriented into sarcomeres and myofibrils with restoration of cross-striations in the immature myofibers (Figure 10.5). Subsequently the central nuclei will migrate to their normal subsarcolemmal location (as seen in mature fibers), and the regenerated muscle fibers may then be indistinguishable from adjacent fibers that have not suffered injury.

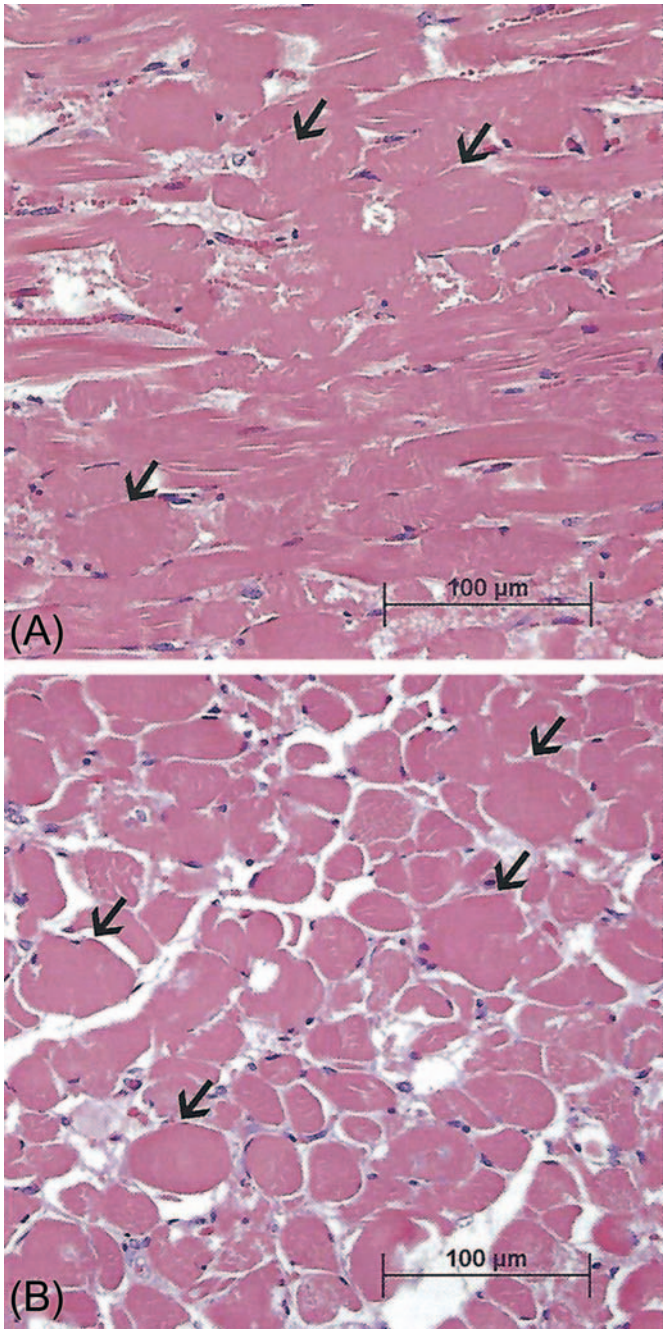

FIGURE 10.5 Acute segmental myofiber necrosis of skeletal muscle from a sheep with monensin toxicosis. (A) Longitudinal and (B) cross-sections demonstrating a monophasic polyfocal reaction characterized by segmental hypercontraction of myofibers, which appear swollen and hyalinized (arrows), with loss of cross-striations and fragmentation. Formalin fixation, paraffin embedding, hematoxylin and eosin (H&E) staining. *Source: Figure reproduced from Haschek, W.M., Rousseaux, C.G., Wallig, M.A. (Eds.), 2010. Fundamentals of Toxicologic Pathology, third ed. Academic Press, Fig. 12.24, p. 372, with permission.*

Pathologic Alterations in Skeletal Muscle

Degeneration and Necrosis. Unlike many tissues the difference between the reversible sublethal alterations of degeneration and the irreversible lethal changes of necrosis is difficult to detect by microscopic study. Skeletal muscle fibers are large multinucleated cells, and it is often not possible to view the entire length of the fiber in the plane of a tissue section to determine

whether the sarcoplasmic damage involves the entire fiber or only a segment of the fiber. It seems likely that segmental degeneration occurs frequently, but necrosis of entire myofibers is uncommon. In any event the causes of both degeneration and necrosis are similar.

Specific morphologic types of skeletal muscle degeneration have been described. The most common type is so-called hyaline-type or waxy degeneration. Affected muscles may be detected grossly by diffuse pallor or scattered pale streaks (i.e., "white muscle disease;" Figure 10.6), especially if secondary calcification has occurred in damaged fibers. Microscopically, affected fibers appear swollen and hypereosinophilic with loss of cross-striations (Figures 10.5 and 10.7). The altered contractile material frequently becomes fragmented into large blocks or disks scattered along the "tube" of persisting external lamina of the degenerating muscle fiber. Within 24 hours the affected areas will be invaded by an occasional polymorphonuclear leukocyte and numerous macrophages. Macrophages are observed in the interstitium and also within injured muscle fibers. Ultrastructurally the affected myofibers show tangled masses of disrupted contractile material with damaged membranes of mitochondria, SR, and sarcolemma. The "tube" of external lamina persists to guide regenerative events and may be focally disrupted to allow entry of macrophages.

Another type of degeneration described in skeletal muscle is granular degeneration. The microscopic appearance differs from hyaline degeneration because the damaged sarcoplasm appears as small basophilic granules that fill the "tube" of external lamina and are identified as mineralized mitochondria by ultrastructural study. The causes of granular and hyaline degeneration are similar and include nutritional deficiencies (such as selenium/vitamin E deficiency), various myotoxic drugs and plants, and metabolic disorders such as azoturia and capture myopathy.

The spatial distribution and temporal pattern of degeneration and necrosis in skeletal muscle have been used to classify reactions as (1) monophasic monofocal, (2) monophasic polyfocal, (3) polyphasic monofocal, and (4) polyphasic polyfocal. Monophasic monofocal reactions result from an isolated, single mechanical injury such as external trauma or needle insertion. In monophasic polyfocal reactions (Figures 10.5 and 10.7) a single insult such as exposure to various myotoxic drugs or chemicals or various metabolic disorders may initiate widespread muscle lesions, but all the lesions are in the same phase of injury. Polyphasic monofocal reactions would be the result of repeated localized mechanical injury. Polyphasic multifocal reactions are frequent in muscular diseases of animals, and result from continued insults applied

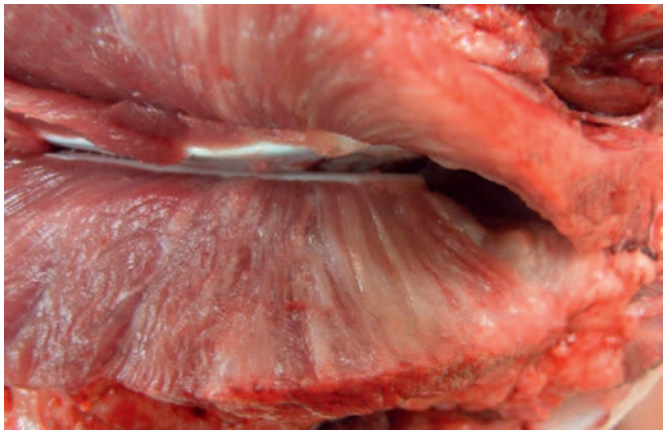

FIGURE 10.6 Necrosis of the muscles of the right neck and shoulder in a pig is indicated by multifocal white streaks running parallel to the direction of the muscle fibers. This gross appearance is consistent with both ionophore-induced myotoxicity (e.g., monensin formulation error) and dietary vitamin E/selenium deficiency. Source: *Courtesy: Dr. Brian G. Caserto, VetPath Services, Stone Ridge, NY, from the Veterinary Pathology Forum blog (https://vetpath.wordpress.com/2010/06/14/skeletal-muscle-necrosis-in-a-pig-2/), with permission.*

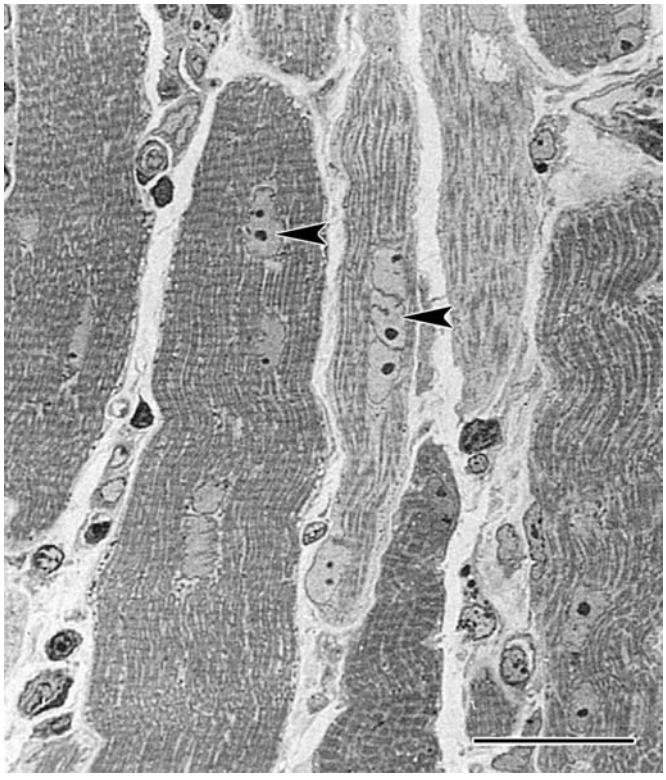

FIGURE 10.7 Acute monensin toxicosis in a pig. Regenerating skeletal muscle fibers show multiple large, vesicular, centrally located nuclei (arrowheads). Formalin fixation, plastic embedding, toluidine blue staining. Bar = 50 μm. Source: *Figure reproduced from Haschek, W.M., Rousseaux, C.G., Wallig, M.A. (Eds.), 2013. Handbook of Toxicologic Pathology, third ed. Academic Press, Fig. 46.26, p. 1647, with permission.*

intermittently or continuously over a prolonged time (e.g., from nutritional deficiencies and from genetic disorders like muscular dystrophies); the lesions are widespread in the musculature, and various pathological reactions indicative of differently timed insults will occur concurrently, including necrosis (acute reaction), leukocyte invasion during resolution (often subacute response), and regeneration (subacute to chronic outcome). Xenobiotic-induced toxic myopathies tend to be monophasic polyfocal responses.

Other less common types of degeneration in skeletal muscle fibers include vacuolar or hydropic degeneration and fatty degeneration. Vacuolar or hydropic-type degeneration occurs with cortisol excess. The affected fibers have vacuolated, lace-like areas in the sarcoplasm. Fatty degeneration is uncommon. It is seen as a nonspecific response to injury, and results in abundant small spherical lipid vacuoles scattered between myofibrils. Similar appearing but less abundant lipid deposits are normally present in type I muscle fibers.

Table 10.2 summarizes the chemical and biological agents that have been associated with necrosis or degeneration of skeletal muscle in animals and humans. Many of these agents also produce myocardial injury.

Drug-Induced Neuromuscular Blockade. A number of drugs may interfere with neuromuscular transmission in human patients. Three clinical syndromes have been recognized: drug-induced myasthenic syndrome, which is uncommon; drug-induced aggravation or unmasking of existing myasthenia gravis; and postoperative respiratory depression from direct effect of the drug or from potentiation of muscle relaxants. Drugs implicated in these syndromes include aminoglycoside antibiotics (neomycin, kanamycin, streptomycin, gentamycin); polypeptide antibiotics (polymyxin B, colistins); other antibiotics (oxytetracycline, rolitetracycline, lincomycin, clindamycin); antirheumatic drugs (D-penicillamine, chloroquine); cardiovascular drugs (oxprenolol, practolol, quinidine, procainamide, propranolol); anticonvulsants (trimethadione, phenytoin); psychotropic drugs (lithium, chlorpromazine, promazine, phenelzine); anesthetics (diazepam, ketamine, propenidid, ether); and other drugs (busulfan, oral contraceptives, methoxyflurane, adrenocorticotropic hormone (ACTH), corticosteroids, thyroid hormones, anticholinesterases, oxytocin, aprotinin, procaine, lidocaine). These drug-induced clinical syndromes have not been associated with morphologic alterations in skeletal muscle. The mechanisms of these drug-induced neuromuscular blockades include (1) presynaptic local anesthetic-like action, (2) postsynaptic receptor blockade, (3) interference with ACh release, and (4) impairment of muscle membrane conductance.

Drug-Induced Myotonic Syndrome. Myotonia is the failure of normal muscular relaxation following contraction. Myotonic syndrome occurs in human patients, rats, and goats administered 20,25-diazacholesterol and its analogs as hypocholesterolemic agents. Propranolol and suxamethonium may precipitate or exacerbate myotonia in human patients.

Drug-Induced Denervation Atrophy. Over 50 drugs used clinically in human patients have been reported to produce peripheral neuropathies. Damage to the nerve supply leads to myofiber atrophy of affected motor units and eventually progression to the distinctive morphologic alteration of "fiber group atrophy" (Figure 10.8). Neurogenic atrophy represents a loss of myofiber mass as an indirect response caused by biochemical or structural interruption that prevents nerve impulses from depolarizing the myofiber. Key morphologic attributes of neurogenic lesions include clusters of small angulated myofibers (i.e., foci of denervation atrophy) intermingled with large oval myofibers (i.e., those retaining an intact somatic nerve supply). Drugs implicated include antimicrobial agents (isoniazid, nitrofurantoin, sulfonamides, clioquinol, metronidazole, amphotericin B); antineoplastic agents (vincristine, procrabazine, nitrofurazone, cytosine arabinoside, podophyllir, chlorambucil); antirheumatic drugs (gold, colchicine, chloroquine, indomethacin, phenylbutazone); hypnotics and psychotropics (thalidomide, methoqualone, glutathimide); cardiovascular drugs (perhexiline, amiodarone, hydralazine, diisopyramide, clofibrate, digitalis); and other drugs (phenytoin, disulfiram, dapsone, ergotamine, methimazole, propylthiouracil, methylthiouracil).

Muscle Repair. Evidence of repair typically is a feature of myopathic lesions (i.e., those in which muscle tissue is directly injured), but usually is not present in neurogenic lesions (i.e., those in which muscle is affected secondarily as a consequence of primary damage at an extra-muscular site) (Figure 10.8). Successful restoration of muscle parenchyma leads to myofiber regeneration within intact external laminae (to restore necrotic muscle cells; Figures 10.4 and 10.7). More extensive myopathic lesions that result in both myofiber necrosis and interruption of external laminae may evoke inflammation (typically mononuclear cells), expansion of interstitial fibrous connective tissue, and sometimes mineralization of damaged myofibers. Over time the inflammatory reaction may recede, but fibrosis and mineralization represent permanent changes.

MECHANISMS OF TOXICITY

Skeletal muscle accounts for a significant portion of total body weight. The normal structure and function of skeletal muscle can be altered by a variety of chemicals and drugs. Skeletal muscle susceptibility to potential toxicants appears in part to be related to high

TABLE 10.2 Toxic Chemical and Biological Agents That Cause Necrosis or Degeneration of Skeletal Muscle in Animals and Humans

Causes	Skeletal muscle		Type I fiber selectivity	Species affected
	Necrosis	Degeneration		
Ionophores—Monensin, lasalocid, narasin, A-204, maduramicin, salinomycin	+	+	+	Horse, cow, pig, sheep, dog, chicken, turkey, rat, mouse
Antivirals—Zidovudine (AZT)	−	+	ND	Rat, human
Quinolone antibacterials—Pefloxacin, levofloxacin	+	+	ND	Rat, human
Antimalarials—Emetine, chloroquine, quinine, plasmocid	+	+	+	Rat, human, rabbit, pig
Immunosuppressive and cytotoxic drugs—Vincristine, azathioprine, doxorubicin	+	+	ND	Rat, human
Corticosteroids—Cortisone, triamcinolone, fluorocortisone	+	+	−	Rabbit, human, dog
Antibiotics—Nitroxoline, thiabendazole	−	+	ND	Mouse, human
Local anesthetics—Bupivaccine, tetracaine, lignocaine	−	+	ND	Human, pig
Analgesics—Pentazocine, paracetamol, salicylates	+	+	ND	Human
Anesthetics—Halothane and others (via malignant hyperthermia)	+	+	+	Rat, human, pig
Agents producing hypokalemia—Carbonoxolone, licorice, corticosteroids, diuretics	−	+	ND	Human, rabbit
Hypocholesterolemic agents—Lovastatin, simvastatin, pravastatin, cerivastatin, rosuvastatin	+	+	−	Rat, human, rabbit
Hypolipidemic agents—Clofibrate	±	±	±	Rat
Cationic amphiphilic drugs—Amiodarone, chlorphentermine, tamoxifen, chlorcyclizine	−	+	ND	Rat
Systemic toxic agents—Alcohol, oxygen, carbon monoxide, organophosphates	+	+	ND	Rat, human
FURTHER AGENTS ADMINISTERED SYSTEMICALLY				
p-Phenylenediamine, diphenylenediamine	+	+	ND	Rat
Iron dextran	+	+	ND	Pig
Brown FK	+	+	ND	Rat
Insulin	+	+	ND	Rabbit
Selenium	+	+	ND	Pig
ε-Aminocaproic acid	+	+	ND	Human
Iodide	+	+	ND	Rat
Iodpacetate, fluoroacetate	+	+	ND	Rat
Imidazole	+	+	ND	Rat
Dimethylsulfoxide	+	+	ND	Rat
Phencyclidine	+	+	ND	Rat, human
Cannabinoids	+	+	ND	Mouse
Colchicine	+	ND	−	Rat
Triethyltin sulfate, triethyltin bromide	−	+	ND	Rat
2,4-Dichlorophenoxyacetate (2,4-D)	−	−	ND	Guinea pig
6-Mercaptopurine	−	+	ND	Rat
Clenbuterol, salbutamol	+	+	ND	Rat, dog
Paraoxon, physostigmine, pyridostigmine, parathion	+	+	ND	Rat
2,4-Dinitrophenol	−	+	ND	Rat
Acrylamide	−	+	ND	Rat

(*Continued*)

TABLE 10.2 (Continued)

Causes	Skeletal muscle		Type I fiber selectivity	Species affected
	Necrosis	Degeneration		
Rolziracetam	+	+	ND	Dog
Thyroxine	−	+	ND	Rabbit
Cassia occidentalis, C. obtusifolia	+	+	ND	Cow, horse, sheep, goat, rabbit
Karwinskia humboltiana	+	+	ND	Goat, sheep
Ageratina altissima (previously *Eupatorium rugosum)*	+	+	ND	Horse, cow
Gossypol	+	+	ND	Pig
Trigonella foenumgraecum	+	+	ND	Cow
Petiveria alliacea	+	+	ND	Cow
Lupine—*Diaporthe toxica*	+	+	ND	Sheep
Snake venom (sea snake, Australian mulga snake, tiger snake, prairie rattlesnake)	+	+	ND	Rat, mouse
Oriental hornet venom	−	+	ND	Human
Stonefish venom	−	+	ND	Mouse
Cicuta douglasii	+	+	ND	Sheep
Thermopsis montana	+	+	ND	Cow
Clostridium chauvoei, C. septicum, C. novyi, C. perfringens	+	+	ND	Cow, sheep, horse, pig
Uremic toxins	+	+	ND	Rat, human

+, present; −, absent; ND, not determined.
Table modified from Haschek, W.M., Rousseaux, C.G., Wallig, M.A. (Eds.), 2013. Handbook of Toxicologic Pathology, third ed. Academic Press, Table 46.6, pp. 1649–1652 with permission.

metabolic activity and the presence of multiple potential sites by which toxicants can interfere with crucial energy generating pathways. In addition, sensitivity to toxic agents may be enhanced because the high rate of blood flow increases exposure to many substances capable of binding to skeletal muscle. Skeletal muscle dysfunction or damage has been induced by both indirect and direct mechanisms.

Altered Neurogenic Function

Muscular atrophy can develop when interruptions occur in peripheral motor nerve function. Usually only some of the motor fibers supplied by the nerve undergo atrophy, while others remain relatively normal (Figure 10.8). The nerve damage may occur centrally in the neuron that innervates a motor unit, or peripherally in either the nerve fiber or at the motor end plate. For example, intramuscular injections to the hind limb may damage the sciatic nerve, leading to primary nerve fiber degeneration and secondary atrophy of muscles supplied by sciatic nerve branches. Botulinum toxin affects muscle function by blocking the release of ACh from presynaptic motor nerve terminals at the motor end plate (i.e., neuromuscular blockade). Magnesium also interferes with neuromuscular transmission by blocking the release of ACh. Muscle weakness also occurs after exposure to a variety of substances that are capable of causing or intensifying neuromuscular blockade. No significant morphologic changes appear during neuromuscular blockade, and the blockade is usually reversed when the causative substance is removed. However, severe prolonged neuromuscular blockade can induce neurogenic muscle atrophy. In some instances, xenobiotics have induced muscle necrosis by dramatically increasing motor nerve activity or by allowing significant amounts of ACh to accumulate at the myoneural junction. In rats injection of paraoxon causes a progressive myopathy, which ultimately leads to necrosis of muscle fibers; the myopathy is attributed to excessive concentrations of ACh at the neuromuscular junction. Acute rhabdomyolysis is a severe necrotizing myopathy associated with heroin addiction, amphetamine overdoses, and phencyclidine abuse. The muscle damage probably occurs as a result of extreme motor nerve excitation rather than direct myotoxicity.

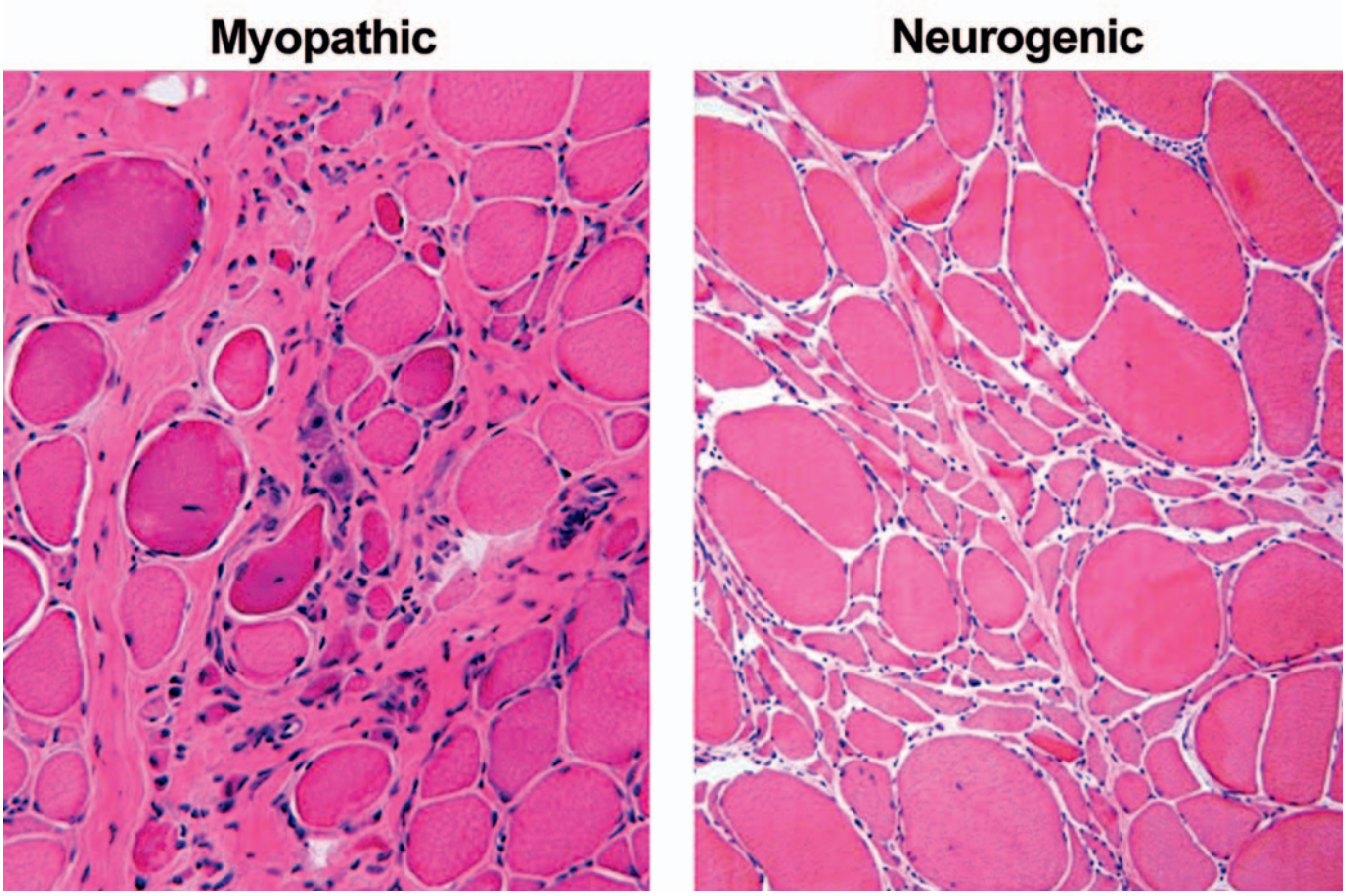

FIGURE 10.8 The spectrum of skeletal muscle lesions differentiates myopathic lesions (left panel) from neurogenic (or denervation) atrophy (right panel). Myopathic lesions, resulting from direct damage to muscle tissue, are characterized by rounded, randomly sized myofibers with central nuclei and variable degrees of myofiber necrosis, regeneration, and/or mineralization sometimes accompanied by inflammation (typically mononuclear cells) and fibrosis. In contrast, neurogenic lesions, which are an indirect effect on muscle tissue secondary to a primary injury the nerve supply, feature groups of angular small myofibers (i.e., foci of denervation atrophy) with peripheral, relatively large nuclei interspersed with large oval myofibers (i.e., those retaining an intact somatic nerve supply), but usually no evidence of myofiber destruction (e.g., myofiber necrosis or regeneration, inflammation or fibrosis). Human skeletal muscle biopsies; formalin fixation, paraffin embedding, hematoxylin and eosin (H&E) staining. Source: *Courtesy: Dr. Mark L. Cohen, Case Western Reserve University, Cleveland, Ohio, with permission.*

Altered Immunologic Function

A xenobiotic may also induce myotoxicity indirectly by provoking immunologic reactions that lead to generalized muscle weakness. D-Penicillamine induces a variety of antibodies, especially an anti-acetylcholine receptor antibody. Experimentally, high doses of D-penicillamine given to guinea pigs over a prolonged period of time cause a mild level of neuromuscular blockade. The slow onset of muscular weakness and the identification of anti-acetylcholine receptor antibodies suggest that the pathogenesis is immune-mediated. Clinical use of D-penicillamine has been associated with adverse effects such as dermatomyositis (inflammation of the skin and muscles) and polymyositis. There is evidence to indicate that autoimmune reactions play a role in the etiology of these types of inflammatory myopathies. A form of myositis may also develop as part of a drug-induced, lupus-like reaction during treatment with procainamide. Rare adverse effects, such as myasthenia gravis and myositis, have been reported in patients given interferon-α. Evidence of dermatomyositis and polymyositis has been reported in some patients treated with statin drugs. These cases responded to steroid treatment, suggesting that statins either initiated immune-mediated skeletal muscle alterations or unmasked a latent subclinical autoimmune condition.

Direct Localized Injury

Some xenobiotics may exert localized toxicity when injected into or near the muscle. Focal damage (i.e., degeneration, necrosis, and hemorrhage) may occur following intramuscular injection of narcotic analgesics and oxytetracycline. Fibrosis of overlying connective tissue,

fascia, and skin has been noted after frequent repeated intramuscular administration of agents such as pentazocine and meperidine. Experimentally, all local anesthetics have been found to induce injury to skeletal muscles with procaine causing the least and bupivacaine the most myotoxicity. Other xenobiotics can produce diffuse damage when given systemically. It is apparent that myopathic effects can occur when a substance directly alters critical structural or functional components of the muscle fiber.

Cell Membrane Alterations

The sarcolemma represents an important cellular component that is usually exposed to the highest concentration of a substance. Some xenobiotics may change the electrical properties of the membrane. Muscle weakness, which occurs when concentrations of potassium are reduced, is apparently the result of a decrease in membrane excitability. Severe hypokalemia may lead to muscle fiber necrosis. In contrast, increased membrane excitability is the likely mechanism by which a number of agents (lithium, cimetidine, salbutamol, danazol, and captopril) cause muscle cramping.

The use of lipid-lowering drugs (statins and fibrates) may elicit a myopathy in both clinical and experimental situations. The precise mechanism by which these types of agents induce muscle fiber necrosis has not been completely elucidated, but there is evidence that the function of certain sarcolemmal ion channels is affected. Ion channel alterations may occur because these drugs inhibit the biosynthesis of important cholesterol-related membrane components. In addition, the lipid-lowering drugs also have important intracellular effects, which likely contribute to the muscle toxicity.

The hypocholesterolemic agent 20,25-diazacholesterol (no longer in clinical use) interferes with the biosynthesis of cholesterol and, as a result, causes accumulation of the cholesterol precursor desmosterol in the serum, the sarcolemma, and the SR. The presence of excessive amounts of desmosterol in the sarcolemma leads to excessive chloride permeability and myotonia (i.e., inability to relax voluntary muscles). Myotonia also occurs following exposure to the herbicidal compound, 2,4-dichlorophenoxyacetic acid (2,4-D). This agent causes metabolic alterations by inhibiting glucose-6-phosphate dehydrogenase, an effect that leads to membrane and subcellular changes; alterations in ion transport are also provoked. Advanced lesions induced by this agent include vacuolization and muscle fiber necrosis.

Alcohol consumption has been associated with skeletal muscle myopathy. Many pathogenic mechanisms are thought to be responsible for this toxicity, one of which appears to involve alterations in membrane control of electrolyte homeostasis.

Monocarboxylic acids, capable of inhibiting chloride conductance, also produce myotonia. Monensin, a carboxylic acid ionophore that selectively interacts with the voltage-dependent sodium (Na_v) channel, consistently causes both skeletal and cardiac muscle necrosis in a variety of animals. Evidence suggests that these effects are due to calcium overloading in myofibers.

Injection of Type A *Clostridium perfringens* toxin (CPA) induces a unique myopathy. This toxin initially causes alterations in the sarcolemma. Subsequently, changes occur in the mitochondria and SR, and ultimately lesions are found in certain contractile components (I and Z bands, A-band filaments). These changes arise through the phospholipase activity of CPA, which breaks down cellular membranes. *Clostridium chauvoei* toxin A (CctA) is a potent cytotoxin that is a key hemolytic and necrotizing component responsible for inducing "blackleg," an infectious hemorrhagic necrosis affecting the hind quarters of cattle (Figure 10.9) and other ruminants.

Sarcoplasmic Reticulum Alterations

Intraperitoneal injection of doxorubicin damages the diaphragm, an effect which is characterized by dilatation of the SR (appears as cytoplasmic vacuolization), myofibrillar degeneration, interstitial edema, and alteration of mitochondrial membranes. Exposure to doxorubicin has been associated with clinical and experimental evidence of respiratory muscle weakness. Vacuolar myopathic alterations have also been observed in rabbits treated chronically with doxorubicin. The vacuolization and other cellular changes noted in skeletal muscle are similar to those that are well known to be induced, either clinically or experimentally, in cardiac myocytes by anthracycline-type agents such as doxorubicin.

Microtubular Alterations

There are similarities in the overt myotoxic effects of colchicine and vincristine. Both of these agents interfere with the function of microtubules by interacting with tubulin and inhibiting microtubular polymerization. The most common adverse effects reported in patients after treatment with colchicine are generalized myopathy and painful neuromyopathy. Vincristine may initiate proximal muscle weakness and myalgias (i.e., muscle pain) that include denervation and varying degrees of muscle fiber necrosis. Both agents cause comparable vacuolar myopathy, which includes the aggregation of lysosomes and the appearance of autophagic vacuoles. These chemicals cause alterations in one or more other organ systems—an effect that may influence the pathogenesis of the myopathy. It is

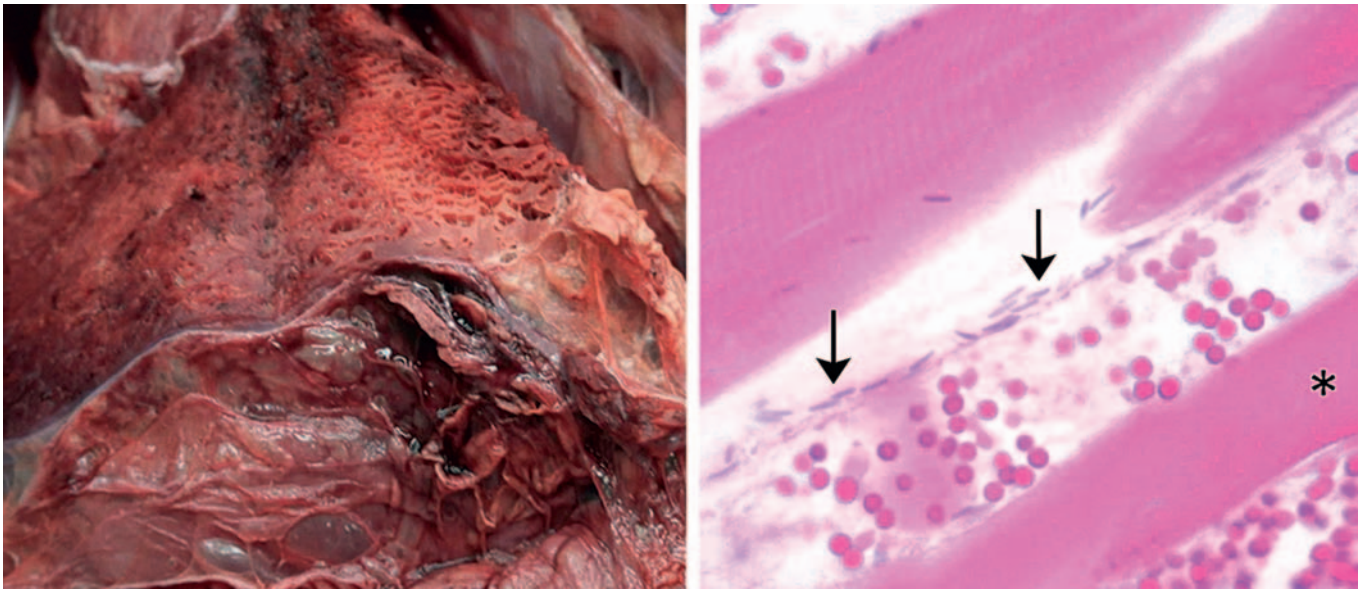

FIGURE 10.9 Hemorrhagic necrosis (blackleg) of the skeletal muscles in the hind quarters of a steer is indicated by multifocal dark red foci with emphysema (i.e., gas bubbles). Tissue sections demonstrated acute myofiber necrosis, shown by loss of striations and nuclei (*), in association with interstitial expansion by edema fluid (clear space with flocculent eosinophilic protein) and hemorrhage. The causative bacillus, *Clostridium chauvoei*, also is visible in the interstitium (arrows). Source: *Image provided courtesy of Dr. Brian G. Caserto, VetPath Services, Stone Ridge, NY, from the Veterinary Pathology Forum blog (https://vetpath.wordpress.com/page/13/?archives-list=1), with permission.*

possible that the tubulin inhibitors share a mechanism with the cationic amphiphilic inducers of phospholipidosis (described below) by inhibiting cellular autophagy and inducing cellular toxicity.

Myofilament Alterations

Myofilament degeneration in certain striated muscles occurs following treatment with plasmocid. In the rat diaphragm, plasmocid initially causes selective loss of actin filaments together with muscle cell Z and I bands. These effects precede the onset of localized myofiber necrosis. It has been suggested that skeletal muscles that are in continual use, such as the masseter, external ocular muscles, and the diaphragm, are most likely to be injured by plasmocid. In cardiac muscle, plasmocid induces mitochondrial dysfunction prior to myocyte necrosis.

Emetine, a constituent of ipecac, produces a pattern of myotoxicity that is similar to the muscle fiber breakdown seen in certain human myopathies. In humans, high doses of emetine cause profound, predominately proximal, myopathy, and cardiomyopathy. In humans and animals, emetine has been found to induce atrophy in both types of striated muscle fibers. Emetine affects intermediate filaments, resulting initially in disruption of the Z discs and subsequently the breakdown of myofilaments in conjunction with accumulation of myofibrillar protein. Multifocal loss of muscle cell cross-striations has been reported to occur in animals treated with emetine. In some areas, loss of oxidative enzyme activity was associated with muscle necrosis. Emetine inhibits protein synthesis, but it is not clear what role this action plays in the myotoxicity. Clinically, some improvement in the myopathy has been reported when use of emetine is terminated.

Lysosomal Alterations

Cationic amphiphilic drugs (CADs) are those whose structure includes both a hydrophilic domain and also a hydrophobic domain that includes a primary or substituted positively charged amine group. These features can facilitate interactions with anionic phospholipids that are constituents of the membranes that surround the sarcolemma and organelles. Drug binding to these phospholipids leads to their intracellular accumulation, which can occur in a variety of cell types and organs including skeletal myofibers. Certain of these cationic amphiphilic agents with diverse pharmacologic actions cause a skeletal myopathy characterized ultrastructurally by lysosomal phospholipid accumulation in the form of large masses of concentric lamellar and curvilinear bodies (i.e., drug-induced phospholipidosis) (Figure 10.10). Type I (slow twitch) myofibers are more frequently affected. The antimalarial chloroquine is associated with this type of myopathy. Chloroquine-induced myopathy is mostly painless, is slowly progressive, and is more pronounced proximally and in the lower extremities.

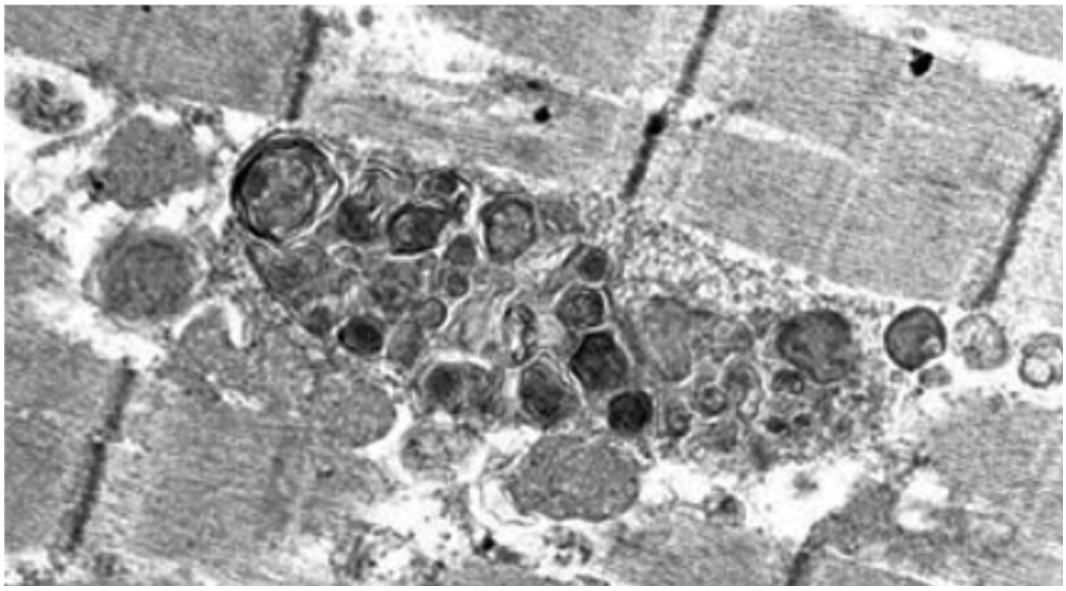

FIGURE 10.10 Transmission electron micrograph of drug-induced phospholipidosis demonstrating multiple lamellar bodies, produced by lysosomal phospholipid accumulation, located between two skeletal myofibrils. Source: *Figure reproduced from Nonoyama, T., Fukuda, R. 2008. Drug-induced phospholipidosis—pathological aspects and its prediction. J. Toxicol. Pathol. 21, 9–24 with permission of the Japanese Society of Toxicologic Pathology.*

Cardiomyopathy can also occur. Examples of other amphiphilic agents associated with myopathy are amiodarone and perhexiline. The myopathy caused by these substances is part of a more general form of intracellular lipid accumulation, which, in addition to skeletal muscle, affects cells in other tissues such as the peripheral and central nervous systems. These agents are both water- and lipid-soluble, and therefore readily diffuse through the plasma membrane. After passing through the sarcolemma, they become adsorbed onto intracellular membranes and form stable drug–lipid complexes that progressively accumulate within the lysosomes of skeletal muscle cells and other tissues. Apparently, such drug–lipid complexes are resistant to degradation by lysosomal enzymes, which fosters the formation of the autophagic vacuoles that are filled with lamellar material.

Altered Intracellular Calcium Concentration

A potentially serious drug-induced myopathic condition, characterized by muscular rigidity and myoglobinuria, hypermetabolism, and metabolic acidosis, occurs in genetically susceptible individuals undergoing routine surgery. Nonspecific observations obtained from muscle biopsy specimens include variability in fiber size, increased size of internal nuclei, "moth-eaten" fibers, and muscle cell necrosis. Malignant hyperthermia is commonly precipitated in these individuals by exposure to halothane and succinyl choline. Other halogenated anesthetic agents, nitrous oxide, muscle relaxants, and certain local anesthetic agents also may induce this reaction. A condition similar to the human syndrome has been described in certain breeds of pigs. Susceptible pigs are sensitive to stress and develop muscle rigidity, acidosis, and hyperkalemia. Death ensues due to heart failure if these pigs are subjected to stress. These sensitive pigs also react to halothane and depolarizing neuromuscular blocking agents. The malignant hyperthermia reaction appears to result from an excessive release of calcium by the ryanodine receptor (a SR calcium channel). Acute increases in this cation cause contracture of muscle fibers, decreased ATP levels, increased cellular metabolism and core body temperature, and secondary changes in a variety of cellular components.

Altered Protein Synthesis

Prolonged corticosteroid therapy is known to cause a skeletal muscle myopathy. Steroids that are fluorinated in the 9th position (triamcinolone, dexamethasone, and betamethasone) are most likely to be myotoxic, but continuous treatment with any of the corticosteroids will also lead to a myopathy. Clinically, steroids induce proximal weakness and atrophy of the lower and upper limbs. The clinical syndrome tends to be less severe than experimentally induced skeletal muscle alterations. According to some definitions, the steroids do not cause a true myopathy but only atrophy of type II fibers. Slow recovery of muscle function usually occurs when administration with the offending

steroid is terminated. Corticosteroids bind to specific target cell receptors and eventually are transported into the nuclei, where they affect the transcription of certain genes. The mechanism of steroid-induced myopathy has been explored in a number of animal studies. These hormones are found to alter multiple myocyte functions, such as protein synthesis (decrease) and degradation (increase), carbohydrate metabolism, sarcolemmal excitability (reduce), and electrolyte homeostasis (yielding hypokalemia). However, the primary mechanism responsible for muscle fiber atrophy appears to be suppression of protein synthesis. This has been attributed to enhancement of the production of myostatin, a protein that inhibits muscle anabolism and promotes proteolysis. Activation of the ubiquitin−proteosome system may also play a role.

Altered Mitochondrial Function

Chronic treatment with nucleoside analog reverse transcriptase inhibitors (NRTIs) such as zidovudine (AZT) has been associated with skeletal and cardiac muscle pathologies. Other NRTI agents, such as zalcitabine (ddC), didanosine (ddI), and lamuvidine (3TC), cause neuropathy while stavudine (d4T) and fialurdine (FIAU) induce myopathy and/or neuropathy and lactic acidosis. Clinical signs of AZT myopathy include progressive proximal muscle weakness, myalgias, and fatigue. In some instances, it has been difficult to separate the effects of human immunodeficiency virus (HIV) disease on skeletal muscle from drug-induced myotoxicity. NRTIs exert clinical activity by competing with certain innate substrates of HIV reverse transcriptase. These agents lack specificity and also block the action of a key skeletal muscle mitochondrial DNA replication enzyme (mitochondrial DNA polymerase gamma). Characteristics of the AZT-induced myopathy include "ragged red" fibers (resulting from accumulation of abnormal mitochondria beneath the sarcolemma), multiple cytochrome c oxidase-negative fibers (indicating reduced mitochondrial capacity for ATP production), biochemical cytochrome oxidase defects, and structurally abnormal mitochondria (when viewed by electron microscopy). Animals given AZT and cells in culture exposed to NRTIs develop similar changes. AZT-induced myopathy is reversible following termination of drug treatment.

Mitochondrial dysfunction has also been implicated in the pathogenesis of statin myopathy. The hypocholesterolemic effect of these agents is related to inhibition of the key enzyme in cholesterol biosynthesis (3-hydroxy-methylglutaryl CoA (HMG-CoA) reductase), which converts HMG-CoA to mevalonate. Clinical expression of myotoxicity in human patients varies from asymptomatic elevations of serum CK activity (i.e., a key cytosolic enzyme found at high levels in skeletal myofibers) to myalgia, cramps, exercise intolerance, fatigability, and rarely muscle fiber necrosis as well as potentially fatal rhabdomyolysis.

Animal studies of the mechanism and lesions produced in skeletal muscle by statin treatment show selective damage to Type IIB fibers. Early ultrastructural alterations involve mitochondrial damage with subsarcolemmal accumulations of myelinoid whorls with fragments of mitochondria. Although multiple mechanisms of muscle fiber injury have been advanced, a central role of mitochondrial function impairment with resulting alterations in intrafiber calcium homeostasis is likely.

The histopathologic alterations produced in rats by treatment with statins showed scattered myofiber necrosis with or without infiltration of inflammatory cells and evidence of myofiber regeneration. Many muscles were affected, but some muscles including the soleus, tongue, masseter, diaphragm, and flexor carpi ulnaris were spared.

In addition to its role in cholesterol biosynthesis, mevalonate is a precursor for intermediates that are key substrates of coenzyme Q10 (ubiquinone), which plays a key role in the mitochondrial electron transport chain. Accordingly a proposed mechanism for statin myopathy has been reduction in coenzyme Q10 leading to impaired muscle energy metabolism. Clinical testing of that hypothesis has seen mixed results. Other proposals focused on mitochondrial energy metabolism include carnitine palmitoyltransferase II deficiency and carnitine abnormalities.

Skeletal muscle atrophy is a recognized consequence of advanced neoplasia (i.e., "cachexia of cancer"). This condition is attributed to induction of inflammatory cytokines. Evidence also suggests that the drugs used to treat cancer may be culprits. Clinically, patients may experience muscle pain and weakness, exercise intolerance, and persistent fatigue. Since several classes of cancer drugs, such as alkylating agents (cisplatin), antitumor antibiotics (e.g., anthracyclines), and antimetabolites (e.g., 5-fluorouracil, capecitabine, gemcitabine), act directly or indirectly but nonselectively to interfere with DNA or RNA replication or synthesis, mitochondria may be targets.

Altered Muscle Cell Differentiation

Information regarding the possible effect of exposure to xenobiotics during pregnancy on subsequent growth and development of skeletal muscle in the fetus is inconclusive. In tissue culture studies, some drugs seem to interfere with certain aspects of muscle

cell differentiation. For example, prenatal exposure of rats to 6-mercaptopurine (a purine analog that disrupts nucleic acid synthesis in rapidly dividing cells) leads, after a latent period, to a continuous and progressive degeneration of muscle cells. These myotoxic effects are not seen when 6-mercaptopurine is administered during the postnatal period. Intrauterine exposure of pregnant rats to low doses of chloroacetonitrile causes fetal skeletal muscle tissue alterations in which the fibers were distorted, smaller in size, and widely separated by connective tissue. Skeletal muscle mitochondrial myopathy has been observed in fetal monkeys whose mothers were exposed to zidovudine (AZT) during pregnancy.

SUMMARY

The skeletal muscle system is an important and potentially less appreciated target of xenobiotic-induced injury. However, its contribution to overall body mass and important roles in structural conformation and locomotion significantly impact general health and well-being. Though important elements of structure and physiology of skeletal and cardiac myocytes are shared, skeletal myocytes have an important regenerative capability that cardiomyocytes do not. Accordingly, mechanisms of xenobiotic-induced injury often are common between the two muscle types, but the consequences to the individual's overall health typically are very different.

Contraction and relaxation of skeletal myocytes are initiated by changes in action potentials across cell membranes influenced by neuromuscular signals and facilitated by intracellular calcium gradients and mitochondrial energy production. All of these activities are important targets that may lead to skeletal muscle toxicity. Basic cellular maintenance functions like protein and nucleic acid synthesis as well as protein degradation and membrane production are also targets. The long-term consequences of xenobiotic-induced skeletal muscle injury are influenced by the severity and duration of injury as well as the impact on the regenerative capacity of the myocytes. Pathologists tasked with evaluating skeletal muscle for potential toxic effects will need to be able to differentiate one-time (i.e., monophasic) from intermittent or continuous (i.e., polyphasic) lesions, and to recognize the attributes of damaged tissue in the midst of repair.

Further Reading

Berridge, B.R., Van Vleet, J.F., Herman, E., 2013. Cardiac, vascular, and skeletal muscle systems. In: Haschek, W.M., Rousseaux, C.G., Wallig, M.A. (Eds.), Haschek and Rousseaux's Handbook of Toxicologic Pathology, third ed. Elsevier, Inc., Academic Press, pp. 1567–1665.

Cooper, B.J., Valentine, B.A., 2016. Muscle and tendon. In: sixth ed. Maxie, M.G. (Ed.), Jubb, Kennedy, and Palmer's Pathology of Domestic Animals, vol. 1. Elsevier, St. Louis, MO, pp. 164–249.

Jones, J.D., Kirsch, H.L., Wortmann, R.L., Pillinger, M.G., 2014. The causes of drug-induced muscle toxicity. Curr. Opin. Rheum. 26, 697–703.

Mastaglia, F.L., 1982. Adverse effects of drugs on muscle. Drugs. 24, 304–321.

Pasnoor, M., Barohn, R.J., Dimachkie, M.M., 2014. Toxic myopathies. Neurol. Clin. 32 (3), 647–674.

Sirvent, P., Mercier, J., Lacampagne, A., 2008. New insights into mechanisms of statin-associated myotoxicity. Curr. Opin. Pharm. 8, 333–338.

Sorensen, J.C., Cheregi, B.D., Timpani, C.A., Nurgali, K., Hayes, A., Rybalka, E., 2016. Mitochondria: inadvertent targets in chemotherapy-induced skeletal muscle toxicity and wasting? Cancer Chemother. Pharmacol. 78, 673–683.

Warren, J.D., Blumbergs, P.C., Thompson, P.D., 2002. Rhabdomyolysis: a review. Musc. Nerv. 25, 332–347.

CHAPTER

11

Urinary System

Kanwar N.M. Khan[1], *Gordon C. Hard*[2], *Xiantang Li*[1], *and Carl L. Alden*[3]

[1]Worldwide R&D, Pfizer, Groton, CT, United States [2]Toxicologic Pathology Consulting, Tairua, New Zealand
[3]Mayflower Consulting, Wrenceburg, IN, United States

OUTLINE

PART 1: KIDNEY

INTRODUCTION

The urinary system is a common target site for toxicity of drugs and environmental chemicals. The kidney is particularly susceptible because of the high blood flow to this organ relative to its mass and the unique property of renal tubular epithelium in concentrating urine and its constituents including drugs and chemicals. Three main clinical entities in humans associated with drug effects on kidney are the nephrotic syndrome (NS), acute renal failure (ARF), and chronic renal failure. It is estimated that about 20% of all ARF cases in humans are related to pharmaceutical agents and that 2% to 5% of patients admitted to the hospital will develop drug-induced acute renal insufficiency. An estimated 500,000 new patients exposed to drugs on a worldwide basis each year

Fundamentals of Toxicologic Pathology.
DOI: http://dx.doi.org/10.1016/B978-0-12-809841-7.00011-3

develop end-stage renal disease. The estimated annual costs of dialysis and transplants are substantial, representing a major challenge to the pharmaceutical and chemical industries for developing safer molecules.

The gold standard method for identification of toxicity to the urinary system is light microscopic examination, supplemented with renal function tests and biochemical markers of cell injury in blood and urine. To refine the risk assessment, establishment of the cellular and subcellular organelle targets of xenobiotic injury by the pathologist forms a cornerstone in expanding the mechanistic understanding of the injury process. Through identification of cellular and subcellular targets, the most sensitive biomarkers can be identified to noninvasively monitor for the presence of a specific xenobiotic insult in laboratory animals and eventually in humans. This chapter emphasizes the structural and biochemical changes and the potential mechanisms involved in urinary tract toxicity.

STRUCTURE AND FUNCTION OF THE KIDNEY

The urinary system plays many important and sometimes vital functions to maintain normal homeostasis in the body. The major contributions include excretion of waste products of metabolism, regulation of body water and salt, maintenance of extracellular fluid volume, maintenance of acid–base balance, and elimination of foreign substances such as drugs and chemicals and their breakdown products. Alterations in renal functional capacity can affect any of these functions and have a detrimental effect on the body. The kidney is recognized as one of the target organs most vulnerable to the toxic effects of drugs and environmental chemicals. The kidney is particularly susceptible because of the high blood flow to this organ relative to its mass and the unique property of the renal tubular epithelium in concentrating urine and its constituents (e.g., drugs or chemicals) through the countercurrent mechanism. Thus, the kidney is typically exposed to a more localized and a higher concentration of drugs and chemicals than other tissues.

In the safety assessment of new molecular entities, the concordance in responses to xenobiotics in rat and human strongly support the rat as a good predictor for human renal hazard. The exceptions in concordance include two categories, immune-mediated drug injury in humans and the xenobiotic-associated unique alpha$_{2u}$ globulin nephropathy syndrome in male rats. The safety assessment based on data from healthy laboratory animals can also be challenging because of the frequency of complexing factors in human drug-induced renal injury, such as age-associated variability in renal structure and function, or concomitant conditions affecting renal functions such as hydration status, hypertension, heart failure, and cirrhosis. The toxic effects of exposures are therefore difficult to precisely extrapolate from laboratory animals to humans because of these variable risk factors for renal toxicity.

Renal Structure

The kidney of the mature rat is bean-shaped and weighs approximately 0.51%–1.08% (with a mean of 0.65%) of the body weight, varying with age and sex. It has a basic unipapillary architecture, the simplest type of mammalian kidney. Other architectural types in other species can be regarded as adaptations to larger body sizes. Each adult rat kidney contains roughly 30,000–35,000 nephrons. In transverse section, the cortex and outer stripe of the outer medulla (OSOM) can be differentiated from the inner stripe of the outer medulla (ISOM) and the inner medulla with the papilla extending into the renal pelvis (Figures 11.1 and 11.2). Furthermore, the arcuate vessels are readily visualized in this section. The renal pelvis represents a dilatation of the ureter.

In the adult kidney, the renal artery branches at the hilus into 6 to 10 interlobar arteries, giving rise in turn to arcuate arteries coursing parallel to the capsule along the corticomedullary junction (Figure 11.1). Interlobular arteries arise from the arcuates, coursing perpendicular to the capsule, each supplying a cortical labyrinth. Each interlobular artery gives rise to 6 to 11 afferent arterioles. All renal artery branches are end arteries without significant collateral supply. The renal circulation is a portal system since glomerular capillary beds reunite into an efferent arteriole, running for a varying distance before again forming a capillary bed surrounding portions of the lower nephron. All circulation to the medulla is of postglomerular capillary derivation. Veins run parallel to the main arterial and arcuate system. Lymphatics run parallel only to the cortical vasculature. Efferent arterioles of subcapsular nephrons are long, breaking into capillary beds that supply the same nephron, then subsequently coalescing to form an interlobular vein. Efferent arterioles of midcortical and juxtamedullary nephrons, in contrast, give rise to descending vasa recta which break up into capillary plexuses, forming the exclusive blood supply to the medulla. Capillary plexuses reunite, forming ascending vasa recta. Capillary plexuses are dense in the inner stripe, but sparse in the outer stripe and inner medulla. Ascending vasa recta join the arcuate veins at the corticomedullary junction. Mammalian kidneys are richly innervated with postganglionic sympathetic fibers to the afferent and efferent renal arterioles, juxtaglomerular apparatus (JGA), proximal tubule, loop of Henle, and distal tubule.

The glomerulus is composed of a capillary network lined by a thin layer of endothelial cells; a central

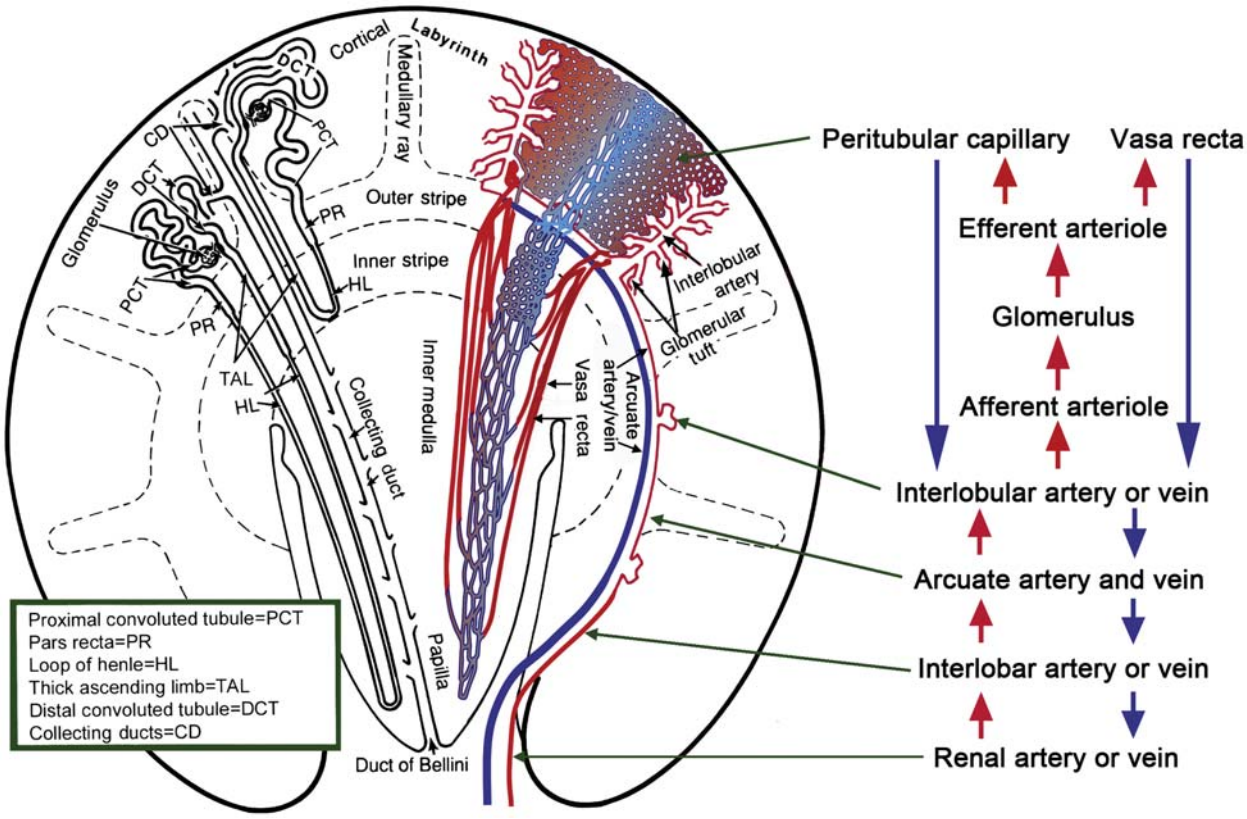

FIGURE 11.1 Schematic drawing of the nephron and vasculature, denoting subtopographical anatomic relationships. *Figure modified from Haschek and Rousseaux's Handbook of Toxicologic Pathology (2013), third ed. (W.M Haschek, C.G. Rousseaux and M.A. Wallig, eds.), Academic Press (Elsevier), Figure 47.1, p. 1671, with permission.*

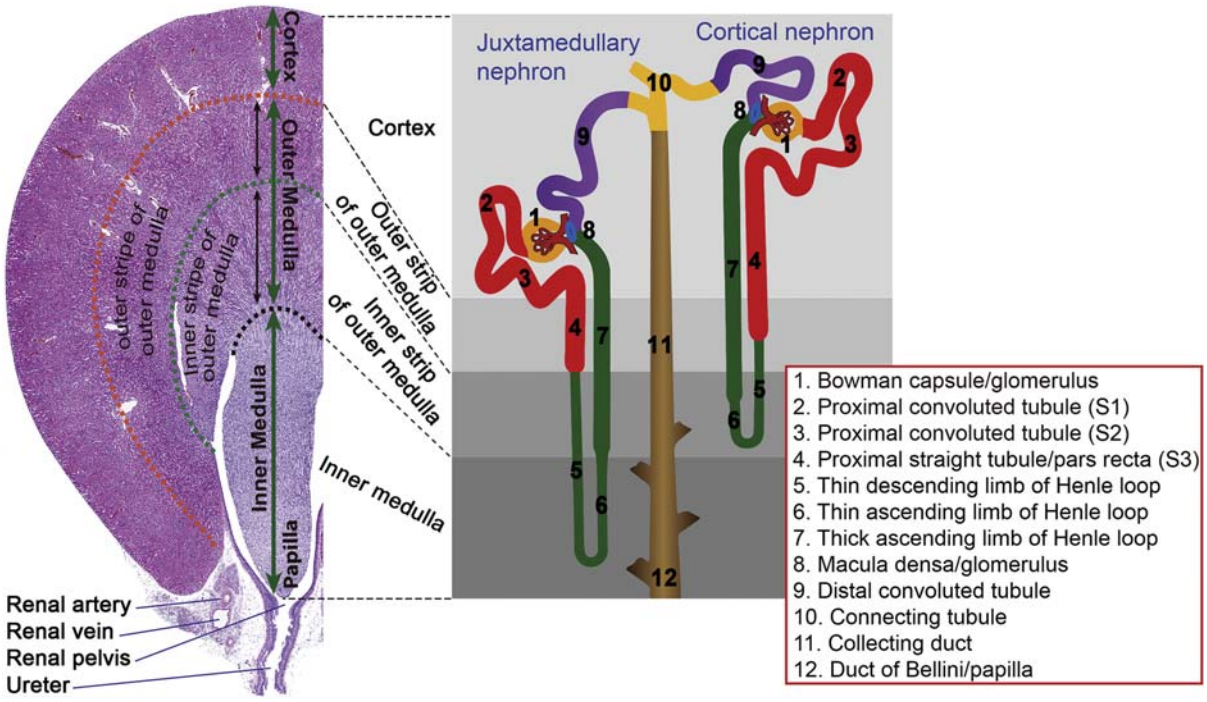

FIGURE 11.2 Subgross topographical anatomy of the rat kidney, illustrating the zones of the kidney and correlative distributions of renal tubules.

region of mesangial cells and mesangial matrix; and the visceral epithelial cells or podocytes and parietal epithelial cells (PECs) of Bowman's capsule and the associated basement membranes. The glomerulus represents the filtering unit for blood through which the plasma filtrate is derived in the first part of the uriniferous space. The filtering membrane of the glomerulus consists of fenestrated capillary endothelial cells, a glomerular basement membrane, and the podocytes (Figure 11.3). Podocytes are postmitotic highly differentiated cells with a unique architecture that includes a cell body, major processes and foot processes bridged by slit diaphragms. The PEC of Bowman's capsule and its basement membrane are continuous with the proximal convoluted tube (PCT).

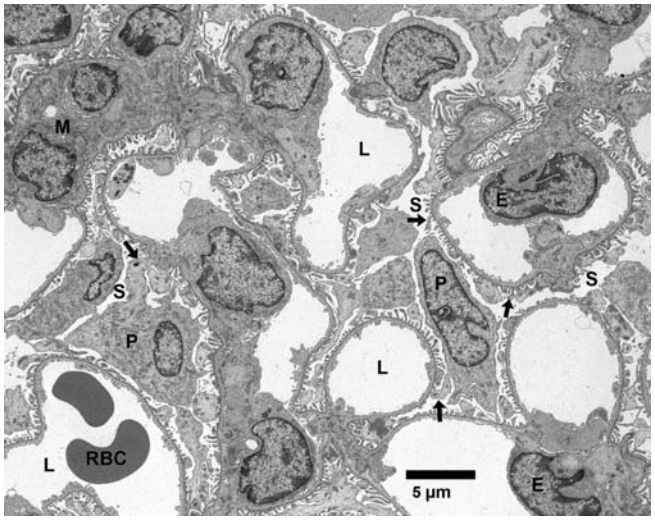

FIGURE 11.3 Ultrastructure of the rat glomerulus, illustrating podocytes (P) and their foot processes (arrows) adjacent to the basement membrane, endothelial cells (E) of capillary loops (L), red blood cells (RBC), and glomerular filtration space (S). *Figure from Haschek and Rousseaux's Handbook of Toxicologic Pathology (2013), third ed. (W.M. Haschek, C.G. Rousseaux and M.A. Wallig, eds.), Academic Press (Elsevier), Figure 47.4, p. 1673, with permission.*

The proximal tubule begins at the urinary pole of the glomerulus and consists of an initial convoluted portion, the PCT, which is a direct continuation of the parietal epithelium of the Bowman's capsule and a straight portion, the pars recta, which is located in the outer stripe and medullary ray (Figure 11.2). The proximal tubule is approximately 8, 10, and 14 mm long in the rat, rabbit, and human, respectively. The vast majority of structural subunits in the cortex represent PCTs. The proximal tubule morphologically is divided into three segments (S_1, S_2, and S_3) in several animal species including rat, rabbit, mouse, and the rhesus monkey (Figure 11.2). The S_1 segment is short, connecting with the glomerular filtration space. The cells of this segment have the highest rate of oxidative metabolism in the kidney. The S_2 segment represents the vast majority of the PCT and extends into the pars recta (S_3). The pars recta, the straight portion of the proximal tubules of the juxtamedullary nephron, are located in the OSOM (Figures 11.2 and 11.4), while pars recta of short-looped (subcapsular) nephrons are found within the medullary rays or within the outer stripe.

The transition from the proximal tubule to the thin descending limb of the loop of Henle is abrupt and it marks the boundary between the outer and the inner stripes of the outer medulla. The length of loop of Henle varies with subcapsular nephrons having a very short loop (thus short-looped nephrons) extending only into the outer stripe. Juxtamedullary nephrons (or long-looped nephrons) extend deep into the papilla (Figures 11.1 and 11.2). However, only about 250 nephrons reach the last millimeter of the tip of the papilla.

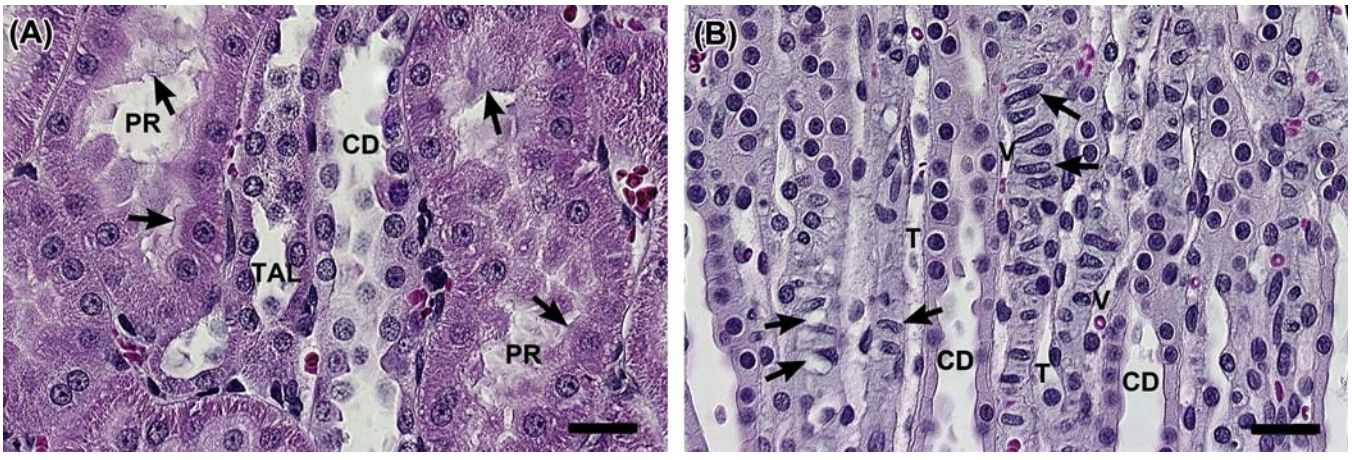

FIGURE 11.4 Light micrograph of a rat kidney. (A) The outer stripe of the outer medulla illustrates normal pars recta (PR) or straight portion of the proximal tubule, with prominent brush borders (arrows), thick ascending loop (TAL) of Henle and collecting duct (CD). Bar = 20 µm. (B) Inner medulla illustrating stellate cells (arrows) and collecting duct (CD). The elongated nuclei of stellate cells are arranged like rungs of a ladder between the thin loop (T) of Henle and vasa recta (V). Bar = 25 µm.

The distal tubule comprises three structurally distinct segments: The thick ascending limb of the loop of Henle (TAL), the macula densa, and the distal convoluted tubule (DCT). The TAL is found in the outer zone of the medulla and in the cortex, ending near its own glomerulus, just past the macula densa (Figure 11.2). The JGA is located at the vascular pole of the glomerulus, where a portion of the distal tubule comes into contact with its parent glomerulus (Figure 11.2). The main components of JGA are the macula densa of the thick ascending limb, the renin producing granular cells of the afferent arteriole, and the extraglomerular mesangial cell (Goormaghtigh cell, lacis cell). The macula densa is a region of the specialized DCT epithelial cells adjacent to the hilum of the glomerulus.

The DCT is approximately 1 mm in length and begins at a variable distance beyond the macula densa and extends to the connecting tubule that connects the nephron with the collecting duct (Figure 11.2). Cytologically the DCT cells are taller but otherwise similar to those of the thick ascending limb of loop of Henle. The collecting ducts progressively anastomose and extend from the connecting segment in the cortex through the outer and the inner medulla to the tip of the papilla (Figures 11.2 and 11.4). The collecting ducts can arbitrarily be subdivided into three regions based on their location in the kidney including the cortical collecting ducts, the outer medullary collecting ducts, and the inner medullary collecting ducts. The cells lining the collecting duct are low cuboidal in the cortex, increasing in height to low columnar in the papilla. In most nonhuman primate species, there are multinucleated syncytial cells lining the medullary collecting ducts (Figure 11.5). In the papilla, collecting ducts form the ducts of Bellini which empty into the pelvis. The cortex in the rat consists of 7% interstitium by volume, of which only 3% represents the interstitial cells. By contrast, in the medulla the amount of interstitium continuously increases toward the tip of the papilla, reaching up to 29% by volume. The corticomedullary junction connective tissue and outer stripe apparently serve to isolate the increasingly hypertonic medullary interstitium from the cortex.

FIGURE 11.5 Light micrograph of the renal medulla of a young male cynomolgus monkey illustrates spontaneous syncytial cells (arrows) in the collecting tubules. Bar = 25 μm.

Interspecies differences in renal structure and function are summarized in Table 11.1. Pig and human kidneys are anatomically quite similar both being characterized as multilobular and multipapillary and with many similarities in anatomical relationships between intrarenal arteries and the collecting duct system. In both species, an elaborate system of interlobar and segmental arteries is present to supply the numerous kidney lobes whereas in dogs and rodents, segmental arteries are not present nor needed because of the lack of multiple medullary pyramids.

Renal Function

The primary functions of kidneys can be divided into four major categories: (1) control of the body's fluid and electrolytes, (2) elaboration of hormones, (3) excretion of the waste products of metabolism, and (4) selected metabolic activities. Most importantly, nitrogenous waste products consisting of urea, creatinine, and ammonia ion are excreted in the urine; thus any significant alterations in renal function are manifested as retention of these waste products in the body.

Normal renal function is predicated on adequate perfusion (pressure and volume). The kidneys typically receive 25% of the cardiac output but only about 10% of oxygen consumption occurs in the kidneys. Approximately 85% of renal blood flow is associated with the cortex, 14% with the outer medulla, and 1% with the inner medulla, reflecting heterogeneity in intrarenal distribution. Filtration is the basic determinant in urine formation and a key measurement of kidney function.

The proximal tubule represents the site of reabsorption of the most sodium. The water reabsorption is passive, accompanying active reabsorption of solutes. The kidney is responsible for controlling the concentration of potassium in the body. A marked decrease in urinary potassium clearance does not occur until body potassium stores are depleted 20%–40%. An increase in potassium load, however, results in a prompt rise in urinary potassium clearance. There is a connection between sodium reabsorption and potassium excretion, reflecting passive K^+ transport. A connection also exists between urinary potassium and hydrogen ion excretion. Potassium excretion is also influenced by aldosterone. The proximal tubule is the site of 70% of potassium reabsorption. Alkalosis results from increased excretion of potassium in urine, whereas acidosis results in diminished renal potassium excretion.

Ca and PO_4 balance is profoundly influenced by active transport in the proximal tubule. The glomerular

TABLE 11.1 Comparative Renal Structure and Functional Characteristics to Aid in Understanding and Interpretation of Responses to Nephrotoxicants

Parameter	Rat	Monkey[a]	Dog	Pig	Man
Body weight (kg)	0.24	3.8	9.1	46	70
Single kidney weight (g)	0.75	9	31	77	157
Nephrons (per g body weight)	128	49	45	26	16
Number of nephrons (000s)	30	103–123	340–490	400–1196	300–1100
Glomeruli radius (μ)	61	83	90	83	100
Proximal tubule length (M)	12	NA	20	NA	16
Tubule radius (μ)	29	NA	33	NA	36
Long loops (%)	28	NA	100	3	14
Medullary thickness (relative)	5.8	NA	4.3	1.6	3.0
Maximum osmolality (mOsmol/kg)	2610	1900	2610	1080	1400
Inulin clearance (mL/min/kg)	6.0	1.9	4.3	NA	2.0
Maximal GFR (mL/min m^2)	35	NA	104	72	75
Renal organization	Unipapillary	Unipapillary	Uniapillary	Multilobular	Multilobular
Medullary structure	Complex	Simple	Simple	Simple	Simple

[a]*Cynomolgus monkey kidney is unipapillary while Rhesus monkey kidney is multilobular.*
NA, data not available.
Table reproduced from Handbook of Toxicologic Pathology (2013), third ed. (W. M. Haschek, C. G. Rousseaux, and M. A. Wallig, eds.), Academic Press, Table 47.3, p. 1678, with permission.

filtrate concentration of calcium is 50%–75% of the plasma level. Calcium is 99% reabsorbed, 60% in the PCT, two-thirds of which is passive in exchange for sodium. The phosphate glomerular filtrate concentration is 90% of the plasma level. Two-thirds of the phosphate is reabsorbed in the proximal tubule, whereas 20% typically is cleared in the urine.

Nitrogenous waste products consisting of urea, creatinine, and ammonia ion are excreted in the urine. The concentration of urea and creatinine in blood represents dynamic production and excretion. During health, the kidney has remarkable functional reserve as the excretion of these nitrogenous waste products is unaffected until approximately 60% reductions have occurred in the glomerular filtration rate (GFR). Beyond this, urea levels are dependent on both GFR and its production, affected by protein intake and tissue catabolism. Creatinine is a better guide to GFR than urea as it is less dependent on diet but can be influenced by age, sex, and muscle mass.

Of the amino acids in the glomerular filtrate, 99% are actively reabsorbed in animals and humans, with the unique exceptions of the male mouse urinary protein and the male rat $alpha_{2u}$ globulin protein. The male mouse and rat are physiologic proteinurics. Fractional excretion of most amino acids is between 0.2% and 2.5%, although this proportion may increase in various pathologic conditions. Fanconi syndrome that causes impaired reabsorption of filtrated molecules, including amino acids, small proteins, and glucose, is a disorder of the proximal tubules. The etiology of the syndrome is associated with tyrosinemia.

On the basis of the preferential substrate selectivity, transport systems responsible for renal tubular secretion of endogenous or exogenous substances in the PCT can be divided into organic anion and organic cation transport systems. By molecular cloning, several families of multispecific organic anion transporters (OATs) and cation transporters have been identified (Table 11.2). The OAT family consists of six isoforms (OAT1–4, URAT1, and rodent OAT5) representing the main renal secretory and reabsorptive pathway for organic anions. The OAT family is also involved in the distribution of organic anions in the body, drug-drug interactions, and toxicity of anionic substances such as nephrotoxic drugs and uremic toxins.

The kidney plays an important role in the synthesis, metabolism, and secretion of hormones, metabolism of drugs and xenobiotics, and the excretion of the waste products of metabolism, drugs, hormones, and xenobiotics. The major metabolic activity is present in the cytoplasm of proximal tubules and specifically in microsomes. Cytochrome P-450 content of the kidney is only 10%–20% of liver content. However, at the cellular level, the cells of the pars recta are comparable with hepatocytes in concentration of P-450 enzymes. In instances of renal impairment, the clearance of a drug can be compromised, resulting in increased

TABLE 11.2 Organic Anion Transporters in the Kidney

Transporter	Substrate examples
OAT-1	*p*-Aminohippurate, urate, PGE2, NSAIDs, ochratoxin-A, β-lactam antibiotics, ACE inhibitors, uremic toxins
OAT-2	PGE2
OAT-3	Estrone sulfate, cAMP, cGMP, dehydroepiandrosterone sulfate, PGE2, ochratoxin-A, cimetidine, tetracycline, uremic toxins
OAT-4	Estrone sulfate, DHEAS, PGE2, PGF2α, ochratoxin-A, tetracycline, methotrexate
URAT-1	Urate
OAT5	Estrone sulfate, ochratoxin-A, dehydroepiandrosterone sulfate

Table reproduced from Handbook of Toxicologic Pathology (2013), third ed. (W. M. Haschek, C. G. Rousseaux, and M. A. Wallig, eds.), Academic Press, Table 47.5, p. 1683, with permission.

systemic levels with continuing administration, subsequently achieving toxic levels. Compounds with low molecular weights, low lipophilicity, and preferentially ionic at pH 7.4 are eliminated effectively. Substances with high molecular weight, avid protein binding, lipophilicity, and/or almost completely nonionic will not be effectively cleared in the urine.

EVALUATION OF RENAL TOXICITY

Routine methodologies comprising standard biomarkers in blood and urine followed by gross and microscopic pathologic evaluations are considered appropriately sensitive in standard preclinical testing. Once nephrotoxicity potential is recognized, additional *in vitro*, *ex vivo*, or specialized *in vivo* studies can be done to gain further understanding on mechanisms of toxicity, or to screen a library of test articles if availability of test material limits assessment in standard toxicology studies.

Clinical chemistry screens with blood urea nitrogen (BUN), creatinine, and electrolytes, urinary excretion of protein and electrolytes, and routine urinalysis (with volume, specific gravity, and microscopic sediment evaluations) supplemented with kidney weights and histology provide adequate information on the physiologic status of the kidney or any significant perturbations in renal functions in a well-designed toxicology study. There are a variety of highly sensitive biomarkers of renal toxicity that can be additionally incorporated into toxicology studies if kidney is considered to be a potential target organ. For robust assessments of urinary biomarkers, it is essential to collect urine specimens of good quality over a 16–24-hour period and consider the age of animals being evaluated. In rats, the urinalysis results may become more variable because of development of spontaneous age-related renal diseases.

Physiologic Considerations

Age, gender, and species-related differences in anatomy and physiology should be thoroughly considered in translating preclinical toxicity data for humans (Figure 11.6). Drug-response differences in patients of various ages including children and the elderly are common, often leading to challenges in optimizing dosages and duration of use. For example, developmental changes in renal function can dramatically alter the plasma clearance of compounds with extensive renal elimination and thus can enhance renal and systemic toxicity of these drugs. Because of the challenges presented for pediatric clinical trials, attention has turned to the supportive preclinical data that accompany clinical trials. It has been recognized that there are circumstances where the existing toxicology studies in adult animals may need to be supplemented by added investigation using juvenile animals. However, the juvenile animal data can only be useful to inform the pediatric human populations if evaluated in the most appropriate species at the most relevant age considering comparability of specific organ system development in question coupled with the disease indication, existing toxicological data and likely route of human exposure. In humans, before 34 weeks of gestational age, the functional demands on the fetal kidney are minimal, but these increase dramatically in the last part of the third trimester and with birth. While the adult kidney receives 20%–25% of the cardiac output, the human fetal kidney receives only 4%, which increases to 10% by the end of the first postnatal week. Renal function in neonates remains different from that of adults, and GFR and renal blood flow corrected for body size are not comparable to adult values until the child is 12 months old. GFR gradually increases until adolescence, where it is maintained at adult levels. After the age of 40 in humans, there is a progressive decrease in renal function, which is primarily the result of progressive loss of renal mass and nephron number.

Age-related renal damage contributes significantly to abnormalities in GFR and tubular function resulting in different susceptibility of the aged population to nephrotoxic response as compared to neonates, juveniles, and young adults. Similarly, in rats, GFR

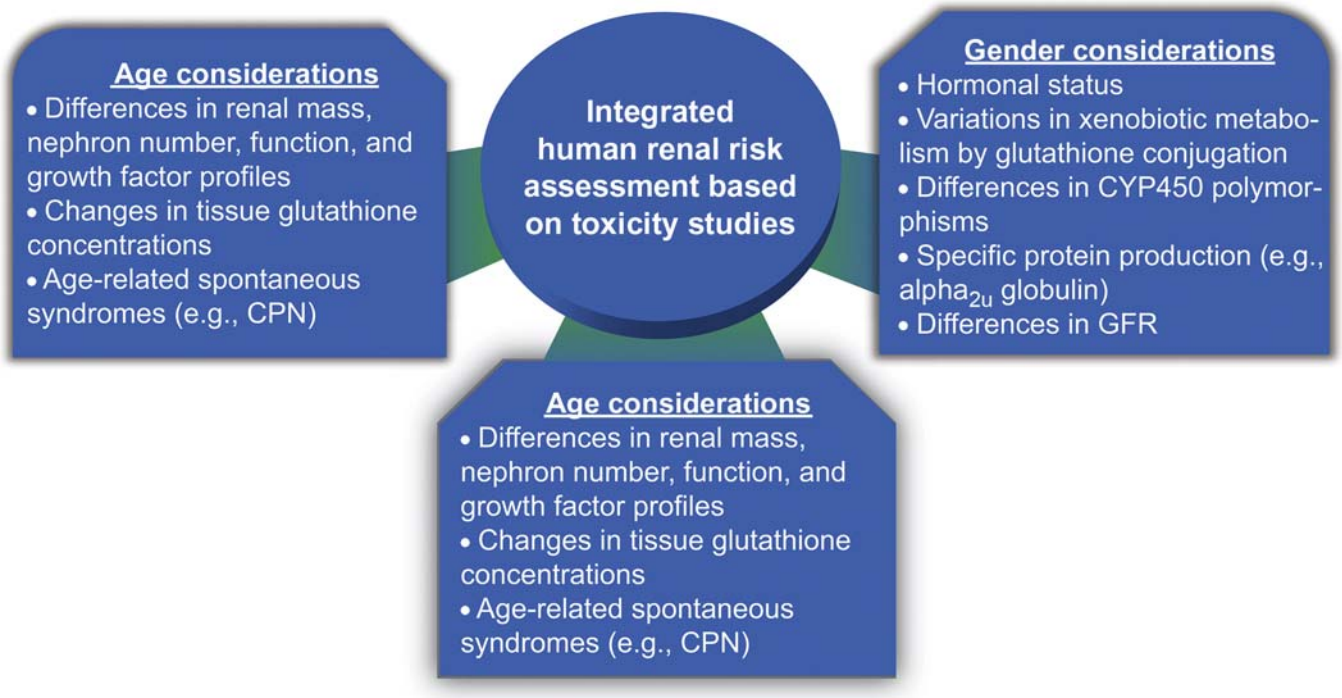

FIGURE 11.6 Age, gender, and species considerations for integrated human renal risk assessment of nephrotoxicity. *Figure reproduced from Haschek and Rousseaux's Handbook of Toxicologic Pathology (2013), third ed. (W.M. Haschek, C.G. Rousseaux and M.A. Wallig, eds.), Academic Press (Elsevier), Figure 47.13, p. 1691, with permission.*

gradually decreases with age, and by 18 months, the GFR is decreased to approximately 68% of its rate compared to young adult rats. These age-related changes are manifested in increased serum levels of urea, creatinine, sodium, and chloride, decreased serum levels of albumin, decreased creatinine clearance, decreased urine output and sodium excretion, and proteinuria. Proteinuria along with urinary loss of albumin is evident in male rats as early as 6 months of age. In dogs, there is a gradual increase in GFR in the first 3 weeks postnatally. This increase in GFR is primarily the result of continuing glomerular differentiation in the outer cortical region. With progressive nephron loss in older dogs, there are decreases in GFR, similar to those in rats and humans.

Changes in tubular function, similar to GFR, occur with age and are important in age-dependent differences in susceptibility to nephrotoxicity e.g., aminoglycosides and vancomycin. Fetuses and neonates have inefficient urine-concentrating ability, as a result of both short proximal tubules and inefficient tubular transport. The tubular function in human kidney reaches adult capacity by 18 months of age and in rat kidney by 6 weeks of age. Although the relatively low tubular transport capacity of the neonate is generally of no clinical significance, it may be more vulnerable in disease than glomerular functions. The neonatal renal tubular function for the transport of organic ions is low and thus so is the accumulation of nephrotoxic substances in the proximal tubular epithelial cells. Therefore, neonates are generally less likely to have drug-induced nephrotoxicity. Examples of specific compounds, in which adults have a higher risk of nephrotoxicity than neonates, include aminoglycosides, vancomycin, cadmium, cisplatin, and acetaminophen.

In humans, tubular transport efficiency is greatly reduced in the aged kidney as a result of progressive nephron loss, decreased mitochondrial function, and reduced numbers of proximal tubular ion transporters. Defects in tubular transport with increasing age are demonstrated by decreases in *p*-aminohippuric acid (PAH) uptake by proximal tubular cells. Rats also develop age-related changes in normal tubular transport function. This is characterized by progressive decreases in urinary concentrating ability and decreased chloride, calcium, and potassium retention. Changes in tubular transport function are evidenced by a 5%–10% decrease in urine osmolality in rats as early as 6 months of age and, between the age of 12 and 27 months, there is a 40% decrease in active renal tubular transport. Renal tubular function in dogs does not reach adult levels until after 1 to 2 months of age, as evidenced by reduced renal amino acid reabsorption. With age, dogs develop reductions in urinary concentrating capacity, similar to rats and humans.

Physiologic Adaptation to Demands for Altered Function

The kidney adapts to altered demands by functional and structural changes. Compensatory hypertrophy occurs in the kidney after extirpation of the contralateral kidney. Hypertrophy is recognized by an increase in the volume of the cortex, primarily involving PCTs, without an increase in nephron numbers but with some increase in glomerular volume. Measurement of the cross-sectional area of PCTs parallels functional adaptation measurements more precisely than does organ weight. The PCT response primarily represents hypertrophy with only slight hyperplasia.

Several stimuli are recognized as the causes of renal hypertrophy, including administration of increased protein, amino acids, urea, or NaCl. Testosterone treatment, ACTH-mediated hyperadrenocorticism, and diabetes mellitus also cause renal hypertrophy. Potassium depletion results in an increase in lumenal membrane area and altered mitochondrial content of collecting duct intercalated cells. Chronic furosemide treatment results in increased sodium loss, with a persistent need for increased sodium reabsorption in the DCT to compensate. Xenobiotics metabolized by the kidney can cause renal enlargement, presumably through adaptive increase in metabolizing-enzyme synthesis activity. Cyclosporine A treatment is associated with renal enlargement and glomerular hyperfiltration in rats. Decalin, a propellant, results in renal hypertrophy across species and sexes.

Biochemical and Biomarker Evaluations

In preclinical toxicology studies, microscopic evaluation of kidney remains the gold standard, but its limitation is that it cannot be monitored effectively in clinical investigations. Among the basic requirements for a renal biomarker besides noninvasiveness specificities for kidney are reliability, noncomplexity, inexpensive, and low interindividual variability. An ideal marker would also reveal the location of tubule segment or compartment where the injury occurred (e.g., cortical renal tubules, pars recta, collecting duct, renal pelvis, or interstitium); provide a quantitative reflection discriminating different pathophysiologic processes (e.g., sepsis, ischemia, tubular epithelial necrosis, inflammation, chronic kidney disease); predict injury progression; and monitor response to therapeutic intervention with prognostic significance. The application of different renal biomarkers to predict the location of renal injury is summarized in Table 11.3. Baseline renal function values for various ages of Sprague-Dawley (SD) rats and of young adult Beagle dogs are summarized in Tables 11.4 and 11.5, respectively.

TABLE 11.3 Urinary Biomarkers of Nephrotoxicity

Biomarker	Site of renal injury
β_2-Microglobulin	Proximal tubule
Albumin	Glomerulus and tubule
Clusterin[a]	Tubular epithelial regenerative response
Creatinine	General kidney injury and disease
Cystatin C	Glomerular and tubular filtration
GSH-π[a]	Distal tubule
GSH-α[a]	Proximal tubule
Interleukin-18	Tissue inflammation
Kidney injury molecule-1 (KIM-1)[a]	General kidney injury and disease
Lipocalin 2 (NGAL)[a]	Proximal tubule
Microalbumin	Proximal tubule
Podocin[a]	Glomerulus (podocyte)
Renal papillary antigen-1 (RPA)[a]	Renal papilla & collecting duct
Total protein	Glomerulus and tubule
Trefoil factor-3 (TFF3)[a]	Tubule dedifferentiation in response to injury
Urinary*N*-acetyl-β-(D)-glucosaminidase (NAG)[a]	Proximal tubule

[a]*Methods available to assess levels in formalin-fixed tissues by immunohistochemistry.*
Table reproduced from Handbook of Toxicologic Pathology (2013), third ed. (W. M. Haschek, C. G. Rousseaux, and M. A. Wallig, eds.), Academic Press, Table 47.7, p. 1694, with permission.

Evaluation of Traditional Biomarkers

Traditional biomarkers of renal injury used for many years in laboratory animals and humans include serum creatinine (sCr), BUN, glucose, leakage enzymes such as urinary *N*-Acetyl-β-(D)-glucosaminidase (NAG) and glutathione *S*-transferases (GST), total urinary protein, albumin and low molecular weight proteins such as β2-microglobulin (β2-M). These analytes can be evaluated in routinely collected serum and urine samples.

Serum Creatinine and Urea Nitrogen: In the clinic, the traditional biomarkers, sCr and BUN are late indicators of renal injury, and do not become significantly elevated until at least one half of the kidney mass has been compromised. This can be due in part to the fact that the acute phase of injury may not have been recognized or assessed, since sCr and BUN are consistently elevated in the acute stages of injury in toxicology testing of laboratory animals. Furthermore, in chronic stages of injury, typically in toxicology studies, other parameters than sCr and BUN are affected such as GFR and urine albumin levels. In addition, sCr and BUN do not provide any indication concerning the region of kidney affected in the clinic or in preclinical studies. The normal sCr and BUN values in the

TABLE 11.4 Baseline Renal/Function Parameters over the Lifespan of Sprague-Dawley Rats

Parameter	Age (months)			
	≤2	6	12	≥18
Kidney weight (g)	2.13 ± 0.23	3.46 ± 0.35	3.97 ± 0.36	5.22 ± 2.12
Body weight (g)	115 ± 6.0	645 ± 38	773 ± 109	914 ± 88
Urine output (mL/22 h)	26 ± 9.5	23 ± 8.5	26 ± 6.8	21 ± 9.8
Urine osmolality (mOsm/kg)	853 ± 328	791 ± 468	745 ± 332	816 ± 329
Sodium excretion (mmol/22 h)	0.58 ± 0.2	0.6 ± 0.3	0.37 ± 0.2	0.33 ± 0.2
Potassium excretion (mmol/22 h)	1.6 ± 0.3	1.9 ± 0.3	2.0 ± 0.2	1.9 ± 0.6
Chloride excretion (mmol/22 h)	0.61 ± 0.2	0.7 ± 0.2	0.63 ± 0.2	0.42 ± 0.3
Calcium excretion (mg/22 h)	0.6 ± 0.2	1.6 ± 0.9	1.8 ± 0.9	2.5 ± 1.3
Phosphorus excretion (mg/22 h)	17 ± 4.2	18 ± 3	17 ± 4.8	18 ± 5.4
Protein excretion (mg/22 h)	7.3 ± 1.9	9.4 ± 2.4	18.5 ± 8.9	103.4 ± 122
Creatinine clearance (mL/min/100 g b.wt.)	0.383 ± 0.07	0.367 ± 0.07	0.331 ± 0.07	0.26 ± 0.10
Urinary NAG (U/L)	10.1 ± 3	14.6 ± 4	16.3 ± 4	22.6 ± 12
Urinary alkaline phosphatase (U/L)	3 ± 4	1 ± 1	2 ± 3	4 ± 7
Serum urea (mg/dL)	19 ± 1	17.3 ± 1	16.9 ± 1	22 ± 13
Serum creatinine (mg/dL)	0.6 ± 0.03	0.7 ± 0.06	0.7 ± 0.07	1 ± 0.6
Serum total protein (mg/dL)	6.2 ± 0.3	6.4 ± 0.1	6.5 ± 0.2	6.1 ± 0.2
Serum albumin (mg/dL)	4.6 ± 0.2	4.2 ± 0.2	4.3 ± 0.2	3.7 ± 0.4
Serum sodium (mmol/L)	144 ± 1.6	146 ± 1.2	148 ± 1.8	148 ± 1
Serum potassium (mmol/L)	6.4 ± 0.5	5.9 ± 0.7	5.5 ± 0.3	6.2 ± 0.7
Serum chloride (mmol/L)	102 ± 1.8	106 ± 0.9	107 ± 1.9	108 ± 2.5
Serum calcium (mg/dL)	11.3 ± 0.5	10.2 ± 0.3	10.6 ± 0.4	10.7 ± 0.6
Serum phosphorus (mg/dL)	11.1 ± 0.8	8.3 ± 1.7	12 ± 2.6	11.6 ± 2.1

Table reproduced from Handbook of Toxicologic Pathology (2013), third ed. (W. M. Haschek, C. G. Rousseaux, and M. A. Wallig, eds.), Academic Press, Table 47.8, p. 1695, with permission.

TABLE 11.5 Baseline Renal Function Values in Young Adult Beagle Dogs

Parameter	Mean ± SD
Urine output (mL/18 h)	235 ± 58
Urine flow rate (mL/min)	0.9 ± 0.25
Urine osmolality (mOsm/kg)	541 ± 52
Plasma osmolality (mOsm/kg)	308 ± 15
Sodium excretion (mmol/18 h)	35 ± 12
Potassium excretion (mmol/18 h)	14 ± 4.7
Chloride excretion (mmol/18 h)	25 ± 7.7
Calcium excretion (mg/18 h)	17 ± 6.1
Phosphorus excretion (mg/18 h)	59 ± 33.8
Protein excretion (mg/18 h)	20 ± 11.5
Creatinine clearance (mL/min/100 g b.wt.)	3.5 ± 0.4
N-Acetyl-β-D-glucosaminidase (U/L)	1.1 ± 2.65
β-2 Microglobulin (μg/18 h)	6.3 ± 2.6
Renal blood flow (mL/min)	104 ± 17.1
Renal vascular resistance (vru)	68 ± 16
Filtration fraction	0.20 ± 0.06

Table reproduced from Handbook of Toxicologic Pathology (2013), third ed. (W. M. Haschek, C. G. Rousseaux, and M. A. Wallig, eds.), Academic Press, Table 47.9, p. 1696, with permission.

presence of chronic renal injury reflect the functional reserve of the kidney. In addition, normal sCr levels are affected by multiple nonrenal factors, including age, gender, muscle mass, hydration status, nutritional status, and in humans, medications.

Urinary β-(D)-Glucosaminidase: NAG is a lysosomal brush border enzyme of 140 kDa present mainly in the proximal tubule cells. It is the most active glycosidase in proximal tubule cell lysosomes, which tend to be concentrated in the S_2 segment of PCTs. As NAG is too large to be filtered through glomeruli, its urinary excretion reflects increased lysosomal activity and tubule cell injury. NAG has proved to be a sensitive biomarker of proximal tubule cell injury associated with a wide variety of drugs and environmental toxicants in animals, as well as in a cross section of human renal conditions.

Urinary Glutathione *S*-Transferases: GSTs are mainly cytosolic dimeric enzymes involved in detoxification of xenobiotic compounds through addition of glutathione. Several isoforms exist but in the kidney there are two main classes, GSTα and GSTπ. GSTα is highly expressed in proximal tubule cells, whereas GSTπ is localized to the DCT, thin limbs of Henle, and the collecting ducts. Therefore, application of these parameters raises the possibility of discrimination between damage to the proximal tubules and damage to the distal nephron and collecting system. In a cross-sectional study of human patients with proteinuria, the highest levels of urinary GSTα were in patients still in an early phase of their proteinuric renal disease, whereas the highest levels of GSTπ were in patients with more compromised kidneys undergoing renal failure.

Proteinuria and Albuminuria: The classical paradigm of glomerular capillary leakage as the primary cause of proteinuria/albuminuria is currently challenged by increasing recognition that the glomerulus exerts mainly size selectivity in the process of protein filtration, implying that physiological levels of filtered protein such as albumin have been significantly underestimated in the past. Beyond the glomerulus, albumin is efficiently retrieved through megalin and/or cubulin

binding and endocytosis into proximal tubule cells where the protein is catabolized to small peptides, some of which may then be secreted back into the urine. Thus, an increase in albumin in the urine can signal impairment of the degradation pathway when there is proximal tubule injury. Consequently, proteinuria can now be regarded as a reflection of two separate mechanisms (1) abnormal transglomerular passage of large proteins due to increased permeability of the glomerular capillary wall and/or (2) the subsequent impaired resorption of proteins by epithelial cells of the PCTs.

Urinary β2-Microglobulin: β2-M, a single polypeptide chain of 12 kDa, is expressed on the surface of all nucleated cells and is freely filtered through the glomerulus, and almost entirely reabsorbed and catabolized in the PCTs. An increase in its urinary excretion has been considered to reflect impairment of the PCTs resorption process, and thus tubule injury. The usefulness of this polypeptide as a biomarker is limited by its instability in pathological urine due to pH-dependent enzymatic degradation. β2-Microglobulin is highly species-specific and its assays may not be readily available across laboratory animal species.

Evaluation of Novel Biomarkers

Traditional markers of renal toxicity primarily indicate impaired kidney function rather than tissue injury, thus do not fulfill the requirements for an efficient safety biomarker in the clinic that will predict acute or progressive renal injury in an accurate and timely fashion. Novel biomarkers of kidney injury have been developed to aid in monitoring acute renal insult in humans and laboratory animal species including kidney injury molecule-1 (KIM-1), clusterin, cystatin C, trefoil factor 3 (TFF3), neutrophil gelatinase-associated lipocalin (NGAL), and liver-type fatty acid-binding protein (L-FABP).

Kidney Injury Molecule-1: KIM-1, a type 1 transmembrane glycoprotein, is not detectable in normal kidney tissue, but increases substantially in kidney following injury. It has a central role in the renal tubule repair process by removing dying cells and cell debris from the injured tubule. It is expressed at very high levels in dedifferentiated proximal tubule cells after toxic or ischemic renal insult. KIM-1 can be measured in urine with a microsphere-based Luminex xMAP technology using monoclonal or polyclonal antibodies raised against rat or human KIM-1 ectodomain. Dipsticks for assaying KIM-1 in urine have also been developed for rapid diagnosis and monitoring at the bedside or in the laboratory. In a rat study, KIM-1 was tested under conditions of nephrotoxicity induced by gentamicin, inorganic mercury, or chromium. KIM-1 proved to be more sensitive in detecting proximal tubule damage regardless of whether it affected cortical or outer medullary proximal tubules, and was more rapidly elevated than NAG. In the clinical setting, studies have indicated that KIM-1 is most efficient at distinguishing acute tubular necrosis from other types of renal injury, such as chronic kidney disease. KIM-1 seems to have many of the characteristics preferred for a genuinely useful biomarker, including the fact that it is stable in urine.

Neutrophil Gelatinase-Associated Lipocalin (NGAL): NGAL, also known as lipocalin-2, is a 25-kDa polypeptide chain that is secreted in a bound state with gelatinases from neutrophils, macrophages, and other cells involved in inflammation. Because of its iron-carrying function, it is believed to have both antimicrobial activity and a role in epithelial growth, differentiation, cell survival, and proliferation. Because NGAL was rapidly induced in mouse kidney urine after acute cisplatin tubule necrosis, it was proposed as a sensitive marker of acute kidney injury. Subsequently, it has been investigated in a series of studies covering a wide spectrum of human renal disease with promising results, but with better predictive ability in pediatric cases than in adults. NGAL, however, is not specific for kidney as serum levels are also raised in the presence of liver injury, acute bacterial infections, and chronic obstructive pulmonary disease. The predictive performance of NGAL is considered low compared with that of KIM-1 or NAG in animals with nephrotoxicity.

Clusterin: Clusterin, a 75−80-kDa disulfide-linked heterodimeric glycoprotein, is involved in the clearance of cellular debris and apoptosis. Clusterin is expressed in most mammalian tissues and appears to be associated with a range of conditions in humans. It is elevated in the kidney and urine of rats, dogs, and primates in association with the acute injury induced by ischemia/reperfusion, nephrotoxicants, and other causes of renal damage. In a rat model of unilateral urethral obstruction, clusterin α elevation in urine and strong positivity for clusterin β in tubule epithelium are shown as early changes of tubule injury.

Renal Papillary Antigens (RPAs): Few biomarkers have been discovered capable of detecting damage to the distal collecting system of the kidney. In particular, it is critical to detect any potential of a newly developed drug for causing renal papillary necrosis (RPN), a specific type of kidney injury that has been well documented in humans as a drug-induced entity. RPN risk is effectively identified in routine toxicology testing, but in humans, severe degrees of RPN can occur without detection. Monoclonal antibodies to rat renal papillary tissue termed RPA-1 and RPA-2 have been used as a diagnostic tool for identifying damage to the rat papilla. The amount of RPA-1 is increased in rat urine following exposure to classical papillotoxins, including single doses of 2-bromoethanamine (2-BEA), propyleneimine, and single or repeated doses of indomethacin.

Morphologic Evaluation

Histopathology is recognized as the single most appropriate screen for evidence of renal injury. An evaluation strategy that uses unambiguous descriptive terminology and that is free from the many restraints of traditional diagnostic concepts could enhance communication in toxicologic pathology. Such a scheme must include subtopographical anatomy, description of the basic pathologic process, modifiers, and quantitative measures of lesion distribution and extent (Table 11.6). Familiarity with spontaneous diseases occurring in animal models is essential for the establishment of the nature and cause of morbidity or mortality in an individual animal. In acute toxicity studies, recognition that death from renal toxicity with renal failure typically takes 3 days in the rat is important. Death within 24–48 hours of initial treatment probably cannot be attributed to nephrotoxicity with renal failure as the primary mechanism. On a group basis in the execution of a hazard identification protocol in rats, the most minimal expression of nephrotoxicity may occur simply as a slight exacerbation of the severity of a spontaneously occurring lesion. Spontaneous disease may also mask or mimic a toxicologic response.

Common Spontaneous Lesions in Rats: The background incidence of spontaneous lesions varies by research laboratories and by the strain of rats used in preclinical toxicology studies. A majority of rats in chronic and carcinogenicity studies exhibit several age-related inflammatory, degenerative, and proliferative lesions in the kidney predominated by chronic progressive nephropathy (CPN). In standard 2–13 week toxicology studies, approximately 50%–60% of SD rats exhibit histologic changes in the kidney. The most common (≥2%) microscopic changes include: CPN (Figure 11.7), mineral deposits (Figure 11.8), and interstitial mononuclear cell infiltrates. The incidence of CPN is higher in males (~30%) than in females (~20%) in 2- to 13-week studies and can have two or more of the histologic features discussed above. Incidence of CPN in 4–5-month-old male F344 rats is 100%. Renal parenchymal mineralization is more frequent in females and incidence and severity increase

TABLE 11.6 Suggested Descriptive Nomenclature for Reporting Common Nonproliferative Alterations of Kidney

Congenital lesions	**Cell death**
Renal agenesis	Single cell death
Renal hypoplasia	Tubular necrosis
Polycystic kidney	Renal papillary necrosis
Adrenal rest	Infarct
Hydronephrosis	
Disturbances of cell growth/differentiation	**Degenerative changes**
Glomerular atrophy	Tubular epithelial vacuolation
Tubule atrophy, cell/tubule hypertrophy, tubule regeneration	Hyaline droplet accumulation
Karyomegaly/karyocytomegaly/multinucleation	Intracellular inclusion bodies
Bowman's capsule metaplasia/hyperplasia	Cytoplasmic pigmentation
Squamous cell metaplasia of pelvic epithelium	Tubular dilatation, tubular casts (hyaline, pigmented or granular)
Osseous metaplasia	Crystal formation
	Mineralization (tubular, vascular, or renal pelvic)
	Renal calculi
	Amyloidosis
	Glomerulosclerosis
Inflammatory changes	**Vascular changes**
Glomerulonephritis (membraneous, mesangioproliferative, or crescentic)	Vascular thrombosis, Infarction (acute or chronic)
Pyelonephritis, microabscesses	Periarteritis, fibrinoid necrosis
Interstitial nephritis, interstitial fibrosis	
Miscellaneous changes	**Special disease processes**
Tubular regeneration/basophilia	Chronic progressive nephropathy (CPN)
Extramedullary hematopoiesis	$Alpha_{2U}$-globulin nephropathy
	Obstructive nephropathy
	Immune complex glomerulopathy

Severity modifiers: minimal (<1%); mild (1%–10%); moderate (10%–25%); moderately severe (25%–75%); and severe (75%). Duration modifiers: acute, subacute, or chronic. Distribution modifiers: focal, multifocal/segmental, or diffuse/global.

Table reproduced from Handbook of Toxicologic Pathology (2013), third ed. (W. M. Haschek, C. G. Rousseaux, and M. A. Wallig, eds.), Academic Press, Table 47.10, p. 1700, with permission.

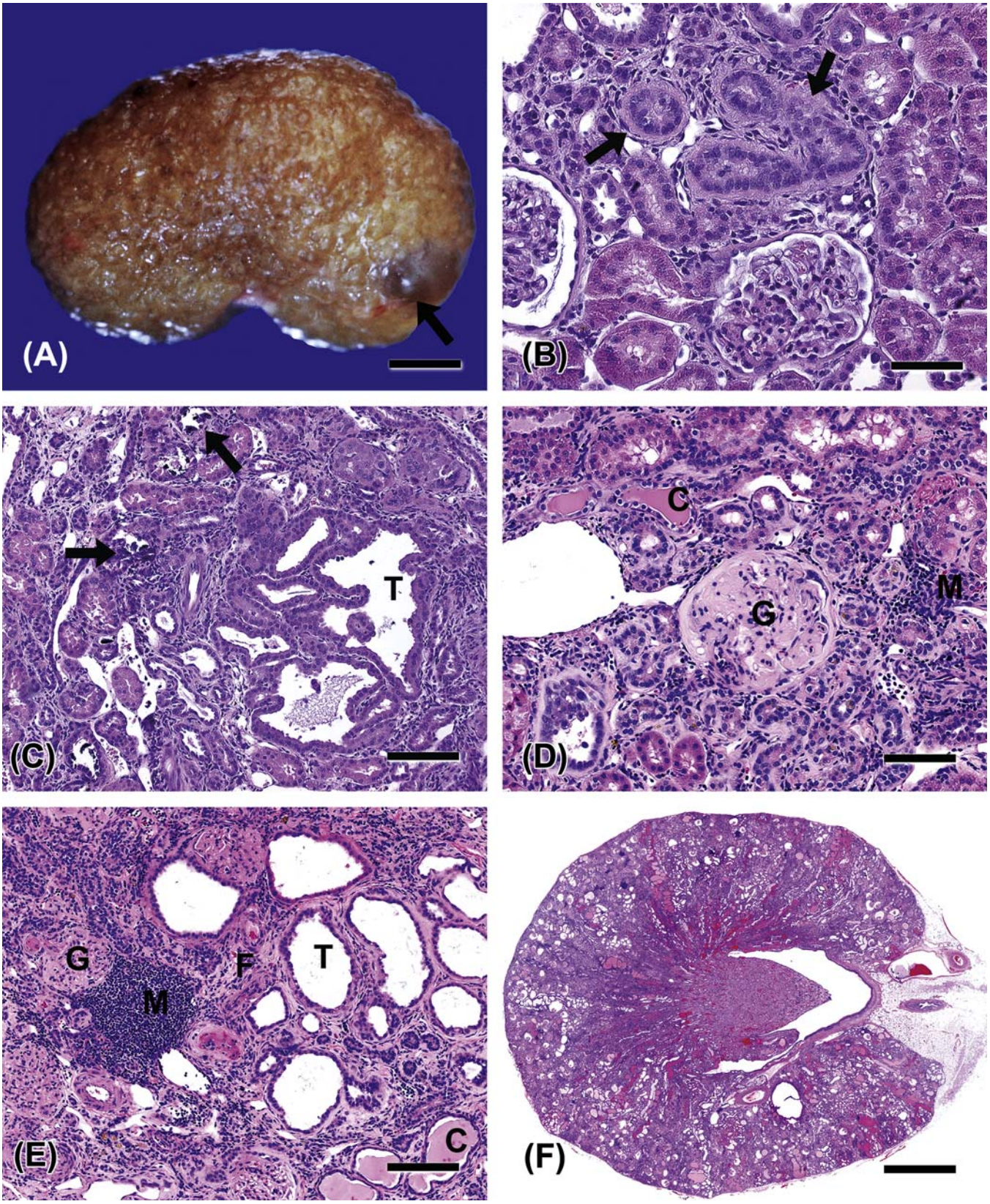

FIGURE 11.7 (A) CPN in Sprague-Dawley rats. Gross photograph (A) illustrates the cystic or granular surface of a kidney in late stage of CPN. Bar = 3 mm Light micrographs (B)–(F) illustrate the hallmarks of CPN. (B) Illustrating tubular epithelial hyperplasia and thickened basement membrane (arrows) Bar = 45 μm; (C) illustrating tubular and interstitial mineralization (arrows) and tubular dilation and hyperplasia (T), bar = 55 μm; (D) illustrating glomerular sclerosis (G), interstitial mononuclear or inflammatory cell infiltration (M), and tubular casts (C), bar = 55 μm; (E) illustrating glomerular sclerosis (G), interstitial fibrosis (F) and mononuclear or inflammatory cell infiltration (M), and tubular dilation (T) and casts (C), bar = 110 μm; and (F) subgross micrograph shows the late stage of CPN of a 2-year-old Sprague-Dawley rat. Bar = 1 mm. *Figure reproduced from Haschek and Rousseaux's Handbook of Toxicologic Pathology (2013), third ed. (W.M. Haschek, C.G. Rousseaux and M.A. Wallig, eds.), Academic Press (Elsevier), Figure 47.14, p. 1702, with permission.*

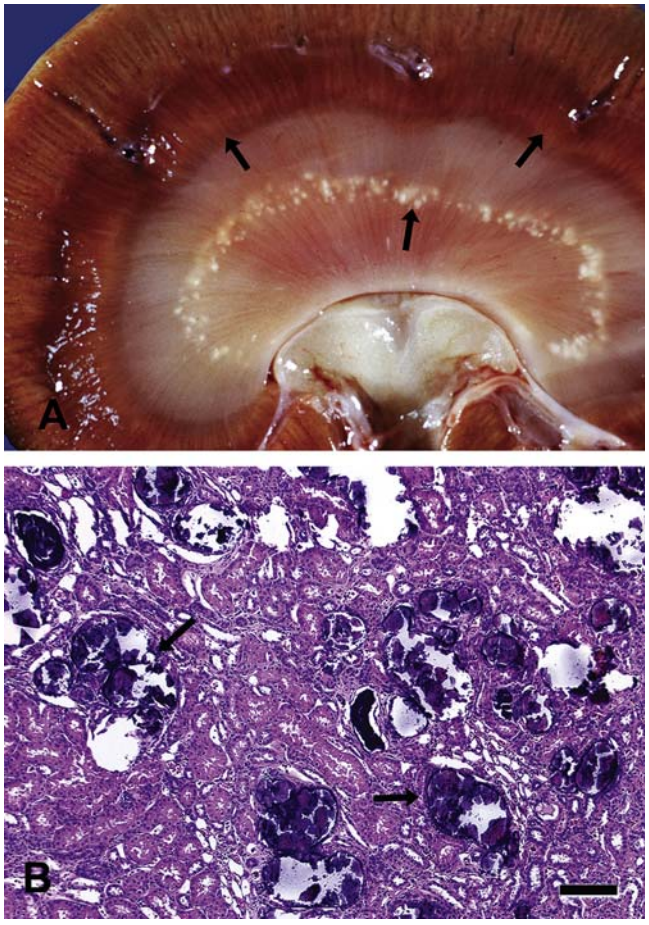

FIGURE 11.8 Spontaneous nephrocalcinosis. (A) Gross photograph of a dog kidney illustrating pale to white linear to granular mineral deposits in medulla (arrows). (B) Light micrograph of a rat kidney illustrates mineral deposition that effaces the renal architecture (arrows). Bar = 90 μm. *Figure reproduced from Haschek and Rousseaux's Handbook of Toxicologic Pathology (2013), third ed. (W.M. Haschek, C.G. Rousseaux and M.A. Wallig, eds.), Academic Press (Elsevier), Figure 47.15, p. 1703, with permission.*

with age. Less common (≤2%) microscopic changes in SD rat kidney include: Intratubular casts, increased hyaline droplet accumulation, focal tubular dilatation, focal interstitial fibrosis, tubular epithelial vacuolation, glomerular lipidosis, focal infarcts, renal pelvic dilatation, and karyomegaly. Multilamellar bodies representing reduplicated basement membranes that occur in PCTs are also seen rarely.

The background incidence of microscopic changes in Wistar-Han rats is significantly lower than that of SD rats due primarily to the lower incidence of CPN. Approximately 35%–45% of Wistar-Han rats in standard 2–13 week toxicology studies exhibit histologic changes in the kidney. Most common (≥2%) microscopic changes include: CPN, renal pelvis dilatation, increased hyaline droplet accumulation, tubular epithelial vacuolation, mineral deposits, and interstitial mononuclear cell infiltrates. Similar to SD rats, the incidence of CPN is higher in males (~20%) than in females (~10%) in 2- to 13-week studies. Less common (≤2%) microscopic changes in Wistar-Han rat kidney include: intratubular casts, focal tubular dilatation or cysts, focal interstitial fibrosis, and rarely chronic infarcts, congenital anomalies, focal segmental vasculopathy, dystroglycans in glomeruli or tubules, and nephroblastomatosis.

Simple tubular epithelial hyperplasia, atypical hyperplasia, adenoma, and carcinoma are seen in longer term rat studies (Figure 11.9). Renal tubular neoplasm occurring as a result of xenobiotic exposure cannot be morphologically differentiated from spontaneously occurring tubular tumors. Renal mesenchymal tumor (RMT) occurs in young rats associated with genotoxic insult at an immature age. The predominant cell type is a fibroblastic spindle cell, with predisposition to encircle sequestered preexisting tubules. Smooth muscle fibers, vascular structures, and occasionally striated muscle and cartilage can be found in these tumors. Nephroblastoma is a tumor of the young rat, rarely occurring spontaneously, but inducible with specific *in utero genotoxic* xenobiotic insult. This tumor consists of islands of densely packed blastema-like basophilic cells with scant cytoplasm and ill-defined cytoplasmic margins, often with a tubular structure at their center. The glomeruloid formation is found in about 50% of cases. Lipomatous tumors (Figure 11.10) are spontaneous tumors that are slow growing and usually appear in old animals, appearing to arise at the corticomedullary junction. Cells appear as mature fat cells, with some tumors also containing lipoblasts.

Chronic Progressive Nephropathy: CPN is a spontaneous disease of laboratory rats that represents a significant complexing factor for interpretation of renal histopathology in toxicology studies (Figure 11.7). Rodent CPN is characterized by basophilic tubules with conspicuously thickened basement membranes, tubules in the medulla (and later cortex also) filled or dilated with hyaline proteinaceous casts, and with time, glomerulosclerosis (Figure 11.7). The disease progresses relentlessly, at least in rats of the SD and F344 strains, from a solitary affected tubule in the earliest stage, to formation of multiple foci, ultimately involving the whole kidney sometimes leading to death through chronic renal failure in rats typically over 18 months of age. Male gender is a primary risk factor for developing CPN, this male sex predisposition having been linked to the presence of androgen rather than to an absence of estrogen.

CPN is an age-related disease modulated by numerous extrinsic factors such as diet and chemical exposures (Figure 11.11). A number of factors, such as dietary manipulations, have been shown to significantly modify the expression of CPN. Among these, restriction of caloric intake is the most effective

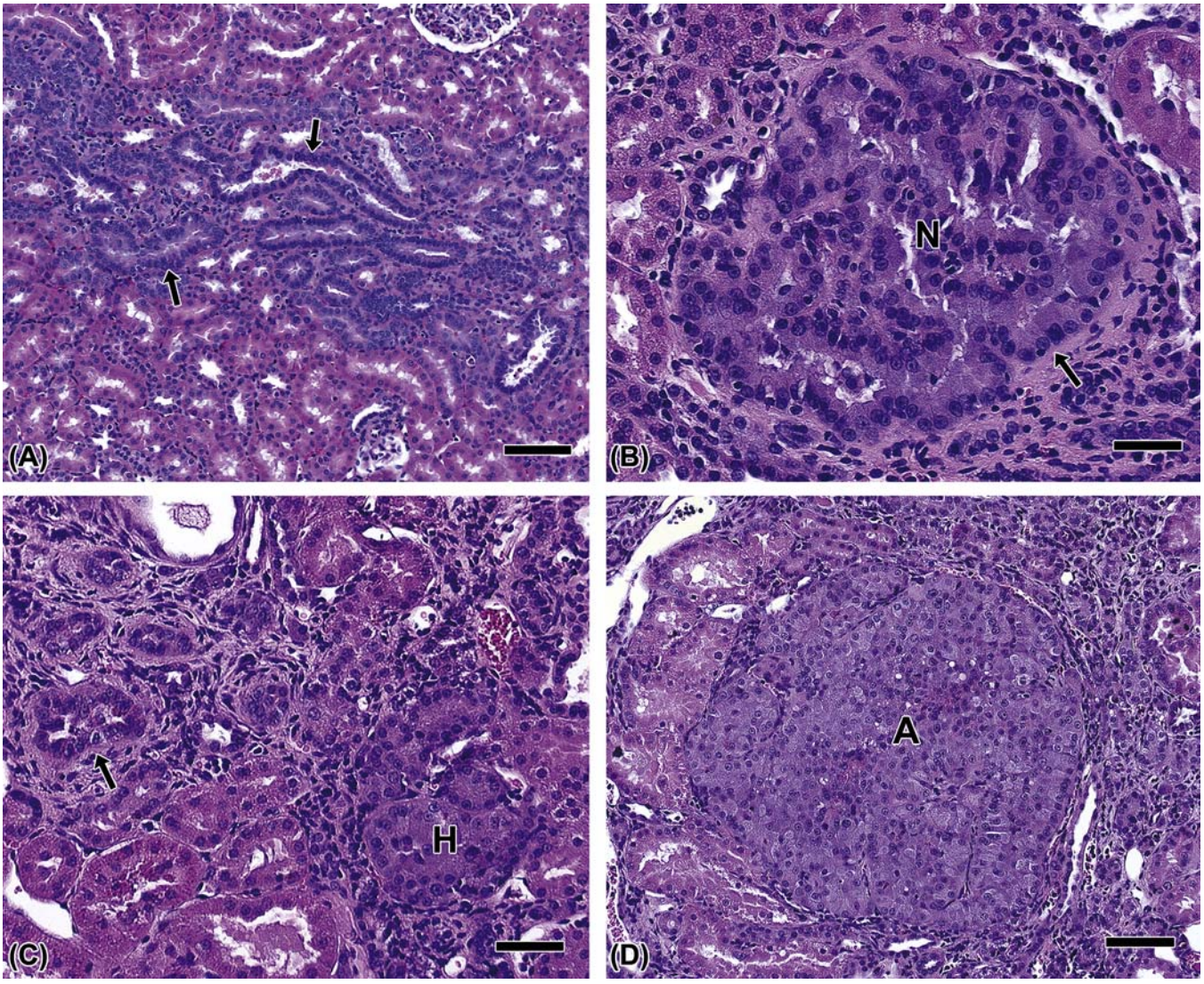

FIGURE 11.9 Proximal tubule proliferation and neoplasia. (A) Focal tubular epithelial cell hyperplasia with variable luminal dilation (arrows). Bar = 70 μm. (B) Atypical tubular epithelial cell hyperplasia (H) and basement membrane thickening (arrow). Bar = 55 μm. (C) Adenomatous or papillary nodular hyperplasia (N) with cellular basophilia and basement membrane thickening (arrow). Bar = 35 μm. (D) Tubular adenoma (A) with cellular proliferation and loss of the tubular lumen and basement membrane. Bar = 50 μm. *Figure reproduced from Haschek and Rousseaux's Handbook of Toxicologic Pathology (2013), third ed. (W.M. Haschek, C.G. Rousseaux and M.A. Wallig, eds.), Academic Press (Elsevier), Figure 47.16, p. 1704, with permission.*

method for inhibiting the disease process. Reducing protein intake after the rapid growth phase also significantly reduces the incidence and severity of CPN. The precise etiology of CPN and the mechanism(s) underlying its pathogenesis remain unknown. CPN is not only a degenerative disease, but also has regenerative aspects with a high cell proliferative rate in affected tubules. Accordingly, evidence exists that advanced, particularly end-stage CPN, is a risk factor for a marginal increase in the background incidence of renal tubule tumors. Many chemicals are known to exacerbate the severity of CPN to an advanced stage, and this interaction between chemical and CPN can result in a small increase in the incidence of renal adenomas in 2-year carcinogenicity bioassays. Since the risk factor is of weak potency, with the standard group size and duration, often the risk cannot be identified. Since the cancer bioassay is not powered to identify tumor differences of less than 10%, not all agents demonstrated to exacerbate CPN result in renal tumorigenesis. Because CPN is a rodent-specific entity, the finding of a small, statistically significant increase in renal tubule tumors, linked to exacerbation of CPN by a test chemical in a preclinical study for carcinogenicity, can be regarded as having no relevance for extrapolation in human risk assessment.

Microscopic lesions of CPN can be seen in rats as early as 2 months of age. Toxicologic pathologists should

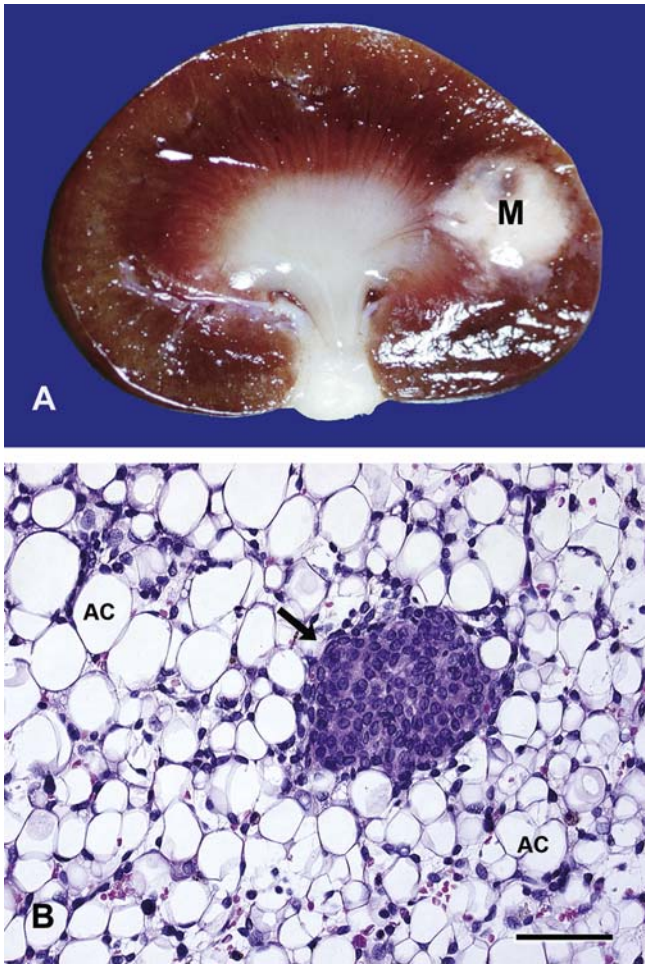

FIGURE 11.10 Lipomatous tumor in the kidney of a rat. (A) A well-demarcated pale mass (M) in the renal cortex with infiltration into medulla. (B). Well-differentiated mature adipose cells (AC) with entrapped renal epithelial cells (arrow). Bar = 60 μm. *Figure reproduced from Haschek and Rousseaux's Handbook of Toxicologic Pathology (2013), third ed. (W.M. Haschek, C.G. Rousseaux and M.A. Wallig, eds.), Academic Press (Elsevier), Figure 47.17, p. 1705, with permission.*

use a consistent approach in recording these lesions as a new molecule progresses through various stages of development. Because CPN is a complex of a number of individual morphologic changes, including tubule basophilia, simple tubule hyperplasia, hyaline casts, interstitial fibrosis, and glomerulosclerosis, it is recommended that study pathologists recognize the complex as a single entity, and record it as such under the term spontaneous nephropathy or CPN. In other words, the individual components of the disease process should not be recorded separately. However, if tubule basophilia, hyperplasia, casts, or glomerular change occurs in the rat kidney unrelated to the CPN disease state, such changes must be differentiated and reported as unique findings. Severity of CPN can be recorded on a scale of 0 to 4, by estimating the percentage of parenchyma affected by CPN recognizing minimal, mild, moderate, and marked stages of CPN progression.

Common Spontaneous Lesions in Beagle Dogs: The laboratory beagle at less than 3 years of age has healthy kidneys. Immature glomeruli especially in outer cortex often occur in dogs up to 6 months of age. Approximately 50%–60% of Beagle dogs in standard toxicology studies exhibit histologic findings in the kidney. The most common (≥2%) microscopic changes include: mineral deposits in cortex and medulla (Figure 11.8), interstitial mononuclear cell infiltrates, focal pigment deposition, and chronic interstitial nephritis. Less common (≤2%) microscopic changes include: focal tubular dilatation, focal eosinophilic hyaline cast, focal interstitial or capsular fibrosis, and tubular epithelial vacuolation, lipid deposition in glomeruli, focal hemorrhages, granulomas, and transitional cell hyperplasia of the renal pelvis. Mineralization is more common in females and can be seen in as many as 60% of animals in a given study.

Common Spontaneous Lesions in Monkeys: Background histologic changes have been reported in kidneys at an incidence of 75% of control cynomolgus monkeys in toxicology studies. The most common (≥2%) microscopic changes include: Interstitial mononuclear cell infiltrates, segmental, focal or diffuse glomerulosclerosis, focal vasculopathy, mineral deposits in cortex and medulla, and tubular epithelial degeneration and regeneration. Focal vasculopathy is characterized by mononuclear cell infiltrates surrounding blood vessels with rare vessel wall hyalinosis. Less common (≤2%) microscopic changes in cynomolgus monkey kidney include: hypercellular immature glomeruli, focal tubular dilatation, focal interstitial fibrosis, tubular epithelial vacuolation, granulomas, chronic infarcts, and rarely unilateral atrophy. Multifocal segmental to global glomerulosclerosis is often noted in older marmosets. Mononuclear cell infiltrates in interstitium, focal glomerulosclerosis, and focal vasculopathy are seen more commonly in Chinese origin cynomolgus monkeys than Mauritius origin cynomolgus monkeys. This difference may partly be related to relatively high background incidence of spontaneous infections in the Chinese origin monkeys.

Common Spontaneous Lesions in Other Laboratory Animal Species: Common nonneoplastic lesions in the kidney of the CD-1 mouse include amyloidosis (Figure 11.12A), interstitial mononuclear cell infiltrates, chronic nephropathy, and mineralization and rarely cytoplasmic vacuolation for example due to lipidosis (Figure 11.12B and C). Chronic nephropathy in mice is characterized by regenerative tubules, thickened tubular basement membranes, and interstitial mononuclear cell infiltrates. Occasionally, tubular protein casts and focal glomerulosclerosis with dilated Bowman's space are seen in older animals. The incidence is higher in males than females. The severity of renal involvement and extrarenal secondary effects are modest compared with

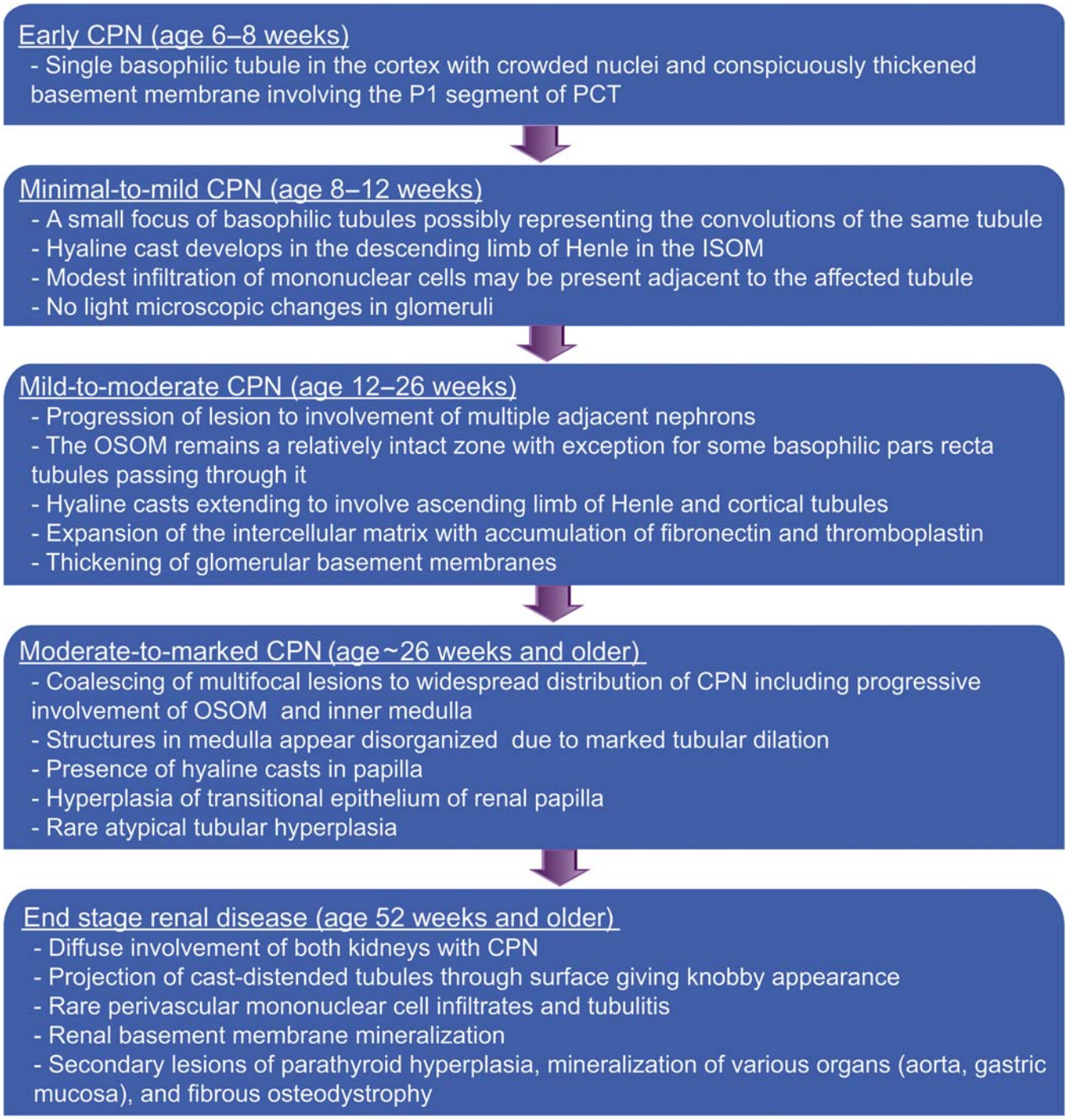

FIGURE 11.11 Chronology of age-related progressive CPN in rats. *Figure reproduced from Haschek and Rousseaux's Handbook of Toxicologic Pathology (2013), third ed. (W.M. Haschek, C.G. Rousseaux and M.A. Wallig, eds.), Academic Press (Elsevier), Figure 47.18, p. 1706, with permission.*

that seen in rats with CPN. The proliferative lesions reported in the mouse kidney include tubular epithelial cell hyperplasia, tubular adenoma (Figure 11.13A), carcinoma, nephroblastoma (Figure 11.13B), histiocytoma, and transitional cell carcinoma of the renal pelvis. Spontaneous membranous or membranoproliferative glomerulonephritis, accompanied by secondary tubulointerstitial damage is reported in minipigs. The most common disease of Syrian hamsters is amyloidosis. The kidney is typically involved, with an incidence at 2 years usually over 50% in both sexes. In Syrian hamsters, end-stage renal disease is usually the major cause of death. Typically, renal amyloidosis is causative while nonamyloid-related end-stage renal disease can also be

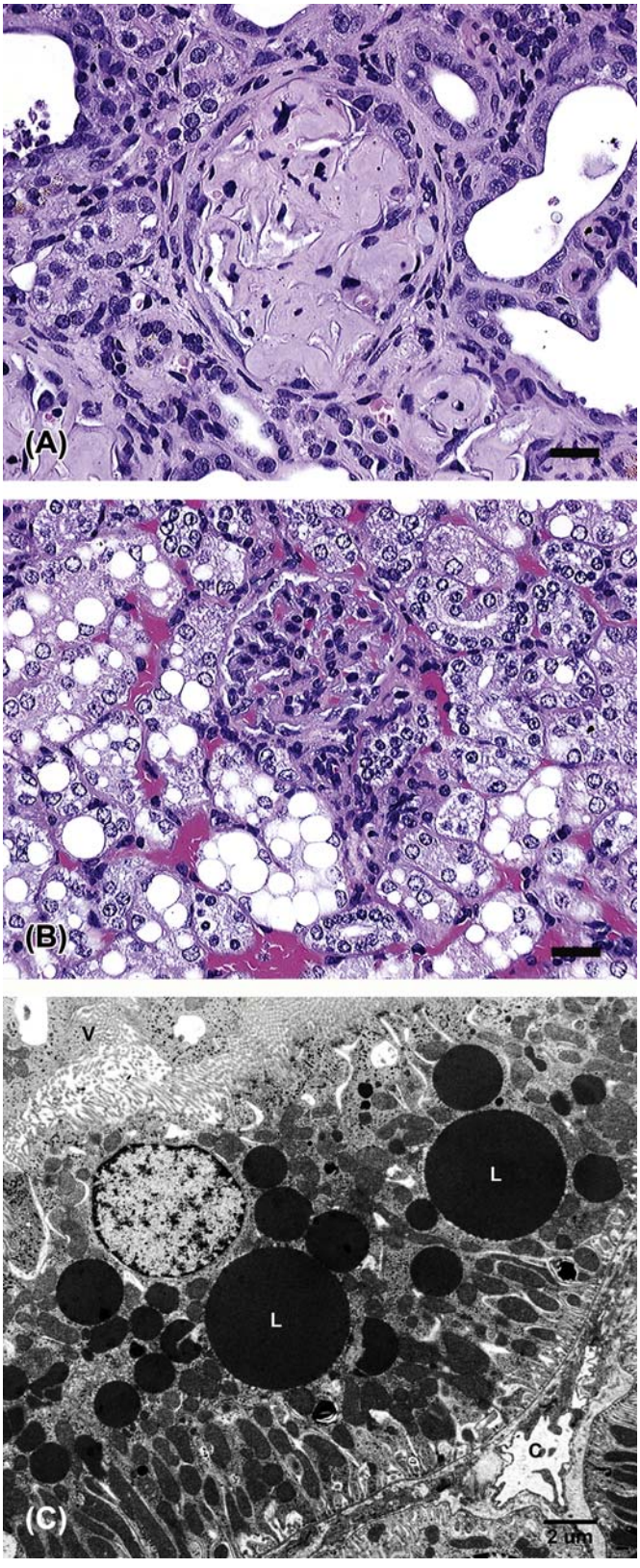

FIGURE 11.12 (A) Light photomicrograph illustrating (A) Renal amyloidosis in an old CD-1 mouse kidney. Bar = 20 μm. (B) Light photomicrograph illustrating renal lipidosis in an old CD1 mouse kidney. Bar: 20 μm. (C) Electron micrograph illustrating intracytoplasmic lipid droplets (L) in a proximal renal tubular epithelial cell of a Wistar rat. Note microvilli (V) projecting into the tubular lumen and a capillary (C) subjacent to the basement membrane. *Figure reproduced from Haschek and Rousseaux's Handbook of Toxicologic Pathology (2013), third ed. (W.M. Haschek, C.G. Rousseaux and M.A. Wallig, eds.), Academic Press (Elsevier), Figure 47.19, p. 1708, with permission.*

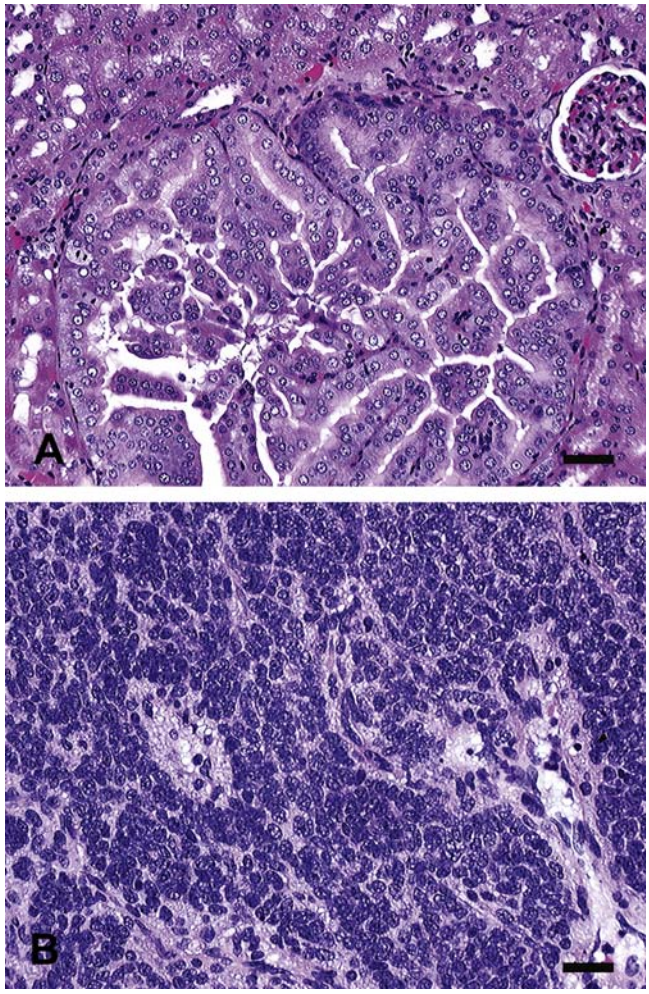

FIGURE 11.13 (A) Light photomicrograph illustrating a tubular adenoma in an old CD-1 mouse kidney. Bar = 40 μm. Light photomicrograph illustrating nephroblastoma in an old CD-1 mouse kidney. Bar = 20 μm. *Figure from Handbook of Toxicologic Pathology, second ed. W. M. Haschek, C. G. Rousseaux and M. A. Wallig, eds. (2002) Academic Press, Figure 35, with permission. Figure reproduced from Haschek and Rousseaux's Handbook of Toxicologic Pathology (2013), third ed. (W.M. Haschek, C.G. Rousseaux and M.A. Wallig, eds.), Academic Press (Elsevier), Figure 47.19, p. 1708, with permission.*

important. Cellular infiltration of the kidney, nephropathy, and mineralization represents the other common age-related lesions found in the hamster kidney. In New Zealand White rabbits, granulomatous nephritis caused by Encephalitozoan cuniculi can be frequent, even in young rabbits, with a reported incidence of 20% at ages under 1 year. Mineralization also occurs commonly

in young animals, with higher incidence in females than in males.

Testing for Renal Carcinogenic Potential

The 2-year chronic bioassay conducted in rats, mice, and rarely hamsters has been the tactic for determining the carcinogenic potential of drugs, industrial chemicals, agrochemicals, and food-related substances for over 4 decades; however, the 2-year mouse bioassay is being eliminated in favor of the rasH2 transgenic mouse alternative. Because criteria are somewhat arbitrary and since progression can occur from benign to malignant, little merit exists in the differentiation of benign and malignant renal epithelial tumors. In other words, benign and malignant neoplasm should be added together in the reporting activity for the risk assessment. By contrast, urothelial tumors, since of different embryonic derivation and of different etiopathogenesis, should not be combined with tubular tumors in reporting.

Carefully studied models of renal tumor development in the rat, regardless of mechanism, demonstrate a dose-responsive increase in hyperplastic tubules, morphologically representing a continuum of change up to and including neoplasm development (Table 11.7). Furthermore, the increased incidence and severity of CPN has been demonstrated to parallel an increase in regenerative and hyperplastic tubules, again up to and including neoplasm formation. When studying tumorigenic events and when searching for evidence of tumorigenic events in instances of low tumor incidence, it becomes important to record the incidence and severity of foci of atypical tubule hyperplasia. Cytologic features per se are not sufficient for sharply differentiating hyperplasia from benign neoplasia and benign neoplasia from malignancy. Size of lesion is an important determinant (although not the only one) in this differentiation. The most important determinant is whether the lesion extends beyond the integrity of a single tubule (or its convolutions). Karyomegaly or cytomegaly especially associated with genotoxic xenobiotics or heavy metals observed in subchronic or chronic toxicology studies should lead to prediction that lifetime studies may yield tubular tumors.

Renal tumor development can be associated with direct damage to the genetic material and/or regenerative response to cytotoxic injury to the renal tubule. A retrospective analysis of 16 chemicals that had been tested for both carcinogenicity and subchronic toxicity by the National Toxicology Program (NTP), 5 of them produced renal tubule tumors in the 2-year studies. Of the 5 chemicals, 4 were associated with histopathologic alterations in the respective 13-week toxicity studies, including hyaline droplet accumulation (anthraquinone, decalin), apoptosis (fumonisin B1), regeneration (benzophenone, decalin, fumonisin B1), or exacerbated

TABLE 11.7 Classification of Renal Tubular Proliferative Lesions in Rodents

Designation	Subclass	Criteria
Tubular regeneration		Tubule lined by cells with basophilic cytoplasm and often increased numbers but without increase in size of the tubule[a]
Simple tubular hyperplasia	Predominantly basophilic, also eosinophilic, clear, or oncocytic	Definite increase in cross-sectional diameter of the tubule and number of cells lining the tubule; single layer of cells lining the tubule
Atypical tubular hyperplasia	Predominantly basophilic, also eosinophilic, clear, oncocytic, or amphophilic Cystic or solid	Tubules increased in size because of increase in cell number with multiple layers and orderly growth in relation to nephron basement membrane; cellular atypia may occur
Adenoma	Cell type is basophilic, eosinophilic, clear, oncocytic, or amphophilic Predominantly growth pattern is tubular, lobular, or solid	Unequivocal loss of continuity with original nephron unit; often with compression of adjacent parenchyma; synthesis of new basement membrane; frequent cellular atypia; typically greater in cross-sectional diameter than twice a normal glomerular tuft
Adenocarcinoma/ carcinoma	Cell type is predominantly basophilic, also eosinophilic, clear, or amphophilic; predominant growth is tubular (more or less distinct formation of tubules), lobular (nests of cells separated by scanty connective tissue), or solid (continuous sheets of cells) Scirrhous response (prominent dense fibrous connective tissue proliferation)	Disorderly basement membrane synthesis and invasiveness or growth without regard to limiting basement membranes; frequently necrosis; neovascularization; size typically greater than 3 mm in diameter; usually marked cellular atypia or pleomorphism

[a]*Regenerative, simple, and atypical hyperplasia occurs on a nephron basis as several adjacent affected tubules typically are noted in cross-section with perpendicular orientation to the medulla. Neoplasm and atypical hyperplasia are enumerated whereas simple hyperplasia is graded.*

Table reproduced from Handbook of Toxicologic Pathology (2013), third ed. (W. M. Haschek, C. G. Rousseaux, and M. A. Wallig, eds.), Academic Press, Table 47.13, p. 1709, with permission.

CPN (anthraquinone). All those five chemicals were associated with increased kidney weights at 13 weeks. However, there were also false positives in this analysis. The approach using the histopathology and organ weight to evaluate renal tumor development in subchronic studies may require rigorous validation.

RESPONSE TO RENAL INJURY

Physiologic, Molecular, and Biochemical Responses

Drugs and chemicals can have direct toxic effects on cells of the renal vasculature, tubules, and glomeruli, and/or induce inflammation of the renal interstitium, leading to acute intrinsic renal failure. A major concept in toxicologic pathology of the kidney is the propensity for the nephron to respond to injury as a unit rather than respond only at the subtopographical site of injury. Morphologic presentation of nephrotoxicity at the cellular level can occur as cellular degeneration, necrosis, apoptosis, or hyperplasia. Renal cellular hyperplasia can be a reparative response to tubular injury with intact basement membranes or can be part of a response to long-term exposures to xenobiotics including neoplasm development in some cases.

Increased apoptosis can be recognized in microscopic sections as increased apoptotic cells in urine or uriniferous spaces and further demonstrated with immunohistochemical stains. In addition, expression levels of messenger RNA (mRNA) and protein of apoptosis-related genes such as bax, Bcl-2, cytochrome c, caspase-9, and caspase-3 can be used in nephrotoxicity assessment. Apoptosis can be initiated via an intrinsic pathway that involves changes in subcellular organelles including mitochondria, lysosomes, or endoplasmic reticulum, or apoptosis can be initiated via an extrinsic pathway, also called death receptor pathway, that involves the activation of death receptors in response to ligand binding. Nephrotoxic drugs are said to act mainly through the intrinsic pathway. The role of proapoptotic Bcl-2 like proteins in drug-induced apoptosis in renal cells is well documented for gentamicin and cyclosporine A. At least four pathways are shown to be involved in renal cell apoptosis induced by cyclosporine A. Caspases might be the final common pathway as shown in *in vitro* studies with cyclosporine A. Drugs and toxic agents with apoptotic potential are summarized in Table 11.8.

Increased apoptosis occurs in the steady state kinetics of healthy adult tissue. Apoptosis plays an important role in nephron development in fetal kidney and in tubular repair following renal insult. Accelerated apoptosis has been defined as a pivotal feature in renal toxicity such as observed in fumonisin-induced injury in rats (Figure 11.14). Numerous toxicants (heavy metals, drugs, and naturally occurring toxins) have been implicated to trigger or block important intracellular processes, thus resulting in abnormal regulation of apoptosis mediating a

TABLE 11.8 Drugs and Toxicants with the Potential to Induce Apoptosis in the Kidney

Inducing agent	Chemical/Drug class
Acetaminophen	Analgesic
Adriamycin	Anthracycline antineoplastic
Alternaria alternata lycopersici toxin	Mycotoxin
Aminoglycosides	Antibiotic
Amphotericin	Antifungal
Cadmium	Heavy metal
Ceramide	Sphingolipid metabolite
Cidofovir	Antiviral
Cisplatin	Antineoplastic drug
Curcumin	Dietary pigment/spice
Cyclophosphamide	Antineoplastic drug
Cyclosporin A	Immunosuppressant
Diclofenac	NSAID
Doxorubicin	Antineoplastic drug
Dithiothreitol	Reducing agent
Endotoxin	Bacterial toxin
Fumonisin B_1	Mycotoxin
Gliotoxin	Mycotoxin
Hygromycin	Antibiotic
Hydrochlorothiazide	Thiazide diuretic
Melphalan	Antineoplastic drug
Mercuric chloride	Heavy metal
Metolazone	Thiazide diuretic
Microcystin LR	Cyanobacterial toxin
Ochratoxin A	Mycotoxin
Okadaic acid	Polyether fatty acid
Ricin	Plant toxin (ribosome inactivating protein)
s-(1,2-Dichlorovinyl)-L-cysteine	Reducing agent
Verocytotoxin	*E. coli* enterotoxin
Zolendronate	Bisphosphonate

Table reproduced from Handbook of Toxicologic Pathology (2013), third ed. (W. M. Haschek, C. G. Rousseaux, and M. A. Wallig, eds.), Academic Press, Table 47.19, p. 1717, with permission.

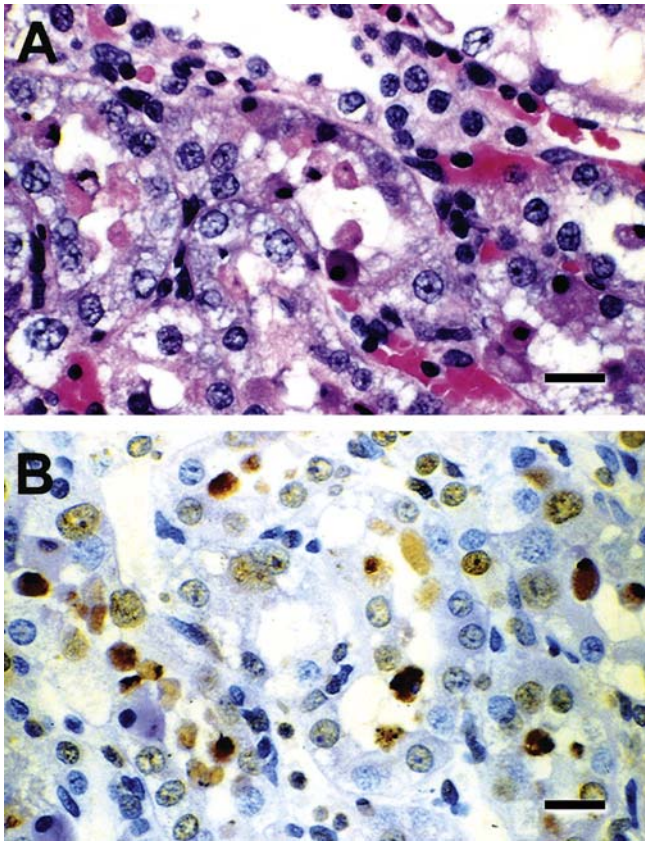

FIGURE 11.14 Tubular epithelial apoptosis. Rat kidney following subchronic treatment with fumonisin B_1, exhibiting outer stripe apoptosis. (A) H&E stain. (B) TUNNEL stain. *Courtesy of Drs. Tom Bucci and Paul Howard, NCTR. Figure reproduced from Handbook of Toxicologic Pathology, second ed. W. M. Haschek, C. G. Rousseaux and M. A. Wallig, eds. (2002) Academic Press, Figure 20, with permission.*

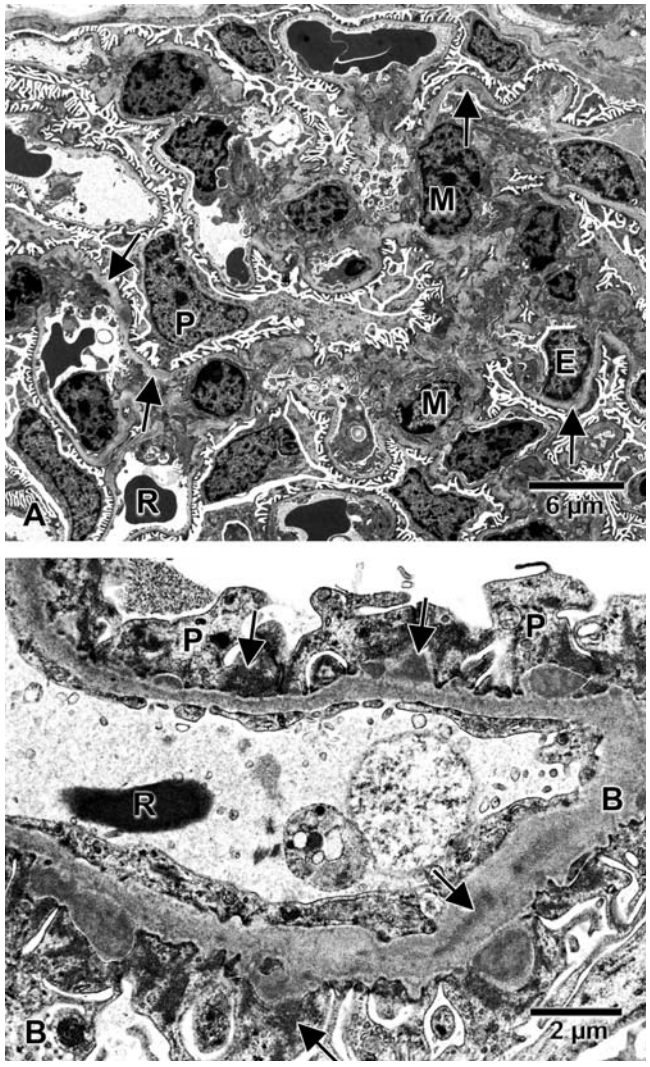

FIGURE 11.15 Ultrastructural glomerular lesions in a monkey treated with a protein therapeutic. (A) Increased mesangial cells (M), podocyte hypertrophy (P) and thickened basement membrane (arrows). Note endothelial cells (E) and erythrocytes (R) in the capillary loops. (B) Thickened basement membrane. 1000× (B) and swelling and fusion of podocyte foot processes (P) with multifocal electron dense deposits of presumably immune complexes (arrows). 10,000×. *Courtesy of Dr. Tom Brown at Pfizer. Figure reproduced from Haschek and Rousseaux's Handbook of Toxicologic Pathology (2013), third ed. (W.M. Haschek, C.G. Rousseaux and M.A. Wallig, eds.), Academic Press (Elsevier), Figure 47.22, p. 1720, with permission.*

wide range of pathologic consequences ranging from renal agenesis to neoplasia.

Morphologic Response

Injury to Glomerulus

Glomeruli should be evaluated for cellularity, patency of capillary lumena, changes in GBM, and the mesangium. The microscopic lesions of nephrotoxicity in the glomerulus can simply manifest as thickening of GBM (Figure 11.15) or can include inflammatory cell infiltrates. It is important to note that, unlike humans, GBM thickening by itself in nonhuman primates does not necessarily imply evidence of an induced glomerular disease state. Approximately 10% of cynomolgus monkeys exhibit the spontaneous occurrence of GBM thickening of varying severity under the light microscope. Ultrastructurally, about 20% of control cynomolgus monkeys may exhibit electron dense deposits (subendothelial, intramembranous, subepithelial, or mesangial) and occasionally separation of podocytes from GBM and podocyte foot process fusion. These changes have been seen more frequently in Chinese origin macques than those from Mauritius.

Glomerular injury can be inflammatory or noninflammatory. A combination of histologic, immunohistochemical, and ultrastructural evaluations provide valuable information in distinguishing between spontaneous and induced lesions and between inflammatory and noninflammatory processes. The relevant ultrastructural observations may include the presence or

absence of electron dense deposits and their location, thickened GBM, podocyte hypertrophy as defined by increased cytoplasm and/or formation of villi, podocyte foot process fusion, increased podocyte densities, and tubuloreticular inclusions in the capillary endothelial cells. Increased cytoplasmic densities in podocytes can be seen following a septicemic process and are characterized by multiple discrete irregularly shaped, nonmembrane bound, electron dense deposits.

NONINFLAMMATORY GLOMERULAR INJURY

Podocyte injury underlies most forms of proteinuric glomerular diseases of the kidney. A noninflammatory glomerular injury of potential importance in toxicologic pathology is designated "focal segmental glomerulosclerosis" (FSGS).

Podocyte Injury: Four major types of podocytopathies are described, all of which are associated with variable degrees of foot process effacement: (1) Minimal change nephropathy, with normal morphology by light microscopy and preserved podocyte number; (2) FSGS, characterized by segmental thickening of the tuft, occasionally accompanied by hyalinosis, foam cells or adhesion to Bowman's capsule, and decreased number of podocytes; (3) Diffuse mesangial sclerosis, defined by the presence of mesangial sclerosis with or without mild mesangial cell proliferation, and mildly increased proliferative activity of podocytes; and (4) Collapsing glomerulopathy (CG), characterized by segmental or global collapse of the glomerular basement membranes and glomerular tufts, proliferation of podocytes, and pseudocrescent formation.

Focal Glomerulosclerosis: "Focal" denotes absence of involvement of all nephrons in contrast to diffuse involvement. The term "segmental" denotes involvement of only part of an individual glomerulus, in contrast to global involvement. Aminonucleosides exemplify agents inducing this effect. Light microscopically, increased PAS-positive staining occurs in the affected tuft with increased silver staining of the thickened basement membrane. Ultimately the tuft becomes sclerotic or scarred (>3 weeks) and may stain positively with Masson's trichrome for collagen. Occasionally, immune-complex trapping can be demonstrated, but this is considered secondary.

Membranous Nephropathy: Membranous nephropathy is primarily associated with immune complex deposition in the glomerular tuft and should be appropriately investigated to differentiate the drug-induced from background lesions, especially in monkeys (Figures 11.15 and 11.16). Repeated (chronic) injection of soluble antigens or biopharmaceutical products causes this lesion, characterized by subepithelial immune-complex (IgG and C3) deposition, and recognized light microscopically with silver stains as spikes of argyrophilic material on the epithelial surface of the basement membrane. Rarely aggregates of intravenously administered biopharmaceutical products may lodge in glomeruli without the typical antigen–antibody complexes and initiate in situ immune-mediated glomerular injury. In routine H&E stained sections, the capillary walls of the affected glomeruli are slightly thickened as a diffuse change.

Amyloidosis: Amyloidosis is a spontaneous disease characterized by the extracellular deposition of polypeptide fragments of serum proteins (often defective immunoglobulin fragments) appearing in routine section as a lightly eosinophilic amorphous material within glomerular tufts (Figure 11.12A). Confirmation

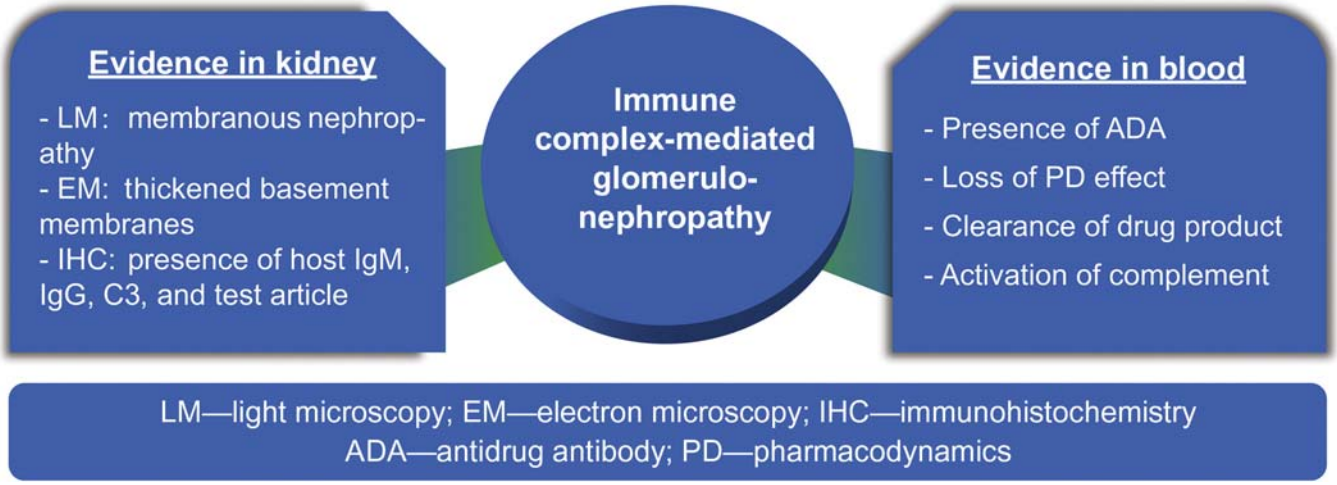

FIGURE 11.16 Evidence for immune complex-mediated glomerulonephropathy following treatment with protein therapeutics. *Figure reproduced from Haschek and Rousseaux's Handbook of Toxicologic Pathology (2013), third ed. (W.M. Haschek, C.G. Rousseaux and M.A. Wallig, eds.), Academic Press (Elsevier), Figure 47.23, p. 1721, with permission.*

of the deposits as amyloid can be accomplished with light microscopy using, for example, Congo red stains. Amyloid appears apple green under polarized light with this stain.

INFLAMMATORY GLOMERULAR INJURY

Cell proliferation is the hallmark of an inflamed glomerulus termed glomerulonephritis and is sometimes seen following treatment with immunosuppressive agents, especially if an infectious process followed the treatment. If the proliferating cell is mesangial, the process is designated mesangioproliferative glomerulonephritis. If neutrophils are increased within the tuft, the process is designated intracapillary proliferative or exudative glomerulonephritis. Postinfectious glomerulonephritis (e.g., poststreptococcal glomerulonephritis) is an example of exudative glomerulonephritis which can stem from an immunomodulatory phenomenon. Severe tuft inflammation may lead to proliferation of mesangial and epithelial cells, with formation of crescents, thus, crescentic glomerulonephritis. Crescents represent sites of adhesion between the visceral and parietal layers of Bowman's capsule. Membranoproliferative glomerulonephritis denotes a combination of mesangial cell proliferation and basement membrane thickening. Each of these morphologic types suggests different disease syndromes when occurring in human medicine. These diseases typically have a primary immunologic etiology and are of relevance in diagnostic laboratory animal pathology and experimental pathology.

Injury to Renal Tubules

TUBULOINTERSTITIAL DISEASE

In humans and dogs, injury to the tubules and interstitium are typically lumped together under the heading tubulointerstitial disease. Disorders that affect the tubules cause immediate reaction in the interstitium and vice versa. Also, in humans and dogs, in advanced stages tubulointerstitial diseases tend to resemble each other, and are given the common morphological designation of chronic interstitial nephritis. By contrast, in rats, primary interstitial disease is poorly documented, other than in purposeful attempts to induce immunologic disease models. Furthermore, the consistent minimal expression of renal toxicity in the rat is designated as exacerbated CPN. This species difference in interstitial response is exemplified by direct comparison of the chronic renal effects of a diphosphonate drug at high dosages in the dog and the rat. The dog response is that of chronic interstitial nephritis, whereas the rat response is characterized as increased incidence and severity of CPN.

Chronic interstitial nephritis is characterized by interstitial fibrosis, interstitial inflammatory infiltrates, tubular atrophy, and glomerular sclerosis. If interstitial inflammation occurs without evidence of tubular injury, is severe and appears early in the process, contains eosinophils or polymononuclear leukocytes, or occurs with peritubular immune complex deposition, the process should be regarded as a primary interstitial nephritis. Focal areas of tubular necrosis may accompany the interstitial reaction. The process most commonly producing this pattern of renal injury in humans is hypersensitivity to methicillin. The response typically has a delayed onset and is not dose responsive.

TUBULAR DEGENERATION AND NECROSIS

Acute alteration of proximal tubular epithelium, induced by xenobiotics in the human and laboratory animals, can lead to acute tubular necrosis (Figure 11.17). Several patterns of specific alterations occur, depending on the inciting agent and thus on the mechanism. Various nephron segments differ in their capacity to withstand hypoxic insults. Proximal tubules have little capacity for anaerobic glycolysis; hence, they are particularly sensitive to total cessation of renal blood flow and oxygen delivery, as occurs in the model of transient clamping of the renal artery. The pathophysiology of renal tubular damage includes a clear direct toxic effect (gentamicin, cisplatin), hypoxic damage induced by altered medullary microcirculation or enhanced metabolic requirements (NSAIDs, radiocontrast agents, cyclosporine) or both, or injury caused by free radical generation (heme pigments). These mechanisms often work in concert. For instance, amphotericin B

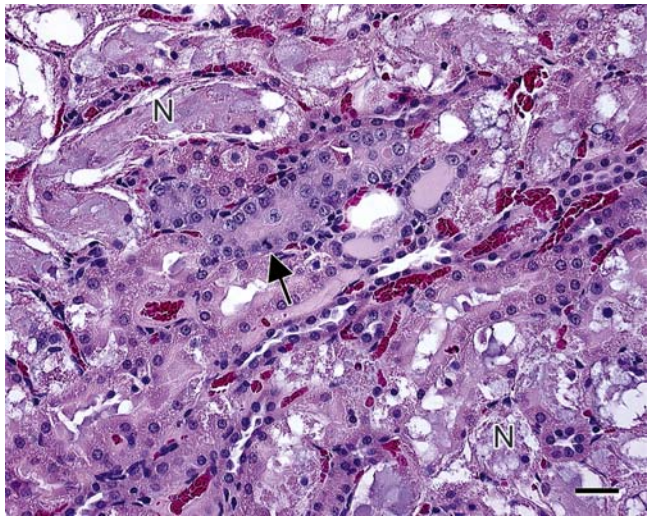

FIGURE 11.17 Multifocal acute tubular necrosis (N) and regeneration (arrow) in a rat treated repeatedly with nanoparticles of a small molecule therapeutic. *Figure reproduced from Haschek and Rousseaux's Handbook of Toxicologic Pathology (2013), third ed. (W.M. Haschek, C.G. Rousseaux and M.A. Wallig, eds.), Academic Press (Elsevier), Figure 47.24, p. 1721, with permission.*

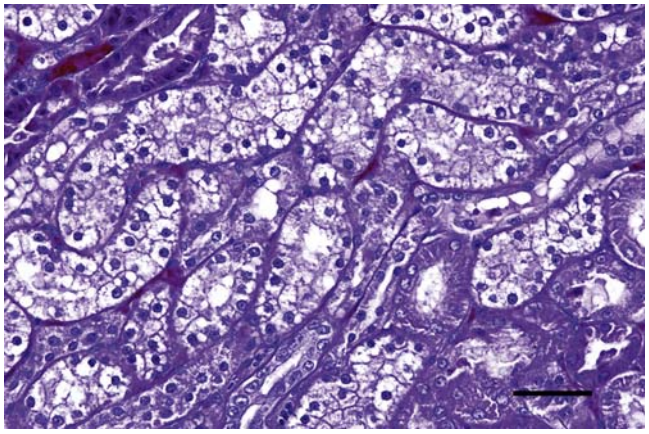

FIGURE 11.18 Osmotic nephrosis. Kidney from a Sprague-Dawley rat administered sucrose intraperitoneally. Note the prominent proximal convoluted tubular cell cytoplasmic vacuolation which, upon ultrastructural evaluation, is confirmed as osmotic nephrosis due to hydropic lysosomal swelling. Bar = 33 μm. *Figure reproduced from Fundamentals of Toxicologic Pathology, second ed. W. M. Haschek, C. G. Rousseaux and M. A. Wallig, eds. (2009) Elsevier, Figure 11.12A, p. 289, with permission.*

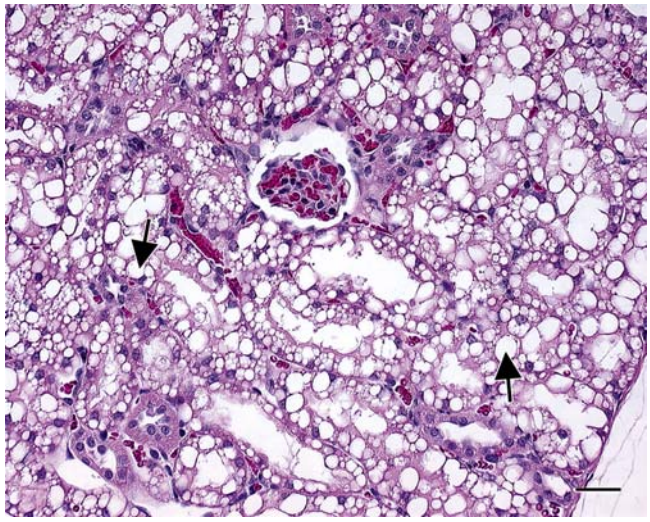

FIGURE 11.19 Renal tubular epithelial cell vacuolation (arrow) in a rat treated with pegylated monocloncal antibody therapeutic. Bar = 40 μm. *Figure reproduced from Haschek and Rousseaux's Handbook of Toxicologic Pathology (2013), third ed. (W.M. Haschek, C.G. Rousseaux and M.A. Wallig, eds.), Academic Press (Elsevier), Figure 47.26, p. 1722, with permission.*

directly injures tubular cell membranes, induces hypoxic tubular damage by profound renal vasoconstriction, and enhances oxygen consumption to maintain cellular transmembrane electrolyte gradient. Rapid accumulation of neutrophils and monocyte/macrophages in injured kidney is an essential feature of the innate immune response induced by ischemia-reperfusion injury.

Osmotic nephrosis occurs in rats after exposures to osmotically active agents such as mannitol and sucrose. Microscopically, the change is diffuse in PCTs and is characterized by cytoplasmic vacuolation (Figure 11.18). The hydropic change is limited to the phagolysosome. Osmotic nephrosis or hydropic change occurs in ethylene glycol toxicity, but here the swelling may also occur between the proximal tubular cell and basement membrane. Diffuse cytoplasmic vacuolation of tubular epithelium is seen with protein therapeutics containing polyethylene glycol of various molecular weights, especially in rodents (Figure 11.19).

Hyaline droplet nephrosis represents phagolysosomal protein overload (Figure 11.20). Increased glomerular filtrate protein, derived via glomerular disease, primarily represents albumin and typically stains positive with PAS. By contrast, the protein overload associated with the inducible alpha$_{2\mu}$-globulin nephropathy syndrome results in hyaline droplets that are PAS-negative, but Mallorys Heidenhain positive. Mallorys stain is not specific for alpha$_{2\mu}$-globulin, but it is specific to the biochemical attributes of this and other proteins.

Lipidosis of proximal tubular epithelium occurs spontaneously in the rat and the mouse (Figure 11.12). These cytoplasmic fat droplets can be confirmed by oil red-O staining of frozen sections. Increased fat or lipid

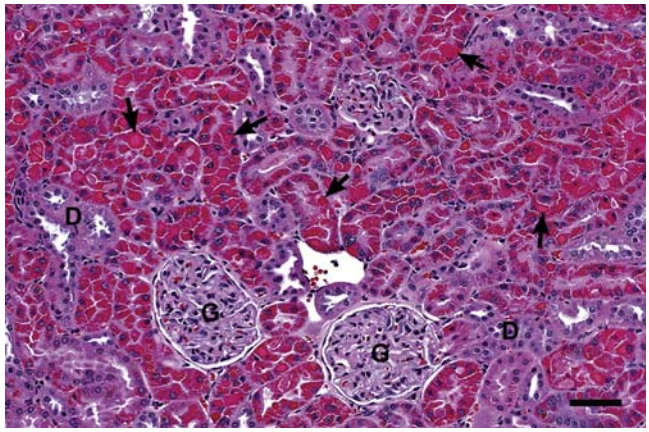

FIGURE 11.20 The kidney from a rat illustrates eosinophilic droplets of variable size and shape in the cytoplasm of the proximal tubular epithelial cells (arrows). The glomeruli (G) and distal convoluted tubule (D) are not affected. Bar = 40 μm.

nephrosis is not a common toxicologic response but can be observed, for example, as a transient acute change when the solvent decalin is given by gavage in corn oil to rats. Subtle light microscopic differences exist between osmotic nephrosis and fatty degeneration, enabling differentiation between the two in routine sections. In humans, lipid glomerulopathy is a rare disorder characterized by proteinuria, renal insufficiency, and disturbances in lipoprotein metabolism closely related to that observed in type III hyperlipidemia. Treatment with fibrates is shown to improve renal pathologic alterations and may result in the complete clinical remission of the disease.

Phospholipidosis in the kidney is typically induced by aminoglycoside antibiotic therapy. Light microscopically, in routine section, the proximal tubular epithelial cells may have subtly increased cytoplasmic lucency. In toluidine blue-stained plastic sections, cytoplasmic bodies are readily apparent by light microscopy. Ultrastructurally, the hallmark of phospholipidosis is the presence of concentric multilaminated phospholipid membrane whorls in the phagolysosome, designated myelin figures.

Ischemia, heavy metals, and xenobiotics requiring metabolic transformation to exert their toxic potential typically induce tubular cell necrosis. Ischemic injury, certain metals (such as mercury) affecting cell respiration, and xenobiotics requiring metabolic transformation to exert their injury preferentially affect the pars recta. This propensity may require time and dose studies for demonstration since, with increased severity, all segments of the proximal tubule may be injured. Other heavy metals, such as lead, and xenobiotics bound to circulating proteins and xenobiotics requiring transport, such as organic acids or bases, preferentially injure the PCT because organic ion and protein reabsorption activity predominates in this part of the nephron.

Agents that induce proximal tubular necrosis at higher doses typically induce accelerated apoptosis at lower doses. For example, gentamicin and mercury, at high doses (but below the dose sufficient for inducing light microscopic lesions), cause replicative and apoptotic rate increases in PCT. Increases in proximal tubular cell replicative rate and urine apoptotic cell count may reflect a more sensitive indication of cell injury than light microscopic examination in short-term studies. Additional factors contributing to renal dysfunction include tubular obstruction, loss of tubular cell polarity, reflux of tubular fluids, and inflammatory processes, which lead to compromised renal microvasculature. The ultimate indicator of renal dysfunction, reduced GFR, may reflect primarily altered glomerular hemodynamics, as occurs during hypovolemic shock or endotoxemia, or may be secondary to a tubular injury with obstruction of the lumen and increased intratubular pressures and activation of tubuloglomerular feedback mechanisms. Chemical warfare agents such as organophosphates can produce acute renal damage. Nonlethal acute exposure to sarin has been associated with significant reduction in GFR, oliguria, retention of electrolytes, hematuria, and glucosuria.

Poorly soluble sulfonamides can crystallize in the tubules and cause direct toxicity to the tubular epithelium via mechanical means. Crystals are usually detected on gross but not always histological examination since they dissolve with tissue processing. Proximal tubular degeneration and nephrosis occur in oxalate nephrosis which can be induced by ingestion of ethylene glycol or some plants. The specific findings

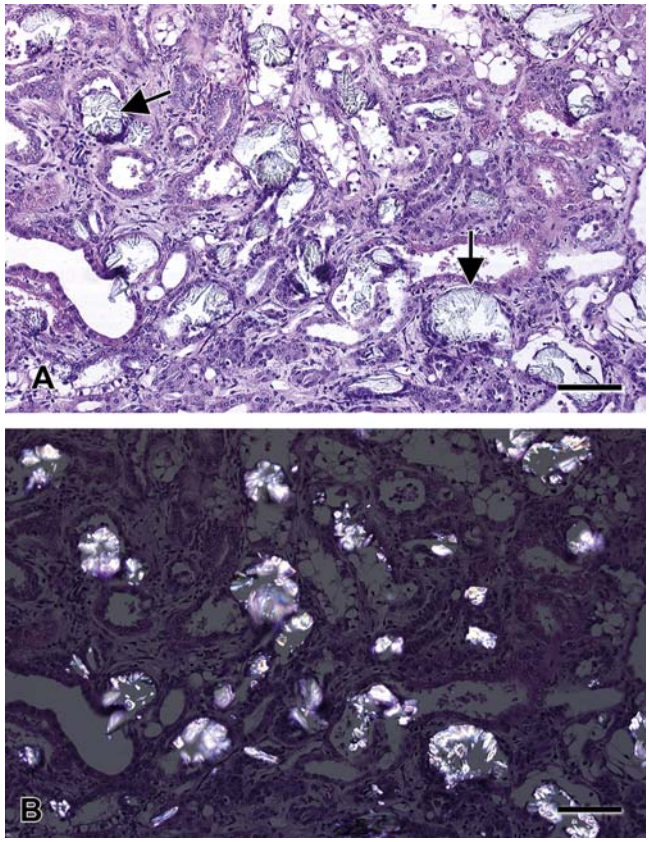

FIGURE 11.21 Kidney of a pig with ethylene glycol (antifreeze) toxicity. (A) Tubular dilation and epithelial regeneration with prominent refractile oxalate crystals in the lumen of proximal tubules (arrows). (B) Prominent refractile oxalate crystals in the lumen of proximal tubules under the polarized light. Bar = 75 μm. *Figure reproduced from Haschek and Rousseaux's Handbook of Toxicologic Pathology (2013), third ed. (W.M. Haschek, C.G. Rousseaux and M.A. Wallig, eds.), Academic Press (Elsevier), Figure 47.36, p. 1748, with permission.*

are pale yellow, birefringent, calcium oxalate crystals in the tubular lumens, and sometimes also in the tubular epithelium and interstitium (Figure 11.21). These crystals are arranged in rosettes or sheaves and can be readily identified with polarized light. Distal tubular necrosis is reported in cats and dogs following ingestion of pet food contaminated by melamine and cyanuric acid. Crystals are pinwheel shape and granular and readily visualized without the need for polarized light (Figure 11.22).

RENAL MINERALIZATION

Xenobiotics exerting a vitamin D-type activity at sufficiently high doses cause mineralization of renal basement membranes, both vascular and tubular (Figure 11.8). Perturbation of calcium phosphorus ratios, for example, through the use of certain commercially available synthetic rodent diets, results in severe tubular lumenal mineralization, predominantly restricted to the pars recta. Special stains, such as

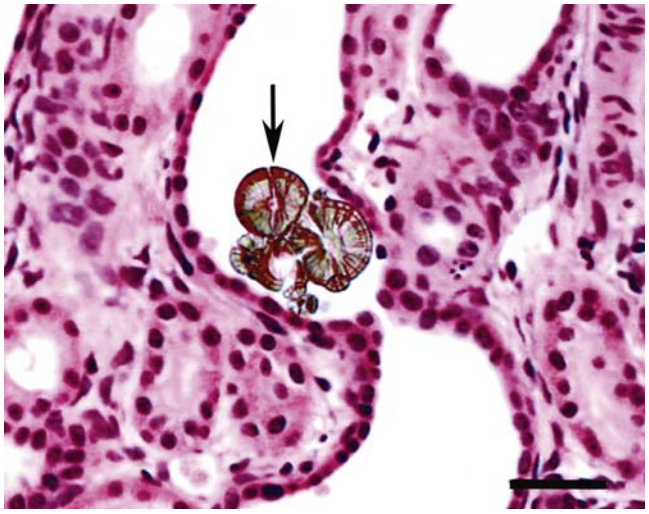

FIGURE 11.22 Dilated distal tubule containing a cluster of crystals with radiating spokes and concentric striations (arrow) from a cat with pet food toxicity. H&E stain. Bar = 45 μm. *Figure reproduced from Brown. et al. (2007)* J. Vet. Diagn. Invest. *19: 525–531, with permission.*

Alizarin Red S or Von Kossa's, can be used for better demonstration of mineralization.

RENAL PAPILLARY NECROSIS

Nephrotoxicity can be manifest as RPN as is the case with NSAIDs. Severe cases of RPN are visible grossly as pale areas involving the tip of, or the entire papilla (Figure 11.23). Microscopically the severity of RPN can be graded as follows. Grade one is characterized by loss of microvasculature, loops of Henle, and interstitial cells, with replacement by eosinophilic homogenous substrate. This occurs with complete preservation of collecting ducts. The transitional cell lining of the papilla may be intact or focally disrupted. In grade two, focal necrosis of all structures occurs, but is limited to the tip of the papilla. In grade three, confluent necrosis extends to midpapilla. In grade four, confluent necrosis extends to the base of the papilla. In grade five, confluent necrosis extends into the outer medulla. The necrotic papilla may become mineralized or the mineralization may be restricted to a transverse band (the abscission zone) at the junction with viable medulla. Sloughing of the necrotic papilla into the renal pelvis may occur, followed by reepithelization over the remaining viable medulla. Secondary cortical changes develop as a consequence of nephron obstruction, reported as glomerulosclerosis. Reepithelialized medulla or urothelium in proximity to nonviable tissue may become hyperplastic. Neoplasia may ultimately develop from this hyperplastic urothelium if the rat survives into old age. Neoplasia occurring secondary to RPN is possibly of limited relevance in risk assessment, since RPN is uncommon in humans and typically linked with analgesic abuse.

TUBULAR HYPERPLASIA AND NEOPLASIA

Drug and chemical nephrotoxicity can be manifested as a proliferative lesion of the tubular epithelium. The renal tumor that is the most relevant to humans with respect to risk assessment is of tubular origin, termed renal tubule tumor in rodents, and renal cell carcinoma in humans.

MECHANISMS OF RENAL TOXICITY

Xenobiotic-associated kidney injury typically depends on selective concentration of the toxic moiety in the target cell or subcellular organelle. This concentration is favored by the normal function of the kidney. The magnitude of blood flow per gram of renal parenchyma is higher than for any other tissue. Glomerular filtration with tubular reabsorption serves to further concentrate potentially toxic moieties. Tubular transport occurs via protein binding and subsequent endocytosis, through active or passive links with ATP hydrolysis-dependent transport such as the sodium pump, or organic anion or cation transport. Concomitantly, selective membrane permeability may serve to maintain critical concentrations of molecules obtained via transport. Furthermore, the kidney has the capacity to dissociate protein-bound toxins; such binding serves to protect other tissues from the injurious agent. The kidney also has the capability to alter the pH of tubular fluid, which can serve to transform solutes into reactive forms. Finally, the kidney participates in the metabolism of xenobiotics (Figure 11.24). Renal metabolism with derivation of reactive electrophilic intermediates causes injury following covalent or peroxidatic reactions with the target cell macromolecules.

Nephrotoxicity can be categorized according to functional and structural characteristics of compounds, morphologic presentation of lesions, mechanism of renal damage, and subtopographical location of injury (Table 11.9). The compounds for which kidney injury occurs as a major toxic host response are listed in Table 11.10. Obscure chemicals or chemicals that cause functional perturbation without overt evidence of morphologic alteration are excluded. Nephrotoxicants categorized by their subtopographical or subcellular organelle target site are listed in Table 11.11. Target site identification is a prerequisite in understanding functional impact, as well as in developing the most sensitive premonitory indicator of injury from nephrotoxicants. In the following sections, well-characterized nephrotoxicants are discussed to exemplify specific mechanisms of injury in different segments of the nephron.

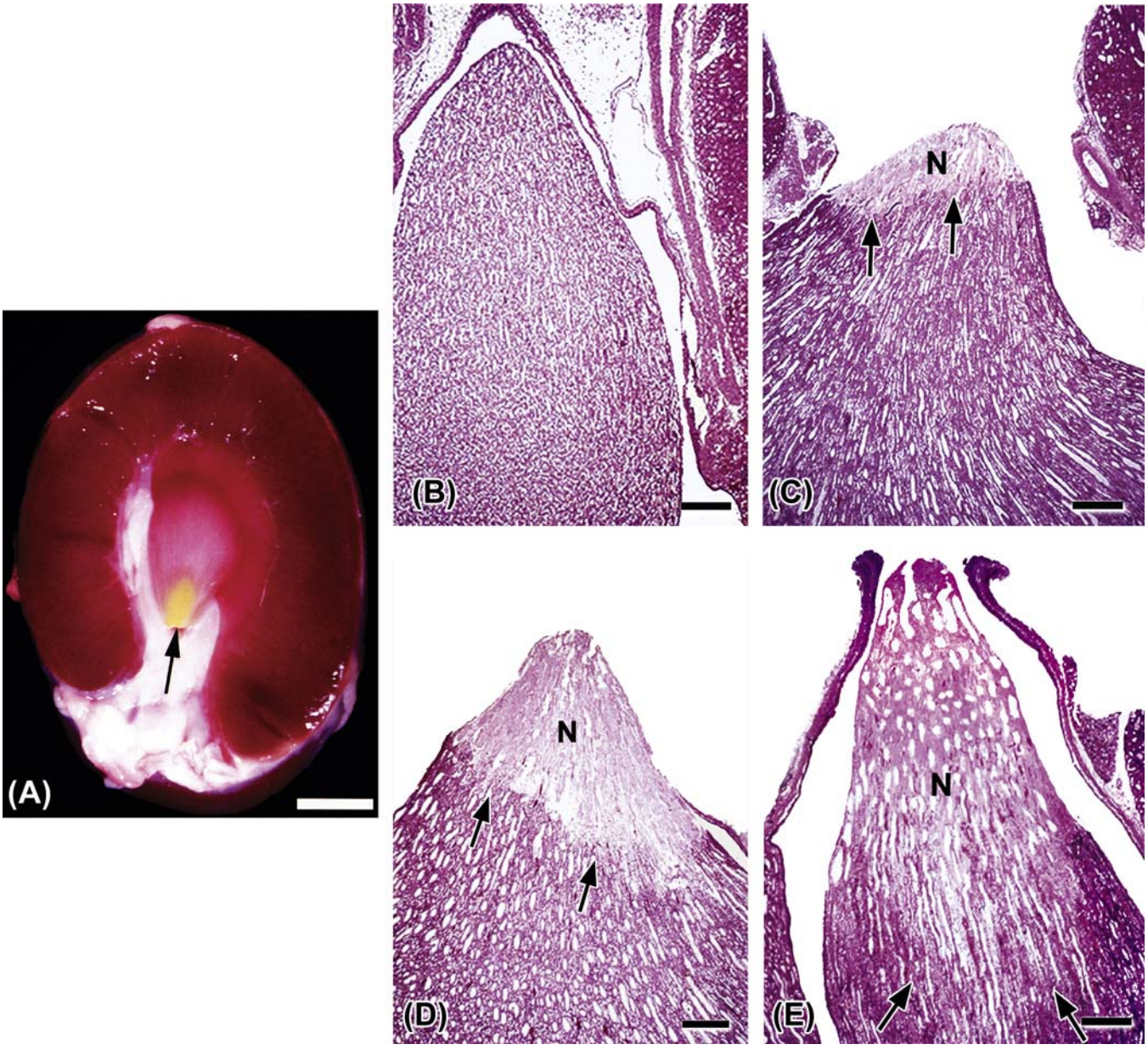

FIGURE 11.23 Nonsteroidal antiinflammatory drug-induced renal papillary lesions. (A) Gross appearance of renal papillary necrosis (arrow). Bar = 5 mm. Photomicrographs show the normal renal papillae (B), and Grade I (C), II (D) and III (E) renal papillary necrosis (N and arrows). Bars = 350 μm. *Figure reproduced from Haschek and Rousseaux's Handbook of Toxicologic Pathology (2013), third ed. (W.M. Haschek, C.G. Rousseaux and M.A. Wallig, eds.), Academic Press (Elsevier), Figure 47.28, p. 1725, with permission.*

Mechanisms of Glomerular Injury

Direct Xenobiotic Perturbation of Cell or Subcellular Organelle Function

Glomerular Podocyte Injury: Podocyte injury is an essential feature of progressive glomerular diseases including direct damage by infectious agents such as human immunodeficiency virus (HIV) and drugs such as adriamycin (doxorubicin). In podocytopathies, many molecules/proteins are involved in the crosstalk between different glomerular cells during disease progression (Figure 11.25). Initial local podocyte damage can spread to induce injury in otherwise healthy podocytes and further affect both glomerular endothelial and mesangial cells, implying that even limited podocyte injury might initiate a vicious cycle of progressive glomerular damage. Injured podocytes may have foot process effacement and slit diaphragm alterations as an early manifestation of injury and subsequently undergo detachment, apoptosis, and dedifferentiation.

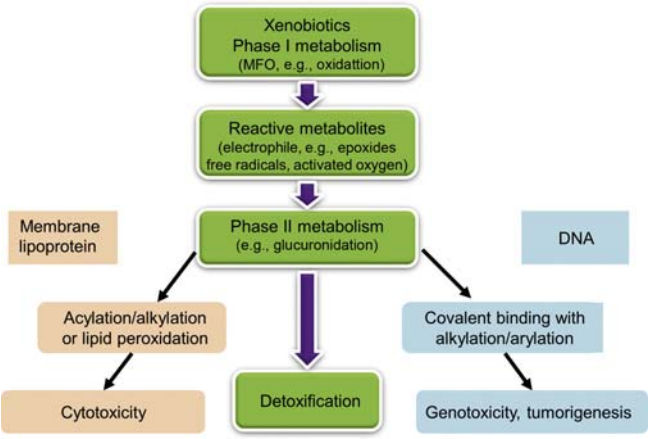

FIGURE 11.24 Mechanistic scheme for xenobiotics injuring kidney by renal metabolism to reactive intermediates. *Figure modified from Haschek and Rousseaux's Handbook of Toxicologic Pathology (2013), third ed. (W.M. Haschek, C.G. Rousseaux and M.A. Wallig, eds.), Academic Press (Elsevier), Figure 47.33, p. 1743, with permission.*

TABLE 11.9 List of the Basis for Classification of Nephrotoxicants

Functional/structural characteristics of the xenobiotic
Subtopographical target
Mechanism of injury
Direct perturbation of cell or subcellular organelle function
Injury via metabolic activation
Perturbation of endogenous or nutritive substrate
Perturbation of renal hemodynamics
Exacerbation of spontaneous age-related chronic progressive nephropathy
Obstructive nephropathy

Table reproduced from Handbook of Toxicologic Pathology (2013), third ed. (W. M. Haschek, C. G. Rousseaux, and M. A. Wallig, eds.), Academic Press, Table 47.21, p. 1726, with permission.

A reclassification of podocyte diseases into four major types of podocytopathies including CG was discussed in the previous section. CG also referred to as collapsing FSGS or malignant FSGS is of specific interest in toxicologic pathology. CG is a proliferative disease defined by segmental or global wrinkling of the glomerular basement membranes associated with podocyte proliferation, pseudocrescent formation, and sometime tubulointerstitial injury. Podocyte injury results in a dedifferentiated phenotype, reflected by the loss of expression of maturity markers and reexpression of proliferative markers, dysregulation of the phenotype reflected by loss of expression of WT-1, and trans-differentiation toward a macrophage-like phenotype. While there is genetic predisposition in some populations, especially African Americans, CG has been observed in immunocompromised states in association with HIV, autoimmune diseases, or following treatment with bisphosphonates, interferon-alpha, or valproic acid. The mechanism of podocyte injury following HIV or other viral infections may be a direct cytopathic effect, with intracellular expression of the viral genome or proteins, and/or indirect effects mediated by release of cytokines by inflammatory cells in the circulation or in the renal parenchyma. Other mechanisms include dysregulation of vascular endothelial growth factor expression and acute ischemic processes, such as thrombotic microangiopathy after therapy with calcineurin inhibitors (Figure 11.26).

Adriamycin is a well-known inducer of renal injury in rodents, which mirrors that seen in human chronic kidney disease due to primary FSGS. Adriamycin induces injury by direct toxic damage to the glomerulus with subsequent tubulointerstitial injury. Changes occur in the glomerular filtration barrier, affecting podocytes, glomerular endothelial cells, glycocalyx, and glomerular basement membrane. Changes are characterized by reduced thickness of glycocalyx, increased size of glomerular endothelial cell pores, reduced glomerular charge selectivity, and fused podocyte foot processes. These changes are associated with reductions in glomerular cell production of proteoglycans and glycosaminoglycans contained within the glycocalyx.

The target site for another animal model of podocytopathies, specifically puromycin aminonucleoside nephrosis has been critically examined with detailed sequential ultrastructural evaluation of glomeruli in a daily low-dose rat model. The earliest change occurs as effacement of podocytic foot processes by broad expanses of epithelial cytoplasm, followed by proteinuria. With persistent proteinuria, puromycin induces FSGS characterized by podocytopenia, focal sclerosis of the tuft, and adhesions to Bowman's capsule.

Bisphosphonates, including pamidronate, alendronate, and zoledronate in animal models, have been associated with nephrotoxicity, the spectrum of which includes collapsing and noncollapsing forms of FSGS, minimal change disease, and tubulointerstitial nephritis. Morphologically, there is an increased podocyte proliferation index and decreased expression of synaptopodin, suggesting a mechanism of direct podocyte toxicity. Mitochondrial perturbations in podocytes with pamidronate and iron overload with other bisphosphonates have also been reported.

In nonclinical toxicity studies, monkeys may be especially susceptible to glomerular lesions similar to FSGS because of the presence of background subclinical infections and concomitantly administered immunomodulatory therapeutic agents (Figure 11.15). Loss of podocytes (viable and apoptotic cells) in the urine precedes proteinuria thus podocyturia can serve as the first noninvasive marker of active glomerular damage. In addition to light microscopic and ultrastructural evaluations, immunohistochemical methods can be

TABLE 11.10 Nephrotoxicity Classification Based on the Functional Characteristics of the Specific Potentially Injurious Agent

Functional characteristics of the inducing xenobiotic	Specific potentially injurious agent
Hemodynamic and prerenal factors	Angiotensin-converting enzyme inhibitors, hypertension, hydropenia
Inotropic and vasodilator cardiotonics	Digoxin, lsoproterenol, ischemia, shock
Proteins and amino acids	Albumin, $Alpha_{2u}$ globulin, Bence-Jones, D-serine, dietary protein, hemoglobin, lysinoalanine, lysozyme, maleic acid, myoglobin, rapeseed
Naturally occurring organic toxins	Aflatoxin, aristolochic acids, bacterial toxins, broom weed, Chinese tallow tree, citrinin, furan derivatives, greasewood, halogeton, lantana camara, monocrotaline, mushroom, pigweed (*Amaranthus retroflexus*), rhubarb
Synthetic biological toxicants	Fumigants/nematocides, 1,2-dibromomethane, 1,2-dibromethane-3-chloropropane, *n*-succinimide
Germicides	*O*-Benzyl-*p*-chlorophenol
Herbicides	Bipyridium compounds
Insecticides	Chlorinated hydrocarbons, hexachlorocyclohexane, organophosphorous compounds, toxaphene
Normal endogenous substrates	ACTH, bilirubin, calcium, fluoride, glucose, iron, magnesium, phosphate, potassium, sodium, serotonin, vesicourethral reflux, vitamin D_2, zinc
Physical agents	Electrical shock, heat stroke, radiation
Metals	Aluminum, antimony, arsenic, beryllium, bismuth, cadmium, copper, gold, lead, lithium, mercuric chloride, nickel, rubidium, trimethyltin, uranium
Glycols	Diethylene glycol, diethylene glycol monoethyl, ethylene dichloride, ethylene glycol, ethylene glycol dinitrite, propylene glycol
Industrial chemicals involved in plastics and resins manufacture	Acrylonitrile, hexachloro-1,3-butadiene, organonitriles
Chelators	Diphosphonates (Cl_2 MDP, EHDP), bisphosphonates, ethylenediamine tetraacetic acid (EDTA), nitrilotriacetic acid (NTA)
Anesthetics and anticonvulsants	Halothane, methoxyflurane
Antibiotics/antifungals/antimalarials	Amikacin, ampicillin, amphotericin B, bacitracin, beta-lactam compounds, cephaloridine, chloroquine, colistin, gentamicin, kanamycin, methicillin, netilmicin, neomycin, polymixins, streptomycin, sulfonamides, tobramycin, vancomycin
Immunomodulatory agents	Adalimumab, basiliximab, calcineurin inhibitors (cyclosporin, tacrolimus), cyclophosphamide, dactinomycin, daclizumab, etanercept, infliximab, methotrexate, sirolimus
Osmotic agents and diuretics	Carbonic anhydrase inhibitors, dextran, ethacrynic acid, furosamide, mannitol, sucrose, thiazides, torasemide
Organic solvents	Carbon tetrachloride, chloroform, halogenated aliphatics, toluene, trihalomethanes, trichloroethylene
Cancer therapeutics	Alemtuzumab, adriamycin, bevacizumab, capecitabine, cetuximab, *cis*-platinum, crizotinib, dasatinib, gemtuzumab ozogamicin, hydroxyurea, imatinib, interferon alfa, isotretinoin, lapatinib, letrozole, melphalan, ofatumumab, paclitaxel, puromycin mononucleoside, rituximab, sorafenib, streptozotocin, sunitinib, tamoxifen, trastuzumab, vincristine
Diagnostic agents	Diatrizoate iodide
Hyperuricacidemia therapeutics	Allopurinol
Male antifertility agents	α-Chlorohydrin
Nonsteroidal antiinflammatories	Acetaminophen, celecoxib, diclofenac, diflunisol, ibuprofen, indomethacin, ketoprofen, meloxicam, nabumetone, naproxen, oxaprozin, paracetamol, paracoxib, peroxicam, phenacetin, rofecoxib, salicylates, sulindac, valdecoxib
Miscellaneous agents	Melamine, raisins, grapes, interferon, IV γ-globulin, acyclovir, cimetidine, foscarnet, probenecid, captopril, clofibrate, propanolol, isoniazid, methyldopa, azathioprine, ACTH, bilirubin, calcium, fluoride, glucose, iron, lilium, magnesium, phosphate, potassium, sodium, serotonin, zinc

Table reproduced from Handbook of Toxicologic Pathology (2013), third ed. (W. M Haschek, C. G. Rousseaux, and M. A. Wallig, eds.), Academic Press, Table 47.22, p. 1728–1729, with permission.

TABLE 11.11 Nephrotoxicant Classification Based on Subtopographical Site of Injury or the Functional Effect Causing Injury in the Kidney

Target/Functional activity	Associated nephrotoxicants or inducting agent
GLOMERULUS	
Direct effects on podocytes	Puromycin, bisphosphonates, interferon-α, valproic acid
Direct effect on glomerular endothelium	VEGF and VEGF-R inhibitors
Oxidative activation	Adriamycin
Increased GFR	Hypertension, aldosterone, high protein diet
Decreased GFR (via efferent arteriole constriction)	Cyclosporin, tacrolimus, amphotericin-B, radiocontrast media, NSAIDs
Decreased GFR (via systemic effects)	ACE inhibitors, inotropic and vasodilator cardiotonics
PROXIMAL CONVOLUTED TUBULE	
Sodium pump-linked transport	Phosphate, lithium
Endocytosis, pinocytosis, protein-linked update	Aminoglycosides, α2μ globulin, Bence-Jones protein, hemoglobin, myoglobin, lead, cadmium, bismuth, sucrose, manitol, nitrilotriacetic acid
Obstructive nephropathy	Folic acid, ethylene glycol, glycolic acid, oxalic acid, methotrexate, sulfonamides, peptide mimetics (e.g., integrins receptor antagonists)
PARS RECTA	
Oxidative stress	Chloroform, acetaminophen, acetamide, paracetamol, *p*-aminophenol, 1,1-dichloroethylene, bromobenzene, epichlorhydrin, 1,2-dichloropropane, *n*-succinimide
Activation by glutathione system	1,2-Dibromomethane, trisphosphate, 1,2-dibromo-3-chloropropane, 1,2-dichloroethane
B-lyase-mediated bioactivation	Trichloroethylene, hexachlorobutadiene, trichloroethane, tetrachloroethane, chlorinated, and fluorinated olefins
Organic acid transport (with metabolism to reactive intermediate)	Carbapenems, cephalosporin, citrinin, procainamide, methotrexate
Organic base transport (with oxidative activation)	Cisplatin
Cell respiration	Mercury salts, ischemia/hypoxia reperfusion injury
Distal nephron	Fluoride, methoxyflurane, 5-azacytidine, furosemide (thick ascending tubule), thiazide-like diuretics (distal convoluted tubule), amiloride (cortical collecting ducts)
RENAL PAPILLA	
Interstitial concentration via countercurrent exchanger and oxidative activation via endoperoxide synthase	NSAIDs, phenacetin, 2-bromoethylamine, 5-nitrofurans

Table reproduced from Handbook of Toxicologic Pathology (2013), third ed. (W. M. Haschek, C. G. Rousseaux, and M. A. Wallig, eds.), Academic Press, Table 47.23, p. 1730, with permission.

used to characterize podocyte toxicity including markers of podocyte plasma membrane proteins (podocalyxin, glomerular epithelial protein-1, GLEPP-1), slit-diaphragm-associated protein (nephrin), cytoskeleton-associated pedicel protein (synaptopodin), protein synthesized by podocytes (VEGF), PEC markers (paired box gene 2, PAX2), transcription factors (Wilms tumor protein-1, WT-1) and cytoskeleton intermediate filaments. In FSGS, a progressive loss of podocyte markers (synaptopodin, podocalyxin, GLEPP-1, and VEGF) is noted, while PAX2 and cytokeratin in PECs may exhibit an increase in staining intensity. WT-1 staining is shown to be variable but usually parallels PAX2 staining in PECs.

Glomerular Endothelial Cell Injury: Glomerular endothelial cells are a component of the normal glomerular permeability barrier, modulating adhesion and infiltration of circulating cells, and producing factors that regulate intraglomerular hemodynamics and hemostasis. The glomerular endothelial cell is both a target in injury and a contributor to perpetuation of injury. These cells closely interact with podocytes and mesangial cells, and are modulated by key angiogenic factors derived from these cells. Therefore, indirect

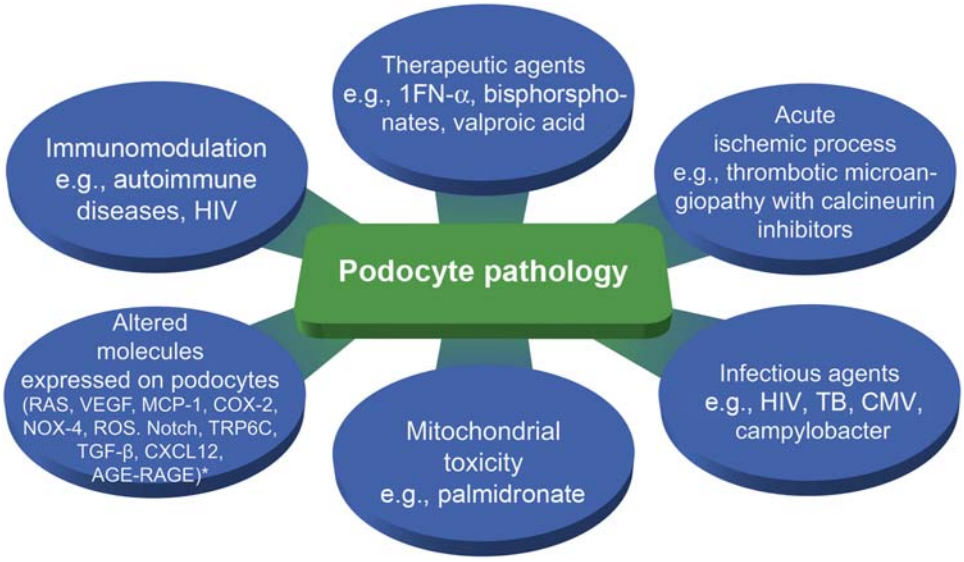

FIGURE 11.25 Potential causes of podocyte pathology include therapeutic agents, infectious agents, and secondary to immunomodulation. Four major patterns of morphologic changes are seen following podocyte injury including foot process effacement, apoptosis, arrested development, and dedifferentiation. Injured podocytes could spread injury to other neighboring healthy cells resulting in a vicious cycle. *Many molecules/proteins are involved in the "crosstalk" between glomerular cells including glomerular endothelial cells, mesangial cells, and podocytes and alterations in one can affect functions in the other cells. *Figure reproduced from Haschek and Rousseaux's Handbook of Toxicologic Pathology (2013), third ed. (W.M. Haschek, C.G. Rousseaux and M.A. Wallig, eds.), Academic Press (Elsevier), Figure 47.29, p. 1731, with permission.*

glomerular endothelial injury is observed when podocytes are severely injured, resulting in loss of key angiogenic factors necessary for maintenance of endothelial cell survival and function. Endothelial cells respond to injury by increased elaboration of prothrombotic substances, including plasminogen activator inhibitor-1. Markers of endothelial dysfunction include elevated serum levels of von Willebrand Factor. Specific disease states where glomerular endothelial cell injury directly or indirectly contributes to the disease pathogenesis include hemolytic uremic syndrome (HUS), diabetic nephropathy, obesity, preeclampsia/eclampsia, transplant nephropathy, and immune complex/crescentic glomerulonephritides.

Mesangiolysis, capillary endothelial cell loss, capillary fibrin deposits, and glomerular capillary cysts (aneurysms) occur as acute phase responses to snake bites, croton oil, glomerular ischemia, hypertension, HUS, thrombotic thrombocytopenic purpura, transplant rejection, radiation, and immune-mediated glomerulonephritis (Figures 11.15 and 11.26). Hemolytic-uremia syndrome represents a serious complication of bacterial endotoxemia. The increased susceptibility of children with diarrhea-positive HUS has been proposed to be due to increased glomerular expression of globotriaosylceramide (Gb3). This receptor binds shiga toxin and is preferentially expressed on glomerular endothelium. Hemolytic-uremia can be produced in the rabbit by injection of *Shigella* endotoxin and prevented by pretreatment with busulfan (causing leukopenia). Hemolytic-uremia is characterized by leukocyte-mediated intravascular fibrin deposition in, and occlusion of glomerular capillaries with resultant renal cortical necrosis (generalized Schwartzman reaction model). Medications such as cyclosporin, mitomycin-C, and estrogen-containing contraceptives have been associated as risk factors for hemolytic-uremia in humans.

Direct injury to the glomerular endothelium is observed in immune complex disease with subendothelial deposits (Figure 11.15) where activation of complement and membrane attack complex occurs in the subendothelial space. TNF-α is increased in a variety of inflammatory conditions, and causes increases in endothelial cell adhesion molecule expression and expression of IL-6. TNF-α disrupts the glycocalyx and also directly increases endothelial permeability.

Mesangiolysis: Mesangial cells generate their own extracellular matrix and together they constitute the central stalk of the glomerulus. In close partnership with endothelial cells and podocytes, they form the functional glomerular unit and are in continuity with the extraglomerular mesangium and the JGA. Mesangial cell injury directly or indirectly contributes to a wide variety of glomerular diseases. Mesangioproliferative diseases are typically associated with mesangial immunoglobulin deposition and comprise primary diseases such as IgA nephropathy, mesangioproliferative

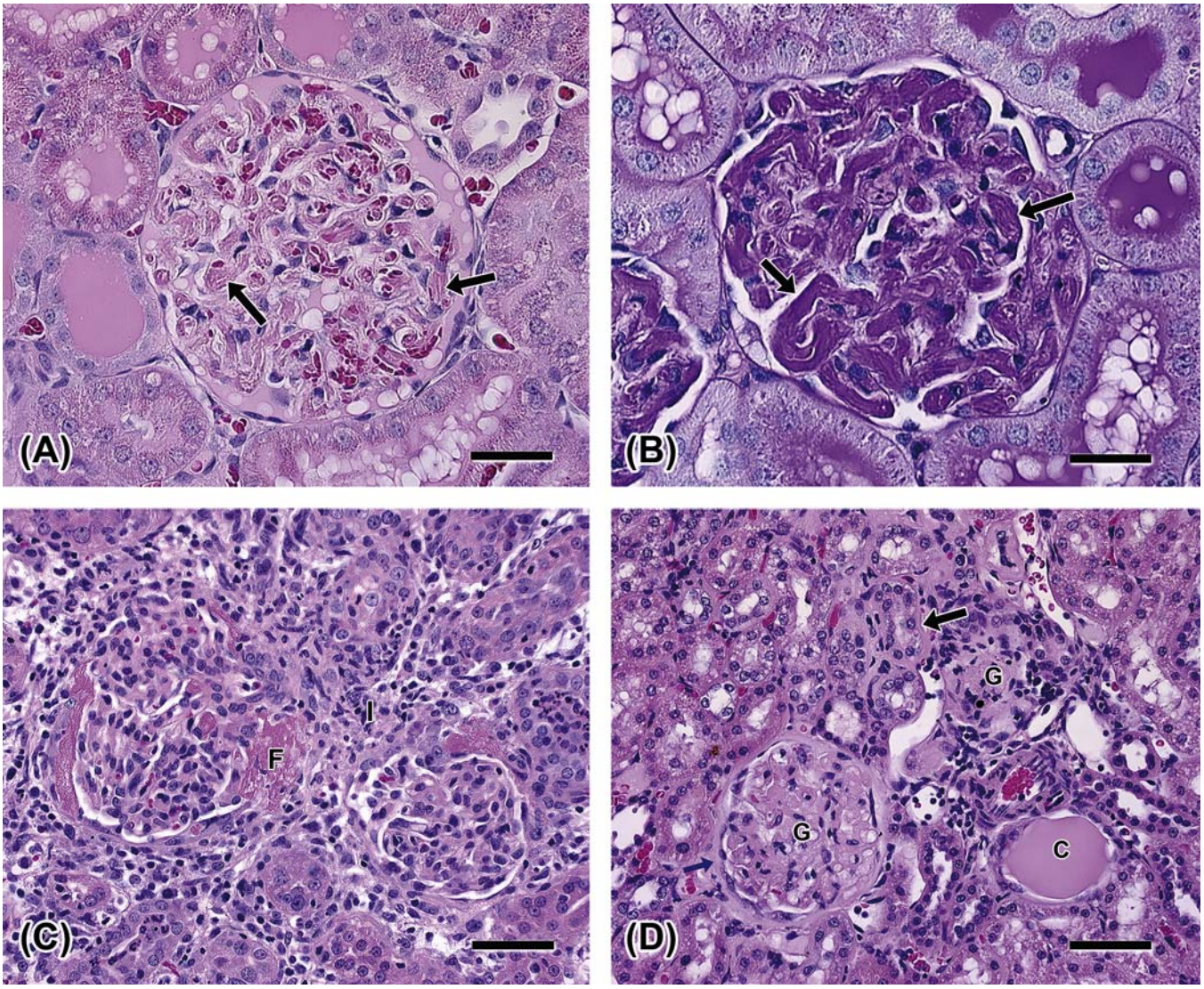

FIGURE 11.26 Thrombotic glomerulopathy in a rat treated with a nanoparticle formulation illustrates fibrinous thrombi in the capillary loops (arrows) stained with H&E (A) and PAS (B), respectively. Bar = 30 μm. (C) Glomerulonephritis in a monkey treated with a protein therapeutic illustrates effacement of glomeruli by inflammatory cells and fibrin (F) deposition. Bar = 55 μm. (D) Glomerulosclerosis in a young spontaneously hypertensive rat fed a high salt diet, which accelerated glomerular sclerosis (G) and nephropathy processes such as tubular regeneration (arrow) and casts (C). Bar = 60 μm. *Figure reproduced from Haschek and Rousseaux's Handbook of Toxicologic Pathology (2013), third ed. (W.M. Haschek, C.G. Rousseaux and M.A. Wallig, eds.), Academic Press (Elsevier), Figure 47.30, p. 1733, with permission.*

glomerulonephritis, and systemic diseases such as lupus nephritis. Mesangial matrix expansion with diffuse or nodular glomerulosclerosis is a typical feature of diabetic nephropathy. The induction of HUS by bevacizumab, an antibody against VEGF, in the treatment of patients with cancer is associated with proteinuria, mesangiolysis, glomerular endothelial damage, and basement membrane duplication.

Mesangiolysis occurs following acute insults with toxins (e.g., Habu snake venom) or directly through destruction of mesangial cells by antibodies directed against a mesangial antigen (Thy 1.1. in rats). The resultant pathologic effect is characterized by mesangiolysis and replacement of capillary loops with capillary balloons, similar to the congenital defects observed in knockouts for endothelial PDGF-B or mesangial PDGFR-β. Some of these observations suggest that mesangial cells may act as specialized pericytes supporting glomerular capillary loops.

Reflux Nephropathy: Reflux nephropathy arising as mesangial injury occurs in humans with vesicoureteral reflux. The mechanism of injury is not well defined but does not require infection. Early factors include expansion of mesangial matrix, possibly because of tubular secretory antigenic proteins, normally restricted to uriniferous space, reaching the mesangial matrix or interstitial space because of back pressure, with subsequent immune-mediated tissue injury.

Laboratory rats can have reflux upon micturition, evident by retrograde flow of dye placed in the urinary bladder under physiologic pressure. The pathologic consequence of reflux is not defined in the rat. Retrograde nephropathy characterized by tubular dilation extending from the papilla to the cortex has been reported in rats treated with melamine (Figure 11.22). This is thought to be due to melamine precipitation in the lower urinary tract creating pressure effects through transient obstruction. These renal changes are similar to human reflux nephropathy of early childhood when urinary tract infection is superimposed on congenital vesiculouretral reflux. Microscopic changes of human reflux nephropathy primarily involve the tubules and interstitium and are characterized by tubular atrophy and dilation, and corticomedullary fibrosis. The epidemic of infant kidney disease in China linked to melamine adulteration of milk products may have a similar etiology. Affected infants developed urinary tract calculi.

Changes in Polyanionic Binding Sites in the Glomerular Filtration Barrier: Protamine (a heparin antagonist) induces charge reduction in the glomerular filtration barrier followed by functional evidence of injury, manifested as proteinuria. Fixed polyanionic binding sites in the filtration barrier serve to retain anionic plasma proteins such as albumin in the circulation. Nontoxic doses of circulating polycationic agents such as protamine cause protein leakage, which secondarily induces morphologic lesions. Podocyte injury in this model is a consequence of albuminuric or protein overload.

Interference in Formation of Crosslinks in Glomerular Basement Membrane Collagen: D-Penicillamine affects glomerular basement membrane directly in rats, possibly by interfering with collagen crosslink formation. Adverse effects of the drug which is used in the treatment of rheumatoid arthritis include development of membranous glomerulonephritis as an apparent consequence of defective basement membrane synthesis.

Perturbation of Renal Hemodynamics

Increased Glomerular Filtration Rate: Persistent elevation of glomerular capillary flow causes glomerular injury, characterized by mesangial expansion and proteinuria, progressing to focal glomerular sclerosis. Two interrelated, but potentially independently acting, hemodynamic functional alterations causing injury include increase in single nephron GFR (SNGFR) and increase in glomerular capillary hydraulic pressure (GCHP). Increased SNGFR and GCHP can be induced by deoxycorticosterone injection and by saline as the drinking water source, which is a model for inducing hypertension. Prednisone treatment in humans for 2 weeks is associated with increased GFR. Methylprednisolone in dogs results in increased GFR and RPF and decreased filtration fraction. It is also associated with reduced renal vascular resistance (RVR) after short-term exposures and increased RVR after long-term exposures in dogs. The morphologic changes in kidneys following subchronic and chronic administration of glucocorticoid agonists can therefore be attributed to alterations in local hemodynamics or effects on insulin metabolism. These could mimic early stages of diabetic nephropathy. Dogs, following chronic glucocorticoid agonist treatment, develop an increased size of kidneys and individual glomeruli. Histologically, glomerular lesions may be comprised of a combination of nodular (Kimmelstiel–Wilson type nodules) or diffuse intercapillary glomerulosclerosis, accumulation of eosinophilic material within Bowman's capsule (capsular drop), eosinophilic material within capillaries (fibrin cap), glomerular synechia, parietal cell hyperplasia and arteriolosclerosis. Renal lesions are less prominent in rats treated with glucocorticoid agonists and may include increased kidney weights, basophilic staining of tubular epithelium and intracytoplasmic clear vacuoles in tubular epithelium.

A decrease in dietary protein in the normal rat leads to decreased SNGFR and GCHP. Dietary protein plays an important role in the development and progression of kidney injury. An increase in dietary protein can cause an increase in kidney size and GFR, with subsequent glomerular injury, accumulation of mesangial deposits, and eventually, glomerulosclerosis. Associated at least in part with protein overnutrition, CPN occurs in nearly all 2-year-old male laboratory rats (Figure 11.7). Female rats have a similar change but lower incidence and slower progression, possibly because of lower food consumption. These lesions in the rat are substantially reduced by limiting either protein or total diet consumption. Susceptibility to CPN can be influenced genetically, but is not recognized to be strain specific in the rat, though severity varies among laboratories and among strains. Elevation in circulating aldosterone levels has been associated with an increase in cellular replicative rate in rat kidney which is considered to play a role in the development of CPN.

Reduction in renal mass also results in an increase in SNGFR and GCHP in renal parenchyma as a compensatory response to maintain renal function. The increased SNGFR and GCHP can occur even with insufficient loss of renal mass for development of reduced GFR and ARF, indicating that GFR values do not necessarily reflect SNGFR. Hormones such as glucagon and prostaglandins (PGs) are suspected as mediators of these intrarenal hemodynamic changes. Reduction in renal mass results in nephron injury morphologically similar to that associated with hypertension and protein overnutrition. Reduction of dietary protein significantly reduces the severity

and rate of progression of disease in the remnant parenchyma.

Reduced renal mass with individual nephron hyperfiltration, subsequent mesangial expansion, and sclerosis with further nephron loss thus represents the final common pathway to progressive renal failure regardless of the primary injury mechanism. Restriction of dietary protein is universally beneficial in ameliorating chronic progressive kidney disease regardless of the instigating factors.

Decreased Glomerular Filtration Rate: Transmembrane signal transduction refers to the process whereby a ligand binds to the external surface of the cell and, without necessarily penetrating the cell membrane, elicits a physiological response specific for that hormone and cell type. Cyclosporine may cause renal toxicity via signal transduction. Cyclosporine, used in transplant patients to prevent rejection, causes two forms of toxicity. The first is an acute decrement in the GFR which is reversible on cessation of treatment. Cyclosporine markedly augments the glomerular vasoconstrictor response to vasoactive hormones. Thus, cyclosporine induces an unfavorable perturbation in transmembrane signaling response, serving as a prototype for a transmembrane signaling disorder. The second form of toxicity is a chronic and reversible attrition of nephron function following chronic exposure. It is believed that episodes of acute vascular effect, when sustained, eventuate in a chronic form of tubulointerstitial disease. The chronic disease is characterized by areas of multifocal tubulointerstitial fibrosis, tubular atrophy, and efferent arteriolopathy, beginning in the outer medulla with extension into the medullary rays. In Gottingen minipigs, acute cyclosporine exposure is associated with glomerular hyperfiltration whereas chronic treatment results in patchy interstitial fibrosis, glomerulosclerosis, and renal enlargement.

NSAID-related Nephrotoxicity: Conditions that may reduce actual or effective circulation volume, e.g., plasma volume contraction (hemorrhage, salt loss, hypoalbuminemia), congestive heart failure, cirrhosis, and ascites, cause a homeostatic increase in vasoconstrictors including norepinephrine and angiotensin-II (Figure 11.23). Vasodilatory effects of PGs at the afferent arteriole counterbalance this vasoconstrictor effect to maintain GFR and renal perfusion. Inhibition of PGs by NSAID inhibition of cyclooxygenase (COX) (especially at the afferent arteriole) results in pronounced vasoconstriction and a decrease in glomerular capillary pressure resulting in a decline of GFR. ARF induced in humans with NSAID treatment is caused by this hemodynamic effect as a result of loss of counter-regulatory PGs.

NSAIDs either selectively inhibit COX-2 or are nonselective inhibitors of both COX-1 and COX-2 isoforms (Figure 11.27). The most frequent renal side effects of

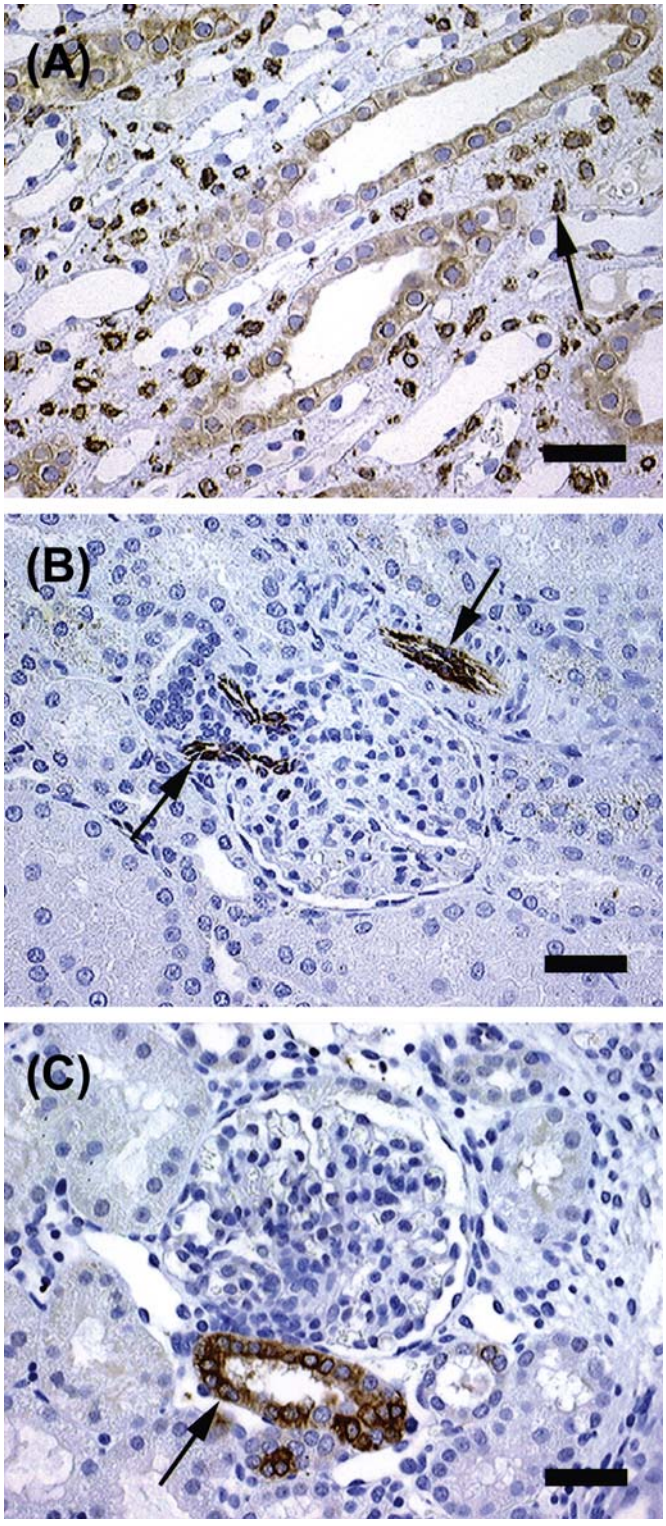

FIGURE 11.27 Immunohistochemical staining showing COX-1 immunoreactive protein in (A) the collecting ducts and the papillary interstitial cells (arrow). Bar = 25 μm (B) The efferent and afferent arterioles and a small artery, and (C) COX-2 immunoreactivity in the macula densa (arrow) in the dog kidney (arrows). Bar = 30 μm. *Figure reproduced from Handbook of Toxicologic Pathology, second ed. W. M. Haschek, C. G. Rousseaux and M. A. Wallig, eds. (2002) Academic Press, Figure 12, with permission.*

NSAIDs are functional, and include interference with fluid and electrolyte homeostasis that is generally mild and transient. The less frequent, but clinically significant, renal side effects include ARF, interstitial nephritis, NS, and RPN. These adverse effects, excluding interstitial nephritis in humans are associated with the simultaneous presence of other risk factors, e.g., age, atherosclerotic heart disease, congestive heart failure, concomitant use of diuretics, and analgesic abuse. The mechanism for interstitial nephritis is unknown, but up to 5% of renal lesions in humans are attributed to conventional NSAIDs treatment.

The clinical laboratory changes in subjects developing ARF in response to conventional NSAIDs include oliguria, decreased fractional excretion of sodium, decreased GFR, and increased BUN and creatinine. Withdrawal of NSAIDs results in complete reversal of ARF; however, if not recognized early in the course of therapy, prolonged renal ischemia may cause acute tubular necrosis and permanent renal damage.

Acute interstitial nephritis (AIN) with or without NS occurs following months to years of NSAID treatment. AIN alone is more common than AIN with NS and NS alone. The clinical laboratory changes in this syndrome include elevated BUN, creatinine (often >6 mg/dL), oliguria, proteinuria (>3.5 g/24 hours with NS), microscopic hematuria, and pyuria. Histopathologic evaluations reveal severe interstitial edema and multifocal infiltrates of lymphocytes and plasma cells surrounding proximal and distal tubules. Lymphocytes are predominantly CD-8^+ T-cells with small numbers of B-cells. Eosinophiluria, eosinophilia, rash, and fever are absent. Ultrastructurally, patients with NS show minimal change glomerulopathy with marked epithelial foot process-fusion.

PGs exert modulatory influences on many ion transport sites along the nephrons and are important in sodium and water homeostasis in the kidney. Thus NSAID inhibition of renal PGs interferes with PG-mediated sodium chloride transport, antidiuretic hormone, and distribution of blood flow from cortical to juxtamedullary nephrons. The sodium and water retention manifests clinically as edema. The clinical laboratory changes may include oliguria, decreased urinary sodium and chloride excretion, and increased serum chloride levels.

PGs also regulate renin release and thus indirectly affect aldosterone production. NSAID treatment may result in hyporeninemic hypoaldosteronism. Aldosterone is important in potassium excretion from the DCTs and collecting ducts. However, it is rare to see hyperkalemia with NSAIDs in the absence of other defects in potassium homeostasis. Elevated serum potassium and decreased urinary potassium excretion are observed in the clinical laboratory profile of NSAID-associated adverse effects.

In experimental studies, RPN is produced readily in rats, occasionally in rabbits and dogs, and rarely in monkeys. As a chronic consequence of RPN, rats develop urothelial neoplasia. Multifocal RPN occurs in the clinical setting in horses and calves and is associated with butazolidin or, occasionally, other NSAID treatment. Since RPN only develops in humans after prolonged high-level use, and in the presence of chronic renal disease, the pig could be presumed to be similarly refractive to RPN. The pig has not been shown to develop RPN at levels substantially exaggerated over those causing RPN in rats (1 g/kg/day of salicylate in the pig for 10 months with no effect versus 250 mg/kg as a single dose causing RPN in rats). Several interrelated differences in rats compared to humans and other species influencing the integrity of inner medullary blood flow include presence of well-developed inner medulla, unipapillary kidney, high urine-concentrating capacity, exclusive postglomerular tuft blood supply to the papilla, and increased NSAID or metabolite papilla concentration on an mg drug/kg body weight basis. These factors along with interspecies differences in COX isoform distribution may explain the enhanced susceptibility of rats to develop RPN.

The isoform and species variations in renal distribution of COX may, in part, explain the renal effects of NSAIDs in humans and laboratory animals. The renal medulla and papilla predominantly express COX-1, and are the major sites of PG production in the kidney. PGs at these sites are considered to be involved in modulating various aspects of urine-concentrating ability and to antagonize vasopressin-mediated water and solute reabsorption. PGs also have direct effects on distal tubular potassium secretion and they promote vasa recta dilation to maintain medullary blood flow. Thus, it is likely that the inhibition of COX-1-mediated PGs by NSAIDs at the above sites is responsible for promoting fluid and electrolyte disturbances and interference with the actions of arginine vasopressin.

Immune-Mediated Injury

Immune-mediated kidney injury accounts for the most common forms of primary glomerular disease in humans. Drug-associated immune-mediated kidney injury represents an important differential etiologic diagnosis in all renal diseases in humans. An occasional industrial or environmental chemical has also been implicated by association in the development of immune-mediated kidney disease. Drug-induced immune-mediated renal toxicity can appear as interstitial inflammation characterized by infiltration of lymphocytes, monocytes, eosinophils, and plasma cells within the interstitium, urinary sediment with pyuria and/or white blood cell casts, eosinophiluria, hematuria, and mild-to-moderate proteinuria. This type of renal disease has been induced with a variety of drugs

in humans including penicillin, methicillin ampicillin, rifampin, sulfonamides, thiazides, cimetidine, phenytoin, allopurinol, cephalosporins, cytosine arabinoside, furosemide, interferon, NSAIDs, ciprofloxacin, clarithromycin, telithromycin, pantoprazole, omeprazole, and atazanavir.

Mercurials and drugs with a sulfhydryl group, such as gold salts, pencillamine, and captopril, are associated with membranous glomerulopathy. NSAIDs and lithium are responsible for the NS with minimal glomerular change considered as a T-cell-mediated disease. Hydralazine causes a lupus-like syndrome. A myriad of drugs have been implicated in immunologically mediated AIN without the NS. In considering an exhaustive list of drugs that have been identified as injurious to human kidneys, AIN would be the most frequent expression. That is not to say that AIN is the most important but rather to say that the list of agents associated with AIN would be longer than that associated with any other mechanistic category.

Drug-associated immune-mediated kidney injury in humans depends on host factor variability for expression, as well as interaction with preexisting disease. Immune-mediated kidney injury in animals represents an important consideration in establishing causality of spontaneous disease especially in diseased animal models. In routine toxicology studies, primary immune-mediated renal toxicity is rare; however, recently there is greater recognition of immune-mediated renal toxicity in nonhuman primates and rodents following chronic treatment with protein therapeutics. The mechanisms may involve deposition of systemically circulating immune complexes or immune complexes formed in situ comprising antidrug antibody with or without the elicitation of glomerular or interstitial inflammation. It should be noted that there may be light microscopic, electron microscopic, and/or immunohistochemistry evidence of glomerular immune complexes in clinically normal cynomolgus monkeys which may significantly increase following treatment with protein therapeutics.

Other Mechanisms of Glomerular Injury

Reactive oxygen intermediates (ROI) have been implicated in the pathogenesis of inflammatory, immune, and toxic insults in glomerular injury. ROI mediate inactivation of NO and modify the metabolism of PGs. With continuous treatment, cytotoxic properties of adriamycin may arise from metabolism to a quinone by PG endoperoxide synthetase (in the glomerular tuft endothelial cells). An electron reduction, catalyzed by flavoenzymes such as NADPH-cytochrome and P-450 reductase, produces semiquinone electrophilic intermediates, with covalent binding and injury, or production of superoxide anions, and transformation into more deleterious oxygen species, the hydroxyl radical and singlet oxygen.

Diabetic hyperglycemia is associated with glomerular and mesangial basement membrane thickening, characteristics of diabetic glomerulopathy. Glycosylation of basement membrane protein proportional to the level of glucose in the local environment has been hypothesized as a mechanism of the basement membrane injury. Xenobiotics perturbing glucose levels could thus potentially act through this mechanism.

Mechanisms of Proximal Tubular Injury

Proximal tubular toxicants frequently affect both convoluted and straight segments. One factor relevant to expression of injury in the proximal tubule is the unique portal system. There is a marked cortical medullary gradient with relative hypoxia in the outer medulla. This is related to the lower medullary blood flow, the countercurrent exchange of oxygen, and the high metabolic requirements of the thick ascending limb and pars recta. Blood flow to the outer stripe is via postglomerular capillary venous efferent vessels. The number of mitochondria is significantly higher in the S3 segment compared to that in the S1 and S2 segments in the rat (Figure 11.2). The outer stripe, hence, is the most sensitive in the rat kidney to hypoxia and is a site for synergism between toxicity and hypoperfusion (Figure 11.28). Synergism between compromised perfusion and toxicity occurs clinically where the majority of cases of human drug-induced nephrotoxicity occur in the presence of compromised renal perfusion.

The importance of primary xenobiotic injury to the distal segments of nephron including the loops of Henle, the TAT, or the DCT is not well established. Tilorone, an interferon inducer, causes phospholipidosis in the DCT as a limited example of a primary toxic response for the distal nephron. Other reports of distal nephron perturbation are often based on functional tests without concomitant demonstration of the site of specific structural change.

Direct Perturbation of Cell or Subcellular Organelle Function

Nephrotoxicity due to direct perturbation of cellular or subcellular organelle function occurs most commonly in the highly metabolically active proximal tubules and less so in the distal tubules and collecting ducts. The injury can be related to accumulation of xenobiotics or their metabolites in subcellular organelles e.g., aminoglycoside antibiotic lysosomal overload. Lysosomal overload of gentamicin and phospholipid membranes results in compromised lysosomal membrane integrity. Lysosomal enzyme leakage occurs as a consequence and possibly

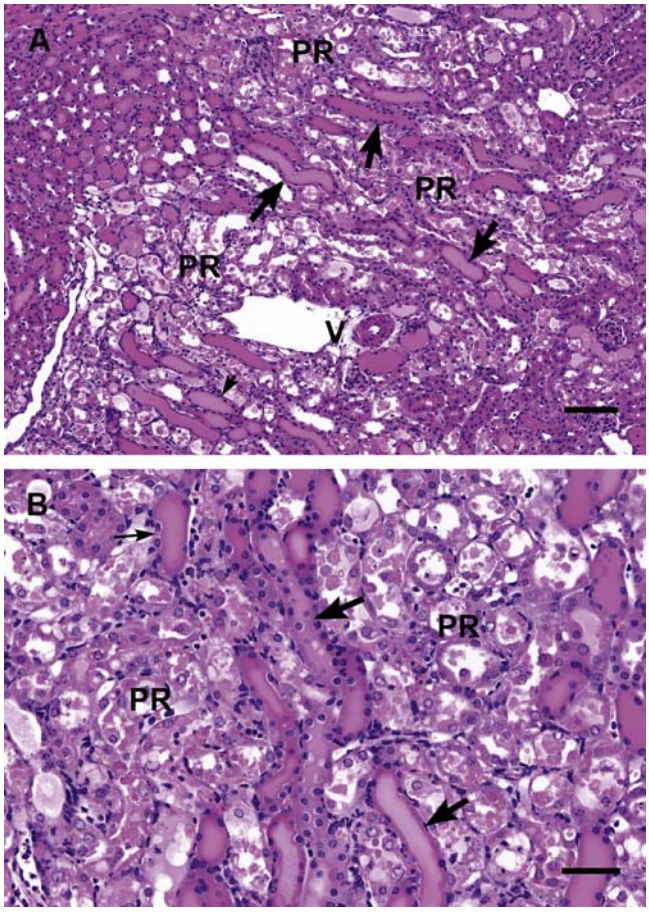

FIGURE 11.28 Necrosis of pars recta (PR) in a male SD rat kidney treated with a chemical molecule. (A) Low magnification showing multifocal tubular necrosis and tubular dilatation with intratubular protein casts in thick ascending loops of Henle and/or collecting ducts (arrows) along the corticomedullary junction and in the outer stripe of the outer medulla (note the arcuate artery/vein, V). Bar = 125 μm. (B) Higher magnification showing pars recta necrosis (PR) and tubular dilatation with intratubular protein casts (arrows). Bar = 45 μm.

explains cell necrosis as the overt manifestation of toxicity. Heavy metals usually accumulate in the kidney, liver, bone, and brain. The injury in the kidney typically involves the pars recta. The common examples of heavy metals resulting in direct cellular toxicity in the kidney include cadmium, mercury, manganese, and lead.

Aminoglycoside Antibiotic Lysosomal Overload: Gentamicin, a prototypical aminoglycoside antibiotic, has a low molecular weight, binds only weakly to plasma proteins, and is freely cleared into the glomerular filtrate as the primary route of excretion. Serum half-life is inversely correlated with GFR. Serum half-life is 30 minutes with normal GFR. Within minutes after administration, intense binding of drugs to brush border can be demonstrated. This binding is specific and receptor mediated. A charge interaction exists between cationic sites on the gentamicin molecule and anionic sites on the brush border. Propensity for binding phospholipids, charge, and toxic potential are strongly correlated when comparing different aminoglycoside antibiotics. After binding, gentamicin is taken into the cell by endocytosis, followed by fusion of the endocytic vesicles with phagosomes. Within the phagolysosome, gentamicin inhibits phospholipases and sphingomyelinase responsible for the degradation of phospholipid-rich cell membranes. Thus, the drug and phospholipid membranes are sequestered and accumulate in the phagolysosome. This phenomenon is reflected ultrastructurally by the appearance of myeloid bodies occurring at all levels of the proximal tubule but with a predilection for the PCT. Calcium competes with gentamicin for binding sites; thus, calcium loading ameliorates gentamicin toxicity. Lysosomal overload of gentamicin and phospholipid membranes results in compromised lysosomal membrane integrity. Lysosomal enzyme leakage occurs as a consequence and possibly explains cell necrosis as the overt manifestation of toxicity. The chronic effect of gentamicin toxicity in the absence of overt tubular necrosis consists of increased incidence and severity of lesions of chronic CPN compared with controls. Females, including rats and humans, may be more severely affected than males at comparable tissue levels of the drug. A myriad of risk factors predisposing to gentamicin injury has been identified clinically. A severe degree of acute renal toxicity and reduced GFR with gentamicin can be explained by tubular obstruction. However, in mild cases and early stages of severe cases where tubular obstruction has not yet occurred, GFR reduction is likely the result of extratubular mechanisms within the kidney including tubular glomerular feedback, direct mesangial and vascular contraction caused by gentamicin, and indirect mesangial and vascular contraction produced by inflammation and paracrine mediators. Therefore an integration of tubular, glomerular, and vascular effects of aminoglycosides may be involved in the pathogenesis of nephrotoxicity of this class of drugs.

Heavy Metals: Heavy metals typically are injurious to the proximal tubule and nervous system. They tend to accumulate in the kidney, liver, bone, and brain. The spectrum of heavy metal renal effects, as well as pathogenesis, can be appreciated by considering the effects of cadmium, mercury, manganese, and lead. Other heavy metals are less studied, but share features of injury with one or more of these chemicals.

Cadmium: Cadmium is a widespread environmental and occupational contaminant. Upon uptake from digestive or respiratory portals of entry, cadmium binds to albumin and other high molecular weight proteins, and then is taken up by the liver. In the liver,

cadmium is bound to the low molecular weight metal transport protein metallothionein and released into the blood stream.

Plasma levels of cadmium bound to metallothionein remain low since this complex passes freely into the glomerular filtrate. The complex is reabsorbed, as are many low molecular weight proteins, in the proximal tubules by endocytosis. Metallothionein is hydrolyzed in the phagolysosome, releasing cadmium, which stimulates metallothionein synthesis de novo. Cadmium rapidly binds newly synthesized or reabsorbed metallothionein. The renal toxicity of cadmium occurs upon the intralysosomal release of free ligand, which also may interact with proteins other than metallothionein. Cadmium accumulates in the kidney, bound to metallothionein in a time and dose-responsive manner. The biological half-life in humans is approximately 10 years.

Threshold levels of cadmium must accumulate prior to induction of overt tubular injury. The threshold varies widely in experimental animals from 10 to 200 μg Cd/g wet weight because of variations in dose rate, route, and form of cadmium administered. Impaired reabsorption of beta$_2$-microglobulin is a sensitive marker of cadmium injury to the proximal tubule. The earliest ultrastructural alteration of cadmium toxicity occurs as phagolysosomal change. Tubular necrosis or increase in incidence or severity of lesions of CPN forms the light microscopic changes in cadmium injury in the rat.

Mercury: As with cadmium, the toxic potential of mercury depends on dose, form, and route of administration. Toxicity of the inorganic salts is quantitatively different from organic mercurials because of differential solubility. Mercurial nephrotoxicity in humans today is almost always a consequence of chronic occupational exposure. Acute mercury poisoning represents the classical cause of proximal tubular cell necrosis. This response preferentially occurs in the pars recta, but with increased time and dose all segments may be affected. The mechanism of proximal tubular cell injury traditionally has centered on uncoupling of oxidative phosphorylation in mitochondria. Mercury does inhibit mitochondrial enzymes. Furthermore, this mechanism is consistent with subtopographical localization in pars recta, the site of predilection for hypoxic injury.

As with other heavy metals, mercury also reacts with free sulfhydryl groups and thus leads to depletion of glutathione. Peroxidative processes also can be considered a cause underlying tubular cell injury. Male rats are significantly more sensitive to mercury-induced tubular cell injury; this is associated with correlative sex differences in renal levels of sulfhydryl groups. Chronic exposure of rats to mercury results in increased incidence and severity of lesions of CPN. Chronic mercury poisoning has been reported to occur because of immune-mediated mechanisms of injury. These reports of immune-mediated renal injury in chronic mercury poisoning fail to differentiate chronic cytotoxicity with an expected secondary immune-mediated component in the spectrum of injury from a primary immune-complex disease, independent of cytotoxicity.

Lead: Rapid and selective accumulation of lead occurs in the kidney, initially isolated to the cytosolic fraction of proximal tubular epithelium. Lead is highly reactive with the sulfhydryl group of two cytosolic proteins having molecular weights of 11,500 and 63,000 Da accounting for the accumulation. These high-affinity lead-binding proteins regulate the bioavailability of lead, as well as transport into the nucleus. Lead pretreatment results in a 30%–40% decrease in binding of lead to renal mitochondria. Through specific cytosolic protein binding, the renal toxicity of this metal is reduced.

Acute or subchronic lead nephrotoxicity is characterized by the presence of intranuclear inclusions visible by routine or special stains in proximal tubular epithelial cells in most species. In the kidney, 80%–90% of lead is concentrated in nuclei, suggesting that the intranuclear inclusions represent a storage site. Extrusion of the nuclear inclusion into the cytoplasm and increasing tubular lysosomal activity may represent a sequence of lead metabolism by the proximal tubule. Cytoplasmic lead can bind to mitochondria, inhibiting mitochondrial respiration, with resultant mitochondrial swelling as a potential mechanism of injury. Acute lead exposure is also characterized by increased apoptotic necrosis and proximal tubular cell replication. This stimulated replication may be related to the carcinogenic potential of lead in the rat. A sensitive morphologic indication of lead toxicity in the rat kidney in routine histopathology is karyomegaly, with males significantly more susceptible than females. Chronic lead exposure may result in increased incidence and severity of lesions of CPN in rats or induction of a chronic nephropathy in humans. Chronic exposure at dosages which show cytomegaly and karyomegaly is associated with eventual renal tubule tumor formation in the rat. However, lead exposure does not appear to represent a risk for renal tumorigenesis in humans.

Antisense Oligonucleotide Nephropathy: Antisense oligonucleotide-based therapeutics are 18–21 nucleotides in length and are designed to bind to target RNA through base pairing. The kidney is frequently a target organ because of the accumulation of this type of drug in rodents and monkeys in nonclinical safety studies. At early time points after injection, these molecules

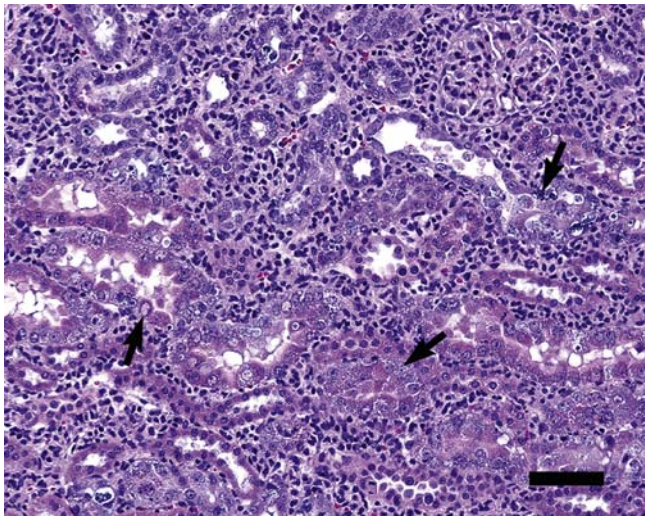

FIGURE 11.29 Antisense oligonucleotide nephropathy in a rat kidney; note accumulation of basophilic material (black arrows) within tubular epithelial cells, intranuclear accumulation of eosinophilic homogeneous material within proximal tubular epithelial cells, and interstitial infiltration of predominantly mononuclear cells. Bar = 50 μm. *Figure reproduced from Haschek and Rousseaux's Handbook of Toxicologic Pathology (2013), third ed. (W.M. Haschek, C.G. Rousseaux and M.A. Wallig, eds.), Academic Press (Elsevier), Figure 47.32, p. 1741, with permission.*

appear to be associated with extracellular matrix as well as within epithelial cells; however, by 24 hours, almost all of the oligonucleotide is found within tubular cells. It is suggested that oligonucleotides are filtered by the glomerulus and are reabsorbed from the tubular lumen into proximal epithelial cells. Microscopic evaluations reveal granular material in both the cytoplasm and the nuclei (Figure 11.29). Immunohistochemistry studies using antibodies against oligonucleotide antisense compounds, as well as the measurement of tissue levels of these agents, shows the material to be consistent with the test agent or a related compound. Histologically, basophilic granules are seen within proximal tubular epithelium which at high doses may be visible at low magnification. Sometimes there is also tubular epithelial degeneration characterized by cellular swelling, cytoplasmic vacuolation, and rarely intratubular hemorrhage. No significant changes in renal function tests are seen in animals. As yet, there is no evidence of a significant adverse renal effect in humans given antisense oligonucleotides.

Chemotherapeutics-induced Nephrotoxicity: Chemotherapeutics typically have no margin of safety and often are used in patients with altered or diminished function of drug metabolism and clearance systems. Patients often have renal abnormalities necessitating pretreatment screening and monitoring of kidney functions and sometimes dose modulation based on individual patient tolerance. Nephrotoxicity is an inherent adverse effect of certain anticancer drugs in humans and animals. Renal toxicity can be manifested by primarily tubular-limited dysfunction, glomerular injury with proteinuria, full-blown acute kidney injury, and long-term chronic kidney injury. In humans, renal pathologic alterations in most cases develop from innate toxicity of the chemotherapeutic agents, but underlying host risk factors and the renal handling of drugs can increase the likelihood and severity of nephrotoxicity. A survey compared toxicity prediction for twelve platinum analogues that had both preclinical (mice, rats and/or dogs) and clinical data from matching drug administration schedules. Nephrotoxicity was observed in human Phase-1 clinical trials for 3 of 12 drugs. Corresponding nephrotoxicity was seen for all human nephrotoxic drugs in dogs and for 2 of 3 in rats. Nephrotoxicity was seen for another 4 drugs in rats and 5 drugs in dogs without any corresponding nephrotoxicity signal in humans. Therefore, predicting nephrotoxicity potential for humans based on nonclinical toxicology studies in animals can be useful but also challenging because of the use of relatively high doses in nonclinical studies. In addition, prophylactic measures can be used in humans to prevent nephrotoxicity (e.g., hydration and forced diuresis), whereas toxicology studies in experimental animals are devoid of such measures.

Mechanisms of chemotherapy-induced nephrotoxicity generally include damage to nephron components or renal vasculature, HUS, or prerenal perfusion deficits. Nephrotoxicity of certain chloroethylnitrosourea compounds (carmustine, semustine, and streptozocin) is characterized by increased sCr levels, uremia, and proteinuria. Cisplatin and carboplatin therapy is associated with increased sCr levels, uremia, and electrolyte abnormalities and rarely HUS with cisplatin. Ifosfamide therapy is linked to proximal tubular damage, urinary loss of electrolytes, glucose, and amino acids (Fanconi syndrome), rickets, and osteomalacia. Azacitidine renal effects are characterized by tubular acidosis, polyuria, and urinary loss of electrolytes, glucose, and amino acids. ARF and HUS are reported following high doses of methotrexate.

Nephrotoxicity with anticancer molecular-targeted therapies can be directly related to perturbation of targets expressed in the normal kidney. Three categories of nephrotoxic agents can be identified for targeted anticancer therapies: (1) high risk of nephropathy, in terms of frequency and severity, mainly represented by the anti-VEGF/VEGFR agents, (2) intermediate risk of nephropathy, with the c-kit inhibitors, and (3) low-risk of nephropathy, including EGFR inhibitors. The VEGF inhibitors can cause thrombotic microangiopathy (TMA), glomerulonephritis, proteinuria, and hypertension. The VEGFR inhibitors can produce

interstitial nephritis, glomerulonephritis, proteinuria, and hypertension. EGFR inhibitors can induce proteinuria, IgA nephropathy, and acute tubular necrosis. c-Kit inhibitors can result in TMA, glomerulonephritis, proteinuria, and hypertension.

B-raf is the main activator of the mitogen-activated protein kinase pathway and is involved in cell proliferation and differentiation. Aberrant activation of this pathway is associated with cellular hyperplasia and neoplasia. Experimental anticancer therapeutics targeting B-raf have been evaluated as a potential therapy for various tumors. Repeated dose toxicity studies only up to 4 weeks in duration for these potentially targeted molecules have shown proliferative lesions in rats including in renal pelvis and urinary bladder.

Xenobiotics Which Cause Injury via Metabolic Activation With or Without Organic Ion Transport

Xenobiotic-metabolizing enzymes, including CYP-450-dependent mixed-function oxidases, are present in the kidney. Mixed-function oxidase activity occurs primarily in the pars recta or S_3 segment in the rat. CYP-450 content of the kidney is only 10%–20% of liver content; however, at the cell level, the concentrations in the cells of the pars recta in the outer stripe are comparable to hepatocytes (Figures 11.2 and 11.4A). A xenobiotic may be metabolized in the kidney to a reactive intermediate (Tables 11.12 and 11.13). Cells of the pars recta contain a much greater proportion of smooth endoplasmic reticulum than any other portion of the nephron. Thus the outer stripe is typically the primary site of injury for xenobiotics, mediated by metabolic activation (Figure 11.28). It is in these cells that cytochrome P-450 and mixed-function oxidases catalyze reactions to produce a more readily excretable form of the parent xenobiotic. The same family of enzymes responsible for metabolism and detoxification catalyze metabolic activation. Phase I reactions involve oxidation, reduction, or hydrolysis to produce more water-soluble metabolites facilitating excretion. In Phase II metabolism, a reactive

TABLE 11.12 Experimental Manipulation of the Rat for Implicating Renal P-450 Microsomal Metabolism with Derivation of a Reactive Intermediate as the Mechanism of Toxicity

Pretreatment modulating factor	Influence	Nephrotoxic response to xenobiotic metabolite
Butathionine sulfoximine	Inhibits glutathione synthesis	↑
Diethylmaleate	Depletes renal glutathione	↑
Cysteine	Increases renal glutathione	↓
Polybrominated biphenyl	Stimulates renal metabolism	↑
Piperonyl butoxide	Blocks renal metabolism	↓
Phenobarbital	Stimulates hepatic metabolism	No influence
Cobalt	Blocks hepatic metabolism	No influence

Table reproduced from Handbook of Toxicologic Pathology (2013), third ed. (W. M. Haschek, C. G. Rousseaux, and M. A. Wallig, eds.), Academic Press, Table 47.25, p. 1744, with permission.

TABLE 11.13 Criteria for Including Xenobiotics as Inducers of the $Alpha_{2u}$ Globulin Nephropathy Syndrome

Criteria for consideration
1. The xenobiotic or its metabolites bind reversibly and specifically with $alpha_{2u}$ globulin in the kidney
2. $Alpha_{2u}$ globulin bound with the xenobiotic or its metabolite accumulates in the mature male rat kidney in hyaline droplets (other proteins do not accumulate)
3. Subchronic treatment results in injury to the male rat kidney, consistently characterized by a specific spectrum of lesions, including exacerbated hyaline droplets formation, granular casts in the outer medulla, and exacerbated changes undifferentiable from those of chronic progressive nephropathy
4. Chronic treatment (≥1 year with sacrifice after 2 years) consistently results in a specific triad of injury, including linear inner medulla mineralization (descending Loops of Henle's lumena), urothelial hyperplasia, and exacerbated CPN plus low incidence of renal tubular tumors in male rats
5. Renal injury, including tumor formation, cannot be forced in the female rat or mice of either sex in short-term or in long-term testing; furthermore, the xenobiotics or their metabolites do not accumulate, nor does protein accumulate in the exposed female rat or mouse kidney
6. The xenobiotics or their metabolites are not considered genotoxic

Table reproduced from Handbook of Toxicologic Pathology (2013), third ed. (W. M. Haschek, C. G. Rousseaux, and M. A. Wallig, eds.), Academic Press, Table 47.26, p. 1751, with permission.

intermediate can conjugate with glutathione to form a stable metabolite protecting the cell from damage. However, certain xenobiotics that are metabolized to sulfur-containing metabolites conjugated with glutathione can be further metabolized to cysteine S-conjugates, and then metabolized by cysteine conjugate beta-lyases to reactive thiols. Xenobiotic injury via the beta-lyase pathway is preferentially expressed in the outer stripe. The metabolism to cysteine conjugates may sometimes occur in the liver with subsequent transport to, and uptake by, pars recta, the cellular site of the highest concentration of beta-lyases.

In addition to cell metabolism in considering proximal tubule toxicity, the organic acid/base transport systems must be considered. Several xenobiotics require transport as an organic ion to initiate cell injury, including cephalosporin antibiotics, citrinin, mercuric anion, and cysteine conjugates. The organic ion transporter has been well characterized and may be the most important for renal toxicity. This transporter is localized in the basolateral cells at all levels of the proximal tubule. Organic anion transport, for which *p*-aminohippuric acid (PAH) represents a model organic anion, is presumed to be involved in the transport of important proximal tubule nutrient substrates such as succinate. Transport of PAH is inhibited by organic anions such as probenecid and penicillin. PAH and probenecid have been demonstrated to reduce toxicity of drugs requiring transport as an organic anion in mechanistic studies. Mepiperphenidol, quinine, and quinidine have been used as inhibitors of organic base transport.

Organohalides: Organohalides form a class bridging three functional categories: synthetic biologic toxins, organic solvents, and chemicals involved in plastics and resin manufacturing. The kidney is a primary target organ for toxic organohalides. A significant portion of the American population is chronically exposed to small amounts of these chemicals in water. The acute necrotizing effects, as well as teratogenic and carcinogenic effects at high doses in the laboratory animal, are dependent on the conversion of the parent compound to toxic metabolites. Species, sex, and tissue differences in susceptibility to injury are expected, related to differences in pharmacokinetic behavior of each specific chemical.

Chlorine disinfection of drinking water results in the formation of trihalomethanes, primarily chloroform. Chloroform is considered a prototypical organohalide; its mechanism of injury has been extensively studied. Renal metabolism of chloroform results in derivation of phosgene as the potential reactive intermediate. Prerequisite renal metabolism can be demonstrated by enhanced toxicity following pretreatment with drugs such as polybrominated biphenyls, known to stimulate renal MFOs.

Phenobarbital, the classical stimulator of hepatic MFOs, does not induce rat renal MFOs and, thus, does not enhance rat chloroform nephrotoxicity. Pretreatment with inhibitors of renal metabolism, specifically piperonyl butoxide reduces chloroform nephrotoxicity. In the mouse, renal toxicity may occur in the absence of hepatotoxicity, further suggesting intrarenal metabolic activation. Furthermore, subcutaneous administration of chloroform causes greater renal toxicity than oral dosing at comparable levels of systemic absorption, presumably because the liver "first pass effect" is avoided.

Species, strain, and sex susceptibility to chloroform nephrotoxicity is proportional to renal MFO activity. The location and distribution of radiolabeled chloroform are also proportional to the extent of nephrotoxicity. Mature male mouse kidneys have significantly higher MFO activity than females or neutered males. The intact male DBA/2 J mouse is significantly more susceptible than the C57BL/6 J mouse and other species, correlating with increased capacity of the kidney to metabolize chloroform. Irreversible binding, measured by covalent adduct quantitation, correlates with the severity of tissue injury. The putative chloroform metabolite phosgene depletes renal glutathione, subsequently initiating an autocatalytic peroxidative degradation of membranes. Glutathione conjugation with the injurious chloroform metabolite reduces or prevents covalent binding with tissue macromolecules. Thus, pretreatment with diethylmaleate, which reduces renal glutathione, significantly enhances chloroform nephrotoxicity.

Cephalosporin: Cephalosporins and other β-lactam antibiotics cause proximal tubular necrosis in humans and laboratory animals. Selective toxicity to the PCT occurs because of high intracellular concentrations achieved by active transport by the OAT. Cephaloridine, as a model cephalosporin, is metabolized in the proximal convoluted tubular cell and, at sufficiently high concentrations, induces lipid-peroxidation-type injury to membranes. Evidence for oxidative stress as a mechanism of injury include (1) inhibition of injury by superoxide dismutase, by catalase, by the hydroxyl radical scavenger mannitol, and by the singlet oxygen scavenger histidine; (2) increase in malondialdehyde production *in vitro*; (3) superoxide anion generation *in vitro*; (4) glutathione depletion of renal cortex from treated animals; and (5) potentiation of injury by pretreatment with antioxidant-deficient diets (vitamin E and selenium). Importance of metabolism and generation of reactive intermediates is further indicated by demonstration of covalent binding of renal-cortex-homogenate microsomal fraction by

cephalosporin in a quantity proportional to their toxic potential. In addition, piperonyl butoxide, a well-known inhibitor of renal MFOs, reduces cephalosporin nephrotoxicity. Predictably, species-, strain-, sex-, and age-related differences in the toxic potential of cephalosporin occur as they do for other xenobiotics requiring metabolism for induction of injury. Species differences in transport have also been demonstrated as the explanation for differences in injury potential.

Mycotoxins: Mycotoxins represent an important class of xenobiotics (in terms of morbidity) which cause renal injury in humans and food animals. Ochratoxin A, an organic anion, causes proximal tubular injury which first appears as cytoplasmic vacuolation with phagolysosomal hydropic swelling and myelin figure formation followed by tubular necrosis. Ochratoxin A was thought to be the cause of Balkan endemic nephropathy, an important urologic syndrome of humans in Eastern Europe, although the etiologic agent is now believed to be aristolochic acid. Ochratoxin A is an important cause of chronic kidney injury in swine and a potential renal carcinogen in humans. Ochratoxin A is actively transported via the OAT, resulting in tubular accumulation. Blocking transport with probenecid modulates toxicity. Furthermore, ochratoxin A is probably metabolized to a reactive intermediate as the mechanism of injury. Balkan endemic nephropathy is associated with an increased incidence of renal pelvic cancer, but in laboratory rodents, ochratoxin induces only renal tubule tumors. Fumonisin causes renal injury in several species and cancer in rats. The most sensitive target tissue in rats, the pars recta, develops accelerated apoptosis in subchronic studies and tubular neoplasms in chronic studies. Fumonisin perturbs renal sphingolipid profiles (Figure 11.14). Deoxynivalenol is a toxin produced by the fungus *Fusarium graminearum* in the heads of small grains. Experimentally, this mycotoxin has been shown to produce IgA nephropathy.

Halogenated Alkenes: Conjugation in Phase II metabolism, for example, with glutathione (GSH), typically decreases the reactivity of the metabolic intermediate, correspondingly reducing toxicity potential. There is now evidence, however, that stable GSH conjugates which are degraded to cysteine conjugates may be subsequently bioactivated to a toxic metabolite by a renal cysteine conjugate β-lyase (β-lyase pathway). β-Lyase cleaves *S*-cysteine conjugates to putative reactive thiols. Hexachloro-1,3-butadiene, tetrafluoroethylene, and chlorotrifluoroethylene, trichloroethylene, and dichlorovinyl cysteine may produce nephrotoxic effects via such a mechanism. These agents correspondingly produce selective necrosis in the pars recta (Figure 11.28).

Xenobiotics Perturbing Endogenous or Nutritive Substrate

Examples of nephrotoxicity from perturbation of an endogenous or nutritive substrate include phosphate toxicity, iron toxicity, zinc toxicity, osmotic nephrosis, oxalate nephrosis, light chain nephropathy, amino acid toxicity, synthetic diet induced nephrocalcinosis, melamine-related pet food nephropathy, inducible alpha$_{2\mu}$-globulin nephropathy syndrome, myoglobin nephropathy, and hemoglobin nephropathy.

Osmotic Nephrosis: Osmotic nephrosis refers to a nonspecific histopathologic finding rather than defining a specific entity characterized by vacuolization and swelling of the renal proximal tubular cells. Glucose and sucrose are reabsorbed by pinocytosis, leading to vacuolization of PCTs representing hydropic swelling of the phagolysosome (Figure 11.18). Postprandial phagolysosomal vacuoles occur normally in all species. Mannitol, hydroxyethyl starch, dextran, and contrast media induce the same change. The functional impact of this change is minimal and the vacuolization actually may be a transient adaptive response. Acute kidney injury and chronic kidney failure have been reported in rare cases, for example, after surgical placement of an antiadhesive barrier of macromolecular polysaccharides in the peritoneal cavity. Lifetime rodent studies of mannitol have not revealed toxic or tumorigenic consequence of the osmotic change.

Oxalate Nephrosis: Ethylene glycol is a prototype for chemicals causing oxalate nephrosis. Nonmetabolized ethylene glycol has similar toxicity to ethanol. Ethylene glycol or its metabolites can be associated with osmotic nephrosis which is unassociated with oxalate deposition. Reduced renal function may occur in acute exposure without oxalate deposition.

A metabolic derivative of ethylene glycol oxidized via alcohol dehydrogenase is oxalic acid. Oxalic acid is also normally found in the liver. Oxalic acid in the renal tubular lumen sequesters calcium, precipitates, and obstructs the nephron, leading to oxalate nephrosis (Figure 11.21). The consistent finding in the fatal cases of acute ethylene glycol poisoning in animals with renal failure is marked oxalate deposition.

Melamine-Related Nephropathy: Melamine, 1,3,5-triazine-2,4,6-triamine, is used primarily for manufacturing melamine resins and melamine-based resins that are used in production of a wide variety of products including laminates, adhesives, molding compounds, textiles, and flame retardants. The addition of melamine, which is high in nonprotein nitrogen, to food constituents in order to boost the apparent protein content has been a widespread practice in China. In 2007, an outbreak of renal failure in domestic cats and dogs associated with renal tubule crystalluria resulted in a major recall of pet

food in North America. The outbreak was traced to wheat gluten imported from China. Analysis of the pet food and gluten demonstrated the presence of simple triazine compounds, primarily melamine and cyanuric acid. Experimentally, a mixture of melamine and cyanuric acid produced melamine cyanurate crystalluria and acute renal toxicity in cats, fish and rodents. Cyanuric acid complexing with melamine was critical for the precipitation of crystals in the kidney. A similar outbreak in Asia in 2004 resulted in deaths of 6000 dogs and fewer cats due to renal failure. This outbreak was the result of pet food contamination which was incorrectly attributed to mycotoxins at the time. Retrospective analysis for melamine and cyanuric acid in paraffin sections from affected animals was positive.

Clinically, animals ingesting pet food contaminated with melamine and cyanuric acid were azotemic with hyperphosphatemia, and urinalysis revealed isosthenuria and crystalluria. In acute cases, the kidneys were pale and swollen with congested vasculature. Crystals could be identified on impression smear. Histologically, distal nephron injury was characterized by tubular dilation, epithelial tubular degeneration and necrosis, and intratubular crystal deposition. Unique striated crystals were present in distal tubules and collecting ducts (Figure 11.22). These dissolved over time in neutral buffered formalin so timely processing is important. Tubular rupture with inflammation can occur. In more chronic cases, intratubular crystals may be found in the medulla. Inflammation, fibrosis and sometimes granulomatous lesions may be present.

The major differential for melamine cyanurate nephrotoxicity in dogs and cats is oxalate nephrosis. Hypocalcemia is prominent in oxalate nephrosis but absent with melamine/cyanurate toxicity. Crystal morphology and location within the nephron differs. Oxalate crystals are pale yellow, occur as sheaves and rosettes, are stable and prominent on polarization, and are located primarily in proximal tubules (Figure 11.21). Melamine/cyanurate crystals are gold to brown, occur as pinwheels or granules, and are located in the distal nephron. Sulfonamides have also caused crystal nephropathy affecting the distal nephron in domestic animals and humans. Crystals may be observed grossly but have poor stability in formalin and during processing. Currently used sulfonamides have good solubility and do not form crystals unless predisposing factors are severe.

Inducible Alpha$_{2\mu}$-Globulin Nephropathy Syndrome: Normal mature male rats spontaneously develop hyaline droplets in PCT epithelial cell cytoplasm, observable by light microscopy (Figures 11.30 and 11.31). Ultrastructurally these hyaline bodies represent phagolysosomal proteinic reabsorption droplets, and biochemically consist of alpha$_{2\mu}$-globulin. Hyaline droplets reflect normal glomerular filtration with PCT uptake and cytoplasmic accumulation of this poorly hydrolysable low molecular weight protein. The mature male rat synthesizes abundant alpha$_{2u}$ globulin in the liver, secreting approximately 50 mg per day, which is rapidly cleared in the glomerular filtrate. Approximately 15–20 mg of alpha$_{2\mu}$-globulin is lost in the urine each day in the normal mature male rat, creating a physiologic proteinuria. Normal humans or humans with perturbed urinary protein profiles do not excrete significant levels of proteins migrating as an alpha$_{2\mu}$-globulin. The male mouse also is physiologically proteinuric because of mouse urinary protein, which has similar electrophoretic characteristics but is not reabsorbed by the proximal tubule.

Exacerbated hyaline droplet accumulation in PCTs was reported to be one of the most common renal findings in a recent histopathological survey of 42 90-day toxicity studies conducted by the NTP. Several chemicals of societal importance affect the male rat through perturbation of alpha$_{2\mu}$-globulin. These include the nongenotoxic agent D-limonene and unleaded gasoline. D-Limonene is widespread in natural foods, with average daily adult consumption estimated at over 2.5 mg/kg body weight. In the male rat, 10 mg/kg body weight per day is injurious to the kidney. Unleaded gasoline and D-limonene induce a specific triad of subchronic renal lesions in the male rat. The primary response in the male rat kidney is exacerbated hyaline droplet formation, consisting specifically of alpha$_{2\mu}$-globulin, which causes PCT cell injury. Granular casts are recognized as a hallmark feature of alpha$_{2\mu}$-globulin nephropathy and occur at the junction of the OSOM and ISOM representing lodgment of cellular debris where the lumen of the S_3 tubule narrows into the thin descending limb of the loop of Henle (Figure 11.30). Granular casts are composed of exfoliated cortical cells engorged with protein resulting in marked dilation of solitary tubules. The lining tubular epithelium is flattened and the basement membrane slightly thickened. The third subchronic study component of the triad, pathognomonic for this unique male rat syndrome, is linear mineral deposits in the descending limb of Henle, representing fragments of the granular casts that lodge in the prebend segment. This leads to the granular cast formation in the outer medulla and linear mineral deposits, subsequently increased incidence or severity of CPN.

The chemicals causing a high incidence and severity of this specific subchronic triad of lesions in the rat over a life time cause renal tubular tumors in male rats, but not in female rats or mice of either sex. Thus, a specific spectrum of chronic injury includes linear papillary mineralization, increased incidence and severity of CPN, and tubular tumorigenesis

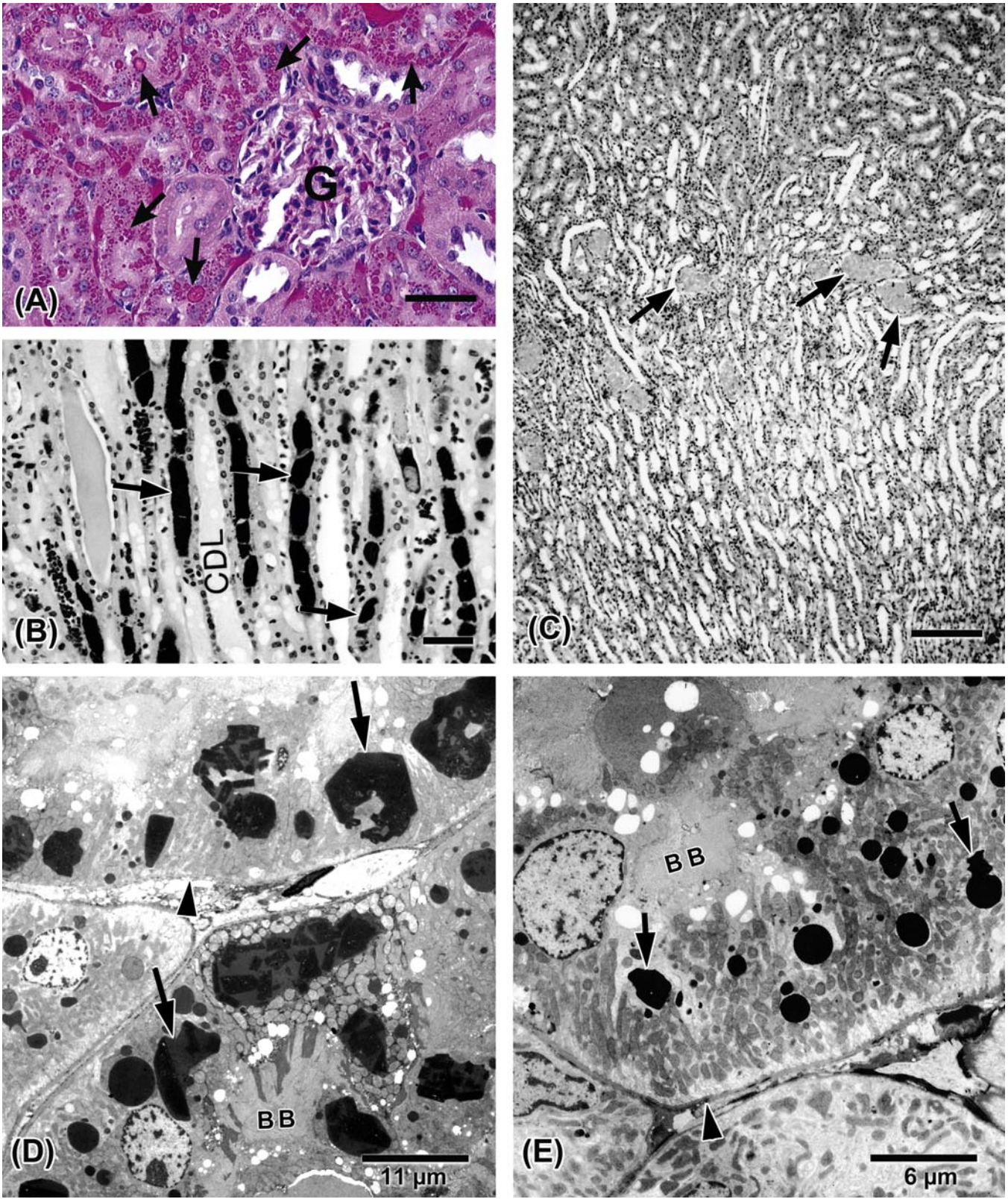

FIGURE 11.30 Inducible alpha$_{2u}$ globulin nephropathy syndrome in male rats. (A) Exacerbated hyaline droplet formation in the cytoplasm of proximal convoluted tubular cells (arrows). Bar = 40 µm. (B) Linear mineral deposits (arrows) in the prebend segment of the loops of Henle, considered a consistent characteristic feature of the chronic changes (>3 months treatment) in this syndrome. Collecting duct lumen (CDL). Bar = 50 µm. (C) Granular casts (arrows) entrapped at the junction of inner and outer stripe, considered a subchronic pathognomonic lesion of this syndrome. Bar = 250 µm. (D) Decalin-treated and (E) control animals: Ultrastructural correlate of the hyaline droplets observed by light microscopy. Note the increased size and propensity for crystalloid change of phagolysosomes (arrows) with decalin treatment. Basement membrane of the proximal tubules (arrowhead); brush border (BB), Bar = 50 µm. *Figure (B–E) reproduced from Handbook of Toxicologic Pathology, second ed. W. M. Haschek, C. G. Rousseaux and M. A. Wallig, eds. (2002) Academic Press, Figure 24, p. 297–299, with permission.*

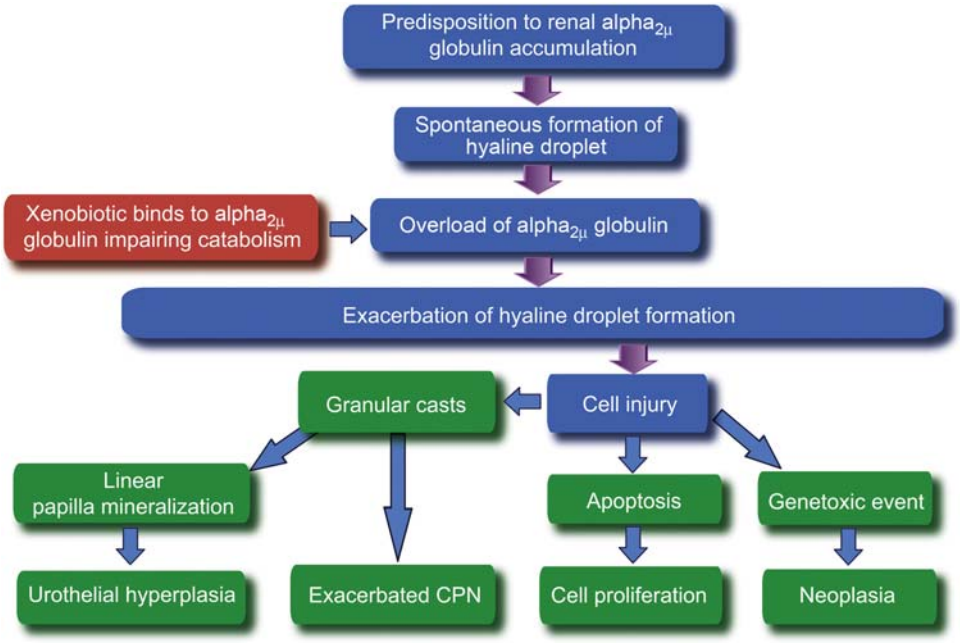

FIGURE 11.31 Schematic pathogenesis of the specific lesions occurring in inducible male rat alpha$_{2u}$ globulin nephropathy syndrome. *Figure reproduced from Haschek and Rousseaux's Handbook of Toxicologic Pathology (2013), third ed. (W.M. Haschek, C.G. Rousseaux and M.A. Wallig, eds.), Academic Press (Elsevier), Figure 47.38, p. 1752, with permission.*

TABLE 11.14 Examples of Xenobiotics Which Produce the Alpha$_{2u}$ Globulin Nephropathy Syndrome and Associated Renal Proliferative Lesions in Male Rats[a]

Xenobiotics producing alpha$_{2u}$ globulin nephropathy and proliferative lesions
β-Myrcene
Dimethyl methylphosphonate
Ethyl and methyl *tert*-butyl alcohol
Hexachloroethane
Hexachlorobenzene
Jet fuels: JP-4, JP-TS, JP-7, RJ-5, JP-10
Nitrotoluene
Isophorone
D-Limonene
Lindane
Paradichlorobenzene
Pentachloroethane
Tert-Butyl alcohol
Unleaded gasoline

[a]*Test system specific response.*
Table reproduced from Handbook of Toxicologic Pathology (2013), third ed. (W. M. Haschek, C. G. Rousseaux, and M. A. Wallig, eds.), Academic Press, Table 47.27, p. 1752, with permission.

(Tables 11.13 and 11.14). Following chromatographic separation of kidney proteins in male rats treated with radiolabeled injury-inducing xenobiotics such as D-limonene and unleaded gasoline, a distinct peak of radioactivity coelutes specifically with alpha$_{2\mu}$-globulin. These results indicate a direct and specific interaction between alpha$_{2\mu}$-globulin and the inducing xenobiotics or metabolites. This reversibly bound conjugate resists hydrolysis to a greater extent than alpha$_{2\mu}$-globulin alone, thus accumulating to a pathologic degree. Finally, the alpha$_{2\mu}$-globulin PCT cell overload results in cell loss with a replicative response persisting through the first year of treatment of the male rat. This replicative response has been demonstrated to be linked with the subsequent tubular tumor development. The alpha$_{2u}$ globulin considered alone is injurious and has been demonstrated to injure the kidney upon infusion in female rats and also to cause cell transformation in the Syrian Hamster Embryo test system.

Although considered a pathognomonic feature of alpha$_{2\mu}$-globulin nephropathy, granular casts are not always found in association with chemically induced hyaline droplet accumulation in rat toxicity studies if the chemical is a weak inducer of alpha$_{2u}$ globulin nephropathy and such chemicals do not cause male rat kidney cancer via this mechanism.

Because abundant liver synthesis of alpha$_{2u}$-globulin is specific to the male rat, this response is not considered predictive for female rats or other common mammalian species such as mice, dogs, monkeys, and humans. This has been confirmed, for example, with D-limonene treatment of female rats, and mice and dogs of both sexes. The concept is further reinforced by identification of an inbred male rat, the NBR (NCI-Black-Reiter) that does not express the genes for alpha$_{2\mu}$-globulin synthesis in the liver. Consequently,

NBR rats are resistant to the toxicologic effect associated with agents binding to alpha$_{2\mu}$-globulin. The recognition of male rat specificity of this nephropathy resulted in the FDA and EPA not exerting regulatory restrictions relative to the unique male rat tumorigenic response to D-limonene and unleaded gasoline.

Light Chain Nephropathy: In the normal human, 5 mg/kg of κ light chain is filtered daily, of which 0.04 mg/kg/day is excreted in the urine. Much larger amounts of light chain molecules (approximately 22,000 Da) termed Bence Jones proteins, may be excreted in the urine of patients with multiple myeloma, primary amyloidosis, or monoclonal gammopathies. Light chain proteinuria is seen in 40%–80% of myeloma patients because of overproduction by neoplastic cells. The capacity of the proximal tubular epithelium to reabsorb and catabolize the protein may be exceeded. Approximately 50% of patients with multiple myeloma have renal impairment, of which one-third is due to Bence Jones protein nephrosis. The Bence Jones protein in these cases resists normal lysosomal proteolytic degradation, and thus accumulates in the phagolysosome. These spontaneous cases, as well as experimentally induced cases of Bence Jones nephrosis, are characterized by phagolysosomal protein overload, with propensity for crystalloid change in proximal tubular epithelium, cast formation, and nephron atrophy or regeneration. This nephropathy is important to the toxicologic pathologist because it illustrates the nephrotoxic potential of endogenous proteins and presents similarities to the renal changes in the inducible alpha$_{2\mu}$-globulin nephropathy syndrome.

Myoglobin and Hemoglobin: Myoglobin can induce ARF as a result of myoglobinuria and pigmented cast nephropathy secondary to rhabdomyolysis. Causes of rhabdomyolysis include trauma, ischemia, hyperpyrexia, electrolyte disturbance, and toxins. Hemoglobin can also induce a morphologically comparable pigmented cast nephropathy (Figure 11.32). Hemoglobin excess occurs at injurious levels in glomerular filtrate after intravascular hemolysis. Causes of intravascular hemolysis include exogenous chemicals, such as phenothiazine. The concentration of hemoglobin sufficient to injure the kidney typically is associated with red discoloration of plasma. By contrast, in myoglobinuria, because of smaller molecular weight, renal clearance is sufficiently high to maintain normal colored plasma. The mechanism of renal injury is not defined, but may include nephron obstruction as well as proximal tubular phagolysosomal overload.

Amino Acid Toxicity: Lysinoalanine, an amino acid formed during alkali treatment of protein, may be found in processed foods for human consumption. Lysinoalanine induces nephrocytomegaly and/or karyomegaly in the pars recta of rat and mouse, but this effect has not been observed in hamsters, monkeys, or rabbits. The change seems largely reversible. Furthermore, long-term studies with lysinoalanine have not led to recognition of renal tumor formation or any other adverse change. Lysine, a component of some parenteral nutrition therapies, and D-serine injection in the rat induce necrosis of the proximal tubule. In the case of D-serine, the induced necrosis is restricted to the pars recta. Serine is also normally synthesized *in vivo* in the rat as well as in the human kidney.

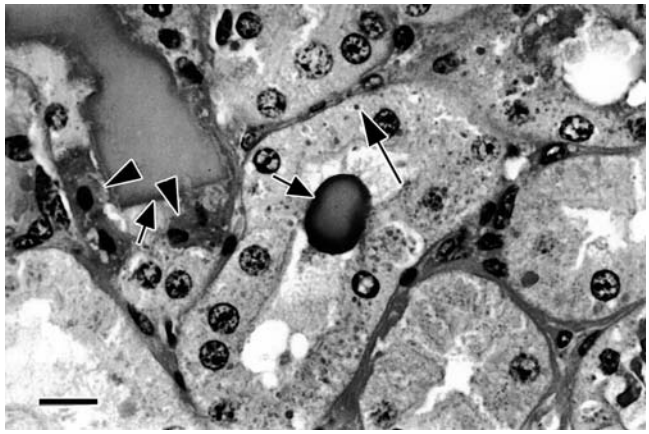

FIGURE 11.32 Hemoglobin casts and crystals (small arrows) in the proximal tubular lumen of horses in red maple poisoning. Hyaline droplets (large arrows) and proximal tubular cell degeneration and necrosis (arrow heads) are evident. Bar = 17 μm. *Courtesy of Dr. W. Crowell, University of Georgia. Figure reproduced from Handbook of Toxicologic Pathology, second ed. W. M. Haschek, C. G. Rousseaux and M. A. Wallig, eds. (2002) Academic Press, Figure 25, p 300, with permission.*

Xenobiotics Perturbing Renal Hemodynamics

Ischemia and Hypoxia: Renal ischemia is a component of many renal insults in humans including nephroangiosclerosis, renal artery stenosis, and renal vascular lesions occurring in the course of glomerular or interstitial nephropathies. The common outcome of renal ischemia is renal fibrosis followed by atrophy and chronic renal failure. This process is self-perpetuating, as ischemia promotes fibrosis and fibrosis aggravates ischemia. Endothelin-1 antagonists are shown to reduce renal fibrosis following ischemia. Nephroangiosclerosis is commonly associated with hypertensive end-stage renal disease. The spontaneously hypertensive rat exhibits vascular lesions of nephroangiosclerosis, precipitated by a sodium-rich diet or infusion of angiotensin (Ang) II.

The similarity in renal architecture, physiology, and immune systems between humans and minipigs makes the latter species a suitable model of human kidney disease such as renal transplantation and ischemia-reperfusion injury to the kidney. In both humans and pigs, an elaborate system of interlobar and segmental arteries is present to supply the numerous kidney lobes whereas in dogs and rodents,

segmental arteries are bypassed due to the lack of multiple medullary pyramids. As in the human kidney, there are free anastomoses between the intrarenal veins in the pig. Prolonged ischemia (over 2 hours) results in infarction. When induced by temporary clamping of the renal artery it results in cortical infarction, whereas occlusion of the venous return results in medullary infarction. Obstruction of an arcuate artery results in a wedgeshaped area of cortical necrosis.

Obstructive Nephropathy

Most nephrotoxic drugs are excreted by the kidneys and accumulate in tubular cells as a result of increased local drug concentration and the presence of cell-specific transporters. Obstructive nephropathy is a relatively common condition in animals and humans, the causes of which may be intra or extrarenal, and may be congenital or acquired. Among acquired intrarenal causes, accumulation of drugs and chemicals in the urinary tract is an important condition especially in susceptible populations. Risk factors for xenobiotic or endogenous crystal precipitation within the kidney tubules include true or effective intravascular volume depletion, underlying kidney disease and certain metabolic disturbances that promote changes in urinary pH favoring crystal precipitation. Intrarenal obstruction occurs secondarily to accumulation of poorly soluble materials within the tubules such as following high dosages of xemilofiban, naproxen, methotrexate, acyclovir, and triamterene. In veterinary medicine, the most common cause is oxalate nephrosis which is most frequently induced by ethylene glycol (antifreeze) ingestion in dogs and cats and by oxalate containing plants in large animals (Figure 11.21). Melamine adulteration of food products has also been associated with crystalline nephropathy (Figure 11.22). Uric acid crystal deposition can occur with acid urine usually after cancer chemotherapy with alkylating agents; the risk of its development is related directly to plasma uric acid concentrations.

Obstructive nephropathy is classified according to the degree, duration, and site of the urinary tract obstruction. Obstruction can occur anywhere from the level of renal tubules to the urethral meatus. In the adult human kidney, approximately 2 L of urine flows through the renal papilla daily. Any obstruction to this unidirectional flow can lead to build up of urine flow and pressure affecting renal functions. Urinary symptoms may or may not occur along with changes in urine output. Mild episodes of polyuria may alternate with periods of oliguria or occasionally anuria. A complete obstruction of short duration results in profound alterations in renal hemodynamics and glomerular filtration with minimal anatomic changes.

Exacerbation of Spontaneous Age-Related Nephropathy

CPN is a confounding factor in both subchronic toxicity studies and chronic bioassays because the tubular basophilic lesions have to be discriminated from chemically induced toxicity and some chemicals are capable of exacerbating the severity of CPN in a dose-related fashion (Figure 11.7). Depending on the xenobiotic, evidence of active injury may also persist with continuing treatment, as is typical for the toxic tubular tumorigens. Persistence of the active injury may then give some specificity to the chronic process. Nephrotoxicant dose levels that do not induce light microscopically overt acute tubular injury can still produce adverse renal effects in rodents, manifested only as increased incidence or severity of CPN. The aminoglycoside antibiotics typify this concept.

Manifestation of exacerbated CPN in rats does not necessarily predict susceptibility of humans to nephrotoxicity. In humans, chronic renal disease has many causes and associations. The apparent increase in end-stage renal disease in humans observed recently is due to an increase in the proportion of renal failure attributed to arteriopathic and diabetic nephropathies. Together, diabetes, hypertension, and the glomerulonephritides make up >75% of the incident cases of treated end-stage renal disease. There is no significant entity in human that has the singular features of CPN in the laboratory rat. Moreover, in contrast to humans, rat CPN is characterized by the early appearance of proteinuria and maintenance of a normal GFR until very advanced age.

Mechanisms of Injury to Collecting Ducts and Renal Papilla

2-Amino-4,5-diphenyl thiazole HCl is of interest as a model for the induction of polycystic kidney disease because it may help to clarify factors prerequisite for cyst development in the absence of tubular obstruction and in the presence of a normal transtubular pressure gradient. Specifically, this model chemical causes a structural defect of the basement membrane as an integral step in the pathogenesis. The primary site of basement membrane injury is in the collecting duct of the outer medulla. Tubular basement membrane is principally responsible for limiting distensibility of the renal tubule.

Renal papillary injury can occur under various conditions that affect medullary blood flow or solute concentration, e.g., amyloidosis, diabetic nephropathy, dehydration, and treatment with various chemicals and drugs. Among drugs, renal papillary injury is widely recognized following treatment with NSAIDs in both animals and humans. In addition to renal papillary injury, other renal effects of NSAIDs include ARF, interstitial nephritis, and fluid and electrolyte

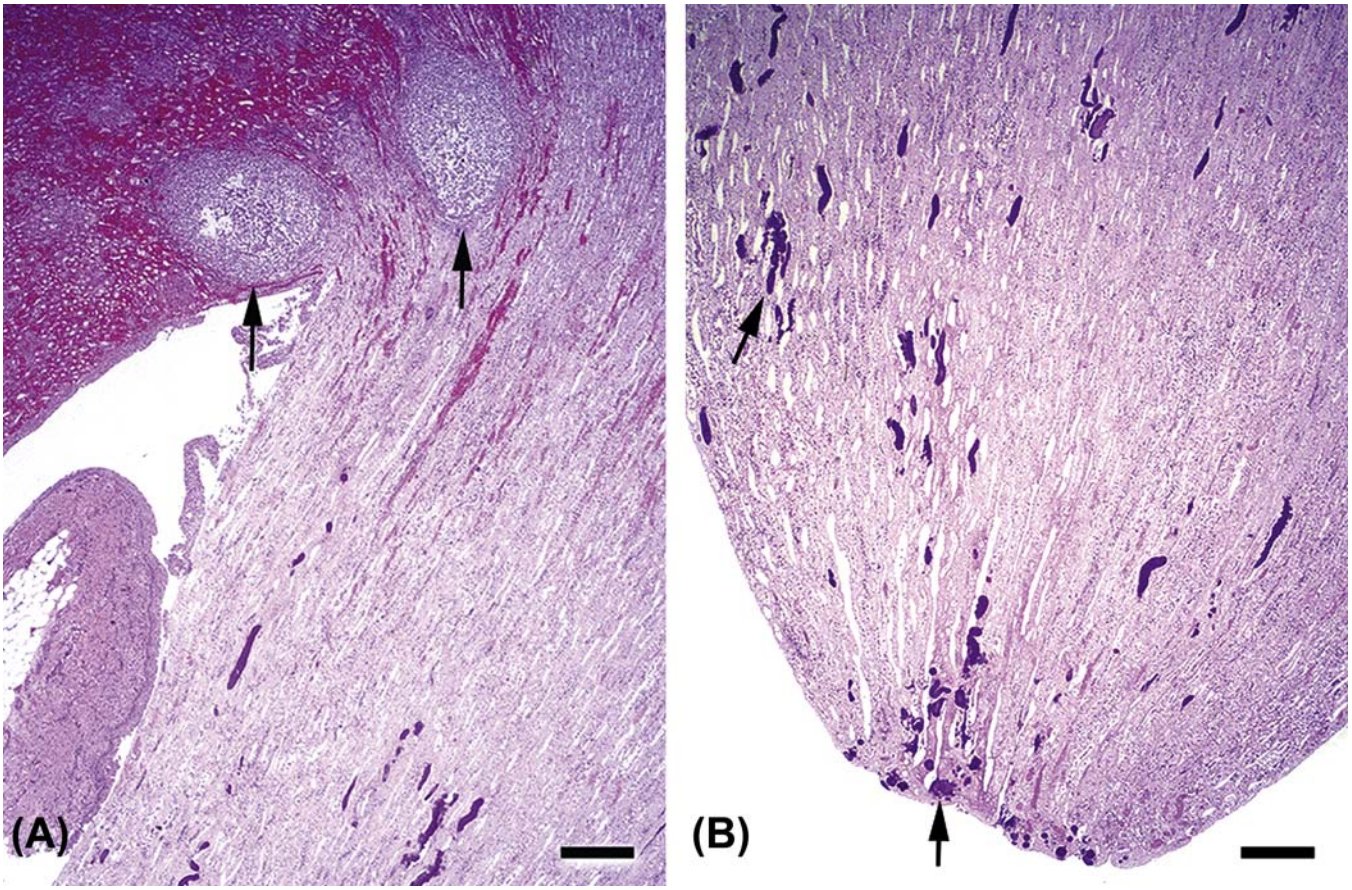

FIGURE 11.33 Kidney from a dog treated with an antiinflammatory drug resulting in gastrointestinal ulceration and secondary septicemia. (A) Note corticomedullary thrombosis (arrows) and perivascular hemorrhages secondary to septicemia. (B) Note diffuse acute necrosis involving the papilla along with multifocal bacterial colonies (arrows). Bar = 450 μm. *Figure reproduced from Haschek and Rousseaux's Handbook of Toxicologic Pathology (2013), third ed. (W.M. Haschek, C.G. Rousseaux and M.A. Wallig, eds.), Academic Press (Elsevier), Figure 47.40, p. 1758, with permission.*

disturbances in humans, monkeys, rats, and dogs; NS, interference with hypertensive and diuretic therapy, and allergic type interstitial nephritis with peripheral eosinophilia, and eosinophiluria in humans; and outer cortical atrophy with interstitial fibrosis in dogs, monkeys, and human infants. With the exception of renal papillary injury, the above NSAID-related renal effects are most commonly reported in humans.

Depletion of effective plasma volume or increased solute load increases the propensity for RPN occurrence. Decreased flow may be mediated by renin release. The homozygous Brattleboro rat, devoid of endogenous ADH, is resistant to RPN, but becomes susceptible with ADH injection, supporting the concept of an interactive influence of urine flow and papilla solute concentration on RPN development. Dogs, following septicemia, can develop renal abscess at the corticomedullary junction and diffuse RPN (Figure 11.33). Chemically induced RPN has also been associated with other agents including cyclophosphamide, dapsone, radiocontrast media, 2-BEA hydrobromide, ethyleneimine, and jet fuel petroleum in laboratory animals.

Mechanisms of Renal Carcinogenesis

Nephrotoxicity due to drugs and chemicals can manifest itself as a proliferative lesion. The renal tumor that is the most relevant to humans with respect to risk assessment is of tubule origin, termed renal tubule tumor in rodents, and renal cell carcinoma in humans. Renal cell cancer primarily arising in the PCT constitutes approximately 2% of all noncutaneous malignancies in humans. Renal adenomas are much more frequent, with incidence as high as 20% of randomly autopsied patients. Over 85% of these adenomas occurred in kidneys with glomerulosclerosis. Established risk factors for renal tumors in humans include cigarette smoking, obesity, chronic inflammation and hypertension while association with other risk factors such as caffeine, carbonated soft drinks,

hydrocarbon solvents, and gasoline has not been substantiated.

Understanding of the potential mechanisms underlying the development of chemically associated cancer has increased markedly over the years, often stimulated by carcinogenicity bioassay results (Table 11.15). In particular, it has been the accumulation of knowledge on key, often histopathologic, events occurring on a causal pathway leading to cancer in target organs during subchronic phases of study, which are now referred to as modes-of-action (MoA). In the rat kidney, MoA can include evidence of cytotoxicity, increased cell proliferation, and hyaline droplet nephropathy due to chemical binding to the protein $alpha_{2u}$ globulin. The latter MoA is rat-specific and been judged not relevant to humans by regulatory and authoritative bodies. Because of the long duration and expense of the 2-year rodent bioassay, and increasing concern regarding its relevance to human carcinogenic risk for non-DNA-reactive chemicals, there have been numerous calls for a modified *in vivo* test. The latest is the suggestion that an enhanced 90-day toxicity study would be sufficient for identifying carcinogens relevant to humans. The new approach involves a short-term screen, in which the *in vivo* segment would rely on organ weight evaluation and histopathology including a labeling assay for cell proliferation. Such an approach might be applicable to kidney but would require rigorous validation to determine false-positive/false-negative rates.

A retrospective analysis of chemicals that had been tested for both carcinogenicity and subchronic toxicity by the NTP, focusing on 3 organ systems including kidney, indicated that 5 of the 16 chemicals had produced renal tubule tumors in the 2-year studies and 4 of these 5 were associated with histopathologic alterations in the respective 13-week toxicity studies. The histologic findings included hyaline droplet accumulation (anthraquinone, decalin), apoptosis (fumonisin B_1), regeneration (benzophenone, decalin, fumonisin B_1), or exacerbated CPN (anthraquinone). In addition, all 5 experimental renal carcinogenic chemicals cited above and including methyleugenol were associated with the nonspecific finding of increased kidney weight, both absolute and relative, at 13 weeks. The combination of kidney weight and histopathologic change at 13 weeks for this series of chemicals identified all of the renal carcinogens. However, there were also false positives in this analysis as some chemicals that did not produce renal tumors after 2 years were associated with renal lesions or organ weight increase at 13 weeks. These analyses concluded that 13-week studies using conventional endpoints were not adequate to identify all nongenotoxic chemicals with the potential to produce tumors by 2 years in rats. Additional endpoints, such as bromodeoxyuridine (BrdU) labeling for cell turnover or a measure of apoptosis were suggested as possible complements to the routine evaluation. However, these assessments do not address the utility of this strategy in predicting for human carcinogenesis. Traditional life-time rodent bioassays are recognized to have a substantative false negative rate and an egregious false-positive rate in predicting for human pharmaceutical cancer risk.

On the basis of the evidence accumulating from studies with chemical agents, a list of mechanisms is proposed by which chemicals are believed to produce, or be associated with, an increase in renal tumors in the rodent. This mechanistic approach has been used to analyze and categorize the chemicals in the NTP database. The possible mechanisms of xenobiotic-induced carcinogenesis are summarized in Table 11.16. These mechanisms include direct or indirect DNA reactivity, multiphase bioactivation usually involving glutathione conjugation in liver, and subsequent enzymatic activation in kidney, direct or indirect cell damage stimulating a sustained regenerative response (toxic tubular tumorigenesis), or association with exacerbation of CPN. Renal carcinogenesis associated with direct or indirect cytotoxicity and CPN involves nongenotoxic chemicals.

TABLE 11.15 Mechanisms of Xenobiotic-Induced Renal Carcinogenesis

Potential mechanisms
1. Direct DNA reactivity
2. Indirect DNA reactivity exemplified by oxidative stress pathways
3. Multiphase bioactivation usually involving glutathione conjugation in liver and subsequent enzymatic activation in kidney
4. Direct cytotoxicity stimulating a sustained regenerative response
5. Indirect degenerative/regenerative response associated with perturbation of a physiological process, such as lysosomal digestion
6. Exacerbation of CPN again associated with a sustained regenerative response

Table reproduced from Handbook of Toxicologic Pathology (2013), third ed. (W. M. Haschek, C. G. Rousseaux, and M. A. Wallig, eds.), Academic Press, Table 47.28, p. 1759, with permission.

Genotoxic Xenobiotics

Current knowledge of chemical renal carcinogenesis has its foundations in early work in developing chemical induction models of renal cancer, and studying tumor pathogenesis. For the renal tubule tumor, these earlier models employed genotoxic carcinogens such as *N*-nitrosomorpholine, *N*-nitrosodimethylamine, *N*-(4′-fluoro-4-biphenylyl) acetamide, and *N*-ethyl-*N*-

TABLE 11.16 Chemicals with Mutagenic or Genotoxic Potential and Requiring Metabolic Activation for Expression of Their Renal Carcinogenic Potential

Xenobiotic	Comment
Nitrofuran derivatives (3-hydroxymethyl-1-hydantoin)	Antibacterial agents
Azoxymethane	Carcinogen active in cycasin from the cycad plant
Ochratoxin	Feed grain mycotoxin contaminant
Citrinin	Feed grain mycotoxin contaminant
Tris (2,3-dibromopropyl)-phosphate	Fire retardant
Adriamycin	Human cancer chemotherapeutic
Bleomycin sulfate	Human cancer chemotherapeutic
Daunomycin	Human cancer chemotherapeutic
Streptozotocin	Human cancer chemotherapeutic agent; model chemical for induction of diabetes
Trichloroethylene	Industrial chemical
Urethan	Industrial chemical
Hexachlorobutadiene	Industrial chemical by-product
Anthraquinones	Industrial dye intermediate
2-Acetylaminoflorene	Model chemical carcinogen
Dimethylnitrosamine (DMN)	Model chemical carcinogen
Formic acid 2-[4-(5-nitro-2furyl)-2-thiazoly] hydrazide	Model chemical carcinogen
N-Nitrosomorpholine	Model chemical carcinogen
N-(4-Fluoro-4-biphenyl) acetamide	Model chemical carcinogen
Alkyl aryltriazenes	Model chemical carcinogen
N-Butyl-*N* (4-hydroxbutyl) nitrosamine	Model chemical carcinogen
Niridazole	Schistosomal therapeutic
N-Nitrosobis (2-oxopropyl) amine	Schistosomal therapeutic

Table reproduced from Handbook of Toxicologic Pathology (2013), third ed. (W. M. Haschek, C. G. Rousseaux, and M. A. Wallig, eds.), Academic Press, Table 47.29, p. 1760, with permission.

hydroxyethyl nitrosamine. These various studies provided evidence that the renal tubule tumor is preceded by a stage of tubule alteration involving hyperplasia of the lining epithelium. It is now generally accepted that this alteration, known as atypical tubule hyperplasia, is a precursor of, and on a continuum with, renal tubule adenoma and carcinoma. It has also been shown recently that atypical tubule hyperplasia has the morphological characteristics of an expansive lesion. Foci are surrounded peripherally, at least partially, by attenuated fibroblasts and/or capillaries, and they have a high DNA synthesis labeling rate, indicating that the lesion is expanding in size, and on the pathway to becoming an adenoma. Consequently, induction of foci of atypical tubule hyperplasia by a chemical in a truncated bioassay predicts that the test chemical is a rodent renal carcinogen, when administered over a life time.

Many chemicals require metabolic conversion to exert their genotoxic and consequent carcinogenic potential (Figure 11.24). Resultant electrophilic intermediates covalently bind renal macromolecules, including nucleic acids. Aflatoxin B_1, dimethylnitrosamine, daunomycin, and 2-aminofluorene exemplify this concept. Genotoxic renal carcinogens share the propensity to exert their biologic effect in multiple species, strains, sexes, and tissues. Tissue site, strain, sex, and species differences in response to exposure parallel the capability of the target site to accumulate and metabolize the xenobiotic, as shown with nitridazole and dimethylnitrosamine. Furthermore, genotoxic renal carcinogens typically induce tumors rapidly, in high incidence, and with minimal duration of exposure. Rodent experiments with bleomycin sulfate, 1,2-dimethylhydrazine, ENU (*N*-ethyl-*N*-nitrosourea), azoxymethane, and dimethylnitrosamine demonstrate this potential. Some genotoxic renal carcinogens (ENU), when administered in utero, induce nephroblastoma which is a counterpart of Wilm's tumor in juvenile humans. Other genotoxic chemicals administered prenatally (during renal immaturity) typically induce RMTs in the rat. By contrast, after onset of sexual maturity, agents inducing RMT during immaturity primarily induce tubule neoplasia. Dimethylnitrosamine is a model agent for this age of exposure factor. Nephroblastoma has been induced in rats only by genotoxic chemicals and mostly by direct-acting nitrosoureas administered transplacentally.

Xenobiotics inducing renal tumors in multiple species and both sexes suggest the presence of human renal carcinogenic potential (e.g., ochratoxin A), if comparable exposures are achieved in humans. Variations in tumor response can be quantitative, based on varying levels of metabolic conversion and adduct formation at the target cell level. Species and sex variability frequently exists in metabolism of xenobiotics. Correlative differences in sensitivity to the toxic and carcinogenic effect of xenobiotics causing injury following derivation of reactive metabolites can be observed. Genotoxic renal carcinogens are nephrotoxic; however, the cytotoxic event and associated repair processes usually are not considered essential factors in the eventual tumor development. The cytotoxic responses typically include proximal tubular cell

necrosis, and sometimes karyomegaly of proximal tubular epithelium. These genotoxic xenobiotics also can cause increased relative kidney weight in animals upon repetitive exposure. This is presumably associated with stimulated renal mixed-function oxidase activity.

Heavy Metal Carcinogens

Several heavy metals share structural and functional renal effects in the rodent species. Metals that have been carefully scrutinized, including chromium, mercury, nickel, and lead, induce genetic injury and may interact or bind directly with DNA. Several metals are carcinogenic in rodent kidneys, for example, lead, nickel, gold, chromium, and mercury (organic). The carcinogenic response typically is not species or strain specific. The accumulation of the metal at the tissue target site is prerequisite to the carcinogenic response. The solubility of the metal complex, the vehicle for the metal, and the dose level and duration of treatment all influence the metal's carcinogenic potential in rodents. Each of these latter factors presumably influences the critical target tissue level of the metal. Similarly, the chemical form of the metal influences its carcinogenic potential.

Carcinogenic heavy metals have nephrotoxic potential, characterized by acute tubular necrosis if administered at sufficiently high levels. Increased tubular replicative rate occurs, even at doses failing to induce cell necrosis, presumably associated with increased apoptosis. In subchronic and chronic studies at carcinogenic levels these metals induce karyomegaly and cytomegaly in proximal tubular epithelium. The karyomegalic cell has not been demonstrated as a precursor cell (preneoplastic change) in the cancer response. Nonetheless, karyomegaly may represent a useful short-term marker of renal events occurring relevant to the carcinogenic process. Heavy metals that induce nephrotoxicity, interact with DNA, or accumulate in the nucleus, and that are nephrotoxic (with karyomegaly) in subchronic studies, can be predicted to be rodent renal carcinogens if tested in lifetime studies at doses inducing these short-term effects. The relevance of this rodent response for higher species, including humans, has not been demonstrated. In part, this may be because the high levels required to induce precursor lesions are unlikely to be encountered outside the laboratory setting.

Nongenotoxic Rodent Renal Carcinogenesis

Several chemicals exert a nephrotoxic response which apparently forms a prerequisite event in the tumorigenic process. The toxic injury is manifested by increased apoptosis, replicative rate increase, and hyperplastic response in tubular epithelium. Exposure must occur over the majority of the rodent's lifespan and tumors appear late, usually well after 1 year of treatment. Tumor incidence often is low and toxic tubular tumorigens typically do not interact directly with DNA and are not considered genotoxic, as evaluated in short-term assays. However, several chemicals tested in rodent cancer bioassays have not been demonstrated to cause tumors despite the presence of chronic toxic injury, possibly because of the limitations of the bioassay to detect weak tumorigens. The tumor potential of nephrotoxic antibiotics such as netilmicin and gentamicin has not been assessed with the duration criterion for chemicals in this mechanistic class.

Lysosomal Enzyme Release: Several mechanisms by which toxicity occurs can be conceptually linked to cancer induction. For example, lysosomal overload may destabilize lysosomal enzymes, resulting in release into the cytosol and opportunity to interact with nucleic acid. Lysosomal enzymes RNAse and DNAse have been demonstrated to have genotoxic potential. This enzyme leakage may not only be relevant in tumorigenesis but also represents a potential toxicity mechanism wherein the cell undergoes necrosis. Two models of extensively studied rodent toxic tubular tumorigens include the inducible alpha$_{2\mu}$-globulin nephropathy syndrome and the nitrilotriacetic acid (NTA)-treated rodent. In both of these syndromes, phagolysosomal swelling occurs. In the alpha$_{2\mu}$-globulin nephropathy syndrome, the swelling occurs because of alpha$_{2\mu}$-globulin accumulation. In the NTA model, the swelling is osmotic in nature, associated with zinc overload. In both models, the chronic toxicologic response has been demonstrated to be inexorably linked with the renal tumor response.

Oxidative Stress/Chronic Inflammation: Oxidative stress can be mediated chemically and has been linked to genetic injury. Active oxygen species clearly have the potential to interact with nucleic acid or any protein in their milieu. Reactive oxygen species derived in oxidative stress bind covalently with DNA, creating promutagenic DNA modifications with 8-hydroxy-2-deoxyguanosine (8-OHdG) as an example. Increased levels of oxidative stress can be quantified by determining 8-OHdG levels in the urine. A potential model for this mechanism is the rodent treated with xenobiotics inducing peroxisomal proliferation, potassium bromide, and the ferrous salt of NTA administered parenterally. Nitric oxide and its derivatives produced in inflamed tissues can contribute to carcinogenesis. Following reaction of NO with oxygen and superoxide, electrophiles are formed. Specifically, peroxynitrite-induced adducts and single strand breaks of DNA can result from increased tissue NO concentration. Chronic

inflammation in the kidney of rodents can clearly be linked with increased risk for renal cancer.

Sustained Increase of Replicative Rate and Apoptosis: Sustained replicative rate increase, as well as perturbed rate of apoptosis, have been suggested as risk factors for carcinogenesis in the kidney. Chronic toxicity can be presumed to be associated with a persistent replicative increase and perturbed apoptotic rate. Examples include β-cyclodextrin, folic acid, agents inducing the unique alpha$_{2u}$-globulin syndrome, and fumonisin B_1 (Figure 11.30).

Several converging data bases support this concept. First, rat nongenotoxic renal carcinogens for which sufficient data have been published are injurious to the kidney at carcinogenic doses in subchronic studies. Chronic toxicity can be presumed to be associated with persistent replicative increase and perturbed apoptotic rate. Second, alternative mechanisms to direct injury of DNA for heritable genetic change have been identified. Although the specific molecular pathways explaining nongenotoxic agent carcinogenesis are unknown, it remains certain that heritable genetic change is prerequisite in carcinogenesis.

Heritable Change without Direct Xenobiotic Effect on DNA: DNA methylation plays a role in the regulation of gene activity. Hypomethylated genes possess an increased potential for expression as compared to a hypermethylated gene. Changes in the methylation status of a gene via xenobiotic exposure provide a mechanism by which its potential for expression can be altered in a heritable but epigenetic manner. A second example of an alternative mechanism is the selective loss of the p53 gene reported to occur via intensive selection pressure associated with persistently unregulated apoptosis.

Exacerbation of Rodent CPN and Renal Tumors

Recent work has shown that advanced CPN in control rats is a risk factor for developing renal tubule tumors (strictly adenomas) and their precursors, foci of atypical tubule hyperplasia (Figures 11.7, 11.11, and 11.34). This may be because of the high rate of cell turnover that characterizes some of the CPN-affected tubules throughout its progression. In the F344 male rat with end-stage CPN, the incidence of these precursor and neoplastic lesions combined can exceed 20%. In cases where chemicals exacerbate this spontaneous process to advanced stages (including end-stage kidney) there may be a dose-related increase in renal tubule tumors in the 2-year carcinogenicity bioassay. In an investigation, assessing the predictiveness of CPN exacerbation in NTP studies, there was a statistically significant increase in renal tubule tumors at 2 years, where CPN had been exacerbated by the chemical at 13-weeks, and that early CPN exacerbation had predicted renal tumor outcome with 100% sensitivity and 88% specificity. Such a finding does not necessarily indicate that the chemical is a renal carcinogen, as the risk for spontaneous development of adenomas will increase with increasing exacerbation of the severity of CPN. As a potential MoA in rodents, CPN exacerbation is unlikely to be relevant for species extrapolation in risk assessment.

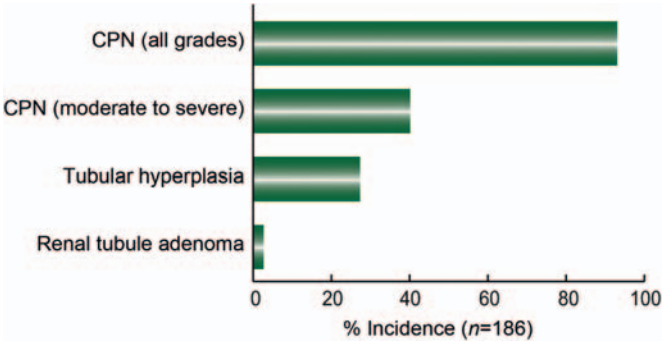

FIGURE 11.34 Close association between severe chronic progressive nephropathy, hyperplasia, and neoplasia seen in male control Sprague-Dawley rats in a 2-year carcinogencity study. *Figure reproduced from Haschek and Rousseaux's Handbook of Toxicologic Pathology (2013), third ed. (W.M. Haschek, C.G. Rousseaux and M.A. Wallig, eds.), Academic Press (Elsevier), Figure 47.41, p. 1763, with permission.*

PART 2: LOWER URINARY TRACT

INTRODUCTION

The lower urinary tract includes the renal pelvis, ureters, urinary bladder and urethra all of which are lined by a unique epithelium, the urothelium. Urothelial toxicity occurs predominantly due to urinary exposure rather than blood-borne exposure. After being excreted and concentrated in the urine, xenobiotics and their metabolites come into direct contact with the urothelium. Thus, the urothelium is a frequent target of toxicity, particularly that of the urinary bladder. Furthermore, many xenobiotic agents can alter urine pH or composition, resulting in the formation of urine solids or calculi, which can also produce toxicity or increase susceptibility to microbial infections.

STRUCTURE AND FUNCTION OF LOWER URINARY TRACT

The structure and function of the lower urinary tract are similar among most mammalian species. The

urothelium (i.e., transitional epithelium) is a highly specialized epithelium serving primarily as a barrier to the absorption of urine. The urothelium is composed of variable thickness in layers, depending on animal species and extent of luminal distention. Generally, the urothelium can be divided into three layers: basal, intermediate and superficial layers (Figure 11.35A). The basal layer is composed of cuboidal cells resting on a basement membrane attached via hemidesmosomes. The intermediate layer is composed of slightly larger cells. The superficial cell layer is composed of large, flat, polygonal cells with a scalloped surface, the so-called umbrella cells. Nonhuman primate urothelium has distinct intracytoplasmic keratohyaline granules which are round to oval, homogenously eosinophilic, and located mostly in the superficial and intermediate cells.

Ultrastructurally there is a circumferential band of tight junctions between superficial urothelial cells, which contributes to the barrier function of the urothelium (Figure 11.35B). The luminal surface of the superficial cells has numerous scallop-shaped membrane plaques, especially in the urinary bladder. The plaque consists of four different uroplakins and integral membrane proteins and acts as an exceptional barrier to water and toxic materials in urine. In the urinary bladder, there are intracytoplasmic fusiform vesicles in the superficial and intermediate urothelial cells. In the superficial cells, the vesicles can connect to the luminal surface and are believed to represent foldings in the luminal membrane for expansion and contraction of the bladder.

MECHANISMS OF LOWER URINARY TRACT TOXICITY

Lower urinary tract toxicity is primarily related to the excretion and concentration of xenobiotics or their metabolites in the urine and/or to the concentration of constitutive metabolites and nutrients. Xenobiotics or their metabolites in the urine may directly interact with urothelial cell DNA, protein, organelles or cell membranes, or may indirectly alter urine pH or composition. Interaction with DNA is the basis for formation of DNA adducts or mutations potentially leading to carcinogenicity. Interactions with proteins, organelles or cell membranes can lead to urothelial cell degeneration, necrosis or urothelial hyperplasia. Alterations in urine pH or composition may lead to urine solid formation, including mineral precipitates, crystals or calculi. Microbes, cellular debris or cells may be present in the solids if urothelial necrosis and infections occur. Large urine solids can obstruct the urinary tract and lead to hydroureter and hydronephrosis.

Urine and Urinary Solids

Alterations in urine pH, osmolality and composition can have considerable influences on the solubility, ionization and solids formation of normal constituents in the urine, such as calcium, magnesium and phosphate, and of various xenobiotics or their metabolites. Rodent urine pH ranges from 5.0 to 8.0 and can be influenced greatly

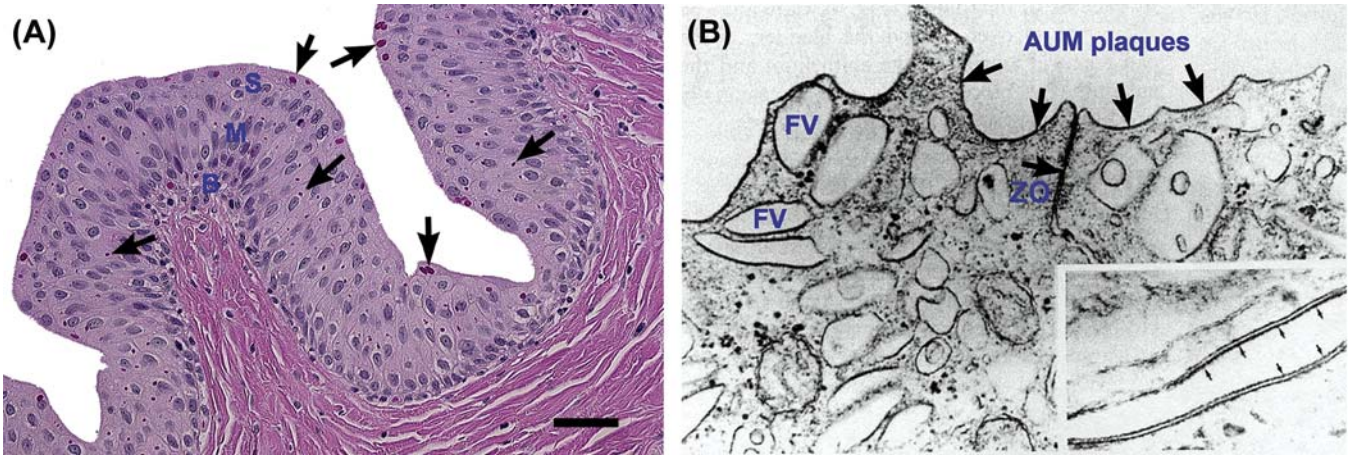

FIGURE 11.35 (A) The urothelium of monkey bladder illustrates the basal (B), intermediate (M) and superficial (S) cell layers. Nonhuman primate urothelium has distinct intracytoplasmic keratohyaline granules (arrows) that are round to oval, homogenously eosinophilic, and located mostly in the superficial cells. Bar = 45 μm. (B) Luminal surface of two superficial cells of the urinary bladder, joined by zonular occludens intercellular junction (ZO) (tight junction). The luminal membrane has a scalloped appearance due to the presence of rigid, curved, asymmetric unit membrane (AUM) plaques alternating with short segments of symmetric membrane, which serve as "hinge" areas. Intracytoplasmic fusiform vesicles (FV) are lined by AUM plaques. Inset: The thicker leaflets of the AUM plaque of fusiform vesicles face inward, lining the intravesicular space. This leaflet contains particulate membrane components (arrows). *Figure B reproduced from Handbook of Toxicologic Pathology, second ed., W. M. Haschek, C. G. Rousseaux and M. A. Wallig, eds. (2002) Academic Press, Fig. 1, p. 339; originally from Alroy (1979) Ultrastructure of canine bladder carcinoma, Vet. Pathol., 16, 693–701, Fig. 5, with permission.*

by diet. By altering urine pH, the toxicity of xenobiotics or their metabolites can be significantly modified, even for genotoxic carcinogens such as aromatic amines. There are species differences in the urine osmolality and composition, particularly between rodents and humans. Rodent urine is usually highly-concentrated and osmolalities range from 1200 to 2000 mOsmol/L.

Species differences in the urine composition have been noted in both protein and mineral components. Rodents have higher urine protein concentrations in males than females, due to the production and excretion of alpha$_{2\mu}$-globulin in male rats and mouse urinary protein in male mice. Differences in the concentration of calcium, phosphate, and magnesium can influence the formation of various urine solids. Calcium precipitates frequently in rodent urine as the phosphate salt, whereas in monkeys and humans it precipitates as calcium oxalate. Urinary calcium, phosphate, and magnesium are present at considerably higher concentrations in rats than in mice, which might explain the greater susceptibility of rats to formation of urine solids. In rats, small amounts of microcrystals are normally present in the urine, usually as magnesium ammonium phosphate (struvite) crystals. The calcium phosphate-containing precipitate does not occur in mouse urine due to the much lower urine concentrations of calcium and phosphate, nor in nonhuman primates and humans due to the much lower urine osmolality and protein levels.

Urinary solids can be formed, dissolved, reformed or excreted, depending on the urinary pH, osmolality, composition, and exposure and physicochemical property of xenobiotic agents or their metabolites. Some xenobiotics or their metabolites can cause excess excretion of calcium and phosphate in the urine, leading to calcium phosphate calculi. In rats, large amounts of calcium phosphate-containing precipitate are formed after administration of high doses (≥2.5% of the diet) of various sodium or potassium salts (Table 11.17). Urine solids can form when xenobiotics or their metabolites are excreted in urine in high concentration, such as sodium saccharin, oxalate and melamine (Figures 11.21 and 11.22).

Crystals and calculi can form in the urine of most animal species. In general, rodents are considerably more susceptible than are humans and nonhuman primates. Crystals and calculi can form following administration of numerous xenobiotic substances in rodents (Table 11.18). In rodents, xenobiotics are often given at maximal tolerated toxic doses and precipitates or calculi can be formed readily. In quadruped animals, such precipitates or calculi can accumulate for long periods of time in the bladder and potentially result in urothelial injury and tumors (Figure 11.36). In contrast, in humans, pharmaceutical agents are given at low or therapeutic doses and precipitates or calculi rarely form and/or will be removed surgically. Similarities in the dose response to calculi formation between rodents and humans have been exemplified by adulteration of baby formula with melamine (Figure 11.22). In rats, melamine in the diet produces urinary tract calculi and urothelial tumors at high concentrations of four or five orders of magnitude of human environmental exposures. With adulteration of baby formula, however, formation of urinary calculi and consequent obstructive urinary syndrome occurred when melamine exposures in babies were similar to the high exposures achieved in the rat studies.

TABLE 11.17 Sodium Salts Administered Orally at High Doses to Rats that Produce Urothelial Proliferation

Ascorbate	Glutamate
Aspartate	Phosphate
Chloride	Saccharin
Erythorbate	Succinate

Table modified from Handbook of Toxicologic Pathology, second ed. W. M. Haschek, C. G. Rousseaux and M. A. Wallig, eds. (2002) Academic Press, Table II, p. 343, with permission.

TABLE 11.18 Substances Producing Urinary Calculi When Administered to Rodents and/or Humans

Acetazolamide	Indinavir
Amoxicillin	Melamine
Ampicillin	Orotic acid
Biphenyl	Oxamide
Calcium phosphate	Polyoxyethylene-8-stearate
Cysteine oxalates	Silicates
Diethylene glycol	Sulfonamides
Dimethylterephthalate	Sulfosulfuron
4-Ethylsulfonylnaphthalene-1-sulfonamide	Terephthalic acid
Fosetyl-al	Thymine
Glafenic acid	Triamterene
Glycine	Uracil
Homocysteine	Urate

Table modified from Handbook of Toxicologic Pathology, second ed. W. M. Haschek, C. G. Rousseaux and M. A. Wallig, eds. (2002) Academic Press, Table I, p. 342, with permission.

Carcinogenesis

Urothelial neoplasms can be induced in most species by two basic mechanisms, direct genotoxic damage to DNA or nongenotoxic increase in cell proliferation. Some genotoxic xenobiotics are

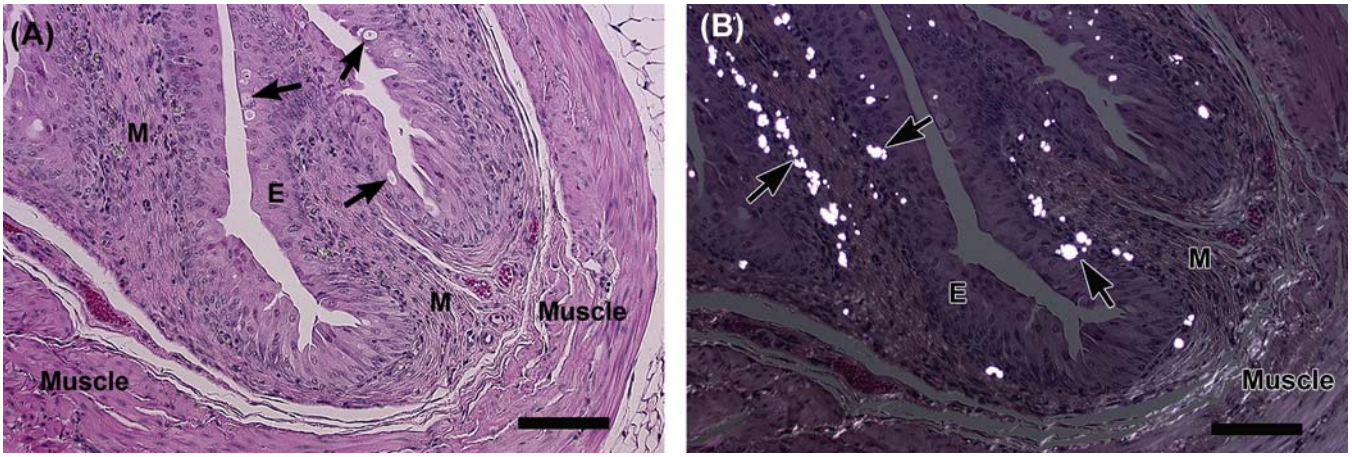

FIGURE 11.36 Bladder from a rat treated with a small molecule therapeutic illustrates crystals of the test article in the mucosa. (A) Hematoxylin-eosin stained section illustrates the epithelial hyperplasia (E), intracytoplasmic vacuoles or inclusions (arrows), and inflammatory reaction in the mucosa (M). Bar = 70 μm. (B) Polaroid light field illustrates crystal precipitation of urine constituents and/or test article (arrows) in the urothelium and submucosa. Bar = 70 μm.

metabolically activated to reactive electrophiles which covalently bind to DNA, leading to gene mutation and carcinogenesis. Most DNA-reactive xenobiotics often are cytotoxic at high doses and induce cell proliferation. They may induce tumors in rodent carcinogenicity studies if administered at cytotoxic concentrations.

Animal models of urinary bladder cancer have been extensively used for the identification of numerous xenobiotics and mixtures that produce bladder cancer in humans, including aromatic amines, cigarette smoking, cyclophosphamide and inorganic arsenic. Aromatic amines are present in relatively high concentrations in cigarettes, and are likely a major contributor to the carcinogenicity of cigarette smoke for the urothelium. Many aromatic amines, such a 2-acetylaminofluorene, produce bladder and other tissue tumors in rodents. Several urothelial-specific carcinogens have been identified, including *N*-butyl-*N*-(4-hydroxybutyl) nitrosamine (BBN), nitrofurans, and other nitroaromatics, nitrosoureas, or cyclophosphamide.

In contrast, a large number of agents may produce bladder tumors in rodents by a mode of action involving increased cell proliferation due to cytotoxicity. The nongenotoxic or non-DNA-reactive mode has a threshold-level fortoxicity and carcinogenicity. Urothelial cell proliferation or direct mitogenesis can be produced by urinary solids, reactive xenobiotics or their metabolites, and altered urinary constituents, such as propoxur and peroxisome proliferator-activated receptor/PPAR agonists.

Rodent carcinogenicity studies show that the PPARγ agonist such as pioglitazone and dual PPARα/γ agonists such as ragaglitazar, muraglitazar, and naveglitazar may increase the risk of bladder cancer. Bladder cancer shows a species- and sex-specificity, has a dose-responsive pattern, and tends to occur in the ventral dome of the bladder in rats. For example, bladder tumors occur more in male than female rats, but not in mice of either sex. Since most PPAR agonist compounds and their metabolites are not genotoxic, PPAR receptor-modulated cell proliferation and cell proliferation in response to "urolithiasis" injury had been hypothesized in rats.

Clinical associations between PPAR agonists and bladder cancer have been contradictory. Increased risk of bladder cancer has been observed with pioglitazone in a cohort of 145,806 patients. The risk rises with longer duration of use and increased cumulative dose. However, some clinical studies showed that pioglitazone did not increase or even decreased the risk of bladder cancer. Rosiglitazone, also from the thiazolidinedione class, was not associated with an increased risk of bladder cancer, suggesting that the increased risk is drug-specific and not a drug-class effect. It was hypothesized that pioglitazone might be a dual PPARα/γ agonist, and rosiglitazone a PPARγ agonist. Paradoxically, some PPARγ agonists, e.g., methylene-substituted diindolylmethanes, had been shown to inhibit tumor activity in bladder cancer cells through activation of proapoptotic proteins.

LOWER URINARY TRACT RESPONSE TO INJURY

Nonneoplastic Response of the Lower Urinary Tract

The lower urinary tract has limited responses to injury. Cytoplasmic vacuolation of the urothelium has been noted as a common and early response to toxic injury, including potential injury by certain peroxisome proliferator-activated receptor agonists. Vacuolation related to cytotoxicity frequently occurs initially in the superficial and intermediate cell layers

(Figure 11.36). The vacuoles often represent swollen organelles such as lysosomes, endoplasmic reticulum or other cytosolic elements, and may contain fluid, lipid, or xenobiotics or their metabolites. However, immediate and proper tissue fixation is necessary to avoid artifactual or autolytic changes.

Acute toxic injury to the urothelium typically begins with urothelial degeneration and necrosis and underlying tissue hemorrhage and inflammation, depending upon the nature and exposure of the causative agent (Figure 11.37A). For example, cyclophosphamide can cause hemorrhagic cystitis in dogs and cats, due to the toxic effect of its metabolite, acrolein. If the extent of injury is not extensive, the lesion can be repaired completely and the urothelium returns to normal. If the full thickness of the urothelium and basement membrane are damaged, toxic materials can be absorbed from the urine and induce injury to the mucosa and deep tissues. If the damage is more extensive or severe, chronic inflammation can persist and fibrosis may occur. In the rat and mouse, the time-course of this process is consistent regardless of the chemical or physical stimuli. Necrosis or ulceration usually is present within hours to a few days of the inciting stimulus, with a peak proliferative and inflammatory response within 5–7 days. Usually the lesion is repaired within approximately 3 weeks, with the bladder returning to normal within 3–5 weeks. Complete resolution of the damage is dependent on removal of the inciting stimulus, the overall condition of the animal, and the composition of the urine.

Inflammatory infiltrates can be observed occasionally in the mucosa of the lower urinary tract in both rodents and nonrodents as a background finding, which is typically minimal or mild in severity and focal or multifocal in distribution. The lymphocytic infiltrate must be distinguished from a lymphomatous/leukemic infiltrate in aged mice. Granulomatous inflammation has been associated with urinary crystalline solids. Severe inflammation can result from ascending bacterial infection from the urethra or descending bacterial infection from pyelonephritis. Squamous metaplasia of the urothelium can be induced by chronic inflammation, certain urothelial toxicants or Vitamin A deficiency.

Urinary solids are present in small quantities in normal urine of rodents and composed typically of calcium phosphates or calcium carbonates, with variable magnesium. In quadrupeds, urinary solids can accumulate in the ventral bladder since they are horizontal. Toxicity of urinary solids depends on their quantity and physicochemical property. Mineralization of the lower urinary tract is commonly seen at the fornix of the rodent kidney, accompanied by chronic inflammation and epithelial hyperplasia. Large crystals or calculi can cause urothelial necrosis, inflammation and urinary obstruction leading to hydronephrosis and hydroureter. Urothelial ulceration and/or calculi may result in hematuria if hemorrhage occurs in the lower urinary tract. Urinary calculi or crystals have been associated with proliferative and neoplastic lesions in rodents.

If the stimulus incites chronic damage, urothelial hyperplasia in the lower urinary tract may occur. Urothelial hyperplasia can be focal, multifocal, or diffuse, with or without an inflammatory reaction. The urothelial hyperplasia may be accompanied by underlying stromal or capillary proliferation. This stromal or capillary proliferation reverses upon reversion of the urothelial proliferation. In the bladder, urothelial hyperplasia can be simple, nodular or papillary (Figure 11.37B). Simple hyperplasia is an increase in

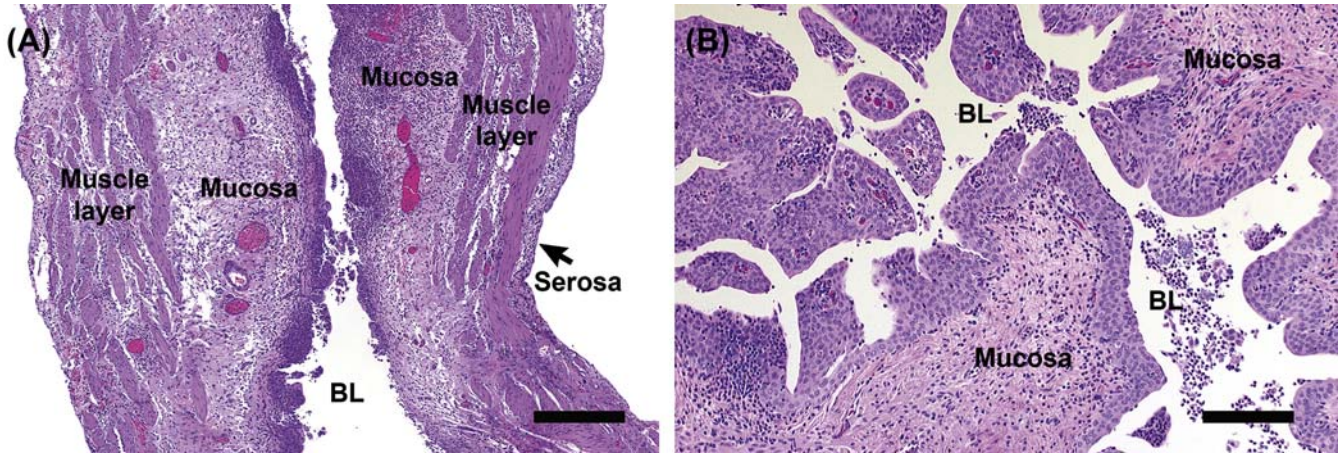

FIGURE 11.37 (A) Bladder from a rat illustrating acute inflammation involving the mucosa, muscle and serosa, with urothelial ulceration, inflammatory cells and necrotic debris in the mucosa and the bladder lumen (BL). Bar = 1.4 mm. (B) Bladder from a rat illustrating chronic inflammation characterized by urothelial hyperplasia, mucosal fibrosis, and inflammatory cell infiltrates in the urothelium, mucosa and bladder lumen (BL). Bar = 120 μm.

the number of cell layers normally present without formation of nodules or papillary projections into the lumen. Nodular hyperplasia represents an endophytic growth of epithelial cells with fibrovascular stroma similar to the mucosal connective tissue. Papillary hyperplasia is an exophytic growth and consists of fronds of well-differentiated epithelial cells layered on a central fibrovascular core. The lining epithelium is usually three to five layers thick. Rarely, urothelial hyperplasia can become preneoplastic or neoplastic in rats as in the case of certain peroxisome proliferator-activated receptor agonists or urinary crystal solids.

Mesenchymal proliferative lesions have been observed in mice. This lesion appears to be strain-specific, e.g., common in Swiss Webster mice but absent in B6C3F1 mice. The etiology is unknown, but similar to decidual-like reactions noted in male accessory sex glands of older mice. The lesions are mostly located in the caudal bladder near the trigone and often protrude into the bladder lumen. They tend to be solitary, well demarcated, and not encapsulated. The lesion often consists of large pleomorphic epithelioid cells and spindle cells. Epithelioid cells have homogenously eosinophilic cytoplasm with distinct cytoplasmic borders. Spindle cells resemble fibroblasts or smooth muscle cells. Local invasion is occasionally seen and mitoses are variable.

Other spontaneous nonproliferative lesions include congenital aplasia or agenesis of the ureter in association with renal aplasia. Certain rat (SD/cShi) and mouse (NON-Shi) strains develop a high incidence of hydronephrosis. Diverticula have been reported in mice and rats and other species, including humans, and consist of urothelial invagination into the mucosa or through the muscle wall. The diverticula can be lined by normal or hyperplastic urothelium and may be accompanied by squamous metaplasia. Brunn's nests have been observed in the bladder of dogs, monkeys and humans. These are solid nests of benign urothelial cells often having regular contours and are located mostly in the mucosa of the trigone region. Brunn's nests are considered a reactive change or a normal variation of the urothelium.

Neoplastic Lesions of the Lower Urinary Tract

Although certain strains of rats (SD/cShi) and mice (NON-Shi) have a higher incidence of tumors of the upper urinary tract, urothelial tumors occur mostly in the urinary bladder in laboratory animal species (Figure 11.38). Bladder cancer in humans has been associated with a number of risk factors, such as life style and other environmental factors. In humans, bladder cancer may represent two distinct disease types. The common type consists of a low-grade, papillary neoplasm which does not invade or metastasize, but tends to recur. The other type is nonpapillary, high grade, and is frequently invasive and metastasizes. In the rat, papillary neoplasms occur most commonly, and can further evolve to high-grade and invasive lesions. In mice, nonpapillary neoplasms are most common.

Urothelial papillomas are benign epithelial tumors in the renal pelvis or bladder. Papillomas may appear to be polypoid and project into the lumen. Papillomas usually have stalks with prominent fibrovascular cores. The epithelial lining of the papillary fronds and nodules is generally limited to three to five cell layers in thickness. There is no cellular or nuclear pleomorphism or anaplasia. Mitoses are uncommon.

Spontaneous urothelial carcinomas are rare in laboratory animal species, but have been associated with chemical carcinogens. Urothelial carcinomas of the prostatic urethra have been reported in beagle dogs. Carcinomas are usually solitary, poorly demarcated, and locally invasive. Neoplastic cells are well-differentiated to anaplastic, mitoses are variable; and squamous and glandular metaplasia can be observed. Cytokeratin stains and uroplakin structures can be useful markers in detecting urothelial lineage in tumors.

Adenocarcinomas have been induced experimentally by bracken fern and nitrosamine. Major morphologic features include the presence of glandular elements and/or tubules, lined by pleomorphic to anaplastic cuboidal cells in the tumors, which may contain mucous.

Spontaneous squamous cell carcinomas are rare, but have been induced by carcinogenic agents. Squamous cell carcinomas have irregular growth patterns and are invasive. Mitoses increase as malignancy increases and metastases are common. The main differential criterion distinguishing carcinoma and squamous cell carcinoma is the keratinization or keratin "pearl" formation in squamous cell carcinoma.

Mesenchymal tumors are uncommon in rodents, but most types of benign or malignant mesenchymal tumors have been reported in the lower urinary tract or bladder, such as leiomyomas and leiomyosarcomas, hemangiomas and hemangiosarcomas, fibrous and lipomatous tumors, and fibrous histiocytomas or fibrosarcomas.

EVALUATION OF LOWER URINARY TRACT TOXICITY

Urinalysis and morphologic evaluation are essential tools to evaluate lower urinary tract toxicity. Specific analyses of the administered agents or their metabolites in the urine may be useful under certain circumstances.

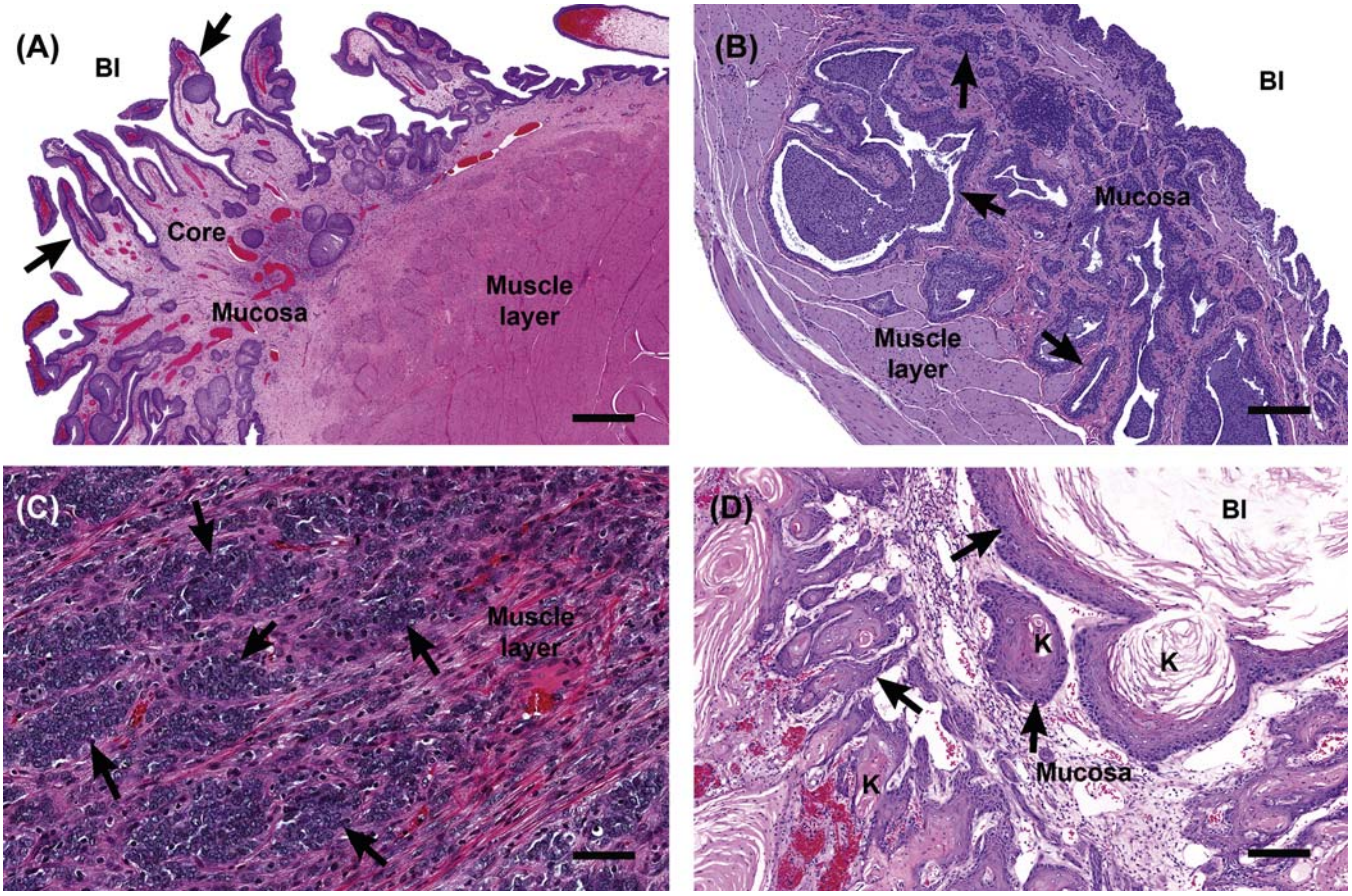

FIGURE 11.38 Urinary bladder illustrating urothelial hyperplasia, papilloma, carcinoma and squamous cell carcinoma. A. Bladder from a dog illustrating a papilloma projecting into the bladder lumen (Bl), with prominent fibrovascular cores or stalks. The papillary fronds (arrows) are generally lined by 3–5 cell thick epithelial layers. There is no cellular or nuclear atypia and no or very few mitotic figures. Bar = 400 μm. (B) Bladder from a rat illustrating an inverted papilloma extending down to the mucosa (arrows). The papillary fronds are generally lined by a 3–5 cell thick epithelial layer without cellular or nuclear atypia and few mitoses. Bar = 350 μm. (C) Bladder from a rat illustrating a poorly demarcated carcinoma (arrows). Neoplastic cells are poorly differentiated with variable mitoses and invade into the muscular layer. Bar = 60 μm. (D) Bladder of a mouse illustrating a squamous cell carcinoma that had an irregular and invasive growth pattern (arrows), with prominent squamous cell differentiation and keratin "pearl" formation (K). Bar = 110 μm.

Urinalysis

Urinalysis has become a critical tool for the lower urinary tract toxicity and many factors may influence the analysis. Variations in diet and water intake may affect urinary composition, pH, osmolality, and xenobiotic excretion. Species differences and diurnal variations in urine composition, including electrolytes, protein, pH, and osmolality, should be kept in mind when evaluating urinalysis data. Some changes in the urothelium and formation of urine solids can be rapid or transient after administration of test agents. Some urinary solids, especially organic components, may not be detectable in the sediment microscopically as they may be lost during sample processing. Thus, it is critical to collect and process urine samples in a timely, consistent and appropriate manner to avoid artifactual changes. Frequently, multiple collections during the day may be necessary to examine urine composition because of marked variability in urine due to diurnal variation.

Morphologic Evaluation

Morphologic changes in the urothelium can occur directly by urine exposures to toxicants or in response to urine solids. Morphologic evaluation is routinely accomplished by light microscopy of hematoxylin and eosin-stained sections, as well as special stains. Subtle or specific urothelial cytotoxicity may require other morphologic tools, including histochemistry, immunohistochemistry and electron microscopy. For example, subtle or early cell proliferation can be detected by DNA replication with immunohistochemistry before the microscopic evidence of hyperplasia.

Morphologic evaluation of the bladder is best performed on appropriately fixed and uniformly distended bladder. As rodents are quadripeds, urine solids may settle down in the ventral dome of the bladder. Thus, the ventral portion of the bladder should be included for evaluation, in addition to the dome and trigone regions.

Special Evaluation

Mechanistic assessments of specific lower urinary tract toxicity findings may require additional and special evaluation. For example, potential genotoxic agents and their reactive metabolites can be identified by genotoxicity assays and rodent carcinogenicity studies. Cytotoxicity of specific agents or their metabolites can be assessed utilizing primary urothelial cells or well-characterized urothelial cell lines from animals or humans. Comparing the LC50 *in vitro* to the urinary concentration following *in vivo* administration of the agent may provide some perspective for assessing the relevancy and dose response. Further analyses of the specific components of urine solids may require special tools and techniques, including xenobiotics, test agents or their metabolites.

Most importantly, the dose response and relevance to human risk regarding the lower urinary tract should be assessed based on the knowledge of mechanisms and effects of the agent on humans and animals. The dose response relationship determination is critical as pharmaceutical agents are given to humans at low or therapeutic doses and to animals at maximal tolerated doses.

Acknowledgments

Our thanks to Dr. Samuel M. Cohen who authored the chapter titled "Lower Urinary Tract" in the 2nd Edn of the *Handbook of Toxicologic Pathology* which was used as a basis for the corresponding section in this chapter.

Further Reading

Alden, C.L., Lynn, A., Bourdeau, A., Morton, D., Sistare, F.D., Kadambi, V.J., et al., 2011. A critical review of the effectiveness of rodent pharmaceutical carcinogenesis testing in predicting for human risk. Vet. Pathol. 48, 772–784.

Anderson, T.D., Khan, K.N., Tassinari, M.S., Hurtt, M.E., 2009. Comparative juvenile safety testing of new therapeutic candidates: Relevance of laboratory animal data to children. J. Tox. Sci. 34, SP209–SP215, Special Issue II.

Coca, S.G., Yalavarthy, R., Concato, J., Parikh, C.R., 2008. Biomarkers for the diagnosis and risk stratification of acute kidney injury: a systematic review. Kidney Int. 73, 1008–1016.

Cohen, S.M., 2004. Human carcinogenic risk evaluation: an alternative approach to the two-year rodent bioassay. Toxicol. Sci. 80, 225–229.

Cohen, S.M., 2013. Lower urinary tract. In: third ed. Haschek, W.H., Rousseaux, C.G., Wallig, M.A. (Eds.), Haschek and Rousseaux's Handbook of Toxicologic Pathology, Vol. 2. Elsevier/Academic Press, London UK, Walthama MA and San Diego CA, pp. 1775–1793.

Cohen, S.M., Ohnishi, T., Clark, N.M., He, J., Arnold, L.L., 2007. Investigations of rodent urinary bladder carcinogens: collection, processing, and evaluation of urine and bladders. Toxicol. Pathol. 35, 337–347.

Ennulat, D., Adler, S., 2015. Recent successes in the identification, development, and qualification of translational biomarkers: the next generation of kidney injury biomarkers. Toxicol. Pathol. 43, 62–69.

Frazier, K.S., Seely, J.C., Hard, G.C., Betton, G., Burnett, R., Nakatsuji, S., et al., 2012. Proliferative and nonproliferative lesions of the rat and mouse urinary system. Toxicol. Pathol. 40 (4 suppl), 14S–86S.

Hard, G.C., Khan, N.K., 2004. A contemporary overview of chronic progressive nephropathy in the laboratory rat and its significance for human risk assessment. Toxicol. Pathol. 32, 171–180.

Hard, G.C., Seely, J.C., 2005. Recommendations for the interpretation of renal tubule proliferative lesions occurring in rat kidneys with advanced chronic progressive nephropathy (CPN). Toxicol. Pathol. 33, 641–649.

Heyen, J.R., Rojko, J., Evans, M., Brown, T.P., Bobrowski, W.F., Vitsky, A., et al., 2014. Characterization, biomarkers, and reversibility of a monoclonal antibody-induced immune complex disease in cynomolgus monkeys (*Macaca fascicularis*). Toxicol. Pathol. 42, 1–9.

Khan, T.M., Khan, K.N., 2015. Acute kidney injury and chronic kidney disease. Vet. Pathol. 52, 441–444.

Khan, N.M., Hard, G.C., Alden, K.L., 2013. Kidney. In: third ed. Haschek, W.H., Rousseaux, C.G., Wallig, M.A. (Eds.), Haschek and Rousseaux's Handbook of Toxicologic Pathology, Vol. 2. Elsevier/Academic Press, London UK, Walthama MA and San Diego CA, pp. 1667–1773.

Sellers, R.S., Senese, P.B., Khan, K.N., 2004. Interspecies differences in nephrotoxic response to cyclooxygenase inhibitors. Drug Chem. Toxicol. 27 (2), 111–122.

Waanders, F., Navis, G., van Goor, H., 2010. Urinary tubular biomarkers of kidney damage: potential value in clinical practice. Am. J. Kidney Dis. 55, 813–816.

This page intentionally left blank

CHAPTER

12

Immune System

Christine Ruehl-Fehlert[1], *George A. Parker*[2], *Susan A. Elmore*[3,*], *and C. Frieke Kuper*[4]

[1]Bayer AG, Wuppertal, Germany [2]Charles River Laboratories, Inc., Hillsborough, NC, United States [3]National Toxicology Program/NIEHS, Research Triangle Park, NC, United States [4]TNO, Zeist, The Netherlands

OUTLINE

INTRODUCTION

The primary concern of immunotoxicology is to assess the undesired interactions of substances with the immune system. Toxic responses may occur when the immune system is a passive target of chemical insults, leading to altered immune function. This can result in an increased susceptibility to infection or to the development of allergy, autoimmune disease, or neoplasia. Alternatively, toxicity may arise when the immune system responds to the antigenic specificity of a substance, which can lead to substance-specific allergy (hypersensitivity) or autoimmune disease. The immune system may be especially sensitive during immune development, as in the fetus and neonate, but also in adult life during pregnancy, glucocorticoid-related stress, and aging.

To interpret undesired alterations of the immune system, comprehension of the histophysiology of the system is required. Table 12.1 gives an overview on histophysiology and compartments of the thymus, spleen, lymph nodes, mucosa-associated lymphoid tissue (MALT), tertiary lymphoid tissues, and lymphoid cells in omental adipose tissue. In addition, the immune histophysiology of nonlymphoid organs is described, exemplified by the liver. For the blood and bone marrow, the reader is referred to Chapter 13, Hematopoietic System. T- and B-lymphocytes of lymphoid organs reside in different compartments (Table 12.2).

A schematic presentation of antigen processing and recognition is given in Figure 12.1. The antigen is ingested and degraded by immature antigen-presenting (dendritic) cells, which reside in the targeted tissue (Figure 12.1A,B). The antigen is then carried to local/draining lymph nodes, where the dendritic cells (DCs) present the antigen to T-lymphocytes.

By autophagy, cells can eliminate intracellular pathogens by lysosomal degradation of cell constituents.

*Susan A. Elmore contribution is in Public domain.

Fundamentals of Toxicologic Pathology.
DOI: http://dx.doi.org/10.1016/B978-0-12-809841-7.00012-5

TABLE 12.1 Compartments, Cells, and Functions of Lymphoid Tissues

Organ	Function	Organization	Compartments/ subcompartments	Main type of resident cells	Main type of mobile cells
Thymus	Mechanical stability	Capsule and trabeculae (forming two lobes divided into lobules)		Fibrocytes	
	Proliferation and maturation of T-cells		Cortex (containing epithelium-free areas)	TEC	Immature T-cells
			Corticomedullary junction/zone	TEC, IDC	T-cells in transition
			Medulla	TEC (can form Hassall's bodies); IDC	T-cells (and B-cells)
Spleen	Mechanical stability	Capsule		Fibrocytes	
	Contraction	Trabeculae		Smooth muscle cells	
	Blood storage, filtration of blood and hematopoiesis	Red pulp	Sinuses	Endothelium	Lumen: blood components, wall: macrophages
			Splenic cords	FRC	Macrophages
			Ellipsoids (nonrodent)	FRC	Macrophages
	Immune responses to blood-borne antigens and generation of antibodies	White pulp (lymphoid tissue)	Follicles	FRC, FDC	B-cells
			PALS—inner part	FRC, IDC	T-cells
			PALS—outer part	FRC	B-cells, T-cells
			Marginal zones	FRC	Specialized macrophages (rodent: marginal metallophils), B-cells, T-cells in marginal zone bridging channels
Lymph nodes	Mechanical stability	Capsule		Fibrocytes	
	Filtration of lymph	Vascular spaces	Sinuses	Endothelium	Macrophages
	Recirculation of lymphocytes		HEV of interfollicular areas and paracortex, pigs mostly via normal vasculature	Endothelium	Lumen: blood components, wall: migrating lymphocytes
	Immune reactions related to local stimulation of tributary and generation of antibodies	Lymphoid tissue arranged in lobules	Cortex—follicles	FRC, FDC	B-cells
			Paracortex/ interfollicular cortex	FRC, IDC	T-cells
			Medullary cords	FRC	B-cells, macrophages
Malt	Immune reactions related to mucosal Antigens	Lymphoid tissue	Follicles	FRC, FDC,	B-cells
			Interfollicular areas	FRC, IDC	T-cells
		Specialized covering epithelium		M (microfold)-cells	Migrating lymphocytes
	Recirculation of lymphocytes	Vasculature	HEV of interfollicular areas	Endothelium	Lumen: blood components, wall: migrating lymphocytes

(*Continued*)

TABLE 12.1 (Continued)

Organ	Function	Organization	Compartments/ subcompartments	Main type of resident cells	Main type of mobile cells
Tertiary lymphoid tissue	Response to continued exposure to local antigen	Lymphoid tissue	Follicles	FRC, FDC	B-cells
			Interfollicular areas	FRC, IDC	T-cells
	Recirculation of lymphocytes	Vasculature	HEV of interfollicular areas	Endothelium	Lumen: Blood components, wall: Migrating lymphocytes
Omental adipose tissue	Restoration of peritoneal tissue integrity, reaction to immunogenic stimuli in the abdominal cavity	Adipose tissue with high content of diverse immune cells	Clusters of immune cells (milky spots)	Fat cells	Mixture of lymphocytes, macrophages, and other immune cells
Liver	Immune reactions, phagocytosis, and waste sink for immune cells and molecules, extrathymic T-cell generation, hematopoiesis	Associated with liver sinuses and oriented at lobular organ structure		Sinusoidal endothelial cells, stellate (Ito) cells	Pit (NK) cells, KCs, T-cells, aggregates of mixed immune cells

FDC, follicular dendritic cell; FRC, fibroblastic reticulum cell; HEV, high endothelial venules; IDC, interdigitating cell (derived from hematopoietic progenitor cells but act as fixed cells in lymphoid organs); TEC, thymic epithelial cell.

TABLE 12.2 Anatomical Structure and Distribution of T- and B-Cells in Compartments of Lymphoid Organs

Organ	Structure of lymphoid tissue	T-cell region	B-cell region
Thymus	Cortex, medulla	Cortex, medulla	Not present but a specific B-cells population exists in medulla
Bone marrow	Not applicable	Not present but T-cells proven	Not present but B-cells proven and lymphoid follicles may develop
Spleen	White pulp	PALS	Follicles, marginal zones
Lymph nodes	Lymphoid lobules	Paracortex, interfollicular cortex	Follicles, medullary cords
MALT	Follicles and interfollicular areas	Interfollicular areas	Follicles

MALT, mucosa-associated lymphoid tissue; PALS, periarteriolar lymphoid sheath.

Autophagy moderates inflammation by contributing to antigen presentation via proinflammatory cytokines or by suppressing inflammasome activation. Autophagy also enhances major histocompatibility complex (MHC) class II antigen presentation and is required for homeostasis of T- and B-cell populations. Defective autophagy can be associated with tissue inflammation and autoimmune disease. Drugs like rapamycin and 3-methyladenine target autophagy by influencing central mechanisms. Aberrant or foreign protein structures undergo proteasomal degradation leading to antigenic peptides, which are finally presented together with MHC-I molecules on the cell surface.

After antigen presentation, and activation of T-cells, a choice of effector reactions (response) enables the optimal destruction or inactivation ("immune elimination" and "immune exclusion") of the antigen/pathogen (Figure 12.1C,D). In the antibody (immunoglobulin)-mediated reaction, activated T-cells induce B-cells to become antibody-producing plasma cells (Figure 12.1C). In the cellular effector reaction, T-cells activate cytotoxic (Tc) cells and other effector T-cells. The immune response needs to be downregulated properly, to prevent unnecessary tissue and organ destruction.

DCs play a prominent role in immune responses as interface between innate and adaptive immunity. Different populations have been recognized in humans and mice regarding their provenience—either from bone marrow (conventional DCs, plasmacytoid DCs, monocyte-derived DCs) or yolk sac (Langerhans cells)—and function. Conventional DCs are involved in the selection of T-cells in secondary lymphoid organs and have a short half-life. Monocyte-derived DCs develop in the context of inflammation. Nonphagocytic, follicular DCs of B-cell areas have to be differentiated from phagocytic DCs. Follicular DCs interact with B-cells by long-term presentation of

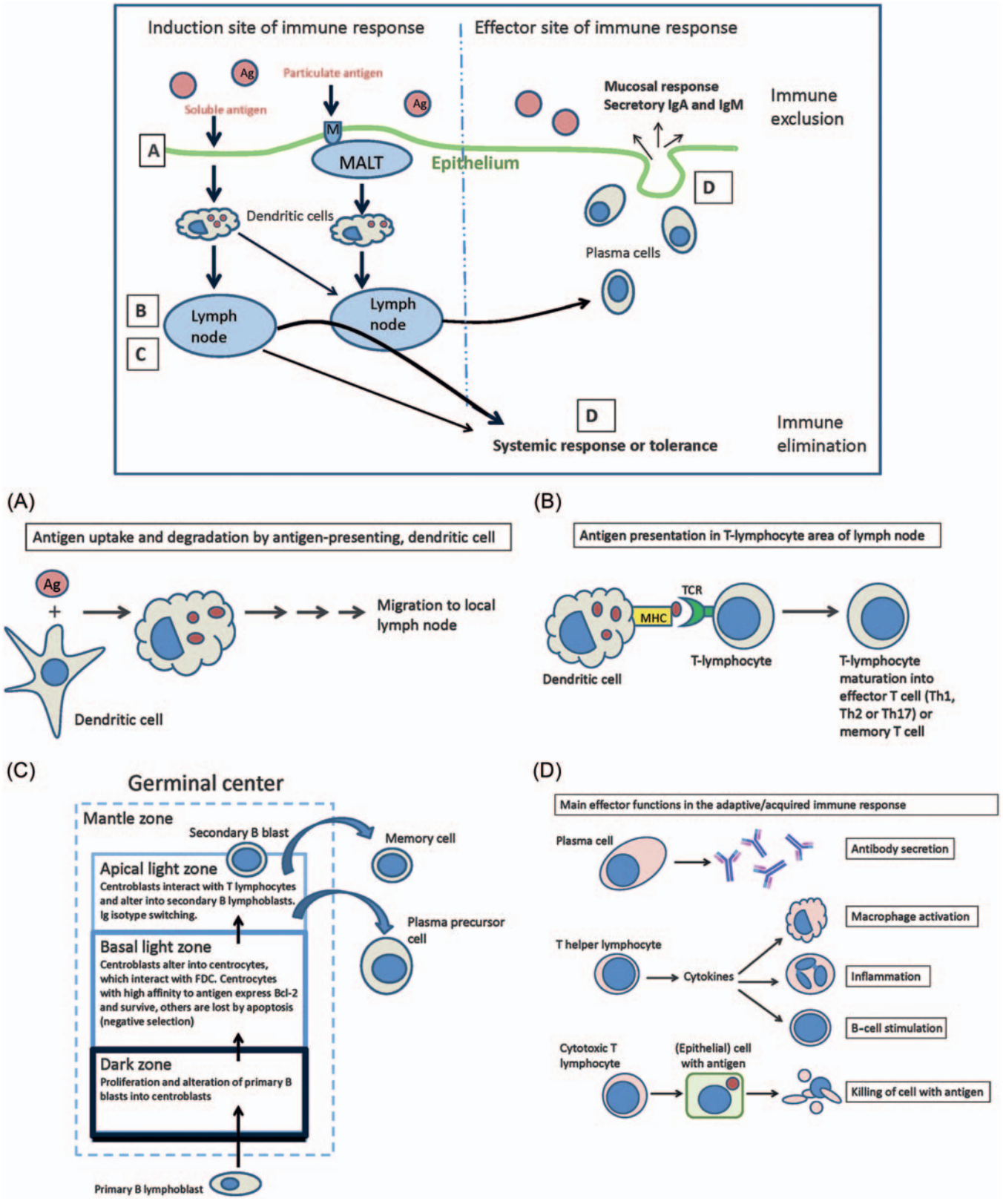

FIGURE 12.1 Schematic presentation of the generation of antigen-specific local and systemic immune responses via mucosal epithelium: overview and detailed figures. (A) Soluble antigens preferentially enter via the normal epithelium, whereas particulate antigen preferentially is taken up by microfold or M cells. DCs capture and degrade antigens/pathogens. (B) Subsequently they migrate and present the antigen to T-lymphocytes. T-cells can recognize antigens only when presented on MHC molecules. Antigens processed by endocytosis are presented predominantly on MHC class II molecules, whereas endogenous antigens (viral antigens, self-peptides) are predominantly presented on MHC class I molecules (MHC; also known in humans as HLA). B-cells can directly recognize antigen. As a result of contact with an antigen, antibodies can be produced by plasma cells, via maturation of immature B lymphoblasts into plasma cell precursors. (C) The maturation of B blasts takes place in the GC, which develops in a primary or resting follicle. (D) Finally, effector reactions are generated, including secretion of specific antibodies (secretory Ig) into the lumen, to bind to antigen and exclude it. Source: *From Haschek, W.M., Rousseaux, C.G., Wallig, M.A. (Eds.), 2013. Haschek and Rousseaux's Handbook of Toxicologic Pathology, third ed. Academic Press (Elsevier), San Diego, CA, Figure 49.1, p. 1798, with permission.*

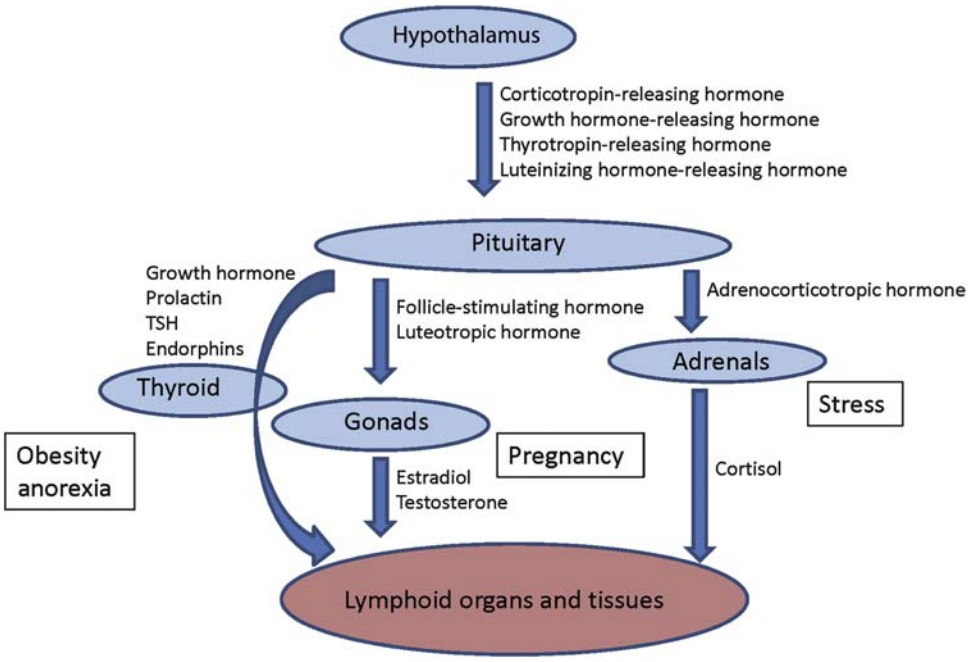

FIGURE 12.2 The influence of the neuroendocrine system on the immune system. TSH, thyroid-stimulating hormone. Source: *From Haschek, W.M., Rousseaux, C.G., Wallig, M.A. (Eds.), 2013. Haschek and Rousseaux's Handbook of Toxicologic Pathology, third ed. Academic Press (Elsevier), San Diego, CA, Figure 49.2, pp. 1801, with permission.*

complement-fixed antigens and production of iccosomes (immune complex-coated bodies).

The immune system aims at a continuous state of homeostatic balance, whereas the introduction of an antigen/pathogen disturbs this balance due to activation of antigen-specific T- and B-lymphocyte clones. The system not only allows the proliferation and amplification of relevant clones to cope with the antigen, but also searches for (and reaches) a state of newly defined homeostasis.

The communication with other homeostatic mechanisms in the body is an important aspect of immunoregulation. Communication and cooperation of the immune system with the neural and endocrine systems is particularly important. Their interaction is mediated by a network of hormones, cytokines, and receptors (Figure 12.2).

Structure and Physiology of Lymphoid Organs and Tissues

Components of the immune system are present throughout the body (Figure 12.3). The lymphoid organs can be divided into primary or central (lymphocyte generation from progenitor or stem cells), secondary or peripheral (interaction with antigen and activation and development of naive lymphocytes into mature T-lymphocytes and plasma cells) such as lymph nodes (Table 12.3), and tertiary lymphoid organs and tissues. As the immune system is ubiquitously represented throughout the organism, classification of organs and tissues into lymphoid and nonlymphoid organs/tissues is somewhat artificial. The liver plays an important role in fetal lymphopoiesis. Later, it is active in the clearance of immune complexes by Kupffer cells (KCs), removal of immunologic signaling and effector molecules by sinusoidal endothelial cells, removal of activated T-cells, in IgA transport, and in the regulation of immune responses in the intestines (see Chapter 8: Liver and Gall Bladder). Although the liver is often not perceived as an immune organ, it is the organ that is most commonly affected by xenobiotics, and is mentioned here to demonstrate its importance in immune function.

Thymus

The thymus is a primary lymphoid organ assigned to the development of a repertoire of immunocompetent T-lymphocytes (Figure 12.4). Its organization into the compartments cortex and medulla is highly consistent throughout mammalian species. During embryofetal development (Figure 12.5A,B) the thymus quickly matures to its final "adult" morphology with a highly cellular cortex and less densely populated medulla (Figure 12.5C). In particular in young animals the thymic cortex has a high level of cellular proliferation (Figures 12.5C and 12.6) that is most pronounced in

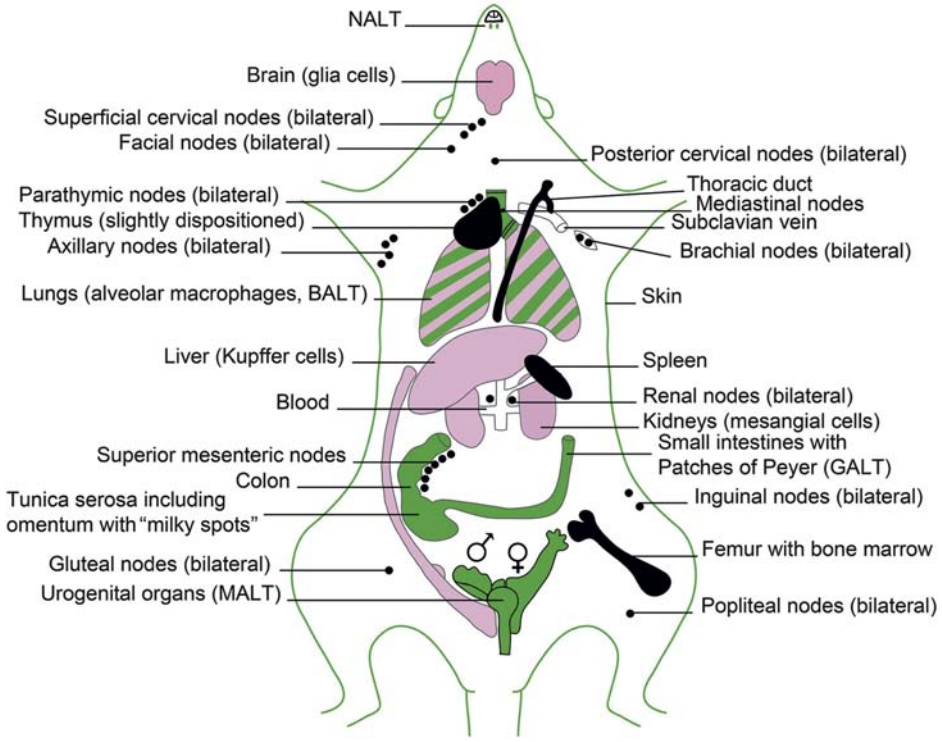

FIGURE 12.3 Lymphoid organs and tissues in the rat. Classic lymphoid organs (bone marrow, thymus, spleen, and lymph nodes) are in black; mucosae and skin are in green; special mononuclear systems are in pink. Data on lymph nodes that drain the genital tract in the rat are unknown. In mice, the lumbar/iliac/caudal/para-aortic lymph nodes drain the uterus. Source: *Courtesy: World Health Organization, EHC no. 180, 1996, with permission.*

the subcortical zone. In active thymuses of certain strains of rats areas free of epithelium with high proliferative activity may be observed as a normal finding in the outer cortex (Figure 12.7A). Physiologically reduced activity of the thymus is encountered in the context of aging (Figure 12.5E); activity is also altered during pregnancy and stress.

T-cell progenitors are formed in the bone marrow, and then migrate to the thymic cortex. Here, they undergo extensive proliferation and selection processes to form single positive CD4+ CD8− and CD4− CD8+ T-cells (Figure 12.4). Cells that fail to recognize self-MHC (major histocompatibility genes; in humans designated HLA or human leukocyte antigens) or have an excessively high affinity with self-MHC, and cells that have an affinity for self-antigens, are eliminated by apoptosis. It is estimated that 95%–99% of immature T-lymphocytes undergo apoptosis due to negative selection. The population that survives migrates to the medulla, where maturation continues. Maturation of T-cells involves an orchestrated movement of cells from the entry point of venules at the corticomedullary junction, then outward to the subcapsular region, and subsequently exit from the medulla of the thymus.

While the thymus is considered to be a "T-cell organ," it is not uncommon to encounter clusters of B-cells or plasma cells in the thymus of various animal species. The B-cell population tends to be more plentiful in aged animals.

Spleen

The structure of the spleen is complex due to its hematopoietic, storage, and defensive functions. The red pulp consists of venous sinuses lined by endothelium and cords containing a mixed population of immune cells including highly active macrophages filtering the blood and removing worn erythrocytes. In dogs and pigs, the red pulp is a major blood reservoir, which is reflected by a thick splenic capsule and strong trabecular muscle. The splenic compartments are outlined in Tables 12.1 and 12.2.

The spleen's main immunological function is to guard the body's vascular compartment by generating, among others, T-cell-independent IgM antibody responses to bacterial polysaccharides and by exerting an enormous phagocytic power. Together with the hepatic phagocytic system, splenic macrophages synthesize the majority of components involved in the complement cascade. The marginal zone plays a key

TABLE 12.3 Areas Drained by Lymph Nodes in Rodents

Lymph node (group), rat[a]/mouse[b]	Area drained	Efferent drainage
HEAD AND NECK		
Superficial cervical/(accessory) mandibular	Tongue, nasolabial lymphatic plexus, brain[b]	Posterior cervical lymph nodes
Facial/superficial parotid	Head: ventral aspect and sides of neck	Posterior cervical lymph nodes
Internal jugular	Pharynx, larynx, proximal part of esophagus	Posterior cervical lymph nodes
Posterior cervical/cranial deep cervical	Superficial cervical, facial and internal jugular nodes, pharynx, larynx, proximal part of esophagus, NALT[c]	Cervical duct
UPPER AND LOWER EXTREMITY, TRUNK		
Brachial/proper axillary	Upper extremities, shoulders, chest	Axillary nodes
Axillary/accessory axillary	Upper extremities, trunk, brachial nodes	Subclavian duct
Inguinal/subiliac	Thigh, flanks, scrotum, lateral tail	Axillary nodes
Popliteal/popliteal	Foot, hind leg	Lumbar, inguinal nodes
Gluteal/external iliac	Tail	Caudal, lumbar, inguinal and popliteal nodes
THORAX		
Parathymic/cranial mediastinal	Peritoneal cavity, liver, pericardium, thymus, lung	Mediastinal duct
Posterior mediastinal/ tracheobronchial; caudal mediastinal	Thoracic viscera, pleural space, pericardium, thymus	Mediastinal duct
Paravertebral	Diaphragm, thoracic viscera	Posterior mediastinal nodes
PELVIS AND RETROPERITONEUM		
Caudal	Ventral tail, anus, rectum, gluteal nodes	Iliac nodes
Iliac/medial iliac	Pelvic viscera, popliteal, gluteal, caudal nodes	Renal nodes
Para-aortic/lateral iliac; lumbar aortic	Pelvic viscera, popliteal, gluteal, caudal nodes	Renal nodes
Renal/renal	Kidney, suprarenal, lumbar lymphatics	Renal duct to cistern chyli
External lumbar	Fat pad, psoas muscles, pelvic viscera	Lumbar lymphatics
ABDOMEN		
Splenic	Splenic capsule and trabeculae	Posterior gastric nodes
Posterior gastric/gastric	Distal esophagus, stomach, pancreas, splenic node	Portal nodes
Portal	Liver, splenic, posterior, gastric nodes	Portal duct to cistern chyli
Superior mesenteric/jejunal	Duodenum, small bowel, cecum, ascending and transverse colon, PP	Superior mesenteric duct to cisterna
Inferior mesenteric/colic	Descending and sigmoid colon	Inferior mesenteric duct to cisterna

[a]*Nomenclature according to Tilney (1971).*
[b]*Nomenclature according to Van den Broeck et al. (2006).*
[c]*Hameleers et al. (1990), Koornstra et al. (1991).*

role in the antibody responses of the spleen, via trapping of blood-borne antigens/pathogens by marginal zone macrophages and marginal metallophilic macrophages (MOMA-1+ cells; interferon alpha/beta-producing cells). Following antigen trapping, marginal zone B-cells proliferate and IgM antibodies against the pathogen are produced. The marginal zone also retains B-lymphocyte memory. In the fetus, the spleen is an

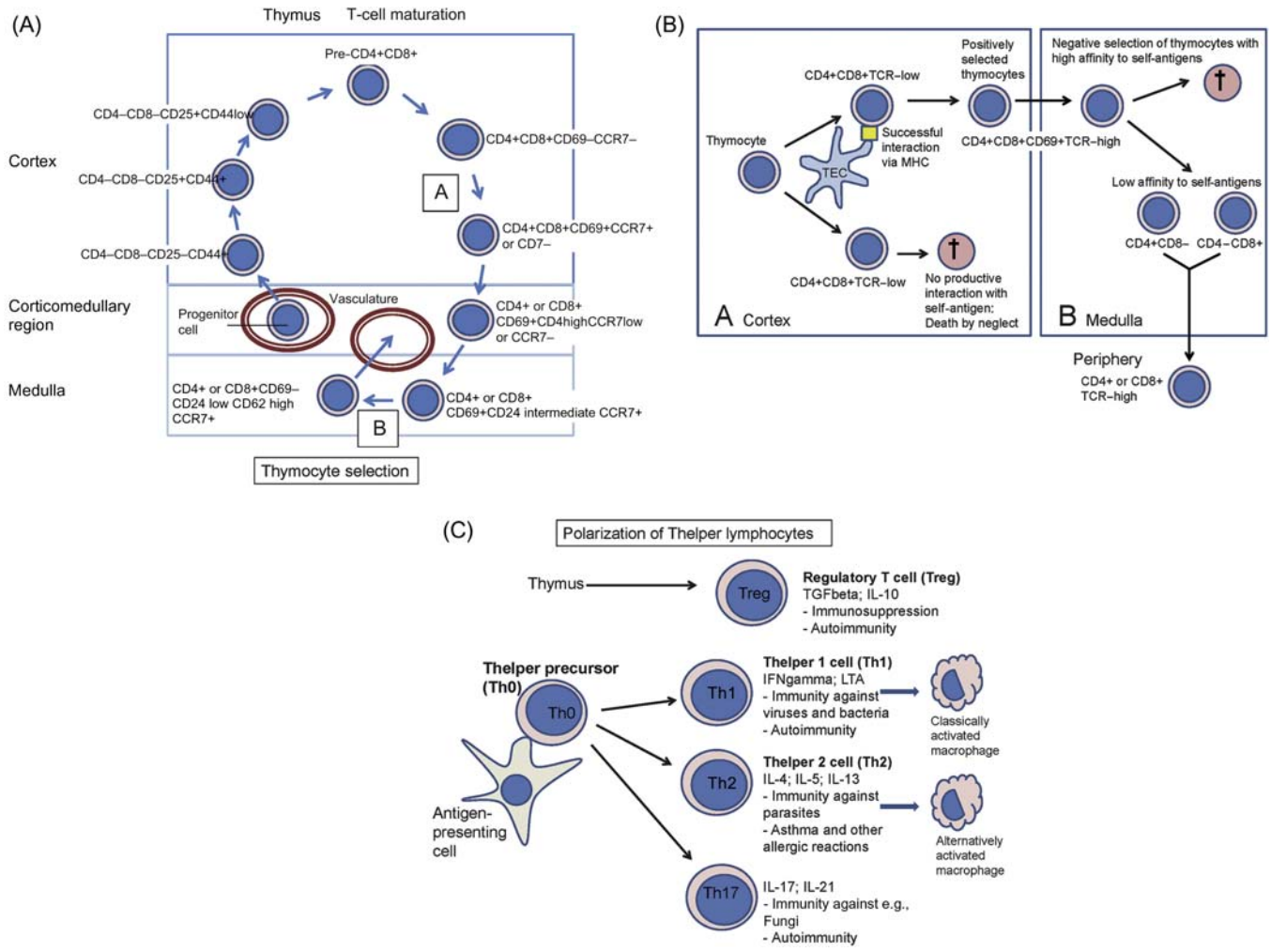

FIGURE 12.4 (A) T-lymphocyte maturation in the thymus. Bone marrow–derived progenitor cells enter the thymus through blood vessels in the corticomedullary zone and, after maturation and selection, leave the thymus as mature T-lymphocytes. The vasculature involved in emigration of T-cells is yet not precisely known. (B) Positive and negative selection of thymocytes takes place in the thymus. (C) In the periphery, T-lymphocytes differentiate further into a number of subpopulations. This differentiation process is directed partly by antigen contact, and depends upon the genetic make-up of the animal (strain and species). Source: *From Haschek, W.M., Rousseaux, C.G., Wallig, M.A. (Eds.), 2013. Haschek and Rousseaux's Handbook of Toxicologic Pathology, third ed. Academic Press (Elsevier), San Diego, CA, Figure 49.7, p. 1805, with permission.*

important site of hematopoiesis. This function is maintained in rats and mice throughout adulthood, but in other species it is resumed only in certain diseases. Figure 12.8A shows a periarteriolar lymphoid sheath (PALS) from the rat spleen with adjacent marginal zone embedded in the red pulp. Figure 12.8B–D give an overview of the pig spleen, which has prominent ellipsoids containing macrophages ensheathing vessels of the marginal zones. Ellipsoids are also seen in dogs, pigs, and nonhuman primates, but not in rodents.

Lymph Nodes

Lymph nodes are widely distributed throughout the mammalian body, and are typically located at points where there is confluence of lymphatic vessels from a major anatomic area such as a limb. Patterns of lymphatic drainage in the laboratory rat have been systematically investigated (Table 12.3). Lymph nodes are composed of a variable number of contiguous lymphoid lobules, each of which consists of a cortex, paracortex, and medulla (Tables 12.1 and 12.2; Figures 12.9, 12.10, and 12.11).

Following antigenic stimulation, the primary follicles of the lymph node enlarge to form secondary follicles (Figure 12.12). Each lobule of the lymph node drains a specific region, and therefore different lobules within a lymph node commonly exhibit different levels of reactivity. This is particularly noticeable in mesenteric lymph nodes of rodents, which form a long chain of contiguous lymphoid lobules, often with striking variation in histomorphology. High endothelial venules (HEVs) are postcapillary venules and the site

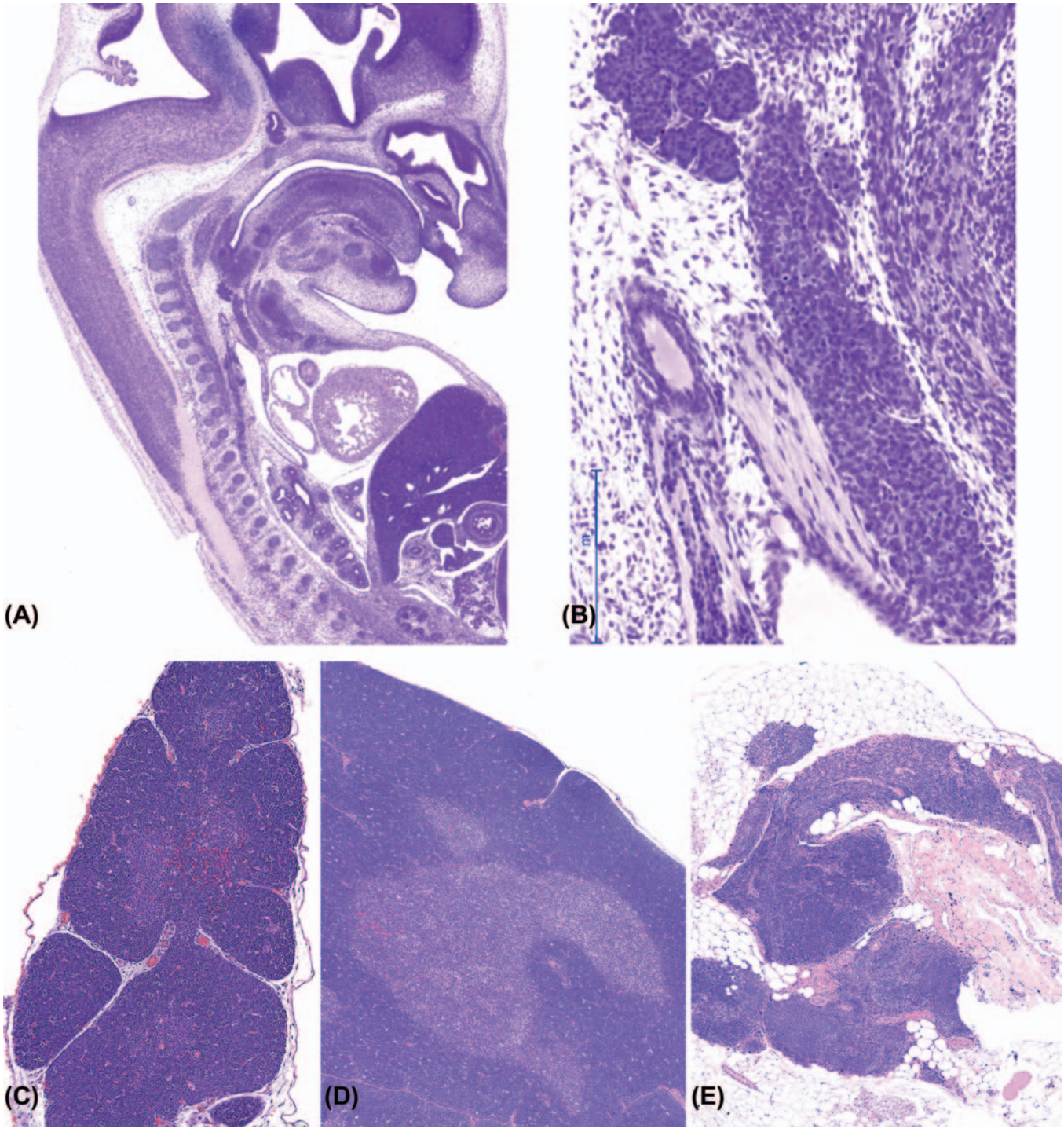

FIGURE 12.5 Age-related changes in the thymus. (A) Thymus from a Wistar rat at day 15 of fetal life. The organ is a small band of epithelial cells, located mainly in the neck region and close to the thyroid. (B) Detail of fetal thymus and thyroid. The thymus lacks any organization and is almost devoid of lymphocytes. H&E stain. (C) Thymus from PND0 (newborn) Sprague–Dawley rat. Cortex and medulla are distinguishable, but medullary areas are less distinct than in young adult. H&E stain, ×100. (D) Thymus from PND42 Sprague–Dawley rat. Note dense cellularity of cortex and distinct medullary regions. H&E stain, ×50. (E) Thymus from aged male Wistar rat. Note clusters of epithelial cells and absence of distinct cortical and medullary areas. H&E stain, ×50.

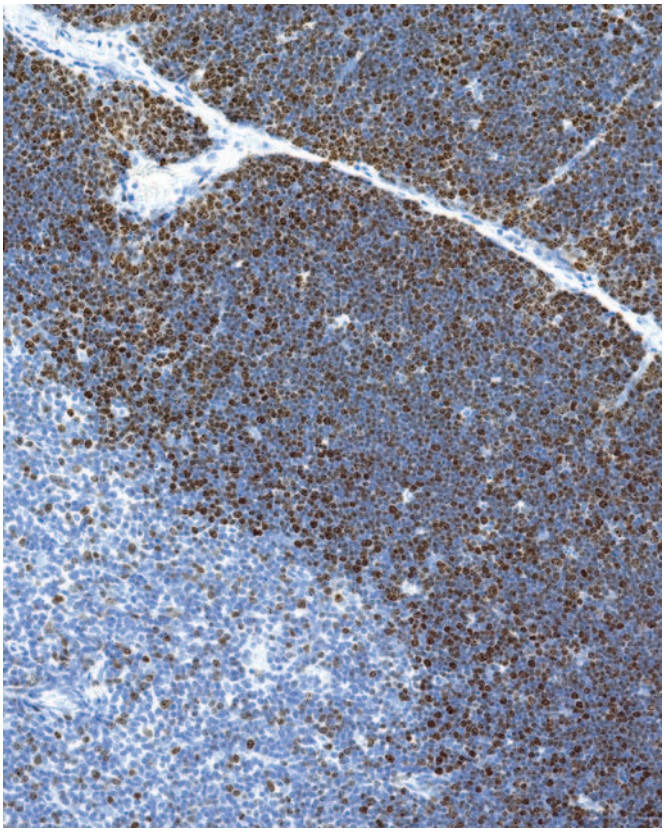

FIGURE 12.6 Sprague–Dawley rat, postnatal day (PND) 42. Thymus is stained by immunohistochemistry for Ki67 proliferation marker, using diaminobenzidine (DAB) chromagen, counterstained by hematoxylin. Note pronounced population of brownstained proliferating cells in cortex. ×200.

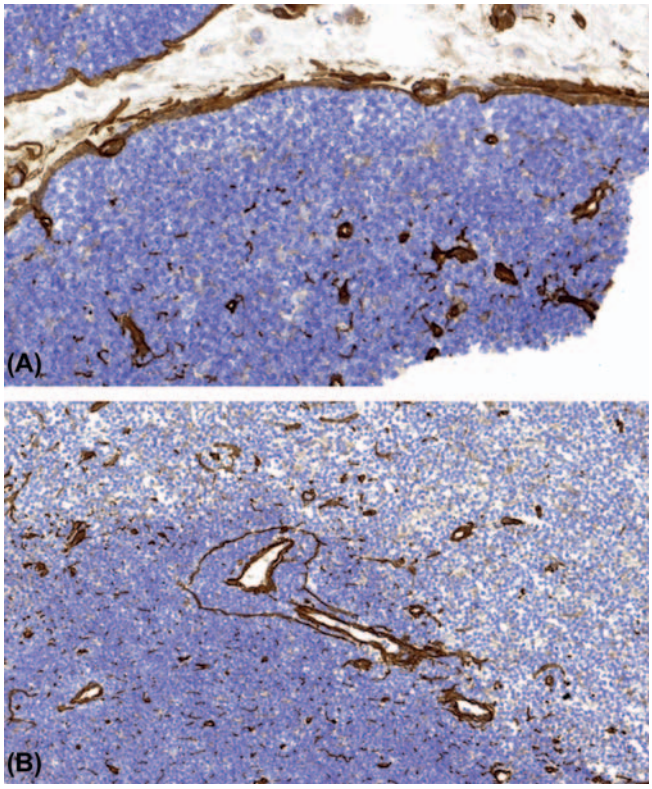

FIGURE 12.7 Laminin staining (brown color; DAB chromagen, counterstain hematoxylin) of thymus. (A) Epithelium-free area-intrathymic region that is mostly subcapsular, free of thymic epithelium, and filled with double-positive, immature thymocytes. The area is only distinguishable from the surrounding thymic cortex by a higher density of thymocytes and because it lacks a capsule/laminin-positive layer. *Epithelium-free area. (B) Perivascular space—extrathymic region that is filled with lymphocytes with a peripheral, mature phenotype, concentrated at the border of the cortex and the medulla (corticomedullary zone), and surrounded by a laminin-positive layer.

of lymphocyte migration from blood into the lymph node (Figure 12.13). HEVs serve as a storage pool for lymphocytes entering the lymph node, and in pigs HEVs may also be exit sites for lymphocytes. Lymphocytic migration from blood into stimulated lymph nodes can increase lymphocyte exiting 10-fold over that seen with nonstimulated lymph nodes. The increase in lymph node cellularity due to local lymphocytic proliferation and "lymphocyte trapping" from the blood results in the "reactive" lymph nodes that are commonly seen in association with inflammatory lesions.

Lymph nodes have a filtering function, and provide a matrix that allows the immune system to interrogate and, when appropriate, respond to incoming pathogens and antigenic epitopes. Lymph nodes and other secondary lymphoid organs as, for example, the inner PALS of the spleen have a specific population of (myo) fibroblastic reticular cells that limit the circulating lymphocyte population by controlling the production of lymphocyte survival factors such as IL-7. The chain of events that results in lymph node stimulation and expansion of specific T-cell populations is initiated by DCs. Upon stimulation by antigen, the B-lymphocytes undergo clonal expansion, forming a secondary follicle with a germinal center (GC). Selective processes result in apoptosis of a large percentage of the proliferating cells. Surviving antigen-specific cells form memory B-cells and plasma cells. Plasma cell precursors migrate to medullary cords, where they produce (predominantly IgM) antibody that is secreted into the efferent lymph (Figure 12.14). Of note, plasma cells producing high-affinity antibodies elocate to the bone marrow.

Mucosa-Associated Lymphoid Tissue

Organized lymphoid tissues are found in the mucosae of the gastrointestinal, respiratory, and urogenital tracts as well as the conjunctiva; they are referred to as MALT (Figure 12.15). MALT in the oronasal region in

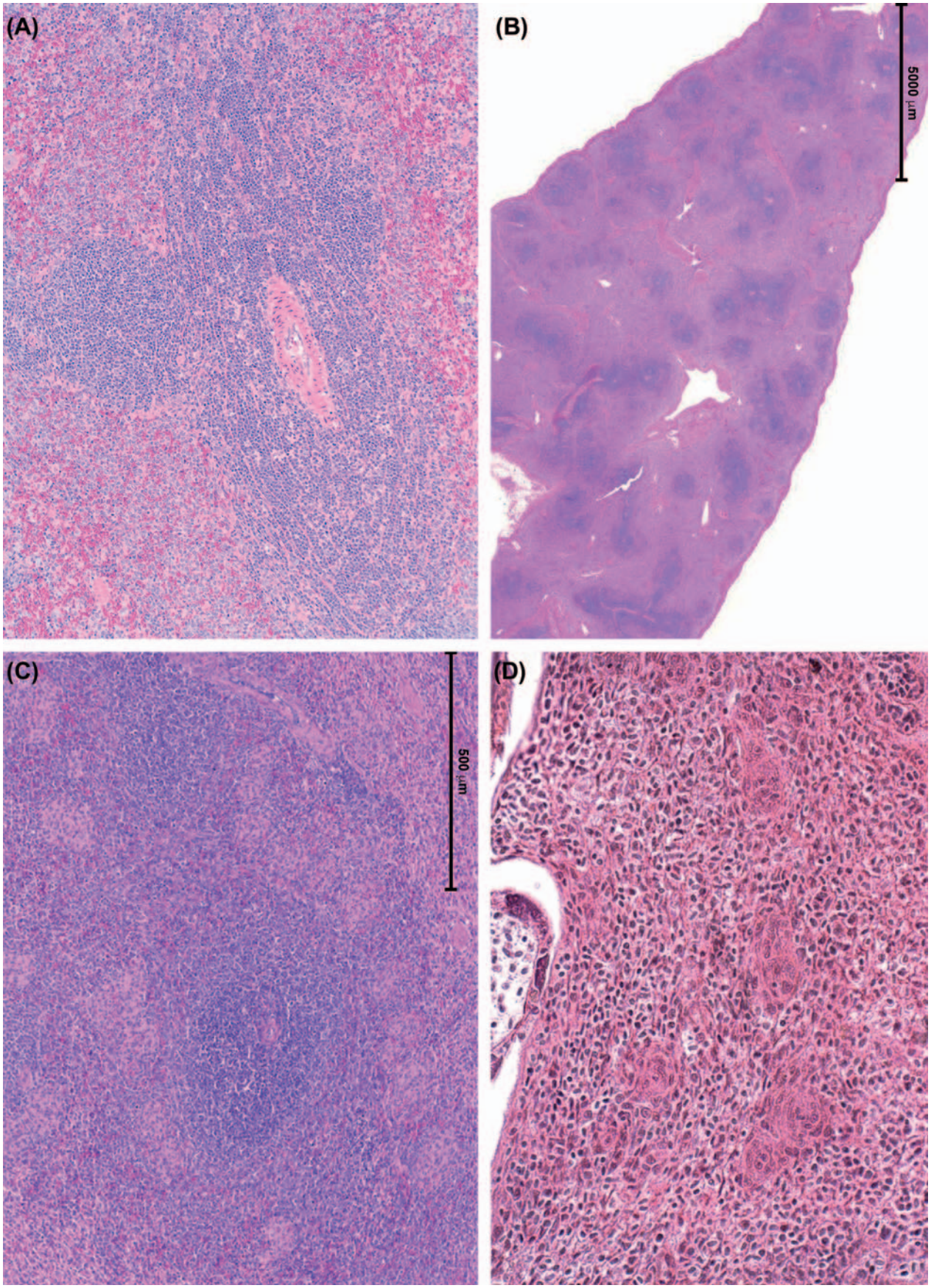

FIGURE 12.8 (A) Spleen rat, with the densely populated PALS oriented around an arteriole at the center of the image and surrounded by the paler marginal zone. (B) Overview of spleen of minipig showing the numerous basophilic PALS with (C) detail to show "ellipsoids," which are pericapillary macrophage sheaths and which are especially abundant in the marginal zone between the basophilic PALS and the red pulp containing brightly eosinophilic erythrocytes. The capillaries of the ellipsoids continue as terminal arterial capillaries. The ellipsoids are visible as pale-staining macrophage clusters (D). Source*: From Haschek, W.M., Rousseaux, C.G., Wallig, M.A. (Eds.), 2013. Haschek and Rousseaux's Handbook of Toxicologic Pathology, third ed. Academic Press (Elsevier), San Diego, CA, Figure 49.8, p. 1806, with permission.*

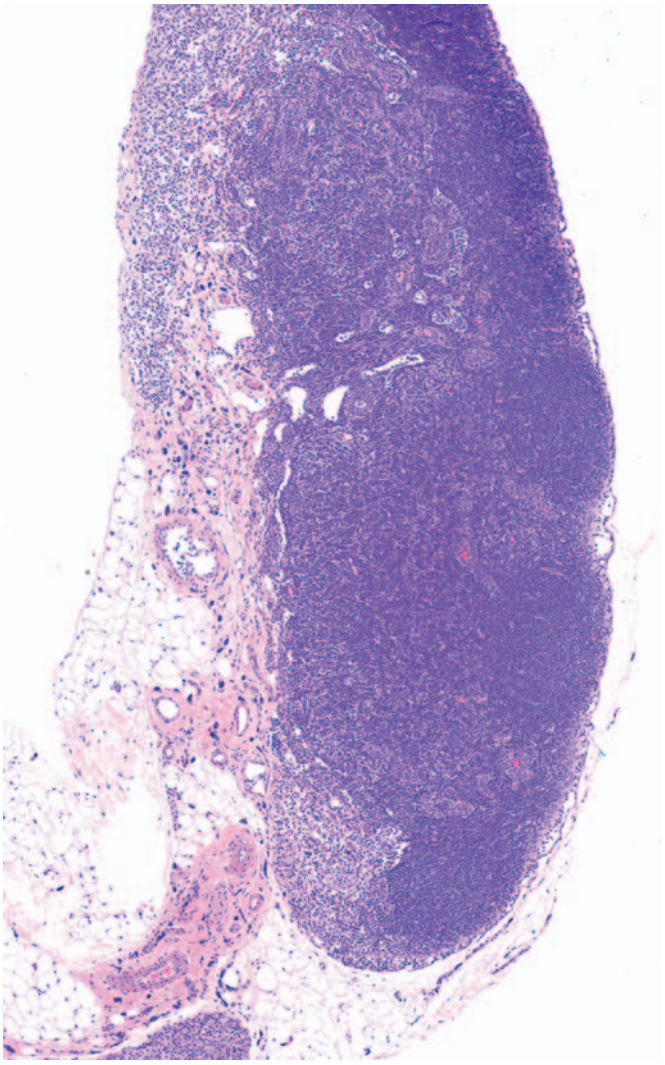

FIGURE 12.9 Mesenteric lymph node from 10-week-old Sprague–Dawley rat. Lymph nodes are composed of a variable number of contiguous lymphoid lobules, each of which consists of a cortex, paracortex, and medulla. Here prominent cortical follicles and paracortex are shown. H&E stain, ×50. Source: *From Haschek, W.M., Rousseaux, C.G., Wallig, M.A. (Eds.), 2013. Haschek and Rousseaux's Handbook of Toxicologic Pathology, third ed. Academic Press (Elsevier), San Diego, CA, Figure 49.10, p. 1810, with permission.*

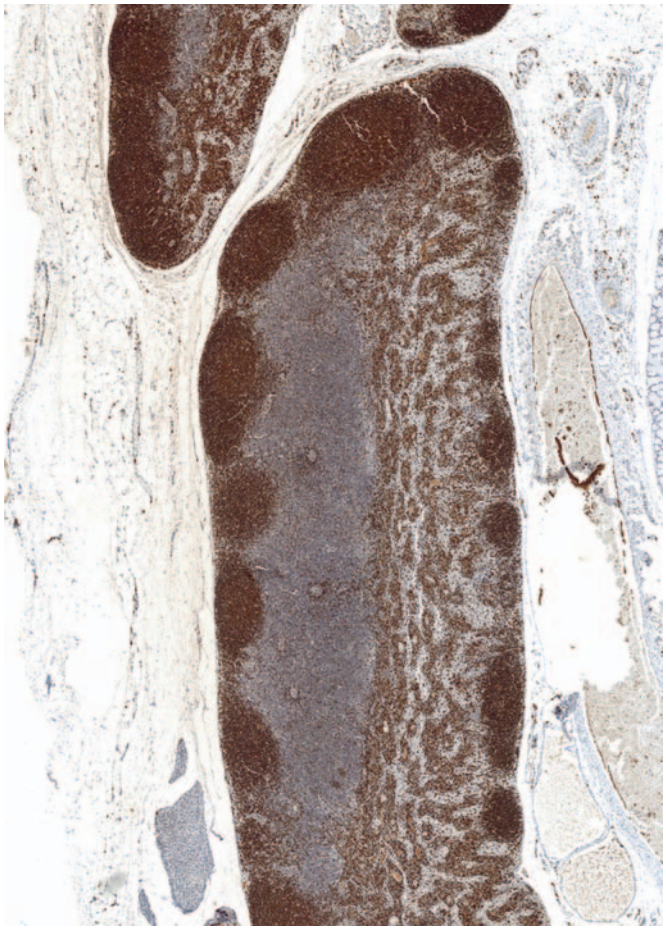

FIGURE 12.10 Mandibular lymph node from PND42 Sprague–Dawley rat. The superficial cortex is a predominantly B-cell zone that consists of primary lymphoid follicles, macrophages, follicular DCs, and diffuse interfollicular cortex. Dark brown cortical follicles indicate a predominance of B-cells. Immunohistochemical staining for CD45RA, a B-cell marker, with DAB chromagen, counterstained by hematoxylin. ×25. Source: *From Haschek, W.M., Rousseaux, C.G., Wallig, M.A. (Eds.), 2013. Haschek and Rousseaux's Handbook of Toxicologic Pathology, third ed. Academic Press (Elsevier), San Diego, CA, Figure 49.11, p. 1811, with permission.*

man, domestic animals, and minipig is quite extensive (Waldeyer's ring); the larger lymphoid nodules in the pharyngeal region are called tonsils and represent lympho-epithelial organs. In the mouse and rat it is limited to nasopharynx-associated lymphoid tissue (NALT) (Figure 12.16). In addition, larynx-associated (LALT), bronchus-associated (BALT), and gut-associated (GALT) lymphoid tissues are observed in rat. In other species, like mice and humans, BALT is present when stimulated or induced (iBALT). Peyer's patches (PP, small intestinal GALT) and tonsils in primates and dogs often feature prominent follicles with GCs. Numerous single T-lymphocytes are disseminated in the covering epithelium (intraepithelial lymphocytes) and lamina propria (lamina propria lymphocytes or LPL) of the gastrointestinal tract; in fact, these lymphocytes form the body's largest single T-lymphocyte pool.

The epithelial surfaces of the body form the major route of entry for antigens. Upon antigen contact an immune response is generated in MALT, which is passed on to the draining lymph nodes, such as the mesenteric lymph nodes of the gastrointestinal tract. Nonspecific lymphocyte-like killer cells in the

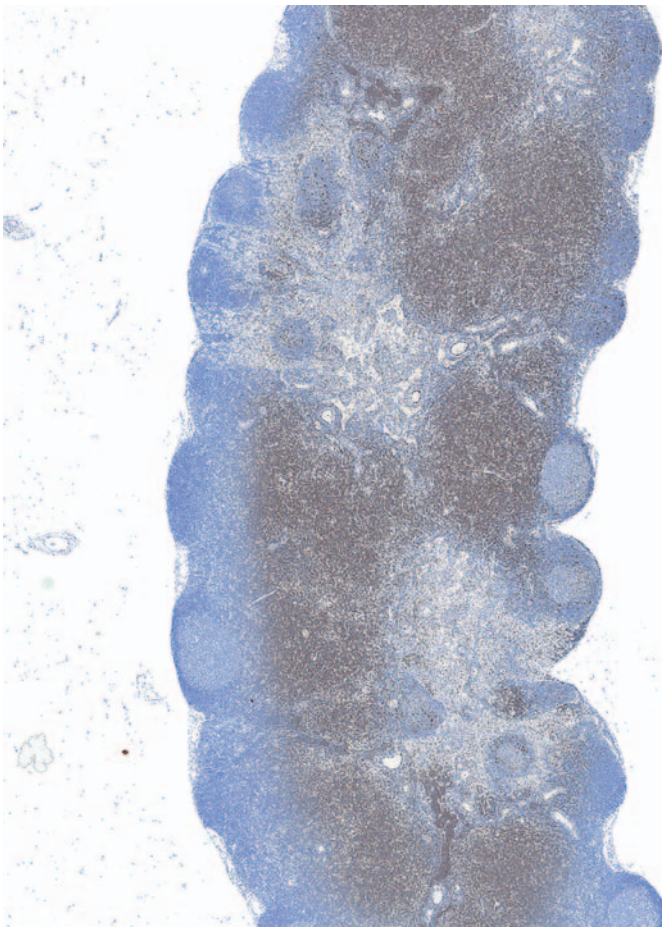

FIGURE 12.11 Mesenteric lymph node from PND42 Sprague–Dawley rat shows CD3-positive staining in the paracortical region. The paracortex consists of a single deep cortical unit (DCU) that is populated by mostly T-cells and interdigitating DCs. Immunohistochemical staining for CD3 with DAB chromagen, counterstained by hematoxylin. ×25. Source: *From Haschek, W.M., Rousseaux, C.G., Wallig, M.A. (Eds.), 2013. Haschek and Rousseaux's Handbook of Toxicologic Pathology, third ed. Academic Press (Elsevier), San Diego, CA, Figure 49.13, p. 1812, with permission.*

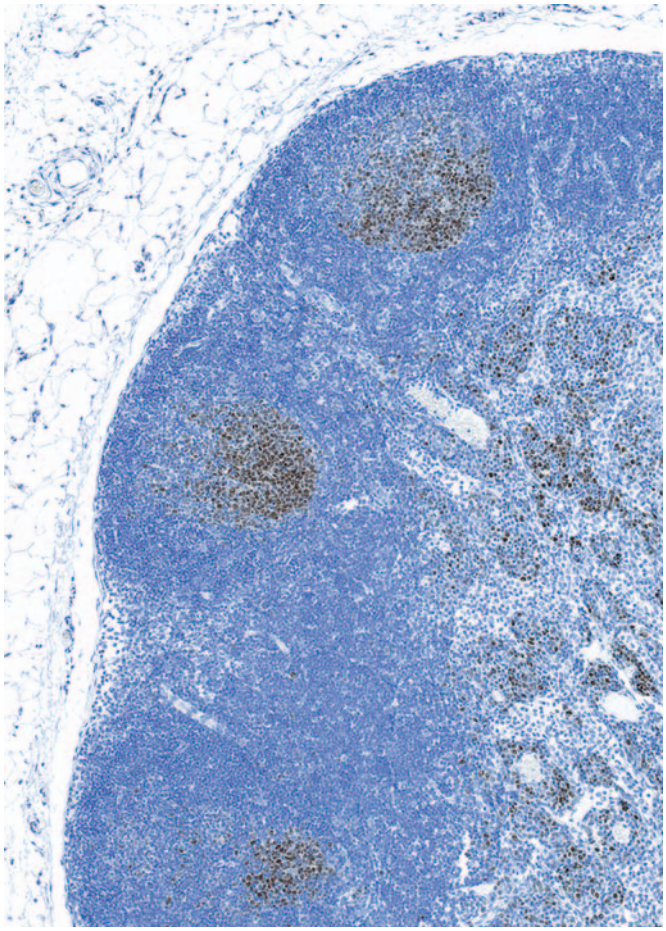

FIGURE 12.12 Mandibular lymph node from PND42 Sprague–Dawley rat. Following antigenic stimulation, the primary follicles enlarge to form secondary follicles containing GCs. Intense proliferative activity (dark brown staining) is seen in the deep aspect of follicular GCs. Immunohistochemical staining for Ki67 proliferation marker with DAB chromagen, counterstained by hematoxylin. ×100. Source: *From Haschek, W.M., Rousseaux, C.G., Wallig, M.A. (Eds.), 2013. Haschek and Rousseaux's Handbook of Toxicologic Pathology, third ed. Academic Press (Elsevier), San Diego, CA, Figure 49.12, p. 1811, with permission.*

epithelium have been found to kill pathogens, presumably without prior sensitization. In mice, these cells have been characterized as T-cells with a specific receptor, T cell receptor (TCR)gd, which, in contrast to TCRab Tc cells, kill targets in an MHC nonrestricted manner. They may serve also as initiators of TCRab T-mediated responses.

The immune response in MALT differs from that at other sites of the body, being especially devoted to the generation of an (secretory) IgA-antibody response. The main function of secretory IgA is to prevent the entry of potentially pathogenic substances into the body, a specific antigen exclusion function whereby the epithelium is coated with "antiseptic paint" that prevents binding and uptake.

Tertiary Lymphoid Tissue

Tertiary lymphoid structures are ectopic-organized lymphoid structures that typically consist of follicles often with active GCs and surrounded by T-cell aggregates with HEVs. The microarchitecture of the GCs resembles that of GCs in lymph nodes and spleen (Figures 12.1C and 12.12). Like MALT, tertiary lymphoid structures are not supplied by afferent lymph vessels and are not encapsulated, indicating that they are directly exposed to antigens from the surrounding environment. Tertiary lymphoid tissues can form at any time and lack site specificity (Figure 12.17).

Tertiary lymphoid structures are the result of lymphoid neogenesis in the course of chronic

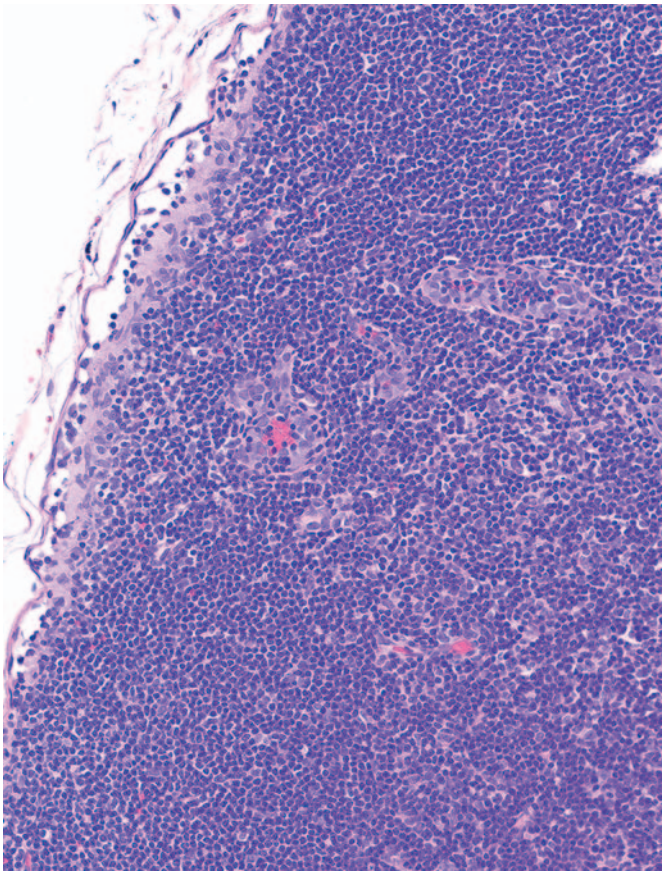

FIGURE 12.13 Mesenteric lymph node of female Sprague–Dawley rat (age 10 weeks) showing prominent HEVs within highly cellular paracortex. H&E stain, ×200. Source: *From Haschek, W.M., Rousseaux, C.G., Wallig, M.A. (Eds.), 2013. Haschek and Rousseaux's Handbook of Toxicologic Pathology, third ed. Academic Press (Elsevier), San Diego, CA, Figure 49.14, p. 1812, with permission.*

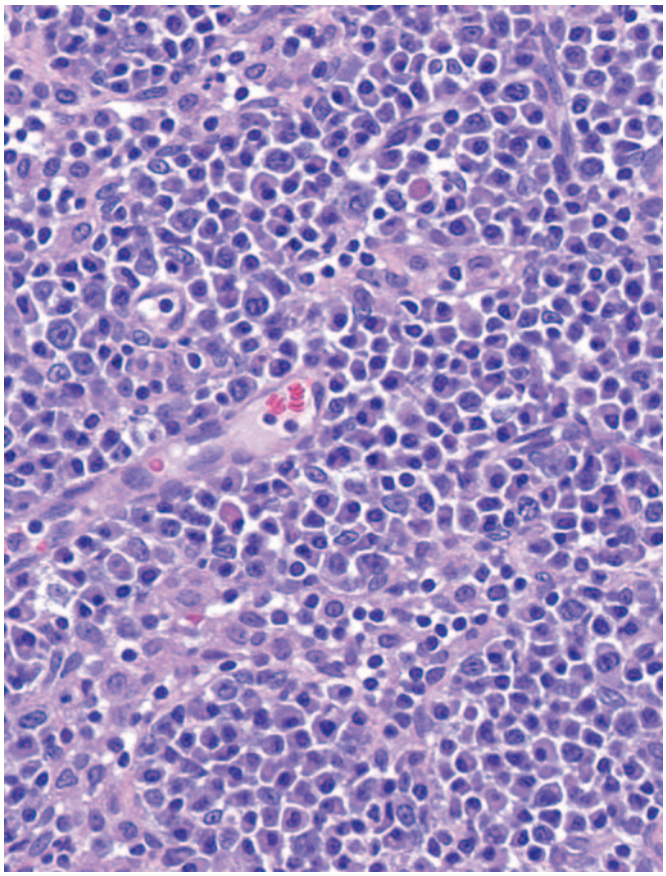

FIGURE 12.14 Mandibular lymph node from PND42 Sprague–Dawley rat showing medullary cords that contain large numbers of plasma cells with occasional eosinophilic Mott cells. Plasma cell precursors migrate to medullary cords where they produce antibody that is secreted into the efferent lymph. H&E, ×400. Source: *From Haschek, W.M., Rousseaux, C.G., Wallig, M.A. (Eds.), 2013. Haschek and Rousseaux's Handbook of Toxicologic Pathology, third ed. Academic Press (Elsevier), San Diego, CA, Figure 49.16, p. 1814, with permission.*

inflammation. Many of the same signaling pathways that are involved in inflammation, for example, the tumor necrosis facto-α family of cytokines and receptors, are involved in the organogenesis of lymph nodes, spleen, and MALT. As with the formation of lymph nodes, formation of tertiary lymphoid tissues involves collaboration between lymphoid tissue initiator cells of bone marrow origin and lymphoid tissue organizer cells that are derived from adipocyte precursors. Once formed, further cytokines and chemokines are produced along with antibodies directed against specific antigens in the inflamed tissue. In some cases the selection process in the GCs is disturbed and negative selection does not function properly (as evidenced by a low number of apoptotic bodies in the basal light zone; Figure 12.1C). This has the potential to lead to the generation of detrimental antibody responses, including unwanted responses against self-antigens. Tertiary lymphoid structures can keep a chronic infection in check, but in autoimmunity they can exacerbate deleterious inflammatory changes.

Omental Adipose Tissue

The omentum connects visceral organs like the spleen and the stomach. It is enriched in macrophages, B and T-lymphocytes, DCs, and natural killer (NK) cells. At certain locations, the leukocytes are organized into clusters (milky spots). Omental milky spots collect fluids, particulates, bacteria, and cells from the peritoneal cavity and can induce an immune response or support immune suppression. The

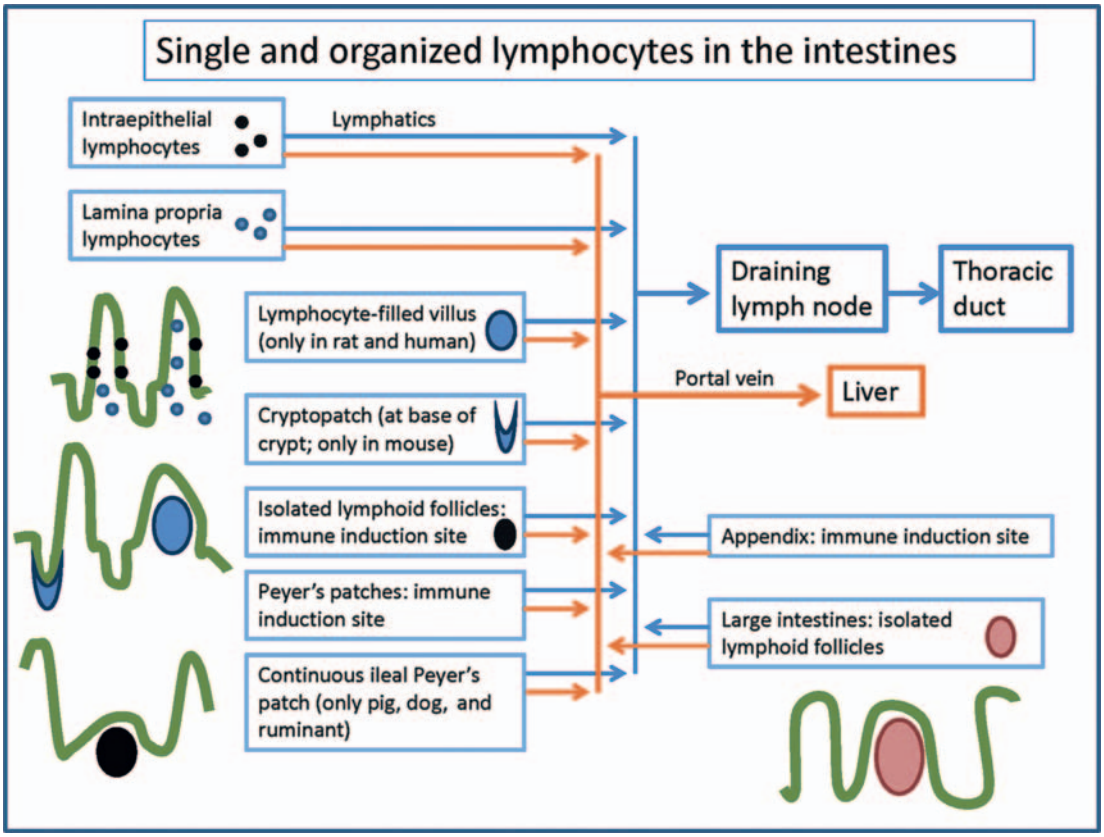

FIGURE 12.15 Scheme of MALT tissues in the gastrointestinal tract, after Brandtzaeg and Pabst (2004).

omentum helps to restore tissue integrity in the peritoneum by connecting tissue repair with immunological defense. Upon intraperitoneal immunization, follicles and GCs can be formed.

Liver (See Also Chapter 8: Liver and Gall Bladder)

The liver contains a substantial population of immunologically active cells, including T- and B-lymphocytes, KCs, liver-adapted NK-cells (pit cells), NKT cells, stellate cells, and DCs. Hepatic T-cells are phenotypically different from T-cells in blood, lymph nodes, or spleen. There may be a concentrated population of highly active KCs in the region of the lobule that is the first point of contact for incoming, potentially pathogenic microorganisms. A liver-specific population of NK-cells, also known as pit cells, comprises intrasinusoidal cells that are defined morphologically as large granular lymphocytes (LGLs) and functionally as liver-associated NK-cells. Pit cells are located inside sinusoidal lumina, where they adhere to endothelial cells and KCs. Pit cells and KCs have a symbiotic relationship, with each cell producing cytokines that potentiate the effects of the other cell. Hepatic stellate cells ("Ito cells" or "perisinusoidal fat-storing cells") were first described by Kupffer in 1876, and have historically been known for their ability to store lipoid materials, including vitamin A. Activated stellate cells produce mononuclear cell and neutrophil chemoattractants, complement protein C4, and a plethora of chemokine and immunomodulatory molecules that participate in both innate and acquired immune functions.

The liver is the primary hematopoietic organ during the fetal stage (Figure 12.18). Hematopoiesis undergoes constant reduction in rats until PND 21 (Figures 12.19 and 12.20) but can be reactivated in case of demand even during adult life. The postnatal liver retains immunologically important functions. Major hepatic contributions to innate and adaptive immunity are summarized in Table 12.4.

Developmental and Aging Changes

Developmental Changes

The immune system of rodents develops from a population of pluripotential hematopoietic stem cells

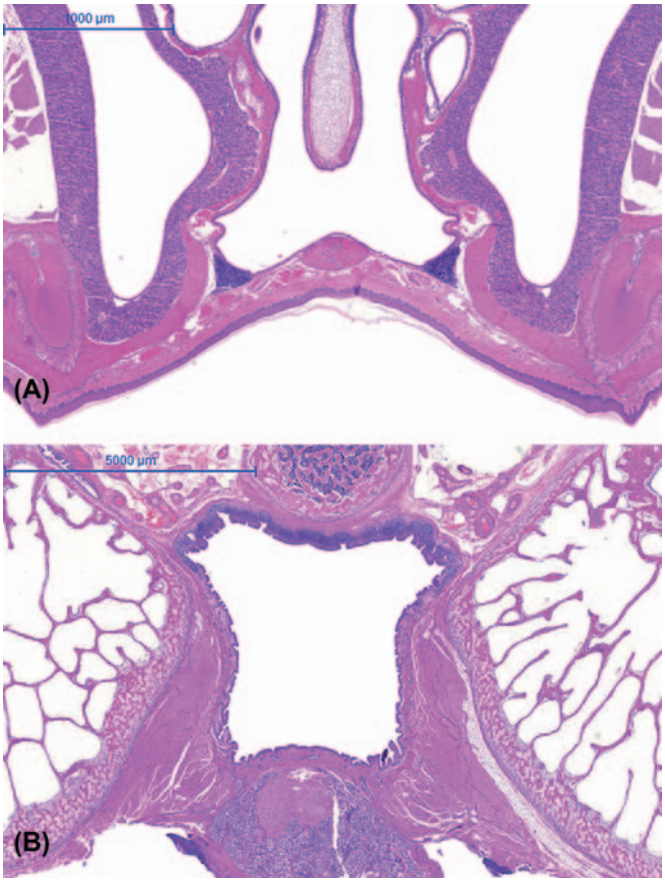

FIGURE 12.16 NALT of (A) rat and (B) minipig. NALT in rat is a paired organ, located at the base of the nasopharynx; in the minipig NALT is a single organ (as in man) at the roof of the nasopharynx. H&E stain. *Source: From Haschek, W.M., Rousseaux, C.G., Wallig, M.A. (Eds.), 2013. Haschek and Rousseaux's Handbook of Toxicologic Pathology, third ed. Academic Press (Elsevier), San Diego, CA, Figure 49.18, p. 1816, with permission.*

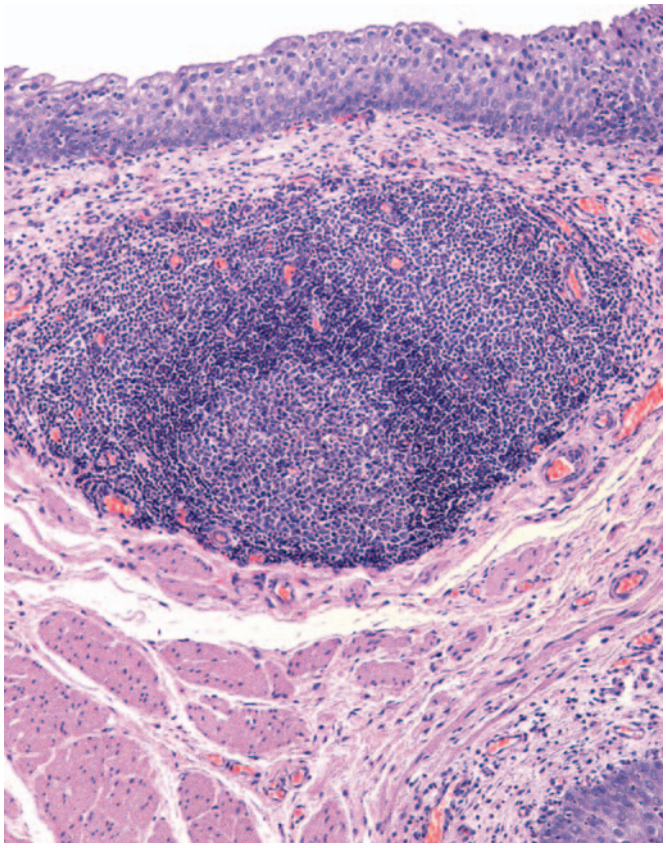

FIGURE 12.17 Tertiary lymphoid tissue in the urinary bladder mucosa of a dog with chronic inflammation. The mucosa of the lower urinary tract is prone to the development of lymph follicles during ascending chronic inflammation. In this case, a diffuse infiltrate is present in the transitional epithelium, and organized lymphoid tissue resembling a secondary follicle with GC formation is present in the propria mucosae. H&E stain, ×10. Source*: From Haschek, W.M., Rousseaux, C.G., Wallig, M.A. (Eds.), 2013. Haschek and Rousseaux's Handbook of Toxicologic Pathology, third ed. Academic Press (Elsevier), San Diego, CA, Figure 49.19, p. 1816, with permission.*

(HSCs) generated early in gestation from uncommitted mesenchymal stem cells in the intraembryonic splanchnoplure surrounding the heart. HSCs give rise to all circulating bone marrow cell lineages, including cells of the innate and adaptive immune system. Definitive hemopoietic progenitors have been shown to emerge in the aorta–gonad–mesonephros region before the fetal liver develops. Methodological and interspecies/strain differences, however, lead to a certain variation in the reported time points of pre- and postnatal development of immune organs and functions. Nevertheless, subsequent stages of development of the immune organs follow a chronological sequence, which is highly similar in laboratory species and man (Table 12.5).

Aging changes

Aging leads to a progressive reduction in weight and size of the thymus (Table 12.9), the delineation between thymus cortex and medulla becomes indistinct, proliferative areas in the outer cortex vanish, and the lymphocyte population is replaced by univacuolar adipocytes. Remnants of thymic tissue can still be detected in old animals. Secondary lymphoid organs do not undergo related involution but a functional shift from naïve to memory T-cells takes place. The altered functional status of secondary lymphoid organs is accompanied by histologic changes that are less spectacular than age-related thymic involution, but nevertheless important in histopathological evaluation of immune system organs. The bone marrow

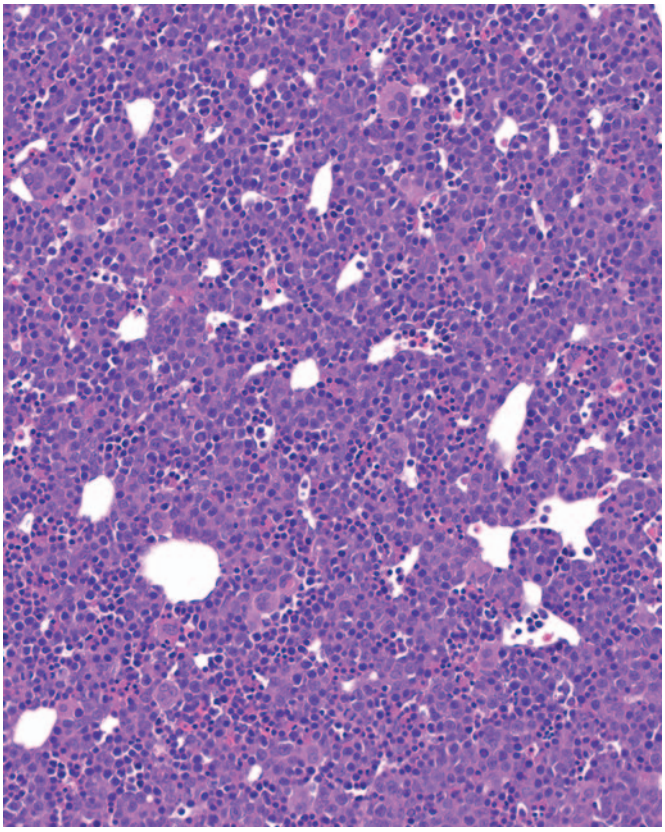

FIGURE 12.18 Liver from gestation day (GD) 15, Sprague–Dawley rat. Note diffuse hematopoietic activity. H&E stain, ×200. Source: *From Haschek, W.M., Rousseaux, C.G., Wallig, M.A. (Eds.), 2013. Haschek and Rousseaux's Handbook of Toxicologic Pathology, third ed. Academic Press (Elsevier), San Diego, CA, Figure 49.20, p. 1817, with permission.*

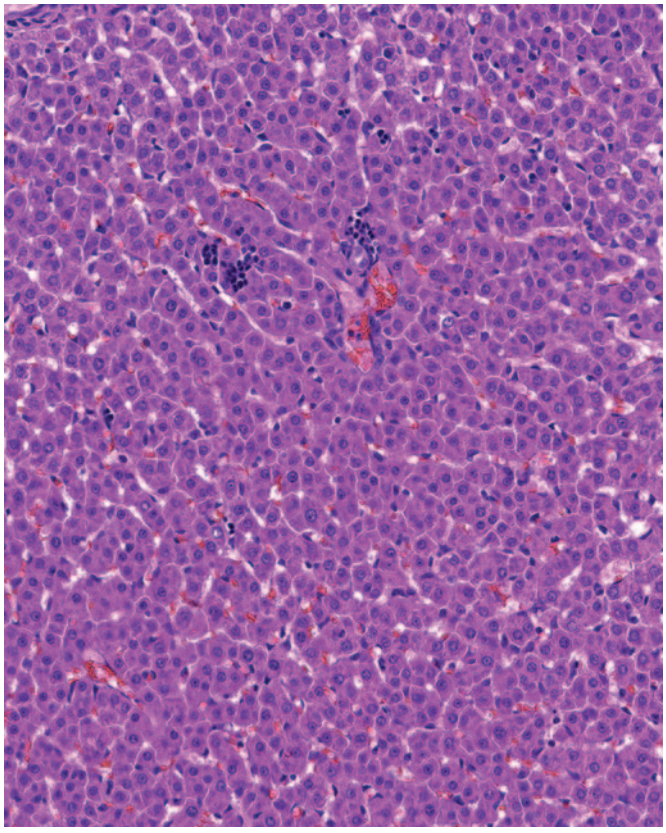

FIGURE 12.19 Liver from Sprague–Dawley rat on day of birth (PND0). The hematopoietic activity is diminished, when compared to the liver at GD15 (see Figure 49.18 of Haschek et al. 2013). H&E stain, ×200. Source: *From Haschek, W.M., Rousseaux, C.G., Wallig, M.A. (Eds.), 2013. Haschek and Rousseaux's Handbook of Toxicologic Pathology, third ed. Academic Press (Elsevier), San Diego, CA, Figure 49.22, p. 1821, with permission.*

gradually releases increased numbers of myeloid cells at the expense of B-lymphocytes. In mice, it has been shown that total numbers of peripheral B-cells remain constant, related to the increased lifespan of B-cells and the expansion of existent antigen-experienced cell populations, in particular of CD5+ B1 cells. Immunosenescence leads to production of antibodies with low affinity and polyspecificity, as well as to increased autoantibodies, resulting in a proinflammatory status (inflammaging), which contributes to the pathogenesis of various diseases such as atherosclerosis, diabetes, and Alzheimer's disease. Spontaneous inflammatory lesions of old animals may thus be triggered by age-related changes of B-cell subpopulations. It should also be noted that B-cell lymphoid follicles are frequently encountered in the thymic medulla of healthy beagle dogs and older rats without any evidence of a pathological background. Lymphoid nodules are also seen with some frequency in the bone marrow of cynomolgus monkeys (*Macaca fascicularis*). Figure 12.5 illustrates the profound age-related changes of rat thymus from fetal life to old age.

MECHANISMS AND EVALUATION OF TOXICITY

Mechanisms of Toxicity

The primary aim of the immune system is to recognize exogenous agents; therefore, it interacts with many compounds in an antigen-specific fashion.

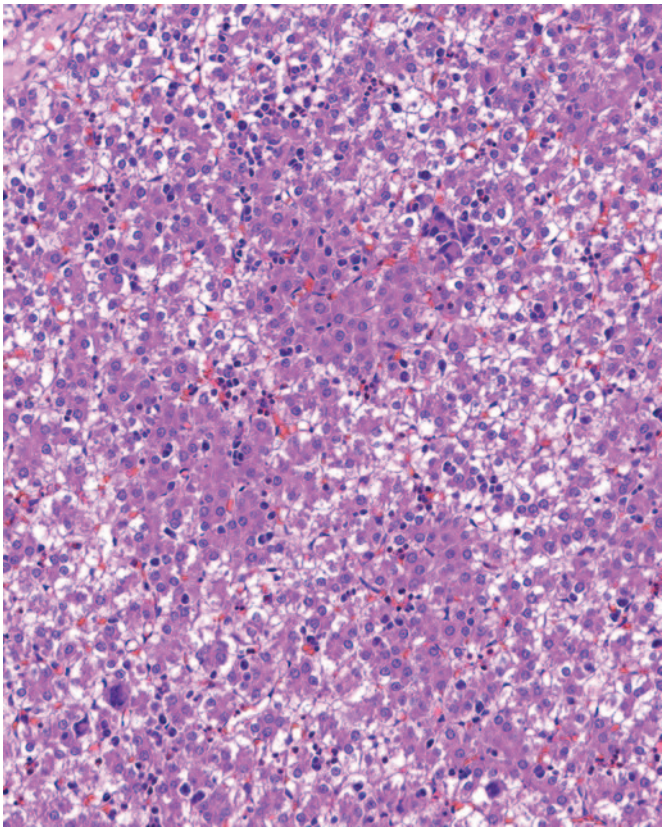

FIGURE 12.20 Liver from Sprague–Dawley rat on PND10. Note multifocal low-level hematopoietic activity. The liver becomes progressively less prominent as hematopoietic organ through PND10. Note increased fat content of the liver before weaning. H&E stain, ×200. Source: *From Haschek, W.M., Rousseaux, C.G., Wallig, M.A. (Eds.), 2013. Haschek and Rousseaux's Handbook of Toxicologic Pathology, third ed. Academic Press (Elsevier), San Diego, CA, Figure 49.23, p. 1822, with permission.*

TABLE 12.4 Immune Roles of the Liver

INNATE (NONSPECIFIC) IMMUNITY INVOLVEMENT
Production of acute phase proteins
Nonspecific phagocytosis
Nonspecific cell killing
Disposal of waste molecules of inflammation and nonspecific immunity
Nonspecific immunoregulation
ADAPTIVE (SPECIFIC OR ACQUIRED) IMMUNITY INVOLVEMENT
Deletion of activated T-cells
Induction of tolerance to ingested and self-antigens
Extrathymic proliferation of T-cells
Disposal of waste molecules of specific immunity
Specific immunoregulation

From Haschek, W.M., Rousseaux, C.G., Wallig, M.A. (Eds.), 2013. Haschek and Rousseaux's Handbook of Toxicologic Pathology, third ed. Academic Press (Elsevier), San Diego, CA, Table 49.4, p. 1818, with permission.

Usually, immune responses to exogenous agents are beneficial to the host. Undesired, exaggerated responses are allergies/hypersensitivities and autoimmune diseases (antigen-specific toxicity). Compounds also can affect the immune system in an antigen-nonspecific fashion either via direct toxicity to components of the immune system, which can lead to malfunctioning of the system, or by indirect toxicity, namely via other organ systems, especially the nervous and endocrine systems. Compound-specific allergy, autoimmunity, and nonspecific toxicity often are set wide apart (Table 12.6). Yet compound-specific allergy and autoimmunity can result in malfunctioning of the immune system, which in turn can lead to exaggerated responses to nonrelated substances (Figure 12.21). Examples of immune-modulating compounds are presented in Table 12.7.

Antigen-Specific Toxicity

Adverse-specific responses of the immune system to compounds are consequences of inadvertent sensitization. The classification system of Gell and Coombs distinguishes four types of hypersensitivity, although in practice the distinction is often less strict than suggested. New classifications are suggested because drug allergies do not easily fit into one of the three categories; these are (1) pseudoallergic reactions, (2) primarily antibody-mediated reactions, and (3) cell-mediated reactions.

Nonantigen-Specific Direct Toxicity

The dynamic and complex nature of the immune system renders it vulnerable to toxic compounds, in particular the "passenger" cells (lymphocytes, macrophages, DCs of bone marrow and thymus). The framework constituents of the lymphoid organs, on the other hand, appear relatively resistant to toxic substances. Immature T-cells (thymocytes) are quite susceptible, due to their fragile composition and to their development, which involves gene amplification, transcription, and translation. The disappearance of lymphoid cells from blood and tissue is often the first sign of this type of toxicity. The stromal framework constituents may respond to this disappearance by degeneration, ending in atrophy and fibrosis. It should be kept in mind that suppression of one immune cell type can result in overall immune

TABLE 12.5 Time Sequence of Immune Organ Development in Rodents and Human

Development phase	Rat/mouse	Human
Critical window of HSC formation	GD 7 to 11	GW 5
Critical window of cell migration to liver and thymus—liver as predominant hematopoietic organ—precursor T-cells in thymis	GD 10 to 16—start GD 12—start GD 9 to 10	GW 5 to 7—start GW 5—start GW 7
Sequential development of lymph nodes	GD 9 to 17	GW 15 to 38
Formation of bone marrow vascular mesenchyme	Start GD 15 to 18	Start GW 20
Critical window of colonization of thymus and bone marrow	GD 11 to 16	GW 16
Differentiation of thymic cortical and medullary epithelia	GD 15	GW 16
IgM-expression by hepatic B-lymphocytes	Start GD 16 to 17	Start GW 10 to 12
Formation of PP	GD 17	GW 11
Thymus: morphological distinction of cortex and medulla	GD 20	GW 16
Demarcation of splenic architecture (red and white pulp)	PND 6	GW 26
Compartments in lymph nodes discernible	PND 3	Until GW 38
Development of NALT	PNW 1 to 2	At birth
Critical window of developed immunoreactivity—occurrence of GCs in follicles	Postnatal—PND 21 to 28	Prenatal—GD 270
Critical window of establishment of immune memory	PND 30 to 60	PNY 1 to 13

GD, gestational day; GW, gestational week; PND, postnatal day; PNW, postnatal week; PNY, postnatal year.

TABLE 12.6 Deranged Immune Reactions, Immunity, and Toxicity

Condition	Mechanism	Antigen source	Result
Allergy/hypersensitivity	Immunologic	Foreign	Disease
Autoimmunity	Immunologic	Self (altered)	Normal: homeostasis and regulation of immunity Deranged: disease
Immunity	Immunologic	Foreign	Prophylaxis
Nonimmune toxicity	Toxic	Not applicable	Adverse changes/disease

From Haschek, W.M., Rousseaux, C.G., Wallig, M.A. (Eds.), 2013. Haschek and Rousseaux's Handbook of Toxicologic Pathology, third ed. Academic Press (Elsevier), San Diego, CA, Table 49.5, p. 1822, with permission.

enhancement—for instance, when T suppressor cells are affected and immune responses are subsequently not properly checked or regulated. The immune cells can be stimulated as well—for instance, by compounds that act as adjuvants (nonspecific enhancers of the immune system). Adjuvants are often used in vaccines to help generate a protective immune response. The immune system has a great regenerative capacity, and it occurs in a relatively short time: depleted lymphocyte populations can be restored within weeks. Regeneration following destruction of the white blood cell system does not occur when stem cells in the bone marrow are affected—for example, after sublethal irradiation.

Indirect Toxicity

Compounds can have an effect on the immune system via effects on other organ systems—for instance, via induction of acute phase proteins like C-reactive protein and transforming growth factor beta as a result of liver injury. The immune system is especially sensitive to imbalances in the endocrine and neural systems, because these three systems are so closely intertwined with each other. This is exemplified by the profound influence of sex and stress hormones on immune reactivity. Autoimmune diseases like systemic lupus erythematosus (SLE) and rheumatoid arthritis of humans are linked to sex steroid hormone

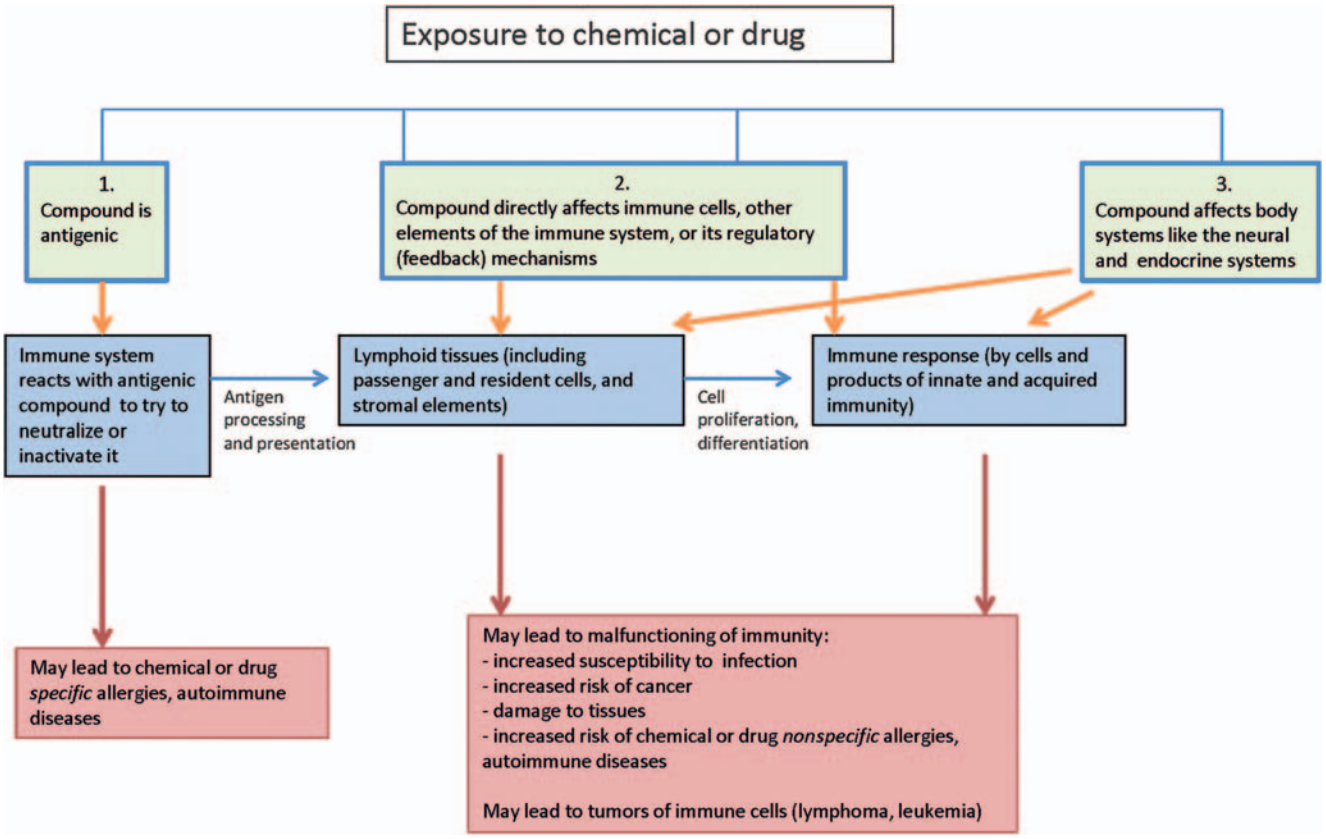

FIGURE 12.21 Mechanisms of immune system toxicity. Source: *From Haschek, W.M., Rousseaux, C.G., Wallig, M.A. (Eds.), 2013. Haschek and Rousseaux's Handbook of Toxicologic Pathology, third ed. Academic Press (Elsevier), San Diego, CA, Figure 49.24, p. 1823, with permission.*

balance. They occur more frequently in females, and the course of the disease may be exacerbated when the sex hormone ratio shifts toward a higher estrogen to androgen ratio.

Animal models of autoimmune disease, such as (NZB-NZW)F1, B/W, and MLR/lpr mice, have provided further evidence for this sex (hormone)-dependent intrinsic disturbance of the immune system. This autoimmunity mainly concerns (auto) antibody formation, since cell-mediated effector immune reactions can be depressed in females or in males with enhanced estrogen levels. Estrogen receptors are present in the thymus, both on thymocytes and epithelial cells; thymocytes also have androgen receptors. Glucocorticosteroid hormones have a pivotal position in the homeostasis of the immune system and their increased synthesis often leads to suppression of the immune system with lymphopenia (see "Stress" section, later in this text, for a description of the histology). The toxicologic pathologist should be aware of stress-associated thymic involution in rodents and other species in order to correctly interpret the effects of xenobiotics in short-term high-dosage toxicity studies.

Immune Derangements and Neoplasia

The risk of lymphoma is significantly increased in congenital or acquired immunodeficiency and certain autoimmune diseases, in particular collagen vascular diseases. The relationship with immunodeficiency is based on the "immune surveillance" theory that assumes a continuous guarding function for the immune system against, and elimination of, potentially neoplastic cells in the body. However, the association between neoplasia and immunodeficiency cannot be explained solely by reduced immune surveillance. Some viruses may act as neoplastic agents, and a defective host resistance facilitates the oncogenic potential of viruses. Epstein–Barr virus of humans is a well-known example, producing polyclonal B-lymphocyte activation that shifts from polyclonal into oligoclonal and monoclonal B-cell malignancies. Cytomegalovirus can also manifest oncogenic potential in such situations. Finally, a shared pathway of expression (e.g., DNA repair mechanisms in human ataxia telangiectasia) may underlie both, immunodeficiency and cancer, without necessarily a causative relation between the two phenomena.

TABLE 12.7 Examples of Compounds and Agents That Can Affect the Immune System

Compounds and other agents	Experimental data	Biomarkers
1. COMPOUND-SPECIFIC ALLERGY/HYPERSENSITIVITY/AUTOIMMUNE DISEASE		
Heavy metals	Nickel ions: contact dermatitis; mercury chloride: glomerulonephritis in Brown Norway rats, resembling immune complex hypersensitivity; gold therapy for rheumatoid disease: hypersensitivity/autoimmune-like pathology in humans	– Compound-specific immunoglobulins – Compound-specific T-cells in blood. – Compound-specific positive skin prick test – Autoreactive T-cells and antibodies, like antinuclear antibody (ANA) and antineutrophil cytoplasmic antibody (ANCA), in blood
Diisocyanates; acid anhydrides	Asthma; allergic alveolitis; contact dermatitis	
Penicillin	Anaphylactic shock; urticaria; hemolytic anemia; immune complex disease; contact dermatitis; immune neutropenia	
Propylthiouracil	Systemic lupus erythematosis; Wegener's disease	
Therapeutic proteins	Potential immunogenicity of the drugs (dependent on size of protein). Drug-specific antibodies can, upon repeated exposure, neutralize drug and thus decrease efficacy, but also provoke hypersensitivity reaction against drug. Potential induction of cytokine storm, unchecked acute phase response and vascular leak syndrome.	
2. DIRECT TOXICITY		
Dexamethasone (immunosuppressant drug)	Compound has glucocorticosteroid activity. Target cells are small-sized CD4+/CD8+ thymocytes in cortex	– Altered immune function, e.g., altered delayed type hypersensitivity response in skin against a model contact allergen like dinitrochlorobenzene (DNCB) – Altered number and functions of leukocytes from blood – Altered level of antibodies/presence of autoantibodies in blood – Altered cytokines in body fluids and/or exhaled air
Cyclosporin A (immunosuppressant drug)	Target cells are epithelial and DCs in thymus medulla	
Azathioprine (cytostatic drug)	Antiproliferative effect. Lymphocyte depletion in lymphoid organs, especially thymus cortex.	
Procainamide, hydralazine	Polyclonal activation and/or disruption of tolerance and/or disruption of lymphocyte recognition	
Polychlorinated dibenzo-*p*-dioxins (e.g., TCDD); dibenzofurans (PCDFs); biphenyls (PCBs)	TCDD target cells are lymphoblasts in outer cortex and epithelial cells in cortex of thymus; bone marrow cellsSome PCBs can also act as endocrine disruptors	
Polycyclic aromatic hydrocarbons (mainly air pollutants, e.g., exhaust fumes)	Affect especially humoral immunity; besides being directly carcinogenic, induction of neoplasia may be helped by their suppression of immune surveillance	
Organotin compounds	Main target organ is thymus. Exposure of very young rats leads to more severe immunosuppression than does exposure of 1-year-old rats. Some fish species also sensitive.	
Heavy metals	Complex immune-modulating effects on immune system. Immunosuppression as well as immunostimulation.	
Chlorinated hydrocarbons; zearalenone (mycotoxin); 9-tetrahydrocannabinol; diethylstilbestrol (DES)	All compounds have estrogenic activity. Animals exposed in utero to DES have abnormal B- and T-cell responses, persisting and progressing during life. Humans do not demonstrate severe immune effects, but their propensity to develop autoimmune diseases appears increased.	
NO_2, SO_2, and O_3 air pollution		

(*Continued*)

TABLE 12.7 (Continued)

Compounds and other agents	Experimental data	Biomarkers
	Associated with increased susceptibility to airway infection in humans and test animals	
Irradiation	Antiproliferative effect; death of lymphocytes; immunomodulation/tolerance induction. Target cells are cells in lymphoid organs, including bone marrow.	
UV-B light	Immunomodulation, induction of suppressor cells; decrease of Langerhans cells in skin	
Crystalline silica (quartz)	Exposure associated with increased risk of the autoimmune diseases scleroderma, rheumatoid arthritis, SLE, and vasculitis	
3. INDIRECT TOXICITY		
Ethylene, 1,1-dichloro-2,2-bis(*p*-chlorophenyl)	Antiandrogenic compound; induces Bursa of Fabricius atrophy in birds	
Marked food deprivation	Immune modulation via adrenal activation	

From Haschek, W.M., Rousseaux, C.G., Wallig, M.A. (Eds.), 2013. Haschek and Rousseaux's Handbook of Toxicologic Pathology, third ed. Academic Press (Elsevier), San Diego, CA, Table 49.6, pp. 1824–1825, with permission.

Evaluation of Toxicity

Biomarkers

Biomarkers help in the translation of results from experimental animals to humans, and to monitor human exposure and immune reactions to biopharmaceuticals, which have high species specificity. An array of methods to assess immune function is available in humans, but most of these assays pertain to blood analysis (Table 12.7).

Morphologic Evaluation

Conventional histopathology enables evaluation of the effects of xenobiotics on main cell subsets by assessing their distinct cytomorphology or tissue location. In this way, the effects on lymphocytes of T and B lineage, or on components of the supporting stroma, can be investigated. The sensitivity of histopathologic assessment can be increased by combination of immunohistochemistry with quantitative methods such as morphometry, cell counts, and flow cytometry to investigate subpopulations. As histopathological slides represent a static time point, the dynamic events of the immune system should be carefully considered in the assessment of immunotoxicity. For example, histologic structure of lymph nodes is highly dependent on (local) antigenic stimulation. Normally, lymph nodes draining antigen-rich tributaries are in a state of chronic stimulation indicated by prominent secondary follicles with GCs, well-developed paracortex, considerable numbers of macrophages in the sinuses and paracortex, and plasma cells in the medullary cords. Histologic assessment of MALT such as gut-, bronchus-, nose-, larynx-, skin-, vascular-, and eye-associated lymphoid tissue gives information concerning the mucosal, secretory immune system. Splenic histology reflects the systemic immune system, which is directly associated with blood. When evaluating hematoxylin and eosin (H&E)-stained slides, "enhanced histopathology" provides higher accuracy and sensitivity of histopathological diagnostics. The core points of this structured assessment are that the compartments of lymphoid organs should be evaluated individually as they support specific immune functions and that a semiquantitative descriptive (rather than interpretative) terminology should be used (Table 12.8).

Immunotoxic compounds may have an effect on one compartment while leaving other compartments unaffected. This is of interest for the evaluation of the mode of action of a compound because distinct compartments within a lymphoid organ reflect one or more specific functions, and each houses lymphoid and nonlymphoid cells of different lineages and in different ratios. One of the problems in the detection of alterations in cell numbers is discrimination from "normal" morphology, since the range of normal appearance for lymphoid organs may be wide. Once the normal range is established, tissues from treated animals can be compared with those of control animals. This requires that "blind scoring" of tissue sections not be done at the beginning of the morphologic evaluation, although it can be useful at a later stage of the evaluation to confirm subtle changes. Enhanced histopathology may not be helpful in chronic studies due to the variability of normal aging changes that occur in

TABLE 12.8 Terminology of Enhanced Histopathology

Organs and compartments	Changes
All lymphoid organs, all compartments	Increased or decreased sizeIncreased or decreased cellularity of passenger cells (lymphocytes, plasma cells, blast cells) Increased numbers of cells otherwise not present or in low numbers: – Tingible body macrophages – Phagocytosing or pigmented macrophages – Mast cells – Granulocytes – Apoptotic cells – Necrotic cells (micro) Granulomata or macrophage aggregates
Thymus	Increased or decreased cortex: medulla ratio Effects on number or size of epithelium-free areas Increased epithelial cords and tubules Presence of follicles/GCs
Lymph nodes, spleen, and MALT	Increased or decreased GC development
Lymph nodes and MALT	Prominent HEVs
Lymphatics, lymph nodes, MALT	Lymphatic ectasia

From Haschek, W.M., Rousseaux, C.G., Wallig, M.A. (Eds.), 2013. Haschek and Rousseaux's Handbook of Toxicologic Pathology, third ed. Academic Press (Elsevier), San Diego, CA, Table 49.8, p. 1830, with permission.

long-term studies. Though procedures such as enhanced immunohistopathology are valuable in accurately defining specific effects on individual immune system organs, the overall interpretation of immunomodulation or immunotoxicity should be based on integration of the observations in the whole animal or, preferably, the group of animals.

Animal Models

Immunotoxicity of a compound is generally assessed in the framework of standard, guideline-driven toxicity studies. In this way, effects on the immune system can be evaluated against effects on other organ systems. Histopathology of lymphoid organs is crucial in these studies, but immune function tests are needed to interpret the consequences of observed histopathological changes on immune function. Special attention should be paid to juvenile immunotoxicity because of proven high sensitivity as well as different modes of reactivity, latency, or longer persistence of effects in the developing immune system. A test strategy for juvenile exposure is implemented in guidelines for reproductive and developmental toxicity and called developmental immunotoxicity testing (DIT). Within the critical developmental windows gestation, postnatal development, and weaning, there are specific critical windows of immune system development (Table 12.5). Their sequence shows similarities across mammalian species but may vary with respect to the time point in intrauterine or postnatal life. DIT should address all windows of immune development. Principal transferability of DIT to human has been shown for compounds such as methylmercury, ethanol, arsenic, or polychlorinated biphenyls (PCB). Besides for chemical entities in the environment, DIT is used in investigational drug development, depending on the causes of concern, or in pediatric drug development. When using mouse models, a completely anatomically intact morphology can be found on PND42 with maturation of T-cell compartments prior to B-cell compartments. Importantly, histological signs of maturity have to be distinguished from functional maturity.

Most immunotoxicity studies are performed in rodents, usually the mouse or the rat. Other species, like monkeys, minipigs, and fish, are used less often, but may be valuable or even better alternatives in some cases. Specialized studies looking at a specific arm of the immune system have used spontaneously occurring mutants or artificially constructed laboratory animals such as the congenitally athymic (nude) rodents. In athymic animals, lacking production of T-lymphocytes, T-cell compartments are devoid of lymphocytes. In addition, single-gene animal models of immunodeficiency are now available to extend such studies for the evaluation of effects on specific arms of the immune system. An interesting model of immunodeficiency in this respect is the mouse with the severe combined immunodeficiency (SCID) mutation, which results in severe combined immunodeficiency. The lack of immunocompetent T and B-cells permits engraftment of tissues from other species without being rejected. This extends also to cells of the human immune system allowing the investigation of human immune reactions

specifically in a model organism without functional T, B, and NK-cells (SCID-hu mouse).

Genetically modified animals are another generation of laboratory animal constructs. Examples are mice expressing frequent Caucasian HLA-alleles. Histopathological evaluation of toxic effects in lymphoid organs of these animal models requires a thorough knowledge of their histophysiology. A major challenge is the safety and immunotoxicity testing of monoclonal antibodies (mAbs). The primary toxicity of mAbs lies in their ability to block or enhance the activities of the target molecule on the target cells, or target molecules on nontarget cells or crosslinking with nontarget molecules, which may lead to cytokine/eicosanoid "storms," immune suppression, and autoimmune diseases. Unfortunately, these effects are often highly species-specific, and animal models may either exaggerate (reactions against foreign, namely human, proteins; induction of neutralizing antibodies) or severely underestimate the effects in humans. Formation of neutralizing antibodies, though not per se a toxic effect, may lead to sights of immune activation including GC formation in follicles, lymphocyte proliferation or increased compartment sizes. Routine toxicity studies are thus often inadequate to detect the side effects of MAbs and often a valid second species normally required in toxicological investigations may not be available. Main reasons are absence of the intended human target in animal species, neutralizing antidrug antibodies directed to foreign protein structures and inherent differences between the immune systems of humans and selected test species. An example of the complexity of changes in the immune system that can be induced is natalizumab, a humanized mAb against human α integrin. In monkeys, due to its intended pharmacological mechanism in humans, trafficking of leukocytes was likewise impeded in this closely related species. In addition, immunogenicity leads to individually differing amounts of neutralizing antibodies associated with immune stimulation, and variable lowering of serum concentrations of the test article.

Typically, tissue cross-reactivity studies are needed to identify target structures in animal tissues in comparison to human. In the conduct of studies, monitoring of antidrug antibody formation is required and high levels may cause an increase of dose or even termination of the study. In general toxicity studies, enhanced histopathology is recommended. In the case of positive results, immune phenotyping is recommended for further characterization of the effect. In long-term studies in nonhuman primates, activation of endogenous viruses such as lymphocryptovirus, cytomegalovirus, Epstein–Barr virus, and polyomavirus may occur. Virus activation can be monitored serologically and may eventually lead to lymphoma.

Embryo-fetal and peri-/postnatal development toxicity studies are required for immunomodulatory MAbs for treatment of women with child-bearing potential and include investigation of the fetal immune system. Positive results have been reported for an antiCD11a surrogate antibody of efalizumab, which caused prolonged immune function effects in the treated offspring of CD-1-mice and reduced CD11a-expression. Also Rituximab, an anti-CD20 antibody, showed prolonged B-cell depletion in the offspring of treated cynomolgus monkeys.

With nanoparticles immune compatibility is a main issue and often the immune system is affected at lower doses than other target organs. Small particle sizes seem to be particularly prone to elicit immune reactions. As there is only partial correlation of *in vitro* and *in vivo* studies, *in vivo* investigations including histopathology are indispensable and contribute to the investigation of organ distribution, clearance, disposition, or degradation of nanoparticles. As with other classes of potentially immunomodulating entities, a combination of functional (e.g., macrophage function tests) and structural investigations is needed. An example of immunotoxicity is the intravenous administration of silver nanoparticles in rats in a 28-day repeat-dose study with accumulation of particles in liver, spleen, and lymph nodes associated with a suppression of splenic NK-cell activity. In children exposure to diesel exhaust particles has been associated with pronounced allergic airway reaction.

RESPONSE TO INJURY

The immune system represents multiple organs but one system. Hematological investigations, weighing of selected lymphoid organs, histopathology of the immune organs, and bone marrow cytology belong to the core investigations when screening for immunotoxicity in standard repeat-dose studies. The focus of these investigations is on immunosuppression, although signs of immunostimulation can be detected as well (see also "Autoimmune Diseases and Hypersensitivity Reactions" section).

Nonneoplastic Changes

Lymphoid Organ Weight and Gross Pathology

Assessment of lymphoid organ weight and gross changes at necropsy give a first indication of immune effects although there may be influences by a variety of unspecific factors including feeding status, aging, and stress phenomena near the maximum tolerated dose (Table 12.9). These have to be differentiated from

TABLE 12.9 Effects of Aging, Feed and Stress on Organ Weights, Immune Functions, and Histology of Lymphoid Organs

Species	Organ weights	Immune cells/functions
AGING		
Rat	Spleen ↑, thymus ↓	Proliferative response to mitogens ↓, lymphokine production ↓
Mouse	Spleen ↑, thymus ↓	B-cells: proliferative response to mitogens ↓, affinity response ↓, monoclonal gammopathies ↑, autoantibodies ↑T-cells: age-related shift of subsets depending on strain, bone marrow production of pro-T-lymphocytes ↓NK cell function ↓
Hypocaloric status/feed restriction		
Rat	Spleen ↓	Proliferative response to mitogens ↑, IL-2 receptors on splenic T-lymphocytes ↓, white blood cells/granulocytes ↓
Mouse	Spleen ↓	NK cell function ↑, B-cell subpopulations ↑, T-precursor cells ↑
STRESS		
Rat	Spleen and thymus (most sensitive parameter) ↓ (along with deteriorated condition or reduced body weight gain)	Granulocytes ↑
Mouse	Spleen and thymus↓ (along with deteriorated condition or reduced body weight gain)	Granulocytes ↑, lymphocytes (T:CD4 + and CD8 +) ↓, B-cells expressing MHC class II protein (most sensitive parameter) ↓, spleen cell number ↓

From Haschek, W.M., Rousseaux, C.G., Wallig, M.A. (Eds.), 2013. Haschek and Rousseaux's Handbook of Toxicologic Pathology, third ed. Academic Press (Elsevier), San Diego, CA, Table 49.9, p. 1835, with permission.

immunotoxicity. Figure 12.22A–D shows normal lymph node morphology and examples of alterations.

STRESS

Under physiological conditions, glucocorticoids support thymic homeostasis. Death by neglect of CD4+ CD8+ thymocytes is mediated by glucocorticoids (Figure 12.4). Hence, in adrenalectomized mice increased numbers of CD4+ CD8+ and CD4+ CD8− thymocytes could be found in the thymus. However, the mechanism of glucocorticoids' role in thymocyte apoptosis is still not clarified. Investigations in mice with glucocorticoid receptor deficiency did not show changes in thymic lymphoid cellularity. Any stress reaction leading to an increase of corticosterone (in rodents, or closely related glucocorticosteroids in other species) causes increased apoptosis of CD4+ CD8+ thymocytes; these particular thymocytes are most susceptible to apoptosis due to abundant expression of glucocorticoid receptors. The acute stress response is very fast. Within a few days, histological cortical changes in thymus progress from increased apoptosis of cortical thymocytes with increased amounts of tingible body macrophages (Figure 12.23A, minipig) to lymphocyte depletion (Table 12.9), which can be such that a reversed pattern of lymphocyte density is observed in the medulla (Figure 12.23B, minipig). Under experimental conditions such as administration of dexamethasone to rats or mice, significant apoptosis of cortical lymphocytes is underway in the thymus at 6 hours postdosing, and by 24 hours postdosing the thymic cortex is largely depleted of lymphocytes. B-cells are also influenced by glucocorticoids and show reduced expression of MHC class II. In 28-day studies in mice, investigations of habituation to different stressors have shown that tolerance to stress depends on the nature of the stressor. The magnitude of the response after habituation correlates well with respective corticosterone levels. In moribund animals, the splenic red and white pulp can become severely depleted (Figure 12.24A,B). Indications of stress imply, besides decreased thymic weight and decreased lymphoid cellularity, increased adrenal weight, increased glucocorticoid levels, and adrenocortical hypertrophy.

Histopathology

THYMUS

The thymus is often the first organ to be affected by immune-modulating compounds (Table 12.7; Figure 12.25A–C). Sensitivity of cortical thymocytes to immune-modulating compounds differs between the stages of T-lymphocyte development in the thymus. Immature thymocytes of the thymic cortex are very susceptible to toxic injury and prone to apoptotic cell death, which can be distinguished

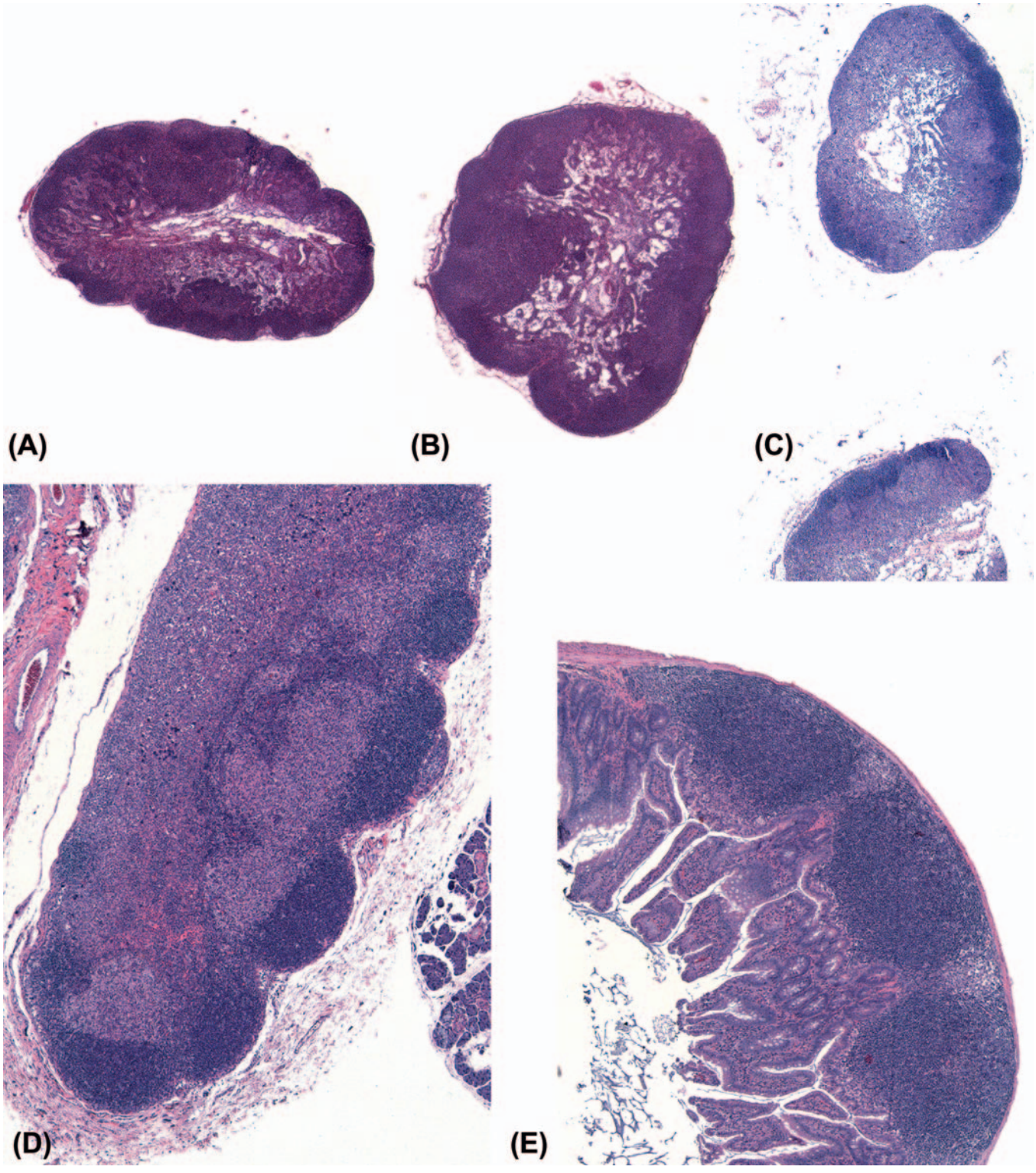

FIGURE 12.22 Differences in weight and size of lymphoid organs have to be investigated for underlying histopathology. Examples: Popliteal lymph nodes of young adult rats at an age of about 10 weeks—(A) untreated control; (B) treated with 150 mg/kg HCB for about 4 weeks, showing a generalized enlargement by increased populations of lymphocytes in all compartments; (C) athymic nude rat with depleted paracortex. H&E stain, ×1.6. (D) Mandibular lymph node and (E) PP of an athymic nude rat. In the T-cell areas of both organs, only nonlymphoid cells are present. In athymic animals, the B-cell areas are either unstimulated with normal size and density, as seen here, or show increased stimulation and increased size to compensate for the immune defect of the T-cell arm. H&E stain, ×5. Source*: From Haschek, W.M., Rousseaux, C.G., Wallig, M.A. (Eds.), 2013. Haschek and Rousseaux's Handbook of Toxicologic Pathology, third ed. Academic Press (Elsevier), San Diego, CA, Figure 49.235, p. 1837, with permission.*

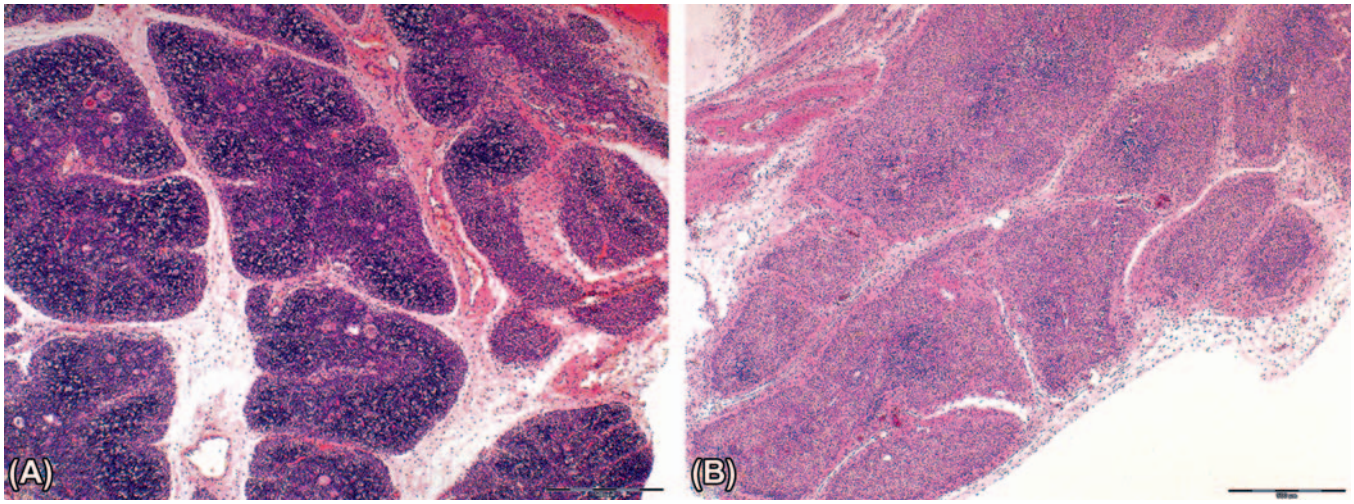

FIGURE 12.23 Thymus of minipig; stress-related changes are mimicked by dexamethasone (a glucocorticoid drug) treatment. (A) Acute stage, presented by an increase in lymphophagocytosis (increase in tingible body or "starry sky" macrophages), mainly in the cortex; (B) prolonged stage, in which a lymphocyte-poor cortex is observed, leading to an inverse density of the cortex and medulla. H&E stain, ×25. Source: *From Haschek, W.M., Rousseaux, C.G., Wallig, M.A. (Eds.), 2013. Haschek and Rousseaux's Handbook of Toxicologic Pathology, third ed. Academic Press (Elsevier), San Diego, CA, Figure 49.26, p. 1840, with permission.*

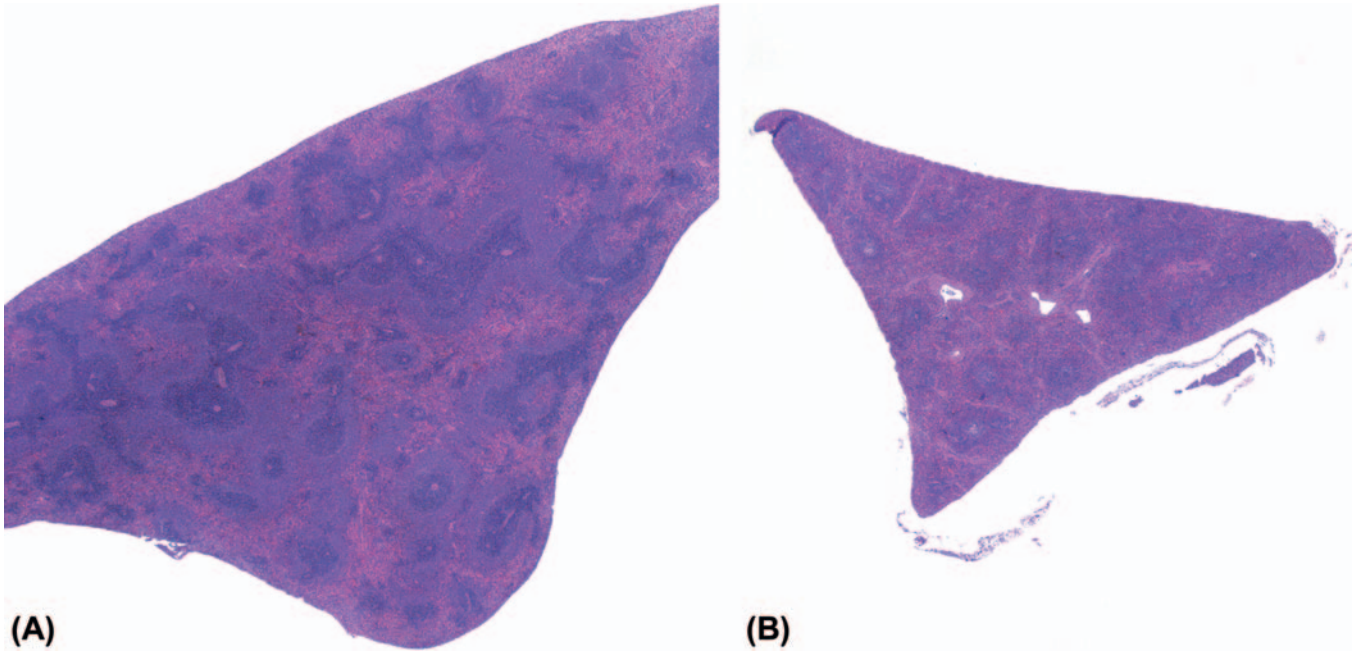

FIGURE 12.24 (A) Normal rat spleen and (B) spleen of an animal with a severely reduced general condition, showing decreased cellularity in the white pulp including the marginal zones, and a reduction in red pulp. This finding is regarded as nonspecific and not as evidence of primary immunotoxicity. H&E stain, ×1.6. Source: *From Haschek, W.M., Rousseaux, C.G., Wallig, M.A. (Eds.), 2013. Haschek and Rousseaux's Handbook of Toxicologic Pathology, third ed. Academic Press (Elsevier), San Diego, CA, Figure 49.27, p. 1834, with permission.*

from necrosis by presence of apoptotic bodies and immunohistochemically by cleaved caspase 3-positivity or TdT-mediated dUTP-Biotin nick end labeling (TUNEL) staining. With necrosis, contiguous cells are often affected; karyolysis, pyknosis, and karyorhexis, cell swelling with disruption of the cell membrane, and release of cytoplasm into the surrounding tissue are observed. Apoptosis and necrosis can occur simultaneously when apoptosis mediators are depleted.

Signaling pathways leading to chemically induced thymocyte apoptosis often involve the FAS/FAS ligand. Aromatic hydrocarbons such as dioxins are ligands of AhR. They cause apoptosis of thymocytes and affect all subsets, probably by activation of the FAS/FAS ligand system. TCDD toxicity of the thymus of mice showed apoptosis only up to 12 hours after treatment. Thymic atrophy started at 72 hours after treatment. This indicates that investigations of early time points after exposure have to be taken into account since transient apoptosis may be missed due to rapid clearance of apoptotic cells by thymic macrophages. Cytostatic agents such as azathioprine and 5-fluorouracil as well as irradiation affect DNA synthesis and hence diminish cell proliferation in the outer cortex. In such cases, reduced cellularity may be not accompanied by a clear increase of tingible body macrophages. Administration of xenoestrogens, such as diethylstilbestrol, genistein, or methoxychlor, caused lymphocyte depletion of the thymic cortex. An arrest early in thymocyte development was observed at the stage of CD4− CD8− CD3− CD44+ CD25−, which is mediated by estrogen receptors α or β, both present in the thymus. Thus, estrogen antagonists abolished changes mediated via estrogen receptors. Some organotin compounds caused thymic atrophy at doses, which did not lead to overt toxicity in other organs. Perfluorated compounds such as perfluorooctane sulfonate exerted immunomodulating effects as ligands of peroxisome proliferator-activated receptor (PPAR)-α. As a consequence, thymic and splenic atrophy have been observed. The cellular decreases in the thymic cortex affected, in particular, CD4+ CD8+ thymocytes. Ultrastructurally, lipofuscin granules were observed in thymic lymphocytes. Structural changes similar to aging have been induced in the thymus and less obviously in the spleen of mice treated with D-galactose, a compound known to accelerate the aging process by formation of advanced glycation end-products. Cytotoxicity to cells in the bone marrow may reduce the flow of progenitor cells from the bone marrow into the thymus. The immune-modulating sphingosine 1-phosphate agonist FTY720 reduced the entrance of thymic progenitor cells and led to reduced numbers of early double negative thymocytes in mice after short-term treatment. The cross-talk between epithelial and lymphoid cells in the thymus may lead to changes in epithelial cells when primarily lymphoid cells are affected and vice versa. Staining for the different cytokeratins allows the identification of medullary and cortical thymic epithelial cell (TEC) subpopulations and Hassall's bodies (rodents: CK5 and CK14 in medullary TEC, CK8 in cortical, and medullary TEC including Hassall's bodies). With flow cytometry, or with electron microscopy, TECs were found to be reduced in mice treated with different immunosuppressants, including dexamethasone, cyclophosphamide, and cyclosporine A. The depleted TECs included those producing the autoimmune regulator, AIRE. The depletion of AIRE-producing cells compromises immunological self-tolerance. The changes were reversible within a few weeks.

Induced cortical atrophy may be accompanied by a high cellularity of the thymic medulla, leading to an "inverse" appearance (Figure 12.25B), where the cortex has fewer lymphocytes than the medulla. When assessing medullary cellularity, however, one must consider whether the observed increases are absolute—due, for example, to increased transition of T-lymphocytes into the medulla—or to decreased emigration of thymocytes from the thymus because of arrest of T-cells in the thymic medulla. Increases in medullary cellularity can be relative as well, where absolute medullary cellularity remains constant but cortical cellularity is decreased. An increased ratio of cortex−medulla lymphocytes seen after treatment with cyclosporine in rats is a rare finding (Figure 12.5C), since generally cortical thymocytes are most susceptible to induced apoptosis. Effects on the thymus such as this can lead to reduced lymphocyte emigration into the periphery, whereupon T lymphocyte-dependent areas in peripheral lymphoid tissues are reduced in cellularity and size. Immune-modulating compounds such as cyclosporine, cyclophosphamide, corticosteroids, and dioxins influence regulatory T-cells either *in vivo* or *in vitro*. Unwanted effects are difficult to predict in preclinical studies, and even if manipulation of function of regulatory T-cells is the therapeutic goal, investigation in preclinical studies is challenging. If physiological tolerance is disrupted, for example, inflammation in response to normally tolerated microflora of the gastrointestinal tract will result, and changes in the thymus in response to this can be seen by the pathologist. Xenobiotic-related alterations in the intestinal microbiome may have far-reaching effects such as the known interactions between the intestinal microbiome, cytokine production, and development of *Candida albicans* infections in the oral cavity.

PERIPHERAL LYMPHOID ORGANS: SPLEEN AND LYMPH NODES

Reduced generation, maturation, and/or emigration of thymocytes to the periphery subsequently lead to depletion of T-cell−dependent areas of peripheral lymphoid organs. The spleen has the highest frequency of lymphocyte recirculation; therefore, reduced lymphocyte cellularity secondary to reduced thymic lymphocyte output is commonly seen in splenic white pulp. In lymph nodes, which have generally lower rates of lymphocyte recirculation, atrophy/reduced cellularity of T-cell regions can be less pronounced or even absent.

Compounds associated with suppression of T-lymphocytes can cause, as a secondary effect,

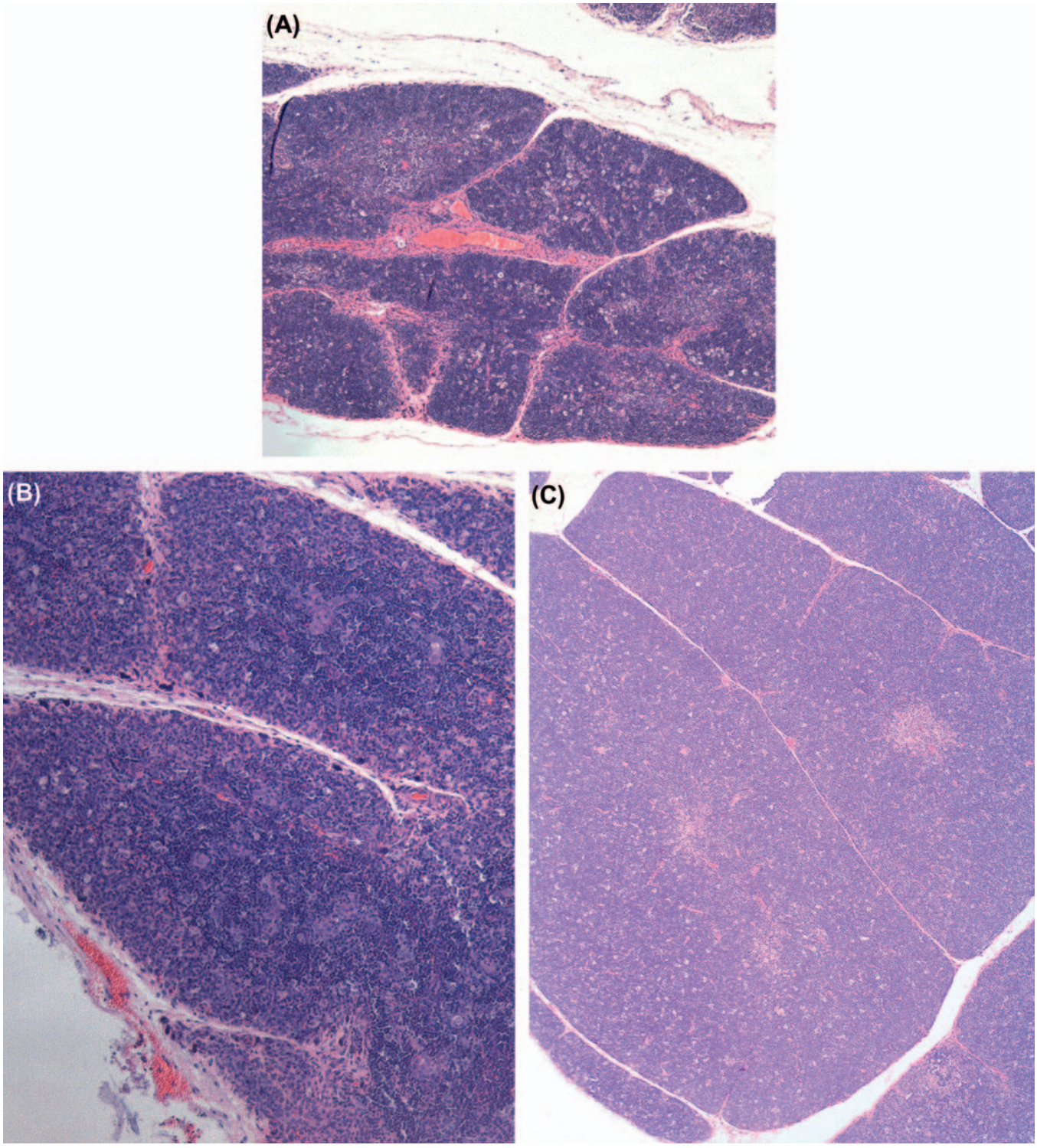

FIGURE 12.25 Thymus after 28 days of treatment with (A) 150 mg/kg benzo[*a*]pyrene, showing reduced cortex size and numerous tingible body macrophages. H&E stain, ×5. (B) Chemically induced thymic atrophy can lead to a reversal of lymphocyte density between cortex and medulla. Whereas the cortex is depleted, the medulla is hypercellular. (C) Increased ratio of cortex/medulla lymphocytes, as seen here, can occur with treatment by certain compounds such as cyclosporine. H&E stain, ×10. Source*: Courtesy: Dr. Maike Huisinga, BASF AG.*

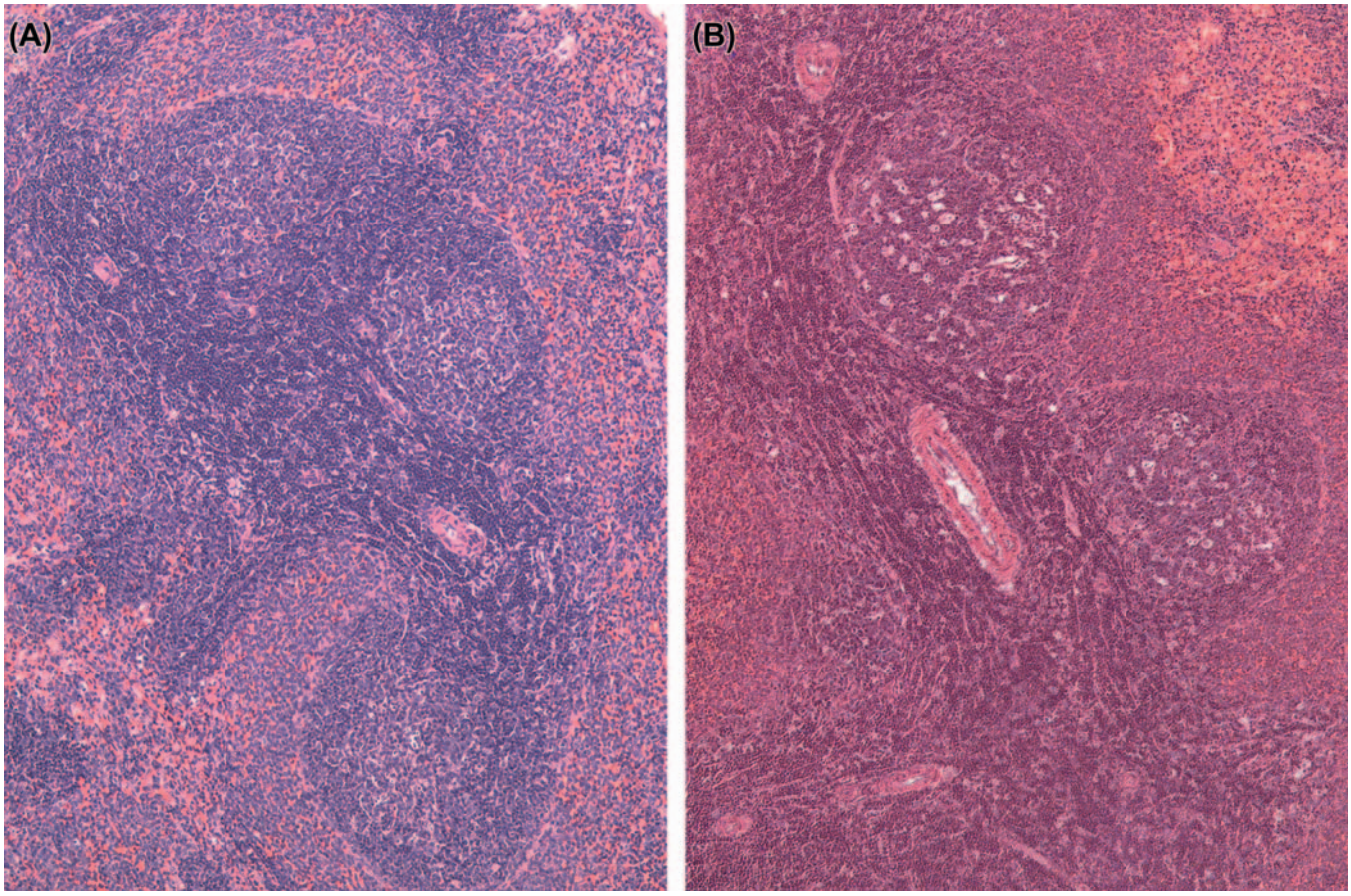

FIGURE 12.26 The spleen responds to antigenic stimulation with GC formation in the follicular B-cell areas. (A) GC formation in a rat immunized with sheep red blood cells 5 days before necropsy. (B) Secondary follicles with a thin mantle zone and markedly enlarged GCs containing an increased amount of tingible body macrophages in a rat treated for 8 weeks with a developmental compound. H&E stain, ×10. Source: *From Haschek, W.M., Rousseaux, C.G., Wallig, M.A. (Eds.), 2013. Haschek and Rousseaux's Handbook of Toxicologic Pathology, third ed. Academic Press (Elsevier), San Diego, CA, Figure 49.29, p. 1844, with permission.*

morphological changes in B-cell areas as well. Short-term treatments of organotin compounds in mice showed marked decreases of peripheral lymphocytes within a few hours after injection. Besides a decrease in peripheral T-lymphocytes, a marked decrease in B-lymphocytes has also been observed. Histological findings related to immunosuppression are decreased lymphoid cellularity of splenic white pulp follicles and marginal zones, lymph node cortex and medullary cords, and follicles of PP. Often the development of secondary follicles with active GCs from primary follicles is decreased, although at very low doses GC development can be increased. This may be due to an early effect on T suppressor cells, which leads to an overall stimulation of the immune response. As an example of B-cell responses to injury, cannabinoids have an immunosuppressive potential mediated by interaction with cannabinoid 2 (CB2) receptors found on various types of immune cells, including B-lymphocytes. CB2 agonists and antagonists influence the retention of immature B-cells in bone marrow sinuses. Thus, CB2 antagonism with SR144528 reduced the number of B-lymphocytes in bone marrow sinuses and splenic marginal zones. A specific effect on the shuttling of marginal zone B-cells in the spleen has been described for FTY720, an immunosuppressing sphingosine 1-phosphate receptor agonist which prevents egress of lymphocytes from lymphoid organs, and of plasma cells from secondary lymphoid organs, to blood and bone marrow. In the spleen, a displacement of marginal zone lymphocytes to splenic follicles was observed. A similar displacement of marginal zone lymphocytes was reported to occur after LPS treatment. Marginal zone B-cells represent a specific subset, which produces high levels of soluble IgM and expresses the complement receptors CD21 and CD35. Antigens and chemically inert substances, which enter the body by chance or are administered on purpose, can lead to increased cellularity of peripheral lymphoid organs (Figure 12.26A,B). Substances migrate

with the lymph with different velocities depending on their size. For example, in lymph nodes, unbound small molecules reach the tributary lymph node within a few minutes, but antigens transported by DCs need several hours to travel the same distance. In the subcapsular sinus, specialized macrophages are the first immune cells to encounter unbound antigenic material. They are located in the sinus wall, and their cytoplasm contacts the subcapsular sinus as well as the underlying cortical B-cell region. Capture of antigens is followed not by degradation but by transport along the cell body into the B-cell area. Small antigens, which are not taken up by macrophages, enter the lymphoid tissue through so-called conduits, tracts of collagenous fibers ensheathed by projections of stromal cells. Circulating antigen evokes lymphocyte trapping, which is increased recruitment of lymphocytes through HEVs combined with reduced release of lymphocytes through efferent lymphatics. This leads to gross enlargement and weight increase of lymph nodes.

Microscopically, prominent HEVs with increased transmigration of lymphocytes as well as increased cellularity of lymph node compartments are visible. Within a few days, the immune response to T-cell–dependent antigens causes formation of GCs in follicles. As a consequence of stimulation, an increase in plasma cells is observed in the medulla of lymph nodes. Immunostimulatory effects can occur even after exposure to compounds without obvious immunogenicity, but which nevertheless cause malfunction of the immune system. Vanadium pentoxide inhalation over 12 weeks in mice caused increased spleen weights and GCs, which could become very large and not clearly delimited. Antigen challenge showed that high-affinity antibodies were diminished in treated mice when compared to control. Oncostatin M (OM), a member of the IL6 family, caused thymic atrophy and had a paracrine effect as well. It supported T-cell maturation from hematopoietic progenitor cells to mature T-cells in lymph nodes, which then functioned as primary lymphoid organs. Both effects of OM—thymic atrophy and enhanced T-cell maturation in the lymph nodes—have been detected in OM-transgenic mice. The extrathymic T-cells in these mice were, however, functionally different from thymic T-cells because of higher responsiveness to antigen stimulation and increased susceptibility to apoptosis. Histopathologically, the lymph nodes of OM-transgenic mice showed an increased number of HEV. This angiogenic effect seemed to be necessary for extrathymic T-cell development under OM influence, and was induced by cyclooxygenase-2. Increased weight and lymphoid cellularity of lymphoid organs mediated by increased macrophage activity were seen after treatment with hexachlorobenzene (HCB) in rats. The effect seemed to be mediated by increased recirculation of lymphocytes via HEVs (Figure 12.27) to peripheral lymphoid organs. Functional tests revealed no clear evidence of immunostimulation in this investigation in Wistar rats, whereas in Brown Norway rats, T-cell activation was observed. HCB toxicity demonstrates that effects on cells of the innate immune response have to be taken into account when effects on lymphocytes are observed.

PERIPHERAL LYMPHOID ORGANS: MALT

Reports about chemically induced changes of the immune system of the mucosae with its MALT are relatively scarce. This is remarkable, since it houses the majority of the body's immune cells and is particularly complex with MALT and large pools of diffuse, single lymphoid cells. Moreover, the mucosae (together with the skin) are the main contact sites of the body with the environment. The cause of this discrepancy is likely the predominance of tolerance induction by MALT; however, MALT and the single intraepithelial and LPL are also more difficult to examine critically. Even inherited immunodeficiency related to IgA secretory function of PP as observed in the wasted mutant mouse do not cause morphological or morphometric differences when compared to wild-type controls. The different MALT tissues share structural and functional features, but differences in cellular composition regarding the T-cell/B-cell ratio and CD4+/CD8+ T-cell ratio are known to exist; these are as yet relatively undefined. They are thought to reflect adaptation to the anatomic location. For example, in the intestinal PP (part of the GALT), M cells continuously perform transcytosis of bacteria, particulate matter, and macromolecules, which they deliver to macrophages of the dome area. Pathogens can lead to inflammation and macrophage aggregates in the PP. Although pathogenic bacteria are uncommon in toxicity studies, their potentially confounding effects have to be taken into account when assessing the effects of potent immunosuppressive compounds. In immunosuppression, there could even be pathogenicity of normal mucosal microbiota.

The immune response of MALT, and in particular GALT, is mainly the formation of secretory IgA. IgA does not interact with complement, and thus has only low proinflammatory potential. However, divalent secretory IgA has a critical role in the incapacitation of microbes in the intestinal lumen. Reduced GALT tissue is reported, for example, in specific pathogen-free animals after parenteral nutrition, administration of oral antibiotics, in immunodeficient animals such as SCID and nude phenotypes, and in aging animals. Reference compounds for the investigation of immunotoxic

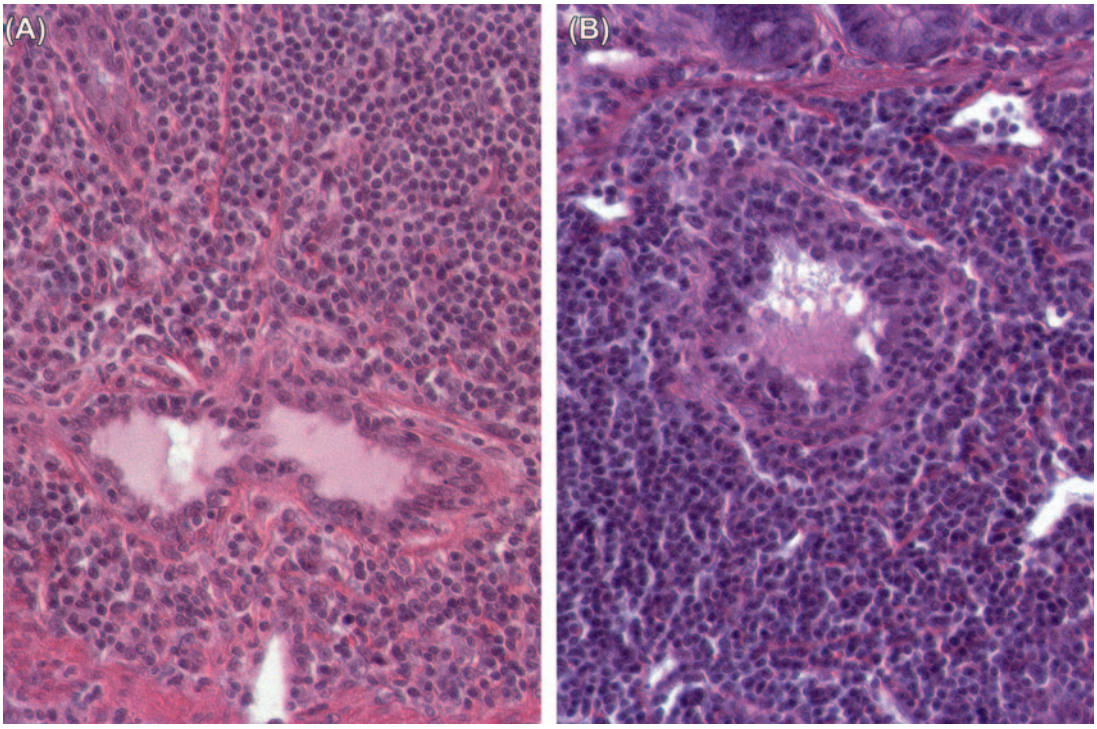

FIGURE 12.27 In a 28-day collaborative study with HCB in rats, morphologically increased size and weight of spleen, mesenteric, and popliteal lymph nodes (see Figure 12.22) were found. Histopathology revealed increased cellularity of splenic marginal zones and of the medullary region of lymph nodes, as well as hyperplasia and evidence of increased recirculation of lymphocytes in HEVs of lymph nodes and PP. (A) HEV from the PP of a control and (B) HEV from the PP of a dosed animal showing increased size and marked transmigration of lymphocytes. H&E stain. Source: *From Haschek, W.M., Rousseaux, C.G., Wallig, M.A. (Eds.), 2013. Haschek and Rousseaux's Handbook of Toxicologic Pathology, third ed. Academic Press (Elsevier), San Diego, CA, Figure 49.30, p. 1846, with permission.*

effects such as cyclosporine or HCB induced changes in the PP concomitantly with similar changes in other secondary lymphoid organs. Some compounds (azaspiracid, nivalenol, dimethyl sulfoxide) have been shown to cause degeneration, necrosis, and subsequent mineralization of PP in toxicity studies in rodents. The specialized M cells covering all MALT structures can be affected directly as well.

Inhalation of ozone induced increased vacuolation of these cells in BALT, together with increased proliferation of BALT lymphocytes. BALT hyperplasia is a common observation subsequent to chronic inflammatory stimuli such as infection by constitutive androstane receptor bacillus or mycoplasma species in rodents. BALT increase, especially in subacute and subchronic studies, can be a physiological response or direct evidence of immunotoxicity. Since lymphocytes from MALT migrate to their draining lymph nodes, these nodes should be evaluated together with MALT.

Preneoplastic Changes and Neoplasia

Tumors of Resident Cells

The incidence of tumors derived from resident mesenchymal and vascular cells of lymphoid and hematopoietic tissues is generally low in rodents, but unanticipated increases may be seen depending on genetic background. Reactive proliferations involving the stromal and vascular compartments of lymphoid organs or bone marrow and blood are more common, and often related to circulatory disorders in aging rodents. In the splenic red pulp, long-term treatment with hematotoxic compounds such as aniline leads to stromal fibrosis, fibroma, and fibrosarcoma. Hyperplasia and neoplasia of TECs (thymoma) have a strong interconnection with the proliferation, maturation, and release of lymphoid cells from the thymus. The spectrum of thymomas ranges from cases with low proportions of proliferating epithelial cells and high number of thymocytes, thus resembling T-cell lymphoma, to purely epithelial tumors resembling squamous cell carcinoma (Figure 12.28A–D). In rodents, females are generally more prone to thymoma than males. Thymomas with high amounts of lymphocytes often lead to concomitantly increased lymphoid cellularity in secondary lymphoid organs. As a differential diagnosis, epithelial hyperplasia of branchial remnants forming tubules, cords, and cysts has to be taken into account. The latter finding is common in both aging rats and mice, and more frequently seen in

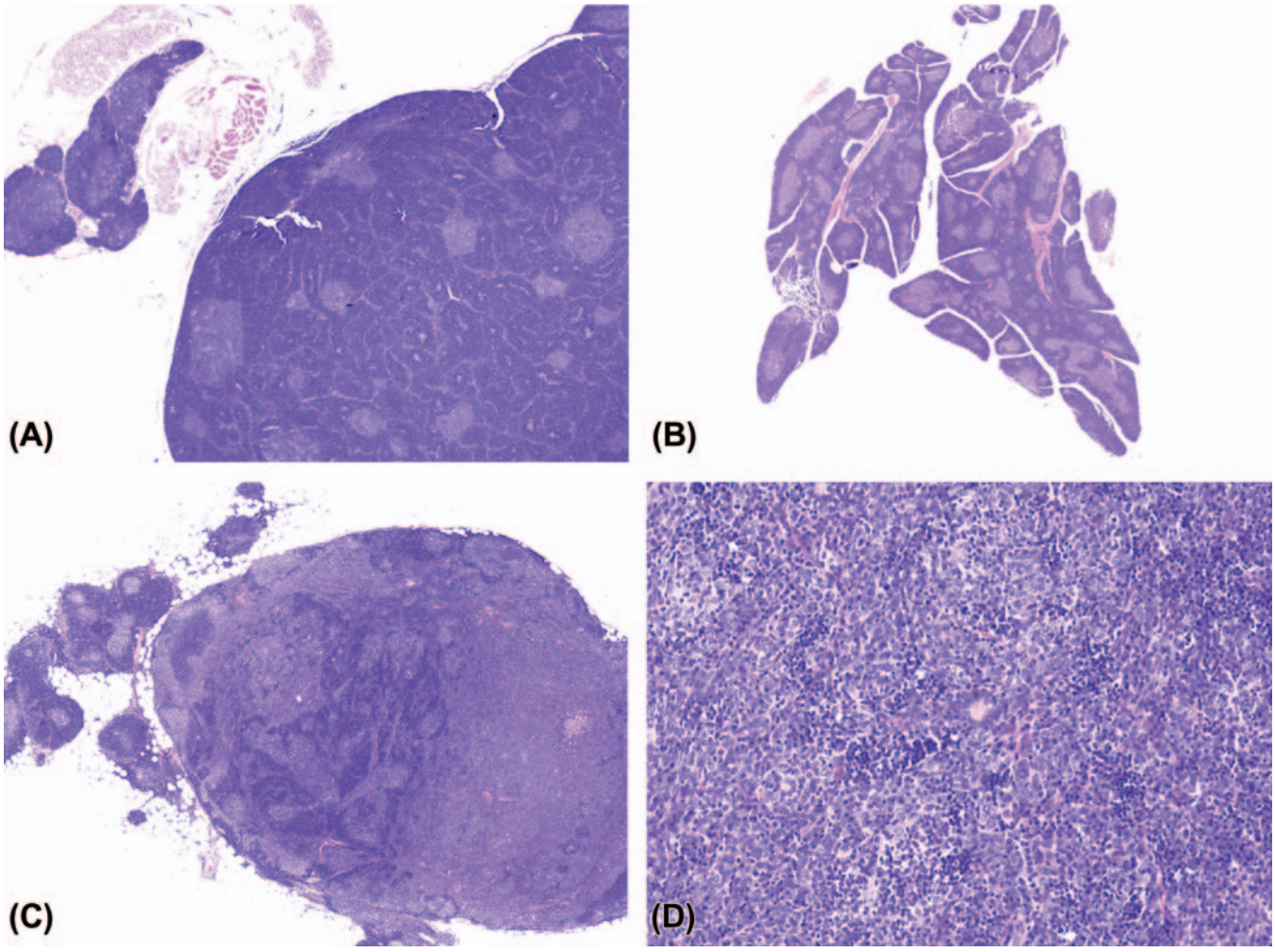

FIGURE 12.28 Thymomas are epithelial tumors, in some cases with massive involvement of lymphocytes. (A) Thymoma from an aged Wistar rat in which the presence of cortex and medulla plus numerous lymphocytes suggests a certain organization. The tumor is located in one of the lobes, while the contralateral lobe (in the upper left corner) is involuted, and uninvolved. These tumors should not be mistaken for a hyperplastic thymus. (B) Hyperplastic thymus from an aged male Wistar rat. In contrast to thymoma with organoid appearance, hyperplasia involves the entire thymus. (C) Thymoma in one lobe of the thymus of an aged Wistar rat. This thymoma contains considerably fewer lymphocytes than the thymoma with organoid appearance. (D) In a higher magnification image of the tumor, neoplastic epithelial cells are slightly spindle-shaped. H&E stain. Source: *From Haschek, W.M., Rousseaux, C.G., Wallig, M.A. (Eds.), 2013. Haschek and Rousseaux's Handbook of Toxicologic Pathology, third ed. Academic Press (Elsevier), San Diego, CA, Figure 49.31, p. 1847, with permission.*

females. This finding does not influence the lymphoid compartment. In aging female mice of some strains (in particular CD-1), a B-cell hyperplasia is frequently observed and has to be differentiated from thymoma or lymphoma (Figure 12.29A–C).

Tumors of Hemopoietic Cells

Hemopoietic cell tumors include myeloid leukemia, lymphoma, and histiocytic sarcoma. They represent frequent spontaneous and induced tumor entities in rodents. The spontaneous background incidences of these tumor entities are highly strain-specific. Induced tumors in rodents have been observed due to viruses, irradiation, and chemical carcinogens (Table 12.10).

For nonclinical research in mice, the Bethesda proposals for classification of lymphoid neoplasms in mice in 2002 parallel the structure of the WHO classification of 2001 for humans. For rodent carcinogenicity studies, the IARC classification can be used in order to standardize nomenclature and diagnostic criteria in regulatory studies (Table 12.11). Figures 12.30–12.33 illustrate the morphology of lymphoma and histiocytic sarcoma in rodents. For further differentiation, the application of immunohistochemical markers is recommended. The interpretation of immunohistochemical

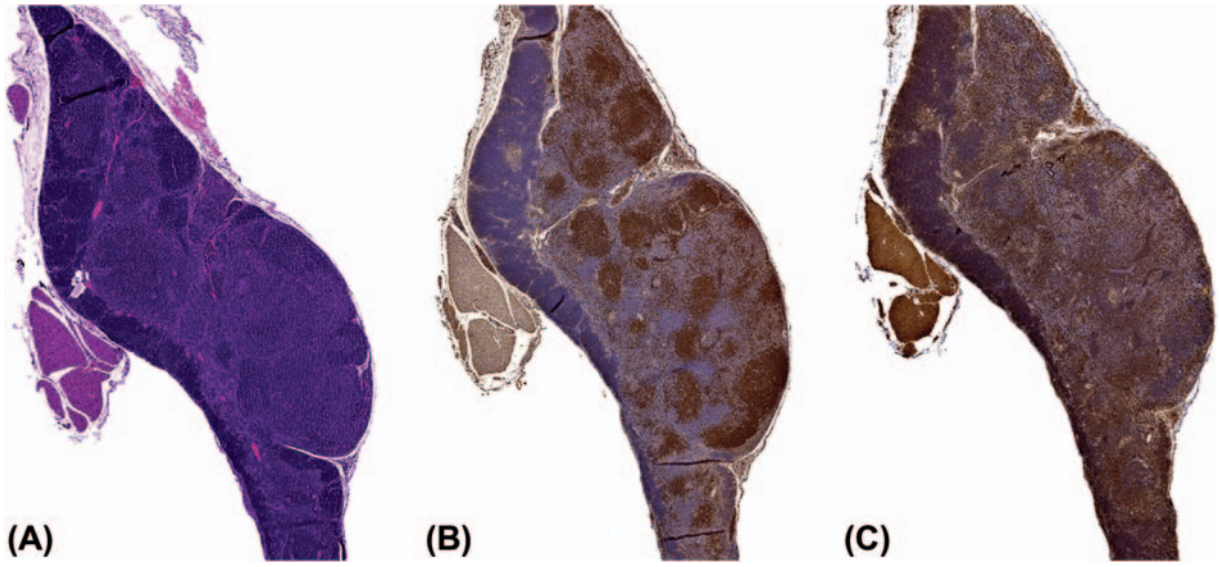

FIGURE 12.29 In the thymus of old mice (typical for CD-1 mouse) from carcinogenicity studies, (A) diffuse or follicular lymphocyte proliferation is observed in the thymic medulla leading to distorted architecture in H&E stained sections. (B) Immunohistochemically, the proliferations are of B-cell origin as PAX-5 immunohistochemistry for B-lymphocytes indicates. (C) In the residual cortex and interspersed in the B-cell infiltrate, T-cells can be demonstrated with CD3 immunohistochemistry. Source*: From Haschek, W.M., Rousseaux, C.G., Wallig, M.A. (Eds.), 2013. Haschek and Rousseaux's Handbook of Toxicologic Pathology, third ed. Academic Press (Elsevier), San Diego, CA, Figure 49.33, p. 1854, with permission.*

TABLE 12.10 Induced Hemopoietic Tumors

Causative agent	Mouse	Rat	Relevance for humans[a]
ONCOGENIC VIRUSES			
	Lymphoma, erythroleukemia	Low susceptibility	Various leukemias
RADIATION			
	Myeloid leukemia and lymphoma	Low susceptibility	Various leukemias
IMMUNOSUPPRESSION AND ACTIVATION OF LATENT VIRUSES			
	Lymphoproliferative disorder and lymphoma (mostly B-cell type)		Lymphoproliferative disorder and lymphoma (mostly B-cell type)
ANTICANCER DRUGS			
– Estradiol mustard	Lymphoma		Known human carcinogen (HC)
– Isophosphamide	Lymphoma[b]		Known HC
– *N*-Ethyl-*N*-nitrosurea compounds[c]	Lymphoma, myeloid leukemia[d]	Lymphoma, myeloid leukemia	Known HC
– Procarbazide	Lymphoma, leukemia	Lymphoma	Anticipated HC
– Thiotepa	Lymphoma		Known HC
OTHER DRUGS			
– 2-Amino-5-nitrothiazole		Lymphoma, granulocytic leukemia[e]	–[f]
– Anthraquinone	Lymphoma[b]		–[f]
– Beta-2′-deoxy-6-thioguanosine monohydrate	Lymphoma, leukemia		–[f]
– Phenolphthalein (also occupational exposure)	Lymphoma, histiocytic sarcoma		Anticipated HC

(*Continued*)

TABLE 12.10 (Continued)

Causative agent	Mouse	Rat	Relevance for humans[a]
HORMONALLY ACTIVE COMPOUNDS			
– Diethylstilbestrol	Uterine histiocytic sarcoma[b,g,h]	Not investigated	Known HC
– Estrogen	Lymphoma		Known HC
CHEMICALS WITH EXPOSURE VIA NUTRIENTS			
– Allyl isovalerate	Lymphoma[b]	Mononuclear cell leukemia[e]	–[f]
– Citral	Lymphoma[b]		–[f]
– Lasiocarpine	Not investigated	Lymphoma, leukemia	Anticipated HC
– *N*-bis(2-hydroxypropyl) nitrosamine	Histiocytic sarcoma[g,i]	Not investigated	Anticipated HC
Urethane		Lymphoma	Anticipated HC
CHEMICALS WITH OCCUPATIONAL EXPOSURE			
1,3-Butadiene	Lymphoma		Known HC
2,4,6-Trichlorophenol		Lymphoma[e], leukemia[e]	Anticipated HC
3,3′-Dimethoxybenzidine-4,4′-diisocyanate		Leukemia, lymphoma	Anticipated HC
4,4-Methylenedianiline dihydrochloride	Lymphoma[b]		Anticipated HC
Benzene	Leukemia, lymphoma		Known HC
Benzylbutylphthalate		Mononuclear cell leukemia[b]	–[f]
Coal tar	Histiocytic sarcoma[g]	Not investigated	Known HC
Dimethyl methylphosphonate		Mononuclear cell leukemia[e]	Possible HC
Ethylene oxide	Lymphoma[b]		Known HC
Formaldehyde			Known HC, increased lymphoma[j]
Furan		Mononuclear cell leukemia	Anticipated HC
Glycidol	Histiocytic sarcoma[e,k]		Anticipated HC
σ-Nitroanisole		Mononuclear cell leukemia	Anticipated HC
Tetrachloroethylene		Mononuclear cell leukemia	Anticipated HC
VAT yellow 4	Lymphoma[e]		–[f]

[a]*Known or suspected carcinogens according to NIEHS data (Report on Carcinogens, 12th edition, 2010).*
[b]*In females.*
[c]*Hemopoietic tumors also induced in rodents by other carcinogens of this chemical class.*
[d]*NUP98-HOXA9 transgenic mice.*
[e]*In males.*
[f]*Inadequate knowledge, no positive information.*
[g]*Only females investigated.*
[h]*CBA mice.*
[i]*P53-knockout mice.*
[j]*Under debate, because of lack of plausible mode of action.*
[k]*p16Ink4a/p19Arf tumor suppressor-gene haplo-insufficient mice.*
From Haschek, W.M., Rousseaux, C.G., Wallig, M.A. (Eds.), 2013. Haschek and Rousseaux's Handbook of Toxicologic Pathology, third ed. Academic Press (Elsevier), San Diego, CA, Table 49.11, p. 1848, with permission.

TABLE 12.11 IARC Nomenclature of Tumors of the Immune System in Rodents

Type	Modifier	Characteristics	Predilection sites
Lymphoma	Lymphocytic	Small to medium-sized lymphocytes, noncohesive, well differentiated	Spleen, thymus, lymph nodes
	Lymphoblastic	Noncohesive, large cells, nuclear pleomorphism common, growth in sheets, mitotic figures frequent	
	Pleomorphic	Cohesive growth pattern, nuclear pleomorphism, mixed cell population, altered architecture of affected lymphoid organs	
	Immunoblastic	Rare, large, noncohesive cells with large nuclei/nucleoli, mitotic figures frequent, plasma cell differentiation may be present	
	Plasma cell	Differentiation to plasma cells	
	Cutaneous T-cell	Infiltrate of skin by small to medium-sized lymphocytes, may be intermingled with other cell types such as histiocytes and plasma cells, Pautrier's microabscesses in epidermis and hair follicles	Skin
	Marginal zone	Small lymphocytes, arises in the splenic marginal zone	Spleen
LGL leukemia		Medium-sized lymphocytes, granules containing perforine and lysozyme (visible in imprints or smears only with special staining), leukemic, high incidences in F344 rats	Spleen
Histiocytic sarcoma		Pleomorphic or indented nuclei, varying amounts of eosinophilic cytoplasm, multinucleated cells, hyaline droplets in renal proximal tubules	Liver, uterus (mice), frequently spreading to lungs
Myeloid leukemia	Neutrophilic	Neutrophilic type is most frequent, others very rare, immature myeloid cells with ring or doughnut-shaped nuclei, kidneys: hyaline droplets in renal proximal tubules	Bone marrow, spleen, liver
	Eosinophilic		
	Basophilic		
Erythroid leukemia		Erythroid precursor cells	Spleen, liver
Megakaryocytic leukemia		Megakaryoblasts and atypical maturing megakaryocytes	Bone marrow, spleen

results may be challenging due to issues such as varying fixation periods, variations in the expression of markers, coincidence of systemic tumors, and mixtures of neoplastic and nonneoplastic cells in certain tumor entities.

Autoimmune Diseases and Hypersensitivity Reactions

Target Organs

Antigen-specific deranged processes like autoimmune disease and allergy lead to tissue damage, protein (immune) complex deposits, and/or inflammatory cell infiltrates in predominantly nonlymphoid, target organs. Well-known targets are vasculature, kidneys, synovial membranes, thyroid (Figure 12.34), skin, liver, and lungs. Figure 12.35 depicts an allergy-related mononuclear cell infiltrate in rat nasal passages, similar to allergy-related inflammation in the lungs. The morphological hallmark of autoimmune (-like) disease and allergy is inflammation. Unfortunately, there are at present no morphological criteria to identify antigen-specific inflammatory responses. Antigen-specific inflammation in nonlymphoid organs includes changes such as granulocytic and lymphocytic cell infiltrates, granuloma, necrosis, and fibrosis. These infiltrates are also common in nonspecific inflammation, and therefore their interpretation is difficult.

Typical changes like vasculitis, inflammation at dermal–epidermal interfaces, fibrinoid necrosis (Figure 12.36), and expansion of extracellular matrix are suggestive of an allergic- or autoimmune-related inflammation. In subacute and subchronic toxicity studies signs of full-blown autoimmune diseases are rarely encountered, because the time of exposure is too short and the number of animals per group is small, and relatively insensitive animal species or strains may be used. Therefore, in most cases only early indicators of such a disease may be present—for instance, lymphocytic infiltrates in the pancreatic islets as a symptom of early diabetes. The histology of clinically manifest, antigen-specific inflammatory reactions depends on the type of immune reaction, which can be

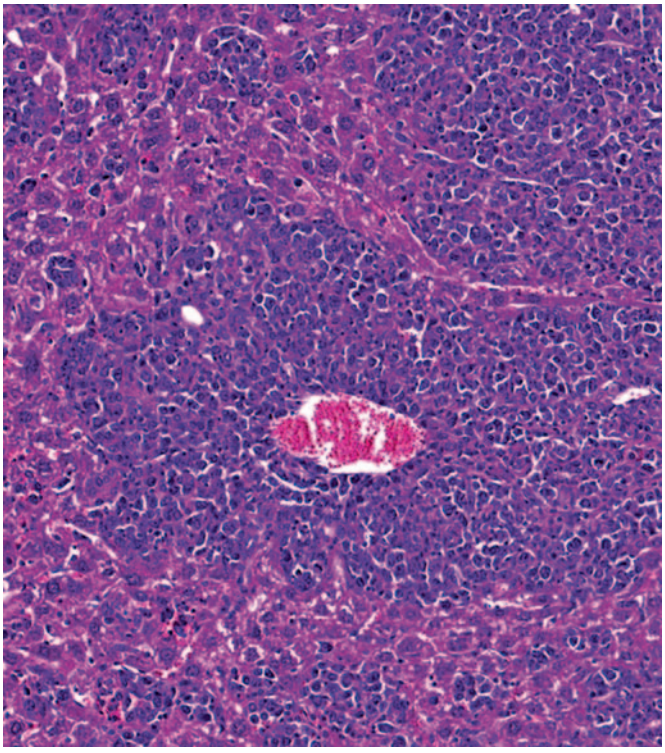

FIGURE 12.30 Lymphomatous infiltrate with nodular appearance in the liver of a mouse from a 2-year carcinogenicity study. H&E stain, ×20. Source: *From Haschek, W.M., Rousseaux, C.G., Wallig, M.A. (Eds.), 2013. Haschek and Rousseaux's Handbook of Toxicologic Pathology, third ed. Academic Press (Elsevier), San Diego, CA, Figure 49.32, p. 1853, with permission.*

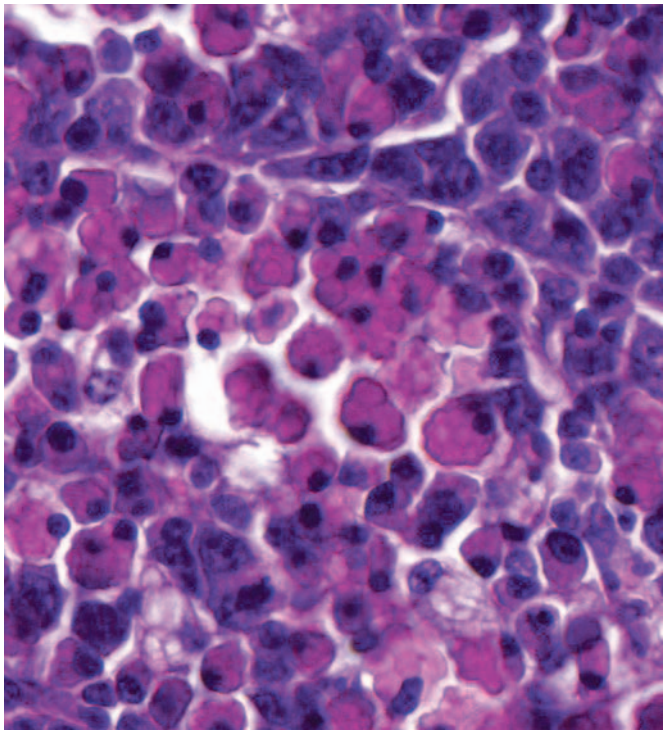

FIGURE 12.32 Plasmacytic lymphoma from a CD-1 mouse with prominent Russell bodies. Source: *From Haschek, W.M., Rousseaux, C.G., Wallig, M.A. (Eds.), 2013. Haschek and Rousseaux's Handbook of Toxicologic Pathology, third ed. Academic Press (Elsevier), San Diego, CA, Figure 49.35, p. 1854, with permission.*

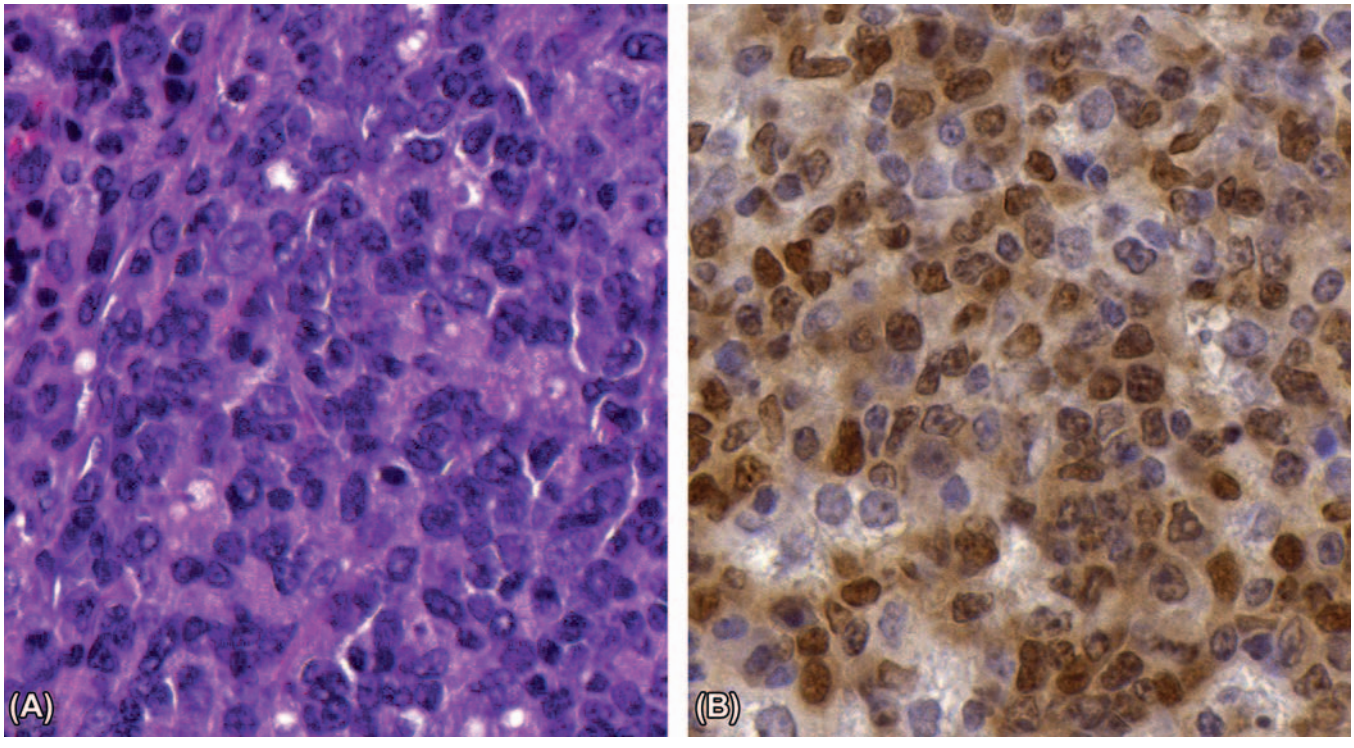

FIGURE 12.31 (A) Pleomorphic lymphoma arising in the splenic white pulp of a CD-1 mouse from a 2-year carcinogenicity study, showing cohesive cells with variable morphology. (B) Neoplastic cells are positive for the B-cell marker PAX-5. Source: *From Haschek, W.M., Rousseaux, C.G., Wallig, M.A. (Eds.), 2013. Haschek and Rousseaux's Handbook of Toxicologic Pathology, third ed. Academic Press (Elsevier), San Diego, CA, Figure 49.34, p. 1854, with permission.*

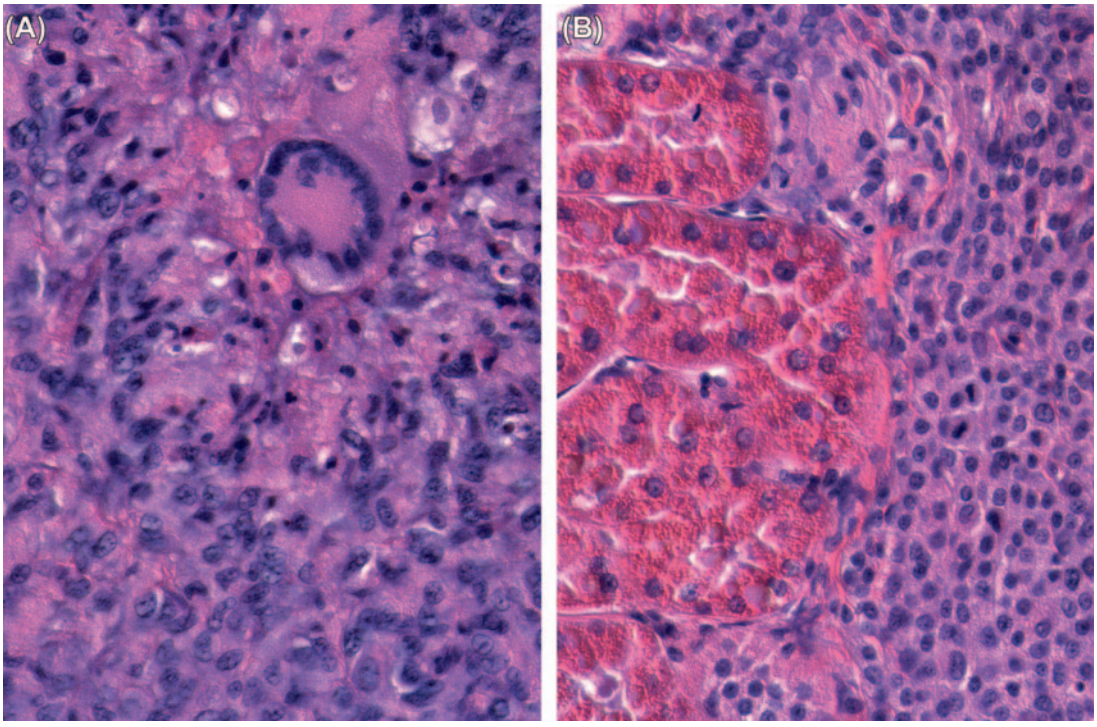

FIGURE 12.33 (A) Histiocytic sarcoma, Wistar rat, exhibiting multinucleated giant cells. Observation of giant cells is helpful for diagnosis in unclear cases. H&E stain, ×40. (B) Histiocytic sarcoma, Wistar rat. Half of the image shows a tumor infiltrate in the kidney, which is very typical. The infiltrate is a monomorphic infiltrate of small cells with eosinophilic cytoplasm. Renal proximal tubules with abundant hyaline droplets are visible; this is often observed with histiocytic sarcoma infiltration, even if it occurs elsewhere in the body. Source: *From Haschek, W.M., Rousseaux, C.G., Wallig, M.A. (Eds.), 2013. Haschek and Rousseaux's Handbook of Toxicologic Pathology, third ed. Academic Press (Elsevier), San Diego, CA, Figure 49.36, p. 1856, with permission.*

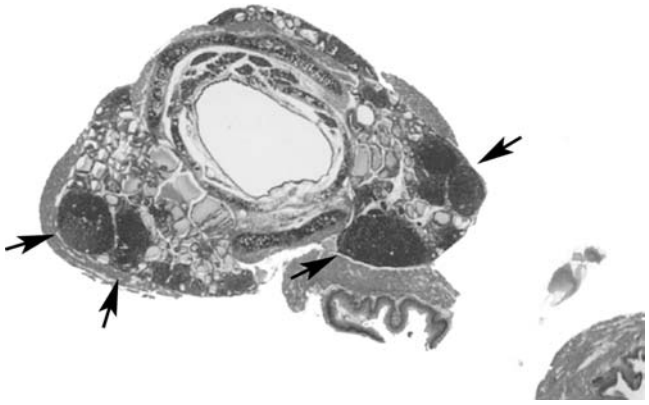

FIGURE 12.34 Lymphoplasmacytic thyroiditis in a 27-month-old female Praomys (Mastomys) nataliensis. Thyroiditis in Mastomys is associated with the presence of autoantibodies to colloid. There is no GC development. Source: *Courtesy: Dr. C. Zuercher, Voorschoten, The Netherlands. From Haschek, W.M., Rousseaux, C.G., Wallig, M.A. (Eds.), 2013. Haschek and Rousseaux's Handbook of Toxicologic Pathology, third ed. Academic Press (Elsevier), San Diego, CA, Figure 12.21, p. 640, with permission.*

categorized according to the Gell and Coombs classification. It should be kept in mind that an antigen often induces more than one type of reaction, and this is reflected by the morphology of the inflammation.

Figure 12.34 presents an example of lymphoplasmacytic infiltrates in the thyroid of the mastomys (*Mastomys natalensis*), which in this case occurred spontaneously. The infiltrates were associated with autoantibodies to colloid and were therefore considered to represent autoimmune thyroiditis. Histologic changes of this type are also seen with some frequency in the thyroid glands of beagle dogs. Another example of antigen-specific inflammatory reactions is beryllium-induced granulomatous inflammation in the lungs as the result of persistent antigenicity of inhaled beryllium. In dogs, beryllium induces so-called immune granulomas, while in rats nonspecific irritation by beryllium induces so-called foreign-body granulomas. The immune granulomas induced in dogs are complex, discrete, and highly organized, with a central region of epithelioid cells surrounded by significant numbers of lymphocytes and a few multinucleated giant cells of Langham's type. Coinfiltrating lymphocytes are beryllium-specific T-lymphocytes. The foreign-body granulomas in rats are simpler and more loosely organized than the immune granulomas in dogs, and contain monocytes, enlarged, and vacuolated macrophages, and multinucleated foreign-body giant cells. Few to no lymphocytes are present in the

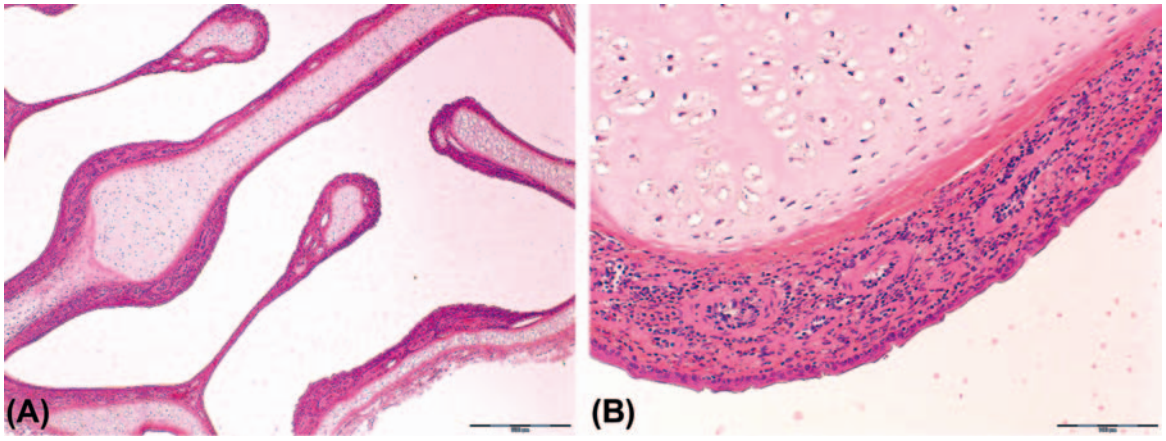

FIGURE 12.35 Inflammatory responses in nasal tissues of Brown Norway rats, sensitized dermally with dinitrochlorobenzene, and challenged by inhalation. (A) Overview of cross-section through the nasal passages, with a diffuse mononuclear (predominantly lymphocytic) inflammatory cell infiltrate. H&E stain, ×25. (B) Detail of infiltrate in the lamina propria of the septum. H&E stain, ×200. Source: *Courtesy: Dr. J.J. van Triel, TNO Triskelion, The Netherlands.*

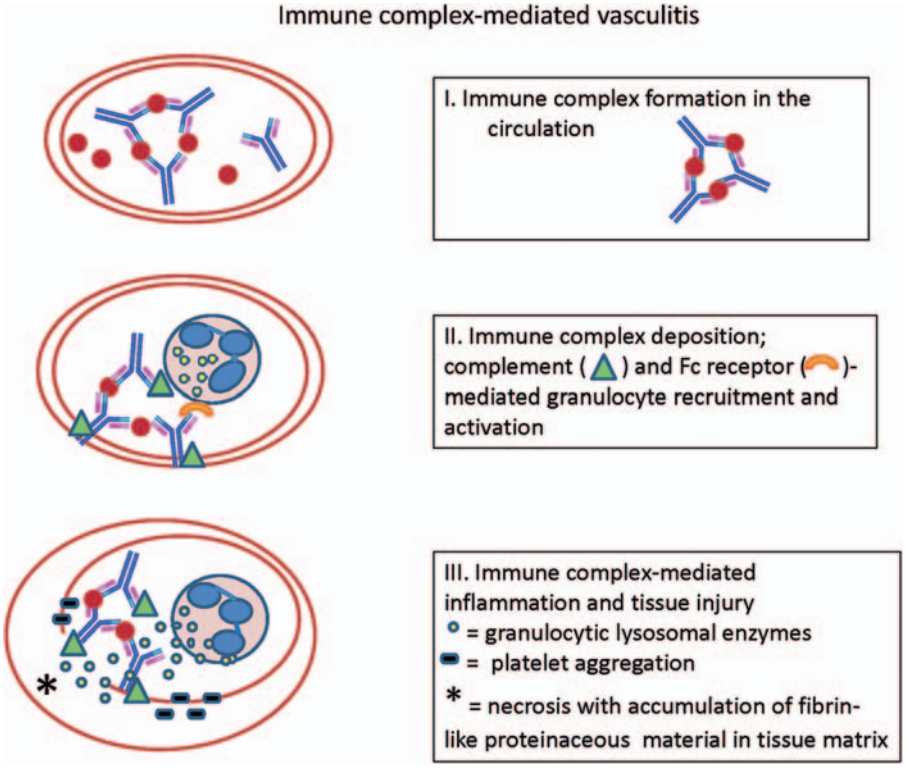

FIGURE 12.36 Immune complex-mediated vasculitis (Type III hypersensitivity). The morphologic manifestation is necrotizing vasculitis, with necrosis of the vessel wall and neutrophilic inflammation. The necrotic tissue, immune complex deposits, complement and plasma protein lead to an eosinophilic deposit. The microanatomy of the vessel is thus obscured and the phenomenon is designated fibrinoid necrosis. Source: *From Haschek, W.M., Rousseaux, C.G., Wallig, M.A. (Eds.), 2013. Haschek and Rousseaux's Handbook of Toxicologic Pathology, third ed. Academic Press (Elsevier), San Diego, CA, Figure 49.39, p. 1858, with permission.*

lesions. In a third example, inhaled crystalline silica may continuously be mobilized from macrophages and granulomas, in the lung and draining lymph nodes, even long after initial exposure to the silica, producing progressive lesions. In these lesions, alterations in extracellular matrix were the characteristic features. Silica may disseminate via lymph and blood, leading to granulomas in organs outside the

respiratory tract and its local lymph nodes. The continuous stimulation and degradation of inflammatory cells by silica has been associated with autoimmune (-like) diseases such as antineutrophil cytoplasmic antibodies (ANCA)-associated glomerulonephritis and vasculitis. Recently, it has been suggested that "frustration" of macrophages by partial ingestion of long nanotubes (Figure 12.37) may eventually lead to induction of autoimmune phenomena.

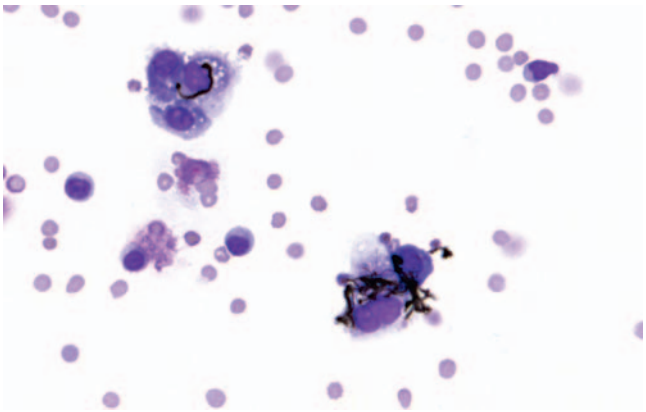

FIGURE 12.37 Macrophages from a bronchoalveolar lavage taken from rats exposed by inhalation to multiwalled carbon nanotubes (MWCNT). The length of the nanotubes prevented adequate uptake by the macrophages, leading to frustrated macrophage activity. Frustrated macrophages contribute to local inflammation, and might lead to immune derangements. Source: *From Haschek, W.M., Rousseaux, C.G., Wallig, M.A. (Eds.), 2013. Haschek and Rousseaux's Handbook of Toxicologic Pathology, third ed. Academic Press (Elsevier), San Diego, CA, Figure 49.40, p. 1858, with permission.*

Lymphoid Organs

Changes in lymphoid organs can alert the pathologist to potential autoimmune effects (Table 12.12). Alterations in lymphoid organs often accompany autoimmune inflammation at the nonlymphoid target sites; the most well-known examples in humans are thymoma and thymic follicular hyperplasia in myasthenia gravis. Comparable thymic proliferative changes are found in the autoimmune disease-prone mastomys and (NZB-NZW)F1 mouse. Mercuric chloride induces autoimmune disease in Brown Norway rats, with concomitant follicular hyperplasia in the thymus. The effect of exposure to mercuric chloride depends on the genetic make-up of the animal (and individual), because it induces immunosuppression in Lewis rats.

Alterations in lymphoid organs are not only associated with overt manifestation of autoimmune disease but have also been found to precede it; for example, follicular hyperplasia in the NZB mouse is observed before the onset of SLE or SLE-like disease. Moreover, thymectomy or cyclosporine-induced partial thymus depletion in very young animals can result in autoimmune (-like) disease. Therefore, follicular hyperplasia and certain forms of lymphoid organ depletion can be early indicators of autoimmune disease.

SUMMARY

The inherent characteristics of the immune system are its ubiquitous distribution (multiple sites but

TABLE 12.12 Lymphoid Organ Alterations in a Selection of Animal Models With Autoimmune (-Like) Inflammation

Animal species and strain	Autoimmune (-like) inflammation	Lymphoid organ alterations
BB rat	Pancreatic islets inflammation (diabetes mellitus); thyroiditis	Blood lymphopenia; thymus epithelial defects; liver increased apoptosis of recent thymic emigrants
Mercuric chloride in BN rat	Nephropathy; Sjögren syndrome-like adenitis	Thymus follicle formation
(NZB × NZW) F1 mouse	Chronic glomerulonephritis; vasculitis; SLE	Thymus decreased cellularity and follicle formation; lymph nodes and spleen lymphocyte proliferation; spleen follicular hyperplasia, erythropoiesis and hemosiderosis
NZB/Lac mouse	Chronic glomerulonephritis; vasculitis	Thymus decreased cellularity; lymph nodes plasma cell accumulations and increased cellularity; spleen increased cellularity, erythropoiesis, and hemosiderosis
NOD mouse	Pancreatic islets inflammation (diabetes mellitus); Sjögren syndrome-like adenitis	Thymus decreased cellularity, plasma cell infiltration and epithelial cell defects

From Haschek, W.M., Rousseaux, C.G., Wallig, M.A. (Eds.), 2013. Haschek and Rousseaux's Handbook of Toxicologic Pathology, third ed. Academic Press (Elsevier), San Diego, CA, Table 49.14, p. 1859, with permission.

one system) and multifaceted constituents jointly interacting within the organism. Under physiological conditions, the immune system aims at a status of homeostatic balance, which is constantly challenged by a variety of external influences.

Changes in lymphoid organs and in immune function can be related to beneficial effects like protection against pathogens by vaccination and intended suppression of immune function to try to cure autoimmune disease. Immune changes can also be related to adverse effects leading to an increased rate of infections or even tumors, to allergy and autoimmune disease.

Investigation of the immune system in toxicology needs a specific understanding of its structure and physiology. Moreover, species- and age-related changes and the interaction with the endocrine and nervous systems have to be taken into account. Histopathology has a pivotal role in the detection of immune changes in nonclinical toxicology studies, but additional assays are commonly required for elucidation of underlying immunological mechanisms. For interpretation of immune-related findings, a synopsis of findings in immune and nonimmune-related organs, hematological and immunological biomarkers is necessary. Furthermore, mechanistic studies in animal and *in vitro* models represent a relevant tool to investigate the translatability of immune findings to humans.

Further Reading

Bhogal, N., 2010. Immunotoxicity and immunogenicity of biopharmaceuticals: design concepts and safety assessment. Curr. Drug Safety. 5, 293–307.

Brandtzaeg, P., Pabst, R., 2004. Let's go mucosal: communication on slippery ground. Trends Immunol. 25, 570–575.

Brayton, C.F., Treuting, P.M., Ward, J.M., 2012. Pathobiology of aging mice and GEM: background strains and experimental design. Vet. Pathol. 49, 85–105.

Brennan, F.R., Morton, L.D., Spindeldreher, S., Kiessling, A., Allenspach, R., Hey, A., et al., 2010. Safety and immunotoxicity assessment of immunomodulatory monoclonal antibodies. Monocl. Antibodies. 2, 233–255.

Collinge, M., Burns-Naas, L.A., Chellman, G.D., Kawabata, T.T., Komocsar, W.J., Piccottio, J.R., et al., 2012. Developmental immunotoxicity (DIT) testing of pharmaceuticals: current practices, state of the science, knowledge gaps, and recommendations. J. Immunotoxicol. 9, 210–230.

Deretic, V., Kimura, T., Timmins, G., Moseley, P., Chauhan, S., Mandell, M., 2015. Immunologic manifestations of autophagy. J. Clin. Investigat. 125, 75–84.

EMEA, 2006. ICH Topic S8 Immunotoxicity studies for human pharmaceuticals EMEA/CHMP//167235/2004-ICH.

Everds, N.E., Snyder, P.W., Bailey, K.L., Bolon, B., Creasy, D.M., Foley, G.L., et al., 2013. Interpreting stress responses during routine toxicity studies: a review of the biology, impact, and assessment. Toxicol. Pathol. 41, 560–614.

Finch, G.L., Hoover, M.D., Hahn, F.F., Nikula, K.J., Belinsky, S.A., Haley, P.J., et al., 1996. Animal models of beryllium-induced lung disease. Environ. Health Perspect. 104, 973–979.

Gopinath, C., Mowat, A., 2014. The lymphoid system. Atlas of Toxicological Pathology. Springer Verlag, New York, pp. 197–213.

Haley, P., 2003. Interspecies differences in the structure and function of the immune system. Toxicology 188, 49–71.

Hameleers, D.M., van der Ven, I., Sminia, T., Biewenga, J., 1990. Anti-TNP-forming cells in rats after different routes of priming with TNP-LPS followed by intranasal boosting with the same antigen. Res. Immunol. 41, 515–528.

Koornstra, P.J., de Jong, F.I., Vlek, L.F., Marres, E.H., van Breda Vriesman, P.J., 1991. The Waldeyer ring equivalent in the rat. A model for analysis of oronasopharyngeal immune responses. Acta Oto-Laryngol. 111, 591–599.

Kuper, C.F., Koornstra, P.J., Hameleers, D.M.H., Biewenga, J., Spit, B. J., Duijvestijn, A.M., et al., 1992. The role of nasopharyngeal lymphoid tissue. Immunol. Today 13, 219–224.

Kuper, C.F., Ruehl-Fehlert, C., Elmore, S.A., Parker, G.A., 2013. Immune system. In: Haschek, W.M., Rousseaux, C.G., Wallig, M. (Eds.), Handbook of Toxicologic Pathology, vol. III. Academic Press Elsevier Inc, San Diego, CA, Chapter 49.

Kuper, C.F., Schuurman, H.-J., Bos-Kuijpers, M., Bloksma, N., 2000. Predictive testing for pathogenic autoimmunity: the morphological approach. Toxicol. Lett. 112-113, 433–442.

Leifer, C.A., Dietert, R.R., 2011. Early life environment and developmental immunotoxicity in inflammatory dysfunction and disease. Toxicol. Environ. Chem. 93, 1463–1485.

Mohr, U., Dungworth, D.L., Capen, C.C., 1992. Pathobiology of the Aging Rat, vol. I. ILSI Press, Washington, DC.

Monograph, W.H.O/I.P.C.S., 2006. Principles and Methods for Assessing Autoimmunity Associated with Exposure to Chemicals. Environmental Health Criteria 236. WHO, Geneva.

Pabst, R., 2007. Plasticity and heterogeneity of lymphoid organs: what are the criteria to call a lymphoid organ primary, secondary or tertiary? Immunol. Lett. 112, 1–8.

Parker, G., Picut, C., Swanson, C., Toot, J., 2015. Histologic features of postnatal development of immune system organs in the Sprague-Dawley rat. Toxicol. Pathol. 43, 794–815.

Pichler, W.J., Naisbitt, D.J., Park, B.K., 2011. Immune pathomechanism of drug hypersensitivity reactions. J. Allergy Clin. Immunol. 127, S74–S81.

Pruett, S.B., Fan, R., Zhang, Q., Schwab, C., 2009. Patterns of immunotoxicity associated with chronic as compared with acute exposure to chemical or physical stressors and their relevance to the role of stress with regard to immunotoxicity testing. Toxicol. Sci. 109, 265–275.

Rehg, J., Bush, D., Ward, J., 2012. The utility of immunohistochemistry for the identification of hematopoietic and lymphoid cells in normal tissues and interpretation of proliferative and inflammatory lesions of mice and rats. Toxicol. Pathol. 40, 345–374.

Sainte-Marie, G., Peng, F.S., Belisle, C., 1982. Overall architecture and pattern of lymph flow in the rat lymph node. Am. J Anatomy. 164, 275–309.

Tilney, N.L., 1971. Patterns of lymphatic drainage in the adult laboratory rat. J. Anatomy. 109, 369–383.

Van den Broeck, W., Derore, A., Simoens, P., 2006. Anatomy and nomenclature of murine lymph nodes: descriptive study and nomenclatory standardization in BALB/cAnNCrl mice. J. Immunol. Methods. 312, 12–19.

Vohr, H.W., 2015. Encyclopedia of Immunotoxicology. Springer, Berlin, ISBN 978-3-642-54595-5.

Ward, J.M., Rehg, J.E., Morse III, H.C., 2012. Differentiation of rodent immune and hematopoietic system reactive lesions from hyperplasias. Toxicol. Pathol. 40, 425–434.

This page intentionally left blank

CHAPTER

13

Hematopoietic System

Lila Ramaiah[1], *Denise I. Bounous*[2], *and Susan A. Elmore*[3,*]

[1]Bristol-Myers Squibb Co., New Brunswick, NJ, United States
[2]Bristol-Myers Squibb Co., Princeton, NJ, United States
[3]National Toxicology Program/NIEHS, Research Triangle Park, NC, United States

OUTLINE

INTRODUCTION

The hematopoietic system is one of the largest organs in the body. Its primary function is hematopoiesis, a highly regulated, complex, and dynamic process that continuously produces highly specialized circulating blood cells responsible for respiratory, immune, and hemostatic processes. The hematopoietic system is particularly susceptible to toxic insult owing to its rapid metabolic and proliferative rate, extensive vascularization, local metabolism of xenobiotics, and lifelong reliance on a limited pool of self-renewing stem cells. As such, it ranks alongside liver and kidney as one of the most important target organs of toxicity.

This chapter provides a mechanistic and morphologic foundation for understanding the broad range of hematotoxicities. Topics pertaining to the myeloid, erythroid, and megakaryocytic/platelet compartments of bone marrow (BM) include normal hematopoiesis as well as mechanisms of, and responses to, hematotoxicity. The lymphoid compartment is discussed in Chapter 12, Immune System. Abbreviations used in this chapter are listed in Table 13.1.

*Susan A. Elmore contribution is in Public domain.

Fundamentals of Toxicologic Pathology.
DOI: http://dx.doi.org/10.1016/B978-0-12-809841-7.00013-7

TABLE 13.1 Abbreviations

ALAS	Aminolevulinic acid synthase
AhR	Aryl hydrocarbon receptor
AIHA	Autoimmune hemolytic anemia
AITP	Autoimmune thrombocytopenia
ARID5B	AT-rich interactive domain-containing protein 5B
ATP	Adenosine triphosphate
AGM	Aorta-gonad-mesonephros
BFU-E	Erythroid burst-forming units
BM	Bone marrow
BMP	Bone morphogenetic protein
CEBPE	CCAAT/enhancer binding protein, epsilon
CD	Cluster of differentiation
CDK	Cyclin-dependent kinase
CDKN2A/B	Cyclin-dependent kinase inhibitor 2 A/B
CLP	Common lymphoid progenitor
CFU-E	Erythroid colony-forming units
CMP	Common myeloid progenitor
CMLP	Common myeloid/lymphoid progenitor
DIC	Disseminated intravascular coagulation
DMS	Demarcation membrane system
DNA	Deoxyribonucleic acid
DPG	Diphosphoglycerate
EDTA	Ethylenediaminetetraacetic acid
EMP	Erythroblast macrophage protein
EKLF	Erythroid Kruppel-like factor
EMH	Extramedullary hematopoiesis
EPC	Endothelial precursor cells
EPO	Erythropoietin
FGF	Fibroblast growth factor
FLT3	Fms-like tyrosine kinase-3
FLVCR	Feline leukemia virus, subgroup C, receptor
FoxO	Forkhead Box O
GATA3	GATA binding protein 3
GADD	Growth arrest and DNA damage
G-CSF	Granulocyte colony-stimulating factor
GMP	Granulocyte/monocyte progenitor
GMT	Gelatinous marrow transformation
IGF	Insulin-like growth factor
IL	Interleukin
IMHA	Immune-mediated hemolytic anemia
ITP	Immune-mediated thrombocytopenia
JAK	Janus kinase
IKZF1	Ikaros family zinc finger protein 1
KLF1	Kruppel-like factor 1
LMPP	lymphoid-primed multipotent progenitors
LTBR	lymphotoxin-β receptor
M-CSF	Macrophage-colony-stimulating factor
MDSC	Myeloid-derived suppressor cells
M:E	Myeloid to erythroid ratio
MEP	Megakaryocytic/erythroid progenitor
MGDF	Megakaryocyte growth and development factor (TPO)
MK	Megakaryocyte
MPL	Myeloproliferative leukemia (virus oncogene)
MPP	Multipotent progenitor
MSC	Mesenchymal stem cell
NRTI	Nucleoside reverse transcriptase inhibitor
PDE	Phosphodiesterase
PDGF(R)	Platelet-derived growth factor (receptor)
PGE	Prostaglandin E
PHD	Prolyl-4-hydroxylase domain
PTP	Protein tyrosine phosphatase
O	Oxygen
Rb	Retinoblastoma
RBC	Red blood cell
REPOS	Renal erythropoietin producing and oxygen sensing
RNA	Ribonucleic acid
ROS	Reactive oxygen species
SCF	Stem cell factor
SCL/TAL1	Stem cell leukemia/T-cell acute leukemia 1
SDF	Stromal cell-derived factor
SERPIN	Serine protease inhibitor
SOD	Superoxide dismutase
Scfr1	Stem cell frequency regulator 1
TGF	Transforming growth factor
TIMP	Tissue inhibitors of metalloproteinases

(*Continued*)

TABLE 13.1 (Continued)

GM-CSF	Granulocyte/monocyte-colony stimulating factor	TNF	Tumor necrosis factor
HCK	Hemopoietic cell kinase	TPO	Thrombopoietin
HDAC	Histone deacetylase	TRAIL	TNF-related apoptosis-inducing ligand
Hgb	Hemoglobin	UTS	Untranslated sequence
HIF	Hypoxia-inducible factor	VEGF(R)	Vascular endothelial growth factor (receptor)
HO-1	Heme oxygenase 1	VLA	Very late activation antigen
HSC	Hematopoietic stem cell	vWF	Von Willebrand factor
HSP	Hemoglobin stabilizing proteins	WBC	White blood cell
ICAM	Intercellular adhesion molecule		

Table modified from Haschek, W.M., Rousseaux, C.G., Wallig, M.A. (Eds.), 2013. Handbook of Toxicologic Pathology, third ed. Academic Press, Table 50.1, pp. 1866–1867 with permission.

PHYLOGENESIS AND ONTOGENESIS

Phylogeny (Evolutionary Origin) of the Hematopoietic System

Most primitive multicellular organisms have primitive hematopoietic cells between the ectoderm and endoderm and hematopoietic clusters appear as specialized vascular domains in the coelomate splanchnopleure. True hematopoietic organs developed in vertebrates with the emergence of primitive and definitive hematopoiesis. Lower vertebrates and ectotherms have foci of lymphopoiesis and myelopoiesis in mesodermal tissue, such as kidney or spleen. Bony fish have a rudimentary BM while amphibians, reptiles, birds, and mammals have both a thymus and BM. Permanent separation between lymphoid and myeloid tissues is first observed in birds (lymph nodules, lymph nodes (some species), and bursa of Fabricius).

Respiration is present in all aerobic organisms. Nonvertebrate gas transport metalloproteins range from single-chain globins to multidomain and giant hemoglobins with a heme moiety (for reversible binding of oxygen). Most vertebrates have tetrameric hemoglobins (pairs of globin chains α and β), for cooperative oxygen binding and sigmoid-shaped dissociation curves, as opposed to the hyperbolic curves of monomeric hemoglobins of invertebrates. Vertebrate hemoglobin is sequestered in erythrocytes (RBCs), conferring longevity and efficiency. Regression of tubulin marginal bands, nuclear loss, and 2,3-bisphosphoglyceric acid (2,3-BPG) production have further enhanced the RBC's circulatory and respiratory capabilities in mammals. The resultant RBC is a radially symmetrical, biconcave disk that has low inertial forces while in circulation and a high deformability for easy migration through capillaries. Hemostasis arose alongside the hematopoietic and circulatory systems in invertebrates (hemocytes) and vertebrates (thrombocytes/platelets).

Innate immunity exists in all living organisms. Discrimination of self and nonself uses pathogen-recognizing receptors encoded in the genome (see Chapter 12: Immune System. Innate immune responses are further enhanced by programmed hyper-variability at genetic loci involved in immunity. The transition to multicellularity necessitated recognition of compromised or altered self. Peptides that destroy cell membranes emerged in lower invertebrates and evolved to a complex, highly regulated complement cascade of about 30 proteins in mammals. Specialized immune cells (phagocytes) that used reactive oxygen species (ROS) to kill pathogens arose in the earliest multicellular organisms. Vertebrates developed adaptive pathogen recognition, based on clonal expansion of lymphocytes bearing specific immune receptors of unlimited variability, though primitive forms of adaptive immune recognition also exist in bacteria and prokaryotes.

Ontogenesis (Embryonic and Postembryonic Origin) of the Hematopoietic System in Mammals

Hematopoietic ontogeny parallels phylogenetic events in the evolution of the hematopoietic system. Mammalian hematopoietic development occurs in two distinct phases: (1) primitive hematopoiesis, which supports blood cell production during embryogenesis, and (2) definitive hematopoiesis, which generates committed hematopoietic progenitors necessary to foster all lineages in the fetus onward into postpartum existence.

In primitive hematopoiesis, hemangioblasts (mesothelial progenitors arising in the inner layer of the visceral yolk sac) aggregate into blood islands comprised of a central core of hematopoietic progenitors (hemocytoblasts), surrounded by an outer rim of endothelial progenitors.

Most cells produced during primitive hematopoiesis are erythroid, though primitive megakaryocytes (MK) and macrophages are also encountered. Hemocytoblasts differentiate into erythroid colony-forming cells and then into primitive erythroblasts, which enter the bloodstream. Colony-forming erythroid cells eventually regress, leaving circulating primitive erythroblasts as the sole source of RBCs until definitive hematopoiesis takes hold (late-stage embryo). Consequently anemia observed during mid-stage embryogenesis is due to a defect in primitive erythropoiesis.

Definitive hematopoiesis begins in mid-stage embryogenesis. Cytopenia occurring in late-stage embryos, fetuses, and neonates is due to a defect in definitive hematopoiesis. Definitive pluripotent hematopoietic stem cells (HSCs) arise from the aorta-gonad-mesonephros (AGM) region, allantois, chorion, definitive placenta, umbilical arteries, and yolk sac. HSCs migrate to hematopoietic stromal cell niches where they commit to a more limited range of lineage options. During late embryogenesis the liver is the primary site of definitive hematopoiesis. From the liver, HSCs migrate to thymus, spleen, lymph nodes, or BM. Primary lymphoid development first begins in the thymus, with subsequent development in other tissues. The BM is first colonized early in fetal life, and becomes the primary site for hematopoiesis soon after birth. Foci of hematopoiesis are still present in the liver of pigs at birth, and persist in the spleen of mice and, to a lesser extent, rats, throughout life. In other mammals, hematopoiesis may return to the spleen under conditions of heightened demand.

STRUCTURE, FUNCTION, AND CELL BIOLOGY

Anatomy of the Bone Marrow

BM is the major site of hematopoiesis in the body and is the largest primary lymphoid tissue. All cells of the blood and the immune system are initially derived from the BM. Consequently following severe toxic insult, the regenerative capacity of blood cells and most peripheral lymphoid organs depends on BM stem cells. An inflammatory reaction, hemorrhage, or other stressors that "consume" erythroid, myeloid, or lymphoid cells, may also be reflected in the BM as peripheral need increases. Therefore evaluation of the BM is integral to any investigation of hematotoxicity, and proper evaluation requires an understanding of its normal structure and function.

This section discusses BM anatomy. Histomorphology of individual cellular components is discussed later in this chapter ("Morphologic evaluation of the bone marrow" section). Splenic and hepatic extramedullary hematopoiesis (EMH) are discussed Chapter 8, Liver and Gall Bladder and Chapter 12, Immune System.

The intertrabecular spaces of axial and long bones are filled with marrow, a highly vascular loose connective tissue stroma, which contains maturing blood cells and their precursors. Hematopoietically active "red marrow" is commonly found in young animals due to a predominance of mature RBCs. With time, this red marrow is slowly replaced by adipocytes, becoming yellow in color.

Anatomically BM can be subdivided into vascular, stromal, and hematopoietic compartments. The vascular compartment is well organized and complex (Figure 13.1). Nutrient and periosteal arteries supply the highly vascular marrow. The larger nutrient artery traverses cortical bone via the nutrient canal (located mid-shaft) and then branches to run parallel to the long axis in the central part of the marrow cavity. This artery further divides into radial arteries, which ultimately produce a system of capillaries that permeate the marrow. Smaller periosteal arteries, derived from arteries in surrounding muscles, also traverse the cortical bone to form capillaries that anastomose with the vessels derived from the nutrient artery, thus forming a sinusoidal plexus throughout the marrow cavity.

Hematopoietic tissue exists within the spaces of this blood-rich capillary network. Blood from the sinusoidal plexus drains into the large central vein and exits the bone as the nutrient vein via the nutrient canal. This provides a circular pattern of blood flow, with blood moving from the center of the marrow cavity toward the periphery, then back toward the center. Most vessels in the BM are thin-walled, permitting cellular egress to the blood and lymphoid tissues. Though the thin-walled vessels of BM appear morphologically similar to lymphatic capillaries, immunohistochemical staining with specific lymphatic endothelial cell markers (LYVE-1/podoplanin) indicates that lymphatic capillaries are absent from bone and BM. Lymphatic circulation does not appear to play a role in normal bone and BM fluid drainage, and lymphatic vessels are only observed in connective tissue overlying the periosteum. Even in malignant neoplasia, lymphatic capillaries are generally not observed in bone or BM (exceptions include lymphangiomatous hyperplasia, lymphangioma, lymphangiosarcoma, and hemangioendothelioma).

The stroma supporting the vasculature and hematopoietic cells consists of adventitial reticular/barrier cells (fibroblasts), reticulin fibers, adipocytes, macrophages, nerves, and components of the extracellular matrix such as collagens, laminin, fibronectin, hemonectin, and proteoglycans. Reticular cells produce argyrophilic reticulin fibers (Type I and II collagen) that cross-link to form a fine meshwork, which acts as a highly ordered physical support system for the marrow. Marrow adipocytes are thought to originate from

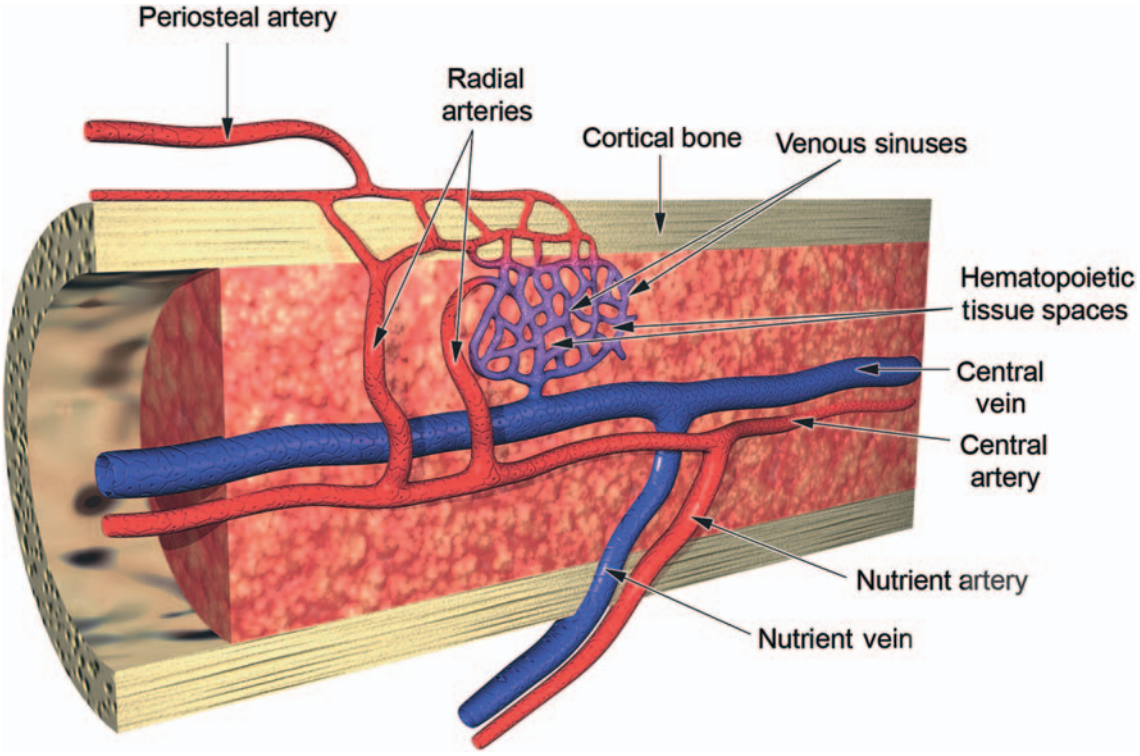

FIGURE 13.1 Diagrammatical representation of the bone marrow (BM) vascular supply. Source: *Drawing by David Sabio, in Travlos, G. 2006. Normal structure, function, and histology of the bone marrow,* Tox. Path. *Adapted from Abboud, C.N., Lichtman, M.A. 2001. Structure of the marrow and the hematopoietic microenvironment. Figure reproduced from Williams Hematology, sixth edition. Copyright McGraw-Hill, used with permission from SAGE Publications.*

these reticular cells. The hematopoietic compartment is separated from circulation by vascular sinus endothelium, basement membrane, and adventitia. Myelinated and nonmyelinated nerves serving the smooth muscle of the vessels can be found adjacent to the arterioles, and may occasionally be found within the hematopoietic tissue.

Hematopoiesis

Stem Cell Biology

Pluripotent stem cells (e.g., hemangioblasts) have unlimited self-regenerative capacity while multipotent hematopoietic stem cells (MHSC) have limited self-regenerative capacity. MHSC can divide symmetrically to maintain a population of undifferentiated cells within the stem cell pool for months to years, or divide asymmetrically to generate committed oligopotent progenitors (HSCs, mesenchymal stem cells (MSCs), and endothelial precursor cells (EPCs)). HSC can be loosely subdivided into three pools: (1) the quiescent stem cell pool (nondividing or slowly-dividing long-term repopulating cells), (2) the mitotic pool (rapidly dividing short-term repopulating cells), and (3) the postmitotic pool (maturing or differentiating cells).

Under the classical view of hematopoiesis, HSC progressively become lineage restricted as they differentiate through a succession of divisions. However, this hierarchical model (Figure 13.2) is not immutable (exhibits plasticity) or universal (varies between species and cell types). For example, mice have a common myeloid/lymphoid progenitor whereas humans exhibit strict separation of myeloid and lymphoid lineages. Surface antigen expression at each developmental stage also differs among species. Some fully differentiated cells (macrophages, dendritic cells, lymphocytes, and mast cells) still have proliferative capacity in extramedullary tissues. Furthermore cells such as dendritic cells and mast cells follow a graded lineage commitment model, where cells arise from progenitors of varying differentiation stage and lineage. Finally seemingly committed cells can be induced to convert into cells of another lineage, i.e., lineage reprogramming.

Hematopoietic Microenvironment

The hematopoietic microenvironment maintains multipotent quiescent pools and orchestrates the activities of proliferating and differentiating pools through direct cell−cell interactions, paracrine interactions, elaboration of the extracellular matrix, and

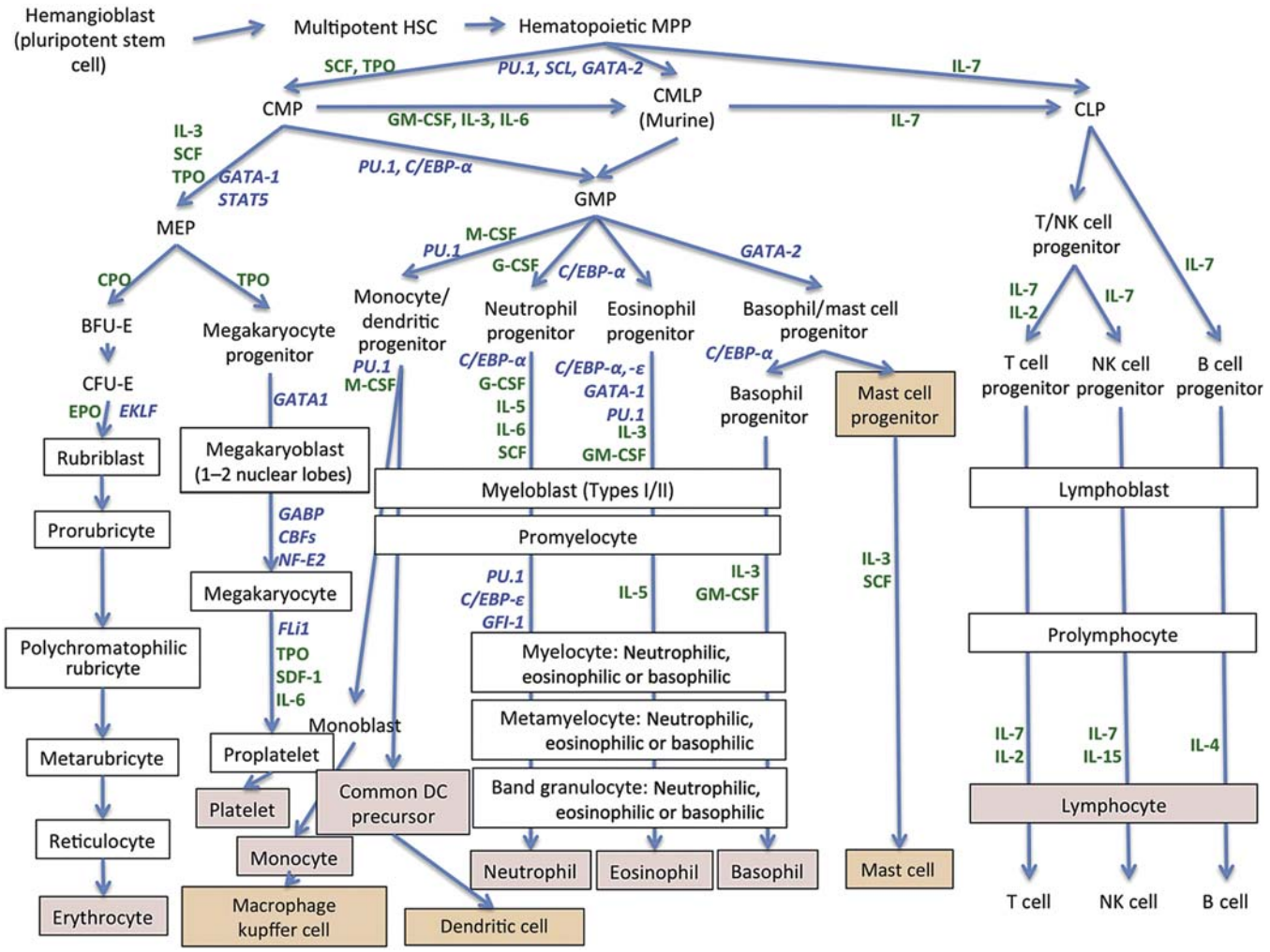

FIGURE 13.2 Schematic of Hematopoiesis. Lineage differentiation varies with species and is more plastic than this linear model implies. Cell types shown in boxes can be recognized by light microscopy; Orange box: tissue cell; Pink box: circulating cell; Green font: stimulatory cytokines; Blue font: transcription factors. Source: *Figure reproduced from Haschek, W.M., Rousseaux, C.G., Wallig, M.A., (Eds.), 2013. Handbook of Toxicologic Pathology, third ed. Academic Press, Fig. 50.2, p. 1874 with permission.*

reciprocal molecular interactions with hematopoietic cells. Specialized microanatomical units (niches) provide the matrix to support the self-renewal, differentiation, and proliferation of hematopoietic cells. The subendosteal/osteoblastic niche sustains and regulates quiescent stem cells by virtue of its low oxygen and ROS levels, which suppresses proliferation, differentiation, and mobilization. It is at the lowest (1% O_2) end of an oxygen gradient arising from capillaries in the vascular niche (20% O_2). HSC in the subendosteal niche eventually migrate to the perisinusoidal vascular niche, where increased perfusion provides nutrients and oxygen required to maintain proliferation. MK development begins in the subendosteal niche, where low oxygen, type I collagen and fibronectin promote MK spreading and inhibit proplatelet production. The vascular niche promotes fibrinogen and von Willebrand Factor (vWF) expression, terminal differentiation, and production of proplatelets. MK are also present in other high oxygen compartments such as spleen and lung capillaries. Erythroblastic islands, located near venous sinuses, consist of single macrophages (nurse cells) that support the maturation of 10–30 surrounding erythroid cells. These macrophages are essential for iron transfer and phagocytosis of extruded nuclei and defective RBC.

Life Cycle of Blood Cells

ERYTHROPOIESIS

In most mammalian species, each HSC produces approximately 2×10^7 RBCs over a period of months. Multipotent hematopoietic progenitors differentiate into megakaryocytic/erythroid progenitors (MEPs), followed

by Erythroid Burst-Forming Units and Colony-Forming Units (BFU-E and CFU-E). In culture, BFU-E take 7–9 days to develop into CFU-E, which take 3–5 days to develop into rubriblasts. Over approximately 5 days and 5 mitotic divisions, rubriblasts differentiate into prorubricytes, polychromatophilic rubricytes, metarubricytes, and reticulocytes. There are normally about 50 rubricytes and 113 reticulocytes for every rubriblast. In most species, reticulocytes spend 2–3 days maturing in BM before being released into circulation.

Erythropoietin (EPO) is an evolutionarily conserved glycoprotein hormone that shares structural homology with growth hormones and hematopoietic class 1 cytokines. As the principal erythropoietic hormone, it stimulates the survival, proliferation, and maturation of erythroid cells. During development, hepatic EPO supports erythropoiesis in the fetal liver. After birth, specialized Renal Erythropoietin-Producing and Oxygen-Sensing (REPOS) cells become the primary source for EPO production. REPOS cells are peritubular, interstitial fibroblast-like cells located in the corticomedullary oxygen gradient of the juxtamedullary cortex of the kidney. Decreased regional blood oxygen levels can induce a 150- to 1000-fold increase in EPO production, proliferation of REPOS cells, and EPO mRNA stabilization. The liver can also contribute to EPO production in response to hypoxia (up to 50% of total EPO in adult rodents).

The EPO receptor is expressed at low levels on early erythroid progenitors (BFU-E), at high levels in late progenitors (CFU-E) and early committed erythroid cells and is then down regulated as cells become increasingly differentiated. EPO receptors are also expressed in endothelial, neural, muscle, cardiovascular, and renal tissues, where it protects against tissue ischemia by promoting vasoconstriction and stimulating angiogenesis and nerve regeneration. Strength and duration of EPO pulses, receptor expression, and the activity of kinases relative to phosphatases, all regulate the kinetics of red blood cell (RBC) maturation.

Terminal differentiation of erythroid cells requires tight regulation of DNA synthesis, nuclear division, chromatin condensation, cytokinesis, organelle loss, and hemoglobinization. The pace of cell division and chromatin maturation generally follows that of hemoglobin synthesis. As hemoglobin accumulates, overall transcriptional activity diminishes and cells become smaller. Heme accumulates earlier and faster than globin, and regulates its own synthesis as well as that of globin. When a specified level of nonfree heme is reached, iron uptake and cell division are halted and the nucleus is extruded. In reticulocytes, globin mRNAs are protected from degradation by mRNA–protein (mRNP) complexes, and continue to be translated for as long as 1 week following nuclear extrusion. The successful protracted synthesis of hemoglobin relies on the survival of globin mRNA (half-life of 10–60 hours) and on the stabilization of free globin chains by hemoglobin stabilizing proteins (α-HSP). Hemoglobin synthesis persists at a low rate for 3–4 days until it reaches a finite concentration. Excess free heme is rapidly exported or degraded by heme oxygenase to minimize generation of ROS.

Reticulocyte maturation occurs in the BM, spleen, and circulation. Young reticulocytes have a high metabolic rate, synthetic function, and fragility. Maturing reticulocytes lose organelles, surface area, and surface proteins by exosome formation and blebbing, as membranes are remodeled and cytoskeleton is stabilized.

Reticulocyte migration from BM into circulation results from loss of surface adhesion molecules, small size, heightened deformability, pressure gradients along BM sinus wall, and EPO-induced increases in endothelial pore number and size. The maturity of cells entering circulation varies with species and age. During basal erythropoiesis, humans, dogs (aggregate), cats (punctate), and rodents primarily release reticulocytes, while ruminants and horses release mature RBC into circulation. Basal reticulocyte counts are high in young rodents and decrease substantially as they mature. In response to an erythropoietic stimulus, cats release aggregate reticulocytes, ruminants release reticulocytes and horses release large RBCs. Reticulocyte responses are robust in rodents. Reticulocytes released in response to erythropoietic stimulation are less mature and have a longer circulating life span (3–5

TABLE 13.2 Normal Blood Cell Life Span by Species

	RBC (days)	Platelet (days)	Neutrophil (h)
Mice	30–52	3–5	12.5
Rats	42–69	3.7–8	6
Guinea pigs	60–80		
Hamsters	60–70		
Rabbits	60–70	3	
Cats	60–80		
Dogs	100–120	4–9	7
Swine	80–100	5–7	8
Sheep	114		
Goat	125		
Nonhuman primates	85–105	6.5	
Humans	120	7–10	6.6 h to 5.4 days
Horses	140–150		
Cattle	160		

Table modified from Haschek, W.M, Rousseaux, C.G., Wallig, M.A. (Eds.), 2013. Handbook of Toxicologic Pathology, third ed. Academic Press, Table 50.4, p. 1879 with permission.

days vs 1−1.5 days). Dramatic age-related changes in reticulocyte counts can occur in pigs (increase at 3−7 days, decrease at approximately 3 weeks, increase at 8 weeks, and decrease at approximately 3 months of age). It is not uncommon to observe abrupt changes in reticulocyte numbers even in 6-month-old minipigs.

The life span of mature circulating RBCs is determined by eryptosis and senescence-based clearance, and varies according to basal metabolic rate in each species (Table 13.2). Eryptosis in RBCs is analogous to apoptosis in nucleated cells and is characterized by cell shrinkage, blebbing, phospholipid scrambling of the cell membrane, and cell surface expression of phosphatidylserine. It is associated with a wide variety of diseases and is also triggered by osmotic shock, oxidative stress, energy depletion, hyperthermia, and many small molecules. RBC senescence involves receptor-mediated removal of aged or damaged RBCs by splenic and BM macrophages and hepatic Kupffer cells.

MEGAKARYOPOIESIS AND THROMBOPOIESIS

Within the subendosteal niche, thrombopoietin (TPO) and platelet-derived growth factor (PDGF) induce MEP differentiation into lineage-committed MK progenitors. MK progenitors undergo endomitosis, a highly specialized form of mitosis in which there is chromosome duplication but no true cell division from the progenitor stage to the MK stage. This facilitates the synthesis of massive quantities of platelet cytoskeletal, cytoplasmic, and membrane components. Due to an altered mitotic spindle, there is a failure of anaphase, telophase, and cytokinesis, resulting in polyploidy ranging from 16N (mice and humans) to 32N (dogs and rabbits) and 32−64N (cats and cattle) after multiple rounds of endomitosis occurring over approximately 2 days. Ploidy determines MK cytoplasmic volume, platelet production, and circulating platelet size and count. Cytoplasmic MK maturation involves production of membrane receptors (CD41/61, CD42, and glycoprotein V), α- and dense granules, protein synthetic apparatus, and an internal demarcation membrane system (DMS). The DMS is an elaborate network of tubular plasma membrane invaginations that provide a reservoir for the formation of proplatelet processes.

After completion of endomitosis and cytoplasmic maturation, MKs migrate to the vascular-rich niche, bind to endothelial cells, and begin elaborating proplatelets (pseudopod membrane projections). Platelets are shed into vascular sinusoids by proplatelet fragmentation, taking with them a full complement of membranes, organelles, granules, and soluble macromolecules. Each MK produces 1000−3000 platelets before the residual nucleus is degraded by macrophages.

TPO stimulates proliferation and differentiation of MEPs, endomitosis and maturation, proplatelet formation and stimulation of erythroid proliferation and differentiation. TPO also acts together with several cytokines to promote the growth of primitive stem cells and granulocyte/monocyte progenitors (GMPs) and induces splenic EMH. TPO is primarily synthesized in the liver, but also in kidney, skeletal muscle, BM stromal cells, spleen, testis, muscle, and brain. Its expression is enhanced by inflammation (IL-6). TPO receptors are expressed on platelets, MKs, MK precursors, and endothelial cells. Circulating levels of TPO are regulated via platelet receptor−mediated uptake and degradation. Platelets also produce platelet factor 4 (PF4), which inhibits megakaryopoiesis.

MYELOPOIESIS

Myelopoiesis varies among species and cell types. Monocytes/macrophages, granulocytes, and mast cells arise from a common myeloid progenitor (humans) or a common myeloid/lymphoid progenitor that differentiates into a granulocyte/monocyte progenitor (mice). Common progenitors then differentiate into lineage-committed monocyte, neutrophil, eosinophil, basophil, and mast cell progenitors. In a synchronous sequence of division and maturation, cells acquire lineage-specific cytoplasmic granules and nuclear conformations.

Myelopoiesis is regulated by the coordinated up- or down-regulation of transcription factors and myelopoietic cytokines. The default pathway for myeloid progenitors is the monocytic/macrophage lineage; transcription factors and cytokines direct cells toward a granulocyte or mast cell lineage. Developing granulocytes can be subdivided into mitotic, maturing, and storage pools. The proliferating pool constitutes 10%−30% of BM granulocytes, while the maturation and storage pools constitute 65%−90% of BM granulocytes. Each myeloblast produces 16−32 metamyelocytes in approximately 6 days. Metamyelocytes and band granulocytes no longer divide but undergo nuclear and cytoplasmic maturation into segmented granulocytes. In some species, neutrophils are released in a cyclic or pulsatile fashion (∼every 3 days in mice, ∼14 days in dogs, and ∼20 days in humans). Under conditions of increased demand, cytokines shorten maturation time from 6 days to 2−3 days, stimulate the release of neutrophils from BM, and prevent apoptosis. As cytokine concentrations increase, more immature myeloid cells are released into circulation. Mammalian (human) granulocyte life span in circulation is short (neutrophils: 5.4−8 hours; basophils: <6 hours; eosinophils: <1 hour). As granulocytes circulate, nuclear maturation continues, resulting in increased nuclear condensation and segmentation. Granulocytes that exit the blood vascular system do not reenter circulation, but are utilized and removed in situ.

Mast cell hematopoiesis is not fully understood. Lineage-committed mast cell progenitors may be

derived directly from multipotent progenitors instead of the common myeloid progenitor. Progenitors enter circulation and migrate to peripheral tissues including skin, heart, lung, and gastrointestinal submucosa, where they proliferate and differentiate. Mature mast cells distinguish themselves by expression of high-affinity IgE receptors (FcεRI), c-Kit, and characteristic secretory granules. Basophils, which also express high-affinity IgE receptors, may arise from a common basophil/mast cell progenitor. In the BM, they mature into basophils under the direction of transcription factor CCAAT/CEBPα.

The lineage-committed monocyte/dendritic progenitor (MDP) is the precursor to a heterogeneous group of mononuclear cells, phagocytes, and antigen-presenting cells (APC) including monocytes, most macrophages, dendritic cell (DC) subsets, and osteoclasts. Like mast cells, they have the capacity to proliferate at extramedullary sites. Within the BM, MDPs differentiate into monocytes and common DC precursors (CDPs) which differentiate into plasmacytoid DCs or pre-DCs. Pre-DCs then enter circulation to mature into classical DCs in the spleen and lymph nodes, or mucosal DCs in the lamina propria. Regulatory T cells, FMS-like tyrosine kinase-3 (Flt3), and the lymphotoxin-β receptor (LTBR) control pre-DC proliferation and maturation within lymphoid organs. Classical DCs have a short half-life and are rapidly replaced by BM precursors. Some DCs arise directly from HSCs, common myeloid progenitors, or common lymphoid progenitors. Differentiation of MDP into monocytes is poorly understood and differentiation stages in the BM are not readily identified. Monocytes may be considered to be circulating precursor cells that give rise to tissue macrophages (M-CSF), inflammatory DCs (GM-CSF and Flt3L), and osteoclasts (M-CSF and RANKL). They remain in circulation for approximately 25 hours. In tissues, they divide at a slow rate and have a long life span (years). Inflammatory cytokines stimulate tissue macrophages to differentiate into a variety of inflammatory tissue macrophages, multinucleated giant cells, syncytial cells, and epithelioid macrophages. Inflammatory DCs have a half-life of 3−5 days. Common myeloid progenitors also give rise to a population of phenotypically heterogeneous myeloid-derived suppressor cells (MDSC), which resemble immature monocytes/granulocytes. In response to factors such as glucocorticoids, VEGF, PGE2, GM-CSF, TGF-β, IL-1β, IL-10, IL-6, and M-CSF these immature myeloid cells accumulate and proliferate at sites of inflammation or neoplasia and suppress immune responses by inhibiting T-cell proliferation and cytokine production. Not all tissue macrophages originate from monocytes. Tissue-specific macrophages such as hepatic Kupffer cells, microglia in the central nervous system, dermal macrophages, dermal and mucosal Langerhans cells, splenic marginal zone macrophages, and metallophilic macrophages, colonize tissues during embryogenesis, differentiate in situ, proliferate during the first week of life and continue to divide in situ during adulthood.

LYMPHOPOIESIS

In the BM, HSCs differentiate into multipotent progenitors that give rise to lymphoid-primed multipotent progenitors (LMPP). LMPP lack MK/erythroid potential, but maintain combined lymphoid and myeloid potentials. The lymphopoietic lineage begins as CFU-L, which differentiate into either a CFU-B or CFU-T cells, followed by Pre-B and Pre-T lymphocytes, B and T lymphoblasts, and finally mature B and T lymphocytes. B cells and NK cells are generated in the BM. T cells and some NK cells are generated in the thymus from multipotent progenitors and common lymphoid progenitors that migrate to the thymus from the BM. Lymphocytes in peripheral blood consist primarily of T cells. The lymphoid system is further discussed in Chapter 12, Immune System.

EVALUATION OF HEMATOTOXICITY

BM and peripheral blood are evaluated in concert in a functional precursor/product relationship, and interpreted in light of changes occurring in other tissues. In the nonclinical drug safety setting, the first tier assessment of the hematopoietic system entails a complete blood count in conjunction with a concurrent histologic BM examination. Unexplained or inappropriate effects require further characterization by cytology or flow cytometry (second tier). Hematopoiesis can also be investigated using *in vitro* or *in vivo* culture and animal models.

Because hematotoxicity may also occur indirectly through injury to other organ systems, considerations must be given to all other organ systems as well as the general condition of the animal. Other organs that have a lymphoid or hematopoietic component might also be affected including the lymph nodes, mucosa associated lymphoid tissue, thymus, liver, and spleen. These are discussed in Chapter 12, Immune System.

Morphologic Evaluation of the Bone Marrow

Histologic evaluation is important to assess overall hematopoietic cellularity and architecture and to identify the type and distribution of lesions. Increases or decreases in hematopoietic cells may be identified by estimating the percentage of fat versus hematopoietic cells in the marrow cavity compared to concurrent control animals. The amount of hematopoietic tissue relative to fat varies by age, species, and site. Younger animals

and rodents have less adipose tissue when compared to older animals and nonrodents (e.g., dogs and monkeys). In rodents the best sites for histologic evaluation are the proximal femur, proximal humerus, and sternum.

Histologic evaluation of hematoxylin and eosin (H&E)–stained BM should begin at low magnification with an overall assessment of tissue architecture, cellularity, lineage proportions, and/or stromal cell proliferations. Definitive identification of lymphoid cells is usually difficult (except in lymphoma), and may require immunohistochemical B and T-cell stains. Higher magnification is needed for identification and evaluation of erythroid, myeloid, and megakaryocytic lineages, estimation of M:E ratio, MK cellularity and iron stores (hemosiderin-laden macrophages), and evaluation of vasculature (venous sinuses, radial arteries, nutrient vein, nutrient artery) and other features such as neoplasia, inflammation, infectious agents, etc. The cells that can be identified include the maturing stages of erythroid, myeloid, and megakaryocytic cells, as well as adipocytes, hemosiderin-laden macrophages, and mast cells. The ratio of myeloid to erythroid cells (M:E ratio) may be estimated and maturation sequence may be estimated as based on the presence/predominance of immature cell types. Severe disturbances in maturation sequence may be seen histologically as changes in the ratio of proliferating cells to maturing cells, generally 1:4 in rodents. Asynchronous maturation observed histologically should be confirmed by cytologic evaluation.

Erythroblastic islands may be evaluated histologically, though they are not always readily apparent without the aid of immunohistochemistry. The more mature erythroid cells within these islands are smaller and more hyperchromatic than the larger immature erythroid cells with large round nuclei and deeply basophilic cytoplasm. Granulopoiesis is also compartmentalized but the sites are less distinct foci. Histologically, immature myeloid cells are large, with bean-shaped nuclei and finely granular, vesicular chromatin. Segmented and band neutrophils can be easily identified. MKs are frequently located adjacent to sinus endothelium to facilitate release of mature platelets into the circulation. These are the largest and thus easiest cells to identify with abundant pale eosinophilic cytoplasm and multilobulated nuclei.

Cytologic Evaluation of the Bone Marrow

In toxicologic studies, cytologic evaluations are indicated when there is an inappropriate or unexplained histologic BM change and altered peripheral blood counts or morphology. Cytology rarely adds useful information when there is evidence of an appropriate response to peripheral demand or when the cause of changes is known (e.g., decreased food consumption or known cytotoxicity). It is not useful to investigate granulocyte or platelet dysfunction, and may not be helpful to investigate decreased lymphocyte counts or BM architecture or cellularity. In toxicologic studies, BM smears may be collected at necropsy and stored for future evaluation as needed on a case-by-case basis. BM cytology entails a qualitative assessment of cell maturation and cytomorphology. It may include a quantitative assessment (differential count of 100–500 cells) to characterize alterations in lineage proportions (including M:E ratio) or incomplete/asynchronous maturation of a given lineage.

Flow Cytometry

The biggest limitation to quantitative evaluation of cytologic specimens is that relatively few cells are counted. Flow cytometry is an investigative tool that can be applied to any hemolymphatic tissue including peripheral blood, lymph node, and spleen. Although technically challenging, it allows for high-throughput, reproducible, and precise differential counting of many cells (10,000–35,000). A rodent's entire long BM can be harvested to provide absolute cell counts. Flow cytometry cannot be used to obtain a complete differential count or to assess cytomorphology, and thus cannot replace cytologic assessments. Therefore cytospin preparations of cell suspensions should always be prepared simultaneously. Other applications for flow cytometry include assessment of *in vivo* genotoxicity/clastogenicity; proliferative activity; MK maturation; evaluation of platelet, granulocyte, and macrophage function and activation; characterization of clonal disorders; detection of subcellular particles; and isolation and enrichment subpopulations of cells for *in vitro* applications.

In Vitro Techniques

In vitro methods are useful to investigate mechanisms and to screen compounds in early discovery toxicology. In addition, they enable translation of results between species and compounds, and facilitate dose setting and maximum tolerated dose (MTD) prediction. *In vitro* cytogenetic analysis can be used to investigate genotoxicity, clastogenesis, myelodysplasia, and leukemogenesis. Clonogenic assays evaluate stem cell to proliferation and differentiation in selective media when exposed to potential toxicants. Colony-forming assays are time consuming to perform and rely on the subjective and technically demanding manual enumeration of colonies. Promising techniques for high-throughput *in vitro* hematotoxicity testing include automated nonclonogenic fluorometric microculture cytotoxicity assays (FMCA), quantification of

intracellular ATP concentration, and coculture of hematopoietic progenitors with stromal or "feeder" cells.

Animal Models

Animal models have historically relied on naturally occurring susceptibilities or exposure to classic hematotoxicants. Other approaches have included BM transplantation, *in vivo* clonogenic assays in lethally irradiated mice, IL-21-induced anemia in monkeys, humanized mice, transgenic knockout and targeted "knockin" mice, mutant mice (hypotransferrinemic, erythropoietin-deficient, thalassemic, and hemojuvelin and hepcidin knockout), and mice harboring single nucleotide polymorphisms. The hematopoietic system can also be studied in zebrafish (*Danio rerio*) embryos, which are easy to manipulate genetically, permeable to water-soluble chemicals, and amenable to high-throughput screening. Zebrafish kidney marrows are functionally equivalent to the BM niche of mammals.

MECHANISMS OF TOXICITY

Most adverse xenobiotic-induced reactions are predictable, dose-dependent reactions that result from the direct effect of a xenobiotic or its metabolite (Type A). Less commonly, they may be unpredictable and nondose-related events that are idiosyncratic or attributable to hypersensitivity (Type B). They can also act indirectly through systemic effects.

BM toxicity most often manifests as hematopoietic suppression, though responses vary depending on the injured cell type. Xenobiotics may target a broad spectrum of blood cells or cells of a specific cell type (erythroid, myeloid, platelet) or stage of maturity (stem cell, progenitor, maturing, circulating). Injury to uncommitted stem cells generally produces aplastic pancytopenia (aplastic anemia), while injury to committed myeloid or erythroid progenitors produces agranulocytosis or pure red cell aplasia, respectively. Injury to the mitotic pool results in generalized BM hypoplasia or aplasia, with recovery supported by surviving quiescent stem cells. Death of maturing cells may produce maturation arrest and/or increased proportions of immature cells. Altered nuclear or cytoplasmic maturation usually leads to dysplasia. Altered nuclear maturation due to interference with DNA synthesis or mitosis results in atypical mitotic figures, nuclear fragmentation, and bi/multinucleation. Altered nuclear maturation with spared protein synthesis and cytoplasmic maturation, results in macrocytosis, megalocytosis, or granulocyte hypersegmentation. Altered cytoplasmic maturation with spared nuclear maturation results in microcytosis with hypochromasia and indistinct or scalloped plasma membranes (RBC) and retention of RNA (basophilia). Agents that inhibit heme synthesis (ethanol, isoniazid, pyrazinamide, cycloserine, chloramphenicol, copper chelation/deficiency, zinc, lead, trichloroethylene, and gallium arsenide) cause iron and ferritin to precipitate in mitochondria of maturing erythroid cells, producing siderocytes. Injury to circulating cells generally produces peripheral cytopenia with the appropriate BM hyperplastic response.

Mechanisms of hematopoietic injury are similar between species, and hematopoietic toxicity in animals holds high concordance with and predictivity for human toxicity. However, species differences do modulate the hematotoxic effects of some compounds. For example, mice and cats are particularly susceptible to the hematotoxic effects of nitrosoureas while rats, guinea pigs, and sheep appear to be somewhat resistant. Cytosine arabinoside and busulfan induce thrombocytopenia in a wide variety of animal species, but not humans. In BALB/c mice, vincristine produces thrombocytosis without prior thrombocytopenia, whereas in rats, it produces a transient thrombocytopenia.

Direct Nonimmune Injury to Hematopoietic Cells

Xenobiotics can injure blood and BM cells by directly altering molecular bonds (frank breaks, alkylation, cross-linking, and oxidation of nucleic acids, proteins, carbohydrates, and lipids), disrupting membrane integrity, inducing apoptosis, or inhibiting essential cellular functions, (e.g., quiescence, division, differentiation, motility, mitochondrial function, and cytoskeletal function). Injury to the extracellular matrix, supportive stromal cells, and vasculature of the BM is also an important contributor to hematopoietic toxicity. Classes of common hematotoxic agents include antineoplastic, antimicrobial and immunosuppressive chemotherapeutics, kinase inhibitors, antibiotics, antiretrovirals, antifungals/parasiticides, hormones and hormone antagonists, cytokines, environmental contaminants, physical injury, heavy metals, mycotoxins, and plant toxins (Table 13.3).

Although BM susceptibility is generally attributed to the rapidly dividing mitotic pool, xenobiotics can injure nondividing cells at all stages of maturity, from quiescent stem cells to maturing and fully differentiated circulating cells. Circulating blood cells are particularly prone to direct injury from high exposures to circulating xenobiotics.

Some agents show specificity for self-renewing stem cells. Alkylating agents target resting pluripotent stem cells as well as proliferating cells (phase-specific), leading to severe BM suppression with delayed recovery.

TABLE 13.3 Classes of Agents Causing Injury to Hematopoietic Cells

Class		Examples	Mechanism of action	Hematotoxicity
Cytotoxic agents	Alkylating agents	Nitrogen mustards: Mechlor-ethamine, cyclophosphamide, ifosfamide, melphalan, Chlorambucil	DNA cross-linking	Myelosuppression with neutropenia and thrombocytopenia Chromosomal aberrations, aneuploidy, poikilocytosis, macrocytosis, hypersegmentation Myelodysplastic syndrome, leukemia
		Methylhydrazine derivatives: Procarbazine		
		Alkyl sulfonate (Busulfan)		
		Nitrosureas: Carmustine (BCNU), streptozotocin, bendamustine		
		Triazenes: Dacarbazine (CTIC), temozolomide		
		Platinum coordination complexes (platinum analogs): Cisplatin, carboplatin, oxaplatin		
		Mitomycin-C	Bioreductive alkylation DNA cross-linking	
	Vinka Alkaloids	Vinblastine, vinorelvine, vincristine	Inhibit microtubule function	
	Taxanes	Paclitaxel, docetaxel		
	Topoisomerase inhibitors and DNA intercalators	Acridines (Pyrazoloacridine)	Intercalate DNA Inhibit topoisomerase	
		Epipodophyllotoxins: Etoposide, teniposide		
		Camptothecin, topotecan, irinotecan	Inhibit topoisomerase	
		Actinomycin D	Intercalates DNA Inhibit topoisomerase	
		Fluoroquinolone	Inhibit topoisomerase	
		Anthracyclines: Daunorubicin, doxorubicin, idarubicin	Inhibit topoisomerase Intercalate DNA Oxidative injury	
		Hydroxyurea	Intercalates DNA Inhibits ribonucleotide reductase Inhibits topoisomerase Increases synthesis of γ-globin chains (fetal globin), increasing oxygen affinity	
		Anthracenediones: Mitoxantrone	Inhibit topoisomerase Intercalate DNA	
	Radiomimetics	Bleomycin	Oxygen-mediated DNA double strand breaks	
		Enediynes		
		Ecteinascidin		
Nucleoside/ Nucleotide antagonists	Folic acid analogs/ antagonists	Methotrexate (Amethopterin), pemetrexed	Inhibit DNA synthesis	
	Pyrimidine analogs	Fluorouracil, cytarabine (cytosine arabinoside), gemcitabine, fludarabine, 2-chlorodeoxy-adenosine, clofarabine, capecitabine, gemcitabine, 5-azacytidine, deoxy-5-aza-cytidine, flucytosine		
	Purine analogs and related inhibitors	Mercaptopurine, pentostatin, flurabine, clofarabine, nelarabine, azathioprine		
	Nucleoside reverse transcriptase inhibitors (NRTI)	Ribavirin, zidovudine (Azidothymidine, AZT)	Inhibit cellular and mitochondrial DNA polymerase	

(*Continued*)

TABLE 13.3 (Continued)

Class		Examples	Mechanism of action	Hematotoxicity
Antibiotics	Sulfonamides	Sulfanilamide, sulfadiazine, sulfamethoxazole, sulfoxazole, sulfacetamide	Immune mediated	Agranulocytosis, aplastic anemia Acute hemolytic anemia
	Chloramphenicol	Chloramphenicol	Inhibit synthesis of mitochondrial proteins critical for aerobic metabolism and incorporation of iron into heme	BM suppression (Type A): Anemia, reticulocytopenia, leukemia Aplastic anemia (Type B): immune mediated Dog: Ringed sideroblasts
	Oxazolidinones	Linezolid, eperezolid	Inhibit protein synthesis	Myelosuppression: Pancytopenia, thrombocytopenia Dogs: Megakaryocyte hypersegmentation
	Cephalosporins	Cefonicid, cefazedone	Mitochondrial injury Possibly immune mediated	Myelosuppression and maturation arrest
Antifungals		Fluconazole, itraconazole, voriconazole	Reduce ergosterol synthesis by inhibiting fungal cytochrome P450 enzymes	Myelosuppression, leukopenia, thrombocytopenia
		Terbinafine	Reduce ergosterol synthesis by inhibiting the fungal enzyme squalene epoxidase	Myelosuppression, leukopenia, thrombocytopenia
		Griseofulvin	Inhibit cell wall synthesis	Myelosuppression in cats
Antivirals		Gancilclovir	Inhibit viral DNA synthesis	Myelosuppression: Neutropenia, thrombocytopenia
		Interferons	Inhibit paracrine production of hematopoietic growth factors Immune mediated	Myelosuppression: Neutropenia, thrombocytopenia
Antiparasitics		Levamisole, albendazole, metronidazole, fenbendazole, thiacetarsamide	Levamisole: Immune mediated in humans Idiosyncratic	Agranulocytosis Pancytopenia, BM hypoplasia
Hormones and hormone antagonists	Adrenocortical suppressants	Mitotane		BM necrosis
	Estrogens	Diethylstilbestrol, ethinyl estradiol, esters of estradiol (benzoate, cypionate, propionate, valerate, enanthate, and undeclynate)	Induction of a thymic factor that suppresses hematopoiesis	Rats: Anemia Dogs and ferrets: Fatal pancytopenia
Differentiating agents		HDAC inhibitors	Decrease the transactivation function of GATA-1, inhibiting GATA binding protein-1 (GATA-1) gene expression in megakaryocytes leading to a delay in megakaryocyte maturation	Thrombocytopenia
Agents directed at specific molecular targets	Tyrosine kinase inhibitors	Pazopanib, lestaurtinib (CEP-701), imatinib (Gleevec), nilotinib	Inhibits signaling by c-Kit, Flt3, PDGFR, ephrin receptor, Btk, and Jak2 (involved in signaling by the EPO/TPO receptor)	Myelosuppression with neutropenia, thrombocytopenia, anemia, macrocytosis, and lymphopenia
		Sunitinib, Sorafenib	Inhibit signaling by c-Kit, Flt3	
		Dasatinib	Inhibits Src kinases expressed in megakaryocytes	Thrombocytopenia
	TPO agonists	First generation	Immune mediated	Thrombocytopenia
		Second generation: Romiplostim and eltrombopag	Excessive stimulation of megakaryocytes and PDGF/TGF-β-induced stimulation of fibroplasia	Myelofibrosis and hyperostosis
CNS drugs	Anticonvulsants	Phenytoin, primidone, phenobarbital	Phenytoin in humans: Binds and inhibits intestinal conjugase, which converts monoglutamates into folic acid Phenobarbital/Phenytoin in dogs: Destroy mature granulocytes	Phenytoin in humans: Aplastic anemia, neutropenia, thrombocytopenia, macrocytosis, neutrophil hypersegmentationPhenobarbital/Phenytoin Dogs: Aplastic anemia, neutropenia, thrombocytopenia, myelonecrosis/fibrosis

(*Continued*)

TABLE 13.3 (Continued)

Class		Examples	Mechanism of action	Hematotoxicity
	Atypical antipsychotics	Clozapine	Oxidative injury: Bioactivation to a chemically reactive nitrenium ion	Agranulocytosis
Ionizing radiation			DNA damage (strand breaks, cross-links, mutagenesis), oxidative injury	Myelosuppression with neutropenia and thrombocytopenia. Chromosomal aberrations. Myelodysplastic syndrome, Leukemia
Plant and fungal toxins	Mycotoxins	Trichothecene mycotoxins (T-2 toxin, deoxynivalenol, stachybotryotoxicosis in horses and cattle), ochratoxin, zearalenone in humans		Aplastic anemia
	Bracken fern (*Pteridium aquilinum)*	Ptaquiloside	Thiamine deficiency due to thiaminase DNA adduct formation	Myelosuppression, pancytopenia, leukemia
Environmental Contaminants	Chlorinated polycyclic aromatic hydrocarbons	Benzene, benzene derivatives (chlorophenothane (DDT), lindane, pentachlorophenol)Carbon tetrachloride, hexachlorophene, chlordane, chlorobenzene, chlorinated dioxins, trichloroethylene, DMBA, benzopyrene, TCDD	Mutagenic AhR agonism Oxidative injury Protein alkylation Initiation of redox cycling Immune dysfunction Growth factor inhibition	Aplastic anemia Dysmyelopoiesis Myelodysplastic syndrome AML
		Trichloroethylene	Inhibits heme synthesis (inhibits delta-aminolevulinate dehydratase) in rats	Dyserythropoiesis, metarubricytosis, microcytosis, hypochromasia, basophilic stippling
	Heavy metals	Lead	Inhibits heme synthesis (γ-ALA dehydratase and ferrochelatase) and RNA depolymerization (pyrimidine 5′-nucleotidase)	
	Inorganic arsenic		Oxidative injury DNA damage, lipid peroxidation Induced release of heme from hemoglobin	Aplastic pancytopenia, dyserythropoiesis with karyorhexis, megaloblastosis *and* multinucleation, Hemolytic anemia

Table modified from Haschek, W.M., Rousseaux, C.G., Wallig, M.A. (Eds.), 2013. Handbook of Toxicologic Pathology, third ed. Academic Press, Table 50.6, pp. 1891–1895 with permission.

In contrast, cyclophosphamide affects stem cells with low self-renewal potential and high proliferative activity. Cycle-specific agents induce cell synchronization, resulting in a higher proportion of cells susceptible to subsequent exposures, depending on the timing of exposures relative to cell cycle. Therefore the frequency and duration of exposure can be important determinants of toxicity.

Injury to Hematopoietic Progenitors

Chlorinated polycyclic aromatic hydrocarbons such as benzene and its derivatives are genotoxic, mutagenic, and cytotoxic to pluripotent stem cells and progenitor cells. Benzene is hematotoxic even at low doses (<1 ppm, the current occupational standard), causing aplastic pancytopenia, myelodysplastic syndrome, and leukemia. Its reactive intermediates and metabolites (hydroquinone, *p*-benzoquinone, catechol, phenol, and muconaldehyde) induce myelosuppression by direct interaction with DNA and proteins, initiation of redox cycling, protein alkylation (tubulin, histones, topoisomerases), induction of chromosomal aberrations, aryl hydrocarbon receptor (AhR) agonism, immune dysfunction (TNF-α, INF-γ), and growth factor inhibition.

Toxic benzene metabolites are produced locally in the BM due to its expression of cytochrome p450 enzymes (e.g., CYP2E1 and CYP1B1). Benzene metabolites are also oxidized by peroxidases and converted to several biologically reactive quinones. Peroxidase and/or phenoxy radical–mediated oxidation of hydroquinone initiates redox cycling, glutathione conjugation, and formation of 1,4-benzoquinone, a reactive electrophile considered to be one of the ultimate hematotoxic metabolites of benzene. The production of ROS near DNA strands results in DNA backbone cleavage and cell cycle arrest, and defective maturation of precursor cells. Benzene metabolites also indirectly suppress hematopoiesis via injury to EPO-producing REPOS cells. In addition, benzene injures the microenvironment and triggers a sustained stress response that alters paracrine regulation of hematopoiesis, activates quiescent cells, and depletes the stem cell pool.

Agonism of the AhR has recently been identified as a mechanism of myelosuppression by polycyclic

hydrocarbons (primarily dioxin and benzene). AhR is a ligand-activated cytoplasmic transcription factor expressed in HSCs that regulates cell cycle entry to prevent premature exhaustion of the quiescent stem cell pool. AhR also regulates the expression of enzymes involved in xenobiotic activation and the responses to altered microenvironment, hypoxia, redox states, and circadian rhythms. AhR knockout mice fail to develop benzene hematotoxicity.

Injury to the Mitotic Pool Inhibition of DNA Synthesis and Cell Division

Chemotherapeutic agents have well recognized, direct, predictable, and dose-limiting cytoreductive effects leading to myelosuppression. Reversible neutropenia and thrombocytopenia may be observed initially, with aplastic pancytopenia, myelodysplastic syndrome, myelofibrosis, and/or leukemia occurring with prolonged exposure. Because chemotherapeutics inhibit DNA replication, their greatest impact is on the mitotic pool, whereas quiescent cells and postmitotic cells are relatively resistant. However, the deleterious effects of a single exposure can induce quiescent cells to enter the cell cycle, rendering them susceptible to subsequent exposures. The inhibition of DNA synthesis can result in macrocytosis with or without granulocyte hypersegmentation. Myelotoxicity is usually accompanied by lymphoid, gastrointestinal, and testicular toxicity.

Alkylating agents and ionizing radiation cause DNA interstrand cross-links and strand breaks, inducing cell cycle arrest, and possibly apoptosis if the damage is complex and difficult to repair. Topoisomerase-targeting antineoplastic agents inhibit DNA unwinding, causing strand breaks. Some topoisomerase inhibitors can intercalate themselves within DNA and thereby inhibit DNA replication and RNA synthesis. Hydroxyurea also inhibits conversion of ribonucleotides into deoxynucleotides.

Vinca alkaloids, taxanes, and colchicine are phase-specific cytotoxic agents that inhibit microtubule assembly and mitotic spindle formation. Since only a proportion of hematopoietic cells are in the susceptible part of the cycle (late S and early G2) at any given time, increasing the dose beyond an effective threshold does not increase the number of affected cells and results in a saturated dose-response curve.

Antimetabolite analogs of folic acid, pyrimidines, and purines inhibit DNA replication and cell division by inhibiting the synthesis of nucleotides and nucleosides. In cats treated for FeLV/FIV with azidothymidine (AZT) for several weeks there is erythroid hypoplasia as well as a transient or progressive nonregenerative macrocytic anemia, and there can also be Heinz body formation in this oxidant-susceptible species. In humans, drugs that contribute to vitamin B_{12} or folate deficiency reduce thymidine synthesis, resulting in suppression of DNA synthesis and megaloblastic anemia affecting all lineages.

Bracken fern contains thiaminases and ptaquiloside. Thiaminases cause thiamine deficiency and aplastic pancytopenia in cattle, sheep, pigs, horses, rats, and mice as well as polioencephalomalacia in ruminants, retinal degeneration, and blindness in sheep, and beriberi in nonruminants. Ptaquiloside is an alkylating and adduct-producing agent linked to myelosuppression, pancytopenia, and leukemia.

Zearalenone is a nonsteroidal estrogenic mycotoxin produced by *Fusarium* fungi that contaminates the food chain. Injury to hematopoietic cells occurs due to its genotoxic effects (chromosomal aberrations, DNA fragmentation).

Injury to the Maturing Pool Inhibition of Protein Synthesis

Cells of the maturing pool are most susceptible to inhibition of protein synthesis since they are actively synthesizing cytoplasmic constituents. Mammalian erythropoietic cells are particularly sensitive to chloramphenicol, which inhibits synthesis of proteins critical for aerobic metabolism and incorporation of iron into heme. Inbred mice are more susceptible than outbred mice, which are more susceptible than rats. Neutropenia and thrombocytopenia may also be observed in mice, rabbits, dogs, and cats.

Oxazolidinone antibiotics (e.g., linezolid, eperezolid) block the initiation step of mRNA translation, inducing mild, reversible, duration-dependent and dose-related myelosuppression, anemia, and thrombocytopenia, with or without neutropenia. In dogs, eperezolid alters regulation of MK endomitosis and increases MK numbers and mitoses, nuclear hypersegmentation, and multiple separate or satellite nuclei.

Trichothecenes are toxic fungal metabolites in contaminated food products. Trichothecene mycotoxins are small, amphipathic molecules that can be easily absorbed via integumentary and gastrointestinal systems. They are directly toxic without metabolic activation, allowing for rapid toxic effects on proliferating tissues. Their primary mode of toxicity is preventing peptide bond formation at the peptidyl transferase center of the 60S ribosomal subunit and activation of ribotoxic stress. Trichothecenes also disrupt DNA and RNA synthesis, cell division, mitochondrial function, membrane integrity, and immune cell-to-cell interactions, contributing to their radiomimetic, hemolytic, and immunosuppressive properties.

Lead inhibits γ- and δ-aminolevulinate dehydratase and ferrochelatase (required for heme synthesis), and

pyrimidine 5′-nucleotidase (required for reticulocyte ribosomal RNA depolymerization), resulting in failure of nuclear extrusion and RNA retention, respectively. Lead toxicity is characterized by BM dyserythropoiesis and increased myeloid to erythroid ratio, and circulating microcytosis, hypochromasia, metarubricytosis, and basophilic stippling.

Agents Directed at Specific Molecular Targets

Novel agents providing enhanced efficacy and reduced toxicity have been targeted toward growth factor receptors, intracellular signaling pathways, epigenetic processes, angiogenesis, DNA repair, and apoptotic pathways. Myelotoxicity and myelodysplasia are common and potentially severe consequences of treatment with kinase inhibitors, which may have off-target inhibitory effects on hematopoietic kinases (VEGFR, PDGFR, Flt3, Jak2, Kit, Axl, Mer, CSF-1R, Lyn, and HCK). For example, tyrosine kinase inhibitors of VEGFR commonly induce myelosuppression of varying frequency and severity through off-target inhibition of Flt3 and c-Kit. Inhibitors of Bcr-Abl tyrosine kinase nonspecifically inhibit Src kinases expressed in MKs, preventing MK migration along the SDF1-α gradient from the proliferative osteoblastic niche to the vascular niche, resulting in decreased proplatelet formation and thrombocytopenia.

Second-generation thrombopoietic agents produce reversible myelofibrosis, hyperostosis, and increased BM reticulin due to exaggerated pharmacology (see "Myeloproliferative Lesions" section). It is hypothesized that induction of megakaryopoiesis and thrombopoiesis by TPO agonists results in increased production of fibrogenic growth factors (platelet-derived growth factor (PDGF) and transforming growth factor-β (TGF-β) and osteoprotegerin). PDGF stimulates fibroblast proliferation, and TGF-β has stimulatory effects on fibroblasts and osteoblasts. In rats given a PEGylated peptide mpl (myeloproliferative leukemia virus oncogene) agonist, >threefold increases in platelet counts were associated with myelofibrosis and hyperostosis. Other consequences of TPO agonism include thromboembolic complications, myeloblast proliferation, and malignant transformation.

Oxidative Injury to Hematopoietic Cells

ROS are among the major determinants of cellular senescence, cytotoxicity and genotoxicity, and play a primary role in the development of myelofibrosis, myelodysplastic syndrome, and leukemia. ROS constitute a heterogeneous group of inorganic molecules and free radicals (superoxide (O_2^-), hydrogen peroxide (H_2O_2), singlet oxygen ($^1O_2$), nitric oxide (NO), peroxynitrite ($ONOO^-$), and hydroxyl radical (*OH)) endogenously produced at low levels as products of aerobic respiration. ROS are also important cell signaling intermediates that govern the oxidoreductive (redox) state of signaling proteins. The major source for ROS in hematopoietic cells is superoxide from the mitochondrial electron transport chain and from a variety of oxidases expressed throughout hematopoietic development. Superoxide is short-lived but can dismutate to hydrogen peroxide, a long-lived species from which all other physiologic ROS molecules are derived. Maturing erythroid precursors also generate ROS when incorporating iron into heme in mitochondria. In this process, hydrogen peroxide is spontaneously converted by ferrous iron ions (Fenton reaction) to the highly reactive hydroxyl radical.

Oxidative stress can be caused by increased ROS production, disturbances in cellular redox cycling of signaling intermediates, or antioxidant depletion/inhibition. In hematopoietic tissues it induces a variety of disease states ranging from BM failure to leukemia. In most cells ROS-generating systems are coupled to a network of antioxidant systems and functionally organized redox circuits that compartmentalize and scavenge ROS. Antioxidants that regulate ROS levels and/or mediate signal transduction by ROS include reducing enzymes (superoxide dismutase, catalase, glutathione peroxidase, thioredoxin, peroxiredoxin), nonenzymatic small molecule scavengers (ascorbic acid (vitamin C), uric acid, bilirubin, glutathione, zinc, selenium, tocopherols (vitamin E), β-carotene, ubiquinol-10 (coenzyme Q), lycopene), and proteins (albumin, haptoglobin, ferritin, ceruloplasmin).

Agents that have ROS-generating electron transfer functionalities can produce hematotoxicity through oxidative injury. These include ionizing radiation, ultraviolet light, drugs and their metabolites (especially chemotherapeutics, 5-fluorouracil, adriamycin, barbiturates, phorbol esters, peroxisome-proliferating compounds, captopril), cigarette smoke, ozone, and environmental and industrial chemicals (arsenic, benzene, chlorinated compounds, acrylonitrile, butoxyethanol). Chemical drug classes include quinones (or phenolic precursors), metal ions and metal complexes (or complexors), aromatic nitro compounds (or reduced derivatives), and conjugated imines or iminium species.

ROS exert their damaging effects by reacting with and altering the structure and function of all biological molecules, directly modifying macromolecules, altering the redox state of signal transduction factors and denaturing critical proteins such as hemoglobin and thiol-dependent enzymes. Lipid peroxidation severely damages cell membranes, causing alterations in membrane fluidity, cell shape, enzyme systems, receptors, and ion channels. Increased permeability to calcium and other ions may initiate inflammation and apoptosis. Injury to mitochondria reduces ATP production. The spectrum of DNA lesions caused by oxidative stress is

similar to that for ionizing radiation (base modifications, apurinic/apyrimidinic sites, protein−DNA cross-links, single and double strand breaks).

Oxidative stress disrupts homeostatic redox cycling in hematopoietic cells, resulting in activation of quiescent cells and premature stem cell exhaustion. ROS buildup drives stem cells out of quiescence to allow for DNA repair, leading to accelerated aging of HSCs, apoptosis or mutagenesis. In the proliferating pool, ROS-induced DNA damage causes cell cycle arrest. Failure of DNA repair results in apoptosis or chromosomal instability, mutagenesis, and altered gene expression. ROS-generating agents are considered complete carcinogens since they contribute to all stages of carcinogenesis (initiation, promotion, progression, and malignant conversion).

Several mechanisms limit oxidative stress in mammalian HSCs. Quiescent HSCs are protected from oxidative stress thanks to their reliance on anaerobic glycolysis and low oxygen levels in the subendosteal niche. FoxO (Forkhead Box O) transcription factors maintain HSC quiescence and induce expression of SOD (superoxide dismutase), catalase and GADD45 (Growth Arrest and DNA Damage) in hematopoietic stem and erythroid cells.

Chronically elevated ROS effectively limit the life span of HSCs, resulting in premature exhaustion of HSCs, hematopoietic dysfunction, and eventual myelodysplastic syndrome. Since many of the conserved pathways regulating stem cell self-renewal and differentiation are also stress-response pathways, activation of stress-response pathways by oxidative stress alters regulation of cell fate. The repeated activation of quiescent stem cells over a life span can have cumulative cell-autonomous effects including epigenetic dysregulation, mutations, and telomere erosion.

Direct Nonimmune Injury to Circulating Cells

Peripheral blood cells come into direct contact with circulating xenobiotics. Nonnucleated cells (platelets and RBCs) are most sensitive because they have limited repair capacity and no self-regenerative capacity. Platelets are also susceptible to functional alteration or inappropriate activation. Nucleated cells tend to be much more resistant to direct injury. Lymphocytes have self-regenerative capacity but are susceptible to immunomodulation and are predisposed to apoptosis when exposed to stressors. Monocytes and macrophages are highly resistant thanks to robust self-regenerative capacity, though numerous agents can alter their function. Agents that cause direct, nonimmune injury to circulating cells are listed in Table 13.4.

Highly reactive compounds or those that interfere with ATP production can rapidly cause intravascular hemolysis while the slow, unchecked accumulation of damage causes extravascular hemolysis and shortened RBC life span. The most common causes of premature RBC destruction or death are oxidative injury, nonoxidative chemical injury, and immune-mediated destruction (discussed in "Immune-Mediated Destruction" section).

Free hemoglobin (from intravascular hemolysis or exogenous hemoglobin infusion) is inherently harmful due to its vasoactive and redox-active properties. When normal protective mechanisms (e.g., haptoglobin, α_1-microglobulin, heme oxygenase ferritin, transferrin, CD163 receptors on monocytes/macrophages) are exceeded, free hemoglobin irreversibly binds nitric oxide (NO), resulting in vasoconstriction and vascular dysfunction. Free heme also induces formation of ROS, which result in hemoglobinuric nephrosis, acute renal failure, hepatic necrosis, and blood−brain barrier disruption. Ferric iron may react with chloride to form hemin, a hydrophobic molecule that intercalates in RBC membranes and causes rapid lysis upon accumulation. Hemin also promotes lipid peroxidation and mitochondrial dysfunction, and can lead to vasculitis, phlebitis, and coagulopathy.

RBD life span is reduced by the accumulation of RBC damage such as membrane alterations (e.g., unmasked antigens, carbohydrate epitopes, externalized phosphatidylserine, Band 3 clustering, CD47 alterations) that stimulate phagocytosis or removal of altered membrane (producing spherocytes), or cause autoagglutination due to antibody binding. Eryptosis (RBC apoptosis) may also be triggered by osmotic shock, oxidative stress, energy depletion, hyperthermia, lead or mercury intoxication, and a number of small molecules. Small molecules generally trigger eryptosis by increasing cytosolic calcium (Ca^{2+}), stimulating ceramide formation, depleting ATP, causing oxidative stress, and/or activating caspase 3.

Oxidative Injury to Circulating Cells

Circulating RBCs experience some of the highest levels of oxidative stress in the body because they carry large quantities of oxygen and are exposed to oxidizing agents in plasma. Source of oxidants may be exogenous (foods, chemicals, drugs, and environmental contaminants) or endogenous (normal processes and many disease states). In mature RBCs, endogenous ROS arise from spontaneous conversion of oxyhemoglobin to methemoglobin and from anaerobic glycolysis. In maturing erythroid cells, highly reactive hydrogen peroxide is also produced from incorporation of iron into heme.

Oxidoreductive enzymes (methemoglobin reductase, copper/zinc-superoxide dismutase, catalase, glutathione peroxidase, thioredoxin reductase, thioredoxin, and peroxyredoxins) and nonenzymatic scavengers (reduced glutathione, vitamin E, ascorbic acid,

TABLE 13.4 Agents Causing Direct (nonimmune) Injury to Circulating Cells

Mechanism		Cell	Xenobiotic
Oxidative injury	Methemoglobinemia (oxidation of heme iron)	Erythrocytes	Aliphatic esters of nitrous acid (N-hydroxylamines), aliphatic esters of nitric acid (glyceryl trinitrate), amyl and butyl nitrite, local anesthetics (e.g., lidocaine, benzocaine, prilocaine), nitrate-contaminated water, nitrites, nitroaromatics (nitrobenzene, phenylhydroxylamine, dinitrotoluene), Plants (*brassicaceae*, capeweed, pigweed, sorghums, tribulus, variegated thistle), potassium chlorate, aminophenols, anilines, sulfonamides, chlorine dioxide
	Heinz Bodies (oxidation of globin)		Aspirin, phenacetin, phenylhydramine, phenylhydrazine, phenothiazine, phenazopyridine, primaquine, propofol, ecabapide, benzocaine, dapsone, menadione, methylene blue, crude oil (marine birds), and naphthalene Plants (onions, garlic, *Brassica*, *Acer rubrum*) Acetaminophen (cats, dogs); propylene glycol (cats); zinc (dogs); copper (ruminants, Bedlington terriers)
	Sulfhemoglobin		Acetaminophen, acetanilide, aniline, chlorate salts, hydroxylamine, dimethyl disulfide, methylene blue (In G-6-PD deficient individuals), naphthalene, nitrobenzenes, phenols, primaquine, sulfites, sulfonamides, onions and garlic (dogs and cats), microcystin-LR, sulfanilamide, phenazopyridine, propylene glycol, phenothiazine (horses), Red maple (*Acer rubrum*) (Horses), *Brassica* Spp., and rye grass in ruminants
	Membrane damage		Acetaminophen, arsine, copper, dapsone, primaquine, ribavirin, snake venom (vipers)
	Induced apoptosis	Leukocytes	Clozapine
Direct lysis	Membrane damage	Erythrocytes	Insect and snake venoms; 1-tryptophan and indoles; arsine
		Platelets	IL-2, valproate, phenytoin, GM-CSF, and snake venom
	Complement-mediated destruction	Neutrophils	Clozapine, rituximab, 5-azacytidine (hypomethylation-induced apoptosis), and propythiouracil
		Erythrocytes	Benzene, vitamin C, antithymocyte globulin
Altered function	Enzyme inhibition	Erythrocytes	Lead, zinc (pennies, metallic hardware), chromium, copper, and mercury
	Altered cooperative binding of globin units		Methemoglobinem, carbon monoxide, clofibric acid, bezafibrate, aromatic benzaldehydes, hydroxyurea
	Inhibition of serotonin reuptake	Platelets	Fluoxetine, some tricyclic antidepressants
	Inhibition of thromboxane synthesis (antithrombotic)		COX-1 inhibitors
	Inhibition of prostaglandin synthesis (prothrombotic)		COX-2 inhibitors
	Membrane receptor antagonism		β-Lactam containing antibiotics (penicillin, ampicillin, cephalosporins)
	Ca channel antagonism		β-Blocker cardiac drugs (propranolol), β-lactam antibiotics
	Risk of thrombosis		Clopidogrel, anti-GP IIb/IIIa inhibitors Antiestrogens (tamoxifen, toremifene); progestins (hydroxyprogesterone caproate, medroxyprogesterone acetate, megesterol acetate); aromatase inhibitors (anastrozole, letrozole, exemestane); EPO
	Altered adherence and motility	Neutrophils	Colchicine, dextran, ethanol, glucocorticoids, iron oxide, rifampicin, macrolide antibiotics
	Impaired superoxide production		Methadone
	Inhibits kinase signaling		Dasatinib
	Impaired phagocytosis		Ethanol, glucocorticoids

Table modified from Haschek, W.M., Rousseaux, C.G., Wallig, M.A. (Eds.) 2013. Handbook of Toxicologic Pathology, third ed. Academic Press, Table 50.7, pp. 1902–1903 with permission.

and carotenoids) protect RBCs against oxygen radicals. NAPDH provides reducing equivalents needed for catalase function and for maintenance of the reduced states of glutathione and thioredoxin. Older RBCs are most susceptible to hemolysis because glucose-6-phosphate dehydrogenase (reduces NADP + to NADPH) decreases as RBCs age.

Oxidants damage hemoglobin, enzymes, iron, cytoskeleton, and membranes, resulting in abnormal oxygen carrying capacity, cell shape, and membrane

fluidity. Oxidative stress also triggers eryptosis by different but converging pathways: (1) caspase activation, (2) formation of prostaglandin E_2 leading to Ca^{2+} channel activation, and (3) phospholipase A_2–mediated release of platelet-activating factor, which activates a sphingomyelinase and leads to formation of ceramide. Activation of Ca^{2+} channels induces phosphatidylserine externalization, marking cells for phagocytosis, and activates K^{2+} channels leading to cell hyperpolarization and shrinkage, calpain activation, degradation of cytoskeletal proteins, and cell membrane blebbing.

Clozapine-induced neutropenia is caused by its oxidation to a reactive nitrenium ion by myeloperoxidase-hydrogen peroxide of activated neutrophils and BM cells. The accumulation of this reactive metabolite depletes ATP and reduced glutathione renders neutrophils and their precursors highly susceptible to oxidant-induced apoptosis.

OXIDATION OF IRON IN HEMOGLOBIN: METHEMOGLOBIN

The spontaneous but reversible oxidation of ferrous iron (Fe^{2+}) to ferric iron (Fe^{3+}) results in methemoglobin ($HgbFe^{3+}$) and superoxide formation (Eq. 13.1). A direct interaction of reduced hemoglobin with hydrogen peroxide also results in methemoglobin formation (Eq. 13.2). The rate of iron oxidation is enhanced by increased temperature, decreased pH, organic phosphate, metal ions, nitrites, partial oxygenation of hemoglobin, and superoxide anions (Eq. 13.3).

$$HgbFe^{2+} + O_2 \rightarrow HgbFe^{3+}O_2^- \rightarrow HgbFe^{3+} + O_2^- \quad (13.1)$$

$$2HgbFe^{2+} + 2H_2O_2 \rightarrow 2HgbFe^{3+} \rightarrow H_2O + O_2 \quad (13.2)$$

$$HgbFe^{2+} + O_2 + O_2^- + 4H^+ \rightarrow 2HgbFe^{3+} + 3O_2^- \rightarrow HgbFe^{3+} + O_2 + H_2O \quad (13.3)$$

Methemoglobin is normally maintained below 1% of total hemoglobin by cytochrome b_5 methemoglobin reductase (NADH dehydrogenase) and its cofactor flavin adenine dinucleotide (FAD). However, oxidizing agents can facilitate the oxidation of heme to metheme, and substantially increase methemoglobin concentrations.

Methemoglobin cannot bind oxygen but increases the oxygen affinity of other hemoglobin molecules within the tetramer, thus impairing oxygen delivery to tissues. Methemoglobin levels $<10\%$ are asymptomatic while levels $>10\%–20\%$ (>1.5 g/dL) may be associated with anoxia, cyanosis, reduced oxygen saturation, lethargy, and brown-colored arterial blood and levels $>70\%$ are life threatening. Methemoglobin is a reactive molecule that further increases oxidative stress and causes osmotic fragility and intravascular hemolysis. Oxidation of methemoglobin and hemoglobin can also produce hemichromes, which may precipitate and induce membrane protein Band 3 clustering, opsonization and RBC phagocytosis.

In grazing domestic animals (especially cattle), nitrate-containing plants (e.g., *Brassicaceae*, *Silybum*, *Amaranthus*, *Cryptostemma*, and *Tribulus*), plants treated with potassium chlorate (herbicide), and water supplies containing nitrites and nitrates are prime causes of methemoglobinemia. Methemoglobinemia has also been reported in horses, alpacas, and zebras after ingestion of red maple (*Acer rubrum*) and in a dog exposed to skunk spray. A variety of therapeutic drugs and environmental chemicals have also been shown to induce methemoglobin formation. Most of the chemical agents that cause methemoglobinemia can also cause sulfhemoglobinemia. The oxidation of ferric iron by hydrogen sulfide (H_2S) irreversibly produces sulfhemoglobin, a denatured, nonfunctional form of Hgb.

OXIDATION OF GLOBIN

Oxidation of sulfhydryl groups on the globin moiety of hemoglobin results in cross-linking between hemoglobin molecules as well as oxidative denaturation of globin with dissociation of heme. Aggregation and precipitation of denatured hemoglobin results in Heinz body formation and premature RBC phagocytosis. Removal of Heinz bodies by the mononuclear phagocyte system can lead to abnormally shaped RBCs.

Heinz body anemia secondary to oxidative damage to hemoglobin has been identified in domestic animals in association with exposure to a wide variety of plants, drugs, chemicals, and diseases (Table 13.5). Species differences in xenobiotic metabolism and antioxidant defense account for differences in susceptibility to Heinz body formation. More Heinz bodies are observed in cats (up to 5% in healthy cats) because the spleen does not remove damaged RBCs as efficiently and because feline hemoglobin has 8 reactive sulfhydryl groups per hemoglobin tetramer (vs 4 in dogs and 2 in humans). Rodents are less susceptible because they have more reactive cysteine residues, which compete and cooperate with glutathione, acting as a sink for ROS. In mice heightened sensitivity has been associated with β globin gene complex allelic variations.

OXIDATION OF CYTOSKELETON AND MEMBRANE PROTEINS AND LIPIDS

The RBC cytoskeleton and membranes are also prone to oxidative injury. Lipid peroxidation and cytoskeletal injury results in phospholipid cross-linking, membrane stiffening, decreased deformability, and enhanced fragility, resulting in RBC fragmentation. Oxidative injury to cytoskeleton and membranes

TABLE 13.5 Agents Causing Heinz Body Anemia in Animals

Class	Agent	Mechanism	Species	Outcome
Plants	*Allium* family (onions, garlic)	Aliphatic sulfides decrease glucose-6-phosphate dehydrogenase activity	Most domestic species Shiba dogs	Heinz body hemolytic anemia
	Brassica (cabbage, kale, rape)	1. S-methyl-L-cysteine sulfoxide metabolized to dimethyl sulfide (oxidant) by rumenal bacteria 2. High sulfur content reduced copper availability 3. Low copper and zinc content	Ruminants	Heinz body hemolytic anemia
	Acer rubrim (wilted red maple leaves)	Rapid glutathione depletion	Horses and zebras	Eccentrocytosis with or without Heinz bodies, methemoglobinema
Drugs/ Chemicals	Acetaminophen	Low acetaminophen UDP-glucuronosyltransferase activity in cats results in increased levels of oxidant acetaminophen metabolites	Cats Dogs	Heinz body hemolytic anemia
	Propylene glycol (food additive)		Cats	Heinz body hemolytic anemia
	Zinc (pennies, hardware, ointments)	Band 3 clustering	Dogs	Spherocytosis Heinz body hemolytic anemia
	Copper (subterranean clover, copper plumbing)	Acute release from liver	Ruminants (especially sheep) Bedlington terriers	Intravascular hemolysis, Heinz bodies, methemoglobinemia

Table modified from Haschek, W.M., Rousseaux, C.G., Wallig, M.A. (Eds.) 2013. Handbook of Toxicologic Pathology, third ed. Academic Press, Table 50.8, p. 1906 with permission.

frequently causes adhesion of opposing membrane bilayers to form eccentrocytes and pyknocytes.

Membrane lipid peroxidation alters membrane permeability to potassium and alters Na/K gradients. Severe membrane damage may impair ion gradient maintenance, leading to swelling or intravascular hemolysis. Copper is notoriously damaging to RBC membranes, especially in sheep. Snake venom also causes membrane damage, as does arsine (arsenic hydride), a byproduct of certain industrial processes, and the aniline-based drugs, dapsone and primaquine. The antiviral drug ribavirin causes methemoglobin formation and promotes hemolysis via oxidative membrane damage and ATP depletion.

Nonoxidative Injury

Some xenobiotics cause hemolysis without significant oxidative injury. Arsine gas can cause severe intravascular hemolysis, with anemia, jaundice, and hemoglobinuria. Arsine's hemolytic potential is thought to result from dissociation of heme and hemoglobin and its interaction with Na/K pumps, which disrupts ion homeostasis, resulting in osmotic hemolysis.

Metals such as lead, zinc, chromium, copper, and mercury inhibit enzymes required for RBC maturation and function. While some effects may be observed in maturing cells of the BM, peripheral destruction is also observed. Sideroblastic anemia is common in lead and zinc toxicity, and has also been associated with isoniazid, chloramphenicol, linezolide, penicillamine, triethylene tetramine dihydrochloride, and with chemotherapy-related myelodysplasia. The damaging effects of lead result in reduced RBC life span, dyserythropoiesis, and an increased BM myeloid-to-erythroid cell ratio. Lead interferes with heme synthesis resulting in a nonregenerative, sideroblastic, hypochromic, microcytic anemia with metarubricytosis due to failure of nuclear expulsion. Lead also inhibits pyrimidine 5′-nucleotidase leading to retention of RNA in reticulocytes and basophilic stippling and promotes oxidative stress by inhibiting antioxidants. Common sources of lead include lead-containing paints, batteries, industrial contaminants in pastures, and lead shots.

Copper inhibits enzymes involved in the hexose monophosphate shunt and Embden-Meyerhof pathway, causing acute intravascular hemolytic anemia, icterus, and hemoglobinuric nephrosis in ruminants. Pyrrolizidine alkaloid hepatotoxicity is associated with excessive release of hepatic copper stores into circulation and secondary hemolytic crisis. Ingestion of excess chromium may also result in a hemolytic anemia and thrombocytopenia. Mercury inhibits glutathione reductase, G-6-PD, and acetylcholinesterase, and is associated with anemia, dysmyelopoiesis and increased BM cellularity, idiosyncratic IMHA, and immunotoxicity.

Hemolysin toxins found in insect and snake venoms can cause hemolysis, either by direct (polypeptidic "direct lytic factor") or by indirect (phospholipase) action on RBC membranes. ATPases in snake venoms deplete

ATP, resulting in osmotic hemolysis. Phospholipase A2 promotes lysolecithin incorporation in the outer layer of the RBC membrane, causing disproportionate expansion of the outer layer and formation of echinocytes and spheroechinocytes. Similarly 1-tryptophan and indoles are readily incorporated into red cell membranes due to their lipophilic properties, resulting in acute hemolytic anemia and hemoglobinuria.

Thrombocytopenia due to direct cytotoxicity and/or increased clearance by the reticuloendothelial system (RES) has been reported in association with IL-2, valproate, phenytoin, GM-CSF, and snake venom. Drug-induced neutropenia can occur in association with clozapine, rituximab, and 5-azacytidine, which cause hypomethylation-induced apoptosis, and with propythiouracil, which causes complement-mediated destruction of neutrophils. Clozapine is metabolized by neutrophil myeloperoxidase to a reactive nitrenium ion metabolite that appears to initiate an immune response and accelerate neutrophil apoptosis.

Altered Blood Cell Function

Xenobiotics can alter cooperative binding of globin units and hemoglobin oxygen affinity, impacting respiratory RBC function. Effects may also occur secondary to changes in blood pH, 2,3-BPG (2,3-bisphosphoglycerate) concentrations, body temperature, or induced expression of fetal globins. A large number of drugs directly affect platelet function. Cyclooxygenase (COX)-1 inhibiting nonsteroidal antiinflammatory drugs (NSAIDs) exert their effects by reversibly (nonaspirin NSAIDs) or irreversibly (aspirin or acetylsalicylic acid) inhibiting acetylation of COX-1, resulting in inhibition of thromboxane A_2 synthesis, vital for proper platelet function. In contrast, COX-2 inhibitors have prothrombotic effects since they inhibit production of prostacyclin, which inhibits platelet function. Acidic phospholipase (snake venom) inhibits platelet aggregation and selective serotonin reuptake inhibitors (SSRI) block deplete platelet serotonin and impair platelet aggregation.

Calcium channel blockers and β-lactam antibiotics interfere with agonist-stimulated calcium release from endoplasmic reticulum necessary for platelet aggregation. Penicillin is also postulated to irreversibly attach to the platelet surface, causing impairment of agonist (ADP, collagen, thrombin) binding to platelet receptors. Residual impairment of receptor function may be observed even after the antibiotic is discontinued. Hypoalbuminemia enhances the effect because higher levels of unbound drug interact with the platelet surface.

Agents that inhibit platelet function generally do not cause clinical bleeding unless there is a coexisting hemostatic defect, such as uremia, marked thrombocytopenia, von Willebrand's disease, or vitamin K deficiency. Other indirect causes of altered platelet function include hyperglobulinemia, increased fibrin degradation products (disseminated intravascular coagulation (DIC) or liver failure), uremia, and colloidal plasma expanders. Clinically, defects in platelet function produce prolonged bleeding times and gastrointestinal bleeding but may not be associated with overt bleeding or alterations in platelet count or morphology.

Thrombotic microangiopathies (e.g., thrombotic thrombocytopenic purpura and hemolytic-uremic syndrome) occur secondary to excessive platelet activation (direct, immune-mediated, or endothelial injury). They are associated with thrombocytopenia, microangiopathic hemolytic anemia, and symptoms of microvascular occlusion. Thrombotic microangiopathy in humans has been reported with exposure to cyclosporine, mitomycin-C, gemcitabine, cisplatin, α-interferon, tacrolimus, thienopyridines, ticlopidine, clopidogrel, and quinine.

Impaired neutrophil function has been reported with numerous agents. Some agents impair superoxide production (methadone) while others suppress expression of integrins and receptors to alter adherence, mobility, and/or chemotaxis (macrolide antibiotics). Dasatinib, a potent tyrosine kinase inhibitor chemotherapeutic, inhibits neutrophil activation by blocking Src family kinases and inhibiting integrin-dependent and Fc-receptor-dependent neutrophil activation and downstream signaling, resulting in decreased spreading, adhesion, and exocytosis of secondary granules. Impaired neutrophil phagocytosis (ethanol and glucocorticoids) leads to premature neutrophil death, neutropenia, and susceptibility to infection. Enhanced neutrophil function has been reported in association with sodium sulfite, mercuric chloride, chlordane, and toxaphene.

Immune-Mediated Destruction

In contrast to Type A drug reactions, which are predictable and dose-dependent, Type B, are unpredictable and nondose-related events that are attributable immune-mediated hypersensitivity reactions, nonimmune hypersensitivities, or idiosyncratic reactions. Immune-mediated hypersensitivities are antibody mediated. Antibody binding can trigger direct complement-mediated lysis or sequestration and phagocytosis of complement C3- or immunoglobulin-coated cells. Immune-mediated hypersensitivities are typically classified as Type I (immediate, IgE mediated), Type II (IgG or IgM mediated), Type III (IgG/IgM immune complex mediated), and Type IV (delayed type or cell mediated). Nonimmune hypersensitivities resemble allergic

reactions clinically but arise via direct complement activation (C activation-related pseudoallergy (CARPA)). Idiosyncratic reactions are rare, unpredictable reactions that are hypothesized to arise from a combination of immune mediated, genetic, and environmental factors.

Drug-induced immune-mediated hematologic disorders are most commonly due to Type II hypersensitivity and are associated with four types of antibodies: hapten (neoantigen)-dependent antibodies, drug-dependent antibodies, drug-induced (drug-independent) autoantibodies, and drug-specific antibodies. Hapten-dependent antibodies recognize drug−protein adducts on RBC or platelet membranes, resulting in anemia or thrombocytopenia, respectively. Hapten-dependent drug-induced hemolytic anemia is associated with penicillins, cephalosporins, levamisole, sulfonamides, vaccination, and heparin.

Drug-dependent antibodies require soluble drug to bind their cellular targets but do not recognize drug-coated cells. Rather the drug promotes Fab binding to its target without linking covalently to either of the reacting macromolecules. Cytopenia is usually drug-specific and resolves after drug withdrawal. Drug-dependent antibodies have been reported to cause immune-mediated hemolytic anemia (IMHA) (cefotetin, ceftriaxone, ceftizoxime, tolmetin, etodolac, chlorpropamide, carboplatin, cisplatin, ibuprofen, oxaliplatin, poperacillin, probenecid, quinine, quinidine methyldopa, and fludarabine), and immune-mediated thrombocytopenia (quinine, many antibiotics, NSAIDs, anticonvulsants, and ocreotide).

Drug-induced (drug-independent) autoantibodies are responsible for the classic, true autoimmunity disorders of autoimmune hemolytic anemia (AIHA), and autoimmune thrombocytopenia (AITP). In these cases the drug induces antibodies that react with cells in the absence of drug (positive antiglobulin test) and after drug withdrawal. Drugs associated with AIHA or AITP include α-methyldopa, levodopa, procainamide, piperacillin, cefotetan, ceftriaxone, penicillamine, sulfamethoxazole, and gold salts.

Type III hypersensitivity is characterized by formation of drug−antibody complexes (immune complex disease). In patients chronically treated with heparin, antibodies specific to heparin-bound PF4 (platelet α granule component) form immune complexes, which activate platelets via Fc receptors (in contrast to drug-dependent antibodies that bind their targets via the Fab domain). The resultant immune complex-mediated platelet activation and aggregation may result in thrombosis, but the thrombocytopenia is usually not severe enough to cause clinical bleeding.

The normal removal of aged or damaged cells involves antibody-mediated identification and removal by phagocytes of the RES. Drug-induced opsonization by antibodies also leads to increased clearance of the-coated cells by RES macrophages. Immune-mediated destruction usually involves circulating cells, producing disorders such as immune-mediated anemia, immune-mediated thrombocytopenia, and immune-mediated neutropenia. However, antibody-mediated destruction can extend to hematopoietic cells of the BM, resulting in pure red cell aplasia, agranulocytosis, or aplastic pancytopenia. The causes and the mechanisms of immune-mediated destruction are highly varied, and it is suspected that genetic and environmental factors play an important role. Specific drugs may cause different types of hypersensitivity reactions in different individuals and multiple mechanisms may operate in a single individual. In addition, temporal associations of exposure and onset of hematologic disorders are not always consistent. In general, there is a delay between exposure and onset of the adverse reaction. Anamnestic immune responses, characterized by rapid onset of hypersensitivity after a rechallenge, confirm that the effect is immune-mediated. However, immune-mediated hypersensitivities may not have an amnestic response if the hypersensitivity has a strong autoimmune component that results in deletion of autoimmune memory cells after drug withdrawal.

Drug-induced immune-mediated hemolytic anemia (IMHA or DIHA) is characterized by destruction of RBC by antibodies acting against membrane antigens. Antibody-mediated RBC destruction results in decreased hematocrit with or without anemia, hyperbilirubinemia, a positive Coombs test, and an inflammatory leukogram. Onset is abrupt, and frequently the hematocrit plunges precipitously. In the dog, e.g., the hematocrit declines by $\geq 50\%$ in ≤ 30 days. Spherocytosis and agglutination may be observed if the blood sample is obtained soon after onset. The reticulocyte count is normal to increase if sufficient time for a regenerative response (i.e., 4−7 days) has elapsed, and the direct antiglobulin test may be positive. Erythrophagocytosis may also be prominent in the spleen, BM, and liver.

IMHA, can often be difficult, if not impossible, to distinguish clinically from idiosyncratic reactions. However, some classes of drugs seem to produce IAHA on a somewhat more consistent basis. Drugs most often associated with AIHA include propylthiouracil, penicillins, cephalosporins, sulfonamides, phenacetin, quinidine, and α-methyldopa.

In drug-induced IMTP, platelets are bound by antibodies and cleared by the RES. Thrombopoiesis may also be decreased due to immune-mediated suppression of MKs and proplatelets. Thrombocytopenia is typically observed 6−8 days after exposure, and may

be asymptomatic or accompanied by purpura on mucosal and skin surfaces. Platelet counts rapidly return to normal upon drug withdrawal. Laboratory confirmation by identification of platelet-associated immunoglobulin gives inconsistent results. Causes include quinine and quinine-like drugs, antimicrobials, antiinflammatory drugs, antineoplastic drugs, antidepressants, benzodiazepines, anticonvulsants, and cardiac and antihypertensive drugs.

In IMTP, most common are drug-dependent antibodies that bind platelet membrane glycoproteins IIB/IIIa or Ib/IX. Antifibrotic agents Abciximab (a chimeric Fab fragment) and fibans (RGD mimetic inhibitors) induce a conformational change in GPIIb/IIIa that may be recognized by drug-dependent antibodies, resulting in severe thrombocytopenia. First generation TPO receptor (mpl) agonists (PEG-rHuMGDF and recombinant human TPO (rhTPO)) designed to treat thrombocytopenia instead produce paradoxical thrombocytopenia due to immune-mediated production of anti-TPO antibodies and inhibition of binding to mpl, the TPO receptor. Drug-induced immune-mediated thrombocytopenia has also been reported in a dog after amiodarone administration. Thrombocytopenia that is drug-related should be distinguished from pseudothrombocytopenia, a spurious finding that occurs when the EDTA anticoagulant exposes neoantigens on platelet membranes as blood samples cool in the laboratory prior to analysis.

Drug-induced immune-mediated neutropenia is a rare disorder caused by hapten-dependent, drug-dependent and autoantibodies against neutrophil-specific glycoproteins (FcγIII, CD177, GP70-95, CD11a, CD11b). Drugs most commonly associated with agranulocytosis are antithyroidals, antibacterials, and anticonvulsants. Drug-induced immune-mediated neutropenia has also been reported in a dog after the administration of quinidine gluconate. Neutropenia or agranulocytosis is acute and profound and associated with infection and possible mortality. In toxicity studies a single or occasional dog is affected, a graded dose-response is absent, neutrophil counts are decreased markedly, a neutrophil "left shift" is not present unless infection supervenes, and the BM is normo- or hypercellular at the nadir of the neutropenia. Neutrophil counts rapidly return to normal following cessation of drug treatment, and there is no decrease in CFU-GM (granulocyte macrophage) cloning activity in BM cell cultures, indicating intact neutrophil stem cell proliferative capacity. The diagnosis is generally made on the basis of the clinical and hematologic features due to the technical complexity, frequency of false negatives, and lack of specificity of *in vitro* confirmatory tests (drug-dependent antineutrophil antibody test, drug-dependent test for immune complexes, demonstration of leukoagglutinin).

Idiosyncratic Reactions

Idiosyncratic toxicities comprise a complex group of rare nondose-related adverse events that are not predictable based on an inciting agent's pharmacology. Due to their infrequent occurrence, animal models are not predictive and evidence for mechanisms is primarily based on epidemiologic studies. The pathogenesis of idiosyncratic drug reactions is hypothesized to involve the combined effects of hypersensitivity, immunomodulation, reactive metabolites, oxidative stress, and genetic predisposition. Many cases are believed to be immune-mediated based on a delay between the initial exposure and the onset of the adverse reaction, as well as rapid onset upon rechallenge (amnestic response). However, antibodies are not always documented. Reactive drug metabolites formed in target organs are hypothesized to form immunogenic conjugates with cellular proteins. For example, drugs oxidized to reactive metabolites by myeloperoxidase may thus induce immune-mediated neutropenia. The hapten hypothesis proposes that the interaction of the drug with the cell membrane of the affected cell produces a neoantigen (hapten). The danger hypothesis proposes that reactive metabolites or their covalent binding to proteins induce stress and cellular expression of danger signals that trigger an immune response. The pharmaceutical interaction hypothesis proposes that the drug directly targets immunoregulatory mechanisms by up regulating costimulatory signals in antigen-presenting cells that activate T cells. Drug-dependent antibodies may also play a role when less reactive metabolites enter the circulation and induce hypersensitivity.

Idiosyncratic cytopenias have many of the characteristics of an immune-mediated process, such as abrupt onset due to rapid clearance or premature removal of affected cells from the circulation, rapid recovery when the drug is withdrawn, shortening of induction time upon re-exposure to the drug and, in many instances, reinduction of the cytopenia with a lower dose than the inciting dose. It usually affects one or two animals in a study or population, and occurs most often in dogs. It involves neutrophils, RBC, or platelets, singly or in combination, with one cell type often being much more affected than other cell types in a given individual, and may also involve the marrow.

Indirect Injury

Xenobiotic-related indirect effects on the hematopoietic system are exceedingly common, and they often reflect the systemic effects and homeostatic responses. Indirect effects can be broadly classified as causing

suppression of hematopoiesis, injury to the microenvironment, and/or decreased cell survival.

Suppression of Hematopoiesis

Suppression of hematopoiesis is commonly observed secondary to decreased food consumption, iron deficiency, chronic disease, and inflammation. Causes of iron deficiency include repeated phlebotomy, chronic blood loss, low dietary iron, and copper deficiency. Inflammation decreases iron availability (hepcidin disorders) and increases hematopoiesis-suppressing cytokines (e.g., IL-12, IFN-γ).

Natural and synthetic estrogens indirectly induce production of a myelopoiesis-inhibitory factor by thymic stromal cells, causing myelosuppression, as well as fatal pancytopenia (dogs and ferrets) and anemia (rats). Some drugs suppress hematopoiesis via exaggerated pharmacology (IL-12) or off-target suppression (nonselective kinase inhibitors).

Chronic treatment with recombinant human erythropoietin (rhEPO) induces production of anti-EPO antibodies that neutralize exogenous and endogenous EPO, resulting in profound erythroid hypoplasia and nonregenerative anemia. Exposure to rubber leachates from prefilled Eprex (EPO) syringes with uncoated rubber stoppers also causes pure red cell aplasia due to the formation of antierythropoietin antibodies. Finally suppression of thrombopoiesis has been reported with histone deacetylase (HDAC) inhibitors.

Damage to the Microenvironment

Damage to BM microenvironment and microvasculature suppresses hematopoiesis by disrupting blood supply, nurse cell function and cytokine expression, matrix and cellular adhesion molecule interactions, and by displacing hematopoietic cells with nonhematopoietic cells, or extracellular matrix. Acute microvascular injury and sinusoidal endothelial cell degeneration increases vascular permeability, resulting in sinusoidal dilatation, interstitial edema, hemorrhage with fibrin exudation and infiltration by neutrophils, inflammation, and ischemia. Chronic injury leads to necrosis and myelofibrosis. Other stromal lesions include serous fat atrophy, myelophthisis (replacement of hematopoietic tissue by nonhematopoietic tissue), fibrous osteodystrophy, osteosclerosis, and microangiopathy.

Causes of acute marrow stromal injury in dogs and/or cats include inflammatory diseases, DIC, leukemia/lymphoma, and drugs (cyclophosphamide, carprofen, metronidazole, and fenbendazole). Expansion of adipocytes (as seen with aging) is associated with suppression of hematopoiesis.

Agents that injure HSCs also injure stromal stem cells, their progeny, and surrounding extracellular matrix through direct and bystander effects. Benzene-induced aplastic pancytopenia is hypothesized to result from damage to the microenvironment, since benzene-treated lethally irradiated marrow is not reconstituted by transplantation with normal marrow. IL-6 antagonists decrease myelopoiesis, resulting in transient neutropenia. IL-6 is constitutively expressed by and required for proliferation of BM stromal cells, and is essential for production of extracellular matrix that induces osteoblastic differentiation of MSCs. Microenvironment alterations also contribute to stem cell aging, myelodysplasia, malignant transformation, and metastasis.

Decreased Life span

The life span of mature circulating RBC is determined by basal metabolic rate, senescence-based clearance, and eryptosis. Inappropriate eryptosis is associated with a wide variety of diseases and is also triggered by osmotic shock, oxidative stress, energy depletion, hyperthermia, and many small molecules. RBC senescence involves receptor-mediated removal of aged or damaged RBCs by splenic macrophages and hepatic Kupffer cells.

Decreased RBC survival due to increased senescence occurs secondary to accumulation of injuries, such as oxidative injury, microangiopathy, membrane lipid changes, decreased deformability, mitochondrial dysfunction (lack of ATP to maintain Na/K gradients and repair mechanisms), and Band 3 clustering (IgG opsonization and complement binding). Membrane lipids may change as a consequence of plasma lipid abnormalities (hypercholesterolemia and hypotriglyceridemia) as observed with liver disease and lipid-modulating therapeutics. Age-related decreases in antioxidant status result in 0%–60% shorter life span in old rodents when compared to young rodents. Neoplasia and inflammation may, in rare instances, induce excessive erythrophagocytosis due to hemophagocytic syndrome.

Circulating cell counts may change secondary to indirect induction of lysis. Indirect causes of intravascular hemolysis include hypophosphatemia (cattle), acute hyponatremia (water intoxication), and rapid administration of 40% DMSO (horses). Species with small RBCs appear to be most susceptible to hypotonicity-induced hemolysis.

RESPONSES OF HEMATOPOIETIC TISSUES TO INJURY

Changes in Peripheral Blood Cells

The hematopoietic system encompasses multiple tissues (i.e., peripheral blood, BM, and spleen) that cooperate with other organs to maintain homeostasis. Hematopoietic organs are capable of responding to changes in all other organs and organ systems

TABLE 13.6 Responses to Injury in Blood and Bone Marrow (BM)

Change in blood	Change in bone marrow	Cause	Examples
Increased erythrocytes	None	Relative erythrocytosis	Reduced water intake (fasted mice) Fluid Loss Splenic contraction (dogs)
Increased platelets		Relative thrombocytosis	Muscular activity Excitement
Increased neutrophils and lymphocytes		Physiologic leukocytosis	Excitement in dogs and macaques (epinephrine-induced shift within blood vessels from the marginal pool to the circulating pool)
Increased neutrophils		Neutrophil demargination	Glucocorticoids (stress) Ethanol, colchicine, epinephrine (excitement)
Increased RBC	Erythroid hyperplasia ± left shift	Physiologic (appropriate) erythrocytosis due to tissue hypoxia	Decreased tissue oxygenation (abnormal Hgb:MetHgb) Systemic hypoxia due to lung disease Systemic alkalosis (increased hemoglobin affinity for oxygen)
	Erythroid hyperplasia	Secondary inappropriate erythrocytosis	Erythropoietin excess Activation of erythropoietin receptors Endocrinopathy (cortisol, androgen, thyroxin, and growth hormone)
	(Inappropriate) Erythroid hyperplasia, dyserythropoiesis	Primary erythrocytosis due to myeloproliferative disease	Polycythemia vera
Increased platelets	Megakaryocyte hyperplasia	General bone marrow stimulation	Blood loss, iron deficiency, hemolytic anemia, inflammation, growth factors
Leukocytosis with band neutrophils	Myeloid hyperplasia ± left shift	Stimulation of Myelopoiesis	Inflammation Growth factor or cytokine-stimulating compounds (GM-CSF)
Decreased RBC and/or platelets	None	Splenic congestion	Barbiturate-induced splenic congestion (nonrodents) Reversible thrombocytopenia due to antisense oligonucleotide (ASO) therapy in mice, monkeys, and humans
Decreased neutrophils		Margination	Histamine, iron oxide, dextran
Decreased RBC	Erythroid hyperplasia	External blood loss	Repeated or excessive blood collection (common) External hemorrhage
		Intravascular hemolysis	Complement-mediated lysis Direct contact (saponin, phenylhydrazine, arsine, naphthalene) Oxidative injury Copper toxicity Inhibition of mitochondrial function or glucose metabolism Excess dietary cholesterol in guinea pigs
		Extravascular hemolysis	Antibody mediated (autoimmunity, hapten-induced, LGL leukemia of F344 rats) Erythrocyte fragmentation (microangiopathy, disseminated intravascular coagulopathy) Oxidative and structural damage Internal hemorrhage
Decreased Platelets	Megakaryocyte hyerplasia	Loss/destruction	Acute blood loss Immune mediated Consumptive coagulopathy
Neutropenia ± band neutrophils	Myeloid hyperplasia ± left shift	Inflammation	
Decreased erythrocytes	Erythroid hypoplasia	Myelosuppression	>20% Decrease in food consumption, stress, decreased oxygen demand
		Absolute iron deficiency	Dietary iron deficiency, prolonged hemorrhage
		Functional iron deficiency	Chronic inflammation, Hepcidin overexpression, ferroportin suppression
		Chronic disease	Chronic kidney or liver failure
		Dyserythropoiesis	Altered nucleic acid synthesis
Pancytopenia	Erythroid and myeloid hypoplasia	Direct injury to hematopoietic precursors	Ionizing radiation, benzene, chemotherapy
		Bone marrow infiltration (myelophthisis)	Leukemia, myelofibrosis

Table modified from Haschek, W.M., Rousseaux, C.G., Wallig, M.A. (Eds.) 2013. Handbook of Toxicologic Pathology, third ed. Academic Press, Table 50.9, pp. 1916–1917 with permission.

including the kidney, lung, cardiovascular system, hemostatic system, and immune system. As such, its diseases are best interpreted from a functional perspective.

Appropriate responses to systemic insults indicate normal hematologic function. Examples include reticulocytosis in response to anemia, leukocytosis in response to tissue inflammation, and thrombocytosis in response to blood loss. When evaluating BM responses, it is essential to bear in mind rate of injury, cellular life span, and kinetics of BM production, and to confirm that sufficient time has elapsed to observe the appropriate response. For example, after an acute loss of RBC, it takes approximately 3–5 days for reticulocytes to increase in circulation.

An inappropriate BM response to a systemic change indicates a primary abnormality of the hematopoietic function (e.g., pancytopenia secondary to marrow failure). Changes in circulating cell counts can be broadly classified as due to redistribution/sequestration, destruction/loss/consumption, or decreased production. The BM generally does not respond to small magnitude changes in circulating blood cells or transient changes due to redistribution or sequestration. Destruction, consumption, or loss of circulating cells should elicit a physiologic proliferative BM response, reflecting normal hematopoietic function.

The number and variety of BM responses are numerous. The literature in humans, and to a lesser degree experimentally in rodents and other laboratory species, is vast. Some specific responses are discussed later and presented in Table 13.6.

Redistribution, Sequestration, and Demargination/Margination

In dogs and monkeys circulating counts of RBCs, reticulocytes, and platelets may transiently increase secondary to splenic contraction (due to catecholamines, exercise, stress, physical restraint in rodents) and decrease secondary to splenic congestion (barbiturate-induced splenomegaly). Stress and excitement are also commonly associated with neutrophil increases due to glucocorticoid- and epinephrine-induced demargination, respectively. Xenobiotics that alter granulocyte adherence to vascular endothelium alter the proportions of circulating and marginated leukocytes. Ethanol, colchicine, and adrenergic agonists can rapidly increase the circulating granulocyte pool by inducing demargination of mature granulocytes from the vascular endothelium. In contrast to inflammation, demargination typically does not cause marked leukocytosis or a left shift. Histamine, iron oxide, and dextran produce an apparent granulocytopenia by increasing the size of the marginated pool. In humans, splenic sequestration of platelets with splenic enlargement and thrombocytopenia has been associated with portal hypertension secondary to oxiplatin-induced liver sinusoidal injury.

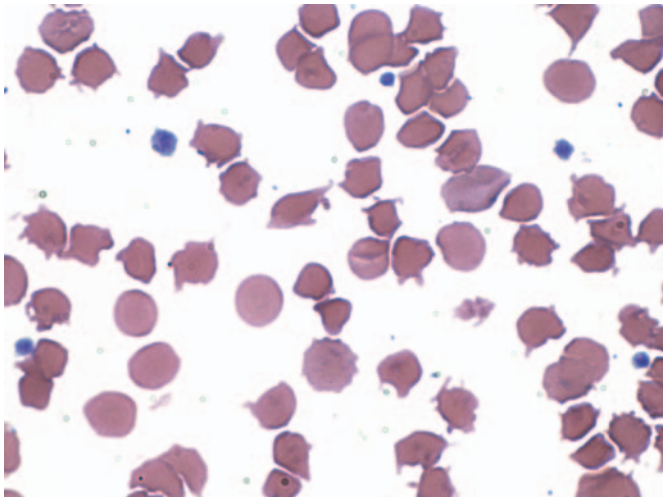

FIGURE 13.3 Severe drug-induced poikilocytosis (abnormally shaped RBCs) in a peripheral blood smear from a cynomolgus macaque. Wright's stain. Source: *Figure reproduced from Haschek, W. M., Rousseaux, C.G., Wallig, M.A. (Eds.), 2013. Handbook of Toxicologic Pathology, third ed. Academic Press, Fig. 50.7, p. 1918 with permission.*

Hemolytic Anemia

Acquired hemolytic anemia is among the most frequently reported drug reactions in humans. Decreased RBC life span defines hemolytic anemias. Injury can range from subtle membrane changes resulting in premature removal from circulation (extravascular hemolysis) to life-threatening intravascular hemolysis. Hemolytic anemias are often accompanied by a regenerative response (reticulocytosis and BM erythroid hyperplasia). The peripheral blood smear may show morphologic evidence of RBC destruction, including schistocytes and spherocytes, and occasionally Heinz bodies, and other forms of poikilocytosis (Figure 13.3), depending on the pathogenesis of the anemia. A regenerative response may not be present with acute intravascular hemolysis. A rapid decline in red cell mass in the absence of overt hemorrhage is compatible with hemolytic anemia.

Intravascular hemolysis is dramatic and often life threatening, due to the sudden drop in hemoglobin and oxygen carrying capacity of the blood, as well as the release of RBC contents into circulation. Intravascular hemolysis is typified by hemoglobinemia, hemoglobinuria, and hyperbilirubinemia. Drug-induced intravascular hemolysis is most often immune mediated, typically due to a type II reaction with fixation by complement (membrane attack complex), and lytic pore formation.

Extravascular hemolysis is more insidious in its presentation. Extravascular hemolysis can be due to direct injury or immune-mediated (type II with nonlytic

fixation of complement or type III with removal of immune complex-coated RBCs). Damaged, fixed, or coated RBCs are removed by mononuclear phagocytic cells. Since affected RBCs are not lysed within the vascular space, hemoglobinemia and hemoglobinuria are not observed, and hyperbilirubinemia is variable, depending on the rate of hemolysis. Splenomegaly is frequently encountered in chronic hemolytic anemia because of sequestration of damaged RBCs by fixed macrophages within the red pulp. These cells can hypertrophy and can become quite large and prominent, giving the spleen a solid "meaty" appearance grossly. Widespread and marked EMH is also common, along with hemosiderin-laden macrophages (siderophages).

Blood Loss Anemia

In toxicity studies, decreases in red cell mass due to blood loss are typically the result of repeated phlebotomy or, less commonly, hemorrhage. Hemorrhage due to hemostatic dysfunction occurs secondary to suppression of thrombopoiesis, impaired platelet function, or coagulopathy (most commonly vitamin K antagonists). Severe thrombocytopenia may be associated with petechiae, ecchymoses, melena, and prolonged bleeding from small wounds (e.g., venipuncture). When these clinical manifestations are observed in the absence of decreased platelet counts, alterations in platelet function may be involved.

Inflammation

Inflammation in toxicity studies is commonly incidental (e.g., abscesses) or secondary to procedure-related effects (infection of catheterization site), though it may also be observed with immunomodulatory compounds or those affecting myelopoiesis. The leukogram or pattern of change in blood, including cells affected and direction and magnitude of change, depends on the inciting agent, site of inflammation, and chronicity.

Changes in Bone Marrow Hematopoietic Cells

Lesions in BM can reflect disturbances in growth, degenerative changes, inflammatory changes, and neoplasia. For practical purposes, these may be classified into physiologic responses, nonproliferative lesions, clonal diseases, and proliferative lesions.

In toxicology studies the most frequently observed BM changes are physiologic responses to changes/lesions elsewhere in the body. These are characterized by the appropriate release of cells stored in the BM into circulation with peripheral increases in the affected cell type. Less frequent are primary hematologic diseases due to BM dysfunction. These are characterized by inappropriate responses to peripheral cytopenia (nonregenerative anemia, thrombocytopenia, leukopenia), inappropriate cytosis (polycythemia vera, essential thrombocytosis, leukemia) and/or qualitative changes (i.e., abnormalities in function and/or morphology).

Physiologic Responses

A physiologic response to increased cell demand (e.g., anemia or infection) may result in increased BM hematopoietic cells but unaffected cell morphology and maturation synchrony. Increased erythropoietic cells generally indicate a response to anemia (e.g., early blood loss or hemolytic anemia), or stimulation of erythropoiesis (hypoxia, exogenous rhEPO). In the case of anemias the development of erythroid hyperplasia

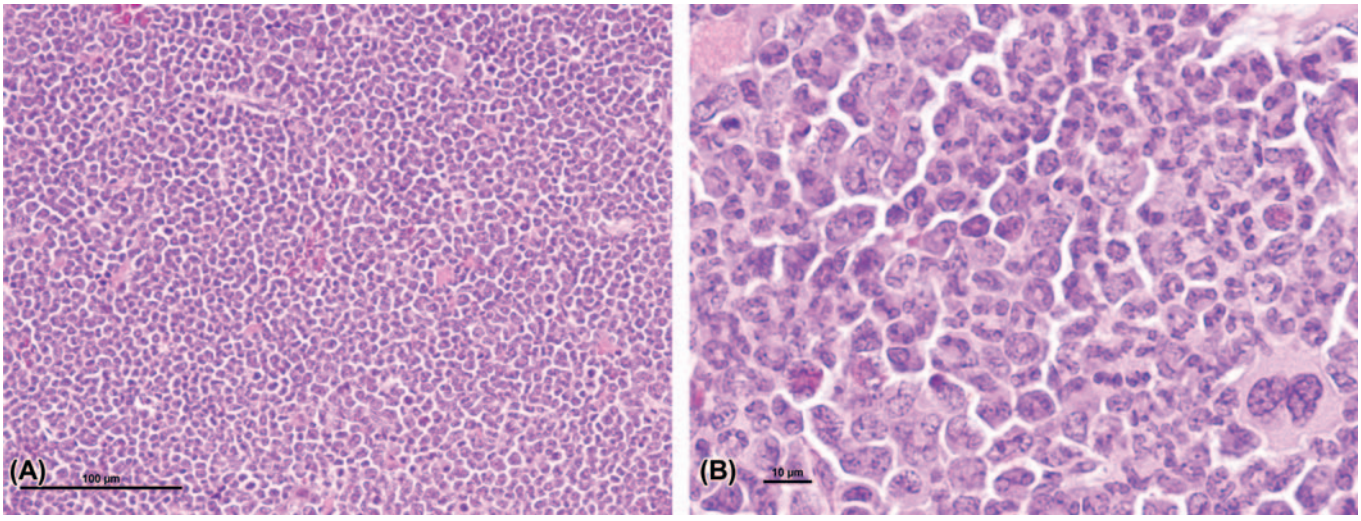

FIGURE 13.4 Myeloid (neutrophil) hyperplasia in a mouse. (A) Low resolution. (B) High resolution. Proliferation of granulocytes has displaced erythroid islands, resulting in a markedly elevated M:E ratio. H&E. Source: *Figure reproduced from Haschek, W.M., Rousseaux, C.G., Wallig, M.A. (Eds.), 2013. Handbook of Toxicologic Pathology, third ed. Academic Press, Fig. 50.8, p. 1920 with permission.*

will depend on the type, duration and severity of the anemia and on the age of the animal. EMH may be seen in the spleen and liver, particularly in mice. Rubricytes and metarubricytes generally predominate but there may also be an increase in rubriblasts and prorubricytes.

Increased numbers of granulopoietic cells are frequently associated with an inflammatory response. Although there is an increase in all immature forms, metamyelocytes, bands and segmented granulocytes predominate. In acute inflammation, BM segmented neutrophils may be decreased due to release from the storage pool. Myeloid hyperplasia (Figure 13.4) due to leukemoid responses (leukemia-like extreme inflammatory leukocytosis) may be distinguished from myeloid neoplasia based on maturation asynchrony and atypia observed with neoplasia. Increased mast cells may be observed with inflammation, particularly with parasitic infection secondary to immunosuppression.

Increased MKs are associated with platelet consumption/destruction and regenerative anemias. MK hyperploidy may occur with MK hyperplasia but cytomorphology is otherwise normal.

Nonproliferative Lesions

The most common manifestations of BM suppression are decreased circulating platelet, granulocyte, or reticulocyte counts (with or without RBC decreases depending on duration and severity of effect). Persistent granulocytopenia is one of the most sensitive indicators of myelotoxicity. Because of the short

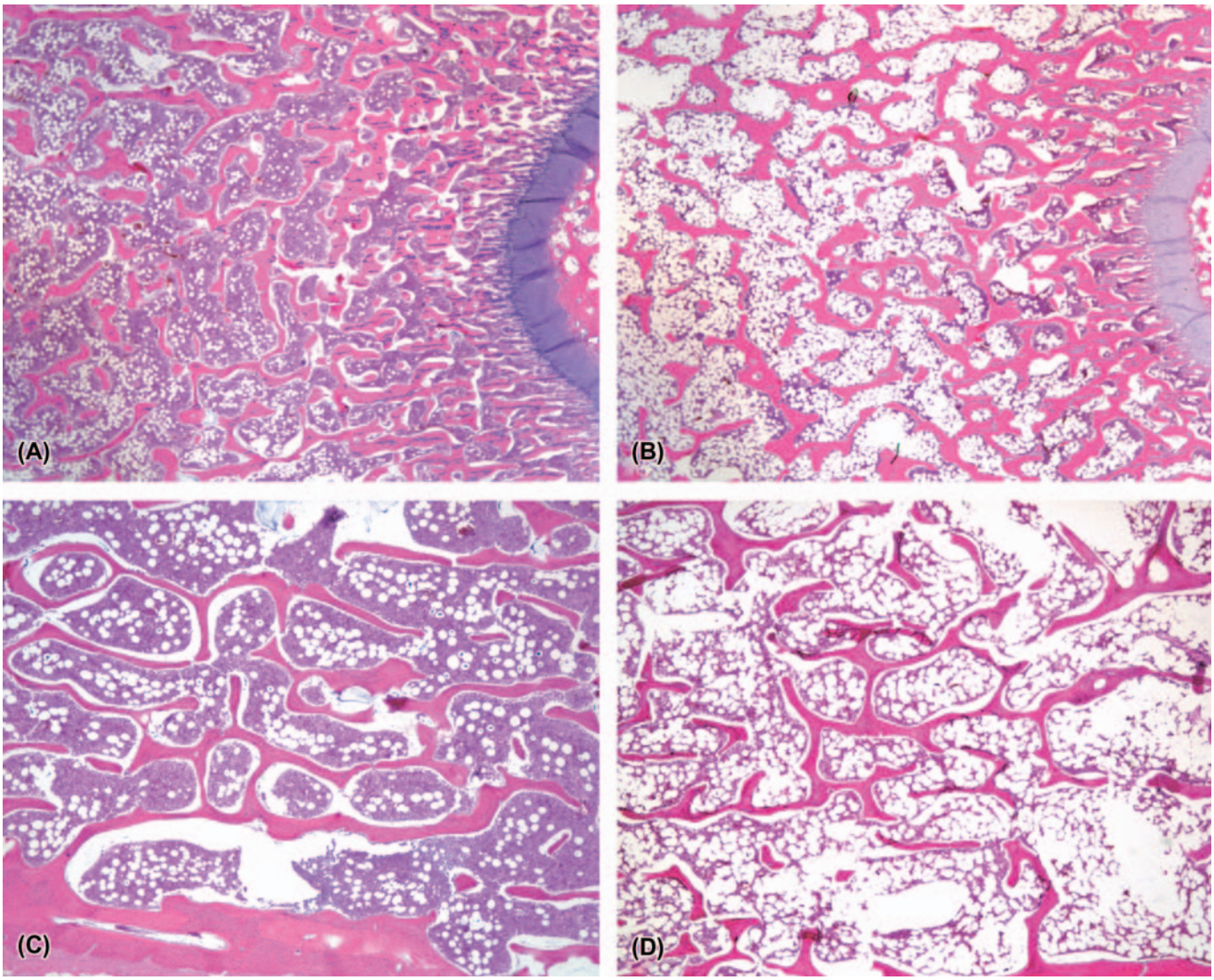

FIGURE 13.5 Bone marrow (BM) hematopoietic hypocellularity. (A and C) Control dog. (B and D) BM hematopoietic hypocellularity and replacement by adipocytes in a dog given a corticotropin releasing factor-2 receptor (CRFR2) agonist. This change was accompanied by mild decreases in reticulocyte counts and red cell mass, and associated with decreased food consumption, body weight loss, decreased thymic weight, and thymic lymphoid depletion. H&E. Source: *Figure reproduced from Haschek, W.M., Rousseaux, C.G., Wallig, M.A. (Eds.), 2013. Handbook of Toxicologic Pathology, third ed. Academic Press, Fig. 50.9, p. 1921 with permission.*

life span of neutrophils in the circulation (hours), neutropenia is usually the earliest detectable sign of myelotoxicity, occurring as early as 1–3 days postexposure with high doses of cytotoxic agents, and somewhat later (7–14 days) with lower doses or agents with reduced toxicity profiles. Decreased peripheral reticulocyte and platelet counts may be detected as early as 2–3 days and 9–14 days postexposure, respectively. Red cell mass may not be decreased, at least initially, because of the much longer life span of RBCs.

Nonspecific stresses or systemic toxicity can transiently alter cell cycle kinetics in proliferating BM populations, producing wide fluctuations in circulating granulocyte numbers. Rodents and rabbits are especially susceptible to stress-induced leukopenia. Similarly, decreases in reticulocytes can also occur with nonspecific myelosuppression secondary to inflammation or chronic disease.

With hypoplasia, marrow cellularity is reduced in both hematopoietic area and in cellular density, and adipose tissue is diffusely increased. These decreases must be distinguished from age-related increases in marrow adiposity in all species and from spontaneous multifocal hypoplasia in rats. Decreases in BM nucleated cells may involve all lineages or individual cell lines. The M:E ratio (normally ranging from 0.6–2.3 in monkeys, 0.45–2.87 in dogs, and 1.07–1.93 in rats) may be increased (erythroid hypoplasia) or decreased (myeloid hypoplasia). If all cell lines are affected (panhypoplasia), the hematopoietic tissue in the marrow cavity may be replaced with

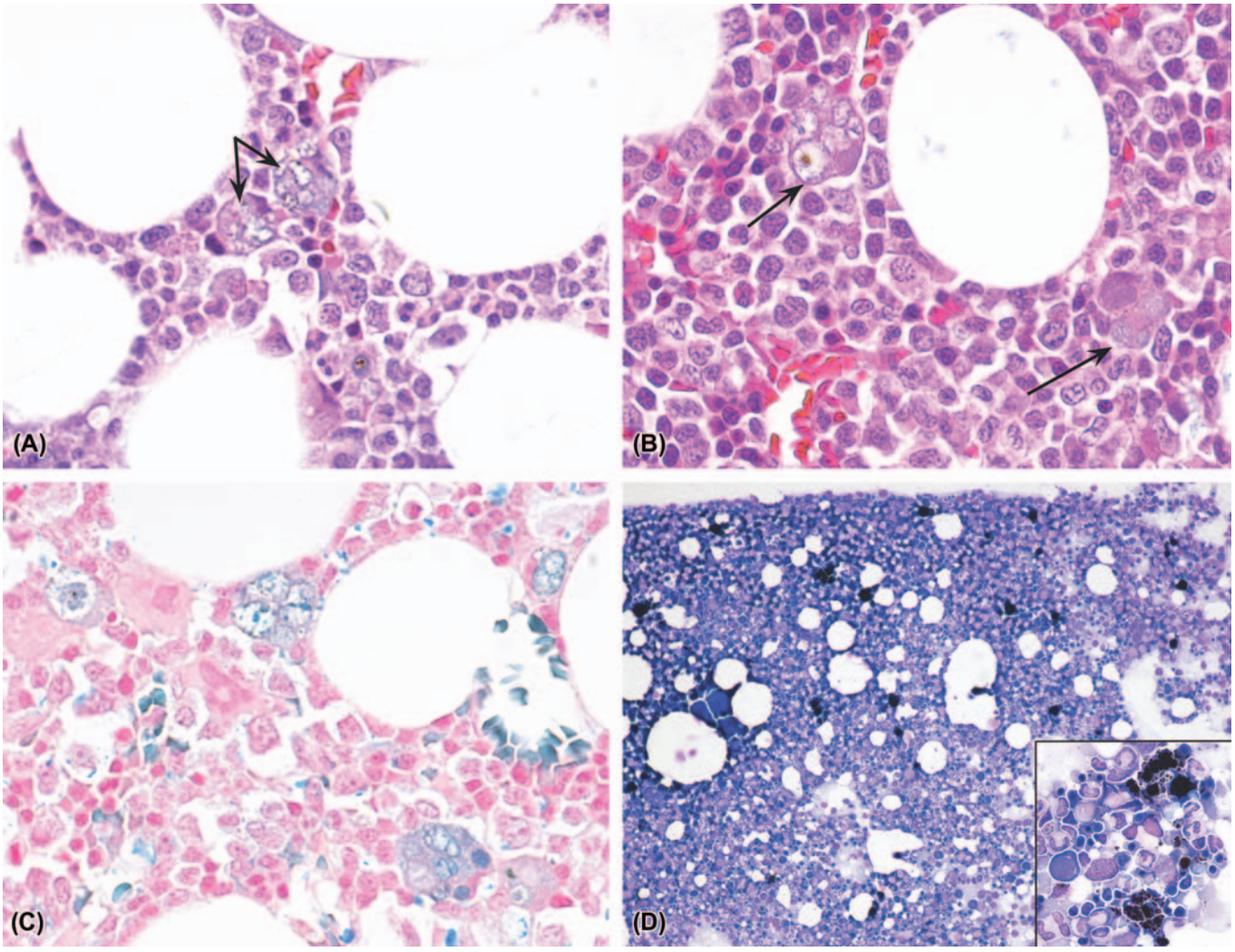

FIGURE 13.6 Iron overload. (A and B) Minimally increased iron pigment (pale brownish-gray due to decalcification) within macrophages (arrows) (H&E). (C) Prussian blue staining confirms presence of ferric iron. (D) Cytologic smear demonstrates increased intracellular and extracellular iron stores in the absence of increased erythrophagocytosis. Inset: Extracellular iron pigment is visible in large clumps and scattered as small granules (Wright's stain). Source: *Figure reproduced from Haschek, W.M., Rousseaux, C.G., Wallig, M.A. (Eds.), 2013. Handbook of Toxicologic Pathology, third ed. Academic Press, Fig. 50.10, p. 1922 with permission.*

adipose tissue (Figure 13.5) and pancytopenia may be observed. It is also important to note that a single lineage may be decreased even though BM cellularity is normal or increased. Decreased thrombopoiesis is most commonly associated with an overall BM suppression. With megakaryocytic hypoplasia, MK numbers and ploidy are reduced.

Erythroid hypoplasia/suppression may be due to a direct drug effect (e.g., estrogen, antivirals, chemotherapeutics, etc.) or to an indirect effect (e.g., tumor necrosis factor, hypothyroidism, emaciation, inflammation, neoplasia, chronic renal or liver disease, etc.). Morphologically, BM sections appear hypocellular, the M:E ratio may be increased, and there may be a shift in the maturation sequence to mature cells.

BM iron stores typically stain as a golden brown (H&E) or blue (Prussian blue) pigment (Figure 13.6). The evaluation of iron stores may be useful in distinguishing anemia of chronic inflammation (normal cellularity and morphology with increased iron) from iron deficiency anemia (decreased iron) and anemia of chronic renal disease (normal to hypocellular marrow with normal iron stores).

Severe stress, malnutrition, inanition, or cachexia may lead to gelatinous marrow transformation (GMT), a diffuse or focal degeneration/necrosis of marrow adipocytes (fat necrosis, serous atrophy of marrow fat). Adipocytes and hematopoietic tissue are replaced by hyaluronic acid-rich mucopolysaccharides without reticulin fibers. Fat necrosis is thought to result from inadequate trophic stimulation from BM microenvironment. Lesions are reversible after return to adequate nutritional status. Fat necrosis been reported in male Gottingen minipigs and rabbits, as well as miniature horses, ruminants, reindeer, swans (lead toxicity), and calves (fluoride toxicity in dams).

BM necrosis may occur with severe injury caused by chemotherapeutic agents, phenobarbital, estrogen, carprofen, metronidazole, fenbendazole, colchicine, cephalosporins, and mitotane. Necrosis may also occur with vascular occlusion (infarction) or with severe malnutrition. It is usually accompanied by refractory anemia with or without leukopenia and thrombocytopenia. Necrotic areas of BM have an eosinophilic tint and indistinct margins. Degenerating hematopoietic and stromal cells may be vacuolated or necrotic, with nuclear pyknosis and karyorhexis. Vacuolated macrophages phagocytizing cellular debris and containing ceroid or lipofuscin may be increased. Depending on severity and chronicity, there may be extensive replacement of normal stroma by necrotic debris and hemorrhage with or without blue foci of mineralization. BM necrosis is usually coagulative and only the eosinophilic outline of the marrow cells and structure may remain (Figure 13.7, Panels C and D).

Pure red cell aplasia is characterized by normocytic anemia, reticulocytopenia, normal leukocyte and platelet counts, and absence of mature marrow erythroid progenitors. Since granulocytes and MKs are not affected, the overall marrow cellularity may not be dramatically altered. The M:E ratio is markedly increased and hemosiderin-laden macrophages may be increased as well. Pure red cell aplasia is a persistent, chronic refractory anemia that tends to develop after prolonged exposure to recombinant erythropoietin, as well as with a variety of drugs including immunosuppressants, antibacterials, antivirals, fludarabine, anticonvulsants, as well as chloroquine, allopurinol, ribavirin, and gold.

Aplastic pancytopenia (BM aplasia, aplastic anemia) is a syndrome associated with BM failure, characterized by pancytopenia, BM hypocellularity and grave prognosis (in the absence of successful BM transplantation, approximately 40% of all affected humans die within 6 months of diagnosis). This condition should not be confused with pure red cell aplasia, which involves decreased production of only the erythropoietic cell lineage. The marrow may be completely devoid of hematopoietic cells, with only adipose tissue, fibrous stromal cells, and vascular sinuses remaining. There may be small isolated islands of hematopoietic or other cells scattered about, such as lymphocytes, plasma cells, macrophages, and mast cells. Aplastic pancytopenia is a disorder of stem cell regulation, though stromal cell defects and immune-mediated destruction of stem cells may also play an important role. In some cases there is evidence to support a clonal origin. Aplastic pancytopenia may arising secondary to chemotherapy or xenobiotic exposure carry an even more dismal prognosis. Though rare in domestic animals, it has been reported with exposure to antimicrobials, chemotherapeutics, phenylbutazone, estrogen, bracken fern, and aflatoxin B1. Xenobiotic-associated aplastic pancytopenia is usually acute, with severe neutropenia within 1 week and severe thrombocytopenia within 2 weeks. Animal models of aplastic pancytopenia are relatively few, and have been largely restricted to those induced by viruses, busulfan, ionizing radiation, or benzene.

Ionizing radiation produces both transient and prolonged BM suppression, depending on the dose, dose rate, and exposure conditions. Local irradiation of rats with 2000 rad results in a transient hypoplasia and recovery. This pattern of suppression followed by regeneration is also observed in other species. Twice the dose results in a transient hypoplasia with a latent period, followed by a prolonged hypoplasia. Aplastic anemia resulting from either busulfan treatment or irradiation is characterized by a marked reduction in most proliferating cell populations in mice.

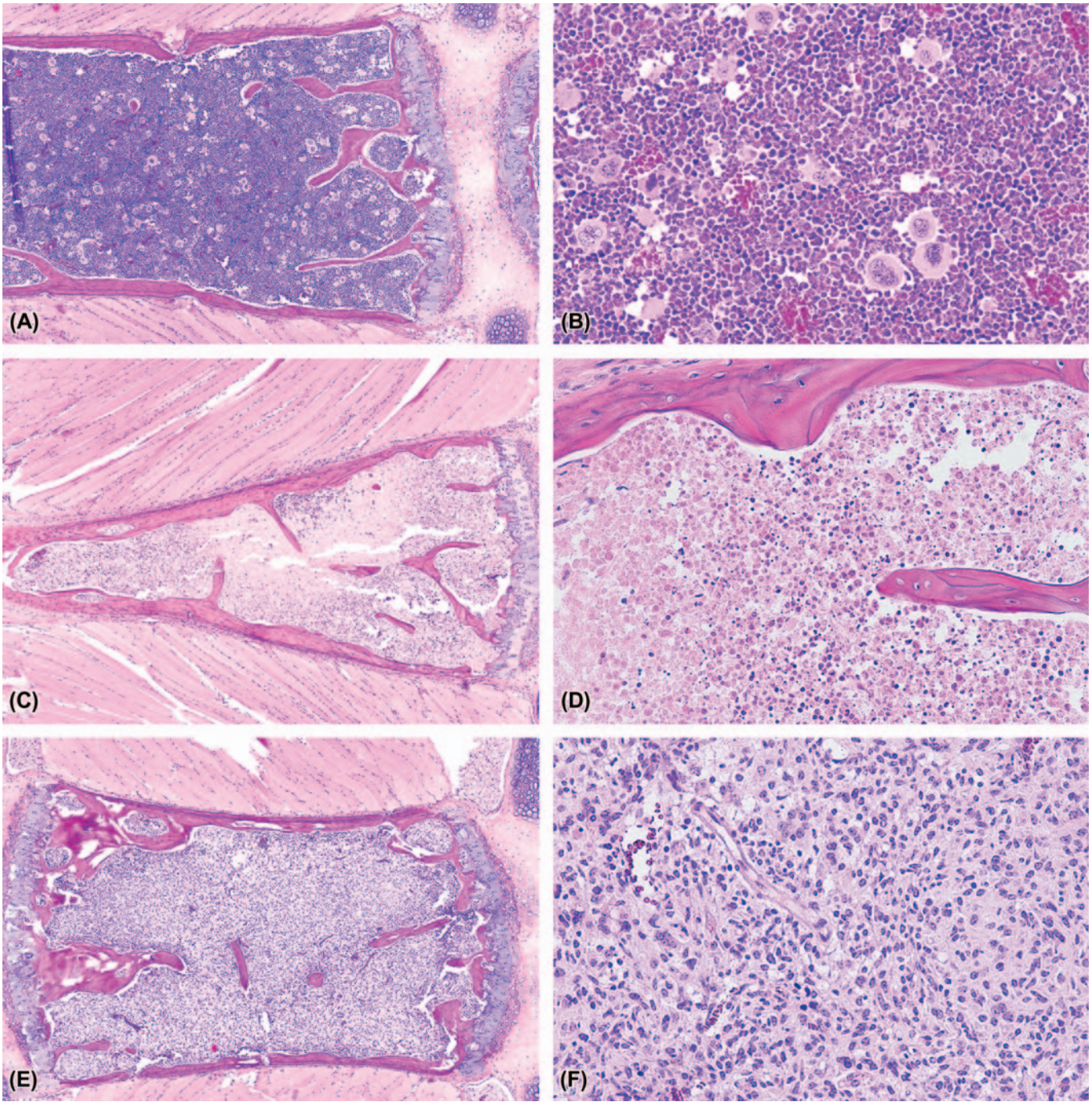

FIGURE 13.7 Drug-induced severe stromal hyperplasia and necrosis in mice. (A and B) Control mouse. (C and D) Necrosis. (E and F) Stromal hyperplasia, note the lack of associated collagen. H&E. Source: *Figure reproduced from Haschek, W.M., Rousseaux, C.G., Wallig, M.A. (Eds.), 2013. Handbook of Toxicologic Pathology, third ed. Academic Press, Fig. 50.11, p. 1923 with permission.*

Clonal Hemopathies

Erythropoiesis is more sensitive to chemical disruption than granulopoiesis. However, anemia may not be observed or may be a late manifestation, since RBC have a long life span relative to leukocytes. Consequently bone marrow suppression-related anemias are usually clonal disorders of erythropoiesis accompanied by morphologic changes suggestive of maturational alterations. They may initially manifest only as megaloblastic, sideroblastic, or hemolytic anemias, but can also eventually progress to myelodysplasia and secondary acute leukemia.

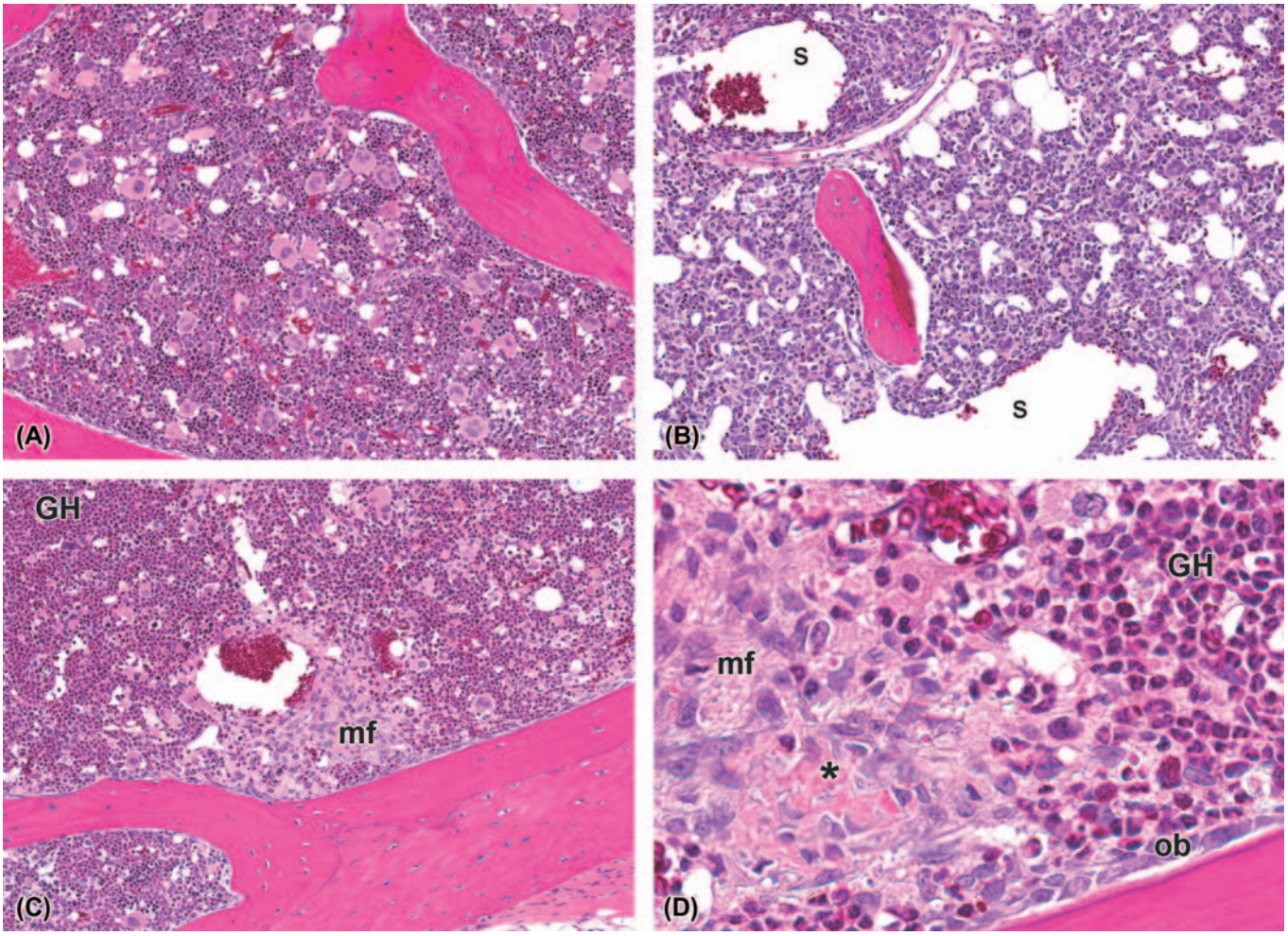

FIGURE 13.8 Drug-induced megakaryocyte hypocellularity with secondary myelofibrosis in rats. (A) Control rat. (B) Mild generalized hematopoietic hypocellularity with severe megakaryocyte hypocellularity and slight dilation of medullary sinusoids (**s**) (end of dosing for 7 days). (C and D) Focal myelofibrosis (**mf**) and granulocytic hyperplasia (**GH**) with a predominance of late-stage granulocytes (end of 7-day recovery). Myelofibrosis was characterized by activation and extension of osteoblasts (**ob**) into areas of fibrosis and the formation of new woven bone (*). Myelofibrosis and woven bone formation were secondary to induction of TPO production and prolonged bone marrow (BM) megakaryopoiesis. H&E. Source*: Figure reproduced from Haschek, W.M., Rousseaux, C.G., Wallig, M.A. (Eds.), 2013. Handbook of Toxicologic Pathology, third ed. Academic Press, Fig. 50.12, p. 1926 with permission.*

Megaloblastic anemia is clonal RBC disorder characterized by macrocytic or microcytic peripheral RBCs, BM hypercellularity, and megaloblasts (large, abnormal hematopoietic progenitor cells). Causes include drugs that interfere with RNA/DNA synthesis, decrease vitamin B_{12}, folate, or cobalamin levels.

Sideroblastic anemia is a clonal disorder of erythropoiesis caused by altered heme synthesis and precipitation of iron and ferritin in mitochondria of maturing erythroid cells. It is characterized by ringed sideroblasts (rubricytes containing iron-positive granules surrounding the nucleus) in the BM and peripheral microcytosis. Causes include ethanol, isoniazid, pyrazinamide, cycloserine, chloramphenicol, copper chelation/deficiency, zinc, lead, trichloroethylene, linezolid, penicillamine, triethylene tetramine dihydrochloride, and gallium arsenide.

Paroxysmal nocturnal hemoglobinuria (PNH) is a clonal HSC disease reported only in humans exposed to benzene, vitamin C, antithymocyte globulin and in some animal models (calves and mice). It may be also observed with aplastic anemia and myelodysplasia. PNH results in episodic or chronic, complement induced, intravascular hemolytic anemia, hemoglobinuria, and thrombosis. It is hypothesized to be due to the clonal expansion of a mutated HSC that lacks a membrane anchor protein (glycosyl-phosphatidyl-inositol anchor protein, or GPI-AP). Affected cells consequently do not express cell surface proteins that use the GPI anchor for attachment to the cell membrane, including proteins that prevent complement-mediated lysis such as decay-accelerating

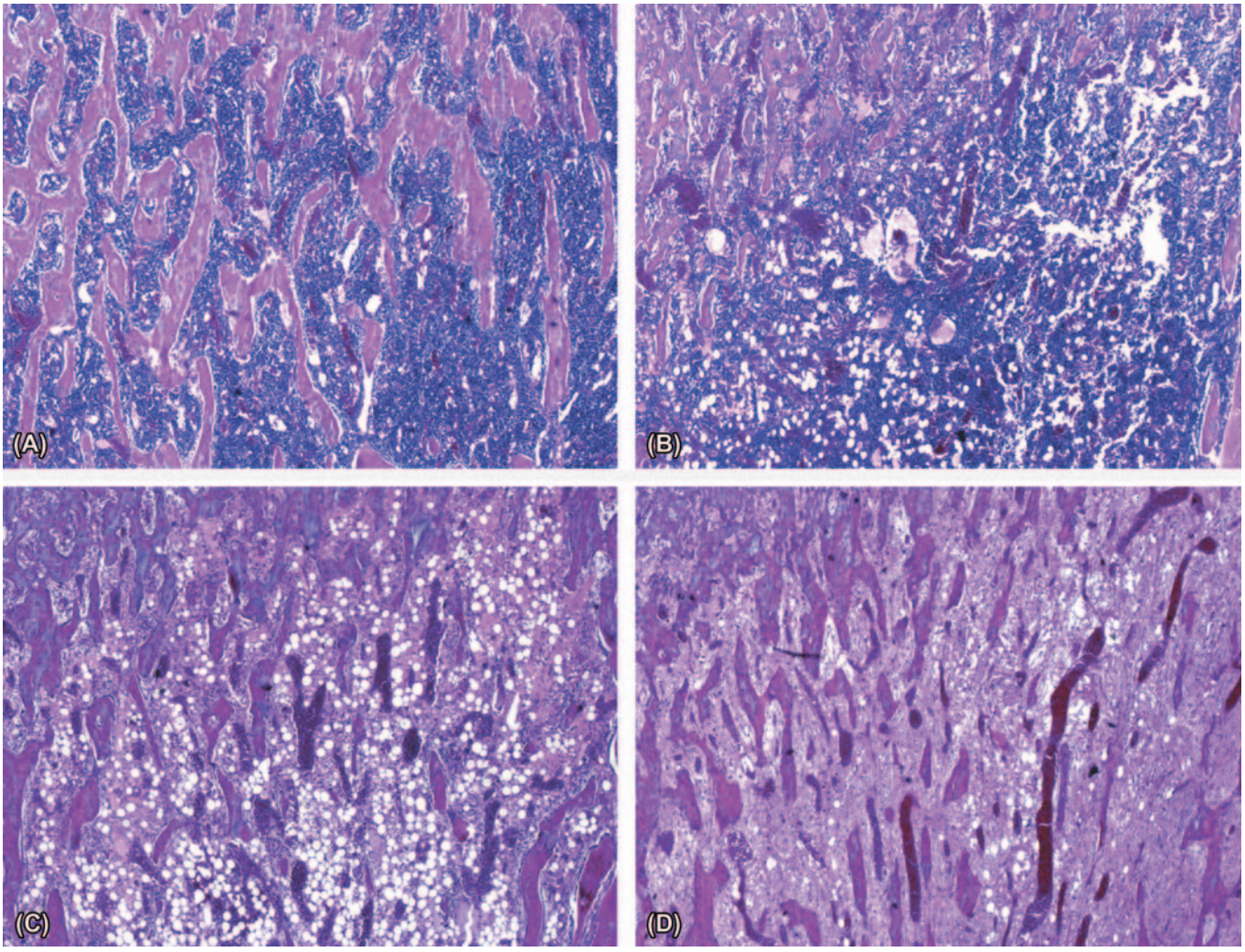

FIGURE 13.9 Drug-induced acute marrow hypoplasia in a dog given an anticancer agent (p53 enhancer) for 2 weeks. (A) 0 mg/kg (control); (B) 25 mg/kg (mild hypocellularity); (C) 75 mg/kg (moderate hypocellularity); (D) 150 mg/kg (severe hematopoietic hypocellularity with fibrosis). Source: *Figure reproduced from Haschek, W.M., Rousseaux, C.G., Wallig, M.A. (Eds.), 2013. Handbook of Toxicologic Pathology, third ed. Academic Press, Fig. 50.13, p. 1927 with permission.*

factor (DAF or CD55), which disrupts C3 convertase formation, and protectin (CD59), which binds the membrane attack complex and prevents C9 binding to the cell.

Myeloproliferative Lesions

Myelofibrosis involves active fibroblast proliferation (i.e., "stromal hyperplasia") in marrow spaces and deposition of large amounts of reticulin, interfering with blood supply and eventually resulting in replacement of hematopoietic cells with inactive fibrous tissue. (Figure 13.7, Panels E and F). Hematologic findings in myelofibrosis vary considerably, depending on species and severity; EMH and myeloid metaplasia are common. Primary myelofibrosis is a myeloproliferative disease primarily observed in humans but also reported in dogs. Its pathogenesis is linked with MK secretion of growth factors that induce fibroplasia and reticulin deposition, such as transforming growth factor-β (TGF-β), platelet-derived growth factor (PDGF), and fibroblast growth factor (FGF) (Figure 13.8).

Secondary myelofibrosis results from replacement of necrotic marrow with fibrous connective tissue (i.e., "scar tissue"). Necrosis may be due to chronic renal disease (rats, fibrous osteodystrophy), IMHA, inflammation, dysmegakaryopoiesis, neoplasia, and long-term treatment with hematotoxic drugs. Drug-induced secondary myelofibrosis has been most frequently reported dogs exposed to compounds that produce generalized myelosuppression (e.g., estrogen) (Figure 13.9).

Myelodysplastic syndromes (MDS, dysmyelopoiesis) are clinically heterogeneous clonal HSC disorders characterized by ineffective hematopoiesis (impaired differentiation) of one or more nonlymphoid lineages, associated with peripheral cytopenia(s), BM dysplasia, and risk for progression to acute myeloid leukemia. MDS have been described in dogs, cats, and humans. Peripherally, there is anemia with macrocytosis, leukopenia, and/or thrombocytopenia. Histologically, BM is hypercellular, though hypocellularity with proliferation of one or more cell lineages can be observed. Dysplasias include dyserythropoiesis, dysgranulopoiesis, dysmegakaryopoiesis. Immature forms or blast cells may be increased but represent less than 20% of nucleated cells. Diagnosis requires cytological (qualitative and quantitative) evaluation of BM smears. MDS may be classified as leukemia if >20% of nucleated hematopoietic cells are immature forms or blasts and/or if there is metastasis to nonhematopoietic tissues. Leukemia, primarily acute myelogenous leukemia, is often preceded by a "preleukemic" or prodromal state of chronic BM insufficiency. The rate of progression from MDS to frank leukemia in humans appears to be particularly high in cases arising secondary to chemotherapy or benzene exposure. Clonal abnormalities may be present for years prior to the onset of leukemia. MDS carries a grave prognosis, with reported mortalities of 30%–84%.

Leukemias are among the most widely recognized and feared malignancies. Derived from BM, they usually disseminate via blood. The hematopoietic lineage involved depends on cause and genetic susceptibility. For example, genetic susceptibility to pediatric acute lymphoblastic leukemia has been associated with coding polymorphisms at loci such as CDKN2A/B (cyclin-dependent kinase inhibitor 2 A/B), GATA3 (GATA binding protein 3), ARID5B (AT-rich interactive domain-containing protein 5B), IKZF1 (Ikaros family zinc finger protein 1), and CEBPE (CCAAT/enhancer binding protein, epsilon). In another example, CBA/H mice are susceptible to radiation-induced acute myeloid leukemia while C57BL/6 mice are resistant. Susceptibility in CBA/H mice has been attributed to variants at the stem cell frequency regulator 1 (Scfr1) locus. In humans xenobiotic-induced leukemias are predominantly of the acute myeloid type. Leukemias consisting predominantly of immature or blast cells tend to be aggressive and proliferate rapidly whereas more differentiated phenotypes tend to take a more protracted course. Reports of drug-induced leukemia in domestic animals are exceedingly rare, though myelodysplasias have been reported with somewhat more frequency (see earlier).

Lymphoid cells account for <30% of nucleated hematopoietic cells in normal nonrodent marrows (higher proportions in rodents). In contrast, lymphoma or leukemia is likely when lymphoid cells account for >30% of nucleated BM hematopoietic cells. In lymphoid hyperplasia involving the BM, there may be focal or diffuse increases in lymphocytes; small mature lymphocytes predominate, though lymphoblasts and prolymphocytes may be increased. In contrast, lymphoma presents with focal aggregates primarily in the thymus, lymph nodes, or splenic white pulp whereas leukemia tends to present as sheets in the BM, and spleen, with neoplastic cells also in the blood. As an exception, murine lymphomas do form space-occupying lesions in BM, but also spill into the blood, rendering the distinction difficult.

Secondary Hematopoietic Organs

Any physiological demand for blood cells may result in EMH in tissues other than the BM, such as the spleen, liver, and perirenal adipose tissue. Increased EMH may be seen as a reaction to injuries such as hematotoxic insult, anemia or infections elsewhere in the body. The spleen and liver are most often involved since they normally have foci of EMH to increase production when needed. However, other organs, such as the lymph nodes and kidneys, may also be involved via hematogenous spread and tissue infiltration by multipotential stem cells from the BM. In all organs that support EMH, hematopoietic cells are composed of varying numbers of myeloid, erythroid, or megakaryocytic cells, depending on the need and inciting cause. Cell lines sharing a common progenitor may also be affected (RBC and platelets). The erythroid component may predominate secondary to hemorrhage or RBC destruction, and the myeloid component may predominate secondary to inflammatory or immunoproliferative conditions. The diagnosis (erythroid, myeloid, or granulocytic hyperplasia) is based on the most prominent lineage involved. Some degree of EMH is normally present in the livers and spleens of rodents. Marked EMH with a predominant myeloid component (e.g., response to severe inflammation) shares some histological similarities with granulocytic leukemia. Increases in lymphocytes are best identified by immunohistochemistry since the morphologic appearance of lymphocytes is similar to that of HSCs.

In the spleen, EMH is characterized by varying numbers of MKs as well as clusters of myeloid and erythroid precursors throughout the red pulp. In severe cases the entire red pulp may be occupied by erythroid precursors. Extensive splenic EMH occurs secondary to anemia, blood loss, or hypoxia. In the spleen, EMH is more common in mice, young compared to old rodents, and in females compared to males. EMH as a response to injury may be seen as an increase in the number

and/or size of foci of hematopoiesis or as a diffuse (nonneoplastic) hyperplasia of the red pulp.

EMH is abundant in the fetal and neonatal liver but small, scattered foci still exist in adults and are typically found within the sinusoids, around central veins, and around portal vessels. In response to injury, foci of EMH may be scattered within the hepatic sinusoids as well as around central veins and portal vessels, and may increase in size and/or number.

SUMMARY

The hematopoietic system is responsible for the continuous production of highly specialized mature circulating blood cells with functions in oxygen transport, hemostasis, and immunity that are vital to an organism's survival. It is highly susceptible to direct and indirect xenobiotic-induced injury and adverse effects. Identifying and interpreting hematotoxicity requires an understanding of normal hematopoiesis, mechanisms of hematotoxicity, and hematopoietic tissue responses to injury. This chapter provides a functional, mechanistic, and morphologic background for understanding the broad range of toxic effects on the hematopoietic system, and describes how alterations in blood and blood-forming tissues can point to the mechanism of injury.

Further Reading

Elmore, S.E., 2006. Enhanced histopathology of the bone marrow. Toxicol. Pathol. 34 (5), 666–686.

Frith, C.H., Ward, J.M., Tyler, R.D., Chandra, M., Stromberg, P.C., 1996. Proliferative lesions of the hematopoietic and lymphatic systems in rats, HL-1. Guides for Toxicologic Pathology. STP/ARP/AFIP, Washington, DC, pp. 1–20.

Frith, C.H., Ward, J.M., Chandra, M., Losco, P.E., 2000. Non-proliferative lesions of the hematopoietic system in rats, HL-1. Guides for Toxicologic Pathology. STP/ARP/AFIP, Washington, DC, pp. 1–22.

MacKenzie, W.F., Eustis, S.L., 1990. Bone marrow. In: Boorman, G.A., Eustis, S.L., Elwell, M.R., Montgomery, C.A., MacKenzie, W.F. (Eds.), Pathology of the Fischer Rat. Academic Press, Inc, San Diego, Ca, pp. 395–403.

Mintzer, D.M., Billet, S.N., Chmielewski, L., 2009. Drug-induced hematologic syndromes. Adv. Hematol. 2009, 1–11.

Orkin, S.H., Zon, L.I., 2008. Hematopoiesis: an evolving paradigm for stem cell biology. Cell 132 (4), 631–644.

Reagan, W.J., Irizarry-Rovira, A., Poitout-Belissent, F., Bolliger, A.P., Ramaiah, S.K., Travlos, G., et al., 2011. Best practices for evaluation of bone marrow in nonclinical toxicity studies. Vet. Clin. Pathol. 40 (2), 119–135.

Travlos, G.S., 2006. Histopathology of bone marrow. Tox. Pathol. 34, 566–598.

Weiss, D.J., 2012. Drug-associated blood cell dyscrasias. Compendium: Continuing Education for Veterinarians. 34 (6), E1–E8.

Weiss, D.J., Wardrop, K.J., 2011. Schalm's Veterinary Hematology. Wiley-Blackwell.

This page intentionally left blank

CHAPTER

14

Respiratory System

Jack R. Harkema[1], *Kristen J. Nikula*[2], *and Wanda M. Haschek*[3]

[1]Michigan State University, East Lansing, MI, United States [2]Seventh Wave Laboratories, LLC, Maryland Heights, MO, United States [3]University of Illinois at Urbana-Champaign, Urbana, IL, United States

OUTLINE

INTRODUCTION

The mammalian respiratory system is susceptible to injury caused by either air- or blood-borne toxicants. Susceptibility of the lung to injury caused by inhaled toxicants is due in large part to the extensive interface between the alveolar surface area and inspired air. Likewise, the extensive interface between the alveolar capillary surface area and circulating blood makes the lung susceptible to blood-borne toxicants.

The respiratory tract comprises the largest mucosal surface of the body, with an internal surface area that is 25 times greater than the external surface of the body covered by skin. In contrast to other mucosa-lined organs found in the digestive and reproductive tracts that are only periodically exposed to the external environment, the respiratory organs are constantly in contact with large amounts of inhaled air that may contain airborne xenobiotic compounds, such as gaseous and particulate air pollutants. At rest, the adult

Fundamentals of Toxicologic Pathology.
DOI: http://dx.doi.org/10.1016/B978-0-12-809841-7.00014-9

human takes in 10,000–15,000 L of ambient air through the nasal passages each day. Likewise, the pulmonary circulation receives the total cardiac output from the heart's right ventricle, making the lung also vulnerable to blood-borne toxic agents. Targeted toxicity of air- or blood-borne toxicants within the upper or lower respiratory tract is dependent on numerous factors, but most importantly the physical and chemical character of the chemical agent, site-specific tissue dosimetry and sensitivity, and host-dependent factors such as health status, gender, and age.

The respiratory system is a structurally complex arrangement of organs designed principally for the intake of oxygen and the elimination of carbon dioxide, i.e., respiratory gas exchange or "respiration." Though its main function is gas exchange, the respiratory tract is composed of specialized tissues and cells that have other important functions, such as the production of glycoproteins (e.g., mucus) and phospholipids (e.g., surfactant), the activation and inactivation of circulating hormones, and the metabolism of xenobiotic compounds entering the body through inhalation or other routes. Another important function, especially of the upper respiratory tract, is host defense against exposure to inhaled infectious agents (e.g., viruses, bacteria) and noxious chemical agents (e.g., respirable dusts and gaseous pollutants). In addition, parts of the nasal airways are lined by a unique neurosensory olfactory epithelium (OE) that connects directly to the brain, allowing the detection of odors (e.g., sense of smell or olfaction) but also providing an alternative route for some airborne agents (e.g., viruses, metals, nanoparticles) to enter the brain, bypassing the blood–brain barrier.

Exposure to respiratory toxicants can occur in occupational settings (e.g., silica, asbestos, chronic acid fumes); during medical treatment (e.g., bleomycin, cyclophosphamide, X-rays); in self-inflicted injury (e.g., cigarette smoking and cocaine use); and during the course of everyday activities, such as inhalation exposure to common air pollutants (e.g., ozone, particulate matter) or ingestion of toxic agents in food (e.g., toxic rapeseed oil, pyrrolizidine alkaloids). Pulmonary diseases linked to chemical injury range from acute reversible diseases (e.g., metal fume fever following inhalation of zinc) to chronic irreversible diseases (e.g., fibrosis following inhalation of silica, lung cancer caused by cigarette smoking). A variety of defense mechanisms, such as the mucociliary apparatus in the conducting airways and alveolar macrophages in the pulmonary parenchyma, can prevent contact of the injurious agent with vulnerable alveolar tissues in the deep lung. Unfortunately, sometimes these defenses are inadequate, and toxic lung injury occurs.

The location and type of injury are the result of complex interactions between the agent and the host. Determining factors are the physicochemical characteristics of the agent, the severity of insult (dose), and the metabolic capabilities present in the cellular components of the host respiratory tissue. Characteristics of the host response and severity of insult will determine whether the injury is reversible or irreversible, and whether long-term health effects will occur.

STRUCTURE, FUNCTION, AND CELL BIOLOGY

Macroscopic and Microscopic Anatomy

Although there is considerable variation among mammalian species in the macroscopic and microscopic anatomy of the respiratory tract (Figure 14.1; Table 14.1), the general principles involved in gas exchange are identical. The respiratory tract can be divided into two portions based on gross anatomy and physiology: (1) the proximal conducting (nonrespiratory) airways that include the nose, pharynx, larynx, and tracheobronchial airways (trachea, bronchi, and bronchioles) and (2) the distal respiratory portion comprised of the respiratory bronchioles, alveolar ducts, and alveolar sacs. The conducting portion of the respiratory system serves not only as a conduit moving air in and out of the lungs, but also to warm, moisten, and filter the inspired air. Gas exchange between air and blood is restricted to the respiratory portion located in the delicate alveolar parenchyma of the lung. The upper conducting airways must be sufficiently open to the distal alveolar regions for the system to function properly, allowing adequate delivery of oxygen to the lungs, red blood cells, and the rest of the body to sustain life.

The Nose

In both humans and laboratory animals, the nose is the primary portal of entry for the respiratory system. Besides serving as the major sensory organ for smell, the nose also functions as an air conditioner and a defender of the lower respiratory tract by humidifying, heating, and filtering, the inhaled air. In addition, it protects the delicate gas-exchange regions of the lung by absorbing water-soluble and reactive gases and vapors, trapping inhaled particles, and metabolizing airborne xenobiotics.

The nasal cavity is divided into two main air passages by the nasal septum. Each nasal passage extends from the nostrils to the nasopharynx. The nasopharynx is defined as the airway posterior to the termination of the nasal septum and proximal to the termination of the soft palate. Inhaled air flows through the nostrils,

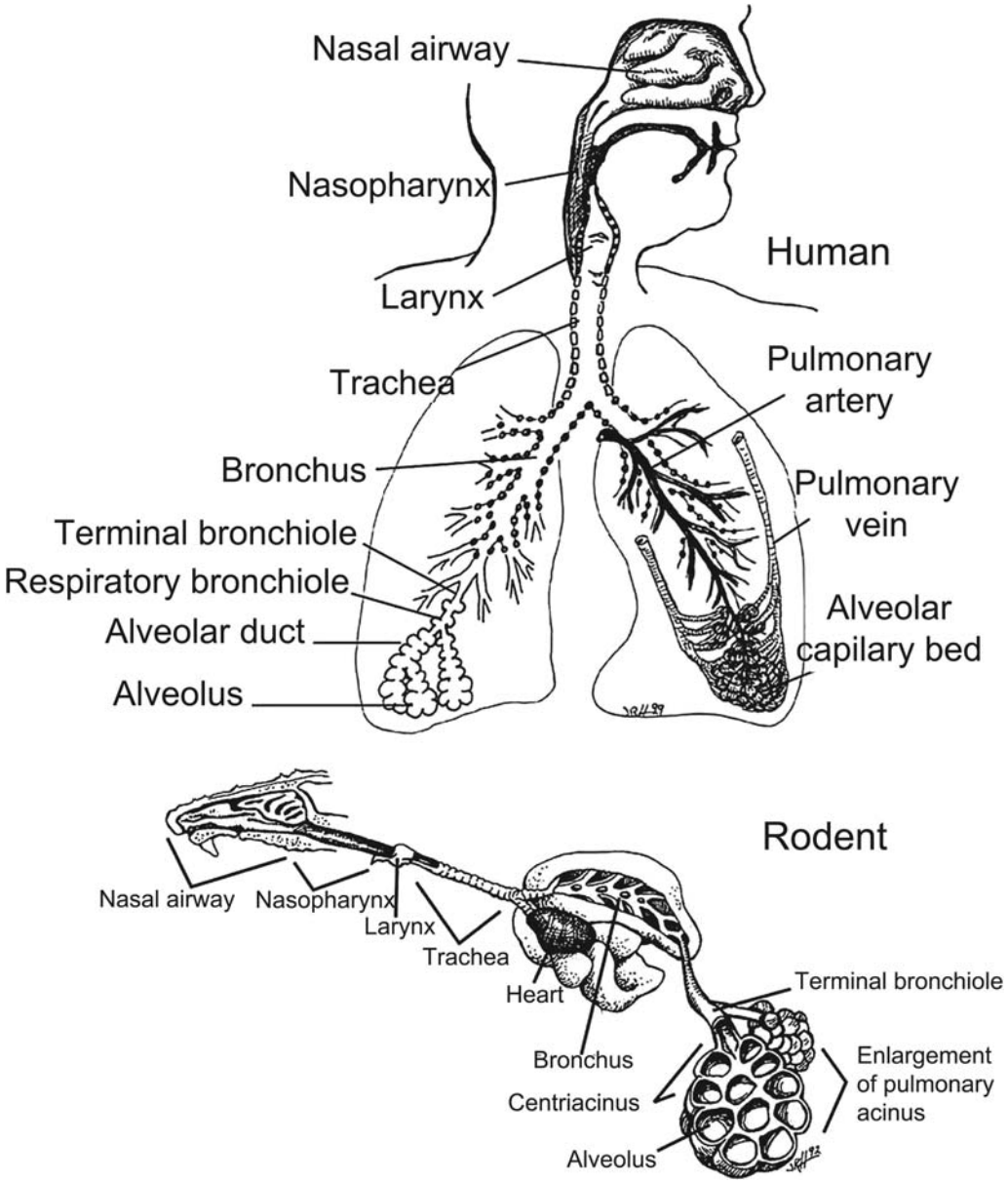

FIGURE 14.1 Diagrammatic representation of the human and rodent respiratory tracts. Dots along the laryngeal and tracheobronchial airways indicate intramural cartilage. *Figure reproduced from* Haschek and Rousseaux's Handbook of Toxicologic Pathology *(2013), third ed. (W.M Haschek, C.G. Rousseaux and M.A. Wallig, eds.), Academic Press (Elsevier), Figure 51.1, p. 1937, with permission.*

TABLE 14.1 Interspecies Comparison of Pulmonary Anatomy

Anatomical characteristics	Mouse, rat, hamster	Dog, cat, rhesus monkey	Minipig	Human
Pleura	Thin	Thin	Thick	Thick
Secondary lobulation	Absent	Absent	Present	Incomplete
Pulmonary veins	Cardiac muscle in media	Thin, mainly fibrous wall	Thick, smooth muscle in intima	Thin, mainly fibrous wall
Cartilage and submucosal glands in intrapulmonary bronchi	Absent	Present	Present	Present
Respiratory bronchioles	None/minimal	Extensive	None/minimal	Present

Table reproduced from Handbook of Toxicologic Pathology *(2013), third ed. (W. M. Haschek, C. G. Rousseaux, and M. A. Wallig, eds.), Academic Press, Table 51.1, p 1937, with permission.*

or nares, into the vestibule, a slight dilatation just inside the nares, before it enters the main chamber of the nose. Unlike the more distal main chamber, which is surrounded by bone, the nasal vestibule is surrounded by flexible cartilage. The luminal surface is lined by a squamous epithelium (SE) similar to that of external skin.

After passing through the nasal vestibule, inhaled air courses through the narrowest part of the entire respiratory tract, the nasal valve, and then into the main nasal chamber. A lateral wall, septal wall, roof, and floor define each nasal passage of the main chamber. The lumen of the main chamber is lined by well-vascularized and innervated mucous membranes (nasal mucosa) that are covered by an "epithelial lining fluid" containing a continuous surface layer of mucus. The nasal mucous layer is moved distally, by the synchronous beating of motile cilia, to the oropharynx, where it is swallowed into the esophagus.

Turbinates, bony structures lined by the well-vascularized mucosal tissue, project into the airway lumen from the lateral walls into the main chamber of the nose (Figure 14.1). Turbinates increase the inner surface area of the nose, which is important in the conditioning of the inhaled air. Though there are some general similarities among the nasal passages of laboratory rodents, nonhuman primates, and humans, there are also striking species differences in nasal architecture. From a comparative viewpoint, humans have relatively simple noses with breathing as the primary function (microsmatic), while rats, mice, and dogs have more complex noses with olfaction as the primary function (macrosmatic). The relative surface area (i.e., surface area/volume) of the nasal cavity is approximately five times greater in the laboratory mouse than in humans, due principally to the greater complexity of its nasal turbinates. In addition, the nasal and oral cavities of humans, and most nonhuman primates, are arranged in a manner to allow for both nasal and oral breathing. In contrast, laboratory rodents and rabbits are obligate nose breathers, due to the close apposition of the epiglottis to the soft palate.

Luminal surfaces of the nasal mucosa, with the exception of the most proximal regions of the nasal vestibule, are lined by a watery, sticky material called mucus that is secreted from mucous cells in surface epithelium and from underlying glands in the lamina propria. Its physical and chemical properties are well suited for its role in upper airway defense by trapping inhaled particles and removing certain reactive gases. The synchronized beating of airway surface cilia propels the nasal mucus at different speeds and directions depending on the intranasal location.

Nasal mucus containing entrapped materials ultimately is propelled by beating cilia to the naso- and oro-pharynx, and then swallowed into the esophagus and cleared through the digestive tract. The nasal mucociliary apparatus (i.e., mucus and cilia) exhibits a range of responses to inhaled xenobiotic agents and can be a sensitive indicator of toxicity. As this upper airway apparatus is one of the first lines of defense against inhaled pathogens, dusts, and irritant gases, toxicant-induced compromises in its defense capabilities could lead to increased nasal infections and increased susceptibility to lower respiratory tract diseases.

Nasal Epithelium

Besides differences in the gross architecture of the nose between laboratory animals and humans, there are also species differences in the surface epithelial cell populations lining the nasal passages. These differences among species are found in the distribution of nasal epithelial populations and in the types of nasal cells within these populations. There are, however, four distinct nasal epithelial populations in both animals and humans. These include the squamous epithelium (SE), which is primarily restricted to the nasal vestibule; ciliated, pseudostratified, cuboidal/columnar epithelium, or respiratory epithelium (RE), in the main chamber and nasopharynx; poorly ciliated cuboidal/columnar epithelium that is often termed transitional epithelium (TE), lying between SE and RE in the proximal aspect of the main chamber; and OE, located in the dorsal or dorso-posterior aspect of the nasal cavity. Figure 14.2 illustrates these airway epithelia that line the nasal cavity.

The nasal vestibule in both animals and humans is completely lined by SE. This region of the nasal mucosa probably functions similarly to the epidermis of skin, to protect the underlying tissues from potentially harmful environmental agents.

Distal to the stratified SE and proximal to the ciliated RE is a narrow zone of poorly or nonciliated, microvilli-covered, cuboidal/columnar surface epithelium, which has been referred to as nasal non- or scantly-ciliated RE, or nasal TE (Figure 14.2). Common, distinctive features of TE in mice, monkeys, and humans include: (1) an anatomical location in the proximal aspect of the nasal cavity between the SE and the RE; (2) the presence of numerous nonciliated cuboidal or columnar surface cells and basal cells; (3) few ciliated cells and a scarcity of mucous (goblet) cells; and (4) an abrupt morphological border with SE but a less abrupt border with RE.

Luminal, nonciliated cells in the TE of mice rarely contain secretory granules but do have abundant smooth endoplasmic reticulum (SER) in their apices. SER is an important intracellular site for xenobiotic-metabolizing enzymes, including cytochromes P450

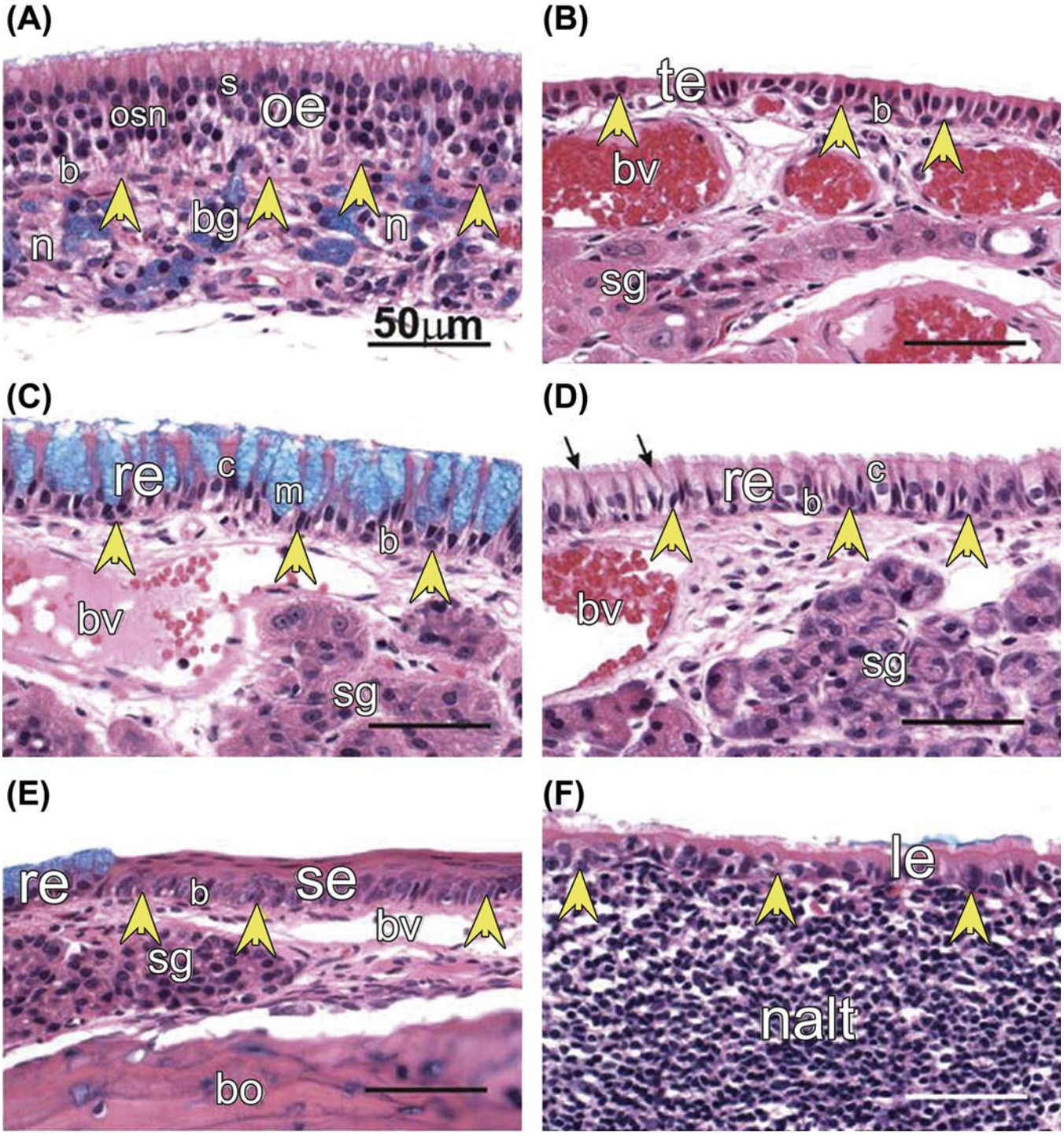

FIGURE 14.2 Light photomicrographs of the rat's nasal mucosa containing (A) olfactory epithelium (oe), (B) transitional epithelium (te), (C) respiratory epithelium (re) with numerous mucous cells (m), (D) respiratory epithelium with serous cells, (E) squamous epithelium (se), and (F) lymphoepithelium overlying nasal-associated lymphoid tissue (nalt). Arrows identify the basal lamina between surface epithelium and underlying lamina propria; *n*, nerve bundles; *bg*, Bowman's gland; *s*, sustentacular cell nuclei; *osn*, nuclei of olfactory sensory neurons; *b*, basal cells; *bv*, blood vessels; *sg*, secretory glands in lamina propria; *bo*, bone; H&E/Alcian blue stain. *Figure reproduced from Harkema et al. (2006). The nose revisited: a brief review of the comparative structure, function, and toxicologic pathology of the nasal epithelium*, Toxicol. Pathol. *34, 252–269 (Figure 4, p. 256), with permission.*

mixed function oxidases. The prominent presence of this organelle in these cells, as well as in the sustentacular cells of OE, suggests metabolizing capability for certain inhaled and noninhaled xenobiotics.

The lamina propria beneath the TE and RE, described below, is a highly vascularized and innervated loose fibroelastic connective tissue containing serous and seromucous secretory glands. Cavernous venous plexuses, sometimes referred to as "swell bodies," are also present in the lamina propria of the nasal mucosa and located in distinct regions along the nasal airway. Dilation of these vessels is thought to alter nasal airflow by thickening the mucosa, narrowing air passages, and diverting inhaled air. Prominent swell bodies in the mouse are found in the maxilloturbinates and lateral wall in the proximal nasal passage.

The majority of the nonolfactory nasal epithelium is RE. It is a pseudostratified, cuboidal/columnar, ciliated epithelium (Figure 14.2). Numerous secretory glands, containing serous and/or mucous cells, are located in the lamina propria beneath RE, predominantly in the proximal septum and lateral walls of mice. The largest nasal secretory gland in the mouse and rat is the bilateral lateral nasal gland, also referred to as Steno's gland, which surrounds the maxillary sinus located in the lateral wall adjacent to each nasal passage (in the standard T3 nasal section). Similar nasal glands are also found in the primate nose, including that of humans.

The most prominent difference in nasal epithelium between laboratory animals and humans is the amount of the main nasal airway chamber that is lined by OE (Figure 14.2A). OE lines a greater percentage of the nasal cavity of mice, which have an acute sense of smell, as compared to that of monkeys or humans, whose sense of smell is not as well developed. OE is a pseudostratified, columnar neuroepithelium containing three principal epithelial cell types. These are the olfactory sensory neurons (OSNs), sustentacular cells, and basal cells. OSNs are bipolar neuronal cells interposed among the sustentacular cells. Mature OSNs immunohistochemically express olfactory marker protein (OMP), which is used for light-microscopic detection of these unique neuroepithelial cells found in both rodents and primates, including humans. The cellular composition and epithelial thickness are remarkably similar among primate and rodent species.

Dendritic portions of the OSN extend above the epithelial surface and terminate in a bulbous olfactory knob from which protrude 10–15 immotile cilia which provide an extensive surface area for reception of odorants. These knobs harbor the olfactory receptors (ORs), a series of G-protein-coupled receptors encoded by several hundred genes. Each OR can interact with many different odor molecules, while a given odor molecule binds to multiple ORs (though with variable affinities). The axon of the OSN originates from the base of the cell and passes through the basal lamina to join axons from other OSNs to form unmyelinated nerve fascicles, or bundles, in the lamina propria. These olfactory nerves perforate the boney cribiform plate that separates the nasal cavity from the brain, and form the outer olfactory nerve layer of the olfactory bulb. Axons of OSNs converge on "glomeruli" within the olfactory bulbs. Glomeruli are relatively large spherical neuropils (100–200 μm in diameter) in which the axons of OSNs form synaptic connections on the dendrites of mitral and tufted cells, the output neurons of the olfactory bulb. Transmission of olfactory information is further sent through the axons of the mitral and tufted cells to the olfactory cortex.

Sustentacular (supporting) cells are columnar epithelial cells that span the entire thickness of the OE from the airway surface to the basal lamina. The distinct oval nuclei of the sustentacular cells are aligned in a single row along the apical aspect of the OE, and are the most apically located epithelial nuclei within the mammalian OE (Figure 14.2A). These supporting cells surround the OSNs, making multiple contacts with OSNs through fine cellular extensions. The apical surfaces of sustentacular cells are lined by numerous long microvilli that intermingle with the thin cilia of the OSNs along the surface of the airway lumen. The supranuclear cytoplasm of sustentacular cells has abundant SER and xenobiotic-metabolizing enzymes (e.g., cytochromes P450, flavin-containing monooxygenases, *N*-acetyltransferases). The metabolism in these cells may be important in detoxification of inhaled xenobiotics and in the function of smell. Sustentacular cells are also thought to contribute to the regulation of the ionic composition of the overlying mucous layer that undoubtedly affects the chemical interactions between odors and their ORs. In addition to these principal epithelial cells in the OE, there are substantial numbers of different types of apically located microvillous cells whose function(s) are not fully understood. The production and secretion of mucus covering the luminal surface of OE is restricted to the subepithelial Bowman's glands (BG; Figure 14.2A). Like the sustentacular cells, both the acinar and duct cells of BG also contain many xenobiotic-metabolizing enzymes.

Besides the OE in the main nasal chamber described above, there are three accessory olfactory organs found in the nasal airways of mice, but not well developed or functional in the human nose. These include the vomeronasal organ (VNO), the septal organ of Masera (SOM), and the septal organ of Grüneberg (SOG). A primary function of the VNO is to detect pheromones, airborne chemical messages or signals, sent between

individual rodents and essential for normal reproductive physiology and behavior. The SOM may have an alerting function by sensing airborne odors during quiet breathing when intranasal airflows do not reach the main OE in the more dorsal regions of the nasal cavity. Though the function of SOG is unknown, its rostral location suggests that it may have a special function for early detection of distinct odorants.

Nasal-Associated Lymphoid Tissue

In addition to the four principal nasal epithelia already described, there is another specialized epithelium, lymphoepithelium (LE), which covers discrete focal aggregates of nasal-associated lymphoid tissue (NALT) in the underlying lamina propria (Figure 14.2F). In rats and mice, NALT with associated LE is restricted to the ventral aspects of the lateral walls at the opening of the nasopharyngeal duct (in the T3 nasal section). The overlying LE is composed of cuboidal ciliated cells, a few mucous cells, and numerous nonciliated, cuboidal cells with luminal microvilli (so-called membranous or M cells) similar to those in the gut- and bronchus-associated lymphoid tissues (GALT and BALT) in the intestinal and lower respiratory tracts, respectively (see Chapter 12: Immune System). M cells are thought to be involved in the uptake and translocation of inhaled antigens from the nasal lumen to the underlying lymphoid structures.

NALT, with its specialized LE, has also been described in the nasopharyngeal airways of nonhuman primates. The correlate of NALT in humans is Waldeyer's ring, the oropharyngeal lymphoid tissues composed of the adenoid, and the bilateral tubal, palatine, and lingual tonsils.

The location of NALT at the entrance of the nasopharyngeal duct is a very strategic position as most of the nasal secretions and inhaled air, both presumably laden with antigenic material, flow over this area. Though the function of NALT and its place in the general mucosal-associated lymphoid system are not fully understood, these mucosal lymphoid tissues may have an important function in regional immune defense of the upper airways.

Nasal Nerves and Blood Vessels

Inhaled chemicals may neurogenically stimulate not only the OE in the main chamber and accessory olfactory organs, but also chemoreceptors of nasal trigeminal nerves, which are part of the somatic sensory system for the eyes, nose, and mouth. Trigeminal chemoreceptors are present throughout the nasal epithelium lining the murine and human nasal cavities. Stimulation of trigeminal nerve fibers produces sensations described as irritating, painful, burning, cooling, tingling, stinging, or pungent. Chemical stimulation of these sensory nerves may also result in protective reflexes causing increased secretions (e.g., nasal mucus), decreased respiration rate (e.g., apnea), and reduction in the nasal airways due to vascular congestion and mucosal swelling. Nasal trigeminal nerve fibers that respond to irritants release neuropeptides, such as substance P and calcitonin gene-related peptides, and are presumably polymodal nociceptors. These sensory nerve fibers ramify repeatedly in the nasal mucosa, and their intraepithelial nerve endings extend close to the airway surface, just below the apical tight junctions connecting epithelial cells.

The Pharynx and Larynx

The pharynx connects the nasal and oral airways with the laryngeal airway (Figure 14.1). In humans and nonhuman primates, the pharynx is situated posterior to the nasal cavity, mouth, and larynx. In many other laboratory animal species (e.g., dogs, rats, mice), the pharynx is distal to most of the nasal airway and dorsal to the oral cavity and larynx. The pharynx is a musculo-membranous tube that is anatomically divided into nasal, oral, and laryngeal regions. The nasopharynx is lined with ciliated RE with mucous goblet cells, while the oro-pharynx and laryngopharynx are lined by nonkeratinized SE.

One of the more conspicuous anatomical differences in the pharyngeal region of the upper airway among mammalian species is the angle of the dorsoventral bend in the nasopharynx (Figure 14.1). Rodent and canine species have a slight nasopharyngeal bend (e.g., 15° and 45° in rats and dogs, respectively), while primates have a marked bend (e.g., 80° and 90° in rhesus monkeys and humans, respectively) due to their more erect stature. The degree of this bend in the upper airway impacts the regional dosimetry of some inhaled agents.

The larynx is the part of the upper respiratory tract between the pharynx and trachea (Figure 14.1). The airway lumen of the human larynx is lined for the most part by pseudostratified ciliated RE, except for a small area on the vocal folds where it is stratified SE. In laboratory rats and mice, a transitional zone of nonciliated epithelium extends between the squamous and ciliated respiratory epithelia. In terms of inhalation toxicology, the larynx is a major resistive element to airflow and a potential site for inhaled particle deposition. The rapid expansion and contraction of this organ of phonation creates turbulence and inspiratory air jets that may lead to additional particle impaction on the wall of the trachea.

The Trachea, Bronchi, and Bronchioles

The trachea is continuous with the larynx in the neck and extends distally into the thoracic cavity to the carina, where it bifurcates to form two primary, or "mainstem," bronchi (Figure 14.1). The airway wall of the trachea and more distal conducting airways (bronchi and bronchioles) is composed of three distinct layers: the mucosa, submucosa, and adventitia. The mucosa lining the airway lumen is composed of a pseudostratified, ciliated RE and a thin subepithelial lamina propria compared to the thick lamina propria in the nasal mucosa. A fine smooth muscle layer divides the mucosa from the submucosa. These conducting airways are connected to the surrounding tissue by a loose connective tissue, the adventitia.

The distal end of the trachea divides, at the carina within the thoracic cavity, into two extrapulmonary mainstem bronchi (Figure 14.1). These large bronchial airways further divide into smaller bronchi. In the human respiratory tract, there are seven generations of bronchi and the tracheobronchial branching system is relatively symmetrical—i.e., the parent airway divides into two smaller airways with relatively equal diameter. This dichotomous branching pattern is in contrast to the monopodial branching pattern of most mammals, such as monkey, dog, rat, and mouse, where daughter branches are of unequal diameter.

As the bronchi divide into smaller and smaller diameter airways within the lung, there is a point (airway diameter of ~1 mm in humans) where intramural cartilage and submucosal glands are no longer present and the conducing airways are referred to as bronchioles. The human respiratory tract contains several generations of nonrespiratory bronchioles, i.e., no alveolar outpocketings along the bronchiolar airway. Considerably fewer generations of these intrapulmonary airways are present in other mammalian species, such as the dog, cat, and monkey. The number of generations of nonrespiratory bronchioles in rodents and rabbits is similar to that in humans.

The most distal nonrespiratory bronchiole is defined as the terminal bronchiole. The distal end of this conducting airway connects to alveolarized (respiratory) airways. This junction, where conducting and respiratory airways join, is called the centriacinus. It is a common site of injury from inhaled gases and particles that reach the lung. In humans and some laboratory mammals, such as dogs, cats, and monkeys, the terminal bronchioles end into several generations of respiratory bronchioles containing widely scattered intramural alveoli, often referred to as alveolar outpocketings. In contrast, the terminal bronchioles in smaller laboratory animals, like rats, mice, hamsters, and rabbits, end directly into one short segment of respiratory bronchioles or into small airways completely lined by alveoli and designated as alveolar ducts (Figures 14.3 and 14.4).

Epithelial Cells Lining Tracheobronchial Airways

The pseudostratified RE lining the tracheobronchial airways varies from a tall columnar ciliated epithelium in the proximal trachea to a low cuboidal epithelium in the distal bronchioles, and a simple SE lining the alveolar outpocketings of the respiratory bronchioles (Figure 14.4). Surface epithelial cell type and abundance varies among species and airway generations (see Harkema et al., 2013).

CILIATED CELLS

Ciliated cells are the most abundant epithelial cells that line the conducting airways of the respiratory tract in all mammalian species. Along with airway secretory cells, they comprise the cellular components of the mucociliary defense apparatus that is important in clearing various inhaled foreign agents (e.g., dust, bacteria) which deposit on a moving layer of mucus that lines the luminal surfaces. The primary function of ciliated cells is to generate the flow of airway mucus with synchronized beating of numerous motile cilia that extend from the apical aspects of these dynamic cells. Cilia beat at a high frequency of 12−15 beats/second. The synchronous beating of cilia along the airway moves the mucous in a specified direction depending on the location in the respiratory tract. Nasopharyngeal mucus is moved distally towards the orifice of the esophagus, where it is constantly swallowed. In the tracheobronchial tract, the mucus flows proximally up the airways towards the esophageal opening where it, too, is swallowed into the gastrointestinal tract.

In general, ciliated cells are terminally differentiated or "end-stage" cells with limited capacity to divide and proliferate. They originate from progenitor basal or secretory cells. Ciliated cells are particularly sensitive to injury from inhaled chemical irritants, such as chlorine, nitrogen dioxide, sulfur dioxide, ozone, and tobacco smoke. Toxicant-induced injury to ciliated epithelial cells may be manifested as ciliostasis (loss of motility), detachment or resorption of cilia, or cell death with exfoliation. The end result is impairment of mucociliary clearance, which can be reversible or can lead to secondary bacterial bronchitis and bronchopneumonia, which are potentially life-threatening situations.

SECRETORY CELLS

Secretory epithelial cells are interspersed among the ciliated cells in the surface epithelium of conducting airways. The three principal secretory cells in RE lining

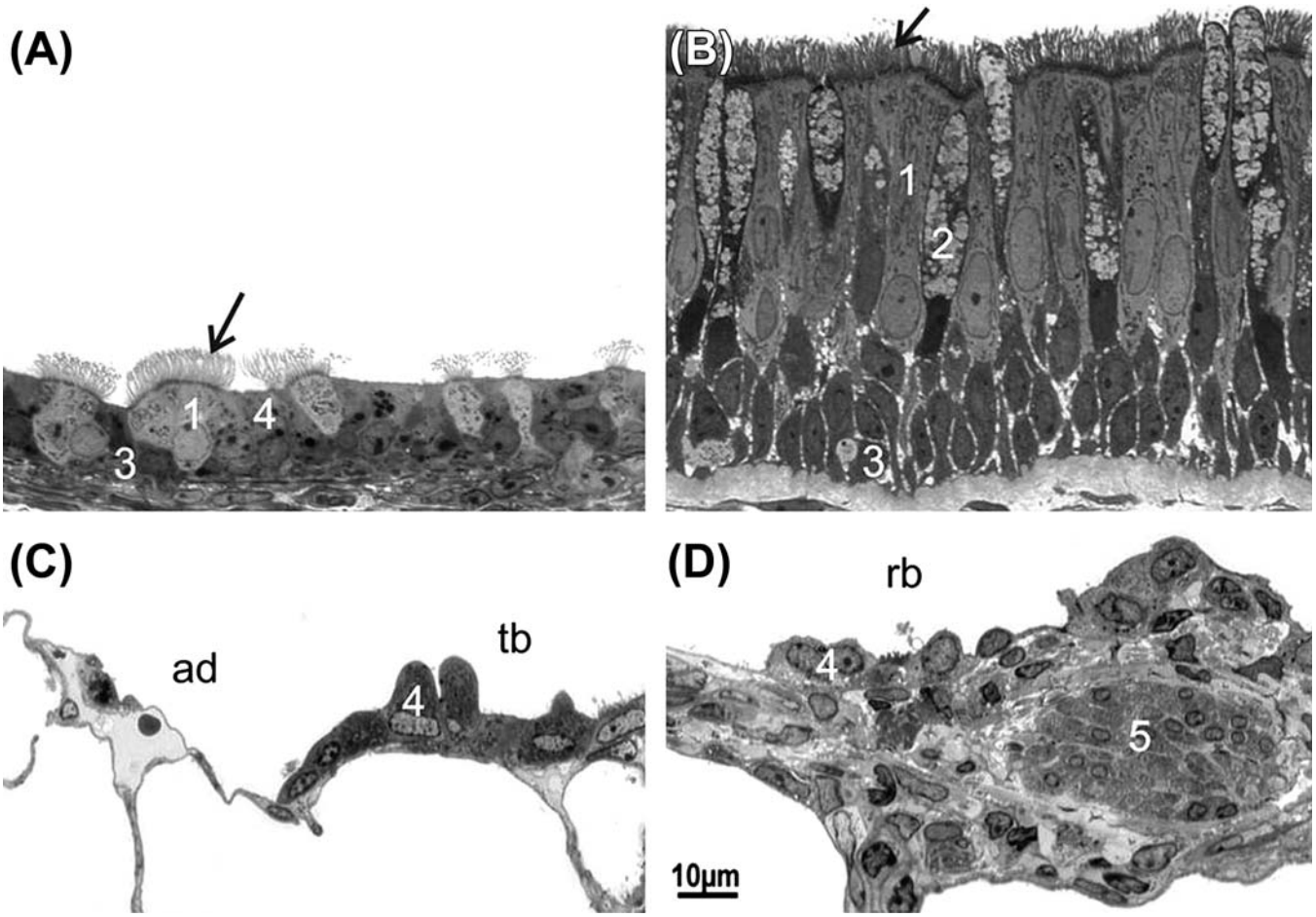

FIGURE 14.3 Transmission electron photomicrographs of the surface epithelium lining tracheal (A, B) and distal bronchiolar (C, D) airways in the mouse (A, C) and rhesus monkey (B, D). 1, ciliated cells; 2, mucous cells; 3, basal cells; 4, nonciliated club (or Clara) cells; 5, intramural smooth muscle; arrows, cilia; ad, alveolar duct; tb, airway of terminal bronchiole; rb, airway of respiratory bronchiole. *Figure modified from* The Laboratory Primate: The Handbook of Experimental Animals, *first ed. Wolfe-Coote, ed. (2005) Academic Press, pp. 503–506, with permission.*

the tracheobronchial airways are the mucous, club (Clara), and serous cells. The cytoplasm of all these cells contains unique, spherical, membrane-bound secretory granules in the apical portion of the cell or "theca." Secreted materials from these surface epithelial cells, and those from the secretory cells in submucosal glands, provide the air–tissue interface with a moisturizing, lubricating and protective fluid layer, often referred to as "epithelial lining fluid."

Mucous cells secrete mucus, a hydrated sticky gel made up primarily of water but also containing distinctive carbohydrate-rich glycoproteins or "mucins," lipids, proteins, salts, and other small dialyzable components. Production and secretion of the airway mucus is important for maintaining the mucociliary defense apparatus of the conducting airways. Inhalation exposure to chemical and physical irritants, like inhaled cigarette smoke, ozone, chlorine, and particulate matter, often causes hypersecretion of mucosubstances resulting in excess airway mucus.

CLUB CELLS

Club cells (previously named Clara Cells) are nonciliated, nonmucous, secretory cells in RE. These epithelial cells secrete several distinctive proteins, including club cell 10-kDa secretory protein (CCSP). By light microscopy, club cells are morphologically columnar to cuboidal with a distinctive dome-shaped luminal surface and contain small periodic acid-Schiff (PAS)-positive secretory granules. In the laboratory mouse, the club cell is the principal secretory cell type throughout its tracheobronchial airways. In contrast, club cells are most predominant in the terminal and respiratory bronchioles of humans and monkeys.

The primary functions of club cells are: (1) to provide secretory surfactants (surfactant proteins A, B, and D) and other specific proteins (e.g., CCSP) that contribute to the airway epithelial lining fluid; (2) to serve as progenitor cells for ciliated and secretory epithelial cells; and (3) to metabolize xenobiotic compounds through cytochromes P450-dependent

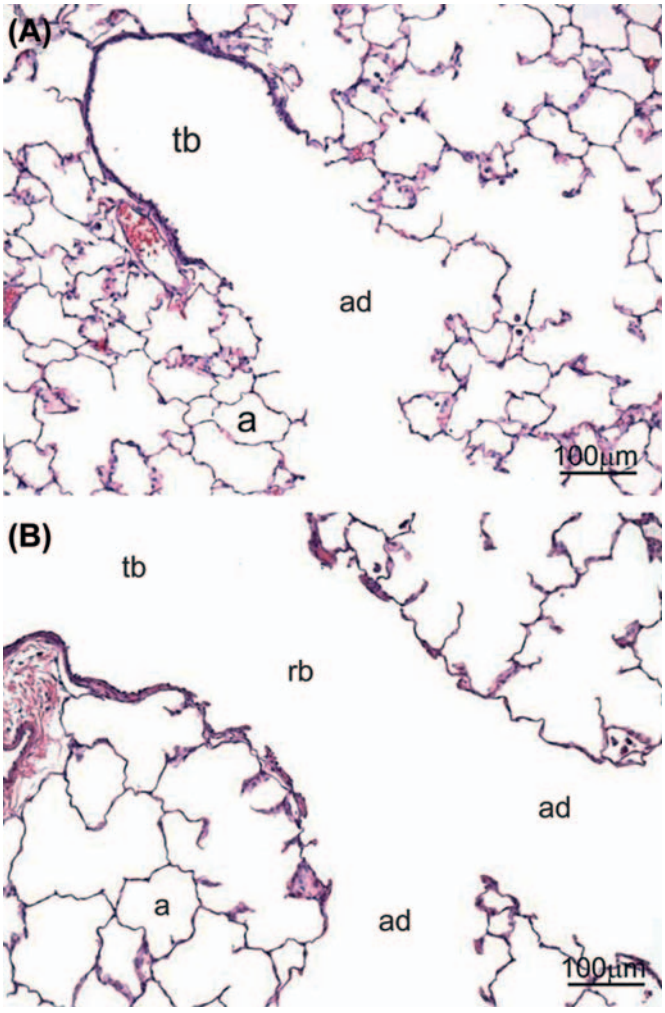

FIGURE 14.4 Light photomicrographs of the centriacinar region in the laboratory rat (A) and rhesus monkey (B). Respiratory bronchioles (rb) are present in the monkey, but not the rat. tb, terminal bronchiole; ad, alveolar duct; a, alveolus; H&E stain. *Figure reproduced from* Haschek and Rousseaux's Handbook of Toxicologic Pathology *(2013), third ed. (W.M Haschek, C.G. Rousseaux and M.A. Wallig, eds.), Academic Press (Elsevier), Figure 51.5, p.1948, with permission.*

mixed-function oxygenases associated with the SER. Through the latter metabolizing process certain inhaled or ingested xenobiotic agents, like naphthalene, styrene, acetaminophen, and ipomeanol, may generate toxic metabolites that can damage the club cell, causing degeneration and necrosis.

SEROUS CELLS

Serous cells are secretory cells in the RE that are phenotypically distinct from mucous and club cells. Like club cells, serous cells can produce seromucous or mucous granules after exposure to certain inhaled irritating or allergic agents (e.g., bacterial endotoxin, ovalbumin), thus differentiating into mucous cells without the need for cell division.

BASAL CELLS

The primary support cells in the RE are the basal cells. These epithelial cells are small, flattened cells that are closely attached to the basal lamina and do not extend to the airway lumen. It is the presence of these epithelial cells located in the larger conducting airways that accounts for the pseudostratified classification given to RE. Basal cells are a population of multipotent stem cells that are important in regeneration and homeostasis of the respiratory epithelial cell population.

NEUROENDOCRINE CELLS

Neuroendocrine cells are relatively rare in the RE lining the conducting airways of most mammalian species. These cells occur individually or in small clusters called neuroepithelial bodies, display endocrine, paracrine, and secretory mechanisms, and are often associated with intraepithelial nerve fibers. Neuroendocrine cells and neuroepithelial bodies have multiple proposed physiological functional roles, including modulation of early lung development and airway chemoreceptors. Neuroepithelial bodies may be sensors for hypoxia. Another novel role for these cells, as guardians of lung stem cell niches, has recently emerged.

BRUSH CELLS

Other relatively rare epithelial cells in the conducting airways are brush cells. Their name comes from the border of long microvilli that is present on their apical surface. Brush cells are found in the RE lining both nasal and tracheobronchial airways. Some of these cells are solitary chemosensory cells that utilize the chemoreceptive transduction cascade first described in taste buds.

Bronchus-Associated Lymphoid Tissues

Some, but not all, mammalian species contain nodules of bronchus-associated lymphoid tissue (BALT): well organized, densely packed aggregates of lymphoid cells in the bronchial mucosa. Like NALT, BALT belongs to the body's mucosa-associated lymphoid tissue system (MALT) (see Chapter 12: Immune System). Morphologically, it resembles NALT in the upper respiratory tract or Peyer's patches in the intestinal tract.

BALT is a prominent airway tissue in laboratory rats and rabbits, but absent in the lung of mice. BALT is also absent from the pulmonary airways of healthy dogs, cats, nonhuman primates and humans. In these species, though BALT is not constitutively expressed,

microbial stimulation or airway inflammation can induce its formation in the bronchial airways. Morphologically, the classically defined BALT is covered by a specialized LE that is composed of nonciliated, cuboidal epithelial cells that are interspersed with lymphocytes. This LE is devoid of ciliated or mucous epithelial cells. The absence of a mucociliary barrier facilitates the transport and presentation of inhaled antigenic agents to the underlying BALT, providing immune surveillance of the inhaled air.

BALT is organized as a dome-like aggregate of tightly packed lymphoid cells underlying the luminal LE. A follicular region dominated by B cells lies directly beneath the airway epithelium. T cell-dominated parafollicular regions make up the ablumenal periphery of this subepithelial lymphoid tissue.

Gas-Exchange Regions of the Lung

Lobation of the lung varies greatly among species: the human has two lobes on the left and three on the right; the monkey, dog, and cat have three left lobes and four right lobes; and the mouse, rat, and hamster have a single left lobe and four right lobes. Depending on species, lobes may be divided into bronchopulmonary segments, subsegments, and lobules by interlobular tissue (Table 14.1). The lobule consists of a lobular bronchiole with its branches and associated structures.

Visceral pleura covers the outer surfaces of the lung lobes, and the parietal pleura covers the walls of the thoracic cavity. Communication between the two pleural cavities (right and left) and pleural thickness (Table 14.1) are species-dependent. Vessels (pulmonary artery and veins, bronchial artery, and lymph vessels) and nerves enter the lungs with the bronchi at the hilus; the tracheobronchial lymph nodes are also found in this area.

Respiratory Bronchioles

Bronchioles that have a few alveolar outpockets arising from their walls are defined as respiratory bronchioles. These poorly alveolarized bronchioles are the transitional airways between the conducting (nonrespiratory) bronchioles and alveolarized ducts that are completely lined by alveolar outpockets. There are major species differences in respect to respiratory bronchioles (Table 14.1). The luminal surface of the nonalveolarized portion of respiratory bronchioles is lined by ciliated cells and club cells, but normally lacks mucous cells and basal cells. The cellular and acellular structures of the alveolarized outpocketing of the respiratory bronchiole resemble those of alveolar ducts and alveoli that are described below.

Alveolar Parenchyma of the Lung

The basic unit of ventilation in the mammalian lung consists of alveoli and alveolar ducts distal to the transition from one bronchiole to an alveolar duct system. Alveoli and alveolar ducts of these "ventilator units" occur in a highly interconnected pattern which forms distinct subdivisions of the alveolar parenchyma that do not overlap. The ventilator unit is functionally important because it is the smallest common denominator in determining the distribution of inspired air to the gas-exchange surfaces of the lung. Though there are distinctive species-related differences in the branching patterns of the small airways and in the presence or absence of respiratory bronchioles, all mammalian species have the interconnected terminal bronchiole to alveolar duct junctions that serve as the portals of entry for distinct ventilator units where gas-exchange occurs.

The "pulmonary acinus" consists of all the gas-exchange structures distal to a single terminal bronchiole, and is composed of two or more ventilator units. The average number of alveoli per acinus is relatively constant among mammalian species. The ventilator unit size and the size of an individual alveolus are directly proportional to the size of the animal species (e.g., human alveolus > mouse alveolus). The pulmonary parenchyma (gas-exchange region of the lung) comprises 90% of the total volume of the mammalian lung. The most prominent structures in the lung parenchyma are the alveolar ducts and alveoli. Alveolar ducts arise from the most distal (terminal) bronchiolar airways, i.e., respiratory or nonrespiratory bronchioles, depending on the species. The walls of alveolar ducts are composed of a linearized arrangement of alveoli (Figure 14.4). The proximal alveolar duct branches into secondary alveolar ducts, each of which ends in a blind outpouching composed of two or more small clusters of alveoli called alveolar sacs.

The alveoli are the primary functional and structural units of the lung parenchyma where a very thin tissue barrier separates the surface of the airspace from the luminal surface of capillaries (Figure 14.5). This extremely thin air–blood barrier in mammalian lungs allows for efficient gas transfer between the inspired air and the circulating blood.

The interconnected capillaries within the alveolar wall form a single vascular bed that is separated from the alveolar air space by a thin structural barrier of epithelial, interstitial, and endothelial tissues. The integrity of the alveolar septa is maintained by interstitial connective tissues composed of collagen and elastin fibers that interweave around the capillaries, forming what are called "thick" and "thin" regions within the wall. The thick regions of the septa contain the extracellular matrix of collagen and elastin fibers intermixed with interstitial cells

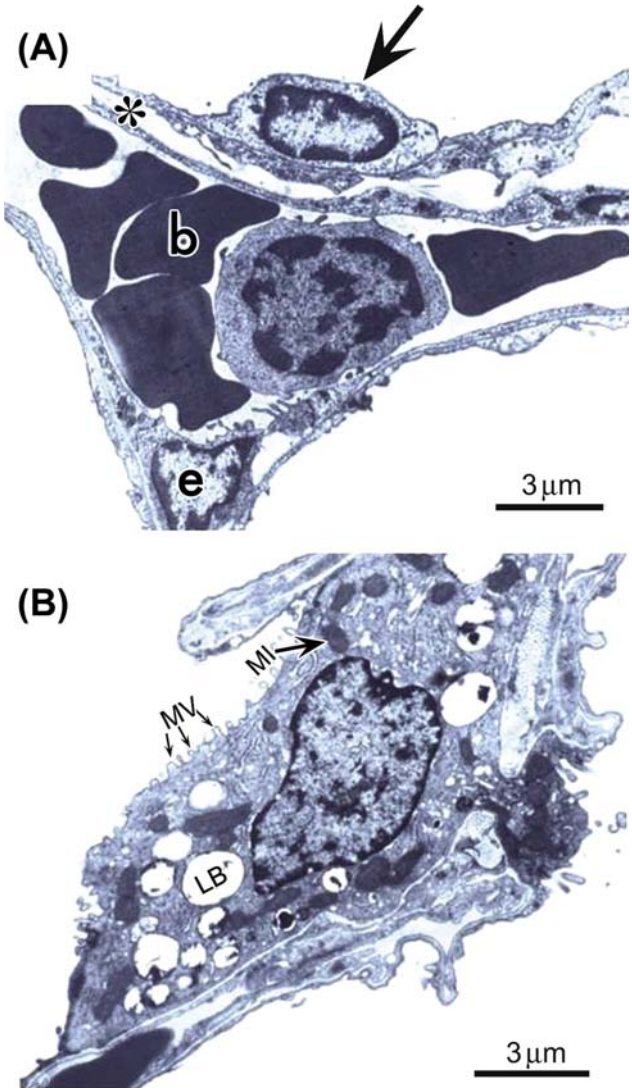

FIGURE 14.5 Transmission electron photomicrographs of the alveolar septum. Alveolar airspaces are lined by type 1 (panel A, arrow) and type 2 (panel B) epithelial cells. b, red blood cells in the alveolar capillary lumen; e, endothelial cell lining the capillary lumen; MI, mitochondrion; MV, microvilli on apical surface of the type 2 cell; LB, cytoplasmic lamellar bodies in type 2 cell; asterisk, single basement membrane located between the epithelial and endothelial cells in the thin portion of the alveolar wall (i.e., forming a minimal barrier between alveolar air and capillary blood). *Figures reproduced from* Pulmonary Immunotoxicology, *M. Cohen, J. Zelikoff and R. Schlesinger, eds. (2001) Springer, with permission.*

(e.g., fibroblasts, myofibroblasts), all of which lie between the epithelial lining of the alveolar air space and the endothelial lining of the capillary lumen. The thin portions of the septa represent the air−blood barrier and are formed by epithelial and endothelial single cell layers that are separated only by a thin single basement membrane.

Epithelial Cells of the Alveolus

The alveoli arise from the respiratory bronchioles and the alveolar ducts. The alveolar septum or wall consists of three components: epithelium (which lines the alveolus or air space), interstitium, and capillary endothelium. Gas exchange occurs in the alveoli across the thin epithelial lining and adjacent endothelium (air−blood barrier).

The major cell types are the epithelial type I and type II cells, the pulmonary endothelial cells, interstitial cells, and macrophages. Type I cells constitute 8%−11% of all cells found in the alveolar region, and type II epithelial cells constitute 13%−16%. Tight junctions are present between epithelial cells. Epithelial cells lie on a continuous basement membrane, as do endothelial cells. In many places, the basement membrane of epithelial cells and endothelial cells is fused, forming an extremely thin air−blood barrier. In other areas, the cells are separated by interstitium that consists of scant connective and elastic tissue and resident interstitial cells, macrophages, lymphocytes, plasma cells, and mast cells.

Alveolar type I epithelial cells are attenuated, highly differentiated cells that do not divide; they cover approximately 90%−95% of the alveolar surface. Since these cells have a large surface area, they are highly susceptible to injury. The main function of the type I cell is the maintenance of a barrier to prevent leakage of fluid and proteins across the alveolar wall into the air spaces, while allowing gases to cross the air−blood barrier freely.

Alveolar type II epithelial cells are cuboidal in shape, located in corners or niches between capillaries, and contain lamellar bodies in which surfactant is stored. The functions of type II cells include the synthesis, storage, and secretion of pulmonary surface-active material; the reepithelialization of the alveolar wall after lung injury; and transepithelial solute transport to limit the volume of and perhaps regulate the composition of alveolar fluid.

Capillaries, lined by endothelial cells (30%−42% of all alveolar cells), are of the closed type without openings or fenestrations. Intercellular junctions between endothelial cells are characterized by *zonulae occludens* but are less tight than the epithelial junctions. Therefore, unlike other tissues, the major permeability barrier in the lung is the alveolar epithelium.

Macrophages have been identified in three distinct locations in the lung: the interstitium, alveoli, and capillary lumen. Macrophages present in the alveolar interstitium are derived from bone marrow, can divide, and can either phagocytize particulate material that crosses the alveolar walls or move into the alveolar compartment to become alveolar macrophages (AMs). Another macrophage-like cell in the interstitium is the dendritic cell, which is specialized for antigen presentation and accessory function.

AMs are derived from the interstitial compartment. However, they do divide and are a self-renewing

population of cells. The intravascular macrophage (IVM) is present in humans, pigs, cats, horses, ruminants, and marine mammals, but not in rodents or dogs. It is a fixed macrophage of the capillary bed, has specialized junctional complexes with adjacent endothelial cells, and is morphologically and, presumably, functionally similar to hepatic Kupffer cells. IVMs function similarly to AMs. IVMs account for some of the species differences that occur in response to pulmonary injury.

Fibroblasts are the major cell type present in the interstitium. Apart from maintaining the structural integrity of the lung and production of collagen and other matrix components, such as fibronectin, fibroblasts produce a variety of enzymes, including collagenase, and other factors, such as prostaglandins and plasminogen activator, that may modulate the function of other cell types. Fibroblasts and myofibroblasts play a major role in disease processes that result in fibrosis.

Pulmonary Blood Vessels, Lymphatics, and Nerves

Blood reaches the lungs through two separate systems, the pulmonary vessels and the bronchial vessels. The pulmonary arterial system differs from other organs in that it is derived from the low-pressure pulmonary arteries, supplying blood for gas exchange in the pulmonary capillaries. It carries high volumes of poorly oxygenated, venous blood from the right heart, and supplies the distal portion of the respiratory bronchioles, the alveolar ducts, and alveoli, where it is oxygenated. The bronchial system is a high-pressure arterial system derived from the aorta, and carries oxygenated blood to meet the metabolic needs of the larger airways, visceral pleura, and large pulmonary vessels.

The pulmonary arteries differ morphologically from the smaller muscular bronchial arteries. However, because of the reduced pressure, pulmonary arteries and veins may resemble each other fairly closely, especially in large animals. The muscular layer of the pulmonary arteries and veins varies with the species (Table 14.1). In rodents, pulmonary veins have an adventitial coating of cardiomyocytes extending from the left atrium into the lung tissue.

Lymphatics are confined to the extraalveolar interstitium (i.e., peribronchial, interlobular, and pleural interstitium). Lymph flows centripetally through a subpleural network that is joined by perivascular and peribronchial lymphatics at the hilus. Afferent lymphatic vessels from the lungs drain into the lymph nodes, and then into the thoracic, right, and left lymphatic ducts, and the bloodstream.

The sympathetic and parasympathetic divisions of the autonomic nervous system provide motor (efferent) innervation to the lungs, including bronchial smooth muscle, blood vessels, submucosal glands, and lymphatics. Sensory (afferent) innervation is maintained by way of several types of chemo- and mechanoreceptors that respond to inhaled irritants and other stresses.

TESTING FOR TOXICITY

Evaluation of pulmonary function, chest radiographs, cytology of lavage fluid or sputum, and morphologic examination of respiratory tissues (biopsy) are common tests conducted in a clinical setting. Experimentally, respiratory toxicity can be evaluated *in vivo*, *in vitro*, or in combined *in vivo–in vitro* systems. An understanding of the strengths and weaknesses of the various systems or models is critical to interpreting experimental results. Consideration for whole animal studies includes selection of the appropriate routes of exposure for the xenobiotic being studied, species differences in xenobiotic metabolism or respiratory tract anatomy, and cell susceptibility to toxic injury.

There are many ways in which injury and the response to injury can be characterized and quantified. A combination of morphology, physiology, biochemistry, and molecular biology is often the most useful way to evaluate toxic lung injury. *In vivo*, acute and chronic respiratory damage can be evaluated by noninvasive and nondestructive respiratory function tests; by morphological methods such as histology, quantitative morphometry, cell kinetics and immunohistochemistry; and by biochemical techniques such as analysis of bronchoalveolar lavage (BAL) fluid and lung collagen content. Similar biochemical and morphological evaluations can be performed in some *in vitro* systems. Qualitative observations are useful for the characterization of the type and severity of response, while quantitative data allow statistical analyses and descriptive modeling that can be used to extrapolate results across studies and species.

Methods of Testing

Whole Animal Exposure

Reproduction and study of lung damage caused by bloodborne agents in appropriate animal models usually does not present any special problems or technical difficulties, except where there are marked species differences in metabolism. To duplicate human inhalation, exposure is more demanding, and requires special techniques and equipment. Furthermore, most small rodents are obligatory nose-breathers, and many aerosolized noxious agents are deposited and filtered in the upper respiratory passages. Despite potential complications regarding regional deposition and

dosimetry, inhalation studies are usually the best means to study responses to materials that people may inhale intentionally or unintentionally, especially when the exposures are repeated.

INHALATION EXPOSURE

Though inhalation is often the most appropriate way to expose experimental animals to airborne toxicants, it is also technically the most demanding. Generation of gases and aerosols, measuring exposure concentrations and particle sizes or numbers, maintaining adequate chamber concentration and homogeneity of the agents examined, and avoiding accumulation of ammonia, carbon dioxide, and heat requires investments in equipment and trained personnel.

Most inhalation studies are conducted in a dynamic mode. In a dynamic system, the test agent is mixed with the air that flows through the inhalation chamber and a constant concentration of the agent within the chamber is maintained throughout the entire experiment. Animals may be exposed to airborne test agents in whole-body chambers, in nose-only exposure chambers (rodents), or by using oral-nasal facemasks or helmets (dogs and primates). These methods most closely mimic the way humans are exposed to inhaled materials.

Dose estimation, both as the total inhaled dose or exposure to the respiratory system and the pulmonary deposition fraction, is an important consideration for extrapolation of findings from experimental animals to humans and for setting the maximum allowable dose for clinical trials of inhaled drugs.

Intratracheal instillation and pharyngeal aspiration are acceptable alternate routes of exposure in some cases, such as mechanistic studies where dose–response is not the issue. The major disadvantages are that the test agent, delivered at a high dose rate, becomes unevenly distributed, and the animals must be individually and repeatedly treated. The dose rate to the lung is several orders of magnitude greater than that achieved in experimental, occupational, or environmental inhalation exposures, which greatly confounds interpretation of lung responses. Aspiration of test material droplets placed on the nares of rodents and use of nasal sprays in dogs are standard methods for studying nasal effects of pharmaceutical agents intended for delivery by nasal spray.

In Vitro Methods

In vitro studies are indispensable tools for characterizing and understanding respiratory tract toxicity. *In vitro* models facilitate the precise application of toxicants, quantification of pathways and kinetics of toxicant interactions, generation of data from specific cells or anatomic compartments, and integration of studies performed at different organizational levels. A major drawback to the use of *in vitro* systems is the inability to study chronic injury and repair.

Isolated perfused lungs have been used to study the metabolic fate of foreign chemicals processed by the lung, characterize effects on lung function, characterize interactions between lung toxicants and circulating inflammatory cells, and evaluate the distribution and extent of toxicant-induced cellular perturbations. Lungs from such diverse species as rabbits, rats, mice, and guinea pigs have been used. The toxicant under study can be administered by either the circulatory or the ventilatory route.

Whole lung tissue slices, airway rings, isolated or microdissected airways, and arterial rings or strips have all been used to maintain a degree of structural or organizational integrity of targeted respiratory components. These systems have been used to study metabolic activity and biochemical response to toxicants. Embryonic and fetal lung organ cultures have been used extensively in the study of embryonic and fetal development of the lung, and effects of toxicants on gene expression and airway branching morphogenesis.

Isolated cells provide a powerful approach to the understanding of the biology of individual cell types. Cultures of individual cell types, including type I and type II cells, various airway epithelial cells, fibroblasts, endothelial cells, and macrophages, have been used to determine cell composition, biochemical activity, control mechanisms, and responses to toxicants. These cells may be cultured in isolation or as cocultures. Epithelial cells require maintenance at the air–medium interface to preserve polarity and differentiation. Numerous commercially available cell lines provide alternatives to harvesting and primary cell culture.

Pulmonary Function

Pulmonary function tests, which are easy to use and noninvasive, are used in epidemiological studies of air pollution effects, in some workplace exposure monitoring programs, and in preclinical and clinical studies of inhaled pharmaceutical agents. Physiological measurements provide useful information in intact animals regarding adverse health effects, especially in relation to ventilatory function or gas exchange. In humans and laboratory animals, these tests are advantageous because they are noninvasive, may not interfere with other toxicologic tests, and can be repeated on the same subject. Many of the same parameters are measured in humans and animals, which aids cross-species comparisons and extrapolations. In addition, pulmonary function tests may detect functional changes in cases where there is no alteration in structure (e.g., during bronchoconstriction).

The disadvantage is that handling, stress, and other factors may affect the results. Therefore, sham-treated or sham-exposed animals should also be included in the test groups. In small laboratory animals, some of these tests are performed in anesthetized animals, as terminal procedures, or using excised lungs.

Bronchoalveolar Lavage

Bronchoalveolar lavage (BAL) can be used to evaluate toxicant-induced alterations in pulmonary epithelial integrity, cell damage, inflammatory infiltrates and mediators, and surface release of cellular secretory products. It is also a convenient way to recover macrophages and other cells for *in vitro* studies. If the animal is large enough, BAL can be performed in the living animal, either as a single test or sequentially to monitor changes. In smaller animals, such as the rat and mouse, BAL is usually performed after euthanasia either in the lung in situ or following excision.

The aspirated fluid can be analyzed for its cellular profile, protein content, enzymes, cytokines and chemokines, and lipids. Increased activity of marker enzymes such as lactate dehydrogenase, alkaline or acid phosphatase, or angiotensin-converting enzyme usually is an indicator of cell damage, and increased serum albumin is indicative of pulmonary edema. Similar changes are not detectable in the serum unless there is a significant inflammatory process within the lung tissue, in which case there may be a systemic leukocytosis and increases in serum chemistry biomarkers such as C-reactive protein and fibrinogen.

Biochemical Evaluation

The biochemistry of lung cells, lining fluid, and matrix has been extensively studied with methods ranging from analysis of whole homogenized lung tissue to defined lung cell types *in vitro*.

Advantages of biochemical measurements are that they are quantitative and may provide mechanistic information. A major disadvantage is the difficulty of localizing or relating specific biochemical events to a defined cell population.

Morphological Evaluation

Morphological evaluation of the respiratory tract begins at the macroscopic level, proceeds through light microscopy, and may include ultrastructural examination. Light microscopy must precede ultrastructural examination as it is easy to miss focal lesions if ultrastructural samples are taken without prior localization of changes. Outline drawings of the respiratory tract may be useful to record the location of lesions. A number of incidental background findings occur in experimental animals, and awareness of these findings is necessary to avoid incorrect association of findings with test article exposure.

Nasopharyngeal and Laryngeal Regions

In laboratory animals, gross examination of this region is usually limited to the exterior, with internal examination performed on histologic sections. Nasopharyngeal structures are generally fixed in situ with the rest of the nose and a portion of the skull, in 10% buffered formalin solution. Optimal fixation is achieved using retrograde flushing of the nasal cavity with the fixative through the nasopharyngeal orifice. Decalcification follows, preferably using the slow formic acid–sodium citrate method. For large animals, selected nasal regions are placed in the decalcification solution. For ultrastructural studies, a glutaraldehyde-formaldehyde fixative is preferred, as is demineralization in 10% ethylenediaminetetraacetic acid (EDTA) in 0.1 M cacodylate buffer.

For light microscopic examination, standard cross-sections from decalcified tissue should be made. Because of the distribution of different types of epithelium within the nasal cavity, it is imperative to examine sections from exactly the same location in both control and treated animals (see "The Nose" section). Mapping of the location, type, and severity of lesions may be useful, especially in rodents, because the nasal passage of rodents is very complex and lesions may occur in small but distinct regions. This method allows the susceptible site and cell type to be identified.

Standard cross-sections of the larynx should also be examined because the larynx is also an important target site for inhaled materials, especially in rodents. A major target site in rodents is located on the ventral floor of the larynx near the base of the epiglottis.

Tracheobronchial Airways and Pulmonary Parenchyma

The macroscopic examination determines the topographic distribution of abnormalities and, especially in larger animals, provides the basis for sample selection. The lungs are examined visually, and palpation is a useful adjunct in larger species; care must be taken, however, not to induce artifactual changes that interfere with morphological and especially ultrastructural examination. The pleural cavity should be examined for the presence of fluid or abnormalities of the pleura. Determination of lesion distribution can be useful in differentiating toxicant-induced findings from spontaneous disease, aspiration, or experimental accident.

Lung weight, a useful parameter for initial determination of whether or not the test agent causes a

pulmonary effect, is determined prior to fixation. Both wet and dry weight information may be useful because lung weight may be increased by edema, inflammation, fibrosis, or neoplasia. If dry lung weights are to be measured, a separate subset of animals or weighing of individual lobes is required.

Buffered 10% formalin is the usual fixative for light microscopy, while formaldehyde-glutaraldehyde fixatives are preferable for combined light and electron microscopic studies. The lungs from laboratory animals should generally be fixed by intraairway instillation of fixative. Intravascular fixation may be the method of choice for ultrastructural examination of pulmonary vasculature, or in situations when it is critical to not move epithelial lining fluid, intralumenal cells, or particles in the lung airways. Fixation by immersion may be the method of choice when lung tissue is no longer aerated, as with severe edema (see "Response to Injury" section and Figure 14.10A).

Fixation by airway instillation is the best method when lung tissue is still aerated. The quality of fixation is high and the alveoli are open, allowing detection of subtle lesions. Airway fixation can be done simply with a syringe and blunt needle inserted into the trachea in small animals, or into a selected lobar bronchus in larger animals (if only a portion of lung is to be fixed). The fixative is instilled at a relatively constant rate and pressure until the periphery of the lobes is uncurled and the visceral pleura is smooth. The airway should be ligated after fixative instillation to maintain inflation. With practice, this method is highly reproducible and satisfactory for routine light microscopic examination. If morphometric studies are to be performed, fixation at a constant pressure (e.g., 25 cm of hydrostatic pressure for rodents) is required. The final volume of intratracheally fixed lungs is measured as a prelude to most stereological studies of lung structures.

The protocol for sampling lung tissue for microscopic evaluation is of critical importance and should be standardized for each study. Lesions may be focal rather than diffuse, and may affect airways, parenchyma, or both. In addition, the sections examined represent a very small part of the total lung. Typically, the proximal trachea is examined and, in inhalation studies, the tracheobronchial bifurcation. The tracheobronchial lymph nodes should also be examined. In small animals, for simple qualitative morphological examination, the lung lobes should be separated at trimming and a longitudinal section should be acquired cut parallel to the axis of the main bronchus for each major lobe. This section should include the bronchus, major vessels, main axial airway, and pulmonary parenchyma. For large animals, multiple samples are required to adequately sample central and peripheral airways, multiple alveolar regions, and the pleura. Appropriate sampling is essential to the design of most quantitative and stereological studies. Microdissection of airways so that specific generations and locations of airways are sampled is another technique that may be employed. In many studies, lung samples are divided for biochemical analyses, gene expression, and morphological examination.

Paraffin sections, approximately 5 μm thick, are sufficient for routine histopathology. For greater resolution, 1-μm-thick sections impregnated with plastic resin are preferred. A variety of special histological and immunohistochemical staining techniques, and in situ hybridization, are available. Transmission and scanning electron microscopy, and confocal microscopy are useful for special studies.

Quantitative Techniques

Quantitative information on changes in structure of the respiratory tract may be obtained by morphometric techniques. Measurements made from two-dimensional sections can be used to quantify structures as they exist in three dimensions by stereologic techniques.

Cell turnover and cell kinetics have been studied by autoradiographic and immunohistochemical techniques. Whatever method is used, it must be noted that it is not possible to clearly differentiate type I cells from interstitial cells using standard 4- to 5-μm-thick paraffin sections. Thinner (usually 1 μm) sections of lung embedded in plastic resin such as methacrylate are used when differentiation of cell types is required. Animals may be given a single injection or a constant infusion (using a minipump) of [^{3}H] thymidine or the thymidine analog 5-bromo-2′-deoxyuridine (BrdU) so that radiolabeled thymidine or BrdU incorporated into DNA are detected in tissue sections using autoradiography or a specific antibody to BrdU, respectively. Endogenous markers of cell proliferation, such as proliferating cell nuclear antigen (PCNA) or Ki67 can also be used to identify proliferating cells. These markers are particularly useful for evaluating cell proliferation in archived tissues. Proliferative activity can be expressed as labeling index, that is, the number of labeled cells within a defined cell population (e.g., type II alveolar cells) or within the overall cell population (e.g., number of labeled terminal bronchiolar epithelial cells per total number of terminal bronchiolar epithelial cells counted, or number of alveolar cells labeled per total number of cells counted in the alveolar zone).

Animal Models

Models of human disease are developed in laboratory animals to study the mechanisms involved in the

initiation and progression of the disease as well as to test potential treatments. In addition, mouse strains with differing disease phenotypes are used to study the genetic bases of differential responses. To test potential treatments, the choice of disease or mechanistic model is determined by similarity to the pathophysiology of the human disease of interest or whether the drug target is key to the disease mechanism. The choice of animal species for the testing of compounds potentially toxic to the respiratory tract may be made on the basis of species similarity to humans and the type of response anticipated. However, for nonclinical safety assessment inhalation studies are conducted using two species, one of which is a rodent and one a nonrodent. Similarities across species include the diversity of cell types, cell size of major alveolar cell types, the allometry of lung volume and alveolar surface area with respect to body mass, and thickness of air to blood–tissue barrier. Species differences include nasal cavity morphology, airway branching patterns, airway composition, epithelial cell distribution, club cell composition and metabolic function, transition from airways to alveolar duct, and alveolar number, surface area, and size. Other criteria for species selection include existence of a large or appropriate database, cost, and ease of animal handling.

RESPONSE TO INJURY

Factors Affecting Toxic Injury and Host Response

Responses of the respiratory tract to air- and blood-borne toxicants depend primarily on the nature, dose, and exposure duration or treatment regimen of the xenobiotic agent. Host factors such as age, genotype, gender, epigenetics, nutrition, and previous exposure history will also influence the airway and alveolar responses to toxicant-induced injury. The pattern, distribution, and severity of respiratory tract lesions depend to a large measure on the interplay of local dosimetry and tissue sensitivity at various anatomic sites along the respiratory tract. As noted previously, anatomic, physiologic, cellular, and biochemical differences of the respiratory system among animal species may result in differences in response to toxicant injury, and make the estimation of human health risk from results of animal toxicology studies difficult.

In general, inhaled highly water-soluble chemicals and large particles (mean aerodynamic diameters $>2.5-10\,\mu m$—e.g., coarse ambient particulate matter [PM_{10}]) will generally cause toxicity to the upper respiratory tract, while poorly soluble chemicals and small particles ($\leq 2.5\,\mu m$—fine ambient particulate matter [$PM_{2.5}$]) will target the lower respiratory tract and/or alveolar parenchyma. Once defense mechanisms at specific airway sites are overwhelmed by the toxic insult, injury ensues followed closely by acute inflammatory and epithelial responses to repair the damage caused by the toxicant.

Patterns of Respiratory Tract Injury to Inhaled Toxicants

Two principal gradients of damage are often observed in the respiratory tract upon exposure to inhaled toxicants. At each site, the gradient is a proximal to distal decrease in lesion severity. The physicochemical nature of the airborne toxicant and the inhalation exposure conditions dictate whether one or both gradients of airway toxicity occur, as well as the severity and distribution of the injury (and response to injury) within each site. The first gradient is in the upper respiratory tract extending from the nasopharyngeal passages through the tracheobronchial airways. The second is in the lower respiratory tract, and extends from the terminal bronchioles (proximal centriacinus) to the alveolar ducts and adjacent alveoli (distal centriacinus) in the pulmonary parenchyma. The gradient in the upper airways occurs most often with inhalation exposure to the highly water-soluble chemicals (e.g., sulfur dioxide) or large particles (e.g., PM_{10}), while the second gradient of injury in the centriacinar region of the lung is caused by inhaled poorly soluble chemicals (e.g., nitrogen dioxide) and small particles (e.g., $PM_{2.5}$).

Gases or aerosolized chemicals that are of low water solubility but highly reactive (e.g., ozone, chlorine), as well as certain nanoparticles (e.g., ≤ 20-μm carbon black nanoparticles), cause gradient injury at both upper and lower respiratory sites with repeated long-term exposures in laboratory rodents. Interestingly, both the nasal and centriacinar sites of injury are also predicted dosimetric "hot spots" for ozone and nanoparticles, based on computational deposition modeling.

Cell-Specific versus Nonspecific Injury

Exposure of the respiratory tract to a wide variety of agents results in epithelial cell injury and cell death. Injury to individual cells may be reversible, such as altered mucus production or loss of cilia, or irreversible, leading to cell death. Chemical agents may nonspecifically affect all epithelial cells within a region or may selectively injure a single cell type (Table 14.2).

TABLE 14.2 Specificity of Cell Damage by Selected Compounds which Undergo In Situ Metabolic Activation Within the Respiratory Tract

Compound	Primary cell type affected	Species	Route
Acetaminophen	Olfactory mucosa, transitional epithelium, club cell	Rat, mouse	Oral, ip
Bromobenzene	Club cell	Rat, mouse	ip
Butylated hydroxy toluene (BHT)	Type I epithelial cell, capillary endothelial cell	Mouse (not rat)	ip
Carbon tetrachloride	Club cell	Guinea pig Rat	Inhalation ip
4-Ipomeanol	Club cell (also causes pulmonary edema)	Rat, mouse	ip
3-Methylfuran	Olfactory mucosa, club cell	Mouse, rat, hamster	Inhalation
Naphthalene	Club cell	Mouse, rat	ip, inhalation
Alpha-naphthylthiourea (ANTU)	Capillary endothelial cell	Rat	Oral
Trialkyl phosphoro-thioates	Type I epithelial cell, club cell	Rat	Oral, ip
Phenacetin	Olfactory mucosa	Rat	Oral

ip, intraperitoneal.
Table modified from Handbook of Toxicologic Pathology, *second ed. W. M. Haschek, C. G. Rousseaux and M. A. Wallig, eds. (2002) Academic Press, Vol. 2, Table VI, p. 32, with permission.*

In general, the most vulnerable cells to toxic injury are the ciliated cells of the RE lining the conducting airways and the type I epithelial and capillary endothelial cells of the alveolar gas-exchange region in the deep lung. These cells are damaged nonselectively by toxicants because of their functional and morphological characteristics, for example the large surface area of type I epithelial cells and endothelial cells presented to air- and blood-borne toxicants, respectively. Nonspecific injury may also occur when agents are so toxic that all cells in contact with the agent are injured. An example of this type of injury would be aspiration of a caustic solution or exposure to high airborne concentrations of a warfare/terrorist agent such as chlorine or mustard gas, which would cause diffuse necrotic damage with exfoliation of airway and alveolar epithelium.

As mentioned previously, susceptibility of other cell types to injury is dependent on the nature of the toxicant and its interaction with a unique function of the cell. For example, cells and tissues containing high concentrations of cytochromes P450 enzymes, such as the olfactory sustentacular cells and bronchiolar club cells, are susceptible to injury by toxicants which require metabolic activation, such as 3-methylfuran, acetaminophen, styrene, naphthalene, and 4-ipomeanol.

Cell Proliferation, Regeneration, and Repair Processes

Irrespective of the mechanism of toxicity and cell type affected, relatively stereotyped repair processes that include proliferation of stem cells and inflammation follow initial damage. Proliferation of resident cells generally occurs as a regenerative response following cell necrosis. This is an acceleration of the normal cell renewal process by which tissue integrity is maintained. In some situations, cell proliferation can be initiated by the migration of inflammatory cells into the lung. In addition to repair processes, cell proliferation is also associated with lung growth and neoplasia.

Chemical damage to the nasal OE can be repaired by regeneration if sufficient basal cells survive to initiate this repair process. If injury occurs to the ciliated RE, surviving cells spread to cover the denuded basal lamina. This is accompanied by proliferation of surviving immature secretory cells or basal cells. These cells may divide and differentiate into ciliated cells, resulting in a restoration of the surface epithelium. In the smaller bronchiolar airways, the club cell is the progenitor cell responsible for reparative regeneration in response to toxicant-induced bronchiolar injury. Proliferating club cells may differentiate into either mature club cells or ciliated cells.

Injury to the alveolar epithelium is followed by proliferation of type II epithelial cells whose normal function is surfactant secretion. Newly divided type II cells can differentiate into end-stage type I cells, which are incapable of division, or mature type II cells. Proliferation of type II cells may also follow migration of inflammatory cells from the capillary bed into the alveoli. Injury to capillary endothelium within the lung is repaired by proliferation of remaining endothelial cells or by circulating stem cells. AM proliferation is also commonly seen. In response to injury, mediators

are released that result in an influx of polymorphonuclear cells and monocytes into the lung. These monocytes differentiate into AMs, replenishing and augmenting the AM population.

Proliferation of fibroblasts located in the walls of the airways and in the pulmonary interstitium frequently follows injury. This proliferation is usually not due to direct injury to the fibroblast but related to the loss of overlying epithelium and basement membrane, as well as to the production of mediators and growth factors by AMs and inflammatory cells. Excessive fibroblast proliferation and collagen production can lead to fibrosis or "scarring," which compromises normal pulmonary elasticity or compliance and gaseous diffusion.

Under most conditions of injury, proliferation of epithelial cells begins within the first day of injury and peaks over the next few days. Proliferation of other cell types occurs at later times. Inhibition of epithelial cell proliferation can delay or inhibit normal repair, resulting in chronic damage or secondary bacterial infections. Remodeling of tissue may occur with chronic injury if repair mechanisms are unable to keep pace. This structural remodeling may be beneficial or have adverse consequences. In addition, inhibition of cell differentiation—for instance, under conditions of chronic exposure—can result in large numbers of undifferentiated cells. These cells may be less susceptible to the original injury and tolerance may develop. These cells may also play a role in the development of neoplasia.

Thus, mild epithelial or endothelial injury without basement membrane damage, severe inflammation, or persistence of the inciting agent may be resolved by simple cellular regeneration. With more severe damage, a significant inflammatory component may be elicited which may be followed by tissue destruction or fibrosis. In some cases, persistence of the inciting agent within the tissue may lead to the development of granulomatous disease, as observed with inhalation exposure to crystalline silica or carbon nanotubes.

Nasopharyngeal and Laryngeal Responses to Injury

Important factors in the pathogenesis of toxicant-induced nasal lesions include airflow, absorption, tissue susceptibility, mucociliary apparatus, and metabolism. The distribution of damage is dependent on regional deposition of inhaled chemicals and on tissue or cell susceptibility to individual agents. Regional deposition of inhaled chemicals is dependent on airflow and, in the case of particles, on particle characteristics such as size and aerodynamic shape. Species differences in regional airflow play a role in lesion distribution. Nasal uptake of gases is dependent on the partition coefficient of the gas and, in the case of reactive gases, on the rate of reaction. For example, in the dog, nasal uptake is 100% for formaldehyde, 40%–70% for ozone, and 1% for carbon monoxide. Distribution of nasal lesions is also dependent on cell or tissue susceptibility. For example, OE is damaged by xenobiotics that require metabolic activation, such as methylbromide, 3-methylfuran, 3-methylindole, carbon tetrachloride, naphthalene, and acetaminophen. This usually occurs irrespective of the route of administration. On the other hand, ciliated cells and perhaps mucous cells are the targets of toxicity caused by other nasal toxicants such as formaldehyde.

Substances affecting nasal function may impair mucociliary flow, change nasal airflow resistance, and irritate or damage the nasal mucosa. Damage to the OSNs of the OE can result in anosmia (loss of smell). Chemically induced nasal epithelial lesions fall into one or more of the following categories: degeneration and necrosis, inflammation, repair, adaptation, and proliferative lesions, including neoplasia (Table 14.3).

Degeneration and necrosis are usually followed by inflammation and cell proliferation to repair damaged epithelium. Excessive proliferation can result in epithelial hyperplasia. Increased cell turnover can potentially predispose to carcinogenesis since enhanced DNA synthesis will increase the probability of mutation. Continued low-level toxic exposure may result in

TABLE 14.3 Classification of Nonneoplastic Alterations to the Respiratory System

Alteration	Xenobiotic
NASAL CAVITY AND AIRWAYS	
Degeneration/necrosis	Acetaminophen, 3-methylfuran
Inflammation	Acetaldehyde, formaldehyde, cigarette smoke, ammonia
Metaplasia/hyperplasia	Acetaldehyde, formaldehyde, cigarette smoke, ammonia
Fibrosis	Nitrogen dioxide (NO_2), methyl isocyanate
Chronic bronchitis	Chronic exposure to cigarette smoke, irritant gases
PULMONARY PARENCHYMA	
Edema	Phosgene, α-naphthothiourea, endotoxin
Inflammation	Hyperoxia, radiation, bleomycin, paraquat, silica
Fibrosis	Hyperoxia, radiation, bleomycin, paraquat, silica
Emphysema	Smoking, cadmium chloride ($CdCl_2$)

Table reproduced from Fundamentals of Toxicologic Pathology, *second ed., W. M. Haschek, C. G. Rousseaux and M. A. Wallig, eds. (2010) Elsevier, Table 6.6, p. 110, with permission.*

adaptive responses such as squamous or mucous cell metaplasia, or mucous cell hyperplasia. The presence of exudate in the nasal cavity is a valuable indication of nasal toxicity and is readily detected by light microscopy at low magnification. However, nasal exudate is also a hallmark of microbial infections caused by mycoplasma and Sendai virus. The relatively stereotyped nature of the response of tissues to injury, independent of etiology, needs to be reemphasized.

In the larynx, the transitional zone, between the stratified SE cranially and the RE caudally, is the most sensitive site for inhaled xenobiotic-induced injury resulting in degeneration, squamous metaplasia, or hyperplasia. Xenobiotics affecting the larynx include tobacco smoke and cobalt sulfate. These lesions must be differentiated from aging changes, thus emphasizing the need for age-matched controls in evaluating xenobiotic-induced changes.

Nonneoplastic Lesions

ACUTE LESIONS

In the nasal epithelium, the mildest change may be loss of motile cilia from ciliated cells, or immotile cilia from OSNs, with little change in the underlying or adjacent cells. Similarly, loss of OSNs may occur without apparent disruption of the overall structure of the OE. Acute necrosis and loss of OE may be seen following inhalation or bloodborne exposure to toxicants requiring metabolic activation by the cytochromes P450 system, such as 3-methylfuran and acetaminophen, respectively. Once the basement membrane is exposed, cytokines are released and inflammation takes place. Acetaminophen also causes selective necrosis of nasal TE, which is also the target site of ozone toxicity.

More severe nasal epithelial lesions, such as segmental loss of basal lamina or ulceration, cause damage to the underlying lamina propria and even the bone or cartilage. This can lead to turbinate atrophy or perforation of the nasal septum. With extensive nasal epithelial damage, the affected area may be covered by an exudate indicating marked rhinitis. Repair may take place or, if repeated exposure occurs, squamous metaplasia of respiratory or even olfactory regions may result, occasionally with extensive keratinization.

SUBACUTE/CHRONIC LESIONS

Subacute/chronic nonneoplastic changes of the olfactory mucosa following inhalation of irritant substances such as acrolein, formaldehyde, acetaldehyde, and cigarette smoke may include atrophy of the OE or even loss of the entire olfactory mucosa, including nerve bundles and Bowman glands in the lamina propria. In the latter case, the olfactory mucosa may be replaced by squamous or respiratory metaplasia. The dorsomedial region of the nasal cavity appears to be the most vulnerable to these changes. Cessation of exposure may lead to recovery, but the regenerated OE may still appear disorganized and relatively thin.

Common changes of the transitional and RE following inhalation of irritant substances such as formaldehyde and cigarette smoke are epithelial hyperplasia and/or squamous metaplasia of the nasal mucosa in the proximal nasal airways. Mucous cell metaplasia or hyperplasia may also occur (Figure 14.6C). Repeated ozone exposures cause epithelial hyperplasia followed by mucous cell metaplasia/hyperplasia in the proximal nasal airways of monkeys, mice, and rats. The mucus produced by these cells may have an increased concentration of acidic mucous glycoproteins, resulting in altered viscoelastic properties that modify mucous flow, thus affecting airway clearance mechanisms.

Stratified squamous metaplasia, with or without keratinization, is also frequently observed and may interfere with mucociliary clearance (Figure 14.6D). This metaplastic change is often reversible following cessation of exposure. If normal epithelial adaptive or repair processes cannot take place because of severe injury with complete loss of epithelial cells, including progenitor cells, excessive fibrin will accumulate in the nasal exudates, followed by intraluminal fibrosis. In rodents, excessive hyperkeratosis, severe inflammatory exudation, or fibrosis may lead to obstruction of the nasal cavity and even death of these obligate nasal breathers.

In summary, chemically induced injury of the nasal epithelium may be followed by regenerative hyperplasia or metaplastic changes such as respiratory metaplasia of the OE and mucous or squamous cell metaplasia of the transitional and RE. Severe hyperplastic and squamous metaplastic changes from persistent mucosal injury may be a prelude to nasal neoplasia.

Nasal Neoplasia

In spite of the rare occurrence of spontaneous nasal tumors in rodents, the nasal cavity is highly sensitive to environmental carcinogens, irrespective of the route of administration, and thus should be examined in all carcinogenicity studies using inhalation as the route of exposure. Grossly, these neoplasms appear as gray-white to yellowish infiltrative masses partially occluding the nasal cavity, often with necrotic areas and with destruction of adjacent tissue. These may occasionally extend into the brain or metastasize to other organs. The larynx is also a target site for carcinogenic xenobiotics, and should be routinely examined.

Nasal tumors have been induced experimentally in rodents following inhalation of a variety of important industrial chemicals, such as formaldehyde, acrolein,

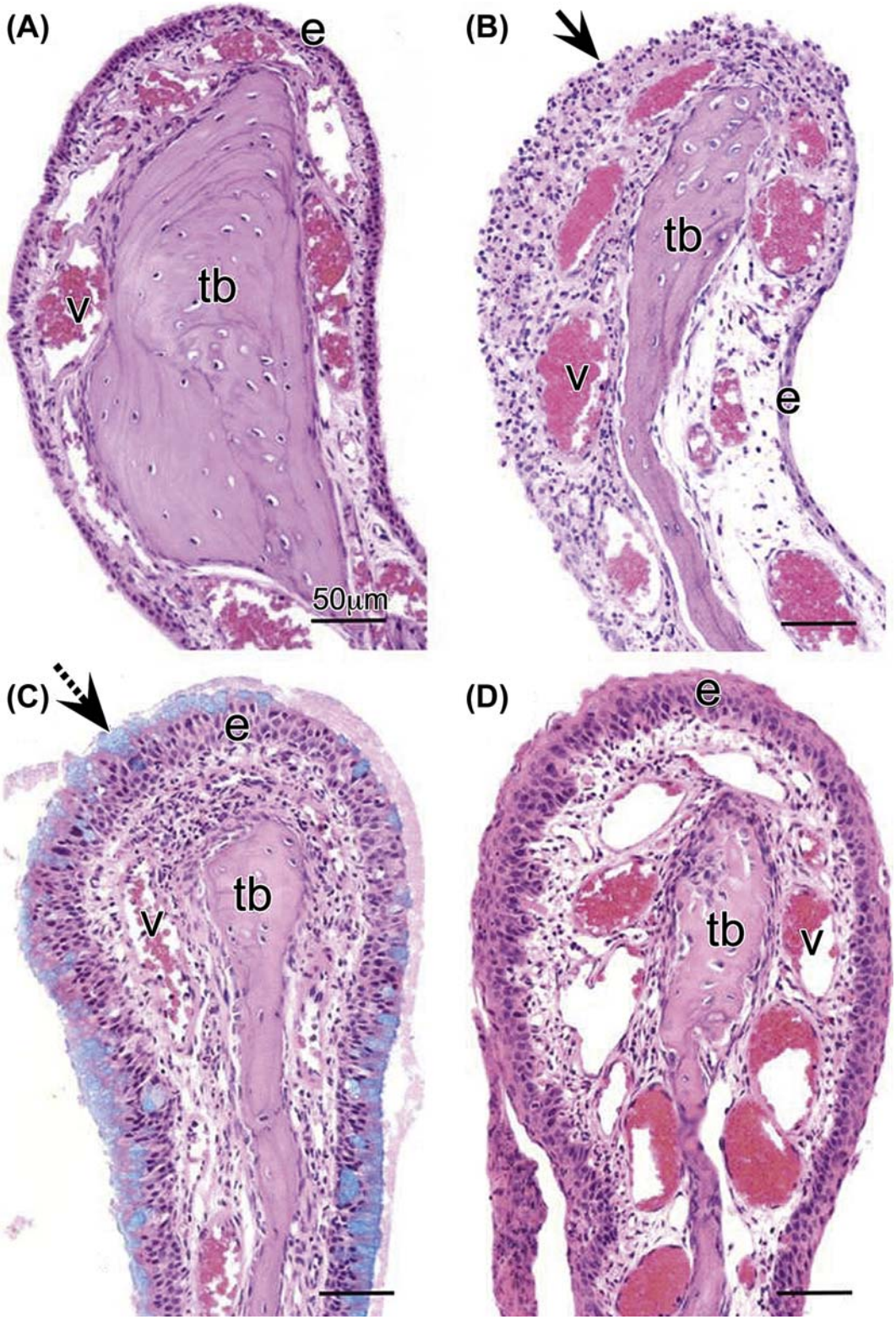

FIGURE 14.6 Light photomicrographs of the maxilloturbinates in the proximal nasal airways of rats that were exposed to either filtered air alone (A; controls), short-term inhalation exposure to a high concentration of mainstream cigarette smoke (B), or long-term exposures to a high concentration of ozone or cigarette smoke (C and D, respectively). Tissues were stained with hematoxylin and eosin, and Alcian blue (AB). The transitional epithelium (e) lining the maxilloturbinate in (B) has exfoliated (arrow), and a conspicuous acute inflammatory cell influx is present in the lamina propria. The ozone-exposed maxilloturbinate (C) is remarkably thickened due to epithelial hyperplasia and mucous cell metaplasia (stippled arrow, mucous cells with AB-stained [pale blue] mucosubstances). Numerous inflammatory cells are also present in the underlying lamina propria. Long-term cigarette exposure (D) exhibits squamous metaplasia of the transitional epithelium along with inflammation in the lamina propria. The turbinate bones (tb) are atrophic in the maxilloturbinates of the rats exposed to these inhaled toxicants (B, C, D). v, blood vessels. *Figures 14.3 (A) and (C) reproduced from Harkema et al. (2006) The nose revisited: a brief review of the comparative structure, function, and toxicologic pathology of the nasal epithelium*, Toxicol. Pathol. *34, 252–269, with permission.*

acetaldehyde, bis(chloromethyl) ether, hexamethylphosphoramide, and vinyl chloride. Obligate nasal breathing and complexity of the nasal turbinates may explain why nasal tumors develop in rodents but have not been reported in association with exposure to these chemicals in humans. Nasal tumors have also been induced following parenterally administered chemicals such as nitrosamines. Malignant nasal neoplasms are rare in humans, except for six occupational groups: chromate workers, nickel refiners and workers, mustard gas makers, isopropyl alcohol workers, makers of wooden furniture, and boot and shoe workers. In addition, welders, flame cutters, and solderers have an increased risk of nasal cancer. Animal studies have incriminated certain hexavalent chromium compounds and metallic nickel as carcinogenic agents.

Tumors of the rat nasal cavity have been classified as adenomas, adenocarcinomas and carcinomas of squamous cell, adenosquamous and neuroepithelial type. These mainly arise from the lining epithelium, but may also arise from the submucosal glands. Squamous cell carcinomas and adenocarcinomas have also been reported in the larynx of rats and hamsters.

In humans, squamous cell carcinoma is the most common spontaneous tumor (75%), while adenocarcinomas and undifferentiated tumors are less common (10% each). In the dog, adenocarcinoma, squamous cell carcinoma, and undifferentiated carcinoma are equally prevalent.

Tracheobronchial and Pulmonary Responses to Injury

As in the upper airways, toxic injury to the lower respiratory tract may nonspecifically affect most epithelial cells or be limited to a single cell type. Injury may be mild and reversible, with minimal inflammation and complete repair by epithelial regeneration. More severe injury, with nonspecific necrosis or following chronic toxicant exposure, can induce severe inflammation and fibrosis, which is irreversible. The epithelial lining of the bronchiolar region is exquisitely susceptible to injury by oxidant gases (NO_2, sulfur doxide [SO_2], and ozone [O_3]) and toxicants (3-methylindole).

Injury to airway epithelium invariably impairs mucociliary clearance due to changes in mucus or to injury of ciliated cells. Changes in the ciliated cells may range from ciliostasis or ciliary loss to cell death. An increased rate or amount of mucus secretion is a common response to inhaled toxicants such as SO_2, O_3, NO_2, and ammonia (NH_3). Mucus hypersecretion from surface epithelial cells may be stimulated by direct irritation. Hypersecretion and an increase in glycoprotein content from submucosal glands may follow parasympathetic stimulation or parasympathomimetic drugs such as acetylcholine and pilocarpine. A change in the glycoprotein fraction affects the viscosity of mucus. Excess mucus has an irritant effect on sensory nerve endings, often triggering the cough reflex. Release of acetylcholine from irritated synapses of the autonomic innervation present in the bronchiolar epithelium causes bronchiolar constriction and mucus secretion. Mast cell mediators, as well as prostaglandins and lipoxygenase products, also appear to stimulate mucus secretion.

Morphologically, mucus may be readily observed in airways of affected animals, whereas in normal animals it is not. In some cases of chronic exposure, increased numbers of mucous cells (hyperplasia) or abnormally located mucous cells (mucous cell metaplasia) may be observed. If these changes persist, they can result in blockage of mucus-producing glands and ducts, airway obstruction, and alveolar injury. Debris can accumulate and incite an inflammatory response. Inflammation, if present, may be confined to the airway wall or spill over into the lumen. Neutrophils predominate in the early stages of inflammation, whereas mononuclear cells are prominent in later stages. Eosinophils may be associated with allergic conditions.

Injury to epithelium may result in epithelial degeneration, detachment and exfoliation of cells. This loss is normally followed by inflammation and repair. If the basement membrane is not damaged and the injurious agent does not persist, the epithelium will regenerate within a few days by proliferation of immature secretory stem cells or club cells in the small airways. Differentiation of these cells is followed by recovery. If basement membrane is damaged, fibroblast precursors may migrate from the ulcerated airway wall into the lumen, particularly when a fibrinous exudate is present. Organization can occur within 7–10 days, resulting in intraluminal fibrosis (bronchiolitis obliterans; Figure 14.7). This type of lesion has been reported with highly reactive volatile chemicals such as methyl isocyanate, with NO_2 in silo filler's disease, and with diacetyl in microwave-popcorn factory workers. Fibroblast proliferation may also occur in the lamina propria or peribronchially. If severe inflammation is present, in addition to basement membrane damage, bronchiectasis (destruction of airway wall with dilation) or abscess formation, following infection, may occur.

If clearance is sufficiently impaired and spontaneous resolution does not take place, obstruction of airways with concomitant bronchoconstriction and hypoxic vasoconstriction may occur and lead to death from hypoxia, or alveolar injury and emphysema. In the event of continued irritation, squamous metaplasia may occur. Both squamous metaplasia and

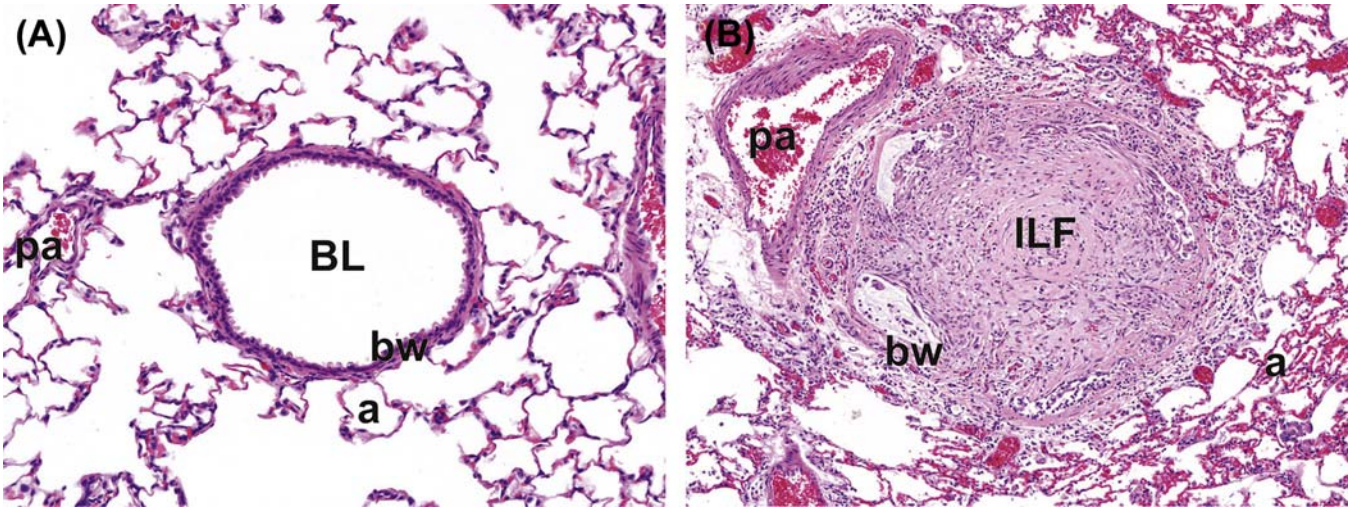

FIGURE 14.7 Light photomicrographs of small-diameter, preterminal bronchioles in the lungs of mice that received repeated, daily inhalation exposures to either filtered air (A; control) or a butter flavoring agent, 2,3 pentanedone (B). The bronchiolar lumen (BL) in (B) is almost completely obliterated by fibrotic tissue (intraluminal fibrosis; ILF), the distinguishing histologic feature of bronchiolitis obliterans. Tissue sections were stained with hematoxylin and eosin. bw, bronchiolar wall; a, alveolar parenchyma; pa, pulmonary artery. *Photographs courtesy of Drs. Crystal Johnson, Gordon Flake, and Daniel Morgan at the U.S. National Toxicology Program, National Institute of Environmental Health Sciences, Research Triangle Park, NC, USA. Figure reproduced from* Haschek and Rousseaux's Handbook of Toxicologic Pathology *(2013), third ed. (W.M Haschek, C.G. Rousseaux and M.A. Wallig, eds.), Academic Press (Elsevier), Figure 51.14, p. 1974, with permission.*

uncontrolled cell proliferation may potentially be followed by neoplasia.

Cell-Specific Injury

Ciliated cells lining the tracheobronchial airways may be selectively damaged by inhaled toxicants. For instance, loss of cilia is a stereotyped response to inhalation of acidogenic gases such as SO_2 and NO_2, while cigarette smoke slows ciliary beat frequency. Ozone selectively damages ciliated cells in the terminal and respiratory bronchioles, causing loss of cilia or cell death. This is followed by conspicuous hyperplasia of club cells in both rodents and monkeys.

As mentioned previously, selective toxicity to the club cell is also induced by agents that require metabolic activation to their putative toxicant by the cytochromes P450 enzymes (Table 14.2). Damage may be limited to the club cells or may be followed by more extensive pulmonary injury, depending on the specific compound, dose, and species. Examples of selective club cell toxicants are 4-ipomeanol, naphthalene, 3-methylfuran, carbon tetrachloride (CCl_4), styrene, and acetaminophen. Movement of remaining bronchiolar cells to cover the denuded basement membrane follows necrosis of club cells and rapid proliferation of remaining club cells to regenerate normal epithelium (Figure 14.6).

Selective damage to club cells, unrelated to their cytochrome P450 content, has also been reported. This selectivity is presumably related to other unique features of the cell. For instance, methylcyclopentadienyl manganese tricarbonyl, which is detoxified in the liver by the cytochromes P450 enzymes, causes mitochondrial damage in club cells, presumably due to the high oxidative enzyme content of these cells. In addition, some polychlorinated biphenyl (PCB) congeners affect club cell secretory functions.

Hyperreactive Airway Disease

Hyperresponsive airways are a possible sequel to bronchiolar injury. Hyperactive airway disease can develop following transient and often innocuous viral infection, from exposure to certain allergens, or from exposure to inhaled or ingested respiratory toxicants. Sustained inhalation of dust particles may play a role by upregulating the production of cytokines (interleukin-8 [1L-8]) and monokine-inducible protein 2 (MIP-2) by AMs, attracting neutrophils into the bronchoalveolar region and causing secondary bronchiolar injury. Airway hyperresponsiveness is characterized by exaggerated bronchoconstriction following exposure to mild stimuli such as cold air. Typically, increased numbers of mast cells, eosinophils, and T lymphocytes are present in the airway mucosa.

Chronic Obstructive Pulmonary Disease

Chronic bronchitis, emphysema, and asthma comprise the clinical entity known as chronic obstructive pulmonary disease (COPD). Asthma can be clinically differentiated from chronic bronchitis and emphysema

because the obstruction is reversible. Chronic bronchitis and emphysema are difficult to distinguish clinically, but they are distinguished postmortem based on morphologic criteria. A distinction is often made between disease of the larger airways (chronic bronchitis) and disease of bronchioles (bronchiolitis or small airways disease). However, most patients with chronic obstructive lung disease show evidence of both conditions because the etiologic agents, such as cigarette smoke, affect the lung at all airway levels. Emphysema also frequently accompanies chronic bronchitis and contributes to small airway obstruction.

Asthma

Asthma is recognized clinically as episodic, reversible airway bronchoconstriction. Pathologically, it is a chronic inflammatory disease of airways. Episodic acute inflammation corresponds to clinical exacerbations of asthma. In asthmatics, the control of airway muscle shortening is abnormal. It is thought that chronic inflammation causes the airways of asthmatics to narrow when stimulated in ways that have minimal effects on nonasthmatics.

Asthma is generally categorized as being intrinsic (idiosyncratic) or extrinsic. Intrinsic asthma is initiated by nonimmune mechanisms and is seen in some patients after ingestion of aspirin, pulmonary (usually viral) infections, cold, inhaled irritants, stress, and exercise. Extrinsic asthma starts as a type I hypersensitivity reaction to an extrinsic antigen and includes atopic (allergic) and occupational asthma. Allergic or atopic asthma, which is an IgE-mediated sensitivity primarily to inhaled antigens (allergens) and resulting in bronchoconstriction, is the most common form. Examples of antigens include dusts, pollens, animal dander, and foods. Initial sensitization (priming) by the antigen induces T-helper lymphocytes that produce IL-4 and IL-5 (Figure 14.8).

These cytokines support an antibody-drive (T_H2) immunity characterized by the production of IgE by B lymphocytes, increased numbers of mast cells with antigen-specific IgE bound to their receptors, and recruitment of eosinophils. Subsequent exposure to antigen results in an acute response (immediate phase, in minutes) and a late-phase (hours) reaction. On reexposure to inhaled antigen, antigen-induced crosslinking of IgE bound to mast cells on the airway surface causes release of preformed mediators that open tight junctions between epithelial cells. Antigen then enters the mucosa and activates mucosal and submucosal mast cells and eosinophils that release additional mediators. These mediators, either directly or indirectly through neural reflexes, induce bronchospasm, increased vascular permeability and edema, mucus production, and recruitment of additional inflammatory cells from the blood. The recruitment of neutrophils, eosinophils, basophils, lymphocytes, and monocytes marks the start of the late phase. During the late phase, there is additional mediator release from leukocytes, endothelial cells, and epithelial cells. Endothelins from endothelial and epithelial cells are potent bronchoconstrictors and inducers of airway smooth muscle cell proliferation and fibrosis. Release of eotaxin from airway epithelial cells results in eosinophil recruitment and activation. During this phase, eosinophilic cationic protein and major basic protein released from eosinophils damage the epithelium and cause bronchoconstriction. Ambient air pollutants, such as ozone and particulate matter, are now thought not only to cause exacerbation of preexisting asthmatic conditions but also to act as adjuvants during initial sensitization to enhance the development of this common airway disease.

Occupational asthma has been associated with exposure to fumes such as epoxy resins, organic and inorganic dusts such as wood, cotton, and platinum, and gases such as toluene diisocyanate and formaldehyde. The mechanisms underlying occupational asthma may vary according to the stimulus. Occupational asthma due to low molecular weight antigens such as toluene diisocyanate appears to be IgE-independent and most likely is mediated by CD8+ T cells, IL-5 secretion, and eosinophils.

The morphologic features of asthma include excess mucus and eosinophils in the bronchial lumen, goblet cell metaplasia/hyperplasia of the surface epithelium, epithelial desquamation, hypertrophy and hyperplasia of the submucosal mucous glands, congestion and edema of the bronchial mucosa, chronic airway inflammation, basement membrane thickening, structural remodeling of airway longitudinal elastic bundles, and hypertrophy/hyperplasia of smooth muscle. The smooth muscle thickening is seen throughout the bronchial tree, but is most pronounced in the segmental airways and terminal bronchioles. The inflammatory cells in the airway walls include eosinophils, lymphocytes, neutrophils, macrophages, and mast cells. Eosinophils are prominent and may comprise 5%–50% of the infiltrating cells. This characteristic eosinophilic infiltrate differentiates asthma from other chronic inflammatory conditions of the airway.

Proliferative Lesions

Squamous metaplasia and hyperplastic lesions occur in the rat trachea, most frequently at the carina, and in the larynx, particularly at the ventral and lateral aspects. The rat larynx appears to be uniquely sensitive to induction of these lesions by various industrial chemicals, pharmaceuticals, and propellants. Papillomas are the main spontaneous neoplasms reported within the airways of rats. Benign

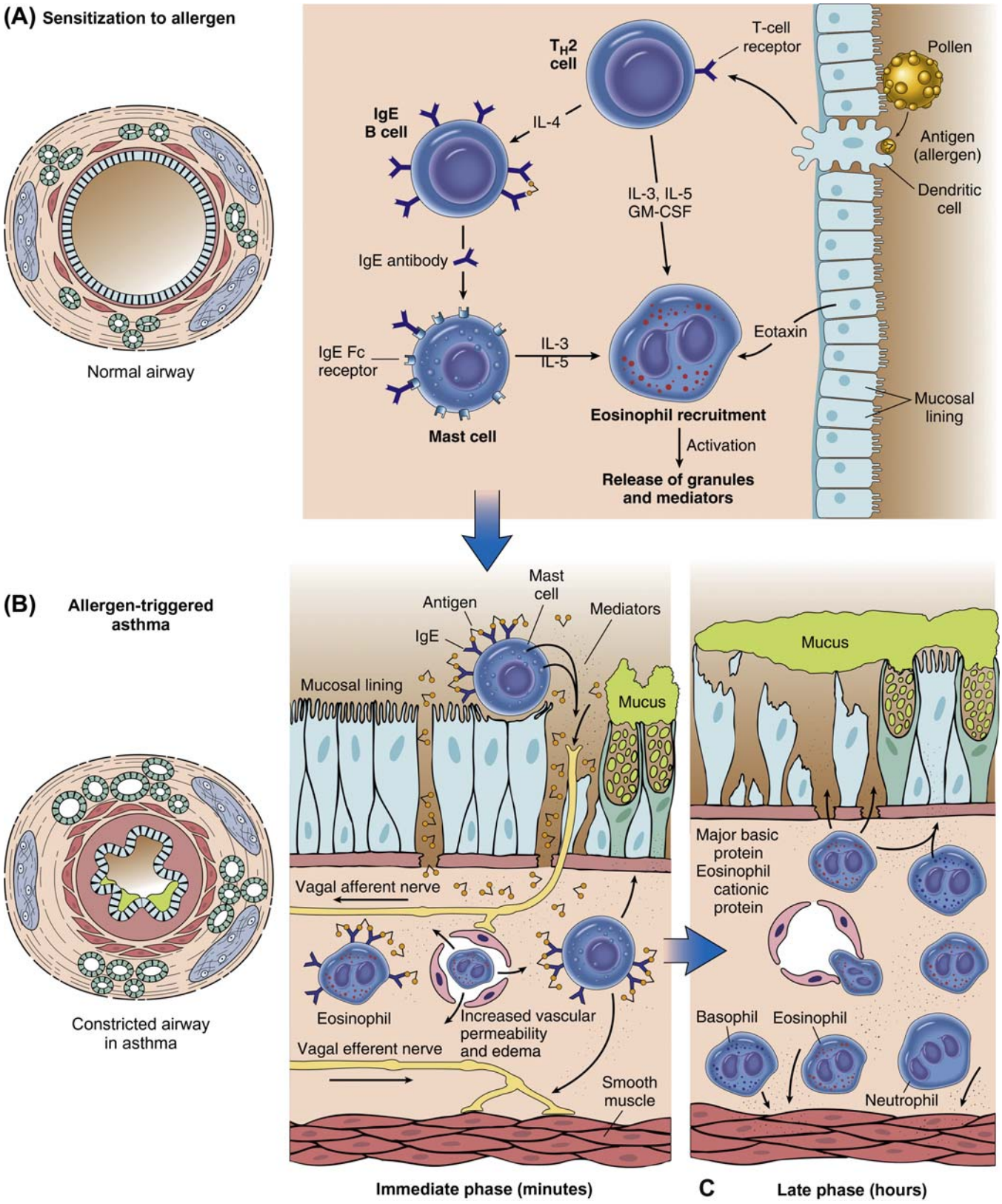

FIGURE 14.8 Allergic asthma. (A) Inhaled allergens (antigen) elicit a T_H2 dominated response favoring IgE production and eosinophil recruitment (priming or sensitization). (B) On reexposure to antigen (Ag), the immediate reaction is triggered by Ag-induced crosslinking of IgE bound to IgE receptors on mast cells in the airways. These cells release preformed mediators that open tight junctions between epithelial cells. Antigen can then enter the mucosa to activate mucosal mast cells and eosinophils, which in turn release additional mediators. Collectively, either directly or via neuronal reflexes, the mediators induce bronchospasm, increased vascular permeability, and mucus production, and recruit additional mediator-releasing cells from the blood. (C) The arrival of recruited leukocytes signals the initiation of the late phase of asthma and a fresh round of mediator release from leukocytes, endothelium, and epithelial cells. Factors, particularly from eosinophils (e.g., major basic protein, eosinophilic cationic protein), also damage the epithelium. *Figure reproduced from Hussain and Kumar (2005). The lung. In:* Robbins and Cotran Pathologic Basis of Disease, *seventh ed. (Kumar, V, Abbas, A.K. and Fuasto, N., eds), Elsevier Saunders, Fig. 15-11, p. 725, with permission.*

neuroendocrine tumors, though uncommon, must be considered when papilloma-like tumors are found.

Pulmonary Parenchymal Responses to Injury

Although it would be of great diagnostic convenience if specific agents elicited a characteristic response, the lung responds in a similar way to a wide variety of infectious and toxic agents. Viral and chemical agents frequently incite a similar type of interstitial pneumonia, and both need to be considered as differentials for diffuse spontaneous pulmonary diseases. Particulates such as silica may incite a granulomatous response similar to that induced by tuberculosis and some mycotic agents. In some cases the etiologic agent can be identified, although methods other than the routine hematoxylin and eosin (H&E) stained paraffin sections are usually required for detection. The response does vary to some degree, depending on the nature of the agent and on the severity and persistence of injury, as well as on the particular cell type affected and the reparative processes initiated by the injury.

Endothelial and type I epithelial cells are especially susceptible to toxic injury. When endothelial cells are injured or die, there is an increase in vascular permeability. Platelets may adhere to the exposed basement membrane, resulting in release of vasoactive agents. Complement activation, coagulation, and fibrinolysis may also occur before the basement membrane is repopulated. Increased vascular permeability allows the leakage of fluid into interstitial spaces and lymphatics, and eventually into alveolar spaces. If damage is more severe, edema may be followed by interstitial inflammation.

Epithelial damage is accompanied by the acute exudative phase of inflammation characterized by fibrin, neutrophils, and edema. Type II epithelial cells start to proliferate within 12–24 hours and, after a few days, may line alveoli; by light microscopy, this appears as a cuboidal epithelial lining. With time, the inflammatory component will consist of increased numbers of mononuclear cells and macrophages. If damage is not too severe and the basement membrane is intact, resolution may occur by transformation of type II cells into type I cells and subsidence of the inflammatory component. However, if alveolar epithelium has been denuded and the basement membrane has been damaged, fibroblast precursors move rapidly into the alveolar space and, particularly in the presence of fibrin, will result in intraalveolar fibrosis. Similarly, fibrosis may be a consequence of severe endothelial cell damage and fibrin deposition. Interstitial fibrosis may occur after distortion of the normal cell–cell contacts by inflammation or edema. Fibroblast proliferation can be noted within 72 hours of initial injury, and fibrosis may be evident in as little as 7 days. Atypical type II cells may persist in these areas.

Continued inflammation of the alveolar wall implies persistence of the causative agent or injurious mechanisms, and is an important feature of chronic interstitial pneumonia. The characteristic components of chronic alveolar irritation are proliferation and persistence of type II epithelial cells, interstitial thickening due to fibrosis, and accumulation of mononuclear cells. An intraalveolar exudate largely comprised of macrophages may be present. Sustained or recurrent injury to capillary endothelium can lead to progressive vascular remodeling and chronic pulmonary hypertension (see Chapter 9: Cardiovascular System). Pulmonary hypertension has been reported after ingestion of certain plants or medicines, including the leguminous plant *Crotolaria spectabilis*, indigenous to the tropics and used medicinally in "bush tea" and the appetite depressant agent aminorex.

Pulmonary Edema

Pulmonary edema can occur as a result of altered hemodynamics or increased permeability of the air–blood barrier. Altered hemodynamics can result from increased capillary hydrostatic pressure due to cardiac failure, acute injury to the nervous system (neurogenic pulmonary edema), or decreased plasma oncotic levels due to decreased plasma protein levels.

The constituents of the lung that are important in fluid homeostasis are the vascular bed, endothelial barrier, interstitial space, lymphatics, alveolar epithelial barrier, and alveolar surface tension (Figure 14.9). Altered hemodynamics or increased endothelial permeability will result in fluid loss through the moderately leaky endothelium into the adjacent interstitium. Interstitial fluid normally percolates along the interstitium until it reaches the lymphatics that are located adjacent to airways and associated vessels, within interlobular septa (in species that have these) and beneath the pleura. Alveolar fluid clearance across the alveolar epithelium is also a mechanism of fluid removal from the lung. Dilated lymphatics and increased lymph flow are good early indicators of edema. If lymphatic capacity is overwhelmed, interstitial edema will occur. When the capacity of the interstitium is overwhelmed, or if there is damage to alveolar epithelial cells, fluid will leak into the alveoli causing alveolar edema, which interferes with diffusion of gases and results in impaired gas exchange. Because of their tight junctions, alveolar epithelial cells provide a tighter barrier to exudation of fluid than do endothelial cells. Depending on the extent of increased permeability, fibrin and low molecular weight proteins such as albumin will accompany the fluid loss. Pleural

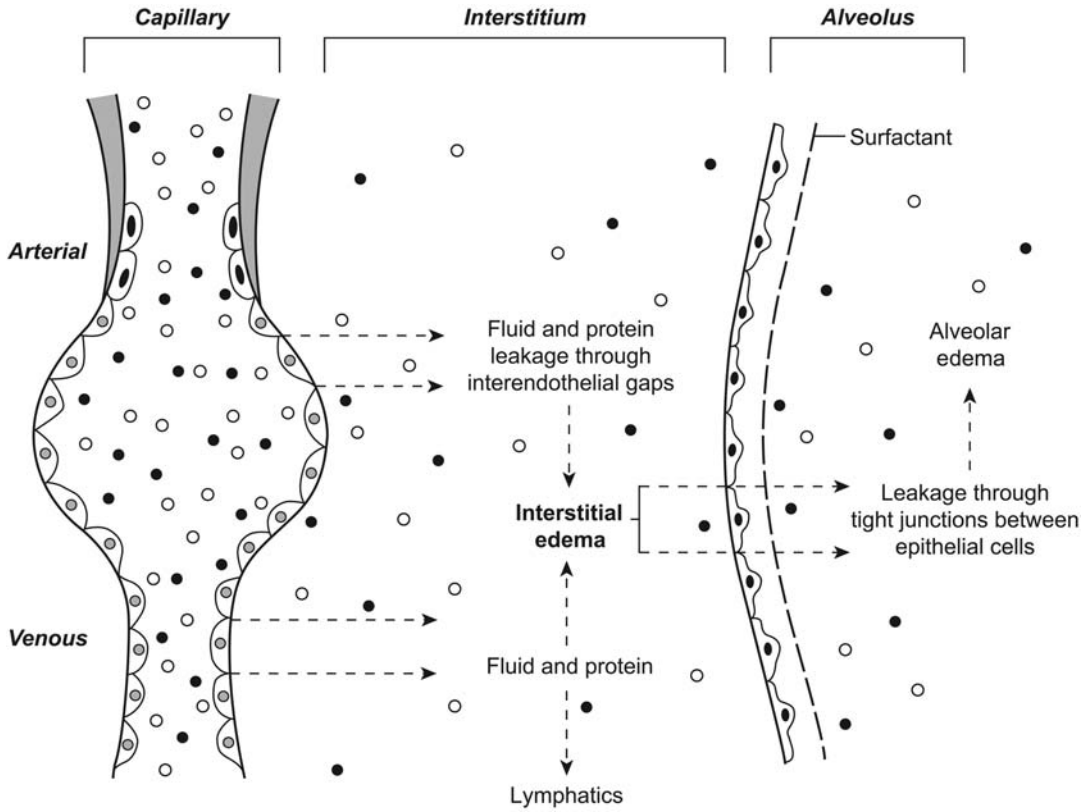

FIGURE 14.9 Pulmonary edema. Interstitial edema occurs when excess fluid enters the interstitium from the pulmonary vasculature. Alveolar edema occurs when interstitial fluid enters the alveolar lumen either following direct alveolar epithelial damage or following a build-up of interstitial fluid. *Figure reproduced from* Handbook of Toxicologic Pathology, *second ed. W. M. Haschek, C. G. Rousseaux and M. A. Wallig, eds. (2002) Academic Press, Vol. 2, Fig. 20, p. 53, with permission.*

effusion is a common feature of pulmonary edema in rodents; interstitial fluid passes from the subpleural interstitium into the pleural cavity through stomata in their very thin pleural mesothelium.

The edematous lung is larger and firmer than normal and does not collapse. Fluid oozes from the cut section. The pleura and interlobular septa are thickened by clear fluid, and pleural effusion (hydrothorax) may be present. Froth in the airways without other findings may be due to agonal change. These changes are easy to detect in large animals but more difficult to identify in rodents. Lung wet weight and, more specifically, the wet-to-dry-weight ratio are useful in determining the presence of edema. More sensitive and specific techniques for measuring pulmonary edema are available in order to discriminate between simple edema and increased blood content (congestion or hemorrhage) or cellular components. On light microscopic examination, early/mild edema is characterized by dilated lymphatics, widening and separation of interstitial tissue (especially perivascularly), and, if alveoli are affected, expansion of the alveolar lumen. This should not be confused with artifacts that can be induced by intratracheal fixation. If the fluid contains protein, it will have a homogeneous eosinophilic appearance on H&E-stained sections (Figure 14.10).

PATHOGENESIS OF PULMONARY EDEMA

Permeability edema occurs when there is excessive opening of endothelial gaps or damage to the air–blood barrier (type I epithelial cells or endothelial cells). Changes in capillary permeability may be due directly to endothelial cell injury or to the effect of cellular or humoral "mediators" of inflammation. Numerous inhaled or circulating toxicants, bacterial toxins, anaphylactic shock, and drugs are believed to cause pulmonary edema by a direct effect on the endothelium or type I epithelial cells. Mediators that alter endothelial permeability may be released from mast cells (histamine) during allergic responses, from aggregated platelets, and from phagocytic cells as they migrate through the endothelium. Since type I epithelial cells are highly vulnerable to toxicants such as NO_2, SO_2, H_2S, and 3-methylindole as well as to free radicals, alveolar edema accompanies many toxic pulmonary diseases.

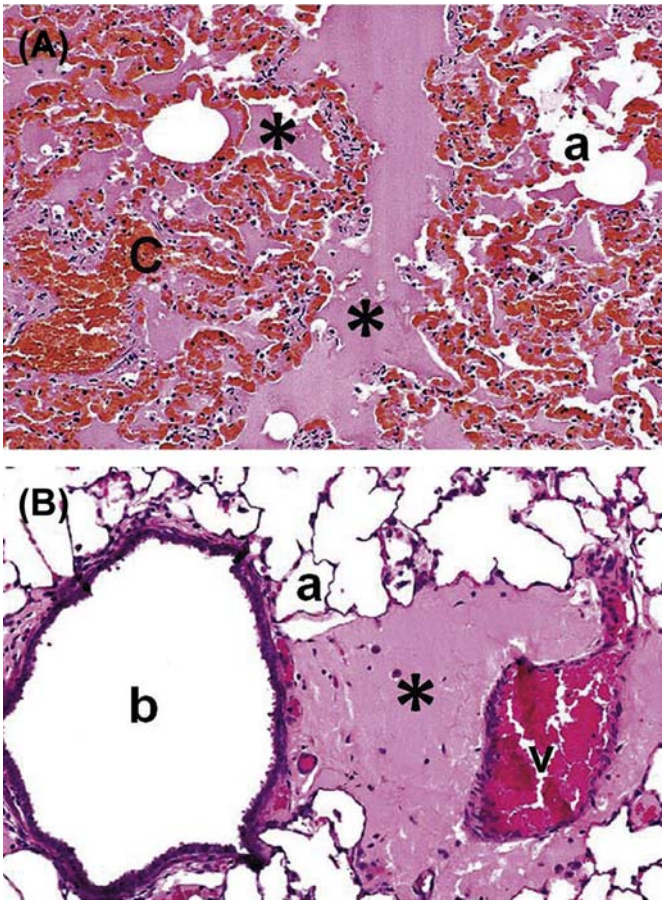

FIGURE 14.10 Light photomicrographs of pulmonary edema located in bronchiolar and alveolar airspaces (asterisks in A) along with congestion (C) of capillaries in the septal wall, and in the perivascular interstitial spaces (asterisk in B) of the rat; H&E stain. *Figure reproduced from Renne et al. (2009) Proliferative and nonproliferative lesions of the rat and mouse respiratory tract*, Toxicol. Pathol. *37, 5S–73S (Figures 99 and 100), with permission.*

Pulmonary edema interferes with the respiratory gas-exchange function of the lung. With mild injury, repair processes can result in a return to normal. However, with severe or prolonged injury, inflammation and eventually fibrosis may follow.

SPECIFIC ETIOLOGIC AGENTS

The classic example of toxicant-induced pulmonary edema is that induced by α-naphthylthiourea (ANTU), a rodenticide. The rat is extremely sensitive to ANTU; massive pulmonary edema and pleural effusion occur as a consequence of endothelial damage to capillaries and venules. Inflammation does not occur. In animals that survive, edema is resolved by 48 hours, without permanent lung damage. Although the mechanism by which this agent damages the lung is not known, it appears that ANTU is metabolically activated to a toxic oxidative species.

Many other toxicants also cause pulmonary edema. These include bacterial endotoxin, which injures endothelial cells; paraquat, which damages epithelial cells (both type I and II); oxygen, which damages both endothelial and epithelial cells; and 4-ipomeanol, which damages club cells. In most cases, pulmonary edema occurs as an acute response and then resolves or is followed by an inflammatory response. In the case of phosgene and smoke inhalation, the edema is characteristically delayed for 1–2 days. Delayed edema is also produced by intravenously administered opiates, such as heroin and methadone. These opiates may act through the central nervous system. Delayed onset of severe proteinaceous edema, the "exudative phase" of radiation pneumonitis, occurs after ionizing radiation exposure. Many cardiovascular toxicants ultimately cause pulmonary edema, which may be lethal (see Chapter 9: Cardiovascular System). Permeability edema due to epithelial and endothelial or microvascular damage is seen with a number of gases, including smoke from fires, endotoxemia, drugs, and chemicals such as paraquat. The lung is the target organ for anaphylactic shock in most domestic animals (those with IVMs); however, the portal–mesenteric vasculature is the primary target in dogs and rodents.

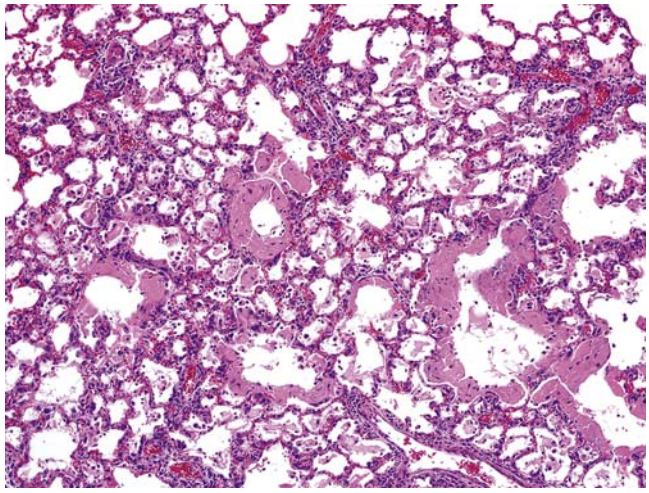

FIGURE 14.11 Light photomicrograph of the lung from a mouse that received repeated, daily inhalation exposure to the butter flavoring agent, 2,3 pentanedone. Airspaces of alveolar ducts and alveoli are lined by hyaline membranes; H&E stain. *Photograph courtesy of Drs. Crystal Johnson, Gordon Flake, and Daniel Morgan at the U.S. National Toxicology Program, National Institute of Environmental Health Sciences, Research Triangle Park, NC, USA. Figure reproduced from* Haschek and Rousseaux's Handbook of Toxicologic Pathology *(2013), third ed. (W.M Haschek, C.G. Rousseaux and M.A. Wallig, eds.), Academic Press (Elsevier), Figure 51.20, p. 1982, with permission.*

Diffuse endothelial and alveolar damage leading to fulminating edema is termed acute respiratory distress syndrome (ARDS). It is an important condition in humans, characterized by intravascular aggregation of neutrophils, diffuse alveolar damage, permeability edema, and formation of hyaline membranes (Figure 14.11). The diffuse alveolar damage results from systemic diseases as well as

direct injury to the lung, where macrophages generate overwhelming amounts of cytokines (mainly tumor necrosis factor-alpha [TNF-α]) and neutrophils aggregated in capillaries release destructive enzymes and toxic oxygen metabolites. ARDS can occur due to direct lung injury caused by oxygen toxicity, radiation therapy, inhalation of toxicants and other irritants, such as smoke; or by systemic conditions resulting from shock, pancreatitis, narcotic overdose, and other drug reactions. ARDS is difficult to treat and is frequently fatal. This type of lesion also occurs in domestic animals, and is considered to be a very early stage and severe form of interstitial pneumonia.

Pulmonary Inflammation

Inflammation, also referred to as alveolitis or interstitial pneumonia, results from diffuse or patchy damage to alveolar septa caused by blood-borne or inhaled toxicants. In humans, the etiology in the majority of cases of interstitial pneumonia is unknown. Inflammation is also a component of pneumoconiosis and other granulomatous diseases, although once the disease is well established the fibrotic component is most prominent.

Pulmonary inflammation is a highly regulated process that involves a complex interaction of leukocytes that arrive via the circulation, and resident leukocytes and pulmonary cells (Figure 14.12). Once in the lung, imported leukocytes communicate with pulmonary and vascular cells through adhesin and other inflammatory molecules such as the complement system (C3a, C3b, C5a), coagulation factors (factors V and VII), arachidonic acid metabolites (interleukins, monokines, chemokines), adhesin molecules, enzymes and enzyme inhibitors (elastase, antitrypsin), oxygen metabolites (O_2, OH, H_2O_2), antioxidants (glutathione), and nitric oxide. These and other molecules can initiate, maintain, and resolve the inflammatory process.

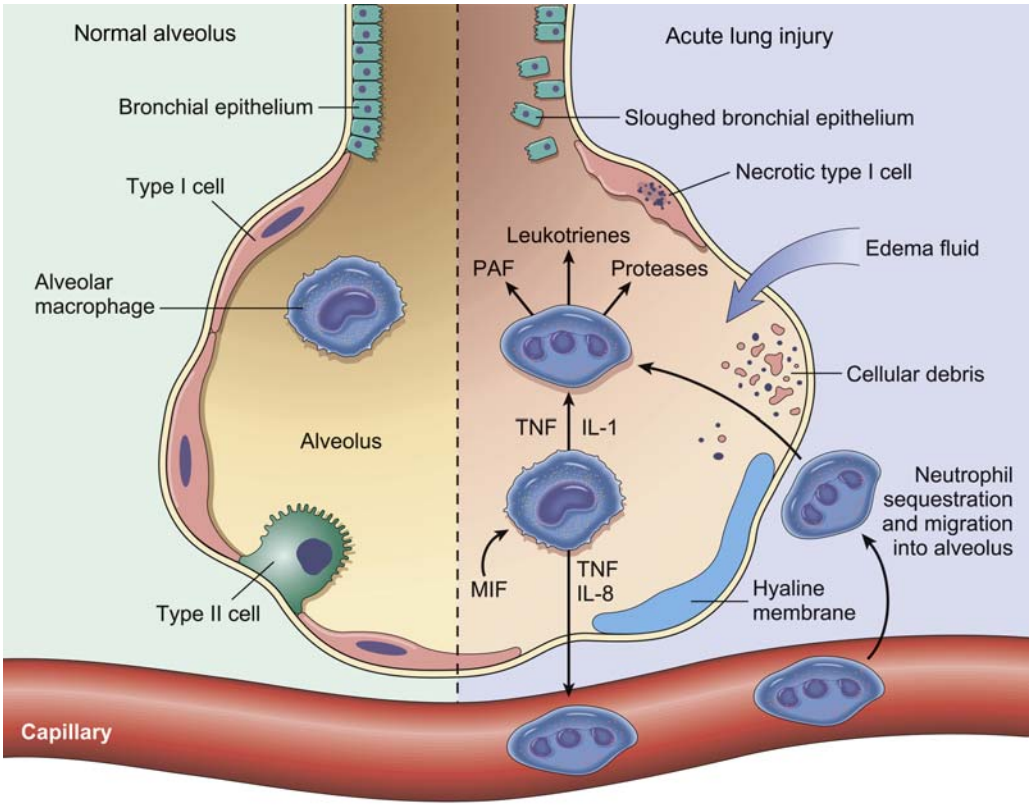

FIGURE 14.12 Normal alveolus (left side) compared with injured alveolus in the early phase of acute lung injury and acute respiratory distress syndrome (ARDS). Proinflammatory cytokines, such as interleukin-8 (IL-8), interleukin-1 (IL-1), and tumor necrosis factor (TNF) (released by macrophages), cause neutrophils to adhere to pulmonary capillaries and extravasate into the alveolar spaces, where they undergo activation. Activated neutrophils release a variety of factors, such as leukotrienes, oxidants, proteases, and platelet activating factor (PAF), which contribute to local tissue damage, accumulation of edema fluid in the airspaces, surfactant inactivation, and hyaline membrane formation. Macrophage migration inhibitory factor (MIF) released into the local milieu sustains the proinflammatory response. Subsequently, the release of macrophage-derived fibrogenic cytokines such as transforming growth factor β (TGF-β) and platelet-derived growth factor (PDGF) stimulate fibroblast growth and collagen deposition associated with the healing phase of injury. *Figure originally modified from Ware and Matthay (2000); reproduced from Hussain (2010). The lung. In:* Robbins and Cotran Pathologic Basis of Disease, *eighth ed. (Kumar, V., Abbas, A. K., Fuasto, N. and Aster, J.C., eds), Elsevier Saunders, Fig. 15-4, p. 682, with permission.*

The pulmonary macrophages are the single most important effector cell and source of cytokines for all stages of pulmonary inflammation. They modulate the recruitment and tracking of circulatory leukocytes in the lung through the secretion of chemokines. Nitric oxide regulates the vascular and bronchial tissue, and modulates the production of cytokines and the recruitment and trafficking of neutrophils in the lung. Uncontrolled production and release of cytokines can result in ARDS, pulmonary fibrosis, and asthma.

INTERSTITIAL PNEUMONIA

Infectious and chemical agents can cause interstitial pneumonia. It may occur following hyperoxia, ingestion of paraquat, administration of chemotherapeutic drugs such as bleomycin and busulfan, and radiation exposure that damages epithelial and/or endothelial cells, or basement membrane. Pulmonary hypersensitivity reactions can also manifest as interstitial pneumonia. Since interstitial pneumonia is a diffuse lesion, it can be difficult to identify on gross examination, especially in smaller animals. Failure to collapse to the extent of a normal lung (best identified prior to removal from the thoracic cavity) and firmness on palpation are the key gross features. In most cases it is impossible to determine the causative agent from the histological changes in the lung. However, in a small percentage of cases, identifying features may be present.

In the acute phase, the capillary endothelial and alveolar epithelial cells are injured, with subsequent flooding of alveoli with serofibrinous exudate. Occasionally, if injury is especially severe, hyaline membranes formed from serum proteins and components of surfactant line the airspaces. They have a hyaline appearance (eosinophilic, homogenous, amorphous) on microscopic examination (Figure 14.11). This is followed by leukocytic infiltration of both alveolar lumina and interstitium. In human medicine, this stage of the disease is frequently referred to as the acute respiratory distress syndrome (ARDS).

Inhalation of manure ("pit") gases such as H_2S and NH_3, inhalation of NO_2 from silos, and ingestion of paraquat can cause similar injury in humans and animals. Resolution of acute injury occurs by proliferation of stem cells to replace damaged endothelium and epithelium, and by resolution of the inflammatory component. This proliferative stage is characterized by type II epithelial cell hyperplasia with thickening of the alveolar wall.

If injury is more severe or consists of multiple episodes or chronic exposure, inflammation persists and normal regeneration is inhibited. The chronic phase is characterized by intraalveolar accumulation of various mononuclear cells (mostly macrophages), proliferation and persistence of increased numbers of alveolar type II cells, and interstitial thickening due to accumulations of lymphoid cells, fibroblast proliferation, and collagen deposition. Examples of toxicants causing chronic interstitial pneumonia include paraquat, some chemotherapeutic drugs like bleomycin, and radiation. Once established, fibrosis is irreversible and frequently progressive. Extensive tissue destruction may also occur, resulting in so-called "honeycomb" lung. Honeycomb lung is the end result of severe chronic interstitial lung disease, with both fibrosis and cicatricial ("scar") emphysema as major components.

Pulmonary Fibrosis

The definition of fibrosis is difficult, but, for all practical purposes, relates to one or more of the following: an increased amount of collagen, an abnormal location of the deposited collagen or an abnormality in the nature of the collagen itself. Morphologically, fibrosis is defined as an increase in observable connective tissue at the microscopic level; special stains may be required to demonstrate its presence. Biochemically, fibrosis is defined as an increased amount of collagen, which can be estimated from the hydroxyproline content of the lung, or differences in relative concentration of the different collagen types. Fibrosis can be distributed diffusely or focally throughout the lungs; this will affect the sensitivity of the biochemical and morphological evaluations. Functionally, there is a reduction in compliance and an impairment of gaseous diffusion.

Fibrotic lung disease in humans is a heterogeneous group of chronic disorders that may be produced by a variety of toxic agents, including inhaled silica, asbestos, and beryllium; ingested paraquat; and chemotherapeutic drugs or thoracic irradiation. Fibrosis may also be produced in infectious and immune-mediated disorders; in many cases, the fibrosis is idiopathic (idiopathic pulmonary fibrosis, IPF). It is possible that IPF is toxic in origin, or the result of interaction between several toxicants or between infectious and toxic agents.

Fibrosis may occur following diffuse alveolar damage, as in interstitial pneumonia, in which case collagen is distributed relatively uniformly throughout the lungs. Collagen is deposited within the interstitium of the alveolar walls and may also be present within the alveolar lumen. Grossly, if the lung is severely affected it will not collapse when the thoracic cavity is opened, and will be paler and firmer than normal. It is difficult to induce severe pulmonary fibrosis in laboratory animal models.

Fibrosis is also a major component of pneumoconiotic diseases such as silicosis and asbestosis. In such cases, collagen is distributed multifocally throughout

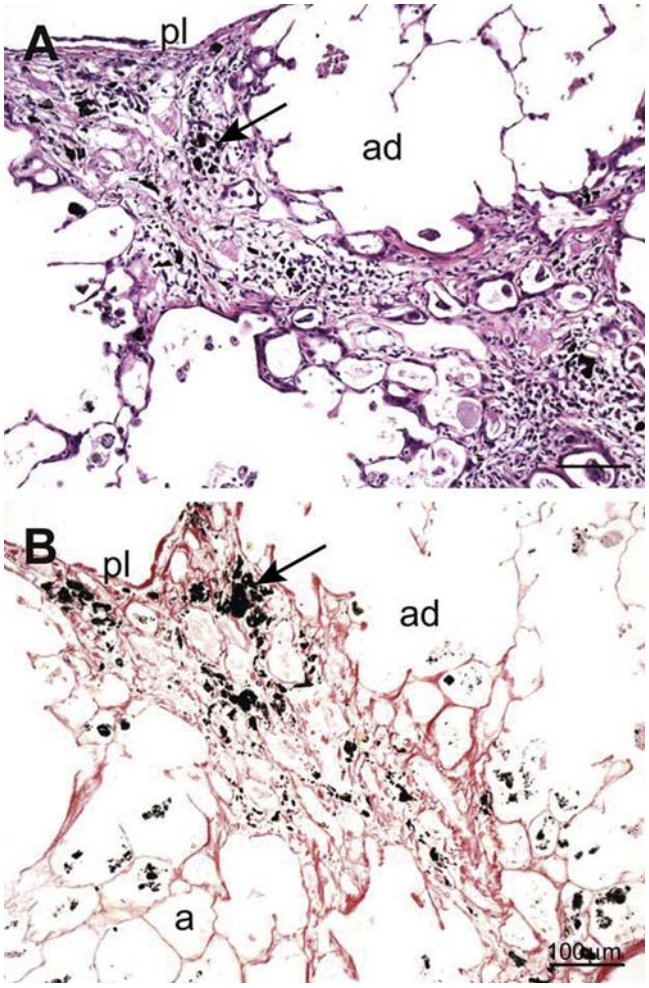

FIGURE 14.13 Light photomicrographs of an area of pulmonary fibrosis in the lungs of a rat subchronically exposed by inhalation to a large concentration of carbon black particles. One section was stained with hematoxylin and eosin (A), and the other was histochemically stained with picrosirius red for collagen (B). The scarred areas have effaced a large area of the alveolar parenchyma and caused enlargement of adjacent air spaces of alveolar ducts (ad). Large and small aggregates of the inhaled particles (arrows) are embedded in the fibrotic tissue. pl, pleural surface of the lung lobe. *Figure reproduced from* Haschek and Rousseaux's Handbook of Toxicologic Pathology *(2013), third ed. (W.M Haschek, C.G. Rousseaux and M.A. Wallig, eds.), Academic Press (Elsevier), Figure 51.22, p. 1985, with permission.*

the lung as a component of the chronic inflammatory response to inhaled particles (Figure 14.13). In the affected human lung, multiple firm nodules, sometimes coalescing, develop in severe cases (Figure 14.14). At autopsy, these may be found on visual examination but may be more evident on palpation. Pigment may be associated with the lesions, such as in coal miners' pneumoconiosis ("black lung"). The presence of silica in dust inhaled by coal miners is the major cause of the pneumoconiosis.

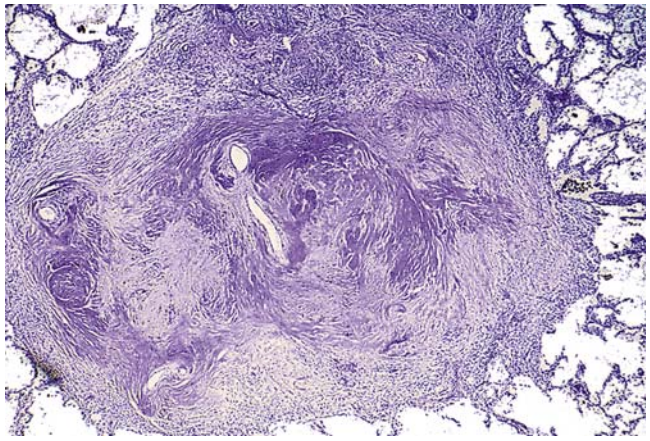

FIGURE 14.14 Several coalescent collagenous silicotic nodules. *Photograph courtesy of Dr. John Godleski, Brigham and Women's Hospital, Boston, MA; reproduced from Hussain (2010). The lung. In:* Robbins and Cotran Pathologic Basis of Disease, *eighth ed. (Kumar, V., Abbas, A. K., Fuasto, N. and Aster, J.C., eds), Elsevier Saunders, Fig. 15-19, p. 682, with permission.*

PATHOGENESIS OF PULMONARY FIBROSIS

The development of fibrosis is a very complex process that has been studied extensively both *in vivo* and *in vitro* in numerous experimental animal models as well as in humans. Pulmonary fibrosis can occur if there is disruption of the normal repair mechanism following interstitial injury. Such interstitial injury can result from one or more of the following: alteration in number, properties, or differentiation of parenchymal cells; inflammatory and immune responses; modification of connective tissue destruction; or acellular expansion of interstitium by edema fluid.

Most forms of fibrosis are biologically complex and can be mediated through effector cells of the inflammatory and immune systems, platelets, the complement cascade, and in situ factors. Interaction of these components is exceedingly complex. The macrophage appears to play a central role, although neutrophils, eosinophils, and mast cells may also be involved. However, both neutrophils and macrophages can stimulate as well as suppress the fibrotic response, and both contain collagenases.

SPECIFIC ETIOLOGIC AGENTS OF PULMONARY FIBROSIS

Experimentally, pulmonary fibrosis has been studied following administration of silica, hyperoxia, radiation, bleomycin, and combinations of agents such as butylated hydroxytoluene (BHT) or bleomycin with oxygen. Ozone, endotoxin, and particulate matter induce parenchymal inflammation that can also be followed by fibrosis. In general, however, rodents are not

considered good models for pulmonary fibrosis in humans.

Fibrosis is also an important component of the pneumoconioses, at least those caused following occupational exposure to mineral dusts such as asbestos, silica, and beryllium. Inhalation of dust containing crystalline-free silica leads to a progressive pulmonary disease characterized by extensive formation of granulomatous lesions and fibrosis throughout the lung parenchyma. Silicosis is mostly an occupational disease found in rock miners, sandblasters, stonecutters, and foundry workers, and generally presents decades after exposure. Silica particles that reach the deep lung are phagocytized by AMs and taken up into phagolysosomes. Contrary to many other dusts, which may remain within the phagolysosomes, silica has the potential to destroy lysosomal membranes, resulting in release of digestive enzymes and chemical mediators. These mediators, and other products of destroyed cells, stimulate the migration of additional macrophages to the lesion and may incite fibroblasts to proliferate and to synthesize increased amounts of collagen. Silica also causes activation and release of mediators by viable macrophages, including IL-1, TNF, fibronectin, lipid mediators, oxygen-derived free radicals, and fibrogenic cytokines. The developing silicotic nodules may eventually undergo hyaline degeneration, enlarge slowly, and coalesce into larger lesions (Figure 14.14). In humans, the disease is often associated with tuberculosis.

Coal worker's pneumoconiosis ("black lung") results from deposition of coal particles in the deep lung. The simple form of the disease (accumulation of pigment with macrophage infiltration) usually does not produce serious symptoms, although the inhaled coal dust may produce chronic bronchitis. The disease usually does not progress once exposure has ceased. Coal miners' pneumoconiosis may become more severe if large amounts of dust are inhaled or if silica is present in the inhaled coal dust. Improved underground mining technology that allows miners to spend more time underground and newer mining methods that are thought to decrease the size of silica particles in dust may be increasing the amounts of coal dust and silica inhaled by miners, resulting in increased severity of disease at exposure concentrations (limits) that were formerly considered protective. Anthracosis, the simple accumulation of carbon pigment without a cellular response, is present in coal miners and urban dwellers.

Inhalation of asbestos fibers in mining, milling, and manufacturing operations is another occupational health hazard that may lead to the development of chronic interstitial lung disease (asbestosis). Initially, inflammation develops at the respiratory bronchiolar–alveolar duct junction, a preferred site for deposition of inhaled asbestos fibers. Eventually, diffuse interstitial fibrosis develops. Deposition of iron on deposited fibers gives rise to asbestos bodies, a marker of asbestos exposure. The more important risk following exposure to asbestos is the development of cancer, either from the bronchial epithelium (bronchogenic carcinoma) or from the pleura (malignant mesothelioma). There is a synergistic interaction between asbestos and cigarette smoking in the development of bronchogenic carcinoma but not of malignant mesothelioma.

Several metals, such as cadmium and beryllium, also may produce interstitial lung disease. Acute beryllium disease is characterized by acute interstitial pneumonia, and is usually associated with accidental exposure to high concentrations of beryllium. Although comparatively rare, it may be rapidly progressive and has been fatal in 10%–15% of cases. Chronic beryllium disease is caused by induction of cell-mediated immunity, and is characterized by multiple granulomas in the pulmonary parenchyma. Modern industrial hygiene methods have been successful in eliminating acute but not chronic beryllium disease. Beryllium is a known human carcinogen, and beryllium compounds are carcinogenic in rats and monkeys after inhalation or intratracheal instillation. Preliminary studies of materials developed for new technologies, such as carbon nanotubes and microspheres, suggest that they may induce granulomatous inflammation and fibrosis.

Pulmonary Emphysema

Pulmonary emphysema is defined as abnormal permanent enlargement of the air spaces distal to the terminal bronchiole, accompanied by destruction of air space walls. Emphysema is one of the causes of COPD (see "Tracheobronchial and Pulmonary Response to Injury" section). There are two main reasons for the airflow obstruction: the destruction of parenchyma decreases the elastic recoil that is normally used for expiration, and the lumena of small airways that have lost the structural support and radial tension imparted by normal parenchyma collapse prematurely during expiration. While pressure–volume curves document decreased elastic recoil and increased compliance, a definitive diagnosis of emphysema requires morphologic assessment.

At autopsy or necropsy, the emphysematous lung is larger than normal and often does not collapse completely when the thoracic cavity is opened. Air space wall destruction is recognized microscopically by an increase in the number and size of fenestrations in the alveolar septa, with the alveolar septa appearing as isolated detached segments in later stages

(Figure 14.15). Fibrosis is not a component of emphysema, but is often present in emphysematous lungs because cigarette smoking, the most common cause of emphysema in humans, also causes bronchiolitis with fibrosis of respiratory bronchioles.

There are two main anatomic types of emphysema, classified according to the distribution of the air space enlargement within the acinus: panacinar emphysema, and centrilobular (sometimes called proximal acinar) emphysema. In panacinar emphysema, the enlargement of airspaces is distributed throughout the acinus and involves the respiratory bronchioles, alveolar ducts, and alveolar sacs. In centrilobular emphysema, the air space enlargement primarily involves the respiratory bronchioles, with lesser involvement of the alveolar ducts and relative sparing of the alveolar sacs. In humans, approximately 95% of the symptomatic cases of emphysema are centrilobular. Another type of emphysema, irregular emphysema, is primarily associated with fibrous scars and is sometimes called cicatricial emphysema (Figure 14.13). Distal acinar emphysema, also called paraseptal emphysema, spares the alveolar ducts. The latter two types, irregular and paraseptal emphysema, are not associated with airflow obstruction.

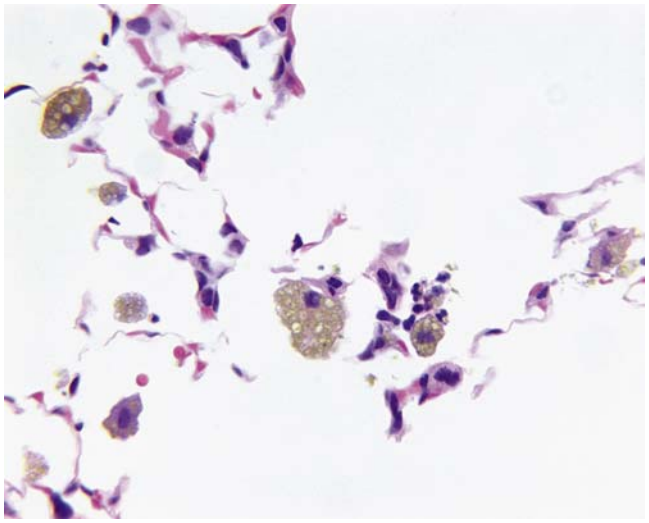

FIGURE 14.15 Alveolar parenchyma from a cigarette smoke-exposed mouse. Pigmented macrophages, inflammation, and septal breaks and fragments, which are features of emphysema, are illustrated. *Photograph courtesy of Dr. Thomas March. Figure reproduced from* Haschek and Rousseaux's Handbook of Toxicologic Pathology *(2013), third ed. (W.M Haschek, C.G. Rousseaux and M.A. Wallig, eds.), Academic Press (Elsevier), Figure 51.24, p. 1987, with permission.*

PATHOGENESIS OF PULMONARY EMPHYSEMA

The pathogenesis of emphysema is summarized by the protease/antiprotease hypothesis, which states that the susceptibility of the lung parenchyma to proteolytic degradation is determined by the relative balance between elastases and other proteases and their inhibitors (Figure 14.16). The principal protease activities are derived from inflammatory cells. The principal antiprotease activity in serum and interstitial tissue is α_1-protease inhibitor (PI), but secretory leukoprotease inhibitor in bronchial mucus and α_1-macroglobulin in serum may also be important to lung protection. Lung destruction occurs when protease activity predominates due to excessive proteases or inhibition of antiproteases. Evidence supporting this theory comes from

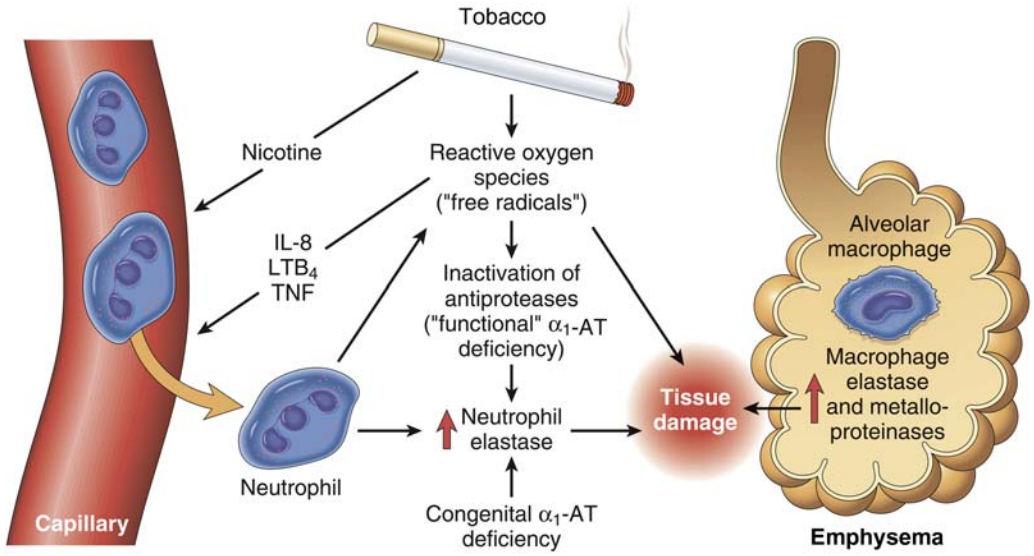

FIGURE 14.16 Pathogenesis of emphysema. Excessive protease activity and reactive oxygen species are additive in their effects and contribute to tissue damage. α_1-antitrypsin (α_1-AT) deficiency can be either congenital or "functional" as a result of oxidative inactivation. See text for details. *IL-8*, interleukin 8; *LTB_4*, leukotriene B_4; *TNF*, tumor necrosis factor. *Figure reproduced from Hussain (2010). The lung. In:* Robbins and Cotran Pathologic Basis of Disease, *eighth ed. (Kumar, V., Abbas, A. K., Fuasto, N. and Aster, J. C., eds), Elsevier Saunders, Fig. 15-8, p. 682, with permission.*

observations of severe emphysema in patients with α_1-PI deficiency and experimental models that use inhaled or intratracheally instilled proteases to induce emphysema or animals with antiprotease deficiencies.

Genetic and environmental factors determine the risk for developing COPD including emphysema. Genetic deficiency of α_1-PI is associated with an increased risk for emphysema. Other genes may also influence risk for COPD. Cigarette smoking is the most important risk factor for developing emphysema. Smokers have increased numbers of neutrophils and macrophages in their lungs, and smoking stimulates release of elastase from neutrophils and enhances elastolytic protease activity in macrophages. There is also decreased antielastase activity in the lungs of smokers. Another risk factor for emphysema is occupational exposure to a dusty environment, such as in underground coal- or gold-mining, or exposure to cadmium oxide fumes.

Pulmonary Neoplasia

LUNG CANCER IN HUMANS

Lung cancer was a rare disease at the turn of the century, but its incidence increased after World War I until, by the end of the 20th century, it had become the leading cause of death from cancer in both men and women. The most important risk factor in lung cancer is smoking cigarettes and exposure to products from other inhaled tobacco or plant products. Tobacco use may be responsible for approximately 85%–90% of all lung cancers. Lung cancer and other tobacco smoke-induced diseases (cardiac disease, pulmonary disease) constitute a public health problem of major proportions.

Lung cancer also is found in nonsmokers. One possible risk factor is exposure to environmental tobacco smoke, a mixture of smoke emanating from the lit end of a cigarette and the smoke exhaled into the surrounding air by active smokers. An additional risk factor is air pollution present in urban areas. Inhalation of common air pollutants, particularly small particles emanating from the combustion of fossil fuels and loaded with carcinogens such as polycyclic aromatic hydrocarbons and nitroarenes, is a risk factor.

In humans, there are four major lung tumor types: squamous cell carcinoma (about 30% of all lung cancers), adenocarcinoma (just over 30%), small cell carcinoma (20%–25%), and large cell carcinoma (poorly differentiated carcinomas that do not have features of the three other types). Lung cancer continues to have a notoriously poor prognosis. Most of the tumors appear to originate from the bronchial epithelium, and are often referred to as "bronchial cancer." In laboratory rodents, intratracheal instillation of polycyclic aromatic hydrocarbons has produced such tumors, while inhalation exposure produces lung tumors located much more peripherally and resembling human bronchioloalveolar tumors rather than bronchogenic carcinoma. With the increasing use of molecular techniques, it has become apparent that many of the peripherally located adenomas and adenocarcinomas in animals might represent useful models for human lung cancer. Small cell lung cancer, comprising 30%–40% of all lung cancers found in smokers, has not been reproducibly induced in experimental animals.

Pleural mesothelioma is associated with exposure to asbestos and other fibrous materials, although it occasionally occurs in individuals without such known exposure. While the association with asbestos exposure is unequivocal, it is less certain to what extent manmade mineral fibers, widely used in insulating materials, constitute a risk factor. Mesotheliomas have a long latency period and are invariably fatal. They can be produced in experimental animals by exposing them to fibers via the inhalation route or by intrapleural or intraperitoneal suspensions of fibers. Fiber physical characteristics like size and shape, more so than chemical composition, are important determinants of carcinogenicity.

LUNG CANCER IN ANIMALS

Spontaneous lung cancers in animals are rare, although certain mouse strains (A/J strain) may have a comparatively high lung tumor rate. An international project (INHAND) to develop standardized diagnostic criteria and nomenclature for lesions in rats and mice has proposed the following classification for lung neoplasms in mice and rats: broncho-alveolar adenoma, carcinoma [bronchoalveolar, acinar (mice only), adenosquamous, squamous cell] and epithelioma (rat only; cystic, keratinizing, and nonkeratinizing). Most lung tumors found in rodents are found peripherally, originating from the lung parenchyma, including bronchioles. This seems to differentiate lung tumors in rodents from human lung cancer. A second difference is metastasis. Human lung cancer frequently metastasizes to organs such as liver, bone, and brain. In contrast, distant metastasis is much less frequent for rodent lung cancers, although they are able to invade adjacent tissues, lymphatics, and blood vessels. Two rodent lung tumors are described in more detail below because of their particular significance in toxicology.

LUNG TUMORS IN MICE

The most common spontaneous lung tumor found in mice originates in the peripheral lung from either the type II alveolar epithelial cells or the bronchiolar club (Clara) cells. A/J mice or Swiss-Webster mice have a very high spontaneous incidence with exposure to carcinogens greatly increasing the number of lung tumors per animal, whereas other strains, such as

C57BL, are very resistant and rarely develop lung tumors. B6C3F1 and CD1 mice, two strains commonly used in carcinogenicity studies, have a fairly high spontaneous incidence of broncho-alveolar adenomas and carcinomas. In both strains, adenomas are more common than carcinomas, and the incidence of neoplasms is higher in male than female mice.

These lung tumors are now accepted to represent a valid model of human adenocarcinoma. Many gene mutations found in human lung adenocarcinoma, particularly in the ras family of oncogenes, also occur with very high frequency in mouse lung tumors. Alterations in signal transduction pathways and other biochemical parameters in human and mouse tumors are also similar. Thus, lung tumors in mice allow the study of the carcinogenic process from hyperplasia to adenoma to carcinoma in situ—stages practically inaccessible in man (Figure 14.17).

TUMORS IN RAT LUNG EXPOSED TO HIGH CONCENTRATIONS OF PARTICULATE MATTER

Rats exposed by inhalation to high concentrations of diesel exhaust, oil shale dust, talc, titanium dioxide, or carbon black develop adenomas, adenocarcinomas, squamous cell carcinomas, or adenosquamous carcinomas in the peripheral lung (Figure 14.18). In addition, lesions labeled as keratin cysts, cystic epithelioma, or benign keratinizing squamous cell tumor originate from foci of alveolar metaplasia. The tumors consist of whorled keratin masses surrounded by well-differentiated layers of stratified SE. They often arise adjacent to fibrotic foci, and a large bronchiole with

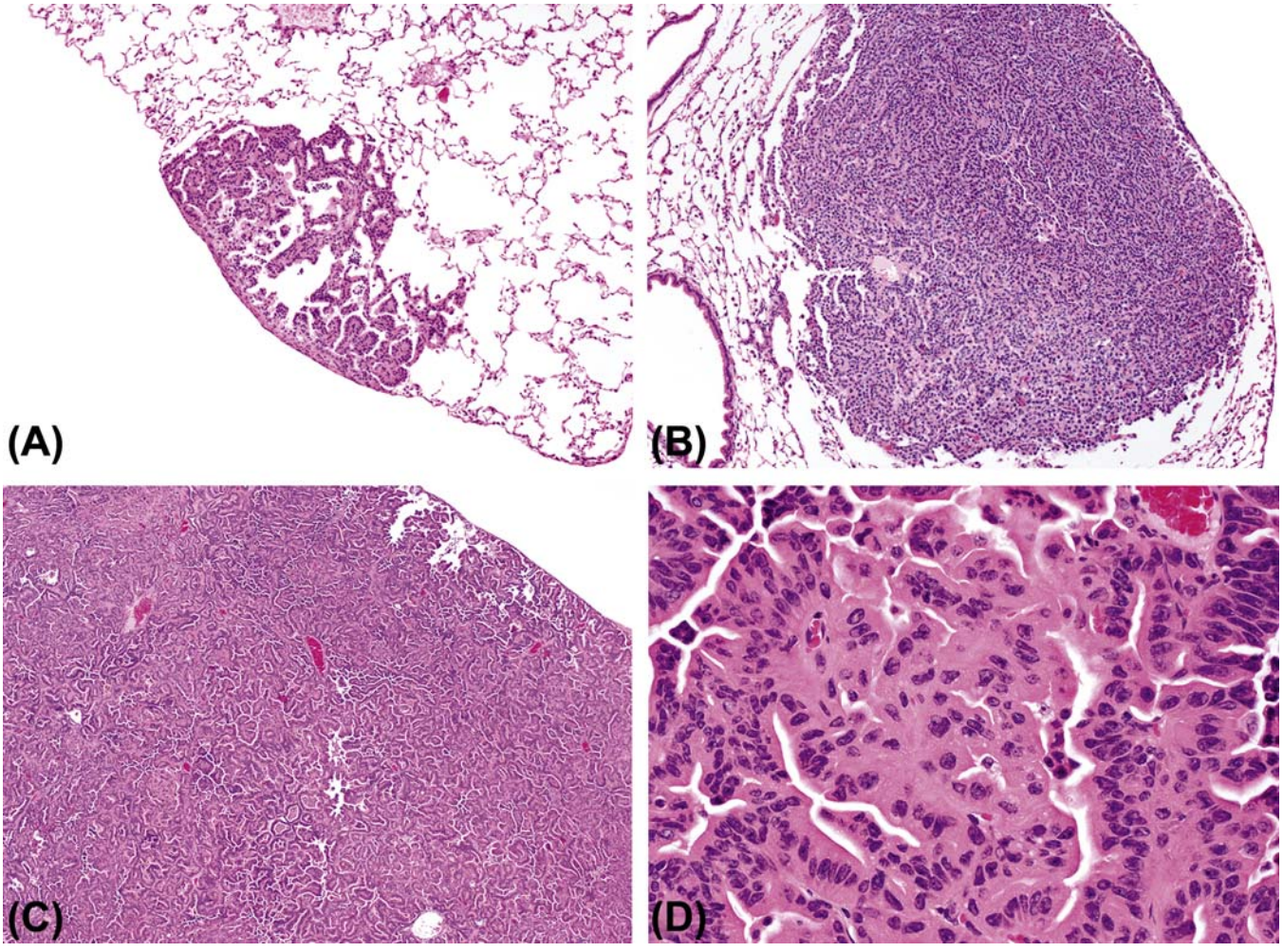

FIGURE 14.17 Light photomicrographs of hyperplastic and neoplastic lesions in mice exposed to cigarette smoke. Focal bronchiolar–alveolar hyperplasia, which forms a wedge shape but does not obscure the alveolar architecture (A). Bronchiolo-alveolar adenoma showing typical features including small size, high cell density that obscures the alveolar architecture, sharp demarcation from the surrounding lung, and convex border (B). Bronchiolo-alveolar carcinoma illustrating typical large size and architectural distortion (C). Higher magnification of the carcinoma showing nuclear atypia and lack of polarity (D). H&E stain. *Photographs courtesy of Dr. Julie Hutt. Figure reproduced from* Haschek and Rousseaux's Handbook of Toxicologic Pathology *(2013), third ed. (W.M Haschek, C.G. Rousseaux and M.A. Wallig, eds.), Academic Press (Elsevier), Figure 51.26, p. 1990, with permission.*

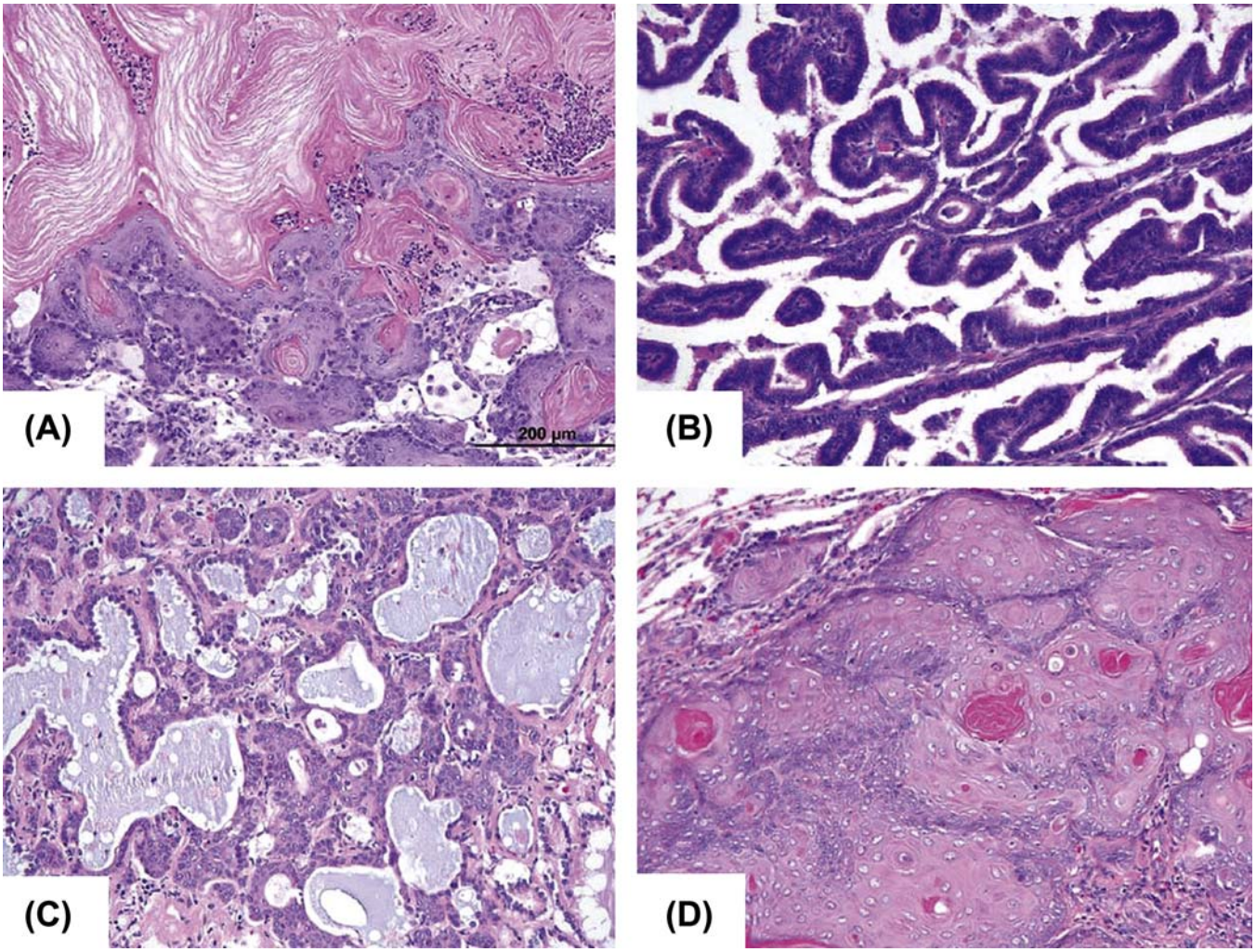

FIGURE 14.18 Light photomicrographs of a cystic keratizing epithelioma (A), bronchioloalveolar carcinoma (B), adenosquamous carcinoma (C), and squamous cell carcinoma (D) in the lungs of rats; H&E stain. *Figure reproduced from Renne et al. (2009) Proliferative and nonproliferative lesions of the rat and mouse respiratory tract*, Toxicol. Pathol. *37, 5S–73S (Figures 113, 115, 117, and 118), with permission.*

hyperplastic epithelium often opens into the lesion. These tumors only develop when the macrophage-mediated clearance mechanism of the lung is overwhelmed and there is excessive retention of particles in the alveoli ("particle overload"). Excess particulate matter may lead to secondary inflammatory and proliferative lesions, eventually leading to tumors by nongenotoxic mechanisms.

LUNG TUMORS IN DOGS

Dogs have been used fairly widely in inhalation studies due to their convenient size, cooperative temperament, and similarity to the human in respect to bronchiolar structure and pulmonary deposition of inhaled aerosols. Pulmonary tumors of dogs are also of interest since dogs, as companion animals, are exposed to a similar environment to humans. Bronchioloalveolar carcinomas are the most prevalent type of pulmonary neoplasm. Unlike in humans, bronchogenic carcinomas and anaplastic small and large cell carcinomas are infrequent. K-ras mutations (GGT to GGA transitions at codon 12) have been detected both in spontaneously occurring and in $^{239}PuO_2$-induced malignant canine lung tumors.

MECHANISMS OF TOXICITY

Toxic lung damage is an exceedingly complicated series of interdependent events. Primary lung injury may be initiated by mechanisms such as osmotic or cytolytic membrane injury, oxidative damage to cell constituents mediated through the formation of reactive oxygen species, or metabolism of foreign chemicals to reactive intermediates that are potentially able to interact with intracellular targets (Table 14.4).

Primary lung injury is often amplified through secondary events such as formation and release of

TABLE 14.4 Mechanisms of Toxicity to the Respiratory System with Selected Examples

Mechanism	Xenobiotic
Direct toxicity	Oxygen, ozone, phosgene, hydrochloric acid, other fumes and gases
Metabolic activation	
In situ metabolic activation	Acetaminophen, bromobenzene, butylated hydroxytoluene (BHT), carbon tetrachloride, 4-ipomeanol, 3-methylfuran, naphthalene
Activation outside the lung	Pyrrolizidine alkaloids (e.g., monocrotaline)
Cyclic reduction/oxidation with production of reactive oxygen species	Paraquat, nitrofurantoin
Immune-mediated	
Hypersensitivity reaction:	
Type I hypersensitivity	Toluene, diisocyanates, trimellitic anhydride, ozone
Type II hypersensitivity	Trimellitic anhydride, mercury, organic dusts, beryllium
Immune suppression	Oxidant gases, asbestos, tobacco smoke, benzene, toluene, cadmium, zinc, lead
Nonimmune secretion of inflammatory mediators can cause hyperreactive airway syndrome	Isocyanates, formaldehyde, trimellitic anhydride, ozone
Xenobiotic interactions through simultaneous or sequential exposure	Oxygen enhances toxicity of paraquat, bleomycin, butylated hydroxytoluene (BHT), $CdCl_2$

Table reproduced from Handbook of Toxicologic Pathology, *second ed. W. M. Haschek, C. G. Rousseaux and M. A. Wallig, eds. (2002) Academic Press, Vol. 2, Table V, p. 29, with permission.*

mediators (e.g., vasoactive amines and leukotrienes), activation of the kinin and complement cascades, release of lysosomal enzymes, release of cytokines, and activation of inflammatory cells. Activation of phagocytes results in release of reactive oxygen species, which contributes to an imbalance of the oxidant/antioxidant defenses and further amplifies the cascade, leading to injury. M_1 macrophages, which are activated by interferon-γ, are key players in promoting inflammation, with important functions such as phagocytosis, antigen presentation, and production of T-helper cytokines. In contrast, M_2 (alternatively activated) macrophages, which are activated by stimuli such as IL-4 and IL-13, may have an antiinflammatory role or play a major role in chronic airway diseases, including COPD and asthma. Toxicity may also be directly related to the physicochemical properties of inhaled agents or their ability to induce immune-mediated responses.

Direct Toxicity

Many agents produce respiratory injury by a direct interaction of the reactive molecule with its respiratory tract target. Examples include oxidant and irritant gases such as oxygen, ozone, chlorine, phosgene, ammonia, hydrochloric acid, and many other fumes and gases. These gases and many acidic or alkaline irritants may produce cytolytic changes directly at their site of primary interaction, the exposed cell membrane, or increase the generation and accumulation of reactive oxygen species and thus trigger cell injury. (See "Patterns of Respiratory Tract Injury to Inhaled Toxicants" section for a discussion of gradients of injury due to inhaled toxicants.)

Injury mediated by reactive oxygen species appears to be an important mechanism in toxic respiratory damage for oxygen, ionizing radiation, and bleomycin. Ozone is so highly reactive that it likely produces aldehydes and hydroxyperoxides through ozonolysis of substances in the airway and lung lining fluid, as well as reactive oxygen species from free radical reactions. It is these reaction products that damage cells.

As a consequence of either direct or indirect cell injury, inflammatory cells, particularly macrophages and polymorphonuclear leukocytes, may be recruited into the lung parenchyma. Upon appropriate stimulation, these cells can undergo activation and produce a burst of reactive oxygen species, especially hydrogen peroxide, which in turn may also damage respiratory cells (Figure 14.12). Platelet aggregates localized to sites of pulmonary microvascular injury may also generate reactive oxygen species.

Common consequences of exposure to toxicants that directly damage the upper respiratory tract are damage to ciliated cells, inflammation, and mucus cell hypertrophy or hyperplasia. Inhaled direct toxicants that reach the alveolar region at high concentrations may induce acute or delayed pulmonary edema due to necrosis of type I epithelial cells or endothelial cells. Following inhalation of phosgene, hydrochloric acid,

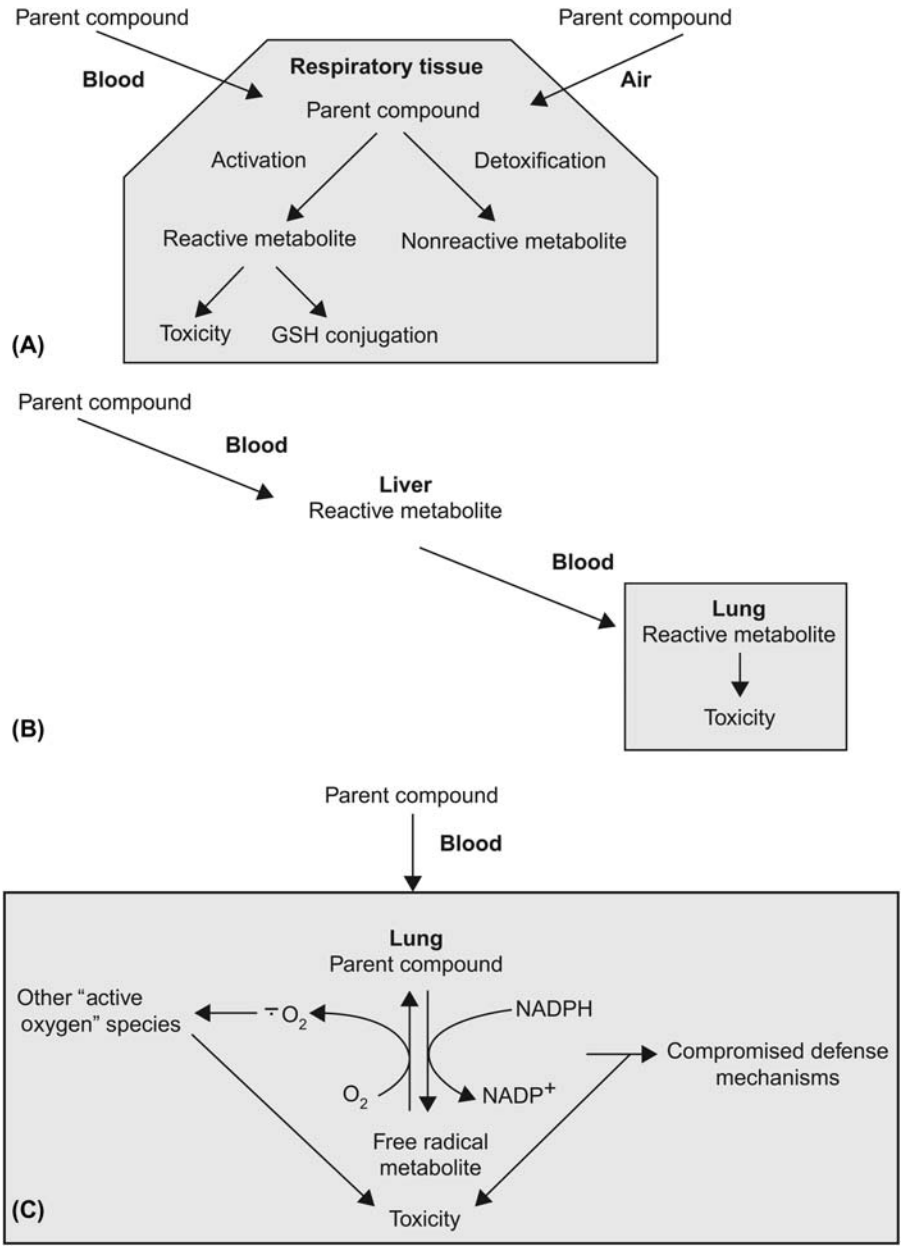

FIGURE 14.19 Mechanisms of respiratory injury involving metabolic activation. (A) In situ metabolic activation of parent compound. (B) Activation of parent compound in liver; metabolite produces toxicity in lung. (C) Parent compound undergoes cyclic reduction/oxidation, indirectly inducing toxicity. *Figure reproduced from* Handbook of Toxicologic Pathology, *second ed. W. M. Haschek, C. G. Rousseaux and M. A. Wallig, eds. (2002) Academic Press, Vol. 2, Fig. 11, p. 31, with permission.*

ammonia, or smoke, a latent period of several hours may occur prior to the appearance of lung damage. Fatal pulmonary edema may then develop, even in the absence of further exposure to the offending agent.

Metabolic Activation

A great deal of information is now available describing the role of metabolic activation of xenobiotics in respiratory toxicity (see "Cell-Specific Injury" section). Three different mechanisms may be involved. In the first scenario, the parent compound itself reaches the respiratory tract, either through the blood following systemic administration or as an inhalant. The compound then undergoes metabolic activation to the proximate toxicant (Figure 14.19).

Interaction with the target is often manifested as covalent binding of the reactive metabolite to cell macromolecules. Activation by microsomal mixed-function

oxidases, especially the cytochromes P450 enzymes, is a key element in the process; on the other hand, protective systems such as intracellular levels of glutathione (GSH) and enzymes involved in maintaining reducing equivalents within the cell are crucial components in protection. Cell types that contain high concentrations of cytochrome P450s are particularly important in the detoxification of xenobiotics; however, these cells are vulnerable to injury caused by the reactive metabolites they form. Examples of chemicals that cause respiratory damage following in situ metabolic activation include phenacetin, bromobenzene, 4-ipomeanol, BHT, CCl_4, 3-methylindole, acetaminophen, and 3-methylfuran (Tables 14.2 and 14.4). 3-Methylindole (3MI) is formed in ruminants by bacterial degradation of tryptophan in the rumen, and is also present in cigarette smoke and in the human intestinal tract. 3MI is absorbed into the circulation, taken up by the lung, and metabolized by the cytochromes P450 enzymes, resulting in toxicity. In cattle, severe damage to alveolar cells results in an acute interstitial pneumonia, which is identical to that caused by the ingestion of moldy sweet potatoes containing 4-ipomeanol. In mice, both 3MI and 4-ipomeanol cause club cell necrosis; 3MI also causes necrosis of OE.

The second mechanism involves uptake of a systemically administered foreign compound by the liver, or any other organ, where the agent is metabolized to a highly reactive and toxic metabolite(s) (Figure 14.19B). This metabolite(s) may cause liver injury, but also may escape into the circulation via the hepatic veins and caudal (inferior) vena cava. The next capillary bed encountered is in the lung, and widespread damage may occur. The best studied examples of chemicals causing this form of lung damage are the pyrrolizidine alkaloids.

The pyrrolizidine alkaloid monocrotaline (MCT) is found in the plant *Crotalaria spectabilis*. Human toxicity has occurred from consuming contaminated grain or herbal teas made from such plants, whereas animal toxicity can occur following grazing on such plants. At high doses, MCT rapidly causes severe liver injury and death. At lower doses, it produces mild liver injury and delayed pulmonary injury characterized by pulmonary hypertension. MCT is bioactivated in the liver to pyrrolic metabolites by the cytochromes P450 enzyme system. The "putative" reactive metabolite dehydromonocrotaline (MCTP) is toxic to both liver and lung. It is stable enough to reach the lung, which is itself incapable of the bioactivation of MCT. The target cell in the lung is the endothelial cell. Injury is delayed and progressive, both *in vivo* and *in vitro*. The first phase is characterized by vessel leakage; the later hypertensive phase is characterized by vessel smooth muscle hypertrophy and perivascular fibrosis, elevated vascular pressure, and hypertrophy of the right heart. *In vitro*, MCTP results in delayed and progressive injury to endothelial cells and a decrease in their proliferative capability. It has thus been suggested that *in vivo*, MCTP, in addition to causing endothelial cell injury, also prevents normal repair processes which allows progressive injury to take place.

The third mechanism involves what has been called "futile redox cycling" (Figure 14.19C). It is best exemplified by the pulmonary toxicity of the herbicide paraquat. Paraquat is selectively taken up by alveolar epithelial cells via an energy-dependent transport system. It is not metabolized but undergoes cyclic oxidation and reduction with concomitant production of reactive oxygen species such as superoxide anion, hydrogen peroxide, and hydroxyl free radicals. Direct evidence for the formation of lipid peroxides in paraquat toxicity remains more elusive. This is partly due to the pulmonary antioxidant defense mechanisms, including vitamins C and E, which make it difficult to obtain reliable measurements of peroxidative processes. A second event in paraquat toxicity is excessive oxidation, glutathione oxidation, and eventual depletion of cellular reducing equivalents, particularly of NADPH. The extent to which this mechanism contributes to the development of toxic lung damage is unknown. Acute pulmonary edema may occur within a few hours of ingestion of paraquat, and pulmonary fibrosis and death typically occurs 1–3 weeks after ingestion of lethal amounts of paraquat.

Immune-Mediated Toxicity

Both physical and immunological mechanisms are important in pulmonary defense against chemical and infectious agents. However, the immune response may result in an adverse effect if hypersensitivity reactions, immune suppression, or nonimmunological enzymatic injury occur (Table 14.4). Hypersensitivity diseases or allergies are the most common types of immune-mediated respiratory disease caused by inhaled agents. The four types of hypersensitivity reaction are discussed in Chapter 12, Immune System. Type I (anaphylactic), Type II (cytotoxic), and Type III (Arthus type) are antibody-mediated reactions, whereas Type IV (delayed hypersensitivity) is a cell-mediated reaction.

The most common types of hypersensitivity reaction documented in the respiratory tract are Types I and III. Exposure to pulmonary sensitizers, either foreign proteins or simple chemicals that act as haptens, at sufficiently high concentrations induces the formation of specific antibodies. Type I hypersensitivity is primarily manifested as rhinitis (inflammation of the nasal mucosa) or asthma (bronchoconstriction and airway inflammation; see *Asthma* section below), although

life-threatening bronchospasm and edema can occur in severe anaphylaxis. Initial exposure to the allergen or sensitizer induces production of IgE antibodies, which bind to mast cells and basophils. Subsequent exposure to the allergen cross links the cell-bound IgE and triggers mast cell degranulation with release of vasoactive amines and other mediators (Figure 14.8). Platelet activation factor causes platelet aggregation and release of histamine, heparin, and vasoactive amines, thus further amplifying the response. Eosinophils and neutrophils, attracted by eosinophil chemotactic factor of anaphylaxis and neutrophil chemotactic factors, release hydrolytic enzymes that cause tissue necrosis. Chemicals that produce a Type I reaction include toluene diisocyanates, trimellitic anhydride, and platinum salts. However, the Type I reactions due to small chemical molecules may be mediated by CD8+ T cells, IL-5 secretion, and eosinophils through an IgE-independent mechanism. Numerous pharmaceutical agents have been implicated in Type I reactions, but β-lactam antibiotics and sulfa-containing drugs are the most common causes of drug-induced Type I reactions. Penicillin is thought to cause approximately 75% of fatal anaphylactic reactions in the United States.

Type III hypersensitivity manifests as hypersensitivity pneumonitis, also called "extrinsic allergic alveolitis," and results from deposition of antigen–antibody complexes plus complement in the lungs, which in turn causes inflammation. Chemicals that produce Type III hypersensitivity include trimellitic anhydride and mercury. Organic dusts containing spores of thermophilic bacteria, true fungi, or animal proteins are the most common cause of hypersensitivity pneumonitis in people. Examples such as farmer's lung, humidifier lung, mushroom picker's lung, and pigeon breeder's lung are named for the settings in which the antigens are encountered. The initial alveolitis may progress to chronic fibrotic lung disease with granulomas. Type IV hypersensitivity is likely involved, along with the Type III response, in the formation of granulomas. Type IV hypersensitivity occurs when sensitized T lymphocytes induce a cell-mediated response after a latent period. An example of a primary Type IV response is the granulomatous reaction induced by beryllium in dogs and people. In rats, however, the granulomas induced by beryllium are considered foreign-body type granulomas, and beryllium-specific T cells are not found.

Immune suppression due to inhaled air pollutants has been documented in humans through epidemiological studies and in experimental animals, primarily through bacterial infectivity models, for agents that include oxidant gases such as ozone, nitrogen dioxide, and sulfur dioxide (see Chapter 12: Immune System), tobacco smoke, benzene, toluene, and metals such as arsenic, cadmium, nickel, zinc, and lead. Effects on the physical and innate (nonspecific) lung defense mechanisms frequently cannot be separated in these studies, but various studies have demonstrated adverse effects on the mucociliary apparatus, pulmonary surfactant, and macrophage function. As an underlying potential mechanism for immune suppression, decreased macrophage function, including phagocytosis and antigen presentation, has been the most commonly studied and documented suppressive effect on the immune system of experimental animals exposed to oxidant gases, aerosols, and particulate air pollutants. Effects on the adaptive immune system have been documented less frequently, but immunosuppression in experimental animals exposed to dioxin has resulted in decreased cell-mediated immune responses and depressed antibody production in response to T-dependent antigens.

Toxicity and Responses to Inhaled Particles

Pulmonary toxicity and responses to inhaled particles are influenced by the dose of material, size and surface area of the particles, chemical composition of the particles, and the dynamics of their deposition, retention, and clearance in the lung. For inhaled drugs in particle form, pharmacologic mechanisms may modulate the expression of toxicity. Responses to inhaled particles may include adaptive, nonadverse physiological responses or inflammatory and immune-mediated responses, cell injury, and repair. For particulate chemicals, metabolism also affects toxicity. Highly soluble particles leave the lung rapidly, and the dose is delivered in a pattern that is similar to inhaled gases. In contrast, poorly soluble particles persist in the lung after cessation of exposure, thus delivering a protracted dose to the lung. Historically, crystalline silica (quartz) and coal dust have been the most important inhaled, nonfibrous particles causing occupational lung disease (see the above section on pulmonary fibrosis).

After a single inhalation exposure to particles, the amount of particulate material in the lung decreases with time due to dissolution and/or mechanical clearance. Dissolution is the major route of clearance of soluble particles. Phagocytosis by macrophages and clearance via the mucociliary escalator or lymphatics is a major mechanism for removal of poorly soluble particles, other than nanomaterials, from the lung. However, this mechanism may be abrogated by highly toxic particles. Silica particles, for example, are toxic to macrophages and, as part of the cytotoxic response, macrophages release cytokines that stimulate fibroblasts to replicate and synthesize collagen. In addition, silica also causes activation and release of mediators

by viable macrophages, including IL-1, TNF, fibronectin, lipid mediators, oxygen-derived free radicals, and fibrogenic cytokines. The macrophage cytotoxicity and ensuing inflammatory and fibrotic responses retard particle clearance.

Depending on the physicochemical properties of the particle, concentration, duration of exposure, and species exposed, nonneoplastic parenchymal responses to particles may include infiltrates of AMs, alveolar epithelial hyperplasia (Figure 14.20), inflammation, bronchiolization, proteinosis, and fibrosis (Figure 14.13). After cessation of exposure, lesions may regress, persist, or progress.

Numerous studies in rats using inert, insoluble, fine particles, particularly titanium dioxide and carbon black, have led to a consensus that, for these nonfibrous particles, the quantity of material in the lung is the key determinant of the lung pathology. Furthermore, evaluation of data across multiple studies indicates that a lung burden of approximately 0.1 mg/g lung is required for findings to be detectable in histologic sections by light microscopy. When that burden is achieved in rats, increased numbers of AMs are observed. Chronic and reversibility studies have shown that with exposures resulting in lung burdens of these relatively "inert" particles below approximately 1 mg/g lung, the adaptive increase in AMs does not progress to more complicated lesions and is reversible. When lung burdens exceed approximately 1 mg/g lung, inflammation, epithelial hyperplasia, and fibrosis are observed, and these findings may persist or progress after cessation of exposure. Very large lung burdens, approximately 50–100 mg/g lung, result in "lung overload" in which macrophage-mediated clearance is reduced and lung lesions typically progress after cessation of exposure.

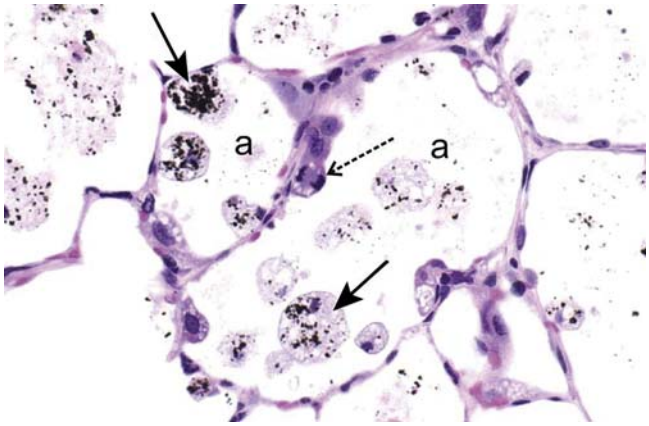

FIGURE 14.20 Light photomicrograph of the alveolar parenchyma from a rat that received a 90-day inhalation exposure to a large airborne concentration of carbon black particles. Numerous enlarged, particle-laden alveolar macrophages (solid arrows) are present in the alveolar airspaces (a). Type 2 epithelial cell hyperplasia is present along the alveolar septa with a mitotic figure (stippled arrow) in one of these epithelial cells, indicating cell proliferation. H&E stain. *Figure reproduced from* Haschek and Rousseaux's Handbook of Toxicologic Pathology *(2013), third ed. (W.M Haschek, C. G. Rousseaux and M.A. Wallig, eds.), Academic Press (Elsevier), Figure 51.29, p. 1997, with permission.*

There are a number of nongenotoxic, poorly soluble particles, such as titanium dioxide, talc, and carbon black, that induce lesions in rats that are exposed under conditions resulting in overload of macrophage-mediated clearance. Chronic inhalation of these poorly soluble particles by rats can result in pulmonary inflammation, fibrosis, alveolar epithelial hyperplasia, bronchiolization, squamous metaplasia, and squamous cysts. Neoplastic lesions that occur late in life (usually between 24 and 32 months of age) include squamous epitheliomas, bronchiolar–alveolar adenomas, squamous cell carcinomas, and bronchiolar–alveolar adenocarcinomas. In contrast to rats, mice and hamsters develop less severe lesions and do not develop lung tumors even with particle lung burdens that are similar to that produced in the rat. These findings have raised questions concerning the appropriate use of data from rats, exposed under conditions resulting in clearance overload, for hazard identification in humans.

The preceding discussion of particle toxicity applies to particles greater than 100 nm in size. Particles with at least one dimension in the nanoscale (less than 100 nm) are referred to as nanomaterials if they are engineered, man-made materials, and as ultrafine particles if they are air pollutants. The majority of ultrafine particles are produced by incomplete fuel combustion in engines and industrial furnaces; however, natural sources include volcanic activity and sand storms. Concern for the potential toxicity of nanoparticles initially came from epidemiological data showing a relationship between exposure to ultrafine particulate air pollution and increased cardiovascular and respiratory morbidity and mortality in sensitive populations. Subsequent studies in animals using air pollution condensates, as well as a number of *in vivo* and *in vitro* studies using manufactured nanoparticles, have helped describe potential mechanisms of nanoparticle-related toxicity.

Inhalation is the major route of entry into the body for nanoparticles. Nanoparticles have a high surface area per unit mass and thus have a large catalytic surface for formation of free radicals that drive oxidative stress. This capacity is especially important for nanoparticles with bound transition metals and metal-based nanoparticles (such as silver and cadmium nanoparticles), which can be highly toxic. Additionally, the large surface per unit mass of nanoparticles may lead to adsorption of organic toxicants in air pollution and

increase their interaction with cells. Soluble metals and aromatic hydrocarbons on the surface of nanoparticles may interact with lung lining fluid and undergo cyclic redox reactions that produce reactive oxygen species. Inhaled nanoparticles may agglomerate in the lung lining fluid or become coated by opsonins. Agglomerated or opsonized nanoparticles are phagocytosed by macrophages, and may induce oxidative stress and inflammatory processes similar to those induced by other respirable particles. Nanoparticles that are not phagocytosed by AMs efficiently enter lung epithelial cells and fibroblasts in the interstitium as well as cross the alveolar–capillary barrier to enter the circulation, whereby they are distributed to other organs. Nanoparticles deposited on the olfactory mucosa may translocate to the brain through sensory nerves and the olfactory bulb. When nanoparticles gain entrance to cells, they may induce oxidative stress and cause protein, DNA, and membrane injury as well as activate inflammatory and growth factor cascades and the oxidant-induced transcription factor nuclear factor-κB; these processes potentially may lead to inflammation and fibrosis. Inflammation and oxidative stress in the lung indirectly promote atherothrombosis and atherosclerosis through effects on the endothelium, cardiac blood flow, platelet activation, and coagulation. An area of active research is in understanding the risk for nanoparticle-induced genotoxicity and carcinogenesis.

Toxicity and Responses to Inhaled Fibers

Fibers are a special type of particle defined as having a length to diameter ratio greater than 3:1. The fibers of toxicological concern are asbestos (chrysotile, crocidolite, anthophyllite, amosite, actinolite, and tremolite), synthetic vitreous fibers (SVF; glasses and ceramics in fibrous form), and, more recently, nanotubes. Epidemiological studies in humans and experimental studies in animals using asbestos and SVF have led to general agreement that four interrelated factors—dose, particle dimensions, surface properties, and biopersistence—largely determine the toxicity of inhaled fibers. Iron ions on amphibole types of asbestos react with epithelial lining fluid in the lung and generate reactive oxygen species that induce toxicity, and oxidant stress may lead to DNA damage. There is a direct relationship between biopersistence, which is determined by fiber length and chemical composition, and toxicity. Longer, thinner fibers are more toxic because they are not cleared by AMs and therefore persist in the lung. Fibers longer than approximately 15 μm are particularly toxic and bioactive. They are not completely engulfed by macrophages, leading to release of lysosomal contents, cytotoxicity, oxidant stress, and stimulation of inflammatory and growth factor pathways.

Inhaled asbestos causes asbestosis, which is a fatal interstitial fibrosis, lung cancer, and pleural disease consisting of pleural fibrosis, plaques, and mesothelioma. Fibers must be thinner than 0.5 μm to translocate to the pleural surface. Inhaled asbestos and erionite, which is a nonasbestos, long fiber, are the only known causes of mesothelioma in humans.

Nanofibers are a diverse group of materials. Their potential for toxicity will likely be determined by dimensions, surface properties, bioreactivity, and biopersistence. Carbon nanotubes are among the most commonly manufactured nanomaterials. Inhaled carbon nanotubes have been shown to penetrate AMs, the alveolar wall, and the pleura in mouse studies. They induce an inflammatory response, oxidant stress, granulomatous pneumonia, and interstitial fibrosis. *In vitro* experiments have shown that carbon nanotubes can induce mitotic disruption. The toxicology of nanomaterials is a relatively new field, and further studies are needed to develop screening strategies to evaluate potential hazards and set safe exposure limits.

Xenobiotic Interactions

Toxicological interactions may play a role in the pathogenesis of lung injury. Simultaneous exposure to a blood-borne pulmonary toxicant and to an inhalant may also greatly enhance the development of untoward effects in the lung. Well-known examples are enhancement of paraquat, bleomycin, or BHT toxicity by oxygen species. In humans with diffuse alveolar damage (e.g., in ARDS), oxygen therapy, although necessary, may enhance the later development of fibrotic changes. Finally, the risk for lung cancer in uranium miners or asbestos workers is greatly increased by cigarette smoking.

SUMMARY

The respiratory tract is a complex organ system both macroscopically and microscopically, with many different functions and cell types localized throughout the nasopharyngeal, tracheobronchial, and pulmonary segments. Exposure to xenobiotics occurs via inhalation and via the blood following ingestion, dermal exposure, or parenteral administration. Xenobiotics vary from particles of variable size to gases to plant toxins, so dosimetry and site of injury are critical in interpreting the response to injury. In addition, species differences in respiratory tract anatomy and physiology must be considered

in interpretation of data to be used in risk assessment. In naturally occurring disease, because the pulmonary response to injury is often nonspecific, it is important to consider the gross distribution of pulmonary lesions and to use detailed history and ancillary test results in conjunction with histological evaluation to determine potential etiologic agents.

Acknowledgment

We acknowledge the contributions of Dr. Hanspeter Witschi, coauthor of the chapter on respiratory tract toxicology in earlier editions of the *Handbook of Toxicologic Pathology*.

Further Reading

Beers, M.F., Morrisey, E.E., 2011. The three R's of lung health and disease: repair, remodeling, and regeneration. J. Clin. Invest. 121, 2065–2073.

Byers, D.E., Holtzman, M.J., 2011. Alternatively activated macrophages and airway disease. Chest. 140, 768–774.

Dixon, D., Herbert, R.A., Sills, R.C., Boorman, G.A., 1999. Lungs, pleura, and mediastinum. In: Maronpot, R.R. (Ed.), Pathology of the Mouse. Cache River Press, Saint Louis, MO, pp. 293–332.

Dixon, D., Herbert, R.A., Kissling, G.E., Brix, A.E., Miller, R.A., Maronpot, R.R., 2008. Summary of chemically induced pulmonary lesions in the National Toxicology Program (NTP) toxicology and carcinogenesis studies. Toxicol. Pathol. 36, 428–439.

Green, F.H., Vallyathan, V., Hahn, F.F., 2007. Comparative pathology of environmental lung disease: an overview. Toxicol. Pathol. 35, 136–147.

Harding, R., Pinkerton, K.E., Plopper, C.G., 2003. The Lung: Development, Aging and the Environment, First ed. Academic Press, Amsterdam, The Netherlands.

Harkema, J.R., Carey, S.A., Wagner, J.G., 2006. The nose revisited: a brief review of the comparative structure, function, and toxicologic pathology of the nasal epithelium. Toxicol. Pathol. 34, 252–269.

Harkema, J.R., Cary, S.A., Wagner, J.G., Dintzis, S.M., Liggitt, D., 2012. Nose, sinus, pharynx, and larynx. In: Treuting, P.M., Dintzis, S.M. (Eds.), Comparative Anatomy and Histology: A Mouse and Human Atlas. Academic Press, Amsterdam, The Netherlands, pp. 71–94.

Harkema, J.R., Nikula, K., Haschek, W.M., 2013. In: Haschek, W.M., Rousseaux, C.G., Wallig, M.A. (Eds.), Respiratory system In: "Haschek and Rousseaux Handbook of Toxicologic Pathology,", third ed. Academic Press (Elsevier), San Diego, pp. 1935–2003.

Herbert, R.A., Leininger, J.R., 1999. Nose, larynx, and trachea. In: Maronpot, R.R. (Ed.), Pathology of the Mouse. Cache River Press, Saint Louis, MO, pp. 259–292.

Hubbs A.F., Porter, D., Mercer R., Castranova V., Sargent L.M., Sriram K. Nanoparticulates In: "Haschek and Rousseaux Handbook of Toxicologic Pathology," third ed. (Haschek WM, Rousseaux CG, Wallig MA, eds.). Academic Press (Elsevier), San Diego, pp. 1373–1420.

Hussain, A.N., 2015. The lung. In: Kumar, V., Abbas, A.K., Aster, J.C. (Eds.), Robbins and Cotran Pathologic Basis of Disease, Ninth ed. Elsevier Health Sciences, New York, NY, Ch 15.

Khalil, N., Churg, A., Muller, N., O'Connor, R., 2007. Environmental, inhaled and ingested causes of pulmonary fibrosis. Toxicol. Pathol. 35, 86–96.

Leikauf, G.D., 2013. Toxic responses of the respiratory system. In: Klaassen, C.D. (Ed.), Casarett and Doull's Toxicology: The Basic Science of Poisons, eighth Ed McGraw Hill, New York, NY, pp. 691–732.

Mortaz, E., Masjedi, M.R., Allameh, A., Adcock, I.M., 2012. Inflammasome signaling in pathogenesis of lung diseases. Curr. Pharm. Des. 18 (16), 2320–2328.

Mowat, V., Alexander, D., Pilling, A., 2017. A comparison of rodent and non-rodent laryngeal and tracheal bifurcation sensitivities in inhalation toxicity studies and their relevance for human exposure. Toxicol. Pathol. 45, 216–222.

Nikula, K.J., McCartney, J.E., McGovern, T., Miller, G.K., Odin, M., Pino, M.V., et al., 2014. STP position paper: Interpreting the significance of increased alveolar macrophages in rodents following inhalation of pharmaceutical materials. Toxicol. Pathol. 42, 472–486.

Parent, R.A. (Ed.), 2015. Comparative Biology of the Normal Lung. second ed. Academic Press, Elsevier, London, UK.

Prasad, R., Gupta, P., Singh, A., Goel, N., 2014. Drug induced pulmonary parenchymal disease. Drug Discov. Ther. 8 (6), 232–237.

Renne, R., Brix, A., Harkema, J., Herbert, R., Kittel, B., Lewis, D., et al., 2009. Proliferative and nonproliferative lesions of the rat and mouse respiratory tract. Toxicol. Pathol. 37 (Suppl. 7), 5S–73S.

Renne, R.A., Gideon, K.M., Harbo, S.J., Staska, L.M., Grumbein, S.L., 2007. Upper respiratory tract lesions in inhalation toxicology. Toxicol. Pathol. 35 (1), 163–169.

Rock, J.R., Hogan, B.L., 2011. Epithelial progenitor cells in lung development, maintenance, repair, and disease. Annu. Rev. Cell. Dev. Biol. 27, 493–512.

Sells, D.M., Brix, A.E., Nyska, A., Jokinen, M.P., Orzech, D.P., Walker, N.J., 2007. Respiratory tract lesions in noninhalation studies. Toxicol. Pathol. 35, 170–177.

Suttie, A.W., Leininger, J.R., Bradley, A.E. (Eds.), 2017. Boorman's Pathology of the Rat. Academic Press, in press.

Yost, G.S., 2010. Toxicology of the respiratory system. In: Second ed. McQueen, C. (Ed.), Comprehensive Toxicology, vol. 8. Elsevier Ltd, Kidlington, UK.

This page intentionally left blank

CHAPTER

15

Digestive System

Matthew A. Wallig

University of Illinois at Urbana-Champaign, Urbana, IL, United States

OUTLINE

INTRODUCTION

This chapter will present the basic mechanisms by which toxic xenobiotics produce their deleterious effects and describe the consequences of toxicity on the integrity of gastrointestinal (GI) structure and function. The intrinsic ability of the GI tract to resist toxic chemicals has led to a paucity of data regarding GI toxicologic pathology, yet this organ system can be readily perturbed, leading to easily identified toxic responses such as emesis or diarrhea. Other perturbations such as insufficiency of enzymes (e.g., lactase, lipase); the presence of localized inflammation, polyps, or neoplasms; changes in function such as excess production of mucus or delayed gastric emptying; or structural damage such as ulcers are more difficult to identify and attribute to toxicologic processes. For these reasons, it is necessary to identify those functions and structures of the GI tract that are subject to direct or indirect chemical toxicity.

When considering the potential toxic activity of various agents on the GI tract, a number of signalments are possible. Acute effects may result from direct irritants (e.g., strong acids and bases), whereas chronic

Fundamentals of Toxicologic Pathology.
DOI: http://dx.doi.org/10.1016/B978-0-12-809841-7.00015-0

effects may be observed, such as increased muscular layer thickness from bulking agents. Importantly, delayed effects can be expressed years after exposure to ulcerogenic or carcinogenic agents. In addition to the array of tissue responses, interpretation of functional and morphological alterations can be complex. For example, increased mucosal thickness can occur when toxic compounds induce cellular proliferation and hyperplasia (e.g., enterochromaffin cell-like hyperplasia) or when nontoxic foodstuffs such as fiber induce generalized mucosal growth. The focus of this chapter is the examination of developmental, structural, and functional components of the GI tract that are important in understanding mechanisms involved in the toxicologic pathology of this organ system.

The principal functions of the GI tract that are subject to toxic effects of metals, toxicants, toxins, and xenobiotics include storage, propulsion, digestion, absorption, secretion, barrier activity, and elimination. Due to the importance of nervous reflexes and hormones in regulation of the GI tract, this organ system is relatively unusual in that toxic effects of a particular toxic molecule at one site (e.g., stomach) maybe expressed at another site (e.g., colon).

The GI tract is the entry site into the body of orally administered compounds that maybe highly toxic to other internal organs yet have little or no noticeable effect on the GI tract. A distinctive feature of the GI tract is the high proliferative and metabolic rate of the mucosa. In addition, the GI tract mucosa is a complex barrier that must exclude bacteria and their molecular toxins and, at the same time, absorb nutrient molecules that are vital for homeostasis. These two functions alone make the GI tract unique. Furthermore, this organ system cannot sustain widespread toxicity without serious direct and indirect consequences to the rest of the body, if for no other reason than nutrient malabsorption with consequential malnutrition or starvation.

The GI tract is the only internal organ system that contains endogenous biotransforming and toxigenic bacteria, as well as inert drug-binding materials. Consequently, when a compound is present in the GI milieu, the ultimate toxicity to this organ system will be determined by interactions of the chemical with both bacterial and mammalian enzymes, and by the extent of respective detoxification and bioactivation processes. The ability to evaluate genomic, proteomic, biochemical, or morphological changes in the GI tract can be complicated because of the matrix of interactions and the GI tract's exquisite sensitivity to autolysis and postmortem alterations. Many subtle toxicologic events that occur at cellular and subcellular levels may only be observed by careful and proper handling of the GI tissues immediately after death.

STRUCTURE AND FUNCTION OF THE GASTROINTESTINAL TRACT

Macroscopic and Microscopic Structure and Function

Although many of the basic features of the GI tract are similar for various species (Figures 15.1 and 15.2), major interspecies variations are present in the fore- and hindgut (Table 15.1). This notwithstanding, within each major macroscopic variation, the cell types composing the mucosal lining of the GI tract are remarkably similar (Figure 15.1 and Table 15.2).

Esophagus

The function of the esophagus in all species is to act as a conduit for food materials in the oral cavity to enter the GI tract. Interspecies esophageal variations occur related to the presence and extent of smooth and striated muscle, the gastroesophageal junction, and caudal sacculated adaptations (forestomachs). In all species, the esophagus is lined by stratified squamous epithelium with varying degrees of keratinization.

The extent of keratinization of the esophageal and nonglandular gastric epithelium is dependent on the amount and type of dry foodstuff ingested. Consequently, hyperkeratosis of the mucosa can indicate anorexia or an increase in roughage content of the feed in both ruminants and rodents. This keratinized epithelium imparts a whitish color to the mucosa when the esophagus is viewed macroscopically. Keratinization is also a normal feature of the nonglandular portion of the rodent stomach.

The tunica muscularis of the esophagus has two muscle layers composed of striated, smooth, or a mixture of both types of muscle, depending on the species. Variations in esophageal musculature account for the ability or inability of an animal to vomit or regurgitate. The absence of significant amounts of striated muscle in the esophagus of rats and the presence of a limiting ridge (margo plicatus) in the stomach separating the nonglandular and glandular regions explains why these animals are unable to vomit. The ability of dogs and guinea pigs to vomit and ruminants to regurgitate is dependent upon the presence of striated muscle in the esophagus, which permits esophageal contractions that allow retrograde transit of gastric contents.

Regurgitation, not vomiting, in nonruminants indicates esophageal dysfunction or obstruction. If the esophagus is perforated by caustic compounds, chronic drainage of saliva and ingested foodstuffs into the esophageal submucosa or intrathoracic regions leads to severe inflammatory reactions, fibrosis, and strictures. The esophagus does not heal as rapidly or

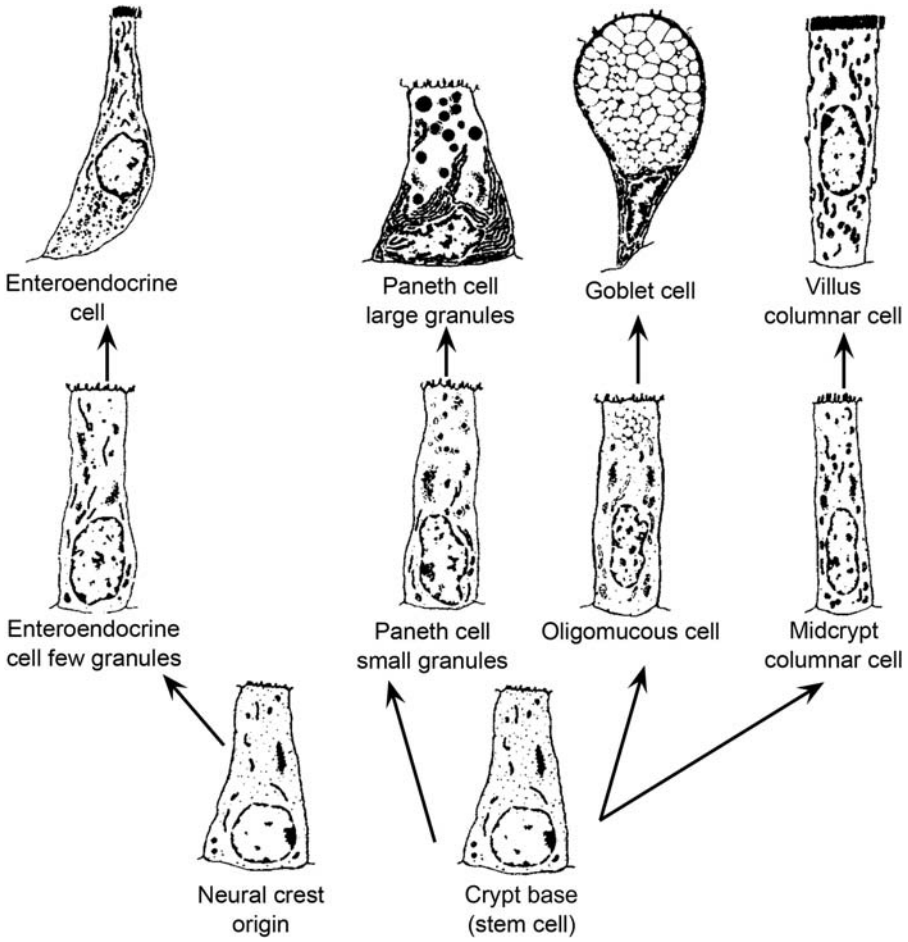

FIGURE 15.1 Epithelial cells of the gastrointestinal tract are derived from clonal stem cells. Toxic injury to these stem cells will disrupt the functional and structural development of the crypt–villus unit. *Figure reproduced from* Handbook of Toxicologic Pathology, *second ed. W. M. Haschek, C. G. Rousseaux and M. A. Wallig, eds. (2002) Academic Press, Fig. 1, p. 123, with permission.*

achieve structural restoration as completely as other portions of the GI tract because of a marginal blood supply and a minimal amount of adventitial and serosal connective tissue.

Stomach

Anatomical and functional variations are important considerations when designing animal studies. Compound absorption and enzyme exposure (e.g.,-ruminal bacteria or inflammatory cell proteases) often vary from species to species, and sites of storage (e.g., nonglandular stomach) may provide prolonged contact between the host mucosa and a toxic compound.

FUNCTION

The stomach functions to store and macerate food—a necessary early phase of food digestion. Some phylogenetic orders have a highly sacculated forestomach (e.g., some artiodactyls and primates). Entrapment of food within saccules aids in food digestion by extending the exposure of ingested materials to digestive acids and enzymes. In ruminants, the ruminal portion (rumen) of the forestomach, which is actually a modification of the esophagus, is highly permeable to volatile fatty acids released from the microbial metabolism of complex carbohydrates and also is capable of active sodium and chloride absorption.

Several mammalian orders, including rodents and perissodactyls (horses, tapirs and rhinoceroses), have a nonglandular stratified squamous portion of the stomach proximal to the fundic mucosa. This squamous portion of the stomach is separated from the glandular stomach by a limiting ridge (margo plicatus) and serves as a storage organ for ingested material. Various inflammatory cells (lymphocytes, plasma cells, and eosinophils) maybe present in the lamina propria of the limiting ridge of rodents as a normal characteristic and should not be interpreted as an inflammatory process.

STRUCTURE

The topographical organization of the gastric mucosa varies widely among species. As monogastric simple-stomached mammals, humans and dogs have the cardia as the first glandular portion of the stomach following the esophagus or squamous forestomach; the cardiac mucosa is macroscopically red. This portion of the stomach has foveolae (gastric pits) and tortuous mucous glands. The fundus is the next glandular region and is characterized by mucosal convolutions called rugae. The distal portion of the stomach, the pylorus, also has rugae, but they are smaller than those of the fundus and are arranged obliquely in the direction of the antrum. Unlike other portions of the stomach, the foveolae of the antrum are deeper and make up as much as 50% of the mucosal thickness.

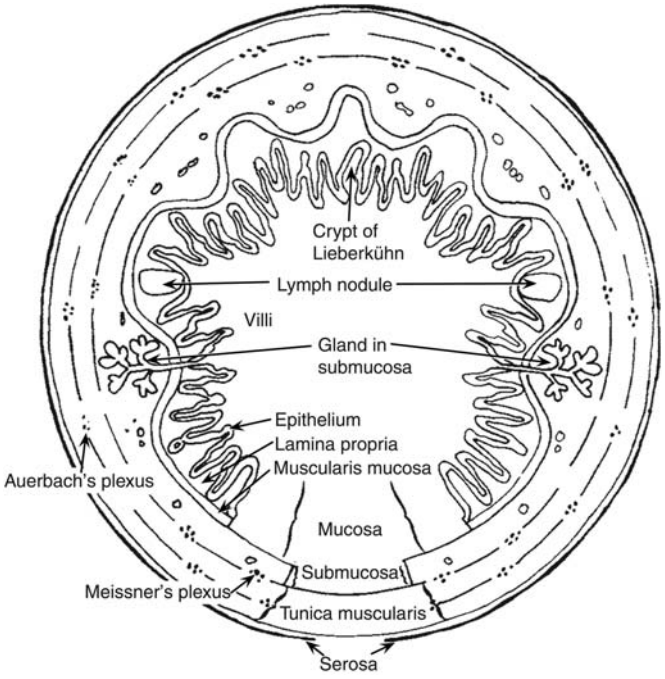

FIGURE 15.2 Schematic drawing of the intestinal tract. This basic tissue organization demonstrates the general organization of the entire gastrointestinal tract. Brunner's glands are located in the submucosa of the duodenum only. Villi are present in the small intestine only. *Figure reproduced from* Handbook of Toxicologic Pathology, *second ed. W. M. Haschek, C. G. Rousseaux and M. A. Wallig, eds. (2002) Academic Press, Fig. 2, p. 124, with permission.*

In spite of many macroscopic variations, the microscopic arrangement of the stomach is similar in all species. The mucosa rests on the submucosa, and these two layers are surrounded by a muscular coat (tunica muscularis) that is, covered by the single mesothelial cell layer of the serosa.

The fundic mucosa contains glands that are composed of mucous surface neck cells, parietal (oxyntic) cells, chief (zymogen) cells, and enteroendocrine (enterochromaffin) cells (Table 15.2). Chief cells are cuboidal and have a basally placed nucleus. The apical portion of the cytoplasm is filled with pepsinogen-filled zymogen granules. The primary function of the chief cell is to release enzyme precursors into the gastric lumen; once in contact with the acidic extracellular environment, the enzymes become activated to begin the process of gastric digestion. Parietal cells are larger but generally less numerous than chief cells. Parietal cells have a centrally located nucleus, and the smooth endoplasmic reticulum (SER) and mitochondria-laden cytoplasm stains intensely eosinophilic. Parietal cells release hydrochloric acid (HCl), to maintain gastric pH, and chymosin (or rennin) in young animals, to facilitate digestion of milk. Carbonic anhydrase in the parietal cells acts on carbon dioxide (CO_2), thereby producing carbonic acid that dissociates to provide H^+ for excretion. Both Cl^- and H^+ are actively secreted into the lumen, with water following the osmotic

TABLE 15.1 Variations in Dietary Consumption Related to Gastrointestinal Structure in Various Mammals[a]

				Stomach		Large intestine	
Order	**Carnivore**	**Omnivore**	**Herbivore**	**Sacculated**	**Stratified squamous epithelium**	**Cecum**	**Sacculated colon**
Carnivora	+	+		−	−	±	±
Rodentia	+	+	+	±	±	±	±
Lagomorpha			+	−	−	+	+
Primates	+	+	+	±	±	+	±
Artiodactyla		+	+	±	±	±	±
Marsupialia	+	+	+	±	±	±	±
Perissodactyla			+	−	+	+	+

[a]*Modified from Stevens (1980).*
Table adapted from Handbook of Toxicologic Pathology, *second ed. W. M. Haschek, C. G. Rousseaux and M. A. Wallig, eds. (2002) Academic Press, Table I, p. 124, with permission.*

TABLE 15.2 Cells Composing the Epithelial Lining of the Gastrointestinal Tract[a]

Cell type	Shape	Location	Product
Absorptive cell (enterocyte or colonocyte)	Columnar	Small intestine to colon	Nutrient absorption
Mucous cell	Cuboidal to columnar	Stomach to rectum	Mucus
Chief cell	Pyramidal	Stomach (fundic)	Pepsin, rennin, lipase
Enterochromaffin cells	Pyramidal	Stomach to rectum	Endocrine (at least 10 types)
Goblet cell	Columnar	Small intestine to rectum	Mucin
M cell	Membranous	Dome of Peyer's patches	Processed antigens
Paneth cell	Pyramidal	Small intestine	Lysozyme, peptidase
Parietal cell	Cuboidal	Stomach (fundic)	HCl, intrinsic factor
Undifferentiated crypt cell	Cuboidal	Small intestine to rectum	Progenitor cell
Vacuolated cell	Columnar	Colon to rectum	Progenitor cell

[a]*The number of these individual type cells in any given anatomical location in the gastrointestinal tract can vary with animal species and diet. Additionally, toxicologic agents can markedly influence the distribution and relative ratios of each cell type.*
Table adapted from Handbook of Toxicologic Pathology, *second ed. W. M. Haschek, C. G. Rousseaux and M. A. Wallig, eds. (2002) Academic Press, Table II, p. 128, with permission.*

gradient. Food material in the stomach, vagus nerve stimulation, gastric distension, and gastrin released from G-cells in the glands of the pylorus and duodenum stimulates the parietal cells to release H^+. Stimulation of chief cells to release pepsinogen comes from a combination of vagal nerve stimulation, H^+ concentrations, gastrin, and secretin (released from duodenal secretin cells).

In the antrum, the mucosal glands produce mucus. Gastric mucus is a composite of mucin, electrolytes, sloughed cells, enzymes, nucleic acids, lipids, plasma proteins, secreted immunoglobulins, bacteria, and bacterial metabolites. The composition of gastric mucus is 90%–95% water, 5%–10% mucin, 1% electrolytes, and approximately 5% all other components. Mucin, the principal component of gastric mucus, is synthesized by and secreted from mucus-producing cells resident within mammalian gastric mucosa. MUC5AC and MUC6 are the main mucins secreted by surface or glandular mucous cells of the human stomach. Mucins are high-molecular-weight polymers composed of glycoprotein subunits joined by disulfide bridges. Each glycoprotein subunit has a central peptide core flanked by carbohydrate side chains. Hydrogel formation by aqueous mucin polymers leads to formation of a protective layer over the gastric mucosa, which further assists in lubrication of the mucosal surface and digestion. Cells of the gastric glands also release arachidonic acid metabolites (e.g., prostaglandins of the E series) that facilitate protection of the mucosa.

Cellular composition of gastric glands in the fundic mucosa varies among animal species. Intermixed with the gastric gland epithelium are enteroendocrine cells, of neural crest origin. Enteroendocrine cells, which are usually located between the basement membrane and chief cells, synthesize, store, and secrete hormones in response to autonomic and intraluminal stimuli. There are at least 10 different enteroendocrine cell populations in the mucosa. Enteroendocrine cells secrete serotonin, histamine, enteroglucagon (A cells), and gastrin (G cells), among other factors.

Replication of the mucosal cells in the stomach is somewhat different from that of the rest of the GI tract. Unlike the replication of crypt cells of the intestines and basal cells of the esophagus, gastric mucosal cell replication occurs in the neck of the gastric glands.

The next layer of the gastric mucosa, immediately below the epithelium, is the lamina propria, which is separated from gastric epithelial cells by a basement membrane. The lamina propria of the cardia and pylorus contains high numbers of lymphocytes and plasma cells. These immune cells are abundant throughout the gastric mucosa and submucosa, and the pyloric lamina propria may contain numerous lymphoid follicles even in a healthy animal. This lymphoid tissue can markedly enlarge in disease states where there is antigenic stimulation (Figure 15.4).

The lamina muscularis mucosae separate the mucosa from the submucosa. The submucosa is composed of a loose connective tissue matrix supporting many nerves and blood and lymphatic vessels. Three smooth muscle layers constitute the tunica muscularis, which encircles the stomach in overlapping layers and functions to mix food and move contents from storage in the stomach into intestine for

continued digestion and nutrient absorption. The muscle fibers are oriented in circumferential (middle layer), longitudinal (outer layer), and oblique (inner layer) bundles to massage the ingesta from as many angles as possible, which facilitates physical disruption of intragastric solids.

Small Intestine

FUNCTION

This segment is primarily responsible for secretion and absorption of nutrients. In addition, the small intestine functions to biotransform compounds, resulting in bioactivation or detoxification (Table 15.3), as a barrier to luminal contents (bacteria and nonabsorbed compounds), and as a conduit for indigestible ingesta to pass out of the body. Numerous anatomical modifications increase the functional capacity of the small intestine, including its long length, linear plicae, circular plicae, villi, and microvilli. These characteristics influence mucosal surface area and can modify the transit time of a compound through the GI tract. Relative to the stomach and large intestine, passage time through the small intestine is relatively rapid (i.e., a few hours).

Between the proximal and distal small intestine, a functional gradient of ion and water transport occurs, which controls the movement of fluids and electrolytes across the mucosa. In the proximal small intestine, passive movement of sodium and water is from the blood to the GI tract lumen. In contrast, fluid and sodium movement is from the lumen to the blood in the distal small intestine. Net secretion occurs in the ileum and jejunum of guinea pigs, the ileum of rabbits, and the proximal portion of the jejunum in neonatal swine. The jejunum absorbs sodium, chloride, and bicarbonate against an electrochemical gradient; however, this decreases as the animal ages. Bile salts are primarily reabsorbed in the ileum.

TABLE 15.3 Mucosal Metabolic Conjugation of Selected Chemicals

Chemical	Glucuronidation	Sulfation
o-Aminophenol	+	+
Anthranilic acid	+	+
Buprenorphine	+	
Dihydromorphine	+	
Ethinylestradiol	+	
Etorphine	+	
Isoprenaline		+
Midaglizole	+	
Morphine	+	
p-Nitrophenol	+	+
Phenol	+	+
Salicylamide	+	+
Salicyclic acid	+	+
Thyroxine analogs	+	+
Xamoterol	+	+

Table adapted from Handbook of Toxicologic Pathology, *second ed. W. M. Haschek, C. G. Rousseaux and M. A. Wallig, eds. (2002) Academic Press, Table III, p. 129, with permission.*

STRUCTURE

The small intestine constitutes the majority of the GI tract's length. Major structural features of the small intestine vary little among species. The general microscopic organization of the small intestine is similar to that of the stomach, with three distinct layers (mucosa, submucosa, and tunica muscularis) surrounded by the serosa.

Small-intestinal morphology reflects its absorptive function and can be artificially divided into two zones: villi for absorptive and enzyme release, and crypts for secretion and mucosal replication/replacement (Figure 15.2). Crypt-depth-to-villus-height ratios vary from species to species but tend to remain constant within a species; hence, they can be used to assess the degree of intestinal damage resulting from exposure to a toxic compound. The distance from the base of the crypt to the tip of the villus is divided by a "shoulder" at the crypt–villus junction (Figure 15.3D). This juncture is the transition between the crypt and villus functionally as well as anatomically. The crypt-depth-to-villus-height ratio in the proximal small intestine ranges from a small 1:7 ratio in the pig to a larger 1:2 ratio in the dog. Within a species, this ratio also will vary with the amount of food material in the lumen, luminal distension, and diet.

Villus height progressively decreases from proximal to distal small intestine. Villi are covered by mature but senescent cells that have migrated along the basement membrane up from the crypts and are supported by a connective tissue core, the lamina propria. The center of the villus has blind-ended lymphatic vessels, or lacteals (Figure 15.3D), that are surrounded by an elaborate capillary bed; both these vascular beds are located subjacent to the epithelial basement membrane. The lacteals serve to carry fat-soluble compounds to the systemic circulation, thus bypassing hepatic metabolism.

Cells lining the mucosa of the small intestine are primarily composed of simple tall columnar epithelium (enterocytes) on the villi and cuboidal epithelium in the crypts (Table 15.2). Villous epithelial cells have a

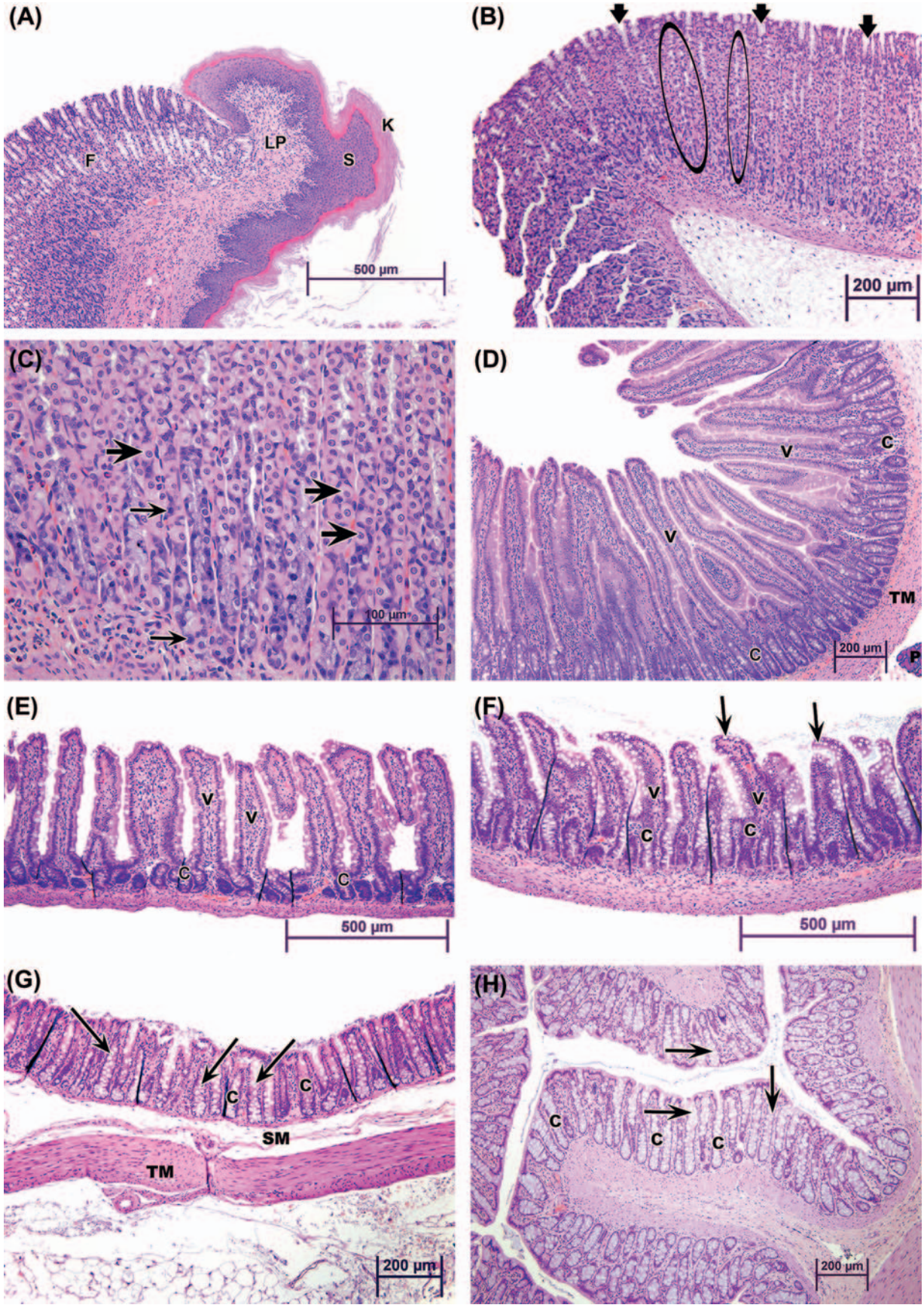

FIGURE 15.3 Normal histology of the rat GI tract. (A) Nonglandular (squamous) portion of the stomach (S) from a rat at the junction (limiting ridge) with the fundus (F) with its deep gastric glands. The stratified squamous epithelium of the forestomach is covered by a layer of keratin (K), and the underlying lamina propria (LP) is infiltrated by a resident population of inflammatory and immune cells. (B) Fundic (oxyntic) mucosa of the glandular stomach. Gastric pits (arrows) are lined by columnar epithelium and are the outlet for fundic gland (ellipses)

thick microvillar apical membrane (approximately 11 nm in height) and have multiple biotransforming and metabolizing enzymes at the luminal surface. The thickness and composition of this enzyme-rich apical membrane is maintained by cytoskeletal elements (microtubules) and the presence of tight junctions at the lateral membrane–junctional complexes near the apices of the cells. Enterocytes absorb simple carbohydrates, amino acids, and some xenobiotics and then actively transport them, with little processing, into subjacent capillaries for transportation to the liver.

Each villus consists of 2000–8000 enterocytes and is surrounded by 6–14 crypts. The crypt is the proliferative unit of the intestinal mucosa, as cell division is confined to the crypts. Each crypt generates four types of terminally differentiated cells: enterocytes, goblet cells (to secrete mucus), enteroendocrine cells, and Paneth cells (to produce lysozymes); all these cells serve as a barrier to bacteria. Each crypt produces 300–400 cells per day, and each epithelial cell has an average life of 3 days. Most extensive replication occurs in the cells immediately above the bottom four to six cells. Each crypt has committed stem cells that divide rapidly to produce daughter cells. Daughter cells may themselves divide several times in the lower and middle portions of the crypts, but their mitotic capabilities are limited. Negative feedback mechanisms coordinate the rate of cell proliferation in the crypts. The cells differentiate and mature during an orderly and rapid migration from the crypt to the apex of a surrounding villus. As the cells migrate up the villus, they differentiate both structurally and functionally. Enterocytes (absorptive cells), by far the majority cell type, have a microvillous "brush border" on their apical surface. Goblet cells secrete mucus, and their apical cytoplasm is typically distended with mucus-filled secretory granules. Closely related to goblet cells are the epithelial cells lining submucosal (Brunner's) glands present in the cranial duodenum of most mammalian species. These highly branched glands produce mainly mucin but also serve an endocrine function (see below). Enteroendocrine cells (themselves composed of many individual subtypes) are smaller and secrete various digestive hormones, such as catecholamines. Once these three cell types reach the apex of a villus, they are exfoliated. This process of proliferation, upward migration, and subsequent exfoliation is completed in 2–5 days.

Relative to other cell types in small intestinal crypts, Paneth cells exhibit several unusual traits. They remain anchored in the lower portion of the crypt rather than migrating up villi. They are long-lived, surviving for approximately 21 days. Finally, Paneth cells are a critical component of the mucosal defense system because they secrete antibacterial proteins (lysozyme, defensins) that provide local control of luminal microbiota. Paneth cells are found in monkeys, mice, rats, hamsters, guinea pigs, ruminants, and horses, but not in dogs, cats, swine, or raccoons. Paneth cell numbers increase in number from duodenum to ileum. The Paneth cell secretes mercury and other heavy metals into the intestinal lumen. These cells become necrotic in chronic methylmercury intoxication of primates.

Intestinal crypt cells secrete fluids and electrolytes, which are reabsorbed by intestinal villus cells. The transport of electrolytes across epithelial cell apical membranes occurs by multiple mechanisms. Uniport mechanisms move a single ion (e.g., sodium), symport systems move two ions simultaneously in the same direction (e.g., sodium and chloride), and antiport elements are ion exchangers which move two ions with the same charge in opposite directions (e.g., sodium and hydrogen). These systems are "active" processes that frequently require energy (ATP) and are stimulated by cAMP, cGMP, or increased levels of intracellular calcium. Fluid transport is also modulated by neurotransmitters such as serotonin (increases secretion) and neuropeptide Y (increases absorption).

Toxicant-induced damage to membrane-bound proteins can influence the viability of the mucosal epithelial cells and as a consequence the nutritional status of the animal. Within the apical membrane are proteins that consist of intimately membrane-associated calcium–magnesium-dependent ATPases and alkaline phosphatases, and less tightly held disaccharidases (i.e., lactases, sucrases, and maltases), and leucine aminopeptidases. The less tightly held enzymes are responsible for digestive processes, while the more tightly held ATPases control cellular homeostasis and viability. In the thinner lateral membranes

secretions. (C) In a higher magnification view of the fundus, eosinophilic, pyramidal parietal cells (large arrows) as well as smaller, more basophilic chief cells (small arrows) lining the gastric glands are indicated. Identification of the enteroendocrine cells that are also present in lower numbers requires special staining techniques (e.g., Grimelius stain). (D) Duodenal portion of the small intestine. Villi (V) are very long in relation to the crypts (C). Tunica muscularis (TM) and attached pancreas (P) are indicated. (E) Jejunal portion of the small intestine. Villi (V) are lined by columnar epithelial cells and have a central lacteal. Crypts (C) are composed of proliferating epithelial cells. (F) A section of ileum illustrates the shortness of the villi (V) in relation to the crypts (C). Numerous goblet cells (arrows) are also evident. (G) The cecal mucosa in the rat (as well as other species) is relatively thin, with only crypts (C) and numerous goblet cells (arrows) but no villi. The submucosa (SM) is rather "loose" and the tunica muscularis (TM) is thin. (H) Colonic mucosa in the rat is highly folded and has abundant goblet cells (arrows). Colonocytes are not as tall as enterocytes, and no villi are present, only crypts (C). *Figure reproduced from* Fundamentals of Toxicologic Pathology, *second ed. W. M. Haschek, C. G. Rousseaux and M. A. Wallig, eds. (2007) Academic Press, Fig. 8.2A–H, pp. 166–167, with permission.*

(approximately 7 nm thick) of mucosal epithelial cells, ouabain-sensitive sodium−potassium ATPase is found in concentrations that are higher than in the apical surface. This enzyme is tightly linked to glucose absorption.

Less numerous goblet cells are scattered among enterocytes of the villi. The numbers of goblet cells increase in the villous mucosa from proximal to distal small intestine. Lysozyme- and peptidase-rich Paneth cells are found near the base of the crypts, associated with the proliferating cells, but there is no known dietary or environmental factor that controls this distribution (Table 15.2).

M cells are located in the surface epithelium overlying the lymphoid tissues (Peyer's patches, see below) of the intestinal tract. These cells are recognized histomorphologically by the microfolds on their luminal surface (folds are not present in rats), and they are highly phagocytic. M cells are responsible for sampling antigens from the lumen contents and for transfer of the antigen to T lymphocytes and dendritic macrophages. The M cells can also function as an access route for pathogenic microbes and particulate toxic agents (e.g., asbestos).

Enterocytes may also function as antigen-presenting cells, especially for soluble proteins. Enterocytes express Class II major histocompatibility complex antigens and are capable of stimulating T lymphocytes to activate and proliferate. While enterocytes may process soluble antigens, M cells seem to be primarily responsible for processing particulate antigens.

The lamina propria is the neighboring loose connective tissue layer that nourishes the mucosal epithelium and its associated mucosal glands. Lymphocytes, plasma cells, and to a lesser extent, mucosal mast cells and eosinophils are present throughout the lamina propria, both within the villi and around the crypts. The numbers of these cells increase with age in all species. Although most of the immune cells in the lamina propria function in a similar manner to those in other regions of the body, the mucosal mast cell is functionally distinct from mast cells in other tissues (Section 2.3, Enteric Nervous System).

The muscularis mucosae separates the mucosa from the underlying submucosa. The muscularis mucosae is a thin smooth muscle layer that functions to move luminal contents in a single (distal) direction by modulating the sizes and shape of small intestinal mucosal folds (rugae). Motor activity in the muscularis mucosae exhibits considerable variations among regions and across species. Intracellular signaling pathways to control motor activity in this layer differ from those of smooth muscle in the tunica muscularis (muscularis externa). Since the submucosal area is a major source for eicosanoid production, abnormality of muscularis mucosae motor activity may link with abnormality of mucosal absorption and secretion functions.

The submucosa is found between the muscularis mucosae and the tunica muscularis. This layer consists of loose connective tissue and contains comparatively large vascular and lymphatic elements.

The tunica muscularis is usually a thin, double layer of smooth muscle. The smooth muscle cells are oriented circularly or helically within the inner layer, and longitudinally in the outer layer. This is typically the most substantial layer of the intestinal wall.

The adventitial layer on the outer surface of the small intestine is covered by mesothelium derived from the peritoneum in which the organ is suspended and hence is called the tunic serosa. This layer is composed of loose collagenous and elastic tissue in which adipose tissue can be found in well-nourished animals. The serosa is also the entry point for major arteries originating from the mesenteric arterial system. These arteries arborize longitudinally within the serosa but also penetrate the muscularis to form a second longitudinal arborization in the submucosa. Smaller arteries radiate outward into muscularis and mucosa, respectively, from these two major vascular supplies. Veins and lymphatics that drain the intestine follow the arterial supply back to the serosa to mesenteric venous and lymphatic drainage systems. There are extensive anastomoses between the various branches of the mesenteric arterial system and similar anastomoses between the various branches on the venous side as well.

Large Intestine

FUNCTION

Major functions of the large intestine include storage of digesta, water and electrolyte absorption, and secretion. One of the main electrolyte-absorbing processes is through the Na^+/K^+-dependent ATPase pathway of the mucosal epithelium. Herbivores secrete large volumes of salivary, pancreatic, and biliary fluids, and in perissodactyls (horses), the large intestine secretes additional fluids equivalent to 40% of the extracellular fluid volume. However, 98% of the fluid and ions secreted in the upper GI tract is reabsorbed in the cecum and colon. It is critical that this reabsorptive process is taken into account when attempting to investigate toxicant-induced diarrheas.

The colon has protein-absorbing activity. However, relative to the small intestine, the large intestine absorbs a small proportion of total body protein needs. The large intestine instead serves as the major site of digesta retention; however, the duration and primary site of retention varies between species. The rate of

passage is inversely related to the degree of colonic compartmentalization. Additionally, retrograde propulsions of the colon, associated with absorption of water and electrolytes, may help delay the passage of a toxic compound and prolong exposure of a toxicant to various biotransforming enzymes.

The high concentration of bacteria in the colon facilitates roughage digestion and compound biotransformation. Although bacterial metabolism is critical for nutrition and influences toxicologic processes, the role of bacteria in colonic physiology has received limited study (Table 15.4).

STRUCTURE

Macroscopic morphology of the large intestine varies widely among species. Anatomical modifications of basic structure include marked variations in relative length, diameter, volume, and compartmental complexity of this organ. The secretory and absorptive capacity of the large intestine is related to both its anatomical complexity and the need for the animal to conserve water.

TABLE 15.4 Metabolic Reactions by Intestinal Microflora[a]

Reaction	Representative substrate
HYDROLYSIS	
Glucuronides	Bilirubin glucuronide
Glycosides	Cycasin
Sulfamates	Cyclamate
Amides	Methotrexate
Esters	Acetyldigoxin
DEHYDROXYLATION	
C-hydroxy groups	Bile acids
REDUCTION	
Nitro groups	*P*-Nitrobenzoic acids
Double bonds	Unsaturated fatty acids
Azo groups	Food dyes
Aldehydes	Benzaldehydes
Alcohols	Benzyl alcohol
N-Oxides	4-Nitroquinoline-1-oxide
Decarboxylation	Amino acids
Deamination	Amino acids

[a]*Modified from Simon and Gorbach (1984) Intestinal flora in health and disease,* Gastroenterology *85, 144–193, Table p. 175, with permission.*
Table adapted from Handbook of Toxicologic Pathology, *second ed. W. M. Haschek, C. G. Rousseaux and M. A. Wallig, eds. (2002) Academic Press, Table IV, p. 132, with permission.*

Cecum

Although considered separately here, the cecum is an extension of the colon arising at the ileo–eolic junction. Cecal structure varies considerably among different animal species, as a rule quite small in carnivores and very large in herbivorous animals that rely heavily on ceco-colonic breakdown of cellulose for energy needs (e.g., rabbits and to a lesser extent rodents). The cecal lumen contains many bacteria that are metabolically active in detoxifying or bioactivating ingested compounds and producing essential vitamins. Some aspects of antimicrobial toxicity are directly related to the modification of normal cecal microflora.

The cecal mucosa is anatomically similar to that of the colon (see below), and the submucosa contains abundant lymphoid nodules that function like Peyer's patches of the small intestine. The primary function of the cecum is for microbial fermentation and storage of ingesta. Intraluminal ingesta can be passed back and forth from the cecum to the proximal colon several times before continuing its passage down the remaining distal segments of colon.

Animals with large and functionally active ceca (e.g., rats, ruminants, swine) may have significantly different passage rates for ingesta and toxic compounds than do species with a rudimentary cecum (e.g., dogs, primates). Such information must be incorporated into the design of animal model studies and considered when interpreting toxicokinetic and drug metabolism data.

Colon

The mucosa of the colon and cecum is significantly different from the mucosa of the small intestine. Goblet cells are abundant in the colonic mucosa and are responsible for adding mucus to the dehydrated ingesta. Inflammation of the colon can lead to epithelial Paneth cell metaplasia, which reduces mucus production and renders the mucosa prone to bleeding.

The submucosa, tunica muscularis, and serosa of the large intestine are similar to those of the small intestine. The terminal end of the large intestine (rectum) is located retroperitoneally in the pelvic canal and is not covered by a serosa.

Enteric Lymphoid System

The GI immune response is multifactorial and involves both cellular and humoral immune mechanisms. Immunologic response of the GI tract is predominantly mediated by immunoglobulin isotype A (IgA) with and without secretory component (sIgA). The GI tract mucosa contains many IgA-producing plasma cells. Additionally, cell-mediated immune mechanisms

are involved in the mucosal response to toxic compounds. Cell-mediated immunity of the mucosa is distinctly different from that of nonmucosal sites. This difference is exemplified by the enterocytes of the small intestine, which can function as antigen-presenting cells, IgA-antigen carriers, and activators of T lymphocytes. Consequently, immune mechanisms in the GI tract involve multiple pathways for response to toxic compounds, which may include hypersensitivity.

Located throughout the small intestine are deep mucosal/submucosal lymphoid aggregates called Peyer's patches (Figure 15.4). Peyer's patches represent the organized portion of the GI immune system and are part of the gastrointestinal (gut)-associated lymphoid tissue (GALT). GALT composes over 25% of the body's total lymphoid organ mass and is most extensive in the small intestine. Peyer's patches can be composed of only a few lymphocytes or maybe well-developed lymphoid nodules with many active secondary follicles. Well-developed nodules have both follicular and parafollicular regions. Follicles are composed of B cell-rich germinal centers located in the lamina propria or submucosa. Germinal centers are surrounded by parafollicular T cells and are capped by a dome of small lymphocytes that extends into the specialized M cell-rich mucosal epithelial covering. The stronger the antigenic stimulus, the more extensive will be the response and development of the nodules.

Lymphoglandular complexes of the colon are an important part of the GALT complex. Lymphoglandular complexes have germinal centers in the submucosa with deep mucosal epithelial invaginations projecting into them. As in Peyer's patches, M cells partially line the surface of these complexes, and lymphocytes are closely apposed to these phagocytic cells. Epithelial cells lining true Peyer's patches in the rat colon function like M cells but do not have the characteristic morphological appearance of microfolds on their luminal surfaces.

When GALT is activated, lymphocyte traffic through Peyer's patches increases. Primed and activated T and B lymphocytes migrate to mesenteric lymph nodes via the thoracic duct to postcapillary venules lined by high endothelial cells (high endothelial venules, HEV), and then into intestinal lymphoid tissue. Tissue specificity of the T and B cells is determined by interaction with the endothelial cells of the HEV. The ability of the immune system in the GI tract to respond to microbial, chemical, and dietary antigens helps prevent these agents from entering the body. GI tract mucosal hypersensitivity can be induced by circumventing the normal process in which a toxic compound is handled by GALT. This can be done, for example, by coadministering a mucosa-damaging agent and the antigenic compound concomitantly.

Lymph flows from the central lacteal to Peyer's patches and then to many different lymph nodes, including mesenteric, pancreatic, gastric, hepatic, splenic, and colonic nodes. Intestinal lymph contains absorbed lipids, fat-soluble xenobiotics, and recirculating lymphocytes. Some of the circulating lymphocytes have been primed by antigen exposure and are migrating to other mucosal sites, including respiratory and genital tracts. This allows immune cells exposed to antigens in the GI tract to localize at other sites of the common mucosal immune system that may also be exposed to environmental toxicants.

The T-lymphocyte population in the GI lamina propria consists primarily of CD4 helper/inducer cells. These cells play a major role in the development of the initial immunologic response to a new antigen, which is consistent with the concept that the gut represents a site of primary exposure of the host to many new antigens. Cytotoxic/suppressor (CD8) cells are less frequently seen in this location. For more specific information regarding GALT, and the immune system as a whole, and their responses to toxic substances, refer to Chapter 12, Immune System.

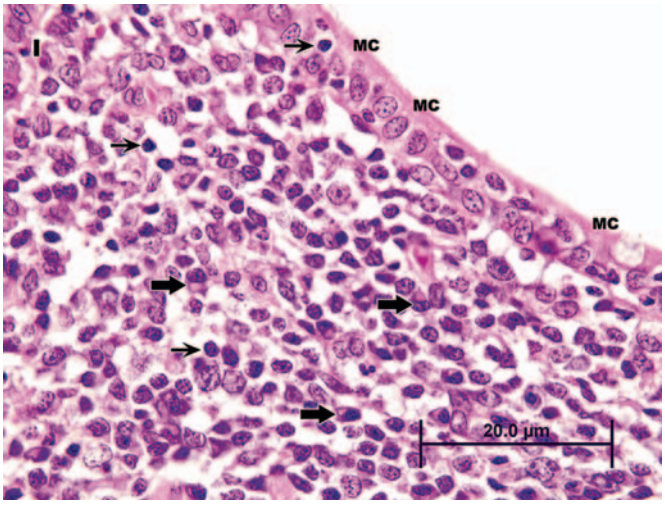

FIGURE 15.4 Peyer's patch from the ileum of a dog-illustrating M cells (MC) and the mixture of lymphocytes (small arrows) and plasma cells (large arrows) in the lamina propria. *Figure reproduced from* Fundamentals of Toxicologic Pathology, *second ed. W. M. Haschek, C. G. Rousseaux and M. A. Wallig, eds. (2007) Academic Press, Fig. 8.2I, p. 166, with permission.*

Enteric Nervous System

The nervous tissue of the GI tract is highly organized but diffuse in nature. These elements are components of the autonomic nervous system (ANS). Various motor and sensory neurons ramify throughout the wall of the GI tract and form multiple plexuses. Nerve fibers emanate from these plexuses and vary in

thickness, carrying information from one ganglion to another and from intrinsic to extrinsic neurons. The nervous tissue of the GI tract differs from other portions of the ANS because many of its neurons do not receive direct input from the central nervous system. However, neural information does come from autonomic motor neurons that are both sympathetic and parasympathetic, and from GI sensory neurons. This results in reflex activities that act independently of the brain or spinal cord. Yet the central nervous system can regulate the rate of turnover of GI mucosal cells.

Neurons of the parasympathetic ganglia are in both the submucosal (Meissner's) plexus and myenteric (Auerbach's) plexus. The myenteric plexus is responsible for the electrical rhythms of the GI tract but is not needed for propagation of the myoelectric complex that controls intestinal function. The myenteric and submucosal plexuses are interconnected to form a single functional unit, so integration of electrical activity occurs at multiple locations in the GI tract.

Parasympathetic stimulation of the GI tract leads to increased blood flow, enhanced secretion, and increased muscular activity. Stimulation by the sympathetic nervous system has the opposite effects. The enteric nervous tissue is also composed of integrative circuits that consist of interneurons within ganglia that process information from intramural and mucosal sensory receptors. Sensory neurons detect fluidity, volume, chemical composition, and temperature of the luminal contents. The appropriate motility of the GI tract is affected via motor neurons. Specific motor neurons release neurotransmitters in the proximity of mucosal effectors, blood vessels, and muscle layers. In addition, receptors for neurotransmitters are present on and near epithelial cells. The spatial density of myenteric neurons decreases with age. Additionally, toxic substances such as anthraquinone injure the nerve fibers and may alter the number of neurons. Topical application to the GI tract of cationic surfactants, such as benzalkonium chloride (a mixture of compounds) or benzyldimethyltetradecylammonium chloride, destroys intrinsic neurons in the myenteric plexus of the small intestine as well as damages smooth muscle. After nearly complete regeneration of the smooth muscle, the damage to nerves persists.

The small intestine contains small-diameter sensory nerve fibers in the mucosa and tunica muscularis, which can be stimulated by capsaicin to release substance P and calcitonin gene-related peptide (CGRP). These sensory nerve fibers have the potential when hyperstimulated to initiate a cascade of proinflammatory events and transmit nociceptive information to the central nervous system. The contractile effects of intragastric capsaicin via release of substance P and CRGP in the colon can be inhibited by muscarinic antagonists, implying that cholinergic neural pathways are involved in this sensory-motor pathway of reflex motility.

There are three principal motility patterns of the GI tract: storage, mixing, and propulsion. Movement of a swallowed bolus from the mouth to the stomach and into the intestinal tract is a propulsive event, caudally progressing in front of a contraction wave of the circular muscle layers in various digestive tract segments. Effective gastric emptying requires coordinated propulsive contractions in the antrum that progress to the pyloric canal, as well as properly timed relaxation of the upper duodenum. Some drugs and toxicants reduce the rate of gastric emptying by producing contractions of the duodenum that abolish the antral-duodenal pressure gradient required for effective emptying.

Contractions of the circular muscle occur more or less randomly but are somewhat fixed in timing and location by the electrical slow waves or electrical control activity generated initially in interstitial cells (of Cajal), which serve as bioelectrical pacemakers for smooth muscle. Clusters of propulsive contractions associated with contractile rings migrate 5–30 cm caudally, thereby propelling content toward the cecum. Toxic agents that induce excessive migrating clustered contractions would abnormally speed propulsion through the small intestine, which can impact electrolyte, nutrient, and water absorption.

Migrating motor complexes are bands of contractile activity that move caudally over the stomach and small intestine during fasting to sweep digested food remains out of the stomach. These motor complexes are active during periods of fasting and continue until another meal is consumed. The central nervous system exerts some degree of control over the activity of these complexes, but the actual complexes are initiated in the enteric nervous system. Premature migrating motor complexes can be induced by opiates and erythromycin.

Biotransformation

The mucosa of the GI tract is a site of high enzymatic activity and compound conjugation. The mucosa is exposed to the highest concentration of orally administered compounds and can modify these compounds prior to their entry into the blood. The consequences of mucosal biotransformation can be compound activation or deactivation (detoxification) (Figure 15.5).

Intestinal mucosal enzymes that metabolize xenobiotics can prevent systemic absorption of many potentially toxic substances such as peptides (via peptidases), esters (via esterases), and alcohols [via alcohol dehydrogenase (ADH)] present in the gastric

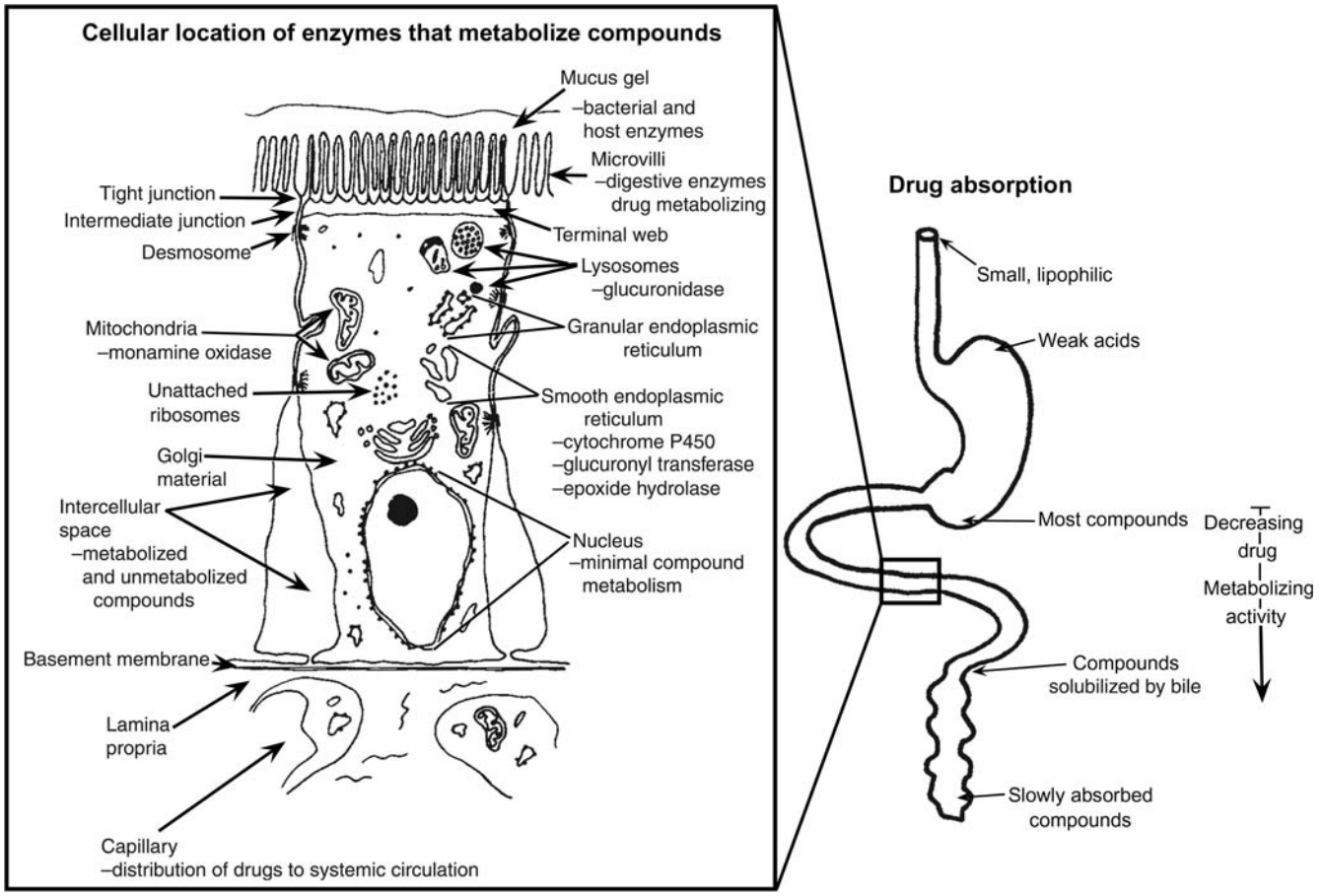

FIGURE 15.5 Biotransformation of compounds is a complex event involving absorption and metabolism gradients. Different sites of absorption will lead to different enzyme exposures. Compound solubility and transport mechanisms will result in contact with different enzymes. *Figure reproduced from* Handbook of Toxicologic Pathology, *second ed. W. M. Haschek, C. G. Rousseaux and M. A. Wallig, eds. (2002) Academic Press, Fig. 8, p. 138, with permission.*

mucosa. Xenobiotic metabolism also can be carried out by luminal microorganisms; furthermore, luminal organisms can affect mucosal enzyme activity. Factors affecting the metabolic activity of the intestinal microflora must be taken into account in studies of the biotransformation of orally ingested xenobiotics. Marked differences exist in microbial composition and metabolism of the gut flora of different species of animals, and environmental factors such as drugs (especially antibiotics), diet, and xenobiotics can modify microbial metabolism, and thus the toxicity, of foreign compounds. Presystemic clearance can occur for some toxicants either within the enterocyte or within the gut lumen itself. This gut-associated first-pass effect represents the irreversible extraction and/or biotransformation of toxicants passing through enterocytes on their way into the lacteals or portal venous blood. Metabolites produced by enterocyte biotransformation can enter the intestinal lumen, the portal venous system, lacteals, or simply remain stored in the cell. Conjugated water-soluble compounds formed during transport into enterocytes tend to be excreted relatively quickly into the intestinal lumen, and therefore are cleared from the body (Table 15.3). After oral administration, when the concentration of a xenobiotic within the enterocyte is very high, intestinal biotransformation reactions will generally be capacity-limited.

The colon is three- to fivefold more active than the small intestine in certain enzymatic processes (e.g., demethylation). Compared to the liver, jejunum has a higher monoamine oxidase activity. Several compounds, such as polychlorinated biphenyls (PCBs) and phenobarbital, increase cytochromes P450 (CYP) levels in intestinal mucosa 2–4 days after exposure; the effect is greatest after oral administration of the compound. This augmentation of enzyme activity is similar to that which occurs in the liver. As occurs in the liver, chronic intake of ethanol will also increase the level of activity for several intestinal enzyme pathways.

Several biotransforming and toxicant-metabolizing gradients exist in the GI tract (Figure 15.5).

Monooxygenase (CYPs) and uridine diphosphate (UDP)-glucuronosyl transferase activities are higher in the upper duodenum than in the lower small or large intestines. Sulfation proceeds more rapidly in the proximal than in the distal small intestine and colon.

CYP activity in the small intestine provides the principal, initial biotransformation of ingested xenobiotics. Enzymes of enterocytes are fully competent to carry out oxidative, reductive, hydrolysis, and conjugation reactions. The oxidative reactions are largely catalyzed by CYP isozymes. The intestinal mucosa also contains nonspecific esterases and amidases, (UDP)-glucuronosyltransferases, and reductases. Some enzyme activities, such as nitroreductase and dechlorinase, maybe attributable to both mucosal enzymes and luminal microflora. Most CYP isozyme activity increases in enterocytes during their migration from crypt to villus. Nearly all CYP activity is attributable to villous cells, and NADPH CYP 450 reductase is expressed constitutively only in villus cells. Both glucuronidation and sulfation reactions increase solubility of xenobiotics and thus play a major role in intestinal first-pass clearance for various xenobiotics. Intestinal presystemic elimination of a dopamine prodrug, *N*-(*N*-acetyl-L-methionyl)-*O*,*O*-*bis*(ethoxycarbonyl)dopamine, indicates that catechol ester hydrolysis, amido hydrolysis, and catechol *O*-methylation can also occur in enterocytes. A biotransformation gradient from the apical to the basal surface of enterocytes is present; it is controlled by enzyme-rich drug-metabolizing organelles (e.g., SER) and active transport systems in the apical cell membrane. However, the gradient varies with the cellular location in the GI tract and route of exposure. Compounds entering from the blood (basal) side can be found in the GI tract lumen independent of enterohepatic circulation. Many toxicants enter the intestinal contents by direct transfer from blood or when released out of the enterocyte. In general, intestinal excretion is a relatively slow process that is important for chemicals having low rates of biotransformation and/or low renal or biliary clearance.

Although passive diffusion is an important mechanism for intestinal excretion, active secretion of organic acids and bases has been demonstrated in the gut. The transepithelial elimination of ciprofloxacin in rabbits and rats is probably due to active transport. It has been shown that P-glycoprotein (Pgp) mediates efflux of etoposide out of intestinal cells, and this efflux is inhibitable with quinidine. Pgp is the 170-kDa product of the ABCB1 gene in humans and is an ATP-powered efflux pump which can transport hundreds of structurally unrelated hydrophobic amphipathic compounds, including therapeutic drugs, peptides, and lipid-like compounds. An organic cation transporter, originally identified in kidney and liver that is responsible for translocation of hydrophobic and hydrophilic organic cations of different structures has also been identified in the intestine. As an adaptive response to renal failure, the intestine can excrete chemicals such as oxalate. In addition, epithelial cells of the GI tract can absorb and export compounds from the circulating blood and the intestinal lumen, indicating that many intestinal transport systems are likely "two-way streets."

Disposition of highly lipophilic chemicals in an organism often requires consideration of lipid transport. The two important mechanisms that contribute to the nonbiliary intestinal excretion of lipids are (1) exfoliation of intestinal cells and (2) exudation of lipids across the mucosa.

Besides altering the biological activities of toxicants, biotransformation reactions in enterocytes may influence the postabsorptive fate of xenobiotics. Metabolites maybe excreted by enterocytes into the intestinal lumen and eliminated as fecal matter, thereby permitting escape from enterohepatic circulation. Metabolites maybe either excreted across the mucosal membrane, back into the lumen, or secreted across the serosal membrane into portal venous blood.

Blood supply to the mucosa is a critical component of mucosal biotransformation. Provision of oxygen to the epithelium is important in oxidation and reduction reactions. The microvascular anatomy of the mucosal villi provides a countercurrent exchange system, which can reduce entry of a toxicant into the portal circulation. As the toxicant is picked up in the villus and moved to the crypt, exchange with blood going to the villus occurs, resulting in slower compound absorption and increased time for biotransformation (Figure 15.6).

Fecal excretion is a major route of elimination for many lipophilic chemicals, with most toxicants probably being transferred by passive diffusion and a number excreted into the feces by nonbiliary pathways. Direct mucosal-to-serosal transport into the feces occurs for some nonpolar, lipophilic xenobiotics that undergo little or no biotransformation. However, rapid exfoliation of intestinal cells may also contribute to fecal excretion of some toxicants. The intestinal excretion rate of some lipophilic chemicals can be substantially enhanced by increasing the lipophilicity of the GI contents by, for example, adding mineral oil to the diet.

Enterohepatic Circulation

Enterohepatic circulation allows for recycling of metabolized and nonmetabolized compounds, and is of critical importance in toxicologic processes involving the GI tract. This circulatory route is active when ingested compounds that are absorbed in the GI tract enter the portal circulation, go to the liver, and then return to the

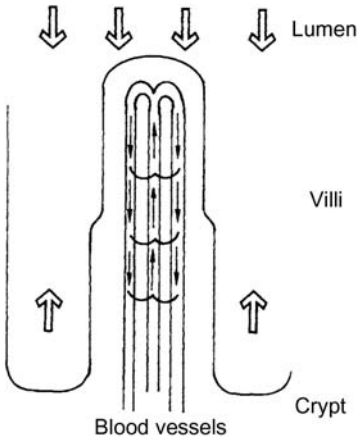

FIGURE 15.6 Countercurrent mechanism that is active in the individual villi. Blood is carried into the villi from the lamina propria. A countercurrent exchange mechanism is established by blood going to the villus tip and blood returning toward the crypt region of the lamina propria. The exchange operates primarily through passive diffusion and allows absorbed compounds, obtained in the lumen, to be carried back to the villus tip against a concentration gradient. This process is active for nutrients, diffusible compounds, and gases (e.g., O_2 and CO_2). *Figure reproduced from* Handbook of Toxicologic Pathology, *second ed. W. M. Haschek, C. G. Rousseaux and M. A. Wallig, eds. (2002) Academic Press, Fig. 9, p. 140, with permission.*

GI tract via biliary excretion. The enterohepatic circulatory pathway can also be utilized by dermally absorbed or inhaled materials that are excreted in the bile.

A compound leaves the enterohepatic circulation if it passes in the feces before being reabsorbed or into the urine before being cleared by the liver. The ultimate destiny of a compound is dependent on its chemical composition and the species. The importance of species differences is best illustrated by the nonsteroidal antiinflammatory drug (NSAID) indomethacin, which undergoes enterohepatic circulation; it is excreted in the feces of dogs but in the urine of rats. The duration of enterohepatic circulation is most extensive for this drug in dogs and rats, and least extensive in rabbits and humans. This observation impacts resulting species-specific variability in the toxic response of the GI tract to NSAIDs, with dogs being less tolerant of NSAID administration when compared to rats, rabbits, or humans.

The amount of a compound that is excreted in the feces is controlled by the lipophilicity of the chemical and the extent of metabolism that alters this lipophilic character. Processes that increase the aqueous nature of a compound include dealkylation, glucuronidation, and sulfation. One process that increases lipophilicity is glucuronide hydrolysis, often by microbial glucuronidases. Increasing lipophilicity is associated with higher excretion of the compound in feces.

The rate at which a chemical is excreted in the feces is limited by the time it takes for a compound to be excreted in the bile and reabsorbed by the intestine. Increasing metabolism of the chemical will raise the rate of excretion. Factors that modify this excretion rate include motility of the intestine, distance of the site of (re)absorption from the major duodenal papilla (site of common bile duct entry), rate of conjugate hydrolysis by GI bacteria, transport rate across the intestinal wall, and motility of the gall bladder (in species which have this structure). With the exception of gall bladder motility, all factors influence intestinal transit time.

Combined biotransformational processes in the liver and intestine can substantially affect the toxicity of a compound. For example, the activation of diphenolic laxatives by microbial metabolism in the GI tract, and conjugate hydrolysis by these microbes has been clearly established. Bacteria can also modify dinitrotoluene by nitro-reduction and give rise to elevated hepatic levels of the carcinogenic metabolite dinitrobenzyl alcohol. Arylamines formed from the biliary metabolite of chloramphenicol maybe responsible for the goitrogenic effect of this antibiotic in rats. Hydrolysis of polycyclic aromatic hydrocarbon glucuronide metabolites demonstrates how enterohepatic circulation can reactivate a detoxified compound. These are just a few of many instances of how enterohepatic circulation can affect toxicity.

During enterohepatic circulation, compounds may interact with intestinal contents. This is demonstrated by the binding of bile salts to dietary fibers. Such binding will decrease the reabsorption of bile salts, and maybe partially responsible for the healthful effects of soluble fibers. Alteration of bile acid circulation can influence the hepatobiliary level of several compounds that are bile-soluble (cholephils). In addition, the bile salt taurocholate promotes motor activity in the colon, thereby reducing intestinal transit time. Bile salts also increase the transport of compounds across the intestinal mucosa, and may consequently enhance the toxic properties of a compound.

Enterohepatic circulation will increase the toxicity of a compound to organs in the enterohepatic circuit if the compound remains active during circulation. The concentrating capacity of enterohepatic recycling may play an important role in the ulcerogenic effects of NSAIDs (such as indomethacin) in dogs. This same process maybe important in the carcinogenic effects of 3,3-dimethoxybenzidine and tris(2,3-dibromopropyl) phosphate in the colon. Biliary excretion and enterohepatic circulation have a role in colon carcinogenesis of rats induced by 2,3-dimethyl-4-aminobiphenyl (DMAB). Rats treated orally with this compound excrete mutagenic agents in the bile. However, rats injected subcutaneously with DMAB do not develop colonic neoplasms.

The Microbiome

Ingested materials are metabolized not only by digestive and intestinal enzymes but also by resident bacteria (Table 15.5). These bacteria have metabolic activities that include reductases, hydrolases, demethylases, β-glucuronidases, and β-glucosidases. Since there are approximately 10^9–10^{12} bacteria per gram of feces in humans and animals, the potential enzymatic activities of this compartment of the GI tract cannot be ignored. The microfloral composition in mammals depends on the nutritional and health status of the host, and also the host's dietary composition.

Microorganisms have an active metabolic function promoting a wide variety of biochemical reactions important in normal vertebrate as well as bacterial physiology. With the exception of ruminants, most bacteria are present in the lower small intestine, cecum, and colon. There is a gradual transition from sparse gram-positive microflora in the stomach to a mixture of gram-positive and gram-negative bacteria in the ileum and finally a preponderance of gram-negative bacteria in the large intestine. Bacterial concentrations in excess of 10^{12}/mL of ingesta are common. Anaerobic bacteria outnumber aerobic species by a factor of 10^2–10^4. Frequently identified anaerobic microorganisms include Bacteroides, Bifidobacteria, and Eubacteria, anaerobic gram-positive cocci, and *Clostridium* sp. Aerobic isolates include species of Enterobacteriaceae, enterococci and other streptococci, staphylococci, and also the fungus *Candida*.

The influence of intestinal microbes on the host's nutritional status has been clearly demonstrated. Weight of the GI tract and mucosal thickness are markedly reduced in animals without bacteria in their gut contents. Conversely, bacterial overgrowth can modify lipid and carbohydrate absorption. Overgrowth of intestinal bacteria can lead to steatorrhea due to hydrolyzing bile-acid conjugates and altering micelle-forming abilities of the microflora. Bacterial proteases also remove maltase from brush border membranes, which results in carbohydrate malabsorption. Consequently, compounds altering microbial populations can lead to altered nutritional status. The composition of the GI microbiome may influence the onset and progression of degenerative processes in more distant systems (e.g., neurodegenerative diseases).

TABLE 15.5 Microbial Density in Different GI Compartments of Humans and Mice

	Human		Mice	
Organ/ tissue	**pH gradient**	**Microbial mass (cells/mL)**	**pH gradient**	**Microbial mass (cells/g)**
Stomach	1.5–5.0	10^2–10^3	3.0–4.5	10^7–10^9
Duodenum	5–7	10^3–10^4	4.5–5.0	10^7–10^9
Jejunum	7–9	10^4–10^5	4.5–5.5	10^7–10^9
Ileum	7–8	10^8	4.5–5.5	10^7–10^8
Cecum	–	–	4.3–5.0	10^7–10^8
Colon	5–7	10^{11}–10^{12}	4.5–5.0	10^9–10^{10}

Table adapted from Handbook of Toxicologic Pathology, *third ed. W. M. Haschek, C. G. Rousseaux and M. A. Wallig, eds. (2011) Academic Press, Table 56.5, p. 2298, with permission.*

Bacteria produce and release compounds that have local effects or, if absorbed, systemic impacts. Mammalian metabolic pathways generally require oxygen, so injurious compounds are generally detoxified by oxidation and conjugation pathways. However, gut bacteria are active in oxygen-free environments and thus utilize reduction and hydrolysis reactions, resulting in different metabolites with potentially harmful side effects. The role of bacteria in modifying host responses is most marked in the lower segments of the GI tract. For example, the pharmacologic activity of digoxin is dependent upon bacterially mediated hydrolytic removal of a trisaccharide, which releases digoxigenin. In some individuals, however, there is a further reduction in the double bond of the lactone ring by *Eubacterium lentum* present in the colon, which results in the formation of a pharmacologically inactive substance, dihydrodigoxigenin. Diet appears to play a role in the presence of this bacterial species and the frequency of digoxin inactivation in humans.

Bacterial deamination is another important metabolic activity that is mediated by the bacterial flora. The breakdown of urea into carbon dioxide and ammonia is catalyzed by bacterial urease. Approximately, 40% of the urea synthesized by the liver is degraded by a variety of aerobic and anaerobic bacteria.

The role of bacteria in GI toxicity is most clearly defined for carcinogen activation. Many indirectly acting chemical carcinogens require enzymatic activation before they can cause cellular transformation. Bacterial β-glucuronidases can deconjugate glucuronides and lead to the release of carcinogenic aglycones. Additionally, fecal flora nitroreductases can activate procarcinogens. Bacteria also have a direct role in the detoxification process. Bacteria can deactivate carcinogens by *N*-dehydroxylation.

Antibiotics can not only modify bacterial populations in the GI tract but also depress neuroeffector and neuromuscular transmission in the walls of digestive organs. *In vitro* studies have demonstrated that ampicillin, lincomycin, erythromycin, and clindamycin depress contractions of the muscularis mucosa. Clindamycin and erythromycin depress the responses of the muscularis mucosa to acetylcholine. As an example, impaired GI motility after administration of

oral antibiotics can facilitate the proliferation of *Clostridium difficile* in the lower GI tract and lead to pseudomembranous colitis.

Microbial metabolism in the gut also serves to detoxify many toxic xenobiotics and protect or suppress the harmful effects of the xenobiotic metabolites on the host. Examples of such metabolized drugs/additives that are degraded by microflora include digoxin, diethylstilbesterol, estrogens, cyclamate, azulfidine, 3,4-dihydroxyphenylalanine, amygdalin, metronidazole, caffeine, propachlor, morphine, buprenophine, oxazepum, phenolphthalein, warfarin, and dichlorodiphenyltrichloroethane (DDT).

Intestinal microbiota, however, also have many bacterial enzymes that can catalyze the production of mutagens, carcinogens, and tumor promoters. Examples of these enzymes include β-glucuronidase, β-glucosidase, β-galactosidase, nitroreductase, azoreductases, tryptophanase, and 1-α-steroid dehydrogenase, to name a few. These enzymes can act on a variety of substrates, including nonnutritive plant material, as well as metabolize administered drugs/toxicants and supplements/additives. Some examples of substrates that are acted upon by gut microfloral enzymes to become mutagenic include cycasin (a plant-derived β-glucoside; carcinogenic), 2-nitofluorene, trypan blue, tryptophan, and dimethylamine.

EVALUATION OF GASTROINTESTINAL TOXICITY

The ability of the GI tract to adapt to various diets and nontoxic compounds is well established. Both adaptational and toxicologic processes can be manifested by altered structure or function. Evaluation of these processes requires a basic understanding of the mechanism or suspected pathogenesis of the toxic injury or response. Routine approaches involve *in vitro* and *in vivo* methods. Because alterations in numerous other organ systems can occur as a result of GI toxicity, whole animal studies are generally required in order to properly interpret GI toxicity. As a result of this complex interrelationship among organ systems and the inherent complexity of the GI tract, animal models have been developed to study various GI diseases and toxicities. This section will focus on conventional morphologic assessments of injury as applied to animal models (including knockout/transgenic models) of GI toxicity.

Morphological Methods

Evaluation of the GI tract for toxicity should be conducted using macroscopic, microscopic, and ultrastructural methods. Macroscopic evaluation includes identification of ulcers, enlarged lymphoid tissues (e.g., Peyer's patches), neoplasms, and foreign bodies. Microscopic studies should be conducted on all lesions observed macroscopically, and also at preselected sites in macroscopically normal organs. Proper tissue fixation is essential for structural studies. In an attempt to standardize communications, specialty organizations are adopting harmonized nomenclature for the description of microscopic lesions in certain portions of the GI tract (Table 15.6). The most current terminology, including representative images of common lesions, developed by the International Harmonization of Nomenclature for Diagnostic Criteria in Rats and Mice, is now available on the Society of Toxicologic Pathology website (http://www.toxpath.org/inhand.asp).

Assessment of morphological alterations of the GI tract should consist of close evaluation of the mucosa and its specializations. The mucosa consists of surface epithelium, crypts/glands, lamina propria, and a thin layer of muscle (the muscularis mucosae) separating the mucosa and submucosa. Specializations of the mucosa include glands of the esophagus, foveolae of the stomach, villi of the small intestine, and glands of the large intestine. The submucosa and the tunica muscularis (outer muscle layers) also should be examined for changes in thickness and cellularity.

Villi should be evaluated critically when assessing small intestinal toxicity. Since villi bend in various directions, and have shapes that vary with species (e.g., tongue-like in rats and finger-like in humans) and location (longer in the duodenum than in the ileum), close comparisons with control animals is required to prevent misinterpretation.

Changes in the lamina propria will be detected by assessing alterations in the normal cell population. Neutrophil, eosinophil, lymphocyte, and plasma cell populations may change. An increase in any of these populations is a potential indication of an underlying toxic or disease process. Inflammatory cell infiltrates frequently occur secondary to epithelial cell toxicity. Lymphoid follicles may develop and be associated with an extensive increase in lymphocytes and plasma cells. These follicles may occur in the lamina propria or submucosa. Additionally, lymphomas maybe indicated by a substantial number of abnormal lymphocytes expanding the lamina propria. Additional sites of potential injury in the lamina propria include blood vessels and lacteals (lymphatic capillaries). Common lesions associated with GI toxicity include vascular blockage (thrombosis), dilation (e.g., lymphangiectasia), and rupture.

Changes in the submucosa may involve blood vessels, nerves, and lymphatics. Alterations in these

TABLE 15.6 Nomenclature for Describing Lesions of the Gastrointestinal Tract

Location	Term	Definition	Term	Definition
Oral cavity	Proliferative lesions		Inflammatory and ulcerative lesions	
	Hyperplasia	Broad areas of thickened and differentiated epithelium especially the keratin layer; which may have prominent papillary endophytic projections	Stomatitis	Initial lesions frequently begin as ulcerative processes followed by neutrophilic exudative phase; established lesions have lymphocyte and plasma cell accumulation; advanced lesions can be associated with alveolar bone loss; dietary content influences extent; severity and frequency of lesion
Esophagus	Proliferative lesions		Degenerative lesions	
	Hyperkeratosis/ parakeratosis	Thickened mucosal layer with retraction of nuclei; absence of cellular atypia	Megaesophagus	Esophageal enlargement; degeneration of muscle and nerve cells in the wall
Stomach	Degenerative lesions			
	Mucosal atrophy	Results from ulceration, inflammation, mineralization, or infarction; glandular ectasia and inflammation or fibrosis of lamina propria		
	Chief cell atrophy	Age-related decrease in size and number of chief cells		
	Intestinal metaplasia	Focal crypt and villous formation with goblet cells and Paneth cells; complete forms have a small intestinal morphology while incomplete forms have a large intestinal morphology		
	Nonneoplastic lesions of the glandular mucosa		**Neoplastic lesions of the glandular mucosa**	
	Erosion	Area of superficial necrosis of the mucosa that does not extend beyond the muscularis mucosa	Adenoma	Adenomatous polyps are usually located in the antrum and are composed of basophilic columnar epithelium organized into glandular structures; mass maybe pedunculated or endophytic and arise in areas of reactive hyperplasia
	Ulceration	Area of mucosal necrosis that extends to or through the muscularis mucosa	Adenocarcinoma	Lesions invade into the submucosa and may metastasize or locally infiltrate; cytologically, cells range from dysplastic to anaplastic with pleomorphic nuclei and increased mitotic index
	Glandular dilation	Distention of the basal portion of the gastric gland; distention maybe sufficiently large to form a microcyst	Neuroendocrine cell tumor	Also called carcinoids; rarely spontaneous; characteristic lesion of potent gastric antisecretory agents causing hypergastrinemia; agyrophilic cells forming the tumor are reactive for nerve specific enolase and chromagranin-A; maybe intramucosal or invasive
			Nonneoplastic lesions of the nonglandular mucosa	
	Eosinophilic chief cells	Infrequent spontaneous lesion that maybe associated with lymphoma of gastric mucosa or other disease; induced by antisecretory drug treatment; reversible, nonprogressive alteration only reported in rats	Hyperplasia	maybe a focal or diffuse thickening characterized by increased numbers of one or more cell types (basal, spinous, or granular); focal hyperplasia is differentiated from papilloma by the absence of a connective tissue core containing blood vessels and the presence of an intact muscularis mucosa
	Hyperplasia (focal)	Most common type is associated with erosions or ulcers and found primarily in the antrum; hyperplastic glands may extend through the muscularis mucosae forming persistent adenomatous diverticula	Hyperkeratosis	Increased thickness of nonnucleated keratin layer
			Neoplastic lesions of the nonglandular mucosa	
	Hyperplasia (fundic)	Also called hypertrophic gastritis or adenomatous hyperplasia; associated with administration of antisecretory compounds; result of endocrine stimulation of the oxyntic region; generalized increase involving all cellular compartments	Papilloma	Pedunculated with a prominent connective tissue core; evidence of localized invasion through the muscularis mucosa near base of papilloma should be considered evidence of carcinoma formation

(*Continued*)

TABLE 15.6 (Continued)

Location	Term	Definition	Term	Definition
	Hyperplasia (neuroendocrine)	Specific neuroendocrine cell hyperplasia in response to endocrine alterations; in rats, enterochromaffin-like (ECL) cells are the main cell types responsive to hypergastrinemia; in mice; basal portions of gastric glands may normally be lined by pure populations of neuroendocrine cells	Adenoma	Circumscribed areas of dysplastic epithelium that distorts adjacent normal mucosa and is confirmed by a basement membrane; same tumors maybe sessile or pedunculated
			Carcinoma	Locally invasive lesion that is a neoplastic proliferation of squamous epithelium
Small and large intestine	Proliferative lesions		Neoplastic lesions	
	Reactive hyperplasia	Epithelial cells are basophilic and depleted of mucus with enlarged nuclei containing prominent nucleoli; crypt herniation may occur especially if the muscularis mucosae has been disrupted; in the small intestine, reactive hyperplasia can be accompanied by villous atrophy	Adenoma	Circumscribed areas of dysplastic epithelium that distort adjacent normal mucosa and are confirmed by a basement membrane; same tumors maybe sessile or pedunculated
	Focal atypical hyperplasia	Crypts are elongated and have dilated lumens and may have a tortuous contour; architecture of the adjacent mucosa is not distorted by compression; epithelial cells lining the crypts are normal to markedly dysplastic and may forma single layer or be pseudostratified with many mitotic figures; goblet cell numbers are reduced; severe inflammatory reactions maybe associated with these foci	Adenocarcinoma	Dysplastic epithelium with clear evidence of invasion past the basement membrane into the lamina propria or submucosa; the invasive characteristics of adenocarcinomas must be differentiated from tangential cuts of glands in the lamina propria found at the base of adenomas; there maybe a scirrhous (desmoplastic) and/or inflammatory response which can help differentiate invasive epithelial nests from cryptal herniation; adenocarcinomas of the small intestine are more invasive and metastasize more frequently than those of the large intestine

Information adopted and modified from Nolte, T., Brander-Weber, P., Dangler, C., Deschl, U., Elwell, M.R., Greaves, P., Hailey, R., Leach, M.W., Pandiri, A. R., Rogers, A., Shackelford, C.C., Spencer, A., Tanaka, T., and Ward, J.M. (2016). Nonproliferative and proliferative lesions of the gastrointestinal tract, pancreas and salivary glands of the rat and mouse (review). J. Toxicol. Pathol. *29 (1 Suppl), 1S–124S.*

structures in this region are frequently characterized by lymphangiectasia and inflammatory or neoplastic cell infiltrates.

Different fixatives are used for histologic evaluation of GI organs, depending on the purpose of the study and the technique being used. A routinely used multipurpose fixative is neutral buffered 10% formalin. Because of rapid postmortem autolysis, GI tract tissues must be placed into the fixative within 1–2 minutes of death for optimal preservation. In some laboratories, it is routine to immerse the entire segment of GI tract of interest overnight in neutral buffered 10% formalin. Upon completion of fixation, the GI tract is opened longitudinally and flushed extensively with sterile water to remove any fecal matter. Segments of the fixed GI tract may then be dissected out and embedded in polymer resin prior to sectioning and histological analysis. Alternatively, fecal matter maybe removed from the mucosa prior to fixation by flushing the surface with physiological saline (rather than water, which may promote osmotic rupture of epithelial cells).

Ultrastructural studies can be conducted using scanning or transmission electron microscopy (TEM). Scanning electron microscopy provides information on surface alterations. This technique is particularly useful for examining altered villus structure in the small intestine. TEM, although not utilized as extensively as in the past, is valuable for identifying subtle changes in organellar structure that precede later, more "generic" histologic changes and thus give an indication of possible mechanism(s) of injury. Morphometric and stereological analyses at the light microscopic and electron microscopic level are powerful morphological methods that can combine biochemical and morphological data.

Normal cellular proliferation, differentiation, and senescence are processes that have distinctive phenotypic and genotypic characteristics. These molecular alterations can be examined phenotypically by using a variety of histo- and immunohistochemical marker. For example, for enterocytes various disaccharidases, Intestinal Fatty Acid Binding Protein, Enterocytin, MDM4, Epithelial Cell Adhesion Molecule (EpCAM) and various cytokeratins (CK 8, CK 18, & CK 20) can be used, whereas in colonocytes Carbonic Anhydrases 1 & 2 (CA-1 & CA-2) as well as the plant lectin DBA have been utilized to identify these "mature"

nonproliferating cell populations. For proliferative crypt cell populations, the nonspecific Proliferating Cell Nuclear Antigen as well as more specific Lysozymes 1 & 2 (Lyz1 & Lyz2), α-defensins (Defa 5 & Defa 22), β-catenin and Epbh2 can be used of identification. Paneth cells express a combination of markers seen in both proliferative crypt cells and nonproliferative enterocytes, including MDM4, α-defensins and Epbh2. An understanding of the genetic control of proliferation and differentiation via Wnt and Notch signaling pathways, for example, can be obtained using techniques such as in situ hybridization and rtPCR.

Animal Models

General Considerations

Variations in mammalian GI tract morphology show closer correlation with diet, body weight, and the need for water consumption than with taxonomical classification. The capacity of the GI tract to hold digesta decreases with decreasing body weight in herbivorous animals; however, the rate of metabolism increases with decreasing body weight. Smaller animals may have various strategies to compensate for this phenomenon. These adaptive mechanisms include an increase in cecal volume or the practice of coprophagy by lagomorphs and rodents. Because of these modifications, the GI tract in these species may render them unsuitable as animal models for humans.

Nutritional issues must be considered when extrapolating results from GI studies performed in healthy animals to humans. Generally, compounds of therapeutic importance are administered to human patients who are ill and consequently malnourished. In contrast, toxicologic effects of therapeutic or other beneficial compounds are tested in healthy animals. These animals are fed nutritionally balanced commercial diets for their lifespan, and are allowed to grow and develop under ideal conditions of lighting, temperature, and humidity. Since macronutrients in the diet markedly affect the drug-metabolizing enzyme systems associated with the GI tract, such modifications may alter the maximally tolerated dose in test animals relative to a tolerable dose for sick humans.

Evaluation of the GI tract for toxicity must involve consideration of dietary effects on the mucosa. All diets support normal growth and health conditions of rats, yet the absorption site (mucosa) in the animals fed a semipurified diet varies significantly among the various formulated diets. This indicates that structural and functional results that are observed maybe independent of a compound's toxic or biological effects.

Since many mammalian systems (including humans) have similar mechanisms of response to toxic compounds, animal models serve as ideal test systems for the evaluation of toxic potential, pathophysiological responses, and systemic complications of an ingested or injected compound. In contrast to toxicity testing of compounds for human or animal use, animal models of human diseases are generally defined only on the basis of specific pathologic criteria. The specific lesions may be subtly or markedly different, but the general character of the disease process is usually similar to that observed in the human disease; otherwise, the animal model would be discarded.

The few examples below demonstrate the significance and problems of using models for investigating the toxicity and efficacy of any compound that could produce lesions in the GI tract. Animal models allow the testing of the structure–function activity of chemical compounds, as well as the identification of chemical therapeutics for human and animal disease. Additionally, basic information on the pathogenesis of the underlying cellular and biochemical processes important to lesion development can be identified. Finally, animal testing provides a substantial and significant bridge between *in vitro* testing and the ultimate application of any compound for human use.

Specific Models

ULCERATIVE LESIONS OF THE STOMACH AND SMALL INTESTINE

Propionitrile, cysteamine, 3,4-toluenediamine, and 1-methyl-4-phenyl-1,2,3,6-tetrahydro-pyridine produce acute and chronic gastric and duodenal ulcers in rodents. The morphological appearance of duodenal ulcers produced by these compounds in rats is similar to that seen in humans (Table 15.7).

COLITIS AND TYPHLITIS

Experimental models of colitis have been created in a number of laboratory animals (e.g., rats and guinea pigs) with ricinoleic acid, bile acids, poligeenan, melphalan, formaldehyde, alcohol, dextran sodium sulfate, and acetic acid. Some of the lesions observed in these models maybe mediated by mechanisms involving hypersensitivity or alterations in prostaglandin synthesis, and are frequently associated with colon cancer if the compound induces an inflammatory process that is longstanding (e.g., poligeenan). Intracolonic administration of the hapten trinitrobenzene sulfonic acid (TNBS) will also lead to an immunologically based colitis. This model is best demonstrated if damage to the mucosal barrier occurs prior to compound exposure (Figure 15.7).

TABLE 15.7 Selected Characteristics Comparing Cysteamine-Induced Duodenal Ulcers of Rats to the Natural Disease of Humans[a]

	Rat duodenal ulcer	Human duodenal ulcer
Location of ulcer	Anterior and posterior wall	Anterior and posterior wall
Tendency to perforate	+	+
Occurrence of massive bleeding	+	+
Chronic and active ulcers	+	+
Pyloric ulcers	+	+
Increased gastric acid release	+	+
Elevated gastrin levels	+	±
Responds to therapy:		
Antisecretory agents	+	+
H_2 receptor antagonists	+	+

[a]*Modified from Cheville, N.F. (1980) Discussion: Period 3, from "Criteria for development of animal models of diseases of the gastrointestinal system." Am. J. Pathol. 101, S77–S89.*
Table adapted from Handbook of Toxicologic Pathology, *second ed. W. M. Haschek, C. G. Rousseaux and M. A. Wallig, eds. (2002) Academic Press, Table XIV, p. 179, with permission.*

COLON CANCER

Colon neoplasia represents a leading cause of cancer-related death in Western civilization, but is relatively rare as a spontaneous lesion in laboratory animals. Consequently, a number of experimental models have been generated to evaluate this process. In addition, various animal species and dosing regimens have been used to produce colon cancers in animals (Figure 15.8). Both genotoxic and nongenotoxic models of colon cancer are used, but the chemically induced genotoxic models are most consistent (Table 15.8).

Of the various chemical models available, the hydrazine derivatives have several properties that make them useful for evaluating the two-step mechanisms of colon carcinogenesis. Unlike the skin, colon carcinomas can be obtained in 1,2-dimethylhydrazine (DMH)-treated rats without a preliminary benign tumor stage. The incidence rate is constant and directly proportional to total dose, with an average of one carcinoma per colon per year. This hydrazine derivative produces the promutagenic DNA lesion of *O*-6-methylguanine. In general, hydrazine models demonstrate that dysplastic or adenomatous changes are not obligatory stages before cancer; however, these lesions do indicate an increased risk of cancer development. The models may also be used to determine whether the major factors in determining

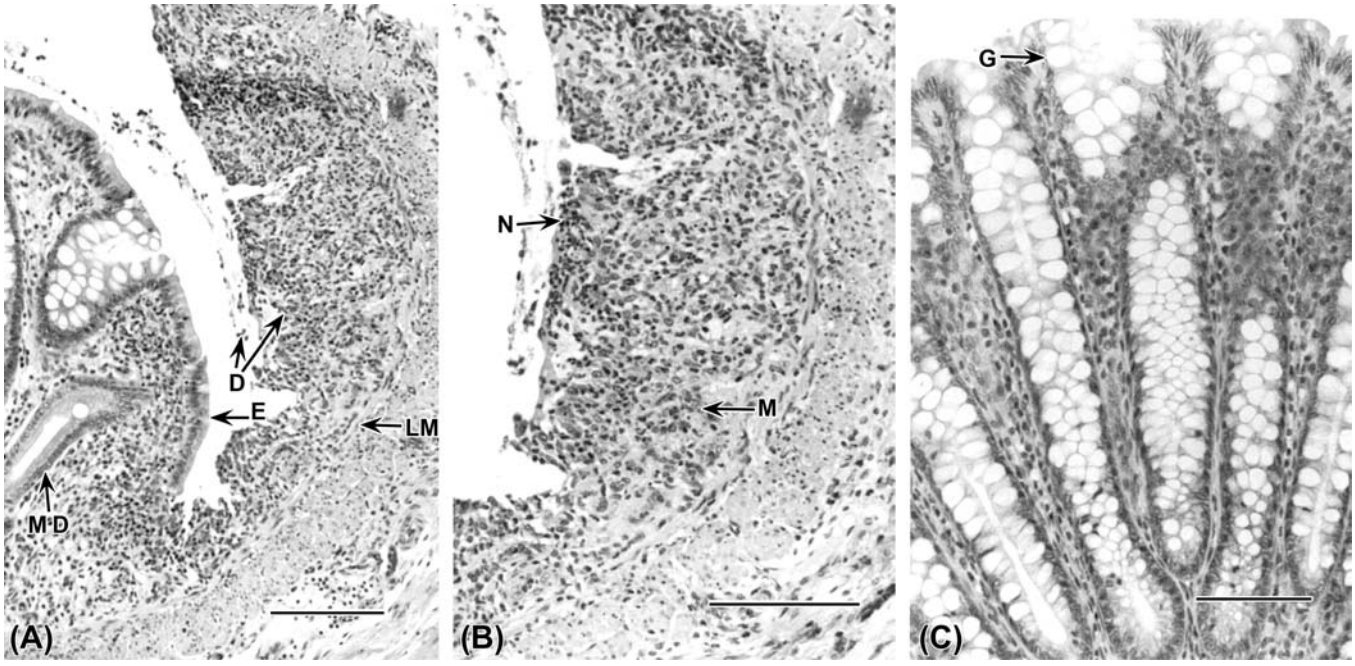

FIGURE 15.7 Dextran sodium sulfate (DSS)-induced ulceration and inflammation in rat large intestine. (A) Transmucosal ulceration extends to lamina muscularis (LM). Lamina propria is thickened by inflammatory cells. Surface epithelium (E) is replaced by a covering of necrotic tissue embedded in proteinaceous and inflammatory-cell-rich exudate (D). Mucus is depleted in epithelial cells (MD) in crypts near ulcer. Bar = 200 μm. (B) Higher magnification of (A) demonstrating many neutrophils (N) and macrophages (M) that characterize the infiltrating inflammatory cells in the lamina propria. Bar = 100 μm. (C) Normal colonic mucosa has a goblet cell (G)-rich epithelial mucosa. Note the lack of leukocytes in the colonic lamina propria of the normal animal. Bar = 50 μm. *Figure reproduced from* Handbook of Toxicologic Pathology, *second ed. W. M. Haschek, C. G. Rousseaux and M. A. Wallig, eds. (2002) Academic Press, Fig. 22, pp. 180–181, with permission.*

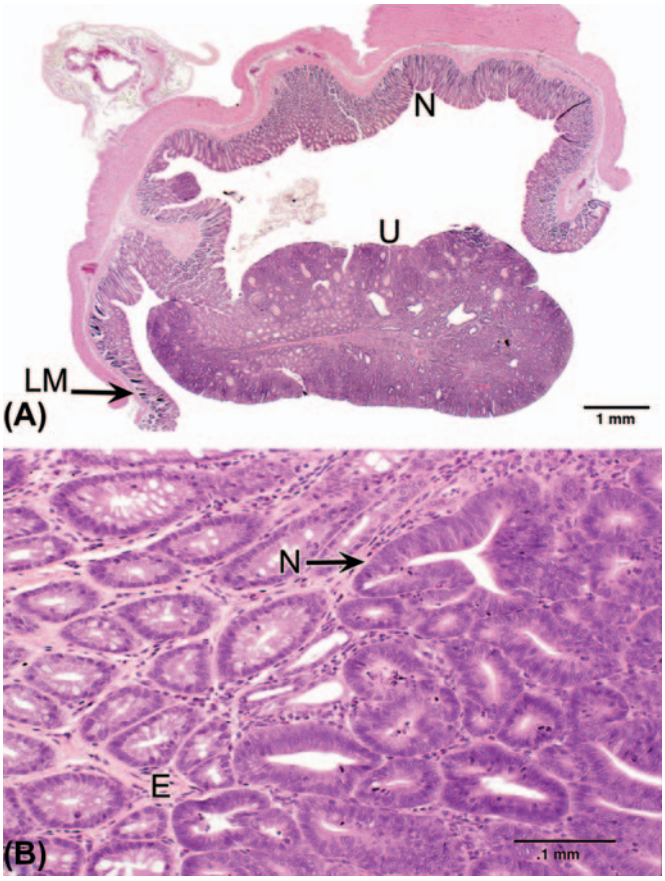

FIGURE 15.8 Adenocarcinoma in colon of a rat orally dosed with bromodichloromethane. (A) Neoplastic tissue has thickened the wall of the colon by penetrating through the lamina muscularis mucosae (LM) and infiltrating into the submucosa. Neoplastic tissue exposed to the lumen is ulcerated (U) and inflamed. Compare the architecture of the neoplasm to that of the more normal adjacent colonic mucosa (N). (B) Neoplastic cells (N) in a loose fibrous-tissue stroma infiltrated by inflammatory cells (E). *Figures provided courtesy of Dr. Susan Elmore, National Toxicology Program, NIEHS. Figure reproduced from* Handbook of Toxicologic Pathology, *third ed. W. M. Haschek, C. G. Rousseaux and M. A. Wallig, eds. (2013) Academic Press, Fig. 13, p. 2323, with permission.*

malignancy are ones that cause benign lesions to become larger, or ones that initiate specific procancerous changes in the DNA.

The rat is widely used as a rodent model of colon carcinogenesis. The F344 strain has a colon with many of the same structural and histochemical features of the human colon. The rat model maybe better than the mouse since colon structure and epithelial-cell histochemical composition in the mouse differs from that of the human. In F344 rats, azoxymethane produces colon cancer within 3 months, and the neoplasms readily metastasize to regional lymph nodes and the liver. This biological behavior is similar to that of certain human colorectal carcinomas.

TABLE 15.8 Animal Models of Colon Carcinogenesis

Chemical	Dose (mg/kg)	Animal
Aflatoxin B_1	0.1[a]	Rat
3,2-Dimethyl-4-aminobiphenyl (DMAB)	20	Rat
	100	Hamster
1,4-*bis*(4-fluorophenyl)-2-propynyl-*N*-cyclooctylcarbamate (FPOC)	125–500[a]	Rat
N-Methyl-*N*-nitrosourea	2–2.5[b]	Rat, mouse, guinea pig
N-Methyl-*N*-nitro-*N*-nitrosoguanidine (MNNG)	2	Rat
Methylazoxymethanol acetate (MAMA)	35	Rat
1,2-Dimethylhydrazine (DMH)	40–200	Rat, mouse, hamster
Azoxymethane	8	Rat

[a]*Dose in ppm.*
[b]*Dose is in mg/week.*
Table adapted from Handbook of Toxicologic Pathology, *second ed. W. M. Haschek, C. G. Rousseaux and M. A. Wallig, eds. (2002) Academic Press, Table XV, p. 183, with permission.*

ENTEROHEPATIC CIRCULATION

Species differences in enterohepatic circulation are primarily determined by variations in biliary excretion. Since the rat is a very good biliary excretor, extrapolation of toxicity data on drugs undergoing enterohepatic circulation from rats to other species may result in over-estimation of a compound's safety or toxicity.

The metabolism and toxicity of drugs maybe influenced by enterohepatic circulation, especially in species, such as rats, deer, and horses, that lack a gall bladder. Because of the concentrating capacity of the gall bladder, compounds maybe concentrated to levels 10 times greater than in hepatic bile. Such concentrating activity, coupled with prolonged biliary retention, may favor passive reabsorption of compounds through the gall bladder mucosa. Additionally, reabsorption would be markedly enhanced by concomitant mucosal injury to the gall bladder epithelium. These factors must be taken into consideration when considering selection of a model for compounds that may enter the enterohepatic circulation.

Knockout/Transgenic Models

Transgenic and targeted gene recombination have been used to study the basic biology and toxicology of the gut in a wide variety of systems. These animal models have been used to study cell growth and regulation, metabolism, mutagenesis, and carcinogenesis.

CELL GROWTH AND REGULATION

TRANSFORMING GROWTH FACTOR-ALPHA In the small intestine and colon, there is regional variation in the production of epidermal growth factor (EGF) and transforming growth factor-alpha (TGF-α). Transgenic mice expressing TGF-α regulated by a metallothionein-inducible promoter/inducer have been created which have a phenotype similar to human Menetrier's disease, including hypertrophic gastric folds with foveolar hyperplasia and cystic dilation, increased neutral mucin staining, and reduced basal and histamine-stimulated rates of gastric acid secretion. Overexpression of TGF-α in the mouse duodenal epithelium results in a pronounced increase in crypt epithelial cell proliferation and increase in crypt–villus dimensions, and suggests that TGF-α maybe a physiological regulator of small intestinal epithelium proliferation.

β-CATENIN A critical component of the Wnt/Wingless signal transduction pathway and an important effector of cell–cell adhesion through cadherins, β-catenin has been implicated in human colorectal carcinogenesis via its association with the *APC* (adenomatous polyposis coli) gene product. However, attempts to genetically engineer mice homozygous for the null allele resulted in early embryogenic death. Recently, chimeric mice were generated with amino-terminal truncated β-catenin to study the effects on proliferation, cell fate specification, adhesion, and migration within the intestinal epithelium. The resulting mice showed marked increases (fourfold) in cell proliferation and apoptosis in the small intestinal crypts, augmentation of cell–cell junctions, and interference with normal cellular migration along the crypt–villus axis, occasionally resulting in abnormal architecture. The significance of these abnormalities to the pathogenesis of colon cancer is still being explored as elevated neoplastic transformation was not observed.

MUTAGENESIS AND CARCINOGENESIS

Investigations of the mutagenicity and carcinogenicity of benzo(*a*)pyrene [B(*a*)P; 75 and 125 mg/kg orally for 5 days] in transgenic lacZ mice (MutaMouse) have demonstrated that the mutation frequency (MF) is increased 37-fold in colon, followed by increases in MF in the ileum > forestomach > bone marrow, spleen > glandular stomach > liver, lung > kidney and heart cells 14 days after the last dose of B(a)P. The main target organs for carcinogenicity in this transgenic mouse strain were the forestomach and lymphatic organs. These studies demonstrate that mutation data reflect carcinogenicity outcome, but not all organs with high frequencies of induced mutation in the lacZ transgene develop tumors, nor does the magnitude of the induced MF in the different target organs correlate with the their carcinogenic responsiveness. Although there is no clear rationale for these discrepancies between MF and cancer susceptibility, possible explanations include (1) the nature of the target gene and type of mutations detected by the transgenic assay (the lacZ gene is neutral and is mainly sensitive to point mutations, which may not reflect the mutations in the cancer genes associated with these tumors); (2) inadequate selection of target cells within the target organs; and (3) the importance of factors such as cell proliferation, turnover, and apoptosis in tumorigenesis at specific organ sites.

Transgenic and knockout models for a wide range of cancer genes, such as *p53* (tumor suppressor gene), *APC* (a tumor suppressor gene), and *ras* (oncogene), have also been created and used to investigate both spontaneous and environmentally induced tumorigenesis in the intestine. Although these models allow for understanding of specific gene changes within the context of a genomic environment of the model species, it is clear from the complexity of gene regulation in different species that extrapolation of carcinogenic vulnerability from one species to another requires information which is currently beyond state-of-the-art interpretation of genomic and proteomic information.

METABOLISM

HEAVY METALS Metallothioneins are low-molecular-weight-inducible proteins, rich in cysteine (~33%), that bind heavy metals. They are associated with the homeostasis of essential heavy metals such as zinc, and also provide protection from exposure to toxic heavy metals such as cadmium. Metallothionein knockout and transgenic mice have been developed to study the expression, distribution, regulation, and function of these proteins, and to investigate heavy metal metabolism and toxicity. Mice transgenic for metallothionein have elevated levels in many tissues, including liver and intestine, and are resistant to dietary zinc deficiency. Knockout mice, in contrast, have delayed renal development and increased sensitivity to zinc and cadmium toxicity.

CYTOCHROME P450 Transgenic and knockout mice of various CYP genes (e.g., CYP1A2, CYP2E1) and the aryl hydrocarbon (Ah) receptor have been constructed to investigate the role of these proteins in phase 1 metabolism of various tissues, including intestine, and their contribution to embryonic development. Proposals have been made to use genetic modification to "humanize" rodent models with human P450s for toxicological studies *in vivo*.

RESPONSE OF THE GASTROINTESTINAL TRACT TO INJURY

Most responses that occur in GI intoxication are ulcerative, proliferative, or inflammatory (Table 15.9). Because of variations in structure and function, each segment of the GI tract is affected by toxic compounds in a slightly different manner. In addition, each segment has a different range of pathophysiological responses to a toxic compound. Clinically, most alterations of the GI tract are manifested clinically as abnormal function, such as vomiting (if the animal is capable of it), diarrhea, constipation, or nutrient malabsorption. Additionally, occult bleeding or large amounts of hemorrhage into the GI lumen may occur and blood, maybe present in the stool. Of these possible manifestations, diarrhea is the most commonly observed sign.

TABLE 15.9 Gastrointestinal Reaction to Various Chemical and Elemental Toxins

Toxic agents	Gastrointestinal pathology
Corrosive agents Mineral acids Iodine Sodium fluoride Strong bases Phenol	Ulcerative gastritis and esophagitis
Volatile organic agents Ethanol Methanol Chloroform Gasoline and kerosene	Gastritis and gastric ulceration
Nonvolatile organic agents Dimethylhydrazines Nitrosoguanidines Nitrosamines	Esophageal, stomach, and intestinal cancer, and/or acute gastritis
Metallic inorganic agents Arsenic Bismuth Copper salts Gold salts Iron salts Lead Manganese Mercury Nickel Thallium Vanadium Zinc salts	Ulcerative, hemorrhagic, and necrotic gastroenteritis and/or colitis
Nonmetallic inorganic agents Phosphorus Nitrites	Ulcerative, hemorrhagic, and necrotic gastroenteritis

Table adapted from Handbook of Toxicologic Pathology, *second ed. W. M. Haschek, C. G. Rousseaux and M. A. Wallig, eds. (2002) Academic Press, Table XI, p. 155, with permission.*

Responses of the GI tract to toxic compounds must be considered on an organ, tissue, and cellular basis. Two specific processes, the inflammatory response and the immune response, are discussed in detail here because many of the disease processes resulting from chemical injury involve these two host reactions. Finally, the response of the enteric nervous tissue is discussed. Although the GI tract has a large amount of autonomic nervous tissue, most neural responses are manifested only on a functional basis.

Pathophysiological Responses

Diarrhea

Identification of mechanisms responsible for diarrhea should focus on the small and large intestine separately as well as collectively. Small intestinal diarrheas are generally associated with increased mucosal permeability, hypersecretion, and/or malabsorption. Major mechanisms of large intestinal diarrhea include hypersecretion, large-bowel malabsorption, and/or direct colonic mucosal injury. Small intestinal malabsorption allows fermentable nutrients to enter the colon, where bacteria generate osmotically active products that hold water in the lumen. Mucosal damage and inflammation lead to release of prostaglandin E_2 (PGE_2), which stimulates electrolyte secretion, and activation of mast cells, with subsequent release of histamine to enhance vascular permeability. Inflammatory cells can also release mediators that stimulate nerve activity, which may lead to localized GI tract hypermotility. Consequently, the pathogenesis of diarrhea can be generally divided into four major categories: (1) increased mucosal permeability and exudation; (2) hypersecretion; (3) malabsorption; and (4) abnormal GI motility.

The exact pathogenesis of diarrhea can vary, but some of the most injurious mechanisms involve toxins or toxicants that affect the GI tract's ability to transport fluid. Since a major function of the GI tract is both to secrete and then absorb large amounts of fluid, such intoxications are life-threatening even though little morphological damage maybe present. This process, and the extent of the resulting diarrhea, is best demonstrated with cholera toxin. Cholera toxin activates adenylate cyclase, resulting in the secretion of large amounts of fluid into the small intestinal lumen, overloading the large intestine's ability to absorb intraluminal water. This process leads to severe diarrhea and death, with little morphological evidence of mucosal damage.

Malabsorptive diarrheas associated with loss of enterocytes, crypt cells or both, often accompanied by

mucosal hemorrhage and inflammation, are commonly associated with GI toxicosis. This type of diarrhea is more often accompanied by morphologic changes, although they are relatively nonspecific. These lesions maybe site-specific, however, providing a clue to the type of toxicant involved. For example, corrosive agents are far more likely to cause necrosis and inflammation in the pharynx and esophagus than lower down in the GI tract.

Coordinated peristalsis can be altered by bulking agents such as fiber. By causing distension, these compounds elicit contractions that occur in either direction along the bowel. In a few cases, for example, organophosphate-insecticide toxicosis, diarrhea is via prolonged stimulation of muscarinic receptors due to inhibition of acetylcholinesterase at the synapse. The greatly enhanced peristaltic activity, combined with stimulation of secretion, leads to decreased transit time through the GI tract and resultant diarrhea.

The consequences of diarrhea are systemic in nature, and include dehydration, acidosis, and electrolyte alterations. Direct loss of bicarbonate in the feces is a major cause of acidosis. Intracellular hydrogen ion concentrations increase and potassium concentrations decrease. This electrolyte imbalance leads to improper maintenance of intracellular pH ranges, and reduces the activity of multiple enzyme systems. Reduced intracellular potassium is the result of a failure in cellular electrolyte transport. Consequently, there is inadequate maintenance of electrochemical gradients, which leads to increased extracellular potassium and mass excretion of this electrolyte in the urine and feces.

Vomiting

Vomiting is a clinical response that occurs in some animal species. Vomiting requires the presence of skeletal muscle in the wall of the esophagus. Vomiting maybe stimulated by direct mucosal irritation or by stimulation of the vomiting center in the central nervous system. Vomiting may also occur if the esophageal or pyloric lumen is obstructed by a scar or neoplasm. Toxic substances can act on the GI mucosa to induce emesis via activation of sensory nerves that travel over vagal and sympathetic afferent pathways to brain medullary centers that control vomiting. One mucosal sensory emetic pathway involves activation of 5-hydroxytryptamine 3 (5-HT3) receptors at the peripheral ends of these sensory nerves in the GI mucosa. 5-HT3 receptors are ligand-gated ion channels that mediate depolarization of nerves, and the vagus nerve is densely populated with 5-HT3 receptors. Cyclophosphamide, carmustine, dactinomycin, and cisplatin interact with mucosal enterochromaffin cells to promote release of large quantities of 5-HT, which leads to emesis. Bilateral abdominal vagotomy and bilateral splanchnic nerve transection completely inhibit emesis induced by these anticancer drugs. Emesis induced by cancer chemotherapeutic agents can be reduced or prevented by administration of 5- HT3 antagonists, such as granisetron, or those that block both dopamine D_2 receptors and 5-HT3 receptors, such as metoclopramide. However, 5-HT3 antagonists are not effective against some other emetogenic substances, such as copper sulfate, protoveratrine, or apomorphine.

Cisplatin appears to act by effects on the central nervous system that promote release of 5-HT and subsequent activation of 5-HT3 receptors. Evidence for this mode of action comes from observations that combined vagal and splanchnic nerve transections do not completely prevent vomiting in response to peripherally administered cisplatin, whereas emesis is reduced by administration of 5-HT3 antagonists. The highest concentration of 5-HT3 receptors in the mammalian brainstem is located in the area postrema of the brain. Activation of vagal sensory neurons by 5-HT3 receptor-mediated events causes release of proemetic neurotransmitters from the central terminals of sensory fibers in the solitary nucleus and in the area postrema. 5-HT3 receptors in the brainstem appear to be associated with presynaptic sites and serve primarily to modulate release of neurotransmitters. Presumably, activation of the central 5-HT3 receptors enhances release of proemetic substances, thereby activating the chemoreceptor trigger zone of the area postrema and the nearby emetic center.

Agonists of dopamine D_2 receptors such as apomorphine, L-dopa, and bromocryptine act in the chemoreceptor trigger zone of the brainstem area postrema. Phenothiazine drugs with significant dopamine D_2 antagonists properties, such as chlorpromazine and promethazine, block the emetic actions of dopamine D_2 agonists. Emetine, the principle ingredient of ipecac, and opiates, such as morphine, act nonspecifically at the chemoreceptor trigger zone to initiate an emetic response. The area postrema is unprotected by a complete blood–brain barrier, thus allowing chemicals in blood to penetrate with relative freedom into this brain area.

Constipation

Constipation is both a structural and a functional disease. Compounds that bulk the stools (e.g., fiber) may lead to constipation if there is concomitant reduction in water intake. Polyps and neoplastic masses induced by carcinogenic agents as well as partly or completely circumferential scars may result in physical obstruction. The constipating effects of certain analgesic compounds (e.g., morphine) have a neurological component to their pathogenesis.

Gastrointestinal Nervous Tissue and Motility

Nervous tissue responses are generally identified by functional abnormalities that are initially detected clinically. Normal intestinal motility consists of peristaltic activity, which moves intraluminal contents down the GI tract. This activity represents contraction of both longitudinal and circular muscle layers. Neuronal networks involved in peristalsis are complex and incompletely understood; however, cholinergic excitation mechanisms play a major role. Such coordinated peristaltic activity can be altered by bulking agents. These compounds cause intestinal distension and elicit contractions that occur in either direction along the bowel.

Opiate (e.g., morphine) toxicity is manifested clinically as a nonpropulsive and constipating pattern of segmentation motility. Segmentation movements accomplish mixing of intraluminal contents. This activity involves reciprocal neural inhibition and disinhibition of adjacent muscle segments; it maybe preprogrammed into the internuncial circuitry of the GI nervous system. Endogenous opioid peptides maybe involved in segmentation motility, since morphine locks the intestine into a continuous segmentation pattern of motility. In morphine-dependent rats, diarrhea, which is the opposite of the acute effects of morphine, is a primary withdrawal event. PGE_2 and 5-HT may also contribute to a secretory type of diarrhea.

Extrinsic nervous input affecting motility includes both stimulatory and inhibitory nerve fibers. Both vagal and sacral innervation to the large intestine is especially active during defecation. Sympathetic nerves are active in reducing blood flow and motility of the GI tract. Inhibitory nerve input into the GI tract leads to reduction or cessation of muscle motor activity (ileus). Tonically active inhibitory neurons can account for a low responsiveness of circular muscles to myogenic pacemakers. A model toxicity of inhibitory nerve input that leads to suppression of both cholinergic and serotoninergic synaptic transmission is norepinephrine overdose. Peritoneal irritation can also cause this effect and lead to ileus.

Spasm is a functional disorder, the opposite of ileus, and consists of accelerated activity of circular muscles with no activity on inhibitory neurons. Intoxication by various cholinergic agents can cause spasms of the GI tract. The model for this disorder is aganglionic megacolon of piebald mice. In these animals, the terminal segment of the large intestine lacks inhibitory neurons.

Inflammatory Response

Because of the high number of bacteria and the physicochemical nature of the luminal contents, inflammation is frequently involved in many lesions of the GI tract regardless of the underlying mechanism of injury. However, the inflammatory response is generally less severe in primary toxicologic lesions than in primary infectious (bacterial and viral) diseases.

Inflammation of the stomach (gastritis) is essentially a process that is restricted to the mucosa. Gastritis is usually catarrhal (with large amounts of mucus), and may involve ulceration, hemorrhage, and lymphoid hyperplasia. "Gastritis glandularis," a disease of primates, is characterized by mucosal hyperplasia and mucus-filled cysts in the mucosa and submucosa. This lesion maybe induced by ingestion of PCBs.

Inflammation of any part of the intestinal tract can be termed *enteritis*, but in practice this term is frequently used to designate only small intestinal inflammation. In contrast, the term *colitis* is used to designate large intestinal inflammation. Direct irritants usually cause more severe inflammation of the proximal intestine (duodenum) and less inflammation of the distal tract (ileum and large intestine). However, mercury can cause lesions of the large intestinal mucosa as a result of transport from the blood into the colonic lumen.

Chronic inflammatory reactions can be a primary or secondary effect in toxicologic lesions. Immune-mediated responses are characterized by accumulation of chronic inflammatory cells (lymphocytes, plasma cells, and macrophages), although they may have an active cellular component consisting of neutrophils and eosinophils.

Diseases that result in chronic inflammation or injury to the lamina propria or lymphatic vessels cause malabsorption of fatty acids and weight loss. Fatty acids and monoglycerides are packaged into chylomicrons by the enterocytes before being exported to the central lacteal and into the lymphatic circulation. Consequently, longstanding damage to the lymphatic circulation can result in significant malabsorption-related disorders. Systemic complications such as septicemia and bacteremia may develop as a result of chronic inflammation and ulceration of the GI tract. Secondary lesions maybe present in the liver (e.g., abscesses), skin (e.g., perianal ulcers that develop secondary to chronic diarrhea), or urinary tract (e.g., females can develop an ascending infection of the urethra from malabsorption-induced diarrhea).

Mucosal Response

General

The intestinal mucosa separates the body from the GI tract's luminal contents (including bacteria and nonabsorbed toxic compounds). This lining is also responsible for selective absorption of ingesta to obtain

the proper nutrients that will maintain homeostasis. The mucosal lining is the first site of exposure to an ingested toxicant, and the cells lining the GI tract have the capacity to respond to these toxigenic compounds.

The exposure of the rapidly proliferating GI mucosal epithelial cells to toxins would suggest that the GI tract should be a frequent site of toxicologic injury. The actual frequency of toxicity in commonly used laboratory animals is lower than one might expect, primarily due to the high rate of cellular proliferation that can occur in the reparative response to any loss of mucosal epithelium. Factors that account for the GI tract's ability to escape damage include its capacity for compound biotransformation and the large surface area that permits extensive contact between the toxic compound and multiple toxin-metabolizing enzymes. Additionally, mixing an injurious compound with luminal contents dilutes the toxin and its effects. Finally, mucosal barrier components (e.g., mucus) are protective, and the short half-life of GI epithelial cells rapidly removes those cells that have suffered molecular damage (e.g., DNA mutations).

Since the epithelium of the GI tract is the first layer of host cells to contact ingested compounds, these cells can respond to toxic compounds before they enter the circulation. Epithelial cells can also undergo biochemical changes that allow them to functionally reconstitute mucosal integrity after a toxic insult. Modification of several enzyme pathways—including the CYP 450, ADH, monoamine oxidase, epoxide hydrolases, esterases, amidases, glucuronidases, sulfatases, and various conjugation pathways—allows epithelial cells to maintain a barrier function. Many of these same enzymes are involved in compound metabolism and biotransformation. Interestingly, transgenic mice that carry a mutant dihydrofolate reductase (*DHFR*) gene display resistance to methotrexate toxicity of the GI tract. Methotrexate interferes with DNA replication via inhibition of DHFR bioactivity and consequent reduction of de novo thymidine and purine biosynthesis.

Mucosal epithelial cells interact with reactive compounds via both membrane-bound and cytoplasmic enzymes. Although the CYP 450 pathway can generate cell-damaging and reactive intermediate epoxides, mucosal cells can form nontoxic dihydrodiols and glucuronide conjugates from these intermediates. This process occurs via mucosal cell enzymes, including epoxide hydrolases and glucuronosyl transferases.

Unique forms of adaptive mucosal protection occur after exposure of the mucosa to mild irritants. Under these conditions, increased levels of PGE_2 are elaborated and protect the mucosa from strong irritant damage by increasing blood flow and stimulating local bicarbonate secretion in the small intestine.

Sublethally injured GI epithelial cells are able to reseal damaged membranes and can participate in covering discontinuities in the epithelial barrier. Repaired cells at the margins of ulcers and erosions become active participants in GI barrier restitution by "flattening," then spreading out and migrating over denuded basal lamina. Membrane resealing is a key process in maintaining an intact epithelial layer if the injury does not cause widespread and severe loss of epithelial cells. GI epithelial cells are protected from injury by an apical membrane enriched with viscosity-enhancing glycosphingolipids, a microvillar surface that can be sloughed if damaged, and a circumferential apical cytoskeleton that can contract and seal off the apical surface of enterocyte, preventing further injury. Resealed or healed cells may remain viable for up to 24 hours in the stomach and 48 hours in the intestine.

Rapid epithelial restitution is one of the mucosa's primary defense mechanisms throughout the GI tract (esophagus to anus). Each segment of the GI tract has a basal rate of mucosal cell proliferation, which varies with species, age, diet, and disease state. Under normal dietary conditions and health, the range of proliferation rates for the most actively dividing mucosal cells (stomach to colon) is 3−6 days. When the intestine encounters a noxious agent, enterocyte half-life is reduced to quickly replace injured cells. If the damage is transient, mucosal replacement, and normal microarchitecture will recover within 3 days.

Arachidonic acid metabolites from the cyclooxygenase (COX) and lipoxygenase pathways are elevated during GI inflammation and after acute colonic injury in which an inflammatory process has not yet developed. These inflammatory mediators have many effects on the structure and function of the GI tract, particularly with regards to blood flow.

Bile salts (e.g., deoxycholate) induce the release of arachidonic acid and COX and lipoxygenase metabolites of this fatty acid, and lead to the generation of active oxygen radicals Bile salts also induce increased colonic secretion and permeability, but this occurs by mechanisms independent of endogenous arachidonic acid metabolism. However, prostaglandins of the E series suppress enzyme release and superoxide anion production by neutrophils. Thus, the interaction of these chemical mediators may be important in controlling the inflammatory response of the GI mucosa and the final outcome of injury.

Nitric oxide (NO) can be beneficial or toxic, depending on circumstances. It is synthesized from the amino acid L-arginine by at least two different NO synthases. The two major isoforms of NO synthase are a constitutive enzyme, which is calcium- and calmodulin-dependent, and an inducible form, which is calcium-independent. The constitutive form has been identified in endothelium, nerves, and brain. It seems to be active continuously, generating small amounts of NO. The

inducible form has been identified in macrophages and is probably present in other tissues, such as GI and vascular smooth muscle and vascular endothelium.

NO in low concentrations is thought to protect the GI mucosa from injury and to enhance restitution of injured mucosa. It produces vasodilation of gastric microvessels and exerts an antiaggregation effect on platelets. These actions tend to maintain adequate mucosal blood flow. It also stimulates secretion of mucus by surface mucous cells and helps maintain protection against luminal acid. Laboratory studies indicate that functional repair of the epithelial barrier after acute injury is enhanced by NO. While NO confers many benefits to the GI tract by protection of the mucosa, maintenance of mucosal blood flow, and regulating contractions of smooth muscle and propulsion, it can also be responsible for GI toxicity. This dual nature of NO appears to be related to the relative expression of the two major isoforms of NO synthase. In general, the NO produced by the constitutive form of the enzyme produces beneficial effects, while the NO produced by the inducible form of the enzyme has often been implicated in vascular or epithelial cell injury. Excess production of NO in the GI mucosa by the inducible form of NO synthase is linked to initiation of secretory diarrhea. Diarrhea induced in rats by castor oil or bile salts (e.g., sodium choleate) is blocked by inhibitors of NO synthase. Castor oil and bile salts also induce direct mucosal damage, but the damage is ameliorated by coadministration of NO synthase inhibitors. These results suggest that NO mediates, at least in part, the diarrheal effect of these compounds, presumably by increasing secretion of fluid into the intestinal lumen, even though, simultaneously, NO exerts a protective effect on the intestinal mucosa. This suggests that bile acids and castor oil directly damage intestinal mucosa and activate the inducible isoform of NO synthase to produce large amounts of NO linked to production of diarrhea. Although laxatives, such as phenolphthalein and bisacodyl, are also associated with electrolyte secretion, changes in mucosal histology, and abnormal motility, their effects have yet to be linked to NO production remains to be established.

Stomach

Mucosal defense and protection, initially termed *cytoprotection*, was originally described as the ability of prostaglandins to prevent macroscopic evidence of gastric mucosal injury. This protective phenomenon is partially dependent on the antisecretory activity of prostaglandins, and is dose- and route-dependent.

It is currently understood that several mechanisms besides prostaglandin-mediated pathways are responsible for preventing mucosal damage by both normal digestive processes and injurious compounds. These include increased amounts or modifications of mucous gel covering the mucosal epithelial surface, increased secretion of bicarbonate, increased resistance to acid back-diffusion, and increased blood flow. Several of these processes are mediated by prostaglandin synthesis in mucosal and submucosal tissues (Figure 15.9). Additionally, mucosal protection is mediated in part by lipids (neutral lipids and phospholipids) within the mucous gel layer. These lipids increase the hydrophobicity of the mucous gel, leading to repulsion of water-soluble compounds (including many toxicants).

Mucosal damage can occur with or without mucous-layer damage. The adherent mucous gel is not extensively disrupted by mucosal-damaging agents such as dilute HCl or indomethacin (an NSAID). These agents permeate the mucous barrier and directly damage the underlying epithelium. Since the mucous layer remains intact, it facilitates epithelial repair in these situations. However, mucus is lost when the stomach is exposed to mucosal-damaging agents such as pepsin, bile acids, and ethanol, and also mechanical trauma (Figure 15.10). With persistent mucosal damage, mucous-gel secretion is impaired and mucous-gel loss will exceed production. Additionally, mucus composition can be modified by epithelial cell metaplasia, leading to chemical changes in the mucous gel and loss of functional integrity.

These types of direct injuries will ultimately lead to collapse of the mucous barrier because the mucous gel alone, without constant renewal, cannot protect the mucosa and support rapid recovery after epithelial cell damage. The damaging effects of mucus loss are manifested by further loss of surface epithelial cells, reduced mucus release, vascular occlusion in underlying lamina propria, and, ultimately, ulceration and scar formation (Figure 15.11).

Repair of chemically or mechanically induced gastric epithelial cell discontinuities can be complete within 30–90 minutes of injury. The rate of repair will vary with location in the GI tract (stomach, small intestine or colon) and extent of initial damage. Repair can be very rapid. For example, gastric mucosa experimentally damaged by exposure to high concentrations of sodium chloride, which produces direct structural damage, can be repaired over a period of 6 hours by a gradual process of restitution of epithelial integrity via migration of cells from the gastric glands.

Cellular proliferation is a key epithelial cell mechanism in maintaining mucosal barrier function. The extent of general mucosal damage resulting from an insult can be anticipated based on the amount of damage the compound inflicts on proliferating cells of the mucosa. Minor damage to the proliferative compartment leads to mild gastritis or enteritis, and any increased loss of surface cells is readily compensated

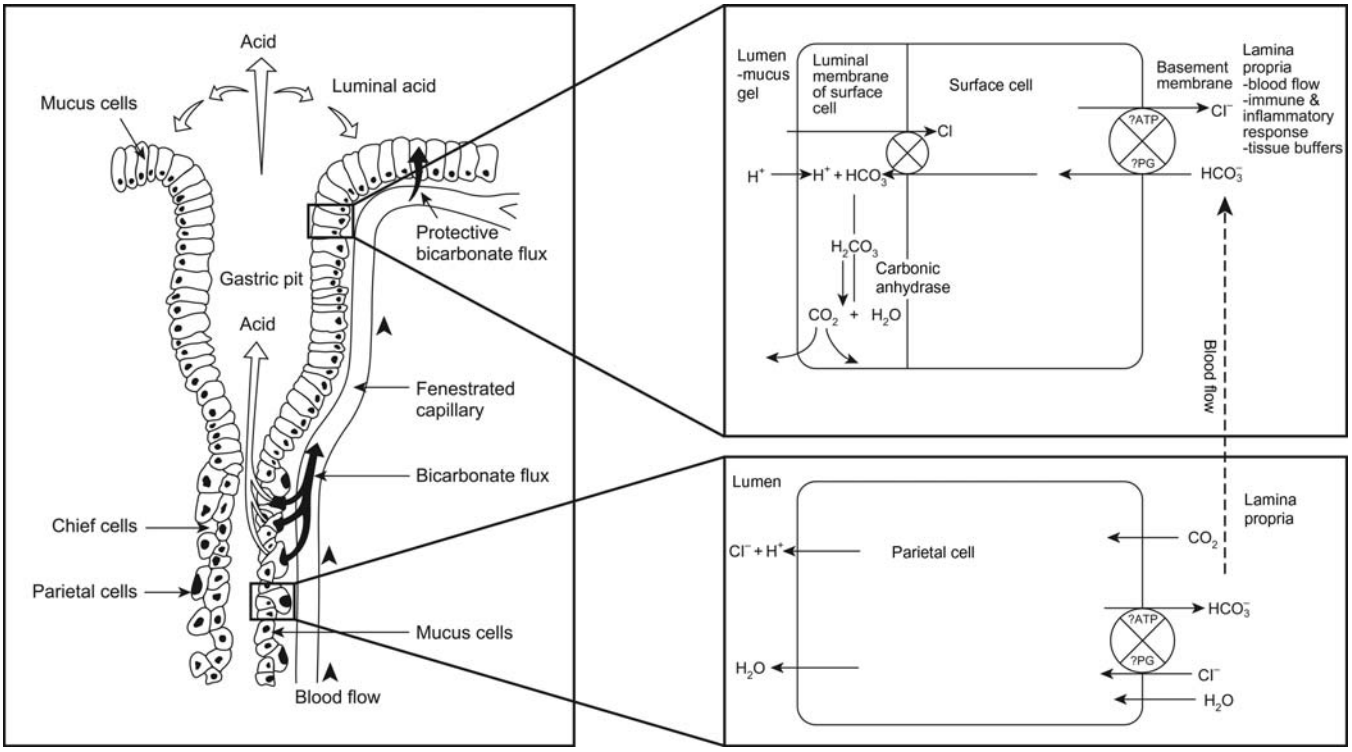

FIGURE 15.9 Schematic drawing demonstrates the interactions of acid production, blood flow, and bicarbonate release. These various interactions allow the gastric mucosa to resist the damaging effects of the low pH environment and toxic compound exposure. *Figure reproduced from* Handbook of Toxicologic Pathology, *second ed. W. M. Haschek, C. G. Rousseaux and M. A. Wallig, eds. (2002) Academic Press, Fig. 10, p. 146, with permission.*

by the undamaged proliferative cells that remain in the glands. However, severe mucosal damage will occur when the proliferating unit of the mucosa is destroyed. Such injury develops after irradiation, exposure to some mycotoxins, or administration of cytotoxic drugs. One of the mechanisms by which PGE_2 enhances healing of the mucosa is by protecting the cells in the isthmus of the gastric pits and allowing these replicative cells to reconstitute the surface epithelium.

Modifications of epithelial cell proliferation maybe the only morphological indication of mucosal injury. Low doses of indomethacin and aspirin (an NSAID) increase epithelial proliferation in rat gastric glandular mucosa but have no effect in the antrum and duodenum; they do not cause inflammation. In contrast, corticosteroids depress epithelial cell proliferation in fundic, antral, and duodenal mucosa of rats, and hydrocortisone predisposes to gastric ulcers. Proliferative rates are also modified by starvation, and pharmacologic and toxicologic doses of mineralocorticoids, glucocorticoids, and adrenocorticotropic hormone.

Intestines

Damage to small intestinal mucosa by toxicants results in a variety of changes depending on the degree and extent of injury. Damage to enterocytes without damage to underlying lamina propria or to the proliferative epithelial cell population lining the crypts will result in a temporary shortening of villi and decrease in height of remaining enterocytes as they flatten out to cover the denuded mucosal surface. Restitution of the lost enterocytes can happen within a matter of a few days. As proliferative rate of crypt cells increases and the cell cycle time decreases, crypts will elongate as the number of newly formed epithelial cells increase. Complete cell differentiation and restoration of function generally takes longer than cell replacement since newly formed epithelial cells must leave the proliferative compartment and develop the specialized biochemical and morphologic features associated with absorptive enterocytes.

Damage to the crypt cells by toxicants is a more serious matter, leading to "mucosal collapse." The mechanisms of restitution after proliferative unit ablation are not well understood. Death of crypt cells without underlying damage to lamina propria, in particular the vasculature, will eventually result in complete restitution of cryptal and villous epithelium, provided that complicating factors associated with loss of the mucosal barrier are minimized. Secondary events such as fluid loss from the denuded mucosal surface, leakage of

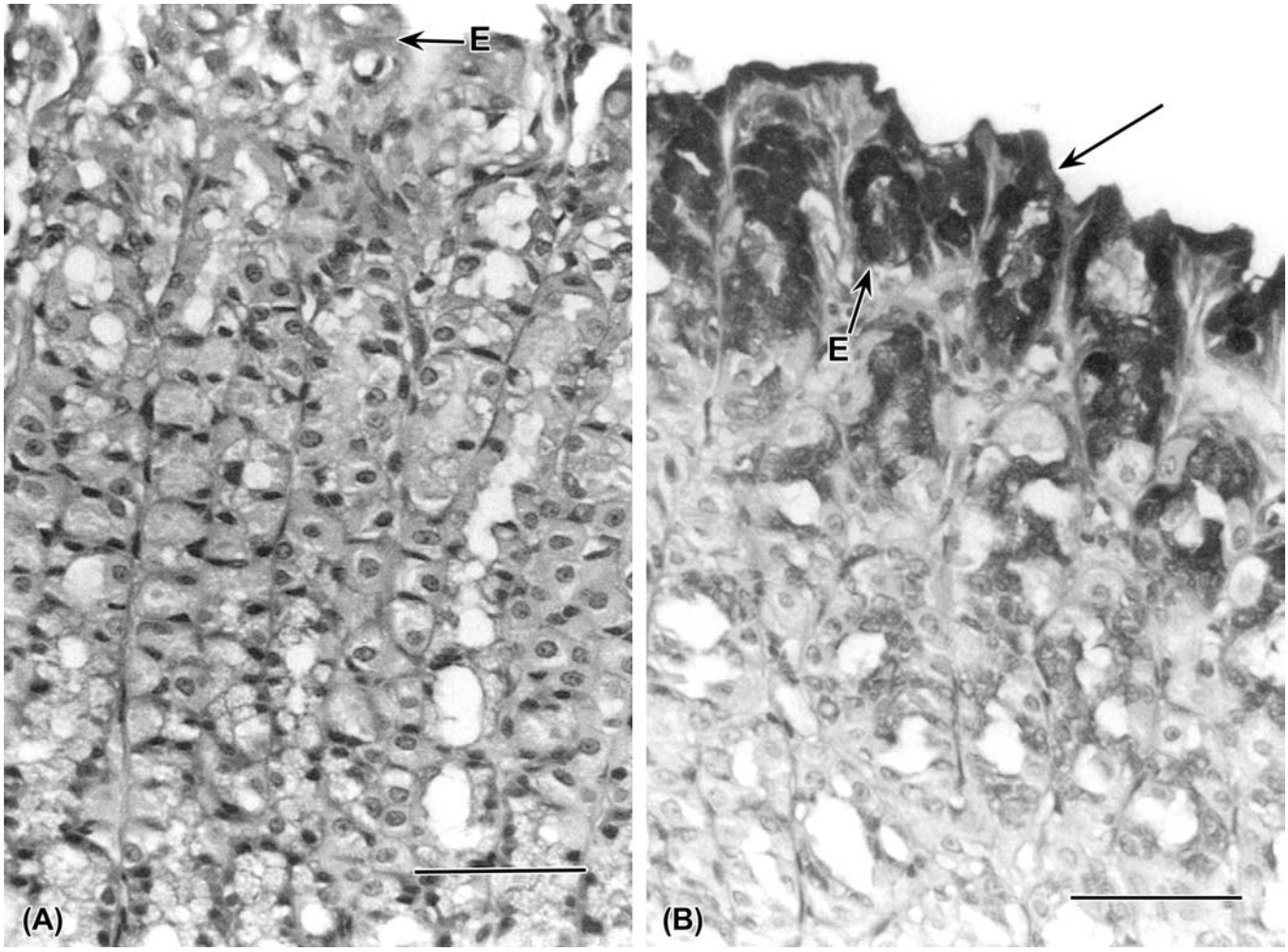

FIGURE 15.10 Taurocholate (bile acid)-induced gastric damage in a rat 1 hour after oral gavage. Bar = 50 μm. (A) Periodic acid-Schiff (PAS) staining reaction demonstrates that glycoprotein loss in foveolar mucous-epithelial cells (E) of the fundic mucosa is one of the earliest injuries induced by agents which disrupt the mucous lining of the stomach. (B) Normal control fundic mucosa with abundant PAS staining for neutral mucosubstances is gastric surface and pit epithelial cells (arrow). *Figure reproduced from* Handbook of Toxicologic Pathology, *second ed. W. M. Haschek, C. G. Rousseaux and M. A. Wallig, eds. (2002) Academic Press, Fig. 14, p. 161, with permission.*

ingesta into the lamina propria, colonization of the lamina propria by resident gut bacteria (Figure 15.11), and the inevitable inflammatory response are minimized. Any one of these complicating factors, if unchecked, can lead to severe systemic consequences and defective restitution of the mucosal barrier. Damage to underlying vasculature, especially if thrombosis occurs, can exacerbate injury even further and lead to ulceration and hemorrhage as well. It is thought that maintenance of regional blood flow in areas of damage is essential for the minimization of ongoing damage and enhancement of repair and restitution in all sections of gut.

By contrast, the colonic mucosa is covered by relatively flat mucus-secreting cells and crypts. Several substances serve as growth factors that can positively stimulate epithelial growth. These include gastrin, TGF-α, and transforming growth factor-beta (TGF-β). The influence of these growth factors is exerted on the stem cell. The ingestion and digestion of food appear to be important in maintaining growth of the intestinal mucosa. Mucosal toxicity can be exhibited by decreased cell production or increased cell loss, which can lead to atrophy or ulceration. Increased cell production in excess of the rate of sloughing can lead to hyperplasia. This latter response is characteristic of mucosal repair, where it is transient, or certain infectious (bacterial) and preneoplastic conditions.

Rapid epithelial restitution is now considered one of the primary defense mechanisms of not only the stomach and small intestine but also colon. However, this occurs only under conditions in which damage is confined to the superficial mucosa. In the colon, for example, epithelial restitution is associated with migration

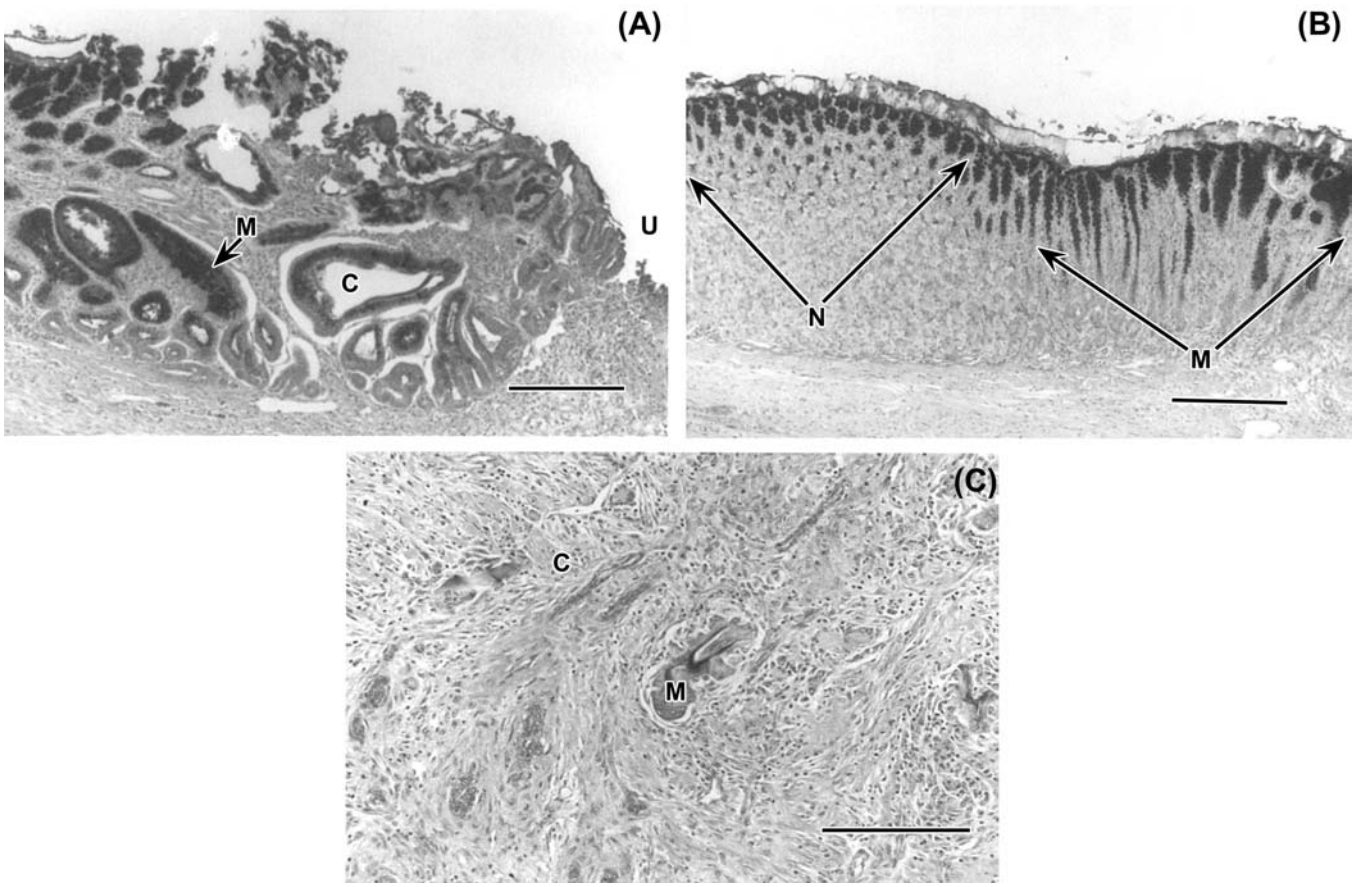

FIGURE 15.11 Acid pH-induced gastric injury. (A) Ulceration (U) of mucosa leads to cystic dilatation of associated gastric glands (C) and marked proliferation of neutral mucosubstance (PAS-stained)-containing mucous cells (M). Cells that are positive for the PAS reaction at the margins of the ulcer have been demonstrated to release epidermal growth factor (EGF). These cells have been proposed to have a significant role in controlling the healing and reepithelialization process of the ulcer. Bar = 500 μm. (B) Mucous cell (M) proliferation occurs around margins of cystic glands and the transition to a more normal mucosa (N) is abrupt. Bar = 500 μm. (C) The base of the ulcer contains fibrous connective tissue at the base of the ulcer, trapped nests of mucous cells (M), and few inflammatory cells. Bar = 100 μm. *Figure reproduced from* Handbook of Toxicologic Pathology, *second ed. W. M. Haschek, C. G. Rousseaux and M. A. Wallig, eds. (2002) Academic Press, Fig. 15, pp. 162–163, with permission.*

of cells at a speed of approximately 2 μm/minute. On the other hand, regions of the mucosa with gross hemorrhagic lesions heal by a lengthy process of tissue replacement involving cell mitosis. It is thought that maintenance of regional blood flow in the area of damage is important for repair of lesions (as well as prevention thereof). Indirect damage to epithelium may occur as a result of hypoxia when blood flow to the area of damage is compromised.

Three mechanisms influence restitution of the mucosal barrier after toxic damage: (1) the rate of increased epithelial cell production; (2) the reduced cell cycle time (the period between two successive divisions of proliferating cells); and (3) an increased proliferative compartment via an increase in the proportion of cells in the proliferative cycle or an increase in the absolute number of cells that are replicating at any given time. In contrast, under adaptive conditions (e.g., intestinal resection or dietary change), only one mechanism is operative: increased cell production rates via increased numbers of cells that are proliferating. The intestinal mucosa can also be induced to proliferate as a healing response near areas of cellular toxicity and ulceration. PE_2 and fermentable fibers (e.g., guar) are examples of inducers of mucosal proliferation in the intestinal tract. Mechanisms of restitution after proliferative unit ablation are not well understood.

Organ-Specific Response

Esophagus

Various species have unique anatomical adaptations of the esophagus (e.g., forestomachs of ruminants), but

the lining mucosa and its response to injury are similar among species. Both neoplastic and ulcerative processes can lead to a reduction in the esophageal lumen by the physical obstruction of a space-occupying mass (neoplasm) or a stricture from scar contraction. If highly caustic agents are fed to animals, severe mucosal damage is followed by ulceration, inflammation, fibroplasia, and scar formation. Ulceration can be restricted to the esophagus, or may involve the stomach, small intestine, and/or large intestine.

Spontaneous esophageal cancer is rare in animals and humans living in Western civilizations. However, esophageal cancers are commonly found in humans living in regions of China, reportedly due to high levels of aflatoxins in contaminated grains. When rats are exposed to chemical carcinogens (*N*-methyl-*N*-nitrosoaniline), their esophageal mucosae undergo a progression of changes, a sequence of hyperplasia and hyperkeratosis leading to dysplasia, papillomas, and finally to carcinoma. Esophageal cancer can also be induced in rats with dihydrosafrole, and in mice with gamma irradiation. Additionally, zinc-deficient rats treated with carcinogens may develop multiple neoplasms of the esophageal mucosa.

Stomach

ULCERATION AND INFLAMMATION

Gastric ulceration and associated inflammation and mucus loss are responses to stress (unrelated to compound administration) and various mucolytic agents (Figure 15.12). Active ulcerogens include NSAIDs, alcohol, taurocholate (bile acids), nitriles, thiols, and amines (Table 15.10). In addition to these direct GI irritants, which also affect the stomach, antimitotic and antineoplastic agents (e.g., colchicine and 5-fluorouracil) cause ulceration in various parts of the GI tract. Mechanisms of ulceration are discussed extensively in Section 5.

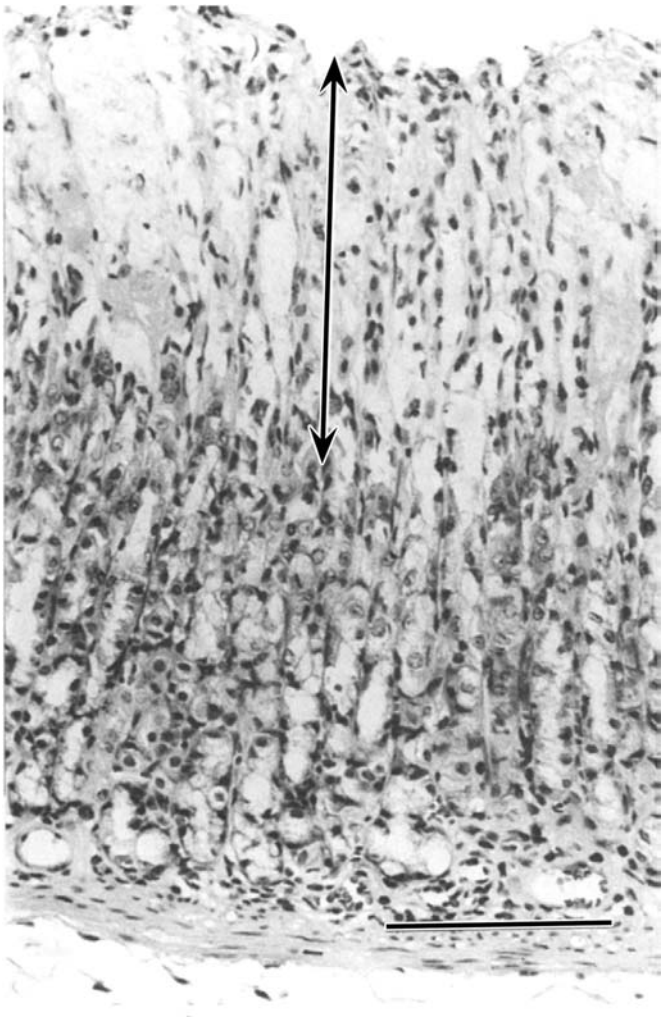

FIGURE 15.12 Early injury to fundic gastric mucosa (bile salts) that disrupts the mucous blanket. Coagulative necrosis (arrow-bar) of the foveolar region occurs prior to the development of ulceration. Necrotic zones can extend deep into the fundic mucosa. Bar = 100 μm. *Figure reproduced from* Handbook of Toxicologic Pathology, *second ed. W. M. Haschek, C. G. Rousseaux and M. A. Wallig, eds. (2002) Academic Press, Fig. 16, p. 165, with permission.*

PROLIFERATIVE RESPONSE

Epithelial cells maintain normal anatomical boundaries (i.e., do not infiltrate into submucosal tissues) in hyperplastic conditions. However, if hyperplasia is of sufficient duration, it may in certain situations increase the risk of a neoplastic process developing. Adenomas are the result of a benign proliferative response that is neoplastic, and they can potentially progress to malignancy. Determination of the malignant potential of adenomas should include evaluation for evidence of epithelial dysplasia, proliferative activity, cysts, blood capillary organization, stromal infiltration of epithelial components, and inflammation. Intestinal metaplasia can occur in adenomas, as can tissue invasion and distortion. If the neoplasm being examined has morphologically demonstrable tissue invasion or areas of severe epithelial atypia, metaplasia, or dysplasia—with or without extensive proliferative activity—the lesion should be considered malignant (i.e., an adenocarcinoma).

A hormone-mediated proliferative response of the stomach is demonstrated by hyperplasia of enterochromaffin-like cells and an increase in neuroendocrine-cell tumors ("carcinoids"), which develop after prolonged gastrin release (Figure 15.13). Hyperplasia of these enteroendocrine cells has been demonstrated after exposure to ranitidine and substituted benzimidazoles like omeprazole, both of which produce hypergastrinemia. Animals with gastric hyperplasia have abnormal mucosal maturation that is characterized by a decrease in the number of cells with cytoplasmic zymogen granules, a decrease in mature

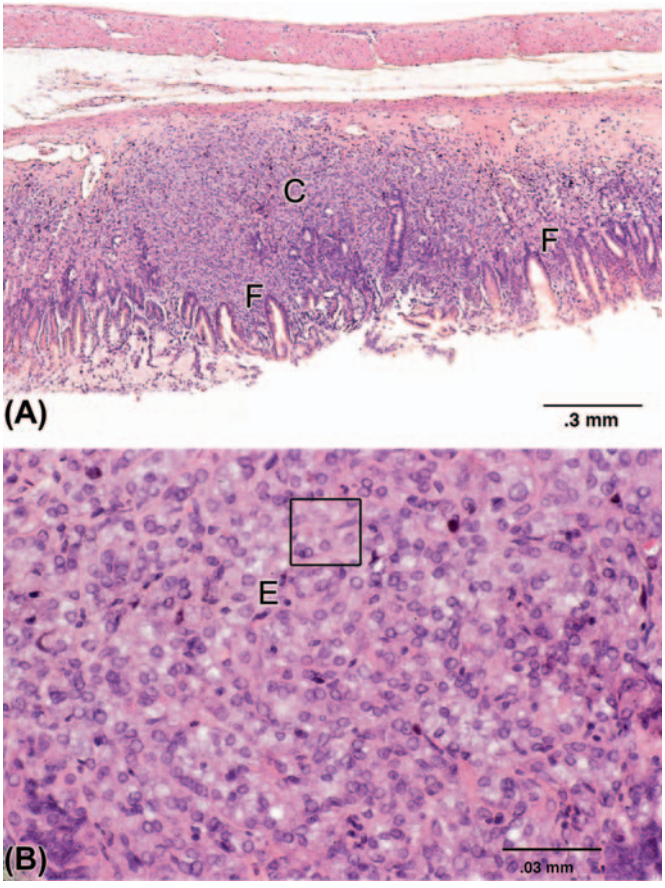

FIGURE 15.13 Enterochromaffin-like (ECL) cell carcinoid and hyperplasia in the glandular stomach of a F344/N male rat treated with methyleugenol. (A) Carcinoid (C) compressing the adjacent fundic (F) mucosa (arrows). (B) Higher magnification of carcinoid showing the peritheliomatous and nesting arrangements (box) of the neoplastic ECL cells (E) within a delicate fibrovascular stroma. Neoplastic cells have large, round, centrally located nuclei and pale cytoplasm. *Figures provided courtesy of Dr. Susan Elmore, National Toxicology Program, U.S. National Institute of Environmental Health Sciences [NIEHS]. Figure reproduced from* Handbook of Toxicologic Pathology, *third ed. W. M. Haschek, C. G. Rousseaux and M. A. Wallig, eds. (2013) Academic Press, Fig. 19, p. 2336, with permission.*

TABLE 15.10 Selected Mechanisms of Toxicity to the Gastrointestinal Tract

Mechanism	Toxic entity
ALTERED ABSORPTIVE FUNCTION	
Reduced nutrient absorption	Alcohol Antimitotic agents Cholestyramine Karacine Neomycin Heavy metals
Altered solute transport	*E. coli* toxins Shigatoxin Laxatives
Increased absorption of allergens	Polyvinyl chloride Metallic iron Asbestos
Decreased blood supply, hypoxic uncouple oxidative phosphorylation	NSAIDs Arsenates
DAMAGE MUCOSAL BARRIER	
Block protective prostaglandins	NSAIDs
Alter mucus synthesis	NSAIDs Steroids
Direct cytotoxicity	Bile acids Ethanol
Damage proliferating cells	Radiation T-2 toxin Ricin
Hypersensitivity	Trinitrobenzene Sulfuric acid
Genotoxicity	1,2-Dimethylhydrazine Azoxymethane

Table adapted from Handbook of Toxicologic Pathology, *second ed. W. M. Haschek, C. G. Rousseaux and M. A. Wallig, eds. (2002) Academic Press, Table V, p. 143, with permission.*

surface cells, glandular atrophy, loss of regular parietal cell distribution, and an increase in cellular proliferation. The initiation of a carcinoma is demonstrated by loss of cellular differentiation, abnormal gland structure, invasion of mucosal elements into surrounding tissue, abnormal glycoprotein expression, and displacement of normal tissue.

Small Intestine

Damage to the small intestinal mucosa frequently results in villus atrophy and crypt-cell hyperplasia. If ulceration occurs, an associated inflammatory reaction ensues. Duodenal sites are more frequently found to have ulcers than other small intestinal segments. The same ulcerogens that affect the stomach frequently damage the duodenum. The distal small intestine is a frequent site of functional abnormalities, such as diarrhea, rather than a location for morphological damage. The small intestine is an infrequent site of neoplastic formation. However, lymphosarcomas may originate in the lymphoid nodules of the lamina propria and submucosa. Adenocarcinomas induced by a carcinogenic agent or natural causes may originate from the mucosal epithelium and invade the submucosa and tunica muscularis mucosa (Figure 15.14).

Large Intestine

ULCERATION AND INFLAMMATION

The response of the large intestine to toxic injury can be studied using models that induce acute and chronic lesions. Acute erosive injury to the colonic mucosa can be induced in rat and pig. using the bile salt deoxycholate. Damage to the surface cells is mediated by reactive oxygen species, and complete ablation

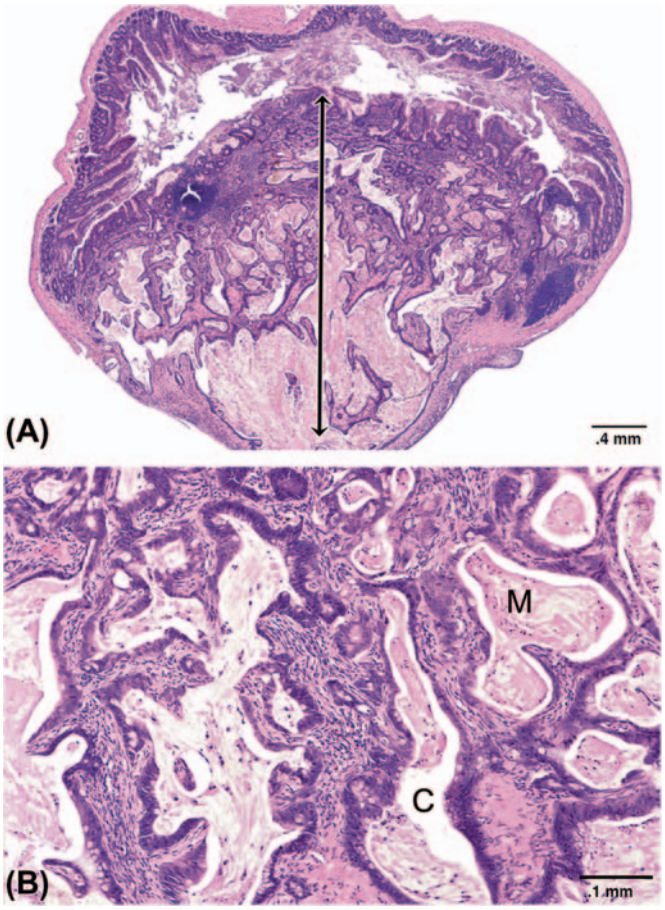

FIGURE 15.14 Mucinous adenocarcinoma in a male F344/N rat treated with 2,3-dibromo-1-propanol. (A) Neoplastic tissue (arrow–bar) extends from the mucosa through the submucosa into tunica mascularis mucosa. (B) Cystic spaces (C) are lined by neoplastic cells and contain mucus (M). *Figures provided courtesy of Dr. Susan Elmore, National Toxicology Program, U.S. National Institute of Environmental Health Sciences [NIEHS]. Figure reproduced from* Handbook of Toxicologic Pathology, *third ed. W. M. Haschek, C. G. Rousseaux and M. A. Wallig, eds. (2013) Academic Press, Fig. 20, p. 2337, with permission.*

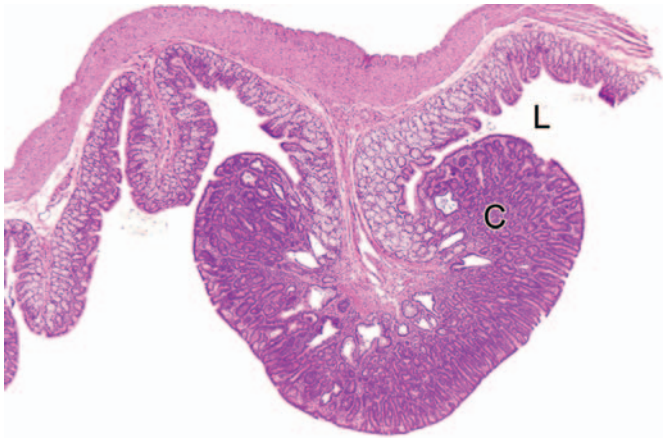

FIGURE 15.15 Polyp in colon of a male F344/N rat treated with 0-nitroanisole. The polyp almost completely occluded the lumen (L) of the colon. The mass is supported by a mucosal stalk and is composed of multiple cystic glands (C). *Figure provided courtesy of Dr. Susan Elmore,* National Toxicology Program, *U.S. National Institute of Environmental Health Sciences [NIEHS]. Figure reproduced from* Handbook of Toxicologic Pathology, *third ed. W. M. Haschek, C. G. Rousseaux and M. A. Wallig, eds. (2013) Academic Press, Fig. 21, p. 2338, with permission.*

of the surface epithelium occurs within 8 minutes. Mucosal permeability is regained after 40 minutes, and recovery of absorptive activities occurs when the epithelium is restored to a columnar phenotype (2 hours). The reparative process of the mucosa occurs by active cell migration from the proliferative zone to the surface. This process will be delayed or is unable to take place if damage to the mucosa is severe enough to damage stem cells, in which case ulceration and inflammation will be observed.

PROLIFERATIVE RESPONSE

One common response seen in the colon is mucosal hyperplasia and polyp formation. Hyperplastic polyps of the colon maybe either inflammatory or regenerative in nature. Benign lymphoid polyps, not necessarily associated with toxicity, also occur in the colon or rectum as a result of lymphoid hyperplasia. Proliferative polyps of epithelial origin can be classified as adenomatous polyps or adenomas. Adenomatous polyps are composed of tubules of neoplastic epithelium with little stroma (Figure 15.15). In contrast, villous adenomas have multiple projections of epithelial-lined lamina propria. Regardless of classification, the mucus content of neoplastic epithelial cells is reduced, and mitotic figures are common in these polyps. The presence of multiple polyps should be regarded as an early cancerous event in rodents, since there is an established adenoma–carcinoma sequence in the colon.

CECAL ENLARGEMENT

Cecal enlargement is a response in several rodent species to various compounds and food additives in the digesta. These materials include antibiotics, modified starches, polyols (sorbitol and mannitol), some fibers, and lactose. Cecal enlargement, for example, is associated with increased death losses in rats fed raw potato starch. Enlargement of rodent ceca has been interpreted as both a toxic and an adaptive phenomenon.

Compounds that are poorly absorbed and are osmotically active are frequently associated with cecal enlargement. The mechanism for the distension has been proposed to be the attraction of fluid into the lumen. However, when the luminal contents are removed, tissue weights remain elevated, so other mechanisms are also operative. Other processes involved in cecal enlargement and dilatation include

mucosal hypertrophy and hyperplasia. This morphologic response is associated with functional changes that lead to soft stools, diarrhea, and increased large-bowel mucosal permeability. These functional alterations are likely to be mediated by the increased osmotic activity of the cecal contents. Morphological changes probably represent an adaptational process, since the changes are reversible when the diets are returned to normal.

Large intestinal enlargement is a common change observed with incompletely digested and poorly absorbed substances that are subjected to microbial metabolism in the cecum and colon. The increased microbial metabolism leads to an increase in osmotically active material, and results in soft stools and cecal distension. One functional change in rats fed sugar alcohols and lactose is increased absorption of calcium. Sequelae to this process are increased calcium excretion in the urine and nephrocalcinosis.

Regenerative Response

Repair vs Regeneration

Tissue response to injury maybe divided into two classes: repair and regeneration. Repair refers to the physiologic alteration of an organ after injury for the purpose of restoring stability without exact replacement of lost or damaged tissue. Repair often results in fibrosis. In contrast, regeneration signifies the replacement of lost or damaged tissue with a precise duplicate, such that both morphology and functionality are completely restored. Conditions required for regeneration are sometimes in direct contrast to those favoring repair. For example, a prolonged inflammatory response needed for repair will not allow for regenerated tissue to form due to the granulation bed that forms at the injured site. Likewise, contraction at the site during repair will further inhibit replacement with duplicate tissue. Many tissues are not overtly capable of regeneration, so the only response to injury is repair.

Injuries involving the inner mucosal layer of the small intestine can result from chemical and radiation exposure during treatment for cancer, changes in gut microbiology in response to antibiotics, and inflammation or necrosis due to parasitic or autoimmune disease. In contrast, blunt force injuries to the small intestine, due to automobile accidents, stabbings, or gunshot wounds, often compromise the entire structure of the organ, involving both the inner and outer tissue layers. Since the inner mucosal layer is crucial for the nutrient absorption function of the small intestine, the following subsections will provide a broad overview of some of the key components involved in repair and regeneration of the epithelial cells lining this organ.

Stem Cells

It is reasonable to assume that any injury to the small intestine will require repopulation of the injured area by one or more cell types. Adult stem cells are multipotent and can differentiate into a limited number of cell types. These are capable of maintaining, generating, and replacing terminally differentiated cells within their own specific tissue in response to physiological cell turnover or tissue injury. The multipotent properties of adult stem cells makes them easier to coax into replacing lost or damaged adult tissue with exact copies of defective cells, thereby reconstituting original function. Pluripotent stem cells from embryonic sources require more controls during the differentiation process, to reduce the occurrence of neoplastic transformation.

Stem cells may differentiate into fibroblasts and myofibroblasts in response to connective tissue growth factor (CCN2) and platelet-derived growth factor, respectively, thus contributing to tissue repair of GI epithelial layers. Multipotent adult stem cells may ameliorate colitis by exerting an antiinflammatory effect in the affected tissue by reducing expression of cytokines such as tumor necrosis factor-alpha (TNF-α), interleukin-1beta (IL-1β), and COX-2.

Activation and proliferation of stem cell reservoirs within the crypts of the intestine are modulated by Wnt signaling. Proliferation appears to be dependent upon activation of nuclear β-catenin/T-cell factor transcriptional activity. Expression of Ephrin B receptors and ligands, critical for establishing the migratory path from the crypt to the villus, is modulated by the β-catenin/T-cell factor transcriptional complex. Without Wnt signaling, β-catenin, needed by resident epithelial cells for regulating growth and adhesion between cells, becomes targeted for destruction, thereby contributing to fibrosis. Transcription factor 3 (TCF3, also known as E2A immunoglobulin enhancer-binding factors E12/E47) is another TCF regulated by Wnt signaling. TCF3 can repress expression of the embryonic stem cell gene, *nanog*, potentially downregulating stem cell pluripotency and self-renewal.

Signaling Pathways

In addition to Wnt, which has been discussed above, bone morphogenic protein (BMP) signaling also plays an important role in regulating intestinal development and epithelial homeostasis in normal, nondiseased tissue. BMPs generally function as a negative regulator of cell proliferation in the small intestinal crypts. In so doing, they effectively act as a brake to intestinal epithelial cell regeneration in normal gut. A BMP antagonist, called noggin (NOG), is expressed in the submucosal region adjacent to the crypts,

providing a feedback mechanism for proliferation control. NOG binding to BMP receptors removes the negative effect of BMP, resulting in an increase in intestinal stem cell proliferation, thereby removing the brake to tissue regeneration. Under normal circumstances, BMP inhibits intestinal fibrosis by downregulating TNF-α and by inhibiting TGF-β-mediated epithelial-to-mesenchymal transition. Without such BMP inhibition, activated fibroblasts would be generated, which are a key component in tissue repair and scarring.

Hormones

Endocrine cells can be found throughout the mucosa of the GI system, in particular gastric glands and crypts of the cranial small intestine (duodenum and jejunum). Peptides released by these cells not only regulate secretion, absorption, digestion, and motility but also affect the pathogenesis of several GI diseases, such as cancer. The hormones discussed below have been implicated in regulating mucosal cell growth and regenerative responses either positively or negatively.

GASTRIN-RELEASING PEPTIDE AND GASTRIN

Gastrin-releasing peptide (GRP) functions primarily as a stimulator of gastrin release and subsequent gastric acid secretion. Gastrin also stimulates gastrointestinal mucosal cell growth in the small intestine. Recent evidence suggests that gastrin can modulate the function of cells involved in immune and inflammatory responses. This proinflammatory function must be downregulated during repair of the intestinal epithelium resulting from colitis, perhaps by affecting the activity of another proinflammatory factor, TNF-α.

GHRELIN

Ghrelin is produced largely in the stomach, and to a lesser degree in the small intestine and colon. This peptide plays an important role in regulating food intake, gastric emptying, and gastric acid secretion. Reports in the recent literature support a role for ghrelin in suppressing inflammatory and apoptotic pathways activated by GI injury, enhancing intestinal motility, and promoting mucosal epithelial cell proliferation. Mechanistically, ghrelin has been shown to inhibit cellular apoptosis by regulating the ratio of the apoptotic regulator protein Bcl2 with the proapoptotic protein BAX.

SOMATOSTATIN

Somatostatin (SST) is arguably the master controller of all GI hormones, capable of inhibiting gastric acid secretion, motility, and mucosal cell growth. SST accomplishes this feat either directly via interaction with specific receptors, or indirectly by antagonizing the function of other trophic hormones, such as gastrin. It has been demonstrated that radiation injury of intestinal mucosal cells can be alleviated by administration of an SST analog. This may imply that SST functions in a "proliferative capacity" by inhibiting apoptosis to enable maintenance of the surface epithelium.

Growth Factors

EPIDERMAL GROWTH FACTOR

EGF consists of a family of peptides, of which EGF and TGF-α are two of the most studied members. EGF is produced by epithelial cells located in the submucosal (Brunner's) glands of the duodenum, while TGF-α is produced by epithelial cells lining the small intestine. Both EGF and TGF-α are mitogens stimulating cell division in multiple cell types within the gastrointestinal tract. Hence these growth factors enhance mucosal healing after injury by increasing cell proliferation and stimulating angiogenesis.

FIBROBLAST GROWTH FACTORS

The family of fibroblast growth factors (FGFs) also regulates growth and differentiation of intestinal epithelial cells, in addition to the proliferation of stem cells during the process of tissue regeneration. Acting as a mitogen, FGFs promote mucosal and epithelial cell proliferation in the small intestine in addition to mediating angiogenesis. FGFs stimulate fibroblast and endothelial cells, two key building blocks for angiogenesis and granulation tissue development. Together, angiogenesis and granulation tissue increase blood supply to the area and fill the injured site with well-oxygenated cell mass during the tissue repair process.

INSULIN-LIKE GROWTH FACTORS

There are two members of the insulin-like growth factor (IGF) family, designated IGF-I and IGF-II. Following interaction with their receptors, these growth factors upregulate epithelial cell and fibroblast proliferation while downregulating apoptosis. During the tissue repair process, IGF also stimulates intestinal epithelial cell migration so that cells can quickly be redistributed over a damaged area. In so doing, the barrier between the intestinal lumen and submucosa is rapidly restored while epithelial cell proliferation is being initiated to more completely repair the damaged area with new cells.

TRANSFORMING GROWTH FACTOR-BETA

The TGF-β family functions to inhibit the growth of GI mucosal cells. Following epithelial cell injury in the small and large intestine, increased levels of this

growth factor can be found in the mucosa, resulting in an inhibition of epithelial cell proliferation. There appears to be a synergistic relationship between TGF-β and GRP, in that together they negatively regulate intestinal epithelial cell proliferation and differentiation better than each does individually. Similar to IGF, TGF-β also stimulates intestinal epithelial cell migration to restore a barrier quickly during tissue repair.

MECHANISMS OF GASTROINTESTINAL TOXICITY

Basic functions of the GI tract include acting as a barrier, digesting and metabolizing ingested material, secreting enzymes, and absorbing needed nutrients (including water). Any impairment of these basic functions will result in functional or structural alterations and disease (Table 15.10). Because the GI tract is involved in transport of nutrients, it is especially prone to injury by processes that alter absorptive functions. Additional mechanisms that can cause severe GI pathology include reduced blood supply or hypoxia, acid build-up with damage to the mucosal barrier, hypersensitivity reactions, and genotoxicity, which potentially leads to neoplasia. At a cellular level, injury to the plasma membrane and mitochondria of mucosal epithelial cells represents an irreversible loss of cellular viability from which there is little likelihood of return. At the tissue level, the difference between development of a superficial or a deep mucosal lesion depends on the extent of involvement of subepithelial capillaries. In this section, general toxicologic mechanisms are discussed, and several model toxicants are used to illustrate these processes.

Intestinal Barrier Function

Most ingested toxins enter the systemic circulation through the small intestine, either by passing through the enterocytes or by passive paracellular diffusion. Contents of the gut are mainly in an aqueous phase, with a 35-μm unstirred water layer next to the mucous layer of the surface epithelial cell. The ability of a xenobiotic to traverse the mucosal barrier depends upon its solubility in water for diffusion through the unstirred water layer, its size and charge for paracellular flow, and its lipid solubility for transcellular diffusion. Large and polar molecules pass poorly through epithelial tight junctions unless the epithelial barrier is disrupted (as with high doses of ethanol). Small electroneutral molecules pass easily around the epithelial cells and into the portal circulation, but polar molecules cannot pass through the lipid barrier of the cell. Weak acids or bases are in equilibrium, with both ionized and nonionized states present, making them simultaneously soluble in water and lipids. The nonionized molecules can diffuse through the membrane into the enterocyte. Once in the enterocyte, a xenobiotic maybe pumped out of the cell by a multipurpose transporter (e.g., Pgp) on the luminal surface of villus cells, metabolized by various enzyme systems within the cell to either a toxic or nontoxic metabolite, or transferred into the portal blood or lymph. Intestinal metabolism may play an important role for some medications, including lidocaine and cyclosporine, or maybe the site of drug interactions. Some compounds also have direct toxic effects on the enterocyte without being systemically absorbed, such as toxins produced by the blue green algae *Microcystis*.

Substrates that do not have specific transporters are absorbed passively around epithelial cells. Tight junctions are very permeable in the proximal intestine, becoming less permeable in the ileum. Electrolytes are absorbed either by paracellular bulk flow or by electrogenic transport and exchange processes, depending upon the permeability of the tight junctions of the specific segment of the intestine. Net secretion of fluid is quite large; for example, in the human there is a net secretion of approximately 7 L of fluid into the jejunum, originating from biliary, pancreatic, and intestinal secretions. Fluid secretion via intestinal tissue is due to the paracellular flow of water drawn into the lumen by the high osmotic load of ingesta. This fluid is then absorbed in the ileum and colon as nutrients and electrolytes are absorbed against a concentration gradient. A variety of ion pumps, exchangers, and channels are involved in the electrogenic transport of electrolytes in the distal small and large intestine. As electrolytes are transported out of the gut, water is also reabsorbed passively to maintain electrochemical gradients. When nutrients or electrolytes are not absorbed, there is an increase in luminal liquid volume that results in diarrhea.

Intestinal Malabsorption

A number of transport pathways exist in the GI tract to carry materials across the mucosal epithelium. These mechanisms include active transport, facilitated diffusion or solvent drag, passive diffusion, pinocytosis, and phagocytosis. Most nutrients are absorbed by active transport mechanisms, in contrast to most toxicants, which are transported by a passive diffusion process. Consequently, greater lipid solubility of a toxicant will enhance absorption, smaller molecules will diffuse more rapidly, and the nonionized forms of

acids and bases will be absorbed more rapidly than the ionized forms. A significant exception to this generalization includes the active transport of inorganic ions, as typified by calcium carrier mechanisms present in the GI tract.

Malabsorption results from alterations in epithelial transport mechanisms, reduction in surface area (e.g., villus blunting from antimitotic agents), or the binding of nutrients or compounds to unabsorbed intestinal contents (e.g., modified bile salt absorption by cholestyramine) (Table 15.11). Reduced nutrient absorption can be mediated by various toxicants, including heavy metals and plant extracts. Cadmium interferes with or inhibits the absorption of calcium and alters digestion of protein and fat. Tobacco-leaf extracts reduce the activity of the loosely held intestinal brush border enzymes lactase, sucrase, maltase, and alkaline phosphatase. When enzymes involved in the metabolism of complex carbohydrates are damaged, the GI epithelial cells are unable to absorb carbohydrate-derived nutrients. Malabsorption results in malnutrition, vitamin deficiencies, and diarrhea.

Toxic compounds can alter solute transport across or between mucosal epithelial cell membranes. By damaging junctional complexes between enterocytes, interfering with hydrostatic pressure gradients, or causing high luminal osmotic pressure, a toxic compound can contribute to net water loss from the body into the feces and lead to diarrhea. Some bacterial toxins (*E. coli* toxins and shigatoxin) and laxative compounds act as secretagogues and promote active sodium and water loss into the lumen. Toxic doses of these secretagogues eventually lead to diarrhea.

GI toxicity can also be mediated by an increased absorption of nutrients or toxic compounds. Glycogen content increases in the midgut epithelium of cockroaches fed pyrethrum. Degeneration of fish intestine is observed as a consequence of water and electrolyte transport alterations which occur from exposure to DDT. Increased toxicity of organophosphates in young mice compared with older mice is the result of an increased rate of absorption of the toxic compound.

Particulate materials maybe taken up by pinocytosis (nanometer-sized particles) or phagocytosis. In mice, phagocytosis is limited to particles smaller than 6 μm in diameter. Particulate uptake plays an important role in pathological responses to polyvinyl chloride, metallic iron, and asbestos. The passage of these particles through the protective mucosal epithelium of the GI tract can lead to allergic hypersensitivity reactions or the entry of unmetabolized compounds directly into the lymphatic and blood circulations.

Hypoxia

Hypoxia is a key factor in the pathogenesis of GI mucosal injury. This is typified by the development of mucosal lesions in various types of shock. The degree of mucosal damage in shock is correlated with the extent of reduced GI blood flow. Decreased blood flow and oxygen exchange increases the susceptibility of the mucosa to injury. A local reduction in blood flow can occur with vascular thrombosis; this mechanism is a major process in gastric injury induced by absolute ethanol.

Stomach

Hemorrhagic shock in rats leads to uniform blanching of the glandular mucosa of the stomach and a generalized reduction in blood flow. Small, white, ischemic foci develop on the gastric mucosa, which will ulcerate and bleed as necrotic tissues slough after the restoration of blood pressure or flow. Ischemia predisposes the stomach to HCl-mediated mucosal lesions because blood flow is sufficiently reduced to cause a build-up of hydrogen ions in the tissue. A decrease in local blood flow or an increase in acid back-diffusion can lead to mucosal injury and erosion. This combination of events may cause severe mucosal damage (Figure 15.9).

Arachidonic acid metabolites are inflammatory mediators that can induce gastric damage. Thromboxane A_2 (TXA_2), formed by platelets, is a potent vasoconstrictor and causes extensive mucosal damage in the presence of topical taurocholate. Platelet aggregation is also promoted by TXA_2 and can lead to vascular thrombosis and mucosal infarction. Both mechanisms are active when there is tissue hypoxia, and both are involved in the ulcerogenic

TABLE 15.11 Intestinal Malabsorption Induced by Drugs and Chemical Agents[a]

Surface active agents that block fat and vitamin absorption: alcohol, cholestyramine
Antibacterial agents that block fat, protein, electrolyte, and vitamin absorption: kanamycin, neomycin, polymycin
Miscellaneous agents that block fat, vitamin, protein, and carbohydrate absorption: calcium carbonate, clofibrate, colchicine, indomethacin, methotrexate, phenformin, phenytoin, phenolphthalein, quinacrine, sulfasalazine, and triparanol

[a]*Modified from Banwell (1979)* Environ. Health Perspect. *33, p. 111.*
Table adapted from Handbook of Toxicologic Pathology, *second ed. W. M. Haschek, C. G. Rousseaux and M. A. Wallig, eds. (2002) Academic Press, Table VI, p. 144, with permission.*

effects of TXA_2. In contrast, some prostaglandins protect the mucosa from injury. Protective processes mediated through prostaglandins are thought to be increased mucosal blood flow, and therefore an improved supply of oxygen. Modification of blood flow, prostaglandins, and the mucosal barrier, coupled with tissue-damaging bile acids and activated neutrophils, are the basis for gastric ulceration observed with NSAIDs (Table 15.12).

Intestines

Ulcerative mucosal lesions can develop as a result of impaired villus microcirculation during hypotension. Hypoxia develops as a result of increased mean transit time for blood in the villus vascular loop, which increases the efficiency of the countercurrent exchange mechanism in the villi of the GI mucosa (Figure 15.6). When blood flow is sluggish, the time available for oxygen diffusion back into the blood is increased, resulting in reduced availability of oxygen at the villus tip. Rheological factors such as intravascular aggregation of erythrocytes and platelets can contribute to compromising oxygen transfer, especially when blood flow is already significantly reduced. Hypoxic injury is compounded by epithelial and intraluminal enzymes, such as trypsin, that contribute to mucosal lesion development under these conditions.

TABLE 15.12 Chemical Agents and Drugs That Can Induce Gastrointestinal Ulcers

Antiinflammatory agents (steroids and NSAIDs): corticosteroids, phenylbutazone, indomethacin, flunixin, oxyphenbutazone, sulindac, flurbiprofen, tolmetin, ketoprofen, fenoprofen, naproxen, and ibuprofen
Inflammatory mediators: histamine, serotonin
Antihypertensive agents: reserpine
Hormone analogs: gastrin-like compounds
Catecholamines: epinephrine
Antimicrobial agents: polymyxin B
Antimetabolic agents
Sympatholytic agents: priscoline
Antihistamines: dimaprit (H2 blocker)
Amines: ethylamine, cysteamine, and cystamine
Nitriles: propionitrile and butyronitrile
Short-chain alkanes and alkenes
Miscellaneous agents: caffeine, KCl, gold thioglucose, and haloperidol

Table adapted from Handbook of Toxicologic Pathology, *second ed. W. M. Haschek, C. G. Rousseaux and M. A. Wallig, eds. (2002) Academic Press, Table VII, p. 146, with permission.*

Mucosal Barrier Damage and Cytotoxicity

Nonsteroidal Antiinflammatory Drugs

NSAID-induced mucosal damage follows a temporal course of events, starting early with neutrophil-independent toxicity and progressing later to neutrophil-dependent toxicity. The time course of the cascade is approximately 6 hours. Early changes include alterations in mitochondrial oxidative functions and inhibition of COXs. Once absorbed into the mucosa, NSAIDs interact with epithelial cell mitochondria to cause uncoupling of oxidative phosphorylation, leading to energy depletion and decreased mitochondrial enzyme activity. Energy depletion leads to disruption of ATP-dependent epithelial cell junctions, thus increasing intestinal epithelial permeability.

The increase in permeability due to altered epithelial barrier functions reduces protection from hostile gastric and/or duodenal luminal factors such as bile acids, hydrogen ions, and bacteria. The presence of bacteria will attract and activate neutrophils, which increase the ulcerogenicity of NSAIDs. Activated neutrophils attracted to the mucosal microvessels and lamina propria release reactive oxygen species, lysosomal proteases, and leukotriene B_4 (LTB_4). Myeloperoxidase is a hemoprotein peroxidase released by activated neutrophils into the extracellular medium, where it interacts with hydrogen peroxide (H_2O_2) to form an enzyme–substrate complex with great oxidizing potential. Activated neutrophils produce large quantities of hypochlorous acid (HOCl), a powerful oxidizing agent, leading to OCl^- generation by means of myeloperoxidase-catalyzed oxidation of Cl^-. Active oxygen species and lysosomal enzymes cause direct damage to epithelial cells, especially membranes. The LTB_4, released by neutrophils, is a powerful chemoattractant for additional neutrophils. In addition, LTB_4 causes vasoconstriction of arterioles. As a result of this cascade, GI epithelial cells become targets of attack by bile acids, hydrogen ions, active oxygen, and lysosomal enzymes.

NSAIDs are also directly cytotoxic to the mucosal epithelium through reduction of cytosolic ATP as well as by blocking COX activity and the synthesis of mucosal protective prostaglandins. NSAIDs stimulate membrane-bound sodium ion pumps and alter acid production by the gastric mucosa. Lesions occur after oral or parenteral administration of NSAIDs. The lesions caused by these compounds are erythema, hemorrhage, erosions, and ulceration of the GI mucosa, especially in the stomach and throughout the small intestine. When NSAIDs are administered at toxic levels, the same types of mucosal lesions are present regardless of route of administration or anatomical location.

The two major COX isoforms, COX-1 and COX-2, differ in their sensitivity to inhibition by individual NSAIDs. COX-1 is the constitutive form of the enzyme found in healthy tissues, while COX-2 is an inducible form that can be stimulated by several cytokines and mediators of inflammation. Most NSAIDs inhibit activity of both isoforms of COX. Inhibition of COX-2 maybe associated with most of the beneficial effects of NSAIDs, while inhibition of COX-1 maybe associated with many of their adverse effects. Inhibition of COX by NSAIDs results in two significant toxicological effects: reduction in formation of prostaglandins, and increased formation of leukotrienes. The loss of endogenous prostaglandin protection may then render the stomach prone to damage by other agents that are normally only mild ulcerogens, and leaves lipoxygenase metabolites like hydroperoxyeicosatetraenoic acid and leukotrienes without the counterbalancing effects of endogenous prostaglandins.

PGE_2 and prostacyclin are vasodilators, so blockade of PGE_2 and prostacyclin synthesis may favor some degree of vasoconstriction and oppose prostaglandin-mediated tonic vasodilation. Increased metabolism of arachidonic acid by the 5-lipoxygenase pathway with concomitant inhibition of COX may contribute to NSAID-induced GI toxicity, since leukotrienes C_4 and D_4 are vasoconstrictors and LTB_4 is a powerful chemoattractant of neutrophils. LTB_4-stimulated attraction and activation of neutrophils leads to release of lysosomal enzymes and microvascular occlusion. Cellular damage to epithelial cells is further exacerbated by a reduction in mucosal blood flow, brought about by a combination of vasoconstriction caused by leukotrienes, and occlusion of microvessels by activated neutrophils.

As potent vasoconstrictors, lipoxygenase metabolites indirectly deprive the mucosa of oxygen. This relative hypoxia may then predispose the mucosa to other damaging agents. Support for this pathogenesis is demonstrated by studies in which lipoxygenase and COX coinhibition and antioxidant agents decrease the incidence of gastric ulcers compared with COX-inhibitor-only exposed controls.

Another important process that contributes to damage when these agents are given by an oral route is direct mucosal irritation by the chemical itself. NSAIDs also directly decrease mucus and bicarbonate release, independently of prostaglandin inhibition. The mucous layer and presence of bicarbonate contribute to mucosal protection from endogenously produced acids. Damage to the mucosal barrier also causes intramucosal histamine release by mucosal mast cells, with resultant vascular congestion, edema, and plasma exudation.

Aspirin inhibits COX activity and is rapidly deacetylated to salicylate. Both aspirin and salicylate are toxic toward mucosal epithelial cells but with differing potencies; furthermore, salicylate is toxic to mucosal epithelial cells at different gastric sites. Salicylate also affects mucosal barrier function, reduces cellular ATP, stimulates sodium ion pumps, and increases proton (H^+) loss. Thus, NSAIDs like aspirin and salicylate reduce production of protecting substances and increase production of damaging substances.

Species differences exist with regard to NSAID-induced GI toxicity. Dogs are more sensitive than rats, which are more sensitive than monkeys. However, although monkeys do not develop lesions after oral exposure to ibuprofen (300 mg/kg/day), gastric ulcers occur when the same dose is given intravenously. Species differences maybe related to the plasma half-life of the active compound, since the propionic acid NSAID flurbiprofen has a half-life of approximately 40 hours in dogs, 6 hours in rats, and 3 hours in monkeys, which correlates with the relationship to ulcerogenic sensitivity.

Alcohol (Ethanol)

Ethanol, like NSAIDs, causes hemorrhagic erosions in the gastric mucosa. The rate-limiting step in this lesion development is the extent of microvascular damage. Vascular injury is the result of cell membrane injury, mast cell degranulation, leukotriene release, and increased mucosal permeability. As occurs with other mucosal-damaging agents, injured epithelial cells are rapidly replaced if blood flow is maintained and the basement membrane remains intact.

Gastrotoxic effects of alcohols like ethanol are related to their ability to increase cell membrane fluidity. Osmolality and lipid solubility are also involved, but to a lesser extent. Depletion of intracellular glutathione (GSH) has been implicated in alcohol injury to mucosal cells. The levels of GSH decline in proportion to the degree of alcohol injury, while treatment with PGE_2 can essentially abolish alcohol injury. *N*-ethylmaleimide, which causes profound GSH depletion, abrogates prostaglandin-induced protection against alcohol injury.

Chronic administration of alcohol is also associated with enhanced expression of a number of growth factors, including EGF and TGF-α. These growth factors are thought to protect the gastric mucosa against acute injury, and may explain the observation that adaptation of the gastric mucosa to chronic alcohol administration is associated with increased cell proliferation and increased expression of mucosal EGF and TGF-α. The ability of chronic alcohol exposure to lead to hyper-regeneration of the gastric mucosa could be responsible for the suspected carcinogenic effect of alcohol in the stomach, and likely is mediated by peptide growth factors. Generation of acetaldehyde (which

can alkylate nucleotides in DNA) by endogenous CYP isozymes, has also been implicated, thus suggesting a potential role of gastric mucosal ADH in deleterious effects of alcohol on GI mucosa.

Alcohol increases the permeability of the mucosa and causes back-diffusion of H^+ and a rise in luminal Na^+ concentrations. At low alcohol concentrations (10%), mucus synthesis and bicarbonate secretion are inhibited. At higher concentrations (12%−15%), alcohol releases surface mucus, depletes intracellular mucus, and promotes leakage of bicarbonate and electrolytes into the gastric lumen. At concentrations above 20%, the severity of gastric erosions increases with rising concentrations of alcohol. At concentrations above 40%, there is dose-dependent damage to the mucosal blood vasculature.

Steroidal Compounds

Steroids, like NSAIDs, also induce gastric and large intestinal mucosal alterations and damage by altering cytoprotective mechanisms and the mucosal barrier. Long-term or high-dose steroid administration induces gastric ulceration. Dogs given toxic levels of dexamethasone, a phospholipase inhibitor, develop gastric bleeding, erosions, and melena (black, tarry stools due to gastric hemorrhage). These findings indicate that the mechanism for steroid-induced gastric lesions is partially mediated through inhibition of prostaglandin synthesis. Since the prostaglandin synthetase (COX) substrate arachidonic acid is reduced by inhibiting phospholipase activity, the mucosal protection provided by prostaglandins (PGE_2) is lost and gastric acid activity proceeds without inhibition. This mechanism of gastric damage is in distinct contrast to that demonstrated by cysteamine, which inhibits somastatin activity but enhances gastrin production, leading to hyperacidity and delayed gastric emptying (due to altered duodenal motility), followed by mucosal damage.

Bile Acids

Bile acids are synthesized from cholesterol, and can damage the GI mucosa. Bile acids are usually ionized and occur in two forms: monomeric and micellar. Of the excreted bile acids, over 97% are reabsorbed in the ileum and returned to the liver via the enterohepatic circulation. The remaining 3% undergo bacterial degradation in the colon and are excreted in the feces or reabsorbed in the colon. GI bacteria deconjugate and desulfate bile salts, leading to the production of toxic and even carcinogenic metabolites. Bile salt malabsorption during certain ileal diseases is implicated in colonic mucosal damage and diarrhea. Bile salts in the stomach break down gastric mucosal permeability and solubilize the outer lipid bilayer of surface epithelium; deoxycholate inhibits active sodium ion transport from mucosa to submucosa. The basic mechanism of mucosal barrier damage is similar for ethanol and deoxycholic acid. Bile salts stimulate colonic epithelial cell proliferation and are capable of acting as tumor promoters in the colon.

Radiomimetic Agents

Radiomimetic compounds result in substantial cytotoxicity in mucosal epithelial cells, and the mitotic mucosal cells of the crypt are at high risk. Ingestion of a trichothecene mycotoxin, T-2 toxin, results in widespread crypt epithelial necrosis and mucosal injury that resembles the effects of radiation exposure (Figure 15.16). Contributing to the mucosal injury is

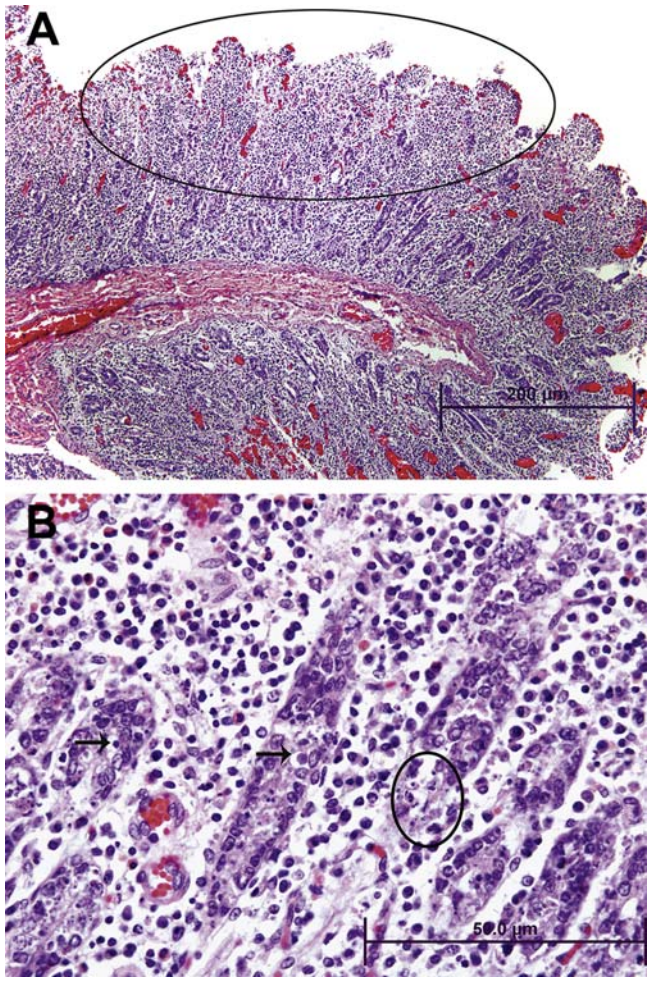

FIGURE 15.16 (A) T-2 mycotoxin-induced loss of intestinal villous epithelium (encircled) secondary to crypt necrosis in a pig. Also present is engorgement of underlying capillaries and larger blood vessels in the underlying lamina propria. (B) Higher magnification image illustrating ongoing crypt cell apoptosis (arrows) and necrosis (circle). *Figure reproduced from* Fundamentals of Toxicologic Pathology, *second ed. W. M. Haschek, C. G. Rousseaux and M. A. Wallig, eds. (2007) Academic Press, Fig. 8.7, p. 180, with permission.*

necrosis of proliferating crypt cells. This eventually leads to loss of remaining mucosal epithelium lining the villi as a result of continued cell senescence in the absence of replacement. Consequently, there is collapse of the mucosa, ulceration, hemorrhage, and secondary inflammation along with bacterial invasion. Chemotherapeutic agents such as the fluropyrimidines floxuridine and 5-fluorouracil as well as plant toxins (e.g., ricin) can cause similar lesions.

Dioxins

Gastrin, EGF, TGF-α and other endogenous growth factors can stimulate GI crypt cells to proliferate. Mucosal hyperplasia can be associated with ingested chemicals, such as 2,3,7,8-tetrachlorodibenzo-*p*-dioxin (TCDD) and probably other related polychlorinated dioxins. TCDD binding converts the Ah receptor to its activated functional form, which binds to DNA of the CYP1A1 gene and increases the rate of CYP1A1 transcription; this CYP isozyme is an important player in phase I xenobiotic and drug metabolism. The intestinal mucosa contains significant levels of Ah receptors and CYP1A1. TCDD can induce mucosal hyperplasia in some animal species, possibly by exerting a disinhibitory effect on gastrin release, which can then stimulate crypt cell proliferation and result in mucosal hyperplasia. TCDD intoxication also induces a "wasting syndrome" that is characterized by hypophagia and severe loss of weight. Most species given lethal doses of TCDD die within 2 weeks.

Cytotoxic Agents and Heavy Metals

Compounds that react by 1,4 addition at the β-olefinic carbon of some cellular nucleophiles (e.g., ethyl acrylate) are cytotoxic. These compounds are typically biotransformed/detoxified by conjugation to GSH, which is the dominant nonprotein sulfhydryl-containing constituent of epithelial cells that protects them from oxidative damage. Cytotoxicity occurs because GSH is consumed in the biotransformation process for inactivating the compounds. The cell is therefore more susceptible to the oxidation products that are produced during normal metabolism. Ethyl acrylate, for example, causes forestomach damage through depletion of GSH and other sulfhydryl-bearing (cysteine) groups found in thiol-containing peptides.

Cellular damage can also occur by inhibiting oxidative metabolism. Arsenates uncouple oxidative phosphorylation in the mitochondria, possibly by substituting for inorganic phosphate and forming unstable esters. Arsenic is stored in several body sites, one of which is the wall of the GI tract. Inorganic arsenicals cause hyperemia of the GI blood vessels, which, coupled with endothelial cell damage, leads to submucosal hemorrhage. Suppression of epithelial cell proliferation accentuates the damage, and hemorrhagic enteritis develops.

Cadmium causes irritation of GI epithelial cells leading to vomiting, salivation, and diarrhea. Ingestion of ionic inorganic mercury leads to precipitation of mucosal proteins and a corrosive effect on the GI mucosa. Acute inorganic mercury intoxication causes vomiting.

Hypersensitivity

Immune-mediated hypersensitivity mechanisms of toxicity require as a predisposing factor some form of damage to the mucosal barrier. Mucosal damage leads to inadequate clearance of an antigenic or haptenic compound by the mucosal immune system. Although multiple examples of immune-mediated GI toxicity exist, specific antigen models provide the clearest evidence of the interaction between the mucosal barrier and GI tract-associated immune responses. Antigens can enter enterocytes by pinocytosis or by interactions with nutrient transport systems, or can cross the mucosal barrier by paracellular pathways to interact with immune cells in the lamina propria. Antigen-presenting cells release IL-1, which activates T cells to express IL-2 and release a number of cytokines, including TNF-α, and several interferons, including interferon-gamma (IFN-γ). Activated macrophages also release IL-6, which activates lymphocytes; IL-8, which attracts neutrophils; colony-stimulating factors that activate immune cells; and prostaglandins that maintain blood flow. B cells are stimulated by antigens and interleukins to proliferate and differentiate into plasma cells that synthesize and secrete immunoglobulins. Immunoglobulin-E is one of a number of regulators (cytokines, complement 3a) that can activate GI mast cells. Activated mast cells release neurotransmitters (substance P, CGRP), histamine, interleukins, and platelet-activating factor.

These proinflammatory and immune system regulatory factors can induce changes in mucosal transport and GI motility. Increased fluid secretion stimulated by immune mediators maybe involved in regulating stimulatory effects on enteric nerves, with subsequent neural-mediated activation of mucosal secretory mechanisms. Secretory products of mast cells may act both directly on muscle fibers and indirectly by means of enteric neurons to increase contractile activity of GI smooth muscle. Cytokines released from immune and epithelial cells during the GI tract immune response may affect mucosal blood flow, induce a chronic inflammatory response, and/or promote generation of reactive oxygen species.

Experimental hypersensitivity in the GI tract is best exemplified by using ethanol to break down the mucosal barrier and increase permeability toward luminal antigens. By administering trinitrobenzenesulfonic acid (TNBS, which acts as a hapten) after ethanol preadministration, a severe transmural granulomatous inflammation (a model of ulcerative colitis) develops in the distal colon of mice (and rats). The inflammatory response is characterized by mucosal and submucosal infiltrations of neutrophils, macrophages, Langhans-type multinucleated giant cells, lymphocytes (T>B), and mast cells, and represents an example of delayed (Type IV) hypersensitivity. Such immune-mediated inflammatory responses lead to severe colonic ulceration. Once an animal is sensitized to an antigenic compound, an immune reaction can be generated on subsequent hapten exposures without first causing damage to the mucosal barrier. Such "intact barrier" reactions are likely the result of hapten transport through the barrier by mucosal epithelial cells or leukocytes that engage in transepithelial migration through the mucosa. How such low-molecular-weight luminal antigens gain access to the intestinal lumen across the epithelial barrier remains unclear. One mechanism of action may involve paracellular diffusion across pores in tight junctions connecting epithelial cells.

Acetylcholinesterase Inhibitors

Acetylcholinesterase is an enzyme normally responsible for inactivation of the excitatory neurotransmitter, acetylcholine, at synaptic and neuroeffector endings of cholinergic motor and secretomotor neurons in the enteric (autonomic) nervous system. Inhibition of enzyme activity allows accumulation of acetylcholine, leading to increased motor activity in the GI tract via stimulation of smooth muscle M3 muscarinic receptors. The accumulated acetylcholine also acts at M1 and M3 muscarinic receptors in other digestive tract domains to increase salivary, gastric, pancreatic, and intestinal secretions. Extensive inhibition of acetylcholinesterase leads to the secretion of large volumes of fluid and electrolytes into the lumen of the intestine, which results in profuse, watery diarrhea. Anticholinergic drugs such as neostigmine, edrophonium, and pyridostigmine; organophosphate insecticides that include parathion, malathion, and paraoxon; and toxic nerve gases including tabun, sarin, and soman all are capable of causing severe diarrhea and death as a result of reversible or irreversible inhibition of acetylcholinesterase.

Microfloral Effects

Administration of antibiotics has a profound effect on the colonic and fecal flora, depending upon the specific antimicrobial activity of the agent involved, the route of administration, and the local luminal concentration of the drug. A marked reduction in the concentration of intestinal bacteria can be achieved with oral antibiotics, although this effect is usually short-lived. The effect of antibiotics in reducing the bacterial concentrations leaves a void in the bacterial ecosystem that can be filled by pathogenic bacteria. For example, a toxin-producing anaerobic bacterium, *Clostridium difficile*, colonizes the large intestine and produces pseudomembranous colitis, usually after prolonged treatment with antibiotics. Clindamycin and ampicillin are most frequently implicated, but virtually any antibiotic can cause this syndrome. The organism elaborates protein toxins that cause ulceration and necrosis of the intestinal mucosa.

The plethora of gut microbiota is mostly beneficial to the host by virtue of the various symbiotic physiological associations between the microflora and the host. However, this association can also be detrimental to the host under conditions in which gut microbial homeostasis is disturbed, such as in immunodeficient states, after exposure to antibiotics, toxins/carcinogens, or copathogens, or after mechanical damage to the GI tract (especially the mucosa). Subtle but important differences in microfloral composition among individuals may determine the outcome and severity of many pathological conditions and the host's subsequent response to therapy. Increasingly, the GI microflora is thought to be an important determinant in the pathogenesis of many human and similar animal conditions such as inflammatory bowel disease (IBD), celiac disease, type 1 (insulin-dependent) diabetes, obesity, cardiovascular disease, atherosclerosis, autoimmune disease (rheumatic disorders), allergy, cancer, and some neurological and psychiatric diseases and viral diseases.

In IBD (e.g., Crohn's disease and ulcerative colitis) of humans and similar experimentally induced conditions in laboratory animals, the disruption of regulatory T-cell functions and associated abnormal mucosal immune (T-cell) responses to normal intestinal commensal bacterial flora are considered as key elements in sustaining chronic immune-mediated intestinal inflammation and injury. Genetically manipulated rodents such as IL-10 knockout or IL2 knockout mice are common models of chronic intestinal inflammation. Interestingly, under germ-free conditions these mice do not develop chronic colitis, highlighting the vital role of GI microflora in aggravating immune-mediated GI injury.

The intestinal microbiota are vital for GI physiology, including the development and functionality of the gut–brain axis, a bidirectional communication nexus composed of neural, immunological and endocrine

mechanisms that aid the brain in monitoring and modulation of GI function. As a result, the gut microbiota is now increasingly being explored for its roles in some autoimmune neurological and demyelinating diseases like multiple sclerosis, Parkinson's disease, and autism.

Carcinogenicity

Stomach

Naturally occurring tumors of the forestomach are rare in rats and mice (1%), although hamsters can have an incidence as high as 12%. Many agents are capable of inducing or modulating forestomach neoplasia in laboratory animals. For induction of carcinogenic activity, nongenotoxic carcinogens must be in contact with the epithelium of the forestomach for extended periods of time. The absence of a forestomach in humans complicates translational decisions when conducting risk assessments for rodent forestomach neoplasms.

Morphologically, both genotoxic and nongenotoxic agents lead to dysplastic areas of the forestomach (Table 15.13). However, early lesions induced by the prototypical forestomach nongenotoxic carcinogen, butylated hydroxyanisole, are reversible, whereas those induced by genotoxic agents are irreversible. Epithelial dysplasia and metaplasia with glandular distortion is a consistent feature of chemically induced precancerous lesions in rodents. The metaplastic process is also associated with changes in epithelial cell enzymes (alkaline phosphatase, β-glucuronidase) and glycoprotein (neutral and acid mucopolysaccharides) content. Glandular atrophy occurs near neoplastic sites as a result of compression and expansion of the adjacent neoplastic process. In humans, "intestinalization" should be considered a precancerous condition if it is part of a longstanding chronic process; it is not established if the same criteria exist in laboratory animals. The intestinalization process is characterized by gastric-gland neck-region elongation. These regions are replaced by a metaplastic mucosa composed of goblet cells and tall columnar absorptive-type cells of the intestine.

TABLE 15.13 Compounds that Induce Forestomach Neoplasia in Rodents[a]

Chemical	Class	Species affected
N-Ethyl-*N*-nitrosourea	Nitroso	Rat
Butylated hydroxyanisole (BHA)	Aliphatic/aromatic hydrocarbon	Rat, hamster
8-Nitroquinoline	Nitro	Rat
Benzo[*a*′]pyrene	Polycyclic/aromatic hydrocarbon	Hamster, mouse
Allyl chloride	Halogenated hydrocarbon	Mouse
Sodium saccharin	Miscellaneous	Rat

[a]*No genotoxic properties have been demonstrated for BHA, allyl chloride, or sodium saccharin.*
Table adapted from Handbook of Toxicologic Pathology, *second ed. W. M. Haschek, C. G. Rousseaux and M. A. Wallig, eds. (2002) Academic Press, Table VIII, p. 152, with permission.*

Intestines

Spontaneous intestinal tumors in laboratory rodents are rare. However, the high incidence of colon cancer in humans nonetheless has led to the development of animal models that utilize chemical carcinogens to initiate colon tumors (Table 15.14). Chemically induced tumors of the colon are polypoid or sessile. The more dangerous tumors are the sessile variants, which are usually mucinous and can progress to malignancies that are characterized by local invasion, metastasis to mesenteric lymph nodes, lung, or liver, and intussusception.

Several aromatic amines induce intestinal cancers in laboratory animals through genotoxic processes (Table 15.15). However, extensive metabolism is generally required before many of these chemicals become carcinogenic. Target specificity is associated with chemical structure and animal species. Many nitrosamines induce tumors of small and large intestine in rats, hamsters, or guinea pigs. Additionally, the rat esophagus is sensitive to the carcinogenic effects of

TABLE 15.14 Experimental Compounds for Induction of Colon Cancer[a]

Chemical class	Compound
Cholanthrenes	1,2,5,6-Dibenzanthracene 20-Methylcholanthrene
Aromatic amines	4-Aminodiphenyl 3,2′-Dimethyl-4-aminodiphenyl *N*,*N*″-2,7-fluorenylenebisacetamide
Hydrazine derivatives	1,2-Dimethylhydrazine Methylazoxymethanol Azoxymethane 1-Methyl-2-butylhydrazine Methyl-azoxybutane
Alkylnitrosamides	*N*-Methyl-*N*′-nitrosoguanidine *N*-Methyl-*N*-nitrosourea *N*-Nitroso-*bis*(2-oxypropyl)amine
Miscellaneous agents	Poligeenan Dextran sodium sulfate (DSS) Bracken fern extracts Aflatoxin B_1

[a]*Modified from Maskens (1983).*
Table adapted from Handbook of Toxicologic Pathology, *second ed. W. M. Haschek, C. G. Rousseaux and M. A. Wallig, eds. (2002) Academic Press, Table IX, p. 152, with permission.*

TABLE 15.15 Compounds That Induce Intestinal Neoplasia in Rats

Agent	Duodenum	Jejunum/ ileum	Colon
Azoxymethane	−	−	+
Ethylazoxymethane	−	+	+
Nitroso-hydroxypropyloxopropylamine	−	−	+
bis-Oxopropylamine	−	−	+
bis-2-Hydroxopropylamine	−	−	+
Ethylurea[a]	+	+	+
Hydroxyethylurea[a]	+	+	+
Methoxyethylurea[a]	+	−	+
Phenylethylurea[a]	+	+	−
Allylurea[a]	−	+	+
Butylurea[a]	−	−	+
Amylurea[a]	−	+	+
Hexylurea[a]	−	−	+
3-Hydroxypropylurea[a]	+	+	+
Diethylurea[a]	+	+	+
Ethylmethylurea[a]	−	+	+
Ethyl-hydroxyethylurea[a]	−	−	+
Hydroxyethyl-ethylurea[a]	−	−	+

[a]*The proportion of animals that will develop tumors of the large and small intestine after exposure to the nitrosourea compounds ranges from 10% to 50%; females have the lowest and males the highest frequency of lesions. The median time to death ranges from 25 to 70 weeks.*

Table adapted from Handbook of Toxicologic Pathology, *second ed. W. M. Haschek, C. G. Rousseaux and M. A. Wallig, eds. (2002) Academic Press, Table X, p. 153, with permission.*

some nitrosamines. The organ specificity for many nitrosamines may relate to the affinity of these compounds for enterocyte or nonenterocyte receptors or alternatively site-specific cellular biotransformation pathways (Figure 15.17). Duration of mucosal exposure to the chemical is also critical. Azoxymethane is an alkylating agent that only methylates DNA in colonic epithelium of rats and hamsters, which likely partially accounts for the site-specific carcinogenic activity of this compound. In the large intestine of the rat, tumors induced by certain genotoxic carcinogens (e.g., dimethylhydrazine) are associated with lymphoid aggregates, with at least two distinct neoplastic processes occurring in the colonic mucosa. If the target epithelial cell is not associated with a lymphoid aggregate, polypoid adenocarcinomas and adenomas develop; if the target cell is near lymphoid tissue, sessile tumors develop. The reason for this dichotomous lesion pattern is not understood.

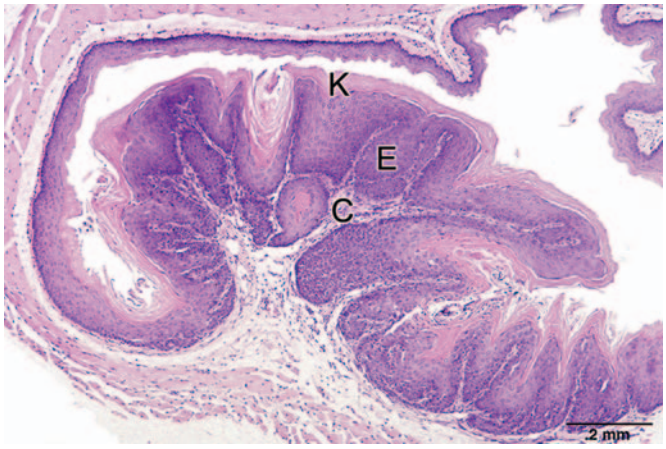

FIGURE 15.17 Esophageal papilloma in a male B6C3F1 mouse treated with azathioprine/interferon (AZT/IFN). Note the connective tissue core (C) for the supportive stalk of the proliferating epithelial cells (E), which are invading subjacent tissue. Surface of papilloma is covered by a thick, hyperkeratinized layer (K). *Figure provided courtesy of Dr. Susan Elmore,* National Toxicology Program, *U.S. National Institute of Environmental Health Sciences [NIEHS]. Figure reproduced from* Handbook of Toxicologic Pathology, *third ed. W. M. Haschek, C. G. Rousseaux and M. A. Wallig, eds. (2013) Academic Press, Fig. 21, p. 2355, with permission.*

Organ-specificity of cancer development in the GI tract also relates to the sites of specific genetic mutations. An example is the dominant mutation that occurs in the germline of mutant, $APC^{min/+}$ mice, which predisposes the animals to multiple intestinal tumors. The propensity for tumor development is dependent on a single allele, and tumors develop in the duodenum, ileum, and colon. Since all cells of these mice carry the mutation and tumors occur only in the intestinal tract, somatic events as well as genetic predisposition are needed for neoplasia to develop. Mutation of this gene may involve loss of function at a genetic site important for normal intestinal development, gain of function in a gene that has an unknown activity, or a complex interaction of both gene suppression and activation.

Genotoxic carcinogen-induced changes in rat colonic epithelium are similar to those observed in spontaneously developing colorectal cancer in humans. In rats, sulfomucins are the primary glycoprotein of the normal colonic epithelium. Shortly after treatment with azoxymethane and *N*-methyl-*N*-nitro-*N*-nitrosoguanidine, cryptal epithelium mucus changes to express primarily sialomucins. Normal intestinal biopsies are characterized by the predominance of sulfomucins. These features support the de novo histogenesis of colon carcinoma.

Aberrant crypt foci (ACF), which represent individual glands or clusters of glands lined by hypertrophic and hyperplastic epithelial cells, are present in the carcinogen-treated rodent colon. The two most

common colon-specific carcinogens, azoxymethane and DMH, have been used in rats and mice to induce ACF. Aberrant crypts are observed topographically on whole mounts of colonic mucosal surfaces stained with methylene blue, where these foci are easily distinguishable from the surrounding normal crypts because they take up increased amounts of blue stain.

ACF are purported to be preneoplastic lesions. This is supported by a number of studies into the biology of ACF. A carcinogenic dose of azoxymethane or 1,2-dimethythydrazine induces a large number of ACF. A systematic and sequential analysis of the number and growth features of ACF has demonstrated that ACF appear in the colon of rats and mice within 2 weeks after carcinogen injection, and that their number increases with time. At early time points, ACF contain one or two crypts (i.e., crypt multiplicity of 1 or 2); however, as time progresses many of the foci expand clonally and contain several crypts in the foci. ACF display proliferative atypia and dysplasia, a preneoplastic phenotype, and also show biological heterogeneity both among individual ACF and within a focus. Some ACF expand clonally without exhibiting dysplasia, whereas others start exhibiting dysplasia with or without clonal expansion; not all crypts in foci exhibit dysplasia, however. Crypt "budding" (the fission and multiplication of intestinal crypts) is evident in both types of foci. These findings support the hypothesis that dysplasia arises in ACF as a result of clonal selection. A number of genotypic atypias also occur in ACF. These genetic differences are indicated by variable resistance to apoptotic cell death induced by azoxymethane and sometimes by elevated levels of GSH-*S*-transferase isoforms.

Compounds that are carcinogenic to the GI tract of laboratory animals may act by direct or indirect actions. Direct-acting (genotoxic) carcinogens lead to initiated cells without prior metabolic activation, with subsequent persistence of neoplastic cells that can grow to become morphologically verified tumors. Indirect-acting (nongenotoxic) compounds, requiring biotransformation or additional promotional interactions to incite a carcinogenic response, may result in a prolonged stimulus of proliferation leading to a substantial increase in the number of dividing (stem) cells. Intestinal stem cells maybe identified by expression of the stem cell markers Lgr5 and EphB2. Single Lgr5 + stem cells isolated from intestine are capable of forming intestinal organoids recapitulating the three-dimensional crypt/villus organization *in vitro*. Expression of Lgr5 and EphB2 has been shown to define a cancer stem cell niche within colorectal tumors, and is predictive of disease relapse in colorectal cancer patients; consequently, a tissue containing such stem cells is more vulnerable to background initiating stimuli. The exact relationships between the genetic alterations and the phenotypic expression of cancer for nongenotoxic carcinogens are incompletely understood. Regardless of mechanism, carcinogenic compounds can act on all tissues of the GI tract.

Gut Microflora and Cancer

The role of gut microflora in the promotion of inflammation-associated cancers, like *Helicobacter pylori* (Hp)-associated gastric cancer and IBD-associated colorectal cancers, is now an active area of research. In Hp-induced gastric ulcers, gastritis, and its subsequent promotion to gastric cancer, the role of other gastric microflora, at least in experimental models, is now believed to play an important role in the severity of initial gastric lesions and also lesion progression over time. Of note, in the hypergastrinemic transgenic insulin-gastrin mouse model [INS-GAS (where the rat insulin 1 promoter drives overexpression of human gastrin in the pancreas)] of Hp infection, the lack of commensal flora in germ-free mice resulted in a decreased severity of Hp-induced gastritis and delayed the progression to GI intraepithelial neoplasia (GIN) as compared to their infected conventional specific pathogen-free (SPF) counterparts. Interestingly, Hp-infected SPF mice showed a significant increase in the amount of *Frimicutes* and a decrease in the levels of *Bacteroidetes* in their stomach as compared to non-Hp-infected SPF mice. This microfloral signature implies a potential role of gut microflora in the copromotion of Hp-associated gastritis and gastric cancer. Intestinal bacteria are capable of degrading dietary components into toxic byproducts with genotoxic, carcinogenic and tumor-promoting activity, and hence are also considered to play a role in the development of colon cancer. Germ-free rats and mice have lowered abilities to activate dietary procarcinogens or chemical tumor initiators like DMH and induce DNA adduct formation as compared to their conventional counterparts, which is indicative of the role that a complex intestinal microbiota may play in carcinogenesis. The microbiota in general is important in bile metabolism and formation of secondary bile acids (which are considered to be possible tumor promoters) and other toxic dietary metabolites like *N*-nitroso compounds which are associated with an increased risk for colon cancer. Intestinal bacteria, depending upon the species, can cause intestinal tumor promotion or suppression based on their ability to express enzymes such as β-glucuronidase, β-glucosidase, and nitrate- and nitro-reductases. Intestinal *Bacteriodes*, *Eubacteria*, and *Clostridia* are associated with enhanced carcinogen formation and metabolism, whereas some *Lactobacillus* spp. and *Bifidobacterium* spp. have beneficial tumor protective effects.

SUMMARY

For many toxic substances, the GI tract is the first portal of entry. Many of these pass through the GI tract without causing harm, but a significant number directly or indirectly damage the GI tract itself. When considering the potential toxic activity of various agents, one must take into account a number of potential mechanisms and the various cell populations (and their unique physiologies) present in each GI segment. For example, acute toxic effects may result from direct irritation (e.g., strong acids and bases), whereas chronic effects maybe manifest as increased muscular layer thickness (e.g., bulking agents). Delayed effects also maybe expressed years after exposure to the initial ulcerogenic or carcinogenic toxic agents. In addition to an array of tissue responses, the interplay of toxicant-induced functional abnormalities and subsequent morphological alterations can be complex and must be taken into account when assessing the proximate cause of the injury. In this chapter, structural and functional components of the GI tract important for understanding mechanisms involved in the toxicologic pathology were discussed, including the role of gut microflora in the genesis, evolution and resolution of lesions caused by toxic substances. Hence, a thorough knowledge of core structures and functions, basic mechanisms of toxicologic damage and specific responses to toxicologic insult is essential before tackling the complex issues of determining whether the GI lesion observed in a particular situation is a primary, secondary or even tertiary effect of the substance to which the animal (or cohort) was exposed.

Acknowledgments

Timothy A. Bertram
RegenMed (Cayman) Ltd., Grand Cayman, Cayman Islands

John W. Ludlow
JWLudlow Consulting, LLC, Carrboro, NC, United States

Joydeep Basu
RegenMed (Cayman) Ltd., Grand Cayman, Cayman Islands

Sureshkumar Muthupalani
Massachusetts Institute of Technology, Cambridge, MA, United States

Further Reading

General

Bertram, T.A., Ludlow, J.W., Basu, J., Muthupalami, S., 2013. Digestive tract. In: Haschek, W.H., Rousseaux, C.M., Wallig, M.A. (Eds.), Handbook of Toxicologic Pathology, third ed. Vol. III. Academic Press (Elsevier), San Diego, USA, pp. 2277–2359. (Chapter 56).

Coruzzi, G., 2010. Overview of gastrointestinal toxicology. Curr. Protoc. Toxicol. (43:21.1.1-21).

Gad, S.C., 2007. Toxicology of the Gastrointestinal Tract. CRC Press, Boca Raton, FL.

Gastrointestinal toxicology. In: second ed Hooser, S.B., McQueen, C.A. (Eds.), Comprehensive Toxicology, Vol. 10. Elsevier:, Amsterdam, The Netherlands.

Gut Microflora

Kinross, J.M., Darzi, A.W., Nicholson, J.K., 2011. Gut microbiome–host interactions in health and disease. Genome Med. 3, 14.

Moos, W.H., Faller, D.V., Harpp, D.N., Kanara, I., Pernokas, J., Powers, W.R., et al., 2016. Microbiota and neurological disorders: a gut feeling. Biores. Open Access. 5 (1), 137–145.

Reading, N.C., Kasper, D.L., 2011. The starting lineup: key microbial players in intestinal immunity and homeostasis. Front. Microbiol. 2, 148.

Tlaskalova-Hogenova, H., Stepankova, R., Kozakova, H., Hudcovic, T., Vannucci, L., Tuckova, L., et al., 2011. The role of gut microbiota (commensal bacteria) and the mucosal barrier in the pathogenesis of inflammatory and autoimmune diseases and cancer: contribution of germ-free and gnotobiotic animal models of human diseases. Cell. Mol. Immunol. 8, 110–120.

Animal Models

Chandra, S.A., Nolan, M.W., Malarkey, D.E., 2010. Chemical carcinogenesis of the gastrointestinal tract in rodents: an overview with emphasis on NTP carcinogenesis bioassays. Toxicol. Pathol. 38, 188–197.

Cheville, N.F., 1980. Criteria for development of animal models of diseases of the gastrointestinal system. Am. J. Pathol. 101 (3 Suppl), S77–S88.

Merchant, H.A., McConnell, E.L., Liu, F., Ramaswamy, C., Kulkarni, R.P., Basit, A.W., et al., 2011. Assessment of gastrointestinal pH, fluid and lymphoid tissue in the guinea pig, rabbit and pig, and implications for their use in drug development. Eur. J. Pharm. Sci. 42, 3–10.

Tissue Regeneration and Healing

Iizaku, M., Konno, S., 2011. Wound healing of intestinal epithelial cells. World J. Gastroenterol. 17, 2161–2171.

Reider, F., Brenmoehi, J., Leeb, S., Scholmerich, J., Rogler, G., 2007. Wound healing and fibrosis in intestinal disease. Gut 56, 130–139.

Pathophysiology of the GI Tract

Fortun, P., Hawkey, C.J., 2007. Drug-induced gastrointestinal disorders. Medicine 35 (4), 210–215.

Rainsford, K.D., 1988. Gastrointestinal damage from nonsteroidal anti-inflammatory drugs. Toxicol. Pathol. 16, 251–259.

Response of GI Tract to Injury

Dixon, D., Heider, K., Elwell, M.R., 1985. Incidence of nonneoplastic lesions in historical control male and female—344 rats from 90-day toxicity studies. Toxicol. Pathol. 23, 338–348.

Nolte, T., Brander-Weber, P., Dangler, C., Deschl, U., Elwell, M.R., Greaves, P., et al., 2016. Nonproliferative and proliferative lesions of the gastrointestinal tract, pancreas and salivary glands of the rat and mouse (review). Toxicol. Pathol. 29 (1 Suppl), 1S–124S.

Rao, J.N., Wang, J.-Y., 2011. Regulation of gastrointestinal mucosal growth. In: Granger, D.N., Granger, J.P. (Eds.), Integrated Systems Physiology: From Molecule to Function to Disease. Morgan & Claypool Life Sciences, San Rafael, CA.

Society of Toxicologic Pathology. International Harmonization of Nomenclature and Diagnostic Criteria (INHAND). <https://www.toxpath.org/inhand.asp> (last accessed May 2016).

Carcinogenesis

Brambilla, G., Mattioli, F., Martelli, A., 2010. Genotoxic and carcinogenic effects of gastrointestinal drugs. Mutagenesis 25, 315–326.

Hoenerhoff, M.J., Hong, H.H., Ton, T.V., Lahousse, S.A., Sills, R.C., 2009. A review of the molecular mechanisms of chemically induced neoplasia in rat and mouse models in National Toxicology Program bioassays and their relevance to human cancer. Toxicol. Pathol. 37, 835–848.

Rosenberg, D.W., Giardina, C., Tanaka, T., 2009. Mouse models for the study of colon carcinogenesis. Carcinogenesis 30, 183–196.

Tammariello, A.E., Milner, J.A., 2010. Mouse models for unraveling the importance of diet in colon cancer prevention. J. Nutr. Biochem. 21, 77–88.

CHAPTER

16

Exocrine Pancreas

Matthew A. Wallig[1] *and John M. Sullivan*[2]

[1]University of Illinois at Urbana-Champaign, Urbana, IL, United States
[2]Eli Lilly & Company, Indianapolis, IN, United States

OUTLINE

INTRODUCTION

The exocrine pancreas is an organ that is seldom prominently involved in toxicity in laboratory and domestic animals. Similarly, it is generally not considered to be a target organ for most xenobiotics and is not routinely considered to be involved in xenobiotic metabolism or bioactivation. Yet, when the pancreas is injured directly in a toxic process affecting islet or exocrine cells, vascular or endothelial injury, or secondarily in concert with damage to the liver, stomach, intestinal tract, or anterior abdomen (via trauma), the consequences can be devastating. Injury can be quite variable, ranging from acute hemorrhagic and necrotizing pancreatitis, with dramatic and rapid clinical onset, to recurrent, subchronic, and low incidence single cell necrosis with slowly evolving subacute to chronic inflammation leading to lobular atrophy and fibrosis that may be clinically silent. The triggers that regulate or modify responses to pancreatic injury have been the object of intensive study over the past decades. Reports link exposure to various drugs or xenobiotics to both acute and chronic pancreatitis. In humans, this is especially true in developing countries, where chronic pancreatitis is endemic. The incidence in these locales parallels environmental pollution

Fundamentals of Toxicologic Pathology.
DOI: http://dx.doi.org/10.1016/B978-0-12-809841-7.00016-2

(smoke from kerosene stoves, wood fires, and cigarettes); contaminated food supplies (especially by mycotoxins); and consumption of ethanol. These examples highlight the importance of predictive and/or correlative biomarkers for onset of pancreatic injury that ultimately can be predictive of a patient's prognosis.

NORMAL STRUCTURE AND FUNCTION OF THE EXOCRINE PANCREAS

Gross and Microscopic Anatomy

The pancreas can vary widely in location and compactness among species, although microscopic anatomy is remarkably uniform. In most mammals, at least one major component of the pancreas is concentrated along the greater curvature of the stomach near the pylorus and proximal duodenum. This allows the outflow of digestive juices through the major pancreatic duct to empty at or near the same location in the duodenum as the common bile duct. In humans, dogs, cats, ruminants, and horses the pancreas is compact and elongated, and easily distinguished from surrounding tissues. In rodents, major components of the pancreas include a prominent head and body, but also a less distinct and less compact duodenal segment, dispersed within the duodenal mesentery. The main pancreatic duct is generally visible in all species; an accessory duct occurs in humans and multiple ducts may occur in rodents, all entering into the duodenum.

Microscopically, the pancreas is described functionally and morphologically as having two distinct parts, the exocrine pancreas or acini comprising lobules; and the endocrine pancreas or islets of Langerhans that exist within the exocrine parenchyma. The major "functional unit" of the exocrine pancreas is the acinus and the interconnecting ductal network of intra- and interlobular ducts leading to the main pancreatic duct (Figure 16.1). In the acinus, the apical portion of each cell is stained brightly eosinophilic (via hematoxylin and eosin) due to abundant zymogen granules, which contain the precursors (zymogens) of digestive enzymes. Discussion of the pancreas would not be complete without acknowledging the fibrovascular supporting stroma and circulation. The islets are vascularized by afferent arterioles that pass directly through the exocrine pancreas to the islets. The efferent venules exit the islets and bathe the peri-insular exocrine tissue at what has been termed the "endocrine–exocrine interface (EEI)."

The EEI has been extensively reviewed by Brenneman et al. (2014) and defines the conjunction of islet-acinar portal system (venous outflow from islets) with venous connections of postlobular arterioles that primarily supply the non- or tele-islet acini of the lobule. To date the rat EEI has been characterized the most extensively compared to other species. Capillaries are highly fenestrated in both the exocrine and endocrine pancreas, and the greatest fenestration occurs within pancreatic islets, allowing rapid uptake of endocrine hormones into efferent capillary beds, which then bathe neighboring acini or tele-acinar pancreas as well as distant organs after exiting the pancreas. Digestive zymogens pass from acini along with the ductal secretions directly into the duodenum by arborized pancreatic ducts. Ductular cells (Figure 16.1) form a single layer along a basement membrane beginning at the acinus and are surrounded by minimal to moderate amounts of richly reticulo-vascular stroma depending on the caliber of the duct. Centroacinar cells are aligned with the ductular lumen and acinus.

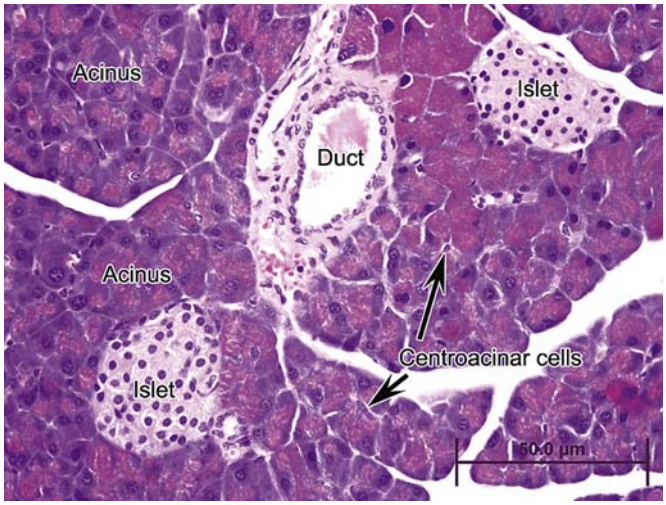

FIGURE 16.1 Pancreas from a rat showing zymogen-rich acinar cells, centroacinar cells (thought to function as precursor cells for regeneration of damage exocrine pancreas), ducts, and islets. Hematoxylin and eosin. Source: *From Haschek, W.M., Rousseaux, C.G., Wallig, M.A. (Eds.), 2007. Fundamentals of Toxicologic Pathology, second ed. Academic Press, San Diego, CA, Figure 10.1, p. 236.*

Physiology

The exocrine pancreas synthesizes and secretes digestive enzymes for lipid, carbohydrates, and protein. Except for amylase, the various proteins within zymogen granules remain inactive until proteolytic cleavage, initiated by enterokinase (enteropeptidase) in the gut lumen. Cholecystokinin (CCK) modulates zymogen release from acini in concert with cholinergic stimulation. Feedback loops involving trypsin and CCK-releasing protein shut down or amplify enzyme release. Secretin similarly modulates submucosal glands in the duodenum and ductal epithelium, triggering the release bicarbonate-rich fluid from ductal

cells and gut epithelium. The alkaline pH of ductal secretions (generally 8–9) serves to neutralize the acidity of the chyme entering the duodenum and produce the appropriate near-neutral pH and appropriate ionic balance for maximal activity of chymotrypsin, lipase, and amylase.

EVALUATION OF TOXICITY

Histologic Evaluation

Typically, in most nonclinical toxicity bioassays, a single section of pancreas usually taken as a cross section through the body of the pancreas is examined histopathologically. Evaluation of lipase or amylase measurement is only done if the target has the potential for pancreatic modulation. However, in toxicologic pathology assessment of molecules with known modulation of the acinar or islet pancreas, or in diagnostic cases, correlation of biomarkers with the extent and time course of exocrine injury should include histologic evaluation of the major pancreatic duct and exocrine parenchyma adjacent to the duodenum and surrounding the duodenal papilla, as well as sections through each major component of the pancreas. Particular attention to the peri-insular or peri-islet exocrine tissue should be considered. The peri-islet exocrine pancreas (similar to and extending beyond the EEI) tends to have the highest density of zymogen granules/acinar cell compared to distant exocrine sites. The primate pancreas should be sectioned to include the head, body, and tail. In the dog, sections should include the body of the pancreas (adjacent to the duodenal papilla), the gastric limb (left lobe) and duodenal limb (right lobe). In the rat and mouse, the pancreas is a more diffuse organ that is generally divided into three parts: biliary, duodenal, and gastrosplenic. The gastrosplenic portion along the dorsal aspect of the stomach toward the spleen is the largest section of rat pancreas (analogous to the body of the pancreas in other species). Sectioning oriented perpendicular to the major pancreatic duct is most diagnostic when multiple or step sections are taken. In rodents, islets are heavily distributed along the major pancreatic duct, and recent publications suggest the highest distribution of islets occurs within the tail of the rodent pancreas (Brenneman et al., 2014).

Immunohistochemistry and Histochemistry

In localized mild pancreatic injury, the only evidence of injury may be short-lived increases in either apoptosis as assessed by terminal deoxynucleotidyl transferase dUTP nick end labeling and antiactivated caspase 3 (apoptosis) immunohistochemistry (IHC), or in cell proliferation as evaluated by antibromodeoxyuridine and anti-Ki67 IHC. Routine histochemical stains (periodic acid-Schiff for zymogen granules and Masson's trichrome for fibroplasia) can be useful in grading subtle injury. In addition, the peri-islet or EEI component of exocrine pancreas should be evaluated for acinar, ductal, and vascular continuity and the presence or absence of inflammation. IHC is useful in identifying proteins specifically expressed by mature acinar and ductal epithelium, and tubular complexes; for example, mature acinar cells uniquely express *Reg1*, and mature ductal epithelium expresses cytokeratin 19. Similarly, IHC markers may be helpful in identifying specific inflammatory cells such as macrophages and lymphocytes.

In summary, biopsies or postmortem samples, as well as potential immunohistochemical and in situ hybridization techniques are useful in identifying cellular characteristics of affected tissue (ductal and/or acinar), and can guide understanding the pathogenesis of injury and relative significance and mechanism of the biomarker excursions. In most cases the magnitude of exocrine injury can be correlated with the timing of biomarker elevations and biomarker half-life. Postmortem evaluation and excisional biopsies from human surgical cases allow correlations between humans and animals in translating morphological injury with biomarker signals. Definition of chronic injury and regeneration may be aided by IHC identification of unique protein markers in affected cell populations. Importantly, localized or global vascular injury leading to ischemia can be a causative factor that usually drives coagulative necrosis, and/or severe liquifactive injury.

Clinical Chemistry

In acute pancreatitis, previously uninjured or naïve tissue has a greater propensity to elicit rapid elevations in leakage enzymes (biomarkers) based solely on the higher population of acinar epithelial cells proximate to the locus of injury. In cases of prolonged or recurrent pancreatic injury, concentrations of circulating biomarkers may poorly reflect extensive atrophy, fibrosis, or concurrent active inflammation. The most common markers of confined exocrine pancreatic injury are amylase and lipase activity, lipase immunoreactivity, trypsin-like immunoreactivity (TLI), trypsinogen-activated peptide (TAP) concentrations, and carboxypeptidase B activation peptide (CAPAP) concentrations. Micro-RNA shows promise in early and specific prediction of acinar cell injury; however, additional work on precision and translatability is ongoing concurrent shifts in the leukogram, coagulation markers,

concentrations of C-reactive protein (CRP), neutrophil elastase activity, phospholipase A2 activity, and concentrations of cytokines interleukin (IL)-6 and IL-8 activity, procalcitonin (a marker of survival in humans), and macrophage chemoattractant proteins (MCP-1 and MCP-2) further define pathogenesis and multiorgan involvement. Similarly, in acute necrotizing pancreatitis, consumption of fibrinogen can suggest fibrin activation, clot formation, and extension beyond the pancreas. A many-fold increase in serum lipase and amylase activities can occur in widespread acute inflammation or acute hemorrhagic pancreatitis, whereas, no or only marginal increases occur in animals or humans with recurring bouts of chronic pancreatitis.

Serum amylase is released from pancreas, liver, small intestine, and parotid salivary gland (man and pig). Typically increases in serum pancreatic amylase are most sensitive for diagnosing exocrine pancreatic injury. Yet total amylase activity has been shown in human diagnostics to be as effective in diagnosing pancreatic injury as the isotype alone. In any case, total amylase is reabsorbed by the renal tubular epithelium and inactivated by the normal nephron, so decreased glomerular filtration or proximal tubular renal injury may increase circulating amylase separately from pancreatic injury by up to 3 times the reference interval for all subspecies of amylase. Therefore, diagnosis of pancreatic injury must be considered in the context of serum lipase elevations, which are most specific. Most serum lipase activity is of pancreatic origin, although hepatocytes and intestinal mucosal cells also contribute to circulating levels. Typically, increases in serum lipase three to fourfold above the reference interval are suggestive of pancreatic injury. Acute injury causes increases in lipase activity within 24 hours, which peaks in 2–5 days. Since lipase concentrations in zymogen granules are approximately 4.5 times those of amylase, recurring injury is more likely to be recognized by leakage of lipase into the circulation. Lipase is less frequently increased by hepatobiliary and intestinal injury or renal failure than is amylase, and is considered more specific for mild localized exocrine injury in dogs. Lipase normally passes through the glomerular filtration barrier and is inactivated by the kidney in the proximal tubules, so hyperlipasemia can occur as a nonspecific finding with severe renal disease. Since pancreatic lipase requires calcium (Ca^{2+}), colipase, and bile salts as cofactors for digestion, elevated lipase with concurrent decreases in serum Ca^{2+} may suggest accompanying peri-pancreatic injury and abdominal steatitis. Lipase concentrations are usually measured as serum lipase activity; however, measurement of pancreatic lipase immunoreactivity may be more specific for exocrine injury than serum lipase activity alone.

Other markers of pancreatitis consist of TAP as a cleavage product of trypsinogen, and CAPAP as a peptide fragment of procarboxypeptidase B, a large cytosolic protein in acinar cells. Both TAP and CAPAP are released with protease activation. They are uniquely sensitive due to low circulating concentrations in healthy animals. Both pro-peptides are stable but short-lived in circulation; urine presents the preferred matrix for measurement. In a published study in dogs with clinical pancreatitis, urinary TAP, the urinary TAP–creatinine ratio, TLI, and serum lipase activity had the highest specificity for severe versus mild pancreatic necrosis. Procarboxypeptidase B is also present in serum, and with a longer serum half-life is useful in diagnosing necrosis several days after the primary insult is resolved. In combination, urine TAP and CAPAP, serum procarboxypeptidase B, serum amylase, and serum lipase can be diagnostic of the longitudinal nature or chronicity, severity, and progressivity of injury.

TLI measures both circulating trypsinogen and trypsin, which in healthy animals is comprised almost entirely of trypsinogen. TLI is increased in acute exocrine injury; however, rapid excretion by the kidney results in a short circulating half-life. Elevations can occur quickly with necrosis, but serum sampling can easily miss insults of short duration. As such, it is considered an effective marker of exocrine mass, and decreases are highly correlated with exocrine pancreatic insufficiency. Decreased glomerular filtration with impaired renal function can also impair TLI interpretation.

Other Markers of Injury

Whether exocrine injury occurs as activation of digestive enzymes within acinar cells alone, through retrograde efflux of bile acids into the pancreatic ductal system, or due to an acute or subacute ischemic event, biomarkers are defined by increased circulating concentrations of activated pancreatic proteases and their by-products. Concurrent increases in concentrations of acute phase reactants, activated leukocyte proteases, cytokines, chemokines, and traditional clinical chemistry and hematology markers of multiorgan injury express the magnitude and distribution of the lesion. Qualification of a reference interval for each biomarker and the linearity of each assay serve to define both sensitivity (the statistical ability to detect pancreatic injury) and specificity (the statistical ability to discriminate a true negative effect).

Experimental trials in animal species and assessment of diagnostic cases have collectively defined our current knowledge of pancreatic injury. As pancreatic

injury develops into peri-pancreatic inflammation and pancreatitis, an influx of activated neutrophils and macrophages releases leukocyte-derived enzymes including neutrophil elastase, phospholipase A2, procalcitonin, peroxidases, and cytokines at the site of injury. Localized lipid peroxidation releases malonyl dialdehyde, and activated macrophages release interleukins (IL-1 and IL-6) and tumor necrosis factor-alpha (TNFα). IL-6 is a potent inducer of acute phase protein synthesis by the liver, and increases in serum concentrations are correlated with disease severity. Increased IL-6 induces acute phase protein synthesis by the liver, CRP being the most prominent. Increases in serum concentrations of CRP, IL-6, procalcitonin, and neutrophil elastase are correlated with progressive abdominal inflammation and are predictive of a poor prognosis.

Animal Models

Studies of normal pancreatic physiology and models of experimental pancreatitis have primarily used rats and dogs although mice are now being used more frequently as transgenic and strains of knock-out mice are developed that exhibit a predisposition to pancreatic injury or pancreatitis. Nevertheless, the rat is still used more often than mouse, because the rat's larger size makes more pancreatic tissue available for study and permits readier surgical manipulation. Rats also appear to be sensitive to a wider variety of xenobiotics, in particular those that cause hyperstimulation (see later). The guinea pig has also been used in the past in some of the classic *in vivo* studies of acinar cell biology.

Models of Acute Pancreatitis

Investigators who want to study mechanisms of acute pancreatitis using noninvasive techniques typically use secretagogues that elicit some sort of hyperstimulation, such as supraphysiologic doses of CCK (or CCK analogs such as caerulein). These secretagogues produce many of the early biochemical and morphologic changes observed in acute pancreatitis in humans. Although hyperstimulation models are noninvasive, inexpensive, and relatively easy to implement, the responses can be variable and highly dose and species dependent, unless they are used concurrently with priming or synergizing agents or procedures (e.g., duct ligation or retrograde instillation of bile acids).

Given that overconsumption and abuse of ethanol is the most commonly identified trigger of pancreatitis in humans, numerous ethanol-based animal models of pancreatitis have been proposed and used in rats, cats, and dogs, most notably for studying the impact of oxygen free radical stress on acinar cells and pancreatic microcirculation. Unfortunately, these models tend to be inconsistently reproducible without concomitant hyperstimulation (caerulein), ductal ligation, or retrograde instillation of bile acids into the pancreatic ductal tree.

Models of Chronic Pancreatitis

Noninvasive models of chronic pancreatitis use repeated doses of hyperstimulatory compounds such as caerulein or L-arginine, in essence producing repeated bouts of relapsing acute pancreatitis. This activates pancreatic stellate cells (PSC) to produce the interstitial extracellular matrix (ECM) and elicit fibroplasia. Variations in which additional toxic stimuli such as cyclosporin D, lipopolysaccharide, or ethanol are coadministered enhance or accelerate the generation of chronic pancreatitis. Invasive techniques once used extensively in studying acute and chronic pancreatitis mimicked bile acid reflux and/or increased intraductal pressure, which are prominent features in the pathogenesis of alcoholic and cholelithiasis-induced pancreatic disease. These techniques are less commonly used now that noninvasive techniques can reliably induce pancreatic injury.

A slightly different model utilizes retrograde infusion of the main pancreatic duct at the pancreatobiliary-duodenal opening with bile salts or with bile salts plus activated pancreatic enzymes. While technically less challenging, this model is difficult to reproduce in part because there is poor precision in measuring and maintaining consistent retrograde pressure.

In conclusion, no singular animal model of pancreatitis or pancreatic injury to date meets all the criteria as an optimal model of human disease. A careful assessment of the study goals, for example, elucidation of mechanism, definition of early changes, measurement of impact on regeneration and healing must be made prior to selecting an *in vivo* model for investigating pancreatic injury by a xenobiotic.

Genetically Engineered Models of Pancreatitis

Enhanced predisposition to enhancement of either acute or chronic pancreatitis has been identified in many knock-out strains, including those with loss of inflammatory mediators. Additional knock-out strains that have an impact on pancreatitis include peroxisome proliferator-activated receptor *gamma*, metallothionein-1, and phospholipase A2. While the knock-out strains are useful for studying pancreatitis in the context of primary disruption of inflammation, the loss of these genes has a wider impact on other tissues and the body as a whole, making it difficult to ascribe changes specifically to induction of pancreatic injury.

More specific knock-out models, linked to known genetic predispositions to pancreatitis, an array of mutated or knock-out models for the cystic fibrosis transmembrane conductance regulator gene (*CFTR*), and the pancreatic secretory trypsin inhibitor (*Kazal Type I*) gene (*SPINK1*) knock-out models, have allowed for additional targeted research into the pathogenesis of acute recurrent and chronic pancreatitis. The *CFTR* knock-out mouse has been used to study the role of altered duct secretions in chronic pancreatitis while *SPINK1* knock outs have been used to study the role of autophagy and premature intracellular trypsin activation in the evolution of pancreatitis.

Models of Pancreatic Carcinogenesis

Of the various long-term models for chemical induction of pancreatic carcinomas, only two have been extensively characterized and described. The first of these uses azaserine as a pancreatic carcinogen in rats. Azaserine induces microscopically detectable acinar adenocarcinomas in the exocrine pancreas that can become grossly visible nodules 1 mm in diameter or larger.

The second model uses *N*-nitrosobis (2-oxopropyl) amine (BOP) in the Syrian golden hamster. The dominance of acinar cell tumors in the rat versus the dominance of ductal tumors in the hamster is striking. This disparity in tumor phenotype apparently represents a fundamental difference in the response of pancreatic cells in the two species to initiating agents. Since the vast majority of human pancreatic cancer is ductal in phenotype, the Syrian hamster is the species that has been used more frequently in the past as a model for modeling human pancreatic carcinogenesis. The Syrian hamster, however, has rarely been used in studies not involving pancreatic carcinogenesis, the rat and mouse being the preferred model animals for studying acute and chronic pancreatic injury.

RESPONSES OF EXOCRINE PANCREAS TO INJURY

Response to injury may be localized to individual cells, affect entire lobules, localize uniquely in peri-islet exocrine zones, or involve extensive effacement of the majority of the pancreas, ultimately extending into the anterior abdomen to include peri-pancreatic tissues and organs.

Nonlethal Injury and Autophagy

Beginning at the cellular level, acinar cells may undergo swelling or accumulate lipids in the cytoplasm as a direct or indirect effect of oxidative injury, ischemia, or derangement of cell metabolism. At the ultrastructural level, cell swelling is accompanied by vesiculation of the rough endoplasmic reticulum (RER) and dilatation of RER and SER cisternae, giving the acinar cell a pale, "feathery" appearance histologically. Lipid accumulation and swollen mitochondria may also occur separately or concurrently with free radical injury and oxidative stress. With starvation, acinar cells may fail to synthesize zymogens and lose the apical hyper-eosinophilia of zymogen granules over time; concurrently individual acinar apoptosis can reduce overall pancreatic mass or weight. With overstimulation, acinar cells may "degranulate," particularly when hypersecretion or supramaximal stimulation by a secretagogue (e.g., caerulein or CCK) is the pathogenesis of the injury. With intense stimulation, inappropriate trafficking of autophagic vacuoles (AV) and zymogen granules to the basolateral membrane occurs and elicits localized autodigestion. Large AV adjacent to the basal lateral portion of the cell are often surrounded by a thin clear halo (Figure 16.2), and in later stages may condense and resemble residual bodies.

In stable autophagy, cathepsin L released from the lysosome into the newly formed autophagolysosomes degrades any trypsinogen and prevents its activation to trypsin, hence short-circuiting any inappropriate activation of other zymogen proenzymes. However, cathepsin B (another lysosomal hydrolase) can activate trypsin, which could initiate an autodigestive cascade. A balance of cathepsins B and L within the AV during normal autophagy suggests that cathepsin B activity

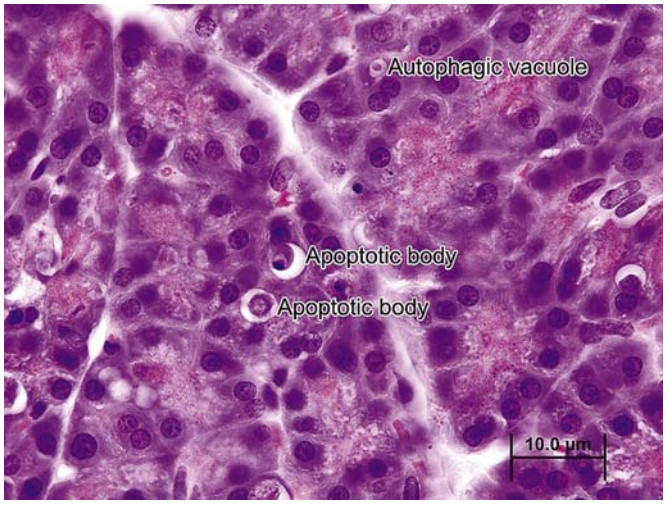

FIGURE 16.2 Pancreas from a rat treated with crambene showing generalized loss of zymogen granules (as evidenced by general pallor), AV, and apoptotic bodies affecting acinar epithelial cells. Hematoxylin and eosin. Source: *From Haschek, W.M., Rousseaux, C.G., Wallig, M.A. (Eds.), 2007. Fundamentals of Toxicologic Pathology, second ed. Academic Press, San Diego, CA, Figure 10.6A, p. 246.*

does not predominate; hence, only residual lipids, membranous and granular debris, remain after physiologic or "normal" autophagy. Examples of xenobiotics causing increased AV with dense inclusions in the endoplasmic reticulum (intracisternal granules) have been noted in rats following exposure to puromycin and 1-cyano-2-hydroxy-3-butene (crambene), and other agents that induce acinar cell death. These inclusions represent indigestible cellular remnants from the AV.

Another, somewhat unique process termed "zymophagy" is a modified form of autophagy involving *Bcl-1* and *VMP1*. Zymophagy results in a smaller AV containing only defective zymogen granules and surrounding cytoplasm. It is proposed that this is the process whereby acinar cells regulate their zymogen content. Experimental evidence is accumulating that "normal" autophagy is deregulated in injured acinar cells; dysregulation of zymophagy is at least partially responsible for the inappropriate activation of excessive trypsin, causing acute necrosis. The triggers modulating cellular autophagy versus apoptosis are unclear.

Apoptosis and Acinar Injury

Apoptosis is a more frequent occurrence in the exocrine pancreas than previously supposed, and involves mainly acinar cells, especially in cases of mild injury such as starvation or moderate food restriction, or with persistent low-grade injury. In pigs, for example, the mycotoxins fumonisin B_1 and T-2 toxin (vomitoxin) frequently induce vacuolation and "single cell necrosis" consistent with what is now interpreted to be apoptosis (Figure 16.3).

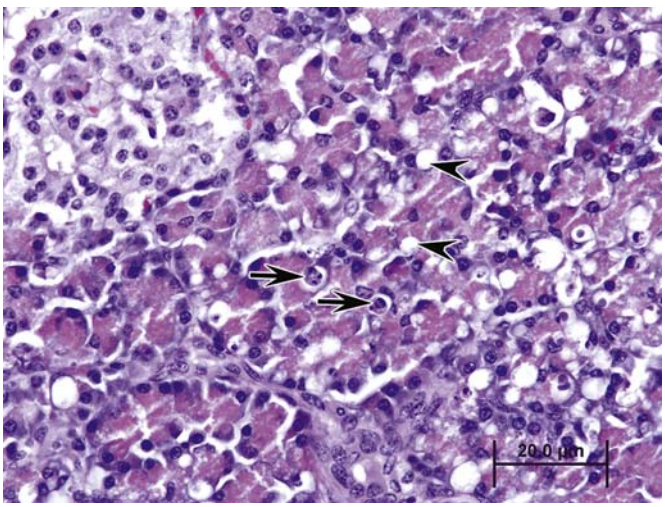

FIGURE 16.3 Acinar cell apoptosis (*arrows*) and vacuolation (*arrowheads*) in a porcine pancreas after exposure to T-2 mycotoxin. Hematoxylin and eosin. Source: *From Haschek, W.M., Rousseaux, C.G., Wallig, M.A. (Eds.), 2007. Fundamentals of Toxicologic Pathology, second ed. Academic Press, San Diego, CA, Figure 10.7, p. 246.*

Apoptosis in a sense is the "preferred" response to acinar cell injury since subsequent inflammation is usually minimal or absent, and dead acinar cells are eliminated before they can release their pro-inflammatory contents, which are highly attractive to neutrophils. Acinar cells express high levels of the pro-apoptotic protein *Bax* (localized in mitochondria) but express very little *Bcl-2*, which is the prime antiapoptotic protein and regulator of *Bax*. Acinar cells also express death receptors for FAS-ligand induced apoptosis, including the TNFα receptor and CD95. An inverse relationship between apoptosis and necrosis with acinar cell injury has been described in various experimental models. Stimulation of apoptosis appears to protect against acute necrotizing reactions from cellular toxicants, whereas inhibition of apoptosis leads to a necrosis, severe inflammation, and progression to pancreatitis.

Acinar cell apoptosis is classically manifested in many cases of xenobiotic-induced injury (Table 16.1). Typically only one or two cells per acinus may appear apoptotic at any one time without any neutrophil recruitment. In contrast, engorged macrophages containing apoptotic cells or residual bodies can increase with progressive tissue injury that leads to recruitment of neutrophils and macrophages through cytokine release (Figure 16.4). Even with large-scale apoptosis, inflammation and fibrosis may be minimal and contained locally. Biomarker elevations would not be expected.

Edematous Pancreatitis

The progression of unique mechanisms of acinar or islet injury usually causes apoptosis as defined in the above paragraph. As injury progresses to cause expansion of the pancreatic parenchyma, by edema (initially), followed by influx of inflammatory cells and the cascade of events listed in subsequent sections, it is more appropriate to use pancreatitis as a diagnostic term.

Pancreatitis in its mildest presentation occurs as "edematous pancreatitis (EP)," and has been described as increased numbers of histiocytic macrophages (often engorged with apoptotic bodies), few neutrophils, prominent inter- and intralobular interstitial edema, and expansion of the fibrovascular stroma. Often only apoptosis, edema, and histiocytic infiltrates are present after the initial wave of injury, and release of circulating pancreatic biomarkers does not occur.

Necrosis and Acute Necrotizing Pancreatitis

Necrosis of acinar cells is more widespread throughout single or multiple lobules, often involving

TABLE 16.1 Classification of Pancreatic Alterations with Selected Examples of Causative Agents

Alteration	Xenobiotic
Vacuolation and autophagy (degeneration)	Crambene, ethanol, fumonisin B_1, organophosphates, puromycin, T-2 toxin
Acinar cell apoptosis	Arginine, crambene, organophosphates, *p*-chloro-phenylalanine, scorpion venom (Central and South America),T-2 toxin
Acinar cell necrosis followed by inflammation	Actinomycin D, arginine, azaserine, crambene, ethioinine, GLP 1 analogs, 4-hydroxyaminoquinoline-1-oxide (4-HAQO), lysine, organophosphates, puromycin, sitagliptin, zinc
Acute inflammation with variable acinar cell necrosis	Alcohol, azathioprine, L-asparaginase, chlorthalidone, chlorothiazide, furosemide, 6-mercaptopurine, methyldopa, oral contraceptives, pentamidine, riftampicin, sulindac, tetracycline, thiazide diuretics, valproic acid
Chronic interstitial inflammation with fibrosis	Ethanol, dibutyl tin
Duct cell degeneration/necrosis	Dibutyl tin, zinc
Neoplasia (experimental animals)	
Well characterized	Azaserine, 7,12-dimethylbenz[α]anthracene, 4-hydroxyaminoquinoline-1-oxide (rat); *N*-nitroso (2-hydroxypropyl) (2-oxypropyl) amine, *N*-nitrosobis (2-hydroxypropyl) amine (rat and hamster), *N*-nitrosobis (2-oxypropyl) amine (hamster)
Weak or sporadic association	Aflatoxin B_1 (monkey); colfibrate, nafenopin, nitrofen, *N*-nitrosodimethylamine (rat); N_δ-(*N*-methyl-*N*-nitrosocarbamoyl)-L-ornithine (rat, hamster); *N*-nitroso-2,6-dimethylmorpholine, *N*-nitrosomethyl (2-oxopropyl) amine (hamster); *N*-methyl-*N*-nitrosourea (guinea pig, mouse), *N*-ethyl-*N*′-nitro-*N*-nitrosoguanidine (dog)

From Haschek, W.M., Rousseaux, C.G., Wallig, M.A. (Eds.), 2007. Fundamentals of Toxicologic Pathology, second ed. Academic Press, San Diego, CA, Chapter 10, Table 10.4, p. 244.

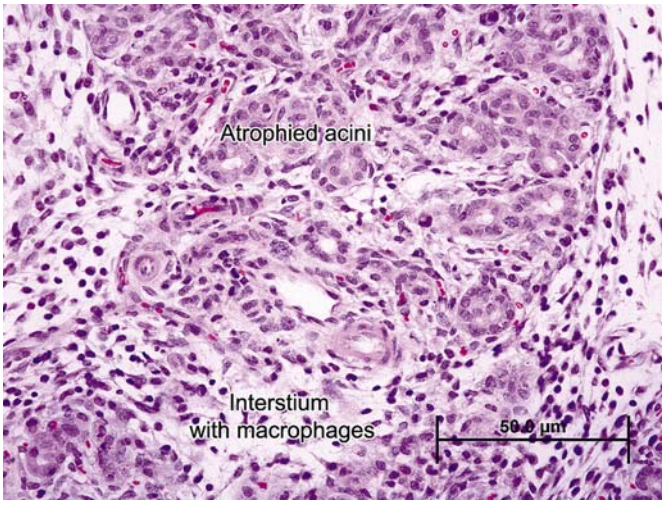

FIGURE 16.4 Pancreas from a rat after repeated crambene exposure, with persistent acinar cell apoptosis leading to exocrine atrophy, increased interstitial space and prominence of tissue macrophages. Hematoxylin and eosin. Source: *From Haschek, W.M., Rousseaux, C.G., Wallig, M.A. (Eds.), 2007. Fundamentals of Toxicologic Pathology, second ed. Academic Press, San Diego, CA, Figure 10.6B, p. 246.*

large clusters of acini and, in severe cases, the entire lobule. Necrosis often occurs initially at the periphery of the lobule, and progresses centripetally toward the center of the lobule. The changes differ from acinar cell apoptosis such that membrane disruption and release of cellular contents in the adjacent parenchyma initiates localized edema and cytokine recruitment. The context of pathogenesis to higher grade injury has significance in relation to the diffusion of activated zymogen proteins not only into lobular interstitium but also into surrounding peritoneal adipose tissue, triggering fat necrosis and peritonitis. Furthermore, the abundance of venules at the periphery of the lobules allows for rapid accumulation of neutrophils, which enhance the severity of the lesion (see later). With necrosis, acinar cells release zymogen contents within the interstitial stroma, and cell death quickly passes through the morphologic stage of coagulation necrosis and progresses to liquefaction as seen grossly (Figure 16.5A,B). This is because of the high content of hydrolytic enzymes activated and released into interstitial space. An intense neutrophilic inflammation is incited, and the classic microscopic appearance of acute necrotizing pancreatitis (Figure 16.6) can be observed. At this stage of injury, biomarkers of acinar cell injury are released and can be detected peripherally as elevated serum amylase and lipase activities within a time-dependent window. Necrosis is best recognized serologically 12–48 hours after insult, which corresponds temporally with concurrent vascular engorgement (congestion) of the pancreas (especially around the margins of the lobules) and intense chemoattraction of neutrophils. Intense neutrophil infiltration is likely responsible for the transition between cases of EP to fulminant necrotizing pancreatitis.

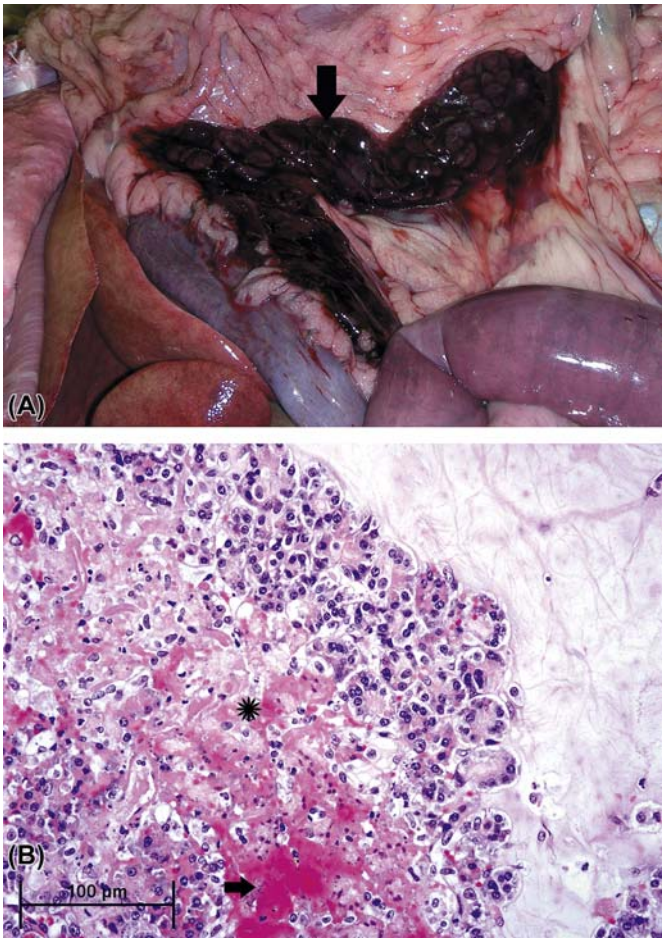

FIGURE 16.5 (A) Gross image of necrotizing pancreatitis in a dog. The *arrow points* to the necrotic and hemorrhagic pancreas. Liver and duodenum are in the lower left and lower right portions of the image, respectively. (B) Histologic image from the same case, illustrating necrotic acinar cells in the process of liquefaction (*) and lysed red cells (*arrows*). Early saponification of omental adipose tissue can be seen on the right-hand side of the image. At the time of death, neutrophils had not yet flooded the necrotic areas. Hematoxylin and eosin. Source: *From Haschek, W.M., Rousseaux, C.G., Wallig, M.A. (Eds.), 2013. Handbook of Toxicologic Pathology, third ed. Academic Press/Elsevier, London, Figure 57.5, p. 2378.*

Once necrosis has begun, tissue breakdown products enter the general circulation through the local capillary network, inducing generalized depression of cellular respiration, vasodilation and shock in concert with injury to the myocardium and pulmonary vasculature. Accompanying localized hemorrhage adjacent to the pancreas, with concurrent necrosis of adjacent mesentery and gastrointestinal tissues, leads to localized abscessation and potentially sepsis. If pancreatic necrosis is contained, regeneration follows a defined course of increased mitosis in both acinar and ductal cells; ducts regenerate from acinar cell metaplasia and centroacinar cell proliferation. Acinar cells are regenerated and zymogen granules appear with intact ductal connections. This restorative capacity occurs provided

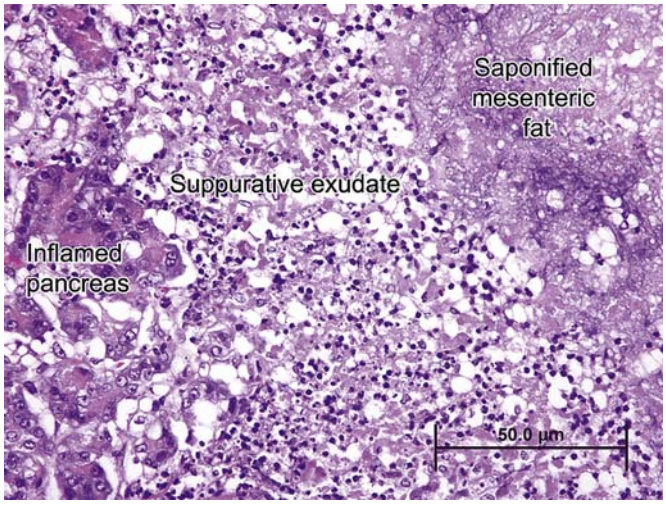

FIGURE 16.6 Acute necrotizing pancreatitis in a dog with an intense suppurative exudate and necrosis of mesenteric fat with saponification. Hematoxylin and eosin. Source: *From Haschek, W.M., Rousseaux, C.G., Wallig, M.A. (Eds.), 2007. Fundamentals of Toxicologic Pathology, second ed. Academic Press, San Diego, CA, Figure 10.8, p. 246.*

necrosis has not been widespread and damage to preexisting stroma has not been profound.

Interface Pancreatitis

EEI pancreatic injury is a unique type of pancreatitis reported in certain strains of rats (most notably Sprague–Dawley) in response to a variety of test articles. To date, this type of pancreatic injury has not been reported in other species. Initially necrosis is localized around intact islets; sometimes just a few islets are involved, while other times there is widespread involvement of islets. The necrotizing lesions spread centrifugally often to involve the entire lobule, with eventual fibrosis of the entire exocrine portion of the lobule beginning at the peri-islet interface. The pathogenesis is unknown but observations suggest endothelial toxicity or potential extensive congestion at the EEI, with subsequent interactions between damaged venule endothelium and inflammatory cells, which subsequently induces venous dilation, attraction of more inflammatory cells, and localized progressive peri-islet injury (Brenneman et al., 2014).

Chronic Pancreatitis

Chronic pancreatitis can be progressive, severe, relapsing, and persistent. The hallmark feature of chronic pancreatitis is marked fibrosis, which is active and progressive. The severity of fibrosis often varies from lobule to lobule and may be relatively mild in one lobule and very profound and exuberant in another. Initially fibrosis is primarily perilobular and periductal, surrounding major interlobular ducts. This

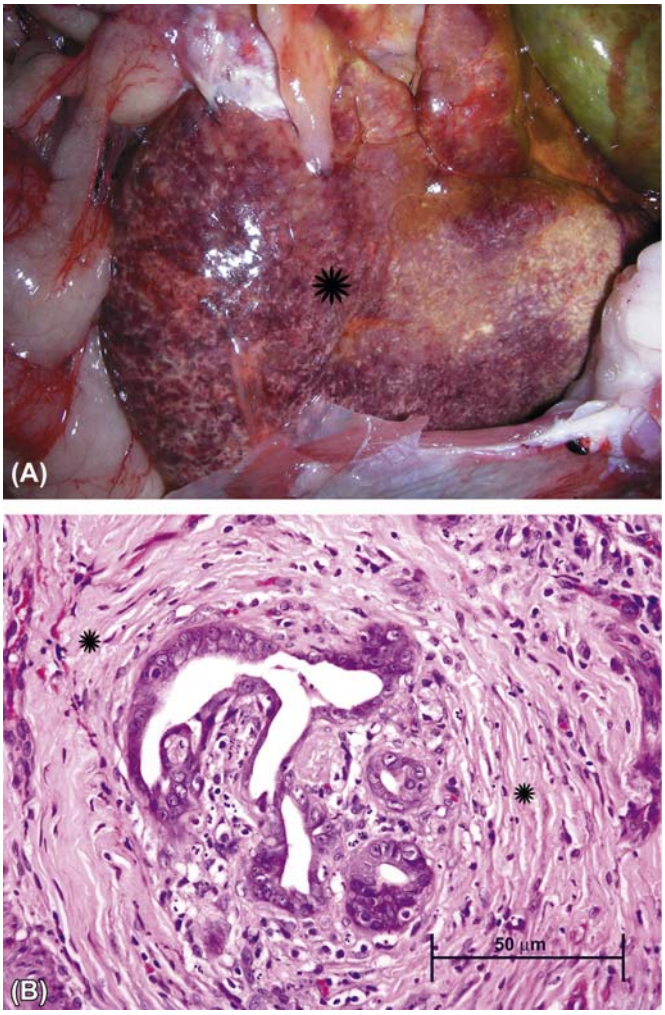

FIGURE 16.7 (A) Gross image of a pancreas in a dog with severe chronic pancreatitis. Note the pale areas of fibrosis throughout the affected pancreas (*). (B) Histologic image of fibrotic pancreas from a dog with severe chronic pancreatitis. Note the concentric layers of dense collagenous scar tissue (*) trapping residually inflamed ductules and acini. Hematoxylin and eosin. Source: *From Haschek, W.M., Rousseaux, C.G., Wallig, M.A. (Eds.), 2007. Fundamentals of Toxicologic Pathology, second ed. Academic Press, San Diego, CA, Figure 10.3, p. 240.*

fibrosis isolates lobules and traps remnant acinar cells and associated ductules within the shrinking lobule (Figure 16.7). With time, fibrosis becomes more intralobular, centering around small ducts and ductules, with subsequent atrophy of trapped ductal remnants and acinar cells. Much of the fibrosis is mediated by PSC, which share many features with myofibroblasts, in concert with recruited neutrophils and macrophages. In cases of mild pancreatic injury, apoptosis of PSCs occurs with reversal of injury and complete regeneration. However, if injury is severe, active, or relapsing, PSCs continue to actively produce ECM proteins. Long-term relapsing injury increases local pancreatic matrix metallo-protease 2, which is secreted by PSCs. Among its substrates is type IV collagen in lobular basement membranes, and this presumably elicits progressive acinar necrosis and atrophy with accompanying progressive inflammation.

Clinically, chronic pancreatitis manifests in most species as persistent low-grade pain associated with recurrent inflammation. Inflammation is primarily lymphocytic, comprised mainly of T-cells with proportionately fewer plasma cells. Macrophages are also present, as in any chronic lesion with fibrosis. Distribution of the inflammatory cells is concentrated in areas of active necrosis and early fibrosis. Pathogenesis and progression are often complex, compounded by impairment of ductal patency, reflux of biliary or pancreatic secretions, and low-grade adjacent lobular inflammation, necrosis, and fibrosis. As fibrosis progresses, zonal atrophy of ductular epithelium occurs and ducts are distorted (with the epithelium typically appearing folded and irregular).

Progression of inflammation and subsequent fibrosis beyond the thin pancreatic extracellular capsule causes perilobular fat necrosis due to the diffusion of activated hydrolytic enzymes released from dead acinar cells and the intense neutrophilic response that follows. Eventually there will be profound fibrosis and formation of pseudocysts (dilated structures adjacent to but separate from the main body of the pancreas). The cysts may be filled with proteinaceous fluid and debris and most likely reflect former foci of fat necrosis. Pseudocysts can become quite large and grossly resemble pancreatic neoplasms.

Immune-mediated pancreatitis in most species is a form of chronic pancreatitis with morphologic features that are somewhat different. Periductal fibrosis is profound and often partially occlusive, pushing the trapped ductal epithelium into star-shaped folds. Inflammation in these cases is centered mainly around large- and medium-sized pancreatic ducts, with degenerative features in ductules and acini reflective of impairment of outflow. The intensity of periductal inflammatory infiltrates is also greater in this condition, with thick cuffs of lymphocytes and plasma cells, sometimes with macrophages and granulocytes present as well. The main biliary ducts are also involved in this condition. Examples of each type of pancreatic injury are included in Table 16.1.

Proliferative Responses to Injury and Carcinogenesis

Benign pancreatic tumors in domestic and laboratory animals are rare, although pancreatic adenomas in dogs and cats do occur. These tumors can be acinar, ductular, or a combination of morphologies; many also elicit a dense fibrotic (scirrhous) stromal response. Aged rats spontaneously develop a low incidence of well-differentiated, apparently benign acinar cell neoplasms (adenomas).

The vast majority of pancreatic neoplasms (excluding rare spontaneous tumors) in laboratory animals occur as malignant neoplasms resulting from treatment with carcinogenic xenobiotics. Rats and mice exposed to pancreatic carcinogens characteristically develop acinar cell neoplasms that exhibit several histologic variants. Hamsters characteristically develop neoplasms with a ductal phenotype. The incidence and number of acinar cell adenomas is often dramatically increased among rats after treatment with carcinogens such as azaserine and 4-hydroxyaminoquinoline-1-oxide. Acinar cell carcinomas in rats have been classified as well-differentiated, poorly differentiated, and undifferentiated. Duct-like, cystic, and microcystic foci can be encountered in tumors in which the dominant phenotype is acinar; mucin secretion is rare in rat pancreatic carcinomas. In contrast, duct-like carcinomas predominate in hamsters and often show evidence of mucin secretion and admixed increases in goblet cells resembling the early preneoplastic changes seen in human patients with developing malignant pancreatic neoplasms. In nonrodents, pancreatic adenocarcinomas are uncommon, and their relation to environmental carcinogen exposure (if any) is unknown. As with adenomas and adenocarcinomas in rodents, pancreatic neoplasms in nonrodents can be acinar or ductular in pattern, often with a marked scirrhous stroma (Figure 16.8).

Background histologic findings accompany pancreatic neoplasia in all species. These incidental changes include necrosis of both normal acinar epithelium and tumor tissue, resulting in separation of cells and loss of distinguishing morphologic features and arrangements between the neoplastic and nonneoplastic phenotypes, sporadic focal lobular atrophy with variable fibrosis, telangiectasia (usually involving islets), mixed mononuclear cell infiltration, sporadic autophagy and apoptosis, and hyperplastic nodules. These hyperplastic lesions seldom evolve into neoplastic foci.

Background or Confounding Changes

Recognition of autolysis is important when assessing microscopic pancreatic appearance. Occurring rapidly after death, this artifact can be reduced through rapid collection and immersion into fixative of the pancreas at necropsy. In cases where pancreatic lesions are expected, collection of this tissue should occur directly after opening of the abdomen.

Both autophagy and apoptosis can be observed sporadically in "normal" pancreas of animals that have been fasted for long periods, have experienced chronic anorexia, or have been starved. Autophagic vacuoles, often containing protein inclusions, in pancreata from fasted or starved animals are substantially smaller than those in animals in the early stages of pancreatic injury and are also much fewer in number. Apoptosis also may be seen in starved animals but in much lower numbers than in animals with xenobiotic injury.

Aged dogs and cats occasionally develop hyperplastic nodules within the exocrine pancreas, composed entirely of acinar cells, which are often somewhat larger and more intensely stained than surrounding normal acinar cells (Figure 16.9). The nodules are irregularly distributed and seldom if ever develop into true neoplasms. The pathophysiologic significance appears

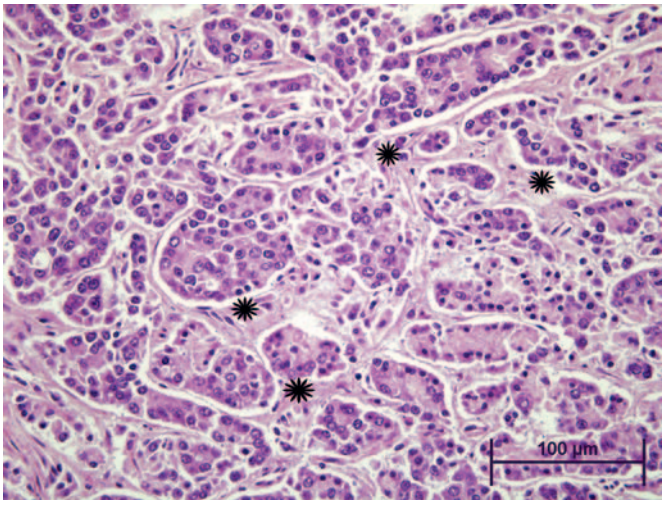

FIGURE 16.8 Pancreatic adenocarcinoma (ductular type) in the dog. Note the abundant dense fibrous stroma [i.e., early scirrhous response (*asterisks*)] which are often a feature of these neoplasms. Hematoxylin and eosin.

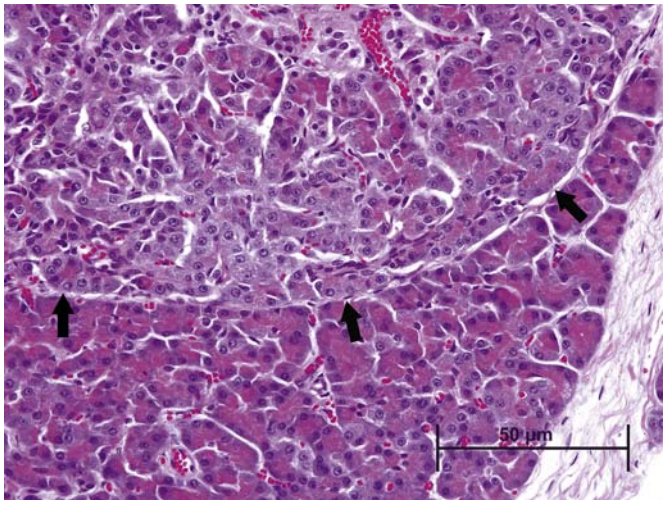

FIGURE 16.9 Nodular acinar cell hyperplasia in a dog. The *arrows* define the border between the paler hyperplastic cells and normal pancreas. Hematoxylin and eosin. Source: *From Haschek, W. M., Rousseaux, C.G., Wallig, M.A. (Eds.), 2007. Fundamentals of Toxicologic Pathology, second ed. Academic Press, San Diego, CA, Figure 10.10, p. 248.*

negligible, and a connection to toxin exposure has not been established.

MECHANISMS OF EXOCRINE PANCREATIC TOXICITY

Numerous chemical agents are known or suspected to induce acinar cell damage or necrosis, can alter acinar cell or duct cell function, or can induce neoplastic change in the exocrine pancreas. Medical literature contains numerous reports of acute pancreatitis in association with specific therapeutic products (Table 16.2). The risk of pancreatitis, although low, seems well established for some of these agents, for example, asparaginase and azathioprine. For other suspected pancreatic toxicants, however, only rare sporadic cases have been reported, and the connection between the agent and the cause of pancreatitis is often circumstantial.

Experimentally, rodents are susceptible to pancreatic damage by an overlapping but somewhat different spectrum of xenobiotics (Table 16.3). In contrast, relatively few xenobiotics are clearly linked to pancreatic injury in common domestic animals (Table 16.4) even though there are sporadic anecdotal reports in the veterinary literature.

For simplification, xenobiotic-induced injury can be categorized by the morphological characteristics of the injury they induce. These basic mechanisms are:

1. perturbation of zymogen granule trafficking,
2. oxidant stress,
3. localized ischemia,
4. pancreatic ductal stenosis or occlusion,
5. immune-mediated disease,
6. exposure to carcinogens.

Altered Zymogen Trafficking

Under normal conditions, secretion of zymogen granules is limited to the apical membrane area of the acinar cell, with tight apical cellular junctions between neighboring acinar cells. Any disruption of these tight junctions results in the leakage of zymogen into intercellular spaces. Apical secretion can be blocked in an acinar cell injury. Disruption of the plasma membrane leads to excessively high intracellular calcium (Ca^{2+}) concentrations, which trigger a signaling cascade that allows release of intact zymogen granules into the intercellular space. Colocalization of cathepsin B from lysosomes at the basolateral membrane or between acinar cells will further acinar cell injury by activating trypsinogen to trypsin and releasing cytokines that recruit inflammatory cells, leading to pancreatic inflammation.

TABLE 16.2 Agents and Drugs Reported to Cause Pancreatitis in Humans

Association with pancreatitis	Agent
Strong causative association with pancreatitis	Alcohol (ethanol)
	Azathioprine
	L-Asparagiuase
	Corticosteroids
	Cytarabine
	Didanosine
	Estrogens
	Furosemide
	GLP I analogs
	Mercaptopurine
	Mesalamine
	Opiates
	Pentamidine
	Pentavalent antimonials
	Sitagliptin
	Sulfasalazine
	Sulindac
	Trimethoprim-associated sulfonamides
	Valproic acid
Probable causative association with pancreatitis	Acetaminophen
	Carbamazeprine
	Cisplatin
	Cyclopenthiazide
	Enalapril
	Erythromycin
	Hydrochlorothiazide
	Interferon α-2β
	Lamuvidine
	Methyldopa
	Octreotide
	Phenformin
	Procainamide
	Rifampin
Other agents associated with pancreatitis	Clozapine
	Cyclosporine
	2′,3′-Dideoxyinosine
	Lisinopril
	Metronidazole
	Salicylates
	Zalcitabine

From Haschek, W.M., Rousseaux, C.G., Wallig, M.A. (Eds.), 2007. Fundamentals of Toxicologic Pathology, second ed. Academic Press, San Diego, CA, Chapter 10, Table 10.1, p. 242.

TABLE 16.3 Selected Agents Reported to Cause Toxic Effects in Exocrine Pancreas Experimentally in Rodents

Agent	Species
2-Acetaminofluorene and 4-acetaminofluorene	Rat
Aflatoxin	Rat
β-3-Thienyl-DL-alanine	Rat
Arginine	Rat
Azaserine	Rat
Carbon tetrachloride	Rat
Chloraquine	Rat
Crambene	Rat
Dibutyl tin	Rat
Diethanolamine	Rat
Ethanol	Rat
GLP 1 analogs	Rat
5-Fluorouracil	Rat
Lysine	Rat
Manganese	Rat
N-Nitrosomethyl(2-oxopropyl)amine	Rat
Puromycin	Rat
Triparanol	Rat
Zinc	Rat
Actinomycin D	Mouse
Chlorothiazide	Mouse
Neutral red	Mouse
Vinblastine	Mouse
Cobalt chloride	Guinea pig
Diazinon	Guinea pig
N-Nitrososbis(2-oxopropyl)amine	Hamster
Cortisone	Rabbit
Ethionine	Rat, mouse, guinea pig, hamster
4-Hydroxyaminoquinoline-1-oxide	Guinea pig, rat
Methionine	Hamster, rat
N_6-(*N*-Methyl-*N*-nitrosocarbamoyl)-L-ornithine	Rat, hamster
N-Nitroso(2-hydoxypropyl)(2-oxypropyl) amine	Hamster, rat

From Haschek, W.M., Rousseaux, C.G., Wallig, M.A. (Eds.), 2007. Fundamentals of Toxicologic Pathology, second ed. Academic Press, San Diego, CA, Chapter 10, Table 10.2, p. 242.

TABLE 16.4 Selected Agents Associated with Exocrine Pancreatic Toxicity in Common Domestic Animals[a]

Agent	Species
Chocolate[b]	Dog
Corticosteroids	Dog
Deoxyvalinol (DON)	Pig
Diazinon	Dog
Dichloroacetate	Dog
Ethanol	Dog
DL-Ethionine	Dog
Fumonisin B_1	Pig
Organophosphates (especially diazinon)	Dog
T-2 toxin (vomitoxin)	Pig
Trimethoprim-enhanced sulfonamides	Dog
Scorpion venom (Central and South America)	Dog
Zinc	Dog, cow, sheep, pig, chicken

[a]*Experimental and "naturally occurring" reports, idiosyncratic occurrences not listed.*
[b]*Associated with the high fat content of chocolate rather than toxicosis.*
From Haschek, W.M., Rousseaux, C.G., Wallig, M.A. (Eds.), 2007. Fundamentals of Toxicologic Pathology, second ed. Academic Press, San Diego, CA, Chapter 10, Table 10.3, p. 243.

Under physiologic conditions, CCK stimulates both protein synthesis of zymogens and secretion of mature zymogen granules. Secretion generally outpaces protein synthesis, and as a result zymogens tend not to accumulate within the acinar cell. With "supramaximal" doses of CCK (or analogs like caerulein that induce hypersecretion), protein synthesis outpaces secretion. Excessive accumulation of zymogens overwhelms the zymophagy pathway and triggers large-scale autophagy. A potential "autophagic traffic jam" then can lead to formation of dysfunctional autophagolysosomes and uncoordinated activations of lysosomal cathepsins L and B. As previously stated, when cathepsin B predominates, trypsonigen is activated to trypsin, which can activate other pro-zymogen proteins in the zymogen granules. The subsequent autodigestive cascade elicits membrane destruction in the local pancreas. Localized pancreatic autophagy is balanced by continued local membrane destruction by activated digestive enzymes and contained by acinar cell apoptosis at the margin of the lesion with recruitment of inflammatory cells that together contain the injury.

"Prototypical" xenobiotics that cause pancreatic injury via altered zymogen trafficking include caerulein, crambene, carbachol, organophosphates, and scorpion toxin. Ethanol is a "sensitizer," enhancing the sensitivity of acinar cells to altered zymogen trafficking by enhancing hyperstimulation.

Oxidant Stress

The pancreas, unlike many other nonhepatic tissues, has active glutathione-synthesizing machinery including

the inducible, rate-limiting enzyme of glutathione synthesis, glutathione cysteine ligase. Hence, the pancreas can increase its baseline level of glutathione if the oxidant stress evolves slowly. Similarly, both acinar and ductal cells contain phase II enzymes such as the glutathione S-transferases (GSTs). The lower magnitude of GSTs in acinar cells compared to duct cells is postulated to make acinar cells more prone to damage by bioactivated xenobiotics. GSTs are also secreted into pancreatic juice, and this is postulated to play a protective role against xenobiotics present in ingested materials.

Active transsulfuration complements the antioxidation pathway, allowing the acinar cell to derive cysteine from methionine. These can be used to produce more glutathione if needed. Nicotinamide adenine dinucleotide phosphate quinone reductase, another antioxidant enzyme, is also expressed significantly in pancreatic acinar cells and can have increased induction under conditions of oxidant stress, most notably glutathione depletion. The pancreas contains not only phase II drug-metabolizing enzymes but also phase I metabolizing enzymes, although the levels/activities of cytochromes P450 (CYP) and related Phase I enzymes are quite low compared to liver (as little 1% of hepatocyte concentrations). CYP enzyme activity appears to be present in roughly equal proportions in both acinar cell and duct cells, although there is some variation in isoform expression, making both cell types more prone to bioactivation of xenobiotics and injury by reactive intermediates. The low overall activity of CYPs within the pancreas compared to liver makes CYP induction less common in the pancreas. As with CYP enzymes in any tissue, some pancreatic CYP isoforms are inducible. However, variability in isoforms across species requires assessment of respective CYPs important in predicting xenobiotic transformation within pancreatic tissue.

Localized Ischemia

Arteriolar and capillary blood flows are affected by parasympathetic and sympathetic ganglia in the organ and adjacent mesentery. EP in generalhas increased capillary blood flow, and necrotizing pancreatitis is often associated with local pro-coagulant activity and decreased capillary blood flow within the organ. A role for interactions of the renin-angiotensin system in pancreatic necrosis has recently been postulated, and supported by the discovery of angiotensin receptors in pancreatic capillary beds and acini. Binding of angiotensin results in renin-induced vasoconstriction, decreased capillary perfusion, and increases the potential to exacerbate local ischemia.

Impaired Ductal Outflow or Obstruction

Impairment of ductal outflow is a major predisposing factor for pancreatitis both in humans and experimentally in rodent models, in particular in relation to chronic pancreatitis. One of the most important functions of the pancreas is regulation of bicarbonate and chloride flux in acinar and ductal epithelial cells, most importantly the ductal epithelium. Since bicarbonate secretion is important in modulating the pH of ductal secretions and pancreatic juice for appropriate activation of pancreatic digestive enzymes, modest perturbations in the pancreatic microenvironment caused by acute gastritis or alcohol consumption can result in localized activation of digestive enzymes just as blockage of the common bile duct can induce retrograde efflux of bile acids into the pancreatic ductal tree. Collectively, modulation of ductal secretion and/or reflux of bile acids (e.g., with cholelithiasis, or bile duct fluke migration) can induce acute widespread induction of duct injury. Cell membranes are destroyed by bile acids, contents leak into the parenchyma, cathepsin B activates trypsinogen to trypsin, and lipase is activated within the acini of the affected lobule(s) to induce progressive pancreatic necrosis. Predisposing factors include excessive cortisol (endogenous or exogenous sources) and persistent hypercalcemia or hypertriglyceridemia. If ethanol is removed as an etiology of exocrine injury, many of the causes of pancreatitis remain idiopathic.

Immune-Mediated Disease

Immune-mediated pancreatitis is a recently defined entity in humans that originated with characterization of sclerosing cholangitis and sclerosing pancreatitis. These conditions occur with concurrently increased serum γ-globulins (IgG1 or IgG4 autoantibodies), diffuse pancreatic enlargement, obstruction or narrowing of the pancreatic ducts (sclerotic change), and mixed lymphocytic and plasmacytic infiltration of the exocrine pancreas. Typically affected pancreata exhibit stenosis of the major pancreatic duct and common bile duct with capillary thrombosis. An animal model of autoimmune pancreatitis has been developed using the neonatal BALB/c mice that have undergone thymectomy and then are immunized with carbonic anhydrase II (an important enzyme in ductal epithelium) or lactoferrin. These mice express increases in CD4+ Th1 cells (which enhance cell-mediated inflammatory process) as the syndrome develops with subsequent depletion of regulatory T-cells. It is likely that T-helper 2 cytokines (which promote humoral immunity) are involved in the progression of the disease with recruitment and proliferation of B cells and plasma cells.

Exposure to Carcinogens

Nonlethal mutations occur both in acinar and ductal cells exposed to mutagens or carcinogens. The induction of DNA damage in these cells by carcinogens has been documented in hamsters and rats. For example, the β-oxidized di-*n*-propylnitrosamines are activated to form mutagens by pancreatic microsomal cell fractions. There are significant species differences in the effect of carcinogenic xenobiotics on the pancreas. Short-term *in vitro* assays for screening pancreatic carcinogens, most of which involve short-term cell culture assays, have been attempted but often are problematic to perform. Similarly, maintaining long-term cell cultures, in particular with acinar cells, has proved challenging, since the precise factors needed for maintenance of viability and differentiation have been difficult to identify. The most intensively studied rodent pancreatic carcinogens, azaserine, 4-hydroxyaminoquinoline 1-oxide, and BOP, besides being directly mutagenic, have poorly characterized cytotoxic effect as well as assessed through measurement of decreased protein synthesis. At present, it is not possible to determine whether or not a focal lesion has the potential to progress to a neoplasm, except by observation in long-term studies, or potentially genetically altered species (transgenic mice, for example). It has been estimated that fewer than 1% of such foci actually complete the progression to neoplasia although recent studies have shown that *Kras* mutations are present early in pancreatic carcinogenicity, often in preneoplastic lesions, and p16 is mutated early in the progression from benign to malignant, invasive tumors. A wide array of chemical carcinogens with widely divergent structures has been shown to affect the pancreas (Table 16.5).

TABLE 16.5 Summary of Chemicals that Cause Carincoma in the Exocrine Pancreas of Experimental Animals

Agent	Species
Group A (well-characterized model carcinogens)	
Azaserine	Rat
7,12-Dimethylbenz[*a*]amhracene	Rat
4-Hydroxyaminoquinoline-1-oxide	Rat
N-Nitroso(2-hydroxypropyl)(2-oxopropyl)amine	Hamster, rat
N-Nitroso(2-oxopropyl)amine	Hamster
N-Nitroso(2-hydroxypropyl)amine	Hamster, rat
Group B (reported as carcinogens once or in a limited number of studies)	
Aflatoxin B_1	Monkey
Clofibrate	Rat
4-Hydroxy-3-nitrobenzenearsonic acid (Roxarsone)	Mouse
N^6-(*N*-methyl-*N*-nitrosocarbamoyl)-L-ornithine	Rat, hamster
N-Methyl-*N*-nitrosourea	Guinea pig, mouse
Nafenopin	Rat
Nitrofuran	Rat
N-Ethyl-*N*′-nitro-*N*-nitrosoguanidine	Dog
N-Nitrosodimethylamine	Rat
N-Nitroso-2,6-dimethylmorpholine	Hamster
N-Nitrosomethyl(2-oxopropyl)amine	Hamster
2,3,7,8-Tetrachlorodibenzo-*p*-dioxin	Rat

From Haschek, W.M., Rousseaux, C.G., Wallig, M.A. (Eds.), 2007. Fundamentals of Toxicologic Pathology, second ed. Academic Press, San Diego, CA, Chapter 10, Table 10.5, p. 247.

SUMMARY

The pancreas is a unique and dynamic organ with endocrine and exocrine functions. The location of the pancreas within the anterior abdomen, rich blood supply, and role in synthesis of proenzymes of digestion, along with limited ductal outlets to the intestinal tract, has allowed evolution into a generally stable organ with a variety of adaptions (e.g., autophagy and apoptosis) to limit progression of injury. Disruption or excessive stimulation of digestive proenzyme trafficking to the ductal system can elicit colocalization of zymogen granules and lysosomes within AV eliciting cathepsin B activation of trypsinogen to trypsin leading to localized or global organ injury. Similarly, oxidant stress can induce excessive apoptosis or necrosis in acini and ductal epithelium, and ischemia with reperfusion can elicit thrombosis, localized acidosis, membrane breakdown, and enzymatic digestion. The proximity of the bile duct and bile acids can move retrograde up the pancreatic ducts leading to tissue necrosis and further activation of trypsinogen. Like other tissues, the pancreas is also susceptible to carcinogens and immune−mediated diseases. Its remarkable ability to limit injury through the propensity for acinar cell apoptosis versus necrosis helps manage excessive digestive enzyme activation and minimize injury in many cases. The inherent regenerative capacity of acinar cells and ductal epithelial allows maintenance of organ function in the face of toxicity.

However, the pancreas is very susceptible to recurring injury leading to a loss of ductal patency, fibrosis, and continued attempts to regenerate acinar cells and zymogen granules. Thus, multiphasic and relapsing injury collectively may lead to excessive and permanent glandular or islet destruction. In severe cases, the injury and subsequent inflammation can spread to

the peritoneum and liver, causing an acute abdominal crisis. For assessment of pancreatic injury due to toxic insult, a large group of serum biomarkers are available for peripheral evaluation of pancreatic toxicity at in its early stages; however, almost all of these serum biomarkers need to be measured within 24–48 hours after a single-source injury to be effective in detecting pancreatic necrosis, assessing the severity of the insult, or defining clinical or preclinical prognosis.

Further Reading

Wallig, M.A., Sullivan, J.M., 2013. The exocrine pancreas. In: third ed. Haschek, W.H., Rousseaux, C.M., Wallig, M.A. (Eds.), Handbook of Toxicologic Pathology, vol. III. Academic Press (Elsevier), San Diego, CA, pp. 2362–2390. Chapter 57.

Anatomy and Physiology

Beger, G.R., Warshaw, A., Buchler, M., Kozarek, R.A., Lerch, M.M., Neoptolemos, J.P., et al., 2008. The Pancreas: An Integrated Textbook of Basic Science, Medicine, and Surgery, second ed. Blackwell Publishing Limited, Malden, MA.

Go, V.L.W., DiMagno, E.P., Gardner, J.D., Lebenthal, E., Reber, H.A., Scheele, G.A. (Eds.), 1993. The Exocrine Pancreas: Biology, Pathobiology, and Diseases. Raven Press, New York.

Ulrich, A.B., Standop, J., Schmied, B.M., Schneider, M.B., Lawson, T.A., Pour, P.M., 2002. Species differences in the distribution of drug-metabolizing enzymes in the pancreas. Toxicol. Pathol. 30, 247–253.

Evaluation of Toxicity

Aghdassi, A.A., Mayerle, J., Christochowitz, S., Weiss, G.U., Sendler, M., Lerch, M.M., 2011. Animal models for investigating chronic pancreatitis. Fibrogen. Tissue Repair 4, 26–42.

Lippi, G., Valentino, M., Cervellin, G., 2012. Laboratory diagnosis of acute pancreatitis: in search of the holy grail. Critical Rev. Clin. Lab. Sci. 49, 18–31.

Takahashi, M., Hori, M., Mutoh, M., Wakabayashi, K., Nakagama, H., 2011. Experimental animal models of pancreatic carcinogenesis for prevention studies and their relevance to human disease. Cancer 3, 582–602.

Walgren, J.L., Mitchell, M.D., Whiteley, L.O., Thompson, D.C., 2007. Evaluation of two novel peptide safety markers for exocrine pancreatic toxicity. Toxicol. Sci. 96 (1), 184–193.

Responses to Injury

Bhatia, M., 2004. Apoptosis versus necrosis in acute pancreatitis. Am. J. Physiol. (Gastrointest. Liver Physiol.). 286, G189–G196.

Brenneman, K.A., Ramaiah, S.K., Messing, D.M., O'Neil, S.P., Gauthier, L.M., Stewart, Z.S., et al., 2014. Mechanistic investigations of test article–induced pancreatic toxicity at the endocrine–exocrine interface in the rat. Toxicol. Pathol. 42, 229–242.

Hashimoto, D., Ohmuraya, M., Yamamoto, A., Suyama, K., Ido, S., Okumura, Y., et al., 2008. Involvement of autophagy in trypsinogen activation within the pancreatic acinar cells. J. Cell Biol. 181, 1065–1072.

Klöppel, G., 2007. Chronic pancreatitis, pseudotumors and other tumor-like lesions. Mod. Pathol. 20, S112–S131.

Nolte, T., Brander-Weber, P., Dangler, C., Deschl, U., Elwell, M.R., Greaves, P., et al., 2016. Nonproliferative and proliferative lesions of the gastrointestinal tract, pancreas and salivary glands of the rat and mouse (review). J. Toxicol. Pathol. 29 (1 Suppl), 1S–124S.

Voronina, S., Sherwood, M., Barrow, S., Dolman, N., Conant, A., Tepikin, A., 2009. Downstream from calcium signaling: mitochondria, vacuoles, and pancreatic acinar cell damage. Acta Physiol. 195, 161–169.

Mechanisms of Toxicity

Gaisano, H.Y., Gorelick, F.S., 2009. Insights into the mechanisms of pancreatitis. Gastroenterology 136, 2040–2044.

Saluja, A.K., Lerch, M.M., Phillips, P.A., Dudeja, V., 2007. Why does pancreatic overstimulation cause pancreatitis? Ann. Rev. Physiol. 69, 249–269.

Thrower, E.C., Gorelick, F.S., Husain, S.Z., 2010. Molecular and cellular mechanisms of pancreatic injury. Curr. Opin. Gastroenterol. 26, 484–489.

CHAPTER

17

Male Reproductive System

Dianne M. Creasy[1] *and Robert E. Chapin*[2]

[1]Dianne Creasy Consulting, Diss, Norfolk, United Kingdom
[2]Retired, Pfizer Global R&D, Groton, CT, United States

OUTLINE

INTRODUCTION

Recent concerns about falling sperm counts and the likely involvement of environmental endocrine disruptors in the declining reproductive health of human and wildlife populations has galvanized public awareness of the potential for environmental contaminants, occupational exposures, and therapeutic drugs to pose a significant hazard to male fertility. This whole field was underappreciated prior to 1977, when the salutary lesson of dibromochloropropane (DBCP)-induced testicular toxicity became public knowledge. The clear and profound effects produced by DBCP, and the fact that these effects had been noted in animals several years earlier and then overlooked, was a wake-up call about the potential vulnerability of the male reproductive system to environmental exposures.

From 1977 until the mid-1990s, the focus in human male reproductive health was primarily on occupational exposures to adult men and animal models of such exposures. Heavy metals such as cadmium, lead, and copper along with pesticides such as Kepone, ethylene dibromide, and carbaryl have all adversely impacted sperm measures (mostly count but also

Fundamentals of Toxicologic Pathology.
DOI: http://dx.doi.org/10.1016/B978-0-12-809841-7.00017-4

structure or motility) and/or fertility in men, mirroring their effects previously seen in animals. Solvents, such as the glycol ethers, were prominent tools in preclinical reproductive toxicology in the early 1980s, and two glycol ether congeners (2-ethoxyethanol and 2-methoxyethanol) were eventually found to affect sperm counts in occupationally exposed men, consistent with the effects noted earlier in animals.

Then, in the early 1990s, prenatal exposure to diethylstilbestrol was linked to malformations of the male reproductive tract in the offspring (its effects on females had been noted much earlier). It soon became clear that such effects could be produced by compounds which altered hormonal signaling in the fetus. Further work revealed that there were numerous ways to disrupt the endocrine system, from direct receptor interaction to reduced hormone synthesis. The pervasiveness of these endocrine disruptors has led to significant increases in regulatory oversight, and large new testing programs have been instituted by regulatory agencies. While the impacts of fetal and neonatal exposures will be touched on briefly, the bulk of this chapter will concentrate on the evaluation of tissue from adults after postpubertal exposures.

Male fertility can be impacted by disturbances at sites other than the testis, and it is necessary to evaluate the system as a whole and consider the functions of the individual components. In addition to the testis, this includes the excurrent ducts which transport, modify, and store sperm prior to ejaculation, the accessory sex glands, and the hypothalamic–pituitary–gonadal (HPG) axis, which provides overall regulation of the reproductive system.

Broadly speaking, reproductive embryology, anatomy, and physiology are similar between mammalian species, but there are detailed differences, some of which may have a significant impact on a species response to toxicants. Since the rat is the most common species studied in toxicologic pathology and for which most is known regarding reproductive physiology, it will be the primary species discussed in this chapter, but important species differences will be covered where relevant and when known.

Identification and evaluation of male reproductive toxicity requires integration of information from a variety of endpoints other than morphology. Male infertility can be mediated through alterations in sperm function that are not associated with any alterations in testicular or epididymal morphology, and so, an integrated assessment of as many endpoints as possible (organ weights, histomorphology, sperm parameters, hormonal measurements, and fertility endpoints) provides the most thorough and holistic evaluation. In most cases, multiple endpoints will be affected. The profile of changes identified often allows valuable insight into the possible site and mechanism of toxicity, and the likely relevance of the changes to man.

Morphologic evaluation of the testis is accepted to be the most sensitive method for identifying most male reproductive toxicants, but that sensitivity is directly proportional to the level of knowledge and understanding that the pathologist has of the spermatogenic process and spermatogenic organization within the seminiferous tubules. Subtle morphologic changes in germ-cell morphology or in germ-cell organization can result in dramatic effects on fertility, and frequently the only way a pathologist is able to recognize such subtle changes is by conducting a "stage-aware" evaluation. This means having a general knowledge of the shape and size of the different germ cell types as they progress through spermatogenesis, as well as which cell types occur in association with one another.

Light microscopic examination of the entire reproductive tract is the foundation of identifying male reproductive toxicity. Once identified, there is often a desire to provide a mechanistic explanation for the toxicity, but due to the complexity of cellular interactions within the testis and the interdependence of the various cell types, isolating and probing specific cell types outside of their normal *in vivo* environment is beset with problems. Even separating the individual cell types is technically challenging, and, certainly, once isolated and purified these cells are no longer the same as they were in situ. Such purified preparations are of limited usefulness in identifying the rich intercellular mechanisms of toxicity.

STRUCTURE, FUNCTION, AND CELL BIOLOGY

Embryonic Development

The primordial gonad develops as the genital ridge, which grows along the coelemic surface of the mesonephros. Primordial germ cells migrate from the yolk sac endoderm and combine with somatic (Sertoli) cells from the mesonephros to form the seminiferous (medullary) cords. Once these cords are formed, the fetal Leydig cells begin differentiating from mesenchymal cells, which are present in the interstitial tissue between the cords. This differentiation is thought to be under the control of the Sertoli cells (Figure 17.1).

Testosterone, secreted by fetal Leydig cells during the fetal and neonatal period is responsible for the masculinization of various processes and systems, including the central nervous system and sexual behavior. Around postnatal day 10, the fetal Leydig cells regress and are gradually replaced by a different

generation of adult Leydig cells, which also differentiate from interstitial mesenchymal cells.

The excurrent duct system, comprising the rete testis, efferent ducts, epididymis, and vas deferens, develops from the Wolffian duct system. The seminal vesicles develop from lateral buds of this duct. However, the prostate and bulbourethral (Cowper's) glands, along with the urethra and external genitalia, have a different embryologic origin, developing from the urogenital tubercle (Figure 17.1).

In mammalian species, the default phenotypic sex is the female; i.e., for a phenotypic male to develop, a whole series of events must be triggered and coordinated to form the male reproductive system and associated secondary sexual characteristics (Figure 17.2). The failure of certain genes or hormones to be expressed will normally result in a female phenotype. As the gonad emerges in the genital ridge in the embryo, it has the potential to become either a female or a male gonad. The critical event controlling maleness is the expression of the sex-determining gene (Sry), the expression of which is regulated by numerous proteins including Wt1, members of the insulin-receptor family, and a Gata4/Fog2 complex, amongst others. This in turn elicits a whole cascade of events to enable the fetal gonad to develop into a testis. In the fetal gonad, the development of the Sertoli cells plays a major role in how the reproductive system develops. The Sertoli cell synthesizes factors that drive the formation of an extensive vasculature and seminiferous cords. One of the most important of these is Müllerian-inhibiting substance which initiates the removal of the female structures (the Müllerian ducts) that would have formed the oviducts, uterus, and vagina. Sertoli cells also control the normal development of the testosterone-secreting Leydig cells, which then play an important role in the development of the epididymis, vas deferens, and seminal vesicles from the Wolffian ducts (Figure 17.2). Dihydrotestosterone, the testosterone metabolite produced locally from testosterone by the enzyme 5α-reductase, appears crucial

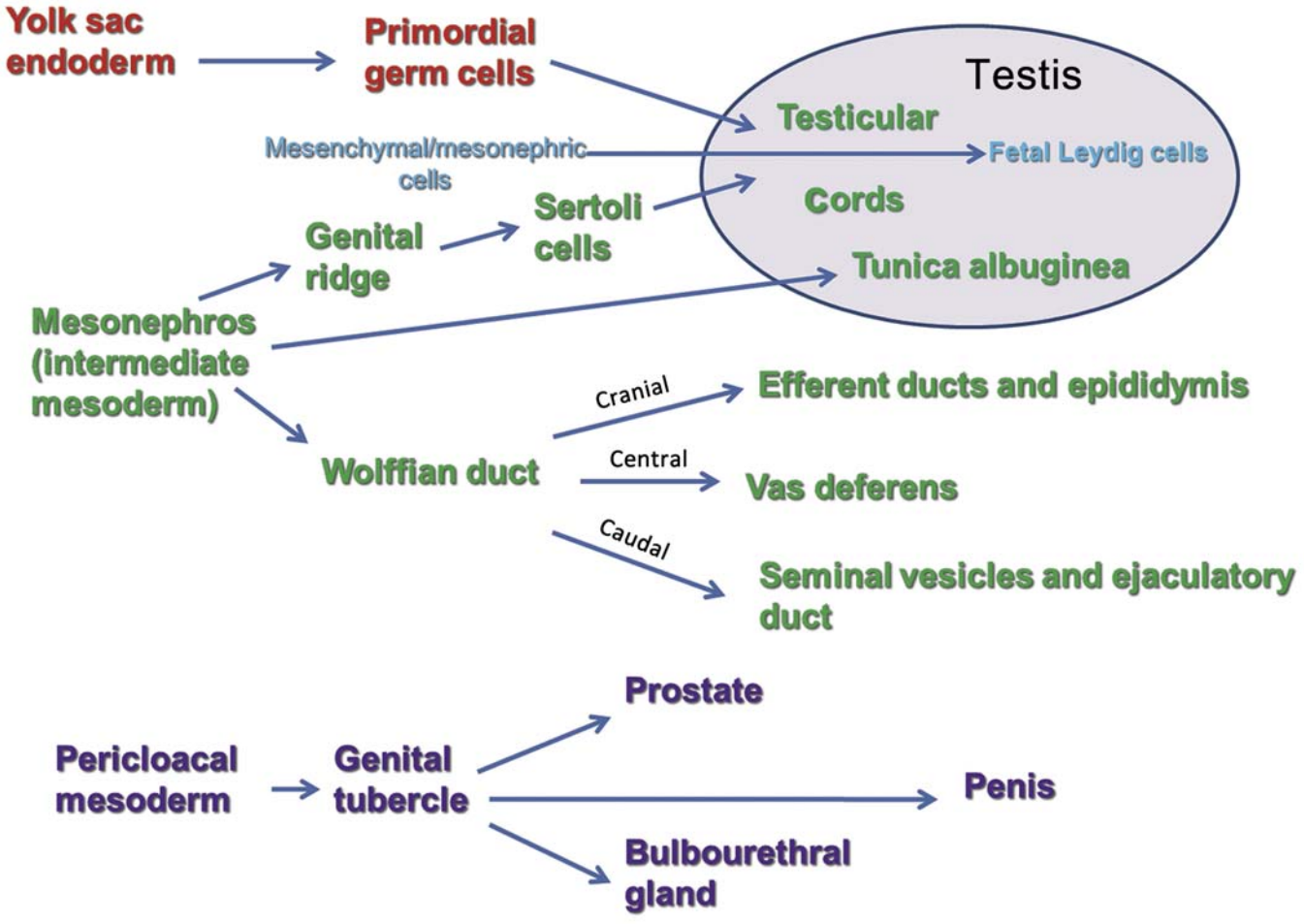

FIGURE 17.1 Embryological derivation of the tissues and cells of the male reproductive tract. Source: *Figure reproduced from* Haschek and Rousseaux's Handbook of Toxicologic Pathology *(2013), third ed. (W.M. Haschek, C.G. Rousseaux and M.A. Wallig, eds.), Academic Press (Elsevier), Figure 59.1, p. 2496 with permission.*

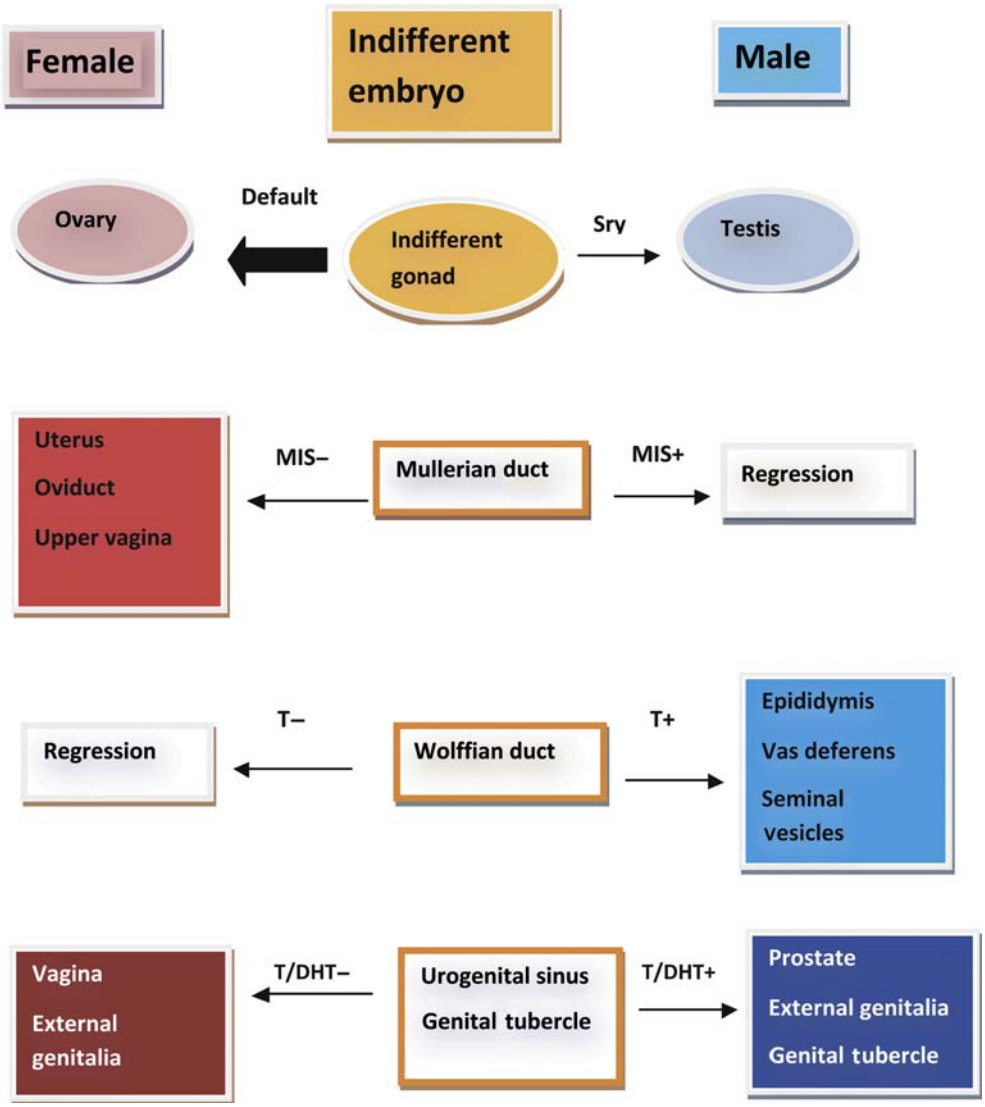

FIGURE 17.2 Factors regulating sexual differentiation of the embryonic reproductive tract. *Sry*, sex determining gene; *MIS*, Müllerian inhibiting substance; *T*, testosterone; *DHT*, dihydrotestosterone. Source: *Figure reproduced from* Haschek and Rousseaux's Handbook of Toxicologic Pathology *(2013), third ed. (W.M. Haschek, C.G. Rousseaux and M.A. Wallig, eds.), Academic Press (Elsevier), Figure 59.2, p. 2497 with permission.*

for the development of the prostate and external genital structures from the urogenital sinus. The basic developmental processes are quite similar between species, but the timing of certain events show significant species differences. In rodents most of these events take place in late gestation (for the rat, gestation days 12–20), whereas in the human fetus most events occur in the first trimester of pregnancy. Some events show dramatic differences in timing—for example, descent of the testis into the scrotal sac occurs during gestation in the human and is a postnatal event in most other species. Table 17.1 illustrates the various time lines (where known) for some major developmental landmarks of the male reproductive tract in rats, dogs, monkeys, and humans.

Postnatal Development of the Reproductive Tract

With the increased concern regarding juvenile toxicity, it is becoming a more common requirement for the pathologist to examine tissues from juvenile animals. The morphologic characteristics of the postnatal developing rat testis have been described by Picut et al. (2015) and a more thorough discussion of postnatal development is provided in Creasy and Chapin (2013). The rate of development and maturation of the reproductive tissues varies greatly between species. In rodents, the initiation of spermatogenesis begins immediately at birth and is slightly accelerated compared with the adult, so that sperm are starting to be released from the testis by 6–7 weeks of age in the rat

TABLE 17.1 Approximate Timelines and Hormonal Control for the Development of the Male Reproductive Organs in Rodents, Dogs, Primates, and Humans

Rat	Dog	Monkey	Human	Event (hormone responsible)
GD 8–10	GW 3	GW 4–6	GW 5–6	Migration of germ cells, precursor Sertoli cells, and interstitial cells to indifferent gonad
GD 14	GW 4	GW 6	GW 7–8	Start of sex cord development, Sertoli cells identifiable
GD 15–20	GW 5–6	GW 7–9	GW 8–9	Fetal Leydig cell proliferation and androgen secretion begins, Wolffian duct development (T), Müllerian duct degeneration (MIS)
GD 19.5–PND 10	N/A	GW 7–20	GW 16–24	Seminal vesicles develop (T)
GD 15.5–19.5	GW 5–6	GW 9–14	GW 9	External genitalia start to masculinize; continues through late gestation (DHT)
GD 15.5–PND 15			GW 5–10	Prostate develops from walls of urogenital sinus (DHT); most development occurs postnatally in rat
GD 19–PND 4		GW 9–12	GW 18–38	Regression of fetal Leydig cells
GD 21	GW 9	GW 22	GW 40	Birth
PND 13–15	PNW 8	PNM 32	PNY 12	Sertoli cells stop dividing
PND 22	PND 3–42	Birth and PNY 3	GW 24–36	Testis descent; in monkeys, testes descend at birth and again at ~3 years, returning to the inguinal canal in between (IL3)
PND 2–4	PNM 4.5–5	PNM 4–5	PNY 1–10	Spermatogonia begin to divide
PND 15	PNM 5–6	PNY 3–3.5	PNY 11.8–12.2	Tubular lumen develops
PND 15	PNM 6–7	PNY 3–3.5	PNY 11.8–12.2	Primary spermatocytes appear
PND 26	PNM 6–8	PNY 3.5–4	PNY 11.8–14	Spermatids appear
PND 42–45	PNM 7–10	PNY 3.5–5	PNY 11.8–15.3	Spermatozoa start to be shed

GD, gestation day; *GW*, gestation week; *PND*, postnatal day; *PNW*, postnatal week; *PNM*, postnatal month; *PNY*, postnatal year; *T*, testosterone; *DHT*, dihydrotestosterone; *MIS*, Müllerian duct inhibiting substance, *IL3*, insulin-like growth factor 3. Data have been assimilated from various sources.
Table reproduced from Handbook of Toxicologic Pathology *(2013), third ed. (W. M. Haschek, C. G. Rousseaux, and M. A. Wallig, eds.), Academic Press, Table 59.1, p. 2498, with permission.*

and 4–5 weeks of age in the mouse. In contrast, larger animals such as the dog, monkey, and human go through a period of dormancy before spermatogenesis begins. The testes will not begin spermatogenesis prior to 5 months of age in the Beagle dog or 3 years of age in the cynomolgus monkey. Even though this is the age at which sperm starts to be produced, it should be appreciated that the efficiency of spermatogenesis and therefore the number of sperm and size of the reproductive organs will continue to increase over a longer period of time. In general, maturation follows a very consistent and predictable time line in rodents, with most animals reaching sexual maturity at the same age ±1 week, but there is significant individual variation in the rate of maturation in dogs and monkeys. In dogs, the age of sexual maturation can be anywhere between 7 and 12 months of age; in the cynomolgus monkey, it can be anywhere between 3.5 and 5.0 years of age. This has very important implications when attempting to evaluate the effects of test materials on sexual development and maturation in the small group sizes used for large animal studies. Table 17.1 provides an approximate timing for some major postnatal maturational changes in the testis of the rat, dog, monkey, and human.

Sertoli Cell Division and Maturation

In all species, Sertoli cells have a limited period in which they divide. In the rat, division starts at GD 12 and ceases (*in vivo* and *in vitro*) after approximately post natal day (PND) 13–15. This period of Sertoli cell division is critical, because the final sperm output is a function of the number of Sertoli cells in the testis. If division ceases too soon (due to juvenile or maternal hyperthyroidism, for example), it can result in smaller testes and reduced sperm output. Sertoli cell proliferation can also be reduced by too much estrogen, insufficient testosterone, and insufficient follicle-stimulating hormone (FSH). On the other hand, hypothyroidism delays the cessation of Sertoli divisions, which results in enlarged adult testis size and increased overall sperm output. Sertoli cell numbers are decreased in

mice with inactivated androgen receptors, including the androgen receptor knockout and the testicular feminized mouse. Around this same time (PND 15) the Sertoli cell begins to produce seminiferous tubular fluid and androgen binding protein (ABP) and also undergoes significant maturational changes in its function and its regulation. FSH is the main regulatory hormone in the testis up until about PND 18, when its secretion peaks, after which time FSH levels decline and luteinizing hormone (LH) secretion increases with a commensurate increase in testosterone, androgen receptors, and ABP. By PND 25, testosterone is the major regulatory hormone in the testis.

In the rat, tight junctions between adjacent Sertoli cells, which will form the major part of the blood–tubule barrier, begin to develop 15–18 days after birth, which is coincident with the beginning of fluid secretion into the tubular lumen. Prior to this age, gap junctions join the Sertoli cells and substances permeate the tubular epithelium freely.

The dog and the cynomolgus monkey both have long postnatal quiescent periods (up to 4–5 months in the dog and 3–4 years of age in the monkey) with no activity in the seminiferous tubules other than the very slow final expansion of the stem cell spermatogonia and Sertoli populations.

Structure and Function of the Testis

Seminiferous Tubules

The testicular parenchyma is composed of convoluted seminiferous tubules separated by interstitial tissue and enclosed in a capsule. The seminiferous tubules are long, highly convoluted tubes that empty at both ends into the rete testis, which is a sac like reservoir. In the rat there are approximately 30 separate tubules that are arranged in a transverse circumferential organization. In the dog, monkey, and man the individual seminiferous tubules are grouped into lobules.

Leydig (Interstitial) Cells and Testicular Macrophages

Leydig cells comprise about 17% of the interstitial tissue in rats, in contrast to pigs, where Leydig cells make up around 50%. Mice have more and larger Leydig cells than rats, amounting to 35% of the volume of the interstitial tissue. Leydig cells are the major site for the synthesis of the predominant male steroid hormone, testosterone. Following secretion from the Leydig cell and entry into the peripheral circulation testosterone is metabolized further in the liver, androgen-dependent tissues (e.g., epididymis, seminal vesicles, and prostate) and a variety of peripheral tissues.

Testicular macrophages are a unique subset of the mononuclear phagocyte system that have close physical and functional interactions with the Leydig cells and participate in paracrine regulation and in the immuno-endocrinology of the testis.

Sertoli Cells

STRUCTURE

Sertoli cells provide the supporting framework in which the germ cells are embedded. The size and shape of the Sertoli cell are difficult to appreciate in conventional sections viewed by light microscopy. The germ cells are embedded into apical or lateral invaginations of the Sertoli cells (Figure 17.3). The Sertoli cell is connected to the germ cells by a variety of cell junctions, some of which are unique to this cell type. Adjacent Sertoli cells are joined at their basolateral aspect by specialized occluding junctions, which form the major component of the blood–testis barrier and help shield the nonself germ cells from the interstitial macrophages.

Normal Sertoli cell function is critical for the integrity of the seminiferous epithelium. Generally speaking, these functions include regulation of spermatogenesis, structural and metabolic support of the germ cells, sperm release, secretion of tubular fluid for sperm transport, and maintenance of a permeability barrier between interstitial and tubular compartments. Disturbance of any of these functions is likely to impair spermatogenesis and, in turn, sperm production.

ROLE IN STRUCTURAL SUPPORT AND GERM CELL TRANSLOCATION

The structural support and movement of germ cells is central to the process of spermatogenesis. As germ cells develop from spermatogonia to spermatids they are gradually moved up to the luminal surface, and then, as elongating spermatids, they are pulled back down towards the Sertoli cell nucleus before returning to the surface to be released. The cytoskeleton is thought to have a major role in this process along with the specialized junctions between the Sertoli and germ cells. Disruption of the cytoskeletal filaments and retraction of the lateral processes that surround germ cells are associated with sloughing of germ cells into the lumen.

ROLE IN METABOLIC SUPPORT OF GERM CELLS AND FLUID PRODUCTION

Germ cells in the adluminal compartment rely entirely on the Sertoli cell for their supply of nutrients and oxygen. Spermatocytes and spermatids are unable

to utilize glucose and must be provided with lactate and/or pyruvate by the Sertoli cell as a substrate for energy production. Similarly, the metabolism of amino acids occurs within the Sertoli cell to produce α-keto acids that are utilized by the germ cells. In addition, the Sertoli cells secrete fluid which carries the newly released sperm to the epididymis for their acquisition of motility.

ROLE IN PHAGOCYTOSIS

Phagocytosis is another important function of the Sertoli cell. During spermatid development (spermiogenesis), the cytoplasmic volume of the spermatid is reduced by up to 70% and a large proportion of its organelles are discarded. This is accomplished by formation of the residual body, which contains redundant organelles, nucleic acids (various RNA species), and cytoplasm; it is shed from the spermatozoon at the time of spermiation, phagocytized by the Sertoli cell and merged with lysosomes while being moved down to the basal Sertoli cell cytoplasm, where digestion is completed. Apoptotic germ cells, which are a normal feature of spermatogenesis as well as a result of toxic injury, are also removed rapidly by phagocytosis.

ROLE IN BLOOD–TESTIS BARRIER FORMATION

Spermatogenesis occurs in a specialized and protected environment in the adluminal compartment of the seminiferous epithelium. The specialized conditions are maintained and protected by the presence of a blood–tubule barrier that shares some of the same exclusion properties as the blood–brain barrier. The main exclusion barrier is formed by the basolateral occluding cell junctions between adjacent Sertoli cells, situated at a level above the spermatogonia and below the spermatocytes (Figure 17.3). The interstitial compartment is exposed to all substances transported through the capillary endothelium, including toxicants. Although the peritubular cells may exclude some very large molecules, the basal compartment of the tubule, which contains the spermatogonia, is also readily accessible to virtually all bloodborne substances. In contrast, the adlumenal compartment, which contains all meiotic and postmeiotic cells, is only exposed to bloodborne

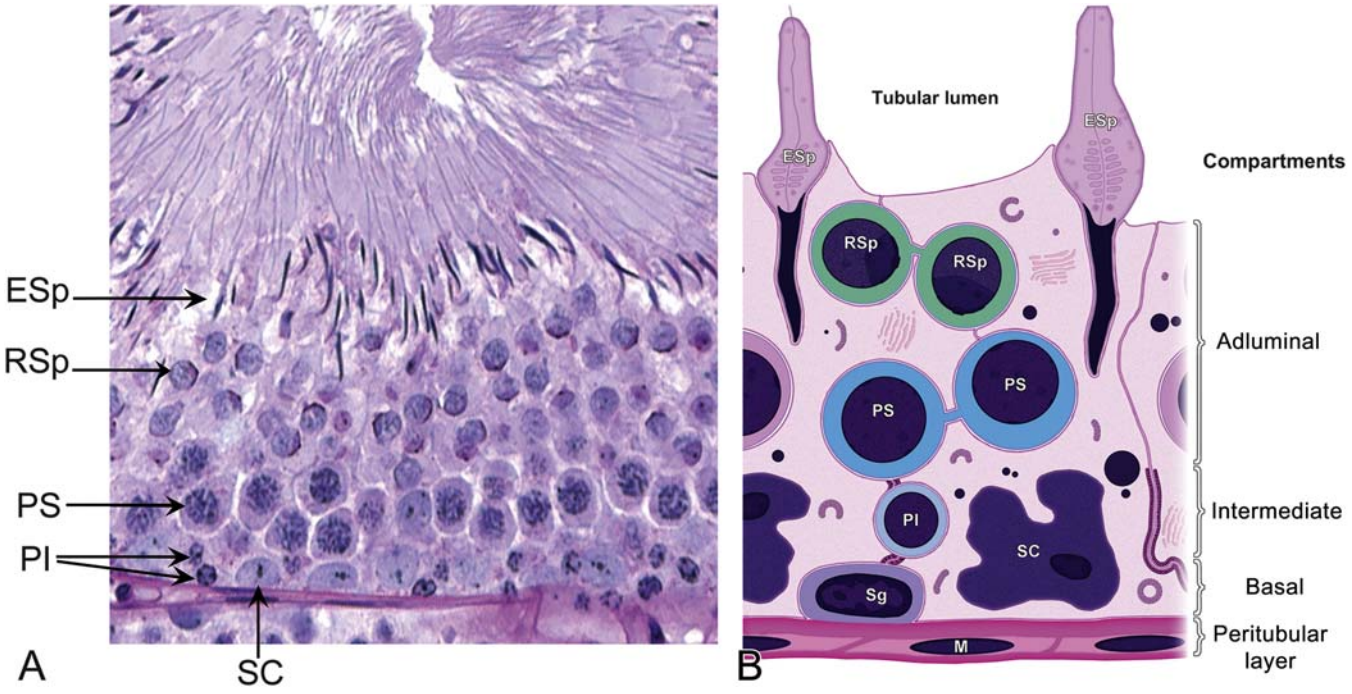

FIGURE 17.3 Organization and compartmentalization of the seminiferous tubule in the rat. (A) Section of a tubule in early stage VII of the spermatogenic cycle (methacrylate embedded, PAS, ×40). (B) Labeled representation of the same stage tubule, showing the relationship of the compartments and cell types to one another. The tubule is surrounded by myoepithelial peritubular cells (M); Sertoli cell (SC) nuclei lie on the basement membrane interspersed with type A spermatogonia (Sg). There are very few of these in a stage VII tubule, and they cannot be seen in the histological section on the left. Tight junctions between adjacent Sertoli cells form the blood–testis barrier separating the basal from the adluminal compartment. An intermediate compartment is formed when the developing preleptotene spermatocytes (PI) move through the tight junction during this stage. Pachytene spermatocytes (PS) and round spermatids (RSp) form layers of germ cells within the adluminal compartment. Maturation phase elongating spermatids (ESp) are embedded within lumenal Sertoli cell cytoplasmic processes while their tails project into the lumenal compartment. Source: *Figure reproduced from* Haschek and Rousseaux's Handbook of Toxicologic Pathology *(2013), third ed. (W.M. Haschek, C.G. Rousseaux and M.A. Wallig, eds.), Academic Press (Elsevier), Figure 59.7, p. 2504 with permission.*

substances that have been transported through the Sertoli cell. This might provide some protection against genetic damage or death of the gamete by toxicants.

Spermatogonia

Spermatogonia represent the stem-cell population of the germ cells. There are three classes of spermatogonia: stem cell spermatogonia, proliferative spermatogonia, and differentiating spermatogonia. Stem cell and proliferative spermatogonia are responsible for renewing their own cell number and producing a pool of spermatogonia that are committed to differentiation. Six mitotic divisions of these differentiating spermatogonia result in the main expansion of the spermatogonial population. As the cells undergo mitosis, cytokinesis is incomplete, leaving the descendent population of spermatocytes linked together in a syncytial arrangement. This is maintained throughout spermatogenesis and is believed to enable the synchronized development and differentiation of the individual populations of cells. It also underlies the generation of multinucleated giant cells after treatment with toxicants (below).

Spermatocytes

Preleptotene spermatocytes are formed from the final mitotic division of the differentiating spermatogonia. The cells then enter a 3-week-long meiotic prophase, passing through the leptotene, zygotene, pachytene and diplotene stages, and diakinesis, and the first meiotic division to produce secondary spermatocytes. The second meiotic division follows rapidly to produce the haploid spermatid.

Spermatids

The second meiotic division of the spermatocytes results in the formation of the haploid spermatid. The spermatid begins life as a conventional round cell, but the nucleus and cytoplasm undergo a number of extremely complex morphological modifications including the development of an acrosomal cap on the nucleus, profound shape changes, and condensation of the nucleus to form an elongated head, while the cytoplasm and mitochondria are totally rearranged to form a motile-tail section. The process of spermatid transformation is termed spermiogenesis.

In the final maturation phase of spermiogenesis, the cytoplasmic volume of the spermatid is greatly reduced by the condensation and expulsion of the spermatid cytoplasm including many of the redundant organelles and mRNA to form the residual body, which is shed to the Sertoli cell at the time of spermiation. One metabolic function retained by the spermatozoa is energy production by the sheath of mitochondria enveloping the tail to permit motility. Most of the other metabolic requirements of the mature spermatid within the testis are met by the Sertoli cells; outside the testis, the quiescent spermatozoon is sustained by the complex mixture of fluids secreted by the epididymis and accessory sex organs.

Spermatogenesis and the Spermatogenic Cycle

The process whereby primitive stem cell spermatogonia develop to form highly specialized spermatozoa is termed spermatogenesis. The process of spermatogenesis comprises a series of successive mitotic divisions by the spermatogonial population, meiosis by the spermatocytes, extensive cellular remodeling, and differentiation throughout the haploid–spermatid development (spermiogenesis) (Figure 17.4). Four generations of germ cells develop simultaneously within the seminiferous epithelium of the rat; their synchronous development gives rise to specific cellular associations that follow each other in a precisely defined sequence. One unit of repetition of the sequence of cellular associations is termed a cycle of the seminiferous epithelium (often abbreviated to spermatogenic cycle), whereas individual cell associations within this cycle are referred to as stages of the cycle (Figure 17.5A).

Detailed classification of the rat spermatogenic cycle into stages is largely based on the developing morphology of the spermatid acrosome, which is visualized using periodic acid Schiff (PAS) stain. In the rat, 19 different steps of spermatid development, which are denoted by Arabic numerals (1–19) are used as a marker to identify 14 different cellular associations (or stages), referred to by roman numerals (I–XIV) (Figure 17.5A). (For more detailed guidance on staging, see Russell et al., 1990; Creasy, 1997; Creasy and Chapin, 2013) The number of stages into which the cycle is divided is arbitrary and depends on the classification criteria used by the originator of the particular scheme. The most commonly used schemes divide the mouse cycle into 12 stages, the dog cycle into 8 stages and the cynomolgus monkey cycle into 12 stages (Table 17.2). Maps similar to the one depicted in Figure 17.5A have now been devised for most of the common laboratory species. Although accurate staging of testes requires examination of the spermatid acrosome at high magnification in PAS-stained testes, an easier method of staging can be performed on H&E-stained sections of testes using the position and shape of the elongating spermatid as it moves from a luminal position to a basal position and back again (Figure 17.5B). This approximate staging of the cycle is generally adequate for most routine examinations and will allow the pathologist to readily distinguish between early, mid, and late stages of the spermatogenic cycle (Figure 17.6). Also see Creasy and Chapin (2013).

Dynamics of the Spermatogenic Cycle

In all species, the entire process from stem cell spermatogonium to spermatozoal release spans approximately 4 cycles (depending when the start of spermatogenesis is defined). As each cycle is completed and the mature spermatozoa are released, another generation of spermatogonia divides and becomes committed to maturation (Figure 17.5A). The duration of the cycle and thus of spermatogenesis is fairly constant for a given species and strain of animal (Table 17.2). Once committed to undergoing spermatogenesis, it takes about 8 weeks in the rat (timing is species-specific) for spermatogonia to complete their development into spermatozoa that are ready to be released into the tubular lumen (Figure 17.5A and B). This process involves an individual spermatogonium passing through four spermatogenic cycles (each cycle lasting approximately 2 weeks) as it develops into a mature spermatid. The practical implications of this process are important when evaluating spermatogenesis. For example, take the development of one spermatogonium in a mid-stage (VII) tubule: on Day 1 it starts spermatogenesis as a type A spermatogonium. Two weeks later that segment of tubule will have passed through the other 14 stages of the spermatogenic cycle and will reenter stage VII, during which time the type A spermatogonium will have developed into a preleptotene spermatocyte. After another 2 weeks the tubule will reenter stage VII and the preleptotene spermatocyte will have developed into a mid-pachytene spermatocyte, and following another 2 weeks it will be a round spermatid. A further 2 weeks will see the cell become a fully mature elongated spermatid (step 19) that is about to be released into the lumen. This timing is important when evaluating cell degeneration and depletion in studies of different durations. Another important concept to bear in mind is the progressive expansion of each population of cells as it develops. Beginning with a single stem cell spermatogonium, by the time it has completed its multiple mitotic divisions, in theory it will produce 512 spermatocytes and, following another two meiotic divisions,

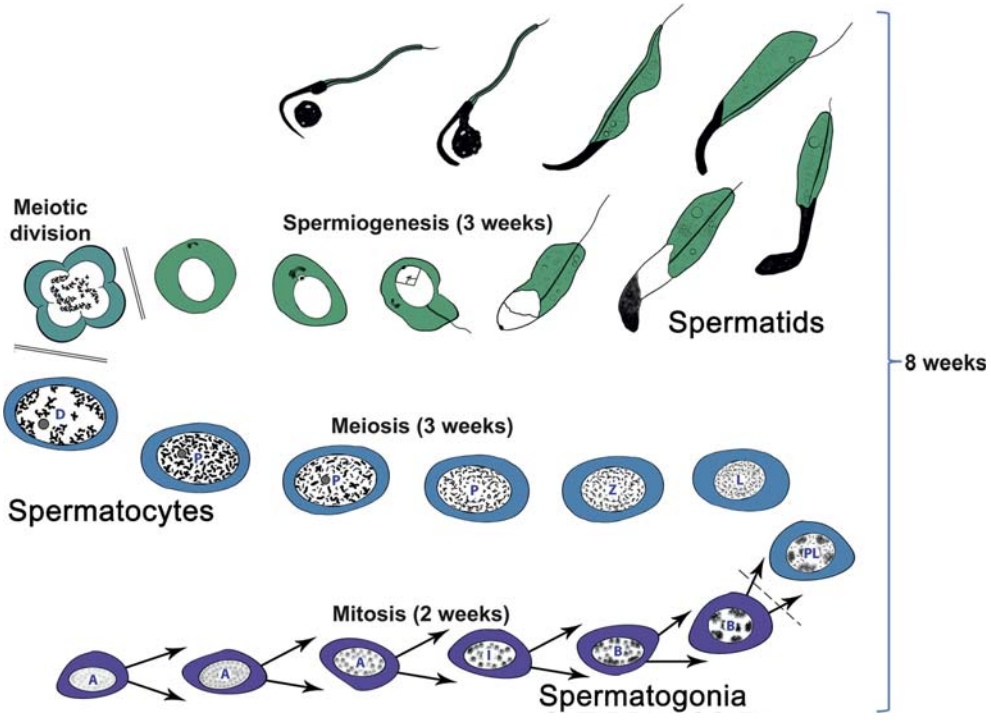

FIGURE 17.4 Spermatogenesis involves multiple-mitotic divisions of spermatogonia, beginning with type A spermatogonia (A) (pale-staining nuclei with fine chromatin) through intermediate (I) spermagonia, and finishing with type B spermatogonia (B) (darker staining nuclei with peripheral clumps of chromatin). Division of B spermatogonia produces the spermatocyte which undergoes meiotic prophase where DNA replication occurs to produce a tetraploid cell. This comprises preleptotene (PL), leptotene (L), zygotene (Z), a long phase of pachytene (P) that can be split into early, mid, and late. This is followed by diplotene/diakinesis (D) and then two reduction divisions, the first producing diploid secondary spermatocytes and the second producing the haploid spermatid. The spermatid then undergoes morphological transformation from a regular round cell into a sperm with an elongated head made up of condensed chromatin and a tail comprising a flagellum surrounded by mitochondria. The transformation has been divided into 19 steps of spermiogenesis based on the development of the acrosome and the shape of the developing spermatid (only a few are illustrated here). In the rat, the process takes approximately 8 weeks. Source: *Figure reproduced from Sahota, P.S., Popp, J.A., Hardisty, J. F., Gopinath, C., (Eds.), 2013. Toxicologic Pathology: Nonclinical Safety Assessment, CRC Press, Figure 18.3, p. 722 with permission.*

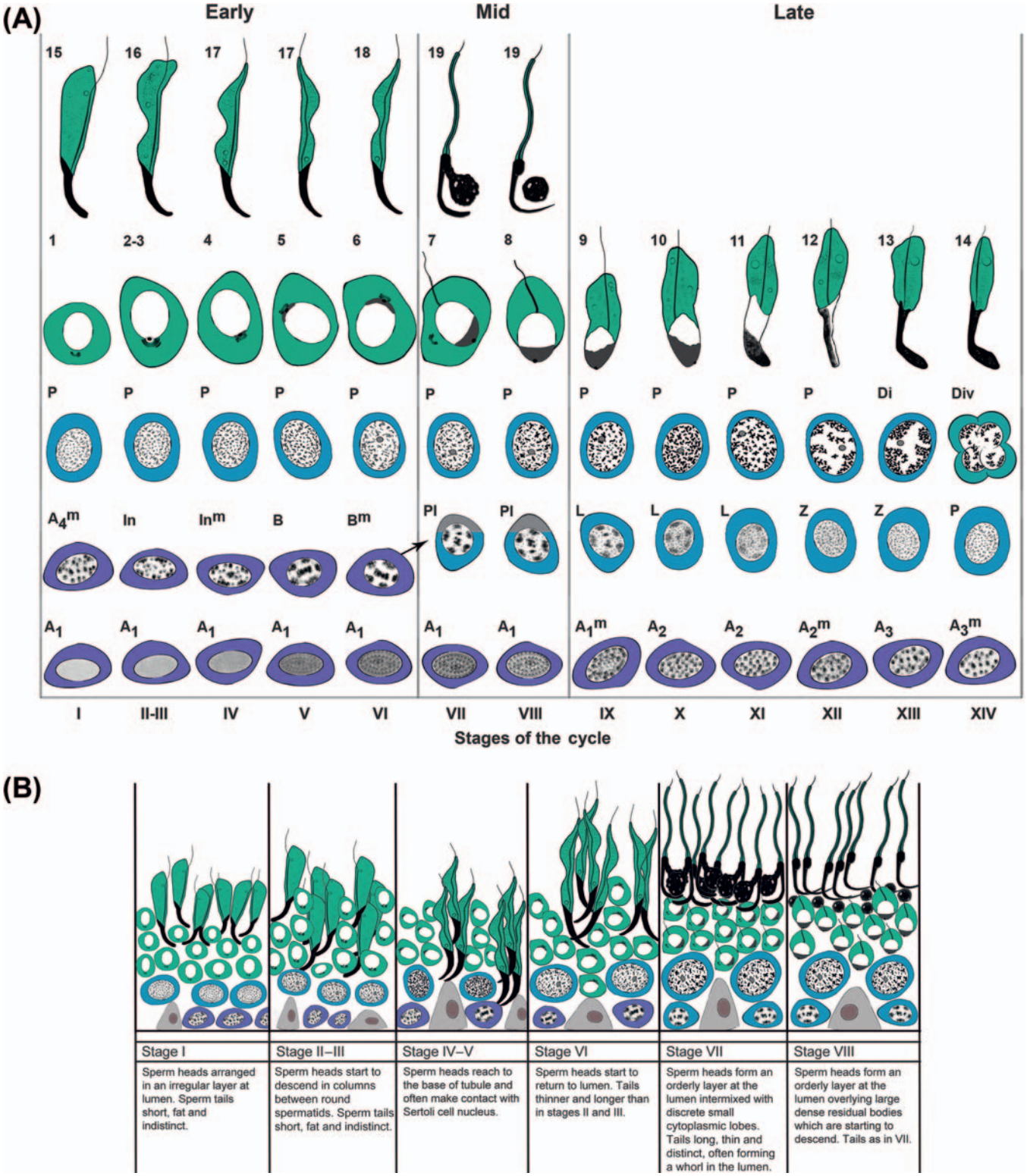

FIGURE 17.5 (A) Diagram illustrating the cellular composition of the 14 stages of the spermatogenic cycle in the rat. Each column represents a stage (I–XIV). The stages are defined by the morphological characteristics of the accompanying spermatid. Spermatid development is divided into 19 steps (1–19), the first 14 of which are in numerical agreement with Stages I–XIV. It is these 14 steps that are the most important. In stages I–VIII, the detailed morphology of the spermatid acrosome (stained with PAS) is used to distinguish between stages. In stages IX–XIV, the shape of the elongating nucleus is used. In a given location in any tubule, the cellular associations (stages) will succeed one another over time, proceeding from the left to the right of the diagram. Stage XIV is followed by stage I to begin another cycle. One complete sequence of the 14 cellular associations represents one complete "cycle of the seminiferous epithelium," whereas the developmental sequence

TABLE 17.2 Species Differences in the Spermatogenic Cycle and Sperm Output[a]

Species	Daily sperm output ($\times 10^6$/g)	# Stages/cycle	Cycle duration (days)	Duration of spermatogenesis	% Abnormal sperm
Rat	21	14	13	52	<5
Mouse	54	12	8.6	35	<5
Beagle dog	20	8	13.6	54	≥50
Minipig/pig[b]	20–30	8	8.6–9.0	38–41	<20
Cynomolgus monkey	23	12	10.5	42	<25
Human	3.1–4.25	6	16	72	≥50

[a]*Values are an approximation based on data derived from various sources.*
[b]*Relatively few data are available for the Göttingen minipig. The numbers provided are based on data published for the minipig, and domestic and wild boars.*
Table reproduced from Handbook of Toxicologic Pathology *(2013), third ed. (W. M. Haschek, C. G. Rousseaux, and M. A. Wallig, eds.), Academic Press, Table 59.2, p 2512, with permission.*

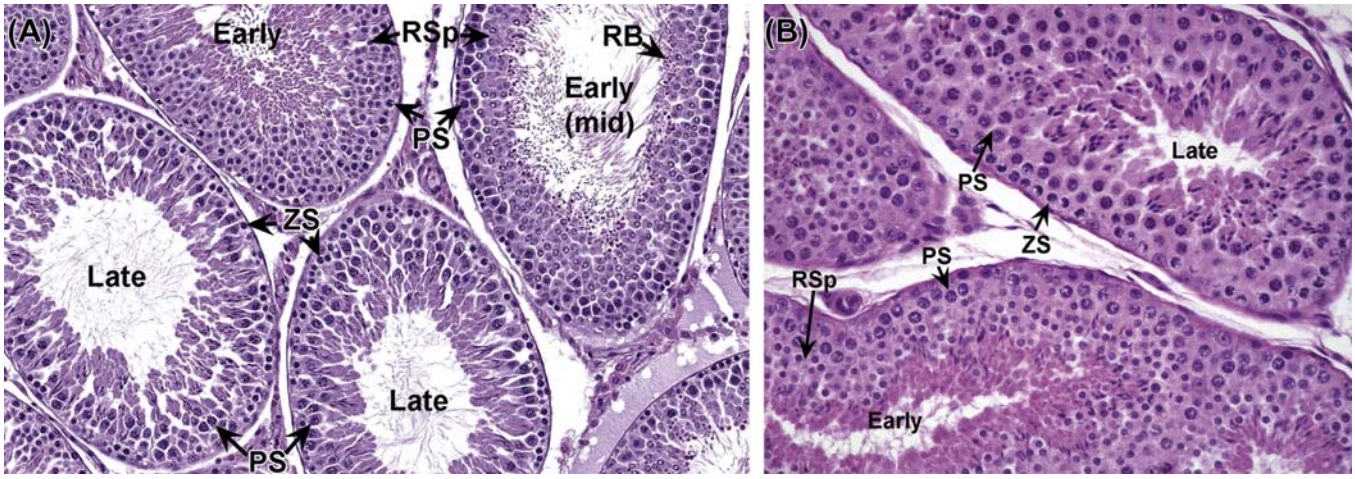

FIGURE 17.6 (A) Rat testis. There are obvious differences in the cell populations between early-stage tubules (stages I–VIII) and late-stage tubules (stages IX–XIV). The early-stage tubules have multiple layers of round spermatids (RSp) overlying a single layer of pachytene spermatocytes (PS), while the late-stage tubules have multiple layers of pachytene spermatocytes overlying a single layer of early (zygotene) spermatocytes (ZS). Both have a luminal layer of elongating spermatids, but they are fat and short in the late-stage tubules and long and thin in the early-stage tubules. Within the early-stage tubules, mid-stage (stages VII and VIII) tubules can be distinguished by the presence of basophilic granular residual bodies at the luminal surface (RB). Rat, H&E, ×20. (B) Dog testes. There are only eight stages in the dog spermatogenic cycle, but the same distinction between early (stages I–V) and late (VI–VIII) tubules can be distinguished as in the rat cycle. Dog, H&E, ×20. Source*: Figure reproduced from* Haschek and Rousseaux's Handbook of Toxicologic Pathology *(2013), third ed. (W.M Haschek, C.G. Rousseaux and M.A. Wallig, eds.), Academic Press (Elsevier), Figure 59.10, p. 2511 with permission.*

from spermatogonia through to step 19 spermatid represents the process of spermatogenesis. As the diagram is read from the bottom and from left to right, the spermatogonia go through a number of mitotic (m) divisions developing through type A (A1–4), intermediate (I), and type B (B) spermatogonia. These give rise to spermatocytes, which proceed through meiotic prophase, including preleptotene (Pl), leptotene (l), zygotene (z), pachytene (P), and diplotene/diakinesis (Di), and through two meiotic divisions (Div). The haploid spermatids produced from the meiotic division undergo the morphological progression through the 19 steps of spermiogenesis (1–19). As the cells develop from spermatogonia to spermatids, they gradually move up through the epithelium. As the mature spermatid is released during stage VIII, another generation of spermatogonia becomes committed to spermatogenesis from the slowly dividing pool of stem cells.
(B) Approximate staging of the spermatogenic cycle can be conducted in H&E stained sections by using the shape and position of the elongating spermatids in the epithelium rather than the detailed acrosome morphology of the round spermatids in a PAS section. In general, this is adequate for routine screening of testes for spermatogenic disturbances. Source*: (A) Figure reproduced from* Haschek and Rousseaux's Handbook of Toxicologic Pathology *(2013), third ed. (W.M. Haschek, C.G. Rousseaux and M.A. Wallig, eds.), Academic Press (Elsevier), Figure 59.9B, p. 2510 with permission. (B) Figure reproduced from* Haschek and Rousseaux's Handbook of Toxicologic Pathology *(2013), third ed. (W.M. Haschek, C.G. Rousseaux and M.A. Wallig, eds.), Academic Press (Elsevier), Figure 59.9C, p. 2511 with permission.*

there will be 4096 round spermatids for every one spermatogonium that enters the maturation sequence. Although there are regulatory processes that utilize apoptosis to reduce the population to an appropriate number that can be supported by each Sertoli cell, the important message is that there will be relatively few spermatogonia (they will be difficult to find), many more spermatocytes and a lot more spermatids, which will be about four times more numerous than spermatocytes. In practical terms, this means that it will be a lot easier to identify germ cell loss if it affects or has reached the spermatid population than if it is only affecting the spermatogonial or early spermatocyte population (see the "Germ Cell Depletion" section).

It is important to appreciate the dynamics of germ-cell development when evaluating toxicity because toxicity to a cell type at the beginning of a study will translate into depletion of a different cell type at the end of the study, and the cell type depleted will depend on the duration of dosing. Similarly, if certain cells have been affected by a drug during the dosing phase, the degree of recovery will depend on the duration of the recovery period and the cell type originally damaged by the drug. This progressive loss of more mature germ-cell types due to failed development of removed early germ cell types, explains why testes often appear to have more severe depletion of cells at the end of a 2- or 4-week recovery period than at the end of the dosing period (see "Recovery and Reversibility of Injury" section).

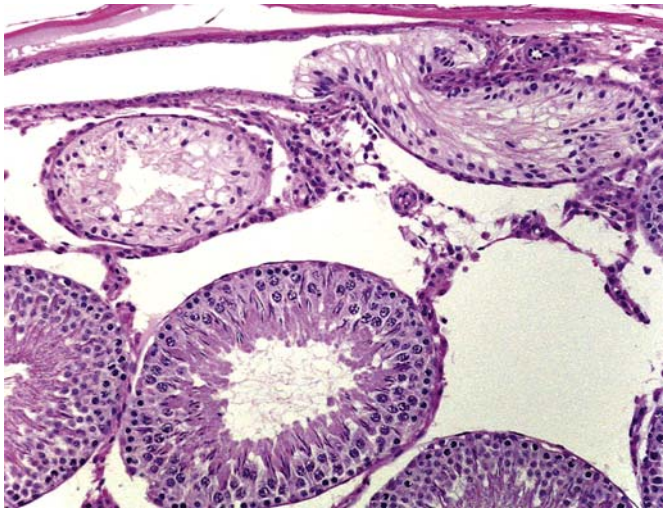

FIGURE 17.7 Tubulus rectus is the transitional part of the seminiferous tubule as it enters the rete testis. It is lined only by Sertoli cells and can be mistaken for an atrophic tubule in cross-section. The cytoplasmic protrusion into the rete also acts as a one-way valve for the propulsion of sperm and fluid out of the tubule. Rat, H&E, ×10. Source: *Figure reproduced from* Haschek and Rousseaux's Handbook of Toxicologic Pathology *(2013), third ed. (W.M. Haschek, C.G. Rousseaux and M.A. Wallig, eds.), Academic Press (Elsevier), Fig 59.28 A and B, p. 2513 with permission.*

Structure and Function of the Rete Testis, Efferent Ducts, and Epididymis

When sperm are released into the lumen of the seminiferous tubule they are transported into a common collecting duct within the testis, termed the rete testis (Figure 17.7). Sperm then pass into a network of efferent ducts, which in the rat are located within the epididymal fat pad, and these in turn lead into a single highly coiled duct to form the epididymis. The epididymis is divided into four major parts: the initial segment, the caput (head), corpus (body), and cauda (tail) epididymis. The coiled epididymal duct then leads into a straight portion termed the ductus or vas deferens, which extends through to the urethra. Various glands empty their secretions into this duct.

When sperm leave the testis, they are incapable of fertilization and are barely motile. They are transported out of the testis in seminiferous tubule fluid (STF) that is secreted by the Sertoli cell. Most of the fluid (up to 96%) and many of the proteins in the STF are reabsorbed by the rete testis and efferent ducts and the initial segment of the epididymis. During their passage through the epididymis the sperm are bathed in the secretions of the cells of the epididymal epithelium and thus, mature and acquire progressive forward motility and the ability to undergo capacitation and fertilize an oocyte. Maturation involves extensive remodeling of the sperm plasma membrane with the binding and incorporation of proteins synthesized by the epididymal epithelium. Once in the cauda epididymis, the sperm are stored for days (humans) or weeks (rodents) prior to being released by ejaculation through the vas deferens into the penile urethra.

Rete Testis and Efferent Ducts

The rete testis comprises a single or series of interconnected channels, lined by simple cuboidal or columnar epithelium, into which the seminiferous tubules open and which leads into the efferent ducts. In some species, such as the rat and mouse, the rete is situated in a subcapsular position at the cranial pole of the testis, but in other species, including the dog, rabbit, and monkey it forms a series of ducts running through the center of the testis.

The efferent ducts (ductuli efferentes) are a series of convoluted tubules that empty into the initial segment of the epididymis. In the case of the rodent, almost all of the long and tortuous efferent ducts (proximal and distal sections) are located within the epididymal fat pad, making it difficult to sample them, and so they are rarely examined. The final distal portion may

occasionally be seen in standard sections of the rodent epididymis. In contrast, the efferent ducts of the dog are much shorter, being almost entirely located within the head of the epididymis and forming a large proportion of the epididymal head. This is also the case in man. In cynomolgus monkeys, the efferent ducts are enclosed within the same connective tissue capsule as the head of the epididymis but are located slightly proximal to the head and may or may not be sampled in a routine section of epididymis.

The main function of the efferent ducts is to transport sperm from the rete testis to the epididymis and to concentrate them by reabsorbing most of the fluid and the proteins from the accompanying STF. Over 90% of the fluid and protein is reabsorbed as the sperm suspension passes through the rat efferent ducts. Estrogen and endothelin 1 appear to be the major regulator for the fluid reabsorption. Active transport of water out of the lumen is accomplished in a similar manner to reabsorption of water from the renal nephron.

Epididymis

Superficially, the epididymis appears to be a histologically simple tissue comprising a convoluted, epithelial lined duct that carries sperm from the testis to the vas deferens. In reality it is surprisingly complex, both in the structural diversity of its epithelial cell types and in the number of critical functions it performs in the maturation and transport of sperm.

Functions of the epididymal epithelium include the synthesis and secretion of a wide range of proteins, and the transport of ions and small organic molecules across the epithelium to create a slightly basic luminal environment which is conducive to protein uptake into the sperm membranes. After early secretion into the lumen of the caput, the corpus is where the sperm incubate in the specialized luminal environment, followed by the selective absorption of luminal contents in the distal corpus and cauda. Thus, the epididymis provides the specialized environment required for the progressive maturation of sperm as they pass from the initial segment to the tail of the epididymis, during which time the sperm acquires the ability to fuse with, and fertilize, an oocyte. Newly motile sperm must then be maintained in a quiescent state by the caudal secretion of immobilin, which prevents sperm from swimming in the epididymis. This thick glycoprotein is stripped off the sperm by the process of ejaculation and the mixing with the proteases in the accessory organ secretions, resulting in ejaculated sperm which are motile.

Storage of the sperm prior to ejaculation is also an important function of the cauda epididymis. Depending on the species and the frequency of ejaculation, sperm reach the cauda 1–2 weeks after release from the seminiferous tubule. Sperm production is a continuous process; if the stored sperm are not removed by frequent ejaculation, they are voided in the urine.

Structure and Function of the Accessory Sex Organs

The accessory sex organs in rodents are the seminal vesicles, prostate, coagulating gland, bulbourethral gland, and preputial gland. They are located along the route of the urethra as it relays sperm from the vas deferens out through the penis. The glands secrete a variety of complex fluids that transport and sustain the sperm during their lengthy journey out of the male and through the female genital tract. Their structure is typical of active exocrine secretory glands, although the characteristics of the individual secretions are markedly different. Because the secretory activity of the accessory sex glands is extremely sensitive to androgen levels, weight change and altered cellular activity in the ventral prostate and seminal vesicles can be used as a good, and relatively rapid, indicator of altered circulating androgen levels. There are major species differences in the complement of accessory sex glands.

Prostate

The prostate is the only accessory sex gland that is present in the dog. In all species the glandular tissue forms multiple lobes around the urethra, but in the nonhuman primate the glandular tissue is only present on the posterior surface of the urethra and there are no anterior lobes. In the rodent, a discrete pair of ventral lobes and a smaller group of dorsal and lateral lobes are situated around the neck of the bladder. Also in rodents, a pair of anterior lobes, otherwise known as the coagulating glands, is situated along the inner curvature of the seminal vesicle. The prostatic fluid secretion constitutes 15%–30% of the ejaculate. It is a colorless fluid rich in proteolytic enzymes (e.g., acid phosphatase). The fluid also contains relatively high levels of zinc, inositol, transferrin, and citric acid.

Seminal Vesicles

The mucosa of the seminal vesicles has a honeycombed structure formed by complex folding. The seminal vesicle fluid is a viscous secretion constituting approximately 70% of the seminal fluid and about 50% of the ejaculate. The alkaline fluid is thought to neutralize the acid pH of the vagina; it contains citric acid as well as fructose and lactoferrin. Lactoferrin is one of the sperm-coating antigens and, as its name suggests, is also involved in iron binding and transport. In the

rat, fluid from the coagulation gland, secreted immediately after ejaculation, mixes with vesicular fluid to form the copulatory plug within the vagina. This prevents loss of sperm and further copulation. The dog does not have seminal vesicles or coagulating glands. Primates have seminal vesicles but do not have coagulating glands.

Bulbourethral Glands

Bulbourethral glands (Cowper's glands and Mery glands) are paired compound tubuloalveolar glands that secrete a mucoid material into the penile urethra during ejaculation. In rodents, it is secreted immediately before ejaculation of the sperm, to clear the urethra of urine and provide lubrication. It is not present in the dog.

Preputial Glands

Preputial glands are paired sebaceous glands located in the subcutaneous tissue of rodents near the tip of the penis in the mouse and along the ventral midline in the inguinal region of the rat. Ducts leading from the sebaceous acini are lined by squamous epithelium. The ductular secretion and the intracellular secretory granules are intensely eosinophilic, resembling keratin in appearance. Secretion from the preputial gland contains pheromones (aliphatic alcohols) and glucuronidase.

Hormonal Regulation of Reproductive Function

Overall hormonal control of the testis is maintained by the hypothalamic–pituitary axis and is mediated by gonadotropin-releasing hormone (GnRH) secreted by the hypothalamus, which regulates secretion of the gonadotropins, LH and, FSH, by the pituitary (Figure 17.8). These major hormones are overlaid by paracrine, autocrine, and inacrine control mechanisms, which "fine tune" or modulate the endocrine effects.

Gonadotropin-Releasing Hormone

GnRH which is secreted in a pulsatile manner by the GnRH neurons located within the paraventricular nucleus of the hypothalamus, orchestrates the entire endocrine regulation of reproductive function by controlling gonadotropin (FSH and LH) secretion from the pituitary, which in turn regulates secretion of testosterone from the Leydig cells. Secretion of GnRH is regulated not only by negative feedback of the sex steroids but also by a myriad of other chemicals, many of which are involved in other pathways such as maintenance of energy status and regulation of the stress response. Recent research has provided strong evidence that the critical regulatory gatekeeper integrating these various inputs and controlling GnRH secretion involves the kisspeptin/GPR54 ligand–receptor complex, which is present in multiple hypothalamic nuclei adjacent to the GnRH secreting neurons. Kisspeptin/GPR54 also mediates the negative feedback of circulating sex steroids on the GnRH neurons and has recently been shown to be pivotal in the timing of pubertal onset in many species.

Follicle-Stimulating Hormone

FSH is produced and exported from the pituitary to act principally on the Sertoli cells. It is secreted in a pulsatile manner in response to GnRH, also referred to as luteinizing-hormone releasing hormone (LHRH), from the hypothalamus. Inhibin, secreted by the Sertoli cell, is believed to be involved in a feedback loop from the testis to the pituitary to inhibit FSH production. The action of FSH on immature and mature animals is profoundly different. FSH is often considered to be the hormone of puberty, as rising levels of FSH act as a trigger for testicular growth, junction formation between adjacent Sertoli cells and ABP secretion from the Sertoli cells, and generally initiates spermatogenesis and the expansion of the seminiferous tubules. Once this has occurred, the Sertoli cell switches its responsiveness from FSH to testosterone as many of the FSH-regulated functions in the immature animal are taken over by testosterone in the adult.

The primary impact and effects of FSH in the adult are poorly understood, although its importance seems to vary between species. Suppression of FSH in the adult rat has a negligible effect on spermatogenesis, whereas in nonhuman primates, it results in considerable suppression of spermatogenesis and sperm output.

Inhibin and Activin

Inhibin is a protein that is secreted by both testis and ovary and decreases FSH but not LH secretion by pituitary cells. In the male, inhibin is secreted by Sertoli cells and appears to have both endocrine (via its effect on the pituitary) and paracrine (other effects on cells within the testis) properties. Activins have a similar structure to inhibin but possess FSH-stimulating activity in pituitary cells. As well as regulation of FSH, dual opposing roles for activin and inhibin have been demonstrated for the regulation of steroidogenesis in the Leydig cell. The main source of circulating inhibin is the gonads, but activins are synthesized in a broad range of tissues. Although circulating activin has FSH-modulating abilities, the main role for activin is now considered to be as a paracrine rather than an endocrine regulator of reproductive function.

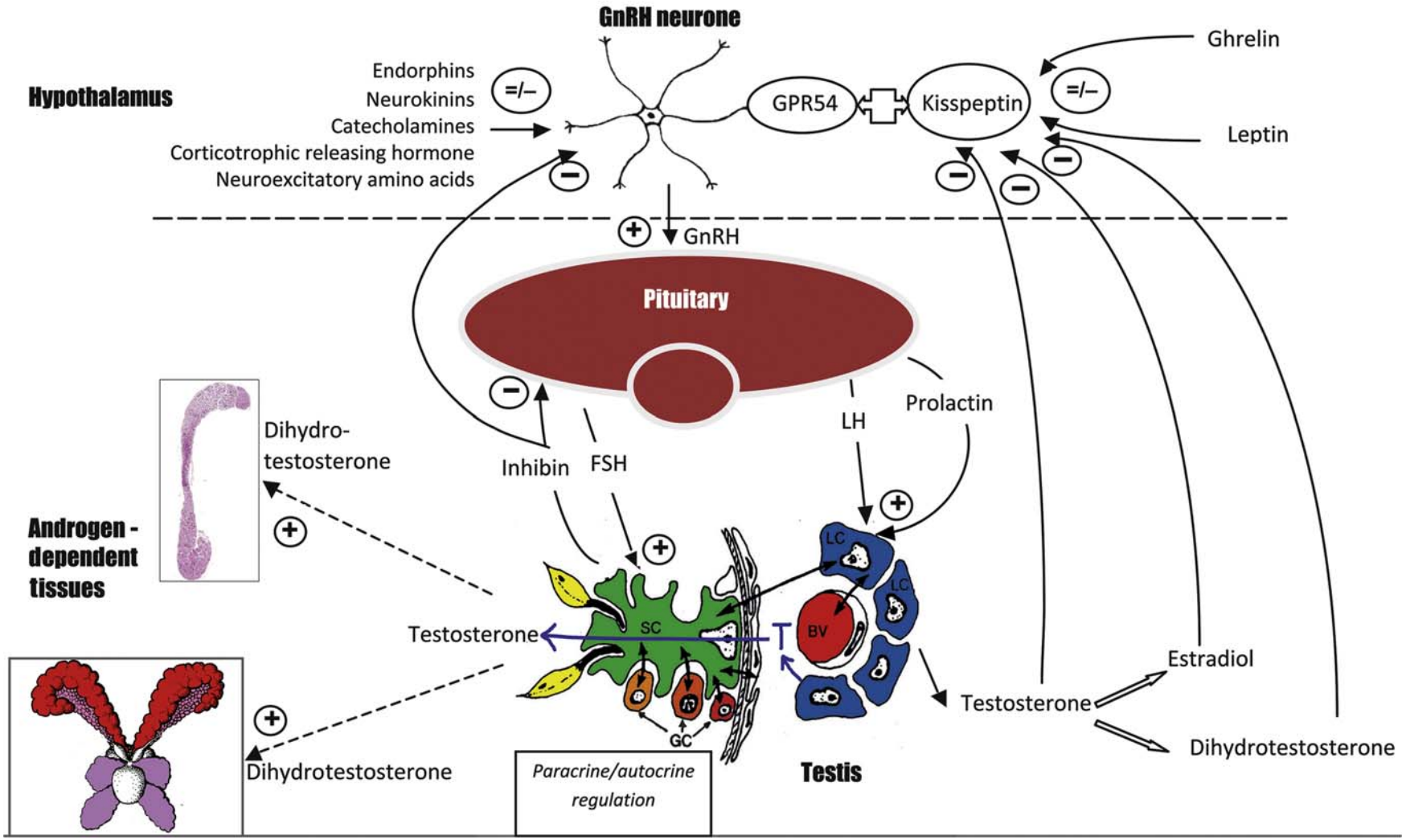

FIGURE 17.8 Endocrine and paracrine regulation of the testis. GnRH secreted from the hypothalamus stimulates secretion of FSH and LH from the pituitary. LH stimulates testosterone (T) production from the Leydig cell (LC), and FSH acts on the Sertoli cell (SC), regulating a number of cellular processes, including inhibin secretion, which negatively feeds back to the hypothalamus and pituitary to control GnRH and FSH release. Prolactin secreted from the pituitary increases LH receptor sensitivity on the Leydig cell. Testosterone, secreted by the Leydig cell, is important for spermatogenesis within the testis, but is also transported into the peripheral circulation and into the seminiferous tubule fluid, where it is further metabolized to dihydrotestosterone by 5α-reductase, and to estradiol by aromatase. Estradiol has important regulatory functions, particularly in the efferent ducts and epididymis, while dihydrotestosterone is the main androgen regulating epididymal and accessory sex organ function. Testosterone and its metabolites regulate GnRH and LH secretion through negative feedback to the hypothalamus. GnRH is secreted from neurons within the paraventricular nucleus of the hypothalamus and its secretion is modified and regulated by many different chemicals, including those involved in energy balance and stress responses. The GPR54 receptor and its ligand, kisspeptin, form the critical gateway that modulates the actions of leptin and ghrelin and circulating steroids on the GnRH neurons. Overlaid on this endocrine regulation is a complex autocrine and paracrine regulation, where a multitude of factors are secreted by Sertoli cells, peritubular cells, Leydig cells, germ cells (GC), and blood vessel endothelial cells (BV) to provide local signaling and regulation to neighboring cells. Source: *Figure reproduced from* Haschek and Rousseaux's Handbook of Toxicologic Pathology *(2013), third ed. (W.M. Haschek, C.G. Rousseaux and M.A. Wallig, eds.), Academic Press (Elsevier), Figure 59.15, p. 2520 with permission.*

Luteinizing Hormone

LH, like FSH, is a glycoprotein hormone secreted in a pulsatile fashion by the pituitary under GnRH control. In rats it acts on Leydig cells and is the primary regulator of testosterone secretion, which is also secreted in a pulsatile manner. Circulating plasma testosterone (or its metabolites) completes the feedback loop via the kisspeptin/GPR54 complex, to modulate LH secretion.

Prolactin permits LH-stimulated testosterone secretion in the rat by increasing the number of LH receptors on the Leydig cell. The Leydig cells of other species do not appear to possess prolactin receptors, which has important implications with regard to species-specificity/sensitivity to chemically induced Leydig cell tumors.

Testosterone

The major androgenic steroid in males, testosterone, is synthesized primarily in the Leydig cells in rats and has both intratesticular effects (on spermatogenesis) and peripheral effects (on accessory sex organs as well as nonreproductive organs such as brain, muscle, bone, and skin). There is also significant testosterone metabolism in many peripheral tissues—for example, the aromatization of testosterone to estradiol which is an important reaction in nonrodent species.

Testosterone is not stored within the Leydig cell but is secreted into the interstitial fluid as it is synthesized. From here it is either (1) taken up by the Sertoli cells and bound to ABP, which is then secreted by the Sertoli cell and transported through the seminiferous epithelium into the STF and on into the epididymis; or (2) diffuses into the interstitial capillaries, where it binds quickly to steroid hormone binding globulin (SHBG) for transport through the body, where it has wide-ranging effects on all other tissues of the body. In the rat, ABP is synthesized by the Sertoli cell, whereas SHBG is synthesized in the liver. The main known effects of testosterone in supporting spermatogenesis are to stimulate STF production by the Sertoli cell, to regulate release of the mature spermatids from the Sertoli cell (spermiation) and to support the development of pachytene spermatocytes and later germ cell types through stage VII of the spermatogenic cycle.

The major stimulus for testosterone production comes from blood levels of LH from the pituitary. It is important to recognize that this connection varies widely across species: in dogs and primates, a pulse of LH is followed closely by a pulse of testosterone. In rats, this connection is much less predictable, and several LH pulses may elicit no rise in testosterone or there may be a significant delay before a testosterone pulse occurs.

Feedback inhibition of LH and hypothalamic GnRH is mediated through circulating levels of testosterone and its metabolites, dihydrotestosterone (DHT), and estradiol, but the relative importance of the various molecules is species-dependent. In the rat, testosterone is the main feedback molecule, whereas DHT is thought to have more importance in the mouse, and estrogen feedback is more important in the dog, monkey, and man.

Estrogen

Estrogen is an important metabolite of testosterone that plays a role in spermatogenesis and in fluid reabsorption in the efferent ducts. Aromatase, which irreversibly converts testosterone to estradiol, is expressed in Leydig cells, Sertoli cells, and germ cells, with the highest functional activity being present in spermatids. Estrogen receptors are also expressed in germ cells, Sertoli cells, and Leydig cells. Aromatase activity/estrogen has been shown to contribute to spermiogenesis and sperm motility. In addition, strogen is a major regulator of fluid reabsorption in the efferent ducts, with high concentrations of estrogen present in the epididymal fluid and high concentrations of estrogen receptor-α in the efferent ducts. Endothelin receptors are also present in high concentrations, and endothelin is also thought to be involved in the process of fluid resorption in humans. Reabsorption is achieved through an active sodium−chloride pump with aquaporins regulating membrane permeability.

Dihydrotestosterone

The major regulatory androgen in the epididymis (and in the accessory sex organs) is not testosterone, but the more potent 5-hydroxy metabolite DHT which is synthesized within the epididymal epithelium by 5α-reductase and binds to the androgen receptor with higher affinity than testosterone.

ANDROGEN-BINDING PROTEIN

ABP is synthesized by the Sertoli cell in the testis, where $\sim$80% is secreted into the luminal fluid and the other $\sim$20% is secreted into the interstitial compartment and taken up into the systemic circulation. ABP binds testosterone and transports it in the STF to the epididymis, where it is taken up by a receptor-mediated process into the principal cells of the initial segment and caput epididymis. Once released from ABP, the testosterone is converted to DHT by the epithelial 5α-reductase. ABP is very similar in structure to SHBG, which is synthesized in the liver and binds testosterone in the peripheral blood. ABP has been identified in rat, dog, monkey, and human.

Paracrine Regulation of Testicular Function

As already discussed, testosterone is the major regulatory hormone within the testis, but its secretion is modified by a variety of substances produced by the Sertoli cells, the blood vessels, the peritubular cells, the interstitial macrophages, and the Leydig cells themselves. These paracrine and autocrine hormones provide a faster response time and allow more sensitive control of testosterone secretion as well as providing a cascade of cell-to-cell chemical communication. The list of these secreted "hormones" is growing continuously and rapidly and includes glycoprotein and steroid hormones, peptide growth factors, cytokines, proopiomelanocortin derivatives, and neuropeptides. The receptors for most of these molecules have been identified *in vitro*, although their physiological function and significance are unknown in most cases. The production of such a variety of pharmacologically potent molecules within the testis has obvious potential for being toxicologically important.

REGULATION OF PROTEIN SECRETION BY THE SERTOLI CELL

The Sertoli cell secretes hundreds of different proteins and proteases, most of which have unknown functions. These include transport proteins, which bind metal ions, lipids, hormones, and vitamins; proteases and protease inhibitors; basement membrane glycoproteins; growth factors; and paracrine factors. Their production is stimulated by testosterone and the presence of germ cells in the adult and by FSH in the prepubertal animal. The Sertoli cell also secretes STF, which maintains patency of the tubules and transports sperm out of the testis to the epididymis. Secretion is also androgen regulated and is influenced markedly by the germ cell complement and if elongating spermatids are missing, STF production is inhibited and tubule diameter is decreased.

REGULATION OF BLOOD FLOW AND INTERSTITIAL FLUID

Interstitial fluid has a very specific composition, compared with plasma, and is responsible for providing the oxygen and nutrients required by the metabolically active Sertoli and germ cells, which are otherwise located in an avascular environment. Interstitial fluid is thought to be produced as a result of rhythmic alterations in arteriolar blood flow (vasomotion), which brings about movement of fluids from the blood through the unfenestrated capillaries into the interstitial space. Androgen receptors are present on the muscular wall of the small testicular arteries, and testosterone is able to regulate overall testicular blood flow as well as the volume of interstitial fluid and the degree of vasomotion.

EVALUATION OF TOXICITY

The effects of toxicants on male reproductive function can occur through disturbances at one or more tissue sites, including hypothalamus, pituitary, testis, efferent ducts, epididymis, accessory sex organs, or penis. In most cases, effects at one site will cause knock-on (secondary) changes at other sites; therefore, in general, the more endpoints examined, the better the chance of detecting toxicity, the more information available for distinguishing the primary cause of toxicity versus the secondary consequences of toxicity, and the greater chance of detecting a single random change occurring in isolation with no biological consequence.

Physiologic Evaluation

Organ Weights

Although organ weights are a standard parameter measured in any regulatory toxicity study, they can provide unique and mechanistically important information for male reproductive tissues because the weight of the accessory sex organs is androgen-dependent (Table 17.3). It is particularly important that the seminal vesicles and prostate (including secretions) be sampled in *all* studies, since these provide a relatively sensitive indication of androgen status. More importantly, they smooth out, or integrate, the peaks and valleys of testosterone secretion, providing a much more reliable assessment of testosterone status than a single hormone assessment. The epididymis is also an androgen-dependent tissue, but nearly 50% of its weight reflects sperm content, which is a function of the efficiency of spermatogenesis. When measuring testis weight in rodents, it is important to use absolute rather than relative weight since the testis, like the brain, is conserved despite decreased body weight gain and even modest body weight loss (up to ~70% of normal body weight). Because of that fact, decreased body weight gains will generally lead to increase in relative testis weight (testis weight as a percentage of body weight). Decrease in absolute testis weight is generally due to decreased germ cell content and/or decreased fluid content. Increased absolute testis weight is generally due to increased STF content (Table 17.3).

Sperm Analysis and Spermatid Head Count

Sperm assessment is performed most often at the end of the study and after a mating trial which

TABLE 17.3 Rapid Reference Guide for Evaluation and Interpretation of Weight Changes in the Reproductive Tract

Finding/observation	What to look for	Possible causes
Increased testis weight	Seminiferous tubular lumen dilatation	Increased seminiferous tubule fluid which may be due to obstruction of outflow, decreased emptying of tubules, decreased resorption of fluid by rete/epididymis, increased production by Sertoli cell
	Increased interstitial fluid (interstitial edema)	Altered hemodynamics, injury to vascular endothelium, reduced lymphatic drainage
Decreased testis weight	Germ cell depletion	Disruption of spermatogenesis through effects on germ cells, Sertoli cells, hormonal disturbance, or blood supply
	Seminiferous tubule lumen contraction	Decreased production of seminiferous tubule fluid which may result from loss of elongating spermatids and/or decreased testosterone production
Increased epididymal weight	Increased interstitial fluid	Altered hemodynamics, injury to vascular endothelium, reduced lymphatic drainage
	Increased ductular fluid	Decreased resorption of fluid by rete, efferent ducts, and caput epithelium
	Sperm granulomas	Maybe spontaneous, but maybe induced by any agent causing inflammation or damage to the epididymal epithelial lining
Decreased epididymal weight	Reduced sperm content and contraction of ductular lumen size	Disruption of spermatogenesis resulting in reduced sperm production or release from the testis
Decreased weight of seminal vesicles and/or prostate	Atrophic changes in the secretory epithelium and decreased secretory product	Reduced levels of circulating testosterone, inhibition of 5α-reductase, or disruption of androgen receptor binding
Increased weight of seminal vesicles and/or prostate	Increased secretory product	Androgenic activity of a treatment; hyperprolactinemia

Table reproduced from Handbook of Toxicologic Pathology *(2013), third ed. (W. M. Haschek, C. G. Rousseaux, and M. A. Wallig, eds.), Academic Press, Table 59.5, p. 2526, with permission.*

assesses the actual fertility of the male (Table 17.4). Measurement of sperm parameters (count, motility, morphology of epididymal sperm, and a count of testicular spermatid heads) can provide important information which can also add to mechanistic interpretations (Table 17.4). In many cases, the sperm measurements may serve to confirm and support the morphologic findings identified in the testis. Indeed, if spermatogenesis declines, all three sperm endpoints will decline. However, there are other situations, such as long-term, low-dose exposures, that result in spermatogenic disturbances that produce no visible lesion in the testis but where the sperm output is detectably compromised when measured as epididymal sperm count, and this will also impact fertility endpoints.

Measuring the number, motility, and morphology of sperm in the epididymis or vas provides an integrated readout of the efficiency and overall health of testicular spermatogenesis as well as epididymal maturation and transport. It is unusual but not unheard of to see a selective effect on count, morphology, or motility in the absence of a change in at least one other measure. These sperm endpoints are all *components* of fertility, but none of them is sufficiently strongly correlated with, or drives, fertility that it may substitute for a functional assessment of how well the sperm work in a fertility test. Thus, while normal values in a treated group of animals offer some degree of assurance that an exposure did not produce severe damage to the male reproductive system, one should not be misled into assuming that fertility is normal in those animals.

Testicular spermatid head count (homogenization resistant spermatid head count) is an additional measurement that provides an indication of testicular sperm production. Contrast this with caudal epididymal sperm count which reflects both the production of sperm from the testis *and* storage of sperm by the epididymis. This is always a useful adjunct to the epididymal sperm data.

In rodents, sperm measurement is a terminal procedure conducted at necropsy, but since it is possible to collect ejaculates from most other species there is the potential for examining longitudinal samples, including predose, during dosing, and during recovery, thus providing regular monitoring of any significant effects

TABLE 17.4 Rapid Reference Guide for Evaluation and Interpretation of Sperm Parameters in the Reproductive Tract

Finding/ observation	What to look for	Possible causes
Decreased epididymal sperm count	Is there any evidence of testicular injury? Is there a similar decrease in testicular homogenization resistant spermatid (HRS) head count? Is there any decrease in accessory sex organ (ASO) weight? Are the other sperm parameters normal?	If there is no testicular injury and no decrease in HRS, the epididymis maybe the primary site of toxicity. If other sperm parameters are normal, decreased count maybe due to reduced (quicker) epididymal transit time. If ASO weight is decreased, low sperm count maybe due to low testosterone (T)
Increased epididymal sperm count		Increased (slower) epididymal transit time
Decreased testicular spermatid head count (HRS)	Are there abnormalities in epididymal sperm parameters? Can you see degeneration/reduction in spermatogenesis or in the number of step 19 spermatids (stage VII/VIII tubules)? Is there any decrease in ASO weight?	Decreased numbers of HRS means reduced testicular spermatogenesis and should be accompanied by reduced epididymal sperm count. Any spermatogenic disturbance will usually result in decreased HRS. If ASO weight is decreased, low T could be the cause
Increased testicular spermatid head count (HRS)	Is there evidence of spermatid retention—i.e., presence of step 19 spermatids at the lumen of stage XI tubules or at the base of stage XII tubules? Is this correlated with a decrease in epididymal sperm count or changes in motility or morphology?	An increased count for HRS can only be caused by spermatid retention because spermatogenesis cannot increase its output of sperm. There may be a decrease in epididymal sperm count (but this may be less sensitive). Spermatid retention is usually associated with an increase in abnormal sperm and decreased motility
Decreased motility	Is there any evidence of testicular injury or changes in HRS? Is there any decrease in ASO weight? Are the other sperm parameters normal?	Decreased motility can be caused by testicular or epididymal toxicity. If it is associated with changes in other sperm parameters, it is likely of testicular origin. Frequently accompanies spermatid retention
Increased numbers of abnormal sperm	Is there any evidence of testicular injury or changes in HRS? Is there any decrease in ASO weight? Are the other sperm parameters normal?	An increase in the number of morphologically abnormal sperm is usually due to spermatogenic disturbance. It is a very sensitive indicator in the rat

HRS, homogenization resistant spermatids; *T*, testosterone; *ASO*, accessory sex organs.
Table reproduced from Handbook of Toxicologic Pathology *(2013), third ed. (W. M. Haschek, C. G. Rousseaux, and M. A. Wallig, eds.), Academic Press, Table 59.6, p. 2527, with permission.*

on spermatogenesis and reversibility. For large animals (rabbits, dogs, and monkeys), sperm evaluation is also a useful hallmark of sexual maturity. A problem with sperm count is its degree of variability, resulting in large standard deviations and relatively wide ranges for normal background data. Variability exists not only between individual animals but within the same animal on different sampling occasions which is why multiple ejaculates are often collected per time point (either within 1 day or on adjacent days during a long study). Fortunately, both the number of morphologically abnormal sperm in rodents and their motility is fairly consistent from animal to animal, and therefore provides sensitive parameters for evaluation.

SPERM COUNT

Sperm count is generally taken from the cauda epididymis and since the function of the cauda is mostly to store sperm, this count reflects both sperm production by the testis and also the storage function of the epididymis. Reduced sperm count is generally due to reduced production but can also be caused by decreased transit time in the epididymis (i.e., the sperm move through more quickly, for example, with **2,3,7,8-Tetrachlorodibenzo-*p*-dioxin** (TCDD) exposure and some estrogenic compounds).

SPERM MOTILITY

Sperm motility is a functional measurement of the sperm themselves. Sperm are sampled either from the cauda or the vas deferens and assessed for motility. In rats, motility is generally high and fairly consistent between animals: with control values in the 85%–96% range for rodents, dogs, and monkeys. Sperm motility can be affected by disturbances in testicular spermatogenesis or by effects on the epididymis.

SPERM MORPHOLOGY

Sperm morphology, especially the head or nucleus, reflects the integrity and quality of the sperm. The number of abnormal sperm produced spontaneously, varies dramatically with species. In rodents

(depending on the laboratory and strain), normal sperm values between 94% and 99.7% are common. In dogs, the percentage of normal sperm varies between 50% and 90%; in cynomolgus monkeys, the value is around 80%. For comparison, the number of normal sperm in normal fertile humans is generally around 50%. Increases in the number of abnormal sperm reflect disturbances in testicular spermatogenesis.

TESTICULAR SPERMATID HEAD COUNT

Testicular spermatid head count is a convenient way of quantifying spermatogenesis in the testis. It is much less labor-intensive than manual counting of testicular germ cells using a microscope. One testis is macerated sufficiently to destroy everything except the highly condensed, most mature heads of the elongating spermatid population (steps 16–19 in rats). This is a defined cell population that represents the final 6 days of spermatid development prior to release. It can therefore be used to provide a value for daily sperm production (when divided by ~6) or the number of spermatid heads per gram of tissue. Spermatid head count will decrease in response to anything that decreases spermatogenic efficiency (as long as the injury has had time to work through to the mature elongating spermatids). The count can also be increased if mature spermatids are not released, as in the case of low-testosterone induced spermatid retention. Integration of this measurement with that of epididymal sperm count provides powerful insight into the site of an effect and an integrated view of the toxicity of a treatment (Table 17.4).

Hormone Analysis

Measurement of hormones can be a powerful and informative tool if it is incorporated into a well-designed study that has adequate numbers of animals or samples to make the data statistically valid (reviewed by Chapin and Creasy, 2012). The most commonly measured hormones are testosterone, LH, FSH, and inhibin B. Additional hormones that can be useful in specific situations are estradiol and DHT, both metabolites of testosterone and important for specific functions of the reproductive tissues. In addition, prolactin which is secreted by the pituitary and has a regulatory role in the secretion of testosterone, may also provide useful information. Most of the reproductive hormones have a pulsatile secretory pattern, are affected by stress, and may also have circadian rhythms. Study design needs to take these factors into consideration if the results are to be trusted.

WHEN TO MEASURE HORMONES

Hormone measurements can be useful to provide mechanistic support for the hypothesis that a reproductive toxicant is acting through a primary disturbance of hormonal regulation, and/or to identify potential biomarkers for that toxicity in man. Since relatively few toxicants act through a hormonally mediated mechanism, it is necessary to identify those that do before embarking on hormonal measurements. In theory, any disruption of spermatogenesis could result in a secondary response in hormone levels (e.g., an increase in testosterone or FSH levels to compensate for a decline in spermatogenesis); however, such hormonal responses are inconsistent in nature and magnitude, late in occurrence, and unlikely to provide a sensitive marker of testicular injury. Thus, it is essential for the pathologist to identify those cases of reproductive toxicity that are caused by a primary hormonal event which can be done using the morphologic profile (see "Patterns of Change Associated with Loss of Androgen Support" section).

One reason for embarking on hormone measurements is when Leydig cell tumors are encountered in a carcinogenicity study. In the rat, Leydig cell tumors are generally caused by any treatment that causes a prolonged increase in LH. This can occur through many different mechanisms, and there is a wide variety of drugs and chemicals that will trigger this response. Although such mechanisms have negligible risk for inducing Leydig cell tumors in man, their occurrence in rodents does reflect a hormonal disturbance which may have other toxicologic implications; therefore, it can be important to establish the cause of this disturbance.

Another, and arguably the most common, trigger for hormone measurements is when the major effects in a study are atrophy or weight loss in the accessory sex organs with or without altered spermatogenesis. If these changes are seen in the absence of significant body weight loss and moribundity, a mechanism involving decreased androgenic stimulation should be considered.

Fertility Assessment

A detailed review of fertility testing and evaluation of fertility endpoints is outside the scope of this chapter, but it is important to appreciate the basic concepts and the fact that fertility is an important endpoint for consideration by the toxicologic pathologist. Fertility is the final-integrated endpoint of the successful functioning of the male and female reproductive processes, and in that sense it sums all the related processes into a single integrated output.

Fertility can be impacted by morphological or biochemical injury in any of the reproductive tissues, by hormonal disturbances anywhere in the HPG axis, or by neurobehavioral alterations in sexual behavior (reduced libido means no or fewer litters). Due to the massive reserve capacity of spermatogenesis in

rodents, fertility is relatively insensitive for identifying testicular toxicity, particularly when compared with morphology or sperm parameters. An often quoted observation is that rats can remain fertile (they can produce offspring) with less than 2% of their normal sperm numbers. Even though they may remain fertile, other fertility endpoints, such as total litter size, pup weight, or time to pregnancy, will show significant alterations. In comparison with rodents, humans have vastly less reserve to maintain fertility when reproductive function is compromised. This is due to the relative inefficiency of spermatogenesis (sperm output/gram of testis) in humans, which is significantly lower than most other species, and a high proportion of abnormal sperm (over 50%) produced as compared with less than 1% abnormal forms in rodents (Table 17.2). The fact that rodents have such high fecundity means that fertility (number of pregnant females per group) may remain high or unaffected in a group of 20 females, despite detectable histopathological changes or changes in sperm parameters. Aggregate data from many multigenerational studies have shown, however, a remarkably good correlation between overall fertility and sperm count and motility; even modest reductions in sperm count (e.g., 10%) in rodents will translate into reduced fertility in a *population* of rodents. Note that this may not be seen in a small group of 20 animals.

Morphologic Evaluation

Histopathology is often cited as being the most sensitive method for detecting disturbances in spermatogenesis, and indeed it is, if conducted on well-fixed tissue and by a pathologist with a clear understanding of spermatogenesis, the cell associations (stages) that make up the spermatogenic cycle and the dynamics of the overall process (Table 17.5). If these requirements are not met, important lesions will be missed, especially in short-term studies of 2–4 weeks. This can be critical for human safety, since in the case of pharmaceutical development, "first into man" clinical trials are often based on the results from such short-term studies.

Importance of Fixation

Testes fixed in conventional 10% neutral buffered formalin (NBF) causes severe shrinkage of the Sertoli and germ cells within the tubules. This seriously compromises the pathologist's ability to detect subtle changes such as tubular vacuolation, shape changes in the head of the elongating spermatids, spermatid retention, and displacement of germ cells from their normal position within the seminiferous epithelium. Fixation of testes with Bouin's or Modified Davidson's fixative overcomes this problem and should be used for all studies if possible, or at least for studies of ≤ 13 weeks. The epididymis and accessory sex organs are best fixed in conventional NBF.

Testes need to be fixed whole to maintain the architectural integrity of the seminiferous tubules and prevent disruption of the delicate germ cell–Sertoli cell junctions. This includes large animal testes as well as rodents, and so penetration and protein crosslinking properties of the fixative are particularly important. Although formalin is a rapidly penetrating fixative, it is slow in its abilities to crosslink proteins, even when tissues are trimmed to an ideal thickness. When testes are fixed whole in formalin, it is likely that proteins are never fully crosslinked and are therefore susceptible to distortion during subsequent processing and paraffin embedding. Bouin's and Modified Davidson's both contain formalin, but they also contain acetic acid which causes swelling of cells, counteracting the shrinkage induced by formalin. Both Bouin's and Modified Davidson's provide excellent cellular and nuclear morphology of the germ and Sertoli cells; the main disadvantage of Bouin's fixative is its tendency to cause excessive shrinkage of tubules and a graininess to the cytoplasm (in addition to the fact that the waste is explosive and requires special handling methods), whereas the main disadvantage of Modified Davidson's is that it results in pale PAS staining of the acrosome. A recommended recipe for Modified Davidson's is provided in Box 17.1.

Fixation of testes for immunohistochemistry (IHC) may require different fixatives and shorter fixation times, depending on the antigen being stained and antigen retrieval techniques employed. Trials are recommended to optimize for each antigen. Fixation of testes for electron microscopy and/or embedding in plastic (epoxy resin or glycol methacrylate resin) requires special fixation to provide optimal morphology. In the case of electron microscopy, perfusion fixation is essential if detailed ultrastructural evaluation is the goal. Successful perfusion of the testis can be challenging, and following specific published methodology relating to testicular perfusion is recommended. Perfusion fixation can also be used for glycol methacrylate embedding, although immersion fixation provides acceptable results. Surprisingly, NBF provides good results with this water-soluble embedding medium, and fixation is not improved when the fixative is perfused.

Importance of Sampling

Sampling of the testis should always incorporate part of the rete testis so that this can be evaluated for changes. In rodents, the testes can be sampled to provide a transverse or longitudinal section or one of each type can be taken from each testis. In large animals, the size of the testis may preclude obtaining an entire

TABLE 17.5 Rapid Reference Guide to Evaluation and Interpretation of Histopathologic Findings in the Reproductive Tract

Finding/observation	What to look for	Possible causes
Testicular germ cell loss	Is a specific cell type(s) affected? Does the germ cell loss fit into a pattern of maturation depletion, or is it nonspecific? Is it focal or diffuse, is it partial or generalized?	The pattern of the germ cell loss will provide valuable clues as to the likely mechanism of injury, but this will also be very much influenced by the duration of the study (see main text for detail). The pathogenesis of germ cell loss is best investigated in a short time-course study
Loss of elongate and elongating spermatids	Degeneration of step 7 spermatids and pachytene spermatocytes in stage VII tubules	Disruption of testosterone secretion, which may be caused by direct effects on the Leydig cells or endocrine-mediated effects. Direct effects on elongating spermatids
Degeneration/apoptosis of germ cells	Is a specific cell type affected? Are the dying cells restricted to a specific tubular stage? Are the affected cells forming multinucleate aggregates?	The cause maybe direct toxicity to the affected germ cell, but may also be mediated through a stage-specific disturbance to the Sertoli cell. Apoptotic cells are rapidly removed. Multinucleate aggregates suggest a slow, nonspecific degenerative process
Germ cell exfoliation	Presence of exfoliated germ cells in the rete and epididymal lumens	Disruption of Sertoli/germ cell junctions leading to loss of adhesion. Disruption of Sertoli cell cytoskeletal fibers leading to sloughing of apical Sertoli cell cytoplasm and attached germ cells
Macro/microtubular vacuolation (in the absence of severe germ cell injury/loss)	Is this located in the basal Sertoli cell cytoplasm, or scattered as large vacuoles throughout tubule? Look for accompanying or additional focal germ cell loss (suggesting focal Sertoli cell damage)	Disturbance of Sertoli cell function leading to vacuolation of organelles or disturbance of fluid balance. *NB: Do not confuse with osmotic induced fixation artifact*
Necrosis and disorganization of tubular contents (including Sertoli cells)	Evidence of acute inflammatory infiltrate around affected tubules	Disturbance in hemodynamics or damage to the vascular endothelium leading to ischemic necrosis
Spermatid retention	Alteration in epididymal sperm parameters (morphology, motility and count) and possible increase in HRS. Are ASO weights reduced?	Reduced ASO weights → disturbance in testosterone secretion. No change in ASO weights implies disturbance in Sertoli cell function or in spermatid development
Dilated seminiferous tubule lumens	Blockage of efferent ducts or epididymal duct. Evidence of pressure-induced germ cell loss	Increased seminiferous tubule fluid due to obstruction of outflow, decreased emptying of tubules, decreased resorption of fluid by rete/epididymis, or increased production of fluid by Sertoli cell

ASO, accessory sex organs; *HRS*, homegenization resistant spermatids.
Table reproduced from Handbook of Toxicologic Pathology *(2013), third ed. (W. M. Haschek, C. G. Rousseaux, and M. A. Wallig, eds.), Academic Press, Table 59.7, p. 2540, with permission.*

BOX 17.1

RECIPE FOR MODIFIED DAVIDSON'S FIXATIVE

140 mL Ethyl alcohol (95%+)
62.5 mL Glacial acetic acid
375 mL Commercial formaldehyde solution: (37%)
422.5 mL Distilled water

Box reproduced from Handbook of Toxicologic Pathology *(2013), third ed. (W. M. Haschek, C. G. Rousseaux, and M. A. Wallig, eds.), Academic Press, Box 59.1, p. 2541, with permission.*

cross-section of testis unless using oversize slides. The section should at least contain a portion of the rete testis and also incorporate peripheral as well as the central regions of the tubule-containing lobules. Since the matrix of Sertoli cells and germ cells that constitutes the seminiferous epithelium is delicate and easily disrupted, it is important that the testes are handled gently at necropsy. Care should be taken to keep the capsule intact and not puncture or nick it when removing the epididymides. It is *not* necessary to puncture the capsule prior to immersion in fixative, even with nonrodents, since this often causes more damage than benefit.

Sampling of the epididymis should include all regions (initial segment, caput, corpus, cauda, and junction with the vas deferens). This is best achieved by taking a longitudinal section through the entire organ. Lesions are often region-specific in the epididymis and sperm density varies significantly depending on location, so consistent and complete sampling is important.

Sampling the accessory sex organs is relatively straightforward. In the case of rodents, it is important to ensure that the different lobes of the prostate are adequately sampled because they respond differentially to different endocrine-disrupting scenarios.

Stage-Aware Evaluation of Spermatogenesis

Whenever a pathologist examines a testis with the intent to identify changes in spermatogenesis, it needs to be done with an awareness of the stages of spermatogenesis. Failure to do this will result in important changes being missed. A stage-aware evaluation should not be considered a "special" evaluation; it should be the routine way that any toxicologic pathologist examines a testis. Ideally, a pathologist should have a thorough knowledge of spermatogenesis, as well as the cellular associations in each of the different stages of the spermatogenic cycle, in each of the species routinely evaluated, and a clear understanding of the dynamics of the process (reviewed by Creasy, 1997). In reality, most changes can be readily identified as long as the pathologist can recognize the different appearance and cell types within tubules that are at the beginning, in the middle, or at the end of the cycle (Figures 17.5B and 17.6). Having this level of knowledge allows detection of relatively subtle changes in any routine regulatory study using conventional H&E sections.

If there is a suspicion that a drug or chemical belongs to a class of known testicular toxicants, then a more detailed stage-aware evaluation maybe requested. In these situations it is recommended that the testes be stained with PAS-hematoxylin to stain the spermatid acrosome. This allows accurate placement of any tubule with respect to its precise stage within the spermatogenic cycle (Figure 17.5A). This is not the case with dog spermatogenesis, where the acrosome fails to stain with PAS.

The value of examining the testis in a stage-aware manner is that it allows recognition of when a cell that should be present is in fact missing, or, conversely, is present when it should not be. This can be surprisingly difficult to see unless the observer is familiar with the correct number of layers of cells and their general appearance in the different (early, mid, and late) phases of the cycle (Figures 17.9 and 17.10). Another advantage of examining the testis with a knowledge of stages is that it enables recognition of stage-specific cell degeneration (Figure 17.11B) or stage-specific Sertoli cell vacuolation. Stage-specificity of changes is only likely to be seen in short-term studies (≤4 weeks duration). Many testicular toxicants show stage-specific changes at the earliest time points, but as the affected tubule continues through consecutive stages of the spermatogenic cycle and the repeat dosing regimen continually damages more tubules in the sensitive stage, the appearance of stage-specificity is lost.

Using the same basic principles, a stage-aware evaluation can be conducted regardless of species, but the pathologist should be aware of the differences in cell associations between species. Staging maps are readily available for all the major species (see the "Further Reading" section) and should be referred to when examining testes. Using these maps, staging of tubules in the cynomolgus monkey is relatively straightforward as long as the monkey is mature. Staging spermatogenesis in the dog is much more difficult than in the rat or the monkey because the layering of the germ cells is less regular and the overall appearance of the seminiferous epithelium is less compact. Additional difficulties include the fact that the spermatid acrosome does not stain with PAS, the spatulate head of the elongating spermatid presents a variable profile in the same stage tubule depending on its plane of section, and mature spermatids maybe released from tubules (spermiation) in two consecutive stages (stage IV and V), resulting in significant numbers of "mid-stage" tubules that are missing their complement of elongating spermatids. Nevertheless, early mid- and late-stage tubules (Figure 17.10) can still be distinguished and can be examined to identify whether the main cell types are present in their expected proportions.

Nomenclature and Grading of Lesions

As with any organ or tissue, using consistent nomenclature and severity grading for findings is important. There is an added degree of complexity with respect to nomenclature and grading of changes in the testis because many of the early toxicant-induced disturbances in spermatogenesis are cell- and/or stage-specific and may only affect one cell type or only affect one or a few stages of the spermatogenic cycle.

NOMENCLATURE

The recently published International Harmonization of Nomenclature and Diagnostic Criteria for Lesions in Rats and Mice nomenclature system for the male reproductive system in rodents (Creasy et al., 2012) recommends using cell- and stage-specific terminology

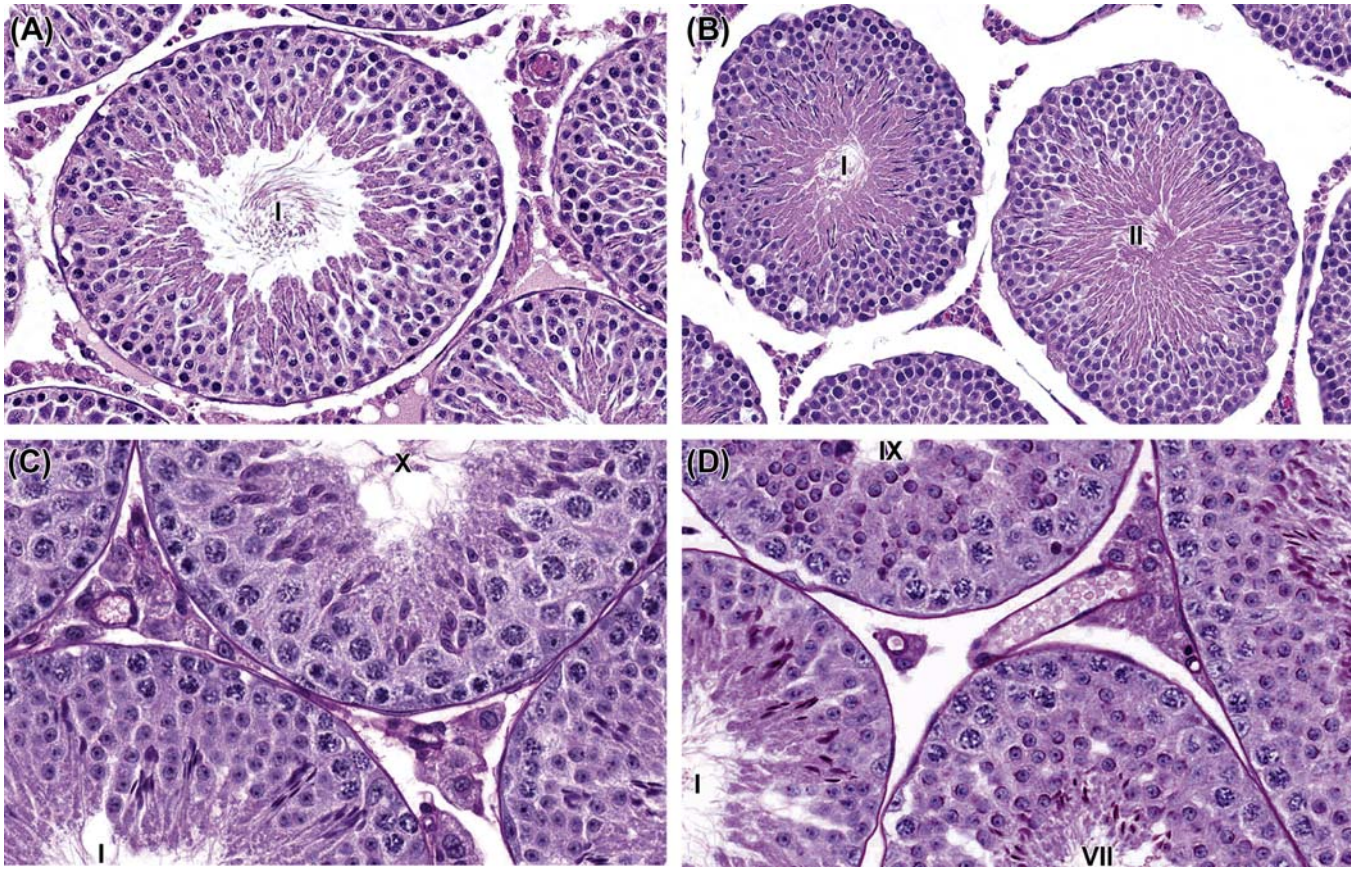

FIGURE 17.9 (A) Normal stage I tubule from control rat. (B) Stage I tubule (left) and stage II tubule (right) after 2 days' dosing with a testicular toxicant that kills stage I pachytene spermatocytes. The stage I tubule shows swelling and early apoptosis of its pachytene spermatocytes. The stage II tubule shows complete absence of all pachytene spermatocytes (which were killed when the tubule was in stage I on Day 1 of dosing). Rat, H&E, ×20. (C) Testis from a control mouse showing normal cellular associations in a stage I and stage X tubule. (D) 14 days' dosing with a spermatogonial toxicant. The stage I tubule is missing its spermatogonia and its pachytene spermatocytes. The stage IX tubule is missing spermatogonia and zygotene spermatocytes. Notice that the stage VII tubule still has its pachytene spermatocytes but is missing its preleptotene spermatocytes. If dosing was continued, the "front" of germ cell depletion would continue to move through the stages and cell types. Mouse, PAS, ×40. Source: *Figure reproduced from* Haschek and Rousseaux's Handbook of Toxicologic Pathology *(2013), third ed. (W.M. Haschek, C.G. Rousseaux and M.A. Wallig, eds.), Academic Press (Elsevier), Figure 59.16, p. 2543 with permission.*

when such changes are seen, and using generalized terminology (e.g., tubular degeneration/atrophy) for nonspecific changes (Figure 17.11). It is often important to capture the cell- and stage-specificity of a finding because it can provide important mechanistic information or important information for risk assessment. For example, a finding of "degenerating round spermatids and pachytene spermatocytes, stage VII/VIII" indicates that reduced testosterone is the probable cause of the degeneration, especially if the change was associated with reductions in accessory sex organ weight. Alternatively, if the change only involved elongating spermatids (e.g., "degeneration and depletion elongating spermatids"), this would signify that the toxicity is limited to the final stages of spermatid development, which would suggest it is likely to be a rapidly reversible change with only transient effects on fertility (although this would need to be tested). Cell- and stage-specific changes are most likely to occur in short-duration studies (≤4 weeks of dosing), and the longer the study duration, the more cell types and the more stages are likely to be affected. In these situations, nonspecific terminology (such as tubular degeneration/atrophy) is more appropriate.

Epididymal lesions are frequently also region-specific, and if this is the case the nomenclature should reflect the anatomic location because the information can have important mechanistic implications. Reductions in sperm content can even be region-specific depending whether the reduction in sperm output from the testis occurred within the past few days of dosing (low sperm in the caput, normal sperm in the cauda) or occurred over the previous 1−2 weeks of dosing (low sperm throughout the epididymis).

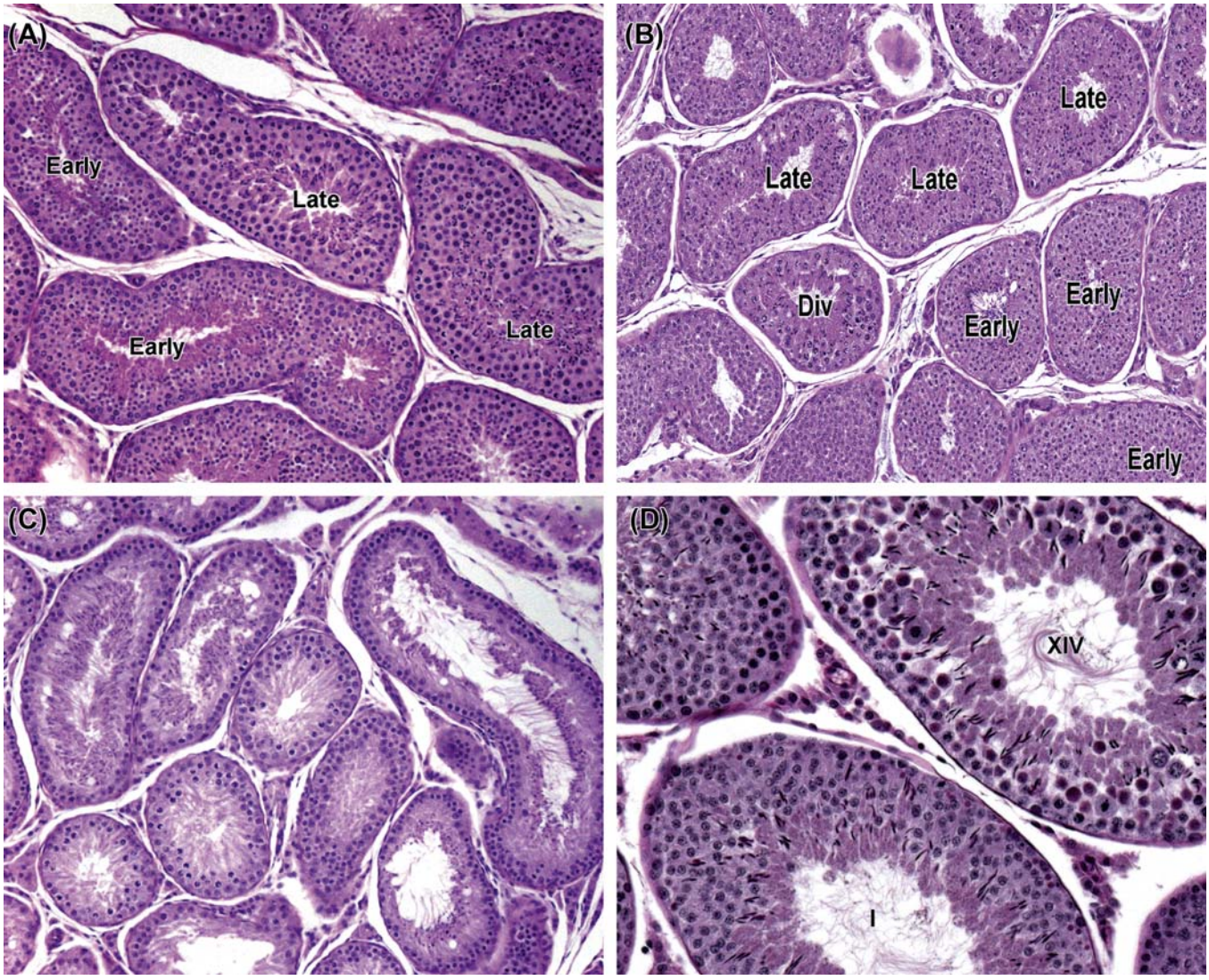

FIGURE 17.10 (A) Testis from a control dog. Note the cell associations in the early- and late-stage tubules. Dog, H&E, ×10. (B) Testis from a dog after dosing for 4 weeks with a spermatogonial toxicant. Most of the spermatogonia, prepachytene, and pachytene spermatocytes are missing from early- and late-stage tubules. The "front" of depletion has not yet affected the dividing spermatocytes in the stage VIII tubule (Div). Dog, H&E, ×10. (C) Testis from a dog following a 4-week recovery period after dosing for 4 weeks with a spermatogonial toxicant (see B). Maturation depletion has now progressed to deplete most of the round and elongating spermatids such that the severity of the lesion appears worse than at the end of dosing. However, spermatogonia and prepachytene spermatocytes have recovered in all tubules. When an 8- to 10-week recovery period was used, spermatogenesis returned to normal. Dog, H&E, ×10. (D) Rat testis treated with a single dose of ethylene glycol monomethyl ether (EGME). Target cells are stage I pachytene spermatocytes and dividing spermatocytes. Dividing spermatocytes are undergoing apoptosis in the stage XIV tubule while early pachytene spermatocytes have already died and been phagocytized from the stage I tubule. Rat, H&E, ×20. Source: *Figure reproduced from* Haschek and Rousseaux's Handbook of Toxicologic Pathology *(2013), third ed. (W.M. Haschek, C.G. Rousseaux and M.A. Wallig, eds.), Academic Press (Elsevier), Figure 59.17, p. 2544 with permission.*

SEVERITY GRADING

Grading the severity of disturbances in testicular spermatogenesis can present a challenge. Severity grading for nonspecific testicular changes such as tubular degeneration/atrophy is generally not a problem and can be based on the proportion of affected tubules. However, severity grading for cell- and stage-specific changes needs to take into account the number of cells affected as well as the number of tubules affected. For example, spermatid retention only involves the retention of step 19 spermatids in stage IX–XI tubules, which constitute a very small proportion of the total tubular profiles but may involve a very high proportion of the step 19 spermatids. Should the change be

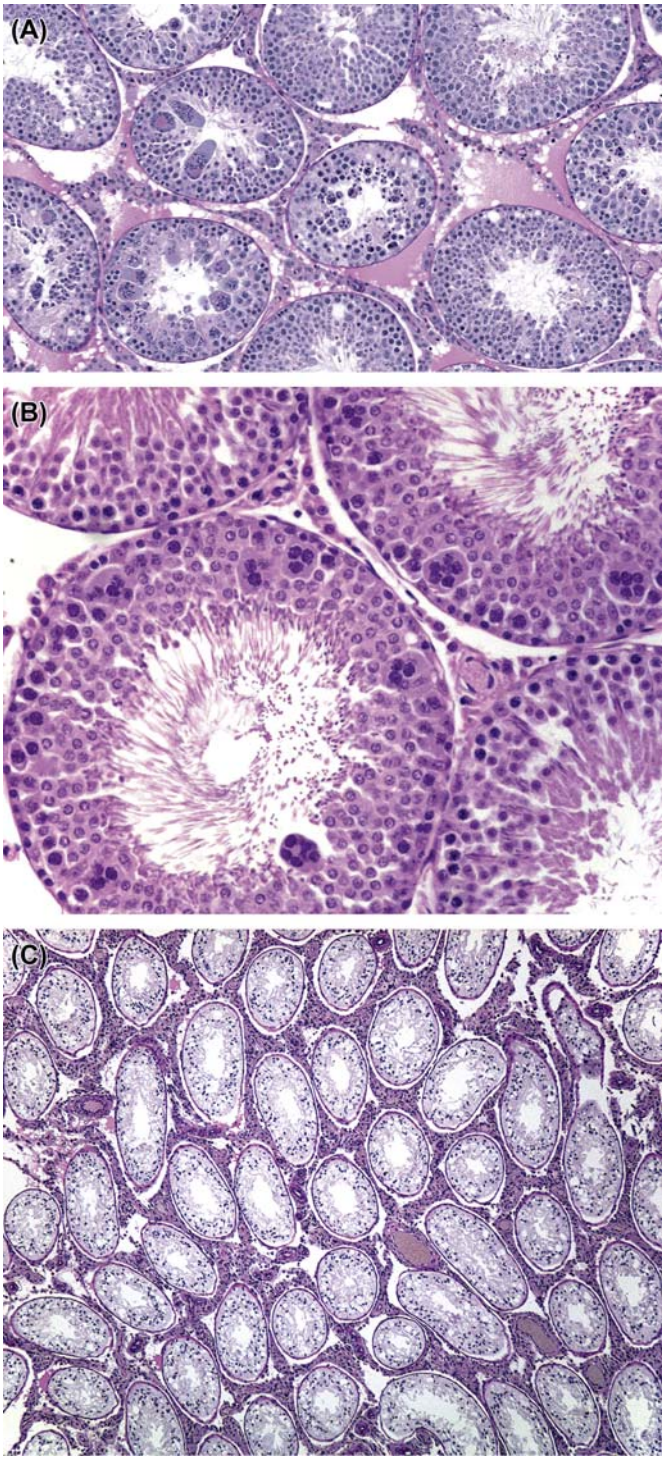

FIGURE 17.11 (A) Nonspecific tubular degeneration/atrophy. Some tubules contain multinucleate degenerate cells; others are partially depleted of germ cells. Rat, H&E, ×10. (B) Stage-specific (stage VII) multinucleate degeneration of pachytene spermatocytes. Rat, H&E, ×20. (C) Tubular atrophy. Contracted tubules, totally depleted of germ cells and lined only by Sertoli cells. Rat, H&E, ×4. Source: *Figure reproduced from* Haschek and Rousseaux's Handbook of Toxicologic Pathology *(2013), third ed. (W.M. Haschek, C.G. Rousseaux and M.A. Wallig, eds.), Academic Press (Elsevier), Figure 59.19A,B, p. 2552, Figure 59.20B, p. 2553 with permission].*

considered minimal or severe? The decision has to be made on a case by case basis and explained in the text of the report if needed.

Special Techniques

Immunohistochemistry

The testis lends itself to IHC as well as any other tissue, although a word of caution is in order. We have the perception that the testis has its own isoforms of proteins; although the protein is present in the testis, it maybe as a splice variant which reduces or eliminates the ability of that protein to be recognized by the antibody which works perfectly well in other tissues. Investigators should be aware of the testis' penchant for protein uniqueness, and guard their interpretations appropriately.

Staining for Proliferating and Apoptotic Cells

There are staining methods which will specifically highlight dividing cells (predominantly spermatogonia) and apoptotic cells. Proliferating cells can be stained using IHC methods. The most common methods include proliferating cell nuclear antigen (PCNA), Ki67 antigen, or administration of bromodeoxyuridine which will be taken up by the dividing cell and then visualized using subsequent immunohistochemical methods. PCNA is an antigen that is expressed for relatively long periods of time after cell division and is less specific than Ki67, which only stains recently divided cells. Both are technically easier than administering bromodeoxyuridine (BrDU). Since spermatogonia can be difficult to visualize and count, this relatively simple IHC method provides a good way of visualizing the spermatogonial population in different stages of the spermatogenic cycle and can be useful in confirming a suspected treatment-induced reduction or cessation in spermatogonial divisions.

Apoptotic cells can be stained using TUNEL (terminal deoxynucleotidyl transferase-mediated deoxyUTP-biotin nick end labeling) or Caspase 3 staining. TUNEL is a method which labels the ends of a DNA strand with a visualization tag. It was thought that this method labeled only that DNA cleaved by endonucleases between the histone solenoids. It is true that this method will visualize cells undergoing apoptosis in situ and will do it with significant sensitivity. However, it has also been shown to stain cells undergoing necrosis (the more disorderly cell death process), as well as cells undergoing DNA repair or damaged by mechanical or shearing forces. Thus, it might be appropriate to use TUNEL staining to identify DNA damage, but then to defer the decision on a specific mode of death to another technique, such as DNA

electrophoresis, to look for the "ladder pattern" so characteristic of apoptosis. Methods are widely available to visualize cells stained with this method; the main message here is to remind us that TUNEL is *not* specific for apoptosis. If a conclusion about apoptosis is important, staining for Caspase 3 should be performed. Caspase 3 is a lysosomal enzyme involved in the apoptotic pathway and is more specific in the detection of apoptotic cells than TUNEL.

In Vitro Methods

Cell culture models are often used academically to investigate specific aspects of cell biology. Although there is increased effort to create engineered-tissue-culture models which would accommodate the long-term growth and maintenance of highly polarized epithelium characteristic of the seminiferous tubules (with the eventual production of mature sperm), no successful methods have been published outside of a few unreplicated academic reports. Thus, all *in vitro* models of testis or epididymis are short-term (a couple of days) or transformed cell lines which lack various metabolic capabilities. Cell lines can be a useful tool if they retain the features and pathways of interest to a project but this knowledge is required upfront.

RESPONSE TO INJURY

Organ Weight Changes

Table 17.3 provides guidance on the evaluation of organ weight changes. Growth and maintenance of the testis, like brain, is preserved despite body weight loss; thus, absolute rather than relative weight should be used for evaluation. As might be expected, a decrease in body weight gain will result in an increase in testis to body weight ratio when compared with controls. A decrease in absolute testis weight generally reflects a loss in germ cell number and STF, which will usually be reflected by a decrease in epididymal weight since sperm content is responsible for approximately 50% of its weight. An increase in the weights of testis or epididymis generally indicates increased fluid content. In the case of the testis, this is usually due to increased tubular fluid and is accompanied by obvious tubular dilation. It is most likely due to blockage of the efferent ducts, while in the epididymis, interstitial edema or possibly a sperm granuloma is the most likely cause.

In the rat, decreased weight of the seminal vesicles and ventral prostate is a relatively sensitive indicator of reduced androgen status, is more sensitive than morphological evaluation of atrophic changes and is less variable than measuring hormone levels. Indeed, these weights are the best integrative indicator of androgen status currently available. Most of the weight change is due to a reduction in the stored secretion, and therefore it is important that this is captured when the tissues are weighed—i.e., weigh the tissues with their stored secretions. The combined weight of the seminal vesicles, coagulating gland, and prostate can be used, or each organ can be weighed separately. In practice (and when allowed by the protocol), it is just as sensitive and much easier to lift the aggregate tissue mass by the bladder, cut the urethra immediately below the prostate, place the whole unit (bladder, prostate, and seminal vesicles) intact on the balance and then trim off the bladder. It is easy and fast and guarantees retention of the fluid.

In endocrine-disruptor screening studies, the ventral prostate is sometimes dissected and weighed separately since it is the most androgen-sensitive portion of the gland. Increased weight and secretory content of the accessory organs can occur if androgens are administered, or expulsion of secretion is inhibited, which has been reported with some alpha-adrenergic agents. Hyperprolactinemia has also been reported to cause enlargement of accessory sex organs in rodents.

Weight change of the accessory sex organs is not as sensitive a parameter in the dog and monkey because of the inter-animal variation, smaller group sizes, and the fact that comparatively little secretion is stored in these organs.

Morphologic Changes (Nonproliferative)

The most common appearance of the testis following dosing with any testicular toxicant is varying degrees of germ cell degeneration, depletion, and disorganization of the germ cell layers within the seminiferous epithelium (Table 17.5). This reflects the fact that the germ cells are exquisitely sensitive to any disturbance of their support, be it mechanical, biochemical, nutritive, or regulatory. So, whether a toxicant acts through the Sertoli cell to disrupt a biochemical pathway that regulates or supplies energy to the germ cells, or acts on the Leydig cells to decreases testosterone levels, or even on the vasculature to cause anoxia, it will be the germ cells that are most affected and show evidence of cell degeneration, death, and depletion. Although the Sertoli cells are very sensitive to disturbances due to their multiplicity of biochemical pathways, for the most part this is not reflected by morphological changes that are evident by light microscopy. It is not until they are severely damaged that morphological changes are recognizable. In fact, there are very few toxicants or injuries that actually kill Sertoli cells; one of the few examples is ischemia. This robustness maybe related to the fact that the

Sertoli cell is incapable of division once it has passed its postnatal proliferative phase (day 15 rat, week 15 dog, and month 32 cynomolgus monkey), and because the Sertoli cell forms the blood–testis barrier that protects the seminiferous epithelium from the destructive/protective actions of the immune system. Once the Sertoli cell barrier is broken, the tubule is generally destroyed and replaced by granulation tissue and fibrosis. Apart from the few occasions where the Sertoli cell barrier is breached, inflammation is rarely seen as a response to injury.

Since all types of injury cause the same morphologic response, how can the pathologist gain insight into how and where the toxicant is acting? The answer is to look at the earliest morphological changes and concentrate on the *pattern* of toxicity (see "Morphological Patterns of Response to Different Types of Injury" section). Table 17.5 also provides a rapid reference guide on specific features to look for and how they can be interpreted. This may mean looking at the cell-specificity or stage-specificity of the early changes, as well as the character of the morphological changes (germ cell degeneration versus germ cell depletion versus tubular vacuolation or necrosis). It means taking into consideration the effects on the rest of the reproductive tissues (epididymis and accessory sex organs and sperm endpoints if available). This kind of detailed morphologic examination of early changes relies heavily on the pathologist's knowledge of spermatogenesis and the ability to detect when a particular stage of the spermatogenic cycle is abnormal. This can be surprisingly subtle even when there are multiple cell types missing (Figures 17.9 and 17.10).

In reality, it is our evolving appreciation that almost all testicular toxicants probably produce disruption of spermatogenesis through a final common pathway due to effects on the Sertoli cell. This is because the Sertoli cell (also known as the nurse cell) provides almost all the needs of the germ cells and the regulation of spermatogenesis. Even testosterone, as a major regulator of spermatogenesis, is believed to have its main effects through interaction with androgen receptors on the Sertoli cell, which, in turn, controls functions such as the rate of spermatogonial differentiation, the processing of spermatocytes and round spermatids through androgen-dependent stages (stages VII and VIII), and the release of mature step 19 spermatids from the Sertoli cell cytoplasmic recesses (spermiation). Similarly, some spermatogonial toxicants act through disruption of the complex cascade of factors that involve the Sertoli cell stem cell factor (SCF)–c-kit system rather than a direct (cytotoxic) effect on the spermatogonia. Nevertheless, it is possible for the pathologist to distinguish between these different types of toxicity by characterizing the early pattern of changes, thereby providing important information that maybe useful for risk assessment, biomarker identification, or further mechanistic investigations. In addition, because of the central role the Sertoli cell plays in spermatogenesis, it is important to distinguish a toxicant that is producing its effects through disturbance of a biochemical pathway from one that is producing effects through overt structural damage of this critical cell.

Germ Cell Degeneration (Apoptosis)

Although the term "germ cell degeneration" suggests a potentially reversible effect on the germ cell, it is the recommended terminology that is applied to germ cells undergoing cell death (apoptosis). In the testis, apoptosis provides the important physiologic function of limiting the size of the germ cell population to numbers that can be supported adequately. The Sertoli cell regulates this function utilizing the FAS gene system. Germ cells express Fas, a transmembrane receptor protein that, when bound by Fas ligand (FasL) secreted by the Sertoli cell, transmits an apoptotic signal within the cell. All chemically induced germ cell death investigated so far also appears to occur through the process of apoptosis. This is true for both direct germ cell toxicity, as occurs with radiation, and indirect germ cell death resulting from Sertoli cell injury. It is even true for death that appears pyknotic (Figure 17.10D), such as the spermatocyte death induced by glycol ethers in rats. The precise mechanism triggering apoptosis appears to be different in each case. With Sertoli cell toxicants there is upregulation of Fas and FasL, but with germ cell toxicants there is only upregulation of Fas. Although DNA laddering electrophoresis might indicate that germ cell death occurs by apoptosis, for the bench pathologist looking at dying germ cells microscopically, the only dying cells that fit the classic morphologic appearance of apoptosis (DNA fragmentation and clumping at the periphery of the nucleus within an eosinophilic cytoplasm), are spermatogonia. These can often be seen undergoing normal attrition, particularly at the outside of stage XII tubules.

In cases of testicular toxicity, one of the most obvious and common manifestations of degeneration is that of the "multinucleate giant cell" (see Figure 17.11A and B). These generally comprise round spermatids or occasionally pachytene spermatocytes that have fused together into one large cell. Recall the earlier notation that as spermatogonia proceed through their successive divisions, they remain connected to their siblings via cytoplasmic bridges (incomplete cytokinesis). These cytoplasmic bridges remain intact through the rest of spermatogenesis and are thought to allow for coordinated development between the

progeny of a spermatogonial division. The multinucleate germ cells are believed to form when the cytoplasmic bridges between adjacent cells open and allow fusion of the cytoplasm. When round spermatids are involved, the nuclear acrosomic caps often appear to adhere to one another. Multinucleate giant cells appear to be a relatively slow form of germ cell death, since the nuclear and cytoplasmic characteristics often retain normal staining and morphology, are TUNEL negative and elicit very little response from the surrounding Sertoli cell. They can be seen as an occasional focal or diffuse background finding in rodents and dogs (Figure 17.11A), but when a dose-related increase is seen in number and incidence they are a good indication of toxicity. They can also be seen as a cell- and stage-specific change (Figure 17.11B).

Germ cells with eosinophilic, slightly shrunken cytoplasm and nuclei with condensed or pyknotic chromatin are a different manifestation of apoptosis, and probably represent a much more rapid type of cell death. Such cells are rapidly phagocytized by the surrounding Sertoli cell cytoplasm, and evidence of their demise is rapidly removed, generally within 24 hours. If this type of death occurs within a specific cell population (e.g., pachytene spermatocytes in stage I tubules), examination of the testis on the following day would show absence of stage II pachytene spermatocytes because the tubule will have progressed to the next stage and the pachytene spermatocytes will have been removed (Figure 17.9A and B).

Germ Cell Depletion

Once germ cells undergo apoptosis they are rapidly phagocytized by the Sertoli cell and all evidence of their previous existence disappears. If an entire generation (layer) of germ cells dies and the testis is examined soon afterwards, the resulting depletion can be difficult to detect (Figures 17.9 and 17.10). If the study is a repeat dose study and the same cell type is continually killed with each repeat dose, the depletion will probably appear relatively nonspecific by the end of the study (see the "Patterns of Change Associated with Germ Cell-Specific Toxicity" section). Death and depletion of a specific germ cell type suggests interference with a specific process, either within the affected germ cell or affecting a specific pathway in the Sertoli cell that is critical for the survival of that stage of germ cell development. More commonly, germ cell depletion occurs with a patchy, multifocal distribution and is accompanied by disorganization with some degeneration of the remaining germ cell layers. In this situation, the term "degeneration/atrophy" might be more appropriate (Figure 17.11). This pattern of change often suggests structural damage to the Sertoli cell, compromising its ability to support the survival of its entire cohort of cells.

Tubular Degeneration/Atrophy, Testis

Tubular degeneration/atrophy is a nonspecific term that can be used to describe any situation where there is a mixture of tubules containing degenerating germ cells, partial loss of germ cells, disorganization of germ cell layers, and tubules lined only by Sertoli cells. It is the most common pattern of change seen in repeat-dose studies with testicular toxicants (Figure 17.11A). If there is diffuse loss of all germ cells, leaving tubules lined only by Sertoli cells, the term "tubular atrophy" might be more appropriate (Figure 17.11C). When the change is diffuse, it is an end-stage lesion that provides no information about likely cause. Occasional atrophic or degenerate tubules (e.g., one to five tubular profiles per section of testis) is a relatively common background finding and represents a focal or segmental loss of germ cells from a part of one or a few seminiferous tubules. Tubules that are depleted of germ cells and lined only by Sertoli cells are often seen adjacent to the rete testis (Figure 17.7). In fact, these are sections through the tubulus rectus which is where the seminiferous tubule empties into the rete testis. These normal structures should not be mistaken for "atrophic tubules."

Tubular Necrosis, Testis

Tubular necrosis differs from tubular degeneration/atrophy in the fact that it involves coagulative necrosis (rather than apoptosis) of the germ cells and generally involves disruption and necrosis of the Sertoli cells lining the tubule (Figure 17.12A). If there is significant disruption of the Sertoli cells, the blood–testis barrier will be breached, resulting in an inflammatory infiltrate around and invading the affected tubule. There are very few other cases where toxicant-induced testicular injury gives rise to an inflammatory response. Tubular necrosis is a relatively uncommon finding and most often occurs in response to ischemic injury. Necrosis of large areas, or of the entire testis (testicular necrosis), can be seen following torsion or infarction of the testis (Figure 17.12B).

Tubular Dilation, Testis

Enlarged testes containing seminiferous tubules with dilated lumens and thinned seminiferous epithelium (Figure 17.13A) can be seen as incidental lesions but can also be chemically induced (see with "Patterns of Change Associated Disturbance of Fluid Production, Resorption or Efferent Duct Obstruction" section). The finding is generally unilateral but can sometimes be bilateral. The change is generally due to efferent duct

obstruction and, with time, will usually progress to total tubular atrophy, generally with dilated lumens (Figure 17.13B).

Tubular Vacuolation

Tubular vacuolation can represent a primary response of the Sertoli cell to toxicant-induced injury (Figure 17.14A and B) or it can be a secondary response due to loss of the space-occupying germ cell (Figure 17.14C). When it is a primary change, it can appear as microvesicular vacuolation in the basal Sertoli cell cytoplasm (Figure 17.14A) or as larger discrete vacuoles part way up the seminiferous epithelium (Figure 17.14B). The primary-response type of vacuole often displaces the germ cells lying adluminal to it.

For the larger primary-response vacuoles, it is usually difficult to identify whether they are intra- or

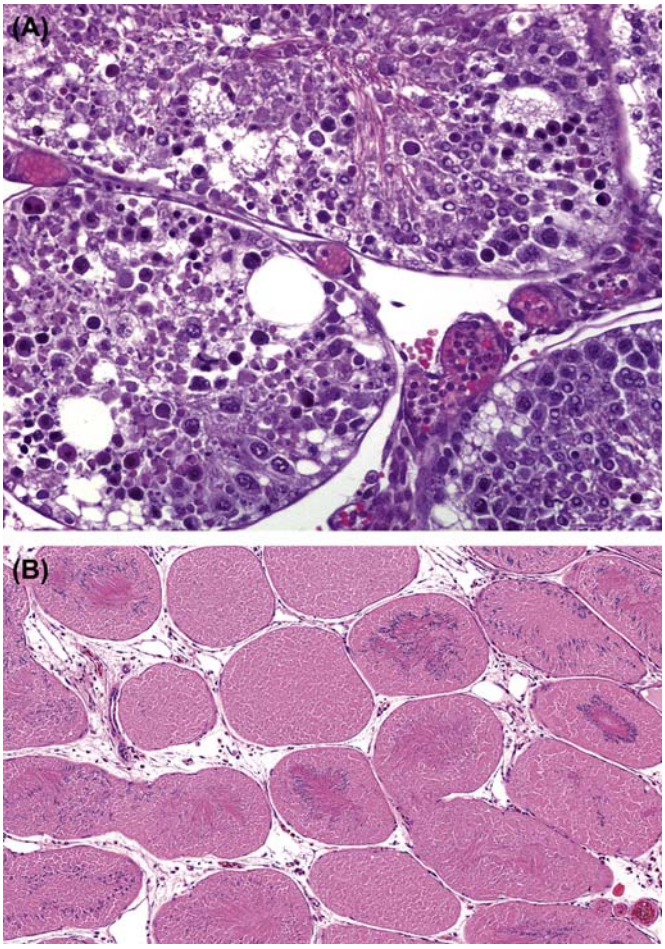

FIGURE 17.12 (A) Tubular necrosis. This is an uncommon change in the testis that is usually caused by anoxia/ischemia. It is characterized by a coagulative necrosis of the germ cells with severe disruption of the organization of the germ cells. Death of the Sertoli cells or disruption of the tight junctions between them, often causes breakdown of the blood–testis barrier leading to stimulation of a neutrophilic inflammatory response. Note the accumulation of neutrophils in the congested interstitial blood vessels. Rat, H&E, ×20. (B) Testicular necrosis. Diffuse coagulative necrosis of all tubular elements caused by ischemia. Rat, H&E, ×4. Source: *Figure reproduced from* Haschek and Rousseaux's Handbook of Toxicologic Pathology *(2013), third ed. (W.M. Haschek, C.G. Rousseaux and M.A. Wallig, eds.), Academic Press (Elsevier), Figure 59.22, p. 254 with permission.*

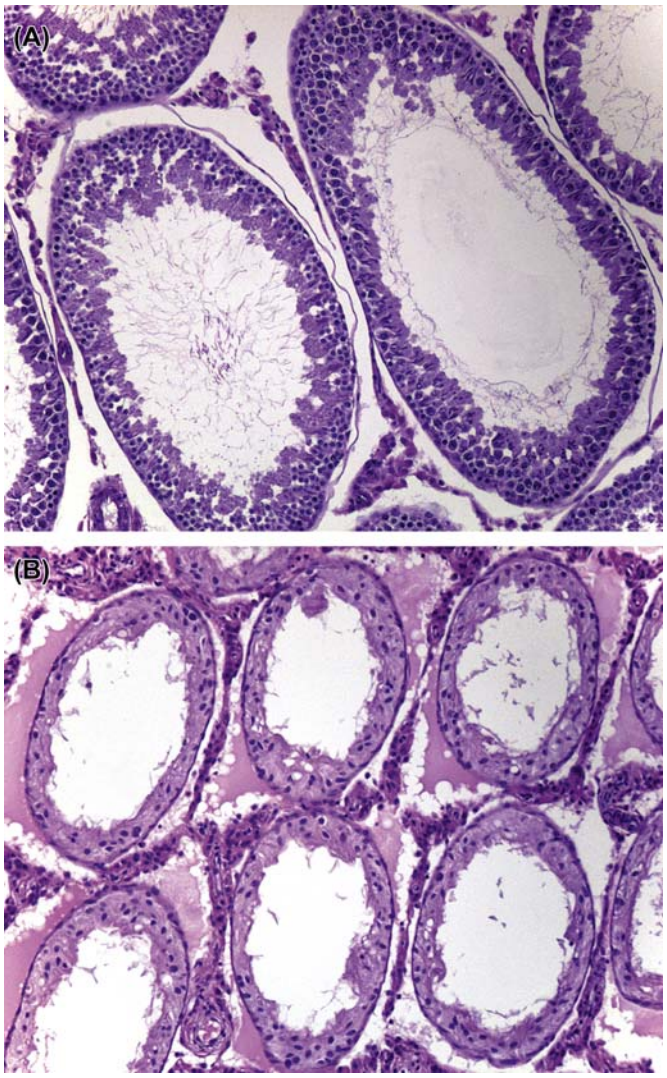

FIGURE 17.13 (A) Tubular dilation. Tubules with dilated lumens caused by increased fluid content. The seminiferous epithelium is thinned, but the normal layers of germ cells are present. The increased fluid content is frequently caused by obstruction of the efferent ducts. Rat, H&E, ×10. (B) Tubular atrophy with dilated tubular lumens. This is frequently the sequel to prolonged tubular dilation and is caused by pressure atrophy from the increased fluid pressure on the epithelium. There is also edema in the interstitial space. (Compare the dilated lumens with the contracted lumens in Figure 17.11C.) Rat, H&E, ×10. Source: *Figure reproduced from* Haschek and Rousseaux's Handbook of Toxicologic Pathology *(2013), third ed. (W.M. Haschek, C.G. Rousseaux and M.A. Wallig, eds.), Academic Press (Elsevier), Figure 59.23, p. 2554 with permission.*

intercellular. When examined, the basal vacuoles have been found to be intracellular and may represent expansion of cytoplasmic organelles (SER), phospholipididosis, or intracellular edema. These are generally an early toxicant-induced change associated with Sertoli cell disturbance and usually progress to tubular degeneration/atrophy with continued dosing. Occasional large vacuoles can be seen in normal testes, but they are generally few in number (Figure 17.14D).

Spermatid Retention

Step 19 mature spermatids should be released from the luminal Sertoli cell cytoplasm during Stage VIII of the spermatogenic cycle. If spermiation fails (which can occur due to disturbances in Sertoli cell processes and reduced testosterone levels or abnormal spermatid development), then step 19 spermatids fail to be released and are still seen at the tubular lumen in stage IX, X, and XI tubules (Figure 17.15A). By the time the tubule reaches stage XII, the spermatid heads have

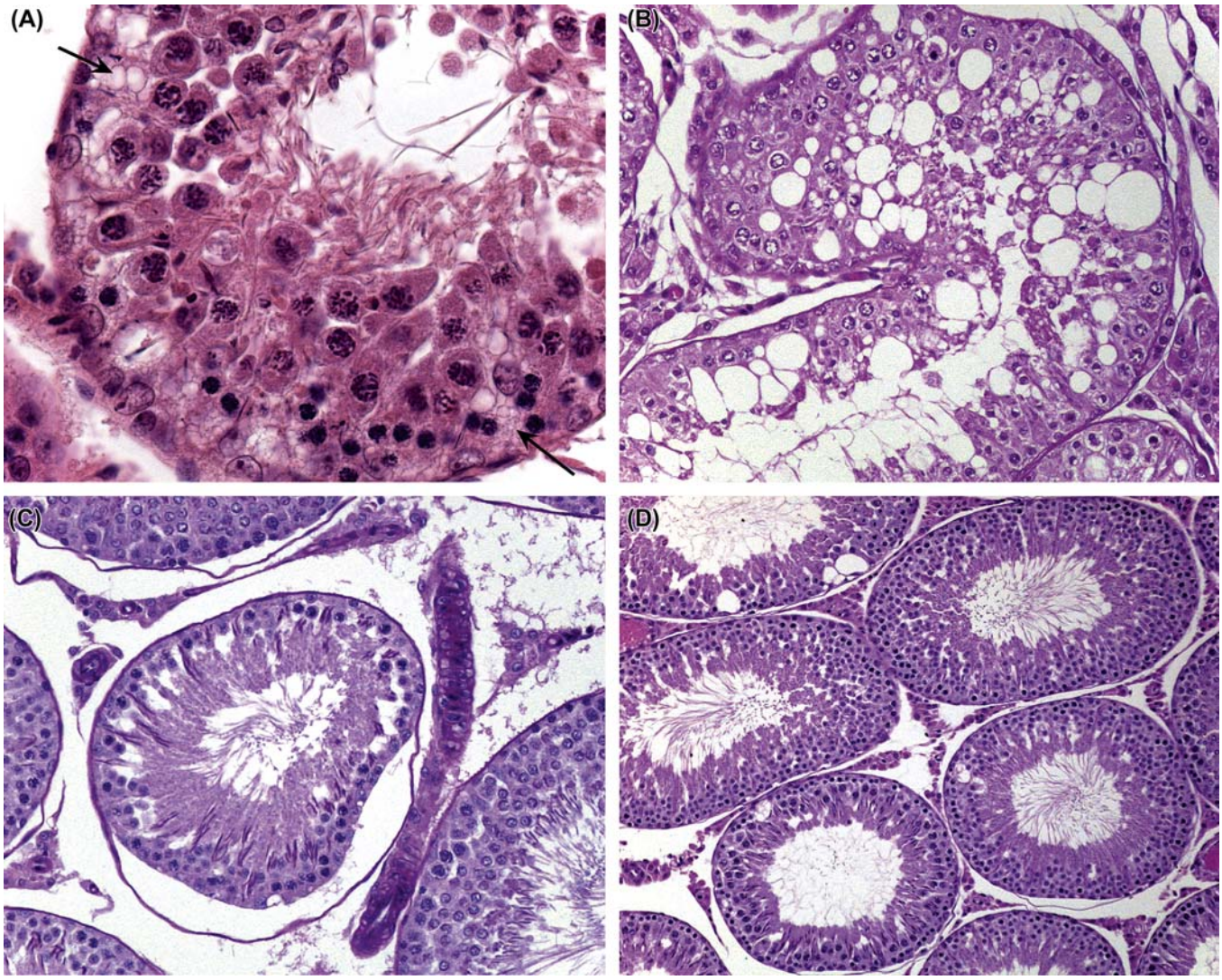

FIGURE 17.14 (A) Tubular vacuolation. Microvacuolation of the basal Sertoli cell cytoplasm (arrowed) with displacement of the overlying germ cells. Note that the cytology of the germ cells appears mostly normal, suggesting that the primary change is in the Sertoli cell. This was caused by a drug that produced phospholipidosis in multiple tissues including the testis (Sertoli cell) and epididymis. Rat, H&E, ×40. (B) Tubular vacuolation in dog testes. The vacuolation is macrovesicular and maybe within or between Sertoli cells. Dog, H&E, ×20. (C) Vacuolation due to loss of space-occupying germ cells. These vacuoles are due to the substantial loss of round spermatids and not a primary degenerative change in the Sertoli cells. Rat, H&E, ×20. (D) Occasional vacuoles in the tubules of normal rat testes is a common background finding, but an increase in the number of these vacuoles can be caused by test article-administration. Rat, H&E, ×10. Source: *Figure reproduced from* Haschek and Rousseaux's Handbook of Toxicologic Pathology *(2013), third ed. (W.M Haschek, C.G. Rousseaux and M.A. Wallig, eds.), Academic Press (Elsevier), Figure 59.24, p. 2555 with permission.*

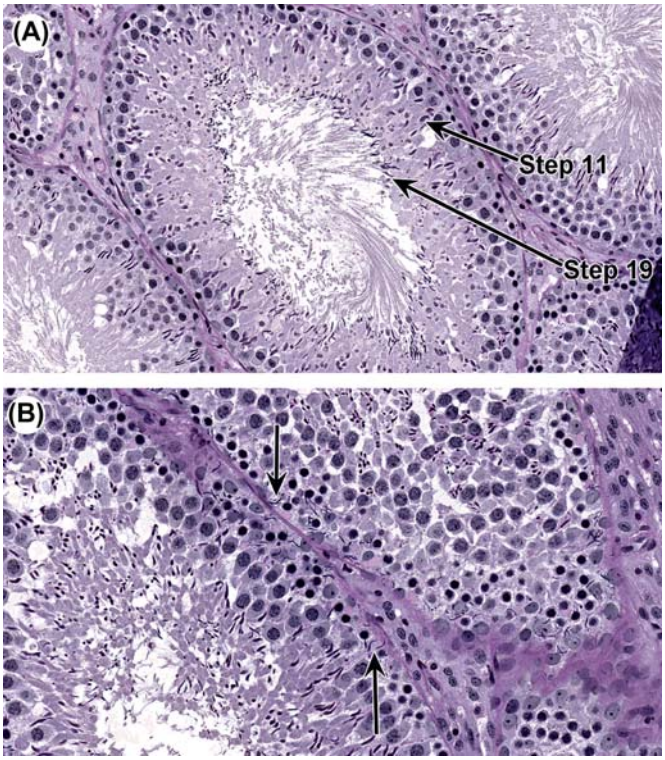

FIGURE 17.15 (A) Spermatid retention occurs when mature step 19 spermatids fail to be released during stage VIII and are retained at the luminal surface or phagocytized by the Sertoli cell and moved to the basal cytoplasm in stage IX–XII tubules. In this stage XI tubule there is a normal layer of step 11 spermatids with an abnormal layer of step 19 spermatids on top. Rat, methacrylate, PAS, ×20. (B) Spermatid retention: the step 19 spermatids have been phagocytized into the basal cytoplasm of these stage XII tubules (arrows). The normal (step 12) spermatids can be seen at the lumen. Rat, methacrylate, PAS, ×20. Source: *Figure reproduced from* Haschek and Rousseaux's Handbook of Toxicologic Pathology *(2013), third ed. (W. M. Haschek, C.G. Rousseaux and M.A. Wallig, eds.), Academic Press (Elsevier), Figure 59.25, p. 2556 with permission.*

generally been pulled down into the basal Sertoli cell cytoplasm where they are phagocytized (Figure 17.15B). By Stage XIII, they have generally disappeared. Therefore, this subtle lesion will only be seen in a relatively small proportion of tubules within an affected testis. Although morphologically subtle, the finding is generally associated with significant changes in sperm parameters (particularly motility and morphology) and potential fertility. If there is significant spermatid retention, testicular spermatid head count should increase while epididymal sperm count decreases.

One *aide memoire* to help in identifying inhibited or delayed spermiation is that in a normal testis there is only a single generation of elongating or elongated spermatids in any tubule. A tubule that has two generations of elongating or elongated spermatids is an adversely affected tubule. A few tubules with mild spermatid retention may also be seen in normal testes.

Leydig Cell Atrophy, Testis

Leydig cells undergo atrophy in response to decreased LH stimulation or as a result of decreased testosterone synthesis (see the "Patterns of Change Associated with Loss of Androgen Support" section). Due to the variability in size of Leydig cells and the effects of fixation on their normal appearance, it can be quite difficult to evaluate size by qualitative examination unless the effect is marked. Image analysis combined with immunohistochemical markers can be used to quantify more subtle alterations in size/volume.

Cell Debris, Intraluminal, Epididymis

The presence of cells and cell debris admixed with sperm in the lumen of the epididymis generally reflects sloughing of germ cells from the testis (Figure 17.16). In the mature rat there are normally very few sloughed cells, making this a very sensitive indicator of spermatogenic disturbance in the testis. Sloughed cells are seen more frequently in the normal mouse and are quite common in the dog. They are also common in peripubertal animals of any species, which reflects the higher background level of germ cell degeneration and exfoliation during the first wave of spermatogenesis. In some cases the sloughed cells seen in peripubertal epididymal lumens also represent

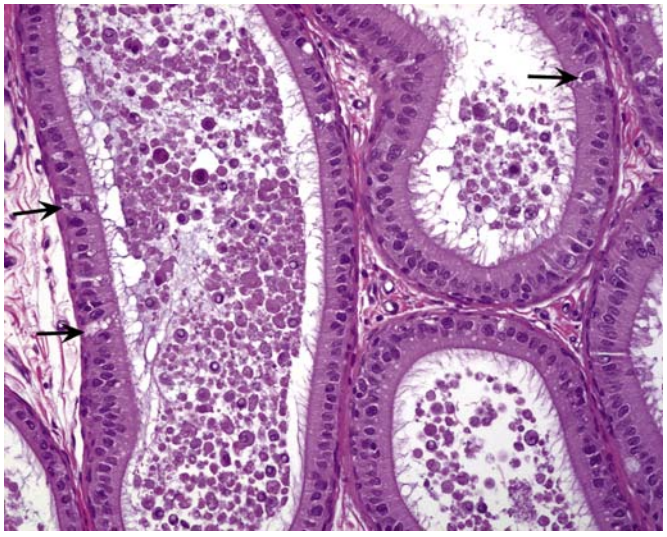

FIGURE 17.16 Intraluminal cell debris/germ cells in the epididymis of a rat. The presence of sloughed germ cells and cell debris in the rat epididymis is a very sensitive indicator of testicular damage. The normal adult rat epididymis contains very few sloughed germ cells. The mouse and dog have a low number as a normal background finding. Increased numbers of clear cells (arrows) often accompany increased debris. Rat, H&E, ×20. Source: *Figure reproduced from* Haschek and Rousseaux's Handbook of Toxicologic Pathology *(2013), third ed. (W.M Haschek, C.G. Rousseaux and M.A. Wallig, eds.), Academic Press (Elsevier), Figure 59.27, p. 2557 with permission.*

exfoliated epididymal cells. Thus, while most round cells in the epididymis of an animal treated with a testis-toxicant are exfoliated germ cells, be aware that in a prepubertal animal these round cells can also be of epididymal origin.

Sperm Granuloma, Epididymis

Sperm are antigenically foreign, due to the genetic exchange between chromosomes that occurred during meiosis. A granuloma is a foreign-body reaction whereby a tissue recruits many immune cells from the blood to surround and wall off foreign bodies with inflammatory cells and fibroblasts. The mechanism of formation of most epididymal granulomas is unknown. The most popular belief is that there is a rupture of the epididymal tubule, and eruption of the sperm from the break into the interstitium, followed by a responsive inflammation which forms a nodule encapsulating the sperm. This is supported by the fact that ligation of the vas deferens in rats invariably results in sperm granulomas developing at sites proximal to the ligation (and also occurs in a high proportion of men undergoing vasectomy). Moreover, the fact that sperm granulomas develop at the vas–cauda junction in rats that have had the sympathetic autonomic nervous supply chemically blocked using guanethidine has been explained on the basis of rupture due to the increasing pressure of sperm build-up in the cauda. Thus, there is some evidence for pressure-induced granuloma formation. However, this seems unlikely to be the only mechanism by which they form.

Consider this alternative explanation. The epididymis is filled with foreign bodies (sperm), which it must nurture and support and store . . . but they *are* foreign. To accommodate this, the epididymis must exist in a dynamic equilibrium between immune tolerance and activation. It would be possible, then, for a treatment to alter the internal biochemistry driving that balance. For example, a treatment that rendered the epididymis more tolerant would show no pathology, but an alteration that activated the epididymis would recruit neutrophils and macrophages from the circulation and would show interstitial inflammation. These recruited cells would eventually damage the interstitium and a tubule. The leakage of some sperm antigens would exacerbate the inflammatory stimulus and progress to ductular damage and granuloma formation. There are emerging data to support this "immune balance" theory, which is presented here primarily to broaden the thinking of those charged with investigating etiology. Although sperm granulomas can be quite large, in most cases there are sperm in the duct distal to the granuloma, which suggests continued flow of sperm down the epididymis. This implies that a granuloma does not necessarily obstruct the flow of sperm through the epididymal duct and therefore may not impact fertility. They can occur anywhere in the epididymis but are most frequently seen in the distal corpus or cauda.

Atrophy: Prostate or Seminal Vesicles

This change is characterized by decreased secretion and reduced size of the epithelial lining of the prostatic acini or seminal vesicular epithelium. It is pathognomonic of decreased androgen stimulation, which can be due to low testosterone, low conversion of testosterone to DHT, or interference with the androgen receptor in the affected tissue. As with Leydig cell atrophy, subtle changes can be difficult to recognize by qualitative morphologic evaluation, and organ weight is usually a much more sensitive endpoint. Atrophy of the accessory sex organs is a common age-related finding.

Morphologic Changes (Proliferative)

With the exception of Leydig cell hyperplasia and Leydig cell tumors, there are very few nonneoplastic or neoplastic proliferative lesions in the testis (For detailed review see Creasy et al., 2012). Leydig cell hyperplasia can occur as a focal or diffuse lesion. Focal Leydig cell hyperplasia and Leydig cell adenomas form a continuum of change, making it difficult to separate hyperplasia and adenoma (Figure 17.17A and B). In the absence of any significant morphological differences in cellular appearance, a size that is equal to or greater than the diameter of three seminiferous tubules is generally used as the main but arbitrary classification criterion in rats. Diffuse Leydig cell hyperplasia is generally a physiological response to hormone imbalance and may accompany severe atrophy of the seminiferous tubules. Diffuse hyperplasia (and tumors) can also be seen in response to estrogen administration in mice. One other relatively frequent proliferative lesion in the mouse is hyperplasia of the rete testis epithelium, which is a common age-related finding that can occasionally progress to adenoma. Although testicular tumors (Sertoli and Leydig cell tumors and, less commonly, seminomas) occur as spontaneous tumors in aging dogs, they are seen only occasionally in laboratory-maintained dogs, where the lifespan is normally restricted.

Reparative hyperplasia of the prostatic epithelium or, less commonly, the seminal vesicle epithelium often accompanies inflammatory lesions associated with urogenital infections in rodents, but tumors in the accessory sex organs are uncommon except in some transgenic mouse strains.

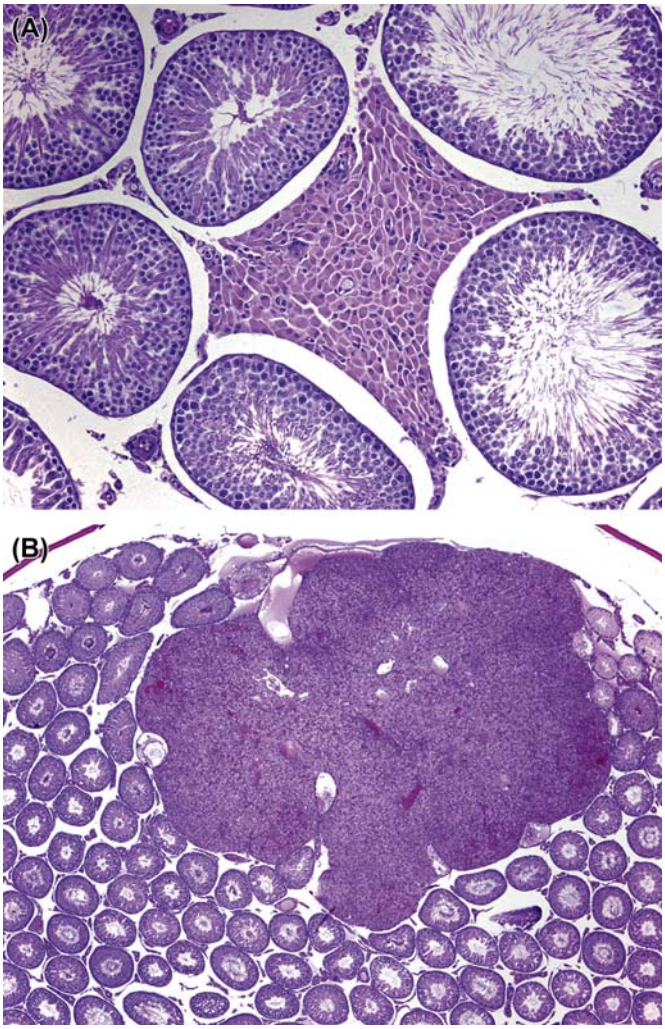

FIGURE 17.17 (A and B) The continuum between Leydig cell hyperplasia and adenoma makes diagnosis difficult. Size is the most common criterion used. Aggregates of Leydig cells less than the diameter of three seminiferous tubules is recommended as a criterion for hyperplasia. (A) This aggregate is on the border of adenoma and hyperplasia. Rat, H&E, ×10. (B) Leydig cell adenoma with growth between tubules. Rat, H&E, ×2. Source: *Figure reproduced from* Haschek and Rousseaux's Handbook of Toxicologic Pathology *(2013), third ed. (W.M. Haschek, C.G. Rousseaux and M.A. Wallig, eds.), Academic Press (Elsevier), Figure 59.28, p. 2559 with permission.*

Proliferative Lesions of the Testis

LEYDIG CELL HYPERPLASIA AND TUMORS

Diffuse Leydig cell hyperplasia can develop in response to decreased spermatogenesis. The Leydig cells are generally increased in size as well as number, but it is important to distinguish real hyperplasia from an apparent increase in Leydig cell volume caused by shrinkage of the atrophic tubules. The spontaneous incidence of Leydig cell tumors in rodents is species- and strain-specific, but they are more common in the rat (up to 100% in aged F344 rats and generally <6% in Sprague Dawley and Wistar rats). In mice the incidence is generally lower (B6C3F1 <1%, CD1 <2%).

Prolonged disruption of the pituitary–gonadal hormone axis in rodents is very likely to result in Leydig cell tumors. In the rat, focal Leydig cell hyperplasia and Leydig cell tumors (Figure 17.17A and B) can be readily induced by a wide range of chemically diverse drugs and chemicals, including dopamine agonists, antiandrogens, LHRH analogs, peroxisome proliferators, and histamine receptor antagonists (Table 17.6). The proposed mechanism of action for these various classes of compounds is through interference with Leydig cell control mechanisms at a variety of points along the hypothalamic–pituitary–testicular axis. A major impetus for Leydig cell tumorigenesis in the rat is considered to be high circulating levels of LH. In human and mouse, persistent elevation in LH is not mitogenic; in the rat, they eventually cause Leydig cell mitosis and then hyperplasia, continuing to adenomas. Interestingly, a significant number of Leydig cell tumorigens have no effect on circulating levels of LH but do alter intratesticular testosterone (and other hormones), thereby affecting the paracrine feedback control of Leydig cell proliferation, presumably through local growth factors. Another interesting fact is that Leydig cell proliferation in the fetal testis occurs in the absence of circulating LH and is thought to be controlled by Sertoli cell factors.

In contrast, the chemical induction of Leydig cell tumors in the mouse is less common and is generally associated with high circulating levels of estrogen or administrations of estrogenic compounds such as diethylstilbestrol. In general, the range of chemicals producing Leydig cell tumors in the rat is ineffective in mice. Furthermore, estrogen administration to the rat appears to be inhibitory to the development of spontaneous and chemically induced Leydig cell tumors, although in at least one case (ammonium perfluorooctonate) the major detectable hormonal change leading to Leydig cell tumors is an increase in plasma estradiol levels. Aromatase inhibitors such as formestane and letrozole reduce plasma estradiol levels by inhibiting the conversion of testosterone to estrogen. In the dog, but not rodents, this results in Leydig cell hypertrophy and hyperplasia. This is thought to be due to the differential sensitivity of the pituitary feedback mechanism to estrogens and androgens in the different species. The aromatization of testosterone plays a significant role in the control of gonadotropins in dogs, nonhuman primates, and man, whereas in rodents, testosterone and DHT are the main regulatory molecules.

The testicular tumor profile and the physiology of Leydig cell tumorigenesis in rodents and humans appear to be very different, and on this basis it has

TABLE 17.6 Chemicals Known to Produce Leydig Cell Hyperplasia and Tumors in Rats

Chemical	Class/action	Putative mechanism of induction
Cimetidine	Histamine receptor antagonism	Androgen receptor antagonism, testosterone biosynthesis inhibition
Flutamide	Antiandrogen	Androgen receptor antagonism
Finasteride	5α-Reductase inhibitor	Decreases androgen feedback
Buserelin/Leuprolide	GnRH agonists	Binds to Leydig cell LHRH receptors
Mesulergine	Dopamine agonists	Decreases prolactin which decreases Leydig cell LH receptor sensitivity
Isradipine	Calcium channel antagonist	Inhibition of testosterone biosynthesis
Gemfibrozil	PPAR-α/hypolipidemic	Decreases prolactin which decreases Leydig cell LH receptor sensitivity
Lansoprazole	Proton pump inhibitor	Inhibition of testosterone biosynthesis
Linuron	Phenylurea herbicide	Androgen receptor antagonism
Procymidone	Systemic plant fungicide	Androgen receptor antagonism

Table reproduced from Handbook of Toxicologic Pathology *(2013), third ed. (W. M. Haschek, C. G. Rousseaux, and M. A. Wallig, eds.), Academic Press, Table 59.8, p. 2561, with permission.*

been argued that chemical induction of Leydig cell tumors in the rat is a species-specific effect with limited relevance for risk assessment to man (reviewed by Cook et al., 1999). Indeed, the antipsychotic dopamine agonists which produce Leydig cell tumors in rats by lowering prolactin levels, are taken by many for treatment of schizophrenia and there has been no observable increase in Leydig cell tumors, an otherwise extraordinarily rare tumor in humans. Similarly, the widely prescribed H2 histamine antagonist cimetidine which also produces Leydig cell tumors in rats through its antiandrogenic properties, also has shown no evidence of Leydig cell tumorigenesis in man. Nevertheless, claims of irrelevance need to be supported by careful investigations into the mechanism of hormonal disruption.

Proliferative Lesions of the Epididymis

Proliferative lesions of the epididymis are almost nonexistent. The epididymal epithelium does not respond with a true hyperplastic response. Cribriform change, where the epithelium folds in on itself and forms pseudoglandular structures, is sometimes considered a hyperplastic lesion, but because it is generally associated with collapse of the ductal lumen it is difficult to distinguish from epithelial folding. The only primary tumors that have been described in the epididymis are Leydig cell adenomas and histiocytic sarcomas; both occur in the mouse, but they are rare. Since Leydig cells are not normally found in the epididymis, the occurrence of Leydig cell adenomas is unexplained, but there are a number of reports describing these tumors in mice. The epididymis can also be a primary site for the development of histiocytic sarcoma in mice.

Proliferative Lesions of the Accessory Sex Organs

In contrast to man, where hyperplasia and neoplasia of the prostate are extremely common, spontaneous neoplasia of the prostate in other species is rare. Reactive (reparative) hyperplasia of the prostatic epithelium commonly accompanies inflammatory lesions resulting from urogenital infections. This is particularly common in mice and generally located in the dorsolateral lobes of the prostate. In more severe urogenital infections, the seminal vesicle epithelium may also respond. Hyperplasia of the accessory sex glands is not often seen as a response to inflammation in the dog or the monkey.

Focal hyperplasia in the absence of inflammation is most commonly seen in the ventral prostate of rats and mice. The diagnosis of hyperplasia in the rodent prostate is mainly based on the occurrence of multilayered normal epithelium in a few adjacent acini of otherwise normal glands without architectural disturbance. There appears to be a morphologic continuum between focal hyperplasia and benign adenoma of the prostate, and the distinction between the two is not always clear. Adenomas and adenocarcinomas of the ventral prostate and seminal vesicles are occasionally seen as a background finding in rodents, more commonly in some of the transgenic mouse strains. Dorsolateral prostatic adenomas appear to be rare as spontaneous lesions but have been chemically induced. Experimental models of prostate carcinogenesis have been developed in the rat using *N*-nitrosobis (2-hydroxypropyl)amine, *N*-methylnitrosourea, and 3,2′-dimethyl-4-aminobiphenyl. Invasive carcinomas of prostate and seminal vesicles can be induced when these carcinogens are coadministered with high doses of testosterone. Prostate carcinoma has also been induced by testosterone administration to a strain

of rat (Noble rat) that has a genetic susceptibility to prostate cancer. Transgenic mouse models such as Transgenic Adenocarcinoma of Mouse Prostate have also been developed to study human prostate cancer.

Recovery and Reversibility of Injury

The reversibility of infertility is a very important consideration for risk assessment in male reproductive toxicology, and the potential for complete recovery is largely dependent on the site and the severity of the toxic insult. This puts additional importance on identifying the primary cell of toxicity and the pathogenesis of the lesion.

Following germ cell-specific damage or depletion (in the absence of significant Sertoli cell damage), the chances of regeneration of the entire germ cell population and recovery of functional spermatogenesis are good. Although many of the germ cell types are sensitive to physical and chemical disturbances, the renewing stem cell spermatogonial population is relatively resistant. This has been well illustrated using varying doses of radiation. The order of cell sensitivity to increasing doses of radiation shows that although the generations of differentiating spermatogonia are very sensitive to radiation, primitive stem cell spermatogonia require a much larger dose to cause death.

When choosing the duration of a recovery period, it is usually advisable to make it equal to the timing of the spermatogenic process for the test species (e.g., 8 weeks for the rat and dog, 5 weeks for the mouse, and 6 weeks for the cynomolgus monkey). However, if most of the spermatogonia have been affected it may be necessary to extend this to two or even three times the duration of spermatogenesis to allow sufficient time for the slowly dividing stem cell population to repeatedly cycle and replenish the differentiating spermatogonial population to allow recovery of the rest of spermatogenesis. When short-duration recovery periods (e.g., 2–4 weeks) are employed in studies where there has been germ cell-specific toxicity (particularly in studies of $\leq$28 days of dosing), it is quite common for the degree of germ cell depletion to appear more severe at the end of the recovery period than at the end of the dosing period. This can easily be misinterpreted as progression or irreversibility of the lesion, but this would be an incorrect conclusion. It is entirely predictable due to the progression of maturation depletion through the later (and more numerous) round and elongating spermatid population, which cannot be replenished until sufficient recovery time has elapsed to allow the spermatogonia and/or spermatocytes to replace them (see "Patterns of Change Associated with Germ Cell-Specific Toxicity" section). For example, if spermatogonia are the target cell in a 14-day study, the only cells that will be missing at the end of the dosing period will be spermatogonia and early spermatocytes. This will be detectable but will be a relatively subtle lesion (Figure 17.9C and D). If the animals complete a 4-week recovery period, that "hole" of missing cells will consist of absent spermatocytes and round spermatids as a result of "maturation depletion" caused by the loss of their precursor cells (Figure 17.10A–C). Although spermatogonia and early spermatocytes will probably have recovered, the overall severity of the germ cell depletion will appear greater and the weight and size of the testes will appear much less at the end of recovery than at the end of dosing. However, if the recovery period is extended to 8 weeks, full recovery will likely be witnessed, or, at least, significant evidence of recovery seen.

If the Sertoli cell is injured and the damage is mild, then full recovery may be possible. If Sertoli cells are destroyed or, as more often happens, permanently functionally compromised, regeneration is not possible because these cells are unable to replenish themselves in the adult. However, they are remarkably resistant to cell death and are often found as the only remaining cell type in the seminiferous epithelium when all germ cells have been lost. Toxicant-induced atrophy frequently manifests as an end-stage lesion where the only cells in the tubules are the Sertoli cells and the stem cell spermatogonia. For example, in the case of 2,5-hexanedione toxicity, where the Sertoli cell is believed to be the primary cell affected, the end-stage lesion comprises tubules that contain Sertoli cells and dividing spermatogonia, yet spermatogenesis never recovers. Investigations have suggested that this is due to the lack of a Sertoli cell-derived growth factor called SCF, which binds the c-kit receptor on spermatogonia. Reestablishment of SCF and reversibility of the lesion can be accomplished by administration of exogenous SCF or stimulation of endogenous SCF by treatment with the GnRH agonist, leuprolide.

Most effects of androgen deficiency, including spermatogenic disruption and atrophy of the epididymis and accessory sex organs, are also readily reversible with the reestablishment of normal hormone balance. An obvious exception to this is the Leydig cell tumor, which, once established, is androgen-independent and irreversible. Effects on the epididymis that result in granulomatous inflammation and sperm granulomas are generally progressive and irreversible. The presence of persistent inflammation in close proximity to viable sperm runs the additional risk of leukotriene-induced genotoxic damage to the sperm, as seen with methyl chloride.

TABLE 17.7 Age of Sexual Maturation Versus Typical Age of Animal Used in Toxicity Studies

Species	Typical starting age for routine studies	Age of sexual maturation
Rat	Soon after weaning (6–7 weeks after acclimation)	9–10 weeks
Mouse	Soon after weaning (6–7 weeks after acclimation)	7–8 weeks
Dog	4–6 months	7–12 months
Minipig	3–4 months	3–4 months
Cynomolgus monkey	Young adults (often 2–3 years)	4.5–5.5 years

Table reproduced from Handbook of Toxicologic Pathology *(2013), third ed. (W. M. Haschek, C. G. Rousseaux, and M. A. Wallig, eds.), Academic Press, Table 59.11, p. 2565, with permission.*

Immaturity and Peripuberty as Confounding Factors for Identifying Toxicity

Regardless of mechanism, the most obvious feature of testicular toxicity is death and depletion of germ cells. If an animal is immature and at a stage where spermatogenesis has not started or has only barely started (5- to 6-month-old dogs or 3- to 4-year-old cynomolgus monkeys), then testicular toxicity, however severe, will go undetected. If spermatogenesis is progressing but the animal has not reached puberty or is on the cusp of puberty (7- to 8-month-old dogs and 3.5- to 4.5-year-old cynomolgus monkeys), then the testes will likely contain significant numbers of degenerating germ cells and have partially depleted seminiferous tubules which will be indistinguishable from a degenerative response to a testicular toxicant. This presents a real risk of producing a false positive result if a greater proportion of the peripubertal animals are in the high-dose group. Table 17.7 provides a summary of the approximate age that animals attain sexual maturity compared with the age of animal commonly used in routine regulatory studies.

Rodents

Rats are able to sire a litter from around 8 weeks of age, but the testes do not appear morphologically "normal" until around 10 weeks of age. Rats aged 8–9 weeks often have low numbers of elongating spermatids in the testes with occasional evidence of degenerating cells. In addition, the epididymis contains increased numbers of degenerating germ cells and has relatively few sperm in the cauda epididymis. These features can be mistaken as evidence of testicular toxicity and reduced spermatogenesis if, by chance, there is a higher incidence in the high-dose group. A similar situation exists in 5- to 6-week-old mice. To overcome this problem, rats should be at least 10 weeks of age by the end of the study and mice should be at least 8 weeks old.

Dogs

The use of immature and peripubertal dogs represents the most common cause of confusion to pathologists when evaluating testicular toxicity. Dogs vary in the age they reach sexual maturity; at 7 months of age one dog may have testes that appear fully mature with expanded epididymal ducts filled with sperm, while other dogs of the same age have testes with partially depleted seminiferous tubules and frequent degenerating germ cells, and epididymides that have contracted ducts containing large numbers of sloughed degenerate germ cells and no sperm (Figures 17.18 and 17.19). Spermatogonial proliferation and fluid secretion begins at around 5–6 months in the dog. This results in gradual lumen formation and progressive expansion of the tubules as secretion increases. In dogs of this age, it is common to see tubular (Sertoli cell) vacuoles accompanying the start of lumen formation. These are likely fluid-filled vacuoles related to the initiation of fluid production by the Sertoli cell and should not be considered abnormal (Figure 17.18B and C).

Most dogs have normal appearing testes with significant sperm content in the cauda epididymis by 10 months of age, but the efficiency of spermatogenesis and the size of the testes will continue to increase until the animals are 12–18 months of age. With this degree of variability, small group sizes, and the fact that maturing and peripubertal testes are indistinguishable from testes undergoing toxicant induced degeneration, there is a risk that immaturity will mask a toxicant induced lesion or that immaturity will be mistaken for testicular toxicity. At the very least, it will add an additional layer of complexity to the evaluation of a tissue that is already difficult to evaluate.

The variation in age of maturation is reflected by dramatic differences in testicular weight and testicular size from animals that are the same age and same body weight. Prostatic development cannot be used as an indicator of sexual maturity because this tissue often develops at a different rate from the testis, presumably due to differential development/expression of androgen receptors between the two organs. It should also be borne in mind that size of dog and age of sexual maturation vary with the source (supplier) of the dogs.

The best way to avoid confusion and avoid the possibility of missing an important toxicant induced lesion is to use dogs that are *at least* 10 months of age by study termination. If there is a suspicion that the test article may affect spermatogenesis, it would be prudent to ensure the animals are 12 months of age at

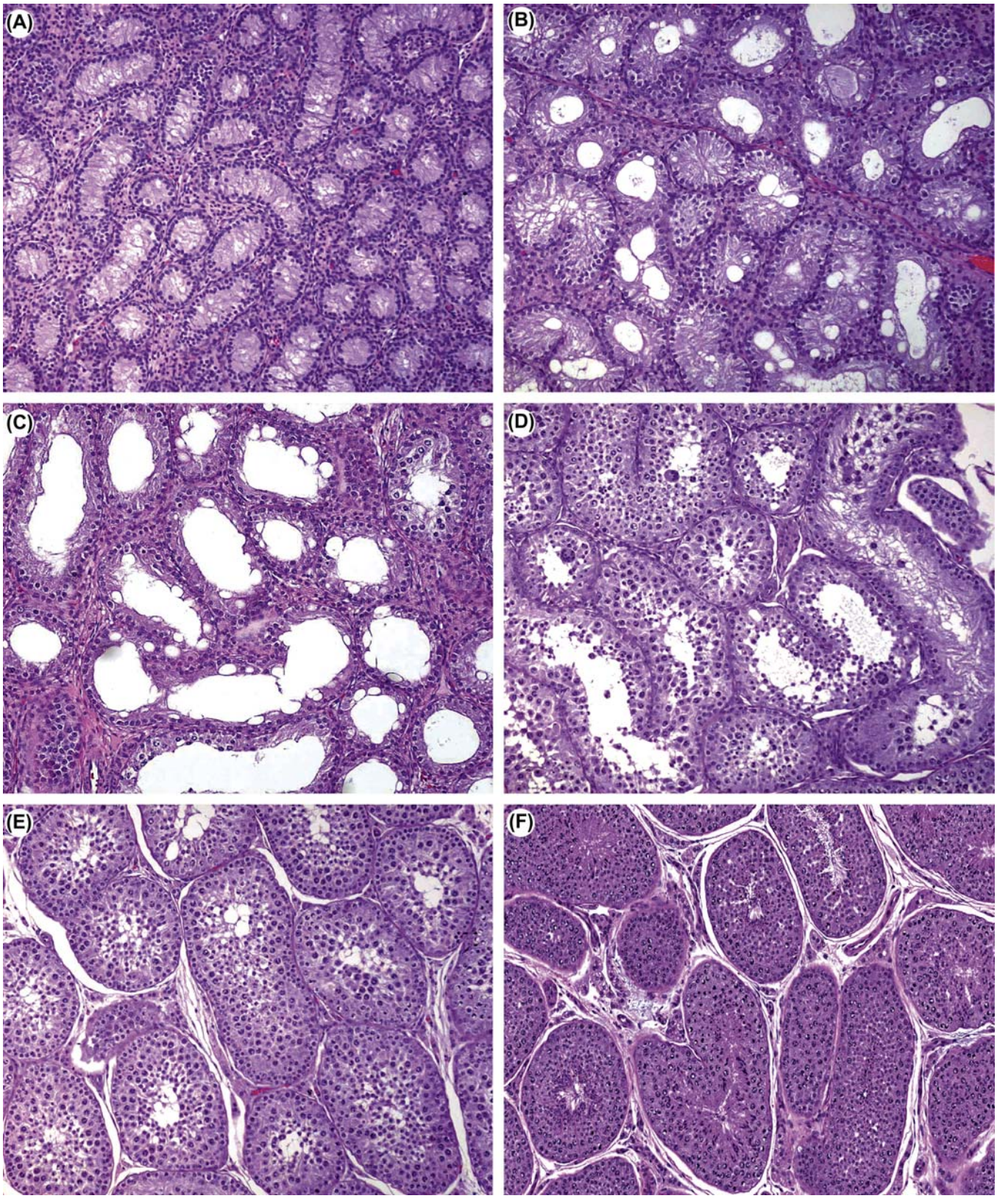

FIGURE 17.18 (A) Immature testis from a 5- to 6-month-old dog. Tubules are contracted with no lumen and lined by Sertoli cells and spermatogonia. Dog, H&E, ×10. (B) Immature testis from a 5- to 6-month-old dog that has just started fluid secretion. Fluid filled vacuoles are present in the epithelium and a lumen is beginning to develop. Dog, H&E, ×10. (C) Immature testis from a 6- to 7-month-old dog. The lumen has started to expand and spermatogonial proliferation is beginning with occasional spermatocytes formed. Dog, H&E, ×10. (D) Immature testis from a 7- to 8-month-old dog. Spermatogenesis is proceeding at different rates in different tubules, and there are

termination to guarantee sexual maturity. The same rule should be applied to any juvenile study that is conducted in the dog. Dosing should be continued until the dogs are at least 10 months of age to avoid misinterpretation of changes in the developing testis.

Cynomolgus Monkeys

The majority of studies undertaken in cynomolgus monkeys utilize animals that are immature or are a mixture of immature, peripubertal, and mature. As with dogs, the animals mature over a relatively wide age range. There are numerous references regarding the age and body weight of male cynomolgus monkeys in relation to attainment of sexual maturity, and most put the minimum age at around 4.5–5 years and a body weight of approximately 5 kg. In studies where sexually mature monkeys are needed, minimal criteria should be based on age and body weight. Even then, additional measurements and endpoints, such as sperm evaluation, testicular volume, and testosterone measurements, are generally needed to gain a high degree of confidence that the animals are sexually mature. Due to the size, cost, and limited supply of mature cynomolgus monkeys, it is not practical to use them for routine regulatory toxicity studies. Accepting that, it should be borne in mind that studies conducted with immature or mixed maturity status animals will not be able to detect testicular toxicants.

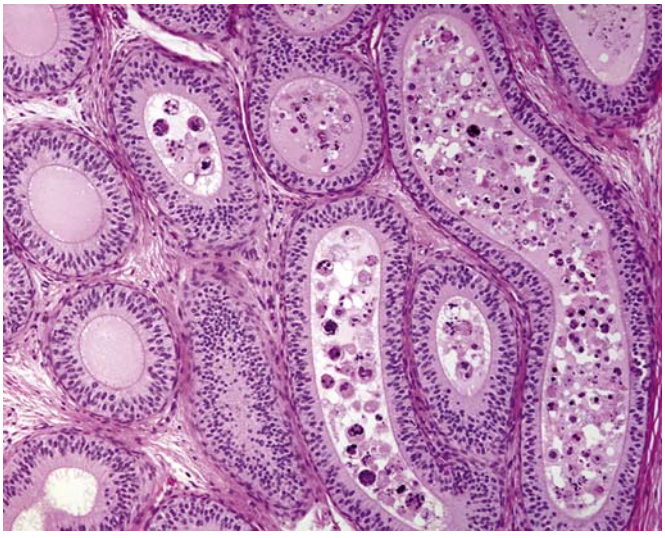

FIGURE 17.19 Epididymis from a 6- to 7-month-old dog with intra luminal cell debris/sloughed germ cells but no sperm. Dog, H&E, ×10. Source: *Figure reproduced from* Haschek and Rousseaux's Handbook of Toxicologic Pathology *(2013), third ed. (W.M. Haschek, C.G. Rousseaux and M.A. Wallig, eds.), Academic Press (Elsevier), Figure 59.32, p. 2567 with permission.*

Minipigs

Use of the Göttingen minipig as a preclinical species is becoming more common. Boars become sexually mature at 3–4 months of age with a body weight of 7–9 kg. A characteristic feature of pig testes is the large size and volume of Leydig cells in the interstitial compartment. This increases with age and can be quite variable in peripubertal animals (3–4 months of age) such that the more mature animals can appear to have Leydig cell "hyperplasia" when compared with the less mature animals. Similarly, the regularity and efficiency of spermatogenesis will continue increasing with age, and there maybe variability in pigs that have recently attained maturity.

Background Pathology as a Confounding Factor for Identifying Reproductive Toxicity

In addition to immaturity, background pathology can cause significant problems for detecting toxicity, particularly in the dog. This is rarely a problem when examining rodents, because they have relatively few background lesions and group sizes are large enough to be able to distinguish between test article-related changes and background changes.

Rodents

Spermatogenesis is very efficient and consistently normal between animals. Even though there may be an occasional animal that shows degenerative testicular changes, the incidence is low and the group sizes large enough that distinguishing them from test article-induced changes is generally not a problem. Unilateral or bilateral severe, diffuse tubular degeneration/atrophy is occasionally seen as a background finding in young adult rats and mice. When unilateral, the finding is likely associated with obstruction of the efferent ducts. The incidence is generally low, and should not amount to more than 1 or 2 rats in any one study of 40 males. If the number is significantly more than this, a relationship to the test article should be considered.

◀ numerous apoptotic and multinucleate germ cells in this first wave of spermatogenesis. Dog, H&E, ×10. (E) Immature testis from a 7- to 9-month-old dog. Spermatogenesis has proceeded to produce round spermatids, but there are no elongating spermatids. Dog, H&E, ×10. (F) Mature testis from 10- to 12-month-old dog. The tubules are fully expanded with all germ cell types present and a full complement of mature spermatids. Dog, H&E, ×10. Source: *Figure reproduced from* Haschek and Rousseaux's Handbook of Toxicologic Pathology *(2013), third ed. (W. M. Haschek, C.G. Rousseaux and M.A. Wallig, eds.), Academic Press (Elsevier), Figure 59.31, p. 2566 with permission.*

Dogs

Background pathology in dogs presents much more of a problem. Spermatogenesis in the Beagle dog is relatively inefficient, and it is very common to see tubules with partial depletion of one or more generations of germ cells (hypospermatogenesis) or focal areas of undeveloped tubules (hypoplasia). Almost all dogs will have scattered degenerating (multinucleate) germ cells and abnormal appearing, swollen spermatocytes (Figure 17.20). The incidence and severity of these lesions seem to vary with the cohort of dogs, suggesting a possible genetic component, but the high incidence of the findings combined with small group sizes make these changes problematic for distinguishing them from testicular toxicity (reviewed by Rehm, 2000).

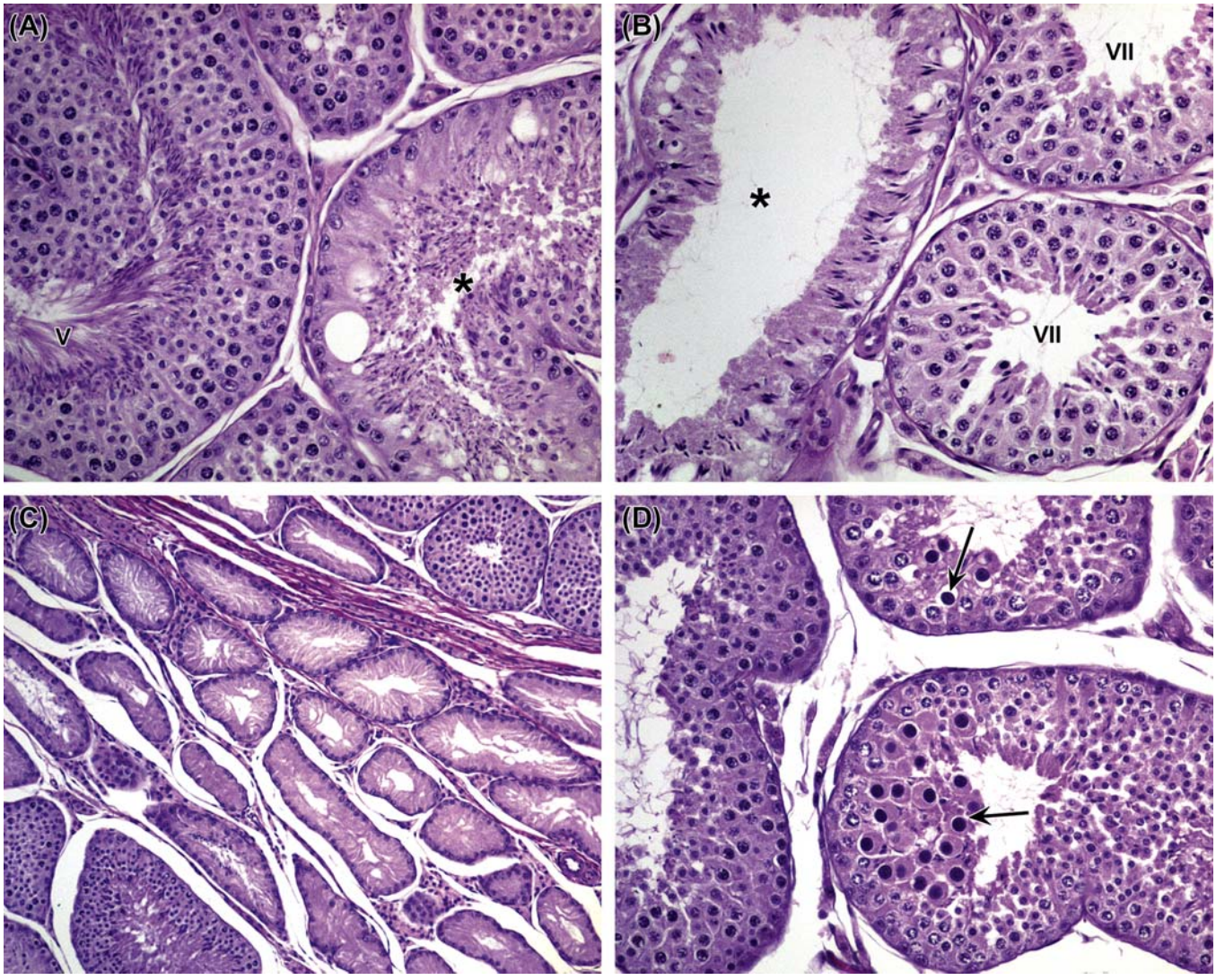

FIGURE 17.20 (A and B) Segmental hypospermatogenesis in dog testes is characterized by the partial depletion of one or more layers of germ cells with no accompanying germ cell degeneration. (A) The depleted tubule (*) is in the same stage as the adjacent tubule (stage V). Although it still has its normal luminal layer of elongating spermatids, it is missing the underlying round spermatids, pachytene spermatocytes, and preleptotene spermatocytes. (B) The depleted tubule (*) is in the same stage as the adjacent tubule (stage VII). It has its normal layer of luminal elongating spermatids but is missing the underlying layers of pachytene spermatocytes and zygotene spermatocytes. Dog, H&E, ×20. (C) Segmental tubular hypoplasia in the dog testis. This is a common background finding in dog testes and typically forms a wedge shape of contracted tubules lined only by Sertoli cells and surrounded by otherwise normal tubules. The affected tubules appear to have never supported spermatogenesis, thus, the term tubular hypoplasia. Dog, H&E, ×10. (D) Swollen spermatocytes (arrows) are a common background finding in dog testes. They are generally larger in size and have densely staining nuclei with a tightly packed chromatin pattern. They appear to be secondary spermatocytes that did not complete their second meiotic division during stage VIII but survived into later stages. Dog, H&E, ×20. Source: *Figure reproduced from* Haschek and Rousseaux's Handbook of Toxicologic Pathology *(2013), third ed. (W.M. Haschek, C.G. Rousseaux and M.A. Wallig, eds.), Academic Press (Elsevier), Figure 59.33, p. 2570 with permission.*

The typical characteristics of segmental hypospermatogenesis in the dog are the absence of one or more generations of germ cells (e.g., pachytene spermatocytes and round spermatids) combined with the presence of earlier (spermatogonia) and later (elongating spermatids) germ cells in the tubule. Characteristically, there are very few actively degenerating germ cells associated with this lesion, and the pattern suggests failure of the spermatogonial division over two to three cycles in this part of the tubule. This is effectively "maturation depletion" as seen with spermatogonial toxicants, but tubules are affected in a segmental and patchy distribution rather than a diffuse manner. Another finding that seems largely unique to the dog is focal or segmental hypoplasia. The characteristics of this lesion are contracted tubules lined only by Sertoli cells, with the appearance of never having supported germ cells. This is different from atrophic tubules, which are usually lined by Sertoli cells with disorganized and vacuolated cytoplasm and evidence of residual germ cells or debris. Hypoplastic tubules generally form a wedge-shaped area which is often subcapsular. Segmental hypospermatogenesis and hypoplasia are specific diagnostic terms that have been defined and described in detail in the literature (see Suggested Reading). It is important to use the same terminology and diagnostic criteria for these lesions when seen in dog toxicity studies, so that the cited literature can be used to support any conclusion relating to their relationship to test article-administration. A final cautionary note is that hypospermatogenesis can also be caused or exacerbated by test article-exposure; thus, if the incidence and/or severity of this common background finding appears to be dose-related, a relationship to treatment should be considered.

The difference between immaturity, hypospermatogenesis, and tubular degeneration/atrophy is subtle, but it is extremely important for the interpretation of a study and for distinguishing test article-related testicular toxicity from either background degenerative changes or prepubertal degenerative changes. Table 17.8 lists the main features and a recommended approach for addressing this issue.

Distinguishing testicular toxicity from background pathology and immaturity is difficult and ultimately comes down to a weight-of-evidence approach. This is where having multiple measures of the same thing can be most helpful (organ weights, sperm measures, and histology). Since hypospermatogenesis can be exacerbated by chemical exposure, an important part of that evidence is the background incidence and severity of hypospermatogenesis in the laboratory conducting the study. This calls for consistent grading and recording of the main background changes so that the historical control database is an accurate reflection of these changes.

Cynomolgus Monkeys

Relatively few studies employ mature cynomolgus monkeys, so there is comparatively little information on background lesions. Compared with the dog, there appear to be relatively few background degenerative changes and spermatogenesis appears more regular and efficient in this species. Focal tubular dilation with thinning of the seminiferous epithelium is quite commonly seen, especially in peripubertal animals. In addition, animals with focal areas of atrophic and vacuolated tubules are sometimes seen. A lesion that has become prevalent in the testes of cynomolgus monkeys in recent years is a congenital/developmental abnormality whereby varying proportions of the seminiferous tubules are replaced by dense collagen (Figure 17.21). This can be seen in immature and mature monkeys.

TABLE 17.8 Distinguishing Immaturity from Testicular Toxicity in Dogs and Primates

Maturity status	Epididymal caudal duct expansion	Epididymal sperm content	Testis: presence of degenerate/ multinucleate germ cells
Immature; normal	Contracted	None	None
Prepubertal; normal	Contracted	None	Few—frequent
Peripubertal; normal	Partial expansion	Few in corpus, none in cauda	Frequent
Mature; normal	Expanded	Plenty in distal corpus and cauda	Infrequent
Mature with testicular degeneration	Expanded	Some in distal corpus and cauda	Increased—frequent
Mature with hypospermatogenesis	Expanded	Usually normal but maybe low in severe hypospermatogenesis	Infrequent

Table reproduced from Handbook of Toxicologic Pathology *(2013), third ed. (W. M. Haschek, C. G. Rousseaux, and M. A. Wallig, eds.), Academic Press, Table 59.12, p. 2568, with permission.*

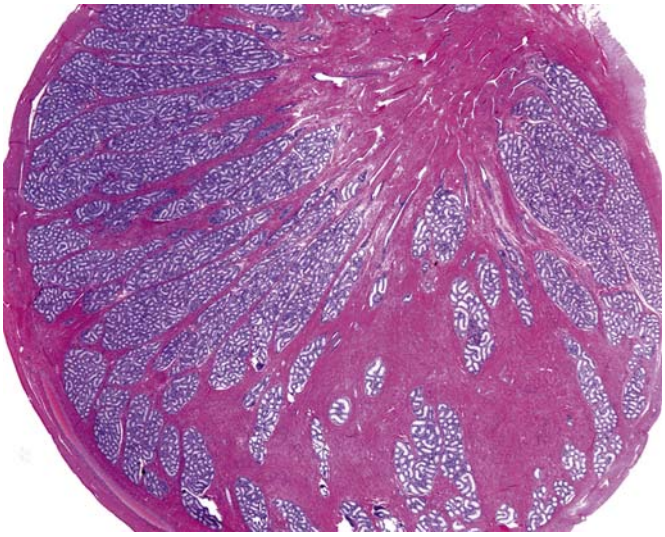

FIGURE 17.21 Fibrotic hypoplasia of an immature cynomolgus monkey testis. This appears to be a congenital condition where there is a reduction in the number of seminiferous tubules and an increase in the amount of dense collagen. This is particularly prominent around the rete. Monkey, H&E. Source: *Figure reproduced from* Haschek and Rousseaux's Handbook of Toxicologic Pathology *(2013), third ed. (W.M. Haschek, C.G. Rousseaux and M.A. Wallig, eds.), Academic Press (Elsevier), Figure 59.34, p. 2571 with permission.*

Minipigs

Tubular hypoplasia or tubular atrophy is a very common background change in adult minipig testes. It occurs in approximately 25% of untreated pigs. The affected tubules are generally contracted, devoid of germ cells, and lined only by Sertoli cells. In some cases they may contain a layer of spermatogonia and early spermatocytes, and in other cases there may be a patchy and partial depletion of germ cells. In most cases (approximately 60% of affected animals) the number of tubules affected is small (minimal severity) and the affected tubules are scattered throughout the testis, but in some cases a large proportion or the majority of tubules are affected. In these more severe cases, there is a reduction or absence of sperm in the epididymis. The change is generally bilateral and often associated with an apparent increase in the number of Leydig cells surrounding the affected tubules. If the incidence or severity appears to show a dose relationship it makes it very difficult to distinguish this common atrophic lesion from a test article-related effect. One criterion that maybe useful is whether the atrophic tubules are accompanied by a significant number of actively degenerating germ cells. Active germ cell degeneration is often a good indicator of ongoing toxicity and is less commonly associated with a long-standing background lesion. One final consideration when evaluating pig testes is the variable volume of the Leydig cell population. Since pigs are generally examined at an age where they have only just attained sexual maturity, the size of the Leydig cell compartment and the efficiency of spermatogenesis can vary significantly between different individuals. Differences should not necessarily be interpreted as test article-related findings.

Stress and Body Weight Loss as a Confounding Factor for Identifying Reproductive Toxicity

Reproductive success is tied to food availability, adequate metabolic reserves, and suitable environmental conditions. In general, activation of the hypothalamic–pituitary–adrenal axis by stress results in suppression of the HPG axis. Many of the neurotransmitters involved in energy homeostasis, such as leptin, ghrelin, cholecystokinin, and vasoactive intestinal peptide, as well as mediators of the stress response, such as corticotropin-releasing hormone, arginine-vasopressin, glucocorticoids, and β endorphins, are also major regulators of the GnRH neurons in the hypothalamus and will decrease reproductive capability in times of low food availability and/or stress (reviewed by Everds et al., 2013). In nonclinical studies, decreased food intake, decreased body weight, and nonspecific stress are common consequences of dosing animals near the maximum tolerated dose, and therefore effects on reproductive parameters are relatively common.

GnRH suppression will result in reduced testosterone secretion from the Leydig cells and reduced plasma testosterone levels, and this largely dictates the morphological changes seen in the reproductive tissues. In rodents, the most sensitive endpoint is a decrease in the weight of the accessory sex organs (prostate and seminal vesicles). Epididymal weight may also be decreased, but testis weight is generally unaffected except in mice. There are generally no detectable histopathological changes in any of the tissues. Exceptions include minimal tubular degeneration in the testes of mice and focal tubular degeneration in the testes of rats subjected to repeated immobilization in restraint tubes.

Dogs and monkeys are generally less susceptible to the effects of stress and body weight decrease, and few changes are seen. An exception to this is the effect of social stress on cynomolgus monkeys, particularly relating to hierarchical status. It is becoming common practice to house monkeys in social groupings during nonclinical safety assessment studies, but introduction of individuals to one another naturally leads to a ranking of dominant and subordinate individuals. High-ranking males will be those animals with the highest body weight, and they will also maintain the highest testosterone levels, while the low-weight monkeys will

generally be the subordinate animals and will have low testosterone levels. Reductions in testicular size of up to 45% from baseline in subordinate males have been observed follow introduction to social groupings.

MECHANISMS OF TOXICITY

Molecular and Biochemical

There have been numerous in-depth discussions of mechanisms of specific toxicants in recent years (see Boekelheide et al., 2005), so rather than duplicating these in detail a relatively high-level overview of some selected compounds will be provided, followed by a view of the emerging involvement of oxidative stress or damage in the male reproductive system. First, though, a frequently used mechanistic concept of "the target cell" will be considered.

Reporter Cell versus Target Cell

In the early 1980s, the term "target cell" was frequently used to indicate the cell type that showed the first visible changes during the development of a lesion in the testis (Table 17.9). This was done with the tacit understanding that there would be preceding biochemical changes which would be invisible to the pathologist, and these could be in any of the cells in the testis, not necessarily only in the first to be visibly affected. This subtlety is easily overlooked, and can lead to misguided investigational approaches and narrow interpretations regarding the nature of the

TABLE 17.9 Site/Cell-Specific Changes Associated with Male Reproductive Toxicants

Reporter/target cell	Toxicant	Effect
Leydig cell	Ethane dimethane sulfonate	Leydig cell necrosis with secondary germ cell death and depletion and atrophy of accessory sex organs
	Lansoprazole (Prevacid)	Inhibition of testosterone synthesis and increased plasma clearance of testosterone resulting in Leydig cell hyperplasia and tumors in rats
Sertoli cell	2,5-Hexanedione, phthalate esters	Sertoli cell vacuolation with subsequent death or exfoliation of germ cells
	Carbendazim, colchicine	Disruption of apical Sertoli cell cytoskeleton resulting in shedding of germ cells and Sertoli cell cytoplasm
Spermatogonia	Busulfan, cyclophosphamide	Spermatogonial death with subsequent maturation depletion of later germ cells
Spermatocytes	Glycol ethers, nitroaromatics	Stage-specific death of pachytene spermatocytes, mediated through disturbances in Sertoli cell
Round spermatids	Ethyl methane sulfonate, methyl chloride	Damages the round spermatid and leads to depletion and abnormalities in the elongating spermatid head shape
Elongating spermatid	Boric acid, dibromoacetic acid	Retention and phagocytosis of step 19 spermatids, abnormalities in the released sperm
Testicular blood vessels	Cadmium chloride	Damages endothelium of testicular blood vessels causing ischemic necrosis of all testicular cell types
Epididymis	Phosphodiesterase 4 inhibitor, α-chlorohydrin	Inhibition of fluid reabsorption in efferent ducts resulting in sperm granulomas and secondary testicular atrophy
	Methyl chloride	Epithelial degeneration resulting in sperm granulomas
Epididymal sperm	Ornidazole, α-chlorohydrin	Inhibition of glycolysis resulting in loss of sperm motility
Vas deferens	Guanethidine	Inhibition of ejaculation due to adrenergic receptor blockade, resulting in rupture at vas epididymal junction and sperm granulomas
Prostate and seminal vesicles	Flutamide	Androgen receptor blockade resulting in secretory inhibition and atrophy
	Finasteride	Inhibition of metabolism of testosterone to dihydrotestosterone resulting in secretory inhibition and atrophy
	α-Adrenergic receptor antagonists	Inhibit contraction/secretion of fluid from the seminal vesicles resulting in dilation

Table reproduced from Handbook of Toxicologic Pathology *(2013), third ed. (W. M. Haschek, C. G. Rousseaux, and M. A. Wallig, eds.), Academic Press, Table 59.13, p. 2573, with permission.*

toxicity. For example, a toxicant causing cell-specific death in the spermatocyte population may well be mediated through disturbances of cellular processes in the Sertoli cell that are critical to spermatocyte survival. Any mechanistic investigations into events leading up to cell death would benefit from looking not only at the spermatocytes but also at the cells required to keep the spermatocytes alive—the Sertoli cells.

Rather than "target cell," we propose the use of the term "reporter cell." This carries with it an implicit acknowledgment that the altered cell is merely reporting a lesion and does not imply that this cell is necessarily the main site of the biochemical events leading up to the lesion. Using "reporter cell" removes the potential confusion and assumptions associated with the term "target cell," and additionally accommodates the complexity that is likely to be uncovered by toxicogenomics (see below).

In some cases the reporter cell and target cell are indeed the same cell, and in a very few cases this has been demonstrated. One such example is 2,5-hexanedione which was extensively investigated by Boekelheide et al., whose results implicate the Sertoli cell as the initial cell showing morphologic and biochemical evidence of injury, following exposure. In addition, the extensive sloughing of the adluminal third of the seminiferous epithelium caused by intratesticularly administered colchicine can plausibly be explained by the fact that colchicine targets microtubules, and the Sertoli cells are the site of microtubules in the epithelium. These two lesions are unlikely to be changed by the use of a "reporter cell" term. However, the involvement of the Sertoli cell in the germ cell death lesion seen after ethylene glycol monomethyl ether (EGME) exposure would not be so readily overlooked. We expect that the Sertoli cells will be found to play an etiologic role in other lesions of germ cells, and the *reporter cell* term should help remind us of the limits of our knowledge about how these lesions develop.

Nitroaromatics

The testis is sensitive to multiple nitroaromatics, including nitrofurantoin, nitrofurazone, nitroimidazoles, di and trinitrotoluene, chlorodinitrobenzene, and 1,3-dinitrobenzene (DNB). Since the first description of its toxicity in 1981, DNB has been the subject of numerous in-depth investigations. Some of these studied key events in the development of this specific lesion. Others used DNB as a tool to explore the nature of response to toxic exposures and the testis' recovery after varying degrees of insult. Others looked for differences between a single administration and multiple administrations, and added biochemical measures of effect, or evaluated fluid production or hormonal effects.

The first morphologically identifiable effects produced by DNB are ultrastructural vacuolation in the Sertoli cells and, in fixed tissue sections, the appearance of space between the Sertoli cells and germ cells, interpreted as retraction of Sertoli cells from the germ cells. Perhaps predictably, when mixed-cell cultures are made with Sertoli cells and germ cells and DNB is added to the cultures, this retraction translates to a release of the germ cells into the medium. This is dose-related and quantifiable. The Sertoli cells catabolize DNB *in vitro*, creating more polar metabolites through the reactive nitrosonitrobenzene, which produces a similar type of germ cell loss when applied to the cultures and appears more potent than the parent DNB. The hypothesis was put forward that the local production of this metabolite was responsible for the observed toxicity and is one of only three or four compounds whose testicular metabolism is thought to play a central role in the observed testicular toxicity. Collectively, these data above led to defining the Sertoli cell as the target of DNB's toxicity, and its site of metabolism. Another important aspect of the toxicity caused by DNB is the role of the glutathione detoxification pathway in determining species sensitivity to DNB. The hamster is resistant to testicular toxicity when exposed to the same blood levels or cumulative exposure of DNB as is toxic to the rat. This is despite the fact that mitochondrial preparations of hamster testicular tubular mitochondria are more efficient in catabolizing DNB to its active metabolite. However, cellular levels of glutathione and ATP are depleted more rapidly in rat mitochondria than in hamster, resulting in oxidative stress within the Sertoli cell of the rat but not the hamster. This has been proposed as the probable cause of the differential species sensitivity.

In the case of DNB, toxicogenomics has led to several interesting insights, not least of which is the complexity of the response to a toxic insult. First, as expected, there are numerous significant gene expression changes that occur before any lesion is visible in the tissue. The earliest gene reductions (and by far the largest) were those enriched in pachytene spermatocytes, which were the site of the first visible change by light microscopy (spermatocyte apoptosis), even though the initial ultrastructural changes were seen in the Sertoli cell. Those authors focused on the cell adhesion genes and found that the genes coding for the cell-cell adhesion molecules (many of them Sertoli cell based) were all significantly increased at times when cells were beginning to be sloughed from the testis, and even trended insignificantly upwards at 4 hours after exposure, before there were any observable lesions. There were also changes in genes responding to oxidative stress and nitro metabolism,

though these last were not explored. In this situation, we are left considering how to relate an upregulated Sertoli adhesion gene to the release and death and sloughing of germ cells. The most likely possibility is that this increase responds to an earlier effect on the function of those adhesions. If that is true, it demonstrates how genomics, as inclusive and insightful as it is, does not capture nongene-based functions of proteins. Adhesions malfunctioning because of an oxidative damage-induced change in intracellular signaling will not be revealed by an array analysis. This demonstrates the need for additional biochemical assays which evaluate the function of subcellular components. To obtain a full and balanced picture of the events in lesion development will require relating biochemical, genomic, and structural changes to each other over time.

Glycol Ethers

The glycol ethers were also used as investigative toxicants in the emerging field of male reproductive toxicology in the early 1980s. This included explorations of the structure−activity relationships, and many studies using the two most potent congeners (EGME and ethylene glycol monoethyl ether) as tool compounds to visualize various patterns of response. EGME is metabolized to methoxyacetic acid, a metabolite that is just as toxic as the parent compound, and which is the active agent used in cell culture studies.

Numerous pathogenesis studies identified the early and late pachytene spermatocytes (but not mid pachytene spermatocytes) and the dividing spermatocyte as the most sensitive germ cell for this family of toxicants, with cell death being stage-specific and occurring within 12 hours of a single dose. Numerous follow-on studies have used this compound as a tool, based on that observation and on the assumption of the spermatocyte being the specific target. Despite this collective tunnel vision, it is important to remember that several other studies have reported either small vacuoles at the ultrastructural level in Sertoli cells which resolved by 24 hours after a single administration, or early changes in Sertoli cell enzymes or receptors or kinases. The Leydig cells never appeared abnormal, although prostate weights were occasionally reduced in some studies.

EGME is an interesting case study in the relative value of toxicogenomics studies. Work in the 1980s and 1990s regarding various mechanisms had explored several separate avenues: (1) that methoxy acetic acid (MAA) could form an MAA−CoA metabolite which could disturb carbohydrate metabolism, (2) that calcium channel blockers and kinase inhibitors could prevent many of the testicular (and other) toxicities observed after EGME treatment, (3) that Sertoli cells were required for the full expression of the cell death program in the spermatocytes, and (4) that kinase activity plays a central role in the spermatocyte death. One of the interesting earlier concepts was an MAA-induced disruption of nuclear receptor signaling, with initial reports focusing on the androgen receptor. This helped to identify early responses in Sertoli cells. Subsequent work on this and another short-chain fatty acid (valproic acid) found early and specific dysregulation of multiple nuclear receptors through activating the mitogen-activated protein kinase (MAPK) and inhibiting histone deacetylase, although neither were sufficient to account for all the receptor-potentiating effects reported for MAA.

Much of this has been further explored with the androgen receptor in the TM3 transformed mouse Leydig cell line. Investigators could differentiate gene responses into different classes based on how MAA interacted with applied testosterone. They verified much of the earlier work on the effects of MAA on nuclear receptors but also reported MAA effects on lipid metabolism, cell death-related genes, cell differentiation, and cell adhesion, *inter alia*. The fact that such gene sets were upregulated in a transformed line of a cell type which shows no pathology or visible change after EGME exposure *in vivo* is perplexing. On the one hand, it is reassuring that genes presumably underlying (or at least consistent with) the *in vivo* lesion are altered *in vitro*. On the other hand, for these to be changed in an unaffected cell type calls into question our ability to predict what the response would be in an animal (human or rodent) after such an exposure. How would we be able to predict that spermatocytes would be the responding cell based on these data from a Leydig cell line? Although confusing, a possible way to view these data is that they may imply a future where pathway testing is done in any available cell type (or perhaps multiple cell types), and then a yet-to-be-discovered method is applied to identify which cell types will be the ones responding. It is encouraging to think that multiple cell types would give the same response, but daunting to consider how much more we have to learn in order to predict a real *in vivo* response. The other thing this calls into question is the current common practice of linking gene response data from affected cells to the lesions in those cells.

More recent toxicogenomics work with MAA has found significant response of oxidative stress responsive genes, which leads into our next proposal for considering mechanisms.

Oxidative Stress

Oxidative stress has been known as a mechanism of toxicity for decades, with initial work focusing on

unstable epoxides formed by the metabolism of specific chemical structures. Its occurrence appears to be much more widespread than the initial focused work might imply.

All cells of obligate aerobes (this would include all major laboratory species as well as humans) use mitochondria to pass electrons from metabolic end-products (lactate and pyruvate, among others) down the electron transport chain and combine them with oxygen to form water. Not all electrons will be fully controlled, and if the estimated 2%–3% of these electrons are not fully reduced, their uncontrolled recombinations would produce reactive oxygen species (ROS). It has been estimated that, under normal metabolic conditions, the mitochondrion and membrane-bound NADPH oxidase are the two significant sources of oxidation damaging agents in the cell. A survey of the literature shows there is good evidence that oxidative stress is a regular feature of testicular toxicants or toxic exposures.

The following have been found to produce testis lesions and either upregulate oxidative stress responsive genes or have that lesion be ameliorated by antioxidant treatment: experimental diabetes, cadmium, cryptorchidism, sasanguasaponin, Di(2- ethylhexyl) phthalate (DEHP), chlorpyrifos, lead, TCDD, and EGME. Each of these reports has its shortcomings, but the strongest papers individually, and the whole of them collectively, lend support to the concept of oxidative damage as an early, even initiating, factor in testis damage. But the question must be asked: How might a general feature such as oxidative damage manifest as a lesion in one tissue and not others?

The mitochondria are the main source of ROS in the cells, and the mitochondria from different tissues express their own unique suite of proteins. Oxidative damage is more than lipid peroxidation and membrane damage. Oxidant molecules (superoxide and hydrogen peroxide much more than the hydroxyl radical) can impact signaling systems and either act as signaling molecules themselves or impact several critical intracellular control systems. Chief among these are MAPK, the Jun N-terminal kinases (JNKs), and members of the p38 family. In most other cell types, these proteins are key to cell survival or death, and help control cell migration and division … in short, they control many key cell outcomes. These are all found in the testis, and the excellent review by Wong and Cheng (2005) demonstrates how these help control not only cell life and death but also the junctions that attach the germ cells to the Sertoli cells as well as the junctions forming the blood–tubule barrier between adjacent Sertoli cells. Disrupted blood–testis barrier structure or function has been associated with severe testis lesions, and certainly sloughing of prematurely released germ cells is a key feature of many acute testicular toxicants. Given our evolving appreciation of the complexity of these junctions and their control by kinases and numerous intracellular activities, it appears very plausible that oxidation of, for example, a controlling cysteine residue on a MAPK or a JNK or p38 protein would then disassemble the junctions holding the germ cells to the Sertoli cells. Even if this was not followed by FasL synthesis and release, the loss of junctional attachment should result in the death of that cell, given the dependence of the germ cells on the Sertoli cell for nutrition and maintenance. Such release would then produce the familiar sight of an epididymal lumen with increased numbers of sloughed round germ cells in varying stages of death and degradation.

It is unlikely that all testicular toxicants would produce an increase in ROS, but the increase in oxygen consumption and mitochondrial activity which indicates compensated toxicity (the hormetic response) is seen for an astonishing number of toxic exposures and conditions. If this increased mitochondrial activity does lead to increased flow through the electron transport chain, and if some proportion of those are poorly controlled or produce ROS, it is easy to see how there would be oxidative damage and likely changes in intracellular signaling after exposures which do not produce epoxide intermediates. Moreover, the tissue-specific mitochondrial proteome provides a plausible mechanism to begin to explain why one tissue might respond to a toxicant and others would not. Altogether, the data appear more convincing that some degree of oxidative damage or stress is at least a component of, if not a cause of, many testis lesions.

Morphologic Patterns of Response to Different Types of Injury

It would be truly rewarding for the pathologist to be able to examine the reproductive tissues in a short-term or time-course study, identify the true target cell for toxicity, postulate a mechanism for injury based on the known pharmacology or biological activity of the test material, and utilize this in the overall risk assessment or mode of action (MOA) evaluation for exposure in man. In reality, complete understanding of any mechanism of testicular toxicity is rare and the information is difficult to generate (Tables 17.9–17.12). As discussed earlier, the complexity of cell–cell signaling in the testis is such that morphologic injury, even of a specific cell type within a specific stage of spermatogenesis, generally reflects a downstream effect of disturbed cell signaling in a different cell type. Thus,

as suggested above, the use of the term "reporter cell" rather than "target cell" is probably a more valid concept.

Nevertheless, the terms "Sertoli cell toxicants" versus "germ cell toxicants" and "hormonally mediated toxicants" are commonly used to distinguish between different manifestations of toxicity within the testis (reviewed by Creasy, 2001). This classification is based largely on the reporter cell, as indicated above: the cell type that shows the earliest morphological changes, along with the characteristics of the lesion as it progresses with time (Table 17.9). Taking that one step further, toxicants can be classified into broad categories based on their overall pattern of morphologic change. This is useful since it allows the design of additional biochemical or molecular investigations, and because it provides useful information for risk assessment or MOA evaluation. There are a number of different patterns of change that the pathologist can recognize, but these depend on whether the lesion is very early in its development or has been developing for some time, or whether it has reached its end stage (see Tables 17.10–17.12 for a summary of the major features of the different patterns). If an end-stage or advanced stage of a lesion is present in the high-dose group of a study, it is often possible to see the early stages of lesion development in the lower-dose groups, because in many cases lower exposure levels take longer to begin exerting their effects—so in some cases the same information can be gained from a routine toxicity study without doing an actual time-course study. When considering a time-course study to identify early changes, the duration of dosing will depend on the toxicant and the dose level, and the speed of onset of the lesion. Changes can be seen within hours of a single dose for some toxicants but can take weeks to develop for others.

The following patterns of change are based largely on the responses seen in the rat which is an ideal species for detecting subtle changes. The same broad principles apply across species, but it is much more difficult to identify specific changes in the dog and monkey.

Patterns of Changes Associated with Sertoli Cell Injury

When the Sertoli cell is the primary site of morphological damage, the pattern of subsequent germ cell death and depletion is frequently multifocal and affects numerous or all different germ cell types when examined in a repeat-dose study (Table 17.10). However, if the earliest signs of the lesion are examined, it is common to see stage- and cell-specificity associated with the germ cell death. For example, DNB is a Sertoli cell toxicant that produces Sertoli cell vacuolation in stages VII and XI within 24 hours of dosing, which is followed by apoptosis of late pachytene spermatocytes in stages VI–XIII 24–48 hours after dosing. With repeat dosing and examination at a later time point, this stage- and cell-specificity will obviously expand through more cells and more stages.

FOCAL GERM CELL LOSS

Each Sertoli cell supports a specific cohort of germ cells as they develop through spermatogenesis. If that Sertoli cell suffers significant injury, all of the germ cells it supports will likely die and disappear. In the earliest stages of lesion development, this leads to an

TABLE 17.10 Patterns of Change Associated with Sertoli and Germ Cell Injury

	Pattern of change		
Injury	**Testis**	**Epididymis**	**Prostate/seminal vesicles**
Sertoli cell injury (early)	Foamy vacuolation in Basal Sertoli cell cytoplasm or solitary large discrete vacuoles. Focal drop out of germ cells. Spermatid retention. Disorganization of germ cell layers	Sloughed testicular Germ cells present in lumen (initially confined to caput, later in the cauda)	Normal
Sertoli cell injury (later/late)	Partial/patchy loss of germ cells. Progressive diffuse degeneration of germ cells (without cell-or stage-specificity). Sloughing of germ cells into lumen	Larger numbers of sloughed germ cells. Decreased sperm content	Normal
Germ cell injury (early)	Degeneration or depletion of a specific germ cell population(s) with remaining germ cell layers appearing normal (cell- and stage-specific)	Normal	Normal
Germ cell injury (later/late)	Progressive depletion of more mature germ cell layers (maturation depletion)	Decreased sperm content, but not until the maturation depletion has reached step 19 spermatids	Normal

Table reproduced from Handbook of Toxicologic Pathology *(2013), third ed. (W. M. Haschek, C. G. Rousseaux, and M. A. Wallig, eds.), Academic Press, Table 59.14, p. 2577, with permission.*

TABLE 17.11 Patterns of Change Associated with Efferent Duct Obstruction and Anoxia/Ischemia

Injury or lesion	Testis	Epididymis	Prostate/seminal vesicles
Efferent duct obstruction/ disturbed fluid reabsorption	Mixture of tubular dilation and severe tubular atrophy. Frequently unilateral. Dilated testes are increased in weight. Rete testis maybe dilated. Atrophic tubules frequently have patent or slightly dilated lumens. Interstitial edema maybe present. Incidence of affected testes often sporadic with poor dose relationship	Sperm stasis and granulomatous inflammation in the efferent ducts. Epithelial apoptosis of the initial segment. Cribriform change in the caput epididymis. Epididymis associated with testis that has dilated tubules may or may not have sperm content. No sperm and generally no sloughed germ cells in epididymis of atrophic testis	Normal
Anoxia/ischemia (testis)	Initial anoxia causes increased apoptosis of spermatogonia and early spermatocytes. Early ischemia causes separation of germ cells (similar to autolysis). Later progresses to necrosis (coagulative) of germ cells and Sertoli cells. Generally, associated with an interstitial inflammatory response to necrotic tubules. Affected tubules often become mineralized and may proceed to fibrosis. May affect individual tubules or affect focal areas	Sloughed testicular germ cells and reduced sperm	Normal

Table reproduced from Handbook of Toxicologic Pathology *(2013), third ed. (W. M. Haschek, C. G. Rousseaux, and M. A. Wallig, eds.), Academic Press, Table 59.15, p. 2583, with permission.*

TABLE 17.12 Patterns of Change Associated with Androgen Imbalance in Rodents

Type of androgen imbalance	Pattern of change		
	Testis	Epididymis	Prostate/seminal vesicles
Decreased testosterone (early/mild)	Degeneration of occasional pachytene spermatocytes and round spermatids in stage VII/VIII tubules. Spermatid retention. Leydig cell atrophy (if severe testosterone reduction)	Apoptosis of ductal epithelium (most prominent in the initial segment)	Decreased weight. May see increased epithelial apoptosis
Decreased testosterone (late/severe)	Progressive degeneration and depletion of elongating spermatids. Leydig cell tumors (rat)	Reduced sperm content, reduced weight, ductal atrophy	Reduced weight, reduced secretion, atrophy
Androgen agonist	Same effects as with decreased testosterone due to effects on hypothalamic pituitary feedback. Inverse dose relationship with most severe disruption of spermatogenesis at low doses and less severe effects at high dose	Reduced sperm content, reduced weight, ductal atrophy	Increased weight, increased secretion, enlargement
Androgen antagonist	Leydig cell hyperplasia (early), Leydig cell tumors (late) (rat)	Normal or slightly reduced weight	Reduced weight, reduced secretion, atrophy
Reduced DHT (5α-reductase inhibitor)	Normal (rat). Leydig cell hyperplasia and tumors (mouse)	Normal or slightly reduced weight	Reduced weight, reduced secretion, atrophy
Estrogen agonist	Progressive degeneration and depletion of elongating spermatids. Leydig cell hyperplasia and tumors (mouse)	Apoptosis of ductal epithelium (most prominent in the initial segment). Reduced sperm content, reduced weight, ductal atrophy	Reduced weight, reduced secretion, atrophy

Table reproduced from Handbook of Toxicologic Pathology *(2013), third ed. (W. M. Haschek, C. G. Rousseaux, and M. A. Wallig, eds.), Academic Press, Table 59.16, p. 2584, with permission.*

appearance of focal loss or "dropout" of germ cells from that one Sertoli cell or a patchy partial loss of germ cells from multiple Sertoli cells in affected tubules (Figure 17.22). As the degree of damage progresses and more Sertoli cells become injured, a more generalized germ cell degeneration and depletion will develop, leading to a final end-stage lesion of severe tubular degeneration/atrophy (Figure 17.11A and C). Since

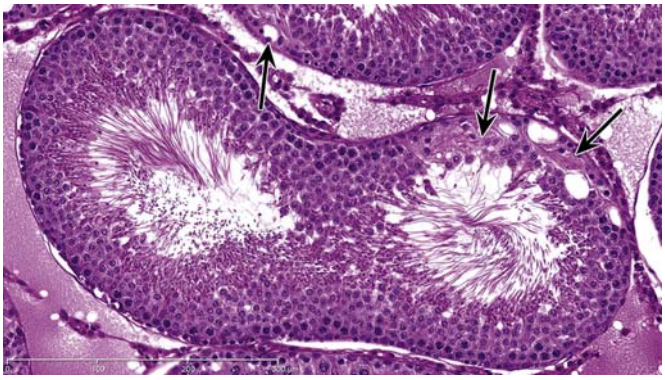

FIGURE 17.22 Patchy partial loss of germ cells affecting multiple Sertoli cells (arrows). This is a typical early pattern of change that occurs when toxicity is mediated through the Sertoli cell. Rat, H&E, ×20. Source: *Figure reproduced from* Haschek and Rousseaux's Handbook of Toxicologic Pathology *(2013), third ed. (W.M. Haschek, C.G. Rousseaux and M.A. Wallig, eds.), Academic Press (Elsevier), Figure 59.35, p. 2578 with permission.*

almost all testicular toxicants produce the same end-stage lesion (severe tubular degeneration/atrophy), it is important to study the earlier changes to gain any insight into pathogenesis. In general, this pattern of change is associated with slow or incomplete recovery.

The other significant insight from such an early lesion is that not all Sertoli cells are equal. If they were a homogeneous population, they would all respond the same way. The fact that they do not must indicate considerable heterogeneity among the cells.

VACUOLATION

Early evidence of Sertoli cell injury can also be reflected by macro- or microvesicular vacuolation of scattered Sertoli cells (Figure 17.14). Microvacuolation is generally present in the basal Sertoli cell cytoplasm and represents swelling and coalescence of membrane-bound organelles such as endoplasmic reticulum or vesicles. This may be accompanied by disorganization or displacement of the regular layering of germ cells. Although there maybe degeneration of germ cells, it is generally infrequent or develops subsequent to the vacuolation of the Sertoli cells. Macrovesicular vacuolation also occurs with some testicular toxicants, such as 2,5-hexanedione. This change is characterized by solitary or multiple large vacuoles at the base or part way up the tubular epithelium (Figure 17.14B). As an early change, this type of vacuolation is generally not associated with germ cell degeneration; however, if treatment continues, it inevitably leads to germ cell death and loss.

GERM CELL SLOUGHING AND SHEDDING

When immature germ cells (spermatocytes and round spermatids) are admixed with sperm in the epididymis, they have been prematurely released from the seminiferous epithelium (Figure 17.16). In most cases the shed germ cells retain relatively normal nuclear and cytoplasmic characteristics, suggesting that they have lost contact with their Sertoli cell processes and been "passively" shed into the tubular lumen. Since the rat epididymis contains negligible round germ cells when there is normal spermatogenesis, this can be a very sensitive and very early indicator of spermatogenic disturbance and often is easier to see than the testicular change that is causing it. Care should be taken not to confuse apocrine cytoplasmic blebs, originating from the normal process of apocrine secretion by the efferent duct or epididymal epithelium, with sloughed testicular germ cells. Apocrine cytoplasmic blebs can be a prominent change, particularly in the dog epididymis.

The Sertoli cell supports and moves the germ cells up and down within the seminiferous epithelium, utilizing a well-developed cytoskeleton of microtubules and intermediate filaments. The germ cells share a variety of specialized junctions with the Sertoli cell, some of them unique to the testis, that hold the germ cells in place and embedded within the Sertoli cell cytoplasmic processes. If those junctions are broken or there is retraction of the cytoplasmic processes, the germ cells can be "cast loose" and shed into the lumen. This can be a very prominent change with some Sertoli cell toxicants, such as the phthalate esters, where retraction of the cytoplasmic processes that support and separate the germ cells has been shown to be an early change (Figure 17.23). Microtubule inhibitors, such as colchicine and carbendazim, cause shedding of the germ cells in sheets that are still attached to the apical cytoplasm of the Sertoli cell. This appears to be a wholesale sloughing of the apical third of the

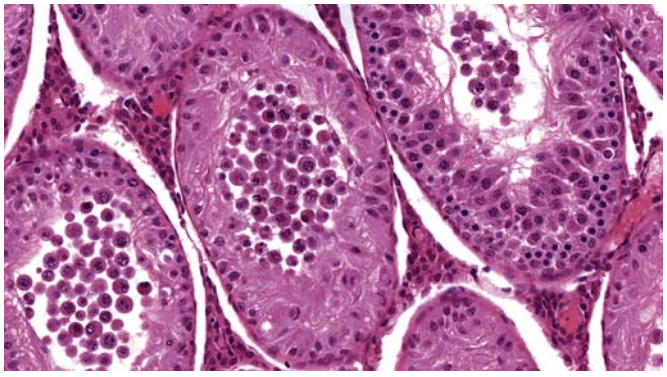

FIGURE 17.23 Sloughed germ cells in the testis of a rat dosed with di-*n*-pentyl phthalate. The toxicity appears to cause loss of contact between germ cells and Sertoli cell processes. Rat, H&E, ×20. Source: *Figure reproduced from* Haschek and Rousseaux's Handbook of Toxicologic Pathology *(2013), third ed. (W.M. Haschek, C.G. Rousseaux and M.A. Wallig, eds.), Academic Press (Elsevier), Figure 59.36A, p. 2579 with permission.*

Sertoli cell and cytoplasm and germ cells, presumably due to disruption/dissolution of the cytoskeletal microtubules.

TUBULAR CONTRACTION AND DECREASED SEMINIFEROUS TUBULAR FLUID

The Sertoli cells continuously secrete STF into the tubular lumen. This transports the sperm out of the tubule and into the rete and the efferent ducts, and is responsible for the patency of the tubular lumens. The size of the tubular lumen is directly related to the amount of fluid within the lumen, so if secretion is decreased the tubule will contract, and if secretion increases, or its exit from the testis is blocked, the tubule will dilate. Reduced secretion of STF has been demonstrated as an early event with a number of Sertoli cell toxicants, including the phthalate esters, 2,5-hexanedione, and indenopyridine exposure. Although qualitative microscopic evaluation is not very sensitive for detecting tubular contraction, particularly when there is differential shrinkage of tubules due to fixation artifact, the volume of STF can be measured. This is done by ligating the efferent ducts of one testis and comparing the weight difference between the ligated testis and the contralateral unligated testis after $\geq$15 hours. Decreased fluid content will also be reflected by a decrease in the weight of the testis; therefore, if there is a significant weight loss in the testis and no obvious germ cell loss, a disturbance in STF should be considered.

Patterns of Change Associated with Germ Cell-Specific Toxicity

When germ cells are the primary cell type damaged, the changes are generally cell- and stage-specific (Table 17.10). If the testes are examined early in lesion development, it is possible to identify apoptotic germ cells in the presence of normal-appearing Sertoli cells. More often, the testes are examined after repeat dosing, and since apoptotic cells are rapidly eliminated, the most characteristic feature of germ cell toxicity is a stage- and cell-specific depletion, which is commonly referred to as "maturation depletion." The number of cell types depleted will depend on the cell type that has died as well as the duration of the dosing regimen. As an example, if a toxicant kills stage I pachytene spermatocytes, and this occurs on day 1 of dosing, by day 2 of the study most (but perhaps not all) of the necrotic cells will have been phagocytized and the tubule will have progressed to stage II, minus its pachytene spermatocyte population (Figure 17.9B). Moreover on day 2, the tubules that were in stage XIV on day 1 of dosing will now have entered stage I and their pachytene spermatocytes will become susceptible to toxicity and die (Figure 17.10D), and the process is repeated. If the testes are examined after 2 weeks of continuous dosing (one complete cycle of spermatogenesis), the death of the stage I pachytene spermatocytes 2 weeks previously will be reflected by the absence of step 1 round spermatids, as well as all of the developmental stages of pachytene spermatocytes in between (i.e., in stages II–XIV). The progress of maturation depletion over time is illustrated in Figure 17.24, and this pattern of germ cell depletion is the hallmark for recognizing germ cell toxicity.

A feature of maturation depletion is that the effect becomes more obvious as the later developmental stages of germ cells (e.g., spermatids) are lost. This is because there are theoretically 4 spermatids for every primary spermatocyte, 2 spermatocytes for every B spermatogonium, and 32 B spermatogonia for every type A1 spermatagonium that enters spermatogenesis. The progressive expansion of the germ cell population means that a compound which targets stem cell spermatogonia will be very difficult to identify in conventional H&E sections during the first 2 weeks of dosing, because very few cells will be lost. By 4 weeks after the onset of dosing, depletion will have reached the much more numerous pachytene spermatocyte population and be more obvious, and by 6 weeks after the start of dosing it will be very obvious because a large proportion of the round spermatids will be missing, in addition to all the earlier cell types.

Another aspect of the dynamics of this progressive maturation depletion is the appearance of the testes at the end of dosing versus the end of recovery. At the end of dosing, maturation depletion may only have caused the loss of spermatogonia and a few stages of pachytene spermatocytes and be difficult to identify (Figure 17.10A and B), but following an additional 2- or 4-week recovery period the progressive depletion of the spermatid population will make the severity of germ cell loss appear much more severe (Figure 17.10C). In these situations, it is important to note which cells are missing at the end of dosing (spermatogonia and certain stages of spermatocytes) versus which cells are missing at the end of recovery (e.g., round and elongating spermatids) but with recovery of spermatogonia and early spermatocytes. Failure to do this will result in an erroneous conclusion that the damage is getting worse rather than recovering.

Degeneration and malformation of elongating spermatids is a form of germ cell-specific toxicity that is occasionally seen. In order to recognize this, the pathologist needs to have a good knowledge of the normal shape changes that the elongating spermatid head goes through as it moves through each of the stages of the cycle. A head malformation is most easily recognized in stages XI–XIII, where the head

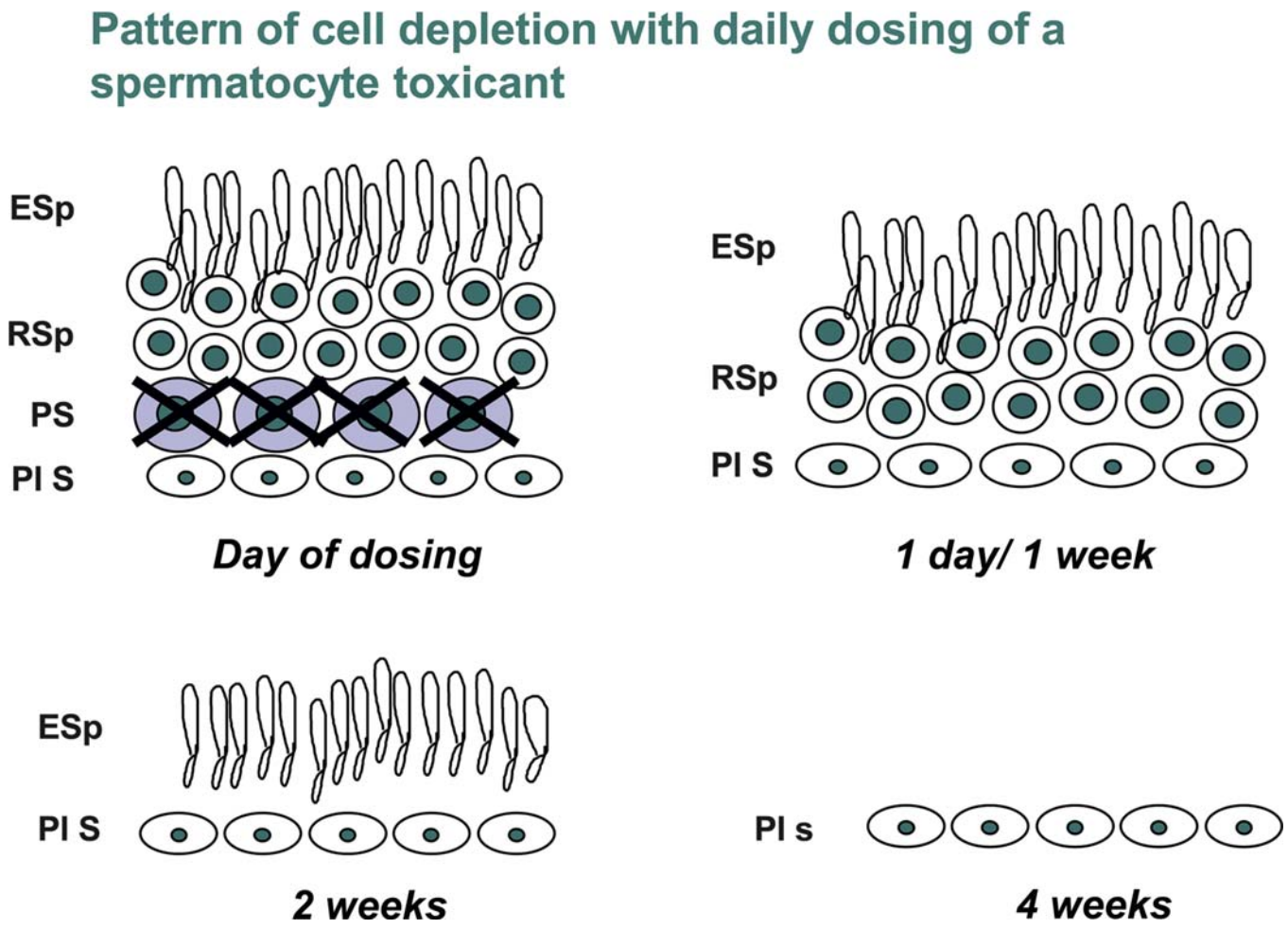

FIGURE 17.24 Typical progression of maturation depletion that occurs following germ cell-specific toxicity in the rat. A Stage VII tubule is illustrated. On day 1, it contains preleptotene spermatocytes (Pl S), pachytene spermatocytes (PS), round spermatids (RSp), and elongating spermatids (Esp). On the day of dosing, the toxicant causes apoptosis of the pachytene spermatocytes. If that stage is examined the following day or after a week of dosing, the pachytene spermatocytes will be missing but the other cell types will appear normal. If the same stage tubule is examined after 2 weeks of dosing (i.e., one complete spermatogenic cycle), pachytene spermatocytes will be missing (because they are still being killed by the toxicant) and round spermatids will be missing because their precursor cell was killed 2 weeks earlier, but preleptotene and elongating spermatids will still be present. After 4 weeks of dosing, the elongating spermatids will also be depleted, leaving the end-stage lesion of tubules containing preleptotene spermatocytes but with all subsequent cell types missing. Source: *Figure reproduced from* Haschek and Rousseaux's Handbook of Toxicologic Pathology *(2013), third ed. (W.M. Haschek, C.G. Rousseaux and M.A. Wallig, eds.), Academic Press (Elsevier), Figure 59.37, p. 2581 with permission.*

loses its long delicate curvature and becomes shortened, clubbed, and condensed (Figure 17.25). There also appears to be abnormal tail formation and retraction of the cytoplasmic coating around the developing flagellum of the tail. These changes are usually accompanied by the presence of cell debris in the head of the epididymis, which appears to consist of prematurely shed heads and tails of malformed elongating spermatids. It is possible that these deformed elongating spermatids are due to disturbances in the formation of the acrosome earlier in spermiogenesis. This has been described in the case of carbendazim.

Germ cell toxicity has been described for a number of toxicants; the best documented is probably EGME or its active metabolite MAA (see "Mechanisms of Toxicity of Glycol Ethers" section). At low doses, this chemical causes very specific death of stage I–V pachytene spermatocytes and stage XI–XIV pachytene and dividing spermatocytes (Figure 17.10D) within hours of dosing. Although there is no visible evidence of Sertoli cell injury, additional investigations indicate that the Sertoli cell is essential in mediating the germ cell toxicity, thus, supporting the concept of the reporter cell. As the dose level increases, pachytene spermatocytes in all stages become susceptible, and at

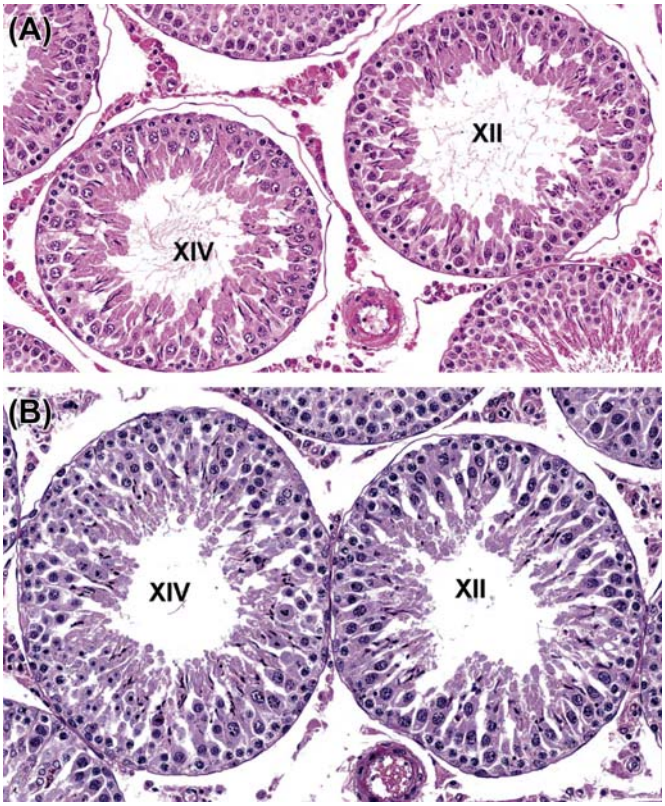

FIGURE 17.25 Degeneration of elongating spermatids. This can be recognized by malformation of the shape of the head of elongating spermatids. To recognize this change, it is essential to know the normal shape of elongating spermatids in the different spermatogenic stages. (A) Normal stage XII and XIV tubules. (B) Stage XII and XIV tubules containing elongating (step 12 and 14) spermatids with condensed and clubbed heads. Rat, H&E, ×20. Source: *Figure reproduced from* Haschek and Rousseaux's Handbook of Toxicologic Pathology *(2013), third ed. (W.M. Haschek, C.G. Rousseaux and M.A. Wallig, eds.), Academic Press (Elsevier), Figure 59.38, p. 2582 with permission.*

even higher doses the toxicity expands into the spermatid population and the prepachytene spermatocyte population. This loss of cell- and stage-specificity as the dose level increases is a common phenomenon.

Patterns of Change Associated with Anoxia or Ischemia

In theory, the seminiferous epithelium should be very susceptible to reduced blood flow, because there are no capillaries within the epithelium and all oxygen and nutrients need to travel from the interstitial capillaries into the interstitial fluid and be transported through the Sertoli cells to reach the germ cells sequestered within the Sertoli cell processes (Table 17.11). An alternative view is that the tubules would likely be resistant to anoxia because they operate normally at such low oxygen levels (3–5 mm O_2 intratubularly). In fact, in early experiments where the blood supply was ligated for varying lengths of time, total ligation for up to 60 minutes resulted in little or no damage but ligation for 90–105 minutes caused selective damage to the spermatogonia and preleptotene spermatocytes. The degree of damage observed depends on whether the testes are examined at the end of the ligation period or whether the blood flow is reinstated (reperfusion). If blood flow is cut off and then reestablished (as is the case for surgically treated testicular torsion in humans), there is often no obvious damage from the ischemic event arising from the torsion, but spermatogenesis generally is severely affected due to the subsequent apoptotic death of a large proportion of the germ cells. This delayed damage appears to be due to the generation of ROS by the leukocytes that infiltrate the ischemic tissue during the torsion phase.

The most sensitive cells to the injurious effects of reduced oxygen tension appear to be the spermatogonia and early spermatocytes, which undergo an increased rate of apoptosis. This is surprising because they are the closest cells to the oxygen-containing interstitial fluid and are outside the blood–testis barrier, whereas the pachytene spermatocytes and spermatids, which are metabolically active and inside the blood–testis barrier, which is further from the source of oxygen, appear less sensitive to reduced blood flow. Studies that examined the effects of graded reductions in testicular blood flow on spermatogenesis have demonstrated an increased level of apoptosis in the spermatogonia and early spermatocytes after 5 hours of blood flow reduced by 70% of its pretreatment level. At this reduced level of flow, the numbers of apoptotic germ cells were increased by approximately 1.8-fold of pretreatment values and kept increasing in direct correlation with a further decrease in blood flow up to 50% of pretreatment values. Further reductions in blood flow resulted in a more generalized disruption, necrosis, and exfoliation of the tubular epithelium rather than germ cell apoptosis (Figure 17.12A). Reduction in testicular blood flow was also accompanied by increased numbers of leukocytes in the blood vessels, with some migrating out into the interstitial space.

A particular pattern of ischemic necrosis is seen with reductions in blood flow produced by some kinds of toxicants. The change has been best described, following a subcutaneous injection of very large doses of human chorionic gonadotropin (hCG) to the rat. The lesion is characterized by a focal area of coagulative necrosis, associated with a leukocytic infiltrate and located specifically in the frontal lower pole of the testis. The mechanism of the hCG-induced necrosis appears to be due to stimulation of the Leydig cells by hCG to synthesize prostaglandins which cause prolonged (>12 hours) contraction and cessation of blood

flow in the intratesticular arteries in the frontal lower pole of the testis, resulting in tubular necrosis in this part of the testis. Although the testicular arteries in the remainder of the testis initially showed the same contraction and reduced blood flow, they recovered much more rapidly and did not cause necrosis of the adjacent parenchyma.

A unique characteristic of blood flow in the testis is its pulsatile nature. This is called vasomotion, and, although its function is not entirely understood, it appears to be very important in the movement of oxygen and nutrients from the capillaries into the interstitial fluid. It has been shown to be reduced or ablated in a number of vascular-induced testicular lesions, including partial arterial obstruction (graded ischemia), hCG-induced testicular necrosis, 5HT-induced testicular vasoconstriction, and testicular torsion. It appears to be a critical component of blood flow when dealing with recovery of the seminiferous epithelium, in that recovery can be compromised if vasomotion is absent, even though blood flow may have returned to normal.

Patterns of Change Associated with Loss of Androgen Support

Recognition of testicular toxicity mediated by androgen withdrawal requires an integrated evaluation of the entire reproductive tract, because changes in the epididymis and accessory sex organs are generally more sensitive than the often subtle cell- and stage-specific changes in the testes (Table 17.12). In addition, there are a number of different mechanisms of reduced androgen status, and each will have a different pattern of effects.

TESTICULAR CHANGES

Androgen status can be reduced by various pathways: (1) decreasing testosterone synthesis, (2) blocking the interaction of androgens with the androgen receptor (antiandrogens, and antagonists), or (3) inhibiting conversion of testosterone to the more potent androgen, DHT. In all cases there will be atrophic changes in the epididymis and accessory sex organs, but the nature of the changes seen in the testes depends on the nature of androgen disruption. Quantitatively normal spermatogenesis requires high levels of intratesticular testosterone, but in the rodent qualitatively normal spermatogenesis can continue despite moderate reductions in testosterone levels. In the dog, reduced testosterone appears to have a more dramatic effect on spermatogenesis.

The effects of testosterone withdrawal have been most fully described in the rat, following ethane dimethane sulfonate administration, which causes Leydig cell necrosis and reduces testosterone to castrate levels. The earliest changes are seen 4 days after destruction of the Leydig cells, and comprise a cell- and stage-specific apoptosis of occasional pachytene spermatocytes and round spermatids in stage VII and VIII tubules (Figure 17.26A). At later times, spermatocytes, and particularly elongating spermatids in later stages (IX–XIV), show degeneration (Figure 17.26B). This reflects the fact that these cells have passed through stages VII–VIII in the absence of testosterone, undergoing lethal damage in the process; however, degeneration is delayed to a later time when

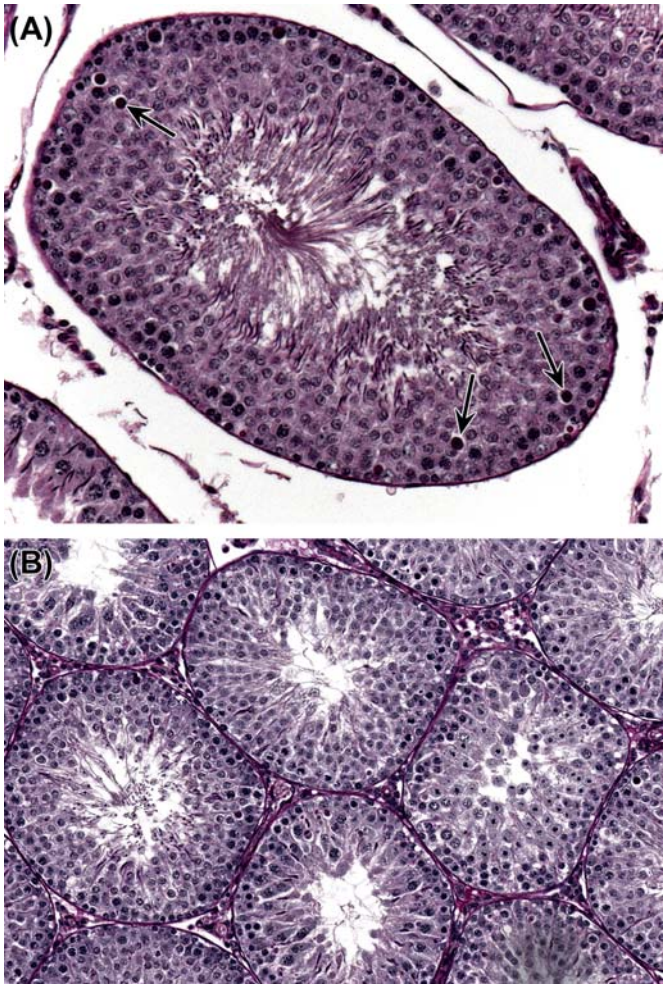

FIGURE 17.26 Characteristic changes caused by low testosterone in the rat. (A) Stage VII tubule with occasional apoptotic round spermatids and pachytene spermatocytes (arrows). This can be the only testicular change seen following mild decreases in testosterone. Rat, H&E, ×20. (B) Generalized depletion of elongating spermatids and contraction of tubular lumens. This is the end-stage lesion in the rat after marked reductions in testosterone. Leydig cell atrophy is also present in both but can be difficult to evaluate qualitatively. Rat, H&E, ×10. Source: *Figure reproduced from* Haschek and Rousseaux's Handbook of Toxicologic Pathology *(2013), third ed. (W.M. Haschek, C.G. Rousseaux and M.A. Wallig, eds.), Academic Press (Elsevier), Figure 59.40, p. 2585 with permission.*

they undergo a critical event, which relies on their previous exposure to testosterone. The endstage lesion for severe testosterone insufficiency in the rat, which is seen after about 2 weeks of treatment, is a slight reduction in the numbers of mid and late pachytene spermatocytes and round spermatids, but an almost complete loss of elongating and maturation phase spermatids (Figure 17.26B). This is accompanied by a marked shrinkage of the tubule, which is partly due to a loss of germ cells but is also caused by a reduction in the secretion of androgen-dependent STF by the Sertoli cell. Testosterone withdrawal also leads to abnormal retention and phagocytosis of step 19 spermatids at stages IX–XII. Although spermatid retention appears to be a common finding with treatments that disturb testosterone levels, it is not unique to this class of compound.

The effects of low testosterone on the dog testis do not show the same cell- and stage-specificity as seen in the rat. With mild reductions in testosterone there appears to be an increased rate of germ cell degeneration and depletion, but with more marked testosterone reduction there is a total loss of spermatogenesis, leaving empty, shrunken seminiferous tubules.

Any morphologic changes in the Leydig cell will depend on the nature of the hormonal disturbance and the species. Increased LH stimulation of rodent Leydig cells will result in hypertrophy of the cell due to an increased volume of smooth endoplasmic reticulum and, if prolonged, may also lead to diffuse hyperplasia of the cell population. Conversely, reduced stimulation of the Leydig cell by LH, or inhibition of the steroidogenic enzymes, will lead to a reduction in the size of the cells and the volume of endoplasmic reticulum (Figure 17.26). In the dog, Leydig cell response is more variable, and Leydig cell vacuolation and hypertrophy is frequently seen accompanying decreased testosterone production.

Administration of exogenous androgens or androgen agonists has an interesting inverse dose–response relationship with regard to its effect on testicular spermatogenesis. Administration of testosterone or other androgen agonists will inhibit LH production from the pituitary, resulting in inhibition of Leydig cell steroidogenesis and decreased intratesticular testosterone levels. There is a marked differential in the concentrations of peripheral versus intratesticular testosterone levels, and, since spermatogenesis requires very high local testosterone concentrations to progress normally, spermatogenesis will decline in response to the locally reduced steroidogenesis. The higher the administered dose of testosterone, the more it is able to compensate for the decrease in testicular steroidogenesis, and the less effect it has on spermatogenesis. The net result is that the lower the dose of testosterone administered, the more severe the degenerative effect on spermatogenesis. The opposite is true for the effect on accessory sex organs, where the increased circulating levels of administered testosterone will be directly metabolized to DHT within the prostate and seminal vesicles and result in enlargement and increased weight of these tissues.

Androgen receptor antagonists (e.g., flutamide) generally have no detectable histopathologic effect on spermatogenesis, but they cause Leydig cell hyperplasia through their stimulatory effect on LH levels (blocked androgen receptor in the CNS leads to increased LH synthesis and release, which produces the Leydig cell hypertrophy). Conversely, 5α-reductase inhibitors (e.g., finasteride) have no detectable effect on spermatogenesis or on Leydig cells in the rat. However, both cause marked atrophy of the accessory sex organs and the epididymis, which are dependent on DHT for their activity and interaction of the androgen with the androgen receptor. In the mouse, finasteride does produce Leydig cell hyperplasia, which is thought to be due to the fact that DHT is more important than testosterone in feedback inhibition of gonadotropin secretion from the pituitary.

EPIDIDYMAL AND ACCESSORY SEX ORGAN CHANGES

In general, the epididymis and especially the accessory sex organs are much more sensitive than the testis to reduced androgen status and rapidly respond with weight loss and epithelial apoptosis and atrophy (Figures 17.27–17.29). In the case of the rat ventral prostate, it loses over 90% of its weight within 4 weeks of androgen withdrawal, while the epididymis loses 80% of its weight in the same time period. The weight loss in the epididymis is due to epithelial apoptosis

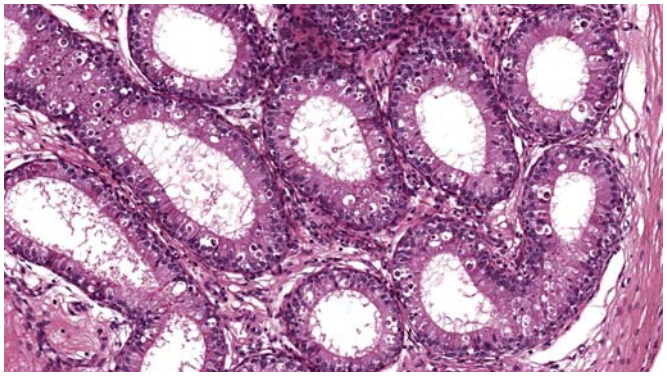

FIGURE 17.27 Apoptosis of the initial segment of the epididymis often accompanies significant reductions in circulating testosterone. Rat, H&E, ×20. Source: *Figure reproduced from* Haschek and Rousseaux's Handbook of Toxicologic Pathology *(2013), third ed. (W.M. Haschek, C.G. Rousseaux and M.A. Wallig, eds.), Academic Press (Elsevier), Figure 59.42A, p. 2587 with permission.*

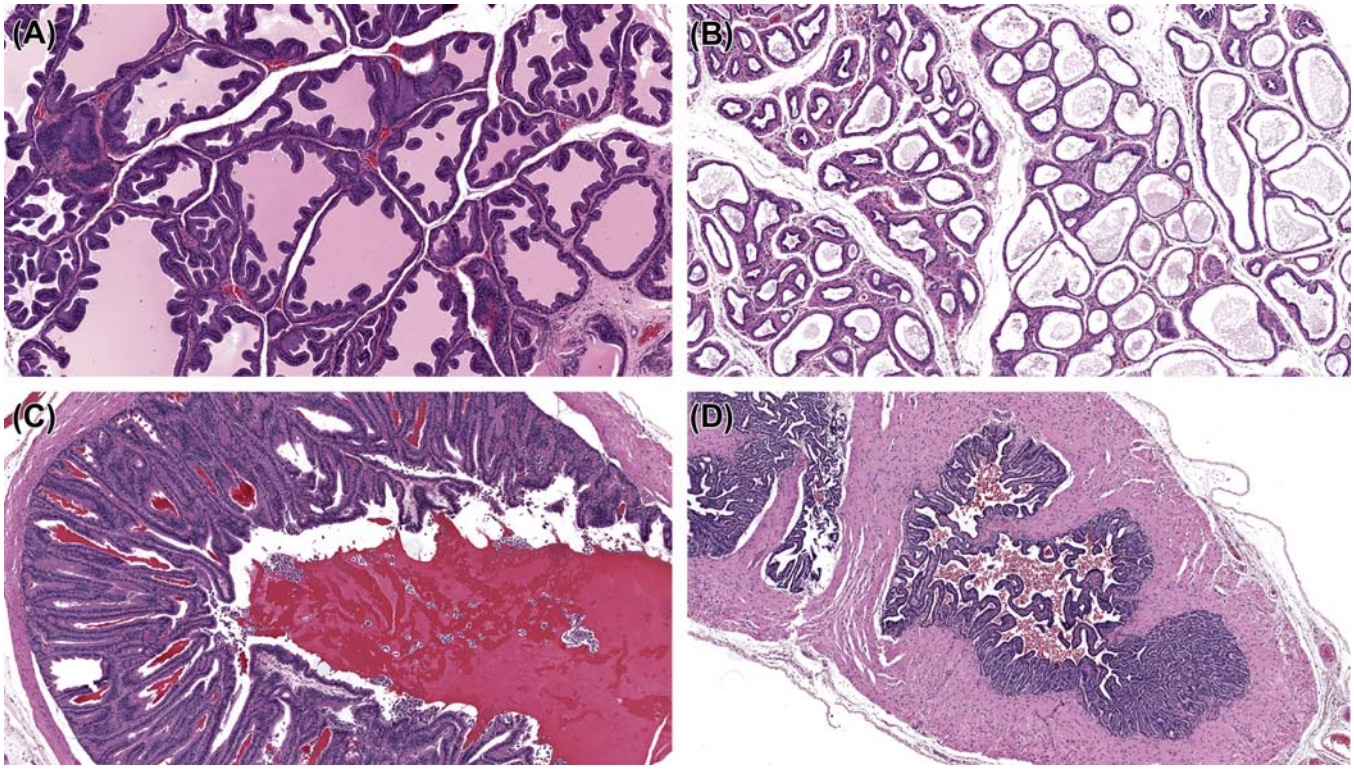

FIGURE 17.28 Loss of organ weight of the accessory sex organs is a sensitive indicator of decreased androgen status. When there is a marked reduction in organ weight, morphological evidence of atrophy can also be seen. (A) Normal ventral prostate. Rat, H&E, ×5. (B) LHRH-treated ventral prostate. Rat, H&E, ×5. (C) Normal seminal vesicles. Rat, H&E, ×4. (D) LHRH treated seminal vesicles. Rat, H&E, ×5. Source: *Figure reproduced from* Haschek and Rousseaux's Handbook of Toxicologic Pathology *(2013), third ed. (W.M. Haschek, C.G. Rousseaux and M.A. Wallig, eds.), Academic Press (Elsevier), Figure 59.43, p. 2588 with permission.*

and atrophy (Figure 17.27), as well as reduced fluid and reduced numbers of sperm from the testis (approximately 50% of epididymal weight is made up of sperm and fluid). Following androgen withdrawal, the epididymal sperm lose their motility and fertilizing ability and die. The rat seminal vesicles are at least as responsive as the ventral prostate, and because of their much greater weight in controls have a larger dynamic range, as well as being easier to dissect if it is necessary to separate these organs from each other.

Withdrawal of androgen results in a wave of apoptosis that starts in the initial segment of the epididymis and moves down the rest of the epididymis with time (Figure 17.27). Many functions of the epididymis are androgen-dependent, including the energy-dependent transport of Na^+ ions across the epididymal epithelium and the activity of the detoxification enzymes glutathione S transferase and gamma glutathione transferase. In the prostate and seminal vesicles, there is epithelial apoptosis and epithelial atrophy (thinning) and decreased secretory content which is roughly proportional to the degree of hormone loss.

Pattern of Change Associated with Disturbance of Fluid Production, Reabsorption or Efferent Duct Obstruction

Patency of the seminiferous tubule lumen and the movement of sperm out of the testis and into the efferent ducts rely on the secretion of STF into the tubular lumen by the Sertoli cell (Table 17.11). The production of STF is continuous, as is the reabsorption of most of the fluid in the efferent ducts. Significant amounts of fluid are produced by the testis in a day (up to 0.8 mL/testis/day in the rat, and approximately 40 mL/testis/day in the boar).

DECREASED FLUID PRODUCTION

Testosterone is a major regulator of STF secretion, but it has also been demonstrated that the presence of elongating spermatids also regulates secretion. Thus, if elongating spermatids are lost from the seminiferous tubules, STF secretion will decrease. This loss of secretory function will result in narrowing of the tubular lumen and general reduction in the diameter of the tubule (tubular atrophy) in addition to the underlying germ cell loss. Fluid content is a significant component of testis

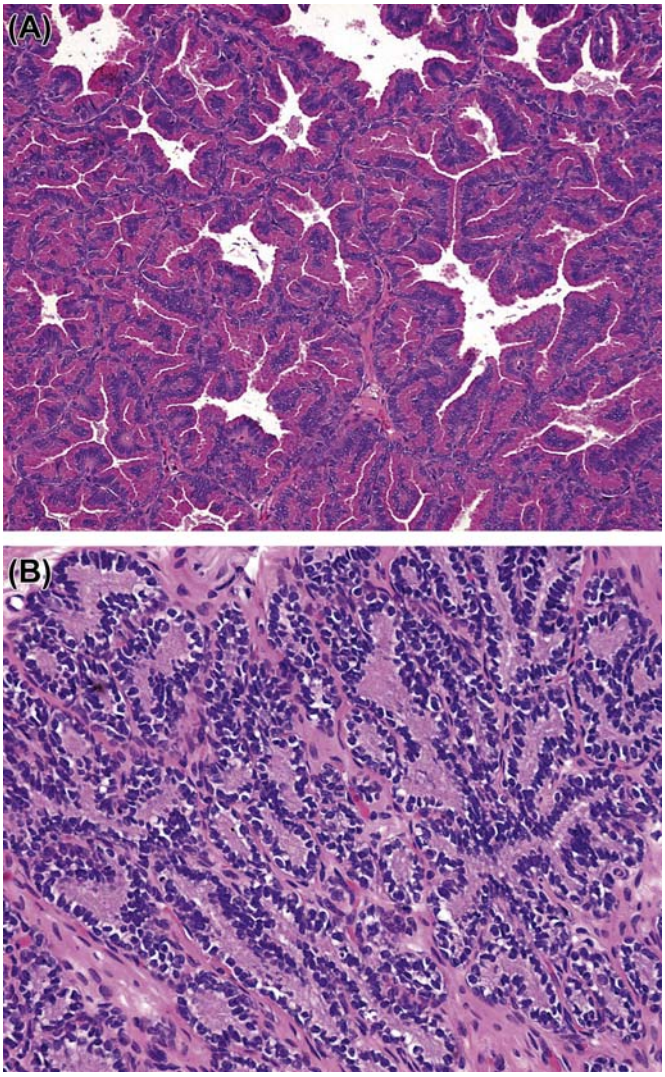

FIGURE 17.29 Dog prostate is also sensitive to decreased androgen status. (A) Normal mature prostate. Dog, H&E, ×10. (B) Mature prostate after antiandrogen administration. Dog, H&E, ×10. Source: *Figure reproduced from* Haschek and Rousseaux's Handbook of Toxicologic Pathology *(2013), third ed. (W.M. Haschek, C.G. Rousseaux and M.A. Wallig, eds.), Academic Press (Elsevier), Figure 59.44, p. 2589 with permission.*

weight, and so decreased testis weight is likely due to reduced STF as well as decreased numbers of germ cells. If a decrease in absolute testis weight is seen in the absence of any significant germ cell loss, a decrease in STF should be considered as a possible cause.

INCREASED FLUID PRODUCTION, OR DECREASED TUBULAR EMPTYING

An increase in absolute testis weight almost always reflects an increase in tubular fluid content and is generally accompanied by an increase in the diameter of the tubular lumen. Although increased fluid secretion by the Sertoli cell is a possible cause, there are no reports of this as a known chemically induced change. Another possibility is reduced emptying of the seminiferous tubules or relaxation of the encompassing peritubular cells. Endothelin antagonists cause increased testis weight and tubular dilation (Figure 17.30), and Endothelin-1 (ET1) has been suggested as a mediator of tubular contraction in the rat. Vasomotion as well as rhythmic contractions of the testicular capsule may also be involved in expulsion of fluid from the seminiferous tubules and interstitial lymph, and these could provide a potential target for disturbance of function. However, the most common *known* cause of increased fluid in the

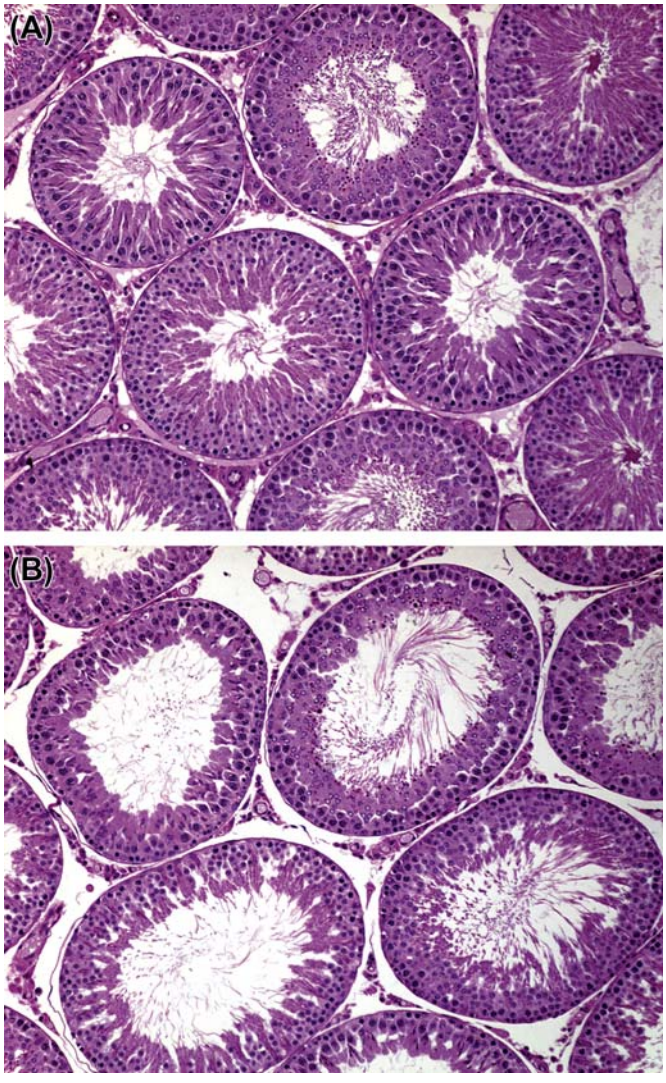

FIGURE 17.30 Tubular dilation produced by an endothelin antagonist in the rat. (A) Normal testis. Rat, H&E, ×10. (B) Treated testis. Note that there is no germ cell degeneration or depletion. Rat, H&E, ×10. Source: *Figure reproduced from* Haschek and Rousseaux's Handbook of Toxicologic Pathology *(2013), third ed. (W.M. Haschek, C.G. Rousseaux and M.A. Wallig, eds.), Academic Press (Elsevier), Figure 59.45, p. 2589 with permission.*

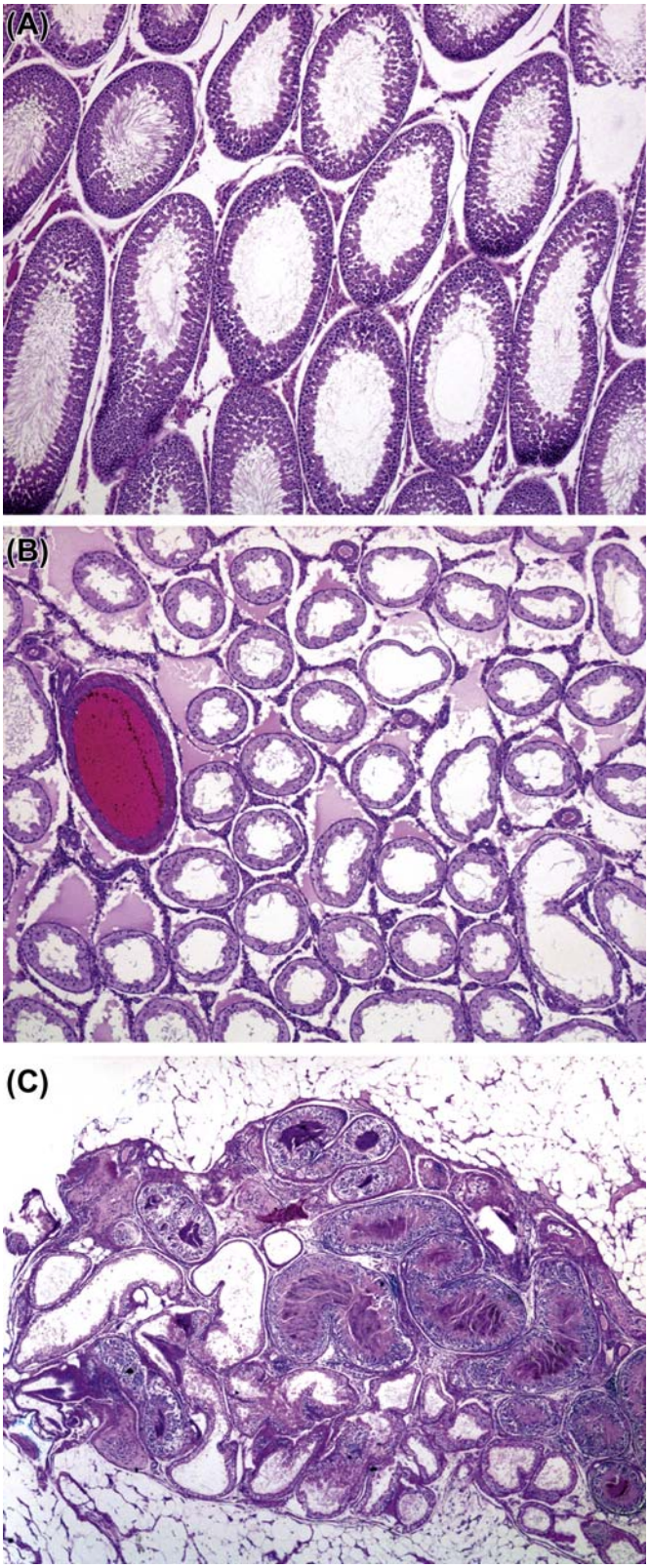

FIGURE 17.31 Testicular and epididymal changes secondary to efferent duct blockage in the rat. (A) Diffuse tubular dilation (this is the early change) Rat, H&E, ×4. (B) Diffuse tubular atrophy with dilated lumens and interstitial edema (this is a progression from tubular dilation). Rat, H&E, ×4. (C) Efferent duct obstruction caused by sperm stasis and granulomatous inflammation. Rat, H&E, ×2. Source: *Figure reproduced from* Haschek and Rousseaux's Handbook of Toxicologic Pathology *(2013), third ed. (W.M. Haschek, C.G. Rousseaux and M.A. Wallig, eds.), Academic Press (Elsevier), Figure 59.46, p. 2591 with permission.*

testis of rodents is obstruction of outflow in the efferent ducts. Although efferent duct obstruction and granulomas can be seen as a background incidental lesion in rats, they can also be caused by a chemically induced disturbance of fluid reabsorption. It is important to identify and elucidate the efferent duct as a target site because an effect on it often leads to severe testicular tubular atrophy, which may otherwise be considered a primary testicular lesion caused by the drug. If the efferent ducts become blocked or the secretion rate of STF exceeds the reabsorption rate, pressure build-up of fluid in the seminiferous tubules will cause severe damage to the testis. The sequence of changes that occurs has been demonstrated using a number of models; the simplest is efferent duct ligation.

EFFERENT DUCT LIGATION

When the efferent ducts are ligated there is a rapid (within hours) build-up of fluid within the testis causing an increase in tubular luminal diameter, thinning of the tubular epithelium, and an increase in testicular size and weight (Figure 17.31A). This reaches a peak at 16–24 hours after the ligation and is then followed by a gradual shrinkage of testicular size and testis weight, due to the progressive degeneration and death of the germ cells from the tubules. By 28 days after ligation the testis has lost 50% of its original weight and the tubules are severely atrophic, having lost all of their organization and most of their germ cells. The end-stage appearance of the testis following this type of injury is tubules lined only by Sertoli cells and occasional spermatogonia, generally having a slightly dilated (rather than collapsed) lumen, possibly accompanied by a dilated rete testis and interstitial edema (Figure 17.31B). The severity of the dilation and atrophy can be modified by ligating only a proportion of the proximal ducts, thereby leaving the common duct and some of the proximal ducts patent.

CHEMICALLY-INDUCED EFFERENT DUCT BLOCKAGE

Efferent duct obstruction, with its secondary testicular effects, can also be induced by exposure to a variety of drugs and chemicals that disturb the process of fluid reabsorption, either by increasing or inhibiting it. If too much fluid is reabsorbed, the sperm become prematurely concentrated and sequestered within the thin tortuous loops of the efferent ducts. Due to the

presence of leaky tight junctions between adjacent epithelial cells, the sequestered sperm will incite a granulomatous inflammatory response, which will permanently obstruct the flow of sperm and fluid through the ducts (Figure 17.31C). If there is inhibition of fluid reabsorption, the upstream ducts dilate with excess fluid and again appear to develop granulomatous inflammation and sperm stasis, possibly due to loss of junctional integrity, and cause occlusion of the ducts and backpressure of fluid to the testes. Inhibition of fluid reabsorption can occur through disturbance of the complex fluid/ion fluxes within the epithelium, or through disturbance of the vasculature that removes the fluid following reabsorption. In the case of a 5HT agonist, experimental evidence to support the latter explanation has been described.

It is important to recognize and distinguish tubular dilation and tubular degeneration/atrophy due to efferent duct blockage from other types of testicular toxicity, because the testicular damage is secondary to build-up of fluid pressure rather than a primary effect on spermatogenesis. Hallmarks of this type of toxicity include the phenomena that the lesions are frequently unilateral, some animals may have one dilated and one normal testis, others may have one atrophic and one normal testis and yet others may have one dilated and one atrophic testis. Another feature is that atrophic tubules often have a patent or slightly dilated lumen (rather than collapsed lumen) and the rete testis maybe dilated. Due to the fact that the testicular lesion (initially dilation, followed by atrophy) will only develop when there are enough efferent ducts obstructed to cause sufficient backpressure to the testis, the incidence maybe sporadic and not show a strong dose relationship (La et al., 2012). In addition, apoptosis of the epithelium of the initial segment and cribriform change in a specific segment of the caput epididymis are frequently seen when the efferent ducts are obstructed.

Further Reading

Boekelheide K., Johnson K.J., Richburg J.H., 2005. Sertoli cell toxicants. In: Skinner, M.K., Griswold, M.D., (Eds.) Sertoli Cell Biology. Elsevier Academic Press: San Diego, CA, pp. 345–382.

Chapin, R.E., Creasy, D.M., 2012. The measurement of male reproductive hormones in laboratory animals. Toxicol. Pathol. 40, 1063–1078.

Cook, J.C., Klinefelter, G.R., Hardisty, J.F., Sharpe, R.M., Foster, P.M. D., 1999. Rodent Leydig cell tumorigenesis: A review of the physiology, pathology, mechanisms, and relevance to humans. Crit. Rev. Toxicol. 29, 169–261.

Creasy, D.M., 1997. Evaluation of testicular toxicity in safety evaluation studies: the appropriate use of spermatogenic staging. Toxicol. Pathol. 25, 119–131.

Creasy, D.M., 2001. Pathogenesis of male reproductive toxicity. Toxicol. Pathol. 29, 64–76.

Creasy D.M., 2012. Reproduction of the rat, mouse, dog, non-human primate and minipig. In: McKinnes, E. (Ed.), Background Lesions in Laboratory Animals: A Color Atlas. Saunders Elsevier: New York, NY, pp. 101–122.

Creasy, D.M., Chapin, R.E., 2013. Chapter 59 Male Reproductive System, Haschek and Rousseaux's Handbook of Toxicologic Pathology, third ed. Elsevier, London.

Creasy, D.M., Chapin, R.E., 2014. Testicular and epididymal toxicity: pathogenesis and potential mechanisms of toxicity. Spermatogenesis. 4 (2), e1005511.

Creasy, D., Bube, A., de Rijk, E., Kandori, H., Kuwahara, M., Masson, R., et al., 2012. Proliferative and nonproliferative lesions of the rat and mouse male reproductive system. Toxicol. Pathol. 40, 40S–121S.

Everds, N.E., Snyder, P.W., Rosol, T.J., Creasy, D.M., Bailey, K.L., Bolon, B., et al., 2013. Interpreting stress responses during routine nonclinical safety studies: a review of the biology, impact, and assessment. Toxicol. Pathol. 41, 560–614.

Lanning, L.L., Creasy, D.M., Chapin, R.E., Mann, P.C., Barlow, N.J., Regan, K.S., et al., 2002. Recommended approaches for evaluation of testicular and epididymal toxicity. Toxicol. Pathol. 30, 507–520.

La, D.K., Creasy, D.M., Hess, R.A., Baxter, E., Pereira, M., Johnson, C.A., et al., 2012. Efferent duct toxicity with secondary testicular changes in rats following administration of a novel leukotriene A_4 hydrolase inhibitor. Toxicol. Pathol. 40, 705–714.

Marty, M.S., Chapin, R.E., Parks, L.G., Thorsrud, B.A., 2003. Development and maturation of the male reproductive system. Birth Defects Res. B Dev. Reprod. Toxicol. 68, 125–136.

Neill J.D., Plant T.M., Pfaff D.W., Challis J.R., de Kretser D.M., Richards J.S., et al., 2005. Knobil and Neill's Physiology of Reproduction, third ed. Elsevier Academic Press: San Diego, CA.

Picut, C.A., Remick, A.K., de Rijk, E.P., Simons, M.L., Stump, D.G., Parker, G.A., 2015. Postnatal development of the testis in the rat: morphologic study and correlation of morphology to neuroendocrine parameters. Toxicol Pathol. 43, 326–342.

Rehm, S., 2000. Spontaneous testicular lesions in purpose-bred beagle dogs. Toxicol. Pathol. 28, 782–787.

Robaire B., Hinton B.T., 2002. The Epididymis: from Molecules to Clinical Practice. Kluwer Academic/Plenum Publishers: New York, NY.

Russell L.D., Ettlin R.A., SinhaHikim A.P., Clegg E.D., 1990. Histological and Histopathological Evaluation of the Testis. Cache River Press: Clearwater, FL.

Seed, J., Chapin, R.E., Clegg, E.D., Dostal, L.A., Foote, R.H., Hurtt, M.E., et al., 1996. Methods for assessing sperm motility, morphology, and counts in the rat, rabbit, and dog: a consensus report. ILSI Risk Science Institute Expert Working Group on Sperm Evaluation. Reprod. Toxicol. 10, 237–244.

Sharpe, R.M., Skakkebaek, N., 2008. Testicular dysgenesis syndrome: mechanistic insights and potential new downstream effects. Fertil. Steril. 89 (Suppl. 1), 33–37.

Wong, C.H., Cheng, C.Y., 2005. Mitogen-activated protein kinases, adherens junction dynamics, and spermatogenesis: a review of recent data. Dev. Biol. 286, 1–15.

CHAPTER

18

Female Reproductive System

Daniel G. Rudmann[1] *and George L. Foley*[2]

[1]Flagship Biosciences, Westminster, CO, United States [2]Abbvie, Chicago, IL, United States

OUTLINE

INTRODUCTION

On Friday, August 10, 1962, *Time* magazine published an article entitled "Medicine: The Thalidomide Disaster," describing one of the most highly publicized drug toxicities in the history of the pharmaceutical industry. The article reported an epidemic of deformities in close to 8000 babies largely from European mothers who took thalidomide as a sleep aid. Fortunately for some regions, widespread use of thalidomide was delayed, which avoided comparable catastrophes in non-European countries. However, germane to this chapter, an important outcome of this crisis was the demand for better supervision of drug development, and more specifically, an increased emphasis on the evaluation of drug effects on the female reproductive system, drug testing in pregnant animals of several species, and proposals for scrutinizing the testing of new drugs in women of child-bearing age.

The gold standard for evaluation of female reproductive system toxicity in general toxicology studies is the assessment of the test article-effects on organ weights, and gross and histologic changes in reproductive tissues in two animal models, generally using a nonrodent and rodent species. For drug development, the safety assessment team (toxicologist, pathologist, and drug disposition scientist) are key contributors to the analysis of the data from these repeat-dose toxicology

Fundamentals of Toxicologic Pathology.
DOI: http://dx.doi.org/10.1016/B978-0-12-809841-7.00018-6

TABLE 18.1 Recommended Female Reproductive System Endpoints for Standard Toxicology Studies[a]

Recommendations
Organ weights: ovary (studies: 6 months in rodents, 12 months in nonrodents); pituitary (all but mouse); uterus (case by case)
Gross pathology: examination of full reproductive tract
Histopathology: ovary, uterus, cervix, vagina, pituitary, adrenal

[a]*See Bregman et al. (2003), Michael et al. (2007), OECD (2008), van Esch et al. (2008b).*
From Haschek, W.M., Rousseaux, C.G., Wallig, M.A. (Eds.), 2013. Handbook of Toxicologic Pathology, third ed. Academic Press, San Diego, CA, Table 60.2, p. 2601, with permission.

studies, which may last up to a lifetime in rodents (2 years) and 1 year in a nonrodent species (usually the cynomolgus monkey or beagle dog). The recommended female reproductive endpoints for these studies are outlined in detail by several excellent multiauthor publications sponsored by the Society of Toxicologic Pathology and summarized in Table 18.1. A summary of the differences between the rat, beagle dog, and cynomolgus monkey with regards to sexual development and reproductive cycle characteristics is given in Table 18.2 and common background findings in Table 18.3.

TABLE 18.2 Differences Between Sexual Development and Reproductive Cycle Characteristics of the SD Rat, Beagle Dog, and Cynomolgus Monkey

	SD rat	Beagle dog	Cynomolgus monkey
Sexual maturity	8 weeks	Approximately 1.5 years	Approximately 4 years
Senescence (S) or menopause (M)	>9 months (S)	Not applicable (S)[a]	>20 years (M)
Cycle length	4 days	3.5e13 months	28 days
Seasonal influence	None	None	Yes, and social influences

[a]*While cycle length can be prolonged in older female beagle dogs, true senescence is not described.*
From Haschek, W.M., Rousseaux, C.G., Wallig, M.A. (Eds.), 2013. Handbook of Toxicologic Pathology, third ed. Academic Press, San Diego, CA, Table 60.3, p. 2602, with permission.

STRUCTURE, FUNCTION, AND CELL BIOLOGY

The Histology of the Rat Female Reproductive Tract During the Estrous Cycle

The cycle of the Sprague–Dawley (SD) and Wister rat is usually 4 days in length; however, occasionally rats will have 5 day cycles or will switch between 4 and 5 day cycles. SD and Wistar rats start entering senescence at 5–6 months of age, which alters the cycle, usually prolonging the portions of the cycle under estradiol influence (late diestrus and proestrus). As the pathologist evaluates the female reproductive system in rat studies of 2 weeks to 3 months, histologic staging is recommended. Table 18.4 lists what we consider are the best distinguishing characteristics of each estrous cycle stage. We believe that the most useful histologic criteria

TABLE 18.3 Commonly Reported Spontaneous Changes in the Female Reproductive Tract of Preclinical Animal Species

Species	Ovary
Rat	Luteal, follicular, or parovarian cysts (Figure 60.21)
Beagle dog	Persistent CL
Cynomolgus monkey	Cortical mineralization; cysts, paraovarian/follicular/rete ovarii; hyperplasia, ovarian surface epithelium
Species	**Uterus**
Rat	Squamous metaplasia (Figure 60.22), cystic endometrial hyperplasia (Figure 60.23), neutrophilic gland infiltrates, endometrial stromal polyps (Figure 60.24)
Beagle dog	Cystic endometrial hyperplasia
Cynomolgus monkey	Endometrial polyps, ectopic ovary, irregular uterine hemorrhage, "inactive," adenomyosis, endometriosis
Species	**Vagina/cervix**
Rat	Squamous metaplasia
Beagle dog	Vaginitis
Cynomolgus monkey	Squamous metaplasia of endocervical glands

From Haschek, W.M., Rousseaux, C.G., Wallig, M.A. (Eds.), 2013. Handbook of Toxicologic Pathology, third ed. Academic Press, San Diego, CA, Table 60.7, p. 2629, with permission.

TABLE 18.4 Key Vaginal Histologic Criteria for the Rat Estrous Cycle

Stage	Histology
Proestrus	Mucified cuboidal epithelium overlying a cornified layer
Estrus	Stratified epithelium with keratin loosely associated or sloughed into lumen
Metestrus (Diestrus I)	Apoptosis of vaginal epithelial cells
Diestrus (Diestrus II)	Increased mitoses of vaginal epithelial cells

From Haschek, W.M., Rousseaux, C.G., Wallig, M.A. (Eds.), 2013. Handbook of Toxicologic Pathology, third ed. Academic Press, San Diego, CA, Table 60.4, p. 2608, with permission.

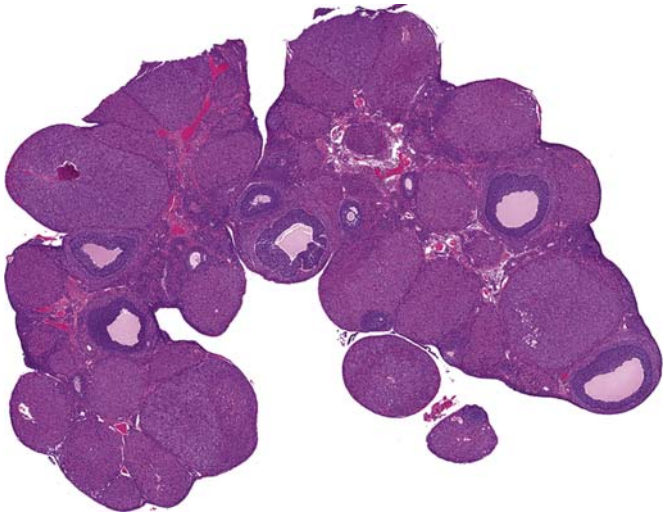

FIGURE 18.2 Ovary, rat, normal ovary. Numerous CL and follicles give the ovary a grape-like appearance. ×15, H&E. Source: *From Haschek, W.M., Rousseaux, C.G., Wallig, M.A. (Eds.), 2013. Haschek and Rousseaux's Handbook of Toxicologic Pathology, third ed. Academic Press (Elsevier), San Diego, CA, Figure 60.1, p. 2603, with permission.*

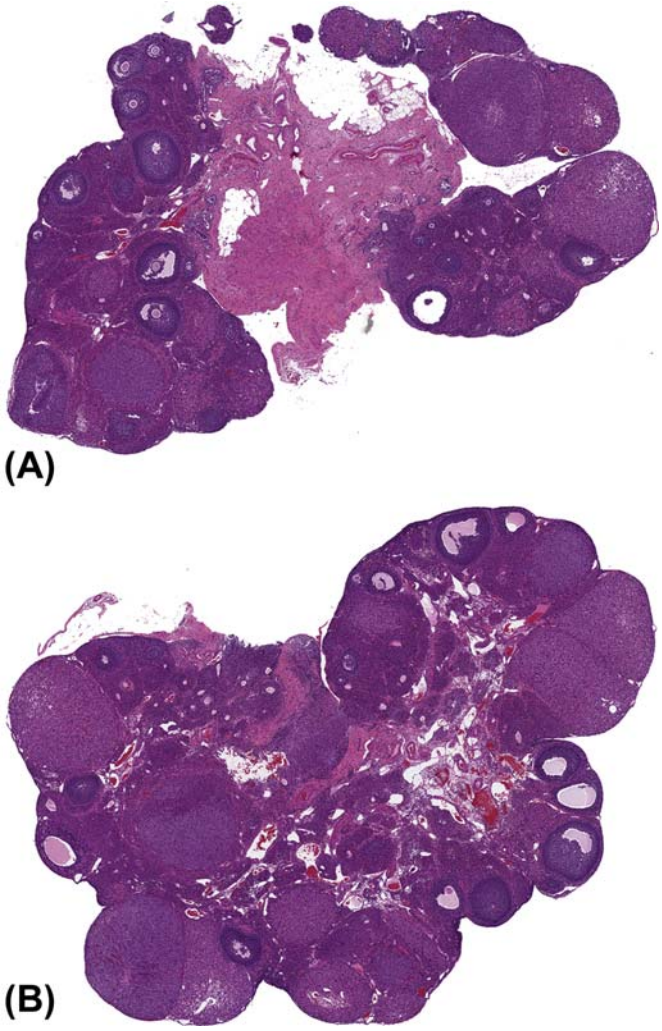

FIGURE 18.1 Ovary, rat, effects of section. Because the section was not optimally processed, the top ovary (A) compared to the bottom (B) appears to have a lower number of follicles and CL. ×15, H&E. Source: *From Haschek, W.M., Rousseaux, C.G., Wallig, M.A. (Eds.), 2013. Haschek and Rousseaux's Handbook of Toxicologic Pathology, third ed. Academic Press (Elsevier), San Diego, CA, Figure 60.6, p. 2610, with permission.*

for differentiating among the various stages of estrous occur in the anterior vagina. While the vagina is very useful in staging, it is important to emphasize that all reproductive tissues should be examined as a unit in the evaluation of a potential effect of a test agent and standardized trimming paradigms should be enforced to protect from artifact especially problematic in the ovary (Figures 18.1–18.6). Note that the most common rat strains used, SD and Wistar, have a similar estrous cycle, and our descriptions of the cycle will be limited to these strains. The information provided in the following will be a compilation of our personal experience, the literature, and the results from a detailed estrous cycle study completed at Eli Lilly in the late 1990s with the Crl:CD (SD) IGS BR SD rat.

On the day of estrus, the ovary usually has four sets of corpora lutea (CL). The new, small basophilic partially luteinized CL are from the most recent ovulation event, basophilic CL from the last cycle are now beginning to appear eosinophilic, eosinophilic CL present from the previous cycles show degenerative changes, and old shrunken CL remain from several cycles ago (Figure 18.7). Dependent on section, one may observe an ovulatory fossa with hemorrhage, mitotic activity, and luteinizing granulosa cells, and oviducts, if present, may have ova or cumulus oophorous cells. The uterus has extensive apoptosis of *both* the luminal and glandular epithelium and there is stromal edema and eosinophil infiltrates (Figure 18.7). The uterine epithelial cells are crowded and tall and the uterine myometrium is thick. The vagina is approximately six to eight layers thick and has characteristic plaques of cornified epithelium that

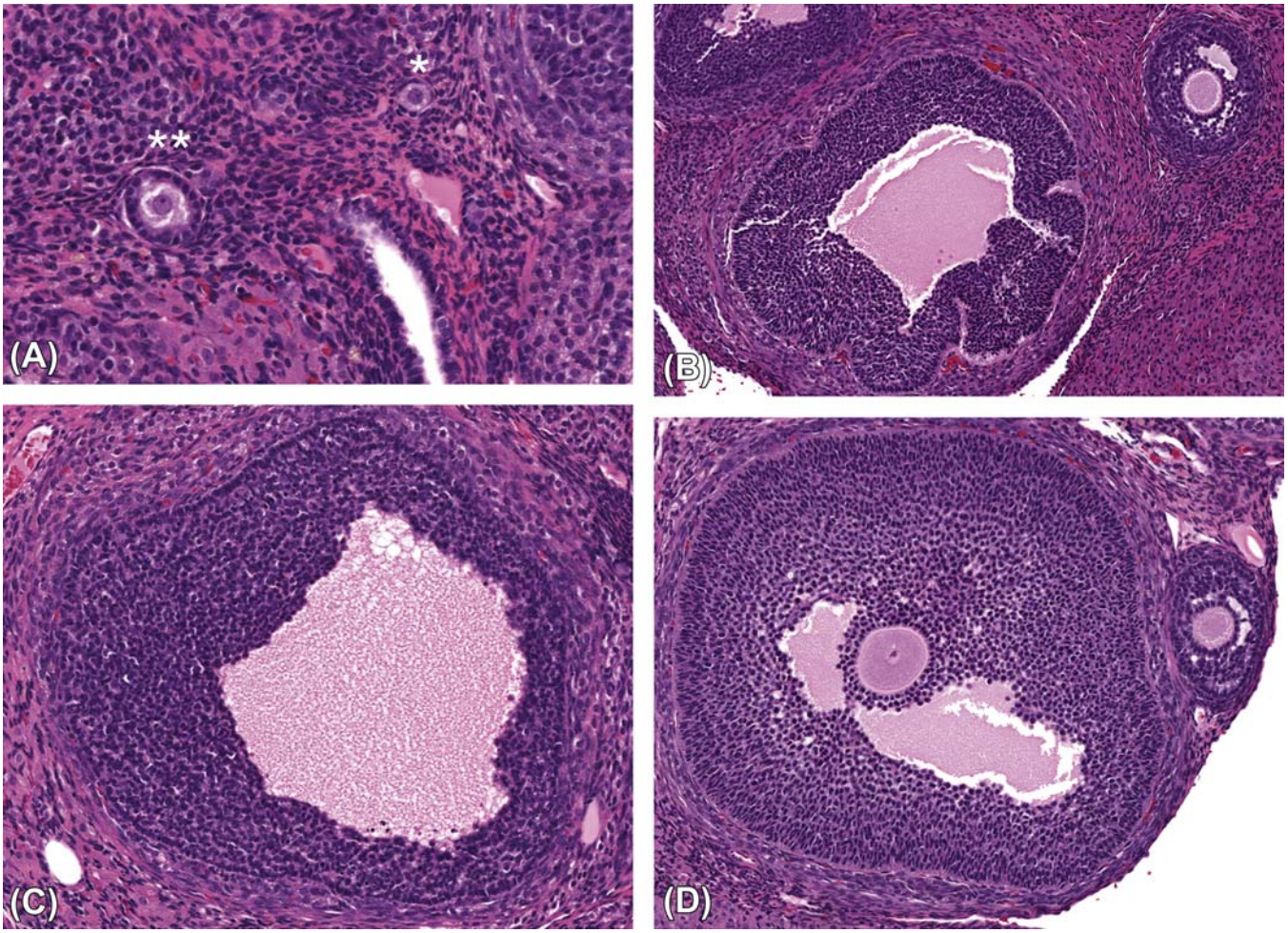

FIGURE 18.3 Ovary, rat, normal follicle maturation. Primary (*) and secondary (**) follicles (A), tertiary follicles (B), and a Graafian follicle without (C) and with a central oocyte (D). ×100 (A), ×50 (B), ×75 (C), H&E. Source: *From Haschek, W.M., Rousseaux, C.G., Wallig, M.A. (Eds.), 2013. Haschek and Rousseaux's Handbook of Toxicologic Pathology, third ed. Academic Press (Elsevier), San Diego, CA, Figure 60.2, p. 2604, with permission.*

are sloughed into the vaginal lumen early in estrus and cleared quickly; therefore, late on the day of estrus very little cornified debris may be left (Figure 18.8).

On the day of metestrus (sometimes referred to as diestrus I), three sets of CL are present: a partially filled basophilic CL with luteolytic changes, an eosinophilic CL from the previous cycle, and old, shrunken CL from past cycles (Figure 18.9). The vagina has a noncornified epithelium, that is, four to six layers in thickness with intraepithelial and luminal leukocytes (Figure 18.6). The uterus still has apoptosis but *only* in the luminal epithelial cells (Figure 18.9). The uterine epithelial cells lining both the lumen and the glands are shorter and more distinct. The uterine myometrium is thinner (Figure 18.9).

On the day of diestrus (sometimes referred to as diestrus II), there are three sets of CL: a filled basophilic CL, an eosinophilic CL with luteolysis, and old CL from past cycles. The filled basophilic CL has luteal cells that are larger with very prominent nucleoli; some containing vacuoles (lipid droplets) in their cytoplasm (Figure 18.9). The vagina is thinner, only three to four cell layers thick, noncornified, and has prominent intraepithelial leukocytes. Mitoses may be observed in the basal layer (Figure 18.6). The uterus is quiescent with a short columnar lining and glandular epithelium and a thinner myometrium (Figure 18.9).

On the day of proestrus, the ovary has mature eosinophilic CL, filled basophilic CL without luteolysis, and old shrunken CL. Large preovulatory follicles are often present in the ovary at this stage of the estrous cycle. Interstitial glands will be the most prominent during proestrus. The uterus has a dilated lumen, stromal edema, a hypertrophied myometrium,

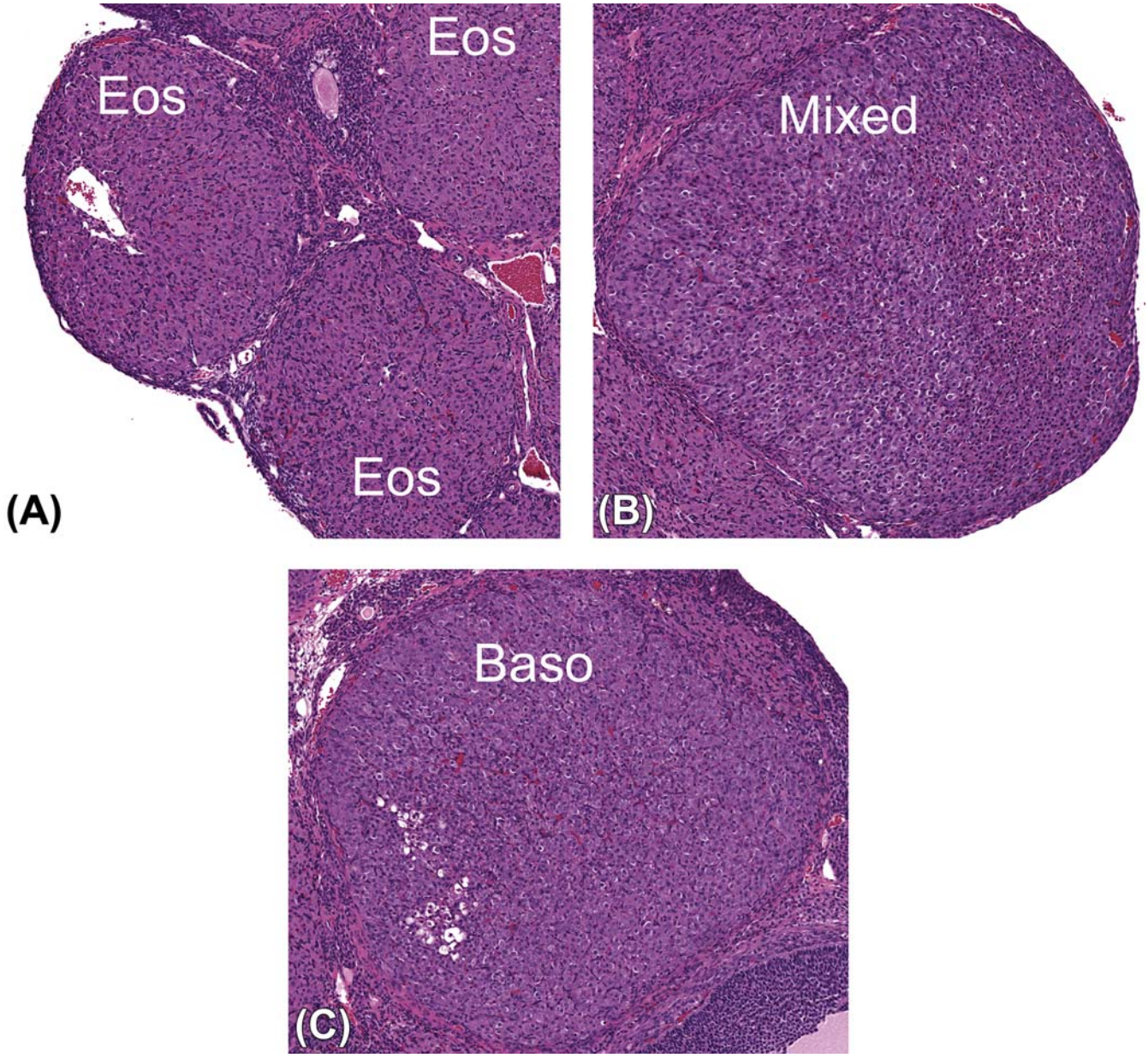

FIGURE 18.4 Ovary, rat, CL types. Normal eosinophilic (Eos) CL (A), mixed esosinophilic and basophilic CL (B), and basophilc (Baso) CL (C). ×50, H&E. Source: *From Haschek, W.M., Rousseaux, C.G., Wallig, M.A. (Eds.), 2013. Haschek and Rousseaux's Handbook of Toxicologic Pathology, third ed. Academic Press (Elsevier), San Diego, CA, Figure 60.3, p. 2605, with permission.*

and mitoses in luminal and glandular epithelial cells (Figure 18.10). Eosinophils in the stroma are most prominent in this stage. Uterine weights are often increased during proestrus and appear larger at necropsy because of intraluminal fluid. Early in proestrus, the vagina is lined by four to eight layers of plump epithelial cells that have a mucoid character to their cytoplasm. Later in proestrus the vaginal epithelium is thicker (up to 10 layers) and overlies a thin layer of cornified cells (Figure 18.6).

The Histology of the Dog Female Reproductive Tract During the Estrous Cycle

The estrous cycle of the dog is very different from the rat. It is markedly longer, more variable in phase length (3.5–13 months), and has a normal "anestrus" phase (for review, see Chandra and Adler, 2008). Evaluating the reproductive tract in dog toxicology studies can be challenging because young, peripubertal dogs may be used in toxicology studies and numbers

in test groups are small (generally 3 or 4) (Figure 18.11). An accurate phasing of the dog estrous cycle will assist in assessing test agent effects on synchronization of the reproductive events in the female dog (bitch) reproductive tract. In fact, in the last several decades, the beagle dog as an animal model has been a very useful predictor of the effects of treatments targeted at human contraception.

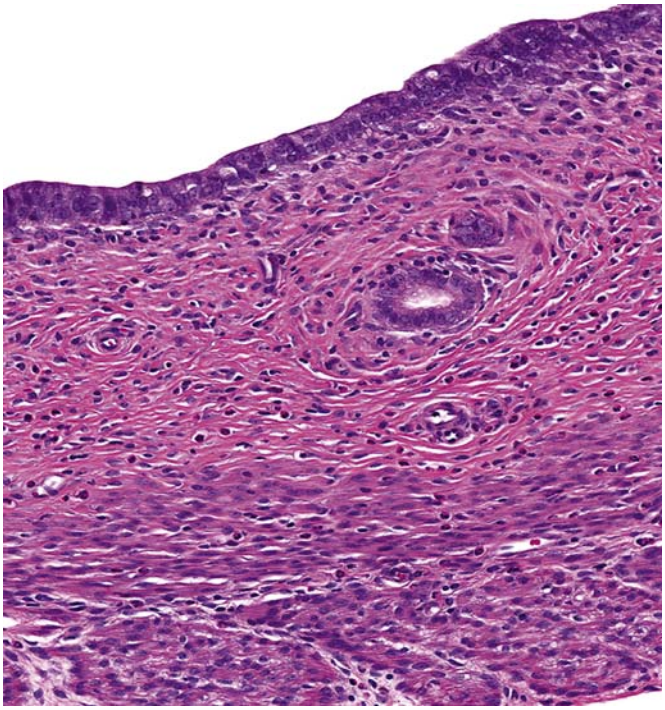

FIGURE 18.5 Uterus, rat, normal: The uterus is composed of an innermost mucosa, the endometrium, a middle muscular layer, the myometrium, and an outer serosal layer, the perimetrium. ×60, H&E. Source: *From Haschek, W.M., Rousseaux, C.G., Wallig, M.A. (Eds.), 2013. Haschek and Rousseaux's Handbook of Toxicologic Pathology, third ed. Academic Press (Elsevier), San Diego, CA, Figure 60.7, p. 2610, with permission.*

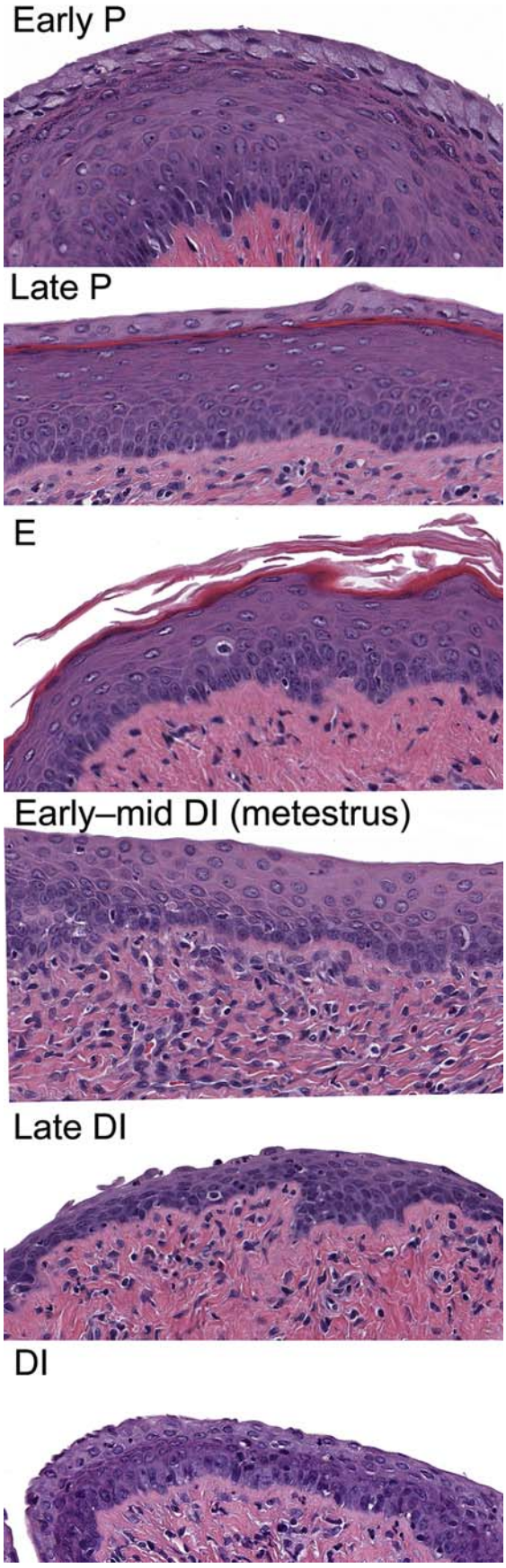

FIGURE 18.6 Vagina, rat, changes with estrous cycle. Proestrus (Early and Late P): Early in proestrus, the vagina is lined by four to eight layers of plump epithelial cells that have a mucoid character to their cytoplasm. Later in proestrus the vaginal epithelium is thicker (up to 10 layers) and overlies a thin layer of cornified cells. Estrus (E): There is no superficial vacuolated layer, the epithelium is approximately six to eight layers thick and has characteristic plaques of cornified epithelium. Diestrus I or metestrus (DI): The vagina has a noncornified epithelium that is four to six layers in thickness with intraepithelial and luminal leukocytes. Diestrus II (DII): The vagina is thinner, only three to four cell layers thick, noncornified, and has prominent intraepithelial leukocytes. ×80, H&E. Source: *From Haschek, W.M., Rousseaux, C.G., Wallig, M.A. (Eds.), 2013. Haschek and Rousseaux's Handbook of Toxicologic Pathology, third ed. Academic Press (Elsevier), San Diego, CA, Figure 60.5, p. 2609, with permission.*

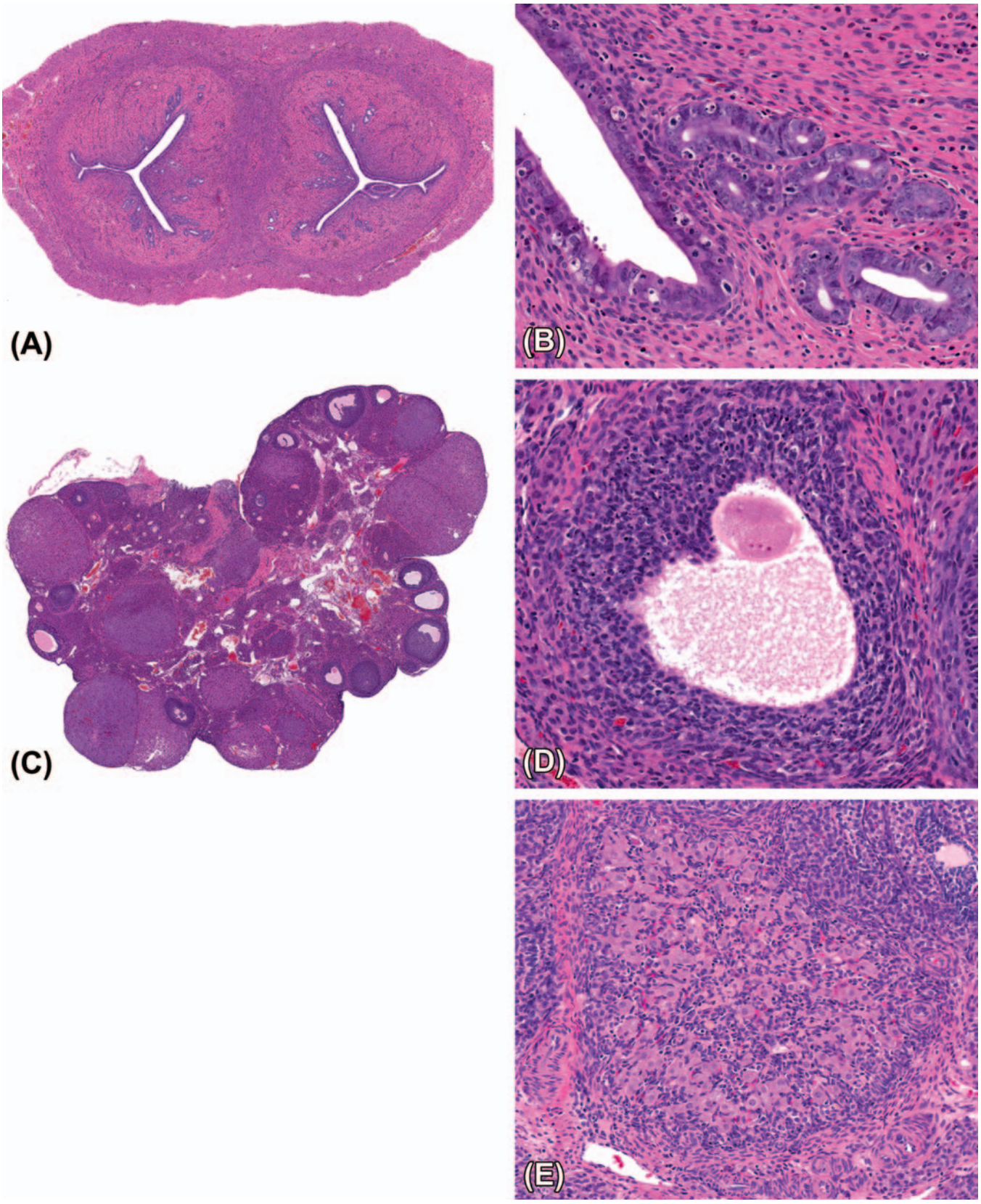

FIGURE 18.7 Ovary and uterus, rat, estrus. The uterus has a thick endometrium and myometrium (A, ×12) and there is apotosis of both luminal and glandular epithelial cells with endometrial inflammatory cell infiltrates (B, ×120). The ovary has four sets of CL (C, ×10) and large antral follicles (D, ×120). The new, small basophilic partially luteinized CL are from the most recent ovulation event, basophilic CL from the last cycle are now beginning to appear eosinophilic, eosinophilic CL present from the previous cycles show degenerative changes, and old shrunken CL (E, ×150) remain from several cycles ago. H&E. Source: *From Haschek, W.M., Rousseaux, C.G., Wallig, M.A. (Eds.), 2013. Haschek and Rousseaux's Handbook of Toxicologic Pathology, third ed. Academic Press (Elsevier), San Diego, CA, Figure 60.9, p. 2612, with permission.*

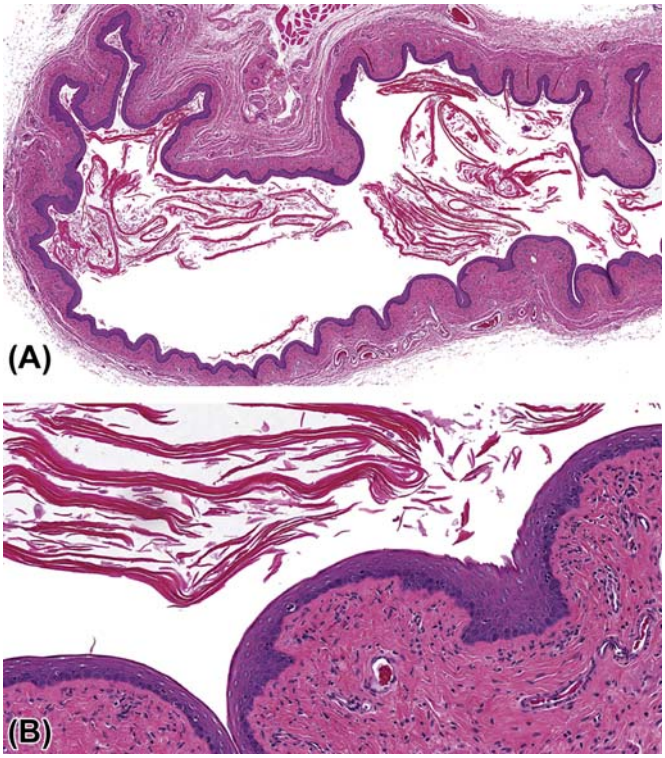

FIGURE 18.8 Vagina, rat, estrus: Cornified material is sloughed into the vaginal lumen; later in estrus there may be very little cornified debris left. ×12 (A) and ×60 (B), H&E. Source: *From Haschek, W.M., Rousseaux, C.G., Wallig, M.A. (Eds.), 2013. Haschek and Rousseaux's Handbook of Toxicologic Pathology, third ed. Academic Press (Elsevier), San Diego, CA, Figure 60.8, p. 2611, with permission.*

Dog ovaries are irregularly ellipsoid. Several follicles and CL may develop during each cycle and polyovular follicles (follicles with two or more oocytes) commonly occur in young bitches. Like the rat, these structures often protrude from the ovarian surface, thus giving rise to the grape-like appearance of the ovary. Dog ovaries also have interstitial glands or granulosa cell cords derived from atretic follicles and stromal cells. Granulosa cells of canine follicles begin to luteinize with extensive infoldings of the granulosa lining prior to ovulation. It is important to note that the infolded luteinized preovulatory follicles in the dog are normal but can often be misinterpreted as abnormal. Unique to dogs at all phases of the reproductive cycle is the presence of invaginated cord-like proliferations of the surface epithelium that extend through the tunica albuginea into the superficial cortex. These structures have been termed subsurface epithelial structures (SES) and are most numerous during anestrus. The SES are hormonally responsive and commonly become cystic in aged dogs. Their functional significance is not known. The dog has a bicornuate uterus with a short body and long and straight uterine horns. The two separate uterine horns open into one common cervical canal. Otherwise, the general histology of the uterus and vagina are comparable to the rat.

Estrus and proestrus phases together account for 1–3 weeks of the estrous cycle in dogs. At estrus the ovary has large preovulatory follicles with luteinization of the granulosa cell layers (Figure 18.12). The uterus has myometrial hypertrophy, stromal cell proliferation, stromal congestion, edema, and hemorrhage (Figure 18.13). The surface and glandular epithelium is increased in height and there are numerous mitotic figures. The vagina is the thickest during estrus and heavily cornified (Figure 18.13). The stroma and smooth muscle are hyperplastic and there are both stromal congestion and edema.

Metestrus or diestrus is up to 100 days in length in the dog. At metestrus the ovary has new CL (Figure 18.12). Uterine luminal glands are proliferative and straight, and abruptly become tortuous toward the basement membrane (Figure 18.13). Often the glandular lumina contain pink secretions, and the stromal edema and congestion are markedly decreased. The upper gland and luminal epithelial cells progressively develop foamier cytoplasm as a consequence of the influence of progesterone. The vagina becomes much

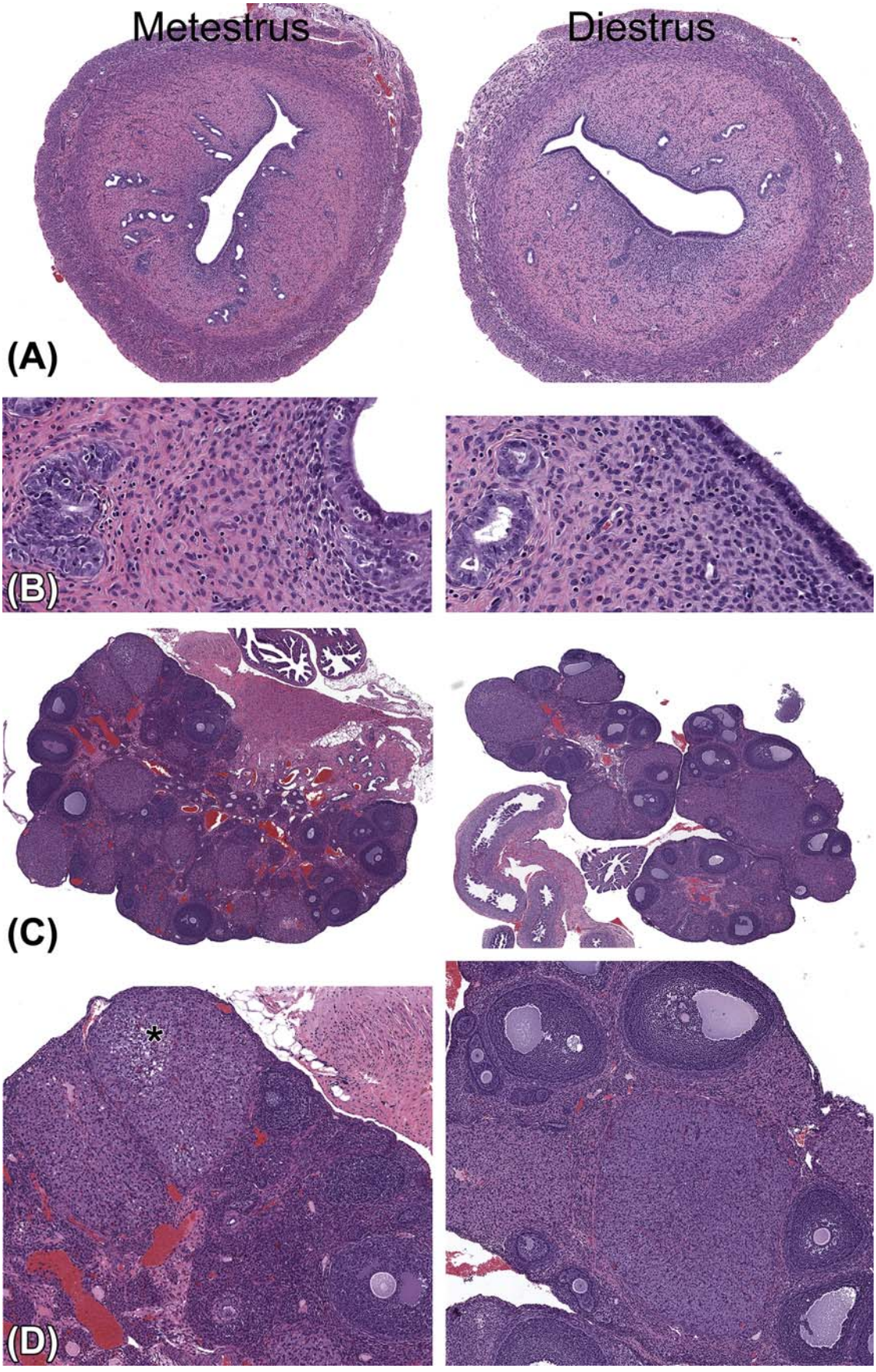

FIGURE 18.9 Uterus and ovary, rat, metestrus (diestrus I) and diestrus (II) (A–D). Metestrus: The uterus (A, B) has apoptotic cells but *only* in the luminal epithelial cells, uterine epithelial cells lining both the lumen and the glands are shorter and more distinct, and the uterine myometrium is thinner. In the metestrus ovary (C, D), three sets of CL are present: a partially filled basophilic CL with luteolytic changes (*), an eosinophilic CL from the previous cycle, and old, shrunken CL from past cycles. Diestrus (or diestrus II): The uterus is quiescent with a short columnar lining and glandular epithelium and also has a thinner myometrium. In the ovary, there are three sets of CL: a filled basophilic CL, an eosinophilic CL with luteolysis, and old CL from past cycles. ×20 (A), ×120 (B), ×15 (C), and ×75 (D), H&E. Source: *From Haschek, W.M., Rousseaux, C.G., Wallig, M.A. (Eds.), 2013. Haschek and Rousseaux's Handbook of Toxicologic Pathology, third ed. Academic Press (Elsevier), San Diego, CA, Figure 60.10, p. 2614, with permission.*

thinner (three to four cell layers) and loses its cornification (Figure 18.13). Because of the long life of the corporal lutea, pseudocyesis (false or pseudopregnancy) with or without clinical signs is common in the dog. In pseudocyesis, dog mammary glands will demonstrate alveolar lobular hyperplasia and increased secretions, which could be interpreted as a treatment-related effect in a toxicology study. Also, the uterus has a hyperplastic endometrium and may have implantation-like areas without the fetal contribution.

glandular epithelium is lined by low columnar cells with basally situated nuclei and the vagina remains three to four cell layers thick (Figure 18.13). The vaginal epithelium is at its thinnest and remains noncornified (Figure 18.13).

At proestrus, there is a gradual increase in ovarian follicular development, and large antral follicles with thick granulosa cell layers are evident (Figure 18.12). Often there are old CL composed of small foci of vacuolated cells and macrophages with intracytoplasmic

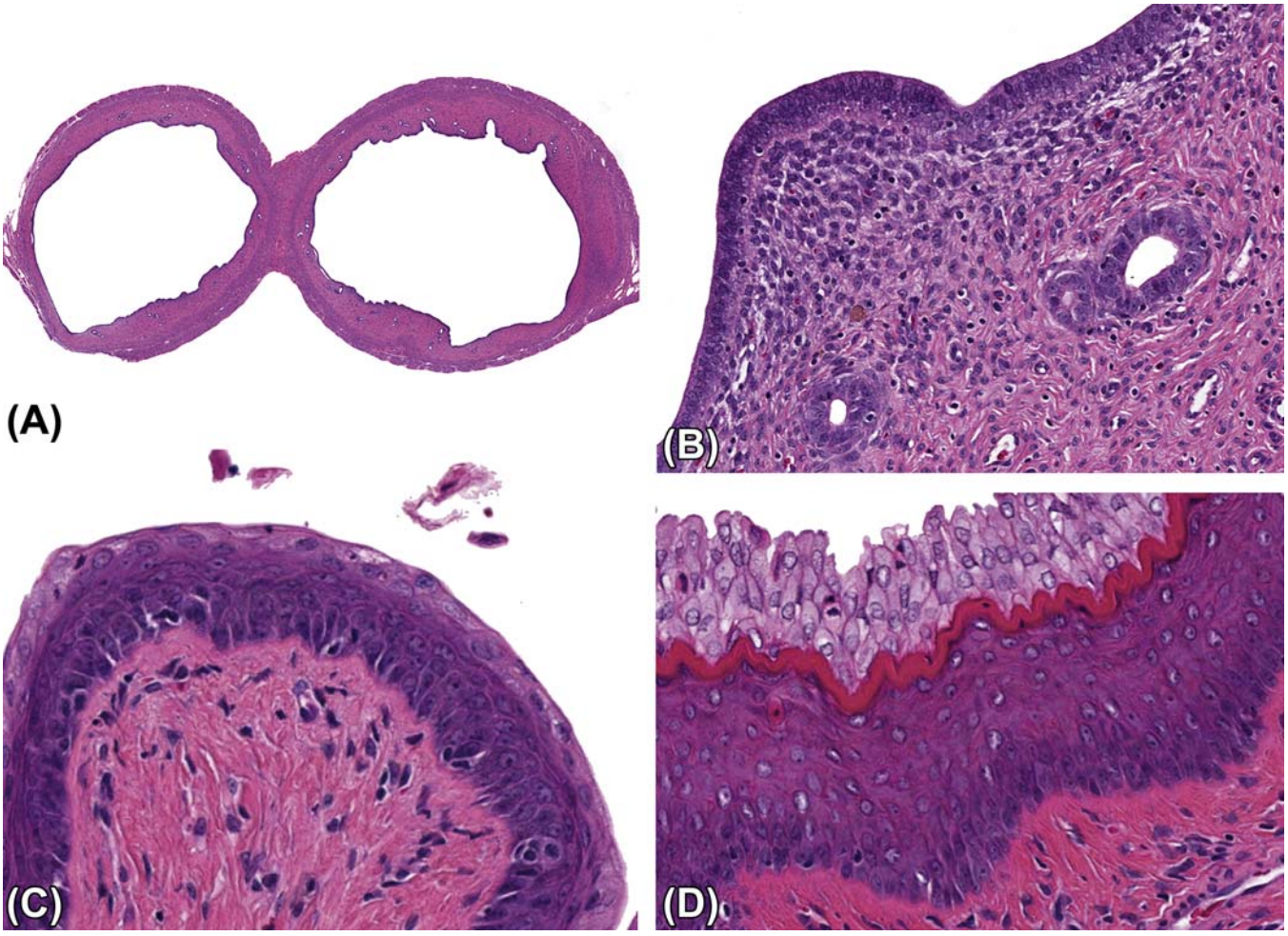

FIGURE 18.10 Uterus and vagina, rat, proestrus. The uterus has a dilated lumen (A), stromal edema, a hypertrophied myometrium, and mitoses in luminal and glandular epithelial cells (B). Eosinophils in the stroma are most prominent in this stage. Early in proestrus, the vagina is lined by four to eight layers of plump epithelial cells that have a mucoid character to their cytoplasm (C). Later in proestrus the vaginal epithelium is thicker (up to 10 layers) and overlies a thin layer of cornified cells (D). ×10 (A), ×80 (B, C), and ×125 (D), H&E. Source: *From Haschek, W.M., Rousseaux, C.G., Wallig, M.A. (Eds.), 2013. Haschek and Rousseaux's Handbook of Toxicologic Pathology, third ed. Academic Press (Elsevier), San Diego, CA, Figure 60.11, p. 2616, with permission.*

Anestrus is the most variable period in the dog, its length partially dependent on the breed. This stage can range from 1 to 6 months in length. During anestrus, the ovary appears quiescent with one or two sets of old CL (Figure 18.12). The uterine surface and

lipofuscin. During proestrus the uterine mucosa becomes more vascular and edematous with occasional small focal areas of erythrocyte extravasation in the zona compacta. The surface and glandular epithelium increases in height, and numerous mitotic figures are

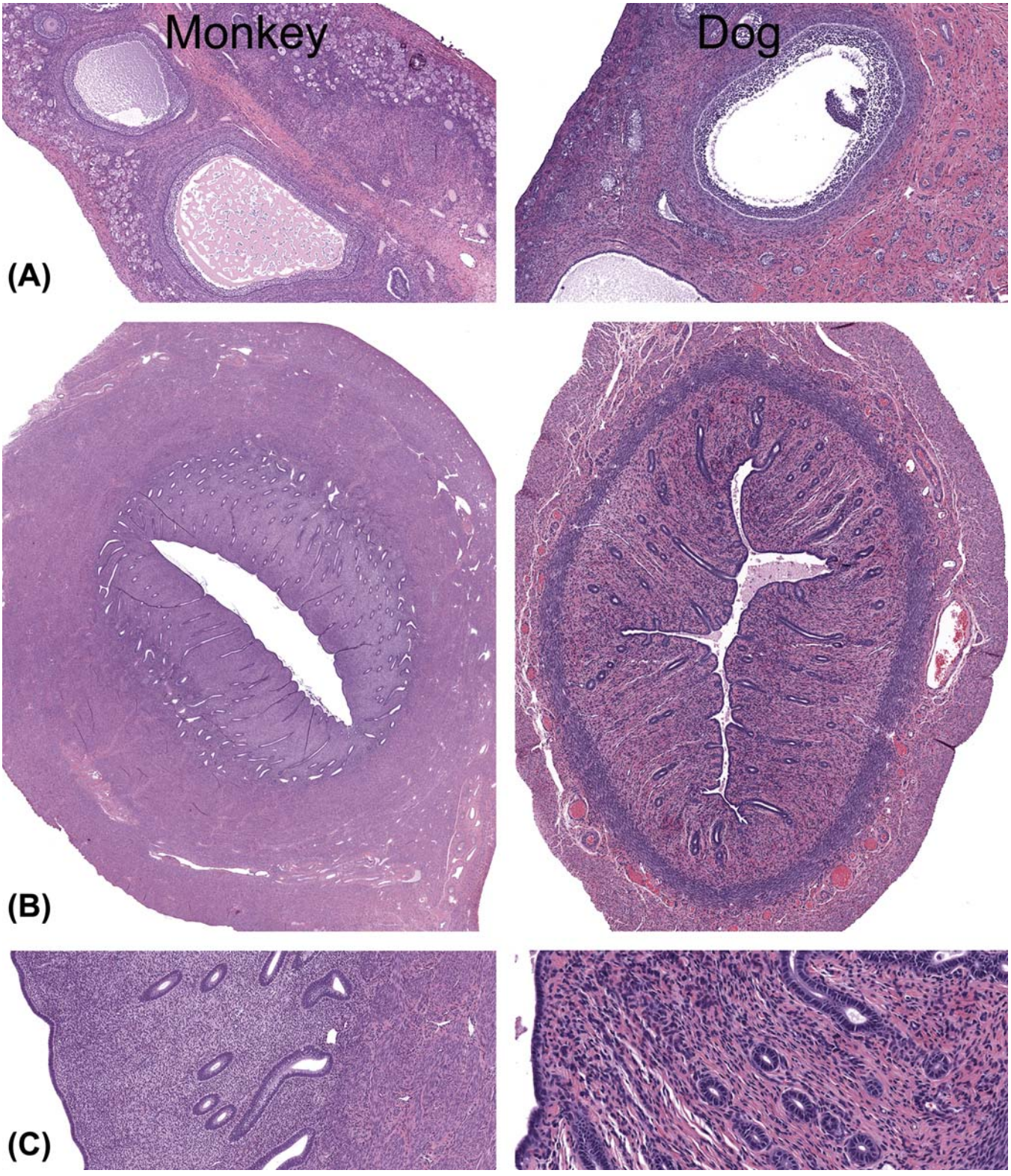

FIGURE 18.11 Ovary and uterus, cynomolgus monkey and dog. Immature. Ovaries and uteri are small grossly (not shown). (A) Ovary: There are no CL and follicles are often immature (×50). (B,C) Uterus: The uterine endometrium and myometrium is thin and endometrial glands are quiescent (×6 and ×20). H&E. Source: *From Haschek, W.M., Rousseaux, C.G., Wallig, M.A. (Eds.), 2013. Haschek and Rousseaux's Handbook of Toxicologic Pathology, third ed. Academic Press (Elsevier), San Diego, CA, Figure 60.12, p. 2617, with permission.*

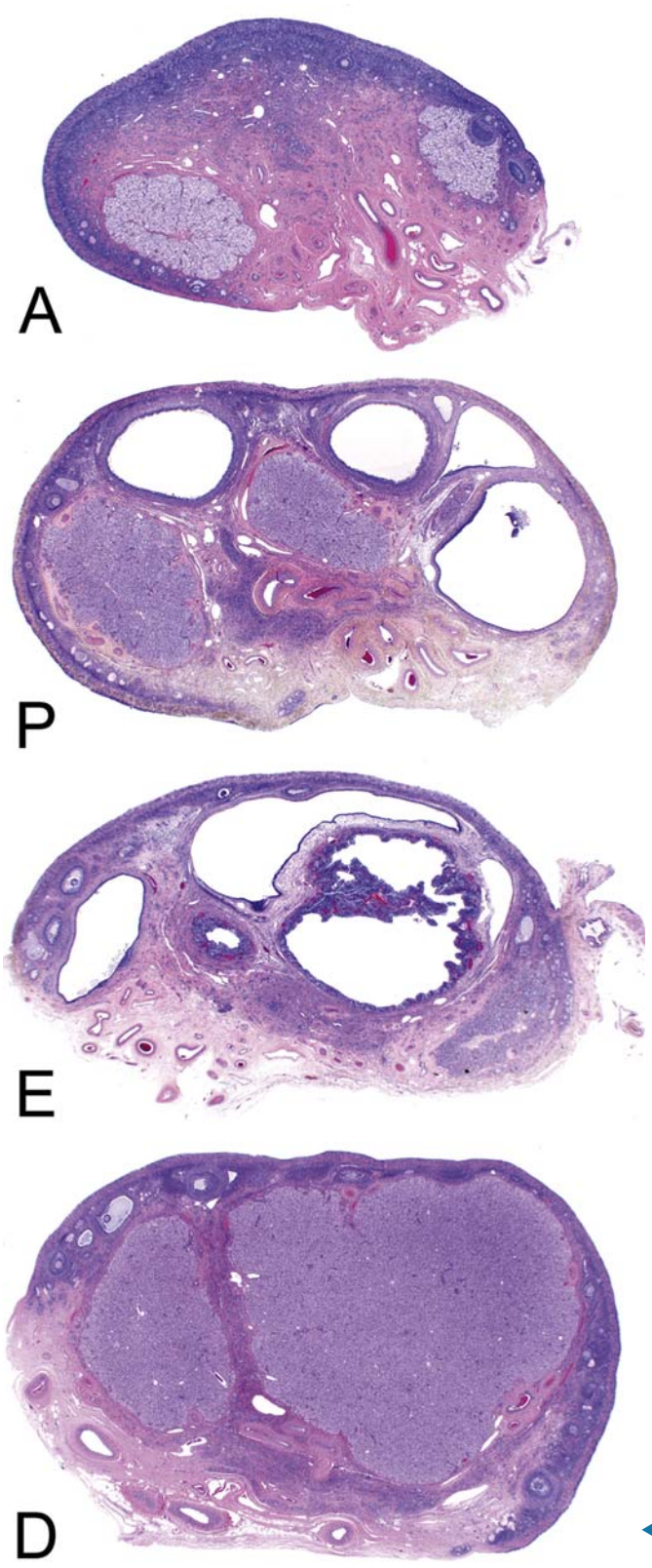

FIGURE 18.12 Ovary, dog, estrous cycle. Typical morphologic features of the ovary during different stages of estrus. Anestrus (A): The ovary appears quiescent with one or two sets of old CL. Proestrus (P): There is a gradual increase in ovarian follicular development and large antral follicles with thick granulosa cell layers are evident. Estrus (E): The ovary has large preovulatory follicles with luteinization of the granulosa cells. Diestrus (D): The ovary has new CL. ×10, H&E. Source: *Courtesy: Dr. Sundeep Chandra. From Haschek, W.M., Rousseaux, C.G., Wallig, M.A. (Eds.), 2013. Haschek and Rousseaux's Handbook of Toxicologic Pathology, third ed. Academic Press (Elsevier), San Diego, CA, Figure 60.13, p. 2618, with permission.*

present (Figure 18.13). The vagina becomes thicker and cornified (Figure 18.13). The stroma and smooth muscle also start to thicken and there are both stromal congestion and edema.

The Histology of the Cynomolgus Monkey Female Reproductive Tract During the Menstrual Cycle

The cynomolgus monkey has a menstrual cycle (and endocrinology) that is very similar to the human. However, as is the case for the dog, assessment of the female reproductive system can be challenging because the numbers of animals used in toxicology studies are small (usually 3–4) and animals are often pre- or peripubertal (Figure 18.11). In the last couple of decades, the attention given to the monkey model has increased because of the large influx of biologics now in preclinical development. Many of these biologics are not amenable to study in rodents and the cynomolgus monkey becomes a key animal model of human relevance. As a result, the use of sexually mature cynomolgus monkey is now more common and it is important for the toxicologic pathologist to be familiar with this model system.

The cynomolgus monkey ovaries are amygdaloid in shape and found in the pelvic cavity. The ovary has multiple primary follicles develop with each cycle but usually only one follicle will be selected to become the preovulatory follicle, resulting in a single protrusion from one ovarian surface. Degenerating primary oocytes are likely the origin of calcified foci found in the ovarian cortex of cynomolgus monkeys. The calcified areas may be multiple and/or bilateral. In the sexually mature cynomolgus monkey, the cervix has a stratified squamous exocervix, squamocolumnar junction (SCJ) and transformation zone, and glandular endocervix with prominent colliculi. The stratified squamous epithelium of the exocervix changes to tall columnar glandular epithelium at the SCJ. In contrast, the cervical mucosa is atrophic in the sexually immature cynomolgus monkey and the SCJ is not distinct. The cervical epithelium in macaques is highly responsive to estrogens. Estrogen stimulation results in marked keratinization of the exocervical epithelium and thickening of the stratified squamous epithelium

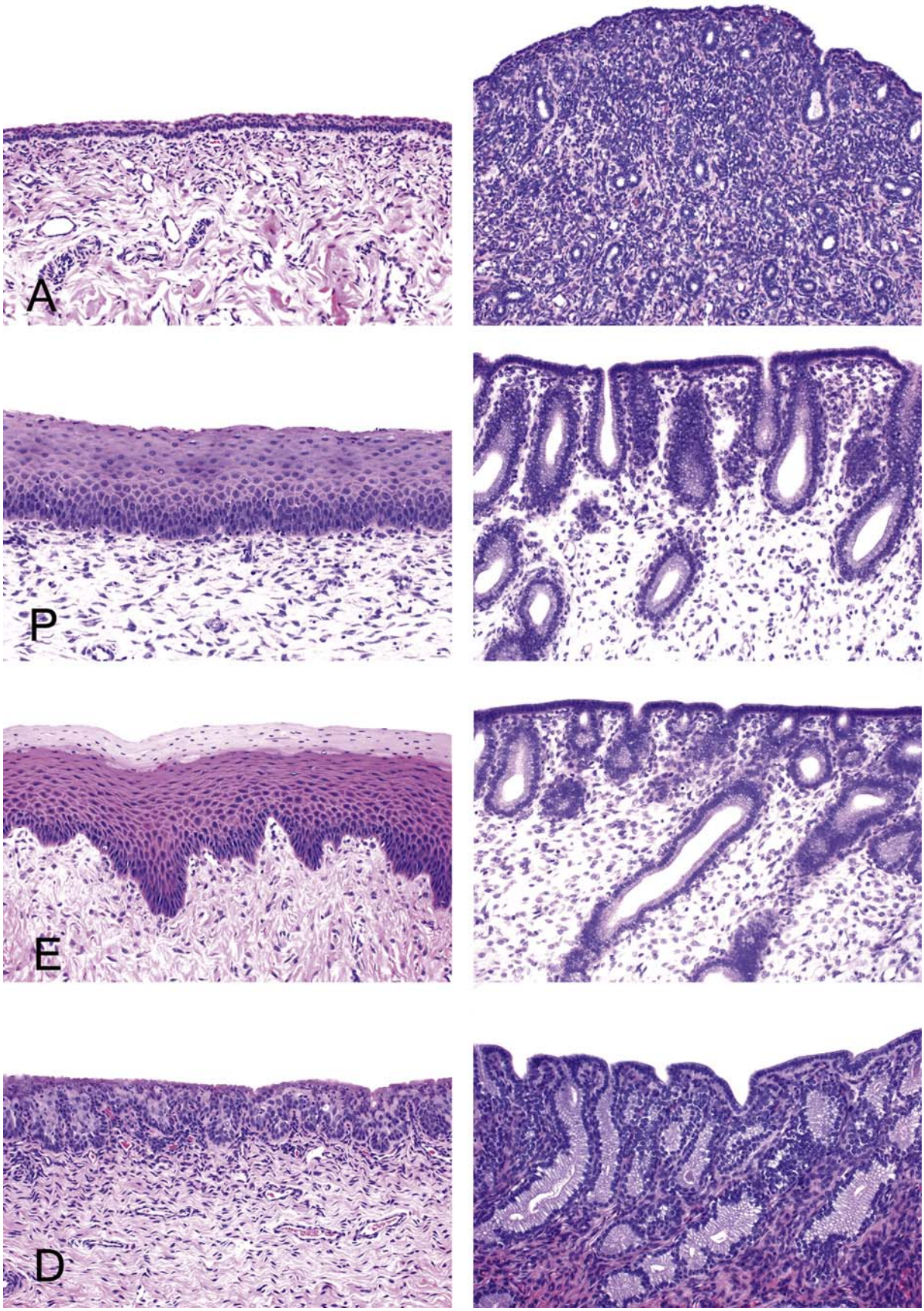

FIGURE 18.13 Uterus and vagina, dog. In anestrus (A), the uterine surface and glandular epithelium is lined by low columnar cells with basally situated nuclei and the vaginal epithelium is thin and underlying stroma compact. In proestrus (P), the uterine mucosa becomes more vascular and edematous with occasional small focal areas of erythrocyte extravasation in the zona compacta. The surface and glandular

near the SCJ, and squamous metaplasia and hypertrophy of the endocervical glands.

The menstrual cycle of the cynomolgus monkey is divided into four major phases: the follicular (or proliferative) phase, the luteal (or secretory) phase, the menstrual phase, and the regenerative phase (Figures 18.14–18.16) (see Van Esch et al., 2008a). The regenerative phase is not included in some descriptions resulting in a three phase menstrual cycle. Cynomolgus monkey endometrial changes are similar to those of women, with menstrual discharge toward the end of each reproductive cycle. The follicular or proliferative stage follows menses. During the follicular (proliferative) phase, the superficial and glandular epithelium, the stroma, and the endometrial vasculature are in varying degrees of physiological proliferation (Figures 18.15 and 18.16B). In effect, the endometrium thickens, spiral arteries develop and the complexity of the uterine glands increases (Figure 18.15). By days 6 to 8, the dominant ovarian

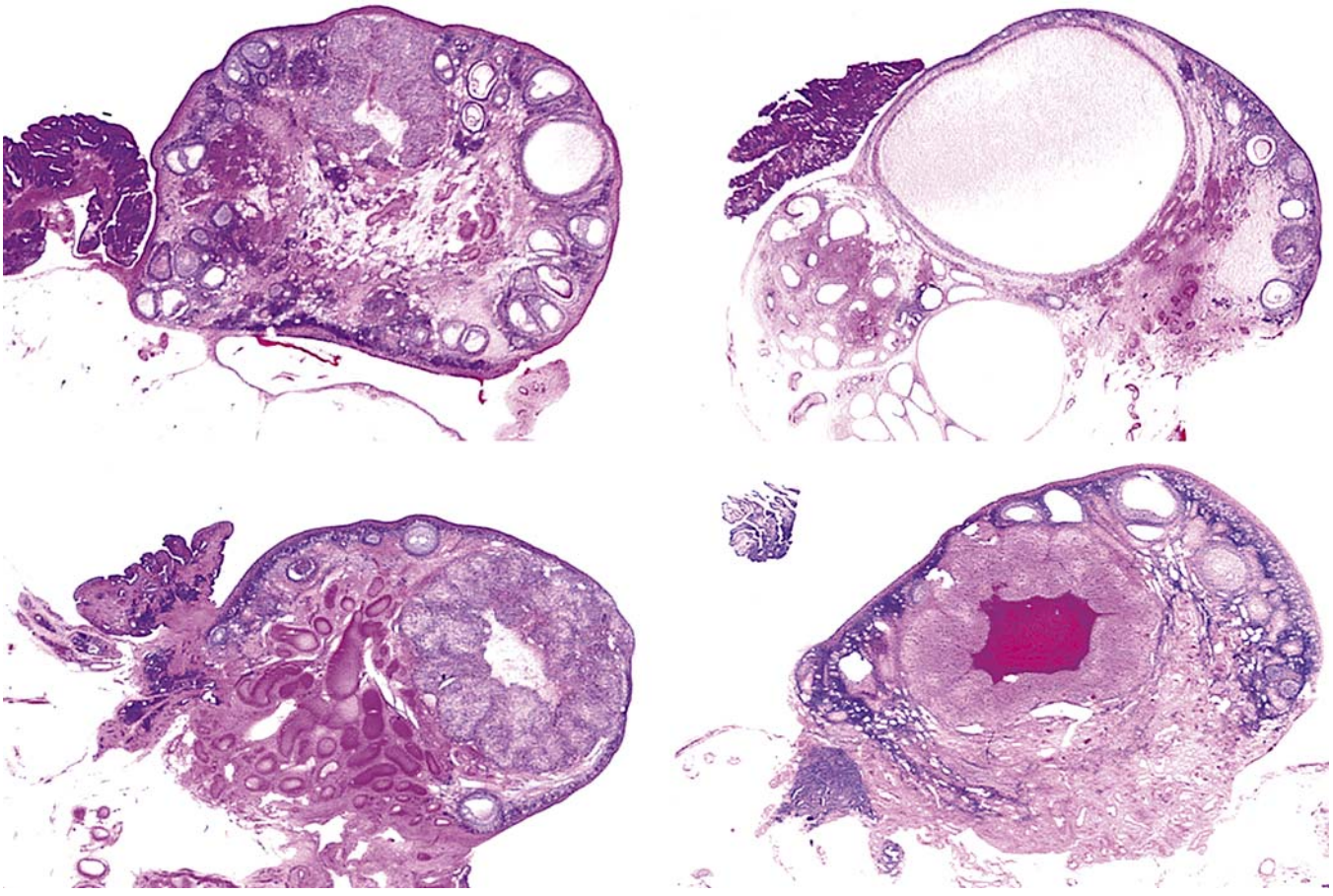

FIGURE 18.14 Ovary, monkey. Ovarian histology during the menstrual cycle of cynomolgus macaques. Clockwise from upper left, the ovaries shown are from early follicular phase (developing follicles and the corpus luteum of the prior cycle); late follicular phase (dominant follicle); ovulation (corpus hemorrhagicum); and luteal phase (corpus luteum). ×10, H&E. Source: *Photograph courtesy: Dr. Mark Cline. From Haschek, W.M., Rousseaux, C.G., Wallig, M.A. (Eds.), 2013. Haschek and Rousseaux's Handbook of Toxicologic Pathology, third ed. Academic Press (Elsevier), San Diego, CA, Figure 60.15, p. 2622, with permission.*

epithelium increases in height and numerous mitotic figures are present. The vagina becomes thicker and cornified. The stroma and smooth muscle also start to thicken and there is both stromal congestion and edema. In estrus (E), the uterus has myometrial hypertrophy, stromal cell proliferation, and stromal congestion, edema, and hemorrhage. The surface and glandular epithelium is increased in height and there are numerous mitotic figures. The vagina is thick and heavily cornified. In diestrus (D), luminal glands are proliferative and straight, but abruptly become tortuous toward the basement membrane. The glandular lumina may contain pink secretions; stromal edema and congestion are decreased. The upper gland and luminal epithelial cells progressively develop foamier cytoplasm as a consequence of the influence of progesterone. The vagina is much thinner (three to four cell layers) and loses it cornification. ×50, H&E. Source: *Photograph courtesy: Dr. Sundeep Chandra. From Haschek, W.M., Rousseaux, C.G., Wallig, M.A. (Eds.), 2013. Haschek and Rousseaux's Handbook of Toxicologic Pathology, third ed. Academic Press (Elsevier), San Diego, CA, Figure 60.14, p. 2620, with permission.*

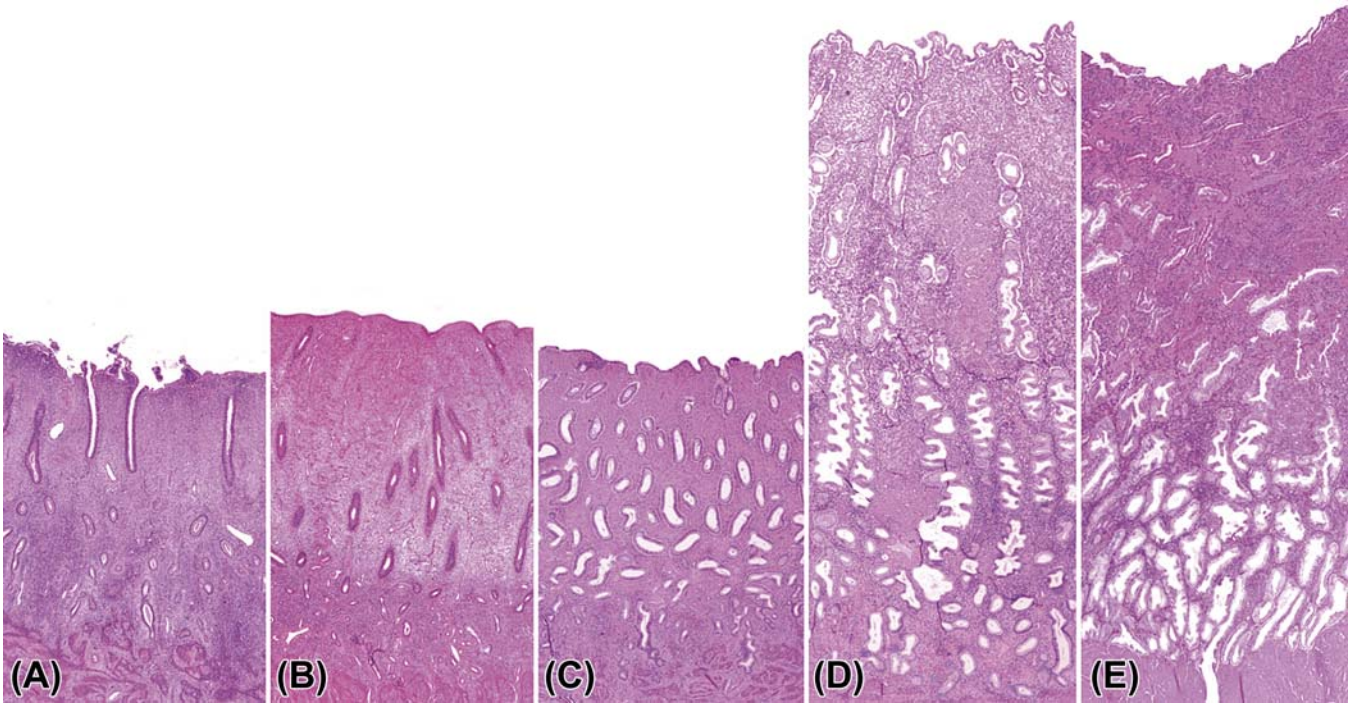

FIGURE 18.15 Uterus, monkey, uterine histology across the menstrual cycle of cynomolgus macaques. Stages shown from left to right are (A) regenerative phase; (B) follicular phase; (C) periovulatory/early-luteal phase; (D) luteal phase; and (E) early menstrual phase. ×25, H&E. Source*: Photograph courtesy: Dr. Mark Cline. From Haschek, W.M., Rousseaux, C.G., Wallig, M.A. (Eds.), 2013. Haschek and Rousseaux's Handbook of Toxicologic Pathology, third ed. Academic Press (Elsevier), San Diego, CA, Figure 60.16, p. 2623, with permission.*

follicle can be identified and will ovulate following the LH surge (Figure 18.14).

Following ovulation, the secretory or luteal phase occurs; the hallmark of ovulation is the appearance of subnuclear vacuoles (Figure 18.16C). The luteal phase lasts approximately 13–14 days and is marked by endometrial glands secreting a glycogen rich material. The glands become coiled and saccular giving a saw-tooth appearance. The spiral arteries become coiled. Implantation typically occurs on days 21–23. If pregnancy is not established, the spiral arteries constrict with declining progesterone levels of the regressing corpus luteum, there is massive apoptosis of endometrial glands (Figure 18.16D), and menses occurs. The postpartum uterus of monkeys may have prominent hyalinized myometrial arteries, which are normal. Cervical intraepithelial neoplasia, endometriosis, ectopic growth of endometrial tissue outside the uterus (endometriosis), and adenomyosis, extension of endometrium into the subjacent myometrium, are reported across the primate order as spontaneous findings.

The Minipig in Toxicology Studies

Of special note is the fairly recent increase in use of the Gottingen, Yucatan, and Troll miniature pigs (minipig) for dermal and medical device toxicity testing highlighted by a recent issue of *Toxicologic Pathology* (Vol. 44, Issue 3, 2016) dedicated to the topic. The female reproductive system of the minipig has a bicornuate uterus with tortuous fallopian tubes and is similar to humans in terms of uterine histology and estrous cyclicity; however, unlike humans and cynomolgus monkeys, the minipig does not menstruate. The minipig estrous cycle includes a follicular/proliferative phase (F/P), early-luteal phase/early-secretory phase (EL/ES), a mid-luteal phase/mid-secretory phase (ML/MS), and a late-luteal phase/late secretory phase (LL/LS). There are several recent reports on normal female reproductive histology as well as spontaneous or experimentally induced female reproductive changes in the minipig. Briefly, stage distinguishing features in the Gottingen minipig for the estrous cycle are best evaluated in the ovary and uterus. In the ovary, whether the Graafian follicles are disrupted or nondisrupted and the size, cell morphology, and structural of CL are used. Uterine endometrial epithelial morphology and secretory activity as well as the level of epithelial mitosis or apoptosis are key differentiators (see de Rijk et al., 2014).

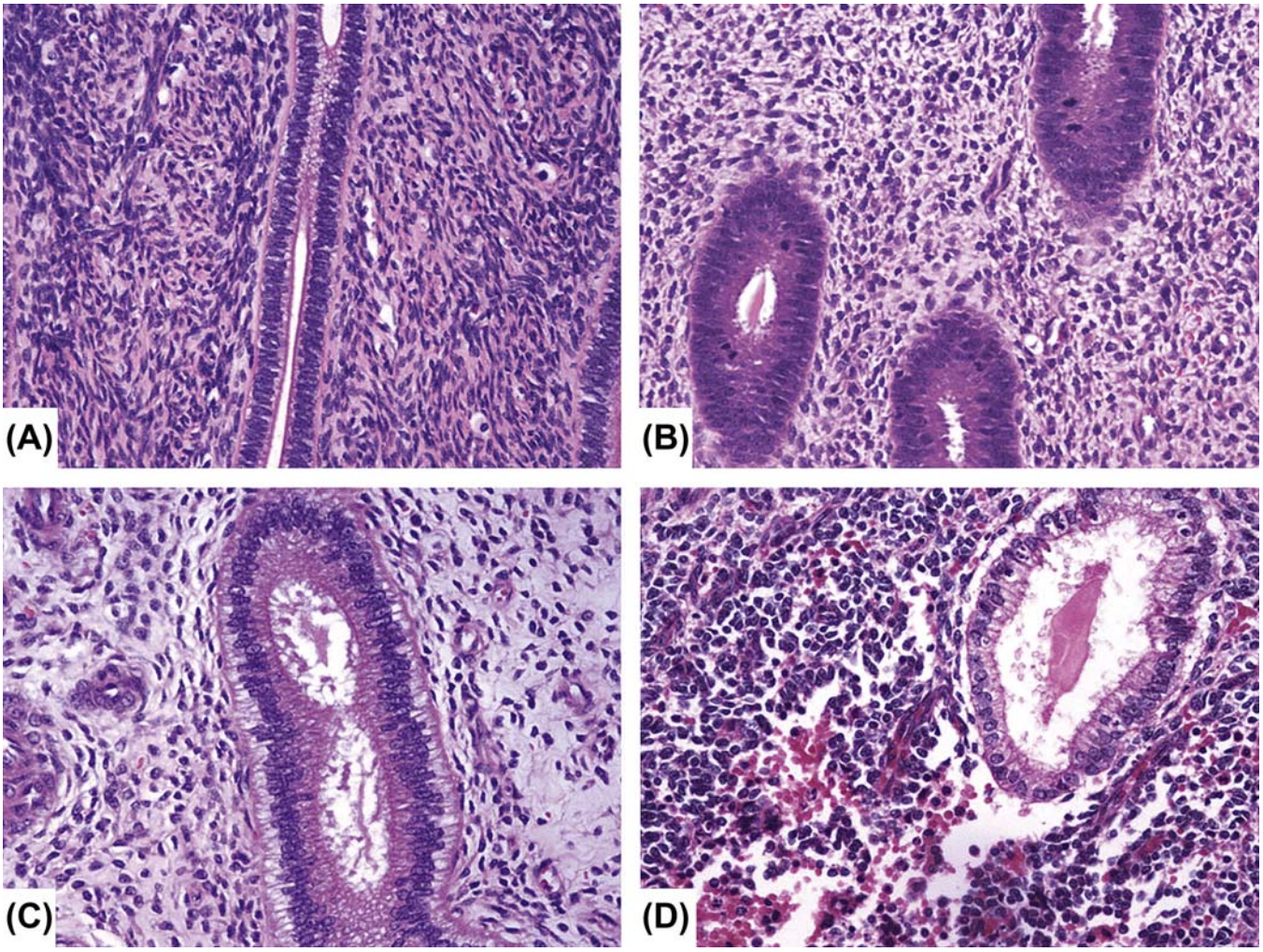

FIGURE 18.16 Uterus, monkey, uterine histology of cynomolgus macaques. (A) Quiescent/atrophic; (B) follicular phase (note mitoses and pseudostratification); (C) luteal phase (subnuclear vacuolation); and (D) menstrual phase (hemorrhage, apoptosis). ×100, H&E. Source: *Photograph courtesy: Dr. Mark Cline. From Haschek, W.M., Rousseaux, C.G., Wallig, M.A. (Eds.), 2013. Haschek and Rousseaux's Handbook of Toxicologic Pathology, third ed. Academic Press (Elsevier), San Diego, CA, Figure 60.17, p. 2624, with permission.*

The Endocrinology of the Estrous Cycle

The cyclic changes within the ovary are mainly regulated by luteinizing hormone (LH) and follicle-stimulating hormone (FSH), whereas the cyclic changes of the uterus and vagina are dependent on ovarian sex steroids. Figure 18.17 provides a relational diagram for the hypothalamic–pituitary–ovarian (HPO) axis. The easiest way to conceptually visualize the HPO axis is as a chemical equation in a cyclic equilibrium composed of a precursor pool of gonadotropins (LH, FSH) stimulating the ovary (also the adrenal in the nonrodent) to synthesize steroidal hormones, which then in turn modulate the physiology of the reproductive end organs (uterus, vagina, cervix, and mammary glands).

Each cycle begins with follicular growth and maturation, followed by ovulation, and the subsequent formation and regression of the corpus luteum. Although the recruitment and growth of a primordial follicle to the stage of an early tertiary follicle occurs spontaneously and does not require hormonal stimulation, the presence of FSH and LH is necessary for continued follicular maturation to the stage of a preovulatory follicle. It has been estimated that it takes 50 days for a primordial follicle to develop into a preovulatory follicle in the adult rat. Selection of follicles to continue onto the preovulatory stage depends on follicles having granulosa cells able to express the necessary gonadotropin receptors at the time of elevated gonadotropin levels. Most follicles undergo atresia and do not reach the preovulatory stage.

LH and FSH are glycoprotein hormones secreted from the anterior pituitary. In polyestrous nonseasonal breeding animals such as the rat, LH and FSH concentrations increase shortly after the end of the preceding cycle. FSH

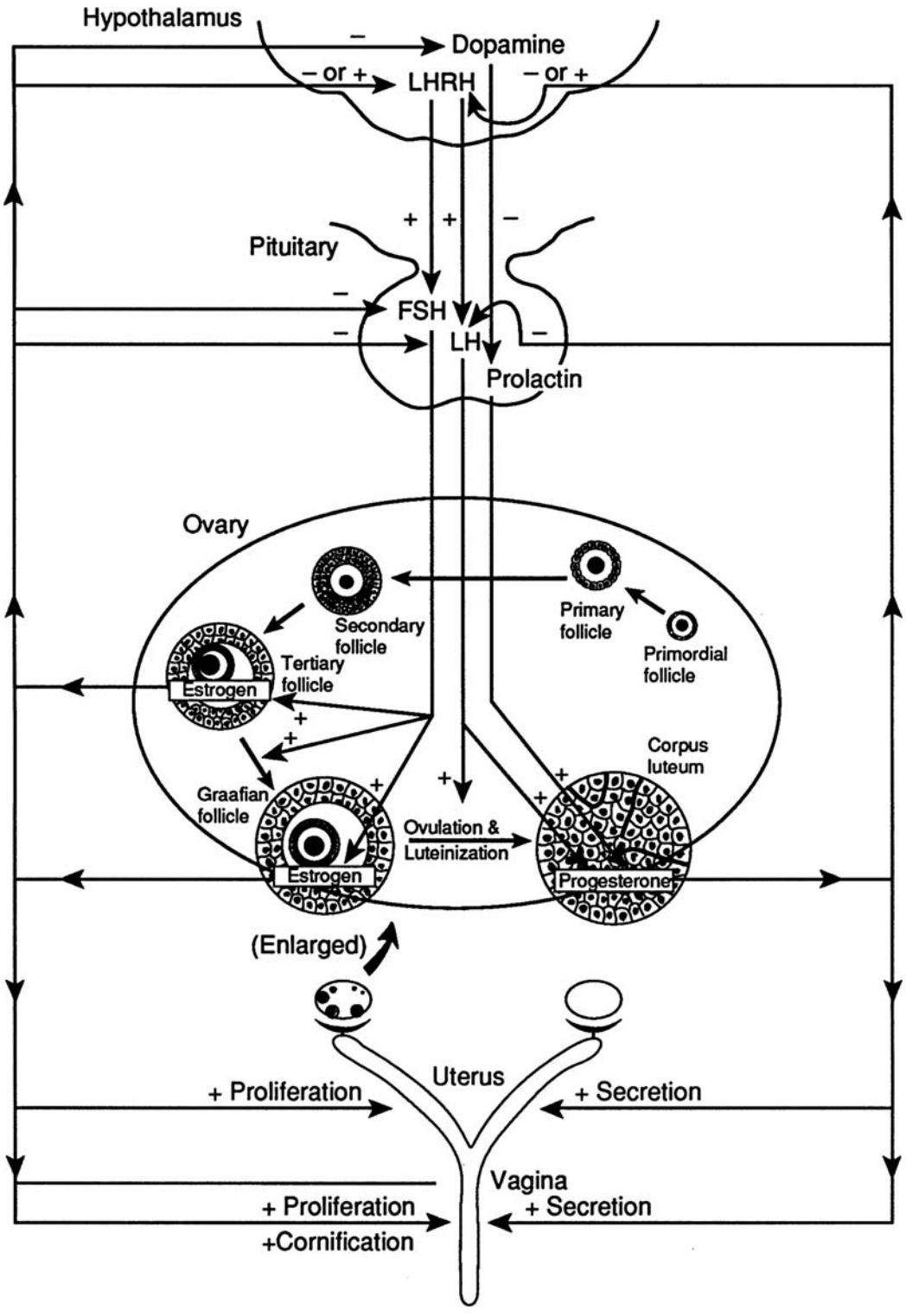

FIGURE 18.17 Schematic drawing of hormonal regulation of reproduction (+, stimulatory; −, inhibitory). Source: *From Haschek, W.M., Rousseaux, C.G., Wallig, M.A. (Eds.), 2002. Handbook of Toxicologic Pathology, second ed. Academic Press, San Diego, CA, Figure 9, p. 863, with permission.*

stimulates the proliferation of granulosa cells and induces receptors for LH on these cells. LH stimulates thecal cells to secrete androstenedione, which serves as a precursor for estrogen and androgen synthesis by granulosa cells through the catalytic function of aromatase.

The estrogen and androgen secreted from growing follicles promote cell proliferation and maturation in both the uterus and vagina. Under the influence of estradiol and androgens, the stromal fibroblasts and epithelial cells of the endometrium proliferate and increase in size. Estrogen and androgen also promote the synthesis of actomyosin and glycogen in smooth muscle cells, resulting in hypertrophy of the myometrium. In addition, estrogen primes the uterus for its response to progesterone. Polymorphonuclear leukocyte migration in the uterus, which may be causally related to intercellular edema and hyperemia, is also attributed to the effect of estrogen. In the vagina, estrogen not only stimulates cell proliferation but also induces epithelial cornification.

In the mature preovulatory follicle, a surge of LH results in ovulation with subsequent formation of the corpus luteum (CL). The newly formed CL incorporates both granulosa and thecal cells and is capable of secreting progesterone for only a certain period of time. Continued function of the corpus luteum requires stimulation by luteotrophic hormones such as LH and prolactin. Prolactin secretion in rats is stimulated by cervical stimulation. The ovarian steroid hormones, including estrogens, progestins, and androgens, exert their influence on the uterus and vagina, and other parts of the body, through the circulatory system.

In primates and dogs, ovulation occurs spontaneously. In the rat, ovulation is also spontaneous and coincides with the preovulatory LH surge that is under photoperiod control. In rabbits and other induced ovulators, the LH surge does not occur until cervical neurons are stimulated by mating or other means to activate the release of luteinizing hormone-releasing hormone (LHRH).

In the newly formed corpus luteum, progesterone secretory activity seems to be autonomous and, in most species, does not require luteotropic factors. For continued CL function, luteotropic hormones from the pituitary are required; LH is considered to be the most important luteotropic factor in most species. However, in rats, prolactin has been identified as the luteotropic factor, whereas in rabbits, estrogen is the only known luteotropic factor.

The functional life of the corpus luteum varies among animal species. In the rat, it functions only for the first 2 days after formation. If cervical stimulation takes place, prolactin continues to be secreted by the pituitary gland and the functional life of CL is prolonged with continued progesterone secretion. If implantation does not take place, the life of CL is terminated 12–14 days after formation. The period during which the corpus luteum is functional is known as pseudopregnancy.

In dogs, luteinization of the preovulatory follicles is accompanied by progesterone secretion prior to ovulation. This is most likely due to the long interval between the LH surge and ovulation. The functional life of CL in dogs is approximately 60 days and is not affected by mating or implantation, and both LH and prolactin are required for their maintenance. Due to the long luteal life span in dogs, pseudopregnancy is common but not always clinically apparent.

In primates, the corpus luteum has a defined functional life span that is unaffected by mating or mechanical stimulation of the cervix. A continuous low level of LH is required to maintain the corpus luteum. If pregnancy occurs, the embryonic trophoblast secretes chorionic gonadotropin as early as 8–9 days after fertilization, thus maintaining the corpus luteum throughout early pregnancy.

Progesterone inhibits cell division and maturation but promotes secretion by the endometrial glands. With prior estrogen priming, it can also cause the endometrial stromal cells to change from the small inactive form with fusiform nuclei to large cells with ovoid nuclei. Progesterone causes myometrial cells to become hypertrophic with prominent myofibrils. In the vagina, when estrogen is also present, progesterone induces mucification by increased production and intracytoplasmic accumulation of sialic acid. In primates, CL secrete estrogen as well as progesterone.

At the end of its functional life, the corpus luteum regresses (luteolysis). The only clearly demonstrated luteolytic factor is prostaglandin F (2-α), produced by the endometrium. Experimental data indicate that this prostaglandin is responsible for luteolysis in large domestic species such as cattle and sheep and in pseudopregnant rodents such as rat and hamster. Prostaglandin F 2-α has also been demonstrated to be luteolytic in rhesus monkeys.

EVALUATION OF FEMALE REPRODUCTIVE SYSTEM TOXICITY

Spontaneous Changes in the Female Reproductive System (Table 18.3)

No matter the mechanism of female reproductive system toxicity, an understanding of the spontaneous changes observed in the female reproductive tract is required for a consistent and accurate evaluation of test agent effects in the preclinical animal model. In addition, there is a great advantage to the consistent use of

TABLE 18.5 Patterns of Toxicity in the Rat Based on Effects on the HPO Axis in Relative Order of Frequency

Primary and secondary hormonal effect	Most common cause	Most characteristic histologic change(s)
↓ LHRH and ↓ LH/FSH, ↓ ovarian steroid hormones	Stress and negative energy balance	Ovarian, vaginal, and uterine atrophy
↑PRL or ↓ dopamine, ↑P4	Central inhibition of pituitary dopamine release; dopamine receptor antagonism	Mammary gland lobular hyperplasia and lactogenesis, persistent vaginal/uterine diestrus
↑P4, ↓ LHRH and LH/FSH	Progesterone receptor agonism	Vaginal hypertrophy and hyperplasia with mucification
↓ P4 or PR blockade	Progesterone receptor antagonism and increased E2:P4 ratio	Persistent vaginal/uterine estrus
↑E2, ↓ LHRH and LH/FSH[a]	Estrogen receptor agonism	Vaginal and uterine epithelial hyperplasia and squamous metaplasia
ER blockade, ↑LHRH and LH/FSH, ↑E and T	Selective estrogen receptor antagonists (e.g., raloxifene)	Ovarian granulosa cell hyperplasia, mammary gland masculinization
↑LHRH, ↑ LH/FSH, ↑E2/P4/androgens	Gonadotropin receptor agonism	Uterine endometrial cystic hyperplasia
↑Androgens	Androgen receptor agonism	Vaginal mucification, uterine hypertrophy/hyperplasia; mammary gland masculinization

[a]*In rodents, exogenous administration of estrogens or ER agonists can cause hyperprolactinemia and persistent diestrus.*

LHRH, luteinizing hormone-releasing hormone; LH, luteinizing hormone; FSH, follicle-stimulating hormone; PRL, prolactin; P4, progesterone; E2, estradiol; T, testosterone.

From Haschek, W.M., Rousseaux, C.G., Wallig, M.A. (Eds.), 2013. Handbook of Toxicologic Pathology, third ed. Academic Press, San Diego, CA, Table 60.9, p. 2637, with permission.

terminology when annotating histologic alterations of the female reproductive tissue. For the latter, a global effort to harmonize terminology (International Harmonization of Nomenclature and Diagnostic criteria or INHAND) for all rodents and nonrodents is underway. The reader is referred to the recently published rodent guidance for female reproductive system terminology (see Dixon et al., 2014). For the former, in Table 18.3, we list some of the most common spontaneous findings in the rat, dog, and rhesus and cynomolgus monkeys by tissue and stage of estrus based on our own experience and that reported in the literature. Note that we limited our list to changes expected to occur in toxicology studies. Therefore, changes reported in older monkeys (>10 years) and beagle dogs (>8 years) are not listed. Also, we have not included "immaturity" as a spontaneous lesion; however, as mentioned previously, beagle dogs and monkeys used in toxicology studies are generally sexually immature or peripubertal and toxicologic pathologists may wish to indicate this in the histopathology raw data as a way to document histologically the reproductive status of the test animal.

Response to Injury

The response of the reproductive system to insult is comparable among different species of laboratory animals because of the similarity of reproductive function control. As described earlier, reproductive end organ growth and development are dependent on numerous trophic factors produced by the pituitary, ovary, and in the nonrodent, the adrenal gland. These trophic factors modulate cell growth, metabolism, and differentiation within the varied compartments of the ovary, uterus, vagina/cervix, and clitoral glands. Not only is the level of individual factors important but the ratio of factors is also critical (e.g., estrogen:progesterone ratio). Therefore, it is not surprising that a major mode of response to injury in the female reproductive system is that of disturbances of growth: atrophy, hypertrophy/hyperplasia, metaplasia, dysplasia, and neoplasia.

Atrophy and hypertrophy/hyperplasia may result from increases or decreases in cell proliferation or apoptosis, both important and normal physiologic processes in the cycling female reproductive tract. As discussed previously in the endocrinology sections, hormones produced by the hypothalamus, pituitary, ovary, and in nonrodents, the adrenal gland, modulate the balance between cell proliferation and apoptosis in the reproductive tract. For example, normally, prolactin extends the life of the CL by preventing regression through apoptotic mechanisms and androgens are anabolic for smooth muscle and increase cell proliferation in the muscular compartment of the female reproductive tract. However, when the balance of trophic factors becomes altered in toxicity, one should expect to

TABLE 18.6 Examples of Preclinical Toxicology Rat Findings Related to the Modulation of Specific Mammalian Targets or Pathways

Compound class	Proposed mechanism	Reported histologic findings
SERM	LH/FSH hypersecretion due to hypothalamic ER antagonism	Ovarian follicular dilation/cysts[a] and granulosa cell hyperplasia/neoplasia; uterine hyperplasia +/−
Estrogen receptor-α or β agonists	Central and end-organ ER agonism, prolactin hypersecretion	Increased tertiary ovarian follicles, decreased CLs; uterine/vaginal squamous metaplasia, hyperplasia and vaginal and cervical mucification; mammary gland lobular hyperplasia
Androgen agonists	Tissue-specific AR agonism	Ovarian follicular cysts, decreased CLs, interstitial gland atrophy; uterine hypertrophy/hyperplasia; vaginal mucification
Dopamine or opioid receptor antagonists	Prolactin hypersecretion	Mammary gland lobular hyperplasia, increased CL size, vaginal mucification, uterine and vagina-persistent diestrus
Progesterone receptor antagonists	Progesterone receptor antagonism (E2−P4 ratio decreased)	Increased ovarian weight-dilated antral follicles, all rats in estrus
Histamine 3 antagonist	Increase in TRH and prolactin hypersecretion; interference in steroidogenesis	Ovarian follicular prominence, decreased CLs, uterine and vaginal atrophy, mammary gland lobular hyperplasia
Mitogen activated kinase inhibitors	Angiogenesis inhibition; StAR inhibition	Ovarian follicular and luteal cysts and hemorrhage, uterine glandular atrophy
Growth hormone secretagogues, receptor agonists	Prolactin hypersecretion	Decrease in ovarian basophilic CLs, uterine atrophy, vaginal mucification
Retinoid activated receptor γ antagonists	Unknown; RAR γ highly expressed in rat uterus and ovary	Cycle asynchrony e vaginal estrus without uterine/ovarian estrus morphology
Peroxisome proliferator activated receptor agonists	Direct PPAR-mediated ovarian effects e aromatase cytochrome P450 and estrogen synthesis inhibition	Decrease in ovarian CLs, increase in atretic ovarian follicles, ovarian follicular dilation, decreased uterine and ovarian weights, cystic endometrial hyperplasia

[a]*Also reported in nonrodent.*

From Haschek, W.M., Rousseaux, C.G., Wallig, M.A. (Eds.), 2013. Handbook of Toxicologic Pathology, third ed. Academic Press, San Diego, CA, Table 60.10, p. 2638, with permission.

observe disturbances of growth as an outcome of an altered homeostasis between proliferation and apoptosis.

The trophic hormones are tumor promoters and potential nongenotoxic carcinogens due, in part, to their effects on cell proliferation in the female reproductive tract of animals and women. Therefore, the incidence of spontaneous tumors in the reproductive tract may increase if the HPO axis is modified or a toxicant has a direct hormone-like effect. For this reason, potential shifts in the incidence of spontaneous tumors from hormone responsive tissues (pituitary, mammary gland, vagina, uterus, cervix, ovary, and clitoral gland) may occur in animal model systems. For example, rats treated with certain Selective Estrogen Receptor Modulators (SERMs) in lifetime bioassays have an increased incidence of granulosa cell tumors as a consequence of hypersecretion of FSH but a decreased incidence of mammary gland neoplasms due to antiestrogenic effects of the SERM on the mammary gland epithelium. Of course, a toxicant may also produce neoplasms through a genotoxic pathogenesis. This is a rare observation in pharmaceutical toxicology, because in almost all cases, genotoxic compounds do not advance to lifetime bioassay studies. A discussion of specific neoplasms is presented later in this chapter.

The estrous and menstrual cycles in healthy adult animals and women are synchronous; the reproductive tissues follow a specific pattern manifested by coordinated morphologic and functional changes. Toxicity may alter estrous or menstrual cycle length or cause asynchronous changes in female reproductive tissues. These changes may be more difficult to recognize without specific study designs that assess cycle length because of several factors including the long, variable estrous cycle in the beagle dog; the small number of nonrodents per group used in toxicology studies (generally 3 or 4); and the use of peripubertal nonrodents. However, for rodent studies, the number of animals and study designs offers an opportunity for the pathologist to recognize toxicity-mediated shifts in the number of animals in different stages of estrous or a lack of coordination between the expected morphologic appearance of the uterus, vagina, and ovary for any specific stage of the cycle (i.e., asynchrony).

Angiogenesis is a key process in the normal cycling of the ovary. Normal development of the CL requires cyclic changes in blood vessels. Toxicity that results in

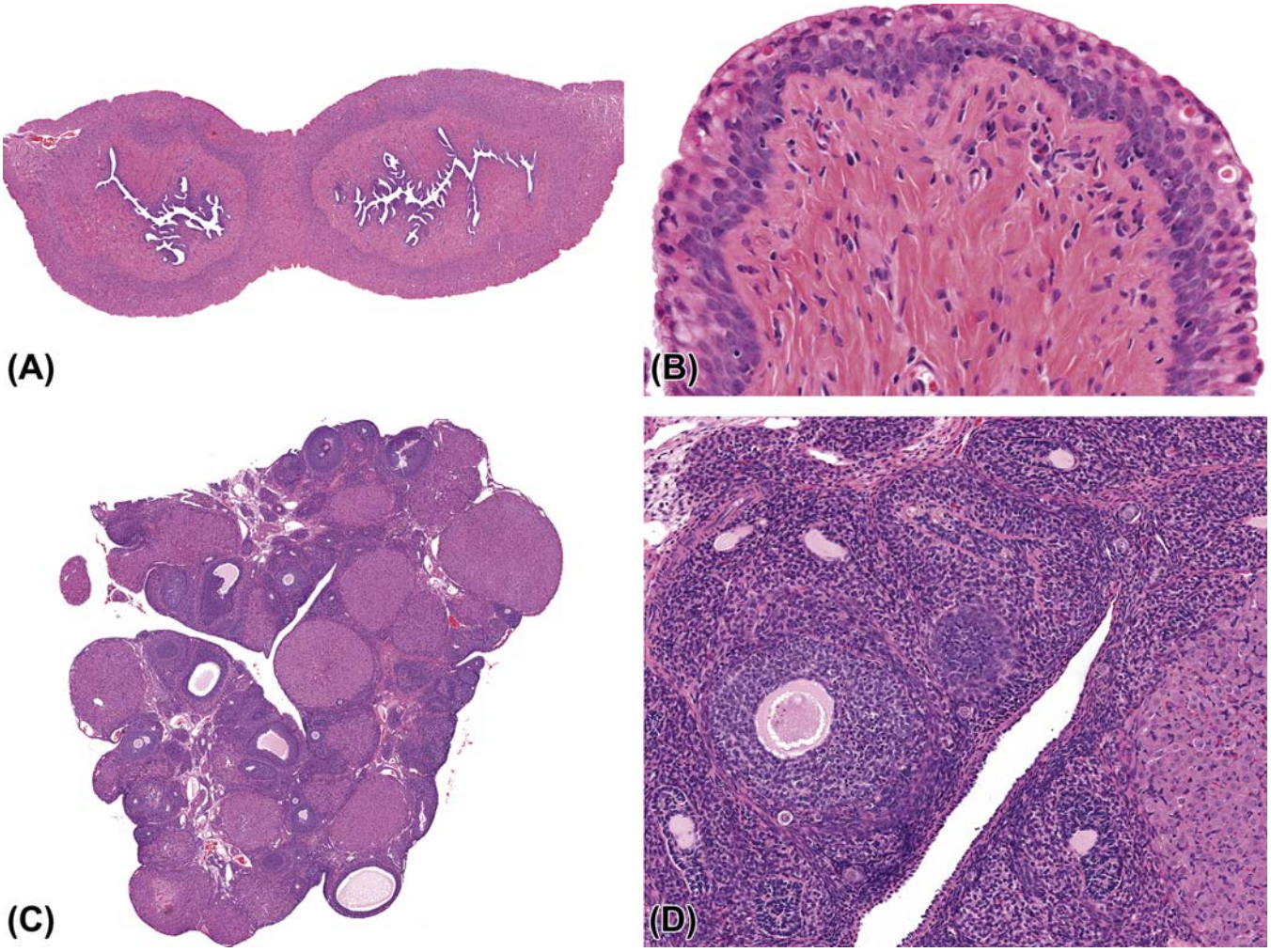

FIGURE 18.18 Uterus, vagina, and ovary, rat. Prolonged diestrus in a rat that is associated with stress and decreased weight gain. The uterine mucosa is quiescent (A). The vaginal mucosa (B) is thin (two or three layers thick) and the superficial epithelial cells have prominent, mucoid cytoplasm. The ovary only has eosinophilic and contracted CL from prior cycles (C) and the follicles are undergoing atresia (D). ×10 (A), ×100 (B), ×10 (C), × and 50 (D), H&E. Source: *From Haschek, W.M., Rousseaux, C.G., Wallig, M.A. (Eds.), 2013. Haschek and Rousseaux's Handbook of Toxicologic Pathology, third ed. Academic Press (Elsevier), San Diego, CA, Figure 60.25, p. 2639, with permission.*

TABLE 18.7 Organ Weight, and Gross and Histologic Changes that may be Associated with Stress and Negative Energy Balance in Animals

Organ weight: decreased thymic, ovarian, uterine weights; increased adrenal weights
Gross pathology: small thymus, decreased visceral fat, large adrenal, reddened gastric/duodenal mucosa
Histopathology: bone marrow hypocellularity, thymic lymphocyte depletion, adrenal cortical hypertrophy, pancreatic zymogen granule depletion, erosion/ulceration of gastric or duodenal mucosa, ovarian/uterine/vaginal/cervical atrophy

From Haschek, W.M., Rousseaux, C.G., Wallig, M.A. (Eds.), 2013. Handbook of Toxicologic Pathology, third ed. Academic Press, San Diego, CA, Table 60.11, p. 2639, with permission.

the modulation of angiogenesis pathways may result in complete failure of CL formation as well as secondary changes in the uterus and vagina (atrophy) due to alterations in ovarian hormone production, a consequence of an interruption in ovarian cycling.

Direct toxicity of components of the female reproductive tract is less common; however, there are some specific examples of degenerative, inflammatory, and immune-mediated responses to injury in the reproductive tract. These include vaginal epithelial degeneration and inflammation as a result of irritation, and degeneration and necrosis of ovarian follicles secondary to chemical toxicants or radiation that target rapidly dividing cell populations.

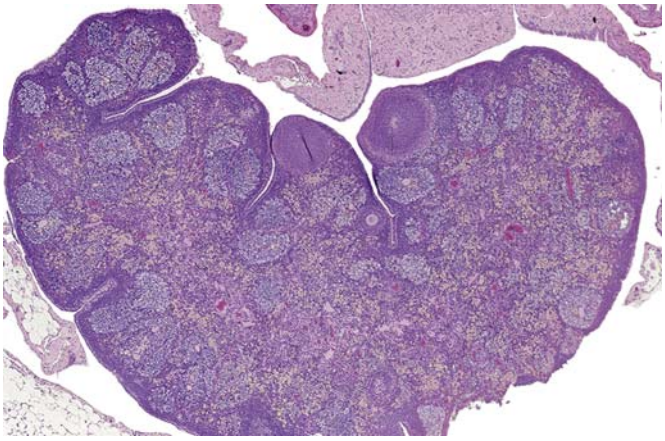

FIGURE 18.19 Ovary, rat. CL depletion. Interstitial cells are prominent and the ovary has marked CL depletion. ×10, H&E. Source: *Photograph courtesy: NTP. From Haschek, W.M., Rousseaux, C. G., Wallig, M.A. (Eds.), 2013. Haschek and Rousseaux's Handbook of Toxicologic Pathology, third ed. Academic Press (Elsevier), San Diego, CA, Figure 60.26, p. 2639, with permission.*

MECHANISMS OF TOXICITY IN THE FEMALE REPRODUCTIVE SYSTEM

Mechanisms of toxicity in the female reproductive tract can be classified into three broad categories: (1) direct disruption of the HPO axis; (2) indirect disruption of the HPO axis; and (3) direct organ-specific pathology. Table 18.5 presents an overview of the types of HPO disruption, a possible cause, and the easiest to recognize and most consistent histologic change (s) observed. The causes are based on our experience and literature reports and are limited to patterns in the rat because of paucity of data due to the use of immature or peripubertal nonrodents. Important to note is that often things are not always this straight forward, as test agents can produce a mixed HPO phenotype based on the biology of nuclear hormone receptors and their tissue-specific cofactors (discussed later). In Table 18.6, we list several classes of compounds that modulate a biological target or pathway, which results in pathologic changes in the female reproductive tract. The examples listed include those cited in the literature and unpublished observations. In almost every case, we only list changes in the rodent because usually the nonrodent toxicologic studies were done in immature or pubescent beagle dogs or cynomolgus monkeys. These classes of compounds include sex hormone receptor ligands, other nuclear hormone receptor ligands, and centrally active neurohormone receptor agents.

Direct organ toxicity is an uncommon cause of female reproductive toxicity; however, there are

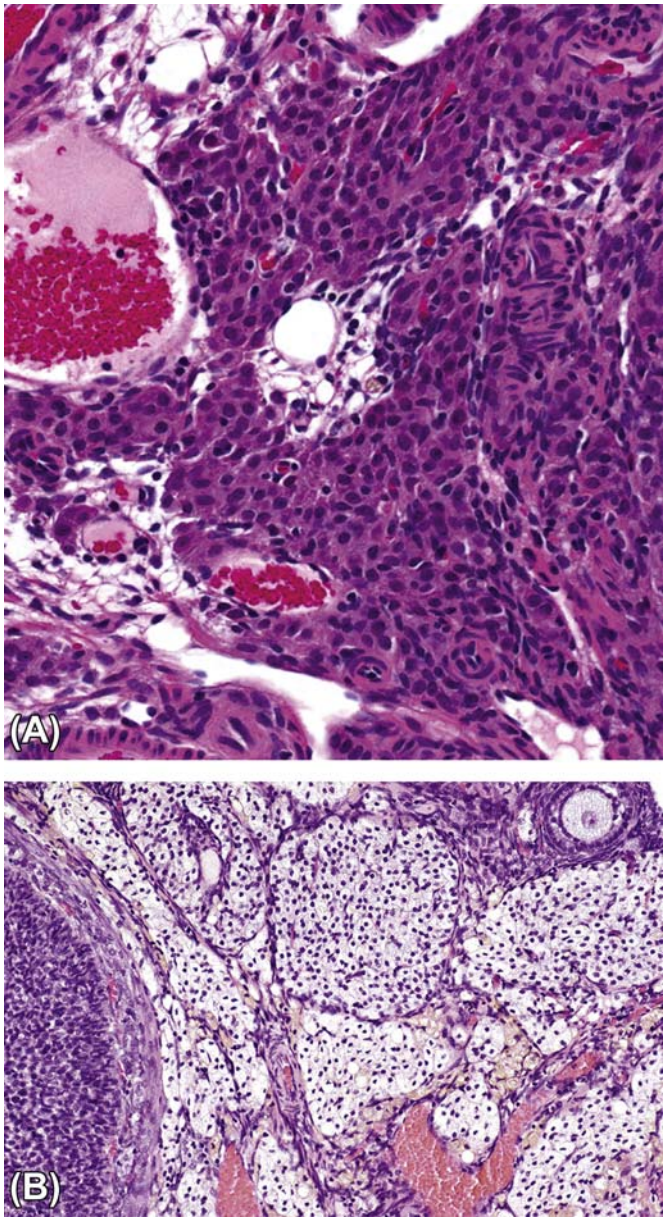

FIGURE 18.20 Ovary, rat. Interstitial glands, normal (A) or hypertrophied (B). ×50, H&E. Source: *Photograph courtesy: NTP. From Haschek, W.M., Rousseaux, C.G., Wallig, M.A. (Eds.), 2013. Haschek and Rousseaux's Handbook of Toxicologic Pathology, third ed. Academic Press (Elsevier), San Diego, CA, Figure 60.27, p. 2640, with permission.*

TABLE 18.8 Histologic Changes Associated with Hyperprolactinemia in the Rat

Mammary gland: lobular hyperplasia with secretions
Ovary: increased size of CL
Uterus: diestral histology
Vagina/cervix: diestral histology with hypermucification

From Haschek, W.M., Rousseaux, C.G., Wallig, M.A. (Eds.), 2013. Handbook of Toxicologic Pathology, third ed. Academic Press, San Diego, CA, 60.12, p. 2640, with permission.

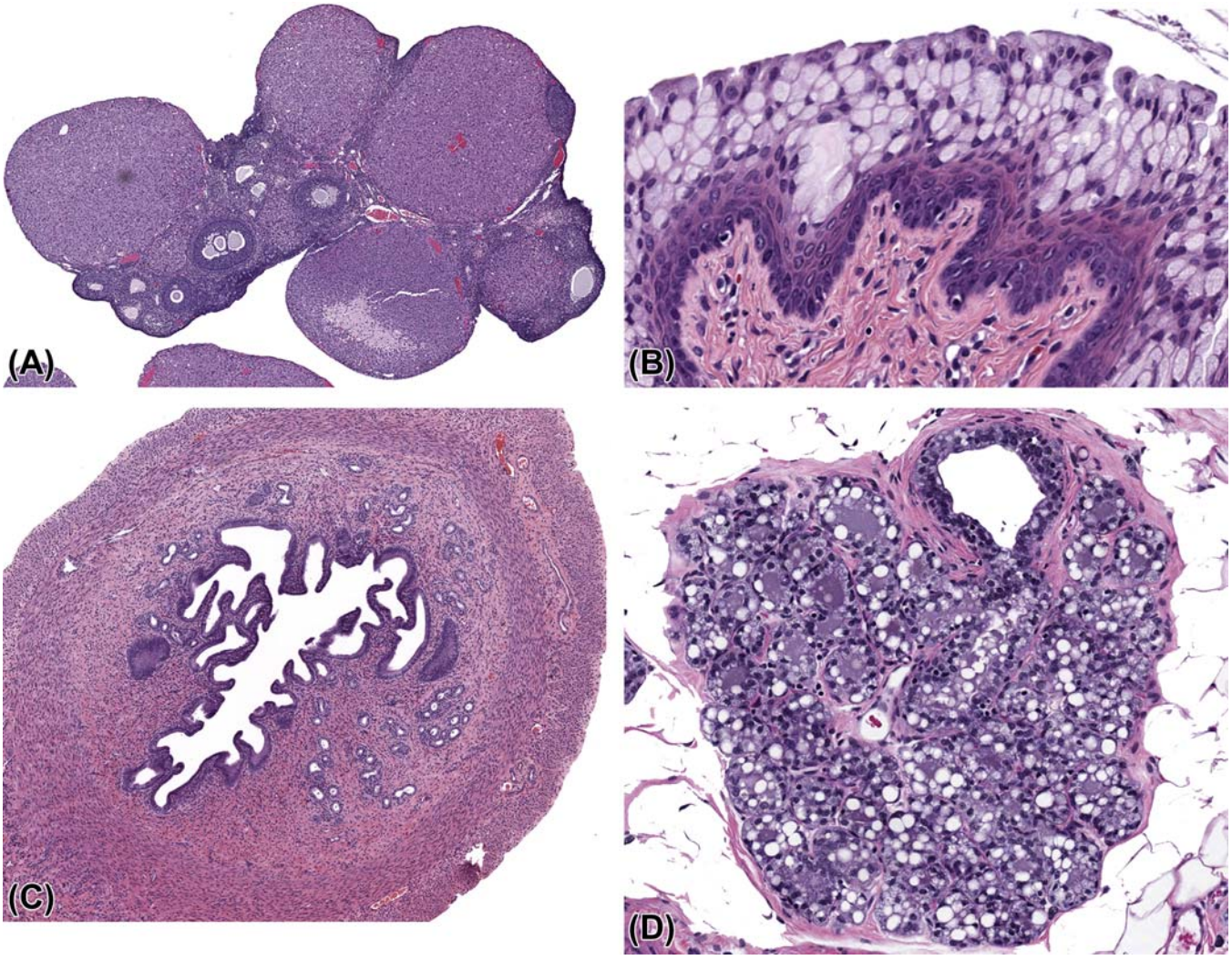

FIGURE 18.21 Ovary, vagina, and mammary gland, rat. Selected female reproductive changes in hyperprolactinemia. (A) Ovary: persistence of eosinophilic CL; (B) vaginal diestrus with mucification secondary to prolonged CL progesterone production; (C) uterus: endometrial folding (hypertrophy/hyperplasia) secondary to prolonged CL progesterone production; (D) mammary gland lobuloalveolar hyperplasia and increased secretions. ×2 (A, C) and ×200 (B, D), H&E. Source: *From Haschek, W.M., Rousseaux, C.G., Wallig, M.A. (Eds.), 2013. Haschek and Rousseaux's Handbook of Toxicologic Pathology, third ed. Academic Press (Elsevier), San Diego, CA, Figure 60.28, p. 2641, with permission.*

examples of xenobiotics that target cell populations in the reproductive tract resulting in specific organ-dependent effects. Examples include bisphenol A for which evidence suggests adverse effects on ovarian meiosis and oocyte quality and the organophosphate pesticide, methoxyclor and its metabolites, which target antral follicles in the rodent and primate ovary resulting in their atresia. Ethylene glycol monomethyl ether is an organic solvent for paints and printer inks and causes CL hypertrophy and progesterone over secretion by luteal cells resulting in a prolonged estrous cycle. As will be mentioned later, xenobiotics that pharmacologically target rapidly dividing cell populations will negatively impact ovarian follicular development, resulting in atresia.

Stress, Negative Energy Balance, and Senescence

A common pattern of reproductive changes observed in toxicology studies is secondary to the effects of stress and reduced food consumption, both common outcomes of administrating high doses of test agents to young, rapidly growing animals used in safety assessment studies. Because reproduction is not an essential process for survival of an animal, when animals enter a negative energy balance, gonadotropin production is reduced and reproductive cycling can be prolonged or delayed, eventually resulting in atrophy of the female reproductive tissues (Figure 18.18). Stress by itself induces excessive secretion of epinephrine, which can depress

TABLE 18.9 Effects of Inhibiting Steroid Metabolic Enzymes on the Female Reproductive Tract

Target enzyme	Example compounds	Pattern of effect
Aromatase	Exemestane	Antiestrogen
Three β-hydroxysteroid dehydrogenase	Troglitazone	Antiprogesterone
17 β-hydroxysteroid dehydrogenase type 1	Various estrone and estrogen derivatives	Antiestrogen
11 β-hydroxysteroid dehydrogenase	PF-877423	Hypercortisolemia

From Haschek, W.M., Rousseaux, C.G., Wallig, M.A. (Eds.), 2013. Handbook of Toxicologic Pathology, third ed. Academic Press, San Diego, CA, Table 60.13, p. 2643, with permission.

the frequency and amplitude of LH secretion and interfere with the reproductive cycle. The organ weight, gross, and histologic changes associated with this common pattern of nonspecific toxicity are listed in Table 18.7.

It is important to note that ovarian atrophy is difficult to assess in short-term rat studies (≤14 days) because the follicular development from primordial to early tertiary stage does not require hormonal stimulation. Also, while expected to decrease with atrophy (Figure 18.19), the CL number can be highly variable and may not be obviously reduced in number or size in these types of studies. The small numbers of animals coupled with the section variability common for ovary also impact assessment of CL number. In short-term studies, we have found that uterine weight and endometrial/myometrial thickness and vaginal epithelial thickness to be very useful and sensitive early endpoints for this pattern. Morphologic changes are easiest to identify in the vagina because the uterine epithelium that lines the luminal and endometrial glands is only a single cell layer that can undergo limited morphological changes under the influence of estrogen, androgens, and progesterone. In contrast, the vaginal epithelium from the anterior 2/3 of the vagina, owing to its multilayered structure and high turnover rate, is able to undergo a variety of changes and is a very sensitive indicator of the hormonal status of the animal. The morphology of the ovarian interstitial glands also changes rapidly with negative energy balance. In a quiescent ovary, normally prominent, large polygonal cells with round nuclei and a moderate amount of deeply acidophilic foamy cytoplasm, become small spindle-shaped cells with dark elongated nuclei and a small amount of lightly acidophilic or basophilic cytoplasm (Figure 18.20).

During the in-life portion of toxicity studies, accommodation may occur to the acute stress and food consumption effects. In these studies, there may be a mixed phenotype at necropsy whereby the histologic pattern of past cycle cessation is combined with a pattern of normal cycling. In these situations, cycle asynchrony in the reproductive tract may be the predominant change. Cycle asynchrony is characterized by an ovary, uterus, and vagina that do not have the histologic characteristics consistent with the same stage of estrus. The toxicologic pathologist should closely evaluate the food consumption and clinical signs in individual animals to appropriately interpret these types of postmortem changes in the female reproductive system.

Differentiating cycle disruption as a result of stress or negative energy balance and primary test agent–related effects can be challenging. It is important that the toxicologic pathologist closely examine the dose-response of the cycle disruption relative to the effects on animal food consumption, clinical signs, and thymic weights and histology, the latter, in our experience, being the most sensitive indicator of previous or ongoing stress in animals. If cycle disruption is only observed at doses that produce decreased food consumption or significant clinical signs or postmortem changes indicative of stress, one may not be able to assess whether there are primary effects on the female reproductive system. However, if this pattern of cycle disruption is observed at doses that cause very little or no changes in food consumption or clinical signs, a primary effect of the test agent should be considered.

In longer term rat studies (>3 months), evaluation of the effects of a xenobiotic may be complicated by reproductive senescence. Early reproductive senescence in the rat may present as persistent estrus (increased antral follicles, decreased basophilic CL, and vaginal cornification) or as persistent diestrus (ovarian and uterine atrophy and diestral vaginal epithelium). These changes can confound the assessment of xenobiotic-related treatment effects.

Hyperprolactinemia

Another common female reproductive toxicity pattern that toxicologic pathologists will likely experience is that manifested by hyperprolactinemia in rats. Female rats are especially sensitive to the effects of hyperprolactinemia, and there are several classes of test agents that induce a hyperprolactinemia phenotype in animals. The most common mechanism of hyperprolactinemia is the excessive prolactin secretion that occurs when dopamine is depleted or antagonized by compounds such as reserpine or phencyclidine hydrochloride. The constellation of changes associated with hyperprolactinemia is outlined in Table 18.8 with the most classic and easily recognized change being that of

mammary gland lobular hyperplasia and persistent vaginal diestrus and mucification (Figure 18.21). It is important to note that the histologic manifestations of xenobiotic-induced hyperprolactinemia may change with the chronicity of the exposure. In our experience the uterine endometrial folding and vaginal mucification is most prominent in studies of up to 1 month where the life span of the eosinophilic CL present in the ovary at study start is extended because of hyperprolactinemia. Because of the inhibitory effects of prolactin on ovarian follicle maturation and ovulation, in longer term studies, the numbers of CL decline and there is follicular atresia and ovarian atrophy. The subsequent decline in ovarian steroid production results in uterine and vaginal atrophy. However, the prolactin-mediated mammary gland changes are maintained.

In our experience, the mammary gland and vaginal changes are most easily recognized in shorter term studies. We recently successfully navigated the structure–activity relationship of a group of compounds, which had a propensity to increase prolactin by only assessing mammary gland and vagina after 4-day repeat-dose studies. In longer term studies, there are histologic changes indicative of prolactin's effect of extending the life span of the ovarian CL (increased size of ovarian CL) and changes in the uterus and vagina consistent with prolonged diestrus (Table 18.9).

While the most common mechanism of hyperprolactinemia in the rat is pharmacologic alterations of the dopamine regulatory pathway for pituitary prolactin production, other possible mechanisms are possible. Opioid receptor biology is also important in prolactin homeostasis. Nonspecific antagonists of opioid receptors (e.g., naloxone) suppress prolactin secretion and natural opioids or synthetic agonists increase prolactin release. Animals given growth hormone develop a prolactogenic phenotype. Increases in the estradiol–progesterone ratio (E2:P4) due to a variety of xenobiotics (e.g., phytoestrogens) can result in hyperprolactinemia.

There are important rat and human species differences with regards to prolactin. For instance, PRL is luteotrophic in rats but not in humans, and, as discussed earlier, the luteotrophic effects of hyperprolactinemia in the rat results in specific uterine (hyperplasia/hypertrophy) and vaginal (mucification) changes that would not be expected in women. Also rats are markedly more sensitive than women to prolactin increases, secondary to estrogen-mediated inhibition of dopamine secretion, and prolactin control is more central (hypothalamic) in rats than in women where peripheral regulation of PRL is more important. Likewise, extrapituitary production of PRL is not important in the nonpregnant rat while in women PRL is produced in mammary gland, the myometrium, and in lymphocytes and adipocytes in both pregnancy and nonpregnancy.

TABLE 18.10 Chemotherapeutic Mechanisms of Female Reproductive System Toxicity

Inhibitory target	Mechanism	Primary effect
VEGF	Antiangiogenesis	Inhibition of CL formation
Tyrosine receptor kinases (e.g., VEGFR, KIT, FLT3, PDGF)	Antiangiogenesis	Inhibition of CL formation, ovarian follicular atresia; uterine endometrial atrophy
FGF receptors	Altered Ca:P metabolism	Ovary mineralization
Cox-2	Prostaglandin inhibition	Impaired ovulation
Cell cycle checkpoint inhibition	Inhibition of rapidly dividing cell populations	Ovarian follicular degeneration/atrophy
erbB receptors	Antiproliferative-epithelial tissues	Vaginal epithelial atrophy

From Haschek, W.M., Rousseaux, C.G., Wallig, M.A. (Eds.), 2013. Handbook of Toxicologic Pathology, third ed. Academic Press, San Diego, CA, Table 60.14, p. 2644, with permission.

While the dogma has been that the effects of hyperprolactinemia in rats are species-specific, there is some controversy as to the significance of the hyperprolactinemic rodent phenotype when assessing the human safety of xenobiotics (see Harvey, 2011). Prolactin is considered a nongenotoxic carcinogen in rodents and some xenobiotics that cause hyperprolactinemia in rodent models are associated with an increased incidence of mammary gland tumors in 2-year carcinogenicity bioassays. Recent retrospective analyses of complex cancer data sets suggest that prolactin may also have an important contributory role in the pathogenesis of human breast cancer. Therefore, as is the case with the safety assessment of all xenobiotics, the potential risk to the exposed population must always be placed into perspective with regards to the benefit to that group.

Altered Activity of Sex Steroid Enzymes and Cholesterol Metabolism

Sex steroid synthesis is a complicated multistep process that requires the activity of numerous substrates and enzymes. In our experience, female reproductive toxicity due to test agent effects on the enzymatic machinery involved in sex steroid synthesis is probably the third most common mechanism

of toxicity, a toxicologic pathologist may observe in preclinical animal models. It is important that the metabolic fate of a test agent is well understood and the drug disposition scientist is an important partner in this assessment. If a chemical structure by its metabolism alters the homeostasis of sex steroid enzymatic activity, female reproductive changes are likely to be observed. The most classic example of this mechanism is the inhibition of the cytochrome P450 enzyme, aromatase, which is necessary for the synthesis of estrogens. The inhibition of this enzyme actually became a major therapeutic breakthrough for diseases like estrogen-responsive breast cancers. Dioxin and dioxin-like compounds, which are common environmental contaminants, produce numerous changes via the aryl hydrocarbon receptor in the female reproductive system, including modulation of the incidence of inflammation and growth disturbances (ovarian and uterine atrophy, hyperplasia, metaplasia, and neoplasia). The mechanism in part for the effects of these compounds appears related to induction of cytochrome P450s, namely 1A1 and 1B1, resulting in an antiestrogenic pattern. Other examples of potential target enzymes and some compounds, which alter their activity, are listed in Table 18.9.

All sex hormone synthesis pathways require a pool of cholesterol substrate therefore test agent effects on cholesterol absorption, synthesis, or metabolism may also have an important downstream impact on sex steroid homeostasis.

The New Generations of Targeted Cancer Therapies

Cancer remains the scourge of modern medicine and efforts to control this complicated disease continue to be a major focus of biotechnology and pharmaceutical companies globally. Historically, the primary focus of chemotherapy was to interfere generically with cells that were undergoing high rates of proliferation using the so-called cytotoxic chemotherapeutics. As a result, toxicity was expected in any noncancer cell that had high turnover such as those present in the bone marrow, gastrointestinal tract, hair follicle, testis, and ovary. Maturation of the ovarian follicle depends on active proliferation of granulosa cells and xenobiotics or radiation that targets a tumor because of its rapid cell turnover can cause direct damage to the oocyte or disrupt granulosa cell proliferation, thus interfering with reproductive function. These include alkylating agents, chemotherapeutic agents, and some heavy metals. In addition to oocyte injury, these xenobiotics may interfere with granulosa cell proliferation, thecal cell differentiation, and active steroidogenesis. For example, cadmium induces necrosis of preovulatory follicles and damages the microcirculation in the uterus of the rat. Radiation causes abnormal mitosis and death of the oocyte and granulosa cells. The result of these processes is a reduction in the total number of oocytes and follicles and an absence of CL in the ovary. This may result in permanent hormonal imbalance due to the loss of negative feedback control from ovarian steroid hormones. If the insult occurs early in life, neoplasms may develop in the remaining hyperstimulated ovarian components.

The age of developing classic cytotoxic agents is for the most part over and therapies that target specific pathways are now the focus of the pharmaceutical industry. Four major approaches used in the last few decades for cancer chemotherapy have involved targeting inflammatory pathways, growth factors, the tumor cell cycle, and the tumor microenvironment, the latter focused on vascular neogenesis and integrity. The structural changes within the female reproductive tract during estrus involve a cascade of events that are highly dependent on cell turnover and angiogenesis; therefore, it is not a surprise that the female reproductive tract is a common target for unwanted toxicologic effects associated with the development of novel

TABLE 18.11 Summary of Uterine and Vaginal/Cervical Histologic Changes for Test Agents that have Estrogen, Progesterone, or Mixed Effects

	Observation		
Hormone pattern	**Endometrial hyperplasia**	**Uterine squamous metaplasia**	**Vaginal and cervical mucosa**
Estrogen dominant	Cystic with leukocytic infiltrates	Present	Hyperplasia
Progesterone or androgen dominant	Noncystic with foamy cytoplasm	Not present	Atrophy with hypermucification
Mixed	Cystic with large cytoplasmic vacuoles	Present	Hyperplasia with hypermucification

From Haschek, W.M., Rousseaux, C.G., Wallig, M.A. (Eds.), 2013. Handbook of Toxicologic Pathology, third ed. Academic Press, San Diego, CA, Table 60.15, p. 2645, with permission.

chemotherapeutics. For this reason, we consider these mechanisms important potential causes of female reproductive toxicity. Table 18.10 lists several chemotherapeutics and associated patterns of toxicities in the female reproductive system.

Modulation of Central Nervous System Biology

Many drugs and chemicals may have a modulatory effect on the central nervous system and the hypothalamus and influence the regulation of gonadotropin secretion. There is an ongoing effort in the pharmaceutical industry to design more effective drugs with better side effect profiles for the treatment of important neurological disorders like schizophrenia, Parkinson's disease, Alzheimer's disease, depression, and anxiety. As the size of the older segment of the population increases, attention to these disorders and their treatment will only increase. For this reason, the toxicologic pathologist should anticipate the potential for female reproductive system toxicities when studying drugs targeted at the central nervous system.

There are several well-studied drugs that modulate cannaboid, dopamine, or opioid pathway physiology, and produce female reproductive toxicity. For example, narcotics such as morphine reduce both serum LH and FSH and block the proestrus surge of LHRH and subsequent ovulation by decreasing the activity of norepinephrine neurons and the storage of hypothalamic norepinephrine. Opioid peptides such as β-endorphin suppress both the amplitude and frequency of the LH pulse and the preovulatory surge of LH, presumably by lowering norepinephrine concentration in the hypothalamus and decreasing the rate of dopamine turnover. Cocaine stimulates LH secretion at low doses, inhibits LH secretion at high doses, and blocks the uptake of dopamine, the latter increasing the secretion of prolactin. Marijuana, containing tetrahydrocannabinol as its principal psychoactive ingredient, depresses LH, FSH, and prolactin secretion at the level of hypothalamus.

Central nervous system toxicants like heavy metals also may produce multiple adverse effects on reproductive function. Inorganic mercury has been reported to block follicular growth and result in anestrus in laboratory rodents, possibly by altering both pituitary gonadotropin and ovarian steroid secretions. In animals treated with lead, atrophy of the ovary, reduction of serum progesterone concentration, and alteration of uterine hormonal receptors have been observed. These toxicities may result from different effects along the hypothalamic–pituitary–ovarian–endometrial axis. Other metals with the potential to affect reproductive function include manganese, tin, and cadmium.

Toxicity Induced by Constituents of the Hypothalamic–Pituitary–Ovarian Axis and Modulators of Nuclear Hormone Receptors

Many naturally occurring and synthetic sex steroid hormones were developed as contraceptives, fertility drugs, and therapeutic agents for the treatment of cancer in the latter half of the 20th century. These include both agonists and antagonists of androgens, estrogen, and progesterone. When sex steroid hormones are given in large nonphysiological quantities in animal toxicity studies, the result is the inhibition of gonadotropin secretion and atrophy of the ovary. However, organs at the bottom of the cascade of control may respond dramatically to the stimulation provided by the massive exogenous doses of these steroids and undergo a high degree of hyperplasia and hypertrophy. Depending on the type of test agent, the changes in these organs will be consistent with what is expected for estrogen, progesterone, or a combination of these two steroids. A summary of the types of test agents and histologic changes that one will observe with an estrogen, progesterone, or mixed stimulus is listed in Table 18.11.

With administration of these various naturally occurring and synthetic sex steroid hormones, the ovary eventually develops atrophy due to the negative feedback of the exogenous sex steroid hormones. However, in dogs and rabbits given estrogenic test agents, ovarian atrophy is accompanied by papillary proliferation of the ovarian surface epithelium. In dogs, there can be metastatic implantation of these epithelial cells onto the capsule of the spleen, kidney, and other abdominal viscera. Since continued growth of these cells is estrogen-dependent, they undergo degeneration, necrosis, and mineralization once these estrogenic compounds are removed. The regression of the canine proliferations has posed the questions if they are true neoplasms since they are not autonomous in growth. Similar regression of granulosa cell "tumors" and hyperplasia following withdrawal of Tamoxifen treatment have been described in the literature. In rabbits, similar transplantation to the splenic capsule is also reported, but dependence on estrogen for continuous growth was not examined.

Another important species difference occurs in dogs, which are very sensitive to stimulation by progestins. In dogs, progestins can cause papillary proliferation of the surface epithelium of the atrophic ovary with occasional thecal-luteal cell hyperplasia. The uterus may become uniformly enlarged and the endometrium is lined by hypertrophic epithelial cells with abundant foamy cytoplasm. Endometrial glands may become hyperplastic and cystic, and exudate may accumulate in glandular lumens. The uterine lumen is

often filled with mucoid material, which may lead to endometritis and pyometra due to superimposed bacterial infection. Cystic glands may also be present in the vagina.

In the last few decades, a more targeted approach has been attempted for hormone therapies by focusing on nuclear hormone receptor physiology and taking advantage of tissue-specific responses that are influenced by the presence of coregulatory proteins. Most of the effort in this area has been focused on tissue-specific modulation of the estrogen receptor with the objective of maximizing the positive outcome of estrogen receptor agonism for bone, metabolic, and peri/postmenopausal symptoms while minimizing the risk for hypothalamic, breast, or uterus endoplasmic reticulum (ER) stimulation. These therapeutics pose an interesting challenge to the toxicologic pathologist because they often produce a mixed female reproductive histologic phenotype due to their disparate effects on estrogen receptors in different tissues and species of animals. Similar modulators have been developed or are in development for several other classes of sex nuclear hormone receptors including the progesterone and androgen receptors and produce other complicated phenotypes. It is important for the toxicologic pathologist to understand the potential for these mixed phenotypes. Data that may help in the interpretation of the changes and their relevance to human risk assessment include the properties of the test agent for the target receptor across species as well as some of the peculiarities of rodents with regards to endocrine physiology as discussed earlier.

SERMs are one class of compounds that may cause upregulation of gonadotropin secretion and abnormally elevated circulating gonadotropins, unresponsive to negative feedback from ovarian steroid hormones. This is due to the SERM acting as an antagonist at the hypothalamic estrogen receptor. The ovary will be hyperactive in these animals and have morphologic changes including follicular cysts and granulosa cell hyperplasia; however, for most SERMs, despite the increased production of ovarian sex hormones including estrogens, progestins, and androgens, the histologic changes in the uterus, vagina, and mammary gland will reflect a lack of estrogenic stimulation because of the SERMs antagonist activity at the level of the estrogen receptor in these tissues. Tamoxifen is a SERM with a slightly different pattern in neonatal and adult mice; whereby, this SERM acts as an ER agonist at the uterus. Interestingly, in adult rats, tamoxifen acts like an ER antagonist in the uterus. These types of observations again underscore the complexity of cross-species comparisons for toxicologic responses of the female reproductive system.

There are many other examples of agents that increase gonadotropin levels. These include direct analogs of LHRH (i.e., Lupron), which are used for the treatment of prostatic cancer and as male contraceptive agents, and human chorionic gonadotropin used for the treatment of infertility in women. In rats, administration of these exogenous gonadotropins will produce continuous stimulation of the growth and maturation of follicles; the formation of CL is not overridden by the elevated levels of ovarian sex steroid hormones. The uterus and vagina will have the expected estrogen-mediated hyperplasia and hypertrophy. As discussed earlier compounds such as reserpine or phencyclidine hydrochloride that elevate prolactin will prolong the functional life of the corpus luteum in rats, thus interrupting the normal reproductive cycle.

CARCINOGENESIS IN THE FEMALE REPRODUCTIVE SYSTEM

Neoplasms in the female reproductive tract are described in detail in the INHAND female reproductive and mammary gland publications (Dixon et al., 2014; Rudmann et al., 2012) and are only summarized here briefly.

The susceptibility to tumor induction in the ovary depends on the strain, species, and age of the animal at the time of exposure. Ovarian gonadotropins are potent growth factors and when their normal hormeostasis is disrupted they can act as nongenotoxic carcinogens. Types of ovarian tumors include granulosa cell tumors, luteoma, tubular adenoma (mouse), Sertoli cell tumor, teratomas, fibroma and fibrous histocytoma, and leiomyoma in the mesovarium.

Endometrial cancer has long been associated with estrogen treatment and more recently with SERMs like tamoxifen that have ER agonist activity in the uterus. The uterus is an estrogen-dependent organ, and endometrial cells proliferate as a result of estrogen stimulation. Early neoplastic growth requires the continuous presence of estrogen. However, once neoplastic growth is established, continuing proliferation or transformation may result in the tumor becoming estrogen independent. Neoplasms induced in the uterus are uncommon or rare and include adenocarcinoma, deciduosarcoma, fibrosarcoma, leiomyoma/leiomyosarcoma, papillary mesothelioma, and squamous cell carcinoma.

A diverse group of chemicals, which includes chemically inert materials such as urea and propylene glycol, is capable of inducing vaginal neoplasms in laboratory animals. The mechanism of tumor induction is not understood but the prolonged exposure may

induce irritation that stimulates epithelial cell proliferation. Extended proliferation has been postulated to progress to uncontrolled neoplastic growth through a transitional stage characterized by epithelial dysplasia. Basal cell carcinomas, leiomyosarcomas, squamous cell papillomas and carcinomas, and tumors of mucin-secreting cells or granular cell tumors have been induced in mice and rats but are all uncommon or rare. Granular cell tumors are relatively common spontaneous tumors in older rats that occur in the vagina and cervix. The incidence of these tumors is reduced in rats treated with an aromatase inhibitor suggesting that estrogen is important in their development.

Clitoral glands are found in multiple species but are most commonly examined in 2-year carcinogenicity rat and mouse studies. They are paired modified sebaceous glands located in the inguinal region adjacent to the vagina. The growth and secretory activity of clitoral glands is regulated primarily by testosterone and the pituitary hormones, adrenocorticotropic hormone, growth hormone, and prolactin. Administration of testosterone, but not estrogens, causes hypertrophy and hyperplasia of clitoral gland acinar cells. In rats, large intracytoplasmic eosinophilic granules are a prominent feature in normal glands. These granules contain pheromones (aliphatic alcohols) and β-glucuronidase that are not present in mice. The degenerative, inflammatory, vascular, and other nonneoplastic changes observed in clitoral glands are comparable to those observed in the mammary gland (see Chapter 19: Mammary Gland). The most common spontaneous lesion observed in these glands is cystic dilation of the duct.

Further Reading

Bregman, C.L., Adler, R.R., Morton, D.G., Regan, K.S., Yano, B.L., 2003. Recommended tissue list for histopathologic examination in repeat-dose toxicity and carcinogenicity studies: a proposal of the Society of Toxicologic Pathology (STP). Toxicol. Pathol. 31, 252–253.

Buse, E., Martina Zöller, M., Van Esch, E., 2008. The macaque ovary, with special reference to the cynomolgus macaque (*Macaca fascicularis*). Toxicol. Pathol. 36, 24S–66S.

Capen, C.C., 2004. Mechanisms of hormone-mediated carcinogenesis of the ovary. Toxicol. Pathol. 32, 1–5.

Chandra, S.A., Adler, R.R., 2008. Frequency of different estrous stages in purpose-bred beagles: a retrospective study. Toxicol. Pathol. 36, 944–949.

Cline, J.M., Wood, C.E., Vidal, J.D., Tarara, R.P., Buse, E., Weinbauer, G.F., et al., 2008. Selected background findings and interpretation of common lesions in the female reproductive system of macaques. Toxicol. Pathol. 36 (suppl 7), 142S–163S.

de Rijk, E., Van Den Brink, H., Lensen, J., Lambregts, A., Lorentsen, H., Peter, B., 2014. Estrous cycle-dependent morphology in the reproductive organs of the female Gottingen minipig. Toxicol. Pathol. 42, 1197–1211.

Dixon, D., Alison, R., Bach, U., Colman, K., Foley, G.L., Harleman, J.H., et al., 2014. Nonproliferative and proliferative lesions of the rat and mouse female reproductive system. J. Toxicol. Pathol. 27, 1S–107S.

Greaves, P., 2011. Female genital tract, Histopathology of Preclinical Toxicity Studies, fourth ed. Academic Press, New York, pp. 667–724.

Harvey, P.W., 2011. Prolactin-induced mammary tumorigenesis is not a rodent-specific response. Toxicol. Pathol. 39, 1020–1022.

Rudmann, D., Cardiff, R., Chouinard, L., Goodman, D., Kuttler, K., Marxfeld, H., et al., 2012. Proliferative and nonproliferative lesions of the rat and mouse mammary, zymbal's, preputial, and clitoral glands. Toxicol. Pathol. 40, 7S–39S.

Rudmann, D., Foley, G., 2013. Female reproductive system. In: Haschek, W.M., Rousseaux, C.G., Wallig, M.A. (Eds.), Haschek and Rousseaux's Handbook of Toxicologic Pathology, third ed. Academic Press (Elsevier), San Diego, CA.

van Esch, E., Cline, J.M., Buse, E., Weinbauer, G.F., 2008a. The macaque endometrium, with special reference to the cynomolgus monkey (*Macaca fascicularis*). Toxicol. Pathol. 36, 67S–100S.

van Esch, E., de Rijk, E.P.C.T., Buse, E., Zoller, M., Cline, J.M., 2008b. Recommendations for routine sampling, trimming, and paraffin-embedding of female reproductive organs, mammary gland, and placenta in the cynomolgus monkey. Toxicol. Pathol. 36 (Suppl.), 164S–170S.

Weinbauer, G.F., Niehoff, M., Niehaus, N., Srivastav, S., Fuchs, A., Van Esch, E., et al., 2008. Physiology and endocrinology of the ovarian cycle in macaques. Toxicol. Pathol. 36, 7S–23S.

Westwood, F.R., 2008. The female rat reproductive cycle: a practical histological guide to staging. Toxicol. Pathol. 36, 375–384.

Wood, C.E., 2008. Morphologic and immunohistochemical features of the cynomolgus macaque cervix. Toxicol. Pathol. 36, 119S–129S.

This page intentionally left blank

CHAPTER

19

The Mammary Gland

Barbara Davis[1] *and Suzanne E. Fenton*[2,*]

[1]Innogenics, Inc., Harvard, MA, United States [2]National Institute of Environmental Health Sciences, Research Triangle Park, NC, United States

OUTLINE

INTRODUCTION

Breast cancer is the most common invasive cancer and the leading cause of cancer-related mortality in women. As such, there remains heightened concern about the potential causes and risk factors, including those from environmental exposures, drugs or dietary intake that may contribute to the development or progression of this deadly disease. Lifetime exposure to estrogens (early age of menarche, older age at menopause, nulliparity, unopposed estrogen) and genetics (family history of breast/ovarian cancer) are major factors that increase risk for breast cancer, and early age of first pregnancy (<22 years old) is associated with decreased risk. Other biological indices, such as obesity and breast density, are highly correlated with risk of breast cancer and may be affected by environmental factors.

This interplay of reproductive and hormonal influences generally holds across species. For example, mammary cancer is the most common malignant cancer in intact bitches (dogs) greater than 6 years old. Neutering prior to first estrus essentially negates the risk, while risk increases with neutering after consecutive cycles. In old world macaques, the role of reproductive status is not clearly defined, but mammary gland biology and breast cancer development are generally comparable to that in women. In a population of captive macaques the lifetime risk for breast cancer was estimated to be about 6% and considered comparable to women (1 in every 8, or 12%). The types of cancer, intraductular carcinomas and invasive and metastatic cancers, are also morphologically like those in women. The role of estrogens and progestins in mammary proliferation are also comparable in macaques and women. In experimental studies in castrated cynomolgus and rhesus macaques, estrogen treatments alone stimulated epithelial proliferation, progesterone treatments alone had negligible effects, while both

*Suzanne E. Fenton contribution is in Public domain.

Fundamentals of Toxicologic Pathology.
DOI: http://dx.doi.org/10.1016/B978-0-12-809841-7.00019-8

estrogen and progesterone treatment together stimulated proliferation exceeding that of estrogen alone.

In rodents, hormonal and reproductive status and genetics have significant effects on the development of mammary cancer. Mammary cancer can be induced with estrogen treatment in both rats and mice and incidence of mammary cancer increases with increasing age in many strains of rats. In rats, as in women, pregnancy is protective, although pregnancy does not have the same protective effect in mice. Mice also deviate from rats, monkeys, and women in that the most common types of mammary cancer in mice are lobuloalveolar, noninvasive, and not metastatic. In contrast, mammary cancers in women, monkeys, dogs, and rats are ductular, derived from the most primitive epithelial cells of the terminal ductal units, and are invasive and malignant.

Animal studies also show that there are windows of increased susceptibility to external influences during gland development, which may enhance the predisposition to cancer later in life. Consequently methods in safety assessment and hazard identification using animal models should be designed to assess developmental abnormalities as well as preneoplastic and neoplastic changes in adults. The purpose of this chapter is to provide an overview of mammary gland biology of different species with relevance to humans, and review models, methods, mechanisms, and definitions of mammary gland toxicity and carcinogenicity.

MAMMARY GLAND STRUCTURE AND FUNCTION

Mammary glands are modified tubuloalveolar glands of the skin (see Chapter 24: The Integumentary System), and are a complex organ composed of epithelial lined ducts and alveoli within an adipose-based fat pad surrounded by fibroblasts, immune/inflammatory cells, lymphatics, and blood vessels. Mammary development resembles that of epidermal appendage sweat glands, but under control of pituitary and gonadal hormones in addition to hormones produced by mammary fat pad components. These hormonal influences transition the gland through numerous phases of growth, differentiation, involution and atrophy, and have varied effects on males and females.

Stages of Mammary Gland Development

Mammary gland development has distinct anatomical and functional changes during embryogenesis and prepuberty that include *bud formation* and early *ductal tree* formation, and during postpuberty and pregnancy that include *ductal elongation*, *lobuloalveolar differentiation*, and *pregnancy and lactation*.

Bud and ductal tree formation: Gland formation begins during embryogenesis with the development of linear bilateral ectodermal thickenings, referred to as the mammary line or ridge, which overlie a specialized mesoderm. The ectodermal cells of the ridge migrate and aggregate, forming "mammary epithelial buds" at the location of the future mammary gland. These solid ectodermal cords grow into the underlying mesenchyme, followed by limited epithelial branching and canalization to form mammary sprouts. Support structures, including adipose tissue, which later forms the fat pad containing blood vessels, lymphatics, and connective tissue, develop from mesenchyme coincidental with mammary bud development. Myoepithelial cells that eventually surround epithelial structures (ectoderm) and nerves (neuroectoderm) differentiate separately, but simultaneously, with the mammary buds. There are some species differences in the number and complexity of sprouts prior to birth as sprouts form the papillary ducts of each gland. Each sprout also communicates externally with epithelium that will form the teat/nipple. Some species have collecting ducts that drain multiple primary ducts into a teat (mice, cows), whereas the human has numerous ducts that drain directly into the nipple.

Ductal elongation: Initial growth of the gland occurs through linear ductal elongation promoted by a distinct bulbous structure at the distal end of the duct called the "terminal end bud" (TEB) (Figure 19.1). TEBs are composed of multiple layers of epithelial cells and myoepithelial cells lining the basement membrane that interact closely with the surrounding mesenchymal stroma of the fat pad to determine length and patterning of the gland. The leading portion of the TEB is covered by a distinct layer of "cap cells" overlying more numerous layers of "body cells," each containing stem cells with the capacity to form ductal or luminal alveolar cell types. Canalization occurs at the trailing end of the duct to form a single layer of luminal cuboidal epithelial cells and basally located myoepithelial cells supported by a distinct basement membrane. A continuous basement membrane is principally composed of type IV collagen, laminin, nidogen, and heparin sulfate proteoglycan. Both luminal epithelial and myoepithelial cells produce laminin subunit chains, distinguished by type: epithelial cells deposit $\alpha 3$ and $\alpha 5$ chains, myoepithelial cells deposit $\alpha 1$ chains. The stroma surrounding the ducts consists of fibroblasts and adipocytes, macrophages and eosinophils. These interstitial cells support ductal elongation and branching. Functionally and microscopically, mammary gland morphology and duct elongation is characterized both as a proliferative and an apoptotic process.

Lobuloalveolar differentiation: In all species, there is extensive growth of the mammary gland and branching of TEBs into lobular structures during

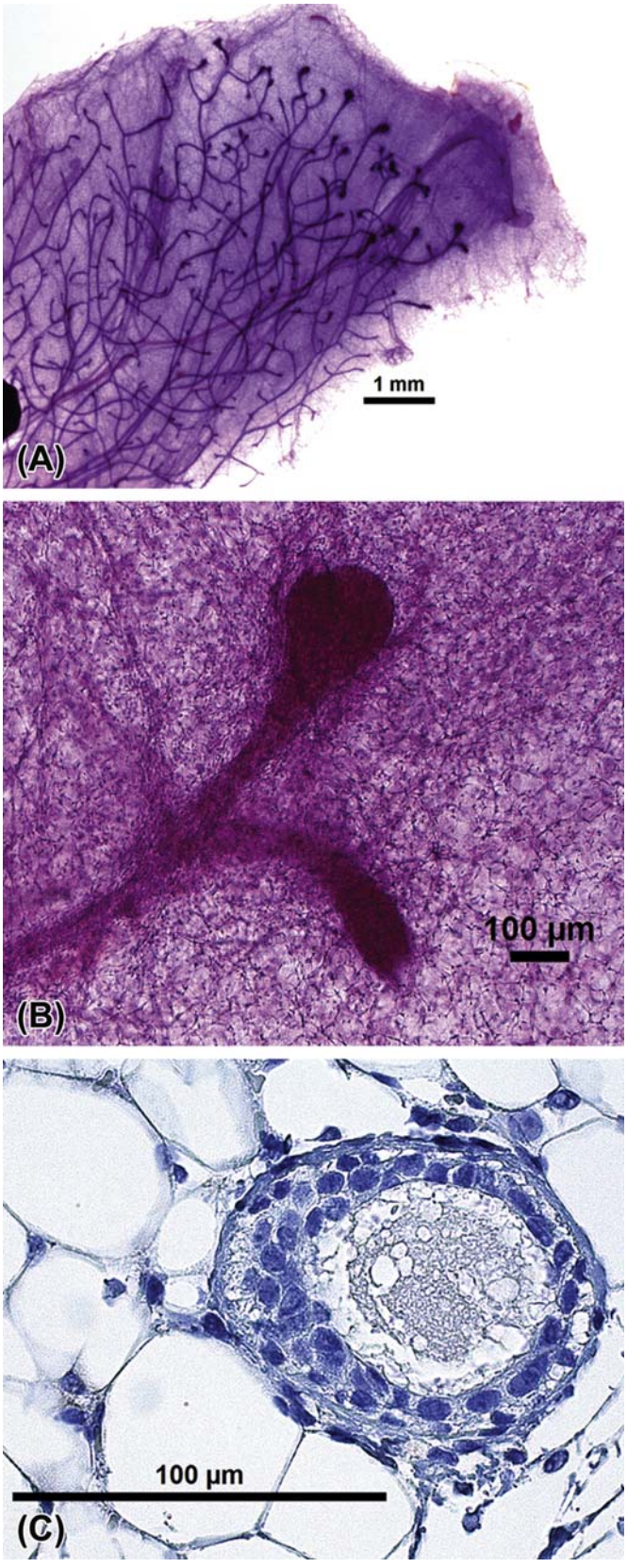

FIGURE 19.1 Mouse mammary gland at 5 weeks showing terminal end bud (TEB) and duct morphology. (A) Carmine alum-stained whole mount of mammary gland with many TEBs at leading edges filling the surrounding fat pad. (B) Higher magnification of the TEBs showing bulbous end and bifurcation. (C) Hematoxylin and eosin-stained section of a TEB showing the single layer of TEB cap cells (outer ring) and multilayered preluminal body cells. The cap cells often appear separate from the body cells but this is an artifact of processing. There is also often an increased stromal cellularity (inflammatory cells and fibroblasts) along the neck. TEBs should not be confused with foci of hyperplasia in young animals. Source: *Figure reproduced from Haschek, W.M., Rousseaux, C.G., Wallig, M.A. (Eds.), 2013. Haschek and Rousseaux's Handbook of Toxicologic Pathology, third ed. Academic Press (Elsevier), Figure 61.1, p. 2667 with permission.*

adolescence. Although there are species differences in promoting growth, in all species exponential mammary epithelial growth and development is ignited just prior to other outward signs of puberty and is coincident with a relative burst of ovarian hormones. In most species, including humans, rapid mammary development occurs prior to cycling, suggesting that more than just ovarian hormones control this process. In the adult, mammary glands are arranged into lobules of compound branched alveolar sacs, separated by dense interlobular connective tissue and fat (Figure 19.2). Lobules are arranged into distinct lobes with its own excretory duct, also called the lactiferous duct, and its own opening on the teat or nipple via the papillary duct. Cuboidal basal and superficial columnar epithelial cells line the lactiferous duct. The secretory units are alveoli, which respond to hormonal signals of lactation. An alveolus is lined by secretory cuboidal or columnar epithelium and an outer layer of myoepithelial cells that lie between the epithelium and the basement membrane.

Pregnancy and lactation: Marked development and differentiation continues through pregnancy and lactation (Figure 19.3). During pregnancy and lactation, extensive growth and alveolar maturation occurs to form milk-producing glands. With growth of the gland, there is a concurrent reduction in the amount of intra- and interlobular connective tissue. The secretory alveoli are lined by cuboidal epithelium, surrounded by a layer of myoepithelial cells, basement membrane, and an intimate network of capillaries and lymphatics. The continued growth of the mammary gland during the second half of pregnancy is due to increases in the height of epithelial cells and an expansion of the lumen of the alveoli. These cuboidal cells produce and secrete the milk components, which are expelled from lobuloalveolar units by contraction of myoepithelial cells. During peak lactation, adipocytes are rarely observed in tissue sections. After lactation or end of suckling the mammary glands undergo an apoptotic process called involution by which remaining milk is phagocytized and epithelial cells degenerate. The few remaining alveoli

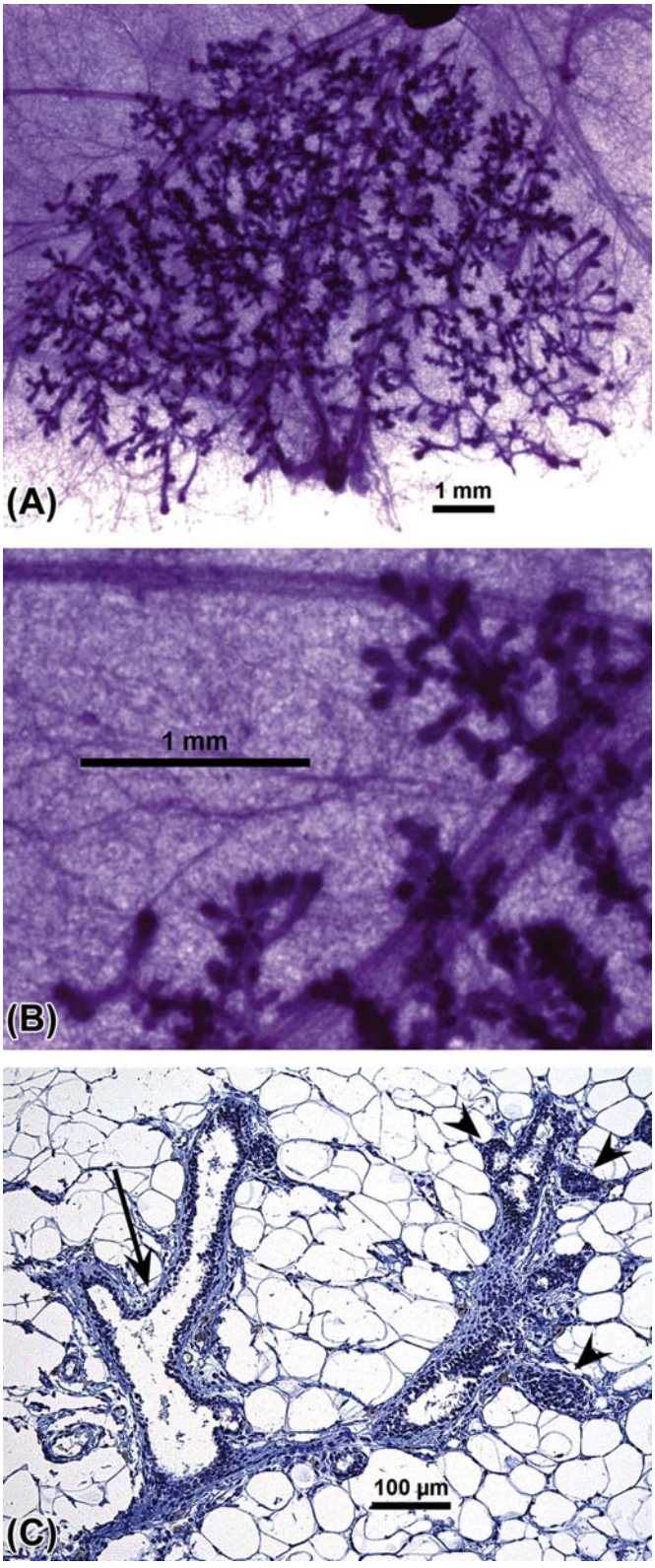

FIGURE 19.2 Rat mammary gland at 3 weeks showing alveolar buds and duct morphology prior to puberty. (A) Carmine alum-stained whole mount of mammary gland with many branching ducts and alveolar buds filling the fat pad. (B) Higher magnification of branching ducts with alveolar buds. (C) Hematoxylin and eosin counter-stained section of duct showing branched ducts (arrow) and ducts lined with numerous buds of various sizes (arrowhead). Source: *Figure reproduced from Haschek, W.M., Rousseaux, C.G., Wallig, M.A. (Eds.), 2013. Haschek and Rousseaux's Handbook of Toxicologic Pathology, third ed. Academic Press (Elsevier), Figure 61.2, p. 2668 with permission.*

are lined by low cuboidal, nonsecretory epithelial cells, and prominent myoepithelial cells. Stromal cells, adipocytes, and the amount of interstitial and connective tissue are increased as involution proceeds. Corpora amylacea, which are small concretions of protein, may be found in alveoli, ducts, or interstitial areas.

Species Variations in Mammary Gland Development

Species differences to consider include the relative timing of development, the extent and complexities of the ductal and lobuloalveolar development, and male mammary characteristics. Understanding these species/sex variations are critical to choosing an appropriate research model and in interpreting the effects of xenobiotics.

Rodents: In the mouse, mammary gland development begins about embryonic day 10.5 with the appearance of 5 placode sets on the mammary ridge. Further development occurs along each of the two mammary lines from embryonic day 11.5 to day 13.5. The mesenchyme adjacent to the mammary epithelium becomes dense and begins to regulate elongation of the mammary buds. Epithelial cords are formed and continue to elongate as terminal ends form and grow into the fat pad through fetal days 15–16.5. Ductal branches and a lumen form just prior to birth.

The rat differs from the mouse in that mammary placode development begins about embryonic day 12.5 with 6 sets of mammary buds present by embryonic day 15.5 that develop into a more complex branched pattern around the time of parturition. Both male and female demonstrate the branched pattern and lumens that are present at the time of birth. Prior to vaginal opening, ductal budding is apparent, and the TEBs begin to cleave into clusters of 3–5 smaller alveolar buds each with a centrally located lumen surrounded by a layer of cuboidal epithelial cells. The glands of the prepubertal female rat are characterized by scattered ducts lined by a single or double layer of cuboidal epithelium, which, after branching several times, becomes multilayered to form the TEBs. TEBs are comprised of 3–6 layers of medium-sized epithelial cells with scant cytoplasm and oval nuclei.

Growth and branching of the mammary structure in rodents continues after birth reaching peak growth rate from 21 to 55 days of age. With each estrous cycle the alveolar buds form complex lobules of smaller diameter with a distinct lumen lined by a single layer

of low cuboidal epithelium. The glands of mature, virgin female rats are tubuloalveolar, characterized by abundant branching, narrower ducts, and more numerous alveolar buds and lobules. As rodents age or experience periods of prolactin and progesterone-prominent pseudopregnancy, glands will have more extensive budding and lobular formation. There are also slight changes in budding/lobule formation depending on the estrous cycle stage, therefore stage of cycle should be determined when evaluating mammary tissue for effects of xenobiotics. When some strains (e.g., Charles River Sprague-Dawley or Fisher 344) become middle aged (from 8 to 14 months of age) and reproductive senescence ensues, prolactin levels increase leading to the development of several morphologic changes including inappropriate secretory activity, ectasia of ducts, formation of cysts or galactocoeles, epithelial hyperplasia, and periductal fibrosis.

Although the mammary gland becomes a vestigial organ in the male, it may be more susceptible to endocrine modulation during development and retains the capacity to develop cancer in the adult. In male mice the mammary rudiment degenerates on or near gestational day 14 in response to androgen-dependent condensation of the surrounding mammary mesenchyme. A small stalk of epithelium may remain. There is no nipple formed in either male mice or rats. However, in male rats mammary glands are difficult to distinguish from female glands prior to puberty, but there is considerable sexual dimorphism in adulthood. Compared to the tubuloalveolar glands in the adult female rat, the adult male has lobuloalveolar glands lined by a single layer of cuboidal vacuolated epithelial cells, and pseudostratified or stratified epithelium. The male rat mammary gland remains responsive to endogenous and exogenous hormone agonists and antagonists throughout its life.

Dogs: When dogs are used in safety assessment studies, they are usually young, sexually immature, which limits the assessment of toxicity. Prior to puberty, dogs have rudimentary glands composed of large interlobular ducts with few laterally projecting TEBs within a dense connective tissue stroma. Like other species, marked proliferation of TEBs, linear growth and tertiary branching into lobes occurs with the onset of puberty and requires the influence of estrogens and progestins.

In cycling bitches the gland of proestrus is characterized by interlobular ducts, a few small lobules and extensive connective tissue stroma. During estrus, there is marked intralobular ductal epithelial proliferation and formation of many small ductules lined by a multilayered epithelium within loose connective tissue. By default in the bitch, corpora luteal function is maintained by prolactin during the 2 months (about 63 days) postovulation regardless of whether the bitch is pregnant or not (see Chapter 18: Female Reproductive System). Mammary gland development during the early half of this period (early diestrus if not pregnant, or early pregnancy) is characterized by greater development of the ducts, the stroma becomes mucinous and fibroblasts within the interlobular stroma demonstrate increased mitotic activity. During the last half of this period, late diestrus or late pregnancy, secretory alveoli begin to develop. Alveoli are filled with bright eosinophilic proteinaceous secretion and lined by cuboidal to flattened cells and elongated or stellate myoepithelial cells and supported by minimal intralobular stroma. Stroma remains prominent around the ducts. If pregnant the mammary gland is stimulated by the hormones oxytocin and prolactin, and becomes secretory. If not pregnant the mammary gland involutes. Involution is characterized as reduction and shrinkage of the alveoli with vacuolated and apoptotic epithelium. Because of such variations, evaluations of cycling females should always be conducted with consideration for cycle stage.

Nonhuman Primates: As in humans a rudimentary ductal tree is formed early in life. TEBs form the leading edge, surrounded by myxoid stroma. Rapid growth and the appearance of "invasive" epithelium are normal in nonhuman primates, particularly macaques. Most of mammary gland development occurs during puberty. In rhesus macaques, puberty occurs between 2- and 3-years old, and in cynomolgus monkeys it occurs slightly later. The epithelial cells are surrounded by myoepithelium and stromal support consisting of fibroblasts and adipocytes. Most of the developing gland is adipose and fibrous connective tissue. The lactiferous ducts are lined by stratified squamous epithelium as they approach the surface, and in the nonlactating animal they are typically filled with keratin. As the mammary gland continues development there is rapid elongation and branching of major ducts to form a dense gland of arborized lobuloalveolar units. Thus even early in puberty with the onset of menstruation, there may be well-differentiated, densely branched lobuloalveolar units lined with secretory epithelial cells.

Toxicology studies of nonhuman primates often employ few and younger animals that may be just entering puberty. Mammary gland development can be quite mixed—varying from dense branching ducts to lobuloalveolar morphologies—which may be misinterpreted as toxicant effects. There are also subtle cycle-related changes characterized by ductal proliferation during the luteal phase of the cycle and alveolar proliferation during the follicular phase. During pregnancy and lactation, extensive alveolar maturation and differentiation to a milk-producing phenotype occurs. Involution is typically extensive with regression of alveoli to a nulliparous

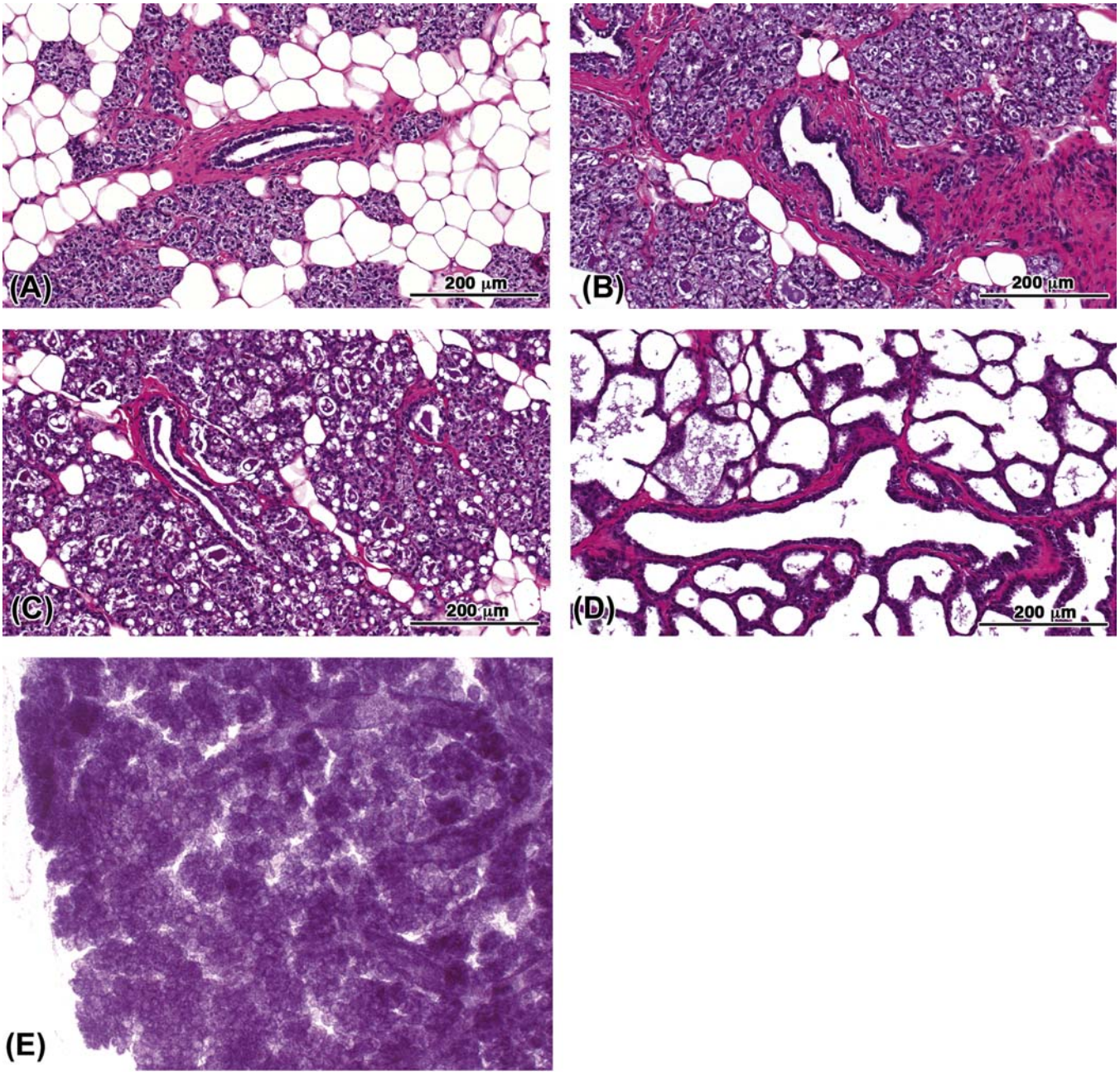

FIGURE 19.3 The pregnant and lactating mammary gland of the rat. Mammary gland H&E representing (A) pregnancy day 15, (B) pregnancy day 17, (C) the day of parturition (21 days pregnant), and (D) the fourth day of lactation. Note increasing epithelium and secretory lipids and proteins as time passes. Adipocytes and stromal cells seemingly disappear and are replaced by cuboidal secretory epithelium. Mammary whole mounts are not an effective tool in evaluating toxicant effects in lactating and pregnant tissue, as the dense staining makes interpretation difficult (E). Source*: H&E figures adapted from Filgo, A.J., Foley, J.F., Puvanesarajah, S., Borde, A.R., Midkiff, B.R., Reed, C.E., et al. 2016. Mammary gland evaluation in juvenile toxicity studies: temporal developmental patterns in the male and female Harlan Sprague Dawley rat. Toxicol. Pathol. 44 (7), 1034–1058 with permission. Whole mount courtesy of A.J. Filgo, NIEHS.*

state. Experimental studies have shown that during aging and menopause, or with surgical castration, atrophic ducts maintain estrogen and progesterone receptors and respond to exogenous steroids for some time. It should also be noted that marmosets do not undergo menopause so older females will maintain more developed glands while rhesus macaques reach menopause at about 22–24 years old, accompanied by atrophic changes in the mammary gland.

Humans: Mammary milk lines develop as early as 4–5 weeks of gestation and form one pair of mammary placodes. The primary ectoderm bud is present by 12 weeks of gestation and small ductal outgrowths as a primitive gland are present at birth. Also, rather than forming a

single ductal tree, each human anlagen forms several trees initiating at the nipple. Before birth the specified mammary epithelium grows from the nipple into the fat pad to form a small, branched ductal network. The advancing margins of undifferentiated TEBs are surrounded by a loose myxomatous connective tissue matrix. TEBs express both estrogen receptors by gestational week 30 and progesterone receptors at birth, evidence of the role that steroid hormones play in normal breast development with implications extending to the potential deleterious influences of endocrine disrupting compounds. During childhood and adolescence, breast growth keeps pace with overall body growth until greatly accelerating at puberty.

Age of puberty in girls is significantly decreasing across continents, with genetics, nutrition, or increasing exposure to natural and synthetic estrogenic compounds all implicated as potential causes. Pubertal development is classified in five Tanner stages, which describe breast and pubic hair growth prior to the onset of menarche. According to median Tanner stages over time, accelerated age of puberty in girls is characterized as menarche occurring possibly a few months earlier, while breast development can occur up to 1–2 years earlier than it did decades ago. Thus breast development is not only significantly advancing in the human population, but there is also dissociation between the pubertal hormonal control of breast development and menarche. These observations underscore the enhanced sensitivity of the mammary gland to genetic and environmental influences compared to other reproductive tissues (see Chapter 18: Female Reproductive System). The advancement of breast development increases the overall time that TEBs remain as susceptible targets, which increases the risk for development of cancer. Indeed, earlier age of menarche and later age of menopause are known risk factors for breast cancers. Thus assessing the maturation of the mammary gland in rodent toxicology studies provides an important means to identify potential human health hazards.

MORPHOLOGIC EVALUATION

Thorough morphological evaluation of mammary glands incorporates routine assessment in histological hematoxylin-eosin (H&E) sections, quantitative morphometric analysis and morphological evaluation of whole mounted mammary glands (see Further Reading for protocols). Factors to consider are the age of the animal and expected developmental maturity of the gland, the species, sex, strain, stage of cycle, pregnancy, lactation, or involution.

In rodent studies, all gross lesions are collected and historically the fifth mammary gland was dissected with or without skin from the same side in both sexes.

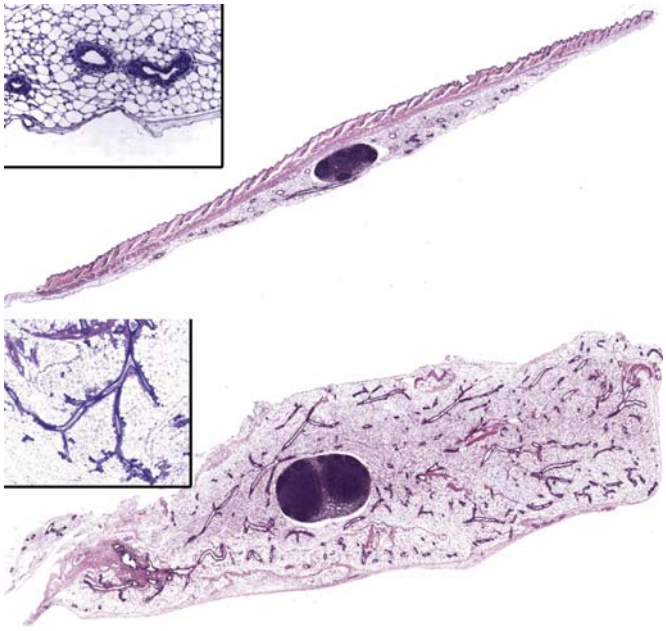

FIGURE 19.4 Mammary gland, rat, H&E prepared in the classical method, which is a cross section or transverse section (top figure) and a contemporary frontal (coronal) method of sectioning (bottom figure). Classical cross sections contained skin, but less mammary tissue compared to the contemporary frontal sectioning, which has greater area of mammary epithelia for evaluation. The frontal sectioning is comparable to whole mount preparations of the contralateral gland and is the suggested method of sectioning for lesion detection. *Source: Figure reproduced from Haschek, W.M., Rousseaux, C.G., Wallig, M.A. (Eds.), 2013. Haschek and Rousseaux's Handbook of Toxicologic Pathology, third ed. Academic Press (Elsevier), Figure 61.5, p. 2677 with permission.*

However, Figure 19.4 demonstrates the major advantage of using the fourth and fifth gland of the rodent, cut in longitudinal sections, allowing a greater chance of detecting a lesion if it exists in the mammary tissue. The contralateral fourth and fifth glands should be isolated for mammary gland whole mounts. Male mice typically lack mammary epithelium, thus would not be evaluated unless nipple/areolae retention is noted early in life. Sampling in dogs includes the nipple and surrounding gland. More extensive collection is needed for nonhuman primates as mammary epithelial growth extends far into the fat. Glands are placed flat in a histocassette or are flattened onto fiberboard or index card and processed through formalin fixation to a 5-micron section on a charged glass slide stained with H&E. Temporal biopsies in nonhuman primates (see Further Reading), add the power of analyzing changes over time without, importantly, the need for sacrifice.

Increasingly, sectioned mammary tissue receives qualitative assessments, coupled with semiquantitative morphometric analysis. Parameters evaluated include length of the ductal tree along the longitudinal axis, total area occupied by epithelial ducts, branching density, total number and size of TEBs all relative to the total

area of mammary epithelium, and total area of the fat pad. These parameters can be measured in the routine sections using image analysis software systems or with eye-piece reticules, but are subjective unless the entire gland is sectioned. Immunohistochemistry end points including cell proliferation and apoptosis measurements are similarly quantified with respect to location of cells (epithelial, myoepithelial, mesenchymal, ductal, bud, alveoli, and fat pad) and total number of cells evaluated. Increases in epithelial density and cell proliferation in early development have been correlated with the development of cancers later in life in both rodents and nonhuman primates. Thus morphometric analysis of glands, coupled with immunohistochemical staining with PCNA or Ki67 cell proliferation markers, provide excellent markers of mammary gland changes.

Whole Mount Preparations: While histologists and pathologists are well versed in light microscopic techniques and evaluation, whole mount preparation (the entire fourth and fifth gland mounted onto a slide) and evaluation is not yet a routine procedure in all laboratories. However, evaluation of mammary gland morphology in whole mounts allows assessment of the branching complexities and glandular densities. Whole mounts are also more amenable to quantitative assessments of TEBs, alveolar buds, duct, and branching development, and growth into the fat pad because the entire gland is represented. Processing mammary gland for whole mounts requires some training, but is relatively inexpensive and does not require pathology experience. Procedures are detailed in Davis and Fenton (2013). The whole mount should be prepared from the contralateral gland processed for standard H&E slide examination. Masses or questionable lesions observed in whole mounts can be excised and reprocessed through paraffin for H&E microscopic examination (Figure 19.5; see Further Reading for protocol). Mammary gland development may be scored according to the criterion detailed in Davis and Fenton (2013) and briefly described here.

Developmental Assessment: To evaluate the whole mounted mammary gland, the normal structures of the mammary gland, including the difference between TEBs and terminal ducts, identification of a bud, lobule, duct, lymph node, and lateral branches, and age-related shifts in morphology should be familiar. Morphology may differ slightly between strains within species, therefore, it is imperative that the slides from the control group are evaluated first, to become familiar with the normal mammary gland morphology for the strain, sex, and age of animal in that particular study. This should include reviewing controls of males and females separately, at the ages evaluated. When assessing the mammary morphological development, determine (1) the number of TEBs relative to the number of duct ends and the morphology of the TEBs, (2) the degree of lateral duct

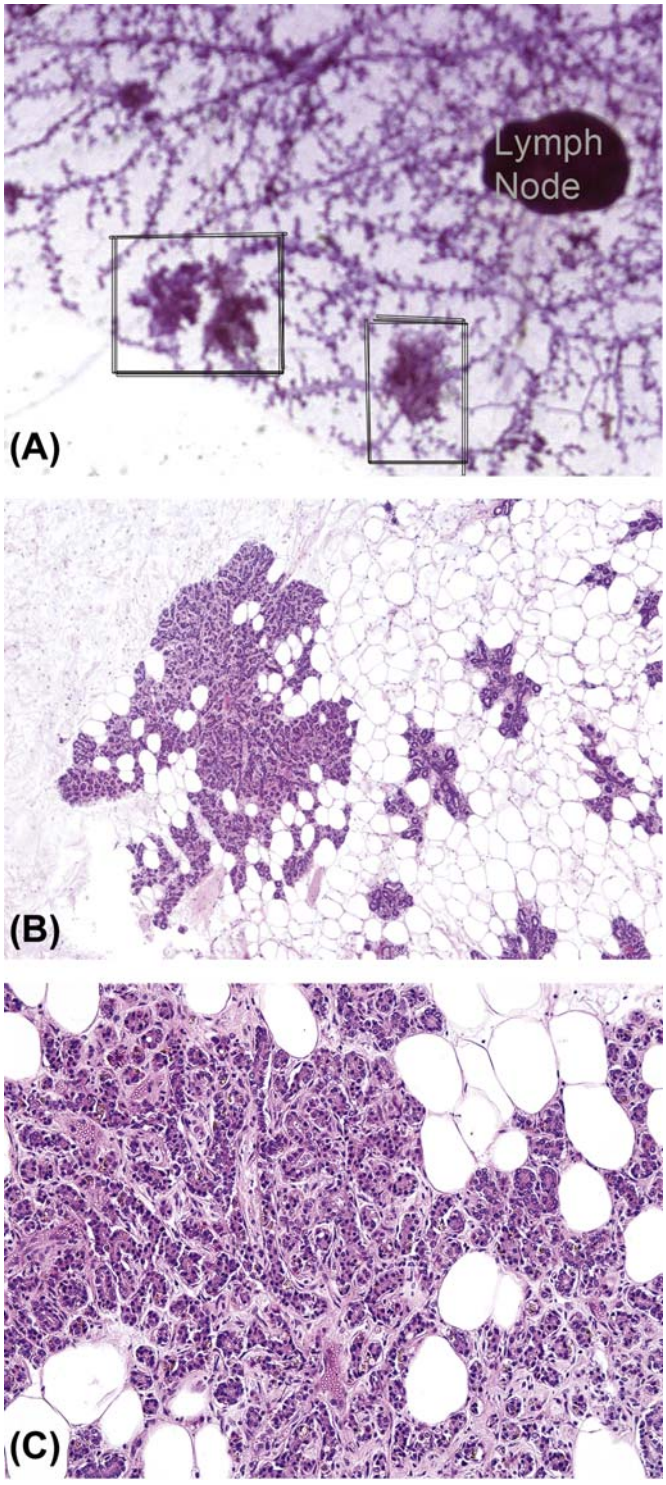

FIGURE 19.5 Identification of lesion/masses in mammary whole mount from CD-1 mouse. (A) Whole mount preparation identified potential lesions (boxed areas) with lymph node designated for reference; Carmine-stained 10× magnification. (B) Whole mount was removed from slide and sectioned/stained as in Tucker et al. (2016, see Further reading). The lesion was diagnosed as alveolar hyperplasia; H&E. 10× magnification. (C) 100× magnification of alveolar hyperplasia. Source*: Photos courtesy of D. K. Tucker, NIEHS.*

branching, (3) the degree of ductal bud and lobule formation, (4) growth of the gland (measure the length and width of the glands), and (5) the glands may be given a morphological developmental "score" as described in Davis and Fenton (2013). In some cases a more quantitative evaluation of the glands may be required. Some suggested methods are provided in Further Reading.

EVALUATION OF TOXICITY

In Vitro Techniques

A variety of *in vitro* techniques are useful as screening assays for mammary toxicants as well as for mechanistic studies. The idea that chemicals can be screened for estrogenic activity *in vitro* was validated by Soto and Sonnescheim and colleagues describing the E-Screen assay. This assay takes advantage of endogenous estrogen receptor–mediated events in breast epithelial cancer MCF7 cells. An "A-screen" has been similarly developed for assessing androgen receptor (AR) activity using prostate carcinoma or MCF7 cells transfected with AR. Yeast-based steroid hormone receptor gene transcription assays and in silico ligand-dependent reporter assays are also used in drug screening, drug development, and toxicology studies. Compounds showing activity in these screening assays should be considered as potential mammary gland toxicants.

Cell culture experiments have provided important mechanistic knowledge of mammary gland biology and cancer. Neoplastic MCF7 and nonneoplastic MCF10 have been widely used, although there are many well characterized mammary (breast) epithelial cells available including cells derived from human breast. Another important and increasingly popular *in vitro* system is the 3-dimensional (3D) mammary gland culture. 3D cultures were originally described by the Bissell lab using MCF10A cells first suspended in medium containing 2% Matrigel and then plated on a solid layer of Matrigel. When mammary epithelial cells (such as MCF10A cells) are cultured on laminin-rich extracellular matrix, they produce a basement membrane and arrange themselves in spherical acini with a centrally located lumen. Modulation of genes or stromal elements can affect the formation of the acini. Such 3D cultures provide an advantage in toxicology studies by providing capabilities to assess both morphological and molecular changes and may demonstrate relevant cell-type interactions.

Animal Studies

Although there are developmental and biological differences between mammary glands of various species of animals and humans, modeling effects of chemicals in animals has proved necessary and critical to advance our understanding of mammary gland biology, response to injury and cancer. The use of animal models (especially rodents) has demonstrated that sensitive life stages (especially fetal development, puberty, and pregnancy) impart a unique sensitivity to some chemical exposures leading to later life disease risk and that toxicants can act by mechanisms other than as frank carcinogens (i.e., as endocrine disruptors) to confer an increased risk of cancer or other late-life effect, such as insufficient lactation (Figure 19.6).

Bioassays in Spontaneous Rodent Animal Models: Bioassays conducted by the NTP have historically relied on B6C3/F1 mice and F344 inbred rats exposed up to maximally tolerated doses of single chemicals from sexual maturity (6–8 weeks old) up to 2 years. However, because of the high background of spontaneous tumors in some strains (Fisher 344), the NTP has recently changed rat strains to the Harlan Sprague-Dawley or Wistar Han. Industry-sponsored studies more often use CD-1 mice and CD-1 Sprague-Dawley, Harlan Sprague-Dawley, or Wistar rats. These different strains of animals have different sensitivities and tumor susceptibilities, which should be considered in study design and study interpretation. For example, mammary gland fibroadenomas are the most common spontaneous tumor in female Sprague-Dawley rats with incidences reported as high at 70% in chronic studies. Female Fischer rats have reported incidences of about 40%. Fibroadenomas are not considered a premalignant lesion in humans nor are rat mammary fibroadenomas considered predictive of carcinoma in women. Spontaneous mammary adenocarcinomas, which are considered relevant to women, are more common in Sprague-Dawley rats, with reported incidences of 11% in Harlan Sprague-Dawley rats. Mice, as compared to rats, have a lower background incidence of mammary tumors. B6C3F1 mice are relatively resistant to spontaneous mammary gland tumor development and the parental strains, C3H/He and C57BL/6, are relatively resistant to spontaneous and carcinogen-induced mammary gland tumorigenesis.

Following an NTP-sponsored expert panel workshop, and with the accumulation of data linking early exposures with later life mammary gland lesions, recent NTP carcinogenicity bioassays have incorporated early life or multigenerational exposures. Morphologic evaluation of the mammary gland includes mammary gland whole mounts and advanced sectioning techniques such as those demonstrated in Figure 19.4. European studies have also modified their protocols in recent years to include mammary gland evaluation of males and females. In addition to

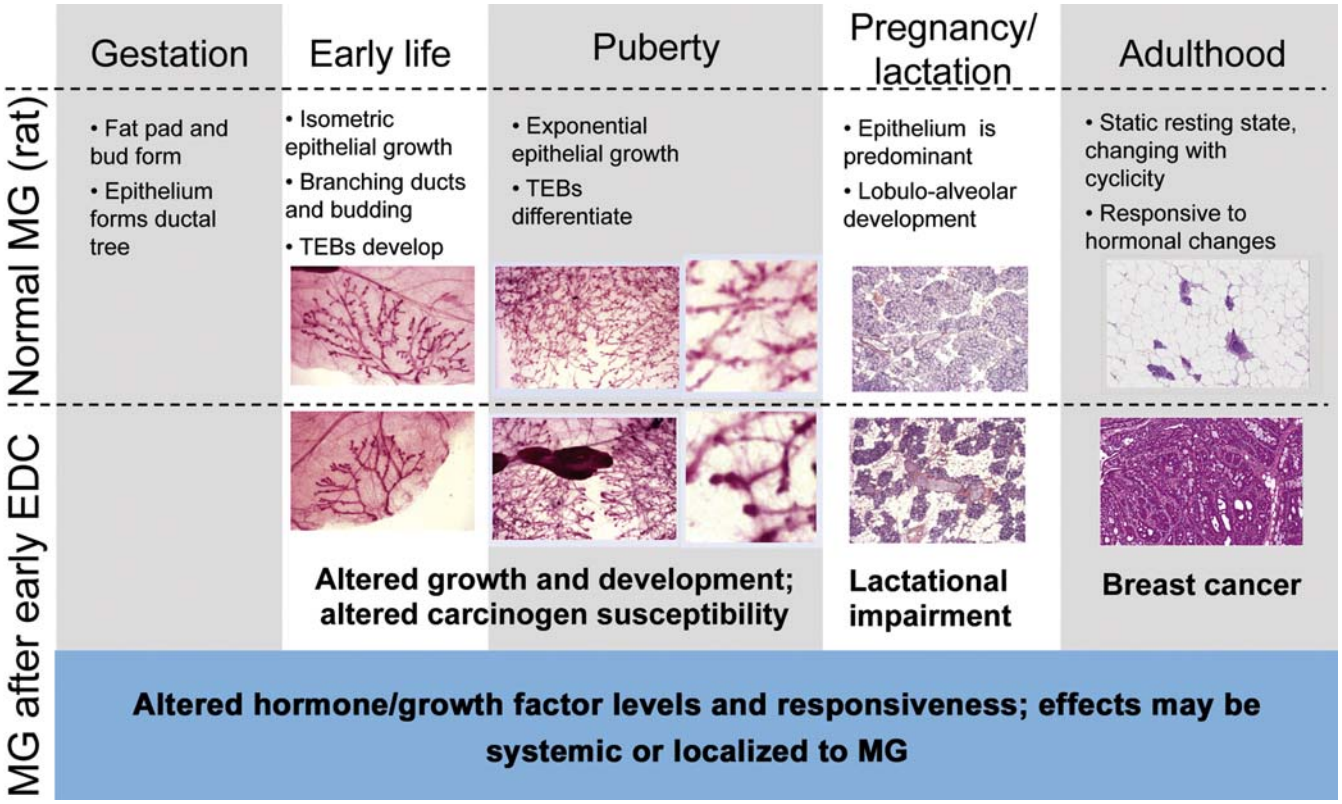

FIGURE 19.6 Stages of mammary gland development in the rat; normal (top) and altered (bottom). Numerous examples of early life endocrine disruptor effects on mammary gland development have been associated with later life adverse outcomes such as altered breast developmental timing during puberty, insufficient lactation or increased risk for mammary tumors. Source: *Figure reproduced from Haschek, W.M., Rousseaux, C.G., Wallig, M.A. (Eds.), 2013. Haschek and Rousseaux's Handbook of Toxicologic Pathology, third ed. Academic Press (Elsevier), Figure 61.7, p. 2684 with permission.*

morphological evaluation of the mammary gland, careful evaluation of serum hormones, and other hormone-related end points in multigeneration studies such as timing of gonadal control of puberty (vaginal opening, heat, first estrus, etc.), cyclicity patterns, retention of nipples/areolae in males, and possibly anogenital distance measurements are important to aid in identification of potential mammary gland toxicants or carcinogens. Finally, a greater emphasis is now being placed on using "environmentally relevant doses" instead of maximum tolerated doses in toxicity studies as our understanding of how endocrine disrupting compounds mediate their effects on cells.

Several chemicals are known to interfere with the full development of a lactational mammary gland (e.g., dioxin, atrazine, perfluorooctanoic acid (PFOA)). Such an effect should be investigated in reproductive studies reporting decreased postnatal survival, decreased litter weights, or altered growth curves in nursing pups. Nursing pups should have stomachs full of milk. When lactation deficiencies are suspected, functional assessments (often referred to as a "lactational challenge") of dam-pup interactions should be made. Such evaluations incorporate timed nursing experiments in which dams are separated from pups from 2–8 hours. Immediately prior to reunion, the litter is weighed, the dam is reintroduced for a fixed amount of time (15–30 minutes), nursing behavior is assessed and postnursing litter weights are measured. The pre- and postnursing litter weights serve as a surrogate for milk volume. Histological examination of the dams' mammary glands is essential to help differentiate underlying morphological alterations versus function alterations (or both). Milk protein measurements from collected milk samples (collected at more than a single time, if possible) may provide valuable biomarkers of effect without having to sacrifice the animal. Lipid profiles, protein content, and other nutritional information may be collected using expressed milk samples.

Chemical carcinogenesis in spontaneous rodent models (also see Chapter 6: Carcinogenesis: Manifestation and Mechanisms): The coadministration of cancer inducing agents with a test article of interest is a commonly used and well-accepted method in toxicology studies to identify potential mammary carcinogens. For example, spontaneous mammary gland cancers in rats, generally adenocarcinomas, can

be enhanced with treatment of genotoxic carcinogens like 7,12-dimethylbenz[*a*]anthracene (DMBA), *N*-nitrosomethylurea (NMU) and *N*-ethyl-*N*-nitrosourea (ENU), or irradiation. DMBA is most effective when administered after puberty. Part of the age-susceptibility pattern to DMBA is attributed to the development of the enzymes necessary to metabolize DMBA to its carcinogenic form after puberty. In contrast, NMU is most effective when administered before puberty due to a deficiency of a DNA repair enzyme in the immature rat gland and the induction of Hras mutations in the mammary epithelial cells. Irradiation is most effective when done in the postpubertal period and enhanced by short-term estrogen treatment during this time. Another consideration for susceptibility to these carcinogens is the relative abundance of TEBs in the gland at the time of administration. The TEBs contain stem cells and have high mitotic indices, thus are susceptible to damage from these chemicals.

Genetically Engineered Mice (GEM): Mice, which tend to have lower incidence of spontaneous mammary cancers that rarely are malignant, have nonetheless been exploited as models for breast cancer. Historically, it was discovered that infection with lactationally transmitted mouse mammary tumor virus (MMTV) caused hyperplastic lesions and mammary tumors through activation of Wnt, fibroblast growth factor, and notch signaling pathways that are also critical in early mammary gland morphogenesis. Hyperplastic lesions and spontaneous tumors that develop in naturally MMTV-infected mice are characteristic of well-differentiated hyperplastic alveolar nodules and alveolar tumors. Some have promoted these lesions to represent preneoplastic lesions comparable to such lesions in women's breast tissue, but others maintain that the biology and morphology of these hyperplasias and benign tumors are features that should be considered mouse specific. Nonetheless, MMTV has also been exploited in the development of many GEM models of mammary cancer by targeting and driving gene expression using MMTV as a promoter. Another commonly used mammary-specific promoter is the whey acidic protein, or WAP promoter.

A tremendous effort has gone into characterizing GEM to bridge morphologic and genotypic variations of mouse mammary cancer to breast cancers in women. More than 40 models have been classified and categorized according to (1) lesions that resemble spontaneous mouse mammary tumors, (2) lesions that are unique and specific for the transgene, and (3) lesions that resemble human breast lesions. However, for most models and transgenes tested, there is limited evidence that these show malignant characteristics and they are not transplantable or immortal. Nonetheless, these models remain informative and recent characterizations further support their importance in understanding mammary gland biology and cancer. There is another effort that is generating diversified outbred mice, genetically unique lines of mice, which will help to identify susceptible subpopulations and allow linking of genetic underpinnings to disease. Phenotypic understanding of their mammary tumor susceptibility is in its infancy, but these may prove to be valuable in testing certain pharmaceuticals/xenobiotics for effect on the mammary gland in the future.

In summary the use of animal models (especially rodents) has demonstrated three critical factors that would have taken decades to discern in humans. First, that sensitive life stages (especially fetal development, puberty, and pregnancy) impart a unique sensitivity to some chemical exposures leading to later life disease risk. Second, that toxicants can act by mechanisms other than as frank carcinogens (i.e., as endocrine disruptors) to confer an increased risk of cancer or other late-life effect, such as insufficient lactation. The use of transgenic, knockout, and other gene modified rodents (primarily mice) have identified highly important details of mechanisms in disease development and progression. Finally, the nonhuman primate is an excellent model to understand pleiotropic effects of toxicants or drugs on mammary gland development as well as carcinogenic potential. It is often overlooked because of costs or availability.

RESPONSE TO INJURY

Physiologic Response to Injury

The most recent emphasis in toxicology has been placed on understanding the direct or modifying effects of endocrine disrupting compounds. These are often reported as causing either accelerated maturation or delayed differentiation of the gland in females (Figure 19.6), or in altering glands in the male from a lobular phenotype to a more female-like tubuloalveolar morphology. Retained nipples in male rodents are also characteristic of antiandrogen effects. Accelerated mammary growth may be characterized as increased TEB formation at early time-points and decreased numbers at later time periods. Delayed maturation may be characterized by the presence of TEBs until much later in development, extending the window of time that these carcinogen-sensitive structures are present in the gland. Inhibition of development may also be reflected as a decrease density of the gland, as well as an overall decrease in TEBs formed. Ductal hyperplasias and dysplasias can be induced with various estrogen-like compounds, but, as mentioned

previously, many of these effects depend on timing of exposure and the extent of mammary gland development within the animal of interest. For example, exposure to estrogenic compounds through the perinatal period in rats, when TEBs are developing, are associated with hyperplasia of the buds, while exposure during the peripubertal period, when ducts are developing, is associated with ductal hyperplasia. Neonatal exposure to estrogen, progesterone, or both in mice causes irreversible effects in adults, including secretory stimulation, dilated ducts, and abnormal lobuloalveolar development. Phytoestrogens, such as genistein and resveratrol, and the mycoestrogen zearalenone act similarly to estrogen agonists in their effects on the gland. Changes include delayed development, ductal hyperplasia, alveolar hypoplasia, reduced apoptosis in TEBs, increased or decreased numbers of terminal ducts or lobules, and accelerated alveolar differentiation, again depending on time of exposure.

Altered mammary gland development following perinatal exposure has also been observed for other endocrine disrupting compounds, including atrazine, bisphenol A (BPA), dibutylphthalate, dioxin, methoxychlor, nonylphenol, polybrominated diphenyl ethers, PFOA, and others. Some of these compounds such as methoxychlor act as estrogen agonists, but most of these compounds have pleomorphic effects on hormone receptors or hormone signaling in many tissues, and thus correlating a specific physiological and morphological response to classes or specific compounds is certainly complex.

Systemic hormonal changes and correlative mammary morphologies related to spontaneous aging and testing of pharmaceutical-based hormone receptor agonists and antagonists have been nicely characterized in rats (see Lucas et al. (2007) in Further Reading). Common changes in the aging adult male rat include a tubular alveolar pattern with formation of central lumens. This is occasionally referred to as mammary gland "feminization" and is attributed to increased prolactin and growth hormone levels. Because both these hormones increase in aging rats, particularly strains with high incidence of pituitary tumors, such changes in male rat morphology can be an indirect effect of a treatment as well as represent an adverse effect of endocrine disruption. In the adult female rat mammary gland, lobuloalveolar hyperplasias with or without ductal ectasia and secretory activity are associated with increased levels of circulating prolactin, growth hormone, or estrogen levels often associated with endocrine disruptors. Lobuloalveolar morphology, sometimes referred to as "virilization" in the female gland, occurs with androgen stimulation or higher levels of circulating testosterone. The varied effects of pharmaceutical agents are consistent and predictable. Thus when such morphologies are observed in the mammary gland of rats in study, careful consideration should be given to determining hormonal effects as well as potential for direct effects on mammary gland development.

Molecular and Biochemical Response to Injury

At the biochemical and molecular levels, complex and varied responses occur after injury. Molecular signaling through hormone and growth factor receptors is altered by changes in hormone receptor expression, receptor levels, receptor affinity to ligands, or receptor localization. These are further altered by production of local growth factors and hormones as well as genetic mutations that result from injury.

Gene expression profiles from chemically induced mammary gland cancers in Sprague-Dawley rats show distinct differences from spontaneous mammary tumors. Compared to spontaneous carcinomas, carcinomas induced by either 2-amino-1-methyl-6-phenylimidazo[4,5-*b*]pyridine (PhIP), DMBA, 2-amino-3,8-dimethylimidazo[4,5-*f*]quinoxaline (MeIQx), NMU, or 4-aminobiphenyl (4ABP) show higher expression of genes associated with mammary epithelial cell growth and proliferation, such as cyclin D1, PDGFα, and relatively lower expression of differentiation marker genes, such as β-casein, WAP, and transferrin. Additionally, several components of the prolactin/prolactin receptor/Stat5a/cyclin D1 signaling pathways are found in the chemically induced rat mammary gland carcinomas. Mammary cancer in DMBA-treated FVB mice show elevated expression of the aryl hydrocarbon receptor (AhR), c-myc, cyclin D1, and hyperphosphorylated retinoblastoma (Rb) protein compared to normal mammary gland tissue. Mammary cancer associated with benzene and ethylene oxide exposure to mice had increased mutations in Tp53 protein and Hras mutations in a chemically related pattern distinguishable from spontaneous mutations. However, for most of the compounds associated with mammary gland injury and dysmorphogenesis, the molecular pathways remain to be defined.

Morphologic Response to Injury

The response of the mammary gland to injury recapitulates a wide spectrum of nonneoplastic and neoplastic changes. Standardized nomenclature provides consistency of diagnoses across studies and captures patterns of lesions that represent xenobiotic effects with biological significance. This is commonly done for rodents used in toxicity studies, but should be done for all species, including nonhuman primates for which there appears to be a propensity for medical

pathologists to diagnose malignancy and veterinary pathologists to diagnose benign.

Rodents: The Mammary Gland Organ Systems Working Group of the International Harmonization of Nomenclature and Diagnostic (INHAND) Criteria for Lesions in Rats and Mice has standardized the nomenclature summarized in this chapter for rodents. An important note is that the various strains of mice and rats will have their own classifications of background lesions for which an effect of chemical needs to be evaluated. Historical background incidences from various studies are often available from the supplier or study site.

Nonneoplastic changes manifest as degenerative, necrotic, inflammatory, and vascular lesions or, in relation to alterations in growth, manifest as atrophy, hypertrophy, or hyperplasia. Degenerative changes affecting the epithelial and myoepithelial cells of the ducts and alveoli are most commonly associated with aging or occasionally observed as a test-article effect. The changes are characterized by epithelial vacuolization, loss of cell layers, and ductal dilation with accumulation of proteinaceous material. Cellular necrosis within the mammary gland is rarely observed but fat necrosis and inflammation occurs as incidental findings. Regeneration of epithelial cells is usually observed in areas of degeneration as well, and degeneration, necrosis, and regeneration typically present together in repeated mammary gland injury.

Inflammation in rodent mammary glands is usually limited to small infiltrates of leukocytes and should be differentiated from the lymphocytic and eosinophilic infiltrates that accompany ductular morphogenesis. Acute inflammation is characterized by epithelial degeneration, vascular congestion, edema, and an admixture of neutrophils, lymphocytes, and few plasma cells. In chronic inflammation, infiltrates of macrophages, and fibrosis will accompany epithelial regeneration, hyperplasia, or metaplasia. Older rats occasionally develop granulomatous inflammation associated with ruptured galactocoeles or dilated/ectatic ducts. Periductular fibrosis is a common age-related change in rats and has been associated with epidermal growth factor treatment in mice. Recent studies have also demonstrated the increasing incidence of toxicants affecting the stromal and adipose-rich areas of the mammary gland, specifically enhanced macrophage infiltration, stromal hyperplasia, and altered fat cell size or number have been noted.

Alterations in growth are commonly associated with age as well as observed as a test article–related effect in younger animals. For example, dilation and ectasia or galactocoeles of ducts or alveolar hyperplasia with or without epithelial hypertrophy or hyperplasia occur as an age-related change in females, but should also be considered as a test article–related effect in younger female rodents. Compared to the female rat in which alveolar hyperplasia may be considered age or test article-related, the normal morphology in male rats is characterized by lobuloalveolar differentiation. Estrogen receptor–α agonists cause lobuloalveolar hyperplasia and secretory activity in female rats, but "feminization" of the mammary gland in male rats. Feminization in the male rat is characterized by a predominance or transformation from tubuloalveolar to ductular morphology. AR agonists have no effect in the male but will cause virilization and increased secretions in the female rat. In contrast, AR antagonists cause atrophy of the male rat mammary gland with no effect on the female rat mammary gland. Progesterone receptor antagonists cause lobuloalveolar hyperplasia and secretions in female rat mammary glands but have no effect on male rat mammary gland, as the male mammary gland does not express these receptors (see Filgo et al. (2016), in Further Reading). Importantly, dopamine receptor antagonists, which stimulate prolactin secretion, will cause hyperplasia in female and feminization in male rat mammary glands—an effect often seen in aging rats with elevated prolactin levels.

However, in the male the normal development and morphology of the glands may be confused with what is diagnosed as the female is not to be confused with what is normal ductular morphology in the adult male. Compared to the tubuloalveolar glands in the adult female rat, the adult male has lobuloalveolar glands lined by a single layer of cuboidal vacuolated epithelial cells, and pseudostratified or stratified epithelium. The male rat mammary gland remains responsive to endogenous and exogenous hormone agonists and antagonists throughout its life. However, ductular ectasia with alveolar epithelial hypertrophy and hyperplasia has been observed. The lesion may be considered secondary to effects on the hypothalamic–pituitary–ovarian (HPO) axis.

Neoplastic changes in rodent mammary glands occur as spontaneous and test article–related benign and malignant tumors. Ductal epithelial atypia a (Figure 19.7) and ductal carcinomas in situ (DCIS) are increasingly being recognized in studies, particularly in studies of rats exposed to chemical carcinogens or endocrine disruptors during development. These lesions are characterized using the same criteria as used for human breast. DCIS show disruption of the epithelial bilayer and atypical disorganized masses of cells bridge across or fill the ductal lumens. The basement membrane remains intact.

Benign neoplasms of epithelial origin include adenomas, fibroadenomas, and benign mixed tumors and malignant tumors include adenocarcinomas, adenocarcinomas arising in fibroadenomas, and malignant

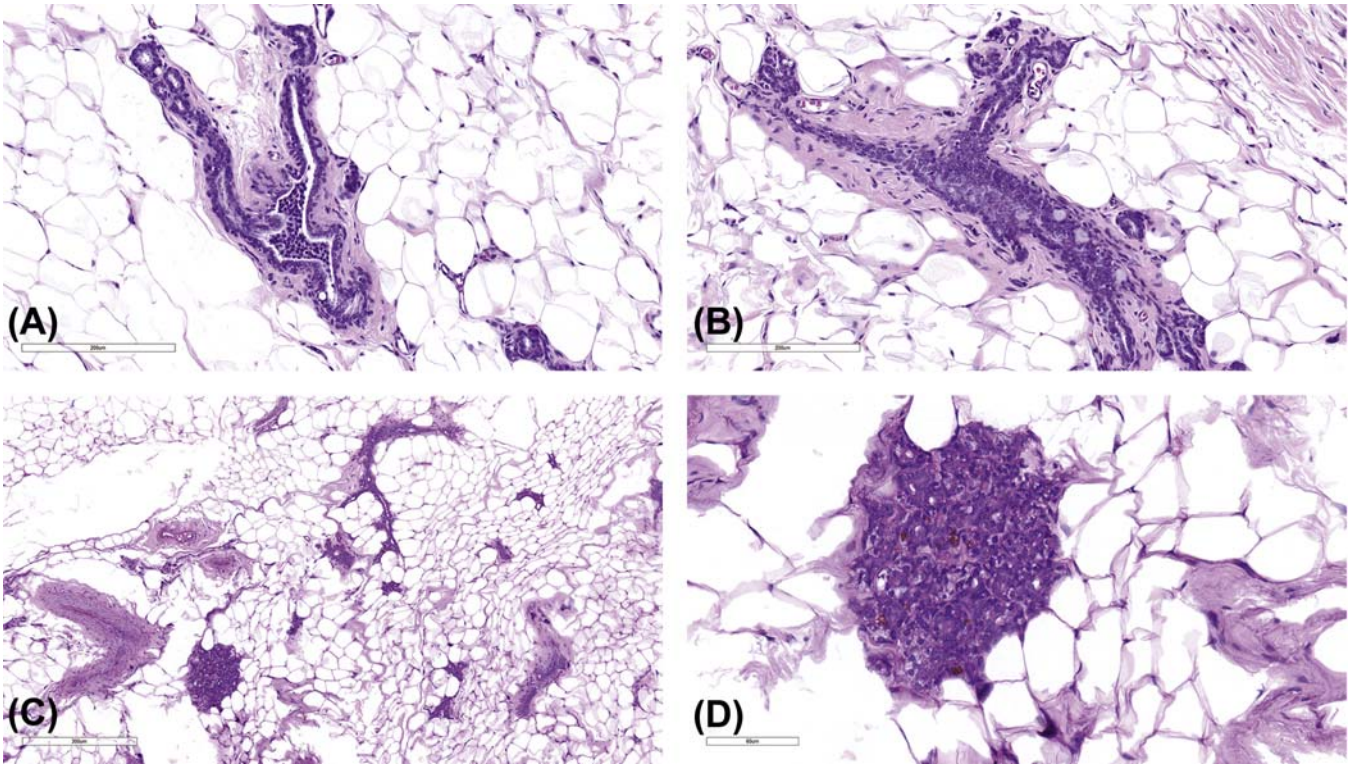

FIGURE 19.7 Mammary gland hyperplasia, rat. H&E stain. (A) Mild ductular hyperplasia with piling of epithelial cells filling lumen (10× magnification). (B) Moderate ductular hyperplasia with ductular closure (10× magnification). (C) Low magnification of a nodule (2× magnification) that at higher magnification in (D) shows tubular alveolar hyperplasia (10× magnification).

mixed tumors (Figure 19.8). In the chemical carcinogen−treated rat model, benign tumors arise from alveolar buds and lobules while carcinomas arise from epithelial cells in less differentiated TEBs and terminal ducts.

Adenomas are usually visible as nodules. Histologically they are characterized as well-demarcated, encapsulated, and expansive masses that compress surrounding normal tissue. They are composed of cysts, alveoli, or papillary fronds of single or multiple layers of epithelial cells aligned on a fine fibrovascular stroma. The epithelial cells are cuboidal, well differentiated, and may show secretory activity. Focal areas of squamous metaplasia may occur. Although there are morphological subtypes, it is not standard to subclassify tumors in toxicity studies.

Fibroadenomas (see Figure 19.8) represent a proliferation of glandular epithelium surrounded by with varying proportions of well-differentiated epithelial tubules or glands and dense fibrous stroma. Mitotic activity is low. Rarely, carcinomas can arise within fibroadenomas and should be diagnosed appropriately as "adenocarcinoma arising in fibroadenoma."

Benign mixed tumors are rare in rodents but are the most common spontaneous tumor in dog. These mammary tumors are neoplastic proliferations of both epithelial and myoepithelial cells with differentiation of the latter into islands of cartilage, bone, adipose, or sometimes hematopoietic marrow and diagnostically classified differently from fibroadenomas because benign mixed tumors do not have a predominant fibrous component. The distinction between benign and malignant mixed tumors is based on the extent of invasion of the surrounding tissues by the epithelial cells or resemblance of the mesenchymal component to osteosarcoma or chondrosarcoma.

Adenocarcinomas are malignant proliferations of pleomorphic columnar or cuboidal epithelial cells arranged in papillary, cystic, tubular, solid, or cribriform or comedo patterns (Figure 19.8). There may be complete loss of lobular−alveolar structures and acini may become cystic or blood filled. Adenocarcinomas can induce a marked schirrous response. These cancers can be locally invasive and are metastatic. If more than about 25% of the tumor has squamous differentiation, then it should be diagnosed as an adenosquamous carcinoma, more commonly seen in mice than rats.

Nonhuman primates: Nonneoplastic lesions manifest as cystic changes in lobules and ducts, and apocrine metaplasia with alveolar dilation and secretory changes

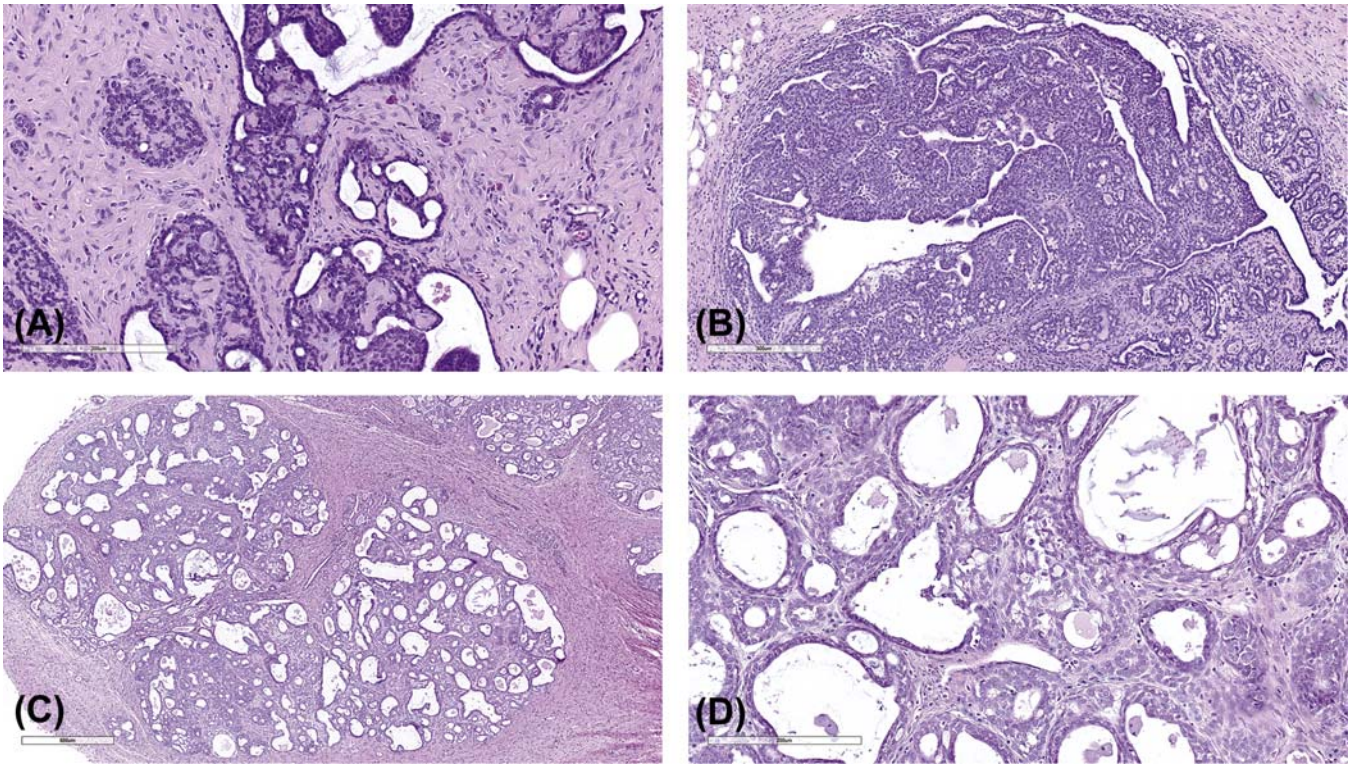

FIGURE 19.8 Mammary gland tumors, rat. H&E stain. (A) Fibroadenoma with epithelia atypia. The predominant component is fibrous matrix (4× magnification). (B) Adenocarcinoma. The predominant component is pleomorphic and atypical epithelial tubules (4× magnification). (C) Adenocarcinoma within a fibroadenoma (4× magnification). (D) Higher magnification showing epithelial proliferation and disorganization within fibrous matrix (20× magnification).

resembling apocrine sweat glands. These are generally incidental, related to aging and reproductive status.

Hyperplastic lesions are focal and multifocal lobular proliferations seen in older rhesus, pigtail, and cynomolgus macaques. The lesions are characterized as enlarged or distinct nodules of well-differentiated alveoli but proliferate independently of hormonal stimulation. They can be found within generalized lobular hyperplasia of lactation or estrogen and progestogen treatment. Ductal hyperplasias are characterized by focal increased epithelial cells into 2–3 layers, with maintenance of polarity and size. These are common spontaneous lesions in intact middle-aged rhesus macaques.

DCIS is distinguished from hyperplasias by increased layers of disorganized, pleomorphic epithelial cells that bridge and occlude the lumens of tubules. The basement membrane remains intact. Loss of basement membrane is diagnostic of intraductular carcinomas, which can be invasive and metastatic. DCIS occur commonly in mammary gland of cynomolgus and rhesus macaques, but development of larger carcinomas are not common.

MECHANISMS OF TOXICITY

Mammary gland toxicity and carcinogenicity have been observed in animal models exposed to a wide variety of agents including estrogens, androgens, antiandrogens, thyroid-active chemicals, aryl hydrocarbon receptor agonists, genotoxic compounds, and mutagens. Several rodent mammary gland carcinogens are epoxides or epoxide metabolites. These include chemicals such as 1,3-butadiene and related chloroprene and isoprene that are metabolized to epoxides. Although the mechanisms related to epoxide-induced mammary cancer are unknown, one hypothesis is that the mammary gland is efficient in metabolizing the chemicals to their epoxides. Epoxides are mutagens and associated with K-*ras* mutations in rodents. Isoprene and 1,3-butadiene also cause chromosomal aberrations, which may be related to mammary carcinogenicity. Brominated species are also associated with rodent mammary cancers. Chemicals, such as 2,2-bis(bromomethyl)-1,3-propanediol are proposed to act either through oxidative damage or formation of DNA adducts and then DNA damage. Many of these chemicals also induce cytochrome P450

metabolizing enzymes, which, like DMBA, can activate chemical reactivity or be metabolized to electrophilic oxygenated species that bind DNA.

Endocrine disrupting chemicals have a variety of effects. Atrazine, brominated diphenyl ethers, and dioxin, all have been shown to delay mammary gland development following neonatal exposures through interactions with hormone responses. Estrogenic compounds like DES or BPA increase protein expression and functional activity of histone methyltransferases, which have been linked to breast cancer risk and epigenetic regulation of tumorigenesis. It is also common for endocrine disrupting compounds to act via indirect mechanisms to induce persistent effects in mammary tissue. Furthermore, recent data suggests that epigenetic mechanisms—those changes to DNA that cause a heritable modification without changing the DNA code—may have important roles in not only mammary, but many cancers over the lifetime.

SUMMARY

The high incidence of breast cancer in women has brought attention to the need to incorporate appropriate and sensitive methodologies with which to evaluate the mammary gland in animal models as applicable to hazard identification for humans. We now have a substantial number of genetically modified and spontaneously occurring mice and rat mammary cancer models to employ and various approaches to assess gland morphology. Evaluation of mammary tissue in studies with nonhuman primates can also serve as an important tool. Of the lessons learned, we know that hormonal perturbations, including chemicals that act as endocrine disruptors, pose a significant risk and that such risk may be increased when exposures occur during development in male and female research models. Given this information, animal studies designed for hazard identification should include exposures during development and include enhanced methods for histological and morphometric mammary gland evaluation, such as whole mount evaluations. *In vitro* screens also continue to serve as important tools for identifying potential hazards and supporting mechanistic understanding of effects. Indeed, discovering genetic and environmental causes of breast cancer go hand-in-hand with discoveries of therapies to treat breast cancer and strategies to prevent breast cancer.

Further Reading

Blacher, S., Gérard, C., Gallez, A., Foidart, J.-M., Noël, A., Péqueux, C., 2016. Quantitative assessment of mouse mammary gland morphology using automated digital image processing and teb detection. Endocrinology 157, 1709–1716.

Blackshear, P.E., 2001. Genetically engineered rodent models of mammary gland carcinogenesis: an overview. Toxicol. Pathol. 29 (1), 105–116.

Cardiff, R.D., Rosner, A., et al., 2004. Validation: the new challenge for pathology. Toxicol. Pathol. 32 (1 suppl), 31–39.

Chandra, S.A., Cline, J.M., et al., 2010. Cyclic morphological changes in the beagle mammary gland. Toxicol. Pathol. 38 (6), 969–983.

Cline, J.M., Wood, C.E., 2008. The mammary glands of macaques. Toxicol. Pathol. 36 (7 suppl), 130S–141S.

Davis, B.J., Fenton, S.E., 2013. The mammary gland. In: Haschek, W. M., Rousseaux, C.G., Wallig, M.A. (Eds.), Haschek and Rousseaux's Handbook of Toxicologic Pathology, third ed. Elsevier, Inc., Academic Press, USA, pp. 2665–2694. (Chapter 61).

Euling, S.Y., Selevan, S.G., et al., 2008. Role of environmental factors in the timing of puberty. Pediatrics 121 (Suppl 3), S167–S171.

Fenton, S.E., Reed, C., Newbold, R.R., 2012. Perinatal environmental factors affect breast development: is precocious thelarche a marker of endocrine disruption? Ann. Rev. Pharmacol. Toxicol. 52, 455–479.

Filgo, A.J., Foley, J.F., Puvanesarajah, S., Borde, A.R., Midkiff, B.R., Reed, C.E., et al., 2016. Mammary gland evaluation in juvenile toxicity studies: temporal developmental patterns in the male and female Harlan Sprague Dawley rat. Toxicol. Pathol. 44 (7), 1034–1058.

Gore, A.C., Chappell, V.A., Fenton, S.E., Flaws, J.A., Nadal, A., Prins, G.S., et al., 2015. EDC-2: the Endocrine Society's second scientific statement on endocrine-disrupting chemicals. Endocr. Rev. 36, E1–E150.

Hoenerhoff, M.J., Hong, H.H., et al., 2009. A review of the molecular mechanisms of chemically induced neoplasia in rat and mouse models in National Toxicology Program Bioassays and their relevance to human cancer. Toxicol. Pathol. 37 (7), 835–848.

Krause, S., Maffini, M., et al., 2010. The microenvironment determines the breast cancer cells' phenotype: organization of MCF7 cells in 3D cultures. BMC Cancer 10 (1), 263.

Lamote, I., Meyer, E., et al., 2004. Sex steroids and growth factors in the regulation of mammary gland proliferation, differentiation, and involution. Steroids. 69 (3), 145–159.

Lucas, J.N., Rudmann, D.G., et al., 2007. The rat mammary gland: morphologic changes as an indicator of systemic hormonal perturbations induced by xenobiotics. Toxicol. Pathol. 35 (2), 199–207.

Rudel, R.A., Fenton, S.E., et al., 2011. Environmental exposures and mammary gland development: state of the science, public health implications, and research recommendations. Environ. Health Perspect. 119 (8), 1053–1061.

Rudmann, D., Cardiff, R., Chouinard, L., Goodman, D., Küttler, K., Marxfeld, H., et al., 2012. Proliferative and nonproliferative lesions of the rat and mouse mammary, Zymbal's, preputial, and clitoral glands. Toxicol. Pathol. 40 (6 Suppl), 7S–39S.

Russo, J., Russo, I.H., 2004. Development of the human breast. Maturitas 49 (1), 2–15.

Sandhu, R., Chollet-Hinton, L., Kirk, E.L., Midkiff, B., Troester, M.A., 2016. Digital histologic analysis reveals morphometric patterns of age-related involution in breast epithelium and stroma. Human Pathol. 48, 60–68.

Son, W.-C., Gopinath, C., 2004. Early occurrence of spontaneous tumors in CD-1 mice and Sprague Dawley rats. Toxicol. Pathol. 32 (4), 371–374.

Souda, M., Umekita, Y., et al., 2009. Gene expression profiling during rat mammary carcinogenesis induced by 7,12-dimethylbenz[a] anthracene. Int. J. Cancer 125 (6), 1285–1297.

Stanko, J.P., Easterling, M.R., Fenton, S.E., 2015. Application of sholl analysis to quantify changes in growth and development in rat mammary gland whole mounts. Reprod. Toxicol. 54, 129–135.

Stanko, J.P., Kissling, G.E., Chappell, V.A., Fenton, S.E., 2016. Differences in the rate of in situ mammary gland development and other developmental endpoints in three strains of rat commonly used in toxicity testing studies: implications for timing of mammary carcinogen exposure. Toxicol. Pathol. 44 (7), 1021–1033.

Thayer, K.A., Foster, P.M., 2007. Workgroup report: National Toxicology Program workshop on Hormonally Induced Reproductive Tumors-Relevance of Rodent Bioassays. Environ. Health Perspect. 115 (9), 1351–1356.

Tucker, D.K., Foley, J.F., Hayes-Bouknight, S.A., Fenton, S.E., 2016. Preparation of high quality hematoxylin and eosin-stained sections from rodent mammary gland whole mounts for histopathologic review. Toxicol. Pathol. 44 (7), 1059–1064.

This page intentionally left blank

CHAPTER

20

Endocrine System

Matthew A. Wallig

University of Illinois at Urbana-Champaign, Urbana, IL, United States

OUTLINE

Fundamentals of Toxicologic Pathology.
DOI: http://dx.doi.org/10.1016/B978-0-12-809841-7.00020-4

INTRODUCTION

A review of the literature of chemically induced lesions of the endocrine organs indicates that the adrenal glands are the most commonly affected, followed in descending order by the thyroid, pancreas, pituitary, and parathyroid glands. In the adrenal glands, chemically induced lesions are found most frequently in the zona fasciculata (ZF), zona reticularis (ZR) and, to a lesser extent, in either the zona glomerulosa (ZG) or the medulla. In a survey of tumor types developing in carcinogenicity studies, conducted by the Pharmaceutical Manufacturers Association, endocrine tumors were observed frequently in rats. The thyroid gland was third in frequency (behind liver and mammary gland), followed by the pituitary gland (fourth), and adrenal gland (fifth).

In the following chapter, basic pharmacological and toxicological effects will be reviewed, with emphasis on the latter. Pharmacologic effects are defined as beneficial and desired drug-related changes with minimal side effects or morphological alterations (often reversible), whereas toxicologic effects are more severe adverse effects that often are irreversible.

PART 1: ADRENAL CORTEX

STRUCTURE AND FUNCTION

Gross and Microscopic Anatomy

In mammals, the adrenal glands are flattened bilobed organs located in close proximity to the kidneys. They receive arterial blood from branches of the aorta or from the phrenic, renal, and lumbar arteries, resulting in a vascular plexus; perfusion occurs by separate sinusoids both to the capsule and to the entire gland, including cortex and medulla. Venous blood flow is derived from a sinusoidal network originating around the cells of the adrenal cortex with eventual flow into the medulla at its periphery. A venous tree is present within the medulla that ultimately flows into the adrenal vein by way of its larger branches.

Midsagittal sectioning of the adrenal gland reveals a clear separation between cortex and medulla. The cortex is firm and yellow and occupies approximately two-thirds of the entire cross-sectional diameter of the organ. In contrast, the medulla is soft, with prominent gray-tan coloration. The ratio of cortex: medulla is approximately 2:1 in healthy laboratory-reared animals.

Defined regions or zones histologically characterize the cortex and include the zona glomerulosa (ZG, multiformis), zona fasciculata (ZF), and zona reticularis (ZR). Zones are not always clearly delineated, as illustrated in the normal rat adrenal cortex (Figure 20.1). The mineralocorticoid-producing ZG (15% of the cortex) contains cells aligned in a sigmoid pattern in relationship to the capsule. Cells of this zone secrete mineralocorticoids (e.g., aldosterone) essential for regulation of body potassium and sodium. The largest zone is the ZF (>70% of the cortex). Cells in this zone are arranged in long anastomosing cords or columns, separated by small capillaries/sinusoids. They are responsible for the secretion of glucocorticoid hormones (e.g., corticosterone in rat, mouse, and rabbit, or cortisol in dog, pig, monkey, and human), which promote the elevation of blood glucose in addition to many other effects. The innermost portion of the cortex is the ZR (15% of the cortex), which normally secretes minute quantities of adrenal sex hormones in some species.

There are structural and functional differences between species and sexes. Accessory cortical tissue is often seen in mice and cynomolgus monkeys, not to be mistaken for proliferative lesions. The marmoset has no obvious ZR, and in the dog the ZF and ZR are poorly demarcated. The mouse develops the x-zone, a prominent fourth cortical layer immediately adjacent to the medulla, which is especially prominent in females (Figure 20.2); this zone degenerates, leaving clumps of brown-yellow lipofuscin at the corticomedullary junction. Primates develop an area of cortical

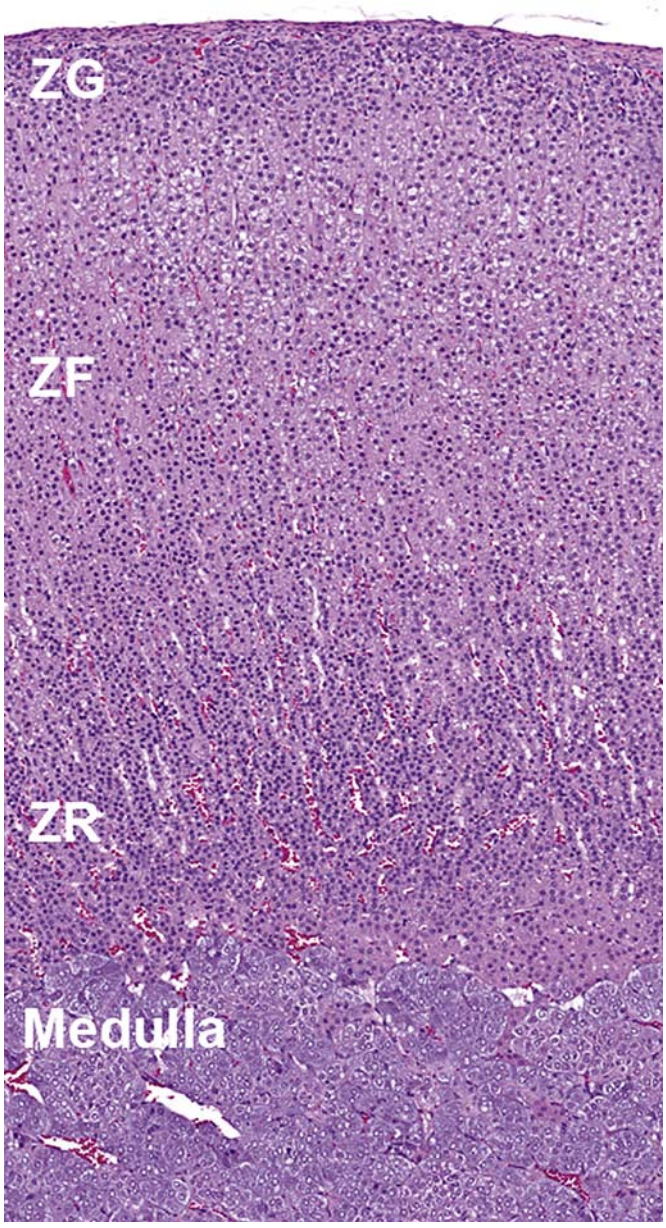

FIGURE 20.1 Zones of the adrenal gland in a normal rat. A thin fibrous capsule surrounds the adrenal cortex. The adrenal cortex consists of three zones, the zona glomerulosa (ZG), zona fasciculata (ZF), and zona reticularis (ZR). The ZG is the thinnest zone of the cortex. The ZF is the thickest zone of the cortex and is composed of columns or fascicles of cortical cells separated by sinusoids. The ZF: ZR boundary is not distinct. The cells of the ZR are smaller and less vacuolated compared to the ZF. The central region is the adrenal medulla composed primarily of chromaffin cells. H&E stain. *Figure reproduced from* Handbook of Toxicologic Pathology, *third ed., W. M. Haschek, C. G. Rousseaux and M. A. Wallig, eds. (2013) Academic Press, Fig. 58.1, p. 2393, with permission.*

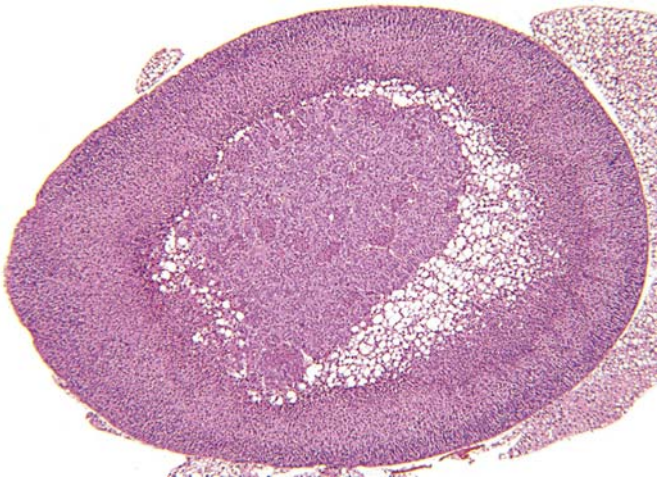

FIGURE 20.2 Corticomedullary vacuolation (X-zone) in female CD-1 mouse. H&E stain. *Figure reproduced from* Handbook of Toxicologic Pathology, *third ed., W. M. Haschek, C. G. Rousseaux and M. A. Wallig, eds. (2013) Academic Press, Fig. 58.2, p. 2394, with permission.*

involution in late fetal life that regenerates after birth. The ZR is three times thicker in male Syrian hamsters than in females.

Ultrastructural Anatomy

Adrenal cortical cells contain large cytoplasmic lipid droplets consisting of cholesterol and steroid precursors. The lipid droplets are in close proximity to the smooth endoplasmic reticulum and large mitochondria, which contain the specific hydroxylase and dehydrogenase enzyme systems required to synthesize the different steroid hormones. Unlike polypeptide hormone-secreting cells, there are no secretory granules in the cytoplasm because there is direct secretion without significant storage of preformed steroid hormones. The three cortical zones have unique ultrastructural characteristics in the rat adrenal cortex (Figures 20.3–20.5).

Physiological and Functional Considerations

All hormones produced by the adrenal cortex are steroids. Steroid-producing endocrine organs such as the adrenal cortex synthesize a major parent steroid compound with 1–4 additional carbon atoms added to the basic 17 carbon-containing steroid nucleus. Because steroid hormones are not stored in any significant amount, a continued rate of synthesis is required to maintain a normal secretory rate. This in turn requires continued stimulation of the adrenal cortex by pituitary derived adrenocorticotropic hormone

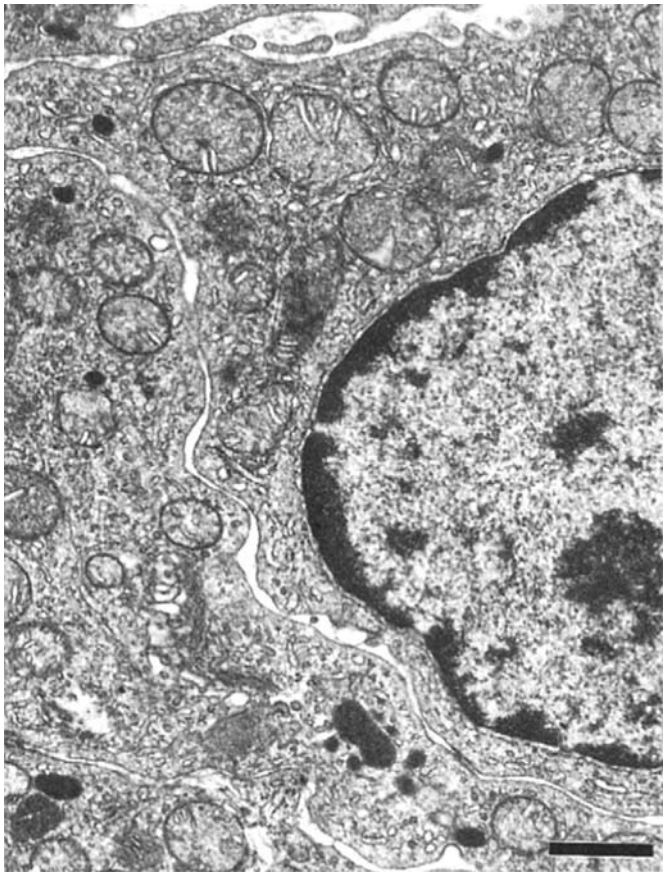

FIGURE 20.3 Adrenal cortical cell from the zona glomerulosa of rat adrenal cortex with mitochondria that have distinct leaf-like cristae. Bar = 1 μm. *Figure reproduced from Yarrington et al. (1985) Degeneration of the rat and canine adrenal cortex caused by α-(1,4-dioxido-3-methylquinoxalin-2-yl)-N-methylnitrone (DMNM),* Fundam. Appl. Toxicol. *5, 370–381, with permission.*

(ACTH; see later) according to physiological requirements. In circulation, steroid hormones (e.g., cortisol or corticosterone) are bound to plasma proteins [e.g., transcortin (CBG, cortisol/corticosterone binding globulin), albumin]. Depending on the nature of the plasma proteins the binding affinity may be high or low, but nonetheless reversible, to allow the steroid to be in a free unbound state when interacting with target cells. Under normal conditions, 10% of the glucocorticoids are in a free unbound state and thus free to interact with target cells either to exert metabolic effects or to be transformed into an inactive metabolite. In conditions of elevated secretion of adrenal glucocorticoid, the free steroid fraction in the blood is increased and available to evoke a response in target cells and tissues.

Adrenal steroids are synthesized from cholesterol, which in turn is derived from acetate. A complex shuttling of steroid intermediates between mitochondria and endoplasmic reticulum characterizes specific

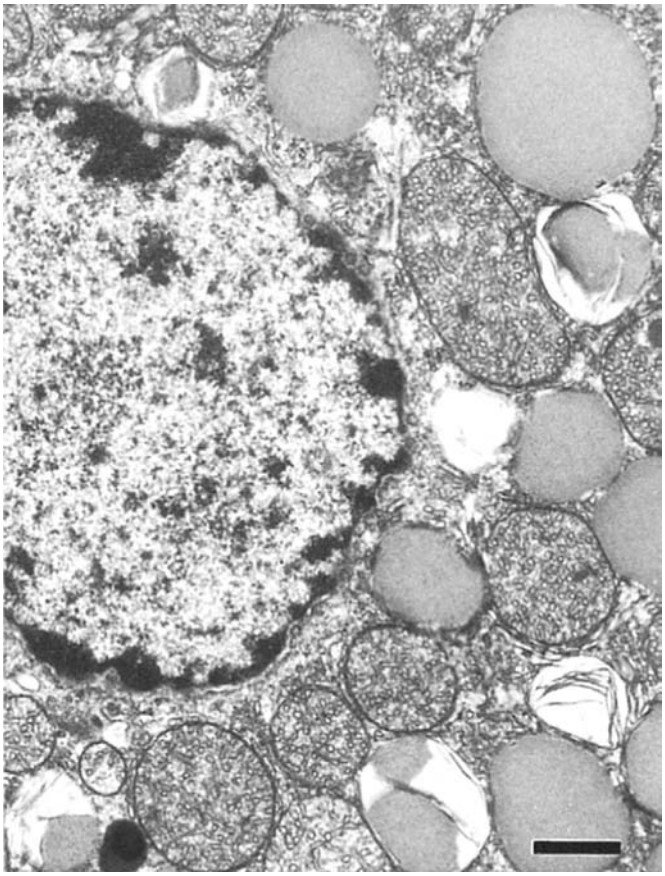

FIGURE 20.4 Cell from the zona fasciculata of rat adrenal cortex with prominent lipid droplets. Mitochondria have vesicular cristae. Bar = 1 μm. *Figure reproduced from Yarrington et al. (1985) Degeneration of the rat and canine adrenal cortex caused by α-(1,4-dioxido-3-methylquinoxalin-2-yl)-N-methylnitrone (DMNM),* Fundam. Appl. Toxicol. *5, 370–381, with permission.*

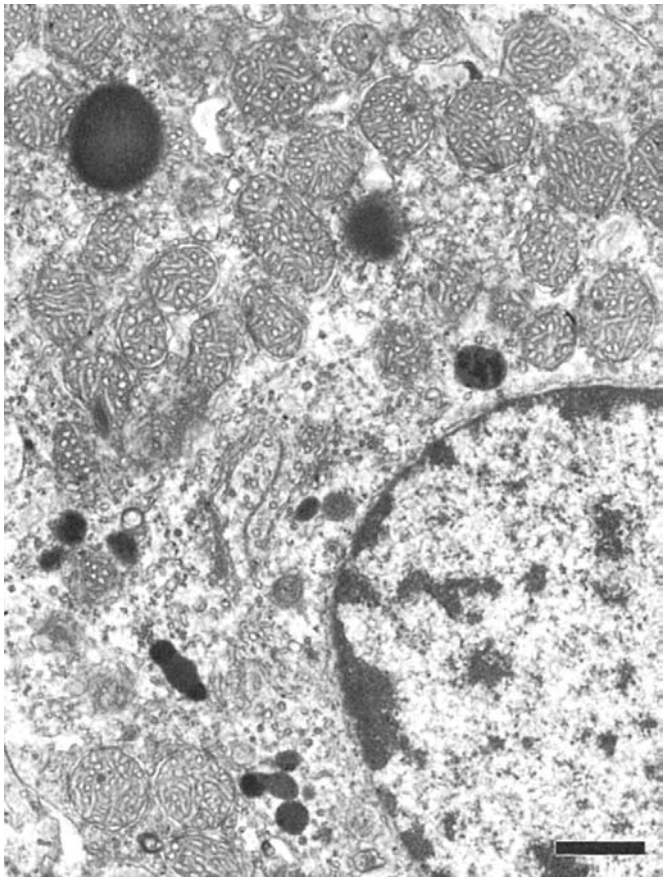

FIGURE 20.5 Cell from the zona reticularis of rat adrenal cortex with mitochondria that have typical tubulovesicular cristae. Bar = 1 μm. *Figure reproduced from Yarrington et al. (1985) Degeneration of the rat and canine adrenal cortex caused by α-(1,4-dioxido-3-methylquinoxalin-2-yl)-N-methylnitrone (DMNM),* Fundam. Appl. Toxicol. *5, 370–381, with permission.*

synthetic processes. The specificity of mitochondrial hydroxylation reactions in terms of the target steroid and the substrate carbon that is hydroxylated is confined to a specific cytochrome P450 (CYP). The common biosynthetic pathway from cholesterol is the formation of pregnenolone, the basic precursor for the three major groups of adrenal steroids (Figure 20.6). Pregnenolone is formed after two hydroxylation reactions.

In the ZF, pregnenolone is first converted to progesterone by two microsomal enzymes, followed by hydroxylation reactions. The resulting steroid is cortisol, which is the major glucocorticoid in teleosts, hamsters, dogs, nonhuman primates, and humans. Corticosterone is the major glucocorticoid produced in amphibians, reptiles, birds, rats, mice, and rabbits. It is produced in a manner similar to the production of cortisol. However, rodents and the above mentioned species lack CYP17 needed to shunt progesterone into the cortisol pathway, and this is an important consideration for toxicology, as compounds that inhibit this enzyme may not be fully detected in rodent species. This may also account for species differences in adrenocortical toxicity between rodent and nonrodent species. Spironolactone and ketoconazole inhibit CYP17 as well as other enzymes in the steroidogenic pathway.

In the ZG, pregnenolone is converted to aldosterone by a series of enzymatic reactions similar to those in cortisol formation; however, the cells of this zone lack 17α-hydroxylase and thus, cannot produce cortisol. Therefore, the initial hydroxylation product is corticosterone. Some of the corticosterone is acted on by 18-hydroxylase to form 18-hydroxycorticosterone, which in turn interacts with 18-hydroxysteroid dehydrogenase to form aldosterone. Because 18-hydroxysteroid dehydrogenase is found only in the ZG, it is not surprising that only this zone has the capacity to produce aldosterone. In addition to the aforementioned steroid hormones, the adrenal cortex also produces small amounts

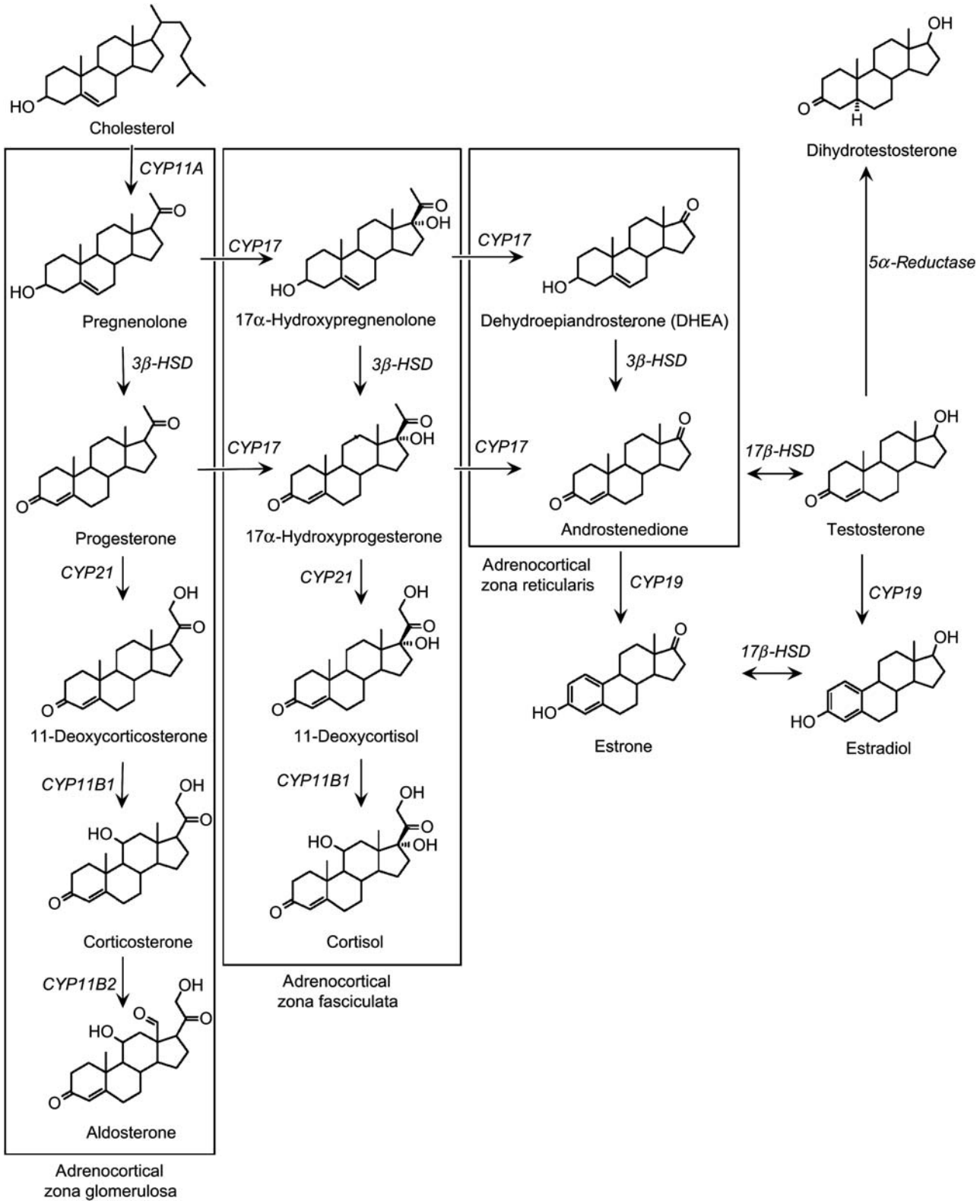

FIGURE 20.6 Adrenocortical steroidogenesis. This diagram shows enzyme expression and steroid production in the zona glomerulosa, zona fasciculata, and zona reticularis of the *human adrenal cortex*. The ability of the cells to produce a specific enzyme conveys the ability to produce a specific steroid and only cells of the zona glomerulosa express CYP11B2 capable of producing aldosterone. CYP17 is required for the production of cortisol and is not expressed in the rat and mouse, which secrete corticosterone as the dominant glucocorticoid. *HSD*, hydroxysteroid dehydrogenase. *Figure reproduced from Sanderson (2009) Adrenocortical toxicology* in vitro*: assessment of steroidogenic enzyme expression and steroid production in H295R cells. In:* Adrenal Toxicology, *(Harvey, P. W., Everett, D. J., and Springall, C. J., eds.), Informa Healthcare, pp. 175–182.*

of sex steroids, including progesterone, estrogens, and androgens. Thus, the adrenal cortex as a whole has all the necessary enzymes to synthesize the full range of steroids, differentially located across the various zones. Rodents do not produce adrenal estrogens and testosterone because they lack CYP17.

After their synthesis, secretion, and interaction with target cells, the adrenal steroid hormones are ultimately metabolized in peripheral tissues. Inactivation occurs in the liver by two main steps that include reduction or side chain removal and conjugation to glucuronic acid or sulfate. In the presence of liver disease, the turnover of steroid hormones, particularly cortisol, may be decreased and can result in abnormal adrenal function tests in patients or test animals without adrenal cortical lesions. Occasionally, peripheral tissues may activate steroid hormones (e.g., testosterone to dihydrotestosterone) or, as in the case of cortisol, convert the steroid to other less active forms of the hormone.

Mineralocorticoids (e.g., aldosterone) are the major steroids secreted from the ZG under the control of the renin–angiotensin II system. Mineralocorticoids have effects on ion transport by epithelial cells, particularly renal cells, resulting in the conservation of sodium (chloride and water) and loss of potassium. In the distal convoluted tubule of the mammalian nephron, a cation exchange exists that promotes the resorption of sodium from the glomerular filtrate and the secretion of potassium into the lumen.

Glucocorticoid hormones increase glucose production with a concomitant breakdown of proteins for purposes of gluconeogenesis. Glucocorticoids also suppress inflammation along with attenuation of fibroplasia and immunological responses. The suppression of the immunological responses is largely related to the stabilization of lysosomal membranes of phagocytic cells, inhibition of a number of lymphoid cell functions, and lysis of lymphocytes. The increase in blood glucose is an important physiological response in adverse situations, but the most important physiological effect of the glucocorticoids in stressful circumstances is to quench the inflammatory response to prevent it developing to the point where it overwhelms the animal.

The principal control for the production of steroids by the ZF and ZR is mediated by ACTH, a polypeptide hormone produced by corticotrophs in the pituitary adenohypophysis. ACTH release is largely controlled by the hypothalamus through the secretion of corticotropin-releasing hormone. An increase in ACTH production normally results in an increase in circulating levels of glucocorticoids, although it can cause weak stimulation of aldosterone secretion as well. Negative feedback control normally occurs when the elevated blood levels of cortisol act on the hypothalamus, anterior pituitary, or both to cause a suppression of ACTH secretion. This negative feedback mechanism can also be involved in adrenocortical toxicity in situations where a compound inhibits a critical enzyme in the glucocorticoid synthesis pathway, with loss of glucocorticoid production leading to less or no feedback inhibition of ACTH. The subsequent persistent overstimulation of the adrenal cortex by ACTH can produce marked adrenal hypertrophy.

In contrast to the normal negative feedback mechanism, abnormally high corticosteroid levels in the plasma, above physiological levels (due to exogenous administration of steroids or cortisol-producing adrenal lesions), will cause marked ACTH suppression. If the suppression is prolonged, secretory cells in the ZF and ZR will undergo atrophy, with a corresponding decrease in their future capability to synthesize and secrete corticosteroid hormones.

EVALUATION OF TOXICITY

When a compound affects steroidogenesis, it is important to define the extent to which it impairs adrenal cortical functional reserve capacity. In some instances, clinical signs of hypoadrenocorticism may be observed in association with lower urinary and plasma corticosteroid levels. When such findings are not obvious, provocative testing for the evaluation of adrenal cortical functional reserves is essential to determine the extent of cortical damage. The most commonly used provocative test is the administration of ACTH to human patients or test animals (the dog is the ideal test animal for evaluation). ACTH has been shown to be a potent stimulus for the synthesis and secretion of naturally occurring glucocorticoids in noncompromised cells of the ZR and ZF.

In Vitro Assessment

In vitro studies are extremely useful in determining the specific cellular consequences of xenobiotic exposure on steroidogenesis. In many instances, the results of these *in vitro* assessments are helpful in correlating the development of adrenocortical degeneration to an inhibited pathway of steroidogenesis. By far, the best available *in vitro* model is the H295R cell line. This is a human adrenocortical carcinoma cell line that retains full adrenocortical steroidogenic enzyme capability and can secrete aldosterone, cortisol, and androgens, estrogens, and progestogens and their precursors in response to appropriate challenge. This system has been used to investigate the majority of chemicals

reported to induce adrenocortical functional toxicity over the past decade, particularly to identify molecular sites of toxicity. It should be noted that rodent cell lines do exist but are deficient in at least CYP17, and the Y1 mouse cell line is only capable of producing progesterone because of deficiencies in numerous other steroidogenic enzymes. Rodent cell lines therefore have little use in establishing mechanisms of toxicity, at least in terms of human relevance.

Morphologic Evaluation

Following the death of a test animal, morphological evaluation commences with macroscopic observation of the adrenal glands to detect changes in size, color, and/or appearance (e.g., nodularity). Subsequent histological examination of adrenal tissue (including both cortex and medulla) on midsagittal sections stained with hematoxylin and eosin (H&E) is performed routinely. The most current terminology for describing various nonproliferative and proliferative lesions of the adrenal cortex, including representative images of common lesions, developed by the International Harmonization of Nomenclature for Diagnostic Criteria (INHAND) in Rats and Mice, will be available at the time of publication of this chapter on the Society of Toxicologic Pathology website (http://www.toxpath.org/inhand.asp).

Microscopic study may be supplemented by the use of special stains and techniques to confirm or identify a particular pigment, cell type, or enzyme. Examples of useful stains are Congo red (amyloid), acid fast stains (ceroid pigment), Sudan black or Oil red O (lipid), Perl's stain (iron), and immunohistochemistry for enzymes (e.g., aldosterone synthase in the ZG; Figure 20.7). Histomorphometric analysis can be used to assess subtle differences in cell size, width of the different cortical zones, and cortical:medullary ratio.

Use of Animals as Models

The adrenal cortex of animals is prone to develop proliferative and degenerative lesions, the etiology of which may be either spontaneous in nature or induced experimentally. Therefore, chemical testing using various domestic or laboratory animals is a valid means of assessing the toxic potential for humans exposed to various xenobiotic chemicals.

Species, Age, and Sex Variables

The correct choice of species of test animal is critical. There often is a variable species susceptibility to toxicity. This observation suggests that differences in metabolism play a role in the development of adrenal cortical toxicity and in the inhibition of steroidogenesis.

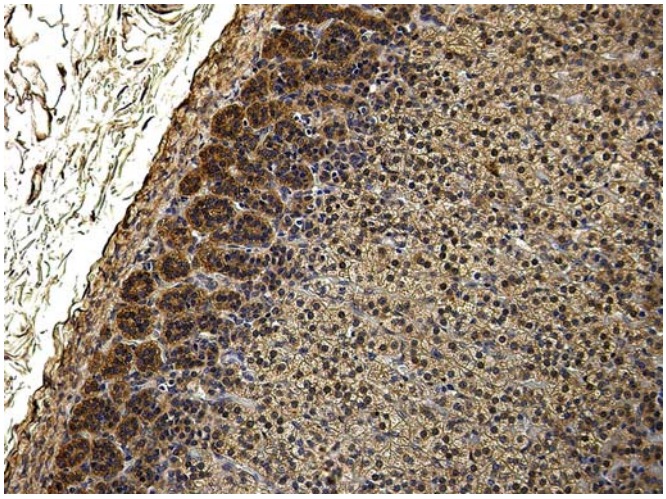

FIGURE 20.7 Cytoplasm of the cells in the zona glomerulosa has strong positivity for aldosterone synthase using immunohistochemistry with K16 antibody in the cortex of a rat. *Figure reproduced from* Handbook of Toxicologic Pathology, *third ed., W. M. Haschek, C. G. Rousseaux and M. A. Wallig, eds. (2013) Academic Press, Fig. 58.23, p. 2415, with permission.*

As mentioned previously, the rodent is deficient in CYP17, and compounds inhibiting steroidogenesis and particularly cortisol production via this enzyme would not be adequately evaluated using the rodent only. However, dog and monkey could be used instead.

Likewise, the age of the test animal, to a lesser degree, may be a factor in the development of chemically induced adrenocortical lesions. For example, adrenal cortical necrosis was induced in rats at 50 days of age but not at 25 days by the administration of 7,12-dimethylbenz[*a*]anthracene.

Stress as a Variable in Animal Models

Although the rat, because of differences in steroidogenesis, is not the best model to fully evaluate adrenal toxicity in terms of human relevance, it often shows adrenal changes in toxicity studies. One of the most common findings in the rat is adrenocortical hypertrophy, which is indicative of ACTH stimulation (Figure 20.8). Adrenal hypertrophy may be a result of stress or indeed may result from functional impairment of the adrenal cortex and reduced capacity to secrete glucocorticoids. It is therefore important, in all cases of adrenocortical hypertrophy induced by excess ACTH stimulation, to establish the mechanism of ACTH elevation (i.e., stress versus adrenal toxicity/insufficiency). Atrophy of the thymus and other lymphoid tissues is a useful surrogate marker for adrenocortical competence, as this atrophy is induced by excess glucocorticoid secretion; similarly, the stress leukogram is useful evidence. Stress is a natural adaptive response designed to better equip the animal to

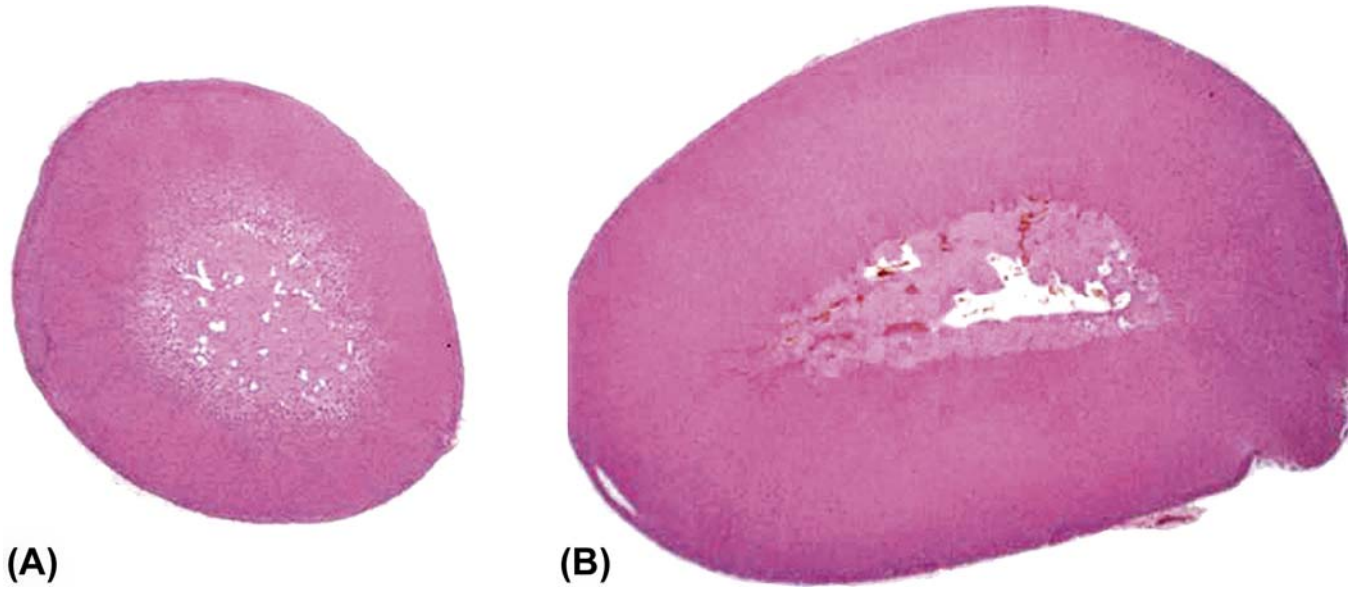

FIGURE 20.8 Adrenal of control rat (A) and rat with grade 3 cortical hypertrophy (B). H&E stain. *Figure reproduced from* Handbook of Toxicologic Pathology, *third ed., W. M. Haschek, C. G. Rousseaux and M. A. Wallig, eds. (2013) Academic Press, Fig. 58.24, p. 2416, with permission.*

survive, and it should result in both elevated ACTH and glucocorticoids. Elevation of the latter is diagnostic and proof of adrenocortical functional competence. Stress, however, should not produce irreversible histopathologic lesions in the adrenal cortex. By contrast, toxicity to the adrenal cortex may be obvious due to marked and often irreversible histopathological lesions (degeneration, necrosis, and fibrosis). However, in cases of pharmacotoxicological inhibition of steroidogenic enzymes there may be no histopathological lesions but grossly impaired glucocorticoid production, clearly a toxicological concern.

If findings are restricted to adrenocortical hypertrophy (i.e., no thymic atrophy, stress leukogram, or other supportive stress-related changes) then stress cannot be confirmed as the cause, and further work to test adrenocortical functionality should be undertaken.

RESPONSE TO INJURY

Disorders of Hyperfunction and Hypofunction

Chemicals can produce functional alterations of the adrenal cortex. Prolonged use of exogenous glucocorticoids can mimic a syndrome of excess adrenal cortical function. Abrupt cessation of steroid use may cause a patient to develop secondary adrenal cortical insufficiency because of the prolonged suppression of ACTH production and the trophic atrophy of cells in the adrenal cortex. More significant from a toxicologic point of view are the degenerative effects of chemicals on the adrenal cortex that result in primary adrenal cortical hypofunction. Disturbances in adrenal–cortical function have been best characterized in the dog. Because of this, and the fact that canine hyper- and hypoadrenocorticism are similar to the corresponding clinical syndromes in humans, the remaining discussion in this section will be principally confined to the dog.

Exogenous glucocorticoid hormone therapy (daily at high doses) often mimics naturally occurring cases of hypercortisolism (e.g., Cushing's syndrome). Clinical observations include polyuria, polydipsia, an enlarged pendulous abdomen, muscular wasting, alopecia, thinning of the skin with cutaneous pigmentation and mineralization, and hepatomegaly. Osteoporosis is an important finding in human patients with cortisol excess but is not a common finding in the dog. Significant laboratory findings include an increase in alkaline phosphatase (steroid-induced isoenzyme), an eosinopenia with marked lymphopenia, and leukocytosis due to the increased formation of neutrophils. Dogs with hypercortisolism infrequently develop significant alterations in serum concentrations of sodium, potassium, or chloride, in contrast to those electrolyte imbalances seen in humans with Cushing's syndrome. With the prolonged use of exogenous glucocorticoids, exogenous ACTH administration results in an inadequate release and blunted increase in blood levels of cortisol. In spontaneous cases of functional adrenal cortical hyperplasia that remains partially under the control of pituitary ACTH, a marked response to the exogenous ACTH challenge occurs, resulting in an exaggerated increase in blood cortisol levels.

In hypoadrenocorticism, caused by natural disease or experimentally by the administration of xenobiotic chemicals, clinical signs often are not pathognomonic and nonspecific. However, there is generally an abnormal electrocardiogram with spiked T waves and flattening of the P wave. These electrocardiographic alterations appear to be due to the prominent increase in serum potassium in dogs with hypoadrenocorticism and subnormal secretion of aldosterone.

Plasma and urinary 17-hydroxycorticosteroids often are at low levels in the resting state. Stimulation tests, including the response to exogenous ACTH challenge, usually reveal a subnormal ("blunted") increase in plasma cortisol due to the reduced number of cortical cells that can respond to the challenge.

Effects During Embryogenesis

It is well documented that synthetic and naturally occurring corticosteroids are potent teratogens in laboratory animals. The principal induced defect is cleft lip or palate; however, there is a paucity of information regarding the direct effect of chemicals on the development of the adrenal cortex. Adrenal aplasia has occurred in a subset of white Danish rabbits when thalidomide was given to their dams.

Morphologic Alterations

Macroscopic lesions of chemically affected adrenal glands are characterized by either enlargement or reduction in size that often is bilateral. Initially, cortical hypertrophy or swelling due to impaired steroidogenesis or hyperplasia due to long-term stimulation often is seen when the adrenal is increased in size. Similar gross findings may be the result of medullary hyperplasia or pheochromocytoma. In contrast, small adrenal glands often are indicative of degenerative changes, resulting in atrophy. Midsagittal longitudinal sections of the glands will reveal a disproportionately wider cortex relative to the medulla, or vice versa, resulting in an abnormal cortical:medullary ratio.

Nonneoplastic Lesions

Histologically, nonneoplastic lesions of the adrenal cortex induced by chemical agents are characterized by changes ranging from acute progressive degenerative to reparative in nature. These may be exacerbations of normal spontaneous findings or directly compound-induced lesions. There is delayed involution of the x-zone in mice after treatment with luteinizing hormone (LH), acetonitrile and the antifungal, ketoconazole (see Figure 20.2). There can be a treatment-related increase in the pigment lipofuscin (formed from lipid products resulting from altered fat metabolism) in the ZR in rats, which increases normally with age, but also can be increased after dosing with estrogens, antithyroid agents, the neurotoxin 1-methyl-4-phenyl-1,2,3,6-tetrahydropyridine, and corticosteroids. It can also be increased after feeding diets high in saturated fats and with Vitamin E deficiency. This pigment can be demonstrated with fuschinophilic stains (Ziehl-Neelson and periodic acid-Schiff), which can help to differentiate it from hemosiderin (a brown blood-breakdown product), which can, in turn, be demonstrated using Perl's stain (for iron) (Figure 20.9).

Early degenerative lesions characterized by enlarged-cortical cells filled with cytoplasmic vacuoles (often lipid) may result in a diffuse hypertrophy of the cortex. Lipid vacuolation is commonly seen in the ZF in normal unstressed animals, with numerous lipid droplets, $\sim$0.5 μm diameter, containing esterified cholesterol. This increases with age and in response to reproductive and physiological changes (Figure 20.10).

However, excessive coalescing lipid droplets have been observed in rats treated with the antibacterial compound, alpha-(1,4-dioxido-3-methylquinoxalin-2-yl)-*N*-methylnitrone (DMNM). This vacuolar type of degeneration is a reflection of impaired steroidogenesis, resulting in excess storage of unmetabolized steroid precursors. More destructive lesions may be observed in the form of hemorrhage and/or necrosis, often in association with an inflammatory response. At the same time, one area of the cortex (e.g., the ZG) may undergo hypertrophy while another area has degenerative lesions (e.g., vacuolar degeneration of the ZF). The ZG remains functional and there are no

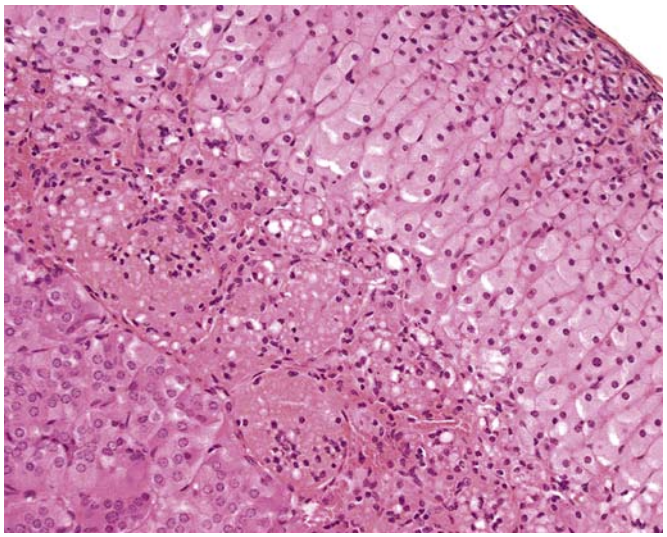

FIGURE 20.9 Lipofuscin pigment at the corticomedullary junction (rat). H&E stain. *Figure reproduced from* Handbook of Toxicologic Pathology, *third ed., W. M. Haschek, C. G. Rousseaux and M. A. Wallig, eds. (2013) Academic Press, Fig. 58.8, p. 2404, with permission.*

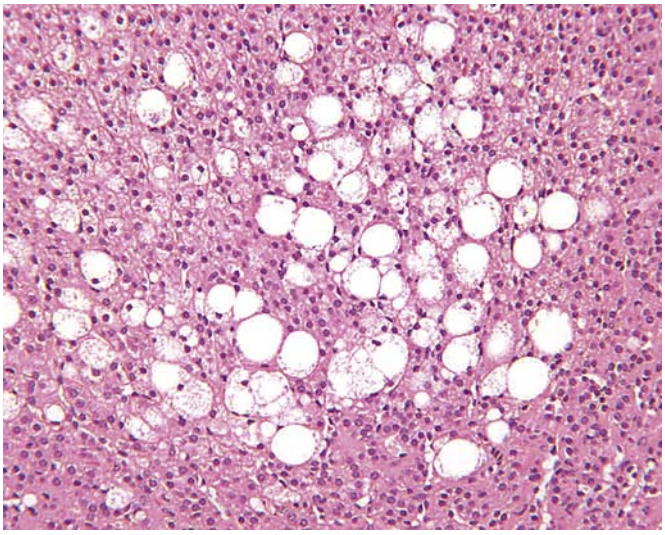

FIGURE 20.10 Lipid droplets in the zona fasciculata of a dog. H&E stain. *Figure reproduced from* Handbook of Toxicologic Pathology, *third ed., W. M. Haschek, C. G. Rousseaux and M. A. Wallig, eds. (2013) Academic Press, Fig. 58.9, p. 2404, with permission.*

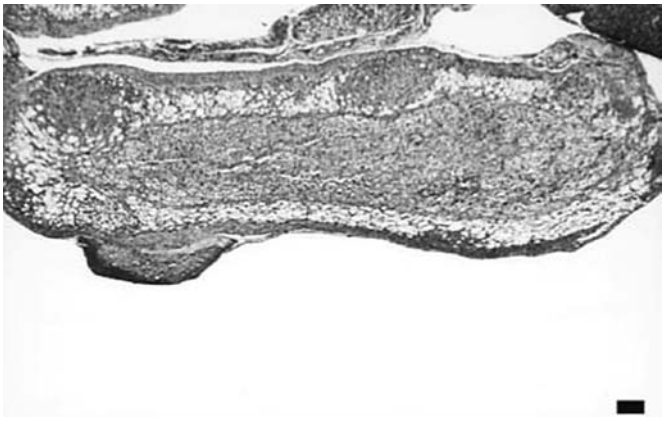

FIGURE 20.11 Atrophy, vacuolar degeneration, and nodular hyperplasia (arrows) of the adrenal cortex from a rat treated with 50 mg/kg/day of DMNM for 90 days. Bar = 100 μm. *Figure reproduced from Yarrington et al. (1985) Degeneration of the rat and canine adrenal cortex caused by α-(1,4-dioxido-3-methylquinoxalin-2-yl)-*N*-methylnitrone (DMNM),* Fundam. Appl. Toxicol. *5, 370–381, with permission.*

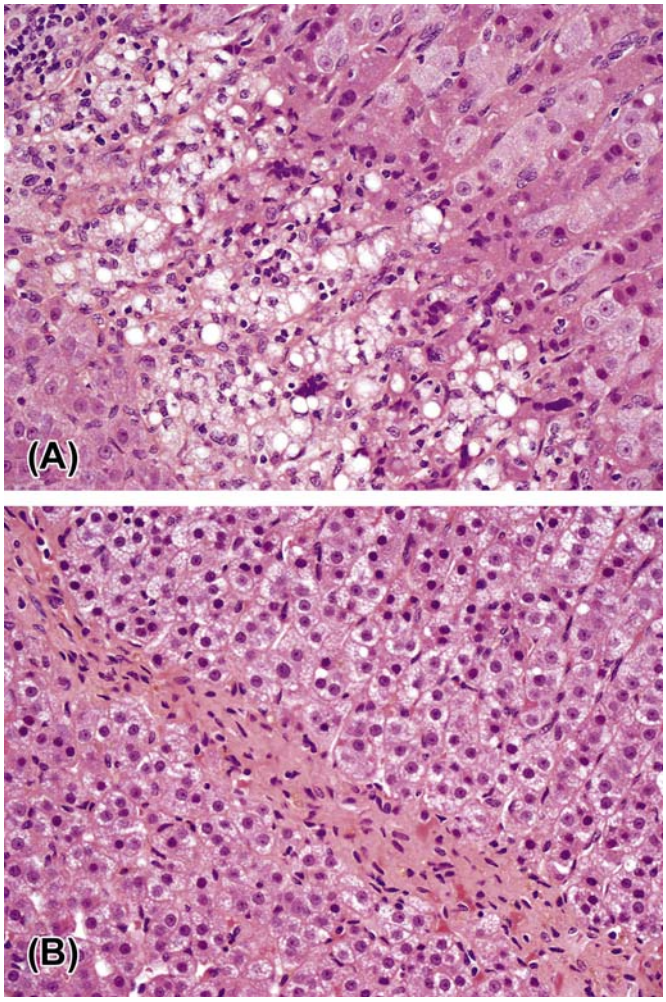

FIGURE 20.12 (A) Adrenocortical cell necrosis and vacuolation in the zona fasciculata of a cynomolgus monkey (treated with PD 132301-2). (B) Adrenocortical fibrosis in a cynomolgus monkey, following a 4-week-treatment-free period. H&E stain. *Figure reproduced from* Handbook of Toxicologic Pathology, *third ed., W. M. Haschek, C. G. Rousseaux and M. A. Wallig, eds. (2013) Academic Press, Fig. 58.14, p. 2406, with permission.*

clinically significant signs of hypoadrenocorticism, and chronic regenerative changes may develop subsequently. Usually, the adrenal cortex will be shrunken or atrophic with fibrosis and areas of multinodular hyperplasia. In the case of chronic DMNM toxicity in rats, fibrosis and occasionally hemosiderin pigment may be found in the ZR. Cortical nodules of presumably functional remnants of the ZF and discernible areas of the ZG were found in rats that survived treatment for 90 days (Figure 20.11).

While many adrenocorticolytic agents affect the adrenal cortex initially at the ZR and inner ZF, some chemicals such as DMNM can cause a progressive degeneration of the adrenal cortex. Occasionally, the effect of a chemical is limited to a specific zone of the adrenal cortex and may be species specific. For example, the compound PD 132301-2, when administered to monkeys, induces a narrow band of degeneration or necrosis of cortical cells in the mid to outer ZF (Figure 20.12). In contrast, all three cortical zones are affected in the adrenal glands of dogs treated with this compound. Xenobiotic chemicals that cause degeneration of the adrenal cortex are summarized in Table 20.1, together with the predilection site of their effects and the most significant lesions. Ultrastructural alterations

TABLE 20.1 Examples of Chemically Induced Microscopic and Ultrastructural Changes of the Adrenal Cortex

Compound	Initial predilection site	Histology	Ultrastructure
Nafenopin	Zona fasciculata	Hypertrophy	SER[a] and peroxisome proliferation
Acrylonitrile	Zona reticularis	Hemorrhage	Damage to vascular endothelium; embolization of medullary cells and cell fragments of capillaries
Aminoglutethimide	All zones; more marked in outer zona fasciculata	Vacuolar degeneration; increased lipid	Mitochondrial hypertrophy and cavitation
o,p′-DDD	Zona reticularis and fasiculata	Vacuolar degeneration; cytotoxic cellular atrophy	Mitochondrial vacuolization; SER dilation
α-(1,4-Dioxido-3-methylquinoxalin-2-yl)-*N*-methylnitrone	Zona reticularis and fasiculata	Granular and vacuolar degeneration; cytotoxic cellular atrophy	Mitochondrial vacuolization; SER dilation
Triparanol	All zones; most marked in zona fasciculata	Increased eosinophilia and inclusions	Decreased lipid droplets; mitochondrial alterations; SER hypertrophy; lysosomal formation
Cysteamine (1-mercaptoethylamine)	Zona reticularis and fasiculata	Hemorrhage and necrosis	Retrograde emboli of medullary cells
Amphenone	Zona reticularis and fasiculata	Fatty degeneration	Mitochondrial alterations
7,12-Dimethylbenzanthracene	Zona reticularis and fasiculata	Necrosis; hemorrhage; calcification	Mitochondrial alterations, including variation in size
Corticosteroids, (e.g., prednisolone, dexamethasone)	Zona reticularis and fasiculata	Atrophy	Increased lipid droplets surrounded by membranous "whorls"; increased myelin figures and lysosomes
Propylthiouracil	Zona reticularis	Ceroid degeneration	Lipid and mitochondrial degeneration
Carbon tetrachloride	Zona reticularis and fasiculata	Necrosis	Swelling of SER
Tamoxifen	Zona reticularis and fasiculata	Degeneration and necrosis; lipid droplets	Necrosis; lipid droplets in macrophages; few lysosomal inclusions
Spironolactone	Zona glomerulosa	Hypertrophy and inclusions	Lipid droplets surrounded by whorls of SER ("spironolactone bodies"); mitochondrial alterations
Hexadimethrine bromide (polybrene)	Zona glomerulosa	Necrosis and infarction	Protein-containing vacuoles and (polybrene) hyalin bodies; microthrombi
RO1-8307, a sulfated mucopolysaccharide	Zona glomerulosa	Condensation	
Captopril	Zona glomerulosa	Atrophy	Decreased mitochondria and SER
1,1′-Thio-diethylidene-ferrocene (MDL 80, 478)	All zones	Granular and vacuolar degeneration; hyperplastic zona glomerulosa	Mitochondrial vacuolation; increased lipid droplets
Aniline	All zones	Hypertrophic cortical cells laden with lipid droplets	Increased lipid droplets; hypertrophic SER; mitochondrial degeneration
Chlorophentermine	All zones	Nothing remarkable	Increased lysosomal alterations in the form of lamellated cytoplasmic inclusions
Triaryl phosphate	All zones	Cytoplasmic lipid droplet	Increased number/size cytoplasmic droplets
PD 132301-2	Zona fasciculata	Coarse vacuolation	SER aggregation; changes of autophagosomes

[a]*Smooth endoplasmic reticulum.*

Table modified from Handbook of Toxicologic Pathology, *second ed. W. M. Haschek, C. G. Rousseaux, and M. A. Wallig, eds. (2002) Academic Press, Vol. 2, Table II, pp. 693–694.*

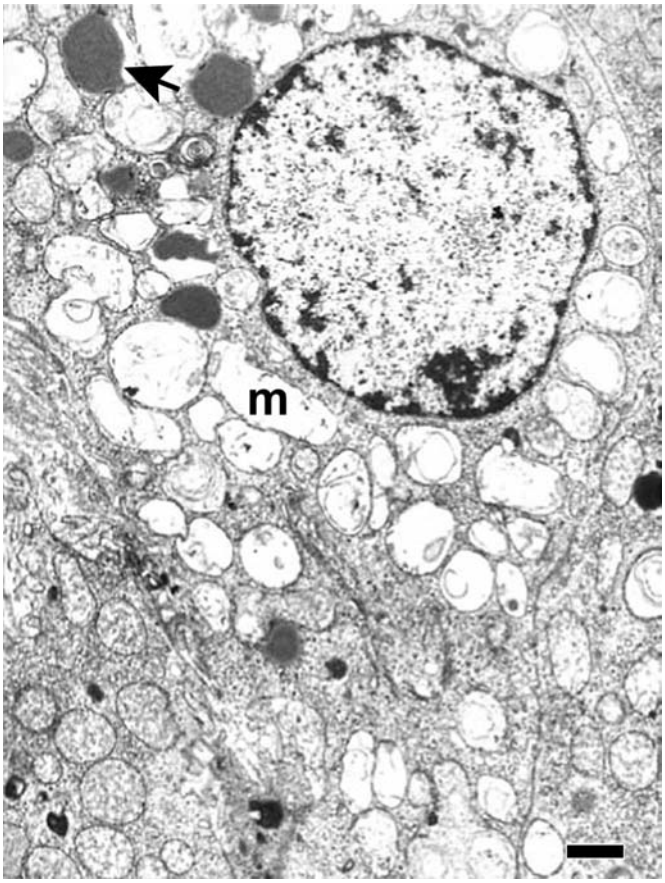

FIGURE 20.13 Cell of the zona fasciculata of the adrenal cortex of a rat treated with 100 mg/kg/day of DMNM for 21 days. Note vacuolated mitochondria (m) and some lipid droplets undergoing lipolysis (arrow). Bar = 1 μm. *Figure reproduced from Yarrington et al. (1985) Degeneration of the rat and canine adrenal cortex caused by α-(1,4-dioxido-3-methylquinoxalin-2-yl)-N-methylnitrone (DMNM),* Fundam. Appl. Toxicol. *5, 370–381, with permission.*

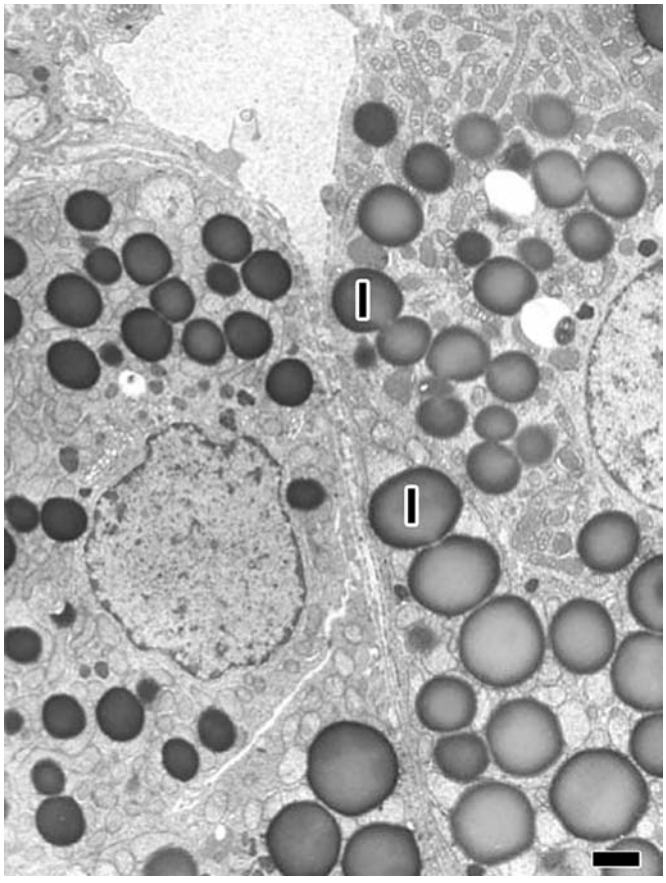

FIGURE 20.14 Numerous lipid droplets (l) in the cytoplasm of cells of the zona fasciculata and glomerulosa from a rat treated with 500 mg/kg/day of MDL 83,478. Bar = 1 μm. *Figure reproduced from Yarrington et al. (1983) Comparative toxicity of the hematinic MDL 80,478: Effects on the liver and adrenal cortex of the dog, rat and monkey,* Fundam. Appl. Toxicol. *3, 86–94, with permission.*

of adrenal–cortical cells associated with chemical injury are quite diverse in nature (Table 20.1). The ZR and ZF typically are most severely affected, although eventually the lesions involve the ZG. These alterations may be classified as follows: endothelial damage (e.g., acrylonitrile), mitochondrial damage (e.g., DMNM, *o*, *p*′-DDD, amphenone), endoplasmic reticulum changes (e.g., triparanol), lipid aggregation (e.g., aniline), lysosomal phospholipid aggregation (e.g., chlorophentermine), and possible secondary effects due to embolization by medullary cells (e.g., acrylonitrile).

Mitochondrial damage with vacuolization (Figure 20.13) and accompanying changes in the endoplasmic reticulum and autophagocytic responses are among the most common ultrastructural changes observed following chemical injury in the adrenal cortex. Because mitochondria and smooth endoplasmic reticulum form an intimate network in cortical cells and important hydroxylases and dehydrogenase enzymes are found in these organelles, it is not surprising that many agents altering the ultrastructural morphology inhibit steroidogenesis. Similarly, increased lipid droplets (Figure 20.13) and lysosomal phospholipidosis (Figures 20.14 and 20.15) are compatible with altered steroid biosynthesis as a result of chemical inhibition of steroid precursors (e.g., cholesterol). The increased accumulation of lipid and severe mitochondrial vacuolization correspond to light microscopic findings of marked cytoplasmic vacuolar and granular degeneration. More severe ultrastructural injury may result with some parenchymal cells of the cortex having an electron-dense cytoplasm, chromatolysis, and disruption of the plasma membranes (necrosis). Frequently, macrophages containing cholesterol clefts, numerous lipid droplets, and membranous debris can be observed among the necrotic cells.

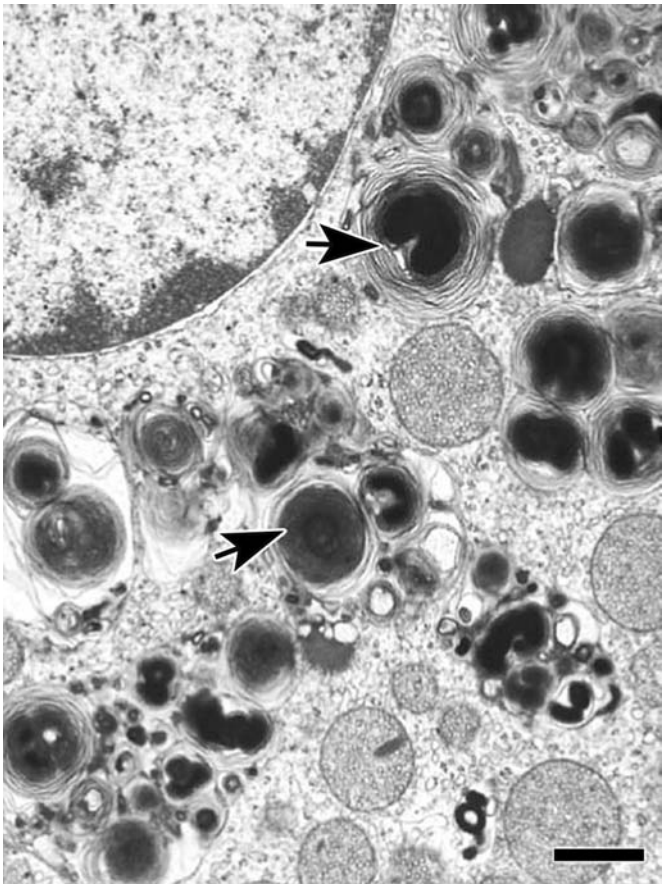

FIGURE 20.15 Large myelinoid bodies (arrows) compatible with lysosomal phospholipidosis in an adrenal cortical cell of a rat treated with a cationic amphiphilic compound. Bar = 1 μm. *Figure reproduced from* Handbook of Toxicologic Pathology, *second ed. W. M. Haschek, C. G. Rousseaux and M. A. Wallig, eds. (2002) Academic Press, Vol. 2, Fig. 13, p. 696, with permission.*

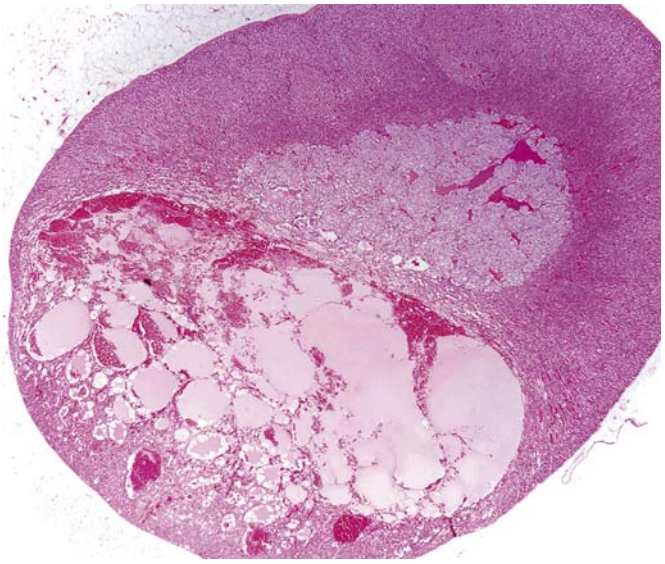

FIGURE 20.16 Eosinophilic nodule in a rat, with cystic degeneration, hemangiectasis, hemorrhage, and large eosinophilic adrenocortical cells. H&E stain. *Figure reproduced from* Handbook of Toxicologic Pathology, *third ed., W. M. Haschek, C. G. Rousseaux and M. A. Wallig, eds. (2013) Academic Press, Fig. 58.19, p. 2412, with permission.*

Proliferative Lesions

Spontaneous hyperplasia of the adrenal cortex is common in the rat, rabbit, golden hamster, mouse, dog, cat, horse, and baboon. Spontaneous proliferative lesions may be found in all zones of the adrenal cortex but are present most frequently in the ZF of adult rats. In these proliferative foci or larger capsule-distorting nodules, there is no change in architectural arrangement of cells and no obvious compression of adjacent cells; however, the cellular aggregates are cytologically different from normal cells surrounding them in terms of size and tinctorial properties. Large eosinophilic nodules in the rat often show vacuolated/cystic degeneration and hemorrhage which can replace many of the large eosinophilic adrenocortical cells (Figure 20.16**)**. Cortical adenomas and, to a lesser extent, cortical carcinomas have been reported in moderately high incidence in certain strains of rat (e.g., Osborne Mendel, *WAG/Rij*, BUF, and BN/Bi strains). The incidence often increases markedly in rats over 18 months of age. A high incidence of cortical adenomas and fewer carcinomas have also been reported in the laboratory hamster (e.g., BIO 4.24 and BIO 45.5 strains). Subcapsular cortical cell proliferation and adenoma are common in laboratory mice; however, neoplasms arising deep within the adrenal cortex are rare but may be induced by gonadectomy. Naturally occurring adrenal cortical tumors are found infrequently in domestic animals, except in adult dogs and castrated male goats.

Less frequently reported are chemically induced proliferative lesions of the adrenal cortex. Unlike the diffuse hyperplasia and hypertrophy associated with the adrenal cortical response to excess ACTH stimulation, chemically induced hyperplasia usually is nodular in type and often multiple in distribution. Each focus or larger nodule is an oval-to-spherical lesion of variable size consisting of enlarged normal or vacuolated cells.

A summary of chemicals causing adrenocortical neoplasms is present in Table 20.2. Most of the reported tumors tend to be benign (adenoma), although an occasional one may be malignant (carcinoma). The ZR and ZF are more prone to develop tumors, whereas the ZG is spared unless invaded by an expanding tumor in the adjacent zones of the cortex. Tumorigenic agents of the adrenal cortex have a diverse chemical nature and use (Table 20.2). Several of the compounds have a steroid nucleus and are natural or synthetic estrogens or androgens.

An adrenal cortical adenoma has characteristics similar to nodular hyperplasia, with the exception that

TABLE 20.2 Examples of Compounds Producing Tumors of the Adrenal Cortex[a]

Compound	Chemical properties	Type of lesion	Animal affected
Aflatoxin/stilbesterol	Fungal metabolite/ steroid	Adenoma and hyperplasia	Rat
Cholesterol	Steroid	Microadenomas	Rabbit
Dibromochloropropane	Soil fumigant	Adenoma	Rat
7,12-Dimethylbenzanthracene	Organic solvent	Adenoma; eosinophilic and basophilic foci	Rat
Estrone, estriol, diethylstilbesterol	Natural and synthetic estrogens	Adenocarcinoma	Rat
Formic acid 2-[4-(5-nitro-2-furyl)-2-thiazolyl]hydrazide	Antimicrobial	Adenoma	Hamster
Parathion	Insecticide	Adenoma; carcinoma	Rat
Tetrachlorovinphos	Insecticide	Adenoma	Rat
Testosterone	Hormone	Adenoma	Hamster
Urethane	Organic solvent; intermediate in organic synthesis	Adenoma	Rat
Linoleic acid	Unsaturated fatty acid	Carcinoma	Rat

[a]*Predilection sites are the zona reticularis and fasiculata.*
Table modified from Handbook of Toxicologic Pathology, *second ed. W. M. Haschek, C. G. Rousseaux, and M. A. Wallig, eds. (2002) Academic Press, Vol. 2, Table III, p. 697.*

adjacent parenchymal cells are compressed and often atrophic due to pressure. Cortical adenomas show loss of the cellular radial architecture but are well differentiated and circumscribed and may be partially encapsulated by a thin band of fibrous connective tissue (Figure 20.17).

Adrenal cortical carcinomas are composed of large polyhedral or pleomorphic cells with an eosinophilic or vacuolated cytoplasm. Tumor cells have prominent nucleoli and variable numbers of mitotic figures, and form different histologic patterns, including sheets, lobules, and cords. The invasive nature of the malignant cells is also apparent by penetration through the capsule, obliteration of the normal architecture of the affected gland, and metastasis to distant sites. Blood-filled spaces and localized areas of necrosis are common in cortical carcinomas (Figure 20.18).

MECHANISMS OF TOXICITY

As mentioned previously, the adrenal is the most common target organ for toxicity in the endocrine

FIGURE 20.17 Adrenal cortical adenoma in a rat showing compression of adjacent parenchyma and loss of radial architecture but well differentiated and circumscribed. *Figure reproduced from* Handbook of Toxicologic Pathology, *third ed., W. M. Haschek, C. G. Rousseaux and M. A. Wallig, eds. (2013) Academic Press, Fig. 58.20, p. 2413, with permission.*

system. First, there is the dependence of the adrenal cortex on the trophic support of hormones from the pituitary and hypothalamus, and also hormones from other endocrine tissues such as adrenomedullary neuropeptides where, for example, adrenomedullin has a role in aldosterone and cortisol secretion. Toxicity in these other sites therefore could ultimately influence the adrenal cortex. Additionally, the adrenal cortex has both anatomic and molecular characteristics that convey vulnerability to toxic insult, and the following factors predispose the adrenal cortex to toxic insult *in vivo*.

1. Functional dependence on the hypothalamus and pituitary and peripheral hormone-carrier molecules (e.g., CBG)

   The large number of potential toxicological targets such as enzymes, receptors, and biochemical functional mediators (e.g., adrenomedullin) of major concern is the sequentially dependent steroidogenic steps in cortisol/corticosterone or aldosterone production and secretion, which are at the end of the pathway and therefore have the highest probability of effect from upstream toxicity.
2. High vascularity and disproportionately large blood volume received per unit mass of adrenal tissue ensuring high exposures to toxicants.
3. The high content of unsaturated fatty acids in adrenocortical cell membranes that are susceptible to lipid peroxidation both directly and indirectly (see below).

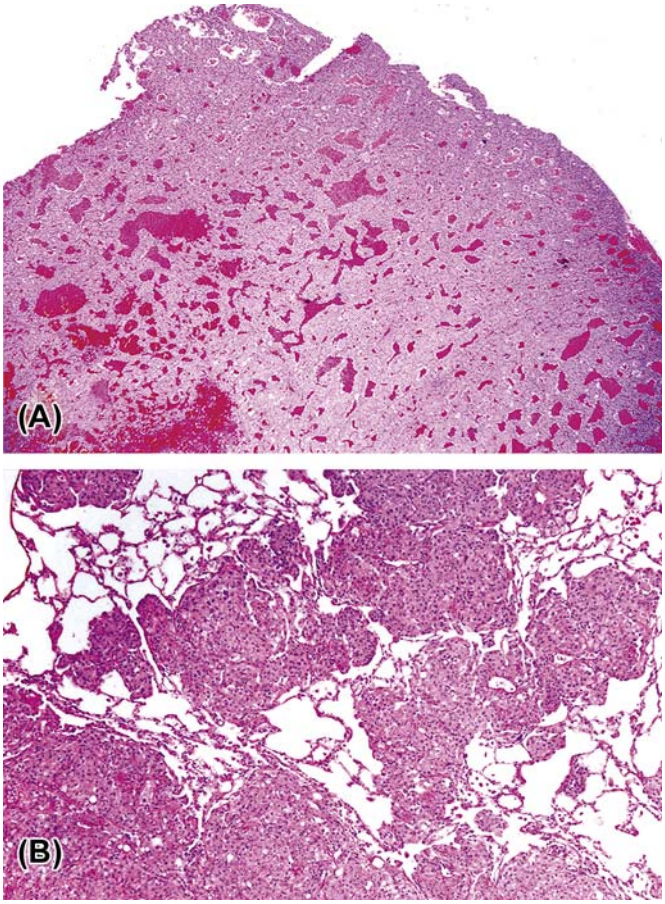

FIGURE 20.18 (A) Adrenocortical carcinoma in a rat with hemorrhage, dilated vascular spaces, and extracapsular invasion. (B) Lung metastases from an adrenocortical carcinoma in a rat. *Figure reproduced from* Handbook of Toxicologic Pathology, *third ed., W. M. Haschek, C. G. Rousseaux and M. A. Wallig, eds. (2013) Academic Press, Fig. 58.21, p. 2413, with permission.*

4. Lipophilicity due to rich cholesterol and steroid content favoring deposition of lipophilic compounds.
5. The high content of CYP enzymes present in the adrenal cortex that can produce—(1) reactive metabolites of toxicants that then mediate toxicity and (2) hydroxylation reactions that may generate free radicals which then damage adrenocortical cells and membrane (as above).

Classes of chemicals known to be toxic for the adrenal cortex include short chain (three or four carbon) aliphatic compounds, lipidosis inducers, and amphiphilic compounds. It would also appear that hormones, especially exogenous steroids, have a direct effect on the adrenal cortex. The most potent aliphatic compounds are of three-carbon length with electronegative groups at both ends. These compounds frequently produce necrosis, particularly in the ZF and ZR. Examples include acrylonitrile, 3-aminopropionitrile, 3-bromopropionitrile, 1-butanethiol, and 1,4-butanedithiol. By comparison, lipidosis inducers can cause the accumulations (often coalescing) of neutral fats, which may be of sufficient quantity to cause a loss of organellar function and cellular destruction. The ZR and ZF appear to be the principal targets of xenobiotic chemicals. Examples of the compounds causing lipidosis include aminoglutethimide, amphenone, anilines, and imidazole antimycotic drugs. Biologically active cationic amphiphilic compounds tend to produce a generalized phospholipidosis that involves primarily the ZR and ZF. They cause microscopic and subcellular phospholipid-rich inclusions. These compounds affect the functional integrity of lysosomes, which appear ultrastructurally to be enlarged and filled with membranous lamellae or myelin figures. Examples of compounds known to induce these types of effect include chloroquine, triparanol, and chlorphentermine.

Another class of compounds that affects the adrenal cortex is certain hormones, particularly natural and synthetic steroids. Some of these steroid hormones (corticosteroids) may cause functional inactivity and morphological atrophy during prolonged exogenous use (Figure 20.19). Other steroid hormones (natural and synthetic estrogens and androgens) have been reported to cause proliferative lesions in the adrenal cortex of laboratory animals.

The final class of compounds represents a miscellaneous group of chemicals that affect hydroxylation and other functions of mitochondrial and microsomal fractions (smooth endoplasmic reticulum). Examples of these compounds include *o,p′*-DDD and -alpha-(1,4-dioxido-3-methylquinoxalin-2-yl)-*N*-methylnitrone (DMNM). Additional compounds in this category cause their effects by means of CYP metabolism and the activation of toxic metabolites. An example is the activation of carbon tetrachloride, resulting in lipid peroxidation and covalent binding to cellular macromolecules of the adrenal cortex. For another example, aminoglutethimide downregulates the ACTH receptor, and inhibits CYP11A1 (cholesterol side chain cleavage) and CYP11B1 (CYP11β/18), which is the terminal enzyme in cortisol synthesis.

Many of the chemicals that cause morphological changes in the adrenal glands can also affect adrenal cortical function (Table 20.3). Chemically induced changes in adrenal gland function result either from blockage of the effects of the adrenocorticoids at peripheral sites or from inhibition of synthesis and/or secretion (steroidogenesis). In the former case, many antisteroidal compounds (antagonists) act by competing with or binding to steroidal receptor sites, thereby either reducing the available receptor sites or altering their functional activity. Cortexolone

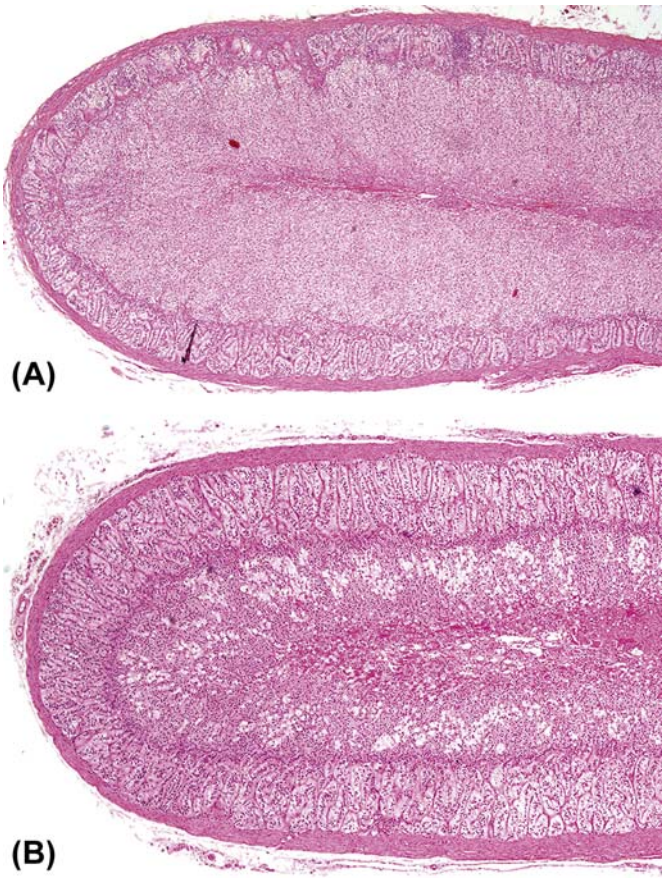

FIGURE 20.19 Adrenal of control dog (B) and adrenal of dog with cortical atrophy (A) following treatment with excessive topical corticosteroids. H&E stain. *Figure reproduced from* Handbook of Toxicologic Pathology, *third ed., W. M. Haschek, C. G. Rousseaux and M. A. Wallig, eds. (2013) Academic Press, Fig. 58.7, p. 2400, with permission.*

(11α-deoxycortisol, an antiglucocorticoid) and spironolactone (an antimineralocorticoid) are two examples of peripherally acting hormone antagonists. Pharmacologically, many of these antagonists are beneficial for either diagnostic or therapeutic purposes.

Most chemicals affecting adrenal function appear to do so by altering steroidogenesis. A study of the effects of these chemicals on the histology and ultrastructure of adrenal cortical cells often can give insight into possible selection sites of inhibition of steroidogenesis. For example, chemicals causing increased lipid droplets may be involved in inhibiting the utilization of steroid precursors, including the conversion of cholesterol to pregnenolone. Chemicals that affect the fine structure of mitochondria and smooth endoplasmic reticulum would be expected to impair the activity of 11α-hydroxylase and 17α- and 2l-hydroxylases, respectively. The previously mentioned examples of impaired steroidogenesis would result in lesions found primarily in the ZR and ZF. However, atrophy of the ZG may reflect specific inhibition of aldosterone synthesis or secretion, either directly (inhibition of 18Q1-hydroxylation) or indirectly (inactivation of the renin–angiotensin system II), by chemicals such as spironolactone and captopril, respectively. The inhibition of steroidogenesis in some situations is nonspecific, as many hydroxylation reactions are affected, such as with carbon tetrachloride and cadmium intoxications.

PART 2: ADRENAL MEDULLA

STRUCTURE AND FUNCTION

Anatomy

The medulla constitutes approximately 10% of the volume of the adrenal gland. In the normal rodent gland and in most other species the medulla is sharply demarcated from surrounding cortex. The bulk of the medulla is composed of chromaffin cells, which are sites of synthesis and storage of catecholamines. In the rat and mouse, norepinephrine and epinephrine are stored in separate cell types that can be distinguished ultrastructurally after fixation in glutaraldehyde and postfixation in osmium tetroxide. Norepinephrine-containing granules appear highly electron-dense, whereas epinephrine granules are less dense with finely granular matrices. In immature rat adrenals, granules of varying densities may be found in the same cell types. Human adrenal medullary cells contain both norepinephrine and epinephrine within a single cell.

In addition to chromaffin cells, the adrenal medulla contains variable numbers of ganglion cells. A third cell type has also been described, and has been designated the small granule containing cell or small intensely fluorescent cell. These cells appear morphologically intermediate between chromaffin cells and ganglion cells. They possibly may function as interneurons.

Adrenal medullary cells also contain serotonin and histamine, but it has not been determined if these products are synthesized in situ or taken up from the circulation. A number of neuropeptides, including encephalin, neurotensin, and neuropeptide Y, are also present in rat chromaffin cells. Another peptide, adrenomedullin, has been shown to modulate function of the adrenal cortex; this peptide has hypotensive actions and as such can influence the renin–angiotensin–aldosterone axis functionally. Pharmacotoxicological effects of a compound on the

TABLE 20.3 Examples of Pharmacological Inhibition of Adrenal Steroid Biosynthesis, Secretion, or Function

Compound	Steroid or conversion site inhibited	Mechanism of action
Aminoglutethimide	Cholesterol to pregnenolone	Competitive inhibition of 20α-hydroxylase
o,p'-DDD	Cholesterol to pregnenolone; 11-deoxycortisol to cortisol	Partial 11β-hydroxylase inhibition
DMNM	Cholesterol to pregnenolone?	Unknown
Triparanol	Desmosterol (24-dehydrocholesterol) to cholesterol	Inhibited reduction of 24, 25 bond
Cyanoketone	δ^5-3β-Ol steroids to δ^4-3-oxo steroids	3β-Hydroxysteroid dehydrogenase inhibition
Trilostane	Δ^5-3β-Ol steroids to Δ^4-3-oxo steroids	3β-Hydroxysteroid dehydrogenase inhibition
Su-9055	Cortisol; aldosterone	Inhibition of 17α-hydroxylase; interference of oxidation at C18
Su-8000	Cortisol; aldosterone	Inhibition of 17α-hydroxylase; interference of oxidation at C18
Metapyrone	11-Deoxycortisol to cortisol	Inhibition of 11β-hydroxylase; inhibition of other hydroxylation reactions depending on species
SKF 12185	11-Deoxycortisol to cortisol	Inhibition of 11β-hydroxylase
Carbon tetrachloride	Nonspecific inhibition	Inhibition of cytochrome P450 portion of microsomal enzymes 17α- and 21-hydroxylases
Cadmium	Nonspecific inhibition	Inhibition of NADPH-cytochrome P450 reductase portion of 21-hydroxylase; other microsomal as well as mitochondrial hydroxylases may also be affected
Amphenone	Nonspecific inhibition	Inhibition of 20α-, 11β-, 17α-, and 21-hydroxylases?
Cortexolone (11-deoxycortisol)	Competitive binding to glucocorticoid receptors	Diminished translocation of glucocorticoid—receptor complex to nucleus of target cell
ROl-8307/heparinoids	Aldosterone	Inhibition of 18-oxidation
Spironolactone	Aldosterone	Competitive inhibition of peripheral receptor sites, resulting in sodium diuresis; possible direct effects on synthesis and secretion
Captopril	Aldosterone; inactivation of renin–angiotensin system	Inhibition of angiotensin-converting enzyme
Triaryl phosphate	Cholesterol ester to cholesterol	Neutral cholesterol ester hydrolase inhibitor
PD 132301-2	Esterification of cholesterol	Inhibition of acyl-CoA; cholesterol acyltransferase
2,3,7,8-Tetrachlorodibenzo-p-dioxin	Cholesterol side chain cleavage	Cytochrome P450s

Table modified from Handbook of Toxicologic Pathology, *second ed. W. M. Haschek, C. G. Rousseaux, and M. A. Wallig, eds. (2002) Academic Press, Vol. 2, Table I, p. 688.*

adrenal medulla can therefore have indirect effects on adrenocortical function.

Biochemistry and Physiology

The catecholamine biosynthetic pathways are in general well known. Tyrosine is acted on by tyrosine hydroxylase to produce L-DOPA (L-3,4-dihydroxyphenylalanine), which is converted to dopamine by aromatic L-amino acid (AA) (DOPA) decarboxylase. In turn, dopamine is acted on by dopamine β-hydroxylase to form norepinephrine, which is converted to epinephrine by phenylethanolamine-*N*-methyltransferase. Tyrosine hydroxylase is the rate-limiting step. The conversion of tyrosine into L-DOPA and dopamine occurs within the cytosol. Dopamine then enters the chromaffin granule, where it is converted to norepinephrine. Norepinephrine leaves the granule to be converted into epinephrine in the cytosol, and epinephrine then reenters the granule. Neuropeptides and chromogranin A proteins are synthesized in the rough endoplasmic reticulum and packaged into granules in the Golgi apparatus.

The role of innervation in regulating the functions of chromaffin cells has been studied extensively. During adult life, stresses such as insulin-induced hypoglycemia or reserpine-induced depletion of catecholamines produce a reflex increase in splanchnic nerve discharge, resulting in both catecholamine secretion and transsynaptic induction of catecholamine biosynthetic enzymes. These effects become apparent during the first week of life, following an increase in the number of nerve terminals in the adrenal medulla. Other environmental influences, including growth factors, extracellular matrix, and a variety of hormonal signals that generate cyclic AMP, may also regulate the function of chromaffin cells.

Physiological effects of adrenaline include an increase in systolic blood pressure and heart rate, diversion of blood to limb muscle beds/away from gut, a decrease in gut motility, bronchodilation, reduced mucus secretion, piloerection, and mydriasis. Noradrenaline only stimulates α and $\beta 1$ receptors so does not cause bronchodilation, which is a $\beta 2$ response, and although it also increases systolic (and diastolic) blood pressure leading to an increased mean arterial pressure, it antagonizes the effects of adrenaline on heart rate and decreases heart rate. Many of these physiological responses become pronounced in pathological conditions affecting the medulla, particularly pheochromocytoma, where excess catecholamine release typically results in hypertension and other distinctive symptoms.

TESTING FOR TOXICITY

Morphologic Evaluation

A variety of techniques may be used for the demonstration of catecholamines in tissue sections. The chromaffin reaction is the oxidation of catecholamines by potassium dichromate solution, and results in the formation of a brown-to-yellow pigment that may be seen both grossly and microscopically. The chromaffin reaction as performed traditionally possesses a very low-level of sensitivity, and should not be used for the routine demonstration of catecholamines. Similarly, both argentaffin and argyrophil reactions, which have been used extensively in the past for the demonstration of chromaffin cells, also possess low sensitivity and specificity. Fluorescence techniques using formaldehyde or glyoxylic acid can be used to demonstrate catecholamines at the cellular level. These aldehydes form highly fluorescent derivatives with catecholamines, which can be visualized by ultraviolet microscopy.

Immunohistochemistry provides an alternative approach for the localization of catecholamines in chromaffin cells and other cell types. Antibodies are now available that permit epinephrine- and norepinephrine-containing cells to be distinguished even in routinely fixed and embedded tissue samples. Tumor cells show positivity for general neuroendocrine markers, including Chromogranin A, synaptophysin, and CD56. Such antibodies are useful for differentiating pheochromocytoma from an adrenal cortical tumor. Catecholamine biosynthetic enzymes can also be demonstrated by immunohistochemical procedures (e.g., tyrosine hydroxylase) and can differentiate a paraganglioma from other neuroendocrine tumors.

RESPONSE TO INJURY

Characteristics of Proliferative Lesions

The adrenal medulla undergoes a series of proliferative changes ranging from diffuse hyperplasia to benign and malignant neoplasia. The latter neoplasms have the capacity to invade locally and to metastasize to distant sites. Diffuse hyperplasia, more common in the rat and strain-dependent, is characterized by symmetric expansion of the medulla with maintenance of the usual sharp demarcation of the cortex and the medulla. The medullary cell cords often are widened, but the ratio of norepinephrine to epinephrine cells is similar to that of normal glands.

Focal hyperplastic lesions are often juxtacortical but may occur within any area of the medulla. The small nodules of hyperplasia in general are not associated with compression of the adjacent medulla (Figure 20.20); however, the larger foci often are associated with medullary compression. Foci of adrenal medullary hyperplasia are typically composed of small cells with round to ovoid nuclei and scant cytoplasm.

Larger adrenal medullary proliferative lesions are accepted generally as pheochromocytomas. These lesions may be composed of relatively small cells similar to those found in smaller proliferative foci. Alternatively, they may be composed of larger cells or a mixture of small and large cells (Figure 20.21). Even in the larger medullary lesions, the chromaffin reaction often is equivocal but catecholamines may be demonstrated both biochemically and histochemically, and the cells generally are synaptophysin positive (Figure 20.22). Invasion of the capsule of the adrenal with or without distant metastases occurs in malignant pheochromocytomas. Detailed criteria for evaluation of proliferative lesions of adrenal medulla have been developed by INHAND for rats and mice and will be available at the time of publication of this chapter on

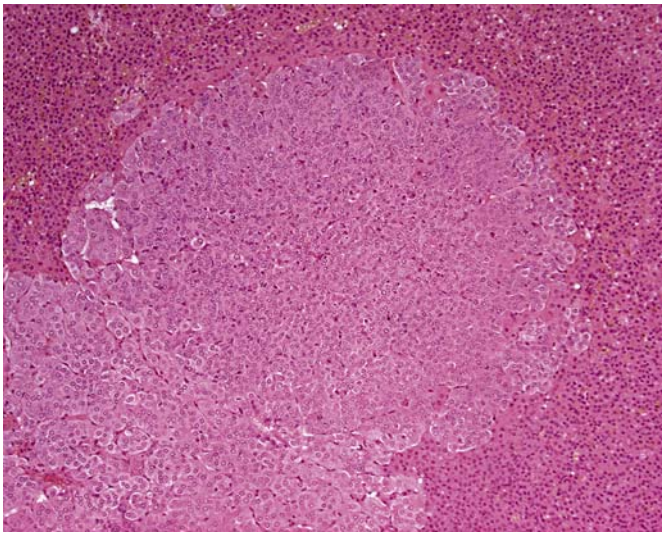

FIGURE 20.20 Focal medullary hyperplasia in Sprague-Dawley rat. H&E stain. *Figure reproduced from* Handbook of Toxicologic Pathology, *third ed., W. M. Haschek, C. G. Rousseaux and M. A. Wallig, eds. (2013) Academic Press, Fig. 58.25, p. 2419, with permission.*

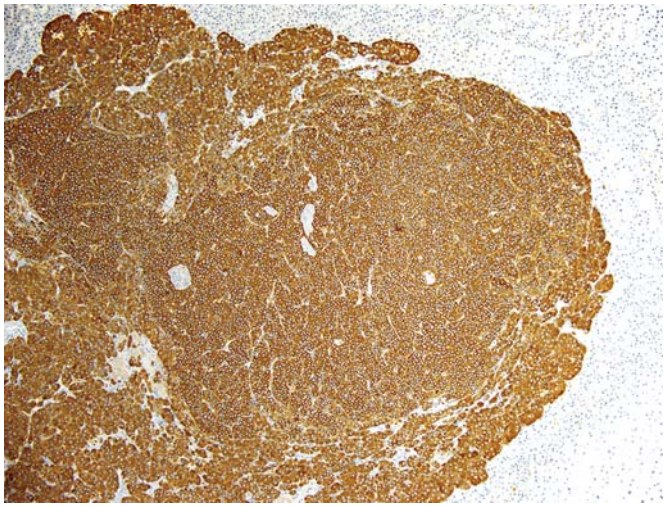

FIGURE 20.22 Pheochromocytoma in a Wistar rat. Synaptophysin immunohistochemistry. *Figure reproduced from* Handbook of Toxicologic Pathology, *third ed., W. M. Haschek, C. G. Rousseaux and M. A. Wallig, eds. (2013) Academic Press, Fig. 58.28, p. 2420, with permission.*

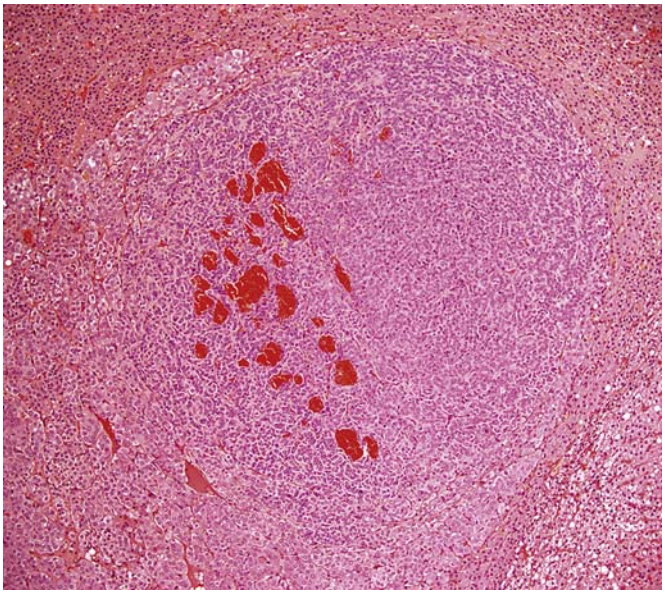

FIGURE 20.21 Pheochromocytoma in a Wistar rat. Note the dilated vascular spaces and compression of the adjacent adrenal cortical and medullary tissue. H&E stain. *Figure reproduced from* Handbook of Toxicologic Pathology, *third ed., W. M. Haschek, C. G. Rousseaux and M. A. Wallig, eds. (2013) Academic Press, Fig. 58.27, p. 2420, with permission.*

the Society of Toxicologic Pathology website (http://www.toxpath.org/inhand.asp).

In contrast to the high frequency of pheochromocytomas, neuroblastomas and ganglioneuromas occur infrequently in the adrenal medulla in rodents and chemical exposure linked to the formation of these tumors has rarely if ever been reported. Neuroblastomas develop as a centrally located expansive mass that compresses the surrounding cortex and are composed of small cells with round to ovoid hyperchromatic nuclei and scanty cytoplasm. Cells comprising neuroblastomas resemble lymphocytes and tend to form pseudorosettes. Ganglioneuromas usually are small benign tumors arising in the medulla and compressing the surrounding cortex. They are composed of multipolar sympathetic ganglion cells and neurofibrils with a prominent fibrous connective tissue stroma (Figure 20.23).

Occurrence of Proliferative Lesions

Proliferative lesions occur with high frequency in many strains of laboratory rats. The incidence of these lesions varies with strain, age, sex, diet, exposure to drugs, and a variety of environmental agents. Studies from the National Toxicology Program (NTP) historical data base of 2-year-old F344 rats have reported that the incidence of pheochromocytomas was 17% and 3.5% for males and females, respectively. Malignant pheochromocytomas were detected in 1% of males and 0.5% of females. In addition to F344 rats, other strains with high incidences of pheochromocytoma include Wistar, New England Deaconess Hospital, Long–Evans, and Sprague-Dawley.

Pheochromocytomas are considerably less common in Osborne-Mendel, Charles River, Holtzman, and WAG/Rij rats. Most studies have revealed a higher incidence in males than in females. Crossbreeding of animals with high and low frequencies of adrenal

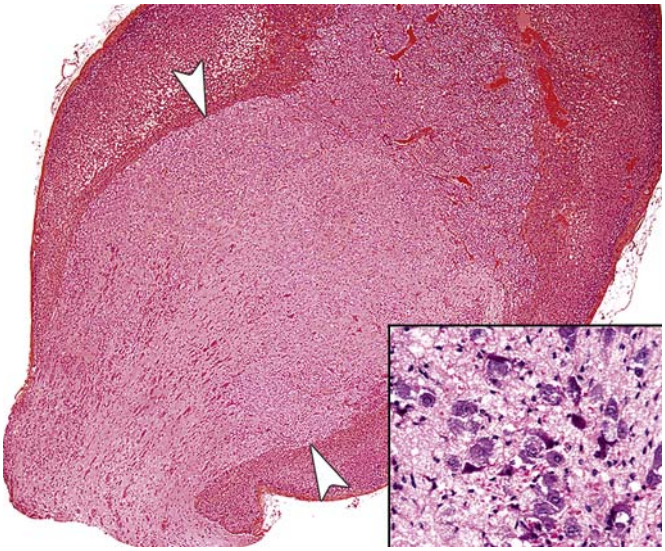

FIGURE 20.23 Ganglioneuroma in a Wistar rat arising from the adrenal medulla with penetration through the adrenal cortex and capsule (arrowheads). The inset demonstrates a higher magnification of ganglion cells (basophilic cells) and Schwann cells (eosinophilic stroma). H&E stain. *Figure reproduced from* Handbook of Toxicologic Pathology, *third ed., W. M. Haschek, C. G. Rousseaux and M. A. Wallig, eds. (2013) Academic Press, Fig. 58.29, p. 2421, with permission.*

medullary proliferative lesions results in first generation (F_1) animals with an intermediate tumor frequency. Pheochromocytomas are less common in the mouse than in most strains of rats.

There is a striking relationship between age and the frequency, size, and bilateral occurrence of adrenal medullary nodules in the rat. In the Long–Evans strain, medullary nodules have been found in less than 1% of animals under 12 months of age. The frequency increases to almost 20% in 2-year-old animals and to 40% in animals between 2 and 3 years of age. The mean tumor size increases progressively with age, as does the frequency of bilateral and multicentric occurrence.

MECHANISMS OF TOXICITY

Proliferative lesions of the medulla, particularly in the rat, have been reported to develop as a result of a variety of different mechanisms. Ionizing radiation has been linked in some studies to adrenal medullary tumors. This has been disputed by others, however.

Some data are available on the relationship of anterior pituitary hormones to the development of adrenal medullary lesions. For example, the long-term administration of growth hormone (GH) is associated with the development of pheochromocytomas as well as tumors in other sites. Some authors have suggested that prolactin (PRL)-secreting pituitary tumors, which occur commonly in many rat strains, may play a role in the development of proliferative medullary lesions. GH and PRL effects may be related because the two hormones are approximately 40% homologous; GH, when present in high concentrations in the circulation, can bind to PRL receptors. Estrogens and thyrotropin-releasing hormone (TRH) also would be expected to stimulate PRL release. Evidence for a role of pituitary hormones in the development of medullary lesions is provided by data suggesting that hypophysectomy eliminates the development of these lesions in a susceptible strain.

Both nicotine and reserpine have been implicated in the development of adrenal medullary proliferative lesions. Both agents may act by a shared mechanism, as nicotine directly stimulates nicotinic acetylcholine receptors, whereas reserpine causes a reflex increase in the activity of cholinergic nerve endings in the adrenal. A short dosing regimen of reserpine administration *in vivo* stimulates the proliferation of chromaffin cells in the adult rat, and the mechanism may involve a reflex increase in neurogenic stimulation via the splanchnic nerve. Treatment with antithyroid drugs such as propylthiouracil (PTU) also may affect chromaffin cells by a similar mechanism, as hypothyroid rats have increased sympathetic activity. An additional component of the action of reserpine occurs through the depletion of hypothalamic dopamine stores.

Several other drugs have been reported to increase the incidence of adrenal medullary proliferative lesions. These include zomepirac sodium (a nonsteroidal antiinflammatory drug), isoretinoin (a retinoid), and gemfibrozil (a hypolipidemic drug). However, the mechanisms responsible for the stimulation of adrenal medullary proliferation by these drugs are unknown.

Chlorinated compounds such as chlorinated paraffins, *P*-chloroaniline hydrochloride, 4-chloro-*M*-phenylenediamine, *P*-dichlorobenzene, hexachloroethane, 4,4′-methylenedianiline dihydrochloride, pentochlorophenol, and 1,1,2-trichloroethane comprise almost half the compounds on the NTP list for chemicals producing treatment-related pheochromocytoma.

Environmental and dietary factors may be more important than genetic factors as determinants of the incidence of adrenal medullary proliferative disorders in rats. The incidence of adrenal medullary lesions can be reduced by lowering the carbohydrate content of the diet. Sugar alcohols, including mannitol, sorbitol, xylitol, and lacitol, have been reported to increase the incidence of all types of proliferative lesions of the adrenal medulla. In view of the fact that sugar alcohols are not mutagenic, it is likely that the increased incidence of adrenal medullary lesions represents a response to metabolic change.

Vitamin D is the most potent *in vivo* stimulus yet identified for chromaffin cell proliferation in the adrenal medulla. Vitamin D_3 (5000, 10,000, or 20,000 IU/kg/day) increases proliferative indices (e.g., BrdU) substantially over the long term in the adrenal medullas of F344 rats. At higher doses, there are focal medullary proliferative lesions. The proliferative lesions are usually multicentric, bilateral, peripheral in location in the medulla and appear to represent a morphologic continuum rather than separate entities.

It has been suggested that at least three dietary factors may lead to hypercalcemia and increased incidence of adrenal medullary proliferative lesions. These are excessive intake of food associated with feeding *ad libitum*; excessive intake of Ca^{2+} and phosphorus, as commercial diets contain two to three times more Ca^{2+} and phosphorus than needed by young rats; and excessive intake of other food components (e.g., vitamin D and poorly absorbable carbohydrates), which predispose to increased Ca^{2+} absorption.

PART 3: PITUITARY GLAND

STRUCTURE AND FUNCTION

Anatomy

The pituitary gland (hypophysis) may be divided into two major compartments: (1) the adenohypophysis (anterior lobe), composed of the pars distalis, pars tuberalis, and pars intermedia and (2) the neurohypophysis (posterior lobe), which includes the pars nervosa or infundibular process, infundibulum, infundibular stem, and tuber cinereum. In most animals and in human fetuses, the thin cellular zone between the adenohypophysis and neurohypophysis is referred to as the pars intermedia or intermediate lobe.

The pituitary lies within the sella turcica of the sphenoid bone. The gland receives its blood supply via the posterior and anterior hypophyseal arteries, which originate from the internal carotid arteries. Arteriolar branches penetrate the pituitary stalk, lose their muscular coat, and form a capillary plexus near the median eminence. These vessels drain into the hypophyseal portal veins, which supply the adenohypophysis. This hypothalamic–hypophyseal portal system transports hypothalamic-releasing and release-inhibiting hormones directly to the adenohypophysis for interactions with their specific target cells.

Functional Cytology

The neurohypophysis is joined to the hypothalamus via the infundibular stalk and is composed of densely packed bundles of nonmyelinated axons and capillaries that are supported by modified glial cells or pituicytes. The capillaries in the pars nervosa are termination sites for unmyelinated axons, which originate from the hypothalamic neurosecretory neurons. Axons that arise from neurons in the infundibular and tuberal regions (tuberohypophyseal tract) terminate predominantly in the median eminence. Axons arising from supraoptic and paraventricular nuclei (supraopticohypophyseal tract) terminate in the pars nervosa. Both oxytocin and vasopressin (antidiuretic hormone) are synthesized in supraoptic and paraventricular nuclei as large precursor molecules, which contain both active hormones and their associated neurophysins. As the biosynthetic precursor molecules travel along the axons in secretion granules from the neurosecretory neurons, the precursors are cleaved into the active hormones and their respective neurophysins. These secretory products can be detected immunocytochemically.

The adenohypophysis represents the largest portion of the pituitary gland. The cells within this lobe are responsible for the synthesis of at least six major hormones: growth hormone (GH), prolactin (PRL), ACTH, follicle-stimulating hormone (FSH), luteinizing hormone (LH), and thyroid-stimulating hormone (TSH) or thyrotropin. With H&E staining, cells of the anterior lobe have been divided into acidophils, basophils, and chromophobes, constituting approximately 40%, 10%, and 50% of the total cell population, respectively.

The GH-secreting acidophils (somatotrophs) constitute approximately 50% of the total cell population in the pars distalis. These cells are distributed throughout the adenohypophysis and are generally round to ovoid in shape. The GH-producing cells stain positively with orange C and eosin. Although most of the GH-synthesizing cells correspond to acidophils, some may be chromophobic, as they are in an actively synthesizing phase of the secretory cycle.

PRL-secreting acidophils (luteotrophs) compose 15%–25% of the total cell population. They tend to be concentrated in the dorsocephalic region of the adenohypophysis. Immunoperoxidase stains reveal that PRL cells have angular cell processes that may be closely applied to the cytoplasm of gonadotrophs. PRL cells, stain positively with erythrosine and carmoisine. However, the sparsely granulated cells with smaller granules often fail to stain with these dyes and appear chromophobic. Pregnancy and lactation are associated with hyperplasia of PRL-secreting cells. These so called "pregnancy cells" are chromophobic by routine staining techniques.

ACTH-producing cells (corticotrophs) are round to ovoid, chromophobic or lightly basophilic (in humans), and stain weakly positive with periodic acid-Schiff (PAS) stain. These cells are widely

distributed within the pars distalis and form the bulk of the pars intermedia. Crooke's hyaline change refers to the intracellular accumulation of an eosinophilic homogeneous material within the cytoplasm of these cells. Immunohistochemical staining reveals that this material represents a keratin-like moiety, which accumulates in conditions associated with glucocorticoid hormone excess.

Thyrotropin-producing (TSH) basophils or thyrotrophs account for about 5% of the cells of the adenohypophysis. These cells tend to occur in small clusters within the pars distalis and have a stellate to polygonal shape. They may be basophilic or chromophobic and are also PAS-positive. "Thyroidectomy cells" are enlarged and vacuolated TSH cells. Large PAS-positive lipofuscin granules often are found within these cells. Conditions, which lead to hypofunction of the thyroid, such as due thyroidectomy, administration of goitrogenic drugs or chemicals that inhibit the biosynthesis of triiodothyronine (T_3) and thyroxine (T_4) or exposure chemicals that increase the hepatic degradation of thyroid hormones, result in the development of thyroidectomy cells in the pituitary gland. Hypertrophy and hyperplasia of TSH cells under these conditions are due to a lack of negative feedback by T_3 and, to a lesser extent, T_4 on the hypothalamus and thyrotrophs.

Gonadotropin-producing basophils or gonadotrophs are relatively large round to oval cells, which account for approximately 10% of the cells in the pars distalis. These cells are responsible for the production of FSH and LH. They tend to be concentrated in the dorsocephalic region of the pars distalis. Immunoperoxidase stains have revealed that some cells contain both FSH and LH, whereas others contain only LH or FSH.

Gonadotroph cells undergo a series of changes following castration, resulting in the formation of "gonadectomy cells." As a result of the lack of negative feedback by gonadal steroids, gonadotrophs are actively stimulated to synthesize and secrete FSH and LH. Gonadotrophs undergo hypertrophy, and the cytoplasm becomes vacuolated due to distention of endoplasmic reticulum with finely granular material in response to long-term stimulation by gonadotropin-releasing hormone (GnRH) from the hypothalamus. In some cells, a single large vacuole occupies most of the cytoplasm, producing cells with a "signet-ring" appearance.

In addition to specific hormone-secreting cells, a population of supporting cells is also present in the adenohypophysis. These cells have been referred to as stellate (follicular) cells and can be stained selectively with antibodies to S-100 protein. Stellate cells typically have elongate processes and prominent cytoplasmic filaments. These cells appear to provide a phagocytic or supportive function in addition to producing a colloid-like material.

The hypothalamus serves as the major regulator of the adenohypophysis. Each cell type within the adenohypophysis is under the control of a corresponding releasing hormone that is synthesized within nerve cell bodies of the hypothalamus. The releasing hormones are transported via axonal processes to the median eminence, where they are released into capillaries and are carried by the hypophyseal portal system to trophic hormone-producing cells in the adenohypophysis. Specific releasing factors have been identified for TSH, FSH, LH, ACTH, and GH. PRL secretion is stimulated by a number of factors, the most important of which appears to be TRH. TRH stimulates the release of PRL with many of the same dose–response characteristics as the stimulation of TSH release.

Multiple influences contribute to the control of adenohypophyseal hormone secretion. Dopamine serves as the major PRL inhibitory factor. This amine suppresses virtually all aspects of PRL secretion and also inhibits cell division and DNA synthesis of this cell type. Dopamine also suppresses ACTH production by corticotrophs in the pars intermedia of some species. A second hypothalamic release-inhibiting hormone is somatostatin (somatotropin release-inhibiting hormone, SRIH). This tetradecapeptide inhibits the secretion of both GH and TSH. In some situations, SRIH also inhibits the secretion of PRL and ACTH. The control of pituitary hormone secretion is also affected by negative feedback loops resulting from the interaction of end-organ hormones, adenohypophyseal hormones, and corresponding hypothalamic-releasing and release-inhibiting hormones.

EVALUATION OF TOXICITY

Immunohistochemical evaluation is an important approach for the functional and morphological analysis of normal and abnormal pituitary glands. Hormones of the various types of adenohypophyseal cells in the rodent gland have crossreactions with antibodies to corresponding human pituitary hormones. However, higher levels of specificity may be achieved with the use of antibodies to the rat pituitary hormones. For most routine toxicological studies, formalin fixation provides adequate preservation of the pituitary hormones for immunohistochemical studies; however, some authors have recommended Bouin's fixation for immunohistochemical staining of the pituitary because this fixative produces more precise localization of the hormones at the light microscopic level. In addition, in situ hybridization techniques have been employed for the identification of messenger RNAs encoding the hormonal peptides.

RESPONSE TO INJURY

Nonneoplastic Lesions

The term "cystoid degeneration" has been used to describe foci of cell loss in the adenohypophysis. Newer nomenclature, developed by the INHAND project (http://www.toxpath.org/inhand.asp), simply refer to these lesions as "cysts," lined by cuboidal or pseudostratified columnar epithelium, or as "pseudocysts," spaces not lined by epithelium. These cystic lesions often measure 50–150 mm in diameter. The edges of these foci are composed of cell types typical of the pars distalis. Occasional cell debris may be found within areas of cystoid degeneration, together with granular eosinophilic material. Occasionally the cysts represent remnants of Rathke's pouch that normally regresses during embryogenesis. Cystic changes may also occur in hyperplastic foci and in neoplasms of the pituitary. The frequency of cystoid degeneration is increased by feeding diets containing diethylstilbestrol to female C3H HeN (MMTV+ mice).

Neoplastic Lesions

Craniopharyngioma

The craniopharyngioma is an uncommon, naturally occurring neoplasm in rodents. The tumor may originate from the craniopharyngeal duct epithelium of Rathke's pouch and is composed of nests and cords of squamous cells with cysts lined by cuboidal or squamous cells that may be focally mineralized.

Pituicytoma

Primary neoplasms of the pars nervosa are extremely uncommon. The tumors that have been reported to occur at this site have been designated as pituicytomas. These tumors are composed of small, closely packed spindle cells arranged in cords and bundles. Most pituicytomas are quite small, but larger tumors may extend into the adenohypophysis and into the adjacent brain tissue. Metastases have not been reported.

Proliferative Lesions of the Adenohypophysis

The histopathological separation among nodular hyperplasia, adenoma, and carcinoma often is more difficult in endocrine glands, such as the pituitary, than in most organs of the body. However, criteria for their separation should be established and applied in a uniform manner. For trophic hormone-secreting cells of the adenohypophysis, there appears to be a continuous spectrum of proliferative lesions between diffuse or focal hyperplasia and adenomas. Prolonged stimulation of pituitary secretory cells predisposes to the subsequent development of a higher than expected incidence of tumors.

Focal ("nodular") hyperplasia usually appears as multiple small areas that are well demarcated but not encapsulated. Cells making up an area of focal hyperplasia in the adenohypophysis closely resemble the cells of origin; however, the cytoplasmic area may be slightly enlarged and the nucleus more hyperchromatic than in normal cells.

Adenomas in rodents usually are solitary nodules that are larger than the multiple areas of focal hyperplasia, with diameters that cover at least half the width of the normal pituitary. They are sharply demarcated from the adjacent normal pituitary glandular parenchyma, and there is a thin, partial to complete, fibrous capsule. Adjacent parenchyma is compressed in at least one quadrant, depending on the size of the adenoma. Cells composing an adenoma may closely resemble the cells of origin morphologically and in their architectural pattern of arrangement; however, there are often histological differences such as multiple layers of cells lining follicles and vascular trabeculae or solid clusters of secretory cells subdivided into packets by a fine reticular stroma.

Carcinomas usually are larger than adenomas in the pituitary and generally result in a macroscopically detectable enlargement. Histopathological features suggestive of malignancy include invasion into adjacent structures (e.g., dura mater, sphenoid bone), formation of tumor cell thrombi within vessels, and, particularly, the establishment of metastases at distant sites. The growth of neoplastic cells subendothelially in highly vascular benign tumors should not be mistaken for vascular invasion. Malignant endocrine cells often are more pleomorphic (including oval or spindle shaped) than normal, but nuclear and cellular pleomorphism is not a consistent criterion to distinguish adenoma from carcinoma in rodents. Mitotic figures may be frequent in malignant cells; however, the degree of background stimulation of the endocrine gland must be taken into account.

Many neoplasms arising in the pituitary are functionally active, secrete an excessive amount of hormone either continuously or episodically and cause clinical syndromes of hormone excess. Quantitation of hormone levels in the serum of plasma in the basal or stimulated state and/or the measurement of the hormone or metabolites in the urine over a 24-hour period of excretion is essential to confirm that an endocrine tumor is functional and releasing hormone at an abnormally elevated rate. Morphologically, an endocrine tumor often can be interpreted as endocrinologically active if the rim of normal tissue around the tumor undergoes atrophy due to negative feedback

inhibition by the elevated target hormone levels. The nonneoplastic secretory cells, especially their cytoplasm, become smaller than normal, and eventually the cells disappear. Functional pituitary neoplasms secreting an excess of a particular trophic hormone (e.g., ACTH or PRL) are associated with striking hypertrophy and hyperplasia of target cells in the adrenal cortex in chronic rodent studies.

Adenoma of Pars Intermedia

Adenomas of the pars intermedia are uncommon in the rat and mouse but common in the horse and dog. These lesions may vary considerably in size. Larger adenomas may compress the adenohypophysis and neurohypophysis, whereas smaller lesions may be of microscopic dimensions. These tumors are nonencapsulated but do compress adjacent normal tissue. The cells often have faintly basophilic cytoplasm with round to ovoid nuclei. Tumor cells in pigmented rats (e.g., Long–Evans) often contain melanin pigment similar to that found in the normal intermediate lobe.

Pituitary Carcinoma

Pituitary carcinomas are uncommon neoplasms compared with adenomas. They usually are endocrinologically inactive but can cause significant functional disturbances by destruction of the pars distalis and neurohypophyseal system, leading to adult-onset panhypopituitarism and diabetes insipidus. Carcinomas are large and invade extensively into the overlying brain, along the ventral aspect of the cranial cavity incorporating cranial nerves (II, III, IV), and locally into the adjacent sphenoid bone of the sella turcica, where they may cause osteolysis. Metastases occur infrequently to regional lymph nodes or to distant sites such as the spleen or liver. Carcinomas are highly cellular and often have large areas of hemorrhage and necrosis. Giant cells, nuclear pleomorphism, and mitotic figures are encountered more frequently than in adenomas.

Functional Characteristics of Pituitary Adenomas

The vast majority of pituitary adenomas in humans and rodents have been described as chromophobic in type; however, many of these tumors have been found to stain for PRL by immunohistochemistry. Of the PRL-producing tumors, most are sparsely granulated with low levels of PRL immunoreactivity by immunohistochemistry. Diffuse hyperplasia of the PRL cells has been noted adjacent to some adenomas.

The development of tumors and hyperplasia of PRL-secreting cells is accompanied by increasing serum levels of PRL. Occasionally, PRL cells within adenomas may be admixed with FSH/LH-, TSH-, or ACTH-positive cells. Infrequent adenomas composed of populations of ACTH or FSH/LH cells have also been reported. Pituitary nodules (focal hyperplasia and adenomas) composed primarily of gonadotrophs occur commonly in male rats of the Lobund-Wistar strain.

Functional (endocrinologically active) neoplasms arising in the pituitary gland of dogs most likely are derived from corticotroph (ACTH-secreting) cells in either the pars distalis or the pars intermedia. These neoplasms cause a clinical syndrome of cortisol excess (Cushing's disease). The pituitary gland is consistently enlarged. Because the diaphragma sella is incomplete in the dog, the line of least resistance favors dorsal expansion of the gradually enlarging pituitary mass, with extension into the overlying brain leading to eventual compression or replacement of the hypothalamus and possible extension into the thalamus. Pituitary corticotroph adenomas are composed of well-differentiated, large or small, chromophobic cells supported by fine connective tissue septa. The cytoplasm of the neoplastic cells stains immunocytochemically for ACTH and melanocyte-stimulating hormone (MSH). Hormone-containing secretory granules can be demonstrated by electron microscopy. Bilateral enlargement of the adrenal glands occurs in dogs with functional corticotroph adenomas due to cortical hypertrophy/hyperplasia, primarily of the ZF and ZR.

Spontaneous Pituitary Adenomas

The high frequency of spontaneous pituitary adenomas in laboratory rats is a well-recognized phenomenon that must be considered in any long-term toxicological study. The incidence of these tumors is determined by many factors, including strain, age, sex, reproductive status, and diet. Studies from the NTP historical data base of 2-year-old F344 rats have shown that the incidence of pituitary adenomas was 21.7% and 44% for males and females, respectively. Corresponding figures for carcinomas arising in the adenohypophysis are 2.4% and 3.5% for males and females, respectively. Studies from 56 NTP rat studies completed between 1983 and 1987 revealed that the incidence of adenomas was 28.6% for males and 43.3% for females, while a diagnosis of pituitary hyperplasia was made in 10.4% of males and 10.3% of females. It should also be noted that numerous studies have called attention to the striking degree of strain variation in the incidence of pituitary tumors in rats, reported to range from 10% to more than 90%.

There is a striking relationship between age and development of pituitary adenomas. These lesions are uncommon in animals less than 1 year of age. When present in this age group, they are generally small and are present as single lesions. Pituitary adenomas are most common in rats at 2 years or more of age and tend to be larger and more frequently multicentric than in younger animals.

Rapid body growth rates and high levels of conversion of feed to body mass in early life or high protein intake in early adult life, predispose any strain of rat to the development of pituitary adenomas. In rats fed a low-protein diet (less than 12.7% crude protein), the overall tumor incidence, incidence of fatal tumors, number of multifocal tumors, and degree of cellular atypia within tumors are significantly lower than in rats fed a standard diet.

MECHANISMS OF TOXICITY

Induction of Pituitary Tumors

Pituitary tumors can be induced readily by sustained uncompensated hormonal derangements leading to increased synthesis and secretion of pituitary hormones. In such a situation, the absence of feedback inhibition of the pituitary cell may lead to its unrestrained proliferation. This effect can be potentiated by the concurrent administration of ionizing radiation or chemical carcinogens.

Hyperplasia of the thyrotrophs occurs concurrently with cellular hypertrophy as a consequence of the absence of normal inhibitory feedback mechanisms. Foci of hyperplasia may progress to the formation of adenomas. The role of gonadectomy in pituitary tumor induction has been studied most intensively in mice. Pituitary tumors induced by gonadectomy in this species are markedly strain-dependent, and they may contain FSH, LH, or both.

The administration of estrogens is a reproducible method for inducing pituitary tumors in some experimental animals. The effect of exogenous estrogen on the rat pituitary includes stimulation of PRL secretion and the induction of PRL-secreting tumors. The administration of estrogens in susceptible strains results in increased serum PRL levels, increased numbers of PRL cells within the pituitary, and increased mitotic activity. There is considerable variation in the inductibility of pituitary tumors by estrogens in different rat strains. For example, F344 rats are more sensitive than Holtzman rats. The precise mechanisms of estrogen-induced PRL tumors are unknown.

The tumorigenic action of estrogen may not be due exclusively to its effect on the hypothalamus because estrogen can produce prolactinomas in pituitaries grafted beneath the renal capsule. Dopamine agonists, including lisuride and bromocriptine, antagonize the direct stimulatory effects of estrogens on the PRL cells. Other agents, including caffeine, have also been implicated in the development of pituitary adenomas. Additionally, the administration of *N*-methylnitrosourea is also associated with the development of pituitary adenomas in Wistar rats. The neuroleptic agent sulpiride has been reported to cause the release of PRL from the anterior pituitary in the rat and to stimulate DNA replication. The administration of clomiphene prevents the stimulation of DNA synthesis produced by sulpiride but does not affect PRL release from the gland. These findings have suggested that the intracellular PRL content of the anterior pituitary plays a role in the regulation of DNA synthesis through a mechanism mediated by estrogens.

Administration of salmon calcitonin for 1 year to Sprague-Dawley and Fisher 344 rats has been associated with an increased incidence of pituitary gland hyperplasia and adenomas. The pituitary tumors also produce the common α subunit of the glycoprotein hormones (LH, FSH, and TSH). This type of tumor has been shown to comprise a significant fraction of pituitary tumors in humans.

Studies have not determined whether the effects of calcitonin are direct or indirect. A striking feature of calcitonin-induced pituitary tumors and elevated serum α-subunit levels is the predilection for male compared with female rats. The basis for sex- and species-specific effects of calcitonin has not been determined. The relevance of the effects of calcitonin in the rat pituitary gland to human pathophysiology is uncertain.

Etiology and Pathogenesis of Spontaneous Pituitary Adenomas

Numerous hypotheses have been invoked to explain the high incidence of pituitary adenomas in certain inbred rat strains. Both hereditary factors and the levels of circulating sex steroids have been suggested as important etiological mechanisms. The hypothalamus has also been incriminated in the development of these tumors. Age-related hypothalamic changes may result in the diminished activity of dopamine, the major PRL inhibitory factor. In this regard, studies of aging male rats have demonstrated abnormal concentrations and metabolism of hypothalamic dopamine, norepinephrine, and serotonin and decreased hypothalamic PRL inhibitory activities. Supporting a role for dopamine in suppression of neoplastic development, dopamine has been found to suppress PRL secretion. The dopamine agonist, bromocriptine, has been

reported to decrease serum PRL levels in female Long–Evans rats with spontaneously developing prolactinomas when compared to untreated age-matched controls, and the mean pituitary weight was reduced in rats treated for 44 days with bromocriptine compared to controls.

PART 4: THYROID C CELLS

STRUCTURE AND FUNCTION

C cells, or parafollicular cells, of the thyroid gland, named after their major secretory product (calcitonin), are located within thyroid follicles between the basal aspects of the follicular cells and the basement membrane of the follicle. They also are present in parafollicular positions. In addition to calcitonin, C cells contain a variety of other peptides, including somatostatin and bombesin, and they are also positive for a wide variety of generic neuroendocrine markers, including chromogranin proteins and synaptophysin. In most mammalian species, C cells are concentrated within the central regions of the lobes, being most prominent at the levels of the parathyroid glands. By light microscopy C cells often have a clear or light appearance, but silver-positive cytoplasmic granules can be demonstrated by argyrophilic staining. At the ultrastructural level, the cells contain variable numbers of membrane-bound secretory granules in which calcitonin is stored prior to its release into the circulation. Although the secretory granules have considerable heterogeneity in terms of size and density, all of the granules contain immunoreactive calcitonin.

Calcitonin is a 32-AA peptide that is derived from a 141-AA precursor (procalcitonin). Ionized calcium (Ca^{2+}) in plasma and extracellular fluids is the major physiologic stimulus for the secretion of calcitonin. The cell membrane Ca^{2+}-sensing receptor, present in both parathyroid cells and C cells, contributes to the regulation of calcitonin secretion. Calcitonin interacts with specific receptors in target cells, principally in bone and kidney. Calcitonin inhibits osteoclast activity in bone, renal tubular resorption of Ca^{2+}, and Ca^{2+} absorption by the intestines. Calcitonin secretion is increased in response to a high Ca^{2+} meal, often before a significant rise in plasma Ca^{2+} levels can be detected. An oral Ca^{2+} load stimulates the secretion of gastrin, cholecystokinin, and glucagon, and these hormones also serve as calcitonin secretagogues. Calcitonin also protects against Ca^{2+} loss from the skeleton during periods of Ca^{2+} mobilization, such as growth, pregnancy, and lactation.

RESPONSE TO INJURY

Proliferative Lesions of C Cells

Hyperplasia of C cells is not usually associated with any macroscopic abnormality in the thyroid gland. Two types of hyperplasia are evident microscopically: diffuse (Figure 20.24) and focal (nodular) (Figure 20.25). In diffuse hyperplasia, the numbers of C cells are increased throughout the thyroid lobes, to a point where they may be more numerous than follicular cells. Diffuse hyperplasia is typically associated with a physiological or pathologic response to chronic stimulation (e.g., persistent hypercalcemia) whereas nodular hyperplasia is generally considered to be a preneoplastic lesion. The relationship of C cells to follicular cells in cases of diffuse hyperplasia is similar to that noted in juvenile thyroid glands. Focal (nodular) hyperplasia of C cells often occurs concurrently with diffuse hyperplasia in the thyroid glands of rats. The follicles become progressively enlarged with increasing numbers of C cells. While normal and hyperplastic C cells are uniformly positive for calcitonin, relatively few also express somatostatin.

C cells are more numerous in rats (compared to mice) and increase in number with age. C cells in rats can be identified in routine H&E-stained tissue sections. Normal and diffuse hyperplasia of C cells in mice typically requires immunohistochemistry for calcitonin to identify the C cells.

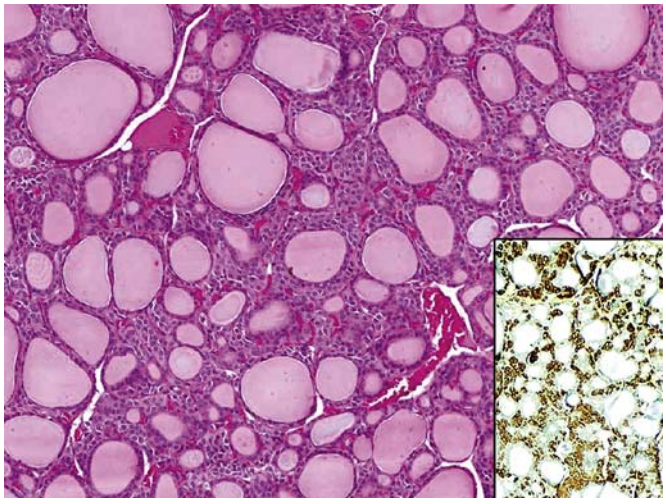

FIGURE 20.24 Diffuse C-cell hyperplasia (rat). There is a diffuse increase in C cells throughout the thyroid lobe (H&E). Inset: Immunostaining for calcitonin. *Figure reproduced from* Handbook of Toxicologic Pathology, *third ed., W. M. Haschek, C. G. Rousseaux and M. A. Wallig, eds. (2013) Academic Press, Fig. 58.34, p. 2433, with permission.*

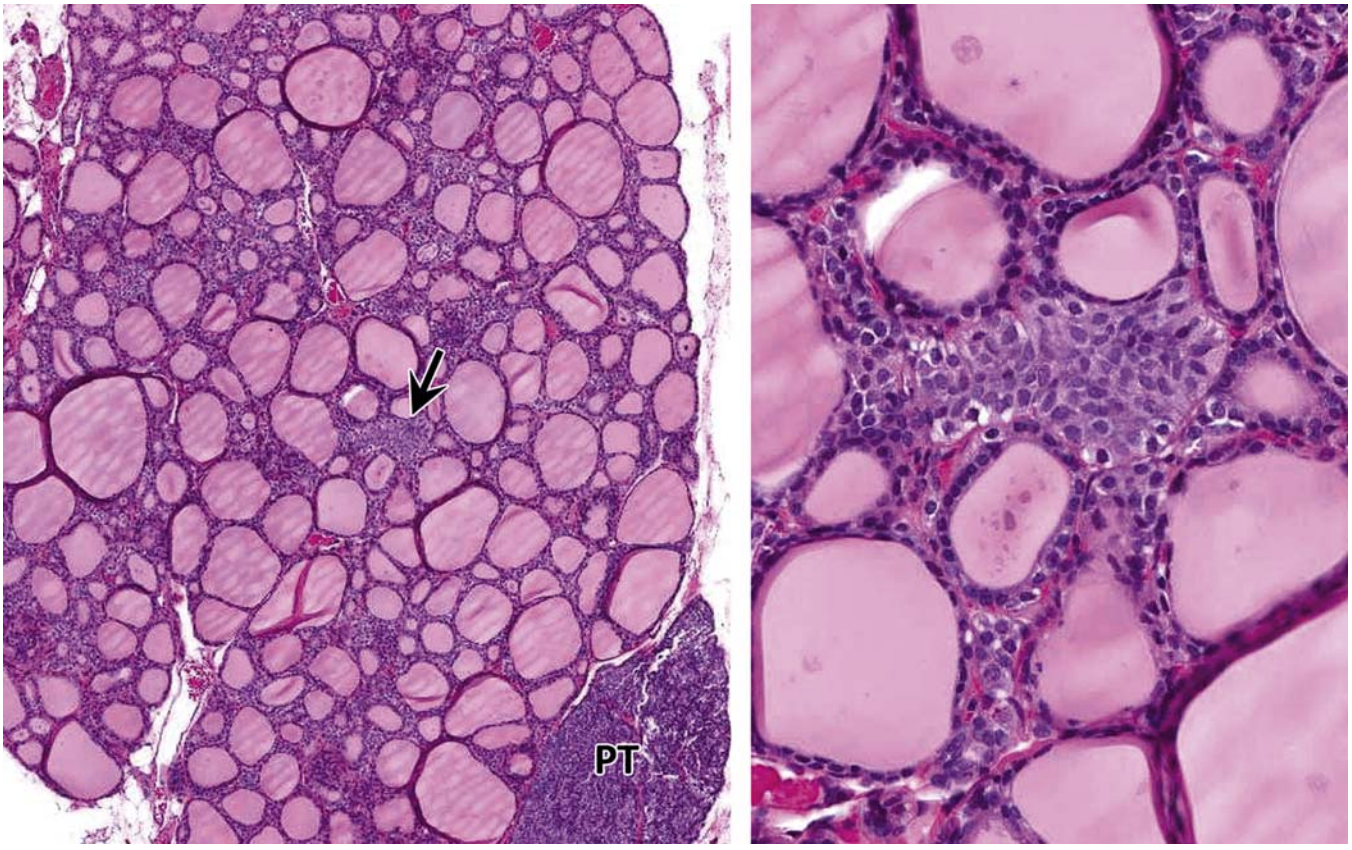

FIGURE 20.25 Diffuse and focal (nodular) C-cell hyperplasia (rat). Low-power view (left) of diffuse and focal (arrow) hyperplasia in the thyroid lobe; PT, parathyroid gland. Higher magnification (right) of focal hyperplasia. A single follicle in this field is expanded by proliferating C cells. H&E stain. *Figure reproduced from* Handbook of Toxicologic Pathology*, third ed., W. M. Haschek, C. G. Rousseaux and M. A. Wallig, eds. (2013) Academic Press, Fig. 58.35, p. 2434, with permission.*

At later stages of development, hyperplastic C-cell "follicles" often assume irregular, twisted, and elongate configurations. Occasional colloid-filled follicles are entrapped among the proliferating C cells. The histological distinction between focal hyperplasia and adenoma of C cells is often difficult to define. Typically, focal (nodular) hyperplasia is characterized by lesions measuring less than five average colloid-containing follicles without compression of the adjacent follicular cells; in addition, there is no compression of adjacent follicles. Cell boundaries are often indistinct.

C-cell adenomas are discrete expansive masses, or nodules of C cells larger than five average colloid-containing follicles (Figure 20.26). Adenomas are either well circumscribed, or partially encapsulated with varying degrees of compression of adjacent thyroid follicles. C cells have relatively abundant cytoplasm that is faintly eosinophilic with a round-to-ovoid nucleus with finely stippled chromatin. Adenomas may be subdivided into small cell groups by fine connective tissue septa and capillaries.

C-cell (medullary) carcinomas are characterized by infiltration of C cells into the adjacent thyroid stroma, extracapsular tissues, and lymphovascular channels (Figure 20.27). Areas of hemorrhage and necrosis may be particularly prominent in larger tumors. The component C cells are often more pleomorphic (cuboidal, oval, or spindle shaped) than those comprising focal hyperplasia or C-cell adenomas. Mitotic activity may be prominent in some cases, and foci of necrosis may be evident. Occasional tumors may contain large cells that may bear a striking resemblance to ganglion cells. Most C-cell carcinoma cells and some C-cell adenoma cells express somatostatin in addition to calcitonin. Amyloid deposits may be present between tumor cells, around blood vessels, and in the interstitium.

Spontaneous C-Cell Lesions

C-cell tumors occur spontaneously in many rat strains. There is a striking correlation between the age of the animals and the extent of C-cell abnormalities.

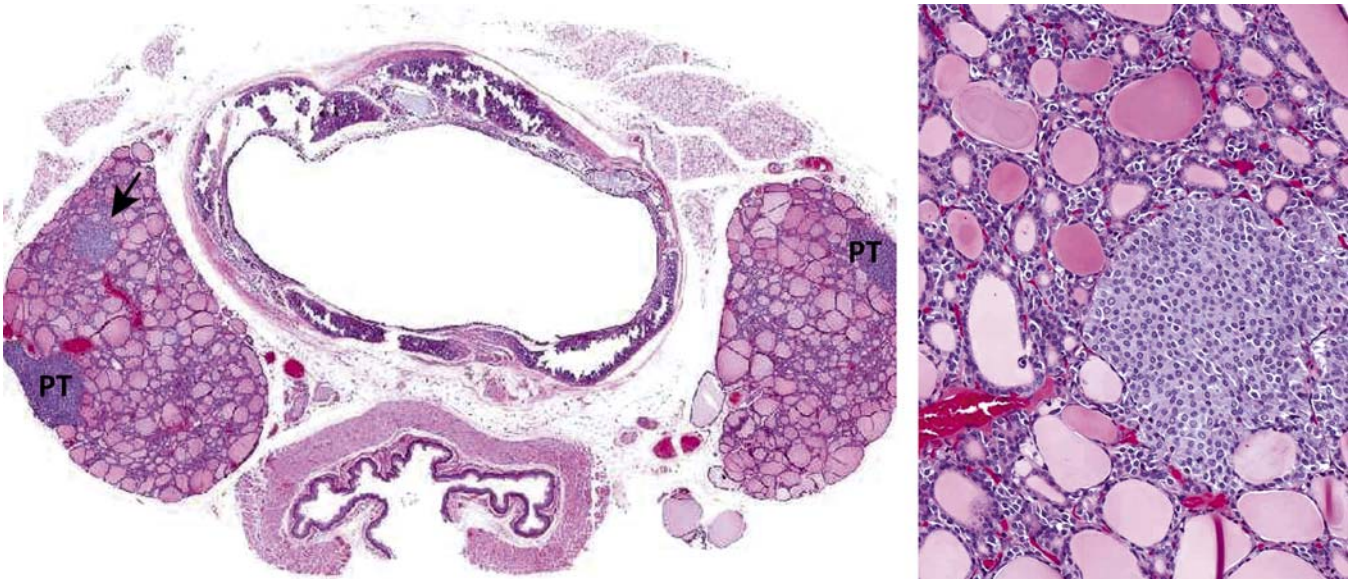

FIGURE 20.26 C-cell adenoma (rat). Low magnification of small C-cell adenoma (arrow) (left); PT, parathyroid gland. Higher magnification of C-cell adenoma (right) with a few follicles entrapped at its periphery. H&E stain. *Figure reproduced from* Handbook of Toxicologic Pathology, *third ed., W. M. Haschek, C. G. Rousseaux and M. A. Wallig, eds. (2013) Academic Press, Fig. 58.36, p. 2434, with permission.*

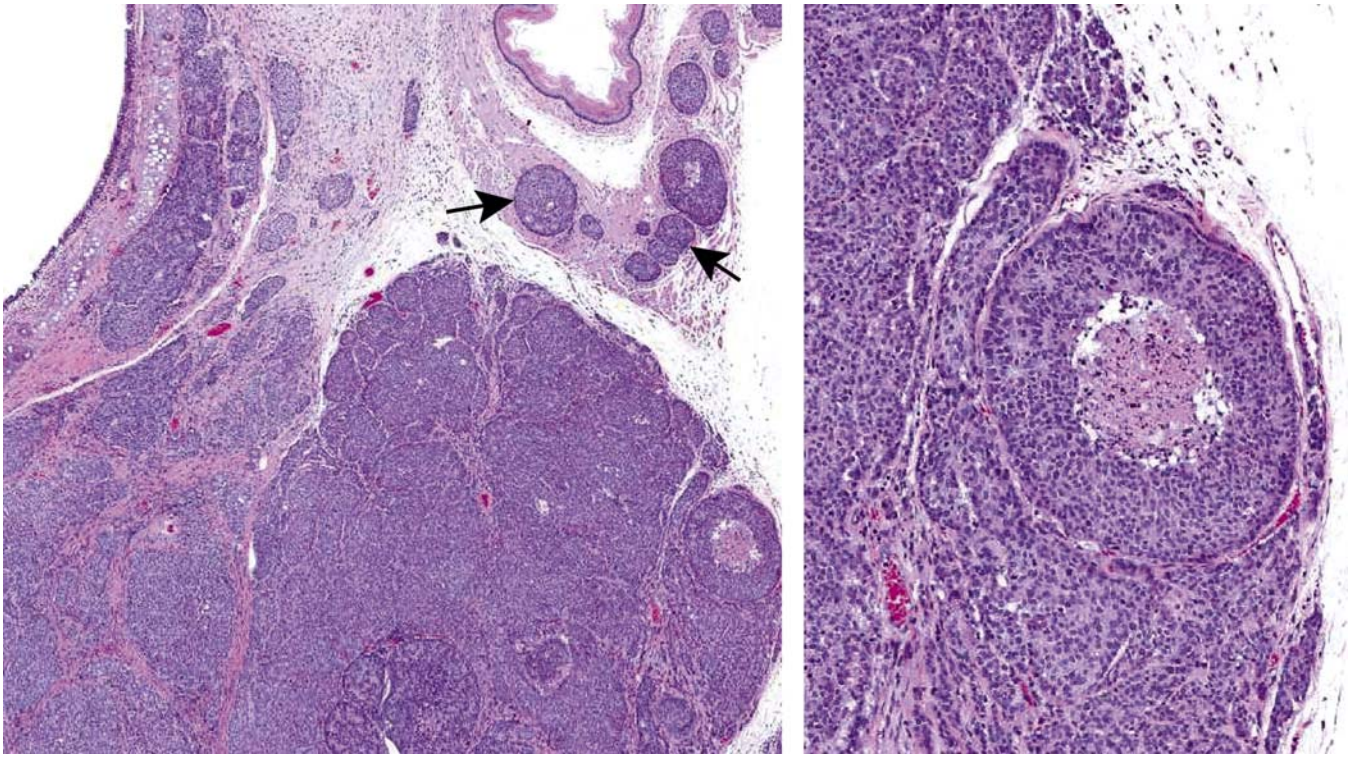

FIGURE 20.27 C-cell carcinoma (rat). Low-magnification view of C-cell carcinoma (left). This tumor involved the entire lobe with foci of lymphovascular invasion of the adjacent tissues (arrows). High-magnification view of tumor (right) with focal central necrosis. H&E stain. *Figure reproduced from* Handbook of Toxicologic Pathology, *third ed., W. M. Haschek, C. G. Rousseaux and M. A. Wallig, eds. (2013) Academic Press, Fig. 58.37, p. 2435, with permission.*

For example, approximately 80% of Long–Evans rats between 12 and 24 months of age have extensive diffuse and/or nodular C-cell hyperplasia, with C-cell adenomas or carcinomas occurring in 14%. By the age of 24–36 months, approximately 25% of the rats have evidence of C-cell adenomas or carcinomas. Rats with C-cell tumors also commonly have adrenal medullary hyperplasia, pheochromocytomas, and pituitary adenomas. In contrast to the high frequency of spontaneous C-cell adenomas and carcinomas in the rat, these tumors are rare in the mouse.

MECHANISMS OF TOXICITY

Radiation administered to newborn rats is followed by a striking reduction in the numbers of C cells. The numbers of C cells increase after 1 year, but their distribution within the gland is often patchy, suggesting a clonal regrowth. Further studies have demonstrated that the incidence of C-cell tumors is increased after irradiation, but high levels of Ca^{2+} in drinking water do not appear to potentiate the carcinogenic effects of irradiation in C cells. However, it has been noted that a significant increase in C-cell tumor incidence has been associated with excess Vitamin D_3 in the diet. These findings suggest that vitamin D or one of its metabolites may affect C-cell growth directly.

The administration of the glucagon-like peptide-1 (GLP-1) analogs, such as liraglutide, results in calcitonin release, upregulation of calcitonin gene expression, and C-cell proliferative lesions in rats and, to a lesser extent, in mice. In long-term rodent studies (104 weeks), C-cell tumors increased in a dose-dependent manner. In contrast to rodents, this effect does not appear to happen in humans and/or monkeys. Other pharmaceutical agents, such as the parathyroid hormone (PTH) analog teriparatide, have been associated with the development of C-cell tumors in rodents.

PART 5: THYROID FOLLICULAR CELLS

STRUCTURE AND FUNCTION

Organogenesis

The thyroid gland originates as a thickened plate of epithelium in the floor of the pharynx. It is intimately related to the aortic sac in its development, and this association leads to the frequent occurrence of accessory thyroid parenchyma in the mediastinum. These nodules are usually 1–2 mm in size and may number from one to five. They are completely lacking in C cells, but their follicular structure and function are the same as that of the main thyroid lobes. This accessory thyroid tissue may undergo neoplastic transformation as, for example, in the adult dog.

Thyroid Histology

The thyroid gland is the largest of the organs that function exclusively as endocrine glands. The basic structure of the thyroid is unique for endocrine glands, consisting of follicles of varying size (20–250 μm) that contain colloid produced by follicular cells. Follicular cells are cuboidal to columnar, and their secretory polarity is directed toward the lumen of the follicles. An extensive network of inter- and intrafollicular capillaries provides the follicular cells with an abundant blood supply. Follicular cells have long profiles of rough endoplasmic reticulum and a large Golgi apparatus in their cytoplasm for the synthesis and packaging of substantial amounts of protein that are transported into the follicular lumen. The interface between the lumenal side of follicular cells and the colloid is modified by numerous microvillar projections.

Thyroid Hormone Synthesis

The biosynthesis of thyroid hormones is also unique among endocrine glands because the final assembly of the hormones occurs extracellularly within the follicular lumen. Essential raw materials, such as iodide, are trapped efficiently by follicular cells from plasma, transported rapidly against a concentration gradient to the lumen, and oxidized by a thyroid peroxidase in microvillar membranes and colloid to iodine (I_2) (Figure 20.28). The assembly of thyroid hormones within the follicular lumen is made possible by a unique protein (thyroglobulin) synthesized by follicular cells.

Thyroglobulin is a high molecular weight (600,000–750,000) glycoprotein synthesized in successive subunits on ribosomes of the endoplasmic reticulum in follicular cells. The constituent AA (tyrosine and others) and carbohydrates (i.e., mannose, fructose, and galactose) come from the circulation. Recently synthesized thyroglobulin (17S) leaving the Golgi apparatus is packaged into apical vesicles and extruded into the follicular lumen. The AA tyrosine, an essential component of thyroid hormones, is incorporated in the molecular structure of thyroglobulin. Iodine is bound to tyrosyl residues in thyroglobulin at the apical surface of follicular cells to form, successively, monoiodotyrosine (MIT) and diiodotyrosine (DIT) (Figure 20.29). The resulting MIT and DIT combine to form the two

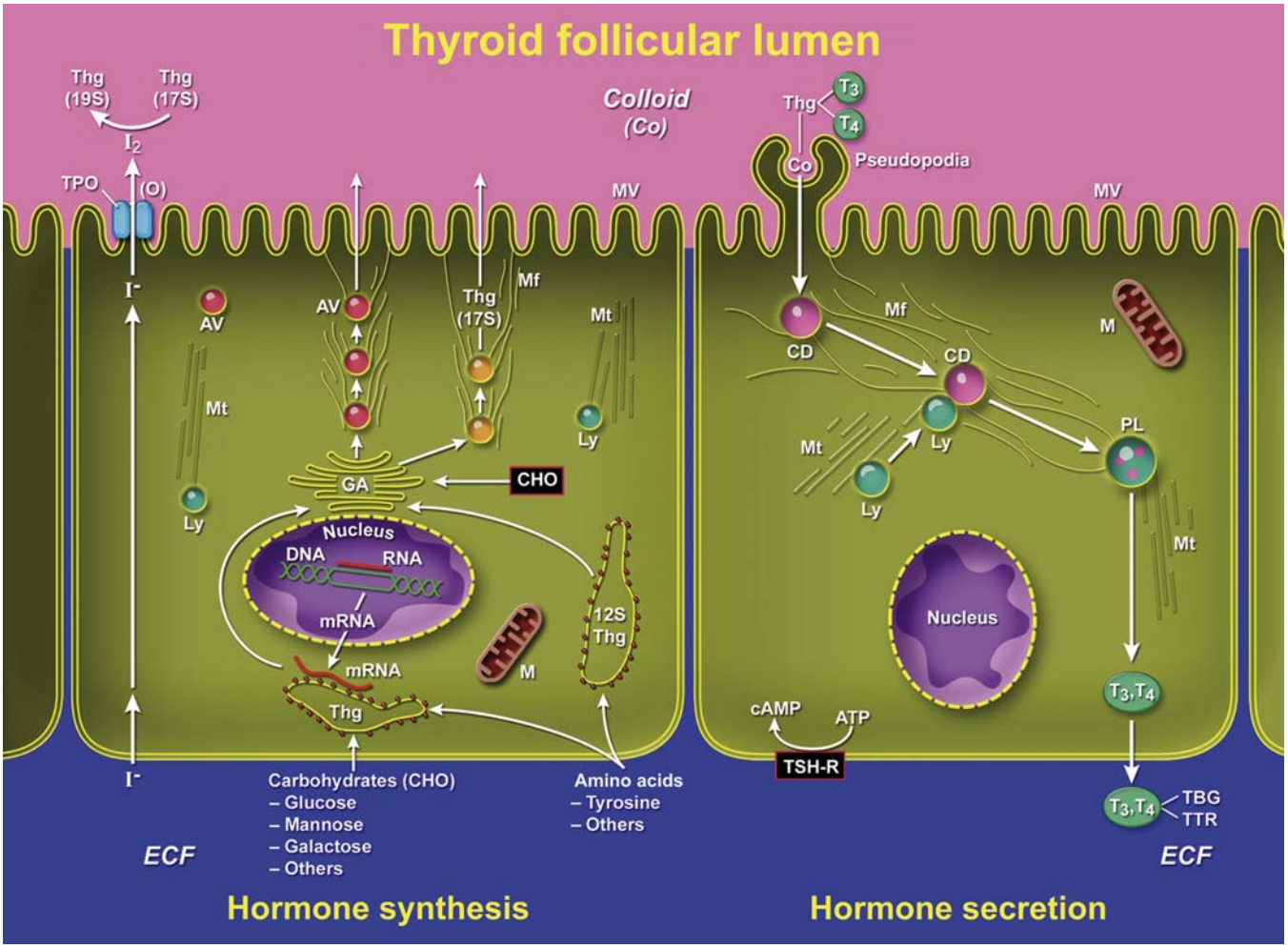

FIGURE 20.28 Normal thyroid follicular cells illustrating two-way traffic of materials from capillaries into the follicular lumen. Raw materials, such as iodide (I^-), are concentrated by follicular cells and are transported rapidly into the lumen (left). Amino acids (tyrosine and others) and sugars (CHO) are assembled by follicular cells into thyroglobulin (Thg), packaged into apical vesicles (AV), and released into the lumen. Iodination of tyrosyl residues occurs within the thyroglobulin molecule to form thyroid hormones in the follicular lumen. Elongation of microvilli and endocytosis of colloid by follicular cells occur in response to TSH stimulation (right). Intracellular colloid droplets (Co) fuse with lysosomal bodies (Ly) and the active thyroid hormone is cleaved enzymatically from thyroglobulin, and free T_4 and T_3 are released into circulation. *Mf*, microfilaments; *M*, mitochondria; *Mt*, microtubules; *TBG*, T_4-binding globulin; *TTR*, transthyretin. *Figure reproduced from* Handbook of Toxicologic Pathology, *third ed., W. M. Haschek, C. G. Rousseaux and M. A. Wallig, eds. (2013) Academic Press, Fig. 58.38, p. 2438, with permission.*

biologically active iodothyronines—T_4 and T_3—secreted by the thyroid gland.

The mechanism of active transport of iodide is associated with a sodium iodide (Na^+I^-) symporter (NIS). The transport of iodide ion across the thyroid cell membrane is linked to the transport of Na^+. The ion gradient generated by the Na^+/K^+-ATPase appears to be the driving force for the active cotransport of iodide. The transporter protein is present in the basolateral membrane of thyroid follicular cells (thyrocytes). Other tissues, such as the salivary gland, gastric mucosa, and lactating mammary gland, also have the capacity to actively transport iodide, albeit at a much lower level than the thyroid. NIS gene expression in the thyroid is upregulated by TSH. The functionally active iodine transport system has important toxicological implications. Radioiodine is used clinically to ablate residual tumor tissues as well as recurrent and metastatic thyroid cancer. Chemicals such as perchlorate and thiocyanate can selectively inhibit the NIS and active transport of iodide, thereby effectively blocking the ability of the gland to synthesize thyroid hormones.

The plasma T_4 half-life in rats is considerably shorter (12–24 hours) than in man (5–9 days). In humans and monkeys, circulating T_4 is bound primarily to T_4-binding globulin (TBG), but this high-affinity

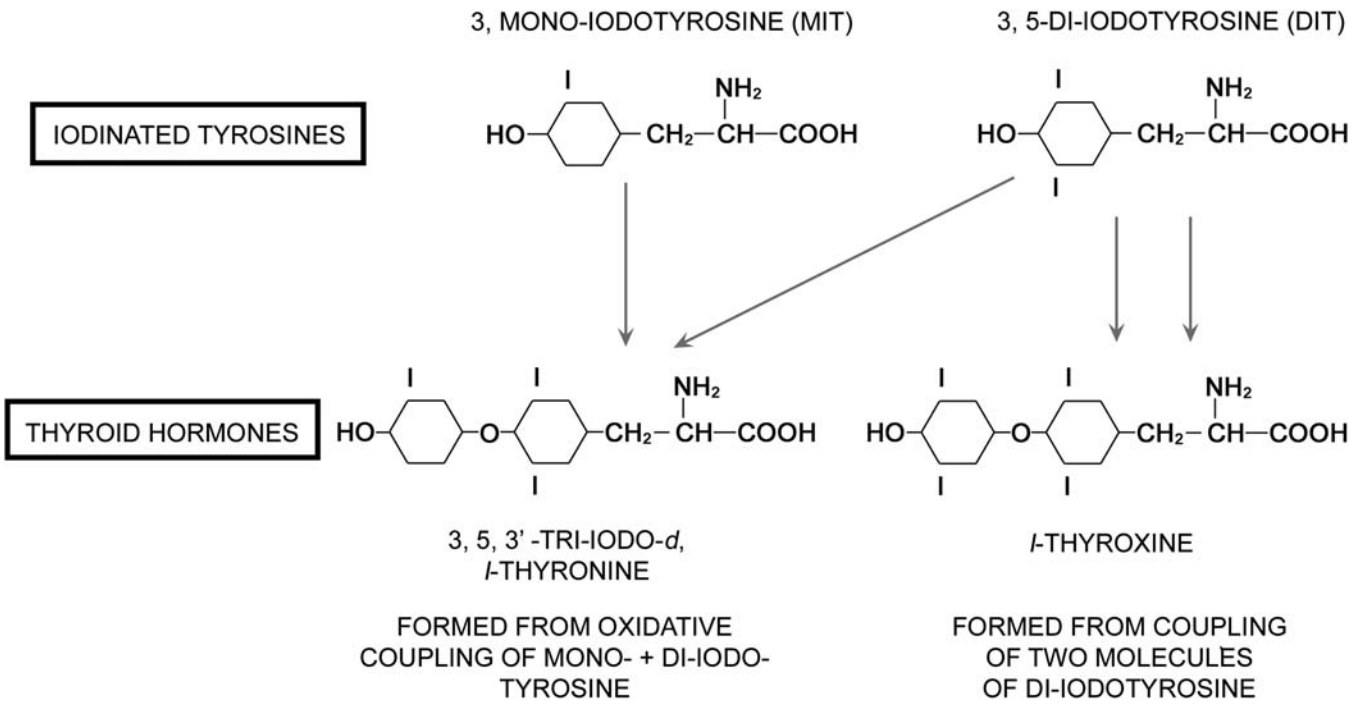

FIGURE 20.29 Formation of thyroid hormones (3,5,3′-triiodothyronine, L-thyroxine) from iodinated tyrosines (MIT and DIT) within the follicular lumen of the thyroid gland. *Figure reproduced from Capen and Martin (1989), The effects of xenobiotics on the structure and function of thyroid follicular cells and C-cells,* Toxicol. Pathol. *17, 266–293, with permission.*

TABLE 20.4 Thyroxine (T_4) Binding to Serum Proteins in Selected Vertebrate Species[a]

Species	T_4-Binding globulin	Postalbumin	Albumin	Prealbumin (transthyretin)
Human	++	−	++	+
Monkey	++	−	++	+
Dog	+	−	++	−
Mouse	−	++	++	−
Rat	−	+	++	+
Chicken	−	−	++	−

[a]*Degree of T_4 binding to serum proteins: + or ++. Absence of binding of T_4 to serum protein: −.*
Table modified from Döhler et al. (1979) The rat as model for the study of drug effects on thyroid function: consideration of methodological problems, Pharmacol. Ther. *5: 305–318.*

binding protein is not present in rodents, birds, amphibians, or fish (Table 20.4).

The binding affinity of TBG for T_4 is approximately 1000 times higher than for transthyretin (prealbumin). The percentage of unbound active T_4 is lower in species with high levels of TBG than in animals in which T_4 binding is limited to albumin, transthyretin, and postalbumin. Therefore, a rat without a functional thyroid requires about 10 times more T_4 (20 μg/kg body weight) for full substitution than an adult human (2.2 μg/kg body weight). T_3 is transported bound both to TBG and albumin in human, monkey, and dog but only to albumin in mouse, rat, and chicken (Table 20.5). In general, T_3 is bound less avidly to transport proteins than T_4, resulting in a faster turnover and shorter plasma half-life in most species. These differences in plasma half-life of thyroid hormones and binding to transport proteins between rats and humans may be one factor in the greater sensitivity of the rat thyroid to develop hyperplastic and/or neoplastic nodules in response to chronic TSH stimulation.

Thyroid Hormone Secretion

The elongation of microvilli and the formation of pseudopods on follicular cells initiate the secretion of thyroid hormones from stores within lumenal colloid. The pseudopods are increased by pituitary TSH, and they phagocytize a portion of adjacent colloid by endocytosis. Colloid droplets within follicular cells fuse with numerous lysosomal bodies that contain proteolytic enzymes and release T_4 and T_3, which diffuse out of the follicular cells and enter interfollicular capillaries. Iodinated tyrosines (MIT and DIT) released from the colloid droplets are deiodinated enzymatically, and the iodide generated under normal conditions either is recycled to the lumen to

TABLE 20.5 Triiodothyronine (T_3) Binding to Serum Proteins in Selected Vertebrate Species[a]

Species	T_3-Binding globulin	Postalbumin	Albumin	Prealbumin (transthyretin)
Human	+	−	+	−
Monkey	+	−	+	−
Dog	+	−	+	−
Mouse	−	+	+	−
Rat	−	−	+	−
Chicken	−	−	+	−

[a]*Degree of T_3 binding to serum proteins: + or ++. Absence of binding of T_3 to serum protein: −.*
Table modified from Döhler et al. (1979) The rat as model for the study of drug effects on thyroid function: consideration of methodological problems, Pharmacol. Ther. *5: 305–318.*

iodinate new tyrosyl residues in thyroglobulin or is released into the circulation.

Negative feedback control of thyroid hormone secretion is accomplished by the coordinated response of the adenohypophysis and certain hypothalamic nuclei to circulating and local tissue levels of T_3. In the rat, 50% or more of the pituitary content of T_3 is generated locally from circulating T_4 by a 5′-deiodinase (type II). A decrease in thyroid hormone concentration in plasma is sensed by groups of neurosecretory neurons in the hypothalamus that synthesize and secrete TRH into the hypophyseal portal circulation. TRH binds to receptors on the plasma membrane of thyrotrophic basophils in the adenohypophysis and activates adenylyl cyclase. Intracellular accumulation of cyclic AMP in thyrotrophic basophils leads to release of TSH-containing secretory granules into pituitary capillaries.

TSH binds to the basilar aspect of the thyroid follicular cell, activates adenylyl cyclase, and increases the rate of synthesis and secretion of thyroid hormones. One of the initial responses by follicular cells to TSH is the formation of cytoplasmic pseudopodia (see above) resulting in the release of preformed hormone stored within the follicular lumen. If secretion of TSH is sustained (hours or days), thyroid follicular cells become more columnar and follicular lumens become smaller. Numerous PAS-positive colloid droplets are present in the lumenal aspect of the hypertrophied follicular cells.

Conversely, in response to an increase in circulating levels of thyroid hormones (T_4 and T_3), there is a corresponding decrease in circulating pituitary TSH. Thyroid follicles become enlarged and distended with colloid due to the decreased TSH-mediated endocytosis. Follicular cells lining the involuted follicles are low cuboidal and have few endocytic vacuoles at the interface with the colloid.

Degradation and Metabolism

Thyroid hormones are degraded primarily by conjugation in the liver. T_4 is conjugated on the outer phenolic ring with glucuronic acid in a reaction catalyzed by T_4 UDP glucuronosyltransferase (UGT), and conjugated T_4 is excreted in the bile. T_3 is conjugated, also on the outer ring, with sulfate in a reaction catalyzed by phenol sulfotransferase. Deamination and decarboxylation of the side chain at the other end of the thyroid hormone molecule and cleavage of the ether linkage are relatively minor pathways of degradation. A wide variety of drugs and chemicals can influence thyroid hormone metabolism by inducing one or more classes of hepatic microsomal enzymes that increase the degradation of thyroid hormones.

The stepwise monodeiodination of T_4 in the liver, kidney, and elsewhere is also important in metabolism of thyroid hormones. The removal of an iodine molecule from the 5 position on the outer phenolic ring by 5′-deiodinase results in the formation of biologically active T_3 (3,5,3′-triiodothyronine; Figure 20.30). However, if a molecule of iodine is removed from the 5 position of the inner phenolic ring of T_4 by another enzyme, 5-deiodinase, reverse T_3 (3,3′,5′-triiodothyronine) is produced, which is biologically inactive. Reverse T_3 subsequently is degraded further by 5′-deiodinase and T_3 by 5-deiodinase; both form DIT (T_2). Chemicals such as FD&C Red No. 3 (erythrosine) and amiodarone disrupt thyroid hormone metabolism by inhibiting the 5′-deiodinase in liver (type I enzyme), thereby inhibiting the conversion of T_4 to T_3.

In dog plasma, T_4 is bound to albumin and three globulin fractions, and T_3 is bound to albumin and one globulin fraction. The overall binding affinity of the plasma proteins for T_4 is lower in dogs than in humans. Most importantly, the affinity of the canine inter-α-globulin fraction for T_4 is much less than that of the human TBG. As a result of this weaker binding, as well as an efficient enterohepatic excretory mechanism, the total T_4 concentration is lower and the rate of thyroid hormone turnover is more rapid in dogs than in humans. Peak concentration usually occurs at about midday and the minimum at about midnight. Both the overall rates of turnover and the loss of hormone in the feces are much higher in dogs than in humans. Fecal wastage substantially reduces the efficiency of hormone utilization but also explains the remarkable tolerance of the dog for excess thyroid hormone.

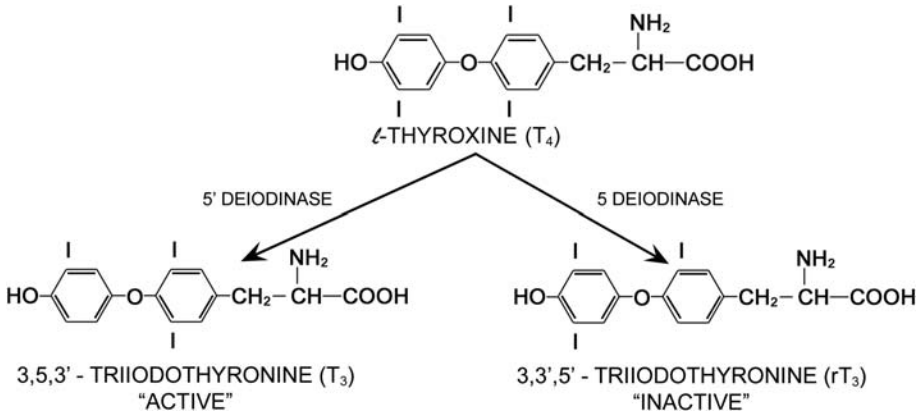

FIGURE 20.30 Monodeiodination of thyroxine to form either active T_3 (left) or inactive (reverse) rT_3 (right) depending on the need for the metabolic actions of thyroid hormone. *Figure reproduced from Capen and Martin (1989), The effects of xenobiotics on the structure and function of thyroid follicular cells and C-cells,* Toxicol. Pathol. *17, 266–293, with permission.*

Biological Action

T_4 and T_3, once released into the circulation, act on many different target cells in the body. The overall functions of T_4 and T_3 are similar, although much of the biological activity is the result of monodeiodination of T_4 to T_3 (3,5,3′-triiodothyronine) prior to interaction with target cells or by the target cells. Under certain conditions (protein starvation, neonatal animals, liver and kidney disease, and febrile illness) T_4 is preferentially monodeiodinated to 3,3′,5′-triiodothyronine (reverse T_3) (Figure 20.30). Because this form of T_3 is biologically inactive, monodeiodination to reverse T_3 provides a mechanism to attenuate the metabolic effects of thyroid hormones. T_4 stimulates oxygen utilization and heat production by many different populations of body cells. It causes increased utilization of carbohydrates, increased protein catabolism, and greater oxidation of fats. The administration of T_4 increases heart rate by a direct effect on heart muscle cells.

Normal function of the central nervous system (CNS) is dependent on T_4. During periods of deficient T_4 levels, the CNS fails to function normally and the animal is lethargic, dull, and mentally deficient. Myelin in fiber tracts is decreased, cortical neurons are smaller and fewer, and vascularity of the CNS is reduced. Neurons are permanently damaged by a deficiency of thyroid hormones in a young growing animal fed a severely deficient iodine diet. However, an excess of thyroid hormone production, as occurs in a hyperthyroid animal or human, stimulates CNS activity to the extent that the animal is nervous, irritable, and hyperactive.

The subcellular mechanism of action of thyroid hormones resembles that of steroid hormones because free hormone enters into target cells and binds to a cytosol-binding protein. Free T_3 either binds to receptors on the inner mitochondrial membrane to activate mitochondrial energy metabolism, or binds to nuclear receptors and increases transcription of mRNA to facilitate new protein synthesis. The overall effects of thyroid hormones are to (1) increase the basal metabolic rate; (2) increase glycolysis, gluconeogenesis, and glucose absorption from the intestine; (3) stimulate new protein synthesis; (4) increase lipid metabolism and conversion of cholesterol into bile acids and other substances, activate lipoprotein lipase, and increase the sensitivity of adipose tissue to lipolysis by other hormones; (5) stimulate heart rate, cardiac output, and blood flow; and (6) increase neural transmission, cerebration, and neuronal development in young animals.

EVALUATION OF TOXICITY

Thyroid Function Tests

Thyroid Hormones

The most sensitive and accurate method for measuring blood T_4 and T_3 levels is radioimmunoassay (RIA). The normal blood level of T_4 in the dog ranges between 1.5 and 3.6 μg/dL (mean: 2.5 μg/dL) and T_3 ranges between 48 and 154 ng/dL (mean: 95 ng/dL). In dogs with hypothyroidism, the T_4 level is usually below 1.0 μg/dL and T_3 is below 50 ng/dL. When the levels are border-line, clearer separation of animals with hypothyroidism from those that are euthyroid can be made by injecting exogenous TSH. In the euthyroid dog, the T_4 level will at least double 8 hours after iv or im administration of TSH. In animals with hypothyroidism, the T_4 and T_3 levels do not change significantly after the injection of TSH. Serum T_4 in the rat is

higher than in the dog with a mean of approximately 4.5 ± 0.2 μg/dL. Serum T_3 in rats is more variable than circulating T_4 levels with a range of 50–100 ng/dL, with T_3 values tending to decrease with advancing age. The serum reverse T_3 level in the normal rat usually ranges between 55 and 75 pg/mL but will increase dramatically and remain elevated following the administration of xenobiotics that inhibit the 5′-deiodinase. The range of values given for serum T_4, T_3, and reverse T_3 should be considered only as a general guideline. A specific range of values for rats of different ages, strains, and sexes should be established in conjunction with the endocrine laboratory performing the assays on serum from a particular experiment. Whenever possible, samples at different intervals from an experiment should be frozen and all assays performed at a single run at the termination of the experiment to minimize interassay variations. Serum collection should be performed during the morning hours, if possible, and rats from control and experimental groups alternated during the collection interval.

Thyroid-Stimulating Hormone

In the evaluation of potential thyroid toxicity of various xenobiotics in rodents, an accurate quantitation of circulating levels of TSH is essential in order to determine whether proliferative lesions of follicular cells are mediated by a chronic hypersecretion of TSH. The immunoassay for TSH is highly species-specific, with considerable interanimal and interassay variation.

Xenobiotics that disrupt thyroid hormone synthesis, secretion, or peripheral metabolism often result in prompt increases in circulating TSH levels. It is important in the design of experiments to evaluate the effect of a xenobiotic on thyroid function to have several early collection intervals. TSH levels are higher in male than in female rats and castration decreases both the baseline serum TSH and the response to TRH injection. Commercial TSH assays are available to measure canine TSH and include immunoradiometric, luminescence, or enzyme-linked immunosorbent assay (ELISA) formats. The β subunit of canine TSH has an 89% homology with the human subunit, and circulating TSH levels in dogs are 10- to 20-fold lower than those in humans. The canine TSH assays have a low diagnostic sensitivity since some hypothyroid dogs do not have increased serum TSH concentrations.

Morphological and Morphometric Evaluation of Thyroid Follicles

Morphological and morphometric evaluations of the follicular cells are sensitive indicators of potential toxic effects of xenobiotics on the thyroid gland. Fixation of the thyroid lobes attached to the adjacent trachea in buffered formalin is the best procedure for routine studies. The combined weight of the right and left thyroid lobes can be expressed as a ratio to total body or brain weight. Changes in thyroid weight are a sensitive overall indicator of the effects of relatively mild goitrogenic chemicals on thyroid structure. Immunohistochemical procedures are particularly helpful with selected proliferative lesions to determine whether they are of follicular cell (thyroglobulin-positive) or C-cell (calcitonin-positive) origin.

Morphometric evaluation of thyroids is a valuable adjunct to histopathological evaluation and determination of thyroid weights to detect and quantitate subtle changes in follicular cells. This is particularly true for rats, where the histology of the normal thyroid (tall columnar follicular cells lining mainly small follicles containing small amounts of lightly eosinophilic colloid) reflects the high baseline TSH levels. Follicle diameter, colloid area, and follicular cell height can be measured from representative follicles in H&E-stained sections using image analysis software. Large, colloid-distended, inactive follicles at the periphery of the lobes are avoided.

Histological examination of a biopsy of the thyroid is a useful and reliable aid in the diagnosis of thyroid disease in larger animals when either the results of serum assays for T_4 and T_3 are equivocal or a nodule is palpated in the thyroid area.

Animals as Models

Much of the significant physiological and pathological data in the literature on thyroid function and structure has come from studies in animals. Although the basic hypothalamic–pituitary–thyroid axis functions in a similar manner in animals and humans, there are differences between species that are important when extrapolating animal data from toxicity and carcinogenicity studies for human risk assessment. Several of these differences have been summarized previously in this section on thyroid follicular cells.

Long-term perturbations of the pituitary–thyroid axis by various xenobiotics or physiological alterations (e.g., iodine deficiency, partial thyroidectomy) are more likely to predispose the laboratory rat to a higher incidence of proliferative lesions in the thyroid (e.g., hyperplasia and adenomas of follicular cells) than is seen in the human thyroid. This appears to be particularly true in the male rat, in which there is higher circulating TSH than in the female.

RESPONSE TO INJURY

Thyroid responses to injury histologically are primarily proliferative in nature, but nonproliferative lesions reflecting disorders of thyroid function also occur.

Species Differences in Response

Long-term perturbations of the pituitary–thyroid axis by xenobiotics or physiologic alterations (e.g., iodine deficiency, partial thyroidectomy, and natural goitrogens in food) are more likely to induce a higher incidence of proliferative lesions (e.g., hyperplasia and adenomas of follicular cells) in the rat, as a response to chronic TSH stimulation, than in the human. This is particularly true in the male rat, which has higher circulating levels of TSH than females. The greater sensitivity of the rodent thyroid to derangement by drugs, chemicals, and physiologic perturbations is also related to the shorter plasma half-life of T_4 than in humans due to the considerable differences between these species in the transport proteins for thyroid hormones.

Histopathological Criteria of Proliferative Lesions

Uniform terminology and more specific criteria for the various proliferative lesions of thyroid follicles, including representative images of common lesions, developed by the INHAND in Rats and Mice project, will be available at the time of publication of this chapter on the Society of Toxicologic Pathology website (http://www.toxpath.org/inhand.asp). Diffuse thyroid enlargement with or without hyperplasia (i.e., "goiter") will be discussed in a later section.

Follicular Cell Hyperplasia

Follicular "cystic" hyperplasia is characterized by single or multiple nodules in the thyroid formed by the coalescence of adjacent colloid-distended follicles. The follicular wall (or remnants) is lined by one or two layers of low-cuboidal epithelium with hyperchromatic nuclei that occasionally form papillary projections. Adjacent thyroid follicles are normal, with minimal evidence of compression and no encapsulation by fibrous connective tissue.

Focal ("nodular") or multifocal areas of hyperplasia of thyroid follicular cells usually only enlarge the affected lobe(s) slightly. The areas of focal hyperplasia are not encapsulated and the adjacent thyroid parenchyma is not compressed. Hyperplastic nodules are composed of irregularly shaped, usually colloid-filled, follicles lined by more basophilic cuboidal follicular cells. The multiple nodules of follicular cell hyperplasia may coalesce to form macroscopically observable thyroid adenomas. Focal hyperplasia is different than the diffuse (TSH-mediated) type of follicular cell hyperplasia observed with iodine deficiency and with a wide variety of xenobiotic drugs and chemicals that disrupt thyroid hormone "economy" to result in increased secretion of TSH.

Follicular Cell Adenoma

An adenoma is a well-circumscribed, usually solitary, benign tumor formed by the autonomous proliferation of follicular cells within the thyroid lobe. Adjacent thyroid follicles are compressed to varying degrees, depending on the size of the adenoma. Adenomas usually do not have a complete fibrous capsule, but larger adenomas may be partially encapsulated by a thin layer of fibrous connective tissue. Neoplastic cells often are more hyperchromatic than the surrounding normal follicular cells and form variably sized colloid-containing follicles, line large cystic spaces, or solid sheets. Neoplastic cells may form papillary structures extending into larger cysts. Neoplastic cells vary from cuboidal to low columnar, and the nucleus:cytoplasm ratio often is high. There is no evidence of vascular invasion. Endocrinologically active thyroid adenomas result in the colloid involution of follicles in the rim of the surrounding thyroid due to the inhibition of TSH secretion by elevated blood T_4 and T_3 levels.

Follicular Cell Carcinoma

Thyroid carcinomas show evidence of intrathyroidal, capsular, or vascular invasion that often enlarges the affected thyroid lobe considerably (Figure 20.31). Malignant follicular cells form colloid-containing follicles of varying size, papillary projections extending into cystic spaces, or solid sheets of cells. The cells are pleomorphic, and nuclei are hyperchromatic with occasional mitotic figures. A desmoplastic reaction often accompanies the infiltration of neoplastic cells into the thyroid capsule. The perithyroidal connective tissue, as well as adjacent trachea and cervical muscles, may be invaded by larger carcinomas.

Disorders of Thyroid Function

Hypothyroidism

Hypothyroidism is a well-recognized clinical entity in dogs, and occurs in many purebred and mixed breed dogs. Subnormal function of the thyroid is recognized less frequently as a naturally occurring entity in other animal species. However, a large number of drugs, chemicals, dietary deficiencies, or excesses can

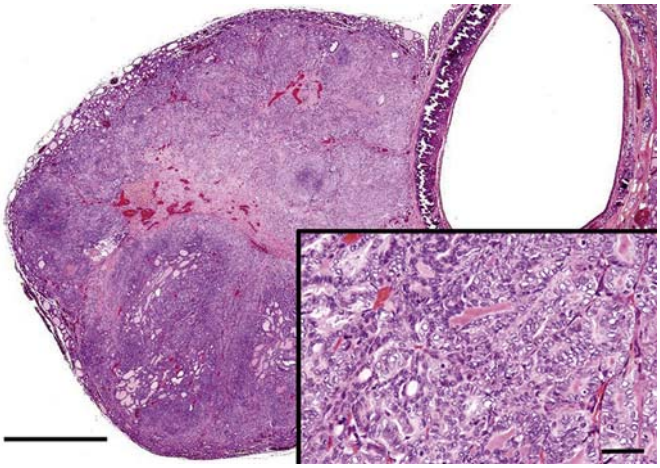

FIGURE 20.31 Follicular cell carcinoma (rat) with enlargement of the thyroid gland, capsular invasion, and growth of neoplastic cells in the perithyroidal connective tissues (Bar = 1 μm). Tumor cells form follicles of varying size and colloid content plus solid areas (Inset: bar = 50 μm). H&E stain. *Figure reproduced from* Handbook of Toxicologic Pathology, *third ed., W. M. Haschek, C. G. Rousseaux and M. A. Wallig, eds. (2013) Academic Press, Fig. 58.38, p. 2438, with permission.*

disrupt one or more steps of thyroid hormone biosynthesis, secretion, metabolism, or degradation and result in subnormal blood levels of thyroid hormones. Hypothyroidism in dogs is often the result of primary diseases of the thyroid gland, especially idiopathic follicular atrophy ("follicular collapse") and immune-mediated lymphocytic thyroiditis. Hypertrophy and hyperplasia of TSH-secreting basophils occur in the pars distalis of dogs with hypothyroidism.

Hypothyroidism may also develop secondary to longstanding pituitary or hypothalamic lesions that prevent the release of either TSH or TRH. The thyroid gland is moderately reduced in size and is composed of colloid-distended follicles lined by flattened follicular cells due to a lack of TSH-induced endocytosis of colloid and secretion of thyroid hormones. Somatostatin inhibits both GH and TSH secretion in the pars distalis of the pituitary gland. Long-acting somatostatin analogs, such as octreotide, have the potential to reduce TSH and serum thyroid hormone concentrations.

Many functional disturbances associated with hypothyroidism are due to a reduction in the basal metabolic rate. A gain in body weight without an associated change in appetite occurs frequently. The rate of lipid metabolism decreases in longstanding cases of hypothyroidism, and blood lipid levels often are elevated because of a decreased rate of intestinal cholesterol excretion and a decreased rate of hepatic conversion into bile acids and other compounds. The elevated blood cholesterol level predisposes to the development of atherosclerosis of small vessels (especially coronary arteries) and deposition of lipid in the liver. The cardiovascular system is further affected by the reduced level of thyroid hormones due to a slowing of the heart rate. The moderate slowing in the heart rate may be difficult to detect unless a normal resting heart rate has been measured previously.

The accumulation of excessive lipid in the liver often results in varying degrees of hepatomegaly with abdominal distension in animals with long-term hypothyroidism. Renal glomeruli may become plugged with lipid in hypothyroid animals with markedly elevated plasma cholesterol, resulting in progressive renal failure.

Abnormalities in reproduction are common when a breeding animal develops hypothyroidism. Lack of libido and reduction in sperm count may occur in males, whereas abnormal or absent estrus cycles with reduced conception rates often result in females. Obesity and changes in behavior resulting from hypothyroidism may have detrimental effects on reproduction.

Hyperthyroidism

Disturbances of growth in the thyroid gland, in which there is secretion of excess thyroid hormones, resulting in hyperthyroidism, are uncommon in animals except in adult to aged cats. Follicular cell adenomas, often developing in a thyroid with multinodular hyperplasia, are encountered more commonly than malignant thyroid tumors. A syndrome of hyperthyroidism has been recognized with increasing frequency since the early 1980s in aged cats associated with multinodular follicular cell hyperplasia, adenomas, or adenocarcinomas. Possible factors in the increasing incidence of functional thyroid lesions in cats include exposure to lawn herbicides or fertilizers, regular treatment with flea sprays or powders, and a canned food diet.

Neoplastic cells release both T_4 and T_3 at an uncontrolled rate, resulting in markedly elevated blood levels of both hormones. Follicles in the rim of the thyroid around a functional adenoma are enlarged markedly and distended by the accumulation of colloid. Follicular cells are low cuboidal and atrophic, with little endocytotic activity in response to the elevated levels of thyroid hormones.

The most common disturbance of function in hyperthyroidism is weight loss, despite a normal or increased appetite. Other clinical signs include polydipsia and polyuria, increased frequency of defecation, increased volume of stools, restlessness, and increased physical activity.

In contrast to cats, thyroid tumors in the dog only occasionally secrete sufficient thyroid hormone to produce clinical signs of hyperthyroidism. Dogs have a very efficient enterohepatic excretory mechanism for

thyroid hormones that it is difficult to overload, either from endogenous production by a tumor or exogenous administration of hormone.

Therefore, the likelihood of developing clinical hyperthyroidism associated with thyroid neoplasms in animals depends on the capability of tumor cells to synthesize T_4 and T_3 (e.g., well-differentiated thyroid tumors that form follicles and produce colloid are more likely to synthesize thyroid hormones than poorly differentiated solid neoplasms), and the degree of elevation of circulating levels of T_4 and T_3, which depends on a balance between the rate of secretion of thyroid hormones by the tumor and the rate of degradation of thyroid hormones. Cats are very sensitive to phenol and phenol derivatives (such as T_4). They have a poor ability to conjugate phenolic compounds with glucuronic acid and hence to excrete T_4-glucuronide into the bile. The capacity to conjugate T_3 to sulfate, an alternative pathway, is limited in all species and easily overloaded.

Diffuse Hyperplasia of Follicular Cells ("Goiter")

MECHANISMS OF GOITROGENESIS

Nonneoplastic and noninflammatory enlargement of the thyroid ("goiter") develops in all laboratory animals, domestic mammals, birds, and other nonmammalian vertebrates. Certain forms of thyroid hyperplasia, especially nodular, may be difficult to differentiate from benign tumors (adenomas). The major pathogenic mechanisms responsible for the development of thyroid hyperplasia include iodine-deficient diets, goitrogenic compounds that interfere with thyroid hormone synthesis, dietary iodide excess, and genetic enzyme defects in the biosynthesis of thyroid hormones (Figure 20.32). All of these seemingly divergent factors result in inadequate T_4 and T_3 synthesis and decreased blood levels of thyroid hormones. The lowered blood levels are detected by the hypothalamus and pituitary to increase the secretion of TSH, which results in hypertrophy and hyperplasia of follicular cells in the thyroid gland.

DIFFUSE HYPERPLASTIC (IODINE-DEFICIENT) GOITER

Dietary iodine deficiency leading to diffuse thyroid hyperplasia is still common in many areas throughout the world, although the widespread addition of iodized salt to animal and human diets has decreased deficiency substantially in recent decades. More often, marginal iodine-deficient diets containing certain goitrogenic compounds result in thyroid follicular cell hyperplasia and clinical evidence of goiter with hypothyroidism. These goitrogenic substances include thiouracil, sulfonamides, anions of the Hofmeister series, and a number of plants from the genus *Brassica*.

Both lateral lobes of the thyroid are enlarged uniformly in animals with diffuse hyperplastic goiter. The enlargements may be extensive and result in palpable swelling in the cranial cervical area. The affected lobes are firm and dark red because an extensive interfollicular capillary network develops under the influence of long-term TSH stimulation. The thyroid enlargements are the result of intense hypertrophy and hyperplasia of follicular cells, often with the formation of papillary projections into the lumens of follicles or multiple layers of cells lining follicles. Endocytosis of colloid usually proceeds at a rate greater than synthesis, resulting in the progressive depletion of colloid.

Under longstanding TSH stimulation, thyroid follicles become smaller than normal and there may be a partial collapse of follicles due to the lack of colloid. Hypertrophic-lining follicular cells are columnar with a deeply eosinophilic cytoplasm and small hyperchromatic nuclei that often are situated in the basilar part of the cell. The follicles are lined by either single or multiple layers of hyperplastic follicular cells that, in some follicles, form papillary projections into the lumen. Similar proliferative changes are present in ectopic thyroid parenchyma in the neck and mediastinum.

COLLOID GOITER

Colloid goiter, or diffuse thyroid follicular dilatation, represents the involutional phase of diffuse hyperplastic goiter in young adults and reflects postproliferation atrophy of follicular cells with persistence of colloid already produced. The markedly hyperplastic follicular cells continue to produce colloid, but the endocytosis of colloid is decreased due to diminished pituitary TSH secretion in response to the return of blood T_4 and T_3 to the normal range. Colloid goiter may develop either after sufficient amounts of iodide have been added to the diet or after the requirements for T_4 have diminished in an older animal. Both thyroid lobes are enlarged diffusely but are more translucent and lighter in color than with hyperplastic goiter. The differences in macroscopic appearances are the result of less vascularity in colloid goiter and the development of macrofollicles distended with colloid. Follicular cells lining the macrofollicles are flattened and atrophic, and the interface between the colloid and the lumenal surface of follicular cells is smooth.

IODIDE-EXCESS GOITER

Although seemingly paradoxical, an excess of iodide in the diet also can result in thyroid hyperplasia in animals and humans. The thyroid glands of the young are exposed to higher blood iodide levels than

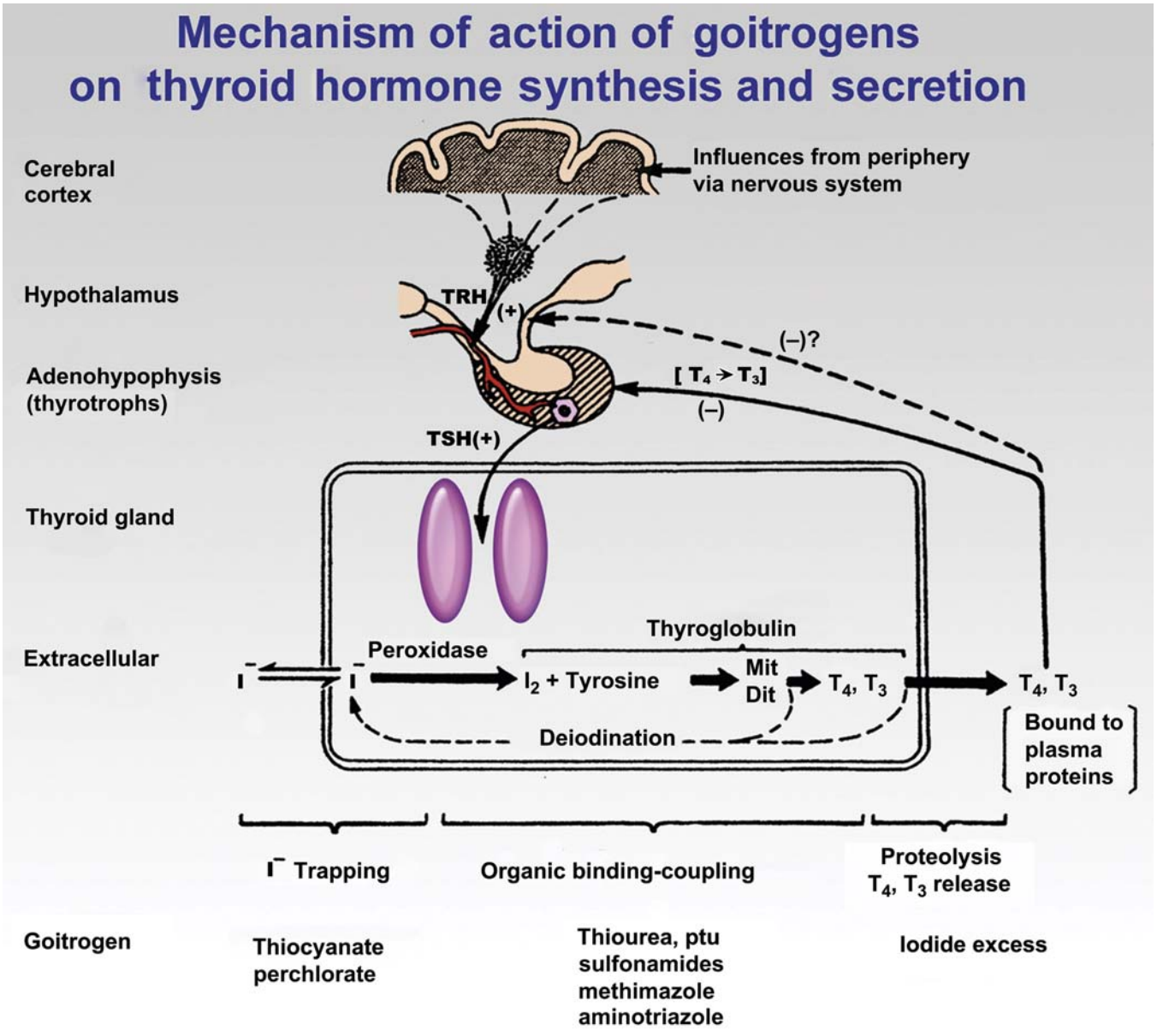

FIGURE 20.32 Mechanism of action of goitrogenic chemicals on thyroid hormone synthesis and secretion. Goitrogens affect iodide trapping, organic binding-coupling, or proteolysis of colloid and release of T_4 and T_3. *Figure reproduced from Capen and Martin (1989). The effects of xenobiotics on the structure and function of thyroid follicular cells and C-cells,* Toxicol. Pathol. *17, 266–293, with permission.*

those of the dam because the placenta concentrates iodide prior to birth and *subsequently*, after birth, the mammary gland also concentrates iodide. High blood iodide interferes with one or more steps of thyroxinogenesis, leading to lowered blood thyroid hormone levels and a compensatory increase in pituitary TSH secretion. Excess iodide appears primarily to block the release of T_3 and T_4 from thyroglobulin by interfering with the proteolysis of colloid by lysosomes, but it also interferes with the peroxidation of 2 I^- to I_2 and disrupts the conversion of MIT to DIT.

NODULAR GOITER

Multinodular hyperplasia ("goiter") in thyroid glands of old animals appears as white-to-tan nodules of varying size in one or both lobes. The affected lobes are moderately enlarged and irregular in contour. Nodular goiter in most animals (except cats) is endocrinologically inactive and encountered as an incidental lesion at necropsy.

Nodular goiter consists of multiple foci of hyperplastic follicular cells that are sharply demarcated from the adjacent thyroid parenchyma, but are not encapsulated, and there is minimal compression of

adjacent parenchyma. Some hyperplastic cells form small follicles with little or no colloid. Other nodules are formed by larger irregularly shaped follicles lined by one or more layers of columnar cells that form papillary projections into the lumen. These changes appear to be the result of alternating periods of hyperplasia and colloid involution in the thyroid glands of old animals. The areas of nodular hyperplasia may be microscopic or grossly visible, causing modest enlargement of the thyroid.

MECHANISMS OF TOXICITY

Direct Thyroid Effect

Inhibitors of Thyroid Hormone Synthesis

BLOCKAGE OF IODINE UPTAKE

The initial step in the biosynthesis of thyroid hormones is the uptake of iodide from the circulation and subsequent transport against a gradient across follicular cells by the NIS into the lumen of the follicle. A number of anions act as competitive inhibitors of iodide transport in the thyroid, the most notable being perchlorate (ClO_4^-), thiocyanate (SCN^-), and pertechnetate (Figure 20.32). Thiocyanate is a potent inhibitor of iodide transport and is a competitive substrate for thyroid peroxidase, but it does not appear to concentrate in the thyroid. Blockage of the iodide-trapping mechanism has a disruptive effect on the thyroid–pituitary axis similar to the effect of iodine deficiency. Blood levels of T_4 and T_3 decrease, resulting in a compensatory increase in the secretion of TSH by the pituitary gland. Hypertrophy and hyperplasia of follicular cells following sustained exposure result in an increased thyroid weight and the development of goiter.

INHIBITION OF THYROID PEROXIDASE (THYROPEROXIDASE)

A wide variety of chemicals, drugs, and other xenobiotics affect the second step in thyroid hormone biosynthesis (Figure 20.32). Classes of chemicals that inhibit the organification of thyroglobulin include: (1) thionamides such as thiourea, thiouracil, PTU, methimazole, carbimazole, and goitrin; (2) aniline derivatives and related compounds such as sulfonamides, *p*-aminobenzoic acid, *p*-aminosalicylic acid, and amphenone; (3) substituted phenols such as resorcinol, phloroglucinol, and 2,4-dihydroxy-benzoic acid; and (4) miscellaneous inhibitors such as aminotriazole, tricyanoaminopropene, and antipyrine and its iodinated derivative, iodopyrine.

Many of these chemicals exert their action by inhibiting thyroid peroxidase, which results in a disruption both of the iodination of tyrosyl residues in thyroglobulin and of the coupling reaction of iodotyrosines (i.e., MIT and DIT) to form iodothyronines (T_3 and T_4). In rats, PTU has been shown to affect each step in thyroid hormone synthesis beyond iodide transport. The order of susceptibility to the inhibition by PTU is the coupling reaction (most susceptible), iodination of MIT to form DIT (moderately susceptible), and iodination of tyrosyl residues to form MIT (least susceptible). Thiourea differs from PTU and other thioamides because it does not inhibit guaiacol oxidation (the standard assay for peroxidase) and does not inactivate thyroid peroxidase in the absence of iodine. Its ability to inhibit organic iodinations is due primarily to the reversible reduction of active I_2 to $2I^-$.

The goitrogenic effects of sulfonamides have been known since the reports of the action of sulfaguanidine on the rat thyroid in the early 1950s. Sulfamethoxazole and trimethroprim exert a potent goitrogenic effect in rats, resulting in marked decreases in circulating T_3 and T_4, a substantial compensatory increase in TSH, and increased thyroid weights due to follicular cell hyperplasia. The dog is also a sensitive species to the effects of sulfonamides, showing markedly decreased serum T_4 and T_3 levels, hyperplasia of thyrotrophic basophils, and increased thyroid weights. By comparison, the thyroids of monkeys and humans are resistant to the development of changes that sulfonamides produce in rodents (rats and mice) and dogs. Concentration of sulfonamide required to inhibit thyroid peroxidase in the monkey is about 500 times that required in the rat. Sensitive species (e.g., rat, mouse, and dog) are much more likely to develop follicular cell hyperplasia and thyroid tumors after long-term exposure to sulfonamides than are resistant species (e.g., nonhuman primate, human, guinea pig, and chicken).

Inhibitors of Thyroid Hormone Secretion

BLOCKAGE OF THYROID HORMONE RELEASE

Relatively few chemicals selectively inhibit the secretion of thyroid hormone from the thyroid gland (Figure 20.32). Excess iodine inhibits the secretion of thyroid hormone, and occasionally can cause goiter and hypothyroidism in animals and humans. Several mechanisms have been suggested for this effect of high iodide levels on thyroid hormone secretion, including a decrease in lysosomal protease activity, inhibition of colloid droplet formation, and inhibition of TSH-mediated increase in cAMP. Circulating levels of T_4, T_3, and rT_3 are decreased by an iodide excess.

Lithium has also been reported to have a striking inhibitory effect on thyroid hormone release (Figure 20.32). The widespread use of lithium carbonate in the treatment of manic states occasionally results in the development of goiter with either euthyroidism or occasional hypothyroidism in human patients. Lithium inhibits colloid droplet formation stimulated by cAMP *in vitro*, and inhibits the release of thyroid hormones.

XENOBIOTIC- (OR METABOLITE-)INDUCED THYROID PIGMENTATION OR COLLOID ALTERATION

The antibiotic minocycline produces a striking black discoloration of thyroid lobes in laboratory animals and humans with the formation of brown pigment granules within follicular cells. The pigment granules stain similarly to melanin and are best visualized on thyroid sections stained with the Fontana-Masson procedure. The pigment appears to be a metabolic derivative of minocycline, and administration of the antibiotic at a high dose to rats for extended periods may result in a disruption of thyroid function and development of thyroid enlargement ("goiter").

Other xenobiotics [or metabolite(s)] selectively localize in the thyroid colloid of rodents, resulting in abnormal clumping and increased basophilia of the colloid. Brown to black pigment granules may be present in follicular cells, colloid, and macrophages in the interthyroidal tissues, resulting in a macroscopic darkening of both thyroid lobes. The altered colloid in the lumen of thyroid follicles appears to be less able to react with organic iodine in a stepwise manner or to be phagocytized by follicular cells and processed enzymatically to release active thyroid hormones. Serum T_4 and T_3 are decreased, serum TSH levels are increased by an expanded population of pituitary thyrotrophs, and thyroid follicular cells undergo hypertrophy and hyperplasia. The incidence of thyroid follicular cell tumors in 2-year carcinogenicity studies in rodents is increased significantly at the higher dose levels, usually with a greater effect in male than in female rats. Similar thyroid changes or functional alterations usually do not occur in dogs, monkeys, or humans.

Effect on Peripheral Metabolism of Thyroid Hormones

Inhibitors of 5′-Deiodinase

FD&C RED NO. 3 (ERYTHROSINE)

FD&C Red No. 3 (erythrosine) is a red dye widely used as a color additive in foods, cosmetics, and pharmaceuticals. The Food and Drug Administration (FDA) peer review panel on Red No. 3 estimated the average quantity of the dye ingested in the United States to be 1.4 mg per person daily (0.023 mg/kg/day for a 60-kg person). FD&C Red No. is a tetraiodinated derivative of fluorescein, and iodine accounts for approximately 58% of the molecular weight of the dye.

Male Sprague-Dawley rats fed high 4% dietary concentrations of Red No. 3 beginning in utero and over their lifetime (30 months) developed a high incidence of thyroid follicular adenomas. Female rats fed similar amounts of the color additive did not have a significant increase in either benign or malignant thyroid tumors. Studies on the absorption, distribution, metabolism, and excretion of FD&C Red No. 3 confirmed earlier reports that the dye is absorbed poorly from the gastrointestinal tract and does not accumulate in the thyroid gland. Subsequent studies revealed that serum T_4 concentrations in rats receiving 4% of the dye are increased from 1 through 6 months while serum T_3 is reduced significantly. Circulating levels of reverse T_3 increase approximately seven-fold after 1 month, and TSH levels are approximately three times baseline. Serum TSH levels in rats fed Red No. 3 and receiving daily T_3 injections were decreased to undetectable levels. T_4 metabolism is altered significantly in liver homogenates prepared from rats fed

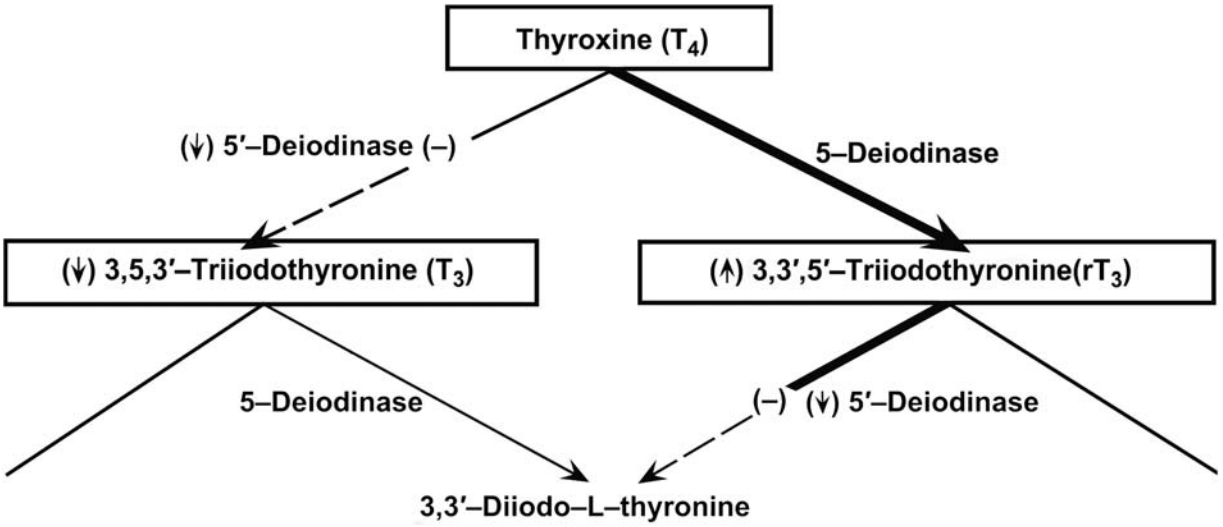

FIGURE 20.33 Effects of FD&C Red No. 3 (Erythrosine) on *in vivo* metabolism of thyroxine by inhibiting the 5′-deiodinase that normally converts T_4 to T_3. *Figure reproduced from Capen and Martin (1989). The effects of xenobiotics on the structure and function of thyroid follicular cells and C-cells,* Toxicol. Pathol. *17, 266–293, with permission.*

4% Red No. 3 (Figure 20.33). Degradation of T_4 is decreased accompanied by a drastic decrease in T_3.

Putting these findings together, an inhibition of 5′-deiodinase in the liver and kidney by Red No. 3 would explain the lower circulating T_3 levels. The monodeiodination of T_4 by another enzyme (5-deiodinase) to reverse T_3 and inhibition of the 5′-deiodinase [which is necessary to further degrade this inactive iodothyronine to 3,3′-diiodothyronine (T_2)] explains the striking accumulation of serum reverse T_3. The pituitary, sensing the lowered circulating levels of T_3, compensates by increasing the secretion of TSH, which results in the morphological evidence of follicular cell stimulation.

Other compounds that are known to inhibit 5′-monodeiodinase in peripheral tissues and disrupt thyroid hormone economy by inhibiting the conversion of T_4 to T_3 include amiodarone and iopanoic acid. These xenobiotics (as well as FD&C Red No. 3) are iodinated compounds, but it is unlikely that their effects are due to the iodide component because even large doses of iodide (5 mg/day) do not affect T_4 metabolism in rats.

AMIODARONE

Amiodarone, an iodinated drug used to treat tachyarrhythmias, inhibits the *in vivo* 5′-monodeiodination of T_4. It blocks the 5′-monodeiodinase (type I enzyme) in rat liver homogenates but not the 5′-deiodinase in the rat pituitary gland. Male and female Sprague-Dawley rats administered amiodarone in long-term carcinogenicity studies had an increased incidence of thyroid follicular cell hyperplasia and adenomas, whereas neither male nor female B6C3F1 mice in similar studies developed increased thyroid follicular cell hyperplasia or tumors. In shorter studies, male Sprague-Dawley rats receiving amiodarone had significant increases in serum TSH, T_4, and T_3, and significantly decreased serum rT_3. These changes are similar to those following administration of Red No. 3. It is likely that amiodarone, like FD&C Red No. 3, produces thyroid follicular cell adenomas in rats through the TSH-mediated secondary mechanism.

IOPANOIC ACID

Iopanoic acid is an iodinated radiographic contrast agent that inhibits both type I and type II 5′-monodeiodinase in rats. Iopanoic acid and FD&C Red No. 3 share the ability to inhibit the T_4 to T_3 conversion and increase serum TSH concentrations in rats. However, iopanoic acid inhibits both type I and type II 5′-monodeiodinase, whereas Red No. 3 inhibits only the type I enzyme in liver and kidney and not the type II enzyme in brain, pituitary, and brown adipose tissue. Iopanoic acid and FD&C Red No. 3 differ in their ability to affect human thyroid hormone economy. Iopanoic acid in doses used commonly in clinical radiographic studies results in increased serum concentrations of T_4 and rT_3, decreased serum T_3 with a compensatory increase in basal serum TSH concentrations, and increased TSH response to TRH after 5–7 days of treatment.

Inducers of Hepatic Microsomal Enzymes

Hepatic microsomal enzymes play an important role in thyroid hormone economy because glucuronidation is the rate-limiting step in the biliary excretion of T_4 and sulfation is the rate-limiting step in the excretion of T_3. Long-term exposure of rats to a wide variety of different chemicals induces these enzyme pathways and results in chronic stimulation of the thyroid by disrupting the hypothalamic–pituitary–thyroid axis (Figure 20.34). The resulting chronic stimulation of the thyroid by increased circulating levels of TSH often results in a greater risk of developing tumors derived from follicular cells in 2-year or lifetime studies with these compounds in rats. Xenobiotics that induce liver microsomal enzymes and disrupt thyroid function in rats include CNS drugs [e.g., phenobarbital (PB), benzodiazepines], Ca^{2+} channel blockers (e.g., nicardipine, bepridil), steroids (spironolactone), retinoids, chlorinated hydrocarbons (e.g., chlordane, dichlorodiphenyltrichloroethane [DDT], 2,3,7,8-tetrachlorodibenzodioxin [TCDD]), and polyhalogenated biphenyls (e.g., polychlorinated biphenyls (PCB), polybrominated biphenyls [PBB]). Most of the hepatic microsomal enzyme inducers have no apparent intrinsic carcinogenic activity and produce little or no mutagenicity or DNA damage. Their promoting effect on thyroid tumors usually is greater in rats than in mice, with males developing a higher incidence of tumors more often than females. In certain strains of mice, these compounds alter liver cell turnover and promote the development of hepatic tumors.

Many of the liver microsomal enzyme inducers in rats [such as PB, pregnenolone-16a-carbonitrile, 3-methylcholanthrene (3MC), and Arochlor 1254 (PCB)] that affect thyroid hormone economy typically induce the activity of T_4-UGT, which is associated with increased excretion of T_4-glucuronide and decreased serum T_4 concentration. Activation of T_3-UGT is more predictive of increased TSH in rats compared to T_4-UGT.

PHENOBARBITAL

PB has been studied extensively as the prototype for hepatic microsomal inducers that increase a similar spectrum of CYP isoenzymes. The activity of T_4-UGT, the rate-limiting enzyme in T_4 metabolism, also is increased by PB, with higher cumulative biliary excretion of T_4. Most of the increase in biliary excretion is T_4 glucuronide due to an increased metabolism of T_4 in PB-treated rats. PB-treated rats develop a characteristic pattern of changes in circulating thyroid hormone levels. Plasma T_3 and T_4 are decreased markedly after

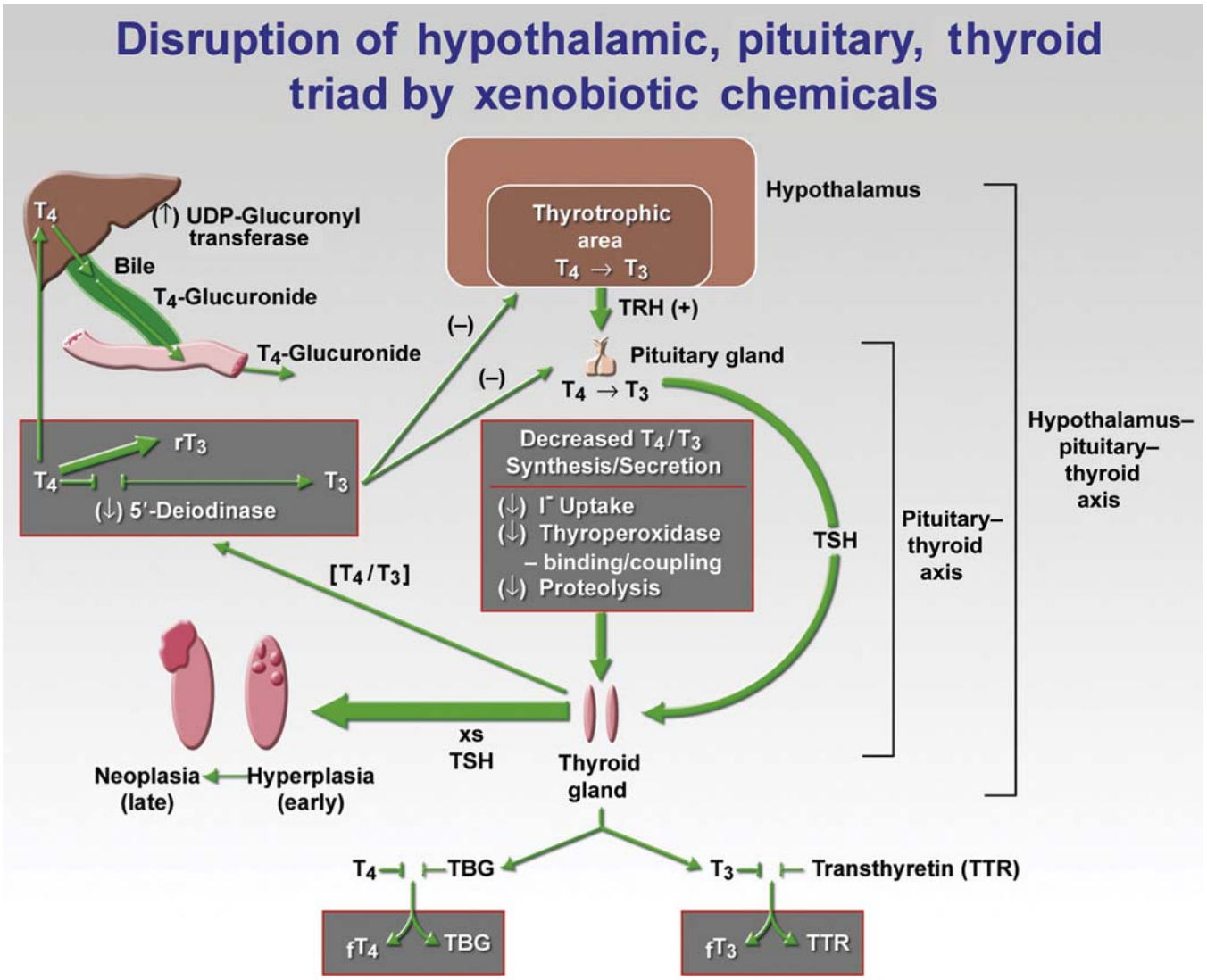

FIGURE 20.34 Multiple sites of disruption of the hypothalamic–pituitary–thyroid triad by xenobiotic chemicals. Chemicals can exert direct effects by disrupting thyroid hormone synthesis or secretion and indirectly influence the thyroid through an inhibition of 5′-deiodinase or by inducing hepatic microsomal enzymes (e.g., T_4-UDP-glucuronosyltransferase). All of these mechanisms can lower the circulating levels of thyroid hormones (T_4 and T_3), resulting in a release from negative feedback inhibition and a compensatory increased secretion of TSH by the pituitary gland. The chronic hypersecretion of excess (xs) TSH predisposes the sensitive rodent thyroid gland to develop an increased incidence of focal hyperplastic and neoplastic (adenomas) lesions by a secondary (epigenetic) mechanism. *Figure reproduced from* Handbook of Toxicologic Pathology, *third ed., W. M. Haschek, C. G. Rousseaux and M. A. Wallig, eds. (2013) Academic Press, Fig. 58.45, p. 2451, with permission.*

1 week and remain decreased for 4 weeks. By 8 weeks, T_3 levels return to near normal due to compensation by the hypothalamic–pituitary–thyroid axis. Serum TSH values are elevated significantly throughout the first month but often decline somewhat after a new steady state is attained. Thyroid weights increase significantly. The prevailing hypothesis is that the promotion of thyroid tumors by PB in rats is not a direct effect of PB on the thyroid gland but an indirect effect mediated by TSH secretion from the pituitary secondary to the hepatic microsomal enzyme-induced increase of T_4 excretion in the bile.

The activation of the thyroid gland during the treatment of rodents with substances that stimulate T_4 catabolism is a well-known phenomenon. It occurs particularly with rodents because (1) UGT can be induced easily in rodent species, and (2) T_4 metabolism takes place very rapidly in rats in the absence of TBG. Despite these findings in rodents, there is no convincing evidence that humans treated with drugs or exposed to chemicals that induce hepatic microsomal enzymes are at increased risk for the development of thyroid cancer. Epidemiologic studies of patients treated with therapeutic doses of PB have reported no

increase in risk for the development of thyroid neoplasia. Likewise, there is no substantive evidence that humans treated with drugs or exposed to chemicals that induce hepatic microsomal enzymes are at increased risk for the development of liver cancer.

POLYCHLORINATED BIPHENYLS

Another classic example of a class of chemical that induces hepatic microsomal enzymes and disrupts thyroid function is the PCB group. PCBs, commonly used industrial compounds, have caused widespread environmental contamination. The disease-producing capability of these compounds includes alterations in reproduction, growth, and development. PCBs cause a significant reduction in serum levels of thyroid hormones due to alterations in thyroid structure, in addition to the well-known induction of hepatic UGT and increased secretion of T_4-glucuronide in the bile.

The most consistent thyroid lesions in follicular cells following chronic feeding of PCB to rats are the accumulation of numerous large colloid droplets and irregularly shaped lysosomal bodies in an expanded cytoplasm. Chronic PCB exposure results in a striking distension of many follicular cells with large lysosomal bodies and colloid droplets, blunt and abnormally branched microvilli, and mitochondrial vacuolation. The principal lesion that contributes to the altered thyroid function appears to be interference with the interaction between colloid droplets and lysosomal bodies, necessary for the enzymatic release of thyroid hormones.

Secondary Mechanisms of Thyroid Oncogenesis

Understanding the mechanism of action of xenobiotics on the thyroid gland provides a more rational basis to extrapolate findings from long-term rodent studies to safety assessment of a particular compound for humans. Many chemicals and drugs disrupt one or more steps in the synthesis, secretion, and peripheral metabolism of thyroid hormones, resulting in subnormal levels of T_4 and T_3, associated with a compensatory increased secretion of pituitary TSH. When tested in a highly sensitive species, such as rats, these compounds result early in follicular cell hypertrophy/hyperplasia and increased thyroid weight, and, in long-term studies, an increased incidence of thyroid tumors by a secondary (indirect) mechanism.

In the secondary mechanism of thyroid oncogenesis in rodents, the specific xenobiotic chemical or physiologic perturbation evokes another stimulus (e.g., chronic hypersecretion of TSH) that promotes follicular cell hypertrophy and then hyperplasia with development of proliferative lesions (initially focal hyperplasia, then adenomas, and less frequently carcinomas). Thresholds for a no effect on the thyroid gland can be established by determining the dose of xenobiotic that fails to elicit an elevation in the circulating level of TSH. Compounds acting by this indirect (secondary) mechanism usually have little or no evidence for mutagenicity or for producing DNA damage.

In humans with markedly altered changes in thyroid function and chronically elevated TSH levels, as in areas with a high incidence of endemic goiter due to iodine deficiency, there is little if any increase in the incidence of thyroid cancer. The relative resistance to the development of thyroid cancer in humans with elevated plasma TSH levels is in marked contrast to the response of the thyroid gland to chronic TSH stimulation in rats and mice.

Initiators of Thyroid Carcinogenesis

Specific chemicals and irradiation appear to have a direct effect on the thyroid gland, resulting in genetic damage that leads to cell transformation and tumor formation. Examples of thyroid initiators include 2-acetylaminofluorene, *N*-methyl-*N*-nitrosourea (MNU), N,N-bis(2-hydroxypropyl) nitrosamine (DHPN), MC, dichlorobenzidine, and polycyclic hydrocarbons. Chemicals in this group often increase the incidence of both benign and malignant thyroid tumors over controls. Iodine status may have a significant impact on development of thyroid tumors; for example, iodine deficiency is a strong promoter of MNU-initiated thyroid tumors in rats. A common component of permanent hair dye preparations, 2,4-diaminoanisole sulfate (2,4-DAAS), dramatically increases thyroid neoplasm incidence in both male and female F344 rats. Follicular cell carcinomas are the principal type of neoplasm induced by 2,4-DAAS in thyroids without a background of diffuse hyperplasia of follicular cells. The carcinomas (papillary, cystic, and solid) were invasive but did not metastasize. 2,4-DAAS has been found to be mutagenic but is not teratogenic. In the thyroid, it results in a dose-dependent accumulation of brown granules in follicular cells that are basic fuchsin positive; PAS, acid fast, and iron negative; and ultrastructurally different than lipofuscin. The thyroid pigment may represent a reaction product of 2,4-DAAS and iodine in the cytoplasm of follicular cells.

PART 6: PARATHYROID GLAND

INTRODUCTION

Parathyroid glands are present in all air-breathing vertebrates. Phylogenetically, parathyroids first appear

in amphibians, coincident with the transition from an aquatic to a terrestrial life. It has been suggested that the appearance of parathyroid glands may have arisen from the need to protect against the development of hypocalcemia and the necessity to maintain skeletal integrity in terrestrial animals, which often are in a relatively low Ca^{2+}-high phosphorus environment.

Ca^{+} plays a key role in many fundamental biological processes, including muscle contraction, blood coagulation, enzyme activity, neural excitability, hormone release, and membrane permeability, in addition to being an essential structural component of the skeleton. Therefore, the precise control of Ca^{2+} in extracellular fluids is vital to health. To maintain a constant concentration of Ca^{2+}, despite variations in intake and excretion, endocrine control mechanisms have evolved that consist of the interaction of PTH, calcitonin, and the active form of Vitamin D (1,25-dihydroxyvitamin D or calcitriol).

STRUCTURE AND FUNCTION

Embryology and Macroscopic Anatomy

Parathyroid glands in most animal species consist of two pairs of glands situated in the anterior cervical region. Rats are the exception because they have a single pair of parathyroid glands located close to the thyroid. Embryologically, parathyroids are of entodermal origin, derived from the third and fourth pharyngeal pouches in close association with the primordia of the thymus (Figure 20.35). The entodermal bud that forms the thyroid gland arises on the midline at the level of the first pharyngeal pouch. This gives rise to the thyroglossal duct that migrates caudally. In the dog and cat, both external and internal parathyroids are close to the thyroid gland. The external parathyroid (III) in the dog is 2–5 mm in length and is found in the loose connective tissue cranial and slightly lateral to the anterior pole of the thyroid. The internal parathyroid (IV) is smaller, flatter, and situated on the medial surface of the thyroid beneath the fibrous capsule.

Functional Cytology

Chief Cells

Parathyroids contain a single type of secretory cell concerned with the elaboration of a single hormone. Parathyroids are composed of chief cells in different stages of secretory activity or in transition to oxyphil cells in certain species (Figure 20.36). Chief cells interpreted to be in an inactive (resting or involuted) stage

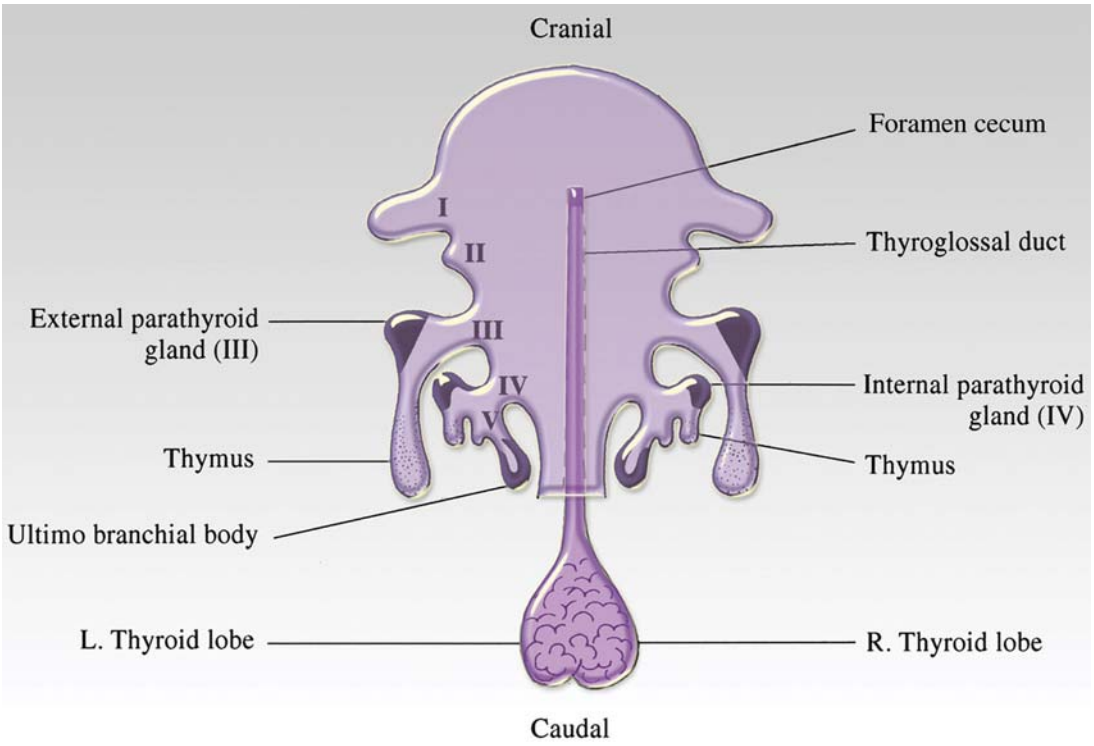

FIGURE 20.35 Embryology of the thyroid and parathyroid glands. The thyroid gland develops from a midline primordia (thyroglossal duct), whereas parathyroid glands develop from the cranial portions of the third and fourth pharyngeal pouch in association with the thymus. *Figure reproduced from* Handbook of Toxicologic Pathology, *third ed., W. M. Haschek, C. G. Rousseaux and M. A. Wallig, eds. (2013) Academic Press, Fig. 58.49, p. 2462, with permission.*

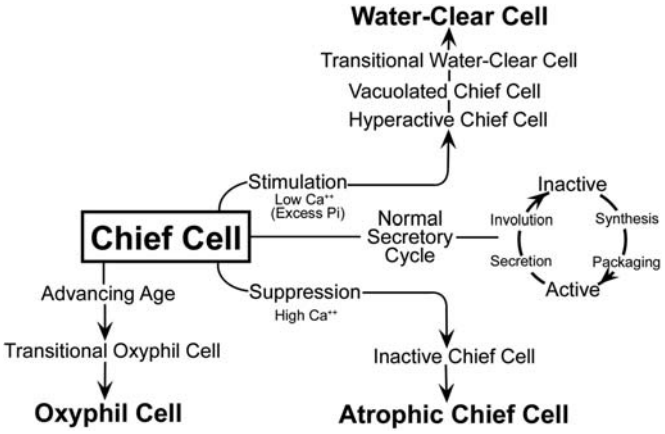

FIGURE 20.36 Functional cytology of parathyroid glands under normal and pathologic conditions. *Figure reproduced from Capen and Rosol (1993) Pathobiology of parathyroid hormone and parathyroid hormone-related protein: Introduction and evolving concepts. In:* Pathology of the Thyroid and Parathyroid Gland: An Update, *(LiVolsi, V. A. and DeLellis, R. A., eds.), Williams & Wilkins, pp. 1–33, with permission.*

of their secretory cycle predominate in the parathyroid glands under normal conditions. Inactive chief cells are cuboidal and have uncomplicated interdigitations between contiguous cells. The relatively electron-transparent cytoplasm contains poorly developed organelles and infrequent secretory granules. The cytoplasm often has either numerous lipid bodies and lipofuscin granules or aggregations of glycogen particles. Chief cells in the active stage of the secretory cycle occur less frequently in the parathyroid glands of most species. The cytoplasm of active chief cells has an increased electron density due to the closer proximity of organelles and secretory granules, increased density of the cytoplasmic matrix, and loss of glycogen particles and lipid bodies.

Oxyphil Cells

The second cell type in the parathyroid glands of certain animal species and humans is the oxyphil cell (Figure 20.36). These cells are absent in parathyroids of the rat, chicken, and many species of lower animals. Oxyphil cells are observed either singly or in small groups interspersed between chief cells. They are larger than chief cells, and their abundant cytoplasmic area is filled with numerous large, often bizarre-shaped, mitochondria. Glycogen particles and free ribosomes are interspersed between the mitochondria. Granular endoplasmic reticulum, Golgi apparatuses, and secretory granules are poorly developed, suggesting that oxyphil cells do not have an active function in the biosynthesis of PTH. Associated with the marked increase in mitochondria, oxyphil cells have been shown histochemically to have higher oxidative and hydrolytic enzyme activity than chief cells. Cells are observed with cytoplasmic characteristics intermediate between those of chief and oxyphil cells suggesting that oxyphil cells are derived from chief cells as the result of aging or some other metabolic derangement.

Parathyroid Hormone

Biosynthesis and Chemistry

The biosynthesis and secretion of PTH is described in detail in Figure 20.37. The biologically active PTH secreted by chief cells is a straight chain polypeptide consisting of 84 AA residues with a molecular weight of 9500. Molecular fragments of PTH are formed in the peripheral circulation and in the liver. The immunoheterogeneity created by the multiple circulating fragments of PTH has caused significant problems in the development and application of highly specific RIA to diagnostic problems in human patients and animals.

Storage and Secretion

Secretory (storage) granules have been demonstrated ultrastructurally within chief cells of the parathyroid glands. The paucity of secretory granules in certain species (e.g., rat) suggests that chief cells, in general, do not store a large concentration of preformed hormone. PTH in the cytoplasm and secretory granules can be stained by immunofluorescent or immunohistochemical techniques. Oxyphil cells do not stain for PTH.

Chief cells synthesize and secrete another major protein, chromogranin A (parathyroid secretory protein I). It is a 70-kDa protein composed of 430–448 AA that is costored and secreted with PTH. A similar molecule has been found in secretory granules of a wide variety of peptide hormone-secreting cells and in neurotransmitter secretory vesicles. Chromogranin A-derived peptides may act locally in an autocrine manner to inhibit the secretion of active hormone by endocrine cells, such as those of the parathyroid gland.

Chief cells in closely related species may vary considerably in the number of storage granules in their cytoplasm, for example, granules are infrequent in rats but numerous in mice. In response to the appropriate stimulus, secretory granules migrate peripherally in chief cells and their limiting membrane fuses with the plasma membrane of the cell. An internal cytoskeleton composed of microtubules and contractile microfilaments (mf) is important in the control of peripheral movement of secretory granules and liberation of secretory products. Colchicine, an inhibitor of intracellular transport and release of secretory products in a number of endocrine organs, also blocks the secretion of PTH from chief cells in rats.

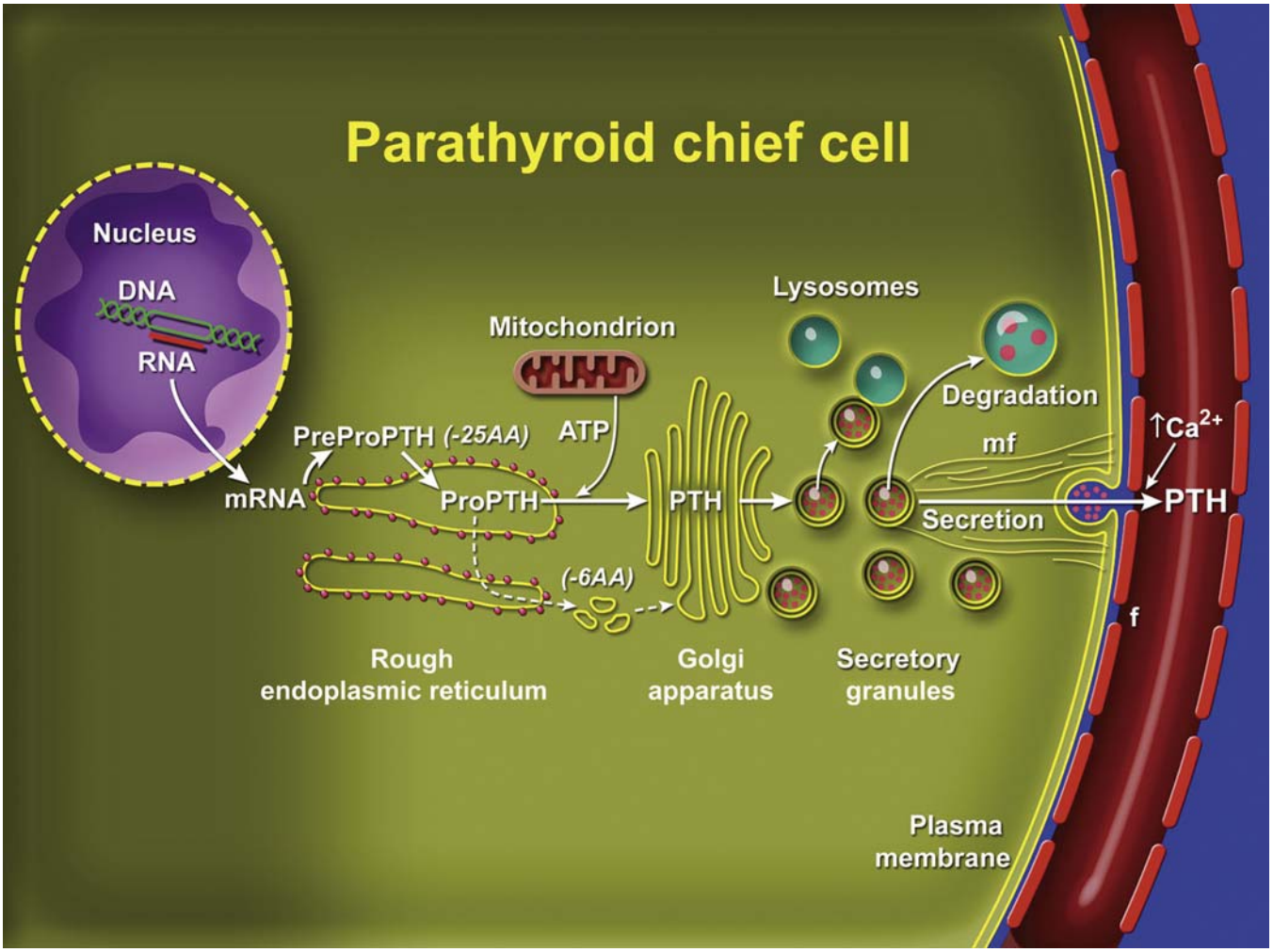

FIGURE 20.37 Subcellular compartmentalization, transport, and cleavage of precursors of parathyroid hormone (PTH). Preproparathyroid hormone (PreProPTH) is the initial translation product from ribosomes of the rough endoplasmic reticulum, which is converted rapidly to proparathyroid hormone (ProPTH). The hydrophobic sequence on the amino-terminal end of the PreProPTH facilitates penetration of the leading portion of the nascent peptide into the lumen of the endoplasmic reticulum. ProPTH is transported to the Golgi apparatus where it is converted enzymatically by a carboxypeptidase to biologically active PTH with a loss of six amino acids (AA). A major portion of the biosynthetic precursors and active PTH is degraded by lysosomal enzymes and is not secreted by chief cells under normal conditions. Extracellular Ca^{2+} binds to a membrane Ca^{2+} receptor (not shown) that induces secretion of mature secretory granules with the participation of microfilaments (mf). PTH enters the blood through capillary fenestrae (f). *Figure reproduced from* Handbook of Toxicologic Pathology, *third ed., W. M. Haschek, C. G. Rousseaux and M. A. Wallig, eds. (2013) Academic Press, Fig. 58.51, p. 2464, with permission.*

Secretory cells in the parathyroid gland store small amounts of preformed hormone but are capable of responding to minor fluctuations in Ca^{2+} concentration rapidly by altering the rate of hormonal secretion and more slowly by altering the rate of hormonal synthesis. In contrast to most endocrine organs that are under complex controls involving both long and short feedback loops, parathyroids have a unique feedback controlled by the concentration of Ca^{2+} (and, to a lesser extent, magnesium) ion in the serum. If the blood Ca^{2+} is elevated by the intravenous infusion of Ca^{2+}, there is a rapid and pronounced reduction in circulating levels of immunoreactive PTH (iPTH). Conversely, if the blood Ca^{2+} is lowered by ethylenediaminetetraacetic acid, there is a brisk and substantial increase in iPTH levels. The concentration of blood phosphorus has no direct regulatory influence on the synthesis and secretion of PTH; however, certain disease conditions with hyperphosphatemia are associated clinically with secondary hyperparathyroidism. An elevated blood phosphorus level may lead indirectly to parathyroid stimulation by virtue of its ability to lower blood Ca^{2+}. Magnesium ion has an effect on parathyroid secretion rate similar to that of Ca^{2+}, but its effect is not equipotent to that of Ca^{2+}.

Recently synthesized and processed active PTH may be released directly in response to increased demand and bypass the storage pool of mature secretory granules in the cytoplasm of chief cells. Bypass secretion of PTH can be stimulated only by a low circulating concentration of Ca^{2+}.

The major inhibitors of PTH synthesis and secretion are increased serum [Ca^{2+}] and 1,25-dihydroxyvitamin D. Inhibition of PTH synthesis by 1,25-dihydroxyvitamin D completes an important endocrine feedback loop between the parathyroid chief cells and the renal epithelial cells because PTH stimulates renal production of 1,25-dihydroxyvitamin D.

Biological Actions

PTH is the principal hormone involved in the minute-to-minute fine regulation of blood Ca^{2+} in mammals. The action of PTH on bone is the mobilization of Ca^{2+} from skeletal reserves into extracellular fluids. The increase in blood Ca^{2+} results from an interaction of PTH with osteoblasts and osteoclasts in bone along with increased tubular reabsorption of Ca^{2+} in the kidney.

BONE

Osteoclasts are primarily responsible for the catabolic action of PTH on bone by increasing resorption. PTH stimulates increased numbers and activity of osteoclasts; however, osteoclasts do not have receptors for PTH. Receptors for PTH are present on osteoblasts. Isolated osteoclasts respond to PTH only with the concurrent presence of osteoblasts. PTH binds to the PTH receptor on osteoblasts and stimulates them to produce RANKL (receptor activator of NFκB ligand), which binds to its receptor, RANK, on osteoclast precursors and osteoclasts to increase the number and function of osteoclasts, respectively. PTH inhibits the production of osteoprotegerin (OPG) by osteoblasts. OPG is a secreted decoy receptor for RANKL, which blocks its action in bone. Therefore, the ratio of RANKL:OPG in the bone microenvironment regulates the level of osteoclastic bone resorption.

KIDNEY

PTH has a rapid and direct effect on renal tubular function, leading to decreased reabsorption of phosphorus and phosphaturia in the proximal tubule of the nephron. PTH binds to a receptor on the basolateral aspect of renal epithelial cells. The hormone stimulates adenylyl cyclase, increases intracellular cAMP, and inhibits phosphorus reabsorption across the brush border through the actions of protein kinases.

PTH also increases the reabsorption of Ca^{2+}, which is of considerable importance in the maintenance of Ca^{2+} homeostasis. The effect of PTH on tubular reabsorption of Ca^{2+} appears to be due to a direct action on the distal convoluted tubule and is coupled to increases in intracellular cAMP. Transcellular transport of Ca^{2+} from the renal tubule lumen to the blood by the kidney involves the Ca^{2+}-selective channels on the luminal (apical) side of the renal epithelial cells, intracellular calbindins to buffer Ca^{2+}, and the $Ca^{2+}-Na^{+}$ exchanger (NCX) and Ca^{2+}-ATPase (PMCA) on the basilar side of the epithelial cells. In addition to PTH, the cell membrane Ca^{2+} receptor, calcitriol, and calcitonin regulate renal Ca^{2+} reabsorption.

Subcellular Mechanism of Action

The receptor for the N-terminal portion of PTH, composed of 34 AA, is considered the most important region in terms of Ca^{2+} regulation. The receptor for N-terminal PTH is a seven transmembrane domain receptor that is expressed in renal epithelial cells, osteoblasts, and dermal fibroblasts and is also found on cells that are not associated with the actions of PTH. Binding of PTH to the receptor results in increased levels of cytoplasmic cAMP and Ca^{2+} by stimulation of the adenylyl cyclase and phosphatidyl inositol pathways.

Degradation

PTH is secreted continuously from chief cells primarily as the intact (1–84 AA sequence) molecule under normal conditions. In the liver (Küpffer cells) PTH is cleaved into the smaller (approximately one-third of the molecule) NH_2-terminal (biologically active) portion and a larger (approximately two-thirds of the molecule) C-terminal (biologically inactive) portion. The kidney is also a major organ for the degradation and excretion of PTH. Biologically active PTH from the peritubular capillaries is degraded by specific proteases on the surface of renal tubular cells. In addition, both biologically active and inactive fragments are degraded intracellularly by lysosomal enzymes in renal tubular cells. C-terminal PTH has a longer circulating half-life compared to full-length and NH_2-terminal PTH.

EVALUATION OF TOXICITY

Morphologic Evaluation

The parathyroid gland is infrequently injured directly by xenobiotics. However, parathyroid function may be altered by a wide variety of chemicals that either elevate or lower the blood Ca^{2+} concentration. In response to hypocalcemia, chief cells undergo hypertrophy and eventually hyperplasia. On formalin- or Bouin's-fixed sections, the expanded cytoplasmic

area is lightly eosinophilic and vacuolated compared with chief cells in normal animals. Perivascular spaces are narrow in a hyperplastic parathyroid and there are few fat cells in the interstitium. In response to hypercalcemia, the cytoplasmic area of chief cells is decreased and more densely eosinophilic, often with a widening of intercellular and pericapillary spaces. If the hypercalcemia is prolonged, there is an overall reduction of glandular parenchyma with increased fibrous or adipose connective tissue in the interstitium. Subtle differences between treated and control groups can be best evaluated by the morphometric evaluation of parenchyma:interstitium and cytoplasmic:nuclear area of chief cells.

Ultrastructural evaluation of chief cells is a sensitive means of assessing morphologically whether a particular drug or chemical affects the parathyroid gland. Perfusion of the thyroid–parathyroid area with glutaraldehyde-based fixatives followed by postfixation with osmium tetroxide results in the best retention of structural detail. Morphometric studies at the ultrastructural level can be used to quantitate total cytoplasmic area and area occupied by a particular organelle (e.g., secretory granule).

In response to an acute lowering of blood Ca^{2+}, a larger percentage of chief cells ultrastructurally will be in the active stage of synthesis and secretion than under steady-state conditions. This is indicated by a peripheral migration of secretory granules and alignment along the plasma membrane, aggregation of the endoplasmic reticulum into lamellar arrays, and enlargement of the Golgi apparatus associated with many small dense granules in the process of formation. Conversely, chief cells in response to hypercalcemia are predominantly in the inactive stage of the secretory cycle as evaluated by electron microscopy, with straight plasma membranes dispersed profiles of endoplasmic reticulum, small Golgi complexes with few granules, and often accumulations of either glycogen or lipid (depending on the species) in the cytoplasm.

Atrophic chief cells develop in response to sustained or more severe hypercalcemia. Their cytoplasm is more electron-dense and irregularly shrunken with widened intercellular spaces. Cytoplasmic organelles are poorly developed and may have early degenerative changes suggested by mitochondrial vacuolation with disruption of cristae, and distension of endoplasmic reticulum, with loss of ribosomes.

Assay of Circulating Parathyroid Hormone

The metabolism of PTH and the formation of multiple circulating forms of PTH have made the development of clinically useful immunoassays challenging. The principal circulating forms of PTH include intact PTH (1–84) and C-terminal peptides (e.g., PTH 35–84). Circulating N-terminal PTH is not present at biologically relevant concentrations, but administration of exogenous PTH (1–34) will nevertheless induce the typical actions of PTH on bone and kidney cells.

Intact serum PTH concentrations are best measured by two-site immunoradiometric assay or N-terminal RIA. Mouse- and rat-specific PTH assays are commercially available. Serum-intact PTH can be measured in dogs and cats with assays developed for human PTH due to the crossreactivity of the antisera used in the assays, but internal validation should be performed for preclinical toxicity studies.

RESPONSE OF PARATHYROID CHIEF CELLS TO INJURY

Parathyroid Cysts

Small cysts are observed frequently as naturally occurring lesions within the parenchyma of the parathyroid or in the immediate vicinity of the glands in rats and dogs, and occasionally in other animal species. Parathyroid cysts usually are multiloculated, lined by a cuboidal to columnar (often partially ciliated) epithelium, and contain a densely eosinophilic proteinic material. Parathyroid (Kürsteiner's) cysts develop from a persistence and dilatation of remnants of the duct that connects the parathyroid and thymic primordia during embryonic development. Similar cysts may be present in the anterior mediastinum when remnants of the embryonic duct are displaced with the caudal migration of the thymus. Parathyroid cysts are distinct from midline cysts derived from remnants of the thyroglossal duct. The latter are lined by multilayered thyroidogenic epithelium that often has colloid-containing follicles. They usually are located near the midline from the base of the tongue caudally into the mediastinum.

Proliferative Lesions of Parathyroid Chief Cells

Incidence

Proliferative lesions of the parathyroid gland include hyperplasia (diffuse and focal), adenomas, and carcinomas. Neoplasms of the parathyroid glands are uncommon in all species of laboratory and domestic animals, but occur at low incidence in rats, Syrian hamsters, dogs, and, rarely, mice. Parathyroid hyperplasia may be primary or secondary. Primary parathyroid hyperplasia or tumors may be functional

(endocrinologically active) or non-functional. Primary hyperparathyroidism is the disorder that results from the excessive and autonomous secretion of PTH from adenomas or chief cell hyperplasia. Atrophy of the remaining normal parathyroid tissue is present with functional tumors and multinodular parathyroid hyperplasia.

Hyperplasia

FOCAL ("NODULAR") HYPERPLASIA

Chief cell hyperplasia may affect the parathyroid in a distinctly focal or multifocal distribution. In focal parathyroid hyperplasia there are single or multiple nodules in one or both glands where there is an increased number of closely packed chief cells often with an expanded cytoplasmic area (Figure 20.38). Focal areas of chief cell hyperplasia are poorly demarcated and not encapsulated from adjacent parenchyma. Chief cells within the nodules have a relatively uniform composition with a high cytoplasm:nucleus ratio and a slightly more hyperchromatic nucleus than adjacent normal chief cells. There may be slight compression of adjacent chief cells around larger focal areas of hyperplasia. Focal chief cell hyperplasia often is difficult to separate from chief cell adenoma using only morphological criteria. The presence of multiple nodules of varying sizes and uniform cellularity in one or both parathyroids with minimal compression and no encapsulation is more compatible with (multi)focal hyperplasia than chief cell adenoma.

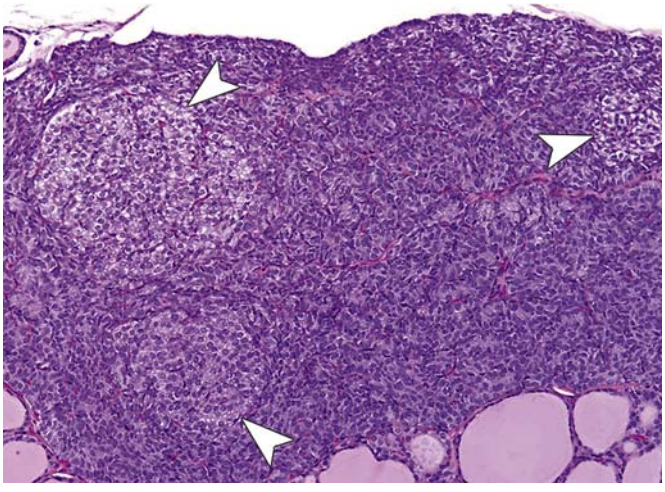

FIGURE 20.38 Multifocal (nodular) hyperplasia (arrowheads) of chief cells in parathyroid glands of a Wistar Han rat. The focal areas of increased cellularity are poorly demarcated and not encapsulated from adjacent parathyroid parenchyma. H&E stain. *Figure reproduced from* Handbook of Toxicologic Pathology, *third ed., W. M. Haschek, C. G. Rousseaux and M. A. Wallig, eds. (2013) Academic Press, Fig. 58.54, p. 2471, with permission.*

Diffuse Hyperplasia

Diffuse parathyroid hyperplasia, as seen with chronic renal failure and long-term dietary imbalances, results in a uniform enlargement of all parathyroid glands. In rats with chronic renal failure, diffusely hyperplastic parathyroid glands may be detected macroscopically as 1- to 2-mm pale nodules projecting from the surface of each thyroid lobe. The uniform enlargement of parathyroid glands is due to both hypertrophy and hyperplasia of chief cells. There is no peripheral rim of compressed atrophic parathyroid parenchyma as seen around a functional adenoma, but there is a uniform population of hyperplastic chief cells extending to the capsule of the gland (Figure 20.39). Chief cells are packed together closely, often with indistinct cell boundaries. The expanded cytoplasmic area of chronically stimulated chief cells is lightly eosinophilic, with occasional distinct vacuoles. A more prominent fibrovascular stroma in some diffusely hyperplastic parathyroids may result in a lobulated appearance. In other hyperplastic parathyroids, chief cells form distinct acinus-like structures in the gland.

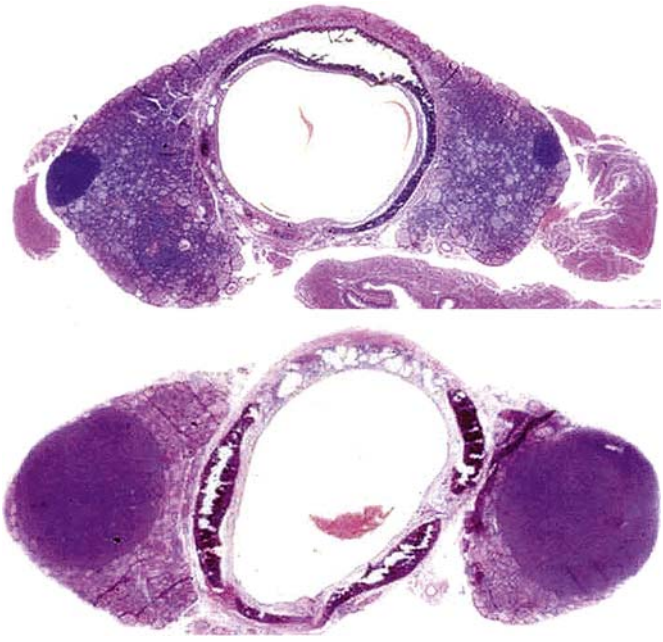

FIGURE 20.39 Bilateral diffuse hyperplasia of parathyroid chief cells with overall enlargement of parathyroid glands of a rat with chronic renal disease (lower image) compared to a normal rat (upper image). There is a uniform increase in cellularity due to hypertrophy and hyperplasia of chief cells. Increased cytoplasm renders the hypertrophic chief cells more eosinophilic compared to normal chief cells with a greater nuclear:cytoplasmic ratio in the control rat. H&E stain. *Figure reproduced from* Handbook of Toxicologic Pathology, *third ed., W. M. Haschek, C. G. Rousseaux and M. A. Wallig, eds. (2013) Academic Press, Fig. 58.55, p. 2472, with permission.*

ADENOMA

Parathyroid adenomas in rats vary from microscopic in size to unilateral nodules several millimeters in diameter. Tumors of parathyroid chief cells do not appear to be sequelae of longstanding secondary hyperparathyroidism of either renal or nutritional origin. The unaffected parathyroid glands may be atrophic if the adenoma is functional, normal if the adenoma is nonfunctional, or enlarged if there is concomitant hyperplasia. In functional adenomas, the normal mechanism by which PTH secretion is controlled by the concentration of blood Ca^{2+} is lost and hormone secretion is excessive, despite an increased level of blood Ca^{2+}.

Adenomas are solitary nodules that are sharply demarcated from adjacent parathyroid parenchyma (Figure 20.40). Because the adenoma compresses the rim of surrounding parathyroid to varying degrees, depending on its size, there may be a partial fibrous capsule, either from compression of existing stroma or from proliferation of fibrous connective tissue. Adenomas are usually nonfunctional in rats but may be functional in dogs, cats, and humans. Chief cells in nonfunctional adenomas are cuboidal or polyhedral and arranged in a diffuse sheet, lobules, or acini with or without lumens. Nuclei are round to oval and often vesicular, and there may be infrequent mitotic figures. Chief cells from functional adenomas often are closely packed into small groups by fine connective tissue septa and have lightly eosinophilic cytoplasm. There is a much lower density of cells in a functional parathyroid adenoma than in the adjacent rim with atrophic chief cells. Some parathyroid adenomas in the rat become cystic.

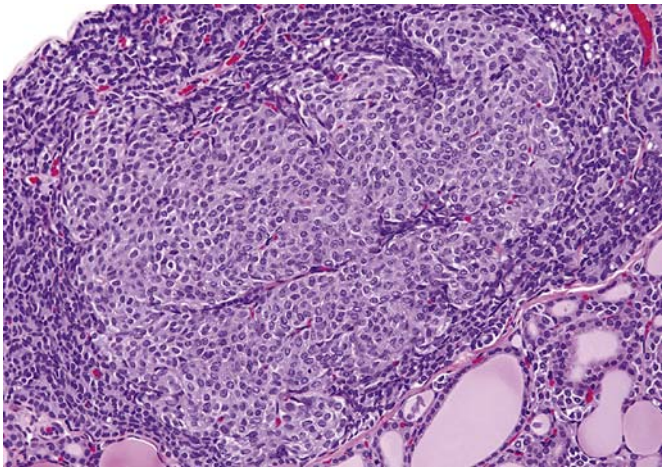

FIGURE 20.40 Chief cell adenoma that is irregular in shape and well demarcated from adjacent parathyroid parenchyma in a Fischer rat. Chief cells in the adenoma have a larger cytoplasmic area than those in the compressed rim of the parathyroid gland. H&E stain. *Figure reproduced from* Handbook of Toxicologic Pathology, *third ed., W. M. Haschek, C. G. Rousseaux and M. A. Wallig, eds. (2013) Academic Press, Fig. 58.56, p. 2473, with permission.*

CARCINOMA

Chief cell carcinomas are encountered rarely. Carcinomas result in a macroscopically detectable enlargement of one gland. Parathyroid carcinomas often are more fixed in position than chief cell adenomas due to invasion of adjacent thyroid or adjacent cervical skeletal muscle. Some of the enlargement may be due to central necrosis and hemorrhage in the carcinoma.

Malignant chief cells are arranged in solid sheets subdivided into lobules by a fine fibrous and richly vascular stroma, often palisading along blood sinusoids. Occasionally, they form acinar structures. There is usually complete incorporation of the affected gland and evidence of invasion through the parathyroid capsule. Evidence of vascular invasion and formation of tumor cell emboli are observed infrequently. Malignant chief cells may be more pleomorphic than those that constitute adenomas, but mitotic figures are infrequent. The cytoplasmic area stains lightly eosinophilic, and boundaries of adjacent chief cells are indistinct.

Multinucleated Syncytial Cells

Parathyroid glands of dogs, rats, and other animals occasionally develop a unique multinucleated syncytial giant cell. Syncytial cells are often more numerous near the periphery of the gland. The number of syncytial cells may account for up to one-half of the parenchyma of the gland. These cells appear to form by the fusion of the cytoplasmic area of adjacent chief cells. The mechanism by which syncytial cells form is uncertain, but it has been suggested that syncytial cells may be an artifact of immersion fixation with aldehydes due to membrane disintegration.

MECHANISMS OF TOXICITY

Agents Influencing the Development of Proliferative Lesions

Age

There are relatively few chemicals or experimental manipulations reported in the literature that significantly increase the incidence of parathyroid tumors. Longstanding renal failure with intense diffuse hyperplasia does not appear to increase the development of chief cell tumors in animals. Parathyroid adenomas in F344 rats are an example of a neoplasm whose incidence increases dramatically when comparing 2-year

studies to lifetime data, where the incidence of parathyroid adenomas increased in males from 0.1% at 2 years to 3.1% in lifetime studies. Corresponding data for female F344 rats was 0.1% at 2 years and 0.6% in lifetime studies.

Irradiation

Irradiation (^{131}I) significantly increases the incidence of parathyroid adenomas in inbred Wistar albino rats of both sexes. However, tumor incidence can be modified by feeding diets with variable amounts of vitamin D, high dietary levels decrease the incidence whereas low levels increase it. Gonadectomy decreased the incidence of radiation-induced (^{131}I) parathyroid adenomas in male rats but had little effect in females. X-irradiation of the thyroid–parathyroid region also increases the incidence of parathyroid adenomas.

Xenobiotics

Parathyroid adenomas have been encountered infrequently following the administration of a variety of chemicals in 2-year bioassay studies in F344 rats. In a study of the pesticide rotenone in F344 rats, there was an increased incidence of parathyroid adenomas in high-dose (75 ppm) males compared with low-dose (38 ppm) males, control males, or NTP historical controls. It is uncertain whether the increased incidence of this uncommon tumor was a direct effect of rotenone feeding or the increased survival time in high-dose males. Chief cell hyperplasia was not present in parathyroids that developed adenomas.

Modification of Parathyroid Function Associated with Metabolic Disorders

Renal Hyperparathyroidism

Secondary hyperparathyroidism as a complication of chronic renal failure is a metabolic state characterized by an excessive, but not autonomous, rate of PTH secretion. The secretion of hormone by the hyperplastic parathyroid gland usually remains responsive to fluctuations in blood Ca^{2+}. The primary etiologic mechanism in this disorder is longstanding progressive renal disease. When the renal disease progresses to the point at which there is a significant reduction in the glomerular filtration rate, phosphorus is retained and progressive hyperphosphatemia develops (Figure 20.41). Hyperphosphatemia contributes to parathyroid stimulation by virtue of its ability to lower blood Ca^{2+} levels. Parathyroid stimulation associated with chronic renal disease also can be attributed to hypocalcemia. Impaired intestinal absorption of Ca^{2+} due to the acquired defect in Vitamin D metabolism associated with loss of tubular mass plays a role in

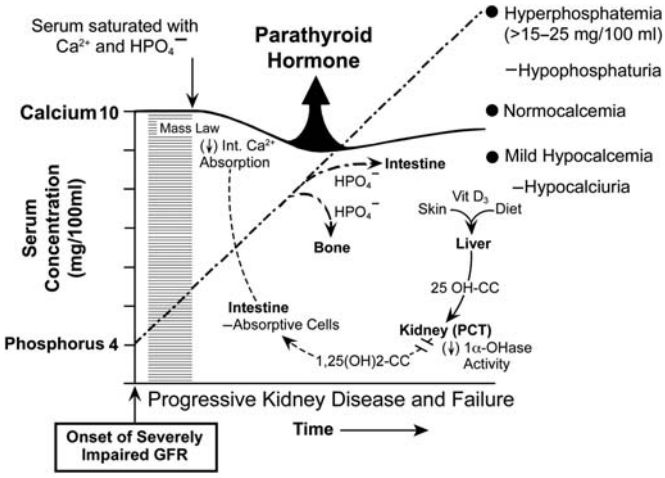

FIGURE 20.41 Alterations in levels of serum calcium and phosphorus during the pathogenesis of secondary hyperparathyroidism associated with chronic progressive renal failure. *Figure reproduced from* Handbook of Toxicologic Pathology, *second ed. W. M. Haschek, C. G. Rousseaux and M. A. Wallig, eds. (2002) Academic Press, Vol. 2, Fig. 53, p. 696, with permission.*

the development of hypocalcemia. Thus, there is diminished production of 1,25-dihydroxyvitamin D_3, in turn leading to diminished intestinal Ca^{2+} uptake. 1,25-Dihydroxyvitamin D_3 also completes an important negative feedback loop with the parathyroid gland since it inhibits the synthesis and secretion of PTH. Decreased 1,25-dihydroxyvitamin D_3 leads to release of chief cells from negative feedback and secondary hyperparathyroidism. All parathyroids are considerably enlarged as a result initially of hypertrophy of chief cells and subsequently due to hyperplasia as a compensatory mechanism.

Nutritional Hyperparathyroidism

The increased secretion of PTH in nutritional hyperparathyroidism is a compensatory mechanism directed against a disturbance in mineral homeostasis induced by nutritional imbalances. The disease occurs in dogs, cats, monkeys, laboratory rodents, and others fed improper diets. Dietary mineral imbalances of etiologic importance in the pathogenesis are a low content of Ca^{2+}, excessive phosphorus with normal or low Ca^{2+}, and inadequate amounts of cholecalciferol (Vitamin D_3) in New World nonhuman primates housed indoors without exposure to sunlight. The significant end result is hypocalcemia which results in parathyroid stimulation (Figure 20.42). A diet low in Ca^{2+} fails to supply the daily requirement, even though a greater proportion of ingested Ca^{2+} is absorbed, and hypocalcemia develops. Ingestion of excessive phosphorus results in increased intestinal absorption and elevation in blood phosphorus levels. Hyperphosphatemia does not stimulate the parathyroid gland directly but

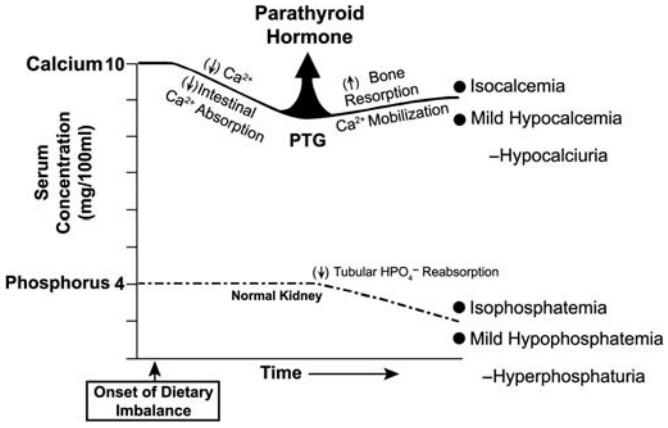

FIGURE 20.42 Alterations in serum calcium and phosphorus in the pathogenesis of nutritional secondary hyperparathyroidism caused by feeding a diet low in calcium or deficient in cholecalciferol but with normal amounts of phosphorus. *Figure reproduced from* Handbook of Toxicologic Pathology, *second ed. W. M. Haschek, C. G. Rousseaux and M. A. Wallig, eds. (2002) Academic Press, Vol. 2, Fig. 54, p. 763, with permission.*

does so indirectly by virtue of its ability to lower blood Ca^{2+} levels and suppress the synthesis of 1,25-dihydroxycholecalciferol by the kidney. In response to nutritionally induced hypocalcemia, all parathyroid glands undergo cellular hypertrophy and hyperplasia.

Hypoparathyroidism

Hypoparathyroidism is a metabolic disorder in which either subnormal amounts of PTH are secreted by pathologic parathyroids, or the hormone secreted is unable to interact normally with target cells. Hypoparathyroidism often is associated with diffuse lymphocytic parathyroiditis, resulting in the extensive degeneration of chief cells and replacement by fibrous connective tissue. In the early stages of lymphocytic parathyroiditis, there is infiltration of the gland with lymphocytes and plasma cells and nodular regenerative hyperplasia of the remaining chief cells. Lymphocytic parathyroiditis appears to develop by immune-mediated mechanisms. The functional disturbances of hypoparathyroidism primarily are the result of increased neuromuscular excitability and tetany. Bone resorption is decreased because of a lack of PTH, and blood Ca^{2+} levels diminish and serum phosphate levels increase progressively.

Primary Hyperparathyroidism

In primary hyperparathyroidism, PTH is produced in excess by a functional tumor in the gland. The normal control of PTH secretion by the concentration of blood Ca^{2+} is lost in primary hyperparathyroidism. Hormone secretion is autonomous, and the parathyroid produces excessive hormone despite the increased blood Ca^{2+}. PTH acts initially on cells in the renal tubules to promote the excretion of phosphorus and the retention of Ca^{2+}. A prolonged increased secretion of PTH results in accelerated bone resorption and increased renal production of 1,25-dihydroxyvitamin D_3. The lesion in the parathyroid gland responsible for the excessive secretion of PTH usually is an adenoma composed of active chief cells.

Cancer-Associated Hypercalcemia

There are three mechanisms by which tumors can induce hypercalcemia: hematologic cancers present in the bone marrow induce hypercalcemia by causing the local destruction of bone; solid tumors can widely metastasize to bone and result in local bone loss associated with the tumor metastases; and humoral hypercalcemia of malignancy (HHM), in which solid tumors that have no or few metastases to bone induce their effects distant from the site of the tumor by the elaboration of one or more factors.

HHM is a syndrome associated with diverse malignant neoplasms in dogs, humans, and cats, and rarely in other animals, although it has been reported in rats and mice. Characteristic clinical findings with HHM include hypercalcemia, hypophosphatemia, hypercalciuria (often with decreased fractional Ca^{2+} excretion), increased fractional excretion of phosphorus, increased nephrogenous cAMP, and increased osteoclastic bone resorption. Hypercalcemia is induced by humoral effects on bone, kidneys, and possibly the intestine.

Malignant neoplasms that are commonly associated with HHM in animals include the adenocarcinoma derived from apocrine glands of the anal sac in dogs, some T-cell lymphomas of dogs, and miscellaneous carcinomas that induce HHM sporadically. Excessive secretion of biologically active PTH-related protein (PTHrP) by cancer cells plays a central role in the pathogenesis of hypercalcemia in most forms of HHM.

PTHrP is produced by a number of normal tissues in neonates and adults, where it functions primarily as a paracrine factor. For example, PTHrP expression by chondrocytes regulates the growth and differentiation of chondrocytes in the growth plate and, indirectly, the length of the long bones. In the fetus, PTHrP regulates Ca^{2+} balance and placental Ca^{2+} transport. Genetic disruption of PTHrP leads to death after birth.

In HHM, PTHrP binds to the common N-terminal PTH/PTHrP (PTH1) receptor in bone and kidney, where it stimulates adenylyl cyclase and increases intracellular Ca^{2+} in bone and kidney. Increased osteoclastic bone resorption with Ca^{2+} release is a consistent finding in HHM. The kidneys play a critical role in the pathogenesis of hypercalcemia, as renal Ca^{2+} reabsorption is stimulated by PTHrP. In some forms of HHM, there are increased serum

1,25-dihydroxyvitamin D_3 levels, which may increase Ca^{2+} absorption from the intestine.

PART 7: ENDOCRINE PANCREAS

INTRODUCTION

The endocrine pancreas consists of a diffusely distributed system of endocrine cells organized mainly into "islets of Langerhans" (islets) but also occurring as small clusters of cells or individual cells in or adjacent to exocrine pancreatic ductules, exocrine acini, or within interstitial connective tissue. Islets are well defined and easily discerned. They range widely in size (100–200 μm in diameter). Islets are not randomly distributed throughout the pancreas but are concentrated in different lobes of the pancreas depending on the species. Each islet consists of multiple different endocrine cells that have separate functions, yet interact in a paracrine manner and by electrical gap-junction coupling. The most numerous endocrine cell type (70%–80%) is the β cell, which is responsible for secretion of insulin and regulation of glucose and fat metabolism. Electrically coupled β cells secrete insulin more effectively than single cells. Other cell types include the α cell (secretes glucagon), δ cell (secretes somatostatin), the PP or F cell (secretes pancreatic polypeptide-PP), and the ε cell (secretes ghrelin). Isolated or small clusters of endocrine cells in the pancreas are usually β cells.

STRUCTURE AND FUNCTION

Functional Cytology

Immunohistochemistry and immunofluorescence are effective techniques to identify the endocrine cell types in the pancreas. In addition, ultrastructure can be used to identify cell types and evaluate cellular pathology. The secretory granules, including their dense cores and submembranous spaces, have distinct sizes and shapes, depending on the cell type and species. For example, in rats, insulin-containing secretory granules have variably sized round dense cores and wide submembranous spaces. In dogs and other species, however, some of the β-cell dense cores of secretory granules are crystalline and elongate.

Islet cells are organized so that β cells have homologous contacts with other β cells and heterologous contacts with α cells. In rats and mice, islet cells are organized in a specific manner. β Cells are the most numerous endocrine cell type and are located in the central region of the islet (Figure 20.43A). However, a small percentage of large islets may have β cells concentrated in the periphery as well. Smaller islets are composed entirely of β cells. The α cells are located in the periphery or mantle of the islet (Figure 20.43B). Small numbers of δ cells and PP cells are also scattered in the periphery of the islets. This pattern is different in humans and nonhuman primates.

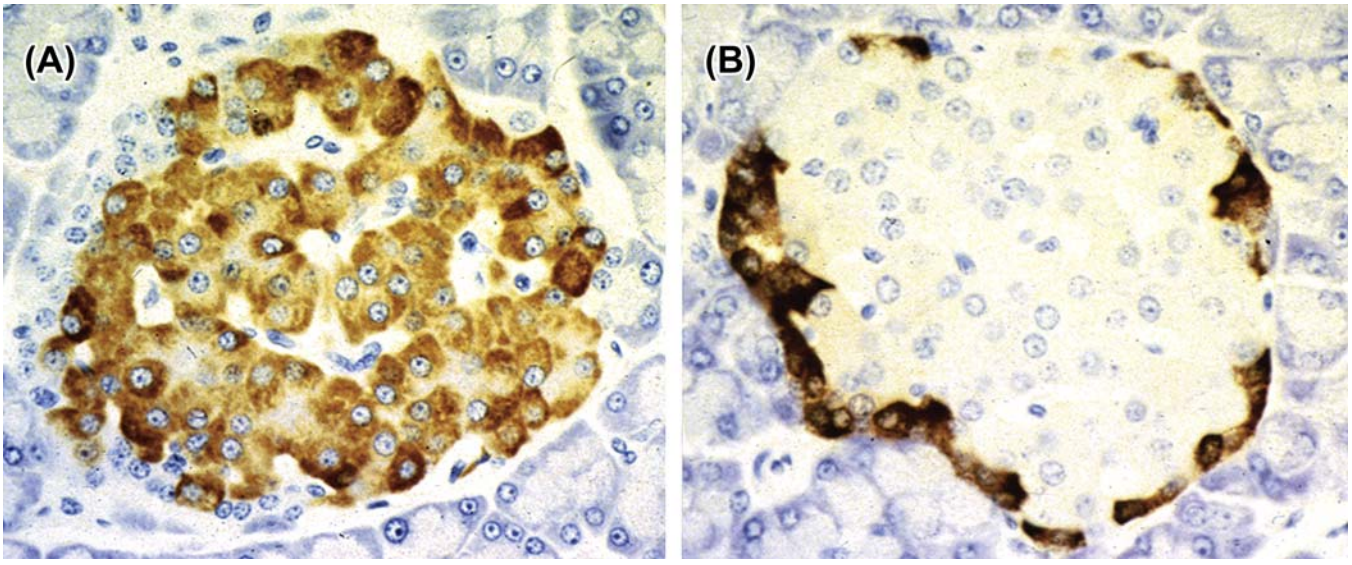

FIGURE 20.43 Immunohistochemistry of a rat pancreatic islet. (A) Insulin-positive cells in the central region of the islet. (B) Glucagon-positive cells in the periphery of the islet. *Figure reproduced from* Handbook of Toxicologic Pathology, *third ed., W. M. Haschek, C. G. Rousseaux and M. A. Wallig, eds. (2013) Academic Press, Fig. 58.58, p. 2476, with permission.*

Physiology

A major role for the endocrine pancreas is to maintain a normal and stable concentration of blood glucose during different physiological states. Insulin decreases blood glucose by increasing the uptake of glucose by muscle, fat, and other cells and promoting the synthesis of glycogen. The liver and brain are not dependent on insulin for glucose uptake. Insulin secretion is regulated by blood glucose, GLP-1, gastric inhibitory peptide, GH, glucocorticoids, and the autonomic nervous system. In contrast, glucagon increases blood glucose by stimulating glycogenolysis in the liver and kidney. Glucagon secretion is stimulated by decreased blood glucose, catecholamines, insulin, and the sympathetic nervous system.

EVALUATION OF TOXICITY

Morphologic Evaluation and Immunocytochemistry

Morphologic evaluation of the pancreatic islets can be assessed using standard sections stained with H&E. Individual cell types can be identified specifically using immunohistochemical stains for hormones, such as insulin, glucagon, somatostatin, and pancreatic polypeptide. Immunohistochemistry also can be used to identify inflammatory cell types or the deposition of collagen in regions of fibrosis. Quantitative pathology or stereology can be used to measure the effects of compounds on the pancreatic islets. However, correct nonbiased sampling is essential because there is normal variability in the size and distribution of islets in the different species.

Assay of Circulating Hormones or Chemicals

Measurement of circulating hormones is used to determine the function and clinical significance of islet cell degeneration, loss, hyperplasia, and neoplasia. Islet cell hyperplasia and neoplasia is usually associated with increased secretion of endocrine hormones. For example, functional β-cell or α-cell hyperplasia/tumors would be expected to be associated with hyperinsulinemia and hyperglucagonemia, respectively.

Glucose challenge or tolerance tests are used to measure the ability of the test subject to reduce serum glucose concentration effectively to an oral or intravenous glucose challenge. Usually, a 2-hour oral glucose tolerance test (with a baseline fasted sample) is adequate to diagnose a state of impaired glucose tolerance or diabetes mellitus (DM). The intravenous glucose challenge is useful for identification of prediabetic states.

Serum glycated hemoglobin (HbA1c) is measured to evaluate the average blood glucose concentration over a prolonged period of time. Effective therapeutics for diabetes are expected to reduce the HbA1c concentrations. Serum HbA1c concentrations can be used to predict the incidence and severity of cardiac, renal, and vascular complications associated with diabetes.

Animal Models

Most animal models that have been developed are associated with the study of DM (see below). The nonobese diabetic mouse is a strain that partially mimics the pathogenesis of Type I DM (T1DM) in humans with similar genetics and autoimmune inflammatory response (see below). Animal models for the study of Type 2 DM (T2DM) include the ob/ob mouse, db/db mouse, Zucker diabetic fatty rat, obese rhesus monkeys, sand rat, streptozotocin-induced adult diabetic animals, complete or partial pancreatectomy, insulin receptor knockout mouse, and mice with knockout of the insulin receptor in β cells.

RESPONSE TO INJURY

Functional Considerations

DM is the clinical condition where there is failure of control of blood glucose, with the development of hyperglycemia and hyperglucosuria; it is the consequence of islet dysfunction. T1DM is a chronic autoimmune disease that results in a primary lack of β cells and decreased insulin production and secretion. T1DM is usually seen in young animals or children and is due to a genetic lack or inflammatory destruction of β cells.

T2DM is the most common form of DM in humans. T2DM is a heterogeneous group of disorders and is associated with obesity, physical inactivity, and genetic predisposition. It is initially due to impaired insulin action from reduced sensitivity of insulin receptors to insulin. Insulin levels may be initially elevated but then are reduced over time when there is failure of the β cells. T2DM occurs in a wide variety of species; some strains of mice and rats are actually predisposed to developing T2DM with obesity. Obese dogs, however, are resistant to development of T2DM.

Islet Inflammation (Insulitis)

Inflammation is important in the pathogenesis of islet cell loss in both T1DM and T2DM. T1DM is due

to autoimmune inflammation of the pancreatic islets. In the occult (early) phase there is a mixed population of leukocytes (lymphocytes and macrophages) in the islets that induce β-cell death. Microvascular leakage occurs in the early phases of the inflammatory response. In the overt phase, when DM is present, there are few β cells and little inflammation. Biomarkers of autoimmune insulitis are serum autoantibodies to a set of β-cell antigens (such as insulin, glutamic acid decarboxylase and protein tyrosine phosphatase-related molecules). In T2DM there are increased macrophages and lymphocytes in the islets associated with increased levels of cytokines (such as interleukin-1β) and chemokines. Fibrosis results from the chronic inflammation. Amyloidosis also may be seen in humans or cats. Hyperglycemia contributes to β-cell apoptosis possibly by induction of the Fas receptor by IL-1β (which is induced by high glucose concentrations). Fatty acids and oxidative stress are also involved in the pathogenesis of inflammation-induced damage to the pancreatic islets.

Islet Cell Amyloidosis

Some species are prone to developing amyloidosis of the islets, which can be confirmed using Congo red to stain the extracellular deposits. Amyloidosis can be exacerbated by inflammation and T2DM (Figure 20.44). The species affected include humans, cats, raccoons, Celebese apes, and the South American degu. The amyloid is formed from the peptide amylin (islet amyloid peptide), which has 37 AA and shares sequence homology with calcitonin gene-related peptide. Amylin is secreted along with insulin and is present in the submembranous clear zone region of the secretory granules. The species that are prone to islet amyloidosis have sequences of AA 20−29 of amylin that favor formation of a β-sheet configuration and amyloid formation in the interstitium of the islets. Overproduction of amylin, decreased catabolism, or aberrant enzymatic processing may also contribute to amyloid formation. Amyloidosis of the islet predisposes to the development of T2DM, but not all individuals with islet amyloidosis have DM.

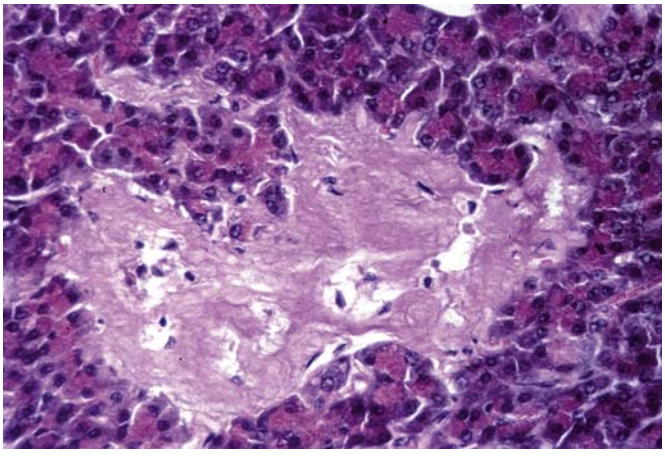

FIGURE 20.44 Islet amyloidosis in a cat. Homogenous eosinophilic amyloid replaces most of the normal islet cells. There are a few hypertrophic, vacuolated islet cells that remain. H&E stain. *Figure reproduced from* Handbook of Toxicologic Pathology, *third ed., W. M. Haschek, C. G. Rousseaux and M. A. Wallig, eds. (2013) Academic Press, Fig. 58.59, p. 2479, with permission.*

Islet Cell Degeneration and Loss

Degeneration of islet cells may occur with certain chemicals or drugs, islet inflammation, or β-cell dysfunction associated with chronic T2DM. Obesity and overeating are common causes of β-cell dysfunction, degeneration, and eventual loss due to apoptosis. In the early stages of obesity and metabolic syndrome there is peripheral insulin resistance with increased total insulin secretion, but the first phase of insulin secretion may be impaired. The pathophysiology of β-cell loss with T2DM is not well understood, but it is insidious. Potential causes of β-cell dysfunction include glucose toxicity, lipotoxicity, increased secretory demand due to insulin resistance, inflammation, and inflammatory cytokines (such as interleukin-1). By the time clinical signs are apparent, approximately 50% of the β-cell mass is gone. Islets in obese animals with T2DM have β-cell hypertrophy, vacuolation, cytoplasmic glycogen accumulation, apoptosis, islet congestion, mononuclear cell infiltration, and fibrosis with collagen deposition. Some islets may have irregular shapes with cellular hypertrophy and hyperplasia in addition to the degenerative, inflammatory and fibrotic changes. Eventually, enough β cells are lost so that the animals develop insulin-dependent DM.

Islet Cell Regeneration

Despite failure of β cells over time in conditions such as obesity and T2DM, islet β cells have a remarkable plasticity and capability to regenerate after injury. New β cells can develop from proliferation of differentiated β cells, neogenesis from uncommitted stem cells in the islets or pancreatic ducts, or by transdifferentiation from other islet cell types, such as α cells. β-Cell regeneration by the three potential mechanisms has been demonstrated in rodents and rodent models of β-cell injury, but the mechanisms and relevance are still controversial. In humans, α cells appear to be more capable of proliferation than β cells in response

to disease or injury of the islets. Some of the regenerative α cells may be positive immunohistochemically for both insulin and glucagon. Proliferation of islet cells can be demonstrated using proliferation markers, such as Ki-67. It has been estimated that β cells survive for about 30 days in growing rats, after which they undergo apoptosis and are replaced by new cells. Proliferation may decrease with age.

Islet Cell Hyperplasia and Neoplasia

Islet cell hyperplasia and adenomas are common age-related lesions found in multiple species. Islet cell carcinomas occur less commonly. There is a continuum of islet cell hyperplasia with progression to adenoma and carcinoma. Proliferative lesions of the islets cells usually affect the β cells but can affect α cells or other cell types. Dietary restriction will reduce the background incidence of islet cell tumors in rats. Pancreatic islet cell hyperplasia is characterized by enlargement of multiple islets (up to 500 μm in diameter), but all islets are not typically involved (Figure 20.45). There is no compression of the adjacent pancreas, and there is lack of fibrous encapsulation. The islet cells usually appear normal but may be elongated. There is low mitotic activity. Adjacent islets may coalesce to form enlarged, irregularly shaped islets.

Adenomas are solitary and grow by expansion, inducing compression of adjacent pancreas; however, they are well differentiated (Figure 20.46). Adenomas may coalesce with adjacent hyperplastic islets. There may be a partial fibrous capsule. Islet cell carcinomas invade into the tumor capsule and adjacent pancreatic tissues (Figure 20.47). Distant metastases may be present in regional lymph nodes or the liver.

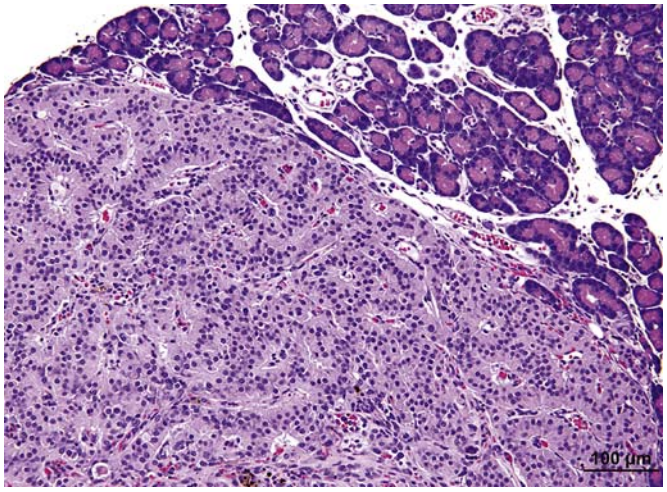

FIGURE 20.46 Islet cell adenoma in a 2-year-old F344 rat. The adenoma is composed of well-differentiated islet cells that have a well-defined margin with mild compression of the adjacent exocrine pancreatic tissue. H&E stain. *Figure reproduced from* Handbook of Toxicologic Pathology, *third ed., W. M. Haschek, C. G. Rousseaux and M. A. Wallig, eds. (2013) Academic Press, Fig. 58.61, p. 2480, with permission.*

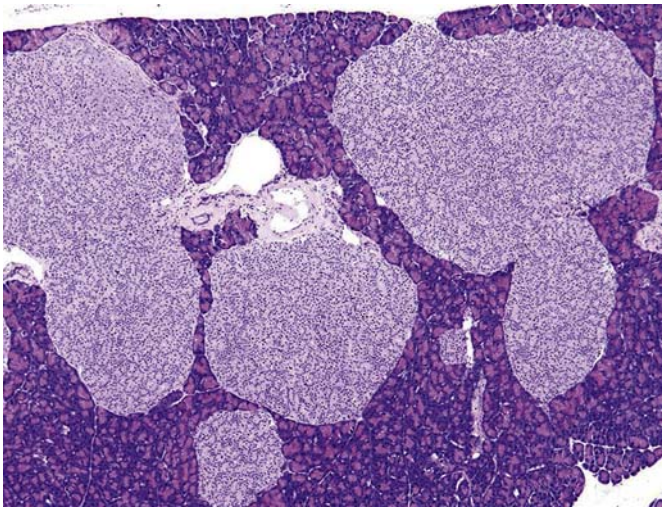

FIGURE 20.45 Islet cell hyperplasia in a 2-year-old B6C3F1 mouse. The islets are variably enlarged due to hyperplasia of β-cells and fusion of multiple islets. Note that some islets remain normal in size. H&E stain. *Figure reproduced from* Handbook of Toxicologic Pathology, *third ed., W. M. Haschek, C. G. Rousseaux and M. A. Wallig, eds. (2013) Academic Press, Fig. 58.60, p. 2480, with permission.*

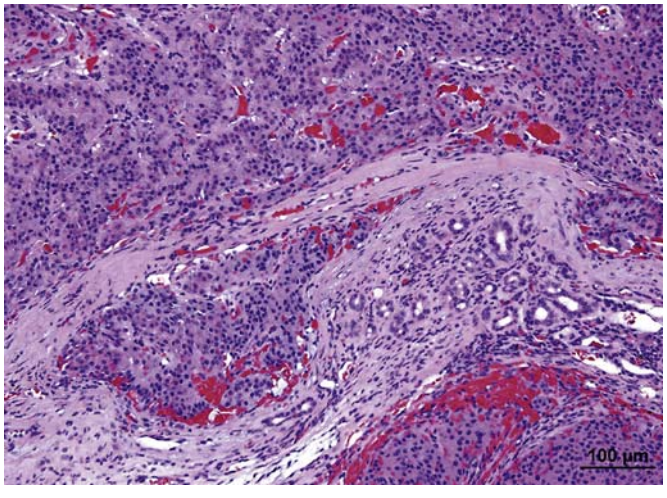

FIGURE 20.47 Islet cell carcinoma in a 2-year-old F344 rat. The islet cell carcinoma is moderately differentiated, invasive into the pancreas interstitium, and has reactive fibrosis, mild hemorrhage, congestion, and secondary proliferation of exocrine ductules. H&E stain. *Figure reproduced from* Handbook of Toxicologic Pathology, *third ed., W. M. Haschek, C. G. Rousseaux and M. A. Wallig, eds. (2013) Academic Press, Fig. 58.62, p. 2480, with permission.*

MECHANISMS OF TOXICITY

Compounds that Cause Proliferation

Glucocorticoids increase blood glucose concentrations and promote insulin resistance. Prolonged administration of glucocorticoids to rats has the potential to increase the incidence of islet cell hyperplasia and neoplasia in 2-year studies. Male rats are particularly sensitive to glucocorticoid-induced islet cell tumors. This effect is not thought to have relevance to humans.

Glucagon receptor antagonists or antireceptor antibodies have the potential for treatment of T2DM due to their ability to decrease blood glucose and hepatic production of glucose. Animals with experimental DM and treated with functional or structural glucagon receptor antagonists develop α-cell hyperplasia with hyperglucagonemia. In addition, GLP-1 levels are increased, which have a beneficial effect in alleviating the DM. Plasma glucagon returns to normal quickly after cessation of antiglucagon receptor therapy even though regression of α-cell hyperplasia is slow.

Compounds that increase PRL secretion increase the incidence of pancreatic islet cell hyperplasia in rats and mice. PRL secretion is inhibited by dopamine. Therefore, dopamine antogonists or dopamine receptor antagonists will increase PRL. Sulpiride (dopamine receptor antagonist) has induced pancreatic islet cell tumors in rats. The combination of naproxen and metoclopramide (structurally related to sulpiride) has induced pancreatic islet carcinomas in male rats.

Nafarelin acetate (nasal solution) is a synthetic analog of GnRH, which increased pancreatic islet cell adenomas in male and female rats in 2-year dosage studies. Leuprolide acetate (depot dosage formulation) increased pancreatic islet cell adenomas in female rats in 2-year studies. The mechanism by which GnRH and its analogs induces islet cell tumors in rats is unknown. However, it has been reported that GnRH and its receptor are present in the rat pancreas and GnRH agonists increase insulin resistance.

Islet cell hyperplasia has been reported in transgenic mice that over express the EAT/mcl-1 gene that is related to Bcl-2. Bcl-2 and its analogs bind to the BAD and BAK proteins to inhibit apoptosis. The islet cell hyperplasia in EAT/mcl-1 mice is due to decreased apoptosis of β and α cells and resulted in a mild increase in serum insulin concentration. A few of the mice also developed islet cell adenomas.

Streptozotocin (Streptozocin) and Alloxan

Streptozotocin is a glucosamine-nitrosourea compound and alkylating agent that damages DNA and which is particularly toxic to islet β cells. Streptozotocin spontaneously degrades to carbonium ions (CH_3^+), which forms DNA adducts by alkylating purine and pyrimidine bases. It is approved by the FDA for use in patients with metastatic β-cell cancer. Streptozotocin is widely used to induce T1DM in animal models, such as rats and mice. A single dose of 50 mg/kg body weight in a rat will cause necrosis of β cells followed by β-cell loss and atrophy of the islets. Alloxan is a cyclic urea analog that is chemically similar to streptozotocin. It is selectively toxic to β cells and can induce T1DM. Alloxan is reduced to dialuric acid in the body and then autooxidized to H_2O_2 and hydroxyl free radicals, which can form hydroxyl adducts with DNA.

The DNA damage and strand breaks induced by streptozotocin or alloxan can be repaired by enzymes (such as poly[ADP]-ribose synthetase) that require nicotinamide adenine dinucleotide (NAD). Depletion of NAD also leads to β-cell damage and death. DNA damage eventually leads to development of β-cell neoplasms. Nicotinamide can be used to maintain NAD levels in β cells and reduce the toxicity of streptozotocin and alloxan.

Zinc

Zinc is an essential micronutrient and is associated with insulin production and metabolism and the normal function of β cells. Zinc is present in the secretory granules of β and α cells. Zinc deficiency predisposes to T1DM and T2DM, and zinc supplementation has a protective effect likely through antioxidant mechanisms and induction of metallothionein.

SUMMARY

The endocrine glands are an important group of organs that are susceptible to chemical-induced changes that occur in short-term and long-term preclinical toxicology studies. It is important to differentiate spontaneous and stress-related changes from compound-induced effects. There are multiple examples of drugs that are approved for human use that have been associated with degenerative or neoplastic changes in the endocrine glands of laboratory animals, but the weight of evidence on the pathogenesis and mode of action has often demonstrated a lack of relevance for humans. Furthermore the mode of action of chemicals on the toxicology of the endocrine glands can be direct or indirect. Therefore, studies on the modes of action require knowledge and experimental interrogation of physiological control and feedback

mechanisms, hormone distribution and receptors on diverse target cells, the primary endocrine cells, and peripheral metabolism and excretion of hormones. In addition, there are significant interspecies differences in the physiology and pathology of the endocrine glands, which makes it imperative to understand the mode of action of chemicals in order to compare preclinical toxicology findings in different species and predict human relevance. This chapter has reviewed the pathophysiology of the endocrine glands in the species typically used for preclinical toxicology studies, and includes toxicologic mechanisms, classic examples of chemical-induced changes and their modes of action, and spontaneous diseases.

Acknowledgments

The contributions of Drs.Thomas J. Rosol, Ronald A. DeLellis, Philip W. Harvey, and Catherine Sutcliffe for the original contribution in *Handbook of Toxicologic Pathology*, 3rd edition are gratefully acknowledged. Also acknowledged are Dr. Charles C. Capen (deceased), Professor Emeritus from The Ohio State University, for the original edition of this chapter in previous editions of *Handbook of Toxicologic Pathology* and *Fundamentals of Toxicologic Pathology*. In addition, the contributions of the Digital Imaging Unit and Dr. Ron A. Herbert of the National Toxicology Program Archives for some of the images are recognized.

Further Reading

Cooke, P., Simon, L., Denslow, N.D., 2013. Endocrine disruptors. In: Haschek, W.H., Rousseaux, C.M., Wallig, M.A. (Eds.), Handbook of Toxicologic Pathology, third ed., Vol. II. Academic Press (Elsevier), San Diego, USA, pp. 1123–1154 (Chapter 37).

Hoyer, P.B., Flaws, J.A., 2012. Endocrine toxicology. In: Klassen, C. (Ed.), Cassarett and Doull's Toxicology, eighth ed. McGraw Hill, pp. 907–930 (Chapter 21).

Jones, T.C., Capen, C.C., Mohr, U. (Eds.), 1996. Endocrine System. Springer-Verlag, Berlin, Germany.

Mete, O., Asa, S.L. (Eds.), 2016. Endocrine Pathology. Cambridge University Press, Cambridge, United Kingdom.

Miller, M.A., 2017. Endocrine system. In: Zachary, J.F. (Ed.), Pathologic Basis of Veterinary Disease, sixth ed. Elsevier, USA, pp. 682–723 (Chapter 12).

Rosol, T.J., DeLellis, R.A., Harvey, P.W., Sutcliffe, C., 2013. The endocrine system. In: Haschek, W.H., Rousseaux, C.M., Wallig, M.A. (Eds.), "Handbook of Toxicologic Pathology, third ed, Vol. III. Academic Press (Elsevier), San Diego, USA, pp. 2391–2492 (Chapter 58).

Society of Toxicologic Pathology. International Harmonization of Nomenclature and Diagnostic Criteria (INHAND). ⟨https://www.toxpath.org/inhand.asp⟩ (last accessed December 2016).

Adrenal

Beuschlein, F., Galac, S., Wilson, D.B., 2012. Animal models of adrenocortical tumorigenesis. Mol. Cell. Endocrinol. 351, 78–86.

Capen, C.C., 2007. Endocrine glands. In: Maxie, M.G. (Ed.), Jubb, Kennedy, and Palmer's Pathology of Domestic Animals, Vol. 3. Saunders, Philadelphia, PA, pp. 325–428.

Everds, N.E., Snyder, P.W., Rosol, T.J., Creasy, D.M., Bailey, K.L., Bolon, B., et al., 2013. Stress during routine nonclinical safety studies: a review of its impact and assessment. Toxicol. Pathol. 42, 560–614.

Gilbert, G., Gillman, J., Loustalot, P., Lutz, W., 1988. The modifying influence of diet and the physical environment on spontaneous tumor frequency in rats. Br. J. Cancer. 12, 565–593.

Harvey, P.W., 2010. Toxic responses of the adrenal cortex. In: McQueen, C.A. (Ed.), Comprehensive Toxicology, Vol. 11. Academic Press, Oxford, UK, pp. 265–289.

Harvey, P.W., Everett, D.J., Springall, C.J., 2007. Adrenal toxicology; a strategy for assessment of functional toxicity to the adrenal cortex and steroidogenesis. J. Appl. Toxicol. 27, 103–115.

Harvey, P.W., Everett, D.J., Springall, C.J. (Eds.), 2010. Adrenal Toxicology. Informa Healthcare, New York, NY.

Petterino, C., Naylor, S., Mukaratirwa, S., Bradley, A., 2015. Adrenal gland background findings in CD-1 (Crl:CD-1(ICR)BR) mice from 104-week carcinogenicity studies. Toxicol. Pathol. 43, 816–824.

Tischler, A.S., Powers, J.F., Downing, J.C., Riseberg, J.C., Shahsavari, M., Ziar, J., et al., 1996. Vitamin D3, lactose, and xylitol stimulate chromaffin cell proliferation in the rat adrenal medulla. Toxicol. Appl. Pharmacol. 140, 115–123.

Tischler, A.S., Powers, J.F., Pignatello, M., Tsokas, P., Downing, J.C., McClain, R.M., 1999. Vitamin D3-induced proliferative lesions in the rat adrenal medulla. Toxicol. Sci. 51, 9–18.

Pituitary Gland

Berry, P.H., 1986. Effect of diet or reproductive status on the histology of spontaneous pituitary tumors in female Wistar rats. Vet. Pathol. 23, 606–618.

Capen, C.C., Martin, S.L., Koestner, A., 1967. Neoplasms in the adenohypophysis of dogs: a clinical and pathologic study. Vet. Pathol. 4, 301–325.

El Etreby, M.F., Lorenz, B., Habenicht, U.F., 1988. Immunocytochemical studies on the pituitary gland and spontaneous tumors of Sprague-Dawley rats. Pathol. Res. Pract. 183, 645–650.

Gilbert, G., Gillman, J., Loustalot, P., Lutz, W., 1988. The modifying influence of diet and the physical environment on spontaneous tumor frequency in rats. Br. J. Cancer. 12, 565–593.

Lee, A.K., DeLellis, R.A., Blount, M., Nunnemacher, G., Wolfe, H.J., 1982. Pituitary proliferative lesions in aging male Long–Evans rats: a model of mixed multiple endocrine neoplasia syndrome. Lab. Invest. 47, 595–602.

Nolon-Noblot, S., Laroque, P., Coleman, J.B., Hoe, C.-M., Kennan, K.P., 2003. The effects of ad libitum overfeeding and moderate and marked dietary restriction on age-related spontaneous pituitary gland pathology in Sprague-Dawley rats. Toxicol. Pathol. 31, 310–320.

Sarkar, D.K., Gottschall, P.E., Meites, J., 1982. Damage to hypothalamic dopaminergic neurons is associated with development of prolactin-secreting pituitary tumors. Science. 218, 684–686.

Satoh, H., Iwata, H., Furuhama, K., Enomoto, M., 2000. Pituicytoma: primary astrocytic tumor of the pars nervosa in aging Fisher 344 rats. Toxicol. Pathol. 28, 836–838.

Thyroid C-Cells

Botts, S., Jokinen, N.P., Isaacs, D.J., Meuten, D.J., Tanaka, N., 1991. Proliferative lesions of the thyroid and parathyroid glands. E-3. Guides for Toxicologic Pathology. STP/ARP/AFIP, Washington, DC.

Capen, C.C., Martin, S.L., 1989. The effects of xenobiotics on the structure and function of thyroid follicular cells and C-cells. Toxicol. Pathol. 17, 266–293.

Gilbert, G., Gillman, J., Loustalot, P., Lutz, W., 1988. The modifying influence of diet and the physical environment on spontaneous tumor frequency in rats. Br. J. Cancer. 12, 565–593.

Thurston, V., Williams, E.D., 1982. Experimental induction of C-cell tumours in thyroid by increased dietary content of vitamin D2. Acta Endocrinol. 100, 41–45.

Thyroid Follicular Cells

Capen, C.C., 1997. Mechanistic data and risk assessment of selected toxic end points of the thyroid gland. Toxicol. Pathol. 25, 39–48.
Coelho-Palermo Cunha, G., van Ravenzwaay, B., 2005. Evaluation of mechanisms inducing thyroid toxicity and the ability of the enhanced OECD Test Guideline 407 to detect these changes. Arch. Toxicol. 79, 390–405.
Curran, P.G., DeGroot, L.J., 1991. The effect of hepatic enzyme-inducing drugs on thyroid hormones and the thyroid gland. Endocr. Rev. 12, 135–150.
Döhler, K.-D., Wong, C.C., von zur Mühlen, A., 1979. The rat as model for the study of drug effects on thyroid function: consideration of methodological problems. Pharmacol. Ther. 5, 305–318.
Hill, R.N., Erdreich, L.S., Paynter, O.E., Roberts, P.A., Rosenthal, S.L., Wilkinson, C.F., 1989. Review: thyroid follicular cell carcinogenesis. Fundam. Appl. Toxicol. 12, 629–697.
Jones, G.N., Manchanda, P.K., Pringle, D.R., Zhang, M., Kirschner, L.S., 2010. Mouse models of endocrine tumours. Best Pract. Res. Clin. Endocrinol. Metab. 24, 451–460.
Kanno, J., Onodera, H., Furuta, K., Maekawa, A., Kasuga, T., Hayashi, Y., 1992. Tumor-promoting effects of both iodine deficiency and iodine excess in the rat thyroid. Toxicol. Pathol. 20, 226–235.
Pickford, D.B., 2010. Screening chemicals for thyroid-disrupting activity: a critical comparison of mammalian and amphibian models. Crit. Rev. Toxicol. 40, 845–892.
Refetoff, S., Robin, N.I., Fang, V.S., 1970. Parameters of thyroid function in serum of 16 selected vertebrate species: a study of PBI, serum T4, free T4, and the pattern of T4 and T3 binding to serum proteins. Endocrinology 86, 793–805.
Zabka, T.S., Fielden, M.R., Garrido, R., Tao, J.H., Fretland, A.J., Fretland, J.L., et al., 2011. Characterization of xenobiotic-induced hepatocellular enzyme induction in rats: anticipated thyroid effects and unique pituitary gland findings. Toxicol. Pathol. 39, 664–677.
Zbinden, G., 1988. Hyperplastic and neoplastic responses of the thyroid gland in toxicological studies: the target organ and the toxic process. Arch. Toxicol. Suppl. 12, 98–106.

Parathyroid Gland

Capen, C.C., 1989. Neoplasms of the parathyroid glands. In: Stinson, S.F., Reznik, G. (Eds.), Atlas of Tumor Pathology in the F344 Rat. CRC Press, Boca Raton, FL.
Kronenberg, H.M., Bringhurst, F.R., Segre, G.V., Potts Jr., J.T., 2001. Parathyroid hormone biosynthesis and metabolism. In: Bilezikian, J.P., Marcus, R., Levine, M.A. (Eds.), The Parathyroids Basic and Clinical Concepts. Academic Press, San Diego, CA, pp. 17–30.
National Toxicology Program, 1986. Toxicology and carcinogenesis studies of rotenone in F344/N rats and B6C3F1 mice (CAS No. 83-79-4). NIH Publ. No. 86-2576. US Department of Health and Human Services, Public Health Service, National Institute of Health, Washington, DC.
Nissenson, R.A., Jüppner, H., 2008. Parathyroid hormone. In: Rosen, C.J. (Ed.), Primer on the Metabolic Diseases and Disorders of Mineral Metabolism. American Society of Bone and Mineral Research, Washington, DC, pp. 123–126.
Rosol, T.J., Capen, C.C., 1992. Biology of disease: mechanisms of cancer-induced hypercalcemia. Lab. Invest. 67, 680–702.
Wild, P., Setoguti, T., 1995. Mammalian parathyroids: morphological and functional implications. Microsc. Res. Tech. 32, 120–128.

Endocrine Pancreas

Buchanan, T.A., 2003. Pancreatic beta-cell loss and preservation in type 2 diabetes. Clin. Ther. 25 (Suppl. B), 32–46.
Carvalho, C.P., Martins, J.C., da Cunha, D.A., Boschero, A.C., Collares-Buzato, C.B., 2006. Histomorphology and ultrastructure of pancreatic islet tissue during *in vivo* maturation of rat pancreas. Ann. Anat. 188, 221–234.
Degraz, R., Bonal, C., Herrera, P.L., 2011. β-cell regeneration: the pancreatic intrinsic faculty. Trends Endocrinol. Metab. 22, 34–43.
Donath, M.Y., Böni-Schnetzler, M., Ellingsgaard, H., Ehses, J.A., 2009. Islet inflammation impairs the pancreatic β-cells in type 2 diabetes. Physiology 24, 325–331.
Jones, G.N., Manchanda, P.K., Pringle, D.R., Zhang, M., Kirschner, L.S., 2010. Mouse models of endocrine tumours. Best Pract. Res. Clin. Endocrinol. Metab. 24, 451–460.
Lin, Y., Sun, Z., 2010. Current views on type 2 diabetes. J. Endocrinol. 204, 1–11.
Lindfors, E., Gopalacharyulu, P.V., Halperin, E., Orešič, M., 2009. Detection of molecular paths associated with insulitis and type 1 diabetes in non-obese diabetic mouse. PLoS ONE. 4, 1–9.
Masiello, P., Broca, C., Gross, R., Roye, M., Manteghetti, M., Hillaire-Buys, D., et al., 1998. Experimental NIDDM: development of a new model in adult rats administered streptozotocin and nicotinamide. Diabetes. 47, 224–229.
Wieczorek, G., Pospischil, A., Perentes, E., 1998. A comparative immunohistochemical study of pancreatic islets in laboratory animals (rats, dogs, minipigs, nonhuman primates). Exp. Toxicol. Pathol. 50, 151–172.

CHAPTER

21

Nervous System

Brad Bolon[1], *Robert H. Garman*[2], *Mark T. Butt*[3], *and David C. Dorman*[4]

[1]GEMpath, Inc., Longmont, CO, United States [2]Consultants in Veterinary Pathology, Inc., Murrysville, PA, United States [3]Tox Path Specialists, LLC, Frederick, MD, United States [4]North Carolina State University, Raleigh, NC, United States

OUTLINE

INTRODUCTION

The linked central and peripheral components of the nervous system (a.k.a., the CNS and PNS) are the instruments by which an animal regulates all other body systems and interacts with the external environment. Neurotoxicants injure (structurally and/or functionally) one or more neural cell types, often acting regionally to produce subtle to calamitous dysfunction. Characterization and prevention of neurological deficits related to xenobiotic exposure is essential to the protection of human and animal health. This chapter largely focuses on methods that are used in regulatory studies designed to assess neurotoxicity in animals. A discussion of other techniques used in neuroscience research such as the use of light to selectively control neural activity (optogenetics), electrophysiological approaches, brain circuit analyses, neural genomics and proteomics, use of *in vitro* techniques and alternative animal models (e.g., *Caenorhabditis elegans*), and other experimental approaches are beyond the scope of this work.

Fundamentals of Toxicologic Pathology.
DOI: http://dx.doi.org/10.1016/B978-0-12-809841-7.00021-6

Many agents have been demonstrated to elicit neurotoxic effects in humans and/or animals (Table 21.1). Humans may encounter neurotoxic chemicals at both home and work, particularly such agents as agrochemicals, metals, and solvents. Some therapeutic agents produce neurotoxic side effects, including cytotoxic (e.g., antineoplastic agents) and neuroactive small molecules (e.g., antidepressants, antiepileptics) and some biomolecules (e.g., natalizumab, an antibody directed against the cell adhesion molecule α_4-integrin). "Life style" chemicals like alcohol (ethanol), nicotine, and "recreational" drugs (e.g., cocaine) tend to have very powerful neurotoxic actions, and many microbes, plants, and animals generate potent neurotoxins.

Neurotoxicity may present as anatomic, chemical, or functional alterations affecting the CNS, PNS, or various effector organs (e.g., muscle). Anatomic indices of neurotoxicity may be observed as structural abnormalities

TABLE 21.1 Common Neural Targets and Neurotoxicants

Site of action	Neurotoxic effect/mechanism	Selected examples
NEURON		
Stem cell, neuronal	Altered migration and/or differentiation	Ethanol
		Methanol
		Methylazoxymethanol (MAM)
		Methylmercury
Mature cell		
Body	Cytotoxicity	
	Alkylating agent	Doxorubicin (alkylating agent)
	Energy depletion (disrupted electron transport)	1-Methyl-4-phenyl-1,2,3,6-tetrahydropyridine (MPTP)
	Excitotoxicity	Domoic acid (marine algal toxin)
		Kainic acid (seaweed toxin)
		Quinolinic acid
		Trimethyltin
	Mitotic inhibitor	Vincristine
	Protein conjugation/inactivation	Methylmercury
		Trimethyltin
Axon	Axonopathy	
	Central (unknown mechanism)	Clioquinol
	Proximal (altered intracellular transport)	β,β′-Iminodipropionitrile (IDPN)
	Distal (macromolecular cross-linking)	Acrylamide
		Carbon disulfide
		n-Hexane
Synapse	Altered neurotransmission	
	Decreased neurotransmitter release	Botulinum toxin
		Tetanospasmin
	Persistent presence of neurotransmitters	Selective serotonin reuptake inhibitors (SSRI)
		St. John's wort (*Hypericum perforatum*)
	Reduced neurotransmitter metabolism	Carbamate insecticides
		Monoamine oxidase inhibitors (MAOI)
		Organophosphorus insecticides

(*Continued*)

TABLE 21.1 (Continued)

Site of action	Neurotoxic effect/mechanism	Selected examples
	Termination of transmembrane ion gradients	Pyrethrin insecticides
		Pyrethroid insecticides
		Tetrodotoxin
GLIA		
Stem cell, glial	Neoplasia (mutation by DNA alkylation)	Acrylonitrile
		Ethylnitrosourea (ENU)
		Ethylene oxide
		Methylnitrosourea (MNU)
Astrocyte	Swelling (Alzheimer Type II cells)	Ammonia
Myelinating cells	Abnormal protein production—Schwann cell	Isoniazid
	Abnormal protein production—Oligodendrocyte	Lead
		Triethyltin
	Anoxia (insufficient oxygen delivery)	Carbon monoxide
	Edema—Oligodendrocyte	Cuprizone
		Hexachlorophene
	Membrane disruption	Lead
		Triethyltin
	Metabolic disturbance	Coyotillo (*Karwinskia humboldtiana*)
	Uncoupling oxidative phosphorylation	Bromethalin
		Hexachlorophene
ENDOTHELIUM (CAPILLARY)		
	Physical penetration of blood–brain barrier elements	Arsenic
	Protein kinase dysfunction	Lead

at the macroscopic, microscopic, or ultrastructural levels. Common chemical lesions induced by neurotoxic agents include changes in neurotransmitter levels and/or neural cell enzyme activities. Functional shifts caused by neurotoxicants include neurobehavioral and neurophysiological (i.e., electrophysiological) fluctuations. Abnormalities in neural chemistry or function secondarily alter neural structure, while structural alterations in the CNS or PNS frequently produce functional deficits. Neurologic alterations produced by chemical exposure are not necessarily adverse. Some chemical actions are pharmacologic, including expected but excessive reactions to neuroactive drugs (i.e., supra-pharmacology) and temporary perturbations in global or regional neurochemistry. Receptor blockade or alteration may result in long-lasting functional effects that may even have structural impacts on neurons, but the therapeutic result (example: analgesia) may justify those alterations. Whether intended or not, local, regional, or widespread effects on nervous system tissues induced by xenobiotic exposure or implanted cells or devices may elicit changes that do impair an individual's ability to survive and prosper in their environment, therefore producing an adverse neurotoxic event.

The nervous system as a whole is predisposed to toxic damage for many reasons. The key factors are the intricate interconnectivity, extensive regional specialization, and restricted ability for cell and tissue repair, especially within the CNS. Locally discrete CNS lesions may produce significant effects in more distant parts of the nervous system due to the close linkage of structure and function in a particular region; neural lesions may affect other body systems since the CNS and PNS act to directly or indirectly regulate the physiological activities of nearly all peripheral organs. The extensive nutritional needs of neural cells embody another key area of neurotoxic vulnerability. The brain is almost entirely reliant on aerobic, glucose-dependent metabolism, which requires

approximately 15% of the total cardiac output and 20% of the body's oxygen-carrying capacity, even though the brain represents only 1%–2% of the total body weight. The limited antioxidant capacity and high quantities of polyunsaturated fatty acids in CNS tissue predisposes neural cell membranes, particularly myelin, to oxidation. Furthermore neural lipids concentrate lipophilic agents—many of which have neuroactive properties—in the CNS, thereby potentiating their possible neurotoxic impact.

The nervous system also features many structures with amplified sensitivity to neurotoxicant exposure. Key factors explaining such site-specific vulnerability include regional variations in biochemistry, metabolism, and vascularization. Another major influence is the capacity for repair following a neurotoxic insult. Injury to the PNS may be repaired, yielding a full or nearly full restitution of function. In contrast, damage to the CNS is met with a minimal ability for structural renovation and functional renewal; instead, brain "repair" typically relies on the recruitment of compensatory processes mediated by other, less affected brain regions. These attributes are impacted by age with older individuals exhibiting less robust structural rebuilding (due to lower neuronogenesis and synaptic plasticity) as well as diminished functional restoration (arising from the inability of adaptive behaviors to fully compensate for deficits produced by damage to other regions). Therefore neurotoxicant-induced CNS damage is likely to engender permanent and often progressive deficits.

NEUROANATOMIC CONSIDERATIONS IN TOXICOLOGIC NEUROPATHOLOGY

Mammals (chiefly rats, dogs, and nonhuman primates) are the favored animal models for neurotoxicity testing because the functional and structural characteristics of their nervous systems are very similar to those of humans. Pathologists require a thorough and integrated knowledge of the connection between regional anatomy, chemistry, and function (i.e., correlative neurobiology) as well as the divergence that exists among species, strains, ages, or genders (comparative neurobiology) in order to effectively identify neurotoxic hazards, assess neurotoxic risks, and diagnose neurotoxic conditions. A detailed consideration of these topics is beyond the scope of this chapter, but further information is readily available in the Further Reading list.

Neural Cell Populations: Key Targets for Neurotoxicity

At the cellular level, neurons are the key functional elements of the CNS and PNS. The adult human brain (weight, 1400 g) holds approximately 130 billion neurons forming 150 trillion synapses. Different populations of CNS neurons may be recognized by many traits, including cell conformation (e.g., pyramidal neurons are large and polygonal, granule cells are small and round; Figure 21.1); axonal length (longer for pyramidal projection neurons, shorter for granule cell interneurons); function (afferent, efferent, or interneuron); neurotransmitter composition; and/or location. In general, neurons, once damaged, do not regenerate, although their processes in the PNS may be rebuilt over time if the cell body remains viable. Neurons are highly vulnerable because they use about 10-fold more oxygen than other neural cells. Typical neuron responses to toxic agents are cell body degeneration leading to necrosis and/or disintegration of its peripheral processes (i.e., axonal degeneration).

Glia are essential support cells in the CNS and PNS, with each CNS neuron being sustained by 10–50 glial cells. Multiple glial cell lineages have been identified.

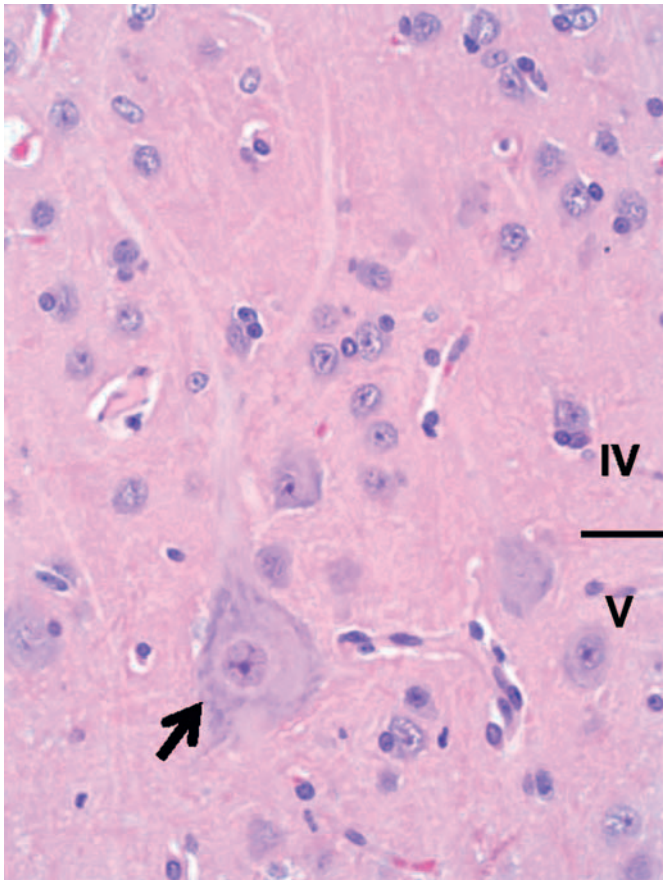

FIGURE 21.1 Common neuronal phenotypes include interneurons (small round cells connecting intracortical neurons, in lamina IV) and pyramidal neurons (large, polygonal cells (arrow) for sending cortical commands outward, in lamina V). Motor cortex from an adult cat. Processing conditions: Formalin fixation by immersion, paraffin embedding, H&E stain.

Astrocytes maintain neuronal processes, remove neurotransmitters from synapses, control chemical and ionic gradients within the brain parenchyma, and form the major protective layer of the blood–brain barrier (BBB). Astrocytes react to neurotoxicants by swelling or vacuolation (if the astrocyte is damaged) or hypertrophy and hyperplasia (reactive astrogliosis) when reacting to structural damage in the CNS. Astrocytes also play a key role in the formation of the "glymphatic system," a recently discovered series of perivascular channels that eliminate soluble proteins and metabolites from the CNS.

Myelinating glial cells are the oligodendrocytes of the CNS, which envelop multiple axons, and Schwann cells of the PNS, which encircle only one axon. The presence of myelin sheaths is required for fast transmission of neural impulses down axons, Myelinating cells respond to neurotoxicants by degeneration and necrosis or by vacuolation due to fluid accumulation between myelin lamellae. Disruption or loss of myelin retards the speed of impulse propagation, especially in thickly myelinated axons in the CNS and somatic (or sensorimotor) PNS required for rapid responses to environmental stimuli.

Unlike other glial cells, which originate from neural stem cells, microglia (the resident CNS immune surveillance and phagocytic cells) arise in peripheral hematopoietic organs from monocytic precursors. Some microglia are also derived from the yolk sac and may be identified in the brain primordium as early as embryonic Day 8. Microglia react to neurotoxicants with hypertrophy and hyperplasia, and they serve as local phagocytic cells clearing debris from the injury of many cell types.

Other classes of glia have been identified. For example, satellite cells in PNS ganglia are thought to serve many of the same metabolic support and barrier functions that their astrocyte counterparts provide in the CNS. In general, the responses of these other glial cell types to neurotoxic agents have yet to be characterized in detail.

Other major cell types in the CNS include choroid plexus epithelium, ependymal cells, and meningeal fibroblasts. The choroid plexus epithelium covers the ventricular surface of the small fibrovascular tufts of choroid plexus that reside, primarily, in the lateral and fourth ventricles. The choroid plexus epithelium actively secretes cerebrospinal fluid (CSF) and also serves as a depot for sequestering neurotoxic heavy metals to prevent their accretion in the brain parenchyma or distribution via the CSF to other portions of the CNS. This epithelium commonly responds to xenobiotic exposures by either vacuolation or degeneration, which may culminate in necrosis and sloughing. Ependymal cells are a special glial derivative that line the surfaces of the brain ventricular system and the spinal cord central canal; the ependyma appears to be resistant to many toxicants (likely because chemicals do not enter the CSF at high levels), although responses similar to those of the choroid plexus epithelium are possible. Meningeal fibroblasts also are resistant to toxicants.

Comparative Neuroanatomy: Basic Principles

Mammalian species used for neurotoxicological hazard identification and risk assessment may be divided into three categories based on reproducible neuroanatomic features. These classes are Rodent (including true rodents like mice and rats but also lagomorphic rabbits), Carnivore (cat and dog), and Primate (monkeys and humans).

While regions and their connections are quite similar across mammalian species, some interspecies variations in neuroanatomic structure are prominent. For example, the weight of this organ increases substantially as the phylogenetic tree is ascended: 1300–1400 g (representing about 1.5%–2% of total body weight) for an adult human versus 1.5–2 g (about 0.8% of total body weight) for an adult rat. The single most conspicuous gross difference among species is the surface contouring of the cerebral hemispheres, which are lissencephalic (smooth) for Rodents but gyrencephalic (convoluted) in Carnivores and Primates (Figure 21.2). The pattern of cerebral gyri and sulci is specific to each species and may be asymmetric between the two hemispheres. Old World primates (e.g., baboon, cynomolgus monkey, rhesus monkey) may be better models for human neurotoxic risk since all these species have bigger brains as well as more and larger gyri relative to New World monkeys (e.g., marmoset, squirrel monkey). Relative to Rodents, brains of gyrencephalic Carnivores and Primates have comparatively more white matter (Figure 21.3) and many more interneurons. The structure–function correlations for major brain domains are similar across mammalian species, but their importance diverges among species. For example, the cerebral surface area mapped to olfactory, motor, and sensory tasks is approximately 80% in Carnivores but 20% in Primates, while the cortical area dedicated to signal integration is nearly 80% in Primates and 20% in Carnivores. Similarly the cerebellar hemispheres (Figure 21.2) and the inferior olivary nucleus are much larger in Primates relative to Carnivores and especially Rodents. Taken together, this species-specific divergence reflects the more elaborate circuitry needed for fine sensorimotor control and efficient cognition (higher thought) in Primates.

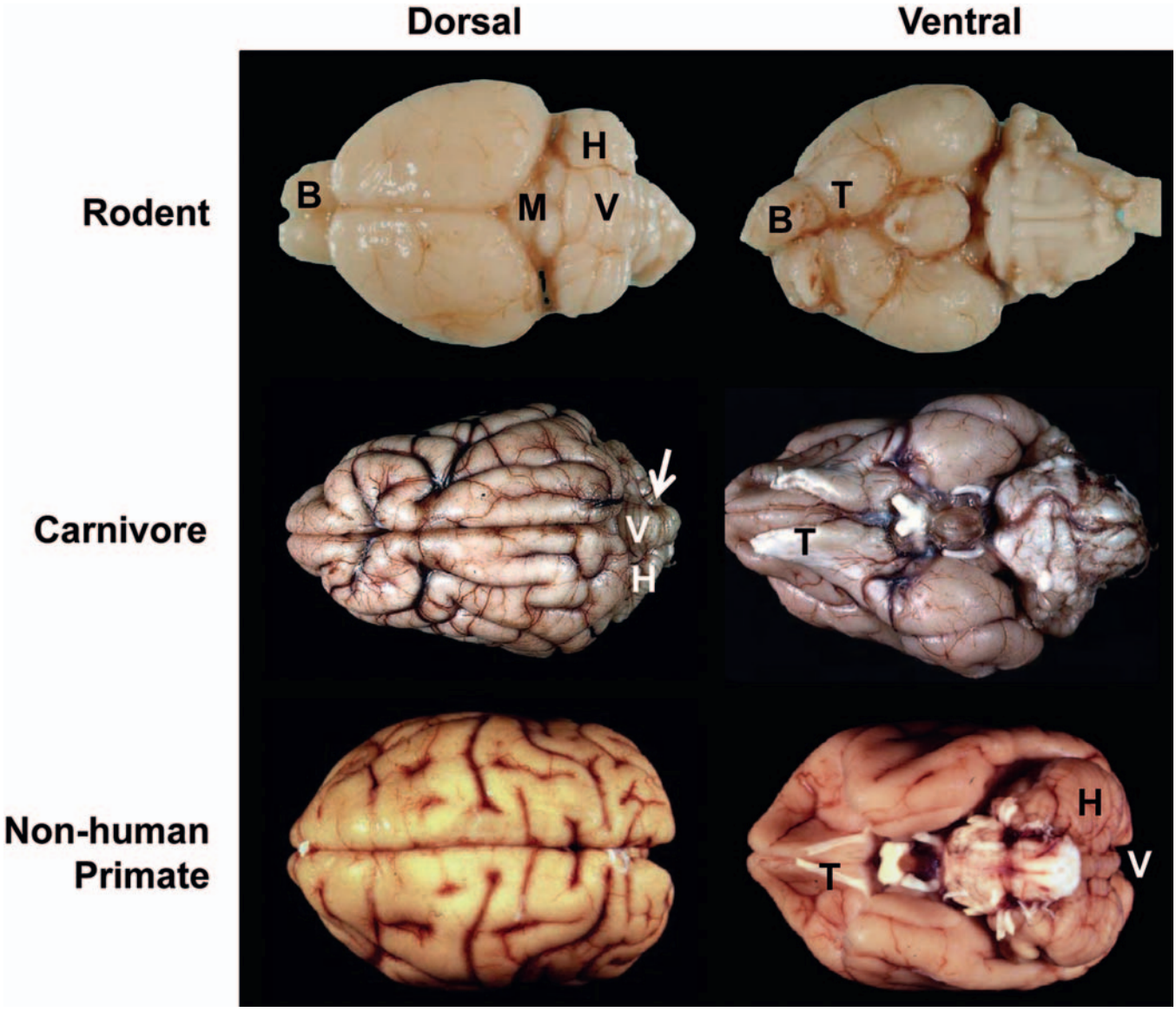

FIGURE 21.2 The prominence of major regions on the external surface of mammalian brains varies considerably in species of neurotoxicological interest. In the Rodent (Sprague-Dawley rat in this case), the midbrain (M) is readily visible on the dorsal surface, while the olfactory bulbs (B), olfactory tract (T), and cerebellum (partitioned as H for hemisphere and V for vermis) are relatively large. In the Carnivore (Beagle dog), the cerebrum partially covers the midbrain, the olfactory bulbs and tract are moderate in size, and the vermis of the cerebellum is serpentine (arrow) rather than straight. In the nonhuman Primate (cynomolgus monkey), the cerebrum is expanded to such a degree that the cerebellum can only be visualized from the ventral surface, the cerebellar hemispheres are much larger than the vermis, and the olfactory tract is quite small.

The basic neuroanatomic pattern of the brain within a species is relatively constant, but several factors may produce structural variations that must be recognized as normal background findings. For example, many Rodent strains exhibit grossly different brain anatomy relative to the expected wild-type configuration, particularly a smaller brain size and a reduced or absent corpus callosum; these architectural changes may or may not be associated with behavioral abnormalities, so it is important to understand the background neuroanatomy and function of specific species and strains/breeds when interpreting data sets for neurotoxic risk assessment. Similarly the sex of the individual may impact regional neuroanatomy. For instance, males tend to have larger numbers of neurons and oligodendrocytes overall, which translates into larger amygdaloid and hypothalamic nuclei (i.e., sexually dimorphic nuclei) and wider white matter tracts. Neural anatomy also evolves throughout development, including final maturation of protective elements like

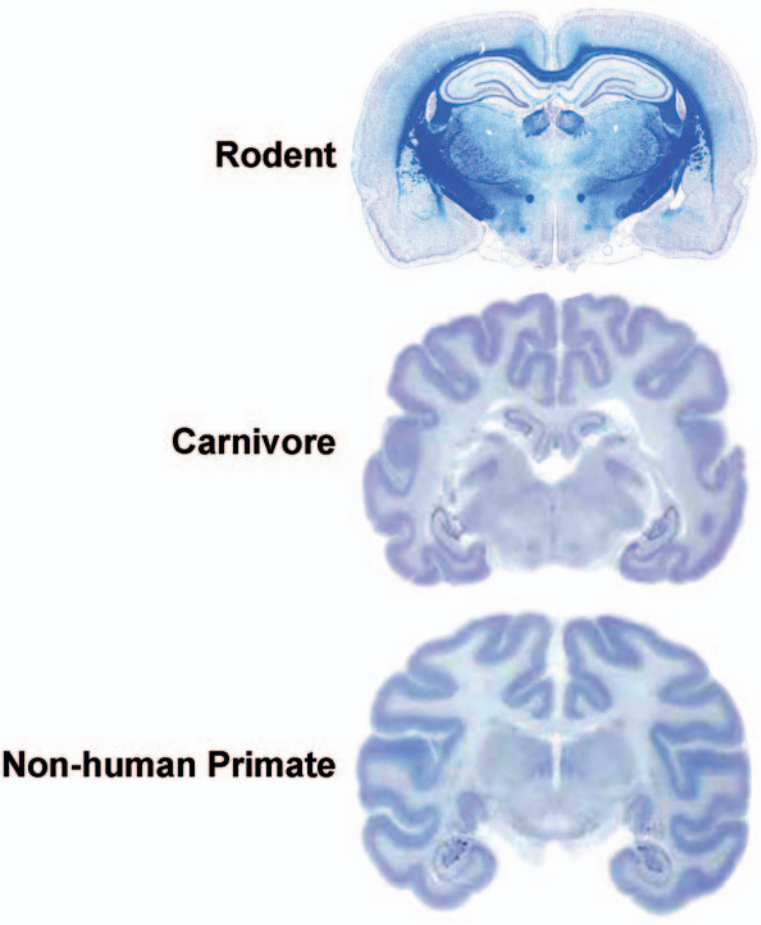

FIGURE 21.3 Coronal sections through the rostral cerebrum highlight the major expansion of both gray matter and white matter as the phylogenetic tree is ascended. The increases result from greatly enhanced associative and cognitive abilities (supported by the neocortex). The Rodent (rat) has a well-defined superficial (cerebral cortex) and deep (basal nuclei) gray matter, and thus exhibits prominent white matter tracts. Carnivores (Beagle dog) and nonhuman Primates (cynomolgus monkey) have large gyri to support the higher number of cerebrocortical neurons (especially interneurons with integrative functions) in the gray matter and even greater complement of myelinated nerve fibers (serving to boost the degree of interhemispheric connectivity). Cresyl violet stain. Source: *Whole-brain sectioning and staining kindly provided by Dr. Robert C. Switzer III, NeuroScience Associates, Inc., Knoxville, Tennessee, United States.*

the BBB and glial cell detoxification pathways well after birth as well as the gradual loss of BBB integrity with age. The complexity of these differences indicates that scientists who design neurotoxicity tests in animals must review the literature and, for novel methods or uncommon endpoints, perform suitable pilot studies with appropriate control animals to confirm that the chosen test species, strain, sex, and age are appropriate.

The spinal cord of mammals is generally comparable, although two species-specific features do need to be considered when extrapolating neurotoxicity data from animals to humans. First, relative to Rodents, the ratio of white matter to gray matter is higher in Carnivores and Primates due to their greater surface areas and larger numbers of interneurons, which require a correspondingly larger supply of axons to innervate the tissue. The volume of white matter is greater in the dorsal funiculus (i.e., proprioceptive and tactile tracts) of Carnivores and Primates compared to Rodents because the extra fibers are predominantly dedicated to sensation in the digits. Second, the organization of the spinal motor tracts that support voluntary motor activities varies among species. In Rodents the main corticospinal tract is located within the ventral portion of the dorsal funiculus, while the equivalent tract in Carnivores and Primates is localized to the lateral funiculus. The rubrospinal tract (which carries subcortical signals from the red nucleus to spinal cord motor neurons) is much smaller in Primates than in Rodents and Carnivores. The spinal cord white matter devoted to such spinal motor activities rises from approximately 10% in Carnivores to between 20% and 30% for nonhuman Primates and humans, respectively.

EVALUATION OF NEUROTOXICITY

Neuropathology assessment is an accepted "gold standard" for identifying neurotoxicants because visible neuroanatomic defects in a critical, minimally reparable system generally are considered to be adverse. Additional methods for identifying neurotoxic risks have emerged (Table 21.2), which can be used together with or occasionally in place of routine neuropathology endpoints. The choice of method(s) used to define neurotoxic risk (Table 21.3) depends on the kinds of

TABLE 21.2 Flow Chart for Toxicologic Neuropathology Endpoints in Conventional Nonclinical Toxicity Testing

- **I.** Gross examination—For general toxicity studies (Tier I "screens") and dedicated neurotoxicity studies (Tier II investigations)
  - **A.** External assessment—Brain, spinal cord (sometimes not performed for survey studies), peripheral nerve Organ weight—brain
  - **B.** Internal evaluation—Brain (on coronal slabs, approximately 0.5–2 cm thick depending on brain size)
- **II.** Light microscopic evaluation
  - **A.** Central nervous system
    - **1.** Technical considerations
      - **a.** Formalin fixation—Neutral buffered 10% (3.7% formaldehyde, approximately pH 7.4)
        - **i.** Immersion for general toxicity studies (Tier I)
        - **ii.** Intravascular perfusion for dedicated neurotoxicity studies (Tier II)
      - **b.** Paraffin embedding—Sections at 4–8 μm
      - **c.** Conventional stains
        - **i.** General architecture—Hematoxylin and eosin
        - **ii.** Neuronal features—Cresyl violet
        - **iii.** Axonal integrity—Silver (Bielschowsky's of Bodian's) stains
        - **iv.** Myelin integrity—Luxol fast blue (LFB)
      - **d.** Special stains
        - **i.** Neuronal degeneration—Amino cupric silver (frozen sections required) or Fluoro-Jade
        - **ii.** Axonal integrity—Neuronal filament protein (NFP) immunohistochemistry
        - **iii.** Myelin integrity—Myelin basic protein (MBP) mmunohistochemistry
        - **iv.** Gliosis
          - **1.** Astrocytic reaction—Glial fibrillary acidic protein (GFAP) immunohistochemistry
          - **2.** Microglial reaction
            - **a.** Ionized calcium-binding adaptor molecule 1 (Iba1) immunohistochemistry
            - **b.** *Griffonia simplicifolia* (GSA I-B4) lectin histochemistry
    - **2.** Regions to consider for sampling
      - **a.** Forebrain—Cerebral cortex, basal nuclei, *corpus callosum*
      - **b.** Diencephalon—Hippocampus, internal capsule, thalamus, hypothalamus
      - **c.** Midbrain—Red nucleus, *substantia nigra*, rostral and caudal colliculi, *tectum, tegmentum*
      - **d.** Hindbrain—Cerebellum, *pons, medulla oblongata*
      - **e.** Spinal cord—Cervical, thoracic, lumbar (emphasizing intumescenses [i.e., the segments giving rise to major nerve trunks that serve the limbs]; cross and longitudinal orientations)
  - **B.** Peripheral nervous system
    - **1.** Technical considerations
      - **a.** Fixation
        - **i.** Formalin—Initial fixative
        - **ii.** Glutaraldehyde, 2.5%, followed by osmium tetroxide (OsO_4), 1%—Postfixation (to stabilize myelin so that it is retained while processing)
      - **b.** Embedding
        - **i.** Paraffin—Sections at 4 μm (suitable for Tier I screening)
        - **ii.** Plastic—Sections at 1 μm (essential for detailed Tier II evaluation; requires the use of hydrophobic resins ["hard plastic"] for optimal resolution)
      - **c.** Conventional stains—General architecture—Hematoxylin and eosin (paraffin) or toluidine blue (plastic)
      - **d.** Sample orientation—Cross and longitudinal orientations
    - **2.** Regions to consider for sampling
      - **a.** Sciatic nerve (proximal trunk and/or distal trunk)
      - **b.** Tibial, peroneal, or sural nerves (distal branches)
      - **c.** Dorsal root ganglia (especially those supplying the sciatic nerve, which vary by species)
      - **d.** Cranial nerves (usually nerve V [trigeminal] as a baseline, possibly with others if indicated by neurological findings)
      - **e.** Autonomic nerves and ganglia (if indicated by neurological findings)
- **III.** Special Procedures—Generally for dedicated neurotoxicity testing (Tier II)
  - **A.** Ultrastructural assessment—Typically requires design of a special nonclinical study
    - **1.** Technical considerations
      - **a.** Fixation—Neutral buffered 10% (3.7% formaldehyde, approximately pH 7.4)
        - **i.** Intravascular perfusion preferred
        - **ii.** Perfusate should include glutaraldehyde at 1%–4%
        - **iii.** Osmium tetroxide (OsO4), 1%—Postfixation by immersion of very small tissue cubes
      - **b.** Embedding—Hard plastic resin to permit thin sectioning (<1 mm)
      - **c.** Stains
        - **i.** Uranyl acetate
        - **ii.** Lead citrate
    - **2.** Regions to consider for sampling—based on light microscopy results

(*Continued*)

TABLE 21.2 (Continued)

- **B.** Immunohistochemistry for additional neural cell markers
  - **1.** Neurons
    - **a.** Tau
    - **b.** Cell type–specific markers (e.g., neurotransmitters, neurotransmitter receptors)
    - **c.** Functional markers (e.g., tyrosine hydroxylase (TH) for catecholamine-synthesizing neurons)
  - **2.** Glia
    - **a.** Oligodendroglia—MBP
    - **b.** Schwann cells—S100
  - **3.** Blood vessels
    - **a.** Presence—Endothelial markers (e.g., Factor VIII-related antigen)
    - **b.** Permeability—Detection of extravasated horseradish peroxidase (HRP) or immunoglobulin (Ig)
  - **4.** Miscellaneous
    - **a.** Leukocyte markers
    - **b.** Degenerating cells (apoptosis)—Anti-caspase-3 immunohistochemistry, or equivalent
    - **c.** Proliferating cells—Anti-bromodeoxyuridine (BrdU) immunohistochemistry, or equivalent
- **C.** Enzyme histochemistry
  - **1.** Cytochrome oxidase—Energy metabolism in neurons
  - **2.** Reporter genes—lacZ (bacterial β-galatosidase), or equivalent, at sites of engineered gene expression
- **D.** Quantitative procedures
  - **1.** Morphometry—Linear or areal measurements in two dimensions
  - **2.** Stereology—Volumetric measurements or object counts in three dimensions

TABLE 21.3 Potential Endpoints of Neurotoxicity

- **I.** Anatomic (structural) indices—Appropriate for mature and developing individuals
  - **A.** Macroscopic changes
    - **1.** Gross abnormalities—Brain, spinal cord, peripheral nerve
    - **2.** Weight alteration—Brain
  - **B.** Microscopic changes
    - **1.** General changes in architecture
    - **2.** Lesions (especially regional destruction of the parenchyma or specific neuronal populations)
    - **3.** Repair reactions (enhanced numbers of reactive astrocytes and/or microglia)
    - **4.** Altered patterns of molecular expression (cell type–specific and functional markers)
- **II.** Behavioral and clinical indices
  - **A.** Overt clinical signs of neurotoxicity
  - **B.** Effector endpoints—Changes (increases or decreases) in:
    - **1.** Learning, memory, and attention
    - **2.** Motor activity
    - **3.** Schedule-controlled behavior (rate or temporal patterning)
  - **C.** Sensory endpoints—Altered sensations of sight, smell, sound, or taste
  - **D.** Developmental deficits
    - **1.** Change in quality—Altered degree or pattern in performing a behavior
    - **2.** Shift in timing
      - **a.** Late onset of behavioral landmarks
      - **b.** Premature onset of behaviors associated with senescence
- **III.** Neurochemical indices
  - **A.** Neurotransmission shifts—Deviations from normal patterns
    - **1.** Neurotransmitter synthesis, release, uptake, and/or degradation
    - **2.** Signal transduction pathways (especially second messenger generation)
    - **3.** Synaptic activity of acetylcholinesterase (AChE) or neuropathy target enzyme (NTE)
  - **B.** Markers of neurotoxicity—At maturity or during development
    - **1.** Neuronal responses
      - **a.** Heat shock proteins (may be upregulated by damage)
      - **b.** Neurotransmitter levels
    - **2.** Glial reactions
      - **a.** Astrocytes—Glial fibrillary acidic protein (GFAP) immunohistochemistry
      - **b.** Microglia—Ionized calcium-binding adaptor molecule 1 (Iba1) immunohistochemistry
- **IV.** Neurophysiological indices—Deviations from baseline
  - **A.** Electroencephalographic (EEG) patterns—Shifts in patterns
  - **B.** Nerve conduction—Altered amplitude, velocity, or refractory period
  - **C.** Sensory-evoked potential—Changed amplitude or latency

effects that investigators suspect and/or follows a menu of regulatory guidelines.

Some modalities for assessing neurotoxicants and their effects are performed during life, like neurological and behavioral evaluations as well as electrophysiological testing. Others are usually confined to the *postmortem* setting, such as macroscopic and microscopic assessment (routine neuropathology). A few can be used in life as well as after death, like noninvasive imaging and assessments of nerve conduction velocities. This section provides an overview of conventional anatomic pathology techniques as well as a brief introduction to other key methods in which toxicologic neuropathology expertise may be important.

Morphologic Evaluation

Basic Patterns for Neurotoxicant-Induced Lesions

Gross observations may reveal toxicant-induced alterations in neural structure at the time of necropsy. An obvious qualitative change that may reveal a neurotoxic effect is discoloration, which demonstrates the presence of necrosis (Figure 21.4) or a neoplasm. More quantitative gross evidence of a neurotoxic outcome is indicated by reduced brain weight (measured at necropsy immediately after organ removal or in fixed organs prior to tissue trimming) or alterations in the dimensions (length, area, or volume) of the brain or a major subregion (Figure 21.4). Generally abnormal absolute brain weights or brain dimensions are judged to be biologically significant markers of neurotoxic damage.

Histopathologic lesions are a common manifestation of neurotoxicant exposure, and indeed microscopic assessment is often the most effective means for identifying many neurotoxicants. The type of histopathological finding will depend on many factors. Perhaps the most important is the age of the lesion. Acute cell death (neuronal necrosis) usually presents as shrunken neurons with hypereosinophilic cytoplasm and dark, condensed, or fragmented nuclei (i.e., classic "red dead" neurons; Figure 21.5). In contrast, chronic lesions typically result in neuronal loss (which may go unrecognized if subtle and in the absence of a glial reaction); coagulative necrosis of the parenchyma (Figure 21.6); neuropil cavitation (i.e., the end-stage finding caused by liquefactive necrosis of the parenchyma); or a prominent glial response (gliosis). The difficulty in detecting small numbers of dead neurons or disintegrating axons microscopically in the "vast pink wasteland" of a large brain section has driven the development of special techniques designed to preferentially label toxicant-injured cells. The two most common methods utilized for this purpose are Fluoro-Jade dyes and silver degeneration procedures (Figure 21.7). These two procedures work best when the cell bodies remain intact, and thus are of most use for detecting acute damage.

Damage to a neuronal population usually is accompanied by an increase in the number of reactive glia in the immediate vicinity of the stricken cells. The typical glial response features astrocytes (Figure 21.8) and/or microglia (Figure 21.9), either or both of which may become larger (hypertrophy) and/or proliferate (hyperplasia). These reactions take place to render the glial cells more adept at filling defects, supporting other

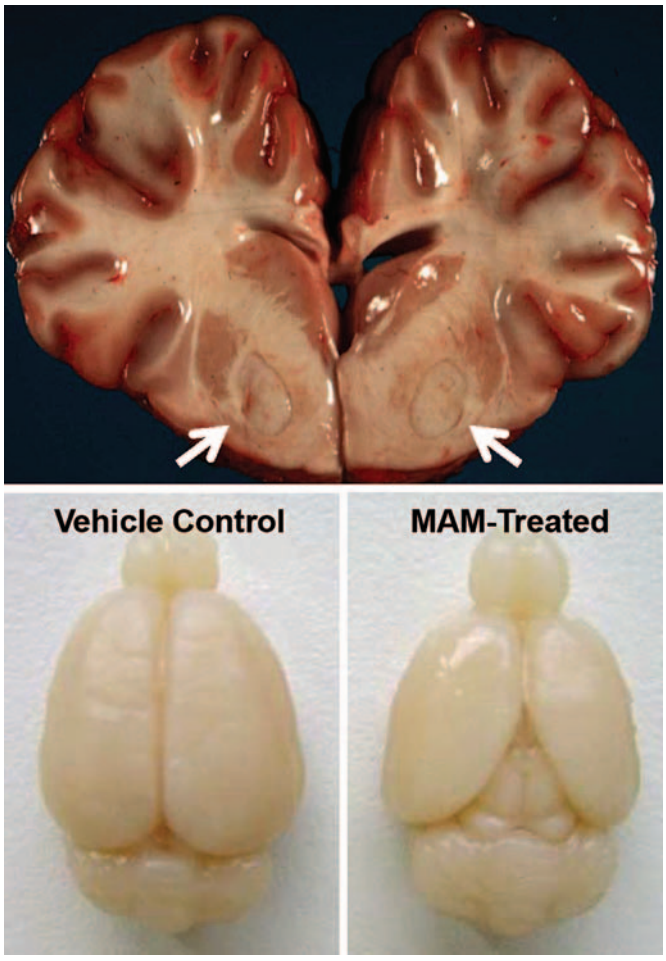

FIGURE 21.4 Macroscopic appearance is an essential tool for identifying neurotoxic lesions. *Upper*: Severe nigropallidal encephalomalacia (arrows) presents as well demarcated, bilaterally symmetrical zones of pallor (cream colored with a thin brown rim, where the adjacent gray matter is light brown) in the affected basal nuclei of this horse that had consumed yellow star thistle (*Centaurea solstitialis*) for an extended period. *Lower*: Pronounced cerebral hypoplasia leading to exposure of the caudal portions of the olfactory bulbs and the entire midbrain in a 21-day-old Wistar rat following maternal treatment with the neuroteratogen methylazoxymethanol (MAM, given at 30 mg/kg body weight by intraperitoneal injection on gestational day 15). Source: *Upper: Image courtesy of Dr. Billy C. Ward from the Noah's Arkive database of veterinary pathology lesions: http://www.vet.uga.edu/vpp/noahsarkive/na.php; image no. 4942. Lower: Images kindly provided by Dr. Wolfgang Kaufmann, Merck KGaA, Darmstadt, Germany.*

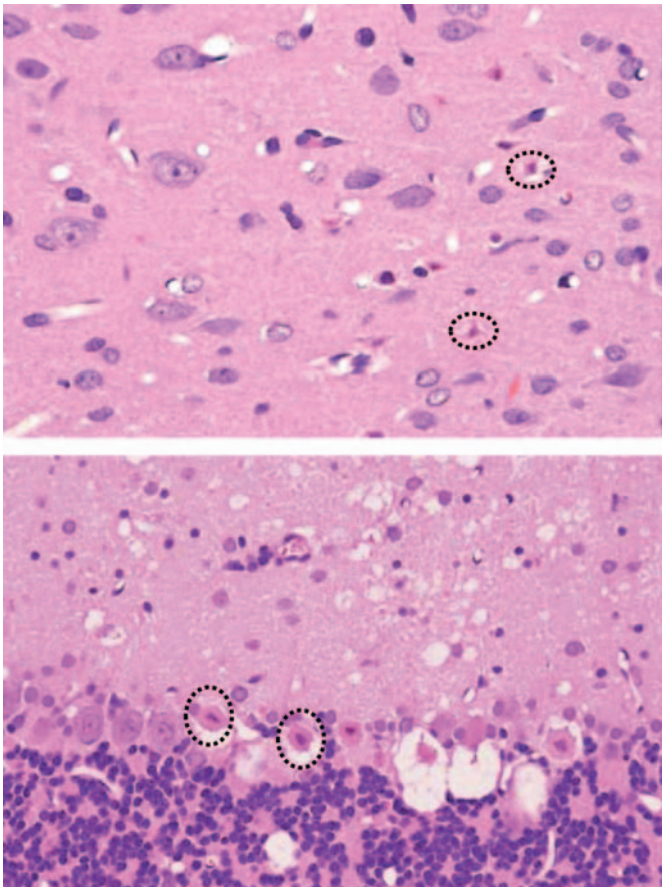

FIGURE 21.5 Acute neuronal death following neurotoxicant exposure typically presents as classic "red dead" neurons. Relative to adjacent cells with normal features, necrotic neurons (circles delineate representative examples) have shrunken, spiky profiles; hypereosinophilic cytoplasm; dark, condensed or fragmented nuclei; and are sometimes bordered by clear retraction spaces. Cerebral cortex (upper) and cerebellum (lower) of a rat exposed to an unspecified neurotoxicant. Processing conditions: Formalin fixation by intravascular perfusion, paraffin embedding, H&E staining.

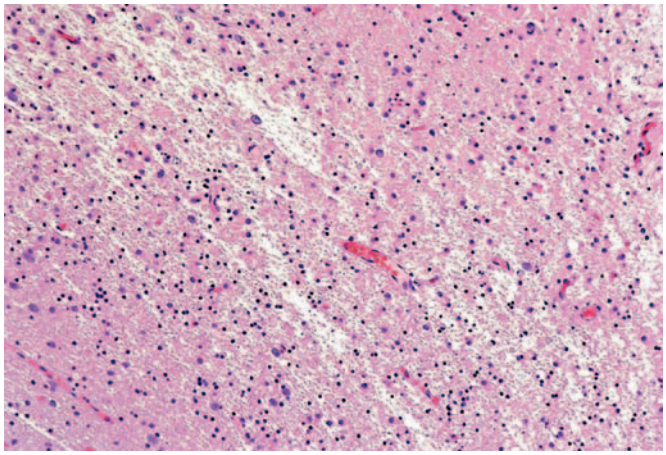

FIGURE 21.6 Substantial areas of neuronal loss or parenchymal necrosis result in variable cavitation of the neuropil and often hypercellularity due to astrocyte hypertrophy and hyperplasia. Processing conditions: Formalin fixation by immersion; paraffin embedding; H&E staining.

local cells, or efficiently removing necrotic neuronal, axonal, and myelin debris. As with injured neurons, reactive glia may be detected more easily if visualized using a special method to reveal the responding cells. The most common means for detecting cell type–specific markers on reactive glia are conventional immunohistochemical (IHC) techniques to detect the astrocyte-specific glial fibrillary acidic protein (GFAP; Figure 21.8) and the microglia-specific ionized calcium-binding adaptor molecule 1 (Iba1; Figure 21.9)

The time during life when exposure occurs will influence both the sensitive cell populations and the potential range of lesions. Different brain regions have unique windows of vulnerability based on when they undergo their peaks of neuronal (Figure 21.10) and glial production and differentiation during development, so transient exposures during different periods of life will elicit divergent outcomes. Adult exposures to neurotoxic agents typically yield necrotic neurons, axonal or myelin degeneration, neuropil vacuolation, and/or reactive gliosis. In contrast, changes usually seen in developing individuals include abnormal cell numbers (termed "dysplasia"; Figure 21.11), displaced (or unmigrated) cells (termed "ectopia" or "heterotopia"; Figure 21.12), and/or aberrant differentiation (indicated by defective myelination or synaptogenesis), but rarely glial reactions; this difference from the adult lesion pattern results from the constant remodeling that occurs during formation of the nervous system. In general, dysplastic and ectopic neurons persist into adulthood. However, some ectopias appear to be transient in nature as indicated by the ability to find aggregates of displaced neural stem cells in brain ventricles of young animals (Figure 21.13) but not adults.

The distribution of lesions among various neural cell populations often depends on cell type–specific architectural or functional factors. For instance the rich synaptic beds in the cerebral and cerebellar cortices as well as the hippocampus make these three regions common targets for neurotoxicants. The cell type–specific factors that direct neurotoxic effects to a particular area also help to explain species differences in responsiveness to various agents. The classic example of this principle is the heightened sensitivity of dopaminergic neurons in the Primate substantia nigra to the prodrug 1-methyl-4-phenyl-1,2,3,6-tetrahydropyridine (MPTP). Conversion of MPTP into the toxic metabolite 1-methyl-4-phenylpyridinium (MPP^+) leads to widespread acute neuronal death, which manifests as acute-onset parkinsonism. The ability of neuromelanin, a dark pigment found specifically in the dopaminergic

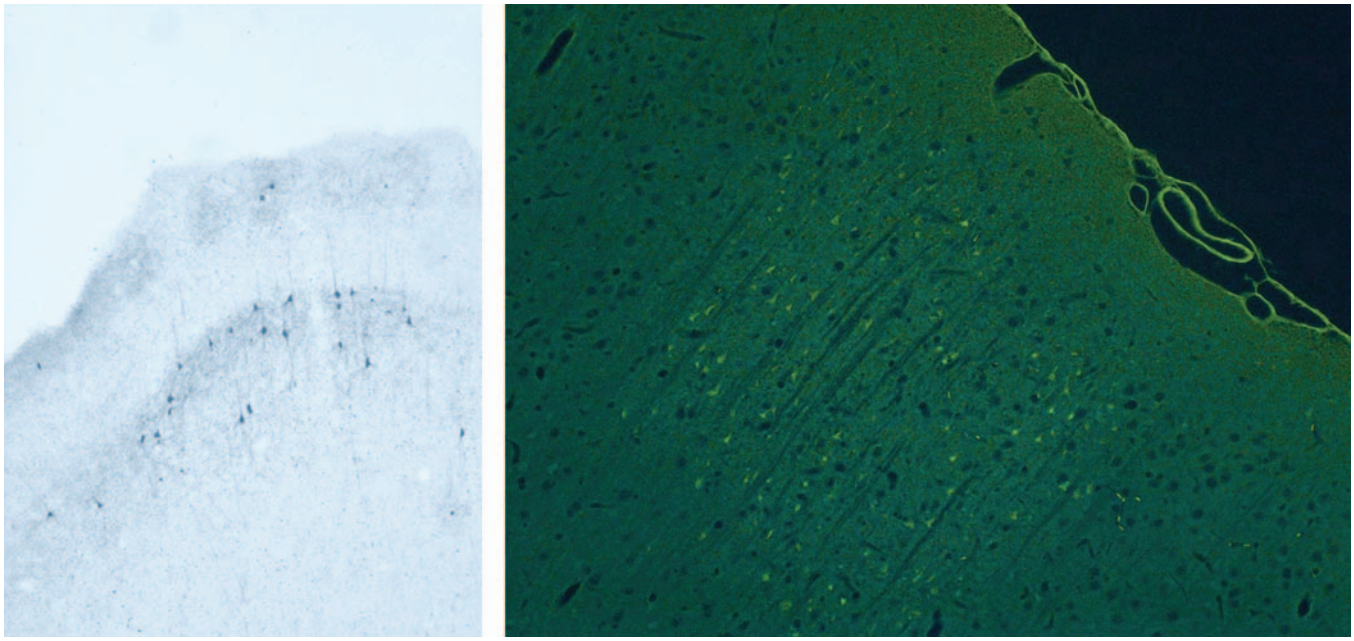

FIGURE 21.7 Special neurohistological techniques to highlight small numbers of degenerating neurons within larger populations of unaffected cells are a standard strategy for speeding the microscopic evaluation of brain tissue. "Dark neuron" artifact (see Figure 21.14) is less likely to present an interpretive problem when using these procedures. While affected neurons are relatively indistinct in H&E-stained sections even at high magnifications (see Figure 21.5), dead cells are easily differentiated at low and intermediate magnifications using amino cupric silver (left; degenerating neurons and processes are black) or Fluoro-Jade B (right; damaged cells are bright green). The amino cupric silver procedure requires frozen tissue, while the Fluoro-Jade method can be performed on routinely processed (i.e., formalin fixed, paraffin embedded) specimens. Cerebral cortex from adult rats given an unidentified neurotoxicant.

neurons of the Primate substantia nigra, to preferentially bind both MPTP and MPP^+ accounts in large part for the higher susceptibility of primates relative to rodents to MPTP-induced neurotoxicity (although some mouse strains are also quite sensitive to MPTP administration).

Study Design

Toxicant-induced structural lesions in the CNS and PNS may be assessed as a stand-alone problem (the usual case in a diagnostic laboratory setting) or as an organized, prospective study of neurotoxic potential (the typical case in the regulated setting for developing new agricultural chemicals or drugs). In general, diagnostic neuropathology is undertaken in a clinical practice (e.g., medical or veterinary medical office) to ascertain whether or not a xenobiotic can be linked to neural damage. The objective of such diagnostic procedures is to facilitate the return of the patient to full (or reasonable) neurological function, so morphological assessment of the nervous system is confined to nonintrusive imaging modalities like computed tomography (CT) or magnetic resonance imaging (MRI), electrophysiology to assess nerve conduction velocities, or to minimally invasive pathology methods like peripheral nerve or skin biopsies (for assessment of intraepidermal nerve fiber density). These techniques are increasingly used in assessing the nervous system in regulatory studies. However, neural evaluation in the majority of regulatory-type nonclinical studies is done either as one aspect of a general screen for toxicity to all organ systems (i.e., "general toxicity studies") or to provide a comprehensive examination of structural damage in many nervous system sites (i.e., "dedicated neurotoxicity studies"). The differing aims of these studies warrant a smaller list of neural tissues for general studies relative to the larger battery of nervous system domains used for studies devoted mainly to a detailed neuropathology analysis.

It is impossible to define a single duration of exposure that is suitable for investigating all neurotoxicants, as different agents elicit a fluctuating spectrum of lesions that peak in incidence and degree at various times after exposure. When known in advance, the timing of necropsies should be arranged to occur when toxicant-induced neural lesions are at their peak, keeping in mind that many agents exhibit multiple peaks characterized by distinct kinds of lesions. This principle is well illustrated by the excitotoxic agent kainic acid, in which neuronal necrosis occurs at 1–4 days following exposure but synaptic terminal disintegration develops at 4–14 days. In many cases, neurotoxicity studies are designed to recapitulate specific requirements listed in regulatory guidelines. Testing

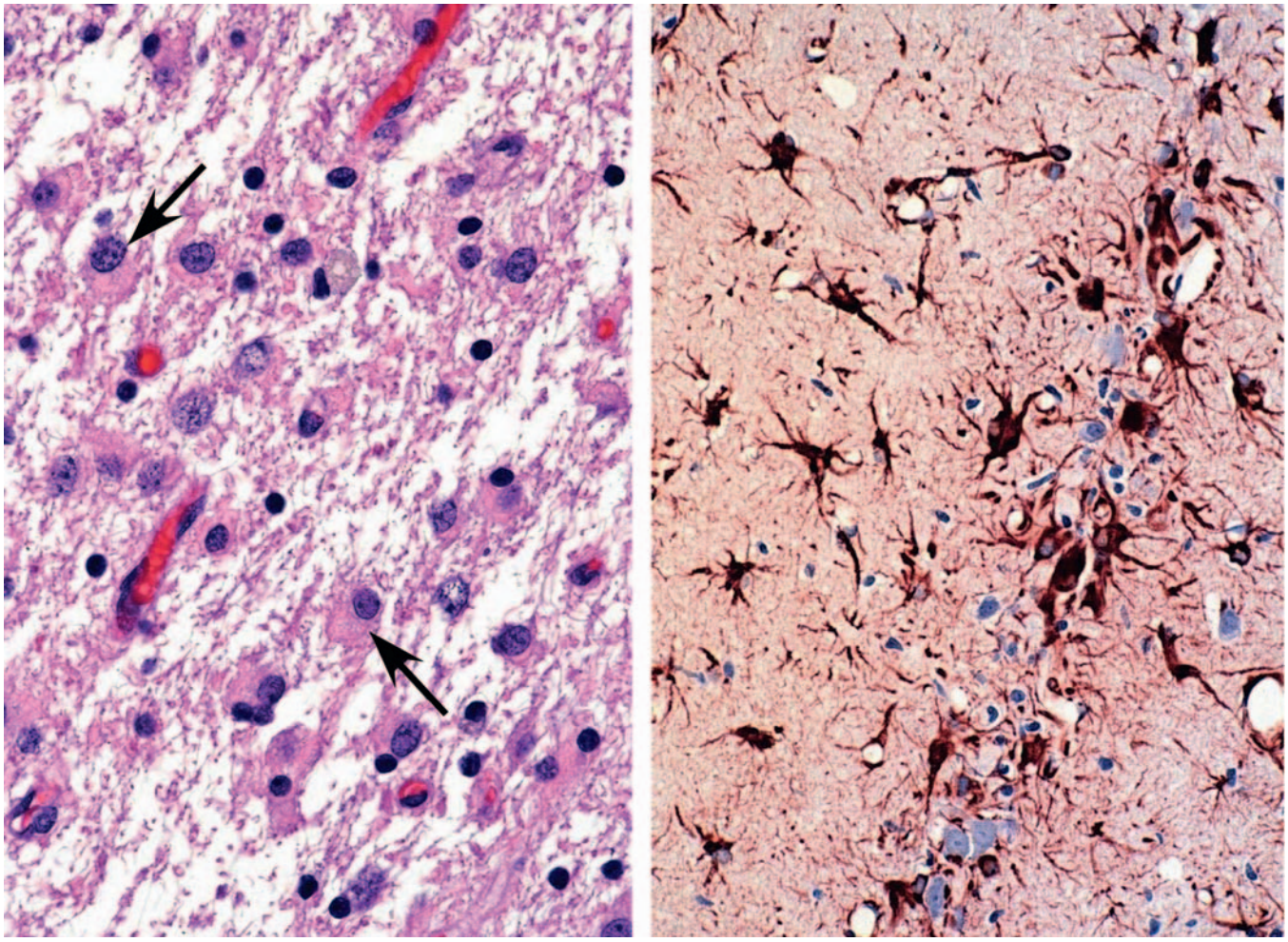

FIGURE 21.8 In most cases, reactive (activated) astrocytes have basophilic, oval to round, often eccentric nuclei and abundant cytoplasm but indistinct cell margins; however, cell borders can be seen when the astrocytes are located in regions undergoing liquefactive necrosis (left). A common means of determining reactive astrocyte numbers is to assess the distribution of GFAP (right), as reactive astrocytes express this protein in large amounts in their hypertrophied cytoplasmic bodies and thickened processes. Brain sections from adult rats; the right micrograph is from the CA_1 hippocampal sector of an adult rat necropsied after a *grand mal* seizure. Processing conditions: Formalin fixation by immersion; paraffin embedding; H&E staining (left) and anti-glial fibrillary acidic protein (GFAP) immunohistochemistry (right).

requirements are relatively specific for dedicated neurotoxicity studies but permit a fair degree of discretion for general toxicity studies.

Tissue Fixation

Neural tissues for general toxicity studies typically are fixed by immersion in neutral buffered 10% formalin (NBF, a 3.7% formaldehyde solution, approximately pH 7.4). This choice is dictated by historical and practical considerations. NBF is available in bulk from many vendors. The small size of the formaldehyde molecule permits it to easily and quickly penetrate dense neural tissues, while the reactive aldehyde group promotes rapid tissue fixation. Nervous system samples fixed in this manner may be processed routinely along with samples from other organs, thus reducing the cost and labor required to prepare tissue blocks for histological sectioning.

For dedicated neurotoxicity studies, the preferred choice for preserving neural tissues for microscopic examination is intravascular perfusion because it offers the best preservation of neural morphology in all CNS and PNS structures (Figure 21.14). Perfusion introduces fixative deep into the nervous system, thus speeding fixation, and it prevents the induction of many artifacts that tend to arise when unfixed CNS tissues are manipulated during necropsy. This method permits the use of fixative mixtures that include methanol-free formaldehyde (often freshly prepared from paraformaldehyde powder) and/or glutaraldehyde. Combinations of formaldehyde and glutaraldehyde are sometimes referred to as McDowell-Trump's fixative (usual composition: 4% formaldehyde and 1%

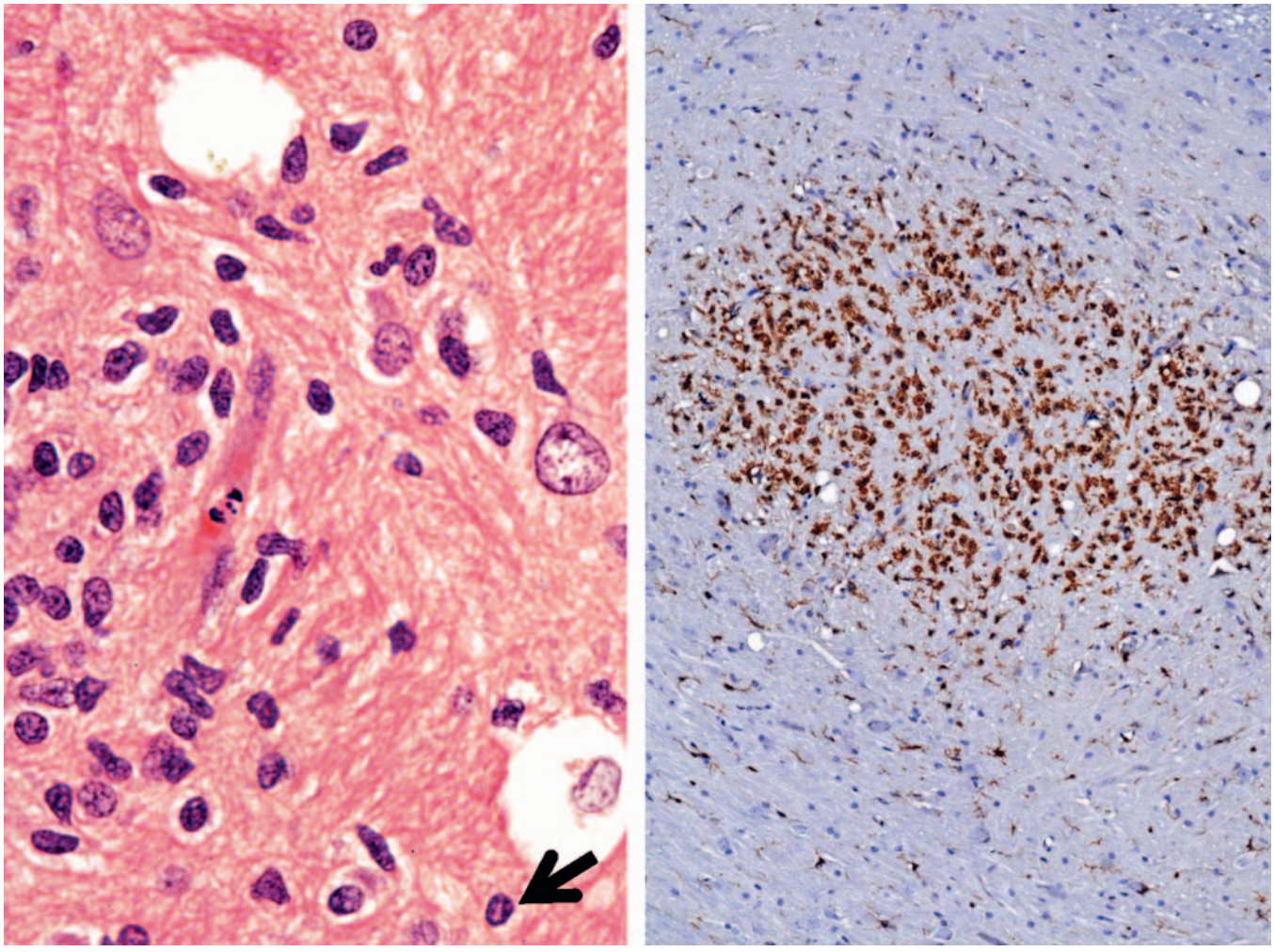

FIGURE 21.9 Reactive microglia also are prominent players in the glial response to neurotoxicant-induced damage in the brain. *Left*: Compared to the small, round to oval, isolated nuclei of resting microglia (arrow), activated microglia have elongated, serpentine- or spindle-shaped nuclei and commonly form small nodules at sites of parenchymal damage. H&E. *Right*: Reactive microglia can be highlighted using immunohistochemistry to detect the cell type–specific marker ionized calcium-binding adaptor molecule 1 (Iba1; done here with a hematoxylin counterstain). Globus pallidus of a rat exposed to an unspecified neurotoxicant.

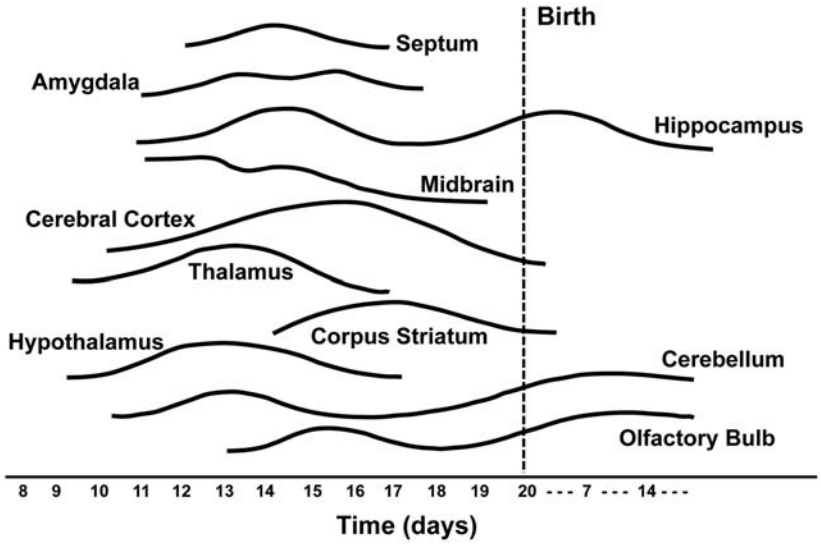

FIGURE 21.10 Peak production of neurons (shown here for the mouse) occurs at distinct developmental stages for different brain regions, with neuronogenesis as a whole extending for a prolonged period during both prenatal and early postnatal life. Some domains experience two peaks, representing the critical periods for forming unique cell classes. Thus acute/short-term neurotoxicant exposures tend to produce targeted damage that is limited to those areas where neuronal production was peaking when the agent was delivered to the developing animal. Source: *Figure adapted from Rodier, P.M., 1980. Chronology of neuron development: animal studies and their clinical implications.* Dev Med Child Neurol. *22, 525–545, with permission of John Wiley & Sons.*

glutaraldehyde) or various modifications of Karnovsky's fixatives (example: modified Karnovsky's fixative, which is typically 2% formaldehyde and 2.5% glutaraldehyde).

Glutaraldehyde is commonly used for preserving cell organelles for ultrastructural analysis. This molecule is a more effective cross-linking agent since it has two aldehyde moieties, but its length greatly slows tissue penetration. Furthermore, glutaraldehyde alone or in combination with formaldehyde enhances the stabilization of lipid-rich membranes, especially myelin. Perfusion fixation typically is conducted at pressures ranging from 70 to 120 mm Hg (i.e., the peak intravascular pressure during systole). Other critical aspects of perfusion fixation—buffering capacity, osmolarity, pH, and temperature—have been discussed in greater detail in other publications (see Further Reading for details). After a suitable period of time following perfusion fixation, neural tissues are removed from the carcass. In general, they are postfixed by immersion for an additional period in NBF. Specimens slated for detailed analysis of myelin and/or electron microscopy analysis are often postfixed a second time in 1% osmium tetroxide (OsO_4) to further stabilize lipid-rich membranes prior to embedding in hard plastic. Osmium postfixation even enhances a pathologist's ability to evaluate myelin sheaths in paraffin-embedded cross-sections of nerve as osmium metal forms dark (and electron-dense) deposits in lipid-rich myelin laminae. Fixation in OsO_4 must be performed in a chemical hood as osmium vapors are highly irritating and also readily bind to and discolor the corneal surface and skin.

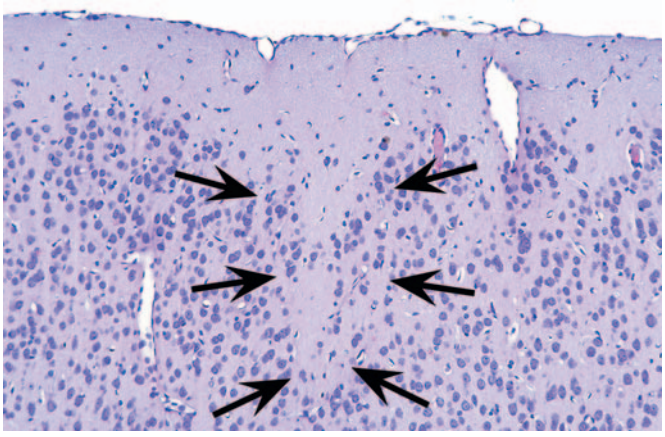

FIGURE 21.11 Neuronal dysplasia, shown as a cell-poor focus (denoted by arrows) in the rat cerebral cortex, is a consequence of abnormal cell production, growth, or differentiation.

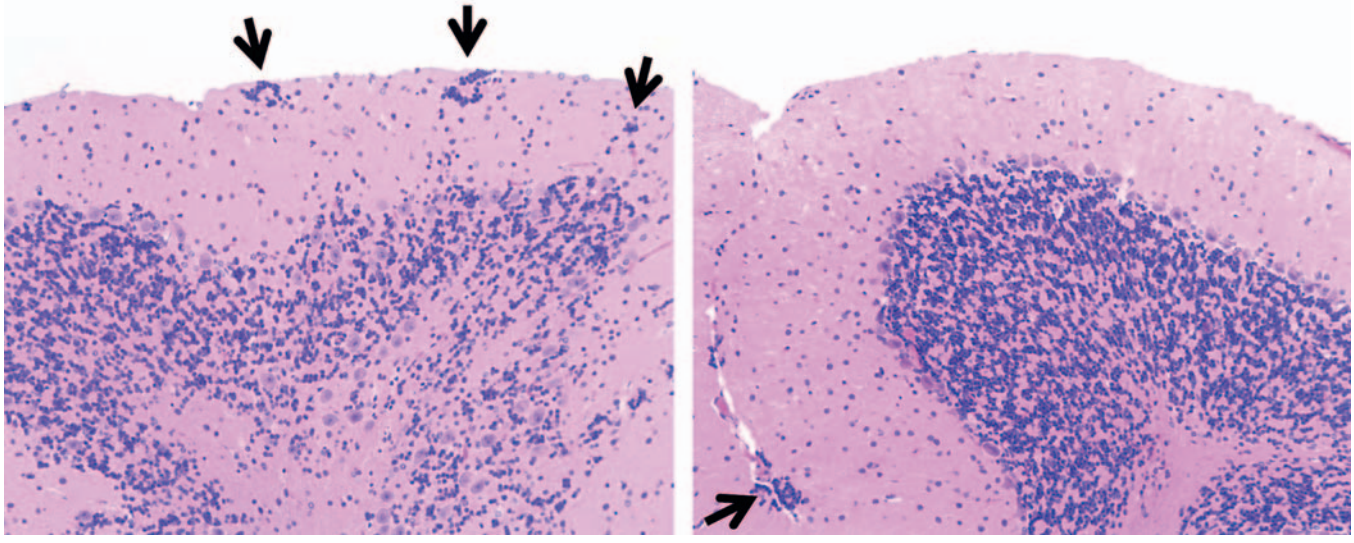

FIGURE 21.12 Neuronal heterotopia (ectopia) results from defective migration of neuronal precursors following developmental exposure to a neuroteratogen. *Left*: This 5.5-month-old, neurologically normal NSG mouse (i.e., nonobese diabetic (NOD) scid gamma, or NOD.Cg-Prkdc^{scid} Il2rg^{tm1Wjl}/SzJ strain) received whole-body irradiation on postnatal day 1 and developed multiple major abnormalities in the laminar organization of the cerebellar cortex: retained external granule cell clusters in the molecular layer (arrows), displacement of numerous Purkinje cells into the granule cell layer and foliar white matter, and reduced thickness and many fewer neurons for the granule cell layer. *Right*: This age-matched C57BL6/J control mouse exhibits the normal organization of the cerebellar cortex. The presence of a persistent focus of external granule cells under the meninges (arrow) is a common incidental finding in mice. Processing conditions: Formalin fixation by immersion, paraffin embedding, H&E staining. Source: *This specimen was kindly provided by Dr. Stefan Niewiesk, The Ohio State University, Columbus, Ohio, United States.*

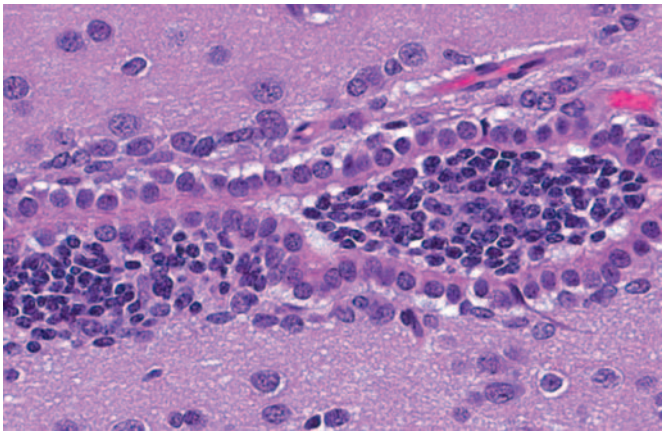

FIGURE 21.13 Ectopic stem cells may be displaced from the subventricular zone (dark cells at left) into the lateral ventricle (dark cells at right) or third ventricle. Over time the displaced cells degenerate and the debris is flushed downstream with the cerebrospinal fluid (CSF). Ventral horn of the lateral ventricle of a 6-week-old control Sprague-Dawley rat. Processing conditions: Formalin fixation by immersion, paraffin embedding, H&E staining. Source:*This image was kindly provided by Dr. Daniel Patrick, MPI Research, Mattawan, Michigan, United States.*

Immersion-fixed neural tissues often exhibit artifacts associated with handling at necropsy and/or suboptimal processing. Examples include dark neurons (Figure 21.14), myelin bubbling, and neuropil vacuolation (all of which are discussed in more detail later). Their presence does not preclude evaluation of neural tissue, but greater care must be taken to avoid false-positive results (i.e., interpretation of artifactual changes as genuine lesions) and false-negative outcomes (i.e., the inability to detect or properly construe modest lesions that may be camouflaged by more widespread artifactual changes).

Many molecular pathology procedures may be performed in NBF-fixed tissues, but certain IHC techniques and polymerase chain reaction (PCR) often require harvesting of unfixed tissue. Intravascular perfusion with ice-cold, buffered physiological saline may decrease the core temperature enough to lessen postmortem autolysis until the specimens can be removed and frozen. In some instances, reduced-strength fixatives (e.g., 1% or 2% formaldehyde) may be used to provide better tissue preservation while retaining the ability to retrieve labile antigens, although a pilot study is recommended to ensure that the altered fixation protocol will support the desired endpoints. In terms of fixative choice, it is best to start with prior knowledge of the required endpoints, then preserve the necessary tissues accordingly.

Brain Weights

Brain weight offers two major advantages as an endpoint for detecting neurotoxicity. First, brain weight is inherently quantitative and objective, which removes a potentially major source of bias in its acquisition and interpretation. Second, weights may be acquired at necropsy to provide a fast and simple clue that a neurotoxic event has occurred. Brain size typically is evaluated both as a measured absolute brain weight and as a calculated "relative weight" (most often reported as a ratio of brain weight to total body weight).

Brain weights may be taken at necropsy on fresh (i.e., unfixed) or perfusion-fixed organs or after some period of fixation. Either option is considered acceptable as long as weights for all subjects in a given study are taken from organs treated in the same fashion. The handling needed for weighing can induce several artifacts in some brain regions, so in dedicated neuropathology studies separate cohorts of animals for each treatment group are needed to obtain brain weights and perform histopathological assessments.

The key to acquiring reproducible brain weight data sets is to ensure that all organs are harvested in a consistent manner. For example, the olfactory bulb of rodents comprises 6%–7% of the brain weight, so this region should always be included or excluded when building a study data set. Similarly the brain should be separated from the spinal cord at a standard position. Typically a visible external landmark, such as the obex (the point on the dorsal *medulla oblongata* at which the fourth ventricle closes to become the central canal of the spinal cord), is used as a visual marker in order to provide long-term consistency in tissue harvesting.

Tissue Collection and Trimming

Neural tissues are prone to artifacts if handled roughly or excessively during necropsy. For instance, prompt removal of the brain from the cranial vault, even shortly after intravascular perfusion with fixative, can increase the propensity for artifactual cell shrinkage and increased amphophilia (i.e., able to bind both acidic [e.g., eosin] and basic [e.g., hematoxylin] dyes) that are the hallmark features of “dark neurons” (Figure 21.14). A better technique for reducing brain microanatomy artifacts is to perfuse the subject with fixative followed by careful removal of the skullcap and submersion of the entire head (with brain left in place) into fresh fixative for at least

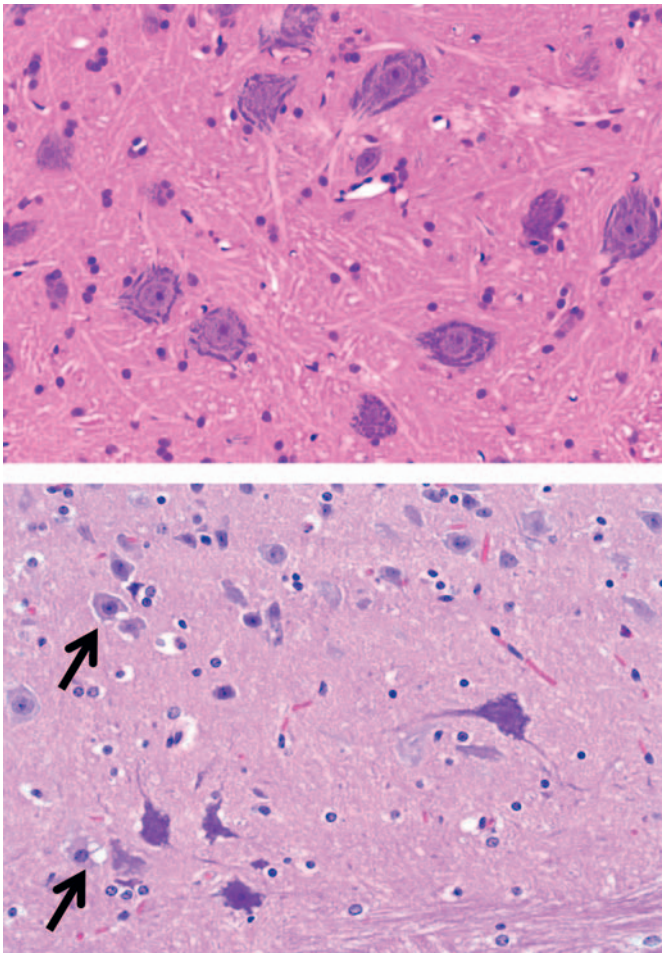

FIGURE 21.14 Neural cell architecture is greatly improved if fixation occurs by intravascular perfusion (upper) rather than immersion (lower). Perfused tissue features neurons with readily distinguished nuclear and cytoplasmic detail as well as improved contrast between neurite (pale eosinophilic) and myelin (darker eosinophilic) elements. Immersed tissue exhibits several artifactual changes that result from delayed penetration of the fixative. First and foremost, clusters of "dark neurons" may be identified by the blending of their darkly amphophilic nuclei and cytoplasm, and often by the presence of a twisted (corkscrew-shaped) and easily visualized dendrite; diagnosing this as a lesion is a typical error by inexperienced individuals, who interpret dark neurons as evidence of toxicant-induced neuronal necrosis. Second, neurons often are encircled by clear retraction spaces. Third, neurons (often small pyramidal cells or stellate cells) may be associated with small, oval, clear vacuoles near the periphery (arrows), which are thought to be swollen astrocyte processes). Finally, the contrast between structures in the neuropil (i.e., the expanse of myelinated neurites between cell bodies) often is minimal. Cerebral cortex of adult rats. Processing conditions: Formalin fixation, paraffin embedding, H&E staining. Source: *Figures reproduced from Bolon, B., Butt, M.T., 2014. Fixation and processing of central nervous system tissue. In: Aminoff, M.J., Daroff, R.B., (Eds.),* Encyclopedia of Neurological Sciences, *second ed., vol. 2. Academic Press (Elsevier), San Diego, pp. 312–316, with permission of Academic Press.*

24 hours before removal. If the brain is removed rather than fixed in situ, immediate immersion into a suitable fixative is preferred relative to delays associated with additional handling (e.g., for weighing).

In general, toxicologic neuropathology requires sampling of the CNS and PNS at multiple sites. The minimal approach to sampling often is a matter of institutional preference. For example, common brain sampling schemes for general toxicity studies are 3–7 full coronal ("cross" or "transverse") brain sections or one mid- or parasagittal (longitudinal) section and 3–5 coronal hemisections. Dedicated neurotoxicity studies typically collect double to triple this number of sections. Trimming the brain and spinal cord using freehand coronal sections, in which planes for sample acquisition are defined using reproducible external or internal anatomic landmarks alone, is a fast and reliable approach for screening studies. Brain molds (i.e., acrylic or metal matrices with multiple parallel slots) may be used if desired when all organs from the test group are of suitable size to fit the apparatus (typically true for adults but not juveniles). The advantage of this latter approach, especially when using fixed brains, is that the slabs can be made quite thin by placing blades in adjacent slots of the mold. However, one caution is that slicing tissue, especially brain, too thin may make it difficult to obtain a full section at microtomy; this is especially true when producing full transverse sections of the brain from primates, canines, and other large animals. The spinal cord and nerves should be examined in both longitudinal (either parasagittal or oblique) and transverse sections as damage to axons in these tissues is often best showcased in the longitudinal orientation.

The keys to proper nervous system sampling are to make sure that critical sites serving major functions and that are targeted by known toxicants are taken. These sites include (as listed alphabetically) the basal nuclei (specifically the caudate/putamen region), cerebellum, cerebral cortex (multiple regions), hippocampus, hypothalamus, *medulla oblongata*, midbrain, olfactory bulb (especially in rodents), pons, and thalamus in the brain; three segments of spinal cord (cervical, thoracic, and lumbar); dorsal root ganglia; peripheral nerves; and the eye (for retina) with attached optic nerve (i.e., cranial nerve II). Additional sites may be taken if warranted by other factors (e.g., the presence of neurological signs or a known tendency for agents with a given structure or mechanism to target a specific neural domain). Organs should be sampled so that the resulting tissue sections are fairly homologous (i.e., exhibit the same structural landmarks) among animals both within and across studies. The tissue dissection strategy, both at necropsy and during trimming, should progress in a similar manner between animals and across studies to enhance consistency and to avoid missing tissue regions.

Neurohistological Procedures

In general, CNS and PNS samples are embedded in paraffin. The advantage of this approach is that neural tissues can be processed along with other organs. Some regulatory guidelines require that PNS tissues instead be embedded in plastic (usually glycol methacrylate (GMA), i.e. "soft plastic") or hard plastic resin (e.g., araldite, epon, Spurr's). Soft plastic or resin embedding allows tissues to be sectioned at thicknesses of 1–2 μm rather than the standard 4–8 μm used for paraffin. If properly fixed and prepared, thinner sections may yield better resolution of fine architectural detail during light microscopic evaluations, especially for nerves (Figure 21.15), but in our experience significantly improved resolution is achieved only using hard plastic. The increase in resolution provided by osmium postfixation and resin embedding is of great benefit whenever there is a need to visualize myelin sheaths (and compare sheath thickness to axon size) or to detect myelin or axon degeneration or regeneration. Many studies rely on paraffin embedding and H&E stains, which at least in longitudinal sections generally provide a suitable screen for the presence of axonal degeneration.

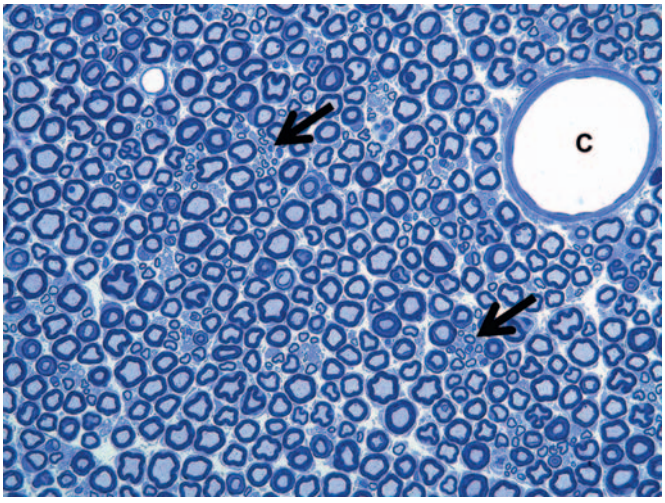

FIGURE 21.15 Embedding in hard resin provides exquisite preservation of fine architectural detail in nerves, which contain numerous myelinated fibers (evident as pale, large axons encircled by thick rings of dark myelin) mingled with scattered clusters (arrows) of unmyelinated fibers (seen as pale, small axons surrounded by thin myelin layers). Myelinated fibers (typically 2–20 μm in diameter) generally serve somatic functions, while unmyelinated fibers (usually 0.2–3.0 μm in diameter) fulfill visceral functions. C, capillary. Cross-section of sciatic nerve from a normal (i.e., control) adult rat. Processing conditions: Perfusion fixation with 4% glutaraldehyde, postfixation by immersion in 1% osmium tetroxide, embedding in hard plastic resin, sectioning at 1 μm in transverse orientation, staining with toluidine blue. Source: *Figure reproduced from Bolon, B., et al., 2008. Current pathology techniques symposium review: advances and issues in neuropathology*. Toxicol. Pathol. *36, 871–889, with permission of SAGE Publications.*

The histological analysis of neural tissues typically is performed in a tiered manner. The examination starts with sections stained using hematoxylin and eosin (H&E), which permits the general evaluation of cytoarchitectural features. Where needed, pathologists will request serial sections stained using special neurohistological methods to reveal additional detail. Such special stains illuminate particular cell populations or probe potential processes that have been shown to be vulnerable to toxicant-induced disruption. Nissl stains (e.g., cresyl violet (Figure 21.16), thionine) used to detect RNA bound to the rough endoplasmic reticulum (Nissl substance) show the fine cellular details of more neuronal populations than does a simple H&E stain although the standard H&E stain also highlights (to a lesser degree) the Nissl substance. Reduced Nissl staining indicates that neuronal function has been impaired.

The health of myelinating cells is examined using methods that label intact myelin, such as Luxol fast blue (LFB, a histochemical method) or myelin basic protein (MBP, a marker protein localized using an IHC method). Neurons and myelin can be visualized in the same section by combining stains (e.g., cresyl violet with LFB (Figure 21.16)). Toxicant-induced neuronal death and/or axonal degeneration can be revealed using fluorescent (e.g., Fluoro-Jade) and metallic enhancement (e.g., amino cupric silver) procedures that collect preferentially in damaged cells (Figure 21.7). Sites of neural injury can also be defined using special techniques to reveal activated glia (e.g., enhanced GFAP (Figure 21.8) or Iba1 (Figure 21.9) expression) collecting at sites of prior neuronal injury.

Contrary to conventional wisdom, labor, money, and time may actually be saved by designing neurotoxicity experiments so that a battery of neurohistological stains are produced automatically as the first tier of the neuropathology examination (e.g., H&E, Fluoro-Jade, and anti-GFAP), if only for the high-dose treatment group and the negative control cohort to start. The reason for this choice is that potential neurotoxic lesions of a subtle character can be more readily identified and rapidly evaluated if sections have already been produced and stained in advance. While the other stains often reveal changes that were not readily seen on the H&E-stained sections, the most important aspect of any evaluation of the nervous system is the preparation and evaluation of an adequate number of sections from multiple CNS and PNS regions to allow for hazard identification and risk assessment. In blunter words, regardless of the special stains used, it is not possible to visualize an abnormality in a portion of

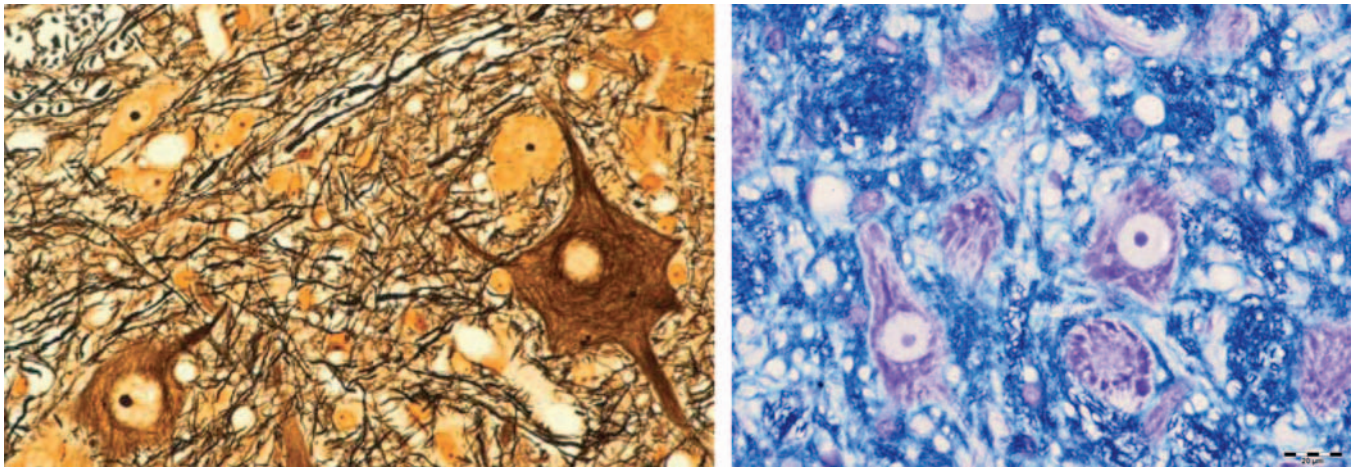

FIGURE 21.16 Features of cellular anatomy often are better highlighted in sections processed with cell type–specific stains rather than H&E (see Figure 21.14 for comparison). For pyramidal neurons, cell bodies are showcased by Bielschowsky's silver stain (left image: neurons have variably darkened cytoplasm, pale yellow nuclei, and black nucleoli) and cresyl violet (right image: neurons have abundant purple Nissl substance (rough endoplasmic reticulum) in the cytoplasm, pale nuclei, and dark nucleoli). Axonal integrity is readily visible in the Bielschowsky's stained preparation (thin black lines). Myelin sufficiency is revealed by the use of Luxol fast blue (LFB) as the counterstain for the cresyl violet–stained section (where myelin sheaths are blue). Cerebral cortex from adult control rats. Processing conditions: Formalin fixation by perfusion, paraffin embedding.

the brain, spinal cord, ganglion, or nerve that is not prepared and examined.

Morphometry

Quantification of neural features in samples that are acceptable for performing measurements in two dimensions (2D)—for instance, fiber diameters in nerve cross sections or thicknesses of brain regions as performed in developmental neurotoxicity studies—is a conceptually simple but moderately laborious means for obtaining objective data during a neuropathology evaluation. Common 2D means for quantification include linear (e.g., lengths, widths, heights, perimeters) and area assessments, typically taken at multiple levels (Figure 21.17). Examples include lengths (e.g., greatest mid-axial length of the dorsal cerebral cortex) and areas (e.g., dimensions of the dorsal profile of the cerebellar hemispheres) of major regions in intact brains; thicknesses or areas of particular domains on histologic sections (e.g., height of the cerebral cortex, width of the basal nuclei); and counts of small structures (e.g., cells in a given nucleus, axonal density). To be valid, such measurements must be gathered on highly homologous samples (e.g., tissue sections with comparable internal landmarks), and ideally using a coded ("blinded" or "masked") analysis in which the investigator does not know the treatment history for the specimens.

Quantification of objects in three-dimensional (3D) structures, such as neuron counts in dorsal root ganglia or in specific brain nuclei, requires a stereological investigation. Investigation design is exceedingly important for this category of specialized analysis. Particular emphasis must be placed on randomly but systematically examining the entire structure, with a sampling parameter that ensures that each and every object of interest has, at the beginning of the study, an equal opportunity of being counted/measured. Stereology generally is employed to answer specific questions rather than as a screening tool for potential neurotoxicity due to the slow and labor-intensive methodology (as described below).

Teased Fiber Preparations

Isolated nerve fibers, consisting of a single axon and its myelin sheath obtained from a nerve, can be evaluated for lesions over long distances (typically 0.5–1 cm). Details of the nerve fiber teasing method are beyond the scope of this chapter, but in brief nerves are fixed by immersion in an aldehyde, separated into individual nerve bundles using forceps, and then postfixed in 1% OsO_4 to stabilize and darken the lipid-rich membranes. Individual myelinated axons are teased apart in cedar wood oil under a stereomicroscope using forceps, mounted on slides, dried, and coverslipped. Features evident for inspection include the myelin integrity, the appearance of the nodes of Ranvier, and the intermodal distance, which can be used to discriminate between degenerative and regenerative processes affecting the axon and its myelin.

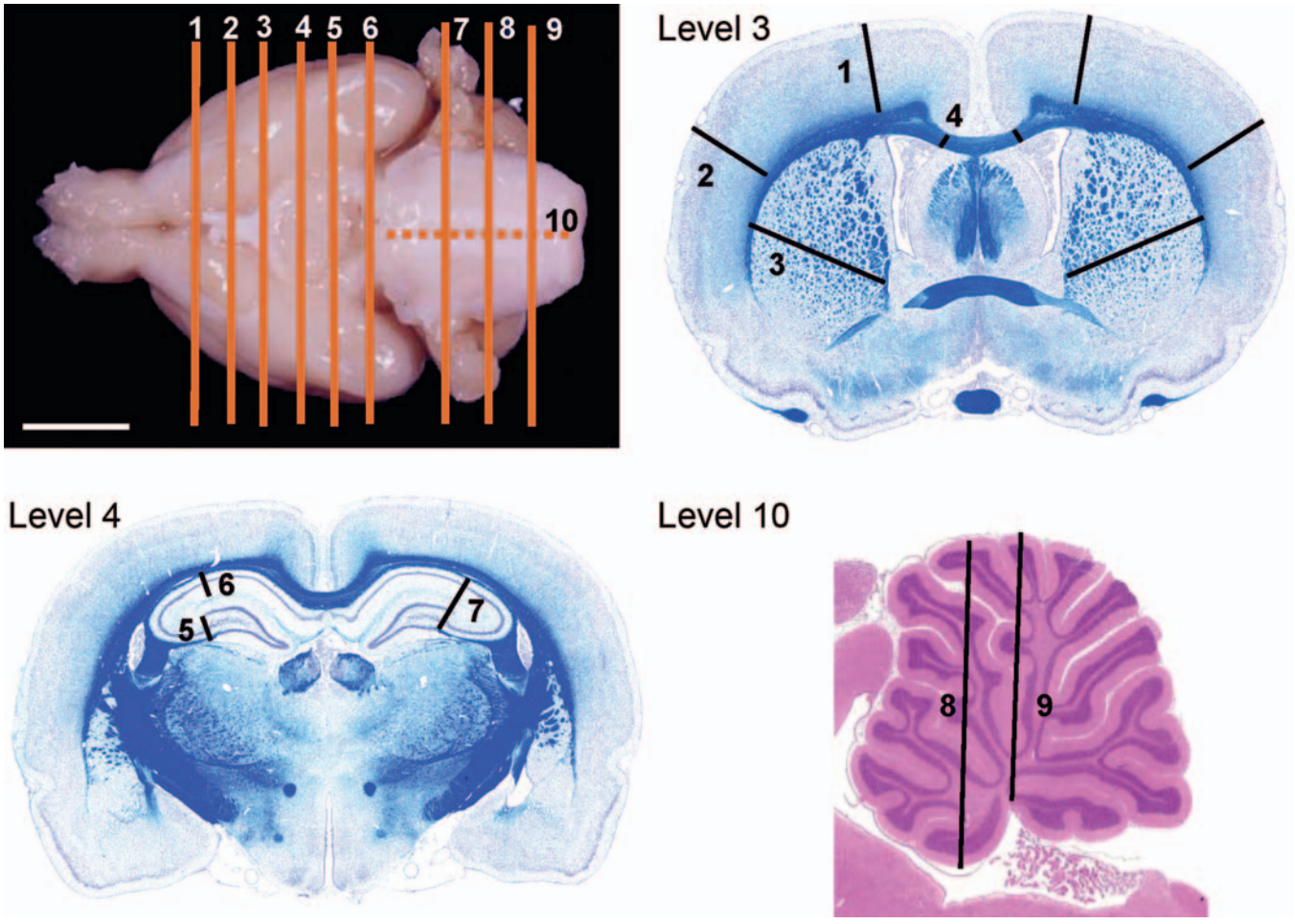

FIGURE 21.17 Simple morphometric measurements may be used to quantify potential neurotoxic injury to particularly critical brain regions with well-known structural–functional correlations, especially the cerebral cortex, hippocampus, and cerebellum. *Upper left*: Ventral surface of a rat brain showing levels at which slices are made using gross neuroanatomic landmarks. Lines 1–6 denote slices that are made from the ventral surface, whereas lines 7–9 indicate cuts made from the dorsal surface. Line 10 (dotted) shows the position of a mid-axial slice if a sagittal orientation is preferred for cerebellar measurements. *Other panels*: Sections demonstrating the most reproducible morphometric measurements for quantitative analysis of rat brain. "Level" numbers reflect those of the labeled lines in the Upper Left panel. Line numbers denote: 1 and 2 = cerebral cortex thickness, motor (1) and sensory (2) areas; 3 = striatum (caudate/putamen) width; 4 = corpus callosum thickness; 5, 6, and 7 = hippocampus thickness for dentate gyrus (5), an individual CA field (6), or the entire domain (7); and 8 and 9 = cerebellum height. The coronal sections (blue hue) were stained with cresyl violet/Luxol fast blue (CV/LFB), which affords especially sharp margins between certain neuroanatomic structures based on their degree of myelination, while the mid-sagittal section (pink hue, lower left panel) was stained with H&E. Source: *Figure reproduced from Garman, R.H., et al., 2016. Recommended methods for brain processing and quantitative analysis in rodent developmental neurotoxicity studies.* Toxicol. Pathol. *44, 14–42, with permission of SAGE Publications.*

Special Anatomy-Based Techniques for Neurotoxicity Assessment

Given the importance of neurotoxicity as a health hazard, considerable effort is ongoing to further refine the battery of tests that are available to diagnose neurotoxic conditions in the clinical setting and/or to identify potential neurotoxicants among newly developed and existing agents to which humans and animals are exposed. Morphological changes again represent the "gold standard" for optimizing these evolving procedures.

Noninvasive Imaging

The multiple whole animal imaging modalities that have been developed in the last two decades exhibit great promise as tools for toxicologic neuropathology. Major advantages include their ability to be used repeatedly during life (albeit at low resolution), thus permitting observations of lesion progression over time, and the capacity to translate both the technology and the findings in test animals directly to humans. The main disadvantage of noninvasive imaging as applied to animal studies is insufficient structural resolution at the

microscopic level, but recent technical advances permit assembly of 3D images from postmortem specimens at fairly high resolutions (down to 20 μm, i.e., magnetic resonance microscopy (MRM)), albeit using very expensive equipment.

Imaging modalities may be used to examine anatomic features or functional attributes, or to correlate functional changes to structural lesions. Technologies that provide anatomic data—computerized tomagraphy (CT), magnetic resonance imaging (MRI), MRM, and ultrasound (US)—form images using endogenous properties of cells and tissues to define the margins between structures. Platforms that yield functional data—optical imaging, positron emission tomography (PET), and single-photon emission computed tomography (SPECT)—reveal features of a specific biochemical or metabolic pathway within a given structure. In particular, PET and SPECT are powerful means of probing neural responses as they depend on selective accumulation of appropriate radiolabeled tracers (e.g., [^{18}F]-fluorodeoxyglucose, a glucose analog) in various CNS structures. A series of 2D images is gathered and assembled into a "z-stack" using an automated algorithm to produce a 3D low-resolution representation showing where the tracers have localized. A more precise anatomic localization may be gained by aligning functional data sets from PET and SPECT in register with CT or MRI images.

Stereology

Precise and unbiased quantitative assessment of the distribution, orientation, number, shape, or size (i.e., volume) of objects in 3D is an important approach for investigating neurotoxic agents. The attraction of this strategy is that stereological methods are quite sensitive to abnormalities in the number of a given class of structures (e.g., neurons, neuronal processes), which generally is not the case for macroscopic and microscopic (including 2D morphometric) procedures that form the basis of conventional neuroanatomic examinations for toxicant-induced neuropathology. The primary disadvantage of stereology is that processing and analysis may be time-consuming. Because one requirement of stereology is the ability to specifically define the limits of the region of interest, structures that are selected most commonly for stereological analysis are domains that are common sites for neurotoxic damage, such as the pars compacta portion of the substantia nigra, basal forebrain nuclear regions (which can be identified by selective staining for choline acetyltransferase), other brain nuclei/neuronal areas whose limits can be defined, PNS ganglia, and nerve cross sections.

In general, stereology for evaluating toxicologic neuropathology focuses on two tasks. The first is defining the region of interest, and determining the size (usually the volume) of that area by measuring area (Cavalieri-based method) and average section thickness. Once the region of interest is defined, the objects of interest can be counted and/or measured using unbiased sampling techniques like the optical disector/fractionator or a physical disector. The goal is typically to count/measure 100–200 objects of a particular kind (example: neurons) throughout the specimen (example: a dorsal root ganglion) in a systematic random manner within 8–10 or more levels (example: serial or step sections of tissue) taken through the region of interest. Optical disector methods use sections with a thickness preferably in excess of 20 microns. Physical disector methods use thinner sections but rely on the use of "look up" sections for comparison to a reference section. Stereology may reveal changes not apparent during standard morphologic evaluations, such as prior neuron loss (detectable as decreased neuron counts), changes in neuron size, and loss of subsets of axons. While slow relative to standard neuropathology evaluation, the discriminative power of quantitative neuroanatomical analysis increases as one moves from gross assessments (e.g., brain weight measurement) to simple microscopic endpoints (e.g., acquisition of areal or linear dimensions using morphometric measurements) to enumeration of specific objects (stereology).

Biomarker Evaluation in Fluids and Tissues

In many cases, the initial neurological changes that might be detected following xenobiotic exposure will not be macroscopic and microscopic structural lesions or functional abnormalities but rather reflect molecular, neurochemical, and/or ultrastructural (i.e., submicroscopic) effects. Recent neurotoxicological research has focused on finding more rapid, less invasive, and less laborious means for identifying neurotoxic risks. Discovery and validation of novel biomarkers has been a particularly active area of inquiry in this regard.

Clinical Pathology

Changes in peripheral blood samples (e.g., whole blood, plasma, serum) generally are uninformative in terms of characterizing neurotoxic changes, but CSF analysis may be of use in certain instances. The utility of CSF as a substrate stems from its link to interstitial fluid (ISF), which is the principal liquid constituent in the brain and spinal cord immediately surrounding neurons and glia. Collection of CSF is less invasive and injurious to the CNS parenchyma than acquiring a neural tissue sample. Common assays include biochemical tests (e.g., protein levels, concentrations of neurotransmitters and their metabolites) and the

evaluation of cell numbers and morphology. In general, CSF collection in rodents is confined to satellite groups of animals as the anesthesia protocols required for this evaluation may impact other endpoints.

Analysis of CSF has reasonable sensitivity but low specificity as an indicator of CNS health. The reason is that the range of aberrant changes in this fluid is narrow relative to the many possible neurological diseases, particularly if the analysis is limited to assessing total and differential cell counts and/or protein concentrations. Diseases in the meninges and neuropil adjacent to the ventricular system (the "CSF compartment") usually produce greater variance in CSF parameters than do diseases in the deep parenchyma of the brain and spinal cord (the "ISF compartment"). Since most neurotoxic lesions affect the deep neuropil, properties of CSF samples from individuals with neurotoxic conditions generally are within normal limits.

Neurochemistry

Neurochemical measurements are common endpoints in neurotoxicological studies. Such tests provide not only evidence that an agent has altered one or more neurobiological parameters but also point toward specific mechanisms of neurotoxic action.

Neurotransmitter systems are classic biomarkers. Their importance during development (as morphogens) and adulthood (as signaling molecules) stems directly from the need to properly maintain their synthesis, release, and removal. Neurotransmitters may be assessed by many means. Chemical assays (e.g., chromatography or microdialysis to define transmitter levels) and molecular biological techniques (e.g., northern analysis of RNA levels, western analysis or enzyme-linked immunosorbent assays (ELISA) for peptide transmitters, receptors, and signaling cascade proteins) can directly detect specific elements contributing to the function of a given transmitter system. The measurements reveal the quality (presence or absence) and quantity of particular elements within a given pathway but do not directly assess the functional integrity of the system. Thus increases or decreases in neurotransmitter levels induced by neuroactive agents are not necessarily indicative of a neurotoxic effect unless they occur with other functional (e.g., behavioral, electrophysiological) or structural (i.e., neuropathological) changes.

Expression of GFAP is another frequent biomarker for CNS damage, including that caused by neurotoxicants. Accumulation of GFAP results from astrocyte hypertrophy; cell expansion requires enhanced production of all cell constituents, and GFAP is key among them as the major intermediate filament protein. Biochemical assays (e.g., radioimmunoassay, sandwich ELISA, and western analysis) or IHC stains (see below) indicating increased GFAP levels are a sensitive, simple approach for confirming the presence of a CNS response to prior damage, although the cause of the change usually cannot be defined without other tests (e.g., histopathology), and sometimes not even then as GFAP expression may rise in the absence of histopathological changes. Therefore stand-alone increases in GFAP above control levels may be indicative of neurotoxicity if a history of exposure is known. An important consideration in interpreting such increases is that GFAP levels will also be higher following injurious events other than neurotoxic damage (e.g., increased corticosteroid levels, normal aging). Interpretation of decreased GFAP levels in adults or any alteration of GFAP expression in developing animals remains uncertain.

Enzyme histochemistry is another common means for detecting changes in biochemical and metabolic pathways that might serve as biomarkers for neurotoxic lesions and their mechanisms. An advantage of these methods is that they detect the presence of a functional protein. Enzyme histochemical tests that are commonly used in neurotoxicologic studies include visualization of extravasated horseradish peroxidase as a probe for xenobiotic-induced damage to the BBB and assessment of acetylcholinesterase (AChE) inhibition in fluids and tissues to indicate exposure to organophosphate (OP) or carbamate insecticides.

Toxicogenomics

The application of various "omics" disciplines including assessments of DNA (genomics), messenger RNA (transcriptomics), or protein (proteomics) responses is increasingly used to define early steps in the pathogenesis of neurotoxicity. The basic principle is that the expression pattern of a molecule can be probed qualitatively or quantitatively in homogenized tissue to determine a molecular signature that may be used in diagnosing the presence and progression of a given disease. These methods provide high-throughput, high-resolution molecular analysis.

The "omics" platforms serve two primary roles in neurotoxicological research. The first is to assess variations in the molecular signature among different cell populations (e.g., neurons vs astrocytes, granule vs pyramidal neurons). The second aim is to examine molecular pathways that play roles in xenobiotic responses that might be used to diagnose or treat particular health conditions (e.g., receptors capable of interacting with antidepressant drugs, signaling cascades impacted by exposure to drugs of abuse). Other roles will be added as this technology matures as a means for neurotoxicological exploration.

"Omics" techniques are quite sensitive to the quality of the starting material. Tissues must be collected as

rapidly as possible after death to prevent artifactual molecular degradation in neural cells (especially in the deep CNS parenchyma) that arise due to *postmortem* acidosis, dehydration, hypoglycemia, and hypoxia. In general, samples should be collected fresh and frozen at −80°C until analysis, but molecular data can often be obtained from fixed or fixed and previously embedded samples as long as the fixation length was relatively short and the blocks were not subjected to extreme temperature fluctuations during their time in storage. Where known in advance, the experimental design can accommodate parallel collection of fresh tissue for "omic" (and other neurochemical) endpoints and fixed tissues for routine neuropathology evaluation.

Success in toxicogenomic studies generally depends on careful experimental design. One critical aspect is that such studies must be built with a clear question in mind. In most cases, this requirement means that experimental subjects should be as nearly identical as possible except for a single variable, such as a manipulation (e.g., genotype or treatment) or physiological state (e.g., age, genetic background, sex). An additional factor that is critical for success is an appropriate sampling strategy, which typically rests on isolating the correct cell population for analysis. Cell harvesting may be done by gross dissection of large tissue blocks where regional homogeneity at the macroscopic level is evident. However, the differential expression of various genes at the cell level invariably results in a readout in which expression data represents an "average" from many neural cell types. The alternative approach is to use laser capture microdissection (LCM), which is more laborious but permits sampling of a defined cell population.

Mammalian Models for Neurotoxicity Research

Neurotoxicity testing is based on the premise that any anatomic, biochemical, or functional effects that develop in the nervous system of animals after exposure to a particular agent would also be likely to occur in exposed humans, in a qualitative sense if not in a quantitative fashion. Accordingly, neurotoxicity bioassays are designed to discover target sites (i.e., cell populations or organ subregions), elucidate dose-response relationships, catalog similarities and differences in sensitivity among species, and determine mechanisms of toxicant action. Another important aspect of neurotoxicity testing is to define any special attributes of certain classes of individuals who are likely to have nervous systems that are particularly vulnerable to neurotoxic agents. Examples of such classes are developing animals (as neural cells and circuits are established over an extended period (Figure 21.10)) and senescent organisms (who theoretically have less functional reserve available to compensate for neurotoxic episodes).

The bulwark of conventional hazard identification and risk assessment *in vivo* involves toxicity studies in young adult rats. This choice is dictated by practical factors (particularly cost), but is permissible because the Rodent nervous system is qualitatively similar to that of other mammals. Rats typically are enrolled on studies at 2–3 months of age, and exposures occur over standard lengths of time (usually 4, 13, or 26 weeks). Neural evaluation occurs as a survey of selected CNS and PNS functions and structures in conjunction with surveys of other major body systems. Such general toxicity studies screen for major effects in key neural regions using a battery of endpoints: in-life observations, collection of gross findings and the brain weight at necropsy, and histopathological assessment of selected critical CNS and PNS regions (Table 21.2). If adverse neural events are not observed using these measures, additional neurotoxicity testing generally is not performed. However, enhanced neurotoxicity testing is undertaken if an agent either impacts a neurological parameter (anatomic especially, but also functional) or has a molecular form that suggests a structure–activity relationship to a known neurotoxicant. Such enhanced testing adds more endpoints (e.g., expanded behavioral testing, electrophysiology, neurochemical measurements, and additional sections for microscopic evaluation) to probe the operational integrity of the nervous system more fully.

Developmental neurotoxicity testing (DNT) is a related but separate strategy that examines the special susceptibility of the immature nervous system. Again, rats are the preferred species for testing due to their fecundity and short gestational length (approximately 20 days). Pregnant animals usually are exposed to a test article from gestational day 6 (the approximate time at which the blastocyst implants in the uterine wall) through postnatal day 11 (the approximate end of major neuronal production in the rat) or postnatal day 21 (the conclusion of neuronal and glial expansion as well as initial circuit generation and myelination). The battery of endpoints is comparable to that used for enhanced neurotoxicity testing in adult rats. A special feature that must be remembered when designing DNT studies is that the appropriate experimental unit is the litter and not the individual offspring, since the dam is the entity that has been exposed to the agent.

Although rats are the most common test species for evaluations of neurotoxicity, they may not always be the most suitable species for predicting specific effects in humans. Different species likely react in diverse ways to the same agent due to species-specific

variations in neural anatomy (especially barriers), developmental timing, pharmacokinetics, and/or inherent pharmacodynamic differences. Since the importance of these interspecies discrepancies often is incompletely or even totally unknown, any neurotoxic effect seen in animals is presumed to foreshadow a risk to humans even though effects seen in animals may not be the same as those produced in humans. Consequently a clear understanding of the pathogenesis and the mechanism(s) of neurotoxicant action that lead to neural damage are critical to produce the best risk assessment decisions.

NERVOUS SYSTEM RESPONSES TO NEUROTOXIC INJURY

The ability of toxic agents to disrupt neural activities depends on many parameters. These factors typically are specific to given entities, such as particular CNS regions or cell populations or subcellular structures. This section describes the most common responses of the nervous system to toxic injury. Frequent artifactual changes are defined where relevant so that they will not be misinterpreted as evidence of neurotoxicity.

Anatomic Lesions

In general, structural damage that manifests in the nervous system may be divided using one of two fundamental approaches. The first is to catalog anatomic changes resulting from injury to a specific cell population (e.g., neuron, myelinating element) or cell part (e.g., axon, synapse). The terms applied to such conditions are commonly designated in broad terms using the name of the targeted cell or cell part followed by the suffix "-opathy." The second option is to diagnose alterations based on the class of lesion that they represent (inflammation, neoplasia, etc.). Basic classes of neural lesions (Table 21.1) are briefly described below.

Cell type–specific lesions

NEURONOPATHIES

Certain toxicants attack specific groups of neurons, usually residing within the CNS. The lesions have been characterized chiefly using rats, but humans typically are vulnerable as well. For instance, 3-acetylpyridine irreversibly destroys the inferior olivary nuclei, thus inducing cerebellar ataxia by decimating the climbing fibers leading to the cerebellum. The neurotoxic effects of MPTP are largely confined to the dopaminergic neurons of the substantia nigra, resulting in cell death in humans, other primates, and some strains of mice (with humans representing the most sensitive species). A mix of cycad toxins have been linked to the induction of amyotrophic lateral sclerosis/Parkinson-dementia complex (ALS-PDC) in natives of Guam with the expanded range of symptoms being attributed to variable blends of toxicants that act individually to target neurons in the cerebral cortex, substantia nigra, and spinal cord. In many instances, the sensitivity of particular neuronal groups to toxic agents first is discerned via their distinct patterns of functional alterations and/or neurochemical changes rather than by morphological analysis.

The basic neuropathology findings associated with a neuronopathy depend on the length of time during which the toxic injury has been taking place. *Degeneration* (alteration of a cell or tissue to a less functional form) may be an acute or chronic condition characterized by a variety of subcellular microscopic changes. For example, a subset of neurons in layers III/IV of the cingulate/retrosplenial cortex targeted by MK-801, a *N*-methyl-D-aspartate (NMDA) antagonist, develop fine cytoplasmic vacuoles within hours of exposure (Figure 21.18), but their nuclei and cell membranes are intact. Neuronal *vacuolation* is caused by expansion of intraneuronal cytoplasm or membrane-bound organelles as a consequence of retained fluid or metabolic byproducts. In principle, degenerative changes may be reversed if exposure to the toxicant ceases in time and/or the dose was below the lethal threshold.

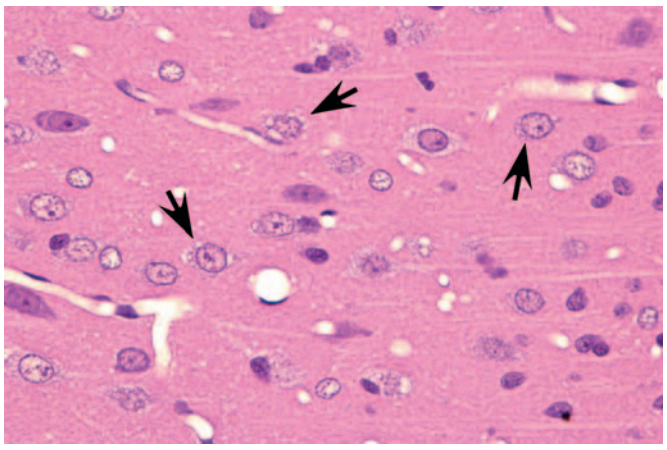

FIGURE 21.18 Peracute neuronal degeneration may present initially as clear, round, cytoplasmic vacuoles (arrows) in affected cells. In this case, the change is evident in granule neurons within the retrosplenial cortex of an adult rat 6 hours after it had been given MK-801, an excitotoxic antagonist of the *N*-methyl-D-aspartate (NMDA) glutamate receptor. This pattern is often termed the "Olney lesion" after its discoverer, American neuropathologist John Olney. Interpretations of this lesion range from a transient perturbation to a precursor of neuronal necrosis to an artifact of aldehyde fixation. Processing conditions: Formalin fixation by intravascular perfusion, paraffin embedding, H&E staining.

Degeneration may, especially within in neurons, progress to necrosis (Figures 21.19 and 21.20). The hallmark features of toxicant-induced neuronal necrosis in the CNS are contraction of the cell (leaving a clear, peri-cellular halo); condensation and/or fragmentation of the nucleus; and loss of the Nissl substance, leading to hypereosinophilic cytoplasm; the latter feature is the classic trait of "red dead" necrotic neuron (Figures 21.5, 21.19, and 21.20). Genuine neurotoxic lesions often harbor an array of affected cells, with responses ranging from acutely injured to dead and disintegrating. Neuronal necrosis may be detected using standard H&E staining, but increased sensitivity is provided by Fluoro-Jade (performed on frozen or paraffin-embedded tissue sections) and cupric silver stains (performed on frozen sections) (Figure 21.7). With time, dead neurons may attract complements of microglia that help to remove the cellular debris in a process termed "neuronophagia" (Figure 21.21). The remnants of necrotic neurons are cleared rapidly. Unless evaluated in the proper (typically early) time frame, quantitative investigations may be required to detect neuron loss. Exceptions to this include areas where neurons are arranged in an orderly manner, including the various CA regions of the hippocampus and the Purkinje cell layers. Even subtle neuron losses in these well-defined brain regions may be detectable as "gaps" in the neuron layer. Stains to detect astrocyte reactions may be particularly helpful to determine if the "gaps" indicate prior neuron loss or are normal anatomic variations.

Neuronal *heterotopia* (or ectopia) is a distinct category of neuronal lesion. Instead of cell loss, the fundamental change is a developmental disturbance leading

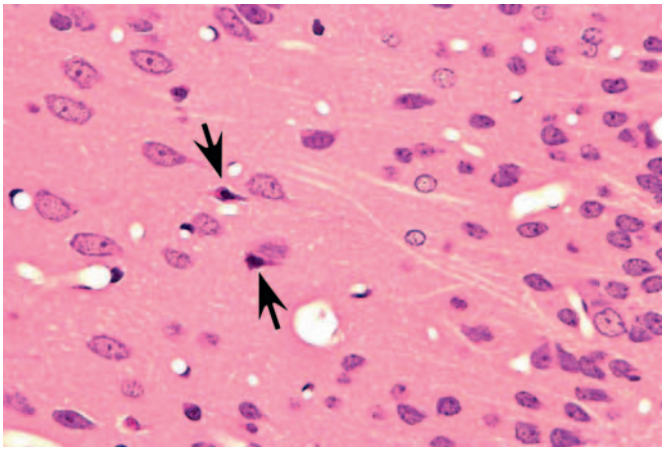

FIGURE 21.19 Acute neuron degeneration (neuronal necrosis) presents as pyknosis (condensed nuclei) with hypereosinophilia (brightly eosinophilic cytoplasm). These "red dead" neurons in the retrosplenial cortex were seen 24 h after treating an adult rat with the excitotoxic agent MK-801, an antagonist of the *N*-methyl-D-aspartate (NMDA) glutamate receptor. Processing conditions: Formalin fixation by intravascular perfusion, paraffin embedding, and H&E staining.

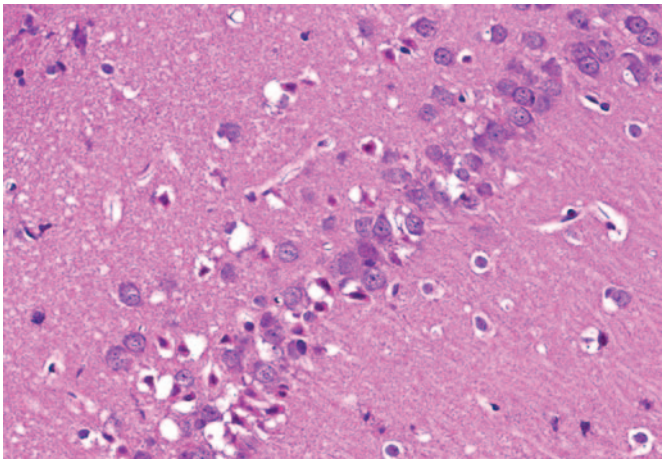

FIGURE 21.20 With time, acute neuronal necrosis progresses by karyorrhexis (nuclear fragmentation) and peri-cellular vacuolation around "red dead" neurons, in this case in the CA_1 field of the hippocampus 48 h after treating an adult rat with the excitotoxic agent kainic acid, an agonist of the kainate-type receptor for glutamate. Processing conditions: Formalin fixation by intravascular perfusion, paraffin embedding, H&E staining. Source: *This image was kindly provided by Dr. Daniel Patrick, MPI Research, Mattawan, Michigan, United States.*

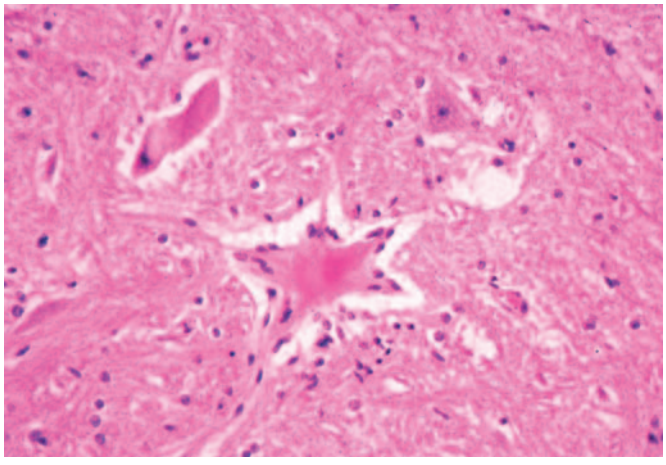

FIGURE 21.21 Satellitosis of small glial cells around toxicant-damaged neurons typically indicates either a final attempt by oligodendrocytes to support degenerating but still living cells or early efforts by microglia to begin scavenging debris from dead cells. This image, from an adult ox exposed to an organophosphorus insecticide, represents the microglial response. Processing conditions: Formalin fixation by immersion, paraffin embedding, H&E staining. Source: *This image was kindly provided by Dr. Patrick Nation, Animal Pathology Services Ltd., Edmonton, Alberta, Canada and obtained from the Noah's Arkive database of veterinary pathology lesions: http://www.vet.uga.edu/vpp/noahsarkive/na.php; image no. 4134.*

to abnormal migration and/or terminal differentiation. A common presentation for ectopic neurons is to see clusters of cells located in atypical sites, leading to disrupted neuronal organization. The misplaced cells exhibit the typical features of the neural site at which they normally would have been found. The most frequent locations for these changes are the cerebral cortex, hippocampus, and cerebellum (Figure 21.12); any layer or multiple layers may be affected. Minor heterotopiae often are seen as isolated cell clusters in grossly unaffected brains, while major lesions frequently occur together with brain malformations like hydrocephalus or microcephaly. Aberrant anatomic development often but not always is accompanied by functional alterations. Alcohols like ethanol, methanol, and methylazoxymethanol (MAM) are potent disruptors of neural cell migration.

Neuronal *storage diseases* result from accumulation of materials in affected cells. Many storage diseases arise from inborn genetic defects that lessen or prevent production of an enzyme needed for normal metabolism. In the absence of functional enzyme, its substrates accumulate within organelles (e.g., Golgi apparatuses, lysosomes) or the cytoplasm. Toxic causes of neuronal storage diseases include cationic amphophilic drugs, which lead to phospholipidosis, and chronic ingestion of swainsonine (the toxic principle in locoweed). Lesions in mild (usually acute) cases of neurotoxicant-induced neuronal storage disease may be reversible if the exposure is halted, but severe (chronic) lesions usually progress to full-blown cell engorgement (Figure 21.22) and eventually to neuronal degeneration.

AXONOPATHIES

Other toxicants do not attack neurons, but rather damage their processes. These lesions may develop within the CNS, where they are typically confined to specific tracts, or in the PNS. In many instances, neurotoxicants with this capability first were discovered following occupational exposures in humans. Three basic lesion patterns can develop.

The first is the *primary axonopathy*, which is produced when the axon itself is the major site of damage. Examples include agents that cross-link macromolecules in distal axons, like acrylamide, carbon disulfide, and *n*-hexane. The fiber proximal to the xenobiotic-induced lesion remains intact while the fiber distal to the lesion disintegrates since it has lost

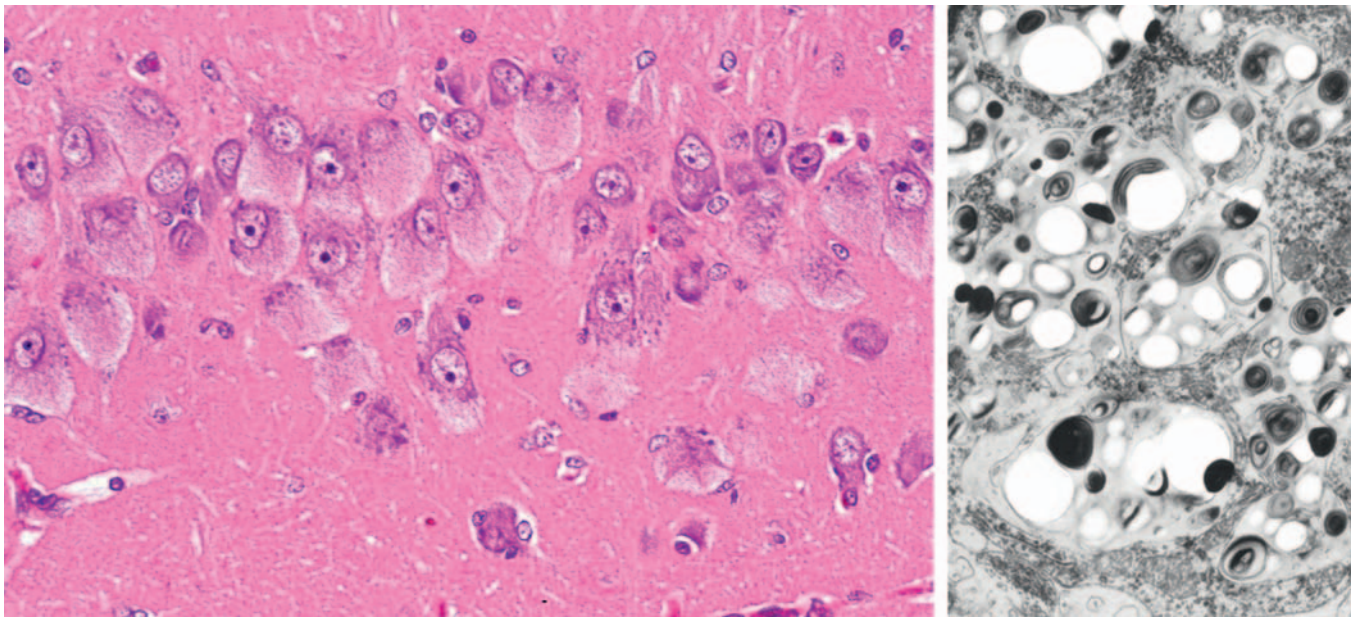

FIGURE 21.22 Drug-induced phospholipidosis (DIPL) is a neuronal storage disorder in which multilamellar (myeloid) bodies fill the cytoplasm of large neurons after chronic ingestion of a cationic amphophilic drug (CAD). *Left*: Typical light microscopic (LM) lesions are pallor and swelling of the cell body. Hippocampus field CA_1 of an adult rat given an undeclared CAD for an indeterminate period. Processing conditions for LM: Formalin fixation by immersion, paraffin embedding, H&E staining. *Right*: Transmission electron microscopy (TEM) is needed to view the myeloid bodies (evident as spaces partially or completely filled with electron-dense, laminated whorls or cores). Cytoplasm of a neuron from the medulla oblongata of a Beagle dog gavaged with the CAD posaconazole (30 mg/kg for 52 weeks). Processing conditions for TEM: Formalin fixation by immersion, other steps specified as "conventional" but not detailed. Source*: The TEM image is reprinted from Cartwight, M.E., et al., 2009. Phospholipidosis in neurons caused by posaconazole, without evidence for functional neurologic effects.* Toxicol. Pathol. *37, 902–910, with permission of SAGE Publications.*

connection to the neuron. The primary changes affecting the distal axon are fragmentation followed by formation of elliptical digestion chambers that hold cellular debris (Figure 21.23). This appearance should be referred to as Wallerian-*like* degeneration as it resembles genuine Wallerian degeneration, which is a sequel to physical (e.g., trauma) rather than chemical nerve transection. Fragmentation may begin within hours of axonal injury, but in practice axon degeneration may require a day or more to appreciate with the light microscope. Over time, macrophages of hematogenous origin (often termed "gitter" cells) are drawn to the site to phagocytize the axonal debris (Figure 21.24).

The next pattern is the *secondary axonopathy*, which occurs when the capacity of a neuron to export materials is compromised below the minimal level needed to sustain its axon and/or nerve terminal. For instance, β, β′-iminodipropionitrile (IDPN) exposure induces a proximal axonopathy because it interferes with slow axonal transport. Continued inability by the neuronal cell body to supply its processes will result in gradual progression of the degenerative changes to more proximal portions of the axon (termed "dying back"); bipolar primary sensory neurons with both central and peripheral axons may exhibit this change in the two processes simultaneously. Morphologic features of the neuronal body and proximal axon may be

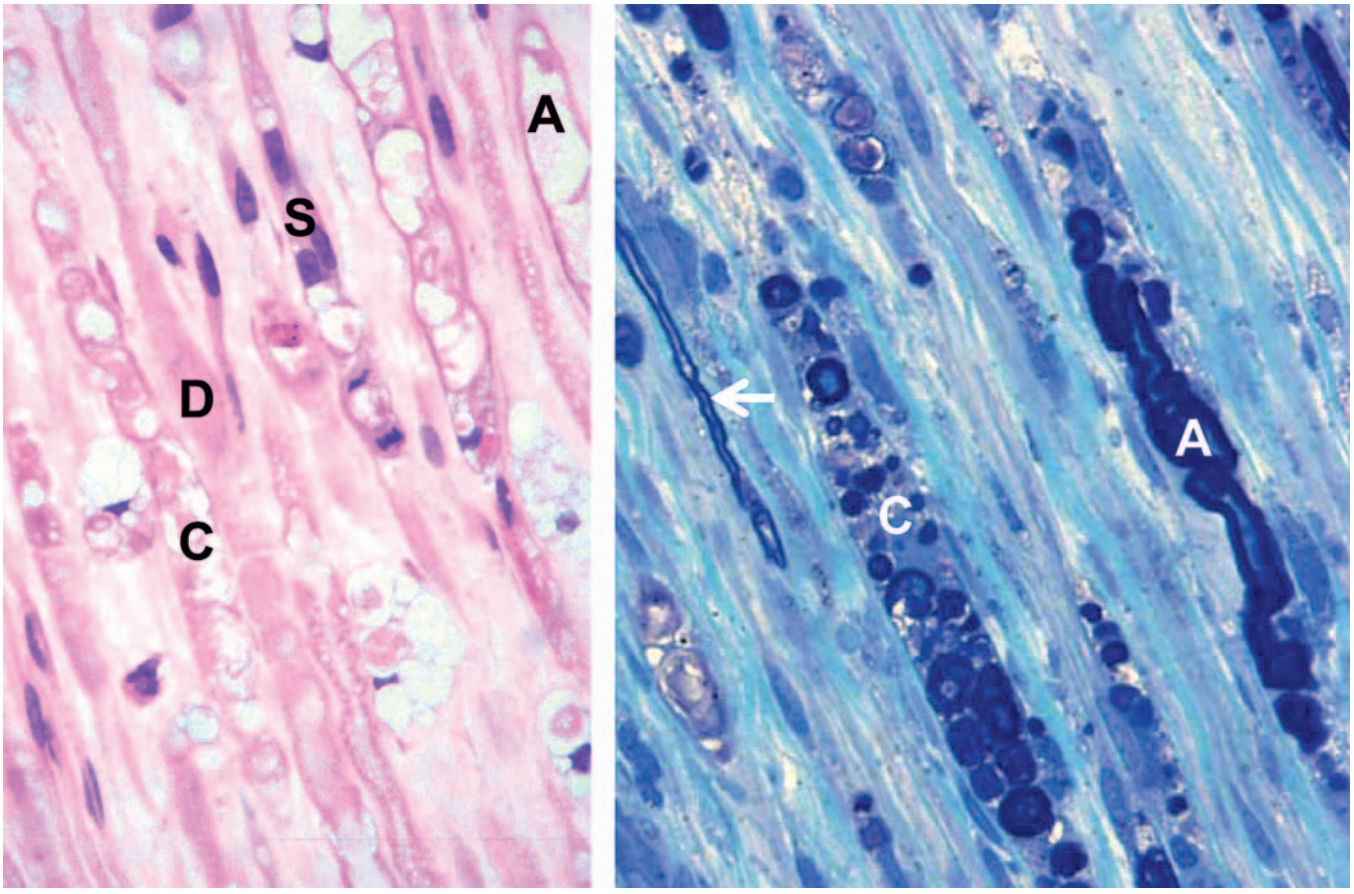

FIGURE 21.23 Primary axonopathies resulting from xenobiotic exposure begin as axonal degeneration (here evident as a swollen fiber (D)) before progressing to axonal disintegration with collection of debris and phagocytic macrophages ("gitter" cells) within dilated spaces (termed "digestion chambers" (C)) confined within the original fiber tract. Advanced lesions (A) result in removal of the myelinating cells as well, leaving a nearly empty fiber tract bordered by the remnant basal lamina (visible as hypereosinophilic lines by H&E). In peripheral nerves, proliferating Schwann cells (S) will fill fiber tracts that retain an intact basal lamina to provide a bed through which the regenerating axon will extend. In most instances, small (so-called "unmyelinated") axons (arrow) are not affected by toxicants. *Left*: Unspecified peripheral nerve of an adult rat given acrylamide for an extended period. Processing conditions: Formalin fixation by immersion, paraffin embedding, H&E staining. *Right*: Sural nerve of a human patient who developed acute ascending polyradiculoneuropathy after combined intravenous and intrathecal chemotherapy to treat leukemia. Processing conditions: Formalin fixation by immersion (presumptive), epon embedding, toluidine blue staining (presumptive). Source: Right: *Reprinted from Rison, R.A., Ascending sensory motor polyradiculoneuropathy with cranial nerve involvement following administration of intrathecal methotrexate and intravenous cytarabine in a patient with acute myelogenous leukemia: a case report*. Cases J. *1, 255 (doi:10.1186/1757-1626-1-255), with permission of BioMed Central Ltd.*

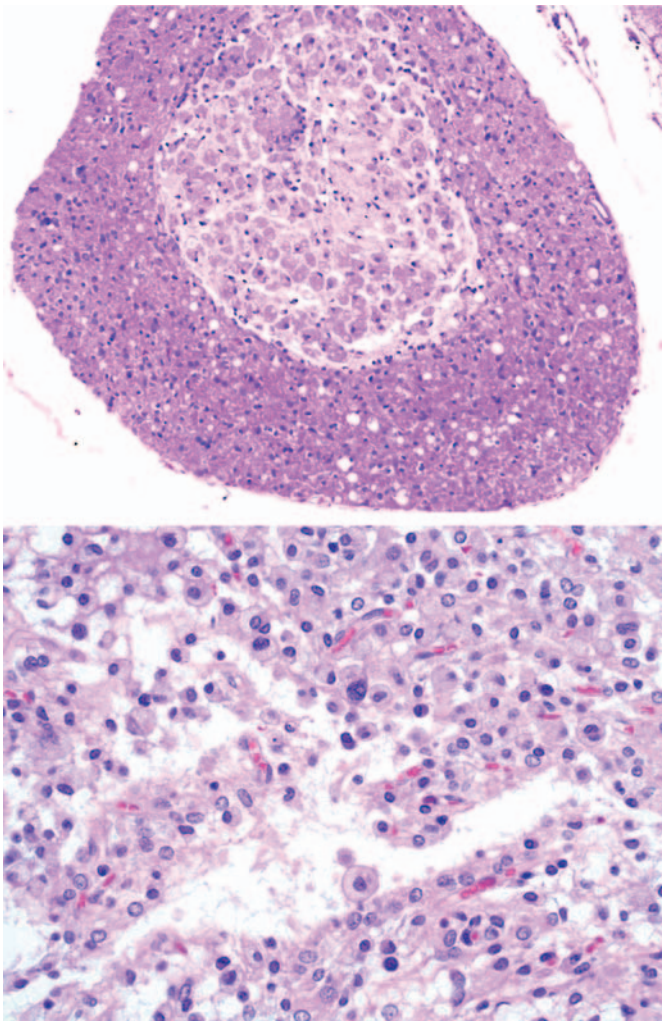

FIGURE 21.24 Destruction of large expanses within the nervous system results in liquefactive necrosis, in which the degenerating lipid-rich cells and cell processes are reduced to fluid and then removed by an influx of myriad macrophages (gitter cells). *Upper*: Optic nerve malacia in an adult rat with gitter cells collecting in the cavity. This lesion arises as an iatrogenic (experimenter-incited) infarct induced in rodents by traumatic blood collection from the retro-orbital venous plexus. White vacuoles in the lower right periphery of the nerve are fiber tracts in which the axons have been lost. *Lower*: Gitter cells have the characteristic traits of large, histiocyte-derived phagocytes: large, oval to reniform (kidney-shaped), often eccentric nuclei with abundant, pale eosinophilic, often vacuolated cytoplasm, and distinct cell borders. These cells were congregating in a cystic cerebral lesion in a nonhuman primate. Processing conditions: Formalin fixation by immersion, paraffin embedding, H&E staining.

morphologically normal even as the changes in the distal axon grow in their extent and severity.

The third pattern is *neuroaxonal dystrophy*, which is characterized by axonal expansion (often termed "spheroids"). In general, widespread neuroaxonal dystrophy is more common as an inherited or acquired neurodegenerative disease in humans and animals than as a consequence of toxicant-induced damage, although a few agents (e.g., aluminum, methylmercury) can produce spheroids as one element of their pathological presentation. These enlarged fibers appear as large, fairly homogeneous, elliptical swellings by light microscopy, which are shown to harbor a tangled web of cytoskeletal elements and cellular organelles by electron microscopy. The swellings are eosinophilic when stained with H&E and black when viewed in silver-impregnated sections (Figure 21.25), and they are much larger in diameter than adjacent "normal" axons. The proposed pathogenesis is a disturbance in retrograde axonal transport that results in progressive accumulation of less flexible materials at points of axonal constriction (i.e., the nodes of Ranvier, which are the gaps formed between the edges of adjacent myelinating cells).

Regeneration of PNS axons can occur once the axonal damage has been cleared provided that the endoneurial tube is intact. The Schwann cells proliferate to form solid columns of cells (termed "bands of Büngner") that reach from the site of the axonal lesion to its distal terminus. At the same time, the proximal axon grows distally into these Schwann cell columns, which guide the axon as it travels to reestablish its link with the site that it originally innervated. Regeneration of the axon requires a transient boost in macromolecular synthesis (mainly proteins) in the neuronal body. This need is accommodated by dispersion of the Nissl substance and translocation of the nucleus to the cell periphery, a change termed "central chromatolysis." This repair response in the neuronal cell body is termed the "axonal reaction," although it is very common to observe axonal degeneration without seeing any associated changes in the neuronal body. Regeneration of axons proceeds at the same velocity as slow axonal transport, and thus is limited to several millimeters a day; full functional recovery takes weeks to months for distant effector organs, especially in larger species. In general, axonal regeneration of differentiated CNS axons is ineffective.

These axonal changes may be recognized in sections stained routinely with H&E, but in many instances special procedures are undertaken to provide additional contrast. The techniques may highlight the axon itself, either by silver impregnation (e.g., Bielschowsky's (Figure 21.25) or Bodian's stains) or IHC labeling to detect an axonal marker (e.g., neurofilament protein (NFP), which is one cytoskeletal constituent). Alternatively the procedure may label the myelin sheath using a histochemical stain (e.g., LFB) that stains lipid, an IHC method to localize a myelin marker (e.g., MBP), or fixation enhancement to increase the contrast between the axon and its sheath (e.g., postfixation in OsO_4) (Figure 21.26). These myelin-detecting procedures may serve as effective

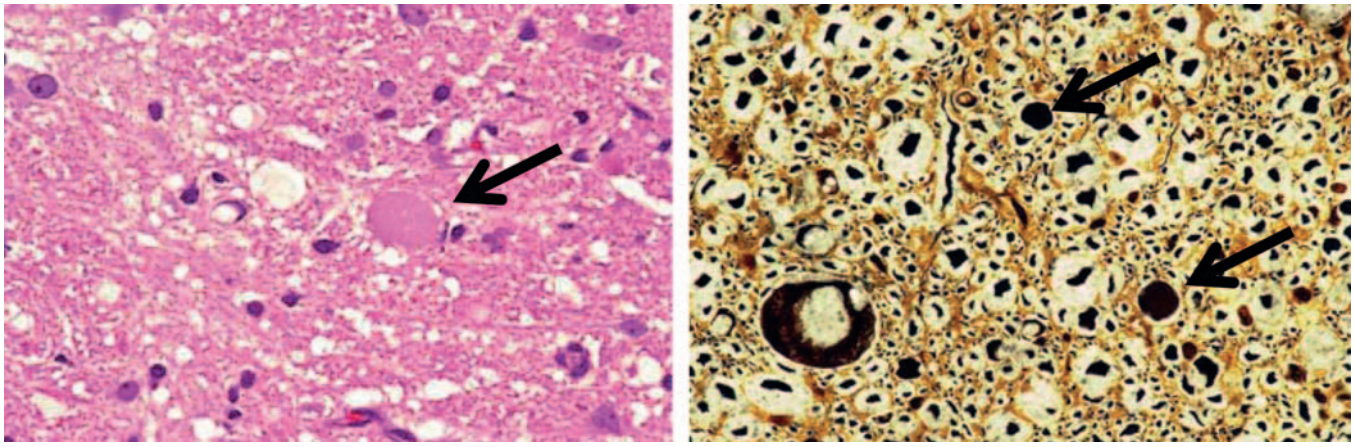

FIGURE 21.25 Axonal expansions termed "spheroids" are the characteristic feature of toxicant-induced neuroaxonal dystrophies. The proposed pathogenesis is reduced axonal transport leading to expanding snarls of cytoskeletal proteins lodged at the narrow nodes of Ranvier. The dilated axons are large, fairly homogeneous, elliptical swellings (arrows), which are eosinophilic when stained with H&E (left) and black when highlighted by silver stains (right; Bielschowsky's silver method). Processing conditions: Formalin fixation by immersion (left) or intravascular perfusion (right), paraffin embedding.

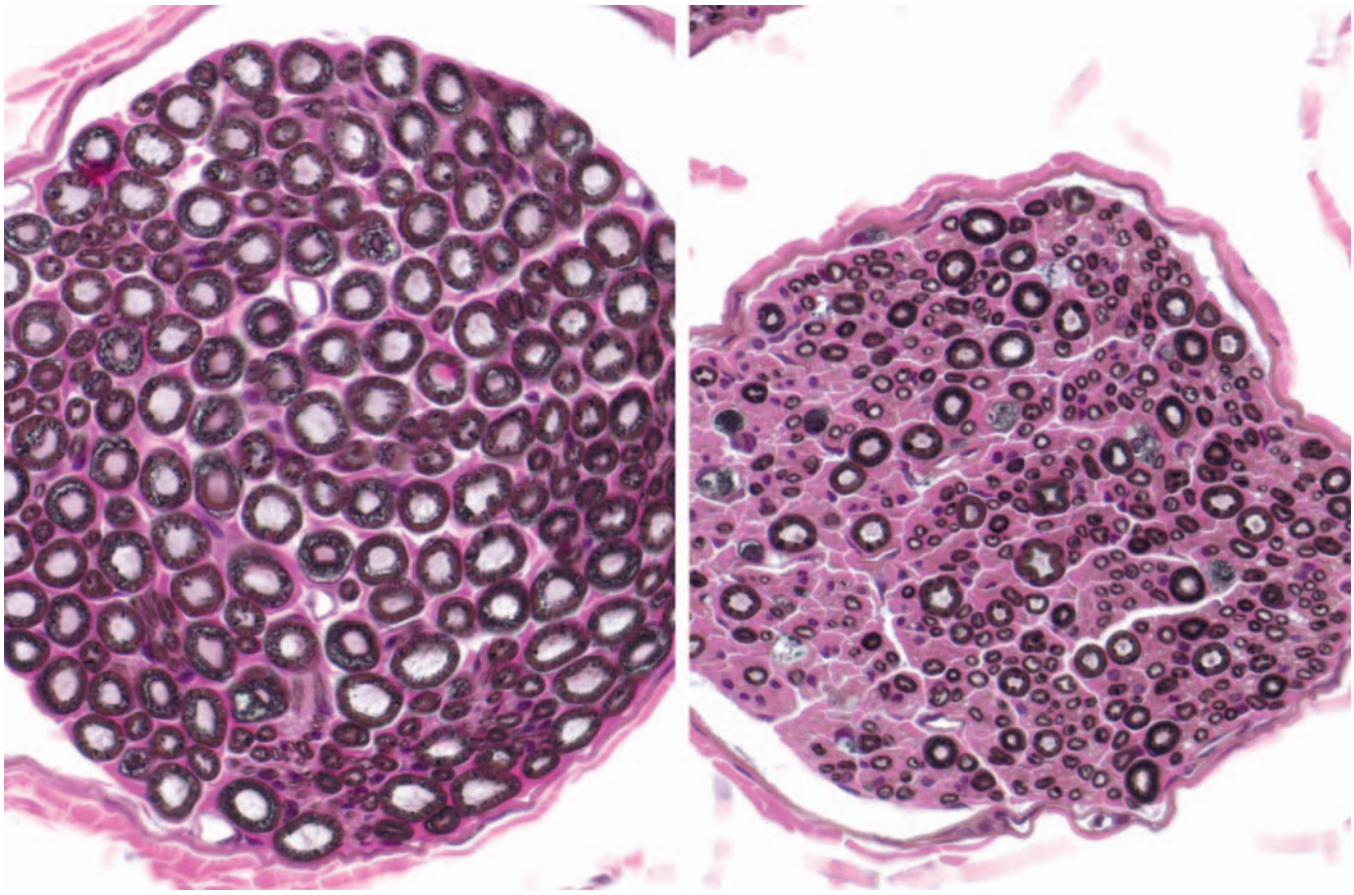

FIGURE 21.26 Myelin integrity as well as the contrast between axons and their myelin sheaths are both improved by metal enhancement using postfixation in osmium tetroxide (OsO_4). Relative to a control nerve with its many large fibers with uniform axonal diameters and thick myelin sheaths (left), nerves with severe primary neuropathy exhibit substantial loss of large fibers and attenuation of their myelin sheaths (right). Unspecified nerve from an adult rat given an unidentified neurotoxicant. Processing conditions: Formalin fixation and OsO_4 postfixation by immersion, paraffin embedding, H&E staining. Source*: This image was kindly provided by Dr. William Valentine, Vanderbilt University, Nashville, Tennessee, United States.*

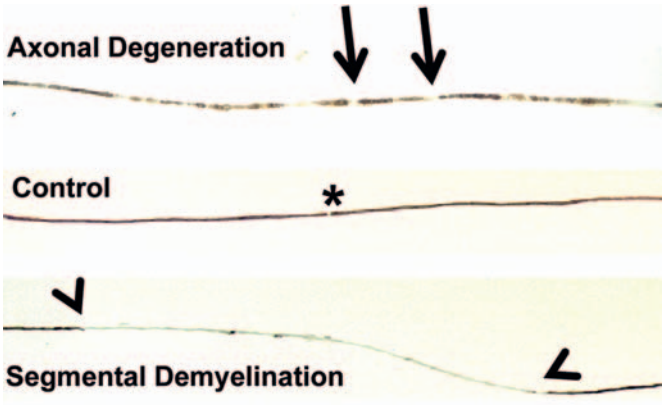

FIGURE 21.27 Teased fiber preparations offer a definitive means of differentiating between the axon and the myelin sheath as the target site for neurotoxicant activity. Axonal degeneration (upper strand; unidentified neurotoxicant) leads to axonal loss (arrows) with secondary attenuation of the myelin sheaths (dark outer layer of the nerve fiber) at multiple points over extended distances. In contrast, primary myelin damage (lower strand; 1% disulfiram in the diet for 4 weeks) results in segmental loss of the myelin sheath (i.e., the length supported by a single Schwann cell (located between the two arrowheads)) while leaving the paleraxon intact. Unaffected fibers (middle strand) have smooth continuous myelin sheaths interrupted only occasionally by nodes of Ranvier (pale transverse band (asterisk)). Isolated fibers from caudal (posterior) tibial nerves of adult rats. Processing conditions: Glutaraldehyde fixation by intravascular perfusion followed by osmium tetroxide postfixation by immersion. Source: *These photographs were provided by Dr. William Valentine, Vanderbilt University, Nashville, Tennessee, United States. The bottom two images have been reproduced with minor modifications from Tonkin, E.G., et al. 2000. Disulfiram produces a non-carbon disulfide-dependent Schwannopathy in the rat. J. Neuropathol.* Exp. Neurol. *59, 786–797, with permission of Wolters Kluwer Health.*

means to indirectly highlight primary axonal damage. A definitive means of differentiating between the axon and myelin as the primary target site is to isolate individual fibers in teased preparations. Axonal lesions are characterized by the absence of the central axon with multifocal attenuation of the Schwann cell profile over long distances, while primary myelin damage leads to segmental loss of the myelinating cell with retention of the denuded but intact axon (Figure 21.27).

SYNAPTOPATHIES

The human nervous system houses trillions of synapses, with each neuron playing host to many thousands. Ultrastructural evaluation may be required to investigate synapses. Their minute size prevents synapses from being observed in standard light microscopy sections except that disintegrating synaptic terminals may be visualized using the cupric silver stain.

One major change in experimental neurotoxicity reports is altered membrane maintenance and turnover in axonal terminals (Figure 21.28). Lesions may affect either the presynaptic or the postsynaptic elements. Agents capable of altering membrane structure include chloromycetin, which targets cerebrocortical motor neurons; diphenylhydantoin (DPH), which impacts cerebellar neurons; and 3,4-methylenedioxymethamphetamine (MDMA), which transforms monoaminergic neurons in the striatum. Common anomalies include thickening of the synaptic membranes or formation of membranous inclusions in the axon terminals. The progressive nature of the inclusions that characterize the DPH-induced lesion suggests that their pathogenesis begins with accretion of interconnected tubules in gradually expanding axon terminals, followed by the buildup of inclusions and the eventual formation of axonal spheroids. Ultimately the affected neurons undergo coagulation necrosis, seemingly as a consequence of excessive synaptic degeneration. The membranous inclusions in the MDMA-injured cells also contain ubiquitin, which provides added confirmation that this finding is an outcome of significant damage to cell membranes.

Other ultrastructural lesions induced by neurotoxicants have also been observed as precursors of degenerative changes in CNS synapses. For instance, simultaneous incubation with amyloid-beta (Aβ), a protein fragment of amyloid precursor protein (APP) thought to be responsible for neural lesions in advanced Alzheimer's disease, and ryanodine induces mitochondrial swelling and a severe reduction in the numbers of small synaptic vesicles and synapse-anchored proteins like synaptophysin and actin in rat cerebrocortical synaptosomes. Depletion of synaptic actin can be reversed by incubation with caspase inhibitors, suggesting that extended abnormalities of synaptic structure can invoke the apoptotic pathway in affected neurons.

MYELINOPATHIES

Toxicant-induced damage to myelin can develop within the CNS or PNS, depending on whether or not the population of injured cells is the oligodendrocyte or the Schwann cell. From a practical standpoint, however, the more important consideration usually is to define the manner in which the lesion is incurred.

Production of myelin to surround axons does not occur at the same time in all parts of the nervous system, but instead develops progressively. In the cerebrum, sizeable white matter tracts and commissures are the first to be insulated, followed in sequence by the major subcortical centers (e.g., thalamic and basal nuclei) and finally the cerebral cortex. Myelination in the cerebral cortex occurs first in projection zones before spreading later to the association areas. In the spinal cord, cervical tracts are myelinated prior to those in the lumbar region. The myelination process is

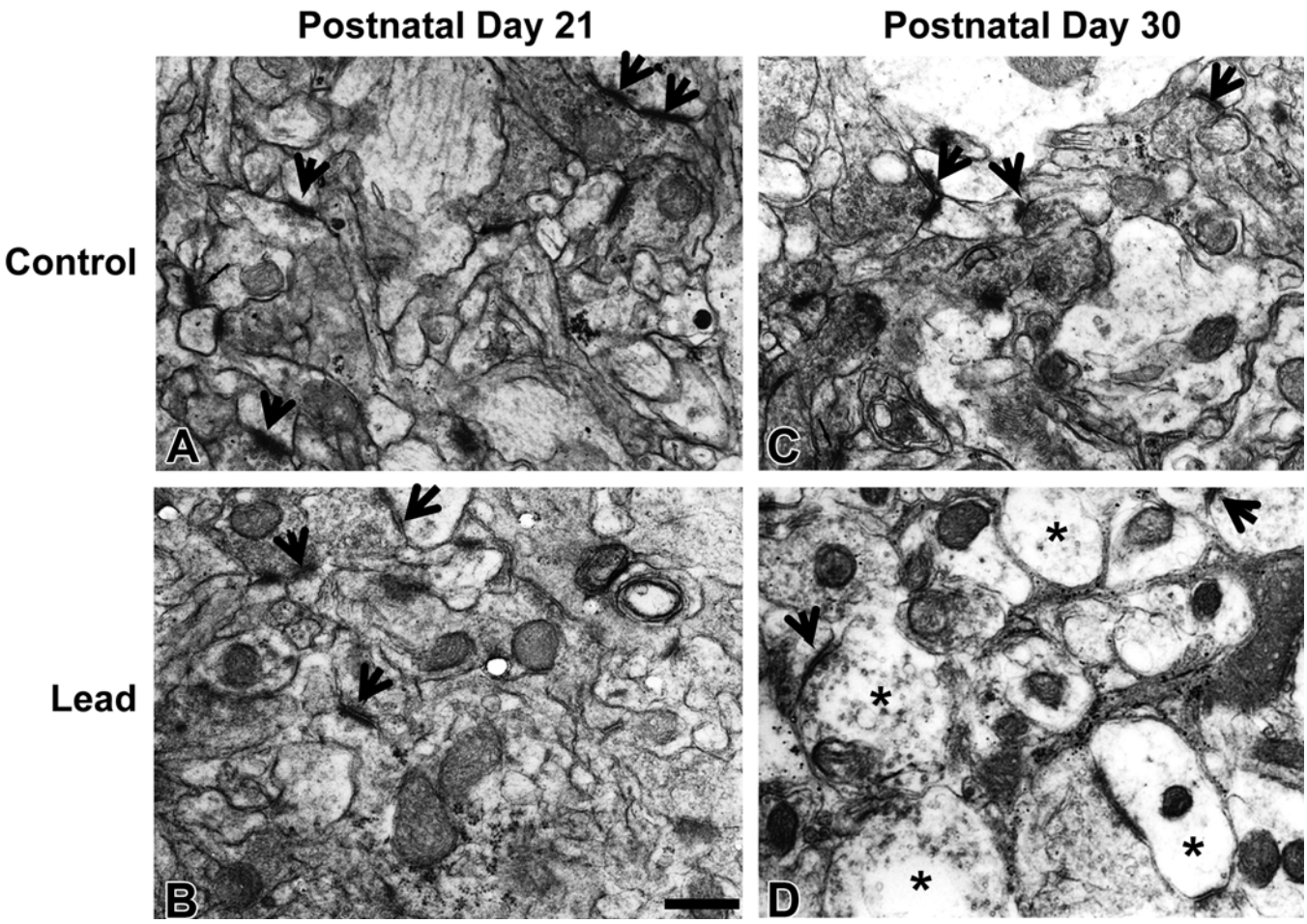

FIGURE 21.28 Synaptic pathology induced by neurotoxicants in either presynaptic or the postsynaptic terminals must be evaluated by transmission electron microscopy (TEM). These electron micrographs compare synaptic and axonal morphology in the molecular layer of the CA_3 region in the hippocampus from control (A, C) and lead (Pb)-exposed (B, D) Wistar rats at 21 (A, B) and 30 (C, D) days of age, following maternal Pb ingestion (0.2% Pb acetate administered in the drinking water) during postnatal days 1–21. (A, C) Synapses (arrows) in control rats have many vesicles and mitochondria in their presynaptic terminals, and the opposing membranes of the presynaptic and postsynaptic cells are equally electron dense. (B, D) Exposure to Pb has markedly reduced synaptic numbers but has not affected synaptic structure. Older Pb-exposed rats (D) also exhibit swollen dendrites (i.e., greatly enlarged cell processes with relatively clear cytoplasm (*)). Processing conditions: Immersion fixation in 4% glutaraldehyde followed by 1% osmium tetroxide, embedding in epoxy resin, sectioning at 70 μm, staining with uranyl acetate and Pb citrate. Scale bar = 500 nm. Source: *These images have been reproduced with minor modifications from Rahman, A., et al. 2012. Over activation of hippocampal serine/threonine protein phosphatases PP1 and PP2A is involved in lead-induced deficits in learning and memory in young rats.* NeuroToxicology *33, 370–383, with permission of Elsevier.*

not fully completed for weeks after birth in rodents, and for years in human infants.

Myelin is particularly sensitive to neurotoxicants during two stages of development. The first is a period of rapid glial cell proliferation (i.e., the first two postnatal weeks in rodents). The second is the time of active myelination, the peak of which occurs on approximately postnatal day 20 in rodents. Therefore the location and extent of myelinotoxic insults will vary with the timing of the exposure.

Primary demyelination is produced when myelin sheaths are the main target of the insult. In such instances the axons are not harmed, and accordingly are preserved intact within the disintegrated myelin sheath. The classic agent responsible for inducing this effect is tellurium. The typical appearance of white matter tracts or nerves with primary demyelination is swelling of the affected sheath segments (where each segment is the product of a single cell) with formation of myelin bubbles (also termed balloons or blebs). These bubbles may be discerned from digestion chambers produced in axonopathies because the bubbles surround continuous (i.e., viable) albeit shrunken axons in close association with myelin debris and macrophages. Primary demyelinating insults generally result in a fairly diffuse distribution of white matter

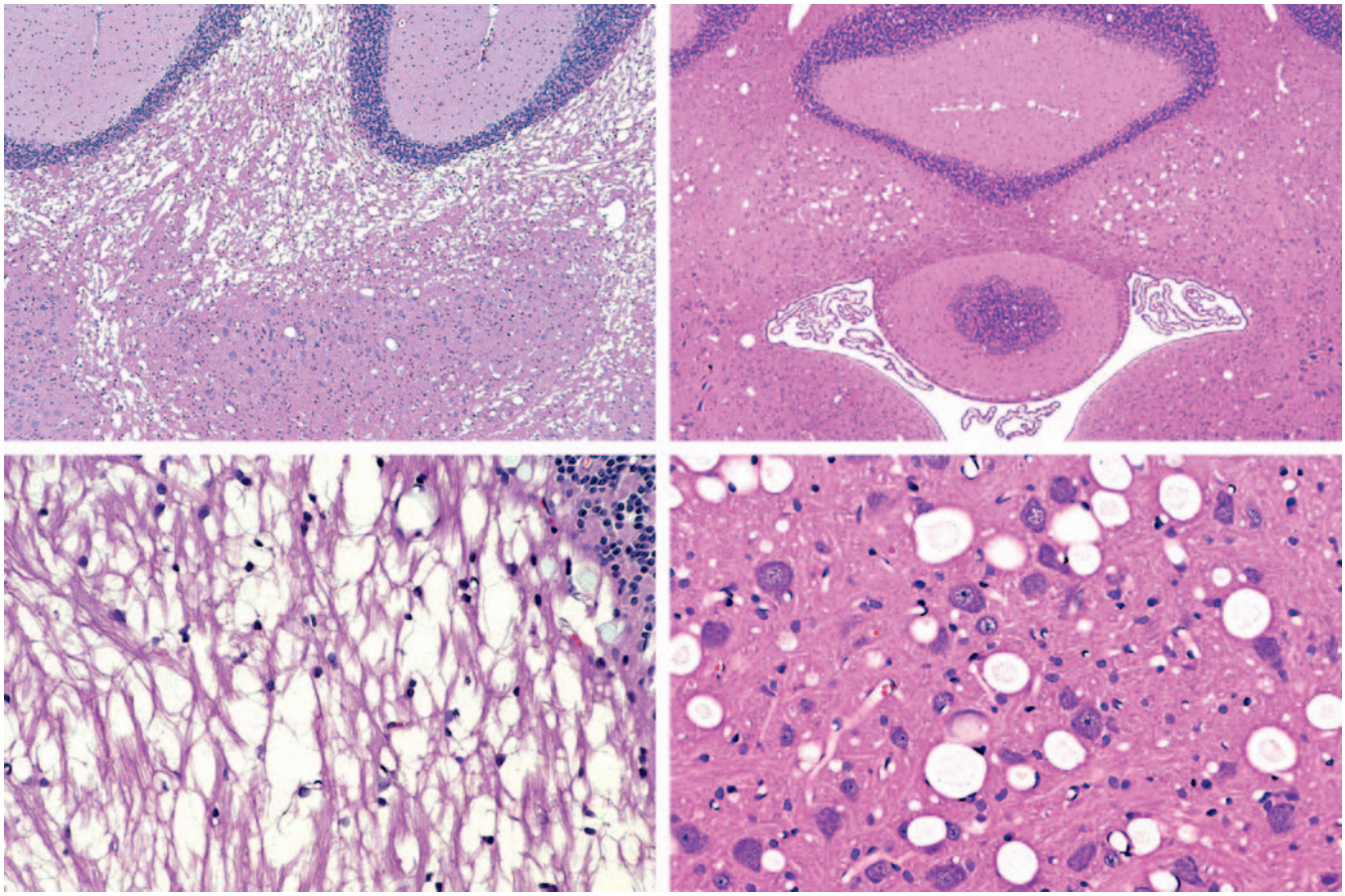

FIGURE 21.29 Distinct patterns of neurotoxicant-induced white matter vacuolation result from the common mechanism of intramyelinic edema. Such lesions are particularly prominent in major white matter tracts in the deep cerebellum (left panels) and cerebrum, although the neuropil is also affected (right panels). Findings typically are bilaterally symmetrical. The pathogenesis is progressive intramyelinic accumulation of fluid, which may be seen at the light microscopic level as clefts in the myelin sheaths (lower left panel) or as vacuoles (lower right panel). The different pathogenic mechanisms between these two similar but morphologically distinct patterns of edema is highlighted by comparing their causes and progressions: the two left panels show lesions in adult rats caused by acute exposure to triethyltin (TET), while the two right panels demonstrate lesions in young rats exposed for approximately 2 months starting on postnatal day 4 to vigabatrin (an antiepileptic GABAergic drug that suppresses neuronal activity) as described in Walzer et al. (2011). (NOTE: Toxicant doses were not specified.) Processing conditions: Formalin fixation by intravascular perfusion, paraffin embedding, H&E staining.

damage, which is readily detected in conventional tissue sections that have been processed to demonstrate myelin in white matter tracts (Figure 21.29).

A variant of primary myelinopathy is *myelin edema*, resulting from fluid accumulation within the myelin sheaths. Hexachlorophene is the prototypic neurotoxicant that induces this lesion. Myelin edema can occur in both the CNS and PNS and usually appears as vacuoles within myelin-rich regions in the absence of myelin degeneration. The volume expansion caused by the increased fluid leads to splitting of the myelin lamellae. Mild cases may be reversible to some extent, but pronounced or chronic lesions typically will lead to secondary axonal damage.

Secondary demyelination results from irreversible degradation of a myelin sheath following the initial loss of its axon. The microscopic appearance of myelin bubbles in this scenario includes loss of the axon, showing that the myelin disintegration follows the prior axonal damage. Conversion of myelin lipoprotein to fully degraded fat typically takes approximately 2 weeks.

Regeneration of myelin sheaths generally is confined to the PNS, and can occur fairly rapidly since it arises from cell precursors already in place at the lesion site. In the PNS, each Schwann cell envelops a single axon, so damage to the Schwann cell will lead to segmental loss of myelin (Figure 21.27) that is more severe at the level of the spinal nerve roots (i.e., where the axons are of larger caliber and thus are encompassed by longer and thicker myelin sheaths). As remyelination proceeds, each gap is filled by a greater number of Schwann cells producing a series of shorter

segments with thinner sheaths than were present in the original.

GLIOPATHIES

In many respects, non-myelinating glia are more resistant to neurotoxic insult than their neuronal and myelin-producing neighbors. Injured glial cells typically respond by swelling. In most instances the affected elements are astrocytes. Lesions of minimal to moderate extent are often reversible if the cause of the change is removed.

The usual appearance of swollen astrocytes is that of cell expansion and/or vacuolation (Figure 21.30), the outcome of fluid or material accumulating in the cytoplasm or a membrane-bound organelle. The change occurs most frequently in the brain, and usually presents most prominently in the gray matter. Microscopically the parenchyma of this region is riddled with small holes, some of which are perivascular in location or appear to compress nearby neurons. In general the effect exhibits bilateral symmetry.

The formation of Type II astrocytes embodies an unusual variant of astrocyte swelling. This cytotoxic response results from nuclear expansion following exposure to elevated levels of nitrogenous waste products (the chief of which is thought to be ammonia); thus, these elements represent a secondary toxic response to primary hepatic disease. Affected astrocytes have swollen clear nuclei with very thin rims of marginated heterochromatin, sometimes with enlarged nucleoli, and indistinct cytoplasm (Figure 21.31). These cells tend to accumulate in the neocortex, basal nuclei, and hippocampus.

GLIAL REACTIONS TO NEURAL INJURY

Glia play prominent roles in the repair response following toxicant- also induced damage to other populations of neural cells. The main responders are the non-myelinating cells of the CNS—astrocytes (i.e., true glia) and microglia (i.e., the bone marrow–derived resident histiocytes of the CNS)—but oligodendrocytes and Schwann cells also participate in such efforts.

Hypertrophy and hyperplasia are the main reactions by activated CNS glia to neural damage. The generic term for this change is "gliosis," which implies enhanced production of multiple cell lineages, but cell type–specific increases (e.g., astrocytosis, microgliosis) are also possible. The presentations and functions served by these reactions are quite distinct. Astrocytosis occurs to fill or encompass damaged regions in the CNS, usually produced as a consequence of neuronal or pan-cellular necrosis. Reactive astrocytes are seen in H&E-stained sections as large, stellate cells with large, pale nuclei and scant to modest amounts of pale eosinophilic cytoplasm (Figures 21.8 and 21.24); they may also be seen in IHC-stained material via their increased

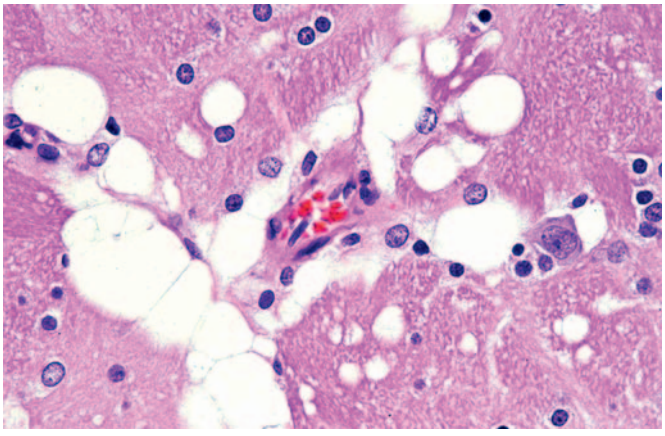

FIGURE 21.30 Vacuolation of the brain gray matter often results from peracute swelling of astrocytes. This finding commonly presents as variably sized but large, oval to round, clear spaces located adjacent to capillaries and/or neurons (with both changes evident here). *Globus pallidus* (a basal nucleus) of an adult rat following exposure to an unspecified pharmaceutical agent. In this case, the vacuolation developed as an agonal event and was probably the result of heightened cell activity or of increased membrane permeability. Processing conditions: Formalin fixation by immersion, paraffin embedding, H&E staining.

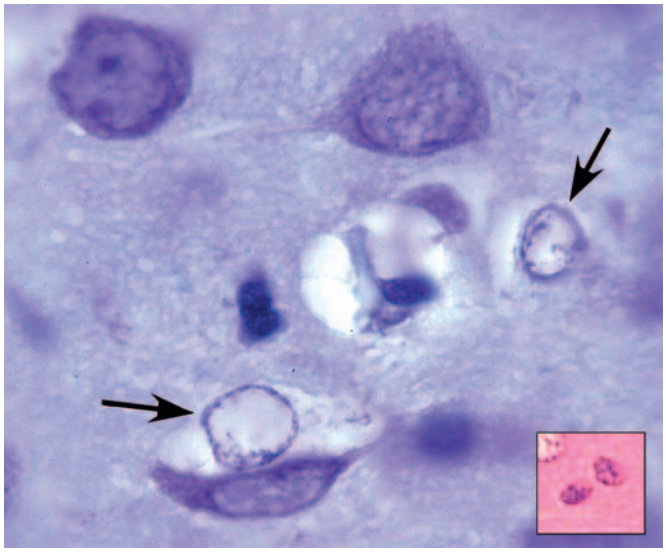

FIGURE 21.31 Alzheimer's Type II astrocytes represent an unusual reaction to hyperammonemia. Affected cells are swollen and have open, pale, swollen nuclei with thin rims of marginated chromatin and pale cytoplasm (arrows), while normal astrocytes have pale basophilic nuclei with clumped chromatin and indistinct cytoplasm (inset). Cerebral cortex of a dog with experimental hepatic encephalopathy. Processing conditions: Formalin fixation by immersion, paraffin embedding, H&E staining. Source*: The figure was kindly provided by Dr. Michael D. Norenberg, University of Miami, Miami, Florida, United States.*

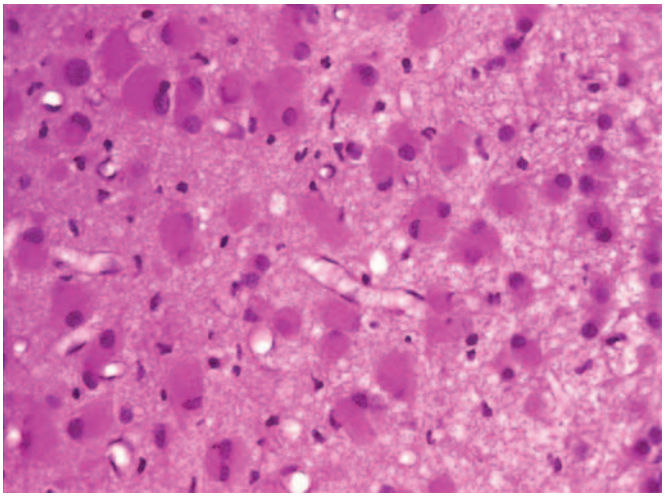

FIGURE 21.32 In certain settings, reactive astrocytes acquire a "gemistocytic" phenotype in which the cytoplasm expands greatly and becomes hypereosinophilic. Primary visual cortex of a macaque monkey after chronic methylmercury intoxication. Processing conditions: Intravascular perfusion with formalin, paraffin embedding, H&E staining.

expression of cytoskeletal proteins like GFAP (Figure 21.8) and vimentin. A variant of reactive cell termed the "gemistocytic" astrocyte may be observed in some CNS lesions as many plump, brightly eosinophilic cells supporting numerous processes (Figure 21.32). The functional basis for the gemistocytic transformation is not clear.

Microgliosis results from proliferation of the resident "immune" elements in the CNS, usually in response to more localized neuronal insults. Microglia can perform both surveillance (e.g., antigen presentation) and effector (e.g., phagocytosis) functions. Reactive microglia are identified in H&E-stained tissue as small, elongate, sometimes twisted nuclei near damaged CNS neuropil (Figure 21.9). Special stains may be used to raise their visibility, such as IHC labeling for Iba1 (Figure 21.9) or histochemistry to detect the lectin *Griffonia simplicifolia*.

The response by reactive oligodendrocytes is termed "satellitosis" as the myelinating cells aggregate around degenerating neurons, presumably in an effort to support their survival and repair. Reactive oligodendrocytes are evident in H&E-stained sections as partial to complete rings of cells encircling abnormal neurons (Figure 21.33). In general, oligodendrocytes are the least reactive population of glia. Pathologists must be careful to avoid undue haste in interpreting the relevance of satellite cells near neurons as neoplastic lymphocytes in a peri-neuronal location may mimic the appearance of oligodendrocytes (Figure 21.33).

Global Classifications of Toxicant-Induced Neural Lesions

Several kinds of toxicant-induced abnormalities that damage the nervous system recapitulate similar processes that occur in non-neural tissues elsewhere in the body. In general, these lesions are categorized as nonproliferative or proliferative based on the prominence of cell division as a mechanism for enhancing the degree of neural damage. The remainder of this section reviews the basic features of the major lesion types in both these categories.

NONPROLIFERATIVE LESIONS

Developmental disturbances as a class are an important outcome following exposure to many neurotoxicants (Table 21.1). The most common macroscopic abnormalities are neural tube defects (NTDs). The NTDs usually result from enhanced cytotoxicity during the period of neurulation, a phase in which the neural folds of the planar embryo progressively elevate and then fuse to form the neural tube (the precursor to the CNS). The spectrum of NTDs ranges from partial to complete nonfusion of the neural tube (see Figure 25.3 for examples) Figure citation. The correct chapter is "Embryo, Fetus and Placenta" by Rousseaux and Bolon. The correct figure is no. 3, which shows 7 yeloow-hued mouse fetuses against a dark blue background. Severe variants include anencephaly (absence of the brain due to complete nonfusion), exencephaly (exposure of the brain due to failure of the cranial vault to close around or over the brain), and/or spina bifida (failure of the spinal cord and/or vertebral arches fuse). Partial closure leads to encephalocele or myelocele (smaller foci of localized nonfusion in which brain or spinal cord tissue, respectively, protrudes through a fissure in the skeleton) or meningocele (only the meninges protrude through the defect). Anencephaly and exencephaly are lethal malformations, while individuals with one of the other NTDs may survive (though often with some degree of lifelong neurological impairment).

Other classes of toxicant-induced developmental defects include microcephaly (presenting as a reduction in cerebrocortical size; Figure 21.4), cerebellar hypoplasia (affecting the entire organ or just the hemispheres), and neuronal heterotopiae (Figure 21.11). These lesions result from toxicant exposure sometime after neural tube closure. The former two changes reflect excessive neuron death and reduced formation of neural circuits, while the heterotopiae generally stem from aberrant migration of newly made neurons and/or defective differentiation of the radial glia that serve to guide migrating neurons to their appropriate positions.

Hydrocephalus results from dilation of one or more channels within the cerebroventricular system. The

change is observed most commonly in the lateral ventricles. The presentation often includes reduced thickness of the overlying brain parenchyma due to increased pressure from the accumulated CSF; the reduction arises by hypoplasia of neural cells if the lesion begins early during development but usually represents atrophy if the change starts after birth. Hydrocephalus is an end-stage lesion that serves as the final common outcome for many different etiologies. In the toxicologic neuropathology setting, hydrocephalus in immature subjects frequently occurs as a compensatory mechanism to fill space within the cranial vault left vacant by xenobiotic-induced reductions in neural cell numbers in the cerebrum. In contrast, in adults the usual cause is CSF blockade by occlusion of the mesencephalic aqueduct (of Sylvius) by a mass such as an abscess (a possible sequel to immunosuppressive therapy or placement of an intrathecal catheter for direct xenobiotic delivery into the CNS) or neoplasm (an occasional finding in rodent carcinogenicity bioassays).

Infarcts (colloquially termed "strokes" in human patients) are characterized by regional necrosis of a neural domain, usually within the brain or spinal cord. The cause is interruption of the blood flow to a particular area as a consequence of blockage or rupture in a larger artery or vein. The absence of blood flow leads to ischemia of all cells within the region supplied by the affected vascular arcade; neurons are most sensitive to ischemia due to their very high basal metabolic rates. A transient disruption in flow typically culminates in neuronal necrosis, which will appear as a reduction or absence of these cells in an otherwise intact region of parenchyma (Figure 21.34). In many instances the numbers of astrocytes and microglia (Figure 21.34) will be enhanced in regions where the neurons used to reside, serving as a lasting marker of previous neuronal damage.

Persistent interference with the blood flow will decimate all cells within the domain, which will finally lead to liquefactive necrosis of the affected parenchyma (Figure 21.24). Eventual removal of the necrotic debris by activated microglia and macrophages recruited from the blood (gitter cells) will leave a cyst that typically has a marginal zone enriched with fibrous (intensely GFAP-positive) astrocytes (i.e., a glial scar). The site and cause of the infarct rarely are seen on gross or histopathologic examination. Potential toxic causes of

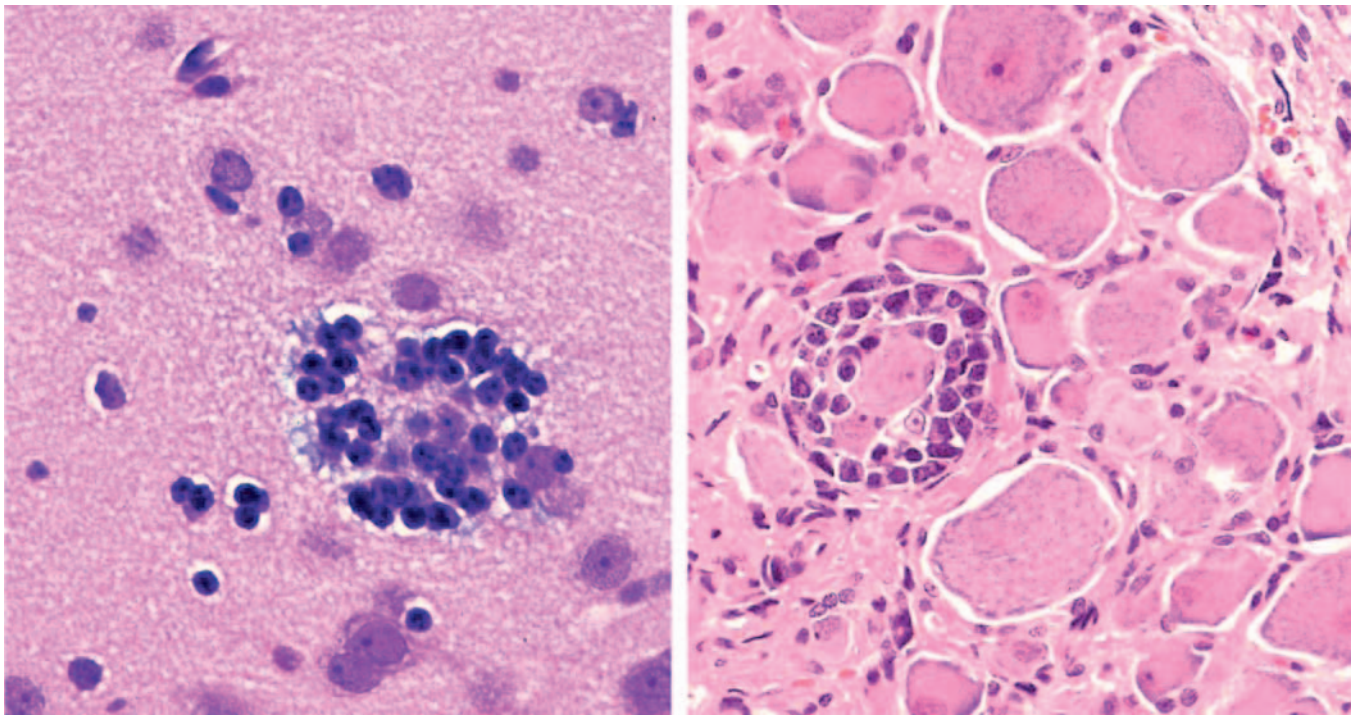

FIGURE 21.33 Satellitosis of oligodendrocytes (left image, unspecified location in the brain) around toxicant-damaged neurons takes place in a final attempt to prevent degenerating cells from dying. The encircling cells have very dark, basophilic, round nuclei and may (or may not) exhibit the peri-nuclear halo that is typical of their nonreactive counterparts within white matter tracts. Differential diagnoses for peri-neuronal round cell aggregates include reactive microglia (Figures 21.9 and 21.34) and neoplastic lymphocytes (right image). In general, microglia collect near intact but dead or disintegrating cells and exhibit the typical elongated, condensed, fairly uniform nuclei of reactive cells. In contrast, the lymphoma cells tend to encircle viable large neurons (as shown here, in a dorsal root ganglion) and display a moderate degree of cellular atypia. Species: Rat. Processing conditions: Formalin fixation by immersion, paraffin embedding, H&E staining.

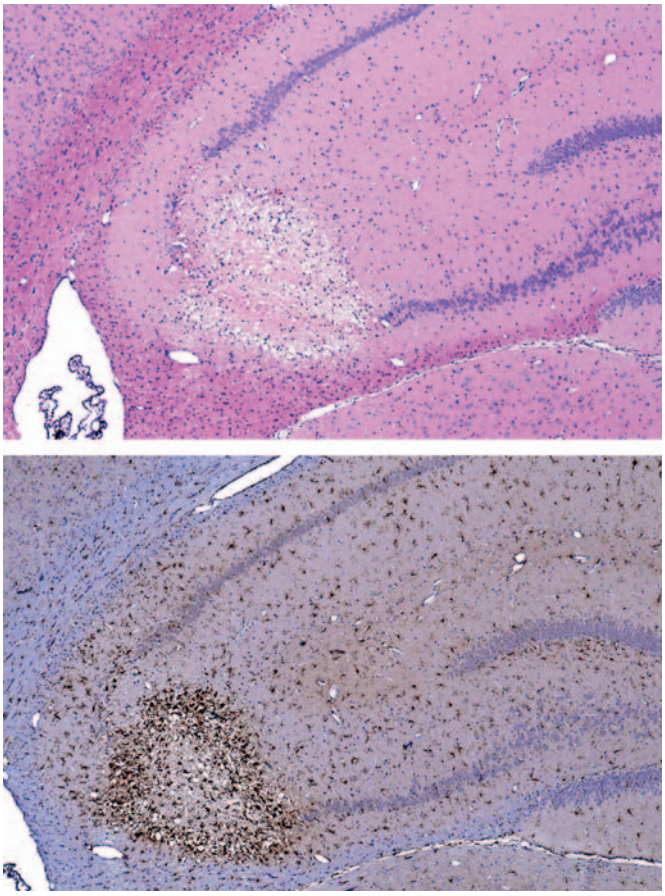

FIGURE 21.34 Neural infarcts (i.e., "strokes") result from ischemia-associated regional necrosis, usually affecting the brain or spinal cord. As demonstrated here in the hippocampal CA_3 field, metabolically active neurons are the most sensitive elements. Oxygen-starved cells will die and disintegrate, and the adjacent neuropil (composed primarily of neuronal processes) will become rarified (upper image; H&E). Over time, reactive glia will accumulate at the edges of the infarct to scavenge the liquefying debris (lower image; IHC method to detect the microglia-specific marker ionized calcium binding adaptor molecule 1 (Iba1), done here with a hematoxylin counterstain). Brain section from a rat model of cardiopulmonary resuscitation (CPR). Processing conditions: Formalin fixation by immersion, paraffin embedding.

infarcts usually are confined to intravascular thrombosis secondary to endothelial cell damage and/or activation of the clotting cascade. Agents that can produce these circulatory injuries include bacterial endotoxins or certain chemicals.

Inflammatory lesions result from damage to the neural parenchyma in the CNS and/or PNS by accumulations of astrocytes and/or microglia in conjunction with circulating leukocytes (of one, a few, or all classes). Because leukocyte infiltrates can occur in the absence of tissue damage (Figure 21.35), the concept of "inflammation" should only be invoked when other evidence of neural injury is evident along with the leukocytes; such features may include neural-specific changes like axonal and/or myelin degeneration or gliosis, or they may be more general findings like edema, hemorrhage, necrosis, and vascular congestion. Neural inflammation as a primary toxic response typically results from direct placement of a drug delivery apparatus into the CNS (Figure 21.35), especially if coupled with delivery of a potentially irritating test article. It may also occur as a secondary consequence of agents that incite another disease processes (e.g., immune dysfunction, neural damage) in which the barriers protecting the nervous system are breeched and the injured cells and newly exposed neural antigens become targets. Examples of this latter class include experimental allergic encephalitis (EAE) in rodents, and perhaps some cases of multiple sclerosis in humans.

Several pigments may be observed within the CNS, either as reactions to administration of a neurotoxic agent or as an incidental finding. Lipofuscin accumulates in the cytoplasm of large CNS neurons (mainly pyramidal cells), astrocytes, and oligodendrocytes via gradual accretion of cell degradation byproducts. This autofluorescent material represents the phospholipid-rich residue of autophagosomal lysosomes produced in cells undergoing substantial lipid peroxidation of their membranes. The microscopic appearance of the granules generally is faint yellow-brown in H&E-stained sections, pink in periodic acid Schiff (PAS)–stained sections, and dark blue to purple in LFB-stained sections (Figure 21.36). In many cases, lipofuscin is stored spontaneously in aged animals, more so for nonhuman primates and humans, and to a lesser extent in carnivores, than for short-lived rodents. These "natural" deposits elicit little if any cytotoxicity in affected cells. In contrast, lipofuscin has been reported to accumulate in rodents given some neurotoxic agents, including alcohol and lead, where its extensive accumulation may be associated with cytotoxicity.

Deposition of hemosiderin within the CNS represents another form of pigment associated with certain neurotoxic treatments. The pattern of deposition depends on the nature of the exposure. For example, Aβ, the endogenous toxicant linked to cerebral amyloid angiopathy (CAA) in Alzheimer's disease, has been associated with microscopic perivascular hemorrhages (Figure 21.36) in affected brain regions of amyloid precursor protein (APP)-transgenic animal models as well as human patients. In contrast, larger foci of hemorrhage and hemosiderin accumulation may be evident at sites where implantation of a direct delivery device has produced microtrauma to the blood vessels coursing through the neuropil. Very small deposits of pigment, presumably hemosiderin, in the Purkinje cell layer can be a hint that there was a prior loss of cells from this neuronal population.

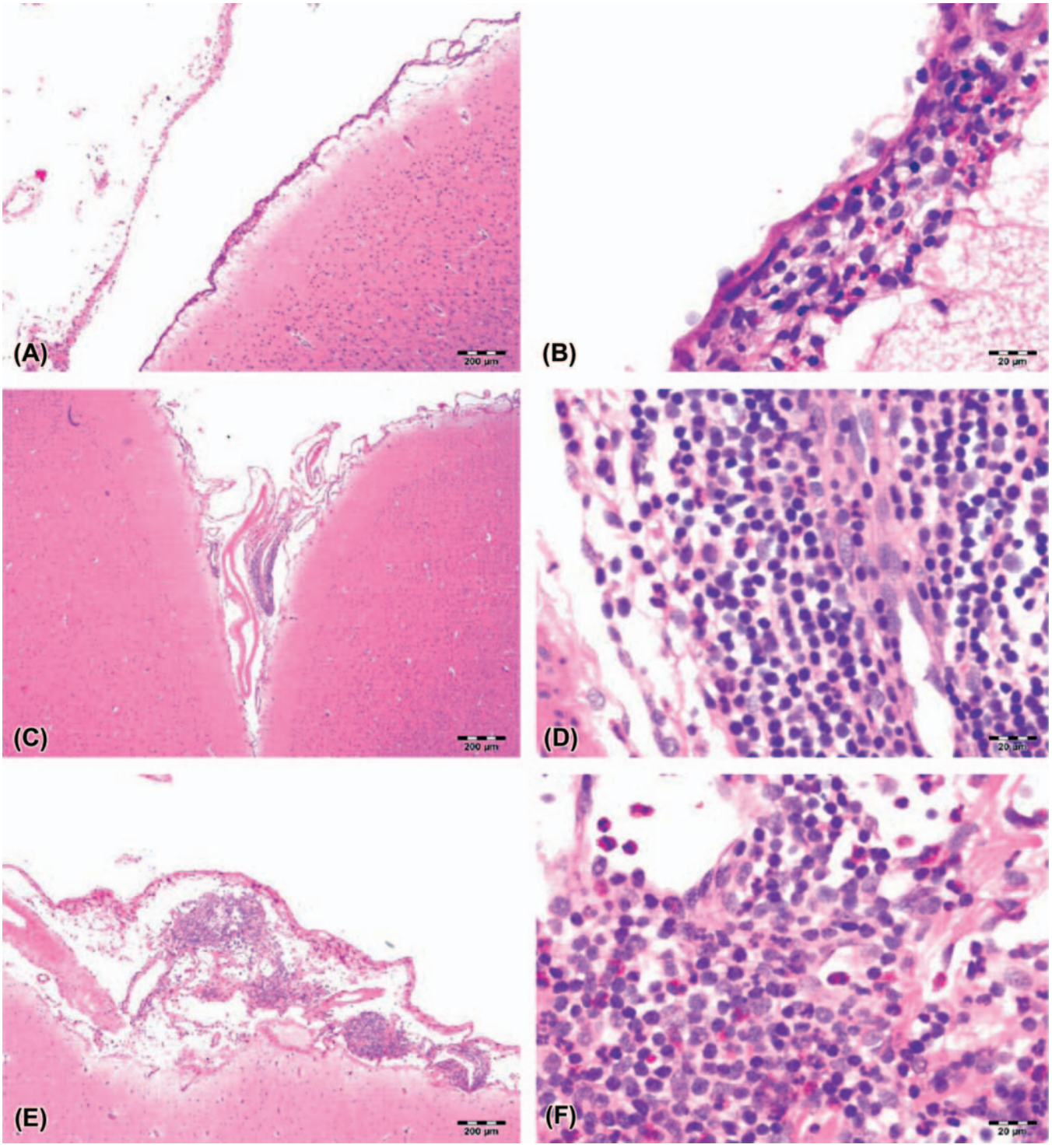

FIGURE 21.35 Leukocyte aggregates within the nervous system may collect at various sites, especially within the loose connective tissues of the choroid plexus and the meninges (shown here). (A, B) This vehicle-treated control animal had a modest mixed infiltrate of lymphocytes and eosinophils, underscoring the fact that small collections (i.e., infiltrates) of leukocytes may collect in the brain in the absence of active leukocyte-mediated tissue destruction (i.e., inflammation). Direct intrathecal delivery of idursulfase at 3 mg/dose (C, D) or 100 mg/dose (E, F) resulted in more pronounced infiltration of leukocytes, but the inflammatory response was reversible once protein instillation was stopped. Scale bars: 200 µm. Processing conditions: Formalin fixation by immersion, paraffin embedding, H&E staining. Source: *Reproduced from Felice, B.R., et al.2011. Safety evaluation of chronic intrathecal administration of idursulfase-IT in cynomolgus monkeys.* Toxicol. Pathol. *39, 879–892, with permission of SAGE Publications.*

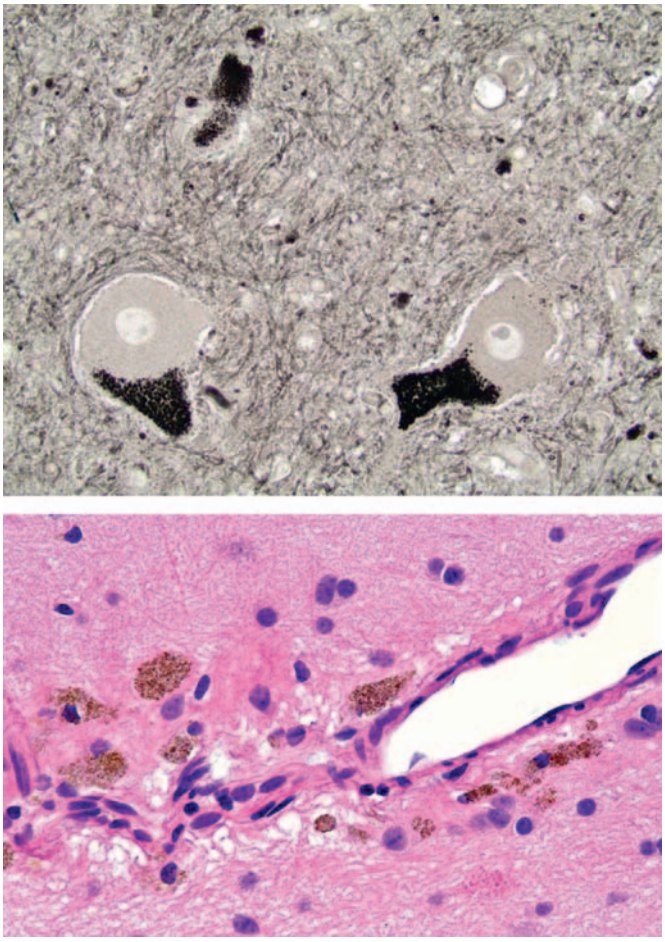

FIGURE 21.36 Pigment deposition in the nervous system occurs in several toxicant-induced processes and as a spontaneous background finding (as here). *Upper*: Large pyramidal neurons in the cerebral cortex of this dog harbor large deposits of lipofuscin, a byproduct of ongoing cell and organelle membrane degradation that gradually accumulates over time. These deposits appear faint yellow-brown by H&E, pink with periodic acid Schiff (PAS), dark blue to purple by LFB, and black using Sudan black (shown here). *Lower*: Phagocytes near small blood vessels in the thalamus of this rat are packed with brown hemosiderin granules, indicating prior episodes of local microhemorrhage. Processing conditions: Formalin fixation by immersion, paraffin embedding, H&E staining.

Storage diseases may occur as a consequence of neurotoxicant exposure, when the active agent reduces or halts the activity of an enzyme required for normal metabolism. The prototypic toxicant-induced neural storage disease is produced by swainsonine, an alkaloid toxin fabricated by plants of the genera *Astragalus*, *Oxytropis*, and *Swainsona* (e.g., locoweed) that inhibits α-mannosidase, a protein involved in the hydrolysis of N-linked glycosides. Affected neurons are observed to have many cytoplasmic vacuoles (representing swollen Golgi bodies) by light microscopy. A variant of xenobiotic-induced storage disease is drug-induced phospholipidosis (DIPL), in which phospholipids accumulate in multilamellar (myeloid) bodies within the cytoplasm (Figure 21.22). Small molecules associated with this lesion are classed chemically as cationic amphophilic drugs (CAD), and they represent essential therapies for treating many indications: angina, depression, hypercholesterolemia, and malaria, to name a few. The usual neural cells targeted by these drugs are large neurons, such as those in dorsal root ganglia and the spinal cord gray matter. In contrast to traditional storage diseases, DIPL results from selective lysosomal uptake and/or retention of the undigested xenobiotic substrate rather than from enzyme inhibition. Confirmation that a molecule has produced lysosomal alterations requires transmission electron microscopy, so in nearly all cases analysis for this finding is limited to experimental animals.

PROLIFERATIVE LESIONS

An infrequent but confirmed consequence of xenobiotic exposure is neurocarcinogenesis, or the induction of neoplasms in the CNS and/or PNS. Most neural neoplasms, including the bulk of xenobiotic-induced lesions, in animals and humans are glial tumors arising in the CNS. These glial neoplasms may evolve from a single cell lineage (e.g., astrocytoma, oligodendroglioma) or from multiple lines (e.g., mixed gliomas, which contain both astrocytic and oligodendroglial elements). In general, chemically induced glial tumors in experimental animals do not evolve into the aggressive glial malignancies (e.g., glioblastoma multiforme) characteristic of lesions observed in human patients. Neural cancers originating from other CNS cell types have been described after exposure to xenobiotics, albeit rarely. These entities include medulloblastoma, a primitive neuroectodermal tumor (PNET) of the cerebellum; granular cell tumors (in rodents) and meningiomas; and ependymomas (typically occurring in the spinal cord central canal).

In the PNS, neural tumors most commonly arise from Schwann cells only or from Schwann cells in combination with endoneurial and perineurial fibroblasts that form the connective tissue sheaths bundling axons within nerves. Traditionally, these neoplasms have been designated as Schwannomas (benign or malignant) and neurofibromas (for benign lesions) or neurofibrosarcomas (for malignant), respectively, but recently some workers have preferred to combine them into a single class as "nerve sheath tumors" (benign or malignant). The PNS axons themselves cannot give rise to neural tumors since they merely represent cell processes, and not cells. However, PNS cell bodies in various ganglia (including the adrenal medulla) can serve as the source of peripheral tumors of neural origin. Chemically induced PNS tumors

usually will possess features of Schwannoma (i.e., originating only from Schwann cells).

Differential diagnosis of neural tumors is complicated by two main factors. The first is the difficulty in discriminating between reactive and neoplastic neural cells, particularly in the PNS. Schwann cells proliferate extensively as a regenerative response to any form of damage, so any connective tissue neoplasm that encompasses a nerve is likely to include a substantial proportion of activated Schwann cells intermingled with the neoplastic tissue. A second factor is that tumor cells often express unusual complements of proteins. Such altered signatures are particularly evident for malignant neoplasms, which may produce greatly reduced amounts of typical marker proteins or manufacture multiple markers that are characteristic of an immature pluripotent cell. From a practical perspective an increase in the number of neoplasms following exposure to a xenobiotic is an adverse event regardless of the cell of origin, so the main focus should be on discriminating between reactive and neoplastic lesions.

Neurocarcinogens include alkylating chemicals, radiation, and certain viruses. In general, exposures leading to carcinogenicity occur during development (e.g., by transplacental or neonatal exposure) or during young adulthood. The same agent (e.g., *N*-ethyl-*N*-nitrosourea (ENU)) can produce increases in the incidences of both glial and non-glial neoplasms in the CNS. Some neural tumors only develop following direct introduction of the toxicant into the CNS (e.g., choroid plexus carcinomas following intracerebroventricular injection), indicating the importance of barrier systems (e.g., BBB) in protecting neural tissues from blood-borne toxic agents.

In the PNS, tumors of peripheral nerve origin must be distinguished from neuromas, which are focal, non-neoplastic lesions that form at the site of a local traumatic injury (commonly transection with displacement or removal of the distal trunk). Neuromas represent the disordered proliferation of elongating proximal axons that have failed to find their former pathways and thus are unable to reestablish connectivity with their effector organ. The presence of numerous axons is a diagnostic feature of neuromas as Schwannomas contain few if any axons. Toxicants cannot induce neuromas as axons cannot become neoplastic. However, toxicants may produce extensive axonal sprouting which collectively may form masses that mimic the effects of tumors.

Background Neuroanatomic Findings and Their Implications

Certain incidental changes are frequently misidentified as neuropathological lesions by inexperienced researchers. The alterations described here are common artifactual findings in vertebrate brains. Identified artifacts typically should not be reported in the pathology data set. However, systematic distribution of a background finding, where one dose group only is involved or the relationship between the lesion incidence and dose is uncertain, may be recognized and noted in the microscopic data or included as a comment to the organ/tissue at the discretion of the study pathologist. The key for such incidental changes is to properly discuss their significance, or more often their lack of significance, with respect to assessing the risk of neurotoxicity.

"Dark neuron" artifact in the brain is the most problematic spontaneous change, as it is misinterpreted as neuronal degeneration with distressing frequency. This artifact occurs more regularly in certain brain regions, particularly the cerebral cortex (Figure 21.14), hippocampus, Purkinje cell layer of the cerebellum, and large pyramidal neurons of many brainstem nuclei and the spinal cord gray matter. Affected neurons typically have darkly amphophilic nuclei and cytoplasm, with larger-sized neurons often having more readably visible cytoplasmic borders. Some dark neurons may exhibit twisted, corkscrew-shaped extensions. Dark neurons have been shown to result from rapid transfer of water out of the neuronal cytoplasm into adjacent glial cells or into the perineuronal neuropil. Within an affected region, all dark neurons have similar features, in contrast to genuine foci of neuronal degeneration in which injured cells exhibit a range (i.e., early to advanced) of neurodegenerative stages (Figure 21.20).

A common presentation for dark neuron artifact is as an asymmetric, focal column of affected cells extending from the deep layers of the cerebral cortex down to the hippocampus. This appearance is consistent with application of superficial pressure to inadequately fixed CNS tissue, leading to localized glutamate release or to other perturbations of neuronal homeostasis. Induction of excitotoxicity *postmortem* may be involved in the pathogenesis of "dark neurons," as administration of glutamate antagonists (MK-801, 6-cyano-7-nitroquinoxaline-2,3-dione (CNQX), etc.) at necropsy has been suggested to reduce their numbers. The usual method for mitigating this artifact is to fix by perfusion and, if time permits, to follow this by an additional period of in situ postfixation (by immersion) following removal of the calvarium.

Neuronal autophagy in ganglia (predominantly dorsal root ganglia, but also occasionally sympathetic ganglia) is the most common form of neuronal death in the PNS and occurs with some frequency in untreated control animals. This change usually is characterized by cell swelling, pale/granular cytoplasm, and the presence of irregular, dark

eosinophilic, globular inclusions (lytic chromatin); infrequently, the affected neuron is encircled by satellite glial cells (Figure 21.37) or lymphocytes. Ganglionic neurons may undergo a more typical necrosis reaction—indeed, this finding typically has been termed "neuronal necrosis" historically—but these PNS cells seldom if ever acquire the classic "red/dead" appearance that develops in necrotic brain neurons (Figures 21.19 and 21.20).

"Myelin bubble" artifact generally involves large myelinated fibers of the spinal cord white matter tracts and PNS major somatic nerve trunks. The finding presents as clear, localized, round to elliptical spaces surrounding an intact axon; the spaces may occur in isolation or in chains (Figure 21.38). The change often is confined to one or a few axons, so it is more readily recognized in longitudinal sections than transverse ones. The main differential diagnosis for this change is axonal degeneration, a true neurotoxic lesion that presents as a string of digestion chambers that contain fragmented axonal and/or myelin debris (sometimes along with phagocytic "gitter" cells). Myelin bubble artifacts tend to develop in immersion-fixed, paraffin-embedded specimens. The mechanism is unknown, but the suggested pathogenesis is manipulation of unfixed tissue leading to tissue fluid accumulation within the traumatized myelin before the fixative solution penetrates the sample.

"Vacuolation" artifact can take several forms in the CNS and PNS (Figure 21.39). Diffuse vacuolation may be observed if fixation is delayed. However, this circumstance is unlikely in experimental studies, and can be managed by careful scheduling of tissue harvesting for diagnostic cases. A more frequent variant in CNS white matter is focally extensive collections of large vacuoles in densely myelinated tracts of the cerebrum, cerebellum, and brainstem. The vacuoles may have irregular borders and be filled with pale, homogeneous material (termed "Buscaino bodies") or have smooth margins and be empty. These vacuoles are more extensive if tissues are retained in alcohol for an extended period—such as holding in the alcohol bath stage on an automated tissue processor over the weekend—possibly as a consequence of excessive lipid extraction. Vacuoles of various sizes are commonly observed in dorsal root ganglia neurons (and less often in sympathetic ganglia neurons) of control animals from many species (Figure 21.40), although they also have been attributed to organophosphate expsoure.

Another form of vacuolar artifact in the CNS results from swollen organelles in particular cell types, especially astrocytes. These may occur as small clear holes in the cytoplasm or as larger, clear vacuoles in the astrocytic processes adjacent to shrunken neurons or blood vessels. The main toxicant-induced differential to this artifact is intramyelinic edema, in which the myelin sheaths encircling intact axons are disrupted by small to large vacuoles (Figure 21.29). Genuine neurotoxic vacuolar lesions usually exhibit a bilaterally symmetrical distribution and are fairly widespread, while the artifactual changes are often limited to one or a few locations.

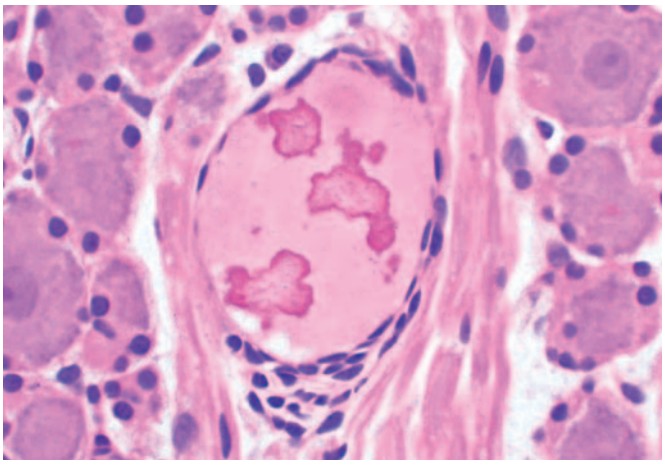

FIGURE 21.37 Neuronal autophagy in dorsal root ganglia (and occasionally sympathetic ganglia) is characterized by cell swelling, cytoplasmic pallor or granularity, and the presence of irregular, dark eosinophilic, globular inclusions (i.e., lysed chromatin). Occasionally, affected neurons are accompanied by satellite glial cells (seen here) or lymphocytes. Dorsal root ganglion of an adult control rat. Processing conditions: Formalin fixation by immersion, paraffin embedding, H&E staining.

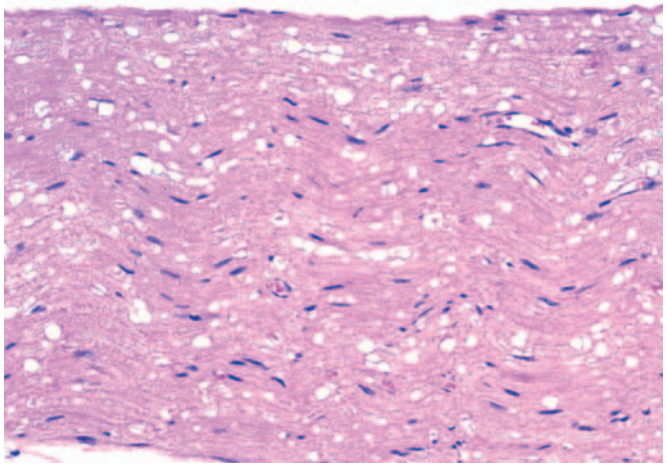

FIGURE 21.38 "Myelin bubble" artifact is readily appreciated in this markedly affected sciatic nerve section from a control mouse. The finding presents as clear, dilated fiber tracts (alone or in chains) surrounding an intact axon in the absence of any Schwann cell or phagocytic reaction. When mild, only a few fiber tracts may be affected, so the change often is recognized more easily in longitudinal sections. The mechanism is unclear but is thought to involve insufficient and/or delayed fixation. Processing conditions: Formalin fixation by immersion, paraffin embedding, H&E staining.

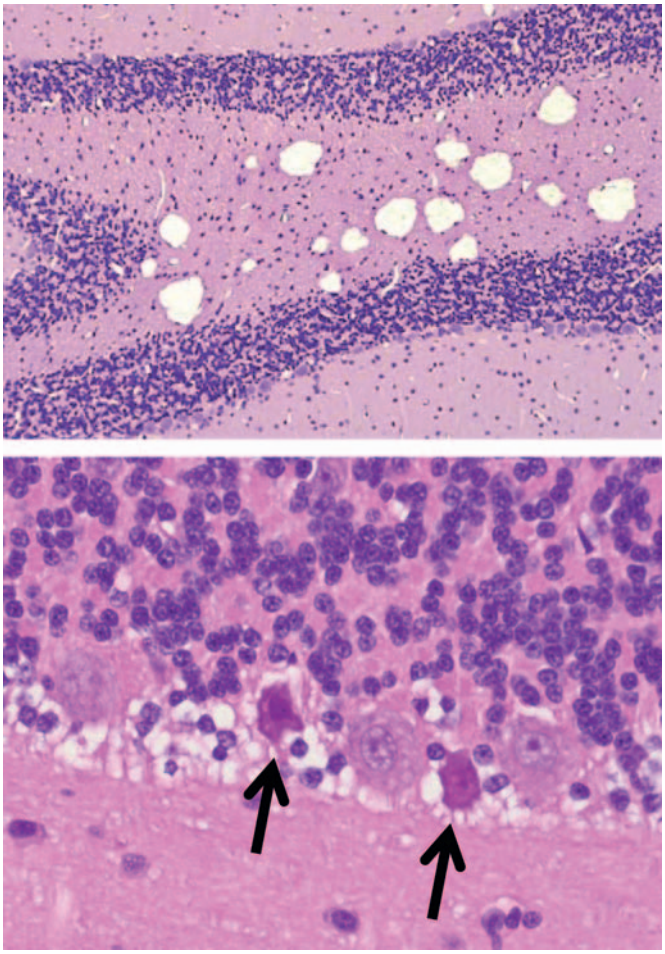

FIGURE 21.39 Vacuolation artifact assumes several forms in white matter tracts of the central nervous system (demonstrated here in the rat cerebellum). *Upper*: A common presentation in deep white matter tracts is focally extensive collections of large vacuoles with irregular margins; in some cases, the vacuoles contain pale, homogeneous material (i.e., "Buscaino bodies"). These vacuoles are more extensive if tissues are retained in 70% alcohol for an extended period—such as retention in the alcohol bath on an automated tissue processor over the weekend—possibly as a consequence of excessive lipid extraction. *Lower*: Markedly swollen astrocyte processes may be responsible for substantial peri-neuronal vacuolation. The adjacent neurons typically are unaffected or may exhibit the early stages of dark neuron artifact (arrows; compare this initial "dark neuron" phenotype to neurons with genuine degenerative changes (Figures 21.5, 21.19, and 21.20) and advanced dark neuron features (Figure 21.14)). Such astrocytic swelling is likely a consequence of hypoxia-associated energy depletion and the inability to actively sustain transmembrane ion gradients and fluid balance during the delay before fixation begins. Processing conditions: Formalin fixation by immersion, paraffin embedding, H&E staining.

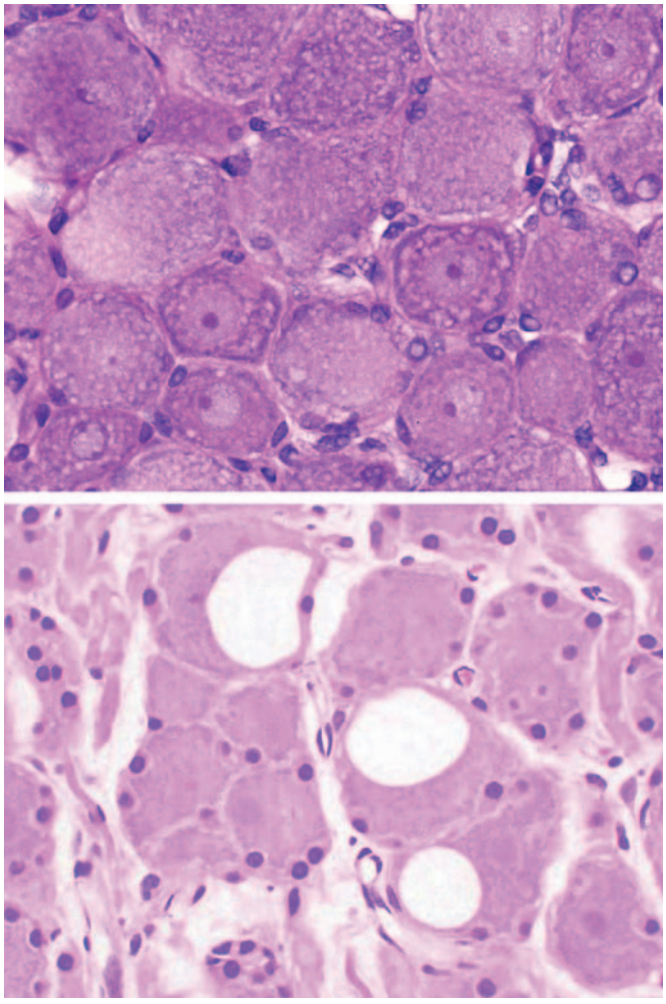

FIGURE 21.40 In the peripheral nervous system, small (upper) or large (lower) vacuoles are commonly seen in neurons of dorsal root ganglia and to a lesser extent sympathetic ganglia. These vacuoles may form by separation of the neuron from the surrounding satellite glial cell processes; another possibility for the large vacuoles is loss of an unknown material from cytoplasmic storage depots. While such vacuoles have been reported to be caused by neurotoxicants, they also occur frequently in control animals of all species. Dorsal root ganglia of adult control rats. Processing conditions: formalin fixation by immersion, paraffin embedding, H&E staining.

Axonal "spheroids" (i.e., focally enlarged axons) are occasionally encountered in white matter tracts of the brainstem and spinal cord as a spontaneous change in older animals. Animals from all treatment groups may be affected, including the negative control cohort, and no relationship to xenobiotic dose is evident. A common site for this finding is the cranial portion of the dorsal funiculus, which is the terminus for the ascending sensory tracts in the spinal cord. Spheroids also can result from neurotoxicant exposure (Figure 21.25), but in such cases their number is higher and they usually exhibit a dose-response relationship.

Melanin occurs as a normal pigment in certain sites within the CNS. This location should not be surprising since melanocytes are derived from precursors of neural crest origin. Typical areas for deposition are the meninges in pigmented mice (Figure 21.41) and certain sheep breeds or the neurons of the *substantia nigra*, the *locus coeruleus*, and some other basal nuclei in

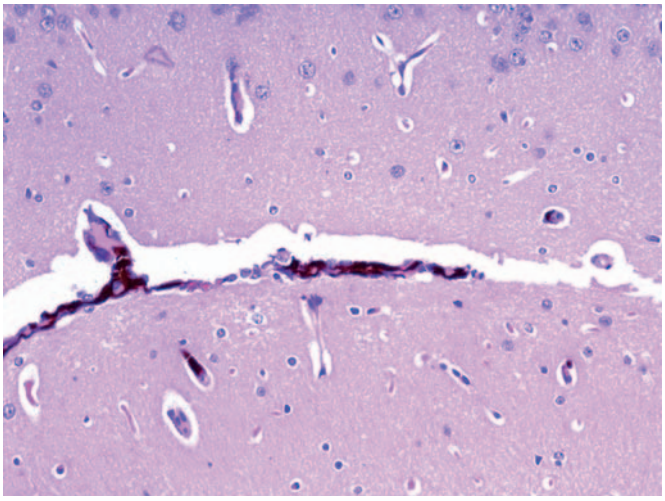

FIGURE 21.41 Melanin pigment is a common incidental background finding in the meninges of mouse strains with pigmented hair. Cerebral cortex of a control C57BL6/J mouse. Processing conditions: Formalin fixation by immersion, paraffin embedding, H&E staining.

primates, including humans. The neuronal form, termed neuromelanin, is minimal at birth but accumulates over time. The meningeal melanin has not been linked to a specific function, nor is its extent altered by exposure to neurotoxicants. The proposed tasks for neuromelanin are protective, such as storage depots for oxyradicals resulting from metabolism of monoamine neurotransmitters (e.g., dopamine (DA) and norepinephrine (NE)) or residual products of autophagy. This role is supported by the ability of neuromelanin to selectively sequester the neurotoxic metabolite MPP^+, a monoamine analog. A more active function for neuromelanin is suggested by the loss of pigmented neurons in basal nuclei in concordance with the onset of certain neurodegenerative diseases.

The ancillary tissues within the CNS are host to two common incidental changes. The first is focal fibrosis of the meninges, which appears as a localized accumulation of fibroblasts and collagen. The second is occasional small aggregates of leukocytes in the choroid plexus, and to a lesser extent near meningeal blood vessels. These foci usually contain mature lymphocytes, mainly of the T-cell lineage, and they are seemingly present to fulfill a surveillance function for the acquired arm of the immune system. Mast cells scattered within the perineurium are a frequent finding in large nerve trunks of the PNS, especially in rodents. In general, none of these changes is impacted by neurotoxicant exposures. In contrast, the presence of granulocyte and/or macrophage aggregates in neural tissues is associated with an immediate response by the innate immune arm to a noxious stimulus, though usually one caused by irritation or bacterial contamination associated with implantation of a direct delivery device into or near the CNS rather than as a direct neurotoxic effect induced by the test article.

One key factor required for success in the practice of toxicologic neuropathology is a solid understanding of normal neuroanatomy. In particular, normal features must be recognized as such and not misdiagnosed as lesions. The typical danger of this sort encountered in the nervous system are the circumventricular organs (CVOs), six small CNS domains (Figure 21.42) containing many small, fenestrated capillary loops located adjacent to the ventricular system. Five are found near the third ventricle (listed from rostral to caudal, and dorsal to ventral): the subfornical organ (SFO), vascular organ of the lamina terminalis (OVLT), pineal gland, subcommissural organ (SCO), and median eminence. The sixth, the area postrema (AP), is in the brainstem near the fourth ventricle. Neurons are found in three CVOs (the AP, OVLT, and SFO); the pineal gland is comprised of pinealocytes, while the SCO consists of specialized ependymal cells. Common misdiagnoses applied to the CVOs by inexperienced investigators include congenital cysts, inflammation, and neoplasia. In contrast to CVOs, genuine cysts (Figure 21.43) have irregular contours, are lined by simple or stratified epithelial linings, and may contain secretory material, while inflammatory and neoplastic lesions appear as disorganized cell aggregates that may penetrate and disrupt the adjacent parenchyma.

MECHANISMS OF NERVOUS SYSTEM INJURY

Neurotoxicants have been shown to produce their effects in many different fashions. Basic mechanisms may target any of several neural elements: particular structures, specific cell types, or certain molecular pathways. The precise nature of the resulting neuropathological lesions will be dictated by the mode of action. Accordingly, the remainder of this section will briefly review basic mechanisms of neurotoxicity using prototypical neurotoxicants (Table 21.1).

Aberrant Cell Migration and/or Differentiation

The typical lesion resulting from abnormal migration and terminal differentiation of neuronal precursors is heterotopia (Figure 21.12), but the mechanisms by which neurotoxicants produce this change are incompletely understood. Experiments with avian and rodent embryos suggest that damage to neuronal stem cells, radial glial (which guide neuronal precursors to their

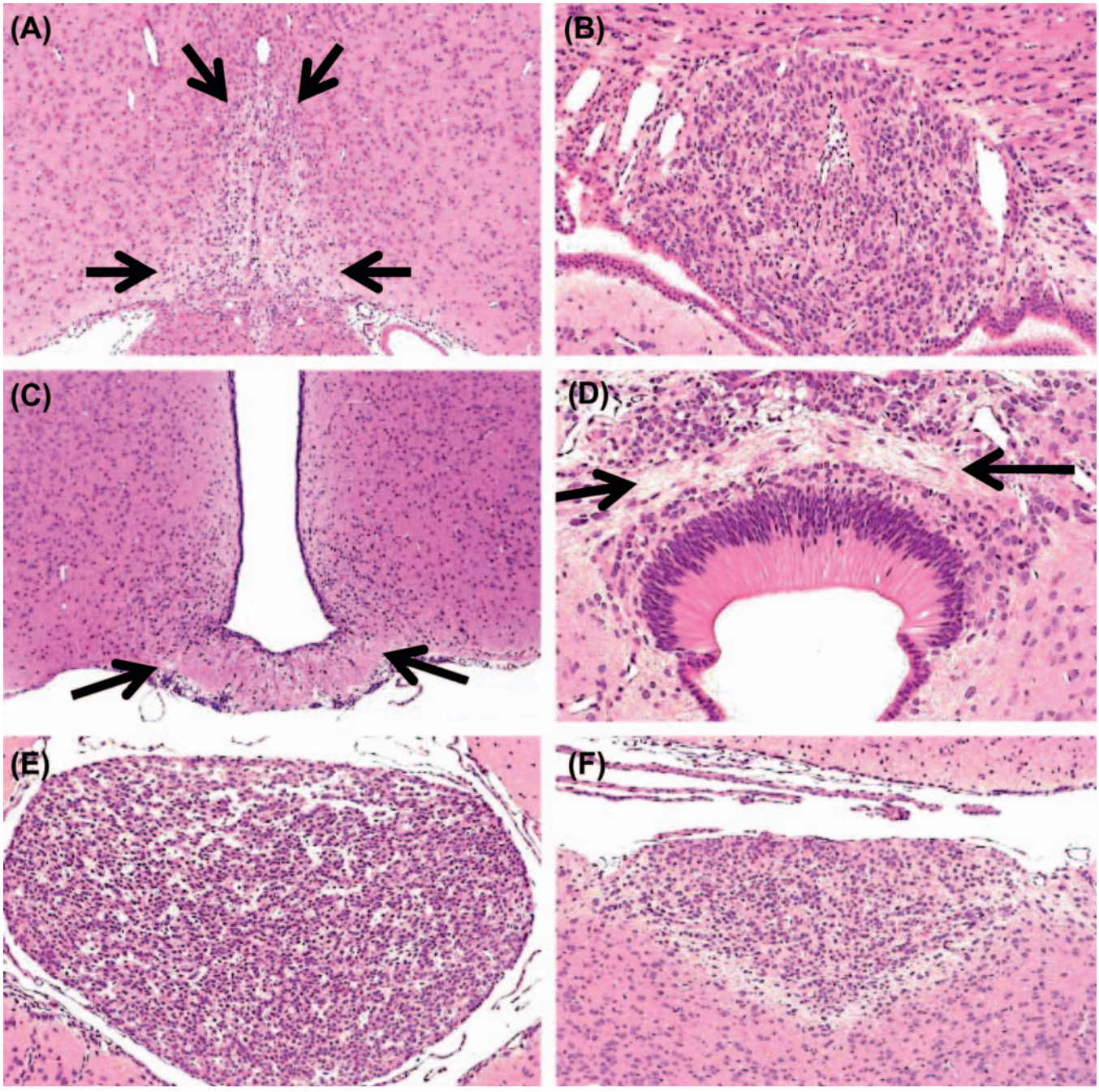

FIGURE 21.42 Circumventricular organs (CVOs) in the adult Rodent brain (specifically rat). These six regions are the organum vasculosum of the lamina terminalis (A, outlined by arrows), subfornical organ (B), median eminence (C, bracketed by arrows), subcommissural organ (D), pineal gland (E), and area postrema (F). Neurons occur only in the CVOs in A, B, and F. The subfornical organ (B) is sometimes mistaken for a lesion (e.g., subependymal granuloma). The posterior commissure (bracketed by arrows in D) appears to be hypomyelinated because the image is from the brain of a weanling at postnatal day 21 (i.e., before myelination is complete). Processing conditions: Formalin fixation by perfusion, paraffin embedding, H&E staining. Source: *Figure reproduced with minor changes from Garman, R.H. 2011. Histology of the central nervous system.* Toxicol. Pathol. *39, 22–35, with permission of SAGE Publications.*

appropriate positions), or both may be factors. Several hypotheses have been advanced to explain the defects.

One alternative is that pluripotent stems cells may be destroyed before they can produce enough daughter cells to populate one or more waves of neuronal migration. This effect may be confined to the neuroepithelium of the neurulating embryo, or it may also impact partially differentiated structures such as ganglia (which are derived from neural crest cells). A second option is that the spatial and/or temporal expression of

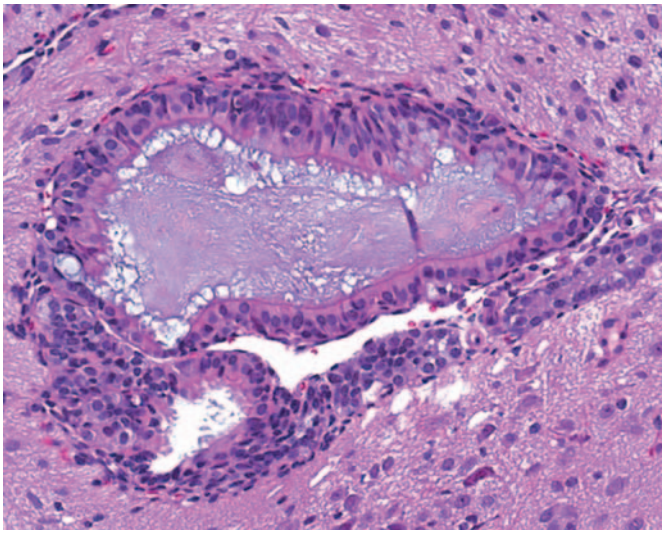

FIGURE 21.43 Congenital cyst (likely originating as a remnant of Rathke's pouch) in the brain adjacent to the ventral portion of the third ventricle. The cyst is lined by simple to occasionally stratified columnar epithelium and contains pale basophilic secretory material. Ventral hypothalamus of a 6-week-old control Sprague-Dawley rat. Processing conditions: Formalin fixation by immersion, paraffin embedding, H&E staining. Source: *This image was kindly provided by Dr. Daniel Patrick, MPI Research, Mattawan, Michigan, United States.*

critical morphogens (growth factors, neurotransmitters, etc.) is disrupted for one or several lineages of neural cell precursors. This consequence may lead to several kinds of functional abnormalities in the affected cells: misdirected migration, reduced movement in the proper direction, and/or incorrectly timed terminal differentiation. In most cases, neurons will seek—and usually succeed, at least in part—to connect with their normal cellular targets. Nonetheless, behavioral or other neurological deficits may be observed since the resulting fiber tracts typically will be too long and insufficiently wired to support normal neural activities.

Altered Intracellular Transport

Toxic agents that disrupt the transfer of essential macromolecules from the cell body to its distant processes will produce degeneration in outlying structures. This finding is typical of axonopathies, in which blocked slow axonal transport results in chemical rather than physical transection of the axon. Axonotoxic chemicals generally induce this effect by promoting the formation of covalent cross-links between macromolecules (e.g., neurofilaments). The resulting disordered filamentous masses will lodge at axonal constriction points like the nodes of Ranvier.

The axon distal to the plug, including the presynaptic terminal, will starve and eventually disintegrate as a primary lesion, to be followed in time by secondary degeneration of the local Schwann cells. The longest axons (e.g., those in long tracts in the spinal cord white matter and in PNS nerve trunks) are affected first. Regeneration can occur in PNS axons if the insult is transient, but affected CNS axons cannot be restored. The neuron generally will survive since the supply of nutrients to its metabolically active body remains intact, although chronic exposure to certain agents (e.g., IDPN) can induce an irreversible loss of CNS motor neurons.

Cell Turnover

Chemical exposure in the rat has been linked to heightened incidences of glial neoplasms (mainly in the deep cerebrum), granular cell tumors (cerebral and cerebellar meninges, chiefly on the dorsal midline), and malignant reticulosis (cerebral and cerebellar meninges). These tumors are thought to evolve from populations of partially committed, oligopotent stem cells that retain the capacity for low-level cell division throughout adulthood. The specific sites are the cerebral subventricular zone adjacent to the lateral ventricles for the glial masses, or fibroblasts or facultative phagocytes in the meninges. These cell populations offer targets for genotoxic carcinogens (discussed later in the "Macromolecular Adducts" section), but cell proliferation is a necessary requirement by which genetic mutations will become fixed in the genome. Cell proliferation occurs in corresponding sites in adult rodents, dogs, monkeys, and humans.

Abnormal cell turnover is also an important factor in neurotoxicity. During development, increased or decreased programmed cell death at an inappropriate time will either reduce or prevent neuronal processes from correctly connecting with their target cells. Such disruptions typically will perturb anatomic and functional maturation. Similarly, toxicants can alter postnatal neuronogenesis in the brains of mature individuals, which can impact behavioral and cognitive abilities (e.g., learning, memory).

Energy Depletion

Reduced availability of energy stores within highly active neural cells, especially neurons, is a common predisposing factor to cell degeneration and eventual cell loss in many brain regions. The mechanism of action involves the capacity of such neurotoxicants to interfere with enzymes in the electron transport chain by which the mitochondria replenish ATP; in the absence of this energy storage molecule, neurons lose their ability to sustain their ionic gradients and thus

fail to produce action potentials. The neurotoxic moiety may reach the target neurons by a circuitous route.

For example, MPTP is converted to the toxic metabolite MPP^+ by peri-synaptic astrocytes in a two-step reaction that requires the enzyme monoamine oxidase B (MAO-B). Subsequently, dopaminergic neurons in the substantia nigra selectively sequester MPP^+ using transporters for the reuptake of monoamine neurotransmitters. Finally, MPP^+ enters the mitochondria where it quenches the activity of reduced nicotinamide adenine dinucleotide (NADH) dehydrogenase, the first enzyme in the electron transport chain. Other agents (e.g., bromethalin, hexachlorophene) damage myelinating cells by uncoupling mitochondrial oxidative phosphorylation, which leads to fluid accumulation in the interlamellar space (Figure 21.29).

Excitotoxicity

Excitotoxic neurodegenerative lesions are thought to result from imbalances in reciprocal feedback between neuronal populations that produce the excitatory neurotransmitter glutamate and the inhibitory neurotransmitter γ-aminobutyric acid (GABA). For example, trimethyltin (TMT) increases glutamate release in the hippocampus while reducing the synthesis and reuptake of GABA and glutamate. Enhanced excitation results in persistent influx of ions across the neuronal plasma membrane, including entry of calcium (Ca^{2+}). The rising Ca^{2+} tide finally floods the neuronal cytoplasm and propels the cell to begin a death spiral. The initial lesion of punctate vacuolation in neurons, consistent with swelling of intracytoplasmic tubular organelles (Figure 21.18), occurs within hours of injury and may progress to full-fledged necrosis (Figures 21.19 and 21.20) over 1 or 2 days.

The vulnerability of various neuronal populations to TMT-induced excitotoxicity is affected by many factors. For example, mice are more sensitive to TMT than rats. However, the lesion pattern diverges in these two species; in the hippocampus, mice preferentially develop dentate gyrus lesions with little involvement of cells in the CA regions, while the converse is true in rats. The sensitivity of the CA neurons is age-dependent in rats with lesions developing only after the hippocampal pyramidal cells mature (i.e., after postnatal day 7). This phenomenon highlights the need to evaluate neurotoxicity under various conditions when seeking to identify and characterize new neurotoxic agents.

Macromolecular Adducts

Known neurocarcinogens in rats (e.g., acrylonitrile, ethylene oxide, nitrosoureas) chiefly produce glial neoplasms following prenatal or prolonged postnatal exposure. These agents are all potent DNA-alkylating chemicals, indicating that the likely mechanism of neural cell initiation is the formation of DNA adducts leading to mutations in critical genes. The typical deep cerebral location of the tumors suggests that the target populations are likely to be retained progenitor cells in the cerebral peri-ventricular zone or subcortical white matter. It is not known whether or not neurotoxicant exposure is responsible for the preponderance of glial tumors in humans, or which chemical(s) or critical developmental periods in people might be most vulnerable to neurocarcinogenic toxicants.

Neurotransmission Disruption

Neurotoxic agents that block synaptic neurotransmission can induce profound neurological dysfunction in the absence of major structural lesions. Classic presentations include altered contraction of skeletal muscles in certain body regions or all major muscle groups, abnormal cognitive abilities, and/or dysfunction of the autonomic nervous system (ANS). Affected subjects can recover if vital functions (e.g., breathing, nutrient intake) can be maintained until the affected synaptic elements are restored. Disruption of synaptic function occurs in several ways.

Decreased Neurotransmitter Release

Attenuated release of neurotransmitters is responsible for botulism and tetanus, both of which are caused by toxins produced by bacteria of the genus *Clostridium* as metabolic byproducts when grown under anaerobic conditions. Botulism develops in fish, birds, and mammals following bacterial colonization in the digestive tract or deep wounds, or by ingestion of the preformed toxin in contaminated food. Botulinum toxin serves as a protease to degrade docking molecules needed for fusion of synaptic vesicles with the presynaptic membrane of the axon terminal. In the absence of vesicle fusion, acetylcholine is not released and the postsynaptic membrane is not stimulated. Skeletal muscles cannot contract, so flaccid paralysis ensues (e.g., limberneck, the manifestation of botulism in waterfowl).

In contrast, tetanus arises when bacteria within infected puncture wounds generate tetanospasmin, which is taken up at neuromuscular junctions in the body periphery and then transported to the CNS by retrograde axonal transport. Tetanospasmin also functions as a protease that thwarts vesicle docking, but affected synapses fail to discharge the inhibitory transmitters GABA and glycine. The removal of feedback control that modulates the excitatory signals to skeletal

muscles results in the characteristic presentation of tetany (i.e., intermittent or constant skeletal muscle contraction).

Persistent Neurotransmitter Activity

Sustained neurotransmission is another recognized route to synaptic neurotoxicity. This effect can be produced in several fashions, and typically occurs in association with CNS neurons. One means is to increase neurotransmitter release from presynaptic terminals. This approach explains the efficacy of mirtazapine (Remeron), a tetracyclic antidepressant that acts as an α_2-adrenergic blocker to promote the discharge of serotonin (5HT) and norepinephrine (NE).

A second, more common way for maintaining neurotransmitter levels in the synapse is to reduce the rate at which transmitters are removed. Inhibition of neurotransmitter reuptake is the desired pharmacological response of several selective 5HT reuptake inhibitor (SSRI) antidepressants, such as fluoxetine (Prozac), paroxetine (Paxil), and sertraline (Zoloft). However, self-medication with two such drugs and/or related pro-serotonergic agents (e.g., amphetamines, monoamine oxidase inhibitors (MAOI), some nutraceuticals (e.g., St. John's wort, *Hypericum perforatum*), and certain opioids) can over-stimulate organs with high numbers of 5HT receptors (e.g., CNS, gastrointestinal tract ANS), resulting in the potentially lethal "serotonin syndrome" (also called "serotonin toxicity"). Some agents can lessen reuptake of two neurotransmitters simultaneously: dopamine (DA) and NE—the effect of bupropion (Wellbutrin); or 5HT and NE—duloxetine (Cymbalta) and venlafaxine (Effexor). St. John's wort is thought to inhibit the uptake of DA, 5HT, and NE, although the exact mechanism remains unclear.

Reduced Neurotransmitter Metabolism

A third strategy is to decrease the degradation of neurotransmitters. This effect is produced by treatment with MAOIs, where the two MAO isoforms are bound to the outer mitochondrial membrane of most cells, including neurons and astrocytes; MAOs promote the oxidative deamination of DA, 5HT, and NE. Similarly, inhibition of synaptic acetylcholinesterase (AChE) by exposure to carbamate or organophosphate (OP) insecticides prevents the hydrolytic removal of acetylcholine from synapses in the CNS and PNS as well as at neuromuscular junctions. The OPs irreversibly phosphorylate the serine residue at the active site of AChE, so any recovery must await the synthesis of new enzyme. Administration of pralidoxime (2-pyridine aldoxime methyl chloride (2-PAM)) early after OP exposure can reduce the extent of neurotoxicity by hydrolyzing the OP−serine bond that inactivates AChE. In contrast, the bond between a carbamate and AChE is reversible, with the hydrolytic removal over several hours leading to the gradual restoration of AChE activity.

Termination of Transmembrane Ionic Gradients

Some agents affect neurotransmission by altering the character of the action potential. The maintenance of normal ionic gradients across the charged membranes of neuronal processes is critical for sustaining the ability to conduct impulses. Neurotoxicants may disrupt the flow of a single ion, or they may impact multiple currents. For example, the type I pyrethroid insecticides allethrin and tetramethrin prolong Na^+ influx, lessen the peak of the Na^+ flow, and decrease the steady-state K^+ efflux, apparently by modulating resting (i.e., closed) Na^+ channels so that they open more slowly than normal. In contrast, tetrodotoxin blocks the extracellular pores of Na^+ channels, thwarting the inward flow of Na^+ ions and thus preventing propagation of any nascent action potential. Neurotoxic effects on ion channels often occur in the absence of structural lesions.

Unknown Impact on Neurotransmission

The pathogenesis for the delayed neurotoxicity in organophosphate-induced delayed neurotoxicity (OPIDN) remains incompletely understood. Certain OP classes (e.g., phosphoramidates and phosphonates) incite central-peripheral distal axonopathy (dying back polyneuropathy) in association with phosphorylation of a second enzyme, neuropathy target esterase (NTE). This molecule is an integral membrane protein in all neurons. Structurally, NTE is unrelated to AChE and other major serine esterases. The physiological role for NTE during adulthood is unknown; in development, NTE appears to control interactions between neurons and glia. Agents that cause OPIDN are postulated to bind covalently to the NTE active site. Ultimately OPIDN results in an abnormal propagation of neural impulses.

Oxidative Damage

Gradual accumulation of free radical-mediated damage to cellular macromolecules is a well-recognized pathway by which toxic agents can produce cell lethality. In the nervous system, the usual cellular targets are neurons due to their high metabolic rates and correspondingly outsized exposure to oxygen. Within neurons, oxidative damage has been postulated to disrupt expression of critical genes, damage cell and organelle membranes, and/or distort signaling pathways. The role of oxidative stress has been examined in the neurotoxicity of copper (Cu),

iron (Fe), manganese (Mn), rotenone, and other redox-active chemicals.

Certain toxicants can become concentrated in susceptible neurons, thereby extending the period during which oxidative injury can occur. For example, Mn is localized in the basal nuclei of primates, including humans, apparently due to efficient blood-borne delivery by the Fe-carrying protein transferrin and/or the strong affinity that Mn has for neuromelanin deposits in certain primate nuclei (e.g., *substantia nigra*). One proposed pathogenesis of Mn-induced neurotoxicity is oxidation of DA. The degree of DA modification may be raised synergistically in neurons with elevated intracellular concentrations of Fe, which is a potent oxidizing agent in its own right. Rodents are much less susceptible to Mn neurotoxicity as their basal nuclei neurons do not contain neuromelanin, and thus are less able to selectively sequester Mn.

Loss of antioxidant molecules in the nervous system is an indirect way of promoting damage by oxygen free radicals. For example, reduced glutathione (GSH), an intracellular reducing agent that protects against oxidative damage to cell macromolecules, is concentrated in the neuropil and white matter tracts of the CNS, especially astrocytes, but is expressed in high levels in only a few neuronal populations (e.g., cerebellar granule and Purkinje cells, sensory neurons in dorsal root ganglia). This distribution overlaps with the expression of xanthine oxidase (XO), an important enzyme that generates reactive oxygen species as a byproduct of purine catabolism; XO activity is present at much higher levels in astrocytes relative to neurons. Thus administration of 1,3-dinitrobenzene (DNB), which is metabolized by XO to form free radicals, injures astrocytes to a much greater extent than it does neurons.

Vascular Impairment

Increased vascular permeability (termed dysoria) resulting from damage to the BBB and/or blood–nerve barrier (BNB) is a common mechanism employed by several neurotoxicants. In this setting the microvasculature is the primary target for toxicity. Nonetheless once the barriers have been breached, other CNS cells may experience direct toxic effects of their own. For example, lead (Pb) neurotoxicity is associated with altered vessel diameters (constricted or narrowed); mural changes (endothelial swelling, necrosis); and thrombosis in CNS capillaries, especially those in the cerebrum and cerebellum. Neuropil near damaged vessels is edematous as a consequence of fluid and protein extravasation. Nearby neurons (cerebrocortical pyramidal cells and cerebellar Purkinje cells) become necrotic, and in chronic lesions there are associated with regional accumulation of reactive astrocytes. At least some neuronal death may arise from direct Pb-induced toxicity to neurons, since dead cells have been observed in CNS regions that lacked evidence of vascular damage. The primary changes induced by Pb in PNS trunks are Wallerian-like axonal degeneration and segmental demyelination mainly affecting motor nerves.

Instead of a definitive "barrier," it may be more useful to view the protection of the brain imparted by the specialized endothelial cells (and to a lesser extent astrocytes) of the BBB and BNB as selective gateways that allow the passage of some essential molecules and attempt to inhibit the passage of others. In fact, due to intended (due to anatomic variation) or unintended disruptions in the "barriers" as well as the numerous areas where the "barriers" are known to be less selective (e.g., some of the CVOs, certain brain nuclei especially hypothalamic nuclei), nearly every molecule, even large biologics, may enter the brain/spinal cord/nerves in some areas.

Multiple Mechanisms

Some neurotoxic agents appear to cause neural damage by several mechanisms at once. Hexachlorophene induces massive intramyelinic edema by uncoupling oxidative phosphorylation from ATP synthesis in oligodendroglia and by altering GABA concentrations in CNS neurons. Methylmercury produces profound neuronal necrosis in many brain regions by disrupting BBB permeability, altering neural cell metabolism, inhibiting synthesis of RNA and protein, and promoting oxidation and denaturation of cell proteins and membranes. Ethanol decreases DNA, RNA, and protein levels in neurons and astroglia and also incites apoptosis of neural cell precursors during development. In our experience, many agents elicit multiple chemical and molecular changes that can be linked to the induction or progression of neurotoxicity, and only careful attention to defining the appropriate study design can permit conclusions to be drawn regarding the primary mechanism of neurotoxic action.

SUMMARY

The regimented arrangement of anatomic and chemical attributes within the CNS and PNS dictate the functional responses by which an individual maintains homeostasis and interacts with his/her external environment. These same stereotypical features are responsible for the patterns of neurotoxic changes produced by numerous xenobiotics. The susceptibility of the CNS is further enhanced by the extraordinary metabolic needs and limited capacity for repair. Taken

together, these characteristics render the possibility of neurotoxic damage among the greatest challenges in navigating the world around us, and in bringing new chemical products to market.

The means for identifying new neurotoxic hazards as well as assessing and managing the risk posed by exposure to such agents are evolving as technical advances increase the affordability, speed, and utility of more detailed neuropathology assessments. The current reliance on limited batteries of functional (e.g., behavior, functional observational battery) and structural (e.g., gross lesions, brain weight, histopathology) endpoints for screening is a reasonable first-tier approach for use with general toxicity studies. More extensive investigations are the norm for second-tier instances where neurotoxicity has been observed or is predicted to be likely based on prior observations. Over time, we predict that current third-tier approaches like noninvasive imaging to follow disease progression throughout life and more extensive "omics" evaluations to explore molecular mechanisms responsible for neurotoxicity will be used on a more regular basis. The next decade or two hold considerable promise for a substantially improved understanding of neurobiology in both health and disease, and the knowledge gained using various toxicants to probe the CNS and PNS will be instrumental in this renaissance.

Further Reading

Bolon, B., Mellon, R.D., 2011. *Fundamental Neuropathology for Pathologists and Toxicologists: Principles and Techniques*. John Wiley & Sons, Hoboken, NJ.

Bolon, B., Bradley, A., Butt, M., Jensen, K., Krinke, G., Mellon, R.D., 2011. Compilation of international regulatory guidance documents for neuropathology assessment during nonclinical general toxicity and specialized neurotoxicity studies. Toxicol. Pathol. 39, 92–96.

Bolon, B., Bradley, A., Garman, R.H., Krinke, G.J., 2011. Useful toxicologic neuropathology references for pathologists and toxicologists. Toxicol. Pathol. 39, 234–239.

Bolon, B., Butt, M.T., Garman, R.H., Dorman, D.C., 2013. Nervous system. In: Haschek, W.M., Rousseaux, C.G., Wallig, M.A. (Eds.), Haschek and Rousseaux's Handbook of Toxicologic Pathology, third ed. Academic Press (Elsevier), San Diego, pp. 2005–2093.

Fix, A.S., Garman, R.H., 2000. Practical aspects of neuropathology: A technical guide for working with the nervous system. Toxicol. Pathol. 28, 122–131.

Garman, R.H., 1990. Artifacts in routinely immersion fixed nervous tissue. Toxicol. Pathol. 18, 149–153.

Garman, R.H., 2011. Histology of the central nervous system. Toxicol. Pathol. 39, 22–35.

Jessen, N.A., Munk, A.S., Lundgaard, I., Nedergaard, M., 2015. The glymphatic system: A beginner's guide. Neurochem. Res. 40, 2583–2599.

Kaufmann, W., Bolon, B., Bradley, A., Butt, M., Czasch, S., Garman, R.H., et al., 2012. Proliferative and nonproliferative lesions of the rat and mouse central and peripheral nervous systems. Toxicol. Pathol. 40, 87S–157S.

Mouton, P., 2002. *Principles and Practices of Unbiased Stereology: An Introduction for Bioscientists*. The Johns Hopkins University Press, Baltimore, MD.

Nayak, D., Roth, T., McGavern, D., 2014. Microglial development and function. Annu. Rev. Immunol. 32, 367–402.

Pardo, I.D., Garman, R.H., Weber, K., Bobrowski, W.F., Hardisty, J.F., Morton, D., 2012. Technical guide for nervous system sampling of the cynomolgus monkey for general toxicity studies. Toxicol. Pathol. 40, 624–636.

Spencer, P.S., Schaumburg, H.H., Ludolph, A.C., 2000. *Experimental and Clinical Neurotoxicology*, second ed. Oxford University Press, New York.

Vernau, W., Vernau, K.M., Bolon, B., 2011. Cerebrospinal fluid analysis in toxicological neuropathology. In: Bolon, B., Butt, M.T. (Eds.), Fundamental Neuropathology for Pathologists and Toxicologists: Principles and Techniques. John Wiley & Sons, Hoboken, NJ, pp. 271–283.

Walzer, M., et al., 2011. Oral toxicity of vigabatrin in immature rats: characterization of intramyelinic edema. Neurotoxicology 32, 963–974.

CHAPTER

22

Special Senses

OUTLINE

Fundamentals of Toxicologic Pathology.
DOI: http://dx.doi.org/10.1016/B978-0-12-809841-7.00022-8

CHAPTER

22a

Special Senses—Eye

Leandro Teixeira and Richard R. Dubielzig
University of Wisconsin-Madison, Madison, WI, United States

INTRODUCTION

The principal means by which most animals are made aware of their surroundings is the reflection or emission of light by external objects and the reception of this light by special cells in the eye called photoreceptors. However, reception of light is only the initial step of vision. Visual perception is the ability to interpret the surrounding environment by processing information contained in the visible light, and for that to be accomplished the whole visual system (eye, optic nerve, and cerebral cortex) needs to be involved. It is reported that humans obtain over 80% of all external information from vision. Visual impairment can have devastating health and socio-economic consequences, so risk assessment for toxicity of new chemicals and drugs with respect to the visual system is extremely important.

The evaluation of ocular tissues for efficacious or toxic effects has many challenges that are shared with nonocular tissues while others are eye-specific. One must understand the special requirements for tissue sampling, trimming, fixation, and histologic processing for eye specimens in general, and for the eyes of different species in particular, in order to obtain histologic sections of suitable quality. From the biologic and anatomic perspectives, one needs to be aware of the differences in ocular anatomy among species in order to differentiate toxicant-induced changes from normal anatomical variations. Because of the accessibility of the intraocular structures to clinical examination and detection of lesions *in vivo*, the accurate identification and diagnosis of microscopic findings requires an awareness and understanding of clinical ocular findings. On the same note, there is an almost complete overlap between the terminology in clinical ophthalmology and ocular pathology, so familiarization with clinical and diagnostic terms is essential for accurate communication. Once identified, ocular findings need to be proper classified as treatment-related, spontaneous, or iatrogenic. A multinational effort involving the Society of Toxicologic Pathology (STP), British Society of Toxicological Pathology (BSTP), European Society of Toxicologic Pathology (ESTP), the Japanese Society of Toxicologic Pathology (JSTP), and the Registry of Industrial Toxicology Animal data (RITA) in Europe is developing standardized nomenclature for classifying microscopic lesions observed in laboratory rats and mice in toxicity and carcinogenicity studies. This project, referred to as the International Harmonization of Nomenclature and Diagnostic (INHAND) Criteria for Lesions in Rats and Mice, has resulted in a list of accepted terms for "Nonproliferative and Proliferative Lesions of the Rat and Mouse Special Sense Organs (Ocular [eye and glands], Olfactory and Otic)," which may be accessed at https://www.toxpath.org/inhand.asp. These terms now are required in product registration packages submitted to the U.S. Food and Drug Administration (FDA) to ensure compliance with the "Standard for Exchange of Nonclinical Data" (SEND) guidance recently implemented by this agency.

STRUCTURE AND FUNCTION

The eye is a highly specialized organ that originates from multiple embryological layers, especially the neural crest, mesoderm, neuroectoderm, and surface ectoderm. This embryological tissue diversity becomes evident in the large spectrum of cellular differentiation as well as the complexity and specialization of the ocular tissues (Figure 22a.1). Table 22a.1 offers timelines for the comparative embryological development of the dog, mouse, and human eyes. The main function of the eye is through the cone and rod photoreceptors located in the retina, which transform light energy into electrical impulses (phototransduction) that are transmitted via the optic nerve to the optical centers of the brain. In order for impulses to be generated in the eye, the light needs to be effectively focused on the retina; proper focusing depends on structural characteristics like size and rigidity of the globe, corneal surface and lens curvature, and locations and optical clarities of the various

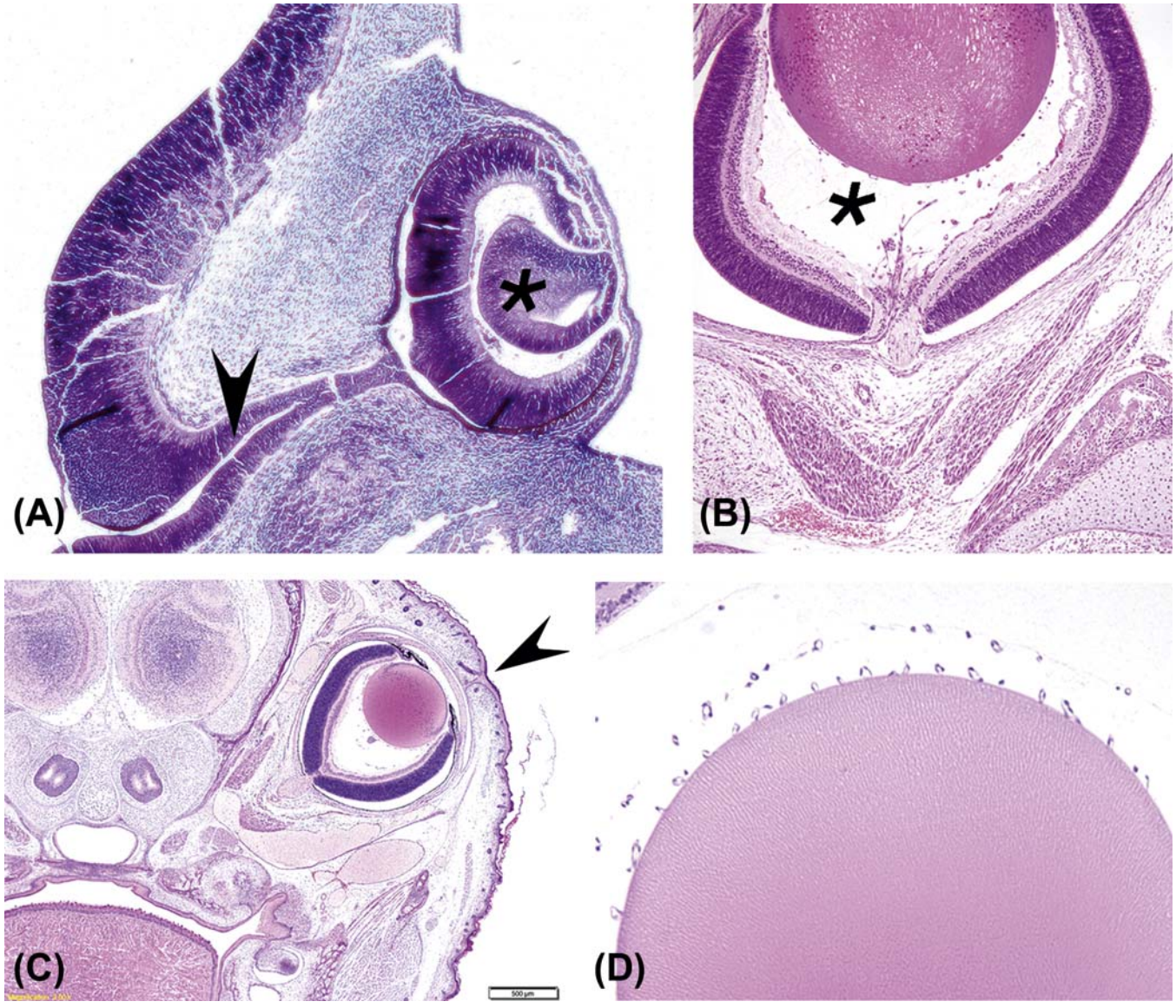

FIGURE 22A.1 Embryology of the mammalian eye. (A) Developing eye from a mid-term (gestational day 128) equine embryo showing the developing neuroretina [thick C-shaped layer lining the deep portion of the globe and encircling the lens vesicle (*)] and the optic stalk [or primitive optic nerve (*arrowhead*)]. (B) Near-term mouse fetus showing the primary vitreous (*) between the lens (pale eosinophilic orb at the top) and retina (thick multilaminar layer at the bottom). (C) Near-term mouse fetus showing the fused eyelids; the *arrowhead* points to the cleft where the palpebrae (eyelids) will eventually separate. (D) Lens from a near-term mouse fetus showing the *tunica vascularis lentis* [as small, regularly spaced capillary cross-sections along the posterior (upper) edge of the lens]. (A) Periodic acid-Schiff (PAS) stain, ×100; (B) H&E, ×200; (C) H&E, ×40; (D) H&E, ×200. Source: *From Haschek, W.M., Rousseaux, C.G., Wallig, M.A. (Eds.), 2013. The Handbook of Toxicologic Pathology, third ed. Academic Press, San Diego, CA, Figure 53.2, p. 2103, with permission.*

ocular tissues. These properties are acquired during development and must be maintained throughout life if the function of the eye is to remain intact.

The eye can be divided into three basic layers or tunics: (1) the fibrous tunic, the external part of the eye composed of the corneal and sclera; (2) the uveal tract, internal to the fibrous tunic and composed of the iris, ciliary body, and choroid, which houses the vascular supply to the eye; and (3) the internal neural layer, composed of the retina and optic nerve head. The eye can be further divided into anterior and posterior segments, the first consisting of the cornea, anterior and posterior chambers, iris, ciliary body, and lens, and the second composed of the vitreous and vitreal space, retina, choroid, sclera, and optic nerve.

Eyelids (Palpebra)

The eyelids' primary function in mammals is protection of the ocular surface from exposure or from the

TABLE 22A.1 Sequence of Ocular Development

Human (approximate postfertilization age)			Mouse (day postfertilization)	Dog (day postfertilization)	Developmental events
Month	**Week**	**Day**			
1	3	22	8	13	Optic sulci present in forebrain
	4	24	9	15	Optic sulci convert into optic vesicles
			10	17	Optic vesicle contacts surface ectoderm
		26			Lens placode begins to thicken
					Optic vesicle surrounded by neural crest mesenchyme
2	5	28	10.5		Optic vesicle begins to invaginate, forming optic cup
					Lens pit forms as lens placode invaginates
					Retinal primordium thickens, marginal zone present
		32	11	19	Optic vesicle invaginated to form optic cup
					Optic fissure delineated
					Retinal primordium consists of external limiting membrane, proliferative zone, primitive zone, marginal zone, and internal limiting membrane
					Oculomotor nerve present
		33	11.5	25	Pigment in outer layer of optic cup
					Hyaloid artery enters through the optic fissure
					Lens vesicle separated from surface ectoderm
					Lens surrounded by intact basement membrane (lens capsule)
					Retina: inner marginal and outer nuclear zones
			11.5	29	Basement membrane of surface ectoderm intact
					Primary lens fibers form
					Trochlear and abducens nerves appear
					Lid folds present
	6	37	12		Edges of optic fissure in contact
			12	30	Tunica vasculosa lentis present
					Lens vesicle cavity obliterated
					Ciliary ganglion present
		41	12	32	Posterior retina consists of nerve fiber layer, inner neuroblastic layer, transient fiber layer of Chievitz, proliferative zone, outer neuroblastic layer, and external limiting membrane
			17	32	Eyelids fuse (dog)
	7				Anterior chamber beginning to form
			12.5	40	Secondary lens fibers present
		48	14	32	Corneal endothelium differentiated
	8	51			Optic nerve fibers reach the brain
					Optic stalk cavity is obliterated
					Lens sutures appear
					Acellular corneal stroma present
		54		30–35	Scleral condensation present

(*Continued*)

TABLE 22A.1 (Continued)

Human (approximate postfertilization age)			Mouse (day postfertilization)	Dog (day postfertilization)	Developmental events
Month	**Week**	**Day**			
	9	57	17	40	First indication of ciliary processes and iris
					Extraocular muscles visible
					Eyelids fuse (occurs earlier in the dog)
	10			45	Pigment visible in iris stroma
					Ciliary processes touch lens equator
					Rudimentary rods and cones appear
				45-	Hyaloid artery begins to atrophy to the disc
3	12				Branches of the central retinal artery form
4				51	Pupillary sphincter differentiates
					Retinal vessels present
				56	Ciliary muscle appears
					Eye axis forward (human)
				56	Tapetum present (dog)
					Tunica vasculosa lentis atrophies
					Short eyelashes appear
5				40	Layers of the choroid are complete with pigmentation
6					Eyelids begin to open, light perception
					Pupillary dilator muscle present
7					Pupillary membrane atrophies
					Rod and cone inner and outer segments present in posterior retina
					Pars plana distinct
9					Retinal layers developed
					Regression of pupillary membrane, TVL, and hyaloid artery nearly complete
					Lacrimal duct canalized

Times represent gestational days (numbers only) or postnatal days (numbers annotated with "P").
From Haschek, W.M., Rousseaux, C.G., Wallig, M.A. (Eds.), 2013. The Handbook of Toxicologic Pathology, third ed. Academic Press, San Diego, CA, Table 53.1, pp. 2099–2101, with permission.

risk of accidental trauma. The lids also have important functions in tear film formation and distribution (see later). In rodents, rabbits, and dogs, the upper and lower lids are fused at birth and separate only after retinal development is adequate for vision (between 12 and 15 days of age in the mouse and rat). In the species commonly used in toxicity studies, the eyelid presents a palpebral (inner) surface lined by conjunctiva, a specialized lid margin that contains openings for multiple meibomian (sebaceous) glands, and haired skin on the outer surface. Carnivores, rabbits, and humans present an almond-shaped eye fissure, while most rodents and nonhuman primates have a round one. Lid closure is moderated by the *orbicularis oculi* (Figure 22a.2) and *levator palpebrae* muscles.

Of the test species of interest the dog, cat, and rabbit possess a *nictitating membrane (third eyelid)*, a large fold of conjunctiva that protrudes from the medial canthus over the corneal surface of the globe. The third eyelid is supported by a curved, T-shaped plate of hyaline cartilage, the base of which is surrounded by a mixed (seromucinous) gland, the gland of the third eyelid. The third eyelid mechanically protects the cornea, aids in tear distribution over the corneal surface, and contributes to 30%–50% of the aqueous portion of the tear film.

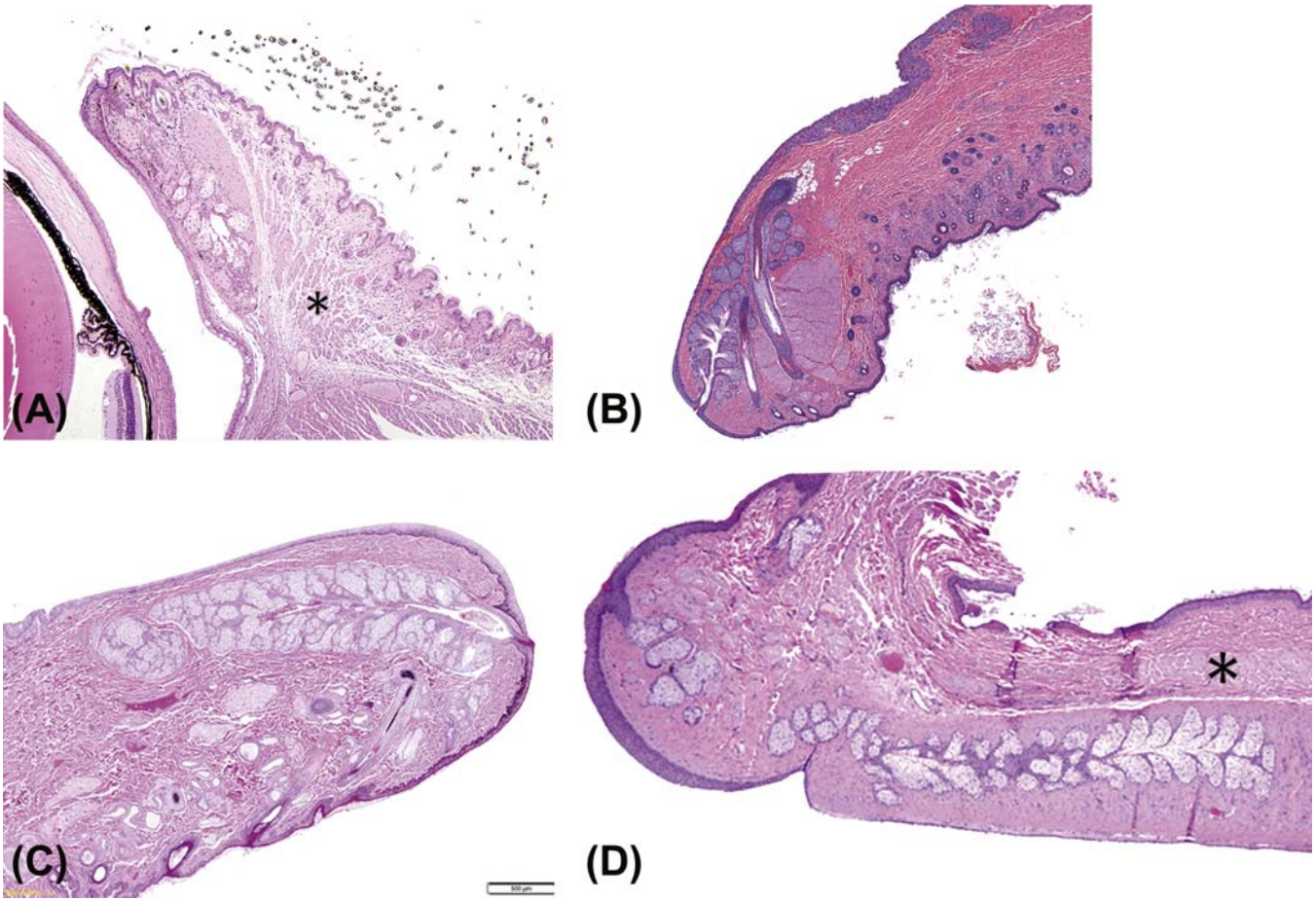

FIGURE 22A.2 **Normal eyelid architecture from various mammalian species used in ocular toxicity testing.** (A) Mouse, (B) rabbit, (C) dog, (D) nonhuman primate. Major features include haired skin on the external surface, nonhaired sebaceous (meibomian) glands with ducts reaching to the inner surface or mucocutaneous junction at the palpebral tip, and *orbicularis oculi* muscle (*). H&E, (A) ×12.5; (B–D) ×40. Source: *From Haschek, W.M., Rousseaux, C.G., Wallig, M.A. (Eds.), 2013. The Handbook of Toxicologic Pathology, third ed. Academic Press, San Diego, CA, Figure 53.6, p. 2114, with permission.*

Lacrimal System

The lacrimal system is comprised of a series of extraocular apocrine glands whose secretions contribute important elements to the tears that lubricate the surface of the eye. Primates (both human and nonhuman) only have one lacrimal gland, which is located dorsal and lateral to the globe. Dogs and cats have both an extraocular lacrimal gland and a gland of the third eyelid. Rodents and rabbits have lacrimal gland systems consisting of extraorbital (i.e., the exorbital lacrimal gland) and intraorbital (i.e., Harderian gland) components (Figure 22a.3). The intraorbital component is located behind the globe, and generally in a medial (nasal) location. The *lacrimal gland* is a seromucinous gland that contributes mainly to the aqueous component of the tears. However, significant quantities of lipid are present in the secretion of Harderian glands, particularly in rabbits. The continual formation of tears that moistens the ocular surface is largely done by the small (minor) lacrimal glands of the conjunctival fornix, with the major lacrimal glands mainly producing the excess tear formation (crying) that results from ocular discomfort. In all species, the glands' secretions contain enzymes and cytokines as well as antimicrobial substances (peptides and proteins) that protect the ocular surfaces.

The normal functions of the cornea are, in part, dependent on the existence of the *precorneal tear film*. This acellular fluid layer is adherent to the most superficial layer of the corneal epithelium and is composed of three main laminae: (1) the inner mucinous layer, secreted by the conjunctival goblet cells with contributions from the lacrimal glands, (2) the middle aqueous layer, secreted by the glands of the lacrimal system,

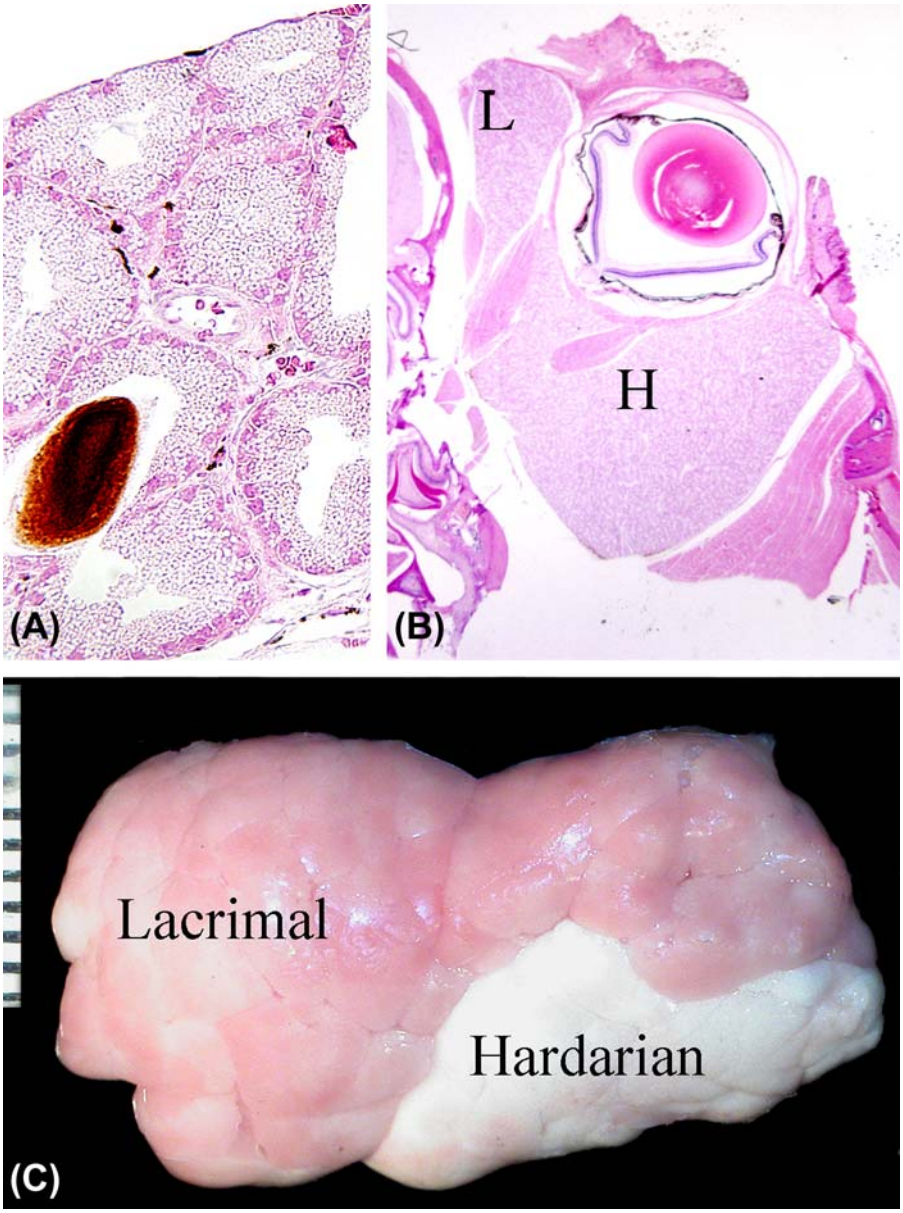

FIGURE 22A.3 Normal architecture of the Harderian and lacrimal glands. (A) High magnification image of the Harderian gland from an adult mouse showing the lipid vacuoles within the acinar epithelium and secreted porphyrin pigment within the lumen. (B) Low-magnification view of the mouse globe in situ showing the relative sizes of the Harderian (H) and lacrimal (L) glands. (C) The lacrimal and Harderian glands dissected from the orbit of a rabbit showing the difference in color. Scale, 1 interval = 1 mm. (A) H&E, ×200; (B) H&E, ×20. Source: *From Haschek, W.M., Rousseaux, C.G., Wallig, M.A. (Eds.), 2013. The Handbook of Toxicologic Pathology, third ed. Academic Press, San Diego, CA, Figure 53.5, p. 2109, with permission.*

and (3) the outer lipid layer, secreted by the sebaceous (meibomian) glands of the eyelid margins and the Harderian glands, particularly in rabbits. The tears are cleared from the ocular surface by a system of drainage ducts, in the conjunctiva near the medial canthus, called the nasolacrimal drainage system.

Cornea and Conjunctiva

Together the cornea and conjunctiva form the ocular surface. The cornea is the central translucent zone through which light reaches the intraocular structures, and the conjunctiva is the opaque mucosal tissue that lines the inner aspect of the eyelids (palpebral conjunctiva), the surface of the sclera (bulbar conjunctiva), and (when present) the inner and outer aspects of the third eyelid.

The *conjunctiva* has several main functions. These are maintenance of the tear film by secreting its mucinous component and aiding in its redistribution during blinking, to provide a loose flexible connection between the globe and the skin, to act as a mechanical barrier, and local immune surveillance through the conjunctiva-associated lymphoid tissue.

The conjunctival epithelium is a thin, multilayered, nonkeratinized epithelium that contains many

unevenly distributed goblet cells. At the limbus (the border between the cornea and the sclera), the conjunctival epithelium forms a specialized, circumferential zone containing the stem cells of the cornea. The cells that migrate and repopulate the corneal epithelium during normal cell turnover and under pathological cell loss that result in corneal defects are derived from these stem cells. The substantia propria, a connective tissue layer beneath the epithelium, contains numerous glands, and is densely populated with both blood and lymphatic vessels. The lymphatic vessels are more common than blood vessels in the underlying loose fibrous connective tissue.

The *cornea* is a highly specialized, highly ordered tissue with many unique anatomical features that render it transparent to light in the visible spectrum. The mammalian cornea is covered on the surface by several layers of nonkeratinizing, stratified squamous epithelium organized into three layers: a deep layer of basal cells resting on a basal lamina, an intermediate layer of "wing" cells, and a surface layer composed of multiple layers of squamous cells, the number of which depends on the species (mice, rats, and rabbits, 3–5 layers, and dogs, cats, and primates, 5–7). This epithelium has a remarkably uniform thickness and structural consistency across the entire surface of the cornea. A modified acellular region of stroma (Bowman's layer) composed of fine, randomly arranged collagen fibers is present posterior to the epithelial basal lamina in humans and nonhuman primates. Although Bowman's layer is not visible by light microscopy in the mouse, a thin layer of randomly arranged collagen fibrils can be seen immediately underneath the corneal epithelium by electron microscopy. The function of Bowman's membrane is not known. The bulk of the cornea is the stroma, which is located deep to Bowman's membrane (if one is present) or to the corneal epithelium (Figure 22a.4). Optical transparency of the cornea stroma is dependent on a precise spatial relationship between stromal collagen fibers, noncollagenous matrix, and the functional stromal cells (keratocytes). A monolayer of low cuboidal epithelial cells (corneal endothelium) separates the cornea from the aqueous humor of the anterior chamber. The corneal endothelium secretes Descemet's membrane, a thick basement membrane positioned between the endothelium and the inner surface of the corneal stroma. Descemet's membrane is composed mainly of laminin, fibronectin, and type IV collagen, which gives it elastic properties. The morphology of corneal endothelium is similar across mammalian species, but cellular density can vary from 2211 cells/mm^2 in the rat to 4450 cells/mm^2 in nonhuman primates and humans. The endothelium actively moves water and electrolytes between the corneal stroma and anterior chamber, thus supplying the cornea with nutritional support from the aqueous while maintaining corneal transparency (Figure 22a.5).

Sclera

The sclera forms the main part of the fibrous tunic of the eye and functions to protect the ocular contents, maintain intraocular pressure (IOP), and preserve the shape of the globe, even during contraction of the extraocular muscles, which have tendons inserted on the globe's surface. The sclera is relatively avascular and possesses great tensile strength, extensibility, and flexibility. It is composed of fibroblasts and dense irregular connective tissue containing mainly collagen type I. Anteriorly the sclera blends with the cornea at the limbus. The sclera surrounds the limbus and extends posteriorly where it is penetrated by the optic nerve exiting the eye at the lamina cribrosa. The sclera merges with dura mater that surrounds the optic nerve.

Uveal Tract

The uveal tract (or uvea) forms the continuous, heavily vascularized middle tunic of the globe. Its main functions are to provide the globe's blood supply and, through its high melanin pigment content, absorb reflected light and prevent glare when light is focused on the retina. The uveal tract can be divided into iris, ciliary body (anterior uvea), and choroid (posterior uvea).

The *iris* is a thin contractile circular tissue analogous to a camera diaphragm. It is cantilevered across the front of the globe where it separates the anterior from the posterior chambers. The anterior chamber represents the space between the cornea and the anterior surface of the iris, while the posterior chamber is the space between the posterior surface of the iris, lens, and anterior face of the vitreous. The chambers are connected by the pupillary space, which is formed within the marginal rim of the iris. Both chambers contain aqueous humor. The anterior surface of the iris has no epithelial lining, so aqueous is free to diffuse from the iris stroma to the anterior chamber with no barrier. The iris stroma consists of a loose connective tissue containing fibroblasts, melanocytes, and collagen fibers. The posterior surface of the iris is lined by simple cuboidal pigmented epithelium (posterior pigmented epithelium), which is in direct contact with the posterior chamber. Tight junctions between these cells create a barrier between the posterior chamber and iris stroma. Contractile

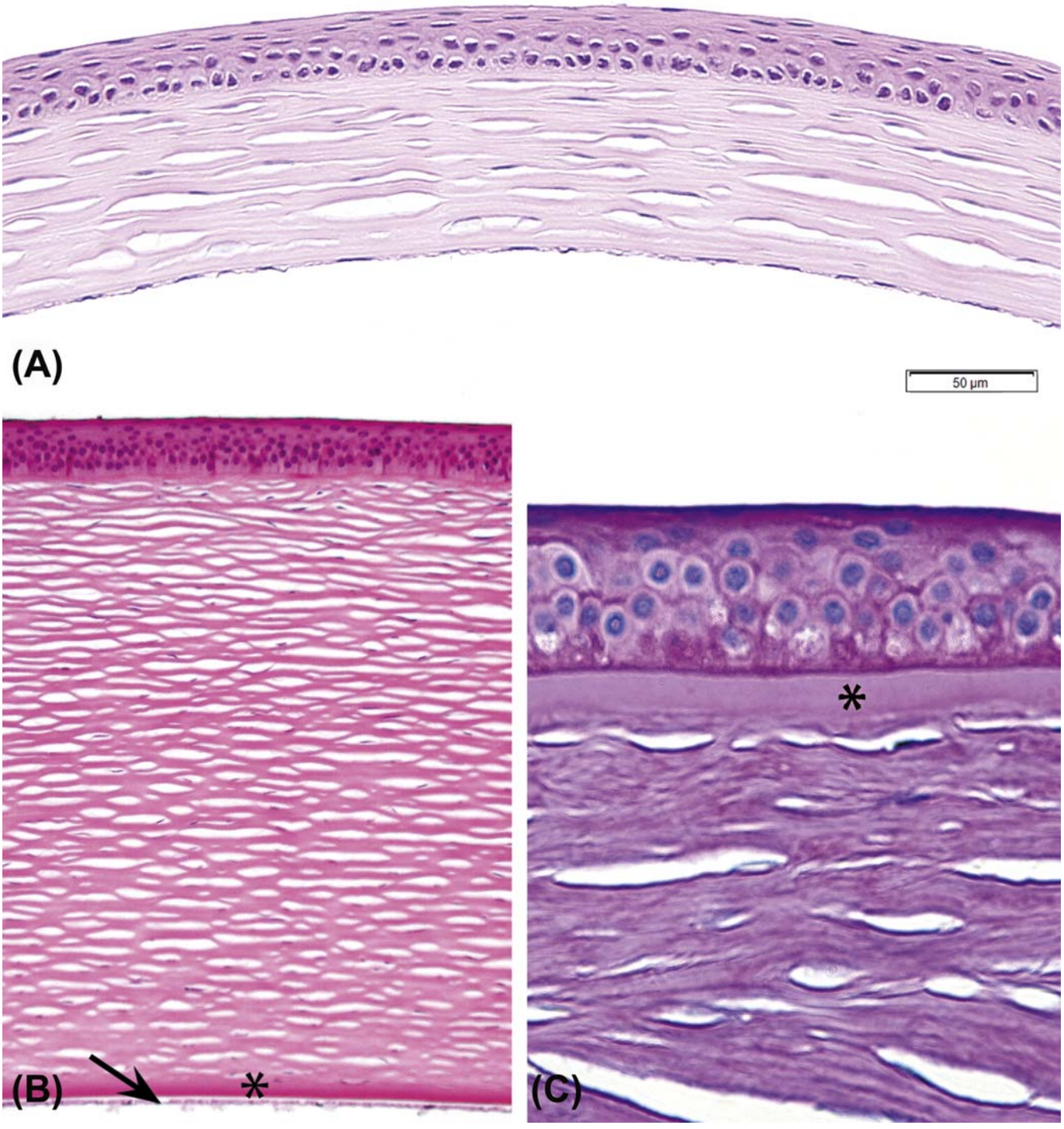

FIGURE 22A.4 Histopathological representations of the cornea. Axial (central) cornea from an adult mouse (A) and an adult dog (B) showing the relative thickness of the epithelium, stroma, Descemet's membrane (*), and corneal endothelium (*arrow*) in these two species. (C) Epithelium and anterior stroma of the cornea from a nonhuman primate stained to show Bowman's membrane (*). In all three images, the clear spaces within the stroma are processing artifacts and not vascular channels. (A) H&E, ×400; (B) H&E, ×400; (C) Periodic acid-Schiff (PAS), ×600. Source: *From Haschek, W.M., Rousseaux, C.G., Wallig, M.A. (Eds.), 2013. The Handbook of Toxicologic Pathology, third ed. Academic Press, San Diego, CA, Figure 53.10, p. 2124, with permission.*

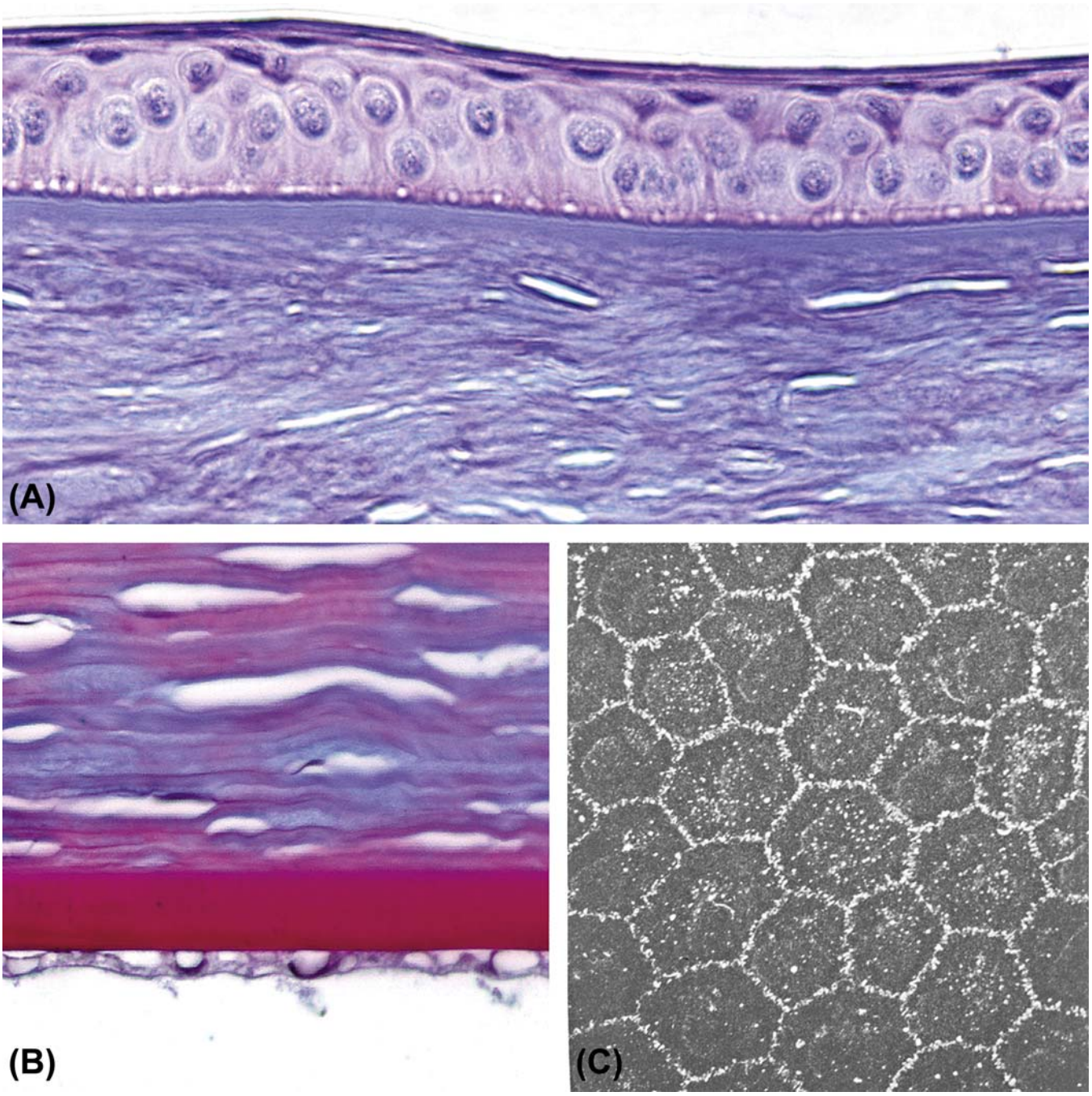

FIGURE 22A.5 **Normal architecture of the cornea.** (A) Epithelium and superficial stroma from a nonhuman primate cornea. (B) Posterior corneal stroma bordered by Descemet's membrane (thick red band) and the corneal (posterior) endothelium from a nonhuman primate. (C) Scanning electron micrograph of the surface of the corneal endothelium from a dog. (A) H&E, ×400; (B) PAS, ×600; (C) ×2500. Source: *From Haschek, W.M., Rousseaux, C.G., Wallig, M.A. (Eds.), 2013. The Handbook of Toxicologic Pathology, third ed. Academic Press, San Diego, CA, Figure 53.9, p. 2123, with permission.*

myoepithelial tissue forms the iris dilator muscle in the posterior iris stroma interior to the epithelium as well as the sphincter muscle that is positioned circumferentially at the leading edge of the iris (Figure 22a.6).

The *ciliary body* is subdivided into (anterior) pars plicata and (posterior) pars plana. In the pars plicata, there are multiple radially arranged folds, known as the ciliary processes. The inner aspect of the ciliary

body is lined by a neural tube-derived double epithelium composed of an inner layer of nonpigmented epithelium and an outer layer of pigmented epithelium. The ciliary epithelium secretes aqueous humor and vitreous glycosaminoglycans and collagen. The zonular ligaments that suspend the lens are also produced by the ciliary epithelium and are anchored on the epithelial apical basement membrane. The ciliary body stroma is similar to the iris stroma and contains the ciliary muscle, a smooth muscle which functions in visual accommodation by controlling the suspension of the lens and thereby its curvature. The ciliary muscle also plays a role in aqueous filtration in primates by regulating the tension of the trabecular meshwork (TM) at the level of Schlemm's canal. The relative tone of smooth muscle within the ciliary body controls the visual accommodation of the lens; thus the relative amount of smooth muscle present in the ciliary body is reflective of visual acuity. The ciliary muscle is robust in primates and accommodation is, by far, more effective in these species than in most other mammals. Accommodation is poor in rodents and dogs.

The *filtration apparatus* is made up of several structural features that function to reabsorb aqueous humor back into the blood. Aqueous is secreted into the posterior chamber, passes through the pupil into the anterior chamber, and is drained laterally though the TM situated within the iridocorneal angle (ICA) (Figure 22a.6). The balance between secretion and drainage of the aqueous humor determines intraocular pressure (IOP). The ICA is formed by the base of the iris and the corneal-scleral tunic. The ICA extends into the anterior ciliary body forming a recession, the ciliary cleft, or ciliioscleral sinus, where the TM is located. The TM is composed of crisscrossing beams of collagen and elastin that are covered by a unique population of endothelial-like trabecular cells. The TM is subdivided into three distinct layers: corneoscleral meshwork (CSM), uveoscleral meshwork, and juxtacanalicular or cribriform meshwork (JCM). There are two major pathways of aqueous drainage: (1) the classic pathway and (2) the alternative pathway. For the classic pathway, aqueous flows through the JCM, collecting ducts [Schlemm's canal, angular aqueous sinus, or

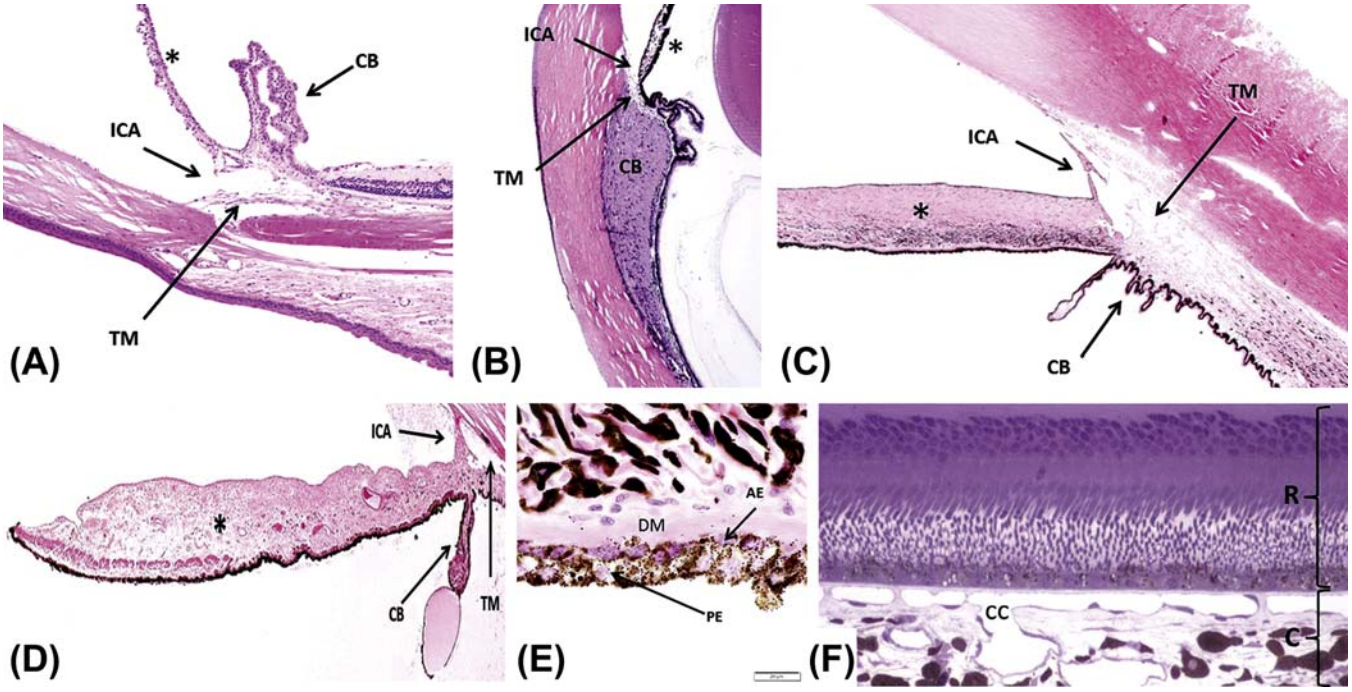

FIGURE 22A.6 Normal architecture of the uvea. The iridocorneal angle (ICA), iris (*), trabecular meshwork (TM), and ciliary body (CB) from an albino mouse (A), nonhuman primate (B), dark-eyed dog (C), and blue-eyed dog (D). Note the marked lack of pigmentation of the iris stroma, characteristic of light-colored eyes, in the mouse (A) and blue-eyed dog (D). (E) Posterior iris epithelium showing the pigmented posterior epithelium (PE), the anterior epithelium (AE) with melanin surrounding its nuclei on the apical (near the posterior epithelium) aspect, and the smooth muscle appearance of its basal aspect, which contains large amounts of myofilaments and forms the dilator muscle of the iris (DM). (F) The outer retina (R) and inner choroid (C) from a nonhuman primate that was perfusion-fixed to allow better observation of the capillary network, the choriocapillaris (cc). (A–D) H&E, ×12.5; (E) H&E, ×1000; (E) Toluidine blue, ×400. Source: *From Haschek, W.M., Rousseaux, C.G., Wallig, M.A. (Eds.), 2013. The Handbook of Toxicologic Pathology, third ed. Academic Press, San Diego, CA, Figure 53.13, p. 2136, with permission.*

angular aqueous plexus (AAP)], intrascleral channels, and exits the eye though the episcleral and conjunctival veins. In primates, rats, and mice, aqueous flows into Schlemm's canal, a continuous circumferential duct lined by endothelium. Schlemm's canal is absent in dogs, cats, and rabbits, which instead have intermittent drainage canals called the AAP that connects the CSM to the intrascleral venous plexus (Figure 22a.7). For the alternative pathway, aqueous flows into a potential space posterior to the TM (i.e., into the anterior face of the ciliary muscle and suprachoroidal space) just inside the sclera and is resorbed by vessels located within the choroid or sclera.

The *choroid* is the posterior portion of the uvea, a layer of blood vessels and connective tissue situated between the sclera and the retina. The main functions of the choroid are to deliver oxygen and nutrients to the high-metabolizing cells located in the outer retina, provide a conduit for vessels traveling to other parts of the eye, and absorb excessive light radiation, thereby reducing the amount of light reflection back to the retina. The choroid supplies oxygen and nutrients to

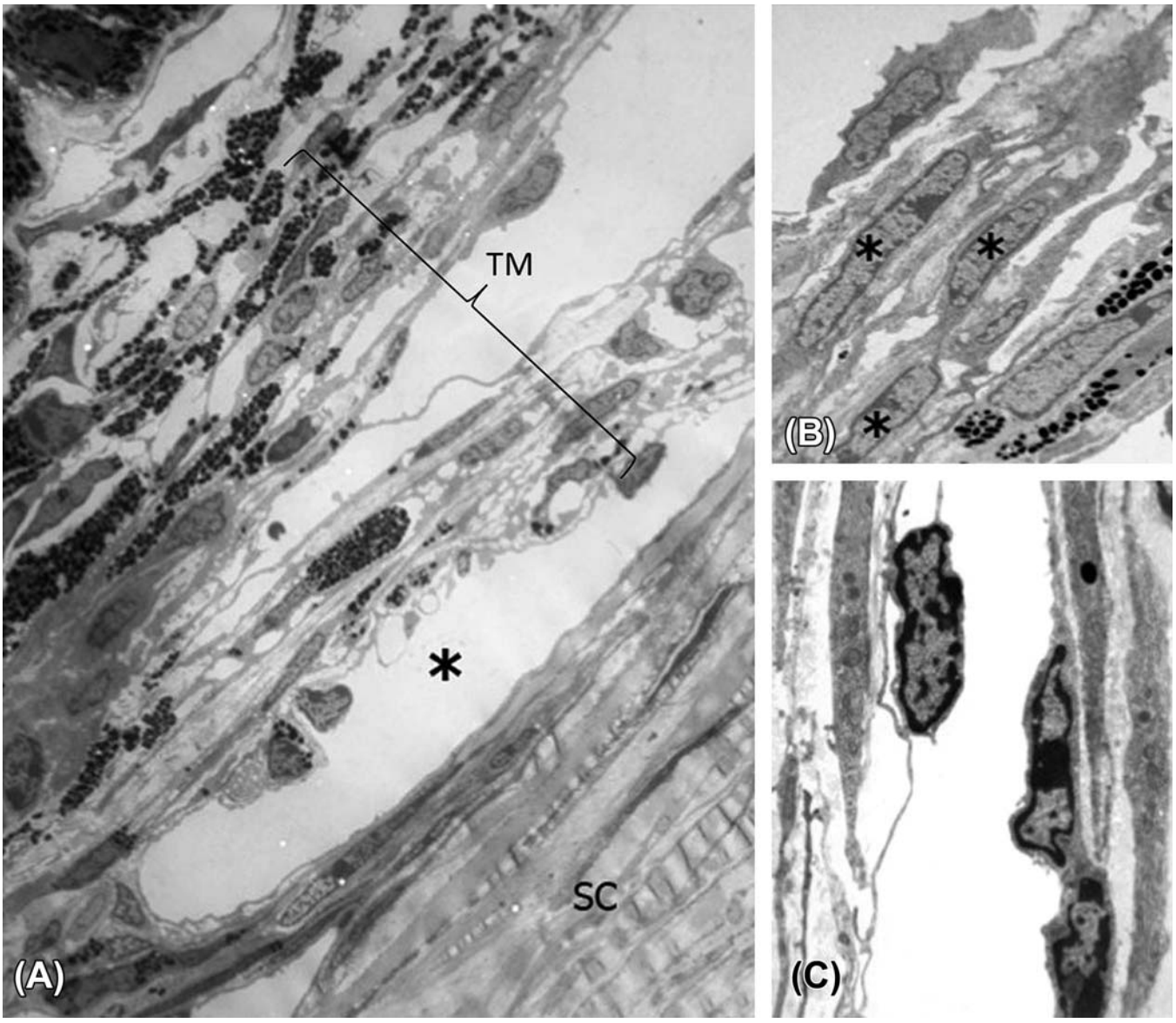

FIGURE 22A.7 Normal ultrastructural architecture of the trabecular meshwork (TM) and Schlemm's canal. (A) In the mouse, the TM, Schlemm's canal (*), and sclera (SC) may be shown to be closely related by transmission electron microscopy (TEM). (B) Trabecular beams composed of trabecular endothelial cells (*) surrounding a core of collagen fibers and small amounts of elastic fibers. (C) Detail of Schlemm's canal with vascular endothelial cells lining the lumen (central clear space). (A) TEM, ×2250; (B) TEM, ×3300; (C) TEM, ×7100. Source: *From Haschek, W.M., Rousseaux, C.G., Wallig, M.A. (Eds.), 2013. The Handbook of Toxicologic Pathology, third ed. Academic Press, San Diego, CA, Figure 53.15, p. 2139, with permission.*

the retina primarily through the choriocapillaris, an extensive interconnected capillary network located posterior to the retinal pigmented epithelial (RPE) cells (Figure 22a.6F). The choriocapillaris is separated from the RPE layer by Bruch's membrane, a structure formed by five layers: the RPE basal lamina, an inner collagenous zone, a middle elastic layer, outer collagenous zone, and the basement membrane of the endothelial cells of the choriocapillaris (Figure 22a.8). Bruch's membrane selectively filters the passage of macromolecules between the retina and choriocapillaris. Vessels of the choriocapillaris have a fenestrated endothelium through which macromolecules leak into the extracellular space of the choroid; this vascular network has the highest perfusion rate of any capillary bed in the body, which is reflective of the high metabolic demands of the ocular tissues. In humans, Bruch's membrane is subject to a variety of senescent changes representing a

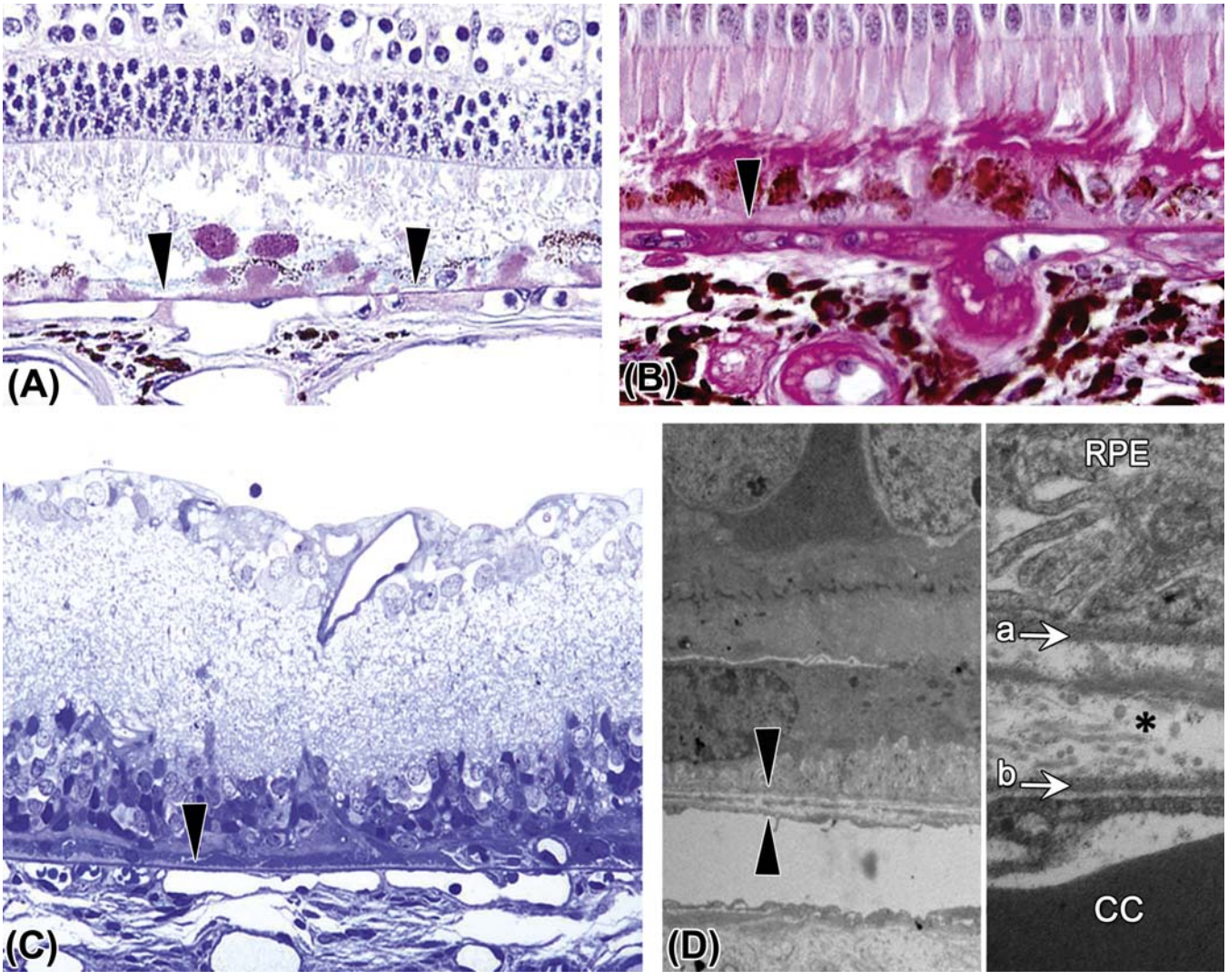

FIGURE 22A.8 **Normal architecture of Bruch's membrane.** This structure lies between the retinal pigmented epithelium (RPE) and uveal capillary bed (choriocapillaris). (A) Image of the outer retina from a dog demonstrating the location and uniform thickness of the normal Bruch's membrane (*arrowheads*). (B) Bruch's membrane (*arrowhead*) from a nonhuman primate with hypertension and diabetes, demonstrating irregular thickening. (C) Bruch's membrane from a rat with outer retinal atrophy, showing an intact Bruch's membrane (*arrowhead*) in spite of the marked outer retinal atrophy. (D) Transmission electron micrograph (TEM) from a rat showing the normal ultrastructural appearance of Bruch's membrane (between the two *arrowheads*). (E) At higher magnification, Bruch's membrane consists of an inner layer (a), formed by the basal lamina of RPE cells, and an outer layer (b), formed by the basal lamina of the choriocapillaris (cc). Between these two basal laminae the membrane contains delicate layers of collagen and elastic tissue (*). (A) Periodic acid-Schiff (PAS), ×200; (B) PAS, ×400; (C) Toluidine blue plastic section, ×200; (D) TEM, ×1025; (E) TEM, ×3100. Source: *From Haschek, W.M., Rousseaux, C.G., Wallig, M.A. (Eds.), 2013. The Handbook of Toxicologic Pathology, third ed. Academic Press, San Diego, CA, Figure 53.14, p. 2138, with permission.*

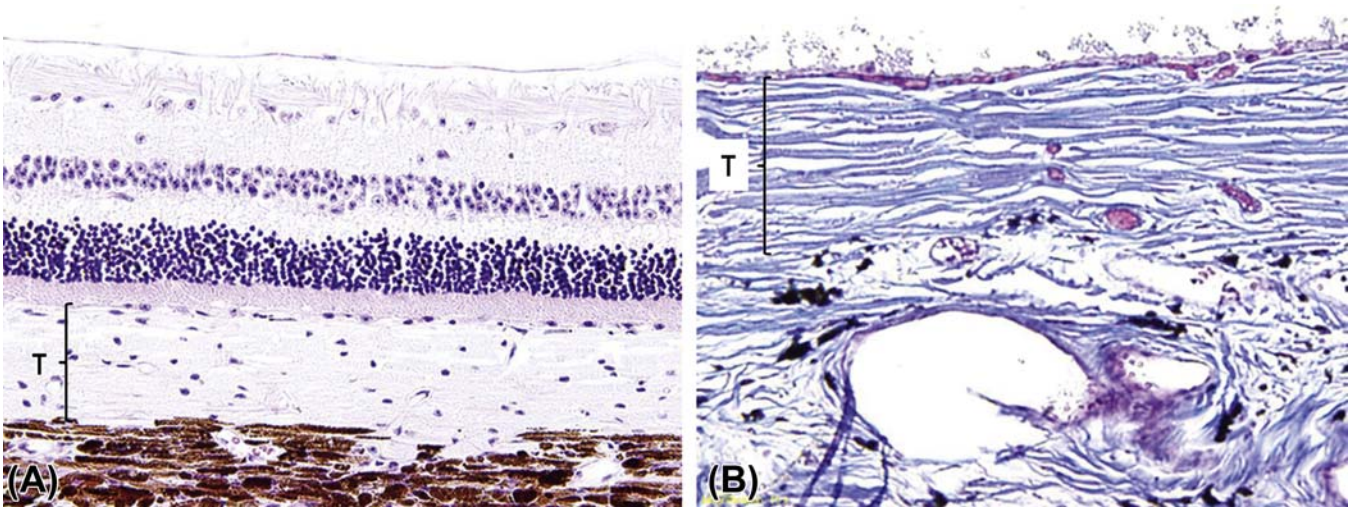

FIGURE 22A.9 **Normal architecture of the tapetum.** (A) Cellular tapetum (T) typical of a carnivore, such as a dog or cat. (B) Fibrous tapetum (T) from a goat, which is made up of collagen. (A) H&E, ×100; (B) Masson's trichrome, ×200. Source: *From Haschek, W.M., Rousseaux, C. G., Wallig, M.A. (Eds.), 2013. The Handbook of Toxicologic Pathology, third ed. Academic Press, San Diego, CA, Figure 53.27, p. 2127, with permission.*

significant cause of age-related visual defects, including age-related macular degeneration (AMD).

Most domestic species, including the dog and cat, have a tapetum lucidum, a layer of reflective tissue interspersed between the choriocapillaris and the mid-sized vessels. The tapetum is composed of a multilayered complex of polyhedral cells (iridocytes) that contain cytosplasmic light-reflective crystals. In the dog, these are composed of zinc cysteine (Figure 22a.9). The tapetum is thought to enhance vision under scotopic (dim light) conditions by reflecting light that has passed through the retina back to the photoreceptors, increasing their activation. The organelles and crystal composition of these cells varies across species, and may have drug-binding characteristics that are also species variable.

Lens

The lens is a transparent, exquisitely organized tissue composed of highly specialized cells (lens fibers) that plays an important role in the ocular optical system by refracting and focusing the light on the plane of the retina. It is suspended in the aqueous humor of the posterior chamber and held in place by the zonular fibers (zonules) and the anterior face of the vitreous body. Structurally the lens is composed of three parts: the lens capsule, the lens epithelium, and the lens fibers. The lens capsule is a thick and elastic basement membrane composed of collagen type IV and sulfated glycosaminoglycans. It is produced by the lens epithelium and completely envelops the lens. The anterior aspect of the capsule is characteristically thicker than the posterior portion. The lens epithelium is composed of simple cuboidal cells that are only present under the anterior and equatorial lens capsule. These cells become columnar and migrate toward the lens equator where they elongate, lose their nuclei, and transform to the relatively homogenous lens fibers that comprise the majority of the lens (Figure 22a.10). As the lens fibers elongate, they expand to become hexagonal structures up to 4×7 μm in cross-section and up to 12 mm in length, extending from the anterior to the posterior pole of the lens.

Vitreous

The vitreous body is an optically clear, viscoelastic, gel-like extracellular matrix that fills the vitreous cavity, the space that spans the distance from the posterior pole of the lens to the inner aspect of the retina. More than 95% of the vitreous gel weight is water, while the remaining balance is comprised of the structural components hyaluronon, heterotypic fibrils of collagens type II, V/XI, and IX; fibronectin; fibrillin; and opticin as well as a small population of resident macrophages (hyalocytes). The anterior face of the vitreous closest to the lens has a more robust collagen structure. The vitreous harbors matrix attachment points to the retinal inner limiting membrane, which help maintain the retina in place. Average vitreous volumes vary by species: human, 4.5 mL; dog, 2.9 mL; cynomolgus macaque, 2.2 mL; rabbit, 1.6 mL; rat, 0.03 mL (30 μL); and mouse, 0.01 mL (10 μL).

Retina

The retina is a highly differentiated and complex multilayered neural tissue derived from an outward

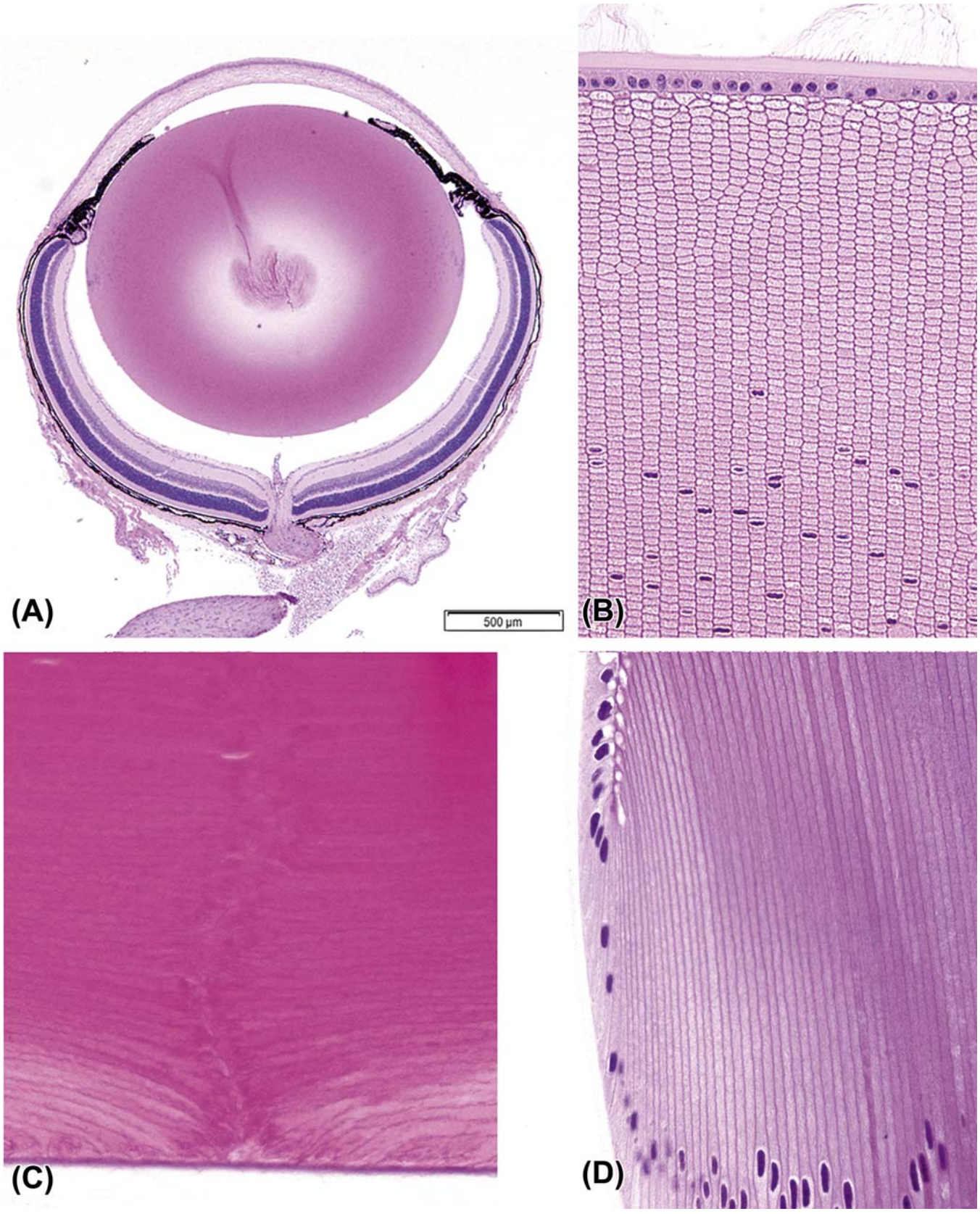

FIGURE 22A.10 **Normal architecture of the lens.** (A) Low-magnification image of an adult mouse eye showing the large relative size of the lens compared to other components of the globe. (B) The anterior pole of a mouse lens fixed with Davidson's fixative showing individual profiles of well-differentiated lens fibers. (C) The posterior pole of the lens from an adult dog showing the posterior suture (curved seam in the middle where fibers meet). (D) The equator of a rabbit lens showing the nuclear bow (*bottom*). (A) H&E, ×40; (B) H&E, ×400; (C) H&E, ×600; (D) H&E, ×600. Source*: From Haschek, W.M., Rousseaux, C.G., Wallig, M.A. (Eds.), 2013. The Handbook of Toxicologic Pathology, third ed. Academic Press, San Diego, CA, Figure 53.16, p. 2144, with permission.*

extension of the rostral neural tube. Vertebrate vision is initiated through the transduction of light energy to neural impulses by the retinal photoreceptors. The retina can be roughly divided into an inner and outer neural retina. The outer neural layer is supported by the retinal pigmented epithelium (RPE). The retina and RPE are not physically attached to one another, but are separated by a potential space. The outer neural retina, particularly the photoreceptor cells, consumes oxygen and nutrients at a higher rate than any other tissue in the body. For this reason, the choroidal blood supply to the RPE is designed to deliver oxygenated blood and remove metabolic wastes for the retina through high-volume, fast-flow rates. The metabolic needs of the inner retina are less than that of the outer retina, and are supplied by an endogenous retinal vasculature, which has a more conventional blood flow rate. Mice, rats, dogs, and nonhuman primates all have an extensive intrinsic retinal vascular bed (i.e., a holangiotic pattern) in addition to the choroidal system (Figure 22a.11). In contrast, rabbits have a limited retinal vascular system (i.e., a merangiotic pattern), and most of the retina lacks an endogenous blood supply. Vessels in the rabbit are located internal to the surface of the medullary rays, and are attached to the retinal surface by glial cell processes. The metabolic needs of the rabbit retina are largely met through diffusion from the medullary ray vasculature.

The *neural retina* is a nine-layered neural tissue responsible for phototransduction, and the signal processing across a three-neuron network that ultimately ends in the transmission of nerve impulses to the brain by the retinal ganglion cells. The layers of the neural retina are listed in the following order, from the inner to the outer layer of the retina (Figure 22a.12).

1. Inner limiting lamina (ILL). A thin, transparent basement membrane, synthesized by the basal foot processes of the Müller cells (retinal glia). The ILL separates the retina and the vitreous body.
2. Nerve fiber layer. Axons from the retinal ganglion cells, interspersed with astrocytes and other glial cells, form the nerve fiber layer that course across the surface of the retina to converge at the optic disc, forming the optic nerve.
3. Retinal ganglion cell layer. Ganglion cells are "third order" neurons that collect integrated signals from interneurons of the inner nuclear layer (INL) and transmit nerve impulses via the optic nerve to the brain. Astrocytes are also present in this layer.
4. Inner plexiform layer (IPL). Synapses between retinal ganglion cells and the interneurons of the INL (bipolar, amacrine, and interplexiform cells) are formed in the IPL.
5. Inner nuclear layer (INL). Nuclei of interneurons ("second order" neurons: bipolar, amacrine, horizontal, and interplexiform cells) and Müller cells (retinal glia) are housed in the INL.
6. Outer plexiform layer (OPL). Houses the synapses between the photoreceptor cells and the interneurons of the INL. Horizontal cells form connections between groups of rods and cones through lateral synapses. Rod spherules and cone pedicles also reside in the OPL.
7. Outer nuclear layer (ONL). Houses the cell bodies and nuclei of the rod and cone photoreceptors. Rod cell nuclei are distributed throughout the layer, while cone nuclei form a row inner to the external limiting membrane. Photoreceptor axons extend into the OPL, while dendrites form the photoreceptor segments.
8. Outer limiting membrane (OLM). Visualized as a line on H&E, the OLM reflects the presence of an anastomosing network of tight junctions formed between photoreceptor cells and Müller cells.
9. Photoreceptor Segments. Photoreceptor dendrites form the inner and outer segments of the retina. The portion of the dendrite residing in the inner segment has a high content of mitochondria, Golgi apparatuses, and rough endoplasmic reticulum, all of which are necessary for high-efficiency protein synthesis. Phototransduction occurs in the outer segment, which houses the discs of the rods and cones.

While the circuitry and function of the retina is remarkably conserved in vertebrates, marked morphological variation in the retina does exist for among species. Perhaps the most important differences to be considered in toxicologic studies are the vascular pattern (described earlier) and distinctive distribution of photoreceptors (rods and cones). As a rule, the cones (which are specialized in the discrimination of color and detail) are concentrated in the central retina, while the rods [adapted for performance in dim light (i.e., for low resolution)] are more common at the peripheral retina. Most primates, including humans, possess a fovea (also termed the *fovea centralis*), which is a small circular region characterized by a higher concentration of cones. The fovea is located in the temporal retina near the optic nerve and is responsible for sharp vision. The fovea in primates in turn is surrounded by the macula, a larger retinal region that exhibits an increased ganglion cell density. In contrast, other laboratory animal species have an *area centralis*, a specialized region that has both more cones and greater retinal ganglion cell density. With the exception of rabbits, the area centralis often is located in the central retina temporal to the optic nerves. Rabbits possess a

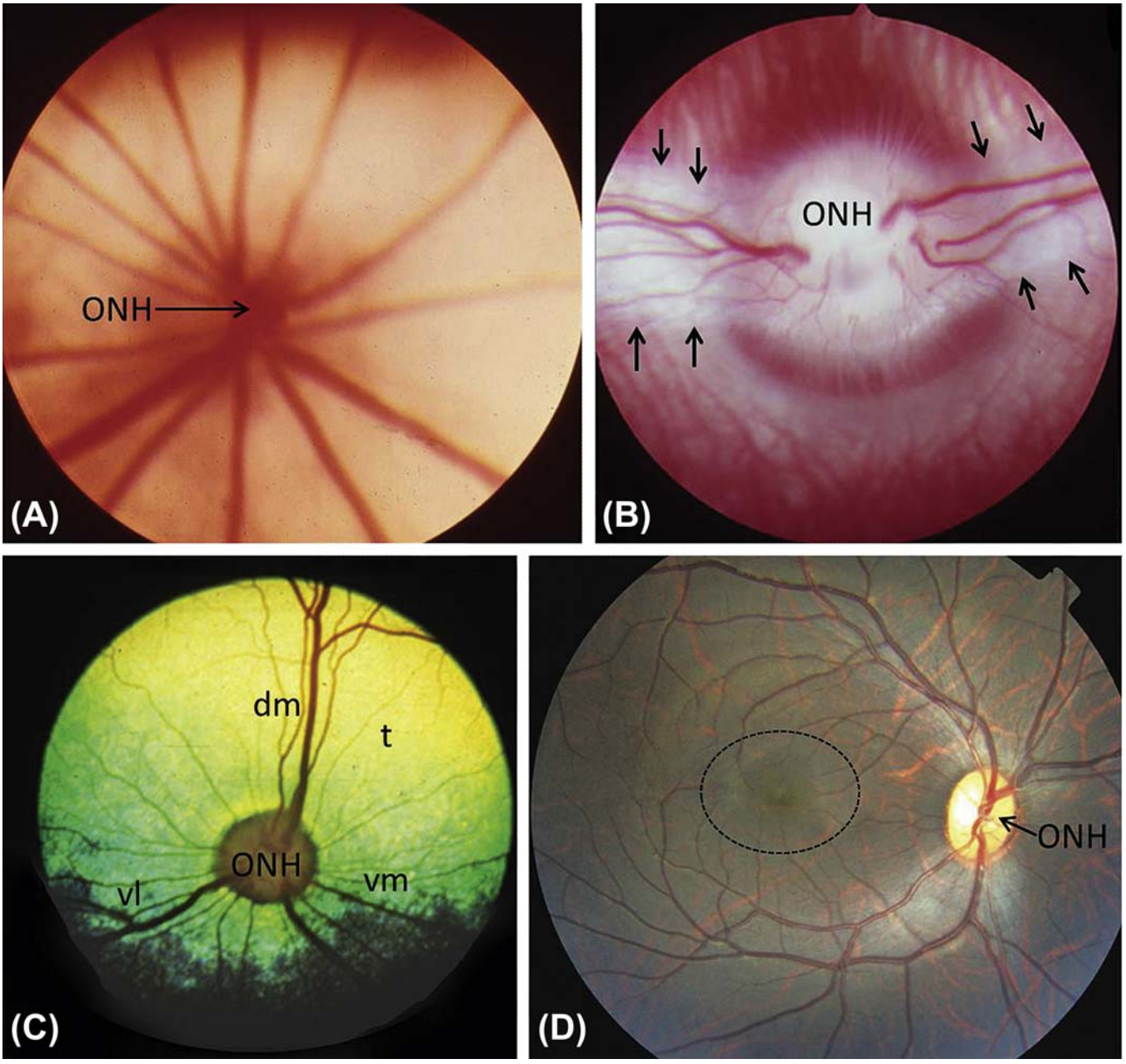

FIGURE 22A.11 **Gross anatomy of the optic fundus.** (A) Albino mouse, holangiotic fundus with blood vessels radiating outward widely from the optic nerve head (ONH). (B) Albino rabbit, merangiotic retina, with retinal vessels emanating from the ONH only in discrete zones along the horizontal plane; these zones, or medullary rays (between *arrows*), represent a thick white band of myelinated nerve fibers that are characteristic of the rabbit. (C) Cat. Holangiotic retina, with retinal vessels departing the ONH in all directions but especially in the dorsomedial (dm), ventrolateral (vl), and ventromedial (vm) directions. The cat has a prominent, highly reflective yellow-green tapetal area (t) dorsally. (D) Nonhuman primate. Holangiotic fundus, with retinal vessels exiting the ONH in all directions but arcing around the relatively avascular—and thus vulnerable—macula (*dotted circle*). This fundus image is almost indistinguishable from a human fundus. Source*: From Haschek, W.M., Rousseaux, C.G., Wallig, M.A. (Eds.), 2013. The Handbook of Toxicologic Pathology, third ed. Academic Press, San Diego, CA, Figure 53.22, p. 2160, with permission.*

visual streak, which is a linear, horizontal band (2−3 mm wide) of increased cone and ganglion cell density. This visual streak is located ∼3 mm ventral to the optic disc, and runs parallel and below the ventral margin of the medullary ray.

Retinal Pigmented Epithelium

The RPE is derived from neural tube ectoderm and is analogous to ependymal cells in form and function. As the optic vesicle folds on itself to form the optic

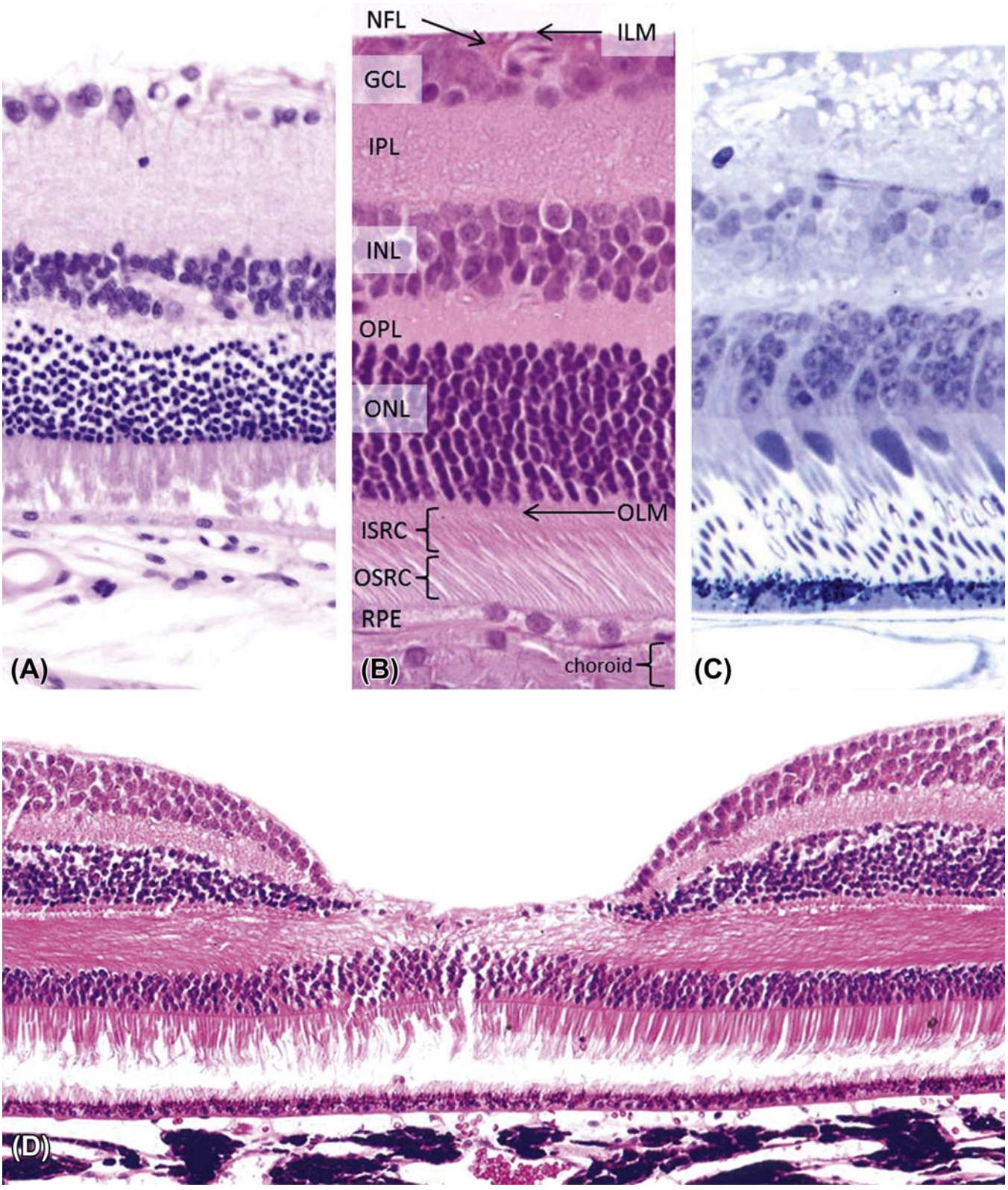

FIGURE 22A.12 **Normal architecture of the retina.** (A) Normal retina from an albino mouse. (B) Area centralis from a normal cat retina, with the retinal layers labeled from outside (bottom) to inside (upper). (C) Plastic section of the retina from a nonhuman primate. (D) Image of the fovea from a nonhuman primate retina. This site contains a heightened number of cone photoreceptors, and thus is critical for proper perception of color and visual acuity in bright light. (A,B) H&E, ×400; (C) Toluidine blue, ×400; (D) H&E, ×200. Abbreviations (listed from top): ILM, inner limiting membrane; NFL, nerve fiber layer; GCL, ganglion cell layer; IPL, inner plexiform layer; INL, inner nuclear layer; OPL, outer plexiform layer; ONL, outer nuclear layer; OLM, outer limiting membrane; ISRC, inner segments of rods and cones; OSRC, outer segments of rods and cones. Source: *From Haschek, W.M., Rousseaux, C.G., Wallig, M.A. (Eds.), 2013. The Handbook of Toxicologic Pathology, third ed. Academic Press, San Diego, CA, Figure 53.20, p. 2154, with permission.*

cup, the RPE remains as a single cell layer in direct contact with the outer cells of the neural retina, which eventually become the photoreceptor cells. The photoreceptor cells and the adjacent RPE function as a unit, and together are responsible for phototransduction.

The RPE cells are smooth and hexagonal in shape when viewed from the inner surface. In histologic sections, the RPE cells consist of an outer nonpigmented basal region with an oval nucleus and an inner, pigmented portion, which extends as a series of straight villous processes between the photoreceptor outer segments. The basal surface of the RPE cells is characterized by extensive infolding. The basal lamina of the RPE cell forms the innermost layer of the five-layered Bruch's membrane, which separates the retina from its rich vascular supply in the choriocapillaris. There is an anastomosing network of tight junctions near the apex of the RPE cell layer that forms the outer blood–retinal barrier, which is similar in structure and function to the blood–brain barrier (Figure 22a.8). The melanin pigment in the RPE protects the outer retina from excessive light reflection and glare, and thus from unrestrained oxidative damage. The RPE also secretes the interphotoreceptor matrix (IPM), a specialized extracellular matrix containing hyaluronan, proteoglycans, glycosaminoglycans, matrix metalloproteases, and growth and immunosuppressive factors that mediates key interactions between the photoreceptors and RPE including adhesion, phagocytosis, outer segment stability, nutrient exchange, development, and vitamin A trafficking in the visual cycle. The IPM also helps prevent vascular proliferation in the surrounding tissues.

Optic Nerve

The term "optic nerve" is a misnomer since this structure actually is a central nervous system (CNS) tract. The optic nerve is composed primarily of the axons from retina ganglion cells (RGC), which extend from the inner retina, coursing posterior, and centripetally within the inner nerve fiber layer to converge into bundles at the optic nerve head (also known as the optic disc) and form the nerve. The position of the optic disc demonstrates some species variation. In dogs, primates, and rodents, it tends to be positioned in the equatorial region, in the rabbit, and in the dorsal posterior pole. The central area of the optic disc is depressed and is supported by a thickening of the retinal inner limiting membrane (called the supporting meniscus of Kuhnt). Before exiting the eye, the RGC axons are arranged into bundles surrounded by retinal astrocytes. As the axon bundles exit the eye posterior to the choroid, they transverse an open meshwork of horizontally oriented collagenous beams or plates continuous with the sclera (lamina cribrosa). The lamina cribrosa (LC) contains elastin and provides structural support for the nerve. In glaucoma, physical distortion of the globe resulting from elevated IOP causes outward bowing of the LC; the physical distortion and misalignment of the laminar plates results in axon compression, atrophy, and subsequent ganglion cell death. The composition of the LC is similar across species, but there are structural differences. Nonhuman primates, pigs, dogs, cats, and rabbits have a robust LC comparable to humans; in rats, single bundles of collagen form the trabeculae, resulting in a delicate LC (Figure 22a.13). Mice do not have a distinct LC. The axons of the optic nerve are myelinated by oligodendrocytes; the extent of myelination varies across species. In dogs, myelination occurs within the optic disc, with variable extension within the peripapillary nerve fiber layer. The rabbit presents a unique arrangement in that it has a medullary ray, a myelinated and vascularized region on either side of the optic nerve. In other species (nonhuman primates, cats, pigs, and rodents), myelination commences at the outer margins of the LC similar to humans. The optic nerve proper is surrounded by extensions of the three meningeal sheaths of the CNS.

The neural signals initially processed by the retina are transmitted to the optical centers of the brain for further integration. Impulses arising in the retina travel via the axons of the ganglion cells through the optic nerves, where they undergo a variable degree of crossing (decussation) before entering the optic tract. Axon crossing is an adaptive feature that allows the brain optical centers to view the same hemispheric visual field from both eyes. Generally, fibers from the temporal retina project to the ipsilateral hemisphere while fibers from the nasal retina cross to the contralateral side. The amount of decussation, however, varies among species. The percentage of axonal crossover is approximately 50% in humans and most primates, 25% in dogs, 33% in cats, and up to 99% in rodents and rabbits. After leaving the optic chiasm and entering the optic tract, signals from the retina reach the lateral geniculate nucleus (LGN), a relay center in the thalamus that exerts dynamic control over the amount and nature of information that is transmitted to the visual processing centers of the brain. Primates and carnivores have a laminated dorsal LGN due to the large number of axons arriving from the contralateral retina, while rodents and rabbits (which have almost no decussation) do not exhibit LGN lamination. Axons from the LGN neurons form the optic radiations that relay visual signals to their final destination in the visual (occipital) cortex, where impulses will be integrated to produce images. In most mammals, the optic

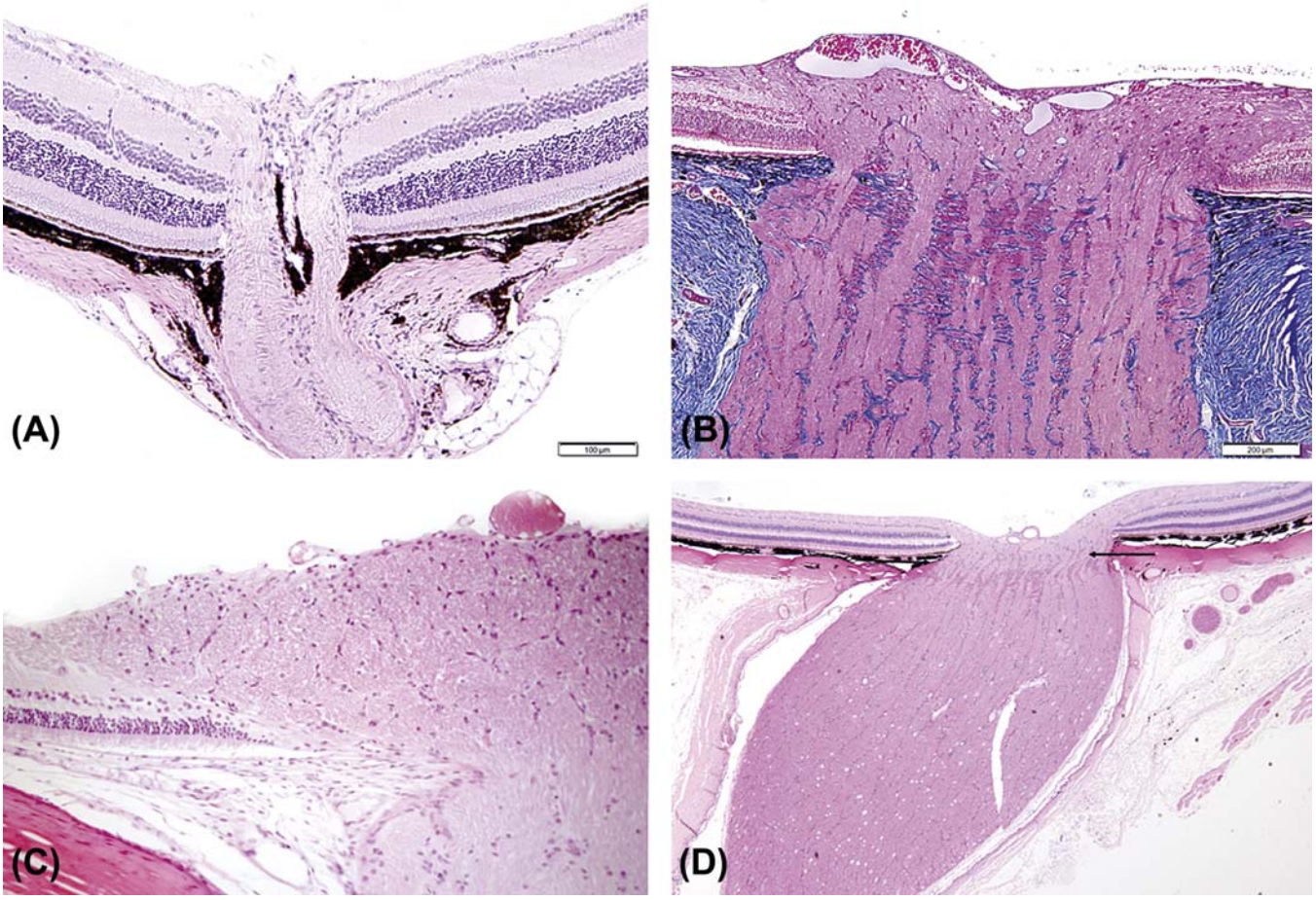

FIGURE 22A.13 **Normal architecture of the optic nerve.** (A) Mouse optic nerve, demonstrating the absence of the lamina cribrosa. The presence of pigmented cells within the optic nerve head is a normal variation. (B) Dog optic nerve, highlighting (in blue) the many parallel collagenous beams of the lamina cribrosa. (C) Rabbit optic nerve, showing the thick optic nerve head is composed of a large concentration of myelinated ganglion cell axons that form the retinal medullary ray and the vessels in the retinal surface (merangiotic vasculature). (D) Nonhuman primate optic nerve, resembling that of humans, has a prominent lamina cribrosa (*arrows*) and a central retinal artery that can be observed as a circular profile on the inner aspect of the optic nerve head. (A,D) H&E, ×12.5; (B) Masson's trichrome, ×100; (C) H&E, ×200. Source*: From Haschek, W.M., Rousseaux, C.G., Wallig, M.A. (Eds.), 2013. The Handbook of Toxicologic Pathology, third ed. Academic Press, San Diego, CA, Figure 53.31, p. 2173, with permission.*

radiations also contain reciprocal fiber tracts of axons from neurons in the visual cortex that descend to the LGN and rostral (superior) colliculus (a midbrain structure, often termed the "optic tectum," that helps direct certain visual-related behaviors), thus enabling feedback control of the visual signal processing.

EVALUATION OF TOXICITY

Use of Animal Models

In preclinical drug development, animal test systems are the backbone of hazard identification and risk assessment. While *in vitro* test systems are being used increasingly to probe relevant questions, none of the current methods for culturing ocular tissues can mimic the whole animal setting in performing these safety assessment functions. When choosing the most appropriate animal test system in an ocular toxicity experiment, many factors need to be considered. The most important of these factors are described here.

The model should be well characterized. The animal species that are commonly used as models in ocular toxicologic pathology are rodents (mouse, rat); rabbits; and larger animals (dog, nonhuman primate). Although there may be specific reasons to choose some other species, the bias for using one of these animal models is founded in the large mass of historic data (with well characterized background changes and expected variations), desirable husbandry characteristics, including knowledge regarding their potential effects on ocular health, and proven and familiar standard operating procedures and handling protocols.

The model should be appropriate for the experimental question. Although small rodents have incalculable value as test models in toxicologic pathology, the small size of the rodent eye and the relatively large size of the lens often preclude the use of such models when certain in-life procedures are a part of the experimental design. Some examples of procedures that are either unachievable or achievable only with great effort and/or risk in rodents are intraocular injections, sampling of aqueous or vitreous, tonometry (measures of IOP), fundoscopy (visual evaluation of the retina), and conventional surgery (e.g., glaucoma filtration procedures). On the other hand, the small eye size in rodents makes it possible to sample the entire eye by making serial or short-interval step sections through the globe.

The model should be anatomically appropriate. The usual species of interest when evaluating the impact of ocular toxicants to the visual system is the human. While eyes of vertebrates share many more similarities than differences regarding structure and function, many experimental hypotheses are most reliably answered using an animal model that best recapitulates the anatomic and functional properties of the human situation. Largely for this reason, nonhuman primates are almost a default favorite as the animal model of choice.

The model should be useful for both acute and chronic studies. It is not efficient to use animal models where aging is an important part of the testing strategy if the animal in question takes 10 years or longer to age. Laboratory rodents achieve advanced age in 2 years, making them useful for chronic toxicity studies.

The model should be cost effective. Small rodents provide obvious cost efficiency, although careful consideration should be given to the likelihood of success if certain protocols and procedures are to be employed.

The model should be appropriate for answering questions about efficacy. Many animal models of disease have been developed to mimic aspects of particular human ophthalmic diseases. These models may be useful in drug testing, particularly when evaluating molecule effectiveness. Some examples are genetically engineered mice models of the distinctive human retinal disease (e.g., Leber's congenital amaurosis) and spontaneous canine models of dry eye.

Ocular Diagnostic and Functional Tests

Multiple experimental endpoints in toxicity and drug development studies are measured by clinicians or an ophthalmologist rather than a pathologist. For example, nonhuman primate models with induced high IOP treated with IOP-lowering drugs can be monitored rapidly and quantitatively by measuring the IOP antemortem using a tonometer without the need to necropsy valuable animals. Many analytical procedures are available for the clinical examination of eyes in live animals (Figure 22a.14). The ophthalmic diagnostic and functional tests most commonly used in toxicology and drug development are described in Table 22a.2.

Morphologic Examination of the Ocular Tissues

Light microscopic examination of the eye requires several factors including: knowledge of the clinical ophthalmic findings, an understanding of comparative ocular anatomy and histology, an awareness of iatrogenic ocular findings and artifacts, an awareness of toxicant-induced changes that may occur in ocular tissues, knowledge of appropriate terminology, and good histologic sections of globes. Of that list, one of the most basic factors, and conversely the one that generates the most enquiries, is the histologic processing of ocular tissues. The basic concepts and procedures for proper ocular tissue fixation and trimming vary from those of other tissues, and so deserve reiteration here.

Tissue Fixation and Handling

Intact globes usually will be fixed by immersion of the entire organ, typically with a portion of the optic nerve. When fixing larger eyes, an intravitreal (IVT) injection of the fixative (0.1−0.3 mL by a 25−27 ga needle) or initially submerging the eye in the fixative for a brief (5−30 minutes) period of time before making a small (5 mm long axis) window in the equatorial sclera are possible (but not necessary) additional steps to insure proper fixation. The excess soft tissues including eyelids, muscles, orbital tissues, and (in rodents) the Harderian glands typically should be removed before fixation. However, there are special circumstances where tissues adjacent to the globe should be kept intact and sampled along with the globe. These might include cases where a surgical field is important (e.g., to define where a glaucoma device was oriented, when analyzing the effects of subconjunctival injections, or to evaluate the invasiveness of a tumors adjacent to the eye). Many options exist for suitable fixation of ocular tissue, each with its own advantages and disadvantages. Regardless of the fixative used, the volume of tissue to be fixed should be kept to a minimum, without sacrificing the integrity of the tissue's anatomic orientation. In most cases, not less than 10 volumes of fixative should be used for one volume of tissue (e.g., 10 mL of solution per 1 gram of tissue). The commonly used fixatives for ocular tissues

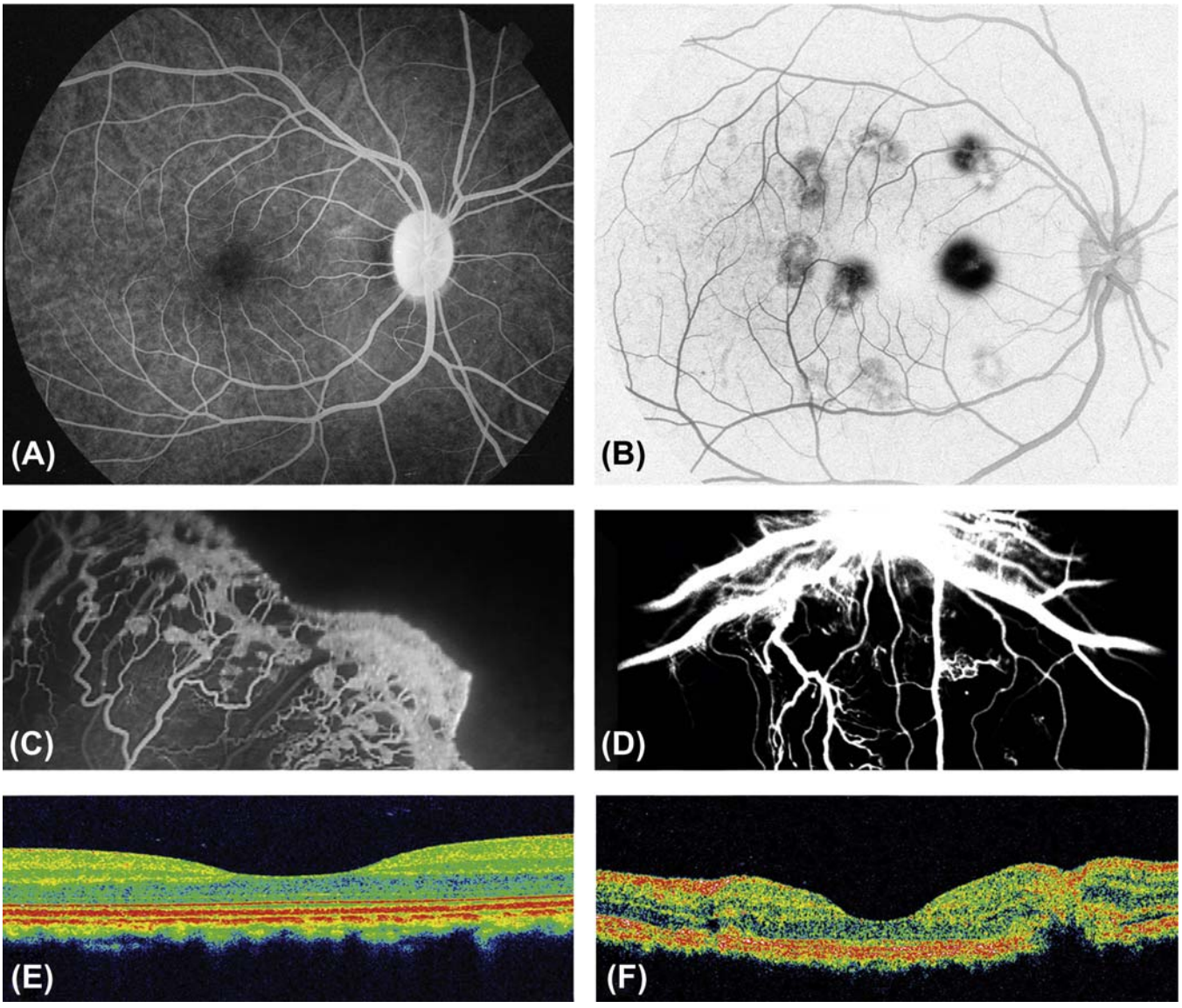

FIGURE 22A.14 **Special techniques for ocular safety assessment.** (A–D) Fluorescein angiography of retinal vasculature. (A) Positive image of fluorescein angiography from a normal (control) nonhuman primate. (B) Negative image of fluorescein angiography from a nonhuman primate in which laser burns (dark spots) were used to destroy Bruch's membrane, causing vascular proliferation and leakage, as a model of age-related macular degeneration (AMD). (C) Fluorescein angiography of the retina of a human infant with vascular proliferation associated with retinopathy of prematurity, demonstrating proliferation of tortuous, newly formed vessels. (D) Fluorescein angiography of retina in a dog model of diabetic retinopathy, showing markedly thickened central vessels and proliferation of tortuous neovascular profiles. (E, F) Optical coherence tomography (OCT), which uses light waves to take high-resolution cross-sectional images of retinal layering. (E) Spectral domain OCT image of the macula from a normal nonhuman primate. The inner surface of the retina is located at the top of the image. The depressed central region represents the *fovea centralis*. (F) Spectral OCT showing an experimentally induced laser burn leading to retinal distortion (disruption of the normal retinal layering) in a nonhuman primate; again, the depressed central region is the *fovea centralis*. Source: *From Haschek, W.M., Rousseaux, C.G., Wallig, M.A. (Eds.), 2013. The Handbook of Toxicologic Pathology, third ed. Academic Press, San Diego, CA, Figures 53.23 and 53.24, pp. 2161, 2162, with permission.*

destined for microscopic evaluation are described in Table 22a.3.

Tissue preparation by frozen sectioning on a cryostat is preferred for processing the eye when immunohistochemistry (IHC) using fixed tissue is not possible due to inadequate preservation of labile antigens or when preservation of enzymatic activity is need for histochemistry. Tissues may be frozen without fixation, or more commonly they may be fixed for a brief period (typically 30 minutes or less) in ice-cold neutral buffered 10% formalin to improve cell morphology. Specimens then should be transferred to 20% sucrose in Dulbecco's phosphate-buffered saline for 15 minutes and then dipped three times into a 1:1 mixture of 20%

TABLE 22A.2 Ophthalmic Diagnostic Tests Commonly Used in Ocular Toxicity Testing

Test	Measurement	Description
Schirmer's tear test	Tear film aqueous production	Absorbent paper placed in the conjunctival fornix measures the amount of tear produced in a defined period of time
Tear film breakup time	Function of mucin and lipid layers of the tear film	Measurement of the time interval following a blink to the occurrence of a break in the tear film
Fluorescein staining	Detection of corneal ulcers	Sodium fluorescein dye applied to the corneal surface bonds to exposed stromal allowing detection of epithelial defects
Tonometry	Intraocular pressure (IOP)	Indirect measurement of the IOP through a tonometer
Pachymetry	Corneal thickness	Corneal thickness measured by a contact ultrasound machine
Confocal microscopy	Morphology of the cornea	*In vivo*, noninvasive microscopic imaging of the corneal epithelium, stroma, Descemet's membrane, and endothelium
Specular microscopy	Morphology of corneal endothelium	*In vivo* noninvasive imaging of the corneal endothelial cells
Gonioscopy	Morphology of the iridocorneal angle (ICA)	Clinical examination of the anterior chamber angle through a goniolens (a special type of contact lens)
Ultrasound biomicroscopy	Morphology of the anterior segment of the eye	High-frequency ultrasound is used to image the cornea, ICAs, iris, ciliary body, and lens. Can be used to determine corneal thickness and monitor changes in the ICA.
Indirect/direct ophthalmoscopy	Morphology of the posterior segment of the eye	Indirect ophthalmoscope provides binocular, inverted, and reversed wide field aerial image of the posterior segment of the eye. Technique of choice for routine screening.
Fluorescein angiography	Vascular integrity of intraocular structures	Intravascular fluorescein dye injection followed by multiple timed images of the iris, choroid, and retina
Electroretinography (ERG)	Retinal function	Measurement of the electrical potential generated by the retina when stimulated by light
Visual evoked potential	Retinal and optic nerve function	Measurement of the brain's electrical response to a light stimulus in the eye
Optical coherence tomography (OCT)	Morphology of the anterior segment, retina, and optic nerve	High-resolution, noninvasive imaging technique that provides real-time cross-sectional imaging of ocular structure (more commonly retina and optic nerve) at an axial resolution of 2–10 μm

sucrose:tissue freezing medium. Next, the sample should be oriented in a cryomold surrounded by 100% freezing medium, frozen by immersion in liquid nitrogen-cooled isopentane, and stored at −80°C until sectioning.

Trimming the Eye

The default orientation for evaluating eyes of animal species other than nonhuman primates is the vertical median (midsagittal) plane, which samples both the tapetal [typically dorsal (superior)] and nontapetal [typically ventral (inferior)] portions of the retina. Exceptions are made in order to sample more effectively known or suspected lesions in the temporal or nasal aspects of the globe. The horizontal plane is the preferred default orientation in viewing eyes of nonhuman primates because the fovea is lateral (temporal) to the optic nerve head. In the extremely small eyes of rodents, trimming is to be avoided. Instead, the whole globe is submitted and oriented at the time of paraffin embedding. Rodent eyes are positioned in the vertical plane, and a central section through the pupil and the optic nerve is obtained by serial sectioning. For best results over time, select a standard technique for trimming globes of each species. This strategy will reliably provide sections with a single orientation and similar morphological features; such standardization will speed the pathologist's histopathological analysis. Generally, the goal should be to obtain an ocular section that includes the optic nerve and passes through the pupil. Below are several techniques that are helpful in obtaining reproducible sections among animals and across studies.

For large globes, make the initial trimming cut near the optic nerve. The lens is sectioned with a quick forceful cut while supporting the globe on the cutting

TABLE 22A.3 Common Ocular Fixatives

Fixative solution	Composition		Fixation	Use	Positive characteristics	Negative characteristics
10% Formalin, neutral buffered (NBF)	Formaldehyde (37%–40%) Distilled water Disodium diphosphate Monosodium phosphate	10% 90% 6.5 g 4.0 g	24–96h[a]	LM, IHC	Readily available, excellent tissue penetration, reasonable histologic detail preservation, preservation of tissue color, gold standard for IHC	Less than adequate tissue rigidity. Can lead to folding and artifactual retinal detachments
Davidson's fixative	Ethanol (95%) Formaldehyde (37%–40%) Glacial acetic acid Distilled water	35% 2% 10% 53%	6–24 h (sg) 24–48 h (lg)	LM	Good histologic preservation of the retina and lens, excellent tissue penetration (better with modified Davidson's), good tissue rigidity	Opaque white discoloration of tissues, (impairs gross identification of landmarks and lesions). Over-fixation can cause artifacts: vacuolation of corneal epithelium and endothelium, oblong spaces in the corneal stroma, shattering of lens fibers and capsule, indistinct photoreceptor segments
Modified Davidson's fixatives	Ethanol (95%) Formaldehyde (37%–40%) Glacial acetic acid Distilled water	15% 30% 5% 50%				
Bouin's fixative	Picric acid Formaldehyde (37%) Glacial acetic acid	75% 25% 5%	12–24 h (sg) 24–48 h (lg)	LM	Good histologic preservation of the retina, decalcifies tissues, excellent tissue rigidity	Opaque yellow discoloration of tissue, corrosive to metal, explosive potential
Glutaraldehyde	Glutaraldehyde 10% NBF	50% 50%	12–24 h (sg)[b] 24–48 h (lg)[b]	EM	Good histologic preservation, preservation of tissue color	Very poor tissue penetration, tissues fixed should be $<1\ mm^3$
Karnovsky's fixative	16% paraformaldehyde 10% glutaraldehyde 0.2 M phosphate buffer (pH7.4) Distilled water	17% 31% 50% 2%	12–24 h (sg) b24–48 h (lg)[b]	EM	Good histologic preservation, preservation of tissue color, better tissue penetration than glutaraldehyde	Still relatively low tissue penetration, tissues fixed should be $<1\ mm^3$
Zenker's	Distilled water Potassium dichromate Mercuric chloride Glacial acetic acid	1 L 25 g 50 g 50 g	12–24 h	LM	Excellent fixation of nuclear chromatin, connective tissue fibers and some cytoplasmic features	Toxic, contains mercury

[a] *If IHC is anticipated, fixation time should be minimized to 24–48 hours.*
[b] *After initial fixation, transfer to 10% NBF for 24 hours to increase ocular tissue rigidity.*
Abbreviations: LM, light microscopy; IHC, immunohistochemistry; EM, electron microscopy; sg, small globes; lg, large globes.

board. A major advantage to this approach is that suitable sections for analysis may be obtained after facing only a few sections from the embedded tissue (just sufficient to reach the optic nerve). Another advantage is that the globe is cut close to the anatomic center, which is appealing for the purpose of macroscopic photography. The disadvantage is that the lens may be misplaced or damaged during trimming. To maximize the chances of preserving good lens morphology when trimming, make an initial off-center cut that avoids the lens. Subsequent step-sectioning once the tissue has been embedded in paraffin can be used to achieve a central cut through the lens and optic nerve. An advantage of this latter approach is that the lens is untouched during trimming and thus is less likely to be artifactually dislodged.

Ensure the inclusion of lesions in the plane of section. The ideal strategy is to have the clinician indicate the location of a focal lesion in the globe with a careful clinical description and/or drawings or photographs, as well as some indication directly on the tissue with a suture or another tissue-marking technique (e.g., insoluble ink applied to the outer surface). Gentle palpation of the globe often is valuable in detecting large localized lesions before sectioning. The orientation of the initial section can be changed in such a way as to sample the palpable lesion. Transillumination (candling) the globe by holding it in front of a bright light in a darkened room can help to localize an opaque focal lesion. Careful examination of the sectioned globe using a dissecting microscope also facilitates the identification of focal lesions. Additional steps may be indicated to sample a focal lesion. The primary calotte (i.e., the term used for an isolated portion of the globe) might be retrimmed so that only the segment of the globe with the lesion is embedded. The histology technician is then instructed to step-section to a specified depth to sample focal lesions. This added step is sometimes essential to fully characterize discrete lesions.

In Vivo Ocular Irritation Test

The Draize test is an acute ocular toxicity test devised in 1944 to provide a method for assessing the irritation potential of materials that might accidentally come in contact with human eyes, such as household and office products, agricultural or environmental chemicals, and volatile organic compounds. Because of the widespread acceptance of this method, it was later adopted for testing eye care products and drugs designed specifically for topical ophthalmic use prior to marketing. The current Draize method involves the instillation of 10 μL of a test liquid (or 10 mg of a test solid) into the lower conjunctival cul-de-sac, followed by a saline rinse. Observations of various criteria (i.e., corneal opacity and area of corneal involvement, conjunctival hyperemia, chemosis, ocular discharges, and iris abnormalities) are taken at predefined intervals: 1 hour, 24 hours, 48 hours, 72 hours, 7 days, and 21 days after administration. The test is usually performed in rabbits due to their large eyes, well-described anatomy, ease of handling, relatively low cost, and ready availability. A slit-lamp examination has been added to allow better assessment of corneal lesions, and topical fluorescein is applied routinely to reveal any cornel ulceration. Optical or ultrasonic pachymetry now is implemented to measure the extent of corneal thickening. Although the Draize test is still the official model for eye irritation and toxicology studies worldwide, it has suffered major criticism in recent years due to the lack of objective quantification within its grading system, its unreliability in predicting chronic toxic reactions, and marked opposition by animal welfare groups.

In Vitro Ocular Toxicity Tests

Several *in vitro* assays have been developed in order to circumvent the aforementioned limitations of the Draize test and to minimize the exposure of animals to potentially irritating materials. No single *in vitro* assay has been validated as a full regulatory replacement for the Draize test.

Key ocular-based platforms may be used for *in vitro* testing. *Isolated rabbit and chicken eyes* (removed immediately after death) are placed in a temperature-controlled chamber and perfused with physiological saline. Test substances are applied topically to the cornea and conjunctiva, and the effects are observed over several days with a slit-lamp biomicroscope. *Isolated corneal preparations* are typically limited to assessments of corneal irritation, and are done using isolated bovine corneas collected from slaughter houses. The corneas are mounted in specially designed holders, incubated in Eagle's minimum essential medium at 32°C, and exposed on the external surface to the test article for 1 hour. Subsequently, changes in the opacity and permeability of the corneal tissue are measured by an opacitometer and by spectrophotometry, respectively. The *corneal cup method* uses isolated fresh bovine corneas to form a "cup" that can be used to assess the local production of leukocyte chemotactic factors. The *corneal fluorescence probe method* measures the degree of epithelium permeability using penetrance of a fluorescent probe after application to fresh rabbit corneas. Cultured conjunctival, corneal, and lens epithelial cells are readily available without the need for specifically

terminating test animals, and in some instances may be of human origin. Methods for assessing cytotoxicity in cell cultures include measurements of plasminogen activation and the ^{51}Cr-release method.

Alternatives exist to the use of eyes and ocular derivatives for *in vitro* ocular irritancy testing. The *Eytex system* is a corneal opacification assay that uses a vegetable protein gel extracted from jack beans (*Canavalia ensiformis*). It predicts ocular irritation of materials based on alterations induced in its vegetable protein matrix. This method is quantitative and reproducible and presents a high degree of correlation to the Draize test.

Substances that irritate ocular tissues also have the potential to cause irritation in other sensitive nonocular tissues. The *chicken egg test (Huhner-Embryonen test)* uses embryonated hens' eggs to demonstrate chemical toxicity through embryo lethality, teratogenicity, and systemic toxicity. It is considered a borderline assay falling between an *in vivo* test and *in vitro* test. Chicken eggs also provide chorioallantoic membrane (CAM) for the *chorioallantoic membrane test*. In this method the vascular CAM is exposed to the test article in multiple dilutions, and the tissue is scored for irritation effects such as hyperemia, hemorrhages, and coagulation activity. *Mucous membranes* from other tissues may be used to assess chemical irritancy. Examples include the rat vaginal mucosa (using prostenoid production as an indicator) and also mouse and rabbit ileum mucosa (using altered contractility as an index).

RESPONSE TO INJURY BY SPECIFIC OCULAR TISSUES

Lacrimal System

All of the glands comprising the lacrimal system are apocrine glands, and they respond to injury much like other apocrine glands throughout the body. They are prone to ductular obstruction secondary to inflammation. This often leads to ascending inflammation affecting the gland acini and can result eventually in atrophy. Lymphocytic clusters among acini are a common background lesion in safety studies, especially in rodents. Viruses such as sialodacryoadenitis virus (SDAV), a coronavirus of rats, can directly infect the acinar epithelium in lacrimal glands as well as salivary glands, leading to necrosis, inflammation (intra- and periacinar), and periacinar fibrosis, which ultimately may lead to atrophy of the remaining parenchyma. Chronic infection with SDAV can cause corneal desiccation [keratoconjunctivitis sicca (KCS)], corneal ulceration and uveitis leading to hyphema (blood accumulation in the anterior chamber), intraocular inflammation, formation of fibrovascular membranes over the iris (preiridal fibrovascular membrane), and eventually to obstruction of the aqueous outflow pathways with secondary (unilateral or bilateral) glaucoma.

Squamous metaplasia of the epithelium lining lacrimal gland ducts is occasionally seen. This change is usually idiopathic, but metaplasia associated with vitamin A deficiency is a possible cause. Ionizing irradiation used for cancer therapy can affect the lacrimal glands, leading to acinar atrophy. The exact mechanism for this atrophy is unclear, but the likely explanation is that cumulative gene damage in irradiated stem cells leads to their apoptosis and a reduced capacity to regenerate gland acinar epithelium.

Like other apocrine glands, lacrimal and Harderian glands are capable of neoplastic transformation. These tumors occur in aged rodents (more common in mice than rats or hamsters), dogs, and cats (the last two presenting only with lacrimal tumors since they do not have Harderian glands). The spectrum of neoplasms seen in lacrimal glands is similar to those that develop in other apocrine glands: acinar, ductular, or solid adenomas (benign) or adenocarcinomas (malignant). When the myoepithelial component that surrounds acini is involved, the architecture can form complex tumors that includes both epithelial and spindle cell components (with the spindle cell element ranging from minimal to major); if there is osseous or cartilaginous metaplasia of the myoepithelial component, truly mixed tumors can arise in lacrimal glands. Rarely, the mesenchymal component will be the predominant malignant cell population so that osteosarcoma or chondrosarcoma may arise as a primary tumor in a lacrimal gland.

Eyelids

The response of eyelid tissue to injury is not complicated. The most common reaction is inflammation secondary to infection or trauma. Subsequent fibrosis (scarring) can have a profound effect on the function of the lid by interfering with its motion or conformation. An inwardly turned lid (entropion), usually affecting the lower lid, can result in hairs contacting the cornea. This abnormal interaction causes pain and irritation and may lead to erosion or ulceration of the cornea. In contrast, an outwardly turned lower lid (ectropion) can invite spillage of tears, which can result in "dry eye" (KCS) and secondary infection. Weakening of the dorsal (superior) tarsal muscle associated with a defect in sympathetic innervation, as in Horner's syndrome, causes ptosis (drooping of the upper eyelid). Blepharospasm, the abnormal contraction or twitching of an eyelid, is a nonspecific response

to painful or irritating stimuli. This clinical abnormality can be triggered by many factors, including conjunctival or corneal irritation or even injury or inflammation in the uvea. The identification of blepharospasm is important when clinically accessing the immediate response to topically administered drugs and ocular discomfort. Neoplasms may develop from any of the structures in the eyelid, including the skin. The most commonly reported tumors include papilloma, squamous cell carcinoma, peripheral nerve sheath tumors, melanocytomas/melanomas, and sebaceous and meibomian gland adenomas.

Conjunctiva

The conjunctiva responds to injury like most mucous membranes of the body. The most common diseases of the conjunctiva are inflammatory (*conjunctivitis*). Most species have viral diseases that affect the conjunctival epithelium, causing epithelial necrosis and ulceration that often lead to secondary bacterial conjunctivitis with suppurative inflammation and tissue destruction. The conjunctiva also is a common site to manifest allergic diseases, presenting as acute eosinophilic inflammation with edema driven by local mast cell infiltration. A varied pattern of inflammatory reactions can be found within the conjunctiva, ranging from dispersed lymphoplasmacytic to granulomatous to perivascular lymphocytic lesions with neutrophilic vasculitis. Infectious agents are hardly ever associated with these inflammatory infiltrates, suggesting that such infiltration results from an immune-mediated reaction of unknown etiology. With chronicity, squamous metaplasia of the conjunctival epithelium can occur. If generalized, this metaplastic change can reduce the numbers of mucus-producing goblet cells leading to a vicious cycle of tear film dysfunction and dry eye that can eventually progress to permanent KCS. The conjunctival surface is exposed to ultraviolet (UV) radiation and thus also can react with dysplastic changes and neoplastic transformation. Tumors typically exhibit squamous cell differentiation, but dogs also may develop vascular endothelial neoplasia. In general, these conjunctival changes are not reported to reflect prior exposure to toxicants.

Cornea

Atrophy of the corneal epithelium is characterized by a decrease in the numbers of corneal epithelial cells and/or a thinning of the epithelial layers. Corneal epithelial atrophy can be secondary to stromal changes, especially edema or a deficiency of the limbal stem cells that replenish the corneal epithelium. The corneal epithelium does not have a native stem cell population, so there is a limited capacity of the epithelium to proliferate in response to injury. After ulceration, the existing epithelial cells disconnect from each other and migrate to cover the wound (a process termed "restitution"). However, newly differentiated corneal epithelial cells are recruited from a stem cell population that exists only in the conjunctiva at the limbus. If this population of cells is destroyed (e.g., by herpes virus, chemical burns, necrotizing inflammation, or some other disease process), the corneal epithelium is at grave risk of permanent deficiency. Conjunctival epithelium will regenerate over the corneal surface, but this scar will not achieve the same optical clarity as normal corneal epithelium since it lacks the differentiation state needed to maintain the proper tissue organization to permit light passage at the proper angle. In addition, the scar will remain thin and at risk of renewed ulceration or even a full-thickness corneal rupture. Limbal stem cell transplantation from the healthy eye to the diseased eye has made it possible for affected humans to regain the function of unilateral eye damage.

Corneal epithelial hyperplasia, *keratinization*, and *melanin pigmentation* are nonspecific responses of the corneal epithelium to chronic injury. These lesions are seen in the late stages of chronic keratitis, corneal surface exposure (exposure keratopathy), and dry eye, and are characterized by thickening and keratinization of the epithelium, along with rete ridge formation and migration of melanocytes leading to pigmentation of the basal layers (Figure 22a.15).

Corneal epithelial ulceration and *erosions* can be associated with trauma, reduced tear production resulting in dry eyes, exposure to topical or gaseous caustic agents, and corneal mineralization. Abrasions may be incidental in rodents, often related to caging conditions or environmental irritants. Direct trauma with epithelial ulceration can provide a portal for bacterial colonization, and an edematous cornea secondary to damage at the corneal endothelium makes the risk of infection and progressive stromal damage all the more serious. Ulcerations are usually associated with corneal stromal *vascularization* and *inflammation (keratitis)*.

Corneal stromal lipidosis. Metabolic disorders, tumors, or hemorrhage can lead to deposition of lipid or the formation of lipid granulomas (often with high cholesterol content) in the corneal stroma. Similar deposits of iron (usually after hemorrhage) and calcium (mineralization) in the superficial stroma may develop if the tear film is allowed to dry (Figure 22a.16).

Corneal subepithelial and stromal mineralization (corneal dystrophy, calcific band keratopathies, dystrophic calcification) is a relatively common lesion that can be associated with hypercalcemia and metastatic

mineralization, or more commonly as a secondary response to chronic corneal irritation and/or ulceration. Mineralization has also been associated with high ammonia levels due to urease-positive bacteria in the bedding. It is a prominent feature of spontaneous corneal pathology in some mouse strains. For instance, BALB/c, C3H, and DBA/2J, mice frequently possess Von Kossa-positive, extracellular, basophilic corneal deposits of mineral that are age-related in incidence and severity and may be associated with focal corneal thinning and ulceration. Interestingly, these mouse strains are also prone to spontaneous cardiac calcinosis.

Corneal edema results from water accumulation in the stroma. The optical clarity of the cornea is dependent on the precise special distribution of keratocytes (i.e., stromal fibroblasts), collagen and proteoglycans in the stroma. Even slight fluid accumulation in the corneal stroma leads to a shift from transparent and colorless to translucent blue (Figure 22a.17). The normal corneal stroma is maintained in a slightly dehydrated state by the intact epithelium, the exclusion of blood vessels from the stroma and, importantly, by the energy-dependent removal of fluid into the anterior chamber across a pressure gradient created by the corneal endothelial cells. Due to the importance of maintaining normal levels of transparency and light refractivity, the cornea presents a very low threshold of tolerance for damage.

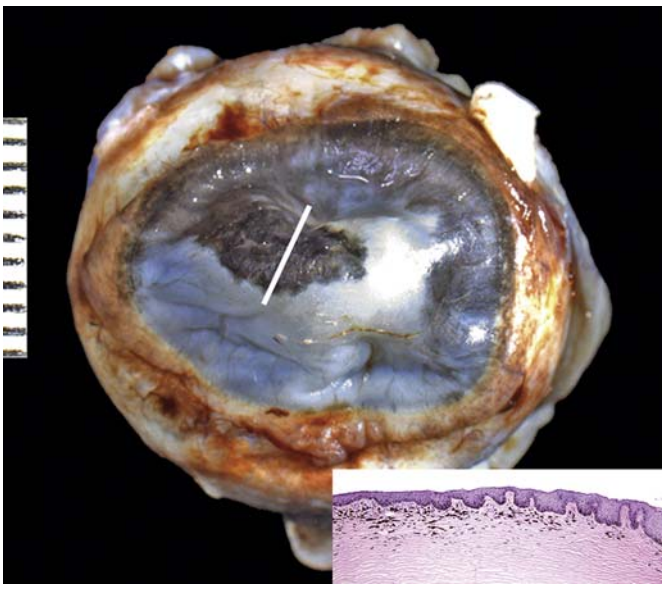

FIGURE 22A.15 **Pigmentary keratitis.** Gross image of a formalin-fixed dog cornea exhibiting marked opacity and dark pigmentation as reactive changes to a chronic inflammatory process. Inset: Histological section corresponding to the region of the cornea marked with a white line. Note the marked corneal hyperplasia and hyperkeratosis and pigmentation of the basal layers of the corneal epithelium and superficial corneal stroma. Scale, 1 interval = 1 mm. Inset: H&E, ×100. Source: *From Haschek, W.M., Rousseaux, C.G., Wallig, M.A. (Eds.), 2013. The Handbook of Toxicologic Pathology, third ed. Academic Press, San Diego, CA, Figure 53.8, p. 2120, with permission.*

Several toxic effects might be associated with corneal edema. For example, permeability of the surface epithelium may be altered. This can occur as a result of physical or chemical damage to the epithelium and is important when irritants come in contact with the ocular surface. Second, the structural integrity of the stroma may be disrupted. This can be caused by damaging the profile of cytokines, which regulate the balance in the arrangement and composition of the stromal elements. Deposition of lipids, mineral, and/or molecules, which might enhance the colloidal pressure in the stroma, can also cause the stroma to become opaque. Third, vascularization of the stroma and/or enhanced permeability of the limbal blood vessels may impact the ability of the cornea to bar the entry of excess fluid. Toxicant-induced changes in vascular permeability can lead to corneal edema even if new blood vessels do not proliferate into the corneal stroma. Finally, malfunction of the corneal endothelium will predispose to fluid accumulation within the corneal stroma due to the cessation of its active transfer from the corneal stroma of excess fluid. Microscopically, corneal stromal edema is characterized by paleness an irregular expansion of the stromal lamellae sometimes associated with edema and spongiosis of the adjacent epithelium and subepithelial cleft formation. It is important, and sometimes challenging, to differentiate stromal edema from artifactual splitting of the corneal lamellae, a very common and almost predictable artifact following conventional histological processing.

Corneal stromal collagenolysis (keratomalacia). Many factors that affect the health of the corneal stroma induce the release of matrix metalloproteinases, which can degrade the stromal collagen. In the worst cases, the collagenolysis is so fast and complete that the corneal stroma can be completely dissolved in a day or less. An example is the "melting" corneal ulcer, a devastating disease that is rare in humans but occurs frequently as a spontaneous condition in dogs, particularly the Shih Tzu breed. Affected dogs present with an acute episode of corneal opacity and edema that is cause by abrupt qualitative changes in the corneal stroma: loss of stromal lamellar architecture and severe liquefaction (collagenolysis) of the tissue, usually associated with marked neutrophilic infiltration. If left unchecked, extensive areas of the corneal stroma are affected, and the lesion evolves to a descemetocele (prolapse of Descemet's membrane through an eroded corneal epithelium and stroma) and eventually corneal perforation.

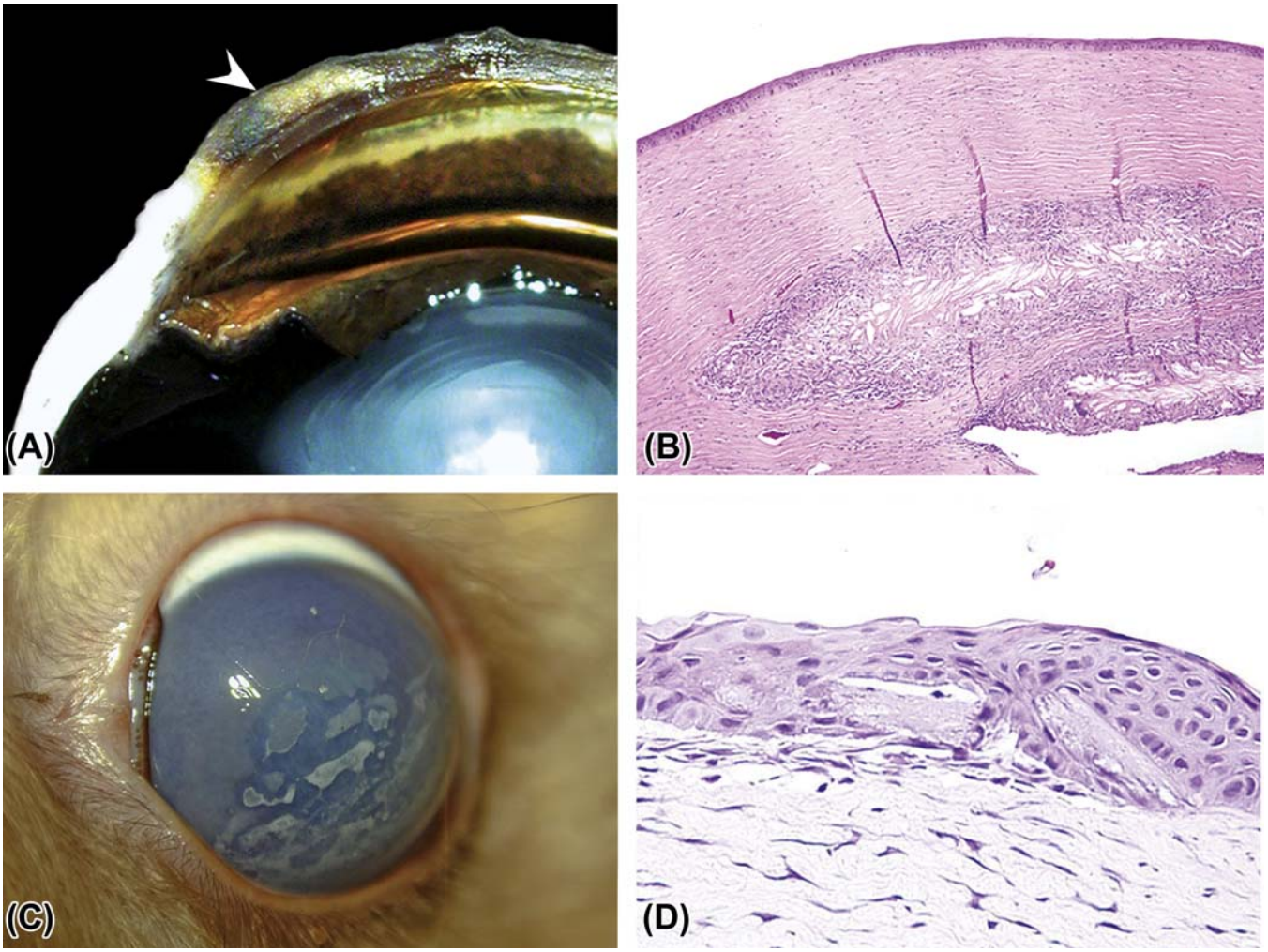

FIGURE 22A.16 **Corneal deposits.** (A) Gross image of a dorso-ventral section of a dog globe showing yellow material, consistent with lipid, deposited in the corneal stroma (*arrow*). (B) Histologic section presenting a large cholesterol granuloma, comprised of numerous cholesterol clefts surrounded by a marked granulomatous reaction, embedded in the deep corneal stroma. (C) Gross image of a rabbit cornea showing white irregular plaques, composed of mineral and lipids deposited in the corneal stroma. (D) Multiple brick-shaped cholesterol crystals embedded in the corneal epithelium of the rabbit in C. (B) H&E, ×100; (D) H&E, ×400. Source: *From Haschek, W.M., Rousseaux, C.G., Wallig, M.A. (Eds.), 2013. The Handbook of Toxicologic Pathology, third ed. Academic Press, San Diego, CA, Figure 53.12, p. 2131, with permission.*

Corneal stroma fibrosis and *neovascularization* are nonspecific responses of the corneal stroma to injury. Neovascularization is usually seen in response to corneal ulceration and inflammation, but it can also be stimulated by intraocular lesions such as endophthalmitis. Vessels start proliferating from the limbus into the peripheral corneal stroma approximately 3 days after the initial stimulus and progress centrally at a rate of approximately one-corneal-thickness (i.e., approximately 100−600 μm) per day. Corneal stromal fibrosis is seen in the late stages of chronic keratitis, corneal surface exposure (exposure keratopathy), and dry eye or as a reparative response after corneal wounds. Histologically, fibrosis is characterized by areas of randomly deposited dense collagen with increase numbers of fusiform cells and loss of the normal parallel arrangement of the corneal stroma—all of which lead to permanent opacity in the affected portion of the cornea.

Corneal inflammation (keratitis) can be present as a response to a variety of possible causes, such as corneal ulceration with or without secondary infections, chronic corneal exposure and dry eye, mechanical irritation, toxic and chemical reactions, photosensitization, immune-mediated processes, and others. The type of leukocyte response varies with the inciting cause, but usually neutrophils predominate in acute and subacute processes while the number of lymphocytes and macrophages increases with chronicity.

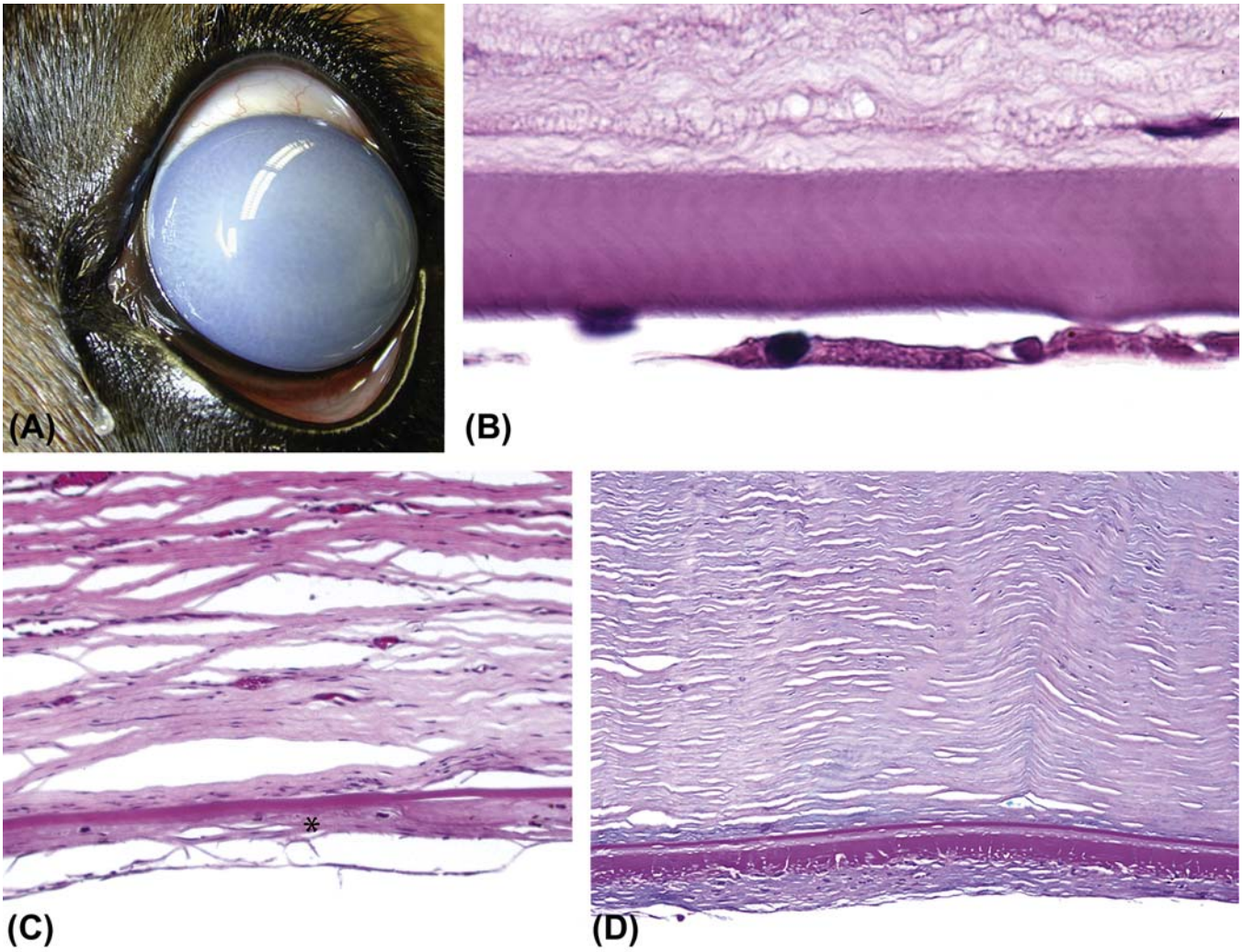

FIGURE 22A.17 **Corneal endothelial lesions.** (A) Clinical image of a dog eye with a diffusely opaque and blue cornea secondary to edema caused by corneal endothelial loss. (B) Attenuated corneal endothelium in a dog with a hereditary endothelial dysplasia. Note the discontinuity and nuclear condensation in the endothelial cell layer beneath the thick eosinophilic band of Descemet's membrane. The stromal connective tissue exhibits an abnormal granular appearance, likely a reflection of fluid accumulation due to disruption of the endothelial barrier. (C) Replacement of the endothelium with a fibrous layer (retrocorneal membrane, *) in a dog secondary to longstanding mechanical disruption of the endothelium. Using Descemet's membrane as a reference, note the increased thickness of the retrocorneal membrane relative to the normal endothelial cell monolayer. (D) Retrocorneal membrane in a dog associated with disorganized deposits of basement membrane proteins. (B) H&E, ×600; (C) H&E, ×200; (D) Periodic acid-Schiff (PAS), ×200. Source: *From Haschek, W.M., Rousseaux, C.G., Wallig, M.A. (Eds.), 2013. The Handbook of Toxicologic Pathology, third ed. Academic Press, San Diego, CA, Figure 53.11, p. 2126, with permission.*

The *corneal endothelium* in most mammalian species presents a very limited proliferative capacity. That said, although rare, the corneal endothelium can respond to injury by proliferating. In such instances, the corneal endothelium migrates over the ICA and anterior aspect of the iris and sometimes produces a Descemet's membrane-like material. This phenomenon is known as endothelialization and is associated with iridocorneal endothelial (ICE) syndrome and some forms of glaucoma in humans. In mice, ICE syndrome occurs in the DBA/2J and AKXD-28/Ty strains and can lead to progressive angle closure glaucoma.

Corneal endothelial attenuation may significantly impact corneal function because of its limited proliferative capacity. When endothelial cells are lost to injury or aging, the tissue attempts to cover the resulting defect by enlargement and stretching of the adjacent cells. Despite this adaptation, with time there is a critical point at which endothelial cells are unable to adequately sustain their function simply because there are too few of them. Microscopically, corneal endothelium attenuation presents as flattened and enlarged cells with an overall decrease in cell numbers and possibly associated corneal stromal edema (Figure 22a.17).

Doubling and *breaks in Descemet's membrane* are usually seen secondary to traumatic events. These lesions can be accompanied by a fibrovascular formation on Descemet's surface (retrocorneal membranes) and/or fibroplasia of the deep corneal stroma. Multiple small breaks in Descemet's membranes can be seen in conjunction with globe enlargement secondary to glaucoma (buphthalmos). In this instance, these breaks are called *Haab's stria*, and they represent linear (usually horizontal) fissures in Descemet's membrane.

Uvea

Fibrovascular membranes result from proliferation of stromal and vascular tissue in the uvea. Because of the need for transparency in the light-transmitting media of the globe, vascular proliferation is tightly regulated. There are many disease states where the release of angiogenic molecules leads to neovascular proliferation associated with the uveal tissue. These membranes are seldom actually within the uveal tissue but rather extend out along the surfaces of the iris, ciliary body, and/or choroid, sometimes extending into the anterior and posterior chambers, vitreous and subretinal spaces. Such fibrovascular membranes can lead to synechiae [i.e., adherence of the iris to either the cornea (anterior synechia) or lens (posterior synechia)], ICA closure, and/or hemorrhage. When severe, the membranes block the aqueous outflow, increase IOP, and initiate glaucoma. Retinal hypoxia as a result of restricted perfusion or retinal detachment and subsequent release of pro-angiogenic factors [e.g., vascular endothelial growth factor (VEGF)] in the ocular chambers is a common cause of fibrovascular membrane formation; two diseases resulting from production of such factors are neovascular glaucoma and choroidal neovascularization in the "wet" form of AMD. Intraocular inflammation, deep ocular trauma, and intraocular tumors are other possible causes. Microscopically, these membranes are characterized by fusiform cells and small vascular sprouts surrounded by collagen fibers. The amount of collagen production and degree of vascular proliferation in these membranes vary markedly.

Uveal inflammation (uveitis). Anterior uveitis refers to inflammation of the iris and ciliary body. Posterior uveitis refers to inflammation of the choroid, which is more commonly denominated choroiditis. When the inflammatory process affects both the anterior and posterior uvea, it is termed panuveitis. Ocular trauma, irritation secondary to intraocular devices, or intracameral injections (i.e., into either the anterior or posterior chamber) may cause uveal inflammation.

Inflammation secondary to a toxic event must be differentiated from leukocyte accumulation as a spontaneous background change. Cynomolgus monkeys exhibit foci of uveal lymphocytic infiltration as an idiopathic background change. A review of hundreds of archival samples shows that these lymphocytic foci are seen in the ciliary body and choroid of approximately 27% of naïve control animals. Such infiltrates usually present as unilateral, focal, minimal to mild, lymphocytic aggregates with few plasma cells, most often in the *pars plana* of the ciliary body. Mononuclear cell infiltration in the iris, ciliary, and ICA is also observed as relatively frequent nonspecific change in rabbits. Rats and aged mice also develop spontaneous leukocyte infiltration of the anterior uvea. This control finding is properly considered an infiltration (i.e., cell accumulation of no pathologic significance) rather than an inflammation (i.e., where the accumulating cells actually damage the affected tissue).

Hyperpigmentation and *depigmentation* of the uvea are nonspecific alterations that can be associated with multiple causes. Hyperpigmentation can occur following systemic administration of compounds such as urethane in neonatal hooded rats or topical application of prostanoid compounds such as latanoprost. Increased pigment deposition occurs in DBA/2J mice homozygous for iris pigment dispersion or iris stromal atrophy. Decreased pigmentation may be associated with uveal inflammation or edema, and can also present as an aging change.

Lens

When reporting lenticular changes, it is important to fully characterize the pathologic changes. Features to describe include the lesion distribution (unilateral or bilateral, focal, multifocal or diffuse), tissues affected (capsule, epithelium, or fibers); and anatomical location in the lens (anterior, equatorial, or posterior; subcapsular, cortical, or nuclear). It is important to recognize that some lenticular opacifications observed clinically are reversible and usually do not present corresponding microscopic lesions. Reversible lens opacification can be induced by cold temperature, dehydration, asphyxia, anoxia, stress, and certain chemicals and drugs (see mechanism of toxicity section).

Cataract (degeneration). Transparency and refraction of light are the main functions of the lens, and toxicity may be manifested by changes in these features. The most readily apparent is a change in transparency, which is defined as a cataract. Not all cataractous changes can be detected microscopically. A good example is changes in the lens nucleus (or core) diagnosed clinically as nuclear cataract. In addition, cataracts may manifest histologically by changes

indistinguishable from certain tissue artifacts related to sectioning and fixation. It is important to identify genuine lenticular changes to avoid misinterpreting lens artifacts as lesions. The most reliable cataract-related lesions that can be demonstrated using a microscope include swelling of lens fibers, formation of Morgagnian globules (large degenerate anuclear fibers) and bladder cells (large degenerate fibers with nuclei or nuclear fragments), liquefaction and mineralization of the cortical lens fibers, migration of the lens epithelial cells (normally only present in the inner aspect of the anterior lens capsule) along the inner surface of the posterior lens capsule, spindle cell (fibrous) metaplasia, and hyperplasia of the lens epithelial cells and wrinkling of the lens capsule (Figure 22a.18).

Posterior migration of the lens epithelium is usually one of the earlier morphologic findings in cataracts. Another early morphologic change that appears to be more specific to mice is internal migration of nucleated lens epithelial cells beyond the nuclear bowl, especially at the lens equator. These initial changes are particularly important to be recognized when screening for

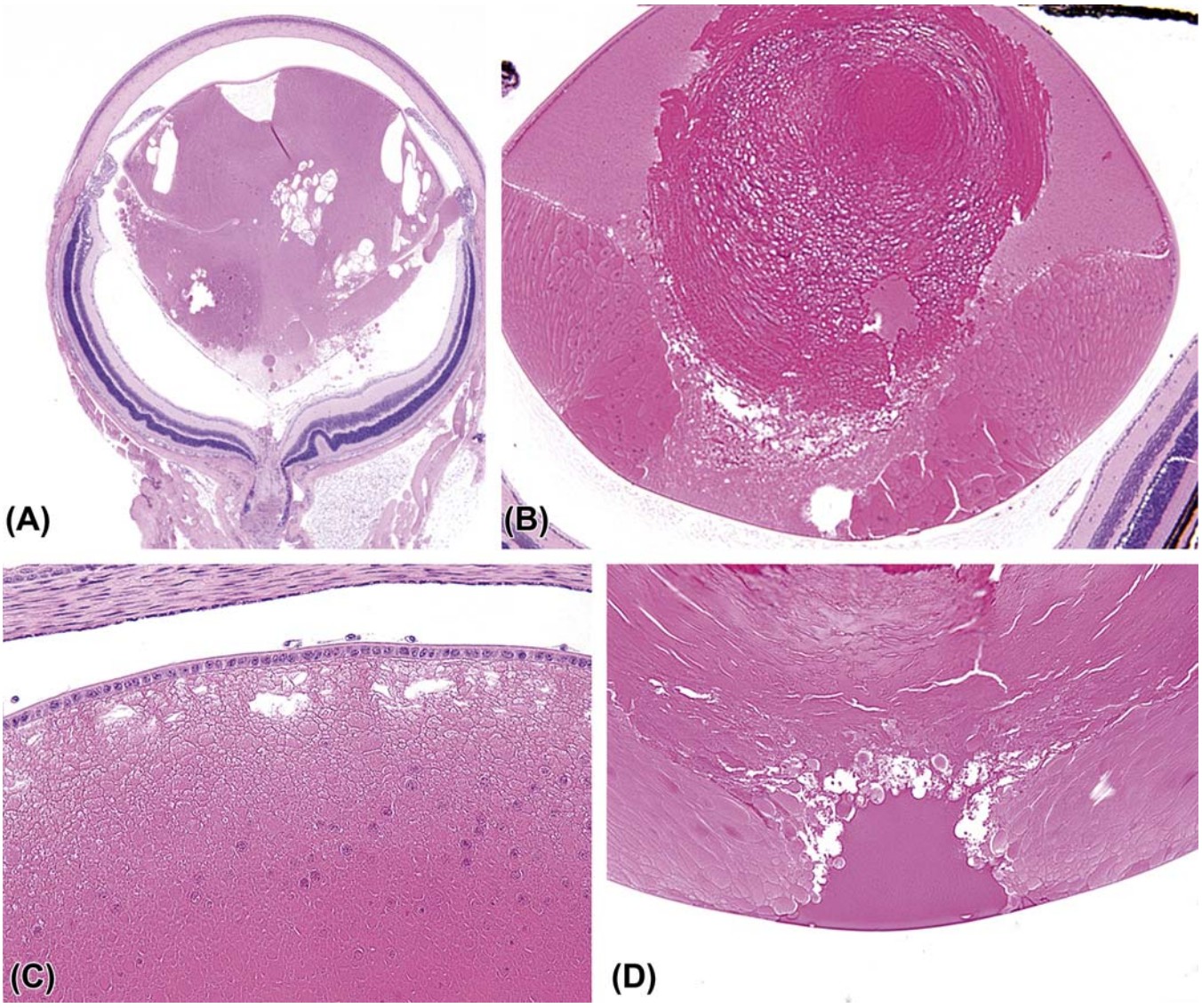

FIGURE 22A.18 **Congenital cataract.** (A) Subgross view of a mouse globe with a cataract distorting the posterior pole of the lens. (B) Lens from a mouse with fairly normal equatorial regions but abnormal nucleus that protrudes caudally to disrupt the posterior pole of the lens. (C) Posterior migration of the lens epithelium (posterior cortical cataract) in a young mouse with persistence of the *tunica vascularis lentis* on the surface of the lens. (D) Cortical cataract at the posterior suture. (A) H&E, ×12.5; (B) H&E, ×100; (C,D) H&E, ×200. Source*: From Haschek, W.M., Rousseaux, C.G., Wallig, M.A. (Eds.), 2013. The Handbook of Toxicologic Pathology, third ed. Academic Press, San Diego, CA, Figure 53.17, p. 2146, with permission.*

morphological phenotypes, especially in developmental cataracts. Morgagnian globules and bladder cells are formed when abnormal cellular metabolism in lens epithelium causes cytoplasmic accumulation of coarse granular material that causes the cells to swell. Mineralization and liquefaction of the lens fibers are often present in advanced (chronic) cataracts. The contents of the liquefied lens fibers have the potential of leaking though the intact lens capsule, where they may incite an intraocular immune-mediated response culminating in uveitis. Lens epithelial cells can undergo spindle cell metaplasia and deposit collagen within the subcapsular space, creating a pattern of opacification clinically referred to as subcapsular cataracts. The metaplastic cells atrophy over time, and often only the collagen remains (Figure 22a.19).

Lens capsule rupture usually affects the posterior lens capsule, which is thinner than the anterior capsule. Lens capsule rupture usually occurs as a posttraumatic event (blunt or perforating trauma, including iatrogenic perforation after intraocular injections) but it can also occur secondary to fast developing (intumescent) cataracts, as seen in diabetic cataracts in dogs, or secondary to granulomatous lenticular inflammation in rabbits infected with *Encephalitozoon cuniculi*. Regardless of the cause, lens protein and fibers are exposed and extruded into the intraocular chambers after capsule rupture usually causing a secondary endophthalmitis and/or uveitis (phacoclastic inflammation). The inflammation associated with release of lens proteins is an autoimmune reaction produced by exposure to "foreign antigens" from the lens interior (which is an immunologically privileged site). Some mutant mouse models develop spontaneous rupture of the lens capsule. These include lens rupture (*lr*), lens opacity 10 (*Lop10*), and lens opacity 12 (*Lop 12*) animals. Unlike traumatic lens capsule rupture in most species, where a granulomatous inflammatory reaction occurs, these genetically mediated ruptures seldom mount an inflammatory response; the reason for this phenomenon is unknown.

It is very important to differentiate real lens capsule rupture from artifactual rupture produced during sectioning of the ocular tissues. The most reliable histologic changes associated with genuine lens capsule rupture are coiling of the free edges of the ruptured capsule away from the site of the break and infiltration of inflammatory cells among the exposed lens fibers. Because of the three-dimensional structure of the lens and the focal nature of some lesions, the exact point of capsule rupture might not be sampled in a given section. In these situations, the presence of inflammatory cells in the intralenticular space interacting with the lens fibers is evidence of lens capsule rupture at another location in the lens.

Lens luxation may present as dislocation either anteriorly or posteriorly. Primary lens luxation occurs in dogs (typically terrier breeds) that carry mutations affecting ADAMTS (a disintegrin and metalloproteinase with thrombospondin motifs) 10, leading to dysplastic zonular fibers and zonular instability (weakness). This ADAMTS 10 mutation also has been described in a colony of beagle dogs that exhibit a primary glaucoma phenotype. These beagles traditionally have been used as an animal model of primary open angle glaucoma in humans.

Lens luxation is more commonly seen in association with trauma, secondary to glaucoma with buphthalmos (enlargement of the globe leading to rupture of the zonular fibers), and hypermature cataracts (where wrinkling of the lens capsule leads to rupture of the zonular fibers). Since the lens can be easily artifactually dislocated while trimming the eye, the adequate diagnosis of lens luxation relies heavily on the clinical and gross identification of a dislocated lens. If the lens is firmly entrapped in the anterior chamber or vitreous, the microscopic diagnosis of luxation is simple. Otherwise, the clinical and macroscopic diagnosis of lens luxation can be supported by the histologic findings of attenuation of the corneal endothelium (suggesting the lens was in contact with the corneal endothelial cells), posterior curving of the iris leaflets, and atrophy of the ciliary body processes.

Vitreous Body

It is tempting to think of the vitreous body as a structural lumen, but it is actually a cell-poor, transparent, extracellular space filled with a gel-like matrix. As such, it responds to injury in the same way other connective tissues do. If there is a stimulus for fibrovascular proliferation, then new blood vessels and spindle cells will move into the vitreous, and deposition of collagen fibrils in the originally rarefied matrix will lead to opacification. Proliferative vitreoretinopathy after retinal detachment, retinopathy, or premature birth are examples of diseases in which fibrovascular proliferation in the vitreous may be profound.

Persistent fetal vasculature (PFV) results from impaired regression if the fetal vitreous vasculature, which normally recedes shortly after birth. In such cases, retained remnants of embryonic vessels accompanied by fibrous connective tissue can be seen in the vitreous and posterior aspect of the lens for extended periods after birth. This condition is referred to as PFV, which is an umbrella term proposed to encompass multiple presentations that can range from persistent hyaloid vessels to persistent hyperplastic primary vitreous and persistent *tunica vasculosa lentis*

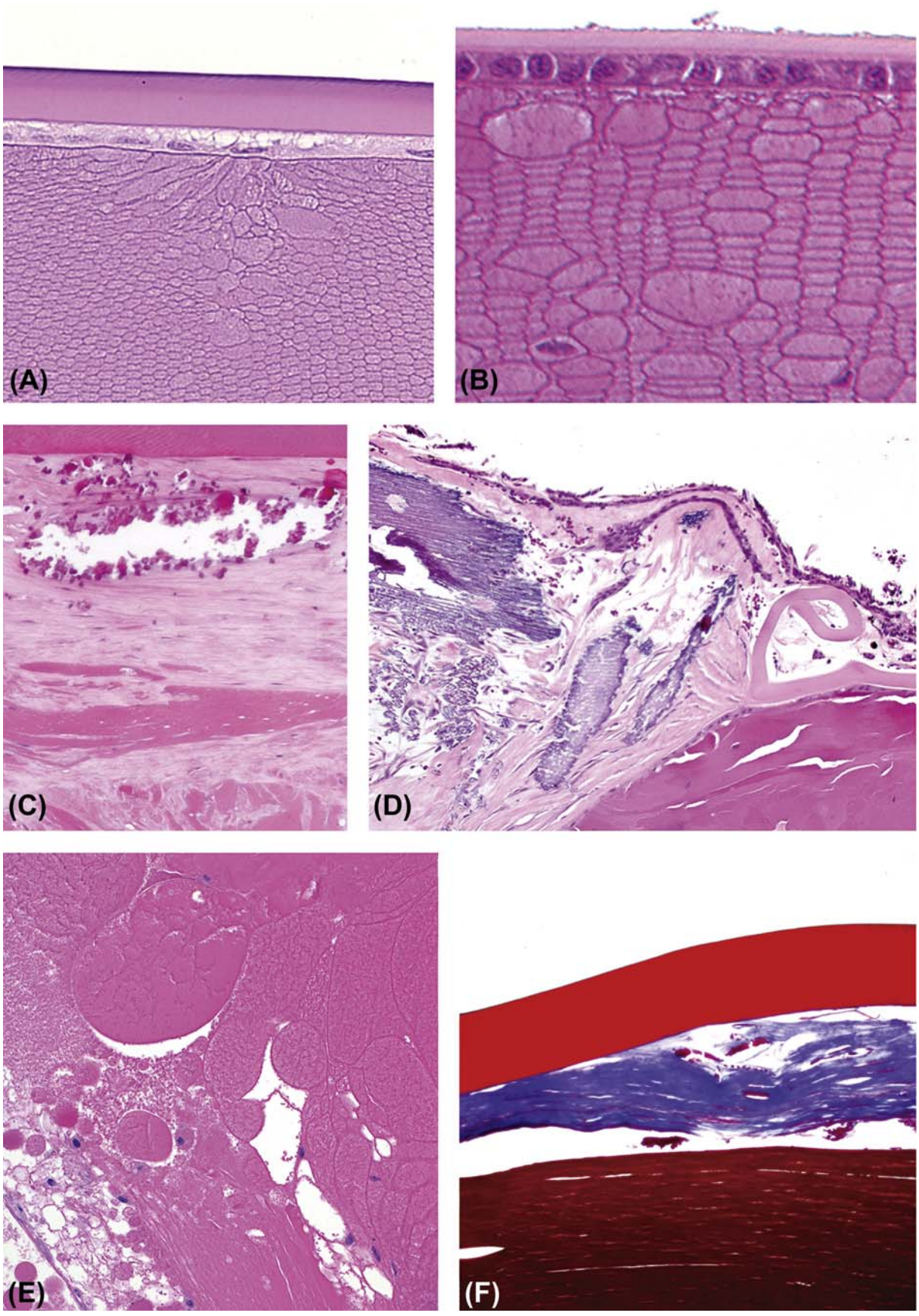

FIGURE 22A.19 **Pathology of the lens.** (A,B) Lens fiber swelling in the anterior cortex of a mouse eye, indicative of cortical cataract; Davidson's fixative. (C,D) Collagen deposition, spindle cell metaplasia of lens epithelial cells, and lens fiber mineralization as part of a subcapsular cataract. The lens capsule is ruptured and coiling in D. (E) Morgagnian globules (round and swollen degenerate lens fibers without nuclei) and bladder cells (swollen degenerate lens fibers with nuclei or nuclear fragments) with extensive disorganization of the lens fibers in a mature cortical cataract. (F) Collagen (blue) subtending the lens capsule (thick upper red band) secondary to spindle cell metaplasia of lens epithelial cells in the formation of a subcapsular cataract. (A) H&E, ×200; (B) H&E, ×400; (C) H&E, ×600; (D) H&E, ×400; (E) H&E, ×100; (F) Masson's trichrome, ×600. Source: *From Haschek, W.M., Rousseaux, C.G., Wallig, M.A. (Eds.), 2013. The Handbook of Toxicologic Pathology, third ed. Academic Press, San Diego, CA, Figure 53.18, p. 2150, with permission.*

(TVL) (Figure 22a.18C). PFV is a relatively common congenital abnormality in human eyes and has been reported as a congenital finding in Sprague–Dawley rats, Swiss mice, Göttingen minipigs, and Yucatan micropigs. PFV is also associated with several different mutant mouse models including the *p53*-null and Norie's disease homologue (*Ndph*) strains, and it can be induced in animals with double null mutations for members of the retinoic acid receptor family. Microscopically, remnants of small vascular profiles admixed with variable amounts of collagen and hemorrhage are present in the central vitreal canal anywhere from the optic nerve head surface to the posterior aspect of the lens.

Degeneration of the vitreous body can be hard to detect microscopically, but it can be seen macroscopically as liquefaction of the gel-like vitreous matrix. Degradation of the vitreous also may be recognized indirectly as the cause of retinal detachment. Liquefaction of the gel-like vitreous causes the retina to be buffeted by energy waves in the fluid media; in the absence of structural protection, the resulting trauma to the neural retina leads to retinal detachment and ultimately retinal degeneration. The formation of fibrovascular membranes (vitreal membranes) in the vitreous is a less common cause of vitreal and retinal traction bands that might promote physical pulling of the retina away from the RPE, and sometimes lead to retinal tearing. With age, changes in the rheologic (i.e., gel-like) features of the vitreous can cause it to separate from the retina spontaneously.

Since substances injected into the vitreous freely diffuse into the retinal tissue, the IVT route has become a popular method of drug delivery to the posterior segment of the eye. The injections are usually made at the level of the equatorial sclera and ciliary body *pars plana*, and are directed into the vitreous body rather than the retina proper. These injection sites usually present histologically as small defects in the ciliary body epithelium, stroma, and sclera, and can be associated with mild fibrosis and minimal infiltration of macrophages and lymphocytes.

Asteroid hyalosis is a degenerative condition characterized by small white opacities in the vitreous. It occurs in humans, dogs, and chinchillas. Clinically, these opacities are quite refractile, giving the appearance of stars (or asteroids) shining in the night sky. Histologically, they present as round, amphophilic, laminated to radiating structures of variable size within the vitreous. Asteroid hyalosis has been associated with aging, diabetes mellitus, hypertension, hypercholesterolemia, and (in dogs) intraocular tumors.

Vitreal inflammation is usually a secondary change rather than a primary response to vitreal disease. Vitritis is more likely to develop as a sequel to corneal ulceration, endophthalmitis, scleral perforations, or systemic infections rather than toxicant exposure.

Retina

Retinal toxicity primarily affects the retinal ganglion cells, photoreceptors, vessels, and the RPE. The RPE is closely integrated with the photoreceptors such that a toxic effect on the RPE will often affect the photoreceptors, and vice versa. It is important to notice that not all functional impairments of the neural retina or RPE will result in morphological alterations. This discrepancy underscores the importance of combined histological and electrophysiological endpoints when evaluating the impact of xenobiotic exposures on the eye, especially when seeking to detect very early stages of toxicity.

Inner retinal atrophy refers to a thinning of the nerve fiber layer and loss of retinal ganglion cells and neuronal nuclei in the inner nuclear layer (INL). The most common causes for loss of retinal ganglion cells and their axons in the nerve fiber layer are increased IOP leading to optic nerve atrophy and compressive lesions on the extraocular portion of the optic nerve, leading to axonal degeneration and ganglion cell death. The retinal ganglion cells can also be targeted by several known retinal toxicants, including carbon disulfide and doxorubicin. A few toxicants, like ethylcholine mustard aziridinium ion (AF64A), preferentially target the interneurons in the INL. Ganglion cell loss can also be spontaneous. Rhesus and cynomolgus monkeys with a condition called idiopathic optic neuropathy present with a loss of ganglion cells in the macular region, which is correlated to atrophy of axons in the temporal portion of the optic nerve.

Outer retinal atrophy is characterized by shortening of the photoreceptor outer segments along with loss of nuclei from the outer nuclear layer (ONL). These features are often seen following exposure to ocular toxicants. Other causes of outer retinal atrophy include inherited genetic defects, aging, light-induced damage, nutritional deficiencies, retinal detachment, and inflammation (Figure 22a.20). A common mistake in designing ocular toxicity studies is to automatically choose rodents as the test species. Hereditary outer retinal atrophy occurs in several strains of mice and rats, such as Royal College of Surgeons (RCS) rats or retinal degeneration (*rd*) mice. These animals are docile and make good experimental animals, but they lose essentially all of their photoreceptors by adulthood as a normal background condition.

Light-induced retinal atrophy/degeneration (usually RPE is not affected) occurs in albino rodents and is

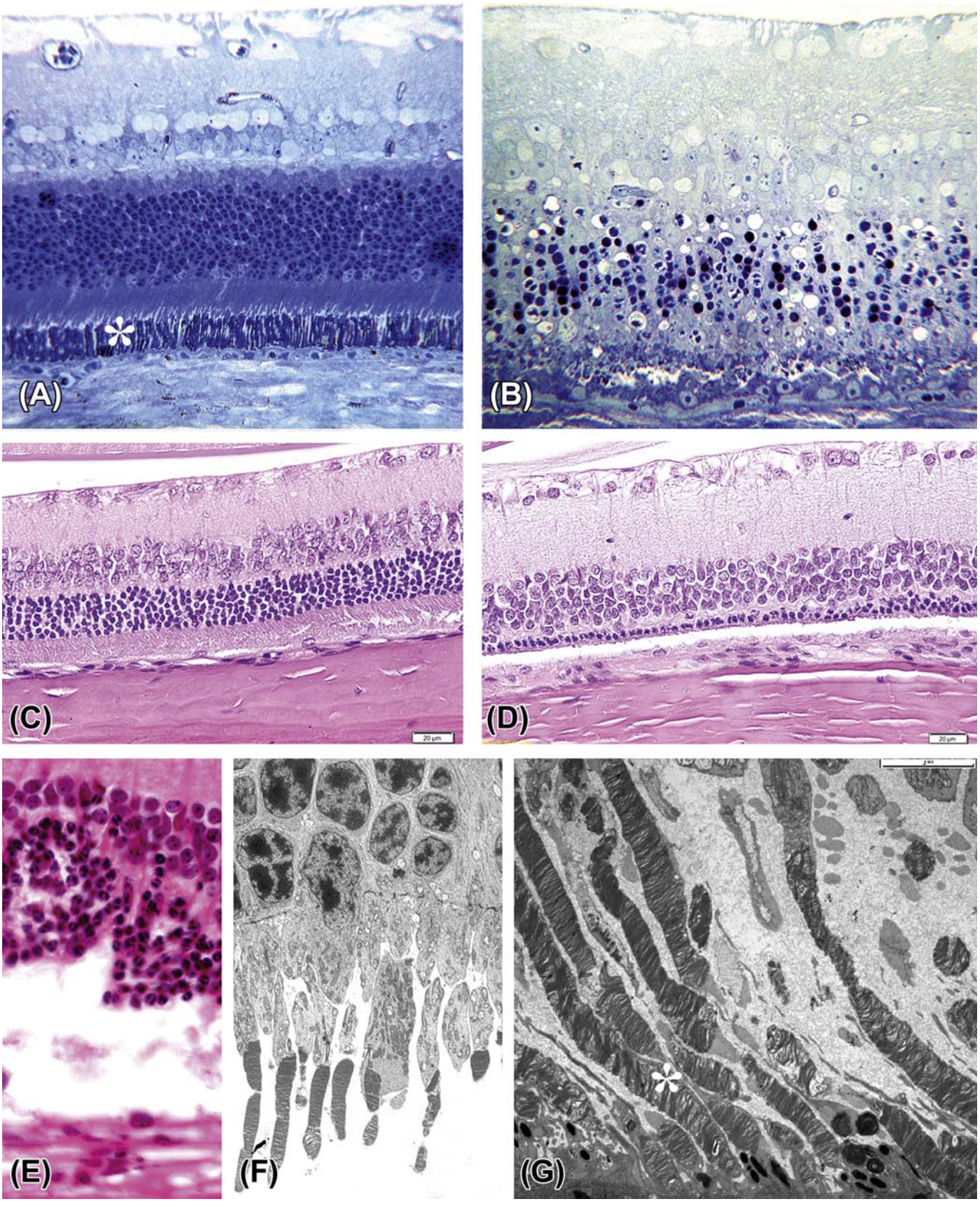

FIGURE 22A.20 Retinal photoreceptor lesions. (A) Plastic section of normal feline retina showing the intact photoreceptor outer segments (*). (B) Plastic section of a feline retina treated with a retinotoxic dose of a fluoroquinolone antibiotic, which manifests as vacuolation, necrosis, and atrophy of the photoreceptors. (C) Normal retina from an albino rat. (D) Photoreceptor atrophy at a toxic response of a test substance resulting in thinning of the outer nuclear layer (ONL) and almost complete absence of the inner and outer layers of the photoreceptor processes. (E) Jumbling of the ONL in another high-dose rat with a retinotoxic dose effect. (F) Transmission electron micrograph (TEM) showing swollen and distorted inner segments in a dog retina. (G) TEM focused on the outer segments from a nonhuman primate retina showing disarray in the expected stacking of the outer segment discs (*) as a response to test material. (A,B) Toluidine blue, ×200; (C,D) H&E, ×100; (E) H&E, ×400; (F) TEM, ×710; (G) TEM, ×2025. Source: *From Haschek, W.M., Rousseaux, C.G., Wallig, M.A. (Eds.), 2013. The Handbook of Toxicologic Pathology, third ed. Academic Press, San Diego, CA, Figure 53.21, p. 2158, with permission.*

caused by prolonged exposure to light or exposure to high-intensity light. These lighting conditions may occur if animals are kept in cages on the top of racks close to the room light source. Study protocols usually take this rodent idiosyncrasy into account. Nonetheless, in 2-year rodent bioassays, phototoxic changes are seen frequently as a background change, especially in females. The authors have seen 2-year studies where phototoxic retinopathy in albino rodents has presented with a pattern suggesting a dose- and sex-dependent toxic effect. We think that this phenomenon is associated with marginally high light levels combined with an otherwise trivial compound-related effect on one of the pathways associated with phototoxicity, such as oxidative stress or apoptosis, rather than to an overt ocular toxicity by the test article alone. In rats, a clue that the change is phototoxic rather than a test article–related retinal toxicity is an unusual vascular proliferation seen in the RPE layer of the retina (Figure 22a.21).

In contrast to a more diffuse outer retinal atrophy, focal atrophy of outer retinal segments may occur following choroidal circular disturbance. This finding is always associated with regional loss of RPE cells.

Global (full-thickness) retinal atrophy is an end-stage retinal lesion. It is characterized by complete collapse of the retinal architecture with extensive gliosis of the remaining retinal tissue.

Retinal detachment refers to the separation of the photoreceptor outer segment from the RPE. Retinal detachment is a very common processing artifact, so differentiation between genuine and artifactual retinal detachment is important. Three microscopic features are associated with true retinal detachment: subretinal deposits, hypertrophy of the RPE cells, and atrophy of the photoreceptor segments. The presence of subretinal deposits, such as blood, protein, or infiltrating leukocytes, represents definitive evidence of a real retinal detachment since these elements could not gain access to this potential space unless an active pathologic process has occurred. Hypertrophy of the RPE cells needs to be distinguished from RPE "tenting," an artifact that results from traumatic shearing of the retina during tissue trimming. In contrast to RPE hypertrophy, "tented" RPE cells present with angular apices with fragments of photoreceptor outer segments still attached to their surfaces.

Photoreceptor nuclei displacement (PDN) occurs in the retinas of many species, including humans. Histologically, it is characterized by typical or pyknotic photoreceptor cell nuclei located external to the retinal outer limiting membrane (OLM) (i.e., between the photoreceptor segments). PDNs, both pyknotic and nonpyknotic, can be found in areas of retinal degeneration or inflammation but also may be seen in control eyes. In rats, these cells are observed in all strains with a frequency of approximately 50% in normal retinas. PDNs are also more frequent in very young (developing) and aged retinas, in retinas of rats exposed to high ambient light levels, and in retinas associated with ocular and systemic diseases.

Retinal dysplasia is a focal or multifocal disorganization of the sensory retina due to faulty development. A common feature is the presence of rosettes (curved profiles of displaced full-thickness retina surrounding a central lumen). In the rat, rosettes appear as linear elevations of the retina, usually unilateral, on ophthalmic examination, and can be induced by the administration of cytosine arabinose, cycasin, *N*-methyl-*N*-nitrosurea, and trimethylin. Beagle dogs sometimes develop focal retinal dysplasia as a background lesion, often in or near the optic disc (Figure 22a.22). The change is usually quite small and does not appear to be associated with any functional abnormalities. Microscopically, focal to occasionally multifocal rosette-like and tubular structures that expand and distort the INL and/or ONL are observed. These structures exhibit variable morphology with a combination of the following features: (1) one to multiple layers of cells with nuclear profiles similar to neurons of the INL and ONL, (2) polarization of the nuclei away from the center or "lumen," (3) eosinophilic linear structures resembling photoreceptors inner segments and/or ciliated cells from primitive neuroepithelial origin in the innermost layer of the rosette, (4) a basement membrane-like structure near the center resembling the external limiting membrane of the retina, and (5) RPE-like cells or macrophages in the center of the rosettes. Rarely lesions can diffusely affect the retina.

Retinal folds have been reported as spontaneous findings in mice and rats (Sprague–Dawley and Wistar). In Sheffield-Wistar rats, these lesions may be congenital and associated with microphthalmia. Microscopically, focal inward projections of the retina with possible separation of the photoreceptor from the RPE are observed. Less severe lesions affect only the outer retinal layers and present as retinal microdetachments with subretinal accumulation of phagocytic cells and no change to the retinal surface contour. More severe folds affect all retinal layers and can be associated with subretinal hemorrhage and photoreceptor outer segments debris. Artifactual retinal folds (Lange's folds) have been described in the peripheral retina of young animals, and especially are associated with tissue fixation using 70% ethanol. When retinal folds are sectioned in a tangential histologic plane, they may resemble rosettes.

Vascular lesions may be induced in the retina by many toxicants. The most common toxicant-induced

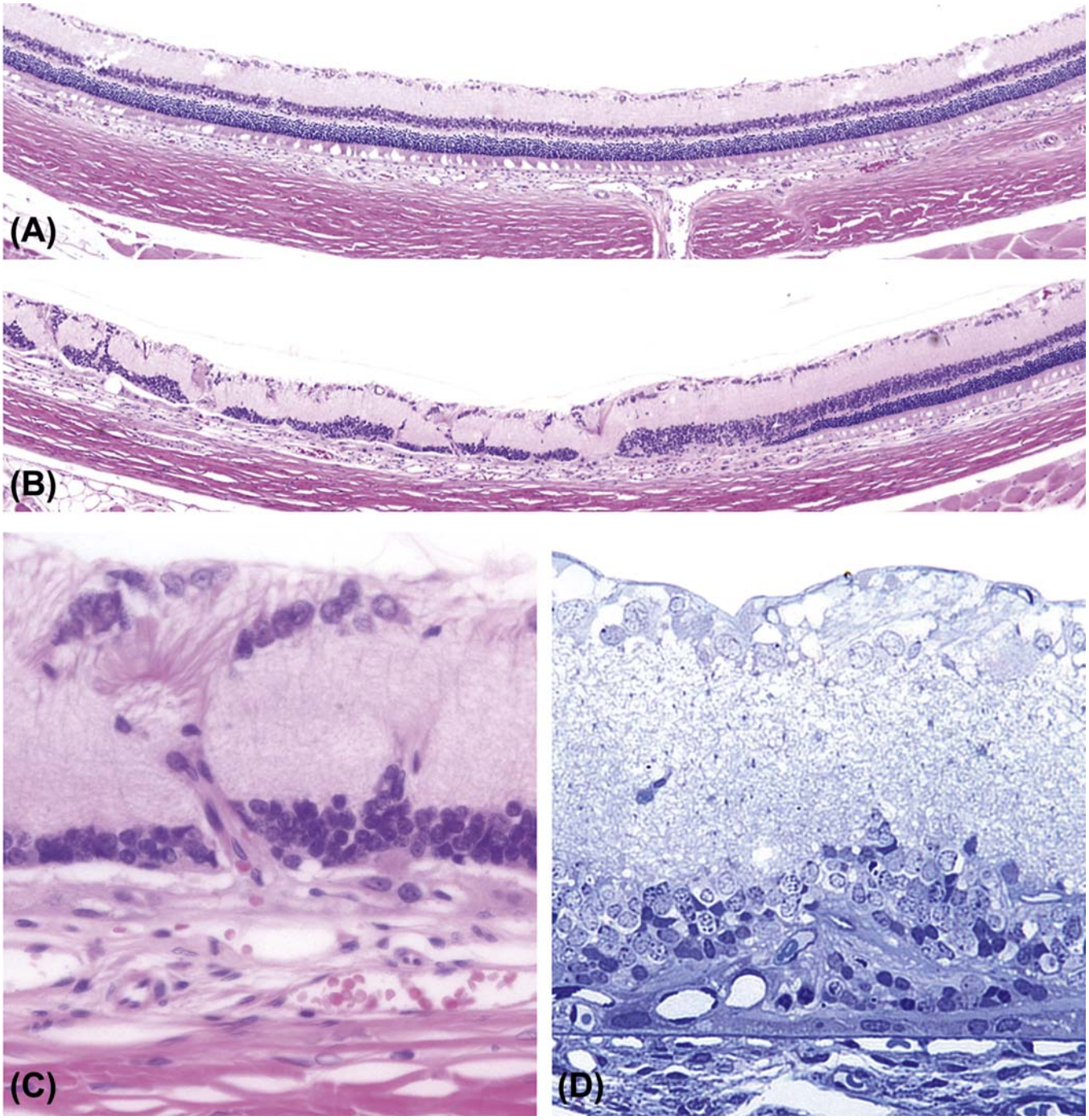

FIGURE 22A.21 **Chronic phototoxicity.** (A) Normal retina of an adult albino rat, showing the distinct alternating layers of nuclei and cell processes. (B) Segmental outer retinal atrophy in adult albino rat caused by phototoxicity, indicated by variable loss of the outer nuclear layer (ONL) and inner nuclear layer (INL) (especially toward the left of the image). (C) Higher magnification of the affected retina showing vascular proliferation into the retina and focal displacement of retinal nuclei. (D) Plastic section of a similarly affected area showing outer retinal atrophy and vessels growing in the RPE layer. (A,B) H&E, ×50; (C) H&E, ×600; (D) Toluidine Blue, ×600. Source: *From Haschek, W.M., Rousseaux, C. G., Wallig, M.A. (Eds.), 2013. The Handbook of Toxicologic Pathology, third ed. Academic Press, San Diego, CA, Figure 53.4, p. 2108, with permission.*

vascular changes in the retina include capillary proliferation, microaneurysms, vessel wall thickening and calcification, edema and hemorrhage, and vascular necrosis. Toxic retinal hemorrhage must be distinguished from other causes such as hypertension, coagulopathies, trauma, primary vascular ocular diseases, and (in rodents) chest compression during handling (Figure 22a.23).

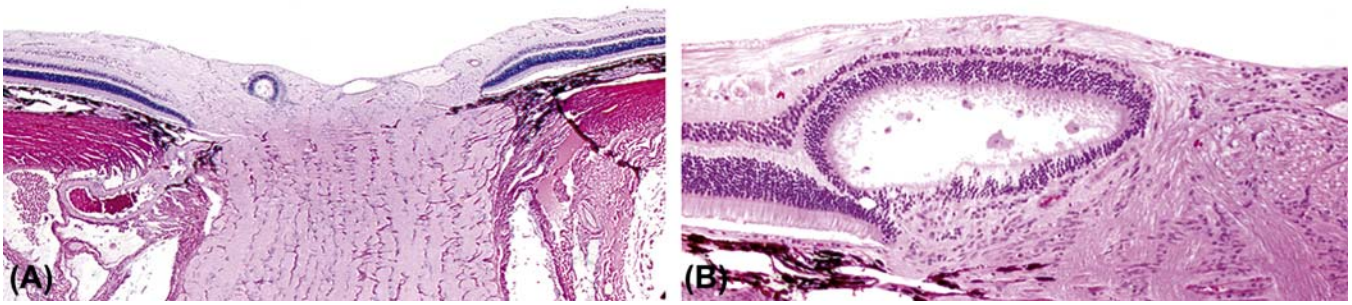

FIGURE 22A.22 **Retinal rosette.** (A,B) Incidental retinal rosette in the optic nerve head as a background lesion in some lines of experimental Beagle dogs. (A) H&E, ×100; (B) H&E, ×200. Source: *From Haschek, W.M., Rousseaux, C.G., Wallig, M.A. (Eds.), 2013. The Handbook of Toxicologic Pathology, third ed. Academic Press, San Diego, CA, Figure 53.30, p. 2168, with permission.*

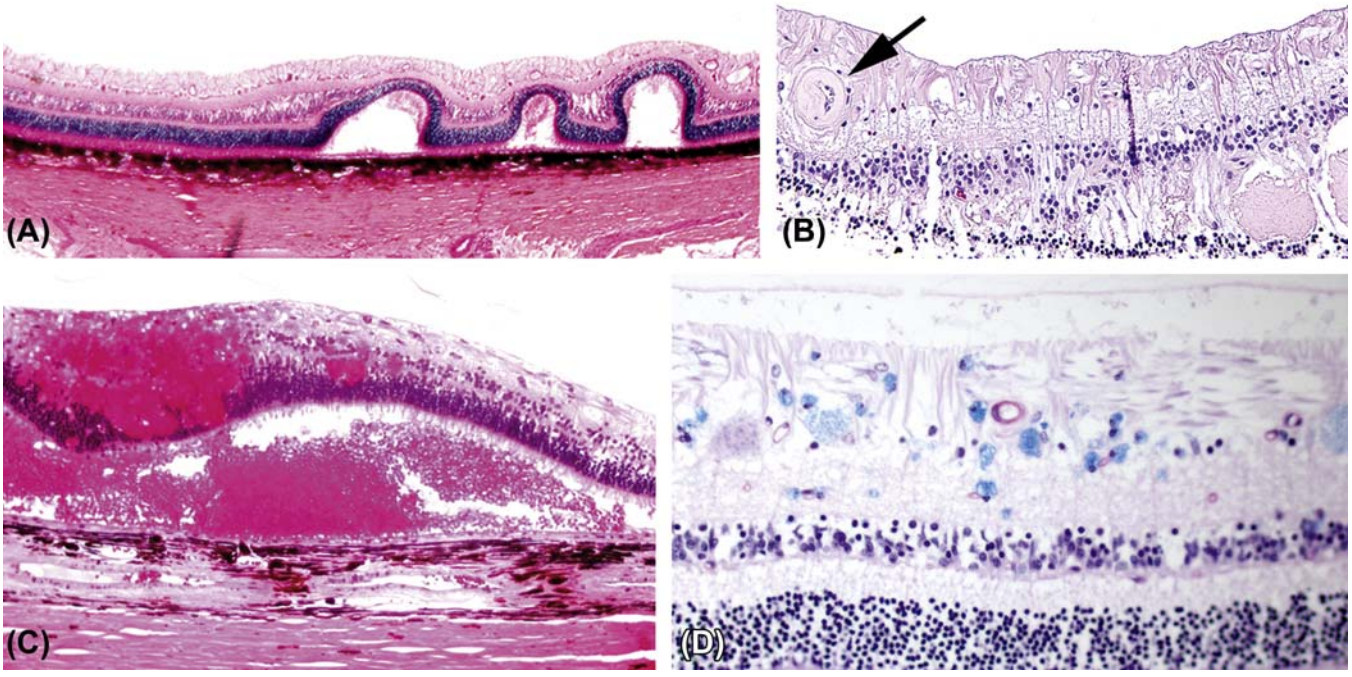

FIGURE 22A.23 **Retinal folds and accumulations.** (A) Retinal folds in a dog after an invasive procedure. (B) Hypertensive vasculopathy [thickened vessel wall (*arrow*)] and ganglion cell loss and outer retinal atrophy in a dog. (C) Extensive retinal and subretinal hemorrhage in a dog following radiation therapy (radiation retinopathy). (D) Accumulation of blue metabolic byproduct in the cytoplasm of neurons from a dog with an undetermined lysosomal storage disease. (A) H&E, ×100; (B,C) H&E, ×200; (D) Luxol fast blue/PAS, ×400. Source: *From Haschek, W.M., Rousseaux, C.G., Wallig, M.A. (Eds.), 2013. The Handbook of Toxicologic Pathology, third ed. Academic Press, San Diego, CA, Figure 53.26, p. 2165, with permission.*

Retinal Pigmented Epithelium

Hypertrophy and hyperplasia of the RPE cells, cytoplasmic accumulation of lipids or lipofuscin, cell atrophy, loss of polarity, and formation of drusen (subretinal lipid-rich deposits) are common changes seen following toxicant exposure. Many compounds bind chemically to melanin and therefore accumulate in pigmented cells and tissues, particularly the RPE. Melanin binding does not predict ocular toxicity. Some drugs can be detoxified by melanin binding (e.g., fenthion and vigabatrin), while others may accumulate locally in the pigmented layers of the eye and thus enhance the toxic effect (e.g., chloroquine and phenothiazines). The pathologist needs to be aware of normal physiologic and background changes on RPE cells when assessing the significance of ocular alterations. Common physiologic changes of RPE that may be misinterpreted as evidence of ocular toxicity include age-related cytoplasmic accumulation of lipofuscin,

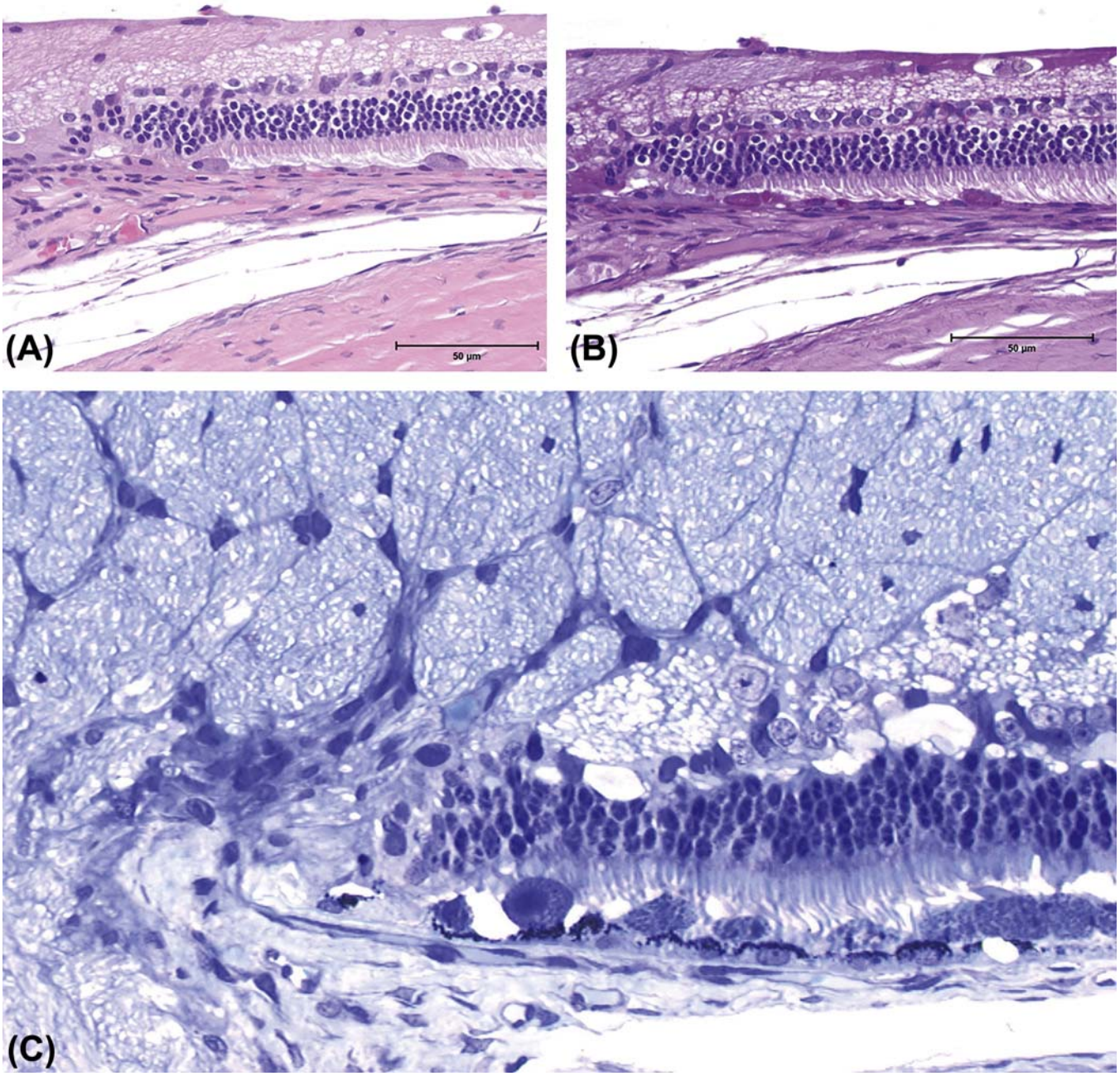

FIGURE 22A.24 **Spontaneous background changes in RPE.** (A,B) Retina of a Dutch-belted rabbit near the optic nerve demonstrating swollen (hypertrophied) RPE cells weakly staining positive for polysaccharides using the periodic acid-Schiff (PAS) stain. (C) Plastic section from another Dutch-belted rabbit showing the same RPE features. (A) H&E, ×100; (B) PAS, ×100; (C) Toluidine blue, ×400. Source: *From Haschek, W.M., Rousseaux, C.G., Wallig, M.A. (Eds.), 2013. The Handbook of Toxicologic Pathology, third ed. Academic Press, San Diego, CA, Figure 53.28, p. 2167, with permission.*

variations in cytoplasmic pigmentation, and focal areas of RPE hypertrophy.

Hypertrophy and hyperplasia of the RPE are common changes associated with toxicant exposure. Hypertrophy of the RPE cells is often associated with detachment of the sensory retina or photoreceptor death. Drug-induced hypertrophy often presents as a uniformly thickened RPE with a closely apposed retina. Dutch-belted rabbits develop an idiopathic hypertrophy of the RPE cells as a common background change. Affected RPE cells are usually located near the optic nerve and appear as cells of increased size with swollen and granular cytoplasm. Focally this change might be associated with secondary atrophy of the outer retina (Figure 22a.24). Hypertrophied RPE cells are recognized on light microscopy as larger-than-normal cells

that may possess unusual melanin pigmentation (reduced numbers or irregular distribution within the cell). In some cases, melanin granules might fuse with lipofuscin granules to form granular conjugates.

Atrophy of the RPE is an age-related lesion that eventually results in cell degeneration and cell death. Chronic atrophy of RPE is associated with degeneration and atrophy of the adjacent outer retina. Microscopically, affected areas have reduced numbers or a complete absence of RPE cells. In these areas, if the retina is not detached, there is direct contact of the outer retina with Bruch's membrane. In an attempt to maintain the blood−retinal barrier and tissue homeostasis, the remaining RPE cells will spread laterally to compensate for any spatial defects, though the RPE cells may appear be attenuated.

Drusen are irregular extracellular deposits composed primarily of apolipoproteins located between the RPE and Bruch's membrane. They likely are derived from RPE metabolism of the outer segments of photoreceptors and members of the complement system, particularly factor H. Zinc present in drusen is thought to have a role in the precipitation and activation of the complement system. Drusen may accumulate due to impaired transport of the debris through Bruch's membrane into the choroidal circulation. Drusen are primarily seen in AMD in humans, and thus are rarely observed in species other than primates. However, "hard" drusen (concentric, nodular masses with well-defined borders) may be observed infrequently in other species.

Intracytoplasmic inclusions can be hosted by RPE. Intracytoplasmic inclusions can be associated with abnormal accumulation of lipofuscin or other pigments that are metabolic byproducts of RPE processing of shed photoreceptor outer segments. Lipofuscin and lipofuscin conjugates (i.e., melanolipofuscin) often accumulate in the base of the RPE cytoplasm as granules. They are generally not observed on light microscopy because they are removed during tissue processing. Instead, clear vacuoles generally remain as residual footprints representing the former presence of cellular accumulations. Lipofuscin accrues spontaneously with age due to impaired ability to properly remove the granules from the cell, and it may also occur with ocular toxicities. Occasionally, cytoplasmic crystals may be observed. Other RPE cytoplasmic inclusions may appear as abnormal organelles containing concentric membranous whorls. On electron microscopy, these membranes may have a lamellated (fingerprint-like) appearance reminiscent of the photoreceptor outer segments (from which they may be derived), and are osmophilic due to their phospholipid content.

RPE depigmentation results from loss of RPE melanin. This change occurs spontaneously as an age-related change. It may also be associated with toxicities in which the toxic agent can bind to melanin, including toxic metals and amines. Melanin may also be taken up by lysosomes of RPE cells and/or fuse with lipofuscin, resulting in apparent diffusion of pigment. Photobleaching of melanosomes also results in diminished pigmentation, although the pigmented granules are still present. Microscopically, a decrease in the amount, distribution, and shape of melanin granules within individual RPE cells can be observed. The distribution of depigmented lesions is usually multifocal to regional.

Optic Nerve

The optic nerve responds to injury in a limited number of ways, and the majority of them are similar to responses in other areas of the CNS. Increased pressure within the cranium can result in clinically apparent swelling and rostral displacement of the optic nerve head into the eye, a protrusion known as papilledema. Gliosis is a common but nonspecific reaction of the optic nerve neuropil to many different insults and can be a sign of early disease. Liquefactive necrosis (malacia) of the optic nerve occurs in association with ischemic (e.g., retrobulbar hemorrhage secondary to blood collection) or inflammatory insults. Necrosis is one of the initial optic nerve alterations seen in acute cases of glaucoma and also is very common in suppurative intraocular inflammation that involves the retina and extends into the optic nerve. As in other parts of the CNS, liquefaction of the optic nerve leads to infiltration with macrophages (gitter cells), many of which may contain eosinophilic intracytoplasmic debris believed to be digested myelin. As a consequence of optic nerve head necrosis in association with high IOP seen in glaucoma, the optic nerve collapses at the lamina cribrosa and the residual nerve tissue is displaced caudally into the sclera (an effect called "optic nerve cupping"). In some cases, a focal loss of optic nerve neuropil allows the vitreous to prolapse into the optic nerve trunk to form a cavitated lesion (termed "Schnabel's cavernous atrophy"). This process is usually associated with glaucoma in dogs and is thought to be an age-related change in humans.

Axonal degeneration occurs in several circumstances in the optic nerve. Loss of retinal ganglion cells, and consequently their axons, secondary to glaucoma is probably the most common cause. On the other hand, lesions in the orbital or intracranial portions of the optic nerve can cause Wallerian degeneration with consequent axon loss and ganglion cell death. Among these lesions are trauma, leading to optic nerve crush, severance or avulsion, and also nerve compression caused by tumors, periosteal proliferation at the optic foramen

(where the nerve enters the calvarium), or granulomatous inflammation. Primary dysmyelination (abnormal formation) and demyelination (pathologic loss) affecting the optic nerve are rare in animals, but multiple mouse models of both processes have been developed to study human diseases like Pelizaeus-Merzbacher disease and multiple sclerosis.

The final stage of optic nerve lesions is characterized by axonal atrophy and varying degrees of fibrosis. At this point, optic nerve function is irreversibly lost.

Rarely, rhesus or cynomolgus macaques develop a bilaterally symmetrical optic nerve atrophy characterized by an absence of retinal ganglion cells from the macula, and therefore an absence of axons in the temporal portion of the optic nerve. Affected animals might have minimal to severe involvement, the extent depending on the degree of ganglion cell loss. Only the most severely affected animals have been able to be detected antemortem by fundoscopic examination (Figure 22a.25).

Tissue Response to Increased Intraocular Pressure and Glaucoma

Contrary to what many believe, increased IOP does not define glaucoma. Rather, glaucoma is a diverse group of diseases united by a common theme in which IOP is too high for the retina/optic nerve to function normally, thus resulting in progressive vision loss. The loss of vision is specific and characterized by atrophy of the optic disc (manifested as cupping) and (in humans) characteristic patterns of visual field dysfunction. Increased IOP is almost always related to an obstruction (partial or complete) of the aqueous drainage pathways. This obstruction can affect the structures of the iridocorneal angle (ICA) directly or adjacent outflow pathway structures like the pupillary space, anterior chamber, and scleral drainage vessels. A primary obstruction of the ICA is usually seen with congenital malformations [goniodysgenesis (abnormal development of the intraocular channels for fluid egress) in dogs and anterior segment dysgenesis/congenital glaucoma in multiple species]. Secondary obstructions can affect all levels of the aqueous drainage pathways and are associated with ocular or systemic diseases. The most common ocular lesions that can obstruct the aqueous pathways and cause glaucoma are intraocular hemorrhage, endophthalmitis, uveitis, anterior uveal fibrovascular membranes and synechiae (iris adhesions), melanin pigment deposition in the trabecular meshwork (TM) (pigment dispersion), anterior lens luxation, and intraocular tumors. Regardless of the cause, the increased IOP can cause global enlargement of the eye (buphthalmos). A number of secondary changes develop subsequently, including corneal stromal edema and neovascularization; multiple breaks in Descemet's membrane (termed "Haab's striae"); scleral atrophy at the limbus, which can evolve to a staphyloma (i.e., outward bulging of the thin atrophic sclera); collapse of the ciliary cleft; and atrophy of the iris, ciliary body and TM. In some cases, animals can develop cataracts and lens luxation due to stretching and breaking of the lens zonular ligaments. One of the central histological features of glaucoma is the loss of ganglion cells in the inner retina and atrophy of the optic nerve.

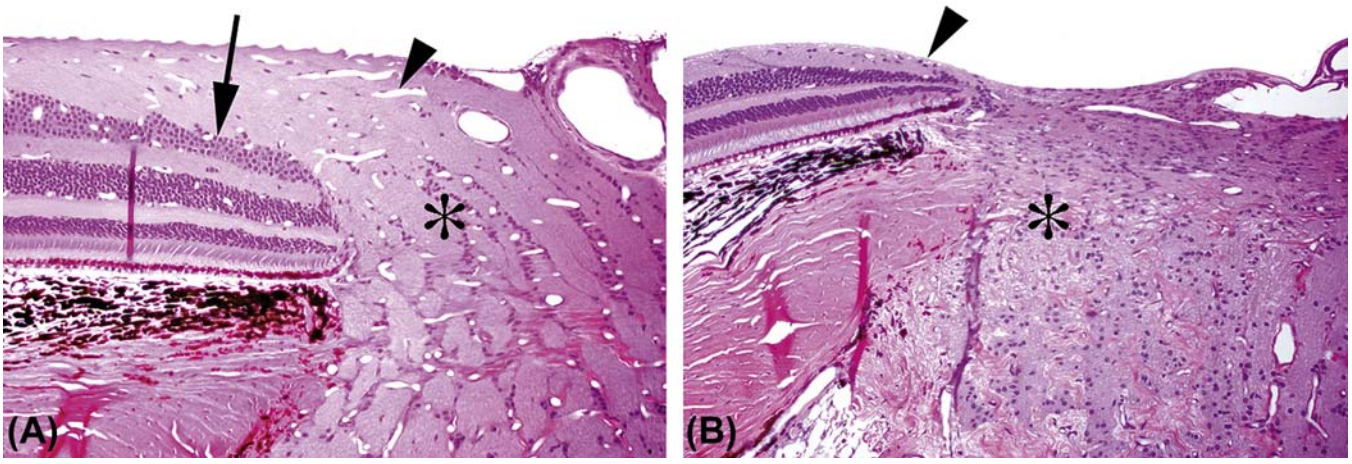

FIGURE 22A.25 **Bilateral optic atrophy.** (A) Image of the temporal aspect of the normal optic nerve head from a control cynomolgus macaque showing a thick nerve fiber layer (*arrowhead*), abundant ganglion cells (*arrow*), and normal appearance of the temporal aspect (*) of the optic nerve within the lamina cribrosa. (B) Image of the same area from an affected macaque. The nerve fiber layer is thin (*arrowhead*), the ganglion cells are reduced in number (*arrowhead*), and the temporal aspect (*) of the optic nerve is atrophic. (A,B) H&E, ×200. Source: *From Haschek, W.M., Rousseaux, C.G., Wallig, M.A. (Eds.), 2013. The Handbook of Toxicologic Pathology, third ed. Academic Press, San Diego, CA, Figure 53.29, p. 2168, with permission.*

The mechanisms of glaucomatous optic nerve and retinal damage remain subject to debate. Of the many proposed mechanisms, the most popular hypotheses are given here:

- Elevated IOP leads to deformation of the optic nerve axons at the lamina cribrosa and blockade of anterograde and retrograde axonal transport. This stoppage, in turn, leads to death of retinal ganglion cells due to an interruption in the supply of neurotrophic factors from the CNS.
- Elevated IOP deforms the lamina cribrosa, resulting in decreased vascular perfusion of the optic nerve head microcirculation. Ischemia produces a loss of axonal integrity and subsequent death of retinal ganglion cells.
- Elevated IOP leads to optic nerve infarction and subsequent gliosis.
- Retinal ganglion cell loss may result from the pathologic release of glutamate from neurons within the damaged retina, which initiates "excitotoxic" neurodegeneration of neighboring neurons.
- Decreased choroidal perfusion causes segmental retinal degeneration affecting both inner and outer retina.

Any or all of these proposed mechanisms might play a role, depending on the species and the underlying pathophysiology of the different glaucoma syndromes. In dogs, the retinal atrophy can affect all retinal layers and is usually more prominent in the nontapetal (ventral) than in the tapetal (dorsal) retina. This phenomenon is called "tapetal sparing," and it is a typical feature of glaucoma in the dog. Necrosis of the optic nerve is an early feature of glaucoma, and it often is followed by malacia, gliosis, and the formation of a deep optic nerve cup. In species other than the dog, the development of gliosis and optic nerve cupping follows a less precipitous course. In glaucomatous optic neuropathy, there is a loss of large-diameter optic nerve axons and consequent optic nerve atrophy (Figure 22a.26).

MECHANISMS OF OCULAR TOXICITY

Developmental Abnormalities

The embryology or the eye is complex and involves numerous inductive relationships in which one component works by proximity to stimulate a developmental event in another component, often one derived

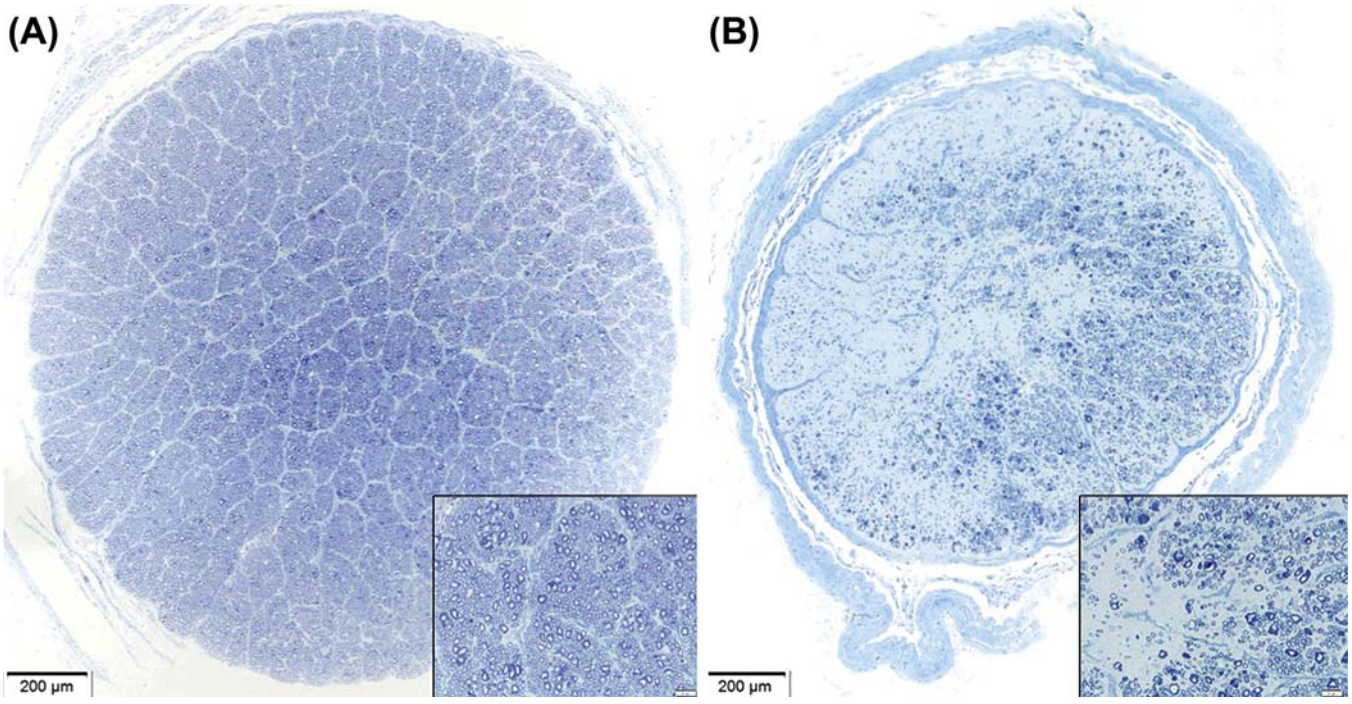

FIGURE 22A.26 **Optic nerve lesions due to congenital glaucoma.** Transverse sections of the orbital portion of the optic nerve from a cat. (A) Control animal, showing the appropriate number of axons highlighted by their thick myelin sheaths. (B) Congenital glaucoma in a 36-month-old cat, with marked atrophy of the optic nerve characterized by a smaller overall size of the nerve trunk and multifocal to coalescing areas (of pallor) due to axon degeneration and fibrosis. (A,B) Toluidine blue, ×100; insets ×600. Source: *From Haschek, W.M., Rousseaux, C.G., Wallig, M.A. (Eds.), 2013. The Handbook of Toxicologic Pathology, third ed. Academic Press, San Diego, CA, Figure 53.32, p. 2179, with permission.*

from a different germ layer. Ocular developmental abnormalities are common in humans, domestic animals, and laboratory animals. They can be a part of hereditary disease processes, or they can be induced by exposure to teratogenic compounds that affect development of the eye in utero without affecting the genome. In either case, ocular abnormalities can be limited to the eye or periocular tissues, but they are often part of systemic syndromes where the effect on ocular tissues is but one of many lesions induced in multiple organ systems sharing a common critical period of development (see Chapter 25: Embryo, Fetus, and Placenta). Toxicity studies often need to evaluate for either genotoxic or teratogenic potential, and evaluation of the developing eye in treated conceptuses has a role in modern toxicologic pathology. Although the mouse model is most often used for this assessment, the zebrafish model has many potential advantages including the rapid pace of embryonic development, the transparency of fish embryos throughout the period of ocular embryogenesis, and the large numbers of offspring. The most common ocular developmental problems encountered in both the teratogenic and genetic scenarios are lesions that involve inductive phenomena such as closure of the optic fissure, separation of the lens vesicle, or replacement of the primary vitreous. Congenital cataract or abnormalities of lens size or position are other frequent problems that may be observed in developmental toxicity studies. We provide a list of known teratogenic substances affecting the eye in Table 22a.4.

Toxicity of the Eyelids and Ocular Glands

Several drugs and chemicals can cause alterations involving the eyelids. Edema of the eyelids can occur from systemic administration of aminodipropionitrile to monkeys. Polychlorinated biphenyl (PCB) poisoning produces chloracne in humans. In this condition, PCBs and similar compounds cause swelling of the eyelids with meibomian gland hypersecretion and abnormal pigmentation of the conjunctiva. Chronic application of topical epinephrine to rabbit eyes results in a syndrome that has been called meibomian gland dysfunction, which is characterized by plugging of the orifice of the glands, formation of microcysts, and enlargement of the gland. Retinoids, like isotretionoin (13-*cis*-retinoic acid), have been recognized to affect the meibomian glands, causing blepharoconjunctivitis in humans and mild conjunctival erythema and crusting of the eyelid margins in New Zealand white rabbits.

Toxaphene administered orally to cynomolgus monkeys has been reported to produce meibomian gland inflammation, enlargement, or both. The pathogenesis involves infected diverticula (arising from the glandular ducts) in both the dorsal (superior) and ventral (inferior) eyelids.

Systemic administration of small molecules that inhibit epidermal growth factor receptor (EGFR) may produce granulomatous inflammation of the meibomian gland. The pharmacologic effect is suspected to be related to a failure to secrete glandular contents. Continued production of secretory material leads to glandular rupture and a substantial lipogranulomatous reaction.

Prostaglandin analogs (latanoprost, travoprost, and bimatoprost) used to decrease IOP can also cause lengthening of the eyelashes (hypertrichosis). The mechanism is unknown but may involve eyelash lengthening during the anagen phase of the lash growth cycle and stimulation of melanogenesis.

Ptosis (drooping eyelids, especially affecting the dorsal lid) and eyelid retraction are relatively common reactions to systemic or locally administered xenobiotics. Snake venoms, especially from elapids (e.g., cobras) and some vipers, succinylcholine, and botulinum toxin can cause ptosis by blocking neurotransmission at the neuromuscular junctions. Other less common drugs associated with ptosis are tetraethylammonium, a ganglion blocker agent; guanethidine, a sympatholytic drug used to reduce lid retraction; penicillamine, a metal-chelator; the sedatives primidone, barbiturates and alcohol; and the chemotherapic agent vincristine. No common mechanism of action has been defined to explain the toxic response to these agents. On the other end of the spectrum, stimulants such as phenylephrine, amphetamine, and cocaine are associated with upper eyelid retraction.

Blepharitis (inflammation of the eyelid) and conjunctivitis (inflammation of the inner lid lining) are common reactions to numerous topical ocular drugs. Drug preservatives such as thimerosal and benzalkonium chloride as well as antiviral agents like vidarabine, trifluridine, and idoxuridine are reported to cause ocular irritation. Most commonly used ophthalmic preparations present the potential for incidentally causing blepharitis and conjunctivitis.

Many inbred mouse strains, including BALB/cJ, BALB/cByJ, CBA/J, and 129P3/J, are reported to develop spontaneous ulcerative blepharitis. Although *Corynebacterium* sp. has been isolated from those lesions, the underlying abnormality and causative agent(s) are not totally clear. Mutations in the desmoglein 3 (*Dsg3*) gene were reported to be the main factor underlying ulcerative blepharitis in $Dsg3^{bal}$ and $Dsg^{3bal\text{-}Pas}$ mice (balding and balding Pasteur, respectively). These animals develop a pemphigus-like reaction with formation of suprabasilar vesicles affecting the mucocutaneous junctions. Such changes are identical to those observed in humans and animals with pemphigus vulgaris.

TABLE 22A.4 Chemicals and Drugs Causing Eye Malformations

Chemical	Animal	Malformation
Actinomycin	Rat	Anophthalmia, coloboma
Adenine	Rat	Anophthalmia, microphthalmia
Adrenalin (epinephrine)	Rat	Cataract
Alcohol	Mouse	Coloboma, open eye
	Rat	Anophthalmia, opaque lens
Alloxan	Mouse, rat	Microphthalmia
6-Aminonicotinamide	Mouse	Microphthalmia, open eye, retinal folds
	Rat[a]	Lens vacuolation, retinal folds
Aminophenurobutane	Rat	Anophthalmia, microphthalmia, no optic nerve
Aminothiadiazole	Rat[a]	Anophthalmia, microphthalmia
Arsenic	Hamster	Anophthalmia
	Mouse	Anophthalmia, open eye
	Rat[a]	Anophthalmia, microphthalmia
5-Bromodeoxyuridine (BrdU)	Mouse	Open eye
Cadmium	Hamster	Microphthalmia
	Mouse	Anophthalmia, microphthalmia
	Rat[a]	Anophthalmia, microphthalmia
Carbutamide	Mouse	Anophthalmia, microphthalmia, cataract
	Rat	Anophthalmia, no optic nerve
Chloraminophen	Mouse	Microphthalmia, no optic nerve
Chloroquine	Rat	Anophthalmia, microphthalmia
Congo red	Rat	Anophthalmia, microphthalmia
Cyclopamine	Rabbit	Cyclopia
Cyclophosphamide	Mouse	Aphakia, open eye
	Rabbit	Coloboma, microphthalmia, retinal folds
	Rat[a]	Cataract, exophthalmos, open eye
Cytosine arabinoside	Mouse	Retinal dysplasia
	Rat	Retinal dysplasia
Diphenylhydantoin	Mouse	Open eye
Dithiocarbamate	Rat[a]	Exophthalmos
1-Ethyl-1-nitrosourea (ENU)	Mouse	Anophthalmia, microphthalmia, exophthalmos
Ethylenediaminetetraacetic acid (EDTA)	Rat[a]	Anophthalmia, microphthalmia
Ethylenethiourea	Rat	Coloboma, exophthalmos
Galactose	Rat	Anophthalmia, cataract
Glucagon	Rat	Glaucoma, microphthalmia
Griseofulvin	Rat	Anophthalmia
Hycanthone	Mouse	Microphthalmia

(*Continued*)

TABLE 22A.4 (Continued)

Chemical	Animal	Malformation
Hydrazine	Mouse, rat	Anophthalmia, microphthalmia
Hydrocortisone	Guinea pig	Open eye
Leucine	Rat	Anophthalmia, microphthalmia
Lithium	Rat	Anophthalmia
Methamphetamine	Mouse	Anophthalmia, microphthalmia
	Rabbit	Cyclopia
Mercury	Rat	Exophthalmos, microphthalmia, opaque cornea, and lens
Niagara sky blue 6B	Rat[a]	Anophthalmia, microphthalmia
Ochratoxin A	Mouse	Anophthalmia, open eye
Perphenazine	Rat	Anophthalmia
Pesticides (aldrin, dieldrin, endrin)	Hamster	Open eye
Phthalic esters	Rat	Anophthalmia
Procarbazine	Rat	Anophthalmia, microphthalmia
Reserpine	Rat	Anophthalmia
Retinoic acid	Hamster	Microphthalmia
	Mouse, rat	Anophthalmia, exophthalmos, microphthalmia, open eye
Ribavirin	Hamster	Anophthalmia, microphthalmia, open eye
Rubidomycin	Rat	Anophthalmia, microphthalmia,
Rubratoxin	Mouse	Open eye
Saccharine	Rat	Lens necrosis, abnormal optic nerve
Salicylate	Rat	Open eye, retinals dysplasia
Serotonin	Mouse	Anophthalmia
	Rat	Anophthalmia
Streptonigrin	Rat[a]	Microphthalmia
Triparanol	Rat[a]	Anophthalmia, microphthalmia
Trypan blue	Mouse	Anophthalmia, microphthalmia,
	Rat[a]	Anophthalmia, microphthalmia, lens degeneration, abnormal optic nerve, retinal dysplasia
Urethane	Rat	Open eye, lens vacuolation
Vinblastine, vincristine	Hamster	Anophthalmia, microphthalmia
	Mouse	Anophthalmia
	Rat[a]	Anophthalmia, microphthalmia

[a]*50% or more of the surviving fetuses have eye malformations.*
From Haschek, W.M., Rousseaux, C.G., Wallig, M.A. (Eds.), 2013. The Handbook of Toxicologic Pathology, third ed. Academic Press, San Diego, CA, Table 53.2, pp. 2106–2107, with permission.

The glands of the lacrimal system are not often the target tissue of toxicants. Few compounds have been reported to be toxic to the lacrimal glands of animals. Among the drugs that do target these organs are phenazopyridine, sulfadiazine, and salicylazosulfapyridine. These drugs are reported to cause marked necrosis of the lacrimal gland, with evolution to fibrosis through an unknown mechanism. Dogs that present with this toxic reaction can later develop KCS (dryness of the conjunctiva and cornea).

Toxicity of the Ocular Surfaces

The corneal and conjunctival epithelium, along with the tear film, are the first tissues to be exposed when a substance is deposited on the surface of the eye. Due to their close proximity, the cornea and conjunctiva are exposed simultaneously. The pathological responses of both tissues usually are also very similar.

One of the most popular routes for clinical administration of ocular therapeutics is via subconjunctival injections. Subconjunctival administration of drugs associated with biodegradable drug implants designed for sustainable drug delivery also is common practice in nonclinical toxicology studies. Poly[D,L-lactide-co-glycolide] (PLGA) or poly[D,L-lactide-co-caprolactone] are among the most common biodegradable polymers used for this purpose; in particular, PLGA has been used extensively in studies to deliver a wide variety of drugs using various forms such as microparticles, emulsions, implants, and hydrogels. These polymers degrade through hydrolysis of their ester bonds into lactic acids, glycolic acids, and caproic acid—and eventually into water and carbon dioxide. In most instances, these subconjunctival implants cause minimal to no tissue reaction, and when one does develop local conjunctival hyperemia and edema are the most common responses. In the rare instances where substantial toxic reactions are observed, they are usually related to failed degradation of the polymer with secondary conjunctival fibrosis of the substantia propria to encapsulate the implants. When subconjunctival injections are part of the study design, the conjunctiva should be evaluated microscopically, especially in the area of the injection.

The conjunctiva and cornea are at great risk from accidental exposure to caustic chemicals such as strong acids and bases, which can easily erode the epithelium to expose the underlying tissues. During chemical burns, the conjunctiva usually develops the earlier changes. In mild acid burns the initial clinical alterations are turbidity and dulling of the conjunctival surface with tissue hyperemia and possibly petechial hemorrhages. With stronger acids, both conjunctiva and cornea become opaque immediately. There is loss of conjunctival epithelium followed in mild cases by rapid regeneration (5–10 days). In severe cases, the conjunctival substantia propria is more affected, and the final result is formation of granulation tissue followed by scaring.

Irritating substances can cause necrosis of the corneal epithelium directly. Acid and alkali burns (described in more detail later) can cause neurotrophic keratitis, a form of corneal degeneration resulting from altered corneal sensory enervation. Surfactants can disrupt the tear film, sensitizing the corneal surface to infection or deep ulceration. Among them, benzalkonium chloride, which is used to increase the penetration of certain drugs to the eye, can cause conjunctival hyperemia, corneal opacification, corneal edema, and occasionally epithelial degeneration and necrosis.

The most common acids that may be involved in ophthalmic injuries are sulfuric and sulfurous acids, chromic acid, nitric acid, hydrochloric acid, sulfur dioxide, and silver nitrate; the most common bases are hydroxides of sodium, calcium, magnesium, ammonium, and potassium. An acid burn to the conjunctiva and cornea will coagulate the proteins from the epithelium, conjunctival substantia propria, and corneal stroma. The precipitation of the protein of the more superficial tissues from the epithelium or substantia propria/stroma prevents acid substances, especially weak acids, from infiltrating more deeply into the tissues, which lessens the severity of the final lesions. This effect does not occur with alkaline substances as they will deeply penetrate the conjunctival and corneal tissues at once, causing more severe damage. The most severe base injuries to the eye are caused by alkalis with pH values greater than 12. On the corneoconjunctival epithelium, alkalis cause saponification of fatty acids, cell membrane dissociation, and acute cell death leading to destruction and penetration of the epithelial layers. In the corneal stroma, alkalis cause hydrolysis of proteoglycans and render the stromal matrix susceptible to enzymatic degradation from neutrophil collagenases and plasmin from damaged epithelial cells and fibroblasts, leading to lysis of the stroma (i.e., stromal collagenolysis or keratomalacia). Interestingly, in contrast to acids and surfactants, alkalis tend to produce multifocal to focally extensive injuries presenting as a pattern of almost normal areas intermingled with deeply affected ones.

Surfactants are also known to cause corneal irritation and tissue damage. Cationic surfactants generally tend to precipitate cellular proteins, while anionic agents cause cell lysis. Nonionic substances can cause either cell lysis or protein precipitation.

The end result of chemical burns to the cornea is extensive scar formation and relatively widespread loss of transparency. The cumulative results of ocular irritation tests performed in rabbit corneas using many agents—acids, alkalis, surfactants, and nonsurfactants like acetone, cyclohexanol, parafluoroaniline, and formaldehyde—suggest that the extent of the initial injury (i.e., the depth to which the corneal tissue is affected) and the final outcome of the ocular irritation is significantly correlated.

Due to the avascular nature of the cornea, substances given by routes other than topical seldom achieve toxic levels in healthy corneal tissues. However, in principle, substances delivered

systemically can be concentrated in the lacrimal glands and thereby secreted locally at high concentrations onto the ocular surfaces. The corneal epithelium is rich in smooth endoplasmic reticulum and functions to metabolize substances, which pass through the epithelium via the direct route. In this fashion corneal epithelial cells might be able to activate or detoxify xenobiotics applied to their apical surfaces.

Some substances can cause thickening of the corneal epithelium. This increase may be reflective of different pathological processes. For example, corneal epithelial hyperplasia has been observed with systemically administered high doses of recombinant epithelial growth factor. Similarly, long-term topical treatment with an immunosuppressive drug like tacrolimus or cyclosporine is correlated with the development of corneal squamous cell carcinoma in dogs, although since these dogs usually also present with chronic keratitis, the degree of risk attributable to the drug treatment relative to persistent inflammation is unknown. Local immunosuppression can also enhance the likelihood of developing opportunistic ocular infections with organisms such as *Toxoplasma* or amoebae.

Eye drops containing irritating preservatives like benzalkonium chloride and, less often, chlorobutanol, thimerosal, sorbic acid, or polyquaternuim ammonium chloride can be associated with a low-grade inflammation of the corneal and conjunctival surfaces when administered frequently over a long period. It has been reported that local anesthetics such as lidocaine, propacaine, and butacaine can cause epithelial damage when applied topically on the ocular surface and may also retard epithelial healing in a dose-dependent manner. For more information on toxic drug reactions affecting the cornea, see Table 22a.5.

Exposure to UV radiation is a significant risk factor for ocular disease in humans and animals. For example, experiments with UV radiation in 129S1/SvImj mice have shown that chronic exposure (over 50 weeks) induces loss of stromal keratocytes. This change leads to stromal thinning, keratoconus, neovascularization, and stromal fibrosis of the cornea as well as a high incidence of posterior cortical cataracts. It is hypothesized that coexposure to low doses of toxic agents and UV light might be able to induce corneal injury in an additive or even synergistic fashion.

In specific strains of mice in which open eyelids at birth are common, severe bacterial keratitis, corneal scarring, and neovascularization of the corneal stroma are common. For example, open eyelids in neonates are associated with strains having a characteristic wavy hair coat and curly vibrissae in the waved-1 ($Tgfa^{wa1}$) and waved-2 ($Egfr^{wa2}$) mutations. The exposure of the eyes as soon as the mice are born makes them prone to trauma induced by contact with bedding debris, parental hairs, and littermates' claws. Traumatic damage is accentuated by several developmental stage-dependent factors that predispose to corneal desiccation (e.g., incompletely evolved tear production systems and inability to blink effectively for several days after birth).

Vascularization of the corneal stroma (neoangiogenesis) is regarded as a secondary phenomenon to corneal inflammation. It can also be seen as a background lesion in nude ($Fox1^{nu}$) and hairless (*hr*) strains of mice. Application of certain pro-angiogenic molecules, such as VEGF, or pro-inflammatory cytokines may also promote corneal stromal vascularization. In general, this response requires the agent to be present for a prolonged period (e.g., by sustained-release drug delivery systems).

Although not directly exposed to the ocular surfaces, toxicity of the corneal endothelium can directly affect the superficial corneal tissues. The corneal endothelium is typically exposed to high concentrations of a substance when the material is introduced into the anterior chamber by either intracameral injections (i.e., directly into the anterior chamber) or introduction during surgical procedures. That said, the flow of the aqueous humor in the anterior chamber normally protects the endothelial cells by quickly removing these substances and preventing its accumulation to high concentration in the aqueous humor. The corneal endothelium has a very limited regenerative capacity, so any toxicity that compromises endothelial function or reduces the total number of corneal endothelial cells seriously impairs corneal integrity. The endothelial cells do not tolerate any sort of contact. In many species, anterior lens luxation leading to contact of the lens capsule with the corneal endothelium will cause attenuation or spindle cell metaplasia of the axial endothelial cells. Similarly, intraocular surgeons go to great lengths to avoid touching the endothelium and to protect these cells by using viscoelastic materials to coat their surfaces. Antimetabolite drugs such as mitomycin C are commonly used as postsurgical treatment in glaucoma surgery in humans and animal models to avoid fibrosis and blockage of implanted aqueous drainage devices. Accidental reflux of these drugs into the anterior chamber and exposure to the corneal endothelial can cause extensive cell degeneration and necrosis.

Intracameral injection of the local anesthetic lidocaine in concentrations higher than 4% and inadvertent injection of benzalkonium chloride in the anterior chamber has been shown to be markedly toxic to endothelial cells in rabbits and humans. Another important endothelial toxic reaction is observed with enzymatic detergents, which are used as sterilization agents on surgical instruments and supplies. These substances

TABLE 22A.5 Topical and Systemic Medications Known to Cause Corneal Toxicity in Humans

Compound	Lesions
Topical aminoglicosides (*tobramycin and gentamicin*)	Superficial punctuate lesion
	Corneal ulceration and conjunctival pseudomembrane (rare)
	Delayed corneal reepithelization
Systemic biphosphonates	Conjunctivitis (also uveitis, episcleritis, and scleritis)
Topical chemotherapics (*mitomycin and 5-fluorouracil*)	Corneal thinning and ulceration
Systemic chemotherapics (*imatinib*)	Delayed corneal healing
Systemic cyclooxygenase-2 (COX-2) inhibitors (*celecoxib*, *rofecoxib*, *valdecoxib*, *etodolac*, and *nimesulide*)	Conjunctivitis
Topical fluoroquinolones (*ciprofloxacin*)	Sterile corneal infiltrates
	Corneal precipitates
Topical glaucoma medications (*latanaprost*, *travaprost*, *timolol*, *brinzolamide*, and *pilocarpine*)	Keratoconjunctivitis
	Keratitis
	Corneal ulcerations
	Corneal opacities
Topical iodine	Chemical keratitis
	Corneal epithelium staining
	Delayed wound healing
Topical non-steroidal anti-inflammatory drugs (NSAIDS) (diclofenac, ketorolac)	Keratomalacia
	Delayed corneal healing
	Prevent corneal reepithelization
Preservatives in eye drops	Direct damage to corneal epithelium
Systemic retinoids/isotretinoin (*isotretinoin*)	Keratitis
	Corneal opacities
	Corneal ulceration
	Dry eye
Topical anesthetics (*tetracaine*, *proparacaine*)	Destruction of superficial cornea epithelium microvilli
	Direct toxicity on stromal keratocytes
	Delayed corneal reepithelization
Topical steroids (prednisolone acetate, dexamethasone sodium phosphate)	Delayed corneal healing
	Prevent corneal reepithelization
	Posterior subcapsular cataract
	Glaucoma

From Haschek, W.M., Rousseaux, C.G., Wallig, M.A. (Eds.), 2013. The Handbook of Toxicologic Pathology, third ed. Academic Press, San Diego, CA, Table 53.3, p. 2133, with permission.

are associated with dose-related corneal thickening and ultrastructural damage to the corneal endothelium in humans and rabbits. Intracameral implementation of medical devices can cause mechanical loss of corneal endothelial cells, leading to focal areas of corneal opacity. The opacity is a consequence of increased water entry and retention in the corneal stroma due to loss of the endothelial barrier.

Functional impairment of the corneal endothelial cells with minimal to no anatomical changes is a phenomenon that must be taken into account whenever a toxic substance is injected directly into the anterior chamber. This effect can sometimes explain variations in corneal thickness observed in toxicologic studies. This phenomenon is usually attributed to inability of the endothelial cells to maintain their normal physiological processes leading often to corneal stromal edema.

Toxicity of the Anterior Ocular Segment

Toxicity that affects the tissues in the anterior segment of the eye—the anterior uvea (iris and ciliary body) and lens—may impact one or several components. The responses of the soft tissues include various degenerative and inflammatory reactions, while direct damage to the lens is predominated by cataract formation.

Anterior Uvea

Toxic Anterior Segment Syndrome (TASS) refers to a sterile inflammatory response affecting the aqueous and anterior uvea that is seen after intraocular surgery. "Uveitic" clinical symptoms like "cell and flare" [the combined presence in the anterior chamber of leukocytes as tiny white specks (clinically termed "cell") and protein as a gray-white haze (clinically termed "flare")] as well as fibrin exudate predominate in TASS, while corneal edema secondary to corneal endothelial compromise might also be seen. TASS is thought to be caused by exposure to irritating irrigating solutions or other fluids or additives placed in the eye during intraocular surgery. Substances such as anesthetics, viscoelastics, and antibiotics have been found to be related to TASS. Chemicals used to clean or sterilize surgical instruments used in eye procedures can also be the cause.

Uveitis induced by minute amounts of endotoxin is a constant worry of the producers of sterile biologic products intended for use within the eye. Profound neutrophilic exudate, vascular leakage, and microthrombosis of ocular vessels are the morphologic hallmarks of endotoxin-induced uveitis. The presumed mechanism is the vigorous immune response raised against the bacterial toxin.

Colchicine, naphthol, and urethane can cause edema, inflammation, or degeneration of the ciliary body. Naphthalene causes degeneration of the ciliary body and choroid, and pyrithione causes edema and degeneration of the choroid.

Darkening of the iris stroma, secondary to an increase in the synthesis of melanin occurs in cynomolgus monkeys and humans that are treated with prostaglandin $F_{2\alpha}$ analogs such as latanoprost, travaprost, and bimatoprost. Phospholipids, disobutamine (a piperidine antiarrhythmic drug), 6-aminonicotinamide (an antimetabolite), and some anticancer agents can cause the vacuolation of the iris and ciliary body epithelium in multiple species. Inflammation of the uveal tract can be secondary to immunologic or toxic mechanisms. Drug-related inflammation of the anterior uvea has been reported in humans associated with administration of ribafutin (an antimycobacterial drugs), palmitic acid, streptokinase, sulfonamides, topical metipranolol, and the antiviral cidocir.

Lens

Cataract, defined as any opacity or loss of transparency on the lens, is the most common and significant abnormality of the lens. Numerous toxic pathways can manifest as cataract. For example, if the chemical environment in the lens differs from the normal state, the lens epithelial cells can undergo an epithelial-to-mesenchymal transformation (EMT) or alter the differentiation path by which lens epithelium transforms to lens fibers. If the external pressure of the zonular ligament is altered, this mechanical change also can cause cataract. The proliferating and differentiating lens epithelium is very sensitive to UV light and to a large number of toxic substances and disease states. Changes in the lens proteins during toxic cataract formation are similar to the changes that occur during aging. The appearance of cataract varies among species, as does the sensitivity to toxic cataract development; these differences are thought to be related to age and different lenticular metabolism profiles among species, and even breed/strains. In addition, cataract features also depend on the nature of the toxicant. For example, glutathione (GSH) is an important lens antioxidant. Chronic corticosteroid exposure can lower GSH levels in the lens and, therefore, increase the risk of cataract associated with oxidative stress. Substances that affect cell mitosis such as radiation or radiomimetic drugs interfere with the organized stepwise differentiation of the lens cortex and can lead to cortical cataract, usually at the nuclear bow. Many photosensitizing agents are thought to cause cataracts. Among them, UV light is the most cited. Some believe UV light exposure alone is not enough to produce lesions and that another photosensitizing agent must also be present simultaneously.

Diabetic dogs and rats but not mice, rabbits, or primates are at high risk of osmotic cataract formation. It is thought that the different risks among species are due to the fact that dogs and rats have relatively high levels of aldose reductase (AR) in the lens. This enzyme reduces various sugars (e.g., glucose to

sorbitol). Because sorbitol does not readily diffuse out of cells and its further oxidation (to fructose via the action of sorbital dehydrogenase) is slow, the accumulation of sorbitol in the hyperglycemic state increases the intracellular osmotic pressure within the lens, leading to water retention and eventual rupture of the lens fiber cells. Similarly, rats and dogs also develop galactose-induced osmotic cataracts, this time by the fast buildup of galactol from galactose reduction by AR. It is also important to recognize that some drugs, including opiates, opioids, and phenothiazine, can induce acute reversible white clouding of the lens in rodents within 1 to 2 hours of administration. This opacification is not apparent microscopically. We provide a list of cataract-causing substances and their mechanisms of action in Table 22a.6.

Toxicity of the Posterior Ocular Segment

The posterior segment of the eye is composed of the vitreous, choroid, tapetum, retina, and optic nerve. Tissue responses for these structures vary depending on their main constituent (e.g., gel vs neural vs vascular).

Vitreous Body

The most common toxic reactions of the vitreous body are the same types of reactions that occur in spontaneous connective tissue diseases elsewhere in the body: cellular and extracellular matrix proliferation. Rabbits are notorious for the formation of spindle cells and collagen membranes in the vitreous and across the retinal surface, favoring the production of traction bands that cause vitreal detachment, retinal folding, and subsequently lead to retinal detachment.

Several aspects of intravitreal (IVT) injections are important when faced with evaluating the consequences in the nonclinical and clinical settings. Delivery by the IVT route has the potential to cause vitreal degeneration and inflammation. Special attention has to be taken when analyzing IVT injection sites of biodegradable drug implants designed for sustainable drug delivery since the nature and size of the

TABLE 22A.6 Biologic Features of Compounds That Cause Cataracts in Rats

Compound	Species	Biologic feature
Chloroquine, chlorphentermine, and iprindole	Rat	Intralysosomal drug-lipid complexes
Diquat	Rat and dog	Formation of free radicals and loss of lenticular ascorbic acid
Methionine sulfoximine	Rat	Interference with protein synthesis
Morphine, morphine-like compounds	Rat, mouse, and guinea pig	Cataracts prevented by simultaneous administration of nalorphine
Myleran	Rat	Prevents lenticular epithelial cell division
Naphthalene	Rat	More consistent, earlier, and severe cataracts in pigmented rats; changes due to a toxic metabolite, 1,2-dihydroxynaphthalene, which is metabolized to 1,2-naphthaquinone and hydrogen peroxide, diminishing the lenticular oxygen and ascorbid acid supply
N^2-Phenyl-β-hydrazinopionnitriles	Rat	Decreased lenticular ATP concentrations
Selenium	Rat, guinea pig, and rabbit	Decreased lenticular concentrations of sulfhydryl groups and GSH, increased lenticular concentrations of insoluble protein, increased amount of lenticular water, interference with GSH metabolism
Streptozotocin	Rat and primate	Cataract due to hyperglycemia of diabetes resulting in lenticular osmotic changes from increased concentrations of sorbitol, glucose, and fructose
Triparanol	Rat, human, and dog	Inhibition of cholesterol biosynthesis with reduction of lenticular sulfhydryl content, accumulation of sudanophilic material causing uptake of water and sodium leading to swelling and disruption
Galactose	Rat	Lenticular accumulation of dulcitol resulting in an osmotic accumulation of water in the lens, decrease in lenticular glutathione (GSH) concentrations, failure of cationic pump, decreased glycolysis, decreased concentrations of ATP

Abbreviations: Diquat = 9,10-dihydro-8a,10a-diazoniaphen-anthrene dibromide.
From Haschek, W.M., Rousseaux, C.G., Wallig, M.A. (Eds.), 2013. The Handbook of Toxicologic Pathology, third ed. Academic Press, San Diego, CA, Table 53.5, p. 2147, with permission.

implants can sometimes induce vitreal inflammation. In general, such reactions are of minimal degree and limited to infiltration of lymphocytes and macrophages. The rate of drug depot dissolution may impact the translucency of the vitreous. Large amounts of opaque and dense substances can stay in the vitreous for extended periods, thereby causing temporary visual impairment. With this in mind, safety studies for assessing IVT products must take into account the animal model that has been used. For examples, rabbits present a denser vitreous, and thus are more inclined to locally retain substances for longer periods. This fact can also influence the rate of diffusion for the drug throughout the posterior globe.

Choroid

The choriocapillaris and adjacent uveal tissues are exposed to focused light in a local environment where lipid membranes are constantly being degraded by phagocytosis. Thus, these tissues are susceptible to toxicity by anything that enhances oxidative stress such as increased fat in the diet, chronic zinc deficiency, or hemochromatosis. Fisher 344 rats, but not Sprague–Dawley rats, develop deposition of adipose tissue in the choroidal stroma adjacent to the sclera as a response to systemic administration of peroxisome proliferator-activated receptor-gamma agonists. As described earlier, many substances that are toxic to the well-vascularized anterior uveal tissues (iris and ciliary body) also affect the choroid.

Tapetum Lucidum

Of the species commonly used in toxicity studies, the dog is the only one that has a *tapetum lucidum*. It is also important to notice that since humans do not have a tapetum, treatment-related findings observed in this tissue are unlikely to be relevant to human safety assessment. If treatment-related tapetal lesions are present, "atapetal" beagles (i.e., dogs with a poorly developed tapetum in which tapetal cells are present but lack intracytoplasmic rodlets) can be used as an alternative animal model to try to define the relevance of such lesions to humans. It has been shown, for example, that administration of imidazoquinoline to normal beagles causes tapetal and retinal lesions, but the same treatment in atapetal beagles results in no retinal changes. Because of the high concentration of zinc in the tapetal cells, this tissue becomes a target for zinc chelators. The severity of the lesions is variable, with some zinc-chelating drugs (pyrithione and hydroxypyridinethione) causing tapetal and choroidal necrosis with secondary retinal detachment while others (ethambutol) produce reversible, velvety-white discolorations of the tapetum. Nonchelating compounds such as enrofloxacin, dithizone, edentate, ethylenediamine derivates, CGS14796C (a potential aromatase inhibitor), and 1192U90 (an antipsychotic agent) also may cause tapetal-specific changes such as edema and degeneration with secondary retinal edema and detachment.

Retina

Retinal toxicity may result from either local or systemic delivery of toxicants. Topical absorption of ocular toxicants may occur through the conjunctiva, cornea, lacrimal system, or sclera. That said, retinal exposure to topically administered compounds is limited by the aqueous humor flow; by physical barriers imposed by the ciliary body, iris, and lens; and by enzymatic systems distributed throughout the ocular tissues. Systemic exposure to toxicants can occur through the uveal and/or retinal circulations; however, the blood–ocular barrier in the uveal circulation limits the vascular delivery of these compounds to the retina. Of the available routes of administration, IVT and subretinal injections offer the greatest opportunity for experimental evaluations of retinal toxicity and efficacy.

Toxic effects to the retina ore often best appreciated with TEM, although light microscopic changes of retinal toxicity may also be appreciated. Selected retinotoxic agents and associated ultrastructural and light microscopic lesions are described in Tables 22a.7 and 22a.8, respectively.

The following substances that affect the retina may be considered as prototypes of the kinds of changes that may be seen when evaluating the retina for toxicity using various morphological techniques. Different toxicants target distinct components of the retina.

Aminophenoxyalkanes are schistosomicidal drugs that induce retinal toxicity in several animal species, including the rat, rabbit, cat, dog, and nonhuman primate. Toxicity appears to affect the RPE, independent of pigmentation. The RPE cells show rapid necrosis that is associated with disruption of photoreceptor outer segments. Remaining RPE cells accumulate disc material and become hyperplastic.

Antidepressant drugs such as amiodarone, chloroamitriptyline, chlorphentermine, clomipramine, imipramine, iprindole, various aminoglycosides, and other cationic amphophilic compounds interfere with the enzymatic degradation of phospholipids. Systemic administration results in accumulation of phospholipids (i.e., phospholipidosis) in retinal cells, including the RPE. Storage is within cytoplasmic inclusions, where the lipids assume a crystal-like conformation. This effect is partially reversible upon discontinuation of treatment.

Desferrioxamine, an iron-chelating agent used to treat hemochromatosis, causes RPE and outer retinal degeneration culminating in vision loss in humans. Retinal

toxicity in rats and rabbits only can be detected by functional testing [electroretinography (ERG)] and not by morphological analysis.

Isopropylamine hydrochloride, an ingredient in some herbicide and plastics formulations, causes retinal toxicity when given in high doses to rats and dogs. The lesion is characterized by loss of photoreceptors and RPE migration into the subretinal space.

Fluoride administered as a sodium salt intravenously at near-lethal doses to rabbits results in fluoride concentration within the eye. These very high concentrations lead to necrosis of the RPE and the photoreceptor outer segments.

Iodates given at high doses by intravenous administration cause retinal damage in several species, including humans. Iodate causes degeneration of the RPE basement membrane, with cytoplasmic swelling and loss of apical microvilli; the end stage is RPE necrosis, which is followed by photoreceptor cell apoptosis. The blood–retinal barrier is compromised, and the choriocapillaris atrophies. The mechanism of toxicity is not clear, but inhibition of lysosomal enzymes may play an important pathogenic role on the RPE lesion.

Iodoacetate, an inhibitor of glycolysis, is highly retinotoxic. High intravenous doses of iodoacetate to rabbits cause injury of rods and also affects phagocytic activity of RPE cells. Recently, a new pig model of inherited retinal dystrophy has been devised by administering a single intravenous dose of iodoacetic acid. Marked photoreceptor degeneration arises after 2–5 weeks.

Lead can cause lipofuscin accumulation in RPE cells of rabbits, leading to outer retinal degeneration. The presumed mechanism is chronic oxidative stress.

Methanol or its toxic metabolite *formic acid* will, if ingested, lead to outer retinal toxicity in humans and nonhuman primates. The presumed mechanism is altered cellular energy metabolism in the highly active retinal cells. In contrast, retinal toxicity can be produced in rats only by inhibiting formate oxidation, which occurs much more rapidly in this species and thus prevents the accumulation of formic acid.

TABLE 22A.7 Ultrastructural Alterations Produced by Selected Retinotoxic Compounds in Rats

Compound	Ultrastructural alterations
Vitamin A	Increased lipid droplets and mitochondrial destruction in RPE, mitochondrial destruction in PRC inner segments
Trimethyltin	Membrane-bound vacuoles and polymorphic dense bodies in PRC inner segments, PRC necrosis, dense-cored vesicles and tubules in ganglion cells, intracytoplasmic dense bodies in INL
Amphiphilic cationic drugs	Accumulation of crystalloid or lamellated inclusions in the cytoplasm of RPE or neuroretina; chloroquine only; multilamellated bodies in PRC inner segments
Fenthione	Loss of PRC outer segments, hypertrophy of RPE, pigment granules in subretinal space and penetrating OLM
Perhexiline maleate	Lamellar and reticular cytoplasmic inclusions in all retinal cell types, crystalloid inclusions in RPE
L-Ornithine hydrochloride	Marked expansion of cytoplasmic matrix and destruction of organelles in RPE → RPE degeneration/hyperplasia → secondary disruption of PRC outer segments
2-Aminoxy propionic acid	Disorientation, vacuolation, and disruption of PRC outer segments → secondary increase in lysosomal bodies and phagosomes in RPE
Zinc chelators	Nonmembrane-bound, electron opaque, scalloped inclusions in basal cytoplasm of RPE
Doxorubicin	Neurofilament accumulation in cell body and proximal axon of ganglion cells
Guanidinoethane sulfonate and β-alanine	Disorganization of PRC outer segment membrane disks
D,L-α-Amino-adipic acids	Decreased electron density, cytoplasmic vacuolation, and necrosis of Müller cells
Lead	PRC necrosis with electron-dense, shrunken inner, and outer segments; necrosis in INL
AY9944	Niemann–Pick disease-like inclusions in various retinal cell types, especially ganglion cells
Glutamate	Swelling of nucleus, cytoplasm, and dendritic processes of ganglion cells; swelling and pyknosis in inner aspect of INL
Hexachlorophene	Vacuolation and tubulovesicular degeneration of PRC outer segment membrane disks

Abbreviations: RPE, retinal pigment epithelium; PRC, photoreceptor cell; INL, inner nuclear layer; OLM, outer limiting membrane; Ay9944, trans-1,4-bis(2-chlorobenzylaminomethyl)cyclohexane dihydrochloride.

From Haschek, W.M., Rousseaux, C.G., Wallig, M.A. (Eds.), 2013. The Handbook of Toxicologic Pathology, third ed. Academic Press, San Diego, CA, Table 53.7, p. 2169, with permission.

Methanol toxicity in rats shows that both mitochondrial disruption and cellular atrophy occur in the outer retina.

4,4′-Methylenedianiline is an intermediate in the production of isocyanates and polyurethanes. It causes retinal toxicity in pigmented and nonpigmented guinea pigs when inhaled, inducing degeneration of the photoreceptor inner and outer segments as well as the RPE. A retinal toxicity of unknown mechanisms also occurs in cats exposed through oral or parenteral routes.

N-ethyl-N-nitrosourea (ENU) is an alkylating agent considered to be mutagenic. It is well known to cause congenital malformations including anophthalmia, microphthalmia, and tumors in various locations, especially the nervous system. Chronic exposure to high doses also is retinotoxic in adult guinea pigs and rats. In rats, photoreceptors undergo degeneration early, with subsequent degeneration of RPE cells. A single high dose of ENU recently has been reported to cause outer retinal atrophy in adult BALB/c mice by inducing photoreceptor cell apoptosis.

Naphthalene is better known to cause cataracts, but it is also retinotoxic. After oral administration to rabbits, the chief lesion is RPE degeneration. It is speculated that the RPE lesion is secondary to increased oxidative stress combined with light-induced oxidative damage.

Nitroaniline, a rodenticide, causes retinal toxicity in humans, rabbits, and hamsters. The changes of note produced by oral administration are related to degeneration in the RPE and photoreceptors. A mechanism of toxicity has not been discovered.

Organophosphates inhibit cholinesterase and are commonly used as pesticides. Retinal degeneration and histological abnormalities of the RPE have been reported in some cases of toxicity, but this finding has been difficult to reproduce. The toxic mechanism remains unknown.

Dibutyl oxalate delivered subcutaneously to rabbits induces the formation of needle-like birefringent crystals in the cytoplasm of RPE cells, as well as in other organs (e.g., kidney, heart, testes). The crystalline

TABLE 22A.8 Microscopic Alterations Produced by Selected Retinotoxic Compounds in Rodents

Compound	Species	Microscopic alterations
Urethane	Rat	Loss of PRC outer segments, decreased melanin granules in RPC, debris in subretinal space→loss of ONL, thinning of INL and focal proliferation of RPE
Trimethyltin	Rat	Pyknotic nuclei in ONL and INL, swollen dark staining PRC inner segments
Vigabatrin	Rat	Disruption of ONL with outward displacement of PRC nuclei
P-1727	Rat	Loss of rods and cones, disorganization of ONL and INL
N-Methyl-*N*-nicrosourea	Hamster	Arcades within the ONL, degeneration of RPE→retinal atrophy
	Mouse	Retinal thinning and rosette formation in offspring following maternal administration
Cycasin	Mouse, rat	Necrosis of the neuroblastic layer of the retina in neonates→retinal rosette formation
Carbon disulfide	Rat	Acute degeneration of retinal ganglion cells
Fenthione	Rat	Thinning of central retina, swelling and disorganization of RPE, melanin pigment about vessels
L-Ornithine hydrochloride	Rat	Degeneration and focal denuding of RPE→secondary disruption of PRC outer segments
2-Aminoxy propionic acids	Rat	Fragmentation of PRC outer segments with outward migration and arcade formation by nuclei of ONL
Kainic acid	Rat	Pyknotic cells in inner aspect of INL and edema in the IPL→thinning and increased mitosis in INL
Glutamate	Mouse, rat	Necrosis and loss of cells in the ganglion cell layer and INL, vacuolation in plexiform layers
Doxorubicin	Rat	Decreased chromatin staining in ganglion cells, swollen axons in NFL→massive loss of ganglion cells
L-Cysteine	Rat	Marked reduction in thickness of the NFL, ganglion cell layer, IPL, and ONL
Cytosine arabinoside	Rat	Retinal dysplasia characterized by rosette formation and retinal disorganization and thinning

Abbreviations: ONL, outer nuclear layer; INL, inner nuclear layer; RPE, retinal pigment epithelium; PRC, photoreceptor cell; NFL, nerve fiber layer; IPL, inner plexiform layer P-1727, *dl*-(*p*-trifluoromethylphenyl) isopropylamine hydrochloride.

From Haschek, W.M., Rousseaux, C.G., Wallig, M.A. (Eds.), 2013. The Handbook of Toxicologic Pathology, third ed. Academic Press, San Diego, CA, Table 53.8, p. 2170, with permission.

deposits in the RPE can be detected as white flecks on the retina by indirect ophthalmoscopy. Histologically, RPE cells exhibit varied numbers of Pizzalato stain-positive (calcium oxalate), intracellular, needle-like crystals that often coalesce to form a single large deposit. The toxic mechanism is thought to be mechanical trauma of cellular membranes but altered calcium metabolism likely also plays a role.

Phenothiazines tranquilizers, including derivatives as piperidylchlorophenothiazine, thioridazine, and chlorpromazine, can cause clinically significant retinopathy in humans. Retinal toxicity also can be induced in cats, but not in rabbits, rats, guinea pigs, or dogs. Photoreceptor cells, particularly the rod outer segments, are the target tissue. The main lesion is degeneration of the outer segments of photoreceptor cells, which leads to thinning of the photoreceptor layer. The RPE cells undergo secondary hypertrophy via cytoplasmic accumulation of lipofuscin, melanolysosomes, and curvilinear bodies. Atrophy of the RPE layer is seen in the end-stage lesion. Phenothiazines bind to melanin and accumulate within the uvea and RPE. Phototoxicity related to photons interacting with the cell-bound chemicals has been postulated as a mechanism for inducing the retinal lesion. Chlorpromazine specifically also has the potential to cause cataract.

Chloroquine and *hydroxychloroquine* are used as antimalarial drugs and for the treatment of extraintestinal amebiasis and autoimmune diseases (rheumatoid arthritis and systemic lupus erythematosus). Chloroquine retinal toxicity occurs in humans, causing vision dysfunction. It is more severe over time and with high doses. In fully developed cases, a depigmented lesion surrounded by a pigmented ring ("bull's eye" depigmentation) is present at the macula. Several animal models of chloroquine-induced retinal toxicity have been developed, including the rat, cat, dog, rabbit, pig, and nonhuman primate. Cytoplasmic accumulation of membranous phospholipid inclusions occurs in retinal ganglion cells, photoreceptors, and the RPE. The RPE cells largely remain intact, but eventually the photoreceptor outer segments degenerate. Chloroquine is thought to inhibit lysosomal degradation. There is a very high affinity of chloroquine for melanin. While this depot effect has been proposed to be an important pathogenic mechanism, the significance of this binding in fact is not well understood.

Taurine is an amino acid that is concentrated in the photoreceptors, and is essential for retinal function. One critical RPE function is to transport taurine to the photoreceptors. Taurine is an essential amino acid for cats, so taurine depletion (by dietary insufficiency) in this species causes outer segment degeneration and loss of photoreceptor cells. The resulting functional defect is a reduced ERG. Guanidinoethyl sulfonate (GES) is an inhibitor of taurine uptake, and GES toxicity leads to a reduction in retinal taurine concentration and causes degenerative changes in the retina of cats.

Different toxicants may induce specific retinal lesions in different species. For examples, some toxicants like benzoic acid can induce retinal detachment in many species, while others like ethylene glycol and hydroxypyridinethione can induce retinal detachment only in cats and dogs, respectively. Others might target specific cell groups or regions of the retina. For example, 1,4-bis(4-aminophenoxy)-2-phenylbenzene(2-phenyl-APB-144) in multiple species and systemic treatment with enrofloxacin in cats have been reported to cause outer retinal atrophy, which is characterized by degeneration of the photoreceptors and the ONL. Other toxicants cause inner retinal atrophy, targeting the retinal ganglion cells [amphotericin B (rabbit), chloramphenicol (human), and carbon disulfide (human, rabbit, and rat)]; cells in the INL [kainic acid (rat), ethylcholine mustard aziridinium ion (multiple species)]; or both [L-cysteine (rat), locoweed (*Astragalus mollissimus*, in cattle and sheep)].

The retinal vasculature is also a potential target for toxic compounds. Retinal hemorrhage has been associated with obvious vascular toxicants like anticoagulants (warfarin) and agents that cause blood hyperviscosity (e.g., dextrans). Some less obvious compounds like prostaglandins, 2-butoxyethanol, and 3,3-iminidopropionitrile also impact retinal blood vessels, although the mechanisms often are not clear.

Vasoproliferative lesions are an important group of retinal and optic nerve lesions. These changes can be induced in primates and rabbits by IVT injections of angiogenic substances like basic fibroblast growth factor and VEGF. Retinal neovascularization can also be a sequela of prolonged exposure to other retinal toxicants like naphthalene.

Retinal Pigmented Epithelium

The RPE is especially sensitive to many toxic compounds because of its high metabolic activity. Distinct agents affect different species. Toxicants that notably impact the RPE are lead (rabbit), methanol (primates and rat), phenothiazines (human and cat), quinolones (rabbit and cat), tricyclic antidepressants (rat), and sodium iodate (mouse). As mentioned in the previous section, the RPE can also develop changes secondary to primary retinal lesions such as photoreceptor degeneration and retinal detachment. These changes develop because a major RPE function is to support photoreceptors (especially the outer segments), so loss of photoreceptors reduces the metabolic demands on the RPE.

Optic Nerve

Toxic reactions of the optic nerve are often secondary to disease processes occurring in the retina (especially to the retinal ganglion cells) or CNS. Primary toxic events to the optic nerve are relatively uncommon.

Congenital optic nerve disease has been reproduced in mouse models by targeted disruption of the sonic hedgehog (*Shh*) gene by genetic manipulation or by exposing pregnant dams during early gestation (approximately gestational day 9.5, just after the neural tube has closed to form the primordial face and brain) to the alkaloid cyclopamine (produced by the poisonous plant *Veratrum californicum*), which inhibits *Shh* gene transduction. Affected offspring will develop cyclopia (a single eye or two fused eyes), holoprosencephaly (a common forebrain rather than twin cerebral hemispheres), and optic nerve aplasia. Optic nerve aplasia and hypoplasia are also observed in the anophthalmic ZRDCT Rax^{ey1} mice and in netrin-$1^{-/-}$ mice. Coloboma, a congenital abnormality in which there is segmental aplasia of optic nerve, retina, and choroid, is found in many mouse mutations; among them are microphthalmia (*Mitf*), belly spot and tail (*Bst*), coloboma (*Cm*), and total cataract and microphthamia (*Tcm*). The variety of these mutations exposes the complexity of the molecular mechanisms involved in specifying the formation and remodeling of the developing optic nerve.

Multiple toxic substances are capable of producing optic "neuritis" in humans and laboratory animals. The common morphological appearance of such lesions is demyelination and degeneration of axons in the optic nerve, with secondary degeneration of retinal ganglion cells and, in severe cases, associated degenerative lesions in the white matter of the brain optical pathway; when present, inflammation is characterized by lymphocytic and less often neutrophilic infiltration. Examples of chemicals that induce optic neuritis include hexachlorophene (humans and rats); arsanilic acid (humans and pigs); carbon disulfide (humans, rabbits, and mice); thallium (humans); cyanide (humans and rats); ethylene glycol (humans); and methanol (humans). Many drugs also may cause optic neuritis, including multiple antimicrobials—chloramphenicol (humans); clioquinol (humans, dogs, and cats); ethambutol (humans, monkeys, rats, and rabbits); and linezoid (humans)—as well as the antiarrhythmia agent amiodarone (humans) and the erectile dysfunction drugs sidenafil, tadalafil, and vedenafil (humans). No common mechanism of action has been found to explain the involvement of the optic nerve in the degeneration and inflammation induced by these agents.

Toxic Elevation of the Intraocular Pressure

Elevated IOP can be considered a significant toxic effect of some drugs. These agents can directly increase IOP, or they can cause intraocular structural damage that will lead to secondary glaucoma. Parasympatholytic drugs such atropine, homatropine, and scopolamine can paralyze the ciliary muscles and increase the IOP in humans, dogs, and cats. Systemic or topical administration of corticosteroids can increase the IOP in humans. It is believed that corticosteroids affect the metabolism of the trabecular meshwork (TM) cells, impairing their ability to degrade glycosaminoglycans and phagocytize debris; the accumulating detritus gets deposited and obstructs the aqueous outflow. This toxic reaction is rare in animals. Transient elevation of IOP was reported in rabbits treated with almost lethal systemic doses of corticosteroids, and there is one report of increased IOP in a cat treated with dexamethasone. Viscoelastic substances injected into the anterior chamber during intraocular surgeries (to protect the corneal endothelium) have been implicated in the induction of significant postoperative increase in IOP in humans and dogs. IOP may be decreased in association with intraocular inflammation and with exposure to cardiac glycosides (via decreased production of aqueous by the ciliary body) and iodacetate and quinine (by direct damage to the ciliary body epithelium).

SUMMARY

The critical nature of vision as a sensory modality for humans renders ocular toxicology pathology, a critical component of nonclinical safety assessment. In many respects, analysis of the eye presents many unique challenges to toxicologic pathologists. Distinctive features of the eye include many interspecies differences in anatomy, and the need for special processing techniques to preserve small and/or delicate structures. In-life evaluations often provide an equal or better assessment to pathology endpoints for some ocular conditions; indeed, in some cases routine pathology parameters will not reveal that a toxicant has produced an adverse effect. Generally, accurate identification and diagnosis of microscopic findings requires an awareness and understanding of clinical ocular findings. Familiarization with ophthalmic terminology and the use of specific clinical and histologic diagnostic terms is essential for accurate communication. Mechanisms of ocular toxicity in animals often are mirrored in humans for those parts of the eye that occur across species.

Further Reading

Chiou, G.C.Y., 1999. Ophthalmic Toxicology, second ed. Taylor and Francis, Philadelphia, PA.

Dubielzig, R.R., Ketring, K.L., McLellan, G.J., Albert, D.M., 2010.). Veterinary Ocular Pathology: A Comparative Review, first ed. Saunders Ltd, Edinburgh.

Fraunfelder, F., Fraunfelder, F., 2004. Adverse ocular drug reactions recently identified by the National Registry of Drug-Induced Ocular Side Effects. Ophthalmology. 111, 1275–1279.

Gellat, K.N., Gilger, B.C., Kern, T.C., 2014. Veterinary Ophthalmology, fifth ed. Blackwell, Ames, IA.

Ramos, M., Reilly, C.M., Bolon, B., 2011. Toxicological pathology of the retina and optic nerve. In: Bolon, B., Butts, M.T. (Eds.), Fundamental Neuropathology for Pathologists and Toxicologists: Priniples and Techniques. Wiley, Hoboken, NJ, pp. 385–412.

Schafer, K.A., Render, J.A., 2013a. Toxicologic pathology of the eye: histologic preparation and alterations of the anterior segment. In: Weir, A.B., Collins, M.J. (Eds.), Assessing Ocular Toxicology in Laboratory Animals. Humana Press, New York, pp. 159–217.

Schafer, K.A., Render, J.A., 2013b. Toxicologic pathology of the eye: alterations of the lens and posterior segment. In: Weir, A.B., Collins, M.J. (Eds.), Assessing Ocular Toxicology in Laboratory Animals. Humana Press, New York, pp. 219–257.

Short, B.G., 2008. Safety evaluation of ocular drug delivery formulations: techniques and practical considerations. Toxicol. Pathol. 36, 49–62.

Smith, R.S., 2002. Systematic Evaluation of the Mouse Eye, first ed. CRC Press, Boca Raton, FL.

Teixeira, L.B.C., Dubielzig, R.R., 2013. The eye. In: Haschek, W.M., Rousseaux, C.G., Walling, M.A. (Eds.), Haschek and Rousseaux's Handbook of Toxicologic Pathology. Elsevier, Waltham, pp. 2095–2185.

Teixeira, L.B.C., Render, J.A., 2013. Methodologies for microscopic characterization of ocular toxicity. In: Gilger, B.C. (Ed.), Ocular Pharmacology and Toxicology. Humana Press, New York, pp. 267–289.

Walls, G.L., 1942. The Vertebrate Eye and Its Adaptive Radiation, first ed. Cranbrook Institute of Science, New York.

CHAPTER

22b

Special Senses—Ear

Kenneth A. Schafer[1] *and Brad Bolon*[2]

[1]Vet Path Services, Inc., Mason, OH, United States [2]GEMpath, Inc., Longmont, CO, United States

INTRODUCTION

The ear is not commonly evaluated in routine nonclinical toxicity studies, either from a functional or morphologic perspective. Most of the ear lesions commonly observed in routine toxicity studies are limited to the pinna and external ear canal. The evaluation of these ear components might be incorporated with the integument and associated adnexal glands (Zymbal's gland in rodents). However, there is much more to the ear than these external features, and failure to consider the potential for ototoxicity—toxic injury in the middle ear and inner ear—may have potentially profound consequences for individuals exposed to certain drugs and environmental contaminants.

The ear serves two functions—hearing and balance. These tasks are centered in the cochlea (hearing) and vestibular apparatus (balance). Sound waves in the air are transmitted as vibrations from the tympanic membrane, through the movements of the three middle ear ossicles, to the fluid-filled cochlea. Waves induced in the fluid by the vibrating tympanic membrane stimulate the hair cells (sensory epithelium) in the organ of Corti within the cochlea. Balance is sensed by the "gyroscopes" of the vestibular apparatus, specifically the semicircular canals as well as the utricle and saccule, which have specialized linings of hair cells to sense changes in fluid inertia and gravity (or linear acceleration), respectively. Neural signals from the cochlea and vestibular apparatus are passed centrally to the appropriate brain centers via separate divisions of cranial nerve VIII (the vestibulocochlear nerve).

Although numerous compounds of diverse type are known to cause toxicity in other organs (e.g., the liver, with thousands of known toxicants), relatively few compounds are known to cause ototoxicity—a little more than a hundred. Due to the infrequency of ototoxicity and the difficulty in assessing the delicate target tissues within the bone-encased ear, this system is not typically evaluated, either grossly or microscopically, in the course of conventional toxicity studies in animals. However, evaluation of the ear will be necessary under

some circumstances. As a practical matter, when defining a program to assess pharmaceutical safety, test substances that are locally applied to the external, middle, or inner ear ought to be the focus of studies that are designed to assess ototoxic potential.

STRUCTURE AND FUNCTION

Gross Anatomy and Function

In laboratory animal species the ear can be divided into three compartments (Figure 22b.1). The external ear includes the pinna and external ear canal. The tympanic membrane (ear drum) is the barrier between the external auditory meatus (ear canal) and the middle ear. The middle ear is housed in the tympanic bulla and contains three small bones (ossicles), which transmit tympanic membrane vibrations to the cochlea. The inner ear is comprised of the cochlea and the vestibular apparatus.

The tympanic bulla is an air-filled space bridged by the middle ear ossicles (malleus, incus, and stapes) (Figure 22b.2). The malleus (hammer) is embedded broadly in the tympanic membrane and articulates with the incus (anvil). The incus has muscular attachments to the wall of the tympanic bulla. The incus articulates in turn with the stapes (stirrup); the footplate of the stapes lies in the oval window of the cochlea. This mechanical apparatus amplifies the tympanic membrane vibrations, possibly providing an increase in magnitude of as much as 20-fold. The auditory (pharyngotympanic or Eustachian) tube originates in the rostral (anterior) wall of the tympanic bulla and extends to the nasopharynx. It allows for drainage of fluid from the middle ear and normalization of pressure across the tympanic membrane.

The cochlea lies on and is embedded in the medial wall of the tympanic bulla (Figure 22b.2). It is almost entirely contained within the temporal bone in primates. The round window of the cochlea is readily visible as a membrane-lined structure adjacent to the oval window. The entire vestibular apparatus (semicircular canals, utricle, and saccule) is contained within the bones of the skull and so is not readily visible during gross examination.

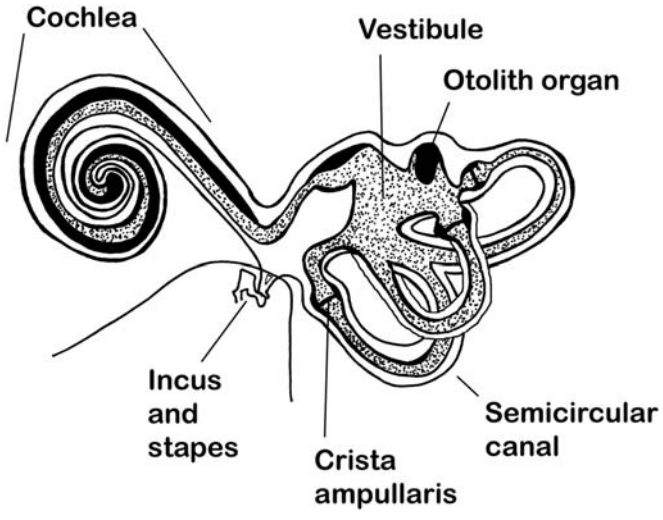

FIGURE 22B.1 Stylized drawing of the components of the human inner ear. The cochlea, semicircular canals, and vestibule form the bony labyrinth, while the membranous structures within form the membranous labyrinth. Areas of dense black ink indicate regions along the walls of the membranous labyrinth that are occupied by sensory epithelia. Stippled areas define the interior of the membranous labyrinth and contain endolymph. White spaces within the bony labyrinth contain perilymph. Source: *Original line drawing by R.M. Blumer.*

Microscopic Anatomy and Function

The pinna has a cutaneous lining on both the external and internal surfaces. The more external areas have a thin epidermis and dermis with a paucity of hair follicles. In the external auditory meatus just outside of the bony collar in the rabbit, but not rodents, the ear canal retains the thin epidermis but has a circumferential zone containing sebaceous glands (ceruminous glands) but lacking hair follicles. Rodents instead have a relatively large compound sebaceous gland, the Zymbal's gland, located cranioventral to the ear canal. Within the more medial portions of the external acoustic meatus, defined by the presence of the bony collar, the dermis is very thin to nonexistent so that the epidermis is almost lying on the temporal bone. The dermis and epidermis of the auditory meatus that abuts the tympanic membrane lack any adnexal structures; in fact, the epidermis continues seamlessly as the external squamous epithelial lining of the tympanic membrane. The auricular cartilage of the pinna is comprised of a fibrocartilaginous core.

The tympanic membrane is lined externally and internally by a thin, simple squamous epithelium. The stroma of the tympanic membrane has areas that are thin, fibrous, and tightly stretched (typically found centrally) as well as areas closer to the periphery, which are fleshy and highly vascularized. The air-filled tympanic bulla is lined by a mucous membrane with epithelium varying from tall columnar with goblet cells to a thin squamous covering. The auditory tube is lined by a columnar ciliated respiratory epithelium with goblet cells.

The inner ear (cochlea and vestibular apparatus) bulges into the lumen of the tympanic bulla but is contained within the temporal bone of its medial wall. The stapes footplate rests within the oval window; the oval window connects with the vestibule of the inner ear. The vestibule communicates with the cochlea and

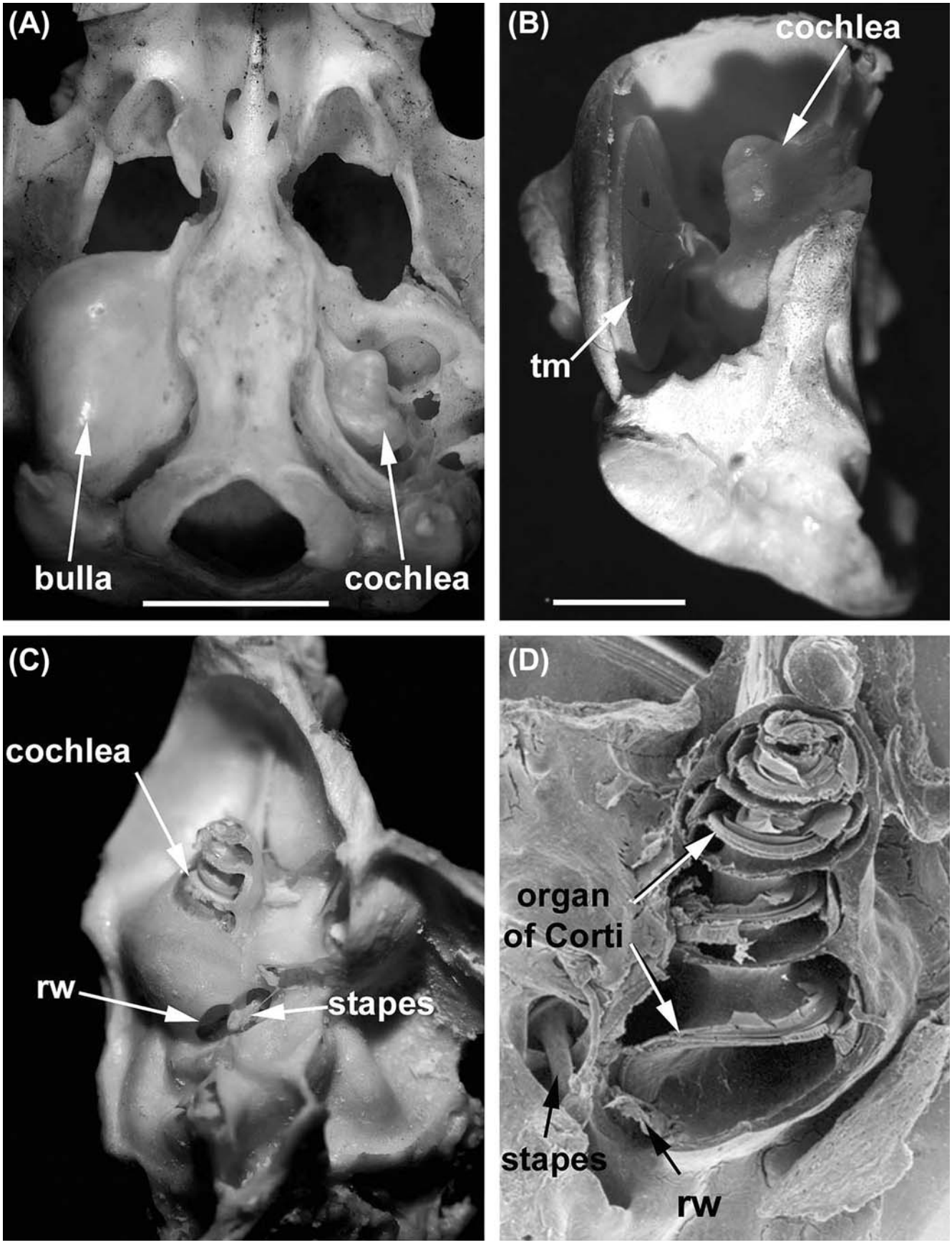

FIGURE 22B.2 Gross structure of the guinea pig bulla and cochlea. (A) Base of the skull (observed from below). The bulla of the right ear (on the left) is intact, while that of the left ear (on the right) has been opened to expose the cochlea. (B) An isolated bulla has been opened to

the semicircular canals of the vestibular apparatus. The utricle and saccule of the vestibular apparatus are contained within the vestibule. The membranous labyrinth is contained within the encasing bony labyrinth. The membranous labyrinth contains endolymph, while the space between the membranous labyrinth and bony labyrinth contains perilymph.

The cochlea is a spiral-shaped structure that has 2.5–3.5 turns, depending on the mammalian species (Figure 22b.3). The three turns are often referred to as apical, middle, and basal turns. The otic capsule is the hard external supporting structure of the cochlea and is part of the temporal bone. There are three fluid-filled spaces in each turn of the cochlea: the scala tympani, scala vestibuli, and scala media (Figures 22b.3 and 22b.4). The scala tympani and scala vestibuli are continuous, meeting at the most apical turn of the spiral, and contain perilymph. The scala media is located between the scala tympani and scala vestibuli and contains endolymph. Perilymph is high in sodium (Na^+) and low in potassium (K^+), while the endolymph is high in K^+ and low in Na^+. The chemical potential, formed by the differential electrolyte concentrations between the canals containing perilymph and endolymph, is essential for the function of the hair cells.

Within the scala media is the organ of Corti (Figures 22b.3 and 22b.4), which consists of the inner and outer sensory hair cells and the associated supporting cells and matrix (Figure 22b.5). The inner hair cells normally occur as a single row running the length of the spiral of the scala media, while the outer hair cells occur as three rows. The inner hair cell is the true otic sensory cell. Deflection of the inner hair cell's stereocilia by sound-induced fluid waves traveling in the endolymph opens transduction ion channels in the apical cell surface that allow influx of K^+ ions into the cell from the endolymph. This flow in turn activates voltage-sensitive calcium (Ca^{++}) channels and Ca^{++}-activated K^+ channels in the lateral and basal membranes, in turn causing release of neurotransmitters at the base of the inner hair cell. Nerve fibers synapse with the inner hair cell and are bipolar neurons of the cochlear (auditory) nerve. The soma of each neuron is located in the spiral ganglion.

Deflection of the stereocilia of the outer hair cells causes the opening of ion channels and results in rapid changes in length and stiffening of the outer hair cell cytoskeleton. These changes in the outer hair cells amplify the wave signal to the inner hair cells. Inner and outer hair cells are terminally differentiated and thus do not proliferate and are not regenerated.

Within the scala media on the lateral wall is the stria vascularis and the spiral ligament. The stria vascularis contains cells with membrane ion pumps and channels that maintain the charge differential between endolymph and perilymph. The spiral ligament anchors

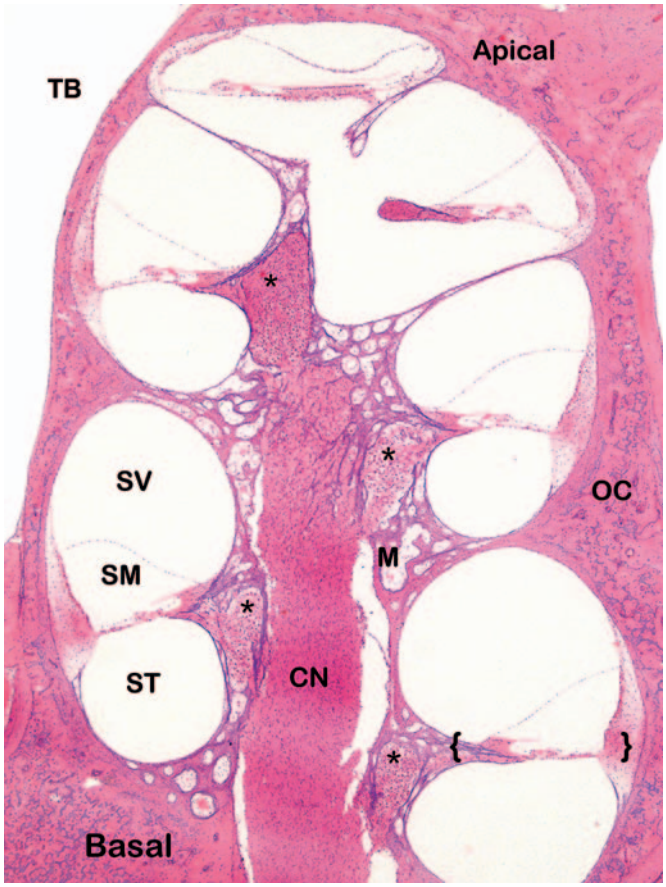

FIGURE 22B.3 Mid-modiolar section of the cochlea from a control chinchilla. The organ of Corti for the basal turn is located between the brackets (at lower right). *CN*, cochlear nerve; *M*, modiolus; *OC*, otic capsule; *SM*, scala media; *ST*, scala tympani; *SV*, scala vestibuli; *TB*, lumen of the tympanic bulla (middle ear), which is normally an air-filled space; *, spiral ganglia. Glycol methacrylate (GMA ["Soft plastic"]) section, H&E stain. 2.5× objective. Source: *Figure reproduced from Haschek, W.M., Rousseaux, C.G., Wallig, M.A., (Eds.), 2013. Haschek and Rousseaux's Handbook of Toxicologic Pathology, third ed., Academic Press (Elsevier), Figure 54.3, p. 2192 with permission.*

◀ reveal the cone-shaped tympanic membrane (tm) and the cochlea (covered in a bony wall). (C) Isolated, opened bulla with the cochlea partially dissected to expose the apical coils of the cochlear spiral. The round window (rw) and stapes (in position in the oval window) at the base of the cochlea are indicated. (D) Scanning electron micrograph of the guinea pig cochlea, with the bony wall opened to expose the interior. The spiraling organ of Corti is indicated, and the tissues that form the lateral wall of the scala media can be seen. The round window (rw) and the stapes (in position in the oval window) are indicated. Scale bars: 0.5 mm. Source: *Figure reproduced from Forge, A., et al., "Toxicological neuropathology of the ear," in: Bolon, B., Butt, M.T. (Eds.), 2011. Fundamental Neuropathology for Pathologists and Toxicologists. Wiley, Figure 23.2, p. 415 with permission.*

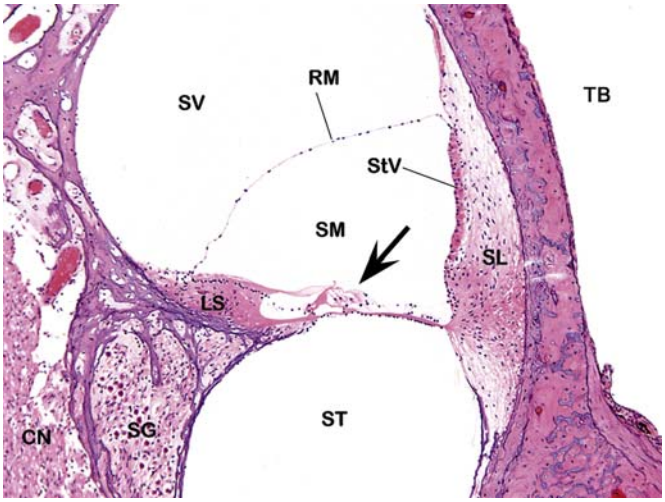

FIGURE 22B.4 Section of one turn from a mid-modiolar section of the cochlea from a control chinchilla. The arrow denotes the organ of Corti. *CN*, cochlear nerve; *LS*, limbus spiralis; *RM*, Reissner's membrane; *SG*, spiral ganglion; *SL*, spiral ligament; *SM*, scala media; *ST*, scala tympani; *StV*, stria vascularis; *SV*, scala vestibuli; *TB*, lumen of the tympanic bulla. GMA plastic section, H&E stain. 10× objective. Source: *Figure reproduced from Haschek, W.M., Rousseaux, C. G., Wallig, M.A., (Eds.), 2013. Haschek and Rousseaux's Handbook of Toxicologic Pathology, third ed., Academic Press (Elsevier), Figure 54.4, p. 2192 with permission.*

the membranous cochlea to the adjacent bony walls of the spiral canal.

As sound is transmitted from the stapes across the oval window, it causes vibratory waves in the perilymph and endolymph to travel through the cochlea. The vibrations in both these fluids trigger the outer hair cells, which amplify the signal transmitted to the inner hair cells by fluid waves carried in the endolymph; the outer hair cells likely act by increasing the vibration in the basilar membrane. The basal turns detect high-frequency sounds, while the apical turns detect low-frequency sounds.

The saccule and utricle (otolith organs) of the vestibular apparatus are located within the vestibule of the inner ear. The saccule and utricle each have a placode of tissue called the macula or otolith membrane (Figure 22b.6). This macula is lined by hair cells and other supporting epithelial cells and rests atop loose connective tissue. These cells are innervated by fibers of the vestibular nerve, the neurons of which are located in the vestibular ganglion. The surface of the macula has an adherent viscous gel in which the hair cells are embedded. Microliths (otoliths) are also entrapped within this gel. The microliths respond to gravity by causing the gel to sag, and the stereocilia on

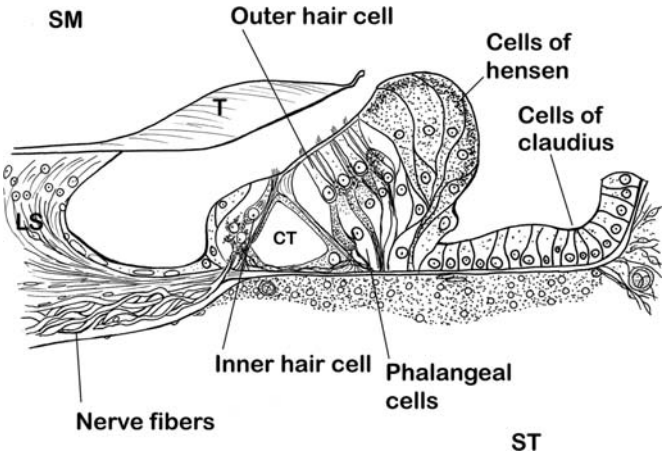

FIGURE 22B.5 Detailed schematic drawing of the organ of Corti. The sensory elements in any given section consist of a single inner hair cell located medially (to the left) and three outer hair cells arranged in a row laterally, with their support cells. The tectorial membrane (T) normally rests on the stereocilia projecting from the apical surfaces of the hair cells, which are bathed in endolymph contained within the scala media (SM). This membrane is supported by the spiral limbus (limbus spiralis, LS). Corti's tunnel (CT) is formed by the pillar cells of the organ of Corti. Phalangeal cells contact the basal portions of the outer hair cells, but the majority of the lateral surfaces of the hair cells are bathed in perilymph of the scala tympani (ST). Source: *Original line drawing by R. M. Blumer.*

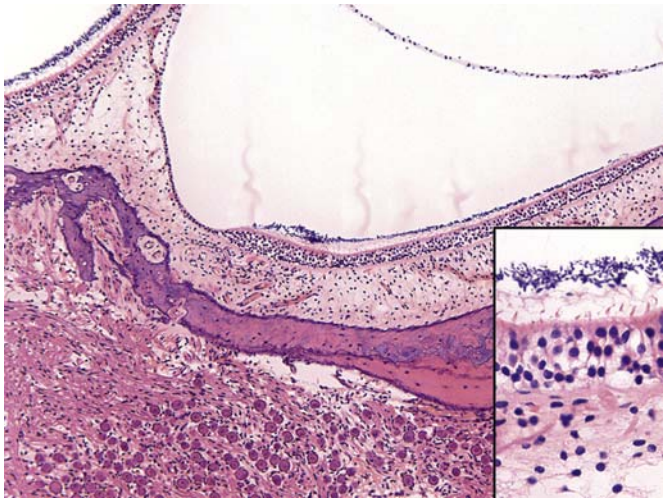

FIGURE 22B.6 A macula of the otolith organs from the vestibular apparatus of a control chinchilla. The surface is covered by a layer of otoliths (shown as dark basophilic granules) embedded in a gel. The sensory epithelia have stereocilia that project into the gel. Underlying the sensory epithelium is a loose connective tissue matrix traversed by nerve fibers. The vestibular ganglion lies within the adjacent bone (at the bottom of the image). GMA plastic section, H&E stain. 10× objective. *Inset*: High magnification of the otoliths resting on the sensory epithelium of the vestibular apparatus. GMA plastic section, H&E stain. 40× objective. Source: *Figure reproduced from Haschek, W.M., Rousseaux, C.G., Wallig, M.A., (Eds.), 2013. Haschek and Rousseaux's Handbook of Toxicologic Pathology, third ed., Academic Press (Elsevier), Figure 54.6, p. 2195 with permission.*

the hair cells to bend. This deflection allows for sensation of the location and orientation of the head relative to the force of gravity based on the distortion of stereocilia within the otolith organs.

The semicircular canals of the vestibular apparatus are membrane-lined bony canals. The membranes have a single crista ampullaris in each canal that protrudes into the lumen and is located near the entrance to the vestibule (Figure 22b.7). The semicircular canals are roughly oriented in three distinct planes representing unique x, y, and z axes, which allows for rotational sensation in all directions. The cupola is the gel-like material on the luminal surface of the cristae in which the stereocilia of the hair cells are embedded. As the head is turned, inertia of the fluid within the semicircular canals causes the stereocilia of the hair cells to flex, thereby allowing the detection of motion.

FIGURE 22B.7 Crista ampullaris from the vestibular apparatus of a control chinchilla. The central mound of tissue is lined by sensory epithelium with stereocilia embedded in the cupola, a gel (the amorphous eosinophilic material) located on the apex. The loose connective tissue underlying the sensory epithelium is traversed by nerve fibers. GMA plastic section, H&E stain. 10× objective. Source: *Figure reproduced from Haschek, W.M., Rousseaux, C.G., Wallig, M.A., (Eds.), 2013. Haschek and Rousseaux's Handbook of Toxicologic Pathology, third ed., Academic Press (Elsevier), Figure 54.6, p. 2196 with permission.*

TESTING FOR OTIC TOXICITY

General Strategy

The clinical health of the ear can be easily assessed during the *in vivo* phase or at necropsy via otoscope, or by various neurological tests that assess the function of the cochlea, vestibular apparatus, or vestibulocochlear nerve. Histologic evaluation of the external ear is best done by taking a section along the longitudinal axis of the pinna and canal to allow for evaluation of the surface features as well as the supporting tissues. However, the usual practice is to focus the histologic analysis on the middle ear and inner ear, or even to limit the entire histologic analysis to the sensory organs in the inner ear if the potential ototoxicant is to be encountered as a blood-borne agent.

Tissue Processing

For routine screening studies, ear specimens are typically fixed by immersion of the entire skull in neutral buffered 10% formalin (NBF), approximately pH 7.4. In general, however, the best preservation of the middle and inner ears requires that fixative be introduced directly into the tympanic bulla by chipping an opening in the bulla at necropsy. Care must be taken not to disturb the ossicle bridge if this dissection approach is chosen.

Difficulties in trimming the ear canal are largely a matter of geometry since the canal is not a straight tube and the inner ear divisions vary considerably in three dimensions over short distances. If sectioned appropriately, sections through the ear canal may include sections of the tympanic bulla (middle ear) including one or more ossicles, the auditory tube, or the inner ear—but not all three in any given section. Any ear canal examination should also strive to include the tympanic membrane. Because the ear is a complex three-dimensional structure, multiple step sections are necessary to sample major middle and inner ear structures. In general the best combination is to evaluate the external and middle ear structures together while leaving the inner ear analysis for another block.

Optimal preservation of ear cytoarchitecture for dedicated ototoxicity studies typically requires embedding in plastic (typically glycol methacrylate (GMA), "soft plastic"), or sometimes "hard plastic" epoxy resins) instead of paraffin because plastic provides sufficient detail to fully evaluate the cellular and subcellular features of the organ of Corti. However, paraffin is used commonly in screening studies where ototoxicity is not expected and the ear is just one of many organs to be examined. Bony specimens are decalcified prior to embedding; calcium chelators like ethylene diamine

tetraacetic acid (EDTA) are preferred over formic acid solutions for this purpose because chelators offer better protection to the fine cytoarchitectural detail of the delicate sensory epithelia.

In evaluating the cochlea for ototoxicity, many laboratories produce cochlear whole mounts, which provide a surface view of hair cell–rich sensory structures, or perform scanning electron microscopy (SEM) of the hair cell surface structure focusing on the arrangement and morphology of the apical stereocilia. For these high-resolution techniques, animals will usually be perfusion-fixed with a combination of methanol-free formaldehyde (made from paraformaldehyde powder) and glutaraldehyde (typically between 1% and 4% of each). Hair cells are subsequently counted, with missing hair cells identified by gaps in the regular arrangement of the hair cells.

Because the inner ear consists of very delicate epithelial and neural sensory elements contained within very tough bony and fibrous supporting structures, it is not readily amenable to routine histologic techniques. This inaccessibility may result in processing artifacts within the fragile elements of greatest interest to the toxicologic risk assessment. In particular the discernment of subtle lesions may be problematic. For this reason, many ototoxicity studies include a positive control group (e.g., one treated with a known ototoxic agent) as a helpful aid to determining the toxicity of the test article. The ability to detect known lesions in a concurrently treated positive control group permits calibration of the artifactual abnormalities that should not be interpreted as test article-induced lesions. Aminoglycosides like gentamicin are popular choices as positive control ototoxicants.

Test Species Selection

Species commonly used for ototoxicity studies include mice, rats, guinea pigs, chinchillas, rabbits, dogs, and nonhuman primates. One potential advantage of rodents is that they are small enough that the entire head, with brain and both ears left in in situ, can be serially or step-sectioned to examine otic and their allied neural tissues. Guinea pigs and chinchillas are preferred for toxicity studies of the inner ear as they have a relatively large tympanic bulla that can be harvested intact, with very little of the cochlea embedded in the temporal bones. Both these species also have 3.5 turns in the spiral of the cochlea, while rats and humans have only 2.5 turns. It is thought that these additional turns provide more tissue as a target for ototoxic agents as well as for detailed histopathologic evaluation.

Mice are very useful animal models for basic research. There are approximately 100 strains with naturally occurring mutations resulting in various auditory or vestibular function defects. However, strain selection in mice can be very important for ototoxicity research due to these inherited background defects and known mutations affecting hearing and/or balance. For example, the 129-related strains, commonly used for producing gene targeted (knockout/knockin) mice, have moderate hearing impairment, while FVB strain animals often used in generating transgenics do not have hearing deficits. Similarly, CD1 mice have complete hearing loss by about 6 months of age, animals with a C57BL/6 genetic background have progressive presenile hearing impairment that is a bit slower in onset, and CBA-derived mouse strains tend to have normal hearing.

Besides chinchillas, guinea pigs, and mice, other species are used less frequently for ototoxicity studies. Rats typically are utilized where dosing is applied to the external or middle ear. Rabbits are a logical choice for dosing to the external ear canal, although rats and dogs are occasionally used for these types of studies as well. Dogs may be used in ototoxicity studies but are not the first choice of species because approximately half of the cochlea is embedded within the temporal bone and requires longer decalcification. Nonhuman primates may be the species of choice for ototoxicity testing based on the pharmacologic activity of the test substance, especially if it is a biotechnology-based material. However, the inner ear of primates is entirely embedded within the temporal bone, making decalcification and preparation of tissue more difficult.

RESPONSES TO INJURY AND MECHANISMS OF INJURY

External Ear

The pinna of the external ear is readily assessed clinically and grossly at necropsy with palpation, observation, and otoscopic examination. Otitis externa is usually not observed in toxicology studies, but, if present, may be associated with bacterial or fungal infections. For rabbits, hemorrhages on the dorsal surface of the pinna are frequently observed at necropsy as the ear veins are a convenient location for blood collection and intravenous dosing during toxicity studies.

Some strains of rats may develop auricular chondritis of the pinna. Sprague-Dawley, Crl:CD, and fawn-hooded rats are particularly susceptible. This well-described syndrome occurs in animals greater than 6 months of age and usually presents bilaterally as single or multiple nodules or diffuse thickening of the pinna. Microscopically the swollen areas consist of granulomatous inflammation centered on the auricular cartilage. The cartilage may exhibit regenerative

hyperplasia in addition to inflammation-induced degeneration, and there may be areas of bone formation within the damaged cartilage.

Neoplasms occasionally occur in the external ear. The most frequent are large Zymbal's gland tumors that arise in rodents, especially rats. These tumors include adenomas and carcinomas that may have squamous cell differentiation, but sebaceous differentiation to some degree is normally identifiable. The Zymbal's gland may also develop ductal cysts that are filled with secretory material, but the epithelial lining remains well differentiated.

Other incidental changes that may be seen on the pinna are wounds from bites or by the placement of identification marks (ear notches or tags). These openings may become infected. Ceruminous plugs filling the ear canal can be observed in rodents. Small foreign bodies such as bedding may be entrapped in the ear canal.

Application of test articles to the external ear canal is often anticipated to produce changes in the canal. Findings are often irritant reactions that may be induced by vehicle alone as well as by the test article. For example, dosing with isotonic saline one or more times per day for multiple days will produce minor changes in the external ear canal, generally consisting of minimal to mild hyperplasia of the epithelial lining. With substances that are more irritating, the subepithelial tissues will in time become edematous and local blood vessels will become congested, producing a reddened and swollen appearance when viewed otoscopically. Frank hemorrhage of the subepithelial tissues may develop as well.

With advancing degrees of irritation the surface epithelium may become eroded or ulcerated (Figure 22b.8), which will often induce fibrosis and a variable degree of inflammation within the underlying tissues. Suppurative inflammation (rich in heterophils (in rabbits)/neutrophils (in other mammalian species)) of the dermis and epidermis may range from minimal to intense, and may contribute to the formation and expansion of serocellular exudates (crusting) in the canal lumen. The epidermis initially may have pustules and transmigrating heterophils/neutrophils (Figure 22b.9), but with chronicity clusters or diffuse infiltrates of lymphocytes and plasma cells will form. As compensatory responses to long-standing inflammation the ceruminous glands will become both hypertrophied and hyperplastic, presumably by secreting increased amounts of cerumin as a protective mechanism. The glands may have heterophilic/neutrophilic infiltrates both around the glands and as plugs within their lumens (Figures 22b.10 and 22b.11). The epithelium lining the external surface of the tympanic membrane may be hyperplastic due to ear canal irritation. Similarly the stroma of the tympanic membrane may become congested, edematous and acquire infiltrates of heterophils/neutrophils. The tympanic membrane is generally a good barrier that prevents materials within the canal from entering the middle ear, so extension of external ear canal changes to the middle ear is infrequent. However, with more severe irritants the tympanic membrane may become necrotic and even rupture (typically in the center rather than at the margins), thereby permitting access of external ear contaminants into the middle ear chamber.

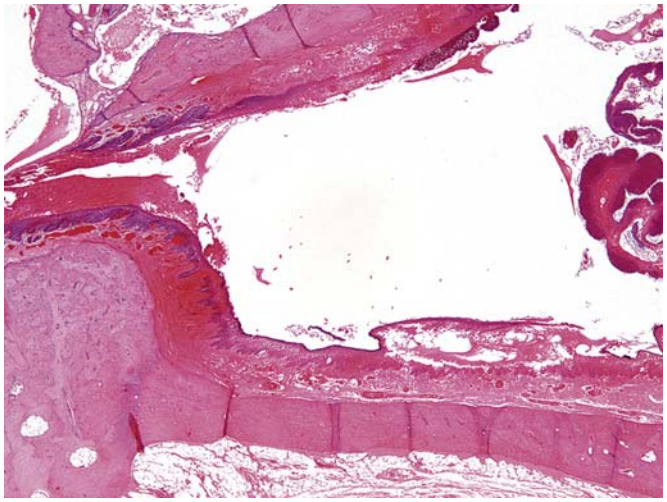

FIGURE 22B.8 Bony portion of the external ear canal from a rabbit dosed with an irritating solution via the external ear canal. The tympanic membrane is to the left. The epidermis in the lower portion of the canal is necrotic and lifting away from the dermis. Adjacent areas of the dermis as well as the dermis of the opposite wall have areas of acute hemorrhage. Paraffin section, H&E stain. 2.5× objective. Source: *Figure reproduced from Haschek, W.M., Rousseaux, C.G., Wallig, M.A., (Eds.), 2013. Haschek and Rousseaux's Handbook of Toxicologic Pathology, third ed., Academic Press (Elsevier), Figure 54.8, p. 2201, with permission.*

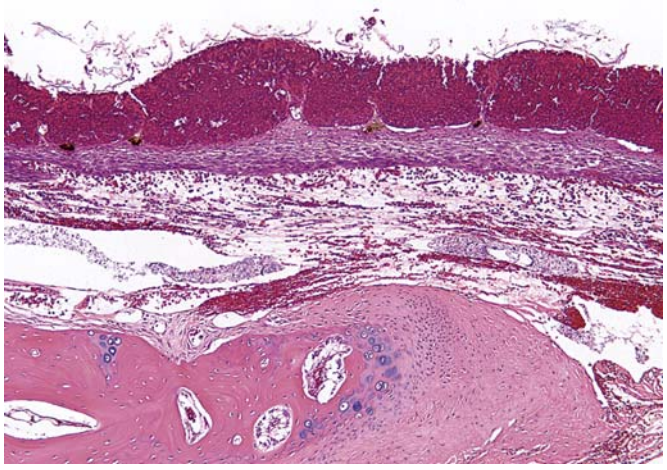

FIGURE 22B.9 External ear canal from a rabbit dosed with an irritating solution via direct instillation into the canal. Extensive heterophilic pustule formation is evident in the superficial epidermis, while the deeper dermis is mildly expanded by edema and hemorrhage but relatively few heterophils (considering the intense degree of the surface reaction). Heterophils are brightly eosinophilic and look like hemorrhage at this low magnification. Paraffin section, H&E stain. 10× objective. Source: *Figure reproduced from Haschek, W.M., Rousseaux, C.G., Wallig, M.A., (Eds.), 2013. Haschek and Rousseaux's Handbook of Toxicologic Pathology, third ed., Academic Press (Elsevier), Figure 54.9, p. 2201, with permission.*

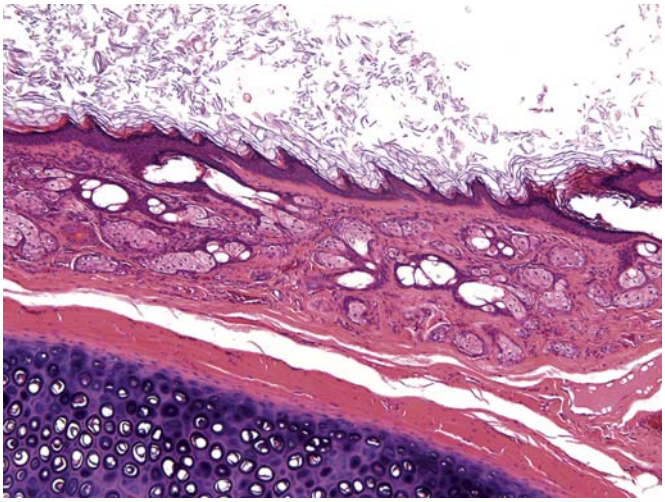

FIGURE 22B.10 Typical sebaceous glands from the external ear canal of an untreated rabbit. Note the relatively small size of the individual sebaceous glands. Paraffin section, H&E stain. 10× objective. Source: *Figure reproduced from Haschek, W.M., Rousseaux, C.G., Wallig, M.A., (Eds.), 2013. Haschek and Rousseaux's Handbook of Toxicologic Pathology, third ed., Academic Press (Elsevier), Figure 54.10, p. 2202, with permission.*

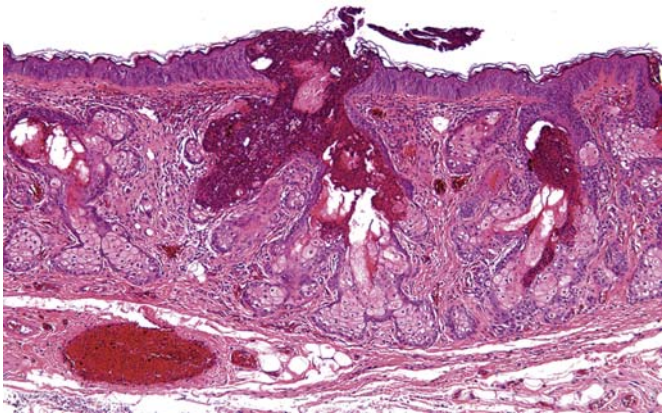

FIGURE 22B.11 Abnormal sebaceous glands from the external ear canal of a rabbit dosed with an irritating solution via the external ear canal. Several glands have large, bright eosinophilic plugs of heterophils and some cerumin (secretion) in the ductular and acinar lumens, while the epithelium of all glands is both hypertrophied and hyperplastic. Inflammatory cells are scattered in the dermis. Paraffin section, H&E stain. 10× objective. Source: *Figure reproduced from Haschek, W.M., Rousseaux, C.G., Wallig, M.A., (Eds.), 2013. Haschek and Rousseaux's Handbook of Toxicologic Pathology, third ed., Academic Press (Elsevier),Figure 54.10, p. 2202 with permission.*

Middle Ear

A variety of spontaneous changes may occur in the middle ear. Germ-free animals have only a few lymphocytes in the mucosal lamina propria of the tympanic bulla. Conventionally raised and housed animals may have minimal to moderate numbers of lymphocytes in the lamina propria (thought to serve a sentinel function) and occasionally a mixed inflammatory infiltrate (which includes plasma cells and a few neutrophils) may be present.

Bacterial otitis media is a relatively common condition in guinea pigs. Accordingly a thorough otoscopic examination should be performed prior to placement of animals on study; infected individuals exhibit reddening of the tympanic membrane, and sometimes outward distortion of its central region due to obstruction of the auditory tube and/or accumulation of inflammatory cells and secretions. Bacterial otitis media is also a frequent finding in immunodeficient mice (Figure 22b.12), but it is reported to be uncommon in wild-type mice and rats. Bacterial otitis media is usually suppurative in nature, leading to an extensive influx of heterophils/neutrophils in response to debris from degenerating cells. The mucosa lining the middle ear will generally be hypertrophied and hyperplastic, consisting of a cuboidal to columnar layer with prominent cytoplasmic vacuolation and goblet cell production. Areas of the mucosa, especially those located ventrally, may develop squamous metaplasia. The mucosal thickness will often be increased by some combination of soft tissue edema, vascular congestion, and formation of glandular structures. Otitis media is often also associated with severe infections of the upper respiratory tract, rupture of the tympanic membrane, or neoplasia in the external ear canal.

Catarrhal otitis media occurs as an acellular exudate in the lumen of the tympanic bulla. The exudate appears to be a mixture of mucous and serous products. The epithelium typically will be hyperplastic while blood vessels in the submucosa will be dilated. Because of the favorable environment, this sterile condition may progress to a suppurative bacterial otitis media with time.

Cholesteatomas occasionally are observed in the middle ears of animals. These masses are neither neoplasms nor are they necessarily rich in cholesterol. They are thought to arise from rupture of the tympanic membrane with migration of squamous epithelium into the tympanic bulla. This epithelium proliferates to form a keratinizing squamous cyst (Figure 22b.13). Breakdown of the entrapped cells releases membrane-bound cholesterol. The hydrophobic nature of this material causes it to condense, so the cholesterol-rich depot will progressively enlarge.

Direct dosing to the middle ear is a viable route for administering pharmaceuticals. Xenobiotics may be injected through the tympanic membrane or via a defect created in the wall of the tympanic bulla; the latter approach is often selected for placement of a cannula to permit repeated dosing. A common alteration following introduction of agents into the tympanic bulla is an irritant response. Many of the middle ear reactions to directly instilled vehicles and test articles are similar to those described earlier for the spontaneous otitides. As with the external ear, treatment with isotonic saline will cause some changes in the middle

FIGURE 22B.12 Tympanic bullae from a 5-month-old mouse contrasting the normal features of an unaffected ear (A) with acute panotitis (B). Protein-rich fluid bearing many degenerate neutrophils fills the external acoustic meatus (EAM) near a large fragment of plant debris (arrow). The keratinized squamous epithelium of the EAM is ulcerated at the base near the transition to the tympanic membrane. The lumen of the tympanic bulla (TB (middle ear)) contains myriad neutrophils, and the ciliated respiratory epithelium lining the bulla is ulcerated segmentally. The incus [I] is visible in both sections. Acute hemorrhage is evident throughout the cochlea (C). Paraffin section, H&E stain, 4× objective. Source: *These panels were provided by Dr. Krista La Perle, Comparative Pathology and Mouse Phenotyping Shared Resource and the Department of Veterinary Biosciences, College of Veterinary Medicine, The Ohio State University. Figure reproduced from Haschek, W.M., Rousseaux, C.G., Wallig, M.A., (Eds.), 2013. Haschek and Rousseaux's Handbook of Toxicologic Pathology, third ed., Academic Press (Elsevier), Figure 54.13, p. 2203, with permission.*

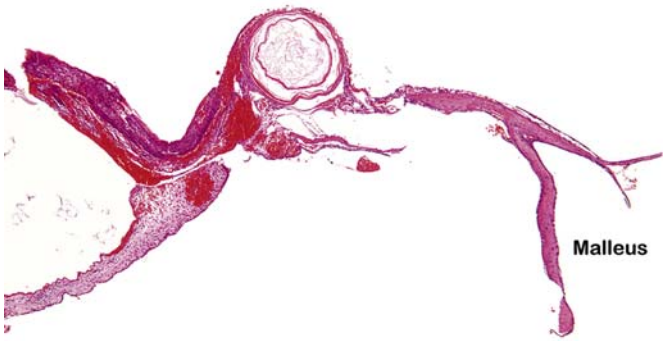

FIGURE 22B.13 Squamous cyst in the tympanic membrane of a rabbit. Given sufficient time, this focal lesion could develop into a cholesteatoma. The malleus (a middle ear ossicle) is to the right. Note the hyperplastic epithelium lining the external surface of the tympanic membrane (to the left in the image). The tympanic membrane is also thickened by multiple foci of hemorrhage. Paraffin section, H&E stain. 5× objective. Source: *Figure reproduced from Haschek, W.M., Rousseaux, C.G., Wallig, M.A., (Eds.), 2013. Haschek and Rousseaux's Handbook of Toxicologic Pathology, third ed., Academic Press (Elsevier), Figure 54.14, p. 2204 with permission.*

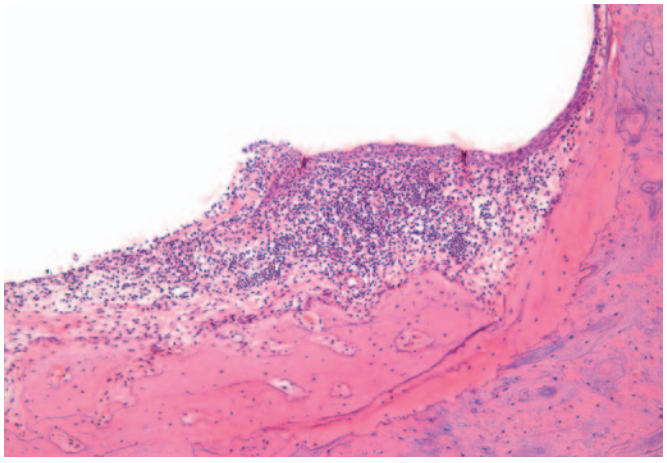

FIGURE 22B.14 Tympanic bulla from a guinea pig in which the test article was introduced directly into the middle ear. The mucosal lining to the right is characterized by squamous metaplasia with underlying suppurative inflammation. The mucosa to the left is ulcerated. GMA plastic section, H&E stain. 10× objective. Source: *Figure reproduced from Haschek, W.M., Rousseaux, C.G., Wallig, M.A., (Eds.), 2013. Haschek and Rousseaux's Handbook of Toxicologic Pathology, third ed., Academic Press (Elsevier),Figure 54.15, p. 2204, globally update with permission.*

ear including minimal to mild hyperplasia and hypertrophy of the mucosal epithelium as well as minimal edema of the lamina propria (Figures 22b.14 and 22b.15). With more irritating substances, heterophilic/neutrophilic infiltrates will develop within the lamina propria and in most cases initiate a suppurative cellular exudate in the tympanic bulla lumen (Figure 22b.16). Over time the lamina propria may also contain numerous lymphocytes, plasma cells, and

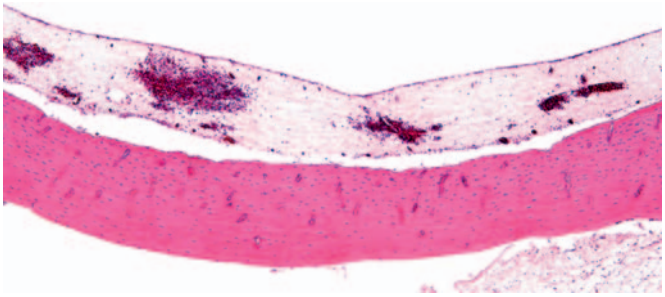

FIGURE 22B.15 Tympanic bulla from a control rabbit in which vehicle was introduced directly into the external ear canal. The mucosa is considerably expanded by edema and has many congested vessels with multiple foci of hemorrhage. Paraffin section, H&E stain. 10× objective. Source: *Figure reproduced from Haschek, W.M., Rousseaux, C.G., Wallig, M.A., (Eds.), 2013. Haschek and Rousseaux's Handbook of Toxicologic Pathology, third ed., Academic Press (Elsevier), Figure 54.16, p. 2205 with permission.*

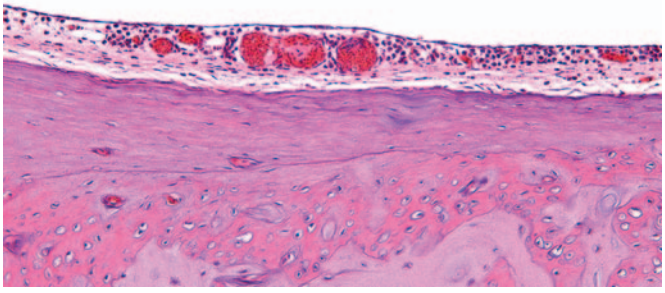

FIGURE 22B.16 Tympanic bulla from the contralateral (untreated control) ear of a rabbit. The diffuse mild infiltrate of heterophils represents a spontaneous change that must be distinguished from an irritant effect if it were observed in a treated ear. Paraffin section, H&E stain. 20X Objective. Source: *Figure reproduced from Haschek, W.M., Rousseaux, C.G., Wallig, M.A., (Eds.), 2013. Haschek and Rousseaux's Handbook of Toxicologic Pathology, third ed., Academic Press (Elsevier), Figure 54.17, p. 2205, with permission.*

macrophages. Within the lamina propria the vessels may be dilated and congested, hemorrhage may occur, and new glands may expand the underlying lamina propria (Figure 22b.17).

Particularly severe and chronic conditions may result in proliferation of fibrous connective tissue and/or bone into the bulla lumen (Figure 22b.18). This osteosclerosis reaction can be extensive and may occur as either new laminar bone formation or as sharp spicules of bone within the markedly thickened mucosa. The middle ear ossicles may become immobilized as they are enveloped in the fibrous and bony outgrowths or become embedded in exudate (Figure 22b.19). While such entrapment would be anticipated to dampen sound transmission to the inner ear, electrophysiological testing will often demonstrate that auditory sensation is partly retained, indicating that the ossicle lesions still allow some vibration to be transmitted. At times

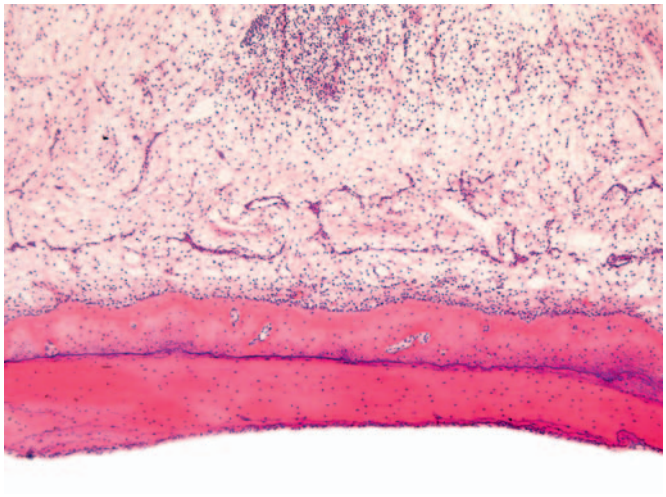

FIGURE 22B.17 Tympanic bulla from a chinchilla in which the test article was introduced directly into the middle ear. The mucosa of the bulla (upper portion of image) is expanded by edema and loose connective tissue to such a marked degree that the entire mucosal thickness cannot be observed in one field even at this low magnification; this can be readily appreciated by comparing this image to the expanse of stroma in Figure 22b.14. The mucosa also harbors multiple large infiltrates of neutrophils as well as diffuse infiltrates of other inflammatory cells types. Paraffin section, H&E stain. 5× objective. Source: *Figure reproduced from Haschek, W.M., Rousseaux, C.G., Wallig, M.A., (Eds.), 2013. Haschek and Rousseaux's Handbook of Toxicologic Pathology, third ed., Academic Press (Elsevier), Figure 54.18, p. 2205 with permission.*

FIGURE 22B.18 Tympanic bulla from a guinea pig in which the test article was introduced directly into the middle ear. The bony wall of the tympanic bulla is markedly thickened by new bone formation (the layer spanned by the double-headed arrow) and loose fibrous connective tissue. *C*, apex of cochlea. GMA plastic section, H&E stain. 2.5× objective. Source: *Figure reproduced from Haschek, W.M., Rousseaux, C.G., Wallig, M.A., (Eds.), 2013. Haschek and Rousseaux's Handbook of Toxicologic Pathology, third ed., Academic Press (Elsevier), Figure 54.19, p. 2206, with permission.*

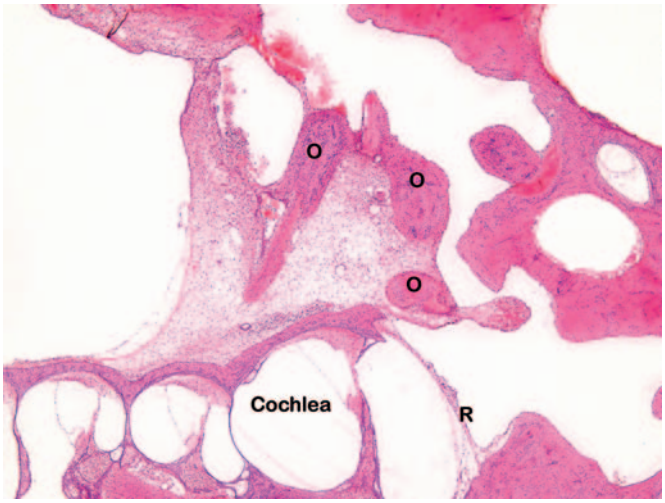

FIGURE 22B.19 Tympanic bulla from a guinea pig in which the test article was introduced directly into the middle ear. A fibrinopurulent exudate extends from the tympanic membrane (at the top of the image but out of the field of view) to the cochlea and has entrapped and immobilized all three ossicles (O). *R*, round window membrane. GMA plastic section, H&E stain. 2.5× objective. Source: *Figure reproduced from Haschek, W.M., Rousseaux, C.G., Wallig, M.A., (Eds.), 2013. Haschek and Rousseaux's Handbook of Toxicologic Pathology, third ed., Academic Press (Elsevier), Figure 54.20, p. 2206 with permission.*

FIGURE 22B.20 Tympanic membrane from a guinea pig with a cannula placed into the tympanic bulla. A translucent, crescent-shaped fragment of tissue glue used to secure the cannula is entrapped within the tympanic membrane and surrounded by macrophages. *E*, external surface (i.e., the external ear canal), *I*, internal surface (i.e., the lumen of the tympanic bulla). GMA plastic section, H&E stain. 10× objective. Source: *Figure reproduced from Haschek, W.M., Rousseaux, C.G., Wallig, M.A., (Eds.), 2013. Haschek and Rousseaux's Handbook of Toxicologic Pathology, third ed., Academic Press (Elsevier), Figure 54.21, p. 2206 with permission.*

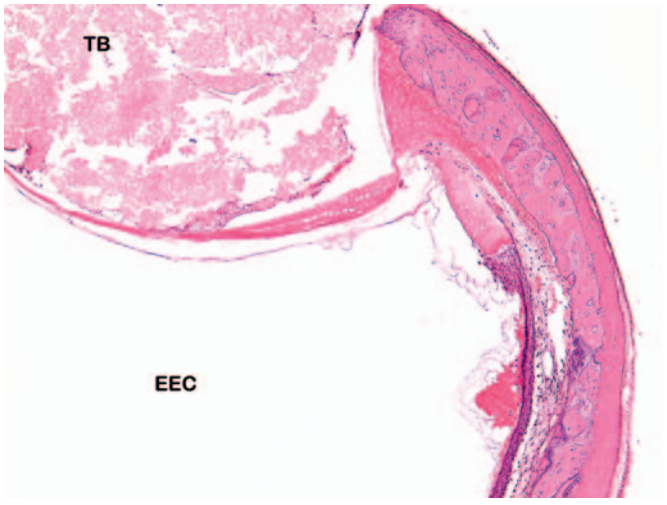

FIGURE 22B.21 Tympanic membrane from a chinchilla in which the test article was introduced directly into the middle ear. The tympanic membrane and its anchoring supports have undergone coagulative necrosis. Acellular debris is in the middle ear space. *TB*, Lumen of the tympanic bulla. *EEC*, Lumen of the external ear canal. Paraffin section, H&E stain. 10× objective. Source: *Figure reproduced from Haschek, W.M., Rousseaux, C.G., Wallig, M.A., (Eds.), 2013. Haschek and Rousseaux's Handbook of Toxicologic Pathology, third ed., Academic Press (Elsevier), Figure 54.22, p. 2206 with permission.*

the ossicles may instead be thinned due to osteoclast formation and subsequent bone degradation. The bone forming the cochlea may also be thickened in chronic middle ear inflammation. With placement of an indwelling cannula, the usual anticipated responses of granulomatous inflammation and fibrosis directed against such foreign bodies as suture material and tissue glue may be observed (Figure 22b.20). Occasionally the cannula will be enveloped by exuberant fibrous connective tissue, which may permit the proliferating tissue to enter into and obstruct the cannula.

The auditory tube often is relatively unaffected by agents instilled in the middle ear, but in some cases luminal cellular debris, hypertrophied and hyperplastic epithelium, or increased lymphoid infiltrates in the lamina propria can be identified in the portion of the tube closest to the tympanic bulla. With extremely severe irritants the tympanic membrane may exhibit erosion of the epithelium in the inner surface, and may even undergo necrosis (Figure 22b.21). When necrosis ensues the tympanic membrane is crusted in serocellular exudate, its stroma is hypereosinophilic (indicative of extensive matrix degradation), and the inflammatory response may drain outward into the external ear canal.

Inner Ear

Ototoxicant-Induced Morphologic Changes

The sense of hearing in the inner ear is susceptible to several classes of ototoxicants following systemic exposures. Prototypical ototoxic agents include aminoglycoside antibiotics, organic solvents, loop diuretics, quinine, salicylates, cisplatins, organometals, and carbon monoxide. High levels of noise also produce otic damage. Combinations of ototoxicants and chronically high levels of ambient noise exacerbate the hearing loss that develops following either source of damage alone. Outer hair cells generally are more sensitive to

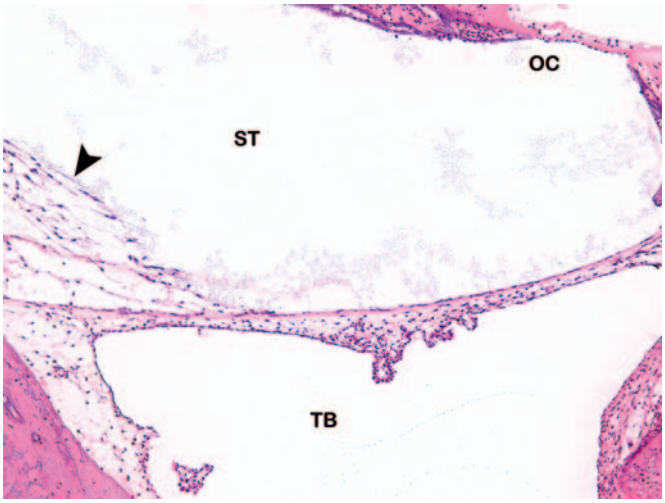

FIGURE 22B.22 Round window from a guinea pig in which the test article was introduced directly into the middle ear. The round window membrane (center) is diffusely expanded by edema and is focally thickened in the center by stromal proliferation. The internal portion of the round window membrane is also thickened adjacent to its attachment to the otic capsule (arrowhead). *OC*, organ of Corti; *ST*, scala tympani; *TB*, lumen of tympanic bulla. GMA plastic section, H&E stain. 10× objective. Source: *Figure reproduced from Haschek, W. M., Rousseaux, C.G., Wallig, M.A., (Eds.), 2013. Haschek and Rousseaux's Handbook of Toxicologic Pathology, third ed., Academic Press (Elsevier), Figure 54.24, p. 2207 with permission.*

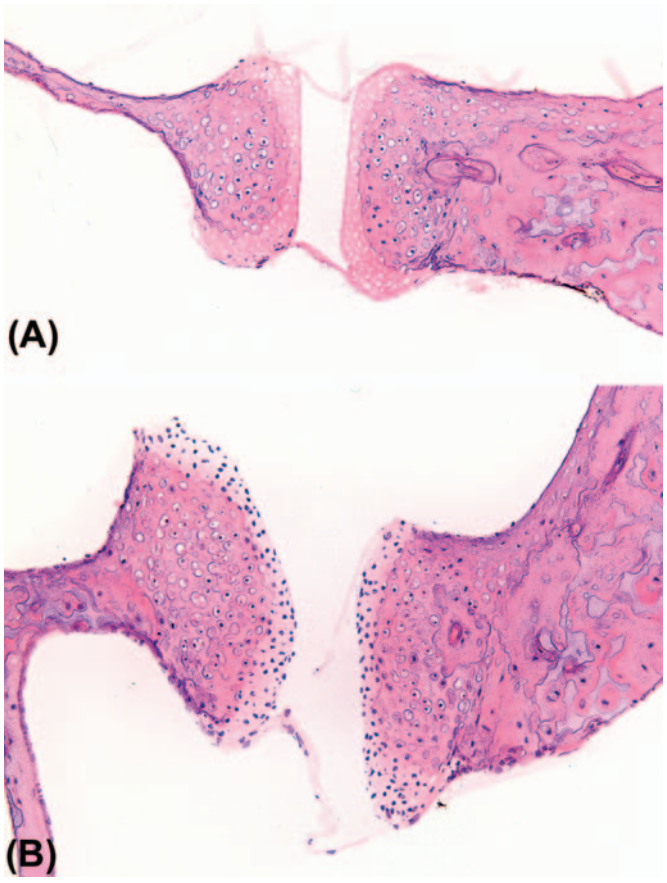

FIGURE 22B.23 Inner ear from a chinchilla 72 hours after test article administration directly into the middle ear. (A) The fibrocartilage of the footplate of the stapes and the oval window are necrotic, as indicated by increased tissue eosinophilia and an absence of chondrocytes within lacunae. The stapes is to the left, and the rim of the oval window is to the right. GMA plastic section, H&E stain. 20× objective. (B) Normal oval window in the same orientation, demonstrating many dark chrondrocyte nuclei. GMA plastic section, H&E stain. 20× objective. Source: *Figure reproduced from Haschek, W.M., Rousseaux, C.G., Wallig, M.A., (Eds.), 2013. Haschek and Rousseaux's Handbook of Toxicologic Pathology, third ed., Academic Press (Elsevier), Figure 54.25, p. 2208 with permission.*

ototoxicants than are inner hair cells. Ototoxic agents typically produce patterns of damage that mimic age-related hearing loss in that the basal (high frequency) areas of the cochlea are affected before the apical (low frequency) areas. However, some animal models, notably mice of the C57BL/6 strain, also develop spontaneous age-related defects in the outer hair cells in the apical and extreme apical regions, but to a lesser degree than the accompanying changes that arise in the basal areas.

Almost any part of the cochlea can present with toxicant-induced histologic changes depending on the agent and the nature of the insult. An irritating xenobiotic or vehicle applied to the middle ear may produce thickening of the bony otic capsule, which is the external structure surrounding the cochlea. Direct middle ear administration of an irritant also can incite inflammatory infiltrates in the round window or near the footplate of the stapes in the oval window. The round window may be thickened by fibroblast proliferation (Figure 22b.22). The footplate of the stapes and the fibrocartilage of the round window membrane may also be affected (Figure 22b.23). If the irritant introduced into the middle ear is able to penetrate into the cochlea, inflammatory cells may infiltrate the lumens or mucosal linings (Figure 22b.24) of the scala vestibuli, scala media, and/or scala tympani; in chronic lesions, proliferation of fibroblasts may lead to expansion and distortion of the inflamed cochlear tissues. In some instances of toxicant-induced cochlear inflammation, hemorrhage may be evident as well. The hemorrhage and inflammation may only be present in dependent (ventrally located) portions of the cochlea, keeping in mind that dependency may be relative to the position of the cochlea during the trimming and embedding processes.

Systemically administered ototoxicants will often affect particular portions of the organ of Corti. Such specificity is generally due either to greater sensitivity of those affected cell populations or to pharmacologic activity. Within the organ of Corti the outer hair cells

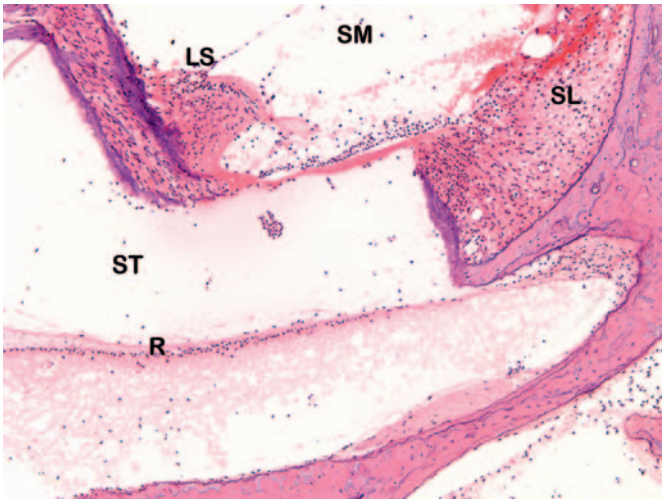

FIGURE 22B.24 Cochlea from a chinchilla in which the test article was introduced directly into the middle ear. Low numbers of neutrophils have infiltrated the scala tympani (ST) and scala media (SM). The round window membrane (R) is necrotic. The stria vascularis is hemorrhagic. The limbus spiralis (LS) and spiral ligament (SL) are necrotic and infiltrated by neutrophils. The organ of Corti is disrupted and eosinophilic (necrotic). GMA plastic section, H&E stain. 10× objective. Source: *Figure reproduced from Haschek, W.M., Rousseaux, C.G., Wallig, M.A., (Eds.), 2013. Haschek and Rousseaux's Handbook of Toxicologic Pathology, third ed., Academic Press (Elsevier), Figure 54.26, p. 2208 with permission.*

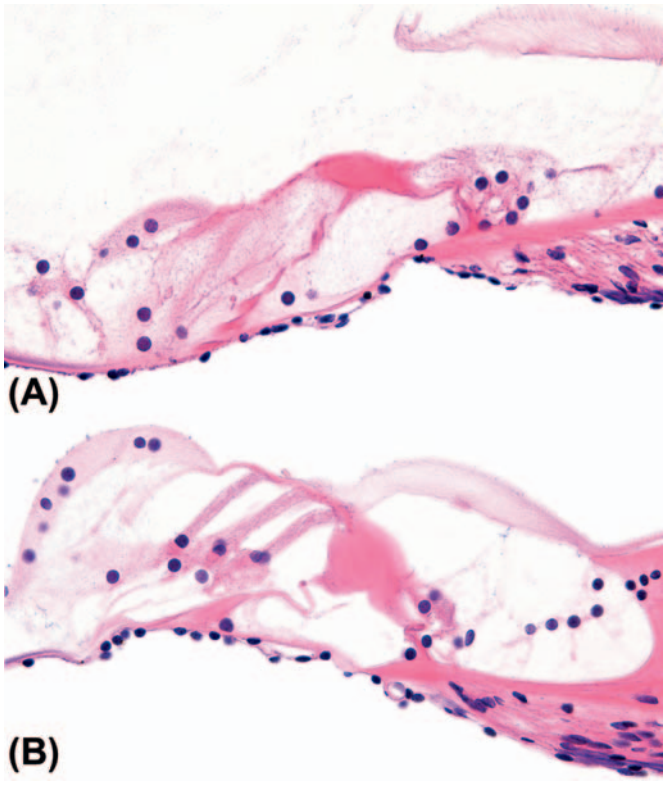

FIGURE 22B.25 Sensory cell damage in the organ of Corti in the cochlea from a chinchilla. (A) Following introduction of gentamicin (a positive control agent) directly into the middle ear, the organ of Corti exhibits loss of all hair cells and the sensory epithelium has been replaced by large cells with pale cytoplasm. GMA plastic section, H&E stain. 40× objective. (B) Normal organ of Corti from a control chinchilla showing the row of three, well defined, outer hair cells (to the left, contacted apically by the tectorial membrane). Due to plane of section, two inner hair cells are visible to the right. GMA plastic section, H&E stain. 40× objective. Source: *Figure reproduced from Haschek, W.M., Rousseaux, C.G., Wallig, M.A., (Eds.), 2013. Haschek and Rousseaux's Handbook of Toxicologic Pathology, third ed., Academic Press (Elsevier), Figure 54.27, p. 2209 with permission.*

are generally much more sensitive to ototoxicants than are the inner hair cells, although there are some compound- and species-specific exceptions. The hair cells of the basal turns of the cochlea, which detect high-frequency sounds, are generally more sensitive to injury than are those of apical regions, which are sensitive to low-frequency sounds. In toxicity studies where agents are given for 2–4 weeks, the outer hair cells will simply be lost and replaced by large vacuolated supporting cells or, if sufficient time has passed, a single row of nondescript epithelial cells (Figure 22b.25). With studies of shorter duration (e.g., 4 days), it may be possible to identify damaged outer hair cells undergoing what morphologically appears to be apoptotic necrosis (Figure 22b.26). In these instances, routine histologic sections will reveal one or more affected outer hair cells with rounded, shrunken profiles and hypereosinophilic cytoplasm, sometimes with pyknotic or karyorrhectic nuclei. With additional time after the outer hair cells are lost, the inner hair cells may also be depleted.

Microscopic changes that can be observed in conjunction with hair cell loss include reduced cellularity of the spiral limbus, necrosis of spiral ganglion neurons, and axonal degeneration of the cochlear nerve. The loss of cellularity in the spiral limbus is of uncertain pathogenesis as the function of the dentate cells within it (a special form of fibroblast) has yet to be

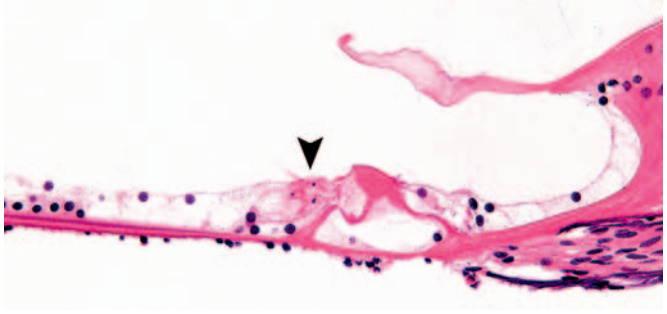

FIGURE 22B.26 Sensory cell damage in the organ of Corti in the cochlea from a chinchilla 4 days after introduction of an ototoxic test article directly into the middle ear. Fragments of necrotic cells (arrow head) remain where outer hair cells would be expected. GMA plastic section, H&E stain. 40× objective. Source: *Figure reproduced from Haschek, W.M., Rousseaux, C.G., Wallig, M.A., (Eds.), 2013. Haschek and Rousseaux's Handbook of Toxicologic Pathology, third ed., Academic Press (Elsevier), Figure 54.28, p. 2209 with permission.*

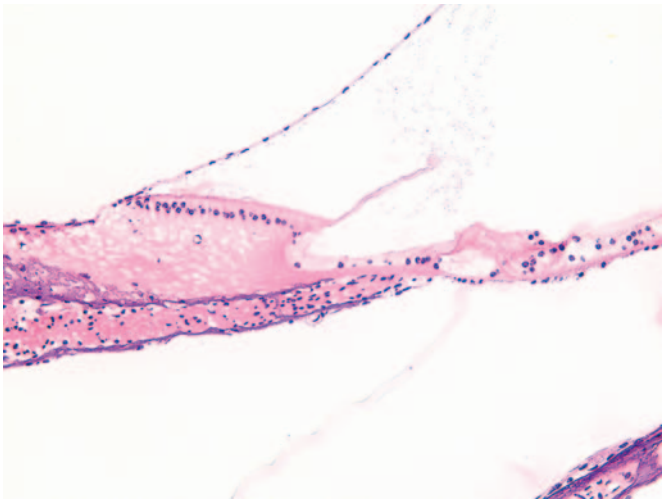

FIGURE 22B.27 Cochlea from a guinea pig following local administration of an aminoglycoside antibiotic directly into the middle ear. Relative to an unaffected organ (shown in Figure 22b.4), the spiral limbus (limbus spiralis, the eosinophilic structure at middle left) has a normal row of cells along the superficial margin but lacks the cells that should be scattered deeper in the stroma. GMA plastic section, H&E stain. 20× objective. Source: *Figure reproduced from Haschek, W.M., Rousseaux, C.G., Wallig, M.A., (Eds.), 2013. Haschek and Rousseaux's Handbook of Toxicologic Pathology, third ed., Academic Press (Elsevier), Figure 54.29, p. 2210 with permission.*

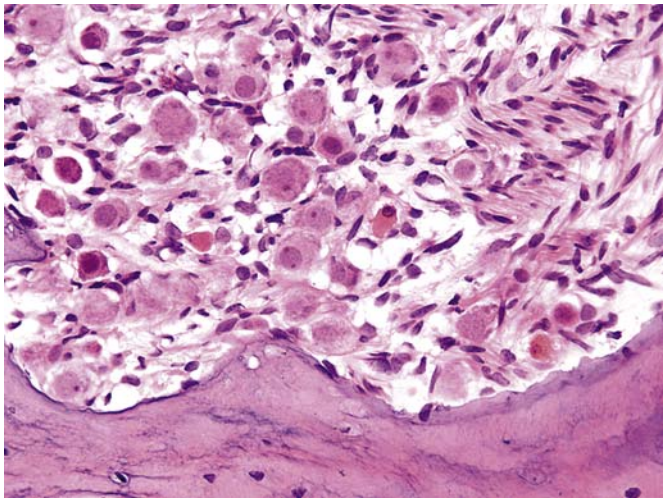

FIGURE 22B.28 Spiral ganglion from a chinchilla following local administration of an aminoglycoside antibiotic directly into the middle ear. Scattered, hypereosinophilic ("red dead") neurons are consistent with acute necrosis. GMA plastic section, H&E stain. 40× objective. Source: *Figure reproduced from Haschek, W.M., Rousseaux, C. G., Wallig, M.A., (Eds.), 2013. Haschek and Rousseaux's Handbook of Toxicologic Pathology, third ed., Academic Press (Elsevier), Figure 54.30, p. 2210 with permission.*

identified (Figure 22b.27). When these cells are lost, readily apparent empty lacunae can be seen.

The spiral ganglion is a primary site of damage for some ototoxicants. This can be surmised in some instances from the loss of spiral ganglion neurons in the absence of inner hair cell loss. Further evidence of this effect may be provided by functional testing. Whether induced by hair cell loss or direct neuronal toxicity, spiral ganglion evaluation is essentially an exercise in standard neuropathology. Dying spiral ganglion neurons will be morphologically identical to the "red dead" neurons observed in other degenerating neural tissues (for example, see Chapter 21, Nervous System, Figure 21.5), appearing as shrunken cells with small, dense nuclei, and bright eosinophilic cytoplasm (Figure 22b.28). The normal cellularity of the spiral ganglion varies highly from apex to base; therefore, a diagnosis of hypocellularity should be made with caution on routine microscopic sections unless the loss of ganglion tissue is marked. Given the appropriate timing of the evaluation after hair cell loss, the "dying back" phenomenon of axons in the nervous system due to loss of functional synapses in the periphery can be readily apparent in the cochlear nerve. With sufficient time and extensive depletion of spiral ganglion neurons, changes in the cochlear nerve trunk may be apparent as pallor of the nerve at low magnification with swelling of axons or their glial sheaths, formation of digestion chambers, and empty spaces on higher magnification.

The stria vascularis is another structure that has a demonstrated sensitivity to ototoxicants. Injury to the stria vascularis will result in functional deficits in hearing, because the stria vascularis is the primary site for maintaining the charge differential (i.e., the endocochlear potential) between the perilymph and endolymph. For example, loop diuretics have been reported to rapidly produce reversible swelling of this tissue. This change may not be sufficient to produce permanent hearing loss, but it is postulated to manifest as tinnitus (transient or persistent ringing in the ears). Loop diuretics may potentiate the injury induced by other ototoxicants, such as aminoglycosides, when the agents are given at the same time. Injury to the stria vascularis, typically elicited by high doses and chronic administration of such agents as aminoglycosides, may lead to permanent atrophy with transformation to a thinner and less complex structure. In these instances the ability to generate the endocochlear potential may be reduced but not ablated. Other manifestations of ototoxicity in the stria vascularis may be degeneration, vacuolation (Figure 22b.29), and apoptosis of the marginal cells.

In the vestibular system the cristae ampullaris and the sensory areas of the utricle and saccule are the main targets of ototoxicants. A variety of lesions may occur,

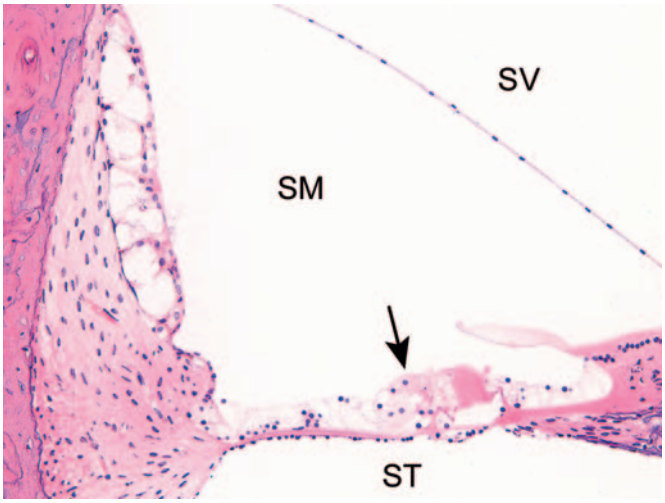

FIGURE 22B.29 Cochlea from a chinchilla in which the test article was introduced directly into the middle ear. In comparison to the normal inner ear features shown in Figure 22b.4, the stria vascularis (vertically oriented tissue on the left) is markedly vacuolated. The organ of Corti (arrow) also exhibits loss of the outer hair cells. *SM*, scala media, *ST*, scala tympani, *SV*, scala vestibuli. GMA plastic section, H&E stain. 20× objective. Source: *Figure reproduced from Haschek, W.M., Rousseaux, C.G., Wallig, M.A., (Eds.), 2013. Haschek and Rousseaux's Handbook of Toxicologic Pathology, third ed., Academic Press (Elsevier), Figure 54.32, p. 2211 with permission.*

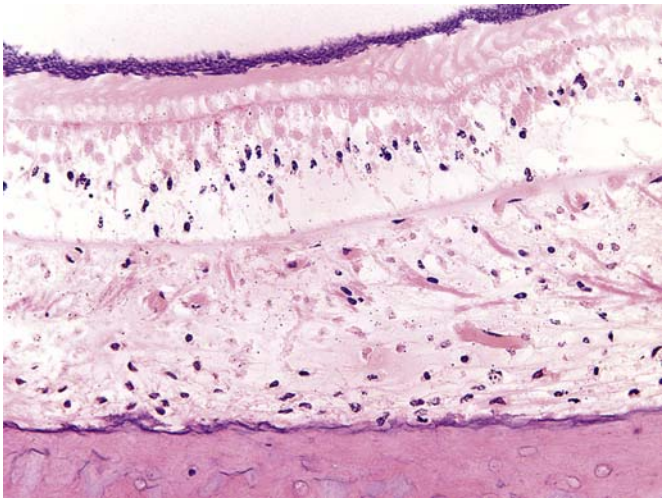

FIGURE 22B.30 Otolith organ from the vestibular apparatus of a chinchilla, 72 hours after test article was introduced directly into the middle ear. The macula has coagulative necrosis as shown by diffuse eosinophilia in association with pyknosis and karyorrhexis of nuclei. GMA plastic section, H&E stain. 40× objective. Source: *Figure reproduced from Haschek, W.M., Rousseaux, C.G., Wallig, M.A., (Eds.), 2013. Haschek and Rousseaux's Handbook of Toxicologic Pathology, third ed., Academic Press (Elsevier), Figure 54.33, p. 2211 with permission.*

including degeneration and loss of hair cells, disruption or disorganization of the sensory epithelium, necrosis (Figure 22b.30) or apoptosis. In the utricle and saccule the otoliths may be lost, displaced, or disorganized.

Specific Ototoxicants

AMINOGLYCOSIDE ANTIBIOTICS

Gentamicin, kanamycin, and neomycin, among others of this antimicrobial class, have long been recognized as ototoxicants. The aminoglycosides have varying propensities to affect either the auditory or vestibular hair cells, but with sufficiently high doses or long schedules they all will affect both populations of sensory cells. Amikacin tends to affect the cochlea more than the vestibular system, while streptomycin affects the vestibular system more than the cochlea. Gentamicin and tobramicin equally affect both the auditory and vestibular systems. In the organ of Corti, aminoglycosides tend to affect outer hair cells before inner hair cells. Some species, such as mice, are notably "resistant" to aminoglycoside antibiotics since dosing produces lethality from renal effects before ototoxicity can be demonstrated. However, ototoxicity can be produced in mice when local or systemic aminoglycoside administration is combined with systemic delivery of a loop diuretic. The toxicity of aminoglycosides is due to generation of reactive oxygen species, with iron being a key player. The basal turn of the ear generally has lower levels of glutathione and other antioxidants, which makes it more susceptible to oxidative damage. Systemic treatment with antioxidants and iron chelators has been shown to attenuate the toxicity of aminoglycosides. The loss of hair cells observed with aminoglycosides appears to be largely by apoptotic necrosis and is permanent.

Aminoglycosides enter the cochlea via the blood vessels of the stria vascularis, which are part of the barrier (analogous to the blood–brain barrier) making the ear a protected site. It was initially thought that aminoglycosides accumulate in the inner ear; however, pharmocokinetic studies have demonstrated that the concentration in the endolymph and perilymph are very low in comparison to that in the serum. The uptake into the inner ear is dose-dependent and has rapid saturation kinetics. However, aminoglycosides are cleared very slowly from the fluids of the cochlea, so even widely spaced doses will result in a long exposure half-life. Aminoglycosides are known to block a variety of ion channels, including Ca^{++}-activated K^{+} channels and transducer channels. At low doses the mechano-electrical transducer channels on hair cell bundles are thought to be permanently blocked by aminoglycosides. These ports may also be one route of antibiotic entry into the outer hair cell; selective pharmacological blockade of these channels prior to dosing with aminoglycosides reduces the extent of ototoxicity. Aminoglycosides are also taken up by hair cells via endocytotic activity at the apical membrane. Mice lacking myosin VIIA are resistant to aminoglycoside

antibiotics, as this myosin variant is necessary for the function of endocytotic vesicles.

In the vestibular organs, aminoglycosides produce greater damage in the cristae with less in the utricular macula and least in the saccular macula. Loss of hair cells in the vestibular organs, as in the organ of Corti, is by apoptotic necrosis and is permanent.

SOLVENTS

Solvents identified as ototoxicants include toluene, xylenes, and styrene, among others. The mechanism of toxicity has not been defined. All solvents are not created equal in their ototoxic capacity. Most solvents that are ototoxicants are aromatic amines, although some nonaromatic solvents such as trichloroethylene are also ototoxic. The ototoxicity of solvents is not dependent on the degree of lipophilicity. Instead, solvent-induced ototoxicity may be related to the shape of a given molecule such as the number, length, and branching of side chains, which appear to have some correlation with the toxicity for aromatic solvents. Such aromatic solvents generally are ototoxic if they have only one side chain. The exception is *p*-xylene, which has two side chains, while neither *o*-xylene nor *m*-xylene is ototoxic.

There are some important species-specific differences for solvent-induced ototoxicity as well. Guinea pigs and chinchillas, which are most often used in ototoxicity studies, are resistant to solvent-induced ototoxicity while rats are sensitive. This selective vulnerability may be due to multiple factors, possibly the most important of which is metabolism. Chinchillas, which have relatively greater expression and activity of cytochromes (CYP) 2E1 and CYP2B—the enzymes most responsible for toluene detoxification—will efficiently metabolize toluene in the liver, resulting in low blood levels. Phenobarbital priming of rats to induce hepatic CYP levels reduces the ototoxicity of toluene. Other proposed explanations for species-specific vulnerability include differences in systemic or local uptake of solvents as well as physiological variation in hair cell membranes.

Solvents also appear to be different from most other ototoxicants in that the hearing deficit is in the mid-frequency range (located in the middle cochlear turn), in contrast to most ototoxicants having toxicity preferentially in basal turns before expanding toward the apex. The reason for this mid-frequency sensitivity is unknown. Styrene causes injury to the outer hair cells and spiral ganglion neurons by independent means. Interestingly the toxicity is limited to the mid-frequency range for both, but the frequencies affected only partially overlap. The spiral ganglion cell loss is not secondary to hair cell loss as lower doses of styrene can produce toxicity with only outer hair cell loss but still elicit spiral ganglion cell loss (90%–95% of which innervate inner hair cells, not outer hair cells). In contrast, aminoglycosides induce spiral ganglion cell loss by damaging inner hair cells, leading to a "dying back" effect on the ganglionic neurons. With styrene and other solvents, the third (most lateral) row of outer hair cells is lost first, then the second row, followed by the first (most medial) row. Although relatively resistant to styrene, inner hair cells can be lost with high doses. The solvent-induced loss of hair cells proceeds from the middle turn of the cochlea into the apical turns, with the basal turns lost last. Although reports are conflicting, some authors have identified injury to the cells of Hensen, an outer hair cell support cell, as preceding the outer hair cell loss. In contrast to styrene, *p*-xylene only affects the outer hair cells; spiral ganglion cell injury has not been identified. On the other end of the solvent spectrum, trichloroethylene decreased numbers of spiral ganglion cells, without changes in the hair cells. For both of these latter agents the injury is limited to the middle turns of the cochlea as the initial insult.

Many of the solvents also produce vestibular effects, which may occur prior to the onset of hearing impairment. These may be related to nerve transmission as well as to effects on the vestibular sensory epithelia, as toluene is thought to also be an antagonist of the inhibitory neurotransmitter gamma-amino butyric acid (GABA).

LOOP DIURETICS

Loop diuretics such as furosemide, ethacrynic acid, and bumetadine (i.e., those with primary action on the loop of Henle in the kidney) produce rapid, acute, but reversible auditory changes. A common clinical complaint is tinnitus, but there are also notable threshold shifts for sound sensation across all frequencies. The stria vascularis is notably edematous; characteristic features include swelling of marginal cells, shrinkage of intermediate cells, and dilation of the intercellular spaces rapidly following intravenous dosing. The loop diuretics directly affect the stria vascularis from the vasculature, resulting in rapid onset. The edema is due to inhibition of ion transport by Na^+/K^+-ATPases at the basolateral membranes of marginal cells, resulting in osmotic expansion of those cells and the intercellular spaces. The toxicologic mechanism of hearing loss related to loop diuretics is due to attenuation of the endocochlear potential and not from injury of the hair cells. Macrolide antibiotics, such as erythromycin, produce similar but less severe changes. The mechanism for erythromycin's effects has not been elucidated.

SALICYLATES AND QUININE

Salicylates and quinine enter the endolymph and act on the hair cells. Salicylates inhibit the amplification

function of the outer hair cells. The concentration of salicylates in the perilymph is directly proportional to serum levels. Salicylates have been shown to produce threshold shifts across all frequencies. The threshold shifts are temporary and reversible and will occur during the dosing phase. Quinine behaves similarly, but is thought to have a different mechanism of action. Salicylates are thought to inhibit the ability of outer hair cells to lengthen. On the other hand, quinine is thought to block Ca^{++} or K^{+} channels and thereby also prevent outer hair cell motility. Morphologic changes related to salicylate and quinine have not been demonstrated.

CIS-PLATINUM

The effects of cisplatins in the inner ear are very similar to those of aminoglycoside antibiotics. The primary sites of toxicity for these compounds are the outer hair cells, the stria vascularis, and the spiral ganglion cells. Dosing with cisplatin will result in a diminished or absent endocochlear potential, likely the result of the strial toxicity. The stria will have morphologic changes that include edema, bulging, rupture, and, eventually, atrophy of the tissue. The outer hair cells are preferentially lost except for the chinchilla, where inner hair cells are preferentially lost at low doses followed by outer hair cells at higher doses. The spiral ganglion cells undergo changes in parallel with the outer hair cell loss, which, like the solvent styrene, suggests two independent mechanisms of ototoxicity. Spiral ganglion cells and their processes will detach from their myelin, appearing as pericellular clear spaces in histologic sections. The toxicity of cisplatins is thought to be due either to reactive oxygen species triggering cell death, as coadministration with antioxidants and free radical scavengers will ameliorate ototoxicity, or to blockade of outer hair cell transduction channels. Whether due to oxidative damage by reactive oxygen species or the cisplatin itself, single-strand DNA breaks have been identified in the stria vascularis.

ORGANOMETALS

Trimethyltin and methyl mercury are both neurotoxicants that are also ototoxicants. Of note is that the chemically related triethyltin is a neurotoxicant but not an ototoxicant. Trimethyltin produces a frequency-specific and dose-dependent auditory impairment. It preferentially affects the outer hair cells of the basal cochlea. Trimethyltin will produce morphologic changes in as little as 12 hours, with vacuolation of the outer hair cells visible by transmission electron microscopy. The guinea pig has swollen spiral ganglion neurons with separation of the myelin from cell bodies by 24 hours. However, there is no correlating inner hair cell damage, indicating that the spiral ganglion cell change occurs independently of hair cell injury. In contrast, rats have loss of spiral ganglion cells only after complete ablation of the cochlea, indicating that neuronal loss is a "dying back" phenomenon in this species. Trimethyltin acts by inhibiting protein synthesis via disruption of ribosomes and rough endoplasmic reticulum.

CARBON MONOXIDE AND CYANIDE

Chemical asphyxiants such as carbon monoxide and cyanide both produce hearing impairment, but likely by different mechanisms. The target of cyanide is the stria vascularis as there is loss of the endocochlear potential with dosing. The stria vascularis is a highly metabolically active site due to the ion transfer that it performs to maintain this potential. In contrast, carbon monoxide likely acts via a direct effect on the inner hair cells, causing glutamate release from this population, and does not affect endocochlear potential. This release leads to excitotoxic death of auditory neurons. However, excitotoxicity will often not manifest in the spiral ganglion as neuronal degeneration or loss, but instead as rupture of the neuronal processes (which is detectable only by electron microscopy).

DEVICES AND BIOTECHNOLOGY PRODUCTS

A wide variety of therapeutic approaches are being used for various types of hearing loss. Implanted devices in the inner ear are becoming a common and viable treatment modality for hearing loss. Biotechnology products are being evaluated as potential therapeutics as well, and some of these are likely to serve as adjuncts to a device for purposes such as preventing further loss of spiral ganglion cells. The biotechnology products currently being developed for otic therapy include monoclonal antibodies, peptides to support neuronal populations (e.g., brain-derived neurotrophic factor [BDNF]), antisense oligonucleotides, viral vectors encoding therapeutic peptides of interest, and stem cells. While the literature is rich with descriptions of their potential uses, reports describing the possible liabilities of these modalities are sparse.

NOISE

High levels of ambient noise are an important source of otic damage. Sound-induced damage is an important safety consideration and is often referred to as acoustic trauma. Loud music, whether from frequent attendance at concerts or from direct piping of high-volume stimuli into the ear canal via earbuds and headphones attached to portable electronic devices, is also an important source of acoustic trauma for the human population. Noise is thought to injure hair cells directly via generation of reactive oxygen species. In addition to being a primary etiology of otic injury,

noise will potentiate or exacerbate the toxicity of many, if not all, of the known xenobiotic ototoxicants.

INFECTIOUS AGENTS

Various disease agents may contribute to hearing loss. In humans, these include chiefly the organisms that induce meningitis, measles, encephalitis, chicken pox, influenza, and mumps. Similar diseases that cause hearing loss in animals have not been well documented except for some bacterial diseases that may extend to the inner ear, but the existence of such pathogens is expected. Gestational cytomegalovirus in guinea pigs can produce deafness, making it important to know the viral status of laboratory animal colonies at animal suppliers.

SUMMARY

As more opportunities arise for development of otic therapies, there will be an increasing need for toxicologic evaluation of the ear—especially the hard-to-reach middle ear and inner ear. Such assessments will require understanding of the anatomy and physiology of the ear (including key species and strain differences), the likely cellular targets for ototoxicants, and what special anatomic and functional methods may be necessary to fully assess them.

Further Reading

Forge, A., Taylor, R., Bolon, B., 2011. Toxicologic neuropathology of the ear. In: Bolon, B., Butt, M.T. (Eds.), Fundamental Neuropathology for Pathologists and Toxicologists: Principles and Techniques. John Wiley and Sons, Hoboken, NJ, pp. 413–448.

Hudspeth, A.J., 1989. How the ear's works work. Nature. 341, 397–404.

Liberman, M.C., 1990. Quantitative assessment of inner ear pathology following ototoxic drugs or acoustic trauma. Toxicol. Pathol. 18, 138–148.

Schacht, J., 1986. Molecular mechanisms of drug-induced hearing loss. Hear Res. 22, 297–304.

Schafer, K.A., Bolon, B., 2013. Ear. In: Haschek, W.M., Rousseaux, C. G., Wallig, M.A. (Eds.), Haschek and Rousseaux's Handbook of Toxicologic Pathology, third ed. Academic Press (Elsevier), San Diego, pp. 2187–2218.

This page intentionally left blank

CHAPTER

23

Bone and Joints

Diane Gunson[1], *Kathryn E. Gropp*[2], *and Aurore Varela*[3]

[1]Novartis Pharmaceuticals Corporation, East Hanover, NJ, United States [2]Pfizer Inc., Groton, CT, United States
[3]Charles River Laboratories, Inc., Senneville, QC, Canada

OUTLINE

INTRODUCTION

Toxicology and research studies in drug discovery and development generally are conducted with young animals that are skeletally immature and in an active state of growth. In contrast, many drug candidates are destined for use in an adult population in which skeletal growth has ceased. This means that compounds which affect bone growth can result in dramatic skeletal changes in test animals that may not be relevant to the intended human patient population. However, if children are included as an intended patient population, skeletal changes in nonclinical studies performed using immature animals become much more important for risk assessment. In such cases, juvenile studies in very young animals may be conducted purposely in addition to other standard nonclinical safety studies.

Choice of Species and Skeletal Sites

Toxicology studies to support nonclinical safety in drug development are mostly conducted in rats, mice, dogs, and cynomolgus monkeys. Sprague-Dawley or Han Wistar rats and CD-1 mice are the usual outbred stocks of rodents used for general toxicity studies in which skeletal toxicity may be identified. However,

Fundamentals of Toxicologic Pathology.
DOI: http://dx.doi.org/10.1016/B978-0-12-809841-7.00024-1

Long–Evans hooded rats are used to study skeletal pharmacology and pharmacokinetics when pigmented animals are required to examine the potential risk posed if compounds bind to melanin. Beagle dogs are the standard nonrodent species used to evaluate skeletal effects of test articles. However, cynomolgus monkeys are an alternative when dogs are not suitable models of human biological processes and/or responses, and are generally used in safety studies for human-derived biomolecules (which often are minimally functional or nonfunctional in nonprimate species).

Studies in drug discovery and basic research for skeletal diseases frequently are conducted in animals not used for safety testing. For example, nude mice may be used for oncology research in bone metastases where intact human tumor explants are placed in the subcutis or isolated tumor cells are injected intravenously. Purpose-bred mongrel dogs are frequently used instead of Beagles in non-GLP efficacy and early toxicity studies.

The choice of which skeletal site(s) to examine depends on the structure, metabolic activity, and biomechanical load. In general, skeletal sites are chosen to permit simultaneous evaluation of bones and bone marrow depots for hematopoiesis. Common sites include an axial long bone (often with a major diarthrodial joint in rodents), the sternum, and sometimes a rib (especially in large animals) or vertebra. In toxicity studies, the femorotibial (stifle/knee) joint along with a length of proximal tibia and distal femur is the standard sample for assessing the structures of bone and diarthroses (freely mobile joints); the sternum is used to examine bone and amphiarthroses (minimally mobile joints) as well as cell-rich bone marrow. Compared to these long bones, lumbar vertebrae in mice contain more cancellous (trabecular or "spongy") bone, and this difference increases with age. In general, synarthroses (nonmobile joints, like skull sutures) are not evaluated specifically during skeletal toxicology studies.

Rats are generally 6–8 weeks of age at the start of nonclinical safety studies and 10–12 weeks old at the end of a 4-week study. At this age these animals still are growing rapidly, so compounds that affect the physis (growth plate) or bone modeling will cause detectable changes in the morphology of the skeleton. In fact, the growth plate of young rodents is a very sensitive detection system for compound-mediated effects on bone growth. It is important to ensure that long bones are examined microscopically, and that for this purpose they must be collected and fixed appropriately (see below).

Bone architecture in male and female Wistar Han and Sprague-Dawley rats and in many strains of mice exhibits sexual dimorphism. Female rats and mice have a greater volume of cancellous bone than males in the proximal tibia, while males have more cortical bone. In both sexes, the amount of cancellous bone in rodents of most strains decreases markedly in the transition from metaphysis to diaphysis in the long bones. Interestingly, hindlimb unloading for a 2-week period in Wistar Han rats results in greater bone loss in males than in females, with a marked decrease in the number of trabeculae in males. It is thought that the higher mass of trabecular bone in females may be related to estrogen levels and the higher mineral mobilization requirements for reproduction in females, especially during lactation.

The growth plate of a normal rat will become narrower as the period of rapid bone growth ends. In addition, the physis of a young intact male rat will be slightly wider than that of an age-matched, young intact female rat during the period of rapid bone growth. These normal age and sex differences can be readily appreciated by comparing long bone physes from control rats at the end of the dosing portion of a 1-month toxicity study with those that are collected from animals which are a few weeks older at the end of a subsequent 2- to 4-week recovery phase.

Dogs, usually purpose-bred Beagles, are generally 6–9 months of age at the start of an efficacy or toxicity study. At this age, young dogs exhibit very little growth in the length of limb long bones even though growth plates may not be completely closed (see Table 23.1). Thus, examination of the standard bone samples in this species, sternum and distal femur, may not reveal compound-related effects on growth plates, metaphyseal new bone quality and quantity, or remodeling bone. Examination of a rib with the costochondral junction as an additional bone specimen will provide an area where active endochondral ossification is still in progress in dogs well into their second year, and possibly longer.

Monkeys [usually cynomolgus (*Macaca fascicularis*)] often are 2–5 years of age at the start of a toxicity study. When sexually mature animals are required, the males will be in the upper end of this age range. If monkeys are selected using a particular weight range, as is often the case, the females usually are more mature than the males (Table 23.1); the practical implication is that females may have closed growth plates, while the males may still have open growth plates. The distal femur with its articular surface and the sternum are the standard bones examined in primates. However, as with dogs, rib samples may provide access to a more active site of endochondral bone growth, and the proximal tibia may provide a more uniform physis to evaluate than the distal femur.

Other species are sometimes used in specialized bone safety studies, including rabbits, guinea pigs, minipigs, and small ruminants (sheep or goats). Large species are utilized especially when seeking to assess the utility of orthopedic devices slated for human use.

TABLE 23.1 Age at Physeal Closure in Usual Laboratory Animals

Species/Sites	Age at physeal closure	
CYNOMOLGUS MONKEY[a]		
	Male	Female
Humerus proximal-distal	6 years–3 years 5 months	4 years 9 months–2 years 3 months
Radius proximal-distal	5 years 3 months–5 years 3 months	3 years 9 months–5 years 9 months
Ulna proximal-distal	5 years–6 years 6 months	4 years 6 months–5 years 9 months
Femur proximal-distal	6 years–5 years 3 months	4 years 9 months–4 years 9 months
Tibia proximal-distal	5 years–5 years 3 months	5 years–4 years 9 months
Fibula proximal-distal	6 years–5 years 3 months	4 years 9 months–4 years 9 months
DOG[b]		
Humerus proximal-distal	10/12 months–6/8 months	
Radius proximal-distal	9/10 months–10/12 months	
Femur proximal-distal	6/13 months–6/11 months	
Tibia proximal-distal	6/11 months–5/8 months	
RAT[b]		
Humerus proximal-distal	52 weeks[c]–6 weeks	
Radius proximal-distal	8/14 weeks–104 weeks[c]	
Femur proximal-distal	104 weeks[c]–15/17 weeks	
Tibia proximal-distal	104 weeks[c]– > 16 weeks	
RABBIT[d]		
Femur proximal-distal	19/24 weeks	
Tibia proximal-distal	22/32 weeks	
Fibula proximal-distal	23/32 weeks	
GÖTTINGEN MINIPIGS[e]		
Femur and lumbar vertebrae start to close at 25 and 21 months of age, respectively, with complete closure occurring around 3.5 years of age		

[a]*Fukuda S, Cho F, Honjo S. Bone growth and development of secondary ossification centers of extremities in the cynomolgus monkey* (Macaca fascicularis). Exp. Anim. *1978:27(4):387–397.*
[b]*Zoetis T, Hurtt ME. Species comparison of anatomical and functional renal development*. Birth Defects Res. B Dev. Reprod. Toxicol. *2003 Apr;68(2):111–120.*
[c]*In rats, rapid growth occurs between 1 and 5 weeks of age, but declines by skeletal maturity at 11.5–13 weeks. Until 26 weeks of age, longitudinal growth still continues, but it virtually ceases thereafter.*
[d]*Kaweblum M, Aguilar MC, Blancas E, Kaweblum J, Lehman WB, Grant AD, Strongwater AM. Histological and radiographic determination of the age of physeal closure of the distal femur, proximal tibia, and proximal fibula of the New Zealand white rabbit*. J. Orthop. Res. *1994 Sep;12(5):747–749.*
[e]*Tsutsumi H, Katagiri K, Takeda S, Nasu T, Igarashi S, Tanigawa M, Mamba K. Standardized data and relationship between bone growth and bone metabolism in female Göttingen minipigs*. Exp. Anim. *2004;53(Jul (4)):331–337.*

Other bone models of interest in these species typically are focused on improved understanding of basic biological processes, such as fracture healing or the pathogenesis of disease [e.g., osteoarthritis (OA)].

STRUCTURE, FUNCTION, AND CELL BIOLOGY OF BONE AND CARTILAGE

The bone and cartilage in the skeleton consist of extracellular matrix, predominantly type I collagen in bone and type II collagen in cartilage. In bone, mineral crystals, mainly calcium hydroxyapatite, have been laid down to provide a strong scaffold.

Structure of Bones and Joints

The basic macroscopic topology of long bones is a cylindrical shell (cortex) comprised of compact (osteonal or Haversian) bone enclosing a cavity supported by an interior scaffold of cancellous (spongy) bone struts (Figure 23.1). Long bones occur in association

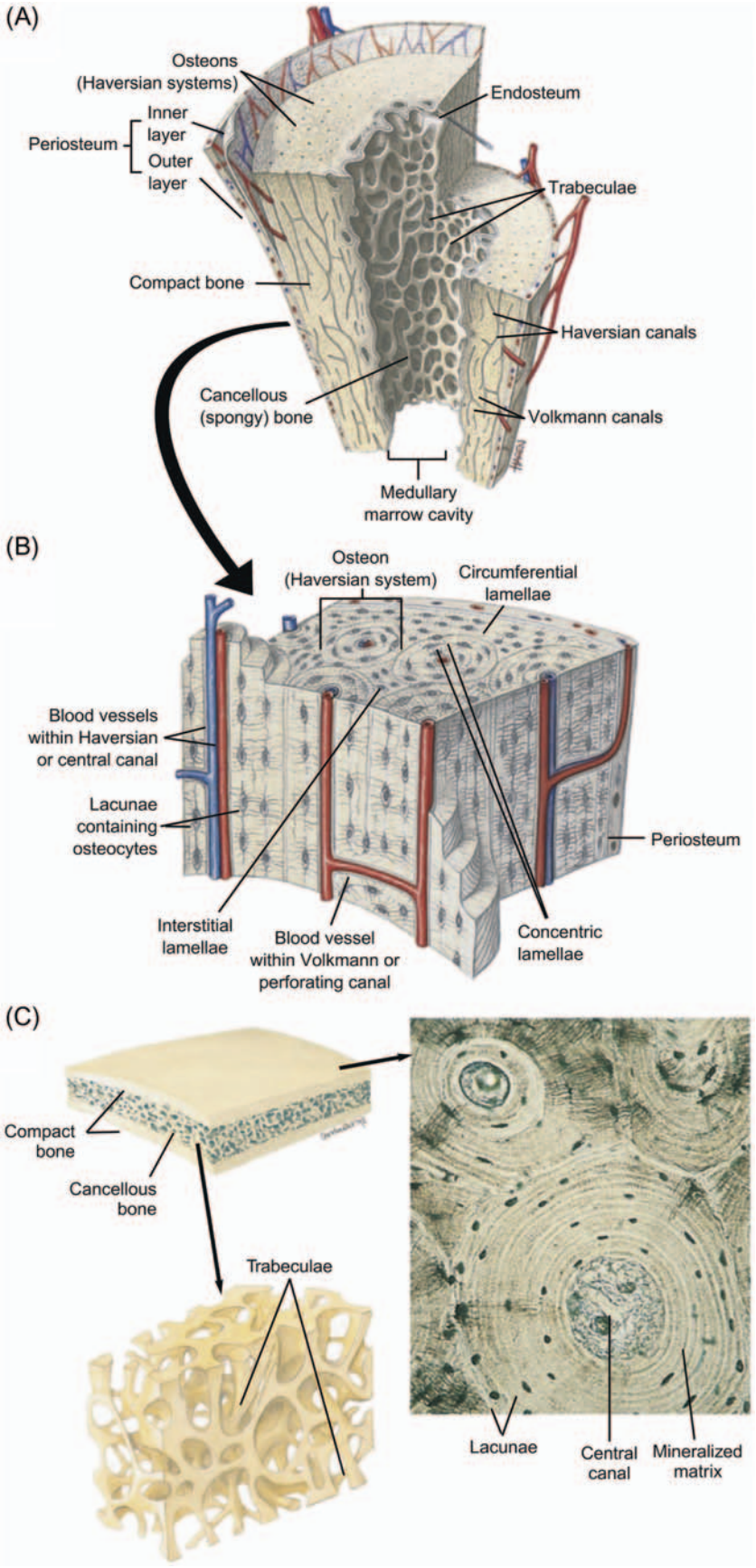

FIGURE 23.1 Schematic diagram of bone structure. (A) Longitudinal section of a long bone showing major bone features. (B) A magnified view of compact bone from the cortical region of the long bone, demonstrating the arrangement of osteons with respect to blood vessels. (C) Anatomy of a flat bone showing the grossly visible structures (upper left schematic section) and the fine structure of the compact and cancellous bone that comprise it. *Reproduced from Thibodeau, G.A., and Patton, K.T., Anatomy and Physiology, fifth ed. Mosby, St. Louis, 2003, with permission.*

with some type of joint surface (articular cartilage, fibrocartilage, etc.) at each end. Bone is anisotropic; its strength is variable depending on the orientation of the load applied, because its structure is not uniform. The cortex is covered by the periosteum on the outer surface and is lined by endocortical bone on the internal surface. Specific areas of cortical bone are termed "envelopes": periosteal on the outer surface, cortical in the middle, and endosteal (endocortical and trabecular bone) lining the inside. The typical long bone contains four main regions (compartments): the epiphysis, the physis (growth plate), the metaphysis, and the diaphysis (shaft). In healthy animals, cavities in the epiphysis, metaphysis, and diaphysis of long bones tend to contain hematopoietic elements in rodents but often also harbor large amounts of white adipose tissue in larger animals, including dogs, primates, and minipigs. Nutrient blood vessels penetrate the cortex and branch to separately supply the epiphysis/physis and the metaphysis/diaphysis.

At the microscopic level, the osteons in the cortex are arranged as concentric lamellar circles of bone around central spaces (Haversian canals) containing blood capillaries and nerve fibers running parallel to the long axis of the bone (Figure 23.1) in most species. Cancellous bone in the epiphysis and metaphysis is composed of trabeculae which form a porous three-dimensional (3D) mesh that supports the cortex and the subchondral bone beneath the articular cartilage. The topology of trabecular bone has been described as an interconnected network of parallel plates or cylindrical rods. Trabeculae are categorized as primary, secondary, or tertiary spongiosa. Trabeculae of the primary spongiosa are located closest to the growth plate and contain the densest number of plates, while tertiary trabeculae extend in small numbers into the diaphysis as long, thin projections. Primary spongiosa are comprised more of calcified cartilage than bone.

The four cell types in bone [osteoclast, osteoblast, osteocyte, and bone-lining cell (BLC)] can be present in a single microscopic field at an active bone remodeling site. Osteoclasts are large cells that undertake bone resorption. Osteoclasts usually are multinucleated except in mice, where they are generally mononuclear. They are located in resorption pits (Howship's lacunae) on the trabecular surface; osteoclast functional polarity is indicated by positioning of the nuclei away from the ruffled border lying on the bone surface. Osteoblasts, which secrete the protein matrix (osteoid) of new bone, line a forming surface of new bone in a single layer and are cuboidal when most active. Some osteoblasts will become BLCs on the newly completed bone surface; other osteoblasts are engulfed by osteoid during the bone formation process and become osteocytes within lacunae of osteons in the bone tissue. Osteocyte signaling by these embedded cells is important for bone maintenance.

The collagen fibrils in most normal, mature bone tissues have a lamellar orientation that is parallel to the contour of the bone surface. Under polarized light, the collagen fibrils have an alternating light/dark appearance (Figure 23.2). The regular organization of collagen fibrils in lamellar bone provides great strength. In rapidly formed bone, such as beneath the growth plate of a young animal or in the bony callus of a healing fracture, the collagen fibrils are randomly oriented because the osteoblasts are not aligned; such bony areas have a crosshatched or woven appearance under polarized light, and thus are termed woven bone. Woven bone is formed quickly during times of maximal osteoblast activity, such as during early fracture healing, but due to the random fibril orientation is not as strong as lamellar bone. Woven bone osteocytes are larger, more numerous, and randomly placed compared to the orderly arrangement of osteocytes in osteons of lamellar bone. When viewed in hematoxylin and eosin (H&E)-stained sections, woven bone is paler than mature lamellar bone.

Diarthrodial (freely mobile) joints are comprised of multiple structures. Articular cartilages and their underlying subchondral plates of epiphyseal bone (which together comprise the articular–epiphyseal complex) from two opposing joint surfaces bear the load. The joint capsule encloses the joint fluid (a lubricant), which is secreted by the synovial membrane lining the capsule. Ligaments, attaching bones to bones, and tendons, connecting skeletal muscle to bones, provide stability to joints. Highly loaded diarthrodial joints like the knee may possess additional shock-absorbing structures, such as the fibrocartilage menisci and pads of white fat. Microscopic synovial villi may project into specialized recesses, such as niches between the large fat folds.

Articular cartilage classically has four zones or layers containing hyaline cartilage and chondrocytes. These zones are (I) the smooth superficial zone, which minimizes friction in conjunction with the lubrication provided by synovial fluid; (II) the transitional zone; (III) the deep radial zone, which absorbs shock; and (IV) the calcified ("mineralized") cartilage zone, which interfaces with the underlying subchondral bone of the epiphysis (Figure 23.3). At the top of the superficial layer is the thin acellular lamina splendens. The chondrocytes and collagen in the superficial layer run parallel to the joint surface, but they change their orientations in the transitional zone to run perpendicular to the joint surface in the deep radial and calcified cartilage layers (Figure 23.3). The tidemark denotes the boundary between the deep radial layer (III) and the calcified cartilage layer (IV). Articular cartilage is

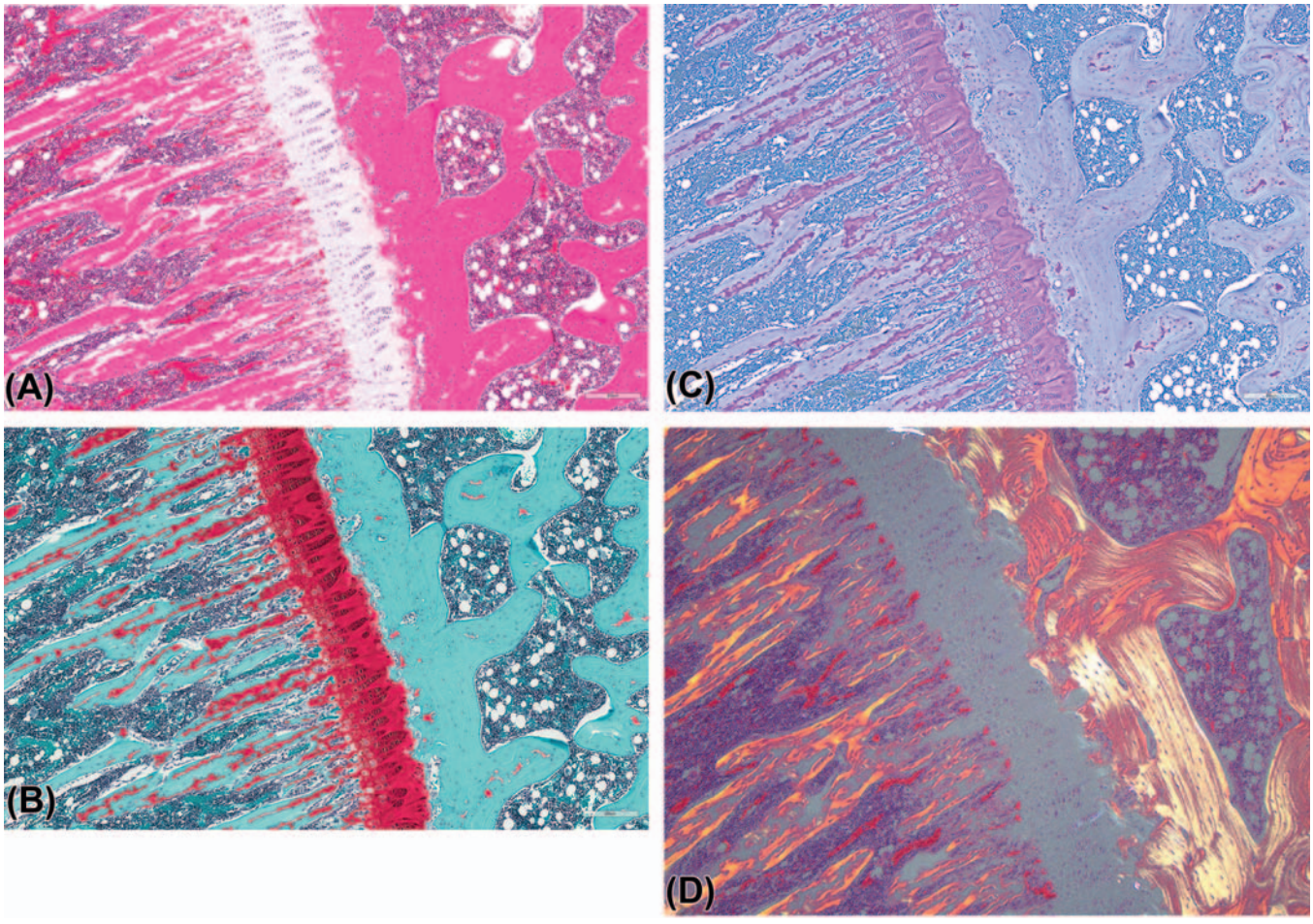

FIGURE 23.2 Sections of physis (growth plate) from a rat femorotibial (stifle or "knee") joint stained with (A) H&E, (B) safranin O, and (C) toluidine blue, showing the staining properties of cells and matrix in bone, cartilage, and hematopoietic cells in bone marrow. Toluidine blue and safranin O are cationic stains (basic dyes) that bind acidic proteoglycans present in cartilage. (D) Slide (H&E stain) viewed with polarized light showing the orientation of birefringent collagen fibers in lamellar and woven bone. Published previously as Figure 63.3 in D. Gunson et al., Bone and joints, in: *Handbook of Toxicologic Pathology, third ed*. (W.M., Haschek, C.G. Rousseaux, and M.A. Wallig, eds), Academic Press, San Diego; volume 3, p. 2768, with permission.

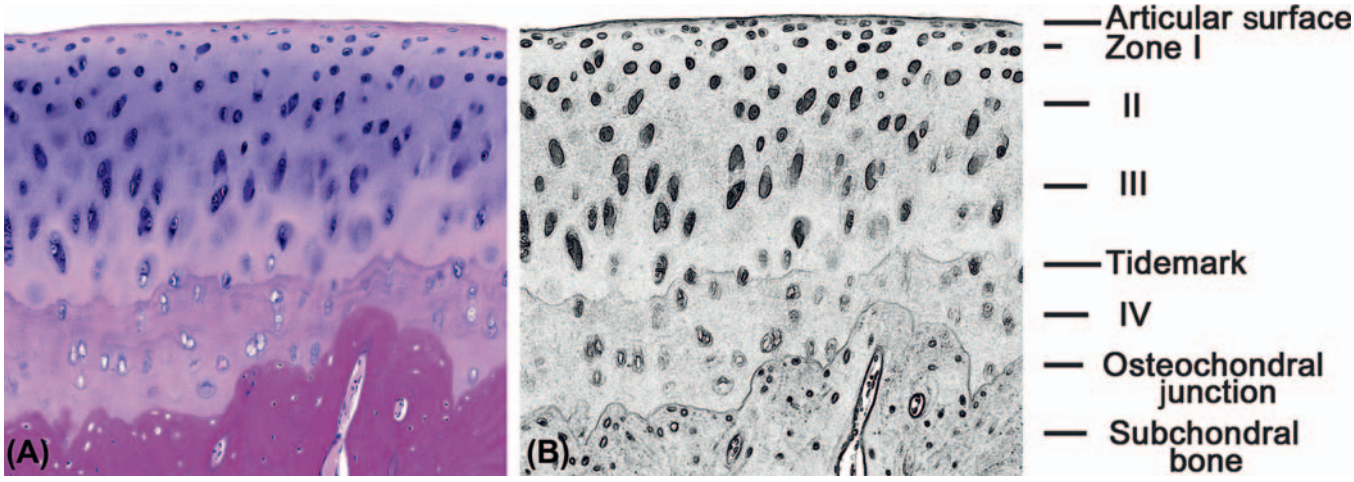

FIGURE 23.3 Structure of articular cartilage of the proximal femur from a cynomolgus monkey. Processing conditions: decalcified section (coronal plane), (A). H&E stain. (B) Black and white reproduction of image (A) demarcating zones I–IV of cartilage and the location of the tidemark, the line at which the cartilage becomes mineralized. Published previously as Figure 63.4 in D. Gunson et al., Bone and joints, in: *Handbook of Toxicologic Pathology, third ed*. (W.M., Haschek, C.G. Rousseaux, and M.A. Wallig, eds), Academic Press, San Diego; volume 3, p. 2769, with permission.

composed of aggrecan (the major proteoglycan in cartilage) and type II collagen.

The synovial membrane is a thin, highly vascular lining covering the inner surface of the articular capsule as well as the surfaces of intraarticular ligaments and tendons. It is usually composed of two layers: a thin internal surface layer that is two to three cells deep, and a deeper subintimal layer of loose or fibrous connective tissue. Synovial cells are of two kinds. Type A (macrophage-like or M) cells have a prominent Golgi apparatus, prominent cytoplasmic vesicles, and little rough endoplasmic reticulum, while type B (fibroblast-like or F) cells have a well-developed rough endoplasmic reticulum but a poorly developed Golgi apparatus. By electron microscopy, synovial cells may be seen to possess filopodia (surface membrane folds, used when the cells serve as opportunistic phagocytes) and, in certain species (rat, rabbit, and calf), cell junctions.

Formation of Bone

Endochondral Ossification

Long bones develop first as cartilage anlagen (primordia) and then grow in length at the physes (growth plates) by endochondral ossification. These plates usually are located at both ends of long bones, but sometimes additional ossification centers are present at other locations. The growth plate consists of a thick layer of cartilage located between the epiphysis and the metaphysis. Chondrocytes in the upper layers of the growth plate divide and move downward toward the lower layer of the plate, where ossification of the matrix occurs. The normal growth plate is arranged in layers ("zones") horizontally and columns vertically (Figure 23.4).

Closest to the epiphysis is the resting zone (also termed the reserve or prehypertrophic zone) of chondrocytes, beneath which lies the zone of proliferation with its flat, compact chondrocytes stacked in neat rows. As they move toward the metaphysis, these chondrocytes enter the zone of hypertrophy, where each chondrocyte is large, approximately spherical, and has an apparent space around the cell. The cartilage matrix becomes calcified at the lower reaches of this zone, resulting in death of the entrapped chondrocytes. Capillaries from the bone marrow invade upward between the spicules of calcified cartilage matrix, and osteoblasts aggregate along these vessels and lay down a thin layer of osteoid on this calcified cartilage scaffold. Mineral (calcium hydroxyapatite) is deposited in the osteoid, which now becomes the primary spongiosa (Figure 23.4), the layer of bone just beneath the growth plate containing many thin trabeculae of woven bone deposited over calcified cartilage cores. This area is rich in osteoclasts, which act to decrease the number of calcified cartilage spicules and the overall number of trabeculae in the primary spongiosa. The layer of secondary spongiosa contains fewer trabeculae, which are thickened by the application of additional bone by

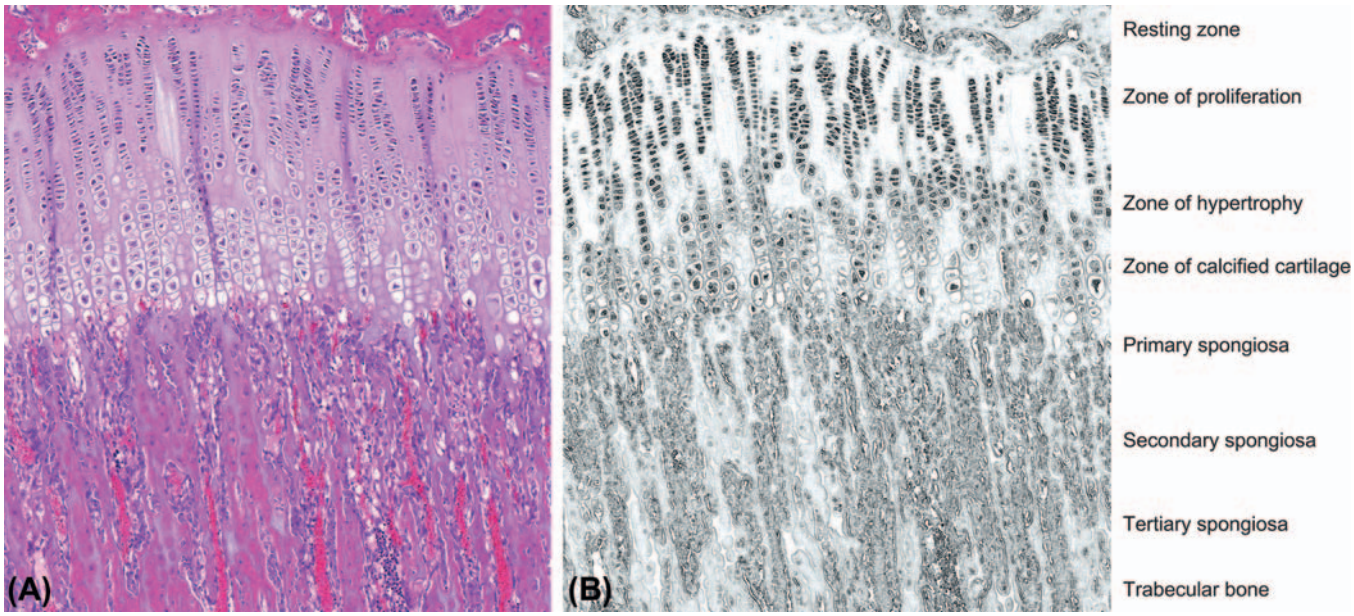

FIGURE 23.4 Zones of cartilage growth and progressive endochondral ossification in the physis (growth plate) of a long bone from a young rat. Processing conditions: decalcified section. (A) H&E stain. (B) Black and white reproduction of image (A) demarcating zones of cartilage and the trabecular spongiosa. Published previously as Figure 63.6 in D. Gunson et al., Bone and joints, in: *Handbook of Toxicologic Pathology, third ed.* (W.M., Haschek, C.G. Rousseaux, and M.A. Wallig, eds), Academic Press, San Diego; volume 3, p. 2771, with permission.

osteoblasts. The woven bone in the primary spongiosa is covered by lamellar bone as the secondary and tertiary spongiosa (mature trabeculae) are formed. This progressive modeling of cartilage to bone provides the engine by which the bone grows in length.

As long bones develop, it is necessary to decrease the bone width from the physis to the diaphysis. This adjustment occurs in the "cut back" zone in the metaphysis in young growing animals, where osteoclasts are plentiful beneath the periosteum and osteoblasts are very active on the endocortical surface. Increases in bone width with age occur from growth at the periosteum as osteoblasts deposit osteoid on the outer surface of the existing cortex.

Intramembranous Ossification

Flat bones [like those of the calvarium (skull) and the scapula] and foci of woven bone are formed by intramembranous ossification. In this process, bone is laid down directly in the mesenchymal collagenous matrix rather than by transmutation of a preformed cartilage model. At such sites, osteoblasts are derived from mesenchymal stem cells, and arranged at random. Woven bone is normally present in few locations in the skeleton: on the surface of calcified cartilage as a result of normal bone modeling, immediately subjacent to the deepest zone of articular cartilage (in small amounts), and at sites of tendon and ligament insertion. It is also formed as part of the initial response to fracture.

Molecular Regulation of Bone and Cartilage Development

Bone and cartilage differentiation, growth, and mineralization are influenced by a variety of hormones, which are systemically available molecules, as well as growth factors, which are produced locally (Table 23.2). Many aspects of this process occur at the growth plate. For example, Indian hedgehog (Ihh) is a master regulator of bone development, serving to control endochondral ossification by coordinating chondrocyte proliferation and differentiation in the growth plate, and osteoblast differentiation in the primary spongiosa. Ihh is synthesized in the growth plate by proliferating chondrocytes as well as early hypertrophic chondrocytes, where a key function is to synthesize parathyroid hormone (PTH)-related peptide (PTHrP), a proproliferative factor for chondrocytes, notably those in the prehypertrophic and early hypertrophic zones. Key hormones include growth hormone (GH), thyroxine (T_4), cortisone, and sex hormones (estrogen and testosterone). Essential signaling molecules include prostaglandin (PG) E_2 and retinoic acid; critical nutrients are vitamin D_3, vitamin K and, in some species (e.g., guinea pigs, monkeys, humans) vitamin C; and other major growth factors such as insulin-like growth factors (IGF) I and II, fibroblast growth factors (FGFs), platelet-derived growth factors (PDGFs), epidermal growth factor (EGF), and vascular endothelial growth factor (VEGF), and bone morphogenetic proteins (BMP). Many of these factors work in combination; for example, activation of GH receptors on osteoblasts enhances chondrogenesis in growth plates via IGF-I and IGF-II. All these ligands have regulatory activity in the growth plate and are essential for normal development of the cartilage centers that presage endochondral ossification. Many factors negatively impact chondrocyte activity when they are deficient, while some (e.g., retinoic acid) also may be toxic when present at excessive levels.

During skeletal growth and repair, cell proliferation and differentiation in cartilage and bone are coordinated by cell–cell signaling. For instance, canonical Wnt signaling (via beta-catenin T-cell factor) is a key regulator of skeletogenesis by accelerating endochondral ossification and suppressing chondrocyte formation, leading to shortening of the growth plate and increased calcification of the hypertrophic zone. In particular, Wnt/beta-catenin signaling works in concert with Ihh signaling in the growth plate, with Ihh stimulating reserve zone chondrocytes to enter proliferation while Wnt acts downstream to promote osteoblast maturation. Similar controlling mechanisms of osteoblast proliferation and differentiation occur in adult mesenchymal progenitor cells during fracture repair, so initiation of bone formation in fracture repair initially requires Ihh signaling and later Wnt signaling in differentiated osteoblasts.

Regulation of Bone Maintenance

Bone metabolism or bone turnover is a dynamic and continuous remodeling process that is normally maintained in a tightly coupled balance between resorption of older (mature) or injured bone and the formation of new bone. Every section will contain both old and new bone, and thus offers a glimpse at the history of the bone. The elements that mediate the set point for this balance include physical forces (i.e., biomechanics); biochemical equilibria (e.g., mineral homeostasis); and molecular signaling. Bone remodeling is divided into two major categories: targeted remodeling in response to injury or changes in biomechanical loading, and stochastic remodeling in response to homeostatic mineral requirements.

Remodeling in large animals (dogs and monkeys) and humans is performed by the basic multicellular unit (BMU) of bone (Figure 23.5). The 3D shape of a

TABLE 23.2 Molecules that Modulate Collagen Biosynthesis in the Skeleton

Factor	Collagens affected	Cellular targets	Type of response
GROWTH FACTORS			
TGFβ$_1$	I, III	Fibroblasts, osteoblasts, hepatoblasts, dedifferentiated chondrocytes	Increases α1(I) + α1(III) mRNA level & stability, enhances translational activity of α2(I) mRNA
	II	Chondrocytes	Suppression of Col2a1 expression
	II	Chondrocytes	Up-regulation of Col2a1 expression
	VI	Fibroblasts	Up-regulates α3(VI), down-regulates α1 + α2(VI)
TGFβ$_3$	α1(I)	Fibroblasts	Stimulates α1(I) mRNA levels; down-regulates in presence of TGFβ1
BMP-2, -3, -4, -7	I (?)	Osteoblasts	Induces osteoblast differentiation, stimulation of collagen I mediated through Smads and Cbfa1β
	II; X	Chondrocytes	Up-regulation of Col2a1 expression in chondrocytic lines
PDGF	V	Gingival fibroblasts	Stimulation of collagen protein synthesis
EGF	I	Osteoblasts	Inhibits collagen synthesis
VEGF	I; IV	Osteoblasts	Promotes vascular invasion of hypertrophy zone
IGF-1	II	Chondrocytes	Stimulates Col2a1 synthesis
CYTOKINES			
IL-1	I, III	Dedifferentiated. Chondrocytes, fibroblasts	Enhanced mRNA levels
	II	Chondrocytes	Suppresses COl12al transcription
IFNγ	I	Fibroblasts	Suppression of collagen synthesis + mRNA levels
	II	Chondrocytes	Suppression of α1(II) mRNA levels
TNFα	I	Fibroblasts	Suppression of α1(I) mRNA
HORMONES AND OTHER FACTORS			
Vitamin D_3	I	Osteoblasts	Active form—1,25$(OH)_2D_3$—decreases α1(I) mRNA and protein levels
Glucocorticoid	α1(I)	Calvaria fibroblasts	Suppresses collagen production in long-term cultures, reduced transcription rate of α1(I), multifactorial complex effects
Growth hormone	I, III	Chondrocytes	Induces IGF in proliferative chondrocytes in growth plate
PTH	I	Fetal rat calvaria	Suppression of α1(I) mRNA levels
	X	Hypertrophic chondrocytes	Reduced α1(X) mRNA levels
Retinoic acid	I, III	Chondrocytes	Induces switch from α1(II) to α1(I), α1(II), and α1(III) mRNA in chondrocytes
	X	Chondrocytes	Transient stimulation of α1(X) expression
Ascorbate (Vitamin C)	All collagens	Fibroblasts, chondrocytes, osteoblasts, etc.	Enhances prolyl and lysyl hydroxylation stimulation of α2(I) mRNA transcription, enhanced mRNA stability
Vitamin K	I	Osteoblasts, chondrocytes	Induces osteocalcin and matrix Gla protein
TRANSCRIPTION FACTORS AND ONCOGENES			
c-fos	I	Osteoblasts	c-fos Overexpression inhibits α1(I) mRNA levels in osteoblasts
Cbfa1/Runx2	I	Osteoblasts	Induces transcription of Col1a1 in osteoblasts by binding to OSE2 elements in the promoter
	X	Hypertrophic chondrocytes	Stimulates Col10a1 expression by binding to OSE2 elements in the Col10a1 promoter
SOX9	II, IX, XI	Chondrocytes	Induces Col2a1 and Col11a1 expression by binding to enhancer
Thyroxine	X	Chondrocytes	Induces Col X mRNA Suppresses clonal expansion & proliferation

Abbreviations: *BMP*, bone morphogenetic protein; *Cbfa1/Runx2*, core binding factor A1/Runt-related transcription factor 2; *c-fos*, FBJ murine osteosarcoma viral oncogene homolog; *Col*, collagen; *EGF*, epidermal growth factor; *IFN*, interferon; *IGF*, insulin-like growth factor; *IL-1*, interleukin 1; *OSE2*, osteocalcin-specific element 2; *PDGF*, platelet-derived growth factor; *PTH*, parathyroid hormone; *OSE2*, osteoblast-specific element 2; *SOX9*, SRY (sex determining region Y)-box 9; Smad, combination name for transcription factors that exhibit homology to both the *Caenorhabditis elegans* protein Sma and the *Drosophila melanogaster* protein Mad; *TGF*, transforming growth factor; *TNF*, tumor necrosis factor; *VEGF*, vascular endothelial growth factor.
Table adapted in part from Dynamics of Bone and Cartilage Metabolism, *second ed., (M.J. Seibel, S.P. Robins, and J.P. Bilezikian, eds). Elsevier, Burlington, 2006; Table 24.1 page 22, with permission.*

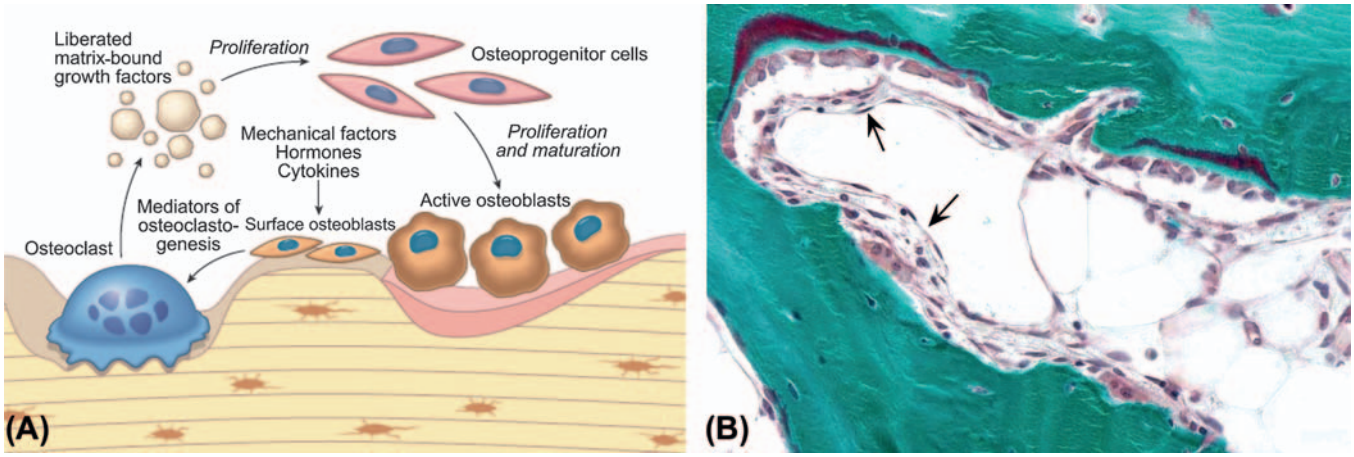

FIGURE 23.5 Bone resorption and formation are coupled processes (A) where the reciprocal actions of osteoblasts and osteoclasts are controlled by systemic factors as well as local cytokines and growth factors, some of which are deposited directly in the bone matrix. (B) Basic multicellular unit (BMU) for coupled bone resorption and formation from the proximal tibia epiphysis of a cynomolgus monkey showing an active resorption surface with two multinuclear osteoclasts on the lower section of trabecula opposite active formation surfaces with cuboidal osteoblasts and red-staining osteoid on the upper section of trabecula. Note the canopy of thin tissue (arrows) separating the BMU from the marrow space. *Processing conditions: undecalcified section, modified Goldner's trichrome stain. Reproduced from Rosenberg (2005) Bones, joints, and soft tissue tumors, In:* Robbins and Cotran's Pathologic Basis of Disease, *seventh ed. (V. Kumar, A.K. Abbas, and N. Fausto, eds.), Elsevier Saunders, Fig. 26.4, p. 1277, with permission.*

BMU is an asymmetric bicone; the osteoclasts resorbing bone line the shorter end of the cone while the osteoblasts laying down new bone line the longer end and act to close the space first created by the osteoclasts. The BMU will be separated from the bone marrow by "BLCs" that have separated from the bone surface, forming a canopy. A blood vessel will be present adjacent to the canopy. The BLCs are thought to play roles in maintaining ion fluxes between fluid in the bone and marrow, initiating BMU activity, and regulating induction of hematopoiesis.

True bone remodeling is minimal in the cortex in rodents. As such, long bones in adult rodents exhibit three major structural features that are not observed in bones of nonrodents. First, cartilage cores persist in trabecular and cortical bone for months or longer in rats. Second, rodent cortical bone contains few osteons. Third, the process of forming and shaping the diaphysis occurs by periosteal bone resorption and endosteal intramembranous bone formation on secondary spongiosa in the "cut back" zone in the metaphysis.

Biomechanics

Physical forces acting on the skeleton constitute a major extrinsic influence on postnatal bone development and maintenance. Cartilage thickness in a mature joint is also affected by local stress and the environment created by physical activity.

Bone responds to an applied force (stress) by undergoing an architectural deformation (a relationship known as Wolff's Law), which depends on the magnitude, frequency, and distribution of the load. Bone can deform because the collagen within it imparts tensile strength. In contrast, the hydroxyapatite mineral crystals within the collagen matrix impart compressive strength. Within the osseous matrix, osteocytes are thought to act in part as a network of mechanical sensory cells. The healthy skeleton is able to continually respond to mechanical stimuli by initiating or inhibiting bone remodeling to maintain bone structure for typical strains within a normal physiological range, a capacity known as the mechanostat. In the context of desirable drug actions and unwanted toxicity affecting bone and cartilage, the concept that mechanical factors may modulate the effects of circulating agents (both endogenous ligands and drugs), genetic programming, and disease on bones (and vice versa) is important.

EVALUATION OF TOXICITY

Toxicity to bone and cartilage can be evaluated in several different fashions. This section explores the common options used for this purpose in conventional product discovery and development programs.

Physiologic Endpoints: Biochemical and Biomarker Evaluation

Biochemical markers of bone turnover [or bone turnover markers (BTMs)] along with hormones and

clinical biochemistry parameters measured in serum or urine provide a rapid, reliable, and dynamic real-time *in vivo* assessment of overall skeletal metabolic activity. BTM immunoassays are noninvasive, simple, specific, and sensitive tools to assess bone metabolism. BTMs represent an important component of nonclinical studies to assess any adverse effects or pharmacological action of compounds on bone metabolism.

The majority of markers used in humans for the diagnosis and monitoring of bone disease and treatment compliance can be assessed in most laboratory animal species with validated analytical methods. Bone markers can be incorporated into routine toxicology studies whenever these data might be able to add perspective to the interpretation of the toxicology endpoints. The storage conditions for samples and the type of assay to be performed must be considered as potential sources of variation. The collection of blood during nonclinical studies should be performed under standardized conditions across all subjects, preferably in the morning (before 10 a.m.) as there are marked circadian variations in biomarker concentrations. In general, blood is collected by intravenous puncture, and serum aliquots are stored frozen until analysis.

Multiple bone formation markers are available. Bone-specific alkaline phosphatase (ALP), which leaks from the osteoblast plasma membrane, is the most specific serum marker for osteoblast activity, but in the absence of intercurrent liver disease total ALP can be used as a surrogate marker for bone-specific ALP, especially in rodents for which no immunoassays are available for the bone isoenzyme. Osteocalcin is a bone matrix protein produced by osteoblasts. Procollagen type I telopeptides, which are cleaved during collagen I formation, also represent a key measure for bone formation, with amino-terminal type I procollagen propeptide (PINP) appearing to be the more sensitive marker of bone formation in most species (Figure 23.6).

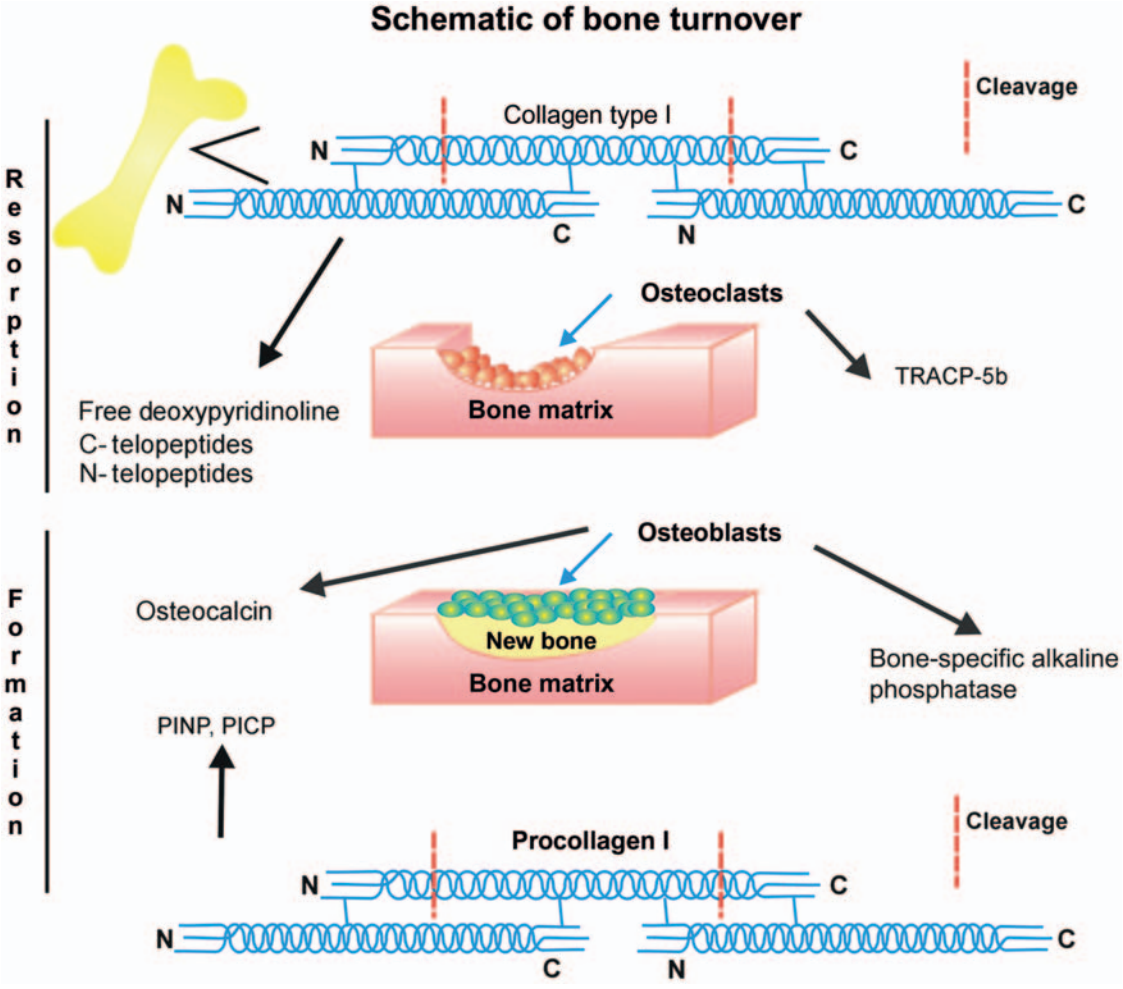

FIGURE 23.6 Schematic diagram of bone turnover illustrating the generation of various bone biomarkers for resorptive and formative processes. Published previously as Figure 63.8 in D. Gunson et al., Bone and joints, in: *Handbook of Toxicologic Pathology, third ed.* (W.M., Haschek, C.G. Rousseaux, and M.A. Wallig, eds), Academic Press, San Diego; volume 3, p. 2782, with permission.

Common bone resorption marker assays of osteoclast activity detect the deoxypyridinoline crosslinks or the N- or C-terminal telopeptide fragments of collagen type I such as deoxypyridinoline (DPD) and type I collagen telopeptide released from the amino (NTx) and carboxyl (CTx) termini. Measurement of tartrate-resistant acid phosphatase (TRAcP5b or TRAP5b), an enzyme expressed by activated (bone-resorbing) osteoclasts, provides a direct assessment of osteoclast numbers. Collagen type I is also present in other tissues such as skin, dentin, cornea, vessels, fibrocartilage and tendons, but the collagen type I turnover rate in nonskeletal tissues is much lower than the process occurring in bone; therefore, nonskeletal collagen type I metabolism contributes very little to the collagen breakdown products in the circulation. Due to the coupling of bone formation and resorption, it is recommended that a panel of bone markers be evaluated in serum samples to fully characterize the skeletal status with respect to these two competing physiologic processes. For nonclinical studies, such panels typically include at least two markers of bone formation (usually osteocalcin and PINP) and two markers of bone resorption (generally CTxI and DPD).

Calcium and phosphorus metabolism and the hormones that govern them are also important to consider. The serum calcium level is regulated closely by homeostatic control mechanisms and thus usually is maintained within the normal range. Since half of serum calcium is bound to protein, either unbound ionized calcium (Ca^{2+}) should be measured or total serum calcium concentrations should be corrected for serum protein levels. The serum phosphorus level fluctuates more widely than does the serum calcium concentration, with phosphorus levels varying based on dietary intake, release from bone, and urinary excretion. Measuring hormones related to calcium metabolism (e.g., calcitonin, PTH and 1,25-dihydroxyvitamin D_3) also may provide useful information regarding calcium utilization.

The effectiveness of these bone biomarkers in short-term and long-term pharmacological studies has been demonstrated in the rat, dog, and monkey. Increases in biochemical markers of bone turnover normally are consistent with histomorphometric indices (see below) of bone turnover. Depending on the class of compound tested and its mechanism of action, different patterns of response can be expected, ranging from an overall increase [bone-building anabolic agents such as PTH (1−34), PTH(1−84), or PTH analogues] or decrease [anti-erosive agents like bisphosphonates or inhibitors of receptor activator of nuclear factor kappa-B ligand (RANKL)] in blood levels of biomarkers to an uncoupling of the response in biomarkers for formation and resorption (antibodies to inhibit sclerostin, an anti-anabolic molecule).

Conventional Evaluation of the Skeleton: Design Considerations and Methods

Production of high-quality bone sections begins at necropsy. If there are pathologic changes in the physis (growth plate), or in very young animals, there may be sufficient skeletal weakness to permit artifactual separation of the epiphysis (end) from the bone shaft at the growth plate with routine handling at necropsy. Therefore, care should be taken to ensure gentle handling of bones and joints during dissection.

Appendicular (long) bones are more frequently assessed during toxicity studies than axial (vertebrae or pelvis) bones. However, evaluation of both bone types may be necessary to fully characterize a disease process or skeletal response to treatment. The most commonly measured compartments are the metaphysis (formed mainly of trabecular bone) and diaphysis (comprised entirely of cortical bone). The epiphysis and its articular surface may be evaluated in arthritides. If the axial skeleton is to be assessed, the most common sites are either a lumbar vertebra (all species) or the iliac crest (in large animals).

One of the primary challenges to the histopathological study of bone biology in experimental animals is obtaining comparable sections from all individuals in a study, and also reproducing this orientation consistently across subsequent studies. This challenge is particularly difficult with respect to major diarthrodial joints [e.g., femorotibial (stifle or "knee") and tibiotarsal (hock or "ankle")], which have curved surfaces that alter shape radically over relatively short distances. The key to attaining this goal is to follow a trimming protocol based on skeletal features that are readily identifiable and can be sampled reproducibly. For example, the physis of the proximal tibia (which is linear) is more uniform and easier to orient than is the physis of the distal femur (which is curved in 3D), so consistent sections of physis are easier to obtain if the tibia is taken.

In rodents, the typical bone and joint specimens are sternum and femorotibial joint. The sternum is commonly used to evaluate bone marrow, but the thin cortical walls and lack of many important bone structures prevents a complete analysis of bone. The femorotibial joint, oriented in a sagittal plane, contains readily obtainable regions of cancellous (trabecular) bone in the epiphyses, primary and secondary spongiosa in the metaphyses, and endocortical and periosteal bone in the "cut back" region of the metaphyses as well as demonstrating other important skeletal features such as the growth plate, subchondral plate, articular cartilage, patella, patellar tendon, cruciate ligaments, and joint capsule. That said, the femorotibial joint often is oriented in the frontal plane to increase the amount of articular cartilage available for evaluation. In older mice, the lumbar

vertebrae cut in a frontal plane will have many more trabeculae than either the distal femur or proximal tibia.

In the larger animal species, either the sternum (to evaluate bone marrow) or the rib (at the costochondral junction) and a long bone are evaluated during general toxicity studies to examine the health of bone. In young animals, endochondral ossification is vibrant at the costochondral junction. The best way of collecting ribs of large animals at necropsy to avoid separation of the bone and cartilage at the costochondral junction is to remove and fix the whole (monkeys) or a portion (several ribs together, for dogs) of one thoracic wall. After fixation, one of the larger ribs can be processed, taking care that the same rib is sampled in each animal. Inclusion of a long bone (typically the proximal tibia, with its linear growth plate) is common; the frontal plane is preferred for trimming because the effect of weight bearing on bone and joint architecture can be appreciated by comparing the medial side versus the lateral side of the joint.

It is critical to proper histological processing to remove as much skeletal muscle and other soft tissue from bones and joints as possible prior to fixation. For nonclinical toxicity studies, bone specimens generally are fixed by immersion in neutral buffered 10% formalin (NBF) at room temperature for at least 24 hours. Fixation time will be longer for large animal specimens with dense cortical bone and may be shorter for thin specimens (3–5 mm thick) of primarily trabecular bone with significant amounts of marrow.

Routine histological processing of bone requires decalcification following fixation. The common approach for nonclinical toxicity studies uses a formic acid-based solution in which the bones are immersed for 1–5 days following fixation, until they become completely decalcified. A solution of up to 10% formic acid, which also contains formaldehyde (approximately 4%) and methanol (5% to 10% by weight) to continue fixation, is commonly used. Alternatively, decalcification may be undertaken using a chelating agent, such as ethylenediaminetetracetic acid. Chelation is a slower and gentler means of removing calcium, and so is employed when special molecular procedures (e.g., immunohistochemistry to detect a labile antigen) is a desirable endpoint. Decalcification by chelation requires multiple transfers of bony specimens into fresh chelating solution (typically one every 24 hours for at least 6 days, depending on the sample size). Production of bone slabs (3–5 mm thick, for large bones) using a diamond saw or cutting a small window through the cortex (for small bones) enhances penetration of the fixative/decalcification solution compared to processing completely intact bones, and so reduces the time needed for fixation. Decalcified bone specimens generally are embedded routinely in paraffin in nonclinical general toxicity studies.

The standard stain for toxicology studies, H&E, is a good choice for general bone examination (Figure 23.2) even though osteoid cannot be differentiated on decalcified sections. Toluidine blue (Figure 23.2) and safranin O (Figure 23.2) commonly are employed to assess the integrity of articular cartilage matrix. Visualization of osteoid requires undecalcified bone sections; the modified Goldner's trichrome stain (Figure 23.5) is suitable for demonstrating osteoid and also permits polarization of collagen. Movat's pentachrome (with modifications) will differentiate mineralized and unmineralized bone and cartilage in undecalcified sections. Von Kossa is commonly used for differentiating mineralized bone from unmineralized osteoid.

Special Techniques for Examining the Skeleton

Nonclinical general toxicity studies in which a skeletal lesion is anticipated or specialized studies dedicated specifically to the assessment of skeletal endpoints often incorporate additional endpoints for skeletal analysis. These may examine morphological features (e.g., bone structure, bone density) or bone function (e.g., biochemical uptake, biomechanical properties). A few of the more common tests used in nonclinical toxicity studies are reviewed briefly here.

Radiological Examination

Conventional radiology is an essential component in examining the skeleton, and provides a commonly available tool for bone analysis *in vivo*. Radiographs also can be performed ex vivo on isolated skeletal segments, often using a high-resolution, bench-top, cabinet-housed, high-resolution radiography system. It is a simple means for examining the size, shape, and density of the entire bony skeleton or large subdivisions thereof, in a stereotypical orientation. Joint contours may be assessed using radiology, as diseases affecting articular cartilage also can impact bone integrity; however, cartilage itself is radiolucent and so cannot be evaluated directly in standard radiographs. Radiography is the method of choice to scan the entire skeleton *in vivo* of small animals before scheduled termination to detect any lesions at skeletal sites that are not routinely harvested and that would not have been detected otherwise. Obtained at intervals in growing animals, serial radiographs provide an accurate record from which to measure bone growth and assess epiphyseal closure in juvenile toxicity studies. Radiographic data are of particular importance for carcinogenicity studies but also are warranted in subchronic and chronic nonclinical studies when direct or indirect effects on bone tissue are suspected (Figure 23.7). Prestudy radiographs in primates can be very useful to document

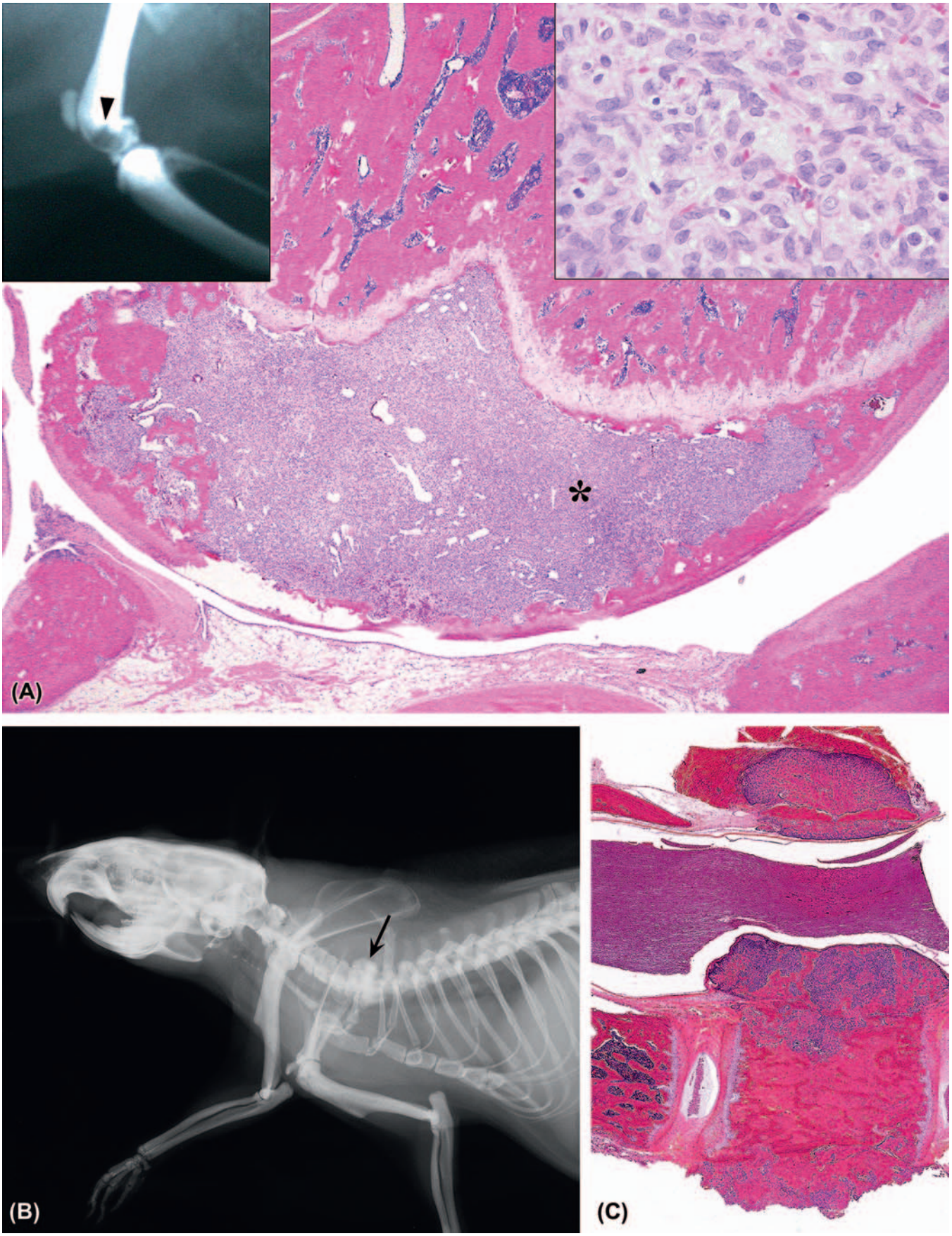

FIGURE 23.7 Occult osteosarcomas in the appendicular and axial skeleton that were detected radiologically in a rat treated for an extended period with recombinant human parathyroid hormone (PTH). (A) Radiograph showing a lytic area (top left inset) in the distal femur (arrowhead) where the bone was effaced (center, asterisk) by an aggressive population of pleomorphic osteoblasts (high magnification inset at

preexisting findings that should not be considered to be a consequence of test article administration.

Specialized imaging technology may provide additional information besides a simple assessment of bone structure. Molecular imaging is the visualization, characterization, and measurement of biological processes at the molecular and cellular levels. The radiotracer approach is used for positron emission tomography (PET) and single photon emission computed tomography (SPECT). Nuclear bone scans such as plain scintigraphy and SPECT radiobisphosphonate bone scans following the administration of ^{99m}-technetium-labeled ethylene diphosphonate may be advantageous as this agent is preferentially incorporated into the skeleton at metabolically active sites associated with bone formation. Bone scintigraphy reveals enhanced radiobisphosphonate deposition due to changes in blood flow or increased osteoblastic activity, and commonly are used to find "hot spots" of metastatic cancer throughout the skeleton. For PET imaging, ^{18}F-fluoride (NaF) is being extensively used for assessing bone metabolism, and it has a similar uptake mechanism to ^{99m}Tc-MDP ^{18}F-FDG (fluorodeoxyglucose) is another PET tracer that can be used as a sensitive functional biomarker indirectly in the skeleton. In general, PET images have a lower resolution compared to other bone-imaging methods, but it has a high molecular sensitivity (nanomolar) with unlimited depth penetration (Figure 23.8). Optical imaging (fluorescence and bioluminescence) techniques are highly sensitive at limited depths (few millimeters), rapid and easy to perform. Fluorescence is used to image the skeleton, with a different bone specific fluorophores (labeled alendronate or other molecule), which are incorporated in the calcified bone matrix at spots with high bone turnover and are therefore good indicators of bone remodeling in sites of bone damage.

Computed tomography (CT), a 3D conventional radiographic technique, and magnetic resonance imaging (MRI), which produces high-resolution 3D representations of skeletal and soft tissues, increasingly are utilized in nonclinical toxicity studies to assess the shape and quantity of various bone compartments.

Osteodensitometry: DXA, pQCT and Micro-CT

Bone mineral density (BMD) can be evaluated *in vivo* or ex vivo using dual energy X-ray absorptiometry (DXA) and/or peripheral quantitative CT (pQCT), or by micro-CT. DXA allows a two-dimensional (2D) assessment, while pQCT and micro-CT provide a 3D volumetric analysis (Figure 23.9). With a nominal resolution (pixel size) of a few microns, micro-CT provides measurements of microarchitecture such as relative bone volume, trabecular number, trabecular surface area, trabecular thickness and trabecular separation (i.e., static parameters traditionally assessed with bone histomorphometry) as well as volumetric and tissue BMD. Baseline or pretreatment data are important to calculate individual animal changes at each time point. The percent change from pretreatment baseline calculated for each individual animal provides a more powerful data set (versus absolute values at each occasion) and helps to overcome limitations due to individual animal variability and the small group sizes normally used in toxicity studies for large animal species. Bone densitometry is a primary endpoint of drug efficacy in both clinical trials and nonclinical studies, and also is employed as a means to quantify any adverse effects on bone mass.

Biomechanical Testing

Bone strength constitutes a critical endpoint in skeletal assessment, serving as the gold standard of bone quality. Biomechanical testing of bone evaluates the functional impact of alterations in bone turnover, bone mass, and bone geometry.

The mechanical competency of a bone depends on multiple factors. These include the direction and magnitude of forces applied, the bone geometry (dimension and shape), and its material properties. Destructive static tests, where the force is applied slowly and gradually until the bone breaks, are most commonly used for animal models and drug testing. Biomechanical strength testing of long bones (in 3- or 4-point bending or in torsion about the long axis), the femoral neck (via shear), and vertebrae (by compression) can be performed to evaluate whether or not treatment has affected any of the properties that define bone strength. The load transmitted through the specimen until failure is recorded by a transducer interposed in the system. Software derives the displacement versus force curves, generating for most biological specimens a typical curve profile.

Common biomechanical endpoints include the force to failure (or peak load), stiffness (extrinsic rigidity of the specimen), and the cumulative energy required to break a bone [area under the curve (AUC)]. Data are normalized for bone size, and calculations of parameters independent of the size of the specimens can be

◀ upper right). (B) Comparable radiograph and corresponding microscopic findings (C) of an occult osteosarcoma affecting a vertebral body. (A, C) H&E stain. *Figure A reproduced from Jolette et al. (2006) Defining a noncarcinogenic dose of recombinant human parathyroid hormone 1–84 in a 2-year study in Fischer 344 rats,* Toxicol. Pathol. *34, pp. 929–940, with permission. Figure B provided courtesy of Dr. Jacquelin Jolette, Charles River Laboratories, Inc., Senneville, Canada. All three figures published previously as Figure 63.13 in D. Gunson et al., Bone and joints, in: Handbook of Toxicologic Pathology, third ed. (W.M., Haschek, C.G. Rousseaux, and M.A. Wallig, eds), Academic Press, San Diego; volume 3, p. 2792, with permission.*

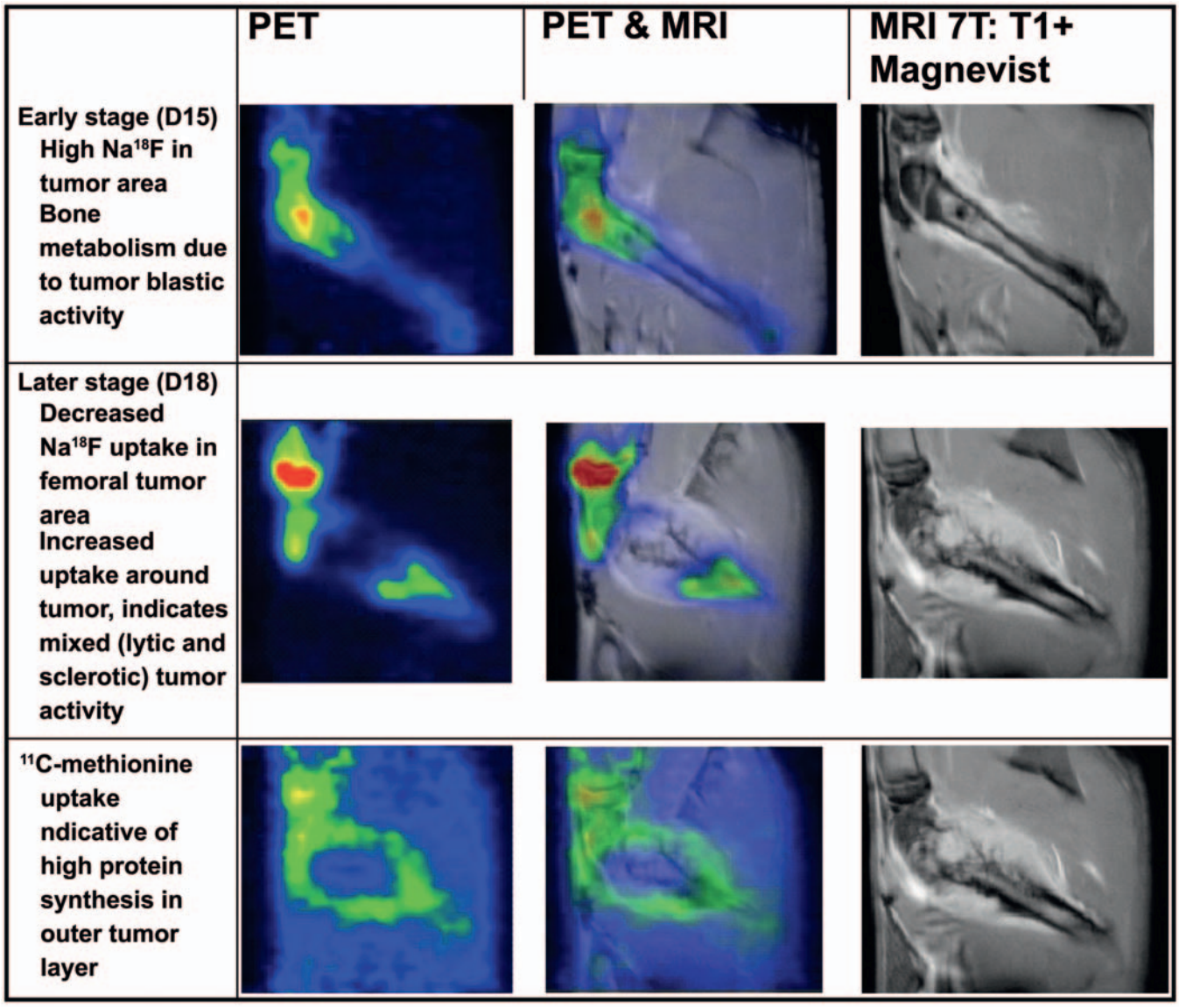

FIGURE 23.8 Magnetic resonance imaging (MRI) and positron emission tomography (PET) for detecting intraosseous foci of metastatic bone neoplasia. *Modified from Doré-Savard et al., Mammary cancer bone metastasis follow-up using multimodal small-animal MR and PET imaging, J. Nucl. Med. 54:944–952, 2014.*

made using the cross-sectional moment of inertia obtained by pQCT scans as a means for defining bone tissue intrinsic parameters: ultimate stress, modulus (intrinsic rigidity of the material when data are corrected for the specimen size), and toughness (a property relating material characteristics to energy absorption, i.e., the AUC corrected for the size of the specimen). Changes in intrinsic properties may reflect an effect of test article treatment on bone quality.

Bone specimens dedicated to biomechanical testing typically are collected at necropsy and cleaned of soft tissue. Without fixation, intact bones are frozen at −20°C until testing. Bones are warmed to room temperature before being subjected to biomechanical stress.

Bone Histomorphometry

Historically, histomorphometric evaluation of bone tissue can be divided into three major analyses: evaluation of bone structure (static parameters), evaluation of bone formation (dynamic parameters), and evaluation of BMU morphology and function. Bone histomorphometry in nonclinical toxicity studies has evolved over the past half century so that parameters, techniques, and nomenclature have become standardized.

Ethanol-fixed, undecalcified, plastic-embedded sections are used instead of standard formalin-fixed, decalcified, paraffin-embedded sections. Decalcification makes evaluation of osteoid impossible. The type of data desired from a histomorphometric examination

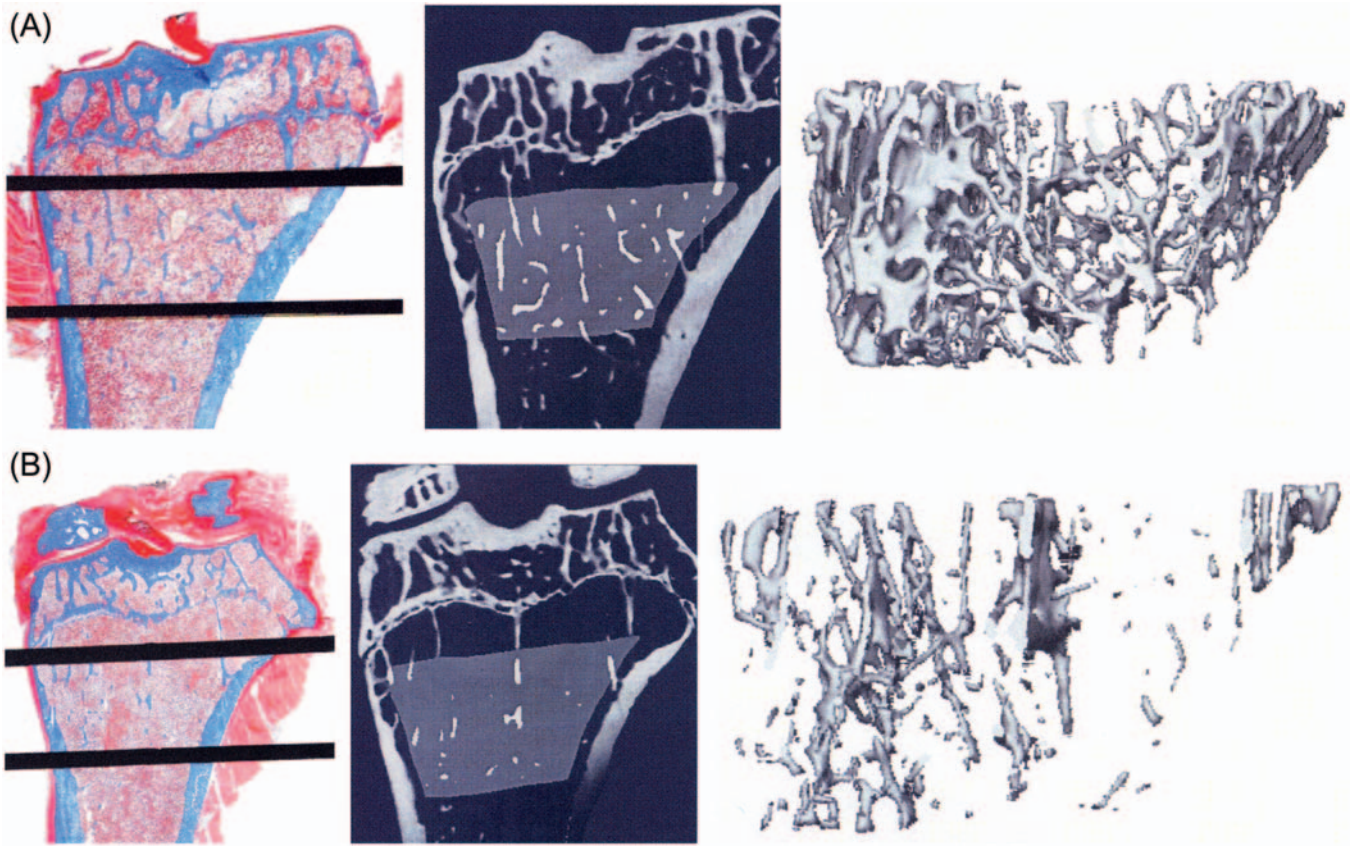

FIGURE 23.9 Comparison of static histomorphometry (left column, modified Goldner's trichrome stain) with high-resolution microcomputed tomography (micro-CT) in two (2D, middle column) or three (3D, right column) dimensions as tools for assessing bone microarchitecture. Relative to an age-matched sham control animal (A), an osteopenic rat (B) has fewer trabeculae in both 2D and 3D representations. Note the similarities of the trabecular representations for histomorphometry and 2D micro-CT of the proximal tibia (coronal orientation). Published previously as Figure 63.15 in D. Gunson et al., Bone and joints, in: *Handbook of Toxicologic Pathology, third ed.* (W.M., Haschek, C.G. Rousseaux, and M.A. Wallig, eds), Academic Press, San Diego; volume 3, p. 2795, with permission.

must be planned in advance since some endpoints require the in-life administration of marker compounds that collect in bone.

When performing a histomorphometric evaluation, the size and location of the region of interest (ROI) depends on the species and type of bone. Some portions of a bone compartment may need to be excluded from analysis if significant, region-specific biological differences exist. As an example, primary spongiosa are routinely excluded from analysis of metaphyseal trabecular bone because primary spongiosa are immature and may not have been exposed to a test-article for the entire duration of a nonclinical study. Similarly, if osteoclast activity is an important endpoint, then measurements should be avoided in regions where osteoclasts are rarely present (such as the mid body of a vertebra).

Static histomorphometry is the direct measurement of the amount of total tissue area, bone area, and bone surface present in the ROI but is increasingly determined using micro-CT. These endpoints may be collected from any nonclinical study, even in the absence of advanced planning for special skeletal endpoints, since in-life treatment with bone-homing compounds is not required to gather such data.

Dynamic bone histomorphometry, which is performed more commonly than static histomorphometry, measures bone formation in trabecular or cortical bone by examining the incorporation of "fluorochrome labels" (fluorescent compounds) administered two or more times during a study (Figure 23.10). Fluorochrome labels that deposit preferentially in bone are given parenterally prior to necropsy. Common agents used for this purpose include calcein green, alizarin red, and doxycycline. Agents are given intermittently to track the rate of new bone formation, which is measured as the distance between any two marker lines (Figure 23.10). Often, multiple agents that emit light at different wavelengths, and thus appear in images as lines of different colors, are utilized to make interpretation simpler.

The other type of histomorphometric evaluation is assessment of BMU cellularity and function on stained

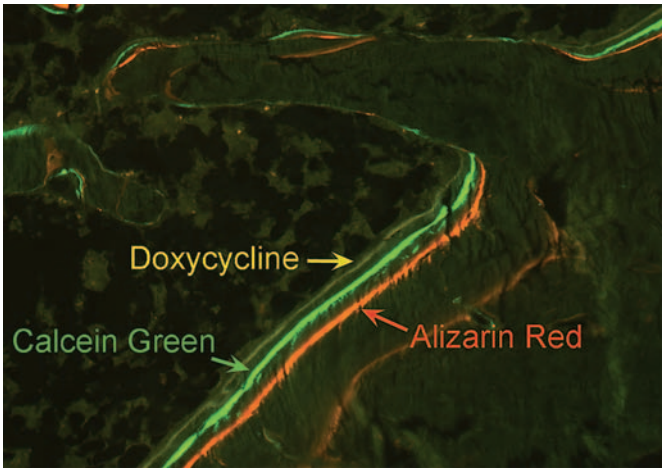

FIGURE 23.10 Multiple fluorochrome labels incorporated at sites of active bone formation in trabecular bone of a rat. The alizarin red label was administered first, followed a few days later by calcein green and then later by doxycycline (which appears yellow). The rate of new bone formation may be calculated by comparing the distance between any two marker lines. *Image courtesy of Dr. Cedo Bagi, Pfizer Inc., Groton, CT. Published previously as Figure 63.17 in D. Gunson et al., Bone and joints, in:* Handbook of Toxicologic Pathology, third ed. *(W.M., Haschek, C.G. Rousseaux, and M.A. Wallig, eds), Academic Press, San Diego; volume 3, p. 2797, with permission.*

(modified Goldner's trichrome, toluidine blue, etc.), undecalcified sections. In this approach, average osteoid width (and extent) are measured. The average orthogonal wall width (WWi) of recently completed BMUs also can be quantified as a means of defining the activation frequency (an indicator of the bone remodeling rate).

Animal Models

Models of Bone Loss

Animal models of bone loss can be produced in many fashions. Surgical procedures include removal of organs (e.g., gonadectomy in rodents and nonhuman primates, hypophysectomy or thyroparathyroidectomy in all species) that produce hormones which serve to either build bone (anabolic) or prevent its resorption (anti-catabolic) and joint manipulations that damage the articular cartilage or disrupt stabilizing structures (ligaments, menescii). Other techniques that may be used experimentally to induce bone loss in rodents include chronic immobilization (tail suspension or limb casting), advanced age, or husbandry adjustments (e.g., dietary or light-cycle manipulations). Use of a calcium-restricted diet enhances ovariectomy-induced bone loss in nonhuman primates and minipigs. Female ferrets can be induced to lose bone by exposure to shortened light cycles (8 hours on/16 hours off). Dogs do not lose bone readily after ovariectomy and are not recommended as a bone loss model, although they are suitable for fracture healing assessments and evaluation of bone anabolic agents. While the number of animals will vary depending upon the endpoints chosen for evaluation and the anticipated effect of a treatment, common group sizes in published reports range from 6 to 25. For instance, higher numbers of animals per group may be needed for histomorphometric studies, while lower numbers are acceptable for biomechanical endpoints and conventional histopathologic evaluation.

Models of Arthritis

Immune-mediated arthritides are inflammatory and erosive joint conditions that affect humans and many animal species as spontaneous or (in animals) genetically engineered and induced diseases. Rodent models of immune-mediated arthritis include adjuvant-induced arthritis (AIA), produced by injection of rats with Freund's adjuvant with or without an additional antigen; collagen-induced arthritis (CIA), produced by immunization of rats, mice, or nonhuman primates with type II collagen from any of several species; and other immune-mediated arthritides, typically produced by injection of bacterial cell wall fragments or other immunogenic proteins or glycoproteins. Genetically engineered animal models of arthritis, in which rats or mice are specifically altered to express a fabricated gene that predisposes them to arthritis, have been generated using various proinflammatory molecules. One example of this strategy is the tumor necrosis factor-alpha (TNF-α) transgenic mouse, which develops a symmetrical polyarthritis that appears first in the tarsus. Similarly, rats engineered to express the HLA-B27 human leukocyte antigen (a major histocompatibility complex, type I antigen carried by many human patients with autoimmune diseases) and human β_2-microglobulin also develop immune-mediated polyarthritis. Immune-mediated joint disease is characterized by diffuse synovial activation (leading to hyperplasia and hypertrophy), extensive infiltration by multiple leukocyte classes (especially lymphocytes and plasma cells), and production of cell-dense fibrovascular tissue (termed pannus) that tends to invade bone and cartilage. The extent of bone loss varies with the arthritis model. In general, AIA models produce rapid and profound bone destruction, while CIA models yield a more slowly progressing dissolution of bone that becomes pronounced over long periods. For this reason, CIA often is considered a preferred choice for investigating immune-mediated joint disease in humans [e.g., rheumatoid arthritis (RA)]. The extent of bone loss is a function of both time (chronic lesions are more severe and destructive) and genetic background (e.g., Lewis rats are more arthritis-prone than are F344

rats). In rodents but usually not primates (including humans) with arthritis, bone loss resulting from marked erosion of preexisiting bones may be obscured to some degree by florid periosteal production of new bone, which may in severe cases result in ankylosis of affected joints.

Osteoarthritis (OA) is another spontaneous disease afflicting humans and various animal species. This condition differs from immune-mediated arthritis (i.e., "inflammatory" arthritis) in that OA (or "noninflammatory" arthritis) tends to exhibit a greater degree of degenerative changes in bone and cartilage in conjunction with a substantially lesser degree of inflammatory cell infiltration. Cardinal features of OA include cartilage degeneration, fragmentation, and loss; degeneration of subchondral bone; and formation of osteophytes (knobs of periarticular new bone produced in an effort to restore some stability to damaged joints). Animal models of OA have been produced in several species (rats, rabbits, guinea pigs, and dogs) via surgical destabilization of the femorotibial joint, which ultimately results in cartilage matrix degeneration and cartilage erosion. Spontaneous OA occurs in many aging animals, including rodents (e.g., STR/ort mice), guinea pigs, and monkeys; these models have been used to study biochemical and molecular mechanisms. Intraarticular injections of iodoacetate (which kills chondrocytes) or systemic quinolone antibiotic treatment also cause cartilage degeneration. Genetically modified mice that over-express or lack bone-regulating molecules also yield OA-like lesions; for example, animals lacking soluble RANKL decoy receptor osteoprotegerin ($OPG^{-/-}$) develop progressive, multifocal degenerative joint disease. A study of T-2 mycotoxin-induced articular cartilage degeneration in the rat has been likened to Kaschin–Beck disease, an endemic form of OA seen in China and considered to be due to an environmental toxin.

Many semiquantitative histopathologic grading schemes are available for macroscopic and microscopic assessment of animal models of immune-mediated arthritis and OA. The scoring schemes may use features that are common to similar conditions across species, or they may emphasize changes that are species-specific. While general morphology is evaluated on routine, decalcified H&E sections, additional sections are stained with either toluidine blue or safranin O to permit grading of cartilage matrix integrity. In general, interpretations of arthritis severity are based not only on pathology lesion scores but also on clinical findings (e.g., number of affected joints); bone densitometry (e.g., DXA or pQCT); or (for immune-mediated models, in which swelling is a prominent feature) joint volumetric measurements (plethysmography).

Study Design Considerations

In nonclinical toxicity studies, evaluation of changes in bone structure, function, and metabolism are evaluated using a number of complementary methods. Some *in vivo* endpoints, such as densitometry and biochemical markers, may be used in humans, so animal data is of clinical relevance. Inclusion of these specialized assessments in the study design will depend on the study objectives and the age of the test animals. Bone biochemical markers and densitometry (DXA or/and pQCT) measurements can be included easily in most toxicity study designs of 28 days' duration or longer in rodents and 3 months' duration or longer for large animals, both for the terminal necropsy and during the recovery phase. For juvenile toxicity studies, pQCT is of particular interest for *in vivo* growth evaluations over time as the evolving geometry of developing bone can be assessed readily with this technique. Pretreatment data are of importance for interpreting densitometry and biomarker data, especially for large animal studies, for two main reasons. These endpoints may be measured intermittently throughout the course of a study, thus giving an idea of progressive skeletal effects, and they can capture changes at much earlier time points (often when structural changes may not be present or quantifiable). Loss or gain in bone mass, alterations in bone geometry, and ultimately shifts in biomechanical properties are cumulative, so important changes that may be detected later reflect the net adjustments in bone metabolism that occurred over the entire study period.

Specialized endpoints are often applied using a tiered strategy. For such an approach to work, provision is made in the study protocol to retain serum or/and urine as well as frozen and fixed samples of specific bones for possible future densitometric and/or biomechanical and/or histomorphometric assessments. Typically, these special samples will be analyzed as a "second-tier" assessment only if the outcome of the "first-tier" analysis (e.g., routine macroscopic and microscopic pathology with conventional serum chemistry parameters) suggest that bone likely is a target or off-target tissue.

RESPONSES TO INJURY

Common Responses of Bone and Cartilage

The numbers of ways in which bone and cartilage can respond to injuries are limited. These responses may include altered metabolism alone (as indicated by changes in the profile of skeletal biomarkers) or the

presence of functional and/or structural changes in bone and cartilage.

An injured region transforms into a special sphere of influence where normal physiologic processes involved in bone growth are accelerated as a means of repair. This phenomenon has been termed a regional acceleratory phenomenon (RAP). Undifferentiated bone marrow mesenchymal stem cells differentiate into osteoblasts, which then produce new (woven) bone. If necrosis has occurred, osteoclasts also will be recruited to resorb the damaged bone. Following the initial healing response, bone remodeling occurs to reshape the microarchitecture of the repair, to conform to biomechanical requirements of the damaged area. The remodeling process is of much greater intensity in juveniles than in adults.

Cartilage has even fewer means than bone for responding to injury. The key feature of repair seen in injured cartilage is clonal proliferation (see below). The cartilage matrix near clonal clusters usually is less dense (stains less darkly) with toluidine blue or safranin O than that of normal cartilage, suggesting that the cartilage proteoglycan composition is altered.

Common Toxicant-Induced Responses in Bone

All the toxicant-related responses of bone following exposure to exogenous chemicals or biologics represent either a normal reparative response or a pathologic condition in which the normal healing process is interrupted. Entities causing metabolic bone disease alter normal bone remodeling, whereas the formation of periosteal or endosteal new bone is similar to the process observed in the formation of a fracture callus. Even neoplasia can be considered in a broad sense as a disruption in the normal processes of cell proliferation and differentiation.

Necrosis

Spontaneous bone necrosis can occur in laboratory animals. Zones of necrotic bone may be encountered in which there is very little response in the surrounding tissue, but areas of a few empty osteocyte lacunae may be present as an artifactual change and should not be interpreted as bone necrosis. Age-related, idiopathic osteocyte necrosis has been observed in normal bone from healthy rhesus monkeys. This change is virtually absent in young animals but is present to some degree in all mature individuals. Common sites to appreciate this finding include the distal femur, femoral head, proximal tibia and vertebral epiphyses. In one mouse study, bone necrosis was observed in up to 4.6% of the test animals, and the incidence in control Wistar rats is $<5\%$. Bony portions of the menisci, which develop by endochondral ossification with age, are necrotic in the femorotibial joint in a large proportion of old rats and mice. Drugs that cause severe anemia, occlusive vascular disease, thrombosis, or pancreatic release of lipolytic enzymes have been shown to induce aseptic bone necrosis in many species, including rats and dogs. Classic bone necrosis not only involves the osteocytes but also the adjacent bone marrow and engenders a vigorous repair response from both osteoblasts and osteoclasts.

Targeted antiresorptive bone therapies, including bisphosphonates and RANKL inhibitors in humans, have been associated with a low incidence of aseptic osteonecrosis of the mandible. A common factor in the early case reports of this condition was a history of a recent invasive dental procedure. Other predisposing factors, including immunosuppression, periodontitis, and/or concomitant bacterial infection in the oral cavity, also seem to be important factors in development of the clinical presentation, and an association with localized areas of acidic pH in the buccal cavity has been reported.

Atypical fractures (e.g., spontaneous metaphyseal femoral fractures) have been associated with long-term use of bisphosphonates and proton pump inhibitors, although the pathophysiology is different for conditions produced by these two drug classes. In the case of bisphosphonates, deposition of the bisphosphonate into the bone matrix may alter biomechanical properties and in the case of proton pump inhibitors (e.g., omeprazole, esomeprazole, etc.), calcium absorption in the gastrointestinal tract is reduced.

Regional Acceleratory Phenomenon

When the RAP has been evoked, most processes in affected bone are quickened above their normal levels. RAP can often hasten longitudinal bone growth following a fracture, denervation, surgical procedure (e.g., periosteal stripping), or tumor. An example of RAP of relevance to nonclinical toxicity studies is local acceleration of the remodeling process to close the wound resulting from a bone biopsy. Unfortunately, the RAP means that intermittent biopsies of the same bone cannot be used to make comparisons of preexisting bony structures and any posttreatment effects. Note that the RAP involves soft tissue adjacent to bone, too. Common RAP features seen in soft tissues include localized fibrosis and chronic inflammation.

Inflammation and Fibrosis

Acute inflammation, formation of granulation tissue, and fibrous repair in the skeletal system do not differ from these processes as seen in other body systems. Inflammatory diseases that weaken or reduce skeletal strength can lead to pathologic fractures (i.e.,

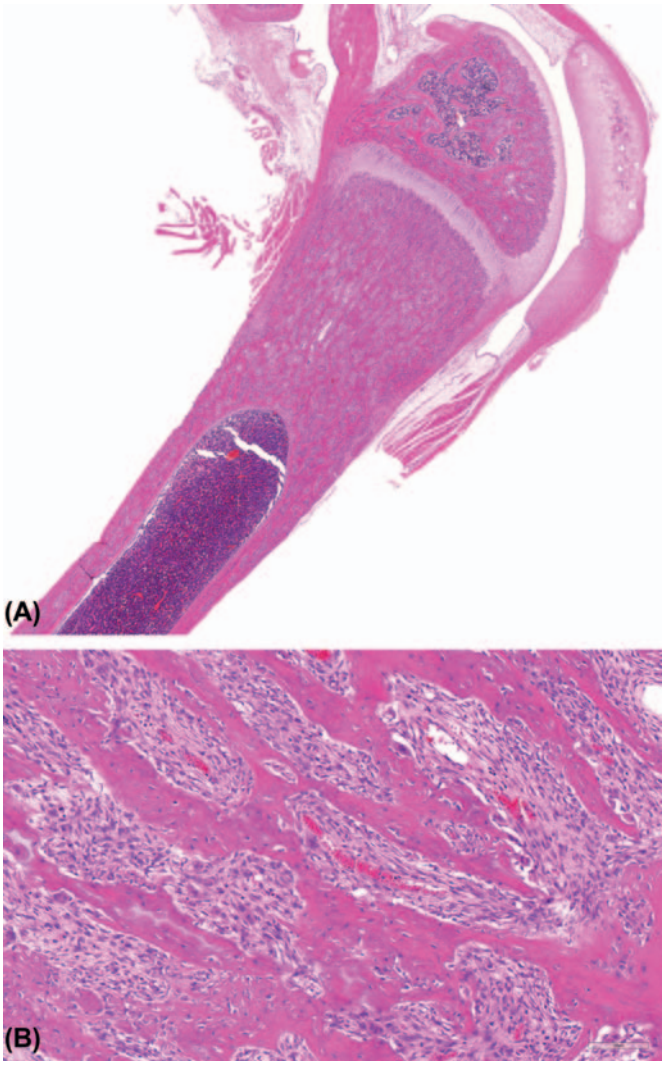

FIGURE 23.11 Myelofibrosis in a young rat after continuous treatment with recombinant human parathyroid hormone (PTH) for an extended period. The apparent consolidation of the marrow space evident between bony trabeculae (A) results from the accumulation of fibrous connective tissue (B). H&E stain. Published previously as Figure 63.19 in D. Gunson et al., Bone and joints, in: *Handbook of Toxicologic Pathology, third ed*. (W.M., Haschek, C.G. Rousseaux, and M.A. Wallig, eds), Academic Press, San Diego; volume 3, p. 2808, with permission.

breaks in bone that is weakened locally by a disease process). Therefore, adaptive reconstruction and reparative processes often predominate in the morphologic picture associated with such conditions. It is frequently necessary to study the progression of a particular lesion, especially by examining early stages, in order to fully understand their pathogenesis.

Fibrous tissue may be deposited as a substitute for bone when disease prevents normal ossification of the tissues filling bone defects. For normal repair, bone fibrosis is characterized by deposition of type I collagen. The fibrosis associated with hyperparathyroidism [i.e., fibrous osteodystrophy (FOD)] probably represents a response that is distinct from the fibrosis used to repair a chronic injury (Figure 23.11). In FOD, fibrous tissue is closely applied to bone trabeculae, particularly at resorptive sites, and contains more reticulin than type 1 collagen.

Growth and Mineralization of Bone

Longitudinal bone growth is determined by events in the cartilage of the growth plate. Extension of a bone's length depends largely on the rate of cell division in the proliferating zone. Circumferential bone growth occurs in the metaphysis and is accomplished by osteoblast division and apposition at the perichondrial ring. Any drug that causes inanition, affects calcium absorption, or produces a negative nitrogen balance can reduce longitudinal bone growth due to insufficient quantities of amino acids to form osteoid and/or minerals to mineralize it. Whenever longitudinal growth slows and the growth plate begins to close, focal degradative changes may be observed in the cartilage of the physis and within the metaphyseal trabeculae, and these trabeculae also appear thickened because osseous tissue is deposited on their surfaces over a longer period. When cessation of growth is severe enough, there may be an attempt at premature growth plate closure; in such cases, a lateral plate of bone termed a transverse bridge is formed beneath the growth plate. If restoration of nutrients permits bone growth to be reinitiated, these transverse bone plates will be left behind in the metaphysis as the growth cartilage recedes from them (Figure 23.12). Such persistent bony plates are termed Harris growth arrest lines. The line is eventually remodeled to remove the bulging ridge. Growth plate closure also occurs when the bone matrix content of osteocalcin is reduced by treatment with warfarin, or by smoothened hedgehog (SHH) inhibition (Figure 23.13). Concurrent treatment with PTH, particularly by continuous infusion, can attenuate growth plate closure caused by SHH inhibition (Figure 23.13).

Normally, longitudinal growth and transverse growth are coupled, but different signaling molecules affect growth in these two directions. For example, GH governs the bone growth rate at both locations indirectly, and a GH deficiency (dwarfism) or excess (gigantism) causes a simultaneous and proportional change in the bone width and length. However, some locally active agents (e.g., sclerostin inhibition and PGE_2) have the potential to alter differentially growth in different bone compartments or portions of the skeleton. If longitudinal growth is inhibited more than transverse appositional growth, then the bones will be short but have a more normal diameter. Such changes can be produced by compounds that induce rickets

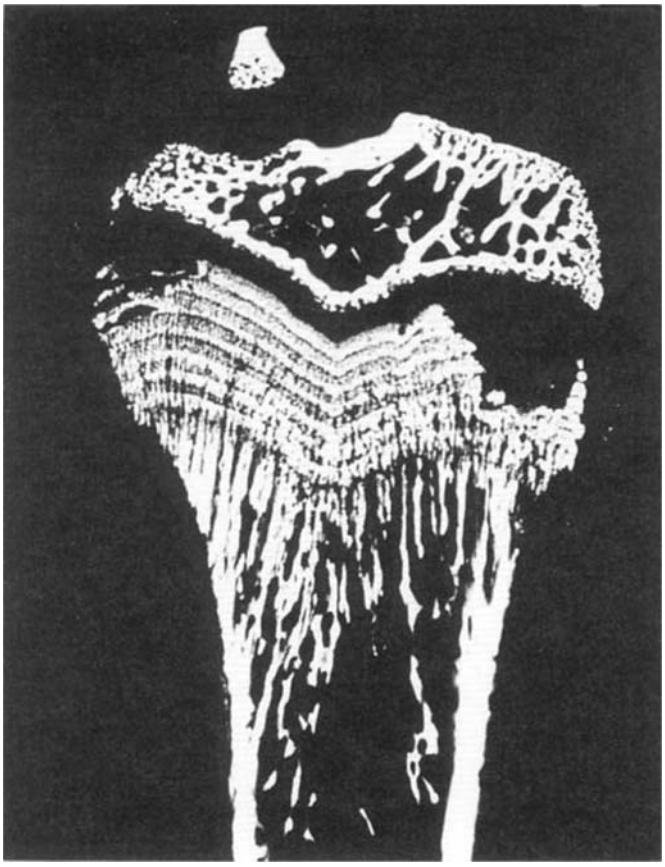

FIGURE 23.12 Growth arrest lines resulting from intermittent episodes of reduced osteoclast activity appear in radiographs as parallel, radiodense regions near the growth plate. Tibial metaphysis from a rat given a daily injection of a bisphosphonate. The peripheral growth plate is enlarged. *Figure reproduced from Miller et al. (1985) Effects of* N,N,N′,N′*-ethylenediaminetetramethylene phosphonic acid and 1-hydroxyethylidene-1,1-bisphosphonic acid on calcium absorption, plasma calcium, longitudinal bone growth, and bone histology in the growing rat*, Toxicol. Appl. Pharmacol. *77, 230–239, with permission.*

(which is characterized by abnormal endochondral ossification with thicker growth plates and unmineralized osteoid) or physeal dysplasia (see below). If transverse growth is inhibited more than longitudinal growth, the bone becomes long and thin. Bones with this characteristic appearance are seen in vitamin A toxicity in rats where pathologic fractures occur in the thin cortices.

The longitudinal growth rate determines the age and amount of trabecular tissue in the metaphyseal zones of different bones. A faster longitudinal growth rate results in an increased amount of cancellous bone of a lesser age (e.g., proximal tibia), whereas a slower growth rate gives less bone of a greater age (e.g., lumbar vertebra). Since an altered longitudinal bone growth rate changes the dynamics of metaphyseal bone modeling and remodeling, studying a drug that alters the quantity of metaphyseal bone in a young animal should determine whether there is an effect on longitudinal bone growth.

Increased Osteoid

Increased osteoid may occur by several mechanisms. These include increased numbers of formation surfaces, an increased thickness of osteoid because of a mineralization defect, or an increased rate of osteoid production. In some cases, osteoid is not mineralized properly because the matrix is abnormal; fluorosis, *Solanum malacoxylon* toxicosis, and penetrating radiation are examples of this phenomenon. In other cases, osteoblast function may be impaired (such as with some early types of bisphosphonate toxicity) so that osteoid matrix is deposited but remains unmineralized.

Increased Bone

An abnormal increase of bone volume or quantity in the skeleton (Figure 23.14) is reported as increased bone with a location identifier (i.e., the increase is trabecular or cortical). Areas of new, woven bone filling part of the medullary cavity of vertebrae, nasal turbinates and tibiae are a spontaneous lesion in aging animals, such as Han Wistar and F344 rats; this finding was previously described as hyperostosis. Aging F344 female rats develop increased bone, but with a somewhat different appearance: thick trabeculae composed of mature lamellar bone partially filling the medullary cavity of a long bone (typically the tibia). Other modifiers may be used to indicate the anatomical site or characteristic appearance, such as exostosis and enostosis to describe increased bone on the periosteal (for exostosis) and endocortical envelopes, respectively. Osteosclerosis has been used for increased bone density without alteration in the gross shape of the affected bone. Under physiological conditions, as an adaptive response, or in disease, bone in adults increases in amount by raising the incremental difference between resorption and formation during remodeling (positive bone balance). An example of this type of increased bone occurs with myelofibrosis, a condition that follows persistent bone marrow depression and has been reported to follow radiation injury or administration of certain toxic chemicals (e.g., benzene, lead acetate).

Increased bone in nonclinical studies may occur in growing animals treated with compounds that affect bone formation or remodeling. For instance, matrix metalloprotease (MMP) inhibitors reduce bone removal while permitting bone formation to continue. Increased bone in the metaphyses of young, fast-growing rats is a classic finding with such compounds (Figure 23.14). This usually appears as thickened metaphyseal trabeculae.

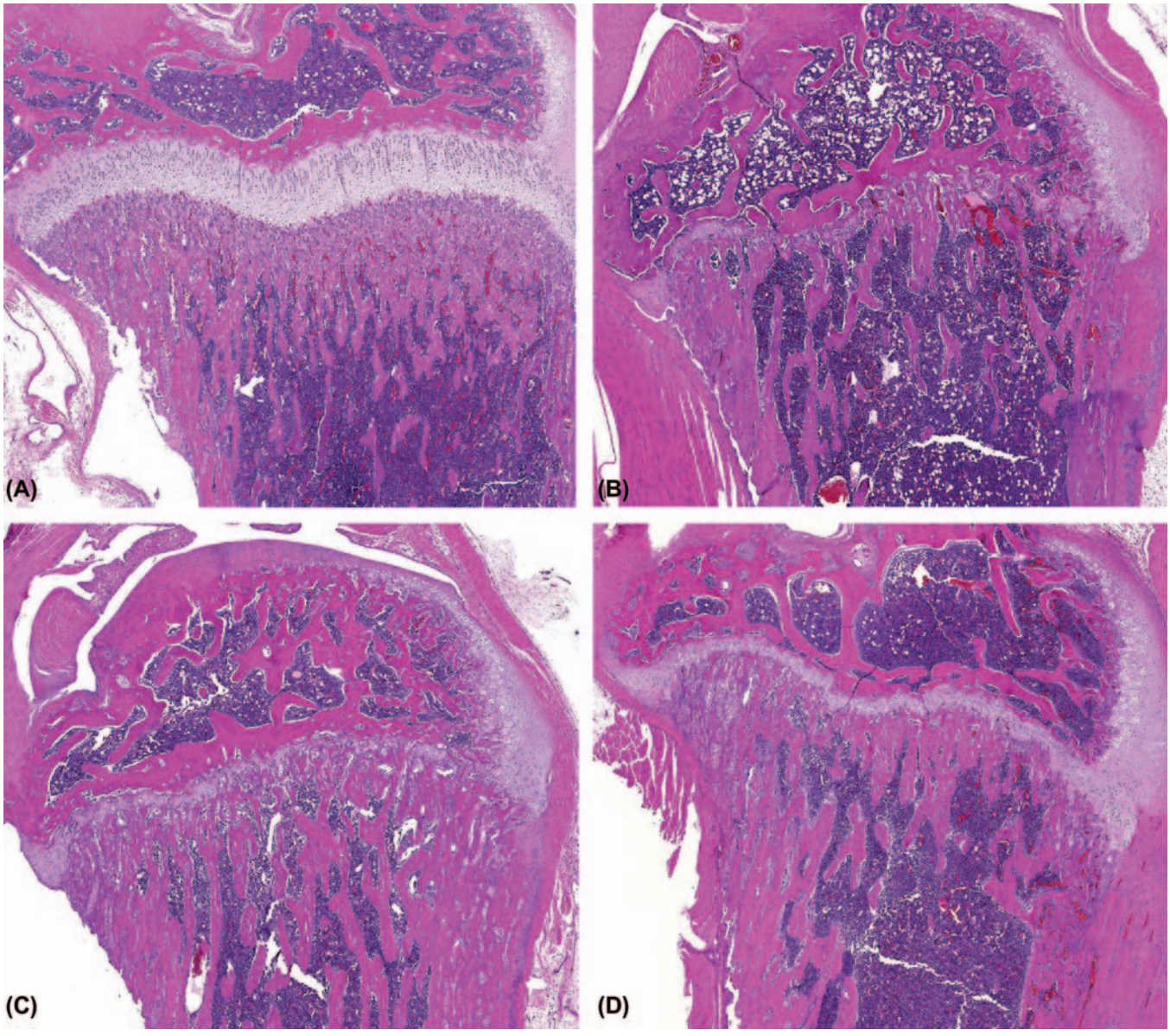

FIGURE 23.13 Proximal tibia with growth plate from young rats treated concurrently with a smoothened hedgehog inhibitor and recombinant human parathyroid hormone (PTH). (A) Control animals exhibit growth plates of uniform thickness with a regular progression of cartilage zones. (B) Treatment with a smoothened hedgehog (SHH) inhibitor only for 14 days results in growth plate closure. (C, D) Treatment with the SHH inhibitor is modulated by simultaneous exposure to PTH, where the growth plate is slightly less closed following a PTH (pulse) for 14 days (C) and even less closed if PTH is given continuously (D) for 14 days. H&E stain. Published previously as Figure 63.21 in D. Gunson et al., Bone and joints, in: *Handbook of Toxicologic Pathology, third ed.* (W.M., Haschek, C.G. Rousseaux, and M.A. Wallig, eds), Academic Press, San Diego; volume 3, p. 2810, with permission.

Neoplasia

In general, primary bone neoplasia in laboratory animals is similar to the phenomenon in humans except that a few morphologic variants of tumors have not been recognized in animals. The vast majority of primary malignant bone tumors in laboratory animals are osteosarcomas, with their typical osteolytic and poorly differentiated features (Figure 23.7). In contrast, primary bone tumors arising from the other major mesenchymal cell types (e.g., chondrosarcomas, fibrosarcomas, liposarcomas) are uncommon. The cause of these neoplasms is not often attributed to toxicants, although long-term treatment of rats with recombinant human PTH has been associated with induction of occult osteosarcomas (Figure 23.7). Osteomas containing C-type retrovirus particles may be found in mice as spontaneous lesions, and increased numbers of osteomas have been observed

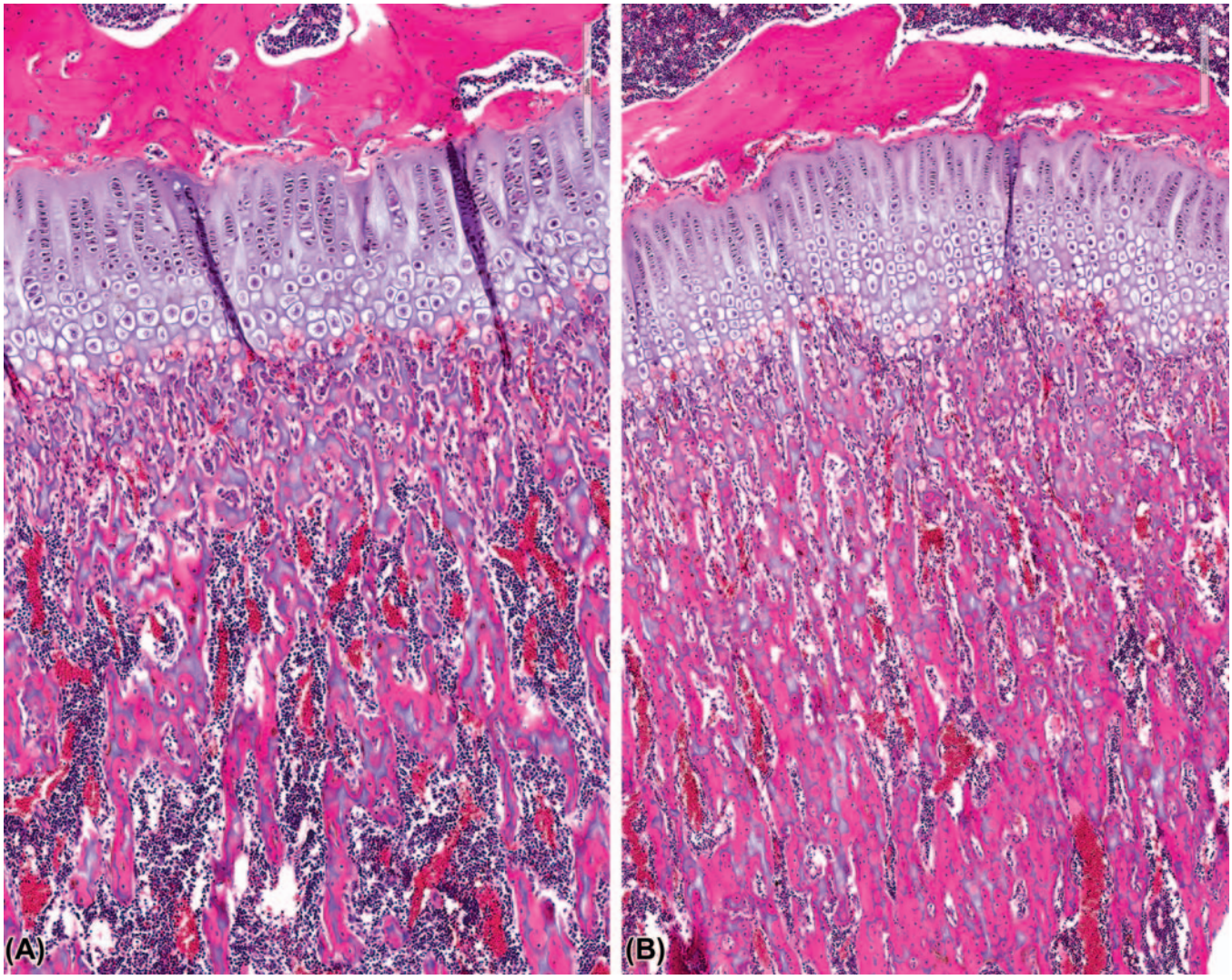

FIGURE 23.14 Metaphyseal hyperostosis in a young rat treated repeatedly with a matrix metalloprotease (MMP) inhibitor by gavage. Relative to an age-matched vehicle-treated control (A), the treated animal (B) has markedly longer primary spongiosa. H&E Stain. Published previously as Figure 63.26 in D. Gunson et al., Bone and joints, in: *Handbook of Toxicologic Pathology, third ed.* (W.M., Haschek, C.G. Rousseaux, and M.A. Wallig, eds), Academic Press, San Diego; volume 3, p. 2819, with permission.

in mice treated for life with fluoride or fluoride-containing compounds. Chordomas are uncommon axial skeleton neoplasms that arise from residual foci of primitive notochord anywhere along the ventral regions of the vertebral column, but they most commonly involve the cranial (skull) and caudal (tail) portions. They are slow-growing but highly infiltrative masses, producing bony destruction and frequently extending into adjacent soft tissues. They have been reported as spontaneous lesions in humans, rats, mice, dogs, ferrets, and mink.

Bone Modeling Alterations

Bone modeling as a process occurs principally during growth, but continues to a small extent throughout life. Toxic responses that depend on altered bone modeling affect compact bone and lead to insufficient or excess accumulations of bone or to mechanically inappropriate architecture. Bisphosphonates interfere with osteoclastic resorption of bone, causing an abnormal metaphyseal contour ("clubbing") in the "cut back" zone and accumulation of unresorbed bone trabeculae in the marrow cavity beneath the growth plate (Figure 23.15).

Reactivation of bone modeling can occur in adult animals, as in the formation of marginal osteophytes in association with joint instability and degenerative arthropathy. Anabolic agents like PTH and PGE_2 add bone mainly by modeling-dependent bone gain (uncoupled de novo bone formation). The production

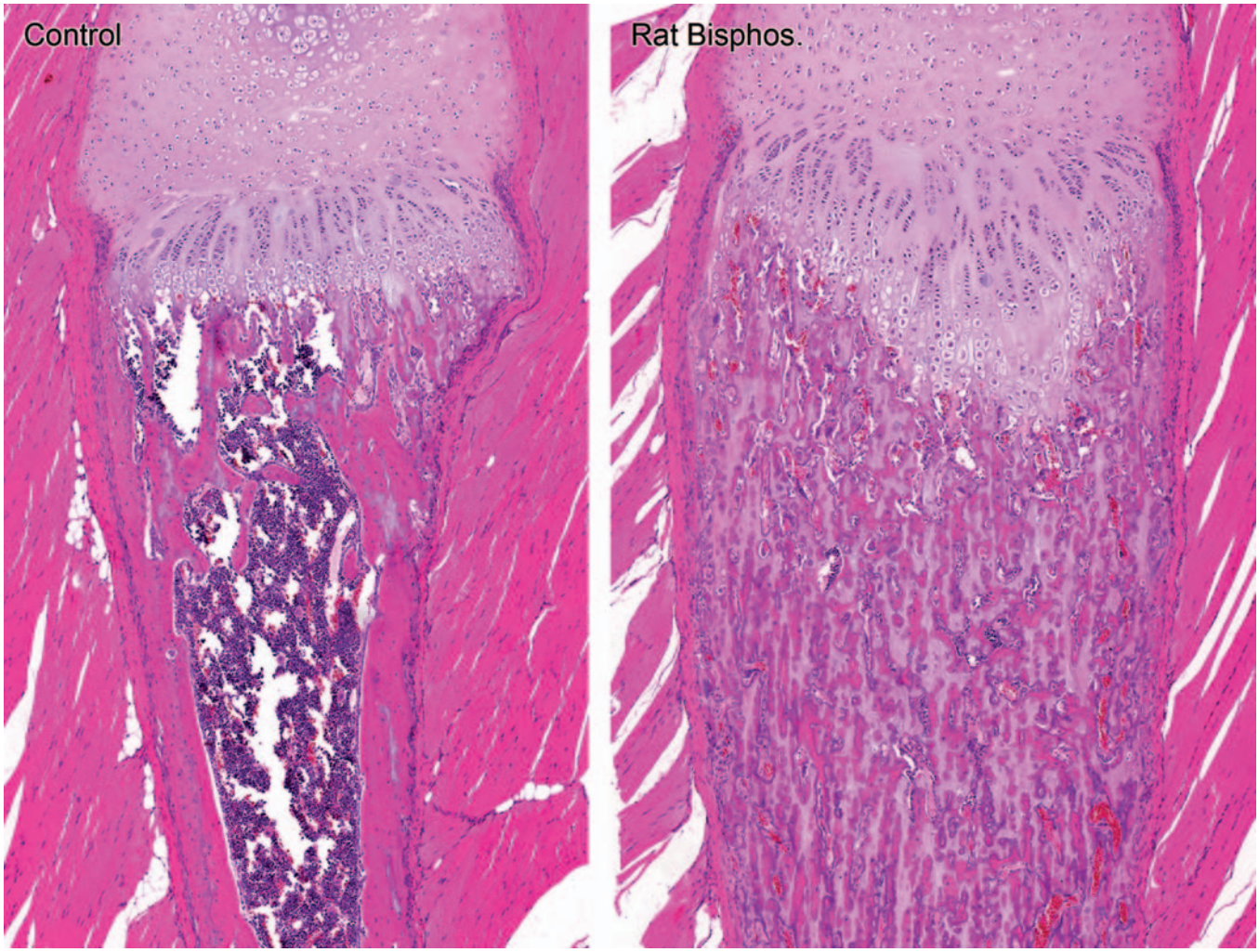

FIGURE 23.15 Agents like bisphosphonates that prevent bone resorption can profoundly raise bone density. Relative to a control animal (left), the rib from a rat given a bisphosphonate (right) exhibits extensive filling of the medullary cavity with retained primary spongiosa with prominent cartilage cores. H&E stain. Published previously as Figure 63.29 in D. Gunson et al., Bone and joints, in: *Handbook of Toxicologic Pathology, third ed.* (W.M., Haschek, C.G. Rousseaux, and M.A. Wallig, eds), Academic Press, San Diego; volume 3, p. 2822, with permission.

of woven bone in the adult or the resorption of bone in association with invasive neoplasia can be considered to be renewed modeling activities. Osteoclast-mediated bone resorption may occur because T-lymphocytes secrete interleukin-1β (formerly known as osteoclast-activating factor). This cytokine has powerful proerosive and proinflammatory properties, and along with TNF-α (another master proinflammatory cytokine) controls many signaling pathways responsible for bone and joint damage in both "inflammatory" (i.e., RA) and "noninflammatory" (i.e., OA) arthritides.

Bone Turnover Alterations

Bone turnover is an ongoing process under the influence of many different factors, both systemic and local. Effects on this process are visualized most readily in the metaphysis. In the growing bone, once the primary spongiosa is formed, the number of trabeculae is reduced by osteoclasts and their thickness increased by osteoblasts. The scalloped cartilage cores and reversal cement lines within metaphyseal trabeculae are evidence of this activity.

Increased bone in the metaphysis may be produced by several mechanisms. If osteoclastic resorption of the metaphyseal trabeculae is inhibited, increased bone results (such as after bisphosphonate administration). Increased bone in the metaphysis is associated with exposure to sodium/glucose cotransporter-2 (SGLT-2) inhibitors (in rats fed a standard laboratory diet), yellow phosphorus, or lead. The amount of metaphyseal bone also may be increased if the biomechanical load is enhanced or anabolic agents are administered.

Usually agents that reduce bone turnover give a transient bone gain.

Any factor, including drugs and toxicants, that increase the rate of bone turnover in the metaphysis will lead to decreased bone. This finding will develop rapidly as reduced numbers and thickness of bony trabeculae since there normally is a loss in the amount of cancellous bone during metaphyseal turnover. In the rat, increased metaphyseal turnover after ovariectomy leads to decreased bone, which can be blocked using antiresorptive agents such as bisphosphonates and RANKL inhibitors. Osteoporosis is a pathologic reduction in bone mass in which the remaining bone is not normal, as indicated by loss of trabecular connectivity in three dimensions. In contrast, osteopenia refers to the state in which overall bone mass is reduced, but remaining bone is qualitatively normal. With aging, the amount of bone removed during remodeling declines, but the amount of bone that refills the resorption pit (i.e., Howship's lacunae) declines even more; therefore, there is accelerated bone loss over time even though there is decreased bone resorption. Any condition or drug that enhances this deficit may cause irreversible bone loss, including malnutrition, high endogeneous levels or exogenous doses of corticosteroids, and chronic metabolic acidosis (which causes preferentially cortical bone loss in rats).

Background Bone Lesions

Most background lesions in animal species used in toxicity studies are more common in older animals and/or are associated with previous bone trauma or infection. Chondromucinous degeneration in the synchondroses of the sternum is the most common nonclinical background finding in rodents. Similar changes can occur in other cartilage locations, including long bone growth plates as well as intervertebral discs. The incidence in older animals can be quite high. The cause is unknown, but the change generally has no relationship to xenobiotic exposures.

Evaluation of new bone production in toxicity studies must consider species-related incidences of spontaneous increased bone. In laboratory rodents, two spontaneous lesions associated with increased bone include enhanced amounts of intramedullary cancellous bone in aged rats, a change traditionally termed hyperostosis. This type of increased bone is uncommon but occurs as a generalized condition, affecting long bones, the sternum, and vertebrae. The other condition, fibro-osseous lesion (FOL) in mice, is seen commonly in old females of certain strains but is rarely seen in males. FOL can be seen in the sternum, facial bones, and long bones, where increased bone begins as a partial replacement of the marrow cavity with undifferentiated mesenchymal cells and matrix. Osteoblasts, osteoclasts, and fibroblasts can be recognized in the lesion, as can fibrous tissue, osteoid, and woven bone. The cause of FOL is unknown. Murine strains with FOL exhibit a high incidence of ovarian cysts and cystic adenomatous hyperplasia of the uterus, suggesting that abnormal regulation of estrogen may play a role. Dietary estrogens have been shown to hasten the development of increased bone and are considered to be one of the many factors predisposing C3H mice to the development of osteosarcoma. Previous trauma or infection can lead to focal areas of decreased or increased bone. Metastatic neoplasms of soft tissues that spread to bone cause focal bone loss that may be detected radiologically. Such metastases may occur by direct invasion, but usually follow hematogenous spread and seeding of the bone marrow.

Common Toxicant-Induced Responses in Joints

Toxicant-related responses in joints following exposure to exogenous chemicals or biologics may affect any of the many intraarticular tissues. Typical joint findings reflect altered disease presentation or progression (e.g., in arthritis models) following xenobiotic treatment or an altered incidence and/or severity of spontaneous changes (many of which are age-related).

Inflammation

Acute synovitis is characterized by periarticular edema, fibrin deposition within the synovial membrane or joint space, and an inflammatory infiltrate (composed principally of neutrophils) that is limited to the synovium. With acute exudative reactions, edema and fibrin deposition in the joint may be considerable, with only a limited inflammatory cell infiltrate. However, in short order neutrophils migrate from the synovium into the joint space; synovial fluid may contain many more neutrophils than may be seen in a synovial biopsy. Even minor joint disturbances, such as saline flushing or instilling the joint with contrast agents, cause an acute inflammatory response with alteration in the surface lining cells.

More substantial reactions representing an escalation of synovitis to arthritis are associated with extension of the inflammatory process into the periarticular soft tissues and/or a substantial inflammatory cell influx into the joint space or other intraarticular tissues (e.g., fat pads). As acute inflammation subsides, the synovial inflammatory infiltrate changes character and becomes composed of mononuclear cells, initially with macrophages predominating. Over time, a lymphoplasmacytic infiltrate characterizes the immune-mediated arthritides (i.e., activation of an acquired immune response). Even

in the face of large lymphoid aggregates in or near the affected joint, germinal centers are rarely seen.

All joint inflammations are accompanied by an increase in intermediate-type and type B (fibroblast-like) synovial cells. These cells alter their phenotypes when challenged to become facultative phagocytes. Fibroblast-like synoviocytes secrete several proinflammatory cytokines, which can sustain arthritis for long periods, and also proteases that contribute significantly to cartilage matrix degradation.

Hyperplasia/Hypertrophy

Synovial cells also can undergo hyperplasia and hypertrophy in response to arthritogenic stimuli (Figure 23.16). When this occurs, the lining cells increase in number, become plump and rounded, and have numerous surface filopodia. The synovial membrane has a tremendous capacity to undergo villous proliferation as a feature of low-grade, persistent inflammation. Villi form when fibrin deposited within the joint space is organized by invading mesenchymal cells, much like an organizing thrombus. Initially, villi that develop by this mechanism appear avascular and hypocellular, but later they become vascularized. Destruction of the articular cartilage occurs with, or more likely because of, synovial inflammation, especially where pannus (see below) arising from the inflamed synovium extend over the cartilage surface. Fragments of articular cartilage that detach or are eroded from the joint surface may lodge in synovial crevices and become incorporated as part of villous proliferation. These cartilage fragments gradually lose their proteoglycans (as shown by their altered staining pattern in histologic sections) and putatively evolve into a nidus for provoking continued inflammation and articular cartilage destruction as the body attacks the liberated proteoglycans and/or type II collagen.

In addition to joint inflammation and villous proliferation, there may be secondary responses within the synovial membrane, especially in chronic arthritis. These changes include rare osteochondral nodules, deposition of hemosiderin pigment within synovial lining cells or macrophages of the synovial membrane or articular capsule, fibrosis and articular capsule hypertrophy. There may also be mineralization within the synovial wall and joint capsule.

Cartilage Degeneration

Too much pressure, or too little, leads to structural and biochemical alterations in articular cartilage. Excess pressure causes cells in the superficial cartilage zone to become necrotic and the adjacent matrix to degrade. In contrast, insufficient pressure leads to cartilage matrix fibrillation. Articular cartilage has a high proportion of both water and proteoglycans, and is viscoelastic and highly deformable. Deformation of articular cartilage due to pressure or loading can lead to cartilage creep (i.e., displacement). The rate of creep depends on how quickly water can be forced out of the solid collagen−proteoglycan matrix. Water loss from the matrix leads to a condensation of the cellular and fibrillar components of cartilage.

Chondromalacia is the macroscopic term used to describe rubbery articular cartilage. Using H&E staining and light microscopy, chondromalacic cartilage often appears normal. However, a loss of cartilage

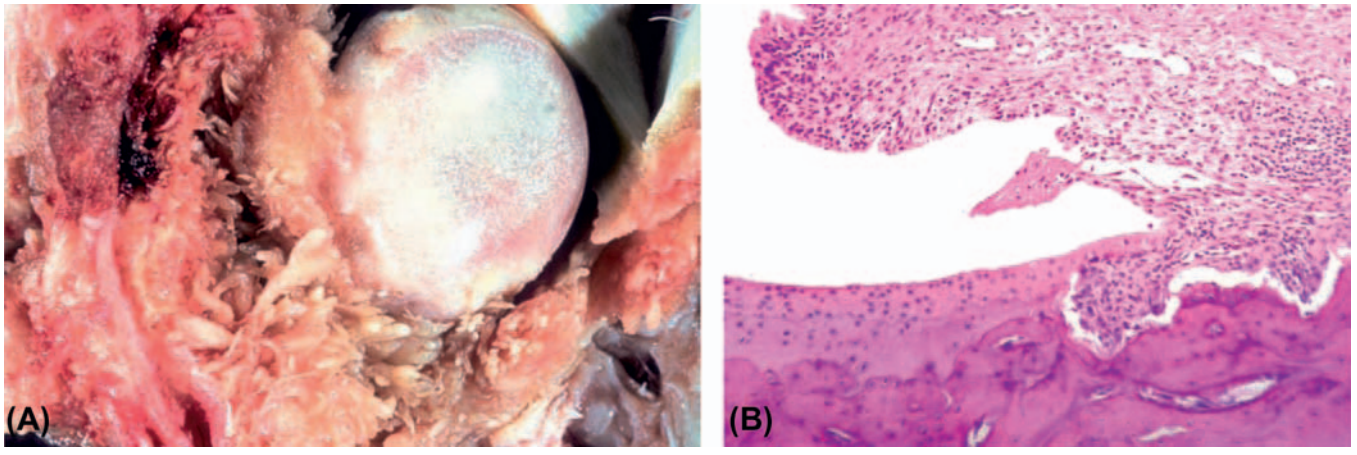

FIGURE 23.16 Synovial responses in arthritis. (A) Marked synovial villous hyperplasia associated with coxofemoral joint (hip) dysplasia in a dog. The extent of this proliferation is unusually severe for canine hip dysplasia. Microscopically, this change routinely is accompanied by variable lymphoplasmacytic inflammation that is independent of the cause of the articular damage. (B) Pannus, a proliferation of fibrovascular tissue that develops in rheumatoid-like arthritis (experimentally induced in this case), affecting the distal tibia of a rat. Pannus originating from the synovium (right) is invading and destroying the articular cartilage and bone. H&E stain. *Figure provided courtesy of Dr S. E. Weisbrode, College of Veterinary Medicine, The Ohio State University; reproduced from Weisbrode (2007) Bone and joints. In:* Pathologic Basis of Veterinary Disease, *fourth ed. (M. McGavin and J. F. Zachary, eds.), Mosby Elsevier, Figs 16.34 and 16.37, pp. 1060−1061, with permission.*

matrix can be identified microscopically by altered matrix staining patterns as visualized by special staining techniques with cationic dyes such as safranin O or toluidine blue. Chondrocyte necrosis may be easily observed in some cases using light microscopy to visualize empty lacunae (Figure 23.17) or pyknotic (dark, shrunken) nuclei within lacunae; due care must be taken to avoid over-interpretation of artifactually empty chondrocyte lacunae since some cell loss is to be expected when trimming and cutting bony specimens. Loss of intercellular matrix, starting superficially and then moving deeper, follows degeneration of chondrocytes. Normal collagen fibrils within the cartilage matrix become more prominent by light microscopy as the proteoglycan matrix is degraded. Cracks and crevices develop and fragment the remaining cartilage into multiple longitudinal clefts (Figure 23.18). In some cases, portions of cartilage may become dislodged and develop into free-floating bodies (or "joint mice") within the joint cavity.

Whenever there is cartilage cell necrosis, or loss of the superficial cartilage layers, the remaining chondrocytes undergo cell division to produce daughter cells. The closely aggregated families of new cells are frequently referred to as clusters, cell clones, or chondrones (Figure 23.17). Under normal circumstances, surface cartilage is worn away by friction and small cartilage clones develop in the middle zone, appearing to migrate toward the surface to be shed into the joint space. The deep margin of cartilage is slowly transformed into bone (chondroid bone). Progressive tidemarks of calcified cartilage form a historical marker of changes in the osteochondral border. While a significant amount of regeneration can occur (more than has been previously appreciated), the restored articular cartilage does not function as well as native tissue.

Associated Subchondral Bone Changes

In certain disease conditions of the adult, the normally slow cartilage modeling process is so exaggerated that the bone contour is altered. This process has been divided into progressive, regressive, and circumferential reactions. In the progressive reaction, there is an initial interstitial proliferation of cartilage leading to an increased thickness of the articular cartilage. The base of the cartilage becomes progressively mineralized, and the deep cartilage layers are invaded by blood vessels and converted into bone, resulting in thickening of the subchondral bone plate. Since the initial reaction represents a growth process, it is followed by remodeling of the tissue. The regressive reaction can be seen whenever loss of the cartilage surface results in the subsequent secondary loss of underlying bone. The cause of regression is unknown, but it may

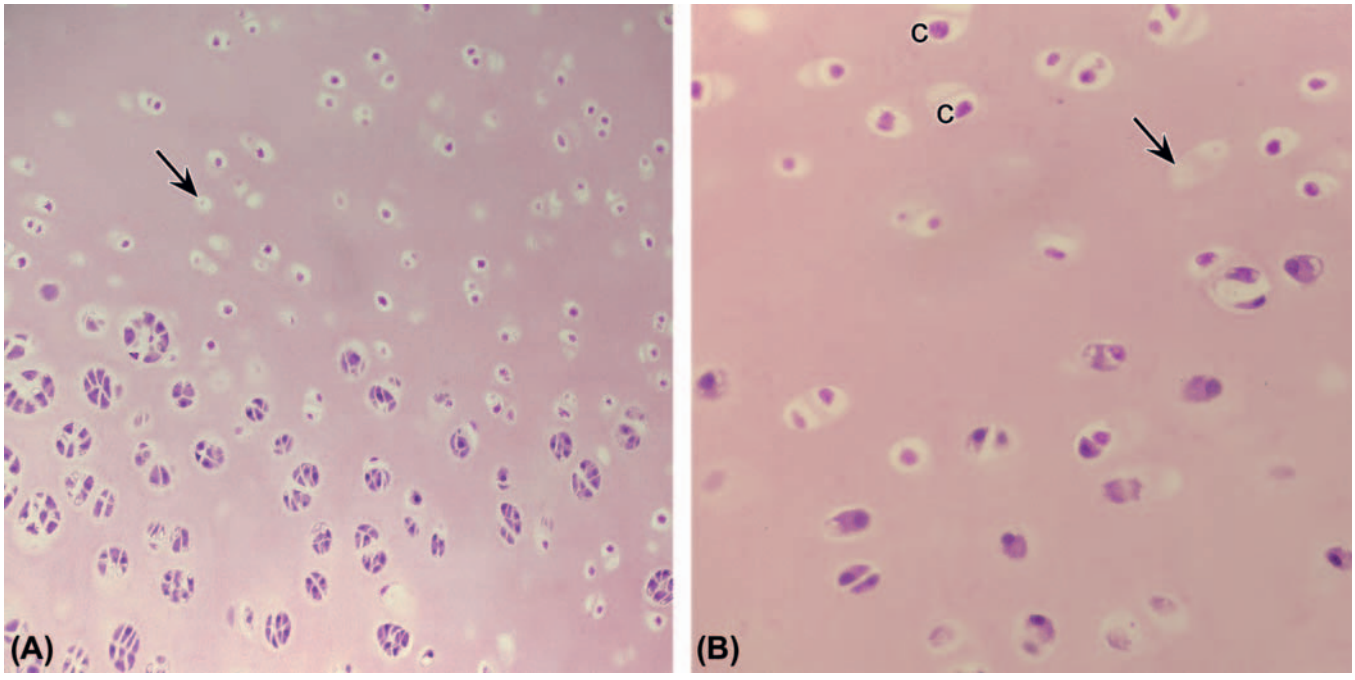

FIGURE 23.17 Ischemic chondronecrosis/osteochondrosis, medial femoral condyle of a 12-week-old domestic pig (A and B). Chondrocyte necrosis is evident as empty chondrocyte lacunae (arrows), or lacunae with degenerate, eosinophilic chondrocytes, lacking cellular detail. Adjacent areas show chondrocyte cloning (A, middle region of left margin). *Images courtesy of Dr. Cathy Carlson, University of Minnesota, St Paul, MN. Published previously as Figure 63.34 in D. Gunson et al., Bone and joints, in: Handbook of Toxicologic Pathology, third ed. (W.M., Haschek, C.G. Rousseaux, and M.A. Wallig, eds), Academic Press, San Diego; volume 3, p. 2828, with permission.*

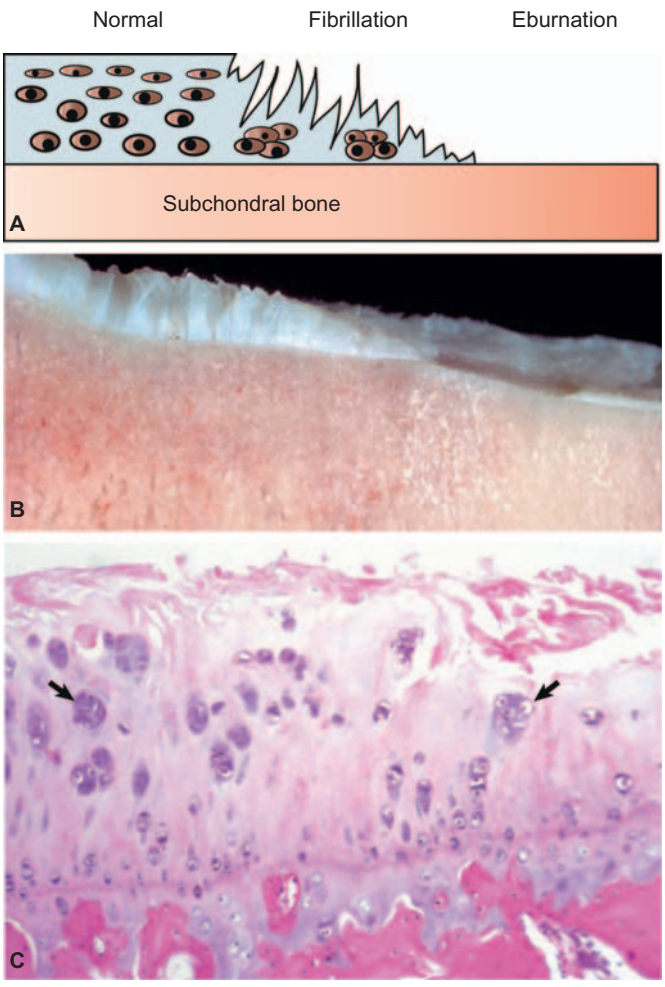

FIGURE 23.18 Degenerative joint disease induces substantial fibrillation, fragmentation, and ulceration of articular cartilage leading to exposure and eburnation of the subchondral bone. (A) Schematic diagram showing fibrillation and erosion of articular cartilage overlying subchondral bone, which has increased in density. (B) The proximal articular cartilage of the tibia from a bull (sagittal section) exhibits fraying (fibrillation) of the cartilage surface to the left and complete cartilage loss (ulceration) to the right. Note that the cartilage is missing from the bed of the ulcer in the plane of the section, but the edge of the ulcer with a rim of normal cartilage is visible at its back. The cartilage to the right of the ulcer is very thin, indicating erosion. (C) The articular cartilage of this dog femoral head exhibits fibrillation and hypocellularity (chondrocyte necrosis) superficially, while clusters of chondrocyes (arrows) represent an ineffectual attempt at repair. *Figures provided courtesy of Dr S. E. Weisbrode, College of Veterinary Medicine, The Ohio State University; reproduced from Weisbrode (2007) Bone and joints. In:* Pathologic Basis of Veterinary Disease, *fourth ed. (M. McGavin and J. F. Zachary, eds.), Mosby Elsevier, Figs 16.30 (A), 16.31 (B), 16.32 (C), p. 1059, with permission.*

be related to mechanical overloading. This change happens during the process of eburnation (i.e., full-thickness, often localized loss of articular cartilage); occasionally, cartilage regenerates over the resulting bare bone surface, but the organization and matrix composition of the new cartilage is abnormal. The circumferential reaction consists of marginal osteophytes. These arise at the boundaries of affected joints due to periosteal bone formation, ossification of tendon or ligament entheses (attachment sites), or upward and lateral growth of cartilage with progressive transformation into bone. Osteophytes may be described as axial if near the center of the joint or abaxial if they are located at the periphery.

Trauma

The response of articular cartilage to trauma is dependent largely upon the depth of the injury. Superficial lacerations evoke only a short-lived metabolic and enzymatic response, failing to provide sufficient numbers of cells or matrix to repair the smallest injury. However, when the injury penetrates the osteochondral border, the response is similar to that occurring in other vascularized tissues, and results in the formation of granulation tissue. This response is similar to that arising in fracture repair except that bone proliferation stops at the cartilage–bone junction, leaving fibrous tissue to bridge cartilage wound edges. The fibrous tissue undergoes progressive hyalinization and chondrification to produce a fibrocartilaginous mass. Continuous passive motion has been shown to assist conversion of fibrocartilage to a more hyaline type of cartilage.

Vascular Changes in Joints

Not only does the vascular reaction occur within the subchondral bone marrow, but synovial vessels also may be stimulated during cartilage remodeling. When this occurs, a fibrovascular membrane (or "pannus") originating from the synovium becomes attached to and invades the cartilage. The response of the subchondral osseous trabeculae is probably due to altered biomechanical stresses and strains resulting in part from decreased shock absorption by the articular cartilage. Trabeculae beneath damaged cartilage vigorously remodel to become thicker. When the trabecular thickness becomes excessive, central Haversian-like canals develop and the subchondral bone acquires an appearance more like compact bone. The chondrification of fibrous tissue filling the subchondral marrow may be deficient, and the tissue exhibits traits that are more characteristic of myxomatous connective tissue. There may be focal bone resorption, surrounding trabeculae may form a wall around the myxomatous reactive tissue, and the lesion can develop into a pseudocyst (i.e., a cavity lacking an epithelial or endothelial lining).

Neoplasia

Synovial sarcomas are the primary neoplasms that arise in joints. Synovial sarcomas typically have a

biphasic cell population of spindle cells (usually in sheets) and epithelial-like cells in H&E-stained sections. However, one typically must examine numerous samples to appreciate the characteristic features of these tumors, which include slit-like spaces or a pseudoglandular pattern. Using immunohistochemical techniques, cells within synovial sarcomas show a biphasic pattern of intermediate filament protein expression, with the spindle cells containing vimentin and the plump epithelial-like cells staining for cytokeratin. Fibrosarcomas rarely develop in the periarticular tissues and can invade joints directly. These can be differentiated from synovial sarcomas because fibrosarcomas do not express cytokeratins.

Background Lesions

Spontaneous OA occurs in several species, including cynomolgus and rhesus monkeys, guinea pigs, mice, and rats. It is typically slowly progressive, and may be present at a high incidence microscopically in older animals. A severe unilateral destructive OA of the hip (idiopathic chrondolysis) in young cynomolgus monkeys has been reported, but the etiology is unknown (Figure 23.19).

MECHANISMS OF TOXICITY

Although the skeletal system is exposed to circulating xenobiotics, it is not known to have a significant role in biotransformation of such substances. Agents reported to have a direct toxic effect on bone and/or cartilage are somewhat limited. It may be that we have not yet learned to evaluate the early primary toxic effects of drugs, chemicals, or other environmental agents on hard tissues. A list of agents and toxic mechanisms causing skeletal pathology are given in Table 23.3.

Bone Toxicity

Primary Toxicity

Aseptic necrosis of the femoral head caused by alcohol consumption or corticosteroid administration is not due to direct drug-induced necrosis of osteocytes, but rather to compromised local circulation in a region of bone that is anatomically vulnerable due to its hemispherical shape and considerable range of motion. In contrast, cyclophosphamide, a cytotoxic antineoplastic agent, directly influences mitotic division of bone cells, thereby inhibiting bone formation and growth. Antibiotics of the quinolone class (e.g., nalidixic acid, ciprofloxacin) have been shown to cause chondrolysis.

Bisphosphonates, which are antiresorptive agents, are rapidly incorporated into mineralized bone and calcified cartilage. When osteoclasts take up bisphosphonates released from mineralized bone and cartilage by acid digestion, their function is impaired. Toxic intracellular metabolites such as ApppI (triphosphoric acid 1-adenosin-5′-yl ester 3-[3-methyl-but-3-enyl] ester), a cytotoxic ATP analog that promotes apoptosis are produced. The osteoclast may undergo apoptosis, have a shortened lifespan, and exhibit morphologic changes such as the formation of giant osteoclasts.

Secondary Toxicity

Since skeletal tissues do not play a major role in biotransformation or elimination of potentially toxic substances from the body, most exogenous chemicals exert their effects on the bone via secondary mechanisms. It has been suggested that secondary toxic effects may be mediated by alterations in blood flow within bones. Increased oxygen tension is thought to stimulate bone resorption locally, while decreased oxygen tension causes bone to accumulate. The close similarity of some drug-induced bone reactions to those observed in spontaneous diseases mediated by a vascular reaction supports the argument for a vascular pathogenic mechanism. Conversely, such reactions could be a manifestation of the limited number of ways in which skeletal tissues can respond to injury.

An example of a tissue reaction that might be mediated by a vascular response is the subperiosteal formation of new bone in dogs following the administration of PGE_2. The drug-induced gross and microscopic lesions are nonspecific but are very similar to those observed in hypertrophic (pulmonary) osteo(artho) pathy (HPO). Substances capable of inducing secondary bone changes usually are hormones, vitamins, or minerals, or affect the metabolism of skeletal-regulating agents. The long-term effects of PTH, corticosteroids, somatotropin, calcitonin, bisphosphonates, and vitamin D and its metabolites on bone resorption and formation are similar in quality but vary in magnitude. When new remodeling units are activated to increase bone turnover (e.g., by PTH or thyroid hormone), the initial bone resorption enlarges the remodeling space and leads to a temporary, nonprogressive bone loss. Conversely, the many agents that depress activation of bone turnover (e.g., calcitonin, increased dietary calcium and vitamin D, estrogens, nonsteroidal antiinflammatory agents, and bisphosphonates) reduce resorption first, leading to a small, nonprogressive net gain in bone.

Some agents act on several or all of the sequential remodeling stages (e.g., corticosteroids, PTH), whereas others act on only one particular stage. This role of a given agent with respect to regulating the turnover

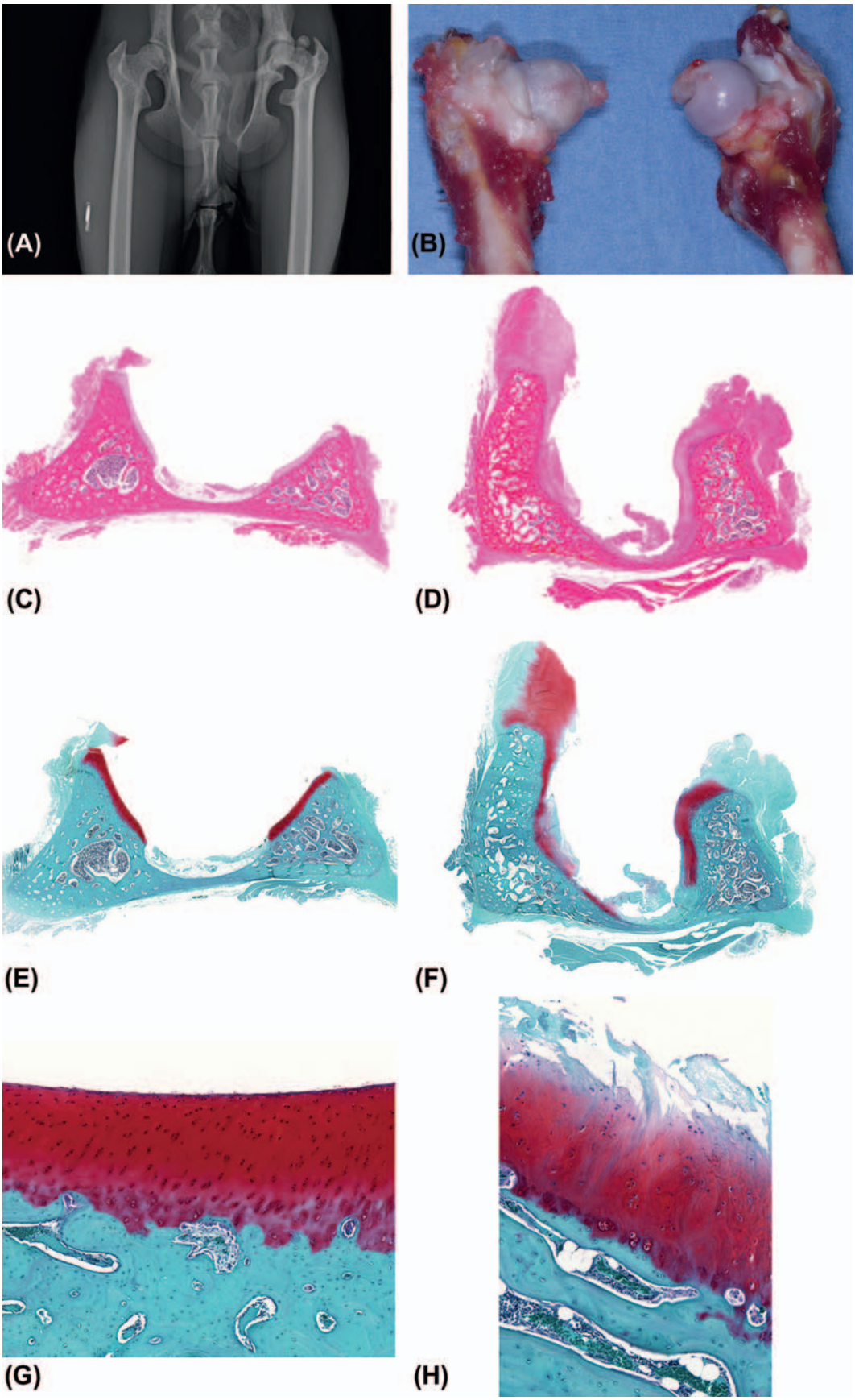

FIGURE 23.19 Chondrolysis of the coxofemoral ("hip") joint in young cynomolgus monkeys. (A) Radiograph demonstrating the irregular surface of the right femoral head compared to the normal conformation of the left side. (B) When examined grossly, the affected right femoral head displays rough dull cartilage relative to the smooth, white, normal articular surface of the left side. The characteristic regular joint surface from the unaffected left acetabulum (C, E, G) lacks fibrillated cartilage and the loss of cartilage matrix integrity of the damaged right side (D, F, H). Stains: C, D = H&E; E–H = safranin O. Published previously as Figure 63.38 in D. Gunson et al., Bone and joints, in: *Handbook of Toxicologic Pathology, third ed*. (W.M., Haschek, C.G. Rousseaux, and M.A. Wallig, eds), Academic Press, San Diego; volume 3, p. 2832, with permission.

TABLE 23.3 Common Mechanisms of Bone and Joint Toxicity

Physiological mechanism	Morphologic change	Biological mechanism	Agent
Hyperparathyroidism	Fibrous osteodystrophy	High serum phosphorus depresses serum calcium	Continuous PTH exposure Excess dietary phosphorus Low dietary calcium: phosphorus ratio Elevated serum phosphorus associated with renal disease
		Skeletal resistance to PTH/renal calcium loss	Gallium
Excessive absorption of calcium	Soft tissue mineralization; sometimes increased bone	Increased serum level of 1.25-$(OH)_2$ Vitamin D_3	Vitamin D intoxication Ingestion of plants containing Vitamin D analogues (*Cestrum diurnum*)
		Increase in dietary osmolarity	Lactose and certain polymers increase calcium absorption
		Direct effect on membrane	Filipin, ionophore A23187
Reduced absorption of calcium	Rickets, osteomalacia	Chelation of dietary calcium	Oxalate
		Reduction in active absorption	Agents that induce renal disease or otherwise interfere with synthesis of 1.25-$(OH)_2$ vitamin D_3 [such as cadmium, vanadium, lead, tin, and strontium; anticonvulsants considered to induce hepatic microsomal enzymes that catabolize vitamin D or its (*Cestrum diurnum*) vitamin D analogues]
		Direct effect on membrane cation transport	Anticonvulsants
Reduced absorption of phosphorus	Mineralization defect	Interference with intestinal transport	Aluminum sulfate High dietary calcium: phosphorus ratio
Decreased renal resorption of phosphorus	Mineralization defect	Decreased suppression of sodium-phosphate cotransporters in renal proximal tubules	Decreased FGF-23
Induction of cartilage call growth	Cartilage hyperplasia	Increased numbers of cartilage cells	Growth hormone (somatotropin) dose-related growth response Somatomedin, diethylnitrosamine (indirect)
Decreased cartilage matrix	Chondromalacia	Lysosomal release of enzymes or production of local factors	Vitamin A; polyene antibiotics cause lysosomal instability
		Inhibition of proteoglycan or collagen synthesis or inhibition of collagen crosslinks	Cadmium inhibits chondroitin sulfate synthesis Thallium inhibits production of acid mucopolysaccharides Cyclophosphamide and methotrexate cause matrix degradation Zinc, cadmium, semicarbizide, and copper antagonists (molybdenum, sulfate) inhibit lysyl oxidase Lathyrism (BAPN)
Decreased bone matrix	Osteopenia, osteoporosis	Reduced synthesis/increased remodeling period	Glucocorticoids, aluminum
		Interference with collagen crosslinks	See "Decreased cartilage matrix"
		Unknown	Heparin
Decreased matrix mineralization	Mineralization defect	Inhibition of matrix mineralization	Fluoride, aluminum, tetracycline, metal ions (strontium, manganese), acid/base balance,

(*Continued*)

TABLE 23.3 (Continued)

Physiological mechanism	Morphologic change	Biological mechanism	Agent
			bisphosphonates, 1,25 dihydroxyvitamin D_3, phenytoin, cadmium
Net bone resorption	Osteopenia	Increased osteoclasts	*Pasteurella* type D toxin causes resorption of turbinates in swine
		Reduced bone mass	Occurs with primary or secondary hyperparathyroidism such as ethylene glycol-induced oxalosis; vitamin A and related retinoids also induced fractures
		Disuse	
Decreased bone resorption	Osteosclerosis (metaphysis during growth)	Inhibition of osteoclast recruitment and/or function	Bisphophonates, DKK-1 inhibitors, RANKL inhibition, calcitonin, actinomycin, gallium, mithramycin, lead, yellow phosphorus, thionaphthene-2-carboxylic acid
		Decreased solubility of bone crystals	Bisphosphonates, fluoride
Accelerated longitudinal bone growth	Gigantism, increased growth plate width	Increased numbers of proliferating cells	Growth hormone (somatotropin), somatomedin, androgens, calcitoninInsulin and thyroid hormones have indirect effects
Decreased longitudinal bone growth	Growth retardation	Decreased cell proliferation	Inanition, tetracycline (premature infants), methylphenidate, furosemide, prostaglandin E2, corticosteroids, GH or IGF-1 inhibition, cyclophosphamide, and methionine
		Interference with cartilage metabolism	Premoline produces growth retardation in children
		Premature closure of growth plate	Quinolones, warfarin, vitamin A, sonic hedgehog inhibition
Increased activation frequency	Reversible bone loss	Increased numbers of active osteons	Thyroid hormone or drugs that induce hyperthyroidism, parathyroid hormone, fluoride
Decreased activation frequency	Maintenance of bone volume	Decreased numbers of active osteons	Estrogens, calcitonin, nonphysiological levels of glucagon, protamine, nonsteroidal antiinflammatory drugs
Increased formation of bone matrix	Increased osteoid	Osteonal bone formation greater than resorption	PTH (1−34), Sclerostin inhibition, estrogens, bone marrow depression
		Bone formation without significant prior resorption	Fluoride, aluminum, prostaglandins E_2, and E_1; also possibly 1,25 dihydroxy Vitamin D_3 and *Solanum malacoxylon*
Marrow fibrosis	Osteomyelofibrosis and sclerosis	Anemia (increased circulating levels of erythropoietin); see "increased formation of bone matrix"	Toxic substances that cause chronic bone marrow depression, such as benzene, lead acetate, bone-seeking radionuclides, and several anticancer drugs
Tumor induction	Osteosarcomas most common	DNA damage	Bone-seeking radioisotopes
		Osteoblast stimulation	PTH, PTH analogs
		Unknown	Beryllium salts, bisphosphonates, methylcholanthrene, cupric-chelate *N*-hydroxy-2′-acetylaminofluorene
Joint degeneration	Loss of articular cartilage	Causes cartilage cell necrosis	Quinolone antibiotics (nalidixic acid, ciprofloxacin, ofloxacin), Mg deficiency
		Causes matrix degeneration/lack of synthesis	See "Decreased cartilage matrix"; corticosteroids, immunosuppressive drugs

(*Continued*)

TABLE 23.3 (Continued)

Physiological mechanism	Morphologic change	Biological mechanism	Agent
Joint inflammation	Synovial inflammation/ hypertrophy	Induces immune-mediated arthritis	Numerous drugs, including penicillin, immunologic stimulants
		Nonimmune mechanisms	Lysosomal membrane destabilizers (streptolysin S, filipin) Charged molecules (poly-D-lysine, dextran sulfate), enzymes (collagenase, papain) Other (zymosan, double-stranded polyriboinosinate-polycytidylate, 6-sulfanilamidoindazole) perfluorocarbon contrast agents
	Deposition of urate crystals	Causes hyperuricemia	Cytotoxic drugs, diuretics, ethambutol, nicotinic acid, pyrazinamide, salicylates
Tendon degeneration	Necrosis of cells/ matrix	Causes tendon rupture	Quinolone antibiotics
	Fibroplasia	Causes contractures	MMP inhibitors, BAPN

These represent known actions that have been well studied. There is a wide divergence in the way many agents produce their effects, which can be observed at different organizational levels (e.g., molecular to whole animal).
Abbreviations: *BAPN*, β-aminoproprionitrile; *DKK-1*, Dickkopf-related protein 1; *FGF-23*, fibroblast growth factor 23; *GH*, growth hormone; *IGF-1*, insulin-like growth factor 1; *MMP*, matrix metalloproteinase; *PTH*, parathyroid hormone; *RANKL*, receptor activator of nuclear factor-κB ligand.
Table adapted from Handbook of Toxicologic Pathology, *second ed. W. M. Haschek, C. G. Rousseaux, and M. A. Wallig, eds. (2002) Academic Press, Table 24.1, pp. 467–470, with permission.*

process will determine whether or not a specific modality of timed drug delivery is effective in eliciting a skeletal response. Since bone turnover events represent a sequence of different biological activities, intermittent, brief, or continuous delivery of the same agent may give distinct skeletal responses. The classic example of this phenomenon is the anabolic action of intermittent PTH administration versus the high bone turnover observed with continuous PTH delivery. Skeletal responses to pharmacologic agents may diminish with time as tolerance develops. Diminution of the skeletal response is seen with longer-term usage of bone anabolic agents such as PTH; the response plateaus because the additional bone activates the negative mechanical usage feedback loop to rid the skeleton of unneeded bone. One probable factor responsible for different drug doses causing varied biological responses is the differential action of drugs on the modeling and turnover stages. For example, a very small dose of 1,25-dihydroxy vitamin D_3 reverses the endochondral growth abnormality associated with vitamin D deficiency, but high doses can produce markedly increased osteoid in the metaphysis.

It is important to recognize that skeletal cell-to-cell and cell-to-matrix interactions involve both bone cells and cells of the bone marrow and are controlled by both systemic and local factors. Therefore, cell functional activities and cellular interactions represent the final common pathway of toxic action rather than a basic mechanism of toxic action. Local events are influenced by circulating agents such as hormones, but the effects of circulating agents are also determined by local factors such as mechanical usage. In addition, the processes active in bone disease are not necessarily the same processes operating in physiologically normal states.

Certain diseases appear to affect one bone envelope (periosteal, Haversian, endosteal) more than others. In general, the endosteal bone envelope is more reactive and responsive than the Haversian envelope because endosteal (endocortical and trabecular) bone possesses a greater cumulative surface area, has cells with higher metabolic activity, and experiences higher bone turnover. The surface-to-volume ratio and turnover rate is three times higher in trabecular bone than cortical bone in both humans and dogs. In the rapidly growing young rat, the endocortical surface of the metaphysis is predominantly formative, while the periosteal metaphyseal surface is predominantly resorptive as the diameter of the bone is progressively reduced from wide at the physis to relatively narrow at the diaphysis. Certain drugs also appear to affect particular envelopes, and there are species differences as well. For example, PGE_2 administration in dogs causes greater subperiosteal proliferation than endosteal proliferation of woven bone (Figure 23.20). In contrast, in rats endosteal proliferation is greater following PGE_2 treatment. Mice treated with estrogens produce much more marrow cancellous bone than do other animals. Bone loss following ovariectomy in rats and nonhuman primates is much greater than in dogs.

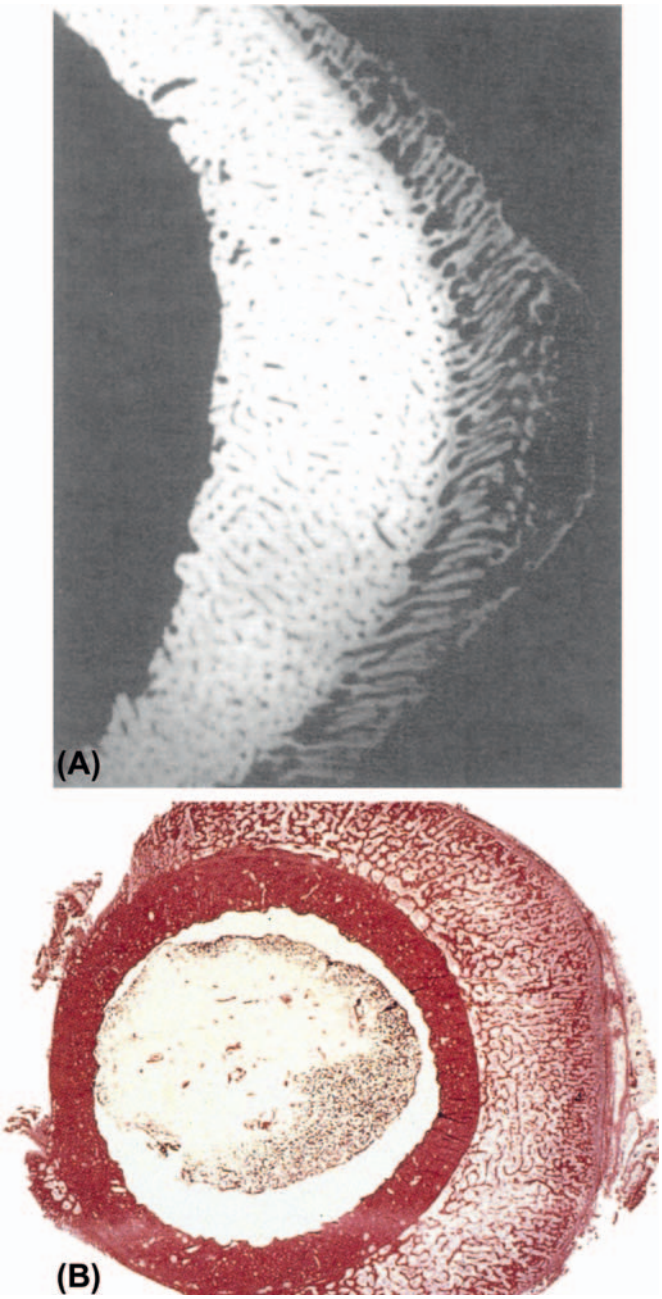

FIGURE 23.20 (A) Subperiosteal osseous proliferation in the long bone of a dog following repeated administration of prostaglandin E_2. Note the parallel trabeculae of reactive bone and surface woven-bone pattern. (B). Hypertrophic pulmonary osteopathy (in this case, from a dog) results in extensive new bone formation beneath the periosteum in long bones. *Image A reproduced from* Handbook of Toxicologic Pathology, *second ed. W. M. Haschek, C. G. Rousseaux, and M. A. Wallig, eds. (2002), Academic Press, Fig. 3, p. 474, with permission. Image B courtesy of Dr. L. Krook, College of Veterinary Medicine, Cornell University; reproduced from* Fundamentals of Toxicologic Pathology, *second ed. W. M. Haschek, C. G. Rousseaux, and M. A. Wallig, eds. (2010) Academic Press, Fig. 14.7, p. 425, with permission.*

Age also affects the responsiveness of the skeletal system. It is well recognized that fracture healing is less vigorous in old animals than in young individuals; the same is true concerning the response of the skeleton to circulating toxicants. The modeling and turnover processes present beneath the growth plates of growing animals respond to xenobiotics to a greater extent than do those in cortical or cancellous bone of older animals. In chronic studies, drug toxicity may influence (or be influenced by) the incidence and severity of spontaneous lesions occurring in the animal strain being used. For example, chronic studies with nitrofurazone show a drug-related effect that greatly increases the distribution and severity of age-related degenerative cartilage changes in rats.

TOXIC EFFECTS ON ENDOCHONDRAL OSSIFICATION AND LONGITUDINAL BONE GROWTH

The active physis of rapidly growing long bones in rats is often affected by both small molecule and biologic pharmaceutical agents. In the context of drug safety risk assessment, it is important to keep in mind that many test article-related effects on the growing physis represent on-target pharmacology and may not be relevant to human safety. Decisions regarding the relevance of such data depend on the proposed indication, exposure margin, and skeletal maturity of the intended population of human patients.

Decreased longitudinal bone growth is a common finding in toxicity studies conducted in rapidly growing young rodents and may be secondary to decreased food intake (inanition) or occur as a consequence of test article activity. There are two main categories of disruption to endochondral ossification: physeal dysplasia and physeal dystrophy. While physeal dysplasia and physeal dystrophy reflect very different toxicologic mechanisms, both lead to functional impairment of the physis and decreased bone production and impaired growth.

INCREASED THICKNESS, PHYSIS (PHYSEAL DYSPLASIA) Toxicity leading to increased physeal thickness is most notably represented by inhibitors of tyrosine kinases (e.g., anti-VEGF agents), MMPs, activin receptor-like kinase 5, and FGFs. Any substance capable of interrupting the transition from hypertrophic cartilage to the calcified cartilage spicules of primary spongiosa, whether by inhibition of angiogenesis, reduced vascular penetration, chondrocyte cell death, or a combination of these processes, can cause physeal dysplasia. Long bone physes are widened, sometimes dramatically, with disorganized and

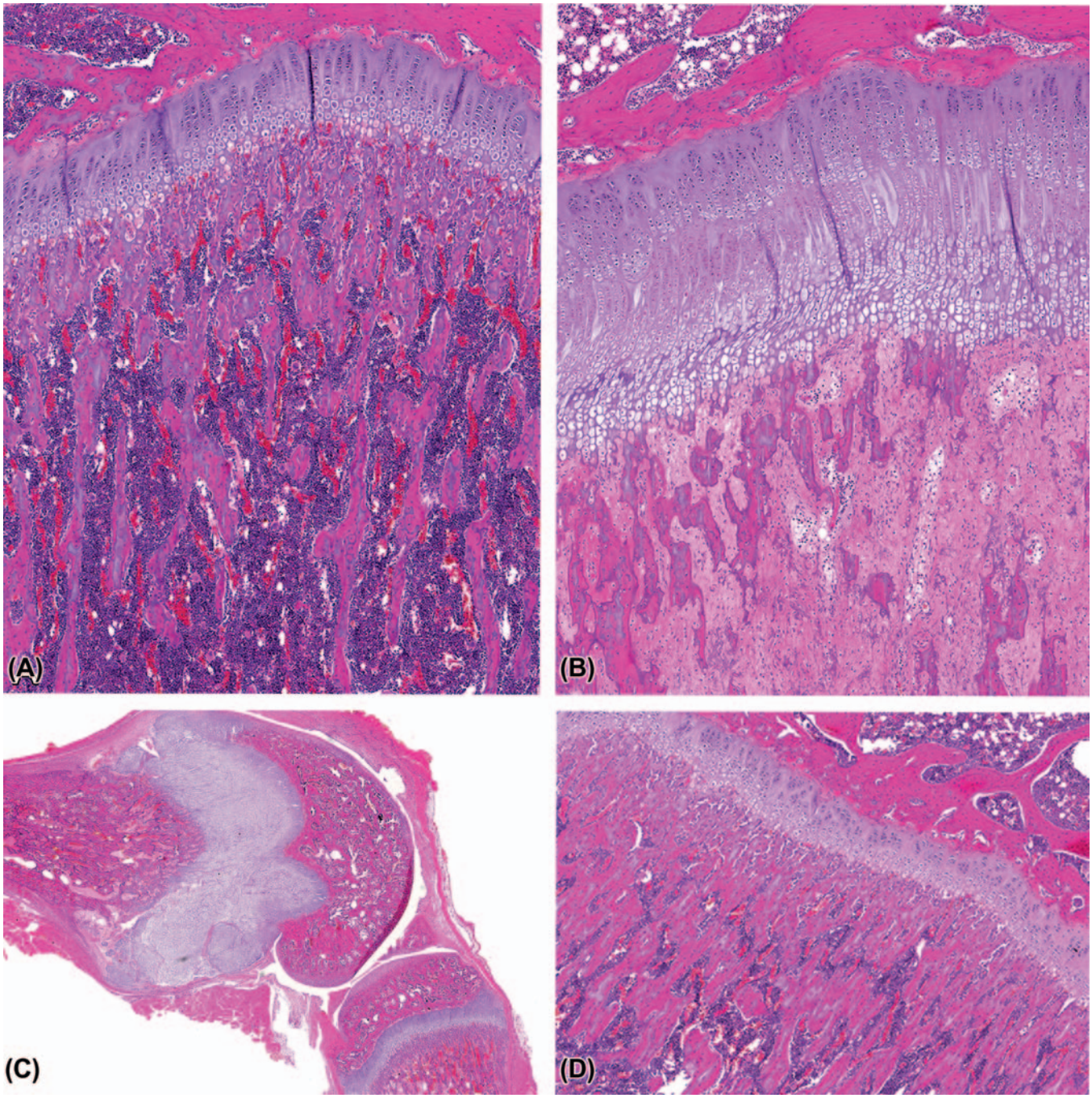

FIGURE 23.21 Physeal (growth plate) disturbances in the proximal tibia of rats typically affects the structure of both cartilage and bone. (A, B) Physeal dysplasia following administration of a vascular endothelial growth factor (VEGF) inhibitor results in marked physeal thickening with lack of normal ossification and primary spongiosa formation (B) relative to an unaffected control animal (A). Unmineralized osteoid has accumulated in the metaphysis. H&E stain; both images are at the same magnification. (C and D) Physeal dysplasia in the femorotibial (stifle) joint of a rat treated with a fibroblast growth factor (FGF) inhibitor. Distal femoral growth plates are sometimes more severely affected than proximal tibial plates, as depicted here (C). Control (D). H&E stain. Published previously as Figure 63.40 in D. Gunson et al., Bone and joints, in: *Handbook of Toxicologic Pathology, third ed.* (W.M., Haschek, C.G. Rousseaux, and M.A. Wallig, eds), Academic Press, San Diego; volume 3, p. 2839, with permission.

expanded chondrocyte columns, particularly in the hypertrophic zone (Figure 23.21). Transverse fractures through the widened (and weak) dysplastic physis can occur through any cartilage zone. When exposure to these inhibitors ceases, these findings usually resolve to a remarkable degree in short order, although some slight residual chondrocyte column disorganization may persist. Physeal dysplasia is most readily

appreciated in the young, rapidly growing rat; it may not be readily apparent in older rodents with little or no longitudinal bone growth. This process has also been reported in skeletally immature nonhuman primates.

DECREASED THICKNESS, PHYSIS (PHYSEAL DYSTROPHY) In decreased physeal thickness, longitudinal bone growth is impaired due to decreased chondrocyte proliferation in the physis, which is characterized by a thin, relatively inactive physis from which fewer and shorter primary spongiosa are produced (Figure 23.22). Secondary spongiosa may be thin if osteoblast function is impaired (e.g., with glucocorticoids), or may be thick if osteoblast function is relatively unchanged. Agents causing this toxicity are most notably represented by inhibitors of the GH/IGF-1 axis, such as glucocorticoids, and somatostatin. Decreased physeal thickness with thicker secondary spongiosa occurs with inanition in rapidly growing rats that have significant weight loss due to the impact of reduced energy availability on the GH/IGF-1 axis. The ultimate manifestation of decreased physeal thickness is physeal closure, which occurs prematurely if the condition develops is manifested in young animals.

TOXIC EFFECTS ON BONE MODELING AND TURNOVER

While bone modeling and bone turnover are processes of bone growth and bone homeostasis, respectively, both processes share common molecular pathways. Thus, both processes may be affected by a large array of pharmacologic agents.

TOXICOLOGIC EFFECTS ON OSTEOCLASTS

Effects of Impaired Osteoclast Formation in the Metaphysis Antibodies to the Wnt pathway inhibitor Dickkopf-related protein 1 (DKK-1) decrease osteoclast formation. Decreased numbers of osteoclasts subjacent to the zone of hypertrophic chondrocytes impair the normal elimination of extraneous calcified cartilage spicules. Primary and secondary spongiosa trabeculae numbers are increased, leading to a markedly increased trabecular bone volume in the metaphysis. Other pharmacologic agents with similar effects on osteoclasts include RANKL inhibitors.

Bisphosphonates are rapidly incorporated into calcified cartilage and mineralized bone, rendering these extracellular hard tissues resistant to acid digestion by osteoclasts. The number of surviving calcified cartilage spicules in the proximal metaphysis (retained primary spongiosa) increases markedly (Figure 23.15). Exposure to bisphosphonates causes characteristic changes to osteoclasts and erosion surfaces. Osteoclasts are typically enlarged with increased numbers of nuclei. Trabeculae of bisphosphonate-treated bone may have slightly undulating surfaces associated with these enlarged osteoclasts, which may reflect the inability of the osteoclast to produce a resorption cavity of normal (more deeply scalloped) size.

Cathepsin K inhibitors produce direct antiresorptive effects on osteoclast function. Cathepsin K, an intracellular enzyme that digests type I collagen, is highly expressed in osteoclasts as a means of degrading demineralized bone matrix. Bone resorption is reduced to a similar degree as with bisphosphonates, but bone formation is enhanced because osteoclast crosstalk to osteoblasts remains intact. Retained primary spongiosa and increased trabecular bone are morphologic features of bones from cathepsin-K deficient mice. Conversely, Wnt inhibition decreases ossification, resulting in reduced trabecular bone formation in the metaphysis of growing animals.

Enhanced Osteoclast Recruitment/Function The classic toxicologic example of increased osteoclast function is represented by continuous exposure to PTH or PTHrP. Bone turnover is markedly increased, especially with continuous PTH exposure, and can occur in inappropriate locations such as directly beneath the osteoid seam or in the middle of the trabecula (so-called "tunneling resorption," Figure 23.23). Misplaced bone removal results in trabecular splitting and a paradoxical increase in trabecular connectivity in the face of decreased trabecular bone volume by this ultimately catabolic process.

TOXIC EFFECTS ON OSTEOBLASTS

Decreased Osteoblast Formation/Function At high doses, first generation bisphosphonate compounds, including etidronate and clodronate, impair osteoblast function as well as osteoclast function, resulting in extremely low or effectively no bone turnover. Osteoid area and volume are augmented (increased osteoid), indicating a mineralization defect. Administration of such agents to young but skeletally mature dogs has been demonstrated to alter the structural integrity of the ribs and vertebral processes, leading to multiple spontaneous fractures. Increased signaling by peroxisome proliferator-activated receptor gamma (PPAR-γ) produced either directly by PPAR-γ agonists or indirectly by modulators of PPAR-γ activity (e.g., FGF-21 in mice) can have profound influence on the differentiation of mesenchymal bone marrow stem cells. Such increases may divert these stem cells toward adipocyte differentiation and away from osteoblast differentiation. Increased adiposity of bone marrow with reduced bone formation occurs as a result of this shift. The resulting decreases in trabecular and cortical bone volume in the mouse can be dramatic.

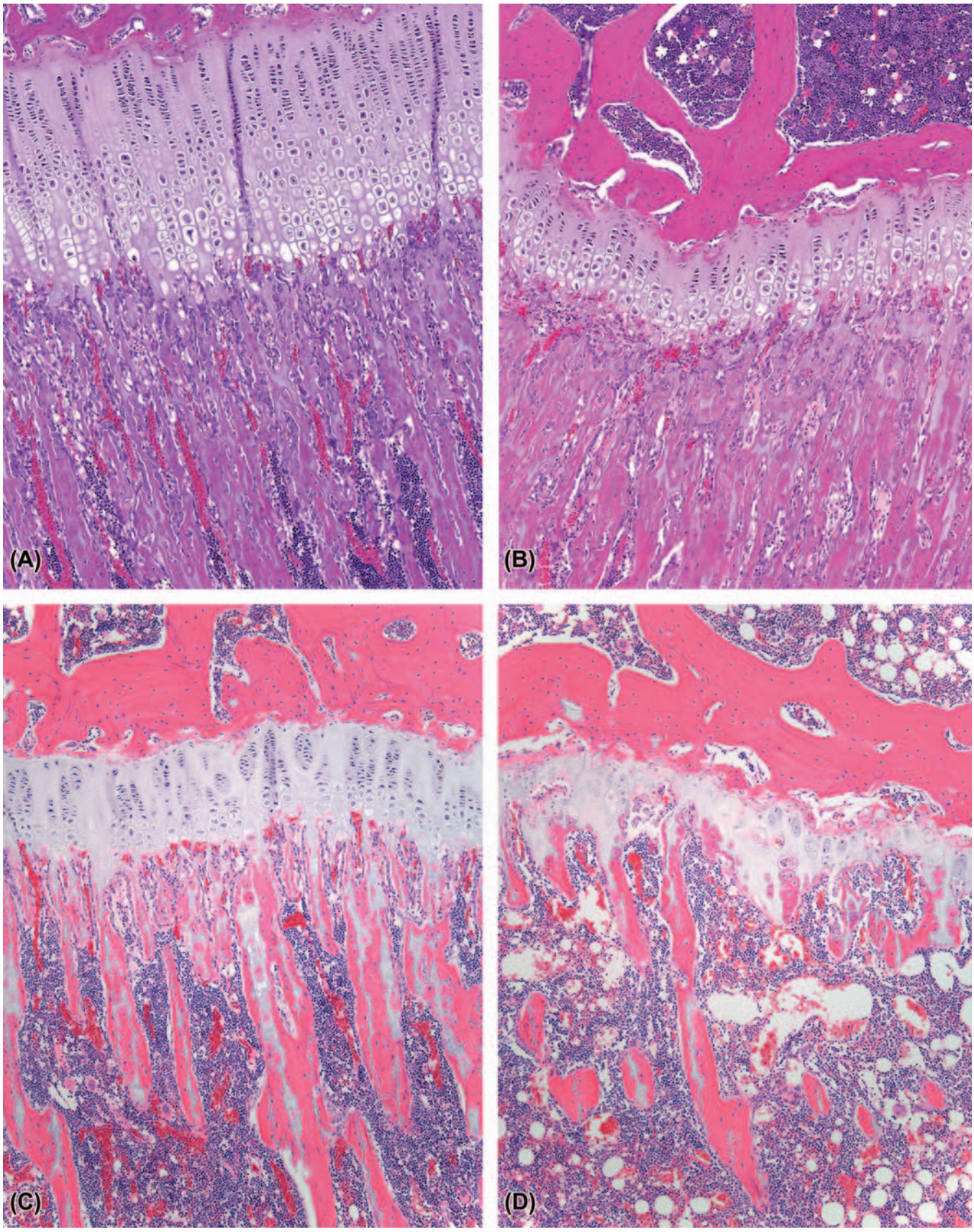

FIGURE 23.22 Physeal dystrophy induced by treating rats with a smoothened hedgehog (SHH) inhibitor for 1 week (B) or 2 weeks (D) leads to marked thinning of the physeal cartilage and reduced (B) or missing (D) primary spongiosa formation and disrupted production of metaphyseal trabeculae (D) compared to control animals (A and C). H&E stain. Published previously as Figure 63.42 in D. Gunson et al., Bone and joints, in: *Handbook of Toxicologic Pathology*, third ed. (W.M., Haschek, C.G. Rousseaux, and M.A. Wallig, eds), Academic Press, San Diego; volume 3, p. 2840, with permission.

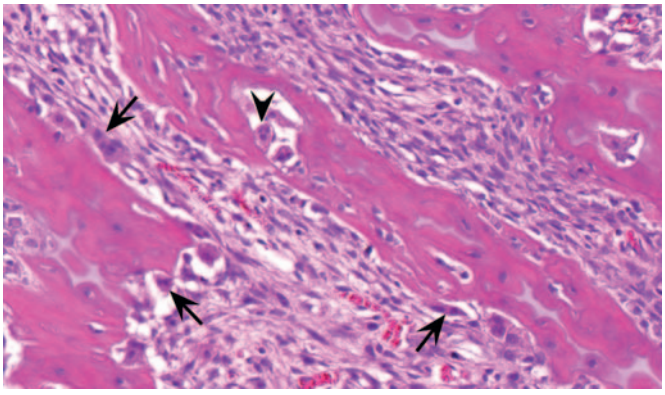

FIGURE 23.23 Rat proximal tibia demonstrating trabecular bone with abundant osteoclast-mediated resorptive activity following continuous exposure to parathyroid hormone (PTH). Many osteoclasts are located in lacunae on trabecular surfaces (arrows) which are normal locations, but other osteoclasts (arrowhead) are present in lacunae within the trabecular bone (i.e., tunneling resorption). Note increased fibrosis in the marrow space. H&E stain. Published previously as Figure 63.45 in D. Gunson et al., Bone and joints, in: *Handbook of Toxicologic Pathology, third ed*. (W.M., Haschek, C.G. Rousseaux, and M.A. Wallig, eds), Academic Press, San Diego; volume 3, p. 2844, with permission.

As noted above, many inhibitors of chondrocyte proliferation, such as glucocorticoids, also inhibit osteoblast function. If these inhibitors have a relatively short half-life compared to the dosing interval (i.e., a pulsatile exposure regimen), variation in the thickness of the secondary spongiosa may occur with sharply linear transverse bands (Harris growth arrest lines) in the proximal metaphysis of a growing animal (Figure 23.12). With respect to homeostatic bone remodeling, the decreased bone formation leads to a net bone loss since the steady state of bone resorption followed by equivalent bone formation is no longer in balance.

Increased cortical porosity and decreased trabecular bone volume are typical findings with bone loss due to glucocorticoids, which can progress to osteoporosis if exposure is chronic. These effects result from the ability of steroids of this class to impair osteoblast activity.

Increased Osteoblast Formation/Function Intermittent exposure to PTH or its analogs increases bone formation by increasing osteoblast numbers. The outcome occurs in part due to inhibition of the Wnt antagonist sclerostin. Marrow fibrosis is another classic feature of continuous PTH exposure, and there is evidence that the cells responsible for this response are collagen-producing mesenchymal stem cells that are destined to become preosteoblasts.

Treatment with anti-DKK antibodies removes Wnt inhibition to osteoblast differentiation. In growing bone, the combination of reduced osteoclast formation (see above) and increased osteoblast numbers by inhibition of DKK-1 results in a metaphysis with greatly increased amounts of trabecular bone and a decreased marrow space resembling the appearance and structure of osteopetrotic bone. Treatment with Wnt inhibitors in animals with actively growing bones leads to a decrease in ossification beneath the growth plate, with a reduction in bony trabeculae within the metaphysis.

Aberrant Bone Production Anticancer pharmaceuticals often have profound effects on bone marrow, with rapid production of woven bone appearing in the bone marrow space secondary to primary deleterious effects on hematopoietic progenitor cells. This new bone is typically noted in the middle of a segment of sternum, or in the deeper metaphysis. The mechanism for this response is thought to be stimulation from local growth factors upregulated in response to myelotoxicity. This woven bone rapidly resolves after cessation of treatment. Aberrant woven bone has also been reported in periosteal, endocortical, and trabecular bone regions in dogs and rats treated with PGE_2. This molecule induces osteoblast differentiation via activation of the prostanoid EP4 receptor. A similar change is observed in trabecular bone of dogs treated with toxic doses of YM175, a bisphosphonate.

A well-known cause of abnormal bone formation is lathyrism in rats fed sweet pea (*Lathyrus odoratus*) or treated with its toxic agent, beta-aminopriopionitrile. This toxin inhibits lysyl oxidase, the enzyme responsible for the hydroxylation of lysine, the normal precursor to crosslinking of elastin and type I collagen fibrils. Reduced fibril crosslinking in connective tissue leads to an abnormal bone matrix and decreased bone growth and strength. Copper is a cofactor for lysyl oxidase, so copper deficiency can also depress lysyl oxidase activity. Pronounced periosteal bone proliferation (increased bone) at the tendon insertion sites of the adductus longus and pectineus on the femur is a classic finding. Distortion of other long bones and spine also occur.

NEOPLASIA

Prolonged stimulation of osteoblasts by some PTH analogs has been shown to produce a spectrum of osseous neoplasms in rats. Lesion types include osteosarcoma (Figure 23.7), osteoma, and osteoblastoma.

Toxic Responses in Joints

Inflammation

The underlying biochemical mechanisms involved in immune-mediated and nonimmune articular reactions to drugs are similar, since the production of local factors in both situations can lead to chondromalacia

or degradation of articular cartilage. Systemic administration of small molecular weight peptidoglycans (typically of bacterial origin for animal arthritis models) can induce acute polyarthritis by a nonimmune-mediated process, an inflammatory response thought to be mediated by mast cell degranulation. Development of immune-mediated arthritis with exposure to peptidoglycans or other antigens requires that the antigenic material be deposited in the joint and the development of delayed hypersensitivity. Nonimmunoglobulin, T cell-derived molecules (e.g., lymphokines) that bind specifically to antigens are the effector molecules. One such protein, albeit incompletely characterized, has been designated "arthritogenic factor" because of its ability to sustain proliferative synovitis when instilled into the joint cavity. The joint lesion that develops following a single injection of arthritogenic factor persists for at least 4 weeks and does not require complement.

The chronicity of antigen-induced arthritis depends on the persistence of a sufficient amount of antigen in the affected joint. Antigen retention is mediated by antibody-dependent trapping. The electronic charge of the antigen also appears to determine the development of arthritis because antigen penetration into cartilage matrix depends on both molecular weight and charge. Immune complexes trapped in collagenous tissues within joints provoke an inflammatory response; the pathologic role of sequestered antigen in maintenance of the chronic inflammatory response lies in long-lasting leakage of antigen into surrounding tissue. Immune complexes can be phagocytosed by macrophages or synovial cells, which then produce IL-1 to perpetuate the inflammation. Alternatively, complement that has leaked into the joint cavity across the inflamed synovium is activated by immune complexes. Production of C3a and C5a components is a further means of inducing IL-1 secretion.

Systemically delivered therapeutic agents that are immune-stimulant compounds have been known to cause destructive arthritis in conventional studies in laboratory animals. Immune stimulants have been designed for therapy of certain systemic diseases, and adjuvants are crafted for a similar purpose with vaccines, to increase the immune response. Such compounds may cause lymphoid hyperplasia with prominent increases in B cells in lymph nodes and other lymphoid organs as well as less prominent T-cell increases in lymph nodes and spleen. It is likely that cytokine production is increased, especially IL-1. Joint lesions produced by immune-stimulant agents (Figure 23.24), which affect mainly the tarsus, carpus, and phalanges, are similar to those seen in animal models of RA, such as AIA. Approximately 10–14 days after introduction of the adjuvant (depending on the adjuvant and antigen), rats develop swollen paws with skin discoloration. Microscopic examination reveals periosteal and synovial inflammation with fibrin deposition in synovial membranes, expansion of joint spaces due to fluid exudation (and sometimes neutrophil accumulation), periosteal new bone formation, and marked osteoclastic erosion with numerous, prominent Howship's lacunae. Visible erosion or loss of articular cartilage is limited to occasional joint surfaces adjacent to thickened synovium that was encroaching into the joint space (Figure 23.24), but the cartilage matrix of the remaining cartilage is degraded. Such synovium often contained inflammatory cells. Articular cartilage was intact and appeared normal in many joints with severe peri-articular reactions although matrix loss can be substantial in apparently normal cartilage in extensively inflamed joints. Cartilage loss would increase after a longer period of disease.

Other systemically delivered compounds cause joint swelling but with a more fibroplastic response. These include bleomycin, in which the fibroplasia is considered to develop because of activation of macrophages. The fibroplasia or "tendonitis" that develops during treatment with MMP inhibitors is thought to occur via blockade of tissue collagenases that play a role in the normal turnover of collagen in tendons, ligaments, and periarticular connective tissue. Rats treated with 6-sulfanilamidoindazole develop an acute exuberant synovitis and periarthritis with arteritis that can resolve in a few weeks. No concomitant changes in bone or cartilage have been demonstrated.

Degeneration

Degradative changes in articular cartilage leading to subchondral bone erosion are a feature of both inflammatory and degenerative joint disease (Figure 23.18). Loss of articular cartilage may result since normal matrix removal continues in the face of decreased synthesis. Lysosomal enzymes (collagenase, cathepsins, elastase, and arylsulfatase) are present in inflammatory, synovial, bone, and cartilage cells. Their release may cause degradation of proteoglycan (as in papain-induced or hypervitaminosis A-associated cartilage matrix degeneration). Free radicals like superoxide (O_2^-) or peroxide (H_2O_2) generated by local enzyme activity can depolymerize polysaccharides and degrade synovial fluid and cartilage. Synovial lining cells from rats with AIA generate H_2O_2 constitutively, whereas cells from corresponding areas of control rats do not.

The cartilage catabolic process also involves aggrecanase or neutral metalloproteases, which act on connective tissue macromolecules (collagenases, proteoglycanases). These enzymes are produced by synoviocytes and chondrocytes. Their secretion into the joint is induced by peptidic factors released from cells of the immune system.

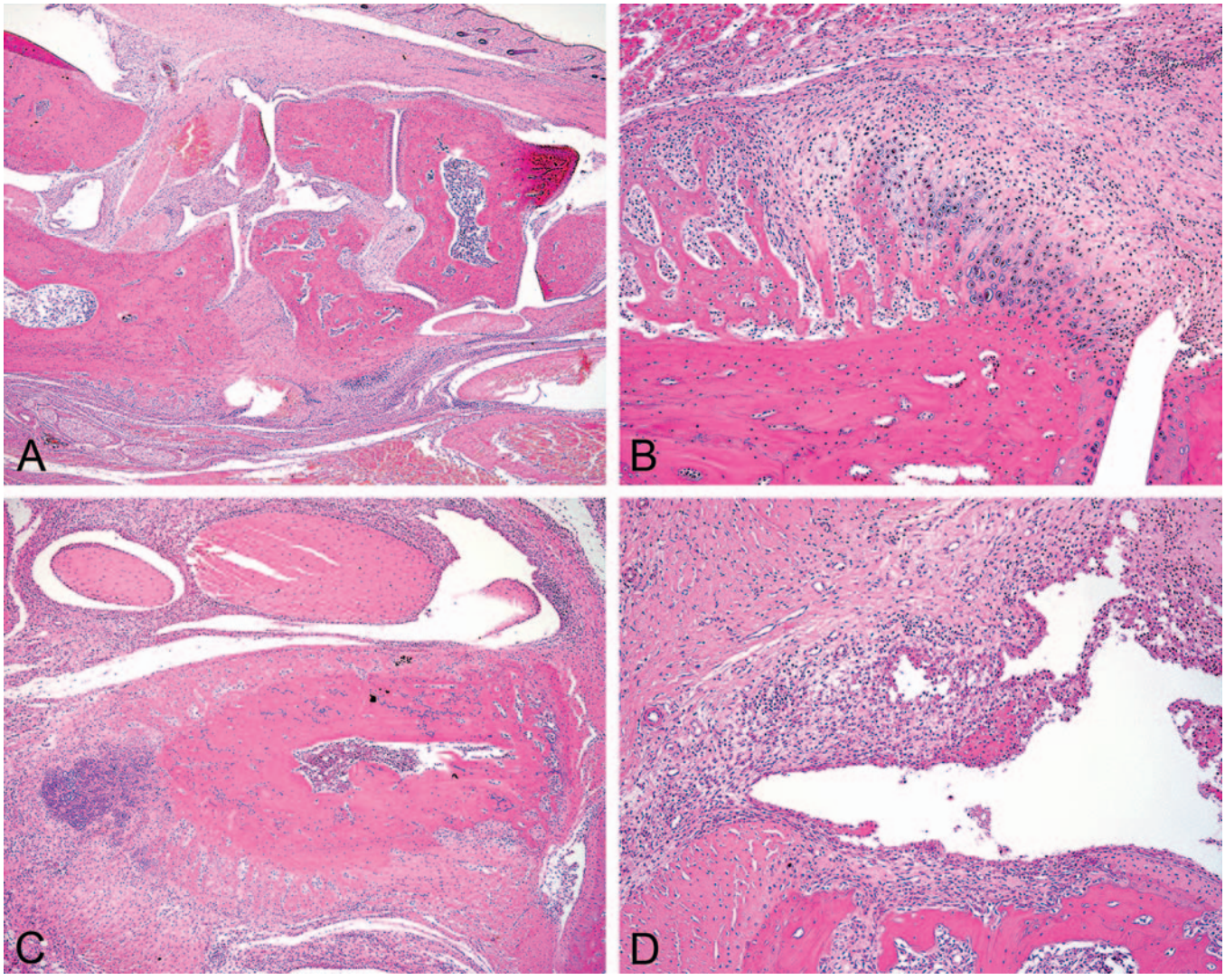

FIGURE 23.24 Immune-mediated arthritis in the tibiotarsal region (hock or "ankle") of a rat after administration of an immunostimulatory compound in a preclinical safety study. (A) Marked thickening and proliferation of synovial membranes. (B) Periosteal periarticular new bone and cartilage formation. (C) Cartilage proliferation on the periosteal surfaces of tarsal bone. (D) True arthritis is characterized by severe inflammation with fibrin deposition in synovial membranes and peri-articular tissues as well as expansion of joint spaces due to fluid exudation. Granulation tissue (pannus) is present within synovial membranes. Periarticular bone is lost due to osteoclast activity and partial loss of the articular cartilage adjacent to affected synovial membrane. All panels, H&E stain. Published previously as Figure 63.46 in D. Gunson et al., Bone and joints, in: *Handbook of Toxicologic Pathology, third ed*. (W.M., Haschek, C.G. Rousseaux, and M.A. Wallig, eds), Academic Press, San Diego; volume 3, p. 2846, with permission.

Among these mediators, IL-1 plays an important role. Since IL-1 is also produced by activated synovial cells, a sustained inflammatory condition does not seem to be necessary for it to be secreted in considerable quantities over an extended period. Degradation of articular cartilage does not necessarily require an exogenous source of enzymes arising from synovial cells or from neutrophils within synovial fluid. Neutral metalloproteases can be released from chondrocytes themselves as latent enzymes requiring activation, probably by serine proteases such as plasminogen activator. IL-1 induces the synthesis of cartilage neutral metalloproteases, stimulates the production of plasminogen activator, and promotes the destruction of cartilage matrix macromolecules. Tissue inhibitors of metalloproteases (TIMPs) are expressed constitutively in cartilage to prevent overactivity of the proteases. Catabolic states within cartilage are characterized by inactivation of TIMPs, resulting in activation of metalloproteases.

Cartilage Necrosis

In the case of drug toxicities, as seen with the quinolone class of antibiotics, the distribution of necrotic chondrocytes in articular cartilage is unique. Necrosis

usually occurs only in animals in which the articular cartilage is still in the process of growth, and begins in the zona intermedia (transitional zone) of the articular cartilage. Necrosis of chondrocytes and subsequent matrix lysis produces a cleft seen grossly as a blister on the articular surface. This bleb quickly ruptures. Tendon ruptures have been associated with fluoroquinolones, which is thought to result from their cytotoxicity (demonstrated *in vitro*) to tenocytes.

Fibroplasia

Rats treated with marimastat and other potent MMP inhibitors, delivered continuously in subcutaneous pumps, develop swollen paws, often with reddening, within 2–3 weeks. Histologically there is fibroplasia, often accompanied by inflammation, in the subcutis, synovium, joint capsules, ligaments, tendons, tendon sheaths and peri-articular skeletal muscles.

The most sensitive site for developing fibroplastic change is the tarsus, followed by the patellar attachment to the quadriceps tendon and the carpal ligaments. Severely affected animals also have fibroplasia in the carpus, and often in the digits of both fore- and hindpaws. Fibroplasia in the joint capsule often extends into the joint space and is associated with substantial angiogenesis, forming "pannus." Occasional foci of cartilage metaplasia and frequently new bone formation also are evident, either at the periosteal surfaces or within the new fibrous tissue. Bone resorption associated with abundant osteoclasts is sometimes present in the cortex of the metatarsals, tibia, and other bones. Inflammation, predominantly lymphocytic, is often present in the proximal part of the gastrocnemius muscle and the distal part of the quadriceps.

SUMMARY

Test articles vary widely in the time needed (weeks to months) to produce an effect on bone and cartilage. The physis and the metaphysis are the most metabolically active sites, and examination of these domains in a fast-growing bone of young animals will give the greatest opportunity to detect xenobiotic-related toxic effects. Many chemical agents affect the skeletal system indirectly via their actions in mediating cell differentiation or modulating cell function. Therefore, skeletal effects may be reflected in the rates at which bone cells function. Evaluation of routine formalin-fixed, decalcified, H&E-stained sections is a suitable first-tier screen for skeletal toxicity, but mechanistic information and a deeper understanding of the pathogenesis often requires such special second-tier techniwues as assessment of bone biomarkers, bone density, bone biomechanical properties, and bone histomorphometry to uncover mechanisms by which skeletal alterations have occurred. Animal models, either naturally occurring or created as a result of genetic, surgical, and/or mechanical manipulation, are useful in assessing the efficacy or toxicity of potential therapeutic agents. Understanding the utility and limitations of each model with respect to predicting human responses is vital to interpretation of the data generated.

Further Reading

Aigner, T. (Ed.), 2010. Osteoarthritis and cartilage histopathology supplement. Osteoarthritis Cart. 18 (Supplement 3), S1–S122.

Baron, R., Kneissel, M., 2013. WNT signaling in bone homeostasis and disease: from human mutations to treatments. Nat. Med. 19, 179–192.

Bilezikian, J.P., Raisz, L.G., Rodan, G.A. (Eds.), 2002. Principles of Bone Biology. Academic Press Inc, San Diego.

Craig, L.E., Dittmer, K.E., Thompson, K.G., 2016. Bones and joints. In: Maxie, M.G. (Ed.), Jubb, Kennedy, and Palmer's Pathology of Domestic Animals, sixth ed Elsevier, St Louis, pp. 17–163.

Eriksen, E.F., 2010. Cellular mechanisms of bone remodeling. Rev. Endocr. Metab. Disord. 11, 219–227.

Fossey, S., Vahle, J., Long, P., et al., 2016. Nonproliferative and proliferative lesions of the rat and mouse skeletal tissues (bones, joints, and teeth). J. Toxicol. Pathol. 29 (3 Suppl), 49S–103S.

Frost, H.M., 1987. Bone mass and the mechanostat, a proposal. Anat. Rec. (1906–2002). 219, 1–9.

Greaves, P., 2012. Musculoskeletal system. Histopathology of Preclinical Toxicity Studies. Elsevier, Amsterdam, pp. 157–206.

Gunson, D., Gropp, K.E., Varela, A., 2013. Bones and joints. In: Haschek, W.M., Rousseaux, C.G., Wallig, M.A., et al., Haschek and Rousseaux's Handbook of Toxicologic Pathology, third ed Elsevier, Amsterdam, pp. 2761–2858.

Gunson, D.E., Carlson, C.S., Gropp, K.E. (Eds.), 2015. Special focus: pathology of bones and joints. Vet. Pathol. 52 (5), 766–984.

Kronenberg, H.M., 2003. Developmental regulation of the growth plate. Nature. 423, 332–336.

McInnes, E.F., 2012. Background lesions in laboratory animals. A Color Atlas. Elsevier, Edinburgh.

Rosen, C. (Ed.), 2013. Primer on the Metabolic Bone Diseases and Disorders of Mineral Metabolism. eighth ed Wiley-Blackwell, Ames.

Seibel, M.J., 2005. Biochemical markers of bone turnover Part I: biochemistry and variability. Clin. Biochem. Rev. (NY). 26, 97–122.

Vahle, J.L., Leininger, J.R., Long, P.H., et al., 2013. Bones, muscle and tooth. In: Sahota, P.S., Popp, J.A., Hardisty, J.F., et al., Toxicologic Pathology: Non-clinical Safety Assessment. CRC Press, Boca Raton, pp. 561–588.

CHAPTER

24

The Integumentary System

Kelly L. Diegel[1], *Dimitry M. Danilenko*[2], *and Zbigniew W. Wojcinski*[3]

[1]GlaxoSmithKline Research & Development, King of Prussia, PA, United States [2]Genentech, South San Francisco, CA, United States [3]Drug Development Preclinical Services, LLC, Ann Arbor, MI, United States

OUTLINE

INTRODUCTION

The integument is one of the most dynamic and important of organs. Having a unique role as a first line defense against numerous environmental insults [e.g., physical trauma, temperature fluctuations, infectious and chemical agents, ultraviolet (UV) radiation], the health of the skin impacts and reflects the health of the organism. Beyond barrier function, the skin is also important as a neurosensory organ, acts as an endocrine organ, is an essential component of the immune system, aids in locomotion, and has essential psychologic/behavioral functions in many species. In toxicologic pathology, the skin may represent a target organ for those compounds that make direct contact with it, but it also may reflect changes in other internal organs (e.g., jaundice), serving as an external reflection of various internal pathophysiologic conditions.

STRUCTURE AND FUNCTION

The structure of the integument of any given species is as unique as the species itself, reflecting the adaptive nature of an organ that very much reflects and reacts to the environment to which it is exposed. It is beyond the scope of this chapter to give details of the integument for all creatures furred, feathered, haired,

Fundamentals of Toxicologic Pathology.
DOI: http://dx.doi.org/10.1016/B978-0-12-809841-7.00025-3

TABLE 24.1 Comparison of Features of Skin From Major Laboratory Animal Species and the Human

Species	Hair follicles per cm^2	Full-thickness skin (μM)	Epidermal thickness (μM)	SC thickness (μM)	Permeability of water $\times 10^{-3}$ cm/h	Permeability of 7-OHC $\times 10^{-3}$ cm/h
Beagle dog	96	2477	16.7	5.0	1.54	0.15
Hamster	402	619	13.8	2.9	1.63	0.45
Guinea pig	498	1438	58.9	22.1	4.73	1.17
Rabbit	229	2311	10.7	2.5	9.7	3.4
Sprague–Dawley rat	342	1242	14.7	4.3	6.6	6.2
Monkey	9	1529	59.9	9.9	3.52	5.13
Piglet	17	1335	36.9	3.5	2.2	0.37
Human	11	3306	49.5	18.4	1.56	1.34

From Haschek, W.M., Rousseaux, C.G., Wallig, M.A. (Eds.), 2013. Haschek and Rousseaux's Handbook of Toxicologic Pathology, third ed. Academic Press (Elsevier), San Diego, CA, Table 55.1, p. 2220, with permission.

horned, scaled, or spined. The following review focuses instead on the essential elements of the skin common to animal models used in toxicity studies and humans: the epidermis, dermis, subcutis, and adnexa.

Although there are aspects of the morphology of the integument that are unique to a given species, there are several generalizations that hold true in comparative dermatology. In general, the thicker the hair coat, the thinner the skin. Since hair is in part protective, the need for a thick epidermis in furred animals is not as great as it is in sparsely haired animals like pigs and humans. The latter tend to have compensatory thick epidermal layers for additional protection in the absence of thick fur. The hair follicle density of the rat is more than 30 times that of the human, while the epidermis of the rat is less than ¼ the thickness of human epidermis. It also follows that a thicker epidermis needs a thicker dermis for support. As epidermal thickness increases, so too increases the dermal contribution to overall skin thickness (Table 24.1).

Another generality is that the thicker the epidermis, the more vascular the upper (papillary) dermis. Essentially, increased vasculature becomes necessary to provide nutrients and flush waste products from thicker overlying avascular epidermal layers. Human skin is a good example, having a rich superficial vascular plexus in the papillary dermis. Of course, having a rich vascular network present superficially also leads to an increased potential for systemic exposure to any material, xenobiotic or other, that can cross through the epidermis into the dermis. A thin epidermis may also increase the risk of systemic exposure to exogenous substances on the skin. However, the thicker hair coat and less vascularized dermis of species with thinner epidermal layers are as such somewhat protective against absorption of chemicals through the skin.

The Epidermis

The epidermis is the outermost layer of the skin, providing the majority of protective barrier function to the body. Morphologically, it is divided into layers named for positional and microscopic/submicroscopic features of cells in each layer: the *stratum basale* (SB), *stratum spinosum* (SS), *stratum granulosum* (SG), *stratum lucidum* (SL), and *stratum corneum* (SC) (Figure 24.1).

Desmosomes adjoining neighboring cells of the SS give rise to artifactual spine-like formations between cells in fixed tissues giving the layer its name. In the SS, synthesis of a number of proteins important to the differentiating keratinocyte begins, including involucrin, profilaggrin, and filaggrin.

Also in the SG, and in the most superficial part of the SS, are lamellar bodies, organelles best classified as secretory lysosomes that contain a number of important substances: lipids that are released to form the lipid portion of the intercellular "mortar" of the corneocyte "bricks" of the SC; hydrolytic enzymes including acid proteases that aid in the process of desquamation; and proteins, for example, defensins, that contribute to barrier defense against pathogens. As the contents of the lamellar bodies are extruded and the nucleus and organelles of the keratinocyte are lost, the corneocyte is formed.

The intricate process of cornification requires complex cell–cell communication and adhesion. The cytoskeleton of the epidermal keratinocyte has complex networks of proteins that include microtubules, actin filaments, and intermediate filaments (i.e., keratin). Synthesis of keratin in any of its forms is an almost exclusive characteristic of epithelial cells.

Desmosomes are formed largely from desmogleins and desmocollins and represent the primary means of cell–cell adhesion in nucleated epidermal layers. Tight

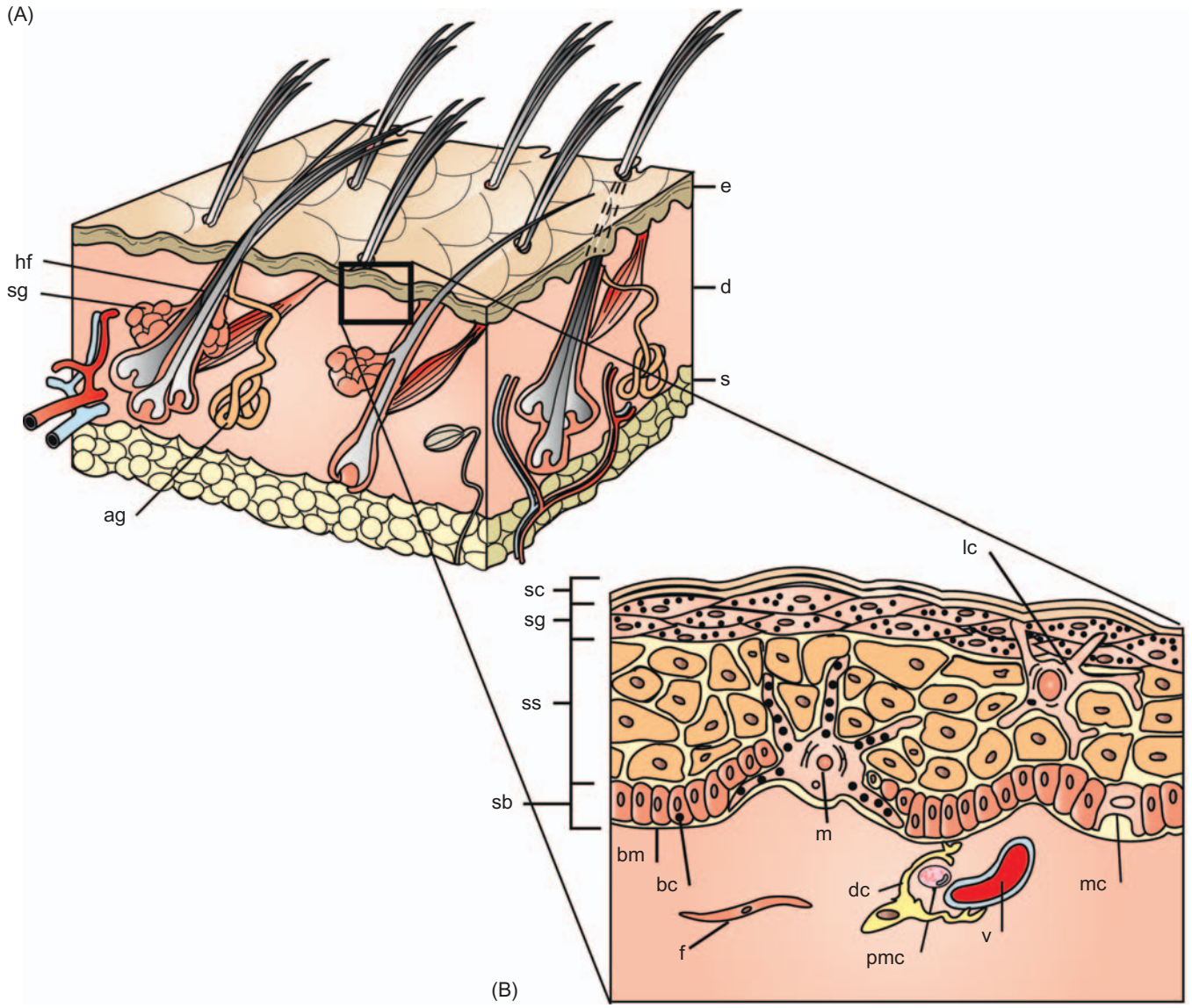

FIGURE 24.1 Microanatomy of the skin: (A) Primary structures include the epidermis (e), dermis (d), subcutis (s), hair follicles (hf), sebaceous glands, (sg), and apocrine glands (ag). (B) Cellular components of the epidermis and dermis. Layers of the epidermis include the *stratum corneum* (sc), *stratum granulosum* (sg), *stratum spinosum* (ss), and *stratum basale* (sb) consisting of basal cells (bc) adherent to the basement membrane (bm). Cells of the epidermis are keratinocytes, Langerhans' cells (lc), Merkel cells (mc), and melanocytes (m). In the dermis, fibroblasts (f), dermal vessels (v), perivascular mast cells (pmc), and dendritic cells (dendrocytes, dc) are pictured. Source*: From Hargis, A.M., Ginn, P.E., 2012. Chapter 17: The integument. In: Zachary, J.F., McGavin, M.D. (Eds.), Pathologic Basis of Veterinary Disease, fifth ed. Mosby Elsevier, St. Louis, MO, Figure 17.3, p. 974, with permission.*

junctions form between neighboring keratinocytes to regulate molecular movement between cells and maintain basolateral cell positioning. Adherens junctions contribute to cell motility and shape via links to internal cytoskeletal components such as actin. Important components of these structures in the keratinocyte include the transmembrane link, E-cadherin, and the intracellular actin-binding α-catenin. Gap junctions are formed from aggregation of connexins into connexons that join adjacent cells to allow intercellular transport of ions and other small molecules.

The keratinocyte life cycle as described earlier ranges from 5 to 30 days, depending on the anatomic site and state of health of the skin. A few specialized cell types present in the skin deserve special mention with respect to function of the skin as an organ.

Melanocytes

The melanocyte provides pigmentation to the skin or fur necessary for behavioral aspects of survival such as camouflage in certain species. Furred species

typically have reduced or absent epidermal melanogenesis (the process of melanin production), instead relying on the hair coat for pigmentation and UV absorption. Sparsely haired species like humans rely on largely on epidermal melanogenesis for protection from UV damage to the skin. In addition to their presence in the epidermis, melanocytes are also found in the eye, cochlea of the ear, the brain/meninges, and the heart. Melanin in melanocytes provides a means by which the skin can defend against the potential genotoxic effects of harmful UV radiation (UVR). Melanin can also bind certain potentially harmful compounds such as cations and metals.

Melanocytes are actively phagocytic, dendritic cells (DCs) derived from the neural crest, and generate pigment in membrane-bound melanosomes. Each melanocyte "serves" about 30–40 keratinocytes in the basal layers of the epidermis. Melanosomes are organelles derived from the endoplasmic reticulum of melanocytes and serve as packages for transfer of melanin. Although the number of melanocytes remains constant, the production and transfer of melanosomes to keratinocytes can be up- or downregulated. Melanosomes form a cap overlying the nucleus of the recipient keratinocyte, protecting the nuclear DNA from harmful UVR.

Merkel Cells

Arranged along the base of the epidermis and outer hair follicle, Merkel cells are DCs thought to be of epidermal stem cell origin. They represent a cell type unique to the skin and oral mucosa, capable of acting as mechanoreceptors with dense granules containing neurotransmitter-like mediators. They also contain cytokeratins, providing evidence for an epithelial origin. These cells form complexes with somatosensory nerve fibers. The dendrites of the Merkel cells contact unmyelinated axons in the epidermis, where they function together as a unit (tylotrich pads) to signal adnexal secretions (sweat), changes in blood flow, tactile sensation, and possibly serve in a paracrine function along with other cells of the skin.

Langerhans Cells and Dermal Dendritic Cells

Langerhans cells (LCs) and dermal dendritic cells (DDCs) are bone marrow monocyte-lineage–derived cells that are key components of adaptive and innate immune defense in the epidermis and dermis, respectively. LCs are the primary epidermal DC populations, and are spaced regularly throughout the suprabasilar epidermal layers, adherent to keratinocytes through desmosomal and tight junction attachments. They represent 1%–3% of total epidermal cell count, varying dependent upon anatomic location. In healthy skin, these cells are relatively inactive and even act to attenuate inflammatory response. They are able to preferentially respond to specific or severe foreign antigens, thereby preventing continual upregulation of inflammatory mediators whenever foreign antigens are sensed, which is nearly constant in the skin.

LCs interact with other DC populations in the skin, some of which are still being characterized. DDCs are also important in cutaneous innate and adaptive immunity. The combined efforts of LCs and DDCs in the skin result in immune defense responses unique to the skin; more detailed information on the role of LCs, DDCs, and other cutaneous DC populations in cutaneous immunity and response to injury is presented in the "Response to Injury" section.

The Dermal–Epidermal Junction and Dermis

The dermal–epidermal junction (DEJ) aids in barrier function (both from and into epidermis), allows for firm attachment of epidermis to dermis, aligns cells of the epidermis, and serves as a base for reepithelialization in wound healing. The outermost DEJ is formed largely by basal keratinocyte plasma membranes and their attachments, hemidesmosomes (Figure 24.2). These link to the *lamina lucida*, the weakest zone of the DEJ. Elements of the *lamina lucida* are attached to the underlying *lamina densa*, a strong collagenous layer derived from collagens IV and V and cross-linking elements. Binding collagens to the dermis are anchoring fibrils (type VII collagen) of the *sublamina densa*, which attaches the DEJ to the dermis and contains a number of collagens, procollagens, and early elastic fiber components.

The dermis gives the skin tensile strength through collagen, contributes to movement by allowing stretch through elastic fibers, has immune regulatory capabilities, contains vascular and neurologic elements important for communication with the epidermis and environment, and forms the matrix for adnexa. The dermis largely determines the thickness of skin and is contiguous. Subregions of the dermis in humans are termed papillary and reticular. In species lacking epidermal rete ridges, these subregions are usually simply described as superficial and deep, respectively. The primary components of the dermis are collagens and elastins, conferring tensile strength, and proteoglycans, glycosaminoglycans, and hyaluronans, which help dissipate pressure forces.

Nerves in the skin are both sensory and motor. Many sensory free nerve endings interact with specialized corpuscular units (mechanoreceptors such as Merkel cells and Pacinian or Meissner's corpuscles, nocioceptors, thermoreceptors) responsible for

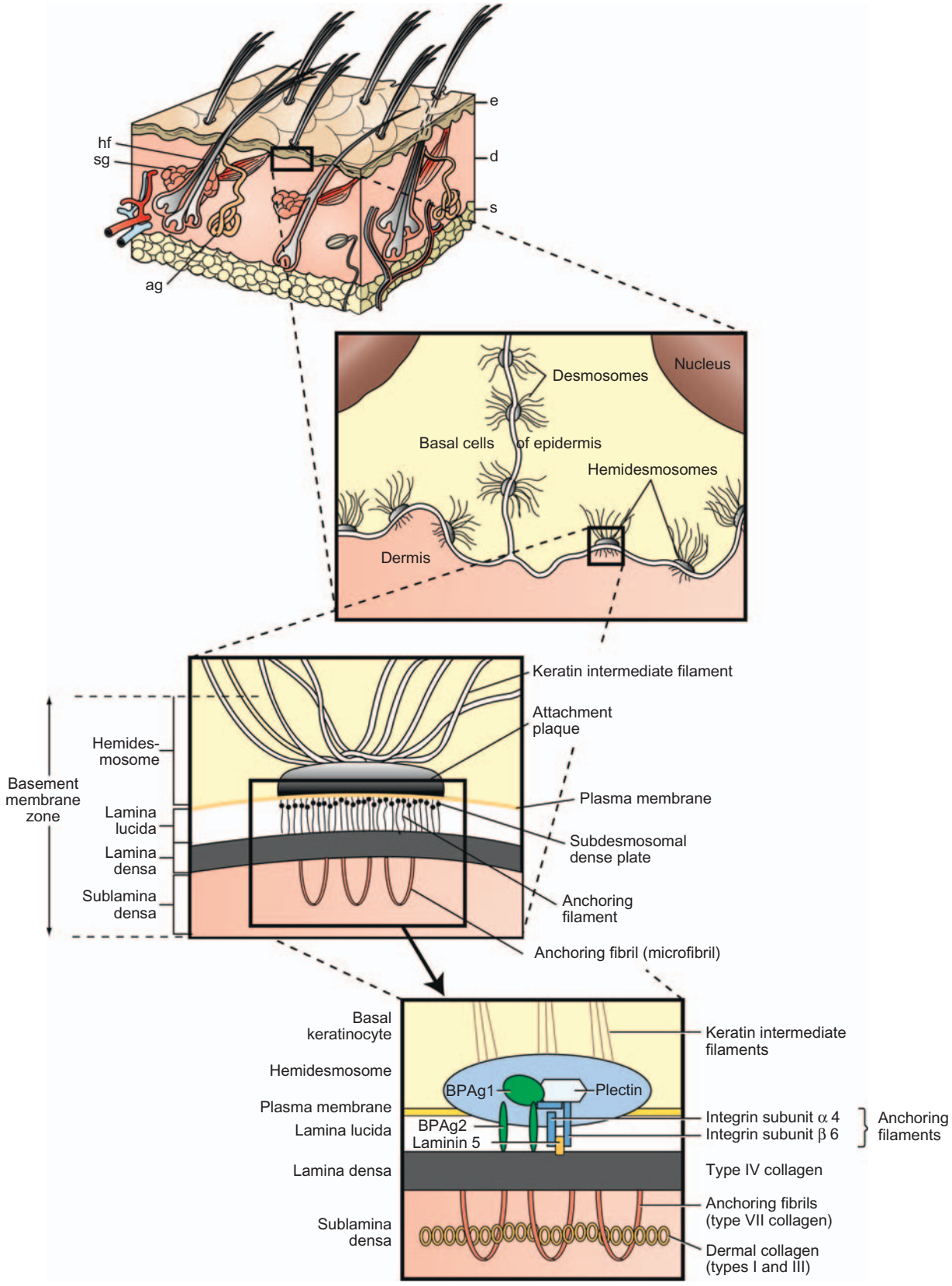

FIGURE 24.2 Detailed structure of the DEJ. Source: *From Hargis, A.M., Ginn, P.E., 2012. Chapter 17: The integument. In: Zachary, J.F., McGavin, M.D. (Eds.), Pathologic Basis of Veterinary Disease, fifth ed. Mosby Elsevier, St. Louis, MO, Figure 17.4, p. 975, with permission.*

pressure, sensing movement, itch/pain, and temperature. The hair follicles are also surrounded by sensory axons. Motor innervation is from sympathetic autonomic nerves and responds to either cholinergic or adrenergic stimuli. Adrenergic responses include vasoconstriction, apocrine gland secretion, and hair follicle positioning. Eccrine sweat glands are under cholinergic control; however, these glands are largely absent in most areas of nonhuman mammalian skin.

Dermal vasculature is rich and complex. Superficial, middle, and deep vasculature plexuses supply corresponding layers of the skin. Arteriovenous anastomoses are common in the skin of the extremities in particular, necessary for adaptation to frequent changes in temperature and blood pressure. These junctions respond to vasoconstrictors and vasodilators such as epinephrine and histamine. Many vessels of the skin have relatively thick walls compared to those of similar size in internal organs, a necessary adaptation for protection against the shear and pressure forces to which the skin is regularly subjected. Also present in the dermis are the fibroblast-like veil cells that define spaces for vessels within the dermis, surrounding microvasculature, and creating a perivascular space.

Cutaneous lymphatics arise as capillaries in the superficial dermis, but below the level of superficial blood capillaries. Gaps within the lymphatic vessels form channels by linking with the dermal matrix, directing excess interstitial fluids from the dermis into the lymphatic system. Lacking smooth muscle and pericytes, lymphatics of the dermis rely on subcutaneous muscle contraction, pressure of the surrounding matrix, and associated blood vessel movements to initiate flow of immunologic, waste, and even degraded pathogenic and xenobiotic materials away from the dermal interstitium. In the deeper subcutis, lymphatics have smooth muscle walls and are actively contractile directly directing flow of lymph to and from the skin.

The Subcutis

The subcutis is the adipose-rich tissue beneath the dermis responsible for attachment to underlying muscle, fascia, or periosteum. Connective tissue septa present throughout the subcutis facilitate movement and support dense vessel and nerve networks in the tissue. This layer also serves to absorb shock to underlying structures, shape the external features of the organism, and regulate temperature. The rich triglyceride stores of the subcutis can be utilized as an energy store and also serve to protect underlying tissues from temperature extremes. Visceral and subcutaneous adipose stores are also important in the secretion and targeting of various hormones and cytokines. In contrast to visceral adipose stores, it appears that the adipose tissue of the subcutis is better equipped for efficient lipolysis and less apt to secrete inflammatory cytokines, making it a compelling target for metabolic disease therapies.

The Adnexa

The cutaneous adnexal unit refers to a hair follicle, the associated *arrector pili* muscle, and associated glands. The hair follicle itself is essentially a down growth of the epidermis (Figure 24.3). The *arrector pili* muscle attaches to the hair follicle and has roles in piloerection and gland secretion that is under cholinergic control. The hair shaft is composed of an inner medulla, a surrounding cortex, and outer cuticle. The hair follicle has subanatomic regions known as the infundibulum (from the surface epidermis to the sebaceous gland duct entrance to the hair follicle), the isthmus (just below the infundibulum, from sebaceous duct to the *arrector pili* muscle insertion), and the inferior segment from the isthmus deep to the dermal papilla. The outer root sheath that contains the hair is contiguous with the surface epidermis.

The inner root sheath is attached to the cuticle of the hair and is distinguishable in tissue sections by the presence of eosinophilic cytoplasmic trichohyalin granules. The dermal papilla at the base of the follicle is a connective tissue-based appendage of the dermis itself that is covered by mitotically active epithelial cells that contribute to hair growth, the cells of the hair matrix. In humans and mice, a structure known as "the bulge" is present and attached to the outer root sheath, near the insertion of the *arrector pili* muscle. The bulge supplies the adnexal unit and, in some instances the surface epidermis (e.g., during wound healing), with pluripotent stem cells for regeneration. The bulge area may be absent in other species, with stem cells being present in infundibular and isthmus regions of the follicle itself, although some research does support bulge cell presence in the dog.

Hair growth is divided into the following stages: anagen (active growth), catagen (transition phase), telogen (resting stage), and exogen (shedding). During hair growth, an ordered array of keratinized cells is gradually pushed upward in the form of hair shafts. These cells give rise to hair by a process of terminal differentiation, analogous to, but more complicated than, the process described for epidermal cornification. Keratinization of hair follicle cells is of four morphologic subtypes: infundibular (like the surface epidermis, featuring keratohyalin), trichilemmal (important in identification of catagen hairs, with dense eosinophilic keratin "flames"), trichogenic/matrical ("ghost cell" keratinization), and medullary/inner root sheath (with deeply eosinophilic trichohyalin granules).

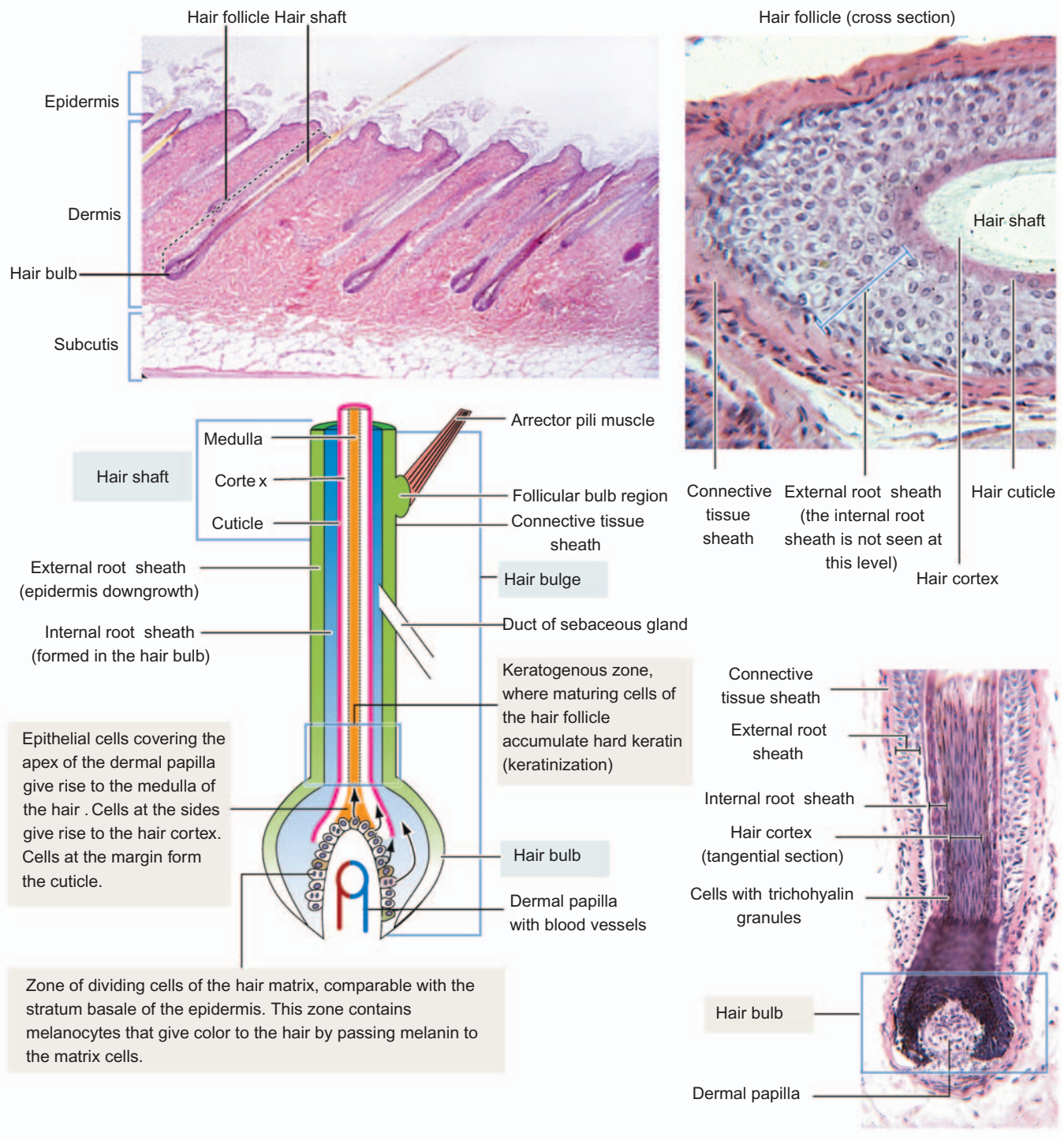

FIGURE 24.3 Detailed structural elements of the hair follicle. Source: *From Kierszenbaum, A.L., Tres, L.L., 2012. Histology and Cell Biology An Introduction to Pathology, third ed., Saunders Elsevier, Philadelphia, PA, Figure 11.15, p. 355, with permission.*

Two types of sweat glands, eccrine and apocrine, have been described in mammals. Eccrine glands participate in thermoregulation by secreting water and salts directly to the epidermal surface. Abundant throughout the skin in great apes and humans, in domestic and laboratory animals, the eccrine sweat glands are largely limited to the foot pads in dogs, and the nasal planum and carpus of pigs. These are merocrine glands composed of a long-coiled secretory tubule and a connecting long excretory duct that ends in the epidermis separate from the hair follicle; the epithelium lining both is simple columnar. The apocrine

glands, which generally empty into the hair follicle at the level of the sebaceous gland, secrete a proteinaceous material that originates from the loss of cytoplasmic blebs from the apices of the simple columnar glandular cells. Their function is not clear, but they are related to accessory scent glands (e.g., porcine mental organ, eyelid/external ear glands, glands of anal sac in dogs, etc.) that produce attractant odors in some species. While distributed generally over the skin of most species, apocrine glands in humans are limited to armpits, groin, and nipples. Mammary glands are also modified apocrine glands specialized to produce milk.

Sebaceous glands develop from the neck or infundibulum of hair follicles and are composed of large polyhedral lipid-laden cells that undergo holocrine secretion after they are sloughed into a short duct. They form sebum, comprised of wax esters, squalene, free fatty acids, and triglycerides. Sebum is discharged into the infundibulum of the hair follicles and spreads to the epidermal surface where it helps to keep the SC moist. It also has antimicrobial function associated with its free fatty acids. There are large sebaceous glands in some species (e.g., chin glands in cats, tail glands in dogs, etc.) that also likely have marking, tactile, or pheromonal roles. Male hamsters have large aural sebaceous glands, making the hamster a popular animal model for testing compounds targeting sebaceous gland activity (Figure 24.4).

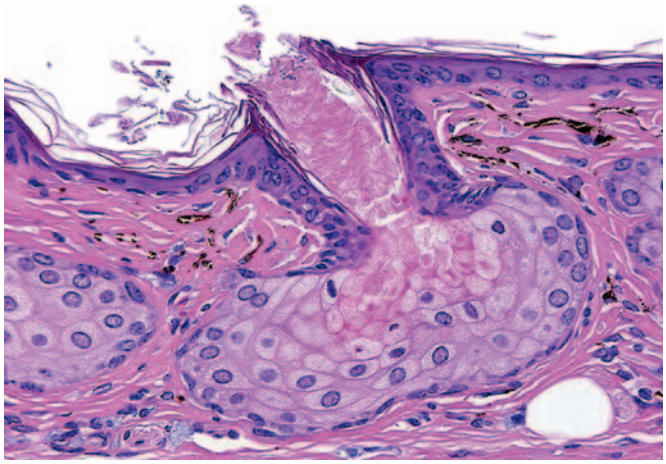

FIGURE 24.4 Sebaceous glands in the ear of a normal male hamster: the large size makes the hamster an attractive model for studies of sebaceous gland physiology/targeting. Source: *From Haschek, W. M., Rousseaux, C.G., Wallig, M.A. (Eds.), 2013. Haschek and Rousseaux's Handbook of Toxicologic Pathology, third ed. Academic Press (Elsevier), San Diego, CA, Figure 55.4, p. 2228, with permission.*

Evaluation of Toxicity

Physiologic and Morphologic Safety Evaluation Strategies and Techniques

Evaluation of cutaneous toxicity is essential for any therapeutic agents intended for use by topical administration. In addition, evaluation of potential adverse effects on the skin is necessary for therapeutic compounds that unintentionally come into contact with the skin (e.g., oral medications), exposure of skin from systemic exposure (i.e., distribution for systemically circulating drugs to the skin), and for nontherapeutic agents (i.e., cosmetics) that are applied to skin. Numerous global regulatory guidances (e.g., FDA, ICH, EMA) are available to provide guidance for the type of toxicity testing recommended for the different types of compounds under investigation. These guidances also extend to the various excipients used in preparation of formulations.

In vivo topical toxicity testing methods have focused on assessing skin irritation, cutaneous sensitization, ocular toxicity, and photosafety testing in various animal species and strains. The animal model selected and type of protocol used will depend on the objective of toxicity test. Unlike many other major organs, there are very distinct differences in skin structure among laboratory animal species and between these species and humans. Consequently, comparative evaluation of skin toxicity can be difficult to accomplish. The rabbit has been used for many years as the animal model of choice for evaluation of topical irritation potential. Although an extensive historical database exists for dermal irritation in the rabbit, this animal model has been shown to be more sensitive to primary irritants than human skin.

Most species used commonly in toxicity evaluations (mice, rabbits, rats, guinea pigs, dogs, and nonhuman primates) have relatively dense fur covering much of their bodies, and as such serve as poor comparators to human skin. The sparse hair covering of the laboratory minipig and the associated thicker epidermis most closely mimics the human skin, making it an attractive model in topical toxicity assessment (Figures 24.5 and 24.6).

The minipig has become the animal model of choice for assessing dermal irritation and tolerability of topical compounds on the basis of the greater similarity of morphologic and physiologic characteristics of pig skin to human skin. There are several breeds of laboratory minipig, but one of the most commonly utilized for regulatory toxicology is the Göttingen, based on its small size (about 45 kg as an adult). Similar to humans, the minipig has a papillary dermis with epidermal rete ridges. The cellular composition of the dermis and subcutis is also similar. Both humans and pigs have a relatively thick dermis with a large elastic fiber component. The dermis tightly adheres to the underlying subcutis and musculature, and the dermal and

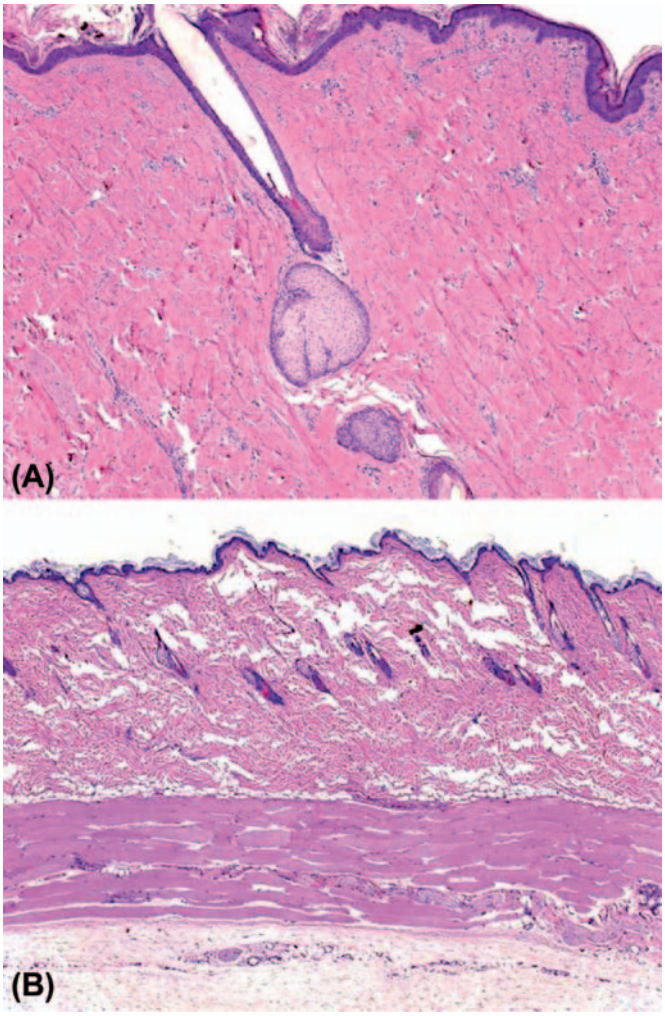

FIGURE 24.5 Comparative photomicrographs of minipig skin (A) and rat (B) skin, are taken at the same magnification. Note the difference in epidermal and dermal thickness, and adnexal distribution. Compare to Figure 24.6. Source: *From Haschek, W.M., Rousseaux, C.G., Wallig, M.A. (Eds.), 2013. Haschek and Rousseaux's Handbook of Toxicologic Pathology, third ed. Academic Press (Elsevier), San Diego, CA, Figure 55.5, p. 2229, with permission.*

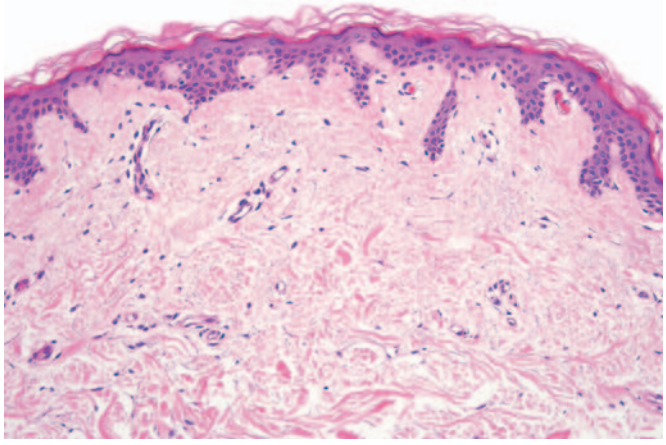

FIGURE 24.6 Normal human skin: Note similarities to minipig skin in Figure 24.5. Source: *Courtesy: Dr. Phillip McKee.*

subcutaneous vasculature and lymphatics are rich and similarly distributed. Also similar to humans, minipig skin thickens and has increased permeability with reduced effectiveness at wound healing with age. Enzymatic properties and drug metabolism in the epidermis and some adnexa also are comparable, as are lipid composition of the epidermis and sebum. Skin pH is slightly higher in the minipig (pH 6–7) compared to human (pH 5). There are even spontaneous models of human skin disease such as melanoma and bullous pemphigoid that exist in minipig strains (the Sinclair and Yucatan, respectively). Yet the thicker SC and increased subcutaneous fat deposition in minipigs are points of dissimilarity with humans. There are also some differences in the enzymatic profile of the skin, in the distribution of eccrine and apocrine sweat glands, and in regulation of exogen as well. Still the minipig appears to be the species best suited for comparative toxicology of the skin.

In addition, other porcine models, in particular the Duroc/Yorkshire model, are considered the best animal models for recreating human wounds. This is based on collagen structure, which is remarkably similar to humans.

However, for certain evaluations, traditional laboratory animal models are still important. For example, the guinea pig is the animal model of choice for assessing allergic contact dermatitis potential of chemicals.

The route of administration selected in assessing the safety of topically applied compounds will depend on the end point of the assessment. Similar to therapeutic agents intended for oral or parenteral administration, in vivo toxicity testing should be evaluated in both rodent and nonrodent species. The rat is the rodent species of choice for evaluation of potential systemic toxicity of topical compounds, whereas the minipig is recommended as the nonrodent species. For topical therapeutic agents, there is also an expectation from regulatory agencies to evaluate both topical toleration and potential adverse systemic effects. For compounds intended for topical application, there have been numerous initiatives to reduce animal use in topical toxicity testing.

Assessment of Cutaneous Irritation

Evaluation of the irritation potential of topically applied compounds has utilized animal models of skin irritation. The Draize scale technique has been commonly utilized for quantitatively determining the degree of irritation caused by topical application of compounds and for providing a quantitative measure of comparison and differentiation of the irritation potential of various compounds (e.g., minor irritants

TABLE 24.2 The Draize Scale—Grading Values for Skin Reactions Following Topical Application of Potential Irritants

Skin reaction	Value
ERYTHEMA AND ESCHAR (CRUST OR SCAB) FORMATION	
No erythema	0
Very slight erythema (barely perceptible)	1
Well-defined erythema	2
Moderate to severe erythema	3
Severe erythema to slight eschar formation	4
EDEMA FORMATION	
No edema (barely perceptible)	0
Very slight edema (raised edges of area well-defined)	1
Slight edema	2
Moderate edema	3
Severe edema (raised more than 1 mm and extending beyond the area of exposure)	4

Modified from National Academy of Sciences (1977). From Haschek, W.M., Rousseaux, C.G., Wallig, M.A. (Eds.), 2013. Haschek and Rousseaux's Handbook of Toxicologic Pathology, third ed. Academic Press (Elsevier), San Diego, CA, Table 55.2, p. 2233, with permission.

TABLE 24.3 Grading Scale in Human Skin Patch Test

Grade	Lesion
0	No response
0.5	Indistinct erythema
1	Well-defined erythema
2	Erythema and edema
3	Vesicles and/or papules
4	Bulla or other severe reaction

Modified from National Academy of Sciences, 1977. From Haschek, W.M., Rousseaux, C.G., Wallig, M.A. (Eds.), 2013. Haschek and Rousseaux's Handbook of Toxicologic Pathology, third ed. Academic Press (Elsevier), San Diego, CA, Table 55.3, p. 2234, with permission.

TABLE 24.4 Assessment of Phototoxic Potential Based on Photoirritancy Factor and Mean Photo Effect

Photoirritancy factor (PIF)	Mean photo effect	Phototoxic potential
<2	<0.1	Nonphototoxic
>2 and <5	>0.1 and <0.15	Probably phototoxic
>5	>0.15	Phototoxic

From Haschek, W.M., Rousseaux, C.G., Wallig, M.A. (Eds.), 2013. Haschek and Rousseaux's Handbook of Toxicologic Pathology, third ed. Academic Press (Elsevier), San Diego, CA, Table 55.4, p. 2234, with permission.

vs major irritants). This technique was adapted in the United States by the Code of Federal Regulations (CFR 1980) and is legislated under provisions of the Federal Hazardous Substances Act. The Draize scale evaluates the degree of redness (i.e., erythema), crust or scab formation (i.e., eschar), and edema (Table 24.2). Human skin irritancy assessment is often required to complement animal irritancy testing in order to more precisely understand human risk (Table 24.3).

Photosafety Testing

Chemicals or drugs that absorb light in the UVA (320–400 nm), UVB (290–320 nm), or the visible range (400–700 nm) are photoreactive. Photoactivation of a chemical may result in adverse effects termed photosensitivity reactions.

Photosafety testing is intended to identify agents with photosensitivity potential. Both in vitro and in vivo assays have been developed to assess the photosensitivity potential of photoreactive chemicals. Key considerations in the assessment of photosensitivity potential in these guidances are: photoirritation, photoallergenicity, photogenotoxicity, photocarcinogenicity, and photococarcinogenicity.

For photoreactive chemicals that absorb light in the UVA/visible light range, the 3T3 NRU assay is a validated in vitro assay for photoirritation potential (Table 24.4). Unfortunately, the 3T3 NRU assay will not work with strictly UVB absorbing chemicals, since UVB irradiation is cytotoxic to 3T3 cells and as such, requires in vivo testing. Human epidermis models (e.g., EpiDerm, EpiSkin, and SkinEthic) are being investigated as alternate in vitro models for utility in phototoxicity testing.

In vivo phototoxicity testing may be conducted in guinea pigs, rabbits, hairless mice, or hairless guinea pigs. In this assay, the application site on the test species is exposed to UV irradiation from a solar simulator. After a period of time to allow for absorption of the test article, the Draize scale is used to determine the phototoxic response by grading of irritation potential. In a review of concordance of toxicity of pharmaceuticals in humans and animals, phototoxicity response in guinea pigs correlated well with that in humans.

Photoallergenicity is typically evaluated in vivo in guinea pigs. The Buehler Guinea Pig Sensitization assay (with exposure to simulated light) is preferred over the Guinea Pig Maximization Assay, which although considered more sensitive than the Buehler assay, is associated with subcutaneous reactions attributed to the use of adjuvant in this assay. It should be noted that although European regulatory guidances

recommend conducting photoallergenicity testing, the FDA does not recommend this assay since convincing data do not support it.

Although photogenotoxicity testing was included in previous regulatory guidance recommendations, it is now generally accepted by regulatory agencies that photogenotoxicity testing not be conducted since there are too many false positives, even with compounds that are not photoreactive.

Photocarcinogenicity testing may be required for topical compounds that are used chronically, are phototoxic, and are topically applied or if there is indication for concern based on the class of compound. However, photocarcinogenicity testing may not be needed for compounds that are photoirritants if a warning is provided in patient information. Photococarcinogenic potential must also be taken into consideration for chemicals that may not be photoreactive but may influence carcinogenicity through immunosuppressive effects (e.g., cyclophosphamide) or altering the optical properties of the skin (e.g., certain emollients). SKH-1 hairless mice are used as models of UVR-induced carcinogenesis and develop skin tumors that are considered relevant to the study of human skin cancer.

RESPONSE TO INJURY

General Mechanisms of Response to Injury

The skin, like other organ systems, has a relatively stereotypic response to injury, regardless of the specific mechanism underlying the insult. Despite the limited range of response, there is still a great deal that can be ascertained from the different morphologic, physiologic, and molecular alterations that arise in response to injury.

One of the skin's primary functions is to serve as a physical and physiologic protective barrier against injury from the external environment and from loss of water and solutes from the body. When the skin is exposed to irritants, such as xenobiotics, infectious agents, or UVR, that may damage or disrupt this barrier, it mounts an inflammatory and proliferative response in order to prevent further damage and to restore a morphologically and physiologically functioning barrier.

This barrier disruption manifests in the form of both morphologic and physiologic alterations that will vary depending on the degree of barrier damage, and to some extent on the specific irritant, although most pathophysiologic responses are generalized and independent of the specific initiating factor(s). A core premise underlying the skin's response to injurious stimuli is that the epidermis, and particularly epidermal keratinocytes and DCs, including LCs, are central to the initiation of the skin's response to injury.

The hypothesis that the epidermal keratinocyte is a primary initiator of the skin's response to noxious stimuli has gained widespread acceptance. Epidermal keratinocytes can recognize pathogen-associated molecular patterns (PAMPs) of microbial origin, and danger-associated molecular patterns (DAMPs), such as xenobiotics and other irritants through Toll-like receptors (TLRs), including TLR-1, TLR-2, TLR-4, TLR-5, and TLR-6 on their surface and TLR-3 and TLR-9 in their endosome, that trigger an inflammatory cascade leading to the generation of antimicrobial peptides such as β-defensins, cathelicidins, and S100 family proteins, pro-inflammatory chemokines such as IL-8, CXCL9, CXCL10, CXCL11, CCL27, and CCL20, and pro-inflammatory cytokines such as IL-1β, TNF, IL-6, and IL-18.

These chemokines and cytokines recruit and activate leukocytes and convert the initial innate immune response to an adaptive immune response. In addition, keratinocytes express nucleotide-binding domain, leucine-rich repeat-containing (NLR) proteins that recognize cytoplasmic PAMPs, DAMPs, and UVR. When engaged, NLRs trigger a pro-inflammatory signaling pathway through a large multiprotein complex termed an inflammasome formed by an NLR, an adaptor protein termed ASC, and pro-caspase 1. Inflammasome assembly activates caspase 1, which in turn cleaves pro-interleukin-1β (pro-IL-1β) to active IL-1β (Figure 24.7).

The immune response triggered by keratinocyte activation is believed to be central to the skin's response to a wide range of stimuli, and leads to the stereotypic morphologic response(s). Even the immune-mediated/autoimmune disease, psoriasis, is now believed to be at least partially caused by inappropriate or poorly regulated activation of epidermal keratinocytes, which in turn leads to inflammation and the hallmark morphologic changes associated with this condition. The ability of cytokines such as IL-22 and oncostatin M to induce morphologic and differentiation features in keratinocytes that mimic those found in psoriatic epidermis in three-dimensional reconstituted human epidermal models skin in the absence of blood vessels and leukocytes reinforces the hypothesis that epidermal keratinocytes are central to the initiation of cutaneous inflammation as well as the initiation of cutaneous response to injury, infection, and toxicity.

Skin-resident DCs, which are bone marrow–derived, have also been implicated as playing an important role in the initiation of the cutaneous inflammatory response to various noxious stimuli. There are several different populations of skin-resident DCs that are defined by their location (epidermal vs dermal), their cell surface antigen expression, and

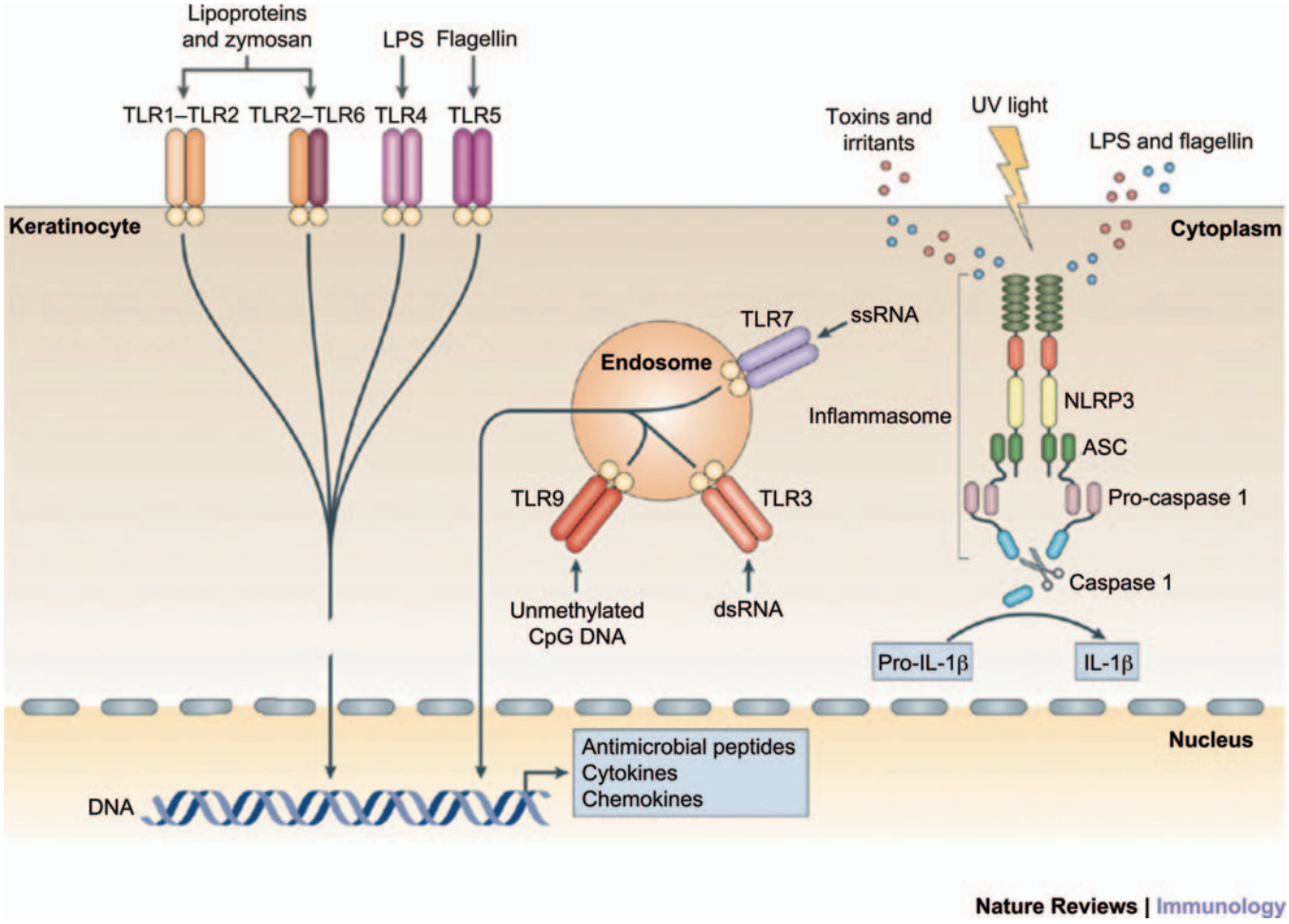

FIGURE 24.7 Keratinocytes as sensors of danger: Keratinocytes are central skin sentinels and can recognize foreign and dangerous agents, for example, PAMPs of microbial origin and DAMPs, such as irritants and toxins, through TLRs and the inflammasome. TLRs are transmembrane receptors that are present on the cell surface or on the surface of endosomal compartments. Lipopolysaccharide (LPS) stimulates TLR-4; bacterial lipoproteins and fungal zymosan stimulate TLR-1−TLR-2 and the TLR-2−TLR-6 heterodimers; bacterial flagellin activates TLR-5. PAMP recognition by TLRs leads to activation of host cell signaling pathways and subsequent innate and adaptive immune responses with antimicrobial peptide, cytokine, and chemokine production. Keratinocytes also express NLR family, pyrin domain containing 3 (NLRP3), which belongs to the newly identified class of proteins encoded by the NLR gene family. These proteins can recognize PAMPs that are in the cytoplasm (such as LPS and flagellin), DAMPs, and UV light, and activate the inflammasome complex. This multimeric complex is formed by an NLR, an adaptor protein termed ASC (apoptosis-associated speck-like protein containing a caspase recruitment domain) and pro-caspase 1, and its assembly leads to the activation of caspase 1, which processes pro-IL-1β into biologically active IL-1β. Source: *From Nestle, F.O., et al., 2009. Skin immune sentinels in health and disease. Nat. Immunol. 9, 679−691 with permission from Macmillan Publishers Limited.*

most importantly, by their functionality. LCs are the primary epidermal DC population, and express CD1a and the c-type lectin, langerin (DC207) in association with ultrastructurally visible racquet-shaped organelles called Birbeck granules. Immature LCs are the immune sentinel cells in the epidermis equipped for antigen capture via TLR and c-type lections such as langerin. Upon antigen capture and activation, these cells become mature LCs, expressing major histocompatibility class (MHC) I and MHC II and costimulatory molecules important in the adaptive immune response, and migrate to the inner paracortex of draining lymph nodes to present antigens to T cells.

Because of their role in cutaneous antigen presentation, LCs are believed to be important in the initiation of cutaneous cell-mediated immune responses, such as those responsible for allergic contact dermatitis. More recently, data from mice deficient in LCs suggest that LCs may decrease rather than enhance inflammation, leading to the hypothesis that LCs may be involved in the generation of tolerance rather than in the initiation of inflammation.

A third set of cells implicated in the initiation of the cutaneous immune response are skin-resident T lymphocytes, found both within the epidermis as well as in the dermis. Epidermal resident T cells are primarily

CD8 + α/β memory T cells, and are often found in close proximity to LCs. Dermal resident T cells are also mostly memory cells, but are roughly equally distributed between CD4 + and CD8 + T cells. Dermal resident T cells express cutaneous lymphocyte-associated antigen, and gain skin-homing properties after contact with resident DCs.

In addition to cutaneous resident T cells, all three major types of CD4 + helper T lymphocytes, Th1, Th2, and Th17 cells have been found in the skin during various inflammatory conditions. Initially, Th1 helper T cells, driven by IL-12 and producing IFNγ and related cytokines, were believed to be the primary T cells involved in the cutaneous immune response and cutaneous response to injury. More recently, IL-23-driven Th17 cells have been recognized as being essential in host immune defense against many bacterial and fungal pathogens at both cutaneous and mucosal surfaces. IL-17 and IL-22, cytokines produced by Th17 cells, upregulate keratinocyte production of antimicrobial peptides. Thus, Th17 cells and their cytokines link the adaptive immune response to the innate immune response of keratinocytes in order to optimize the host immune response to cutaneous pathogens.

Skin-resident T cells are believed to play a major role in skin immune homeostasis and surveillance, and have also been implicated in the pathogenesis of psoriasis and atopic dermatitis. A specific subset of skin-homing T cells that produce IL-22 but not IL-17 or IFNγ, termed Th22 cells, has been recently identified in the skin of patients with atopic dermatitis. Th22 cells produce the epithelial-specific cytokine, IL-22, which induces keratinocyte proliferation, differentiation, and production of antimicrobial peptides such as β-defensins and S100 family proteins, pro-inflammatory chemokines such as IL-8, CXCL1, and CXCL7, and cytokines and growth factors involved in epidermal regeneration such as IL-20 and vascular endothelial growth factor. IL-22 producing Th22 cells provide further evidence for the cross-talk between the adaptive immune system and the innate immune system, particularly epidermal keratinocyte. Thus, the current model for the cutaneous response to injury, regardless of the specific type or etiology of the injury, is initiated by epidermal keratinocyte recognition of PAMP or DAMPs via engagement of TLRs and/or NLRs, thus triggering pro-inflammatory signaling pathways and an inflammatory cascade that leads to the generation of antimicrobial peptides such as β-defensins and cathelicidins, pro-inflammatory chemokines such as IL-8, CXCL1, CXCL9, CXCL10, and CXCL11, and cytokines such as IL-1β, TNF, IL-6, and IL-18. These keratinocyte-derived chemokines and cytokines further recruit and activate DCs and other leukocytes to elaborate additional cytokines and chemokines, such as IFNα from pDCs and IL-12 and IL-23 from dermal DCs. These mediators further recruit and activate T lymphocytes of both the Th1 and particularly the Th17/Th22 lineages to release pro-inflammatory cytokines such as IFNγ, IL-17, and IL-22. These mediators then converts the initial innate immune response to an adaptive immune response, and provide cross-talk between the two arms of the immune system (Figure 24.8). This immune response is believed to be central to the skin's response to a wide range of injurious stimuli, and leads to the morphologic responses that are described in this chapter.

Specific Cutaneous Morphologic Lesions and Patterns of Injury

The histopathologic interpretation of lesions in the integument, is based on the basic morphologic reaction patterns in the integument as much and perhaps more so than in other organ systems. Pattern recognition for the diagnosis of inflammatory conditions in the skin was pioneered by A. Bernard Ackerman in his seminal book *Histologic Diagnosis of Inflammatory Skin Diseases: A Method Based on Pattern Analysis*, and has been extensively used for the recognition and diagnosis of dermatitides in both human and veterinary pathology since.

These basic morphologic reaction patterns serve as a very useful device for the recognition of specific cutaneous morphologic responses to injury. In this section, the INHAND (International Harmonization of Nomenclature and Diagnostic Criteria for Lesions in Rats and Mice) diagnostic classification scheme and nomenclature for proliferative and nonproliferative lesions in mouse and rat integument is followed. The INHAND project is a joint initiative of the societies of toxicological pathology from Europe (ESTP), Great Britain (BSTP), Japan (JSTP), and North America (STP). Its aim is to develop an internationally accepted nomenclature for proliferative and nonproliferative lesions across organ systems in laboratory rodents. The standardized INHAND nomenclature followed here, as well as additional information, is available at Mecklenburg et al. (2013) and at http://www.goreni.org.

Nonproliferative Lesions of the Epidermis

Epidermal atrophy is characterized by thinning of all noncornified epidermal layers with a corresponding decrease in nucleated keratinocytes, such that the distinction between SB, SS, and SG may no longer be apparent. Substances that decrease normal keratinocyte proliferation and metabolic activity, such as topical corticosteroids, are a common cause of epidermal atrophy.

Epidermal erosion and ulceration are characterized by loss of superficial epidermal layers (erosion) or

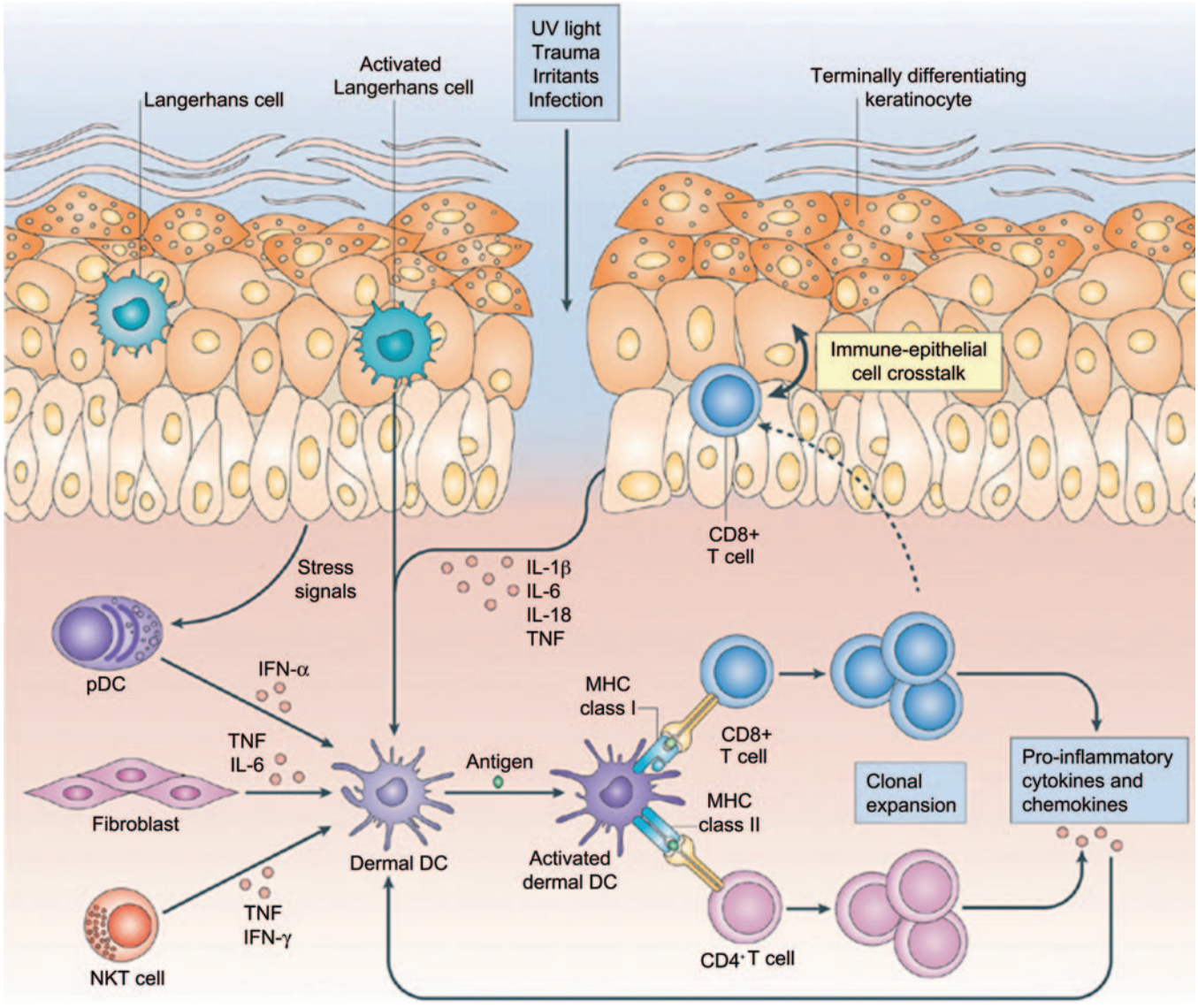

FIGURE 24.8 Skin-resident immune sentinels. UV light, trauma, irritants, or infection (essentially any type of barrier disruption) triggers a coordinated immune response to maintain skin homeostasis. Skin-resident immune cells are key sentinels for restoring homeostasis but can also be effector cells during cutaneous injury. Epidermal LCs are key immunological sentinels. Keratinocytes sense and react to noxious stimuli by producing pro-inflammatory cytokines such as IL-1β, IL-6, IL-18, and TNF, which in turn activate dermal DCs. Innate immune cells, such as pDCs, activated by stress signals derived from keratinocytes, can also contribute to dermal DC activation by releasing IFNα. Fibroblasts can produce TNF and IL-6 and natural killer T (NKT) cells can produce TNF and IFNγ, thereby contributing to the local inflammatory response. Dermal DCs activate and promote the clonal expansion of skin-resident memory CD4 + or CD8 + T cells. T cell-derived pro-inflammatory cytokines and chemokines in turn can further stimulate epithelial and mesenchymal cells, including keratinocytes and fibroblasts, thus forming an amplifying feedback loop for the inflammatory reaction. Moreover, skin-resident T cells can migrate into the epidermis, engaging in cross-talk between immune cells and keratinocytes. Source: *From Nestle, F.O., et al., 2009. Skin immune sentinels in health and disease. Nat. Immunol. 9, 679–691 with permission from Macmillan Publishers Limited.*

complete loss of the epidermis with disruption of the epidermal basement membrane (ulceration). Erosions are always due to superficial epidermal trauma, and are most commonly associated with trauma from scratching. Ulceration is also often caused by superficial epidermal trauma, but may also be the result of toxicity or a necrotizing dermatitis. Ulceration due to toxicity needs to be differentiated from ulcerative dermatitis, which occurs spontaneously in certain strains of mice and rats, most commonly in the C57BL/6 mouse.

Epidermal necrosis can be classified as either single cell or full-thickness necrosis. Epidermal necrosis is a hallmark feature of drug hypersensitivity reactions or drug eruptions, where it can occur as single cell necrosis and is termed *erythema multiforme*, or as full-thickness epidermal necrosis, where it is termed toxic epidermal

necrolysis (TEN). Single cell necrosis of keratinocytes may be further subdivided into apoptosis, or programmed cell death, and dyskeratosis, which is the occurrence of terminal keratinization of individual keratinocytes that has not occurred as part of the orderly process of epidermal keratinization; apoptosis cannot be differentiated from dyskeratosis on H&E stained sections. Apoptotic keratinocytes in UV light-exposed epidermis are often referred to as "sunburn cells."

Vesicular change refers to intracellular edema of keratinocytes and is characterized by increased size and pallor of keratinocytes with peripheral displacement of the nucleus. In the SB, synonyms are hydropic degeneration and vacuolar degeneration, while in the suprabasal epidermis it is often referred to as ballooning degeneration. If vesicular change is severe, keratinocytes may rupture and form intraepidermal vesicles.

In contrast to vesicular changes, spongiosis refers to intercellular edema between epidermal keratinocytes and is characterized by widened intercellular spaces with accentuation of desmosomes. Severe epidermal spongiosis may lead to rupture of intercellular desmosomes and the formation of intraepidermal vesicles. Spongiosis is a common feature of skin inflammation.

A vesicle is an intra- or subepidermal cavity or cleft filled with fluid and is also referred to as a bulla. It occurs following loss of cohesion between epidermal keratinocytes or between epidermis and dermis, resulting in the formation of a fluid-filled cavity. Vesicles that are located between the SB and the underlying mesenchyme are termed clefts.

A pustule, also referred to as a microabscess, is a focal intraepidermal accumulation of leukocytes, and is commonly found as a feature of generalized skin inflammation. In contrast, leukocytes which are diffusely, rather than focally infiltrating throughout the epidermis are referred to as exocytosis. Pustules that are filled with isolated rounded keratinocytes with a normal nucleus are referred to as acantholytic pustules. A predominantly neutrophilic pustule in a $CD45RB^{Hi}$ SCID mouse model of psoriasis is illustrated in Figure 24.9.

Hyperkeratosis refers to an increase in the thickness of the SC, and is classified as either orthokeratotic, composed of normal anucleate corneocytes, or parakeratotic, composed of abnormal nucleated corneocytes. Hyperkeratosis frequently accompanies epidermal hyperplasia and is often associated with chronic epidermal irritation. When the hyperkeratotic SC contains leukocytes or a proteinaceous exudate, it is commonly referred to as a crust.

A squamous cell cyst is an intradermal cyst lined by a wall composed of orderly stratified squamous epithelium with a lumen filled by concentrically arranged lamellar keratin. Squamous cell cysts can spontaneously occur in mice, particularly in the B6C3F1 strain.

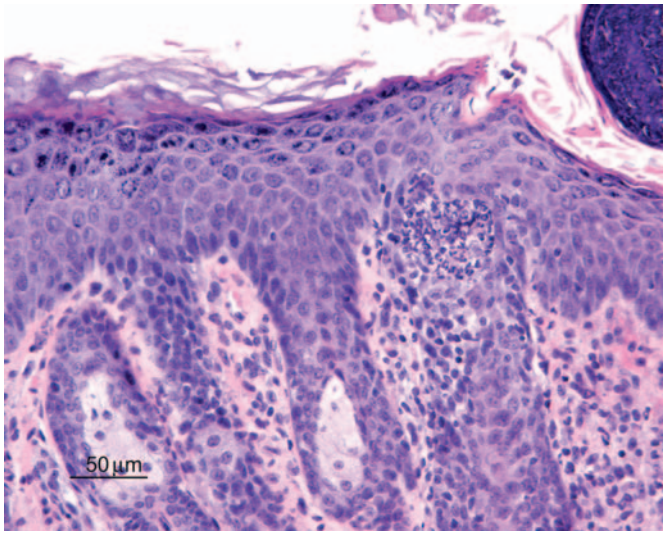

FIGURE 24.9 A predominantly neutrophilic pustule within the hyperplastic epidermis of a $CD45RB^{Hi}$ SCID mouse model of psoriasis. Source: *From Haschek, W.M., Rousseaux, C.G., Wallig, M.A. (Eds.), 2013. Haschek and Rousseaux's Handbook of Toxicologic Pathology, third ed. Academic Press (Elsevier), San Diego, CA, Figure 55.11, p. 2246, with permission.*

Nonproliferative Lesions of the Cutaneous Adnexa

Many of the lesions found in cutaneous adnexa have been previously described under the epidermis, such that only features unique to the adnexal condition will be covered in this section.

Adnexal atrophy is defined by a marked reduction in follicular and sebaceous gland size and cell number well beyond that found physiologically during the normal telogen stage of the hair cycle. It is characterized by small remnants of follicles and sebaceous glands appearing as strands of keratinocytes surrounded by a thickened connective tissue sheath. Most follicles lose their hair shaft, and dermal atrophy or scarring may be present. Hair follicles lose cells when they undergo regression in the catagen stage of the hair cycle. Therefore, hair follicle atrophy must be distinguished from catagen and telogen stages of the hair cycle. Hair follicle atrophy can be caused by a number of different compound classes such as antiproliferatives and steroid hormones.

Follicular dysplasia is an abnormality in the shape of the hair follicle and/or the hair shaft with no evident reduction in size. While for the epidermis dysplasia usually denotes a preneoplastic proliferative change, in cutaneous adnexa it is primarily describing a malformation of the adnexal structure. Many genetically modified mice, including mice null for growth factors and their receptors such as epidermal growth

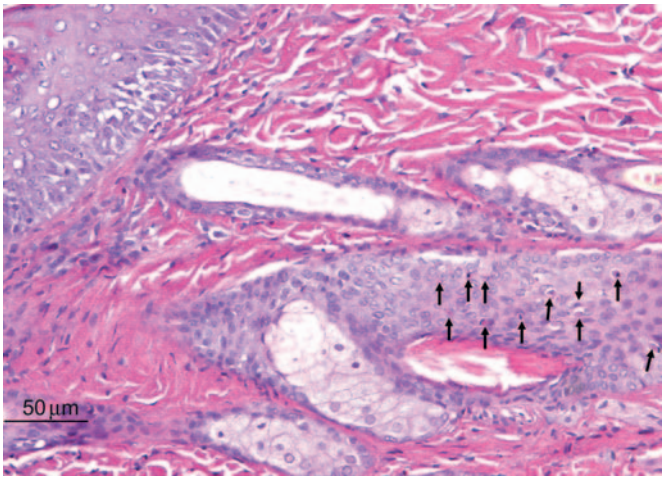

FIGURE 24.10 Keratinocyte single cell necrosis within the hair follicle epithelium of a Lewis rat given a kinase inhibitor systemically. Source: *From Haschek, W.M., Rousseaux, C.G., Wallig, M.A. (Eds.), 2013. Haschek and Rousseaux's Handbook of Toxicologic Pathology, third ed. Academic Press (Elsevier), San Diego, CA, Figure 55.12, p. 2247, with permission.*

factor receptor (EGFR) (termed Waved-2), transforming growth factor-α (termed Waved-1), fibroblast growth factor-5 (termed Angora), and keratinocyte growth factor (termed Rough), have been described that exhibit various forms of congenital hair follicle malformation. The loss of pigment from hair follicles may also be classified as a dysplasia.

Follicular necrosis is similar to epidermal necrosis, and is characterized by degeneration of follicular keratinocytes, either as single cells (single cell type) or as multiple cells (diffuse type). Chemotherapeutic agents such as paclitaxel and doxorubicin induce follicular necrosis of the single cell type, thereby inducing alopecia. Follicular keratinocyte single cell necrosis in a Lewis rat given a kinase inhibitor systemically is illustrated in Figure 24.10. Hair follicle dystrophy can be classified as a form of necrosis, as follicular keratinocytes undergo uncoordinated vacuolar degeneration or apoptosis.

Adnexal, and particularly follicular inflammation, is classified according to its pattern or location (perifollicular, intrafollicular, luminal, mural), similarly to inflammation affecting the dermis. Inflammation can also be subcategorized according to its character (lymphocytic, plasmacytic, neutrophilic, eosinophilic, and granulomatous). Interface folliculitis refers to perifollicular and mural inflammation that is generally associated with distinct necrosis of follicular keratinocytes. Follicular inflammation that has penetrated through the follicular wall leading to follicular rupture and marked inflammation in the surrounding dermis and connective tissue due to a foreign body inflammatory response to the hair shaft and follicular keratins is termed furunculosis.

Proliferative Nonneoplastic Lesions of the Epidermis

Squamous cell hyperplasia is also referred to as acanthosis or epidermal hyperplasia and is characterized by increased epidermal thickness, primarily in the SS and SG, due to an increased number of epidermal keratinocytes, primarily in the SS. As mentioned earlier, hyperplasia is frequently accompanied by hyperkeratosis. In addition, rete ridge formation is often present, but the epidermal basement membrane remains intact. In the dysplastic type of squamous cell hyperplasia, the nonkeratinized layers of the epidermis are irregularly thickened and differentiation between SB, SS, and SG is lost. Cellular atypia is not present, and the epidermal basement membrane still remains intact. Squamous cell hyperplasia typically occurs as a response to a variety of insults including inflammation, toxic irritation, repeated abrasion of the superficial SC, or prolonged exposure to UV light.

Proliferative Nonneoplastic Lesions of the Adnexa

Sebaceous cell hyperplasia is characterized by enlargement of sebaceous glands with maintenance of the normal glandular architecture. Enlarged sebaceous gland acini contain increased cells that are primarily mature, sebum-containing cells. Sebaceous cell hyperplasia frequently accompanies squamous cell hyperplasia, and both are commonly seen with chronic inflammation.

Proliferative Nonneoplastic Lesions of the Dermis

Pigment cell hyperplasia is an accumulation of pigmented melanocytes within the dermis between hair follicles and sebaceous glands. Pigment cell hyperplasia has been observed in some initiation–promotion and skin-painting studies in mice. It can also occur during chronic dermal inflammation, where it needs to be distinguished from the dermal accumulation of pigment-laden macrophages, or melanomacrophages, that have engulfed melanin pigment.

Neoplastic Lesions and Carcinogenesis Models

Carcinogenesis Models

The multistage model of mouse skin carcinogenesis is a very well-established model that has greatly aided in the identification of the underlying cellular, biochemical, and molecular mechanisms associated with the various stages of epithelial carcinogenesis. In this model, tumor development occurs via three distinct stages: initiation, promotion, and progression. Tumor initiation involves induction of a mutation of a critical gene or genes. At the initiation stage, there are no

demonstrable histopathologic alternations present. The *Ha-ras* gene appears to be a primary target gene for the initiation stage in this carcinogenesis model and becomes mutated following exposure to 7,12-dimethylbenz[*a*]anthracene (DMBA). Following initiation, tumor promotion occurs by increased expression of growth regulatory genes and sustained stimulation of epidermal keratinocyte proliferation and hyperplasia. These changes are believed to result from epigenetic mechanisms such as activation of the cellular receptor, protein kinase C.

There are three mouse models that have been commonly used for cutaneous carcinogenesis evaluation, although none are currently approved for stand-alone cutaneous carcinogenicity assessment by regulatory agencies: the Tg.AC (v-Ha-ras) transgenic mouse, the rasH2 transgenic mouse, and the SENCAR mouse. The Tg.AC and rasH2 mouse models are both *rasHa* transgenic lines. Tg.AC mice are hemizygous for a mutant *v-Ha-ras* transgene.

The Tg.AC model was developed using an inducible ζ-globin promoter to drive the expression of a mutated *v-Ha-ras* oncogene, and is regarded as a genetically initiated model. The transgene is transcriptionally silent until activated by full-thickness wounding, UV irradiation, or topical application of specific carcinogens to the shaved dorsal surface of Tg.AC mice to induce epidermal squamous cell papillomas or carcinomas. Hence this is a reporter phenotype that defines the activity of the carcinogen.

The rasH2 mouse, also known as Tg.rasH2, was created by insertion of a human *c-rasHa* transgene driven by its own promoter. Hemizygous *rasH2* mice respond with greater sensitivity to carcinogens than nontransgenic mice and are similarly recommended for genotoxic and nongenotoxic carcinogen identification.

SENCAR mice are not genetically engineered; rather the line was selected over eight generations by for increased skin tumor multiplicity and decreased tumor latency in response to DMBA and TPA treatment. SENCAR mice have an approximately 10 to 20-fold increase in sensitivity to DMBA initiation and 2 to 3-fold increase in sensitivity to TPA promotion compared with the parental CD-1 stock. The SENCAR mouse is a commonly used short-term model system for evaluating the promoting or initiating activity of test items for two-stage skin carcinogenesis in mice. These mice respond rapidly and sensitively with skin tumors following topical application of a single low dose of an initiating agent, typically a mutagenic carcinogen, followed by multiple applications of a tumor promoting agent.

When evaluated for sensitivity and predictability of mouse skin models for carcinogenic hazard identification, all of the three mouse models respond similarly, with mild inflammation and epidermal squamous cell proliferation and hyperplasia, to several weeks of treatment with topical carcinogens. All of the three mouse models are also similar in their development of the reporter phenotype: the development of squamous cell papillomas following extended carcinogen treatment. All have been shown to be fairly predictive of carcinogenic potential in humans.

Cutaneous tumors, particularly those derived from the epidermis and cutaneous adnexa, are not uncommon spontaneous findings in rodents, so attention must be paid to the potential occurrence of spontaneous tumors in the commonly used mouse models of skin carcinogenesis. In these mouse models, the typical carcinogen-induced tumors are squamous cell papilloma with malignant progression to squamous cell carcinoma, such that it is essential to differentiate these carcinogen-induced epidermal keratinocyte-derived epithelial tumors from other spontaneously occurring tumors derived from epidermal keratinocytes as well as spontaneously occurring tumors derived from cutaneous adnexal epithelia.

Neoplastic Proliferative Lesions of the Epidermis

Squamous cell neoplasms are the typical tumors that occur in all mouse skin tumor models, and arise first as squamous cell hyperplasia (described earlier) followed by the development of squamous papillomas, described here, and finally malignant squamous cell carcinomas.

Squamous cell papillomas are benign neoplasms that are derived from epidermal keratinocytes, and are the earliest neoplastic lesion induced by carcinogens in the mouse models of skin carcinogenesis. They can be further characterized into four types: exophytic, endophytic, dysplastic, and nonkeratinizing. The exophytic type has a stalk at its base, and is also often referred to as a pedunculated papilloma. The endophytic type has no stalk, but instead is contiguous with the adjacent epidermis and invaginates to form a depression (Figure 24.11). The dysplastic type contains atypical squamous cells with large hyperchromatic nuclei that are found primarily in the basal and suprabasal layer of the epidermis.

Regardless of type, all papillomas are well-circumscribed papilliform exophytic or endophytic masses with no compression of the surrounding tissue and no capsule. They are composed of keratinizing squamous cells overlying a well-vascularized stroma. Mitotic figures are common. Individual suprabasal cells may show premature keratinization or dyskeratosis, and there is a variable degree of parakeratotic hyperkeratosis.

Squamous cell carcinomas, also referred to as epidermoid carcinoma, are malignant neoplasms derived from epidermal keratinocytes. Squamous cell carcinomas are

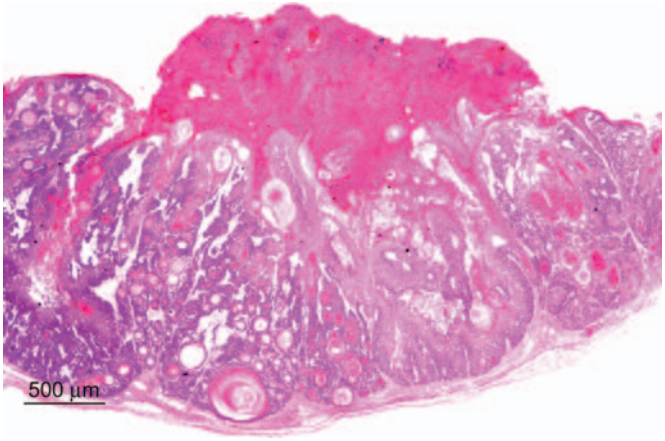

FIGURE 24.11 An endophytic squamous papilloma in a mouse: The endopytic type does not have a stalk, but is instead contiguous with the adjacent epidermis with dermal invagination to form a depression. The invaginated surface is covered by a serocellular crust. Source*: Courtesy: Oded Foreman, Genentech Permission.*

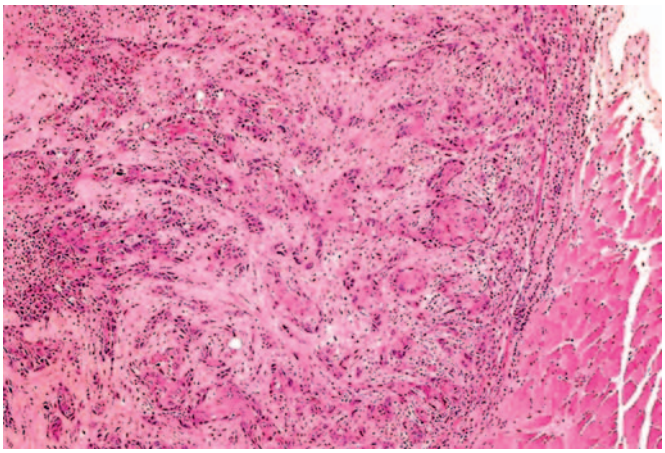

FIGURE 24.12 Cutaneous squamous cell carcinoma in a mouse: The tumor arises from an ulcerated epidermal surface and is composed of islands or cords of cells that invade the dermis, with an accompanying inflammatory and fibroblastic response in the adjacent dermis (desmoplasia). Neoplastic cells demonstrate variable evidence of squamous differentiation and keratinization. Source*: Courtesy: Oded Foreman, Genentech.*

poorly demarcated, generally mostly endophytic, and show no compression of the surrounding mesenchyme, although some tumors elicit a desmoplastic reaction in the surrounding dermis. The tumor is composed of islands or cords of cells that penetrate the basal lamina and invade the dermis, with the neoplastic cells sometimes invading the underlying subcutis or subcutaneous muscle. There is generally some evidence of squamous differentiation (Figure 24.12), although its extent is variable. Centrally located, concentric layers of keratin that are often termed keratin pearls, cancer pearls or horn pearls are also frequently present. Some neoplastic cords may show a central lumen containing individualized (acantholytic) keratinocytes that are surrounded by several layers of neoplastic epithelial cells (pseudo-glandular pattern). Abnormal keratinization (dyskeratosis) of single cells occurs sporadically and intercellular bridges are generally present except in very poorly differentiated tumors.

Benign basal cell tumors are derived from stem cells within hair follicles and/or the interfollicular epidermis and are classified into three distinct types: basosquamous type, trichoblastoma type, and granular type. All basal cell tumors are fairly well circumscribed and multilobulated with some association to the epidermis. The neoplasm is composed of uniform lobules, islands, or cords of closely packed cells that are supported by a variable degree of fibrovascular stroma. Neoplastic basal cells also may be arranged in cords or fine ribbons that may become cystic. There is no invasion of the basement membrane and no compression or desmoplasia of the surrounding dermal mesenchyme. Tumor cells generally resemble normal epidermal basal cells without intercellular bridges, and palisade at the periphery of lobules. Foci of squamous cell differentiation may occur and sebaceous cells may also be present. In the basosquamous type of basal cell tumor, foci of keratinization are present. In the trichoblastoma type, small foci of sebaceous cells and/or follicular differentiation are present. In the granular type, there are basal cells containing periodic acid-Schiff (PAS)-positive granules.

Malignant basal cell tumor is also referred to as basal cell carcinoma or basosquamous carcinoma, and is a malignant tumor derived from stem cells within hair follicles and/or the interfollicular epidermis. Malignant basal cell tumors are poorly circumscribed dermal tumors with some association to the epidermis or adnexa and extensive local invasion. They are composed of lobules and cords of closely packed cells that are supported by a variable degree of fibrovascular stroma. Tumor cells generally resemble normal epidermal basal cells without intercellular bridges, and palisade at the periphery of lobules. Central necrosis in tumor lobules may be present; these necrotic areas are referred to as pseudocysts. In pigmented strains, melanin pigmentation is commonly found, desmoplasia in the surrounding mesenchyme is common, and extensive local invasion may be present.

Benign and malignant basal cell tumor development has been very convincingly linked to upregulated hedgehog (Hh) signaling via several lines of evidence, including genetic mutation analyses, mouse models of basal cell tumors, and the successful treatment of malignant basal cell tumors in the clinic using Hh signaling inhibitors. In addition, many if not all basal cell tumors are believed to derive from hair follicle stem cells.

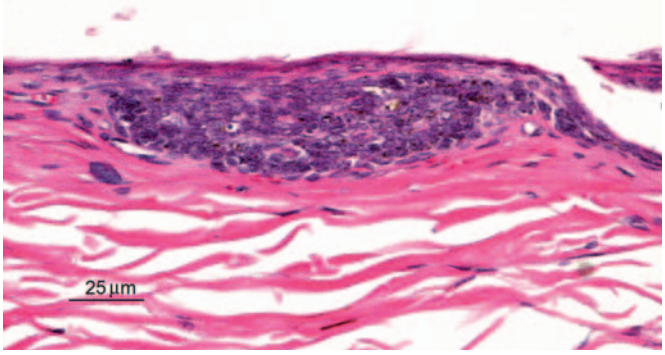

FIGURE 24.13 An early benign cutaneous basal cell tumor arising from the epidermal surface of a patched 1 (*PTCH1)* heterozygous null C57BL/6 mouse to illustrate that the majority of basal cell tumors have identifiable mutations in at least one allele of *PTCH1*, a tumor suppressor gene that encodes a Hh signaling receptor. This early benign basal cell tumor is a very well-circumscribed lobule that is connected to the overlying epidermis and demonstrates no invasion of the basement membrane and no compression or desmoplasia of the surrounding dermal mesenchyme. Tumor cells resemble normal epidermal basal cells without any evidence of intercellular bridges. Source*: Courtesy: Oded Foreman, Genentech.*

In humans, the vast majority of basal cell tumors have identifiable mutations in at least one allele of patched 1 (*PTCH1*), a tumor suppressor gene that encodes a Hh signaling receptor. Hh signaling occurs when Hh ligands bind to PTCH1, specifically through SMO, and relieve inhibition of the Hh pathway. This leads to activation of the Gli family of transcription factors and eventually to cellular proliferation. A basal cell tumor from a *PTCH1* heterozygous null C57BL/6 mouse is illustrated in Figure 24.13.

Adnexal Neoplastic Lesions

Sebaceous cell adenomas are derived from the reserve cells that line the periphery of gland lobules. In contrast to sebaceous gland hyperplasia, in a sebaceous cell adenoma the normal glandular architecture has become distorted, but the tumor is still composed of lobules and acini and is well demarcated from the surrounding tissue. Squamous differentiation and keratinization may be present and mitoses are often seen at the lobular periphery.

Sebaceous cell carcinomas are less differentiated than adenomas and poorly delineated from surrounding tissue, with frequent deep dermal invasive growth. The tumor is composed of lobules and acini containing polygonal cells of variable size and containing variable amounts of intracytoplasmic lipid vacuoles. There is high mitotic activity with numerous atypical mitotic figures. Squamous differentiation and individual cell necrosis, cystic degeneration with the presence of amorphous cellular debris, and melanin pigmentation

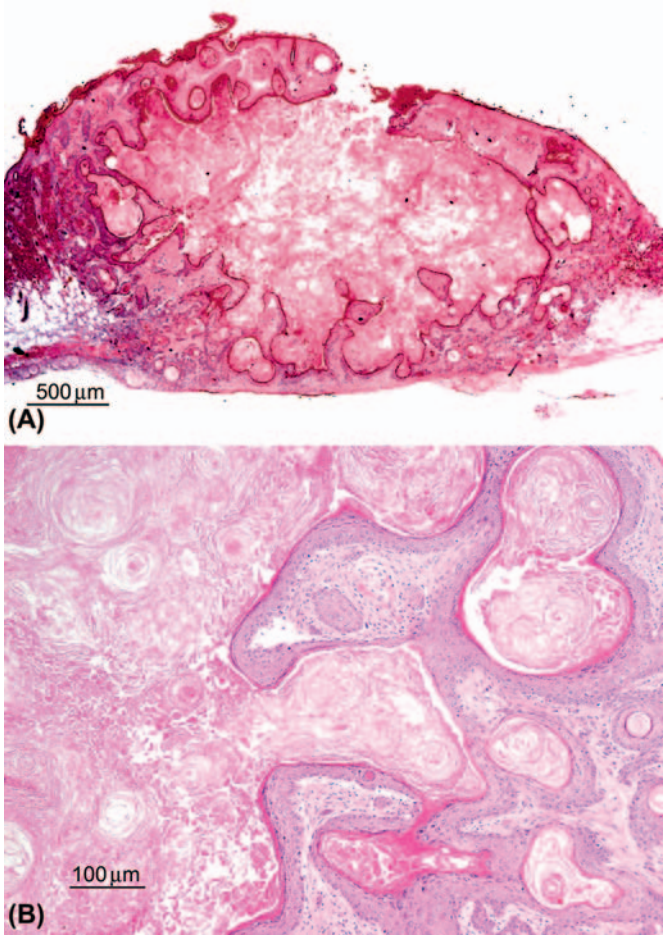

FIGURE 24.14 (A) A low-magnification image of a cutaneous keratoacanthomas in a mouse demonstrating that the tumor is a very well-demarcated mass in the superficial dermis with a prominent pore to the skin's surface. (B) A higher magnification of a keratoacanthoma illustrating the central cavity filled with concentric whorls of keratin (left side of image) lines by well-differentiated squamous epithelium that contains epithelial whorls with central foci of keratinization and resembles the epithelium of the follicular infundibulum. Source*: Courtesy: Oded Foreman, Genentech.*

may be present. Both sebaceous gland adenomas and carcinomas are rare spontaneous tumors in rodents.

Keratoacanthomas arise from squamous epithelial keratinocytes derived from the infundibulum of the hair follicle. They are very well demarcated but generally unencapsulated masses that occur in the superficial dermis and connect to the overlying epidermis, sometimes containing a pore to the skin's surface (Figures 24.14A). The tumor is composed of one to several lobules containing a prominent central cavity filled with concentric whorls of keratin. The cavities are lined by well differentiated squamous epithelium that sometimes contains epithelial whorls with central foci of keratinization (Figure 24.14B). Mitotic figures are uncommon. Experimentally induced keratoacanthomas in mice have been reported to undergo spontaneous

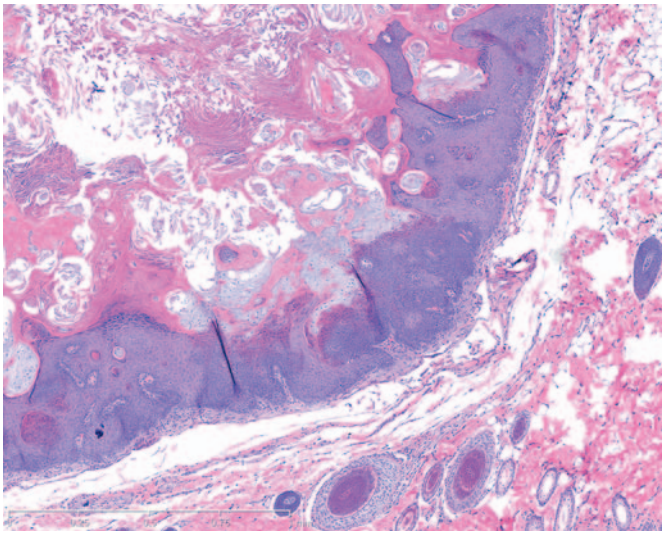

FIGURE 24.15 A pilomatricoma type of benign hair follicle tumor from a rat: The tumor consists of multiple nodules of hair matrix and hair cortex epithelial cells that abruptly keratinize without the presence of keratohyalin granules to a central lumen that contains keratin and keratinized ghost or shadow cells. Source: *Courtesy: Melissa Schutten, Genentech.*

regression, possibly correlated to the normal hair follicle growth and regression cycle.

Benign hair follicle tumors have four distinct types: trichoepithelioma, trichofolliculoma, pilomatricoma, and tricholemmoma. All four types are derived from the hair follicle matrix, and are all well delineated but unencapsulated with no invasion. All have multiple lobules consisting of different stages of follicular trichogenic differentiation, often with one or multiple cysts.

The trichoepithelioma type is derived from the hair follicle matrix epithelium that gives rise to the inner root sheath and hair shafts. They have a fine mesenchymal matrix that resembles the hair follicle dermal papilla and manifests as focal invaginations of the basement membrane.

In contrast to basal cell neoplasms, the epithelium of trichoepitheliomas does not differentiate into sebaceous cells. The trichofolliculoma type is a large cystic neoplasm that has a large central cystic lumen that contains keratin and hair shafts and which is lined by squamous epithelium. This epithelium gives rise to well differentiated hair follicles that radiate peripherally from the cystic center. The pilomatricoma type consists of multiple nodules of hair matrix and hair cortex epithelial cells that abruptly keratinize without the presence of keratohyalin granules and slough into a central lumen that contains keratin and keratinized ghost or shadow cells (Figure 24.15). The tricholemmoma type is a neoplasm derived from the outer root sheath epithelium and thus consists of small epithelial "nests" lined by a prominent basal membrane. Cells at the periphery of nests are basaloid and palisading while the more differentiated suprabasal cells contain PAS-positive glycogen granules similar to those in the external outer root sheath epithelium of normal anagen hair follicles. Suprabasal cells at the center of the nest often demonstrate tricholemmal keratinization characterized by very hyaline amorphous keratin.

Dermal Neoplastic Lesions

Benign melanoma is derived from epidermal and/or adnexal melanocytes and is characterized by a dense nodular accumulation of pigmented cells within the dermis, with or without an epidermal connection. Neoplastic melanocytes are polygonal, epithelioid, or spindle shaped, with variable degrees of intracytoplasmic melanin pigment granules.

Malignant melanoma is also characterized by a dense nodular accumulation of cells within the dermis with or without an epidermal connection, but there is invasive growth and the neoplastic cells are even more pleomorphic in size and shape, and may or may not contain melanin pigment. When they lack pigmentation, they are referred to as amelanotic malignant melanomas. Both benign and malignant melanomas are very rare spontaneous incidental tumors in rats and mice. Amelanotic melanomas in rats occur most frequently in the pinna, eyelid, scrotum, and perianal region.

MECHANISMS OF TOXICITY

Direct Cutaneous Toxicity

Because of its unique role as a first line barrier defense against a number of environmental insults), the skin is exposed to a wide variety of toxic agents. These toxic agents can harm the skin directly, causing irritation or corrosion, or can induce immune-mediated toxic effects, both systemic and cutaneous, that manifest as cutaneous toxicity (Table 24.5).

Direct cutaneous toxicity is caused by direct damage to the skin by any number of external irritants, such as chemical agents, xenobiotics, infectious agents, thermal injury, or UVR that damage or disrupt the skin's barrier function. When this occurs, the skin mounts an inflammatory and proliferative response in order to prevent further damage and to restore a morphologically and physiologically functioning barrier.

Direct cutaneous toxicity activates the innate, but not the adaptive, immune response. For example, reversible damage to the skin by direct contact with toxic agents is referred to as irritation, and results in activation of mast cells, complement, and/or prostaglandin synthesis. Irritation generally occurs within 4 hours following topical application of the irritating substance. Histopathologically, skin irritation is characterized by epidermal hyperkeratosis and hyperplasia

TABLE 24.5 Mechanisms of Skin Toxicity

Type of toxicity	Lesion	Mechanism	Xenobiotic/causative agent
DIRECT TOXICITY			
Irritation	Hyperkeratosis (parakeratotic and orthokeratotic types)	Primary as in seborrhea or secondary to trauma, inflammation, metabolic, or nutritional disorders	Chlorinated naphthalenes, iodine, mercury, sun exposure
	Primary inflammation (e.g., pustules, vesicles, acantholysis, edema)	Disruption of intercellular junctions	Acids, alkalis, organic solvents (mineral spirits, pine oils, essential oils, turpentine), phenol, oxidizing/reducing agents, keratolytic agents
	Secondary inflammation (e.g., dermal or pannicular nodules; sterile pyogranuloma)	Foreign body reaction; injection site reactions	Strong acids, caustic (alkali) agents, oxidizing/reducing agents, foreign bodies, immune reaction
	Epidermal degeneration, necrosis, apoptosis	Direct cellular toxicity, physical injury (e.g., thermal burns), radiation	Acids, alkalis, oxidizing/reducing agents, organic solvents, keratolytic agents, thermal injury, UV, and ionizing radiation
Corrosion/necrosis	Epidermal necrosis, erosion, ulceration, vesiculation	Chemical burn physical injury (e.g., laceration, thermal burns) radiation	Strong acids, caustic (alkali) agents, oxidizing/reducing agents, bleomycin, thermal injury, sulfur mustard, inorganic mercury salts, inorganic arsenic salts, UV, and ionizing radiation
		Vasoactive agents, ischemia, infarction, vasculitis, thromboembolism	Ergot alkaloids
Proliferation	Epidermal hyperplasia (acanthosis, dyskeratosis), dysplasia, or carcinogenicity (e.g., adenoma, carcinoma)	Chronic irritation or factors altering epidermal growth/differentiation (e.g., cytokines and growth factors) or genotoxicity	UVR, inorganic arsenic, sulfur mustard, T-2 toxin, toxic organic agents/metabolites (e.g., polyaromatic hydrocarbons, polyhalogenated hydrocarbons)
Atrophy	Epidermal atrophy	Hormonal imbalances, partial ischemia, malnutrition	Corticosteroids
Immune-mediated toxicity	Acantholysis	Direct activation of immune effectors, disruption of intercellular junctions	Polymyxin B, DMSO, aspirin, phorbol esters, biogenic amines
	TEN	IgE-dependent (Type I hypersensitivity)	Therapeutic agents (e.g., penicillin), foods (urticaria)
	Stevens–Johnson syndrome	Immune complex mediated	Penicillin, aminosalicylic acid, streptomycin
	Erythema multiforme	T-lymphocyte mediated (Type IV hypersensitivity; contact allergens)	Ethyl aminobenzoate, neomycin, metal (e.g., nickel, chromium), metal derivatives (e.g., oligomercurial), plant toxins (e.g., poison ivy)
Phototoxicity		Primary phototoxicity	Tetracyclines, sulfonamides, chlorpromazine, nalidixic acid, phenothiazines, acridine, anthracene, phenanthrenes, fluorocoumarins, fagopyrin, hypericin
		Secondary phototoxicity (e.g., hepatotoxicity mediated by phyllerythrin)	Hexachlrorobenzene, lead, pyrolizidines, pyrrolizidine alkaloids, hepatoxic plants, lantadines A and B, furanosesquiterpenoids, oxalates, mycotoxins, mycrocystin
Photoallergy		Delayed type IV hypersensitivity (light activated)	Sulfonamides, phenothiazides, coumarin derivatives, glyceryl *p*-aminobenzoic acid
PIGMENTATION DISORDERS			
	Hyperpigmentation	Increased amount of melanin or melanocytes due to chronic inflammation, endocrine disorders	Corticotrophin, oral contraceptive drugs, cancer chemotherapeutics (e.g., bleomycin), hydantoins
	Hypopigmentation	Lack of melanocytes or melanin transfer	Fluphenazine, corticosteroids, chloroquine, copper deficiency

(*Continued*)

TABLE 24.5 (Continued)

Type of toxicity	Lesion	Mechanism	Xenobiotic/causative agent
ADNEXAL DAMAGE			
	Hair follicle atrophy	Interference with anagen (rapid growth phase)	Doxorubicin, vincristine, methotrexate, cyclophosphamide, phenylglycidyl ether, dixyrazine, colchicine
	Hair follicle atrophy	Interference with telogen (stationary growth phase)	Chlorinated naphthalenes, propranolol, triparanol, heparin, coumarin, oral contraceptives, phenylglycidyl ether, dixyrazine, thallium, selenium, inorganic arsenic, inorganic mercury, iodine, mimosine
	Alopecia	Loss of hair due to chemical toxicity or hormonal effects	Depilatory agents (e.g., eflornithine), retinoids, androgens, progesterone–estrogen combinations
Acneiform lesions	Hyperkeratinization, chloracne	Comedone formation	Polyhalogenated hydrocarbons (e.g., dioxins)
Anhidrosis	Damage/loss of sweat glands, neutrophilic eccrine hidradenitis	Direct cytotoxicity	Cytotoxic agents (e.g., cytarabine, bleomycin), formaldehyde, arsenic, thallium, lead, fluorine

From Haschek, W.M., Rousseaux, C.G., Wallig, M.A. (Eds.), 2013. Haschek and Rousseaux's Handbook of Toxicologic Pathology, third ed. Academic Press (Elsevier), San Diego, CA, Table 55.5, pp. 2254–2255, with permission.

with dermal inflammation, and is frequently associated with a variety of other epidermal changes such as erosion/ulceration, necrosis, or vesicular change.

When the skin damage induced by direct contact with the initiating agent is irreversible, the lesion is referred to as corrosion. Corrosion is characterized by full-thickness necrosis of the epidermis, leading to ulceration with penetration into the underlying dermis and involvement of the cutaneous adnexa and even the underlying subcutaneous tissue.

When chemical substances or xenobiotics are applied directly to the skin, their effect is determined not only by their primary mode of toxicity but also by the processes of cutaneous absorption and metabolism of the substance. The outer surface of the skin is coated by the lipid sebum, which is secreted from the sebaceous glands and forms a barrier to polar water soluble compounds.

A specific example of direct cutaneous toxicity is direct thermal injury, also referred to as a burn. Burns have classically been classified into three categories: first-, second-, and third-degree burns. First-degree burns have lesions that are limited to the epidermis, and resemble those induced by slight UV irradiation, with the formation of individually necrotic epidermal keratinocytes, or "sunburn cells." First-degree burns are often accompanied by mild dermal erythema and edema.

Second-degree burns epidermal necrosis with epidermal–dermal separation leading to cleft formation, but again with only mild dermal lesions of erythema, edema, and sometimes mild leukocytic infiltration. Third-degree burns are characterized by both epidermal and dermal necrosis. While these classic descriptions are still in common usage, clinical practice and experimental studies frequently use the alternative classification of full- and partial-thickness burns.

Partial-thickness burns are further classified as superficial, which are roughly equivalent to first-and mild second-degree burns, and deep, which are roughly equivalent to severe second-degree burns or less severe third-degree burns. Deep partial-thickness burns are characterized by full-thickness epidermal necrosis with necrosis of superficial cutaneous adnexa and dermal vessels but sparing of deep cutaneous adnexa and vessels. They can be distinguished from full-thickness burns, which exhibit complete epidermal and dermal necrosis, including necrosis of all cutaneous adnexa and dermal vessels, by staining for the presence of proliferation markers (e.g., PCNA), which will be present in partial but not full-thickness burns (Figure 24.16). One can also stain for intact collagen with stains such as Masson's trichrome, which will demonstrate the depth to which dermal collagen fibers have undergone coagulation.

Mild thermal injury is histologically characterized by nuclear and cytoplasmic swelling, generally of epidermal keratinocytes in superficial burns, with later development of individual necrotic keratinocytes. More severe thermal injury is characterized by nuclear rupture, pyknosis, and necrosis of epidermal keratinocytes that exhibit brightly eosinophilic cytoplasm that cannot be morphologically distinguished from premature keratinization, or dyskeratosis. With severe thermal injury, the entire epidermis may undergo necrosis

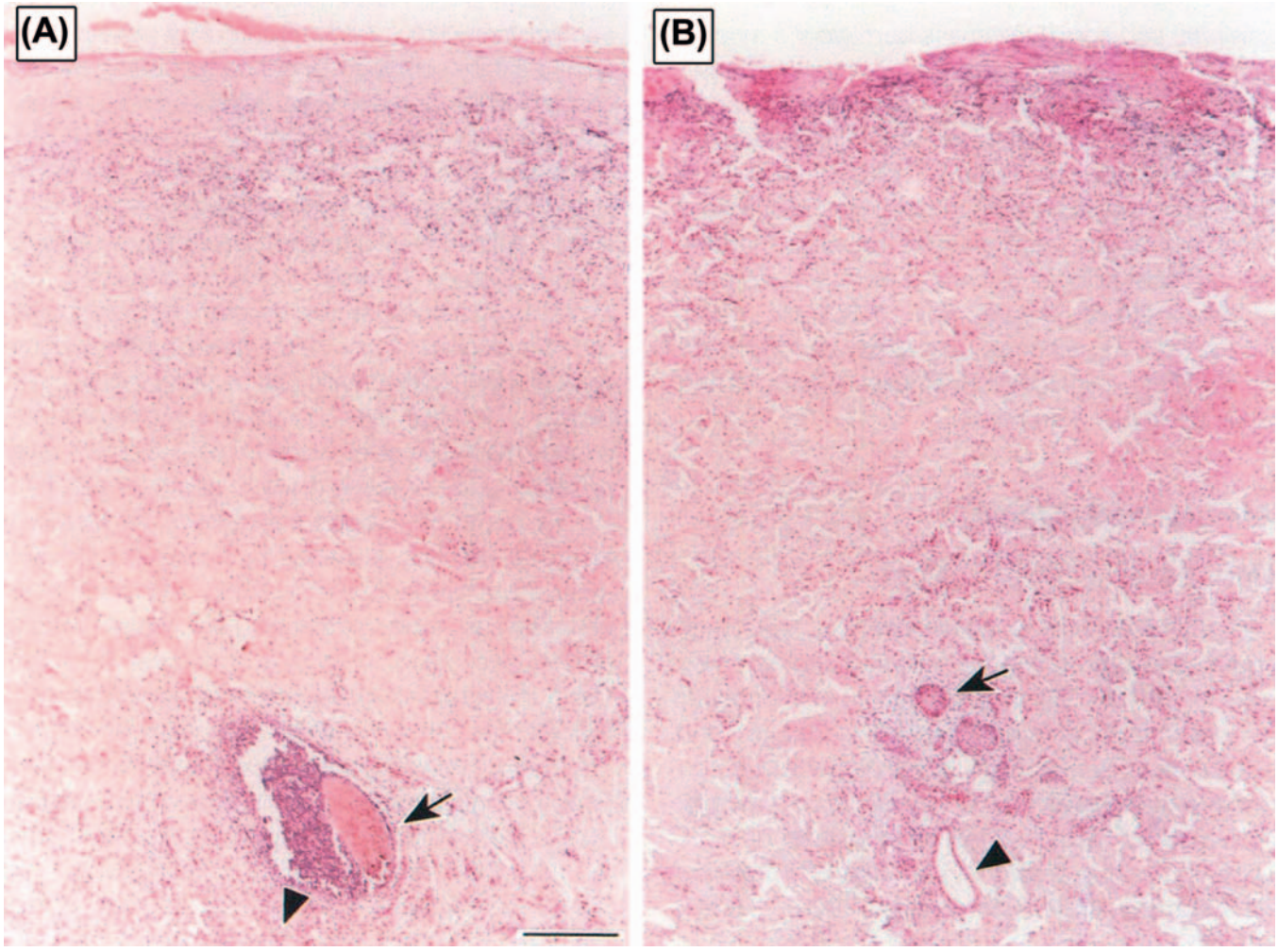

FIGURE 24.16 Representative sections of full (A) and deep partial (B) thickness burns from Yucatan minipigs harvested 4 days postburn and stained for PCNA expression in order to illustrate the depth of cutaneous damage. Both burn sections lack epidermis (the epidermis was fully necrotic and was removed). The full-thickness burn section (A) illustrates a completely necrotic hair follicle deep in the section (*arrow*) with a few PCNA-positive dermal fibroblasts (*arrowhead*) beneath the necrotic follicle. The deep partial-thickness burn section (B) contains PCNA-positive proliferating remnants of a hair follicle (*arrow*) as well as an eccrine sweat gland duct (*arrowhead*). Bar is 250 μm. Source*: From Danilenko, D.M. et al., 1995. Growth factors in porcine full and partial thickness burn repair. Am. J. Pathol. 147, 1261–1277 with permission from the American Society of Investigative Pathology.*

with subepidermal vesicle formation and separation from the underlying dermis (Figure 24.17). Following initial severe thermal damage to the epidermis, adnexa, and dermis, a marked inflammatory reaction generally follows, characterized initially by an infiltration of neutrophils (Figure 24.18), followed subsequently by mononuclear inflammatory cells, including macrophages and lymphocytes.

Another example of direct toxic injury is that induced by the T-2 trichothecene mycotoxin, produced by any one of a number of different fungi of the genus *Fusarium*. T-2 toxicity manifests as degeneration and necrosis of epidermal basal cell layer keratinocytes with progression to full-thickness epidermal necrosis and ulceration. Necrosis of the dermis is also frequently seen (Figure 24.19). The specific mechanism of T-2 toxicity is unknown, although recent studies suggest that the toxin may cause direct damage to cell membranes, with little or no effect on DNA.

A special example of direct cutaneous toxicity is genotoxic injury due to interaction of the toxic agent with DNA, particularly in epidermal keratinocytes, since these cells exhibit a high rate of proliferation and turnover. The initial damage caused by genotoxic agents occurs in the basal layer of the epidermis, where the toxic agent can interact with DNA by a variety of mechanisms such as alkylation, DNA strand breaks, chromosomal breaks, and adduct formation. This results in an increased rate of mutation. At lower doses the only obvious effect may be the induction of neoplasia. At higher doses the probability of lethal mutation increases, and regenerative epidermal

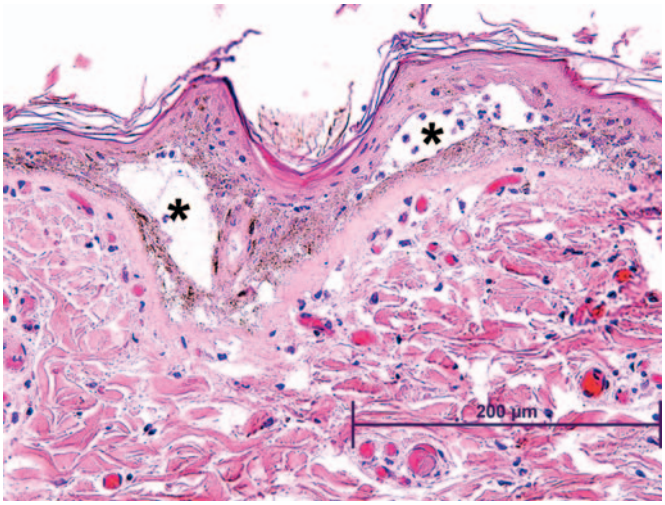

FIGURE 24.17 Full-thickness epidermal necrosis with subepidermal vesicle and cleft formation (*) due to separation of the epidermis and dermis in the skin of a horse with a full-thickness burn: Necrotic cellular debris and neutrophils are present both within the subepidermal vesicles and overlying the necrotic epidermis. Source: *From Haschek, W.M., Rousseaux, C.G., Wallig, M.A. (Eds.), 2010. Fundamentals of Toxicologic Pathology, second ed. Academic Press (Elsevier), San Diego, CA, Figure 7.11, p. 150, with permission.*

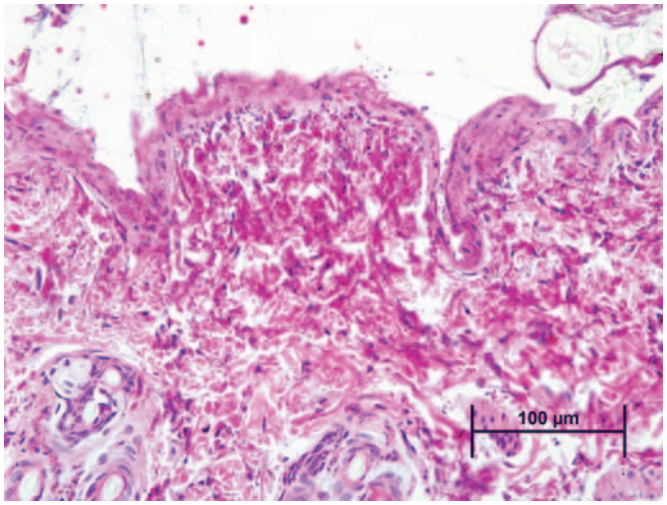

FIGURE 24.19 T-2 mycotoxicosis in a rabbit characterized by full-thickness epidermal necrosis as well as necrosis with coagulation of collagen in the superficial dermis. Source: *From Haschek, W.M., Rousseaux, C.G., Wallig, M.A. (Eds.), 2010. Fundamentals of Toxicologic Pathology, second ed. Academic Press (Elsevier), San Diego, CA, Figure 7.10, p. 150, with permission.*

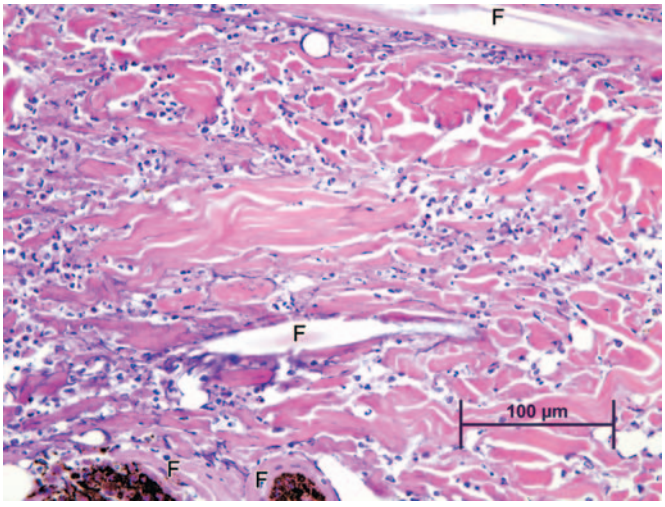

FIGURE 24.18 Full-thickness burn in the skin of a dog illustrating the secondary neutrophilic inflammatory infiltration in the dermis: Hair follicles exhibiting epithelial necrosis (F) are present in the affected dermis. Source: *From Haschek, W.M., Rousseaux, C.G., Wallig, M.A. (Eds.), 2010. Fundamentals of Toxicologic Pathology, second ed. Academic Press (Elsevier), San Diego, CA, Figure 7.3, p. 143, with permission.*

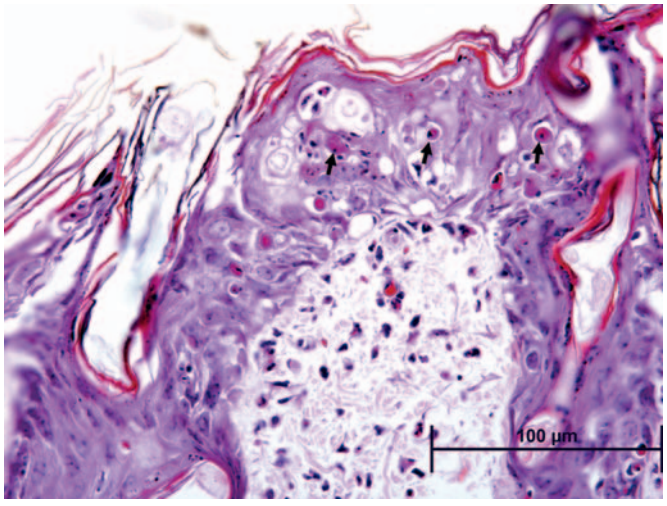

FIGURE 24.20 Skin from a guinea pig exposed to sulfur mustard or mustard gas, illustrating single cell necrosis of epidermal keratinocytes (*arrows*) with secondary inflammation and edema in the underlying superficial dermis. Source: *From Haschek, W.M., Rousseaux, C.G., Wallig, M.A. (Eds.), 2010. Fundamentals of Toxicologic Pathology, second ed. Academic Press (Elsevier), San Diego, CA, Figure 7.4, p. 144, with permission.*

hyperplasia is observed when surviving keratinocytes proliferate in order to replace the cells lost by necrosis due to damage by the mutagen.

In extreme cases, the action of the mutagen impairs the cell renewal process itself, resulting in ulceration since replacement of cells lost to differentiation, as well as replacement of damaged cells, is not possible. This mechanism of toxicity is thought to be the cause of the necrotizing lesions associated with sulfur mustard (mustard gas), which selectively targets basal keratinocytes, causing extensive alkylation of DNA to the point of cell death, leading to necrosis of individual epidermal keratinocytes and epidermal vesicular change, often accompanied by a secondary dermal inflammatory response (Figure 24.20).

Immune-Mediated Cutaneous Toxicity

Cutaneous toxicity that occurs as the result of immune-mediated mechanisms falls into the same categories as systemic immune-mediated diseases. Type I hypersensitivity is acute, and classically manifests cutaneously as urticaria. Type II hypersensitivity is cytotoxicity induced by IgG or IgM antibodies with complement activation. The various forms of pemphigus are an example of cutaneous type II hypersensitivity, with autoantibodies directed against keratinocyte antigens, thus inducing acantholysis, or loss of cell–cell adhesion. Type III hypersensitivity is mediated by IgG or IgM antigen–antibody immune complex deposition. Cutaneous vasculitis and cutaneous *lupus erythematosis* (LE) are examples of type III hypersensitivity. Vasculitis is characterized by inflammation of small cutaneous vessels with or without vascular necrosis and/or thrombosis. Drug-induced cutaneous lupus can have a variety of histologic presentations, but is often characterized by an interface dermatitis consisting of a lichenoid inflammatory cellular infiltrate at the dermal–epidermal interface. Lichenoid drug eruptions have a very similar histopathologic appearance.

In contrast to type I, II, and III hypersensitivities, which are systemic, type IV hypersensitivity is often a local reaction, and in the skin is referred to as allergic contact dermatitis. Different toxic agents can induce more than one immune-mediate mechanism. As an example, penicillin, which is often cited as the classic example of a drug acting as a hapten, can cause both an IgE-mediated type I hypersensitivity reaction manifesting as urticaria, as well as non-IgE-mediated reactions that manifest as variable degrees of epidermal keratinocyte necrosis, ranging from *erythema multiforme* to TEN and Stevens–Johnson syndrome, severe conditions with widespread full-thickness epidermal necrosis and detachment from the underlying dermis.

The pathogenesis of immune-mediated cutaneous toxicity is not completely understood, although current understanding suggests involvement of both the adaptive and innate immune systems. It had long been surmised that drugs and other xenobiotics acted as haptens, as mentioned earlier for penicillin, and when conjugated to proteins were presented to the immune system, which then elicited an immune response. However, there is still much that is not fully understood. As mentioned previously, there is quite a bit of overlap in the mechanisms and lesions that can be induced by any one drug, such as penicillin, which can induce both type I and type IV hypersensitivity reactions. In addition, a single morphologic and diagnostic entity, such as cutaneous LE, can have more than one underlying pathogenesis. As mentioned earlier, the cutaneous LE that is related to therapy with anti-TNF biologics is likely distinct from that induced by nonbiologic drugs. With cutaneous LE induced by biologics, the underlying mechanism is believed to be due to the pharmacologic effect of lowered TNF-α levels. In contrast, LE induced by xenobiotics is believed to be caused by reactive drug metabolites inducing haptens or by direct stimulation of the innate immune system.

The innate immune system, system, and particularly the epidermal keratinocyte, have recently come to the forefront in understanding the pathogenesis of drug-induced immune-mediated skin injury. As described earlier in this section, keratinocytes sense DAMPS through their TLRs, which triggers the release of antimicrobial peptides such as S100A8/S100A9 complexes, as well as cytokines and chemokines that in turn recruit and activate leukocytes. Completing the loop, leukocytes that are recruited to the epidermis then release cytotoxic factors, such as perforin and granulysin from CD8 + cytotoxic cells and NK cells, as well as TWEAK, TRAIL, *Fas* ligand, and other TNF family members from macrophages and DCs. These cytotoxic factors in turn induce the keratinocyte death that underlies drug-induced blistering syndromes such as *erythema multiforme* and TEN.

Drug-induced cutaneous type I hypersensitivity reactions are acute and are mediated by IgE antibodies bound to the surface of mast cells and basophils. When the drug allergen interacts with IgE, the mast cells and/or basophils degranulate, releasing mediators such as histamine and leukotrienes, and manifest cutaneously as urticaria, angioedema, and pruritus. The key to the diagnosis of true urticaria is that the lesions, which consist of raised pruritic erythematous wheals, typically demonstrate the brightest erythema at the outer edge of lesions with rapid paling toward the middle.

Histopathologically, urticaria is characterized by dermal angioedema, often with congestion of dermal vessels. The key differences between drug-induced and nondrug-induced urticaria is that in nondrug-induced urticaria there is often little else to see histologically, while drug-induced urticaria is characterized by the presence of a mononuclear leukocyte infiltrate, often perivascular, with or without eosinophils. The mononuclear cells are T cells, typically with CD8 + cells in the epidermis and CD4 + cells forming the superficial dermal infiltrate. In some cases, lesions of vasculitis may be present; and this is referred to as urticarial vasculitis.

An example of a cutaneous toxicity caused by type II hypersensitivity is drug-induced pemphigus. Pemphigus represents a group of intraepidermal blistering diseases where there is loss of adhesion between keratinocytes due to disruption of desmosomes. Pemphigus features as its hallmark the loss of

keratinocyte adhesion, which is the result of autoantibody binding to various antigens on the keratinocyte cell surface. In *pemphigus vulgaris*, autoantibodies mostly bind to desmoglein 3 while in *pemphigus foliaceous*, they bind primarily to desmoglein 1, the main desmosomal adhesion glycoprotein. While the pathogenesis of pemphigus has been understood to involve autoantibodies against desmoglein 1 and desmoglein 3 for some time, more recently it has been suggested that autoantibodies against keratinocyte acetylcholine receptors are also involved in the initial pathogenesis.

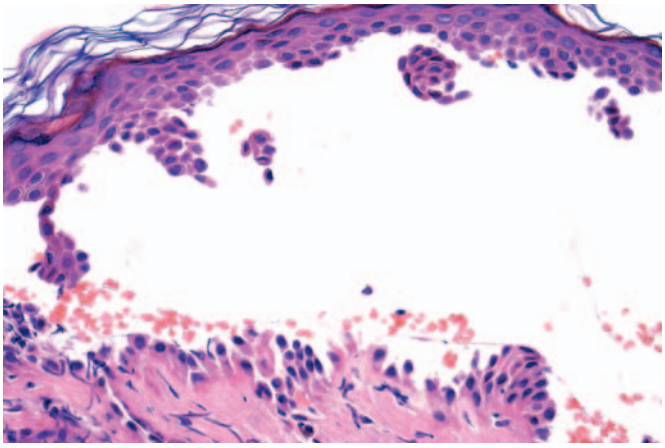

FIGURE 24.21 Skin from a human with *pemphigus vulgaris* illustrating subepidermal separation of epidermal keratinocytes from the underlying dermis (acantholysis) with the resultant formation of a subepidermal cleft containing rounded-up epidermal keratinocytes (acantholytic cells) and occasional red blood cells. Source: *Courtesy: Richard Carr, MD, Department of Histology, Warwick Hospital, United Kingdom.*

In many cases of pemphigus an etiologic factor such as drugs or other environmental factors is known or suspected. Drugs may be involved in as many as 10% of pemphigus cases.

The specific lesions of pemphigus are dependent on where the intraepidermal disruption of keratinocyte adhesion occurs, but all are characterized by intra- or subepidermal separation of keratinocytes (acantholysis), with the formation of intra- or subepidermal clefts, often containing rounded-up epidermal keratinocytes (acantholytic cells) and variable degrees of inflammatory leukocytes, particularly neutrophils (Figure 24.21).

Cutaneous toxicities due to type III hypersensitivity reactions are drug-induced cutaneous vasculitis and cutaneous LE. Approximately 20%–30% of cutaneous vasculitides are drug-induced, generally arising 7–10 days following administration of the inducing drug substance. Vasculitis is also a relatively common drug-induced finding in the nonclinical setting; one particular manifestation is vasculitis that is induced by anti-drug antibodies (ADAs) in an animal model directed against human or humanized therapeutic proteins. While the most common presentation for ADA-induced vasculitis is systemic with occurrence in multiple internal organs ADA-induced cutaneous vasculitis can also occur (Figure 24.22). Cutaneous vasculitis manifests as pruritic, palpable purpura with a purpuric maculopapular eruption. Although eosinophils are not present in all cases of drug-induced vasculitis, when they are

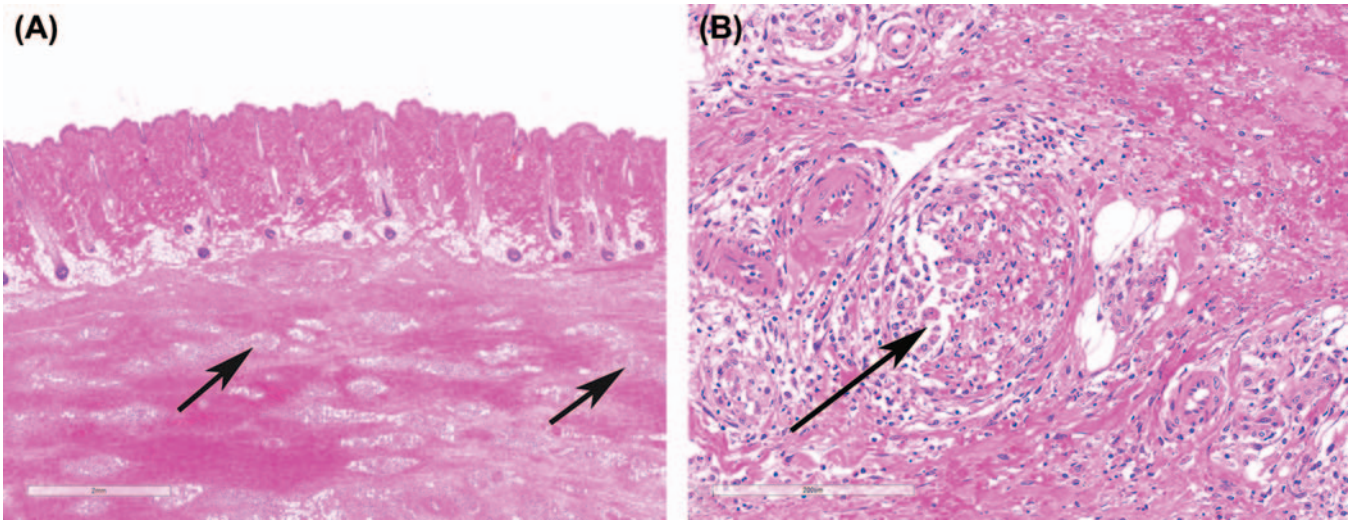

FIGURE 24.22 Skin and subcutis from a cynomolgus monkey administered a humanized therapeutic monoclonal antibody via repeated subcutaneous injections. The injection site subcutis contains relatively marked mixed inflammatory cellular infiltration (*arrows* in A), often surrounding and infiltrating into subcutaneous vessels that sometimes exhibit necrosis and/or thrombosis (perivasculitis and vasculitis; *arrows* in B). This animal had a very high ADA titer of >log 5, strongly suggesting that this subcutaneous vascular inflammation was the result of ADAs directed against the foreign protein. *Figure reprinted from Danilenko, D.M., 2016 An overview of the pathogenesis of immune-mediated skin injury. Toxicol Pathol 44:535–544, Figure 3, page 539 with permission from SAGE.*

present they serve as a valuable clue to the drug-related nature of the vasculitis.

Drug-induced cutaneous LE is another example of a cutaneous toxicity due to a type III hypersensitivity reaction. The cutaneous histological and immunofluorescence findings of drug-induced LE are indistinguishable from those of idiopathic LE. Histopathologically, findings range from an interface dermatitis to a dense lichenoid infiltrate with lymphocytes, macrophages, and eosinophils. Individually necrotic keratinocytes may be present, as dermal edema and vasodilatation.

It has been hypothesized that cutaneous autoimmune inflammation as exemplified in cutaneous lupus is dependent on plasmacytoid DC activation by nucleic acid antigen via the innate immune receptors TLR-7 and TLR-9. In the specific case of cutaneous lupus induced by the TNF-α inhibitor biologics, nucleic acid antigens termed nucleosomes become detectable in the plasma of rheumatoid arthritis (RA) patients after the start of TNF-α inhibitor therapy, suggesting that this rise in plasma nucleosome levels might contribute to a break of tolerance and thereby induce autoantibodies in susceptible individuals. This hypothesis is supported by the finding that antinucleosome antibodies correlated strongly with the presence of antinuclear antibodies, a hallmark of systemic LE in anti-TNF-α-treated RA patients.

Erythema multiforme, toxic epidermal necrolysis (TEN), and Stevens–Johnson syndrome represent a continuum of lesions whose hallmark histological finding is epidermal necrosis ranging from the single cell type in erythema multiforme to the full-thickness type in TEN and Stevens–Johnson syndrome. Inflammatory cellular infiltration may be present, particularly adjacent to individually necrotic keratinocytes in erythema multiforme. Often there is no or minimal inflammatory cellular infiltration during the early stages of TEN or Stevens–Johnson syndrome, which exhibit full-thickness epidermal with epidermal lifting and cleft formation (Figure 24.23).

The pathogenesis of these conditions is not completely understood but is believed to be immune-mediated, as rechallenging an individual with the same drug can result in rapid recurrence of the condition. The clinical, histopathological, and immunological findings in these conditions support the currently prevalent hypothesis that they are specific type IV drug hypersensitivity reactions in which cytotoxic CD8 + T lymphocytes play an important role in the initial pathogenesis of lesions.

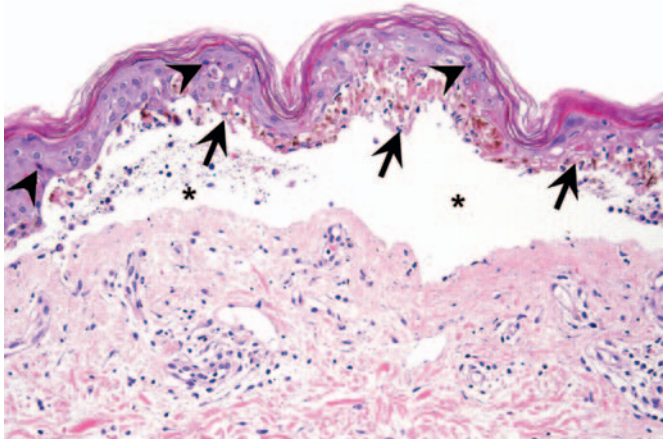

FIGURE 24.23 Skin from a human with TEN illustrating widespread necrosis of the entire basal layer of the epidermis (*arrows*) with scattered necrosis of suprabasal keratinocytes (*arrowheads*) and epidermal–dermal separation and cleft formation (*asterisks*). The cleft is filled with a small amount of cellular debris and amorphous material. There is little or no associated inflammatory reaction in either the epidermis or dermis. Source: *Courtesy: Dr. Phillip McKee.*

Mechanisms of Toxicity: Photosafety

Photosensitivity

Many exogenous chemicals and drugs may absorb UV or visible light. Interaction of a particular wavelength of light with a compound that absorbs UV–visible radiation may lead to an enhanced excitement state for electrons or even the release of free electrons. As electrons return to the less excited state, there is a release of energy, which leads to the generation of free radicals or highly reactive singlet oxygen species. These in turn react with and damage lipid membranes, proteins, and nucleic acids, causing cell injury and death.

Photoactivation of chemicals involves different areas of electromagnetic spectrum including UVA (320–400 nm), UVB (290–320 nm), or the visible range (400–700 nm). Although highly cytotoxic, UVC (200–290 nm) is typically filtered out in the atmosphere and consequently, not considered a significant risk in vivo. Most photoreactions in vivo are caused by less-energetic UVA radiation, whereas more-energetic UVB radiation is involved in fewer photoreactions in vivo since the shorter UVB wavelengths penetrate skin less deeply than the longer UVA wavelengths. Visible light may also induce photoreactions but these are rarely observed. Acute effects of UV irradiation on skin include direct damage to DNA, cell growth arrest, apoptosis, and stimulation of melanogenesis, whereas chronic effects may include photoaging or photocarcinogenesis.

Chemicals or drugs that absorb light are termed photoreactive and the adverse effects of light-induced chemical reactions are termed photosensitivity reactions. Photosensitivity reactions may involve several different mechanisms and are classified as: phototoxicity (photoirritation), photoallergy, photogenotoxicity, and photocarcinogenicity (including photococarcinogenicity). Phototoxic reactions are nonimmunologically

FIGURE 24.24 Secondary phototoxicity in sheep attributed to ingestion of panic grass (*Panicum* sp.?). Ears and nasal plana show marked encrustation and conjunctivae are severely swollen and red. Source: *Courtesy: Dr. John King. From Haschek, W.M., Rousseaux, C.G., Wallig, M.A. (Eds.), 2010. Fundamentals of Toxicologic Pathology, second ed. Academic Press (Elsevier), San Diego, CA, Figure 7.8, p. 147, with permission.*

mediated, whereas photoallergic reactions are immunologically mediated.

Photosensitivity reactions may result from direct contact with the skin, both intentional (i.e., topically applied drugs) and unintentional (i.e., exogenous environmental toxins), or from systemic exposure due to distribution of the photoreactant chemical (e.g., endogenous chromophores such as flavins or porphyrins or xenobiotic compounds) by the circulation to the skin (Figure 24.24).

Phototoxicity may also be caused by endogenous substances through the liberation of photoreactive metabolic by-products into circulation. Porphyria is associated with a disturbance in metabolism of porphyrins resulting in an overproduction of prophyrin intermediates of heme synthesis, most notably protoporphyrin. Porphyria may be hereditary or secondary to hepatotoxicity from exposure to various chemicals, including polychlorinated compounds (e.g., hexachlorobenzene), alcohol, or lead. Distribution of porphyrin to the skin and consequent exposure to light results in a photoactivation of porphyrin, generation of free radicals, and skin lesions.

Compounds that induce photosensitizing reactions include naturally occurring plant derivatives, environmental toxins, and numerous classes of drugs. Furocoumarins constitute an important class of naturally occurring plant photosensitizing agents such as psoralens that are synthesized by common rue, bergamot, sp-fennel, and dill. One such derivative, 8-methoxypsoralen (8-MOPS), also known as xanthotoxin, is used in photodynamic therapy (PUVA) to treat skin conditions such as vitiligo and psoriasis. Coal-tar derivatives are well-known causes of phototoxicity and photodermatitis in industrial and road workers.

Numerous classes of drugs have been implicated in photosensitizing reactions including cardiac antiarrhythmic drugs (e.g., amiodarone), phenothiazines (e.g., chlorpromazine), antimalarials (e.g., quinine, quinidine), thiazide diuretics, tetracyclines (e.g., doxycycline, chlortetracycline), fluoroquinolone antibiotics (e.g., enoxacin, sparfloxacin), antimicrobials (e.g., sulfonamides), fibric acid derivatives (e.g., fenofibrate, gemfibrozil), psychiatric medications (e.g., tricyclics, carbamazepine, benzodiazepines), nonsteroidal antiinflammatory drugs (NSAIDs, e.g., naproxen, tenoxicam), and miscellaneous drugs (e.g., amantadine, dapsone, nifedipine, isotretinoin). Herbal medications (e.g., St. John's wort), sunscreen ingredients (e.g., *para*-aminobenzoic acid), tattoo dyes (e.g., cadmium sulfide), and vitamins (e.g., B6, pyridoxine hydrochloride) have also been associated with photosensitizing reactions.

Phototoxicity

Phototoxic reactions, also referred to as photoirritation, are more frequently encountered than those of photosensitivity, and are characterized by an acute (minutes to hours), nonimmunologic skin reaction occurring in UVR or sun-exposed skin areas, typically resembling exaggerated sunburn. Skin temperature is increased at the site of phototoxicity and in addition to erythema (redness), there may be edema, vesiculation, desquamation, and chronically, hyperpigmentation.

Histopathologically, in affected areas of skin phototoxic reactions are characterized by epidermal keratinocyte apoptosis (apoptotic keratinocytes are termed "sunburn cells"), oncotic necrosis, dyskeratosis, and vacuolation with dermal edema, vascular changes, suppurative inflammation, and/or mononuclear cell infiltrates. Administration of 8-MOPS by gavage to hairless mice followed by exposure to UVA irradiation resulted in dose-related skin reactions ranging from an erythematous phototoxic reaction without subsequent skin lesions to severe burning with subsequent scarring (Figure 24.25). Similarly, oral administration of quinolone antimicrobial drugs to albino Balb/c mice and UVA irradiation in combination but not separately caused a cutaneous phototoxic reaction characterized by auricular degeneration of basal epidermal cells and fibroblasts, edema, and dermal neutrophilic infiltration.

Photoallergy

In contrast to phototoxic reactions, photoallergic reactions are less commonly observed, and are immunologic reactions requiring previous sensitization and manifested 24–72 hours after exposure. Photoallergic reactions are considered delayed-type hypersensitivity

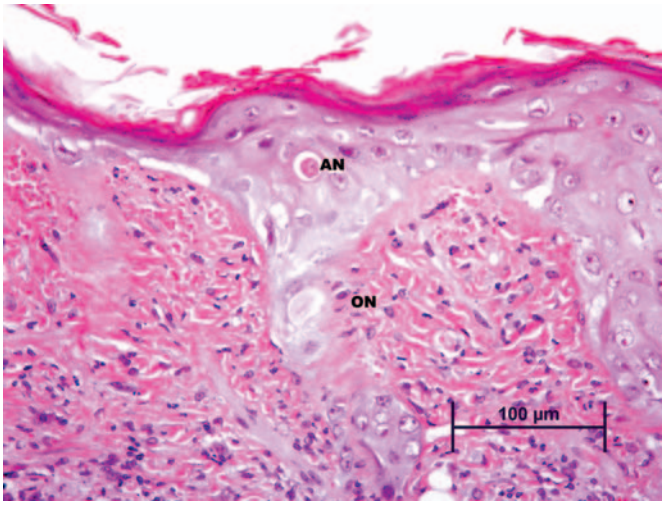

FIGURE 24.25 Primary photosensitization in the skin of a mouse exposed to the phytochemical psoralens followed by UV light exposure. Apoptotic necrosis (AN) and oncotic necrosis (ON) are evident in the epidermis and there is a secondary suppurative inflammation in the underlying superficial dermis. Source: *From Haschek, W.M., Rousseaux, C.G., Wallig, M.A. (Eds.), 2010. Fundamentals of Toxicologic Pathology, second ed. Academic Press (Elsevier), San Diego, CA, Figure 7.7, p. 146, with permission.*

(Type IV) that involves two phases: an induction phase and a challenge phase. Most chemicals involved in photoallergic reactions are small molecular weight, which allows penetration of skin. Yet they are often too small to elicit an immune response by themselves. Combination of the chemical (hapten) with a protein carrier results in formation of hapten-carrier adducts, which are processed by LCs in the skin and transported via lymphatics to regional lymph nodes where a T cell response is triggered. Subsequent exposure to the same chemical triggers a hypersensitivity reaction in UVR exposed areas as well as on unexposed areas of skin. The skin reaction generally recurs upon repeat exposure to UVR even after intake of the initiating agent has stopped. Photoallergic reactions are characterized by dermatitis, pruritus, and may extend beyond sun-exposed areas of skin. Histopathologic changes are typical of allergic contact dermatitis, including epidermal keratinocyte necrosis, epidermal spongiosis, perivascular lymphoid cuffs, and lichenoid infiltrates of lymphocytes with or without neutrophils.

Photogenotoxicity

Numerous chemicals including psoralens, fluoroquinolones, and phenothiazines have been identified as having photogenotoxic potential that may be associated with an increased risk of developing skin cancer. Photogenotoxicity may be the result of direct DNA damage from UVR itself (primarily UVB, rarely UVA) or following photoactivation of chemicals by UV irradiation resulting in generation of DNA-damaging free radical oxygen species. Administration of 8-MOPS in combination with suberythemagenic doses of UVA irradiation is well recognized potent mutagen that forms psoralen-DNA adducts. Factors that may influence photogenotoxicity outcome include binding and retention time of the chemical in different layers of the skin, DNA repair mechanisms, and antioxidant status.

Photocarcinogenicity

Prolonged exposure to UVR is well established as the primary factor responsible for the majority of skin cancers in humans. UVR induces direct DNA damage, but also induces indirect effects on DNA, proteins, and lipids through the generation of reactive oxygen intermediates and chronic inflammation. For example, 8-MOPS administered to mice exposed to sp-suberythemogenic doses of UVA irradiation rapidly develop cutaneous squamous cell carcinomas. UVR can mutate a number of genes that are involved in tumor initiation, promotion, and progression. Many of these genes are tumor suppressors, and include mutated p53 in squamous cell carcinomas and basal cell carcinomas, mutated p16 in malignant melanomas, and mutated PTCH1 leading to unregulated Hh signaling in basal cell carcinomas and some squamous cell carcinomas.

Hairless p53 heterozygote knockout mice exposed to UVB radiation developed squamous cell carcinomas faster and of a more malignant, poorly differentiated variety than wild-type mice supporting the important role of point mutations of p53 genes in skin carcinogenesis. UVR also induces growth arrest and DNA damage-inducible genes such as GADD45, a p53-regulated gene that suppresses cell growth, in keratinocytes and melanocytes. GADD45 is a key protective factor in UV-induced carcinogenesis as UV irradiated GADD45 null mice had reduced apoptotic epidermal keratinocytes but an increase in tumors compared to wild-type mice.

Ras gene activation is frequently seen in squamous cell carcinoma, basal cell carcinoma, and malignant melanoma. This *ras* gene activation is the result of an aberrant repair of UV-induced pyrimidine dimers. In human malignant melanoma specimens, point mutations were found in all *ras* oncogene family members at pyrimidine-rich sequences, implying that these point mutation sites were probably the targets for UV-induced damage that eventually leads to transformation. c-Ha-ras amplification was seen in melanomas. The presence of several *ras* alterations may be due to the accumulation of massive unrepaired, UV-induced DNA lesions. The transcription factor Stat3 has also been shown to play a critical role in UV-induced skin carcinogenesis. BK5.Stat3C transgenic mice overexpressing Stat3 in epidermal basal keratinocytes were more

sensitive to UV-induced skin carcinogenesis compared with wild-type mice, while Stat3-nullmice were much more resistant to UVB-induced skin carcinogenesis compared to wild-type mice.

Certain chemicals that may not be photoreactive may influence cutaneous carcinogenicity through immunosuppressive effects (e.g., cyclophosphamide) or altering the optical properties of the skin (e.g., certain emollients). This reaction is termed photococarcinogenicity and should be considered for drugs that are intended for chronic administration.

Mechanisms of Toxicity: Pigmentation

Pigmentation Disorders

Skin and hair color may be influenced by the presence of hemoglobin and carotenoids, but is primarily attributed to the presence of melanocytes that synthesize melanin pigments. There are two primary types of melanin that influence skin color: eumelanin which is brown-black and phaeomelanin, which confers red−yellow pigmentation. Melanocytes export melanin in melanosomes (melanin-containing granules) to adjacent keratinocytes for distribution to the upper layers of the skin or from the hair bulb to the hair shaft. The number, size, composition, density, and distribution of melanosomes are primarily responsible for variations in pigmentation, whereas the number of melanocytes remains relatively constant. Numerous intrinsic factors may also influence skin pigmentation by acting on melanocytes. These include genetic factors and epigenetic factors derived from keratinocytes (e.g., bFGF, α-MSH, PAR2), dermal fibroblasts (e.g., DKK1, TGFβ1, bFGF, HGF, SCF), endocrine and neural factors (e.g., nitric oxide, α-MSH), and systemic inflammation (e.g., prostaglandins, leukotrienes, thromboxanes, IL-1, IL-6).

Studies on mouse coat color mutants have identified more than 300 genes that may influence skin and hair color. Melanocortin-1 receptor (MC1R) is considered the major determinant of pigment phenotype. α-Melanocyte-stimulating hormone (α-MSH) and adrenocorticotropic hormone are the principle agonists of MC1R that act to increase eumelanin via elevation of cAMP levels. Melanin synthesis is controlled by tyrosinase (TYR) enzymes that initiate melanin synthesis by catalyzing oxidation of L-tyrosine. TYR activity is mediated principally by TYR-related protein 1 (TRP1) and dopachrome tautomerase (TRP2).

Skin pigmentation may also be influenced by extrinsic factors such as UVR. The skin is the main barrier to environmental stresses and noxious stimuli and the melanocytes ability to absorb UVR provides a significant contribution to the protective mechanisms of skin. UVA (320−400 nm) and particularly UVB (280−320 nm) are able to penetrate skin and stimulate melanin pigmentation. Hence, the degree of pigmentation, which is a reflection of degree of photoprotection afforded, is termed skin "phototype" and may be used as a predictor of photoaging and photocarcinogenesis where lighter skin individuals are at higher risk.

Disorders of pigmentation may be classified as hyperpigmentation or hypopigmentation, which may or may not involve alterations in melanocyte numbers. In the extreme, the complete lack of pigmentation, termed albinism, is the result of genetic mutations in the melanin synthesis pathway. More often, however, pigmentation changes are associated with variations in the amount of melanin in skin or hair (i.e., described clinically as normochromia, hyperchromia, and hypochromia), although drug or metal deposits may occasionally be involved.

Drug-induced cutaneous pigmentation disorders that may account for 10%−20% of acquired cases of hyperpigmentation in humans are of particular interest to the toxicologic pathologist. Numerous drugs have been implicated in pigmentation disorders including NSAIDS, antimalarial agents (e.g., chloroquine, quinine), antipsychotic drugs (e.g., chlorpromazine, phenothiazine), anticonvulsants (e.g., phenytoin), amiodarone, tetracyclines, cytotoxic drugs (e.g., cyclophosphamide, busulfan, bleomycin, adriamycin), and heavy metals. The mechanisms involved in pigmentation disorders vary with the type of agent involved. For example, some drugs may react with melanin to form drug-pigment complexes, which may be exacerbated by sunlight stimulation of melanin synthesis. Other types of drugs may either accumulate in the skin or bind to skin components other than melanin. Acute or chronic inflammatory processes may result in nonspecific postinflammatory hypopigmentation or hyperpigmentation through the release of numerous mediators including cytokines and growth factors, which may cause aberrant melanogenesis.

The exact mechanisms involved postinflammatory hypopigmentation are not clearly understood but are thought to be the result of inhibition of melanogenesis rather than overt destruction of melanocytes (although in some instances severe inflammation may result in destruction and loss of melanocytes with permanent pigment change). Heavy metals, on the other hand, may be deposited in the dermis contributing to a pigmentation change by a mechanism other than one involving melanin.

In addition to unintended adverse effects of systemic drugs, many drug development efforts have purposefully pursued hypopigmentation for cosmetic skin lightening. Numerous mechanisms have been targeted for decreasing pigmentation including TYR, TRP1, and TRP2 inhibition (via microphthalmia-associated transcription factor downregulation),

increased TYR ubiquitination, decreased MC1R activity, cAMP inhibition (antiinflammatory agents), interference with melanosome transfer or maturation, and liberation of toxic melanin synthesis intermediates.

Mechanisms of Toxicity: Adnexal Damage

Toxicity of the cutaneous adnexa can be generally categorized into that which affects the hair shaft (follicular atrophy and alopecia), the sweat glands (anhidrosis, hypo- or hyperhidrosis), or the sebaceous glands (xerosis). These changes can occur individually or in combination, depending on the target of the toxicant.

Alopecia is a common cutaneous toxicity secondary to systemically administered drugs, particularly to chemotherapeutic agents that have an effect on disrupting the cell cycle in actively dividing cells, such as those in the hair matrix during hair shaft generation in the anagen phase of the hair cycle. A large number of chemotherapeutic agents can induce alopecia, with four major classes of agents that are classified based on their mechanism of inducing alopecia. Microtubule inhibitors, such as paclitaxel, induce the highest incidence of alopecia at >80% followed by topoisomerase inhibitors such as doxorubicin at 60%–100%, nucleic acid alkylators such as cyclophosphamide at 60%, and 10%–50% for antimetabolites that only damage cells during S phase, when they are actively synthesizing DNA, such as 5-fluorouracil plus leucovorin or methotrexate.

Regardless of the specific agent that induces the alopecia, the histopathologic appearance of lesions is similar, with single cell necrosis or apoptosis of follicular keratinocytes, particularly those in the hair bulb and/or hair matrix epithelium. Toxic effects to the sebaceous glands have also been described for chemotherapeutic agents, and may be associated with or a contributing cause of alopecia, since sebum is an essential component for normal hair growth.

Chloracne is one of the more unique nonimmunologic cutaneous manifestations of systemic toxicity. Chloracne is induced following systemic exposure to 2,3,7,8-tetrachlorodibenzo-*p*-dioxin, commonly referred to as dioxin, and related environmental contaminant compounds. Acneiform lesions that tend to form on the face/head and trunk but generally not on the extremities are typical of the condition. Histopathologically, there are comedones that consist of cystically dilated hair follicles without substantive-associated inflammation. As lesions advance, hyperkeratinization and sebaceous gland atrophy mark the pilosebaceous unit. Outbreaks of chloracne have been described in several populations accidentally exposed to dioxin.

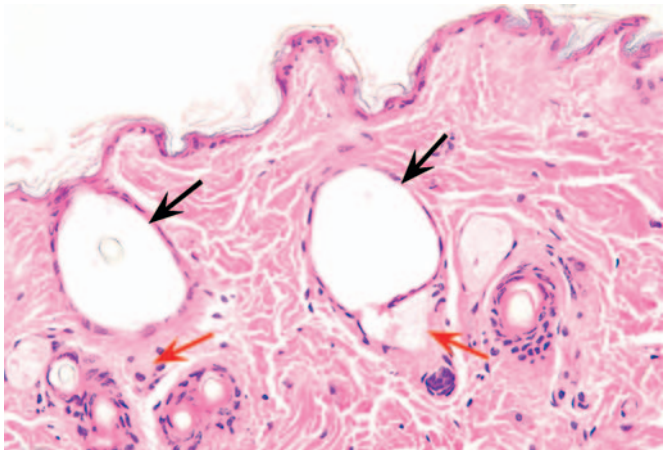

FIGURE 24.26 Histological section from male B6C3F1 mouse treated for 2 years with 30 mg/kg 3,3′,4,4′-tetrachloroazobenzene. Note dilation of hair follicles, flattening of lining epithelium, and atrophy of adjacent sebaceous glands. No infiltration or inflammatory cells can be discerned. *Black arrows* indicate hair follicles. *Red arrows* indicate sebaceous glands. Source: *From Ramot, Y., et al., 2009. Inflammatory and chloracne-like skin lesions in B6C3F1 mice exposed to 3,3′,4,4′-tetrachloroazobenzene for 2 years. Toxicology 265, 1–9, Figure 3F, p. 6, with permission from Elsevier.*

Rabbits, monkeys, rhino mice, and hairless mice (*hr/hr* mutants) have all been used as models for the development of chloracne-like lesions after exposure to dioxin. It was believed that in mice, hairlessness was required for the development of lesions. More recently, however, haired B6C3F1 mice have also been shown to develop chloracne-like lesions following exposure to dioxin-like compounds. Histopathologically, the characteristic lesions of chloracne are similar to those in humans, a cystic dilation of hair follicles with flattening of the lining epithelium and accompanying atrophy of sebaceous glands (Figure 24.26). Inflammation is not a prominent feature, although it is sometimes present.

Another class of compounds frequently clinically associated with acneiform rash is that of the EGFR inhibitors. The rash associated with use of these compounds is pruritic, and may be accompanied by xerosis, hair, and nail changes. Because skin lesions do not occur in all patients responding to treatment, a direct pharmacologic effect of these drugs on the skin is suspected, but exact mechanisms are not entirely understood. Apparent associations with skin lesion development and increasing dose of compound or positive correlation with antitumor effect also suggest direct receptor-mediated pathogenesis. Since EFGRs are present in basilar and proliferative epidermal cells, the lesions most reasonably stem from perturbations in normal proliferation and subsequently in barrier function. Sebaceous glands and hair follicles also express EGFRs and are also known targets in some cases of

toxicity. Histopathologic lesions include hyperkeratosis and folliculitis with perifollicular inflammation, with or without sebaceous gland or dermal vascular changes. EFGR mutant mouse models are all characterized with phenotypic skin changes, and although knockout models are generally lethal, skin of surviving early postnatal knockout mice has also been described as having multiple abnormalities.

Drug-induced changes in eccrine and/or apocrine glands of the skin can be direct or indirect. Indirectly, many neurogenic compounds may lead to suppression or stimulation of sweat gland function through activity on sympathetic innervation of the glands, or by effects on myoepithelial cells also important for sweat production. For instance, anticholinergic and antihistamines may be associated with hypohydrosis via an antimuscarinic pathway. Anticholinesterases cause the opposite effect, increased sweat production or hyperhidrosis. Certain drugs like opioids and some antidepressants can be associated with either increased or decreased sweating, depending on which receptor subtypes are being engaged and thermoregulatory pathway involvement.

Direct toxicity to sweat glands is described for several chemotherapeutic compounds. It is postulated that tendency toward secretion of these compounds in sweat may be at least partially responsible for the targeted gland effect, but a direct toxicity to gland and duct epithelium may also be causative. The change, known as neutrophilic eccrine hyradentitis, features histologic degeneration or necrosis of eccrine and/or apocrine glands sometimes with squamous metaplasia of duct epithelium with or without suppurative inflammation. Neutrophils were originally noted as a key feature of the lesion, but cases without neutrophilic infiltrates in patients that are actually neutropenic are also reported. The most commonly implicated drugs are cytarabine and others that are used to treat acute myelogenous leukemia.

Sebum is rich in lipids, so disruption of lipid synthesis pathways can affect sebum production. The spontaneously occurring asebia mutant mouse is characteristic. This model has defective stearoyl-coA desaturase, an enzyme important in production of monounsaturated fatty acids. Histopathologically, sebaceous glands are hypoplastic and hair follicles are malformed as a result. Sebaceous glands are also rich in nuclear hormone receptors (estrogens, androgen, and progesterone receptors). Testosterone induces sebocyte proliferation and sebum production. Estrogen can also apparently increase sebum, through modulation of the IGF-1 receptor. Beyond hormones, a myriad of receptor subtypes including retinoid/retinoic acid, growth factors, and neurotransmitters characterize sebocytes. This diverse receptor expression suggests the physiologic importance of the sebaceous gland in a number of biologically important pathways.

SUMMARY

The skin constitutes the largest organ in the body and is composed of very distinct components, including innate and adaptive immune systems, that interact and function as a single organ. Since skin may reflect exposure (i.e., drug-induced adverse skin reactions) to both topically applied and systemically administered compounds, it should be considered in any study of toxicity. In addition the species-specific features of skin should always be taken into account in the analysis of any occurrence of comparative cutaneous pathology.

Further Reading

Ackerman, A.B., Boer, A., Bennin, B., Gottlieb, G.J., 2005. Histologic Diagnosis of Inflammatory Skin Diseases: An Algorithmic Method Based on Pattern Analysis, third ed. Ardor Scribendi, New York, NY.

Auletta, C.S., 2004. Current in vivo assays for cutaneous toxicity: local and systemic toxicity testing. Basic Clin. Pharmacol. Toxicol. 95, 201–208.

Bode, G., Clausing, P., Gervais, F., Loegsted, J., Luft, J., Nogues, V., et al., 2010. The utility of the minipig as an animal model in regulatory toxicology. J. Pharmacol. Toxicol. Methods. 62, 196–220.

Diegel, K.L., Danilenko, D.M., Wojcinski, Z.W., 2013. Integument. In: Haschek, W.M., Rousseaux, C.G., Wallig, M.A. (Eds.), Haschek and Rousseaux's Handbook of Toxicologic Pathology. Elsevier, Inc., Academic Press, San Diego, CA, pp. 2219–2275.

FDA (Food and Drug Administration). <http://www.fda.gov/Drugs/default.htm>.

ICH (International Conference on Harmonisation of Technical Requirements for Registration of Pharmaceuticals for Human Use). <http://www.ich.org/>.

Lee, A., Thomson, J., 2006. Drug-Induced Skin Lesions in Adverse Drug Reactions, second ed. Pharmaceutical Press, London.

Mecklenburg, L., Kusewitt, D., Kolly, C., Treumann, S., Adams, E.T., Diegel, K., et al., 2013. Proliferative and non-proliferative lesions of the rat and mouse integument. J. Toxicol. Pathol. 26 (3 Suppl), 27S–57S.

OECD Guideline for the testing of chemicals. (2004). OECD Test Guideline 431. In vitro skin model, Paris, France.

OECD Guideline for the testing of chemicals. (2009). Draft proposal for a new guideline: In vitro skin irritation: Reconstructed human *epidermis* (RhE) model test, Paris, France.

Semlin, L., Schäfer-Korting, M., Borelli, C., Korting, H.C., 2011. In vitro models for human skin disease. Drug Discov. Today. 16, 132–139.

CHAPTER

25

Embryo, Fetus, and Placenta

Colin G. Rousseaux[1] *and Brad Bolon*[2]

[1]University of Ottawa, Ottawa, ON, Canada [2]GEMpath Inc., Longmont, CO, United States

OUTLINE

INTRODUCTION

Until the latter half of the 20th century, congenital malformations were believed to arise solely from genetic or infectious causes. The thalidomide tragedy of the late 1950s and early 1960s showed that xenobiotics also could cause birth defects, and as such sensitized the scientific community and the public to the potential hazards of exposing the developing conceptus to foreign substances. Epidemiological and experimental data indicate that in utero exposure to many xenobiotics can result in structural defects and/or functional deficits within progeny. Humans and animals may be exposed to xenobiotics (e.g., drugs, environmental contaminants, metabolic byproducts, metals) during critical period of development, and at least some of these agents can act as teratogens. Accordingly a more thorough understanding of the processes that drive both normal and abnormal development has assumed increasing importance in toxicologic pathology. This chapter will describe normal and abnormal developmental events in selected vertebrate species, detail methods for determining if and how much such processes may have been disrupted by teratogens, and describe common mechanisms of abnormal development along with factors that may influence the extent and severity of such damage.

Fundamentals of Toxicologic Pathology.
DOI: http://dx.doi.org/10.1016/B978-0-12-809841-7.00026-5

Basic Principles of Developmental Toxicology

Toxicologic pathology of the embryo, fetus, and placenta, termed *developmental toxicology*, assesses the effects induced by xenobiotics, physical agents (e.g., heat, ionizing radiation), or metabolic byproducts. In general the effects of developmental toxicants are manifested as congenital anatomical defects or biochemical/functional deficits that become evident during gestation or soon after birth. However, some toxicant-induced effects initiated during gestation may not become apparent for extended periods after birth, as is the case for transplacental carcinogens.

Developmental toxicity in vertebrates may involve damage to either of the two portions of the conceptus: the embryo (or fetus), and the placenta. The embryonic and fetal periods typically are defined by their relationship to organogenesis, which is the stage during which the organ primordia (or anlagen) first differentiate. The embryonic period is that span of time that precedes and overlaps with organogenesis, while the fetal period is that portion of gestation following the conclusion of organogenesis in which the organs expand toward their adult forms. The fetal period encompasses most of gestation in species with long gestations (e.g., humans), while the embryonic period occupies the major portion of gestation in species with short gestations (e.g., rodents). Indeed the majority of developmental events corresponding to the third trimester of the human fetus actually occur during the first postnatal week of life in rats and mice.

Developmental toxicology is closely allied with *teratology* (derived from the Greek "*teras*" (monster) and "*logos*" (study)), the investigation of manifestations, causes, and mechanisms of developmental anomalies as well as means for their prevention. Thus developmental toxicologic pathologists must command a clear grasp of the six basic principles of teratology, first proposed by James G. Wilson nearly five decades ago.

1. Interactions between the genotype of an embryo or fetus and many environmental factors will influence the onset and degree of teratogenicity;
2. The stage of development during which an embryo or fetus is exposed determines its susceptibility to teratogenic agents;
3. Teratogens induce abnormal development according to specific mechanisms;
4. Physical properties of developmental toxicants determine their access to the embryo or fetus;
5. Death, malformation, intrauterine growth retardation, and postnatal functional abnormalities are all manifestations of teratogenesis; and
6. Expressions of developmental toxicity tend to be dose-related, ranging from slight defects or weight decrements to major malformations or death.

With the exception of Principle 2, these six tenets are identical to those that dictate how adult animals will respond to toxicant exposures. Accordingly, no great adjustment is required when shifting from assessment of toxicologic pathology findings in adults to examination of toxicant-induced effects in developing organisms. It should be noted that not all species are equally sensitive to exposure, and not all littermates show abnormalities, or the same abnormality, following treatment. Maternal toxicity also should be considered and will be discussed later in this chapter.

Incidence of Congenital Anomalies

In developed countries the incidence of major malformation is 2%–4% of births per year. Approximately 3% of congenital defects are considered to arise from maternal exposure to teratogens in the environment.

The incidence of developmental abnormalities in domestic animals ranges from 2% to 12%, depending on the species. Morphologic anomalies in laboratory animals have been well characterized, especially in those species commonly used for teratology studies (particularly mice and rats). In mice, major spontaneous malformations incompatible with postnatal survival (e.g., cardiac septal defects, neural tube defects (NTDs), organ agenesis) occur at a frequency of less than 1%. Minor structural anomalies that do not preclude postnatal viability range in incidence from 1% to 5% for lesions like cranial displacement of the gonads, hemorrhage, sternebral asymmetry, and unossified phalanges, and up to 35% for common variants such as renal pelvic cavitation and supernumerary or wavy ribs.

NORMAL MORPHOLOGIC DEVELOPMENT

The general processes involved in the normal development of humans and most animals are well characterized. Beginning with fertilization, normal morphologic development proceeds through a series of cell expansions and ordered rearrangements that proceed in a stereotypical fashion (Figure 25.1). Terms commonly applied to specific periods during normal development include embryogenesis (the progression of steps needed to form an embryo) and organogenesis (the period in which initial primordia of major organs are formed).

The process of ordered development is guided by multiple factors. Genetic programming, including correct coding and faithful gene transcription and protein translation, is essential to the final differentiation pathway that a cell selects. Accurate intercellular communication is critical to normal development, and occurs via several mechanisms: direct cell contacts, morphogen

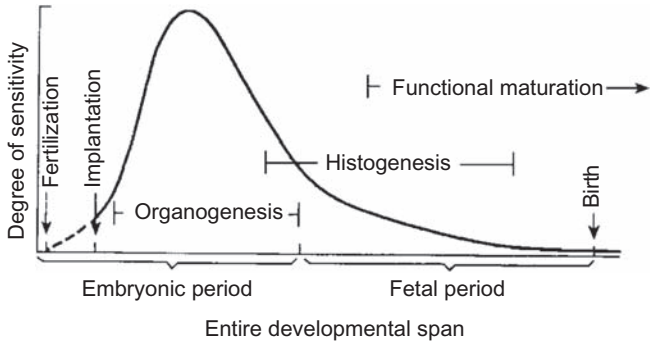

FIGURE 25.1 Sensitivity of the developing mammalian fetus to xenobiotic insults during gestation. Source: *Figure reproduced from the Haschek, W.M., Rousseaux, C.G., Wallig, M.A. (Eds.), 2002. Handbook of Toxicologic Pathology, second ed. Academic Press, Figure 1, p. 897; permission; originally from Wilson, J.G. 1973. Environment and Birth Defects, Academic Press with permission.*

gradients, and tissue interactions (induction). Cell populations respond to their genetic predispositions as well as their internal and external chemical milieus by choosing one or more functional outcomes—cell shape changes, morphogenetic movements, etc.—that will promote ordered differentiation and growth of the organism. An understanding of these processes is essential before the impact of prenatal exposure to teratogens can be fully comprehended. A more detailed consideration of embryonic, fetal, and placental anatomy and physiology is available through excellent developmental biology and developmental pathology texts (see Further Reading).

The zygote (i.e., a one-cell fertilized embryo) divides repeatedly to produce a morula, a grape-like cluster of fundamentally equal, totipotent embryonic stem (ES) cells. Over time, these cells differentiate into two distinct lineages, the trophoblast (a thin layer that encloses the fluid-filled central cavity, or blastocoele), and the inner cell mass, which will become the embryo. These early developmental stages are relatively resistant to toxic insults because of the totipotent nature of ES cells. Toxicant-induced damage that can severely injure these cells will lead to embryonic death prior to implantation, while less serious injury typically will permit the surviving cells to replenish their full complement with little more than a short developmental delay.

In mammalian embryos the process of gastrulation is initiated shortly after the blastocyst (an embryo with a blastocoele) implants within the uterine wall. During this stage the embryonic germ layers (ectoderm, mesoderm, and endoderm) are formed, and the molecular blueprint for the first organs is established. Toxicant exposures at this developmental stage typically do not produce structural malformations, but rather will cause embryonic death and resorption.

Organogenesis, the most complex stage of development, results in specification of all organs within the embryo. The complexity of this developmental stage means that interference by exogenous toxicants can produce devastating effects on the growing organism, usually in the form of major malformations. Teratogenic effects often are produced by interfering with intercellular communication (which guides appropriate connectivity), cell movement, generation of morphogen gradients (where morphogens are molecules that direct structural differentiation when present at the correct concentration), and programmed cell death (needed to sculpt organ primordia into their final form).

As development progresses in a given organ primordium, totipotent stem cells (which express all genes and so can become any cell at need) evolve to pluripotent stem cells (which can develop into many but not all cell types), then to oligopotent stem cells (which can form only a few cell types), and thence to fully differentiated cells (Figure 25.2). The progressive increase in specialization (termed *histogenesis*) renders the cells more capable of performing their specific functions but typically renders them more vulnerable to development toxicants.

DEVELOPMENTAL TOXICITY TESTING AND RISK ASSESSMENT

The toxicologic pathology aspects of developmental toxicity testing are usually performed using various *in vivo* test systems. Fundamental aspects of developmental biology at the cellular and molecular levels have commonly employed both invertebrates, such as fruit flies (*Drosophila melanogaster*) and worms (*Caenorhabditis elegans*), as well as many vertebrates, including zebrafish (*Brachydanio rerio*), avians (e.g., chick (*Gallus gallus*) and quail (*Coturnix* sp.)), and many mammals. The test species used in conventional developmental toxicity testing are generally mammals (mainly rodents and rabbits). This section describes the main principles of such tests and delineates factors that make various mammalian species the subjects of choice for such analyses.

Hazard Identification and Dose-Response Analysis

The first two steps in the risk assessment process for the developmental toxicity potential of any test article are hazard identification and the dose-response evaluation. These steps are difficult to separate, as hazard should always be evaluated in the context of the exposure route, dose, timing, and duration.

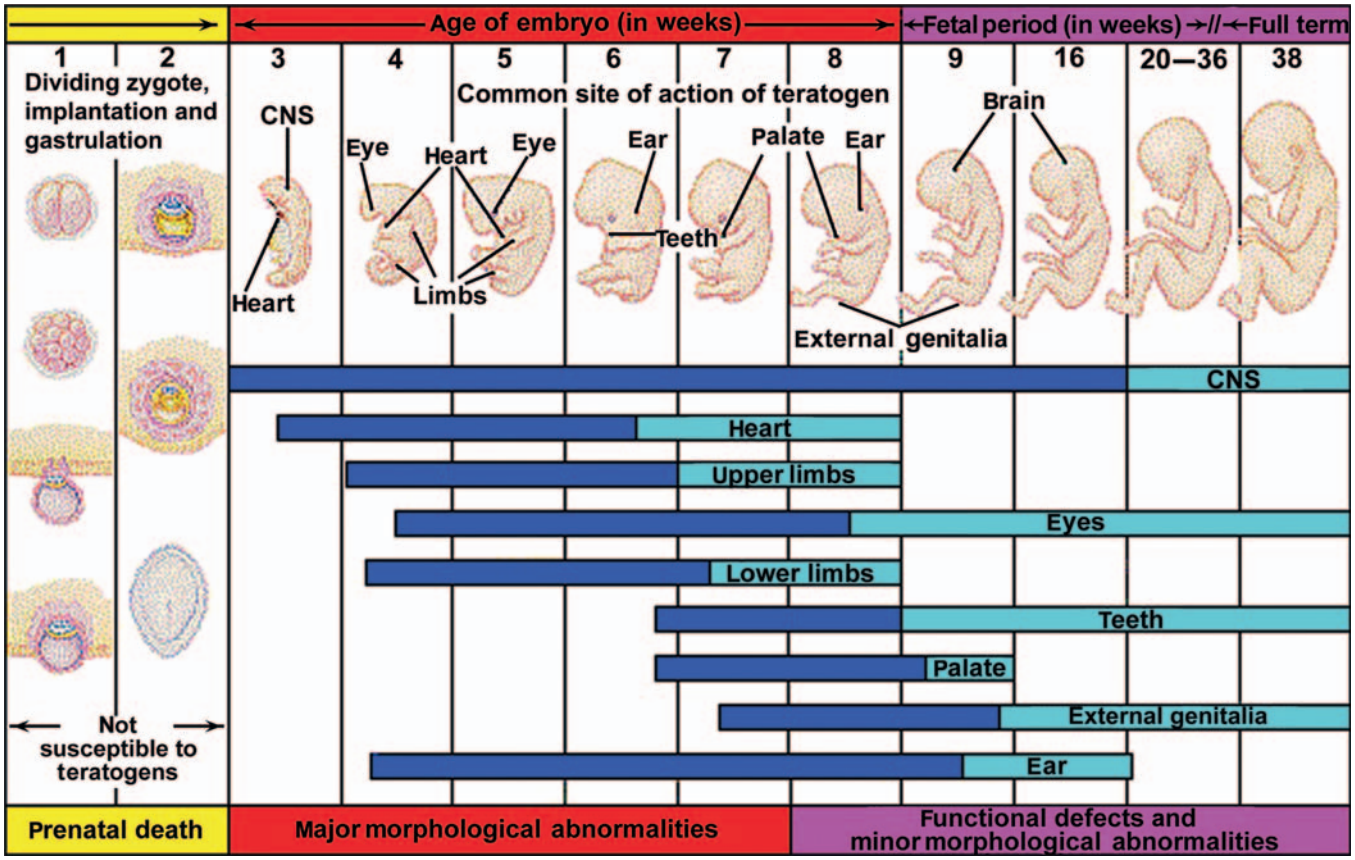

FIGURE 25.2 Schematic diagram of the critical periods of human development. Source: *Figure reproduced from the Haschek, W.M., Rousseaux, C.G., Wallig, M.A. (Eds.), 2002. Handbook of Toxicologic Pathology, second ed. Academic Press, Figure 3, p. 902 with permission, as adapted by Dr. Mark Hill, University of New South Wales, Sydney, Australia (http://embryology.med.unsw.edu.au/Medicine/images/hcriticaldev.gif).*

Default Assumptions

Extrapolation to humans of developmental toxicity data derived from animals is a complex process. A number of general default assumptions can be made to guide the risk assignment process.

The first assumption is that an agent, which produces an adverse developmental effect in experimental animal studies, will pose a potential hazard to humans following sufficient exposure during a susceptible stage of development. This supposition has been confirmed for many developmental toxicants but is not true in all cases. The most glaring example of this discordance is the thalidomide catastrophe, in which the mammalian test species used in developmental toxicity testing (rodents) were insensitive to in utero toxicity while human fetuses were exquisitely sensitive. Rabbits, whose embryos are sensitive to thalidomide, were not used in its safety assessment.

The second assumption is that all four manifestations of developmental toxicity—death, structural malformations, growth alterations, and functional deficits—are of concern in defining whether or not an agent is a potential hazard. The notion is easily confirmed for compounds that significantly reduce the number of viable implantation sites, increase the incidence of perinatal death, or lessen the birth weight or postnatal weight gain. These endpoints are ideal for this purpose as they offer objective (easily quantified) measurements of an effect, with the range of interindividual variation being relatively narrow under normal circumstances.

The third assumption is that the types of developmental effects seen in animal studies are not necessarily the same as those that may be produced in humans. This assumption is made because it is impossible to determine *a priori* which species will be the most appropriate in terms of predicting the specific types of developmental toxicity that might occur in humans, the chief of which are the divergent timing of critical developmental periods (Table 25.1) and fundamental differences in the anatomic, biochemical/molecular, and physiological characteristics of the conceptus (embryo/fetus, placenta, or both). Additional factors such as variations in dose, route, and timing of exposure; unique kinetic and/or metabolic disposition of the test article and its metabolites; and

TABLE 25.1 Timing of Developmental Milestones in Vertebrates[a]

Species		Length of gestation[b]	2-Cell	8-Cell	Morula	Blastocyst	Implantation	Gastrula	Neurula	10-Somite	Embryogenesis completed
Zebrafish	*Brachydanio rerio*	60	0.75	1.25	2	5	N/A[c]	8	10	12	48
Chick	*Gallus gallus*	21	3	4	5	10	N/A[c]	18	24	36	10
Mouse	*Mus musculus*	19	1	2	3	3.5	5	6.5	7.5	8.5	15
Rat	*Rattus rattus*	21	1.5	2.5	4	5	6	8	9.5	11	16
Hamster (golden)	*Mesocricetus auratus*	16	0.75	1	2.75	3.5	5	6	7	8	13
Guinea Pig	*Cavia porcellus*	67	2	3.5	4.5	5.5	6.5	9	12	15	29
Rabbit	*Oryctolagus cuniculus*	32	2	2.5	3	3.5	7	7	8	9	17
Ferret	*Mustela putorius*	42	2	4	5	6	13	13	14	15	20
Cat	*Felis domesticus*	63	3	3.5	4	5	12	12	13	14	28
Dog	*Canis domesticus*	63	4	6	7	8	16	16	17	18	40
Pig	*Sus scrofa*	115	1	2.5	4	5	14	9	14	15	33
Sheep	*Ovis aries*	145	1	2.5	4	6	16	10	15	16	35
Cow	*Bos taurus*	282	1	3	6	8	30	14	19	21	40
Horse	*Equus caballus*	336	1	3	4	6	35	14	18	19	45
PRIMATES											
Rhesus	*Macaca mulatta*	165	1	2	4	5	8	16	20	23	47
Human	*Homo sapiens*	267	1	2	3	5	9	13	16	25	58

[a]*Times are estimated mean values in days postconception except for the zebrafish and chick, where values for all columns (except length of gestation and completion of embryogenesis for chick) are in hours. The day of confirmed mating is designated as the day of conception (gestational day 0).*
[b]*For zebrafish and chicken, the values in this column refer to length of incubation before hatching.*
[c]*N/A denotes not applicable in this species.*
Table reproduced from Haschek, W.M., Rousseaux, C.G., Wallig, M.A. (Eds.), 2013. Handbook of Toxicologic Pathology, third ed., Academic Press, Table 62.1, p. 2706 with permission.

species-specific differences in the mechanisms of action/toxicity also may play a role.

The fourth assumption is that the "most appropriate species" will be used to acquire data for estimating human risk. Ideally translation of animal data to assess human risk is based on evidence permitting a direct cross-species comparison, such as an equivalent pharmacokinetic (PK) profile or similar reactivity of the putative target in animal and human tissues. In the absence of such data, it is presumed that the most sensitive animal species is the most appropriate for use. This supposition is based on epidemiological (in human) and experimental (in animal) observations showing that, relative to the most sensitive animal species, humans are as sensitive or more so to the great majority of human developmental toxicants.

The fifth and final assumption is that developmental toxicants will generally follow a dose-response curve that includes a distinct threshold. This idea is based on the known capacity of the developing organism to either repair or compensate for a certain amount of damage at the cellular, tissue, or organ level.

How Dose Relates to Developmental Defects

The stage of embryonic or fetal development must be considered before attempting to define the correlation between dose and the consequences of abnormal development. Low doses do not necessarily cause functional deficits, and high doses do not always lead to embryonic or fetal death. The outcome also depends on the stage of development at which the agent is administered and the mechanism by which it acts.

During early development, relatively high exposures to xenobiotics may induce death or may elicit few visible changes. These divergent outcomes result from the wide range of fates open to most embryonic cells prior to the start of organogenesis. Once organogenesis is in progress, lesser concentrations of a substance may produce prominent morphological defects. This change in the pattern of anomalies arises because the death of partially committed stem cells tends to

produce cell losses and/or functional deficits, which can no longer be fully reversed by the surviving remnants of the targeted cell population or compensated for by other partly differentiated stem cell collectives.

Toward the end of organogenesis, malformation is less likely and tends to require very large doses. Instead late in embryogenesis xenobiotic exposures are more likely to cause functional deficits and intrauterine growth retardation.

Transplacental carcinogenesis depends on the nature of the carcinogen. Current thinking is that neoplasms can be induced by exposure to very small concentrations during organogenesis or to moderate concentrations after organogenesis. The proposed mechanism of initiation usually is a genotoxic (i.e., mutating) event.

Laboratory Animal Studies

The conventional strategy for developmental toxicity testing programs assesses the ability of the test article to adversely impact development following prenatal exposure during the entire period of organogenesis (i.e., a period spanning the time during which all organs will initially be formed). Program designs commonly test the product in one rodent and one nonrodent species, most often the rat and the rabbit, unless other species (e.g., nonhuman primates) are deemed more relevant (often the case for biomolecules).

The conceptus is exposed to the compound by treating the dam, and the evaluation of toxicity endpoints is performed shortly before parturition. More recent regulatory guidelines recommend longer treatment periods with dosing extending from before or shortly after conception until well after birth (often weaning). Certain study designs have evolved to assess both developmental and reproductive toxicity (DART) endpoints in multiple generations within a single large experiment.

MATERNAL ENDPOINTS OF DEVELOPMENTAL TOXICITY

Many endpoints for assessing the health status of the dam provide data that also provide information regarding the health status of the progeny. In-life measurements of maternal health include clinical signs, food and water consumption, and maternal weight gain (both the amount and the rate) during treatment. Essential parameters to quantify at necropsy are terminal body weight and target organ weights of the dam, and in some cases histopathological analysis of selected target organs; an important consideration is to also measure either the total weight of the gravid uterus or the maternal carcass weight after uterine removal to avoid bias due to different litter sizes. In addition, the number of implantation sites should be counted. Care must be taken when assessing the relevance of such maternal data because some endpoints (e.g., weight gain over time in rabbits) can vary greatly for reasons unrelated to xenobiotic exposure.

PROGENY ENDPOINTS OF DEVELOPMENTAL TOXICITY

In multiparous species the litter is the experimental unit used for statistical analysis of developmental pathology data sets, rather than each individual offspring. Therefore developmental toxicity studies include 10 litters per group (assuming a standard litter size of 8), and not 80 conceptuses. This convention is employed because progeny in a litter are subject to a common environment, resulting from shared influences arising from the specific dam and/or their particular siblings.

Important parameters to measure in all developmental toxicity studies include several measures of litter size—the total number of conceptuses, the numbers of viable and dead conceptuses, and the number of resorptions (abnormal implantation sites)—and the presence of gross structural malformations and incidental variations. The number of dead fetuses and resorptions show a test article's ability to induce prenatal mortality, and both counts are increased by exposure to many developmental toxicants. In near-term fetuses and neonates, total body weights may be acquired, and the sex ratio can be determined using the anogenital distance. In studies that include collection of parturition and lactation data, several other measurements may be taken for the neonates (or juveniles). The easiest measurements are the number of perinatal deaths, incidence of major structural malformations, birth weights, and progressive weight gain over time. If desired, additional endpoints to consider may include clinical signs and symptoms (e.g., abnormal skin coloration, inability to suckle); simple behavioral tests (usually to test progressive motor development); and histopathological examination.

Certain endpoints require special postnecropsy processing. Common techniques of this nature include analysis of internal organs (accomplished by making multiple free-hand cross sections of fixed fetuses (Wilson's technique)) or skeletal anatomy (performed by skeletal double staining with Alcian blue and alizarin red S to highlight cartilage and bone, respectively). These latter techniques are time-consuming and require considerable technical expertise on the part of the personnel.

Careful consideration of the study goal is required when designing developmental toxicity experiments. Major malformations are much more likely to be induced by high-dose, short-term exposures that take place during a particular organ's critical period of development (e.g., in mice, gestational days (GD) 8–9 for NTDs, or GD 10–11 for cleft palate, where the morning after conception is considered to be GD 0). In contrast the typical design used in regulatory studies to assess the risk of developmental toxicity calls for

low-level, longer-term dosing throughout organogenesis, which provides a fairly robust means of evaluating prenatal death and growth retardation arising from substantial damage to any organ system. This latter design is especially desirable when the target organ(s) vulnerable to a test article are not yet known.

ANIMAL MODELS

RODENTS Mice and rats are particularly useful as the initial mammalian test species for most conventional developmental toxicity screens due to their small size, short gestation, large litter size, ease in breeding, and ready availability. Rats have the advantage of producing larger fetuses, thereby enabling easier evaluation. Data are available (both in online databases and from vendors) for rates of spontaneous anomalies in numerous strains and species of rodents. Many inbred mice have a high incidence of strain-specific structural defects. Other mouse strains have low incidences of spontaneous defects and are quite impervious to developing them under the influence of teratogens. This phenomenon means that pairing sensitive and resistant strains of inbred mice in a single study can provide a powerful platform for investigating the influences of genotype and specific molecular mechanisms on the genesis of certain developmental defects, and particularly the potential actions of toxicants in promoting them.

Some institutions use alternative rodent species for teratology studies. In this regard the golden (Syrian) hamster (*Mesocricetus auratus*) is a model of choice. Like other rodents, this species has a 4-day estrous cycle and produces litters averaging 8–10 pups. However, the gestation length of the golden hamster is the shortest known for a placental mammal (16 days, vs 18–20 days for various mouse strains and 20–22 days for rat strains).

RABBITS Rabbits are lagomorphs rather than rodents, and thus represent the nonrodent species of choice for developmental toxicity testing. Factors favoring this choice include their larger size (which provides ample samples for analysis), accuracy in timing the start of conception (since ovulation is induced by copulation, occurring about 10 hours after mating), and large number of progeny (ranging from 4 to 12). The length of gestation is approximately 30 days. Some strains produce a spectrum of malformations similar to those of humans when exposed to thalidomide during gestation, but in general rabbits do not appear to be superior to other animal models in predicting the human response to most developmental toxicants.

NONHUMAN PRIMATES In certain instances the preferred nonrodent species might be a nonhuman primate (NHP). A number of NHP species have been employed for this purpose. Factors dictating this decision include close similarities in maternal kinetics and metabolism of xenobiotics, placental structure, and reproductive physiology—especially anatomic and temporal aspects of early embryogenesis. However, in spite of these resemblances, NHPs are avoided when possible due to their scarcity, high cost, long gestation, and *monoparous pregnancy* (i.e., tendency to produce a single conceptus per pregnancy).

These factors substantially limit sample sizes in treatment groups (typically 3–5 per cohort), and routinely result in a data set in which interactions between the test article and sex cannot be reliably assessed due to the unequal numbers of male and female progeny. Another complicating aspect of developmental toxicity testing with NHPs is that their sensitivity to xenobiotic-induced teratogenicity often differs from that of humans. An example is methotrexate, a folic acid analog, which has been shown to induce skeletal defects (chiefly in the limbs and skull) in humans but produces little or no embryotoxicity in NHPs. Finally, NHPs are commonly not used due to their cognitive abilities and need for substantial environmental enrichment and socialization activities.

OTHER VERTEBRATE SPECIES Other mammals (ferrets, guinea pigs, cats, dogs, swine) are occasionally employed in developmental toxicity studies. However, characteristics such as size, cost, difficulty in handling, long gestation periods, lack of a historical database, and lack of any obvious predictive superiority as well as social acceptability limit their use.

The use of chicken embryos for developmental toxicity screening has the obvious advantages of a readily available, low-cost model with a recognized historical database and short developmental period (21 days at the optimal temperature). However, in the strictest sense, in ovo testing in embryonic chicks is not equivalent to *in vivo* testing as maternal PK processes and placental transfer can play no role in this avian system. In addition, chick embryos have a relatively high sensitivity to many exogenous agents, and significant differences exist in the course of embryogenesis among avian and mammalian species. Together, these factors typically limit the use of chicken (and quail) eggs to mechanistic studies while precluding their use as a system for developmental toxicity testing.

Human Studies

Epidemiological studies are used in two fashions to assess the potential that an agent has for inducing developmental toxicity in humans. The first approach uses such data in an attempt to identify new teratogens based on increased incidences of structural and/or functional abnormalities in exposed individuals. The second tactic is to test the relevance of developmental toxicity data derived from animal studies to

human hazard identification and risk assessment, which is accomplished by determining whether or not the spectrum of defects seen in animals is recapitulated in humans.

Human epidemiological studies have identified many likely human developmental toxicants, including pharmaceutical agents (e.g., anticonvulsants, antineoplastic agents, thalidomide); environmental pollutants (e.g., maternal alcohol abuse or heavy smoking); heavy metals (e.g., methyl mercury); and viral infections (e.g., rubella, Zika). However, such studies by themselves cannot confirm causality and have relatively poor sensitivity.

Maternal Versus Developmental Toxicity

An important question when trying to classify hazards and manage risk is to define whether or not a toxicant-associated developmental defect results from direct damage to the embryo (a primary effect) or is the indirect sequel to some maternal disease process (a secondary effect). The concern arises because mild embryolethality and nonspecific fetotoxicity commonly occur for doses at which dams exhibit more substantial signs of toxicity. The number of possible mechanisms for indirectly inducing maternally mediated effects is probably much lower than the number of direct-acting (i.e., embryotoxic) mechanisms.

Several hypotheses have been suggested to explain this phenomenon. One prominent possibility is failed maternal support of the conceptus (e.g., by anemia or reduced placental circulation), leading to hypoxia in the conceptus. A second prospect is maternal production of some endogenous toxicant by xenobiotic-damaged maternal tissues (e.g., acidosis leading to a precipitous drop in the pH of embryonic tissues); a variant of this scenario is maternal illness leading to an increase in maternal core body (and therefore uterine) temperature—in other words, hyperthermia (fever). Finally, modification of maternal metabolism can intensify or lessen the effects of an agent (e.g., by activation of a nontoxic pro-drug or production of a more toxic or longer-lasting metabolite). Maternal toxicity can promote developmental toxicity by several means, so it is probable that the spectrum of maternally controlled developmental abnormalities in the offspring may be quite broad.

Short-Term Tests

Abbreviated screens for developmental toxicity are often employed to prioritize chemicals for further testing. These tests are typically classified together as "*in vitro*" assays. However, this appellation is a misnomer as many are instead "*ex vivo*" or "*in vivo*" preparations (i.e., utilizing isolated whole organs or intact, viable, nonmammalian organisms, respectively). These short-term assays are not meant to substitute for "*in vivo*" testing in pregnant mammals. Instead, they expose invertebrate organisms (e.g., flies (*D. melanogaster*), hydras (*Hydra attenuata*), worms (*C. elegans*)) or simplified vertebrate systems (e.g., cultured cells, detached body parts (micromass organ cultures), or whole embryos) to xenobiotics for limited periods.

The short-term procedures are particularly relevant for identifying and characterizing *mechanisms* of developmental toxicity due to the ability to observe developmental events over time and the complete exclusion of any confounding maternal influences. These methods are also popular as indicators of developmental toxicant accumulation in polluted aquatic environments.

The short-term screens have several advantages over *in vivo* teratogenicity testing in mammals. The major benefits include their rapidity, low cost, and reduced utilization of sentient laboratory animals. Unfortunately the abbreviated assays also suffer from many significant disadvantages: lack of specificity, inability to model metabolic and PK events, and uncertain applicability of invertebrate models to mammalian species. The lack of metabolic capability may be addressed by partially restoring maternal metabolic function via the addition of cytosolic or S9 microsomal fractions from homogenized liver.

Other Considerations in Developmental Toxicity Testing

As is the case with other toxic effects, developmental toxicity is strongly impacted by PK parameters. The influence of such factors is complicated by the fact that two different organisms are involved, mother and conceptus, both of which have separate and often distinct PK profiles. Maternal uptake, transplacental passage into and away from the embryo, and maternal elimination are critical parameters that govern the access of xenobiotics to the offspring. Biotransformation (metabolism) also plays an essential role in defining the extent of developmental toxicity. In this regard the fully mature maternal metabolic pathways are usually of more importance in dictating the effect of xenobiotics, as enzyme systems in the embryo and fetus usually are incompletely differentiated and/or incapable of high-throughput chemical conversion. Some toxicants may be sequestered within embryonic tissues due to the altered conditions (e.g., lower oxygen tension, reduced glucose stores, pH gradient) relative to those in the dam.

Epigenetic influences (i.e., intrauterine environmental imbalances rather than embryonic genetic anomalies) also may produce long-lasting developmental effects. The classic examples of this phenomenon are maternal metabolic abnormalities, especially diabetes but also some environmental toxicants (e.g., arsenic,

bisphenol A). In humans the incidence of congenital defects in women with preexisting diabetes (about 10%) is higher than that of the general population (approximately 3%), particularly if blood glucose levels are poorly controlled during organogenesis (i.e., the first trimester). The abnormalities occur in multiple systems but are common and severe in the head (e.g., NTDs and craniofacial malformations), heart (often atrial and ventricular septal defects), and caudal trunk (hypoplasia or absence of the caudal trunk and hind limbs). The putative mechanism for functional and structural abnormalities is that nutritional imbalances in cells of the conceptus skew the embryonic programming for many neuroendocrine control systems that regulate energy homeostasis and metabolism. These changes not only alter intrauterine development but may also predispose individuals to developing their own metabolic diseases late in life.

RESPONSES TO INJURY

In many respects a conceptus represents a unique tissue type that just happens to be a transient passenger in its maternal host. The bases for its unique response, particularly during the earlier stages of gestation, are the lesser degree of cellular differentiation and its tolerance for low-oxygen conditions. Both these factors permit more ready repair of damage that would decimate the more differentiated and oxygen-dependent maternal tissues. Nonetheless the fundamental responses of the embryo/fetus and placenta to toxicant-induced damage are similar to the well-recognized reactions that occur in the tissues of toxicant-treated adult animals.

As seen in other tissues the conceptus (and neonate) responds to toxicant-induced injury by initiating a number of mechanisms that either sustains the damaged cells until they can be repaired or tries to mitigate the damage when severely perturbed cells degenerate and die. The basic manifestation of cytotoxicity in the conceptus is cell death, the ramifications of which range from none or slight (in early embryos with pluripotent stem cells) to major structural malformations, growth retardation, or in utero death. Unlike adult animals the developing conceptus seldom mounts an inflammatory response to necrosis (or other insults) until the latter half of gestation, when the immune system has begun to mature.

The plasticity of the early embryo (based on its large complement of totipotent and pluripotent stem cells) allows compensatory growth to completely restore many tissue defects after nonlethal exposure that would induce lethality or major malformations in older individuals. Thus statistically significant growth retardation in many cases is likely to represent a developmental delay rather than a genuine reflection of teratogenic activity per se. To be sure, attempts at repair following developmental toxicant exposure may lead to *deformations*, which are congenital anomalies due to ineffective regeneration (as opposed to *malformations*, which are defects produced by tissue injury). An example of a deformation is intestinal atresia resulting from fibrosis following ischemic injury to the intestine.

Death

Approximately 50%–70% of all human conceptuses are lost during the first 3 weeks of development, and by the end of pregnancy another 78% of the early survivors will have died. Chromosomal anomalies are apparent in 60% of human abortuses occurring at less than 12 weeks of gestation, and have a prevalence of 1 in 160 live births. These aberrations account for many multisystemic malformations in defective fetuses that make it to term. Malformed fetuses are born dead 10 times more often than delivered alive, and many of those that survive birth will die shortly thereafter. Thus a general principle of developmental toxicologic pathology is that major structural defects are usually fatal (assuming no medical intervention to repair them). The most common lethal defects that occur during early gestation are NTDs, cardiovascular malformations, and multisystemic anomalies (that cannot be linked to preexisting chromosomal damage).

Nonviable embryos and fetuses are typically eliminated by spontaneous (natural) causes, a process termed *terathanasia*. However, mortality due to congenital anomalies does not stop with birth. Approximately 8% of human infants with major malformations die during the neonatal and juvenile periods.

Malformations

Embryonic and fetal malformations provide the most spectacular evidence of developmental disaster, and as such have been a source of curiosity and dread for millennia. The modern science of teratology first facilitated investigations of the biological basis of developmental defects, and then expanded to encompass testing for developmental toxicity. The reason for this expanded focus is that numerous xenobiotics are teratogens (i.e., agents capable of inducing malformations) (Table 25.2).

Teratogens often affect multiple species, and induce a similar spectrum of effects across sensitive species. Examples of toxic agents that generate malformations in both humans and laboratory animals include "recreational" (e.g., cocaine, ethanol, nicotine) and therapeutic

TABLE 25.2 Examples of Specific Congenital Defects with Known Etiologic Agents in Mammals

System	Defect	Etiology	Species
Central nervous/axial skeleton	Anencephaly/exencephaly	Colchicine	Mouse
		Injected inorganic arsenic	Mouse, rat, hamster
		Ethylnitrosourea	Rat
		Methylhydrazine	Rabbit
		Retinoic acid	Hamster
		Thalidomide	Rabbit
	Auditory nerve hypoplasia	Quinine	Human
	Cerebellar hypoplasia	Triamcinolone acetonide	Baboon, monkey
	Encephalocele	Ionizing radiation	Mouse
		Hydroxyurea	Mouse
	Hydrocephalus	Ionizing radiation	Mouse, rat
		Vitamin A deficiency	Rat, rabbit, pig
	Iniencephaly	Streptonigran	Rat
	Microcephaly	Hyperthermia	Guinea pig, rabbit
		Methylnitrosourea	Rat
		X-rays	Rat
	Spina bifida	Actinomycin D	Mouse
		7,12-Dimethyl-benz [*a*] anthracene	Rat
		Thalidomide	Baboon, monkey
Craniofacial	Agnathia/micrognathia	Injected inorganic arsenic	Mouse
		Pyrimethamine	Rat
		Retinoids	Hamster, monkey
	Anophthalmia/microphthalmia	Ethylnitrosourea	Rat
		Glycol ethers	Mouse
	Cataracts	Mirex	Rat
	Cleft face	Ochratoxin A	Mouse
	Cheiloschisis/palatoschisis	Dioxin (TCDD)	Mouse
		Diphenylhydantoin	Mouse
		Glucocorticoids	Mouse
		Griseofulvin	Cat
	Cyclopia	*Veratrum californicum*	Ruminants
	Microtia and/or synotia	*Veratrum californicum*	Mouse
	Nasal defects	Griseofulvin	Cat
	Open eye	Methyl salicylate	Mouse
	Retinal defects	X-rays	Rodents
Cardiovascular	Atrial septal defects	Alcohol	Human
		Dextroamphetamine sulfate	Mouse
	Dextrocardia	Actinomycin D	Rat
	Great vessel and *vena cava* anomalies	Valproic acid	Rat
	Tricuspid valve anomalies	Methyl chloride	Mouse
	Various defects	Diethylene glycol dimethyl ether	Mouse
	Ventricular septal defects	Alcohol	Human
		Dextroamphetamine sulfate	Mouse
		Thalidomide	Rabbit
Respiratory	Lung agenesis	Vitamin A deficiency	Rat, pig
	Lung hypoplasia	L-Asparaginase	Rabbit
Gastrointestinal	Absent gallbladder	Nitromifene	Dog
		Retinoic acid	Hamster
	Anal atresia	Colchicine	Mouse
	Diaphragmatic hernia	Nitrofen	Mouse, rat
	Esophageal/duodenal atresia	Thalidomide	Human
	Gastroschisis	Vincristine	Mouse
		6-Azauridine	Rat
	Omphalocele	Actinomycin D	Mouse, rabbit
		Hyperthermia	Rat
Urogenital	Cryptorchidism	Cadmium	Rat
		Vitamin A deficiency	Rat, pig
	Hydronephrosis	Bradykinin	Mouse
	Hydroureter	Vitamin A excess	Rat
	Hypospadias	Chlorambucil	Rat

TABLE 25.2 (Continued)

System	Defect	Etiology	Species
	Intersexuality	Androstenedione	Rat
		Prunus serotina	Pig
	Ovarian hypoplasia	Diethylstilbestrol	Mouse, rat
	Renal agenesis	Chlorambucil	Rat
		Injected sodium arsenate	Rat
		Thalidomide	Human
Musculoskeletal	Arthrogryposis	Anagyrine	Cow, pig, sheep
		Nicotiana glauca	Pig
		Sudan grass	Horse
	Digit malformations	Cyclophosphamide	Human
		Ethylenethiourea	Rat
	Limb reduction defects	Acetazolamide	Mouse, rat
		Caffeine	Mouse
		Hydroxyurea	Rabbit
		N-Methyl-*N*-nitro-*N*-nitrosoguanidine	Mouse
		Thalidomide	Rabbit, monkey, human
	Muscular dystrophy	Vitamin E deficiency	Rat, rabbit
	Polydactyly	Cytosine arabinoside	Mouse
	Rib and/or vertebral defects	Ethylene glycol	Mouse, rat
		Injected sodium arsenate	Mouse, rat
		Hydroxyurea	Rabbit
	Tail shortened and/or malformed	Colchicine	Rabbit
		T-2 toxin	Mouse

Table reproduced from Haschek, W.M., Rousseaux, C.G., Wallig, M.A., (Eds.) 2002. Handbook of Toxicologic Pathology, second ed., Academic Press, Table IX, p. 917 with permission.

(e.g., anticonvulsants, antineoplastics, immune suppressants) drugs as well as many environmental contaminants (e.g., heavy metals, plant toxins, solvents). Indeed, some xenobiotics are so potent, and their constellation of defects so reproducible, that they constitute preferred agents for investigating teratogenic mechanisms (e.g., retinoid-induced cleft palate).

Malformations have been reported in essentially all organs and systems of multiple vertebrate species. This section briefly describes some of the more common anomalies observed in human obstetrical practice and animal developmental toxicity experiments. Unless otherwise noted later, these defects have been linked to many pathogens (usually viruses), physical agents (e.g., heat, radiation), and xenobiotics.

Central Nervous System

DYSRAPHISM

Dysraphism is the generic term for incomplete fusion of the neural tube (i.e., a NTD). Variants of this lesion are typically defined based on the affected site. Common forms are *cranioschisis* (nonfusion of the cranial portion), as exemplified in anencephaly, exencephaly, and encephalocele (Figure 25.3), as well as

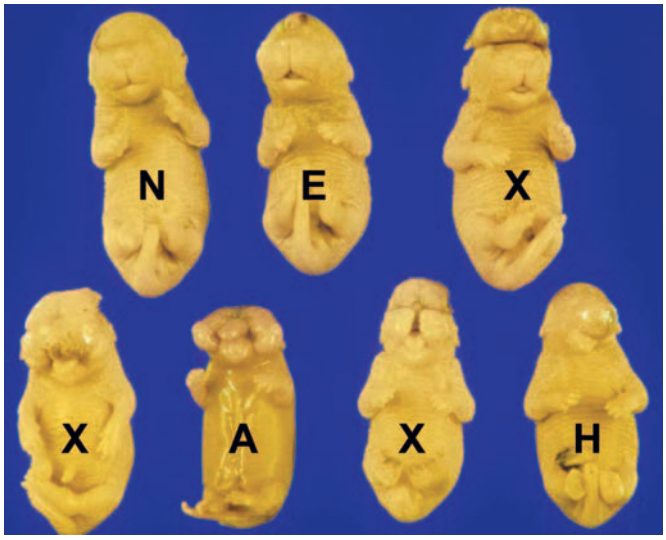

FIGURE 25.3 Neural tube defects (NTDs) represent a continuum of cephalic dysraphism. Relative to an aged-matched control littermate (N), near-term mouse fetuses (gestational day (GD) 17.5) exhibit a spectrum of neural tube and craniofacial defects following maternal inhalation of methanol during neurulation (i.e., the period of neural tube formation and closure, or GD 7–9 in the mouse). The mildest NTD variant is encephalocele (E), in which meningeal-covered cerebral cortex protrudes through a small opening in the frontal region as a consequence of incomplete anterior neuropore closure. Severe defects arising from failure of the anterior neuropore to close include exencephaly (X), in which the exposed cerebrum and midbrain form a tattered cap on the dorsal cranium, and anencephaly (A), where the brain and upper head are absent. The fetus marked by H has holoprosencephaly, or failure of the primary forebrain vesicle to divide into paired secondary vesicles. Craniofacial defects associated with NTD also reflect abnormal closure of the anterior neuropore. Mild effects (relative to the narrow inverted-T conformation of the N (control) fetus) usually present as hypognathism of the maxillae (upper jaw), indicated by the triangular oral openings for the E and X fetuses in the top row. Marked effects include cleft nose (X fetuses of the lower row), aplasia of the cranium (the A and all X fetuses), and aplasia of craniofacial bones (maxillae and mandibles (lower jaws), most prominent in the H fetus) and eyes. Source: *Figure reproduced from Bolon, B., et al., 1994. Methanol-induced neural tube defects in mice: pathogenesis during neurulation. Teratology 49 497–517, 1994 with permission.*

rachischisis (nonfusion of the caudal region) leading to spina bifida (Figure 25.4) and meningocele. Rarely the entire neural tube may remain open, a condition called *craniorachischisis*. The pathogenesis for these lesions is failed elevation and/or fusion of the neural folds, or rarely reopening of a thinly sealed fusion site.

If the head is affected the development of the pituitary gland is often rudimentary. These structural defects are associated with functional abnormalities, which may lead to secondary hypoplasia of endocrine tissues (i.e., adrenal, gonadal, and thyroid) that require pituitary releasing factors for their own maturation.

ANENCEPHALY *Anencephaly* (no brain) is more common in humans than in domestic animals. The usual appearance is absence of neural tissue rostral to the brainstem (Figure 25.3). It has a prevalence ranging between 0.8 and 18/10,000 infants, depending on the locale. Areas with heightened prevalence typically have populations with genetic predispositions or who live in regions with substantial environmental contamination. One factor thought to contribute to the severe loss of brain mass is the long gestational period, which permits lengthier exposure to the destructive effects of amniotic fluid.

EXENCEPHALY *Exencephaly* (external brain) is seen more frequently in laboratory animals than anencephaly. In exencephaly the entire brain is present but is exposed (Figure 25.3). Mechanisms include disruption of tissue interactions, inhibition of cell proliferation, or general cytotoxicity. The occurrence of exencephaly is greatly increased in certain inbred mouse strains, indicating the importance of genetic factors. Preservation of the exposed brain tissue in animal species with short gestations is proposed to result from a shorter exposure to amniotic fluid, although other factors also must contribute as anencephaly is observed occasionally in mice (Figure 25.3).

Encephalocele is the extension of brain tissue (usually cerebral cortex and the overlying meninges) through a small opening in the calvarium (Figure 25.3). These lesions typically present as small round nodules on the midline, often in the frontal region. The masses may be covered by skin, or the brain tissue may be exposed. In general the neural tissue is fairly well differentiated. In mice, encephalocele and exencephaly occur together in litters exposed to various xenobiotics, suggesting that they represent different expressions of the basic NTD phenotype. Encephaloceles are much less common than exencephaly in animal models of NTD.

HOLOPROSENCEPHALY *Holoprosencephaly* (formerly termed *arhinencephaly*) stems from failed division of the prosencephalon (the one primary forebrain vesicle) into the two components of the telencephalon (the two secondary brain vesicles from which the cerebral cortices arise). The resulting single telencephalic ventricle is called a holosphere. The olfactory bulbs and tracts are absent.

The defect typically produces malformations in both the brain and the craniofacial skeleton (Figure 25.3). A common variant is a reduction in the distance between the two eyes, or even their fusion into a single globe located at the midline (i.e., cyclopia). In most instances individuals are so deformed that they expire before birth.

ACRANIA In cases of anencephaly and exencephaly, the corresponding skeletal defect is *acrania* (lack of the calvarium (upper skull)). Associated skeletal reductions or loss affect the petrous temporal bones, sphenoid bone, and internal ear. The base of the skull undergoes normal development. However, the cerebellum, pons, and cranial nerves are usually malformed.

SPINA BIFIDA Spina bifida is a NTD of the caudal axial skeleton resulting from failure of the neural arches of the vertebra to unite (Figure 25.4). Spina bifida has been reported in all species, with a worldwide incidence in humans of 0.5/1000 live births. However, the frequency varies widely depending on the country (e.g., 0.2/1000 in Japan versus 4.1/1000 in South Wales). This divergence in incidence raises questions regarding potential environmental and genetic influences as an etiology for the lesion in humans.

The extent of *spina bifida* is variable. *Myeloschisis*, the most severe form, is characterized by an area of open neural plate with no covering tissues (i.e., the overlying meninges, vertebrae, epaxial muscles, and skin are absent). Pervasive degeneration of the spinal cord results in hind limb paralysis (paraplegia).

FIGURE 25.4 Spina bifida in a neonatal dog. The skin and vertebral column in the lumbar and sacral regions have failed to close. Source: *Figure courtesy of Dr. Wayne Crowell, Department of Pathology, College of Veterinary Medicine, University of Georgia, Athens, GA. Figure reproduced from Haschek, W.M., Rousseaux, C.G., Wallig, M.A. (Eds.), 2013. Haschek and Rousseaux's Handbook of Toxicologic Pathology, third ed., Academic Press (Elsevier), Figure 62.5, p. 2721, with permission.*

FIGURE 25.5 Congenital hydrocephalus presents externally as marked rounding of the skull (foal, left panel) and internally as severe dilation of the lateral ventricles (mouse, right panel). Source: *Figure of the foal reproduced from Haschek, W.M., Rousseaux, C.G., Wallig, M.A. (Eds.), 2010. Fundamentals of Toxicologic Pathology, second ed., Academic Press, Figure 20.5, p 652 with permission. Figure of the mouse kindly provided by Drs. Lisa Berman-Booty and Krista La Perle, The Ohio State University, Columbus, Ohio, USA, and reproduced from Haschek, W.M., Rousseaux, C.G., Wallig, M.A. (Eds.), 2013. Haschek and Rousseaux's Handbook of Toxicologic Pathology, third ed., Academic Press (Elsevier), Figure 52.45, p. 2075 with permission.*

The intermediate form is termed *spina bifida cystica* (due to the cyst-like sac characterizing these defects), which encompasses *myelomeningocele* and *meningocele*. Both usually present as a small, fluctuating mass located on or just beneath the skin surface near the base of the vertebral column. The spinal cord is abnormal by definition in myelomeningocele, but may be structurally altered in meningocele.

The least severe form is *spina bifida occulta*, which is not a NTD in the strict sense and is most commonly asymptomatic. The only indication of its presence may be a sacral skin dimple or abnormally arranged tuft of hair. It is characterized by a gap in one or more vertebral arches, with no protrusion of spinal cord or meninges outside the vertebral canal and no break in the soft tissues or skin covering the area.

Arthrogryposis (multiple joint contractures) is commonly seen in severe forms of spina bifida. The pathogenesis for joint contracture is spinal cord dysgenesis leading to reduced or absent motor activity, which permits soft tissues surrounding joints to become rigid during the course of an extended gestational period.

HYDROCEPHALY (HYDROCEPHALUS) Hydrocephaly (water brain) results from abnormal accumulation of cerebrospinal fluid (CSF) in the ventricular system, usually in conjunction with pronounced ventricular dilation. The typical presentation at birth is an animal with a markedly domed cranium (Figure 25.5). The overlying brain is thinner than normal but still exhibits its normal traits (distinct cortical layers, white matter tracts, etc.). Extreme cases lead to degeneration and loss of the ependymal epithelium with CSF dissection into the neuropil, especially along white matter tracts. This lesion must be differentiated from *hydranencephaly*, in which the cerebral hemispheres are absent and their normal location is filled by fluid.

MICROCEPHALY *Microcephaly* (small brain) is a primary defect in brain development leading to secondary skull involvement. Thus both the brain (Figure 25.6) and calvarium are diminished in size. It has a reported prevalence of 0.6–1.6/1000 live human births, though new agents likely will lead to higher incidences in some locales (e.g., Zika virus in Brazil). Pure cases of microcephaly, in which brain size is decreased but the calvarium is unaffected, are rare.

The cerebral hemispheres of microcephalic brains, and particularly the frontal lobes, are reduced in size and exhibit a simplified and sometimes asymmetric pattern of surface convolutions. Microscopic examination reveals the presence of fewer large, differentiated neurons in the cerebral cortex, with corresponding

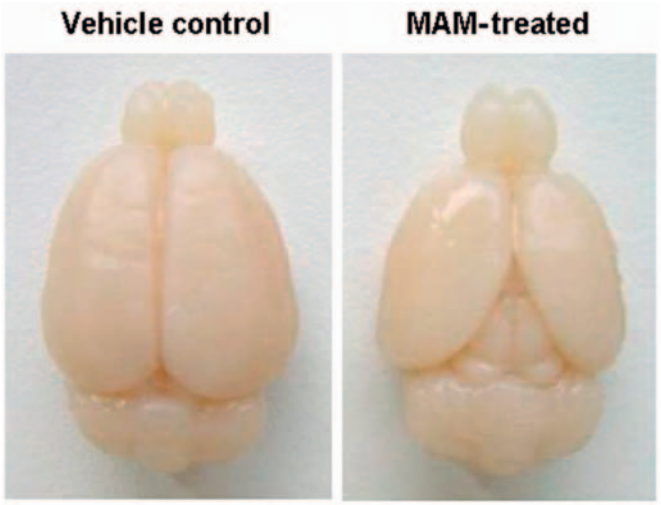

FIGURE 25.6 Microcephaly (right) in a 21-day-old Wistar rat following maternal treatment with the neuroteratogen methylazoxymethanol (MAM, given at 30 mg/kg body weight by intraperitoneal injection on gestational day 15). Relative to an age-matched control animal (left), pronounced cerebral hypoplasia has resulted in exposure of the caudal olfactory bulbs and entire midbrain. Source: *Images kindly provided by Dr. Wolfgang Kaufmann, Merck KGaA, Darmstadt, Germany and reproduced from Haschek, W.M., Rousseaux, C. G., Wallig, M.A. (Eds.), 2013. Haschek and Rousseaux's Handbook of Toxicologic Pathology, third ed., Academic Press (Elsevier), Figure 52.21, p. 2048, with permission.*

increases in neuroblasts and abnormal spindle-shaped cells.

Craniofacial Structures

ANOPHTHALMIA AND MICROPHTHALMIA

Anophthalmia is the complete absence of all optic structures: the globe, optic nerves, optic foramen, and optic chiasm. *Microphthalmia* represents hypoplasia. Both conditions may be either unilateral or bilateral. Microphthalmia is often associated with defects of other eye-associated structures, including congenital cataract, coloboma (a gap due to incomplete development) of the iris and choroid, pupillary obstruction, corneal scarring, and ocular muscle imbalance. The correlation of microphthalmia with facial and cardiovascular defects suggests that this is an anomaly of the first branchial arch. These lesions may represent a primary defect (i.e., total failure of optic vesicle formation) or a secondary anomaly (e.g., suppressed forebrain growth with later partial failure of eye development). Another possible mechanism is destruction of a previously formed optic vesicle.

CYCLOPIA

Cyclopia typically coexists with holoprosencephaly. This ocular lesion may present as complete ocular fusion in a single orbit or as two eyes in a single orbit. Eye defects linked with cyclopia include colobomas

FIGURE 25.7 Cyclopia in a fetal pig. Source: *Figure courtesy of Dr. John King, College of Veterinary Medicine, Cornell University, Ithaca, NY; reproduced from Haschek, W.M., Rousseaux, C.G., Wallig, M.A. (Eds.), 2010. Fundamentals of Toxicologic Pathology, second ed., Academic Press, Figure 20.8, p. 654 with permission.*

(gaps) in the iris, retina, and optic nerve; inconstant optic nerve numbers (either one or two is possible), and an absent or abnormal optic chiasm. Cyclopia occurs when the rostral (anterior) portion of the notochord and adjacent mesoderm are deficient in mass. This shortage leads to the aberrant induction of the forebrain tissues followed by severe derangement of midline facial development.

Cyclopia is uncommon in humans. A well-recognized cyclops syndrome occurs as outbreaks in sheep or cattle that grazed on hellebore (*Veratrum californicum*) at day 13.5 of gestation (Figure 25.7). The responsible toxins are the steroidal alkaloids jervine, cyclopamine, and cycloposine. Several mechanisms of teratogenesis have been proposed: defective craniofacial chondrogenesis, inhibited hedgehog pathway signaling, and altered catecholamine release in the neuroepithelium of the neural tube.

AGNATHIA AND MICROGNATHIA

Total absence of the maxilla or mandible is extremely rare in mammals. *Agnathia* is a common

feature of *otocephaly* (a congenital head malformation featuring marked mandibular hypoplasia or agenesis in conjunction with fusion or close approach of the ears in the throat region) and may accompany cyclopia; hence, it is seen in ruminant fetuses exposed to *Veratrum californicum*. Again, this defect appears to originate in the first branchial arch.

Micrognathia (or *hypognathia*) occurs more often than agnathia. Maxillary micrognathia (Figure 25.3) results from deficient premaxillary tissue during craniofacial development. *Mandibular micrognathia* may occur with cleft palate, glossoptosis (downward displacement of the tongue), microcephaly, and microphthalmia.

CLEFT LIP AND CLEFT PALATE

Palatoschisis, or cleft palate, is an important developmental anomaly of mammals, since the neonate cannot nurse properly without an intact palate (Figure 25.8). A cleft palate usually results in inhalation of milk and aspiration pneumonia. In humans the incidence of cleft palate is 0.5–1/1000 births. The prevalence of cleft palate in animals may be greater than reported, since not all animals that die during or after birth undergo a necropsy (animal autopsy) examination. Cleft palate is commonly bilateral, indicating that neither palatal shelf was elevated.

Cardiovascular System

ATRIAL SEPTAL DEFECTS

Although not fatal malformations, *atrial septal defects* (ASD) account for approximately 17% of all human heart defects. The incidence of ASD in domestic animals is presumed to be similar to that in humans. Experimental induction of ASD is not a commonly reported teratogenic outcome.

FIGURE 25.8 Cleft palate (palatoschisis) in a near-term Simmental cross calf. Source: *Figure reproduced from the SAC VS (Scottish Agricultural College Veterinary Services), 2009. Disease Surveillance Report, Outbreaks of idiopathic haemorrhagic diathesis syndrome in young calves. Vet. Rec. 165 39–42, with permission.*

Four types of clinically significant ASD have been described. First, defects of the oval fossa (the location of the *ostium secundum* in the interatrial septum) account for approximately 70% of ASD in humans, exhibiting a female:male predilection of 3:1. This lesion is characterized by a patent *foramen ovale* with a short or fenestrated primary septum, occurring with or without defective development of the secondary septum. The second form is the *sinus venosus* type, a relatively uncommon condition featuring a high ASD. It results from abnormal absorption of the *sinus venosus* into the right atrium or from abnormal development of the *septum secundum*. Third, a persistent *ostium primum* results from incomplete fusion of the primary septum and the endocardial cushions, with resultant anomalies in the atrioventricular valves. Finally, the least common ASD stems from complete absence of the interatrial septum resulting from a failure of development of both primary and secondary septa.

Many other cardiac malformations have been associated with ASD in humans. Examples include anomalies of the left atrioventricular (AV; also mitral or bicuspid) valve, atresia of the right AV (tricuspid) valve, common ventricle, coarctation (narrowing) of the aorta, noncyanotic patent *ductus arteriosus*, pulmonary stenosis or atresia, tetrology of Fallot, transposition of the great vessels, and ventricular septal defects (VSD).

VENTRICULAR SEPTAL DEFECTS

These malformations occur more commonly than ASD, accounting for an estimated 30%–50% of human congenital cardiac anomalies depending on the screening method used in the survey. *Ventricular septal defects* (VSD) are classified according to their location in the septum as either membranous or muscular (Figure 25.9). The muscular type accounts for approximately 10%–15% of all VSDs in humans. In some cases, absence of both parts of the septum coexists with additional cardiovascular anomalies (e.g., aortic hypoplasia, transposition of the great vessels).

The etiology of VSD is still unclear. In humans, approximately 4% are thought to stem from a chromosomal or genetic defect. Maternal diseases like diabetes mellitus and infections (especially those inducing fever) also may play a role. Experimental treatments that delay closure of the cardiac septae are capable of inducing VSD. Agents include hypoxia; nutritional deficiencies (e.g., folic acid or vitamin A) or excesses (copper or vitamin); and many cytotoxic chemicals.

TRANSPOSITION OF THE GREAT VESSELS

This malformation results from an abnormal spatial arrangement of any of the primary blood vessels: aorta, cranial (superior) and/or caudal (inferior) *vena cavae*, pulmonary artery, or pulmonary vein. The

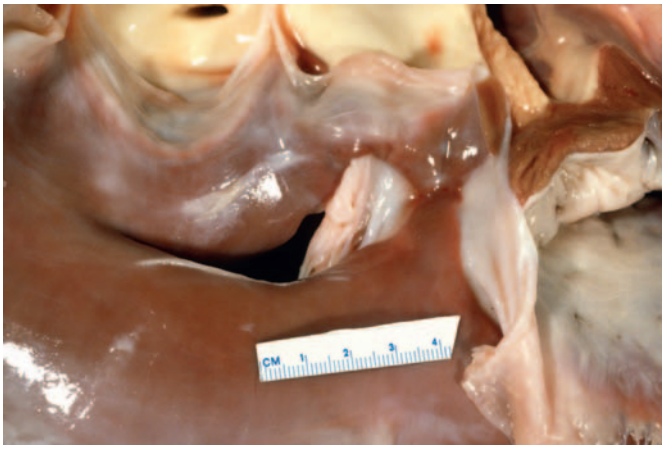

FIGURE 25.9 Ventricular septal defect in the subvalvular region of a horse heart. Source: *Figure reproduced from Haschek, W.M., Rousseaux, C.G., Wallig, M.A. (Eds.), 2010. Fundamentals of Toxicologic Pathology, second ed., Academic Press, Figure 20.10, p. 655 with permission.*

outcomes may range from a change in blood pressure to interruption of the normal right-to-left circulation, depending on the exact location and extent of the malpositioning. Regardless of the cause, survival requires the presence of additional cardiac anomalies, such as septal defects and persistent *ductus arteriosus*, which allow mixing of the two parallel circulations. This disorder appears to be more prevalent in male infants, but in animals it is not recognized as a sex-linked trait.

The pathogenesis by which transposition of the aorta and pulmonary trunk takes place is controversial. Three hypotheses include lack of spiral twisting of the great vessels around each other, abnormal division of the *truncus arteriosus*, and anomalous cardiac looping. The latter possibility has been confirmed in mice exposed to retinoic acid, where altered looping has been linked to hypoplasia of the conotruncal ridges and aorticopulmonary septum, with subsequent delayed fusion of the AV cushions.

Respiratory System

AGENESIS OR HYPOPLASIA OF THE LUNGS

Total absence of the lungs, bronchi, and vascular structures—pulmonary *agenesis* (or aplasia)—is usually unilateral. In rodents, it usually affects the left lung. Aplastic lungs have absent pulmonary and vascular structures with either rudimentary bronchi or abrupt termination of the distal trachea. Agenesis is probably caused by failed interactions between the endodermal components of the tracheobronchial buds and the surrounding mesenchyme.

Pulmonary hypoplasia, commonly associated with renal agenesis, is a more frequent anomaly. The link between these two conditions is explained in part by the ability of fetal urine (an important component of amniotic fluid during late gestation) to promote lung growth as excreted proline directs collagen and mesenchyme formation in the lung. Hypoplastic pulmonary parenchyma resembles fetal lung tissue, having more prominent bronchioles and reduced numbers of underinflated alveoli. Hypoplasia may be primary (e.g., due to genetic defects or a pulmonary viral infection with resulting tissue damage) or secondary (e.g., a consequence of a diaphragmatic hernia following nitrofen administration).

Gastrointestinal System

APLASIA/HYPOPLASIA OF THE CAUDAL ENTERIC GANGLIA

The ganglia of the digestive tract are seeded by migration of neural crest cells. This developmental event is controlled, at least in part, by the glial-derived neurotrophic factor (*Gdnf*) signaling pathway. Mice engineered to have null mutations of either *Gdnf* or in one of the two proteins that contribute to its complex receptor, GDNF receptor α-1 (*Gfra1*) and the RET tyrosine kinase receptor (*Ret*), do not form enteric ganglia in the caudal portion of their intestines; these animals also lack kidneys. The same condition in humans is termed congenital aganglionic megacolon (*Hirschsprung disease*) and occurs in approximately 1/5000 births. This lesion has been linked to maternal hyperthermia. To our knowledge, ganglionic aplasia is not associated with gestational exposure to xenobiotics.

DIAPHRAGMATIC HERNIA

This defect may arise by several mechanisms. These include failed or delayed fusion of the pleuroperitoneal membranes with the *septum transversum* and the dorsal mesentery of the esophagus, premature return of the intestines from the extraembryonic coelom to the abdominal cavity, and weak or abnormal diaphragmatic musculature. Most herniation sites are located in the dorsolateral portion of the diaphragm, thereby leaving room for part or all of the abdominal viscera to enter the thorax. Diaphragmatic hernias occur in about 1/2200 of human infants and are predominately located on the left side.

UMBILICAL HERNIA, OMPHALOCELE, AND GASTROSCHISIS

This trio of related malformations is not rare in humans, and collectively they are common in laboratory animals. *Umbilical hernia* is relatively minor, as one or several loops of intestine are displaced through the abdominal musculature but remain covered by subcutaneous tissue and skin. *Omphalocele* is a more marked lesion in which a variable portion of the

intestines and liver, and occasionally other organs, remain outside the abdomen in a peritoneal sac due to underdevelopment of the abdominal wall muscles. Over half the time, this defect is accompanied by serious malformations in other organs, particularly affecting the heart but often also the urinary tract and/or vertebral column. *Gastroschisis* is the most severe form, presenting as eventration of abdominal contents without a sac. Several mechanisms have been proposed as the pathogenesis for this lesion, including aberrant formation of the lateral folds of the ventral embryonic wall, thereby leading to a persistent defect in the abdominal wall; failure of mid-gestational retraction of the extra-abdominal mass of intestines (a normal physiological event during organogenesis) back into the abdominal cavity; and late-term escape of intestinal loops via an imperfectly closed umbilicus.

Urinary System

RENAL AGENESIS

Bilateral renal agenesis or severe dysplasia is rare in humans, affecting 0.02–0.37 of every 1000 human births. In contrast, *unilateral renal agenesis* is a fairly common finding at postmortem, with an incidence in humans of 1.0–1.8 per 1000. In such cases the remaining kidney is functional but often is deformed as well; common anomalies include altered orientation (ectopia or rotation), hydronephrosis, polycystic disease, or urolithiasis (calculi in the pelvis). Genital defects are another frequent finding in affected individuals, especially in females. The lesion represents a defect in the earliest stages of organogenesis due to altered morphogen expression in the renal primordium.

HYDRONEPHROSIS

Transient closure of the ureters occurs during normal development. If urine secretion by the kidney commences before the reopening of the ureters, the proximal ureters and renal pelvis will become distended (Figure 25.10). Such dilation is often noted in rodents during teratological studies, but this expansion appears to be transient since the incidence in adult animals is much lower than expected based on the number of affected near-term fetuses. Permanent hydronephrosis will result if the obstruction is not reversed. Additional renal defects develop in 40% of individuals with hydronephrosis, including agenesis or hypoplasia of the contralateral kidney, cystic kidney, and hypospadias.

HYDROURETER

This lesion is a common anomaly in laboratory rodents (Figure 25.10). Following obstruction the affected ureter dilates, elongates, bends, and becomes tortuous

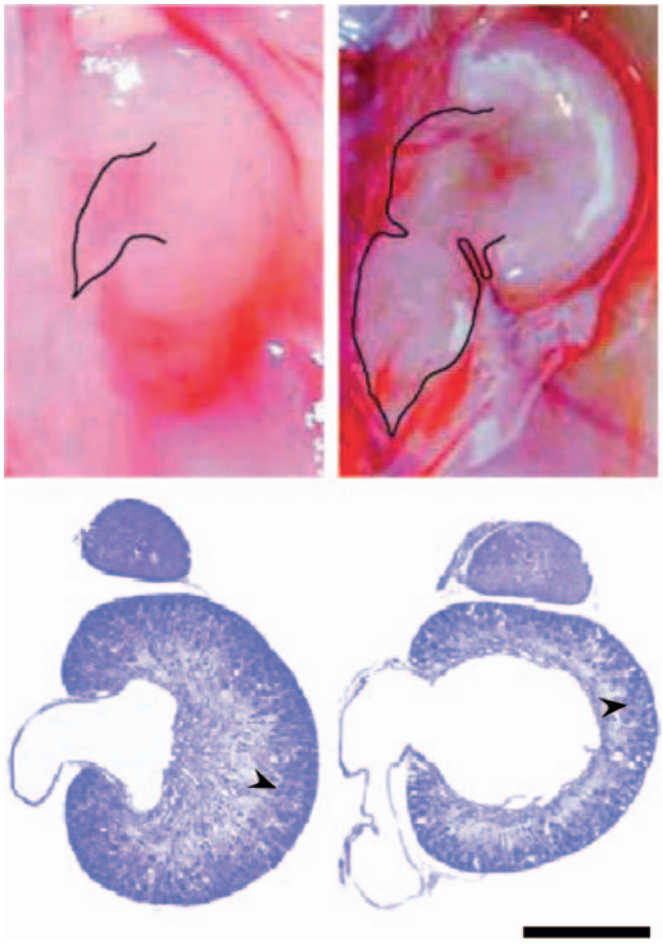

FIGURE 25.10 Hydronephrosis in near-term (gestational day (GD) 21.5) fetal Sprague-Dawley rats, showing the difference between the mild physiological dilation in saline-treated control rats (left side) and the marked renal expansion (right side) in age-matched animals delivered from dams that had been exposed to adriamycin (2.2. mg/kg given on GD 8–9 by intraperitonial injection). The lines (upper panel) indicate the borders of the ureters, while arrowheads show the corticomedullary boundary. Bar = 1 mm. Source: *Figure reproduced from the Gonçalves, A. et al., 2004. Adriamycin-induced fetal hydronephrosis. Int. Braz. J. Urol. 30 508–513 with permission.*

before the development of urinary reflux occurs. Other ureteral abnormalities have been associated with hydroureter, such as duplication, ectopia, ureterocele (i.e., dilation of the distal ureter), and ureterovesicle strictures. Unilateral renal agenesis and renal dysplasia also have been linked to the ureter defect.

HYPOSPADIAS

This urethral defect is the most common urogenital malformation. It presents in males as an abnormally placed external urethral orifice, where the opening is located somewhere along the underside of the penis rather than at the tip. In more than 50% of cases the shift in meatus position is confined to the ventral

surface of the glans, with the remainder opening on the shaft or in the perineal region. The penis may be reduced in size as well, and often exhibits a ventral curvature (termed chordee).

Hypospadias is thought to arise from the incomplete fusion of the urethral folds and/or failed canalization of the glandular plate. The molecular mechanism is posited to be insufficient production of androgens or androgen insensitivity, thereby resulting in a partially feminized phenotype.

Reproductive System

CRYPTORCHIDISM

Failure of one or both testes to descend from their original inguinal position into the scrotum is called *cryptorchidism*. It is the most common genital defect observed in many species, including humans. The condition is usually unilateral but may be bilateral. An undescended testis is evident at birth in approximately 3% of full term and 30% of premature infants. The testis completes its migration in about 80% of cases during the first year of life, making the genuine incidence of this defect around 1% in humans. The term should not be applied to those laboratory animal species (e.g., rodents) in which the wide inguinal rings permit position-dependent translocation of the testes between the scrotum and the abdominal cavity into adulthood. The proposed molecular etiology is deficiency of gonadotropic hormones.

INTERSEXUALITY (PSEUDOHERMAPHRODITISM)

Sexual ambiguity, often referred to as *intersex* or *disorders of sex development (DSD)*, is a reasonably frequent occurrence in humans and various laboratory animal species. The phenotypic sex of developing mammals is defined by three main factors: the genotype, gonadal development, and the genesis of accessory genital organs (Figure 25.11).

Genotypic sex, the genetic designation of gender depends on the expression of several genes. Genotypic sex is determined at fertilization as either male (XY) or female (XX), except in rare instances where an abnormal number of sex chromosomes are transferred (e.g., XXY, XYY, or XO). In contrast, *phenotypic sex* depends on the expression of the *SRY* sex-determining gene; adequate production of the SRY protein results in differentiation as a male, while a lack of SRY leads to a female offspring. If the SRY protein is mutated so that it cannot bind to DNA, sex will be maintained as the default female phenotype.

While numerical and structural aberrations of the sex chromosomes may produce intersex individuals, they are not the only cause of this condition. Gonadal development, and in particular the hormone complement, plays a critical ancillary role in determining the phenotype. Androgens induce male characteristics, while estrogens are responsible for female characteristics. Hyposecretion of appropriate gonadal hormones (androgens for male fetuses, estrogens for females), defective receptors for these hormones, or exposure during gestation to xenobiotics with endocrine-disrupting activities (see later) can produce *pseudohermaphrodites*, individuals in whom the genotype and gonadal development do not agree with the phenotype as expressed in genital structure and secondary sex traits. This condition arises when animals of a given genotype are exposed in utero to excessive quantities of sex steroid hormones appropriate to the opposite sex.

FIGURE 25.11 Male pseudohermaphroditism in a dog. Source: *Figure reproduced from Haschek, W.M., Rousseaux, C.G., Wallig, M.A. (Eds.), 2010. Fundamentals of Toxicologic Pathology, second ed., Academic Press, Figure 20.11, p. 658 with permission.*

Skeletal System

DIGIT ANOMALIES

Malformations of the digit are relatively common in both humans and laboratory animals. Multiple

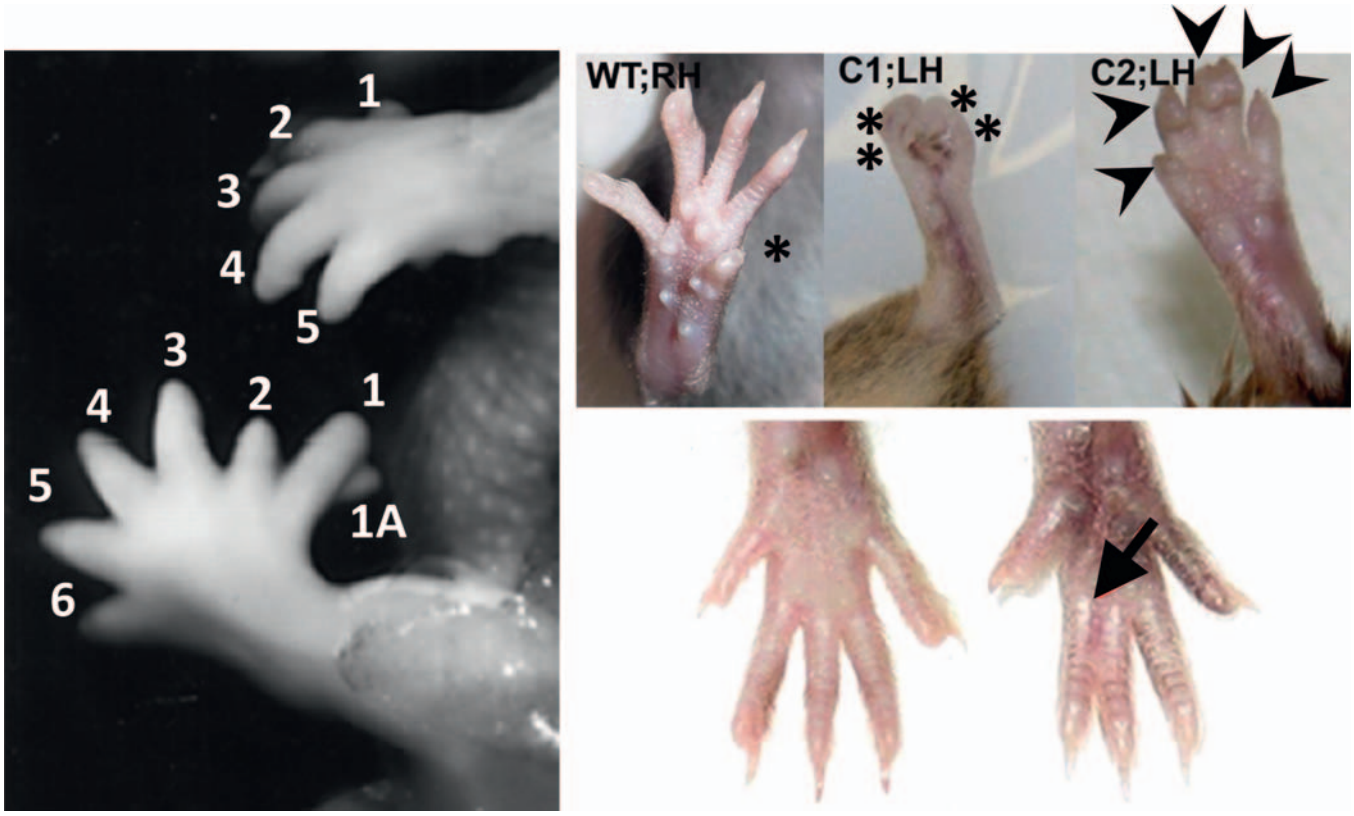

FIGURE 25.12 Common developmental defects of digits observed in mutant or toxicant-exposed animals include adactyly (missing digits (asterisks)), brachiodactyly (short digits (arrowheads)), polydactyly (too many digits), and syndactyly (fused digits (arrow)). In some cases, extra appendages (1A (left image)) that grow from existing digits is a manifestation of polydactyly. *C*, chimera, *LH*, left hind paw, *RH*, right hind paw, *WT*, wild-type. Source: *Original figure compilation reproduced from Bolon, B. (Ed.), 2015. Pathology of the Developing Mouse: A Systematic Approach. CRC Press, Figure 15.A.3, p. 326. Individual figures are reproduced from multiple papers: left panel, from Sinawat, S., et al., 2003. Fetal abnormalities produced after preimplantation exposure of mouse embryos to ammonium chloride. Hum Reprod 18 (10) 2157–2165 with permission of Oxford University Press; upper right panel, from Liu, W., et al., 2012. Deletion of* Porcn *in mice leads to multiple developmental defects and models human focal dermal hypoplasia (Goltz syndrome). PLoS ONE 7 (3) e32331; lower right panel, from Kalcheva, N., et al., 2007. Gap junction remodeling and cardiac arrhythmogenesis in a murine model of oculodentodigital dysplasia. Proc. Natl. Acad. Sci. USA 104 (51) 20512–20516;* © *2007 by the U.S. National Academy of Sciences.*

different abnormalities may occur (Figure 25.12). The common pathogenesis is abnormal remodeling of the apical epidermal ridge (AER) during initial specification of the digital rays early during on limb organogenesis. The type of lesion that develops depends on the manner in which limb differentiation is disrupted.

Ectrodactyly, the absence of part or all of at least one digit, results from interference in normal mesenchymal condensation of digital rays. Possible mechanisms include failed intercellular interactions or cytotoxicity of critical stem cells. The most common type of ectrodactyly in humans is the split hand or foot, where the middle digits (II and III) are absent while normal outer digits (I on one side, and IV and V on the other) border the cleft.

Polydactyly, the presence of extra digits is a common anomaly in mammalian species, including humans. The first and fifth digits are most commonly duplicated in humans. In most instances, only a single extra digit is present. Two mechanisms have been proposed to explain this lesion. The first is a failure of programmed cell death, thereby leading to inappropriate pruning of the digital blastema. The second is formation of a supernumerary digital blastema as a consequence of alterations in the composition, configuration, and quantity of extracellular matrix.

Syndactyly, or fusion of adjacent digits, is a moderately common congenital defect. The mechanism is reduced or failed differentiation between two digits, typically due to interference with programmed cell death that is required to separate the digital rays. In most cases the fusion consists of soft tissue, such as cutaneous webbing; osseous union is rare. Syndactyly often occurs with other limb anomalies, such as *brachydactyly* (digital shortening) and *ectrodactyly* (especially variants with split extremities). The lesion is often linked to *amniotic band syndrome* (i.e., ischemia-related defects, especially of the digits, that arise when limbs

are ensnared in fibrous bands formed following amniotic damage), and it is a part of many malformation syndromes.

REDUCTION DEFORMITIES OF THE LIMBS

The mass of the limbs may be reduced to a variable degree. In many instances the changes affect only a portion of the affected limb. They may be unilateral or bilateral, depending on the cause. Such defects may occur together with malformations of many other skeletal regions.

Amelia is the absence of an entire limb, while *meromelia* is the partial absence of a limb. These defects may occur in isolation, and may affect any of the limbs. However, amelia is also associated with defects in the remaining limbs (e.g., *talipes equinovarus* (club foot)), as well as cleft lip and/or cleft palate and *scoliosis* (curvature of the spine from side to side).

Hemimelia is absence of one side of the distal half of a limb. This anomaly is one of the most common reduction malformations, typically involving the distal forearm and hand.

Phocomelia (seal limbs) results from differential reduction of the long bones in various limb domains. It is typically characterized by greater foreshortening of the upper extremities with relatively more development of distal regions (hands, feet, and digits) (Figure 25.13). This lesion is extremely rare, but known instances are a result of toxicant exposure. The most famous example is *thalidomide*, an antinausea agent given during pregnancy to combat morning sickness; this agent induced phocomelia in thousands of human infants following exposure during the critical period of early limb organogenesis (GDs 35–50). The same lesion occurs in some nonhuman primate species and also in rabbits, but not in rodents, following thalidomide exposure.

The pathogenesis for reduction abnormalities involves interference with regional specification of cell populations in the proximal limb bud. Potential mechanisms are disrupted regional interactions between ectoderm and mesoderm, altered morphogen production, failed morphogenetic movements, or disturbed inductive processes. The reduction or absence of proximal structures coupled with the fairly normal appearance of distal features, as in phocomelia, indicates that limb bud damage induced by toxicants does not thwart limb differentiation. Instead, compensatory processes attempt to repair or bypass reductions in cell mass so that surviving structures can attempt to continue their developmental program.

ARTHROGRYPOSIS

This malformation is characterized by persistent flexure or contracture of one or more joints. Other sequelae include shortened ligaments and fibrous ankylosis of the joints along with reduced amounts of loose connective tissue under the skin. Mechanical compression resulting from increased pressure and/or reduced fetal mobility (e.g., from intrauterine crowding) also can be a cause of this lesion.

Arthrogryposis multiplex congenita, in which multiple joints exhibit ankylosis at birth, occurs in approximately 0.03% of human live births. It is the most common limb deformity in domestic animals, and is often accompanied by defects of the appendicular skeleton (Figure 25.14).

Although usually classified as a skeletal deformity, this malformation typically results secondary to

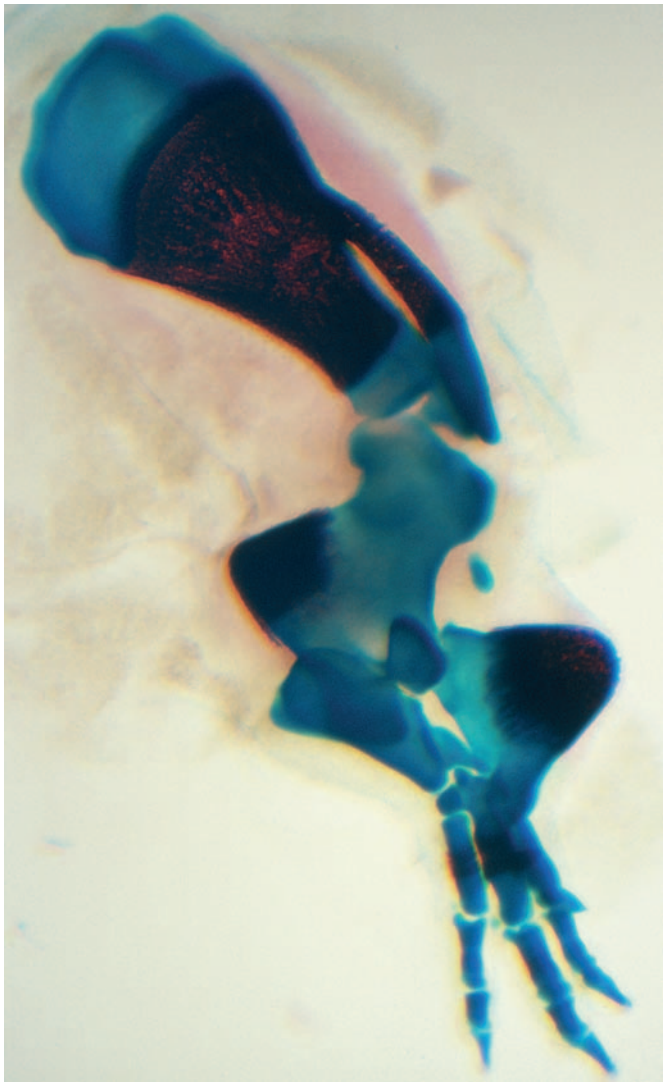

FIGURE 25.13 Phocomelia affecting the forelimb of a CD-1 mouse fetus from a dam treated on gestational day 10.5 with all-trans retinoic acid (200 mg/kg). Source: *Figure reproduced from Haschek, W. M., Rousseaux, C.G., Wallig, M.A. (Eds.), 2010. Fundamentals of Toxicologic Pathology, second ed., Academic Press, Figure 20.13, p. 659 with permission.*

FIGURE 25.14 Arthrogryposis in an Angus calf is indicated by abnormal angling of all four limbs. The altered orientation results from permanent fixation of multiple joints in a contracted position. In cattle, this finding is a common end-stage lesion produced by several etiologic agents, including genetic defects; microbial infections (e.g., the RNA virus that causes bluetongue); and maternal ingestion of some plant-derived teratogens (e.g., lupine (*Lupinus* sp.), poison hemlock (*Conium maculatum*)) between gestational days (GD) 40–75. This congenital malformation often is accompanied by other skeletal defects—especially cleft palate as well as excessive vertebral column deviations like kyphosis (dorsal or ventral displacement) and scoliosis (lateral curvature)—and soft tissue changes, like atrophy of the limb musculature and loss of the motor neurons in the spinal cord that control these muscles. Source: *Figure courtesy of Dr. David Steffen, Veterinary Diagnostic Center, University of Nebraska, Lincoln, NE. Figure reproduced from Haschek, W.M., Rousseaux, C.G., Wallig, M.A. (Eds.), 2013. Haschek and Rousseaux's Handbook of Toxicologic Pathology, third ed., Academic Press (Elsevier), Figure 62.18, p. 2734 with permission.*

insufficient limb movement rather than from a primary failure in skeletal development. Accordingly, more common causes include gestational diseases of the developing CNS, connective tissue, or skeletal muscles. For example, the absence of neural input (typically due to CNS lesions in the motor neurons or motor tracts in the spinal cord) thwarts skeletal muscle activity, which causes denervation hypoplasia and atrophy, and eventually to arthrogryposis.

Intrauterine Growth Retardation

Individuals affected by *intrauterine growth retardation* are not born prematurely, but are born with a small size given the length of their gestation (Figure 25.15). Placental insufficiency has often been considered responsible for intrauterine growth retardation, but this is apparently not the usual cause. The placenta's great physiological reserve capacity means that most placental lesions appear to be functionally unimportant, and do not result in fetal malnutrition.

Intrauterine growth retardation often occurs along with congenital malformations. Common examples include the central nervous system (hydrocephalus, macrocephaly, microcephaly, *spina bifida*); heart (ventricular septal defects); kidney (renal agenesis); and limbs (arthrogryposis, fractures secondary to *osteogenesis imperfecta*). The severity of these defects often is inversely correlated with the fetal body weight.

Placental Abnormalities

Gestational or perinatal mortality have been linked to lesions in many placental elements. Early in gestation the most frequent causes are abnormal yolk sac circulation or failed chorioallantoic fusion. These changes typically are attributed to dysgenesis of hemangioblasts (which serve as precursors for both endothelial cells and erythrocytes in the yolk sac) or mesodermal cells (especially trophoblasts comprising the allantois or in fewer cases the chorion). During late gestation the most common finding is disrupted formation of the placental tissue responsible for gas and nutrient exchange (e.g., the labyrinth in rodents, villi in primates). In general, this change presents as insufficient production and/or branching of capillaries (commonly a consequence of an endothelial defect) or abnormal production of trophoblast (Figure 25.16). Placental tissue also may undergo the same changes observed in other tissues, particularly hemorrhage, necrosis, and thrombosis; these findings typically are linked to acute embryonic or fetal loss only if they are extensive enough to disrupt a large portion of the placenta.

Perinatal Toxicology

Developmental events induced by toxicant exposure during gestation may not be manifested until near or shortly after birth, and then as functional deficits rather than overt malformations. Examples of altered

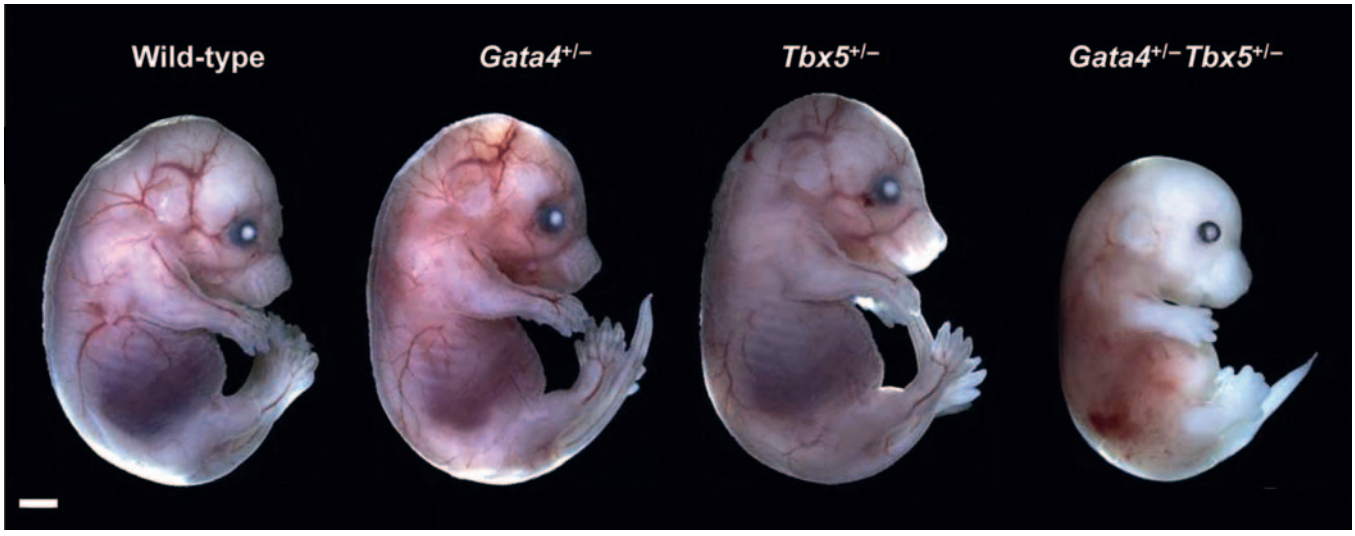

FIGURE 25.15 Intrauterine growth retardation occurs in fetal mice lacking one allele of both *Gata4* (a zinc finger transcription factor) and *Tbx5* (a T-box transcription factor), but not in littermates missing an allele for only one of the genes. The scale bar represents 1 mm. Source: *Figure reproduced from Maitra, M., et al., 2009. Interaction of* Gata4 *and* Gata6 *with* Tbx5 *is critical for normal cardiac development. Dev. Biol. 326 368–377 with permission.*

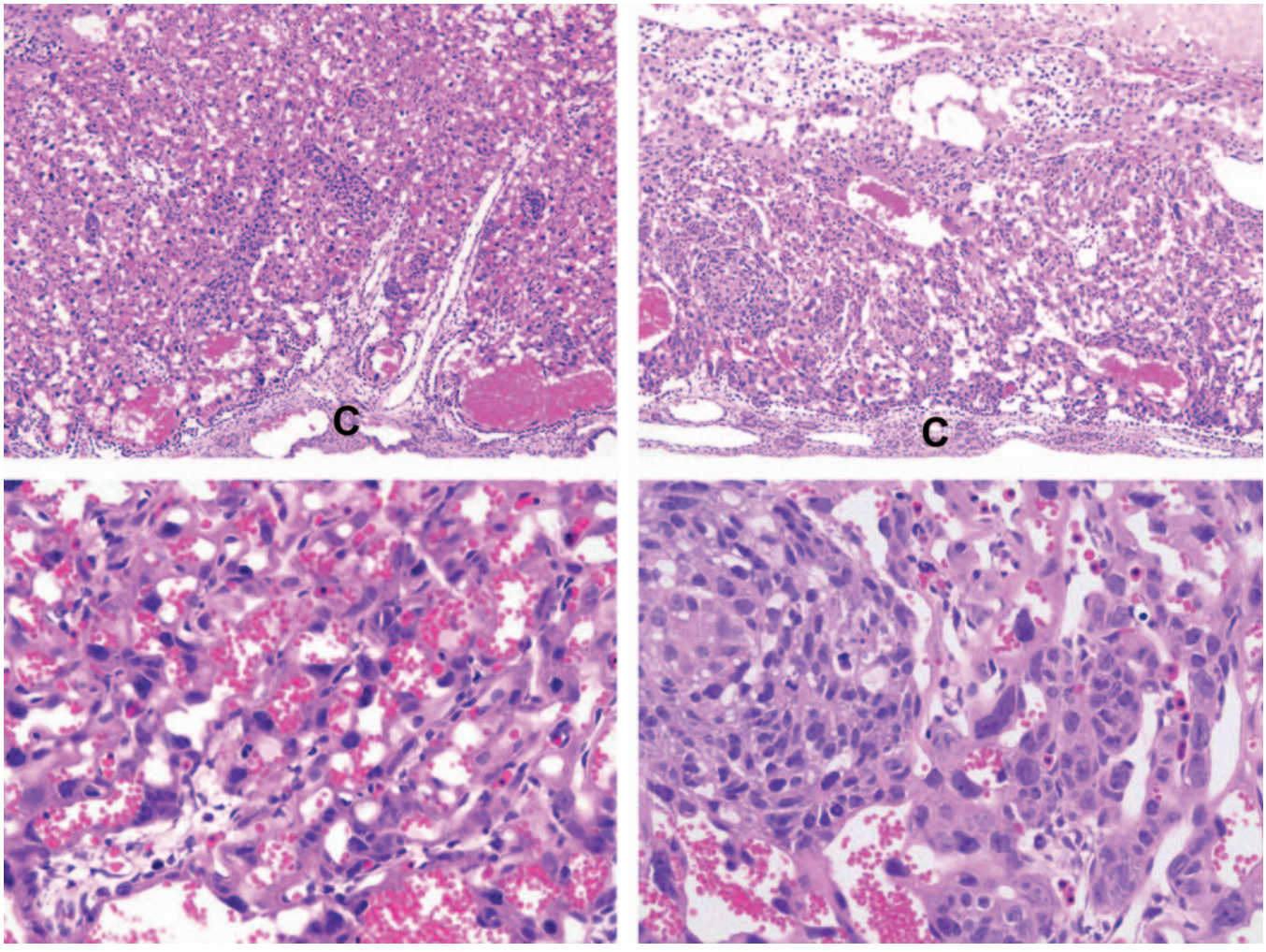

FIGURE 25.16 Placental dysplasia due to aberrant trophoblast formation is a common cause of placental insufficiency. Relative to wild-type mice (left column), placentas from null mutant mouse conceptuses that lack the genes for transcription factors E2f7 and E2f8, which regulate trophoblast differentiation, exhibit a narrow labyrinth comprised principally of large, coalescing aggregates of densely packed, plump trophoblast cells (right column). The distance between embryonic capillaries and maternal sinusoids is increased as a secondary effect. Gestational age = day 13.5, where day 0 is the day of conception. C, chorionic plate. Source: *Images acquired from formalin-fixed, paraffin-embedded, H&E-stained sections that were kindly provided by Dr. Gustavo Leone, The Ohio State University, Columbus, OH. Figure reproduced from Bolon, B., Ward, J.M., 2015. Pathology of the placenta. In: Pathology of the Developing Mouse: A Systematic Approach, Bolon, B., (Ed.), CRC Press (Taylor & Francis), Boca Raton, FL, Figure 16.12, p. 366 with permission.*

function include abnormal cell reactivity (e.g., by immune or reproductive elements), metabolic errors, and neurobehavioral deficits. Although subtle structural defects may be apparent, functional deficiencies are the most common adverse outcomes of this kind. Often these functional changes result from depleted cell numbers due to inadequate repair.

Abnormal cell reactivity in the perinatal period is a common developmental toxicity outcome. The *ontogeny* (i.e., an individual's developmental history) of immune system differentiation is commonly impacted by xenobiotic exposures in utero. The main functional deficits resulting from such exposures are inappropriate immunosuppression and immunostimulation, either of which can permit the onset of inflammatory diseases (especially allergic or autoimmune) or neoplasia later in life. Abnormal reproductive functions can follow intrauterine exposure to many agents, including antineoplastic drugs, hormones, pesticides, and polycyclic aromatic hydrocarbon carcinogens.

Developmental dysfunction associated with errors of metabolism commonly arises from genetic mutations or xenobiotic exposures. Such genetically based "inborn" errors are often not expressed until after birth. An environmentally-caused disease, termed a *phenocopy* because its lesions mimic those of a known genetic ailment, may mirror such congenital genetic conditions. For example, cattle exhibit similar morphologic lesions when afflicted with α-mannosidosis (genetic cause) or locoism (i.e., locoweed toxicity). However, accumulation of α-mannoside in these two conditions results from distinct mechanisms: the inherited disorder arises from the complete lack of functional α-mannosidase protein, while the environmental phenocopy follows α-mannosidase inhibition after ingestion of the alkaloid swainsonine. The existence of phenocopies highlights the difficulty in determining the genuine etiology of congenital defects.

Endocrine Disruption

Xenobiotics classified as *endocrine-disrupting compounds (EDC)* have received much attention in recent years as potential reproductive and developmental toxicants. These agents are exogenous chemicals that are considered to affect the activity of an endogenous hormone by either acting as an agonist or antagonist in place of the native molecule or alternatively by interfering with the endogenous hormone's synthesis, secretion, transport, binding, action, or elimination. The main interest in xenobiotics that mimic endogenous hormones, enhance their actions, or act as hormone antagonists has centered on their potential for disrupting reproductive tract development, altering sexual behavior, and impairing fertility as a consequence of aberrant endocrine pathways in the gonads. However, compounds that affect pituitary or thyroid function are also of concern.

To date, endocrine disruption has primarily been a concern raised in animals. Such effects have been demonstrated in wildlife, a notable example being the feminization of male and "super-feminization" of female alligators in central Florida's Lake Apopka due to accumulation and persistence of pesticide residues in fat. With few exceptions (e.g., diethylstilbestrol (DES) as an etiology of breast and cervical/vaginal carcinomas), causal relationships between exposure to a specific chemical and endocrine disruption have yet to be established definitively in humans. Nonetheless, growing epidemiological evidence suggests that endocrine disruption during development may predispose humans to endocrine-related disorders later in life, as suggested by a global increase in neoplasia of endocrine organs (e.g., adrenal and thyroid glands) and hormone-regulated tissues (e.g., mammary gland, prostate) and metabolic conditions (e.g., noninsulin-dependent (Type II) diabetes, obesity).

Congenital Neoplasia

Tumors in young animals and humans are, by definition, indications of abnormal embryogenesis. Fetal cells are inherently susceptible to carcinogens because of their high rates of proliferation. The incidence of neonatal tumors in humans up to 15 years of age is estimated to be between 98 and 125/million/year. The most common childhood tumors arise from committed stem cells for specific cell lineages, such as leukocytes (leukemia, lymphoma) or mesenchyme (osteosarcoma, rhabdomyosarcoma), although some may be derived from multiple lineages, like nephroblastoma (Wilm's tumor) and neuroblastoma. Many neonatal tumors result from genetic mutations, but others are consequences of in utero exposure to xenobiotic carcinogens.

Transplacental carcinogens may act directly without prior metabolism or require enzymatic bioactivation to reactive intermediates. If bioactivation is required, it takes place in the embryo or fetus as reactive molecules interact immediately with nearby cellular constituents. The long latent period required for neoplastic transformation has been used to support the argument that many if not all cancers that arise during the period from birth to young adulthood are induced by a prenatal initiation event, usually considered to be a mutation (i.e., DNA-reactive event) that becomes fixed due to rapid cell cycling. For this reason, all stages of prenatal development are susceptible to the action of these agents, and the tendency to develop neoplasia can be passed on to any future offspring.

In most instances developmental toxicants act as either teratogen or transplacental carcinogens, but not both. This division is reasonable as most known teratogens do not act by causing mutations. Indeed the genetic causes of malformations are likely to reflect chromosomal abnormalities rather than chemically-induced mutations, while the genomes of animals exposed to transplacental carcinogens will exhibit many aberrations at the DNA level. It is not uncommon to see childhood cancers in individuals displaying defective development, sometimes but not always with the birth defects and neoplasms occurring in the same organ or system. Although some substances (e.g., heavy metals, mycotoxins, solvents) can cause congenital malformations and cancers, it is not known whether intrauterine exposure to any single agent can induce both conditions in a single individual.

PRINCIPLES OF DEVELOPMENTAL TOXICITY

The impact of xenobiotic exposure on the developing organism depends on many interrelated factors. Critical parameters inherent in the conceptus (or neonate or juvenile) include the stage of development during which exposure takes place and the individual's genotype. However, other factors that modify the toxicity of xenobiotics include the parental genotypes, the maternal environment, and the structure and function of placental tissues. These elements are briefly reviewed here. Additional details may be garnered from many supplemental sources (see Further Reading).

Critical Phases of Development

Developmental processes occur in specific locations and at particular times. In many cases the success of subsequent developmental tasks is affected to a greater or lesser degree by the events that have taken place before. The sequence and timing of events generally is consistent for individuals of a given species, and the overall pattern is well conserved across mammalian species. Critical periods for structural development typically occur prior to birth, although certain organs do not fully form until after birth (e.g., the rodent cerebellum). In contrast, both functional and molecular development continues to evolve throughout the neonatal and juvenile periods, not achieving full maturity until puberty. Taken together, these principles indicate that some structure, function, and/or biochemical pathway likely will still be differentiating any time a pregnant individual or her newly born or juvenile offspring are exposed to a xenobiotic agent.

The critical period of intrauterine development is that time during its differentiation and growth during which the conceptus (or any part thereof) has the greatest sensitivity to noxious influences. Critical periods begin during organogenesis, when the structures involved are laying the foundations (i.e., an anlage, or organ primordium) that ultimately determine their final form. Each organ and system has its own critical period or periods. Distinct regions in complex structures (e.g., the CNS) typically have their own critical periods; some (e.g., hippocampus, olfactory bulb) may have more than one such peak of sensitivity (see Figure 21.10 in Chapter 21: Nervous System). Accordingly the same agent may induce different defects depending on when the exposure occurred during gestation.

Modifying Factors

Conceptus

GENETIC BACKGROUND

STRAIN AND SPECIES Species differences in expression of defective development following xenobiotic exposure have been clearly shown experimentally. As previously mentioned the classic example is thalidomide, which is highly teratogenic in humans and certain nonhuman primates but does not readily cause malformations in rodents and chicken embryos. Glucocorticoids are teratogenic in mice but not in rats. Species differences in teratogenic response are probably a manifestation of many species-specific factors. The most important parameters for dictating the teratogenic potential of an agent in any species are thought to be its PK properties—including the individual rate of transplacental transfer—and differences in the distribution and/or sensitivity of the xenobiotic's receptors and target cells. The key means for controlling these response factors are the embryo's complement of genes.

The responses of individuals in outbred species (e.g., humans) are specified chiefly by the person's own allelic complement. In species with multiple highly inbred strains, individuals for a given strain tend to react in a comparable fashion. In contrast, those of distinct strains may respond in divergent fashions depending on how much concordance exists among their complements of genes.

The divergence among strains can represent intrinsic differences, such as unique patterns of protein expression or timing for developmental events, or they can result from extrinsic differences that are defined by unique maternal biotransformation rates or products. For example, cortisone induces a higher

incidence of cleft palate in A/J mice than in either CBA or C57BL/6J mice. The greater vulnerability of the A/J strain appears to reflect both a genetically determined increase in the number of glucocorticoid receptors in the developing maxillary processes as well as the slightly later timing of palatal shelf elevation in this strain. Furthermore, A/J dams metabolize cortisone differently than do CBA dams, thus producing a greater exposure in the A/J embryos.

The importance of the embryonic genotype in determining the response of the conceptus to xenobiotics is readily apparent in the discordant defective development that may occur between dizygotic human twins exposed to a teratogen. This discordance also manifests itself in rodents, since offspring in a single litter are rarely all affected in the same manner or to the same degree following a teratogen exposure. However, such within-litter discordance may arise from other causes. Examples include variations in maternal blood supply to offspring at various locations in the uterine horns and the impact of a sibling's metabolic profile (e.g., hormone production) on nearby conceptuses.

MULTIFACTORIAL THRESHOLD The premise of the multifactorial threshold concept is that the embryo must be genetically predisposed to develop a malformation before the action of a teratogen results in manifestation of the defect. Estimates suggest that approximately 50% of congenital malformations may involve multifactorial inheritance.

Each organ system exhibits a threshold for abnormal organogenesis. Damage below the threshold does not alter the normal developmental program, while damage exceeding the threshold will result in a malformation. The threshold can be impacted by one or more genes as well as by environmental agents. If the genetically determined pathway specifying normal developmental progression is close to the threshold, then only minor noxious stimuli may be necessary to induce an abnormality. A corollary concept is that a higher number of predisposing genes will reduce the severity of the teratogenic insult required to break the threshold. In fact, it is likely that most, if not all, individuals have one or more "weak points" in their genetically programmed developmental plans that are especially vulnerable to influences that could result in abnormal development. The absence of major defects in most individuals speaks to the resiliency of the conceptus.

DEVELOPMENTAL PHARMACOKINETICS

METABOLISM Variability exists among species with respect to the stage in which metabolic systems begin to develop and mature. In general, conceptuses of species with longer gestations (e.g., humans) develop greater metabolic capabilities in utero, while those of species with short gestations (e.g., rodents) typically show little or no enzyme activity until near or after birth, and thus are incapable of extensive in utero metabolism. For a given species, metabolic pathways are much less developed in embryos than they are in fetuses and neonates. Similarly the metabolic proficiency of conceptuses and neonates is less differentiated than is the corresponding set of activities in the dam.

Human hepatic enzyme activities that participate in xenobiotic metabolism begin developing before birth, although the levels vary by enzyme family and subfamily and are well below those of mature adults. For example, hepatic cytochrome P450 (CYP) 3A activity, a critical Phase I enzyme for xenobiotic metabolism accounting for about 30% of fetal CYP content, is about 30%−60% of that found in adults; in contrast, activities of some Phase I enzymes (e.g., CYP2D6 and CYP2E1) are a fraction (10%) of adult levels during gestation and do not begin increasing until adolescence. Thus fetal enzymes can metabolize xenobiotics that have crossed the placenta to make either toxic or nontoxic metabolites. Since these metabolites are water-soluble, they may accumulate in the fetal compartment due to its relatively higher water content. Fortunately, detoxification reactions tend to predominate over activating reactions in fetal tissues. Therefore fetal metabolism usually serves to protect the fetus.

Fetal renal excretion also aids elimination of xenobiotics. During the latter stages of gestation, the glomerular filtration rate increases, resulting in a concomitant increase in the fetal renal drug clearance.

ENZYME INDUCTION Prenatal exposure to known enzyme-inducing agents does increase enzyme activity in laboratory rodents. Both 3-methylcholanthrene and phenobarbital induce effects in conceptuses that are similar to those seen in mature animals. Again the dichotomous risk and benefit regarding whether enzyme-mediated metabolism will result in detoxification versus bioactivation depends on the xenobiotic in question. The ability of conceptuses to respond to xenobiotics that induce Phase I and Phase II reactions depends on the animal strain.

TISSUE ACCUMULATION Preferential sequestration of some teratogens in embryonic or fetal tissues occurs in some species, resulting in higher toxicant concentrations in the offspring than occur in the maternal blood. Lead accumulates in the fetus by binding to mineralizing fetal bone. Methyl mercury is retained in the fetus because it cannot convert the methylated form to inorganic mercury, which is more readily eliminated. Indeed, fetal sequestration of methyl mercury is so complete that pregnant women are protected from

methyl mercury toxicity. Thalidomide is sequestered in the embryos of sensitive species (e.g., rabbit) because embryonic enzymes hydrolyze the parent drug to hydrophilic metabolites that cannot readily cross cell membranes. Many rodent teratogens are weak acids; hence, they tend to concentrate in embryonic and fetal tissues, as the conceptus compartment is more basic than maternal plasma.

Mother

MATERNAL PHYSIOLOGIC STATUS

Alterations in maternal homeostasis must be severe to affect the conceptus, since the needs of the growing organism are usually met even at the expense of the mother. Exceptions do exist, however, since approximately 3.5% of all congenital malformations in humans relate to various metabolic and nutritional imbalances. Examples include diabetes (which results in macrosomia or sacral agenesis); malnutrition (spontaneous abortion, stillbirths, NTDs, neonatal deaths); phenylketonuria (microcephaly, mental retardation, cardiac defects); thyroid disorders (e.g., hypothyroidism, which leads to cretinism, deafness, and retardation); and virilizing tumors (pseudohermaphroditism in females).

MATERNAL PHARMACOKINETICS

Absorption from the gut is altered during pregnancy because of increased gastric emptying time and reduced intestinal motility. These changes increase the residence times in both the stomach and small intestine, with the effect on the amount of uptake depending upon whether a given xenobiotic is more readily absorbed via the stomach or the intestine. The pulmonary tidal volume also increases during pregnancy, resulting in increased uptake of inhaled xenobiotics. In addition, the volume of distribution markedly increases during pregnancy because of increased total body water and body fat. This rise in volume leads to decreases in the initial blood concentration of absorbed xenobiotics. There is also a more rapid maternal elimination of water-soluble compounds because of increased renal plasma flow and glomerular filtration rate.

A progressive gestational decrease in maternal plasma albumin concentration may affect xenobiotic binding by plasma proteins. For example, decreased serum binding of a number of therapeutic drugs has been seen to occur during pregnancy.

Maternal hepatic enzyme activities escalate during pregnancy, probably because of the growing need to metabolize fetal wastes. Unfortunately, drug metabolism may be reduced, at least for certain xenobiotics, because of competitive enzyme inhibition by steroid hormones. These counterbalancing trends are complicated: estrogen decreases the efficiency of some metabolic pathways, while progesterone induces some enzymes. It is probable that the effect of steroids and other hormones on metabolism will depend on the timing of a gestational exposure as well as the physicochemical characteristics of a given xenobiotic. Metabolic capabilities exist between resistant and sensitive inbred strains of mice, showcasing the importance of maternal metabolism in regulating in utero exposure.

Father

DIRECT TOXIC EFFECTS ON SPERM

Teratospermia is the production of morphologically abnormal sperm, which are often functionally deficient as well. This lesion can follow exposure to some toxicants. Direct actions of compounds on sperm may alter their cytoarchitecture and/or their function. The aberrant functional attributes are reported more frequently, and likely are of greater consequence. Examples of functional deficits include altered sperm motility, reduced ribosomal activity (often with decreased RNA content), and impaired protein synthesis. The induction of chromosomal damage is indicative of substantial genetic damage that may be passed to the progeny, and that may result in malformations.

ABNORMALITIES IN SEMINAL FLUID

Xenobiotics dissolved in the seminal fluid can induce secondary morphological abnormalities in sperm, impair sperm motility, and reduce sperm viability. Dissolved toxicants may also have some influence on the uterus, either by directly damaging the endometrial tissue or by impacting more distant maternal functions following systemic uptake. Subsequent adverse effects on the timing of implantation, the number and distribution of implantation sites, and the success of placentation are possible, and some xenobiotics delivered in semen theoretically may be directly toxic to the developing embryo.

Placenta

PLACENTAL BIOLOGY

BARRIER PROPERTIES A major role for the placenta is as the first major physical barrier between the conceptus and any xenobiotics within the surrounding "external" environment (i.e., the maternal circulation). Placental structure evolves over time in mammals. The initial form is comprised of the maternal endometrial (or "decidual") reaction to the newly implanted conceptus. The placental contribution derived from the embryo's extraembryonic membranes builds over time until later in gestation the fully functional placenta becomes responsible for many gestational functions, including hormone production (peptides and steroids),

immunosurveillance, metabolism of endogenous and xenobiotic materials, and nutrient uptake.

The nature of the barrier layers within the placenta varies among species. A "complete" or epitheliochorial placenta contains a full complement of maternal and embryonic layers (three layers for each: epithelial, mesenchymal, and endothelial) between the two blood supplies. Ruminants have evolved this conformation. The dog possesses an endotheliochorial placenta, having retained maternal endothelium and all three embryonic layers. Humans and animals species commonly used in developmental toxicity testing (e.g., nonhuman primates, rats, mice, and rabbits) exhibit a hemochorial structure, in which the three embryonic derivatives are retained but the maternal layers are absent. The conformation in primates and rabbits is hemo-monochorial (having only one layer of embryo-derived trophoblast), while rodents are hemo-trichorial (having three trophoblast layers). The difference in trophoblast layering appears to be inconsequential in terms of embryonic exposure to xenobiotic agents.

The rates at which xenobiotics are transported across the placenta play a great part in determining whether or not toxic levels reach and accumulate in the conceptus. The major factors affecting xenobiotic passage across any membranous barrier—lipid solubility, molecular size, ionic charge, concentration gradients, potential to form complexes with other molecules, and the availability of carrier molecules—also apply to the placenta. Most drugs are transported by passive diffusion. Therefore as lipid solubility increases, the rate of transfer tends to climb. Materials with sizes greater than 1000 Da do not cross the placenta easily, whereas those less than 600 Da (which includes most drugs) travel with ease. Steric hindrance the process by which the shape and size of a molecule may interfere with molecular binding sites, may occasionally play a part in reducing transport across the placenta. Binding of xenobiotics by plasma proteins is also frequently a major influence, as it decreases the amount of the freely diffusible form that is available for transplacental transport.

PHYSIOLOGICAL PROPERTIES Since most drugs cross the placenta by passive diffusion, maturational changes in the barrier structure are unlikely to influence xenobiotic exposure. Thus the rate of transfer of small molecules into the fetus is correlated with the rate of placental blood flow. However, if an agent's permeability is a rate-limiting step in its transfer (e.g., for hydrophilic compounds), physiological changes in the placenta over the full course of gestation may cause significant changes in fetal exposure. Some compounds, mainly vasoactive agents, may alter placental blood flow through their pharmacological activity.

PLACENTAL PHARMACOKINETICS

METABOLISM Placental metabolic capabilities may sometimes play a role in the modulation of embryonic/fetal drug exposure. Enzyme systems in the placenta are subject to induction by xenobiotics. The function of such enzymes is likely to prevent entry of xenobiotics into the embryo or fetus, but the success of this endeavor will depend on the nature of the xenobiotic.

SEQUESTRATION A generalized decrease in nutrient transport has been seen when some xenobiotics bind to the placenta. For example, cortisone exposure decreases glucose transport, and methyl mercury inhibits amino acid transport.

The pH of the conceptus with respect to the dam changes during the course of gestation. During organogenesis the blood and tissues of rodent embryos are more basic than the maternal blood, resulting in accumulation of weak acids in the embryo. Later in gestation, fetal blood is relatively more acidic than maternal blood, leading to "ion-trapping" of basic compounds in the fetal circulation. This trapping can result in a higher concentration of nonionized drug in the maternal circulation and a net transfer to the fetus over a prolonged period.

MECHANISMS OF DEVELOPMENTAL TOXICITY

The pathogenesis and etiology of malformations is quite complex, and many mechanisms have been proposed to explain the genesis of toxicant-induced structural defects. Some represent cellular responses to damage, while others actually represent biochemical and molecular elements that are thought to invoke the cellular reactions. The most important current hypotheses are listed later.

It is often difficult to determine the precise cause of a developmental defect. This problem reflects the multiple potential etiologies of specific lesions due to gestational damage. A particular developmental anomaly can be induced via multiple pathways. In other words, different mechanisms of abnormal development often produce a common lesion. This quandary highlights the limited repertoire of pathologic responses to injury (whether genetic, toxic, or otherwise) that can be expressed by the conceptus.

Excessive Cell Death

Cell populations with a high proliferative rate, or those beginning to differentiate, are the most susceptible to cytotoxicity. This sensitivity may result from the

greater amount of active (or "exposed") genome, yielding greater access to a larger number of genes. Such active DNA is highly susceptible to damage by foreign substances that can form adducts via covalent bonding to nucleotides. The exposed DNA can also be subject to nucleotide substitutions in which native elements are replaced by analogs that distort the annealing of the complementary strands. If left in place, such modified bases can engender point mutations during DNA propagation; in many instances, such damage results in gene inactivation, which is often fatal to the affected cell. Another potential point at which toxicants can inflict damage is by altering energy metabolism, as the internal nutritive requirements of rapidly dividing cells in the G_1 phase may be higher than those of resting (G_0) cells that are common in differentiated tissues of adult animals.

Excessive cytotoxicity is a proven cause of abnormal embryonic development. For example, cell loss localized to a finite region has a dramatic effect on such processes as limb formation and neural tube closure. The pattern of death may encompass large cell groups (i.e., necrosis) or be limited to isolated elements (i.e., single-cell necrosis); importantly, cell loss by necrosis may damage adjacent cells. Early and excessive cell attrition may leave too few cells to initiate critical inductive events at specific stages of development. The lack of positional information associated with this loss will produce incorrect spatiotemporal relationships that can prevent expansion of a given target cell population—and also all future cell collectives that cannot be induced without the help of these affected target cells. Thus small deficits resulting from too much cell death at early points in gestation can cascade into additional deficits affecting many more cell populations later in development. The regenerative capacity of embryonic tissues in compensating for cell death is also vital in defining the extent of toxicant-induced injury.

Interference With Programmed Cell Death (Apoptosis)

Embryonic sculpting by the region- and time-specific activation of *programmed cell death* (PCD) is a normal phenomenon during development and does not damage adjacent cells. Many structures utilize PCD, including the brain (to remove superfluous neurons), digits (to attain the right degree of separation and appropriate size) (Figure 25.16), and hollow organs (to create cavities in solid primordia). The process involves selective suicide (apoptosis) by cells that do not complete their expected developmental program, and it is an active undertaking designed to prune exuberant cell numbers during histogenesis and organogenesis. Signals that can initiate PCD usually are chemical messages, such as hormones or growth factors. Interference with these signaling pathways may prevent timely cell death and lead to supernumerary structures or cells.

Reduced Cell Proliferation

Diminished rates of cell division can occur following an exposure to a dose of developmental toxicant that is lower than the dose that induces cytotoxicity. The diminished cell numbers may cause growth retardation of one or more organs. Growth retardation of an organ can have dramatic effects that resonate throughout the entire period of development, since a critical mass of one tissue is often necessary to induce many secondary structures. For example, if dental anlagen are not of sufficient mass, teeth will fail to develop and their supporting bony structures will be smaller than normal (Figure 25.17).

The growth of various tissues occurs at dissimilar rates, so reduced proliferation of tissues during histogenesis can result in different degrees of abnormal growth depending on the affected organs. This loss of developmental synchrony is a striking feature of hypovitaminosis A in pigs, where piglets are born blind because premature closure of the cranial sutures leads to smaller optic foramina and compression of the optic tracts as they exit the cranium. Similarly, corticosteroids reduce palatal shelf size, resulting in cleft palate formation in mice.

Failed Cellular Interactions

Genetic factors, exogenous agents, or both can cause abortive connections among various cell populations. For example, abnormal cerebellar development in the *weaver* mouse mutant (gene symbol: *wv*) results from a genetically programmed decrease in the numbers of radial glia processes needed to guide the migration of granule cells from the brain surface through the molecular layer to the granule cell layer. Similarly a genetic defect in cattle produces anophthalmia or microphthalmia via reduced or absent contact between the optic cup and overlying ectoderm, thereby preventing induction of the lens placode. Cytotoxic antineoplastic agents as well as ionizing radiation also incite these ocular lesions by the same mechanisms. Hypovitaminosis A disrupts the spatial orientation among cells in mesenchymal condensations through altered cell-adhesion expression, leading to altered shapes of cartilage models and their bony successors.

Impeded Morphogenetic Movements

Cellular migration can be hampered by many mechanisms. Common factors include decreased cell mobility; abnormal quantity or quality of the extracellular matrix

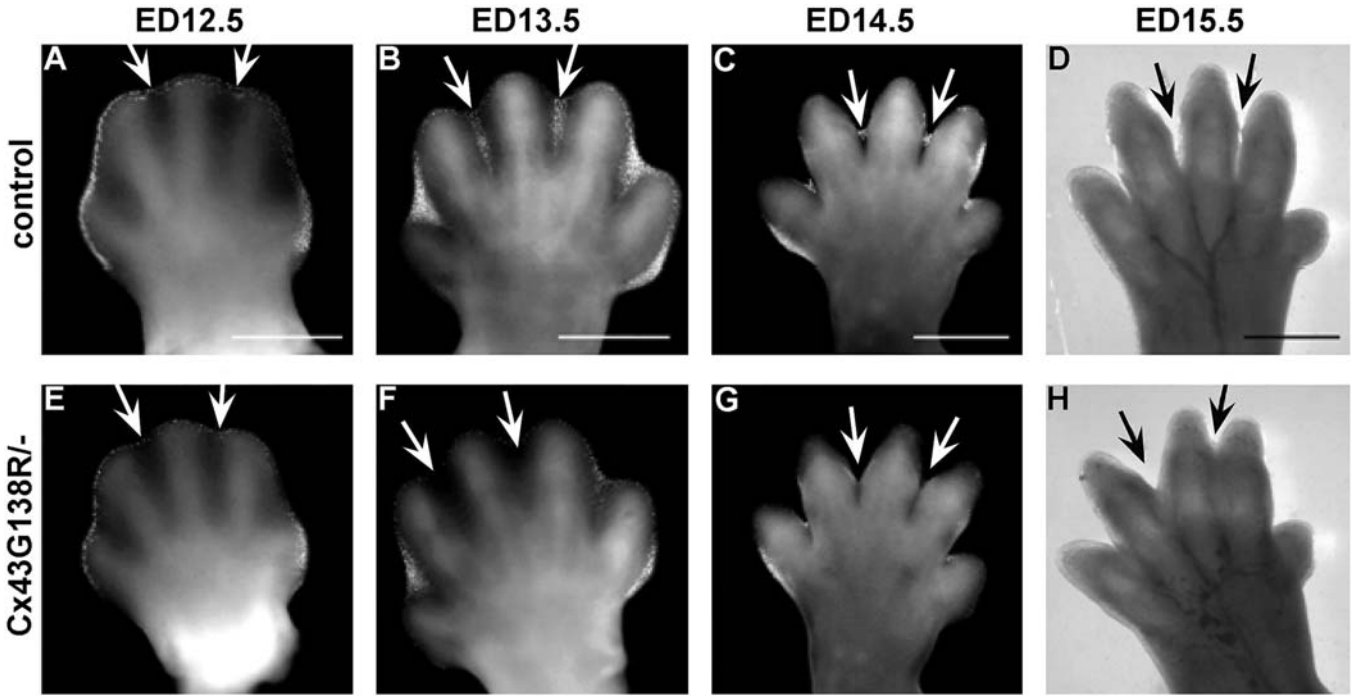

FIGURE 25.17 Paw development in the developing mouse depends on timely programmed cell death at the proper sites. In control animals (top row), the limb bud at gestational day (GD) 12.5 (panel A) is defined by a rise in apoptosis in the soft tissues of the interdigital rays (arrows), which progresses over time (panels B, C) to yield complete separation of the digits by GD 15.5 (panel D). In contrast, stage-matched littermates with a point mutation in connexin-43 (a constituent of gap junctions) have reduced apoptosis (panels E, F, G) that results in a variable degree of syndactyly (persistent fusion of digits, panel H). Scale bars: 500 μm. Source: *Figure reproduced with modified labeling from Dobrowolski, R.M., et al., 2009. Loss of connexin43-mediated gap junctional coupling in the mesenchyme of limb buds leads to altered expression of morphogens in mice. Hum. Mol. Genet. 18 2899–2911 with permission.*

(ECM), especially via altered substrate-adhesion molecules (SAMs); aberrant quality of cell-adhesion interactions as mediated through anomalous patterns of cell-adhesion molecules (CAMs), SAMs, or cell-junctional molecules (CJMs); and disruption of cytoskeletal microtubules or microfilaments. Accordingly, altered perception of critical positional information and/or inability to follow the signals seems to be major themes responsible for such defects.

The ECM is composed of glycosaminoglycans (GAGs) such as chondroitin, chondroitin sulfate, heparan, heparan sulfate, hyaluronic acid, and keratin sulfate as well as abundant collagen. These molecules and other SAMs interact with the integrins on cell membranes, allowing adhesion and ultimately directed motion among tissues in defined planes. The ECM content of these constituents varies during different stages of development. High levels of hyaluronic acid in early morphogenesis encourage cell migration by increasing cell proliferation, inhibiting aggregation, and increasing the fluidity of the ECM. During later differentiation, hyaluronic acid levels decrease as cells begin to aggregate and chondroitin sulfate production is increased.

Diminished cell adhesion can also result in deformities. Cortisone disrupts the synthesis of GAGs and collagen, resulting in reduced production and sulfation of ECM constituents. The decreased adhesive qualities of the ECM may contribute to the inability of the palatine shelves to fuse. In addition, cell surface receptors may be altered, thereby thwarting recognition and induction of certain cell collectives.

Microtubules and microfilaments are essential contractile elements of all cells. Functioning of these elements can be affected by disrupting the synthesis and turnover of tubulin, changing the number and arrangement of microtubule organizing centers, altering the phosphorylation of tubulin-associated proteins, and perturbing tubulin polymerization. Certain antineoplastic agents incite developmental toxicity in this fashion: colchicine and vincristine distort microtubule structures, while cytochalasin B inactivates microfilaments. The actions of these cytoskeletal components can also be impacted by indirect means. Calcium (Ca^{++}) is required for appropriate microtubular and microfilamentous function; therefore, treatment with ethylenediaminetetraacetic acid (EDTA) induces heart malformations by chelating Ca^{++}, which paralyzes

pioneer cells that must move through the cardiac primordium in order to fulfill normal development.

Reduced Biosynthesis of Essential Components

Altered production of many molecules can have profound effects on normal growth and development. In this regard the usual change is decreased synthesis. All the major molecules required to support rapidly expanding tissues—nucleic acids (DNA and RNA), proteins of all kinds, and energy storage molecules (e.g., the complementary molecules adenosine di- and triphosphate (ADP and ATP, respectively)), as well as the native and phosphorylated forms of nicotinamide adenine dinucleotide (NAD and $NADP^+$, respectively)—are subject to such perturbations following xenobiotic exposure during development.

Inhibition of DNA synthesis is not teratogenic per se. However, cytotoxicity is a common outcome of reduced DNA synthesis, and the resulting cell loss can engender teratogenic effects at future stages of embryogenesis. Important factors in the outcome of such inhibition are the time available for cellular repair, which can be minimal in the rapidly dividing cell collectives that are characteristic of the embryo, and the degree of cell necrosis.

A primary reduction in RNA synthesis may inhibit DNA synthesis since some RNA variants are required for nucleic acid replication. However, decreased RNA synthesis more typically interferes with protein production, thereby depriving metabolically active cells of essential building blocks needed for growth. The degree of RNA depletion correlates well with the cytotoxic potential of many antineoplastic agents.

Inhibition of protein synthesis occurs by several mechanisms. Examples include failure to assemble ribosome complexes, which prevents protein translation; misreading of mRNA and/or premature termination and release of peptide chains, both of which results in the release of defective proteins; and the inability to perform posttranslational modification to produce functional proteins. In general, protein synthesis inhibitors yield little cytotoxicity, but they nonetheless are efficient agents for inducing embryolethality or growth retardation.

Abnormal energy metabolism is generally a critical blow to developing organisms. Inadequate reserves of ATP and NAD/$NADP^+$ can have serious effects on biosynthesis by altering the efficiency of glycolysis and electron transport during critical periods of organogenesis. As adequate energy stores are an absolute requirement for many aspects of cellular function, especially in rapidly dividing cells, it is not surprising that agents which block the synthesis of ATP and/or $NADP^+$ can have disastrous effects on the developing embryo, ranging from decreased cell function to cell death. If the degree of cell death is severe, embryonic or fetal death can follow.

Mechanical Disruption

Damage by agents that physically impact normal cytoarchitectural development can profoundly impact the viability of the conceptus. Such disruptions may sever interactions among neighboring cells, impede morphogenetic movements, and decrease proliferation and growth through pressure-induced necrosis. Changes in the local ionic balance can provoke fluid buildup within cells and fluid-filled organs (e.g., brain, eye) that ruins the integrity of these structures. For example, in the chick embryo, both dimethyl sulfoxide (DMSO) and hypoxia precipitate increases in cerebrospinal fluid (CSF) volume, which increase the pressure within the brain ventricles and spinal cord central canal. Over time, distension can exceed the elastic limits of the ependymal lining, thereby permitting escape of the CSF into the adjacent neuropil. This mechanism is thought to explain such congenital defects as *hydrocephalus* and *syringomyelia*.

Altered pressure is also thought to contribute to the genesis of ventricular septal defects (VSD), which are the most common congenital cardiac anomalies. Agents that interfere with aortic arch development can change the blood flow patterns in the heart tube. Over time the distorted flow dynamics increases the intraluminal pressure within the reorganizing heart, thereby preventing normal cardiac partitioning—and in particular, the full closure of the ventricular septum. The chronic pressure overload in the ventricles is commonly accompanied by defects in the atrial septum and/or one or more major cardiac vessels, including *patent ductus* arteriosus, tetralogy of Fallot (of which VSD is an integral component), or the transposition of the great vessels. In addition to certain xenobiotics, other etiologies capable of inducing these changes include infections (e.g., rubella) and maternal diseases (e.g., *diabetes mellitus*).

Mechanical constraint has been linked to many instances of gross malformation in external structures. Examples include mal-positioning, reduction, or amputation of the limbs as well as failed closure of the abdomen, neural tube, palate, or philtrum (middle portion of the upper lip). Abnormalities of placental structure (e.g., umbilical cord bands) or function (e.g., oligohydramnios (deficient production of amniotic fluid)) have been linked to this outcome. In like manner, aberrations of uterine structure (e.g., malformations) or function (prolonged severe contractions) have been associated with such lesions. In all these cases, the putative pathogenesis is an extrinsic increase in the

mechanical pressure applied to the surface of the developing embryo or fetus.

Heightened pressure may disrupt development by mechanisms other than direct trauma to the conceptus. A common pathway for such changes seems to be insufficient circulation to the rapidly evolving tissues. For example, vascular occlusion by tissue compression (e.g., from intense uterine contractions) will decrease organ perfusion. Alternatively, early embryonic trauma through overzealous manual pregnancy testing of cattle can cause *atresia coli* in calves. The presumed pathogenesis of such lesions is hypoperfusion, cell hypoxia, eventual endothelial cell loss, necrosis, with eventual repair by fibrosis. Developmental toxicants such as misoprostol (a synthetic prostaglandin E_1 analog) and phenytoin as well as certain placental manipulations (e.g., chorionic villous sampling) have been shown to induce leg defects in human infants by vascular disruption in limbs that had first formed normally.

Intracellular pH

The hydrogen (H^+) ion concentration in developing cells has been implicated as a common pathogenesis for many developmental toxicants. Decreased intracellular pH interferes with numerous processes, including such critical functions as proliferation, internal signaling, enzyme activity, and cytoskeletal protein polymerization. Thus it is not surprising that toxicant-induced alterations in fetal pH can produce developmental defects. Agents that have been implicated as modifiers of embryonic pH include anticonvulsants (e.g., diphenylhydantoin, sodium valproate), carbonic anhydrase inhibitors (e.g., acetazolamide), and carbon dioxide (which is converted in the body to bicarbonate (HCO_3^-)). These substances cause many types of malformations, including NTDs and postaxial right forelimb ectrodactyly.

SUMMARY

Developmental toxicology studies, including the toxicologic pathology evaluations that comprise a part of the analysis, are essential contributors to the hazard identification and risk assessment processes for novel xenobiotics. The developing embryo or fetus is often the biological system that is most sensitive to xenobiotic exposure. The complexity of developmental processes makes risk assessment for developmental toxicants fairly difficult. Major factors help produce a constantly changing spectrum of functional and structural manifestations of developmental toxicity, including tissue-specific critical periods of organogenesis; the intricate relationship between the spatial and temporal expression of various genes (especially those for morphogens and their signaling pathways); and interactions between the genotype and various metabolic processes and the toxicant. To date, research in this field has predominantly attempted to identify new hazards and develop new methods for evaluating prenatal toxicity. However, the explosion in our understanding of cellular and molecular mechanisms of teratogenesis that has accompanied the rise of bioengineering, coupled with the advent of powerful new bioinformatic and computing platforms, should permit scientists and regulators to increasingly improve their predictive capabilities, thereby allowing society to avoid, reduce, or even reverse the consequences of developmental toxicity.

Further Reading

Bolon, B., 2015. Pathology of the Developing Mouse: A Systematic Approach. CRC Press (Taylor & Francis), Boca Raton, FL.

Gupta, R.C. (Ed.), 2011. Reproductive and Developmental Toxicology. Academic Press (Elsevier), San Diego, CA.

Hood, R.D., 2012. Developmental and Reproductive Toxicology: A Practical Approach, third ed. CRC Press (Taylor and Francis), Boca Raton, FL.

McGeady, T.A., Quinn, P.J., FitzPatrick, E.S., Ryan, M.T., 2006. Veterinary Embryology. Blackwell, Oxford, United Kingdom.

Moore, K.L., Persaud, T.V.N., Torchia, M.G., 2015. The Developing Human: Clinically Oriented Embryology, tenth ed. Elsevier, New York, NY.

Gilbert-Barness, E., Spicer, D.E., Steffensen, T.S., 2014. Handbook of Pediatric Autopsy Pathology, second ed. Springer, New York.

Rossant, J., Tam, P.P.L., 2002. Mouse Development: Patterning, Morphogenesis, Organogenesis. Academic Press, San Diego.

Rousseaux, C.G., Bolon, B., 2013. Embryo and fetus. In: Haschek, W. M., Rousseaux, C.G., Wallig, M.A. (Eds.), Haschek and Rousseaux Handbook of Toxicologic Pathology, third ed. Academic Press (Elsevier), San Diego, pp. 2695–2759.

Shepard, T.H., Lemire, R.J., 2010. Catalog of Teratogenic Agents, thirteenth ed. Johns Hopkins University Press, Baltimore, MD.

Szabo, K.T., 1989. Congenital Malformations in Laboratory and Farm Animals. Academic Press, Toronto, ON, Canada.

Wolpert, L., Tickle, C., Martinez Arias, A., 2015. Principles of Development, fifth ed. Oxford University Press, Oxford, UK.

This page intentionally left blank

Index

Note: Page numbers followed by "*f*," "*t*," and "*b*" refer to figures, tables, and boxes, respectively.

B

C

D

F

H

I

O

P

Q

R

S

T

W

X

Y

Z

FUNDAMENTALS OF

TOXICOLOGIC PATHOLOGY

THIRD EDITION

MATTHEW A. WALLIG WANDA M. HASCHEK
COLIN G. ROUSSEAUX BRAD BOLON BETH W. MAHLER

Fundamentals of Toxicologic Pathology, Third Edition is an essential overview of systems toxicologic pathology presented in a clear and concise manner. Toxicologic pathology integrates toxicology and its interdisciplinary components—biochemistry, pharmacodynamics, and risk assessment—with pathology and its related disciplines—physiology, microbiology, immunology, and molecular biology.

This wholly revised and updated edition presents the newest information in systems toxicologic pathology from the previous edition, while providing context to the practice of toxicologic pathology. It includes a new section describing the application of toxicologic pathology to areas such as diagnostic and forensic toxicologic pathology, environmental toxicologic pathology, and experimental and industrial toxicologic pathology. This section likewise covers pathology issues in the design of toxicology studies. There are also new chapters on special senses (the eye and ear) and the biochemical and molecular basis of toxicity, on top of revisions and updates to all the topic areas.

The new edition is an essential reference for advanced students, early career researchers, toxicologic pathologists, pharmaceutical scientists, medical pathologists and clinicians, as well as anyone involved with drug and device development.

Related Titles

Haschek, Rousseaux, Wallig, *Handbook of Toxicologic Pathology, Third Edition*, 9780124157651, 2013.
Faqi, *A Comprehensive Guide to Toxicology in Preclinical Drug Development*, 9780123878151, 2012.
Greaves, *Histopathology of Preclinical Toxicity Studies: Interpretation and Relevance in Drug Safety Evaluation, Fourth Edition*, 9780444538567, 2011.

ACADEMIC PRESS
An imprint of Elsevier
elsevier.com/books-and-journals